

# PROCEEDING

2018 5<sup>th</sup> International Conference on Electrical Engineering, Computer Science and Informatics

Indexed by:

Scopus<sup>®</sup>

**October  
16 - 18, 2018**

Ijen Suites  
Resort & Convention  
Malang, Indonesia

Co.Organizers:





## **PROCEEDINGS**

2018 5<sup>th</sup> International Conference on Electrical Engineering,  
Computer Science and Informatics (EECSI 2018)

16-18 October 2018, Malang, Indonesia

### **Editors:**

Anton Yudhana, Universitas Ahmad Dahlan, Yogyakarta, Indonesia

Zulfatman, Universitas Muhammadiyah Malang, Indonesia

Deris Stiawan, Universitas Sriwijaya, Palembang, Indonesia

Munawar A. Riyadi, Universitas Diponegoro, Semarang, Indonesia

Imam Much Ibnu Subroto, Universitas Islam Sultan Agung, Semarang, Indonesia

Agus Eko Minarno, Universitas Muhammadiyah Malang, Indonesia

Christian Sri Kusuma Aditya, Universitas Muhammadiyah Malang, Indonesia



# **PROCEEDINGS**

## **2018 5<sup>th</sup> International Conference on Electrical Engineering, Computer Science and Informatics (EECSI 2018)**

Copyright and Reprint Permission: Abstracting is permitted with credit to the source. Libraries are permitted to photocopy beyond the limit of U.S. copyright law for private use of patrons those articles in this volume that carry a code at the bottom of the first page, provided the per-copy fee indicated in the code is paid through Copyright Clearance Center, 222 Rosewood Drive, Danvers, MA 01923. For reprint or republication permission, email to IEEE Copyrights Manager at [pubs-permissions@ieee.org](mailto:pubs-permissions@ieee.org).  
All rights reserved.

Copyright ©2018 by IEEE.

ISBN : 978-1-5386-8401-6 (USB, Part Number : CFP18B51-USB)  
ISBN : 978-1-5386-8400-9 (DVD, Part Number : CFP18B51-DVD)  
ISBN : 978-1-5386-8402-3 (XPLORE COMPLIANT, Part Number : CFP18B51-ART)

Additional copies may be ordered to:  
Lembaga Pengembangan Publikasi Ilmiah (LPPI)  
Universitas Muhammadiyah Malang  
Gedung Perpustakaan Pusat UMM, Jl. Raya Tlogomas No. 246, Malang, 65144.  
+62341-464318 Ext. 243

## EECSI 2018 Partners and Supporters

Organizer:



Sponsored by:



Technical Co. Sponsorship:



Co. Organizers:





## Foreword from General Chair EECSI 2018

### Foreword General Chair

In the name of Allah, the Most Beneficent, the Most Merciful.

Welcome to the 2018 5th International Conference on Electrical Engineering, Computer Science and Informatics (EECSI 2018) in Malang, Indonesia.

The 5th EECSI 2018 is themed “Toward the Next Generation of Technology“. This conference provides academicians, researchers, professionals, and students from various engineering fields and with cross-disciplinary working or interested in the field of Electrical Engineering, Computer Science, and Informatics to share and to present their works and findings to the world.

I would like to express my highly gratitude to all participants for attending, sharing and presenting your ideas and experiences in this interesting conference. Almost 300 papers had been submitted to EECSI 2018. However, the only high quality papers are selected and accepted to be presented in this event. We are also thankful to all the international committee, international reviewers, and steering committee for their valuable support. I would like to give a praise to all partners in publications and sponsorships for their valuable supports, especially for Ministry of Research and Higher Education (Kemenristekdikti) Indonesia.

Organizing a prestigious conference was incredibly challenging and would have been impossible to be held without outstanding committees. Such that, I would like to extend my sincere appreciation to all organizing committees and volunteers from Universitas Muhammadiyah Malang as a host and all colleagues from Universitas Diponegoro, Universitas Ahmad Dahlan, Universitas Sriwijaya, Universitas Islam Sultan Agung, Universitas Gadjah Mada, Universitas Budi Luhur, Universiti Teknologi Malaysia, and IAES Indonesia Section for providing me with much needed support, advice, and assistance on all aspects of the conference. A special thanks also for IEEE Indonesia Section for their contribution as technical co-sponsorship of the conference. We do hope that this event will encourage the collaboration among us now and in the future.

We wish you all find opportunity to get rewarding technical program, intellectual inspiration, renew friendships and forge innovation, and that everyone enjoys Malang.

**Assoc. Prof. DR. Tole Sutikno**  
**General Chair EECSI 2018**



## Foreword from IAES Indonesia Section

Bismillahirrohmannirrahim,

In the name of Allah Al Mighty, The Most Gracious, The Most Merciful

We are pleased to welcome our colleagues in the International Conference on Electrical Engineering, Computer Science and Informatics (EECSI 2018) in Malang, City of Heritage on October 16-18th, 2018.

It must be said proudly that the EECSI has been rolled out for five times since it was firstly initiated on year 2014 in Yogyakarta. Our colleagues all over the world supporting by many tops universities have successfully organized the conference to become the prestigious international annual event in Indonesia.

A highest appreciation is addressed to The Ministry of Research, Technology and Higher Education (Kemenristekdikti) Republic of Indonesia for a worthy technical and financial support during the conference and special thanks for IEEE Indonesia Section for the technical co-sponsorship for this prominent occasion. We do hope that this event will strengthen the collaboration among us now and in the future.

This year, the achievement in this conference is due to valuable contributions from our colleagues from Universitas Muhammadiyah Malang supporting by Universitas Diponegoro, Universitas Ahmad Dahlan, Universitas Sriwijaya, Universitas Islam Sultan Agung, Universitas Gadjah Mada, Universitas Budi Luhur and Universiti Teknologi Malaysia. I would like to express my sincere gratitude and appreciation for all partners, friends, Organizing committee, reviewers, keynote speakers, and participants who have made this event as great as today.

I would also like to extend my gratitude to Rector of Universitas Muhammadiyah Malang who friendly becomes a main host for this great conference. We optimist many following collaborative works will be carried out among us and all participants.

I hope you all had a nice time at the conference where all of you are able to learn something new, renewed and created new networks and at the same time have some fun in Malang City during the conference and Mount Bromo during the cultural tour.

Thank you.



**Assoc. Prof. Mochammad Facta, Ph.D**  
**IAES – Indonesia Chapter**



## Foreword from Rector of Universitas Muhammadiyah Malang

The advent of the next generation of technology, renown as Technology 4.0, is unavoidably incessant. This so-called technology has offered a new horizon in various aspects of man-beings' lives. To be particular in the fields of electrical engineering, electronics, computer science, computer engineering, and informatics, Technology 4.0 plays its potent role to underpin the future advancement of technology for the coming generations. Scientific forum titled as the 2018 5th International Conference on Electrical Engineering, Computer Science, and Informatics (EECSI 2018) hosted by University of Muhammadiyah Malang in collaboration with a number of universities is the manifestation of continuous effort to aim for the ever-changing technology.

Hereby, I would like to congratulate the Faculty of Engineering, University of Muhammadiyah Malang for their effort in organizing the 2018 5th International Conference on Electrical Engineering, Computer Science, and Informatics (EECSI 2018). I appreciate all co-organizers such as Universitas Diponegoro, Universitas Ahmad Dahlan, Universitas Sriwijaya, Universitas Islam Sultan Agung, Universitas Budi Luhur, and Universiti Teknologi Malaysia for their support in this mutual collaboration. Without the full and valuable supports from the international committee, international reviewers, and steering committee, this international conference remains a detached discourse without high commitment to conduct.

The expression of my high gratitude is devoted to the Ministry of Research, Technology, and Higher Education (Kemenristekdikti) Republic of Indonesia, IEEE Indonesia Section, and IAES Indonesia Section for their support to this event as the sponsors and technical co-sponsorship, respectively. Expectantly, this would be the initial and continual collaboration in the future.

To all speakers, presenters, and participants, thank you for participating and welcome to this conference. The success of this conference owes so much on your participation and contribution in promoting the knowledge, information, and robust creativity. To end with, this conference expectedly becomes an arena to build mutual ties among the academicians, researchers, industries, and society.

All the best to EECSI 2018

**Dr. H. Fauzan, M.Pd.**

**Rector**

**Universitas Muhammadiyah Malang - Indonesia**



# ORGANIZING COMMITTEE OF EECSI 2018 CONFERENCE

## Steering Committee

- Adam Skorek, IEEE MGA Awards and Recognition Chair (R7) Trois-Rivières, QC, Canada
- Pekik Argo Dahono, IEEE Indonesia Chapters Chair (EdSoc/EDS/PELS/SPS)
- Mochamad Ashari, Telkom University, Bandung, Indonesia
- Tumiran, Universitas Gadjah Mada, Yogyakarta, Indonesia
- Hermawan, Universitas Diponegoro, Semarang, Indonesia
- Zainudin Nawawi, Universitas Sriwijaya, Palembang, Indonesia
- Rahmat Budiarto, Albaha University, Baha, Saudi Arabia
- Sri Artini Dwi Prasetyowati, Universitas Islam Sultan Agung, Semarang, Indonesia
- Kartika Firdausy, Universitas Ahmad Dahlan, Yogyakarta, Indonesia
- Siti Nurmaini, Universitas Sriwijaya, Palembang, Indonesia
- Ahmad Mubin, Universitas Muhammadiyah Malang, Indonesia

## General Chair

- Tole Sutikno, IAES Indonesia

## Finance Chairs and Treasurer

- Wiwiek Fatmawati, Universitas Islam Sultan Agung, Semarang, Indonesia
- Lailis Syafa'ah, Universitas Muhammadiyah Malang, Indonesia
- Lina Handayani, Universitas Ahmad Dahlan, Yogyakarta, Indonesia

## Program Chairs

- Deris Stiawan, Universitas Sriwijaya, Palembang, Indonesia
- Mochammad Facta, Universitas Diponegoro, Semarang, Indonesia
- Agus Eko Minarno, Universitas Muhammadiyah Malang, Indonesia
- Machmud Effendy, Universitas Muhammadiyah Malang, Indonesia
- Fauzi Sumadi, Universitas Muhammadiyah Malang, Indonesia
- Christian Sri Kusuma Aditya, Universitas Muhammadiyah Malang, Indonesia

## General Co-Chair

- Zulfatman, Universitas Muhammadiyah Malang, Indonesia
- Anton Yudhana, Universitas Ahmad Dahlan, Yogyakarta, Indonesia

## Publication Chairs

- Munawar A. Riyadi, Universitas Diponegoro, Semarang, Indonesia
- Balza Achmad, Universitas Gadjah Mada, Yogyakarta, Indonesia
- Yuda Munarko, Universitas Muhammadiyah Malang, Indonesia
- Wahyu A. Kusuma, Universitas Muhammadiyah Malang, Indonesia

## Publicity Chairs

- Imam Much Ibnu Subroto, Universitas Islam Sultan Agung, Semarang, Indonesia
- Maskur, Universitas Muhammadiyah Malang, Indonesia
- Son Ali Akbar, Universitas Ahmad Dahlan, Yogyakarta, Indonesia
- Sam F. Chaerul, Universitas Islam Sultan Agung, Semarang, Indonesia
- Ahmad Heryanto, Universitas Sriwijaya, Palembang, Indonesia



## Public Relations Chairs

- Aina Musdholifah, Universitas Gadjah Mada, Yogyakarta, Indonesia
- Amrul Faruq, Universitas Muhammadiyah Malang, Indonesia
- Reza Firsandaya Malik, Universitas Sriwijaya, Palembang, Indonesia
- Muhammad Syafrullah, Universitas Budi Luhur, Jakarta, Indonesia
- Muhammad Qomaruddin, Universitas Islam Sultan Agung, Semarang, Indonesia
- Krisna Adiyarta, Universitas Budi Luhur, Jakarta, Indonesia

## Technical Program Members

- Syed Mohsen Naqvi, Newcastle University, UK
- Peter Balazs, Austrian Academy of Sciences, Austria
- Mohammed Alghamdi, Al-Baha University
- Marco Baldi, Università Politecnica delle Marche
- Ihsen Ben Mbarek, National Engineering School of Tunis
- Suryadip Chakraborty, Johnson C. Smith University
- July Díaz, Universidad Distrital Francisco José de Caldas
- Saurabh Dixit, Babu Banarsi Das University, Lucknow
- Wajeb Gharibi, Jazan University, KSA
- Visvasuresh Victor Govindaswamy, Concordia University
- Muhammad Abu Bakar Sidik, Universitas Sriwijaya, Indonesia
- Saied Abd El-atty, Menoufia University-Faculty of Electronic Engineering
- K. M. Mahtab Hossain, University of Greenwich
- Ahmed Mobashsher, The University of Queensland
- Ratan Kumar Mondal, Queensland University of Technology

## Technical Program Chairs

- Munawar A. Riyadi, Universitas Diponegoro, Semarang, Indonesia
- Balza Achmad, Universitas Gadjah Mada, Yogyakarta, Indonesia
- Deris Stiawan, Universitas Sriwijaya, Palembang, Indonesia
- Arief Marwanto, Universitas Islam Sultan Agung, Semarang, Indonesia
- Mudrik Alaydrus, Universitas Mercu Buana Jakarta, Indonesia
- Teddy Mantoro, Sampoerna University, Jakarta, Indonesia
- Sidiq Syamsul Hidayat, Politeknik Negeri Semarang, Semarang, Indonesia

- Kun-Da Wu, HTC Corporation
- Quanxin Zhao, University of Electronic Science and Technology of China
- Tresna Dewi, Polytechnic of Sriwijaya, Indonesia
- David Luengo, Universidad Politecnica de Madrid, Spain
- Maria Chiara Caschera, Consiglio Nazionale delle Ricerche, Rome, Italy
- Amir Nakib, Universite de Paris Est Creteil, Vitry-sur-Seine, France
- Pujianto Yugopuspito, Universitas Pelita Harapan, Indonesia
- Jens Klare, Fraunhofer-Gesellschaft, Munich, Germany
- Ramy Atawia, Queen's University, Kingston, Kingston, Canada
- Maxime Leclerc, Thales Research & Technology (TRT), Canada
- Sanjoy Debbarma, National Institute of Technology Meghalaya, Shillong, India
- Bo Kong, PLA University of Science and Technology, Nanjing, China
- Noha El-Ganainy, Arab Academy for Science & Technology and Maritime Transport, Egypt

- Rodrigo Montufar-Chaveznava, Facultad de Ingeniería, Universidad Nacional Autónoma de México
- Michel Owayjan, American University of Science & Technology
- Ljiljana Šeric, University of Split, Croatia
- Hengky Susanto, Hong Kong University of Science and Technology
- Khoirul Anwar, Telkom University, Indonesia
- Muhammad Raza, HUST Wuhan, China
- Xiaojun Li, Texas A&M University, United States
- Marco Guazzzone, University of Piemonte Orientale, Italy
- Indra Riyanto, Universitas Budi Luhur, Indonesia

### Local Arrangement, Exhibits & Registration Chairs

- Ermanu Azizul Hakim, Universitas Muhammadiyah Malang, Indonesia
- M. Irfan, Universitas Muhammadiyah Malang, Indonesia
- Galih Wasis Wicaksono, Universitas Muhammadiyah Malang, Indonesia
- Lailatul Husniah, Universitas Muhammadiyah Malang, Indonesia
- Ilham Pakaya, Universitas Muhammadiyah Malang, Indonesia
- Novendra Setiawan, Universitas Muhammadiyah Malang, Indonesia

### International Committee

- Lech M. Grzesiak, Warsaw University of Technology, Poland
- Leo P. Ligthart, Delft University of Technology, Netherlands
- Malaoui Abdessamad, University of Beni Mellal
- Muhammad Ishtiaq Ahmad, Beijing Institute of Technology
- Diego Arcos-Aviles, Universidad de las Fuerzas Armadas ESPE
- Eduard Babulak, Fort Hays State University
- Alper Bereketli, ASELSAN Inc.
- Tugçe Bilen, Istanbul Technical University
- Yue Cao, Northumbria University
- Arcangelo Castiglione, University of Salerno, Italy
- Di Chen, University of Rostock, Germany
- Paolo Crippa, Università Politecnica delle Marche
- George Dekoulis, Aerospace Engineering Institut
- Muftah Fraifer, IDC-University of Limerick
- Felix J. Garcia Clemente, University of Murcia, Spain
- Srideep Ghosh, ELTRON Wireless
- Nagendra Kumar Nainar, CISCO
- Abdellah Najid, Institut National des Postes et Télécommunications
- Gabriele Piantadosi, University of Naples Federico II
- Nadia Qasim, King's College London
- Abdalhossein Rezai, ACECR
- Zulhisyam Salleh, Universiti Teknikal Malaysia Melaka
- Hans Schotten, University of Kaiserslautern
- Min Keng Tan, Universiti Malaysia Sabah
- Revak Tyagi, Cisco Systems
- Marcel Wagner, University of São Paulo
- Hao Wu, ZTE Corporation
- Kishore Yalamanchili, Google
- Mohammed Younis, University of Baghdad
- Jing Zhou, University of Science and Technology of China
- Olympia Roeva, Institute of Biophysics and Biomedical Engineering
- Deepika Koundal, National Institute of Technology, Hamirpur
- Domenico Ciuonzo, University of Naples Federico II



- Henry Griffith, Michigan State University
- Berkin Güler, Koc University
- Jun He, University of New Brunswick
- Zhaozheng Hu, Georgia Institute of Technology
- Dimitrios Kallergis, University of Piraeus, Greece
- Fukuro Koshiji, Tokyo Polytechnic University
- Sunil Kumar, The LNM Institute of Information Technology, India
- Takashi Kurimoto, National Institute of Informatics, Japan
- Jia-Han Li, National Taiwan University
- Xiangguo Li, Henan University of Technology, China
- Sukadev Meher, National Institute of Technology, India
- Ronald Mulinde, University of South Australia
- Fernando Mussoi, Federal Institute of Santa Catarina, Brazil
- Ravi Subban, Pondicherry University, Pondicherry, India
- Andrea Fiaschetti, Università degli Studi di Roma La Sapienza, Italy
- Murali Krishna Kadiyala, Wichita State University, United States
- Zhe Zhang, Electrical and Computer Engineering Department, George Mason University
- Parag Chatterjee, Universidad Tecnológica Nacional, Buenos Aires, Argentina
- Mohamed Rehan, AvidBeam Technologies, Cairo, Egypt
- Ahmed Helmy, University of Texas at Dallas, Richardson, United States
- Harikumar Rajaguru, Anna University Chennai, India
- Feng Ouyang, Johns Hopkins University, United States
- Xuanxuan Tang, PLA University of Science and Technology, China

## TABLE OF CONTENTS

Foreword From General Chair EECSI 2018	iv
Foreword From IAES Indonesia Section	v
Foreword From Rector of Universitas Muhammadiyah Malang	vi
ORGANIZING COMMITTEE OF EECSI 2018 CONFERENCE	vii

### KEYNOTE

KN-1 : Optimization of Modified Sliding Mode Control for an Electro-Hydraulic Actuator System with Mismatched Disturbance	1
---	---

### TRACK-1 : Biomedical Engineering and Bioinformatics

T1-1 : OCT for non-destructive examination of the internal biological structures of mosquito specimen	7
T1-2 : Analysis of EMG based Arm Movement Sequence using Mean and Median Frequency	11
T1-3 : Implementation of Myo Armband on Mobile Application for Post-stroke Patient Hand Rehabilitation	16
T1-4 : Development of Embedded System for Centralized Insomnia System	22
T1-5 : Performance Analysis of Color Cascading Framework on Two Different Classifiers in Malaria Detection	27
T1-6 : Monitoring Walking Devices For Calorie Balance In Patients With Medical Rehabilitation Needs	31

### TRACK-2 : Computer Science and Applications

T2-1 : E-Government Maturity Model to Support System Dynamics in Public Policymaking	35
T2-2 : Comparative Analysis of Forensic Software on Android-based Blackberry Messenger using NIJ Framework	43
T2-3 : Semi-reactive Switch Based Proxy ARP in SDN	49
T2-4 : Improvement of Cluster Importance Algorithm with Sentence Position for News Summarization	54
T2-5 : Comparison Between A* And Obstacle Tracing Pathfinding In Gridless Isometric Game	60
T2-6 : Automatic Game World Generation for Platformer Games Using Genetic Algorithm	66
T2-7 : Middleware for Network Interoperability in IoT	70
T2-8 : Face RGB-D Data Acquisition System Architecture for 3D Face Identification Technology	74
T2-9 : Feature Expansion for Sentiment Analysis in Twitter	80
T2-10 : Web-based Campus Virtual Tour Application using ORB Image Stitching	85
T2-11 : Automatic User-Video Metrics Creations From Emotion Detection	89
T2-12 : Real Time SIBI Sign Language Recognition Based on K-Nearest Neighbor	95
T2-13 : Artificial Neural Network Parameter Tuning Framework For Heart Disease Classification	100
T2-14 : Winter Exponential Smoothing: Sales Forecasting on Purnama Jati Souvenirs Center	106

T2-15 : Analysis and Design of Decision Support System Dashboard for Predicting Student Graduation Time	110
T2-16 : Sentiment Analysis Using Support Vector Machine Algorithm	116
T2-17 : Group Formation Using Multi Objectives Ant Colony System for Collaborative Learning	122
T2-18 : Smart Traffic Light based on IoT and mBaaS using High Priority Vehicles Method	129
T2-19 : Correlation Between Bruto Domestic Products (Gdp) With Duty Schools	134
T2-20 : Mobile Learning: Utilization of Media to Increase Student Learning Outcomes	138
T2-21 : Study of the Android and ANN-based Upper-arm Mouse	144
T2-22 : FVEC feature and Machine Learning Approach for Indonesian Opinion Mining on YouTube Comments	150
T2-23 : Clustering human perception of environment impact using Rough Set Theory	156
T2-24 : E-Government Service Evaluation of Batu City Health Dept.using e-Govqual Approach and IPA Analysis	160
T2-25 : Implementation of Obfuscation Technique on PHP Source Code	164
 <b>TRACK-3 : Electrical Power Engineering</b>	
T3-1 : Power Demand Forecasting Considering Actual Peak Load Periods Using Artificial Neural Network	169
T3-2 : A New Algorithm for Designing the Parameter of Damped-Type Double Tuned Filter	175
T3-3 : Comparison of LFC Optimization on Micro-hydro using PID, CES, and SMES based Firefly Algorithm	180
T3-4 : Optimal Power Flow using Fuzzy-Firefly Algorithm	186
T3-5 : Low-Frequency Oscillation Mitigation using an Optimal Coordination of CES and PSS based on BA	192
T3-6 : Computer Aided Model for an Off-grid Photovoltaic System using Batteries Only	198
T3-7 : Computer Aided Model for a Low Voltage Varistor with Increased Thermal Stability	202
T3-8 : Smart Frequency Control using Coordinated RFB and TCPS based on Firefly Algorithm	207
T3-9 : Economic Feasibility Study of Rooftop Grid Connected PV System for Peak Load Reduction	213
T3-10 : Automatic Switching Algorithm for Photovoltaic Power Generation System	218
T3-11 : Rotor Speed Control Maximum Power Point Tracking for Small Wind Turbine	225
T3-12 : Stator Flux Oriented Control of Three-Phase Induction Motor with Improved Decoupling Scheme	231
T3-13 : Sensorless PMSM Control using Fifth Order EKF in Electric Vehicle Application	236
T3-14 : Sizing Optimization And Operational Strategy Of HRES (PV-WT) Using Differential Evolution Algorithm	242
T3-15 : Indoor Agriculture: Measurement of The Intensity of LED for Optimum Photosynthetic Recovery	249
T3-16 : Quasi Z-Source Inverter as MPPT on Renewable Energy using Grey Wolf Technique	255

T3-17 : Analysis of Waveform of Partial Discharge in Air Insulation Measured by RC Detector	260
T3-18 : Application of Ultra-Wideband Double Layer Printed Antenna for Partial Discharge Detection	266
T3-19 : Reliability Analysis of Randu Garut 3 Distribution System Using Section Technique Method	272
T3-20 : Combined Computational Intelligence Approach for the Power System Optimization Problem	278
T3-21 : Partial Discharge and Breakdown Strength of Plasma Treated Nanosilica/LDPE Nanocomposites	284
T3-22 : PSS Design Based on Fuzzy Controller with Particle Swarm Optimization Tuning	288
T3-23 : A Design of Coreless Permanent Magnet Axial Flux Generator for Low Speed Wind Turbine	292
T3-24 : Design of Hybrid System Power Management Based Operational Control System to Meet Load Demand	297
T3-25 : On The Use of Hilbert Transform Method for Enveloping Partial Discharge Signal	303
T3-26 : Circuit Simulation for Wind Power Maximum Power Point Tracking with Four Switch Buck Boost Converter	308
T3-27 : Modulation Strategies for Indirect Matrix Converter: Complexity, Quality and Performance	312
T3-28 : Review on Adjustable Speed Drive Techniques of Matrix Converter Fed Three-Phase Induction Machine	316
T3-29 : A Survey on Topologies and Controls of Z-Source Matrix Converter	322
<b>TRACK-4 : Electronics and Instrumentation</b>	
T4-1 : High Frequency Multiplier by cascading diode with high order bandpass amplifier multiple times	326
T4-2 : Bioelectrical measurement for sugar recovery of sugarcane prediction using artificial neural network	334
T4-3 : Implementation of MEMS Accelerometer for Velocity-based Seismic Sensor	339
T4-4 : Monitoring The Usage of Marine Fuel Oil Aboard Ketapang Gilimanuk Ship	345
T4-5 : Design of Low Noise Micro Liter Syringe Pump for Quartz Crystal Microbalance Sensor	349
<b>TRACK-5 : Information Systems and Technologies</b>	
T5-1 : Appropriate Sets of Criteria for Innovation Adoption of IS Security in Organizations	354
T5-2 : Self-Efficacy a Critical Factor of Information System: An Investigation using DeLone McLean	360
T5-3 : Improvement of Information Technology Infrastructure in Higher Education using IT Balanced Scorecard	365
T5-4 : A Conceptual Framework of Cloud-Based Mobile-Retail Application for Textile Cyberpreneurs	371
T5-5 : Implementation of Winnowing Algorithm for Document Plagiarism Detection	377
T5-6 : Shortest Route at Dynamic Location with Node Combination-Dijkstra Algorithm	383
T5-7 : Analysis of Consumer Confidence on Mobile Commerce in Indonesia	388



T5-8 : Social Media and User Performance in Knowledge Sharing	393
T5-9 : Learning Motivation increased due to a Relaxed Assessment in a Competitive-Learning Environment	399
T5-10 : Development of Mobile Based Educational Game as Learning Media for Basic Programming in VHS	403
T5-11 : Incident and Service Request Management for Academic Information System based on COBIT	408
T5-12 : Applying IT Services Business Relationship Management on Security Outsource Company	413
T5-13 : Implementation of the Culinary Recommendation System Using Sentiment Analysis and SAW in Bengkulu	419
T5-14 : Success Factors of HRIS: A Case of Ministry of State-owned Enterprise	424
T5-15 : Factors Affecting Users' Purchase Intention and Attitudes towards Mobile Advertising	429
T5-16 : Analysis of Electronic Medical Record Reception using Expanded Technology Acceptance Model	435
T5-17 : Implementation Strategy of Knowledge Management System: A Case of Air Drilling Associates	440
T5-18 : The Utilization of Ontology to Support The Results of Association Rule Apriori	446
T5-19 : Determination of Router Location for Optimizing Computer Network Using Dominating Set Methods	452
T5-20 : Evaluating The Semantic Mapping	458
T5-21 : The Role of Social User and Social Feature on Recommendation Acceptance in Instagram in Indonesia	464
T5-22 : User Experience Analysis of The Users Babacucu.Com	471
T5-23 : A Measurement Framework for Analyze The Influence of Service Quality and Website Quality on User Sat	477
T5-24 : Quantitative Strategic Planning Matrix Analysis On The Implementation Of Second Screen Technology	483
T5-25 : Investment Analysis of Smart Connected Motorbike in Machine to Machine Application in Indonesia	488
T5-26 : Efficiency and Reliability Performance's of the Bioinformatics Resource Portal	493
T5-27 : ISO/IEC 9126 Quality Model for Evaluation of Student Academic Portal	499
T5-28 : Measurement of IS/IT Investment on the Implementation of ERP and the Effect on company productivity	505
T5-29 : Analysis on Customer Satisfaction Dimensions in P2P Accommodation using LDA: A Case Study of Airbnb	511
T5-30 : Individual Factors As Antecedents of Mobile Payment Usage	517
T5-31 : Determine supporting features for mobile application of NUSANTARA	522
T5-32 : Knowledge Management Maturity Assessment in Air Drilling Associates using G-KMMM	528
T5-33 : Measuring Knowledge Management Readiness of Indonesia Ministry of Trade	534
T5-34 : Personal Extreme Programming with MoSCoW Prioritization for Developing Library Information System	540

## **TRACK-6 : Networks and Telecommunication Systems**

T6-1 : ML-Optimized Beam-based Radio Coverage Processing in IEEE 802.11 WLAN Networks	545
T6-2 : Single-Tone Doppler Radar System for Human Respiratory Monitoring	552
T6-3 : Dual Frequency Continuous Wave Radar for Small Displacement Detection	557
T6-4 : A New Method for Minimizing the Unnecessary Handover in High-Speed Scenario	561
T6-5 : Automate Snort Rule For Xss Detection With Honeypot	565
T6-6 : Substrate Integrated Waveguide Bandpass Filter with Complementary Split Ring Resonator at 2.45 GHz	570
T6-7 : UUID Beacon Advertisements For Lecture Schedule Information	574
T6-8 : Comparative Performance Analysis of Linear Precoding in Downlink Multi-user MIMO	581
T6-9 : Application of LoRa WAN Sensor and IoT for Environmental Monitoring in Riau Province Indonesia	585
T6-10 : Co-channel Interference Monitoring based on Cognitive Radio Node Station	590
T6-11 : Simulation of Mobile LoRa Gateway for Smart Electricity Meter	596
T6-12 : Rain Attenuation Statistics over 5G Millimetre Wave Links in Malaysia	602
<b>TRACK-7 : Robotics, Control and Automation</b>	
T7-1 : Fuzzy Logic Controller Design for Leader-Follower Robot Navigation	606
T7-2 : Arm Robot Manipulator Design and Control for Trajectory Tracking; a Review	612
T7-3 : Vibration Control of Magnetorheological Elastomer Beam Sandwich	618
T7-4 : Magnetorheological Elastomer Stiffness Control for Tunable Vibration Isolator	622
T7-5 : Improving a Wall-Following Robot Performance with a PID-Genetic Algorithm Controller	626
T7-6 : A Review of Solar Tracker Control Strategies	631
T7-7 : Robust and Accurate Positioning Control of Solar Panel System Tracking based Sun Position Image	636
T7-8 : Robust Adaptive Sliding Mode Control Design with Genetic Algorithm for Brushless DC Motor	642
T7-9 : Active Fault Tolerance Control for Sensor Fault Problem in Wind Turbine Using SMO with LMI Approach	648
<b>TRACK-8 : Signal, Image and Video Processing</b>	
T8-1 : Measurement of Thermal Expansion Coefficient on Electric Cable Using X-Ray Digital Microradiography	653
T8-2 : A Relative Rotation between Two Overlapping UAV's Images	658
T8-3 : Re-Ranking Image Retrieval on Multi Texton Co-Occurrence Descriptor Using K-Nearest Neighbor	664
T8-4 : Human Detection using Aggregate Channel Features with Kalman Filtering Image Processing	669
T8-5 : Automatic Estimation of Human Weight From Body Silhouette Using Multiple Linear Regression	675
T8-6 : Variance and Symmetrical-based Approach for Optimal Alignment of 3D Model	679
T8-7 : The Recognition Of Semaphore Letter Code Using Haar Wavelet And Euclidean Function	685

T8-8 : Adventure Game Show:Audience Involvement, Destination Image and Audience Behavior	690
T8-9 : Visual Emotion Recognition Using ResNet	696
T8-10 : A Feature-Based Fragile Watermarking of Color Image for Secure E-Government Restoration	702
 <b>TRACK-9 : Soft Computing and Intelligent System</b>	
T9-1 : Aspect Based Sentiment Analysis approach with CNN	707
T9-2 : Optimal ANFIS Model for Forecasting System Using Different FIS	713
T9-3 : Automated Diagnosis System of Diabetic Retinopathy Using GLCM Method and SVM Classifier	719
T9-4 : Development of Discrete-Cockroach Algorithm (DCA) for Feature Selection Optimization	726
T9-5 : Narrow Window Feature Extraction for EEG-Motor Imagery Classification using k-NN and Voting Scheme	732
T9-6 : Emotion Recognition using Fisher Face-based Viola-Jones Algorithm	738
T9-7 : IDenet: Inception-Based Deep Convolutional Neural Network for Crowd Counting Estimation	743
T9-8 : Multispectral Imaging and Convolutional Neural Network for Photosynthetic Pigments Prediction	749
T9-9 : Application for the diagnosis of pneumonia based on Pneumonia Severity Index (PSI) values	755
T9-10 : Impact of Matrix Factorization and Regularization Hyperparameter on a Recommender System for Movies	761
T9-11 : Object Detection of Omnidirectional Vision Using PSO-Neural Network for Soccer Robot	765
T9-12 : DSS Scheme Using Forward Chaining-Simple Multi Attribute Rating Technique For Cocoa Beans Selection	770
T9-13 : CountNet: End to End Deep Learning for Crowd Counting	776
T9-14 : Sentiment Analysis Based on Appraisal Theory for Assessing Incumbent Electability	781
T9-15 : Robust Principal Component Analysis for Feature Extraction of Fire Detection System	787
T9-16 : Indonesian Id Card Recognition using Convolutional Neural Networks	791
T9-17 : Sarcasm Detection on Indonesian Twitter Feeds	795

# Optimization of Modified Sliding Mode Control for an Electro-Hydraulic Actuator System with Mismatched Disturbance

Mohd. Fuaad Rahmat  
School of Electrical Engineering  
Faculty of Engineering,  
Universiti Teknologi Malaysia  
Johor Bahru, Johor  
fuaad@fke.utm.my

Siti Marhainis Othman  
Mechatronic Engineering  
Programme,  
School of Mechatronic  
Engineering, Universiti  
Malaysia Perlis  
Perlis, Malaysia  
marhainis@unimap.edu.my

Sahazati Md. Rozali  
Department of Electrical  
Engineering Technology,  
Faculty of Engineering  
Technology, Universiti Teknikal  
Malaysia Melaka  
Melaka, Malaysia  
sahazati@utem.edu.my

Zulfatman Has  
Department of Electrical  
Engineering,  
University of Muhammadiyah  
Malang  
Malang, Indonesia  
zulfatman@umm.ac.id

**Abstract**—This paper presents a modified sliding mode controller (MSMC) for tracking purpose of electro-hydraulic actuator system with mismatched disturbance. The main contribution of this study is in attempting to find the optimal tuning of sliding surface parameters in the MSMC using a hybrid algorithm of particle swarm optimization (PSO) and gravitational search algorithms (GSA), in order to produce the best system performance and reduce the chattering effects. In this regard, Sum square error (SSE) has been used as the objective function of the hybrid algorithm. The performance was evaluated based on the tracking error identified between reference input and the system output. In addition, the efficiency of the designed controller was verified within a simulation environment under various values of external disturbances. Upon drawing a comparison of PSOGSA with PSO and GSA alone, it was learnt that the proposed controller MSMC, which had been integrated with PSOGSA was capable of performing more efficiently in trajectory control and was able to reduce the chattering effects of MSMC significantly compared to MSMC-PSO and MSMC-GSA, respectively when the highest external disturbance, 10500N being injected into the system's actuator.

**Keywords**— *electro-hydraulic, mismatched disturbance, modified sliding mode control, particle swarm optimization; gravitational search algorithm*

## I. INTRODUCTION

The Electro-Hydraulic Actuator (EHA) system, due to its excessive strength to weight ratio and stiffness reaction being more precise, smooth and fast, is one of the crucial force systems in industrial sectors and most engineering practices around the world. Owing to such wide applications, the best overall performance of the electro-hydraulic actuators with regards to its position, force or pressure is necessary. It is however worthy of note that the system is tremendously nonlinear due to many elements, such as leakage, friction, and specifically, the fluid flow expression through the servo valve [1]. Such characteristics, which are prevalent within the system have significantly contributed to the degradation of its overall performance. Upon closely looking into studies such as [2]–[4], it was discovered that the sliding mode control (SMC) as efficient and broadly implemented in comparison

with the nonlinear EHA system. It was particularly observed that most of the existing outcomes on sliding surface design have been focused on the matched uncertainties and disturbances attenuation since the sliding motion of conventional SMC is insensitive to matched uncertainties and disturbance [5]. In other words, the uncertainties and disturbances exist within the identical channel as that control input. However, it has been widely proven in related studies that the uncertainties present in many practical systems may not fulfil the so-called matching condition.

In the present study, the dynamic model and design requirement of electro-hydraulic actuator were taken from the National Institute for Aerospace Research, Romania [6]. Within the dynamic model used, the track input disturbance acts on a different channel from the control input. In the case of such systems, the sliding motion of conventional SMC is critically tormented by the mismatched disturbance and the well-known robustness of SMC may no longer preserve anymore. Owing to the importance of attenuating mismatched uncertainties and disturbances with regards to the practical applications, many researchers have committed themselves to the sliding surface design for uncertain systems with mismatched disturbance. Interestingly, it was also discovered that some related studies in the literature had used conventional SMC with some amendment in its sliding surface. One possible reason for such a change is to help enhance the capability of the modified SMC (MSMC).

In the case of [7], it was learnt that the proportional integral type sliding characteristic was used as a modification of conventional SMC. The proposed modified sliding characteristic is capable of improving the steady state and dynamic performance in DC-DC buck converter application. In the study by [8], the sliding mode control approach was modified from the synchronization of a single dynamic system into the synchronization of a complex network. Besides, there were also studies that had made some modifications into the sliding surface [9], [10]. Owing to some of the significant advantages of the MSMC in dealing with the complex situations, the present study has relied on MSMC in electro-hydraulic actuator with mismatched disturbance.

In addition, parameter estimation has been identified as one of the ways, through which the accuracy of MSMC can be improved. Hybrid optimization is quite well-known in many application [11][12]. Several studies have proposed the combination of GSA and PSO it was through such studies, it was learnt that the combination of PSO and GSA is capable of providing improved results for general mathematical functions [13][14]. However, both have looked into the generic algorithms and it has yet to be specifically applied to estimate the parameters of MSMC controller for mismatched disturbance system such as an electro-hydraulic actuator such as the case in the present study[15][14]. More importantly, no studies, at least to the knowledge of the researcher, have considered looking into parameters estimation for MSMC to enhance its accuracy and performance.

Specifically, the present study concerns the performance comparison between MSMC that had been optimized by using PSO, GSA and PSOGSA. In this regard, comparative assessment of this triple optimization method to the system performance is presented and discussed. The main contents of this article are sequenced in the following order: Section II illustrates the mathematical modelling of the developed system. Section III delineates the MSMC algorithm derivation. Moving on, the optimization algorithms used are presented in section IV. The results from observations are presented, compared and discussed in Section V. Lastly, a brief summary and conclusions are provided in Section VII.

## II. ELECTRO-HYDRAULIC ACTUATOR (EHA) MODELING

The actuator dynamic equation of electro-hydraulic actuator servo system with the external disturbance being injected into its actuator is expressed [6].

$$\dot{x}_1 = x_2 \quad (1)$$

$$\dot{x}_2 = -\frac{k}{m}x_1 - \frac{f}{m}x_2 + \frac{s}{m}x_3 - \frac{F_L}{m} \quad (2)$$

$$\dot{x}_3 = -\frac{s}{k}x_2 - \frac{k_l}{k_c}x_3 + \frac{c}{k_c}\sqrt{\frac{P_a - x_3}{2}}k_v \quad (3)$$

Table 1 shows the parameters of electro hydraulic actuator servo system which are represented by (1), (2) and (3).

TABLE I. TABLE TYPE PARAMETER OF EHA SERVO SYSTEM

Parameters	Value	Unit
Load at the EHA rod ( $m$ )	0.33	$Ns^2/cm$
Piston Area ( $S$ )	10	$cm^2$
Coefficient of viscous friction ( $f$ )	27.5	$Ns/cm$
Coefficient of aerodynamic elastic force ( $k$ )	1000	$N/cm$
Valve port width ( $w$ )	0.05	$cm$
Supply pressure ( $P_a$ )	2100	$N/cm^2$
Coefficient of volumetric flow of the valve port ( $c_d$ )	0.63	—
Coefficient of internal leakage ( $k_l$ )	$2.38 \times 10^{-3}$	$cm^5/Ns$
Coefficient of servo valve ( $k_v$ )	0.017	$cm/V$
Coefficient involving bulk modulus and EHA volume ( $k_c$ )	$2.5 \times 10^{-4}$	$cm^5/N$
Oil density ( $\rho$ )	$8.87 \times 10^{-7}$	$Ns^2/cm^4$

## III. CONTROLLER DESIGN AND STABILITY

The objective of the control design is to achieve a continuous sliding control,  $u$ , such that the output of the system tracks the desired input as closely as possible. At given desired position trajectory,  $x_{id}$  the control objective is to design a bounded control input,  $u$ . Hence the output position,  $x_p$  tracks as closely as possible to the desired position trajectory,  $x_{id}$ . The design of modified sliding mode control involves two main steps. The first step is to select the appropriate sliding surface for the desired sliding motion. The trajectories are enforced to lie on the sliding surface. The desired position of trajectory is as  $x_d = [x_{1d}, x_{2d}, x_{3d}]^T \in R^n$ , and defined as  $\dot{x}_{1d} = x_{2d}$ ,  $\dot{x}_{2d} = x_{3d}$ . In addition, the vector of the system states are assumed measurable and defined as  $x = [x_1, x_2, x_3]^T = [x_p, v_p, P_L]^T \in R^n$ . The state error of the system is defined as

$$e_i = x_i - x_{id} \quad (5)$$

where  $i = 1$  to 3 and  $e \in R^n$ .

In order to ensure that the states of the system successfully tracks the desired trajectories at the same time, the function of a new sliding surface was proposed as in [3].

$$S(t) = x_2 + x_3 + c_1 e_1 + c_2 \int e_1 \quad (6)$$

where  $c_1$  and  $c_2$  are strictly positive constants. The idea behind the designed controller is that a switching gain is designed to force the states to achieve the integral sliding surface, and then the integral action in the sliding surface drives the states to the desired equilibrium in the presence of mismatched uncertainties, nonlinearities or disturbance. The desired dynamic response for the system is given as  $S = \dot{S} = 0$  when the sliding surface is moving. Therefore, it can be obtained as:

$$e_1 = -\dot{x}_2 - \dot{x}_3 - c_2 e_1 \quad (7)$$

The tracking error  $e_1$  is defined as :

$$e_1 = x_1 - x_{1d} \quad (8)$$

In order to obtain the control law, the constant plus proportional reaching law method was applied [16][17]. The reaching law is used to reduce the chattering, since the chattering caused by non-ideal reaching at the end of reaching phase, and also the easy to obtain the control law. The dynamics of the switching function are directly specified by this approach which is described by the reaching function of the form

$$\dot{S} = -Q \text{sign}(S) - KS \quad (9)$$

where  $Q$  and  $K$  are constant with positive value and  $\text{sign}(S)$  representing the signum function which has a piecewise function as below:

$$\text{sign}(S) = \begin{cases} 1 & ; S > 0 \\ 0 & ; S = 0 \\ -1 & ; S < 0 \end{cases} \quad (10)$$

Since the controller is designed to achieve a better tracking accuracy in positioning, a smaller boundary layer is usually required. Hence, an optimal balance between the position error and the level of control chattering can be accomplished by adjusting the thickness of the boundary layer and accordingly, it can be given as



$$\dot{S} = -Qsat(S/\phi) - KS \quad (11)$$

In this regard, that the derivative of (6) gives

$$\dot{S} = \dot{x}_2 + \dot{x}_3 + c_1 \dot{e}_1 + c_2 \dot{e}_1 \quad (12)$$

The control law is obtained by substituting (1) (2) and (3) in (12). Therefore, the control law can be stated as,

$$u = \frac{k_c}{ck_v} \sqrt{\frac{2}{p_a - x_3}} \left[ -Qat(S/\phi) - KS + \frac{k}{m} x_1 + \frac{f}{m} x_2 - \frac{s}{m} x_3 + \frac{F_L}{m} + \frac{s}{k_c} x_2 + \frac{k_l}{k_c} x_3 - c_1 \dot{x}_1 + c_1 \dot{x}_{1d} - c_2 x_1 + c_2 x_{1d} \right] \quad (13)$$

If the initial output trajectory is not on the sliding surface  $S(t)$ , or a deviation of the representative point detected from  $S(t)$  due to variations observed in parameter and/or disturbances, the controller must be designed in such a way that it can drive the output trajectory to the sliding mode  $S(t) = 0$ .

The output trajectory, in such a condition will move towards and reach the sliding surface, and is said to be on the reaching phase. For this purpose, the Lyapunov function can be expressed as

$$V(t) = \frac{1}{2} S^2(t) \quad (14)$$

where  $V(t) > 0$  and  $V(0) = 0$  for  $S(t) \neq 0$ . The reaching condition as presented in (15) is considered as necessary as that will help ensure the trajectory moving from the reaching phase to the sliding phase in a stable condition.

$$\dot{V}(t) = S(t)\dot{S}(t) < 0, \text{ for } S(t) \neq 0 \quad (15)$$

By choosing the Lyapunov function candidate as in (14) and (15), the reaching condition is rearranged as

$$V(t) = \frac{1}{2} S^2(t) = S(t)\dot{S}(t) \leq -\alpha|S(t)| \quad (16)$$

where  $\alpha \in R$  must be a strictly positive design parameter. By means of (6) and (12) by excluding its reaching time function, Equation (16) can be rewritten as

$$\dot{V} = S\dot{S} \leq -\alpha|S| \quad (17)$$

Therefore,

$$S \left[ \left[ -\frac{k}{m} x_1 - \frac{f}{m} x_2 + \frac{s}{m} x_3 - \frac{F_L}{m} \right] + \left[ -\frac{s}{k_c} x_2 - \frac{k_l}{k_c} x_3 + \frac{c}{k_c} \sqrt{\frac{p_a - x_3}{2}} k_v u \right] + c_1 [\dot{x}_1 - \dot{x}_{1d}] + c_2 [x_1 - x_{1d}] \right] \leq -\alpha|S| \quad (18)$$

$$S \left[ \left[ -\frac{k}{m} x_1 - \frac{f}{m} x_2 + \frac{s}{m} x_3 - \frac{F_L}{m} \right] + \left[ -\frac{s}{k_c} x_2 - \frac{k_l}{k_c} x_3 + \frac{c}{k_c} \sqrt{\frac{p_a - x_3}{2}} k_v \left[ \frac{k_c}{ck_v} \sqrt{\frac{2}{p_a - x_3}} \left[ -Qat(S/\phi) - KS + \frac{k}{m} x_1 + \frac{f}{m} x_2 - \frac{s}{m} x_3 + \frac{F_L}{m} + \frac{s}{k_c} x_2 + \frac{k_l}{k_c} x_3 - c_1 \dot{x}_1 + c_1 \dot{x}_{1d} - c_2 x_1 + c_2 x_{1d} \right] \right] + c_1 [\dot{x}_1 - \dot{x}_{1d}] + c_2 [x_1 - x_{1d}] \right] \right] \leq -\alpha|S| \quad (19)$$

$$\text{Let assume } \hat{g} = \frac{c}{k_c} \sqrt{\frac{p_a - x_3}{2}} k_v, X = -\frac{k}{m} x_1 - \frac{f}{m} x_2 + \frac{s}{m} x_3 - \frac{F_L}{m}, Y = \frac{s}{k_c} x_2 + \frac{k_l}{k_c} x_3, Z = -c_1 \dot{x}_1 + c_1 \dot{x}_{1d} - c_2 x_1 + c_2 x_{1d},$$

Therefore;

$$\begin{aligned} S[X + [-Y + \hat{g}[g^{-1}[-Qsgn(S) - KS - X + Y + Z]]] - Z] &\leq -\alpha|S| \\ S[X - Y + \hat{g}g^{-1}[Y - X + Z] - Z] + \alpha|S| &\leq -S[\hat{g}g^{-1}[-Qsgn(S) - KS]] \\ S[-\beta[-X + Y + Z] + [Y - X + Z]] + \beta\alpha|S| &\leq Q|S| + KS \\ S[(1 - \beta)[-X + Y + Z]] + \beta\alpha|S| &\leq Q|S| + KS \\ Q &\geq [(1 - \beta)[-X + Y + Z]] + \beta\alpha - K \end{aligned} \quad (20)$$

The switching gain,  $Q$  help ensure the closed loop system to be robust and asymptotically stable upon the control gain and external disturbance. Therefore, in this study, the value of switching gain,  $Q$  will be determined by using optimization algorithm.

#### IV. HYBRIDIZATION OF PARTICLE SWARM OPTIMIZATION AND GRAVITATIONAL SEARCH ALGORITHM

PSO and GSA share some similarities in relation to their formulation. For that reason, another way to hybridize PSO and GSA are to deal with any particle in the swarm as a particle added through PSO and/or GSA by means of making use of the co-evolutionary technique. PSOGSA, is proposed by means of using cooperative behaviours of the particles tormented by both PSO velocity and GSA acceleration to help enhance the performance of the respective algorithms [13]. Therefore, the two phrases the velocity updating formulation in PSOGSA consists of the cooperative contributions of PSO velocity and GSA acceleration.

$$\begin{aligned} v_i^d(t+1)_{PSO} &= w(t)v_i^d(t) + c_1 r_1^d(t)[pbest_i^d - x_i^d(t)] \\ &\quad + c_2 r_2^d(t)[gbest_i^d - x_i^d(t)] \end{aligned} \quad (21)$$

$$v_i^d(t+1)_{GSA} = rand_i \times v_i^d(t) + a_i^d(t) \quad (22)$$

$$\begin{aligned} v_i^d(t+1)_{PSOGSA} &= wv_i^d(t)_{PSO} + c_a r_1^d(t)_{GSA}[pbest_i^d - x_i^d(t)_{PSO}] \\ &\quad + c_b r_2^d(t)[gbest_i^d - x_i^d(t)_{PSO}] \end{aligned} \quad (23)$$

where Equation (21) is obtained from PSO velocity formulation and Equation (22) comes from GSA velocity formulation and Equation (23) is the PSOGSA velocity formulation updated by PSO velocity and GSA acceleration. Determination of control parameters of the designed controller is considered crucial for accurate tracking performance. Therefore, the PSOGSA are applied to determine the most reliable sliding surface and foremost gain of the designed MSMC. Fig. 1 shows the block diagram of the MSMC with PSOGSA algorithm.

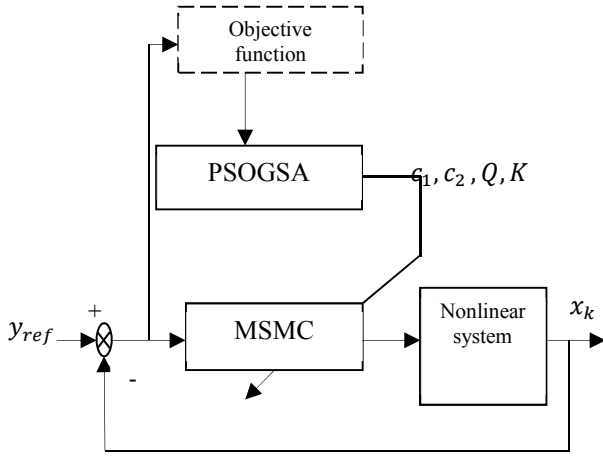


Fig. 1. Block diagram of the MSMC with PSOGSA algorithm

MSMC designed for electro-hydraulic actuator servo system includes four control parameters,  $c_1$ ,  $c_2$ ,  $Q$  and  $K$ . The value of these parameters need to be selected with the intention of minimizing the tracking error. Therefore, in order to enhance the adaptation function of the system, PSOGSA are used to search for the best value of these parameters through the integration of MSMC with this algorithm. PSOGSA caters to this venture primarily based on SSE as an objective function. The formula of SSE is given by

$$SSE = \sum_{k=1}^n (x_k - y_{ref})^2 \quad (24)$$

where  $k$  is the number of iteration,  $x_k$  is the system output at  $k$  iteration and  $y_{ref}$  is the reference input given to the system. The goal of the optimization algorithm is to help minimize SSE.

## V. SIMULATION RESULTS AND COMPARISONS

Simulation was carried out by means of using MATLAB/Simulink 2015 software. MSMC is known to help the system track a shaped square wave signal. The references trajectory and the value of external disturbance, 10500 N which was used in this study is similar to that of [18] and [19].

The implementation of optimization algorithms has used the following parameters, i.e., the number of particles,  $i$  is set at 5, 10, 15, 20 and 25 particles. The initial value of the number of iteration,  $t$  was set at 10 and it was increased to 20, 30, 40 and 50 iterations. As for the presentation of results in this section, the output plot yielded by 5 particles within 10 iterations, 15 particles within 30 iterations and 25 particles within 50 iterations were selected in order to observe the performance of the designed controller with small, medium and bigger number of particles and iterations, respectively. The value of the number of particles and iterations were selected in order to prove that the small number of these parameters will culminate in good tracking performance.

In order to prove the capability of the MSMC, which is not effected on the existence of disturbances for mismatched system, the conventional SMC (CSMC) which was similar to the one used by [20], was utilized for benchmarking and comparison with MSMC. This comparison was performed solely as basic test with the purpose to highlight the primary capabilities of the MSMC. Furthermore, it was designed with the best parameters of CSMC. Parameters for the CSMC were tuned by the same optimization algorithm, namely PSO, GSA

and PSOGSA. Moreover, the analysis was carried out through the comparison between MSMC and CSMC in terms of their performances of employing different optimization.

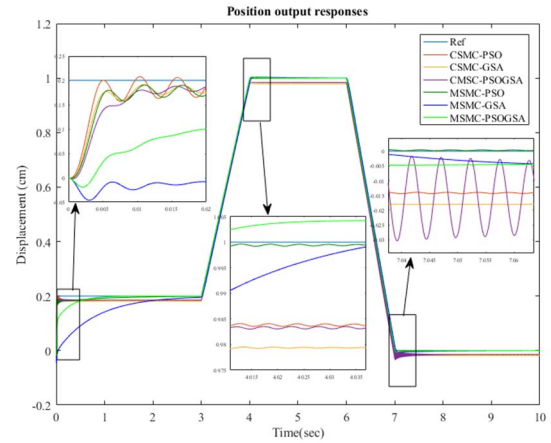


Fig. 2. Position output for CSMC and MSMC, integrated with PSO, GSA and PSOGSA with 5 particles within 10 iterations for external disturbance, 10500N

Based on Fig. 2, through the combination of MSMC with PSO, GSA and PSOGSA, the system output tracked the reference input with different accuracies. Initially, the lowest number of particles and iterations were used, which were 5 and 10 respectively. With this combination, MSMC-PSO was able to exhibit the best system output in comparison to the system output of the MSMC-GSA and MSMC-PSOGSA. This was the inclusion of the values of SSE amounting to 32.4511, 1609 and 147.3797 respectively, as shown in Table 2. In the case of CSMC, the values of SSE for designed controller that which was combined with PSO, GSA and PSOGSA were 232.1030, 370.9705 and 189.8791 respectively. As seen in Fig. 2, at the same external disturbance value, the MSMC shows more accuracy that the CSMC in the aspect of tracking when by 5 particles and 10 iterations are used to find the optimum values of each parameter for both controller. This indicates the lower values of SSE produced by MSMC.

TABLE II. SSE OBTAINED FROM COMBINATION OF MSMC AND CSMC WITH PSO, GSA AND PSOGSA

	CSMC			MSMC		
	PSO	GSA	PSOGSA	PSO	GSA	PSOGSA
<b>i5, t10</b>	232.1050	370.9705	189.8791	32.4511	1609	147.3797
<b>i15, t30</b>	232.1031	308.0041	85.9871	32.5014	746.6484	17.1532
<b>i25, t50</b>	232.1030	234.5374	80.9007	32.7035	881.2971	19.3152

In Fig. 2, even though the MSMC-PSO produces oscillate output at each corner of the output, but the values of SSE is the lowest and capable of tracking the reference input given accurately with minimal error in comparison with the MSMC-GSA and MSMC-PSOGSA. It clearly shows that PSO managed to comprehend the optimum combination of the parameter with the lowest SSE. The output performance of MSMC-GSA was obviously the worst. The SSE value for MSMC-GSA drastically decreased by from 1609 to 746 and then it went up to 881. However, these values still cannot match the performances outputs that had been shown by MSMC-PSOGSA and MSMC-PSO. The SSE value for MSMC-PSO was still around 32 while the SSE value for MSMC-PSOGSA slightly increased to 19.

Fig. 3 and 4 show the position output for CSMC and MSMC, integrated with PSO, GSA and PSO-GSA with 15 particles within 30 iterations and 25 particles within 50 iterations, respectively for external disturbance, 10500N. From both figure, obviously can see chattering occurs along the output response produced by CSMC that been optimized by PSO, GSA and PSO-GSA. MSMC-PSO has the tendency to track reference input given with SSE values being 32.5014 and 32.7035 in both conditions. This situation does not change much with previous MSMC-PSO output response when  $i$  and  $t$  are 5 and 10, respectively.

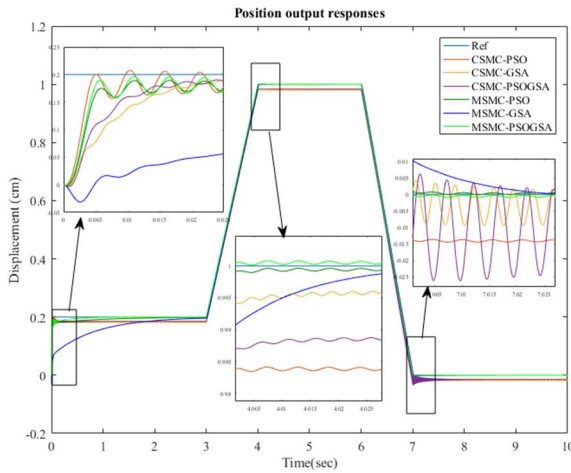


Fig. 3. Position output for CSMC and MSMC, integrated with PSO, GSA and PSO-GSA with 15 particles within 30 iterations for external disturbance, 10500N

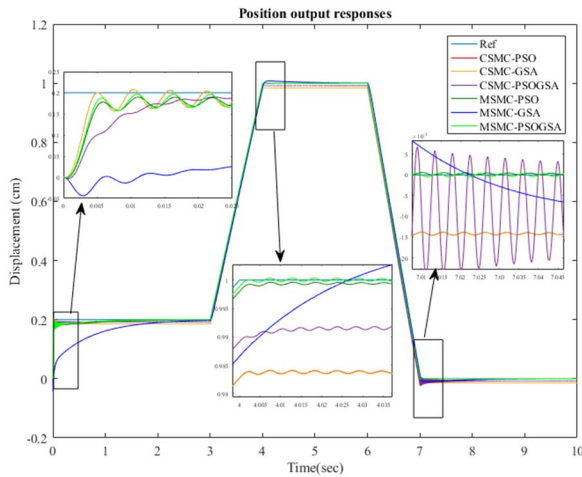


Fig. 4. Position output for CSMC and MSMC, integrated with PSO, GSA and PSO-GSA with 25 particles within 50 iterations for external disturbance, 10500N

Meanwhile, the output response for MSMC-GSA was not found to produce chattering and has shown a smooth and steady output response with respect to the reference input given but the SSE value was the largest with 746.6484 and 881 for both conditions. MSMC-PSOGSA output response showed relatively smaller chattering at each corner when the reference input changed its form and the SSE values given by MSMC-PSOGSA were the smallest with 17.1532 and 19.3152 for both conditions, respectively. Although an increase in SSE value of about 2 was observed, but the value was still too small compared to the MSMC-PSO and MSMC-

GSA. For GSA, even though no chattering produced but the performance output given was the worst compared to MSMC-PSOGSA and MSMC-PSO. MSMC-PSOGSA revealed an excellent improvement in terms of output response in the event of an increase being observed in the number of particles and iterations compared to MSMC-PSO. However, the SSE produced by MSMC-PSO did not show much improvement with a reduction rate and addition of about 0.1 in comparison with the MSMC-PSOGSA with SSE reduction from 147 to 17. By means of increasing the number of particles and iterations from 5 and 10, to 25 and 50, the performance output of MSMC-PSOGSA was seen as the best compared to another two methods. As the researchers were looking for the optimum combination which was capable of producing the lowest SSE value among CSMC and MSMC, integrated with PSO, GSA and PSO-GSA, therefore the optimum combination number of particles,  $i$  and iterations,  $t$  for the best performance output which produced the lowest SSE is shown in Table 3.

TABLE III. OPTIMUM COMBINATION NUMBER OF PARTICLES,  $i$  AND ITERATIONS,  $t$  WHICH PRODUCED THE LOWEST SSE

	CSMC			MSMC		
	PSO	GSA	PSOGSA	PSO	GSA	PSOGSA
Number of particles, $i$	25	25	15	20	20	15
Number of iteration, $t$	50	50	50	40	40	30
SSE	232.10	234.54	72.70	32.66	758.47	17.15

Referring to Table 3, the integration of MSMC and PSO-GSA yielded lower SSE value compared to MSMC-GSA and MSMC-PSOGSA. By means of combining both PSO velocity and GSA acceleration, PSO-GSA managed to obtain the optimum combination of parameters and the best performance of system output compared to PSO and GSA alone. With the lowest SSE value of PSO-GSA (17.1532), the combination of 15 particles/agents within 30 iterations was required. However, compared to PSO, the combination of 20 particles/agents within 40 iterations was required with obtained SSE value of 32.6515, which was almost 15 units bigger than the PSO-GSA. It should be noted that the tracking errors of both PSO and PSO-GSA were almost non-existent. Besides that, PSO-GSA was found to track the given reference smoothly with only minimal chattering at the beginning. This reaffirmed that the optimum combination of parameters can effectively reduce the chattering issue.

## VI. CONCLUSION

In this study, a hybrid algorithm of particle swarm optimization (PSO) and gravitational search algorithms (GSA) based modified sliding mode control (MSMC) for solving tracking control accuracy in the mismatched electro-hydraulic actuator are presented. With the presence of large external disturbance, the integration of MSMC with PSO-GSA potentially enhances the performance and produces relatively higher accuracy in tracking the reference signal given to the system. Such a development clearly indicates that MSMC-PSOGSA has the potentials to overcome the presence of external disturbance for mismatched system, reduce the chattering effectively and enhances the performance based on the lowest SSE, which is 17.1532. Future works may have to consider applying MSMC-PSOGSA and looking into its performance with mismatched electro-hydraulic actuator that is injected with uncertainties

and nonlinearities to help enhance the complexity of the system and at the same time, to verify the robustness of MSMC-PSOGSA to effectively deal with more complex nonlinear systems.

#### ACKNOWLEDGMENT

The authors would like to acknowledge Universiti Teknologi Malaysia (UTM), Universiti Malaysia Perlis (UNIMAP) and Ministry of Higher Education (MOHE) of Malaysia for their support.

#### REFERENCES

- [1] C. Kaddissi and J. Kenn, "Identification and Real-Time Control of an Electrohydraulic Servo System Based on Nonlinear Backstepping," *IEEE Transactions on Mechatronics*, vol. 12, no. 1, pp. 12–22, 2007.
- [2] H. Zhang, X. Liu, J. Wang, and H. R. Karimi, "Robust  $H_\infty$  sliding mode control with pole placement for a fluid power electrohydraulic actuator (EHA) system," *International Journal of Advanced Manufacturing Technology*, vol. 73, no. 5–8, pp. 1095–1104, 2014.
- [3] S. Wang, R. Burton, and S. Habibi, "Sliding Mode Controller and Filter Applied to an Electrohydraulic Actuator System," *Journal of Dynamic Systems, Measurement, and Control*, vol. 133, no. 2, p. 24504, 2011.
- [4] Z. Has, M. F. Rahmat, A. R. Husain, and K. Ishaque, "Robust Position Tracking Control of an Electro-Hydraulic Actuator in the Presence of Friction and Internal Leakage," *Arabian Journal for Science and Engineering*, vol. 39, no. 4, pp. 2965–2978, Nov. 2013.
- [5] H. H. Choi, "LMI-Based Sliding Surface Design for Integral Sliding Mode of Mismatched Uncertain Systems," *IEEE Transactions on Automatic Control*, vol. 52, no. 4, pp. 736–742, 2007.
- [6] I. Ursu, F. Ursu, and F. Popescu, "Backstepping design for controlling electrohydraulic servos," *Journal of the Franklin Institute*, vol. 343, no. 1, pp. 94–110, Jan. 2006.
- [7] B. B. Naik and A. J. Mehta, "Sliding mode controller with modified sliding function for DC-DC Buck Converter," *ISA Trans.*, 2017.
- [8] C. Li, L. Lü, G. Zhao, G. Li, J. Tian, J. Gu, and Z. Wang, "Projective synchronization of uncertain scale-free network based on modified sliding mode control technique," *Physica A*, vol. 473, pp. 511–521, 2017.
- [9] M. M. Ghanbarian, M. Nayeripour, and A. Rajaei, "Design and implementation of a new modified sliding mode controller for grid-connected inverter to controlling the voltage and frequency," *ISA Transactions*, vol. 61, pp. 179–187, 2016.
- [10] M. Soleymani, A. H. Abolmasoumi, H. Bahrami, A. Khalatbari-s, E. Khoshbin, and S. Sayahi, "Modified sliding mode control of a seismic active mass damper system considering model uncertainties and input time delay," *Journal of Vibration and Control*, 2016.
- [11] M. Dehghani, M. Mashayekhi, and E. Salajegheh, "Topology optimization of double- and triple-layer grids using a hybrid methodology," *Engineering Optimization*, vol. 48, no. 8, pp. 1333–1349, 2016.
- [12] L. C. Cagnina, S. C. Esquivel, and C. A. C. Coello, "Solving constrained optimization problems with a hybrid particle swarm optimization algorithm," *Engineering Optimization*, vol. 43, no. 8, pp. 843–866, Aug. 2011.
- [13] S. Mirjalili, S. Zaiton, and M. Hashim, "A New Hybrid PSOGSA Algorithm for Function Optimization," *International Conference on Computer and Information Application (ICCIA 2010)*, no. 1, pp. 374–377, 2010.
- [14] S. Mirjalili, S. Zaiton, M. Hashim, and H. M. Sardroudi, "Training feedforward neural networks using hybrid particle swarm optimization and gravitational search algorithm," *Applied Mathematics and Computation*, vol. 218, pp. 11125–11137, 2012.
- [15] E. Rashedi, H. Nezamabadi-pour, and S. Saryazdi, "GSA: A Gravitational Search Algorithm," *Information Sciences*, vol. 179, no. 13, pp. 2232–2248, Jun. 2009.
- [16] J. Y. Hung, W. Gao, and J. C. Hung, "Variable Structure Control: A Survey," *IEEE Transactions on Industrial Electronics*, vol. 40, no. 1, pp. 2–22, 1993.
- [17] I. M. M. Hassan, a. M. Mohamed, and a. I. Saleh, "Variable structure control of a magnetic suspension system," *Proceedings of the 2001 IEEE International Conference on Control Applications (CCA'01) (Cat No01CH37204)*, pp. 333–338, 2001.
- [18] S. Md Rozali, M. Fua'ad Rahmat, and A. R. Husain, "Performance Comparison of Particle Swarm Optimization and Gravitational Search Algorithm to the Designed of Controller for Nonlinear System," *Journal of Applied Mathematics*, pp. 1–9, 2014.
- [19] S. M. Othman, M. F. Rahmat, S. M. Rozali, Z. Has, and A. F. Z. Abidin, "Optimization of Modified Sliding Mode Controller for an Electro-hydraulic Actuator system with Mismatched Disturbance," *International Journal of Electrical and Computer Engineering*, vol. 8, no. 4, pp. 31–43, 2018.
- [20] Sahazati Md. Rozali, "Optimized Back-stepping Controller for Position Tracking of Electro-hydraulic Actuators," *Phd Thesis*, 2014.

# OCT for non-destructive examination of the internal biological structures of mosquito specimen

Naresh Kumar Ravichandran  
School of Electronics Engineering,  
College of IT Engineering  
Kyungpook National University  
Daegu, South Korea  
nareshr.9169@gmail.com

Jaeseok Park  
School of Electronics Engineering,  
College of IT Engineering  
Kyungpook National University  
Daegu, South Korea  
pjs0307zz@knu.ac.kr

Pilun Kim  
Institute of Biomedical Engineering,  
Kyungpook National University  
Daegu, South Korea  
pukim@knu.ac.kr

Byoung-Ju Yun  
School of Electronics Engineering,  
College of IT Engineering  
Kyungpook National University  
Daegu, South Korea  
bjisyun@ee.knu.ac.kr

Deokmin Jeon  
School of Electronics Engineering,  
College of IT Engineering  
Kyungpook National University  
Daegu, South Korea  
dmjeon@knu.ac.kr

Byeonggyu Jeon  
School of Electronics Engineering,  
College of IT Engineering  
Kyungpook National University  
Daegu, South Korea  
xel700@knu.ac.kr

Kwang Shik Choi  
School of Life Sciences  
Kyungpook National University  
Daegu, South Korea  
kcs@knu.ac.kr

Mansik Jeon\*  
School of Electronics Engineering,  
College of IT Engineering  
Kyungpook National University  
Daegu, South Korea  
msjeon@knu.ac.kr

Junsoo Lee  
School of Electronics Engineering,  
College of IT Engineering  
Kyungpook National University  
Daegu, South Korea  
ljlee5399@knu.ac.kr

Sangbong Lee  
School of Electronics Engineering,  
College of IT Engineering  
Kyungpook National University  
Daegu, South Korea  
emg0218@knu.ac.kr

Hee-Young Jung  
School of Applied Biosciences  
Kyungpook National University  
Daegu, South Korea  
heeyoung@knu.ac.kr

Jeehyun Kim  
School of Electronics Engineering,  
College of IT Engineering  
Kyungpook National University  
Daegu, South Korea  
jeehk@knu.ac.kr

**Abstract**—The Study of mosquitoes and their behavioral analysis are of crucial importance to control the alarmingly increasing mosquito-borne diseases. Conventional imaging techniques use either dissection, exogenous contrast agents. Non-destructive imaging techniques, like x-ray and microcomputed tomography uses ionizing radiations. Hence, a non-destructive and real-time imaging technique which can obtain high resolution images to study the anatomical features of mosquito specimen can greatly aid researchers for mosquito studies. In this study, the three-dimensional imaging capabilities of optical coherence tomography (OCT) for structural analysis of *Anopheles sinensis* mosquitoes has been demonstrated. The anatomical features of *An. sinensis* head, thorax, and abdomen regions along with internal morphological structures like foregut, midgut, and hindgut were studied using OCT imaging. Two-dimensional (2D) and three-dimensional (3D) OCT images along with histology images were helpful for the anatomical analysis of the mosquito specimens. From the concurred results and by exhibiting this as an initial study, the applicability of OCT in future entomological researches related to mosquitoes and changes in its anatomical structure is demonstrated.

**Keywords**—optical coherence tomography, *Anopheles sinensis*, non-destructive imaging, internal morphological analysis.

## I. INTRODUCTION

These mosquitoes are recognized as one of the major vectors of tropical diseases such as malaria, dengue, chikungunya, West Nile virus, yellow fever, lymphatic filariasis, Japanese encephalitis, Zika fever, and many other blood-transmittable diseases [1]. Approximately 212 million cases of malaria occurred in 2015, resulting in the death of approximately 429 000 people [2]. By recent findings, it has been concluded that Zika virus infection in pregnancy can be a cause of microcephaly [3]. Pathogens causing these diseases are transmitted from a mosquito to a host during blood feeding. Thus, research on mosquitoes, their feeding habits [4], probing behavior [5], life cycle [6], and the associated pathogen transmission plays a major role.

To date, many techniques such as micro-computed tomography [7], microscopic and histological analysis [8, 9], and X-ray imaging [10] have been implemented for mosquito studies. However, these techniques require time-consuming sectioning processes, a complex system design, or a long imaging acquisition time. Moreover, the cost of these techniques may be prohibitive for frequent implementation. Thus, a rapid bio-imaging technique would be of considerable advantage to researchers.

Optical coherence tomography (OCT) is a non-destructive imaging modality, which acquires cross-sectional images in real-time [11]. Applications of OCT have been demonstrated in various field of research, including ophthalmology [12, 13], otorhinolaryngology [14, 15], industrial inspection [16], agronomical studies [17-19]. Recently, OCT has been applied in various entomological studies, such as those developing neural morphological analysis and cardiac dynamics in *Xenopus laevis* [20, 21], age estimation of *Calliphora vicina* pupae [22], and

---

This work was supported by Korea Institute of Planning and Evaluation for Technology in Food, Agriculture, Forestry and Fisheries (IPET) through Advanced Production Technology Development Program, funded by Ministry of Agriculture, Food and Rural Affairs (MAFRA) (No. 314031-3). Also supported by BK21 plus project funded by the Ministry of Education, Korea (21A20131600011).



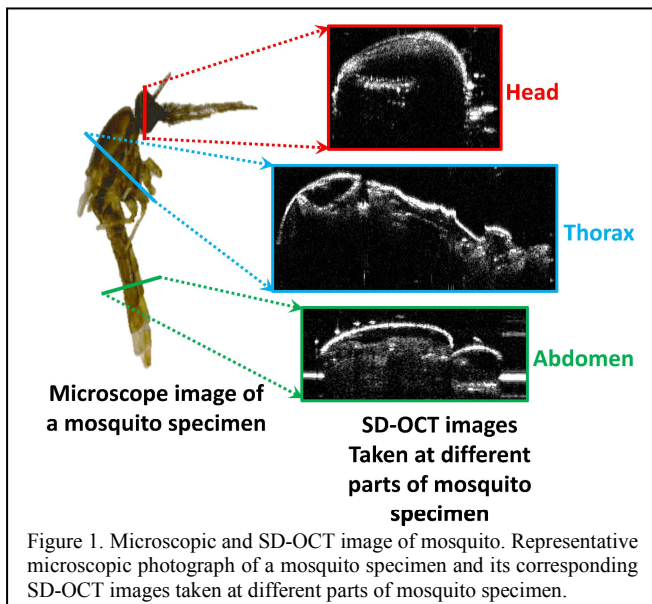
arrhythmia caused by a *Drosophila* Tropomyosin mutation [23]. However, there have been no reports on the use of OCT as a tool for studying the internal organs of mosquito specimens.

In this study, we undertook a morphological analysis of *Anopheles sinensis* mosquitoes using spectral domain OCT (SD-OCT). Thus, we have demonstrated the potential application of OCT for identification of internal morphology in mosquito specimens. This was a feasibility study and by analyzing the results of two-dimensional and three-dimensional OCT images using histological images, we have demonstrated the advantages of using OCT for analysis of mosquito organs and tissue structures for future studies.

## II. MATERIALS AND METHODS

### A. Preparation of Mosquito Specimen for Experiment

Mosquito samples were collected in 2014 at Majeong-ri, Paju-si (37°52'53.52"N, 126°45'24.89"E), Republic of Korea, using a black light trap. Specimens were identified using the molecular method described by [24] (the methods used and the detailed explanation of the procedures followed for identification of specimen has been explained in previously published article). After DNA extraction from a single leg using a genomic DNA extraction kit (Bioneer, Korea). The PCR conditions were as follows: The 12.5- $\mu$ L PCR reaction mixture contained 0.5  $\mu$ L genomic DNA of an individual mosquito, 0.5 units of Taq polymerase, 0.4  $\mu$ M of each primer (see [24] for primer information), 1.5 mM MgCl<sub>2</sub>, 0.2 mM of each dNTP, and 1 X PCR buffer. The PCR cycling conditions were as follows: initial denaturation at 94 °C for 3 min, followed by 30 cycles at 94 °C for 30 sec, 55 °C for 30 sec, 72 °C for 2 min, and a final extension at 72 °C for 7 min. The PCR products were electrophoresed and visualized using ethidium bromide 2.5% agarose gel and a gel imaging system.



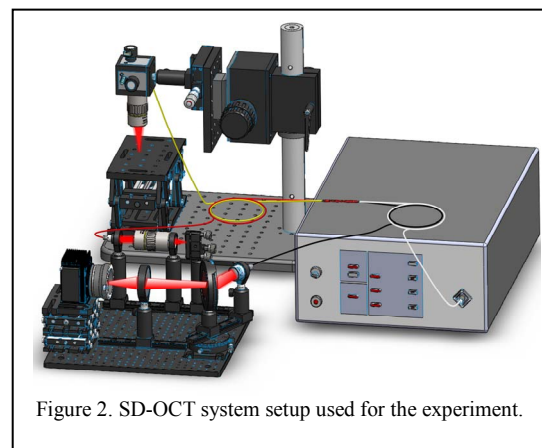
A representative image of a mosquito specimen is shown in figure 1. After being anesthetized, specimens were carefully separated and stored. The experimental environment was maintained at 23 °C and 50% humidity. OCT imaging was carried out immediately after the specimens were anesthetized. For experimental convenience, the wings and the legs were clipped carefully without damaging other parts of the specimen.

### B. Specimen Preparation For Histological Analysis

The specimens were fixed in 2% paraformaldehyde and 2.5% glutaraldehyde in 0.05 M sodium cacodylate buffer for 24 hours under vacuum. Thereafter, the specimens were washed in sterile distilled water and dehydrated in a graded series of absolute ethanol (30%, 50%, 70%, 80%, and 90%) for 30 min. These steps are considered as gold standard methods for histological sectioning analysis [25]. These dehydrated specimens were infiltrated with propylene oxide and then embedded in Spurr's resin. The resin was polymerized in a dry oven at 80 °C for 7hrs. Finally, the samples were accurately sectioned using an ultra-microtome (MT-7000; RMC, Tucson, AZ, USA) and, stained with 2% methylene blue and observed under a light microscope.

### C. SD-OCT System Setup

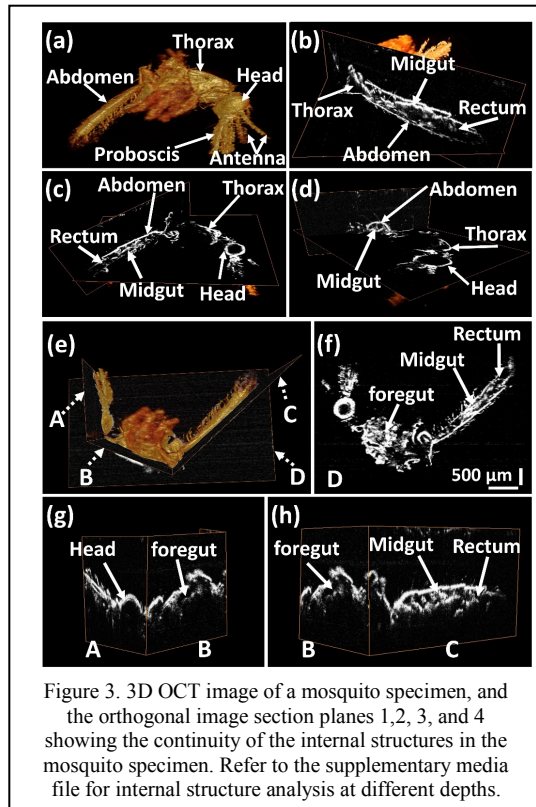
The OCT system was operated with a broadband light source with a center wavelength of 860 nm and a bandwidth of 165 nm. Objective lenses (10X) were used in reference



and sample arms to improve the lateral resolution. The axial and lateral resolution of the OCT were 4 and 10  $\mu$ m. The detailed configurations of the OCT instrumentation are provided elsewhere [19]. The schematic setup of the overall system is shown in figure 2.

## III. RESULTS AND DISCUSSION

### A. Three Dimensional Volumetric Image Analysis



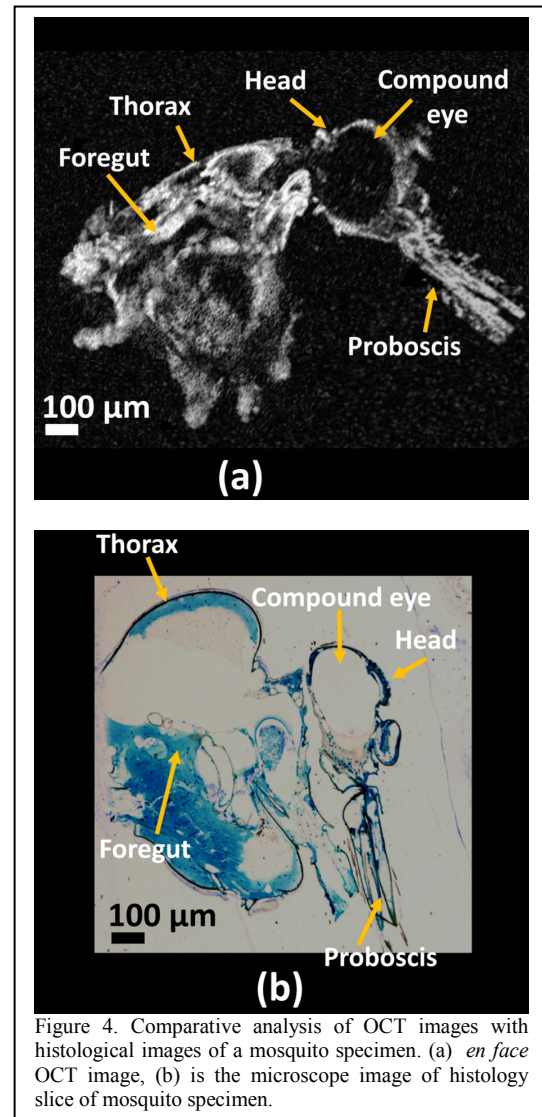
Cross-sectional OCT images were acquired from the head, thorax, and abdominal regions of a mosquito body. Tomograms of the mosquito internal organs were studied by obtaining adjacent 2D-OCT images of all three regions. Using these prominent cross-sectional images, the 3D OCT images of these internal structures were rendered by acquiring adjacent 2D-OCT images and combining these images using volume-rendering software.

The volumetric OCT image is shown in figure 3(a). Figures 3(b), 3(c), and 3(d) show the orthogonal-sectioned images of the 3D images, revealing the internal morphology of head, thorax, and abdominal regions. The midgut and hindgut are shown in figures 3(c) and 3(d). In addition, individual sections of the head, thorax, and abdominal regions are shown in figure 3(e) using orthogonal sectioning planes, which are represented by dotted arrows with representations plane-1, plane-2, plane-3, and plane-4. The foregut, midgut, and hindgut are clearly identifiable through the individually sectioned images. The orthogonal image section planes-1, 2, and 3 helps to visualize the continuity of the internal structures in the specimen, showing the entire cross-section for easier analysis.

#### B. Comparison Of Histology Images With OCT Images

For comparison of OCT images with the obtained histological images, 3D volumetric images were orthogonally sliced at different depths using post-image analysis software, the most correlative OCT image was selected for histological comparison. Figures 4(a) and 4(b) emphasize the comparison between OCT and histology of head and thorax regions. Foregut, head, proboscis, compound eye, and other internal structures in the thorax region are visualized in the OCT image, which are consistent

with the histological image. The midgut and hindgut along with other internal abdominal structures are visible in the OCT image, was also found to be in correlation with the obtained histological image.



#### IV. CONCLUSION

We have demonstrated the benefits of three-dimensional imaging capability of OCT for structural analysis of *An. sinensis* mosquitoes. Internal structures, such as foregut, midgut, and hindgut, were clearly visualized using a customized OCT system supported by histological image verifications. To date, initial morphological studies and analysis of the anatomical structures of mosquitoes using OCT have not been performed. The results of the present study may represent a significant contribution and future in vivo studies on different mosquito vectors of disease-causing pathogens using OCT may help researchers to better understand how diseases are transmitted via mosquito bites. Future experiments can be focused on improving the resolution of the investigating OCT system by increasing the bandwidth of the laser source and detector, by improving the optical transmission of the OCT system for efficient signal

detection [26-28] and for reduction of noise which may improve system sensitivity.

## REFERENCES

- [1] M. A. Tolle, "Mosquito-borne diseases," *Current problems in pediatric and adolescent health care*, vol. 39, no. 4, pp. 97-140, 2009.
- [2] C. A. Guerra *et al.*, "The limits and intensity of Plasmodium falciparum transmission: implications for malaria control and elimination worldwide," *PLoS Med*, vol. 5, no. 2, p. e38, 2008.
- [3] D. Fiorentino and F. Montero, "The Zika Virus and Pregnancy," *Current Obstetrics and Gynecology Reports*, vol. 5, no. 3, pp. 234-238, 2016.
- [4] K. B. Platt, K. J. Linthicum, K. Myint, B. L. Innis, K. Lerdtusnee, and D. W. Vaughn, "Impact of dengue virus infection on feeding behavior of Aedes aegypti," *The American journal of tropical medicine and hygiene*, vol. 57, no. 2, pp. 119-125, 1997.
- [5] L. A. Moreira, E. Saig, A. P. Turley, J. M. Ribeiro, S. L. O'Neill, and E. A. McGraw, "Human probing behavior of Aedes aegypti when infected with a life-shortening strain of Wolbachia," *PLoS Negl Trop Dis*, vol. 3, no. 12, p. e568, 2009.
- [6] W. J. Crans, "A classification system for mosquito life cycles: life cycle types for mosquitoes of the northeastern United States," *Journal of Vector Ecology*, vol. 29, pp. 1-10, 2004.
- [7] Y.-R. Ha, S.-C. Lee, S.-J. Seo, J. Ryu, D.-K. Lee, and S.-J. Lee, "Comparison of the functional features of the pump organs of Anopheles sinensis and Aedes togoi," *Scientific reports*, vol. 5, 2015.
- [8] W. JIRAUNGKOORSKUL, "Larvicidal and histopathological effects of Andrographis paniculata leaf extract against Culex quinquefasciatus larva," *Walailak Journal of Science and Technology (WJST)*, vol. 13, no. 2, pp. 133-140, 2015.
- [9] G. P. League, O. C. Onuh, and J. F. Hillyer, "Comparative structural and functional analysis of the larval and adult dorsal vessel and its role in hemolymph circulation in the mosquito Anopheles gambiae," *Journal of Experimental Biology*, vol. 218, no. 3, pp. 370-380, 2015.
- [10] H. Iwamoto, "X-ray diffraction pattern from the flight muscle of Toxorhynchites towadensis reveals the specific phylogenetic position of mosquito among Diptera," *Zoological letters*, vol. 1, no. 1, p. 1, 2015.
- [11] D. Huang *et al.*, "Optical coherence tomography," *Science*, vol. 254, no. 5035, pp. 1178-1181, 1991.
- [12] M. F. Shirazi, R. E. Wijesinghe, N. K. Ravichandran, P. Kim, M. Jeon, and J. Kim, "Dual-path handheld system for cornea and retina imaging using optical coherence tomography," *Optical Review*, pp. 1-7, 2016.
- [13] R. E. Wijesinghe *et al.*, "Optically deviated focusing method based high-speed SD-OCT for in vivo retinal clinical applications," *Optical Review*, vol. 23, no. 2, pp. 307-315, 2016.
- [14] N. H. Cho, S. H. Lee, W. Jung, J. H. Jang, and J. Kim, "Optical Coherence Tomography for the Diagnosis and Evaluation of Human Otitis Media," *Journal of Korean medical science*, vol. 30, no. 3, pp. 328-335, 2015.
- [15] R. E. Wijesinghe, N. H. Cho, K. Park, M. Jeon, and J. Kim, "Bio-Photonic Detection and Quantitative Evaluation Method for the Progression of Dental Caries Using Optical Frequency-Domain Imaging Method," *Sensors*, vol. 16, no. 12, p. 2076, 2016.
- [16] M. F. Shirazi *et al.*, "Fast industrial inspection of optical thin film using optical coherence tomography," *Sensors*, vol. 16, no. 10, p. 1598, 2016.
- [17] N. K. Ravichandran *et al.*, "In vivo monitoring on growth and spread of gray leaf spot disease in capsicum annum leaf using spectral domain optical coherence tomography," *Journal of Spectroscopy*, vol. 2016, 2016.
- [18] R. Wijesinghe, S.-Y. Lee, N. K. Ravichandran, M. F. Shirazi, and P. Kim, "Optical screening of Venturianashicola caused Pyruspyrifolia (Asian pear) scab using optical coherence tomography," *International Journal of Applied Engineering Research*, vol. 11, no. 12, pp. 7728-7731, 2016.
- [19] N. K. Ravichandran *et al.*, "Depth enhancement in spectral domain optical coherence tomography using bidirectional imaging modality with a single spectrometer," *Journal of Biomedical Optics*, vol. 21, no. 7, pp. 076005-076005, 2016.
- [20] S. A. Boppart, B. E. Bouma, M. E. Brezinski, G. J. Tearney, and J. G. Fujimoto, "Imaging developing neural morphology using optical coherence tomography," *Journal of Neuroscience Methods*, vol. 70, no. 1, pp. 65-72, 1996.
- [21] A. Bradu, L. Ma, J. W. Bloor, and A. Podoleanu, "Dual optical coherence tomography/fluorescence microscopy for monitoring of Drosophila melanogaster larval heart," *Journal of biophotonics*, vol. 2, no. 6 - 7, pp. 380-388, 2009.
- [22] K. Brown and M. Harvey, "Optical coherence tomography: age estimation of Calliphora vicina pupae in vivo?," *Forensic science international*, vol. 242, pp. 157-161, 2014.
- [23] L. Ma, A. Bradu, A. G. Podoleanu, and J. W. Bloor, "Arrhythmia caused by a Drosophila tropomyosin mutation is revealed using a novel optical coherence tomography instrument," *PLoS One*, vol. 5, no. 12, p. e14348, 2010.
- [24] D. Joshi, M. Park, A. Saeung, W. Choochote, and G. Min, "Multiplex assay to identify Korean vectors of malaria," *Molecular ecology resources*, vol. 10, no. 4, pp. 748-750, 2010.
- [25] A. E. Feldstein *et al.*, "Hepatocyte apoptosis and fas expression are prominent features of human nonalcoholic steatohepatitis," *Gastroenterology*, vol. 125, no. 2, pp. 437-443, 2003.
- [26] D. Semrau *et al.*, "Achievable information rates estimates in optically amplified transmission systems using nonlinearity compensation and probabilistic shaping," *Optics letters*, vol. 42, no. 1, pp. 121-124, 2017.
- [27] G. Liga, T. Xu, A. Alvarado, R. I. Killely, and P. Bayvel, "On the performance of multichannel digital backpropagation in high-capacity long-haul optical transmission," *Optics Express*, vol. 22, no. 24, pp. 30053-30062, 2014.
- [28] R. Maher *et al.*, "Spectrally shaped DP-16QAM super-channel transmission with multi-channel digital back-propagation," *Scientific reports*, vol. 5, p. 8214, 2015.

# Analysis of EMG based Arm Movement Sequence using Mean and Median Frequency

B.N. Cahyadi

School of Mechatronic University  
Malaysia Perlis (UniMAP)  
Faculty Engineering of Technology  
Perlis, Malaysia  
basrinoorc@gmail.com

Wan Khairunizam

School of Mechatronic University  
Malaysia Perlis (UniMAP)  
Faculty Engineering of Technology  
Perlis, Malaysia  
khairunizam@unimap.edu.my

M. Nor Muhammad

Center for Diploma Studies, University  
Malaysia Perlis (UniMAP)  
Faculty Engineering of Technology  
Perlis, Malaysia  
matnor@unimap.edu.my

I. Zunaidi

School of Mechatronic University  
Malaysia Perlis (UniMAP)  
Faculty Engineering of Technology  
Perlis, Malaysia  
zunaidi@yahoo.com

S.H. Majid

School of Mechatronic University  
Malaysia Perlis (UniMAP)  
Faculty Engineering of Technology  
Perlis, Malaysia  
saimajid16@gmail.com

Rudzuan M.N

School of Mechatronic University  
Malaysia Perlis (UniMAP)  
Faculty Engineering of Technology  
Perlis, Malaysia  
rudzuan@unimap.edu.my

S.A. Bakar

School of Mechatronic University  
Malaysia Perlis (UniMAP)  
Faculty Engineering of Technology  
Perlis, Malaysia

Z.M. Razlan

School of Mechatronic University  
Malaysia Perlis (UniMAP)  
Faculty Engineering of Technology  
Perlis, Malaysia

W.A. Mustafa

School of Mechatronic University  
Malaysia Perlis (UniMAP)  
Faculty Engineering of Technology  
Perlis, Malaysia

**Abstract** — This paper present the studies of analysis arm movement sequence which dedicated for upper limb rehabilitation after stroke. The recovery of the arm could be optimized if the rehabilitation therapy is in a right manner. Upper limb weakness after stroke is prevalent in post-stroke rehabilitation, many factors that can deficit muscle strength there are neural, muscle structure and function change after stroke. Rehabilitation process needs to start as soon as after a stroke attack, repetitive and conceptualized. On the other hand monitoring of muscle activity also need in the rehabilitation process to evaluate muscle strength, motor function and progress in the rehabilitation process. The objective of this research is to analysis arm movement sequence using the feature frequency domain. In this study deltoid, biceps and flexor carpum ulnaris (FCU) muscles will be monitored by surface electromyography (sEMG). Five healthy subjects male and female become participants in data recording. Mean frequency (MNF) and median frequency (MDF) domain are two signals processing technique used for arm movement sequence analyzing. The analysis result showed that MNF is better than MDF where MNF produced higher frequency than MDF from each segment. From the data analysis, this movement sequence design more focuses on deltoid and FCU muscles treatment. This movement sequence has five condition movements. First undemanding, second difficult, third moderate, fourth moderate and the last cool-down movements. The best movement sequence minimum has four condition movements warming up – moderate – difficult – cool-down.

**Keywords**— Electromyography (EMG), rehabilitation, mean frequency, median frequency, movement sequence

## I. INTRODUCTION

A Stroke is a “brain Attack”. Based on the cause stroke divide into two, the first is hemorrhagic stroke it occurs when there is a blood vessel leak in an area of the brain and the second is a blood vessel carrying blood to the brain is blocked by a blood clot (ischemic). When blood flow to an area of the brain is cut off, so brain cells are deprived of oxygen and begin to die. When brain cells die during a stroke, abilities controlled by that area of the brain such as

memory and muscle control are lost [3]. In 2017 World Health Organization (WHO) published that the second leading of death is stroke accident where more than 15 million people have strokes every year and two-thirds of them have the permanent disability [1]. Rehabilitation after post-stroke is an important and ongoing part of treatment. With the right treatment and the rehabilitation procedures, stroke patients can enjoy normal life is possible. Physical therapy is one of the most important parts in the rehabilitation process where it can help a person relearn movement and coordination. It is important to stay active, even if it is difficult at first [2]. Rehabilitation upper limb after post stroke is indispensable because upper limb motion is very important for the human daily activities such as eating, drinking, brushing teeth, combing hair and washing face [4]. In this time many therapies do the post-stroke rehabilitation using fundamental movement and a play traditional equipment like table and glass. This technique needs more time and there is no feedback from rehabilitations proses.

One of the major objectives of post-stroke rehabilitation is to improve patient’s motor function as it is critically elated to the ability of independent living [5]. The previous scientist explained that motor impairment and muscle strength can be covered or treated with active movement in the oriented and repetitive task, with combinations movement which can improve motor skills and muscular strength by avoiding a muscle and joint pain [6][11]. Studies in post-stroke rehabilitation reported that the most important in process rehabilitation is the monitoring of muscle activity during recovery [7]. Much information can be obtained from the muscle and the researchers can use that information in their study by measuring the electromyography (EMG) signal [8]. This research will analyze of EMG signal based arm movement sequence for post-stroke rehabilitation using mean and median frequency domain.

The outline of this research paper consists of four sections, the first section is an introduction and related



researches, in the second section the proposed research methodologies and the third section discusses the finding of the research. The conclusions of this research are discussed in the last section.

## II. METHODOLOGIES

Fig. 1 shows the workflow for this research from a preparation of the hardware and software until discussion and conclusion.

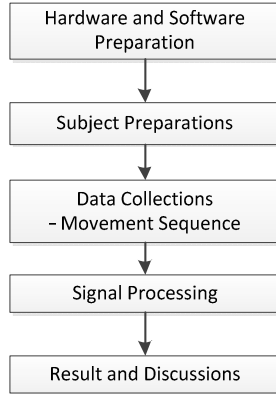


Fig. 1. The flow of the investigation

### A. Hardware and Software Preparations

Data collections in this research used DELSYS Bagnoli EMG system with 8 input channels and EMG works 4.3.2 software used to communicate with a personal computer. Muscle activity in this movement will detect using surface electromyogram sensor type single differential. Raw EMG signal will analyze using software MATLAB r2016a.

### B. Subject Preparation

Five students between the ages of 23 and 30 years old include male and female in good conditions were prepared for this experiment. The participants were graduate or undergraduate students of University Malaysia Perlis. Before data collecting, every subject briefed on experimental procedures and their signature used as approval to be participants. Using healthy subjects caused this research is a laboratory prototype for EMG signal studying and movement sequence were used in this research is applicable for post-stroke patients.

### C. Data Collection

#### I. EMG Signal Acquisition

EMG data were recorded by three surface electrodes on upper limb muscle include deltoid, biceps and FCU muscles. Data recording was done for 30 seconds with frequency 1 kHz using EMG acquisition system.

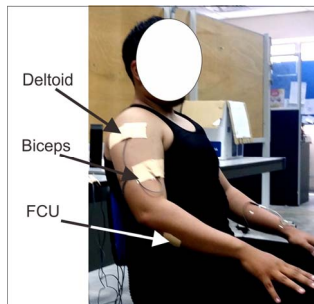


Fig. 2. Sensor placement

## II. Movement Sequence

Arm movement sequences were designed based on the fundamental arm movements to stimulate the weak muscle of post-stroke patient [6]. Repetitive rehabilitation exercise based on fundamental movement is one of the method used in the treatment, the combination of some fundamental movement which produces a movement sequence can increase treatment timing. Motor impairment and coordination between one muscle with another muscle can be treated by movement sequence repetitively [11][14].

Arm movement sequence designed based on fundamental movement which involves flexion, extension and grasp. Design of movement sequence use of three objects as targets, the design of functional movement shows in fig 3. Target number one located on the right patients, target two located on the top of patients and target three located on the left of patients. Firstly participants put their hand at the start point for five seconds after rehabilitation begins, then participants take an object in the start point and move it to target one and back to start point then rest about five seconds. Next targets have the same steps as target one.

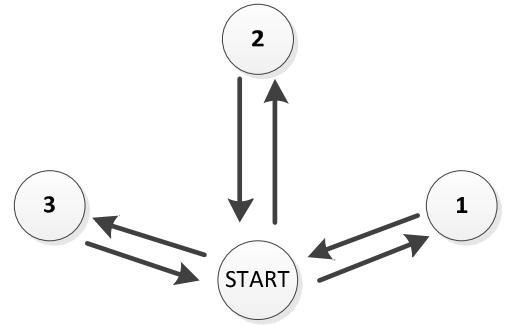


Fig. 3. Movement Sequence [6]

### D. Signal Processing

#### I. Power Spectral Density

Power Spectral Density (PSD) is defined as the amount of power per frequency interval. To transform signal EMG based on time domain to frequency domain need a furrier transform. To search frequency signal components which brought by time domain signal. The most commonly used PSD estimator in the EMG signal analysis is the periodogram. Calculation of PSD in MATLAB used Welch method (1) ie looking for DFT based on calculations with the FFT algorithm, then squaring the magnitude [12][13].

$$P_{xx}(w) = \frac{S(e^{jw})}{2p} \quad (1)$$

Where,

$P_{xx}(w)$  = Power spectrum density at a window

$S(e^{jw})$  = Power spectrum using FFT

$p$  = Estimation of spectrum value using periodogram

$w$  = Sampling window

$f$  = frame window

The estimation of spectrum value ( $p$ ) will be close to the true value if sampling window is very large, this means that the number of periodograms is made as much as possible but the resolution of the observed frequency is decreased.



## II. Mean and Median Frequency

Features-based time domain and frequency domain are two important features. Generally, time domain feature used for the muscle force detection but their performance is a major drawback for detecting muscle fatigue. On the other hand, frequency domain has good performance to detect muscle fatigue [9][10]. Mean frequency (MNF) is an average frequency which is calculated from a total of the product EMG power spectrum and the frequency divided by the total of the power spectrum. The definition of MNF is given by

$$MNF = \frac{\sum_{j=1}^m f_j P_j}{\sum_{j=1}^m P_j} \quad (2)$$

Where,

$f_j$  = frequency value at a data sampling  $j$   
 $P_j$  = EMG power spectrum at a data sampling  $j$   
 $m$  = length of data sampling  $j$

Median frequency (MDF) is a frequency at which the EMG power spectrum is divided into two regions with equal amplitude. The definition of MDF is given by

$$\sum_{j=1}^{MDF} P_j = \sum_{j=MDF}^m P_j = \frac{1}{2} \sum_{j=1}^m P_j \quad (3)$$

Where,

$P_j$  = EMG power spectrum at a sampling  $j$   
 $m$  = length of data sampling  $j$

## III. EMG signal

Raw EMG signal generated by EMG acquisition hardware has a data length of 66000 data. These data were divided into five segments to make it easier to analyze. Segment one is start position, segment two is reached target one, segment three is reached target two, segment four is reached target three and the last segment is finished positions. Fig. 4 showed a sample of Raw EMG signal from a deltoid muscle by subject #1. Fig. 5 showed a sample of power spectrum density (PSD) using the Welch method from a deltoid muscle by subject #1 for the second segment.

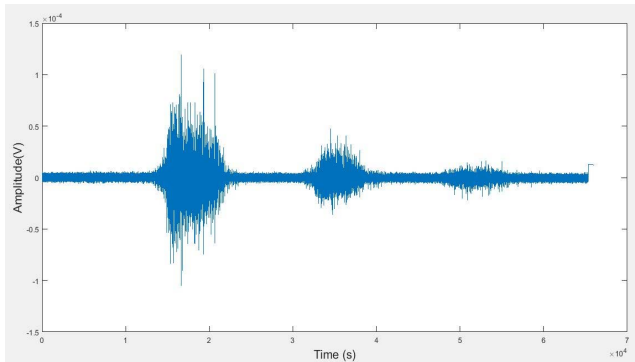


Fig. 4. The sample of Raw EMG signal

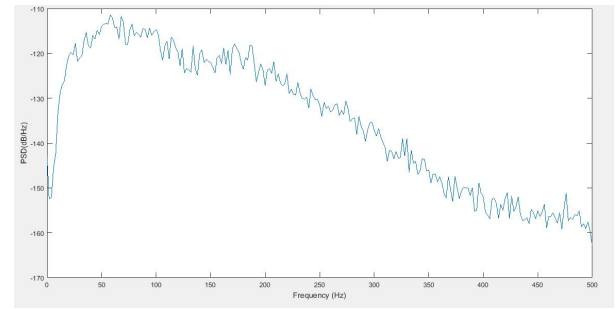


Fig. 5. The sample of PSD using Welch method

## III. RESULT AND DISCUSSION

The EMG signals were analyzed in frequency domain to obtain the feature extraction. A total of two frequency domain features were selected and used to analyze EMG signal from deltoid, biceps and FCU muscles. Table I shows the values of the mean frequency (MNF) for the purpose movement sequence. The frequency at the start position and finish position has almost the same value because in this condition there are no movements so there are no muscle contractions. Deltoid muscle, the biggest frequency when the subjects reach target 1 and the value decreased slowdown when subjects reach target 2 and 3 because when subjects move to target 1 the muscle produces more contractions than subjects move to target 2 and 3. Be evidenced by subject #1, #2 and #5. Biceps muscle, the frequency produced by biceps muscle from this movement sequence inconsistent value where this conditions due to there are not contractions from biceps muscle. FCU muscle, the frequency produced by the FCU muscle from this movement sequence is consistent where this conditions due to there are same contractions from target 1, target 2 and target 3.

TABLE I. VALUE OF MNF DOMAIN FEATURE EXTRACTIONS

Subject		MNF (Hz)				
		Start	Target 1	Target 2	Target 3	Finish
#1	d	38	92	83	65	40
	b	39	53	42	43	41
	f	50	70	82	74	65
#2	d	40	74	69	56	41
	b	37	55	53	49	37
	f	74	84	75	75	65
#3	d	42	73	75	48	42
	b	40	48	45	43	39
	f	48	89	86	86	58
#4	d	42	65	67	58	45
	b	38	48	53	44	34
	f	72	82	77	74	65
#5	d	36	94	85	62	37
	b	37	50	42	40	37
	f	46	75	70	78	67

\*d=deltoid, b=biceps, f=flexor carpi ulnaris (FCU)

Table II shows the values of median frequency domain features for the purpose movement sequence. Median frequency is similar with mean frequency but the value of median frequency is too small than mean frequency so median frequency difficult to analyze.

TABLE II. VALUE OF MDF DOMAIN FEATURE EXTRACTIONS

Subject		MDF (Hz)				
		Start	Target 1	Target 2	Target 3	Finish
#1	d	25	76	67	40	25
	b	25	37	26	30	25
	f	25	54	68	49	26
#2	d	25	63	59	34	25
	b	25	42	39	33	25
	f	34	70	63	64	27
#3	d	25	60	61	35	27
	b	25	27	26	26	25
	f	25	76	73	73	25
#4	d	25	50	53	36	25
	b	25	26	40	26	25
	f	26	66	61	62	26
#5	d	25	81	73	36	25
	b	25	35	31	25	25
	f	25	54	51	55	26

\*d=deltoideid, b=biceps, f=flexor carpum ulnaris (FCU)

Frequency obtained from muscle have inconsistent value depends on arm movement. In this movement sequence design, a frequency obtained from deltoid muscles decreased frequency value, when subjects move their hand to target 1 frequency produced by deltoid muscles is higher than target 2 and 3. Biceps muscles produce inconsistent values but mostly when subjects reach target 2 biceps muscle produce the highest value than the other. At the same time, FCU muscles tend to be more constant, this is due to the same movement ie grasp object.

Difference values of frequency at every target due to the direction of arm movement, the power of contractions and the distance between object and arm. Beside this muscle fatigue also can influence signal which generated by muscle when contractions. Muscle fatigue occurs when muscles contract too long without rest.

Difference value from mean and median frequency feature extraction showed at Fig. 6. Actually in this movement sequence had three condition movements with five segments: warming up, moderate, difficult, moderate and cool-down movement. From the graph forms the following sequence: warming up – difficult – moderate – moderate – cool-down.

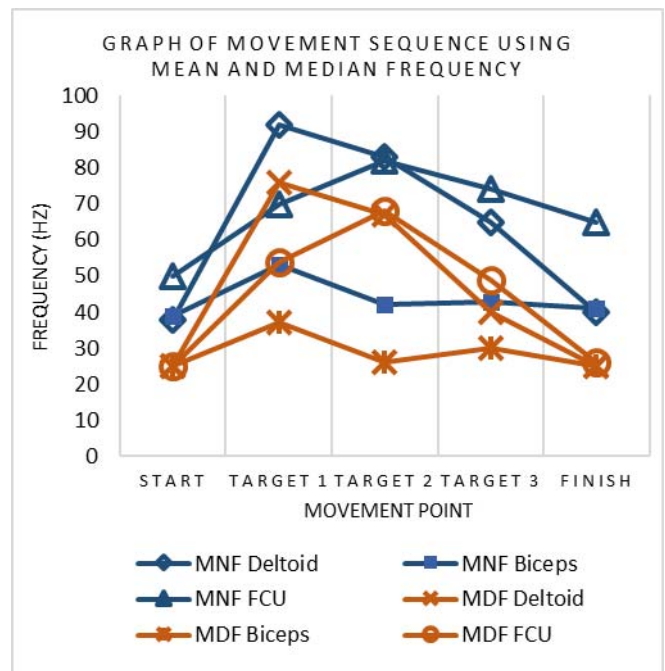


Fig. 6. The sample of graph MNF and MDF from subject #1

#### IV. CONCLUSIONS

The main objective of this research is to analyze movement sequence based on EMG signal using mean and median frequency domain feature extractions. Generally, frequency feature extraction used to analysis of muscle fatigue after post-stroke rehabilitation, in this section mean and median frequency used for analyzing arm movement sequence. From this research obtain some conclusions:

1. Feature extraction using mean frequency domain is better than the median frequency for analyzing movement sequence.
2. From the data analysis, this movement sequence design more focuses on deltoid and FCU muscles treatment.
3. Refer to fig. 6 shows, this movement sequence has five condition movements. First undemanding, second difficult, third moderate, fourth moderate and the last cool-down movements.

Recommendations for the next research (1) Addition virtual reality based on a game in the rehabilitation process can motivate subjects. (2) Showing feedback to screen and saving data to the server can make it easier therapist to data analyzing.

#### ACKNOWLEDGMENT

TUSB Research UniMAP supports this research under the research grant 2017/08/0006.

#### REFERENCES

- [1] 'Malaysia stroke data stroke'. [Online]. Available: <http://www.worldlifeexpectancy.com/malaysia-stroke>.
- [2] J. McIntosh and D. Webberley, "Stroke: Causes, Symptoms, Diagnosis and Treatment", Medical News Today, 2016. [Online]. Available: <http://www.medicalnewstoday.com/articles/7624.php>.
- [3] Statistics of stroke patients in Asia Pacific', 2016. [Online]. Available: <http://www.ncbi.nlm.nih.gov/pubmed/26338106>, 1st ed. 2016.

- [4] Gopura R.A.R.C., "A study on Human Upper-Limb Muscles Activities during Daily Upper-Limb Motions", International Journal of Bioelectromagnetism, vol. 12, No 2, pp. 54, 2010
- [5] Zhang zhe, "Objective Assesment of Upper-Limbs Mobility for Post-Stroke Rehabilitation", IEEE transaction Biomedical engineering, 2015.
- [6] Rashidah Suhaimi and Kamil. S. Talha, "Design of Movement Sequence for Arm Rehabilitation of Post-Stroke", IEEE International Conference on Control System, Computing and Engineering, 2015.
- [7] Zaw Lay Htoon, Shahrul Na'im Sidek, Sado Fatai, " Assessment of Upper Limb MUSCLE Tone Level Based on Estimated Impedance Parameters", IEEE EMBS Conference on Biomedical Engineering and Sciences, 2016.
- [8] Samuel Oluwarotimi Williams, "Patern recognition of electromyography signal on novel time domain features for amputees limb motions clasification", Computer and Electrical Engineering Science Direct, 2017.
- [9] Thongpanja S., "Mean and Median Frequency of EMG Signal to Determine muscle Force based on Time Dependent Power Spectrum", Elektronika IR Electrotecnika, Vol. 19, No. 3, 2013
- [10] Yamamoto Shin-Ichiroh, "A Review of Classification Tehcniques of EMG Signal during Isometric snd Isotonic Contractions", Research Gate 2016.
- [11] Khairunizam Wan, " Design of Arm Movement Sequence for Upper-Limb Management after Stroke", International Workdhop on Nonlinier Circuits, Communication and Signal Processing, 2017.
- [12] Krauss,T.P.,L. Shure and J.N.Little 1995. Signal Processing Toolbox: For Use with Matlab. The Mathworks, Inc.
- [13] A. Phinyomark, "The Usefulness of Mean and Median Frequencies in Electromygraphy Analysis", <http://dx.doi.org/10.5772/50639>
- [14] Rashidah Suhaimi, AR Aswad, Nazrul H Adnan, Fakhrul Asyraf, Khairunizam Wan, D Hazry, AB Shahrman, Abu Bakar, Zuradzman M Razlan (2014): "Analysis of EMG-based muscles activity for stroke rehabilitation," 2014 2nd International Conference on Electronic Design (ICED), pp. 167-170.

# Implementation of Myo Armband on Mobile Application for Post-stroke Patient Hand Rehabilitation

Tri Bintang Dewantoro<sup>1)</sup>, Riyanto Sigit<sup>2)</sup>, Heny Yuniarti<sup>3)</sup>, Yudith Dian Prawitri<sup>4)</sup>, Fridastya Andini Pamudyaningrum<sup>5)</sup>, Mahaputra Ilham Awal<sup>6)</sup>

<sup>1,2,3,5,6</sup>Informatic and Computer Department  
Politeknik Elektronika Negeri Surabaya  
Surabaya, Indonesia

<sup>4</sup>Physical Medicine and Rehabilitation Department  
University Airlangga Hospital  
Surabaya, Indonesia

tribintangd@gmail.com<sup>1)</sup>, riyanto@pens.ac.id<sup>2)</sup>, heny@pens.ac.id<sup>3)</sup>, yudithdianp@gmail.com<sup>4)</sup>, fridastya21@gmail.com<sup>5)</sup>, mahaputrailhamawal@gmail.com<sup>6)</sup>

**Abstract**— Medical rehabilitation is one of the efforts to restore motor function of post-stroke patients, but the biggest factor that makes patients quickly restore motor function by active patient movement exercises. The movement in question is the movement carried out every day outside medical rehabilitation at the hospital. On the other hand, patients are reluctant to do therapy independently outside the hospital, because there is no tool that supports patients to do so. So, we need a device that helps patients to do therapy independently. The device is connected to Myo Armband to read the gestures of the patient by looking at the EMG signal from the patient's hand. Then the system performs matching gestures during therapy with EMG signal data that has been trained. The motion matching is done by calculating the Euclidean distance between the two EMG signal data obtained from the Myo Armband device. From the results of the tests carried out, the accuracy of movement matching results obtained an average accuracy of 89.67 percent for flexion-extension gestures and 82 percent for pronation-supination gestures. It can be concluded that Myo Armband in the Mobile Application can be used for Rehabilitation of post stroke patient hands.

**Keywords**—Rehabilitation, EMG Signal Myo Armband, Post-Stroke

## I. INTRODUCTION

Cerebrovascular accident (CVA) is a disease that is often classified as a deadly disease in Indonesia with 15.9 percent of the causes of death in Indonesia [1]. The World Health Organization (WHO) defines stroke as a rapid onset of clinical symptoms disruption of cerebral function with a symptom lasting 24 or more hours without any apparent power other than from the vascular system [2].

According to data of the Ministry of Health of the Republic of Indonesia, the number of stroke patients in Indonesia in 2013 based on the diagnosis of health workers (Nakes) is estimated as 1,236,825 people (7.0 %), while based on diagnosis / symptoms are estimated as many as 2,137,941 people (12.1 %) [1]. The data is very large for developing countries like Indonesia and each year the number of stroke

patients continues to increase with the unhealthy lifestyles of modern society and underestimate the healthy diet and causes of other stroke.

However post-stroke patients can restore their motoric function by performing regular and regular rehabilitation. Post-stroke rehabilitation is usually performed only in hospitals that have medical rehabilitation facilities with physiotherapy or doctors. Whereas to restore the patient's motoric function efficiently the patient must perform active patient gestures every day outside the rehabilitation time in the hospital. The patient's active motion is self-directed gesture by the patient. It is expected that by actively conducting physical moving the patient in his spare time to increase the level of muscle reconstruction can occur maximally.

The development of tools for post-stroke rehabilitation patients began to emerge much like saddle designs for bicycle stroke patients. Another example is Myo Armband. Myo armband is a device developed by Thalmic Labs company. Myo armband is a bracelet device used on the human arm to identify gesture of arm muscles by using electromyography technique. In addition to the EMG sensor, Myo Armband is also powered with several Accelerometer sensor, Gyroscope, and Magnetometer combination of the three sensors with the Inertial Measurement Unit (IMU) [3]

The research developed a new method for post-stroke patients. The aim of this research is to create an application that helps post-stroke patients in recovering their hands. This will be done with the Myo Armband device used to detect post-stroke patient gesture.

## II. SUPPORTING THEORY

### A. Post-Stroke Rehabilitation

Rehabilitation is a program designed to recover sufferers with physical distress and / or chronic diseases, so that they can live or work fully in their capacity. Post-stroke rehabilitation aims for stroke sufferers to live independently

and productively again. The success rate of post-stroke rehabilitation depends on several aspects, ranging from the extent of brain damage, early handling time, the role of the family, and methods for therapy. Post-stroke rehabilitation therapy is divided into several kinds, ranging from motion exercises, tool modalities, drugs, and psychology [4].

In this research, the authors used post-stroke type of rehabilitation with motion exercises. The motion exercises taken are wrist movement exercises, in which the movement is two wavelengths of flexion-flexion and pronation-supination. The following describes flexion-extension and pronation-supination gestures.

- flexion-extension, i.e wrist movement to the inner side and move the hand back again straight
- pronation-supination, i.e moving the wrist down and back up again.

### B. Manual Muscle Testing (MMT)

Manual Muscle Testing (MMT) itself is one effort to determine or know one's ability to contract muscle or muscle group involuntary. MMT is one of the most popular muscle strength measurement methods and is mostly done by physiotherapy. In MMT, strength is measured on a scale of zero to five points. Table I is the MMT scale and its description.

TABLE I. MANUAL MUSCLE TESTING

Number	Scale	Explanation
1	0	Muscle contraction is undetectable
2	1	The presence of muscle contraction and no movement of the joints
3	2	The presence of muscle contraction and the movement of joints full ROM
4	3	The presence of muscle contraction, the movement of joints full ROM and able to resist gravity
5	4	The presence of muscle contraction, the movement of joints full ROM, able to fight gravity dam minimum resistance
6	5	Ability to resist maximum resistance

In the medical world of post-stroke patients is very complex, in a thousand cases of stroke that each of them is different and unique to each other. So that the handling of rehabilitation must also be done differently to every patient. Therefore, the application is a limited to user who will use the application later. The application will be used for rehabilitation with post-stroke patients with lower arm muscle weakness and Manual Muscle Testing (MMT) more than two.

### III. SYSTEM DESIGN

System design includes the process of making and running applications from the use of Myo Armband hardware,

therapeutic process and application functionality until the applied system diagram.

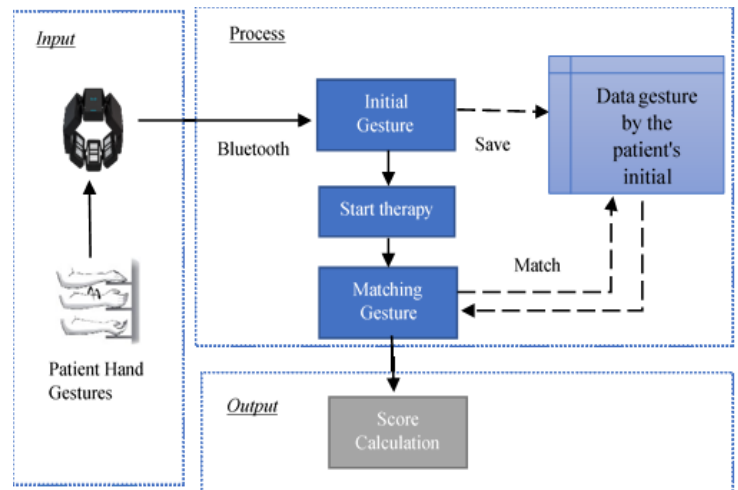


Fig. 1. Diagram System

Figure 1 illustrates the system design block and how the application runs. In general, the system is divided into three stages of input, process and output.

#### A. Input

The input of the hand-therapy application system is the gestures of the patient's hand during a therapeutic motion or not a treatment motion as shown in Table 2. The gesture will then be read by Myo Armband using eight EMG sensors in the device. Given in Myo Armband itself there are some sensors, but researchers only use EMG sensors, because in the therapy system built by the patient's hand does not move coordinately, so the IMU sensor in Myo Armband is not needed.

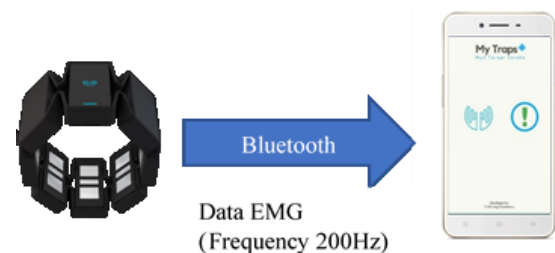


Fig. 2. Communication between devices

The data from myo armband will be sent to the android application using Bluetooth communication. In sending data from the myo armband device to the android application there is a distinction between EMG data and IMU data, where EMG data is flown at 200 Hz frequency while IMU data at frequency 50 Hz. Smartphone used must meet the development requirements of the android version of the Myo android version of SDK.



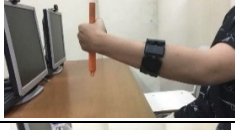
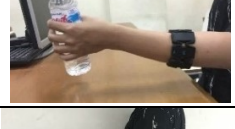




- The smartphone device must have Bluetooth Low Energy (BLE).
- Android version 4.3.

### B. Process

In the application process of this therapy there are several parts that will be run later. Such parts include early therapeutic motion, early gesture storage therapy, initiation of therapy and matching therapeutic gestures. Here's an explanation of each part of the therapy application process.

1) *Early gesture taking* : Once the application can capture the gesture of the patient, then the patient can perform a series of therapies made by researchers. The first thing to do before the therapy in the application begins, patient performs recording or retrieval of early motion data. Each will initiate a series of therapies, the patient must be required to perform initial motion data capture first. Gestures taken based on the motion of therapy performed by patients with gesture as in Table 2 depends on the type of gesture and step chosen by the patient.

TABLE II. GESTURE MODEL ILLUSTRATION

Type of Gesture	Step	Gesture Model Illustration
Flexion - Extension	1	
	2	
	3	
	4	
Pronation-Supination	1	
	2	
	3	
	4	

2) *Storing of early gesture*: After the patient performs the initial gesture of therapy, the application will store the data on a document that is in the internal memory of the smartphone. So the data is easily accessible by the system when matching the gesture later. The type of document used will be of type .dat. The data stored from the patient's gesture is the value of the eight EMG sensors in Myo Armband device, so there are eight data to be stored.

3) *Starting therapy*: When the patient has completed the initial gesture and the gesture data has been stored, the patient can begin therapy, the patient will do the therapy by performing gestures as in Table II and the repetition like the gesture as much as the predetermined number is the number 30.

4) *Gesture matching*: Figure 3 is a flowchart of gesture matchings that exist in the hand-made therapeutic application.

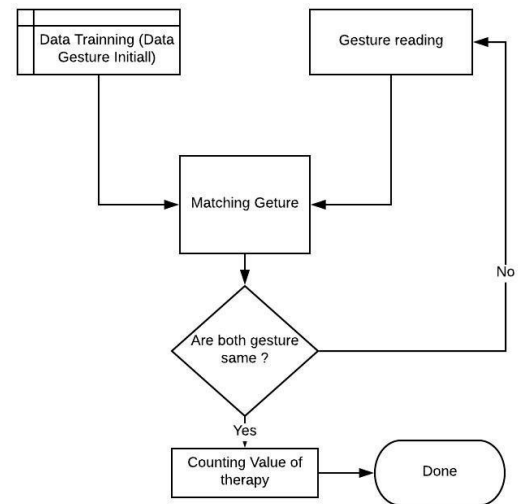


Fig. 3. Flowchart of gesture matchings

The data obtained when the patient performs the initial gesture will be used as training data (x) and motion data will be used as data testing (y). In determining the classification of whether the two gestures are the same or not, the approach by calculating the distance between the two data is called the euclidean distance. Here is the equation of Euclidean distance calculation on the equation 1.

$$D(x, y) = \sqrt{\sum_{i=1}^d (x_i - y_i)^2} \quad (1)$$

Where  $D(x, y)$  is the Euclidean distance or the distance between the two data is x and y. x is the preliminary gestures data of therapy and y is the patient's gestures therapy data. The two variables that are to be classified and i represent the attribute value and n is the attribute dimension. If both data are known the distance between the two then the next system will group the two data together or not. To determine the level of



similarity of researchers using tolerable Euclidean distance limitations.

### C. .Output

The final stage of the system created is output. The output of the created system will then display the value or the therapeutic score, this value is made based on the same amount of gesture performed by the user during therapy with the gesture before the therapy or gesture taken from the beginning before the therapy or in other words the correct calculation of gesture preliminary gesture data. So, if the patient does a lot of the same gesture with the initial gesture, then the value will continue to multiply as well. One gesture of equal value will increase one. The calculation will end if the patient reaches a value of 30. Flowchart calculation of the score or score as in the picture.

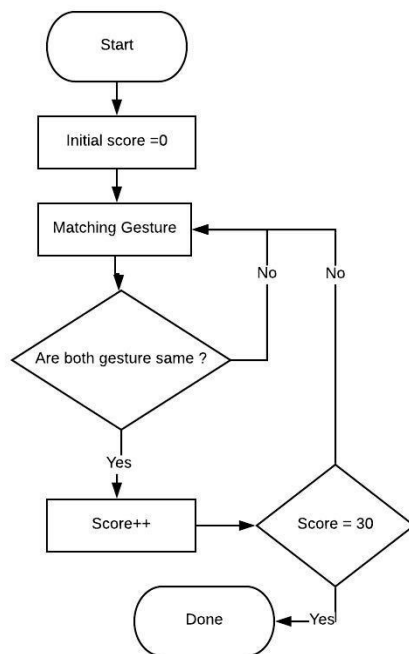


Fig. 4. Flowchart calculation of the score therapy.

Value or score later will be used as a reference for patients to stage therapy (step) or not. The selection of 30 is based on the usual repetition of hospital-based therapies with details of three sets of exercises and each set is ten times the repetition of gesture. In addition to seeing the value achieved by the patient during therapy, the patient's decision to proceed to the next step is determined by the doctor or physiotherapist who handles the patient later.

## IV. RESULT AND DISCUSSION

The applications that have been developed are tested to suit the use in real life. The test conducted in this study is testing about the interface display of the application and matching the gestures performed.

The user interface of the application is tested using multiple users with several types of user mobile devices, where this test is to determine the response of the user

interface that is made to adjust the state of the mobile device. For the example whether the display of buttons and images can adjust from the layer resolution on a mobile device. The following Figure 5 is the result of the application user interface design.

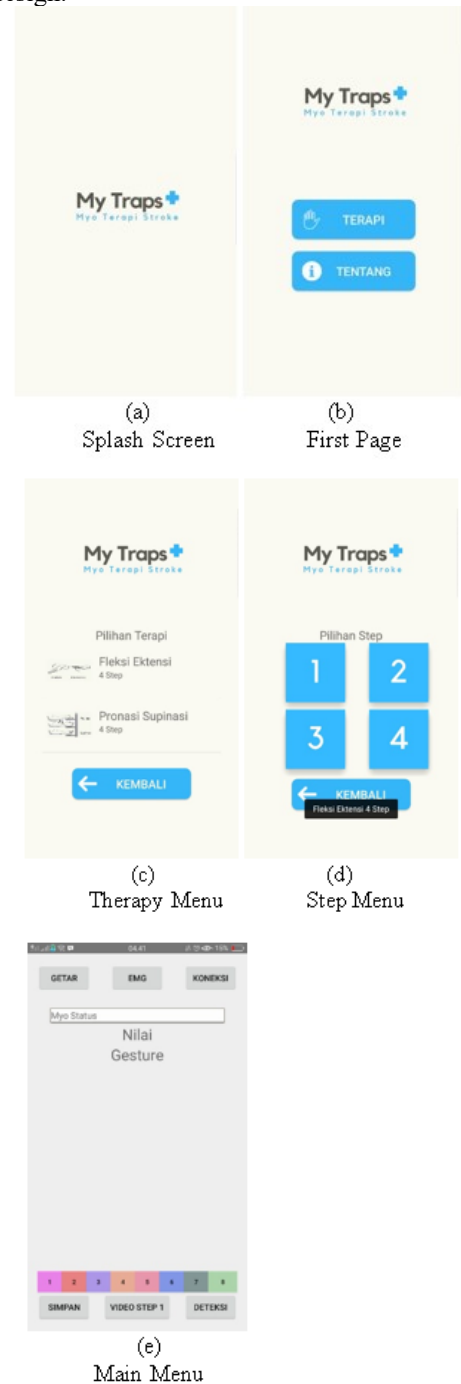


Fig. 5. User interface application.

The user interface test results show that the design is very responsive to other mobile devices. In the application, researchers use Indonesian in the language used, because most users will be Indonesian.



The trial conducted by the next researcher was to test the classification of the forearm movement on users at the Airlangga University Hospital.

The movement being tested is a therapeutic movement consisting of two gestures, including flexion-extension and pronation-supination. Each movement has three types of motion, namely maximum, middle, and relaxed. Each movement was carried out repetition of motion 10 times so that a trial of 30 gestures was obtained. For testing the classification of gestures the researcher took data from 10 users. The following figure 6 is a sensor reading on the flexion motion.

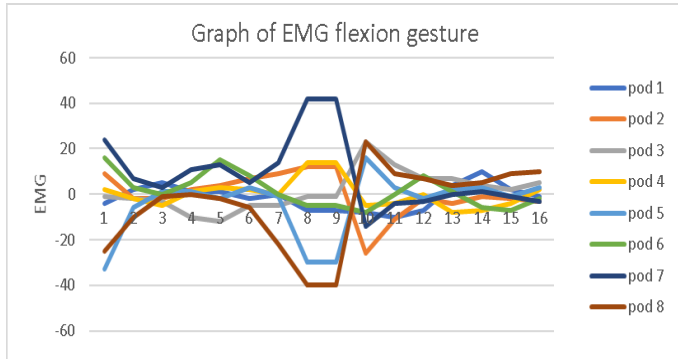


Fig. 6. Graph of EMG flexion gesture.

The researcher carried out 16 EMG sensor data collection in each EMG sensor. It can be seen in Figure 6 the value of the EMG sensor when the user moves, the highest value can reach 42, then the form of each signal on the EMG is almost the same as each other. The following figure 7 is a sensor reading on the pronation motion.

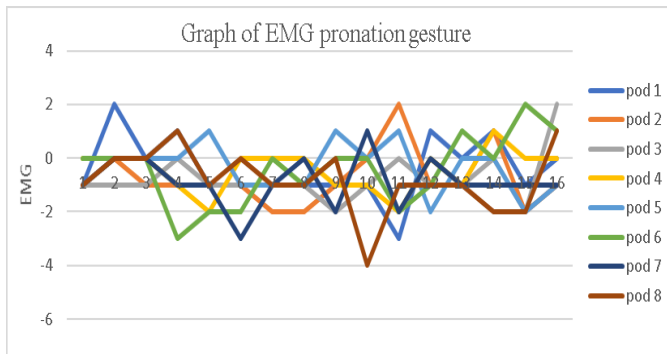


Fig. 7. Graph of EMG pronation gesture.

After the user moves, the researcher records the correct and wrong gestures from the system reading about the user's motion detection. Then the accuracy level of the motion detector is calculated. The formula for calculating accuracy is shown in Equation 2.

$$\text{Accuracy} = \frac{\text{total correct Gesture}}{\text{total overall Gesture}} \times 100\% \quad (2)$$

After calculating the accuracy of the data obtained the accuracy of the movement of each user and the average

accuracy of the movement of each movement. The following table 3 is the result of calculating the accuracy of each user in flexion-extension gestures

TABLE III. CALCULATING THE ACCURACY FLEXION

Number User	Accuracy
1	83.333%
2	86.67%
3	96.67%
4	93.33%
5	86.67%
6	93.333%
7	83.333%
8	93.33%
9	100.00%
10	80.00%
Average accuracy	<b>89.667%</b>

From table 3 it can be seen that the average flex-extension motion matching accuracy results are 89,667 percent of 10 users. Where the smallest accuracy of ten users is 80 percent and the highest reaches 100 percent success in detecting the movement of the user's hand. Next table 3 is the result of calculating the accuracy of each user in the pronation-supination movement.

TABLE IV. CALCULATING THE ACCURACY PRONATION

Number User	Accuracy
1	86.67%
2	83.33%
3	93.33%
4	83.33%
5	80.00%
6	63.33%
7	86.67%
8	76.67%
9	73.33%
10	93.33%
Average accuracy	<b>82.00%</b>

Table 4 shows the level of accuracy of the system in detecting pronation-supination gestures carried out by ten users. From the level of accuracy, the average accuracy value is 82 percent. Where the average accuracy is lower than the average accuracy of flexion-extension gestures. Due to the muscles that work when pronation-supination moves more towards the upper arm muscles instead of the forearm.

## V. CONCLUSION AND FUTURE WORK

Myo Armband on a mobile application can be used to match patient gestures during therapy. The average level of application accuracy in user movement matching is 89.67 percent for flexion-extension gestures and 82 percent for pronation-supination gestures. Based on the results of the experiment, it can be concluded that Myo Armband in a mobile

application can be used as a new tool to help the rehabilitation of the hands of post-stroke patients. In the future, researchers will try application devices to be used by patients directly so that researchers can find out the level of comfort, ease and ergonomics of the application to the rehabilitation of post-stroke patients

#### ACKNOWLEDGMENT

This research was accomplished at Politeknik Elektronika Negeri Surabaya, Surabaya, Indonesia. The authors would like to acknowledge University Airlangga Hospital for the contribution in this research.

#### REFERENCES

- [1] Pusat Data dan Informasi Kementerian Kesehatan RI. 2014. Situasi Kesehatan Jantung.. Kementerian Kesehatan Republik Indonesia. Jakarta.
- [2] Direktorat Pengendalian Penyakit Tidak Menular Kementerian Kesehatan RI, "Pedoman Pengendalian Stroke Kementerian Kesehatan RI", 2013, Jakarta
- [3] Ing. Néstor Mauricio Caro Sánchez, "Gesture Classification Based on Electromyography", Diploma Thesis Czech Technical University In Prague, May 2016
- [4] Okti Sri Purwanti, Arina Maliya, "Rehabilitasi Klien Pasca Stroke", Berita Ilmu Keperawatan ISSN 1979-2697, Vol. 1 No.1, Universitas Muhhamdiyah Surakarta, March 2008.
- [5] Angga Rahagiyanto, "Alat Bantu Komunikasi Tunarungu Menggunakan Hand Gesture Recognition". Tesis Program Studi Magister Terapan Teknik Informatika Dan Komputer, Politeknik Elektronika Negeri Surabaya. 2017
- [6] A. A. Hidayat, Z. Arief and H. Yuniarti, "LOVETT scalling with MYO armband for monitoring finger muscles therapy of post-stroke people," *2016 International Electronics Symposium (IES)*, Denpasar, 2016, pp. 66-70.
- [7] M. Sathiyarayanan and S. Rajan, "MYO Armband for physiotherapy healthcare: A case study using gesture recognition application," *2016 8th International Conference on Communication Systems and Networks (COMSNETS)*, Bangalore, 2016, pp. 1-6.
- [8] M. R. Pambudi, R. Sigit and T. Harsono, "The bionic hand movement using myo sensor and neural networks," *2016 International Conference on Knowledge Creation and Intelligent Computing (KCIC)*, Manado, 2016, pp. 259-264.

# Development of Embedded System for Centralized Insomnia System

Novi Azman  
Faculty Engineering and Science  
Universitas Nasional  
(UNAS)  
Jakarta, Indonesia  
[Novi.azman@civitas.unas.ac.id](mailto:Novi.azman@civitas.unas.ac.id)

Muhammad Haikal Satria  
Faculty of Engineering  
Universiti Teknologi Malaysia  
(UTM)  
Johor Bahru, Malaysia  
[haikalsatria@biomedical.utm.my](mailto:haikalsatria@biomedical.utm.my)

Muhammad Zillullah Mukaram  
Faculty of Science  
Universiti Teknologi Malaysia  
(UTM)  
Johor Bahru, Malaysia  
[azil.utmskudai@gmail.com](mailto:azil.utmskudai@gmail.com)

Mohd Khanapi Abd Ghani  
Universiti Teknikal Malaysia Melaka  
Melaka, Malaysia  
[khanapi@utem.edu.my](mailto:khanapi@utem.edu.my)

**Abstract**— Insomnia is a common health problem in medical field as well as in psychiatry. The measurement of those factors could be collected by using polysomnography as one of the current standards. However, due to the routine of clinical assessment, the polysomnography is impractical and limited to be used in certain place. The rapid progress of electronic sensors to support IoT in health telemonitoring should provide the real time diagnosis of patient at home too. In this research, the development of centralized insomnia system for recording and analysis of patient with chronic-insomnia data is proposed. The system is composed from multi body sensors that connected to main IOT server. The test has been done for 5 patients and the result has been successfully retrieved in real time.

**Keywords**— *Insomnia, Telemonitoring, Portable ECG*

## I. INTRODUCTION

Insomnia is a common health problem in medical field as well as in psychiatry. Insomnia is characterized by a dissatisfaction of the quantity or quality of sleep with a difficulty of falling asleep, difficulty to keep sleeping, and waking up in the morning [1]. Its health impact has always been underestimated and trivialized. Moreover, insomnia could cause a decreased in daytime function [2] and a significant mental and physical disorders for the patients. A research from [5] shows a staggering increase of insomniac patients in developing countries. 16.6% of respondent from Ghana, Tanzania, India, Bangladesh, Vietnam and Indonesia suffered insomnia and other sleeping disorders.

The prevalence of people with chronic insomnia has increase significantly in urban area. The urban life style, requirements and others socio-economy demands are some of the cause for this increment. [3,4,5] This has indirect effect to the socio-economy factors in a country, where about 60% of people in developing countries living in urban area.

As an individual, a patient with chronic insomnia could affect their quality of life and other health comorbidities. [6,7] Several researches have shown that patient with chronic

insomnia will increase their hypertension risk by approximately 350% when compare to people with no sleep disorder. Insomnia is also one of the risk factors for diabetes, anxiety and depression. Further, the patient of chronic insomnia will affect their work performance and social life.

Diagnosis and treatment of patients with chronic insomnia is done individually and respectively. This is due to their individual pattern of sleep and their respective vital signs, such as blood pressure and heart rate, which needs to be monitored continuously. The treatment of each patients will be done based on their insomnia's classification which is based on individual factors, symptoms, frequencies and severity of the insomnia.

The measurement of those factors could be collected by using polysomnography as one of the current standards. However, due to the routine of clinical assessment, the polysomnography is impractical and limited to be used in certain places [8]. A proposed Actigraphy could be used to increase accuracy and mobility from polysomnography for sleep pattern measurement. Unfortunately, the limitation of this device and complexity in its installation along with polysomnography are become their restriction [8]. There is a need of practical device that can overcome these problems.

The classification of insomnia to determine type of the suitable treatment should also be done rapidly. This could be achieved by the continuous monitoring of patient in and out of healthcare facilities or lab. The classification also requires a non-medical input, which is subjective and based on patient qualification, their life style and stress level. The device should support and provide this classification along with taking the patient non-medical record in progressive and structured.

The rapid progress of electronic sensors to support IoT in health telemonitoring should provide above requirements. The implementation of anytime and anywhere concept could give the freedom and manifestation of clinical and non-clinical data continuously for patient with chronic insomnia.

The aim of this research is to provide a reliable telemonitoring system for chronic insomnia with the continuous monitoring of patient's health record as well as the determination of individual insomnia classification to assist medical practitioner for the suitable therapy. The development of a system model of telemonitoring by utilizing IoT technology as the main monitoring devices is need to be done to achieve above objective.

## II. PROTOTYPE DEVELOPMENT

The design of detection devices with vital monitoring based on wireless systems is shown in figure 1. The proposed prototype of this insomnia telemonitoring device should fulfill the specifications of Polysomnography level 2.

Polysomnography level 2 have similar specifications to Polysomnography level 1, with all the required devices and electrodes connected with polysomnography device. The difference on level 2 is the device portability and the absence of environmental conditioning [12]. The selection rationale of level 2 polysomnography is the patient location. The data gather is conducted and installed outside the hospital sleep lab premises and have the convenience of following the patients to their own sleeping premises.

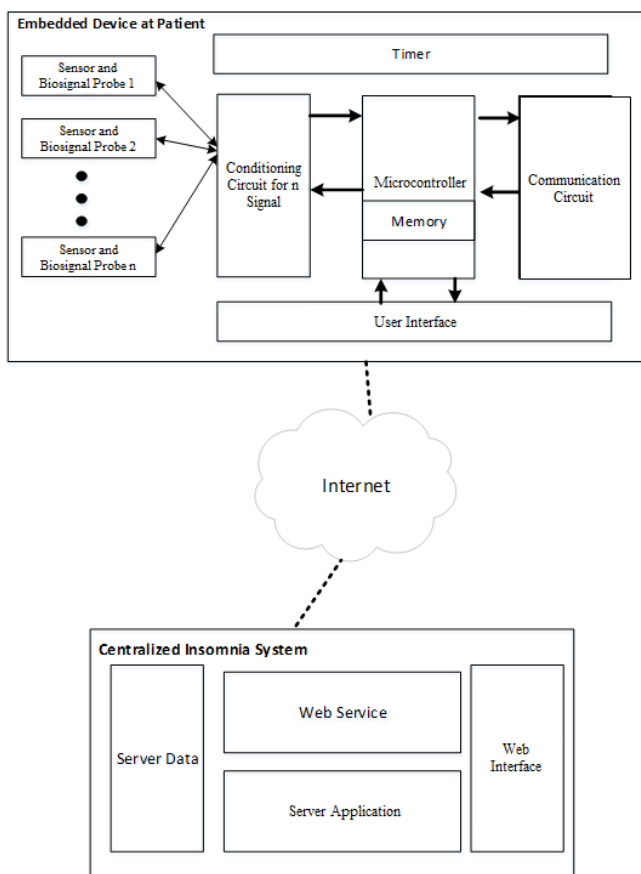


Figure 1. Infrastructure diagram of Embedded system development for centralized Insomnia System

Other specifications are the smaller size and lighter weight of device. The purpose of the embedded device is to

gather the data and sent to the centralized server by using IoT principles. The stored data is then prepared and analyze by researcher at anytime and anywhere.

The centralized insomnia system should provide lightweight data delivery and reception, where multi-sensory devices are connected continuously. The server also needs to provide data processing and automatic analysis of insomnia level where all healthcare and research personnel accessed it. This configuration could minimize the device setup and installation at patient's side.

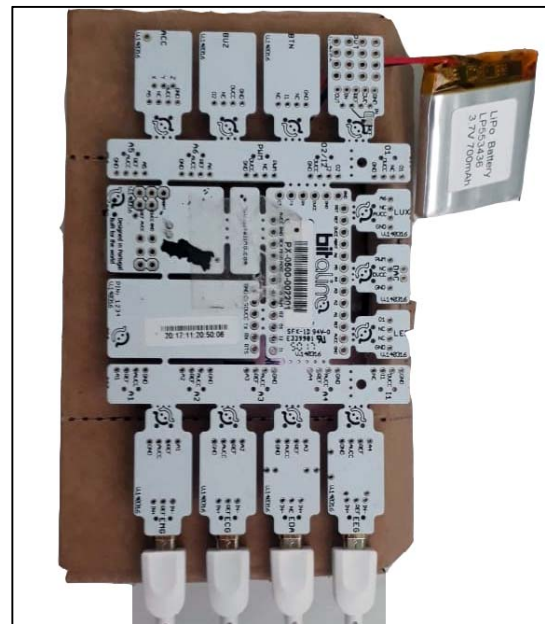


Figure 2. Embedded Device configuration and connection



Figure 3. Load measurement of data sending in the centralized insomnia server.

In this preliminary development, the embedded system is using BITalino solution for physiological computing from Instituto Superior de Engenharia de Lisboa, Portugal [13]. The selection justification of this device is its low-cost and modular biosignal acquisition hardware platform that could provide basic configuration of data acquisition of patient with chronic insomnia disease. It is also has been tested with the standard reference device for ACC, ECG, EEG and EDA data

with high correlation of the raw waveforms [14]. Figure 2 shows the BITalino platform used in this research and its configuration. ECG and EEG are connected to each 4 sensors port in BITalino.

data amount per time sending from the device to the servers. Currently the load balancing mechanism is not being implemented while there are only two connected device.

The RESTapi that being implemented is post mechanism for the data sending from device and get mechanism for the data retrieval at the researcher's computer for analysis.

### III. RESULT AND ANALYSIS

After obtaining the required data as a reference to make the prototype device from the field study stage, at this stage the researchers initiated the manufacture of prototypes of the device used to perform chronic insomnia telemonitoring, which in the manufacture of prototypes is divided into 4 sub-stages.

The data obtained are also required to view system performance as well as reconfiguring or re-tuning which is expected to improve the performance of the prototype device that has been created. Patient's device for patient with chronic insomnia that connected with centralized system for medical practitioner.

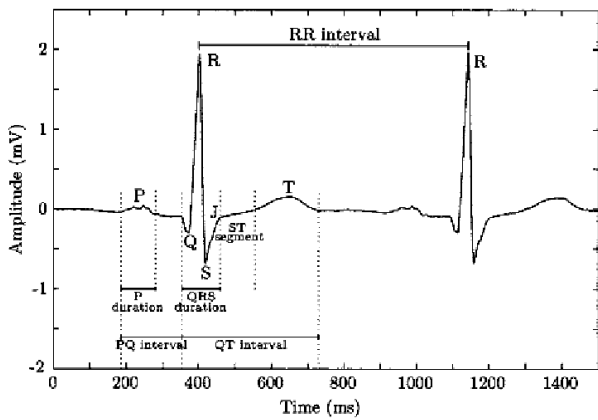


Figure 3. Classic ECG signal characteristics and analysis of its interval [14]

Follow the classic ECG signal characteristics in Figure 4, the analysis of data acquisition results on the server is done. Figure 4 is the snapshot data for 5 second of 3 subjects each subject are recorded for 1 hour.

By observing Figure 4 the RR interval between the 3 subjects differs significantly especially in subject number 2. The same also applied to the P and T wave in all of the subjects. In subject 1 the P and T wave have a miniscule amplitude whereas in the case of subject 3 the amplitude is very significant. The interval of P duration from subject 1 is 0.264. Estimate error compares from ECG reference data is 0.144 for subject 1.

The data is collected through the BITalino sensors and sent to centralized server. The data sending is using RESTapi standard for lightweight communication protocol of continuous connection. Figure 3 shows the screenshot of

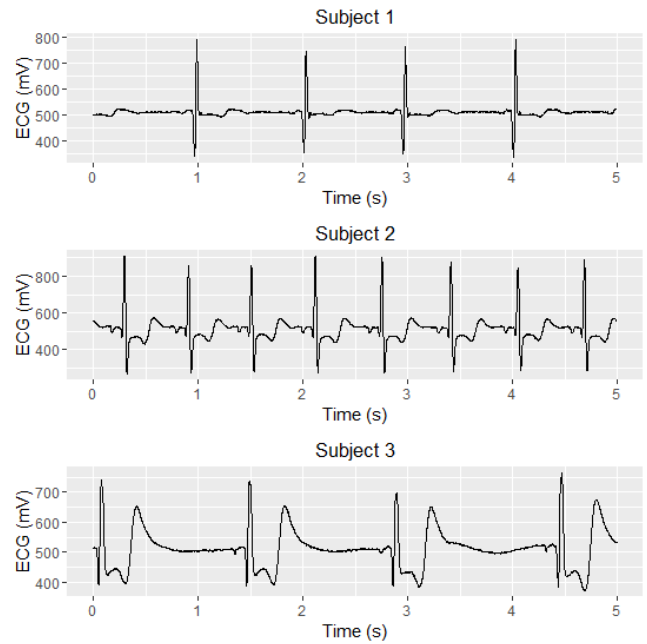


Figure 4. ECG Data Plots

Although the mean and standard deviation of each of the data are almost the same. The data distribution of each subject are difference the kurtosis from each dataset differ by a wide margin and the skewness are also different. T-test and  $\chi^2$ -test of the data also suggest that the data have a different true mean and variance

Subject	Mean	Sd	Min	Max	kurt	skew
1	512.5	67.25	0	1022	33.48	-0.5
2	511.3	72.70	266	932	12.21	1.75
3	511.4	64.41	340	789	4.72	0.89

Table 1. Descriptive Statistics of the ECG Data

Subject	T-test	$\chi^2$ -test
1 and 2	9.625e-05	< 2.2e-16
2 and 3	0.005031	< 2.2e-16
1 and 3	0.8129	< 2.2e-16

Table 2. Statistics Test P-value of the ECG Data

### IV. CONCLUSION

The implementation of embedded device for patient with chronic-insomnia disease has been done. The proposed device is lightweight and could be portably deploy at patient's premises. Current development also successfully implement the centralized insomnia server for data collection and analysis. This server is implemented by using RESTapi for robust and lightweight data sending from the device. Results of ECG data from 3 subjects has been retrieve successfully. The analysis of these data shows that the result

is close to the ECG data references. In the next research, full multi-sensory will be implemented to fulfill the polysomnography level 2 requirements. The auto analysis to determine the insomnia chronic level also need to be done

#### ACKNOWLEDGMENT

This research is supported by Direktorat Riset dan Pengabdian Masyarakat Direktorat Jendral Penguat Riset dan Pengembangan Kementerian Riset, Teknologi, dan Pendidikan Tinggi. Grant number:007/KM/PNT/2018.

#### REFERENCES

- [1] Cunnington, D. & Junge, M., 2016. Chronic insomnia : diagnosis and non-pharmacological management. , 5819(November), pp.1–6.
- [2] Sateia, M.J., 2014. International Classification of Sleep Disorders-Third Edition Highlights and Modifications. CHEST, 146(5), pp.1387–1394.
- [3] A. Zailinawati, D. Mazza, "Epidemiology of Insomnia in Malaysian Adults : A Community-Based Survey in 4 Urban Areas", *Asia Pacific Journal of Public Health*, vol. 20, pp. 224-233, 2008.
- [4] Xiang, Y. et al., 2008. The Prevalence of Insomnia , Its Sociodemographic and Clinical Correlates , and Treatment in Rural and ... The Prevalence of Insomnia , Its Sociodemographic and Clinical Correlates , and Treatment in Rural and Urban Regions of Beijing , China : A General Population- Based Survey. , (December).
- [5] Kidwai, R. & Ahmed, S.H., 2013. Prevalence of insomnia and use of sleep medicines in urban communities of Karachi , Pakistan. , 63(11), pp.1358–1363.
- [6] Daley, M. et al., 1995. The Economic Burden of Insomnia : Direct and Indirect Costs for Individuals with Insomnia Syndrome , Insomnia Symptoms , and Good Sleepers.
- [7] Kyle, S.D. et al., 2014. Insomnia and health-related quality of life Insomnia and health-related quality of life. *Sleep Medicine Reviews*, 14(1), pp.69–82.
- [8] Davila, D. et al., 1995. Practice Parameters for Using Polysomnography to Evaluate Insomnia : An Update.
- [9] Marino, M. et al., 2010. Measuring Sleep : Accuracy , Sensitivity , and Specificity of Wrist Actigraphy Compared to Polysomnography.
- [10] Sciences, M. et al., 2012. Subjective sleep quality in urban population. , (June 2017).
- [11] Weems, Harding, M. & Choi, A., 2016. Classification of the ECG Signal Using Artificial Neural Network BT - Proceedings of the 3rd International Conference on Intelligent Technologies and Engineering Systems (ICITES2014). In J. Juang, ed. Cham: Springer International Publishing, pp. 545–555. Available at: [https://doi.org/10.1007/978-3-319-17314-6\\_70](https://doi.org/10.1007/978-3-319-17314-6_70).
- [12] Chai-Coetzer, Ching Li, et al. "Physician decision making and clinical outcomes with laboratory polysomnography or limited-channel sleep studies for obstructive sleep apnea: a randomized trial." *Annals of internal medicine* 166.5 (2017): 332-340.
- [13] da Silva, H. P., Guerreiro, J., Lourenço, A., Fred, A. L., & Martins, R. (2014). BITalino: A Novel Hardware Framework for Physiological Computing. In *PhyCS* (pp. 246-253).
- [14] Batista, D., Silva, H., & Fred, A. (2017, July). Experimental characterization and analysis of the BITalino platforms against a reference device. In *Engineering in Medicine and Biology Society (EMBC), 2017 39th Annual International Conference of the IEEE* (pp. 2418-2421). IEEE.
- [13] Zhang, H. & Zhu, L., 2011. Internet of Things: Key technology, architecture and challenging problems. 2011 IEEE International Conference on Computer Science and Automation Engineering, 4, pp.507–512.
- [14] Tinati, B. M. M. A. (2005). ECG baseline wander elimination using wavelet packets. *World academy of science, Engineering and technology*, 3(2005), 14-16.





# Performance Analysis of Color Cascading Framework on Two Different Classifiers in Malaria Detection

Cucun Very Angkoso  
Departement of Informatics  
University of Trunojoyo Madura  
Bangkalan, Indonesia  
cucunvery@trunojoyo.ac.id

Yonathan Ferry Hendrawan  
Departement of Informatics  
University of Trunojoyo Madura  
Bangkalan, Indonesia  
yonathan.hendrawan@trunojoyo.ac.id

Ari Kusumaningsih  
Departement of Informatics  
University of Trunojoyo Madura  
Bangkalan, Indonesia  
ari.kusumaningsih@trunojoyo.ac.id

Rima Tri Wahyuningrum  
Departement of Informatics  
University of Trunojoyo Madura  
Bangkalan, Indonesia  
rimatriwahyuningrum@trunojoyo.ac.id

**Abstract**— Malaria, as a dangerous disease globally, can be reduced its number of victims by finding a method of infection detection that is fast and reliable. Computer-based detection methods make it easier to identify the presence of plasmodium in blood smear images. This kind of methods is suitable for use in locations far from the availability of health experts. This study explores the use of two methods of machine learning on Color Cascading Framework, i.e. Backpropagation Neural Network and Support Vector Machine. Both methods were used as classifier in detecting malaria infection. From the experimental results it was found that Color Cascading Framework improved the classifier performance for both in Support Vector Machine and Backpropagation Neural Network.

**Keywords**— Malaria, classifier, Color Cascading Framework, Backpropagation Neural Network, Support Vector Machine

## I. INTRODUCTION

Malaria is a deadly disease. Based on World Malaria Report 2017 organized by WHO, it is stated that 91 countries reported an aggregate of 216 million cases of malaria in 2016. This number increased five million cases compared to the previous year's number. Globally, deaths from malaria reached 445,000 deaths. The number is approximately the same as reported by WHO in 2015. Although the incidence of malaria cases has declined globally since 2010, the rate of decline has stalled in several areas since 2014. The mortality rate follows a similar pattern [1]. The disease is caused by Plasmodium species, which present in the host's blood cells (erythrocytes). Some types of Plasmodium (P) are P. Malariae, P. Falciparum, P. Ovale, and P. Vivax. Each type of Plasmodium experiences different phases during their development cycle within 48 hours. Each stages has a different visual appearance that can be detected using the microscope. It has several phases of life in the human body, including ring, trophozoites, schizonts, and gametocytes [2], [3], [4]. The rapid parasite

development cycle and the slow process of malaria diagnosis, resulting in high mortality due to malaria. The sooner malaria diagnosis is expected to decrease the mortality rate.

There are many methods available to diagnose malaria. The gold standard method of malaria detection in blood smear is the method where technicians or pathologists manually examine thin or/and thick blood smear under a microscope [5], [6], [7]. Other than that, malaria proteins detection [8], host/human antibodies for fighting malaria proteins detection [9], malaria gene based detection [10], [11], and microscopic cell image detection [12] was also used to diagnose malaria. Each method has its advantages and disadvantages. The gold standard method is cheap, but require experienced microscopist and certain set of tools which might be hard to find in remote areas [7]. Human inconsistencies and the difficulty of detecting low infection levels also make it worse [13], [14]. Malaria proteins detection can differentiate species infection, but it needs higher number of parasites/microliter blood sample (above 100) to be reliable compared to only four parasites/microliter for the gold standard detection performed by a skilled medical expert [5], [15]. Host antibodies detection can also discriminate different malarial infection, but the antibodies remain in the blood system after the infection has been cured; making it unreliable if used to test otherwise healthy people [15], [16]. Malaria gene detection can detect mixed infection between more than one malaria species, but needs elaborate sample preparation [10], [17], [18]. Microscopic image detection is fast and cheap method, but unable to detect drug resistance developed by the malaria and unable to capture and use malaria genomic information [7]. In this paper, we explore the detection of Malaria infections using two supervised machine learning: Backpropagation Neural Network (BPNN) and Support Vector Machine (SVM), comparing in accuracy, sensitivity and specificity. Furthermore, we investigate the effect of Color Cascading Framework (CCD-Framework) on both classifier machine.

This paper is organized as follows. Section I provides general information regarding malaria and its current detection method. Section II describes the datasets we used

The authors thank to Balai Besar Laboratorium Kesehatan (Center for Health Laboratory) Indonesian Ministry of Health Surabaya Indonesia (BBLK-dataset). We also thank to The Ministry of Research, Technology, and Higher Education of Republic Indonesia, Directorate of Research and Community Service, who funded this research through the basic research program 2018.



and details of the proposed methods. Next, the experimental results and analysis are presented in Section III. The conclusion of this study in Section IV.

## II. MATERIAL AND METHOD

In this section, we explain the material, proposed method for detecting malaria disease on microscopic blood smear by using two supervised machine learning methods: Backpropagation Neural Networks and SVM.

### A. The Material

Our study used a dataset which composed of 574 microscopy images, consisting of 287 infected images and 287 non-malaria-infected images. The dataset also consisting four types of Plasmodium (P) specifically P. Falciparum, P. Malariae, P. Ovale, and P. Vivax. Each type of Plasmodium has several phases of life including trophozoites, schizonts and gametocytes. All microscopic images of the dataset are using Red, Green, Blue (RGB) colour-space as its baseline colour and resized its dimension to 256 x 256 pixels. The sample data used for the experiment as shown in Figure 1. The data were provided by Balai Besar Laboratorium Kesehatan (Center for Health Laboratory) Indonesian Ministry of Health Surabaya Indonesia (BBLK-dataset).

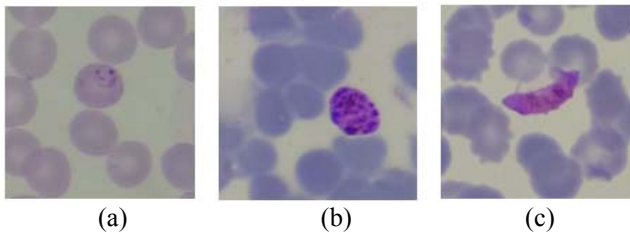


Figure 1. The sample data of Plasmodium Falciparum, (a) trophozoites (b) schizonts (c) gametocytes

### B. Method

We used Color Cascading Framework by Hendrawan et al. as a preprocessing method in preparing the images [19]. The framework involves several processing stages in a sequential step; starting from RGB normalization process, to gamma correction, noise reduction, exposure compensation, edge enhancement, Fuzzy C Means (FCM), and lastly morphological process. In this paper we only utilized the first step (RGB normalization) up to fifth step (edge enhancement). The output from that last step is used as the input for the Neural Network and the Support Vector Machine (SVM). The system's block diagram is shown in Figure 2.

Neural Network is an intelligent system composed of a collection of neurons and the most popular algorithm that has been used by researcher to solve pattern recognition problems [20], [21]. The characteristics method is to minimize the error on the output which generated by the network. The concept of the backpropagation is finding the gradient errors of the network against modified network weights. This gradient error will be used to find the weight value that will minimize the error. In general, neurons are arranged in layers of: input, hidden, and output. In our system the number of input neuron was adjusted to the dimension/size of the images as shown in Figure 3. Since the dimension of our images is 256 x 256 pixels, the input

layer has  $256 \times 256 = 65,536$  neurons. For the hidden layer, we varied the number of neurons: 10, 50, and 100 neurons. For the output screen, we used a single neuron to determine whether the image is infected with malaria or not.

SVM is an intelligent system based on supervised learning. In the training process SVM builds a model that separates each element of input data into different categories. The SVM tries to find the best classifier / hyperplane function to separate two objects. The best hyperplane is a hyperplane located halfway between two sets of objects of two classes. Finding the best hyperplane is equivalent to maximizing margins or the distance between two sets of objects from different classes. In this research we use binary classification system because the problem we want to solve only have two different classes: infected by malaria and not infected by malaria. We used the quadratic programming types of SVM.

The proposed method includes the Color Cascade Framework proposed by Hendrawan et al. which consists of: RGB normalization process, gamma correction, noise reduction, and edge enhancement [19]. Our research focus is on observing the effect of Color Cascade Framework on two different supervised machine learning: Backpropagation Neural Network (BPNN) and Support Vector Machine. The input images are the microscopic images of the blood samples.

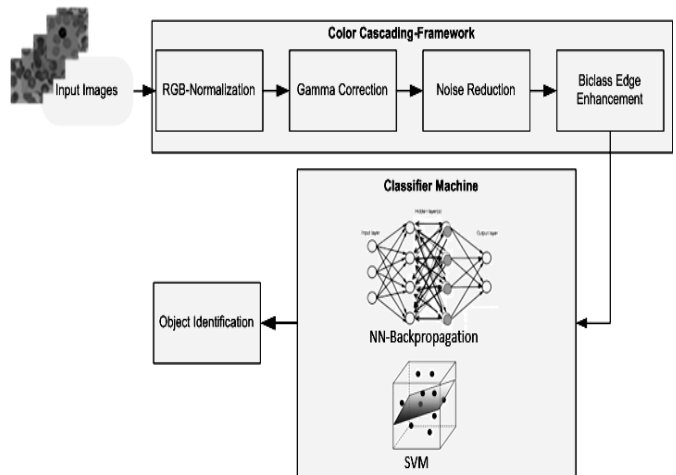


Figure 2. The block diagram of the research

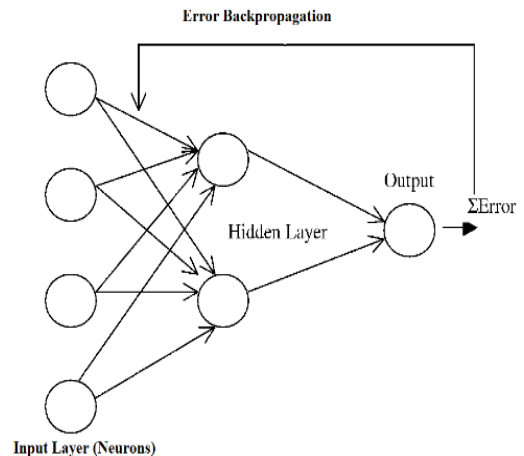


Figure 3. The illustration of BPNN

## III. EXPERIMENT RESULT AND ANALYSIS

The tests were conducted on 574 images in the dataset used as training, validation, and testing data. We made two experiments. The first is using BPNN as its classifier method, and the second is using Support Vector Machine (SVM).

## A. Backpropagation Neural Networks

We choose Backpropagation since it is a popular training method for multi-layer neural networks and has the advantages of accuracy and versatility compared to other methods, such as perceptron. In our experiment, we used several parameters as follows:

- a. Data division : Random pick
- b. Training method : Scaled Conjugate Gradient
- c. Training Performance measurement : Cross-Entropy
- d. Maximum Epoch : 1000
- e. Error target :  $10^{-6}$
- f. Pruning strategy : None

The images were divided into three groups: 70% data as training, 15% data as validation, and 15% data as testing. In the experiment, we used two scenarios: with and without color cascading framework. We also varied the number of hidden layer neurons: 10, 50, and 100. The experiment result is shown on Table 1.

TABLE I. BACKPROPAGATION NEURAL NETWORK CLASSIFIER RESULT

Hidden Layer	Without CCD-Framework			With CCD- Framework		
	A	B	C	A	B	C
100	83.00	80.00	86.60	87.60	80.20	100.00
50	82.40	74.00	100.00	93.20	89.00	98.40
10	87.10	82.20	93.80	83.40	75.10	100.00
AVG	84.17	78.73	93.47	88.07	81.43	99.47

A= Accuracy (%), B= Sensitivity (%), C= Specificity (%)

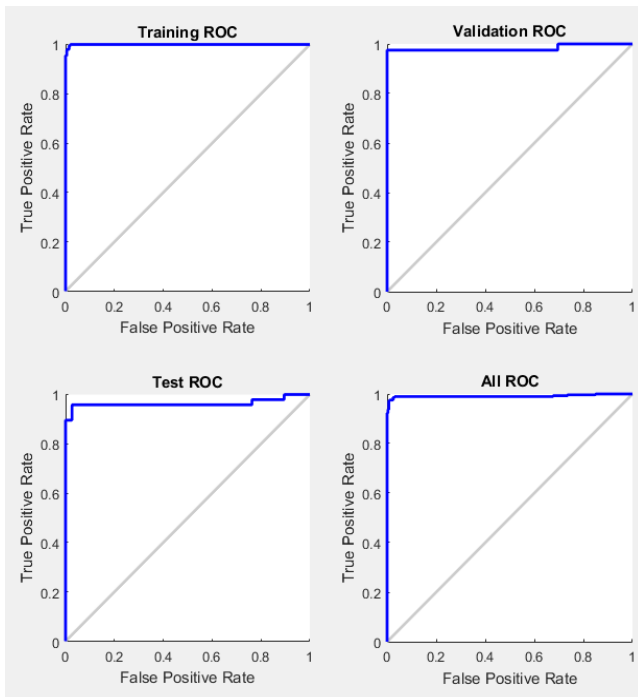


Figure 4. The receiver operating characteristic curve

From the results, it is clear that the use of color cascading framework increased the system's accuracy, sensitivity and specificity. The number of hidden layers did not affect the accuracy, sensitivity, and specificity of the system.

Figure 4 shows the classifier performance for the 50 hidden-layer neuron CCD-Framework experiment. Since the characteristic of ROC curve states that the closer the curve to the main diagonal indicates the less accurate the result, our system performance is favorable since the curve is plotted nearing the (0,1) coordinate.

## B. Support Vector Machine (SVM)

In the SVM experiment, we divided the data randomly into two parts: 70% data as training and 30% data as testing. As in the previous experiment, we also used two scenarios: with and without color cascading framework. We conducted three tests in this experiment. The SVM experiment result is shown on Table 2.

TABLE II. SUPPORT VECTOR MACHINE CLASSIFIER RESULT

SVM	Without CCD-Framework			With CCD- Framework		
	A	B	C	A	B	C
Test-1	91.70	92.50	90.00	97.70	95.50	100.00
Test -2	90.90	90.30	87.60	95.90	94.30	97.60
Test -3	91.50	92.70	87.50	96.50	95.70	97.50
AVG	91.37	91.83	88.37	96.70	95.17	98.37

A= Accuracy (%), B= Sensitivity (%), C= Specificity (%)

From the result, it is also clear that the use of color cascading framework raised the system's accuracy, sensitivity, and specificity of the SVM classifier.

Figure 5 illustrates the two experiments' results. The graph presents the average accuracy, sensitivity, and specificity of 10, 50, and 100 hidden layer neurons from the BPNN experiment. In table 1, the numbers are located in the last row. It also displays the result of the second experiment in the form of average results of the three tests. As in the previous, the numbers are situated in the last row of Table 2.

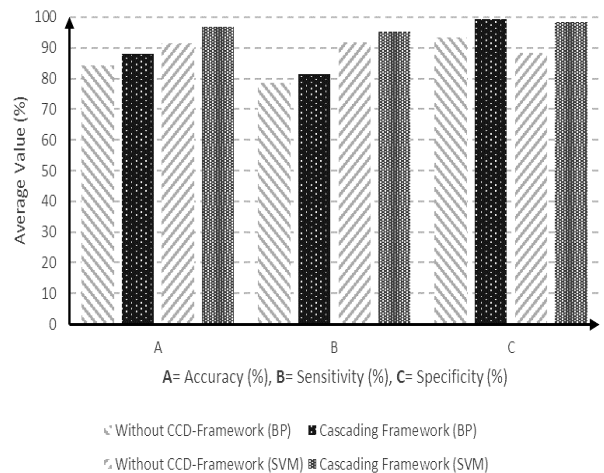


Figure 5. The comparison of experimental result: with and without using Color cascading framework

The system's average value of performance on all classification methods increases with the addition of CCD-Framework. From the results, we can also observe that SVM classifier generates higher performance numbers compared to BPNN classifier in both with and without using CCD-Framework. SVM classifier also has the highest accuracy value (96.70%). It is obtained in the SVM classifier + CCD-Framework test.

In [19], Hendrawan et al used Fuzzy C-Means (FCM) as the CCD Framework's classifier. They achieved their highest results of 98.26% for Accuracy, 97.91% for Specificity, and 98.61% for Sensitivity when they used CCD Framework. Without the framework, they acquired significantly worse results. Whereas for this research, the best results are attained using SVM classifier with CCD framework, that are 96.70%, 95.17%, and 98.37% for accuracy, sensitivity, and specificity. If we compare them, FCM's results are better for all criteria. However, the difference is not large: less than 3% for each measurement component.

#### IV. CONCLUSIONS

The use of CCD-framework has been shown to provide better classifier's performance results. The highest classification results were obtained when applying CCD-Framework with SVM classifier. Its accuracy, sensitivity, and specificity are 96.70%, 95.17%, and 98.37% respectively. So it can be concluded that CCD-Framework is more suitable to be applied in conjunction with SVM classifier in detecting malaria infection in blood smear images. These results are slightly less (<3% for each of the three criteria) than the results of previous study which used Fuzzy C-Means as the classifier. For future studies, we plan to classify the malaria infection into its development phases and species. Correctly identifying the infecting plasmodium species is crucial in determining the appropriate treatment, since it can increase the healing rate.

#### REFERENCES

- [1] "World Health Organization, World Malaria Report 2017." [Online]. Available: <http://www.who.int/malaria/publications/world-malaria-report-2017/en>.
- [2] H. Hiseada, K. Yasutomo, and K. Himeno, "Malaria: immune evasion by parasites," *The International Journal of Biochemistry & Cell Biology*, vol. 37, no. 4, pp. 700–706, 2005.
- [3] M. Poostchi, K. Silamut, R. Maude, S. Jaeger, and G. Thoma, "Image analysis and machine learning for detecting malaria," *Translational Research*, 2018.
- [4] R. T. Wahyuningrum and A. K. Indrawan, "A hybrid automatic method for parasite detection and identification of plasmodium falciparum in thin blood images," *International Journal of Academic Research*, vol. 4, no. 6, 2012.
- [5] M. M. Kettelhut, P. L. Chiodini, H. Edwards, and A. Moody, "External quality assessment schemes raise standards: evidence from the UKNEQAS parasitology subschemes," *Journal of clinical pathology*, vol. 56, no. 12, pp. 927–932, 2003.
- [6] D. K. Das, M. Ghosh, M. Pal, A. K. Maiti, and C. Chakraborty, "Machine learning approach for automated screening of malaria parasite using light microscopic images," *Micron*, vol. 45, pp. 97–106, 2013.
- [7] P. Gascoyne, J. Satayavivad, and M. Ruchirawat, "Microfluidic approaches to malaria detection," *Acta tropica*, vol. 89, no. 3, pp. 357–369, 2004.
- [8] M. T. Makler et al., "Parasite lactate dehydrogenase as an assay for Plasmodium falciparum drug sensitivity," *The American Journal of Tropical Medicine and Hygiene*, vol. 48, no. 6, pp. 739–741, 1993.
- [9] O. Silvie et al., "Potential value of Plasmodium falciparum-associated antigen and antibody detection for screening of blood donors to prevent transfusion-transmitted malaria," *Transfusion*, vol. 42, no. 3, pp. 357–362, 2002.
- [10] M.-A. Lee et al., "Real-time fluorescence-based PCR for detection of malaria parasites," *Journal of clinical microbiology*, vol. 40, no. 11, pp. 4343–4345, 2002.
- [11] K. Ganesan, L. Jiang, and P. K. Rathod, "Stochastic versus stable transcriptional differences on Plasmodium falciparum DNA microarrays," Elsevier, 2002.
- [12] J. Somasekar and B. Eswara Reddy, "Segmentation of erythrocytes infected with malaria parasites for the diagnosis using microscopy imaging," *Computers and Electrical Engineering*, vol. 45, pp. 336–351, 2015.
- [13] C. Di Ruberto, A. Dempster, S. Khan, and B. Jarra, "Analysis of infected blood cell images using morphological operators," *Image and vision computing*, vol. 20, no. 2, pp. 133–146, 2002.
- [14] G. Diaz, F. A. González, and E. Romero, "A semi-automatic method for quantification and classification of erythrocytes infected with malaria parasites in microscopic images," *Journal of Biomedical Informatics*, vol. 42, no. 2, pp. 296–307, 2009.
- [15] J. Iqbal, N. Khalid, and P. R. Hira, "Performance of rapid malaria Pf antigen test for the diagnosis of malaria and false-reactivity with autoantibodies," in *Tropical Diseases*, Springer, 2003, pp. 135–148.
- [16] A. Irion, H.-P. Beck, and T. Smith, "Assessment of positivity in immuno-assays with variability in background measurements: a new approach applied to the antibody response to Plasmodium falciparum MSP2," *Journal of immunological methods*, vol. 259, no. 1–2, pp. 111–118, 2002.
- [17] P. L. Blair, A. Witney, J. D. Haynes, J. K. Moch, D. J. Carucci, and J. H. Adams, "Transcripts of developmentally regulated Plasmodium falciparum genes quantified by real-time RT-PCR," *Nucleic acids research*, vol. 30, no. 10, pp. 2224–2231, 2002.
- [18] C. H. Lai, S. S. Yu, H. Y. Tseng, and M. H. Tsai, "A protozoan parasite extraction scheme for digital microscopic images," *Computerized Medical Imaging and Graphics*, vol. 34, no. 2, pp. 122–130, 2010.
- [19] Y. F. Hendrawan, C. V. Angkoso, and R. T. Wahyuningrum, "Colour image segmentation for malaria parasites detection using cascading method," in *Sustainable Information Engineering and Technology (SIET), 2017 International Conference on*, 2017, pp. 83–87.
- [20] J. Tarigan, Nadia, R. Diedan, and Y. Suryana, "Plate Recognition Using Backpropagation Neural Network and Genetic Algorithm," *2nd International Conference on Computer Science and Computational Intelligence 2017, ICCSCI*, vol. 116, pp. 365–372, 2017.
- [21] Z. Chiba, N. Abghour, K. Moussaid, A. El Omri, and M. Rida, "A novel architecture combined with optimal parameters for back propagation neural networks applied to anomaly network intrusion detection," *Computers & Security*, vol. 75, pp. 36–58, 2018.

# Monitoring Walking Devices For Calorie Balance In Patients With Medical Rehabilitation Needs

Wahyu Andhyka Kusuma  
Informatics Engineering  
Universitas Muhammadiyah Malang  
Malang, Indonesia  
kusuma.wahyu.a@gmail.com

Siti Norhabibah  
Informatics Engineering  
Universitas Muhammadiyah Malang  
Malang, Indonesia  
sitinorhabibah@gmail.com

Zamah Sari  
Informatics Engineering  
Universitas Muhammadiyah Malang  
Malang, Indonesia  
zamahsari@umm.ac.id

Sabrina Nurul Ubay  
Informatics Engineering  
Universitas Muhammadiyah Malang  
Malang, Indonesia  
sabrinarurulubay22@gmail.com

Hardianto Wibowo  
Informatics Engineering  
Universitas Muhammadiyah Malang  
Malang, Indonesia  
ardi@umm.ac.id

Diah Ayu Fitriani  
Informatics Engineering  
Universitas Muhammadiyah Malang  
Malang, Indonesia  
diah.ayyu@gmail.com

**Abstract**—This article presents a measurement system intended to monitor human footsteps. The goal is to guide the user's medical rehabilitation incorrect use to prevent dangerous situations and maximize comfort. Indicators of risk in question: the imbalance of movement in motor coordination and the number of calories to be burned for medical rehabilitation patients by balancing the patient's needs. Measurements are made by placing the sensor on one of the patient's legs. The main sensor accelerometer used in this study. The measurement system comes with an application link that allows patients and therapists to monitor the activity. Calibration and experimental results are presented in this article

**Keywords**— *Walking Devices, Calorie Balance, Medical Rehabilitation*

## I. INTRODUCTION

As the development of science and technology grows, more and more innovations emerge in various sciences. The development also raises the human awareness of the importance of medical rehabilitation especially for patients and parents who need medical rehabilitation. Movements can increase the risk of increasing accidents [1]–[7], especially when walking. The need for medical rehabilitation to perform movements, especially to burn calories into special needs, especially the movement of patients or parents cannot be done in vain.

Walking is a series of straightforward moves. Whatever speed and distance traveled, standing still is the key [8]. Walking is not just anyone can do, walking is also the most comfortable exercise because it is a daily activity. Walking alone has many benefits, and one of them is to lose weight in medical rehabilitation. To lose weight, it needs calorie burning.

Several solutions have been undertaken to address foot step monitoring problems [9]–[12], but the solution of the problem is too expensive to apply in everyday activities and is primarily still theoretical. Some solutions use an accelerometer and Inertial Motion Units (IMU) to obtain kinematic parameters on the movement of human footsteps [13]–[15]. The need in burning calories especially for medical rehabilitation patients and parents is a simple tool that is enough to calculate how many footsteps you have done and how many calories you have burned.

Quoted from the Healthy Food Star, a benchmark to calculate the burning of calories using distance. In taking 1.6 kilometers distance when walking, there are 100 calories burned. The distance is usually taken with 2000 steps. To get 1 pound or 0.45 kilograms of burning, counted must destroy 3500 calories. If you want to lose 1 pound per week, then you have to spend 500 calories per day [16].

Unlike the Healthy Food Star, according [16] to calculate the burning calories the benchmark used is the speed because although the distance traveled the same the speed is different, it can produce different calorie burning. Speed itself is obtained from the calculation of the number of footsteps divided by time (minutes).

Our paper is novel in that we apply accelerometer and gyroscope for calories calculation. In a study conducted using accelerometer and gyroscope sensors contained in the MPU6050 module, the sensor activity is then processed using the Mini Wemos D1 module with a supply of batteries that can last up to one day for continuous activity. The data from Wemos is then processed inside the user's Mobile to find out how many footsteps and calories are burned in one activity.

## II. METHOD

### A. The Human Cycle Walks

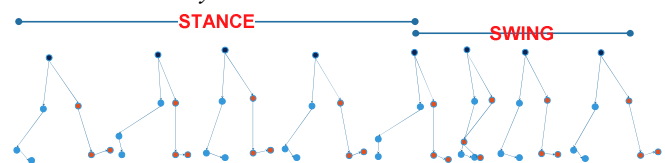


Fig. 1. The Human Cycle Walks

Viewed from the way humans walk shows that the pattern of movement of the human foot during the run has repeated cycles, so by analyzing these patterns detection steps can be done as shown Figure 1. The human pattern of stepping is basically two phases, phase stance and swing phase [2]. Phase stance is a state where one foot treads on the ground. The swing phase is the state in which one leg is raised. By the time one of the legs is in the stance phase, the other foot will be in the swing phase.



### B. Sensor Placement

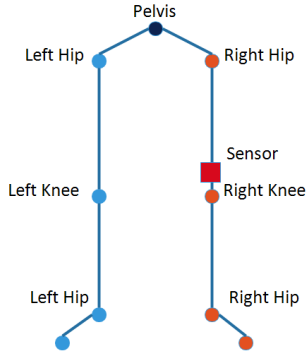


Fig. 2. Sensor Placement

In previous studies several studies have been conducted to find out where to place sensors effectively [17]. Sensor placement depends on the need, the research conducted by the sensor is placed on the right knee. When starting, a calibration process needs to be carried out, where calibration is used to get stable results from foot movements. When calibrating the leg is lifted to form a 90-degree angle with the other leg, then proceed with a relaxed walk. Algorithm 1 as calibration process need raw parameter from gyroscope and accelerometer.

### C. Distance Legs

Humans on foot form a triangle pattern as shown in Figure 3. Before measuring the distance, it should be known how much the average width between the right foot and left foot when stepping. The United States customary units declare that the standardized unit of each human step is naturally calculated from the tip of the foot that is in front of the end of the previous leg.

$$\text{step} = \text{distance} * 0.78 \quad (1)$$

The average step is 78cm or assumed to be a human step along the 0.78m [3]. If it is known the width multiplied by the number of steps that we do then the distance traveled when walking with the formula as Equation (1) The Human Cycle Walks.

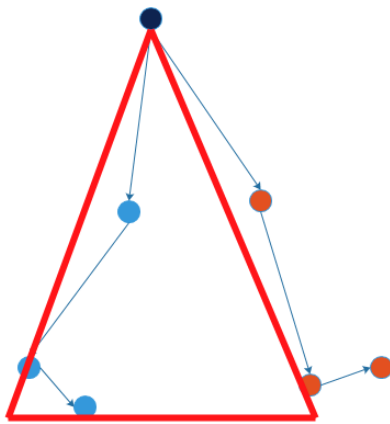


Fig. 3. Triangle Pattern

### D. Calories

Calculation of calorie requirements is needed to determine calories that need to be burned efficiently. Calorie burning, especially for medical rehabilitation, requires burning calories properly.

#### Algorithm 1 Calibration Process

---

**Input:** Accelerometer  $x, y, z$ , Gyroscope  $x, y, z$   
**Output:** Update  $\Delta$  during duration

```

1: if data arrives then
2:   if this is first data then
3:      $\Delta_{min} = \min(x, y, z)$ 
4:      $\Delta_{max} = \max(x, y, z)$ 
5:   end if
6: end if
7: if  $\Delta_{min}$  and  $\Delta_{max}$  is not empty then
8:    $\Delta_{min\_avg} = \sum_n \min(x, y, z) / n$ 
9:    $\Delta_{max\_avg} = \sum_n \max(x, y, z) / n$ 
10:  if  $\Delta_{min\_avg} < \Delta_{min}$  and  $\Delta_{max\_avg} < \Delta_{max}$  then
11:     $\Delta_{min} = \Delta_{min\_avg}$ 
12:     $\Delta_{max} = \Delta_{max\_avg}$ 
13:  end if
14: end if

```

---

#### Algorithm 2 n-Steps Leisurely Walk

---

**Input:** Accelerometer  $x, y, z$ , Gyroscope  $x, y, z$ ,  $\Delta_{min}$ ,  $\Delta_{max}$ , distance  
**Output:** Update Steps during duration

```

1: if data arrives then
2:   if this is first data and distance = 0 then
3:     if  $\Delta_{min} > (x, y, z) > \Delta_{max}$  then
4:       step++
5:     else
6:        $\Delta_{min} = \sum_n \min(x, y, z) / n$ 
7:        $\Delta_{min} = \sum_n \min(x, y, z) / n$ 
8:        $\Delta_{min} > (x, y, z) > \Delta_{max}$ 
9:       step++
10:    end if
11: end if

```

---

#### Algorithm 3 Calories Reduction

---

**Input:** Steps, duration, weight  
**Output:** Update Calories during duration

```

1: if data arrives then
2:   MET = Steps/duration
3:   Calories =
     (MET * 7.8 * (weight * 2.2))/200 * (duration/60)
4: end if

```

---

$$\text{Calories} = (\text{MET} * 7.7 * (\text{weight} * 2.2))/200 * (\text{duration}/60) \quad (2)$$

Medical rehabilitation patients generally cannot carry out too many activities, therefore knowing this can prevent accidents. For calorie calculation as shown in Equation 2 we use Metabolic Equivalent Of Task (MET).

Implementation of MET need three parameters Steps, Duration and Weight, for some problems usually MET needs gender clasification, but in this problem we ignore it. before running the calorie calculation process, it is necessary to calculate footsteps using Algorithm 2. Algorithm 2 will run the footstep calculation process based on the calculation of the threshold specified in the calibration section. After getting the number of steps, the MET calculation can be done by calculating all parameters in Algorithm 3.

### III. RESULT AND DISCUSSION

#### A. Experimental Setup

Before using the footstep monitoring tool, connect the WIFI smartphone with the tool. Tools placed on the thigh then do the monitoring with the application. To detect footsteps, each data has a predefined upper and lower value limits. If the data is less than -20 then there is a marker that the data has reached the lowest point, then the sensor reads the data again. If the data is above 20 and the data marker has read the lowest point, then the number of steps is added 1. After step plus 1, the step multiplied by the average foot width when stepping (0.7m) then obtained the distance.

Ethical Clearance, each test is accompanied by a therapist. All activities have been ensured safe to do. The movements performed are determined by the therapist including the number of calories that need to be burned.

#### B. Design Testing

In design testing, the testing doing by five person to activity leisurely walk, as shown in Table 1 the distance has been determined in advance so that the ground truth can be known the number of footsteps taken.

TABLE I. TABLE ACTIVITY

Activity	Footsteps	Distance
Leisurely Walk	4 Step	2,4 Meter
	8 Step	4,8 Meter
	10 Step	6 Meter
	15 Step	9 Meter
	20 Step	14 Meter



Fig. 4. Device Used

In the research, Wemos D1 Mini was used which was connected directly to the MPU6050, and a 3.3 volt battery as shown in Figure 4.

#### C. Result

From the walking activity conducted by the testers as much as 4, 8, 10 steps as shown in Figure 5 - 8, obtained data from the sensor, convert the data into the sine wave to know the movement of the step to generate how many waves. Wave results are determined by a threshold above and threshold below to detect footsteps that will be displayed on Android applications. Table 2 shows the differences in calculation results performed by tools based on the ground truth in Table 1. In addition, testing was also carried out with equipment that

had been circulating in the market, in this study a comparison was carried out using Mi Band 2. After the result of threshold comparison then detection step is shown .

TABLE II. RESULT AND DIFFERENCE IN COUNTING

Device	Manual	Difference
4	4	0
8	8	0
10	10	0
14	15	1
18	20	2

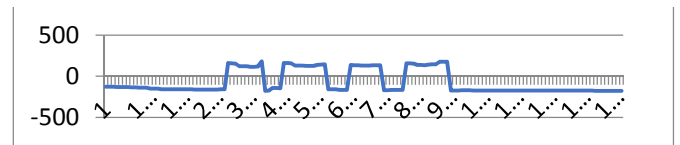


Fig. 5. 4 Steps Leisurely Walk

TABLE III. DIFFERENCE COUNTING WITH MARKET BASED

Steps	Test 1		Test 2		Avg		Diff.
	Mi Band 2	Our	Mi Band 2	Our	Mi Band 2	Our	
5	6	5	4	5	5	5	0
10	17	10	19	10	18	10	8
15	34	14	25	15	29,5	14,5	15
20	43	20	35	19	39	19,5	19,5
25	50	23	56	25	53	24	29

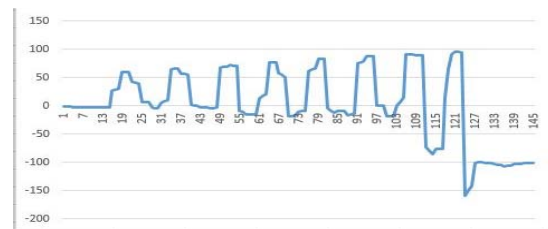


Fig. 6. 8 Steps Leisurely Walk

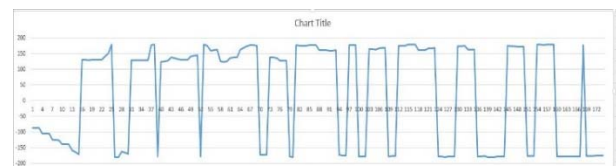


Fig. 7. 10 Steps Leisurely Walk

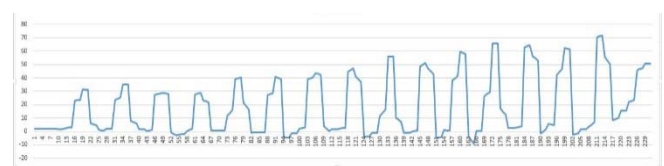


Fig. 8. 15 Steps Leisurely Walk



## IV. CONCLUSION

From the results of tests conducted in detecting footsteps as much as 57 times, obtained an error value of 3.65% means the system is able to detect foot activity with good enough. Monitoring results depend on the laying of the sensor. Use of the tool is very useful to minimize injuries that can occur. The average results obtained for the activity runs smoothly, the movement of each footstep is very regular.

## REFERENCES

- [1] I. Gringauz *et al.*, "Risk of falling among hospitalized patients with high modified Morse scores could be further Stratified," *BMC Health Serv. Res.*, vol. 17, p. 721, Nov. 2017.
- [2] D. J. Clark, "Automaticity of walking: functional significance, mechanisms, measurement and rehabilitation strategies," *Front. Hum. Neurosci.*, vol. 9, p. 246, May 2015.
- [3] Y.-H. Pua, R. A. Clark, and P.-H. Ong, "Evaluation of the Wii Balance Board for Walking Aids Prediction: Proof-of-Concept Study in Total Knee Arthroplasty," *PLoS One*, vol. 10, no. 1, p. e0117124, Jan. 2015.
- [4] M. H. C. Bleijlevens, J. P. M. Diederiks, M. R. C. Hendriks, J. C. M. van Haastregt, H. F. J. M. Crebolder, and J. T. van Eijk, "Relationship between location and activity in injurious falls: an exploratory study," *BMC Geriatr.*, vol. 10, p. 40, Jun. 2010.
- [5] V. Viegas, J. M. Dias Pereira, O. Postolache, and P. S. Girão, "Monitoring Walker Assistive Devices: A Novel Approach Based on Load Cells and Optical Distance Measurements," *Sensors (Basel)*, vol. 18, no. 2, p. 540, Feb. 2018.
- [6] J. A. Stevens, K. Thomas, L. Teh, and A. I. Greenspan, "Unintentional Fall Injuries Associated with Walkers and Canes in Older Adults Treated in U.S. Emergency Departments," *J. Am. Geriatr. Soc.*, vol. 57, no. 8, pp. 1464–1469, Jul. 2009.
- [7] H. Bateni and B. E. Maki, "Assistive devices for balance and mobility: Benefits, demands, and adverse consequences," *Arch. Phys. Med. Rehabil.*, vol. 86, no. 1, pp. 134–145, Jan. 2005.
- [8] T. Z. Sudbury, "Development of biomechanical analysis techniques for fatigue of transtibial prosthetic socket and pylon interactions," 2014.
- [9] M. Alwan, A. Ledoux, G. Wasson, P. Sheth, and C. Huang, "Basic walker-assisted gait characteristics derived from forces and moments exerted on the walker's handles: results on normal subjects," *Med. Eng. Phys.*, vol. 29, no. 3, pp. 380–389, Apr. 2007.
- [10] A. Muro-de-la-Herran, B. Garcia-Zapirain, and A. Mendez-Zorrilla, "Gait analysis methods: an overview of wearable and non-wearable systems, highlighting clinical applications," *Sensors (Basel)*, vol. 14, no. 2, pp. 3362–3394, Feb. 2014.
- [11] E. Sardini, M. Serpelloni, and M. Lancini, "Wireless Instrumented Crutches for Force and Movement Measurements for Gait Monitoring," *IEEE Trans. Instrum. Meas.*, vol. 64, no. 12, pp. 3369–3379, 2015.
- [12] D. D. Ely and G. L. Smidt, "Effect of cane on variables of gait for patients with hip disorders," *Phys. Ther.*, vol. 57, no. 5, pp. 507–512, May 1977.
- [13] L. C. Masse *et al.*, "Accelerometer data reduction: a comparison of four reduction algorithms on select outcome variables," *Med. Sci. Sports Exerc.*, vol. 37, no. 11 Suppl, pp. S544–54, Nov. 2005.
- [14] I.-M. Lee and E. J. Shiroma, "Using accelerometers to measure physical activity in large-scale epidemiological studies: issues and challenges," *Br. J. Sports Med.*, vol. 48, no. 3, pp. 197–201, Feb. 2014.
- [15] S. K. Keadle, E. J. Shiroma, P. S. Freedson, and I.-M. Lee, "Impact of accelerometer data processing decisions on the sample size, wear time and physical activity level of a large cohort study," *BMC Public Health*, vol. 14, p. 1210, Nov. 2014.
- [16] CNN, "Turunkan Berat Badan dengan Berjalan Kaki," 2017, 2017. [Online]. Available: <https://www.cnnindonesia.com/gaya-hidup/20160818115814-255-152171/turunkan-berat-badan-dengan-berjalan-kaki/>.
- [17] A. T. S. Wahyu Andhyka Kusuma, Zamah Sari, "Sensor Fusion Accelerometer dan Gyroscope untuk Pengukuran Perubahan Kinematik Pergelangan Kaki," *Kinetik*, vol. 1, no. 1, pp. 17–22, 2016.

# E-Government Maturity Model to Support System Dynamics in Public Policymaking

Feldiansyah Bakri Nasution  
Department of Computing  
Universiti Teknologi Malaysia (UTM)  
Johor Bahru, 81310 Johor, Malaysia  
feldiansyah2@live.utm.my

Dr. Nor Erne Nazira Bazin  
Department of Computing  
Universiti Teknologi Malaysia (UTM)  
Johor Bahru, 81310 Johor, Malaysia  
erne@utm.my

**Abstract**— In this paper, the main output of e-government is designed to assist a policymaker to create a comprehensive public policy. The policy is developed by studying the political and social issues in holistic way. System Dynamics based on Big Data from e-government infrastructure is suggested as the method for obtaining a comprehensive solution. The solution is selected from some possible scenarios by running simulation on the model of System Dynamics. The policymaker uses this solution as an input for public policymaking. Unfortunately, no E-Government Maturity Model (EMM) has given attention to incorporate Big Data and System Dynamics for Public Policymaking. In this case, a new EMM is proposed. It consists of several stages. Each stage is identified by the range of intensity or level of several criteria or indicators. Some criteria or indicators are proposed by considering technical and non-technical aspect, such as Leadership / Policy, IT Infrastructure, Information Processing (Application), Human Resources and Organization Culture. At the end of this paper, the survey is conducted to identify the current level or stage of EMM of one of government institution in Indonesia. (*Abstract*)

**Keywords**—E-Government, System Dynamics, Public Policy, Big Data (*key words*)

## I. INTRODUCTION

The E-Government Maturity Model (EMM) is used as a guideline to develop e-government from the lowest stage until the highest stage or mature position. The process of movement from the worst position (first stage) to the best position (last stage) is done gradually. To make the movement runs smoothly, it will be broken down into several stages. These multiple stages of EMM are to assist in manageability of the development of e-government. Fath-Allah et al. show that some experts introduce several models [1]. Each model consists of several stages. The total stages of each modal are variety. The most minimum stages are introduced by Reddick Maturity Model [2]. It is 2-stage model which is similar to our basic diagram (see Figure 1).

In designing EMM, the requirement from stage one until the final stage is determined by some criteria or indicators. The objective of each stage is stated. Each objective should align with the main expected output of e-government which is

to achieve the expected result or maturity position. A review can be done to identify if there is any deviation in each stage. It should have its own strategy to accelerate to achieve maturity stage. The establishment of stages in E-Government development is (1) to provide clear direction for e-government development, (2) to facilitate the determination of strategies based on objective of each stage in E-Government development, (3) to solve problem and focus on each stage of E-Government development, and (4) to assist in preparing public policymaking based on data and information.

In this paper, the lowest or first stage is the basic condition of the IT usage in the government. It is the minimum utilization of IT. The final stage is the expected stage and it is usually called as maturity position or stage. The maturity stage is the e-government condition which the public policymaking is created based on system dynamics and Big Data. Nasution et al. [5] gives a good explanation how system dynamics and Big Data contribute for public policymaking. Basically, the Big Data provides the data, information and knowledge to assist in modelling of system dynamics. The model is created to mimic the real system which the issues or problems are situated. After finalizing the model, some scenarios are simulated on the model to find the best outcome to solve the problem. The best outcome of this simulation becomes the input to the public policymaking.

Big Data has more complexity then ordinary data, especially (1) it is involved more technologies and more arrangement of data analytics techniques (2) the data is huge and distributed in several systems. It becomes double complexity if Big Data is used to find a solution of another complex problem, such as public policymaking. At this moment, Big Data has a limitation to assist in solving problem of complex system, such as in public policymaking. In this case, the new method is needed to overcome this limitation. The method should be able to run the analytics on all aspects, not only technical aspects but also non technical aspects which are commonly happened in public policymaking. Multiple factors are studied such as how the new public policy increases satisfaction to group of people and reduce negative sentiment of other group. What the balancing way is to

optimize the outcome of the public policy. It is inclusive the unanticipated side effects of the public policy implementation.

Solving unstructured of complex system and its behaviours need special analytics techniques and methods. One of them which is usually used in the unstructured of complex system is based on the system theory, in more specific, System Dynamics (SD). It becomes our main objective that the output of proposed EMM should be able to support public policymaking by utilizing SD approach and Big Data. Big Data in the e-government is provided to assist in SD model creation. The model is the key in the SD.

Below is the basic diagram of EMM. After defining the first and final stage, the breakdown process is run on it to identify the stages between first and final stage. Each stage is identified with some important criteria and how it's interconnected from previous stage and next stage. It is structurally broken down. The rating of E-Government Maturity is based on the combination capability of criteria or indicators. It could be only in technical aspect or combination between technical and non technical aspect. PeGI stands for Peningkatan e-Government Indonesia (E-Government Indonesia Rating) which is published by Indonesia Government has its own rating [6]. Its rating is based on the criteria of the capability of (1) Planning, (2) Application, (3) Infrastructure, (4) Organization, and (5) Policy [6]. Basically, the functionality of criteria or indicators is related to IT in the government organization. Based on the PeGI, it is not only technical aspect to make the e-government successful. Planning, Organization and Policy are non technical aspect which is considered equally with the technical aspect, such as Application and Infrastructure.

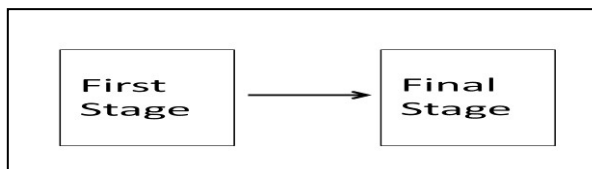


Fig. 1. Basic Diagram of E-Government Maturity Model (EEM)

In our perspective, the main target of a true e-government is its contribution in public policymaking. This aim is the objective of our proposed EMM. It will impact to the way how the stages are designed. In this paper, public policymaking is offered by collaborating Big Data and SD. Big Data has huge capacity to store data and information, and it is used for modelling the issues or problem. Systems dynamics approach uses the model to find its solution by simulating some possible scenarios in multiple perspective [7]. It can look at a problem holistically.

The Big Data are related closely to E-Government. It is only one of the components in E-Government [6]. The success of Big Data implementation should be aligned with E-Government development. Without a proper E-Government development, Big Data will not be utilized optimally. The E-Government development is directed by the selected EMM. Selection of EMM is a critical initiation for long term E-Government development. In the next section, some existing

E-Government Maturity Model (EMM) will be discussed and categorized before proposing a new EMM which is suitable for our requirement.

## II. METHODOLOGY

This research will use comparative and qualitative approach. The results of previous research of EMM are collected and reviewed. The models are compared to understand the outline. The purpose of this comparative study is (1) to discover the similarities and differences of the stages between each EMM, (2) to compare the objective and properties between each EMM (3) to generalize the level of comparison based on the new perspective of the stages of EMM, (4) to determine which one is better or which one should be selected, (5) to investigate the possibility of causal relationships between the stages, and (6) to rediscover new factors that may be the cause the revision.

The main steps in comparative research are used as follows (1) Formulate and define the problem. (2) Examine the existing literature. (3) Formulate the theoretical framework. (4) Develop research design. (5) Conduct survey and analysis. (6) Make conclusions. (7) Arrange the report by scientific writing.

### A. Problem Formulation

E-Government Maturity Model (EMM) has to support public policymaking. Unfortunately, final stage of some models is not stop at public policymaking. They are more focus to technical aspect only. In our perspective, supporting public policymaking is the goal of E-Government. It becomes the main goal. Nasution et al. [7] proposes to use system dynamics to optimize the contribution of Big Data in E-Government for public policymaking. System dynamics could give a holistic and comprehensive perspective in understanding the problem situation. The system dynamics is the mediating variable in this case [8]. Therefore, the readiness of Big Data in E-Government is the most important key factor for public policymaking based on system dynamics. It is in line with a model which is created by Bri [9], where system thinking and system dynamics is put on the highest stage. Although without a clear rating system, at least Bri [9] introduces another perspective of EMM.

### B. Literature Review

Experts have different definitions of E-Government [10][11]. Sometimes, it is defined according to each individual or institution based on its work plan. Here's definition of E-Government by experts:

#### 1) World Bank

E-Government is the use of information technology (such as Wide Area Networks, Internet and other advanced technology) by governments that are able to transform government communications with the public, business or fellow governments.

#### 2) UNDP (United Nations Development Program)

E-Government is the use of Information and Communication Technology (ICT) by government agencies.

### 3) Ministry of Communications and Informatics of USA

E-Government is an Internet-based information technology application and other digital devices managed by the government to communities, business partners, employees, business entities, and other online institutions.

### 4) The Government of New Zealand

E-Government is a new way of using technology by governments to provide easier access to information and government services for the community, to improve the quality of services and open wider opportunities for people to participate in democratic governance.

### 5) Jim Flyzk (US Department of Treasury)

E-Government is about bringing government into the internet world and working in internet time.

In our perspective, E-Government is a system based on IT and its related factors for providing service via internet, intranet and extranet to government officer, citizen and foreigner for the advantage to the country in the secure manner and assist in public policymaking. Everybody such as government officer, citizen and foreigner could participate in the public policymaking via the provided service. It is developed in each stage of EMM until E-Government is mature enough to provide the necessary system. It is in the last stage for some models.

Regardless of the definition, Governments in developed countries that have implemented E-Government, view that E-Government implementation should be done quickly and seriously. E-Government is considered to give a benefit to the country. Benefits of E-Government, among others are:

- E-Government can improve the quality of government services to the community, business partners, industry, business entities and other institutions in terms of effectiveness and efficiency in various aspects of the life of the state.
- E-Government is considered capable of increasing transparency, control, accountability of governmental administration in order to realize good governance.
- E-Government can reduce the administrative costs, relationships and interactions, which are issued by the government and stakeholders in daily activities significantly.
- E-Government is able to provide new sources of revenue for the government through interaction with interested parties.
- E-Government can create a new environmental society that can answer all issues reported quickly and accurately in accordance with the global changes that occur.
- E-Government can empower communities and other stakeholders to become government partners in terms of democratic processes and public policymaking.

### C. Theoretical Framework

Some literatures are discussed about the EMM [1]. They are discussed about the following models: Layne and Lee [12], Andersen and Henriksen [13], United Nations [14], Alhomod et al. [15], Hiller and Belanger [16], Almazan and Gil-Garcia [17], Cisco [18], Baum and Di-Maio [19], West [20], Moon [21], Toasaki [22], Deloitte and Touche [23], Howard [24], Shahkooh et al. [25], Lee and Kwak [26], Siau and Long [27], Wescott [28], Chandler and Emanuel [29], Kim and Grant [30], Chen et al. [31], Windley [32], Reddick [2], Rohleder and Jupp [33], NOA[34], Netchaeva [35], Finn de Bri [9] and PeGI [6].

From many models which are has been discussed before, the minimum of the stages of E-Government Maturity Model are two [2] and the maximum is eight [9]. There are advantages and disadvantages if the total stages are too small or too big. If it is too small, it is more difficult to control the development from one stage to the other stage. If it is too big, it is more complicated to manage because too many stages. If the middle number between two (the minimum) and eight (the maximum) is used, five is the moderate number. This number will be used to categorize all stages of reviewed EMM. It is almost similar as explained by some experts [21][25][27]. The proposed model is called as 5-stage model.

In this paper, all those models are summarized into a table as below. On each model, number 1 – 5 is to represent the stage of the model. Symbol X means Not Applicable (NA) because it is not covered in the discussion of the model.

TABLE I. SUMMARY OF E-GOVERNMENT MODEL IN 5-STAGE MODEL

No	Model	Stage				
		1	2	3	4	5
1	<b>Layne and Lee</b>	1	X	2	3,4	X
2	<b>Andersen and Henriksen</b>	X	X	X	1-4	X
3	<b>United Nations</b>	1,4	2,4	3,4	X	X
4	<b>Alhomod</b>	1	2	3	4	X
5	<b>Hiller and Belanger</b>	1	2	3	4	5
6	<b>Almazan and Gil-Garcia</b>	1,2	3	4	5	6
7	<b>Cisco</b>	1	X	2	3	X
8	<b>Gartner Group</b>	1	2	3	4	X
9	<b>West</b>	1	X	X	3-5	X
10	<b>Moon</b>	1	2	3	4	5
11	<b>World Bank</b>	1	2	3	X	X
12	<b>Deloitte and Touche</b>	1	2	2	3-6	X

No	Model	Stage				
		1	2	3	4	5
13	Howard	1	2	2	3	X
14	Shahkooh	1	2	3	4	5
15	Lee and Kwak	1	2,3	X	4,5	X
16	Siau and Long	1	2	3	4	5
17	Wescott	X	1-3	4	5	6
18	Chandler and Emanuel	1	2	3	4	X
19	Kim and Grant	1,2	X	3	4	5
20	Chen	1	2	X	3	X
21	Windley	1	2	X	X	3,4
22	Reddick	1	X	2	X	X
23	Accenture	1,2	X	X	3,4	5
24	UK	1,2	3	4	5	X
25	Netchaeva	1	2,3	4	X	5
26	Finn de Bri	1-3	X	X	4-7	8
27	PeGI	1-5	1-5	1-5	1-5	1-5

In the table 1, it shows that Layne and Lee [12] is not completely match with the proposed model. Stage 1 of Layne and Lee's model is the same as stage 1 of our proposed model, 5-stage model. Stage 2 of Layne and Lee's model is similar with stage 3 of 5-stage model. Stage 3 and 4 of Layne and Lee's model is similar with stage 4 of 5-stage model. In this case, the symbol X which means Not Applicable is put on stage 2 and 5 of 5-stage model.

Each of the models is compared with the proposed model, 5-stage model. It is categorized into five stages. Stage-1 is for one way information propagation. The information is coming from the government and it is distributed via internet to the society. The Stage-2 is for two ways interaction between government and society. It could be using the email or uploading question via web application. The Stage-3 is for transaction capability, especially in payment which needs interaction with banks or other financial institution. The Stage-4 is for integration between all government units vertically or horizontally. The Stage-5 is the advanced usage of data and information for public policymaking.

The table above is the summary for all discussed models, which are grouped into 5-stage model. The 5-stage model is categorized into Publish (Stage 1), Feedback (Stage 2), Transaction (Stage 3), Integration (Stage 4) and Policy (Stage 5). The stage 4 could be divided into two subcategories: Integration Internal (Stage 4a) and Integration External (Stage 4b). Stage 4a is for integration vertically in the same work unit and Stage 4b is between work units (horizontally). In figure 2, it shows that the stages of maturity growth are not inline. From Stage 1, it will not able to jump directly to Stage 3,

Stage 4 or Stage 5 directly without going through Stage 2. But on Stage 2, it could jump to Stage 4. The Stage 2 is the foundation for Stage 3 and Stage 4. Logically, before doing the transaction, it should have the capability of two way communications. The Stage 3 is the enhancement of Stage 2. In Stage 3, notification, confirmation or feedback is needed after the transaction. In Stage 4, the process of integration between two or more institution must have the two way communications. Transaction is not compulsory in the Stage 4. That's why, it could jump from Stage 2 to Stage 4 directly without through Stage 3. The integration means that all data and information are integrated into one system. It is the baseline for doing business intelligent for public policymaking in the next stage. The Stage 5 is the final stage as the process of public policymaking, which is integrated with the E-Government. Five criteria or indicators are provided to measure the status of each stage. The indicators are a combination between technical and non-technical aspects, such as: Leadership / Policy, IT Infrastructure, Information Processing (Application), Human Resources and Organization Culture [36].

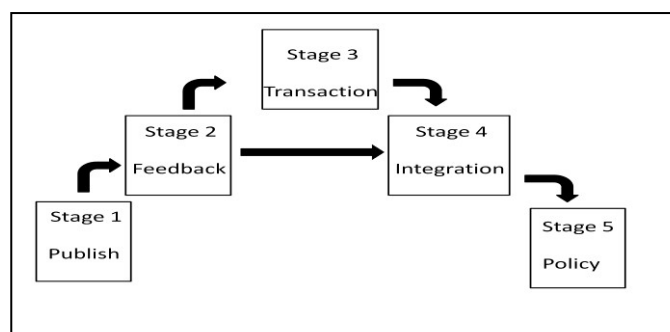


Fig. 2. The 5-stage model of E-Government Maturity Model (EEM)

The stages are:

- Publish (Stage 1),

At this stage, the objective is to give Data and Information in one direction from government to the public. It is published via internet. Leadership / Policy indicator shows that the individual activity is dominance. Self motivation capability is very important. The leader of organization has no interest or capability to utilize the IT for their organization. IT Infrastructure is setup to achieve one way communication only. Information Processing (Application) is not complicated. It is only a static web application to share the data and information to the public. A low skill human resource is needed to support a basic web server. In this stage, the data and information are kept and protected by each department or individual people.

- Feedback (Stage 2),

The objective in this stage is not only to give Data and Information to the public but also receive the feedback. It is supported by the Customer Relationship Management (CRM) System. The CRM is little bit difference with the one in the

private sector, but the main idea is the same. It is to increase the public satisfaction to the government.

Leadership / Policy to motivate others are dominant. The leader of organization has an interest to utilize IT. The Key Performance Indicators are introduced to support this. The IT Infrastructure is supported 24x7 to receive a feedback from public. There are some application suggested at this stage such as Email, Chat and Forum. More skillful human resource is needed, advance in technical and non-technical skill. Service oriented organization is a must. It is because the public is waiting for the action after they give the feedback.

- Transaction (Stage 3),

The objective is to give more services to public such as e-passport, e-licenses, e-payment and others. The transaction financial or non financial are inclusive in stage. The high security level is expected. The PCI DSS, ISO 27001 and ISO20000 / ITIL are considered to be implemented in this stage. Transparency is the key to monitor all business processes.

A dedicated head of Data and Information is needed to manage the operation and project. He/she needs capability to lead the IT group and report to the leader of organization. The IT Infrastructure needs to follow the international standard, especially in security to protect all transactions. The Application has the connection to Banks or Financial Institution for e-payment. Security engineer or expert is another requirement in this stage. Organization culture is to support transparency processes.

- Integration (Stage 4)

A government has many unit organizations, institutions, and departments. It spread over the country. It is very complex and tough challenge to collaborate them together. In this stage, the objective is the integration of all IT-related components in organization. It is not compulsory via stage 3. It could be happened after the stage 2 directly without development of stage 3. By jumping from Stage 2 to Stage 4, it speeds up the process, although it needs to make adjustment in the integration process. Many high skill project managers are needed in this stage to handle each project. For overall, the program or portfolio manager will oversee all projects and lead the function.

IT infrastructure needs more advance control tools such as ID Management, LDAP, Network Management Station (NMS), Policy Servers and others. The application has capability to be customized per profile by the public. It is dynamics web application. The system is more complex, and needs not only person expert in one field but also multiple fields, such as in Server, Network, Security and others. If all integrations run well, the effective and efficient processes will be achieved.

Some cases, the Stage 4 is divided into two sub stages. Stage 4a is for integration on the same department, work unit or institution. Stage 4b is for integration between departments, work units or institutions. Both of them have their own challenges.

TABLE II. INDICATORS OF E-GOVERNMENT MODEL IN 5-STAGE MODEL

No	Indicator	Stage				
		1	2	3	4	5
1	Leadership/Policy	Self motivation	Motivate others	Lead group	Lead function	Lead organization
2	IT Infrastructure	1 way comm.	2 ways comm.	transaction	integration	Business intelligent
3	Information Processing (Application)	Static Web	Web with Email, Chat and Forum	Web with Payment capability	Dynamics Web with public data	Web with provided API
4	Human Resources	Basic capability*	Advance capability	Security capability	Complex capability	Analytics capability
5	Organization culture	Protection	Service	Transparency	Efficiency	Competition

\*) capability in planning, execution and operation

- Policy (Stage 5).

This is the final stage which is the capability of e-government to support for public policymaking. The leader of organization needs to have a good vision and mission to utilize the Data and Information in their public policymaking. The head of Data and Information who reports to the leader of organization should be able support the leader's vision and mission. The IT infrastructure is design to maintain business intelligent application, such as Data Mining, Data Warehouse, Big Data, Data Analytic and others. The application supports to share data and information via API, such as JavaScript Object Notation (JSON) and Extensible Markup Language (XML) in the secured method. Human resource has the analytic capability to learn the data and information before feeding it into the system dynamics software application. It is expected that the competition becomes the culture in the organization.

#### D. Research Design

The objective of this new model of E-Government Maturity is to support the public policymaking. But, how to proof the relationship between them is another challenge. Fortunately, Nasution [8] provides a statistical validation based on Partial Least Square – Structural Equation Modeling (PLS-SEM) to learn the relationship between Public Policymaking (PP), System Dynamics (SD) and Big Data in



the E-Government. As the results of the analysis, System Dynamics (SD) explains 48% of variance in Public Policymaking (PP). E-Government Maturity explains 45% of variance in SD. Overall, the predictive power of factors is moderate or above the average. Therefore, the model gives an adequate predictive power for E-Government Maturity and System Dynamics in Public Policymaking. Next, the research design to evaluate the existing E-Government Maturity based on the proposed model is conducted.

The research is conducted by doing survey to some participant in one of National Application Workshop which is organized by one of ministry in Indonesia. The total respondents with the valid answers are 124. The respondent's profile is male (74%), well educated with university degree (89%) and located in west of Indonesia (56%). In the survey, the conditions of Leadership / Policy, IT Infrastructure, Information Processing (Application), Human Resources and Organization Culture [36] are questioned. Each question has 5 options of answer that will be used to determine the stage of EMM of each institution. The answer a is for stage 1. The answer b is for stage 2. The answer c is for stage 3. The answer d is for stage 4. The answer e is for stage 5. In general, the formula is

$$\text{Level of EMM} = \sum A_i \cdot w_i \quad (1)$$

Whereas  $i$  is to indicate the question 1 until 5,  $A_i$  is the answer of question  $i$ , and  $w_i$  is the weight or contribution of question  $i$ . The total  $w_i$  ( $\sum w_i$ ) is 100%. In this paper, each answer contributes the same which is 20% ( $w_i$ ) of the total answers.

The questions are for:

- Leadership / Policy

E1: The level or power of leadership in the department or organization to support Public Policymaking based on the data? (a. Self motivation or no leadership, b. Motivate others, c. Lead group or department, d. Lead function or division, e. Lead organization)

- IT Infrastructure

E2: The status of Information Technology Infrastructure (Network, Server and Storage) to support functionality in every business process, so that the Government can serve the society well ? (a. One way communication from Government to Society, b. Two ways communication between Government and Society, c. Secure Transaction or Payment is supported via online such as Credit Card and others, d. LAN and WAN Integration in organization to support the communication, e. Business intelligent is utilized)

- Information Processing (Application)

E3: The intensity of data and information processing for the benefit of Government and Society ? (a. Static Web, b. Web with Email, Chat and Forum capabilities, c. Web with Payment capabilities, d. Dynamics Web with public data, e. Web with provided API)

- Human Resources

E4: The expertise of Human Resources (SDM) in the department or organization is determined not only the technical operation of IT, but also Data Analytic capability? (a. Basic capability in operating single alone PC/Notebook, b. Advance capability in LAN, c. Security capability to maintain in the secured IT Infrastructure, d. Complex capability to integration LAN and WAN, e. Analytics capability to run Business Intelligent Application)

- Organization Culture

E5: How good and transparent organizational culture in the department or organization? (a. Protection, each of government employee keep their own data, b. Service, government serve the society, c. Transparency in conducting payment, d. Efficiency in communication between department, e. Competition to provide solution based on data)

The example of returned questionnaire is that if one of the respondents answer a for question 1, b for question 2, b for question 3, a for question 4, b for question 5, then the calculation is conducted based on equation (1) as below

$$\begin{aligned} \text{Level of EMM} &= (1 + 2 + 2 + 1 + 2) \times 20\% \\ &= 1.6 \end{aligned}$$

### III. ANALYSIS

Based on the Survey, all respondents contribute equally to measure the EMM level of their organization. The result is below:

TABLE III. SUMMARY OF RESPONDENT'S RESPONSES

No	Respondents	Results	N
1	<b>Group 1</b>	1	9
2	<b>Group 2</b>	1.2	22
3	<b>Group 3</b>	1.4	49
4	<b>Group 4</b>	1.6	25
5	<b>Group 5</b>	1.8	1
6	<b>Group 6</b>	2.2	10
7	<b>Group 7</b>	2.6	5
8	<b>Group 8</b>	3.2	3

The average of the stage of EMM Level of this ministry between all groups becomes 1.54. The ministry is considered in the Stage 1. In this survey, only 14.5% of total respondents gives a higher (more than 2) stage of EMM Level.

### IV. CONCLUSION

The proposed E-Government Maturity Model (EMM), which is called 5-stage model is valid to support System Dynamics (SD) for Public Policymaking [8]. By conducting the survey, the stage or level of EMM is identified

comprehensively. It is to know the level of Leadership / Policy, IT Infrastructure, Information Processing (Application), Human Resources and Organization Culture in the government [36].

One of the ministries in Indonesia has stage of EMM in the level of 1.54. It means the organization is not adopted the technology very well. Although, the head quarter of ministry in Jakarta has adopted a better E-Government, but unfortunately their work units in province and regency have not yet. Indirectly, it is impacted to the aims for ministry to run public policy effectively to the society [7]. Improvement of the level of EMM is positively related to the effectiveness of the implementation of public policy in the society [8].

### Acknowledgment

Thanks for SIKS team who support me.

### References

- [1] A. Fath-Allah et al., "E-Government Maturity Models: A Comparative Study," *International Journal of Software Engineering & Applications (IUSEA)*, vol. 5(3), pp. 71 – 91, 2014.
- [2] C. G. Reddick, "A two-stage model of E-Government growth: Theories and empirical evidence for US cities," *Government Information Quarterly*, vol. 21(1), pp. 51–64, 2004.
- [3] J. W. Forrester, "Industrial Dynamics," Cambridge, Massachusetts: The MIT Press, 1961.
- [4] Gits, "The 3 Vs That Define Big Data (Volume, Velocity and Variety)," 2016. Available: <http://gitsacademybangalore.over-blog.com/2016/03/the-3-vs-that-define-big-data-volume-velocity-and-variety.html> (Retrieved on Sep 24, 2017)
- [5] F.B.B. Nasution et al., "Big Data's Tools for Internet Data Analytics: Modelling of System Dynamics," *International Journal on Advanced Science Engineering Information Technology (IJASEIT)*, vol. 7(3), pp. 745-753, 2017.
- [6] A. Fitriansyah et al., "Metode Pemeringkatan E-Government Indonesia (PeGI) untuk Audit Tata Kelola Teknologi Informasi," *Seminar Nasional Sistem Informasi Indonesia*, Bali, Indonesia, 2 – 4 Dec 2013.
- [7] F.B.B Nasution et al., "Conceptual Framework for Public Policymaking based on System Dynamics and Big Data," *Proceedings of 2017 4th International Conference on Electrical Engineering, Computer Science and Informatics (EECSI 2017)*, Yogyakarta, Indonesia, 19 – 21 Sep 2017
- [8] F.B.B Nasution et al., "Public Policymaking Framework based on System Dynamics and Big Data," *International Journal of System Dynamics Applications (IJSDA)*, vol. 7(4), 2018.
- [9] Finn de Bri, "An E-Government Stages of Growth Model Based on Research Within the Irish Revenue Offices," *Electronic Journal of E-Government*, vol. 7(4), pp. 339 – 348, 2009.
- [10] D. C. Misra, "Sixty years of development of e-governance in India (1947-2007): Are there lessons for developing countries?," *Proceedings of the International Conference on Theory and Practice of Electronic Government*, Macao, China, 10 – 13 Dec 2007.
- [11] M. Yildiz, "E-Government research: Reviewing the literature, limitations, and ways forward," *Government Information Quarterly*, vol. 24, pp. 646–665, 2007.
- [12] K. Layne and J. Lee, "Developing fully functional E-Government: A four stage model. *Government Information Quarterly*," vol. 18(2), pp. 122–136, 2001.
- [13] K. V. Andersen and H. Z. Henriksen, "E-Government maturity models: Extension of the Layne and Lee model," *Government Information Quarterly*, vol. 23(2), pp. 236–248, 2006.
- [14] United-Nations, "UN E-Government Survey 2012: E-Government for the People," 2012. Retrieved on Sep 30, 2017 from <http://unpan1.un.org/intradoc/groups/public/documents/un/unpan048065.pdf>
- [15] S. M. Alhomod et al., "Best Practices in E government: A review of Some Innovative Models Proposed in Different Countries," *International Journal of Electrical & Computer Sciences*, vol. 12(01), pp. 1–6, 2012.
- [16] J. S. Hiller, and F. Belanger, "Privacy strategies for electronic government," *E-Government*, vol. 200, pp. 162–198, 2001.
- [17] R. S. Almazan and J. R. Gil-Garcia, "E-Government Portals in Mexico," 2008. Retrieved on Sep 30, 2017 from <http://www.igi-global.com/chapter/electronic-government-concepts-methodologies-tools/9818>
- [18] Cisco IBSG, "e-Government Best Practices learning from success, avoiding the pitfalls," 2007. Retrieved on Sep 30, 2017 from [http://siteresources.worldbank.org/EXT/DEVELOPMENT/Resources/20080222\\_Phil\\_eGov\\_workshop.pdf?resourceurlname=20080222\\_Phil\\_eGov\\_workshop.pdf](http://siteresources.worldbank.org/EXT/DEVELOPMENT/Resources/20080222_Phil_eGov_workshop.pdf?resourceurlname=20080222_Phil_eGov_workshop.pdf)
- [19] C. Baum and A. Di-Maio, "Gartner's four phases of e-government model," *Gartner Group*, 2000.
- [20] D. M. West, "E-Government and the Transformation of Service Delivery and Citizen Attitudes," *Public Administration Review*, vol. 64(1), pp. 15–27, 2004.
- [21] M.J. Moon, "The Evolution of E-Government among Municipalities: Rhetoric or Reality?," *Public Administration Review*, vol. 62(4), pp. 424–433, 2002.
- [22] Y. Toasaki, "e-Government from A User's Perspective," *APEC telecommunication and information working group*, Chinese Taipei, 2003.
- [23] Deloitte & Touche, "At the dawn of e-government: The citizen as customer," New York: Deloitte Research, 2000. Retrieved from on Sep 30, 2017 <http://www.egov.vic.gov.au/pdfs/egovernment.pdf>
- [24] M. Howard, "E-Government across the globe: how will e'change government," *E-Government*, vol. 90, pp. 80, 2001.
- [25] K. A. Shahkooh et al., "A proposed model for E-Government maturity," 2008 3rd International Conference on Information & Communication Technologies: from Theory to Applications (ICTTA), Damascus, Syria, 2008.
- [26] G. Lee and Y. H. Kwak, "An Open Government Maturity Model for social media-based public engagement," *Government Information Quarterly*, 2012. Retrieved on Sep 30, 2017 from <http://www.sciencedirect.com/science/article/pii/S0740624X1200086X>
- [27] K. Siau and Y. Long, "Synthesizing e-government stage models—a meta-synthesis based on metaethnography approach," *Industrial Management & Data Systems*, vol. 105(4), pp. 443–458, 2005.
- [28] C. G. Wescott, "E-Government in the Asia-Pacific region," *Asian Journal of Political Science*, vol. 9(2), pp. 1–24, 2001.
- [29] S. Chandler and S. Emanuels, "Transformation not automation," In *Proceedings of 2nd European Conference on E-Government*, St Catherine's College Oxford, UK, 1 – 2 Oct, 2002.
- [30] D-Y. Kim and G. Grant, "E-Government maturity model using the capability maturity model integration," *Journal of Systems and Information Technology*, vol. 12(3), pp. 230–244, 2010.
- [31] J. Chen, Y. Yan and C. Mingins, "A Three-Dimensional Model for E-Government Development with Cases in China's Regional E-Government Practice and Experience," 2011 Fifth International Conference on Management of e-Commerce and E-Government (ICMeCG), Wuhan, Hubei, China. 5 – 6 Nov 2011.
- [32] P. J. Windley, "eGovernment maturity," USA: Windleys' Technolometria, 2002. Retrived on Sep 24, 2017, from <http://www.windley.com/docs/eGovernment%20Maturity.pdf>
- [33] S. J. Rohleder and V. Jupp, "E-Government Leadership: Engaging the customer," Accenture. 2003. Available : <https://www.eldis.org/document/A12464> (Retrieved on Jan 30, 2018)
- [34] NAO, "Government on the Web II," 2002. Retrieved Retrived on Sep 24, 2017, from [http://www.nao.org.uk/publications/0102/government\\_on\\_the\\_web\\_ii.aspx](http://www.nao.org.uk/publications/0102/government_on_the_web_ii.aspx)

- [35] I. Netchaeva, "E-Government and E-Democracy A Comparison of Opportunities in the North and South," *International Communication Gazette*, vol. 64(5), pp. 467–477, 2002.
- [36] Achmad Nizar Hidayanto, Yulia Razila Ningsih, Puspa Indah Sandhyaduhita, and Putu Wuri Handayani, "The Obstacles of the E-Government Implementation: A Case of Riau Province, Indonesia," *Journal of Industrial and Intelligent Information*, vol. 2(2), pp. 126-130, June 2014.

# Comparative Analysis of Forensic Software on Android-based Blackberry Messenger using NIJ Framework

Imam Riadi

Department of Information System  
Universitas Ahmad Dahlan  
Yogyakarta, Indonesia  
imam.riadi@is.uad.ac.id

Sunardi

Department of Electrical Engineering  
Universitas Ahmad Dahlan  
Yogyakarta, Indonesia  
sunardi@mti.uad.ac.id

Arizona Firdonsyah

Department of Informatics  
Universitas Ahmad Dahlan  
Yogyakarta, Indonesia  
arizona.f@gmail.com

**Abstract**— Instant Messaging application is the most widely used application all over the world. Blackberry Messenger is a multiplatform instant messaging application with lots of features that can be a magnet for many people to use it as a tool for committing digital crimes. In the process of investigating digital crime cases, digital evidences are required, and to obtain digital evidence, a set of forensic tools are needed to conduct forensic process on physical evidences. The topic of this research is to describe the forensic process and to compare the current forensic tools used based on acquired digital evidences by using method that refers to mobile device forensic guidelines made by the National Institute of Justice (NIJ). The forensic tools used in this research are Magnet AXIOM, Belkasoft Evidence Center, and MOBILedit Forensic Express. The outcome shows that Magnet AXIOM has the highest capability to obtain digital evidences, Belkasoft Evidence Center has superiority in terms of data text acquisition, and MOBILedit Forensic Express has superiority in physical evidence preserving and cloning.

**Keywords**—*Smartphone, Android, Digital Evidence, Blackberry Messenger, Digital Forensics*

## I. INTRODUCTION

The development of mobile operating system, especially Android is growing rapidly, this can be seen from many types of Android-based gadget with various brands and features that emerges almost every week. The rapid development of Android technology has an impact on the growing number of applications developed for the Android platform, including instant messaging applications. Developers are competing to create instant messaging applications with user friendly features.

There are many free instant messaging application available now which allow people to communicate using texts, phone calls, videos, etc, and to maintain contact with them even internationally. Recent studies have shown that the most popular instant messengers are WhatsApp, Viber, Telegram [1], and Blackberry Messenger (BBM). BBM is one of the multi-platform instant messaging applications that has many users that increase significantly each year. A survey titled “WhatsApp vs LINE vs BBM” that conducted by JakPat Mobile [2] reported that BBM is still a leading instant messaging application in Indonesia. Figure 1 shows the

percentage of BBM users in Indonesia with 89,35%, followed by LINE with 77,42%, and WhatsApp ranked third with 74,19%.

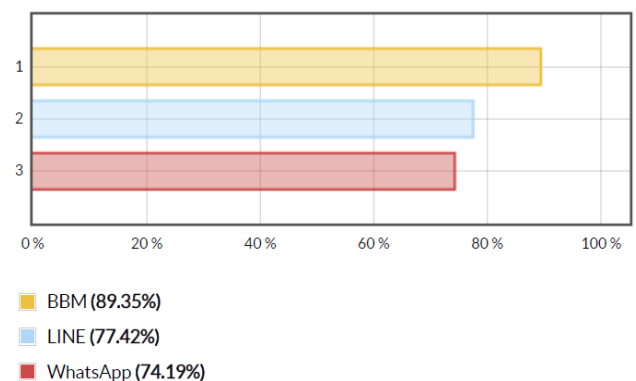


Figure 1. Graphical percentage of BBM users in Indonesia based on JakPat Mobile's Survey.

With the amount of BBM users that rapidly growing, the possibility of digital crimes that occurred is also increased. Information obtained from the web site of Indonesian National Police Public Relations [3] that the crime using the Blackberry Messenger always occurred and are likely to increase, as shown in Table 1.

TABLE I. DIGITAL CRIME THAT USING BBM IN INDONESIA

No	Year	Case
1	2015	Covert prostitution transaction via BBM in Bangka Belitung
2	2016	Cyberbullying in BBM leads to massive fighting at Gorontalo
3	2016	BBM account of DPR members in Jakarta being hacked
4	2017	Online fraud and money laundering at Bangka Belitung
5	2017	Online prostitution transaction via BBM at Pekanbaru

The Increasing number of digital crimes using smartphone's messaging applications such as BBM requires law enforcement agencies to be more thorough in investigating digital crime. This investigative process requires structured analysis and a set of forensic tools to obtain digital evidence from BBM. In this research, the researchers will try to elaborate the investigative steps to obtain digital evidence and

conduct a comparative analysis on forensic tool's performance based on acquired digital evidences and features.

According to Dogan and Akbal [4] that conducted a comparative study using Oxygen Forensic Suite 2014 and MOBILedit Forensics, it can be explained that every forensic tool has its own advantages and disadvantages. This research's result shows that MOBILedit Forensics has advantages in terms of run time, while Oxygen Forensic Suite 2014 has an advantage in terms of artifact analysis.

Other comparative analysis research is conducted by Maurya, Awasthy, Singh, and Vaish [5] by using 2 proprietary forensic tools and 3 open source forensic tools. The conclusion is that many of the features that are present in proprietary forensic tools are also present in open source tools. Even there are certain features that provided by open source tool but proprietary tool does not, for example: SHA-1 hashing is not provided in EnCase but available in open source tools.

Comparison and analysis of proprietary and open source forensic tools also conducted by Padmanabhan, Lobo, Ghelani, Sujana, and Shirole [6] with the tools put into comparison are The Sleuth Kit (TSK) Autopsy, SANS SIFT, MOBILedit Forensics, and Cellebrite UFED. The results of this research are: open source forensic tools have advantages in the number of users, flexibility in terms of use with console commands or GUI- based applications, logging capability, and good in tolerating errors, and proprietary forensic tools are superior in terms of processing speed, the accuracy of data extraction, analytical features, and data restoring ability.

Another comparative research conducted by Salem, Popov and Kubi [7] using Cellebrite UFED and XRY shows that XRY is better than Cellebrite UFED for acquiring most of the artifact types, while Cellebrite UFED is better on preserving the integrity of digital evidence.

## II. RESEARCH METHODOLOGY AND TOOLS

The objective of this research was to describe the forensic process and evaluate forensic tools. Magnet AXIOM, Belkasoft Evidence Center, and MOBILedit Forensics Express will be used and evaluated based on parameters from from researchers in terms of the ability to perform BBM's forensic analysis on Android.

### A. Research Methodology

The U.S. National Institute of Justice (NIJ) has published a process model in the Electronic Crime Scene Investigation Guide, the process model consists of the following steps [8]:

1. Preparation: Prepare the equipment and tools to perform the tasks required during an investigation.
2. Collection: Search for, document, and collect or make copies of the physical objects that contain electronic evidence.
3. Examination: Make the electronic evidence visible and document contents of the system. Data reduction is performed to identify the evidence.

4. Analysis: Analyze the evidence from the Examination phase to determine the significance and probative value.
5. Reporting: Create examination notes after each case.

And the diagram is shown at Figure 2

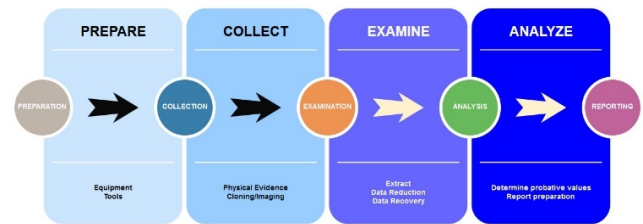


Figure 2. NIJ Forensics Method Diagram.

Based on the framework, the steps of the research are divided into five: software installation, evidence preservation/cloning, extraction experiment, result evaluation and analysis, and the last step is reporting as shown on Figure 3

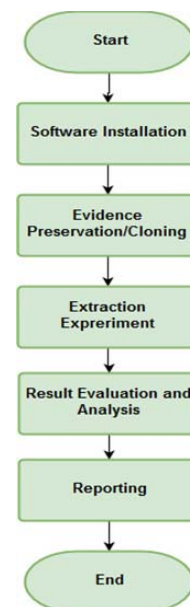


Figure 3. Flowchart of research's steps.

The flowchart can be described as follows:

- Software Installation: The researchers will install forensic tools that will be compared on the notebook.
- Evidence Preservation/Cloning: The researchers will perform the cloning process on smartphone devices to preserve and maintain data integrity.
- Extraction Experiment: The researchers will perform Extraction process on smartphone devices using Magnet AXIOM, Belkasoft Evidence, and MOBILedit Forensic Express.
- Result Evaluation and Analysis: The performance of each forensic tool will then be analyzed based on software features and digital evidence obtained from each device.. The

parameters used are adjusted to the objective of the research, namely, Blackberry Messenger analysis.

- Reporting: The evaluation and analysis of forensic tools are presented..

### B. Research Tools

The research tools used in this research are divided into two parts: Experimental tools and Forensic tools. Experimental tools related to hardware and experimental objects, while Forensic tools are the tools that will be used to acquire digital evidences. Table II describes both tools.

TABLE II. EXPERIMENTAL AND FORENSIC TOOLS

Experimental Tools		
No	Tools	Description
1	Notebook	Asus SonicMaster X450J, OS Windows 10 64bit
2	Data Cable	A data cable that can be used to connect laptop with smartphone
3	Smartphone 1	Sony Xperia SL, OS Android Jellybean
4	Smartphone 2	Samsung Galaxy A5 2015, OS Android Marshmallow
5	Blackberry Messenger	A multiplatform instant messaging application
Forensic Tools		
No	Tools	Description
1	Magnet AXIOM	Windows-Based Applications that can be used to acquire digital evidence on a smartphone
2	Belkasoft Evidence Center	Windows-Based Applications that can be used to acquire digital evidence on a smartphone
3	MOBILedit Forensic Express	Windows-Based Applications that can be used to acquire digital evidence and make smartphone's system copy

## III. RESULTS AND DISCUSSION

### A. Preparation

Preparation stage is a process of preparing physical evidence that will be used to conduct forensic investigation process as shown on Figure 4, and to determine what kind of digital evidences that will be extracted from physical evidence as shown on Table III.



Figure 4. Smartphones as Physical Evidence.



TABLE III. BBM'S DIGITAL EVIDENCE

No	Digital Evidence	Description
1	BBM Profile	Digital Evidence/Artifact related to the owner of BBM Account
2	BBM Contact	A list of BBM Contact, including BBM PIN
3	BBM Chat	Digital Evidence/Artifact related to BBM user's conversation data
4	BBM Transferred Picture/File	Pictures/Files transferred among BBM users
5	BBM Invitation	An invitation to communicate using BBM for other BBM users

### B. Collection

At this stage, physical evidence collection, documentation, and preservation will be conducted. The process at this stage is conducted by checking the type of evidence, specifications, operating system, IMEI, android versions, and other related data. The content of physical evidences may vary depends on the evidence's condition. Table IV shows the results.

TABLE IV. PHYSICAL EVIDENCE SPECIFICATION

Physical Evidence 1		
	Brand	Sony
	Serial	Xperia
	Model	SL
	Model #	LT26ii
	IMEI	353617051988xxx
	OS	Android
	Version	4.1.4 (Jellybean)
	Processor	Dual core
Physical Evidence 2		
	Brand	Samsung
	Serial	Galaxy
	Model	A
	Model #	SM-A500F
	IMEI	-
	OS	Android
	Version	6.0.1 (Marshmallow)
	Processor	Quad core 1.2 GHz Cortex-A53

To maintain the integrity of physical evidence so as not to change, the cloning process of this android smartphone is also conducted by using MOBILedit Forensic Express since this tool is the only tool that have this feature, other tools might do the cloning process while running data extraction. The cloning process and result is as shown on Figure 5.

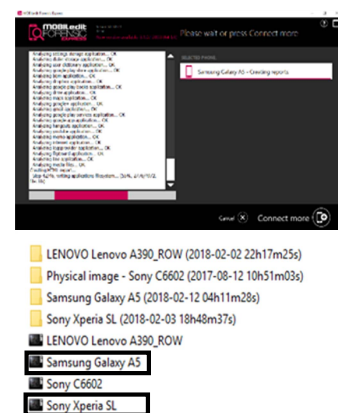


Figure 5. Cloning Process and Results.



### C. Examination and Analysis

Examination and Analysis is the process of retrieving, searching, and analyzing data from physical evidence. In this stage, The examination process is conducted by reducing the search data only on BBM applications. Figure 6 and Figure 7 shows the results of the examination result using Magnet AXIOM for both physical evidences.

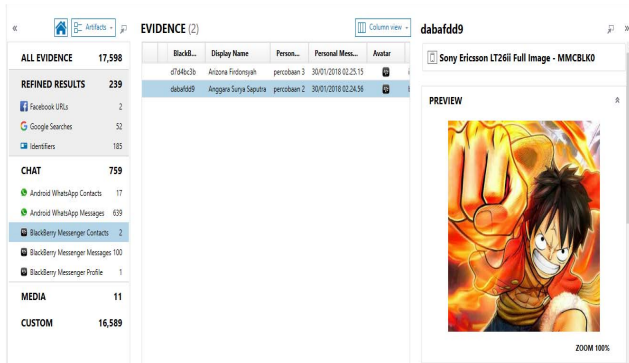


Figure 6. Physical Evidence 1 Examination Result using Magnet AXIOM.

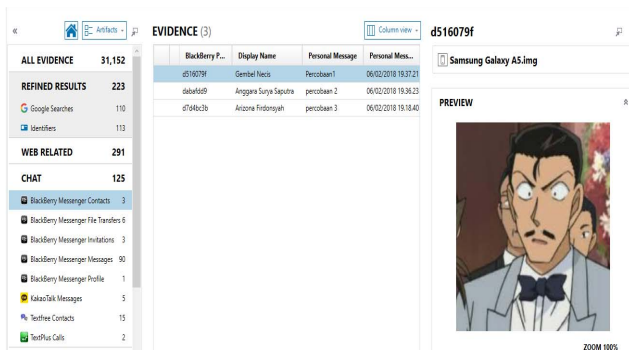


Figure 7. Physical Evidence 2 Examination Result using Magnet AXIOM.

Examination result that acquired using Magnet AXIOM provide a set of Contact List, BBM Invitation, BBM File Transfer, BBM Chat, and BBM Account Owner's Profile. Magnet AXIOM has the ability to conduct physical and logical extraction, so in this research, the researchers did physical extraction on Physical Evidence 1, and logical extraction on Physical Evidence 2.

As shown on Figure 8 and 9, examination process using Belkasoftware Evidence Center resulted in BBM Chat and Pictures.

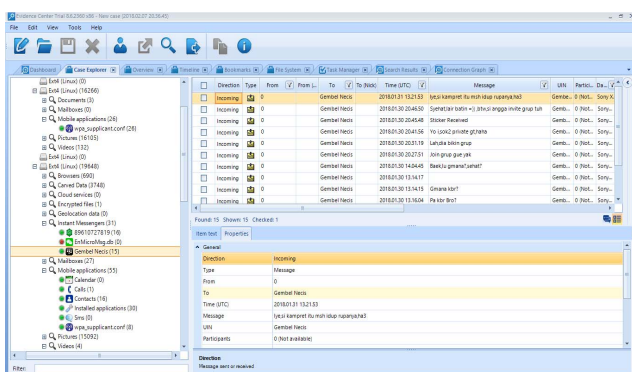


Figure 8. Physical Evidence 1 Examination Result using Belkasoftware.

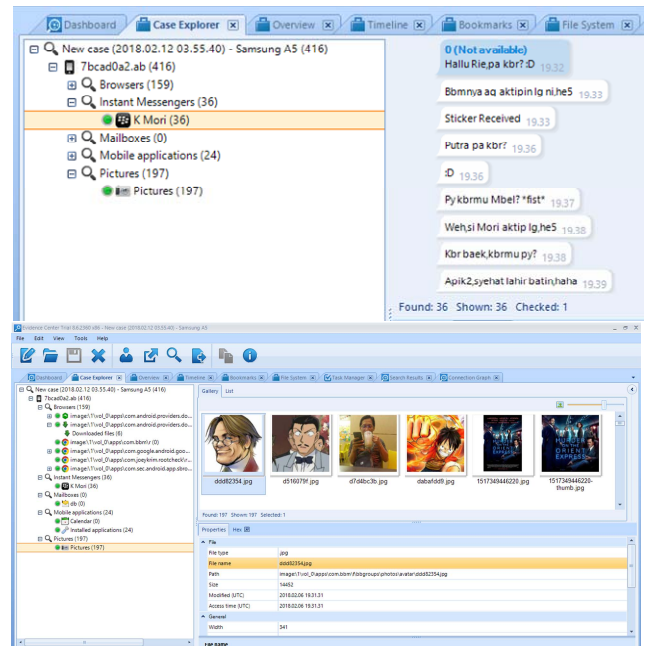


Figure 9. Physical Evidence 2 Examination Result using Belkasoftware.

Belkasoftware Evidence Center also has the ability to do physical and logical extraction, so as well as Magnet AXIOM, the researchers did physical extraction on Physical Evidence 1 and logical extraction on Physical Evidence 2.

MOBILedit Forensic Express is a tool with backup and cloning features, by using this feature, forensic examiners are able to maintain the integrity of physical and digital evidences. Examination process that using MOBILedit Forensic Express resulted in a set of HTML report that can be accessed via browser. The examination result for both physical evidences is shown on Figure 10.

Based on the results of this analysis, a full forensic report contained a summary of acquired digital evidences and performance comparison of forensic tools can be presented.

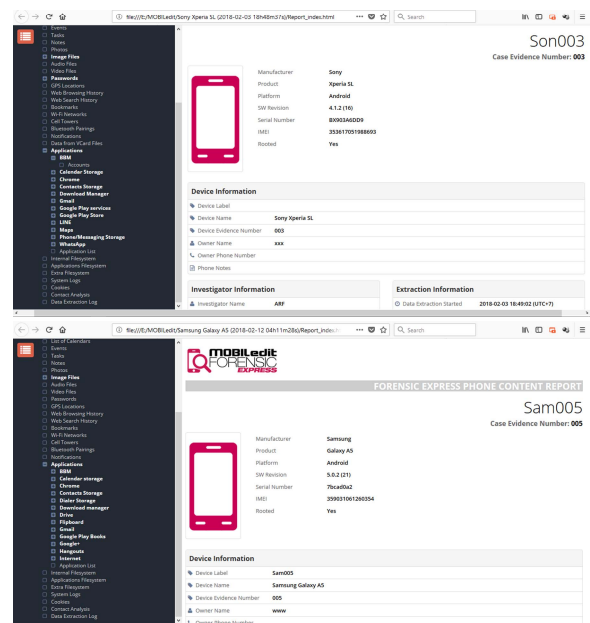


Figure 10. Physical Evidence 1 and 2 Examination Result using MOBILedit Forensic Express.

#### D. Reporting

Reporting [9] is the last stage on NIJ framework. Here, the report will be presented in 2 comparison tables based on software features and based on digital evidence obtained by each device. Feature-based comparison result is as shown in Table V.

TABLE V. FEATURE-BASED EVALUATION RESULT

Measurement Parameters	Forensic Tools		
	Magnet AXIOM	Belkasoft Evidence Center	MOBILedit Forensic Express
Physical Extraction Capability	√	√	√
Logical Extraction Capability	√	√	√
Physical Evidence Preserving and Cloning Capability	-	-	√
Report Generation	√	√	√

The researchers used calculations with index numbers to determine the performance of each forensic tool in accordance with the experiment results. The calculation of index number used is unweighted index as shown in equation 1 [10].

$$Par = \frac{Z_{ar0}}{Z_{arT}} \times 100\% \quad (1)$$

Where:

Par = Percentage of index number

ar0 = Digital Evidence/Artifact gained by Forensic Tool

arT = Total Digital Evidence/Artifact

MOBILedit Forensic Express has superiority in preserving and cloning capability because this tool has the ability to create cloning file that can be read by other tool. By using equation 1 to calculate the index number from each forensic tool, MOBILedit Forensic Express has the highest index number of 100%. Belkasoft Evidence Center and Magnet AXIOM each has an index number of 75%.

TABLE VI. DIGITAL EVIDENCE-BASED EVALUATION RESULT

No.	BBM's Digital Evidence	Forensic Tools		
		Magnet AXIOM	Belkasoft Evidence Center	MOBILedit Forensic Express
1	BBM Profile	√	√	√
2	BBM Contact	√	√	-
3	BBM Chat	√	√	-
4	BBM Transferred Picture/File	√	√	-
5	BBM Invitation	√	-	-

Table VI shows the results of performance analysis conducted on each forensic tool related to the acquired digital evidences. By using the same equation, MOBILedit Forensic

Express got 20% performance index score by only managed to acquire 1 type of BBM Digital Evidence, Belkasoft Evidence Center got 80% performance index score, and Magnet AXIOM got the highest index performance score of 100% because it successfully acquired all 5 types of BBM Digital Evidences.

#### IV. CONCLUSION

Related to Digital Evidence extraction capability, Magnet AXIOM has the highest index number at 100%, followed by Belkasoft Evidence Center with index number at 80%, and MOBILedit Forensic Express with index number at 20%. MOBILedit Forensic Express has weakness in extracting BBM's Digital Evidences. However, related to physical evidence's backup and data preservation, MOBILedit Forensic Express has the highest index number at 100% and manages to make physical evidence backup that can be used by another tool, while Magnet AXIOM and Belkasoft Evidence Center has index number at 75%. The outcome shows that Magnet AXIOM has the highest capability to obtain digital evidences, Belkasoft Evidence Center has superiority in terms of data text acquisition, and MOBILedit Forensic Express has superiority in physical evidence preserving and cloning.

#### V. FUTURE WORK

For future work, there are many comparative study using many forensic tools such as Oxygen Forensic Suite [11], Andriller [12], Cellebrite UFED Physical Pro and XRY [13] that can be conducted. to get an overview on what forensic tool that best for digital forensic investigations. The comparison also can be conducted on forensic frameworks and parameters such as National Institute of Standard Technology (NIST) [14] [15], and Integrated Digital Forensic Investigation Framework (IDFIF) [16].

#### ACKNOWLEDGMENT

This research was supported by Lembaga Penelitian dan Pengembangan Universitas Ahmad Dahlan. We also thank our colleagues from Universitas Ahmad Dahlan who provided insight and expertise that greatly assisted the research.

#### REFERENCES

- [1] T. Sutikno, L. Handayani, D. Stiawan, M. A. Riyadi, and I. M. I. Subroto, "WhatsApp, viber and telegram: Which is the best for instant messaging?," *Int. J. Electr. Comput. Eng.*, vol. 6, no. 3, pp. 909–914, 2016.
- [2] Jakpat Mobile, "WhatsApp vs LINE vs BBM," pp. 1–21, 2016.
- [3] I. Riadi, Sunardi, and A. Firdonsyah, "Forensic Investigation Technique on Android's Blackberry Messenger using NIST Framework," *Int. J. Cyber-Security Digit. Forensics*, vol. 16, no. 4, pp. 198–205, 2017.
- [4] S. Dogan and E. Akbal, "Analysis of mobile phones in digital forensics," *2017 40th Int. Conv. Inf. Commun. Technol. Electron. Microelectron.*, no. October, pp. 1241–1244, 2017.
- [5] N. Maurya and J. Awasthi, "Analysis of Open Source and Proprietary Source Digital Forensic Tools," *Int. J. Adv. Eng. Glob. Technol.*, vol. 3, no. 7, pp. 916–922, 2015.
- [6] R. Padmanabhan, K. Lobo, M. Ghelani, D. Sujana, and M. Shirole, "Comparative analysis of commercial and open source mobile device forensic tools," *2016 9th Int. Conf. Contemp. Comput. IC3 2016*, 2017.

- [7] S. Saleem, O. Popov, and O. K. Appiah-Kubi, "Evaluating and Comparing Tools for Mobile Device Forensics Using Quantitative Analysis," *Stock. Univ.*, pp. 264–282, 2013.
- [8] M. Nur Faiz, R. Umar, and A. Yudhana, "Implementasi Live Forensics untuk Perbandingan Browser pada Keamanan Email," *JISKa*, vol. 1, no. 3, pp. 108–114, 2017.
- [9] I. Riadi, R. Umar, and A. Firdonsyah, "Identification Of Digital Evidence On Android's Blackberry Messenger Using NIST Mobile Forensic Method," *Int. J. Comput. Sci. Inf. Secur.*, vol. 15, no. 5, pp. 156–160, 2017.
- [10] R. Umar, I. Riadi, and G. M. Zamroni, "A Comparative Study of Forensic Tools for WhatsApp Analysis using NIST Measurements," *Int. J. Adv. Comput. Sci. Appl.*, vol. 8, no. 12, pp. 69–75, 2017.
- [11] O. Osho and S. O. Ohida, "Comparative Evaluation of Mobile Forensic Tools," *Int. J. Inf. Technol. Comput. Sci.*, vol. 8, no. 1, pp. 74–83, 2016.
- [12] Andriker, "Andriker – Android Forensic Tools," 2017. [Online]. Available: <https://www.andriker.com/>. [Accessed: 15-Aug-2017].
- [13] A. K. Kubi, S. Saleem, and O. Popov, "Evaluation of some tools for extracting e-evidence from mobile devices," in *2011 5th International Conference on Application of Information and Communication Technologies, AICT 2011*, 2011, no. January 2011.
- [14] W. C. Barker, "Digital Forensics NIST Information Technology Laboratory," 2012.
- [15] National Institute of Standards and Technology, "Mobile Device Tool Test Assertions and Test Plan Version 2.0," 2016.
- [16] R. Ruuhwan, I. Riadi, and Y. Prayudi, "Evaluation of integrated digital forensics investigation framework for the investigation of smartphones using soft system methodology," *Int. J. Electr. Comput. Eng.*, vol. 7, no. 5, pp. 2806–2817, 2017.

# Semi-reactive Switch Based Proxy ARP in SDN

Fauzi Dwi Setiawan Sumadi  
Informatics Department  
Universitas Muhammadiyah Malang  
Malang, Indonesia  
fauzisumadi@umm.ac.id

Diah Risqiwati  
Informatics Department  
Universitas Muhammadiyah Malang  
Malang, Indonesia  
risqiwati@umm.ac.id

Syaifuddin  
Informatics Department  
Universitas Muhammadiyah Malang  
Malang, Indonesia  
saifuddin@umm.ac.id

**Abstract**— In order to achieve high scalability during the network discovery process in software-defined networking (SDN), an extensive method for generating switch-based proxy is essential. This paper investigated the semi reactive solution for guiding the controller to build an OFPT\_FLOW\_MOD message that allowed SDN switch to reply an Address Resolution Protocol (ARP) request directly by deploying the semi-reactive switch-based proxy ARP application in northbound application programming interface (API). We conduct the experiment by using Open Networking Operating System (ONOS) an open-source SDN controller simulated in Mininet environment. As can be seen from the evaluation result, the installed application can reduce the ARP reaction time up to 95% calculated from the sender host. The final result also indicates that our approach can decrease the controller's loads significantly.

**Keywords**— SDN, Proxy ARP, Semi-reactive

## I. INTRODUCTION

Recently, SDN has gained a proper concern among researchers because it boosts the innovation's rate in a networking environment. The main concept of SDN is the separation between the control layer known as controller and the forwarding function which can communicate each other regulated by the southbound API [1]. The network administrator can easily determine the controller's functionality by installing an application directly through the northbound API. This mechanism maintains the network scalability since the proprietary issues originated from the forwarding devices are omitted.

In term of the network discovery process in the IPv4 environment, the controller and the SDN switch may suffer because of the abstraction of centralized networking control and management. The controller will be forced to provide a service to forward the ARP requests which are going to be flooded by the forwarding devices. This problem has been reduced by implementing the reactive based application. It can directly generate an ARP reply packet. However, if there are a lot of end host devices that transmit an ARP request at the same time, the controller still receives the impact for crafting and delivering an ARP reply for every incoming request.

Our proposed research focused on developing a semi-reactive application that can response the ARP request by partially offloading the capability to generate the response into the SDN switch. It can be achieved by defining a single flow rule through an OFPT\_FLOW\_MOD message

which can filter all of the incoming requests. We conduct several scenarios to investigate the effects by calculating the ARP response time and the controller's CPU usage.

The remaining section of this paper is organized as follows. Section II is concerned about the relevant literature review of OpenFlow network and the details of ARP processing in SDN. In section III, we discuss the related works that have been performed before, either in proactive or reactive approach. We illustrate the application workflow and the evaluation scenario in brief in section IV, while section V contains the comprehensive analysis of the proposed simulation. We conclude the paper in section VI.

## II. BACKGROUNDS

This section expounds the details of the relevant information relating to the paper's topic.

### A. OpenFlow Network

One of the prominent southbound API that has been widely utilized in SDN is OpenFlow [2]. It provides a programmatic approach for the controller so it can directly configure the switch's behaviour by defining flow rule for filtering each packet that enters the forwarding device. All of the designed flow rules are stored in the flow table by using OFPT\_FLOW\_MOD message which also can be used for deleting a particular rule. Each of the specific rules has a traffic selector and also a traffic treatment. If there is no rule that can handle the inbound packet, the SDN switch will encapsulate it by using OFPT\_PACKET\_IN message then transmits the packet directly to the controller for further action such as the network initialization process. In response, the controller will send OFPT\_PACKET\_OUT message to the switch for performing the specified action such as broadcast or multicast the inbound packet if the controller does not has a legal route between the source and destination or deliver OFPT\_FLOW\_MOD message for commanding the switch to install the defined flow rule.

### B. ARP Processing in SDN

Generally, the ARP processing in SDN is conducted in a reactive manner. The controller installs an application called ProxyARP on its northbound API. Through the default flow rule deployed in SDN switch, this application can collect OFPT\_PACKET\_IN message contained the incoming ARP request packet and easily break it down by

extracting the essential information including the target protocol address (TPA), target hardware address (THA), sender protocol address (SPA), sender hardware address (SHA), VLAN identification (ID), device ID, and the incoming port's ID. Then the ProxyARP will try to check whether the TPA is mentioned on its ARP cache. If the TPA is listed, the controller will directly craft an ARP reply based on the extracted information enclosed in OFPT\_PACKET\_OUT message which instructs the switch to send the ARP replay directly. However, if there is no information available, the controller will send the ARP request packet encapsulated in OFPT\_PACKET\_OUT. Subsequently, the switch will broadcast the ARP request, then the targeted host will reply. After the SDN switch receives the ARP reply, it will pass the packet to the controller by using OFPT\_PACKET\_IN. Therefore, the controller has a complete route between sender and destination host. Then the controller will send an OFPT\_PACKET\_OUT that intends to tell the switch to forward the packet within the message (ARP replay) back to the sender host. The SDN switch may perform a proactive mechanism for handling the ARP request. The main difference from the previous concept is the processing point. Forwarding device does not have to pass the incoming request since there exists a flow rule that is defined by the network administrator.

### III. RELATED WORKS

Previously, there were several researchers that focused their efforts on implementing either reactive or proactive Proxy ARP in SDN intended to reduce the ARP broadcast storm. [3]-[7] proposed a reactive based Proxy ARP involving the controller for generating ARP reply. Similarly, to the default ProxyARP in ONOS, the controller will store the details of the available host in a specific table or service by obtaining the incoming OFPT\_PACKET\_IN message's information that may contain an ARP request or the Link Layer Discovery Protocol (LLDP) packet. If the controller has a specific information regarding the destination address of the current ARP request, it will directly craft an ARP reply without involving the targeted host.

FSDM [3] initiated a caching scheme for storing the incoming DHCP and ARP information which were used by the controller for crafting both DHCP and ARP reply directly based on the cache information without flooding the request extensively on the network. SEASDN [4] provided a hashing mechanism for storing the request packet's information then responded by sending OFPT\_PACKET\_OUT message containing the reply packet. In the same manner, as FSDM and SEASDN, the authors of [5], [6], and [7] also implemented a reactive approach for handling the ARP request by administering the controller as the ARP proxy. The result from all of the papers indicates that the reactive application can successfully provide scalability to the network. However, this method may exhaust the controller's resource upon receiving a huge amount of requests since it should examine the incoming packets one by one.

Another type of Proxy ARP in SDN is introduced by [8],[9] which deploy proactive scheme for resolving ARP reply generation. [8] extends OpenFlow enabled switch's capability for creating an ARP reply independently while

[9] perform offloading mechanism by injecting several flow rules for generating ARP reply packet manually (hard-coded). This method is restricted by the OpenFlow since it cannot determine the TPA and THA of ARP reply packet. In consequent, [9] applies the broadcast address as the default value. A significant problem that can possibly occur is when a new host joins the network causing the network administrator to install the corresponding rule manually.

### IV. PROPOSED METHOD

Our method intended to create semi reactive mechanism. The proposed approach extended the capability of the current reactive proxyARP application illustrated in figure 1. It could be achieved by partially storing the ARP request information and eventually generating flow rule for the SDN switch. This single rule could handle any incoming ARP request because it could construct the ARP reply's TPA and THA extracted from the incoming ARP request's SPA and SHA. Therefore, the ARP processing would be completely handled by the SDN switch based on the flow rule's selector. The main difference between our method and the proactive Proxy ARP could be clearly pointed during the ARP reply's flow rule generation process.

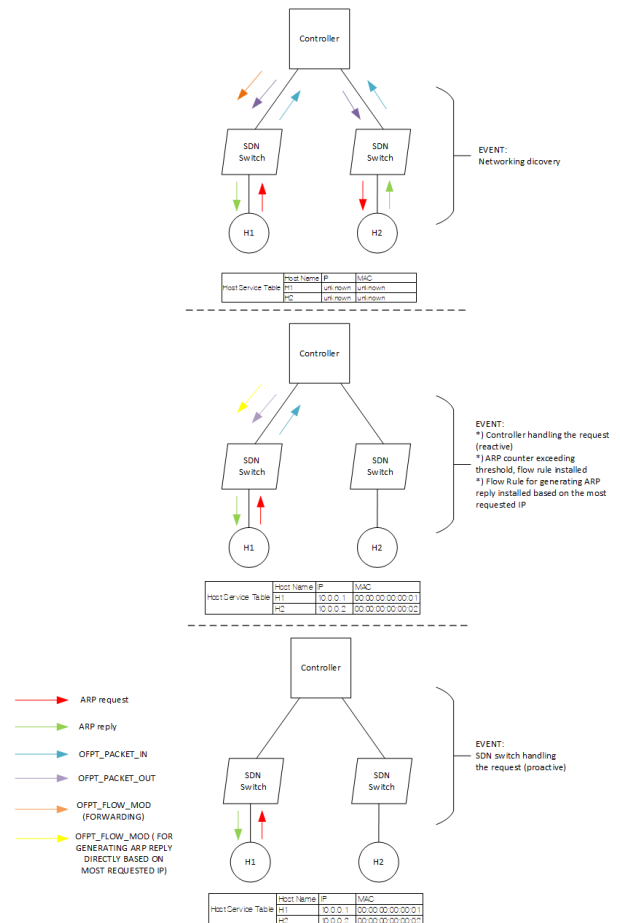


Fig. 1. Semi-reactive proxy ARP scheme

Network administrator requires to manually determine a flow rule for each available host on the network when the proactive proxyARP is implemented. Conversely, the semi reactive approach will assign the flow rule's generation to the application directly which allows it to construct a



single rule based on the information of the most requested IP address during the ARP broadcasting.

## V. SIMULATION SCENARIO

Our experiment was emulated using Mininet [10] version 2.2.2 which specifically implemented tree topology in OpenFlow network (version 1.3). It consisted of 3 SDN switch which used Open vSwitch [11] (OVS) version 2.5.4, 4 virtual hosts separated on each switch and ONOS [12] version 1.13.0 as the SDN controller. We assumed that ONOS applied the default applications including Forwarding, ProxyARP, Host-Provider, Optical-model, Drivers, Mobility, LLDPprovider, OpenFlow, and OpenFlow-base. The simulation was performed on a single Ubuntu 16.04 PC that had the following specification Intel Core CPU i5 3210M Processor 4 GB DDR3 1600 MHz SDRAM.

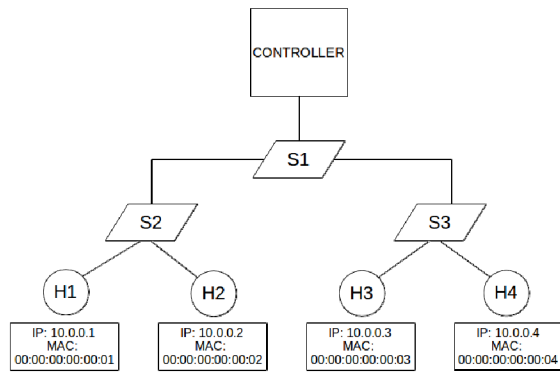


Fig. 2. Simulation topology

We conducted two different scenarios for the experiment. In order to imitate real network environment, the first scenario performed UDP transmission between H2 and H4 that had distinct bandwidth varieties including 2, 50, 100, 500, and 800 Mbps then H1 generated an ARP request to H4 by sending one packet each second. During the UDP transmission, H1 generated a constant ARP request directed to H4 each second. Therefore, the response time between the reply and request could be calculated.

The other emulation scenario performed different ARP request sending rates from H1 to H3 which varied from 500, 1000, 1500, 2000, 2500 packets per second without implementing UDP transmission. The ARP request was originated from H1 which each of the packets consisted of random source IP and MAC address generated by scapy [13] library. The ARP response time could be extracted by subtracting the time when H1 receiving the ARP replay from H3 and H1 sending ARP request to H3. There were two variables that were calculated during evaluation including the controller CPU usage for mapping the controller overhead and the ARP response time for each different sending rates. All of the packets were sent using Tcpreplay [14].

In term of the application's workflow, the controller injected particular flow rule for instructing the SDN switch to transmit incoming ARP packet encapsulated in OFPT\_PACKET\_IN message. Packet service module in ONOS was used to generate the proposed flow rule and

also regulate its priority for only having the standard reactive variable (5). Whenever the SDN switch receiving ARP request packet, it would directly investigate its TPA and THA. If there is a match event between TPA and flow rule's traffic selector originated from the semi-reactive switch proxy application, the SDN switch will craft an ARP reply packet associated with the destination address of the ARP request which is built by imitating the traffic treatment. Therefore, the sender can receive the ARP reply almost real-time without involving the reactive proxyARP application since the semi-reactive application's rule has higher priority.

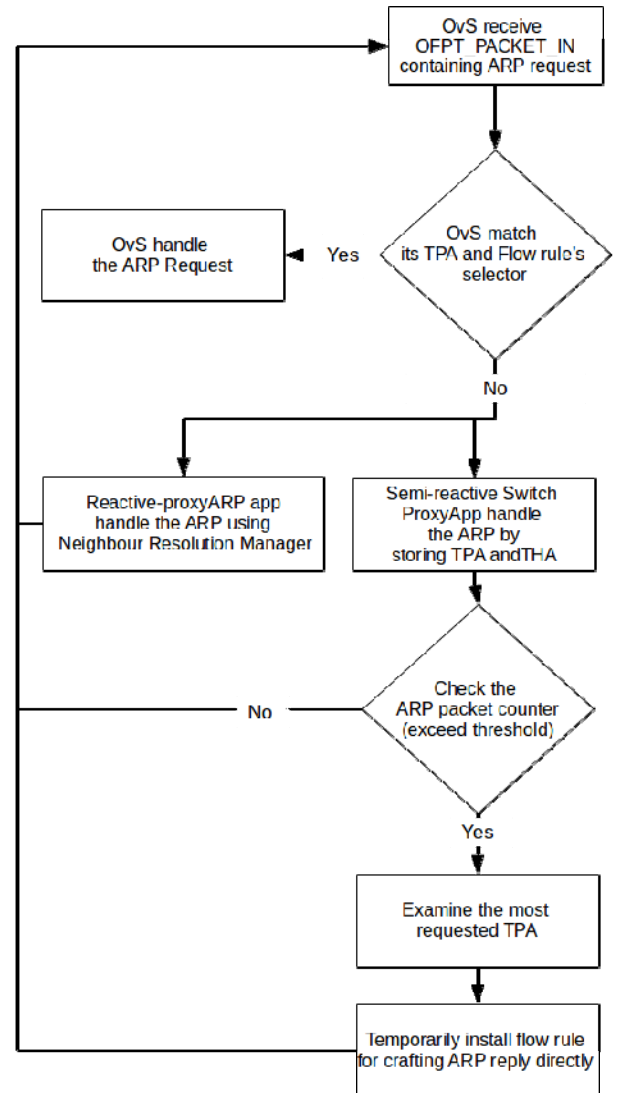


Fig. 3. Workflow of semi-reactive switch proxy application

In contrast, if the TPA doesn't correspond with all of the traffic selector specified in the flow table, OpenFlow switch automatically forward the ARP request to the ONOS controller enclosed in OFPT\_PACKET\_IN message which is handled by reactive proxyARP and semi-reactive switch-based proxy application. Then the NeighbourPacketManager in ONOS will directly send OFPT\_PACKET\_OUT message as described in the 'ARP Processing in SDN' section. In addition, semi-reactive switch proxy application breaks down the packet in message for extracting the TPA and THA which are then stored in HashMap for statistic purpose. If the ARP

counter exceeds the defined value by the application, it will inspect the most requested TPA then temporarily installs the corresponding flow rule with the most occurred TPA as the traffic selector and extends the flow for having the highest priority. The details of the installed flow rule are expounded on table 1.

TABLE 1. FLOW RULE SCHEME

Traffic Selector	
ARP OpCode	1
ARP TPA	The most requested TPA
Traffic Treatment	
ARP OpCode	2
ETH Source	The most requested THA
ETH Destination	ETH of incoming ARP request
ARP TPA	IP of incoming ARP request
ARP THA	ETH of incoming ARP request
ARP SPA	The most requested TPA
ARP SHA	The most requested THA
Output Interface	Incoming packet's port

Traffic selector is set to accommodate TPA of the ARP request packet. This method will filter only an ARP packet with OpCode 1, specifically targeting the specified TPA. SDN switch responds the match event by generating an ARP reply packet based on the traffic treatment which includes transferring both source MAC and IP address of incoming packet into the destination address of the reply packet (THA, TPA, and ETH destination) and changing the source address with the TPA and THA address (SHA, SPA, and ETH source) extracted from the hashmap which has the most occurrence among other TPA. The HostProvider service should have identified the most requested address. Subsequently, the ARP reply is transmitted back to the sender host via incoming packet's port. This scheme will allow the SDN switch for filtering every ARP request destined to particular host only by a single flow rule.

## VI. SIMULATION RESULTS AND ANALYSIS

In term of the effectiveness of the semi-reactive approach, we performed an in-depth analysis between our proposed method and the reactive proxyARP. Therefore, we could infer the ideal scheme for reducing ARP response time significantly. As expected, the results experiment depicted in figure 4 clearly showed a slight difference in the response time of ARP processing between two conditions including without installing the semi-reactive switch application or not. Since the reactive proxyARP maintained the ARP processing, the controller responded rapidly proved by the blue bar exactly at 2.61 ms. It could happen because the Host-provider service in ONOS had already mapped the targeted host after receiving the first ARP request. This method allowed the controller directly to generate ARP replay without sending OFPT\_PACKET\_OUT that contained ARP request for creating a link between the source and the destination. In contrast, after implementing the proposed application, the

ARP response time was dramatically decreased approximately at 0.14 ms indicating that the SDN switch successfully created ARP replay without involving the controller.

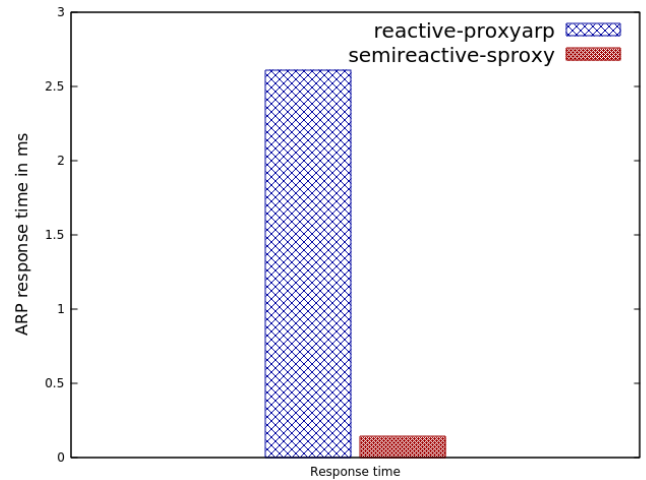


Fig. 4. ARP response time

As far as the first scenario was concerned, the emulation's result during the UDP transmission between H2 and H4 depicted in figure 5, illustrated that the reactive proxyARP still maintained the capability for generating ARP reply encapsulated in OFPT\_PACKET\_OUT message pointed within 1.5 ms and 2 ms.

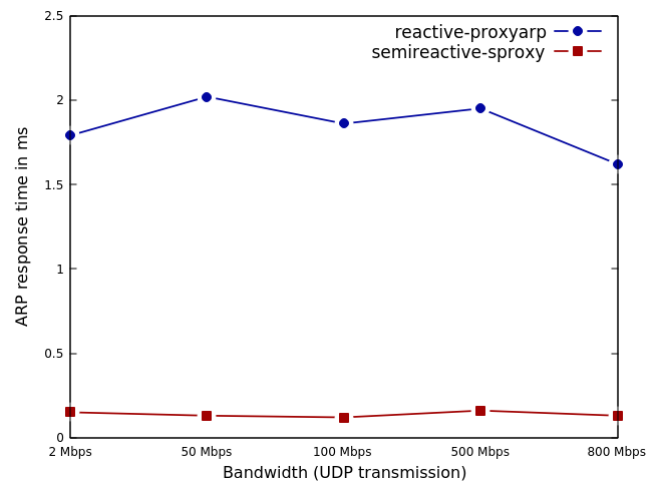


Fig. 5. ARP response time during UDP transmission

Although there was a huge traffics in H4's link, the controller could easily send the replay message to H1 because it had a topological map of the network. On the other hand, the response time of semi-reactive application still pointed in 0.16 ms which still proved that ARP reply was crafted locally by the switch depicted in figure 5. A significant result was shown during the second evaluation scenario. Flooding the controller by using a huge amount of ARP requests which had a different source MAC and IP address could exhaust the controller's resources since it should generate a massive amount of ARP replies within a second interval. The rising trend of ARP response time was described by the figure 6. Along with the growth of the packet sending rate, the response time variable before installing the semi-reactive application showed a gradual rise, which could reach more than 40000ms or 40s.



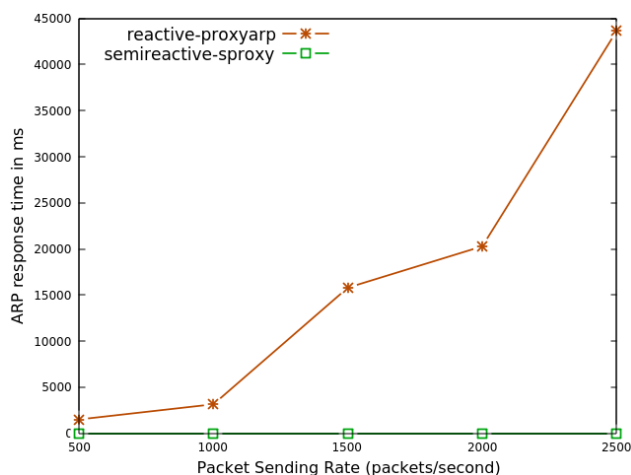


Fig. 6. ARP response time on different packet sending rate

This condition could lead to packet loss event or even worse when the controller didn't have the topological map of the network. In a real network case, a single port on the SDN switch can possibly contain a large number of end-hosts that directly connected in a multi-access network. For instance, a network address 172.16.0.0/22 may contain 1022 hosts on a single subnet. In a worst-case scenario, all of the registered hosts try to contact a single address by sending ARP request. This circumstance will overwhelm the controller which can exhaust the available resources. This problem can be solved by implementing the semi-reactive switch-based proxy application which can handle the problem by directly forwarding the ARP reply packet proven by the result data, approximately below 0.15 ms on each distinct packet sending rate.

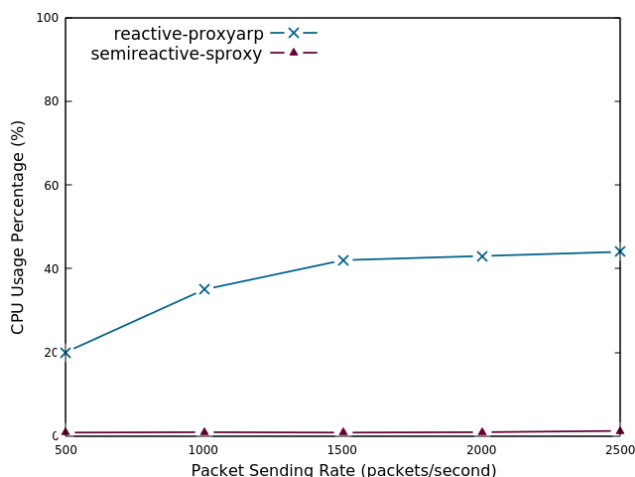


Fig. 7. Controller's CPU usage when receiving a different amount of ARP request

Similarly, a large amount of ARP request could significantly increase the CPU usage of the controller described in figure 7, because it must extract the information of incoming packet as well as transmitting the response packet. The largest packet sending rate could

consume more than 40% of CPU usage. This problem might bring the controller into unpredictable state and caused the sender host not to detect an appropriate link to the targeted host (packet loss). However, after the switch-based proxy rule was installed, the CPU usage stayed below 2% indicating that all of the random ARP requests could be responded accurately by the SDN switch.

## VII. CONCLUSIONS

According to the experiment result, the semi-reactive switch-based proxy application can effectively reduce ARP processing overhead by partially offloading the reply mechanism without involving the controller. This method provides a better option rather than fully hands over the task to the switch. If the network administrator implements the proactive method, whenever a new host entering the network, manual configuration needs to be performed in order to accommodate the request of the new hosts.

## ACKNOWLEDGMENT

This work was supported by the Universitas Muhammadiyah Malang.

## REFERENCES

- [1] H. Kim and N. Feamster, "Improving network management with software defined networking," *IEEE Communications Magazine*, vol. 51, no. 2, pp. 114-119, 2013.
- [2] OpenFlow Switch Specification (Version 1.5.0), O. N. Foundation, 2014.
- [3] W. Jian, Z. Weichen, Y. Shouren, L. Jiang, H. Tao, and L. Yunjie, "FSDM: Floodless service discovery model based on Software-Defined Network," in *2013 IEEE International Conference on Communications Workshops (ICC)*, 2013, pp. 230-234.
- [4] N. Jehan and A. M. Haneef, "Scalable Ethernet Architecture Using SDN by Suppressing Broadcast Traffic," in *2015 Fifth International Conference on Advances in Computing and Communications (ICACC)*, 2015, pp. 24-27.
- [5] C. Hyunjeong, K. Saehoon, and L. Younghee, "Centralized ARP proxy server over SDN controller to cut down ARP broadcast in large-scale data center networks," in *2015 International Conference on Information Networking (ICOIN)*, 2015, pp. 301-306.
- [6] L. Jun, G. Zeping, R. Yongmao, W. Haibo, and S. ShanShan, "A Software-Defined Address Resolution Proxy," in *2017 IEEE Symposium on Computers and Communications (ISCC)*, 2017, pp. 404-410.
- [7] R. d. Lallo, G. Lospoto, M. Rimondini, and G. D. Battista, "How to handle ARP in a software-defined network," in *2016 IEEE NetSoft Conference and Workshops (NetSoft)*, 2016, pp. 63-67.
- [8] F. Schneider, R. Bifulco, and A. Matusiuk, "Better ARP handling with InSPired SDN switches," in *2016 IEEE International Symposium on Local and Metropolitan Area Networks (LANMAN)*, 2016, pp. 1-6.
- [9] T. Alharbi and M. Portmann, "SProxy ARP - efficient ARP handling in SDN," in *2016 26th International Telecommunication Networks and Applications Conference (ITNAC)*, 2016, pp. 179-184.
- [10] Mininet. (Online). Available: <http://mininet.org>
- [11] O. vSwitch. (Online). Available: <http://openvswitch.org>
- [12] ONOS. (Online). Available: <http://onosproject.org>
- [13] Scapy. (Online). Available: <http://www.secdev.org/projects/scapy>
- [14] Tcpreplay. (Online). Available: <http://tcpreplay.synfin.net>

# Improvement of Cluster Importance Algorithm with Sentence Position for News Summarization

Nur Hayatin<sup>1</sup>

Department of Informatics Engineering  
University of Muhammadiyah Malang  
Malang, Indonesia  
noorhayatin@umm.ac.id

Gita Indah Marthasari<sup>2</sup>

Department of Informatics Engineering  
University of Muhammadiyah Malang  
Malang, Indonesia  
gita@umm.ac.id

Syadza Anggraini<sup>3</sup>

Department of Informatics Engineering  
University Muhammadiyah Malang  
Malang, Indonesia  
sasaanggraini.sa@gmail.com

**Abstract**—Text summarization is one of the ways to reduce large document dimension to obtain important information from the document. News is one of information which usually has several sub-topics from a topic. In order to get the main information from a topic as fast as possible, multi-document summarization is the solution, but sometimes it can create redundancy. In this study, we used cluster importance algorithm by considering sentence position to overcome the redundancy. Stages of cluster importance algorithm are sentence clustering, cluster ordering, and selection of sentence representative which will be explained in the subsections below. The contribution of this research was to add the position of sentence in the selection phase of representative sentence. For evaluation, we used 30 topics of Indonesian news tested by using ROUGE-1, there were 2 news topics that had different ROUGE-1 score between using cluster importance algorithm by considering sentence position and using cluster importance. However, those 2 news topics which used cluster importance by considering sentence position have a greater score of Rouge-1 than the one which only used cluster importance. The use of sentence position had an effect on the order of sentence on each topic, but there were only 2 news topics that affected the outcome of the summary.

**Keywords**— *News Summarization; Redundancy; Cluster Importance; Sentence Position*

## I. INTRODUCTION

Information is a notice regarding news that is usually contained in the form of articles, news, scientific papers, and books. However, the information presented is usually quite difficult for some people to understand because much information contained or called information overload [1], and this also occurs to news. In Indonesia, there are more than 43,000 news sites (<https://nasional.kompas.com>), where at a certain moment, some news discuss the same topic. Sometimes, people read news from one site to another to compare the content from the same topic. This will be very time consuming and sometimes there are several sentences that contain the same intent, and this means the reader will repeat the same occupation.

This is why the summarization system is the proper solution to the problem. By using summarization system, some news with the same topic will be summarized into one summary. This will facilitate the reader to get the outline of some news practically.

Summarization is a process to reduce the size of original document to a size which is not more than half of the original document [2]. In document summarization, there are two types of summarization; both of them are extraction and abstraction. Abstraction is a summary produced by changing the sentence but it has same meaning with the original one [3]. Meanwhile, extraction is a summary produced by taking original sentence from the document. Research in this area mostly generates summary with extraction method. A multi-document summary is a summary that involves more than one document. Fabianus [4] conducted a research to create a system of multi-document summarization for news in Bahasa Indonesia by using extraction with TF-IDF method as sentence scoring. But this study does not consider the problem of sentence redundancy. However, the important thing from extraction summary is extracting important textual units from multiple related documents, removing redundancies, and reordering the units to produce the summary [8].

Redundancy is the appearance of similar sentence in a summary. It is one of the most important factors in multi document summarization task [8]. If there is a redundancy in result of a summary, it will make the summary contains a lot of important information with the same meaning. So, it requires a method or algorithm to find similarity between sentences to overcome redundancy and optimize the sentence selection as the material for summary compilation [4]. Since the documents may contain redundant information, the performance of a multi document summarization system heavily depends on the sentence similarity measure used for removing redundant sentences from the summary [5].

Many previous research on extractive summaries used sentence features such as position in the text, words frequency,

or key phrases that indicated the importance words of the sentences. As thought Maximal Marginal Relevance (MMR), the earlier research on extractive summaries is considered redundancy issues by using the sentence level features. Clustering is an alternative approach to ensure good coverage and avoid redundancy that groups the similar textual units (paragraphs, sentences) into multiple clusters to identify themes of common information and selects text units one by one from clusters to the final summary [6][7]. Cluster importance is one of the algorithms on multi-document text summarization system using a similarity histogram based sentence-clustering algorithm to identify multiple sub-topics (themes) from the input set of related documents and selects the representative sentences from the appropriate clusters to form the summary [8]. This algorithm is adapting of a suitable sentence-clustering algorithm, which automatically determines the number of clusters and which is unsupervised in nature. So, this algorithm plays a vital role when the number of clusters is not known in advance.

This study proposes a solution to overcome redundancy by performing multi-document summarization of news in Bahasa Indonesia by using improvement of cluster importance algorithm with sentence position feature. Based on the research [9] explained that in a document, especially news, sentence position is an important feature where the sentence located in the beginning of paragraph has the biggest score than sentence which is located in the end of paragraph. The first phase to summarize is sentence clustering to news sub-topics. Second, the result of clusters that have been formed by weighting each cluster will be sorted. Third, summarization is done by choosing a representative sentence from each cluster by weighting every sentence and choosing a sentence with the highest weight from each cluster as material for summary aggregation.

## II. METHOD

This study was described into figure 1. The picture describes summarization system that covers some processes to build summary. These processes will be explained in the subsections below.

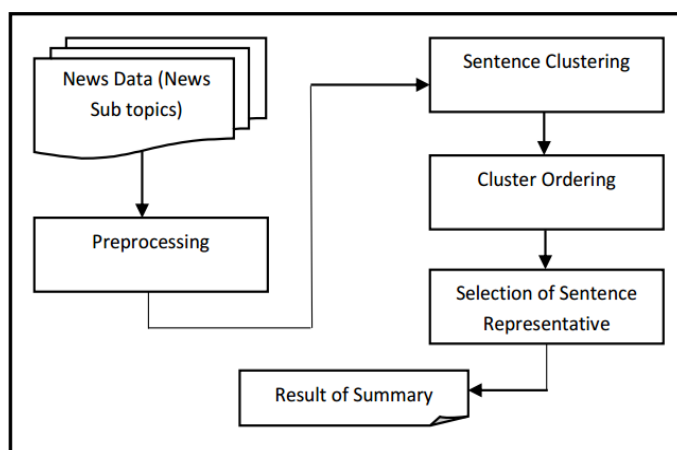


Fig. 1. Schematic of News Multi-Document Summarization System

### News Dataset

The data of this study retrieved online news that as many as 30 topics. 11 topics of news were retrieved from research [9] and

added another 19 topics of news. In one topic of news, there are 5 news sub-topics which every sub-topics were different to each other. The news data used was only the content without using the title of the news.

### Preprocessing

In the news, data preprocessing will be several processes such as splitting the news into individual sentences, case folding, tokenizing, and stop words removal. Splitting the news into individual sentences is a process to split news in paragraph form into individual sentences. After that, every sentences is done case folding to harmonize all alphabets into lowercase and also to delete delimiter such as (.), (,), (!), (?), (:), and etc. Then, proceeding every sentences to perform tokenizing that breaks down each sentence into words carried out before stop words removal process in order to make it easier in removing important words. The list of stop words was taken from research [10].

### Cluster Importance Algorithm

The concept of Cluster importance is that the more sentences that exist in a cluster, the cluster will be considered an important cluster that will be prioritized to appear at the beginning of the summary. Stages of cluster importance algorithm were sentence clustering, cluster ordering, and selection of sentence representative which will be explained in the subsections below. Furthermore, the contribution of this research is to add the position of sentence in the selection phase of representative sentence.

### Sentence Clustering

Sentence clustering is the first stage of cluster importance algorithm. More clearly about the sentence clustering is illustrated in the flowchart of figure 2.

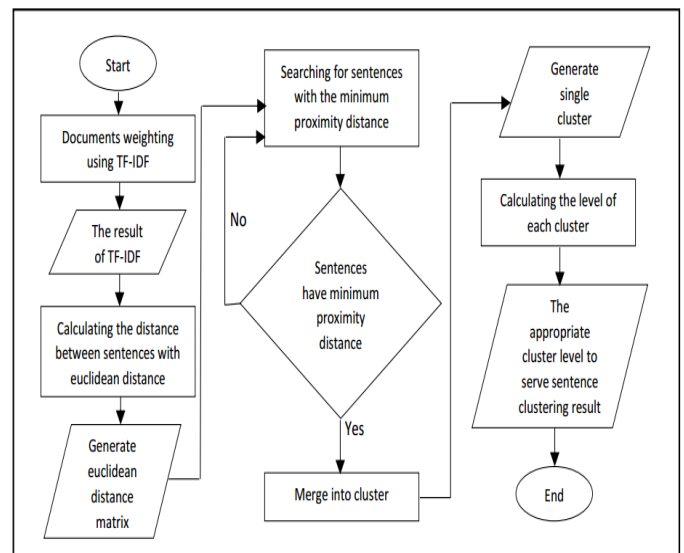


Fig. 2. Schematic of News Multi-Document Summarization System

Based on figure 2 above, the sentence clustering used a single linkage method. However, before using single linkage method, first performed documents weighting using TF-IDF. Term Frequency Inverse Document Frequency (TF-IDF) was weighting by calculating Term Frequency (TF) which was the

frequency or the number of words that appeared in a document. Besides, it also calculated Inverse Document Frequency (IDF) to calculate the importance of a word in a document seen from a number of documents as a whole [11]. The following equations 1 and 2 showed the Term Frequency Inverse Document Frequency (TF-IDF) weighting.

$$IDF(t) = \log \frac{N}{df(t)} \quad (1)$$

$$TF.IDF = TF(dt) * IDF(t) \quad (2)$$

After using TF-IDF as documents weighting, then measure the closeness between sentences by using euclidean distance. The distance between sentences was measured to determine the closeness between them. The following equation 3 shows euclidean distance.

$$Dis(x, y) = \sqrt{\sum (x^i - y^i)^2} \quad (3)$$

The next process after TF-IDF weighting and calculating minimum proximity distance using euclidean distance was sentence clustering by using single linkage. Single linkage is a clustering technique performed by consecutive way of merging begun by searching for two objects (sentences) with a minimum proximity distance. If it had minimum proximity distance, it will merge into a cluster. Next, look for other objects (sentences) that had minimum proximity to the cluster formed. If it had minimum proximity distance, it will merge into cluster formed or form a new cluster with other objects. It was done up to form single cluster. After single cluster was formed, and then choose the right level of cluster to determine the cluster as result of sentence clustering by measuring dissimilarity between them [12]. The following equation 4 calculates dissimilarity.

$$dissimilarity(cluster1, cluster2) = \frac{\sum Euclidian(d1, d2)}{size\ cluster1 \times size\ cluster2} \quad (4)$$

As for the mean of cluster [12] shown by equation 5 below.

$$Sim(X) = \sum_{d \in X} Euclidian(d, c) \quad (5)$$

So, determining the level of cluster or appropriate cluster level as the result of sentence clustering needed to use equation 4 selected by the biggest dissimilarity value.

### Cluster Ordering

Cluster ordering is the second stage of cluster importance algorithm. After completion of sentence clustering, a number of clusters were formed. The purpose of cluster ordering was to show information richness each cluster formed. A cluster consisted of sentences that are less important. Therefore, it needs cluster ordering or cluster sorting [8]. More clearly, cluster ordering can be illustrated by flowchart of figure 3.

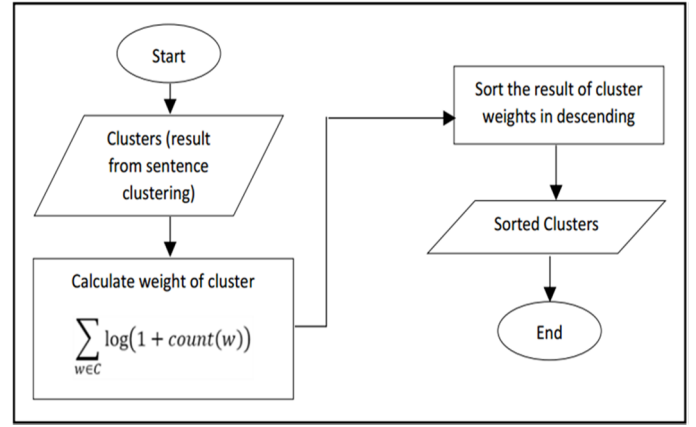


Fig. 3. Flowchart of Cluster Ordering

Based on figure 3, after a number of clusters have been formed from sentence clustering, each cluster was calculated its weight of words. After the weight of each cluster was found, do the sorting from largest to smallest. Cluster ordering is to know which cluster should be in the first as the material of summary aggregation.

### Selection of Sentence Representative

The third stage was representative sentence selection. This stage was a stage to choose a sentence from each cluster which formed by weighting each sentence. More clearly, selection of sentence representative can be illustrated by flowchart of figure 4 above.

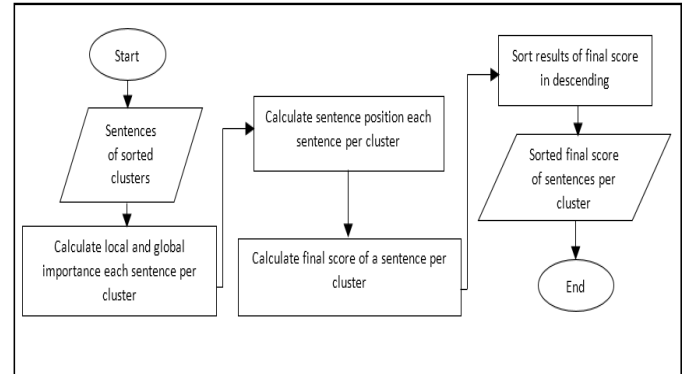


Fig. 4. Flowchart of Representative Sentence Selection

Based on figure 4, selection of sentence representative has two weighting calculation, namely W1 and W2. W1 is the first sentence weighting calculation by calculating local and global importance. Local importance is the word that indicates how many words in the formation of cluster or a number of a word in a cluster. The calculation of local importance was  $\log(1+CTF)$ , Cluster Term Frequency(CTF). While, global importance was the number of clusters that contained a word, the calculation using  $\log(1+CF)$ , Cluster Frequency(CF) [8]. The following equation 6 and 7 show W1.

$$W_1 = \text{Score}(S) = \sum \text{Weight}(w) \quad (6)$$

$$\text{Weight}(w) = \alpha_1 \log(1 + \text{CTF}) + \alpha_2 \log(1 + \text{CF}) \quad (7)$$

$$W_2(S) = \frac{1}{\sqrt{\text{POS}(S)}} \quad (8)$$

Beside calculating first weight,  $W_1$  then calculate second weight,  $W_2$ .  $W_2$  is the calculation of sentence position. From equation 8,  $\text{POS}(S)$  indicated sentence index appeared in a document. Consideration of sentence position within summarization of news multi-document according to study [13] where sentences located at the beginning of document had greater score than at the end of document. Besides, based on science journalism, technical writing in online news used “inverted pyramid”, important sentences were located at the beginning of document and less important sentences of news were located at the end of document [14]

Obtaining the weight of a sentence was done to add up the first and second weight ( $W_1+W_2$ ), in other words, to calculate final score of a sentence shown by equation 9.

$$\text{The last score}(s) = W_1(s) + W_2(s) \quad (9)$$

After the final score had been obtained, scores were sorted from largest to smallest. The greatest final score of a sentence from each cluster was elected as sentence representative of each cluster and also as the material for summary compilation.

## TESTING DESIGN

This study will be tested against the summary result. The following picture explains the testing design.

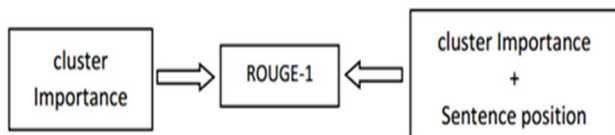


Fig. 5. Schematic of Testing Design

Based on figure 5 above, it showed testing scenario to summary results in which the testing was conducted between summary results of cluster importance and summary results of cluster importance with sentence position. This testing used Recall Oriented Understudy for Gisting Evaluation (ROUGE). ROUGE-N used to calculate the N-gram recall between system summary and reference summary [15]. N value used was 1. The following equation 10 shows ROUGE-N.

$$\text{ROUGE} - N = \frac{\sum_{S \in \text{Summ}_{ref}} \sum_{N\text{-gram} \in S} \text{Count}_{\text{match}}(N\text{-gram})}{\sum_{S \in \text{Summ}_{ref}} \sum_{N\text{-gram} \in S} \text{Count}(N\text{-gram})} \quad (10)$$

As this study used multi-document, the final calculation ROUGE-N was used as follows [15].

$$\text{ROUGE} - N_{\text{multi}} = \text{argmax}_i \text{ROUGE} - N(r_i, S) \quad (11)$$

Equation 11 above was to determine final value of ROUGE-N taken by maximum value of ROUGE-N.

## III. RESULT AND DISCUSSION

The research evaluation was done by testing the summary results between the summary generated by the system and manually by using ROUGE-N based on equation 6 and 7. This evaluation used two ground truth sources. Testing scenarios on these news topics was to compare test results from 30 news topics using cluster importance algorithms plus the position of sentences (CI+POS) with the results of testing 30 news topics only using cluster algorithm of importance (CI). This section explains the results of this study based on the testing results from testing design as described earlier. The following will explain more about the testing results. Examples of summary results are presented below:

Kepala Bagian Kepesertaan, Badan Penyelenggara Jaminan Sosial (BPJS) Sumatera Bagian Utara, Manna Lubis mengatakan pada 2015 BPJS hadir di Gunungsitoli dan Tapaktuan Aceh. Bahkan, sesuai dengan roadmap cakupan kepesertaan yang menyebutkan di tahun 2019 seluruh rakyat Indonesia sudah menjadi anggota BPJS Kesehatan dan apabila ditahun 2019 tersebut sudah tercapai Universal Health Coverage (UHC), BPJS Kesehatan tetap membuka pendaftaran bagi peserta baru khususnya bagi bayi yang baru lahir, warga Indonesia yang baru kembali dari luar negeri, penduduk asing yang baru masuk ke Indonesia, dsb.

"Kami melakukan aksi demo di Kantor BPJS karena pelayanan BPJS yang masih buruk bahkan adanya diskriminasi," kata ketua Federasi Serikat Metal Indonesia Kota Depok Wido Praktikno, Senin (1/12/2014). Bahkan, sesuai dengan roadmap cakupan kepesertaan yang menyebutkan di tahun 2019 seluruh rakyat Indonesia sudah menjadi anggota BPJS Kesehatan dan apabila ditahun 2019 tersebut sudah tercapai Universal Health Coverage (UHC), BPJS Kesehatan tetap membuka pendaftaran bagi peserta baru khususnya bagi bayi yang baru lahir, warga Indonesia yang baru kembali dari luar negeri, penduduk asing yang baru masuk ke Indonesia, dsb.

Summary testing describes the results of testing which will be explained in the table I below:

TABLE I. ROUGE-1 VALUE OF SUMMARY RESULTS

No.	Topic	CI+Pos	CI
1	Air Asia	0.51705	0.51705
2	Angkot Tabrak Grab	0.24103	0.24103
3	Banjarnegara	0.56796	0.56796
4	BBM	0.37888	0.37888
5	BPJS	0.47429	0.42286
6	Countdown Asian Games	0.53498	0.53498
7	Demo Angkot Malang	0.46018	0.46018
8	Dokter Letty	0.43182	0.43182
9	Dolly	0.48831	0.48831
10	Ebola	0.76812	0.76812
11	Gempa Korea Selatan	0.66447	0.66447
12	Gunung Agung	0.49032	0.49032
13	Habib Rizieq	0.38462	0.38462
14	Hari Raya Nyepi	0.41341	0.41341



No.	Topic	CI+Pos	CI
15	Konser Boyband SHINee	0.44872	0.44872
16	Kunjungan Obama	0.50691	0.50691
17	Kurikulum 2013	0.47511	0.47511
18	Ledakan Gudang Mercon	0.54040	0.54040
19	Mahasiswi UI	0.34574	0.34574
20	Palestina	0.41905	0.41905
21	Penasehat KPK	0.35673	0.35673
22	Penutupan Hotel Alexis	0.40462	0.40462
23	Penyanderaan Angkot	0.24725	0.24725
24	Penyiraman Novel Baswedan	0.50459	0.50459
25	Pemilihan Presiden	0.36290	0.36290
26	Pria Pencuri Amplifier	0.64737	0.64737
27	Saksi Kunci E-KTP	0.61290	0.61290
28	Sinabung	0.24171	0.15640
29	Tora Sudiro	0.53333	0.53333
30	U19	0.54113	0.54113

The testing of summary included 30 topics using two ground truth. Based on table 1 above, from 30 topics, there were 2 topics which had different value of ROUGE-1 between cluster importance and cluster importance with sentence position. Those topics are BPJS and Sinabung. However, ROUGE-1 value of cluster importance with sentence position had the greatest value than ROUGE-1 value of cluster importance. While 28 topics had same value of ROUGE-1 between cluster importance and cluster importance with sentence position.

Figure 6 shows the illustration of ROUGE-1 result that representation with graph.

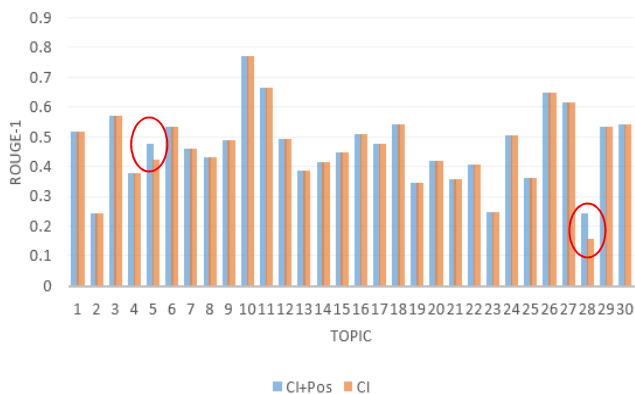


Fig. 6. Comparison Graph for ROUGE-1 Result between CI and CI+POS

The difference of ROUGE-1 value was caused by influence of sentence weight at the selection of sentence representative which affected order of sentence with highest weight as the material for summary compilation. Here is an example from a topic BPJS due to influence of sentence position weighting. From figure 7 and 8 due to changes the

order of sentences, it affects the summary result that also has impact on the value of ROUGE-1 produced.

NO.	CLUSTER	SENTENCES	W1	W2	SENTENCE WEIGHT
4.1		kepala bagian kepesertaan badan penyelenggara jaminan sosial bpjs sumatera bagian utara manna lubis mengatakan 2015 bpjs hadir gunungstolit tapaktuan aceh	9.261	1	10.261
5		melakukan aksi demo kantor bpjs pelayanan bpjs buruk diskriminasi kata ketua federasi serikat metal indonesia kota depok wido praktikno senin 1122014	9.28	0.447	9.727
2.1		ketua asosiasi pengusaha indonesia apindo kota medan rusmin lawin mengatakan program asuransi badan penyelenggara jaminan kesehatan bpjs bagus	8.437	1	9.437
5.8		sesuai peraturan perundangan pekerja penerima upah ppu bumh bumd badan usaha skala besar maupun wajib mendaftarkan pegawainya lambat 1 januari 2015	8.578	0.354	8.932
3.1		pelaksanaan program bpjs badan penyelenggara jaminan sosial kesehatan diajukan kamar dagang industri kadin tahun 2019 mendatang ditunda	7.373	1	8.373
4.4		kata bpjs cabang tapaktuan kedepannya melayani masyarakat kawasan aceh bagian barat kawasan berdekatan unit usaha disana	7.201	0.5	7.701
2.6		rusmin menjelaskan hari sopirnya mengurus bpjs datang pukul 0600 wib antrean kantor bpjs mencapai 100 orang	6.904	0.408	7.312

Fig. 7. An example of Representative Sentence Selection with Sentence Position

NO.	CLUSTER	SENTENCES	W1	SENTENCE WEIGHT
		1.5 melakukan aksi demo kantor bpjs pelayanan bpjs buruk diskriminasi kata ketua federasi serikat metal indonesia kota depok wido praktikno senin 1122014	9.28	9.28
		4.1 kepala bagian kepesertaan badan penyelenggara jaminan sosial bpjs sumatera bagian utara manna lubis mengatakan 2015 bpjs hadir gunungstoli tapaktuan aceh	9.261	9.261
		5.8 sesuai peraturan perundangan pekerja penerima upah ppu bumh bumd badan usaha skala besar maupun wajib mendaftarkan pegawainya lambat 1 januari 2015	8.578	8.578
		2.1 ketua asosiasi pengusaha indonesia apindo kota medan rusmin lawin mengatakan program asuransi badan penyelenggara jaminan kesehatan bpjs bagus	8.437	8.437
		3.1 pelaksanaan program bpjs badan penyelenggara jaminan sosial kesehatan diajukan kamar dagang industri kadin tahun 2019 mendatang ditunda	7.373	7.373
		4.4 kata bpjs cabang tapaktuan kedepannya melayani masyarakat kawasan aceh bagian barat kawasan berdekatan unit usaha disana	7.201	7.201
		2.6 rusmin menjelaskan hari sopirnya mengurus bpjs datang pukul 0600 wib antrean kantor bpjs mencapai 100 orang	6.904	6.904

Fig. 8. An example of Representative Sentence Selection without Sentence Position

#### IV. CONCLUSIONS

From the research that has been done, it can be concluded that there are two topics (BPJS and Sinabung) which have different value of ROUGE-1 between cluster importance and cluster importance with sentence position. ROUGE-1 value from cluster importance with sentence position of those topics has higher value than ROUGE-1 value from cluster importance.

Application of sentence position to cluster importance algorithm as consideration to summarize news document does not give significant result. This is shown on 30 topics that were tested, 28 topics have equal ROUGE-1 value between cluster importance and cluster importance with sentence position. However, application of sentence position shows difference of sentence order at the stage of representative sentence selection, but it does not give big impact to final summary result.

Based on explanation above, summary of application of sentence position is influenced by the news data itself where there is no exact sentence between one and another. So, it causes an influence on the weight of each sentence.

There is also a suggestion for further research that is to use another data research other than news. Therefore, it can be shown to be necessary or not regarding consideration of sentence position to summarize document.



## REFERENCES

- [1] W. E. Waliprana and M. L. Khodra, "Update summarization untuk kumpulan dokumen berbahasa Indonesia," *Cybermatika*, vol. 1, no. 2, 2013.
- [2] N. Munot and S. S. Govilkar, "Comparative study of text summarization methods," *Int. J. Comput. Appl.*, vol. 102, no. 12, pp. 33–37, 2014.
- [3] A. Agrawal and U. Gupta, "Extraction based approach for text summarization using K-Means clustering," *Int. J. Sci. Res. Publ.*, vol. 4, no. 11, 2014.
- [4] Y. S. Fabianus H. Evan, P. W.P, and Pranowo, "Pembangunan perangkat lunak peringkasan dokumen dari banyak sumber menggunakan sentence scoring dengan metode TF-IDF," in *Seminar Nasional Aplikasi Teknologi Informasi*, 2014.
- [5] K. Sarkar, K. Saraf, and A. Ghosh, "Improving graph based multidocument text summarization using an enhanced sentence similarity measure," in *2015 IEEE 2nd International Conference on Recent Trends in Information Systems (ReTIS)*, 2015.
- [6] A. S. Asa, S. Akter, M. P. Uddin, M. D. Hossain, S. K. Roy, and M. I. Afjal, "A Comprehensive Survey on Extractive Text Summarization Techniques," *Am. J. Eng. Res.*, vol. 6, no. 1, pp. 226–239, 2017.
- [7] S. KM and S. R, "Text Summarization using Clustering Technique and SVM Technique," *Int. J. Appl. Eng. Res.*, vol. 10, no. 12, pp. 28873–28881, 2015.
- [8] K. Sarkar, "Sentence Clustering-based Summarization of Multiple Text Documents," *Tech. – Int. J. Comput. Sci. Commun. Technol.*, vol. 2, no. 1, pp. 974–3375, 2009.
- [9] N. Hayatin, C. Fatichah, and D. Purwitasari, "PEMBOBOTAN KALIMAT BERDASARKAN FITUR BERITA DAN TRENDING ISSUE UNTUK PERINGKASAN MULTI DOKUMEN BERITA," vol. 13, no. 1, pp. 38–44, 2015.
- [10] F. Z. Tala, "A Study of Stemming Effects on Information Retrieval in Bahasa Indonesia," Institute for Logic Language and Computation Universiteti van Amsterdam, 2003.
- [11] E. Purwanti, "Klasifikasi dokumen temu kembali informasi dengan K-Nearest Neighbour," *Rec. Libr. J.*, vol. 1, no. 2, 2015.
- [12] Annisa, Y. Munarko, and Y. Azhar, "Peringkasan tweet berdasarkan trending topik twitter dengan pembobotan TF-IDF dan single linkage agglomerative hirarchical clustering," *Kinet. Game Technol. Inf. Syst. Comput. Network, Comput. Electron. Control.*, vol. 1, no. 1, pp. 9–16, 2016.
- [13] J. P. Mei and L. Chen, "SumCR: A new subtopic-based extractive approach for text summarization," *Knowl. Inf. Syst.*, vol. 31, no. 3, pp. 527–545, 2012.
- [14] S. Verdianto, A. Z. Arifin, and D. Purwitasari, "Strategi pemilihan kalimat pada peringkasan multi dokumen," *J. Tek. ITS*, vol. 5, no. 2, 2016.
- [15] C. Y. Lin, "Rouge: A package for automatic evaluation of summaries," *Proc. Work. text Summ. branches out (WAS 2004)*, no. 1, pp. 25–26, 2004.

# Comparison Between A\* And Obstacle Tracing Pathfinding In Gridless Isometric Game

Lailatul Husniah  
Informatics Department

Universitas Muhammadiyah Malang  
Malang, Indonesia  
[husniah@umm.ac.id](mailto:husniah@umm.ac.id)

Rizky Mahendra  
Informatics Department

Universitas Muhammadiyah Malang  
Malang, Indonesia  
[rizky.ade.mahendra@gmail.com](mailto:rizky.ade.mahendra@gmail.com)

Ali Sofyan Kholimi  
Informatics Department

Universitas Muhammadiyah Malang  
Malang, Indonesia  
[kholimi@umm.ac.id](mailto:kholimi@umm.ac.id)

Eko Cahyono  
Informatics Department

Universitas Muhammadiyah Malang  
Malang, Indonesia  
[ekobudi@umm.ac.id](mailto:ekobudi@umm.ac.id)

**Abstract**— The pathfinding algorithms have commonly used in video games. City 2.5 is an isometric grid-less game which already implements pathfinding algorithms. However, current pathfinding algorithm unable to produce optimal route when it comes to custom shape or concave collider. This research uses A\* and a method to choose the start and end node to produce an optimal route. The virtual grid node is generated to make A\* works on the grid-less environment. The test results show that A\* be able to produce the shortest route in concave or custom obstacles scenarios, but not on the obstacle-less scenarios and tight gap obstacles scenarios.

**Keywords**—game, pathfinding, A\*, grid-less, and isometric

## I. INTRODUCTION

Video games genres and styles have evolved in the past decades. The current technologies make it easier for a developer to implement or combine one genre to another. One of the genres that we studied is 2D simulation games with isometric perspective. In the past time, most the 2D isometric games rely on the grid as its base. Almost every game-objects shown on that game has bounded to that grid. Grid usage also makes it easier to implement pathfinding and mapping. Common A\* algorithm could have implemented very well.

Unity3D is a game engine to make a high-quality 3D and 2D games [1]. Although it could produce a 2D game, all game objects occupy a 3D space. Thus a default 2D game would not become a grid based game. However, it still possible to develop a grid-based 2D game by generating the grid itself. Based on such occasion, to solve pathfinding problems, we can either generate a virtual 2D grid to implement basic A\* pathfinding or create a custom pathfinding method to adapt grid-less environment.

“City 2.5” is a grid-less 2D isometric city-building simulation game. Since we are part of the developer who develops this game, we can access and modify every part of this game. City 2.5 use a custom pathfinding method called Obstacle Tracing (OT) [2]. However, this method is not optimal since it cannot always guarantee the shortest path. The tendency of NPC (Non-Player Character) to encircling the obstacle could make the path even longer. NPC is also relying on obstacle collider convex shape which is means when NPC found a concave collider the path taken would be longer.

This previous study [3] use Fuzzy Mamdani Logic to solve navigation problems that made better navigation on the robot hexapod fire extinguisher. Other studies [4] use A\* to solve pathfinding problems in the 2.5D isometric game. The game is grid-based, which preferable for A\* algorithm. The primary goal of that study is to investigate and determine the optimal pathfinding strategy based on several measures such as steps and time have taken to reach the goal using A\* algorithm [5].

A\* itself is favorable as a pathfinding method as it is simple to implement, is very efficient, and has lots of scope for optimization [6,7]. A\* able to generate the shortest path because it uses a heuristic function to estimate the distance of any point to target point [8]. A\* implementation on Unity3D has been done by [9], and so we need to adapt the implementation method for this game.

A\* is an algorithm which measures the heuristic distance between a given point, while the pathfinding itself rely on the search space on how the A\* graph represented in the game. In this study [10,11] there are several ways to represent the search space. Previous research [12] use A\* to solve pathfinding method for a grid-based graph. In this research, we will use the common A\* search space representation, a rectangular grid. The advantage of using the grid is it is easier to generate automatically [13] and easy to implement map representation [14].

Some studies about comparing pathfinding methods have been done by [11,12,13,14,15]. Unfortunately, none of those paper discusses pathfinding on grid-less environment explicitly. What makes this paper different from previous studies is the case study, grid-less environment, and the method Obstacle Tracing, which is rarely used in other paper and research. The goal of this paper is to solve NPC pathfinding problems on a grid-less 2D isometric game. Therefore, A\* is implemented and compare it with current Obstacle Tracing method. This paper also focuses on how to implement A\* properly without altering the unique rules and game design itself. Thus we will limit not to include the computational complexity of the two algorithms, but compare how the path has taken and the speed of computation.

## II. RESEARCH METHODOLOGY

### A. Study on Current Method

*City 2.5* is a city building simulation game developed using the Unity3D engine. It is relying heavily on Unity3D component for everything to works, including its pathfinding method which is Obstacle Tracing. After some studies on this game, we can state the flow of its pathfinding method on Fig. 1 and the predicted result on Fig. 2. At the flowchart in Fig. 1 we can see this method using Raycast [16] to detect the obstacle which blocking its way and move toward it. If the obstacle is not the destination, then it needs to be encircled. Although this method able to find the route, however, if the obstacles have a concave or custom shape, the path taken might be not optimal (not shortest).

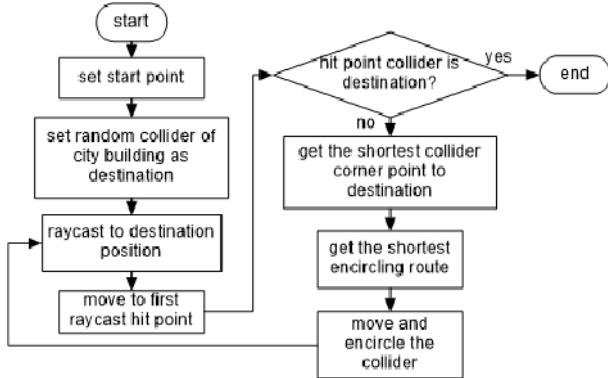


Fig. 1. Obstacle Tracing method flowchart

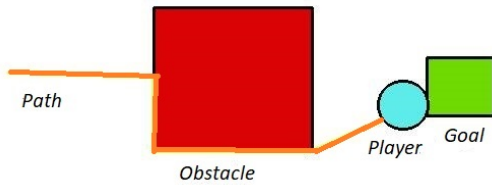


Fig. 2. Pathfinding result using Obstacle Tracing

### B. Design for A\* method

This game requires a dynamic map which able to change when the world itself is changing. To achieve that, a method to generate and validate A\* map has created as seen in Fig. 3. There are three parameters to generate a grid map which is size X and size Y as how much nodes generated on X and Y axis and space between which determine how far the gap between nodes.

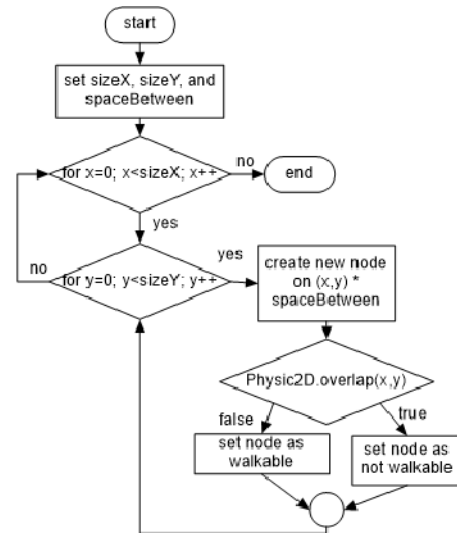


Fig. 3. Map generating flowchart

To validate if the node is either walkable or not, it can achieve by calling Unity method `Physic2D.OverlapPoint` [17]. This method will return true if a point in the game world is inside a 2D collider. Since the obstacles in this game are using 2D collider, so it is possible to determine if the node was walkable when `Physic2D.OverlapPoint` return false, and vice versa.

The conventional A\* path-computing could be applied after the map has generated as shown in Fig. 4. The next problems that need to be solved are how to determine the start and end point for each NPCs. In this game, NPC does not have any collider, which means that it could occupy any node as long as it is walkable. So we could do reverse computing to determine the closest node as the start point as shown in Fig. 5.

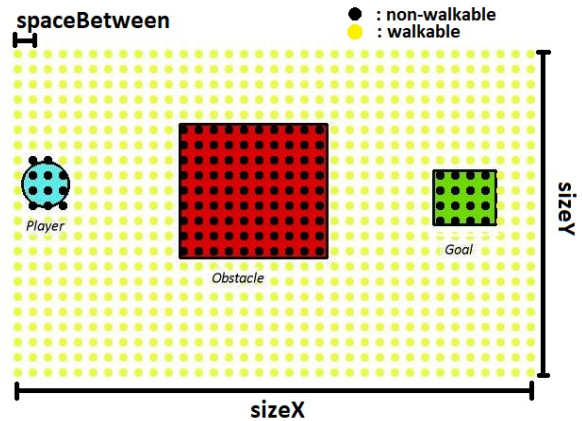


Fig. 4. Map generation result

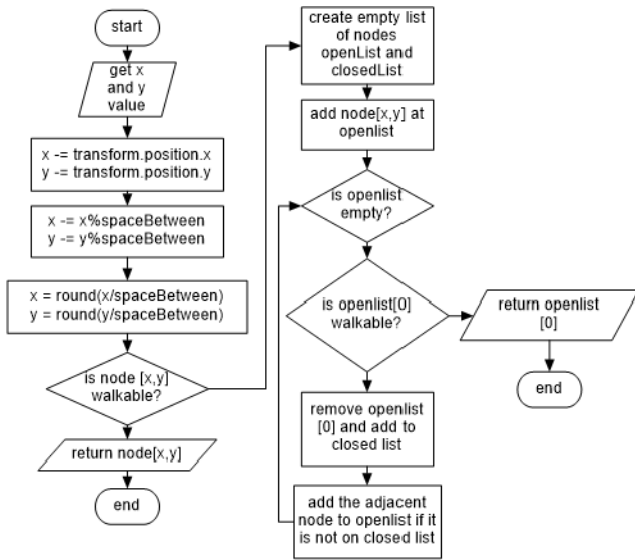


Fig. 5. Find nearest node flowchart

Method on Fig.5 could be used to determine endpoint, but another problem would have occurred like in Fig. 6. The node returned would be always same regardless the NPC start position which would cause less-optimal shortest path.

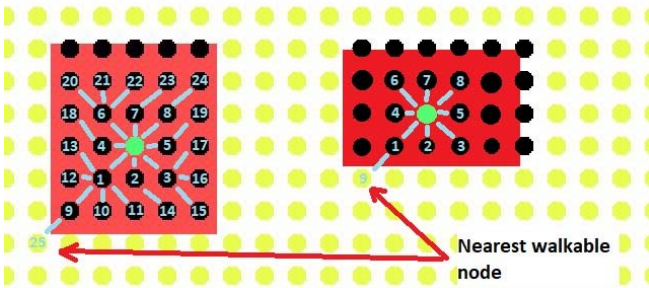


Fig. 6. Current search algorithm always returns the left-bottom side node

To prevent that behavior, it necessary to know which node that closest with destination and start point. It could be achieved by do a Raycast from current position to destination and search the closest node from the hit point, resulting in a method on Fig. 7.

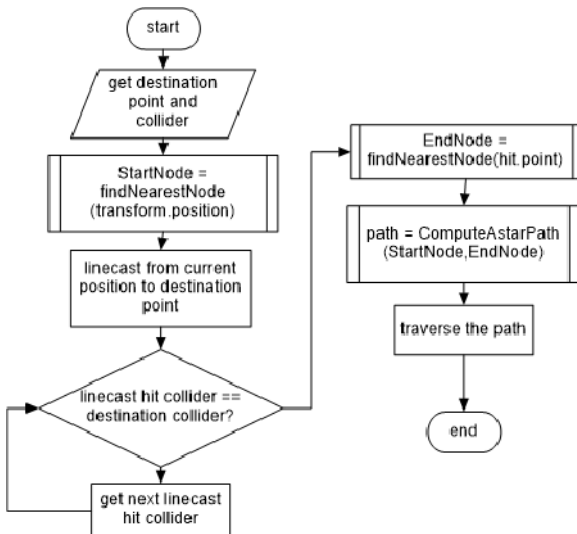


Fig. 7. Determining start and end node

### III. RESULT AND ANALYSIS

The goal of this paper is to compare both methods. A\* pathfinding comparison has been made by [15] using node count and travel length as a parameter. There are ten different scenarios to test. Both NPC with different algorithm placed in the same spot and need to find the path to destination target. A \* map made using the SpaceBetween parameter with a value range of 0.1, 0.2, and 0.3.

A\* map made on three space between parameters value which is 0.1, 0.2, and 0.3. The test parameters are:

Node: Node count need to reach the goal

Actual: Actual distance from start to goal (obstacle ignored)

Travel: Travel distance from start to goal

Error: Difference from target goal point, to an actual goal point

Difference: Algorithm precision score. Where Difference = Actual (Travel + Error). The bigger Difference score is considered better NPC

#### A. Scenario 1: No Obstacles

Table I has shown that OT is better at a Difference score, because of OT NPC able to walk straight to the goal as shown on Fig. 8. While A\* has shorter travel distance, yet the error is too big because A\* movement is dependent on nodes.



Fig. 8. NPC go straight to the destination

TABLE I. SCENARIO 1 RESULT

Obs. = 0	No Obstacle				
	Node	Actual	Travel	Error	Difference
OT	2	2.747102	2.386049	0.361054	<b>-1.1E-06</b>
A* 0.1	21	2.747102	2.487411	0.440114	-0.180423
A* 0.2	10	2.747102	<b>2.340456</b>	0.572451	-0.165805
A* 0.3	7	2.747102	2.381878	0.534509	-0.169285

#### B. Scenario 2: Natural placement

In Fig. 9 obstacles placed naturally as the game behave. Table II shows that A\* able to perform better than OT in



term of the node and travel distance on 0.3 set up. However, the error still significant compared to OT.

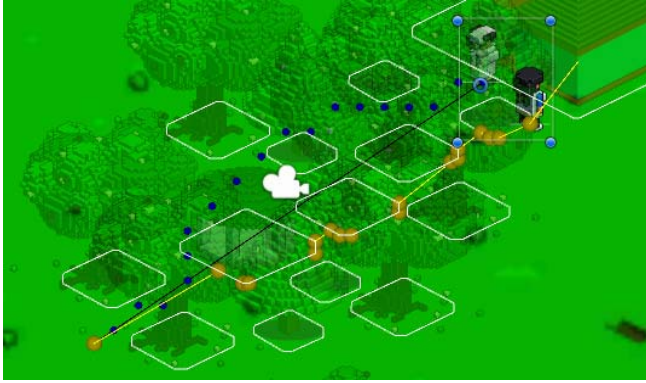


Fig. 9. Scenario 2: both NPCs took a different path

TABLE II. SCENARIO 2 RESULT

Obs. = 13	Normal Placement				
	Node	Actual	Travel	Error	Difference
OT	24	6.817501	6.777603	0.662324	<b>-0.622426</b>
A* 0.1	57	6.817501	6.790489	0.801852	-0.77484
A* 0.2	28	6.817501	6.546429	1.024489	-0.753417
A* 0.3	18	6.817501	<b>6.382557</b>	1.189037	-0.754093

### C. Scenario 3: Tight gap obstacles

In Fig 10, it is clear that A\* unable to make a route through a narrow gap, resulting OT has better scores as shown in Table III. It is possible to generate the shortest path by making node gap smaller, but the nodes count would increase significantly, and more nodes mean more calculating process.



Fig. 10. Scenario 3: OT NPC can go through the narrow gap

TABLE III. SCENARIO 3 RESULT

Obs. = 4	Tight Gap Obstacles				
	Node	Actual	Travel	Error	Difference
OT	17	5.845109	<b>5.730087</b>	0.355027	<b>-0.240005</b>
A* 0.1	73	5.845109	8.620098	0.396763	-3.171752
A* 0.2	36	5.845109	8.638044	0.53361	-3.326545
A* 0.3	25	5.845109	8.580089	0.580986	-3.315966

### D. Scenario 4 : Straight row (horizontal) obstacles

Table IV has shown that A\* is better on every configuration because OT weakness was exposed. OT unable to pre-compute the path, that makes its NPC need to encircle every single obstacle in the path as shown in Fig. 11.

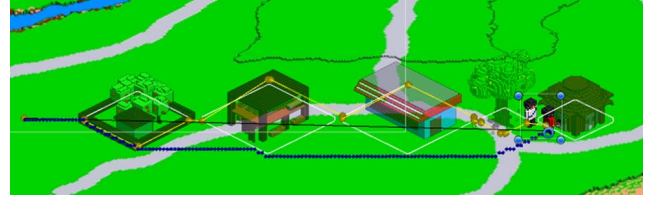


Fig. 11. Scenario 4: A\* NPC has the most efficient path

TABLE IV. SCENARIO 4 RESULT

Obs. = 4	Straight Row Obstacle				
	Node	Actual	Travel	Error	Difference
OT	27	15.12298	16.01473	0.828928	-1.720678
A* 0.1	145	15.12298	15.15446	0.70184	-0.73332
A* 0.2	73	15.12298	15.29319	0.70184	-0.87205
A* 0.3	48	15.12298	<b>14.98526</b>	0.81357	<b>-0.67585</b>

### E. Scenario 5: Wide Obstacle

When the obstacle is modified like on Fig.12, it influences the pathfinding result. Table V shows that A\* is better on travel distance from every configuration. While OT needs a little bit longer path because it needs to go to the nearest Raycast hit point first.

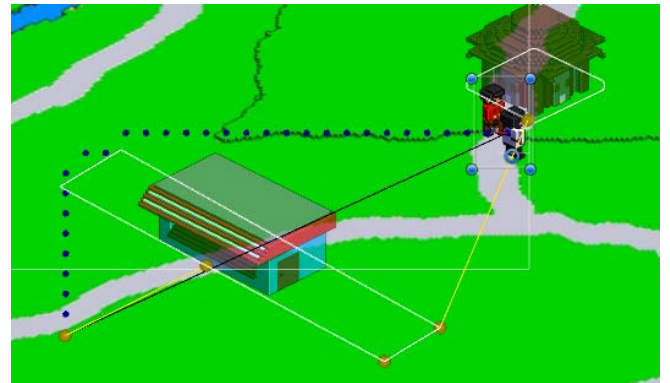


Fig. 12. Scenario 5: NPCs took a different path

TABLE V. SCENARIO 5 RESULT

Obs. = 1	Wide Obstacles				
	Node	Actual	Travel	Error	Difference
OT	6	7.84419	9.709723	0.28821	-2.153743
A* 0.1	91	7.84419	9.507587	0.410222	-2.073619
A* 0.2	44	7.84419	9.553211	0.410222	-2.119243
A* 0.3	31	7.84419	<b>9.274145</b>	0.62037	<b>-2.050325</b>

### F. Scenario 6: River crossing

The more complex and irregular collider shape like a river in Fig. 13, the longer path need to be traversed by OT

algorithm. However, it does not matter for A\* algorithm since it does not depend on obstacle shape. The result on Table VI, A\* is better than OT



Fig. 13. Scenario 6: OT NPC need to travel alongside the river to reach the goal

TABLE VI. SCENARIO 6 RESULT

Obs. = 1	River Crossing				
	Node	Actual	Travel	Error	Difference
OT	21	3.158496	21.97575	0.273512	-19.09077
A* 0.1	156	3.158496	<b>19.12286</b>	0.318549	<b>-16.28291</b>
A* 0.2	80	3.158496	19.46426	0.38832	-16.69408
A* 0.3	54	3.158496	19.69431	0.289024	-16.82484

#### G. Scenario 7: Non-uniform poly obstacles

One of OT weakness is it need to encircle every obstacle that obstructing the view. In Fig 14, many obstacles have been modified thus make OT a bit longer to encircle. The result in Table VII, A\* is the best in every configuration.

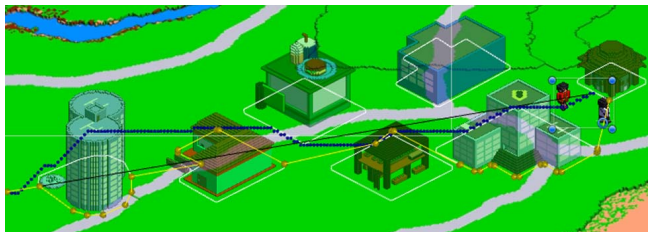


Fig. 14. Scenario 7: OT weakness exposed when the poly is modified

TABLE VII. SCENARIO 7 RESULT

Obs. = 6	Non-Uniform Poly Obstacles				
	Node	Actual	Travel	Error	Difference
OT	38	18.41779	23.21464	0.295155	-5.092005
A* 0.1	177	18.41779	19.26544	0.557314	<b>-1.404964</b>
A* 0.2	88	18.41779	19.20004	0.656201	-1.438451
A* 0.3	59	18.41779	<b>19.41265</b>	0.6772	-1.67206

When comparing about runtime speed, unfortunately, A\* does not perform better than OT. The result in table VIII show runtime speed for each scenario. In Fig. 15, we can see obvious that OT has the stable runtime because OT only counts the corner/vertices of the collider. However, A\* runtime is affected by the traversed node count so the

smaller gap between a node of A\* will increase node count and computing time.

TABLE VIII. SCRIPT RUNTIME COMPARISON

Scenario	OT	A* 0.1	A* 0.2	A* 0.3
1	1.81E-05	0.002579	0.000451	0.000246
2	0.0015984	0.0271087	0.006022	0.004364
3	0.0012391	0.0765834	0.0151963	0.00708
4	0.0014989	0.1833878	0.0280047	0.008471
5	0.0009871	0.0960097	0.0319581	0.006722
6	0.001262	0.8707223	0.1223979	0.078486
7	0.0016031	0.4479461	0.0750437	0.02527

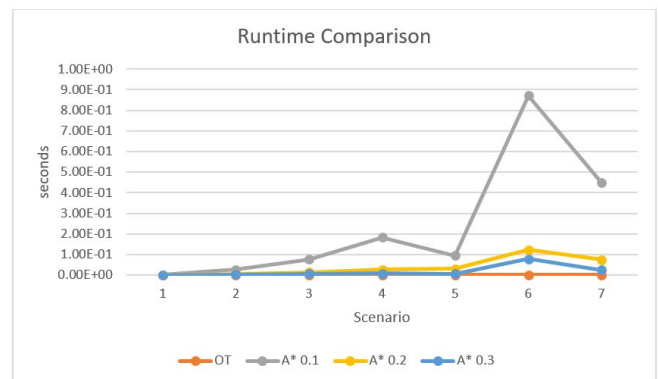


Fig. 15. Runtime comparison graph

## IV. CONCLUSION

The A\* method can be implemented well in isometric non-grid games with the requirement to create a virtual grid for search space. A\* can solve the shortest path regardless of the obstacle shape as long as the generating nodes have not caught in the dead end. The reason A\* lose on the term of shortest path compared to Obstacle Tracing is that of jagged movement pattern caused by the grid or when the gap between A\* node is larger than the gap between obstacles. However, Obstacle Tracing is better on runtime performance.

## V. ACKNOWLEDGMENT

This research supported by Universitas Muhammadiyah Malang.

## REFERENCES

- [1] Unity3D Game Engine, [online] Available : <https://unity3d.com/> [11March 2018]
- [2] M.B. David and S. Glenn, *AI for Game Developers: Creating Intelligent Behavior in Games*, O'Reilly Media, 2014
- [3] Hidayati, Q. Rachman, F. Z., & Yanti, N. "Intelligent Control System of Fire-Extinguishing and Obstacle-Avoiding Hexapod Robot," *Kinetik: Game Technology, Information System, Computer Network, Computing, Electronics, and Control*, vol. 3, no. 1, pp 1-10. 2017
- [4] M. Jason, *Pathfinding Strategy for multiple non-playing characters and agents in a 2.5D Game World*, Athabasca University, Athabasca, Alberta, Canada, 2009
- [5] M. Ian and F. John, *Artificial Intelligence for games*, 2nd ed. Morgan Kaufmann Publisher, pp. 215, 2009



- [6] B. Ray, S.K. Aung, P. Clifford, and N.S. Thet, *Unity AI Game Programming*, 2nd ed. Packt Publishing, pp. 75, 2015
- [7] S. M. LaValle, *Planning Algorithms*, Cambridge University Press, 2006
- [8] H. Zhang, S. Minyong, L. Chunfang, "Research and Application of Path-finding Algorithm Based on Unity 3D", *IEEE ICIS 2016*, June 2016
- [9] C. Xiao and S. Hao, "A\*-based Pathfinding in Modern Computer Games", *IJCSNS International Journal of Computer Science and Network Security*, VOL.11 No.1, January 2011
- [10] C. Xiao and S. Hao, "Direction Oriented Pathfinding In Video Games", *International Journal of Artificial Intelligence & Applications (IJAI)*, Vol.2, No.4, October 2011
- [11] R. Anbuselvi and M.Phil, "Path Finding Solutions For Grid Based Graph", *Advanced Computing: An International Journal ( ACIJ )*, Vol.4, No.2, March 2013
- [12] Y. Bjornsson, M. Enzenberger, R. Holte, J. Schaejfer, and P. Yap, "Comparison of different grid abstractions for pathfinding on maps", In Proceedings of the 18th International Joint Conference on Artificial Intelligence, San Francisco, pp.1511-1512, 2003
- [13] S. Yoppi, S. Hadipurnawan, S. Muhammad, "Comparison of A\* and Dynamic Pathfinding Algorithm with Dynamic Pathfinding Algorithm for NPC on Car Racing Game", *11th International Conference on Telecommunication Systems Services and Applications (TSSA)*, Oktober 2017
- [14] N. Azad, and M. Farzad, "Simulation and Comparison of Efficiency in Pathfinding algorithms in Games", *Ciência e Natura*, v. 37 Part 2, p. 230–238, June 2015
- [15] R.F. Eka, U.M. Siti, and F. Feri, "Comparative Analysis of A\* and Basic Theta\* Algorithm In Android-based Pathfinding Games", *6th International Conference on Information and Communication Technology for The Muslim World (ICT4M)*, November 2016
- [16] Unity Documentation, [online] Available : <https://docs.unity3d.com/Manual/Raycasters.html> [11March 2018]
- [17] Unity Documentation, [online] Available : <https://docs.unity3d.com/ScriptReference/Physics2D.OverlapPoint.html> [11March 2018]

# Automatic Game World Generation for Platformer Games Using Genetic Algorithm

Ali Sofyan Kholimi  
Informatics Department  
Universitas Muhammadiyah Malang  
Malang, Indonesia  
kholimi@umm.ac.id

Ahmad Hamdani  
Informatics Department  
Universitas Muhammadiyah Malang  
Malang, Indonesia  
ahmad\_437256@webmail.umm.ac.id

Lailatul Husniah  
Informatics Department  
Universitas Muhammadiyah Malang  
Malang, Indonesia  
husniah@umm.ac.id

**Abstract**— Most of the games rely on the game designer to design the level and environment. Increasing of game environment space scale followed by increasing of time and cost. Procedural Content Generation (PCG) is a method to solve this problem by generating a game environment space. In this paper, a PCG method proposed using a genetic algorithm approach to solve the problem in generating game environment. Transition graph adapted in the proposed method to make PCG generate difficulty level. The Index-based approach used to display the biome sequence. This approach displays the biome according to its index in the sequence.

**Keywords**— *Procedural Content Generation, Evolutionary Algorithm, Genetic Algorithm, Transition Graph*

## I. INTRODUCTION

The game world is an artificial world in which the game event happen. Mostly, a game word is designed by game designer manually. However, the problem will occur if the game world scale is vast. The longer the development of the game, time and cost will increase. While to finish the game does not take a long time [1], The lack of ability to attract a player to play the game again is also a crucial problem [2]. Especially for an indie game developer that has a limited budget and small fans community, it will be an essential problem to solve.

Procedural Content Generation (PCG) is used to solve this problem. PCG is a content that created by algorithm automatically. PCG itself can accept input from user or game designer to adapt the content it will produce [3]. The game that uses PCG will be more varied, give more challenge and have more attractiveness. Open world platformer or exploration platformer has used in this research. The produced game world divided into biome that consists of land, vegetation, and weather. A transition graph that consists of land, vegetation and weather will be built according to game designer design.

The genetic approach has used in generating game level automatically. The genetic algorithm is a method that adapts from the chromosome evolution in the genes of living things[4]. Previous research [5][6][7][8] used a genetic approach to design game level. While in [9] generating game environment based on the biome. Other research [10] in the game world environment has focused on 3D terrain generation. When working on PCG, it is crucial for the game designer to have the ability to control the difficulty curve of the generated level. So, the game designer can create game level according to their design. The, transition graph [11] is adapted and let the game designer design the

game world or the level using the graph that included in the genetic algorithm proses. The genetic algorithm will provide result according to the transition graph defined by the game designer. In this research, Transition Graph is used to improve the Genetic Algorithm that used for Automatic Game World Generation for Platformer.

## II. RESEARCH METHOD

### A. System Overview

In this research, the genetic algorithm is used to design the game world. First, the difficulty curve is defined and include it in a genetic algorithm. When the genetic algorithm finishes its process, the result then passed to the rendering to generate game world based on the design from a genetic algorithm.

### B. Difficulty Curve

Difficulty curve using Game World Fitness as a base to control the difficulty of the generated game world. The worse value of Fitness, which is further from zero value, increases the level of difficulty. 30 difficulty values defined for 30 level as shown in Fig 1.

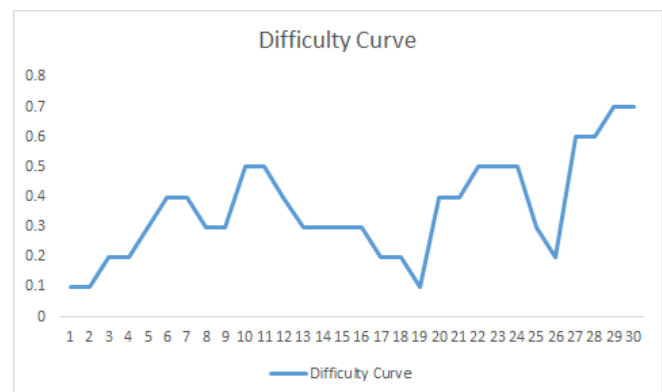


Fig. 1. Difficulty Curve.

### C. Generation of Chromosome

The Chromosome in this genetic algorithm consists of a component set that chosen randomly. The Genes for the chromosome contain the sequence of the component shown in Fig. 2. The component itself is a data container that consists of 3 components, lands, vegetation and weather. Game designer determines the type and amount of biome. So, the biome does not limit to the defined one, but it still can be increased.



Fig. 2. The sequence of a biome.

#### D. Fitness Function

Transition graph is used to calculate the fitness value. The transition graph is a graph that consists of lands, vegetation, and weather. Each transition has each own value as given in Fig. 3.

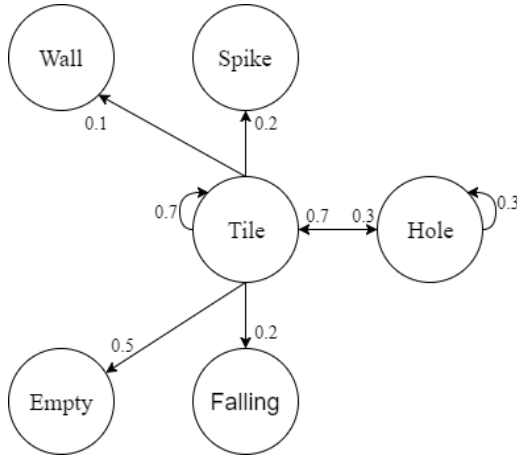


Fig. 3. The transition graph.

Transition graph updated according to the biome used to get better results. The algorithm loops each gene in a chromosome and count the number of chromosomes and divide it by chromosome length calculated by equation (1).

$$d = \frac{\text{numberOfObstacle}}{\text{Chromosome Length}} \quad (1)$$

#### E. Genetic Algorithm Implementation

The genetic algorithm described in Fig 4. It starts by generating an initial population randomly. The parameter of the genetic algorithm defined. The different problem requires a different parameter value. Our method uses the default parameter that already explained in [12]. Those values are two times of the chromosome size for population, 0.7 for crossover rate and 0.001 for mutation rate. Land data has used for the initial population, vegetation and weather have added in runtime to each chromosome. The genetic algorithm halts when maximum generation reached or more than the threshold. The threshold for halt the algorithm is the difficulty value from the difficulty curve. Another termination condition is counter for counting if the algorithm produces a similar population for a certain amount of generation.

The produced initial population entered a crossover process, and the parent is chosen using roulette wheel selection. A random number from range 0 to the total of the transition value of the population has generated. A chromosome is chosen as a parent if the sum of transition value is less than the random number. Next, genes from the middle until the last index of the second parent are swapped with the first parent genes in the middle until the last index.

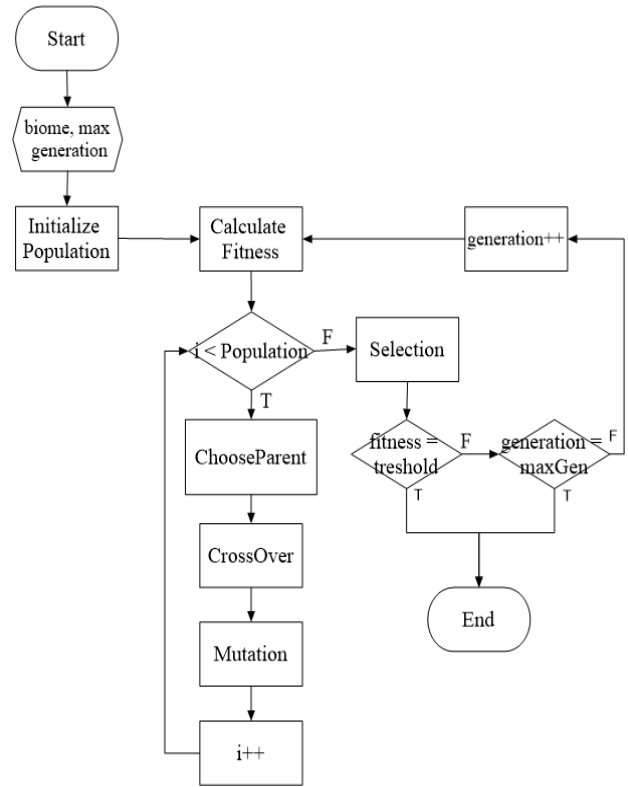


Fig. 4. Genetic algorithm overview.

Child from the crossover process mutate. The probability of mutation happens has decided by mutation rate. There are three mutation operator, that consist of addition, value change, and deletion. It adopts from previous research [11]. A random operator has chosen for the mutation.

1) Value change, choose the value according to the probability in a transition graph.

2) Addition, choose the value to add to the possible value, the value has added to random genes.

Elitism count is used to determine how a chromosome survive to the next generation. It counts N first fittest chromosome in a sorted population that has included in next generation.

#### F. Graphical Representation

Index-based approach [6] is used to show the biome sequence in the chromosome. This method loops through the chromosome and Instantiate game object according to the component position in the chromosome. The game object that used for instantiation changed according to the game environment type or the design. The land component is Instantiated first followed by vegetation and weather. A random walk is also implemented in the land to make the land looks more natural. The random walk works similar to flipping a coin, if the head has obtained then the y-axis value is increased, otherwise tail decrease the y-axis value while the algorithm walks along an x-axis. Random walk makes the generated land or platform more vary. The random walk also becomes a unique point for generating more game world because the same design shown differently. The result of the graphical representation seen in Fig 5.

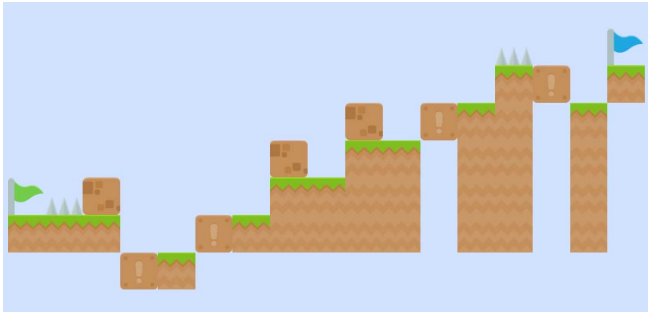


Fig. 5. Generated game world.

### III. RESULT AND ANALYSIS

The research aims to generate a game world that corresponding to game designer design and give vary game world variation. The game world graphical representation created based on the generated chromosome from the algorithm. Our proposed method is tested using six scenarios.

#### A. Scenario 1: Difficulty Curve

Fig. 6 shows the comparison between difficulty curve from designer and the difficulty curve from the generated game world. Root Mean Square Error (RMSE) is also used to compare between difficulty curve from designer and the difficulty curve from our proposed method. RMSE result from our experiment is 0.12.

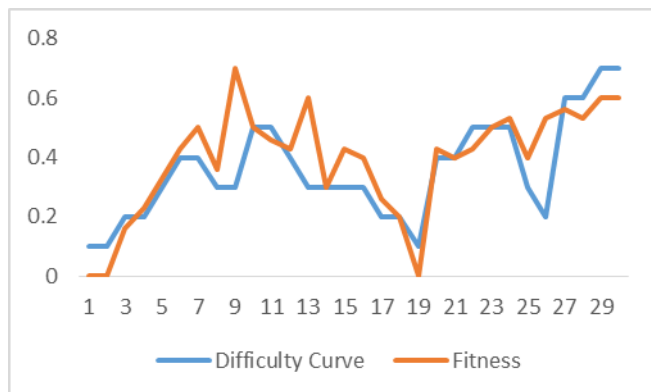


Fig. 6. Comparison between difficulty curve from game designer and generated game world

#### B. Scenario 2: Playability Testing

In order to know if the generated game world is playable, the generated game world is examined using the following criteria [13].

- 1) There is a passage connecting the start and endpoint.
- 2) The passage is fit with the attributes of the player character.

Game played using the generated game world to understand if the generated game world is playable. Table I show that some generated game worlds are not playable although it reaches the given difficulty curve from the game designer. All of the playable game worlds are have fitness under 0.5. However, when difficulty level set higher than 0.6, fitness cannot reach under 0.5.

TABLE I. PLAYABILITY TEST RESULT.

No	Difficulty Level	Fitness	Playtime	Retry	Playable
1	0.1	0	18	0	Yes
2	0.1	0	10	0	Yes
3	0.2	0.16	21	1	Yes
4	0.2	0.23	11	0	Yes
5	0.3	0.33	12	0	Yes
6	0.4	0.43	14	1	Yes
7	0.4	0.5	15	1	Yes
8	0.3	0.36	40	5	Yes
9	0.3	0.7	x	x	No
10	0.5	0.5	18	1	Yes
11	0.5	0.46	23	12	No
12	0.4	0.43	21	4	Yes
13	0.3	0.6	x	x	No
14	0.3	0.3	15	2	Yes
15	0.3	0.43	11	0	Yes
16	0.3	0.4	10	0	Yes
17	0.2	0.26	17	2	Yes
18	0.2	0.2	17	3	Yes
19	0.1	0	8	0	Yes
20	0.4	0.43	19	3	Yes
21	0.4	0.4	53	13	Yes
22	0.5	0.43	9	0	Yes
23	0.5	0.5	x	x	No
24	0.5	0.53	23	3	Yes
25	0.3	0.4	16	0	Yes
26	0.2	0.53	x	x	No
27	0.6	0.56	x	x	No
28	0.6	0.53	x	x	No
29	0.7	0.6	9	0	Yes
30	0.7	0.6	x	x	No

#### C. Scenario 3: Different Population Size

Population size modified in order to know which values that increase the number of Fitness appearance that has value more than 0.5. Table II shows that population size difference does not have an impact on fitness value.

TABLE II. POPULATION SIZE IMPACT ON THE NUMBER OF FITNESS APPEARANCE THAT HAS VALUE MORE THAN 0.5

Population Size	% of Fitness < 0.5
30	30.3
45	20
60	18.7
75	18.5
90	39.3

#### D. Scenario 4: Crossover Rate

Crossover rate is value to calculate the possibility of a chromosome to crossover. Better chromosome will bring out better fitness. Table III shows that cross over difference does not have an impact on fitness value.

TABLE III. CROSSOVER RATE IMPACT ON THE NUMBER OF FITNESS APPEARANCE THAT HAS VALUE MORE THAN 0.5.

Crossover Rate	% of Fitness < 0.5
0.5	17.7
0.6	20.5
0.7	15.2
0.8	29.9

#### E. Scenario 5: Different Mutation Rate

Mutation rate gives a big impact to the genetic algorithm, the higher the value of the mutation rate the algorithm generate more random genes. High mutation rate gives a higher chance to the chromosome in the population to mutate. High mutation rate also gives a negative impact on the fittest chromosome. Because its genes can be mutated and the genetic algorithm loses its fittest chromosome. Table IV shows that the mutation rate difference does not have an impact on fitness value.

TABLE IV. MUTATION RATE IMPACT ON THE NUMBER OF FITNESS APPEARANCE THAT HAS VALUE MORE THAN 0.5.

Mutation Rate	% of Fitness < 0.5
0.001	20.7
0.01	0
0.1	39.8
0.5	8.1
0.25	9.8

#### IV. CONCLUSION

Our proposed method used for difficulty level under 0.5 based on the difficulty curve. For the next research, our proposed method needs to be improved so it can generate a game world that has a higher difficulty level.

#### ACKNOWLEDGMENT

This study has supported by the Informatics Department, Universitas Muhammadiyah Malang (UMM) through Internal Research Grant Scheme 2017. Authors are grateful to the Informatics Department, UMM in supporting the present work.

#### REFERENCES

- [1] E. Adams, *Fundamentals of Game Design 2nd Edition*, 2nd ed. New Riders, 2009.
- [2] J. Ulisses, R. Gonçalves, and A. Coelho, "Procedural Generation of Maps and Narrative Inclusion for Video Games," *Oporto, January*, no. June, 2015.
- [3] N. Shaker, J. Togelius, and M. J. Nelson, *Procedural Content Generation in Games*. Cham: Springer International Publishing, 2016.
- [4] D. S. R. Achmad Arwan, "Optimization of Genetic Algorithm Performance Using Naïve Bayes for Basis Path Generation," *Kinetik*, vol. 2, no. 4, pp. 273–282, 2017.
- [5] L. Ferreira, L. Pereira, and C. Toledo, "A multi-population genetic algorithm for procedural generation of levels for platform games," *Proc. 2014 Conf. companion Genet. Evol. Comput. companion - GECCO Comp '14*, no. November, pp. 45–46, 2014.
- [6] A. B. Moghadam and M. K. Rafsanjani, "A genetic approach in procedural content generation for platformer games level creation," *2nd Conf. Swarm Intell. Evol. Comput. CSIEC 2017 - Proc.*, no. Csiiec20 17, pp. 141–146, 2017.
- [7] F. Mourato, M. P. dos Santos, and F. Birra, "Automatic level generation for platform video games using genetic algorithms," *Proc. 8th Int. Conf. Adv. Comput. Entertain. Technol. - ACE '11*, p. 1, 2011.
- [8] D. F. H. Adrian and S. G. C. Ana Luisa, "An approach to level design using procedural content generation and difficulty curves," *IEEE Conf. Comput. Intell. Games, CIG*, 2013.
- [9] Arttu Martinen, "Procedural Generation of Two-Dimensional Levels," *Metropolis*, 2017.
- [10] P. Walsh and P. Gade, "Terrain generation using an Interactive Genetic Algorithm," *IEEE Congr. Evol. Comput.*, pp. 1–7, 2010.
- [11] K. Hartsook, A. Zook, S. Das, and M. O. Riedl, "Toward supporting stories with procedurally generated game worlds," *2011 IEEE Conf. Comput. Intell. Games, CIG 2011*, pp. 297–304, 2011.
- [12] M. Buckland and A. LaMothe, *AI Techniques for Game Programming*. Premier Press, 2002.
- [13] L. A. Ripamonti, M. Mannalà, D. Gadia, and D. Maggiorini, "Procedural content generation for platformers: designing and testing FUN PLEdGE," *Multimedia Tools and Applications*, vol. 76, no. 4, pp. 5001–5050, 2017.

# Middleware for Network Interoperability in IoT

Eko Sakti Pramukantoro, Fariz Andri Bakhtiar, Binariyanto Aji, Rasidy Pratama  
*Faculty of Computer Science*  
*Brawijaya University*  
 Malang, Indonesia  
 ekosakti@ub.ac.id, fariz@ub.ac.id

**Abstract**—One solution for interoperability issue in IoT is a middleware which is competent on resolving the problems of syntactical, semantic, and network interoperability. In previous study, a middleware capable of addressing semantic and syntactical interoperability challenges has been developed, yet has not responded to network interoperability matter. In this paper we continue our previous research by adding BLE and 6LoWPAN features to the middleware's communication media, so it may communicate with various devices. Interoperability test results show that the middleware is capable of responding to network interoperability challenges and able to receive data from multiple nodes simultaneously.

**Keywords**—Middleware, IoT, Interoperability

## I. INTRODUCTION

Internet of Things (IoT) has rapidly grown and given a quite big impact in daily lives. It enables users to access and manage electronic devices wirelessly through the internet. In the implementation, IoT is facing issues pertaining to device interoperability. The issue arises because IoT is trapped in a “silo” (infrastructure, middleware, and application).

Desai classified this interoperability matter into three: Network Layer Interoperability, Syntactical Interoperability, and Semantic Interoperability. Network Layer Interoperability refers to network protocols used by “things” to connect to other devices; comprising low power networking protocols (Bluetooth Low Energy/BLE, 6LoWPAN) and traditional networking protocols. Syntactical Interoperability refers to the data model or the messaging protocol, e.g. CoAP, MQTT, HTTP, XMPP. Semantic Interoperability refers to the content and data context [1]. To resolve the issue, a middleware supporting interoperability is required. [1] [2].

Previous research has developed a middleware with an event-driven approach that is able to solve semantic and syntactic interoperability issues by providing a gateway to communicate with IoT sensor devices using MQTT and CoAP protocols, and able to communicate with other applications (subscriber) using WebSocket protocol [3]. In its implementation, the communication between the middleware and the sensor still used wireless transmission media, so it has not been able to answer the network interoperability problem.

In an IoT environment, other than Wi-Fi for transmission media, there are BLE and 6LoWPAN which offer low power communication [4]. Communication between the sensor node and gateway using BLE has been implemented in an IoT system prototype by Boualouache. The experimental results showed that the prototype is capable of achieving feasibility, delivery distance up to 6 meters, and efficient power usage[5]. Joshua developed a 6LoWPAN-based sensor node [6], while at other research 6LoWPAN was utilized to arrange communication between a bunch of sensors and a gateway [7]. By evaluating those studies, it then can be concluded that BLE

and 6LoWPAN protocols are reasonable choices in providing communication between sensor nodes and the gateway.

In this paper, BLE and 6LoWPAN communication media will be added to the previous middleware, so that it would be a middleware that can answer the challenge of interoperability in general. The discussion at this paper is organized as follows: I. Introduction, II. Existing IoT Middleware, III. Proposed Middleware, IV. Experiment, and V. Conclusion.

## II. EXISTING IOT MIDDLEWARE

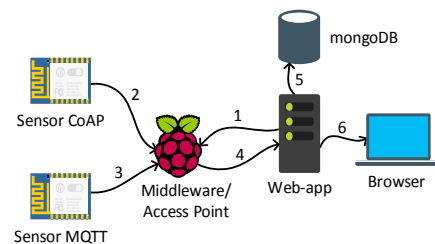


Fig. 1. IoT Environment



Fig. 2. Middleware Prototype

Figure 1 represents an IoT-based network architecture that has been developed in previous research, while Figure 2 is an example prototype of a middleware device built from Raspberry Pi. For sensor nodes, NodeMCU ESP8266 equipped with DHT sensors are used. The middleware software consists of: (1) sensor gateway, which is responsible for handling incoming messages from sensor nodes using both the CoAP and MQTT protocols; (2) service unit, which provides an API for storing published data from sensors to Redis as the broker in the system; and (3) application gateway, which provides a WebSocket protocol-based API for exposing topics to subscriber [3]. From the test results, it was found that the CPU and memory usage are under 13% and the message delivery ratio from the sensor node to middleware was under 1 second [8].

## III. PROPOSED MIDDLEWARE FOR NETWORK INTEROPERABILITY

In this study, two communication media, namely BLE and 6LoWPAN, will be added to existing middleware. There are challenges in this research, where both communication media do not work on IPv4. Hence subsystems need to be added at the sensor gateway. Figure 3 shows a 6LoWPAN subsystem



added to the sensor gateway so that the middleware be able to communicate using IPv6, then GATT and BLE gateway are added so that the middleware may communicate using BLE.

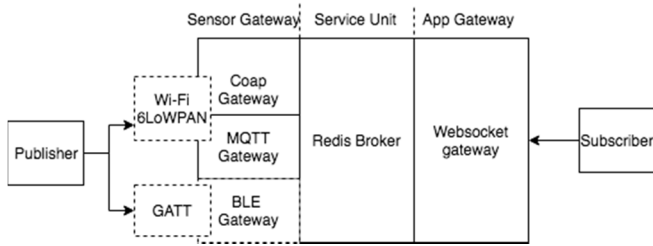


Fig. 3. Adding two communication media to the existing middleware

More detailed discussion will be divided into three parts:

#### A. BLE Interface

The sensor gateway provides an interface for the middleware so that it can read data transmitted by the BLE client and also serves as a bridge to translate the transmitted data using the BLE network into MQTT protocol, so the initial non-IP-based protocol turns IP-based. The design of the BLE gateway serves to provide an interface for the BLE transmission from the sensor so it can be accepted by the middleware and translated into a MQTT transmission. GATT is required because BLE network cannot directly connect to other devices. GATT defines the services and characteristics of the sensor device to be connected. Connections using GATT are exclusive connections where only one BLE communication between sensors and middleware can occur at any one time. The gateway to be embedded on this Middleware is EspruinoHub[9]. First, the sensor will send data to the middleware. Then the data will be forwarded to the EspruinoHub to be translated into MQTT, as BLE network is non-IP (so it cannot directly transmit data using MQTT protocol which is IP-based).

#### B. 6LoWPAN Interface

In order for the middleware to communicate with LoWPAN technology, there are several things need to be done: (1) modifying the CoAP and MQTT sensor gateway to listen to IPv6, (2) adding 6LoWPAN communication module. In this research, the MRF24J40MA/RM module is used for 6LoWPAN. The module works to deliver packets to the middleware over the WPAN network.

Noteworthy matters on the 6LoWPAN network configuration are the use of channels, pan id, and same IP network. Table 1 describes the 6LoWPAN configuration used in our IoT environment.

TABLE I. CONFIGURATION 6LoWPAN

Parameter	Sensor node	Middleware
IP Address	fe80::c030:955d:d2b7:aae5	fe80::c030:955d:d2b7:aae9
Prefix	/64	/64
Channel	11	11
Pan_Id	0x24	0x24

Once the low-level interface is installed, next is to set the middleware software to use the interface. This is done by adding some code so that CoAP and MQTT can listen on IPv6.

#### C. Sensor Nodes

There are three sensor nodes used in this research: (1) NodeMCU ESP8266 as the Wi-Fi network transmitter, (2) NodeMCU ESP32 as the BLE network transmitter, and (3) Raspberry Pi as the 6LoWPAN network transmitter as shown in figure 5. Each sensor node is directly connected to DHT22 and will deliver payload which consists of humidity and temperature data. The semantics of the payload is shown in Figure 4.

```

Var payload = {
  protocol: protocolName
  timestamp: timeSend
  topic: topicPublish
  sensor: {
    tipe: sensorType
    index: sensorIndex
    ip: ipSource
    module: SensorModule
  }
  humidity: {
    value: valueHum,
    unit: unitHum
  }
  temperature: {
    value: valueTemp,
    unit: unitTemp
  }
}

```

Fig. 4. Sensor's payload



Fig. 5. Sensor Nodes

### IV. EXPERIMENT AND DISCUSSION

As discussed in previous research, the middleware was developed on a Raspberry Pi version 3. The version was particularly selected as it already has Wi-Fi and BLE transmission media, so the only additional modules i.e. GATT and EspruinoHub are needed. The experiment is conducted on campus network involving several sensor nodes and one middleware. The sensor nodes will send/publish messages from temperature sensors to middleware. The discussion will be divided into three parts: BLE performance, 6LoWPAN performance, and Network Interoperability Testing.

#### A. BLE Performance

As described in the previous section, in order for the middleware to be able to communicate with BLE devices, additional modules i.e. GATT and espruinihub are needed. The GATT being used is BlueZ GATT which can run on Raspberry Pi having Raspbian OS.

As depicted in Figure 6, the sensor node having MAC Address 24:0A:C4:10:FC:8E will have its data transmitted over the BLE network to be captured by GATT middleware, then forwarded to the BLE gateway that will translate the BLE transmission into an MQTT transmission using IP Address 10.34.8.5. Figure 7 is print out from the pm2 log that indicates published data from node sensor successfully added to Redis.

```
pi@TheMiddleware:~$ sudo hcitool lescan
LE Scan ...
24:0A:C4:10:FC:8E ESP32 SimpleBLE
```

Fig. 6. GATT Middleware has detected BLE sensor

```
0|qoap | 5/30/2018 2:42:52 PM MQTT - Client mqttjs_27f10f1a
publish a message to /ble/advertise/24:0a:c4:10:fc:8e/office/room20

0|qoap | 5/30/2018 2:42:52 PM MQTT - Client mqttjs_27f10f1a
publish a message to /ble/advertise/24:0a:c4:10:fc:8e/rssi
```

Fig. 7. Data from BLE Sensor to Middleware

Next, the distance change test is done to find out the performance of BLE. Delay in the delivery process is measured and used as the parameter in this test.

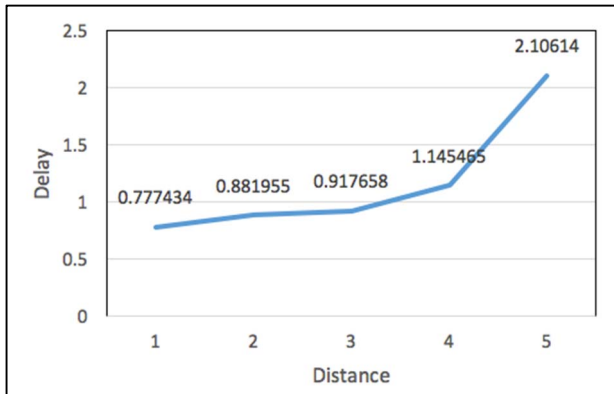


Fig. 8. Influence distance to delay

Figure 8 depicts the test results from the scenario of delay against the distance changes. The test results show that performance on sending data using BLE transmission still has a low delay, even though the distance between Middleware and NodeMCU is different. However, there is a very significant delay change when the distance between Middleware and NodeMCU reaches 5 meters, which is 1 second long. The results of this test indicate that the distance parameter still affects the performance of BLE.

### B. 6LoWPAN Performance

In this section, we will discuss transmission data from sensor nodes to IoT middleware using 6LoWPAN, involving MQTT and CoAP protocols. In this experiment, the first sensor node transmits data using CoAP while the second transmit using MQTT. In addition, tests were performed to determine the effect of transmission distance to the delays. The tests were conducted in a public area where some people occasionally passed by until the 6LoWPAN signal was disconnected. The packets were sent for 10 minutes, once every 10 seconds.

```
0|qoap | 2018-5-30 11:09:13 COAP - Incoming POST request from
fe80::c030:955d:d2b7:aae5 for office/roomA16
0|qoap | 2018-5-30 11:09:23 COAP - Incoming POST request from
fe80::c030:955d:d2b7:aae5 for office/roomA16
```

Fig. 9. Middleware received data using CoAP

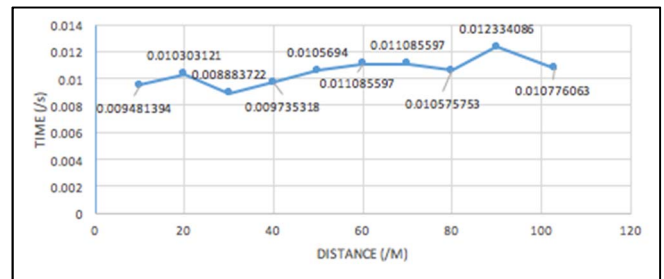


Fig. 10. The effect of distance towards delay in the delivery process using CoAP

The test results showed that 6LoWPAN can reach a distance of 103m. There was an anomaly at a distance of 90m, though. It was due to slight obstruction by an object. 6LoWPAN signals were found to be very weak against objects interference.

In Figure 9, the first sensor node (IP address e80::c030:955d:d2b7:aae5) published data in topic office/room16 to the middleware using CoAP.

```
0|qoap | 2018-5-30 11:09:17 MQTT - Client
fe80::c030:955d:d2b7:aae6 has connected
0|qoap | 2018-5-30 11:09:18 MQTT - Client
fe80::c030:955d:d2b7:aae6 publish a message to office/roomA17
```

Fig. 11. Middleware received data using MQTT

Figure 11 shows middleware received data with topic “office/room17” from node sensor 2.

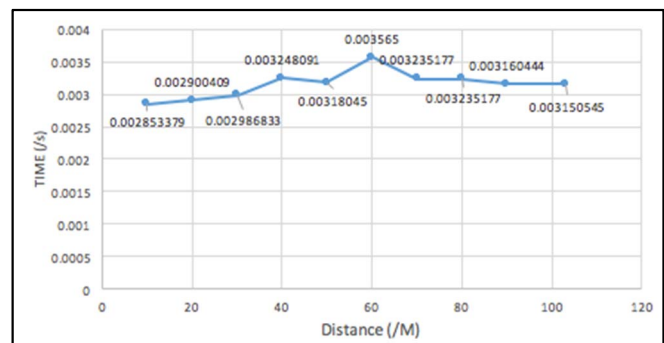


Fig. 12. The effect of distance towards delay in the delivery process using MQTT

In MQTT tests, QoS level 2 was used to focus on average delay, so it needed to take maximum travel time from the amount of data that should be obtained. At a distance of 60m, an anomaly result occurred. It was because the 6LoWPAN module was exposed to direct sunlight during the tests, which decreased 6LoWPAN's performance.

### C. Network Interoperability Testing

The network interoperability tests were done by simultaneously sending data from five sensor nodes to the middleware. Fig. 13 shows that the first node with client id mqttjs\_805d5fda published data from sensor nodes using BLE. The second with client id fe80::c030:955d:d2b7:aae5 published data using MQTT protocol on 6LoWPAN, while the third node with client id fe80::c030:955d:d2b7:aae6 published data using CoAP on 6LoWPAN. The fourth node

with client id 192.168.42.14 published data using CoAP on Wi-Fi, while the last node with id client 8456747 published data using MQTT on Wi-Fi

```

0|qoap | 5/30/2018 3:20:39 PM MQTT - Client mqttjs_805d5fda publish a
message to /ble/advertise/00.15.83:00:33:e5/office/room20
0|qoap | 5/30/2018 3:20:39 PM MQTT - Client mqttjs_805d5fda publish a
message to /ble/advertise/00.15.83:00:33:e5/rssi
0|qoap | 5/30/2018 3:20:39 PM MQTT - Client mqttjs_805d5fda has closed
connection

0|qoap | 5/30/2018 3:20:46 PM MQTT - Client fe80::c030:955d:d2b7:aae5
has connected
0|qoap | 5/30/2018 3:20:50 PM MQTT - Client fe80::c030:955d:d2b7:aae5
publish a message to office/roomA17
0|qoap | 5/30/2018 3:20:51 PM MQTT - Client fe80::c030:955d:d2b7:aae5
has closed connection

0|qoap | 5/30/2018 3:20:53 PM COAP - Incoming POST request from
fe80::c030:955d:d2b7:aae6 for office/roomA17
0|qoap | 5/30/2018 3:20:59 PM COAP - Incoming POST request from
192.168.42.14 for office/roomA14

0|qoap | 5/30/2018 3:23:26 PM MQTT - Client 8456747 has connected
0|qoap | 5/30/2018 3:23:26 PM MQTT - Client 8456747 publish a message to
office/roomA13
0|qoap | 5/30/2018 3:23:26 PM MQTT - Client 8456747 has closed
connection

```

Fig. 13. Print out pm2 logs

The results of interoperability tests show that the middleware can simultaneously receive data from various sensor nodes using heterogeneous transmission media.

## V. CONCLUSION

By observing the experiments' results, it can be concluded that the middleware is able to answer the issue of network interoperability. It means that it is capable to answer overall challenges of interoperability. Some tests were also run to see its performance in messaging. On the parameter of transmission distance, usage of BLE gives a good result at 4 meters with 1 second delay, while 6LoWPAN can reach distance of 103 meters with under 1 second delay. Compared to CoAP, MQTT provides better guarantee in the quality of delivery. This study still limits the communication protocol tests only on the effect of delay, whereas more parameters are notable for testing. In the next study, there will be a more complete comparison between CoAP and MQTT performance to know the quality of data delivery using 6LoWPAN in depth.

## REFERENCES

- [1] P. Desai, A. Sheth, and P. Anantharam, 'Semantic Gateway as a Service Architecture for IoT Interoperability', in *Proceedings - 2015 IEEE 3rd International Conference on Mobile Services, MS 2015*, 2015, pp. 313–319.
- [2] M. A. Razzaque, M. Milojevic-Jevric, A. Palade, and S. Cla, 'Middleware for internet of things: A survey', *IEEE Internet Things J.*, vol. 3, no. 1, pp. 70–95, 2016.
- [3] E. S. Pramukantoro and H. Anwari, 'An Event-Based Middleware For Syntactical Interoperability And Enabling Web-Oriented In Internet Of Things', *Int. J. Electr. Comput. Eng.*, vol. 8, no. 5, 2018.
- [4] R. Tabish, A. Ben Mnaouer, F. Touati, and A. M. Ghaleb, 'A comparative analysis of BLE and 6LoWPAN for U-HealthCare applications', in *2013 7th IEEE GCC Conference and Exhibition, GCC 2013*, 2013, pp. 286–291.
- [5] A. E. Boualouache, O. Nouali, S. Moussaoui, and A. Derder, 'A BLE-based data collection system for IoT', *NTIC 2015 - 2015 1st Int. Conf. New Technol. Inf. Commun. Proceeding*, 2015.
- [6] J. Arndt, F. Krause, R. Wunderlich, and S. Heinen, 'Development of a 6LoWPAN sensor node for IoT based home automation networks', *Proc. - 2017 Int. Conf. Res. Educ. Mechatronics, REM 2017*, 2017.
- [7] R. Xua, S. H. Yang, P. Li, and J. Cao, 'IoT architecture design for 6LoWPAN enabled Federated Sensor Network', *Proc. World Congr. Intell. Control Autom.*, vol. 2015–March, no. March, pp. 2997–3002, 2015.
- [8] E. S. Pramukantoro, W. Yahya, and F. A. Bakhtiar, 'Perform evaluation of IoT middleware for syntactical Interoperability', in *International Conference on Advanced Computer Science and Information Systems (ICACSIS)*, 2017.
- [9] espruino, 'espruino/EspruinoHub'. [Online]. Available: <https://github.com/espruino/EspruinoHub>.

# Face RGB-D Data Acquisition System Architecture for 3D Face Identification Technology

Aldi Bayu Kreshnanda Ismail

Dept. of Informatics and Computer Engineering  
Electronic Engineering Polytechnic Institute of Surabaya  
Surabaya, Indonesia  
aldibayu@ce.student.pens.ac.id

Adnan Rachmat Anom Besari

Dept. of Informatics and Computer Engineering  
Electronic Engineering Polytechnic Institute of Surabaya  
Surabaya, Indonesia  
anom@pens.ac.id

Ihsan Fikri Abdurahman Muharram

Dept. of Informatics and Computer Engineering  
Electronic Engineering Polytechnic Institute of Surabaya  
Surabaya, Indonesia  
ihshan@ce.student.pens.ac.id

Dadet Pramadihanto

Dept. of Informatics and Computer Engineering  
Electronic Engineering Polytechnic Institute of Surabaya  
Surabaya, Indonesia  
dadet@pens.ac.id

**Abstract**—The three-dimensional approach in face identification technology had gained prominent significance as the state-of-the-art breakthrough due to its ability to address the currently developing issues of identification technology (illumination, deformation and pose variance). Consequently, this trend is also followed by rapid development of the three-dimensional face identification architectures in which some of them, namely Microsoft Kinect and Intel RealSense, have become somewhat today's standard because of its popularity. However, these architectures may not be the most accessible to all due to its limited customisation nature being a commercial product. This research aims to propose an architecture as an alternative to the pre-existing ones which allows user to fully customise the RGB-D data by involving open source components, and serving as a less power demanding architecture. The architecture integrates Microsoft LifeCam and Structure Sensor as the input components and other open source libraries which are OpenCV and Point Cloud Library (PCL). The result shows that the proposed architecture can successfully perform the intended tasks such as extracting face RGB-D data and selecting out region of interest in the face area.

**Keywords**—three-dimensional approach, face identification technology, RGB-D data, RGB-D architecture

## I. INTRODUCTION

As three-dimensional face identification technology has been adapted into many applications, there is a high demand of a computationally economic and free-to-customise architecture. Although there are various pre-existing architectures in this particular field, fulfilling the aforementioned criteria is not the case for most of them. High computational cost, and limitation for the developer to access and to experiment with all of the available tools and functions within the architecture are the most common premises which could be seen in most of those architectures. Therefore, to allow more freedom and capability in the development of three-dimensional face identification system, an alternative architecture is needed. This architecture should meet the aforementioned criteria, which is to have a properly optimised performance, while at the same time to remain as customisable as possible to the developer. Therefore, by lowering the computational requirement it will allow more developers to take part in the three-dimensional face technology development. Thus, this paper attempted to provide this alternative by building one of its foundations, which is a data acquisition system. This data acquisition system will rely on open source resources,

including the tools used and the other components utilised in the system.

## II. RELATED WORKS

At its early stage of development, the three-dimensional approach is quite common to be adapted as the standard for many face identification architectures. Zhang et al [1], for example, attempted to propose a better approach to identify facial expression and its variations based on two-dimensional face image. Dadet et al [2], on the other hand, attempted to promote a hypothetically more effective method in estimating facial landmarks which is also applied to two-dimensional face identification system. However, as the requirements and the challenges in the society getting more complicated and demanding, the two-dimensional approach in face identification system have become irrelevant and obsolete. Ruiz and Illingworth [3] revealed that the facial expression change which occurs in face, is actually a challenge for face identification system since it will introduce deformation in the face and will make the system performance suffer. Zhu et al [4] pointed out that besides facial expression, the variety of head pose will also affect the overall face identification system performance because most identification systems use frontal face as the standard identification reference. Moskvich and Osadchy [5] in their research defined the variety of illumination as one of major issues in face identification. Therefore, due to its capability to address the mentioned issues, three-dimensional approach has gained its popularity and have been featured in many researches and regarded as a somewhat today's standard for face identification technology, resulting many researches and papers revolved around three-dimensional approach as the topic of interest [6].

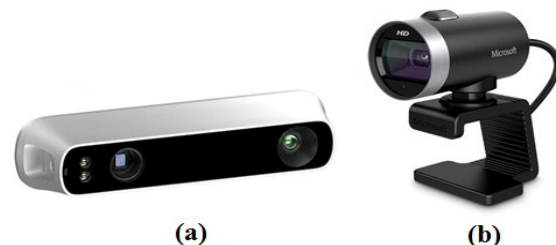


Fig. 1. (a) Structure Sensor [13]; (b) Microsoft LifeCam [14]

Three-dimensional approach in face identification system requires a proper architecture to obtain RGB-D data. RGB-D data is basically a recent development in three-dimensional



approach which is a combination of colour information, commonly in RGB (Red, Green, Blue) format, and depth or three-dimensional information of the face (i.e. the XYZ coordinate of face points). The combination of these data will introduce more flexibility to the system, for example, less sensitive to the illumination variations since the depth data is unaffected by the illumination change. Some of the most commonly used architectures used in recent researches are Intel RealSense as shown in [7][8][9] and Microsoft Kinect as shown in [10][11][12]. These architectures, while being used often, may not be the most accessible architectures out there since it limits user to do complete customisation on its data and its functions due to its nature of being a commercial product. Also, these architectures demand a relatively high computational resource to run properly.

This research aims to propose a state-of-the-art architecture of obtaining RGB-D data of the face for three-dimensional (3D) face identification system. The proposed architecture also aims to be customisable to the user by producing RGB-D data of the face which can be adapted for many purposes at will, while remaining to be accessible to all systems with a reasonable demand for computational resource. This architecture is built upon the principal of open source product by involving open source libraries and features so that user may fully optimise all of its functions. The proposed architecture will include RGB-D data acquisition custom hardware, data structure and also methods. It is expected to be an alternative to the pre-existing architectures and contribute to the development of three-dimensional face identification technology.

The architecture of the RGB-D face data acquisition overall system is constituted from three main components which are the input component, the processing component and the output component. Each component has a distinct role which indicated by its respective name. Figure 2 shows the architecture diagram and the relationship between elements.

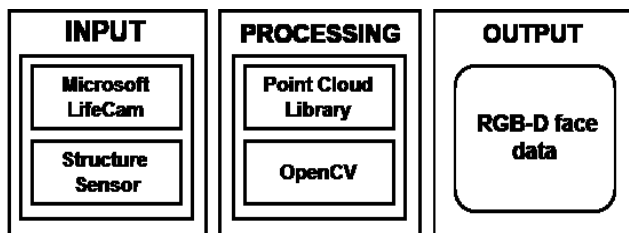


Fig. 2. Architecture diagram

The input component involves the hardware used to acquire RGB-D data of the face, which are Microsoft LifeCam and Structure Sensor. The processing component involves the libraries and functions which are used to process the RGB-D data. The output component is the representation of RGB-D of face data which is the product of this architecture.

### III. HARDWARE ARCHITECTURE

The input component used in this research is a custom built RGB-D data acquisition device which is a product of integration between Microsoft LifeCam and Structure Sensor. Custom built means that such integration has never been attempted to do before. Both of these devices are selected due to their customisable nature which make its functions and features available for user to modify optimally [15]. Microsoft LifeCam is utilised to obtain the colour information from the face in RGB (Red, Green, Blue)

format. On the other hand, Structure Sensor is used to obtain the three-dimensional or depth information of the captured face. In this system, both devices will be integrated and operated simultaneously so that the RGB and the depth data of the same scene could be obtained. It is important to make sure that system really does so, since a difference in the capture time between both devices will cause a mismatch in the RGB and Depth data integration process afterward, resulting in an invalid RGB-D data.

Consequently, since both devices have different perspective, it is also required to align the perspective of these devices so that they will be able to capture the exact same scene at the same time. In doing so, a customised acrylic body as shown in Figure 3 is designed to attach the two devices together and lock them in one position. This body is required to fixate the perspective position of both devices so that the following alignment process could be done easier. It can also be seen that Microsoft LifeCam is placed on the top-centre of the Structure Sensor intentionally because it is expected that the perspectives of both devices will be fixated on the centre of the body. The finalised hardware then attached onto a tripod for a stabilisation

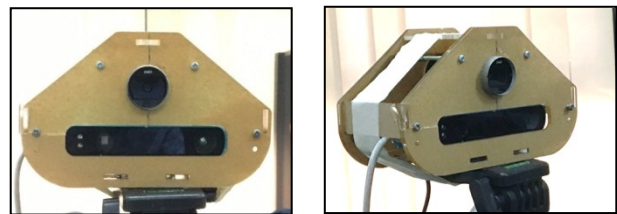


Fig. 3. Front and side view of finalised hardware

### IV. CALIBRATION METHOD

Before any processing could be done, a calibration and transformation process must be carried out to the depth and RGB data. Due to the data similarity used in [16], a similar transformation process is also performed in this research. Although both input devices have been fixated by attaching them to an acrylic body as shown previously, still there is a slight difference of perspective between the two devices. Therefore, a further calibration toward the hardware must be carried out. The calibration in this research is exclusively defined as an attempt to make sure that the perspective of the two devices are perfectly aligned to each other. The difference of perspective merely occurs in the horizontal or x-axis of the captured RGB image from the Microsoft LifeCam. Therefore, utilising OpenCV library, the two-dimensional translation operation is conducted on the captured RGB image from the Microsoft LifeCam to comply with the captured depth data from the Structure Sensor.

An image is fundamentally a matrix with particular dimension. In this case, the RGB image obtained from Microsoft LifeCam is a two-dimensional image hence a two-dimensional matrix. Consequently, the translation operation is a common operation which done to a matrix and in this case such operation is employed to perform translation on the RGB image so that it can be aligned to that of the Structure Sensor. This operation can be described by the following equation:

$$Mx = \begin{bmatrix} x1 \\ y1 \end{bmatrix} + \begin{bmatrix} x2 \\ y2 \end{bmatrix} \quad (1)$$

Where  $M_x$  is the result of translation which is a shifted RGB image,  $x_1$  &  $y_1$  are the horizontal dan vertical position of the initial image RGB respectively, and  $x_2$  &  $y_2$  are the destined horizontal and vertical position of the RGB image. In this case, the value of  $x_2$  and  $y_2$  may vary depending on the hardware architecture itself, which further means depends on how the input devices are configured and installed in the architecture. As for this, the degree of difference between the perspective of both devices will be different for each architecture. After the translation operation has been performed, the result of the translation must be examined thoroughly. A simple method is used to check the result of this translation operation. Identical grids are drawn to overlap the scenery obtained from both devices as a reference to identify whether or not the perspective between the devices differ to one another. Scenery which consists of many linear or rectangular objects (e.g. a box with sharp linear edges) should be chosen since it is easier to identify where the overlapping happens. If the grids on both perspectives overlap at the same particular part of the scenery, it means that the two perspectives have been successfully aligned to one another. Figure 4 shows the captured scenery from the Microsoft LifeCam and Structure Sensor after the translation operation which indicated that it has been successfully performed.

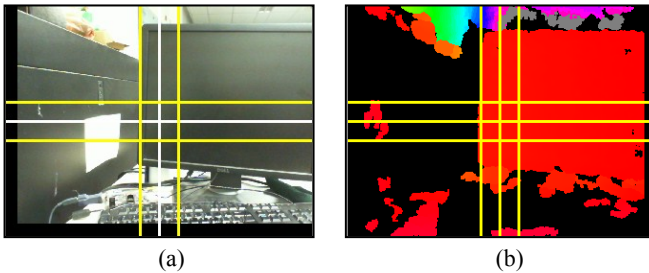


Fig. 4. Side-by-side perspective comparison: (a) The perspective from Microsoft LifeCam after translation; (b) The perspective from Structure Sensor.

## V. RGB-D DATA STRUCTURE

After the perspective of the two devices has been aligned successfully, the hardware now is ready to be implemented in performing the RGB-D data acquisition. However, a proper data structure that can handle the RGB-D data must be established first. In the proposed architecture, the RGB-D data of the face is stored in the point cloud. Point cloud is a data structure which is quite popular among three-dimensional technology researchers, due to its great functionality in terms of representing three-dimensional information of an object [17].

Point Cloud Library (PCL), a novel and powerful open source library to establish point cloud data structure in computing, is utilised within this architecture. Essentially, the RGB-D data is obtained through integrating the colour information of the face, and the depth or three-dimensional information of the face. In this architecture, the colour information is represented by using RGB (Red, Green, Blue) format. On the other hand, the depth information is basically the three-dimensional coordinate information of all the points that represent facial surface. Therefore, the integration of both data will result in a custom data type which is RGB-D data. The structure of such data could be visualised as shown in Figure 5.

Vertex-1	$X_1$	$Y_1$	$Z_1$	$B_1$	$G_1$	$R_1$
	$X_2$	$Y_2$	$Z_2$	$B_2$	$G_2$	$R_2$
Vertex-n	$X_n$	$Y_n$	$Z_n$	$B_n$	$G_n$	$R_n$

Fig. 5. Structure of face RGB-D data in point cloud

The RGB-D data type proposed in this architecture is basically a matrix containing RGB and depth data for each vertices (points). The depth data contains the pixel coordinate in X, Y Z (3D space). Whereas, the RGB data contains the Red, Green, and Blue colour information of each pixel from the image. This data type is to be implemented in point cloud. From a single face capture using the architecture's hardware, thousands of points could be obtained at once. By employing this custom data type, the colour information (RGB) for every point could be acquired too.

## VI. EXPERIMENT RESULT

The experiment in this paper is conducted to demonstrate how the proposed architecture works in reality and to see if it really fulfils the research expectation. The experiment covers the process of obtaining individual RGB and depth data with architecture hardware, until the integration process between both data resulting a proper face RGB-D data, which eventually will be the system output.

### A. Face RGB-D data acquisition

This experiment began with the first step in the system workflow, which the acquisition of RGB data from a calibrated Microsoft LifeCam and depth data from Structure Sensor. The purpose of this experiment is to make sure that the hardware in this architecture could function as intended by acquiring RGB data and depth data respectively.

These data will then be integrated into one custom data type, which is RGB-D data type. The approach of integrating depth data and RGB data is inspired by a similar experiment done in [18], where the difference is instead of using stereo camera, a single RGB camera is used. This experiment is done by situating a subject in the testing environment. This environment is an environment where its environment parameters (e.g. illumination) have been predetermined, or in the other word, with pre-set parameters. A scan of a subject is taken with the architecture hardware until a valid or proper data could be obtained. The definition of valid here means that on both RGB and depth data, there is no failure in acquisition or a missing part in scanning, which are obtained is aligned in perspective. The experiment which has been conducted shows the acquisition of RGB image and depth image could be done successfully as shown in Figure 6.

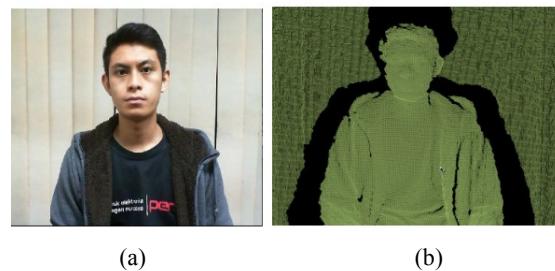


Fig. 6. Face data acquisition: (a) Face RGB data; (b) Face depth data.



### B. Integrating RGB and depth data.

The next experiment is integrating the RGB data and depth data to create RGB-D data of face. The purpose of this experiment is to prove that the architecture can produce RGB-D data of face with only the presence of RGB data and the depth data. Using the calibration method which has been explained previously, the difference of perspectives in this architecture is calculated and translation operation is performed with the following equation:

$$Mx = \begin{bmatrix} x1 \\ y1 \end{bmatrix} + \begin{bmatrix} 20 \\ 13 \end{bmatrix} \quad (2)$$

It can be observed from the equation that, in this architecture, the RGB image needs to be translated 20 pixels to the right and 13 pixels upward. The result from this image is a shifted image as shown in Fig 7.



Fig. 7. Translation operation: (a) Initial RGB image; (b) Shifted RGB image.

After the calibration has been conducted and a shifted RGB image has been acquired, this next phase in this architecture is joining this RGB data and the depth data from the Structure Sensor.

The integration process is done by merging the two data into a new data type which will be stored in the point cloud. Figure 8 shows the visualised RGB-D data which has been integrated successfully. It can be observed that the RGB-D data resembling the output from Structure Sensor, only this time there is a colour information for each point which is extracted from the RGB image. It is also possible to perform three-dimensional transformation to this data, as the example in this experiment, the data is rotated to resemble a side view. This result showed that the integration process between the RGB and the depth data using the custom hardware used in this architecture could be achieved and well implemented.



Fig. 8. RGB-D integration: (a) Face RGB data; (b) Face RGB data (rotated)

### C. Face detection and local area segmentation

The last experiment in this research is to do a detection and segmentation operation which is applied toward the face RGB-D data which have been carried out previously so that the local face area from the face could be selected out and the rest of the data could be eliminated. The face detection

and segmentation are performed by making use of the functions that comes within OpenCV and also Point Cloud library. The face detection method used in this system employs OpenCV HAAR Classifier library [19] whereas the segmentation process done in this experiment is facilitated through the Euclidean Cluster Extraction method which is come equipped with the Point Cloud Library [20]. The purpose of this experiment is to show that the face RGB-D data which is acquired through the proposed architecture is flexible. It means that this data is not only limited to certain procedure to be succeed, but it is possible to implemented in other various method as it is one of the purposes of this research. Figure 9 shows that the local area of face could be selected out from the rest of the RGB-D data which is unnecessary for the processing and may increase the burden of computation since it makes the most part of the RGB-D data.

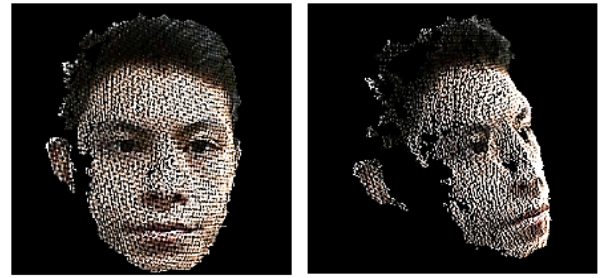


Fig. 9. The localised face RGB-D data in multiple viewpoints







## VII. PERFORMANCE EVALUATION

After successfully conducted the experiments, the performance of the algorithms featured in the system must also be evaluated. Since it is important to see how each algorithm could handle a different kind of dataset, and whether it could still maintain its performance, thus, the performance evaluation is carried out to see the performance consistency of each algorithm despite variation within the dataset.

The evaluation is done by employing specific variety of datasets from several subjects to be processed by the system as the input, and then evaluated. These subjects are consisted of male and female participants to introduce variation into the datasets. The list of subjects used in the evaluation could be seen in Table 1.

TABLE. 1. LIST OF SUBJECTS FOR EVALUATION

Data	RGB Data	Depth Data	Localised Face (RGBD)
A			
B			

Data	RGB Data	Depth Data	Localised Face (RGBD)
C			
D			

The RGB image and depth image of the subjects in neutral expressions are taken. The each of these data are consequently being processed through each algorithm until the localised face of each subject could be obtained. Using the same system which is used to perform the previous experiment, now the processing time of each step is being measured. The system specification is shown in Table 2.

TABLE 2. SYSTEM SPECIFICATION FOR EVALUATION

Hardware	Specification
Processor	Intel Xeon® CPU E3-1225 V2 @ 3.20GHz x 4
RAM	6 GB
VGA	NVIDIA GF108GL (Quadro 600) x64 clock 33Mhz 25.6 GB/s DDR3

The system performance of each dataset as seen in Table 3 is varied depending on the dataset. However, it must be noted that the number of point cloud being processed are also quite different. Therefore, it is important to consider that the amount of point cloud processed will affect directly upon the length of the processing time.

TABLE 3. TIME ELAPSED FOR EACH ALGORITHM

Data	Capture RGBD	RGBD Integration	Face Segmentation	Point Cloud
A	25ms	1046ms	5395ms	14577pts
B	27ms	997ms	6995ms	20320pts
C	25ms	1013ms	5362ms	15283pts
D	27ms	1044ms	7505ms	21348pts

The result further revealed that the time to capture RGBD images is consistent with an average of 26ms processing time.

### VIII. CONCLUSION

In this paper, the RGB-D data acquisition of the face has been presented. This architecture has been proven to be functioning as intended, which is to acquire the RGB-D data from the face. The proposed architecture also exhibited a good integration between the Microsoft LifeCam and Structure Sensor as the custom hardware used to obtain the input. The integration of open source libraries which are OpenCV and Point Cloud Library also enable the

architecture to be modified to meet various preferences since there is no limitation to its features and functions. More importantly, the proposed architecture has also proven that a proper RGB-D data type could be well established and eventually resulting a proper face RGB-D data.

According to the samples, the average time taken to capture to RGB-D data is 26ms, the average time to perform RGBD integration is 1045ms, the average time to perform face segmentation is 4815ms, and the average amount of point cloud obtained and processed in each data acquisition are 17817 points. It shows that the performance of each algorithm is still acceptable despite still needing improvement. One way to do this is by performing downsampling on the RGBD data to reduce the amount of point cloud which could enhance the process speed.

Due to its flexibility and uniqueness, the proposed architecture is expected to be present as an alternative to three-dimensional face identification technology as a stand-alone system, or as a module which could be integrated with other pre-existing 3D face identification architectures.

### IX. FUTURE WORKS

In the following research, we will build general face RGB-D database which will be used to perform various task, including a more advanced testing scenario and identification system, to be equipped within the proposed architecture. This database will include various face RGB-D data including face with expression variance, and pose variance and can be used for various kind of experiments. The overall performance of the system is also expected to be improved.

### ACKNOWLEDGMENT

We would like to thank the Ministry of Research, Technology and Higher Education of Indonesia and EEPIS Robotics Research Centre (E2RC) of Electronics Engineering Polytechnique Institute of Surabaya, for providing the funding and facilities for this research so that this research could be realised and put into implementation.

### REFERENCES

- [1] L. Zhang, N. Ye, E.M. Marroquin and T. Sim, "Expressive deformation profiles for cross expression face recognition," in *2012 21st International Conference on Pattern Recognition (ICPR)*, Tsukuba, Japan, 11-15 November 2012, pp. 1582–1585.
- [2] D. Pramadihanto, H. Wu, M. Yachida, "Invariant face recognition by Gabor wavelets and neural network matching" in *1996 IEEE International Conference on Systems, Man and Cybernetics. Information Intelligence and Systems* Vol. 9 (2017) Vol 1 (1996), pages: 59-63.
- [3] M.C. Ruiz and J. Illingworth, "Expression classification of 3D faces using local deformations," in *IET Conference on Image Processing (IPR 2012)*, London, UK, 3-4 August 2012, pp. 1-6.
- [4] X. Zhu, Z. Lei, J. Yan, D. Yi and S. Z. Li, "High-Fidelity Pose and Expression Normalization for Face Recognition in the Wild," in *2015 IEEE Conference on Computer Vision and Pattern Recognition (CVPR)*, Boston, Massachusetts, USA, 7-12 June 2015, pp. 797-796.
- [5] B. Moskvich and M. Osadchy, "Illumination Invariant representation for privacy preserving face identification," in *2010 IEEE Computer Society Conference on Computer Vision and Pattern Recognition – Workshops*, San Francisco, CA, USA, 13-18 June 2010, pp. 154-161.
- [6] D. Kim, M. Hernandez, J. Choi and G. Medioni, "Deep 3D face identification," in *2017 IEEE International Joint Conference on Biometrics (IJCB)*, Denver, CO, USA, 1-2 October 2017, pp. 133 - 142.
- [7] Zhang, Z. Lu, W. Li and Q. Liao, "A robust and fast 3D face reconstruction method using realsense camera," in 2017

- International Conference on Wireless Communications, Signal Processing and Networking (WiSPNET), Chennai, India, 22-24 March 2017, pp. 2691-2695.
- [8] J. V. Patil and P. Bailke, "Real time facial expression recognition using RealSense camera and ANN," in *2016 International Conference on Inventive Computation Technologies (ICICT)*, Combaitore, India, 26-27 August 2016, pp. 1-6.
  - [9] C. Chih, Y. Wan, Y. Hsu and L. Chen, "Interactive sticker system with Intel RealSense," in *2017 IEEE International Conference on Consumer Electronics (ICCE)*, Las Vegas, NV, USA, 8-10 January 2017, pp. 174-175.
  - [10] R. Siv, I. Ardiyanto, and R. Hartanto, "3D human face reconstruction using depth sensor of Kinect 2," in *2018 International Conference on Information and Communications Technology (ICOIACT)*, Yogyakarta, Indonesia, 6-7 March 2018, pp. 355-359.
  - [11] Z. Cheng, T. Shi, W. Cui, Y. Dong and X. Fang, "3D face recognition based on kinect depth data," in *2017 4th International Conference on Systems and Informatics (ICSAI)*, Hangzhou, China, 11-13 November 2017, pp.555-559.
  - [12] N. N. Kaashi and R. Safabakhsh, "3D constrained local model-based face recognition using Kinect under variant conditions," in *2014 7th International Symposium on Telecommunications (IST)*,
  - [13] H. Lee, J. Seo and H. Jo, "Gaze tracking system using structure sensor & zoom camera," in *2015 International Conference on Information and Communication Technology Convergence (ICTC)*, Jeju, South Korea, October 2015, pp. 830-832.
  - [14] Lievendag, N. 2017, "Structure Sensor 3D Scanner Review", [www.3dscanexpert.com/structure-sensor-review-part-1](http://www.3dscanexpert.com/structure-sensor-review-part-1). Accessed in: 26 May 2018.
  - [15] K. Kadir, M.K Kamarudin, H. Nasir, S.I. Safie and Z.A.K. Bakti, "A comparative study between LBP and Haar-like features for Face Detection using OpenCV," in *2014 4th International Conference on Engineering Technology and Technopreneuship (ICE2T)*, 2014, pp. 335-339.
  - [16] A. Alfarouq, R. Sanggar Dewanto, D. Pramadihanto, "Transformed Stereo Vision and Structure Sensor for Development 3D Mapping on "FLoW" Humanoid Robot in Real Time" in *2017 Journal of Telecommunication, Electronic and Computer Engineering*, Vol. 9 (2017) No. 2-5, pages: 129-133.
  - [17] W. Li, X. Ren, F. Li and W. Wang, "Study on the method of high-precision vehicle-borne lidar point clouds data acquisition in existing railway survey," in *2017 IEEE International Geoscience and Remote Sensing Symposium (IGARSS)*, 23-28 July 2017, pp. 1704 – 1707.
  - [18] D. Pramadihanto, A. Alfarouq, S. A. Waskitho, S. Sukaridhoto "Merging of Depth Image Between Stereo Camera and Structure Sensor on Robot FLoW Vision" in *2017 IEEE International Journal on Advanced Science Engineering Information Technology*, Vol. 7 (2017) No. 3, pages: 1014-1025.
  - [19] L. Cuimei, Q. Zhiliang, J. Nan and W. Jianhua, "Human face detection algorithm via Haar cascade classifier combined with three additional classifiers," in *2017 13th IEEE International Conference on Electronic Measurement & Instruments (ICEMI)*, 20-22 October 2017, Yangzhou, China, pp. 483-487.
  - [20] R. B. Rusu, "Semantic 3D Object Maps for Everyday Manipulation in Human Living Environments". In *KI - Künstliche Intelligenz*, Vol 24 (2010) No. 4, pp. 345-348.

# Feature Expansion for Sentiment Analysis in Twitter

Erwin B. Setiawan, Dwi H. Widyantoro, Kridanto Surendro  
School of Electrical Engineering and Informatics, Institut Teknologi Bandung  
Jl Ganesha No 10, Bandung, Indonesia

Email: [erwinbudisetiawan@telkomuniversity.ac.id](mailto:erwinbudisetiawan@telkomuniversity.ac.id), [dwi@stei.itb.ac.id](mailto:dwi@stei.itb.ac.id), [endro@stei.itb.ac.id](mailto:endro@stei.itb.ac.id)

**Abstract**—The community's need for social media is increasing, since the media can be used to express their opinion, especially the Twitter. Sentiment analysis can be used to understand public opinion a topic where the accuracy can be measured and improved by several methods. In this paper, we introduce a hybrid method that combines: (a) basic features and feature expansion based on Term Frequency–Inverse Document Frequency (TF-IDF) and (b) basic features and feature expansion based on tweet-based features. We train three most common classifiers for this field, i.e., Support Vector Machine (SVM), Logistic Regression (Logit), and Naïve Bayes (NB). From those two feature expansions, we do notice a significant increase in feature expansion with tweet-based features rather than based on TF-IDF, where the highest accuracy of 98.81% is achieved in Logistic Regression Classifier.

**Keywords**—sentiment analysis; feature expansion; twitter

## I. INTRODUCTION

At the end of January 2018, We Are Social and Hootsuite, released data on the number of Internet users and social media in the world [10]. Based on that data, internet users in the world has reached 4 billion, previously, 3.8 billion. Until the first quarter-2017, Twitter users worldwide reached 328 million, an increase of about 14% over the same period in the previous year. From the data released by Twitter Indonesia at the end of 2016, it was noted that 77 percent of Twitter users in Indonesia are active users. In addition, Twitter users in Indonesia are also among the fussiest. This can be seen from the number of tweets generated throughout 2016 which reached 4.1 billion tweets. The number of Twitter users in Indonesia is a promising market, including in five major worlds [11]. It is not surprising that in various fields, e.g., in economics, producers are competing to manage this great potential for their products on the market.

Sentiment analysis is part of opinion mining [1]. Sentiment analysis is the process of understanding, extracting and processing textual data automatically to get sentiment information contained in an opinion sentence. The magnitude of the influence and benefits of sentiment analysis led to research or application of sentiment analysis growing rapidly, even in America approximately 20-30 companies that focus on sentiment analysis services [1].

Less applications and methods of sentiment analysis developed for twitter speak Indonesian. This sentiment analysis research was conducted to find out the sentiments of

a tweet on Twitter by using the approach in machine learning that is Naïve Bayes (NB), Logistic Regression (Logit) and Support Vector Machine (SVM) devoted to Twitter in Indonesian language with various features. Variations that basic features used in this research are unigram, bigram, trigram, POS (Part-of-Speech) Tags, POS Bigram, POS Trigram, and Line Length. In this research, we introduce basic features with feature expansion by using TF-IDF and feature expansion by using tweet-based features. The aim of the paper is to find out the best sentiment analysis models that happened based on accuracy value.

The rest of the paper is organized as follows. Section II discusses issues related to sentiment analysis techniques. Section III describes system model of sentiment analysis on Twitter. Section IV provides the experimental and analysis, followed by the conclusion in section V.

## II. RELATED WORK

The related research on sentiment analysis is abundant. M. S. Neethu and R. Rajasree [2] measured the accuracy of classification process using various classifiers such as Nave Bayes, Maximum Entropy, Support Vector Machine, and Ensemble classifiers. They obtained an accuracy of 90% whereas Naïve Bayes has 89.5%. The feature space used included feature expansion by using tweet-based features, i.e., hashtags and emoticons marks in conjunction with features like unigram.

Celikyilmaz *et al.* [3] used Naïve Bayes, SMO, SVM and Random Forest to classify Twitter data, with F-scores that are relatively 10% better than a classification baseline that uses raw word n-gram features. The features considered by classifiers were pronunciations of words, polarity lexicon from tweets, and extract a set of features based on this lexicon.

Barbosa *et al.* [4] proposed a 2-step sentiment analysis method for classifying tweets. The first step, they classified tweets into subjective and objective and the second phase, the subjective tweets into positive or negative. They use SVM classifier. The feature space used included tweet-based features (retweets, hashtags, link, punctuation) and exclamation marks in conjunction with features like prior polarity of words and POS.

Bahrainian and Dengel [5] used SVM, Maximum Entropy, and Naïve Bayes to examine the performance based on the unigram feature set and compare with a hybrid method that is a combination of the usage of sentiment lexicons with a



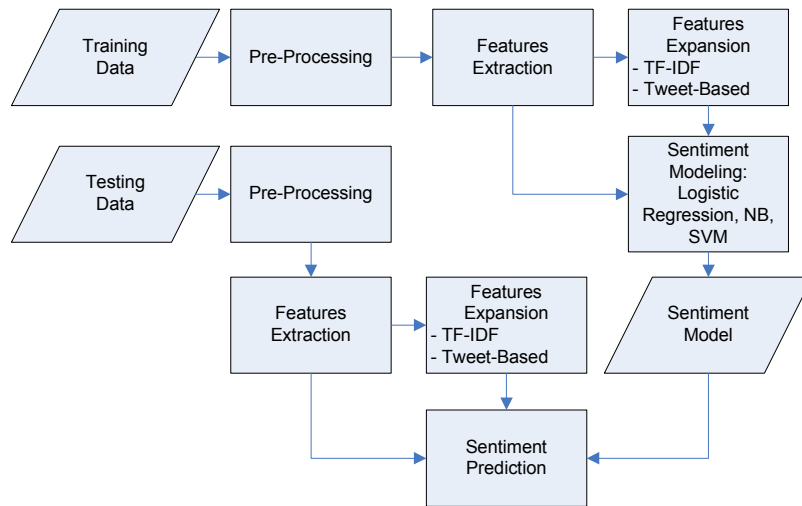


Fig. 1. Sentiment Analysis Model

machine learning classifier for polarity detection of subjective texts in the consumer-products domain. The experimental results indicate that our hybrid method outperforms all other mentioned methods.

In this paper, we introduce a different approach compared to previous research are scope twitter's account of the Indonesian-language, a hybrid method that is a combination between basic features with feature expansion based on TF-IDF and feature expansion based on tweet-based features. We use several classification algorithms, such as Naïve Bayes (NB), SVM, and Logistic Regression (Logit).

### III. SENTIMENT ANALYSIS MODEL AND THE PROPOSED TECHNIQUE

Sentiment Model is shown in Fig. 1. Dataset is divided into two, i.e., training data and testing data. Each data is done pre-processing, feature extraction and feature expansion. Furthermore, the feature extraction or feature expansion results for the training data as input to the modeling process sentiment, the results of this modeling are used to predict the testing data. Last is expected to get Sentiment Class with excellent accuracy.

#### A. Crawling Data

Crawling data on twitter is a process to retrieve or download data from twitter server with the help of Application Programming Integration (API) twitter either in the form of user data or tweet data. The twitter data do be the reference data of this research. Twitter data is divided into two data, training data and testing data.

#### B. Pre-Processing

In the step, we use is pre-processing such as case folding, tokenization, stopwords removal, and stemming. We do pre-processing twitter data automatically with the application that we developed in previous research [6].

#### C. Feature Extraction

Feature extraction is process of taking the feature of a tweet that can describe the characteristics of the tweet. In this phase, we use basic features such as unigram, bigram, trigram, POS (Part-of-Speech) Tags, POS Bigram, POS Trigram, and Line Length.

#### D. Feature Expansion

In this research, we use two feature expansions. Two feature expansions are expansion using TF-IDF and expansion with tweet based feature. Two feature expansions use to improve of accuracy from analysis sentiment.

For TF-IDF as commonly used TF-IDF formula in [7]. The weight of word  $k$  in a tweet  $T$  is calculated as follows:

$$W_{ki} = tf_{kT} * \log \left( \frac{N_T}{n_k} \right) \quad (1)$$

Where  $tf_{kT}$  is the appearance frequency of word  $k$  in the tweet  $T$ ,  $N$  is the number of all the collection of tweets that has been used and  $n_k$  is the number of tweets containing the word.

For feature expansion by using TF-IDF, after we get a unique word that weights for each sentiment (negative, positive, and neutral), the features are as in the research that has been done in [8]. The representation of a  $1\_tfidf$  tweet vector of results can be illustrated as follows, suppose the feature vector encodes the appearance of word in the following order: "good" is 1-top feature in positive sentiment, "bad" is 1-top feature in negative sentiment, and "new" is 1-top feature in neutral sentiment, respectively. A tweet containing "He is a good man" will be represented as  $\{1, 0, 0\}$ .

For feature expansion with tweet-based features, we get 25 features. These features are taken when crawling data and shown in Table I.

#### E. Classification Algorithm

In the research, we use three classifiers used to create classification model, i.e., Naïve Bayes (NB), Logistic Regression (Logit), and Support Vector Machine (SVM).

**Naïve Bayes (NB)** is one of the classification methods based on Bayes theorem by using probability and statistical techniques. The Naïve Bayes algorithm predicts future opportunities based on prior experience with the main characteristic is a very strong assumption of independence from each condition [9].

**Support Vector Machine (SVM)** is a classification method that includes supervised learning that analyzes data and recognizes the data patterns. SVM classification is the process of finding the best hyperplane line that separates two

classes in the input space where the maximum distance or margin to the nearest pattern class points or support vector [9].

**Logistic Regression** (Logit) is a mathematical model that can be used to describe the relationship between variable  $X$  and the dependent variable ( $Y$ ). In Logistic Regression variable  $x$  which is predicted is a function of the probability that an object will be in one category ( $Y$ ) [9].

As shown in Fig. 1, the algorithms of classification are used to create sentiment model during training phase. The sentiment analysis model is then used to classify of new tweets, using the same algorithms as used to create the classification model.

#### IV. EXPERIMENTS AND ANALYSIS

There are 3 (three) objectives of experiment, that is, first to know comparison each labeling technique, second to know influence of feature expansion of TF-IDF and of tweet-based features, and third to know influence of tweet-based features. The classification accuracy is defined as the percentage of correctly classified instances using 10-fold cross validation.

TABLE I. 25 FEATURES OF TWEET-BASED

No	Feature	Description
1	#char	The number of characters from a tweet
2	#emot_happy	The number of emoticons containing expressions of happy
3	#emot_sad	The number of emoticons containing expressions of sad
4	#hashtag	Number of hashtags from a tweet
5	#mention	Number of mentions from a tweet
6	#url	Number of urls from a tweet
7	check_spam	To find out whether in a tweet there are words that are included in the spam list.
8	has_happy	The presence of emoticons that contain expressions of happy
9	has_sad	The presence of emoticons that contain expressions of sad
10	is_favorited	Represented by a small star icon next to a Tweet, are most commonly used when users like a Tweet
11	is_hashtag	The presence of hashtag (#) in a tweet
12	is_mention	The presence of mention(@) in a tweet
13	is_retweet	The presence of retweet (RT) in a tweet
14	is_url	The presence of URL in a tweet
15	tot_negative	The number of negative words from a tweet
16	tot_positive	The number of positive words from a tweet
17	tot_sentiment	The number of sentiment words from a tweet
18	tot_word	The number of words from a tweet
19	length_tweet	Character length or word length of a tweet
20	ratioNegNumtweet	The ratio of the number of negative sentiments to the number of words in a tweet
21	ratioPosNumtweet	The ratio of the number of positive sentiments to the number of words in a tweet
22	ratio_char_tot_word	The ratio of the number of character to the number of words in a tweet
23	ratio_char_length_tweet	The ratio of the number of positive sentiments to the length of words in a tweet
24	retweet_counted	The number of users who retweeted a tweet
25	source	The device that used to share a tweet. Grouped into two, via smartphone or PC Client.

#### A. Data Set and Labeling

We use the same dataset used in [8], which contains 19,401 tweets in Bahasa Indonesia. There are tree data labeling, such as

- Manual labeling  
This labeling involves 20 students. Labeling results can be seen in Table II.

TABLE II. MANUAL LABELING DISTRIBUTION

Label	Sum	Percentage
Positive	8078	41.64%
Negative	2611	13.46%
Neutral	8712	44.90%
Total	19401	

- Labeling by system  
In this labeling, we create a corpus that contains a list of words of sentiment, 354 words, then conducted a survey of each word to get negative, positive and neutral sentiment. This sentiment is obtained by searching for words that belong to negative, positive and neutral groups. Some sample data can be seen in Table III. Labeling results can be seen in Table IV.

TABLE III. EXAMPLE 10 SENTIMENT SURVEY

No	Word	Positive (%)	Negative (%)	Neutral (%)	Weight
1	buruk	0	78.3	21.7	3
2	jelek	0	78.3	21.7	3
3	lama	4.3	30.4	65.3	0
4	lamban	4.3	78.3	17.4	3
5	lambat	13	52.2	34.8	1
6	baik	82.6	0	17.4	4
7	berani	82.6	0	17.4	4
8	benar	82.6	0	17.4	4
9	sudah	56.5	0	43.5	1
10	Ayo	65.2	4.3	30.5	2

TABLE IV. LABELING BY SYSTEM DISTRIBUTION

Label	Sum	Percentage
Positive	9798	50.50%
Negative	1645	8.48%
Neutral	7958	41.02%
Total	19401	

- Labeling by system plus emoticon  
After labeling by system, the next step we do with emoticons. There are two cases handled in this label, first, if the neutral system but positive emoticons then the result is positive, and secondly, if the neutral system but negative emoticons then the result is negative. Labeling results can be seen in Table V.

TABLE V. LABELING BY SYSTEM PLUS EMOTICON DISTRIBUTION

Label	Sum	Percentage
Positive	9797	50.50%
Negative	1655	8.53%
Neutral	7949	40.97%
Total	19401	



### B. Comparison Labeling

As shown in Table VI, labeling by system provides improved accuracy in all conditions. The highest accuracy was achieved at 83.94% on the basic features of Unigram+Bigram+Trigram+Post on logistic regression classifier.

TABLE VI. MANUAL VS SYSTEM LABELING (CORPUS SENTIMENT)

Condition			%		
			NB	Logit	SVM
Unigram	39100	System	67.75	83.42	81.29
	features	Manual	56.68	58.23	56.12
Bigram	37096	System	67.33	82.71	80.98
	features	Manual	56.47	58.13	56.16
Uni+Bi+Tri gram+POS	50779	System	<b>69.01</b>	<b>83.94</b>	<b>82.05</b>
	features	Manual	57.65	58.65	56.60
All	52459	System	68.77	83.68	82.05
	features	Manual	57.50	58.65	56.46

Likewise labeling by system when compared with labeling by system with emoticons. The highest results are still achieved labeling by system. Except one cell of SVM classifier, here is increase accuracy that is equal to 0.14%. The results can be seen in Table VII.

TABLE VII. LABELING BY SYSTEM VS BY SYSTEM WITH EMOTICON

50779 features		
Uni+Bi+Trigram+POS (%)		
System	System with emoticon	
NB	69.01	68.92 (-0.13)
Logit	83.94	83.91 (-0.03)
SVM	82.05	<b>82.17 (+0.14)</b>

In this section, experiments are also performed for labeling by system with some basic features and their combinations, their performances shown in Table VIII. The basic features used include Unigram, Bigram, Trigram, POS Tags, and Line Length. The highest accuracy was seen in the combination of basic features consisting of Unigram, Bigram, Trigram and POS Tags, with accuracy of 69.01% for NB, 83.94% for Logit and 82.05 % for SVM.

TABLE VIII. LABELING BY SYSTEM WITH BASIC FEATURE

Basic Feature	#Features	%		
		NB	Logit	SVM
Trigram	33544	66.85	82.28	80.13
Bigram	37096	67.33	82.71	80.98
Unigram	39100	67.75	83.42	81.29
POS Tags (POS)	39448	67.60	83.23	81.21
Unigram+Line Length	39101	67.66	83.40	81.28
Bigram+POS	43741	68.07	83.49	81.66
Unigram+POS	45745	68.39	83.69	81.68
Uni+Bigram+POS+Line Length	50039	68.77	83.92	82.01
Uni+Bi+Trigram+POS	50779	<b>69.01</b>	<b>83.94</b>	<b>82.05</b>
Uni+Bi+Trigram+POS+Line Length (All)	52459	68.77	83.68	<b>82.05</b>

### C. Labeling by System with Feature Expansion

The baseline row describes the results without performing feature expansion that is accuracy labeling by system using basic features Unigram, Bigram, Trigram and POS Tags. In Table IX, we can see that the effect of feature expansion has significant effect on SVM classifier, the accuracy has increased. From two feature expansions, we do

notice a significant increase in feature expansion with tweet-based features, the highest accuracy of 98.81 % is achieved in logistic regression classifier.

TABLE IX. LABELING BY SYSTEM VS BY SYSTEM WITH FEATURE EXPANSION

Condition	%		
	NB	Logit	SVM
<b>Baseline (B)</b>	69.01	83.94	82.05
B +1_tfidf	68.9 (-0.09)	83.9 (-0.06)	82.2(+0.14)
B+5_tfidf	68.9 (-0.08)	83.9 (-0.06)	82.2(+0.16)
B+10_tfidf	68.9 (-0.08)	83.9 (-0.06)	82.2(+0.19)
B +20_tfidf	68.9 (-0.08)	83.9 (-0.04)	82.3 (+0.25)
B +50_tfidf	70.5 (+2.09)	83.9 (-0.02)	82.1 (+0.04)
B +100_tfidf	68.9 (-0.08)	83.9 (+0.02)	82.3 (+0.34)
<b>B+Tweet-based</b>	<b>82.4 (+19.5)</b>	<b>98.81 (+17.7)</b>	<b>92.1(+12.2)</b>

### D. Influence of tweet-based features

As shown in Table X, the features that positively affect the accuracy are baseline plus tot\_sentiment, tot\_positive, #emot\_happy, #emot\_sad, ratioNegNumtweet, and RatioPosNumtweet. While the negative effect is the feature baseline plus #hashtag, #url, tweet\_length, retweet\_counted and source. The other features (12 features) provide mixed results for three classifiers.

TABLE X. INFLUENCE OF TWEET-BASED FEATURES

Condition	%		
	NB	Logit	SVM
<b>Baseline (B)</b>	69.01	83.94	82.05
B+all	<b>82.4 (+19.5)</b>	<b>98.8 (+17.7)</b>	<b>92.1 (+12.2)</b>
B+#emot_happy	<b>69.1 (+0.13)</b>	<b>84.9 (+1.19)</b>	<b>83.5 (+1.78)</b>
B+#emot_sad	<b>69.0 (+0.00)</b>	<b>83.9 (+0.06)</b>	<b>82.0 (+0.03)</b>
B+#hashtag	68.9 (-0.03)	83.8 (-0.06)	81.9 (-0.14)
B+#url	68.9 (-0.04)	83.9 (-0.02)	82.0 (-0.03)
B+tot_negative	<b>69.9 (+1.36)</b>	<b>85.9 (+2.41)</b>	<b>82.9 (+1.14)</b>
B+tot_positive	<b>74.2 (+7.63)</b>	<b>93.0 (+10.8)</b>	<b>89.4 (+9.05)</b>
B+tot_sentiment	<b>79.2 (+14.7)</b>	<b>98.7 (+17.7)</b>	<b>88.8 (+8.27)</b>
B+ length_tweet	68.8 (-0.22)	83.9 (-0.02)	82.0 (-0.03)
B+ratioNegNumtweet	<b>70.4 (+2.10)</b>	<b>84.5 (+0.76)</b>	<b>88.8 (+8.27)</b>
B+ratioPosNumtweet	<b>76.5 (+10.9)</b>	<b>91.0 (+8.41)</b>	<b>85.6 (+4.32)</b>
B+retweet_counted	68.8 (-0.19)	82.0 (-2.31)	82.0 (-0.04)
B+source	69.0 (-0.01)	83.9 (-0.05)	82.0 (-0.01)

## V. CONCLUSION

We have introduced a hybrid method combining basic feature and feature expansion for improving the accuracy of sentiment analysis in Twitter. We have trained SVM, Logit, and NB to observe the accuracy of sentiment analysis using a series of computation. Expansion features can be used and is proven to increase the accuracy of sentiment analysis. From two feature expansions, we do notice a significant increase in feature expansion with tweet-based features, where the highest accuracy of 98.81% is achieved using logistic regression classifier.

Among tweet-based features, we found that the features that affecting positively the accuracy are tot\_sentiment, tot\_positive, #emot\_happy, #emot\_sad, ratioNegNumtweet, and RatioPosNumtweet. While the negative effect is coming from the feature #hashtag, #url, length\_tweet, retweet\_counted and source.

## ACKNOWLEDGMENT

The author would like to thank to PDD Hibah Dikti 2018, STEI ITB and BPPDN RISTEKDIKTI for the support to this research.

## REFERENCES

- [1] B. Liu, "Sentiment Analysis and Subjectivity," *Handb. Nat. Lang. Process.*, no. 1, hal. 1–38, 2010.
- [2] M. S. Neethu and R. Rajasree, "Sentiment analysis in twitter using machine learning techniques," 2013 Fourth Int. Conf. Comput. Commun. Netw. Technol., pp. 1–5, 2013.
- [3] A. Celikyilmaz, D. Hakkani-Tür, J. Feng, "Probabilistic model-based sentiment analysis of twitter messages," 2010 IEEE Work. Spok. Lang. Technol. SLT 2010 - Proc., hal. 79–84, 2010.
- [4] L. Barbosa and J. Feng, "Robust Sentiment Detection on Twitter from Biased and Noisy Data," *Coling*, no. August, hal. 36–44, 2010.
- [5] S. A. Bahrainian and A. Dengel, "Sentiment Analysis using sentiment features," *Proc. - 2013 IEEE/WIC/ACM Int. Jt. Conf. Web Intell. Intell. Agent Technol. - Work. WI-IATW 2013*, vol. 3, hal. 26–29, 2013.
- [6] E. B. Setiawan, D. H. Widyantoro, K. Surendro, "Detecting Indonesian Spammer on Twitter," 6th Int. Conf. Inf. Commun. Technol. (ICOICT), May 3–4, 2018, no. 10, 2018.
- [7] S. Robertson, "Understanding inverse document frequency: on theoretical arguments for IDF," *J. Doc.*, vol. 60, no. 5, hal. 503–520, 2004.
- [8] E. B. Setiawan, D. H. Widyantoro, K. Surendro, "Feature Expansion using Word Embedding for Tweet Topic Classification," *Inf. Commun. Technol. (ICoICT)*, 2017 5th Int. Conf. Malacca City, Malaysia, 2016.
- [9] T. M. Mitchell, *Machine Learning*. McGraw-Hill Science, 1997.
- [10] <https://www.merdeka.com/teknologi/media-sosial-merajai-penggunainternet-di-dunia.html>, accessed June 2018
- [11] <http://www.beritasatu.com/digital-life/428591-indonesia-masuk-limabesar-pengguna-twitter.html>, accessed June 2018

# Web-based Campus Virtual Tour Application using ORB Image Stitching

Triyanna Widiyaningtyas  
*Dept. of Electrical Engineering*  
*State University of Malang*  
 Malang, Indonesia  
 triyannaw.ft@um.ac.id

Didik Dwi Prasetya  
*Dept. of Electrical Engineering*  
*State University of Malang*  
 Malang, Indonesia  
 didikdwi@um.ac.id

Aji P Wibawa  
*Dept. of Electrical Engineering*  
*State University of Malang*  
 Malang, Indonesia  
 aji.prasetya.ft@um.ac.id

**Abstract**— Information disclosure in the digital age has demanded the public to obtain information easily and meaningful. In this paper, we propose the development of web-based campus virtual tour 360-degree information system application at the State University of Malang, Indonesia which aims to introduce the assets of the institution in an interesting view to public. This application receives a stitched or panoramic image generated through the ORB image stitching algorithm as an input and displays it in virtual tour manner. This paper realizes the image stitching algorithm to present the visualization of the 360-degree dynamic building and campus environment, so it looks real as if it were in the actual location. Virtual tour approach can produce a more immersive and attractive appearance than regular photos.

**Keywords**—web, campus, virtual tour, ORB, image stitching

## I. INTRODUCTION

Information disclosure in the digital age provides space for the public to obtain related information to the public institution services effectively and efficiently. This era demands every public institution to open access for any individual who needs specific public information. Information disclosure can reduce the possibility of asymmetries information that often causes markets to be inefficient [1]. Better disclosure and transparency is essential to help public's encounter their minds on company's activities [2]. To realize this policy, ICT solution becomes a strategic choice. In fact, ICT facilitate the process of collecting, storing, processing, and disseminating of information in a digital format. ICT tools and services play an essential role in improving the availability of market information to the public who need.

Today almost all organization and institution utilize the Internet network to provide information to the public. Web application approach that runs on the Internet network is very appropriate used to introduce the assets of institutions and encourage public information disclosure. The web application approach considerably enhances corporations' ability to deliver their strategies and other relevant information directly to their primary stakeholders. [3]. The web application supports rich content, including multimedia contents such as text, audio, graphics, animation, and video. In fact, we can also include interactive content into web applications that make it more

varied and exciting. Interactive is often used to describe the relationship of two things influencing each other [4]. Therefore, the presentation of public information should also be provide in an interesting, complete, and meaningful way.

In fact, there are still many institutions that provide basic public information system, for example in the State University of Malang (UM), Indonesia. The development of a web-based campus virtual tour 360-degree information system application is considered very appropriate to support the provision of interesting public information. Campus visual navigation is one of an example of a virtual reality application in modern education. This application focus on the campus digitalization and virtualization for optimized management, support campus plan and help decision-making of school development [5]. The virtual tour is emerging approach as an effective tool for destination marketing. To provide information in the virtual tour manner, we can take advantage of established and reliable public service, such as Google Virtual Tour. But there are still deficiencies in the service, among which are unable to uncover specific locations, especially private or indoor places. Therefore, the development of virtual tour applications is still highly relevant to current needs.

In this paper, we propose the development of web-based campus virtual tour 360-degree application. In this work, we utilize the ORB image stitching algorithm which is a combination of several algorithms in the field of computer vision. The result of this application can present the visualization of pictures of buildings and campus environment which moves 360-degree dynamically, so it looks real as if it was in the real environment.

## II. RELATED WORKS

A virtual tour is an interactive simulation of an existing location on the earth, usually composed of a sequence text, still images, and panoramas. The term "panorama" denotes an unbroken tour/view because a panorama usually a series of images captured by the photographer or the video footage [6]. These virtual tours have taken from a series of panoramic photograph known as a vantage point.

Virtual tour basically is a virtual environment in computer which reconstructs a famous places virtually [7]. This method

provides a special sensation to users as if the users visit the area in foregone. Virtual environments are being utilized in a wide range of academic and commercial applications.

The study of virtual tour application has been done and intended for various purposes. Wu et al. [8] proposed a project plan of "Virtual tour at Tsinghua University". In their research, Wu is still limited to produce panoramic images and has not provided supporting features such as rotation and user control. Yang et al. [9] proposed a feasible model and development environment to provide an interactive virtual navigation application for creating and utilizing digital campus approach. However, when considering this scheme in real-time interactivity, especially involved the large-scale data, in-depth research is still necessary. Manghisi [10] proposed a gesture-based interface solution to navigate a virtual tour application on display. This work is also comparing the implemented interface with a traditional mouse-controlled menu with the proposed gesture-based interface to gain the more user engagement.

Referring to the related studies we have mentioned, we can highlight the differences works with our proposed research. To generate stitched images, we utilize a very good-performing ORB algorithm proposed by Wang [11]. The output from this stitch stage we process using HTML and jQuery library to produce a 360-degree panoramic virtual tour. So, here we take advantage of existing and proven performance algorithms and then integrate into a virtual tour campus application that aims to introduce the assets of institutions and encourage public information disclosure.

### III. METHODS

#### A. System Design

This paper describes the implementation of virtual tour 360 applications by utilizing the ORB algorithm. Development of application focus on a web environment that runs on the Internet network. The web app approach is apt as it provides broad access from all corners of the globe and allows various devices to access it, including mobile devices. The architecture of the proposed application shown in Figure 1.

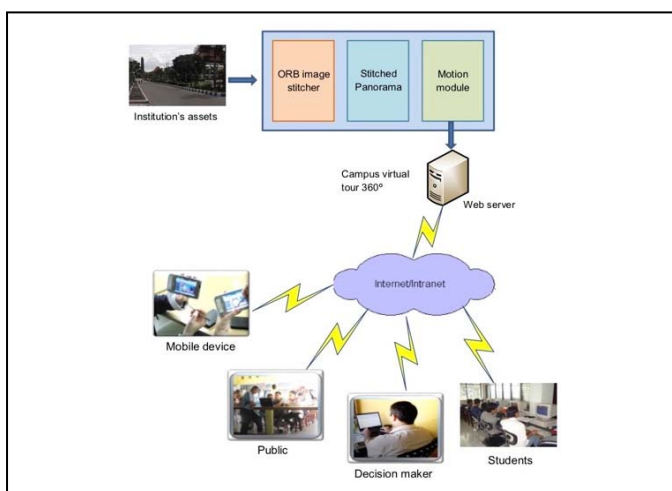


Fig. 1. System architecture

There are two main activities in the development of this system: image stitching, and panorama motion.

#### 1) Stitching

Image stitching is an activity in image processing by combining a set of images into a larger panorama image with a wider field of view of the scene [12]. The goal of this process is to generate natural-looking mosaics free of artifacts that may occur due to some effects, such as relative camera motion, optical aberrations, and illumination changes. [13]. To generate stitched image we use ORB image stitching algorithm.

#### 2) Motion panorama

After a series of stitched images generate an image panorama, the next step is to apply motion techniques to rotate the panoramic image display, so it looks immersive like the original. To implement this module we use the HTML script combined with the jQuery library. The working of this module is to rotate the image left or right to display the entire picture. This approach provides visualization as if the image is moving and the user is like being in its original location.

#### B. ORB Image Stitching

Image stitching is the basic construction process of a series of overlapping images into a single panoramic image with a high resolution. This activity is widely implemented in real-time applications and is an interesting topic in the field of computer vision and computer graphics experts. How the image stitching works are started by matching points that have similarities in two or more images and then produce a composite image form.

Until now there are various techniques in the field of computer vision to realize image stitching, one of which is Oriented FAST and Rotated BRIEF (ORB) developed by Rublee [14]. ORB is principally a combination of the Accelerated Segment Test (FAST), Harris, and Binary Robust Independent Elementary Features (BRIEF) algorithms. The working flow of the ORB algorithm shown in Figure 2.

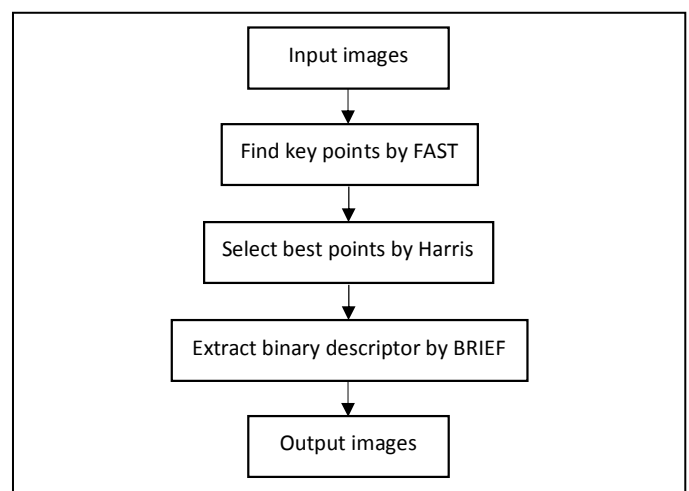


Fig. 2. ORB image stitching stages

The workings of the ORB algorithm start from the comparison and matching of two or more images. ORB builds on the well-known FAST key point detector to find the efficient corner key points. ORB utilize Harris corner filter to reject edges and provide a reasonable score. Finally, it uses a recent feature BRIEF descriptors to produce a smoothed image patch. This descriptor is used for image stitching, and shows good rotational and scale invariance [14].

#### IV. RESULT AND DISCUSSION

##### A. Result

As we mentioned, there are two main modules in this application: stitching and motion panorama. The first stage is the image that will be generated in a stitched image. To ensure the implementation of the algorithm, taking the picture is done using pure cameras without special features, such as panoramic. Examples of the results of two images with overlapping shown in Figure 3.



Fig. 3. Image sources taken by camera

To get a stable shooting result, we use a tripod on the smartphone camera. This technique is essential for obtaining optimal stitching results or reducing unmatched points. Shooting done on bright lighting is also proven to produce excellent stitching. The image stitching results are shown in Figure 4.



Fig. 4. Stitched image result

On taking pictures of locations on campus, we use a smartphone camera. This stage is conducted during the day by targeting places that become the assets of the institution. Shooting on location involves about six camera angles to get enough overlap area. If the stitching result of the series of images still shows a mismatch, then the location is retaken. In

the final step, as a usual panoramic shooting process, we need to cropping the images to get the symmetrical area.

Stitching stage is the primary key to get an excellent panoramic image. The output of this stage will be processed by the panorama motion module to present the visualization of the virtual tour application. The implementation of web technology in this application provides easy and wide access advantages. The appearance of virtual tour web application in the State University of Malang shown in Figure 5.

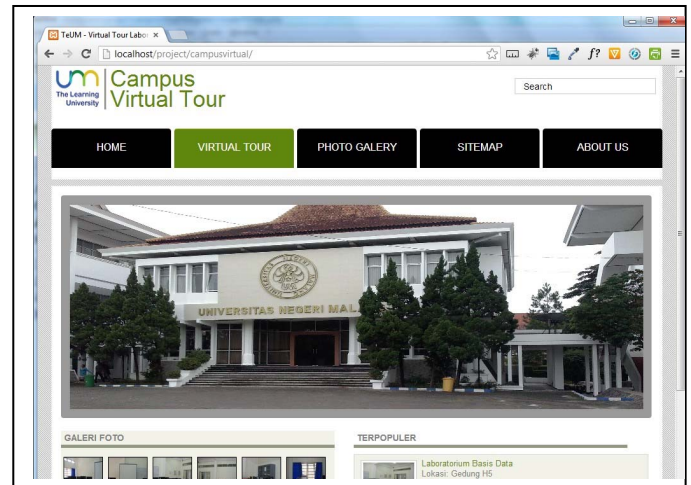


Fig. 5. Virtual tour panorama application

Utilization of web-based information system applications can be a publication media as well as effective promotions that can be accessed widely whenever and wherever without depending on space and time. The main feature provide on this application is a 360 panoramic virtual tour with user control navigation. Through this control interface the user can navigate like start/pause, scroll, and zoom in/out.

Once we succeed in developing the system, the next step is to ensure that the system is correct and properly constructed using a series of tests. Testing conducted using the black-box method and based on the scenario in each subsystem. There are two scenarios that we involve: normal and alternative scenarios. Alternative scenarios arise when there is branching, for example at the stitching stage, the result might be either successful and failure.

There are two main modules that will be a focus on testing, including stitching and motion panorama. The test procedure is performed sequentially from the smallest unit until the finish. The complete testing result is shown in Table 1.

TABLE I. FUNCTIONALITY TEST

Module	Testing		
	Scenario	Methods	Results
Stitch	Normal	Black-box	Accepted
	Alternative	Black-box	Accepted
Motion	Normal	Black-box	Accepted



Module  panorama	Testing		
	<i>Scenario</i>	<i>Methods</i>	<i>Results</i>
	Alternative	Black-box	Accepted

The black-box testing procedure is done by giving input to the system and observing its output. If the outcome has met, by the initial specifications, it can be stated that the product is working properly. Conversely, if the output does not meet, then be repaired and retested to fit. The overall results of the tests on the module, both normal and alternative scenarios, show that the product is working properly and no defects are found.

### B. Discussion

Stitching images is an early stage in computer vision to produce panoramic images. Realization of image stitching is done by employ the ORB algorithm. The process of the ORB algorithm on the shots in bright places using a tripod looks very impressive, in which there is almost no mistake point between one image and the other. This process proves that the ORB algorithm has a good performance and can produce panoramic images.

Implementation of virtual tour application in this research is represented by giving motion effect to a panoramic image. This step is realized through the HTML code combined with jQuery library and PHP programming language. This approach is also used to provide user control, making it easier to navigate the panorama. In order to provide complete information to the public, the panoramic view is also complemented by mapping access to locations. Utilization of web-based applications strongly supports the publication of information widely.

The panoramic image approach is best used in campus virtual tour 360-degree applications aimed at introducing institutional assets and promoting public information disclosure. Compared to the use of static video, virtual tour panorama has several advantages, among which is lighter because in principle only in the form of images. The virtual tour also allows for better interaction supported navigation and user control, such as scroll, zoom in/out, and integration with other interactive menus. The results of the implementation show that the virtual tour approach can produce a more immersive and attractive appearance than regular photos, so it looks real as the original places.

## V. CONCLUSION

A web-based campus virtual tour 360-degree information system application is one of the appropriate strategies to support public information disclosure. The utilization of the ORB image stitching algorithm can produce a quality panoramic image with an excellent level of matching. Implementation of the motion feature makes the application more interesting as the real location. Finally, with the availability of varied information content, including text,

images, and dynamic panorama provide a new experience for the public in obtaining the necessary information in a meaningful manner.

## ACKNOWLEDGMENT

We would like to thank the Department of Electrical Engineering, Faculty of Engineering, State University of Malang (UM), which had full provided support to this research activity.

## REFERENCES

- [1] Tadelis S, Zettelmeyer F. Information disclosure as a matching mechanism: Theory and evidence from a field experiment. *American Economic Review*. 2015 Feb;105(2):886-905.
- [2] Esa E, Zahari AR. DISCLOSURE ON CORPORATE WEBSITES: CORPORATE SOCIAL RESPONSIBILITY IN MALAYSIA & SINGAPORE GOVERNMENT-LINKED COMPANIES. *Journal of Technology Management and Business*. 2017 May 28;4(1).
- [3] Cormier D, Magnan M. The impact of the web on information and communication modes: the case of corporate environmental disclosure. *International Journal of Technology Management*. 2004 Jan 1;27(4):393-416.
- [4] Prasetya DD, Wibawa AP, Hirashima T. An interactive digital book for engineering education students. *World Transactions on Engineering and Technology Education*. 2018 (Vol.16, No.1, pp. 54-59)
- [5] Zhang Weijun etc. Design and Exploitation of Virtual Campus System [J]. *Computer & Digital Engineering*, 2010, VOL38(4): 181-183.
- [6] Cho YH, Fesenmaier DR. A conceptual framework for evaluating effects of a virtual tour. In *Information and Communication Technologies in Tourism 2000* (pp. 314-323). Springer, Vienna.
- [7] Yoo B, Han JJ, Choi C, Yi K, Suh S, Park D, Kim C. 3D user interface combining gaze and hand gestures for large-scale display. In *CHI'10 Extended Abstracts on Human Factors in Computing Systems 2010 Apr 9* (pp. 3709-3714). ACM.
- [8] Wu S, Wang R, Wang J. Campus Virtual Tour System based on Cylindric Panorama. In *Proc. of the 11th International Conference on Virtual Systems and Multimedia (VSMM 2005)*, Ghent, Belgium 2005 Oct.
- [9] Yang WY, Zhang LM, Pan SW, Fan ZX. Interactive digital campus visual navigation system design and development. In *Applied Mechanics and Materials 2013* (Vol. 336, pp. 1422-1425). Trans Tech Publications.
- [10] Manghisi VM, Uva AE, Fiorentino M, Gattullo M, Boccaccio A, Monno G. Enhancing user engagement through the user centric design of a mid-air gesture-based interface for the navigation of virtual-tours in cultural heritage expositions. *Journal of Cultural Heritage*. 2018 Mar 13.
- [11] Wang M, Niu S, Yang X. A novel panoramic image stitching algorithm based on ORB. In *Applied System Innovation (ICASI)*, 2017 International Conference on 2017 May 13 (pp. 818-821). IEEE.
- [12] Chang CH, Sato Y, Chuang YY. Shape-preserving half-projective warps for image stitching. In *Proceedings of the IEEE Conference on Computer Vision and Pattern Recognition 2014* (pp. 3254-3261).
- [13] Lin CC, Pankanti SU, Natesan Ramamurthy K, Aravkin AY. Adaptive as-natural-as-possible image stitching. In *Proceedings of the IEEE Conference on Computer Vision and Pattern Recognition 2015* (pp. 1155-1163).
- [14] Rublee E, Rabaud V, Konolige K, Bradski G. ORB: An efficient alternative to SIFT or SURF. In *Computer Vision (ICCV)*, 2011 IEEE international conference on 2011 Nov 6 (pp. 2564-2571). IEEE.



# Automatic User-Video Metrics Creations From Emotion Detection

Darari Nur Amali<sup>1</sup>, Adnan Rachmat Anom Besari<sup>2</sup>, Ali Ridho Barakbah<sup>3</sup>, Dias Agata<sup>4</sup>

Department of Informatics and Computer Engineering

Politeknik Elektronika Negeri Surabaya (PENS)

Kampus PENS, Jalan Raya ITS Sukolilo, Surabaya, 60111 Indonesia

Email: <sup>1</sup>dararii@ce.student.pens.ac.id, {<sup>2</sup>anom, <sup>3</sup>ridho, <sup>4</sup>diasagata}@pens.ac.id

**Abstract** - In this digital era, digital content especially video, is increasing in number from time to time. Typically, a video service provider like Youtube will perform video analysis based on the video content such as colours, textures, shapes, and other features that exist in video content. The result of this analysis was used to understand user preference and to personalize video for each user. With technological developments, especially in Machine Learning and Computer Vision technology, video analysis can be based on other things beyond the video. In this context, it is the audience's impression. Thus, with the analysis of audience impressions in real-time, it is expected that the video can be analysed using the emotion parameters of the audience while the video is playing, and this can be done automatically and real-time. This system generates impression statistic for each video which concluded from every user who has watched the video and save those data in the database. Method used to analyse the result is by recruiting respondent and give some questionnaires. Respondents were asked to watch some videos and were asked to compare the impression metric which created by the system with user's real impression. The result shows that the automatic video-metric creation from emotion detection has been able to measure user's impression of the video with more than 80% accuracy stated by 75% of 20 respondents of the survey.

**Keywords** — Video Labelling, User-Video Metric Creations, Emotion Detection.

## I. INTRODUCTION

Communications network infrastructure in Indonesia develops rapidly in recent years. Survey of the Indonesian Internet Network Provider (APJII) in 2016 revealed that 132.7 million Indonesians are connected to the Internet [1]. This has led to an increase in the use of digital technology-based facilities in the community, one of them is video streaming platform. This triggers streaming video service providers such as Youtube increasingly preferred by many people.

Youtube-statistic reported that there are 300 hours of videos uploaded to Youtube (refers to Fig.1). The large number of videos on a streaming service such as Youtube will make the video on the service very hard to categorized. This will encourage providers to analyse the video content through the internal content of the video or video features. The features are colour, shape, texture, audio signal model, and others [2]. Then they used the result to determine a video category, get user preference in watching video, and create a personalization for each user.



Fig. 1. Statistic of video uploaded to Youtube in every hour since January 2008 to January 2014.

Their algorithm in analysing video content through its feature was very powerful, with billion videos in numbers as data set, the categorization of the video performed very great in accuracy. So, Youtube can provide many videos with same category as video which played by user, and this system is a part of their recommendation system. But, there are some weaknesses, video which provided based on same feature of its video can't provide variety videos for user, and in some cases, user be bored with the video provided by Youtube recommendation system. In fig. 2 (a), a first case that music video played by user, and Youtube recommend another music video for user. In fig. 2 (b), a second case, reality show video was played by user, and Youtube provide another reality show video. The weakness is, when user wants a video with different category or different content, user cannot find it at video list provided by Youtube and should use search function to get them.

With development of massive artificial intelligence technology, video analysis can now be done through external factors that exist beyond its video, in this case is the impression of the video audience while watching the video. This system is designed to be able to auto-label for each video that is in accordance with the user's impression. Then, after the impression data of each video is obtained, then we will be able to find out whether the video makes the audience laugh, surprised, sad, fear, or even disgust. This will be automated by system and work in real-time. The goal of this research is to create an impression-based label for each video that exist and stored in a database. The result of an impression analysis can be used as a parameter and data set for a new recommender system in further research.

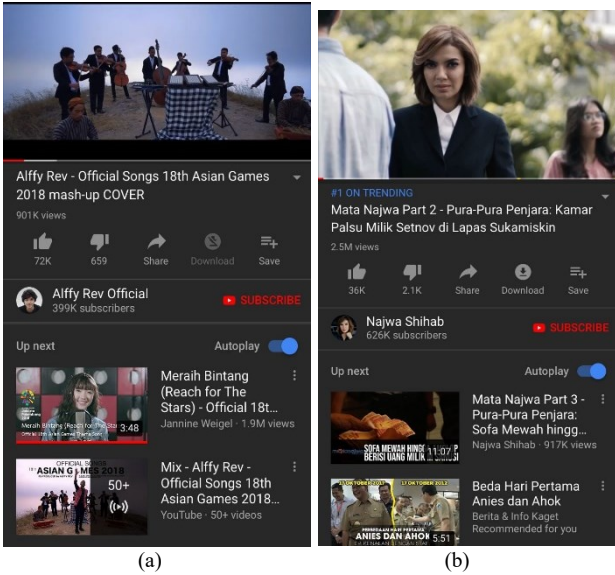


Fig. 2. (a) music video recommendation list, (b) reality show video recommendation list

## II. METHOD

### A. Emotion Detection using Affectiva

Affectiva is one of the projects of the Massachusetts Institute of Technology (MIT) that focuses on machine learning and computer vision. Affectiva Emotion API can perform the scan of a person's facial expression in real-time [3]. In the process of detecting emotions through facial images, Affectiva has 4 stages: 1) Face and facial landmark detection, 2) face texture feature extraction, 3) facial action classification and 4) emotion expression modelling [4]. These four stages can be seen in the Fig.3. This system requires an image as an input which can be obtained from camera stream, video file, video frame stream, or even a picture. To obtain image using camera stream, Affectiva needs camera with minimum specification among them:

1. RGB Camera
2. Minimal Resolution at 320 x 240
3. Minimum video capture speed at 10fps.

This algorithm can run at the background and computational resources which is used to determine an emotion varied based on processing speed. Usually between 1 to 10 FPS (Frame per Second).

As the algorithm shown in Fig.3, Affectiva is able to detect emotions well with accuracy score varied between 0.72 up to 0.9 at ROC (Receiver Operating Characteristic) curve [3]. Here is an example of test data that has been done to get some facial action (Fig. 4).

Facial action describes facial expression of human face. To understand the emotion, Affectiva needs to analyse some facial action that occurs then determine an emotion. Affectiva will generate score 0-100 in determining the emotional score of a person's facial expression. This score determined based on the EMFACS mapping algorithm developed by Friesen & Ekman. The following table I shows the mapping of facial expressions to emotional expressions.

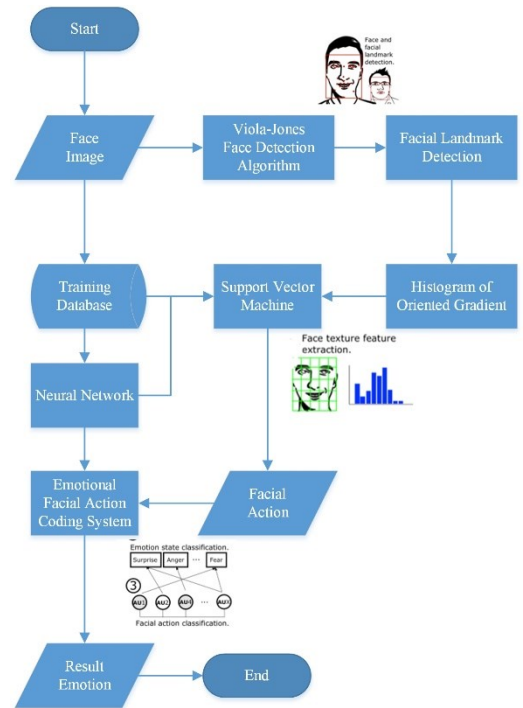


Fig. 3. Emotion detection system flow which developed by Affectiva [4]

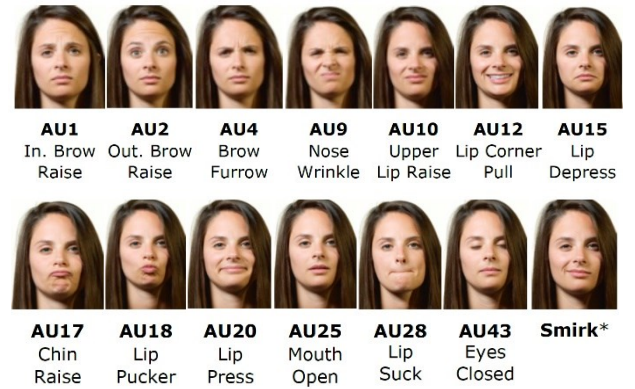


Fig. 4. The facial actions that can be detected. Each action is given a score from 0 to 100. [4]

TABLE I. Expression Mapping to Emotion

Emotion	Increase Likelihood	Decrease Likelihood
Joy	<ul style="list-style-type: none"> <li>Smile</li> </ul>	<ul style="list-style-type: none"> <li>Brow Raise</li> <li>Brow Furrow</li> </ul>
Surprise	<ul style="list-style-type: none"> <li>Inner Brow Raise</li> <li>Brow Raise</li> <li>Eye Widen</li> <li>Jaw Drop</li> </ul>	<ul style="list-style-type: none"> <li>Brow Furrow</li> </ul>
Disgust	<ul style="list-style-type: none"> <li>Nose Wrinkle</li> <li>Upper Lip Raise</li> </ul>	<ul style="list-style-type: none"> <li>Lip Suck</li> <li>Smile</li> </ul>
Fear	<ul style="list-style-type: none"> <li>Inner Brow Raise</li> <li>Brow Furrow</li> <li>Eye Widen</li> <li>Lip Stretch</li> </ul>	<ul style="list-style-type: none"> <li>Brow Raise</li> <li>Lip Corner Depressor</li> <li>Jaw Drop</li> <li>Smile</li> </ul>
Sadness	<ul style="list-style-type: none"> <li>Inner Brow Raise</li> <li>Brow Furrow</li> <li>Lip Corner Depressor</li> </ul>	<ul style="list-style-type: none"> <li>Brow Raise</li> <li>Eye Widen</li> <li>Lip Press</li> <li>Mouth Open</li> <li>Lip Suck</li> <li>Smile</li> </ul>

### B. Combine Emotion Detector with Streamer

The automatic video-metric creations system will be implemented on Android Apps. The apps will develop using Android Studio and Affectiva SDK for Android. Android is chosen because Android OS market share in sales to end users from 1st quarter 2009 to 1st quarter 2018 achieved more than 85% in worldwide [5].

The flow system of this metric will be based on the flowchart in fig. 5 it can be seen that Youtube video will run simultaneously with emotion detection system. The metrics of the user-based impression video will be counted every second. So, the metric results will appear discrete with 1 second interval. Analytics from user-video metrics will be done to determine the impression conclusions on a video.

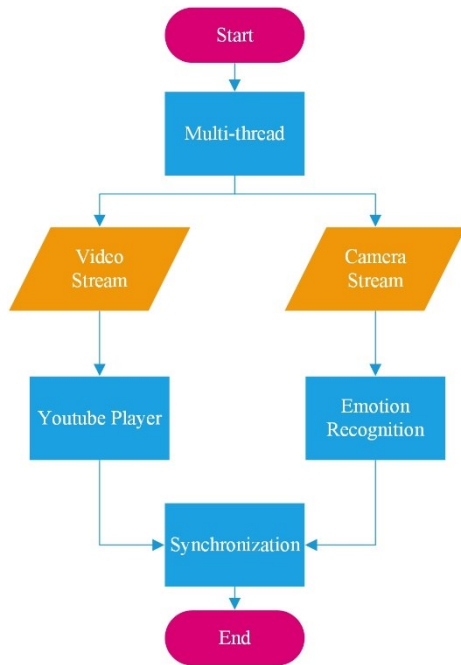


Fig. 5. General system flow of automatic video-metric creations.

Impression details will be stored in databases that have been designed for efficiency and analysed by the system to get an impression of the conclusion of the total impressions of existing video and stored as meta-data that will facilitate the system in accessing data efficiently and quickly [6]. The data to be formed is shown in fig. 5.

TABLE II. Metric data shape shown in table

Video-Metric	V1	V2	....	V(n-1)	Vn
User 1	X 1.1	X 1.2	X...	X 1.(n-1)	X 1.(n)
User 2	X 2.1	X 2.2	X...	X 2.(n-1)	X 2.(n)
.....	X...	X...	X...	X...	X...
User (n-1)	X (n-1).1	X (n-1).2	X...	X (n-1).(n-1)	X (n-1).(n)
User n	X (n).1	X (n).2	X...	X (n).(n-1)	X (n).(n)

Database structure shown in table II was only meta-data structure. The database design will use flat design structure using Firebase Firestore platform. Firebase Firestore was chosen because its speed and reliability. So, the table model

design shown in table II will be converted to flat database design shown in Fig. 6.

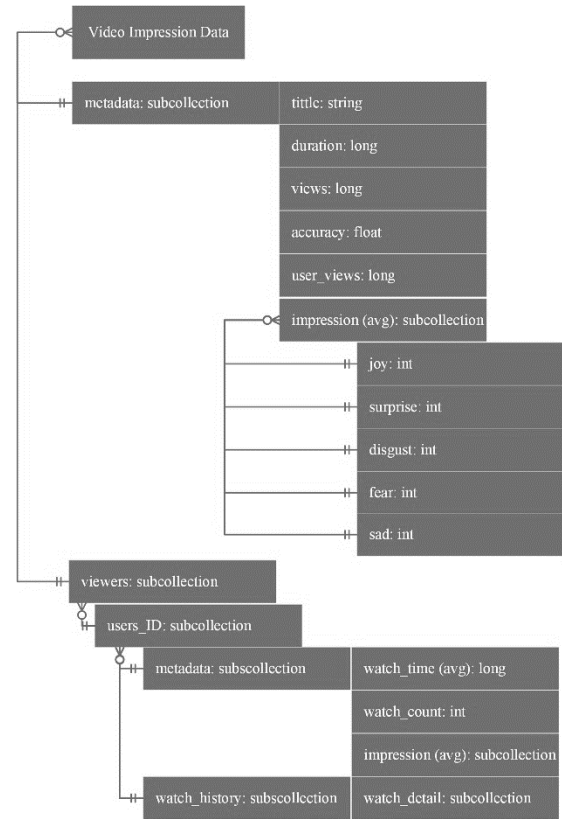


Fig. 6. Video-metric database structure shown in table 2 converted to flat design database which supported by Firebase Firestore.

Flat data structures are chosen because non-SQL data structures have much faster speed compared to table-shaped SQL in very large data conditions (more than 10,000 data). With the above structure, the database will be scalable. So, this database will not be limited by how much the amount of video impression data will be stored later. The database structure for users is also designed scalable, fast and efficient. In this case, using the meta-data technique. Meta-data is used to perform indexing on video data. This is intended to avoid duplication of data so that the storage space used is also efficient.

The value of X in table II is obtained by calculating the accumulation of emotion value which is done by algorithm in fig. 7. The X value is five-dimensional data which contain  $X_{[i=1]}$  to  $X_{[i=5]}$  where i is the five emotions category such as joy, surprised, disgust, fear, and sad.

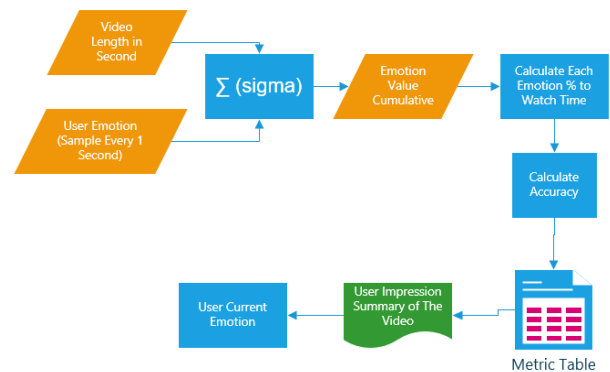


Fig. 7. User-video metric calculation and data storage algorithm

The algorithm in fig. 7. shows that the value to be stored in the metric table is the value of six emotions except the neutral emotion. Value calculations can be done as this equation.

$$\Sigma \text{ Emotion Value} = \sum_k^n (\text{Emotion Value}[k]) \quad (1)$$

The calculation of equation (1) will get the accumulative emotional value. Where n is the amount of emotional data (ideally equal to the video duration in seconds). Emotion Value [k] is the viewer's emotional value on the video on the duration of k. This accumulative value will be compared with the accumulated value of maximum emotions score. So, that it will form the value of emotion percentage to watch time in accordance with calculations of equation 2.

$$\text{Emotion Metric \%} = \frac{\Sigma \text{ Emotion Value}}{\Sigma \text{ Max Possible Emotion Value}} * 100\% \quad (2)$$

The calculation for the maximum emotional value is obtained from the accumulated calculation of the maximum emotional value during the duration of the video. This calculation is in accordance with the following equation 3.

$$\Sigma \text{ Max Possible Emotion Value} = \sum_t^n (\text{Max Value}[t]) \quad (3)$$

Where n is the duration of the video, and t is the index of time of the video. So, max value [t] is the maximum value of the emotion to be detected on the duration of t. Maximum value on this system is 100.

In an automated video-metric manufacturing system, the measured data must meet the requirements to be stored in the database. The requirements are metric data which must have user impression data minimum 70% of video duration. This is intended to maintain the level of measurement accuracy. To measure the accuracy level of this video metric, the system has been able to perform automatically that is by comparing the number of detected expressions with the total duration of the video according to equation 4 below.

$$\text{Metric Accuracy \%} = \frac{\Sigma \text{ Emotion Detected}}{\Sigma \text{ Video Duration}} * 100\% \quad (4)$$

According to equation 4, total count of emotion detected is compared to video duration to calculate Metric Accuracy. This is because system use 1 frame per second in processing rate. So, there will be one emotion value at every second. At 100% accuracy, the total count of emotion value will be the same with the video duration.

### III. RESULT AND ANALYSIS

This test is intended to discover whether the system has been able to display a video gauge based on the audience's impression when viewing it. The test examined several videos with diverse users.

#### A. Validation Method

Validation method for the test result is done by comparing the emotion result calculated by system with the impression characteristic of the video which estimated manually by the authors. If the first step of the validation is valid, then the system can validate the video label by itself,

if the video has been watched in 10 times by some users. The last validation step is by taking feedback from users using questionnaire. In the questionnaire, users will asked to compare the emotion metric statistic which has been created by system to their real emotion feeling while watching the video.

#### B. Test I.

Video Title: Djarum Video Ad – Want to be skinny

Video Duration: 32 Seconds

Video Category: Joy Video/Comedy

Video Characteristics: This video is a comedy video ad such as a video ad of PT. Djarum in general, but the location of this cuteness is located at the end of the video.

Audience Characteristics:

- Age: 20 - 25 years
- Sex: Male and Female
- Mood: Unknown (Unknown)

In this test, it be seen how the user's impression of this video. Video metrics are said to be true if the user's impression of a video has something in common with the video characteristics tested.

From the result of this test, it shows that the total happy impression reached 37.43% which is dominated in the 23<sup>rd</sup> to 32<sup>nd</sup> position in this video. Joy impression at this result test also can be seen at 6<sup>th</sup> to 12<sup>nd</sup> position referred to fig. 8. This is in accordance with the characteristics of the video being tested. Up to this point, based on table III, impression-based video measurement is considered correct.

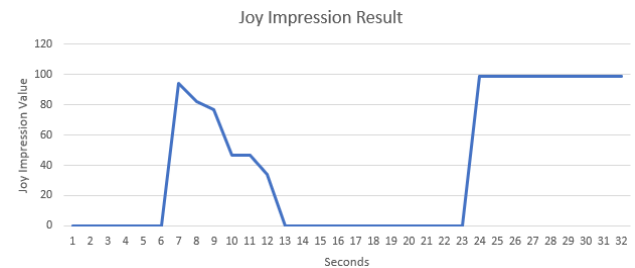


Fig. 8. Users impression detail result of video 1 by user 1 created by automatic video-metric system

TABLE III. Video 1 Impressions Result by 10 Users

No.	Video ID	User ID	% Joy Value
1	b8vhQ-	2zg0xsiPXqZaV8S6SBCboVPHDo23	11,12
2	b8vhQ-	ArL6uaqHvgc3XPlvPCiK40KOJv53	27,25
3	b8vhQ-	bNCD6YWBln6SN6xm4CRzKIOF6n1	8,27
4	b8vhQ-	djasMlryLZemk9SWo9KvGRkvJfg1	39,33
5	b8vhQ-	iEnojOVPPwY75GhC2xGhcrDGVgX2	4,27
6	b8vhQ-	jMF5BIXUUGS79q7byH2yS1Fnpg52	6,26
7	b8vhQ-	P33JdE8VVoejEvWwN246l5Gf3H2	9,31
8	b8vhQ-	St8Xq66JjOWRRqSKVw0zqv6NkeC3	10,92
9	b8vhQ-	YDC5vbkOI06YWQEOBBsPYdf0vJ3	11,61
10	b8vhQ-	zLzIWuam2jWn2Kzz1ST1qzZU7qb2	72,47

#### C. Test II.

Video Title: Asian women eating frog

Video Duration: 59 Seconds

Video Category: Video Log – Disgusting for some people



**Video Characteristics:** This video is a video documentation of a female vlogger who is eating frogs. For most people, frogs are a disgusting animal to eat, so this video is suitable for use as a test for disgusting videos.

From the results of tests conducted for disgusting videos involving 7 users in 10 times views, the results show that this video has an abhorrent label on average of 25% of the expression of disgust detected when users watch the video in accordance with the experimental results listed on the table IV.

TABLE IV. Video 2 Impressions Result by 10 Users

No.	Video ID	User ID	% Disgust Value
1	iDoA9v	kZBvxp7Vx1Q7aYdei3gbk1UePZg1	45,82
2	iDoA9v	dta7oYAJlaZST9CU9Cye0RSb8x13	13,59
3	iDoA9v	dW5ix8hGLYQcgBG2mye5WUP4QUi	19,34
4	iDoA9v	T2MoWeBgu0UMBxOHTiHeteIEDsu2	0,41
5	iDoA9v	dta7oYAJlaZST9CU9Cye0RSb8x13	41,81
6	iDoA9v	S0VjmLrdQgNWQNZ0VcXniee6eH92	14,99
7	iDoA9v	P33JdE8VVoejEvWnS246l5Gf3H2	20,58
8	iDoA9v	9sKjAHYnTjNA9AUHUDQzDaCJYb	18,16
9	iDoA9v	P33JdE8VVoejEvWnS246l5Gf3H2	75,02
10	iDoA9v	P33JdE8VVoejEvWnS246l5Gf3H2	0,47

In one user's experiment, disgusted impression was detected at 74.14% with a disguised impression spread evenly at 0<sup>th</sup> to 50<sup>th</sup> seconds. This appears as shown in Fig. 9. Based on the results of this test, the system has successfully detected a disgusted impression on the disgust category video.

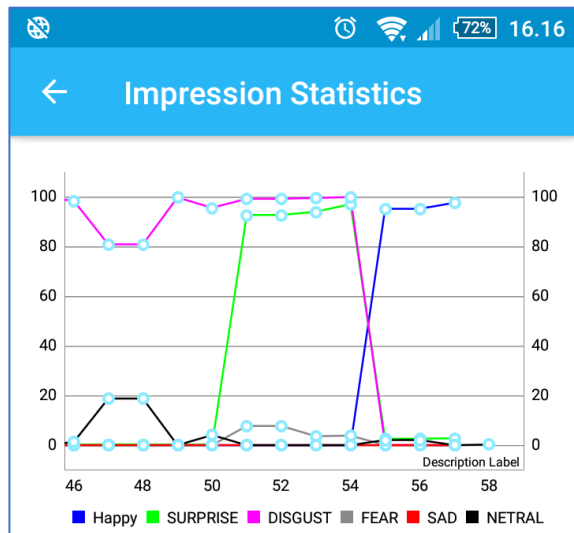


Fig. 9. Users impression detail result of video 2 by user 3 created by automatic video-metric system

#### D. Test III.

**Video Title:** Man Sleep on Rail when Train is Passing.

**Video Duration:** 52 Seconds

**Video Category:** Amateur/Surprising video at first watch.

**Video Characteristics:** This video is an amateur video that is the documentation of a man who is doing a test of guts

by sleeping in a railroad when the train is passing. The surprising thing about this video is that it does not seem at first that there will be a passing train, but suddenly a train passes by the 18<sup>th</sup> second and the man goes straight to sleep on the tracks as the train passes.

From the results of the tests conducted for a surprising video involving 7 users in 10 views, the results show that this video has an astounding average label of 7% of the surprised expressions detected when the user watches the video in accordance with the experimental results listed on the table V.

TABLE V. Video 3 Impressions Result by 10 Users

No	ID	User ID	% Surprised Value
1	aZlA7	2gBcgXWHWgeLvSRs7HwPjIF5	14,83
2	aZlA7	9sKjAHYnTjNA9AUHUDQzDa	4,04
3	aZlA7	HnjBYINrKcPIWb9dsXba0BTsmQ	11,47
4	aZlA7	P33JdE8VVoejEvWnS246l5Gf3	2,33
5	aZlA7	dW5ix8hGLYQcgBG2mye5WUP	4,17
6	aZlA7	P33JdE8VVoejEvWnS246l5Gf3	15,78
7	aZlA7	dta7oYAJlaZST9CU9Cye0RSb8x	3,87
8	aZlA7	P33JdE8VVoejEvWnS246l5Gf3	2,05
9	aZlA7	dta7oYAJlaZST9CU9Cye0RSb8x	7,09
10	aZlA7	kZBvxp7Vx1Q7aYdei3gbk1UePZ	4,81

In the experiment for user 1, the surprised impression can be seen at the 18<sup>th</sup> to the 23<sup>rd</sup> seconds (in figure 10), this is because at that moment, the video shows an incident of a man sleeping directly on the train track as the train passes. And this can make the audience surprised in seeing the action. The surprised expression was also seen in the 44<sup>th</sup> minute to the end of the video, because at that moment the video showed that the man was not hurt even though he slept on the train track as the train passed. It can also make the audience surprised. For the results of experiments on one of the users, can be seen in the following Fig. 10.

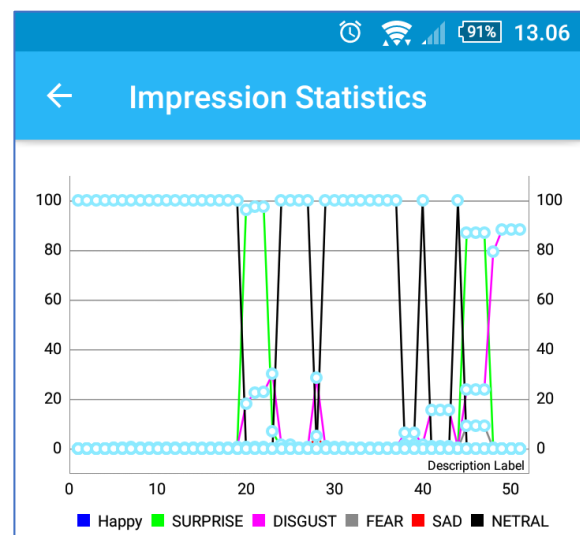


Fig. 10. Users impression detail result of video 3 by user 4 created by automatic video-metric system

### E. Accuracy

The last step of result validation is by getting feedback from users which have watched the videos using this application. By using questionnaire method, users are asked to compare the impression metric which have been created by system with their real feelings. In this research, feedbacks are collected from 20 respondents.

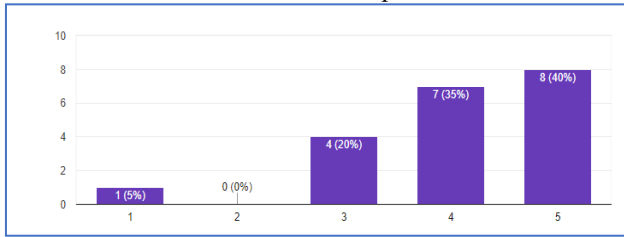


Fig. 11. Survey result from users' real feelings from 20 respondents

Respondents are asked to choose scale 1 – 5 corresponding to measurement accuracy. The scale 1-5 shows measurement accuracy of 20%, 40%, 60%, 80%, and 100% respectively. The accuracy of automatic video-metric measurement system from the results of user's feedback (refers to Fig.11) can be seen that 75% of respondents stated accuracy exceeds 80%, 20% of respondents said the accuracy is only about 60%, while one respondent stated accuracy of less than 20%.

### IV. CONCLUSION

The automatic user-video metric creations system has been able to measure user impressions with an accuracy of more than 80%. This level of accuracy is expressed by 75% of the 20 respondents during the test. In addition, it is known that the ideal distance the system needs to detect the emotions of a user's facial expressions is 20-40 cm from the front of the user's face.

From the results of user impression testing of video using a particular video on different users, the system produces different impressions result. As for things that affect the results of the measurement of the impression is the position of the smartphone to the user, the user's behaviour during watching the video, racial differences between the developer of emotion detection system with the respondents on the test, the difference of the category perception video tested, and the psychological condition of the respondent's influence during the test. In general, automated user-video metric creations systems have been able to work properly, with this result, this system can be used as prerequisite to create an impression-based model video recommender system in the future research.

### ACKNOWLEDGMENT

This research was partially supported by RISTEK DIKTI through Student Creativity Program (PKM). We thank our colleagues from Politeknik Elektronika Negeri Surabaya who provided insight and expertise that greatly assisted and testing the research results, although they may not agree with all of the interpretations/conclusions of this paper.

### REFERENCES

- [1] APJII Infographic Survei Presentation 2016. [Online]. Available: [https://apjii.or.id/downloadfile/downloadsurvei/infografis\\_apjii.pdf](https://apjii.or.id/downloadfile/downloadsurvei/infografis_apjii.pdf). [Accessed: 30-April- 2018].
- [2] Covington, Paul. Jay Adams. Emre Sargin “*Deep Neural Networks for YouTube Recommendations*”. Google Mountain View, CA. 2016.
- [3] D. McDuff, R. el Kaliouby, T. Senechal, M. Amr, J. F. Cohn and R. Picard. *Affectiva-MIT Facial Expression Dataset (AM-FED): Naturalistic and Spontaneous Facial Expressions Collected In-the-Wild*. IEEE Conference on Computer Vision and Pattern Recognition Workshops, Portland, OR, 2013, pp. 881-888. 2013.
- [4] McDuff, Daniel & Mahmoud, Abdelrahman & Mavadati, Mohammad & Amr, May & Turcot, Jay & el Kaliouby, Rana. *AFFDEX SDK: A Cross-Platform Real-Time Multi-Face Expression Recognition Toolkit*. (2016).
- [5] Statista. *Global mobile OS market share in sales to end users from 1st quarter 2009 to 1st quarter 2018*. 2018. [Online]. Available: <https://www.statista.com/statistics/266136/global-market-share-held-by-smartphone-operating-systems/>. [Accessed: 30-May-2018].
- [6] Maksym Petrenko, Amyris Rada, Garrett Fitzsimons, Enda McCallig, Calisto Zuzarte. *Best Practices Physical database design for data warehouse environments*. 2012.
- [7] C. Györödi, R. Györödi, G. Pecherle and A. Olah, "A comparative study: MongoDB vs. MySQL," 2015 13th International Conference on Engineering of Modern Electric Systems (EMES), Oradea, 2015, pp. 1-6.
- [8] Y. Li and S. Manoharan, "A performance comparison of SQL and NoSQL databases," 2013 IEEE Pacific Rim Conference on Communications, Computers and Signal Processing (PACRIM), Victoria, BC, 2013, pp. 15-19.
- [9] McDuff, D.J., Mahmoud, A.N., Mavadati, M., Amr, M., Turcot, J., & Kaliouby, R.E. (2016). *AFFDEX SDK: A Cross-Platform Real-Time Multi-Face Expression Recognition Toolkit*. CHI Extended Abstracts.
- [10] Rolfe Winton, Rana El Kaliouby. *Measuring Emotions Through A Mobile Device Across Borders, Ages, Genders and More*. ESOMAR. 2012



# Real Time SIBI Sign Language Recognition based on K-Nearest Neighbor

Fitrah Maharani Humaira  
Electrical Engineering  
Politeknik Negeri Madura  
Sampang, Indonesia  
humaira1124@yahoo.com

Supria  
Informatics Engineering  
Politeknik Negeri Bengkalis  
Riau, Indonesia  
phiya1287@gmail.com

Darlis Herumurti  
Department of Informatics  
Institut Teknologi Sepuluh Nopember  
Surabaya, Indonesia  
darlis@if.its.ac.id

Kukuh Widarsono  
Electrical Engineering  
Politeknik Negeri Madura  
Sampang, Indonesia  
kukuh@poltera.ac.id

**Abstract**— Persons with disabilities also have the right to communicate between each other, both with normal people and people with other disabilities. People with disabilities will be difficult to communicate with other people. They use ‘sign language’ to communicate. That’s why other normal people will be difficult to communicate with them. Because there are not many normal people that can understand the ‘sign language’. The system can help to communicate with disabilities people are needed. In this paper, we proposed sign language recognition for Sistem Isyarat Bahasa Indonesia (SIBI) using leap motion based on K-Nearest Neighbor. Technology of leap motion controller will generate the existence of coordinate points on each bone in hand. As an input, we used the value of distance between the coordinates of each bone distal to the position of the palm, which were measured using Euclidean Distance. This feature of distance will be used for training and testing data on K-Nearest Neighbor method. The experiment result shows that the best accuracy is 0,78 and error 0,22 with proposed parameter of K = 5.

**Keywords**— dissability, communication, sign language recognition, leap motion controller, K-nearest neighbor

## I. INTRODUCTION

People with special needs or disabilities are also part of society, where they have the same right to interact and socialize with the surrounding environment. Persons with disabilities, such as deaf and speech impaired sometimes looks like a normal person. However, problems arise when communication with others, the deaf cannot hear, whereas speech impaired cannot be answered conversation. Classically, this problem can be answered, in which the deaf using hearing aids. While the speech impaired using sign language, through hand gestures or body movements. While there are many different types of gestures, the most structured sets belong to the sign languages. In sign language, each gesture already has assigned meaning, and strong rules of context and grammar may be applied to make recognition tractable.

However, the constraints, if normal people who talk understands sign language, certainly not all. Therefore, this issue would have to find an alternative solution, need a system that can overcome these problem. In previous research, the technology used is Kinect camera or webcam-based image for sign language recognition. But has built research-based sign language recognition leap motion controller such as American Sign Language (ASL) [1], the introduction of sign language Arabic Sign Language (ArSL)

[2], [3]. In this paper, we proposed an identification of hand gesture alphabet using leap motion controller (LMC). Hopefully the system is able to overcome the weakness of communication with deaf and speech impaired and easier for normal people to communicate with them.

The study proposed a sign language recognition system using leap motion controller and K-Nearest Neighbor (KNN). By using the leap motion controller, every coordinate point bone in the hand will be detected, so that the coordinate points can be used as input feature. The use of distance feature between palm position with type distal measured by Euclidean distance. These features will be used for training and testing data for the k-nearest neighbor classification method. Training data used are 10 samples for each letter, the number of 26 letters of the alphabet, so that the total amount of training data 260 for one person.

Section II of this paper describes the related works. Section III describes the proposed algorithm used for SIBI recognition. The experimental results and conclusions are given in sections IV and V respectively.

## II. RELATED WORKS

### A. Sign Language Alphabet

Sign language alphabet or finger spelled alphabet is the process of spelling out words by using signs that correspond to the letters of the word. Sign language is a technique to interpret the writing alphabet of writing a signal in the form of motion of the fingers, hand shape, orientation and hand gestures. There is a sign language used by the deaf and speech impaired. There has been no successful international signaling alphabet is applied, because in each country have different sign language. Even in Indonesia, there are two types of alphabet sign language, namely: Bisindo (Bahasa Isyarat Indonesia) and SIBI (Sistem Isyarat Bahasa Indonesia) [3].

American Sign Language (ASL) is the dominant sign language used by deaf communities in the United States and most of Canada. Figure 1 is a American Sign Language Alphabet.

### B. Leap Motion Controller (LMC)

Leap Motion Controller (LMC) is a new technology developed by the Leap Motion Company. This USB-based technology is a sensor capable of detecting the movement of the hands and fingers, as well as small objects like a pen. This tool is made to replace the mouse and keyboard to

control or play computer using motion [1]. Figure 2 shows the shape leap motion, Figure 3 is a part-section of the leap motion.

The device is claimed to be even more precise 100x than Kinect, where accuracy in detecting each fingertip position is about 0.01 mm, with a frame rate of up to 200-300 fps. And be able to track all interactions finger of 10 users simultaneously [2]. LMC uses two high-precision infrared camera sensor and 3 LEDs to capture information in the hands of the active range. LMC create 3-dimensional space with the three axes, namely X, Y, and Z as shown in Figure 4 that can extend the distance range from about 1 inch to 2 meters.

Hand gesture detection is the first step in the identification of gesture recognition as the value of the alphabet. This detection task is to extract lines hands formed a whole region of the captured image. LMC is able to capture the image of a hand that can automatically separates the background, then we can ignore the morphological operations and hand detection can be done easily.

Color segmentation generates binary form. Using a binary image with a black area shows the region of the hand and the white area indicates the region of template. Here we consider the image of the hand will always be placed in the middle of a fixed-size frame, so that long-distance image capture of close hand will have no effect. Each image of the alphabet will be trained by 10 different hands image frame based on the long finger; the width of a finger; the position of the x, y, z axis; palms, and so on.

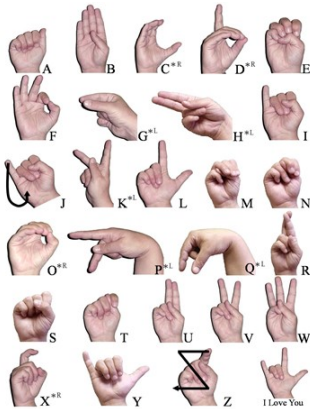


Fig.1. American Sign Language Alphabet



Fig. 2. Leap Motion Controller

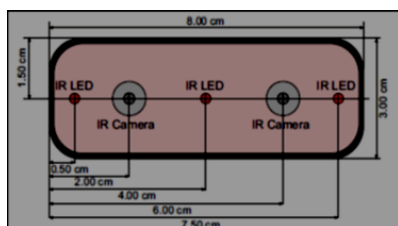


Fig. 3. Part-section of leap motion controller

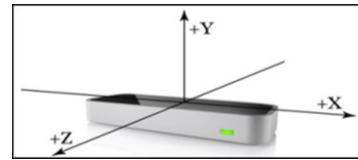


Fig. 4. 3-dimensional space of LMC

### C. K-Nearest Neighbor

Methods K-Nearest Neighbor (K-NN) becoming one of the oldest and popular methods based NN. K values used in here stated number of nearest neighbors were involved in the determination of the class label prediction on the test data. K nearest neighbors were voted then do voting class of the K nearest neighbors. Class with the highest number votes of neighbor given as class labels prediction results on the test data [4].

There are several key issues that affect the performance of KNN, including the vote of the value of K [5]. If K is too small, have consequences of bias prediction result which sensitive to the presence of noise. On the other hand, if K is too large then the selected nearest neighbor might be too much of another class that was not relevant because the distance is too far. To estimate the value of K at its best, can be done by using cross validation. It is important to affirm that  $k = 1$  may perform other K values, in particular for small data sets, including typically when used for research or practice in the classroom. However, if given sufficient samples, then the larger value of K will be more resistant to noise.

Another issue is the approach to combine classes. The simplest method is by majority vote as described above. However, it can be a problem if the nearest neighbor have varying distances, while neighbor closer more reliable shows the class label. More recent approach, which is usually much less sensitive to the choice of K, which is weighted by a nearest neighbor distance. Varying options that could be used e.g. weighting factor that is often taken from the inverse square of the distance, as in:

$$W_i = \frac{1}{d(x_i, z)^2} \quad (1)$$

$W_i$  is weights for the data  $x_i$  selected as nearest neighbors, whereas  $d(x_i, z)$  is the distance (dissimilarity) between data  $x_i$  of the test data  $z$ .

Another important issue on KNN weightlessness is the value of K is used, whether even or odd. For K odd with an even number of classes will facilitate voting because it is guaranteed there will be no two classes received the same voting power. However, if even, there will be the possibility of two classes received the same voting power. For the case when there are two or more classes with the same voting and the majority then the class label can be taken between classes earlier.

The algorithm to calculate the predicted outcome class voting or weighted class voting  $y'$  as in:

$$y' = \arg \max_{v \in C} \sum_{y_i \in D_z} w_i x I(v = y_i) \quad (2)$$

### III. RESEARCH METHOD

In this study, there are several stages in the process of introduction sign language using leap motion controller. The stages are collect distal phalanges coordinate data of each finger and palm position, measure the distance between each distal phalanges on each finger with the palm position and classify testing data towards training data using K-nearest Neighbor method. The general description of the proposed research methods can be seen in Figure 5.

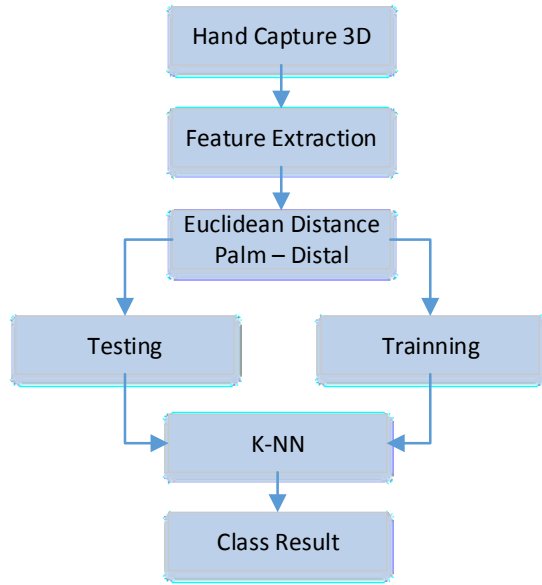


Fig. 5. SIBI recognition diagram

#### A. Preprocessing

Leap motion controller is used to capture hands to get the coordinate points on the hands. The coordinate points generated by a leap motion controller is palm position, the distal phalanges, intermediate phalanges, proximal phalanges, and metacarpals. In this study only used the coordinates of palm position and distal phalanges in each finger. The distance between the palm position and the distal phalanges measured by Euclidean distance, so that the distance is used as the input feature in this study.

#### B. Distance

To measure the distance  $d$  between the palm position and the distal phalanges used Euclidean distance, where measuring the distance from palm position with distal phalanges on every finger, namely the thumb, index finger, middle finger, ring finger and little finger. As for distance measurement using Euclidean distance can be seen in equation 3.

$$d(xyz) = \sqrt{(x_2 - x_1)^2 + (y_2 - y_1)^2 + (z_2 - z_1)^2} \quad (3)$$

#### C. Classification

K-nearest neighbor is the method used to predict the class of testing data which input based on class of training data

that were located closest to the class. Learning data projected onto many-dimensional space, where each dimension represents the features of the data. The space is divided into sections based on the learning data classification. A point in this space marked class  $c$  if class  $C$  is the most common classification  $k$  nearest neighbors on that point. Near or far neighbors are usually calculated based on Euclidean distance.

In the learning phase, the algorithm is simply to store the vectors of features and classification of learning data. In the classification phase, the same features that are calculated to test data (which classification is not known). The distance of this new vector of all learning data vector is calculated, and taken the number of closest  $k$ . New classification point predicted included in the classification most of these points.

The best value of  $K$  for this algorithm depends on the data; in general, a high  $k$  value will reduce the effect of noise on the classification, but makes the boundaries between each classification becomes more blurred. The great value of  $K$  can be selected with parameter optimization, for example by using cross-validation.

K-NN algorithm accuracy is greatly influenced by the presence or absence of features that are not relevant, or if the weight of such features is not equivalent to its relevance to the classification.

### IV. EXPERIMENT AND RESULT

This study focused on the introduction of 26 alphabet on Sistem Isyarat Bahasa Indonesia (SIBI). The data taken using leap motion controller. It is taken from the distal coordinate data on each finger and the data inputted is 15 frames hand training data for each letter of the alphabet so that a total of 390 frames as training data. Then for testing the data needed one hand frame. For an introduction to the alphabet used KNN (k-nearest neighbor) method. The feature used in here is a distance feature.

To measure the success of the proposed system is then measured by calculating the accuracy and error rate. For accuracy by calculating the correctly predicted total data to the total amount of data that is predictable. To calculate the accuracy of the results can be seen in equation 4. As for calculating the error rate (prediction error) is shown in equation 5.

$$Accuracy = \frac{\sum \text{true data prediction}}{\sum \text{all data prediction}} \times 100\% \quad (4)$$

$$Error \text{ rate} = \frac{\sum \text{false prediction data}}{\sum \text{all data prediction}} \times 100\% \quad (5)$$

The Results of SIBI sign language recognition accuracy by using leap motion controller and K-NN performed on the 26-letter alphabet. Testing is done in real-time towards training data. In this paper is determined 3 parameter value of  $K$  nearest neighbor namely 5, 10 and 15. The accuracy of the test results can be seen in Table 1, 2 and 3.

The results of SIBI sign language recognition by using leap motion controller based on KNN method has a very high accuracy. Still in a few letters have low accuracy due to leap motion controller cannot detect the coordinates when the area coordinate point is protected or covered by the toe or the other, and when the letters that have similar data is very high, the system is difficult to distinguish. For several letters

like the letter NR, C, F, L, O, P, W and Y have a very high accuracy, it is because all the coordinates of the finger not covered by sections other fingers, and also does not much similar with another letter.

The test results indicate that the parameter value  $K = 5$  has the highest accuracy compared with the  $K = 10$  and  $K = 15$ . It shows that the parameter value  $K = 5$  has the best average accuracy is 0,78 and error rate is 0,22.

## V. CONCLUSION

The study proposed a sign language recognition system using leap motion controller based on K-Nearest Neighbor. This system allows normal people to understand sign language by hand of the deaf and speech impaired. LMC as the latest infrared sensor technology that can detect the coordinate points on the hands and can facilitate the developer in terms of hand recognition. The results of SIBI sign language recognition by using leap motion controller based on KNN method has a very high accuracy. In the

future, this system is suitable to applied by people with disabilities, especially the deaf and speech impaired to communicate not only the alphabet, but has been able to detect word by word.

## REFERENCES

- [1] C. Chuan, E. Regina, C. Guardino, A. L. M. Controller, and I. Apis, "American Sign Language Recognition Using Leap Motion Sensor," pp. 541–544, 2014.
- [2] M. Mohandes, S. Aliyu, and M. Deriche, "Arabic Sign Language Recognition using the Leap Motion Controller," 2014.
- [3] A. S. Elons, M. Ahmed, H. Shedid, and M. F. Tolba, "Arabic Sign Language Recognition Using Leap Motion Sensor," pp. 368–373, 2014.
- [4] S. Tan, "Neighbor-weighted K-nearest neighbor for unbalanced text corpus," *Expert Syst. Appl.*, vol. 28, no. 4, pp. 667–671, 2005.
- [5] X. Wu, V. Kumar, Q. J. Ross, J. Ghosh, Q. Yang, H. Motoda, G. J. McLachlan, A. Ng, B. Liu, P. S. Yu, Z.-H. Zhou, M. Steinbach, D. J. Hand, and D. Steinberg, *Top 10 algorithms in data mining*, vol. 14, no. 1. 2008.

TABLE 1. Accuracy Result with  $K = 5$

Recognition	Accuracy (%)	Error (%)	Recognition	Accuracy (%)	Error (%)
NR	1,0	0	N	0,4	S(0,2), T(0,4)
A	0,6	G(0,2), O(0,2)	O	1,0	0
B	0,8	W(0,2)	P	1,0	0
C	1,0	0	Q	0,8	L(0,2)
D	0,8	X(0,2)	R	0,8	U(0,2)
E	0,4	G(0,2), M(0,2), T(0,2)	S	0,4	E(0,2), T(0,4)
F	1,0	0	T	0,4	A(0,2), N(0,2), S(0,2)
G	0,6	Q(0,4)	U	0,4	H(0,2), K(0,2), R(0,2)
H	0,4	K(0,2), R(0,4)	V	0,6	K(0,2), U(0,2)
I	0,8	Z(0,2)	W	1,0	0
J	0,8	I(0,2)	X	0,6	D(0,2), Z(0,2)
K	0,6	W(0,4)	Y	1,0	0
L	1,0	0	Z	0,8	D(0,2)
M	0,6	E(0,1), S(0,2)			
Average Accuracy					<b>0.78</b>
Average Error					<b>0.22</b>

TABLE 2. Accuracy Result with  $K = 10$

Recognition	Accuracy (%)	Error (%)	Recognition	Accuracy (%)	Error (%)
NR	1,0	0	N	0,5	A(0,1), S(0,2), T(0,2)
A	0,6	G(0,2), O(0,2)	O	0,6	A(0,1), E(0,3)
B	0,5	NR(0,1), W(0,4)	P	0,6	K(0,4)
C	0,9	O(0,1)	Q	0,6	G(0,2), L(0,2)
D	0,9	P(0,1)	R	0,4	H(0,3), K(0,1), U(0,2)
E	0,6	M(0,2), T(0,2)	S	0,4	A(0,3), E(0,1), N(0,1), T(0,1)
F	1,0	0	T	0,3	A(0,2), M(0,2), N(0,2), S(0,1)
G	0,6	L(0,1), Q(0,2), X(0,1)	U	0,6	H(0,3), K(0,1)
H	0,3	K(0,2), R(0,3), U(0,2)	V	0,7	K(0,2), U(0,1)
I	0,4	J(0,2), Y(0,4)	W	0,9	B(0,1)
J	0,5	I(0,4), Y(0,1)	X	0,7	P(0,1), Z(0,2)
K	0,6	P(0,4)	Y	1,0	0
L	0,6	Q(0,4)	Z	0,8	D(0,2)
M	0,3	E(0,1), N(0,1), S(0,2), T(0,3)			

Average Accuracy	<b>0.63</b>
Average Error	<b>0.37</b>

TABLE 3  
Accuracy Result with K = 15

Recognition	Accuracy (%)	Error (%)	Recognition	Accuracy (%)	Error (%)
NR	1,0	0	N	0,27	A(0,07), E(0,2), M(0,13), S(0,2), T(0,13)
A	0,6	E(0,07), G(0,07), M(0,07), N(0,2)	O	0,47	C(0,13), E(0,2), G(0,07), N(0,13)
B	1,0	0	P	0,4	H(0,2), K(0,27), V(0,07), Z(0,07)
C	0,7	N(0,13)	Q	0,53	G(0,27), L(0,2)
D	0,73	P(0,07), X(0,2)	R	0,33	H(0,13), K(0,07), U(0,13), V(0,33)
E	0,53	M(0,27), S(0,07), T(0,13)	S	0,4	A(0,2), E(0,07), M(0,07), O(0,07), T(0,2)
F	0,93	NR(0,07)	T	0,33	E(0,27), M(0,27), N(0,07), S(0,07)
G	0,73	L(0,07), Q(0,2)	U	0,4	H(0,27), K(0,2), R(0,13)
H	0,33	K(0,2), R(0,27), U(0,2)	V	0,4	H(0,13), K(0,27), R(0,13), U(0,07)
I	0,6	J(0,4)	W	0,67	NR(0,07), B(0,27)
J	0,47	I(0,27), Y(0,27)	X	0,53	Z(0,33), D(0,07), P(0,07)
K	0,47	H(0,07), U(0,07), V(0,4)	Y	0,93	J(0,07)
L	0,67	Q(0,33)	Z	0,53	D(0,33), X(0,13)
M	0,4	E(0,27), N(0,07), S(0,13), T(0,13)			
Average Accuracy				<b>0.59</b>	
Average Error				<b>0.41</b>	



# Artificial Neural Network Parameter Tuning Framework For Heart Disease Classification

M. Haider Abu Yazid  
Faculty of Computing  
Universiti Teknologi Malaysia  
(UTM)  
Johor Bahru, Malaysia  
mhaider04@gmail.com

Muhammad Haikal Satria  
Faculty of Bioscience and  
Medical Engineering  
Universiti Teknologi Malaysia  
(UTM)  
Johor Bahru, Malaysia  
mhaikal@utm.my

Shukor Talib  
Faculty of Computing  
Universiti Teknologi Malaysia  
(UTM)  
Johor Bahru, Malaysia  
shukor@utm.my

Novi Azman  
Faculty of Engineering and  
Science  
Universitas Nasional  
Jakarta, Indonesia  
novi.azman@civitas.unas.ac.id

**Abstract**— Heart Disease are among the leading cause of death worldwide. The application of artificial neural network as decision support tool for heart disease detection. However, artificial neural network required multitude of parameter setting in order to find the optimum parameter setting that produce the best performance. This paper proposed the parameter tuning framework for artificial neural network. Statlog heart disease dataset and Cleveland heart disease dataset is used to evaluate the performance of the proposed framework. The results show that the proposed framework able to produce high classification accuracy where the overall classification accuracy for Cleveland dataset is 90.9% and 90% for Statlog dataset.

**Keywords**—artificial neural network, heart disease classification, artificial neural network parameter tuning, statlog heart dataset, cleveland heart dataset.

## I. INTRODUCTION

Heart disease describes a range of conditions that affect your heart. Heart disease is under umbrella of cardiovascular disease in which are the leading cause of death worldwide where more people die from cardiovascular diseases compared to any other causes annually. Mortality for heart disease is projected to be increase to reach 23.3 million by the year of 2030 where heart disease will remain to be the leading cause of death for human. It became imperative to diagnose the presence of heart disease in the early stages in order to contain the disease from worsening. The early detection of heart disease can help the patient to adjust lifestyle and also help the medical professionals to prescribe appropriate medicine. However, the diagnosing patient with the presence of heart disease can be challenging where it depends on medical professional's experience and intuition [12,13]. It is imperative for medical professionals to have a system that can help them predict and classify the patient who have high risk of getting heart disease.

The implementation of machine learning algorithm can help medical professionals in diagnosing the presence of heart

disease in the patient. Machine learning algorithm have become very popular for solving classification problems where it is capable of mapping the relationship between variables or attributes with minimal human effort

Artificial Neural Network (ANN) are among the most popular machine learning algorithm where it proves to be powerful tools for mapping nonlinear data and are known to be useful in solving nonlinear problems where the rules to solve the problem is difficult to obtain or unknown. However, Artificial Neural Network required a lot of parameter setting where parameter tuning often been done by trial and error. Feed forward back propagation neural network are the most commonly used type of artificial neural network and it requires the users to specify several parameters including the numbers of hidden layer, the numbers of hidden nodes, training algorithm and type of transfer function.

Presently, there are 13 types of training algorithm and 10 types of transfer function. The numbers of possible combination parameters that can be used can range from 1300 up until 130000 depending on the numbers of hidden layers specified by the users. The trial and error approach consuming enormous amount of time and does not guarantee the model to obtain the best possible classification accuracy.

This paper presents the parameter tuning framework for artificial neural network in order to find the optimal artificial neural network parameters for heart disease classification. Statlog heart disease dataset and Cleveland heart disease dataset obtain from UCI machine learning data repository are used to measure the performance of proposed parameter tuning framework.

## II. ARTIFICIAL NEURAL NETWORK MODEL

A neural network consists of an interconnected group of artificial neurons, and it processes information using a connectionist approach to computation. ANN has been implemented in various fields. In healthcare, ANN is implemented for clinical diagnosis, drug development, image analysis and signal analysis [1]. ANN had proven to be useful for modeling complex relationships between inputs and outputs or to find patterns in data. Basically, feed forward

neural network consists three main layers which are input layer, hidden layer and output layer. Input and output are usually consisting 1 layer and hidden layer could consist minimum 1 layer. Figure 1 shows the examples of feed forward neural network architecture. The numbers of input nodes and output nodes depends on the collected data while the numbers of hidden nodes for ANN are based on trial and error.

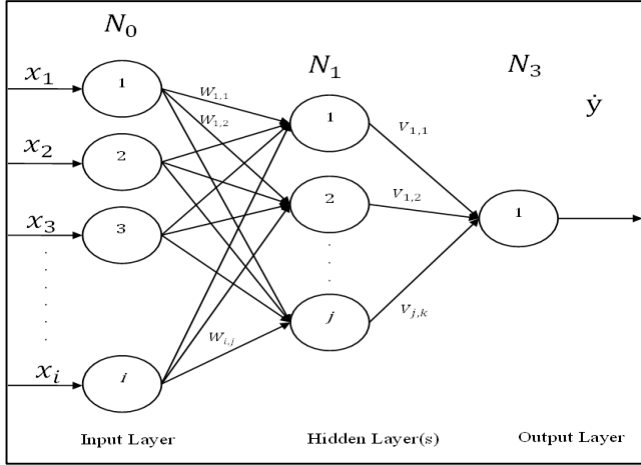


Figure 1 Basic Neural Network Architecture

### III. PARAMETER TUNING FRAMEWORK

Main parameters setting for Feed Forward Backpropagation consist of network structures (number of hidden layer and hidden nodes), training algorithm and types of transfer function. Additional parameter setting will be required depending on types of training algorithm used. Table 1 show the list of main parameters setting for Feed Forward Backpropagation Neural Network.

The numbers of hidden layer usually depending on the user definition. However, most of the previous research only use 1 or 2 hidden layers which enough to obtain the optimum performance. The increase number of hidden layers will increase the run time taken for neural network classification. Low numbers of hidden nodes may result in decreases of neural network classification accuracy. However, the high numbers of hidden nodes may increase neural network accuracy but will increase neural network run time. Previous research has proposed the number of hidden nodes to be at certain numbers depending on the number of input nodes. The number of hidden nodes recommended by previous research is according to “ $n/2$ ”, “ $1n$ ”, “ $2n$ ” and “ $2n+1$ ” where  $n$  is the number of input nodes [33]. However, this guideline does not guarantee the optimum number of hidden nodes required by the neural network to achieve optimum classification accuracy.

The proposed parameter tuning framework consist of several phase. The first phase selects the training algorithm while the second phase select transfer function. The third phase will select the hidden nodes number and the last phase will simulate the neural network using the parameters obtain in phase 1, 2 and 3. In the last phase, the neural network will be simulated numerous time in order to find the best weight and bias that produce the highest classification accuracy.

Figure 2 shows the proposed artificial neural network parameter tuning framework.

Table 1: Feed Forward Backpropagation Parameter Setting

Hidden Layer	Hidden Nodes	Training Algorithm and Additional Parameters	Transfer Function
1-3	10- $\infty$	<ul style="list-style-type: none"> <li>a. BFGS quasi-Newton backpropagation</li> <li>b. Bayesian Regulation backpropagation</li> <li>c. Conjugate gradient backpropagation with Powell-Beale restarts</li> <li>d. Fletcher-Reeves Conjugate Gradient</li> <li>e. Polak-Ribière Conjugate Gradient</li> <li>f. Gradient descent back propagation <ul style="list-style-type: none"> <li>• Learning Rate Parameter</li> </ul> </li> <li>g. Gradient descent with adaptive learning rate back propagation <ul style="list-style-type: none"> <li>• Learning Rate Parameter</li> <li>• Momentum Parameter</li> </ul> </li> <li>h. Gradient descent with momentum <ul style="list-style-type: none"> <li>• Learning Rate Parameter</li> <li>• Momentum Parameter</li> </ul> </li> <li>i. Gradient descent with momentum and adaptive learning rate back propagation <ul style="list-style-type: none"> <li>• Momentum Parameter</li> </ul> </li> <li>j. Lavenberg - Marquadt</li> <li>k. One Step Secant</li> <li>l. Resilient Back propagation</li> <li>m. Resilient Back propagation</li> </ul>	<ul style="list-style-type: none"> <li>a. Hard Limit</li> <li>b. Symmetrical Hard Limit</li> <li>c. Linear</li> <li>d. Saturating Linear</li> <li>e. Symmetric Saturating Linear</li> <li>f. Log-Sigmoid</li> <li>g. Hyperbolic Tangent Sigmoid</li> <li>h. Positive Linear</li> <li>i. Softmax</li> <li>j. Competitive</li> </ul>

The first phase of the framework selects the suitable training algorithm for the each of the dataset. The most commonly used transfer function is used in the first phase. Table 2 shows the setup for first phase of proposed parameter tuning algorithm. In the first phase, all the training algorithm are simulated for five times of iteration to find the best performance from the different training algorithm. Each of the training algorithm will produce five different result for every iteration and the algorithm with the highest average overall accuracy will be chosen as a training algorithm. After the training algorithm is selected, phase 2 simulation is conducted.

For the phase 2, the transfer function combination has to be generated first. The transfer function combination is the possible combination of transfer function that can be use in hidden layer and output layer. This combination depending on the number of hidden layer and the number of transfer function that the users planned to use. This research uses 1 hidden layer with 10 types of transfer function. Table 3 shows the examples of transfer function combination. The initial neural network parameter and simulation parameter is defined after the transfer function combination is generated. Table 4 shows the neural network initial parameters and table 5 shows the simulation parameter. Neural network initial parameters specify the number of initial hidden nodes, training algorithm (selected from phase 1 of the framework), performance function and data partition setup. There 3 types of data used for simulation. Training dataset is used to train the network where the weight and bias is adjusted during training process. The validation dataset is used to validate the performance of the neural network. If the accuracy of validation dataset does not achieve the minimum accuracy desired by the user, the training process will be done again. The test dataset then will be used to evaluate the neural network model

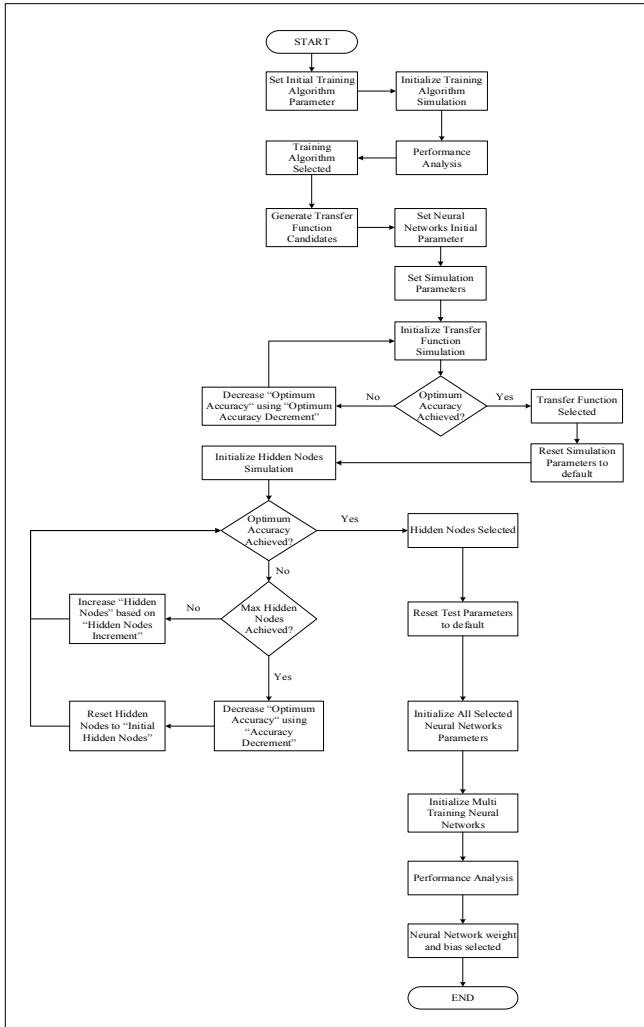


Figure 2. Artificial Neural Network Parameter Tuning Framework

The simulation parameter will be set once the neural network parameter is defined. The simulation parameter includes initial optimum accuracy, accuracy decrement, hidden nodes increment, and iteration for phase 2,3 and 4. Initial optimum accuracy is the user's desired validation dataset accuracy. Accuracy decrement is the decrement of optimum accuracy and iteration is the number of iterations per phase. Hidden nodes increment is the parameter used to increase the hidden nodes value and the maximum hidden nodes is the maximum value of increased hidden nodes.

In phase 2, every combination of transfer function is simulated based on the number of iterations specifies by the users. Any combination of transfer function that achieved the "optimum accuracy" will be stored in the array. Optimum accuracy however will be changed according to "accuracy decrement" if there are no combination of transfer function achieved optimum accuracy during the specified iteration. The new "optimum accuracy" is calculated using equation (1).

$$\begin{aligned} \text{Optimum Accuracy}_i &= \text{Optimum Accuracy}_{i-1} \\ &\quad - \text{accuracy decrement} \end{aligned} \quad (1)$$

Table 2: Initial Training Algorithm Parameter

Hidden Layer	Hidden Nodes	Training Algorithm	Transfer Function		Iteration
			1st Layer	Output	
1	13	n. BFGS quasi-Newton backpropagation o. Bayesian Regulation back propagation p. Conjugate gradient backpropagation with Powell-Beale restarts q. Fletcher-Reeves Conjugate Gradient r. Polak-Ribière Conjugate Gradient s. Gradient descent back propagation t. Gradient descent with adaptive learning rate back propagation u. Gradient descent with momentum v. Gradient descent with momentum and adaptive learning rate back propagation w. Lavenberg - Marquadt x. One Step Secant y. Resilient Back propagation z. Resilient Back propagation	Log - Sigmoid	Log - Sigmoid	5

Where  $i$  is the current cycle of phase 2. The cycle will be repeated until the combination of transfer function that achieved "optimum accuracy" is found. After the phase 2 completed, the simulation parameter will be reset to the initial value specify by the users. The phase 3 will be execute after the simulation parameter is reset and neural network parameter is updated. The updated neural network parameter consists of the combination of transfer function that achieved the optimum accuracy in phase 2 and the training algorithm obtained from phase 1. For the phase 3, the initial hidden nodes values are set according to the number of dataset input. If the optimum accuracy is not achieved during the specifies iteration, the number of hidden nodes will be updated using equation (2).

$$\begin{aligned} \text{hidden nodes}_j &= \text{hidden nodes}_{j-1} \\ &\quad + \text{hidden nodes increment} \end{aligned} \quad (2)$$

Table 3: Examples of transfer function combination

1 <sup>st</sup> Hidden Layer Transfer Function	Output Layer Transfer Function
Hard Limit	Hard Limit
Symmetrical Hard Limit	Hard Limit
Linear	Hard Limit
Saturating Linear	Hard Limit
Symmetric Saturating Linear	Hard Limit
Log-Sigmoid	Hard Limit
Hyperbolic Tangent Sigmoid	Hard Limit
Positive Linear	Hard Limit
Softmax	Hard Limit
Competitive	Hard Limit
Hard Limit	Symmetrical Hard Limit
Symmetrical Hard Limit	Symmetrical Hard Limit
.	.
.	.
.	.
Competitive	Symmetrical Hard Limit

•	•
•	•
•	•
Hard Limit	Competitive
•	•
•	•
•	•
Softmax	Competitive
Competitive	Competitive

Table 4: Neural Network Initial Parameter

Initial Hidden Layer	Initial Hidden Nodes	Training Algorithm	Performance Function	Data Setup
1	13	Selected After Phase 1	Mean Squared Error	1. Training Dataset 2. Validation Dataset 3. Test Dataset

Table 5: Simulation Parameter

Initial Optimum Accuracy	Accuracy Decrement	Hidden Nodes Increment	Maximum Hidden Nodes	Iteration Phase 2&3	Iteration Phase 4
90	5	10	100	50	1000

Where  $j$  is the current cycle of phase 3. However, the optimum accuracy is not achieved even though the number of hidden nodes has increased equal to the number of “maximum hidden nodes”, the optimum accuracy will be updated using equation (1) and the new cycle of phase 3 will be restarted until the optimum accuracy is achieved. Phase 4 will be initiated once the optimum accuracy is achieved and the neural network parameters is updated with the optimum value of hidden nodes.

In phase 4, the neural network model using the parameters obtain in phase 1,2 and 3 will be simulated numerous times. Every iteration will be flagged with an “iteration identification” in order to find which iteration produce the best accuracy. Weight and bias for every iteration also is stored and flagged with “iteration identification”. After all iteration in phase 4 is completed, the algorithm will sort the results according to the validation dataset classification accuracy. The iteration identification will determine which iteration produce the highest accuracy of classification. The weight and bias of iteration with the highest classification will be extracted from the array. The neural network model with optimize parameters and the best weight and bias is simulated using test dataset for evaluation.

The proposed framework uses two sets of heart disease data taken from UCI machine learning data repository. The Statlog dataset and Cleveland Heart dataset is used to evaluate the performance of proposed framework. The result of simulation then compared to the reported results published by the previous research. Dataset is partition into ratio of 80% for training, 10% for validation and 10% for testing.

#### IV. RESULTS

##### A. Parameter Tuning Result

Table 6 shows the parameter obtain from the proposed framework while table 7 shows classification result of heart disease dataset.

Table 6: Neural network parameter obtain by the proposed framework

Dataset	Training Algorithm	Hidden Layer	Hidden Nodes	Transfer Function	
				1st Hidden Layer	Output Layer
Cleveland Dataset	Lavenberg - Marquadt	1	33	Saturating Linear	Linear

Statlog Dataset	Fletcher-Reeves Conjugate Gradient	1	23	Symmetrical Hard Limit	Hyperbolic Tangent Sigmoid
-----------------	------------------------------------	---	----	------------------------	----------------------------

Table 7: Heart disease classification accuracy

Dataset	Training Dataset	Validation Dataset	Test Dataset	Overall Accuracy
Cleveland Dataset	91.1	80	100	90.9
Statlog Dataset	90.7	81.5	92.6	90.0

##### B. Comparison with Previous Research

Table 8 and 9 shows the comparison of classification accuracy for Cleveland and Statlog dataset between previously proposed algorithm and the proposed framework.

Table 8: Cleveland Dataset

Algorithm	Accuracy (%)
Weighted Fuzzy [12]	57.85
Attribute weighted artificial immune system [19]	82.59
Artificial Immune System [19]	84.5
Modified Artificial Immune System [20]	87.43
IB1-4 [22]	50
C5.0 Tree [21]	53.1
J48 [21]	54.4
DKP C [21]	57.6
Random Forest [21]	58
InductH [23]	58.5
SVM C [21]	58.6
RBF [22]	60
FOIL [23]	64
MLP [22]	65.6
T2 [23]	68.1
1R [23]	71.4
IB1c [23]	74
K* [23]	76.7
Logistic regression [24]	77
C4.5 [25]	81.11
Naïve Bayes [25]	81.48
BNND [25]	81.11
BNNF [25]	80.96
AIRS [23]	84.5
AIRS [27]	84.5
Fuzzy-AIRS-Knn based system [26]	87
Artificial neural network (ANN) + Fuzzy neural network (FNN) [29]	86.8
Combining of linear kernel F-score feature selection and ANN [28]	80.74
Combining of RBF kernel F-score feature selection and LS-SVM classifier [28]	83.7
SAS base-Neural networks ensemble [30]	89.01
FDT [31]	77.55
Structural least square twin support vector machine (S-LSTSVM) [32]	87.82
<b>Parameter Tuned ANN</b>	<b>90.9</b>

Table 9: Statlog Dataset

Algorithm	Accuracy (%)
MARS-LR [14]	83.93
Weighted Fuzzy [12]	62
Fuzzy neurogenetic [15]	80
ANN-FNN [16]	87
CHAID [17]	76.6
CRT [17]	76.6
MLP [17]	83.3
RBFN [17]	84.6
ANFIS_LSLM [18]	76.7
ANFIS_LSGD [18]	75.6
1R [18]	71.4
T2 [18]	68.1
FOIL [18]	64
RBF [18]	60
InductH [18]	58.5
<b>Parameter Tuned ANN</b>	<b>90</b>

## V. DISCUSSION

This paper proposed the artificial neural network parameter tuning for heart disease classification. The result shows that the proposed framework able to achieve high classification accuracy with the overall accuracy of 90.9% for Cleveland dataset and 90% of classification accuracy for Statlog dataset. The proposed framework also outperforms previous proposed algorithm. The parameter obtain by the proposed framework is differ from each dataset. It shows that different dataset may have different set of optimal parameters.

## ACKNOWLEDGMENT

This research funded by University Technology of Malaysia (UTM) via Research University Grant (RUG) Tier 1 with vote no (PY/2017/00781).

## REFERENCES

- [1] Remzi M, Anagnostou T, Ravary V, Zlotta A, Stephan C, Marberger M, Djavan B. "An artificial neural network to predict the outcome of repeat prostate biopsies." *Urology*. 2003 Sep;62(3):456-60
- [2] Tu JV: "Advantages and disadvantages of using artificial neural networks versus logistic regression for predicting medical outcomes." *Journal of Clinical Epidemiol*. 1996, 49: 1225-31. 10.1016/S0895-4356(96)00002-9.
- [3] Demuth, Howard, and Mark Beale. "Neural Network Toolbox." For Use with MATLAB. The MathWorks Inc 2000 (1992).
- [4] Lagu, Tara, Penelope S. Pekow, Meng-Shiou Shieh, Mihaela Stefan, Quinn R. Pack, Mohammad Amin Kashef, Auras R. Atreya, Gregory Valania, Mara T. Slawsky, and Peter K. Lindenauer. "Validation and Comparison of Seven Mortality Prediction Models for Hospitalized Patients With Acute Decompensated Heart FailureCLINICAL PERSPECTIVE." *Circulation: Heart Failure* 9, no. 8 (2016): e002912.
- [5] Zhang, Guoqiang, B. Eddy Patuwo, and Michael Y. Hu. "Forecasting with artificial neural networks:: The state of the art." *International journal of forecasting* 14, no. 1 (1998): 35-62.
- [6] Givertz, Michael M., John R. Teerlink, Nancy M. Albert, Cheryl A. Westlake Canary, Sean P. Collins, Monica Colvin-Adams, Justin A. Ezekowitz et al. "Acute decompensated heart failure: update on new and emerging evidence and directions for future research." *Journal of cardiac failure* 19, no. 6 (2013): 371-389.
- [7] Lee, Douglas S., Peter C. Austin, Jean L. Rouleau, Peter P. Liu, David Naimark, and Jack V. Tu. "Predicting mortality among patients hospitalized for heart failure: derivation and validation of a clinical model." *Jama* 290, no. 19 (2003): 2581-2587.
- [8] Amato, Filippo, Alberto López, Eladia María Peña-Méndez, Petr Vaňhara, Aleš Hampl, and Josef Havel. "Artificial neural networks in medical diagnosis." *Journal of applied biomedicine* 11, no. 2 (2013): 47-58.
- [9] Martin T. Hagan , Howard B. Demuth , Mark Beale, "Neural network design." PWS Publishing Co., Boston, MA, 1997
- [10] Demuth, Howard, and Mark Beale. "Neural Network Toolbox." For Use with MATLAB. The MathWorks Inc 2000 (1992).
- [11] Farmakis, Dimitrios, et al. "Acute heart failure: epidemiology, risk factors, and prevention." *Revista Española de Cardiología (English Edition)* 68.3 (2015): 245-248.
- [12] Anooj, P. K. "Clinical decision support system: Risk level prediction of heart disease using weighted fuzzy rules." *Journal of King Saud University-Computer and Information Sciences* 24, no. 1 (2012): 27-40.
- [13] Hedeshi, N. Ghadiri, and M. Saniee Abadeh. "Coronary artery disease detection using a fuzzy-boosting PSO approach." *Computational intelligence and neuroscience* 2014 (2014): 6.
- [14] Y. E. Shao, C.-D. Hou, and C.-C. Chiu, "Hybrid intelligent modeling schemes for heart disease classification," *Applied Soft Computing Journal*, vol. 14, pp. 47–52, 2014.
- [15] K.Vijaya,H. K.Nehemiah,A.Kannan, andN.G.Bhuvaneswari, "Fuzzy neuro genetic approach for predicting the risk of cardiovascular diseases," *International Journal of Data Mining, Modelling and Management*, vol. 2, no. 4, pp. 388–402, 2010.
- [16] H. Kahramanli and N. Allahverdi, "Design of a hybrid system for the diabetes and heart diseases," *Expert Systems with Applications*, vol. 35, no. 1-2, pp. 82–89, 2008.
- [17] Nahato, Kindie Biredagn, Khanna Nehemiah Harichandran, and Kannan Arputharaj. "Knowledge mining from clinical datasets using rough sets and backpropagation neural network." *Computational and mathematical methods in medicine* 2015 (2015).
- [18] Sagir, Abdu Masanawa, and Saratha Sathasivam. "A Novel Adaptive Neuro Fuzzy Inference System Based Classification Model for Heart Disease Prediction." *Pertanika Journal of Science & Technology* 25, no. 1 (2017).
- [19] Polat, K. , Sahan, S. , Kodaz, H. , & Günes, S. (2005). A new classification method to diagnosis heart disease: Supervised artificial immune system (AIRS). In *Proceedings of the Turkish symposium on artificial intelligence and neural networks (TAINN)*.
- [20] Ozsen, S. , & Gunes, S. (2009). Attribute weighting via genetic algorithms for at- tribute weighted artificial immune system (AWAIS) and its application to heart disease and liver disorders problems. *Expert Systems with Applications*, Elsevier, 36 (1), 386–392
- [21] Fern´andez-Delgado M, Cernadas E, Barro S, Amorim D (2014) Do we need hundreds of classifiers to solve real world classification problems? *J Mach Learn Res* 15:3133–3181
- [22] Polat K, G˘unes S, Tosun S (2006) Diagnosis of heart disease using artificial immune recognition system and fuzzy weighted pre-processing. *Pattern Recogn* 39(11):2186–2193.
- [23] Das R, Turkoglu I, Sengur A (2009) Effective diagnosis of heart disease through neural networks ensembles. *Expert Syst Appl* 36(4):7675–7680.
- [24] Detrano R, Janosi A, Steinbrunn W, Pfisterer M, Schmid JJ, Sandhu S, Guppy KH, Lee S, Froelicher V (1989) International application of a new probability algorithm for the diagnosis of coronary artery disease. *Am J Cardio* 64(5):304–310.
- [25] Cheung N (2001) Machine learning techniques for medical analysis. School of Information Technology and Electrical Engineering, BSc Thesis, University of Queensland.
- [26] Polat K, Sahan S, G˘unes S (2007) Automatic detection of heart disease using an artificial immune recognition system (AIRS) with fuzzy resource allocation mechanism and k-nn (nearest neighbour) based weighting preprocessing. *Expert Syst Appl* 32(2):625–631.
- [27] Polat K, G˘unes S, Tosun S (2006) Diagnosis of heart disease using artificial immune recognition system and fuzzy weighted pre-processing. *Pattern Recogn* 39(11):2186–2193.
- [28] Polat K, G˘unes S (2009) A new feature selection method on classification of medical datasets: Kernel f-score feature selection. *Expert Syst Appl* 36(7):10,367–10,373.
- [29] Kahramanli H, Allahverdi N (2008) Design of a hybrid system for the diabetes and heart diseases. *Expert Syst Appl* 35(1-2):82–89.



- [30] Das R, Turkoglu I, Sengur A (2009) Effective diagnosis of heart disease through neural networks ensembles. *Expert Syst Appl* 36(4):7675–7680
- [31] El-Bialy R, Salamay MA, Karam OH, Khalifa ME (2015) Feature analysis of coronary artery heart disease data sets. *Procedia Comput Sci* 65:459–468.
- [32] Xu Y, Pan X, Zhou Z, Yang Z, Zhang Y (2015) Structural least square twin support vector machine for classification. *Appl Intell* 42(3):527–536.
- [33] Zhang, Guoqiang, B. Eddy Patuwo, and Michael Y. Hu. "Forecasting with artificial neural networks:: The state of the art." *International journal of forecasting* 14, no. 1 (1998): 35-62

# Winter Exponential Smoothing: Sales Forecasting on Purnama Jati Souvenirs Center

Fahrobby Adnan  
Faculty of Computer Science  
University of Jember  
Jember, Indonesia  
fahrobby@unej.ac.id

Putri Damayanti  
Faculty of Computer Science  
University of Jember  
Jember, Indonesia

Gama Wisnu Fajarianto  
Faculty of Computer Science  
University of Jember  
Jember, Indonesia

Antonius Cahya Prihandoko  
Faculty of Computer Science  
University of Jember  
Jember, Indonesia

**Abstract**— Forecasting is the process of making predictions of the future based on past and present data and most commonly by analysis of trends. In sales area, an accurate sales forecasting system will help the company to improve the customers' satisfaction, reduce destruction of products, increase sales revenue and make production plan efficiently. Purnama Jati is a typical Jember souvenir place like "prol tape", "pia tape", "brownies tape" and so forth. Every day, sales on every outlet is uncertain so Purnama Jati repeatedly send to the outlets if the stock has run out. This research will focus on "prol tape" cake, "pia tape" cake product as the research object. In this research we will use winter exponential smoothing as a forecasting method due to suitable character with the case.

**Keywords:** forecasting, sales, purnama jati

## I. INTRODUCTION

Forecasting is the process of making predictions of the future based on past and present data and most commonly by analysis of trends[1]. A commonplace example might be estimation of some variable of interest at some specified future date. In sales area, an accurate sales forecasting system will help the company to improve the customers' satisfaction, reduce destruction of products, increase sales revenue and make production plan efficiently[2].

Purnama Jati is one of famous souvenir center in the city. Purnama Jati is a typical Jember souvenir place like "prol tape", "pia tape", "brownies tape" and so forth. Almost all Purnama Jati products are "tape" based. "Tape" is a snack generated from the fermentation process of carbohydrate foods (cassava) as the substrate by yeast. Purnama Jati produces several products every day such as prol tape and pia tape because these two products are the best selling in the market. Then the products will distribute to all outlets. Every day, sales on every outlet is uncertain, so Purnama Jati repeatedly send to the outlets if the stock has run out. As a result, in a day Purnama Jati can perform several times production. Repeated production certainly waste

time and money. This research will focus on "prol tape" cake, "pia tape" cake product as the research object.

This research was conducted to produce the correct forecasting with case study at Purnama Jati souvenir center. In this case, we realize that there is a need of information. An information that figure the amount of "how much stock that they need?". The stock is related with the question "how much the next product sold out?". Based on this need, in this research we will do forecasting for the product sales.

In this research we will use winter exponential smoothing as a forecasting method. We will try to forecast sales for the next day. By doing the forecasting, we will figure out how accurate are the method implementation to the Purnama Jati sales data pattern by calculating the percentage error.

## II. METHODS

Sales data pattern on Purnama Jati are stationary (Fig.1), trend (Fig.2) and seasonal patterns (Fig.3). The stationary data is closely related to the statistical habits of data at a given time and this is often characterized by a constant probability distribution over time[3].

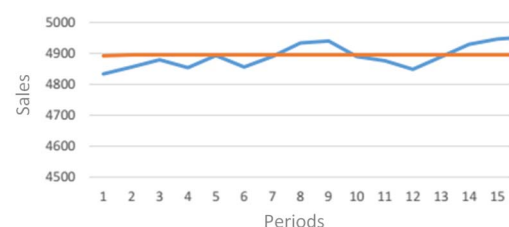


Fig. 1. Stationary data pattern

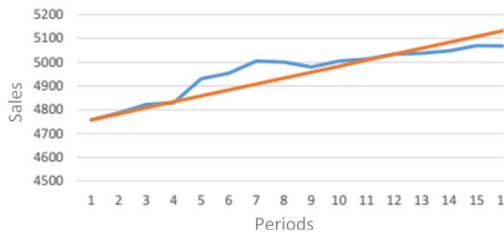


Fig. 2. Trend data pattern

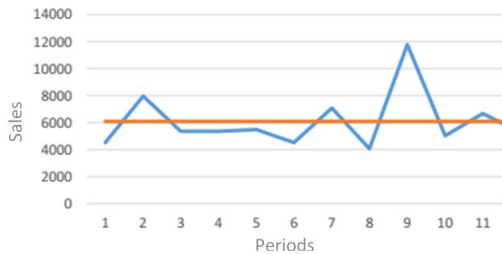


Fig. 3. Seasonal data pattern

Stationary data moves on average data. Data may experience a gradual shift or a relatively higher or lower movement over a longer period of time. Data with these habits is called trend patterned data. Trend data is usually the result of long-term factors such as an increase or decrease in a particular character[4]. Seasonal data can be seen from the existence of repeating patterns in a row in a certain period[5]. Patterns formed by seasonal data can be a significant decrease and increase and fluctuate high.

#### A. Winter Exponential Smoothing

Winter Exponential Smoothing(WES) method is used for data patterns with movements that change following the season or trend[6]. This method is one of the popular methods used for seasonal patterned data. In addition to using the level / stationary factor and Winter method trends also use seasonal factors for each season[7]. Amrit Pal Singh, et al.[8] on their research comparing winter exponential smoothing with Moving Average, Single Exponential Smoothing, and Double Exponential Smoothing. The case studied is a shoe company where there is often a spike in demand or unpredictable demand. And the conclusion of this study after comparing the 4 methods found that the Winter Exponential Smoothing method is suitable for data on case studies. In the method proposed by this winter, it is based on 3 (three) refinement parameters[6], i.e one for element, one for trend, and one for seasonal.

$$A_t = \frac{\alpha Y_t}{S_t - L} + (1 - \alpha) (A_{t-1} + T_{t-1}) \quad (1)$$

$$T_t = \beta (A_t - A_{t-1}) + (1 - \beta) T_{t-1} \quad (2)$$

$$S_t = \frac{\gamma Y_t}{A_t} + (1 - \gamma) S_{t-L} \quad (3)$$

$$F_{t+p} = (A_t + pT_t) S_{t-L+p} \quad (4)$$

$A_t$  = Smoothing Value

$\alpha$  = Smoothing Constant (  $0 < \alpha < 1$  )

$Y_t$  = Actual value in t period

$\beta$  = Smoothing constant for trend estimation (  $0 < \beta < 1$  )

$T_t$  = Trend estimation

$\gamma$  = Smoothing constant for seasonal (  $0 < \gamma < 1$  )

$S_t$  = Seasonal estimates measured as indexes

$L$  = Long season

$p$  = Number of periods to forecast

$F_{t+p}$  = Forecasting results for p period

#### B. Mean Absolute Percentage Error

Mean Absolute Percentage Error (MAPE) is a calculation to measure the accuracy of the results of a forecasting method[9]. This method calculates the average absolute value of the percentage original data error with the data forecasting result[10].

$$MAPE = \frac{\sum \left( \frac{E_t}{Y_t} \right) * 100}{n} \quad (5)$$

$E_t$  = Error Absolute Value

$Y_t$  = Actual value

$n$  = Amount of data

### III. RESULTS AND DISCUSSION

MAPE value able to reflects accuracy level of a forecast. It is said to have very good accuracy if the MAPE value is less than or equal to 10%, has good accuracy if less than or equal to 20%, can be quite accurate if less than or equal to 30% and said less accurate if more than 30%[11].

In this research the forecasting calculation based on last 7 days data. WES method requires the parameter of number of seasons for each calculation, in this study the number of seasons used is 7 because the data provided is the daily data in one month. The calculation of forecasting using the WES Method required 3 constants i.e  $\alpha$ ,  $\beta$ , and  $\gamma$ . In the determination of the value of the constant must consider the constant value that has the smallest MAPE results.

The constants  $\alpha$ ,  $\beta$ , and  $\gamma$  have the provision that  $0 \leq \alpha \leq 1$ ,  $0 \leq \beta \leq 1$ , and  $0 \leq \gamma \leq 1$ . And obtained the value of  $\alpha$ ,  $\beta$ , and  $\gamma$  with the smallest MAPE value for 31 days for “Prol Tape Besar” product is  $\alpha = 0.069$ ,  $\beta = 0.78$  dan  $\gamma = 0.01$ , for “Prol Tape Kecil” products are  $\alpha = 0.23$ ,  $\beta = 0.15$  and  $\gamma = 0.01$  and for “Pia Tape” is  $\alpha = 0.03$ ,  $\beta = 0.99$  and  $\gamma = 0.01$ . According to sales forecasting MAPE from Table 1, 2 and 3 MAPE value is above 20% and below 30%.

TABLE 1. Sales Forecasting Results of “Prol Tape Besar” in October 2016

Dates	Yt (Actual)	Ft	APE
1-Oct-16	227		
2-Oct-16	219		
3-Oct-16	156		
4-Oct-16	150		
5-Oct-16	135		
6-Oct-16	172		
7-Oct-16	249		
8-Oct-16	240	231	4
9-Oct-16	243	229	6
10-Oct-16	183	167	8
11-Oct-16	138	167	21
12-Oct-16	119	151	27
13-Oct-16	152	191	26
14-Oct-16	258	271	5

15-Oct-16	190	245	29
16-Oct-16	302	228	24
17-Oct-16	223	166	26
18-Oct-16	132	165	25
19-Oct-16	127	147	16
20-Oct-16	173	186	7
21-Oct-16	189	266	41
22-Oct-16	0	232	100
23-Oct-16	173	192	11
24-Oct-16	153	123	20
25-Oct-16	122	109	11
26-Oct-16	77	89	16
27-Oct-16	173	100	42
28-Oct-16	144	140	3
29-Oct-16	169	116	32
30-Oct-16	92	109	18
31-Oct-16	199	70	65
		<b>Mean</b>	<b>24</b>

TABLE 2. Sales Forecasting Results of "Prol Tape Kecil" in October 2016

Dates	Yt (Actual)	Ft	APE
1-Oct-16	151		
2-Oct-16	166		
3-Oct-16	175		
4-Oct-16	119		
5-Oct-16	111		
6-Oct-16	120		
7-Oct-16	91		
8-Oct-16	151	140	8
9-Oct-16	202	144	29
10-Oct-16	119	156	31
11-Oct-16	120	92	23
12-Oct-16	99	85	14
13-Oct-16	123	89	28
14-Oct-16	158	69	56
15-Oct-16	147	147	0
16-Oct-16	187	160	14
17-Oct-16	185	173	6
18-Oct-16	118	120	1
19-Oct-16	92	111	20
20-Oct-16	89	114	28
21-Oct-16	114	81	29
22-Oct-16	0	145	100
23-Oct-16	160	117	27
24-Oct-16	98	128	30
25-Oct-16	157	78	50
26-Oct-16	73	88	21
27-Oct-16	93	90	3
28-Oct-16	105	68	35
29-Oct-16	238	124	48
30-Oct-16	95	172	81
31-Oct-16	176	162	8
		<b>Mean</b>	<b>29</b>

TABLE 3. Sales Forecasting Results of "Pia Tape" in October 2016

Dates	Yt (Actual)	Ft	APE
1-Oct-16	69		
2-Oct-16	102		
3-Oct-16	79		
4-Oct-16	40		
5-Oct-16	55		
6-Oct-16	64		
7-Oct-16	74		
8-Oct-16	62	70	13
9-Oct-16	88	104	18

10-Oct-16	68	80	18
11-Oct-16	50	40	19
12-Oct-16	88	56	36
13-Oct-16	96	68	29
14-Oct-16	94	83	12
15-Oct-16	63	80	27
16-Oct-16	118	121	3
17-Oct-16	72	96	34
18-Oct-16	39	49	27
19-Oct-16	54	69	27
20-Oct-16	62	80	29
21-Oct-16	73	91	25
22-Oct-16	0	84	100
23-Oct-16	83	116	40
24-Oct-16	67	85	26
25-Oct-16	65	40	38
26-Oct-16	47	54	16
27-Oct-16	58	60	3
28-Oct-16	75	66	12
29-Oct-16	57	58	1
30-Oct-16	68	82	100
31-Oct-16	92	59	36
		<b>Mean</b>	<b>29</b>

Based on the forecasting result of 3 products Purnama Jati (Prol Tape Besar, Prol Tape Kecil and Pia Tape) in October 2016, the WES implementation is quite accurate. Can be seen in Tables 1, 2 and 3, MAPE values of three products, Prol Tape Besar: 24%, Prol Tape Kecil : 29%, and Pia Tape: 29%.

However, there are some data whose error value is greater than 30% and the forecasting results for the data are said to be inaccurate. This happens because of a spike in data changes that are too high and do not match the pattern. Thus causing chaos on forecasting calculations. Data changes occur because of things that can not be determined. In this case, we analyse deeper on the field. To figure out what happened. And we found out that the possibility of data changes occurs due to holiday outlets or due to declining sales.

#### IV. CONCLUSION

It can be inferred that implementation of WES methods for this case (daily data) is quite accurate. It is indicated by the results of MAPE calculations on all product categories between 20%-30%. This happens because there are some data whose error value is greater than 30% and the forecasting results for the data are said to be inaccurate. Another problem is the limitation from this research is data availability. Purnama Jati only provides data in one month. The data obtained in this study is too small. It is highly recommended to use more complete data. By using more complete data it is possible to produce more accurate forecasting results.

However, the decision to use WES as forecasting method in this case is suitable with the case character (stationary, seasonal and trend data patterns). It is compared with Single Exponential Smoothing that just accommodate stationary data and Double Exponential Smoothing for stationary and trend data pattern.

#### REFERENCES

- [1] R. J. Hyndman and G. Athanasopoulos, *Forecasting: principles and practice*. OTexts, 2018.

- [2] F. L. Chen and T. Y. Ou, "Sales forecasting system based on Gray extreme learning machine with Taguchi method in retail industry," *Expert Syst. Appl.*, vol. 38, no. 3, pp. 1336–1345, 2011.
- [3] P. J. Brockwell and R. A. Davis, *Introduction to time series and forecasting*. springer, 2016.
- [4] D. Anderson, D. Sweeney, T. Williams, J. Camm, and R. Martin, "Time Series Analysis and Forecasting," *An Introd. to Manag. Sci. Quant. Approaches to Decis. Mak.*, pp. 1–896, 2011.
- [5] A. S. Weigend, *Time series prediction: forecasting the future and understanding the past*. Routledge, 2018.
- [6] H. Meyr, "Forecast methods," in *Supply Chain Management and Advanced Planning*, Springer, 2015, pp. 513–523.
- [7] W. L. Winston and S. C. Albright, *Practical management science*, 5th ed. Boston: Cengage Learning, 2015.
- [8] A. Pal, M. K. Gaur, and D. Kumarkasdekar, "A Study of Time Series Model for Forecasting of Boot in Shoe Industry," vol. 8, no. 8, pp. 143–152, 2015.
- [9] U. Khair, H. Fahmi, S. Al Hakim, and R. Rahim, "Forecasting Error Calculation with Mean Absolute Deviation and Mean Absolute Percentage Error," *J. Phys. Conf. Ser.*, vol. 930, no. 1, 2017.
- [10] D. Camm, J., Cochran, J., Fry, M., Ohlmann, J., & Anderson, *Time Series Analysis and Forecasting*, 1st ed. Stamford: Cengage Learning, 2015.
- [11] C. P. Da Veiga, C. R. P. Da Veiga, A. Catapan, U. Tortato, and W. V. Da Silva, "Demand forecasting in food retail: A comparison between the Holt-Winters and ARIMA models," *WSEAS Trans. Bus. Econ.*, vol. 11, no. 1, pp. 608–614, 2014.



# Analysis and Design of Decision Support System Dashboard for Predicting Student Graduation Time

Satrio Wibowo<sup>1</sup>

Information System Study Program  
Telkom University  
Bandung, Indonesia  
satrio.bws@gmail.com

Rachmadita Andreswari<sup>2</sup>

Information System Study Program  
Telkom University  
Bandung, Indonesia  
andreswari@gmail.com

Muhammad Azani Hasibuan<sup>3</sup>

Information System Study Program  
Telkom University  
Bandung, Indonesia  
muhammad.azani@gmail.com

**Abstract**— Information Systems is one of the existing study program at Telkom University that has produced many graduates since it was established in 2008. However, not all graduates produced successfully completed the study period during the four years of normal study. The percentage of graduates on time has some decline between the target and the achievement of the study program. From academic year 2014/2015 to 2016/2017 decrease annually about 1% every year, which is it becomes problems for the credibility and existence of study program and also for academic planners who may have an impact on accreditation assessment process of the study program when it is audited. One of the efforts that can be done by the study program to increase the students on time graduation rate is by making decision support system dashboard that giving early warning to the lecturer or the head of the study program if there are students who are predicted not to graduate on time. By using the C4.5 algorithm to perform the data analysis by looking at the causes of student's graduation time and pureshare methodology to perform dashboard development method. The result of this study is a prototype of decision support system dashboard, because there are lack of analysis in decision making and the dashboard only showing information and temporary prediction. The data model that used on this research is labeling data that has been processed using C4.5 algorithm and data that has been through data cleansing process using Pentaho Data Integration. This prototype is expected to be used as a reference base to support academic planners in order to make this application run with real time data.

**Keywords**— *early warning, dashboard, decision support system, student's graduation target*

## I. INTRODUCTION

The graduation rate of students is very important for an university especially for the study program, because it will affect the credibility and existence of the study program. Information System is the one of study program at Telkom University that has 62% graduation rate on time. This certainly needs to be evaluated, as improvements in graduation rate on time are also assessed as improving the quality of the study program. But there are no valid data to determine the cause of the graduation rate is not timely, and there is no system that can present the graduation rate data and systems that help the head of study programs and lecturers to making a decision for students so they can graduate on time. The official website of Information System Telkom University [1] explained that graduation graph of Information Systems students from 2011 to 2015 are increased as shown in Fig. 1. The x-axis is describe the students school year and the y-axis is describe the number of student who graduated on time.

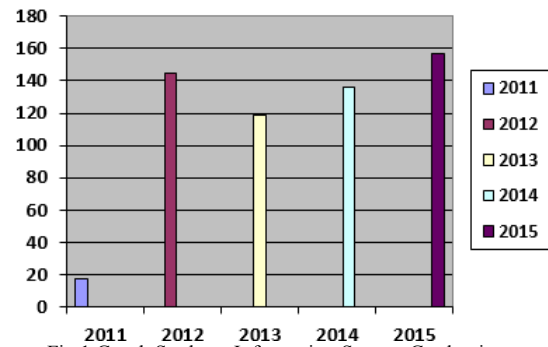


Fig 1 Graph Students Information System Graduation

The graduation of student information system is determined by many factors, such as academic record information, attendance and achievement. But from the graph above, graduation data is calculated not only from graduates on time. The annual report of Information Systems Program shows that the on time graduates each year decreased by 1% from 2014/2015 until 2016/2017. The decrease is seen based on comparison of target and achievement of Information System program. But in 2017/2018 there was an increase of 0.2% with a percentage of 62% in this year. There are several factors that can affect student's graduation time. Based on previous academic records, the researchers conducted an analysis to determine factors that may affect students in achieving on time graduation and design a business intelligence dashboard that used by head of study program and lecture of Information System as an early warning system of student graduation target. In this study, the dashboard is developed by using pureshare dashboard development method.

In order to identify the user requirement, define the key metric, and design the dashboard layout the researchers conducted an interview to the head of study program. The researcher using the previous research to collect data through academic data records of Information system student from 2009 to 2016. Based on the data of previous research, the criteria that affect student's graduation on time are GPA score on 4th Semester, senior high school, the parent's job, the parent's income, selection path, number of credits and SAT points. SAT (student activities transcript) points are obtained from organizational activities that students take as a condition for graduation. But, GPA (Grade-Point Average) is the most influential criterion in student on time graduation.

## II. THEORY AND RELATED WORK

### A. Business Intelligence (BI)

Business intelligence is a set of methodologies, processes, architectures, and technologies that convert raw data into meaningful and useful information used to foster strategic insight and strategic, tactical, and operational effective decision making [2]. The result is a wealth of information and leads to the development of new opportunities for the organization. If these opportunities are identified, and strategies implemented effectively, BI can give the organization a competitive advantage in the marketplace.

There are five dimensions of data quality in BI. First completeness that ensures availability of all required information. Second, consistency that ensures uniformity of information in a table. Third, validity that ensures the correctness of information. Fourth, accuracy that ensures data can be trusted and in accordance with objects in the real world. And the last is integrity that ensures that data are inter-related so as to reduce data duplication rates.

### B. Decision Support System (DSS)

Decision support system is a computer-based system that helps users in assessing and selecting activities. DSS provides data storage and retrieval but to improve traditional access and retrieval function, DSS provides support to create reasoning-based models[3]. Decision support systems can present graphical information and may include artificial intelligence [4]. The decision support system was first used as a Marketing Decision Support System (MDSS), which is as a collection of data, systems, tools and technologies coordinated with software and hardware whereby organizations collect and interpret information from businesses and the environment and transform it into the basis of marketing actions [5].

According to [4] there are five models of decision support systems, that are communication model, data model, document model, knowledge model, and DSS driven model. The communication-based DSS model are targeted to internal teams including partners to produce a set of decisions to implement a strategy or solution. The most common technology used by this DSS model is web based or client server [4]. The data-based DSS model is emphasizes access and manipulation on the internal and external data in real time to fit the needs of the decision maker. This DSS model is used to run database queries or data warehouses to look for specific answers for specific purposes. Data-based DSS is usually created through the main frame system, client server link or via the web [4]. The document-based DSS model uses computer storage and processing technology to provide document retrieval and analysis. The used documents such as text documents, spreadsheets, and database records to generate decisions and manipulate information to improve strategy. The usual technology used to prepare such decision support systems is through web or client server systems [4]. The knowledge-based DSS model can recommend actions to managers to provide management advice in order to choose a product or service. Typical technologies commonly used to set up such this model can be client server systems, web, or software

running on stand-alone PCs [4]. The DSS-driven model are emphasizes access, optimization manipulation and simulation on the financial side. This model are complex systems that help to analyze decisions or choose between different options. The DSS-driven model generally does not require a large database, because it uses only limited data and parameters to assist decision makers in analyzing a situation [4].

The model that used in this research is knowledge model because the aim of this research is to provide management advice in order to choose a decision. And the DSS knowledge-based also can recommend any actions to managers.

### C. Dashboard

The term of dashboard refers to the display of one-page information used to monitor what is going on in some aspects of the business. The dashboard shows key data that users must use efficiently to monitor what's happening in their area of responsibility. Generally, dashboards are used to monitor information on a daily basis, but some jobs require a dashboard to be monitored in real time as monitored activity is currently happening so delay in responding cannot be tolerated. The dashboard can be very useful because it has two capabilities, namely the visual power and the dashboard way to integrate everything the user should remember into one screen even though it is very complex [9]. There are several types of dashboard, namely:

1. Strategic dashboards provide information about the system in general and identify potential benefits for the system. This dashboard does not provide detailed information about what to do to make decisions, but this dashboard helps users identify future benefits for further analysis.
2. Analytical dashboards provide users with information about what might happen in the future using old data compared to various variables. Analytical dashboard gives more detail information than strategic dashboard and operational dashboard.
3. Operational dashboard is used to monitor the current operational conditions. This kind of dashboard needs to be updated in a short time, even real time.

There are several things to avoid in designing the dashboard such as too complicated information, too many warnings, indistinguishable warning, the visual that too big and bassist, inappropriate visual interpretation, incompatibility between information and visual representation, expression of indirect action, and the context are not enough.

In addition, to design an effective dashboard required some principles and positive practices, including using something that can blink and sound to attract attention, encourage users to active for thinking about data, not just passive reactions to alarm, not over-automate the action to the point where people become uninvolved, provide simple and easy way to respond and an overview for the entire team, support projection for proactive responses, and match the mental model

#### D. Pureshare

Pureshare is one of the dashboard development methodologies developed by pureshare vendors. This method aims to facilitate projects related to the measurement and management of organizational performance [6]. In the pureshare development method, the steps taken are planning and design that understanding of user needs and identifying what features will be used on the dashboard. After the user need are identified, the next step is review the system and data to applying a bottom-up approach, such as identification of data sources, how to access data, and the size of a data. After the user needs and the data sources are identified, then the prototype design step is perform to apply a top-down and bottom-up approach together to provide an overview of the final look of the dashboard. After the prototype has a final look, the prototype are reviewed by potential users and perform development according to user needs on prototype refinement step. After the prototype is match with the user needs, the dashboard is implemented on the organization and socialize use through training in release step. The last step is continuous improvement to keep the quality of the dashboard, the dashboard must be developed in various areas of the organization repeatedly.

#### E. C4.5 Algorithm

Algorithm C4.5 is one of the algorithm used to perform the process of data classification by using decision tree technique. Algorithm C4.5 is the development of ID3 algorithm which is also an algorithm to build a decision tree. The C4.5 algorithm recursively visits each decision node, chooses optimal branching, until no more branches are possible [7].

The steps in building the decision tree using the C4.5 algorithm are as follows [8]:

1. Prepare training dataset. Training datasets are usually obtained from pre-existing data history and have been grouped into specific classes.
2. Specifies the root attribute of the decision tree.
3. Create a branch for each attribute.
4. Divide the case in the branch.
5. Repeat the process for each branch until all the cases on the branch have the same class.
6. The decision tree partition process will stop when:
  - a. All records in node N get the same class.
  - b. No attributes or variables in the record are partitioned again.
  - c. No record in the empty branch.

#### F. Related Work

Researchers used the C4.5 algorithm to obtain criteria based on the case studies being conducted. Before the researchers used this method there is some evidence that has been done by other researchers.

Based on the results of research that has been done by David Santiago Rivera & Graeme Shanks [9], in their journal entitled "A Dashboard to Support Management of Business Analytics Capabilities" shows that the successful business analysis capability management are supported by the dashboard prototype. The dashboard has a potential capability to significantly improve the decision support infrastructure within the organization.

And the other result of research that conducted by Adolfo Crespo Marquez & Carol Blanchar [5], in their journal entitled "A Decision Support System (DSS) For Evaluating Operations Investments in High-Technology Business" shows that decision support systems using dynamic simulation system models greatly enhance the analysis of go-to-market strategies, as they can integrate customer knowledge with simulations to analyze tradeoffs of expenditure in service features, support, integration, channel incentives, pricing, and advertising.

By the experiments that conducted by other researchers above, the dashboard decision support system is helpful to improve the organization values. So it can be applied to predicting the students graduation time at Information System study program.

### III. METHODOLOGY

The methodology that used on this research is pureshare methodology that have four steps, there are plan and design, system and data review, prototype refinement and release. At the plan and design stage, the KPI (key performance indicators) of the organization are identified to be improved, then identify the type of dashboard along with its user group and identify the meta information from KPI that has been made. Meta-information here in the form of factors that affect student graduation time. Then at the review system and data stage, the data source to be used are identified, then performs analysis to the data that has been obtained, then data cleansing are performs that can produce the expected information. After the KPI are identified and the data are "clean", the design of the dashboard prototype can be made at prototype refinement stage. Then the prototype will be reviewed periodically and there will be renewal dashboard until the dashboard prototype is approved by the user. Once the dashboard prototype is approved by the user, the dashboard will be implemented to the user at release stage as shown in Fig. 2.

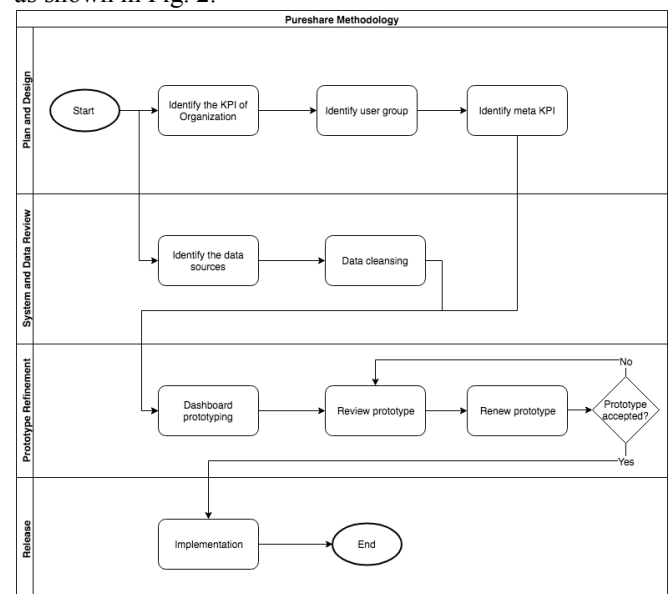


Fig. 2. Pureshare Methodology

In this study, we used data records of students from 2009 to 2012 which is not the data of students who are "drop-out" or "resign" that obtained from the SISFO of Telkom

University. The raw data will be divided into two parts as follows:

1. *Training set*: data are used in the system training process and consists of input data pair and target data. From the total data obtained, 70% - 80% part will be used as training data.
2. *Testing set*: data are used to test the ability of the system and also consists of input data pair and target data. Data testing used amounted to 20% -30% of the data obtained.

The C4.5 algorithm is performed at “Identify the data sources” step on Fig. 2. The C4.5 algorithm train the set by calculating the gain ratio for all attributes that have been determined before, then select with the highest gain ratio to be the root node. And repeat the gain ratio calculation process and form a node that contains the attribute until all data has been included in the same class as shown in Fig 3.

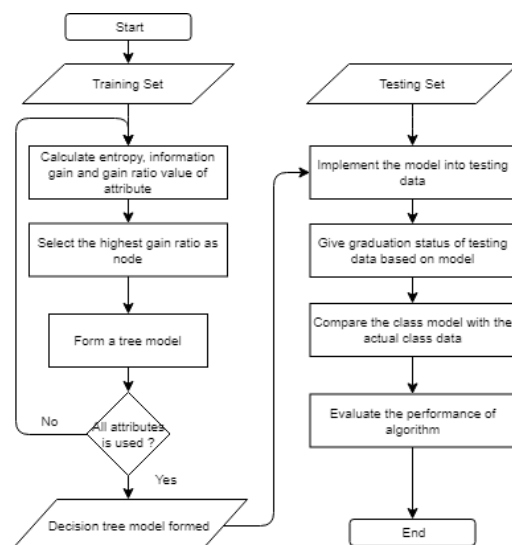


Fig. 3. Flowchart of C4.5. Algorithm

#### IV. RESULT AND ANALYSIS

##### A. Study Case Analysis

In this case, the researcher uses academic record data (SISFO) Telkom University and questionnaires to expert judgment. Based on the academic record, the researcher divides into 7 criteria: GPA (Grade-Point Average) on 4th Semester, senior high school, the parent's job, the parent's income, selection path, number of credits and SAT (Student Activities Transcript) amount of points. Data processing is done based on academic record data from 2009 to 2012. There are 600 students who graduated on time. the percentage shown in the data of the annual report of Information Systems is 62%.

##### B. Dashboard Design

###### 1. Prediction page

The dashboard on Fig. 4 are consists of multiple bar chart that show the prediction of student's graduation level and the target of on time student's graduation. The yellow bar is describe the prediction of student's graduation and the blue bar is describe the target of student's graduation. The card view are used to inform the prediction of total student that may graduate on time, total student that may graduate

not on time, total of the student that ever have a remedial on a subject, and the name of subject that most repeated. Beside the bar chart, there are the top 10 of subject that most repeated.

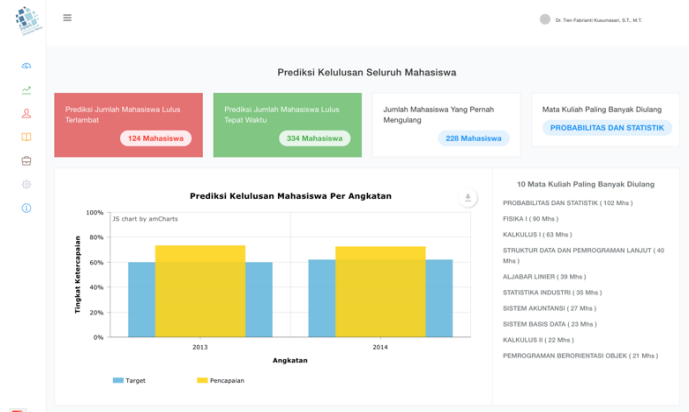


Fig. 4. Prediction page

When the prediction of students who graduated late card in the pressed, it will appear the name of student students who predicted to pass late with a grade 2 GPA of the student, as shown in Fig. 5.

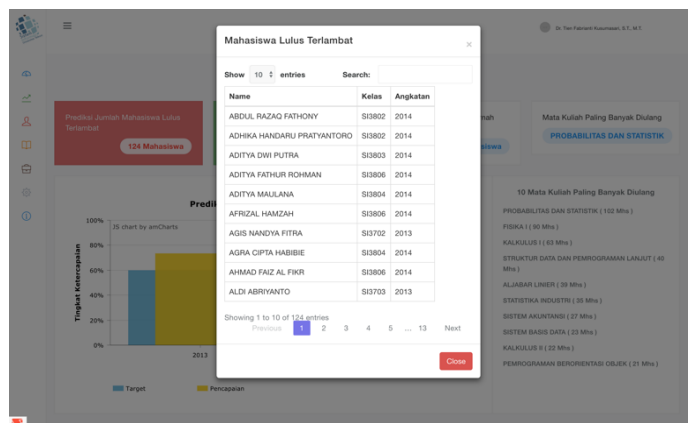


Fig. 5. Prediction of students who graduated late

When the prediction of students who graduated on time card on tap, it will appear the name of student students are predicted to graduate on time along with a grade 2 GPA from the student, as in Fig. 6.

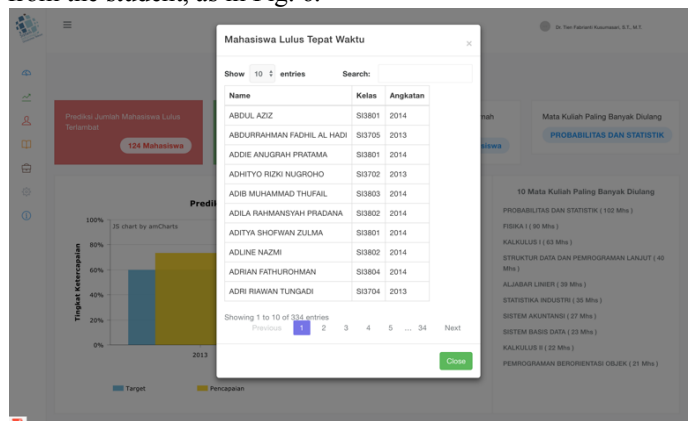


Fig. 6. Prediction of students who graduated on time

When the user presses one of the student's graduation prediction graphs, the user will go to the student's graduation prediction page that is grouped by class according to the student school year, as shown in Fig. 7.

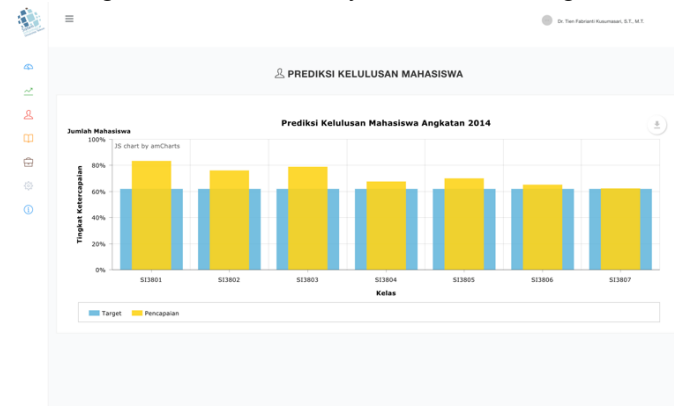


Fig. 7. Prediction of student's graduation that grouped by student school year

When the user presses the predicted graph of a student's graduation of a class, the student's graph will appear late and timely according to the pressed class, as shown in Fig. 8.

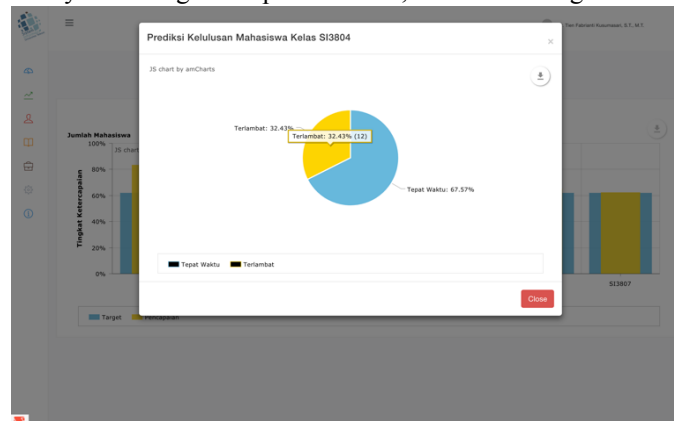


Fig. 8. Prediction of student's graduation that grouped by class

## 2. Student's Performance Page

This page provides information on the performance of classes each semester grouped by force. This page is only accessible by caps. This graph contains data in the form of average grade GPA each semester. This graph provides users with significant increase / decrease in student performance in the third semester. This page is expected to be a reference for head of study program in analyzing the cause of student performance drop in third semester as shown in Fig. 9.

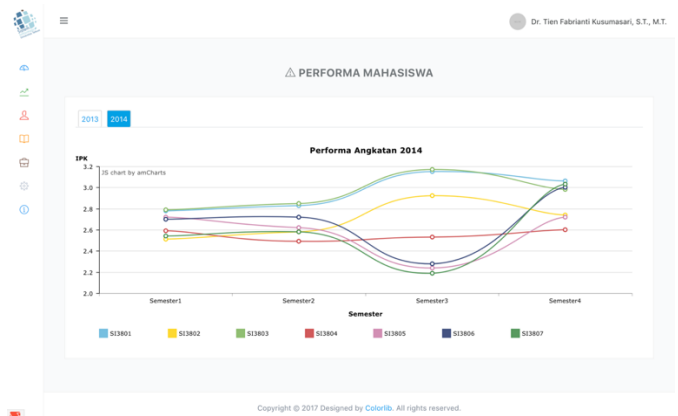


Fig. 9. Prediction of student's graduation that grouped by class

## 3. Most Repeated Subject Page

This page displays the 10 frequently repeated courses in each class. This page is only accessible by caps. To view details of each course, the user can press the desired course chart. With this page is expected to give head of study program action to the courses that are predicted to reduce the number of graduated on time students as shown in Fig. 10.

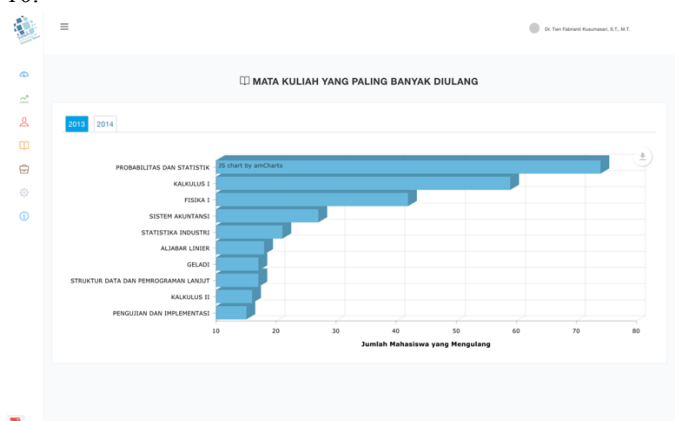


Fig. 10. Prediction of student's graduation that grouped by class

## 4. Testing

The testing method that used for this research are unit testing and usability testing that perform by user using Likert scale for the measurement method. The unit testing is performed by programmer to find bugs of the application. And the usability testing is performed only by head of information system study program, because this application is only used by that user. The usability testing is divided into two categories they are user interface and functionality.

The result of unit testing is there are no bugs found in unit testing. And the result of the usability testing can be seen in Fig. 10.



Tabel 2. Kuesioner

No	Pertanyaan	Skala Likert (Higher is Better)				
		1	2	3	4	5
<b>Pengujian Tampilan Aplikasi</b>						
1.	Apakah tampilan aplikasi ini menarik ?					✓
2.	Apakah tampilan aplikasi ini mudah dipahami?					✓
3.	Apakah tata letak menu serta isi pada tiap menu dalam aplikasi ini sudah rapi?				✓	
4.	Apakah penggunaan warna pada website ini sudah terlihat nyaman oleh user?					✓
5.	Apakah pesan kesalahan yang muncul dapat dimengerti?					
<b>Pengujian Kepuasan Pengguna Terhadap Aplikasi</b>						
1.	Apakah aplikasi ini dapat membantu untuk memprediksi keluhan mahasiswa?		✓			
2.	Apakah kandungan informasi yang tersedia pada aplikasi ini sudah lengkap dan sesuai kebutuhan?			✓		
3.	Apakah aplikasi ini dapat dijadikan sebagai pendukung keputusan untuk meningkatkan angka kelulusan tepat waktu?			✓		

Mohon tulis kritik / saran untuk aplikasi ini pada kotak dibawah

*Aplikasi merupakan prototipe, jika digunakan utk digunakan sebagai dasar / pendukung pengambilan keputusan maka diperlukan analisis tambahan dan pendalaman data lebih lanjut*


Bandung, 28 Mei 2018  
Kepala Prodi Sistem Informasi  
  
**Dr. Tien Fahrianti Kusumawati, S.T., M.T.**  
NIP. 14790008

Fig. 10. Usability testing result

Based on Fig. 10, user is satisfied with the user interface but less satisfied for the functionality to support the decision making.

## V. CONCLUSION

Based on this research can be concluded this dashboard design is just a prototype, because there are lack of analysis in decision making and the dashboard only showing information and temporary prediction. The data model that used on this research is labeling data that has been processed

using C4.5 algorithm and data that has been through data cleansing process using Pentaho Data Integration.

## REFERENCES

- [1] "About Us : Fact & Figure."
- [2] R. F. van der Lans, *Business Intelligence and Data Warehousing*. 2012.
- [3] M. J. Druzdzel and R. R. Flynn, "Decision Support Systems," *Encycl. Libr. Inf. Sci.*, pp. 1–15, 2002.
- [4] G. M. Faculty, C. Science, and B. Management, "Decision support systems Faculty of Computer Science for Business Management , Romanian American University , Bucharest , Romania."
- [5] A. Crespo Márquez and C. Blanchar, "A Decision Support System (DSS) for Evaluating Operations Investments in High- Technology Business," *Proc. 22nd Int. Conf. Syst. Dyn. Soc.*, 2004.
- [6] PureShare Whitepaper, "Proactive Metrics Methodology," 2005. [Online]. Available: [http://pureshare.com/products/proserve\\_method](http://pureshare.com/products/proserve_method). [Accessed: 12-Jan-2018].
- [7] I. Rahmayuni, "Perbandingan Performansi Algoritma C4.5 dan Cart Dalam Klasifikasi Data Nilai Mahasiswa Prodi Teknik komputer POLITEKNIK NEGERI PADANG," *J. Teknol. Inf. Pendidik.*, vol. 7, no. 1, pp. 87–94, 2014.
- [8] E. T. L. Kusriani, *Algoritma Data Mining*. Yogyakarta: Andi, 2009.
- [9] D. Santiago Rivera and G. Shanks, "A Dashboard to Support Management of Business Analytics Capabilities," *J. Decis. Syst.*, vol. 24, no. 1, pp. 73–86, 2015.

# Sentiment Analysis to Measure Celebrity Endorsment's Effect using Support Vector Machine Algorithm

Fransiska Jesinta Pinem  
Faculty of Industrial and System  
Engineering  
Telkom University  
Bandung, Indonesia  
fransiskajp@gmail.com

Rachmadita Andreswari  
Faculty of Industrial and System  
Engineering  
Telkom University  
Bandung, Indonesia  
andreswari@telkomuniversity.ac.id

Muhammad Azani Hasibuan  
Faculty of Industrial and System  
Engineering  
Telkom University  
Bandung, Indonesia  
muhammadazani@telkomuniversity.ac.id

**Abstract**—Celebrity endorsement is a phenomenon in which companies advertise their products by using celebrity services, and celebrities take advantage of their popularity to promote a brand or product of the company through social media. In this study, KFC did a celebrity endorsement to make their menu more popular. KFC choose to work with Raditya Dika to promote their latest menu, KFC Salted Egg Chicken. This study will examine whether in such cases there is a change in public sentiment towards the product after the celebrity endorsement. It can be done using text mining and sentiment analysis. There are several algorithms that can be used to perform sentiment analysis, one of them is Support Vector Machine. Support Vector Machine (SVM) was chosen because this method is quite accurate in various studies. SVM also takes into account various features of the document, including features that often do not appear on the document, so it can reduce the loss of information from the data. The data used in this research are taken from YouTube and Twitter comment about KFC Salted Egg Chicken. Several step was done in this sentiment analysis research, that are preprocessing text, feature extraction, classification, and evaluation. The result model is tested and evaluated before and after endorsement by looking at the value of accuracy, precision, recall, and f1-measure. The test result of accuracy, precision, recall, and f-measure before endorsement were 67,83%, 69%, 68%, and 66%. After the endorsement, the test results were 74.06%, 74%, 74%, and 74% respectively. The results of this study indicate that SVM has an accurate measurement in sentiment analysis studies. Moreover, this study found that there was not significant change in public sentiment regarding the product before and after the celebrity endorsement.

**Keywords**—sentiment analysis, celebrity endorsement, social media, text mining and support vector machine

## I. INTRODUCTION

Celebrity endorsement is a phenomenon in which a company advertises its products by using celebrity services, where the celebrity exploits its popularity to promote a brand or product of the company. By celebrity endorsement, it is expected that new products can be accepted and responded positively by society.

Kentucky Fried Chicken (KFC) is a famous fast food restaurant company in Indonesia. Fried chicken is the main menu of KFC. There are several variations of KFC food menu, one of the variations of the menu is KFC salted egg fried chicken, which is fried chicken with salted egg sauce. KFC salted egg chicken is one of the KFC products themed Taste of Asia. The taste of salted eggs was chosen because according to a survey conducted by KFC, the taste of salted egg is one

of the five most popular flavors in Asia [1]. This menu was launched on February 1, 2018. Since this product was released, this product is reaping controversy on food lovers because of its unique taste. There are various responses to this product, some people like it, some people dislike it, and some people feel neutral about it.

Two weeks after the new menu was launched, KFC endorsed Raditya Dika to promote the menu. Raditya Dika is one of the famous celebrities among young people. He is a writer and also a social media influencer. KFC and Raditya Dika held a contest to make video about review of the new menu. The winner that chosen by him would get a meal voucher at KFC for fifty thousand rupiahs and will also collaborate with Raditya Dika to create video content. This contest encourages people to buy and review the food. However, the effect of celebrity endorsement is unknown regarding public opinion about KFC Salted Egg Chicken. The tendency of public sentiment can be known by sentiment analysis. Sentiment analysis is an approach to classify opinions digitally. Sentiment analysis, also known as opinion mining, is the field of research to analyze sentiments, evaluations, judgments, attitudes, and emotions on entities such as products, services, organizations, characters, topics, and attributes of the entity [2]. Sentiment analysis is often done by various companies to find out whether the product and brand companies have positive or negative responses in communities. Moreover, sentiment analysis can be used to get criticism and suggestions from the public on a product or brand.

Public opinion about a product or brand can be taken from text on social media. Social media is an internet-based application built on the ideology and technology of Web 2.0, which allows users to create content and exchange the content with other users [3]. People use social media as a means to review and discuss various topics, including on food reviews.

This research uses the YouTube and Twitter as a source of data to explore public opinion. YouTube is chosen as the source of opinion in this study because according to Statista's research in the third quarter of 2017[4], YouTube is the most popular social media in Indonesia. YouTube was originally a platform for uploading videos, but now the platform has evolved into social media, as it supports users to interact and conduct social activities, such as commenting, rating, etc. The next data source is Twitter, the seventh most popular social media in Indonesia according to Statista in 2017. The number of Twitter users in Indonesia is quite big. Indonesia is a country with the most users of twitter in Asia Pacific. Every year, the number of Twitter users in Indonesia are always

increase. Twitter was chosen because of the popularity and growth of its users.

After obtaining social media data sources, a text classification using machine learning is done. The algorithm used in this research is Support Vector Machine (SVM). SVM was chosen because it considered quite accurate in various studies. For example, on the comparison of the Deep Recurrent Neural Network algorithm with Support Vector Machine on sentiment analysis based on aspects of Arabic hotel reviews [5]. SVM was rated better than Deep Recurrent Neural Network. In addition, the SVM considers in various features of the document, including a few frequency accuracy features. This ability can reduce the loss of information from the data.

## II. LITERATURE REVIEW

### A. Celebrity Endorsement

Celebrity endorsement is one of the advertising strategies in which a company advertises its products by using celebrity services [6]. Celebrities use their popularity to promote the product to the wider community. Promotion is considered to help company to create a positive image or perception to their consumer towards a brand or product [6]. However, this method is considered very expensive. The effectiveness of celebrity endorsement in several studies has an impact on consumer perceptions of the product. A study of consumer behavior examines the effect of celebrity endorsement on consumer buying interest and consumer responses to a particular product advertised by television [7]. This study uses quantitative methods in which the researchers analyzed the results of questionnaires from 200 respondents from various students from various universities. The results of this study indicate that there is influence of celebrity endorsement to public buying interest. According to the results, celebrity endorsement is more attractive than conventional advertisement. Most consumers involved in the study said they would buy products promoted by celebrities. Some of the factors that make celebrity endorsement more appealing are the physical attraction of celebrities, credibility, and the alignment of celebrities with promoted products. These factors affect consumer perceptions of a product.

### B. Sentiment Analysis

Sentiment analysis or also referred to opinion mining is a field of research to analyze opinions, sentiments, evaluations, judgments, attitudes, and emotions on entities such as products, services, organizations, figures, topics, and attributes of these entities [8].

In the study [9] performed sentiments of analysis on television shows via Twitter using Support Vector Machine and Genetic Algorithm as Feature Selection Method. The study calculated the rating of television shows using sentiment analysis. The dataset used is a tweet of 160, divided into 80 positive tweets and 80 negative tweets. Five experiments were conducted with the ratio of training data and data testing as follows: 90:10, 80:20, 70:30, 60:40, and 50:50. The research process begins by taking a tweet, then do preprocessing. Then the vector term presence is performed. After that, the feature selection is done using genetic algorithm. After that, done classification with Support Vector Machine algorithm and television ratings calculation. Accuracy without feature selection in five experiments is about 90.5%. The accuracy

with feature selection approximates accuracy without feature selection, with an error value of 0.62%, except in the first experiment. The first experiment with feature selection, with training data ratio 90:10, yielded 87.5% accuracy. The result of comparison of television ratings rating based on AGB Nielsen rating and by using sentiment analysis is not much different. Calculation with sentiment analysis has an average error value of 0.562 on AGB Nielsen rating.

There are several approaches in classifying sentiment analysis. Broadly speaking, the approaches are [9]:

- Machine learning approach  
Broadly speaking, the machine learning approach relies on machine learning algorithms to be able to perform sentiment analysis. This algorithm is used to classify texts that have linguistic features. Algorithms commonly used in this approach are Naive Bayes, Neural Network, Support Vector Machine, Decision Tree, and so forth.
- Lexicon based approach.  
Broadly speaking, the lexicon based approach is done by counting the total weight of positive and negative words on a document or sentence to determine whether the document or sentence has positive or negative sentiments.

### C. Support Vector Machine

Support Vector Machine is one of machine learning algorithm. The algorithm was discovered by Vapnik, et al, in about 1960s [10]. Currently support vector machine is often used and is one of the basic algorithms learned in learning machine learning process.

The support vector machine algorithm is basically aimed at finding the best hyperplane to separate the two different classes [11]. Hyperplane maximizes the margin between the closest positive and negative class data from the hyperplane. The closest data of the hyperplane is called support vector [12]. The Support Vector Machine algorithm, in the context of natural language processing, will classify words, phrases, or sentences into categories based on the feature set [13][14]. The entered data will be mathematically transformed by using the kernel function, where this kernel function will create linear separation of data from various categories [13].

## III. RESEARCH METHODOLOGY

### A. Conceptual Model

In this research sentiment analysis is developed to examine the effect of celebrity endorsement on public sentiment by using SVM and had an evaluation phase by doing scenario testing. This research is based on the problem formulation of whether celebrity endorsement affects the public sentiment of the product, especially in the case of KFC salted egg fried chicken. The environment in this research consists of celebrity and social media technology.

The basic knowledge used in this research are sentiment analysis and SVM algorithm. Text mining methodology is also implemented in this research (Fig 1).

### B. Methodology

This research methodology is divided into three stages: problem and solution identification stage, sentiment analysis stage using SVM, result analysis and conclusion stage.

- Problem identification stage.  
The problem identification and solution stage begun by doing problem identification, followed by a literature

study, case study, and algorithm selection. The next process is solution identification. The next process is the identification of research objectives, followed by the

identification of research benefits. The last is problem scoping.

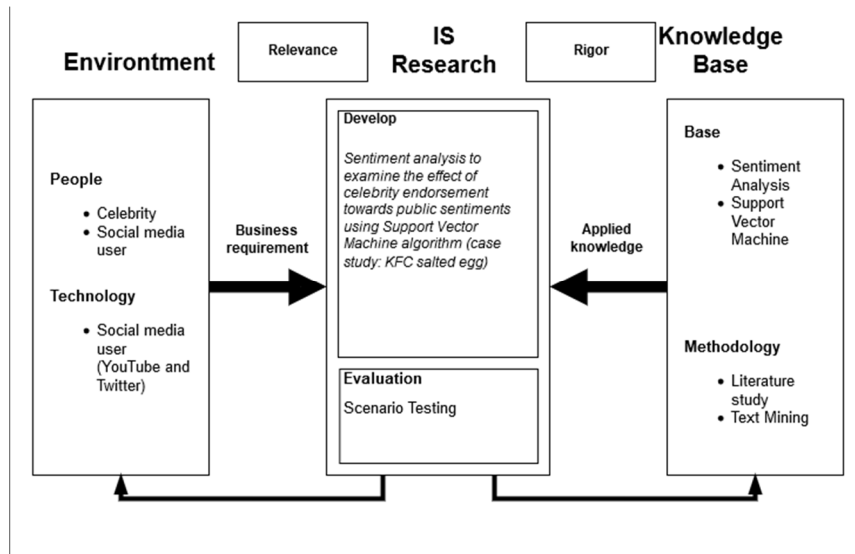


Fig. 1 Conceptual Model

- Sentiment analysis stage**  
 Sentiment analysis stage using the SVM algorithm, began with the data collection [14]. The data collected was obtained from Twitter and YouTube comments from several videos related to case study. After the data obtained, the preprocessing data, i.e. the process of cleaning the data before the text classification is performed. In this process there are four main activities performed: punctuation removal, stop words removal, tokenization, and stemming. Stop words removal is the process of removing the words that have no significant meaning [15]. Tokenizing is the process of breaking sentences into words. Stemming is the process of restoring word into its basic form. The next process is extract features from the data. In the feature extraction process, the frequency of word occurrence is calculated, and comments are converted to vector form. Then, the next process is the classification of sentiment using the SVM algorithm. In this process carried out two activities, namely training data and testing data. The next process is checking the accuracy of machine learning. Python programming language is used in this research.
- Result analysis and conclusion stage**  
 The third and final stage of this research is the result analysis and conclusion stage. In this stage, evaluation and analysis of classification results are performed. Then conclusion and suggestion from this research is obtained.

### C. Dataset

The dataset used in this study are YouTube user's comments and tweets from Twitter that related to the topic of discussion, which is about KFC salted egg chicken. The comments are taken using open source tools. Then the comments are put together in a file with csv format. Then the comments that have been collected are separated according to the date - before and after February 18, 2018. The parameters

used in this study are comments only. Once the data extracted, we labeled the comments based on their sentiments. The data label consists of positive, negative, and neutral.

## IV. RESULT AND ANALYSIS

The dataset contains comments before and after their celebrity endorsement was split into ratio of 75:25. Data is divided randomly. The amount of dataset of comments before celebrity endorsement is 458. Total amount of data training is 343 and total amount of data testing is 115. The amount of data in the dataset of comments after the celebrity endorsement is 737. After divided, total amount of data training is 552 and the total amount of data testing is 185. The feature with the highest value in comment dataset before endorsement can be seen in the following figure 2.

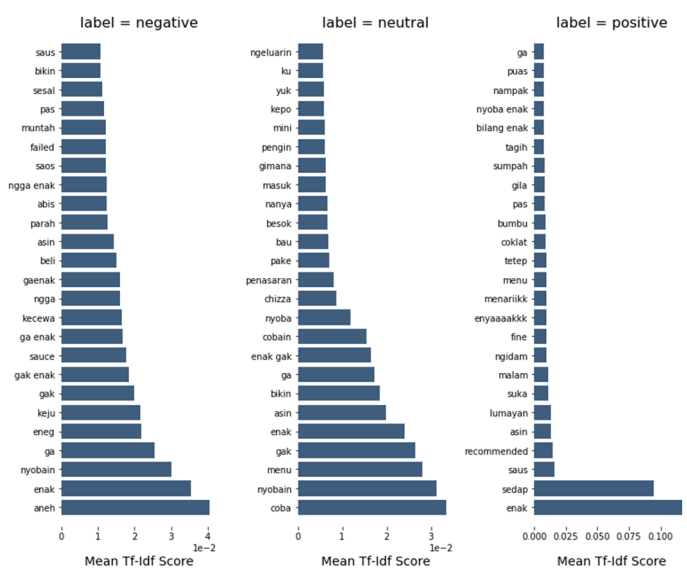


Fig. 2 Feature with Highest Value on Dataset Comments Before Endorsement

While the feature with the highest value in the comment dataset after the endorsement can be seen in Figure 3.

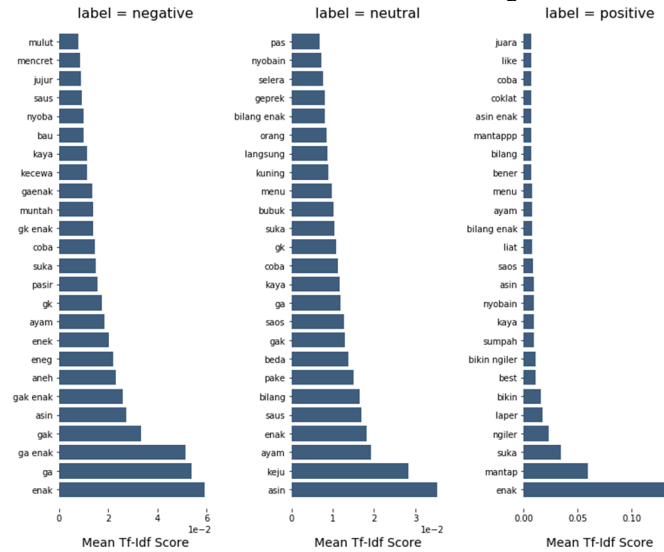


Fig. 3 Feature with Highest Value in Comment Dataset After Endorsement

Details of the amount of data testing based on manual data labeling are as follows (table 1):

TABLE I Details of the amount of data testing

Periode	Positive	Negative	Neutral	Sum
<i>Before endorsement</i>	26	27	62	115
<i>After endorsement</i>	43	73	69	185

The number of comments and tweets analyzed using SVM in the period before celebrity endorsement was 115 with details of 14 positive comments, 19 negative comments, and 82 neutral comments. While the number of comments in the period after celebrity endorsement was 185, with details of 33 positive comments, 78 negative comments, and 74 neutral comments (Fig 4).

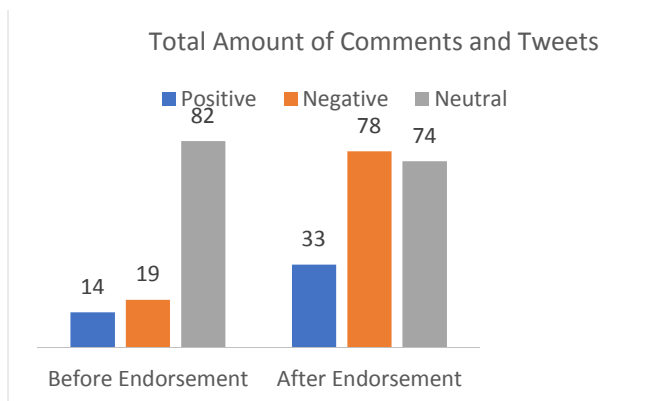


Fig. 4 Total amount of comments and tweets

Details of sentiment proportions before celebrity endorsement were 71% neutral, 17% negative, and 12% positive. The proportion of sentiments in the period before the celebrity endorsement is illustrated in figure 5.

Sentiment Before Celebrity Endorsement

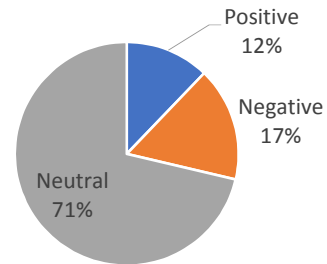


Fig. 5 Sentiment proportions before celebrity endorsement

While the details of sentiment proportions after celebrity endorsement were 40% neutral, 42% negative, and 18% positive. The proportion of sentiments in the period after the celebrity endorsement can be illustrated in figure 6.

Sentimen After Celebrity Endorsement

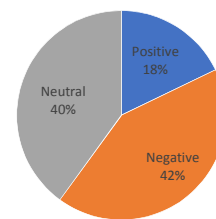


Fig. 6 Sentiment proportions after celebrity endorsement

Based on the illustration, we can see that there was a sentiment shift between the two periods. Prediction results in the period before celebrity endorsement showed that the sentiments on KFC Salted Egg Chicken products were neutral. This prediction caused by not many people who tried the product in the period before the celebrity endorsement. Most commentators ask whether the product is tasty or not. In addition, there were neutral comments that said that the product is ordinary and had no strong feeling towards it.

Prediction results in the period after celebrity endorsement as shown in Fig. 6 showed that most of the sentiments on KFC salted egg chicken products were negative. Most commentators say they dislike the product. In addition, there was a shift in the proportion of neutral sentiments, it can be assumed that already many people had tried the product.

This result showed that the celebrity endorsement of KFC salted egg chicken product by Raditya Dika affected product sentiment. Based on predicted results from both periods, we can see that there is a tendency for greater negative sentiment toward the product than positive sentiment. This is more likely caused by the number of comments that dislike the product is more than the number of comments that likes the product.

Based on this research the accuracy of SVM algorithm in the dataset before celebrity endorsement is 67.83%.



Evaluation of SVM algorithm in dataset of comments before celebrity endorsement is as follows.

TABLE II Evaluation of SVM algorithm on dataset before celebrity endorsement

Label	Precision	Recall	F1-score
Positive	0.48	0.41	0.48
Negative	0.67	0.89	0.76
Neutral	0.86	0.46	0.60
Average	0.69	0.68	0.66

The accuracy of SVM algorithm in dataset of comments after celebrity endorsement is 74,06%. Evaluation of SVM algorithm in comment dataset after celebrity endorsement is as follows.

TABLE III Evaluation of SVM algorithm on dataset after celebrity endorsement

Label	Precision	Recall	F1-score
Positive	0.74	0.79	0.77
Negative	0.72	0.77	0.74
Neutral	0.79	0.60	0.68
Average	0.74	0.74	0.74

## V. CONCLUSION

In this study, the SVM method is used to generate a classifier to classify and predict user comments on a food product. The classification result of this user comment is then used to see how far the endorsement of an artist influences the sentiment of the product being promoted. Based on the results of testing of SVM the accuracy of the support vector machine classifier in performing sentiment analysis before the celebrity endorsement is 67.83% and after the celebrity endorsement is 74.06%.

## REFERENCES

- [1] Maharani, S. (2018, Februari 3). Retrieved from Kumparan: <https://kumparan.com/@kumparanfood/perkenalkan-taste-of-asia-kfc-luncurkan-menu-salted-egg-chicken>
- [2] Liu, B. (2012). *Sentiment Analysis and Opinion Mining*. Chicago, USA: Morgan & Claypool Publishers.
- [3] Kaplan, A. M., & Haenlein, M. (2010). Users of the World, Unite!: The Challenges and Opportunities of Social Media. *Business Horizons*, 59-68.
- [4] Statista (2018) Retrieved from Statista: <https://www.statista.com/statistics/284437/indonesia-social-network-penetration/>
- [5] Al-Smadi, M., Qawasmeh, O., Al-Ayyoub, M., Jararweh, Y., & Gupta, B. (2017). Deep Recurrent Neural Network vs. Support Vector Machine for Aspect-based Sentiment Analysis of Arabic Hotels' Reviews. *Journal of Computational Science*.
- [6] Erdogan, B. Z. (1999). Celebrity Endorsement: A Literature Review. *Journal of Marketing Management*, 291-314.
- [7] Ahmed, R., Seedani, S., Ahuja, M., & Paryani, S. (2015). Impact of Celebrity Endorsement on Consumer Buying Behavior. *Journal of Marketing and Consumer Research*, 12-20.
- [8] Liu, B. (2012). *Sentiment Analysis and Opinion Mining*. Chicago, USA: Morgan & Claypool Publishers.

- [9] Medhat, W., Hassan, A., & Korashy, H. (2014). Sentiment Analysis Algorithms and Applications: A Survey. *Ain Shams Engineering Journal*, 5, 1093-1113.
- [10] Smola, A. J., & Scholkopf, B. (2004). A Tutorial On Support Vector Regression. *Statistics and Computing*, 199-222.
- [11] Khan, A., Baharudin, B., Lee, L. H., & Khan, K. (2010, February). A Review of Machine Learning Algorithms for Text-Documents Classification. *Journal of Advances in Information Technology*, 1(1), 4-20.
- [12] Hotho, A., Nürnberger, A., & Paaß, G. (2005). A Brief Survey of Text Mining. *LDV Forum - GLDV Journal for Computational Linguistics and Language Technology*, 19-62.
- [13] Nadkarni, P., Ohno-Machado, L., & Chapman, W. W. (2011, September 1). Natural Language Processing: an Introduction. *Journal of the American Medical Informatics Association*, 18(5), 544-551.
- [14] Amolik, A., Jivane, N., Bhandari, M., & Venkatesan, D. (2016). Twitter Sentiment Analysis of Movie Reviews using Machine Learning Techniques. *International Journal of Engineering and Technology*, 7(6), 2038-2044.
- [15] Hakim, L., Kusumasari, T. F., & Lubis, M. (2018). Text Mining of UU-ITE Implementation in Indonesia. *Journal of Physics: Conference Series*, 1007(1). <http://doi.org/10.1088/1742-6596/1007/1/012038>



# Group Formation Using Multi Objectives Ant Colony System for Collaborative Learning

Fitra Zul Fahmi<sup>1</sup>, Dade Nurjanah<sup>2</sup>

*School of Computing*

*Telkom University*

*Bandung, Indonesia*

<sup>1</sup>fitradzulfahmi@gmail.com.

<sup>2</sup>dadenurjanah@telkomuniversity.ac.id

**Abstract**—Collaborative learning is widely applied in education. One of the key aspects of collaborative learning is group formation. A challenge in group formation is to determine appropriate attributes and attribute types to gain good group results. This paper studies the use of an improved ant colony system (ACS), called Multi Objective Ant Colony System (MOACS), for group formation. Unlike ACS that transforms all attribute values into a single value, thus making any attributes are not optimally worth, MOACS tries to gain optimal values of all attributes simultaneously. MOACS is designed for various combinations of attributes and can be used for homogeneous, heterogeneous or mixed attributes. In this paper, sensing/intuitive learning styles (LSSI) and interests in subjects (I) are used in homogeneous group formation, while active/reflective learning style (LSAR) and previous knowledge (KL) are used for heterogeneous or mixed group formation. Experiments were conducted for measuring the average goodness of attributes (avgGA) and standard deviation of goodness of attributes (stdGA). The objectives of MOACS for homogeneous attributes were minimum avgGA and stdGA, while those for heterogeneous attributes were maximum avgGA and minimum stdGA. As a conclusion, MOACS was appropriate for group formation with homogeneous or mixed.

**Keywords**— *Collaborative learning, ACS, MOACS, group formation, homogenous group, heterogeneous group, mixed group*

## I. INTRODUCTION

The combination of learning method and social science has led to the development of collaborative learning in which students learn through group learning activities. The objective of group learning activities is that learners can individually gain knowledge by doing group work and interacting with peer learners. Tasks in group learning activities require learners to work together to solve problems, discover information, and complete projects [1]. Collaborative learning is a learning approach to improve social ability, practice skill, and experience, and enhance communication between [2][3][4]. In practicing collaborative learning in a class, teachers are required to perform a number of groups of learners.

Group formation is a key factor for supporting the success of collaborative learning activity [4][5]. The main objective of group formation is to build fair and effective groups [6][7], which can be achieved by finding appropriate attributes and methods. Group formation is important to support fairness and effectiveness of collaborative learning [6][5]. The fairness is related to students' feeling of convenience and happiness when working in a group [6].

The effectiveness refers to the opportunities of students participating in learning activities and gaining benefits from the group work, such as communication skill ability, knowledge, etc. In group formation, several aspects such as psychology, sociology, philosophy and education must be considered.

With the growth of information technology, collaborative learning is influenced by recent technologies of information; it is called computer-supported collaborative learning (CSCL). Group formation in CSCL is not a manual process anymore. The complexity of group formation has been increased because the group formation attributes and constraints are more and more varied. Group formation is an NP-Hard problem [8]. Previous research has studied various methods for group formation, such as rule/inference [9], Multi-agent [10][11], Greedy algorithm [12], Genetic Algorithm [13], Hill Climbing [14], Fuzzy C-Means [15], Ant Colony Optimization [16], and Semantic Web [8].

One of the challenges and issues in group formation system is how to combine learners' attributes which are considered good for performing homogeneous or heterogeneous groups. In this study, we start our work by reviewing and analyzing critical design issues of group formation and organize them according to some classification schemes. So that, it can help teachers to develop group formation system based on their cases. The various criteria or attributes have been applied in group formation, such as knowledge or expertise in a specific domain [9][15], learning goal [10], learners' performance in previous teamwork [10][16], personality traits [16], learning style [8][17][18], thinking style [13], Belbin role and minority [8], and preferred time slots and project [12].

This paper discusses our research on group formation. We applied the Multi Objective Ant Colony System (MOACS). This research accommodates different combinations of attributes for various objectives of grouping that lead to homogeneous, heterogeneous, or mixed groups. The remainder of this paper is organized as follows. Section 2 discusses our study on previous research on group formation. Section 3 explains MOACS for group formation and Section 4 is about the experiments and results. Finally, Section 5 presents conclusions and the future work.

## II. GROUP FORMATION

There are three types of groups: heterogeneous, homogeneous and mixed groups [19]. Homogeneous groups

have members with similar levels or homogeneous values of learners' attributes. Homogeneous groups, however, offer more advantages than heterogeneous groups when applied to skill exercises and guided discovery learning activities. On the other hand, heterogeneous groups consist of members with different levels, values or types of grouping criteria or attributes. Heterogeneous groups are appropriate for in-class problem solving (create journals, project, analysis of some cases) and long-term problem solving projects.

A former study has concluded chances to gain success, as it offers an opportunity for learners to be more innovative and creative [20]. Furthermore, some research has proved that heterogeneous groups support learners more to achieve learning goals than homogeneous groups [17][18][20]. The heterogeneity of the members means the groups have many resources. Every member gains rich and various points of view and opinions in groups rising from different personalities, experience, learning styles, etc. Combining both types has resulted in mixed groups, which are groups that consist of members with a combination of homogeneous and heterogeneous attributes. Homogeneous and heterogeneous attributes are not constraints to be strictly separated. Groups may have both heterogeneous and homogeneous attributes.

Another important attribute that must be considered is group size. Group size becomes an important parameter as it influences communication and relationships between group members. There is a useful point about group size, that is the larger the group size, the more groups can provide resource contribution, knowledge sharing, diversified skills and opportunities to meet other individuals with related interests. On the other hand, when group size increases, new problems tend to appear, such as difficulties in group organizational management, social loafing, free riding, trouble with monitoring behaviour of members, production blocking, evaluation apprehension, reduction in group ability to coordinate and collaborate, and pressure on individuals to conform [21]. Previous studies have revealed that smaller groups have promoted individual participation, greater satisfaction, more time for discussion, and an enhanced perception that contributions of members are vital to the success of the process [21]. Group size should not be based on convenience or instructor preference, but rather the type of tasks and the number of members required in accomplishing the task [21]. Slavin [4] proposed that the size of group formation is four persons with mixed ability members, for example one has high achievement, two have average achievement, and the other has low achievement. Another research [13] formed groups with three members each. Furthermore, another study suggested an optimal size of a group based on learning objectives [22], including skill exercises (teams of two), guided discovery Learning (teams of three), in-class problem solving (teams of four), and long-term problem solving project (teams of five).

There are a number of grouping attributes that have been used in previous studies. Among such group attributes, learning styles, thinking styles, personality types, personality traits and team role are the most used attributes.

### 1) Learning Style

A previous study by Liu et al. [23] used active/reflective dimensions of the Felder and Silverman learning style model to form groups [24]. They applied similar learning styles for doing the first task and diverse learning style for doing the second task. The study showed that applying diverse learning styles mean learners have more meaningful interaction and fewer disagreements in the group collaboration work. Another study [17] used other dimensions of learning styles, active-reflective, and sensing-intuitive. It affected the quality of learners' group work. Diverse learning styles make learners become aware of their own strengths and weaknesses, as well as their team mates' strengths and weaknesses. Knowing their team mates' characteristics made learners honor differences among them, talents and competence [25].

### 2) Thinking Style

Thinking style refers to a way for learners to find a solution to their problem. A previous study [13] found that there is a correlation between learners' attitudes and cooperation with group outcomes. Grouping considering thinking styles resulted in better groups in that they show less variance in group performance than randomly assigned groups do.

### 3) Personality Traits

A previous study found that learners grouped based on the performance level and personality attributes (traits) performed better than randomly-assigned or self-selected groups [20].

### 4) Team Role

Groups in some cases need to assign different roles to their member. It has been proved that the right role assignment resulted in good performance in a group [8].

## III. OUR RESEARCH: GROUP FORMATION USING MOACS ALGORITHM

The idea of using Ant Colony Optimization (ACO) for group formation system has been proposed by [16] and [20]. In previous study, ACO transform all attribute's score become single score, thus making any attributes are not optimally worth. In this study, we apply MOACS that enables to group learners and combine homogeneous or heterogeneous attributes of learners. MOACS tries to gain optimal score of all attributes simultaneously. MOACS consists of five phases, including initialization, exploitation, and exploration, finding the best fitness score, and local / global updating rule.

### A. Group Attributes and Constraints

Grouping attributes is one key aspect to form a group which are gathered from learners. Instructors or teachers must choose the group attributes before starting group formation. However, MOACS can use only attributes that have a score range between 0 and 1 and the attribute has qualitative evaluation by previous literature. Learners' attributes used in group formation in this research consist of:

#### 1) Previous knowledge level

Previous knowledge level is learners' expertise relevant to course or materials. This attribute usually is obtained from the grade in prerequisite course or pre-test before

study. The different levels of knowledge between learners in one group can support interaction between learners with high knowledge and low knowledge [20].

#### 2) Experience

Experience is related to learners' experience about specific cases or projects that learners have to solve it. The similar level of experience in one group can give each learner an opportunity to grow [8]. When learners have an opportunity to grow, learners will do the best together to reach the project goal.

#### 3) Learning style

Learning style has four dimensions: active/reflective, sensing/intuitive, global/sequential, and verbal/visual. Our study applies two attributes, which are active/reflective and sensing/intuitive. Placing different learners with active and reflective learning style can raise meaningful interaction among them [20]. In contrast, placing similar learners with either sensing or intuitive dimension in one group will benefit learners [15][24][25].

#### 4) Interest in a subject [26][27]

Every learner has interests in some subjects. The subjects can be hobbies, knowledge, music, movie, sport, or others. Different interests of learners can enrich group members' knowledge and experience when sharing knowledge or story. Similar interests of learners can motivate the group to engage in a higher level of interaction, that learners with high interest can motivate other learners with low interests.

#### 5) Thinking style in functionality dimension

Thinking style in functionality dimension consists of three attributes: legislative, executive, and judicial. Learners with similar thinking style in functionality dimension can collaborate that will improve learners' attitudes, the collaborative work, and group outcomes [13].

The type and value range of each attribute are shown in Tabel 1.

Table 1 Group Formation Attributes

Attributes	Type, Range Value	Normalized	Labels
Prior knowledge level or score of previous course or task	Heterogeneous, Between 0 and 100	[0..1]	High/ Moderate/ Low
Learning style in Active/Reflective dimension	Heterogeneous, Between -11 and 11	[0..1]	Active/ Neutral/ Reflective
Learning style in sensing/Intuitive dimension	Homogeneous, Between -11 and 11	[0..1]	Sensing/ Neutral/ Intuitive
Thinking style in functionality dimension	Homogeneous, Between 0 and 100	[0..1]	Legislative/ Executive/ Judicial
Learner's interest in a subject	Heterogeneous, Between 0 and 10	[0..1]	Interested/ Medium/ Uninterested

#### B. Algorithm: Multi-Objectives Ant Colony System

Figure 1 shows how group formation is done with MOACS.

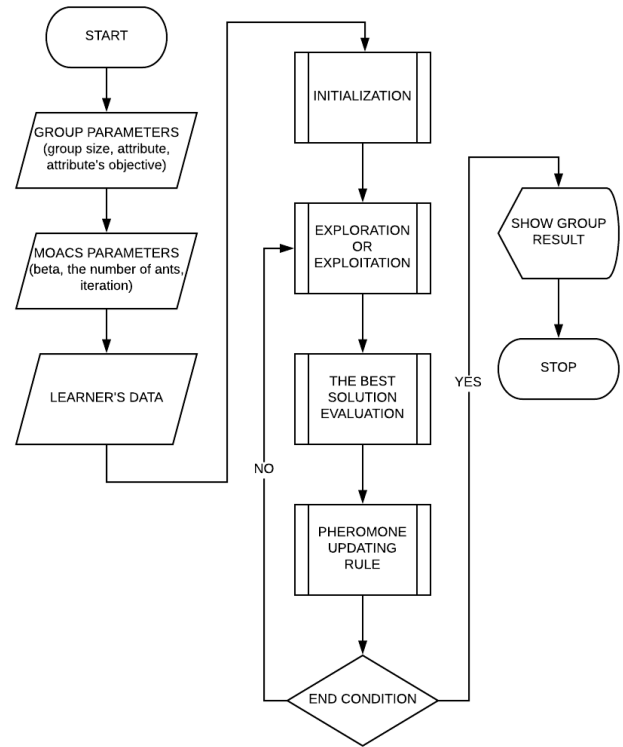


Figure 1 Group Formation using MOACS

#### 1) Initialization Phase

In multi-objective ant colony system (MOACS) problem, every solution by ant is measured according to more than one objective function, each of which must be minimized or maximized [28][29]. In group formation problem using MOACS, the objective function is the objective of attribute that must be heterogeneous (maximized) or homogeneous (minimized). The group formation problem is modelled as a complete graph that represents the closeness among learners. The learner's attributes for learner  $n$ -th that have  $r$  attributes are modelled by  $L_n = [C(0), C(1), \dots, C(r)]$ . The closeness among learners is measured according to each learner's attributes using Euclidean distance and represent by closeness matrices  $[M_{C(0)}, M_{C(1)}, \dots, M_{C(r)}]$ . Here is the formula for calculating distance between two learners for the  $r$ -th attribute.

$$M_{C(r)}(L_n, L_{n+1}) = \sqrt{\sum (C(r)_{L_n} - C(r)_{L_{n+1}})^2} \quad (1)$$

The proposed MOACS uses an ant to simultaneously optimize all objectives: the homogeneous attribute is minimized and heterogeneous attribute is maximized, because all attributes and their objectives are all important. All objectives share the same pheromone trails. In every iteration, an ant  $k$  ( $\forall k \in \{1, 2, \dots, N_{ants}\}$ ,  $N_{ants}$  is the number of ant in a colony that construct one feasible group solution and after ants have solution, the best solution will be chosen. The key of MOACS for group formation is how to determine the state transition rule (exploration and exploitation), group quality function, and the best solution evaluation and global updating rule.

#### 2) Exploration and Exploitation

Every ant does exploration and exploitation to choose group member. An ant selects the first member of the group



using an exploration formula and the second member until the last member in a group using an exploitation formula. If the targeted number of members is four, the ant will do exploration to the first member and then do exploitation to member 2 until 4. After that, for the next group, firstly, the ant does exploration and it continues with exploitation until all learners have been visited. When ant in learner  $i$  and selects the next member (let say learner  $j$ ), the ant will use the exploitation formula given by:

$$j = \begin{cases} \text{argmax}_{j \in N_i^k} \left\{ \tau_{ij} \cdot \left( [\eta_{ij}^{C(0)}]^\lambda \cdot [\eta_{ij}^{C(1)}]^{\frac{1}{r-1}-\lambda} \dots [\eta_{ij}^{C(r)}]^{\frac{r-1}{r-1}-\lambda} \right)^\beta \right\}, \\ \text{when group membership} \\ \text{randomly selected from } N_i^k, \text{ when choose first member (exploration)} \end{cases} \quad (2)$$

$\lambda = \frac{k}{N_{ants}}$  that represent the weight of each attribute and the value depends on the number of attributes  $r$ ;  $\beta$  represents the relative importance of each attribute with respect to the pheromone trail, given by  $\tau$ .  $N_i^k$  is defined as learner  $i$  that has not been chosen by ant  $k$ .  $\eta_{ij}^{C(r)}$  is the visibility for the objective or maximum distance between learner  $i$  and  $j$  in attribute  $r$ -th. In general, it is formulated in.

$$\eta_{ij}^{C(r)} = \begin{cases} \frac{1}{1 - M_{C(r)}(i, j)}, \text{ if } C(r) \rightarrow \text{homogeneous} \\ \frac{1}{M_{C(r)}(i, j)}, \text{ if } C(r) \rightarrow \text{heterogeneous} \end{cases} \quad (3)$$

Homogeneity or heterogeneity is the objective of each attribute. The exploration and exploitation in MOACS correlates to the number of attributes and each attribute's objective.

When an ant does exploration, it will select the learner  $j$  randomly from  $N_i^k$  learners ( $N_i^k$  is learners who have not been chosen by ant  $k$ ), according to the probability distribution given by the following calculation.

$$p_{ij}^k = \begin{cases} \frac{[\tau_{ij}] \left[ [\eta_{ij}^{C(0)}]^\lambda \cdot [\eta_{ij}^{C(1)}]^{\frac{1}{r-1}-\lambda} \dots [\eta_{ij}^{C(r)}]^{\frac{r-1}{r-1}-\lambda} \right]^\beta}{\sum_{j \in N_i^k} [\tau_{ij}] \left[ [\eta_{ij}^{C(0)}]^\lambda \cdot [\eta_{ij}^{C(1)}]^{\frac{1}{r-1}-\lambda} \dots [\eta_{ij}^{C(r)}]^{\frac{r-1}{r-1}-\lambda} \right]^\beta}, \text{ if } j \in N_i^k \\ 0, \text{ otherwise} \end{cases} \quad (4)$$

After an ant has explored and exploited learner's graph and all groups have the same number of members, an ant then checks  $N_i^k$ . If there are still learners in  $N_i^k$ , it means that there are orphan learners or learners who have not assigned to groups. So that, an ant will ignore the rule that limits the number of members in each group and allocate the learners in  $N_i^k$  to appropriate groups. This allocation will happen until there is no member left in  $N_i^k$ . The final activity in exploration and exploitation is local updating rule, which is updating of pheromone value in the route that has been explored and exploited by ant  $k$ .

$$\tau_{ij} = (1 - \rho) \cdot \tau_{ij} + \rho \cdot \tau_0 \quad (5)$$

Furthermore, the initial value of pheromones ( $\tau_0$ ) is also calculated using the following formula.

$$\tau_0 = \frac{1}{n \cdot G_{C(0)}^{\psi^k} \cdot G_{C(1)}^{\psi^k} \dots G_{C(r)}^{\psi^k}} \quad (6) \quad \tau_{ij} = (1 - \rho) \cdot \tau_{ij} + \frac{\rho}{G_{C(0)}^{\psi^{GP}} \cdot G_{C(1)}^{\psi^{GP}} \dots G_{C(r)}^{\psi^{GP}}} \forall (i, j) \in \psi^{GP} \quad (11)$$

Where  $n$  is the number of learners in a graph,  $\overline{G_{C(r)}^{\psi^k}}$ , which represents the average goodness of the  $r$ -th attribute in the initial solution  $\psi^k$ , which is generated randomly.

### 3) Solution Score

The result of an ant tour is a sequence of groups and their members. The quality of every attribute in each group will be measured by calculating the goodness of attribute score [16]. The goodness of attributes of solution given by ant  $k$  ( $\psi^k$ ) for attribute  $r$ -th ( $C(r)$ ) in group  $i$ -th could be computed by calculating the average distance ( $AD$ ) of members in group  $i$ -th for the  $r$ -th attribute.

$$AD_{C(r)}^{\psi^k}(i) = \frac{\max Cscoreof(L_1, L_2, \dots, L_n) + \min Cscoreof(L_1, L_2, \dots, L_n)}{2} \quad (7)$$

Then, the goodness of attributes will calculate by:

$$G_{C(r)}^{\psi^k}(i) = \frac{\max Cscoreof(L_1, L_2, \dots, L_n) - \min Cscoreof(L_1, L_2, \dots, L_n)}{\text{const} + \sum_j |AD_i - scoreof(L_{j(i)})|} \quad (8)$$

Where  $L_{j(i)}$  is the learner-score of the  $j$ -th learner in group  $i$ -th in solution  $\psi^k$  without learner that his score become  $\max Cscore$  and  $\min Cscore$ . Variable const is a constant number that can be set to 1, 0.01, or other. For example, when const is 1, the minimum value of  $G_{C(r)}^{\psi^k}(i)$  is 0 and the maximum value is 1, when const is 0.01, the minimum value of  $G_{C(r)}^{\psi^k}(i)$  is 0 and the maximum value is 100. The  $G_{C(r)}^{\psi^k}(i)$  indicates that the  $r$ -th attribute is in good heterogeneity when the score closes to the maximum value or in good homogeneity when the score closes to the minimum value. Until this phase, every group has goodness of attributes as much as the number of attributes ( $r$ ).

$$F_i^{\psi^k} = (G_{C(0)}^{\psi^k}(i), G_{C(1)}^{\psi^k}(i), \dots, G_{C(r)}^{\psi^k}(i)) \quad (9)$$

After that, the grouping result by an ant is measured by calculating the average goodness of attributes from each group and this result is called Pareto set  $PK$ .

$$PK = (\overline{G_{C(0)}^{\psi^k}}, \overline{G_{C(1)}^{\psi^k}}, \dots, \overline{G_{C(r)}^{\psi^k}}) \quad (10)$$

$\overline{G_{C(r)}^{\psi^k}}$  represent the average goodness of attribute  $r$ -th in solution  $\psi^k$ .

### 4) The Best Solution Evaluation and Global Updating Rule

In each iteration, the solution of each ant is recorded to a Pareto set  $PK$  and it is called local non-dominated set. Pareto-optimal set  $GP$  is called global non-dominated set, which is the best solution found by ants from the beginning of iteration. The solution in  $PK$  will be compared with the solution in Pareto-optimal set  $GP$  in order to check the better solution. When the solution in  $PK$  is non-dominated by  $GP$ , it means that  $PK$  is a new Pareto-optimal set, the value of  $GP$  and  $\psi^{GP}$  is updated by  $GK$  and  $\psi^k$ . Therefore, for each solution in  $\psi^{GP}$  found after one iteration by all ants in one colony, the pheromone information is globally updated according to the following formula.

$\overline{G}_{C(r)}^{\psi^P}$  represents the average goodness of attribute  $r$ -th in solution  $\psi^{GP}$ .

These four steps are done in each iteration (one colony of ant doing tour) until the end of iteration by all colonies or met the targeted condition.

#### IV. EXPERIMENT AND RESULTS

This section discusses the implementation of MOACS for group formation with homogeneous attributes, heterogeneous attributes, or mixed (homogeneous and heterogeneous) attributes. There are three scenarios which apply different types of attributes: homogeneous, heterogeneous, and mixed. Every scenario evaluates orphan learners, the average goodness of attributes (avgGA), and standard deviation (stdGA). MOACS aims to avoid orphan learners, which means that all learners can be grouped. The targeted condition for homogeneous attributes is minimum average goodness of attribute (avgGA) score, while for heterogeneous attributes the targeted condition is the maximum average goodness of attribute (avgGA) score. Standard deviation (stdGA) is used to show the distribution of goodness of attribute score in every group. The more minimum standard deviation, the better the groups resulted. The minimum standard deviation shows that the group result has a balancing goodness of attribute among groups.

The testing scenario was divided into three scenarios according to the types of attributes in group. The three scenarios were group formation using homogeneous for all attributes, group formation using heterogeneous for all attributes, and group formation using homogeneous in some attributes and heterogeneous in some attributes. In every scenario, MOACS was compared with two methods, which were a random method and ant colony by using homogeneous, heterogeneous, and mixed attributes.

##### A. Scenario 1 – Homogeneous Attributes

The objective of the first experiment is to measure the performance of MOACS for homogeneous group formation. MOACS was applied for group formation in Computer Organization and Architecture course with 42 students. It used homogeneous attributes for all attributes. The tasks in Computer Organization and Architecture are multiple choice and essay questions that must be solved by learners individually and then they discuss each solution to find correct answers. The attributes used are learners' interests (I) and learning styles in sensing/intuitive dimension (LSSI). The size of groups was seven as requested by the instructor. The result of grouping was shown in the following chart.

The lowest score in Figure 2 shows a good homogeneous score related to the attributes. MOACS is able to minimize learning style in Sensing/Intuitive dimension (LSSI) attribute. The score variation among learners tends to give a minimum goodness of attribute for homogeneous attribute. On the other hand, for interest in a subject (I) attribute, MOACS result is between the random method and Ant Colony System (ACS). The score variation among learners tends to give a maximum score for homogeneous attributes.

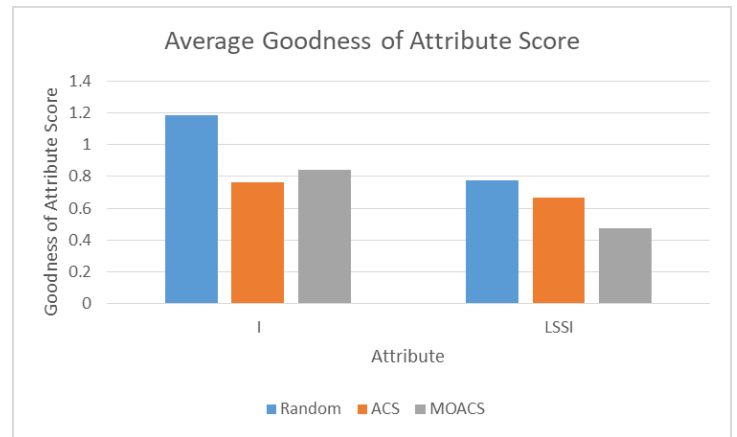


Figure 2 Average Goodness of Attribute Score in Scenario 1

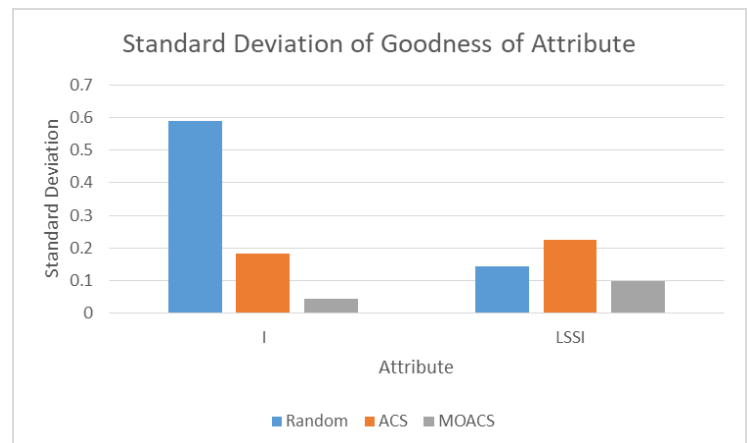


Figure 3 Standard Deviation of Goodness of Attribute in Scenario 1

The lower standard deviation score in Figure 3 shows good group results. MOACS is able to minimize the distribution of goodness of attribute scores in group formation which is better than other methods. The results show the group results have balancing goodness of attributes among groups. The expected result of group formation using homogeneous attributes is minimum avgGA and stdGA. Based on the average goodness of attributes in Figure 2 and standard deviation in Figure 3, MOACS is able to be used for group formation using homogeneous attributes.

##### B. Scenario 2 – Heterogeneous Attribute

The objective of the second experiment is to measure the performance of MOACS for heterogeneous group formation. MOACS was applied in a Design and Analysis Algorithm class with 40 students for grouping learners using heterogeneous attributes. The group task is to create a scientific essay. The attributes used are previous knowledge level (KL) and learning styles in active/reflective dimension (LSAR). The size of group is two. The result of grouping is presented in the figure 4.

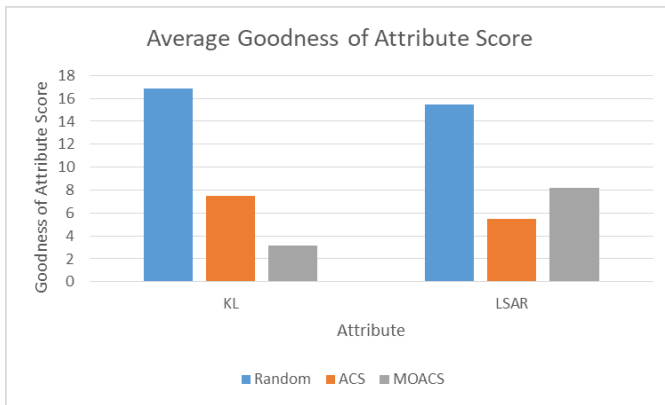


Figure 4 Average Goodness of Attribute Score in Scenario 2

The highest score for heterogeneous attribute in Figure 4 is a good result. MOACS results in low score in knowledge level (KL) and Learning Style in Active/Reflective dimension (LSAR). The knowledge level score has range between 4, 3.5, 3, 2.5, 2 until 1 before normalized to 0-1. The score variation is low, thus making it difficult to gain a maximum goodness of attribute score. Furthermore, LSAR score has range between -11 to 11. Then it is normalized to 0-1. The score variation in each learner tends to give a maximum goodness of attribute for heterogeneous attributes.

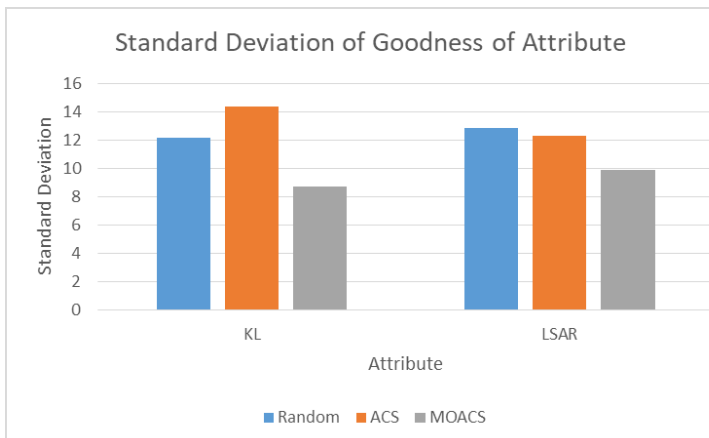


Figure 5 Standard Deviation of Goodness of Attribute in Scenario 2

The result in Figure 5 shows that MOACS is able to minimize the distribution of attribute in every group. MOACS is able to minimize the distribution of goodness of attributes scores in group formation. The result shows balanced goodness of attribute among groups. The expected result of group formation using heterogeneous attribute is the maximum avgGA and minimum stdGA. Based on the average goodness of attribute in Figure 4 and standard deviation in Figure 5, MOACS is not appropriate for group formation using heterogeneous attributes.

### C. Scenario 3 – Mixed Attribute

The objective of the third experiment is to measure the performance of MOACS for mixed homogeneous and heterogeneous group formation. MOACS is used for group formation in a Software Analysis and Design (APPL) class with 38 students using heterogeneous and homogeneous attributes. The main task of the APPL class is document analysis and design. The attributes used are learning style in

sensing/intuitive dimension (LSSI) set to homogeneous and learning style in active/reflective dimension (LSAR) and previous knowledge level (KL) set to heterogeneous. The size of the group was four. The result of grouping is shown in the following chart.

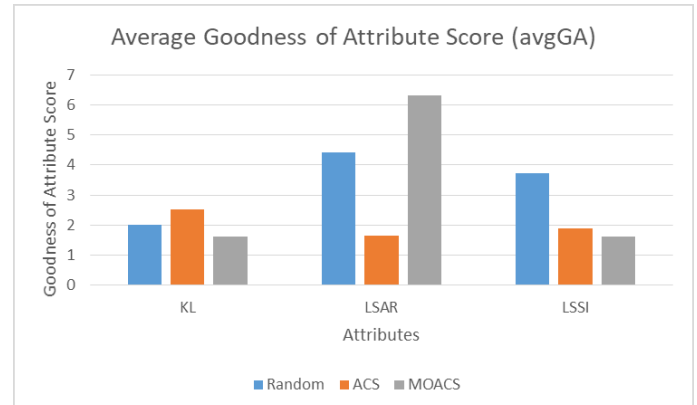


Figure 6 Average Goodness of Attribute Score in Scenario 3

Figure 6 shows that MOACS is able to maximize Learning Style in Active/Reflective dimension (LSAR) and minimize Learning Style in Sensing/Intuitive dimension (LSSI) attributes. The learning style in active/reflective dimension (LSAR) gives maximum avgGA, which means that it is good for heterogeneous attributes. On the other hand, learning style in sensing/intuitive dimension (LSSI) gives a minimum avgGA, which means that it is good for homogeneous attributes. The knowledge level score has range between 4, 3.5, 3, 2.5, 2 until 1 before it is normalized to 0-1. The score variation for each learner is low, thus making it difficult to gain maximum goodness of attribute score. LSAR score has range between -11 to 11 before it is normalized to 0-1. The score variation for each learner tends to give a maximum goodness of attribute score for heterogeneous attribute. Similar to LSAR, LSSI score has range between -11 to 11, then it is normalized to 0-1. The score variation for each learner tends to give a minimum goodness of attribute score for homogeneous attributes.

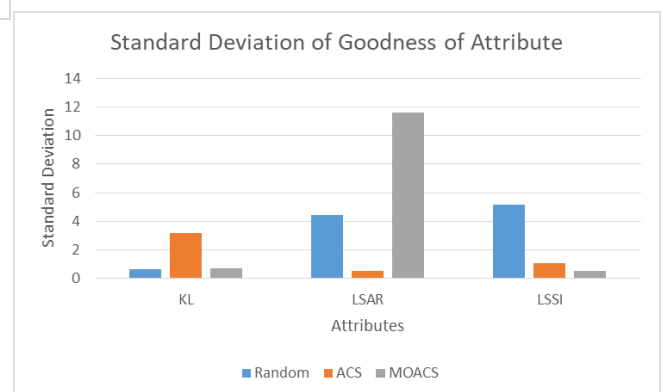


Figure 7 Standard Deviation of Goodness of Attribute in Scenario 3

Figure 7 shows that MOACS is able to minimize the distribution of Knowledge Level (KL) and Learning Style in Sensing/Intuitive dimension (LSSI) in group results. The result indicates that MOACS is able to distribute members among groups with balanced knowledge level and learning style in sensing intuitive attribute scores. The expected results of group formation using mixed attributes are

maximum avgGA for heterogeneous attributes, minimum avgGA for homogeneous attributes, and minimum stdGA for all attributes. Based on the average goodness of attributes in Figure 6 and standard deviation in Figure 7, the MOACS is appropriate for group formation using mixed attributes.

The experiment results show that MOACS gives minimum avgGA and stdGA in homogeneous group formation, which means that the group has member with similar degrees of attributes. The good result is shown in mixed group formation in two of three attributes related to avgGA. MOACS gives a maximum avgGA in learning style in active/reflective dimension for heterogeneous attribute and a minimum avgGA in learning style in sensing/intuitive dimension for homogeneous attribute. Furthermore, it gives a minimum stdGA in knowledge level and learning style in sensing/intuitive dimension. On the other hand, MOACS gives minimum avgGA and stdGA in heterogeneous group formation, which means MOACS is able to distribute members among groups with balanced attribute scores, but does not result in good goodness of attribute score for heterogeneous attributes. To conclude, MOACS is appropriate for group formation using mixed attributes.

## V. CONCLUSION

We have implemented Multi Objective Ant Colony System (MOACS) for group formation. The group formation is dynamic which can be applied to various combinations of attributes. Attributes that can be used in group formation includes learning styles, thinking styles, interests, and learner's knowledge. Considering collaborative learning requires homogeneous groups for some tasks or heterogeneous groups for other cases, we classify learners' attributes into homogeneous or heterogeneous. We test MOACS for homogeneous, heterogeneous, and mixed group formation. The tests show that MOACS is appropriate for homogeneous or mixed group formation.

## REFERENCES

- [1] V. Yannibelli and A. Amandi, "A deterministic crowding evolutionary algorithm to form learning teams in a collaborative learning context," *Expert Systems with Applications*, 39(10), 8584-8592, 2012.
- [2] D. Dansereau and D. Johnson, "Cooperative Learning," In : *Druckman, D., Bjork, R.A. : Learning, Remembering, Believing: Enhancing Human Performance*, National Academic Press, Washington, D.C., pp. 83-111, 1988.
- [3] D. Johnson and R. Johnson, *Leading the Cooperative School*, Edina, MN, 1989.
- [4] R. Slavin, "When Does Cooperative Learning Increase Achievement?," *Psychological Bulletin*, Vol. 94 (1983), pp. 429-445.
- [5] I. Magnisalis, S. Demetriadis and A. Karakostas, "Adaptive and Intelligent Systems for Collaborative Learning Support : A Review of the Field," *IEEE TRANSACTIONS ON LEARNING TECHNOLOGIES*, vol. 4, 2011.
- [6] P. Dillenbourg, "What do you Mean by Collaborative Learning?," *Collaborative Learning: Cognitive and Computational Approaches*, Elsevier Science, pp. 1-19, 1999.
- [7] A. Owens, E. A. Mannix and M. A. Neale, "Strategic formation of groups: Issues in task-performance and team member selection," In D. H. Gruenfeld, editor, *Research on managing groups and teams: Composition*, vol. 1, pp. 149-165, JAI PRESS, 1998.
- [8] A. Ounnas, *Enhancing the automation of forming groups for education with semantics* (PhD dissertation), University of Southampton, 2010.
- [9] H. U. Hoppe, "Use of multiple student modeling to parameterize group learning," 1995.
- [10] A. Inaba, T. Supnithi, M. Ikeda, R. Mizoguchi and J. Toyoda, "How Can We Form Effective Collaborative Learning Groups?," 2000.
- [11] L. K. Soh, N. Khandaker, X. Liu and H. Jiang, "A Computer-Supported Cooperative Learning System with Multiagent Intelligence," 2006.
- [12] M. A. Redmond, "A computer program to aid assignment of student project groups," 2001.
- [13] D.-Y. Wang, S. S. Lin and C.-T. Sun, "DIANA : A computer-supported heterogeneous grouping system for teachers to conduct successful small learning groups," 2007.
- [14] R. Cavanaugh, M. Ellis, R. Layton and M. Ardis, "Automating the process of assigning students to cooperative-learning teams," *AGE*, vol. 9, p. 1, 2004.
- [15] C. E. Christodouloupoulos and K. A. Papinikolaou, "A Group Formation Tool in an E-Learning Context," 2007.
- [16] S. Graf and R. Bekele, "Forming Heterogeneous Groups for Intelligent Collaborative Learning Systems with Ant Colony Optimization," In *Proceedings of Intelligent Tutoring Systems*, pp. 217-226, 2006.
- [17] Alfonseca, "The Impact of Learning Styles on Student Grouping for Collaborative Learning: A Case Study," *User Modeling and User Adapted Interaction*, vol. 16, pp. 377-401, 2006.
- [18] P. Paredes, "The Application of Learning Styles in Both Individual and Collaborative Learning," *Proc. Sixth IEEE Int'l Conf. Advanced Learning Technologies*, pp. 1141-1142, 2006.
- [19] A. Gogoulou, E. Gouli, G. Boas, E. Liakou and M. Grigoriadou, "Forming homogeneous, heterogeneous and mixed groups of learners," In P. Brusilovsky, M. Grigoriadou, K. Papanikolaou (Eds.), *Proceeding of workshop on personalization in learning environments at individual and group level in conjunction with the 11th international conference on user modeling* (pp. 33-40). Corfu, Greece., 2007.
- [20] R. Bekele, "Computer-assisted learner group formation based on personality traits" (PhD dissertation), *Hamburg University*, 2005.
- [21] S. L. Pierzon, "Social loafing and free riding in online learning groups," *PhD Dissertation*, 2011.
- [22] N. Herrmann, "Creativity, learning, and the specialized brain in the context of education for gifted and talented children," *Adapted from an address to the 7th world conference on gifted and talented children*, Salt Lake City, Utah, 1987.
- [23] S. Liu, M. Joy and N. Griffith, "An Exploratory Study on Group Formation Based on Learning Style," *2013 IEEE 13th International Conference on Advanced Learning Technologies*.
- [24] R. M. Felder and L. K. Silverman, "Learning and teaching style in engineering education," *Engineering education* 78.7 (1988), pp. 674-681.
- [25] M. Kyprianidou, S. Demetriadis, T. Tsiatsos and A. Pombortsis, "Group formation based on learning styles: can it improve students' teamwork?," *Educational Technology Research and Development*, Vols. 60(1), 83-110, 2012.
- [26] R. Hubscher, "Assigning students to groups using general and context-specific criteria," *IEEE Transactions on Learning Technologies*, 3(3), 178-189., 2010.
- [27] M. I. Dascalu, C. N. Bodea, M. Lytras, P. O. de Pablos and A. Burlacu, "Improving E-learning Communities Through Optimal Composition of Multidisciplinary Learning Groups," *Computer in Human Behavior*, vol. 30, pp. 362-371, 2014.
- [28] B. Baran and M. Schaerer, "A Multiobjective Ant Colony System for Vehicle Routing Problem with Time Windows. In," *Applied Informatics*, pp. 97-102, 2003.
- [29] L. Wang, J. Shen and J. Luo, "Multi-objective ant colony system for data-intensive service provision," in *Advanced Cloud and Big Data (CBD)*, 2014 Second International Conference on (pp. 45-52). IEEE, 2014.



# Smart Traffic Light based on IoT and mBaaS using High Priority Vehicles Method

Muhammad Izzuddin Mahali  
Department of Electronics and  
Informatics Education  
Yogyakarta State University  
Yogyakarta, Indonesia  
izzudin@uny.ac.id

Eko Marpanaji  
Department of Electronics and  
Informatics Education  
Yogyakarta State University  
Yogyakarta, Indonesia  
eko@uny.ac.id

Satriyo Agung Dewanto  
Department of Electronics and  
Informatics Education  
Yogyakarta State University  
Yogyakarta, Indonesia  
satriyoad@uny.ac.id

Bekti Wulandari  
Department of Electronics and  
Informatics Education  
Yogyakarta State University  
Yogyakarta, Indonesia  
bektiwulandari@uny.ac.id

Umi Rochayati  
Department of Electronics and  
Informatics Education  
Yogyakarta State University  
Yogyakarta, Indonesia  
umi@uny.ac.id

Nur Hasanah  
Department of Electronics and  
Informatics Education  
Yogyakarta State University  
Yogyakarta, Indonesia  
nurhasanah@uny.ac.id

**Abstract**—An increase of the number of vehicles which is not followed by the number of roads can lead to the increase of congestion, especially in big cities. Regulation of law no 22 Year 2009 explains that there are seven types of vehicles prioritized on the road. This research aims to build a Smart Traffic Light as a solution with the goal of making the prioritized vehicle journey smooth when crossing the road with Smart Traffic Light. The proposed system is "Smart Traffic Light on IoT and mBaaS (Mobile Backend As a Service) using High Priority Vehicles Method". The Smart Traffic Light has three important parts, including: (1) Smart Traffic Application; (2) Smart Traffic Controller; and (3) mBaaS. Prioritized vehicle drivers cross the road using the Smart Traffic Application when they are in an emergency situation. Smart Traffic Application and Smart Traffic Controller communicate using mBaaS. Smart Traffic Application has a vehicle track search facility as well as identification of traffic light location. A few meters before crossing, Smart Traffic Application will send the location to mBaaS and continue to be read by Smart Traffic Controller using internet. If it meets the criteria of High Priority Vehicle, then Traffic Light will be changed to green in the same path. The results show that when testing the data rate from Smart Traffic Application to Smart Traffic Controller, it takes no later than 8.15 seconds and 1.2 seconds (the fastest) with the average data transmission time of 3.39 seconds. Smart Traffic Light is able to identify the direction of the vehicle before passing through the Smart Traffic Application.

**Keywords**—smart traffic light, IoT, mBaaS

## I. INTRODUCTION

"Internet of Things (IoT) is a network of physical objects embedded in electronics, software, sensors and connectivity which enables it to achieve greater value and services by exchanging data with manufacturers, operators and / or other connected devices. Each unique thing is identified through an embedded computing system, but it is able to operate within the existing Internet infrastructure. So far, IoT is the most closely related to machine-to-machine (M2M) communications in manufacturing and electricity, petroleum, and gas. Products built with M2M communication capabilities are called smart or smart systems (e.g. smart label, smart meter, smart grid sensor). According to research results obtained from Juniper's study, there is a growth of IoT devices three times greater from 2016 to 2021. According to the results of research

from Juniper, it is estimated that the number of IoT equipment connected to the internet either device, sensor or actuator is approximately more than 46 billion within the next four years.

Mobile Backend as a Services (mBaaS) is one of the categories of cloud computing services that are usually used by mobile application developers. MBaaS helps developers by connecting applications with backend cloud database as well as other features such as user management, push notification and Authentication integration. These services are provided through the support of Software Development Kits (SDK) and Application Programming Interface (API). The Cloud Computing platform, which supports all smart agents, empowers specialized resources [1]. Internet of Things connected with mBaaS is able to create smart systems that can be used with various purposes. Integrated IoT and Cloud computing applications enabling the creation of smart environments such as Smart Cities need to be able to (a) combine services offered by multiple stakeholders and (b) scale to support a large number of users in a reliable and decentralized manner [2].



Figure 1 An Ambulance Stucked In Traffic Jam

According to Law No. 22 of 2009 on Road Traffic and Transportation Article 134 related to road users, those who have the primary right to take precedence are listed as follows: (1) fire-fighting vehicles carrying out duties (2) ambulances carrying sick people (3) vehicles to provide

assistance to Traffic Accidents (4) vehicles led by the State Institution of RI (5) vehicles of leaders and officials of foreign countries as well as international institutions who are guests of the state (5) a funeral parade/procession (7) convoys and / or vehicles for particular circumstances.

A good driving behavior is shown when there is an ambulance, they should give a way to it. However, when at the intersection of roads that have traffic light facing long congestion even up to hundreds of meters, ambulance sirens are not heard up to the vehicle at the end of the traffic light. Then, the ambulance has to wait for its turn to cross the intersection as shown in Fig.1.

## I. RELATED WORK

Another traffic light system is also proposed by [3] who proposes intelligent traffic signal control system by connecting RFID technology system, Microcontroller Unit, Cloud storage and Android App. In a study proposed by [3], when implemented in real terms RFID utilization, it would have difficulty when it is in a junction that had long congestion. RFID technology has difficulty in detecting vehicle distance. In different scenarios, if failing in detecting using RFID, android Application can be used. In the study [3], the number of points passed by the vehicle and how the alternative methods in the detection of lanes and the location of the crossing which is passed are not mentioned.

Firebase usage as mobile Backend as a Service is the use of database in the form of Cloud. The utilization of firebase in the IoT field has been done by [4]. The study discussed the use of cloud databases and authentication used for home automation. Firebase has many features such as Analytical, Authentication, Cloud Messaging, Real-Time Database, Storage, REST, Hosting, Test Lab, Crash Reporting and Cloud Functions [4]–[6]. Utilization of Scientific Cloud (Infrastructure as a Service) in IoT [7] can bridge the communication between hardware that has limited ability in data access. Things in IoT can be either input sensor or output actuator [8], [9].

The research of Smart Traffic Light Solution for High Priority Vehicle has been done by [10]. This study is devoted to ambulance that will be given a priority when crossing the intersection. In the research that has been done using the parameters Amount of ambulance requesting, the ambulance emergency level, minimum distance and waiting time Smart Traffic Light Solution for High Priority Vehicle research have been conducted by [10].

## II. PROPOSED METHODOLOGY

### A. System Diagram

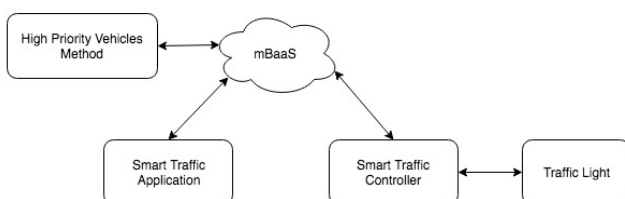


Fig. 2 General System Diagram

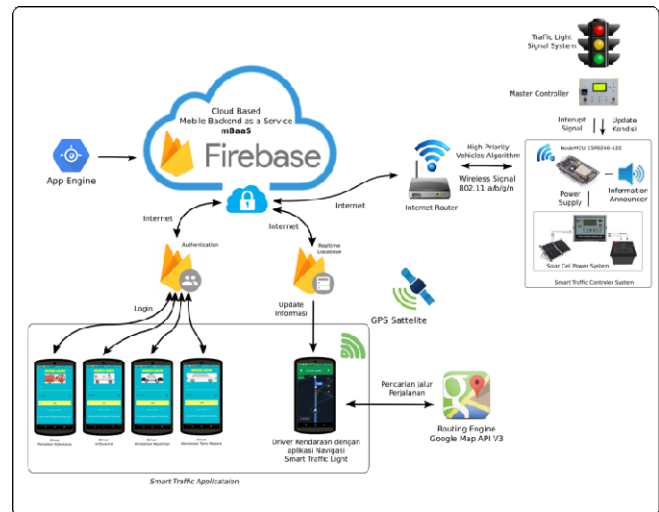


Fig. 3 System Diagram Detail

Broadly speaking, Smart Traffic Light System based on IoT and mBaaS using High Priority Vehicles method has five main parts as in Fig-2. (1) *Smart Traffic Application* (2) *Smart Traffic Controller* (3) mBaaS (4) High Priority Vehicles Method and (5) Traffic Light.

### B. Mobile Backend as a Service

The Smart Traffic Light system uses the Backend as a Service (mBaaS) Firebase mobile service in the form of Realtime Database, Authentication, Android SDK and REST Support services. The firebase usage allows the use of data stored in the cloud. Communications that occur between Smart Traffic Controller System and Cloud utilize API (Application Program Interface) [5]. Smart Traffic Application communicates with Firebase using Android SDK.

### C. Smart Traffic Application

Smart Traffic Application is an Android-based Operating System application used by vehicle drivers. This application has authentication login facility to maintain system security as well as identification of the vehicle type. In addition to using the application authentication feature, smart traffic also has Cloud Database facility that allows storage of cloud-based data (Cloud Database). The use of GPS facility from smart phone is used to know the position of the vehicle in real time. To support the map and navigation path, Smart Traffic Application uses API services from Google Maps [11] that provide digital map data, navigation routing and traffic density.

### D. Smart Traffic Controller

Smart Traffic Controller is a hardware device that plays as Things in the Internet of Things system [3], [4], [12]. Smart Traffic Controller uses nodeMCU main device with base ESP-8266. To support energy independence, this system uses a battery with a solar cell that is used to recharge the battery. Traffic Light on this system is APPL traffic light system that has been installed as a traffic control tool.



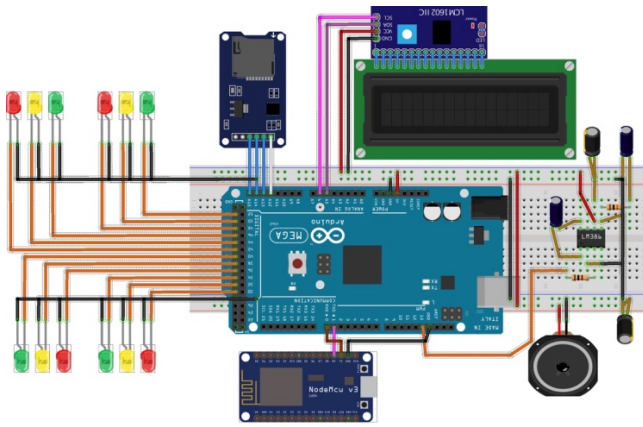


Fig. 4. Smart Traffic Controller System

Smart Traffic Controller Fig 3 is a hardware device used to control Traffic Light. This system consists of Controller Chip based on ESP8266 which has the function to read Realtime Database Firebase data using internet. The system is equipped with speakers used to play sound when there is a vehicle with a High Priority Vehicle crossing the traffic light. Voice mail files are stored in memory cards. The output is in the form of 12 output lines that functioned as input Traffic Light at the time of simulation.

#### E. High Priority Vehicle

Smart Traffic Light can be according to the rules of law requiring the system to apply High Priority Vehicles on App Engine. High Priority Vehicles are the implementation of regulation no 22 of 2009 which give priority of certain vehicles when passing on the road including at the intersection. The algorithm used to determine the most prioritized vehicles passes in the same location was the Analytical Hierarchy Process base. The determination of the value of High Priority Vehicles refers to the Journal written by [10] by introducing High Priority Vehicles (HPV) using 4 parameters while in this study three pieces were used, namely:

1. The type of vehicle is a sequence of priority passing vehicle users grouped in three types (Fire extinguisher, ambulance and vehicles with special interests)
2. The minimum distance is the calculation between the vehicle and the traffic light
3. Traffic Density Level

### III. IMPLEMENTATION OF WORKING

#### A. Smart Traffic Application

Smart Traffic Application is developed using android studio software and Java programming language. The Smart Traffic application has the following features:

- Cloud Database (Firebase)
- SignUp and Login
- Location Determination by using GPS
- Loading Referral Hospital List for Locations
- Selecting a Destination Location using the map
- Displaying the Route of vehicle travel
- Displaying the level of Road density
- Location determination of Smart Traffic Light System

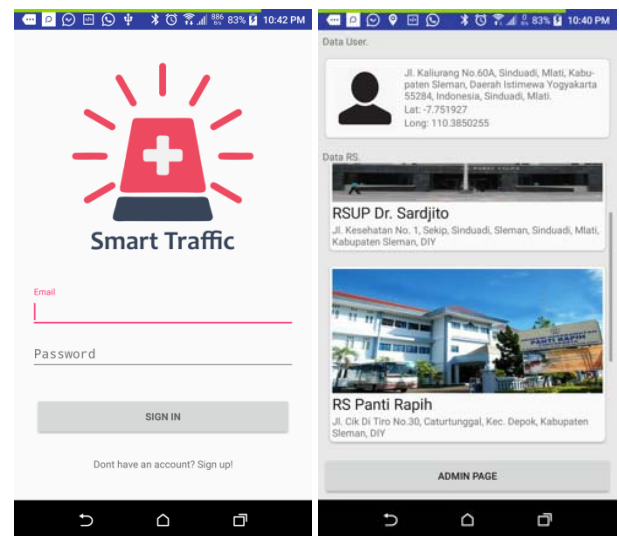


Fig. 5. Smart Traffic Application Authentication

Smart Traffic Application has a service for user account registrar. It aims at facilitating the addition of application users. Smart Traffic Application users should always be connected to the internet because user location updates will always be sent to the Firebase. When the Smart Traffic application is first opened, the user is prompted to enter a login username and password. All Smart Traffic Application users can use the same application simultaneously on the same or different Smart Traffic Light location.

Using the GP in the Smartphone Application will send the vehicle location update data to the Firebase using an internet connection such as a journal written by [8] that mentions that Science Cloud for IOT that we can use servers accommodating calculations on the Internet of Things system. Smart Traffic Application utilizes Google Map API V2 [11] to access digital maps, route searches, distance calculations, Smart Traffic System Location search and Traffic Level Traffic. This application is able to be used jointly by other users with unlimited amount.

#### B. mBaaS

Realtime Database Firebase Services are as Cloud data storage base for the communication bridging Smart Traffic Controller with Smart Traffic Application. Realtime databases on firebase have data structures in the JSON format (Java Script Object Notation) shown in bottom. The data which are saved include: user profile, traffic light location, Hospital location and Trip Log Request. Each location of traffic light that is added in the database is added with the detailed data about the traffic light. The stored data include name, location, coordinates, number of lights, detailed condition of each lamp direction, lamp flame condition, status request, emergency state, voice control and also activation threshold reference distance.

#### C. Traffic Light on Route Vehicle

Smart Traffic Light System has stored all coordinates of the traffic light location. The system will identify the path as well as the amount of traffic light that the vehicle will pass. The best route search takes the Google Maps V2 digital map. Once the route is obtained, it will be followed

by searching the location of traffic light that has been inputted in the database.

Smart Traffic Application continues to update user position and distance with the nearest traffic light. The calculation of the distance between two coordinates of longitude and latitude is calculated using the Harversine formula [13].

$$d = 2r \sin^{-1} \sqrt{\sin^2 \left( \frac{\Delta\phi}{2} \right) + \cos \phi_1 \cdot \cos \phi_2 \cdot \sin^2 \left( \frac{\Delta\lambda}{2} \right)}$$

$d$  is the distance between two point with longitude and latitude ( $\phi, \lambda$ ) and  $r$  is the radius of earth

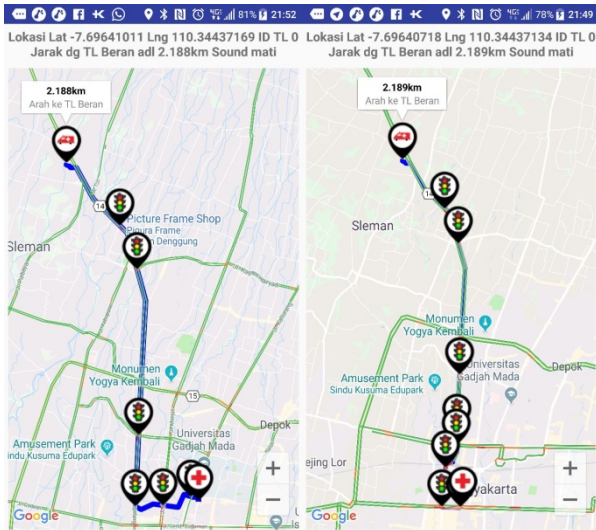


Fig. 6 Smart Traffic Application Route



Fig. 7 Smart Traffic Application Route

High Priority Vehicles algorithm on this system is used to determine the path priority which will cross first. The distance between the vehicle and the nearest traffic light will be shown on the following icon of the nearest Traffic Light when the application is used in emergency conditions as shown in Fig-6. Several meters before the vehicle crossing, the green light signals will be generated on the same line with the vehicle in an emergency so that the path accumulation on the path no longer exists.

#### D. Internet of Things

The Internet of Things Principle on Smart Traffic Controllers uses NodeMCU (ESP8266-12E) devices. NodeMCU has the facility to communicate with other devices by using wireless 802.11 that is able to communicate utilize port 43 (https) so that it makes the communication with Cloud Server becomes more secure. NodeMCU when communicating with mBaaS uses Authentication Key. The Database in Real Time Database with JSON format is translated directly in NodeMCU before send signal control to the actual Traffic Light.

#### E. Data Delivery Speed

Smart Traffic Application and Smart Traffic Controller communicate using internet network. The level of signal stability and internet speed depends on location and internet service provider. Table-1 is the test results of speed data transmission from the application and is received by the hardware Smart Traffic Light. The test of data transmission is done 10 times. Testing is done by utilizing manual configuration form that has been integrated in the application Fig-8. The calculation of time from the change in application happens until the data are received by Smart Traffic Controller. Data were obtained for each direction for north light traffic data with an average of 3,702 seconds, for the average speed of the eastern acceptance of 2.968 seconds, for the average speed of traffic data of the southern light is 1.857 and the last average speed of traffic reception Light west is 5.07 seconds. The fastest time of data transmission is 1.2 seconds and the longest time is 8.15 seconds. The average data transmission speed is 3.39 seconds.



Fig. 8. The Data Delivery Speed Test

Table 1 Speed of data transmission

Test Data	Data Delivery Time (s)			
	North	East	South	West
Data 1	8.15	2.39	3.09	4.03
Data 2	4.05	2.3	1.35	4.75
Data 3	3.05	1.64	1.94	3.1
Data 4	3.53	2.41	1.87	2.39
Data 5	4.29	5.38	1.55	6
Data 6	2.08	3.28	1.36	13
Data 7	2.29	4.05	2.27	5

Data 8	3.26	2.35	1.2	3.27
Data 9	2.62	2.92	2.09	6.16
Data 10	3.70	2.96	1.85	3
Average	3.702	2.968	1.857	5.07

#### IV. CONCLUSION

In this paper, a solution is proposed to reduce the travel time of the vehicle with special criteria (Fire Department, Ambulance, Special Vehicle) prioritized on the road. The travel time of the vehicle due to being trapped in long queues in traffic light can be reduced with Smart Traffic Light technology. Vehicle users can activate the Smart Traffic Application when in an emergency situation to get to a certain location e.g. ambulance that will take the patient to the hospital. Smart Traffic Application will find the fastest route and identify the Smart Traffic Light location to be traversed. Smart Traffic Light Application will send a location update to mBaaS which will be read by Smart Traffic Controller. Smart Traffic Controller will send commands to Traffic Light to provide green light signals before the vehicle passes on the same line. Smart Traffic Light can be used together for the same location or different location.

#### REFERENCES

- [1] G. Fortino, A. Guerrieri, W. Russo, and C. Savaglio, "Integration of agent-based and Cloud Computing for the smart objects-oriented IoT," in *Proceedings of the 2014 IEEE 18th International Conference on Computer Supported Cooperative Work in Design, CSCWD 2014*, 2014.
- [2] J. Gubbi, R. Buyya, S. Marusic, and M. Palaniswami, "Internet of Things (IoT): A vision, architectural elements, and future directions," *Futur. Gener. Comput. Syst.*, vol. 29, no. 7, pp. 1645–1660, 2013.
- [3] B. J. Saradha, G. Vijayshri, and T. Subha, "Intelligent traffic signal control system for ambulance using RFID and cloud," *2017 2nd Int. Conf. Comput. Commun. Technol.*, pp. 90–96, 2017.
- [4] A. Daramas, S. Pattarakitsophon, K. Eiumtrakul, T. Tantidham, and N. Tamkittikhun, "HIVE: Home Automation System for Intrusion Detection," in *Proceedings of the 2016 5th ICT International Student Project Conference, ICT-ISPC 2016*, 2016, pp. 101–104.
- [5] N. Singh, "Study of Google Firebase API for Android," *Int. J. Innov. Res. Comput. Commun. Eng.*, vol. 4, no. 9, pp. 16738–16743, 2016.
- [6] Firebase, "Firebase Realtime Database | Firebase," *April 13*, 2017. [Online]. Available: <https://firebase.google.com/docs/database/>.
- [7] A. Menon and R. Sinha2, "IMPLEMENTATION OF INTERNET OF THINGS IN BUS TRANSPORT SYSTEM OF SINGAPORE," *Asian J. Eng. Res.*, vol. 1, no. 4, pp. 8–17, 2013.
- [8] B. B. P. Rao, P. Saluia, N. Sharma, a Mittal, and S. V Sharma, "Cloud computing for Internet of Things & sensing based applications," *Sens. Technol. (ICST), 2012 Sixth Int. Conf.*, pp. 374–380, 2012.
- [9] E. Marpanaji and M. Izzuddinmahali, "Internet of Things for Survey of Renewable Energy Potential ( SREP ) as the Basis for Hybrid Power Plant Development," vol. 06003, p. 6003, 2016.
- [10] D. Dang, J. Tanwar, and S. Masood, "A Smart Traffic Solution for High Priority Vehicles," in *2015 1st International Conference on Next Generation Computing Technologies (NGCT-2015) Dehradun, India, 4-5 September 2015*, 2015, no. September, pp. 467–470.
- [11] G. Developers, "Google Maps Android API | Google Developers," *Google Developers*, 2015. [Online]. Available: <https://developers.google.com/maps/documentation/android-api/>.
- [12] R. Davies, "The Internet of Things The Internet of Things," no. May, p. 6, 2015.
- [13] N. Chopde and M. Nichat, "Landmark Based Shortest Path Detection by Using A\* and Haversine Formula," *GH Rasoni Coll. Eng. ...*, 2013.

# Correlation Between Bruto Domestic Products (GDP) With Duty Schools Based On Statistics Center Data Using Pearson Correlation Method Case Study : Indonesia 2008 - 2011

1<sup>st</sup> Daroe Iswatiningsih  
*Pendidikan Bahasa dan Sastra  
Indonesia*  
*Universitas Muhammadiyah Malang*  
Malang, Indonesia  
daroe@umm.ac.id

2<sup>nd</sup> Fachrunnisa Firdausi  
*Informatics Engineering*  
Malang, Indonesia  
fachrunnisa.firdausi@gmail.com

4<sup>th</sup> Hardianto Wibowo  
*Informatics Engineering*  
Malang, Indonesia  
ardi@umm.ac.id

3<sup>rd</sup> Wildan Suharso \*  
*Informatics Engineering*  
Malang, Indonesia  
wsuharso@umm.ac.id  
\* Corresponding Author

**Abstract**—This study aims to analyze the linkage of dropout rates with Gross Domestic Product (GDP). The data source of this research is the Central Bureau of Statistics (BPS), with data acquisition of GDP and dropout rate of elementary, junior and senior high school year 2008 until 2011. Data obtained through quantitative approach with secondary data source. The connectedness value between school dropout and GDP at primary level was 0.7294 in 2008, 0.7225 in the year of 2009, 0.4393 in 2010 and 0.3878 in 2011. While the relationship between the number of dropouts and GDP of junior high school level is 0.6095 in 2008, 0.6238 in 2009, 0.3605 in 2010 and 0.2467 in 2011. while the relationship between the drop out rate and GDP of the SMA level was 0.6061 in 2008, 0.5965 in 2009, 0.5321 in 2010 and 0.2606 in 2011.

**Keywords**—dropout, PDB, Pearson correlation

## I. INTRODUCTION

In the Indonesian dictionary, the meaning of education is the process of changing the attitude and behavior of a person or group of people in an effort to mature man through the efforts of teaching and training. It means that education aims to change a group or the whole to become more desirable. In the field of academic education will be related to certain sciences such as mathematics, language, social and others.

Education becomes a unity with culture in one department. This indicates that education is a mirror of a culture that exists in a country [1]. With the education of a culture will be preserved and make a positive value of a country. As well as some of the existing culture in the State of Indonesia is back home every holiday. In addition, there is a regional culture that is preserved by each region through the world of education.

Education is a pillar for a nation in action for the development of a nation [1]. In Indonesia, the education required for all citizens is 9 years of basic education. The same right to education means that there is no social, economic, and cultural background that differentiates in obtaining education for each student.

Implementation of this 9-year compulsory education cannot run smoothly just like that, but there are some

obstacles faced by the government. One of the problems that arise in the achievement of 9-year compulsory education is that students who drop out and who can not continue their education to a higher level. From 2008 to 2010 student dropout rates in Indonesia were relatively stable but in 2011 there was a 56% decline from the previous year [2], this indicates a significant change in 2010.

One of the factors causing dropouts is the economic factor that currently leads to global issues, namely poverty which is directly affected by income, family welfare level and amount of savings [3]. To overcome this global issue, the state has increased education funds up to 20 percent of the state budget. The proportion of government spending on the education sector, both on total development expenditure and Gross Domestic Product (GDP), indirectly indicates the government's reaction to the increasing demand for educational facilities and infrastructure.

In the 1945 Constitution Article 31 states that every citizen is entitled to education, even every citizen is obliged to follow basic education and the government is responsible for financing it. This indirectly shows how far the government realizes the importance of education [4]. So it is important to know the extent of government support for education in the range of 2008 to 2011.

The discovery of the correlation between two variables can be used to determine the relationship between them so that they can be used as a basis for making a causal diagram, in the case of telecommunications companies correlation analysis can be used as a basis for determining customer churn [6]. In the social case, correlation analysis can be used as a basis for determining the relationship between variables that affect public welfare [4]. It is expected that correlation analysis can find a connection between gross domestic product and the drop out rates of school students.

## II. RESEARCH METHOD

### A. Education

Education is a conscious and well-planned effort to create an atmosphere of learning and learning process so that learners actively develop their potential to have spiritual



power, self-control, personality, intelligence, noble character, as well as the skills needed by them, society, nation, and state (UU no. 20 year 2003).

Education is closely related to the quality of human resources (Human Resources) and the progress of the nation, now and in the future.

In the field of education, Indonesia has achieved tremendous progress for the achievement of the MDG (Millennium Development Goals) in the field of universal basic education and gender equality. However, there are still around 2.3 million 7-15-year-olds who are not in school. West Java, Central Java, and East Java provinces, where some of Indonesia's population, there are 42 percent of school children. (UNICEF, Annual Report 2012). The government should follow up on the 9-year compulsory education program and ensure the calibration of opportunities for education for all school-age students in Indonesia.

But not all students in Indonesia can feel the same opportunity because constrained unevenness of 9-year compulsory education program. As a result, many students are still forced to drop out of school. This fact is evident in the high number of poor people in Indonesia whose children drop out of school to no school at all because of lack of motivation and desire for school in the child so decided not to quit school.

Many factors that cause drop out students, economic factors, location factors or distance of school and learning interest is lacking. One of the most dominant main factors is the economic factor.

### B. PDB

According to the Central Bureau of Statistics, one of the important indicators to know the economic condition in a country within a certain period is the data of Gross Domestic Product (GDP), either on the basis of current prices or on the basis of constant prices. GDP is basically the amount of value added generated by all business units within a given country or is the sum of the value of final goods and services produced by all economic units. GDP at current prices illustrates the value added of goods and services calculated using the prevailing prices for each year, whereas GDP at constant prices represents the added value of the goods and services calculated using the prevailing price for a given year as a basis. GDP at current prices can be used to look at economic shifts and structures, while constant prices are used to determine economic growth year after year.

The proportion of government spending on the education sector, both on total development expenditures and Gross Domestic Product (GDP), indirectly shows the government's reaction to the increasing demand for educational facilities and infrastructure. Indirectly it shows how far people realize the importance of education.

### C. Pearson Correlation

Pearson Correlation method or also called Pearson Product Moment Correlation Method. The Pearson Correlation Method is a correlation used for continuous data

and discrete data suitable for parametric statistics. When the data is large and has parameters such as the mean and standard deviation of the population. Pearson correlation calculates correlation using variations of data. The diversity of data can show the correlation. This correlation calculates the data as it is, does not rank the data used. When data are numerical data such as rupiah exchange rate, financial ratio data, economic growth rate, and other numerical data samples, the Pearson product moment correlation is suitable for use. The formula used to calculate the Simple Correlation Coefficient is as follows,

$$r_{XY} = \frac{n \sum XY - \sum X \sum Y}{\sqrt{n \sum X^2 - (\sum X)^2} \sqrt{n \sum Y^2 - (\sum Y)^2}} \quad (1)$$

Explanation (1) includes n which is the number of pairs of data X and Y,  $\sum X$  shows the amount of variables X,  $\sum Y$  shows the amount of variables Y,  $\sum X^2$  shows the squares of total number of variable X,  $\sum Y^2$  shows the squares of total number of Variable Y,  $\sum XY$  shows the squares of total number of variable X and variable Y.

## III. RESULT AND DISCUSSION

### A. Data Collection

To obtain data that is really accurate, relevant and valid then the authors collect data using secondary data analysis. Secondary data is indirect data. These data are Gross Domestic Product (GDP) between 2008 to 2011 and the School Dropout Rate between 2008 to 2011, sourced from the Central Bureau of Statistics.

### B. Data Processing

From several data processing methods that exist and many references, chosen one method that eventually used in this research is Pearson Correlation Method or also called Pearson Product Moment Correlation Method. Pearson correlation method is the correlation used in parametric statistics, while for the data type is continuous data and discrete data.

### C. Education Data

The Department of Education and Culture of the Republic of Indonesia is an institution under the president who deals with and conducts education in the Republic of Indonesia. In the education system in Indonesia is divided into two parts, the first is compulsory education starting from elementary school to high school, the second is higher education that is supervised and managed by the Ministry of Research and Technology. From the data obtained from the Central Bureau of Statistics (BPS) Indonesia, obtained data dropout numbers as shown in table 1,

TABLE I. NATIONAL DROP OUT RATE [1][2]

Year	Dropout Rates
2008	437.608
2009	445.075
2010	439.033
2011	248.988

In table 1 the data of drop out rates every year does not always indicate an increasing number, but there is a decrease especially in 2011.

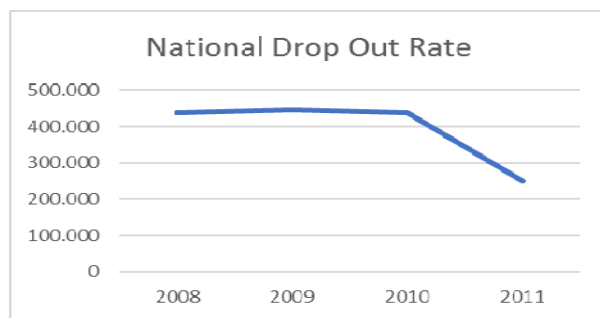


Figure 1. National Drop Out Rate [1][2]

From figure 1, it can be seen that there is a decrease in dropout rates. many things can influence the decline, one of which is a government program to support education or other external causes.

#### D. PDB Data

One of methods for calculating national income is GDP. In the economic field, GDP represents the market value of all goods and services produced by a country in a given period. GDP value data obtained from the Central Bureau of Statistics then processed so as to generate data that will be used to calculate the relationship with the value of drop out of school (table 2).

TABLE II. PDB [2]

Year	PDB
2008	510,2
2009	539,6
2010	755,0
2011	893,0

In table 2 the GDP value of each year is always increasing, in 2008 to 2009 the increase is not too high but then in the next year in the year 2010 to 2011 value of GDP has increased rapidly.

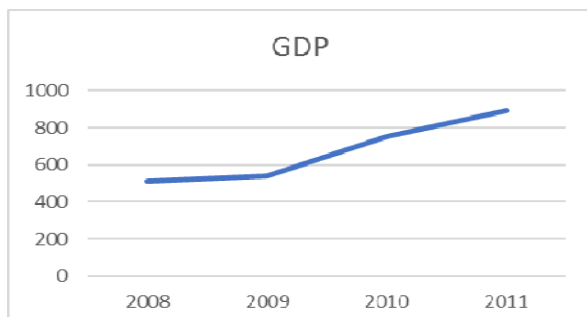


Figure 2. GDP[2]

from figure 2, there is an increase in Indonesia's GDP. In 2009 to 2011 there was a significant increase compared to 2008. Economic growth can be interpreted as a process of changing the economic conditions of a country on a

sustainable basis to a better state during a certain period. Economic growth can also be interpreted as a process of increasing the production capacity of an economy which is realized in the form of an increase in national income.

#### E. Examination

Testing is done by calculating data from BPS. The test result data will be analyzed to get the conclusion of linkage analysis of dropout rate with GDP.

TABLE III. CORRELATION GDP AND NUMBER OF DROP OUT RATES

	2008	2009	2010	2011
Primary School	0,7294	0,7225	0,4393	0,3878
Junior High School	0,6095	0,6238	0,3605	0,3467
Senior High School	0,6061	0,5965	0,5321	0,2606

Table 3 shows the results of the correlation divided into 3 levels, namely Elementary School (SD), Junior High School (SMP) and Senior High School (SMA). The highest score was owned by elementary school in 2008, and the lowest value was owned by Senior High School in 2011

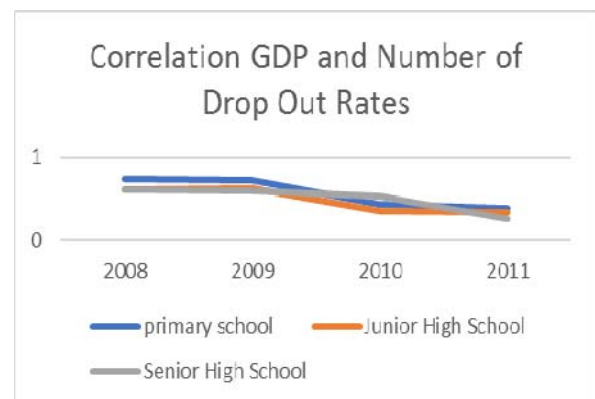


Figure 3. Correlation GDP and Number of drop out rates

#### IV. CONCLUSION

From the results of calculations using the Pearson, Correlation method obtained positive results which means the relationship between two variables are directly proportional or if the variable A rises, then the variable B come up. In other words, if the drop out value will affect GDP or decrease GDP.

The connectedness value between school dropout and GDP at primary level was 0.7294 in 2008, 0.7225 in the year of 2009, 0.4393 in 2010 and 0.3878 in 2011. While the relationship between the number of dropouts and GDP of junior high school level is 0.6095 in 2008, 0.6238 in 2009, 0.3605 in 2010 and 0.2467 in 2011. while the relationship between the dropout rate and GDP of the SMA level was



0.6061 in 2008, 0.5965 at in 2009, 0.5321 in 2010 and 0.2606 in 2011.

The conclusion of the linkage analysis between the number of dropouts and GDP is that the large amount of government aid to education with increasing GDP can not necessarily reduce the number of dropout rates. But the trend of connectedness every year is getting weaker which indicates the beginning of the relationship between the increasing number of GDP with the number of dropouts in Indonesia.

#### REFERENCES

- [1] Kementerian Pendidikan dan Kebudayaan Indonesia, <https://www.kemdikbud.go.id>
- [2] Badan Pusat Statistik Republik Indonesia, <http://www.bps.go.id/>
- [3] Ardiansyah, D., Suharso, W., & Marthasari, G. I. (2018). Analisis Penerima Bantuan Sosial menggunakan Bayesian Belief Network. *Jurnal RESTI (Rekayasa Sistem dan Teknologi Informasi)*, 2(2), 506-513.
- [4] Indonesia, Presiden Republik. "Undang-undang Republik Indonesia nomor 20 tahun 2003 tentang sistem pendidikan nasional." (2003).
- [5] Suharso, W., & Djunaidy, A. (2013). Analisis Customer Churn Menggunakan Bayesian Belief Network (Studi Kasus: Perusahaan Layanan Internet). *SISFO Vol 4 No 5, 4*.
- [6] Iswatiningsih, D., & Sutawi, S. (2016). Ketergantungan Iptek dan Ketidakberdayaan Umat Islam. *Jurnal Bestari*, (35).
- [7] Benesty, J., Chen, J., Huang, Y., & Cohen, I. (2009). Pearson correlation coefficient. In *Noise reduction in speech processing* (pp. 1-4). Springer, Berlin, Heidelberg.
- [8] Benesty, Jacob, et al. "Pearson correlation coefficient." *Noise reduction in speech processing*. Springer Berlin Heidelberg, 2009. 1-4.
- [9] SAHARA, A. Y. Y. (2013). Analisis pengaruh inflasi, suku bunga BI, dan produk domestik bruto terhadap return on asset (ROA) bank syariah di Indonesia. *Jurnal Ilmu Manajemen (JIM)*, 1(1).
- [10] Wicaksono, Galih Wasis, and Muhammad Andi Al-Rizki. "Peningkatan Kualitas Evaluasi Mutu Akademik Universitas Muhammadiyah Malang melalui Sistem Informasi Mutu (SIMUTU)." *Kinetik: Game Technology, Information System, Computer Network, Computing, Electronics, and Control* 1.1 (2018): 1-8.

# Mobile Learning: Utilization of Media to Increase Student Learning Outcomes

1<sup>st</sup> Edy Budiman  
dept. of informatics engineering  
universitas mulawarman  
Samarinda, Indonesia  
edy.budiman@fkti.unmul.ac.id

2<sup>nd</sup> Sitti Nur Alam  
dept. of informatics engineering  
stmik sepuluh nopember jayapura  
Jayapura, Indonesia  
nuralam.aptikom@gmail.com

3<sup>rd</sup> Mohammad Aldrin Akbar  
dept. of Economics Faculty  
university of yapis papua  
Jayapura, Indonesia  
aldrinakbar160@gmail.com

**Abstract**—The low learning outcomes of students from year to year in the department of informatics in the course of data structure affect the learning outcomes. The purpose of this research is to know the difference between Student Learning Result between Using Mobile Media Learning application with Conventional Learning. Using a Quasi-Experimental Design. The sampling technique used is Cluster Purposive Sampling. Samples were divided into two groups: experimental groups taught using media mobile learning apps, and control groups taught using conventional learning. The test result data were tested using the Shapiro-Wilk test to know the data normality, F test for data homogeneity, and t-test to know the difference of learning result value with significant level ( $\alpha = 0.05$ ). Based on the data analysis result, a normality test result with the Shapiro-Wilk test obtained the value of both groups of samples is the normal distribution and the result of the F test is homogeneous. T-test result obtained by probability = 1.830 with  $\alpha = 0.05$  so probability value  $< \alpha = 0.05$  which means  $H_0$  is rejected, hence there is the difference of result of student learning between using application of Mobile learning media with conventional learning.

**Keywords**—mobile learning, data structure, student, learning outcomes, quasi-experimental.

## I. INTRODUCTION

Activity learning environment that goes on is not always the same condition, there is flowing, some are not flowing, there are students who quickly understand what is delivered lecturer, and there are also students who find it difficult to understand what the lecturer presented. Students have high learning motivation and some are difficult to concentrate, and have no motivation, this is often found in the process of teaching and learning.

The data structure is one of the courses that get more attention from the Computer Science Lecturer and students. because this course is a lot of students make a failure in learning [1-2]. Various approaches methods, strategies, pattern, and technologies have been used as a lecturer, but have not been able to be an appropriate solution to be generally applicable [1], [3].

According to [4] data structures is a substantially important foundation course in computer science for computer programming students on account of learning fundamentals of data structures and algorithmic approaches used in software design and development. Further, that

explained data structures is also important for students to have the ability and vision to design and develop fast, active and stable software [4].

In the learning process is very necessary for a lecturer to overcome student learning difficulties. one of the approaches is to develop a mobile learning media. In our previous research, we have designed an instructional framework that focuses on the visualization of content media theory-practice of data structures course [1] and has measured the availability of network and service quality for the application of mobile learning tools of the data structure course. Then, the measurement results become the benchmark in the design and development of online learning software. Data usage, material content, access speed and streaming of learning content [5].

This paper will discuss the effect of mobile media app usage on student learning outcomes. "Is there any influence of the media on student learning outcomes in the course of data structures?", The expected contribution of this research is to become informed about the importance of mobile learning media as one of the methods approaches, become the solution of student's learning difficulties will stimulate students' learning spirit to learn become an easy and fun thing, as improving the teaching and learning process to achieve optimal learning outcomes.

## II. BACKGROUND AND RELATED WORK

### A. Network Availability in East Kalimantan

In order to that the mobile learning process can run well online, the network availability at the location must be available because the successful implementation of the online learning system is largely determined by the availability of the network in the area where the application users live (student habitation). Related to this, in previous studies the author has reviewed the server performance issues and availability of existing networks in the Borneo area, we have also analyzed and discussed them in previous research, among others; the paper [6], the study was conducted using a mobile device and implemented in seven districts and four points in every district in the city of Samarinda, East Borneo. Measurements using the standard quality of TIPHON with some parameters such as end-to-end delay, jitter, packet loss probability and throughput.

Broadband quality of service experience measuring mobile networks from consumer perceived [7], this paper provides an overview of the quality of service experience from the viewpoint of the customer's perceived of mobile broadband services. Using a quantitative descriptive analysis of active testing a number of data packets were sent to the communication line to measure the six Quality of Service parameters using the LIRNEasia Benchmarking approach.

User perceptions of mobile internet services performance in Borneo [8], the study tries to assess the Quality of Service (QoS) for mobile internet services in the ways assessment involves identifying user perception to assess consumer experience of the mobile internet services they were using. A survey led to the gathering of important information on QoS for mobile internet, which has been analyzed further. The information from the survey pertains to the awareness levels among consumers regarding their data plans, overall satisfaction, Indonesia Telecommunication Regulatory Authority (BRTI) and its regulations on QoS.

The network performance measurement related to the content of the application has been discussed in the paper [9], the paper examines the availability of mobile networks and also develops mobile learning software. The app is then implemented directly in the mobile networks, performing measurement and performance testing on the parameter which is the quality of service metrics by internet service providers in locations of the research project. And the paper [10], discussion an availability of mobile networks and develops mobile learning software.

### B. Mobile Learning App for Data Structure Course

Mobile Learning Applications that have been developed contain teaching materials in accordance with the syllabus of the Data Structure course, the material presented in the form of visual animation, along with code-script and theory on each content. The content of teaching materials refers to [1], shown in "Fig. 1.

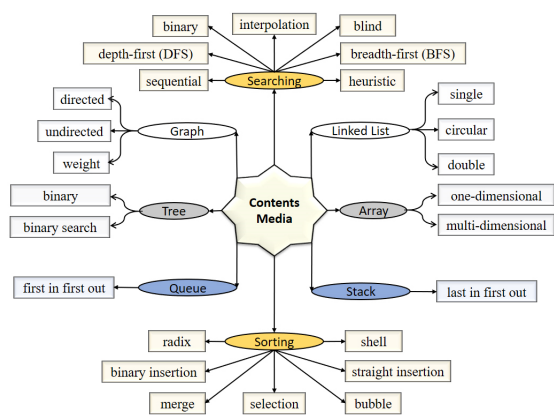


Fig. 1. Mind map diagram of contents media in data structure course app

The user interface of the Mobile Learning App can be seen in "Fig. 2".

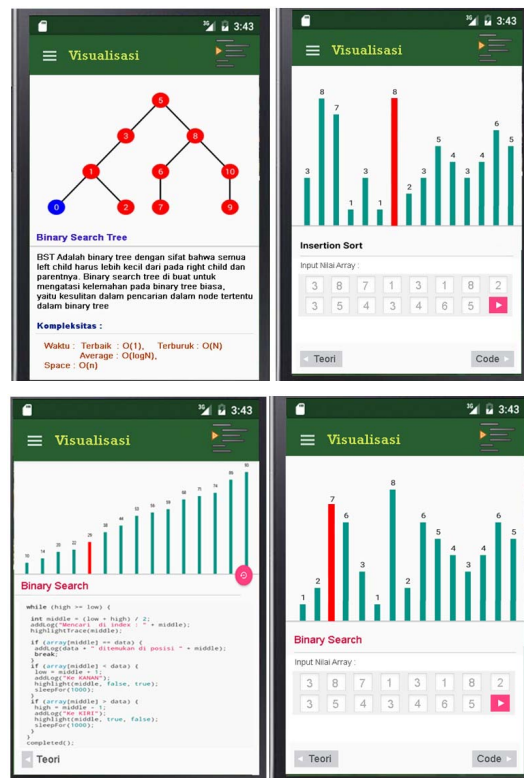


Fig. 2. user interface of the Mobile Learning App.

### C. The Student Learning Outcomes

Reference [11] has perform a survey of some of the literature in the area of learning outcomes shows a number definitions, i.e.:

Learning outcomes are statements of what is expected that the student will be able to do as a result of a learning activity [12]. Learning outcomes are an explicit description of what a learner should know, understand and be able to do as a result of learning [13]. A learning outcome is a statement of what the learner is expected to know, understand and/or be able to do at the end of a period of learning [14].

The student learning outcomes on the object of research have decreased the value of learning, at the end of the lecture many students who have failed in the course learning process. a large number of students who fail to follow this course will affect the quality of learning.

The low student learning outcomes in each year in the informatics department are presented in TABLE I.

TABLE I. THE STUDENT LEARNING OUTCOMES FOR 2 ACADEMIC YEARS

Academic Year	Grade					Sum
	A	B	C	D	E	
2015/2016	11	32	87	79	18	227
2016/2017	22	20	45	81	9	177

<sup>a</sup>. Source: Academic Information System

### III. METHODOLOGY

#### A. Research Design

The design of this research using Quasi-Experimental Design [15]. The research design begins by determining the population and selecting samples from the existing population with Cluster Purposive Sampling. In the design, there are two groups that are each chosen randomly. The same material used for both groups is about Searching and Sorting, but in the experimental class used mobile learning media app, while in the control class applied conventional learning model.

TABLE II. RESEARCH DESIGN WITH CONTROL GROUP DESIGN

Group	treat	Post Test
Experiment	X <sub>1</sub>	Test
Control	X <sub>2</sub>	Test

#### B. Population and Sampling Techniques

The population in this study is all students who program the course Data Structure Academic Year 2017/2018. The population is Student Generation 2017, which consists of 4 classes i.e. class A, B, C and D. Samples taken in this research consist of 2 classes that class A as control class and class B as experiment class. The sampling technique used is a quasi-experimental design. Samples taken in this research using Cluster Purposive Sampling method.

#### C. Conceptual Definition

- Learning using media, Learning uses this media where Lecturers use the media with the tool of Mobile Learning App to explain teaching materials.
- Conventional Learning, Conventional Learning is a lesson that emphasizes the involvement of Students in Lecturer-centered activities. In conventional learning the teacher uses several methods, such as lecture method, practice method and assignment method.
- Learning outcomes, are the abilities that are owned by the Students after receiving their learning experience. Learning outcomes were obtained from the Student's effort after following the learning process by using the learning result test on the subject of Searching and Sorting.

#### D. The Operational Definition of a Aariable

In order not to give rise to multiple interpretations and to avoid misinterpretation of the terms used in this study, the following operational definitions are given:

- (X) The independent variable is a learning model using mobile learning media and Conventional Learning.
- (Y) The dependent variable is the learning outcomes of the Students of the experimental class and control class groups in the Student.

#### E. Data Collection Technique

Methods of data collection conducted in this research are:

- Documentation, the preliminary data on the academic ability of the Student is obtained from the data of daily test results from the lecturers before the

treatment is done. Daily data on the material is the initial capability, and used for the formation of the group in the learning that will take place in the class.

- The test, this data was taken after each group received treatment, using mobile learning media in the experimental class and conventional learning in the control class. The final test result data will be processed and analyzed and then concluded whether there are differences in learning outcomes between the two treated groups.

Before the test is used as a research instrument, the test is first tested and then the item is analyzed. For the analysis of the degree of difficulty [16], [17], distinguishing, and reliability of multiple choice items [17].

#### F. Data Analysis Technique

- Descriptive statistics, used to describe data that is calculate the average value and standard deviation of a data. The data analyzed were preliminary test score data given in the study population, then selected two classes whose mean value of the initial test had significant differences.
- Inferential statistics, to perform hypothesis testing, first testing requirements analysis. before performing t test done first test of normality and homogeneity test two variance.
- Normality test, used to determine whether the data to be analyzed is normally distributed or not abnormally distributed, using the normality test [18]. The technique of calculating the normality test of this data using SPSS program.
- Homogeneity test, t test can be divided into two groups, t test with homogeneous variance and t test of heterogeneous variance. Homogeneous or heterogeneous variance is calculated using the F test [19].
- Hypothesis Testing, When the sample comes from population with homogeneous variance, then t test [20-25] is used.

Statistical Hypothesis in this study using SPSS computer program, then in draw the conclusion as follows:

- If  $\text{sig} > \alpha$  then  $H_0$  rejected, means there are differences in student learning outcomes using mobile learning media applications with Conventional Learning.
- If  $\text{sig} \leq \alpha$  then  $H_0$  accepted, means there are no differences in student learning outcomes using mobile learning media applications with Conventional Learning.

### IV. RESULT AND ANALYSIS

#### A. Initial Value Data

Based on the results of the test obtained descriptive data shown in TABLE III and TABLE IV. TABLE III, it shows that the highest value of the control group is higher than the experiment group value, and the experiment group's lowest value is higher than the control group.

TABLE III. PRE-TEST SCORES

Group	Data Test Value			
	Average	Standard Deviation	Highest Value	Lowest Value
Experiment	53.77	9.62	75.00	34.00
Control	52.27	9.20	76.00	33.00

Based on the post-test results obtained descriptive statistics of experimental class and control group can be seen in Table IV.

TABLE IV. POST-TEST SCORES

Group	Data Test Value			
	Average	Standard Deviation	Highest Value	Lowest Value
Experiment	81.03	11.57	98.00	55.00
Control	75.50	11.84	95.00	50.00

TABLE IV, it shows that the highest value of the experiment is higher than the control group value, and the lowest control value is lower than the value of the experimental group.

### B. Inferential Analysis

- Preliminary Test Data Value Analysis

TABLE V. TESTS OF NORMALITY

Group	Kolmogorov-Smirnov <sup>a</sup>			Shapiro-Wilk		
	Statistic	df	Sig.	Statistic	df	Sig.
Experiment after treat	.105	30	.200 <sup>*</sup>	.950	30	.171
Control after treat	.155	30	.065	.939	30	.085

<sup>\*</sup>. This is a lower bound of the true significance.  
a. Lilliefors Significance Correction

Test Data Normality in TABLE V, from the test results using SPSS 24 obtained value for the test results of the initial experimental group of 0.899 because the value of sig = 0.899 > 0.05 then  $H_0$  accepted. That is, the initial value data is normally distributed. While the results of the initial test of the control group obtained a significant value of 0.555 because the value of sig = 0.555 > 0.05 then  $H_0$  accepted. This means that the initial test data is also normally distributed.

Data Homogeneity Test, homogeneous or heterogeneous two variance were calculated using the F test. Based on the results of manual calculations obtained: F count = 1.119,  $F_{0.05} = 1.85$ . Since F count <  $F_\alpha$  then  $H_0$  is accepted i.e. the two samples of the population with homogeneous variance.

The t test used is a free two-t test that aims to compare two mean values. Based on the results of manual calculations, to determine the differences in the use of conventional learning model and learning using the media of mobile learning app in the data structure course used two-averaged test with the criteria of hypothesis given that  $H_0$  accepted [20].  $T_{table} = \pm 1.699$ ,  $T_{count} = 0.621$ .

$$-1.699 \leq t_{count} \leq 1.699$$

Because the value of T count is less than T table then  $H_0$  is accepted, this means the average of group learning result using conventional learning model there is no difference with mean of learning result using media of mobile learning app.

- Post Test Data Value Analysis

Test Data Normality in TABLE V, from the test results using SPSS 24 obtained value for the test results of the initial experimental group of 0.171 because the value of sig = 0.171 > 0.05 then  $H_0$  accepted. That is, the initial value data is normally distributed. While the results of the initial test of the control group obtained a significant value of 0.085 because the value of sig = 0.085 > 0.05 then  $H_0$  accepted. This means that the initial test data is also normally distributed.

Data Homogeneity Test, homogeneous or heterogeneous two variance were calculated using the F test. Based on the results of manual calculations obtained: F count = 0.955,  $F_{0.05} = 1.85$ . Since F count <  $F_\alpha$  then  $H_0$  is accepted i.e. the two samples of the population with homogeneous variance.

- T test to Determine the Difference between the Experiments group and the Control group

Based on the results of manual calculations, to determine the differences in the use of mobile learning models and conventional learning on the material Searching and Sorting, used two average difference test obtained:

$$T_{count} = 1.830$$

$$T_{table} = 1.699$$

Since the value of t count is more than T table then  $H_0$  is not accepted, this means the average of learning result by using mobile learning media is different with the average of learning result of conventional learning, or there is a real difference between mean of learning result by using mobile learning media with conventional learning. This difference shows that learning outcomes using mobile learning media are better than conventional learning outcomes, this is supported by the average learning outcomes of each group, for the experimental group and the control group.

The low learning outcomes of students from year to year in the field of informatics at the university where the author teaches, various approaches and learning models have been applied, but changes in student learning outcomes are not significant, one of the factors caused by the difficulties of Student learning in the Data Structure Course.

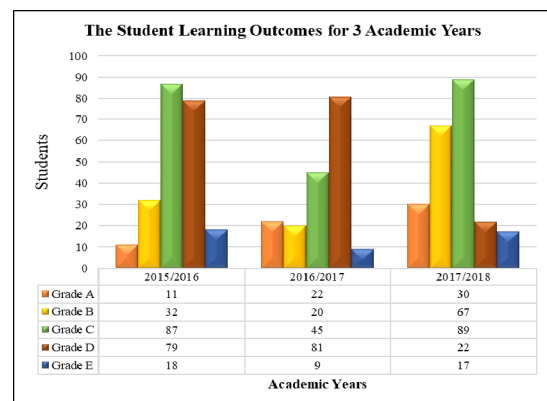


Fig. 3. Comparison of student learning outcomes for 3 academic years

Utilization Mobile-based learning technology to be one solution in helping teachers become teaching tools that can be packaged into a media of learning whenever and wherever students can use, it should be the teachers apply the mobile learning technology.

Since this year (academic year 2017/2018), we have taken advantage of mobile learning media applications that we have developed. And media influence can significantly increase student learning outcomes, particularly in the Data Structure course. Improvements in student learning outcomes are presented in "Fig. 3".

## V. DISCUSSION AND CONCLUSION

This study discusses differences in learning outcomes in the data structure between students taught using mobile learning media and conventional learning on the subject matter of Searching and Sorting Academic Year 2017/2018.

This study required 2 samples of the group, one group as the experimental class and one other class as the control group. In the Informatics department for the class of 2017 consists of 4 classes. Because it takes only 2 classes, then from 4 classes taken 2 classes by looking at the difference in the average value of the exam to be made in the experimental class and control class. From the test results in the previous material, it was found that the results showed that the experimental group and the control group came from the same initial condition, after the normality test and homogeneity test showed that both samples were normal distribution and there was no difference of variance. Then in the experimental group conducted treatment with the given mobile learning media while the control class is given the conventional learning treatment.

This study required 2 samples of the group, one group as the experimental class and one other class as the control group. In the Informatics department for the class of 2017 consists of 4 classes. Because it takes only 2 classes, then from 4 classes taken 2 classes by looking at the difference in the average value of the exam to be made in the experimental class and control class. From the test results in the previous material, it was found that the results showed that the experimental group and the control group came from the same initial condition, after the normality test and homogeneity test showed that both samples were normal distribution and there was no difference of variance. Then in the experimental group conducted treatment with the given mobile learning media while the control class is given the conventional learning treatment.

The learning process in the experimental group is given treatment with mobile learning media, where the students are required to take an active role in teaching and learning process. While the learning process in the control group with conventional learning, Lecturers explain about the material and Students listen to the explanation and asked if there is material that has not or less understood.

After both classes have been treated in the teaching and learning process, both groups are given a test for the evaluation of learning outcomes or final tests in the material. The average final test result obtained for the experimental group was 81.03 and for the 75.50 control group. This means the average experiment group is higher than the control group average. It is also clarified by t-test results where t-

count value is 1.830 with t table 1699, because the value of t-count  $1.830 > t\text{-table } 1.699$ , means  $H_0$  rejected and  $H_1$  accepted means there are differences in student learning outcomes between conventional learning by using mobile learning media.

Based on the normality test and homogeneity test, it was found that the evaluation data of the results of the two groups, namely the experimental group and the control group are normally distributed and the variance of the two homogeneous groups. The results of the analysis show that for the experimental group obtained the probability value 0.171 with a significant level of 0.05. This means the experimental group is normally distributed. For the control class obtained probability value of 0.085 with a significant level of 0.05. This means the control group is normally distributed. For homogeneity test, based on the calculation results obtained values  $F\text{ count} = 0.955$  and  $F\text{ table} = 1.85$  with  $\alpha = 0.05$ . Because  $F\text{ count} < F\text{ table}$  it can be concluded that both groups are homogeneous.

This shows that in teaching and learning process, teachers who teach using instructional media more support in improving student learning outcomes, compared with teachers who use conventional learning model. Based on the results of the above discussion it can be concluded that there are differences in learning outcomes between students who were taught using mobile learning media with students taught with conventional learning. Where learning using media is better than conventional learning.

## ACKNOWLEDGMENT

This research is funded by Non-Tax State Revenues (PNBP) Department of Information and Communication Technology (ICT) Year 2018. Thanks to the Dean of the Faculty of Computer Science and Information Technology.

## REFERENCES

- [1] Budiman, E., Haeruddin, Hairah, U., and Alameka, F., "Mobile learning: Visualizing contents media of data structures course in mobile networks", *Journal of Telecommunication, Electronic and Computer Engineering*, vol. 10 (1-9), 2018, pp. 81-86.
- [2] L. Alzubaidi, A. El Hassan, "Data Structures Learning-A Visually Assisted Approach", In *Proceedings of the International Conference on Computer Graphics and Virtual Reality (CGVR)* Jan, 2013, p. 37.
- [3] S. Patel, A literature review on tools for learning data structures, University of Cape Town, 2014.
- [4] Liu, Xiaojing, Xiaoying Wang, and Rui Wang, "Application of blended learning in data structures and algorithms course teaching." In *2013 the International Conference on Education Technology and Information System (ICETIS 2013)*. Atlantis Press, 2013.
- [5] Budiman, E., Hairah, U., and Saudek, A., *Mobile Networks for Mobile Learning Tools*, *Journal of Telecommunication, Electronic and Computer Engineering*, vol. 10 (1-4), 2018, pp. 47-52.
- [6] Budiman, E., and Wicaksono, O., *Measuring quality of service for mobile internet services*. *Proceeding - 2016 2nd International Conference on Science in Information Technology, ICSITech 2016: Information Science for Green Society and Environment*, Institute of Electrical and Electronics Engineers Inc., 2017, pp. 300-305. DOI: 10.1109/ICSITech.2016.7852652
- [7] Budiman, E., Moeis, D., and Soekarta, R., "Broadband quality of service experience measuring mobile networks from consumer perceived". In *Proceeding - 2017 3rd International Conference on Science in Information Technology: Theory and Application of IT for Education, Industry and Society in Big Data Era, ICSITech 2017*,



- Institute of Electrical and Electronics Engineers Inc., 2018, pp. 423–428.  
DOI: 10.1109/ICSITech.2017.8257150.
- [8] Budiman, E., and S.N. Alam., “User Perceptions of Mobile Internet Services Performance in Borneo.” In Proceedings of the 2nd International Conference on Informatics and Computing, ICIC 2017. Institute of Electrical and Electronics Engineers Inc, 2018. p  
DOI:10.1109/IAC.2017.8280643.
- [9] Budiman. E., and Alam, S.N., “Database: Taxonomy of plants Nomenclature for borneo biodiversity information system”2nd International Conference on Informatics and Computing, ICIC 2017, in Conf. Rec. IEEE Explore 2018, Institute of Electrical and Electronics Engineers Inc, 2018, pp. 1-6.  
DOI: 10.1109/IAC.2017.8280642.
- [10] Budiman, E., Haryaka, U., Watulingas, J.R., and Alameka, F. “Performance rate for implementation of mobile learning in network”. In International Conference on Electrical Engineering, Computer Science and Informatics (EECSI), IEEE Xplore, 2017.  
DOI: 10.1109/EECSI.2017.8239187
- [11] Kennedy D. Writing and using learning outcomes: a practical guide. University College Cork; 2006..
- [12] Jenkins, A. and Unwin, D., How to write learning outcomes, 2001. Available online:  
[www.ncgia.ucsb.edu/education/curricula/giscc/units/format/outcomes](http://www.ncgia.ucsb.edu/education/curricula/giscc/units/format/outcomes)
- [13] Bingham, J., Guide to Developing Learning Outcomes. The Learning and Teaching Institute Sheffield Hallam University, Sheffield: Sheffield Hallam University, 1999.
- [14] Donnelly, R and Fitzmaurice, M. Designing Modules for Learning, in: Emerging Issues in the Practice of University Learning and Teaching, O’Neill, G et al. Dublin: AISHE, 2005.
- [15] Campbell DT, Stanley JC. Experimental and quasi-experimental designs for research. Handbook of research on teaching. pp.171-246.
- [16] Mahjabeen, W., Alam, S., Hassan, U., Zafar, T., Butt, R., Konain, S. and Rizvi, M., Difficulty Index, Discrimination Index and Distractor Efficiency in Multiple Choice Questions. *Annals of PIMS-Shaheed Zulfiqar Ali Bhutto Medical University*, 13(4), 2018. pp.310-315.
- [17] Jandaghi, G. & Shaterian, F. Validity, Reliability and Difficulty Indices for Instructor-Built Exam Questions. *Journal of Applied Quantitative Methods*, vol.3(2),2008, pp.151-15
- [18] Park, H.M., Univariate analysis and normality test using SAS, Stata, and SPSS, 2015.
- [19] Flores, R., Lillo, R. and Romo, J., Homogeneity test for functional data. *Journal of Applied Statistics*, vol. 45(5), 2018, pp.868-883.
- [20] Wang, C. and Weiss, D.J., Multivariate hypothesis testing methods for evaluating significant individual change. *Applied psychological measurement*, 42(3), 2018, pp.221-239.
- [21] Haeruddin., Johan, H., Hairah, U., and Budiman, E. Ethnobotany database: Exploring diversity medicinal plants of dayak tribe borneo. In International Conference on Electrical Engineering, Computer Science and Informatics (EECSI), Institute of Advanced Engineering and Science, 2017, pp. 120–125.  
DOI: 10.1109/EECSI.2017.8239094.
- [22] Hairah, U., Tejawati, A., Budiman, E., and Agus, F. (2018). Borneo biodiversity: Exploring endemic tree species and wood characteristics. In Proceeding - 2017 3rd International Conference on Science in Information Technology: Theory and Application of IT for Education, Industry and Society in Big Data Era, ICSITech 2017, (Institute of Electrical and Electronics Engineers Inc.), pp. 435–440.  
DOI:10.1109/ICSITech.2017.8257152
- [23] Moser, B.K. and Stevens, G.R., Homogeneity of variance in the two-sample means test. *The American Statistician*, 46(1), 1992, pp.19-21.
- [24] Dengen, N., Budiman, E., Widians, J.A., Wati, M., Hairah, U., and Ugiarto, M., Biodiversity information system: Tropical rainforest borneo and traditional knowledge ethnic of dayak. *Journal of Telecommunication, Electronic and Computer Engineering*, vol. 10. No. 1-9, 2018, pp. 59-64.
- [25] Budiman. E., Jamil. M., Hairah. U., Jati. H., and Rosmasari, “Eloquent object relational mapping models for biodiversity information system”, 4th International Conference on Computer Applications and Information Processing Technology 2017, CAIPT 2107, in Conf. Rec. IEEE Explore 2018, Institute of Electrical and Electronics Engineers Inc., 2018, pp. 1-5.  
DOI: 10.1109/CAIPT.2017.8320662.

# Study of the Android and ANN-based Upper-arm Mouse

Hartawan Sugihono  
Informatics Engineering Study Program  
Universitas Ma Chung, Malang,  
Indonesia

Romy Budhi Widodo  
Informatics Engineering Study Program  
Universitas Ma Chung, Malang,  
Indonesia  
romy.budhi@machung.ac.id

Oesman Hendra Kelana  
Informatics Engineering Study Program  
Universitas Ma Chung, Malang,  
Indonesia

**Abstract**— *Disability is a person's condition in the physical, intellectual, mental, and/or sensory limitations in the long term. This study is reserved for those who do not have the lower arm in order to operate the computer normally. This study uses orientation sensor on the smartphone as the main sensor to move the cursor and click. Delivery of data from smartphone to computer is using Bluetooth. This study will compare two gestures from a combination of orientation sensors on the upper arm: gesture 1 using pitch-yaw motion and gesture 2 using pitch-roll motion; to move the cursor on the monitor. Left-click and right-click using ANN is to detect upper arm jerk movements. Evaluation using ISO / TS 9241-411 standard: ergonomics of human-system interaction; which includes performance evaluation and comfort of the gesture. Performance results of throughput, movement time, comfort and fatigue between gestures were not significantly different between those gestures. The result of the effort questionnaire is that gesture 1 has the highest effort on the shoulder and gesture 2 has the highest effort on the hand.*

**Keywords**— Android, ANN, Fitts'law, ISO/TS 9241-411, Pointing device

## I. INTRODUCTION

The Constitution of the Republic of Indonesia number 8 in 2016 [1], describes the disabled as any persons who have limited physical, intellectual, mental, and/or sensory ability in interaction with the environment and may have difficulties to participate effectively. Persons with disabilities have difficulty in the technology processing such as computers. The mouse on the computer becomes one of the obstacles for disabled, especially for those without their forearms (elbows to fingers) to use the computer. Besides the mouse, there is also a cursor triggering tool, that is a remote application in the smartphone. This remote application also uses fingers to move the cursor and click. In this case, the disabled without forearms find problems to use.

Human computer interaction (HCI) is the science in communication between humans and computers. By making use of HCI, an application for the disabled without forearms can be developed; meanwhile, the application of the study itself will use sensors available in a smartphone.

Sensor orientation is used to replace the mouse function. This sensor is available on some smartphones. By using their upper arms to move the computer cursor, the disabled without the forearms can also use it.

Based on the existing problems, there are several similar studies with different methods such as gyro-mouse [2]. It is a study of mouse replacements using the gyro sensors placed on the glasses and how to move it by moving the head. The mouse earphone [3] is a study of mouse alternatives using an accelerometer sensor placed on the earphone and how to move it with head movement. The other references in this study are eye-tracker [4], color pointer detection [5] and voice controller [6]. These studies are carried out by looking for the computer cursor triggering alternative without having to use a finger.

In this study we propose a new method of Android-based mouse alternative for disabled persons with no forearms for both hands. Moving the cursor needs the movement of the upper arm with two gestures. The first gesture uses a pitch-yaw and the second gesture uses pitch-roll. Artificial neural networks (ANN) are used to detect click actions and classify cursor movements (gesture 1 and gesture 2).

## II. METHODS

In general, the system diagram as in Fig. 1. The information flow is 1) orientation sensor is processed by using ANN; 2) ANN result includes left click, right click or cursor movement; and 3) send the command of ANN to PC.

### A. Orientation Sensor

Orientation sensor [7] is a sensor used relatively to monitor the position and orientation of a smartphone to the earth's surface. The orientation sensor obtains its data by processing proximity sensor's data from the accelerometer and geomagnetic field sensors. Using these two sensor sensors, the system provides data for the three orientation angles which are yaw (azimuth), pitch, and roll. Figure 2 shows three orientation angles that work on a smartphone.

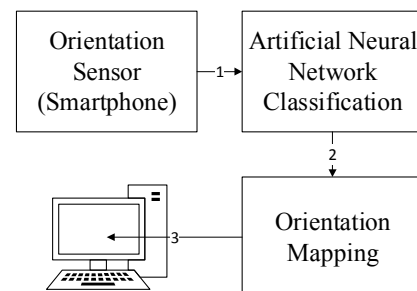


Fig. 1. System diagram

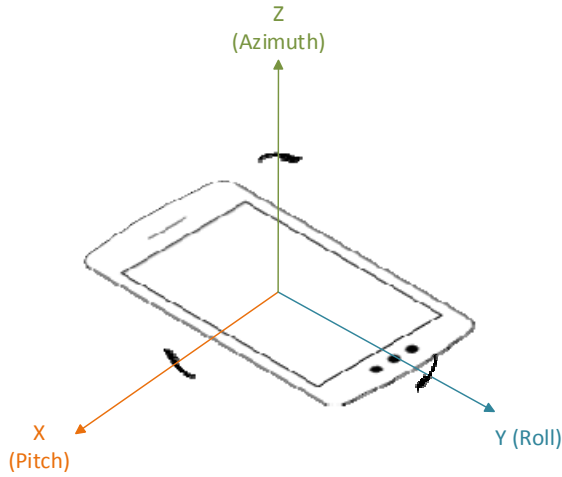


Fig. 2. Orientation sensor angle on the smartphone

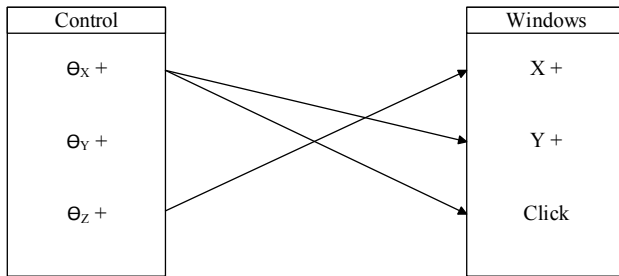


Fig. 3. The sensor-cursor mapping of gesture 1

### B. Upper Arm Movement

The proposed upper-arm mouse uses a smartphone that is placed in the upper arm of a human. This experiment uses two gestures to compare its performance with the mouse. Gesture 1 uses a pitch-yaw angle sensor in which the pitch is for up-down movement and yaw is for left-right movement. Gesture 2 uses a pitch-roll angle sensor in which the pitch is for up-down movement and roll is for left-right movement. The following are the explanations for every gesture examined.

#### 1) Gesture 1

Gesture 1 is mapped as described in Fig. 3. Fig. 3 tells  $\Theta_x +$  to be the initial data to move the cursor on screen in the Y + axis and click method. The  $\Theta_z +$  axis becomes the initial data to move the cursor on screen in the X + axis.

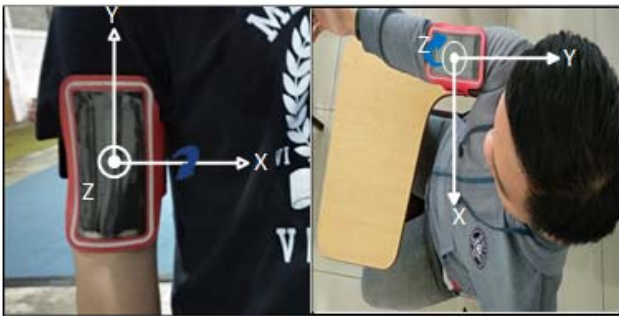


Fig. 4. Gesture 1

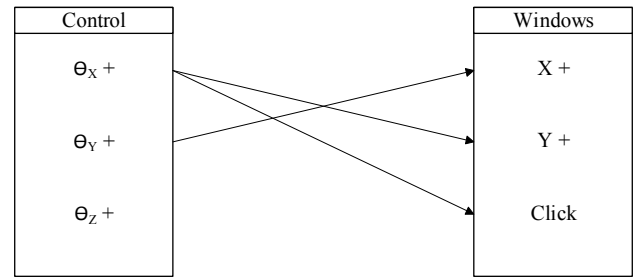


Fig. 5. The sensor-cursor mapping of gesture 2

How to use gesture 1 is illustrated in Fig. 4.

#### 2) Gesture 2

Gesture 2 is mapped as described in Fig. 5. Figure 5 tells  $\Theta_x +$  to be the initial data to move the cursor on screen in the Y + axis and click method. The  $\Theta_z +$  axis becomes the initial data to move the cursor on screen in the X + axis. How to use gesture 2 is illustrated in Fig. 6.

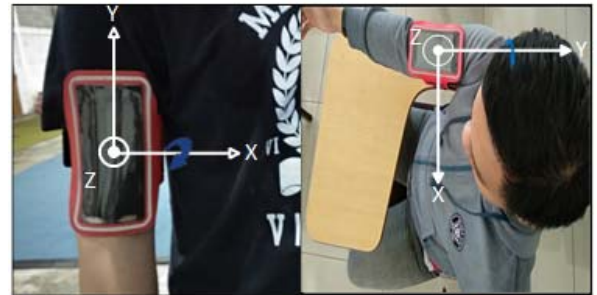


Fig. 6. Gesture 2

### C. Artificial neural network

Artificial neural network (ANN) is a way to demonstrate how neural network in the human brain works in doing a task. Many application used the ANN as an example in measuring the step-length, as in [8]. Neurons are depicting of the human brain's working system in organizing its constituent cells. The goal of organizing these cells is to recognize certain patterns with a very high network effectiveness. The levenberg-marquardt training algorithm is one of the famous due to the speed [9]

Like humans, ANN also needs a learning to recognize patterns. The result of ANN training is the value used for the classification. ANN training requires an activation function to enable or disable neurons. The activation function used in this study is symmetric sigmoid.

We use 200 data in terms of Pitch, which include 100 upward jerks for left click and 100 downward jerks for right click. Figure 7 tells 1 data in terms of pitch has 100 inputs. We use one hidden layer with 14 neurons. The output from ANN is 2 neurons with 01 for left click, 10 for right click, and others counted as cursor movements.

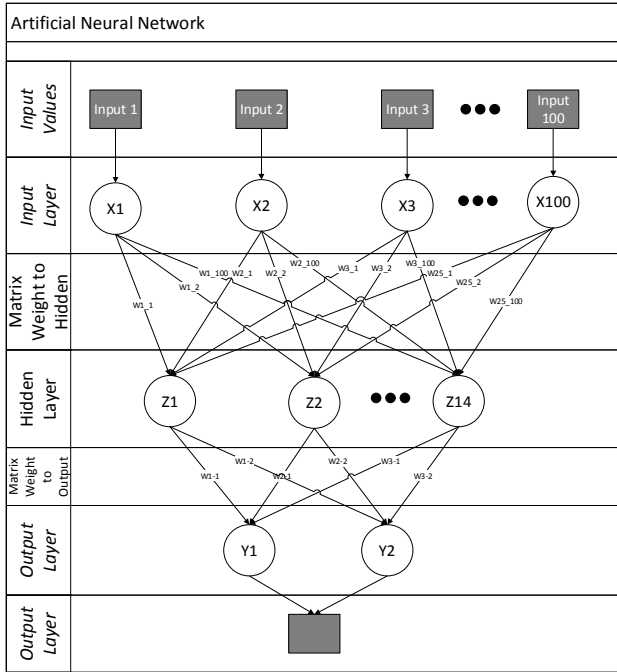


Fig. 7. Artificial neural network architecture

#### D. ISO 9241-411

ISO 9241 is a standard from International Organization for Standardization (ISO) that works on ergonomic human-system interactions [10]. ISO is an international independent agency that sets standards in various fields such as technology, industry, health and others. ISO's objective makes this standard to provide the quality, efficiency, and security of a product or service.

ISO 9241-411 is an evaluation method for input devices. The evaluation method that is utilized used to evaluate the performance of the cursor movement use one directional tapping tests shown in Fig 8. This method uses a block-shaped target in which the color of the target click is red. This evaluation has four difficulty levels:

1. Very easy:  $I_D \leq 3$  (mode 1)
2. Easy:  $3 < I_D \leq 4$  (mode 2)
3. Medium:  $4 < I_D \leq 6$  (mode 3)
4. Hard:  $I_D > 6$  (mode 4)

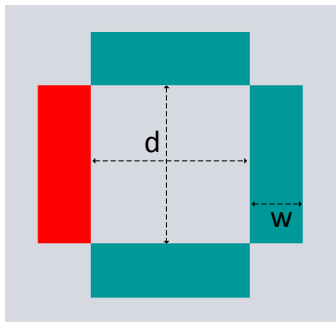


Fig. 8. One directional tapping test

$$\text{Index of difficulty } (I_D) = \frac{d}{w} \quad (1)$$

where  $d$  is distance and  $w$  is width in pixels.

The Effective Index of Difficulty ( $ID_e$ ) is a measurement in the bits of the user's precision achievement during the task.

$$ID_e = \log_2 \frac{d + w}{w} \quad (2)$$

Throughput ( $TP$ ) is used to measure the average velocity of each target shift.

$$\text{Throughput} = \frac{ID_e}{t_{\text{re}}} \quad (3)$$

Movement time is used to measure the average time spent for each target move. Other studies using the other type of tapping test, i.e., multi direction tapping test according to its application and its evaluation of this test, as in [11],[12],[13], and [14]. However, we simplify this study using modified one-directional tapping test as suggested by ISO for horizontal and vertical movement as in Fig. 8.

#### E. Experimental method

Data collection was done at the university under the supervision of the researcher. Each subject is given an explanation or guidance regarding the process of data collection and how to operate of the application. Subjects are given the flexibility to determine the position of the test such as sitting, standing and the distance between the respondent and the computer as long as it is in Bluetooth range.

The number of subjects in this experiment was seven people with an age range from fifteen to twenty-five. The average age of subjects is twenty-one years old with a standard deviation of 2.79. All subjects use the right hand in operation.

The tools needed for this experiment are laptop and smartphone. The Netbeans application and Bluetooth driver is pre-installed in the laptop. Should the laptops do not have bluetooth hardware, the test can still use bluetooth dongle as the replacement. This study uses a screen with a resolution of 1366 x 768. Minimum requirement of smartphone used is to have Bluetooth and sensor: accelerometer, magnetometer, and orientation.

Experimental data were obtained from tapping tests and questionnaires filled or tested by respondents. Trial data from tapping tests contains of coordinates ( $x$ ,  $y$ ), target width and length, distance between targets, errors (if clicks are not on target), time required for each click, and index of difficulty for each trial. The questionnaire consists of several types, i.e.: 1) independent forms, consisting of 7 questions on comfort and 5 questions on fatigue; 2) dependent forms, which are used to compare gesture 1 and gesture 2 in terms of comfort and fatigue; 3)

Borg questionnaire rating of perceived exertion scale, used to determine the effort needed during the use of gestures.

During the test, every subject uses the same rules for each tools, such as the mouse, gesture 1, and gesture 2. Subjects try the test program randomly for the mouse and

both gestures; then, subjects do *tapping tests* for three blocks, with 4 modes on each block, from the easiest to the hardest. The subjects try each mode once. Table 1 shows the detail data of experimental result that will be processed statistically.

TABLE I. DETAILS OF EXPERIMENTAL RESULTS

Block	Mode	Mouse		Gesture 1		Gesture 2	
		<i>tm(s)</i>	<i>TP(bit/s)</i>	<i>tm(s)</i>	<i>TP(bit/s)</i>	<i>tm(s)</i>	<i>TP(bit/s)</i>
1	1	0.94	2.24	13.03	0.15	9.69	0.21
	2	0.96	3.43	16.33	0.18	13.58	0.21
	3	1.06	3.96	20.21	0.18	21.79	0.17
	4	1.58	3.55	40.57	0.15	40.01	0.14
2	1	0.82	2.53	10.39	0.21	8.36	0.22
	2	0.98	3.16	13.80	0.22	13.68	0.21
	3	0.95	4.32	16.21	0.24	15.90	0.25
	4	1.34	4.51	43.57	0.13	43.75	0.13
3	1	0.85	2.39	6.75	0.31	6.57	0.33
	2	1.08	2.82	9.81	0.31	10.15	0.29
	3	1.02	4.09	17.27	0.24	18.34	0.21
	4	1.40	4.14	46.10	0.12	45.37	0.13
Means		1.08	3.43	21.17	0.20	20.60	0.21

### III. EXPERIMENTAL RESULTS

#### A. Quantitative Data

The following are the steps in counting the quantitative data.

##### 1) Fitts'law Calculations

The Fitts' law calculation begins once the data has been filtered in order for the data to be statistically analyzed. The classification of these calculations are type (mouse, gesture 1, gesture 2), block number, and mode to get data in every tool or gesture based on block and mode. We will then determine  $W_e$  and *time* of each mode, using the following equation:

$$W_e = 4.133 * S_x \quad (4)$$

$S_x$  is the standard deviation of the click coordinates with the midpoint of tapping. The next calculation step is to process  $W_e$  and *time* to get  $ID_e$  and Throughput (*TP*). The results of  $ID_e$  and *TP* calculations will be tested by using statistical calculations.

##### 2) Analysis

After Fitts' law calculation is obtained, statistic test can be done to get the difference between the mouse and the two gestures. Quantitative data analysis will be divided into *TP* and movement time (*tm*).

##### a) Throughput (*TP*)

The statistical test for *TP* begins with a normality test using the Shapiro Wilk test. From the result of normalization of *TP* data it can be concluded that *TP* is normally distributed. This conclusion is obtained from the *p* value (mouse:  $p = 0.379$ , gesture 1:  $p = 0.318$ , gesture 2:  $p = 0.483$ ). Since the data is normally distributed, the next test is a homogeneous test with Levene's test.

Levene's test results were statistically significant ( $p < 0.05$ ); means the variant on the mouse and the two gestures are not the same. It can be assumed that the homogeneity of the variant is not fulfilled. Since the variants are not the same on the mouse and the two gestures, the next test is Welch ANOVA used to find out the average difference of *TP* value on the mouse and both gestures.

The results of Welch ANOVA test is  $F(2, 19.593) = 95.055$ ,  $p < 0.05$ , which means there is a significant difference in the transfer speed of the devices. We use Games-Howell post-hoc to see the detail in the significant difference between mouse and the two gestures; this then determines that while there is significant difference of *TP* between mouse and the two gestures, the difference is not significant between the two gestures themselves.

##### b) Movement Time

The statistical test for movement time begins with the normality test with Shapiro Wilk test. From result of normality of movement time data can be concluded that movement time is not normally distributed. This conclusion is obtained from the probability value (mouse:  $p = 0.052$ , gesture 1:  $p = 0.009$ , gesture 2:  $p = 0.012$ ).

Results of Kruskal Wallis test obtained *p* value  $< 0.05$  which means there is significant differences between mouse and both gestures. Mann-Whitney U post-hoc test is used to see details of significant differences.

- The movement time value of the mouse is faster than gesture 1 and gesture 2.
- The movement time value of gesture 1 is not faster than gesture 2.

Therefore, in terms of moving from one target to another, mouse has a faster movement time than the two gestures. Meanwhile, there is no difference in movement time between gesture 1 and gesture 2. Other than that, the





Fig. 9. Graph error rate on each block

comparison of time needed between the two gestures to move from one target to another also do not differ.

### 3) Error Rate Calculations

During the tapping test, we received more than 50 data, which was our target for every trial. This excess data is caused by the click's mistargeting in the subject during the test. The following is a graphic of the error rate for every block.

As seen on Fig. 9, block 3 has less error rate compared to the mouse or two gestures in block 1 and block 2. The data can also be processed statistically in order to prove the conclusion that there is a significant difference in every block. The result of Kruskal Wallis test shows  $p = 0.120$  ( $p > 0.05$ ), which means that statistically, there is no significant difference between the error rate of each block in the mouse and two gestures.

We performed statistical tests on the data showed in Fig. 10 to see the effective modes for gesture 1 and gesture 2. Gesture 1 and gesture 2 were statistically tested using Mann-Whitney U test with mode 1 and mode 2 put in group 1 and mode 3 and mode 4 put in group 2. The result of statistical test of error rate in each mode says that there is significant difference in group 1 and group 2 ( $p < 0.05$ ).

### B. Qualitative Data

The statistical data is obtained from the form filled by the subject after the test. There are seven questions of



Fig. 10. The error rate graph in each mode

comfortability test and five questions of fatigue test questions. Data from each subject will be averaged to determine the level of comfortability and fatigue of the mouse and both gestures.

TABLE II. COMFORTABILITY AND FATIGUE

Assesment	Mouse	Gesture 1	Gesture 2
Comfort	6.95	4.46	4.97
Fatigue	6.61	5.89	5.87

\* Likert scale 7 point

Table II shows the average rate that the mouse has the best levels of comfortability and fatigue. The statistic result of comfortability and fatigue states that there is a significant difference between mouse and the two gestures ( $p < 0.05$ ), whereas it states no significant difference between gesture 1 and gesture 2 ( $p > 0.05$ ). Therefore, we conclude that gesture 1 and gesture 2 are less comfortable, tiring their users much more easily.

Assessment of effort uses Borg rating of perceived exertion scale in which the score 0 indicates the best value and the score 10 indicates the opposite. Mouse has the lowest level of effort for three categories (arm, shoulder, neck). For gesture 1, the highest level of effort lies on the shoulder with a score of 7.29, whereas for gesture 2, it lies on the arm with a score of 7.71. Therefore, we conclude that gesture 1 has more effort on the shoulder, and on the hand for gesture 2.

## IV. DISCUSSION

Statistics shows that there is no difference in the transfer speed of information ( $TP$ ) of gesture 1 and gesture 2, whereas there is a significant difference for transfer rate of information from the mouse to gesture 1 and gesture 2. The same thing happens when we compared the *movement time* between the mouse, gesture 1, and gesture 2. From this, we conclude that gesture 1 and gesture 2 are not different in terms of  $TP$  and *movement time* statistically. We also categorize mode 1 and 2 as group 1, and mode 3 and 4 as group 2 in terms of error rate. The result shows that gesture 1 and gesture 2 are only applicable on mode 1 and mode 2, whereas mode 3 and mode 4 cannot be used for gesture 1 and gesture 2.

In total, the calculated performance of the mouse is much better than gesture 1 and gesture 2 in terms of  $TP$  and *movement time*. The click method which uses jerk movements become one of our obstacles as it requires more effort and that jerk movements, though little, can impact the cursor's accuracy.

To validate the experimental procedure and methodology, the result of performance assessment i.e., *throughput*, revealed that the mouse's  $TP$  is 3.22 bps. This is in line with other studies by researchers which is the range of the mouse's  $TP$  is 3.0-5.0 bps as reported in [15] and [16].

Basically, the method in recognizing jerk movements worked well. From Fig. 9 and 10, we found that the error



rate of gesture 1 and gesture 2 was two times higher than that of the mouse. Possibly, the characteristic of the smartphone's orientation sensor affects the accuracy.

We have 200 test data, where 70% is used for training, and 30% to test the score of the jerk movement detections whether they go smoothly. However, during the implementation, this jerking movement detection affects the cursor position; therefore, we need to reevaluate the click method so that it will not affect the cursor position.

## V. CONCLUSIONS

Based on the result of the research and test, we conclude that.

1. Average calculation of throughput and movement time for mouse is 3.22 bps and 1.14 s, 0.19 bps and 22.18 s for gesture 1, and 0.19 bps and 22.66 s for gesture 2. We conclude that there is a significant difference between mouse and gesture 1 or gesture 2, however, there is no significant difference for gesture 1 and gesture 2.
2. As for the levels of comfortability and fatigue, mouse has the highest level of comfortability and the lowest level of fatigue. Gesture 1 comes on the second position, and gesture 2 on the last in terms of this.

Mouse is the most effective tool in terms to effort. Gesture 1 comes on the second position, and gesture 2 concluded as ineffective.

## REFERENCES

- [1] PUSDATIN, "Kemendagri," [Online]. Available: [http://www.kemendagri.go.id/media/documents/2016/05/11/u/u\\_uu\\_nom%0Aor\\_8\\_tahun\\_2016.pdf](http://www.kemendagri.go.id/media/documents/2016/05/11/u/u_uu_nom%0Aor_8_tahun_2016.pdf). [Accessed: 02-Jan-2018], 2016.
- [2] G. Eom *et al.*, "Gyro-Mouse for the Disabled: 'Click' and 'Position' Control of the Mouse Cursor," *Int. J.*, vol. 5, no. 2, 2007.
- [3] L. Ribas - xirgo and F. López - varquiel, "Accelerometer-Based Computer Mouse for People with Special Needs," *J. Access. Des. All*, vol. 7, no. 1, pp. 1–20, 2017.
- [4] S. Shaikh, P. Gaikwad, A. Prof, and S. Patil, "Eye Tracking For Mouse Processing," no. 5, pp. 1607–1610, 2017.
- [5] D. S. Suresh and I. V Bhavana, "Virtual Mouse Implementation using Color Pointer Detection," vol. 1, no. 5, pp. 23–32, 2014.
- [6] K. K. Kaki, "Mouse Cursor's Movements using Voice Controlled Mouse Pointer," vol. 71, no. 7, pp. 27–34, 2013.
- [7] Google Developer, "Android," [Online]. Available: <https://developer.android.com/guide/index.html>. [Accessed: 05-Jan-2018], 2018.
- [8] R.B. Widodo and C. Wada, "Artificial Neural Network Based Step-Length Prediction Using Ultrasonic Sensors from Simulation to Implementation in Shoe-Type Measurement Device," *J. Adv. Comput. Intell. Intell. Inform.*, Vol.21, No.2, pp. 321–329, 2017.
- [9] H. Yu and B. Wilamowski, "Levenberg–Marquardt Training," pp. 1–16, 2011.
- [10] International Organization for Standardization, 2012. Technical Specification ISO. Switzerland.
- [11] Douglas, S.A., Kirkpatrick, A.E.A.E., MacKenzie, I.S."Testing pointing device performance and user assessment with the ISO 9241, Part 9 standard." *Proc. SIGCHI Conf. Hum. Factors Comput. Syst.* CHI is limit CHI 99 15, p.p. 215–222, 1999. <https://doi.org/10.1145/302979.303042>.
- [12] I.S. MacKenzie, S. Jusoh,, "An Evaluation of Two Input Devices for Remote Pointing." *Eng. Human-Computer Interact.* 2254, 235–250, 2001. <https://doi.org/10.1007/3-540-45348-2>.
- [13] R.M. Quita and R.. Widodo."A Mathematical Proof Concerning the Geometrical Aspect of Very Low Index of Difficulty in Multidirectional Tapping Task of the ISO 9241 - Part 411" *MATEC Web Conf.*, vol. 164, 01036, 2018. <https://doi.org/10.1051/mateconf/201816401036>
- [14] Norman, K.L., Norman, K.D. "Comparison of Relative Versus Absolute Pointing Devices." *Human-Computer Interact. Lab* 1–17, 2010.
- [15] I. S. MacKenzie and S. Jusoh, "An evaluation of two input devices for remote pointing," in *Proc. of the Eighth IFIP Working Conference on Engineering for HCI(EHCI)*, pp.235-249, 2000.
- [16] R.B. Widodo, T. Matsumaru. "Measuring the Performance of Laser Spot Clicking Techniques." *IEEE International Conference on Robotics and Biomimetics (ROBIO)*, 2013.

# FVEC feature and Machine Learning Approach for Indonesian Opinion Mining on YouTube Comments

Aina Musdholifah  
Master Program of Computer Science  
Department of Computer Science and Electronics  
Universitas Gadjah Mada  
Yogyakarta, Indonesia  
aina\_m@ugm.ac.id

Ekki Rinaldi  
Master Program of Computer Science  
Department of Computer Science and Electronics  
Universitas Gadjah Mada  
Yogyakarta, Indonesia  
[ekki.rinaldi@mail.ugm.ac.id](mailto:ekki.rinaldi@mail.ugm.ac.id)

**Abstract**— Mining opinions from Indonesian comments from YouTube videos are required to extract interesting patterns and valuable information from consumer feedback. Opinions can consist of a combination of sentiments and topics from comments. The features considered in the mining of opinion become one of the important keys to getting a quality opinion. This paper proposes to utilize FVEC and TF-IDF features to represent the comments. In addition, two popular machine learning approaches in the field of opinion mining, i.e., SVM and CNN, are explored separately to extract opinions in Indonesian comments of YouTube videos. The experimental results show that the use of FVEC features on SVM and CNN achieves a very significant effect on the quality of opinions obtained, in term of accuracy.

**Keywords**— Machine Learning, CNN, FVEC, Opinion Mining, SVM

## I. INTRODUCTION

Extracting the sentiment from Indonesian YouTube comments is still a challenge. Slangs and various dialect is the main problem. Rinaldi and Musdholifah [1] initiated Indonesian YouTube opinion mining using self-labelled Indonesian comment. The experiment conducted in three type of label given: SENTIMENT, TYPE, and ALL. SENTIMENT label based on overall sentiment given regardless its toward video or product. TYPE label experiment observe the type of comment whether it given toward product or video. ALL label consist the combination of both SENTIMENT and TYPE. This research proves that the overall result of classification using STRUCT method approach is better.

A term called sentiment analysis, or the mathematical taxonomy of statements' negative or positive connotations, gives companies potent ways to analyze cumulative language data across all sorts of communications. Opinion mining and sentiment analysis in the era of big data have been used in categorize the opinion into different sentiment and evaluating the mood of the public in general [2]. Various techniques have been developed over the years in different datasets and applied to various experimental settings and business cases.

Machine learning framework is an integrated system of programs. These programs learn from existing data and capable of predicting new observations. Machine learning learns from data rather than explicitly programmed instructions. Machine learning itself divided into supervised learning which need to learn its predecessor data to make such classification and regression, and unsupervised learning which treat the data as a space to learn the inherent structure of the data without explicitly labelled. This study used machine learning based technique to extract customer's opinion, train and classify on selected key words, named CNN and SVM.

Convolutional Neural Network or known as CNN rise its popularity in image processing with proven capability in various image data like MNIST [4]. CNN uses "neighborhood" method to analyze a pixel value to its surrounding, then extract the important feature from convoluted image. Yoon [5] make a breakthrough by implementing CNN for sentence classification because he see the neighborhood method can be utilized to extract sentiment in the comments. This research proves that CNN can be used in sentence classification with decent performance.

The decent performance and uniqueness of how CNN works bring the curiosity on combining CNN for sentence classification from Yoon [5] with FVEC additional feature from Rinaldi and Musdholifah [1]. Thus this research focused on combining CNN and FVEC then compares the performance with FVEC-SVM.

## II. RELATED WORKS

Severyn [6] introduced FVEC and STRUCT feature in examine opinion mining in YouTube videos in English. The classification method used is SVM using the SHTK kernel function (Shallow Syntactic Tree Kernel). This study uses data from two domains, tablet domain and automobiles domain. The approach taken in classifying is divided into two, namely FVEC-SVM approach using the bag-of-words method and STRUCT-SVM approach using chunking method. Full task category reach 60,3% accuracy with STRUCT approach.

Rinaldi and Musdholifah [1] undertake the research similar to Severyn [6] with the following differences: (1) The comments are in Indonesian, (2) Only use smartphone domain, (3) The kernel functions used include linear, polynomial degree 2, polynomial degree 3, and RBF, (4) In the FVEC approach, lexicon approach is excluded. In this research, the FVEC-SVM performed better than STRUCT-SVM with 62.76% using linear kernel function in full task experiment.

Yoon [5] made a breakthrough by implementing CNN for sentence classification. CNN was popular for image classification by analyzing value of a pixel and its neighborhood using sliding window. This method of finding correlation of a feature with its surrounding undertake the similar problem on sentence classification. Yoon's work put text into word embedding, add padding so each sentence have a same length, and then send it to single-layer convolutional neural network. The performance was respectable compared to other famous text classification methods. Simple CNN with one layer of convolution performs remarkably well instead of tuning on hyper-parameters.

Socher [7] proposed new model called the Recursive Neural Tensor Network (RNTN) Recursive Neural Tensor Networks is able to take input phrases in any length. The phrase transformed into word vectors and parse tree, then by using tensor-based function for higher nodes vector computation. The RNTN accurately captures the sentiment and negation of the sentence. This research also includes two types of analyses: several large quantitative evaluations on the test set, and focuses on two linguistic phenomena that are important in sentiment. The top performance for all models was achieved between 25 and 35 words vector sizes dimensions with batch sizes between 20 and 30.

Socher [8] invented method for paraphrase detection called Recursive Autoencoders (RAE). RAE works by unfolding objective and learn feature vectors for phrases in syntactic trees. These features were used to calculate the similarity of word and phrase-wise between two sentences. This research introduced a novel dynamic pooling layer which computes a fixed-sized representation from the variable-sized matrices as input to the classifier since the length of the sentences vary. This method outperforms other approaches on MSRP paraphrase corpus. The RAE captures syntactic and semantic information as shown qualitatively with nearest neighborhood embedding and quantitatively on a paraphrase detection task. This representation captures sufficient information to determine the relationship of paraphrase on the MSRP dataset with a high accuracy.

Kalchbrenner [9] introduced Dynamic Convolutional Neural Network (DCNN). Dynamic k-Max was used for a global pooling operation over linear sequences. The network is capable to explicitly capturing short and long sentence relations. The network is easily applicable to any language since it does not rely on parse tree. This research conducted small-scale binary and multi-class sentiment prediction, six-way question classification and Twitter sentiment prediction by distant supervision, total four experiments. The model achieves outstanding performance in the first three tasks and more than 25% error reduction in the last task due to the strongest baseline.

Hermann dan Blunsom [10] experiment with learning of vector space representations of sentential semantics and the transparent interface between syntax and semantics provided by Combinatory Categorical Grammar (CCG) to introduce Combinatory Categorical Autoencoders. This research learns high dimensional embedding for sentences and evaluate them in a range of tasks, proving that the incorporation of syntax allows a concise model to learn representations that are both effective and general. This experiment explored a number of models, each of which conditions the compositional operations on different aspects of the CCG derivation. This experiment indicates a clear advantage for a deeper integration of syntax over models that only utilized the bracketing structure of the parse tree thought the most effective way for the compositional operators on the syntax remains unclear.

Wang et al. [11] proposed semantic clustering and convolutional neural network to model short texts based on novel method. The model uses pre-trained word embedding to produce extra knowledge, and multi-scale Semantic Units (SUs). Three pre-trained word embedding for initializing the lookup based on Senna, GloVe, and Word2Vec. The experiments are conducted on two benchmarks: TREC which contains 5,452 training dataset whereas the test dataset consists of 500 questions, and Google Snippets which consists

of 10,060 training snippets and 2,280 test snippets from 8 categories. Three pre-trained words are conducted for each benchmark. This method achieves the highest result of 85.1% on Google snippets by Word2Vec and TREC achieve 97.2% when the GloVe word embedding is employed.

### III. METHODS

This research compares the CNN performance in classifying YouTube comments towards SVM. In addition, FVEC features also added to test if it bring difference to learning model. The main experiment divided into two category: experiment using down-sampled data and experiment using whole data.

#### A. Data

The data used in this research was taken from [1]. This research organizing the data into two groups: whole data group and down-sampled data group. Whole data group uses all data and separated into train-test with 9:1 ratio, while down-sampled data group uses randomly selected comments from comments pool in order to get balanced data. This eliminate possibilities of bias model towards unbalanced data. The distribution of whole data group and down-sampled data group shown on Table 1 and Table 2. TRAIN data in each group k-folded and tested among TEST data to find the best accuracy can be reach for each groups. The down-sampled group TRAIN data folded into 5 while whole group data folded into 10.

Table 1: Down-sampled data group distribution

<i>Label</i>	<i>TRAIN</i>	<i>TEST</i>
Product-Positive	500	400
Product-Neutral	500	400
Product-Negative	500	400
Video-Positive	500	400
Video-Neutral	35	5
Video-Negative	500	400
Uninformative	500	400
<b>Total</b>	<b>3035</b>	<b>2405</b>

Table 2: Whole data group distribution

<i>Label</i>	<i>TRAIN</i>	<i>TEST</i>
Product-Positive	519	64
Product-Neutral	3863	397
Product-Negative	826	89
Video-Positive	850	98
Video-Neutral	35	5
Video-Negative	847	101
Uninformative	5349	612
<b>Total</b>	<b>12289</b>	<b>1366</b>

Since the length of the sentences vary, all sentences in the training data then padded to meet the longest sentence which contain the most word. Each word include padding tranformed into word embedding, replaced each word with numbers and to condition become  $n$ -word length.

For every comment processed, each  $k$ -word replaced with its representative in word embedding and padding is added to sentence to meet the  $n$  length. This transformation enable convolution layer to process the sentence.

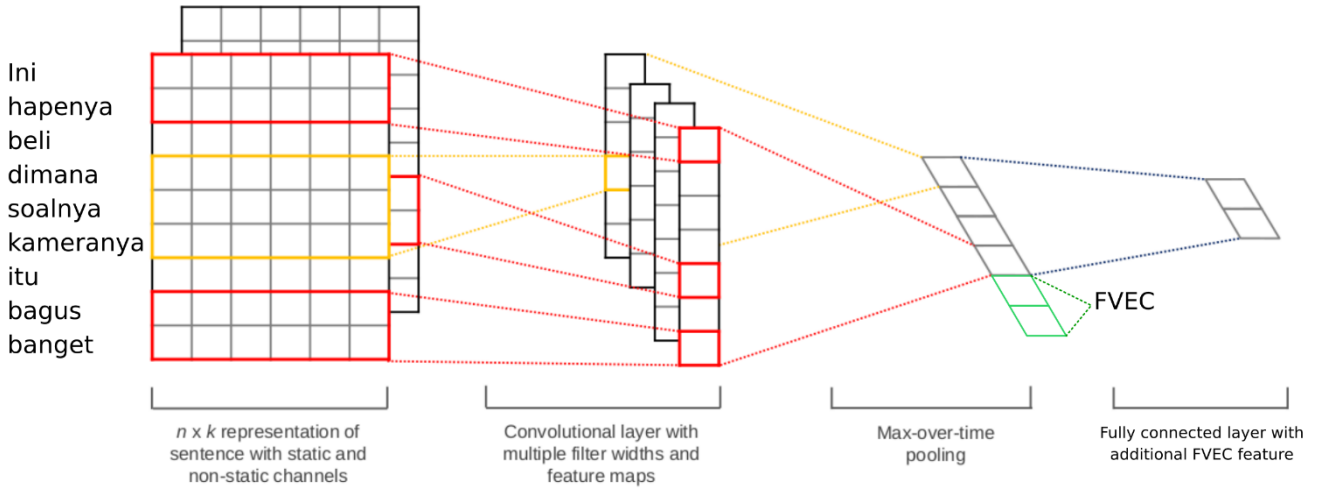


Figure 1: CNN architecture for sentence classification by Kim Yoon, modified by adding FVEC in fully connected layer

### B. FVEC-CNN

CNN for sentence classification was introduced by Yoon [5] in various data. Each sentence tokenized then padding is added to make all sentence have a same length, make it  $n \times k$  word representation. This form enable convolutional layer to process the sentences to learn corellation between sequential word

The model architecture shown in Figure 1, let  $X_i \in \mathbb{R}^k$  be the  $k$ -dimensional word vector corresponding to the  $i$ -th word in the sentence. A length of sentence of length  $n$  (padded if necessary) is represented as:

$$x_{1:n} = x_1 \oplus x_2 \oplus \dots \oplus x_n \quad (1)$$

where  $\oplus$  is the concatenation operator. In general,  $x_{i:i+j}$  refer to the concatenation of words  $x_i, x_{i+1}, \dots, x_{i+j}$ . A convolution operation involves  $w \in \mathbb{R}^{h \times k}$ , which is applied to  $h$  words in order to produce a new feature. For example, a feature  $c_i$  is generated from a window of words  $x_{i:i+h-1}$  by:

$$c_i = f(w \cdot x_{i:i+h-1} + b) \quad (2)$$

here  $b \in \mathbb{R}$  is a bias term and  $f$  is a non-linear function similar to the hyperbolic tangent. This filter is applied to each possible window of words in the sentence  $\{x_{1:h}, x_{2:h+1}, \dots, x_{n-h+1:n}\}$  to produce a *feature map* with  $c \in \mathbb{R}^{n-h+1}$ :

$$c = [c_1, c_2, \dots, c_{n-h+1}] \quad (3)$$

Max-over time pooling operation applied over the feature map and take the maximum value  $\hat{c} = \max\{c\}$  as the feature corresponding to capture the most important feature for each feature map.

Because FVEC has no correlation with the words sequences, additional FVEC feature added in the end of convolutional layer, beginning of fully connected layer. Figure 1 shows the architecture of Yoon's CNN architecture modified by adding FVEC in the beginning of fully connected layer.

For regularization, dropout employed on the penultimate layer with a constraint on  $l_2$ -norms of the weight vectors. Dropout prevents co-adaptation of hidden units by randomly dropping of the hidden units during forward-backpropagation. For output unit  $y$  in forward propagation, dropout uses formula 4 where  $\circ$  is the multiplication operator of element-wise and  $r \in \mathbb{R}^m$  is a *masking* vector. Gradients are back-propagated only through the unmasked units.

$$y = w \cdot (z \circ r) + b, \quad (4)$$

### C. FVEC-SVM

Introduced by Severyn [6] and followed by Rinaldi and Musdholifah [1]. This method combines classic word weighting TF-IDF with additional feature cosine similarity between comments and the video title and counting the negation words in a comment.

Cosine similarity used to detect if a comment contains same product as the title or not because sometimes user name a product on a comment but it does not relate to the title. If it does, then there are probability that the comment talk about the product.

Negation used to inverse the polarity of the comments. If a positive comment contains one negation word, the polarity would be reversed to negative and vice versa.

Lower-cased unigram and bigram used as feature selection to quantify each item present in a comment then classic TF-IDF utilized to turn all features into vector space.

Since the data classified into seven classes, one-versus-rest SVM was performed to find the decision boundary of every class. To find the decision boundary of a class, other class considered as one negative class. Classification is done as much as number of class or seven times.

#### IV. RESULTS

The data made into two groups, whole data groups and down-sampled data groups. Each group separated into two part, training data and testing data. Training data then k-folded in order to get the highest training accuracy. For whole data groups, 10-fold cross validation performed in training data while 5-fold cross validation performed for down-sampled training data.

##### A. Down-sampled Data Group

Figure 2 shows the CNN accuracy for training and validation on each fold for down-sampled data. This shows that FVEC relatively helps model to reach higher accuracy, even it was not significant. For validation data, CNN and SVM creates different slope. This may indicate any over-fitting in high training data accuracy.

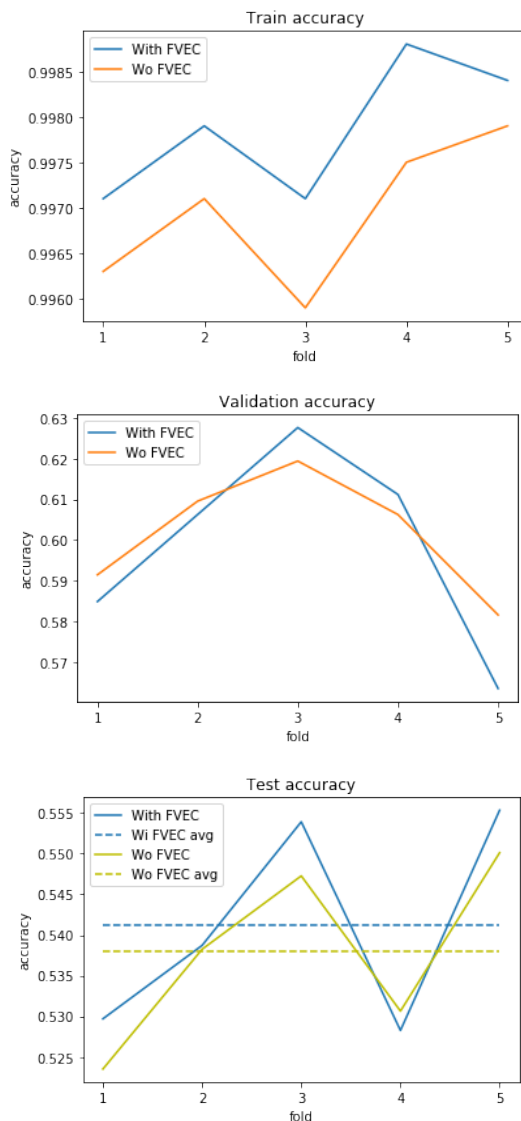


Figure 2: Result of Train, Validation, and Test of CNN performance on down-sampled data group

Figure 3 shows SVM accuracy on down-sampled data on each fold. On training data, FVEC inconsistently helps model to learn. However, FVEC relatively helps increase accuracy on validation data as well as test data. The figure also showed the comparison of SVM with and without FVEC. Once again, FVEC has been proven to increase the accuracy.

Finally, the performance comparison for FVEC-SVM and FVEC-CNN on down-sampled data group shown in Figure 4. FVEC-SVM outperformed FVEC-CNN with slight different around 0.01% difference. Therefore, FVEC-SVM still better than FVEC-CNN for sentence classification.

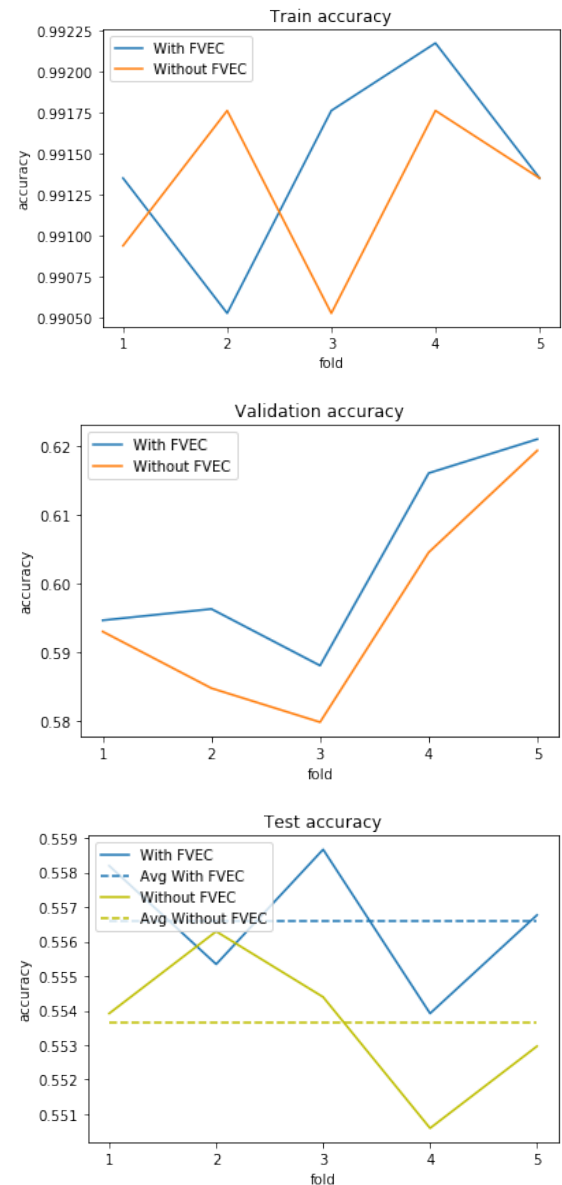


Figure 3: Result of Train, Validation, and Test of SVM performance on down-sampled data group

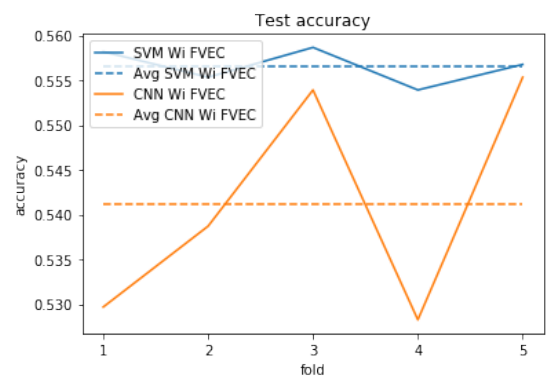


Figure 4: FVEC-SVM vs FVEC-CNN performance on down-sampled

## B. Whole Data Group

Whole data group uses 9:1 ratio for training data and testing data on all data. The data selected randomly and proportionally. The training data then 10-folded in order to find the highest training accuracy. CNN and SVM both performed in this data group.

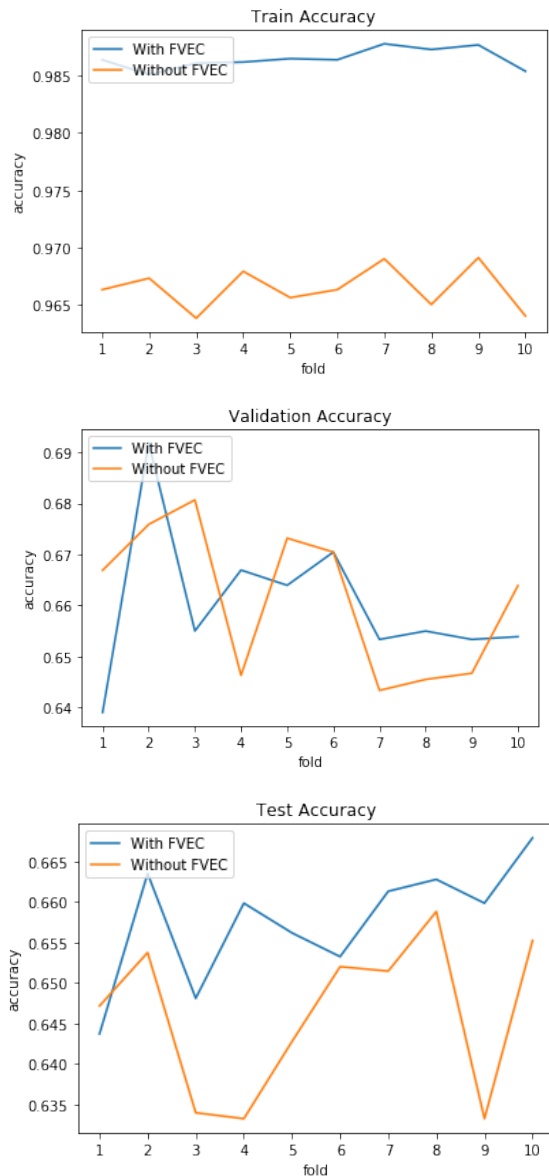


Figure 5: Result of Train, Validation, and Test of CNN performance on whole data group using 10 Fold Cross-Val

Figure 5 shows the result of training, validation, and testing data using CNN. In this case, FVEC has been proven to improve training data accuracy. The result on validation data accuracy seems fluctuate using FVEC, however it really help on predicting test data.

Performance of SVM on whole data group shown on figure 6. On training accuracy, the accuracy increased by utilized FVEC, this applies on validation data and training data as well.

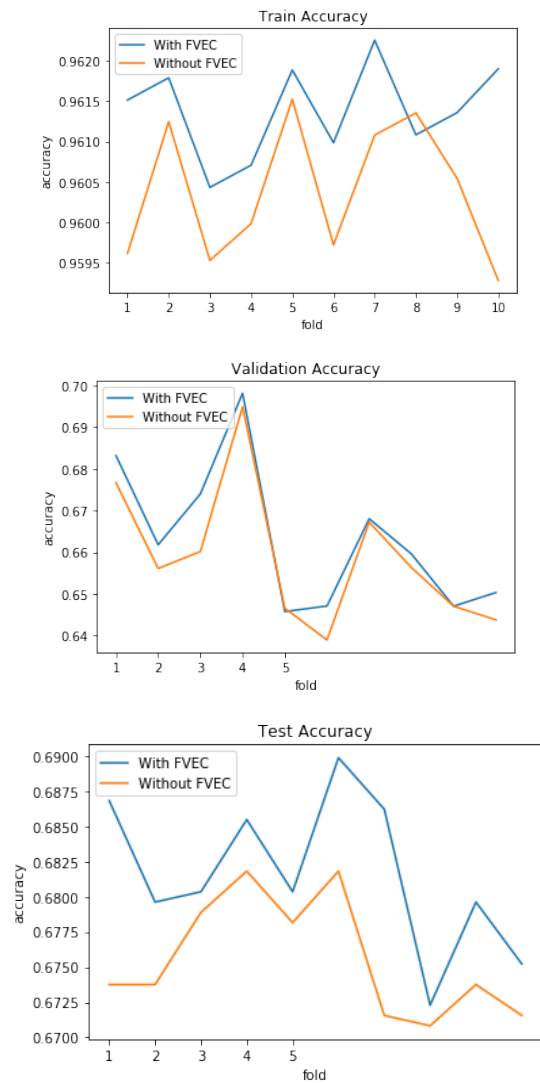


Figure 6: Result of Train, Validation, and Test SVM performance on whole data group using 10 Fold Cross-Val

Lastly, the comparison performance of FVEC-SVM and FVEC-CNN on whole data group shown on figure 7. The result shown that FVEC-SVM accuracy is definitely higher than FVEC-CNN accuracy on every folds.

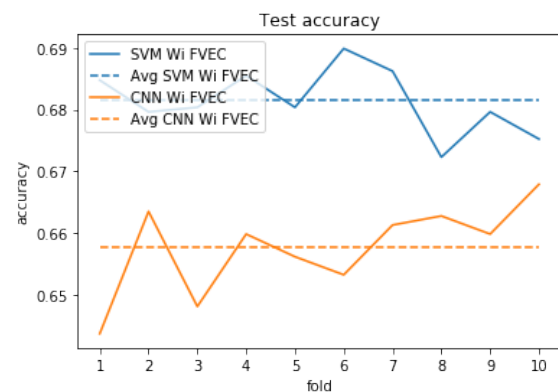


Figure 7: FVEC-SVM vs FVEC-CNN performance on whole data group using 10 Fold Cross Validation



## V. CONCLUSION AND FUTURE WORKS

The proposed FVEC-CNN runs well on both down-sampled and whole data group with decent accuracy. However, FVEC-SVM has been proven to outperformed FVEC-CNN on both down-sampled and whole data group. By this means, CNN neighborhood method is not effective against the data compared to statistical based e.g. TF-IDF. In the future, research continues with method which robust to unstructured data e.g. LSTM, RNN, and Autoencoder.

## REFERENCES

- [1] E. Rinaldi, A. Musdholifah, "FVEC-SVM for opinion mining on Indonesian comments of youtube video" 2017 International Conference on Data and Software Engineering (IcoDSE), 1-2 Nov 2017.
- [2] S. Shayaa et al., "Sentiment Analysis of Big Data: Methods, Applications, and Open Challenges," in IEEE Access, 2018.
- [3] L. Zhang, S. Wang, B. Liu., "Deep Learning for Sentiment Analysis : A Survey". Computation and Language, Cornell University Library, 2018.
- [4] X. Han., and Y. Li., "The Application of Convolution Neural Networks in Handwritten Numeral Recognition," International Journal of Database Theory and Application, Vol.8, No.3 (2015), pp.367-376.
- [5] K. Yoon, "Convolutional Neural Networks for Sentence Classification" Computation and Language (cs.CL); Neural and Evolutionary Computing (cs.NE), 25 Aug 2014.
- [6] A. Severyn, A. Moschitti, O. Uryupina, K. Filippova, and B. Plank, "Opinion Mining on YouTube. In 52nd Annual Meeting of the Association for Computational Linguistics," in Proceedings of the Conference ACL, vol. 1, pp. 1252-1261, 2014.
- [7] R. Socher, A. Perelygin, J. Wu, J. Chuang, C. Manning, A. Ng, C. Potts. 2013. Recursive Deep Models for Semantic Compositionality Over a Sentiment Treebank. In Proceedings of EMNLP 2013.
- [8] R. Socher, J. Pennington, E. Huang, A. Ng, C. Manning. 2011. Semi-Supervised Recursive Autoencoders for Predicting Sentiment Distributions. In Proceedings of EMNLP 2011.
- [9] N. Kalchbrenner, E. Grefenstette, P. Blunsom., "A Convolutional Neural Network for Modelling Sentences," In Proceedings of ACL 2014.
- [10] K. Hermann, P. Blunsom. "The Role of Syntax in Vector Space Models of Compositional Semantics." In Proceedings of ACL 2013.
- [11] P. Wang, J. Xu, B. Xu, C. Liu, H. Zhang, F. Wang, H. Hao. "Semantic Clustering and Convolutional Neural Network for Short Text Categorization". Proceedings of the 53rd Annual Meeting of the Association for Computational Linguistics and the 7th International Joint Conference on Natural Language Processing (Short Papers), pages 352–357, Beijing, China, July 26-31, 2015.

# Clustering human perception of environment impact using Rough Set Theory

Ani Apriani

dept. Geology Engineering  
Sekolah Tinggi Teknologi Nasional  
Yogyakarta, Indonesia  
aniapriani@sttnas.ac.id

Iwan Tri Riyadi Yanto

dept. Information System  
Ahmad Dahlan University  
Yogyakarta, Indonesia, Country  
yanto.itr@is.uad.ac.id

Septiana Fathurrohman

dept. Urban and Regional Planning  
Sekolah Tinggi Teknologi Nasional  
Yogyakarta, Indonesia  
septiana.sttnas.ac.id

Sri Haryatmi

dept. Mathematic  
Universitas Gajah Mada  
Yogyakarta, Indonesia  
s.kartiko@yahoo.com

Danardono

dept. Mathematic  
Universitas Gajah Mada  
Yogyakarta, Indonesia line  
danardono@ugm.ac.id

**Abstract**— Yogyakarta, as the main destination for education, cultural exchange, and tourism in Indonesia has experienced a high demand on physical development. Despite its positive effect, the growth of physical development in Yogyakarta also brings several negative effects. This research aims to figure out the various effect of physical development in Yogyakarta based on the perception of the local residence. To achieve the objective, this research uses two methods based on rough set theory, that are Maximum dependency attribute (MDA) and fuzzy partition based on indiscernible relation (FKP). The results show that the water quality is the important attribute on physical and chemical aspects. Furthermore, on economic aspect, the highest attributes are immigration and employee absorption.

**Keywords**—clustering, environment impact, Rough Set Theory

## I. INTRODUCTION

Development aims to enhance the livelihood of the society by utilizing the available natural and environmental resources. However, the development itself may cause both positive and negative effects to the society. The magnitude of the development effect is influenced by the type of the policy to be implemented, characteristics of the natural environment, the availability of technology and financial resource, and the level of participation in the development process[1]–[5].

Furthermore, the effect of the spatial aspect on the development could not be neglected. This aspect may determine the effect of the development. The effect of development in the urban area, sub-urban area, and rural-area may differ due to the distinct characteristics of the type of economic activity, the intensity of urban development, and the characteristic of the social and natural environment[6], [7].

Yogyakarta, as the main destination for education, cultural exchange, and tourism in Indonesia has experienced a high demand on physical development. It has a potential market for the investment in the trading and hospitality sectors. The hospitality sector itself may contribute 24,88% in the Gross Domestic Product (GDP) of Yogyakarta. This

indicate the positive impact of hospitality sector for the economic development in Yogyakarta.

Despite its positive effect, the growth of hospitality sectors in Yogyakarta also brings several negative effects. The growth of hospitality industry in Yogyakarta has caused a high demand on hotel development. The massive hotels development in Yogyakarta is said to cause several negative effects, for instance, the increase of traffic congestion, the increase of urban temperature, the decline of the groundwater reservoir, and the marginalization of the local architecture [8]. Therefore, this research aims to figure out the various effect of physical development in Yogyakarta based on the perception of the local residence. Thus, a strategic program can be well planned during their period of studies in an institution[3], [9], [10]. An effective way to detect the most its impact is the use of data mining technique[11]. Data mining in general is the process of finding, analyzing a new information that may exist in data and summarizing the results as useful information. There are many outstanding studies on data mining in the areas of clustering, association rules, classification, conflict analysis, and etc [12]–[15]. The field of data mining that concerned with the applications.

In order to achieve the research objective, two method based on rough set theory are used, that are Maximum dependency attribute (MDA) and fuzzy partition based on indiscernible relation (FKP). The MDA method is used to ranking the dependency degrees of attribute and select the most important attribute or features[16]. Furthermore, the FKP as a clustering technique is used for grouping the data selected to the class having similar characteristic[17]. Selecting, identifying the most influential attribute and grouping the data could the police maker to design the proper intervention and take immediate action to improve the quality of social environment.

## II. METHOD

### A. Maximum Dependency Attribute

Maximum dependency attribute (MDA) is proposed by herawan et al, the technique for selecting attribute based on the rough set theory. It uses the dependency of attribute by select the highest dependency respect to all attribute. There are three steps in MDA technique i.e : compute the equivalence classes of attribute, Determine the dependency

attribute, select the attribute based on the degree of dependency [18]–[20].

Equivalence relation can induce a unique partition. The beginning point for formatting partitions is the indistinguishable relationship denoted  $IND(B)$ . Let  $S(U, A, V, f)$  is an information system. Two object  $x, y \in U$  and attribut  $B \subseteq A$  is  $IND(B) \Rightarrow f(x, a) = f(y, a), \forall a \in A$ . The equivalence classes  $U/B$  is the partition of  $U$  by  $IND(B)$  and the  $U/B$  contains  $x \in U$  is denoted  $[x]_B$ . Let  $X \subseteq U$ ,  $\underline{B}(X) = \{x \in U | [x]_B \subseteq X\}$  is the lower approximation called positive region in rough set. Then, the degree dependency  $D$  on  $C$  where  $C, D \subseteq A, C \Rightarrow_k D$  is defined as

$$k = \frac{Pos_C}{|U|}, 0 \leq k \leq 1,$$

$$Pos_C = \sum_{X \in U/D} |\underline{C}(X)|.$$

### B. Fuzzy partition based on indiscernible relation

Fuzzy partition based on indiscernible relation has been proposed by yanto et all. The technique is a parametric approach using likelihood of multivariate distribution function based on indiscernible relation of rough set[21]. The objective function of the technique is maximize the function  $J_m(\mu, \lambda)$ .

$$J_m(\mu, \lambda) = \sum_{i=1}^I \sum_{k=1}^K \mu_{ik}^m \sum_{j=1}^J \ln(\lambda_{ij}^k)$$

by the constrains:

$$\mu_{ik} \geq 0, \sum_{k=1}^K \mu_{ik} = 1,$$

$$\lambda_{ij}^k \geq 0, \sum_{j=1}^J \lambda_{ij}^k = 1.$$

By solving the nonlinear equation system of the first derivate of the Lagrange  $J_m$ , the solution of the problem are found, i.e :

$$\lambda_{ij}^k = \frac{\sum_{l=1}^I \mu_{il}^m \ln(\lambda_{ij}^l)}{\sum_{l=1}^I \mu_{il}^m}, \text{ for } l = 1, 2, \dots, I$$

$$\mu_{ik} = \left[ \sum_{j=1}^J \left[ \frac{\sum_{l=1}^I \mu_{il}^m \ln(\lambda_{ij}^l)}{\sum_{l=1}^I \mu_{il}^m} \right]^{\frac{1}{m-1}} \right]^{-1}$$

## III. RESEARCH METHOD

This research aims to grouping the city having similar impact of environment dataset. There are two phases of the process. Firstly, the selecting the most important of the attribute of the dataset by ranked the degree dependency based on the MDA technique. Size of the dataset are reduced by excluded attribute having the less degree of dependency. Then, the reduced size dataset is grouped using the clustering technique named Fuzzy partition based on indiscernible

relation. This can help the police maker to design the proper intervention and take immediate action to improve the quality of social environment.

The primer dataset was collected by survey involved the 400 respondents consists of 224 females and 176 males. The respondents are fill the questioner regarding the perception of the environment impact in term of Physic and chemical aspects and Economic aspect. The reliability score of the data is 0.953 in Cronbach alpha test. Table 1. Shows the description of the data set.

TABLE I. DATA DESCRIPTION

Data set	Attribute	Description
Physic and chemical aspects	water quantity, water quality, water absorption level, temperature, air pollution level, climate, noise level, land use, availability of public open space	Number of attribute: 9 Mean : 25 SD : 2.95
Economic aspect	immigration, rate of employment, economic structure development, revenue, expenditure, shift of occupation, public health, increasing number of educational facility, increasing number of religious facility, increasing number of health care facility	Number of attribute: 10 Mean : 16 SD : 2.67

## IV. RESULTS AND DISCUSSION

### A. Physic and chemical aspects

Physic and chemical aspects consists nine attributes with mean = 25 and SD = 2.95. The Degree of dependency is shown in table 2. From Table 2, attribute L3, L4, L6, L7, L8 and L9 are the less of dependency thus the attributes are excluded so that the L1, L2 and L5 are selected as an attributes to the next phases. Moreover, the high dependency is L2 that is the water quality as an important attribute.

### B. Economic aspect

Economic aspect consists ten attributes with mean = 12 and SD=1.59. The Degree of dependency is shown in table 3. From Table 3, The highest attributes are E1 (immigration), the movement of the population from outside into the city of

Yogyakarta and E2 (Employee absorption). Attribute E3, E7, E8 and E10 are the less of dependency thus the attributes are excluded so that the E1, E2, E4, E5 and E6 are selected as attributes to the next phase.

TABLE II. DEGREE DEPENDENCY OF PHYSIC AND CHEMICAL ASPECTS

Attribute	L1	L2	L3	L4	L5	L6	L7	L8	L9
Degree of dependency	0.0075	0.0475	0.0025	0.0025	0.0075	0.0025	0.0025	0.0025	0.0025

TABLE III. DEGREE DEPENDENCY OF ECONOMIC ASPECT

Attribute	E1	E2	E3	E4	E5	E6	E7	E8	E9	E10
1stDegree of dependency	1	1	0	1	1	0.015	0	0	0	0
2ndDegree of dependency	0.01	0.01	0	0	0	0	0	0	0	0

### C. Cluster Analysis

The cluster result is analyzed using silhouette coefficient to determine the desirable number of cluster. In the clustering phase, the degree of fuzziness is selected as  $1.2 \leq m \leq 2$  with the variation number of clusters are 2 until 14. The average of silhouette coefficients is summarized in table 4. From table 4. Can be shown that the number of clusters can be determine between 10 -14 number of cluster with significantly value of silhouette coefficients rising 0.9.

TABLE IV. SILHOUETTE COEFFICIENTS IN VARIOUS NUMBER OF CLUSTERS

Number of cluster	Physic and chemical	Economic aspects
2	0.487	0.522
3	0.551	0.614
4	0.632	0.681
5	0.691	0.778
6	0.761	0.810
7	0.830	0.857
8	0.871	0.890
9	0.902	0.909
10	0.925	0.940
11	0.937	0.956
12	0.938	0.973
13	0.954	0.982
14	0.961	0.995

### V. CONCLUSION

This paper studies the utilization of the techniques to cluster the environment impact dataset. The technique

consists two phase i.e feature selection based on the maximum dependency attribute and then clustering using fuzzy partition based on indiscernible relation. Two aspect of environment impact dataset are used to be utilizing using the both techniques. the usefulness of the technique has been demonstrated as an experiment results. This paper can be used to make recommendation to improve the quality of social environment.

### ACKNOWLEDGMENT

This work was supported by Directorate of Research and Community Service Kemenristekdikti no SK 58/STTNAS/P3M/Pen.Dikti/V 12017

### REFERENCES

- [1] P. Clavel and R. Young, "Civics': Patrick Geddes's theory of city development," *Landsc. Urban Plan.*, vol. 166, no. June, pp. 37–42, 2017.
- [2] A. Kumari and A. K. Sharma, "Physical & social infrastructure in India & its relationship with economic development," *World Dev. Perspect.*, vol. 5, pp. 30–33, 2017.
- [3] P. Ashcroft and L. Murphy Smith, "Impact of environmental regulation on financial reporting of pollution activity: A comparative study of U.S. and Canadian firms," *Res. Account. Regul.*, vol. 20, pp. 127–153, 2008.
- [4] J. K. Woo, D. S. H. Moon, and J. S. L. Lam, "The impact of environmental policy on ports and the associated economic opportunities," *Transp. Res. Part A Policy Pract.*, no. xxxx, pp. 0–1, 2017.
- [5] P. Ashcroft and L. Murphy Smith, "Impact of environmental regulation on financial reporting of pollution activity: A comparative study of U.S. and Canadian firms," *Res. Account. Regul.*, vol. 20, pp. 127–153, Jan. 2008.
- [6] K. Howard and R. Gerber, "Impacts of urban areas and urban growth on groundwater in the Great Lakes Basin of North America," *J. Great Lakes Res.*, vol. 44, no. 1, pp. 1–13, 2018.

- [7] A. R. Shahtahmassebi *et al.*, "How do modern transportation projects impact on development of impervious surfaces via new urban area and urban intensification? Evidence from Hangzhou Bay Bridge, China," *Land use policy*, vol. 77, pp. 479–497, 2018.
- [8] P. K. Yogyakarta, "DAMPAK PERTUMBUHAN HOTEL TERHADAP PERUBAHAN KARAKTERISTIK PERWILAYAHAN KOTA YOGYAKARTA Tika Ainunnisa Fitria," vol. 10, pp. 52–57, 2016.
- [9] M. T. Dugan, E. H. Turner, M. A. Thompson, and S. M. Murray, "Measuring the financial impact of environmental regulations on the trucking industry," *Res. Account. Regul.*, vol. 29, no. 2, pp. 152–158, 2017.
- [10] C. Mary Schooling, E. W. L. Lau, K. Y. K. Tin, and G. M. Leung, "Social disparities and cause-specific mortality during economic development," *Soc. Sci. Med.*, vol. 70, no. 10, pp. 1550–1557, 2010.
- [11] T. Woldai and A. G. Fabbri, "The Impact of Mining on The Environment," in *Deposit and Geoenvironmental Models for Resource Exploitation and Environmental Security*, A. G. Fabbri, G. Gaál, and R. B. McCammon, Eds. Dordrecht: Springer Netherlands, 2002, pp. 345–364.
- [12] R. Wardoyo, "A Review on fuzzy multi-criteria decision making land clearing for oil palm plantation," vol. 1, no. 2, pp. 75–83, 2015.
- [13] I. Alwiah, "RETRACTED\*: RCE-Kmeans Method for Data Clustering," p. 26555, 2017.
- [14] M. Muhajir and B. Rian, "Association Rule Algorithm Sequential Pattern Discovery using Equivalent Classes ( SPADE ) to Analyze the Genesis Pattern of Landslides in Indonesia," vol. 1, no. 3, pp. 158–164, 2015.
- [15] D. Ismi, S. Panchoo, and M. Murinto, "K-means clustering based filter feature selection on high dimensional data," *Int. J. Adv. Intell. Informatics*, vol. 2, no. 1, pp. 38–45, 2016.
- [16] N. Senan, R. Ibrahim, N. M. Nawati, I. T. R. Yanto, and T. Herawan, *Soft set theory for feature selection of traditional Malay musical instrument sounds*, vol. 6377 LNCS, no. M4D. 2010.
- [17] I. T. R. Yanto, M. A. Ismail, and T. Herawan, "A modified Fuzzy k-Partition based on indiscernibility relation for categorical data clustering," *Eng. Appl. Artif. Intell.*, vol. 53, pp. 41–52, 2016.
- [18] T. Herawan, I. T. R. Yanto, and M. Mat Deris, *Rough set approach for categorical data clustering*, vol. 64. 2009.
- [19] T. Herawan, M. M. Deris, and J. H. Abawajy, "A rough set approach for selecting clustering attribute," *Knowledge-Based Syst.*, vol. 23, no. 3, pp. 220–231, Apr. 2010.
- [20] N. Senan, R. Ibrahim, N. Mohd Nawati, I. T. R. Yanto, and T. Herawan, *Rough set approach for attributes selection of traditional Malay musical instruments sounds classification*, vol. 151 CCIS, no. PART 2. 2011.
- [21] I. T. R. Yanto, M. A. Ismail, and T. Herawan, "A modified Fuzzy k-Partition based on indiscernibility relation for categorical data clustering," *Eng. Appl. Artif. Intell.*, vol. 53, pp. 41–52, Aug. 2016.



# E-Government Service Evaluation of Batu City Health Dept. using e-Govqual Approach and IPA Analysis

line 1: 1<sup>st</sup> Evi Dwi Wahyuni  
 line 2: *Informatics Engineering*  
 line 3: *University of Muhammadiyah*  
*Malang*  
 line 4: Malang, Indonesia  
 line 5: evidwi@umm.ac.id

line 1: 2<sup>nd</sup> Dharma Surya Pradana  
 line 2: *Informatics Engineering*  
 line 3: *University of Muhammadiyah*  
*Malang*  
 line 4: Malang, Indonesia  
 line 5: dsurya@umm.ac.id

line 1: 3<sup>rd</sup> Yasina Tisha Karina  
 line 2: *Informatics Engineering*  
 line 3: *University of Muhammadiyah*  
*Malang*  
 line 4: Malang, Indonesia  
 line 5: yasinacaca@gmail.com

**Abstract—** E-Government is an application of government information system technology to support public service system and dissemination of information from government to society that used in every element of government. Batu City Health Office website (<http://dinkes.batukota.go.id>) is part of Batu City Government e-Government system that was built to support publication of government information to the public. According to observations, there was a decline in visitors from the number 150 visitors in October 2017 to 50 visitors in November 2017. While in December 2017 stable at the number 50 visitors. Based on the anomaly incident, the aim of this study is to evaluate an e-government in Batu City Health Office by doing the assessment of website service quality from the user side. This evaluation uses e-Govqual and Heuristic Evaluation methods. Assessment of e-govqual attributes on performance values and interests in the IPA quadrant resulted in the conclusion that there are 24 attributes in A and C quadrants in the IPA quadrant that need to improve attribute quality. Suggestions based on quadrant A and C in the form of recommendation improvement in the form of recommendation mockup based on 10 principles of heuristic evaluation. This evaluation is carried out to determine the quality and usefulness of an e-Government in order to improve service to its citizens.

**Keywords—***E-Government, E-Govqual, Heuristic evaluation, Importance-Performance Analysis (IPA)*

## I. INTRODUCTION

Electronic government or e-Government is an application of information technology in government systems supporting the public service system and dissemination of information from government to society that can be used on every element of government [1]. The Government of Indonesia's efforts in implementing e-Government in the system of government is made by the Presidential Instruction of the Republic of Indonesia Number 3 the Year 2003 on Policy and Strategy of e-Government Development which discusses four pillars of e-Government namely content, infrastructure, application, and human resources [2]. Based on these policies, many local governments began to build

and develop a website-based public service. One of them is the government in Batu City.

Batu City Health Office released website (<http://dinkes.batukota.go.id>) in mid-July 2017. This website is part of e-Government system of Batu City government. According to the Batu Municipal Health Office, the construction of a useful website supports the publication of important information from the central government to the local government, then forwarded to the community around the area. According to the results of the analysis of the website <http://similarweb.com>, the website of Dinkes Kota Batu (<http://dinkes.batukota.go.id>) has decreased from 150 visitors in October 2017 to 50 visitors in November 2017. While in December 2017 the number is stable at the number 50 visitors

After conducting interviews with Dinkes website manager staff, the decrease in the number of visitors occurred because the website information is not updated regularly and there is no big activity implemented by the Health Office in those months. So that people feel there is no information missed on the website of Batu City Health Office in the last 3 months in 2017. Referring to the regional regulation No. 4 of 2014, the government has an obligation to evaluate the entire system of public services that include preparation to implementation and community responses to the system. This activity became one of the efforts to improve the quality of service and information dissemination to the community. What is the level of public confidence in e-Government website about freedom from danger risk, doubts during online process, website reliability, quality of e-Government website information and other questions related to website services as a form of e-Government website implementation of Batu City Health Office. It is necessary to evaluate the quality and usefulness of e-Government in fulfilling public service by evaluating the quality of e-Government service with the e-Govqual approach.

E-Govqual is a method of measuring the quality of e-Government services to the community. Thus, the user or society can judge the quality of service by drawing on the dimensions of E-Govqual. E-Govqual has 6 dimensions: Ease Of Use, Trust, Functionality Of The Interaction Environment, Reliability, Content, And Appearance Of Information, Citizen Support [3]. In addition, researchers also used IPA analysis methods to calculate the level of user satisfaction with the system.

Importance-Performance Analysis (IPA) is a method of measuring the level of user satisfaction of goods, services, and services. IPA approach is based on interests or expectations (importance) and performance on products or services [3]. The results of E-Govqual method analysis will be divided into a Cartesian diagram with 4 quadrants ie quadrant A (concentrate here), quadrant B (keep up the good work), C quadrant (low priority), and D quadrant (possible overkill) and x-axis and y-axis. The x-axis of the diagram represents the level of performance and the y-axis represents the degree of importance [4].

Based on these problems, it is necessary to evaluate e-Government in Batu City Health Office by assessing the quality of website services from the user side. This evaluation uses e-Govqual and Heuristic Evaluation methods.

## II. RESEARCH METHODOLOGY

### A. Problem Identification

Problems in e-Government Batu City Health Office do not yet know the quality of service assessments website Batu City Health by the community, so there is no website improvement in accordance with the interests of the people of Batu. Based on the problems and references obtained, then analyzed the evaluation of website services is needed. The method of analysis using e-Govqual and IPA method with the results of this study are able to identify the attributes of 6 E-Govqual dimensions that affect the performance of the Batu City Health Office website based on user needs and can categorize the interests and performance of the website using the IPA method.

### B. Study of Literature

The literature study was conducted to study the related field relevance of this research. Researchers understand all matters relating to e-Government, e-Govqual, IPA method, and all documents related to Batu City Health Office website and other documents.

### C. Initial Data

Stage of initial data collection through direct observation and interviews in the staff of program and report Batu City Health Office. This stage is done to determine the reason for the need for evaluation on the website of Batu City Health Office. The results of observations and interviews show a decrease in the number of visitors because the information on the website is not updated regularly and there is no big activity implemented by the Health Office in those months. There is a behavior that people have read the latest information on the website of Batu City Health Office in the last 3 months in 2017.

### D. Instrument Arrangement

At this stage, the researcher determines the research variables and develops the evaluation questionnaire. The determination of research variables is done as a reference for making a questionnaire. The research variable consists of two, namely the independent variable and the dependent variable. The independent variable is a variable that affects the bound variables while the dependent variable is the variable that becomes the result of the independent variable. The independent variables in this study are e-Govqual

dimensions: Reliability, Trust, Citizen Support, Functionality of the interaction environment, Content and appearance of information, Ease of use. While the dependent variable is E-government Service Quality.

Preparation of questionnaires based on the previous research questionnaire grid. The basis for making the questionnaire is the e-Govqual attribute consisting of 6 dimensions and 47 attributes [5]. Later the questionnaire calculation was done using a Likert scale. The following are the e-Govqual dimensions used in this study.

TABLE I. E-GOVQUAL DIMENSION

Ease Of Use	Trust
Website's structure	Not sharing personal information with others
Customized search functions	Protecting anonymity
Site-map	Secure archiving of personal data
Set up links with search engines	Providing informed consent
Easy to remember URL	Use of personal data
Personalization of information	Non-repudiation by authenticating the parties involved
Ability of customization	A procedure of acquiring username and password
The Functionality of the interaction environment	Correct transaction
The Existence of online help in forms	Encrypting messages
Reuse of citizen information to facilitate future interaction	Digital signatures
Automatic calculation of forms	Access control
Adequate response format	Reliability
	Ability to perform the promised service accurately
	In Time service delivery
	Accessibility of site
Content and appearance of information	Browser - system compatibility
Data completeness	Loading/transaction speed
Data accuracy and conciseness	Citizen Support
Data relevancy	User-friendly guidelines
Updated information	Help Pages
Linkage	Frequently Asked Questions
Ease of understanding/interpretable data	Transaction tracking facility
Colors	The existence of contact information
Graphics	Problem-solving
Animation	Prompt reply to customer inquiries
Size of web pages	Knowledge of employees
	Courtesy of employees
	The Ability of employees to convey trust and confidence

### E. Feasibility Test of Questionnaire

Testing performed includes testing the validity and reliability testing. Valid or not a questionnaire needs validity testing. While the reliability test conducted to measure (accuracy) questionnaire made. Reliable research questionnaires when statements used as a measurement tool can be trusted.

### F. Data Collection

At the data collection stage, the researcher took the research sample. Characteristics of the samples used are all existing staff at Batu City Health Office. According to data until 2018, the number of staff in the health office amounted to 64 people. The entire staff has the same opportunity to be the respondent in this research. This is because the existing system of Batu City Health Office is familiar to staff and employees of Batu City Health Office so that the results of the data will be natural and not biased.

### G. Data Analysis and Recommendations

Data collection was done by distributing a questionnaire directly (offline) to Batu City Health Office staff. The entire staff has the same opportunity to be the respondent in this research. Further processing of IPA data using SPSS application. After knowing the final result of the analysis it will be made document recommendation system based on ten principles of heuristic evaluation.

### H. Preparation Reports

The last stage of making research reports along with suggestions and recommendations of researchers on the improvement of the Batu City Health Office website. Improved performance of website services is expected after the interests of users.

## III. RESULT AND DISCUSSION

### A. Validation Test

The study used a significance value of 5% where  $r$  table value as a reference of 0.361. From the result of validity test with SPSS software get the result that is performance attribute A19 get result count equal to 0,351 where result under  $r$  table specified. At attribute importance, A19 get result above  $r$  table value equal to 0,696. The result can be concluded that the A19 attribute is still needed by the user so that although the performance value of attribute A19 is below  $r$  table value, the attribute is still valid because of the importance value above  $r$  table value. The conclusion that 47 attributes or statements, all attributes are valid. It is known from the calculation  $r$  calculate the value is greater than the value of  $r$  table.

### B. Reliability Test

This test gets the value of Alpha for the interest of 0.971 and the performance of 0.966. The indigo values are then compared with  $r$  table with  $n = 30$  with 5% significance,  $r$  table value of 0.361. Then it can be concluded the value of alpha interest and performance is greater than the value of  $r$  table which means that all statements on the questionnaire have been reliable and reliable as a measuring tool of research.

### C. IPA Method

In the calculation of Importance-Performance analysis, there are 3 stages, the three stages will be described as follows:

1. The first stage in the IPA method is to determine the level of conformity between the level of importance and the level of performance quality attributes studied through the comparison of performance scores with interest scores. By using the formula

$$TK = \frac{x^i}{y^i} \times 100\% \quad (3) [6]$$

By using the formula, it is found that the website suitability level is 92,94% which means that the website is in the category 'SESUAI'. According to Sukardi and Cholis (2006), the level of conformity that is in the range of values close to 100% means that the service or goods used have a good level of conformity

2. The next stage is to calculate the average for each attribute perceived by the user to determine the value staged 3. The formula used is

$$\overline{XI} = \frac{\sum XI}{n} \quad \overline{YI} = \frac{\sum YI}{n} \quad (4) [6]$$

At this stage the calculation of the average value of performance and importance in which the results are used to calculate the boundaries X (performance) and Y (interests) in the IPA quadrant.

3. The third or last stage calculates the average of all attributes of importance (Y) and performance (X) which are the limits in a Cartesian diagram. This means that the results of the average interest and average performance are calculated based on the number of statement attributes in the questionnaire. The result data from this stage is obtained by the formula

$$\overline{XI} = \frac{\sum XI}{k} \quad \overline{YI} = \frac{\sum YI}{k} \quad (5) [12]$$

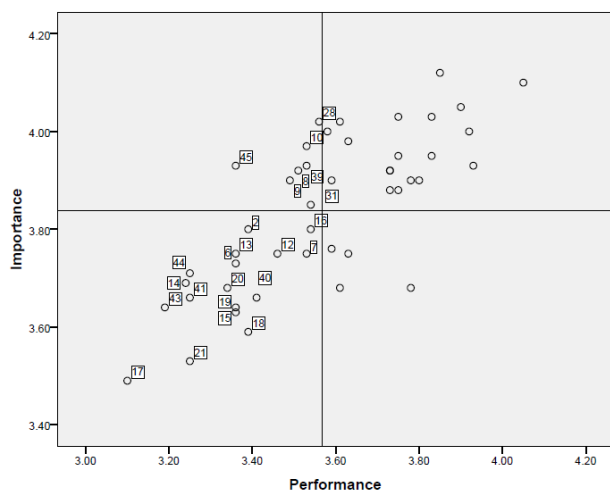
then the result of this staged calculation will be used on the calculation of IPA using SPSS. At this stage, the average of total performance is 3.57 and the average interest is 3.84. These values will then be the boundaries of X and Y in the IPA quadrant where the limit determines which attributes need improvement.

After completing the calculation of phase three, then the process will be taken on the SPSS application to find out how the distribution of e-Govqual attributes in the IPA quadrant.

### D. Calculation of IPA

After the IPA quadrant calculation results are known then the next step is to use the data of stage 3 results from the IPA method on SPSS so that the quadrant results

obtained as shown below. In this picture, it looks at which attribute should get quality improvement.



PICT 1. CALCULATION OF IPA

#### 1. Quadrant A (concentrate here)

High-interest rate values and low-performance levels. This means that attention needs to be paid attention to the improvement and improvement of attributes that are considered less. Service in this quadrant is a top priority for quality improvement. From the research results found that there are five attributes that need to be a priority improvement that is the attribute at number 8 (not the private data part), 9 (protect anonymity), 10 (protection of personal data archives), 28 (completeness of data), 31 (update information), 39 (help pages) and 45 (employee knowledge). According to the user, both attributes are not meet the needs yet of users and performance provided services are still lacking.

#### 2. Quadrant B (keep up the good work)

The high value of importance and high-performance level. It means having an opportunity to maintain attributes that have advantages. Service in this quadrant is considered important by the user so it must be maintained. In this quadrant, there are 18 attributes that can be maintained existence because the service performance is in accordance with the needs of users

#### 3. Quadrant C (low priority)

The value of importance and level of performance is just as low. This means that in this quadrant shows some less important aspects of the effect for the user so that attribute performance in this quadrant is not maximal and tend to be low. To improve it needs to be improved on these attributes. There are 16 attributes that need improvement: number 2 (keyword conformity), 6 (personalization of information), 7 (customization ability), 12 (use of personal data), 13 (identity authentication), 14 (procedure of obtaining account), 15 (access control), 19 (online help), 20 (use of previous information), 21 (automatic form filling), 41 (transaction tracker), 16 (encryption), 43 (problem solving ability), and 44 (the speed of replying to user questions). Attributes in this quadrant have a low priority because they are considered unimportant by users due to poor service quality.

#### 4. Quadrant D (possible overkill)

The low value of importance and high-performance level. This means that all the attributes that exist in this quadrant is considered not too important by the user but has excess resources. So in this quadrant, the existing attributes can be ignored or deleted. In this study, there are 4 attributes that are in quadrant 4.

### IV. CONCLUSION

The conclusions of this study are as follows:

The level of service suitability of Batu City Health Office website is 92.94% which means that the website is in the 'SESUAI' category, but the other consideration is the result of calculating the importance of the users and the value of website performance in the IPA quadrant. According to the results of IPA quadrant calculations, it still needs improvement for users in accessing the website services. The analysis results from the IPA awareness states that of the 47 attributes, there are 24 attributes that need to be improved. With 3 attributes on ease of use dimensions, 10 attributes on trust dimension, 3 attributes on the functionality of the interaction environment dimension, 2 attributes on content and appearance of information dimensions, and 6 attributes on citizen support dimension. This journal still has shortcomings, namely the need to create a prototype website design so that improvements can be made according to the needs of users that have been previously evaluated.

### REFERENCES

- [1] Sosiawan, E. A. (2008). Tantangan Dan Hambatan Dalam Implementasi E-Government Di Indonesia. Seminar Nasional Informatika, 2008(semnasIF), 99–108.
- [2] Republik Indonesia, Instruksi Presiden Republik Indonesia no. 3 tahun 2003 tentang Kebijakan dan Strategi Nasional Pengembangan E-Government
- [3] Wahyudi, S. E., Pinandito, A., & Saputra, M. C. (2017). Penilaian Kualitas Website E-Government Pejabat Pengelola Informasi dan Dokumentasi ( PPID ) Dengan Dimensi e-GovQual (Studi Pada Dinas Komunikasi dan Informatika Pemerintah Kota Probolinggo), 1(2), 108–117.
- [4] Saputra, Rino Agus, dkk. 2018. Penilaian Kualitas Layanan E-Government Dengan Pendekatan Dimensi E-Govqual dan Importance Performance Analysis(IPA) (Studi Kasus Pada Pemerintah Provinsi Nusa Tenggara Barat). Vol. 2, No. 5. 1794-1802.
- [5] Budiaji, W. (2013). LIKERT ( The Measurement Scale and The Number of Responses in Likert Scale ), 2(2), 125–131.
- [6] Santoso, I., Mulyarto, A. R., & Maharani, S. (2011). Persepsi konsumen terhadap kualitas bakpao telo dengan metode importance performance analysis. Jurnal Teknologi Pertanian, 12(1), 23–30.

# Implementation of Obfuscation Technique on PHP Source Code

Maskur Maskur  
Informatics Department

Universitas Muhammadiyah Malang  
Malang, Indonesia  
maskur@umm.ac.id

Zamah Sari  
Informatics Department

Universitas Muhammadiyah Malang  
Malang, Indonesia  
zamahsari@umm.ac.id

Ahmad Sirojul Miftakh  
Informatics Department

Universitas Muhammadiyah Malang  
Malang, Indonesia  
sirojulmiftakh@umm.ac.id

**Abstract**—Source code on web based applications can be altered easily. This occurred because the source code is not compiled into an executable file. Hence, it can be read and copied easily, or be changed without permission from the author. Obfuscation is a technique that commonly used to secure the source code in any websites based application. Obfuscation is a technique to randomize the source code that make the code harder to read but still runnable, but this make the running time increased and the application will run slower then it supposed to. This increased time caused by reverse obfuscation proses to bring back the source code into originally form before interpreted by web server. This studi intended to create an obfuscation technique that keeping the application run time performance as not obfuscated called Wanna Crypt. The methods to create this applications are (1) system design using UML, (2) implementation of the system, which is done by coding or writing scripts using PHP, HTML, JavaScript, CSS to build Wanna Crypt based website, (3) Blackbox and Whitebox testing to compare the execution time. From the tests, it can be concluded that web applications using Wanna Crypt provide a longer response time than web applications without using obfuscation.

**Keywords**— *php, source code, encryption, reverse engineer, obfuscation*

## I. INTRODUCTION

Open source technology used in any software development especially web based application can be build with a fairly low cost in its development. But keep in mind that any open source technology also opens up opportunities for vulnerabilities that can be misused by irresponsible parties due to the source code of software also included into the software deployment. Source code for web based software that is not compiled into executable files allows others to manipulate and even alter malicious code on the application to be built or developed. Application that are processed or executed without being transformed into executable files cause the source code easily known by people and modified or altered without permission[1] [2].

This may result that the software being vulnerable to manipulation, duplication, unauthorized permission, and even unknowingly altered code that can harm to the system when the application is in operation. To overcome the software security case, proposed an approach in the technique of obfuscation by distributing the ciphertext which is the result of the stages of randomization of data or strings in a particular form in accordance with the rules of php language code execution[3][4][5][6]. This research propose a solution through the development of a Wanna Crypt software using a text distribution approach to ciphertext generated through obfuscation process in accordance with the code execution code PHP so that the source code can still be

processed by the web server. Also built a loader which is a new extension in the web server as a support for processing the source code that has been obfuscated using Wanna Crypt application.

Krisma Pradana in [7] was designed an encoder and decoder application intended to obfuscation against a web based software. But the software is focused on pure source code that is purely incompatible with scripts other than the php programming language. This causes problems when the source code has been mixed with other tags such as HTML tags, JavaScript or CSS which are the builder code of a web based software. While, in [8], Oki Setiawan, who also in his research applied the rivest cipher cryptography algorithm to secure the source code of php programming language with obfuscation technique resulted in execution time of 199.86%.

Those previous studies resulted in obfuscation technique that still incompatible to some elements in web based software, and much longer execution time compered to web without obfuscation technique. However, this study tries to solve the problem by designing system that provide obfuscation technique that more compatible with web based software tags and better execution time.

Wanna Crypt is designed and built on web based technology. Wanna Crypt version 1.0.0 is built using Codeigniter's PHP framework which refers to object-oriented programming [9] based approach and Model-View-Controller pattern design. Wanna Crypt is the result of Test Case Code Execution by observing the way of evaluation and execution of PHP code by web server. Wanna Crypt is also designed by building new extensions that will be integrated on the web server. Wanna Crypt designed with the hope of being accessible online on every mobile platform that will have low impact on execution time.

## II. DESIGN AND IMPLEMENTATION

### A. System Design

The design of the system is done to identify the framework or blueprint that can be used as a reference in making the system. System design is done by using flowchart or flowchart approach to arrange system framework. The flow diagram used to build the Wanna Crypt application uses the Unified Modeling Language (UML) scheme to construct the system functionality blueprint scheme to be built. UML scheme used is (1) Use Case Diagram, (2) Activity Diagram, (3) Component Diagram, and (4) Sequence Diagram.



### B. Implementation

Implementation of the system is done by coding or writing scripts using PHP, HTML, JavaScript, CSS to build Wanna Crypt based website. Implementation is done by using Object Oriented Programming (OOP) coding technique using Codeigniter framework which refers to Model-View-Controller (MVC) pattern design.

In addition, to build the loader is done by coding using C programming language and Visual Studio applications to compile the process into a library of Dynamic Link Library (DLL). Implementation of the system is done by referring to the results of the previous system design.

## III. RESULT AND DISCUSSION

Wanna Crypt application testing will be done by applying black box testing techniques and also white box. Black box testing technique is done to ensure that the functionality built in Wanna Crypt application has been running properly and correctly. Furthermore, the white box tested to test whether the ciphertext generated from the obfuscation process can be read or re-executed by the web server and have the most efficient code structure. Other things observed by looking at the comparison of execution time between the source code in plaintext and ciphertext to see the performance comparison between the obfuscated and non-obfuscated web applications.

### A. Obfuscation Steps

This stage is a series of process of transformation and repackaging of ciphertext generated by Wanna Crypt in randomization of source code in accordance with php programming language structure. The scheme of the obfuscation process designed in the Wanna Crypt application can be seen in the schema below.

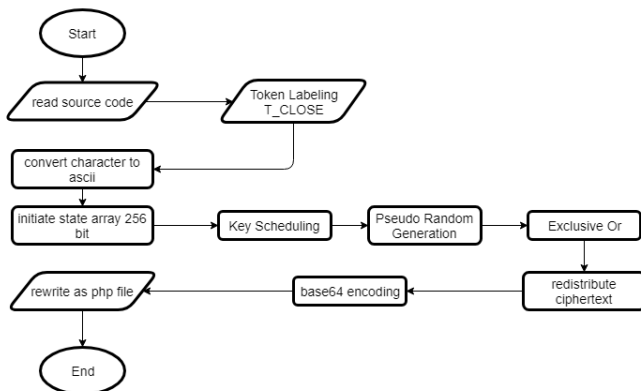


Fig. 1 Schema of obfuscation proses in Wanna Crypt Application

Figure 1 illustrates the path of the obfuscation stage designed in the Wanna Crypt application. The process of obfuscation is done by (1) reading the source code file, (2) tagging the php tag, (3) obtaining the ascii value of each character, (4) initializing the state array with the value 0 to 255, (5) scheduling, (6) running the pseudo random generation method, (7) doing exclusive or encryption (8) compiling the php code execution flow, (9) doing base64 encoding, and (10) rewriting the php source code source into php extension file.

### B. Obfuscated Source Code Proses Steps

This stage is a series of code execution process to source code result of obfuscation by Wanna Crypt application. Here is the scheme of the process execution code results obfuscation using Wanna Crypt application. Obfuscation code processing schemes are described in the following scheme:

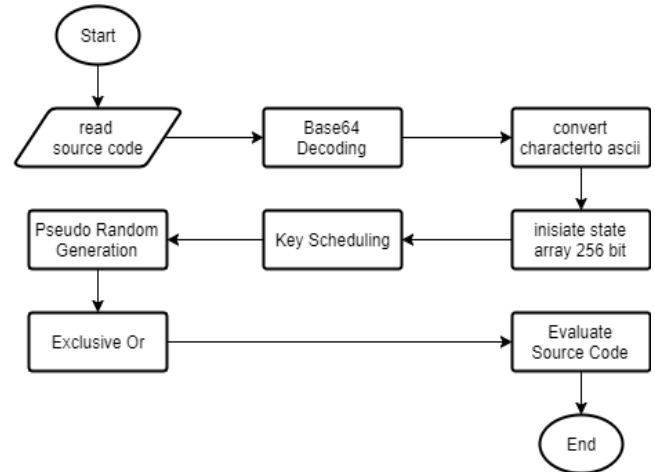


Fig. 2 Schema of Obfuscated Source code execution using Wanna Crypt Application

Figure 2 describes the obfuscation source code execution method using Wanna Crypt with the following paths: (1) reading the source code of the obfuscation result, (2) decoding using base64, (3) obtaining the ascii value of each character, (4) initializing state array (5) executes the key scheduling method, (6) runs the pseudo random generation method, (7) executes the exclusive method or, (8) executes the cipher text source code.

### C. Rivest Chiper 4 Algorithm

Keystream type algorithms that process plaintext changes into ciphertext bytes per byte with simpler and faster computations [10][11][12]. This algorithm can use a key length of 1 to 256 bytes which will be used to initialize the 256 byte substitution key table.

#### 1) Encryption Method

a) Array Initialization: At this stage provided 2 pieces of arrays, each of which is a security key and substitution box. This array substitution box is initialized initially with values from 0 to 255 while the security key array is populated with the decimal value of each character on the security key until it is fully loaded in the array.

b) Key Scheduling Method: At this stage re-initialization process is done on array substitution box or sbx with value along 1 to 256 bit which is repeatedly filling security key that is inputted or used. The results of this stage will be reused in the encryption key generation process. Calculation of key scheduling method can be seen in mathematical calculation below:

$$\begin{aligned}
 & i=0 \text{ dan } j=0 \\
 & j=(j+\text{sbox}[i]+\text{key}[i]) \% 256 \\
 & \text{temp}=\text{sbox}[i] \\
 & \text{sbox}[i]=\text{sbox}[j] \\
 & \text{sbox}[j]=\text{temp}
 \end{aligned}
 \tag{1}$$

Equation 1 contains an explanation of the substitution process of the encryption key generation array that will be used for the transformation of each character in the php source code.

c) Pseudo Random Generation Method: At this stage the encryption key is generated which will be processed using the exclusive method or with each character on the plaintext. The result of this step will be used as an exclusive or encryption key to any character contained in the plaintext or source code. Calculation of this method can be seen in the equation below:

$$\begin{aligned} a &= 0, j = 0, \text{ dan } i = 0 \\ a &= (a+1) \% 256 \\ j &= (j+sbox[a]) \% 256 \\ temp &= sbox[a] \\ sbox[a] &= sbox[j] \\ sbox[j] &= temp \end{aligned} \quad (2)$$

Equation 2 contains an explanation of the calculations performed in the modification process of the state of the security lock generation. The substitution process is performed to randomize the contents of the sandbox data which is then used to generate the encryption key.

d) Exclusive Or Method: After the keystream generation of the specified security key is assigned, each character on the plaintext will be processed bytes per byte or character by character against each keystream that has been exclusively generated or so obtained by the ciphertext of each plaintext. Calculation of this method can be seen in the equation below:

$$\begin{aligned} k &= sbox[(sbox[a]+sbox[j]) \% 256] \\ cipher &= plain[i] \wedge k \end{aligned} \quad (3)$$

Equation 3 contains an explanation of the computations performed in the exclusive or the method for the process of transforming the plaintext into ciphertext by using the xor logic to the bits of each character contained in the plaintext using the previously generated security key.

## 2) Decrypt Method

The method of decrypting or returning ciphertext to plaintext in the rivest cipher 4 algorithm uses the same path as in the encryption process. The security key used in the decryption process also exactly matches the security key used in the encryption process.

### D. Web Application Test without Obfuscation

TABLE I. RESULT OF WEBSITE TEST PERFORMANCE WITHOUT OBFUSCATION

Response Time without Obfuscation		
User	Avg. Time Spent (Ms)	Avg. Click Time(Ms)
5	74.3	74.3
10	53.2	53.2
15	239.2	79.9
20	208.5	104.3
25	453.7	180.3
40	857.5	214.4
50	1340	268
80	3179.1	397.4
100	4811.8	481.1

The data in Table I is the data obtained from the test results of the application without using obfuscation. Testing is done by varying the number of users to observe the performance of the application.

### E. Web Application Test with Obfuscation

Below is the data obtained from the test results of the application without using obfuscation. Testing is done by varying the number of users to observe the performance of the application. Notice Table 2.

TABLE II. RESULT OF WEBSITE TEST PERFORMANCE WITH OBFUSCATION

Response Time with Obfuscation		
User	Avg. Time Spent (Ms)	Avg. Click Time(Ms)
5	65.9	65.9
10	57.8	57.8
15	305.9	101.8
20	214.9	107.5
25	925.3	231.3
40	842.7	210.6
50	1375.8	275.3
80	3120.7	390.1
100	4913.1	491.4

### F. Obfuscation Feature Testing

In this phase, an obfuscation of a PHP source code is mixed with HTML tags in order to see the success of the code execution process. Source code that has been obfuscation using Wanna Crypt placed back into the we server and then observed whether the obfuscated source code successfully processed and executed by the web server as the original source code or cause the source code becomes unreadable by the web server.

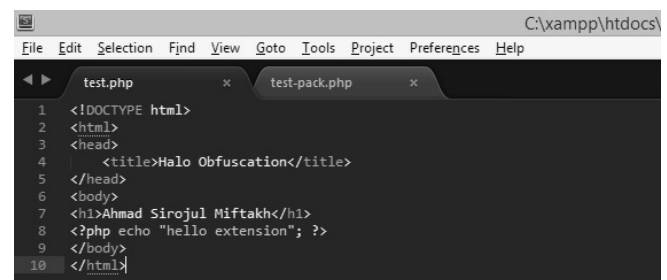


Fig. 3 The original software source code

Figure 3 shows the original source code of a software to be randomized using Wanna Crypt. Obfuscation testing is done by using PHP source code mixed with html tags. Obfuscation process is done by utilizing obfuscation method that has been designed in loader which built before and integrated into web server.



Fig. 4 Result of execution of original source code

Figure 4 contains the source code execution results on the web server. The original source code of a php-based language program that has been mixed with code or html tags is then randomized using obfuscation techniques then executed back into the web server. This test is performed to find out the results of obfuscation performed by Wanna Crypt successfully to be tested again on the web server that has been integrated with the loader.

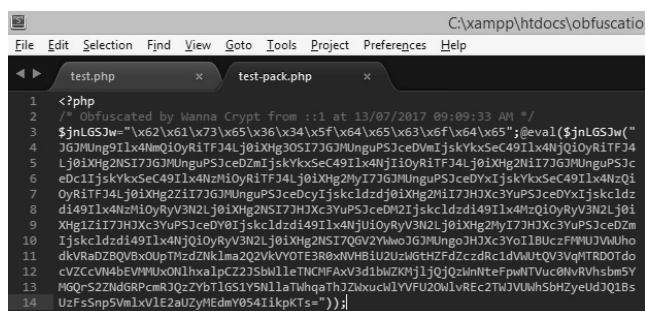


Fig. 5 Source code of obfuscation results using Wanna Crypt

Figure 5 shows the result of the obfuscation process using Wanna Crypt that has performed randomization or obfuscation on the PHP source code. Furthermore the source code generated will be executed again on web server that has been integrated with the loader which is also built in this research.

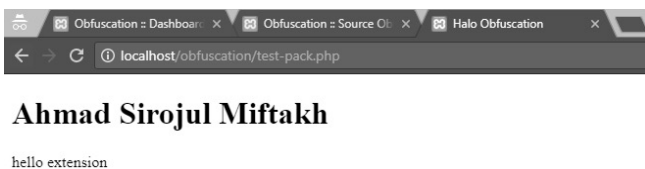


Fig. 6 The result of random source code execution

Figure 6 shows the results of the execution of the randomly generated source code producing exactly the same output as the original non-scrambled source code. This indicates that Wanna Crypt can scramble the source code properly without damaging or changing the program flow compiled in the original software.

Here is a comparison of the reliability of web application that use obfuscation against web application without using obfuscation. The observations in this test comparison are focused on the reliability of web applications that use obfuscation in response to user requests. Notice Table 3.

TABLE III. COMPARISON OF WEB APPLICATION WITH AND WITHOUT

Average Time Spent Analysis				
User	With Obfuscation (ms)	Without Obfuscation (ms)	Performance	Delta (ms)
5	65.9	74.3	Faster	-8.4
10	57.8	53.2	Slower	4.6
15	305.9	239.2	Slower	66.7
20	214.9	208.5	Slower	6.4
25	505.4	453.7	Slower	51.7
40	842.7	857.5	Faster	-14.8
50	1375.8	1340	Slower	35.8
80	3120.7	3179.1	Faster	-58.4
100	4913.1	4811.8	Slower	101.3

OBUSCATION

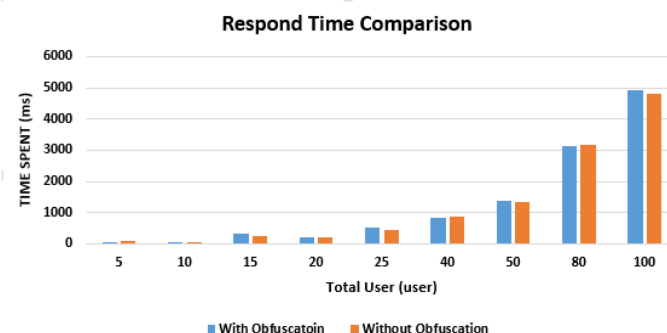


Fig. 7 Comparison Result of Web Application with and without Obfuscation

This longer execution time because of the existence of the obfuscation mechanism first in the source code that has been scrambled before finally processed again by web server.

#### IV. CONCLUSION

Based on the scenarios for testing in observing the performance of web applications using obfuscation and web applications without using obfuscation on Figure 7, it can be concluded that web applications using obfuscation provide longer response time than web applications without using obfuscation. This is due to the existence of deobfuscation mechanism first in the source code that has been scrambled before finally processed again by web server.

#### REFERENCES

- [1] Kurniadi, Irwansyah F. Penerapan Algoritma Rc4 Untuk Enkripsi Keamanan Data ( Studi Kasus : Dinas Pendidikan Dan Kebudayaan Kota Sekayu ). J Ilm R B. 2015;8(12):1-13.
- [2] Rahmatulloh A, Munir R. Pencegahan Ancaman Reverse Engineering Source Code Php Dengan Teknik Obfuscation Code Pada Extension Php. In: Konferensi Nasional Informatika. 2015.
- [3] Ristić N, Jevremović A. An Open Source Solution For Protecting Php Source Code. In: Proceedings Of The 1st International Scientific Conference - Sintez 2014 [Internet]. 2014. P. 616-9. Available From: [Http://Portal.Sinteza.Singidunum.Ac.Rs/Paper/221](http://Portal.Sinteza.Singidunum.Ac.Rs/Paper/221)

- [4] Cimato S, Santis A De, Petrillo Uf. Overcoming The Obfuscation Of Java Programs By Identifier Renaming. 2005;78:60–72.
- [5] Han S, Ryu M, Cha J, Choi Bu. Hotdol: Html Obfuscation With Text Distribution To Overlapping Layers. In: Proceedings - 2014 Ieee International Conference On Computer And Information Technology, Cit 2014. 2014. P. 399–404.
- [6] Nugroho Ps, Ariwibowo E. Pengembangan Modul Enkripsi Dan Dekripsi Pada Php Dengan Modifikasi Metode Kriptografi Vigenere Cipher Dan Cipher Block Chaining (Studi Kasus Pada Geekybyte.Com). In: Jurnal Sarjana Teknik Informatika Universitas Ahmad Dahlan. 2014. P. 1004–12.
- [7] Pradana K. Aplikasi Php Encoder Dan Decoder Menggunakan Algoritma Base64 Dan Kunci Keamanan. 2015;
- [8] Setiawan O, Fiati R, Listyorini T. Algoritma Enkripsi Rc4 Sebagai Metode Obfuscation Source Code Php. In: Seminar Nasional Teknologi Industri Dan Informatika. 2014. P. 113–20.
- [9] Suehring S, Valade J. Php Mysql Javascript Html5 All In One For Dummies. John Wiley & Sons, Inc. 2013. 724 P.
- [10] Setiawan O, Fiati R, Listyorini T. Algoritma Enkripsi Rc4 Sebagai Metode Obfuscation Source Code Php. In: Seminar Nasional Teknologi Industri Dan Informatika. 2014. P. 113–20.
- [11] Miles E, Sahai A, Weiss M. Protecting Obfuscation Against Arithmetic Attacks. Eprint [Internet]. 2014;878:221–38. Available From: [Http://Dx.Doi.Org/10.1007/978-3-642-55220-5\\_13](http://Dx.Doi.Org/10.1007/978-3-642-55220-5_13)

# Power Demand Forecasting Considering Actual Peak Load Periods Using Artificial Neural Network

Yuan Octavia D.P.<sup>1</sup>, A.N. Afandi<sup>2</sup>, Hari Putranto<sup>3</sup>

Electrical Engineering, Universitas Negeri Malang  
Malang, Jawa Timur, Indonesia

<sup>1</sup>yuan.odp@gmail.com, <sup>2</sup>an.afandi@um.ac.id, <sup>3</sup>harput160661@gmail.com

**Abstract**—Presently, electrical energy consumption continues to increase from year to year. Therefore, a short-term load forecasting is required that electricity providers can deliver continuous electrical energy to electricity consumers. By considering the estimation of the electrical load, the scheduling plan for operation and allocation of reserves can be managed well by the supply side. This study is focused on a forecasting of electrical loads using Artificial Neural Network (ANN) method considering a backpropagation algorithm model. The advantage of this method is to forecast the electrical load in accordance with patterns of past loads that have been taught. The data used for the learning is Actual Peak Load Period (APLP) data on the 150 kV system during 2017. Results show that the best network architecture is structured for the APLP Day and Night. Moreover, the momentum setting and understanding rate are 0.85 and 0.1 for the APLP Day. In contrast, 0.9 and 0.15 belong to the APLP Night. Based on the best network architecture, the APLP day testing process generates Mean Squared Error (MSE) around 0.04 and Mean Absolute Percentage Error (MAPE) around 4.66%, while the APLP Night generates MSE in 0.16 and MAPE in 16.83%.

**Keywords**—Artificial Neural Network, Electricity Load, Load Forecasting.

## I. INTRODUCTION

Electrical energy usages continue to increase from year to year. Number of customers Indonesia State Electricity Company (ISEC) from 2011 to 2015 has increased more than 33 percent. Based on the increasing number of customers, ISEC is required to meet all the demand for electrical energy continuously. Continuous distribution of electrical energy is the right of ISEC customers to be prioritized by ISEC as the main provider of electrical energy in Indonesia [1]–[6]. To be able to meet the needs of electrical energy continuously, it is a necessity to balance supply and demand sides. Thus, the power generated must always be equal to the power consumed by the electric power consumer [7]–[15]. Therefore, it is also necessary to estimate short-term electrical loads that can predict the need for the electrical usage. The short-term electrical load forecast (SELF) aims to predict electricity requirements in minutes, hours, days, and weekly hours [2], [8], [10], [16]–[18]. The SELF-brings out to forecast load requirements at a load center switchyard (LCS) and play an important role in the real-time control and security functions of the energy management. An accurate estimation of the electrical load can save operational costs and safe conditions, both can be done by the supply and demand side

management[19]–[22]. The SELF can also be used as a reference to the ISEC's Operational Plan.

In general, the load forecasting is categorized into causal models and time-dependent models. The causal model is based on the relationship between the variables involved, whereas the forecasted model of the forecasting time is based on historical data of variables predicted unaffected by other variables [23]–[27]. Time series electrical load forecast can be applied because load characteristics have the same pattern trend in each period. The time-based electrical load forecast can be applied using several methods. A complicated method does not guarantee a high degree of accuracy of forecasts. One method that can be applied to the SELF is the Artificial Neural Network (ANN) algorithm [16], [23], [25], [28], [29]. These works are concerned in the exploration of ANN backpropagation for defining an effective algorithm as a forecasting method.

## II. PROBLEM STATEMENT

In general, electric consumers are divided into 6 sectors, namely household, industry, business, social, government office building, and street public lighting [2], [30]–[33]. Each consumer of electric energy has different load characteristics based on electric energy consumption patterns in each sector [34]. Determination of electrical load characteristics is very important for evaluation and planning which are needed in distribution substations [35]. In addition, the load studies are crucial in the planning future system development. The description of load characteristics is expressed using a load assessment factors (LAF). This LAF can illustrate load characteristics in terms of quantity and quality. The LAF is also useful for estimating future electrical loads [7], [36], [37]. For the needs of daily electrical load estimation, the LAF covers the based demand, maximum demand, and peak load.

Furthermore, many intelligent methods have been developed to find out the optimal solution for various technical problems [19], [20], [40]–[46]. One of them is the ANN considered the backpropagation. The architecture of the ANN consists of the input layer, hidden layer, and output layer, where each layer consists of one or more neurons [47]–[51]. The backpropagation method uses three steps to perform the training presented in feedforward of the training input pattern, backpropagation of connected error, and weight adjustment [28], [52]. In details, the ANN-Backpropagation architecture is shown in Figure 1. The training procedures of this algorithm are reported in many investigated fields [53]–[56].



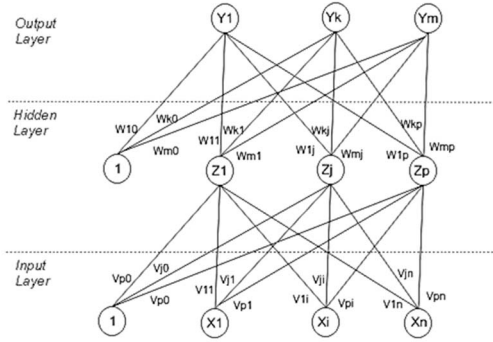


Fig. 1. ANN backpropagation architecture

### III. APPLIED PROCEDURES

As many works, the algorithm is presented in many types of the structures for illustrating steps to get out the solution. This study is also given in a hierarchy to complete the works. This section is used to explain the whole steps of studies which are covered in quantitative processes of the secondary data analysis and all working sequences. Technically, required information is the historical data of daily electrical load on an effective day. The data used for the learning is actual peak load period (APLP) data on the 150 kV system of Buduran Area during 2017. Vulnerable time spent on the APLP Day and Night is also presented. The daily data load power information is obtained from the ISEC for the East Java Area Distribution. Moreover, the data of electrical load usage is covered for the historical data of the electrical load on the 150 kV of the LCS in Buduran, Sidoarjo District. In detail, Figure 2 presents hierarchies of the studies.

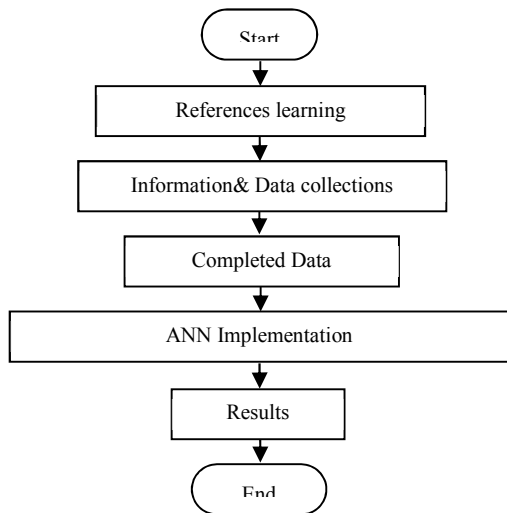


Fig. 2. Block diagram of the whole study

The formation of the best network architecture is structured using a quantitative model which is the most

adaptable to every possibility. Moreover, the level of accuracy is tested on two types covered in Mean Squared Error (MSE) and Mean Absolute Percentage Error (MAPE). The MSE is used to test the error rate of a network architecture in the forecasting, whereas the MAPE is used to test the accuracy of the forecasting results. In this study, the ANN-Backpropagation model is presented in Figure 3 and Figure 4. Figure 3 shows the procedure for the forecasting and Figure 4 shows the ANN network architecture while Table I also shows the composition of this network architecture. In particular, Table II provides the parameter definitions and the MAPE is required as listed in Table III.

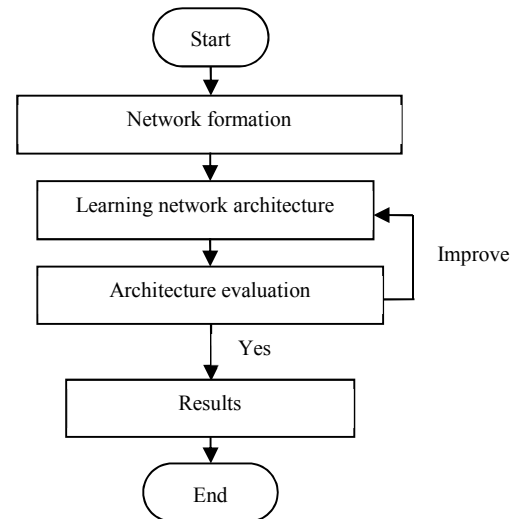


Fig. 3. Load forecasting steps

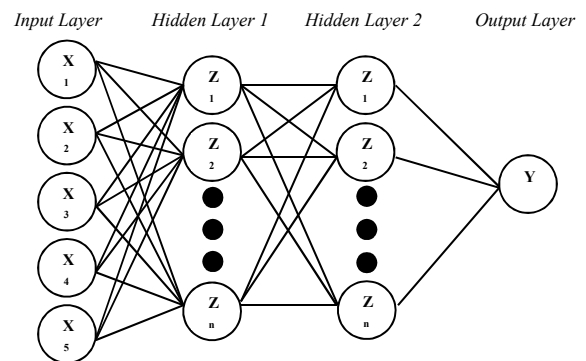


Fig. 4. ANN network architecture

TABLE I. ANN BACKPROPAGATION PARAMETERS

Parameter	Numer	Description
Input Layer	5 neuron	Daily load
Hidden Layer	HL 1-2	Testing data
Output Layer	1 neuron	Prediction
Epoch	10.000 epoch	Maximum setting
Training function	Traingdx	Function
Activation function	Sigmoid Biner	Function

TABLE II. INPUT AND TARGET ALGORITHM

Map	Data Masukan	Target
1.	X <sub>1</sub> -X <sub>5</sub> is a daily load on Monday for 5 weeks, ranged in the 1 <sup>st</sup> week to the 5 <sup>th</sup> week	Load on Monday on the 6 <sup>th</sup> week
2	X <sub>1</sub> -X <sub>5</sub> is a daily load on Tuesday for 5 weeks, ranged in the 1 <sup>st</sup> week to the 5 <sup>th</sup> week	Load on Tuesday on the 6 <sup>th</sup> week
3	X <sub>1</sub> -X <sub>5</sub> is a daily load on Monday for 5 weeks, ranged in week 6 <sup>th</sup> to week 10 <sup>th</sup>	Load on Monday on the 11 <sup>th</sup> week
4	X <sub>1</sub> -X <sub>5</sub> is a daily load on Friday for 5 weeks, ranged in week 16 <sup>th</sup> to week 20 <sup>th</sup>	Load on Friday on the 21 <sup>st</sup> week

TABLE III. MAPE PERCENTAGES

MAPE	Prediction
MAPE ≤ 10%	High
10 < MAPE ≤ 20	Good
20 < MAPE ≤ 50	Reasonable
> 50	Low

Based on Table I, Table II, and Table III, the training results are obtained in the form of network weights that will be used in the testing phase. Training results are applied to the test data pattern while weights and biases can be used to show results for data outside of training input data.

#### IV. RESULTS AND DISCUSSIONS

Based on the preparation of input and target matrices as detailed in Table I, Table II, and Table III, the ANN is processed as the given hierarchies in Figure 2, Figure 3, and Figure 4. The architecture composition of the training and test results are performed in the APLP Day and Night. The momentum setting and rate of understanding are 0.85 and 0.1 for the APLP Day, as well as 0.9 and 0.15 for the APLP Night.

In details, the results are given in following tables and figures. Table 4 shows the results of the training on APLP Day, Table 5 shows the results of the training on APLP Night. Figure 4 shows a graph of error in training.

TABLE IV. TRAINING RESULT OF THE APLP DAY

X1	X2	X3	X4	X5	T	JST
114.90	110.85	109.47	120.48	115.77	120.03	119.243
120.76	120.59	106.59	119.37	119.17	137.07	136.342
110.75	121.24	113.73	121.87	118.47	123.91	123.128
118.82	112.69	114.87	116.32	122.39	119.58	118.816
118.99	115.98	140.75	110.96	120.72	123.84	123.075
120.03	128.24	121.07	120.93	119.93	118.37	118.214
137.07	119.58	122.91	111.51	122.63	126.09	125.33
123.91	122.04	128.86	124.43	136.17	122.49	121.694
119.58	120.83	119.13	121.80	118.75	93.81	93.0896
123.84	126.27	119.58	120.48	121.45	118.37	117.307
118.37	127.69	120.62	119.23	108.32	115.70	114.994
126.09	130.67	123.18	118.30	114.80	122.87	121.99
122.49	130.80	122.91	124.74	115.77	119.30	118.489
93.81	129.56	124.36	124.74	114.32	117.57	116.807
118.37	125.82	122.56	121.35	119.62	118.33	117.127
115.70	113.31	117.54	125.33	122.04	122.73	121.963
122.87	121.76	120.03	121.07	123.29	125.82	125.071
119.30	123.74	128.17	120.38	124.29	128.97	128.276
117.57	123.74	121.00	118.65	122.80	124.33	123.598
118.33	119.17	121.76	118.33	118.33	122.39	121.587

TABLE V. TRAINING RESULT OF THE APLP NIGHT

X1	X2	X3	X4	X5	T	JST
148.71	136.49	135.48	121.66	142.27	135.48	135.241
151.73	140.89	140.54	135.55	129.94	129.97	129.446
150.48	140.30	141.06	144.21	144.73	88.13	88.078
142.65	134.48	141.61	141.20	143.31	135.62	135.982
145.35	144.00	136.73	138.77	143.31	138.25	138.022
135.48	129.35	130.74	133.75	130.63	115.91	115.631
129.97	138.91	141.96	124.92	146.15	147.33	146.945
88.13	135.00	140.82	145.25	140.95	131.15	130.830
135.62	134.96	148.02	145.98	139.29	139.74	139.768
138.25	139.46	137.70	128.31	142.89	134.68	134.498
115.91	138.25	134.86	147.85	139.08	145.80	145.648
147.33	146.64	148.37	151.24	151.03	142.03	141.771
131.15	144.14	148.99	152.11	151.97	146.77	146.254
139.74	136.94	148.75	155.05	148.51	148.26	147.908
134.68	130.94	140.23	163.40	147.50	149.61	149.244
145.80	139.22	137.04	144.18	136.62	142.58	141.867
142.03	111.47	145.53	131.43	142.06	144.70	144.341
146.77	139.19	143.17	139.64	112.90	153.43	152.994
148.26	137.84	145.28	138.91	145.91	149.30	148.084
149.61	145.35	139.33	139.64	126.51	148.30	148.304

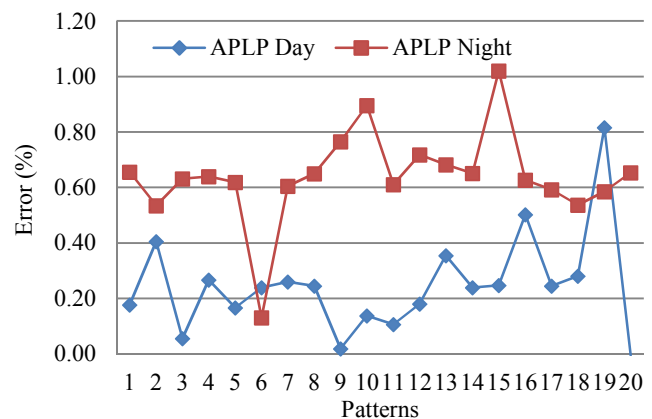


Fig. 5. Training error comparison

In particular, the testing process is conducted to see whether the training pattern can be applied to other patterns outside the training pattern. The best network architecture of the training process is given in Figure 5 for the error. This architecture can be adapted to test the other pattern as shown in Table VI for the APLP Day and Table VII for the APLP Night. Figure 6 shows the graph of the test results and Figure 7 shows the error graph of the test results.

TABLE VI. MAPE CONDITION OF THE APLP DAY

X1	X2	X3	X4	X5	T	JTS	Error
133.33	120.86	134.48	131.25	147.16	143.73	151.395	5.34
143.62	141.09	140.05	112.20	119.68	141.37	158.128	11.85
137.91	135.86	134.75	140.92	148.85	148.58	147.554	0.69
142.06	136.73	136.83	144.18	145.73	146.88	149.72	1.93
142.62	131.71	136.38	136.76	147.16	146.29	146.212	0.05
143.73	138.25	152.28	154.98	143.62	125.09	124.396	0.55
141.37	149.27	151.66	150.13	116.05	147.19	123.993	15.76
148.58	144.66	153.91	146.95	150.72	149.34	146.609	1.83
146.88	151.94	122.73	142.82	141.34	144.97	142.887	1.44
146.29	149.55	153.70	112.86	115.80	150.76	139.941	7.17
Jumlah							46.62
MAPE							4.66%

TABLE VII. MAPE CONDITION OF THE APLP NIGHT

X1	X2	X3	X4	X5	T	JST	Error
120.03	115.49	120.79	138.11	139.98	136.62	101.141	25.9715
117.05	118.02	119.48	134.72	129.59	130.84	102.451	21.697
120.34	119.41	122.32	137.28	139.29	125.85	99.7304	20.755
116.15	117.02	122.18	139.29	131.81	127.65	104.28	18.3091
121.76	115.74	118.61	135.65	130.53	129.18	103.92	19.5518
136.62	128.14	120.93	119.93	118.37	124.95	117.534	5.93564
130.84	128.45	111.51	122.63	126.09	129.04	112.236	13.0205
125.85	126.06	124.43	136.17	122.49	127.41	95.0507	25.3975
127.65	131.50	121.80	118.75	93.81	130.87	138.304	5.6774
129.18	123.81	120.48	121.45	118.37	123.08	108.359	11.9602
JUMLAH							168.27
MAPE							16.82%

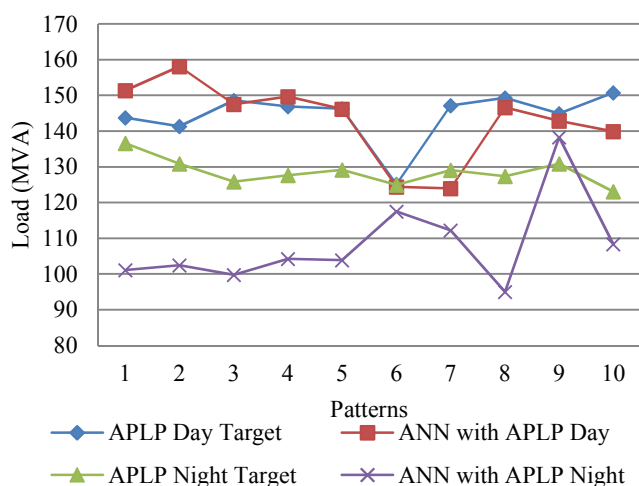


Fig. 6. Testing load results

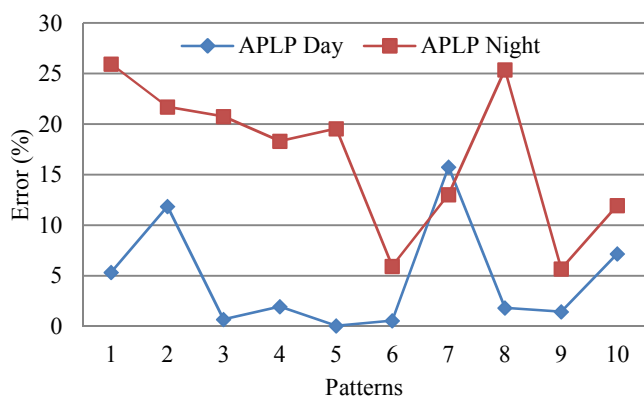


Fig. 7. Error testing results

Based on the results, the best network architecture has the MSE in 0.036084 and MAPE in 4.66% for APLP Day. In contrast, 0.15772 of the MSE and 16.83% of the MAPE belong in the APLP Night. In addition, the networks can adapt well and can produce fairly the accurate forecasting. These results are also shown that the APLP affordability forecasting has a high degree of accuracy, and for the APLP Night accuracy is good. The accuracy rate at the APLP Day is higher than the APLP Night. It can be understood that the 150 kV Buduran Switchyard is mostly for the industrial sector. The pattern of load characteristics in the industrial sector has a similar tendency of loading profiles, and the industrial sector

is dominated by daytime activities, therefore, the load pattern used as input on ANN has the same pattern tendency, so the network is easier to learn patterns. Furthermore, the outcome of the forecasting has a high degree of accuracy.

In contrast, the accuracy of the APLP Night results is lower than that of APLP Day, because the night load is dominated by the household sector. The pattern of load characteristics in the household sector has considerable fluctuations because of the consumption of electrical energy is influenced by behavioral patterns of society which are depended on external factors. The forecasting accuracy on the APLP Night can be improved by adding external factors as input variables, so the network can be better.

## V. CONCLUSION

Based on the results of the studies, the estimation of the electric load for the APLP Day and Night in the 150 kV Buduran Switchyard can be done by using Artificial Neural Network method with backpropagation algorithm model. Based on the best network architecture of the forecasting for the APLP Day and Night, a momentum setting and an understanding rate of 0.85 and 0.1 are produced by the APLP Day, as well as 0.9 and 0.15 for the APLP Night. The APLP Day testing process generates MSE in 0.036084 and MAPE in 4.66%, while for the APLP Night generates MSE in 0.15772 and MAPE in 16.83%. The MSE results indicate that the forecasting on the APLP Day has a high degree of accuracy and the forecasting on the APLP Night has a good level of accuracy. The addition of variables with external factors may increase the accuracy of the forecasting, especially for areas dominated by the household sector. For the future works, additional factor improvements are recommended.

## REFERENCES

- [1] P. J. Burke and S. Kurniawati, "Electricity subsidy reform in Indonesia: Demand-side effects on electricity use," *Energy Policy*, vol. 116, pp. 410–421, May 2018.
- [2] Suhono and Sarjiya, "Long-term Electricity Demand Forecasting of Sumatera System Based on Electricity Consumption Intensity and Indonesia Population Projection 2010-2035," *Energy Procedia*, vol. 68, pp. 455–462, Apr. 2015.
- [3] Wahyuda and B. Santosa, "Dynamic Pricing in Electricity: Research Potential in Indonesia," *Procedia Manuf.*, vol. 4, pp. 300–306, 2015.
- [4] M. El-Shimy, M. A. Attia, N. Mostafa, and A. N. Afandi, "Performance of grid-connected wind power plants as affected by load models: A comparative study," in *2017 5th International Conference on Electrical, Electronics and Information Engineering (ICEEIE)*, 2017, pp. 1–8.
- [5] D. Arengga, W. Agustin, Y. Rahmawati, S. Sendari, and A. N. Afandi, "SPEKTRA fast and smart software for renewable energy management," *IOP Conf. Ser. Earth Environ. Sci.*, vol. 105, no. 1, p. 012077, Jan. 2018.
- [6] Y. Rahmawati *et al.*, "Developing a simulator of renewable energy as a learning media of energy

- conversion,” *IOP Conf. Ser. Earth Environ. Sci.*, vol. 105, p. 012079, Jan. 2018.
- [7] S. Weckmann, T. Kuhlmann, and A. Sauer, “Decentral Energy Control in a Flexible Production to Balance Energy Supply and Demand,” *Procedia CIRP*, vol. 61, pp. 428–433, 2017.
- [8] A. N. Afandi *et al.*, “Designed Operating Approach of Economic Dispatch for Java Bali Power Grid Areas Considered Wind Energy and Pollutant Emission Optimized Using Thunderstorm Algorithm Based on Forward Cloud Charge Mechanism,” *Int. Rev. Electr. Eng. IREE*, vol. 13, p. 59, Feb. 2018.
- [9] J. He, C. Zhao, L. Cai, P. Cheng, and L. Shi, “Practical closed-loop dynamic pricing in smart grid for supply and demand balancing,” *Automatica*, vol. 89, pp. 92–102, Mar. 2018.
- [10] A. N. Afandi, Y. Sulistyorini, G. Fujita, N. P. Khai, and N. Tutkun, “Renewable energy inclusion on economic power optimization using thunderstorm algorithm,” in *2017 4th International Conference on Electrical Engineering, Computer Science and Informatics (EECSI)*, 2017, pp. 1–6.
- [11] E. Pournaras, M. Yao, and D. Helbing, “Self-regulating supply–demand systems,” *Future Gener. Comput. Syst.*, vol. 76, pp. 73–91, Nov. 2017.
- [12] M. D. Leonard, E. E. Michaelides, and D. N. Michaelides, “Substitution of coal power plants with renewable energy sources – Shift of the power demand and energy storage,” *Energy Convers. Manag.*, vol. 164, pp. 27–35, May 2018.
- [13] M. EL-Shimy, N. Mostafa, A. N. Afandi, A. M. Sharaf, and M. A. Attia, “Impact of load models on the static and dynamic performances of grid-connected wind power plants: A comparative analysis,” *Math. Comput. Simul.*, Feb. 2018.
- [14] M. S. Hadi, A. N. Afandi, A. P. Wibawa, A. S. Ahmar, and K. H. Saputra, “Stand-Alone Data Logger for Solar Panel Energy System with RTC and SD Card,” *J. Phys. Conf. Ser.*, vol. 1028, p. 012065, Jun. 2018.
- [15] A. N. Afandi, “Solving Combined Economic and Emission Dispatch Using Harvest Season Artificial Bee Colony Algorithm Considering Food Source Placements and Modified Rates,” *Int. J. Electr. Eng. Inform.*, vol. Vol. 6, p. 267, Jul. 2014.
- [16] G. Cervone, L. Clemente-Harding, S. Alessandrini, and L. Delle Monache, “Short-term photovoltaic power forecasting using Artificial Neural Networks and an Analog Ensemble,” *Renew. Energy*, vol. 108, pp. 274–286, Aug. 2017.
- [17] S. H. A. Kaboli, J. Selvaraj, and N. A. Rahim, “Long-term electric energy consumption forecasting via artificial cooperative search algorithm,” *Energy*, vol. 115, pp. 857–871, Nov. 2016.
- [18] N. Tutkun, O. Can, and A. N. Afandi, “Low cost operation of an off-grid wind-PV system electrifying residential homes through combinatorial optimization by the RCGA,” in *2017 5th International Conference on Electrical, Electronics and Information Engineering (ICEEIE)*, 2017, pp. 38–42.
- [19] A. N. Afandi, I. Fadlika, and Y. Sulistyorini, “Solution of dynamic economic dispatch considered dynamic penalty factor,” in *2016 3rd Conference on Power Engineering and Renewable Energy (ICPERE)*, 2016, pp. 241–246.
- [20] A. N. Afandi, “Weighting Factor Scenarios for Assessing the Financial Balance of Pollutant Productions and Fuel Consumptions on the Power System Operation,” *Wseas Trans. Bus. Econ.*, vol. 14, 2017.
- [21] A. N. Afandi, Y. Sulistyorini, H. Miyauchi, G. Fujita, X. Z. Gao, and M. El-Shimy, “The Penetration of Pollutant Productions on Dynamic Generated Power Operations Optimized Using a Novel Evolutionary Algorithm,” *Int. J. Adv. Sci. Eng. Inf. Technol.*, vol. 7, no. 5, pp. 1825–1831, Oct. 2017.
- [22] L. Labib, M. Billah, G. M. S. M. Rana, M. N. Sadat, M. G. Kibria, and M. R. Islam, “Design and implementation of low-cost universal smart energy meter with demand side load management,” *Transm. Distrib. IET Gener.*, vol. 11, no. 16, pp. 3938–3945, 2017.
- [23] Y. Yang, S. Li, W. Li, and M. Qu, “Power load probability density forecasting using Gaussian process quantile regression,” *Appl. Energy*, vol. 213, pp. 499–509, Mar. 2018.
- [24] K. Berk, A. Hoffmann, and A. Müller, “Probabilistic forecasting of industrial electricity load with regime switching behavior,” *Int. J. Forecast.*, vol. 34, no. 2, pp. 147–162, Apr. 2018.
- [25] P. Singh and P. Dwivedi, “Integration of new evolutionary approach with artificial neural network for solving short term load forecast problem,” *Appl. Energy*, vol. 217, pp. 537–549, May 2018.
- [26] K. B. Debnath and M. Mourshed, “Forecasting methods in energy planning models,” *Renew. Sustain. Energy Rev.*, vol. 88, pp. 297–325, May 2018.
- [27] A. N. Afandi, “Thunderstorm Algorithm for Assessing Thermal Power Plants of the Integrated Power System Operation with an Environmental Requirement,” *Int. J. Eng. Technol.*, vol. 8, pp. 1102–1111, Apr. 2016.
- [28] S. M. Ashraf, A. Gupta, D. K. Choudhary, and S. Chakrabarti, “Voltage stability monitoring of power systems using reduced network and artificial neural network,” *Int. J. Electr. Power Energy Syst.*, vol. 87, pp. 43–51, May 2017.
- [29] M. Talaat, M. H. Gobran, and M. Wasfi, “A hybrid model of an artificial neural network with thermodynamic model for system diagnosis of electrical power plant gas turbine,” *Eng. Appl. Artif. Intell.*, vol. 68, pp. 222–235, Feb. 2018.
- [30] B. Neenan, J. C. Kinnell, M. Bingham, and S. Hickman, “Consumer preferences for electric service alternatives,” *Electr. J.*, vol. 29, no. 5, pp. 62–71, Jun. 2016.

- [31] E. N. Alontseva and P. A. Belousov, "Flexible distributed control and protection system for industrial objects – Consumers of electric power," *Nucl. Energy Technol.*, vol. 1, no. 4, pp. 233–236, Dec. 2015.
- [32] K. Morrissey, A. Plater, and M. Dean, "The cost of electric power outages in the residential sector: A willingness to pay approach," *Appl. Energy*, vol. 212, pp. 141–150, Feb. 2018.
- [33] A. N. Afandi and Y. Sulistyorini, "Thunderstorm Algorithm for Determining Unit Commitment in Power System Operation," *J. Eng. Technol. Sci.*, vol. 48, no. 6, pp. 743–752, Dec. 2016.
- [34] J. C. Maxwell, *A Treatise on Electricity and Magnetism*. Cambridge: Cambridge University Press, 2010.
- [35] M.-J. Kim, "Characteristics and determinants by electricity consumption level of households in Korea," *Energy Rep.*, vol. 4, pp. 70–76, Nov. 2018.
- [36] A. N. Afandi, *Optimal Solution of the EPED Problem Considering Space Areas of HSABC on the Power System Operation*, vol. 7. 2015.
- [37] G. Fernandez, H. Usabiaga, and D. Vandepitte, "An efficient procedure for the calculation of the stress distribution in a wind turbine blade under aerodynamic loads," *J. Wind Eng. Ind. Aerodyn.*, vol. 172, pp. 42–54, Jan. 2018.
- [38] J. Zhou, X. Shi, C. C. Caprani, and X. Ruan, "Multi-lane factor for bridge traffic load from extreme events of coincident lane load effects," *Struct. Saf.*, vol. 72, pp. 17–29, May 2018.
- [39] E. Hartvigsson and E. O. Ahlgren, "Comparison of load profiles in a mini-grid: Assessment of performance metrics using measured and interview-based data," *Energy Sustain. Dev.*, vol. 43, pp. 186–195, Apr. 2018.
- [40] I. Rahman and J. Mohamad-Saleh, "Hybrid bio-Inspired computational intelligence techniques for solving power system optimization problems: A comprehensive survey," *Appl. Soft Comput.*, vol. 69, pp. 72–130, Aug. 2018.
- [41] J. A. Laghari, H. Mokhlis, A. H. A. Bakar, and H. Mohamad, "Application of computational intelligence techniques for load shedding in power systems: A review," *Energy Convers. Manag.*, vol. 75, pp. 130–140, Nov. 2013.
- [42] A. N. Afandi, "Optimal scheduling power generations using HSABC algorithm considered a new penalty factor approach," in *The 2nd IEEE Conference on Power Engineering and Renewable Energy (ICPERE) 2014*, 2014, pp. 13–18.
- [43] Z.-L. Gaing, "Closure to 'Discussion of "Particle swarm optimization to solving the economic dispatch considering the generator constraints,"'" *IEEE Trans. Power Syst.*, vol. 19, no. 4, pp. 2122–2123, Nov. 2004.
- [44] B. Chowdhury and G. Garai, "A review on multiple sequence alignment from the perspective of genetic algorithm," *Genomics*, vol. 109, no. 5, pp. 419–431, Oct. 2017.
- [45] S. D. Dao, K. Abhary, and R. Marian, "An innovative framework for designing genetic algorithm structures," *Expert Syst. Appl.*, vol. 90, no. Supplement C, pp. 196–208, Dec. 2017.
- [46] A. N. Afandi and H. Miyauchi, "Improved artificial bee colony algorithm considering harvest season for computing economic dispatch on power system," *IEEEJ Trans. Electr. Electron. Eng.*, vol. 9, no. 3, pp. 251–257, May 2014.
- [47] A. Shenfield, D. Day, and A. Ayesh, "Intelligent intrusion detection systems using artificial neural networks," *ICT Express*, May 2018.
- [48] M. Manngård, J. Kronqvist, and J. M. Böling, "Structural learning in artificial neural networks using sparse optimization," *Neurocomputing*, vol. 272, pp. 660–667, Jan. 2018.
- [49] X. Wang, C. P. Tsokos, and A. Saghaifi, "Improved parameter estimation of Time Dependent Kernel Density by using Artificial Neural Networks," *J. Finance Data Sci.*, Apr. 2018.
- [50] H. Sebaaly, S. Varma, and J. W. Maina, "Optimizing asphalt mix design process using artificial neural network and genetic algorithm," *Constr. Build. Mater.*, vol. 168, pp. 660–670, Apr. 2018.
- [51] A. N. Afandi, I. Fadlika, and A. Andoko, "Comparing Performances of Evolutionary Algorithms on the Emission Dispatch and Economic Dispatch Problem," *TELKOMNIKA Telecommun. Comput. Electron. Control*, vol. 13, no. 4, pp. 1187–1193, Dec. 2015.
- [52] M. Aladeemy, S. Tutun, and M. T. Khasawneh, "A new hybrid approach for feature selection and support vector machine model selection based on self-adaptive cohort intelligence," *Expert Syst. Appl.*, vol. 88, pp. 118–131, Dec. 2017.
- [53] L. K. Abidoye, F. M. Mahdi, M. O. Idris, O. O. Alabi, and A. A. Wahab, "ANN-derived equation and ITS application in the prediction of dielectric properties of pure and impure CO<sub>2</sub>," *J. Clean. Prod.*, vol. 175, pp. 123–132, Feb. 2018.
- [54] M. Bataineh and T. Marler, "Neural network for regression problems with reduced training sets," *Neural Netw.*, vol. 95, pp. 1–9, Nov. 2017.
- [55] A. Sagai Francis Britto, R. Edwin Raj, and M. Carolin Mabel, "Prediction and optimization of mechanical strength of diffusion bonds using integrated ANN-GA approach with process variables and metallographic characteristics," *J. Manuf. Process.*, vol. 32, pp. 828–838, Apr. 2018.
- [56] S. Panigrahi and H. S. Behera, "A hybrid ETS-ANN model for time series forecasting," *Eng. Appl. Artif. Intell.*, vol. 66, pp. 49–59, Nov. 2017.

# A New Algorithm for Designing the Parameter of Damped-Type Double Tuned Filter

Haposan Yoga Pradika Napitupulu  
Department of Electrical Engineering  
Universitas Trisakti  
Jakarta, Indonesia  
haposan.ypn@outlook.com

Chairul Gagarin Irianto  
Department of Electrical Engineering  
Universitas Trisakti  
Jakarta, Indonesia  
chairul\_irianto@trisakti.ac.id

**Abstract**—Due to harmonics problems generated by converter devices. Currently, passive filter has been widely used in suppressing harmonics distortion. Passive filter which mostly used is double tuned filter. However, double tuned filter doesn't have a damping resistor which can prevent network elements from exposing to harsh condition such as when the system reactance and the filter impedance are conjugated, this condition can cause severe overvoltage harmonics on the filter and other power system components. There is a new configuration of double tuned filter that has damping resistor, called damped-type double tuned filter. Aiming at the question of parameter of damped-type double tuned filter, a new algorithm for designing the parameter of damped-type double tuned filter is proposed based on the relationship between impedance of two single tuned filter and one double tuned filter, and also based on the resonance at tuned frequency one and tuned frequency two are close to zero. Simulation result from MATLAB shows that the impedance of damped-type double tuned filter designed with this algorithm is appropriate. In addition, the simulation result from PSIM shows that damped-type double tuned filter designed with this algorithm works well.

**Keywords**—harmonics, damped-type double tuned filter, filter design

## I. INTRODUCTION

Harmonics distortion is not a new phenomenon in electrical power system, it is caused by non-linear devices in the power system such as converter [1]. HVDC Converter stations usually require ac/dc filters, the main purpose of which is to mitigate current or voltage distortion in the connected networks [2]. In addition, the ac side filters significantly compensate the network demanded reactive power [2]. Passive filter has been widely used in filtering harmonics in power system because it has simple structure, low cost, and high reliability. Double tuned filter is one of passive filters which mostly used. The main advantages of using double tuned over two parallel single tuned filter are double tuned filter has large covering area with one structure, occupies less space and needs only one switchgear, also double tuned filter has a lower cost than the two parallel single tuned filter [3] [4] [5].

Due to phenomenon network resonance takes place when power system reactance and the filter impedance are conjugated, it can cause severe overvoltage harmonics on the filter and other power system components, so last research proposed damping resistor to the conventional double tuned filter in different configuration. Literature [6] has previously put forward an algorithm about parameters calculation of damped-type double tuned filter, but the operation process is complicated and the

characteristic curve impedance-frequency is not clearly differentiate between two resonant frequencies as shown in Figure 1.

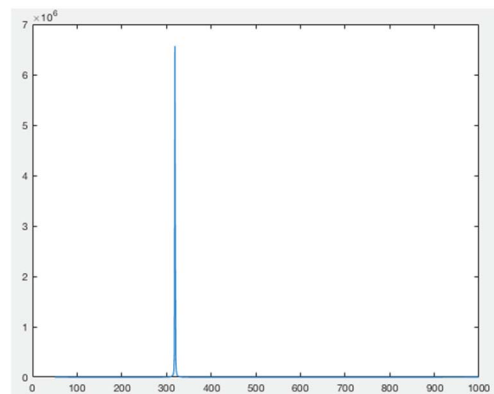


Figure 1. Impedance Response Damped-Type Double Tuned Filter due to impedance for Literature [6]

In order to calculate parameter of damped-type double tuned filter, a new algorithm for designing its parameter is proposed based on relationship impedance of two parallel single tuned filter and one double tuned filter, and also the resonance at the tuned frequency one and tuned frequency two are close to zero.

## II. THE PARAMETER CALCULATION OF DOUBLE TUNED FILTER

There are so many configurations of damped-type double tuned filter as shown in Figure 2.

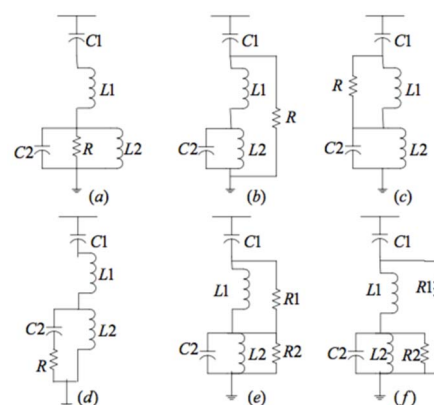


Figure 2. Configurations of damped-type double tuned filter

The most widely-used configuration of damped-type double tuned filter is shown in Figure 2 (a). From that figure, the first



step is to express the relationship between two parallel single tuned filter as seen on Figure 3 and one conventional double tuned filter on Figure 4 into Equations. Then, place a damping resistor on the conventional double tuned filter as shown in Figure 5 and look for the parameter of resistor based on value of impedance at each resonance frequency is close to zero.

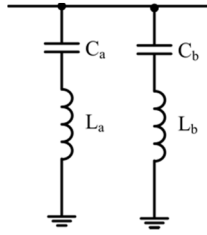


Figure 3. Configurations of two single tuned filter

Each single tuned filter has an impedance that can be expressed at Equation (1).

$$Z_s = j\omega L - j\frac{1}{\omega C} \quad (1)$$

At tuned frequency,  $Z_s$  will decrease to a minimum value. It can be assumed that  $Z_s$  will reach value at 0, so Equation (1) can be changed into Equation (2).

$$\omega L = \frac{1}{\omega C} \quad (2)$$

From Equation (2) above, resonance frequency for single tuned filter can be represented at Equation (3).

$$\omega = \frac{1}{\sqrt{LC}} \quad (3)$$

For two parallel single tuned filter as shown in Figure 3 that has two resonance frequencies, the Equation can be developed from Equation (3) and then can be expressed at Equation (4).

$$\begin{bmatrix} \omega_a \\ \omega_b \end{bmatrix} = \begin{bmatrix} 1/\sqrt{L_a C_a} \\ 1/\sqrt{L_b C_b} \end{bmatrix} \quad (4)$$

The impedance  $Z_{ab}$  of two parallel single tuned filters as shown in Figure 3 above can be represented at Equation (5).

$$\begin{aligned} Z_{ab} &= \left( \left( j\omega L_a - j\frac{1}{\omega C_a} \right)^{-1} + \left( j\omega L_b - j\frac{1}{\omega C_b} \right)^{-1} \right)^{-1} \\ &= \frac{\left( 1 - \frac{\omega^2}{\omega_a^2} \right) \left( 1 - \frac{\omega^2}{\omega_b^2} \right)}{j\omega C_a \left( 1 - \frac{\omega^2}{\omega_b^2} \right) + j\omega C_b \left( 1 - \frac{\omega^2}{\omega_a^2} \right)} \end{aligned} \quad (5)$$

The conventional double tuned filter consists of two capacitors and two inductors, which is composed by series resonance circuit ( $L_1, C_1$ ) and parallel resonance circuit ( $L_2, C_2$ ).

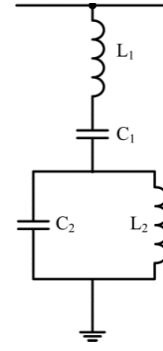


Figure 4. Configurations of conventional double tuned filter

Calculation of series resonance frequency and parallel resonance frequency of conventional double tuned filter can be expressed at Equation (6).

$$\begin{bmatrix} \omega_s \\ \omega_p \end{bmatrix} = \begin{bmatrix} 1/\sqrt{L_1 C_1} \\ 1/\sqrt{L_2 C_2} \end{bmatrix} \quad (6)$$

From Figure 4, the impedance  $Z_f$  of conventional double tuned filter can be represented at Equation 7.

$$\begin{aligned} Z_f &= j\omega L_1 + \frac{1}{j\omega C_1} + \left( j\omega C_2 - j\frac{1}{\omega L_2} \right)^{-1} \\ &= \frac{\left( 1 - \frac{\omega^2}{\omega_s^2} \right) \left( 1 - \frac{\omega^2}{\omega_p^2} \right) - \omega^2 L_2 C_1}{j\omega C_1 \left( 1 - \frac{\omega^2}{\omega_p^2} \right)} \end{aligned} \quad (7)$$

Literature [7] has proposed a method for calculating the parameter of the conventional double tuned filter. The impedance between two single tuned filter at Equation (5) and the conventional double tuned filter at Equation (7) are equivalent. Analyzing the coefficient of  $\omega$ , the parameter of  $C_1$  can be calculated by using Equation (8).

$$C_1 = C_a + C_b \quad (8)$$

The parameter of  $L_1$  can be calculated by using Equation (9).

$$L_1 = \frac{1}{C_a \omega_a^2 + C_b \omega_b^2} \quad (9)$$

Then, the parameter of  $L_2$  can be calculated by using Equation (10).

$$L_2 = \frac{\left( 1 - \frac{\omega_a^2}{\omega_s^2} \right) \left( 1 - \frac{\omega_a^2}{\omega_p^2} \right)}{C_1 \omega_a^2} \quad (10)$$

The parameter of  $C_2$  can be found by using Equation (11).

$$C_2 = \frac{1}{L_2 \omega_p^2} \quad (11)$$

where  $\omega_s$  and  $\omega_p$  can be calculated by using Equation (12) and Equation (13) respectively.

$$\omega_s = \frac{1}{\sqrt{L_1 C_1}} \quad (12)$$

$$\omega_p = \frac{\omega_a \omega_b}{\omega_s} \quad (13)$$

On the other hand, by analyzing the capacitance of two parallel single tuned filter and parallel resonance frequency of conventional double tuned filter, this paper proposes the calculation of the parameter of  $L_1$  by using Equation (14).

$$L_1 = \frac{1}{C_1(\omega_a^2 + \omega_b^2)/2} \quad (14)$$

where the parameter of  $C_1$  can be calculated by using Equation (15).

$$C_1 = \frac{MVAR}{kV^2 \omega} \quad (15)$$

which  $\omega$  is the fundamental frequency. The two results from Equation (8) and Equation (15) are the same, also the two results of Equation (9) and (14) are the same. By using Equation (14) and (15) the calculation to get the parameter of  $C_1$  and  $L_1$  is simpler rather than calculating capacitance for each resonance frequency from two parallel single tuned filter firstly.

### III. THE PARAMETER CALCULATION OF DAMPED-TYPE DOUBLE TUNED FILTER

In order to prevent network elements from exposing severe overvoltage, damping resistor is added to the conventional double tuned filter as shown in Figure 5.

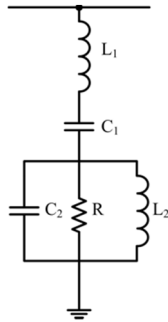


Figure 5. Configurations of conventional double tuned filter

This paper develops impedance of damped-type double tuned filter based on Figure 5, the impedance can be represented at Equation (16).

$$Z_f = j(\omega L_1 - \frac{1}{\omega C_1}) + \left( \frac{1}{j\omega L_2} - \frac{1}{j1/\omega C_2} + \frac{1}{R} \right)^{-1} \quad (16)$$

$$= \sqrt{\left( \omega L_1 - \left( \frac{\frac{L_2^2 R}{C_2^2} (\omega L_2 R - R/\omega C_2)}{\frac{L_2^2}{C_2^2} + (\omega L_2 R - R/\omega C_2)^2} \right) - \frac{1}{\omega C_1} \right)^2 + \left( \frac{\frac{L_2^2 R}{C_2^2}}{\frac{L_2^2}{C_2^2} + (\omega L_2 R - R/\omega C_2)^2} \right)^2}$$

The analysis of impedance frequency characteristic curve from Equation (16) has been done using MATLAB and has been plotted as shown in Figure 6.

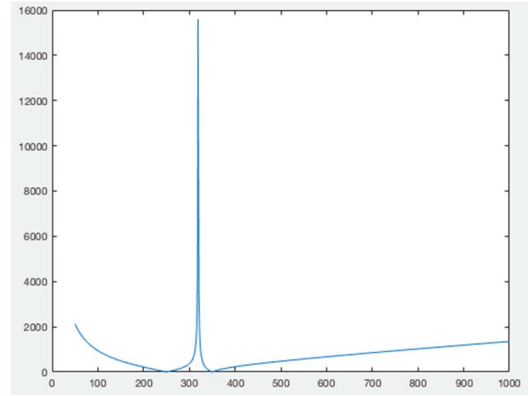


Figure 6. Impedance-frequency Characteristic Curve of New Developing Impedance Damped-type Double Tuned Filter

From Figure 6 above, the characteristic curve between impedance and frequency is clearly different, compared with the impedance from literature [6] shown in Figure 1. Figure 6 shows clearly the resonance frequency at tuned frequency one ( $\omega_1$ ) and tuned frequency two ( $\omega_2$ ) are close to zero because it is suppressed by filter, and the impedance at parallel resonance is too high.

By using the value approach of the resonance frequency at tuned frequency one ( $\omega_1$ ) and tuned frequency two ( $\omega_2$ ) are close to zero, this paper proposed a new algorithm to find out the parameter of damping resistor (R) of the damped-type double tuned filter as shown in Figure 7.

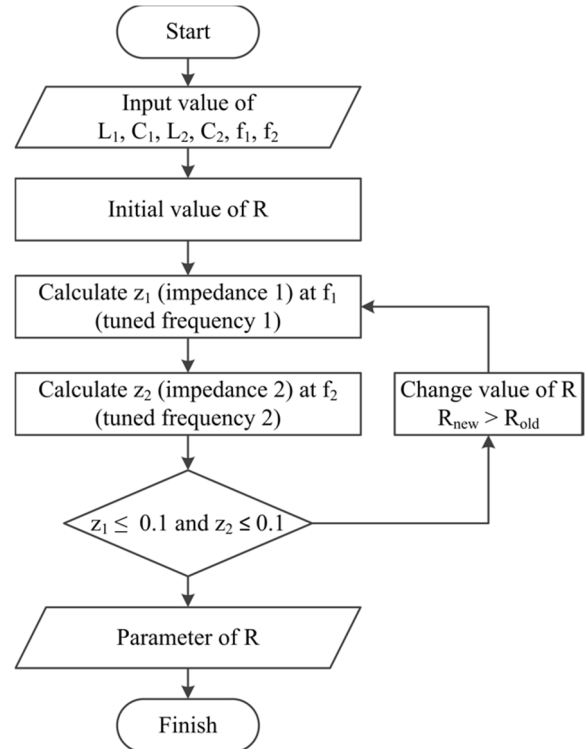


Figure 7. A new Algorithm to find out parameter of damping resistor (R) of damped-type double tuned filter

In conclusion, when the voltage in the network (kV) and demanded reactive power in the network (MVAR) are known, as well as, tuned frequency one ( $f_1$ ), tuned frequency two ( $f_2$ ), series resonance frequency ( $\omega_s$ ), parallel resonance frequency ( $\omega_p$ ) are determined, then the parameter of the damped-type double tuned filter ( $C_1, L_1$ ) and ( $C_2, L_2$ ) can be calculated by using Equation (15, 14) and Equation (11,10) respectively. For the parameter of damping resistor (R), it can be calculated by using an algorithm shown in Figure 7.

For quick calculation of the parameter of damping resistor (R), with the impedance of damped-type double tuned filter at Equation (16), an algorithm as shown in Figure 7 can be written in a language program using MATLAB below:

```
for r=1:1000000
```

$$\begin{aligned} Imp1 = & \sqrt{(((l2 * l2 * r / (c2 * c2)) / ((l2 * l2 / (c2 * c2)) + ((2 * pi * frel * l2 * r) - (r / (2 * pi * frel * c2)))) * ((2 * pi * frel * l2 * r) - (r / (2 * pi * frel * c2)))))) * ((l2 * l2 * r / (c2 * c2)) / ((l2 * l2 / (c2 * c2)) + ((2 * pi * frel * l2 * r) - (r / (2 * pi * frel * c2)))) * ((2 * pi * frel * l2 * r) - (r / (2 * pi * frel * c2)))))) \\ & + (((2 * pi * frel * l1) - (1 / (2 * pi * frel * c1)) - (((l2 * r) / c2) * (2 * pi * frel * l2 * r - (r / (2 * pi * frel * c2)))) / ((l2 * l2 / (c2 * c2)) + (2 * pi * frel * l2 * r - (r / (2 * pi * frel * c2)))) * (2 * pi * frel * l2 * r - (r / (2 * pi * frel * c2)))))) * \\ & ((2 * pi * frel * l1) - (1 / (2 * pi * frel * c1)) - (((l2 * r) / c2) * (2 * pi * frel * l2 * r - (r / (2 * pi * frel * c2)))) / ((l2 * l2 / (c2 * c2)) + (2 * pi * frel * l2 * r - (r / (2 * pi * frel * c2)))) * (2 * pi * frel * l2 * r - (r / (2 * pi * frel * c2))))); \end{aligned}$$
$$\begin{aligned} Imp2 = & \sqrt{(((l2 * l2 * r / (c2 * c2)) / ((l2 * l2 / (c2 * c2)) + ((2 * pi * fre2 * l \\ & 2 * r) - (r / (2 * pi * fre2 * c2)))) * ((2 * pi * fre2 * l2 * r) - (r / (2 * pi * fre2 * c2 \\ & ))))) * ((l2 * l2 * r / (c2 * c2)) / ((l2 * l2 / (c2 * c2)) + ((2 * pi * fre2 * l2 * r) - \\ & (r / (2 * pi * fre2 * c2)))) * ((2 * pi * fre2 * l2 * r) - (r / (2 * pi * fre2 * c2)))))) \\ & + (((2 * pi * fre2 * l1) - (1 / (2 * pi * fre2 * c1)) - (((l2 * r) / c2) * (2 * pi * fre2 \\ & * l2 * r - (r / (2 * pi * fre2 * c2)))) / ((l2 * l2 / (c2 * c2)) + (2 * pi * fre2 * l2 * r - \\ & (r / (2 * pi * fre2 * c2)))) * (2 * pi * fre2 * l2 * r - (r / (2 * pi * fre2 * c2)))))) * \\ & ((2 * pi * fre2 * l1) - (1 / (2 * pi * fre2 * c1)) - (((l2 * r) / c2) * (2 * pi * fre2 * \\ & l2 * r - (r / (2 * pi * fre2 * c2)))) / ((l2 * l2 / (c2 * c2)) + (2 * pi * fre2 * l2 * r - \\ & (r / (2 * pi * fre2 * c2)))) * (2 * pi * fre2 * l2 * r - (r / (2 * pi * fre2 * c2)))))))); \end{aligned}$$

```

    if (Imp1 <= 0.1 && Imp2 <= 0.1)
        fprintf("The parameter of Damping Resistor (R) is %d \n",
r);
        break
    end
end
end

```

#### IV. SIMULATION OF POWER SYSTEM WITH DAMPED-TYPE DOUBLE TUNED FILTER

This paper uses software PSIM to simulate the damped-type double tuned filter designed with this new algorithm. PSIM is one of many software programs to simulate power electronics and power system. The configuration of power system consists of generator, transformer, conductor, six pulse converters, load and some measurement devices. Six pulse converters will raise the harmonic order following Equation (14). Figure 8 shows the power system which has installed damped-type double tuned filter. The parameter of the configuration in Figure 8 before filtering is shown in Table 1.

$$n = kp \pm 1 \quad (14)$$

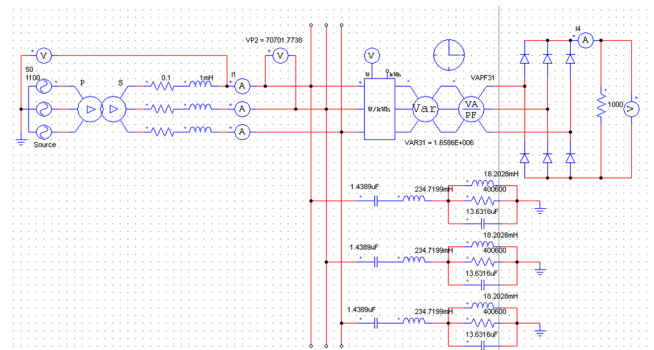


Figure 8. Configuration of Power System

TABLE I. PARAMETER OF THE CONFIGURATION OF POWER SYSTEM

Parameter	Value
U	110kV
F	50Hz
P	20.808.519,00Watt
Pf Existing	0,9552
Pf Target	0,9999

Six pulse converter in this simulation raises the order 5<sup>th</sup>, 7<sup>th</sup>, 11<sup>st</sup>, 13<sup>rd</sup>, 17<sup>th</sup>, 19<sup>th</sup>, and so on. When the damped type filter is not installed in power system, the current that measured by amperemeter 1 at Phase 1 is shown in Figure 9. PSIM provides FFT function that enables engineer to convert time function into frequency function to analyze each component of harmonics. From Figure 10, it can be seen and measured the harmonic distortion for each component. Most harmonics distortions occur at 5th order and 7th order, which has value 25,1563A and 10,7881A respectively.

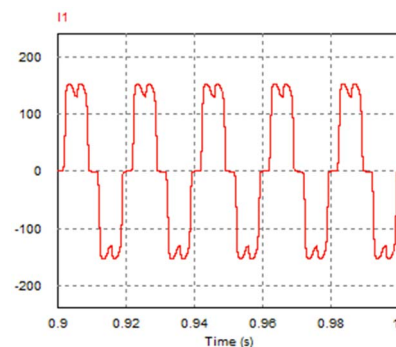


Figure 9. The Waveform Current Phase 1 before Filtering

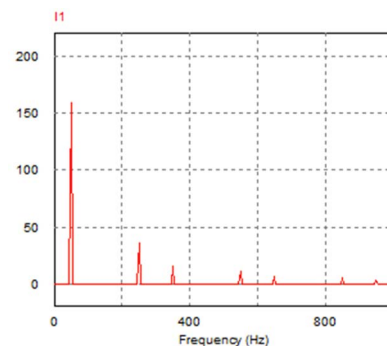


Figure 10. The Harmonic Distortion per Order at Phase 1 before Filtering

The required parameter of damped-type double tuned filter for the power system according to the new algorithm is proposed in this paper as shown in Table 2.

TABLE II. PARAMETER OF THE FILTER

Parameter	Value
C1	1,4389 $\mu$ F
L1	234,7199mH
C2	13,6316 $\mu$ F
L2	18,2028mH
R	400.600ohm

When the damped-type double tuned filter is installed in power system, the current waveform at Phase 1 is shown in Figure 11. Damped-type double tuned filter is designed suppress harmonic 5<sup>th</sup> order and 7<sup>th</sup> order. Then, in Figure 12 shows that the filter effectively works, harmonic 5<sup>th</sup> order and 7<sup>th</sup> order has been suppressed become 0,0036A and 0,0083A respectively.

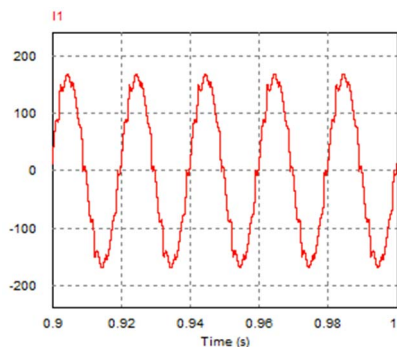


Figure 11. The Waveform Current Phase 1 after Filtering

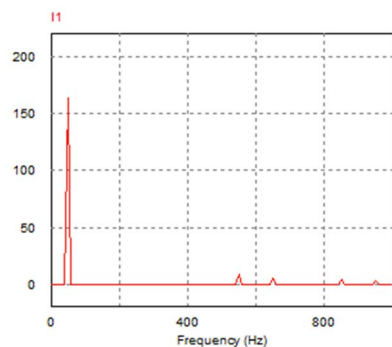


Figure 12. The Harmonic Distortion per Order at Phase 1 after Filtering

In order to summarize the simulation, Figure 11 shows the current waveform after filtering, the form is close to sinusoidal compared with Figure 9 the current waveform before filtering. Then, Figure 12 shows that after damped-type double tuned filter designed with new algorithm proposed in this paper is installed in power system, at 5<sup>th</sup> order and 7<sup>th</sup> order harmonics content are close to zero compare with Figure 10 before filtering. However, after the filter is installed into power system, it is proven that a new algorithm works well and has a good filtering effect.

## V. CONCLUSION

This paper explores the calculation of parameter of the damped-type double tuned filter based on the relationship impedance of two parallel single tuned filter and one double tuned filter, and also the resonance at the tuned frequency one and tuned frequency two are close to zero. The calculation is very simple and the algorithm for calculating the damping resistor can be figured out by making a language program on MATLAB. This paper suggests a new equation of impedance of the damped-type double tuned filter which can be used to give an input for literature [6]. The new impedance and new algorithm proposed in this paper have been proved by simulation using MATLAB and PSIM software and it works splendidly.

## ACKNOWLEDGMENT

Deepest gratitude to Trisakti University for supporting this research and also special thanks to Chairul Gagarin Irianto for his valuable recommendation and guidance on the paper.

## REFERENCES

- [1] Roger C. Dugan, Mark F. McGranaghan, Surya Santoso, and H. Wayne Beaty, "Electrical power system quality - second edition," McGraw-Hill, 2004.
- [2] Cigre WG, "Guide to the specification and design evaluation of ac filters for HVDC systems," Technical Brochure 139, April 1999.
- [3] E. W. Kimbark, "Direct current transmission," John Wiley & Sons, 1971.
- [4] J. Arrillaga, D. A. Bradley, and P. S. Bodger, "Power SYstem Harmonics," John Wiley & Sons, 1985.
- [5] Wang Zhaoan, Yang Jun, "Harmonic suppression and reactive power compensation," China Machine Press, Beijing, 2010.
- [6] M. A. Zamani, and M. Mohseni, "Damped-type double tuned filters design for HVDC systems," 9th International Conference Electrical Power Quality and Utilisation, Barcelona, Spain, 2007, pp. 1-6.
- [7] HE Yi-hong, SU Heng, "A new method of designing double-tuned filter," Proceedings of the 2nd International Conference on Computer Science and Electronics Engineering, Paris, France, 2013, pp. 206-209.

# Comparison of LFC Optimization on Micro-hydro using PID, CES, and SMES based Firefly Algorithm

Kadaryono

Department of Mechanical Engineering  
University of Darul Ulum  
Jombang, Indonesia  
aninanin110@gmail.com

Rukslin

Department of Electrical Engineering  
University of Darul Ulum  
Jombang, Indonesia  
rukslin@gmail.com

Machrus Ali

Department of Electrical Engineering  
University of Darul Ulum  
Jombang, Indonesia  
machrus7@gmail.com

Askan

Department of Mechanical Engineering  
University of Darul Ulum  
Jombang, Indonesia  
askanzamzam@gmail.com

Asnun Parwanti

Department of Civil Engineering  
University of Darul Ulum  
Jombang, Indonesia  
asnunparwanti@gmail.com

Iwan Cahyono

Department of Civil Engineering  
University of Darul Ulum  
Jombang, Indonesia  
cahyonoivan15@gmail.com

**Abstract**—Micro-hydro gets potential energy from water flow that has a certain height difference. Potential energy is strongly influenced by high water fall. Potential energy through pipes, incoming turbines converted into kinetic energy. The kinetic energy of the turbine coupled with the generator is converted into electrical energy. Some components used for micro-hydro power generation, among others; intake, settling basin, headrace, penstock, turbine, draft tube, generator, and control panel. Water flows through the pipe into the turbine house so it can rotate the turbine blades. Turbine rotation is used to rotate a generator at the micro hydro generator. The most common problem with micro-hydro generating systems is inconsistent generator rotation caused by changes in connected loads. Load changes can cause system frequency fluctuations and may cause damage to electrical equipment. Artificial Intelligence (AI) is used to obtain the right constants to obtain the best optimization. In this study compare the control method, namely; Proportional Integral Derivatives (PID), Capacitive Energy Storage (CES), and Superconducting Magnetic Energy Storage (SMES). This study also compared the method of artificial intelligence between Particle Swarm Optimization (PSO) method has been studied with the method of Firefly Algorithm (FA). Overall this study compares 11 methods, namely methods; uncontrolled, PID-PSO method, PID-FA method, CES-PSO method, CES-FA method, SMES-PSO method, SMES-FA method, PID-CES-PSO method, PID-CES-FA method, PID-SMES - PSO, and PID-SMES-FA method. The results of the simulation showed that from the 11 methods studied, it was found that the PID-CES-FA method has the smallest undershoot value, ie -7.774e-03 pu, the smallest overshoot value, which is 4.482e-05 pu, and the fastest completion time is 7.11 s. These results indicate that the smallest frequency fluctuations are found in the PID-CES-FA controller. Thus it is stated that the PID-CES-FA method is the best method used in the previous method. This research will use other methods to get the best controller.

**Keywords**—CES, Firefly Algorithm, micro-hydro, PID, SMES.

## I. INTRODUCTION

In micro-hydro operation, stability issues are of major concern. In order for the frequency to be always stable, the rotational speed of the generator must be fixed. The rotational speed of the generator can be affected by the size or the amount of the load. The addition of a very large load will reduce the rotating density, otherwise a large load reduction will accelerate the generator spin. So that the

frequency will increase and if passing the standard will harm the consumer electrical equipment.

Therefore, to support this micro-hydro performance, setting or controlling the load frequency is required, to always be in the work area. Micro-hydro control is done automatically by governing the governor. Servo motor as governor set the opening height, so that the incoming water flow can be adjusted with the load. So the system can adjust the load power and can reduce the frequency change[1].

Load Frequency Control (LFC) is designed using a controller; Proportional Integral Derivatives (PID), Capacitive Energy Storage (CES) [2], and Superconducting Magnetic Energy Storage (SMES)[3]. All three controllers are tuned using artificial intelligence, namely the method of Particle Swarm Optimization (PSO) and Firefly Algorithm (FA). Because, Artificial Intelligent (AI) is often used to develop various disciplines such as vehicle steering controllers [4][5], as micro-hydro control [6], and others. In this study used the method Firefly Algorithm (FA) [7]. The FA method is used as tuning PID, CES, and SMES controller. With this comparison obtained the best control method. The best results will be applied at micro-hydro plants in Jombang, East Java, Indonesia. This research involves scientists from various disciplines, namely; mechanical engineering, electrical engineering, and civil engineering.

## II. SYSTEM MODELING

### A. Micro-hydro Power Plant

The micro-hydro power plant on harnessing potential energy from the height difference and the amount of water discharge. The potential energy from the water passes through the pipe and rotates the turbine shaft to generate mechanical energy. This mechanical energy drives the generator and generates electrical energy. Micro hydro power plants must have a water source that always flows throughout the year. The electric power generated by the power generator ( $P_{th}$ ) depends on the value of the water discharge ( $Q$ ) and the waterfall height ( $H$ ). The equation can be formulated as follows::

$$P_{th}[W] = Q[m^3 / s].H[m].k[N / kg] \quad (1)$$

The efficiency ( $\eta_{gen}$ ) of the turbine and generator is determined by each manufacturer with a power factor value

of 0.8 causing the actual electrical value to be lower than the generator power ( $P_{th}$ ).

$$P_{real}[W] = Q[m^3/s] \cdot H[m] \cdot k[N/kg] \cdot \eta_{turbine} \cdot \eta_{gen} \quad (2)$$

For pumps used as turbines, the efficiency values varied from 0.6 to 0.8, in this study used 0.8. For cross-flow turbines, values varying from 0.5 to 0.7, in this study are used 0.6. While the generator used in the micro-hydro power plant system here is using an induction generator, a servo motor operated as a governor, and some components are modeled on the simulation using the Matlab-Simulink program. The following figure shows the configuration of the designed micro-hydro power plant.

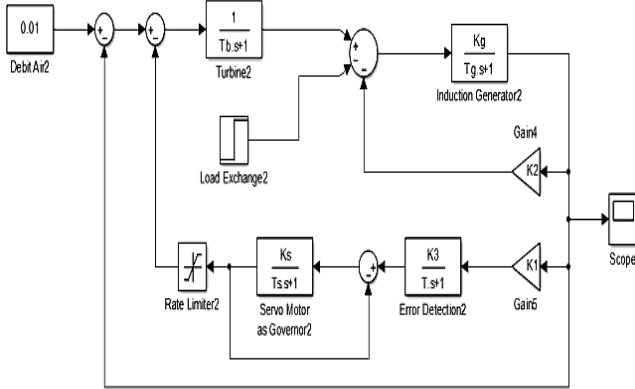


Fig. 1. Block diagram of Micro-hydro System[6]

The signal change ( $\Delta\omega$ ) will be forwarded to the servo motor block functioned as governor. The parameters required for signal strengthening are  $K_s$  and  $T_s$ . The output of the governor is passed to the limiter to limit the signal. Limiter is used to limit the highest and lowest saturation values in order not to exceed the specified value. The limiter output goes to the turbine block. The micro-hydro parameters used in this study can be shown in Table 1..

Table 1. Micro Hydro Parameter [6]

Parameter	Value	Item
Tb	1	Water turbine time response (s)
Kg	1	Reinforcement of inductor generator regulator (s)
Tg	13,333	Response time on generator induction (s)
K1	5	Error Detection confirmation constant
K2	8,52	Frequency of frequency deviation constant
K3	0.004	Strengthening Error Detection
T	0,02	Time response Error Detection
Ts	0,1	The governor's time constant (s)
Ks	2,5	Strengthening governor
Sg	40	Micro-hydro power generator rating (kVA)
pf	0,8	Power Factor
Vg	400/231	Nominal voltage generator (V)
$\omega$	1500	Nominal rotational speed (rpm)
fg	50	The nominal frequency of micro hydro (Hz)

### B. Capacitive Energy Storage (CES)[2]

Capacitive Energy Storage (CES) is a device used to store and release large amounts of electrical power quickly. CES consists of Storage Capacitors (SC) and Power Conversion Systems (PCS). The energy stored by the CES on the capacitor in the form of an electric field, can be shown in Figure 2.

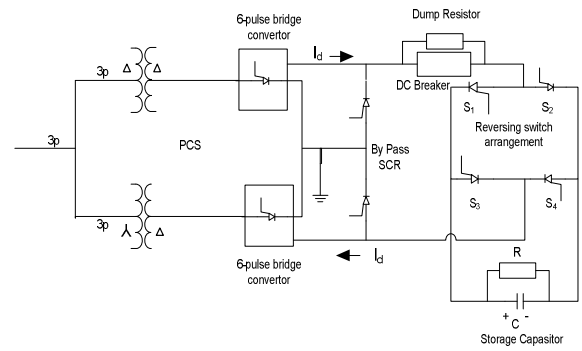


Fig. 2. Capacitive Energy Storage

Storage capacitors consist of discrete capacitors arranged in parallel. Storage capacitors are connected via a 12-pulse Power Conversion System (PCS) to Mesh. The leakage and dielectric energy losses of the bank capacitor at CES are modeled by resistors  $R$  in parallel with the capacitor ( $C$ ). PCS converts to DC and from DC to AC Inverter. Bypass Thyristor serves to provide the current path ( $I_d$ ) when the converter fails. The DC breaker diverts the current ( $I_d$ ) to the resistor point ( $R_d$ ) if the converter fails. The bridge voltage ( $E_d$ ) is shown in equations 3 and 4.

$$E_d = 2E_{d0} \cos \alpha - 2I_d R_D \quad (3)$$

$$E_{d0} = \frac{[E_{d\max}^2 + E_{d\min}^2]^{1/2}}{2} \quad (4)$$

If the system is interrupted, the capacitor voltage becomes too low and the voltage will return to its normal value quickly. The energy will be absorbed by the capacitor and can cause the control to be disconnected. To solve this problem, the lower limit for the capacitor voltage, taken 30% of the rating value ( $E_{d0}$ ). The lower limit of voltage can be seen in equation 5.

$$E_{d\min} = 30E_{d0} \quad (5)$$

The CES voltage will return to its initial value quickly. After the disturbance occurs, the CES unit must be ready to work for subsequent load changes. The voltage deviation of the capacitor is used as a feedback signal in the CES control loop.

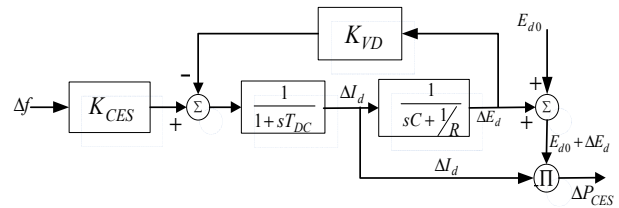


Fig. 3. CES Block diagram

Here's the voltage deviation of the capacitor  $\Delta E_d$ ,

$$\Delta E_d = \left[ \frac{1}{sC + 1/R} \right] \Delta I_d \quad (6)$$

CES output power released to the system during load changes is as follows,

$$\Delta P_{CES} = (E_{d0} + \Delta E_d) \cdot \Delta I_d \quad (7)$$



### C. Superconducting Magnetic Energy Storage (SMES)

SMES stores energy in the magnetic field obtained from Direct Current (DC) into the cryogenic cooled superconducting coil. A SMES connected to a power system, consisting of a cryogenic cooling system, superconducting coil, and Power Conditioning System (PCS) with control and protection functions. PCS is commonly referred to as the power electronics center of the SMES coil. SMES schematic diagram can be seen in figure 4. [3].

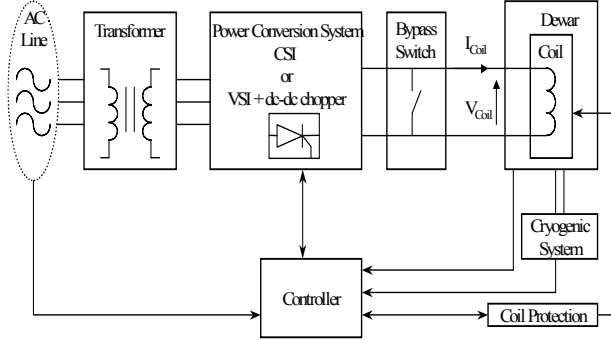


Fig. 4. SMES schematic diagram.

In principle, superconductors have near-zero losses at cold temperatures. The coolant used is Helium liquid which is able to cool to 4 K. PCS is used to transfer energy from the SMES coil to the system. A PCS uses a dc link capacitor to connect a voltage source from the SMES coil to the system. The working principle of SMES is divided into three, namely charging mode, standby mode and discharging mode. The SMES performance setting is performed by adjusting the duty cycle of the converter which in this case uses a Gate Turn Off (GTO) thyristor.

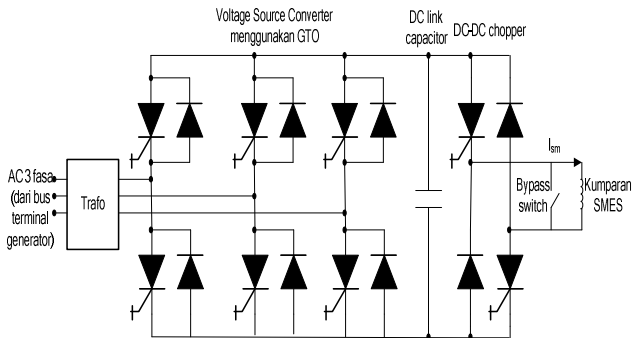


Fig 5. Configure SMES

To effectively control the power balance of the generator, SMES is placed on the bus terminal of the generator. From some SMES equations of reference, a block diagram of the SMES PID controller used is shown in Figure 6.

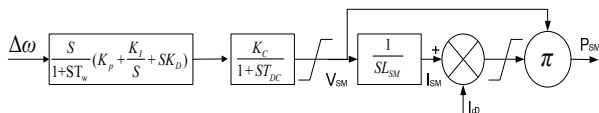


Fig 6. Block diagram PID SMES

In this study, PID-SMES is installed on micro-hydro power system. The PID-SMES installation is on the induced generator bus terminal when there is a burden of changing the load. The SMES parameters can be seen in Table 3.

Table 3. SMES Parameters

Parameters	Tuning Value
Ksmes	90
Tdc	0.0176
tw	7.6616
Kp	8
Ki	6.8462

### D. Firefly Algorithm (FA)[7]

The method used to optimize the PID parameter is the Firefly Algorithm (FA) method. The algorithm was first discovered by Dr. Xin-She Yang at Cambridge University in 2007. The algorithm diagram of the Firefly Algorithm (FA) method used in this research study can be seen in Figure 3. The objective function used to test the stability of the system is with Integral Time Absolute Error (ITAE)[8][7].

$$ITAE = \int_0^t |\Delta\omega(t)| dt \quad (11)$$

The PID parameters set by FA are Kd, Kp, Ki. The data of the standard FA parameters used are shown in Table 4:

Table 4. FA Parameters

Parameters	Value
Alpha	0.25
Beta	0.2
Gamma	1
Dimensi	3
Number of Fireflies	50
Maximum iteration	50
Kp	0 – 50
Ki	0 – 10
Kd	0 – 10

### E. Particle Swarm Optimization (PSO).

his algorithm is inspired by the behavior of swarm in search of food. Particle Swarm Optimization (PSO) is defined as a swarm swarm that can define trajectories by their own best performance and groups. In this paper, swarm partition optimization solves the problem of performance optimization Load frequency control in reducing frequency fluctuations through the description of the algorithm to find the value of the constants PID, CES and SMES.[10][11].

The data of PSO parameters can be seen in Table 5.

TABLE 5. PSO PARAMETERS

Parameters	Value
Number of Particles	30
Maximum iteration	50
Number of Variables	3
C2 (Social Constant)	2
C1 (Cognitive Constant)	2
W (Momentum Inertia)	0.9
Kp	0 – 50
Ki	0 – 10
Kd	0 – 10

## III. RESULT OF SIMULATION AND ANALYSIS

The design of some micro-hydro controllers can be seen in figure 7.

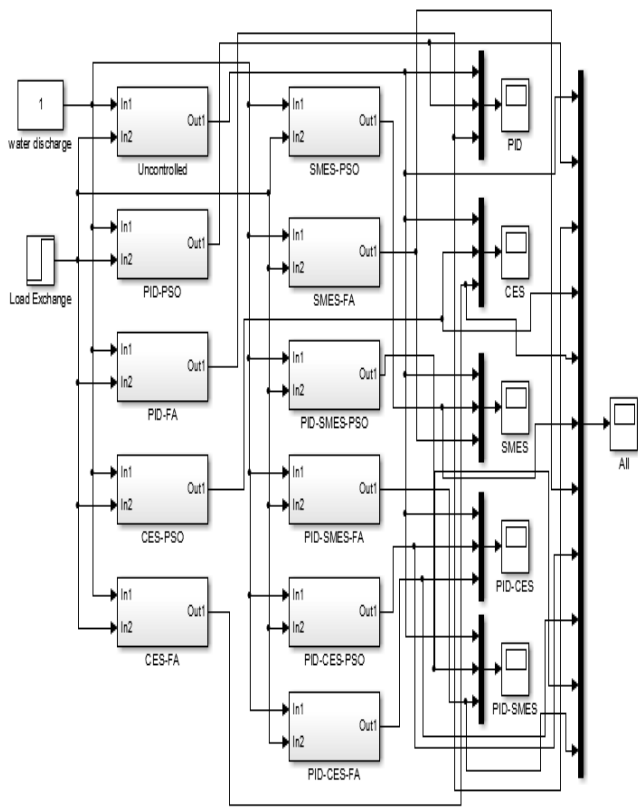


Fig.7. Micro-hydro controller design

Micro-hydro controller constants can be seen in Table 6, table 7, and Table 8;

TABLE 6. OPTIMIZATION RESULTS WITH PID

Parameter	PSO	FA
Kp	16.790915	79.627021
Ki	1.716562	7.161799
Kd	0.091662	6.024251

TABLE 7. PID OPTIMIZATION RESULTS WITH CES

Parameter	PSO	FA
Kces	69.4785	82.1232
Tdc	0.01430	0.0643
Kp	11.7909	49.6827
Ki	1.7165	39.6212
Kd	0.09166	6.1234

TABLE 8. PID OPTIMIZATION RESULTS WITH SMES

Parameter	PSO	FA
Ksmes	81.302	90.634
Tdc	0.02136	0.0176
Twi	7.0321	7.6162
Kp	7.0864	8.8642
Ki	2.6744	6.8463
Kd	0.0083	0.1932

By using the FA method obtained tuning PID controller with a large constant parameter  $K_p = 79.627021$ ,  $K_i = 7.161799$ , and  $K_d = 6.024251$ . With CES method, there are big constants  $K_{ces} = 82.1232$ ,  $T_{dc} = 0.0643$ ,  $K_p = 49.6827$ ,  $K_i = 39.6212$ , and  $K_d = 6.1234$ . With the method of SMES obtained constant  $K_{smes} = 90.634$ ,  $T_{dc} = 0.0176$ ,  $T_{wi} = 7.6162$ ,  $K_p = 8.8642$ ,  $K_i = 6.8463$ , and  $K_d = 0.1932$ .

Figure 8-13 shows the micro-hydro frequency response for each control design.

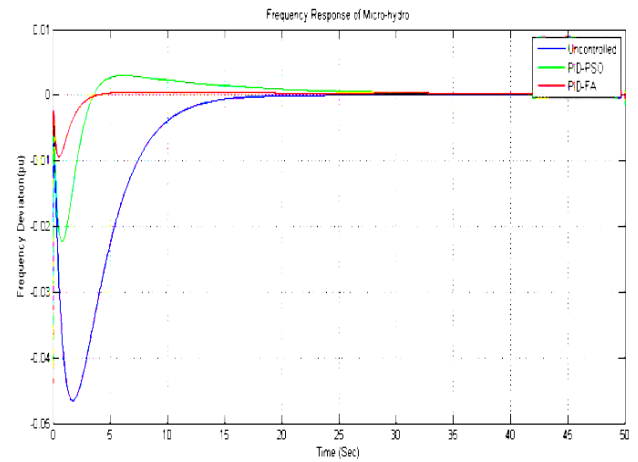


Fig. 8. Micro Hydro Frequency with PID

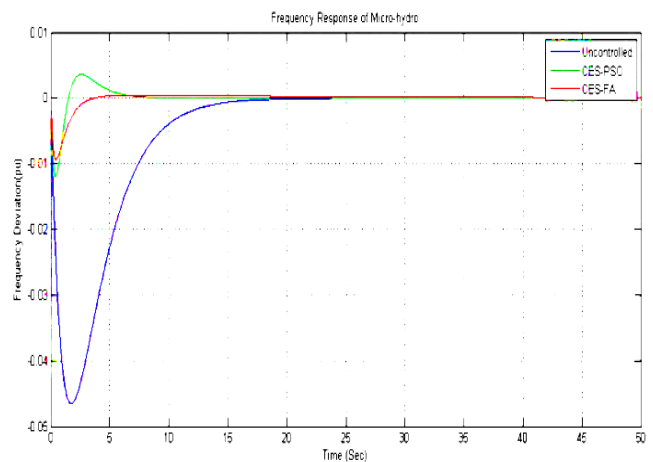


Fig. 9. Micro Hydro Frequency with CES

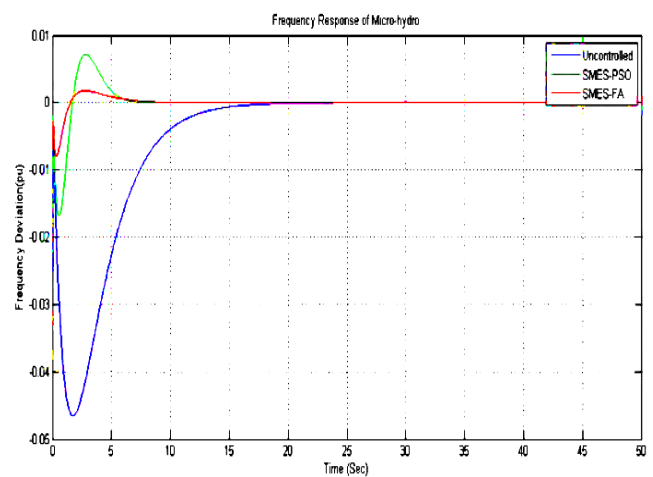


Fig. 10. Micro Hydro Frequency with SMES

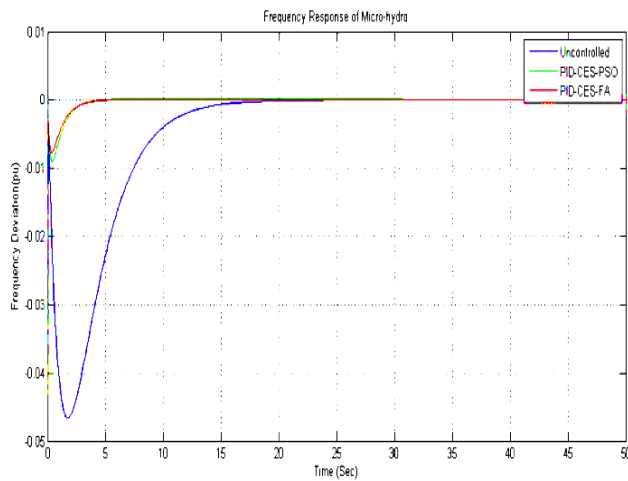


Fig. 11. Micro Hydro Frequency with PID-CES

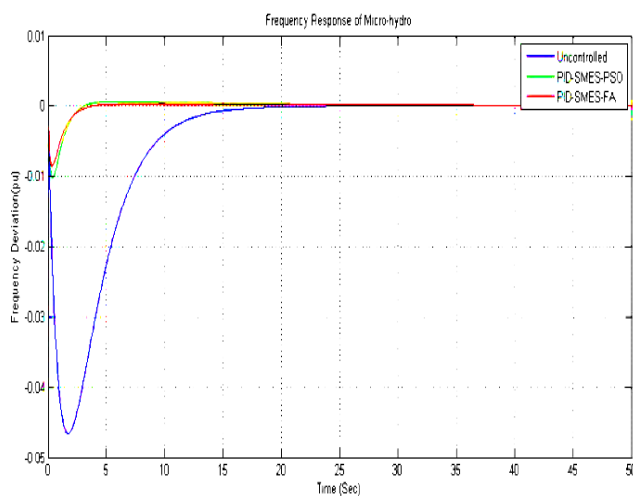


Fig. 12. Micro Hydro Frequency with PID-SMES

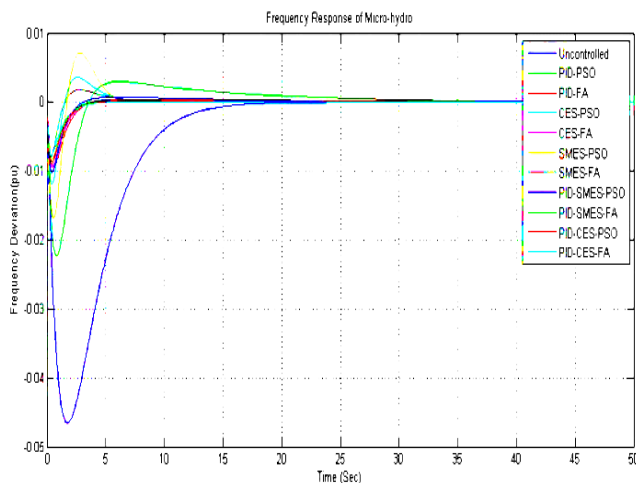


Fig. 13. Plot All Graphic of Control Model

The results of overshoot, undershoot and settling time can be seen in Table 9.

TABLE 9. OVERSHOOT RESULT OF EACH MODEL

Controller	Overshoot (pu)	Undershoot (pu)	Settling time (s)
Uncontrolled	0.0000	-4.661e-02	25.012
PID-PSO	3.945e-04	-2.242e-02	35.653
PID-FA	2.985e-03	-9.448e-03	15.653
CES-PSO	3.582e-03	-1.191e-02	9.883
CES-FA	4.111e-04	-9.375e-03	7.352
SMES-PSO	7.154e-03	-1.701e-02	21.342
SMES-FA	1.961e-03	-8.954e-03	19.763
PID-CES-PSO	1.798e-04	-9.063e-03	7.748
PID-CES-FA	4.482e-05	-7.774e-03	7.11
PID-SMES-PSO	7.000e-03	-1.011e-02	17.863
PID-SMES-FA	1.931e-03	-8.531e-03	11.361

From Figure 8-13 and Table 9 shows that the overshoot, undershoot, and settling time of the method; uncontrolled (0.00, -4.661e-02, 25.012), PID-PSO method (3.945e-04, -2.242e-02, 35.653), PID-FA method (2.985e-03, -9.448e-03, 15.653), CES-PSO method (3.582e-03, -1.191e-02, 9.883), CES-FA method (4.111e-04, -9.375e-03, 7.352), SMES-PSO method (7.154e-03, -1.701e-02, 21.342), SMES-FA method (1.961e-03, -8.954e-03, 19.763), PID-CES-PSO method (1.798e-04, -9.063e-03, 7.748), PID-CES-FA method (4.482e-05, -7.774e-03, 7.11), PID-SMES – PSO (7.000e-03, -1.011e-02, 17.863), and PID-SMES-FA method (1.931e-03, -8.531e-03, 11.361). The simulation results show that the PID-CES-FA method has the smallest undershoot value, ie -7.774e-03 pu, the smallest overshoot, ie 4.482e-05 pu, and the fastest settling time of 7.11 s. thus it is stated that the PID-CES-FA method is the best method used from the previous method..

#### IV. CONCLUSION

By using Firefly Algorithm (FA) as the method of tuning the Capacitive Energy Storage (CES) controller, the result of tuning of CES parameter for Kces 88,8888, Tdc is 0.0563, Kp is 63.6297 and Ki is 43.7886, and Kd is 9.6385. The simulation results show that the PID-CES-FA method has the smallest undershoot value, ie -7.774e-03 pu, the smallest overshoot, ie 4.482e-05 pu, and the fastest settling time of 7.11 s. thus it is stated that the PID-CES-FA method is the best method used from the previous method.

#### V. REFERENCES

- [1] D. Henderson, "An advanced electronic load governor for control of micro hydroelectric generation," *IEEE Trans. Energy Convers.*, vol. 13, no. 3, pp. 300–304, 1998.
- [2] I. T. Yuniahastuti, I. Anshori, and I. Robandi, "Load frequency control (LFC) of micro-hydro power plant with capacitive energy storage (CES) using bat algorithm (BA)," in *Proceedings - 2016 International Seminar on Application of Technology for Information and Communication, ISEMANTIC 2016*, 2017, pp. 147–151.
- [3] M. R. I. Sheikh, S. M. Mueen, R. Takahashi, T. Murata, and J. Tamura, "Minimization of fluctuations of output power and terminal voltage of wind generator by using STATCOM/SMES," in *2009 IEEE Bucharest PowerTech: Innovative Ideas Toward the Electrical Grid of the Future*, 2009.

- [4] M. Ali, F. Hunaini, I. Robandi, and N. Sutantra, "Optimization of active steering control on vehicle with steer by wire system using Imperialist Competitive Algorithm (ICA)," in *2015 3rd IEEE -International Conference on Information and Communication Technology, ICoICT 2015*, 2015, pp. 500–503.
- [5] H. Kusuma, M. Ali, and N. Sutantra, "The comparison of optimization for active steering control on vehicle using PID controller based on artificial intelligence techniques," in *Proceedings - 2016 IEEE- International Seminar on Application of Technology for Information and Communication, ISEMANTIC 2016*, 2017.
- [6] M. Muhlasin, R. Rukslin, A. Raikhani, and M. Ali, "The FA-ANFIS Hybrid Method is used for LFC Optimization in Micro Hydro Power Generation," in *Seminar Nasional Teknik Elektro (FORTEI 2017)*, 2017, pp. 225–229.
- [7] X. S. Yang, "Firefly algorithms for multimodal optimization," in *Lecture Notes in Computer Science (including subseries Lecture Notes in Artificial Intelligence and Lecture Notes in Bioinformatics)*, 2009, vol. 5792 LNCS, pp. 169–178.
- [8] M. Alb, P. Alotto, C. Magele, W. Renhart, K. Preis, and B. Trapp, "Firefly Algorithm for Finding Optimal Shapes of Electromagnetic Devices," *IEEE Trans. Magn.*, vol. 52, no. 3, pp. 1–4, 2016.
- [9] X. S. Yang, "Firefly Algorithm," *Nature-Inspired Metaheuristic Algorithms*, pp. 79–90, 2007.
- [10] T. M. Blackwell, J. Branke, and X. Li, "Particle Swarms for Dynamic Optimization Problems," *Swarm Intell.*, vol. 52, no. 1, pp. 193–217, 2008.
- [11] Z.-H. Zhan, J. Zhang, Y. Li, and H. S.-H. Chung, "Adaptive particle swarm optimization.," *IEEE Trans. Syst. Man. Cybern. B. Cybern.*, vol. 39, no. 6, pp. 1362–1381, 2009.

# Optimal Power Flow using Fuzzy-Firefly Algorithm

Dwi Lastomo<sup>1</sup>, Widodo<sup>2</sup>, Herlambang Setiadi<sup>3</sup>

<sup>1</sup>Department of Automation Electrical Engineering, Institut Teknologi Sepuluh Nopember, Surabaya, Indonesia.

<sup>2</sup>Electrical Engineering Department, University of PGRI Adi Buana, Surabaya, Indonesia

<sup>3</sup>School of Information Technology & Electrical Engineering, The University of Queensland, Brisbane, Australia  
(E-mail: dtomo23@gmail.com<sup>1</sup>, widodo.adibuana@gmail.com<sup>2</sup>, h.setiadi@uq.edu.au<sup>3</sup>)

**Abstract**—Development of Metaheuristic Algorithm in engineering problems grows really fast. This algorithm is commonly used in optimization problems. One of the metaheuristic algorithms is called Firefly Algorithm (FA). Firefly Algorithm is a nature-inspired algorithm that is derived from the characteristic of fireflies. Firefly Algorithm can be used to solve optimal power flow (OPF) problem in power system. To get the best performance, firefly algorithm can be combined with fuzzy logic. This research presents the application of hybrid fuzzy logic and firefly algorithm to solve optimal power flow. The simulation is done using the MATLAB environment. The simulations show that by using the fuzzy-firefly algorithm, the power losses, as well as the total cost, can be reduced significantly.

**Keywords**- Firefly algorithm, Fuzzy logic system, Optimal power flow.

## I. INTRODUCTION

Many power plants such as thermal and hydropower plant are located far away from the load center. Water as a turbine power plant is located either in foothills or mountains as well as in the lake. While petroleum, gas, and coal which is the source of the thermal power plant are generally placed near ports or other places due to the transportation cost [1].

Power plants that located far away from the load center require long transmission line to supply electrical energy to the load center. This long transmission line could cause a huge amount of power loss. This losses resulting in generating units generate power beyond the total load demand that should be borne to compensate for the power loss. The thermal plant is using unrennewable energy such as fuel as the source of energy. The trend in fuel prices on the market fluctuates and the trends continue to increase so that the fuel consumption needs to be minimized due to the high cost for generating electricity [1].

Since the electrical load is a function of generating costs, it is necessary to find solutions to optimally operate the generating units by reducing fuel costs to a minimum and maintaining continuity of service to consumers and still paying attention to the operational constraints. This method is commonly called the optimal power flow (OPF) [2].

The purpose of OPF is to achieve the load demand with a minimum cost production without neglecting physical and operational limits. OPF can be easily done by using

conventional mathematical approach. The application of conventional mathematical approach such as Gaussian Message Passing Iterative detection for solving optimization problems is reported in [3, 4]. However, with the more fluctuation of load demand and the fuel prices, the conventional mathematical approach of OPF sometimes do not give optimal results. Hence solving OPF based metaheuristic algorithm approach can be proposed.

The application of metaheuristic algorithm approach for solving a complex problem in power system application has developed significantly over the few decades. Application of differential evolution algorithm (DEA) for designing battery energy storage systems (BESS) and solving the modal interaction problems are reported in [5, 6]. The application of particle swarm optimization (PSO) for solving load frequency control and optimizing redox flow batteries (RFB) is investigated in [7, 8]. In [9] the application of craziness PSO for mitigating low-frequency oscillatory stability is investigated. Optimizing parameter of blade pitch angle wind turbine using hybrid differential evolution algorithm-particle swarm optimization is explained in [10]. Application of imperialist competitive algorithm for designing capacitive energy storage parameter as load frequency controller of micro hydro is described in [11].

Designing RFB based on ant colony optimization (ACO) approach for solving small disturbance angle stability problems is described in [12]. Optimization of RFB and power system stabilizer (PSS) for small signal stability enhancement of power system using cuckoo search algorithm is presented in [13]. Designing a linear quadratic regulator for enhancing the frequency performance of the power system using artificial Immune System via clonal selection is investigated in [14]. Optimal coordination of superconducting magnetic energy storage (SMES) and PSS using firefly algorithm (FA) for dynamic stability enhancement on the power system is reported in [15]. Among a numerous number of metaheuristic algorithm, FA is becoming more popular due to simplicity and less computational burden. Furthermore, the alpha coefficient in FA is played important role in the firefly algorithm as reported in [16]. So by modified the alpha coefficient of FA, the optimal value can be achieved as the alpha coefficient can reduce the randomness of fireflies [17].

Hence this paper proposed the application of firefly algorithm for solving optimal power flow problems. To get the best performance, the fuzzy logic system is used as a hybrid

with the FA method. The rest of the paper is organized as follows: Section II provides a fundamental theory of optimal power flow, firefly algorithm, and fuzzy logic systems. Section III focused on designing hybrid fuzzy logic and firefly algorithm for solving optimal power flow. Result and discussion are presented in section IV. Finally, section V highlight the contribution, conclusions and future direction of this work.

## II. FUNDAMENTAL THEORY

### A. Optimal Power Flow

The idea of optimal power flow was developed by Carpentier in 1962. OPF is used to determine the optimal set of variables that have various constraint boundaries. The development of OPF has been increasing significantly due to the development of advanced computing technology. The problem of highly complex power system optimization can be solved using OPF without needing any huge amount of time. Conventional OPF is one of the optimization problems in the power system to meet the required load demand at the minimum production cost. The cost of generating electricity has increased significantly, as a result of the increasing fuel prices. It is important to find ways to generate electrical energy at minimum cost in power system as well as achieving the physical and constrained provisions in operation. The mathematical representation of OPF to minimize the cost of generation can be described in (1) [2].

$$\min F(x) = \sum_{i=1}^N C_i(P_{Gi}) = \sum_{i=1}^N (C_2 P_{Gi}^2 + C_1 P_{Gi} + C_0) \quad (1)$$

In (1),  $F(x)$  is the total cost of generation, while  $C_0$ ,  $C_1$ ,  $C_2$  are cost function coefficient. Furthermore,  $P_{Gi}$ ,  $N$  are active power generation and the number of the generator. The concept of OPF has only one restriction that is, the total power generated is proportional to the load plus the loss of power. That restriction can be expressed in the mathematical equation in (2) [2].

$$L = \sum F(P_i) + \lambda (P_{load} + P_{losses} - \sum P_i) \quad (2)$$

The equation that representing “generation equal to load plus power loss” is described in (3) with equality and inequality constraint described in (4) and (5) [2].

$$P_{load} + P_{losses} - \sum P_i = 0 \quad (3)$$

$$P_{Gi} - P_{Di} = V_i \sum_{j=1}^{NB} V_j (G_{ij} \cos(\theta_i - \theta_j) + B_{ij} \sin(\theta_i - \theta_j)) \quad (4)$$

$$Q_{Gi} - Q_{Di} = V_i \sum_{j=1}^{NB} V_j (G_{ij} \sin(\theta_i - \theta_j) + B_{ij} \cos(\theta_i - \theta_j))$$

$$\begin{aligned} P_{Gi\_min} &\leq P_{Gi} \leq P_{Gi\_max} \\ Q_{Gi\_min} &\leq Q_{Gi} \leq Q_{Gi\_max} \\ P_{m\_min} &\leq V_m \leq V_{m\_max} \\ S_L &\leq S_{L\_max} \end{aligned} \quad (5)$$

In (4) and (5)

$V_i$ : Voltage magnitude bus i

$P_{Gi}$ : Active power bus i

$Q_{Gi}$ : Reactive power bus i

$G_{ij}$ ,  $B_{ij}$ : Transmission admittance m-n

$\theta_i$ : Voltage phase angle bus m

$\theta_j$ : Voltage phase angle bus n

### B. Firefly Algorithm

FA is a metaheuristic algorithm inspired by the flashing behavior of fireflies. This algorithm was developed by Dr. Xin-She Yang at Cambridge University to solve optimization problems. FA has three important parts as described in the following rule [18-20]s:

- ❖ All fireflies are unisex, so a firefly will be attracted to other fireflies regardless of their sex.
- ❖ The attraction is proportional to the brightness of the fireflies. Fireflies with lower brightness levels will be attracted and move to fireflies with higher brightness. Brightness may decrease with increasing distance and the absorption of light due to air factor. If there are no fireflies with the most brightness light, the fireflies will move randomly.
- ❖ The brightness or intensity of the firefly is determined by the value of the objective function of the given problem.

There are two things that are related and very important in FA namely light intensity and attractiveness function. In this case, we assume that the attractiveness is influenced by the degree of light intensity. The degree of light intensity on a firefly x can be stated as (6).

$$I(x) = f(x) \quad (6)$$

In (6),  $I$  indicated the level of light intensity on  $x$  fireflies that is proportional to the solution of the objective function ( $f(x)$ ).  $\beta$  is the attractiveness coefficient that has relative value due to the light intensity that must be seen and assessed by other fireflies. Hence, the result of the assessment will differ depending on the distance between the fireflies. In addition, the light intensity will decrease from the source due to the air factor ( $\gamma$ ). Hence, the mathematical representation of the attractiveness function is presented in (7).

$$\beta(r) = \beta_0 * \exp(-\gamma r^m), (m \geq 1) \quad (7)$$

The distance between fireflies  $i$  and  $j$  at the locations  $x_i$  and  $x_j$  can be determined when they are placed at the point



where fireflies are dispersed randomly in the Cartesian diagram as presented in (8). Where the different location of firefly  $i$  to firefly  $j$  is the distance between those two ( $r_{ij}$ ).

$$r_{ij} = \sqrt{(x_i - x_j)^2 + (y_i - y_j)^2} \quad (8)$$

The movement of fireflies that move towards the best level of light intensity can be described as (9) [18-20].

$$x_i = x_i + \beta_0 * \exp(-\gamma r_{ij}^2) * (x_j - x_i) + \alpha * \left( rand - \frac{1}{2} \right) \quad (9)$$

In (9),  $x_i$  indicated the initial position of fireflies located at  $x$ , while  $\alpha$  is a variable that has a range between 0 and 1. All the variables formed on (9) ensure the fast algorithm work toward the optimal solution [20]

### C. Fuzzy logic systems

Fuzzy logic was introduced in 1965 by Lofti Zadeh. The fuzzy or gray concept (vague, unclear) is based on obscurity limits and provides a mechanism for representing linguistic constructions such as “many,” “low,” “medium,” “often,” “multiple”. The fuzzy set provides a meant to model the uncertainties associated with obscurity inaccuracy and lack of information about a problem or plant. Suppose the meaning of a “short” person. For  $X$  individual short people may have a height <4’25”, for  $Y$  individuals <3’90”. The term “short” informs the same meaning as the individuals of  $X$  and  $Y$ , but neither of the gives a distinctive definition [21].

Lofti Zadeh proposed the idea of a set of membership set to make the appropriate decisions when the uncertainty occurred. Like the word “short”, if we take “short” as high equal to or less than 4 feet, then 3’90” easily becomes a member of the “short” set and 4’25” does not belong to the “short” set. The membership value is “1” if a member of the set or “0” if it is not a member of the set. This can be mathematically described as given in (10) [21].

$$X_A(x) = \begin{cases} 1; x \in A \\ 0; x \notin A \end{cases} \quad (10)$$

In (6),  $X_A(x)$  is the member of element  $x$  in the set  $A$ , while  $A$  value itself is the whole set of universes. Membership expanded to have various “degrees of membership” at a real continuous interval [0.1]. Zadeh forms a fuzzy set like the set of the universe  $X$  that can accommodate the “degree of membership” [21].

## III. DESIGN FUZZY-FA FOR SOLVING OPF

### A. Designing Fuzzy for FA

Fuzzy interference is used to set the value of  $\alpha$ .  $\alpha$  value has an important role on FA. Hence, in this research, the  $\alpha$  value is designed as random value based on the Takagi-Sugeno fuzzy formula.

The membership function for fuzzy input is used trapezoidal type and has one input which is the minimum value of total fuel cost at each iteration. The linguistic value of the input variables consists of four fuzzy sets of  $VS$  (very small),  $S$  (small),  $M$  (medium), and  $L$  (large). While the value of crisp output consists of four linear equations. The coefficient values  $a_1$ - $a_4$  and  $J_1$ - $J_6$  are obtained by try and error. The value of  $a_1$ ,  $a_2$ ,  $a_3$  and  $a_4$  are 0.0010465, 0.0021665, 0.003227 and 0.00427 [1]. Table 1 illustrates the membership function of this paper [1].

Table 1 The membership function of fuzzy interference.

Linguistic	Value	Value	Value	Value
Very small	797	801.7	802.9	807.6
Small	802.9	807.6	808.8	813.5
Medium	808.8	813.5	814.7	819.4
Large	814.7	819.4	820.6	825.3

The rule base is used to control the fuzzy adaptation. In this paper the rule base of the fuzzy system can be described in below [1]:

$R_1$ : If  $\min(J)$  very small (VS) then  $u_1 = a_1 \min(J)$

$R_2$ : If  $\min(J)$  small (S) then  $u_2 = a_2 \min(J)$

$R_3$ : If  $\min(J)$  medium (M) then  $u_3 = a_3 \min(J)$

$R_4$ : If  $\min(J)$  large (L) then  $u_4 = a_4 \min(J)$

Furthermore, since the input is just one of the input is directly stated as defuzzification [22]. In the process of defuzzification, the weighted average is used to find the output of fuzzy.

### B. Solving OPF using Fuzzy-FA

Solving OPF using fuzzy-FA includes the following steps:

1. The input parameter of FA, data bus, transmission line,  $P_{min}$  and  $P_{max}$  power output.
2. Start firefly initialization.
3. Firefly is inputted as the parameter of optimal power flow for finding the fitness function.
4. Rank the firefly based on the fitness value and find the best fitness from the firefly.
5. Update firefly movement using Eq. 9 by changing the constant  $\alpha$  value with fuzzy systems
6. Update the best fitness.
7. Update the firefly value.
8. Determine if the characterization is achieved. If not go back in step 3.
9. Print the output (The total generating capacity and cost of the generation).

## IV. NUMERICAL RESULTS

Two cases study is considered in this paper in an attempt to test the effectiveness of the fuzzy-FA for solving optimal power flow problems. Comparison between fuzzy-FA,

conventional FA and Lagrange is done to investigate the efficiency of the fuzzy-FA. All of the simulations are carried out using the MATLAB environment.

#### A. Case study 1

In the first case study, Java-Bali 500 kV is used as the test system. Fig. 1 depicts the one line diagram of Java-Bali system. This system consist of 25 buses with one slack bus, seven generator bus, and 17 bus loads. All of the data was taken from PT PLN (Persero) P3B Java, Bali on April 19, 2011 at 18.30 [23]. Generating units connected to the system Java-Bali 500 kV have limits minimum and maximum power generation as follows [23]:

Suralaya	: $1.703 \leq P_1 \leq 3.287$	(MW)
Muaratawar	: $1.191 \leq P_8 \leq 2.115$	(MW)
Cirata	: $500 \leq P_{10} \leq 1.000$	(MW)
Saguling	: $350 \leq P_{11} \leq 698$	(MW)
Tanjung Jati	: $840 \leq P_{15} \leq 1.321$	(MW)
Gresik	: $238 \leq P_{17} \leq 1050$	(MW)
Paiton	: $1.664 \leq P_{22} \leq 3240$	(MW)
Grati	: $150 \leq P_{23} \leq 827$	(MW)

With the cost function of each generating unit in this system are as follows [23]:

Suralaya	$= -6,99 P_1^2 + 385454,41P_1 + 51229002,4$
Muaratawar	$= 137,924P_8^2 - 873046,208 P_8 + 5375795990$
Cirata	$= 6000 P_{10}$
Saguling	$= 5502 P_{11}$
Tanjung Jati	$= 10,114P_{15}^2 + 284810,35P_{15} + 18527152,74$
Gresik	$= -6,3P_{17}^2 + 1021624,6 P_{17} + 6477009$
Paiton	$= 52,19P_{22}^2 + 37370,67P_{22} + 8220765,38$
Grati	$= -100,79P_{23}^2 + 1726981,41P_{23} + 29938756,61$

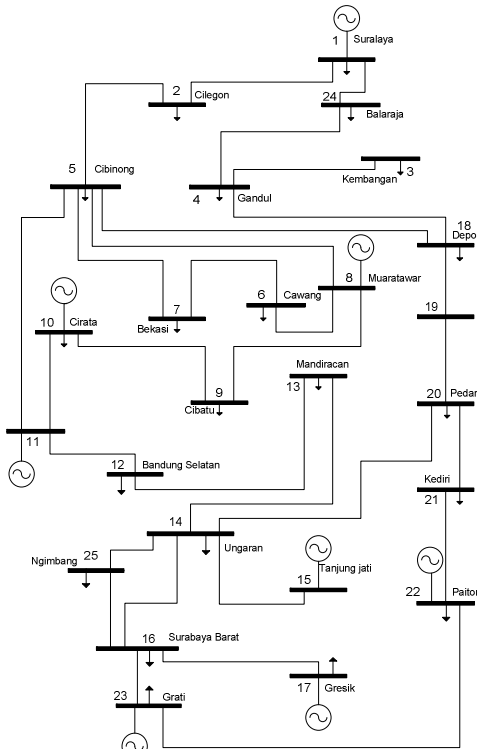


Fig. 1 Java-Bali 500 kV systems.

Table. 2 illustrates the comparison of generating capacity, power loss and cost of the system between a system with Lagrange method, conventional FA method and using the fuzzy-FA method. It is found that by using the Lagrange method, the total cost of the system is 756,570.63 USD and the power loss is 203.34 MW. By using the conventional FA method for solving OPF problems, the total cost can be reduced up to 126,905.87 USD and the power loss can be reduced up to 87.68 MW. Furthermore, the best performance is performed by combining fuzzy and FA. By using fuzzy-FA for solving OPF problems, the total cost becomes 629,664.76 USD.

Table 2. Optimal power flow result on Java-Bali interconnection.

N o	Unit	Lagrange Power output (MW)	Fuzzy-FA Power output (MW)	FA Power output (MW)
1	Suralaya	2006.86	2006.86	2972.69
2	Muaratawar	1673.00	1673.00	2115.00
3	Cirata	1000.00	1000.00	1000.00
4	Saguling	499.00	499.00	660.21
5	Tanjung Jati	1291.00	1291.00	1151.55
6	Gresik	900.00	900.00	238.00
7	Paiton	3198.00	3198.00	2740.74
8	Grati	548.00	548.00	150.00
Total power		11115.85	11029.71	11028.18
Power loss (MW)		203.34	117.19	115.66
Total cost (\$/hours)		756,570.63	629,064.35	629,664.76

#### B. Case study 2

IEEE 30 bus is used as a test system in the second case study. Fig. 2 depicts the single line diagram of IEEE 30 bus systems. This system consists of 30 buses with one slack bus, 5 generator bus, and 24 bus loads. All of the data was taken from reference [24]. The maximum and minimum limits of the power generation in IEEE 30 bus is described as follows [24]:

G1:	$50 \leq P_1 \leq 200$	(MW)
G2:	$20 \leq P_2 \leq 80$	(MW)
G3:	$15 \leq P_5 \leq 50$	(MW)
G4:	$10 \leq P_8 \leq 35$	(MW)
G5:	$10 \leq P_{10} \leq 30$	(MW)
G6:	$12 \leq P_{13} \leq 40$	(MW)

With the cost function of each generating unit in this system are as follows [23]:

$F_1 (P_1)$	$= 0 + 2P_1 + 0.0037P_1^2$
$F_2 (P_2)$	$= 0 + 1.75P_2 + 0.0175P_2^2$
$F_5 (P_5)$	$= 0 + 1P_5 + 0.0625P_5^2$
$F_8 (P_8)$	$= 0 + 3.25P_8 + 0.0083P_8^2$
$F_{10} (P_{10})$	$= 0 + 3P_{10} + 0.025P_{10}^2$
$F_{13} (P_{13})$	$= 0 + 3P_{13} + 0.025P_{13}^2$

Table. 3 illustrates the comparison of generating capacity,

power loss and cost of the system between a system with Lagrange method, conventional FA method and using the fuzzy-FA method. It is found that by using the Lagrange method, the total cost of the system is 803.20 USD and the power loss is 9.59 MW. By using the conventional FA method for solving OPF problems, the total cost can be reduced up to 24.89 USD and the power loss can be reduced up to 3.66 MW. Furthermore, the best performance is performed by combining fuzzy and FA. By using fuzzy-FA for solving OPF problems, the total cost becomes 771.70 USD.

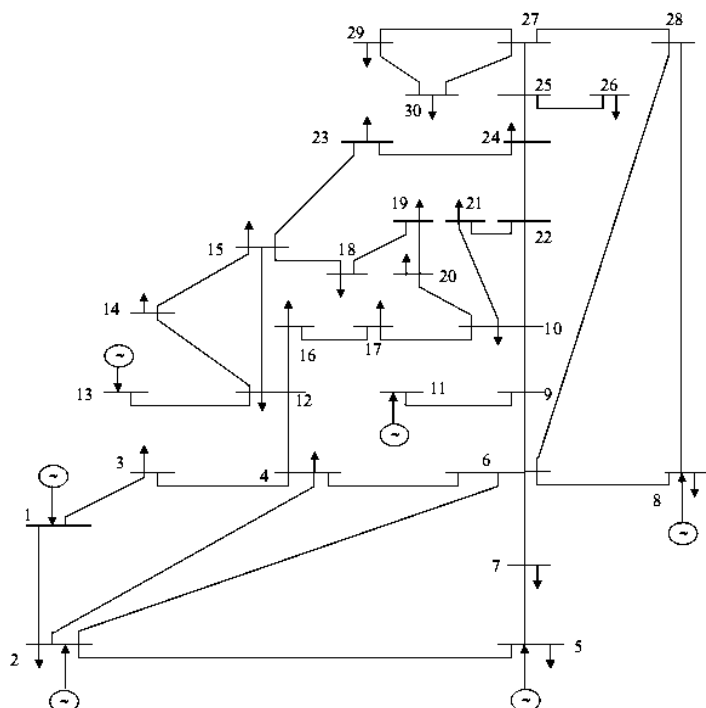


Fig. 2 IEEE 30 bus systems.

Table 3. Optimal power flow result on IEEE 30 bus systems.

No	Unit	Lagrange Power output (MW)	Fuzzy-FA Power output (MW)	FA Power output (MW)
1	G1	193.73	186.28	187.21
2	G2	48.10	47.21	47.40
3	G3	19.47	19.19	19.31
4	G4	11.06	10.43	11.15
7	G5	10.00	10.01	10.00
8	G6	12.00	12.00	12.00
Total power		294.36	285.12	287.06
Power loss (MW)		9.59	1.72	3.66
Total cost (\$/hours)		803.20	771.70	778.31

To test the efficiency of fuzzy-FA for solving optimal power flow, comparative study with another algorithm is essential. Fig. 3 illustrates the comparison of the total cost in IEEE 30 bus systems under different tuning, while Fig. 4

shows the comparison of power loss of IEEE 30 bus systems under different tuning method. From Figs. 3 and 4, it is noticeable that the proposed method (fuzzy-FA) could provide minimum cost and power losses.

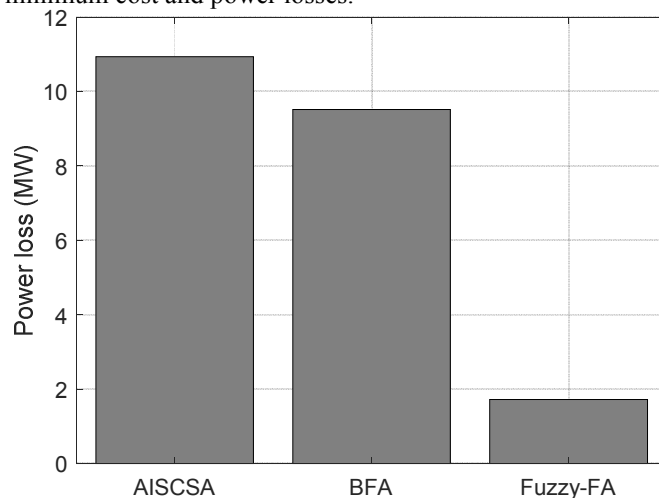


Fig. 3 Power loss comparison.

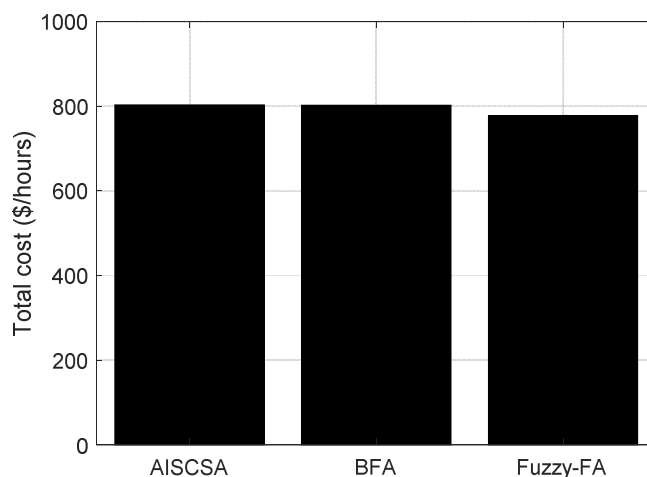


Fig. 4 Total cost comparison.

## V. CONCLUSIONS

This paper proposed a method for solving optimal power flow by combining fuzzy logic and firefly algorithm. From the investigated study case, it is found that by using the proposed method, the total cost of both the Java-Bali and IEEE 30 bus system can be reduced. Furthermore, by using the proposed method, the total power loss can also be reduced in both test systems. However, in the case study one, it is found that the loss of Java-Bali by using regular FA is better than using fuzzy-FA. Further research needs to be conducted by considering the ramp rate of the generator, for analyzing dynamic optimal power flow.

## REFERENCES

- [1] M. R. Fauzi, "The Optimization of Economic Dispatch using Fuzzy-Bacterial Foraging Algorithm," Master, Department of Electrical Engineering, Sepuluh Nopember Institut of Technology, 2011.
- [2] A. J. Wood and B. F. Wollenberg, *Power generation, operation, and control*. John Wiley & Sons, 2012.

- [3] L. Liu, C. Yuen, Y. L. Guan, Y. Li, and Y. Su, "Convergence Analysis and Assurance for Gaussian Message Passing Iterative Detector in Massive MU-MIMO Systems," *IEEE Transactions on Wireless Communications*, vol. 15, no. 9, pp. 6487-6501, 2016.
- [4] L. Liu, C. Yuen, Y. L. Guan, Y. Li, and C. Huang, "Gaussian Message Passing Iterative Detection for MIMO-NOMA Systems with Massive Access," in *2016 IEEE Global Communications Conference (GLOBECOM)*, 2016, pp. 1-6.
- [5] H. Setiadi, N. Mithulananthan, and M. J. Hossain, "Impact of battery energy storage systems on electromechanical oscillations in power systems," in *2017 IEEE Power & Energy Society General Meeting*, 2017, pp. 1-5.
- [6] H. Setiadi, A. U. Krismanto, N. Mithulananthan, and M. Hossain, "Modal interaction of power systems with high penetration of renewable energy and BES systems," *International Journal of Electrical Power & Energy Systems*, vol. 97, pp. 385-395, 2018.
- [7] D. Lastomo, Atmiasri, and H. Setiadi, "Stability enhancement of hybrid energy systems using RFB based on Craziness PSO," in *2017 3rd International Conference on Science in Information Technology (ICSITech)*, 2017, pp. 188-194.
- [8] D. Lastomo, Widodo, H. Setiadi, and M. R. Djalal, "Enabling PID and SSSC for load frequency control using Particle Swarm Optimization," in *2017 3rd International Conference on Science in Information Technology (ICSITech)*, 2017, pp. 182-187.
- [9] H. Setiadi, N. Mithulananthan, A. U. Krismanto, and R. Shah, "Low-Frequency Oscillatory Stability Study on 500 kV Java-Indonesian Electric Grid," in *Industrial Electronics (ISIE), 2018 IEEE 27th International Symposium on*, 2018: IEEE.
- [10] M. Ulum, H. Setiadi, and D. Lastomo, "Design Controller Blade Pitch Angle Wind Turbine Using Hybrid Differential Evolution Algorithm-Particle Swarm Optimization," *Advanced Science Letters*, vol. 23, no. 12, pp. 12396-12399, 2017.
- [11] M. R. Djalal, M. Yunus, A. Imran, and H. Setiadi, "Capacitive Energy Storage (CES) Optimization For Load Frequency Control in Micro Hydro Power Plant Using Imperialist Competitive Algorithm (ICA)," *EMITTER International Journal of Engineering Technology*, vol. 5, no. 2, pp. 279-297, 2018.
- [12] M. Taufik, D. Lastomo, and H. Setiadi, "Small-disturbance angle stability enhancement using intelligent redox flow batteries," in *2017 4th International Conference on Electrical Engineering, Computer Science and Informatics (EECSI)*, 2017, pp. 1-6.
- [13] M. R. Djalal, H. Setiadi, D. Lastomo, and M. Y. Yunus, "Modal Analysis and Stability Enhancement of 150 kV Selselrabar Electrical System using PSS and RFB based on Cuckoo Search Algorithm," *International Journal on Electrical Engineering and Informatics*, vol. 9, no. 4, pp. 800-812, 2017.
- [14] M. Abdilllah, H. Setiadi, A. B. Reihara, K. Mahmoud, I. W. Farid, and A. Soeprijanto, "Optimal selection of LQR parameter using AIS for LFC in a multi-area power system," *Journal of Mechatronics, Electrical Power, and Vehicular Technology*, vol. 7, no. 2, pp. 93-104, 2016.
- [15] H. Setiadi and K. O. Jones, "Power System Design using Firefly Algorithm for Dynamic Stability Enhancement," *Indonesian Journal of Electrical Engineering and Computer Science*, vol. 1, no. 3, pp. 446-455, 2016.
- [16] N. A. Windarko, A. Tjahjono, D. O. Anggriawan, and M. H. Purnomo, "Maximum power point tracking of photovoltaic system using adaptive modified firefly algorithm," in *2015 International Electronics Symposium (IES)*, 2015, pp. 31-35.
- [17] T. Niknam, R. Azizipناه-Abarghoee, and A. Roosta, "Reserve constrained dynamic economic dispatch: a new fast self-adaptive modified firefly algorithm," *IEEE Systems Journal*, vol. 6, no. 4, pp. 635-646, 2012.
- [18] X.-S. Yang, "Firefly algorithms for multimodal optimization," in *International symposium on stochastic algorithms*, 2009, pp. 169-178: Springer.
- [19] X.-S. Yang, *Nature-inspired metaheuristic algorithms*. Luniver press, 2010.
- [20] X.-S. Yang, *Cuckoo search and firefly algorithm: Theory and applications*. Springer, 2013.
- [21] J. R. Jang and N. Gulley, "MATLAB fuzzy logic toolbox," *MathWorks, Inc., Natick, MA*, 1997.
- [22] S. Sivanandam, S. Sumathi, and S. Deepa, *Introduction to fuzzy logic using MATLAB*. Springer, 2007.
- [23] A. Amruddin, "Application Micro Genetic Algorithm to Solve Economic Dispatch at Java-Bali 500 kV Interconnection System," Undergraduate, Department of Electrical Engineering, Sepuluh Nopember Institut of Technology, 2011.
- [24] H. Saadat, *Power system analysis*. WCB/McGraw-Hill, 1999.

# Low-Frequency Oscillation Mitigation using an Optimal Coordination of CES and PSS based on BA

Dwi Lastomo<sup>1</sup>, Herlambang Setiadi<sup>3</sup>, Galih Bangsa<sup>4,5</sup>, Imam Wahyudi Farid<sup>2</sup>, Muhamad Faisal<sup>7</sup>, Peter Go Hutomo<sup>8</sup>, Taurista Perdana Syawitri<sup>10</sup>, Louis Putra<sup>11</sup>, Yongki Hendranata<sup>12</sup>, Kristiadi Stefanus<sup>13</sup>, Chairunnisa<sup>14</sup>, Andri Ashfahani<sup>1,2</sup>, and Ahmad Sabila<sup>9</sup>,

<sup>1</sup>Department of Automation Electrical Engineering, Institut Teknologi Sepuluh Nopember, Surabaya, Indonesia.

<sup>2</sup>PUI-PT Mechatronics and Industrial Automation, Research Center Institut Teknologi Sepuluh Nopember, Surabaya, Indonesia.

<sup>3</sup>School of Information Technology & Electrical Engineering, The University of Queensland, Brisbane, Australia

<sup>4</sup>Mechanical Engineering Department, Institut Teknologi Sepuluh Nopember, Surabaya, Indonesia.

<sup>5</sup>Institute of Aerodynamics and Gas Dynamics, University of Stuttgart, Stuttgart, Germany.

<sup>6</sup>Department of Cybernetics, Graduate School of Engineering Hiroshima University, Hiroshima, Japan.

<sup>7</sup>Non-Installation Top Range Department, Berca Schindler Lifts, Ltd., Indonesia.

<sup>8</sup>Toyota SO Department, Astra International Ltd., Indonesia.

<sup>9</sup>Civil Engineering Department, Universitas Brawijaya, Malang, Indonesia.

<sup>10</sup>Mechanical Engineering Department, Universitas Muhammadiyah Surakarta, Surakarta, Indonesia.

<sup>11</sup>Mechanical Engineering Department, Politecnico di Milano, Milan, Italy.

<sup>12</sup>Mechanical Engineering Department, Texas A&M University, College Station, USA.

<sup>13</sup>Aeronautics Department, Imperial College London, London, United Kingdom.

<sup>14</sup>Department of Aircraft Maintenance Engineering, Politeknik Penerbangan Surabaya, Surabaya, Indonesia.

(E-mail: dtomo23@gmail.com, h.setiadi@uq.edu.au, bangsa@iag.uni-stuttgart.de, d140188@hiroshima-u.ac.jp, andriashfahani@gmail.com, Muhamad.faisal@schindler.com, peter.tianxiang@gmail.com, ariqfihris12@gmail.com, tps123@ums.ac.id, louiszaldhy.purnama@mail.polimi.it, youngkey89@tamu.edu, stefanus.kristiadi16@imperial.ac.uk, nisachairunnisa61@gmail.com)

**Abstract**— Small signal stability represents the reliability of generator for transferring electrical energy to the consumers. The stress of the generator increases proportionally with the increasing number of load demand as well as the uncertainty characteristic of the load demand. This condition makes the small signal stability performance of power system become vulnerable. This problem can be handled using power system stabilizer (PSS) which is installed in the excitation system. However, PSS alone is not enough to deal with the uncertainty of load issue because PSS supplies only an additional signal without providing extra active power to the grid. Hence, utilizing capacitor energy storage (CES) may solve the load demand and uncertainty issues. This paper proposes a coordination between CES and PSS to mitigate oscillatory behavior of the power system. Moreover, bat algorithm is used as an optimization method for designing the coordinated controller between CES and PSS. In order to assess the proposed method, a multi-machine two-area power system is applied as the test system. Eigenvalue, damping ratio, and time domain simulations are performed to examine the significant results of the proposed method. From the simulation, it is found that the present proposal is able to mitigate the oscillatory behavior of the power system by increasing damping performance from 4.9% to 59.9%.

**Keywords**- BA, CES, damping ratio, eigenvalue, low-frequency oscillation, PSS, time domain simulation.

## I. INTRODUCTION

The demand for electrical energy is increasing significantly in the last few decades. Increasing demand for electrical energy has been the main issue for electrical company in order to provide secure, stable and reliable electricity for the consumers. The stability and the security of power system can deteriorate due to perturbation, such as increasing load demand, uncertainty characteristic of the demand and small changes of the systems parameter. One of the stability that can be affected by those perturbations is small-disturbance angle stability.

The ability of power system to maintain the synchronization after small perturbation is called small-disturbance angle stability or low-frequency oscillation is the ability of a power system to maintain the synchronization after being exposed to a small perturbation [1, 2]. This instability characteristic is emerging due to the existence of sufficient damping from the system and can be divided into two categories. The first one is a local oscillation with the frequency ranging from 0.7 to 2 Hz. The other one is a global oscillation (inter-area oscillation) with the frequency ranging from 0.1 to 0.7 Hz [1-3]. If this stability is not well maintained, the magnitude of the oscillation may grow larger

$$\begin{bmatrix} \Delta v_d \\ -\Delta v_F \\ 0 \\ \Delta v_q \\ 0 \\ \Delta T_m \\ 0 \end{bmatrix} = - \begin{bmatrix} r & 0 & 0 & \omega_0 L_q & \omega_0 k M_Q \\ 0 & r_F & 0 & 0 & 0 \\ 0 & 0 & r_D & 0 & 0 \\ -\omega_0 L_d & -\omega_0 k M_F & -\omega_0 k M_D & r & 0 \\ 0 & 0 & 0 & 0 & r_Q \\ \frac{\lambda_{q0} - L_d i_{q0}}{3} & \frac{-k M_F i_{q0}}{3} & \frac{-k M_D i_{q0}}{3} & \frac{-k M_Q i_{d0}}{3} & \frac{k M_Q i_{d0}}{3} \\ 0 & 0 & 0 & 0 & 0 \end{bmatrix} \begin{bmatrix} \Delta i_d \\ \Delta i_F \\ \Delta i_D \\ \Delta i_q \\ \Delta i_Q \\ \Delta \omega \\ \Delta \delta \end{bmatrix} - \begin{bmatrix} L_d & k M_F & k M_D & 0 & 0 & 0 & 0 \\ k M_F & L_F & M_R & 0 & 0 & 0 & 0 \\ k M_D & M_R & L_D & 0 & 0 & 0 & 0 \\ 0 & 0 & 0 & L_q & k M_Q & 0 & 0 \\ 0 & 0 & 0 & k M_Q & L_Q & 0 & 0 \\ 0 & 0 & 0 & 0 & 0 & -\tau_j & 0 \\ 0 & 0 & 0 & 0 & 0 & 0 & 1 \end{bmatrix} \begin{bmatrix} \Delta i_d \\ \Delta i_F \\ \Delta i_D \\ \Delta i_q \\ \Delta i_Q \\ \Delta \omega \\ \Delta \delta \end{bmatrix} \quad (1)$$

and lead to unstable condition. There are several incident (fully and partial black out) happened due to low frequency oscillation problems as reported in [4]. The latest incident related to low frequency oscillation is happened in Continental Europe electricity on December 2016 [5]. Generally, this instability can be overcome by simply adding damper windings into the rotor of the synchronous generator but the performance can deteriorate over the time. Another way to handle this problem is by using power system stabilizer (PSS) as the additional controller [6]. However, PSS alone is out of date to overcome this problem as the load demand is increased over the years and the load demand is tend to have the uncertainty characteristic. Hence, energy storage devices can be considered to handle the increasing capacity of load demand as well as the uncertainty of it.

Energy storage becomes reality in the practical power system. For example, redox flow batteries, battery energy storage, superconducting magnetic energy storage, and capacitor energy storage have been used to solve several problems in power system [7-13]. Among them, capacitor energy storage (CES) is becoming popular due to large capacity and fast response for storing and releasing energy from the grid. However, designing the controller of CES is huge efforts especially if CES is installed in a large power system.

One way out of the above dilemma is by employing an optimization method based on the nature-inspired algorithm which has been utilized to solve complex engineering problems [14-22]. An algorithm such as particle swarm optimization, genetic algorithm, differential evolution algorithm, imperialist competitive algorithm, artificial immune system, firefly algorithm, cuckoo search algorithm and bat algorithm were demonstrated to perform well in solving optimization problems [14-22]. In particular bat algorithm (BA) has shown a good performance finding the optimum parameter for optimization problems [16].

Hence, the main contribution of this paper is to propose a method for mitigating the low-frequency oscillation of a power system using a coordinated control between CES and PSS. Moreover, to obtain the optimum performance, the parameters of CES and PSS are optimized by BA.

## II. FUNDAMENTAL THEORY

### A. Synchronous generator, excitation, and governor model

For low frequency oscillation study, capturing the dynamic characteristic of the synchronous generator is essential. As

consequences, transforming the non-linear model of synchronous machine to linear model and all of the parameters in direct and quadrature (DQ) axis is required. Fig. 1 shows the DQ transformation of the synchronous generator. Furthermore, the mathematical representation of linear model synchronous generator can be described as (1). The detailed linear model of the synchronous generator can be found in [23].

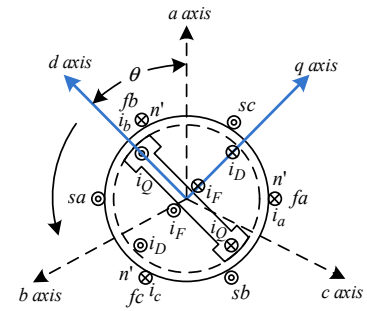


Fig. 1 DQ transformation of the synchronous generator.

The purpose of excitation system is to set the output of the generator such as voltage, current, and power factor. These variables will be adjusted by changing the field in the generator [23, 24]. To handle a small perturbation such as load changing, the exciter increases the current injection magnitude so the terminal voltage will be increased. The purpose of this process is to handle the slow response of the governor to adjust the power input to the generator when the disturbance occurs. In this study, the excitation system can be represented as time delay and gain controller as shown in Fig. 2 [23, 24].

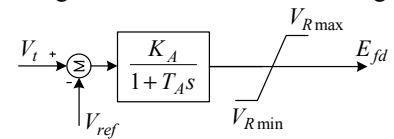


Fig. 2 Block diagram of fast exciter system.

Governor is a controller that serves to set the value of mechanical torque into the input of the generator. For small signal stability study, the governor is represented as a constant gain and first order time delay as illustrated in Fig. 3 [23].

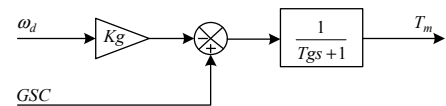


Fig. 3 Block diagram of governor system.



### B. Power system stabilizer

In power system study, PSS is widely used to enhance the dynamic performance of power systems. PSS is applied as an excitation system controller to damp the oscillatory condition of the power system. To produce a damping component, PSS produces an electric torque component corresponding to the rotor speed deviation. It receives inputs in the form of a rotor speed deviation to generate an additional signal to the exciter, which affects the magnitude of the field voltage and the magnetic flux on rotor side. It shall be noted that magnetic flux is directly proportional to the electrical torque generated on the machine. The electric torque that counters the mechanical torque of the engine to reduce the oscillation of frequencies occurring on the machine. Fig. 4 depicts the PSS model used in this study [25].

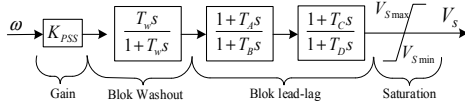


Fig. 4 Block diagram of PSS.

### C. Dynamic model of CES

A device that can release as well as storing power in large quantities is CES. The device consists of storage capacitors and power electronics devices with the associated controller as well as security function. The schematic diagram of CES is illustrated in Fig. 5 [26, 27].

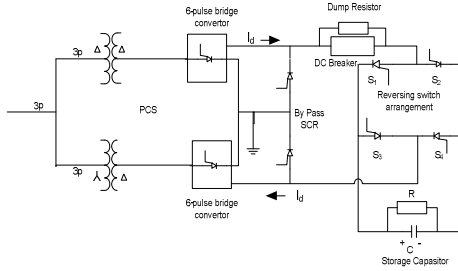


Fig. 5 Schematic diagram of CES.

Several capacitors connected in parallel and denoted by  $C$  capacitance is the representation of storage capacitor in CES. Moreover, resistance that denoted by  $R$  is also connected in parallel with the capacitor. 12 pulse back to back converters are used as an interface between the storage capacitor and grid. When the converters fail, the current  $I_d$  use bypass thyristor as a path. Moreover, if the converters fail, the  $I_d$  current will be diverted to the discharge point of  $R_D$  by the DC-disconnect. The  $E_d$  voltage can then be described as (2) [26, 27].

$$E_d = 2E_{d0} \cos \alpha - 2I_d R_D \quad (2)$$

To vary the capacitor voltage  $E_d$ , changing of phase angle is required  $\alpha$ . The changes in the direction of current during charge and discharge are overcome by arranging switches in reverse using GTO. To operate CES in charging mode, switch 2 and 3 are off, while switch 1 and 4 are on. For discharging operating condition, the switches are operated in the other way around.  $E_{d0}$  can be described in Eq. (3) [26, 27].

$$E_{d0} = \frac{[E_{d \max}^2 + E_{d \min}^2]^{1/2}}{2} \quad (3)$$

It is worth mentioning that capacitor voltage shall not exceed the specified upper and lower limits. When the system is exposed by disturbance, if the capacitor voltage is too low and if another interference emerges before the voltage returns to its normal value, the energy will be rapidly drawn from the capacitor which can lead to a discontinuous condition. To solve this problem, the lower and upper limit for the voltage of the capacitor has to be set as presented in (4) and (5) [26, 27].

$$E_{d \min} = 30E_{d0} \quad (4)$$

$$E_{d \max} = 1.38E_{d0} \quad (5)$$

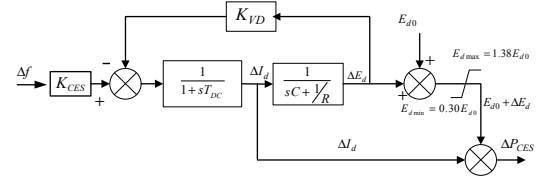


Fig. 6 Block diagram of CES.

After the voltage reaches the rating value, the voltage is maintained at this value with a continuous supply of PCS. Hence, it is sufficient to overcome the resistive drop. Since  $E_{d0}$  is very small, the firing angle of  $\alpha$  is close to  $90^\circ$ . The stored energy is released immediately via power electronics converters as an AC pulse when there is a sudden increase in load. After that to regulate the system in the new operating condition the governor and other control mechanisms start to work. By absorbing some of the excess energy in the system, CES can immediately be recharged to full value. After that, the steady state condition of the system can be achieved [26, 27]. CES can be presented as a second-order differential equation as shown in Fig. 6 [26, 27]. The block diagram of Fig. 6 can be described as using (6)-(8) [26, 27].

$$\Delta I_{di} = \frac{[K_{CES} \Delta f - K_{VD} \Delta E_d]}{1 + sT_{DC}} \quad (6)$$

$$\Delta E_d = \left[ \frac{1}{sC + 1/R} \right] \Delta I_d \quad (7)$$

$$\Delta P_{CES} = (E_{d0} + \Delta E_d) \Delta I_d \quad (8)$$

### III. DESIGN CES AND PSS BASED ON BA

Bat algorithm is a metaheuristic algorithm inspired by bats behavior. This algorithm was first established in 2010 by Yang [28]. Bats use a type of sonar called echolocation to detect food, avoid obstacles and search for a nest in the dark. With the echolocation abilities, bats are able to fly in the night looking for food without crashing. From this characteristic, the bat algorithm can be developed with the following rules:

- Bats use echolocation to sensor distance and distinguish between food and obstacles even in the darkness.
- Bats fly randomly to search for food at a speed  $v_i$  and at position  $x_i$  with a fixed  $f_i$  frequency, wavelength variation  $\lambda_i$  and noise level ( $A_i$ ).
- It can be assumed the noise level varies from that the maximum ( $A_0$ ) to minimum constant ( $A_{min}$ ).

It is noted that  $d_i$  is the dimension to find the space or renewed space. The new solution and speed are indicated by  $x_i^t$  and  $v_i^t$ . The mathematical representation of bat velocity and position can be described in Eq. (9) [28, 29].

$$\begin{aligned} f_i &= f_{min} + (f_{max} - f_{min})\beta \\ v \frac{t+1}{i} &= v \frac{t}{i} + \left( x \frac{t}{i} - x^* \right) f_i \\ x \frac{t+1}{i} &= x \frac{t}{i} + v \frac{t}{i} \end{aligned} \quad (9)$$

where  $\beta$  is a random vector taken from a uniform distribution. Here  $x^*$  is the optimal location of the whole bat solutions after comparing all the solutions among all bats on each iteration  $t$ . As the result of the multiplication between  $\lambda_i$  and  $f_i$  the velocity of the bats increases.  $\lambda_i$  or  $f_i$  can be used to adjust the velocity change and enhance the other factors depending on the type of the problem that will be solved. In the implementation  $f_{min}=0$  and  $f_{max}=1$  are applied depending on the requirement [28, 29].

Noise level ( $A_i$ ) and the pulse emitted from each bat are always updated according to the iteration process. Noise in bats decreases when bats have found their prey, while pulse pants increase. The noise can be selected according to the exact value, for instance,  $A_0=100$  and  $A_{min}=1$  can be used. To make it easier,  $A_0=1$  and  $A_{min}=0$  are also employed. Assuming  $A_{min}=0$  means that bats have just found their prey and temporarily stopped emitting sound. Hence the mathematical representation can be described in Eq. (10) [28, 29].

$$\begin{aligned} A \frac{t+1}{i} &= \alpha A \frac{t}{i}, \\ r \frac{t}{i} &= r \frac{0}{i} [1 - \exp(-\gamma t)] \end{aligned} \quad (10)$$

where  $\alpha$  and  $\gamma$  are a constant value. For every  $0 < \alpha < 1$  and  $\gamma > 0$ , the mathematical representation can be described in Eq. (11) [28, 29].

$$A_i^t \rightarrow 0, r_i^t \rightarrow r_i^0, t \rightarrow \sim \quad (11)$$

In the simplest problem,  $\alpha=\gamma$  and  $\alpha=\gamma=0.9$ . In this paper, BA is used to optimize the parameter of CES and PSS to mitigate the low-frequency oscillation on the power system. To find the optimal parameter of CES and PSS, comprehensive damping index is used as the objective function of the BA which can be calculated using (12) [30].

$$CDI = \sum_{i=1}^n (1 - \xi_i) \quad (12)$$

## IV. RESULTS AND DISCUSSIONS

Investigation of the impact of CES and the proposed method in low frequency oscillation is reported in this paper. MATLAB/SIMULINK environment is used as the software tools to investigate the case study. The test system that use in this paper is well known two-area power plant. A modification has been made by adding 100 MW CES in generator 1. Furthermore, PSS is installed in generator 3. Fig. 5 shows the schematic diagram of the test system. For identifying the efficiency of optimal coordination of PSS and CES using BA in the system, analyzing the eigenvalue and damping performance of electromechanical (EM) mode are conducted. Finally, to verify the eigenvalue as well as the damping value results, comparison of linear time domain analysis is conducted.

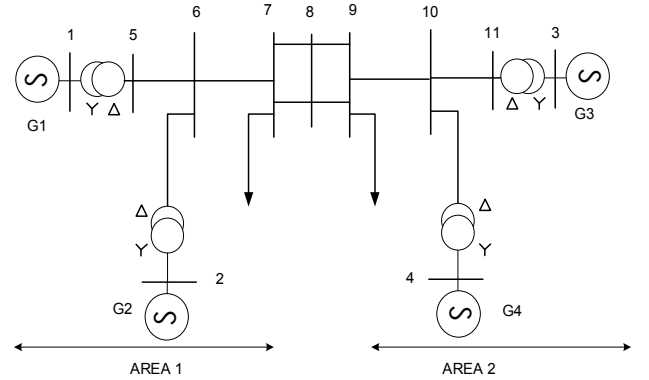


Fig. 5 Test systems.

### A. Case study 1

The comparison of EM mode under different cases is shown in Table 1. It is found that the eigenvalue of inter-area and local mode area-1 are moved towards left-half plane when CES is added in the generator bus 1. This movement is caused by decreasing of generator stress due to the additional active power from CES. It is also monitored that the location of CES has a significant influence in the system dynamic indicated by the movement of local mode area 2 that relatively remain in its position. Furthermore, the proposed method is shown the best eigenvalue performance compared to any other scenario indicated by the more negative eigenvalue.

The damping performance of different scenario is illustrated in Table. 2. It is monitored that by installing PSS in generator-3, the damping ratio of all EM mode are increased gradually. This occurs due to additional signal damping from the PSS to the system. The similar pattern is investigated when CES is installed in the generator-1 bus. The damping of local mode area-1 increases significantly from 4.8% to 36%. Furthermore, the damping of inter-area mode also enhances from 2.6% to 7.7%. However, as mentioned before, that the location of CES has a significant impact to the system. Hence, the damping of local mode area-2 is remained in its position.

The damping performances of all EM modes increase significantly after CES and PSS are installed in the system.

Moreover, the proposed method (coordination between CES and PSS using BA) shows the best performance compared to the other scenarios indicated by the high value of the damping performance. It is also found that the oscillation in local mode area-1 is completely wiped out indicated by the damping value that becomes 100%. This condition takes place due to an optimal coordination between CES and PSS based on BA that can supply large additional signal damping to the system.

Table 1 The comparison of eigenvalue under different cases.

Cases	Local mode 1	Local mode 2	Inter-area
Base case	-0.324+6.77i	-0.342+7.02i	-0.071+2.61i
Considering PSS	-0.324+6.76i	-0.357+7.03i	-0.071+2.61i
Considering CES	-2.67+6.78i	-0.34+7.02i	-0.21+2.67i
Considering CES PSS	-2.63+6.82i	-2.23+9.80i	-0.390+2.96i
Proposed method	-3.7263	-8.26+11i	-0.42+3.41i

Table 2 The comparison of EM mode damping under different cases.

Cases	Local mode 1	Local mode 2	Inter-area
Base case	4.8	4.85	2.6
Considering PSS	4.8	4.88	2.59
Considering CES	36.65	4.85	7.77
Considering CES PSS	36	22.17	13.09
Proposed method	100	59.97	12.25

To verify the eigenvalue analysis, time domain analysis is carried out. To excite the dynamic response of the system, small perturbation is made in the system. Figs. 7 shows the time domain response of rotor speed for generator. Table 3 illustrates the detailed overshoot and settling time comparison of different scenarios. A blue line represents the oscillatory condition of base case system (generic two-area power system) while green line is for the dynamic response of the rotor speed equipped with PSS. The yellow line represents the rotor speed dynamic performance due to small perturbation with CES, while the red line is for the oscillatory condition of the rotor speed with CES and PSS. Furthermore, a system with proposed method is presented with black lines. It is monitored that the best oscillatory condition compared to the others scenario is a system with the proposed method. This time domain simulation also verifies the eigenvalue analysis and damping value analysis by showing that the best performance compared to other scenarios is obtained when the proposed method is applied in the system.

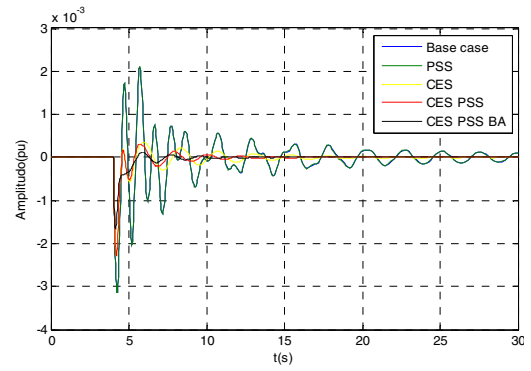


Fig. 7 The time domain response of rotor speed G1.

Table 3 Detailed time domain response of rotor speed G1.

Cases	Overshoot (pu)	Settling time (s)
Base case	-0.003136	>30
With PSS	-0.03134	>30
With CES	-0.02283	16.03
CES PSS	-0.001981	11.74
Proposed method	-0.001658	8.26

### B. Case study 2

In the second case study, comparison of damping performance of the proposed method with other algorithm. In this paper imperialist competitive algorithm (ICA) is used to tune the CES and PSS parameter. Fig 8 illustrates the damping comparison of EM mode between the proposed method and CES and PSS based on ICA.

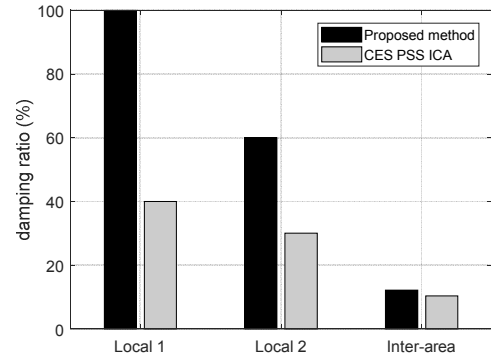


Fig. 8 Damping comparison.

It is noticeable that the proposed method (using BA) provide a better damping ratio compared to CES and PSS based on ICA indicated by higher percentage of the damping.

## V. CONCLUSIONS

This paper investigates the significant impact of installing CES on the small signal stability performance of two-area power system. A method to mitigate the low-frequency oscillation by employing coordinated control between CES and PSS based on BA is proposed. From the simulation results, it is observed that the damping of the system increases when PSS is

utilized in the system. It is monitored that CES enhances the damping performance of the system by injecting additional active power to the grid and the location of CES plays an important role in the system dynamic. By adding PSS and CES to the system, the stability of the power system increases significantly indicated by increasing damping performance of EM mode. The damping performance of EM mode increases from 4.8% to 100 % for local mode area 1, 4.9% to 59.9 for local mode area 2, and 2.6% to 12.3% for inter-area. The reliability of the power system also augments indicated by the time domain results of generator 1 and 4. Furthermore, the proposed method is able to damp the low-frequency oscillation significantly. Further research needs to be conducted by considering high penetrations of renewable energy sources (RESs) such as large-scale wind power system or large-scale PV generation. Installing another PSS such as dual input PSS, and multi-band PSS may be considered to handle low-frequency oscillation from different sources. Another optimization method such as whale algorithm, artificial immune system clonal selection and firefly algorithm can be used for designing a coordinated control between PSS and CES.

#### REFERENCES

- [1] H. Setiadi, A. U. Krismanto, and N. Mithulanathan, "Enabling BES in Large PV Plant for Stability Enhancement on Power Systems with High RES," in *IEEE Innovative Smart Grid Technologies-Asia (ISGT-Asia)*, 2017.
- [2] H. Setiadi, A. U. Krismanto, N. Mithulanathan, and M. Hossain, "Modal interaction of power systems with high penetration of renewable energy and BES systems," *International Journal of Electrical Power & Energy Systems*, vol. 97, pp. 385-395, 2018.
- [3] R. S. Wijanarko, H. Setiadi, and T. A. Nugroho, "Coordination of SPS and CES to Mitigate Oscillatory Condition on Power Systems," *TELKOMNIKA (Telecommunication Computing Electronics and Control)*, vol. 15, no. 4, 2017.
- [4] G. Rogers, *Power system oscillations*. Springer Science & Business Media, 2012.
- [5] entsoe, "Analysis of CE Inter-Area Oscillations of 1st December 2016," European Network of Transmission System Operators for Electricity, 2017.
- [6] N. Mithulanathan, C. A. Canizares, J. Reeve, and G. J. Rogers, "Comparison of PSS, SVC, and STATCOM controllers for damping power system oscillations," *IEEE Transactions on Power Systems*, vol. 18, no. 2, pp. 786-792, 2003.
- [7] D. Lastomo, Atmiasri, and H. Setiadi, "Stability Enhancement of Hybrid Power System using RFB based on Craziness PSO," in *3rd International Conference on Science in Information Technology (ICSITech)*, 2017.
- [8] D. Lastomo, H. Setiadi, and M. R. Djalal, "Optimization of SMES and TCSC using particle swarm optimization for oscillation mitigation in a multi machines power system," *Journal of Mechatronics, Electrical Power, and Vehicular Technology*, vol. 8, no. 1, pp. 11-21, 2017.
- [9] D. Lastomo *et al.*, "The effects of energy storages on small signal stability of a power system," in *International Seminar on Intelligent Technology and Its Applications (ISITIA)*, 2017.
- [10] H. Setiadi, A. U. Krismanto, and N. Mithulanathan, "Influence of BES system on local and inter-area oscillation of power system with high penetration of PV plants," in *International Conference on Applied System Innovation (ICASI)*, 2017.
- [11] M. Taufik, D. Lastomo, and H. Setiadi, "Small-disturbance angle stability enhancement using intelligent redox flow batteries," in *4th International Conference on Electrical Engineering, Computer Science and Informatics (EECSI)*, 2017.
- [12] H. Setiadi, N. Mithulanathan, A. U. Krismanto, and R. Shah, "Comparison of Battery Energy Storage Model for Small Signal Stability in Power Systems," in *IEEE 27th International Symposium on Industrial Electronics (ISIE)*, 2018.
- [13] M. R. Djalal, H. Setiadi, D. Lastomo, and M. Y. Yunus, "Modal Analysis and Stability Enhancement of 150 kV Sulselrabar Electrical System using PSS and RFB based on Cuckoo Search Algorithm," *International Journal on Electrical Engineering and Informatics*, vol. 9, no. 4, pp. 800-812, 2017.
- [14] M. Abdilllah, H. Setiadi, A. B. Reihara, K. Mahmoud, I. W. Farid, and A. Soeprijanto, "Optimal selection of LQR parameter using AIS for LFC in a multi-area power system," *Journal of Mechatronics, Electrical Power, and Vehicular Technology*, vol. 7, no. 2, pp. 93-104, 2016.
- [15] H. Setiadi and K. O. Jones, "Power System Design using Firefly Algorithm for Dynamic Stability Enhancement," *Indonesian Journal of Electrical Engineering and Computer Science*, vol. 1, no. 3, pp. 446-455, 2016.
- [16] N. C. Damasceno and O. Gabriel Filho, "PI controller optimization for a heat exchanger through metaheuristic Bat Algorithm, Particle Swarm Optimization, Flower Pollination Algorithm and Cuckoo Search Algorithm," *IEEE Latin America Transactions*, vol. 15, no. 9, pp. 1801-1807, 2017.
- [17] D. Lastomo, Widodo, H. Setiadi, and M. R. Djalal, "Enabling PID and SSSC for load frequency control using Particle Swarm Optimization," in *3rd International Conference on Science in Information Technology (ICSITech)*, 2017.
- [18] H. Setiadi, N. Mithulanathan, and M. J. Hossain, "Impact of battery energy storage systems on electromechanical oscillations in power systems," in *IEEE Power & Energy Society General Meeting*, 2017.
- [19] M. Ulum, H. Setiadi, and D. Lastomo, "Design Controller Blade Pitch Angle Wind Turbine Using Hybrid Differential Evolution Algorithm-Particle Swarm Optimization," *Advanced Science Letters*, vol. 23, no. 12, pp. 12396-12399, 2017.
- [20] M. R. Djalal, M. Yunus, A. Imran, and H. Setiadi, "Capacitive Energy Storage (CES) Optimization For Load Frequency Control in Micro Hydro Power Plant Using Imperialist Competitive Algorithm (ICA)," *EMITTER International Journal of Engineering Technology*, vol. 5, no. 2, pp. 279-297, 2018.
- [21] H. Setiadi, N. Mithulanathan, A. U. Krismanto, and R. Shah, "Low-Frequency Oscillatory Stability Study on 500 kV Java-Indonesian Electric Grid," in *IEEE 27th International Symposium on Industrial Electronics (ISIE)*, 2018.
- [22] M. R. Djalal, H. Setiadi, and A. Imran, "Frequency stability improvement of micro hydro power system using hybrid SMES and CES based on Cuckoo search algorithm," *Journal of Mechatronics, Electrical Power, and Vehicular Technology*, vol. 8, no. 2, pp. 76-84, 2017.
- [23] P. M. Anderson and A. A. Fouad, *Power system control and stability*. John Wiley & Sons, 2008.
- [24] P. Mitra, S. Chowdhury, S. Chowdhury, S. Pal, and P. Crossley, "Intelligent AVR and PSS with Adaptive hybrid learning algorithm," in *Power and Energy Society General Meeting*, 2008.
- [25] P. Kundur, N. J. Balu, and M. G. Lauby, *Power system stability and control*. McGraw-hill New York, 1994.
- [26] V. Mukherjee and S. Ghoshal, "Application of capacitive energy storage for transient performance improvement of power system," *Electric power systems research*, vol. 79, no. 2, pp. 282-294, 2009.
- [27] P. Bhatt, R. Roy, and S. Ghoshal, "GA/particle swarm intelligence based optimization of two specific varieties of controller devices applied to two-area multi-units automatic generation control," *International journal of electrical power & energy systems*, vol. 32, no. 4, pp. 299-310, 2010.
- [28] X.-S. Yang, *Nature-inspired metaheuristic algorithms*. Luniver press, 2010.
- [29] D. Sambariya and R. Prasad, "Robust tuning of power system stabilizer for small signal stability enhancement using metaheuristic bat algorithm," *International Journal of Electrical Power & Energy Systems*, vol. 61, pp. 229-238, 2014.
- [30] A. El-Zonkoly, A. Khalil, and N. Ahmied, "Optimal tuning of lead-lag and fuzzy logic power system stabilizers using particle swarm optimization," *Expert Systems with Applications*, vol. 36, no. 2, pp. 2097-2106, 2009.

# Computer Aided Model for an Off-grid Photovoltaic System Using Batteries Only

Emil Lazarescu  
POLITEHNICA University of  
Timisoara  
Powers Systems Department  
Timisoara, Romania  
emil\_lazarescu@yahoo.ro

Mihaela Frigura-Iliasa  
POLITEHNICA University of  
Timisoara  
Powers Systems Department  
Timisoara, Romania  
mihaela.frigura@gmail.com

Flaviu M. Frigura-Iliasa  
National Institute for Research and  
Development in Electrochemistry and  
Condensed Matter - LERF  
Timisoara, Romania  
flaviu.frigura@upt.ro

Lia Dolga  
POLITEHNICA University of  
Timisoara  
Mechatronics Department  
Timisoara, Romania  
lia.dolga@upt.ro

Marius Mirica  
National Institute for Research and  
Development in Electrochemistry and  
Condensed Matter - LERF  
Timisoara, Romania  
miricamc@yahoo.com

Hannelore E. Filipescu  
POLITEHNICA University of  
Timisoara  
Mechatronics Department  
Timisoara, Romania  
hannelore.filipescu@upt.ro

**Abstract**— This article will present an off-grid photovoltaic energy system based on a photovoltaic element (PV), or a group of PVs, integrated in a solar battery (SB), directly connected to an electrical battery (EB) having no DC-DC adapter (use of adapters is the most common solution existing now on in this domain). This SB must be properly adjusted to the EB, not only as voltage, but it must provide also the same amount of energy as the system when operating at its classically detected maximum power operating point. This proposed technical solution is more economically justified, compared to the classic one: SB+DC-DC+EB, due to the simple fact that the DC-DC converter is no longer required at all. A simple mathematical model for the current-voltage characteristics is also presented, followed by a comparison between the classic DC-DC converter-based solution and the newly proposed one, without DC-DC converter.

**Keywords**— CAD Model Electric Battery, Maximum Power Point, Solar Battery

## I. INTRODUCTION

Nowadays, all renewable energy sources have gathered more and more importance worldwide. The PV systems are representing a very important and dynamic category from the renewable electric energy generation point of view [1], [2], [3], despite their price and complexity, of course, mostly in countries having many sunny days. But PV systems must operate in many other environments, too.

Within the literature, there are several approaches dealing with solar-electric energy conversions [3], [4], [5], [6]. All these approaches are sustained by the fact that the PV system intends to operate at maximum power operating points [7], [8]. A DC-DC converter is necessary to be installed between the solar battery (SB) and electric battery (EB), to achieve this goal. Thus, the system becomes expensive and, generally, not economically feasible.

By varying the terminal SB equivalent load resistance, it is investigating the operation possibility in the maximum power operating point neighbourhood. However, not knowing this point an operation below the maximum power is achieved [9], [10].

All the equivalent resistance load variation methods are implying high costs, complex electronic equipment meaning DC-DC converters [11]. Thus, in case of several applications these investments are totally unprofitable.

The power provided by the Sun is continuously changing even during daytime, and the system SB+DC-DC+EB (shown in Fig. 1) has to be continuously controlled in such a manner that assures the maximum power operating point.

Cheap and efficient equipment must be realized (as presented in the current paper) in order to reduce the PV systems' costs [2].

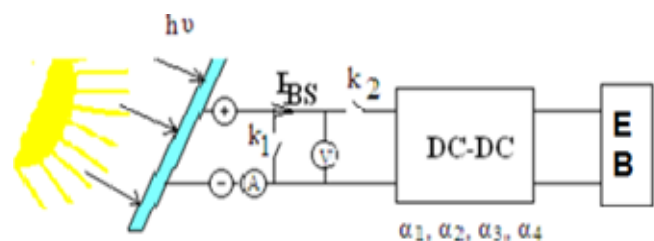


Fig. 1. The complete SB+DC-DC+EB classic solution

By voltage-current characteristics mathematical modelling, SB+EB system operation efficiency estimation is proposed (achieved through computing the obtained energy).

The maximum power operating point  $P_{max}$  coordinates ( $U_{OPTIM}$ ,  $I_{OPTIM}$ ) are changing in time, depending on the environment conditions (solar radiation intensity). Thus, the module terminal equivalent load has to be correlated with the solar radiation intensity [11], [12].

Measuring the solar radiant power  $P_s$  the fundamental quantities characterizing the SB operation in maximum power operating points are able to be determined:

- optimal load resistance  $R_{OPTIM}$  using SB mathematical model or using the simplified version by the ratio between the idle and short-circuit voltages (Fig. 2) [4];
- useful maximum available electric power  $P_{OPTIM}$ ;
- $I_{OPTIM}$  current and  $U_{OPTIM}$  voltage corresponding to the maximum power operating point.

The determination of coordinates for the Maximum power operating point  $P_{OPTIM}$  (Fig. 2) is based on SB (or PV module) external characteristics  $U = f(I)$  that are changing based on atmospheric nebulosity.

These characteristics are valid for regular 44-48 V panels available on the market.

This principle insures optimal operation of the PV system in all weather conditions.

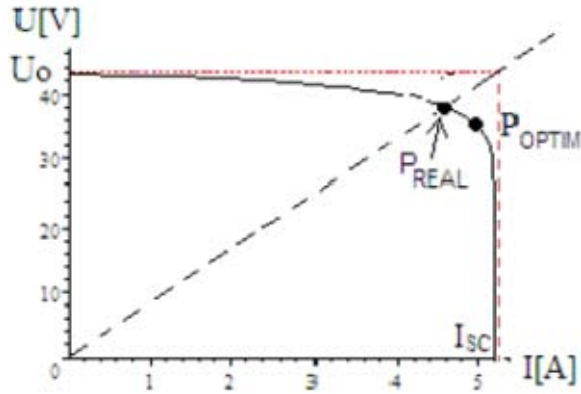


Fig. 2. External characteristics  $U = f(I)$  for a standard PV panel

In the following part of our paper, the difference between the SB obtained energy directly generating on the EB and the available maximum one is computed. Thus, the SB external characteristics  $U(I)$  are mathematically modelled.

## II. MATHEMATICAL MODEL OF THE EXTERNAL PV PANNEL CHARACTERISTICS

The proposed mathematical model for the external characteristics  $U = f(I)$  has the following form:

$$U(I) = (d - T \cdot f) \cdot \left( \cos \left( \frac{a \cdot I - g \cdot T}{P_s^b} \right) \right)^c \quad (1)$$

where:  $a$ ,  $b$ ,  $c$ ,  $d$  and  $g$  – designing constants computed based on the experimental external characteristics [7];  $P_s$  – solar radiant power;  $I$  – generated current. The determination of the maximum power operating point coordinates is performed by cancelling the power  $P = U \cdot I$  derivative:

$$U_{OPTIM} = (d - T \cdot f) \cdot \left( \cos \left( \frac{a \cdot I_{OPTIM} - g \cdot T}{P_s^b} \right) \right)^c \quad (2)$$

and:

$$P_{OPTIM} = U_{OPTIM} \cdot I_{OPTIM} \quad (3)$$

The resulted family of voltage-current characteristics offers us the possibilities for continuous service of that panel for a certain voltage and for a certain current.

Considering the  $T = 273 + 25$  K absolute temperature, the SB external characteristics at 25 degrees Celsius are described by the following functions [4]:

$$U(I) = 41 \cdot \left( \cos \left( \frac{3.14}{8} \cdot I \cdot \frac{883}{P_s} \right) \right)^{0.15} \quad (4)$$

where  $P_s$  – is a certain radiant power (taken as a variable parameter, as presented in Fig. 3).

It is normal that, as well as the solar radiant power is increasing, the converted power also increases, and, for a certain voltage, the panel can provide a higher current, due to a higher converted power (depending on the hour on the day and on meteorological and environmental conditions).

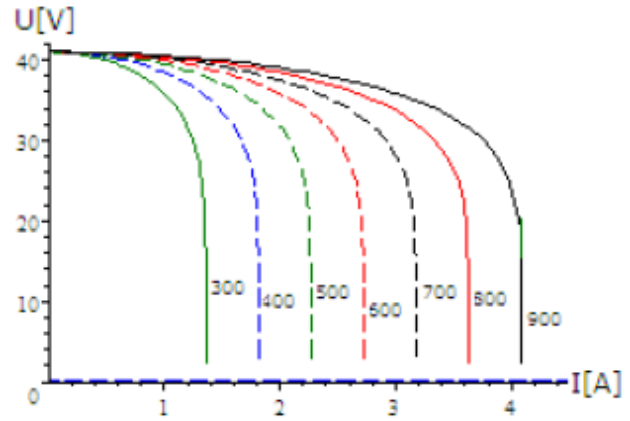


Fig. 3. External characteristics having radiant power as parameter

The main goal of this paper is to determine the maximum power point and to adjust directly the panel parameters, in order to function in these conditions.

## III. MAXIMUM POWER OPERATING POINTS FOR A CLASSIC SYSTEM WITH DC-DC CONVERTORS

The use of a DC-DC converter is requested to operate within the maximum power operating points. It is situated between the SB and the EB. The maximum power operating point coordinates  $(U_{OPTIM}, I_{OPTIM})$  are determined cancelling the derivative [4]:

$$\frac{dP}{dI} = \frac{d}{dI} \left( 41 \cdot \left( \cos \left( \frac{3.14}{8} \cdot I \cdot \frac{883}{P_s} \right) \right)^{0.15} \cdot I \right) \quad (5)$$

This classic structure is shown in Fig.4., which is identical with Fig.1., but with no measuring devices on service.

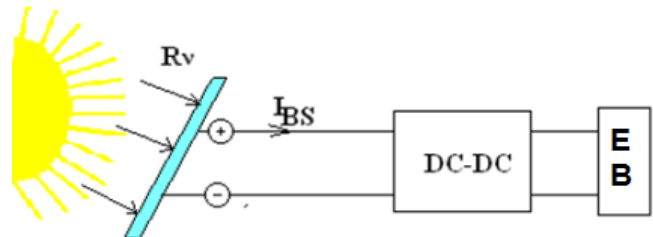




Fig. 4. The simple SB+DC-DC+EB classic solution.

This is the worldwide most common solution for solar energy conversion, tracking, at each moment, the maximum power operating point.

In equations (6) and (7) we will present the computational method for obtaining the optimal charging power. Battery supplying voltage could be easily modified.

For a radiant power  $P_I = 900W$ , we will obtain:

$$\begin{aligned} \frac{dP}{dI} &= \frac{d}{dI} \left( 41 \cdot \left( \cos \left( \frac{3.14}{8} \cdot I \cdot \frac{883}{P_S} \right) \right)^{0.15} \cdot I \right) = \\ &= -1.0 \cdot 10^{-9} \cdot \frac{2.3683 \cdot 10^9 \cdot I \cdot \sin(0.38509 \cdot I) - 4.1 \cdot 10^{10} \cdot \cos(0.38509 \cdot I)}{\cos^{20} 0.38509 \cdot I} = 0 \end{aligned} \quad (6)$$

It provides an optimal current  $I = 3.5533 A$ .

From the next group equations, we will obtain:

$$U = 41 \cdot \left( \cos \left( \frac{3.14}{8} \cdot 3.5533 \cdot \frac{883}{P_S} \right) \right)^{0.15} = 32.232 V \quad (7)$$

In case of the maximum radiant power (for 1 h/day):

For  $P_I = 900 W$  we will obtain:  $P = 114.52 W$ ;

We will consider each effective solar power hour having an average radiant power decreasing with 100 W, applied for  $t_i = 1 \text{ hour}$  (9 effective radiant hours).

- for  $P_2 = 800 W$  it yields:  $P = 101.8 W$ ;
- for  $P_3 = 700 W$  it yields:  $P = 89.080 W$ ;
- for  $P_4 = 600 W$  it yields:  $P = 76.354 W$ ;
- for  $P_5 = 500 W$  it yields:  $P = 63.629 W$ ;
- for  $P_6 = 400 W$  it yields:  $P = 50.902 W$ ;
- for  $P_7 = 300 W$  it yields:  $P = 38.177 W$ ;
- for  $P_8 = 200 W$  it yields:  $P = 25.452 W$ ;
- for  $P_9 = 100 W$  it yields:  $P = 12.726 W$ .

Daily total energy has the following value:

$$W = \Sigma (P_i \cdot t_i) = 3.4587 MJ = 0.96 kWh \quad (8)$$

This is an estimation of the total energy provided by a single panel during an average sunny day with 9 effective radiant hours, when the DC-DC converter is tracking the maximum power point.

#### IV. MAXIMUM POWER OPERATING POINTS FOR A SOLAR BATTERY GENERATING DIRECTLY OVER AN ELECTRIC BATTERY

In some cases, the solar energy storage is performed directly within electric batteries (EB) (SB over EB, as presented in Fig. 5).

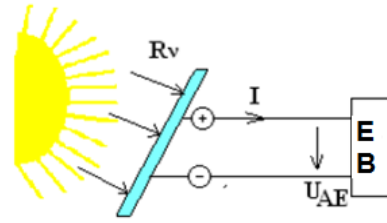


Fig. 5. Solar Battery (SB) over Electric Battery (EB)

For example, the EB voltage could be multiple of ordinary 12 V batteries:  $U_{AE} = k \cdot 12 V$ . In this case the system operation is far from the maximum power operating points, as described in Fig. 6.

The values for  $P_I$  (minimum radiant power) and  $P_2$  (maximum radiant power) operating points are obtained at the intersection between the SB external characteristics  $U = f(I)$  with the ones of the EB voltage  $U = U_{EB} + r \cdot I$ , where  $r$  – EB circuit resistance,  $U_{EB}$  – EB terminal voltage.

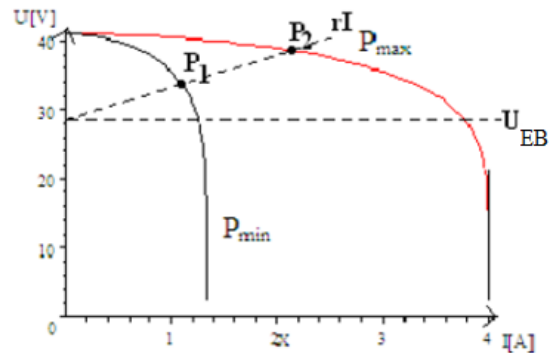


Fig. 6. Operating points of the SB+EB system

Electric battery idle voltage ( $U_{EB}$ ) determination is another important step when using this new system.

The electric batteries' cells have the idle voltage around 2 V. Voltage corresponding to the maximum power operating points for  $P_S = 900 W$  is  $U_{OPTIM} = 32.232 V$ . Thus,  $32 / 2 = 16$  cells are selected for the EB. In case of  $U_{EB} = 32 V$  and EB internal resistance  $r = 0.1 \Omega$ , the same results are obtained as for the maximum power operating point.

The equivalent electric schema is presented in Fig. 7.

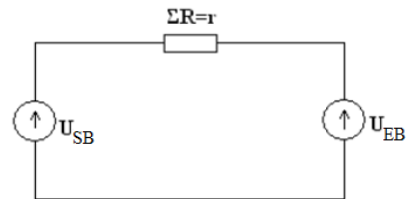


Fig. 7. Electric schema of the SB+EB system

The values for  $P_I$  (minimum radiant power) and  $P_2$  (maximum radiant power) operating points are obtained based on the SB external characteristics  $U(I)$ , is the considered voltage response,  $U = U_{EB} + r \cdot I = 32 + 0.1 \cdot i$ , as presented below:

- for  $P_I = 900 W$  it yields:  $P = 112.11 W$ ;
- for  $P_2 = 800 W$  it yields:  $P = 101.8 W$ ;

- for  $P_1 = 700\text{ W}$  it yields:  $P = 89.079\text{ W}$ ;
- for  $P_3 = 600\text{ W}$  it yields:  $P = 76.353\text{ W}$ ;
- for  $P_4 = 500\text{ W}$  it yields:  $P = 63.628\text{ W}$ ;
- for  $P_5 = 400\text{ W}$  it yields:  $P = 50.901\text{ W}$ ;
- for  $P_6 = 300\text{ W}$  it yields:  $P = 38.175\text{ W}$ ;
- for  $P_7 = 200\text{ W}$  it yields:  $P = 25.449\text{ W}$ ;
- for  $P_8 = 100\text{ W}$  it yields:  $P = 12.724\text{ W}$ .

Daily total energy has the following value:

$$W = \sum (P_i \cdot t_i) = 3.4239\text{ MJ} = 0.95\text{ kWh} \quad (9)$$

The energy difference between these cases is:

$$\Delta W = 3.4587 \cdot 10^6 - 3.4239 \cdot 10^6 = 34800\text{ J} \quad (10)$$

It represents around 1 %, thus a small difference, practically negligible for the common applications, especially if the DC-DC converter efficiency is considered, when introduced, it certainly could overpass the 1 % obtained here for the SB-EB only.

## V. CONCLUSIONS

In this article, a solar battery generating energy over an electrical battery has been analysed in comparison with its operation at maximum power operating point.

The system SB+EB is more economically than the SB+DC-DC+EB system due to its simplicity. We analysed the differences between the amount of energy stored within the EB, for the two cases (having or not a DC-DC convertor), for a standard daylight of 9 radiant hours.

After all calculations, we notice that the difference between these amounts of energies is less than 1 %. It has been demonstrated that the DC-DC converter may be avoided. Thus, a cheaper conversion system has been obtained, operating at increased efficiency conditions.

This study will continue by taking in consideration other radiant power values, different than the average one.

## REFERENCES

- [1] Abbes D., Martinez A., Champenois G., Gaubert J.P., Kadri R., "Estimation of wind turbine and solar photovoltaic energy using variant sampling intervals", 978-1-4244-7855-2/10 ©2010 IEEE, pp. T 12-28-T 12-34.
- [2] Chenni R. et al, "A detailed modeling method for photovoltaic cells", Energy, V32, pp. 1724-1730, 2007.
- [3] DenHerder T., "Design and simulation of photovoltaic super system using Simulink", California Polytechnic State University, 2006.
- [4] Gana O., Prostean O., Vasar C., Babescu M., "Modeling and optimized control of photovoltaic energy conversion systems", Proceedings of the International Conference SACI Timisoara, Romania, 2012.
- [5] Ketjoy N., "Photovoltaic hybrid systems for rural electrification in the mekong countries", University of Kassel, August 2005.
- [6] Petcut F.M., "PV systems mathematical models. Applications within the automatic control systems," PhD Thesis, "Politehnica" University of Timisoara, 2012.
- [7] Posedly P., "Modeling and analysis of photovoltaic generation and storage systems for residential use", Division of Research and Advanced Studies of the University of Cincinnati, 2006.
- [8] Oi A., "Design and simulation of photovoltaic water pumping system", California Polytechnic State University, September 2005.
- [9] Oozeki T., Otani K., Kurokawa K., "An evaluation method for PV system to identify system losses by means of utilizing monitoring data", Proceedings of the IEEE 4th World Conference on Photovoltaic Energy Conversion, Hawaii, vol. 2, pp. 2319-2322, 2006.
- [10] Simons G., Sethi P., Davis R., DeGroat K., Comwell D., Jenkins B., "The Role of Renewable Distributed Generation in California's Electricity System", IEEE PES Summer Meeting, Vol. 1, pp. 546-547, July 2001.
- [11] Sukumar Kamalasadan Khalid Al-Olimat, "Modeling and control of a micro-grid set up using photovoltaic arrays", Department of Engineering and Computer Technology, The University of West Florida, Pensacola, 2013.
- [12] Teodorescu R., Rik W. De Doncker, Marco Liserre, Pedro Rodriguez, "Grid converters for PV and WT systems", Aalborg University, Institute of Energy Technology, 2011.

# Computer Aided Model for a Low Voltage Varistor with Increased Thermal Stability

Adrian F. Olariu  
POLITEHNICA University of  
Timisoara  
Powers Systems Department  
Timisoara, Romania  
adrian.olariu@upt.ro

Flaviu M. Frigura-Iliasa  
National Institute for Research and  
Development in Electrochemistry and  
Condensed Matter - LERF  
Timisoara, Romania  
flaviu.frigura@upt.ro

Florin I. Balcu  
National Institute for Research and  
Development in Electrochemistry and  
Condensed Matter - LERF  
Timisoara, Romania  
ionel\_balcu@yahoo.com

Mihaela Frigura-Iliasa  
POLITEHNICA University of  
Timisoara  
Powers Systems Department  
Timisoara, Romania  
mihaela.frigura@gmail.com

Lia Dolga  
POLITEHNICA University of  
Timisoara  
Mechatronics Department  
Timisoara, Romania  
lia.dolga@upt.ro

Hannelore E. Filipescu  
POLITEHNICA University of  
Timisoara  
Mechatronics Department  
Timisoara, Romania  
hannelore.filipescu@upt.ro

**Abstract**— Metal Oxide Varistors are a very common power electronic device, applied for efficient overvoltage protection at any voltage level. This piece of equipment has a high non-linear current response function of the applied voltage, and, it provides a relatively high heat absorption capacity in case of accidental overvoltage pulse (shock)s. The crossing response current is clearly activated by temperature of that device, and, by consequent, overheating could be disastrous. Actual researches must be carried out both for a new more performant material as well as for new technical solutions for the design of all equipment integrating them, by studying heat extraction and heat transfer inside a new complex varistor device. Our article proposes a totally new device, used basically for low voltage applications, having a supplementary metal mass added to the body of that varistor, shaped as small disk. It actions like a heat pump immediately after the voltage pulse (shock) and as additional radiators at the end of the heating process caused by a transitory overvoltage. A CAD solution combined with a finite element model, followed by some experimental results are also presented, for confirming the performance of that newly design. By placing additional metal alloy masses inside a new varistor structure it will have a higher heat pumping and dissipation capability, in order to reduce temperature stress and all aging effects.

**Keywords**— CAD Model, Low Voltage Varistor, Increased Thermal Stability

## I. INTRODUCTION

Nowadays, Metal Oxide Varistors are often used for overvoltage protection equipment on a large industrial scale. All low voltage sensitive electronic devices are totally exposed to a lot of overvoltage aggressions, caused mostly by lightning (as transitory overvoltage) or caused by internal power network faults (as permanent overvoltage) [1].

The Metal Oxide Varistors are made of a mixture of semiconductor ceramic materials, most of them oxides. The relation between their crossing current and their applied voltage is essentially non-linear and their response time is extremely short, faster than the dielectric breakdown caused by the residual lightning voltage stroke on the sensitive and protected equipment. They have also a relatively high level of energy absorption capacity, but, having a risk of overheating for long time, due to their current which is highly influenced by temperature. Controlling their temperature is crucial for maintaining them in long service.

The current crossing throughout a varistor is highly depending on temperature, as for all semiconductor materials. In case of consecutives lightning strokes applied to the power grid, or in case of a longtime overvoltage, we noticed also an increased risk of overheating for the varistor itself [2].

When temperature increases (also due to environmental causes), the current increases too, due to electrical resistance reduction. An avalanche reaction could possibly appear in this case, with fatal and expensive consequences both for the protection as well as for the protected fragile piece of electronic or electric equipment [3].

Heat quantity produced inside the mass of that varistor is important in any case, and, by consequent, the design of an adequate technical solution, in order to control heat dissipation or evacuation, is mandatory for any varistors involved, at all voltage levels.

There are many practical and simple technical solutions applied mostly to increase the energy absorption capability (capacity) in case of a temporary lightning pulse (shock) (radiators, coating, etc.), not all of them being so effective. Today there is no analytical model which could describe a complex overvoltage incident, both from the electrical as well as the thermal point of view. Only the experimental procedures are suitable for this task [4].

This article describes only models and measurements made in case of the permanent overvoltage service. This permanent (long term) overvoltage service is not completely described in today's literature. In this situation, the varistor is exposed to a longtime accidentally occurring overvoltage, not so high, but enough destructive for the sensitive protected equipment. Heat (heat power, per time unit) produced inside the varistor (only by Joule effect) is provided by:

$$P_{dez} = U \cdot I = U \cdot A(U) \cdot T^2 \cdot e^{-\frac{q_e \cdot \Phi(U)}{kT}} \quad (1)$$

Heat (heat power, per time unit) evacuated by convection and radiation to the environment is provided by [6]:

$$P_{dis} = \alpha \cdot S_t \cdot (\theta - \theta_a) \quad (2)$$

where:

- $I$  – crossing current;
- $U$  – applied voltage;
- $S_l$  – complete external heat exchange surface;
- $\Phi(U)$  – voltage height of semiconductor's junction potential barrier;
- $\theta$  – varistor's own temperature;
- $\theta_a$  – environmental temperature;
- $T$  – absolute temperature, on Kelvin scale;
- $k$  – Boltzmann's constant;
- $A(U)$  – a parametric function depending on voltage and electric field intensity;
- $q_e$  – electric charge of an electron;
- $\alpha$  – the combined convective and radiative heat exchange coefficient;

There is a typical intersection of these two graphs ( $P_{dis}$  and  $P_{dez}$ ) given by (1) and (2), providing two equilibrium points. The situation in which these two graphs do not intersect each other at all is the situation of a permanent fatal overheating regime (when heat produced inside the varistor is too high to be evacuated in the environment) [5].

Thermal stability (and energy adsorption), for a specified varistor, was analyzed only by taking in consideration the temperature of that varistor as the main perturbation, as a direct consequence of the overvoltage exposure [6].

## II. ADDITIONAL METAL MASS PRINCIPLE

As previously explained, the most important issue concerning heat absorption capacity is to maintain the varistor inside the so-called “thermal stability” envelope, by carefully limiting its service temperature [7].

The high voltage exposure of a certain varistor also to a high energy pulse (shock) wave is caused by a short-time overvoltage, (process considered as adiabatic, due to its extremely short time). It means that the whole energy  $Q=W$ , produced by Joule effect remains stored inside its own mass, causing an important increase of its natural temperature  $\Delta\theta_1$ . It's necessary that this temperature increase to not over-pass the temperature stability equilibrium limit, so all heat produced inside the varistor could be dissipated in the environment [8].

The equation of for the varistor temperature increase  $\Delta\theta_1$  due to the  $Q$  heat stored inside, is:

$$W = Q = m_v \cdot c_v \cdot \Delta\theta_1 \quad (3)$$

In practice, after a brief adiabatic process, the whole heat produced inside that varistor by Joule effect,  $Q$ , is stored and kept inside the varistor mass  $m_v$ , having the  $c_v$  specific mass heat. Heat quantity  $Q$  is given by the overvoltage specificity, so it could not be changed, and  $c_v$  is a specific material parameter, which could be slightly increased for higher heat absorption, but with drastic consequences, mostly for the electrical properties of that material. It is considered as a specific constant for a certain varistor type/ material [9].

An efficient and original technical solution (patented in Romania, by the authors), which is strongly recommended for thermal stability control of a certain varistor, consists in attaching some additional masses (made of a conductor material, metal or metal alloy) on the varistor itself. These additional metal based masses must have an excellent thermal and electrical contact with the varistor. The main principle of this idea is briefly synthesized in Fig. 1.

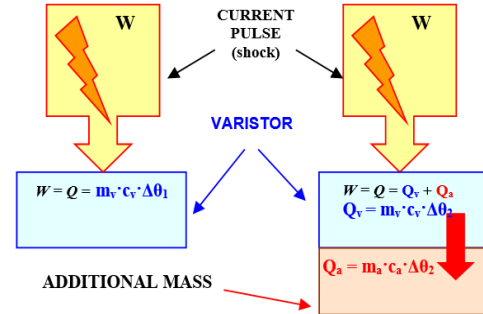


Fig. 1. The additional metal mass principle

The solution of this additional metal mass consists essentially in dividing the heat quantity produced by Joule effect inside the active part of the varistor,  $Q=W$ , in two different fractions. One of these fractions, called in this paper as  $Q_v$  ( $Q_v = m_v \cdot c_v \cdot \Delta\theta_1$ ), remains stored inside the varistor, and the other fraction, called  $Q_a$  ( $Q_a = m_a \cdot c_a \cdot \Delta\theta_2$ ) is naturally sent to and stored inside the additional mass which is well thermo-coupled with the varistor. Of course,  $m_a$  is the additional metal mass and  $c_a$  is its own specific mass heat. In this situation, the corresponding relation is:

$$W = Q = Q_v + Q_a = (m_v \cdot c_v + m_a \cdot c_a) \cdot \Delta\theta_2 \quad (4)$$

Equation (4) is valid and correct because:

- The electrical resistance of that additional mass is nine times smaller than the smallest varistor resistance obtained for the best conduction mode, and, by consequent, the additional mass is a passive conductor, which is not modifying any electric property of the assembly. The heat produced by Joule effect inside this additional mass is totally negligible, and, by consequent, the varistor is considered the only heat source.
- The thermal link between the varistor and the metal additional mass (in our tests is brass) is very well welded, so heat is changed very fast and uniform between those two structural different pieces. By consequent, both pieces involved will have the same temperature increment,  $\Delta\theta_2$ .
- This thermal conduction process is considered as fully adiabatic, very rapid, and we can correctly apply the energy conservation principle [10].
- It is obvious that the newly obtain temperature increase  $\Delta\theta_2$  is smaller then previous  $\Delta\theta_1$ , as given by (4). This simple additional mass is acting, in fact, like a quick and passive “heat pump”, extracting instantaneously a part of the excessive heat stored inside the varistor itself and, by this effect, decreasing its temperature and placing the whole assembly inside a possible thermal stability area.

It is mandatory also to explain that, because of the shape and geometry of these supplementary masses, the whole heat dissipation surface is increasing (not as much as in the case of large dedicated radiators). During the permanent service regime, these additional metal masses could be assimilated as radiators (which is not their main role), having a reduced contribution to the heat dissipation balance. By taking in consideration all these ideas, we can reduce, with a few degrees Celsius, the whole varistors' temperature. But, having a relatively small additional heat dissipation surface, we cannot consider them as dedicated true radiators.

### III. COMPUTER BASED MODEL FOR THERMAL STABILITY ASSESSMENT

The main advantages of placing additional metal masses welded on the varistors could be proved only by using some geometries and numerical models, easily combined and verified by a set of experimental results, in order to perform confirmation of the proposed modeling hypothesis.

All CAD and numerical design procedures were performed at the POLITEHNICA University of Timisoara, Romania. The experimental part was performed at the LAPLACE Laboratory, from the PAUL SABATIER University in Toulouse, France.

All design solutions, simulations and measurements described inside this paper were carried out by using a set of regular 30 mm diameter commercial disk varistors, taken from the market (VARSI V250K30). These devices have reduced 3 mm height and they are applied mainly for a standard 230 V RMS European low voltage (domestic or similar) power supply installations. The varistors involved are not fully covered in epoxy resin, having only the small lateral edge coated with insulator, for about 1 mm. Two Ag alloy based electrodes are deposited by a special solvent technique on both sides. This configuration, having a single varistor alone is called the "A" configuration, in our article.

The additional metallic mass used was a small cylinder made of industrial brass, having a 20 mm diameter and a height of 5 mm. The newly proposed configuration, with a varistor and an additional mass on only one side, centered, is named, in our current article, the "B" configuration.

Analysis based on finite elements software is, nowadays, a powerful tool used for modeling heat transfer, as well as electric or magnetic field problems. For a complete CAD modeling, we used the FLUX 2D software, which provided excellent results for pieces having cylindrical symmetry.

The maximum numerically estimated temperature inside that model for configuration A (for 5300 points network) is:

$$\theta_e = \theta_a + \tau_e = 25 + 9.95 = 34.95 \text{ }^{\circ}\text{C} \quad (5)$$

The maximum numerically estimated temperature inside that model, for configuration B (for 5300 points network) is:

$$\theta_e = \theta_a + \tau_e = 26 + 6.38 = 32.38 \text{ }^{\circ}\text{C} \quad (6)$$

In Fig.2 and Fig.3 we will describe briefly the results of the finite elements approach, at 1 min (60 s) after the overvoltage pulse (shock), for each configuration considered below:

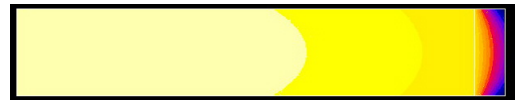


Fig. 2. Temperature repartition for configuration A

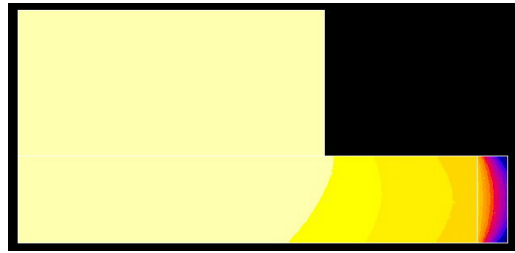


Fig. 3. Temperature repartition for configuration B

The maximal temperature obtained for configuration A was 32.84 °C and the minimal one was 31.77 °C, with a step of 0,09 degrees Celsius for each colour, from yellow to magenta. The time variation graph of the temperature, for a certain random point, located on the top side, where  $H = 3 \text{ mm}$  and having a  $R = 12 \text{ mm}$  radius from the axis, belonging to the configuration A, is shown in Fig.4.

The maximal temperature obtained for configuration B, in the same conditions, was around 31.41 °C and the minimum was 30.62 °C, with a step of 0,07 degrees Celsius for each colour. The time variation of the temperature for that randomly specified point, located on the top side ( $H = 3 \text{ mm}$ ) having a  $R = 12 \text{ mm}$  radius, on the configuration B, is shown in Fig.5.

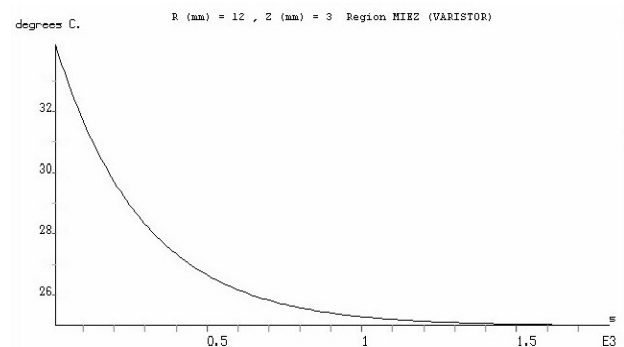


Fig. 4. Time variation of temperature for a point on configuration A

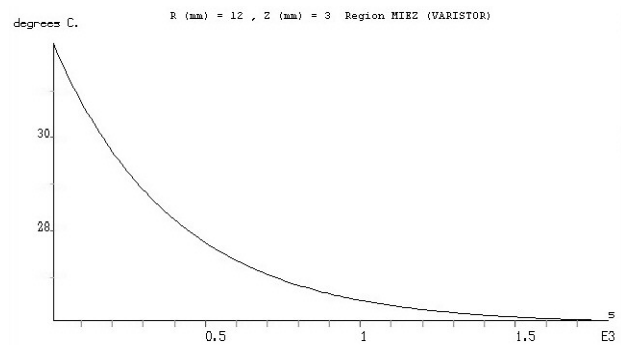


Fig. 5. Time variation of temperature for a point on configuration B

These graphs are only software estimations for the temperature. They must be verified in practice.



#### IV. EXPERIMENTAL RESULTS

Each considered configuration was submitted to an overvoltage test pulse (shock), by using a dedicated standard 8/20 pulse (shock) generator, located at the LAPLACE Laboratory, in Toulouse France. The maximum real measured temperature  $\theta$  for the same random point, numerically and theoretically considered before (3 mm, 12 mm), belonging to the first configuration A was:

$$\theta = 34,44 \text{ }^{\circ}\text{C} \quad (7)$$

We notice that relation (5) offers a very good estimation compared to (7). The time evolution of the temperature, during the “after pulse” cooling process, for the same previous randomly chosen point, is shown in Fig.6. That considered point reference was also used for the other B configuration, too. The maximum physically measured temperature  $\theta$ , on the same considered point position (3 mm, 12 mm), located on configuration B was:

$$\theta = 32,13 \text{ }^{\circ}\text{C} \quad (8)$$

The cooling process graphs are placed below:

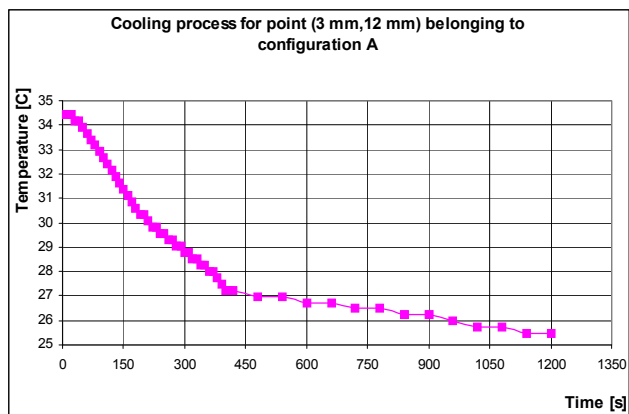


Fig. 6. Cooling process time graph for a point located on configuration A

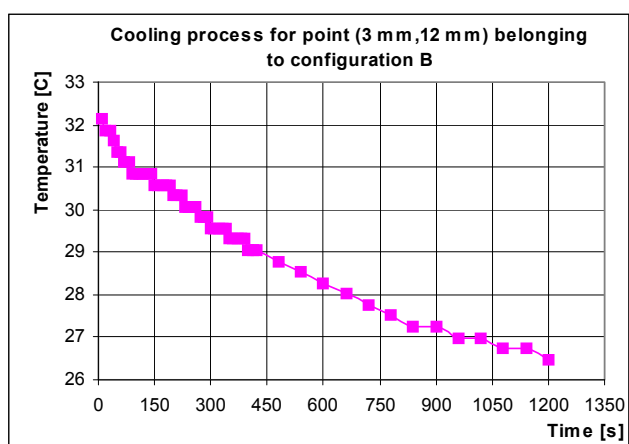


Fig. 7. Cooling process time graph for a point located on configuration B

Equation (6) offers an excellent estimation when compared to (8). The time evolution of the temperature during the cooling process, considered for the same point of configuration B, is described in Fig.7.

All overvoltage pulses applied here were standardized 8/20  $\mu$ s ones, provided by a current pulse generator. All measurements were carried out for at least 60 seconds after applying that current pulse. We observed a very good correspondence between the estimated numerical values and the measured results. These are commonly made measurements which are proving the correct hypothesis considered.

#### V. CONCLUSIONS

After all these studies and taking also in consideration all incidents in service history, we noticed that there is a major risk of overheating a MOV varistor, during both permanent or pulse (overvoltage shock) service regime, because the crossing resulted current throughout that varistor is activated by its temperature.

The newly introduced thermal stability concept is an important issue for the quality assessment of a certain MOV varistor. By eliminating any potential overheating risk, the experiments performed in this paper, are safely placing the varistor inside the thermal stability envelope, in order to avoid its irreversible destruction and, also, to verify the efficiency of the newly proposed technical solution, with additional metal masses.

Potentially, there are plenty of technical solutions concerning the reduction of any overheating risk. From our point of view, the most efficient one involves improvements on the quality of the varistor material itself, which is a study dedicated for chemical or material specialists.

The new and original solution proposed here by the authors, conceived only for existing materials and equipment, consists in an additional metal (brass) mass welded on the varistor surface, which acts like a real heating pump, extracting part of the heat from the electrical active area of the varistor and relocating this heat in corresponding fractions, between the two pieces of equipment (varistor and mass).

This original solution detailed here is part of our Romanian Patent, RO 117052 B, practically proved to be efficient by reducing the varistor temperatures compared to the single varistor configuration. This technical solution offers us a high energy absorption capability, placing the active varistor inside the stability reserve area, for all normal overvoltage pulses (shocks). We observed a very good correspondence between the theoretical estimated models and the measured results. There is a slightly, almost two degrees Celsius difference between the numerical estimated temperature computed by using finite elements model and the real measurements, which is tolerable from the heating point of view (tens of degrees are critical in our case).

This simple principle of additional masses could be successfully applied in industry in order to manufacture “high energy absorption capacity” low voltage varistors or even sensors, suitable mostly for low voltage power or telecommunications applications. We strongly recommend this new varistors for frequent lightning protection.

The use of new and modern surge protection equipment is mandatory also in the field of any automation system or equipment, operating on large areas, especially in the Power and Energy domain.



## REFERENCES

- [1] Sedky A., El-Brolosy T.A., Mohamed S.B., „Correlation between sintering temperature and properties of ZnO ceramic varistors”, *Journal of Physics and Chemistry of Solids*, Volume 73, Issue 3, March 2012, Pages 505-510.
- [2] Loncar B., Vujisic M., Stankovic K., Osmokrovic P., “Stability of Metal-Oxide Varistor Characteristics in Exploitation Conditions”, *Acta Physica Polonica, Series a* 116(6), December 2009, pp.1081-1084
- [3] Cheng L., Li G., Yuan K., Meng L., Zheng L., “Improvement in Nonlinear Properties and Electrical Stability of ZnO Varistors with Bi<sub>2</sub>O<sub>3</sub> Additives by NanoCoating Method”, *Journal of the American Ceramic Society*, Volume95, Issue3, March 2012, pp. 1004-1010.
- [4] Masoumeh D., Azmi Z., Yadollah A., Mansor H., Seyedehtaryam M., “Optimization of Bi<sub>2</sub>O<sub>3</sub>, TiO<sub>2</sub>, and Sb<sub>2</sub>O<sub>3</sub> Doped ZnO-Based Low-Voltage Varistor Ceramic to Maximize Nonlinear Electrical Properties”, *The Scientific World Journal*, Volume 2014, Article ID 741034
- [5] Kulawik J., Skwarek A., “Electrical and microstructural characterization of doped ZnO based multilayer varistors”, *Microelectronics International*, Volume 34, Issue 3, 2017, pp.110-115.
- [6] Li, S.T.; He, J.Q.; Lin, J.J.; Wang, H.; Liu, W.F.; Liao, Y.L. “Electrical-Thermal Failure of Metal-Oxide Arrester by Successive Impulses”. *IEEE Trans. Power Deliv.* 2016, 6, pp. 2538–2545.
- [7] Latiff, N.A.A.; Illias, H.A.; Bakar, A.H.A.; Dabbak, S.Z.A. “Measurement and Modelling of Leakage Current Behaviour in ZnO Surge Arresters under Various Applied Voltage Amplitudes and Pollution Conditions”. *Energies* 2018, 4, 875.
- [8] Tarfulea, N.; Frigura-Iliasa, F. M., Vatau D., Andea Petru, Balcu Florin, Macarie Amalia, “A new Algorithm for the Design of Metal Oxide Varistor Surge Arresters”, *Proceedings of the 2016 IEEE 16<sup>th</sup> International Conference on Environment and Electrical Engineering (EEEIC)*, Florence, Italy, June 7-10, 2016.
- [9] Seyyedbarzegar, S.M.; Mirzaie, M. “Thermal balance diagram modelling of surge arrester for thermal stability analysis considering ZnO varistor degradation effect”, *IET Gen. Transm. Distrib.* 2016, 7, 1570–1581.
- [10] Seyyedbarzegar, S.M. “A new approach to electrical modeling of surge arrester considering temperature effect on V-I characteristic”, *Measurement* 2017, 111, 295–306.

# Smart Frequency Control using Coordinated RFB and TCPS based on Firefly Algorithm

Dwi Lastomo<sup>1</sup>, Arif Musthofa<sup>2</sup>, Herlambang Setiadi<sup>3</sup>, Eddy Setyo Koenhardono<sup>4</sup>, Muhammad Ruswandi Djalal<sup>5</sup>

<sup>1,2</sup>Department of Automation Electrical Engineering, Institut Teknologi Sepuluh Nopember, Surabaya, Indonesia.

<sup>3</sup>School of Information Technology & Electrical Engineering, The University of Queensland, Brisbane, Australia

<sup>4</sup>Department of Marine Engineering, Institut Teknologi Sepuluh Nopember, Surabaya, Indonesia

<sup>5</sup>Department of Mechanical Engineering, State Polytechnic of Ujung Pandang, Makassar, Indonesia  
(E-mail: dtomo23@gmail.com<sup>1</sup>, arifmusthofa1108@gmail.com<sup>2</sup>, h.setiadi@uq.edu.au<sup>3</sup>, eddy-koen@its.ac.id<sup>4</sup>, wandi@poliupg.ac.id<sup>5</sup>)

**Abstract**—The frequency stability enhancement of a power system is proposed in this paper. To enhance the frequency stability, redox flow batteries (RFB) and the thyristor controlled phase shifter are used. Moreover, to get a better performance, the parameter of RFB and TCSC are optimized by the firefly algorithm (FA). Two area load frequency control plant is used as a test system. Time domain simulation is used to assess the performance of the proposed method (adding RFB and TCPS and optimized using FA). From the simulation results, it is found that by installing RFB and TCSC based on FA in the system, the frequency performance can be maintained above the nadir when perturbation emerges.

**Keywords**—Firefly Algorithm (FA), Frequency stability, RFB, TCSC.

## I. INTRODUCTION

The increasing load demand has led to several problems in the power system sector. The problem can come from transmission until distribution sector. The problem in power system is mainly about the stability of the power system. The stability of the power system could also be disturbed by the increasing the capacity of the load. Power system stability itself divided into three categorized which is rotor angle stability, voltage stability, and frequency stability. Rotor angle stability is related to the ability of the power system to maintain stable condition after being subjected to a small perturbation. While voltage stability is the ability of the power system to maintain reactive power in the system. Furthermore, frequency stability related to the ability of the power system to maintain the balance between generating capacity and load capacity [1]. Hence, the frequency stability of the systems is influencing by the increasing load demand capacity.

Maintaining the frequency performance of the system can be done by controlling the generating as well as load automatically. This method commonly called load frequency control (LFC) [2]. The procedure of LFC is putting a feedback signal of a frequency of the system and pass it through the governor controller. Generally, the governor controller is a

simple integral control. However, only used the integral controller to maintain the frequency stability is out of date. Hence, additional devices such as flexible ac transmission systems (FACTS) devices can be considered to enhance the frequency performance of the system.

There have been many types of FACTS devices that already implemented in the practical scenario as well as in the research paper [3-8]. Among them, TCPS is becoming more popular to enhance the frequency stability of the systems [6]. However, due to the increasing load demand as well as the uncertainty of the load, TCPS is not enough to maintain the frequency between the requirements. Hence, it is essential to utilize additional devices to handle the uncertainty of the load demand.

Energy storage can be used as additional devices in the power system. These devices have been shown a better performance as an additional controller to provide as well as store energy when the load changing emerge. Energy storage has shown a promising result for solving stability issue of power system such as rotor angle, voltage as well as frequency stability [9-19]. In recent years, there is a new energy storage that has shown a better response for providing energy in fast response called redox flow batteries (RFB) [17, 20]. This energy storage utilizes the ability of sulfuric acid and vanadium ion for storing electrical energy in the large amount [17, 20]. The major problem here is how to design and optimize the parameter of TCPS and RFB. Designing TCPS and RFB parameters cover a complex mathematical calculation. Hence, artificial intelligence techniques can be used to simplify the problems.

Artificial intelligence can be divided into three categorize, namely artificial neural network (ANN), fuzzy logic system, and metaheuristic algorithm. Metaheuristic algorithm has shown a better performance for solving optimization method. There is a lot of type of metaheuristic algorithm that has been used to solve optimization problems in the last few decades. The application of metaheuristic for solving optimization problems has been developed significantly over the past few decades as reported in [21-25]. The application of cuckoo search algorithm to tuning the parameter of SMES and CES is reported in [21]. In [22], the small disturbance angle stability



Fig. 2 Schematic diagram of RFB.

### C. Thyristor Controlled Phase Shifter

Controlling the power flow between tie-line can be done by installing the TCPS in series with tie-line as depicted in Fig. 3. By controlling the power flow in the tie line, the frequency of the system can be also controlled. Furthermore, the mathematical representation of the power flow deviation in the tie line without TCPS can be described as given (5) [33].

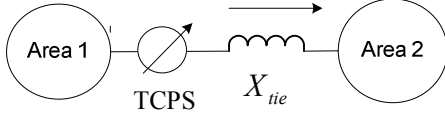


Fig. 3 Schematic diagram of TCPS connected to tie line.

$$\Delta P_{12}^o = \frac{2\pi T^o}{s} (\Delta f_1 - \Delta f_2) \quad (5)$$

In (5),  $T^o$ ,  $P_{12o}$ ,  $f_1$ , and  $f_2$  are the synchronous coefficient transmission line without TCPS, power flow deviation, frequency deviation in area 1 and area 2. The mathematical representation of power flow deviation with TCPC can be described using (6).

$$P_{tie} = \frac{|V_1||V_2|}{X_{12}} \sin(\delta_1 - \delta_2 + \phi) \quad (6)$$

In (6),  $P_{tie}$  is the power in tie line with TCPS in the transmission line, while  $\phi$  is the variable of voltage angle that can be controlled by TCPS. Moreover, the mathematical representation of power flow in the tie line when small perturbation occurs can be described using (7).

$$\Delta P_{tie} = \frac{|V_1||V_2|}{X_{12}} \cos(\delta_1^o - \delta_2^o + \phi^o) (\Delta \delta_1 - \Delta \delta_2 + \Delta \phi) \quad (7)$$

In (7)  $\delta_1^o$  is the nominal condition of voltage angle before the disturbance, while  $\Delta \delta_1$  is the voltage deviation when perturbation emerges. Moreover, the mathematical representation of synchronization coefficient between area can be presented as (8). Hence,  $P_{tie}$  can be calculated using (9) and (10). Furthermore, the Laplace representation of equation (10) can be presented as (11).

$$T_{12} = \frac{|V_1||V_2|}{X_{12}} \cos(\delta_1^o - \delta_2^o + \phi^o) \quad (8)$$

$$\Delta P_{tie12} = T_{12} (\Delta \delta_1 - \Delta \delta_2 + \Delta \phi) \quad (9)$$

$$\Delta P_{tie12} = T_{12} (\Delta \delta_1 - \Delta \delta_2) + T_{12} \Delta \phi \quad (10)$$

$$\Delta P_{tie12} = \frac{2\pi T_{12}}{s} [\Delta F_1(s) - \Delta F_2(s)] + T_{12} \Delta \phi(s) \quad (11)$$

From equation (11), the phase shifter ( $\Delta \theta$ ) angle can be used to control the tie-line power flow. It can be assumed that input of TCPS is an error(s), while the  $K_\phi$  is TCPS gain controller. Furthermore, the phase shifter of TCPC can be calculated using (12).

$$\Delta \phi(s) = \frac{K_\phi}{1 + sT_{PS}} \Delta Error_1(s) \quad (12)$$

In (12),  $T_{PS}$  and  $\Delta Error_1(s)$  are the time constant of TCPS and the input signal from TCPS. Furthermore, by considering equation (11) and (12), the power flow in tie-line can be presented as given in (13) [33].

$$\Delta P_{tie12} = \frac{2\pi T_{12}}{s} [\Delta F_1(s) - \Delta F_2(s)] + T_{12} \frac{K_\phi}{1 + sT_{PS}} \Delta Error_1(s) \quad (13)$$

### III. DESIGN RFB AND TCPS BASED ON FA

Firefly algorithm (FA) is one of the algorithms in the field of metaheuristic approaches. In the heuristic approach, there is the term of swarm intelligence which is defined as a design algorithm or problem-solving tools inspired by the collective social behavior of insect colonies and animal colonies. Hence, FA can be categorized as swarm intelligence [34].

FA is a metaheuristic algorithm inspired by the flashing behavior of fireflies. This algorithm was developed by Dr. Xin-She Yang at Cambridge University to solve optimization problems. There are about two thousand species of fireflies and most of the fireflies produce a momentary and rhythmic blink of light, and for certain species, the blinking pattern is very unique. This light flicker is produced from the bioluminescence process. The actual function of this signal system is still being discussed. However, there are two basic functions of the blinking behavior of fireflies that are to attract the attention of their mates and to attract the attention of their prey [35].

The general formulation of this algorithm is presented together with mathematical modeling analysis to solve problems with the purpose of equivalence function. FA has three important parts as described in the following rules [36]:

- ❖ The fireflies sex is ignored, so regardless of their sex, fireflies will be attracted to each other.
- ❖ The attraction is proportional to the brightness of the fireflies. Fireflies with lower brightness levels will be attracted and move to fireflies with higher brightness. Brightness may decrease with increasing distance and the absorption of light due to air factor. If there are no fireflies with the most brightness light, the fireflies will move randomly.

- ❖ The objective function of the particular problems can be determined as the brightness or intensity of the firefly.

There are two things that are related and very important in FA namely light intensity and attractiveness function. In this case, we assume that the attractiveness is influenced by the degree of light intensity. The degree of light intensity on a firefly  $x$  can be stated as (14).

$$I(x) = f(x) \quad (14)$$

In (14),  $I$  indicated the level of light intensity on  $x$  fireflies that is proportional to the solution of the objective function ( $f(x)$ ).  $\beta$  is the attractiveness coefficient that has relative value due to the light intensity that must be seen and assessed by other fireflies. Hence, the result of the assessment will differ depending on the distance between the fireflies. In addition, the light intensity will decrease from the source due to the air factor ( $\gamma$ ). Hence, the mathematical representation of the attractiveness function is presented in (15).

$$\beta(r) = \beta_0 * \exp(-\gamma r^m), (m \geq 1) \quad (15)$$

The distance between fireflies  $i$  and  $j$  at the locations  $x_i$  and  $x_j$  can be determined when they are placed at the point where fireflies are dispersed randomly in the Cartesian diagram as presented in (16). Where the different location of firefly  $i$  to firefly  $j$  is the distance between those two ( $r_{ij}$ ).

$$r_{ij} = \sqrt{(x_i - x_j)^2 + (y_i - y_j)^2} \quad (16)$$

The movement of fireflies that move towards the best level of light intensity can be described as (17) [34-36].

$$x_i = x_i + \beta_0 * \exp(-\gamma r_{ij}^2) * (x_j - x_i) + \alpha * \left( rand - \frac{1}{2} \right) \quad (17)$$

In (17),  $x_i$  indicated the initial position of fireflies located at  $x$ , while  $\alpha$  is a variable that has a range between 0 and 1. All the variables formed on (17) ensure the fast algorithm work toward the optimal solution [36].

In this paper, FA is used to optimize the parameter of RFB and TCPS to mitigate the low-frequency oscillation on the power system. To find the optimal parameter of RFB and TCPS, comprehensive damping index is used as the objective function of the FA which can be calculated using (18) [37].

$$CDI = \sum_{i=1}^n (1 - \xi_i) \quad (18)$$

#### IV. RESULTS AND DISCUSSIONS

The case study is carried out using MATLAB/SIMULINK environment. Two areas load

frequency control of the power system is considered in this paper as the test system. A modification has been made by adding RFB in area 1 and installing TCPS in the tie line between area 1 and area 2. Fig. 4 shows the schematic diagram of the test system. Observation of a linear time domain is conducted to analyze the frequency response of the system.

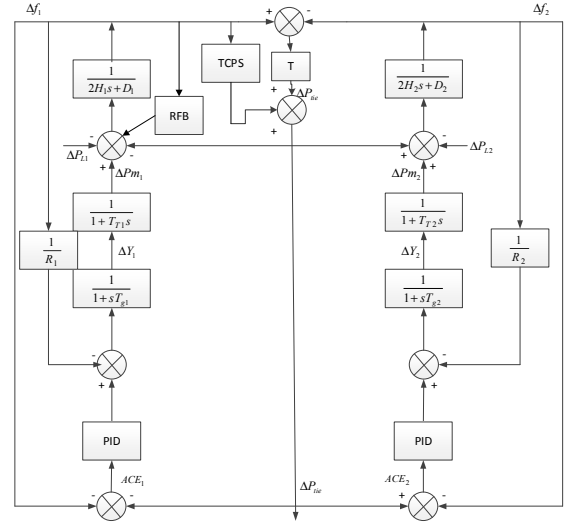


Fig. 4 Test systems.

To analyze the performance, a perturbation is made in the system by giving step input of load change in area 1. Figs. 5 and 6 show the frequency response in area 1 and area 2, while Fig. 7 illustrates the tie line power flow response. It is monitored that, when the load demand is decreased, the frequency response in area 1 and area 2 are started to accelerate. It is noticeable that, due to the accelerated frequency in area 1 and area 2, the tie line power flow is also increased.

Tables 1 and 2 depict the detailed featured of overshoot and settling time of frequency response in area 1 and area 2. While Table 3 shows the detailed featured of overshoot and settling time of tie-line power flow. Moreover, the overshoot and settling time for frequency in area 1 and area 2, as well as tie-line power flow, is decreased when RFB and TCPS are installed in the system. This condition could happen because of RFB is operate in charging condition. Hence, the surplus of electrical energy from the system due to the decreasing of load demand can be stored by RFB (RFB works as additional load). Moreover, TCPS provide the accurate phase shifter to stabilize the tie line power flow. Furthermore, the best response is shown by the system with the proposed response (adding RFB and TCPS based on FA) indicated by small overshoot and fastest settling time. It should be noted that the base case in this study is two area power system with integral control as the governor controller. The base case data is based on the existing scenario in reference [27].

As reported in [29], the frequency of the system has to be

back in the initial condition not more than 10 minutes. As shown in Figs. 5-7, the frequency back to normal less than 25 seconds. Hence the standard minimum of frequency settling time is achieved in all of the cases. Furthermore, 10 % of the load has to be shed if the deviation the frequency is more than  $\pm 0.8$  Hz or pu. If the load shedding procedure emerges, it is not good for the reliability of systems. It can be seen in Fig. 5 and table 1, the overshoot frequency on the base case and systems with TCPS are more than 0.8 pu. It is also observed that a system with RFB, a system with RFB and TCPS and the proposed system can achieve the overshoot of the frequency. Furthermore, it is also noticeable that the proposed systems provide the best frequency response compared to the other cases in this study. It is also noticeable that the proposed system could only reduce the frequency overshoot. This is acceptable as the settling time of the system is already achieved the standard in the base case.

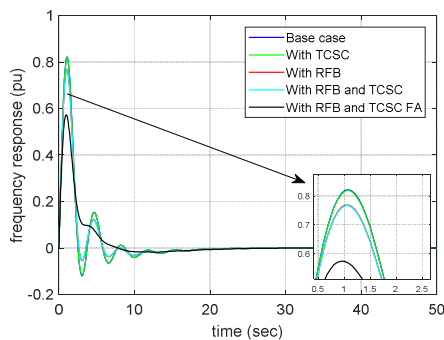


Fig. 5 The frequency response in area 1.

Table 1 Detailed features of Fig.5

Cases	Overshoot (pu)	Settling time (s)
Base case	0.8222	>25
With TCPS	0.8199	>25
With RFB	0.7691	>25
RFB TCPS	0.7669	>25
Proposed method	0.5731	>25

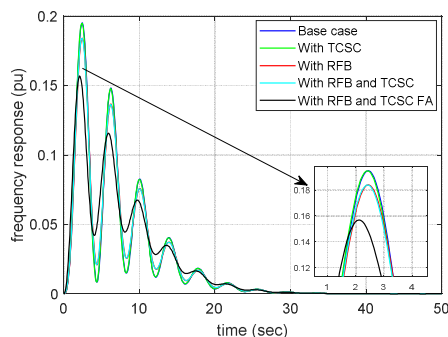


Fig. 6 The frequency response in area 2.

Table 2 Detailed features of Fig. 6.

Cases	Overshoot (pu)	Settling time (s)
Base case	0.1951	>25
With TCPS	0.1949	>25
With RFB	0.1841	>25
RFB TCPS	0.1839	>25
Proposed method	0.1568	>25

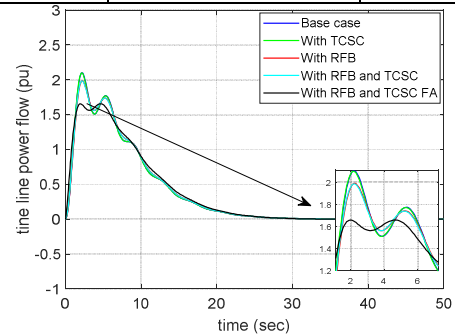


Fig. 7 The tie line power flow response.

Table 3 Detailed features of Fig. 7.

Cases	Overshoot (pu)	Settling time (s)
Base case	2.102	>25
With TCPS	2.099	>25
With RFB	1.989	>25
RFB TCPS	1.985	>25
Proposed method	1.657	>25

## V. CONCLUSIONS

This paper proposed a method for enhancing the frequency stability of a power system by employing coordinated control between RFB and TCPS based on FA. From the simulation results, it is found that by installing RFB and TCPS as well as tune the parameter of the devices simultaneously, resulting in the enhancement of the power system frequency response. It is monitored that RFB enhances the frequency response of the system by releasing energy when the load demand is increased and storing the energy when the load demand is decreasing. The best performance is provided by the system with RFB and TCPS tuned with FA, indicated by the smallest overshoot. Considering renewable energy integration and analyses the impact of frequency stability of a power system can be used as the further research.



## REFERENCES

- [1] P. Kundur *et al.*, "Definition and classification of power system stability IEEE/CIGRE joint task force on stability terms and definitions," *IEEE Transactions on Power Systems*, vol. 19, no. 3, pp. 1387-1401, 2004.
- [2] M. Abdillah, H. Setiadi, A. B. Reihara, K. Mahmoud, I. W. Farid, and A. Soeprijanto, "Optimal selection of LQR parameter using AIS for LFC in a multi-area power system," *Journal of Mechatronics, Electrical Power, and Vehicular Technology*, vol. 7, no. 2, pp. 93-104, 2016.
- [3] N. Mithulananthan, C. A. Cañizares, and J. Reeve, "Hopf bifurcation control in power system using power system stabilizers and static var compensators," in *Proc. of NAPS'99*, 1999, pp. 155-163.
- [4] A. Rahman, L. C. Saikia, and N. Sinha, "Maiden application of hybrid pattern search-biogeography based optimisation technique in automatic generation control of a multi-area system incorporating interline power flow controller," *IET Generation, Transmission & Distribution*, vol. 10, no. 7, pp. 1654-1662, 2016.
- [5] A. T. Al-Awami, Y. Abdel-Magid, and M. Abido, "A particle-swarm-based approach of power system stability enhancement with unified power flow controller," *International Journal of Electrical Power & Energy Systems*, vol. 29, no. 3, pp. 251-259, 2007.
- [6] P. Bhatt, S. Ghoshal, and R. Roy, "Load frequency stabilization by coordinated control of Thyristor Controlled Phase Shifters and superconducting magnetic energy storage for three types of interconnected two-area power systems," *International Journal of Electrical Power & Energy Systems*, vol. 32, no. 10, pp. 1111-1124, 2010.
- [7] R. S. Wijanarko, H. Setiadi, and T. A. Nugroho, "Coordination of SPS and CES to Mitigate Oscillatory Condition on Power Systems," *TELKOMNIKA (Telecommunication Computing Electronics and Control)*, vol. 15, no. 4, 2017.
- [8] N. Mithulananthan, C. A. Canizares, J. Reeve, and G. J. Rogers, "Comparison of PSS, SVC, and STATCOM controllers for damping power system oscillations," *IEEE Transactions on Power Systems*, vol. 18, no. 2, pp. 786-792, 2003.
- [9] D. Q. Hung, N. Mithulananthan, and R. Bansal, "Integration of PV and BES units in commercial distribution systems considering energy loss and voltage stability," *Applied Energy*, vol. 113, pp. 1162-1170, 2014.
- [10] H. Setiadi and K. O. Jones, "Power System Design using Firefly Algorithm for Dynamic Stability Enhancement," *Indonesian Journal of Electrical Engineering and Computer Science*, vol. 1, no. 3, pp. 446-455, 2016.
- [11] D. Lastomo, Atmiasri, and H. Setiadi, "Stability enhancement of hybrid power systems using RFB based on Craziness PSO," in *2017 3rd International Conference on Science in Information Technology (ICSITech)*, 2017, pp. 188-194.
- [12] D. Lastomo, H. Setiadi, and M. R. Djalal, "Optimization of SMES and TCSC using particle swarm optimization for oscillation mitigation in a multi machines power system," *Journal of Mechatronics, Electrical Power, and Vehicular Technology*, vol. 8, no. 1, pp. 11-21, 2017.
- [13] D. Lastomo *et al.*, "The effects of energy storages on small signal stability of a power system," in *2017 International Seminar on Intelligent Technology and Its Applications (ISITIA)*, 2017, pp. 52-57.
- [14] H. Setiadi, A. U. Krismanto, and N. Mithulananthan, "Influence of BES system on local and inter-area oscillation of power system with high penetration of PV plants," in *Applied System Innovation (ICASI), 2017 International Conference on*, 2017, pp. 1-4: IEEE.
- [15] H. Setiadi, A. U. Krismanto, and N. Mithulananthan, "Enabling BES in Large PV Plant for Stability Enhancement on Power Systems with High RES," in *2017 IEEE Innovative Smart Grid Technologies-Asia (ISGT-Asia)*, Auckland, New Zealand, 2017.
- [16] H. Setiadi, N. Mithulananthan, and M. J. Hossain, "Impact of battery energy storage systems on electromechanical oscillations in power systems," in *2017 IEEE Power & Energy Society General Meeting*, 2017, pp. 1-5.
- [17] M. Taufik, D. Lastomo, and H. Setiadi, "Small-disturbance angle stability enhancement using intelligent redox flow batteries," in *2017 4th International Conference on Electrical Engineering, Computer Science and Informatics (EECSI)*, 2017, pp. 1-6.
- [18] H. Setiadi, A. U. Krismanto, N. Mithulananthan, and M. Hossain, "Modal interaction of power systems with high penetration of renewable energy and BES systems," *International Journal of Electrical Power & Energy Systems*, vol. 97, pp. 385-395, 2018.
- [19] H. Setiadi, N. Mithulananthan, A. U. Krismanto, and R. Shah, "Comparison of Battery Energy Storage Model for Small Signal Stability in Power Systems," in *Industrial Electronics (ISIE), 2018 IEEE 27th International Symposium on*, 2018: IEEE.
- [20] D. Lastomo, Atmiasri, and H. Setiadi, "Stability Enhancement of Hybrid Power System using RFB based on Craziness PSO," in *2017 3rd International Conference on Science in Information Technology (ICSITech)*, Bandung, Indonesia, 2017.
- [21] M. R. Djalal, H. Setiadi, and A. Imran, "Frequency stability improvement of micro hydro power system using hybrid SMES and CES based on Cuckoo search algorithm," *Journal of Mechatronics, Electrical Power, and Vehicular Technology*, vol. 8, no. 2, pp. 76-84, 2017.
- [22] M. R. Djalal, H. Setiadi, D. Lastomo, and M. Y. Yunus, "Modal Analysis and Stability Enhancement of 150 kV Sulselrabar Electrical System using PSS and RFB based on Cuckoo Search Algorithm," *International Journal on Electrical Engineering and Informatics*, vol. 9, no. 4, pp. 800-812, 2017.
- [23] M. Ulum, H. Setiadi, and D. Lastomo, "Design Controller Blade Pitch Angle Wind Turbine Using Hybrid Differential Evolution Algorithm-Particle Swarm Optimization," *Advanced Science Letters*, vol. 23, no. 12, pp. 12396-12399, 2017.
- [24] M. R. Djalal, M. Yunus, A. Imran, and H. Setiadi, "Capacitive Energy Storage (CES) Optimization For Load Frequency Control in Micro Hydro Power Plant Using Imperialist Competitive Algorithm (ICA)," *EMITTER International Journal of Engineering Technology*, vol. 5, no. 2, pp. 279-297, 2018.
- [25] H. Setiadi, N. Mithulananthan, A. U. Krismanto, and R. Shah, "Low-Frequency Oscillatory Stability Study on 500 kV Java-Indonesian Electric Grid," in *Industrial Electronics (ISIE), 2018 IEEE 27th International Symposium on*, 2018: IEEE.
- [26] A. Mishra, V. N. K. Gundavarapu, V. R. Bathina, and D. C. Duvvada, "Real power performance index and line stability index-based management of contingency using firefly algorithm," *IET Generation, Transmission & Distribution*, vol. 10, no. 10, pp. 2327-2335, 2016.
- [27] H. Saadat, *Power system analysis*. WCB/McGraw-Hill, 1999.
- [28] D. Lastomo, Widodo, H. Setiadi, and M. R. Djalal, "Enabling PID and SSSC for Load Frequency Control using Particle Swarm Optimization," in *2017 3rd International Conference on Science in Information Technology (ICSITech)*, 2017.
- [29] P. Kundur, N. J. Balu, and M. G. Lauby, *Power system stability and control*. McGraw-hill New York, 1994.
- [30] I. Chidambaram and B. Paramasivam, "Control performance standards based load-frequency controller considering redox flow batteries coordinate with interline power flow controller," *Journal of Power Sources*, vol. 219, pp. 292-304, 2012.
- [31] I. Chidambaram and B. Paramasivam, "Optimized load-frequency simulation in restructured power system with Redox Flow Batteries and Interline Power Flow Controller," *International Journal of Electrical Power & Energy Systems*, vol. 50, pp. 9-24, 2013.
- [32] R. Shankar, K. Chatterjee, and R. Bhushan, "Impact of energy storage system on load frequency control for diverse sources of interconnected power system in deregulated power environment," *International Journal of Electrical Power & Energy Systems*, vol. 79, pp. 11-26, 7// 2016.
- [33] R. J. Abraham, D. Das, and A. Patra, "Effect of TCPS on oscillations in tie-power and area frequencies in an interconnected hydrothermal power system," *IET Generation, Transmission & Distribution*, vol. 1, no. 4, pp. 632-639, 2007.
- [34] X.-S. Yang, "Firefly algorithms for multimodal optimization," in *International symposium on stochastic algorithms*, 2009, pp. 169-178: Springer.
- [35] X.-S. Yang, *Nature-inspired metaheuristic algorithms*. Luniver press, 2010.
- [36] X.-S. Yang, *Cuckoo search and firefly algorithm: Theory and applications*. Springer, 2013.
- [37] A. El-Zonkoly, A. Khalil, and N. Ahmied, "Optimal tuning of lead-lag and fuzzy logic power system stabilizers using particle swarm optimization," *Expert Systems with Applications*, vol. 36, no. 2, pp. 2097-2106, 2009.

# Economic Feasibility Study of Rooftop Grid Connected PV System for Peak Load Reduction

Syafii

Electrical Engineering Department, Engineering  
Faculty, Universitas Andalas  
Padang, Indonesia  
syafii@eng.unand.ac.id

Wati

Accounting Education Department, STKIP PGRI  
Sumatera Barat  
Padang, Indonesia  
tegowati73@gmail.com

Novizon

Electrical Engineering Department, Engineering  
Faculty, Universitas Andalas  
Padang, Indonesia  
novizon@eng.unand.ac.id

Dona Juliandri

Electrical Engineering Department, Engineering  
Faculty, Universitas Andalas  
Padang, Indonesia  
juliandri.tan@gmail.com

**Abstract**— This paper presented the economic feasibility analysis of grid-connected photovoltaic on the roof of building, to reduce peak electrical demand. The Engineering Faculty electrical system is used as case study of PV system economic feasibility. The economic calculation assumptions used are: electricity tariff IDR 1114.74 per kWh based on electricity tariff for medium voltage load, estimated annual module degradation 0.5% and the life expectancy of the solar panels 25 years. The interest rate using of Bank Indonesia (BI) rate for 2018 i.e. 4.25% and inflation rate 3% also considered. The initial investment required to build 117.5 kWp PV system is IDR 2,413 million. The operational and maintenance costs are estimated 1% of initial investment per year. The result of cash flow rate shows that a positive NPV is achievable and payback period less than solar panels life expectancy. The simple payback period is 11 years and discounted payback period calculated by consider multiple parameters to be 14 years. The result of economic analysis using current rate value indicate that the project is profitable.

**Keywords**—grid connected PV system, economic feasibility, peak load reduction.

## I. INTRODUCTION

The Indonesian government encourages the use of renewable energy as a source of energy in office buildings that almost entirely use electricity from National Electricity Company (PLN) grid so as to suppress the use of fuel oil and decrease carbon dioxide (CO<sub>2</sub>) emissions. Utilization of renewable energy suitable for offices is photovoltaic (PV) system installed on the roof of the building [1], because most office buildings use electricity during the day or working hours. The PV system is one of the environmentally friendly power generation technologies and can be a solution to the future electrical energy crisis making it the most widely developed and reliable alternative. In addition to being environmentally friendly, the construction of PV System at the load center can reduce network losses, land investment costs and dependence on fossil energy, thereby enhancing energy sustainability and independence [2].

Several studies of designing PV systems on the rooftop of buildings have been done [3-5]. The hybrid system supply design on an institutional building rooftop of Udayana University, Indonesia and Minia University, Egypt have been presented in [3] and [4]. Another research conducted to design PV system for public building i.e for Ibeno Health

Centre [5]. The design result justified that PV system have a potential and feasible to build on the load area, however the weather condition and actual performance need to consider and improve.

The previous research uses assumption data in the design process so that the treatment will likely differ when installed in certain areas. However, in this study, the grid system design is based on the PV system of the actual small-scale pilot project [6] to obtain important parameters in the design and subsequent economic analysis. The grid connected PV systems have been used in this study. The grid connected PV system have many technical advantages such as flexibility, simplicity to install in any area where the solar irradiation is available, as non-polluting, emitting no noise and requiring little maintenance. The Engineering Faculty of Andalas University electrical demand used as case study of PV system design for peak load reduction and common feasibility criteria used to examine the profitability of this PV system project.

## II. BUILDING PEAK LOAD REDUCTION

Utilization of renewable energy suitable for offices is a solar power plant using photovoltaic solar modules installed on the roof of the building. Rooftop photovoltaic is a reliable solution for energy supply in office buildings because the majority of office buildings use electricity during the day or working hours because the cost of electricity procurement cheaper than diesel or fuel oil [7]. The integration of PV system close to load centers can reduce power losses and increase voltage profile [8]. In addition, maintenance and operation are also easy but significant impact to reduce pollution and greenhouse effect.

Global warming is an environment problem caused by the effect of greenhouses that occur in the Earth's atmosphere. The Kyoto Protocol was formed that agreed to collectively reduce 5.2% of greenhouse gas emissions. One of the biggest contributors to greenhouse gas emissions is carbon dioxide gas. Gas CO<sub>2</sub> produced through the combustion of motorized vehicle fuel, industry, and the biggest is in the process of generating fossil fuel-powered electricity. Through this design study use solar energy as an alternative power plant to reduce the work of fossil fueled power plants so that can reduce CO<sub>2</sub> gas emissions which is released into

the air. Potential reductions of CO<sub>2</sub> emissions can be calculated using factors emissions of carbon dioxide power plant that is equal to 0.73 kg CO<sub>2</sub>/kWh.

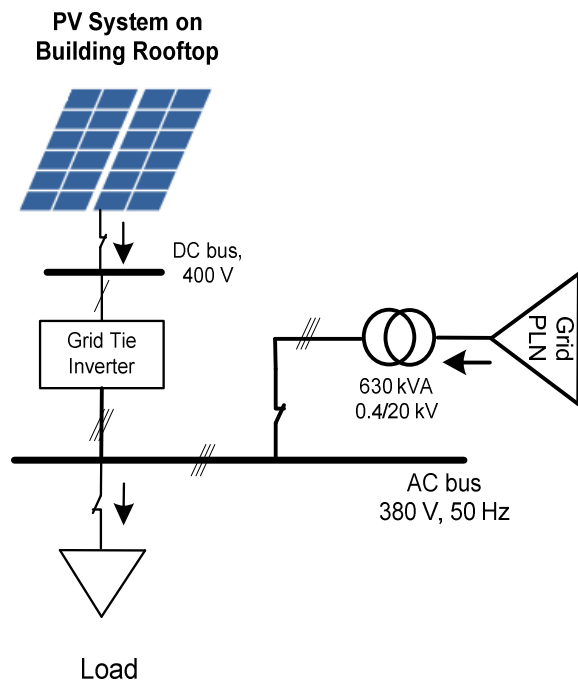


Fig. 1. Grid connected PV system

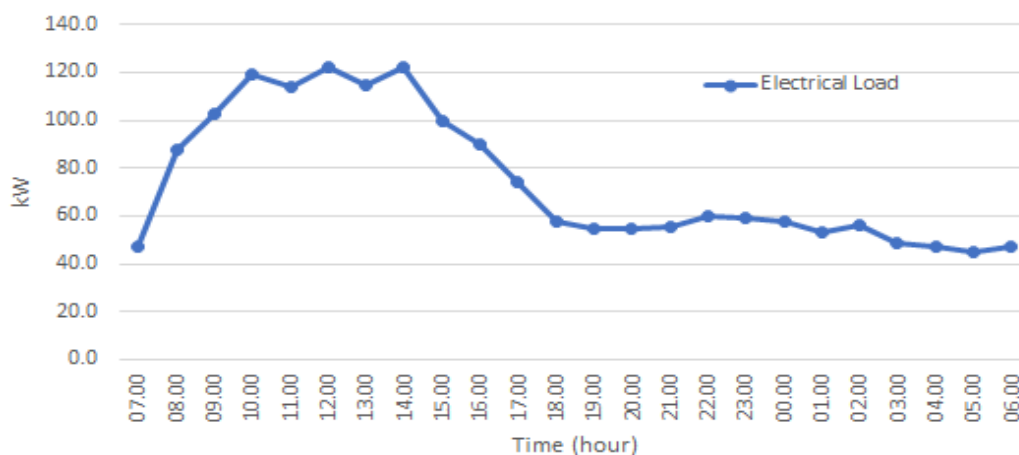


Fig. 2. Electrical load of Engineering Faculty building

The electrical load characteristics of an office building are generally shown in Fig 2. The use of electrical loads as illustrated in Fig 2 is as load characteristic of Engineering Faculty building, Andalas University. The design of grid connected photovoltaic on the roof of the Engineering Faculty building to reduce peak electrical

Grid connected PV as shown in Fig. 1 has been the most popular PV system choice in recent times, because it's can reduce investment funds and battery dependence. Some of the advantages of grid connected PV is the investment and maintenance costs are greatly reduced due to unnecessary battery. When the power of the PV system is greater than the load, the excess power can be send and sold to the power grid. So the electricity bill can be reduced. More environmentally friendly because it reduces battery waste that requires special treatment and not produce CO<sub>2</sub> emissions. In addition to the above advantages, for the case in Indonesia, have supported by appropriate regulation. The scheme will be very helpful for the distribution of targeted electricity subsidies.

A grid connected PV system consists of the following components: solar panels, grid-tied inverter (GTI), solar cables and Mounting. GTI is a special type of inverter that converts direct current (DC) into alternating current (AC) and feeds into an existing electricity network and cannot be used in standalone applications where there is no electricity. Grid-tied PV systems are generally cheaper and simpler to install, as long as the grid is close to the load center. On sunny days, solar panels will usually generate more electricity than consume during the daylight hours. With net metering, the owners can tranfer this excess electricity onto the utility grid rather than store in a battery-bank storage system, which would involve a considerably larger initial investment.

demand have been presented in paper [9]. The result of design study using 470 units of solar module can be shaved maximum load of Engineering Faculty building as shown in Fig 3 with discontinuous line. The load consumed and PV system designed have been used in the study to achieve economic feasibility.

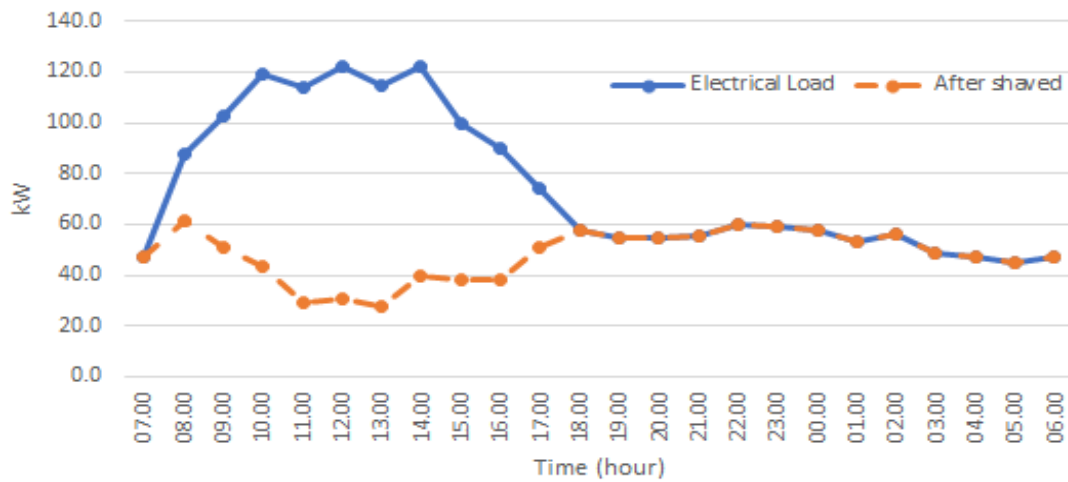


Fig. 3. PV installation reduce EF peak load

### III. ECONOMIC FEASIBILITY CRITERIA

The economic analysis of the PV system for government buildings uses a business feasibility study calculation system to determine investment criteria. These criteria can be used to determine the profitability of a project. The most common criteria used to examine the profitability of a PV project are net present value (NPV), payback period and internal rate of return (IRR). Net present value (NPV) is applied in capital budgeting to analyze the profitability of an investment or project and this formula is sensitive to the reliability of future cash inflows that an investment or project will yield. NPV compares the value of money received today and the value of that same amount of money in the future by taking inflation and rate of return into account. NPV is based on discounted cash flow (DCF) techniques with three basic steps.

The first step is to find the present value of each cash flow, including all inflows, outflows, and discounted at the project's cost of capital. NPV is the ratio between the value of the market investment and the cost itself. The formula for determining NPV is as follows [10]:

$$NPV = \sum_{t=0}^n \frac{CIF_t}{(1+k)^t} - Invest \quad (1)$$

Where:

- k = Discount rate
- $CIF_t$  = Cash in flow for t period
- n = last period of cash flow expected
- Invest = Initial investment

The result can be evaluated that if the NPV value is negative, then the project is not recommended to be implemented, if the value is positive, then the project is feasible to implement. NPV value is zero means there is no difference if the project is still implemented or rejected.

Payback period is a period of time required to recoup the fund expended in an PV investment or to reach the break-even point. The calculation of payback period is done to know the financial risk to the project be done. The smaller payback period will be better, with the risk factor for return on capital will be faster in a short time. In

calculating the payback period is usually called the payback method by dividing the initial capital issued with income received by investors for a year. The use of payback period in calculating the effectiveness of investment still has limits. The payback period does not calculate the profit earned after the payback period and has limitations in comparing the two projects.

The annual maintenance and operational costs for PV system, generally accounted for 1 - 2% of the total initial investment cost [11]. The large percentage of annual maintenance and operational expenses for the PV power plant covering costs for solar panel cleaning work, maintenance and inspection costs of equipment and installations will be set at 1% of the initial total investment because Indonesia only have two seasons i.e. the rainy season and the dry season so that the cost of cleaning and maintaining the solar panel is not as large as the country that have four seasons in one year. In addition, the determination of this percentage is also based on the level of wage labor in Indonesia which is cheaper than the wage rate of labor in other countries.

### IV. ECONOMIC FEASIBILITY OF PV SYSTEM FOR PEAK LOAD SHAVING

The process of economic feasibility analysis is carried out to calculate the feasibility of developing the PV system by comparing the amount of investment cost to income/return (revenue) obtained during the review time (time horizon). In other words, this financial analysis is carried out by forming cash flow from the project plan from the perspective of investors. The time horizon is limited by the estimated of the PV system components lifespan. The review time chosen in this study is 25 years same as solar panel lifespan.

TABLE 1. COST ESTIMATE OF PV SYSTEM INSTALLATION

PV System Components	Total price (IDR)
PV module, 470@250Wp Poly	1,903,265,000
Grid-Tied PV Inverter, 3P	195,000,000
MCB, Cables, busbar and fuses (15 % of PV system cost)	314,739,750
Total cost	2,413,004,750

The initial investment cost estimation used in this study is as shown in Table 1. The amount of electrical energy that can be generated by the 470 units of solar panels for a year is calculated based on actual small-scale PV data for various weather conditions with upscaling factor 94. The weather condition data for Padang city obtained from Meteorological, Climatological, and Geophysical Agency (BMKG) data is shown in Fig 4. Based on the BMKG data the average weather condition can be summarized in percentage/year as show in Table 2. By using this data, the potential of energy of PV system designed can be generated 428.16 kWh/day.

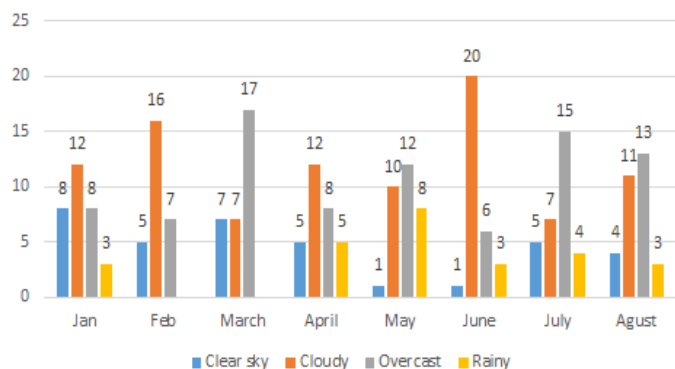


Fig. 4. West Sumatera weather condition

TABLE 2. PV SYSTEM ENERGY GENERATION

Weather	Data Jan-August	Percentage	Energy (kWh)/day
Clear	36 days	15 %	94.60
Cloudy	95 days	39 %	198.55
Overcast	86 days	35 %	119.20
Raining	26 days	11 %	15.82
Total	243 days	100 %	428.16

The electric tariff IDR 1114.74 per kWh based on electricity tariff for medium voltage load 20 kV by PLN 2018 is used. The estimated annual module degradation 0.5% and the life expectancy of the solar panels were assumed to be 25 years as determined by the most of solar companies [11]. The Bank Indonesia (BI) interest rate for 2018 i.e. 4.25% and inflation rate 3% are used in economic calculation based on present value. The result of cash flow rate calculation is shown in Fig 5.

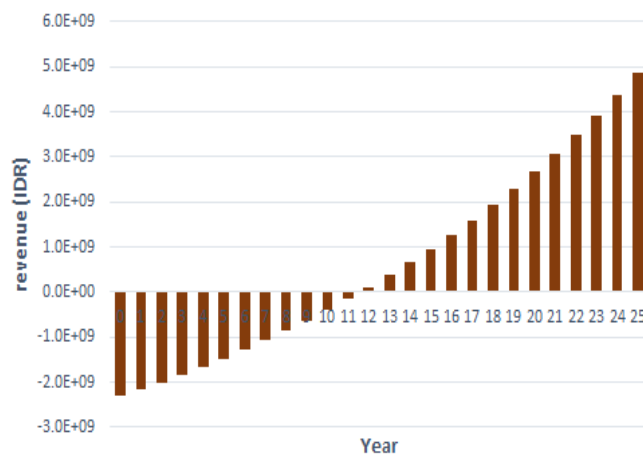


Fig. 5. Cash flow rate

Net present value compares the value of an investment today to the future value of the money based on inflation and returns. NPV is a simple calculation of difference between the present value of cash inflows and outflows using equation (1) as below:

$$\begin{aligned} \text{NPV} &= 3,757,591,476 - 2,413,004,750 \\ &= 1,344,586,726 \end{aligned}$$

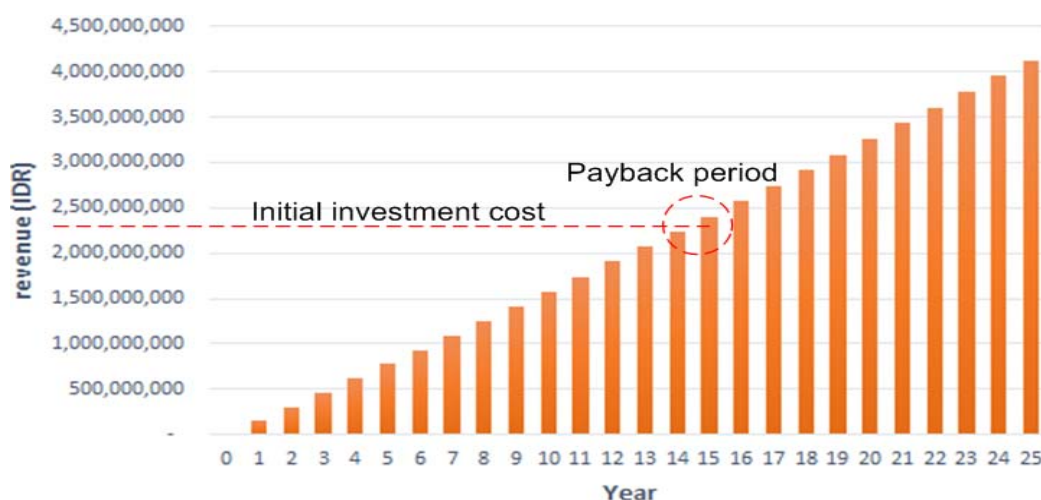


Fig. 6. Present value cumulative Net Cash flow (NCF)

A positive value of NPV indicates a favorable investment. Then, the simple payback period can be calculated by dividing total PV system investment cost by yearly savings. The simple payback period for this PV system is 12 years. The discounted payback period can be

determined from Fig 6 for DF 4.25% is equal to 14 years and 5 months. The simple method for calculating the cost of energy is the ratio of total investment plus the O&M cost over the total energy produced over project period.

The result for both simple and net present value method shown in Table 3.

TABLE 3. ECONOMIC FEASIBILITY

Feasibility Criteria	DF = 4.25%	DF=7.25%
Simple Payback period	11 years	11 years
Payback period	14	18
NPV	1,344,586,726	456,709,878

By knowing the amount of energy that can be generated by PV system and the factor of carbon dioxide gas emission of 0.730 kg CO<sub>2</sub>/kWh [12], it can be known amount of emissions that can be reduced. The design results show that the potential of solar energy which can be generated by the PV system in one year amounted to 156,280 kWh, so that can be obtained the potential of CO<sub>2</sub> emissions that can be reduced in one year is 118.08 tons.

#### V. CONCLUSION

The economic feasibility study of grid connected photovoltaic on the roof of the building for electrical peak load shaving have been done. The potential of energy of PV system designed can be generated 428.16 kWh/day. The economic feasibility study have used actual data of PV system of 1.25 kWp with upscaling factor 94 times, and considering weather conditions from BMKG data per year. The result of economic analysis shows that NPV for Engineering Faculty is IDR 1,344,586,726, simple payback period is 11 years and discounted payback period is 14 years. The result of cash flow rate shows that a positive NPV achievable and payback period less then PV panels life time. The economic feasibility results indicates that the development of PV system in the Faculty of Engineering, Andalas University building is feasible.

#### ACKNOWLEDGEMENTS

The author gratefully acknowledge the assistance rendered by Universitas Andalas for publication funding support of this research paper.

#### REFERENCES

- [1] Hagerman, S., Jaramillo, P. & M Granger Morgan, 2016. Is rooftop solar PV at socket parity without subsidier?, *Energy Policy*, 89, pp.84-94.
- [2] Tyagi, V. V., Rahim, N. a. a., Rahim, N. a., & Selvaraj, J. a. L. (2013). Progress in solar PV technology: Research and achievement. *Renewable and Sustainable Energy Reviews*, 20, 443–461.
- [3] IAD. Giriantari, Rina Irawati, Smart Microgrid System with Hybrid System Supply: Udayana University Pilot Project Design, ICSGTEIS Proceeding, 6-8 Oct 2016, Bali
- [4] Hassan, M.S and Elbaset, A.A, Comparative Study for Optimum Design of Grid Connected PV System based on Actual System Specifications, *International Journal of Computer Applications*, Volume 116, No. 3, April 2015.
- [5] Anyanime Tim Umoette, Emmanuel A. Ubom, Mbetobong Udo Festus, Design of Stand Alone Floating PV System for Ibeno Health Centre, *Science Journal of Energy Engineering*, 4(6), 2016, pp. 56-61.
- [6] Syafii, Refdinal Nazir, Performance and Energy Saving Analysis of Grid Connected Photovoltaic in West Sumatera, *International Journal of Power Electronics and Drive System (IJPEDS)*, Vol. 7, No. 4, December 2016, pp. 1348~1354.
- [7] Ferial, 2015. PLTS Rooftop Untuk Gedung Perkantoran. Available at: <http://ebtke.esdm.go.id/post/2015/03/11/800/plts.rooftop.untuk.gedung.perkantoran>.
- [8] Syafii & Nor, K.M., 2015. Unbalanced Active Distribution Analysis with Renewable Distributed Energy Resources. *Telkomnika*, 13(1)
- [9] Syafii, Dona Juliandri, Zaini, "Design of PV System for Electricity Peak-Shaving: A Case Study of Faculty of Engineering, Andalas University," 2018 International Conference on Computing, Power and Communication Technologies, Galgotias University, Greater Noida, UP, India. Sep 28-29, 2018.
- [10] Tze San Ong dan Chun Hau Thum, "Net Present Value and Payback Period for Building Integrated Photovoltaic Projects in Malaysia," *International Journal of Academic Research in Business and Social Sciences*, Februari 2013.
- [11] J.Lee, B. Chang, C. Aktas, R. Gorthala, Economic feasibility of campus-wide photovoltaic systems in New England, *Renewable Energy*, Vol. 99, 2016, pp. 452-464
- [12] Moien A.Omar, Marwan M.Mahmoud, Grid Connected PV- Home Systems in Palestine: A Review on Technical Performance, Effects and Economic Feasibility, *Renewable and Sustainable Energy Reviews*, Volume 82, Part 3, February 2018, Pages 2490-2497



# Automatic Switching Algorithm for Photovoltaic Power Generation System

Ivan C A P Husain, Canny Dahlia, Feri Yusivar

Department of Electrical Engineering  
Faculty of Engineering, Universitas Indonesia  
Depok, Indonesia

IvanChristianto.husain@gmail.com, dahliacanny@yahoo.com, yusivar@yahoo.com

**Abstract**— within remote area worldwide, solar panel is still considered as an alternative despite its low efficiency rate and complex system. Backup source and storage such as battery are substantially needed to keep Solar Panel working effectively. PI MPPT controller is equipped to remarkably improve the efficiency rate of the solar panel by maintaining it on its Maximum Power Point (MPP) reference. However, tackling the complexity of photovoltaic generator for remote area require another solution. This paper provide a simple yet applicable solution by presenting an algorithm to automatically control the photovoltaic generator system for remote area. The algorithm logic is determined by the key parameters from each system inside, which are solar panel, PI Boost Converter, Battery, and Load. The simulation proves that the algorithm is able to provide an appropriate result with all condition working properly. Thus, the algorithm is eligible to be applied and to be developed further.

**Keywords** - Solar Panel; Switching Algorithm, MPPT; Boost converter; Power electronics; Simulations;

## I. INTRODUCTION

Electric energy demand worldwide is gradually increasing following the development of technology. These days, renewable energy such as solar panel has been developing and being used. Not only sun provides an infinite amount of energy [1], it is also clean and safe to use. Remote area is an area with less population and development, thus resulting in less human resources whereas electricity is a necessity for development [2]. Therefore, solar panel as power source has started to become first choice for developing remote area because of its flexibility and unlimited resource.

Using solar panels as energy source is a complex system which require battery bank, switchboard, and controller to maximize its output [3]. Since the system is complex, the failure of solar panel pilot project sustainability is often occurred. Those problems are mainly caused by the inabilities to do maintenance and improvement when needed. When operating, problem may occur from its components, it may be an overcharge or short in battery bank, or the inabilities of the solar panels to generate sufficient amount of power, or maybe a malfunction within its transmission system [4]. If there are malfunctions as such, great cost and a number of technicians are needed just to repair, moreover to improve the work of solar panel. Since, researchers have been tackling problems one by one, for example MPPT for efficiency, BMS (Battery Management System) for safety, or Converter for adaptability,

there are so little research focusing the complexity of the system. Therefore, an algorithm to make the whole system automatic is needed to secure and improve whole system.

MPPT is an algorithm to maximize the output of a solar panel by giving reference and allowing it to operate on its maximum power point. To improve its results, PI controller is added for whole controller [5]. Battery bank as a supporting source as well as a storage is connected parallel to the Load. This modelled system is connected by three main switches, which are *main switch* to separate solar panel system from the rest, *battery switch* to separate battery bank from the rest, and *load switch* to separate the whole controlled system from the load. Those three switches are automatically controlled by logic algorithm derived by key parameters provided in this paper. Combining the MPPT, Battery, and Solar Panel system, a model of solar panel system complexity can be derived. The algorithm is applied and simulated into the model using MATLAB Simulink S-Function under random irradiance, temperature, and load. This Paper is mainly focused on the algorithm that is tested by using basic and existing methods by other references to prove the eligibility of the switching algorithm.

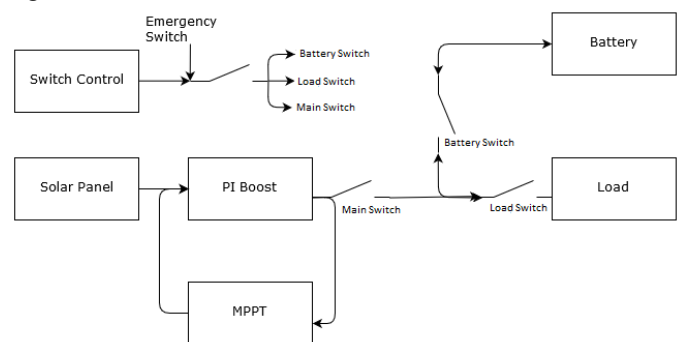


Figure 1 Whole System Design

## II. STATE FLOW AND KEY PARAMETERS

Algorithm is used to control the switching mechanism between three switches, *main switch*, *battery switch*, and *load switch*. The purpose of these three switches is to optimize and secure the system from malfunctioning or overworking. To allow the algorithm to correctly gauge the change needed, there are key parameters obtained from the system used, which are:

1.  $V_{Boost}$  = Voltage measurement from *boost converter* as the Solar system Voltage output (Volt)
2.  $V_{Batt}$  = Voltage measurement from Battery as the Battery System Output (Volt)
3.  $SoC$  = Battery *State of Charge* derived from  $V_{Batt}$  using *Coulomb Counting Method*
4.  $I_{PV}$  = Current measurement from Solar Panel as the solar panel input from conversion between irradiance to current (Ampere)
5. Duty Cycle = Switching state to measure the working percentage of the controller
6. Emergency Switch = A manual switch to disable all the switches.

Resulting in a state flow such as:

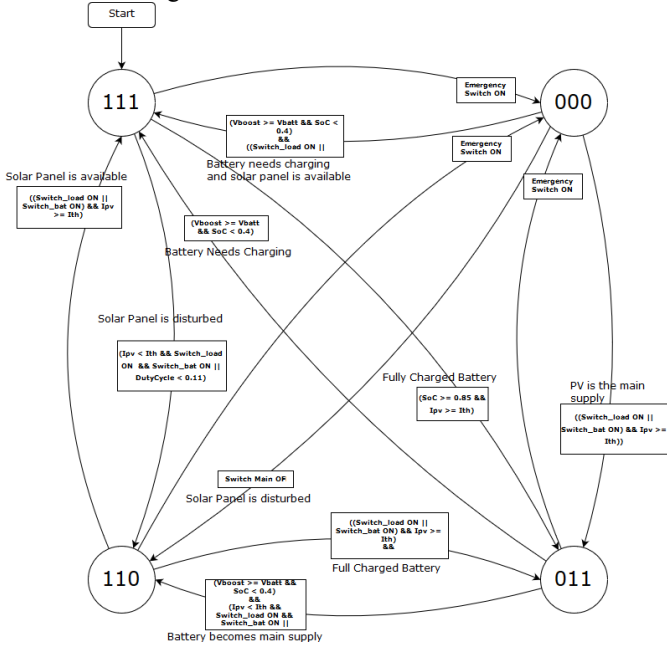


Figure 2 State Flow

With 1<sup>st</sup>, 2<sup>nd</sup>, and 3<sup>rd</sup> binary digits represent the condition of the *main switch*, *load switch*, and *battery switch* corresponding to chronological order.

The algorithm works in four main states interchanging one to another by logically comparing some key parameters to others.

For *battery switch* ( $S_3$ ), the logic goes as:

Battery is activated when:

- $V_{Boost} > V_{Batt}$  &  $SoC$  < standard

This condition stated that system is able to charge the battery and battery needs charging.

- $S_1 = 0$

This condition stated that Solar panel system is unavailable so battery has to be used, even if the battery is already empty.

Battery is deactivated when:

- $V_{Boost} < V_{Batt}$  &  $SoC < 0.10$

This condition stated that system is not able to charge the battery when the battery is empty, system then decide to fully support only the Load.

- $SoC > 0.9$  &  $I_{PV} > I_{threshold}$

This condition stated that Solar panel system is able to supply the load by itself while the battery is full and does not need charging

For *Load switch* ( $S_2$ ), the logic goes as:

Load is activated when:

- $S_2 = 0$

This condition stated that load is not connected previously, so system immediately reconnects it

For *Main switch* ( $S_1$ ), the logic goes as:

Solar Panel system is activated when:

- $I_{PV} > I_{threshold}$  & ( $S_2$  or  $S_3 = 1$ )

This condition stated that system is able to become the main supply, whether to charge the battery or supply the Load

Solar Panel system is deactivated when:

- ( $S_2$  and  $S_3 = 1$ ) &  $I_{PV} < I_{threshold}$

This condition stated that solar panel system is not able to be a supply but the battery is already connected, even if the battery is empty. System then decide to let the battery support the Load.

- Duty Cycle < 0.1

This condition stated that the controller is underwork (not operated as *boost*) so the system let the battery takes charge of being a supply.

If *Emergency Switch* is activated, the whole system is forcefully deactivated until it is reset by reconnecting the emergency switch.

### III. COMBINED SOLAR PANEL, PI MPPT, BOOST CONVERTER, AND BATTERY MODEL

The Solar Panel with PI MPPT, *Boost Converter*, Battery, and Switch Control are represented and modelled into single electrical circuit diagram to simulate the system and test the algorithm

#### A. Solar Panel System

Solar panel is a device that absorbs sunlight as its source and converts it into electricity. Solar panel uses MPPT to maximize its power output by using voltage reference to keep it working in its maximum power point. The Solar Panel using PI MPPT and *Boost Converter* can be represented as single electrical circuit which is shown by fig 3

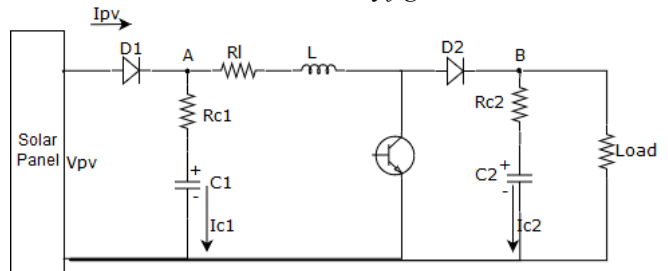


Figure 3 Boost-PI MPPT - PV System Equivalent Circuit

$C_{1,2}$ , and  $R_{C1,2}$  are the capacitance and internal resistance of capacitors,  $L$  and  $R_L$  are the inductance and internal resistance of the inductor,  $D_{1,2}$  are the diodes represent the working states of Boost Converter, and  $V_{PV}$ , and  $I_{PV}$  are solar panel output, voltage and current.

As a current source, the current generated by solar panel is represented as:

$$I_{pv} = N_p I_{ph} - N_p I_s \left( \exp \left( \frac{q \left( \frac{V_{pv} + R_s I_{pv}}{N_s} \right)}{A K T_c} \right) - 1 \right) - \frac{\left( \frac{N_p V_{pv}}{N_s} + R_s I_{pv} \right)}{R_{sh}} \quad (1)$$

$I_{PH}$  is determined by the environment condition such as irradiance and temperature while  $I_s$  is the saturated current of the cell represented as (2) and (3)

$$I_{ph} = \left( I_{sc} + \alpha (T_c - T_{ref}) \right) \frac{\lambda}{\lambda_{ref}} \quad (2)$$

$$I_s = \frac{I_{sc}}{\left( \exp \left( \frac{q V_{oc}}{A K T_c} \right) - 1 \right)} \left( \frac{T_c}{T_{ref}} \right)^3 \exp \left( \frac{q E_g \left( \frac{1}{T_{ref}} - \frac{1}{T_c} \right)}{K A} \right) \quad (3)$$

Since the *boost* IGBT is controlled by Duty Cycle, the voltage transformation increase proportional to the value of Duty Cycle. Summing the equation from ON state and OFF state of the IGBT, the system can be simplified as (4), thus resulting (5)

$$\frac{V_{PV} D T}{L} + \frac{(V_{PV} - V_{Boost})(1-D)T}{L} = 0 \quad (4)$$

$$V_{Boost} = \frac{V_{PV}}{1-D} \quad (5)$$

MPPT controller used in this system is an ICM (Incremental Conductance Method), a method that uses the shift in solar panel P-V curve to calculate error which then improved by PI (Proportional Integral) algorithm to reduce the settling time needed. Equation (6) shows the error calculation

$$\frac{d(V.I)}{dV} = \frac{V.dI + I.dV}{dV} = error \quad (6)$$

## B. Battery System

Battery is a device that can store electrical energy by storing electric charge in the form of chemical reaction. A battery can be modelled as a voltage source that gradually decreasing (discharge) or increasing (charging) with certain parameters. Figure 4 shows a battery system which is modelled as a Two Time Constant (TTC) Internal Resistance model, a simple representation of battery as a voltage source with internal resistance and dynamic state from two capacitors. The voltage value is a function of Battery State of Charge calculated with coulomb counting method. Equation (7), (8) and (9) show the calculation of  $I_{BATT}$ ,  $V_{SOC}$  and dynamic state of the battery while (10) shows coulomb counting method to derive the momentary State of Charge (SoC).

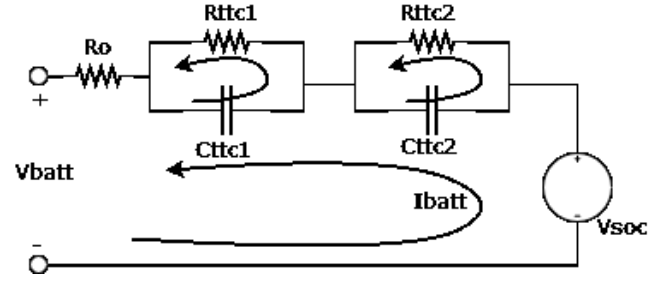


Figure 4 TTC Battery System Equivalent Circuit

$$V_{TTC1,2} = -\frac{V_{TTC1,2}}{R_{TTC1,2} C_{TTC1,2}} + \frac{I_{batt}}{C_{TTC1,2}} \quad (7)$$

$$I_{batt} = \frac{V_{SOC} - V_{TTC1} - V_{TTC2}}{R_o} \quad (8)$$

$$V_{SOC} = N_s * (V_{OC} + k_{SOC} \ln(SOC) - k_{LC} \ln(LC)) \quad (9)$$

$$\Delta SOC = SOC(t) - SOC(t_0) = \frac{1}{C_{rated}} \int_{t_0}^t i(\tau) d\tau \quad (10)$$

$K_{SOC}$  and  $K_{LC}$  represent the relationship between State of Charge and Life Cycle to battery open circuit voltage. These constants are obtained from battery testing and may differ for each type of battery.

## C. Combined System

Whole system of combined solar panel with PI MPPT – Boost Converter and battery bank is represented by circuit diagram shown by Figure 5 with two diodes D1 and D2 (where D2 is a diodes contrary to the state of IGBT) and three switches. Thus, there will be  $2^5$  or 32 states represented shown by Table 1, although there are some states that will due to its possibility. The system works by giving calculation for momentary states happening that time and constantly changing. Active condition is shown as 1 while inactive is shown as 0.

TABLE 1. SWITCHING CONDITIONS

State	Diodes		Switches		
	D1	IGBT' (D2)	Main	Load	Battery
0	0	0	0	0	0
1	1	0	0	0	0
2	0	1	0	0	0
3	1	1	0	0	0
4	0	0	1	0	0
5	1	0	1	0	0
6	0	1	1	0	0
7	1	1	1	0	0
8	0	0	0	1	0
9	1	0	0	1	0
10	0	1	0	1	0
11	1	1	0	1	0
12	0	0	1	1	0
13	1	0	1	1	0
14	0	1	1	1	0
15	1	1	1	1	0
16	0	0	0	0	1
17	1	0	0	0	1
18	0	1	0	0	1
19	1	1	0	0	1
20	0	0	1	0	1

21	1	0	1	0	1
22	0	1	1	0	1
23	1	1	1	0	1
24	0	0	0	1	1
25	1	0	0	1	1
26	0	1	0	1	1

27	1	1	0	1	1
28	0	0	1	1	1
29	1	0	1	1	1
30	0	1	1	1	1
31	1	1	1	1	1

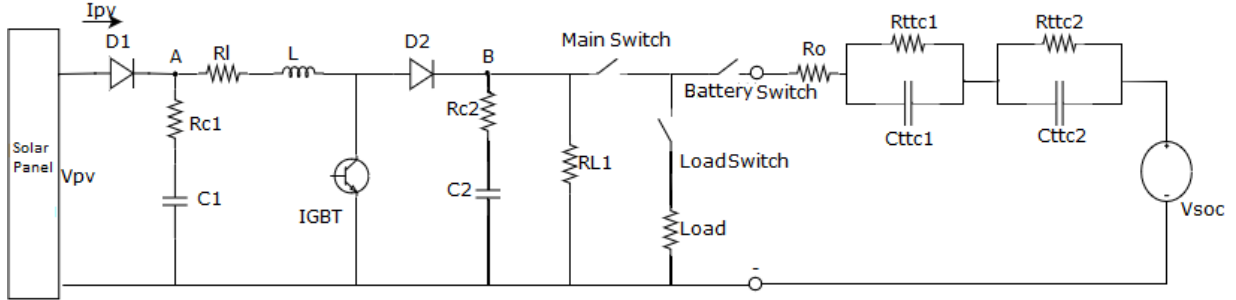


Figure 5 Full System Equivalent Circuit

For state number 27, where D1 is 1 (PV is actively generating power), D2 is 1 (IGBT is open), main load and battery switch is 1 (connected) while main switch is not (state value 0), the system can be derived by analyzing the circuit and put into matrices as follows:

State Matrix:

$$\begin{bmatrix} \frac{dV_{C1}}{dt} \\ \frac{dV_{C2}}{dt} \\ \frac{dI_L}{dt} \\ \frac{dV_{TTC1}}{dt} \\ \frac{dV_{TTC2}}{dt} \end{bmatrix} = \begin{bmatrix} 0 & 0 & -\frac{1}{C_1} & 0 & 0 \\ 0 & a_{22} & a_{23} & 0 & 0 \\ \frac{1}{L} & a_{32} & a_{33} & 0 & 0 \\ 0 & 0 & 0 & a_{44} & a_{45} \\ 0 & 0 & 0 & a_{54} & a_{55} \end{bmatrix} \begin{bmatrix} V_{C1} \\ V_{C2} \\ I_L \\ V_{TTC1} \\ V_{TTC2} \end{bmatrix} + \begin{bmatrix} 0 \\ 0 \\ 0 \\ 0 \\ 0 \end{bmatrix} + \begin{bmatrix} 0 \\ 0 \\ 0 \\ 1 \\ 1 \end{bmatrix} V_{SOC} \quad (11)$$

Output Matrix:

$$\begin{bmatrix} V_{PV} \\ V_{Load} \\ I_{Batt} \end{bmatrix} = \begin{bmatrix} 0 & 0 & 0 & 0 & 0 \\ 0 & 0 & 0 & 0 & 0 \\ 0 & 0 & 0 & -\frac{1}{(R_O+Load)} & -\frac{1}{(R_O+Load)} \end{bmatrix} \begin{bmatrix} V_{C1} \\ V_{C2} \\ I_L \\ V_{TTC1} \\ V_{TTC2} \end{bmatrix} + \begin{bmatrix} 1 \\ 0 \\ 0 \end{bmatrix} V_{D1} + \begin{bmatrix} R_{C1} \\ 0 \\ 0 \end{bmatrix} I_{PV} + \begin{bmatrix} 0 \\ 0 \\ 1 \end{bmatrix} V_{SOC} \quad (12)$$

Where

$$a_{22} = \frac{-1}{C_2(R_{C2}+RL1)} \quad (13)$$

$$a_{23} = \frac{1}{C_2} - \frac{R_{C2}}{C_2(R_{C2}+RL1)} \quad (14)$$

$$a_{32} = \frac{R_{C2}}{L(R_{C2}+RL1)} - \frac{1}{L} \quad (15)$$

$$a_{33} = \frac{R_{C2}^2}{L(R_{C2}+RL1)} - \frac{(R_{C1}+R_L+R_{C2})}{L} \quad (16)$$

$$a_{44} = -\left(\frac{1}{R_{TTC1}C_{TTC1}} + \frac{1}{C_{TTC1}(R_O+Load)}\right) \quad (17)$$

$$a_{45} = -\frac{1}{C_{TTC1}(R_O+Load)} \quad (18)$$

$$a_{54} = -\frac{1}{C_{TTC2}(R_O+Load)} \quad (19)$$

$$a_{55} = -\left(\frac{1}{R_{TTC2}C_{TTC2}} + \frac{1}{C_{TTC2}(R_O+Load)}\right) \quad (20)$$

#### IV. SIMULATION RESULTS

The proposed algorithm in this paper is tested using a combined model of three systems working altogether, PI MPPT, Battery, and Boosted PV. These three systems is modeled as an electrical circuit equivalent to the complex combined system. The algorithm is simulated using MATLAB S-Function Block. The test is done within 2 segments, which are the specific condition testing and random condition testing. For the 1<sup>st</sup> segment, system is tested by manually state the input of the switch according to the state flow from Figure 2. This test is run for showing the key results of each condition before combining. If the test is proven to be working optimally, then the 2<sup>nd</sup> test is conducted to see whether it is possible to combine all the condition and make them interchange if a certain condition occur. The 2<sup>nd</sup> segment is tested with random irradiance changing each second for 15s, random temperature changing every 2.5s and a load of 50Ω

##### A. Condition Testing

Figure 6, 7, and 8 shows the output of testing where the whole system works on each condition shown by state flow. The test is using varied irradiances of 1000W/m<sup>2</sup> to represent the standard irradiance that change to 700W/m<sup>2</sup> in the 2<sup>nd</sup> second and varied temperature of 298 kelvin that change to 315 kelvin in the 3<sup>rd</sup> second.

- 011 condition (PV with Load)

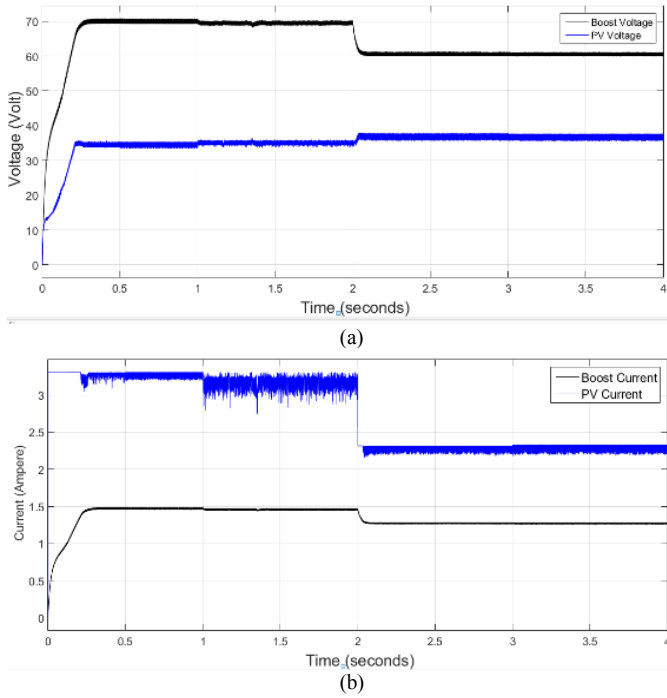


Figure 6 Voltage (a) and Current (b) between PI-MPPT and Boost

- 111 condition (Full System Working)

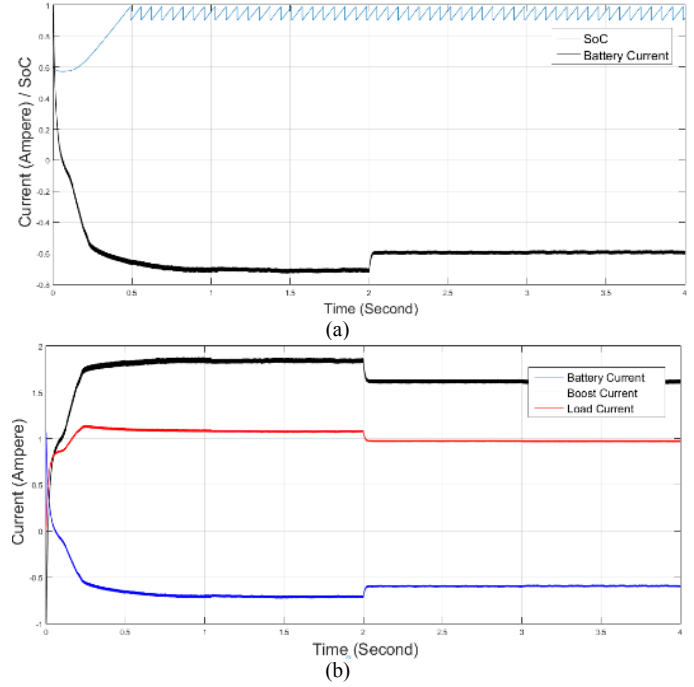


Figure 8 Current and SoC of the battery (a) and Load-PV-Battery current (b) from the system

- 110 condition (Battery with Load)

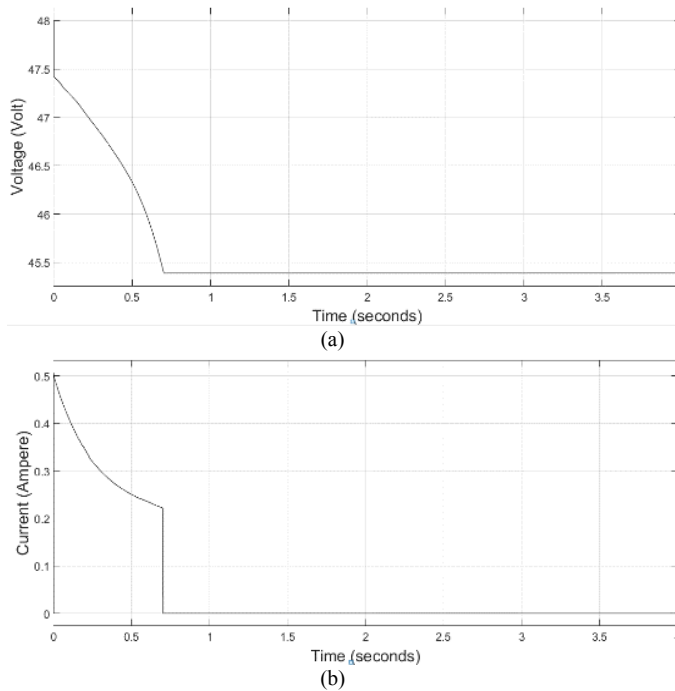


Figure 7 Voltage (a) and Current (b) of Battery Output

## B. System Testing

Figure 9 shows the testing output where the switching algorithm is applied to the system. The test used varied irradiances of [1000 400 1300 600 200 950 1200 1500 300 800 150 2000 1700 550 650] W/m<sup>2</sup> that changed each second and varied temperature of [298 320 250 280 400 270] kelvin that changed once every 2.5 second.

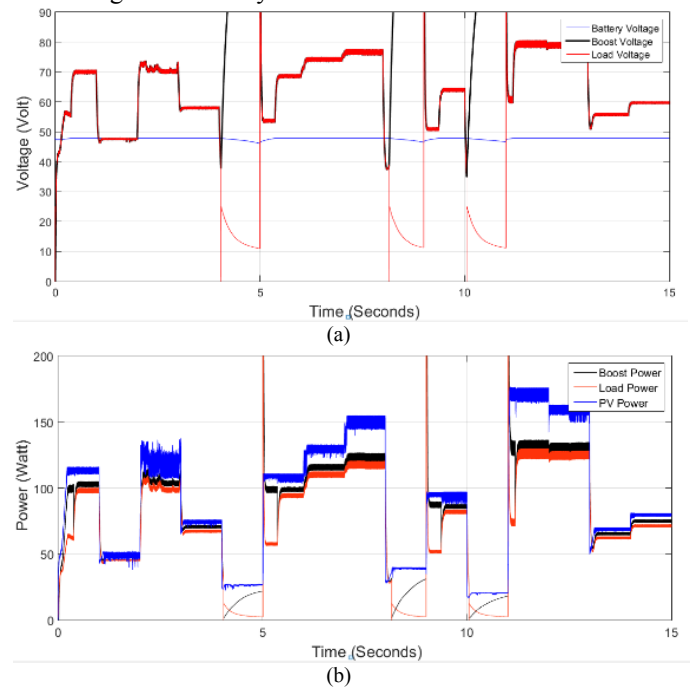


Figure 9 Voltage (a) and Power (c) comparison between PV-Boost, Battery and Load and Switch

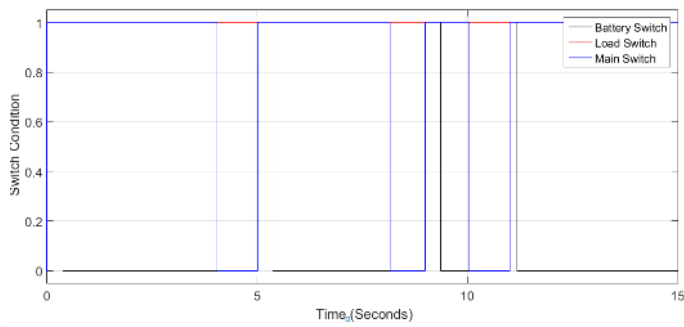


Figure 10 Automatic Switching Algorithm Pattern

Figure 10 shows that the system is working properly and performed good results by working optimally according to irradiance and temperature condition. The MPPT maximizes the output, the battery can either be a storage or a source, and therefore, switch is able to interchange between each condition whenever needed. However, model is generated with parameters from combined sources with little adjustment.

## V. CONCLUSION

This paper proposed a switching algorithm to control a Photovoltaic Power Generation System automatically. System is modelled using MATLAB and being tested on random condition of irradiance and temperature. The simulation for either condition testing and system testing give good results where it is working properly as PV-MPPT-Boost, Battery source, or fully functional system. When the algorithm is applied to the system and simulation is run, algorithm is able to keep the system working properly and interchange the state whenever needed with an acceptable error. Therefore, with great result, it is eligible to say that the algorithm is working and applicable, although it needs further improvement.

## ACKNOWLEDGMENT

This research is funded by Universitas Indonesia research grant of the *Publikasi Internasional Terindeks untuk Tugas Akhir Mahasiswa UI* (PITTA) 2018 Nomor: 2439/UN2.R3.1/HKP.05.00/2018.

## GLOSSARY OF SYMBOLS

$V_{PV}$  = Solar Panel Voltage (V)  
 $V_{Boost}$  = Boosted Voltage (V)  
 $V_{OC}$  = Open Circuit Voltage (V)  
 $R_{C1,2}$  = Capacitor Internal Resistance ( $\Omega$ )  
 $D_{1,2}$  = Diode Voltage (V)  
 $R_L$  = Inductor Internal Resistance ( $\Omega$ )  
 $L$  = Inductor (H)  
 $C_{1,2}$  = Capacitor (F)  
 $I_{C1,2}$  = Capacitor Discharge/Charge Current (A)  
 $I_{PV}$  = Solar Panel Current (A)  
 $I_{PH}$  = Solar Panel Conversion Current (A)  
 $I_s$  = Saturated Current (A)  
 $I_{SC}$  = Short Circuit Current (A)  
 $Q$  = Electron Charge (Coulomb)  
 $E_g$  = Energy Gap (eV)  
 $A$  = Correction Factor

$\lambda$  = Irradiance captured (lambda)  
 $\lambda_{Ref}$  = Sun Irradiance (lambda)  
 $K$  = Boltzmann Constant  
 $R_s$  = Solar Panel Internal Resistance ( $\Omega$ )  
 $R_{SH}$  = Solar Panel Shunt Resistance ( $\Omega$ )  
 $N_p$  = Number of Cells Connected Parallel  
 $N_s$  = Number of Cells Connected Series  
 $T_c$  = Current Temperature (Kelvin)  
 $T_{ref}$  = Environment Temperature (Kelvin)  
 $D$  = Duty cycle percentage (%)  
 $V_{TTC1,2}$  = Time Constraint Voltage (V)  
 $R_{TTC1,2}$  = Time Constraint Resistance ( $\Omega$ )  
 $I_{TTC1,2}$  = Time Constraint Current (A)  
 $C_{TTC1,2}$  = Time Constraint Capacitance (C)  
 $I_{BATT}$  = Battery Current (A)  
 $V_{BATT}$  = Battery Voltage (V)

## REFERENCES

- [1] V. Quaschnig, Understanding Renewable Energy Systems, Canada: Earthscan, 2005.
- [2] Z. Wani, "Quora," 8 May 2017. [Online]. Available: <https://www.quora.com/What-is-the-difference-between-rural-and-remote-areas>. [Accessed 18 June 2018].
- [3] M. Newkirk, "Clean Energy Reviews," 2 April 2014. [Online]. Available: <https://www.cleanenergyreviews.info/blog/2014/5/4/how-solar-works>. [Accessed 18 June 2018].
- [4] M. Pervaz and L. Rahman, "Review and Evaluation of Successful and Unsuccessful Renewable Energy Projects in South Asia," in *IPCBE*, Singapore, 2012.
- [5] M. A. Ramadhan, B. W. Harini, N. Avianto and F. Yusivar, "Implementation of Maximum Power Point Tracker Algorithm based Proportional-Integrator Controller on Solar Cell with Boost Converter Circuit," in *ICSEEA*, 2018.
- [6] F. Yusivar, M. Y. Farabi, R. Suryadiningrat, W. W. Ananduta and Y. Syaifuddin, "Buck-Converter Photovoltaic Simulator," *International Journal of Power Electronics and Drive System (IJPEDS)*, vol. 1, pp. 156-167, 2011.
- [7] F. Yusivar and S. Wakao, "Minimum Requirements of Motor Vector Control Modelling and Simulation Utilizing C MEX S-Function in MATLAB/Simulink," in *IEEE*, Japan, 2001.



# **AUTHORS' BACKGROUND**

Your Name	Title*	Research Field	Personal website
Ivan C A P Husain	Master Student		-
Canny Dahlia	Master Student		-
Feri Yusivar	Associate professor		

\*This form helps us to understand your paper better, **the form itself will not be published.**

\*Title can be chosen from: master student, Phd candidate, assistant professor, lecture, senior lecture, associate professor, full professor

# Rotor Speed Control Maximum Power Point Tracking for Small Wind Turbine

Ni Luh Gayatri Dharmaraditya, Lazarus Stefan and Feri Yusivar

Department of Electrical Engineering  
Faculty of Engineering, Universitas Indonesia  
Depok, Indonesia

Gayatri.niluh@gmail.com, lazarusstefan@yahoo.com, yusivar@yahoo.com

**Abstract**— Due to the change of energy source to renewable energy, the trend of wind turbine is increased in last 5 years. Small Wind Turbine that convert kinetic energy to electric energy needs a rectifier to convert AC to DC. Rectifier used in this paper is active rectifier. Because of its power characteristics, wind turbine needs maximum power point tracking (MPPT) to track its maximum power. This paper shows that by using active rectifier, the algorithm of tracking a maximum power able to be tracked by controlling its rotor angular speed. The simulation result proves that the speed control and MPPT algorithm, perturb and observe, is able to be implemented in various wind speed.

**Keywords**- Wind turbine, Active rectifier, Permanent Magnet Synchronous G, speed control, MPPT

## I. INTRODUCTION

The transition of energy source from fossil fuel to renewable energy is continuously executed by the decrease of fossil fuels. The most common renewable energy system is solar cell and wind turbine. Nowadays, wind turbine system is one of solution to produce renewable energy for both low power and high power. In last five years, the trend of the wind turbine system market has shown an aggressive 20% annual increase in worldwide and the industry predict approximately 750 MW of installed capacity in 2020 [1].

Essentially, wind turbine is a machine system for converting kinetic energy to electric energy. Wind turbine system consist of blade, rotor, generator and AC-DC converter. The type of wind turbine used is variable speed horizontal wind turbine. For generator, this paper uses permanent magnet synchronous generator (PMSG) because PMSG is becoming very common among small scale wind turbines as it provides good efficiency at low speed.

AC-DC converter is needed to control the generator's output. The most common AC-DC converter is diode rectifier but it give the high harmonic. Thus, active rectifier is proposed because the rectifier is fully controlled by space pulse width modulation (SPWM) thus the harmonic can be controlled. Active rectifier consist of 6 switch controlled by PWM. This SPWM is controlled by voltage oriented control, where the input for S<sub>1</sub> PWM is the reference voltage. The reference voltage is controlled by current control which the reference is the output of the speed control. Then, a maximum power point tracking (MPPT) algorithm allows the turbine to find and operate at its maximum power point by giving speed reference to speed control. The illustration about this overall system is shown in Figure 1. This study will discuss the model and simulation of MPPT and speed controller on a small-scale wind turbine that has been tested through simulation on Simulink MATLAB software.

## II. WIND TURBINE, PMSG, ACTIVE RECTIFIER MODEL

### A. Previous Work

There was many methodologies to control active rectifier, Voltage Oriented Control (VOC) and Direct Power Control

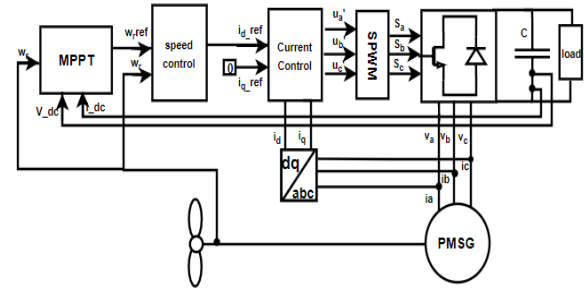


Figure 1. Small Wind Turbine System

(DPC). VOC guarantees high dynamic and static performance via an internal current control loop [2]. But the quality depends mainly on the current control strategy. However, the problem was founded when combined it to the MPPT. It's hard to find the right maximum power by using VOC. This methodology using speed as the control variable where the speed reference will update continuously by the MPPT.

### B. Wind Turbine Model

Turbine mechanical power generated by wind turbine expressed as [3]

$$P = \frac{1}{2} \rho C_p A V_w^3 \quad (1)$$

Where  $\rho$  is air density ( $kg/m^3$ ),  $A$  is rotor blade swept area ( $m^2$ ),  $V_w$  represent wind velocity ( $m/s$ ). Power coefficient,  $C_p$ , can be represented as [3]:

$$C_p = C_1 \left( \frac{C_2}{\lambda_i} - C_3 \beta - C_4 \right) e^{-C/\lambda_i} + C_6 \lambda \quad (2)$$

$$\frac{1}{\lambda_i} = \frac{1}{\lambda + 0.08\beta} - \frac{0.035}{\beta^3 + 1} \quad (3)$$

$$\lambda = \omega_m * \frac{R}{V_w} \quad (4)$$

The value of  $C_1$  to  $C_6$  depend on the type of rotor. In this paper, the value of  $C_1$  to  $C_6$  determined as follow,  $C_1 = 20$ ;  $C_2 = 140$ ;  $C_3 = 0.4$ ;  $C_4 = 28$ ;  $C_5 = 21$ ;  $C_6 = 0.068$

### C. PMSG Model

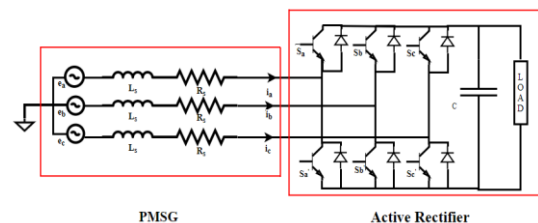


Figure 2. PMSG and Active Rectifier Circuit diagram

The PMSG and active rectifier are represented into single electrical circuit diagram as shown in Fig.

Phase voltage of PMSG represented as:

The electromagnetic force of each phase [4] can be obtained as follows:

$$e_a = p \Psi_f = -N\omega_r \Psi_f' \sin\theta_e \quad (5)$$

$$e_b = p \Psi_f = -N\omega_r \Psi_f' \sin(\theta_e - \frac{2}{3}\pi) \quad (6)$$

$$e_c = p \Psi_f = -N\omega_r \Psi_f' \sin(\theta_e + \frac{2}{3}\pi) \quad (7)$$

$\Psi_f$  is the flux linkage, and N is number of pole pairs of generator,  $\theta_e$  is rotor angular angle

$$V_a = e_a - (i_a * R_s) - \left( L_{sd} * \frac{di_a}{dt} \right) + \left( \frac{1}{2} * M * \frac{di_b}{dt} \right) + \left( \frac{1}{2} * M * \frac{di_c}{dt} \right) \quad (8)$$

$$V_b = e_b - (i_b * R_s) - \left( L_{sd} * \frac{di_b}{dt} \right) + \left( \frac{1}{2} * M * \frac{di_a}{dt} \right) + \left( \frac{1}{2} * M * \frac{di_c}{dt} \right) \quad (9)$$

$$V_c = e_c - (i_c * R_s) - \left( L_{sd} * \frac{di_c}{dt} \right) + \left( \frac{1}{2} * M * \frac{di_b}{dt} \right) + \left( \frac{1}{2} * M * \frac{di_a}{dt} \right) \quad (10)$$

Through Park transformation, generator voltage can be expressed in  $dq$  rotating reference frame [4].

$$\begin{bmatrix} v_{ds} \\ v_{qs} \end{bmatrix} = \begin{bmatrix} \cos\theta_e & -\sin\theta_e \\ \sin\theta_e & \cos\theta_e \end{bmatrix} \sqrt{\frac{2}{3}} \begin{bmatrix} 1 & -\frac{1}{2} & -\frac{1}{2} \\ 0 & \frac{\sqrt{3}}{2} & -\frac{\sqrt{3}}{2} \end{bmatrix} \begin{bmatrix} V_a \\ V_b \\ V_c \end{bmatrix} \quad (11)$$

The current in  $dq$  reference frame represented as

$$\frac{d}{dt} \begin{bmatrix} i_{sd} \\ i_{sq} \end{bmatrix} = - \begin{bmatrix} \frac{R_s}{L_{sd}} & -\frac{L_{sq}}{L_{sd}} \omega_e \\ \frac{L_{sd}}{L_{sq}} \omega_e & \frac{R_s}{L_{sq}} \end{bmatrix} \begin{bmatrix} i_{sd} \\ i_{sq} \end{bmatrix} + \begin{bmatrix} \frac{1}{L_{sd}} & 0 \\ 0 & \frac{1}{L_{sq}} \end{bmatrix} \begin{bmatrix} v_{sd} \\ v_{sq} \end{bmatrix} \quad (12)$$

Therefore, the electromagnetic torque and machine equivalent mechanical torque can be expressed as

$$T_e = N\{\Psi_f + (L_{sd} - L_{sq})i_{sq}\}i_{sq} \quad (13)$$

$$T_m = \frac{P}{\omega_r} = \frac{1}{2} \rho \pi R^2 C_p \frac{V_w^3}{\omega_r} \quad (14)$$

Hence the rotor speed can be calculated

$$\frac{d\omega_r}{dt} = \frac{T_e - T_m - B\omega_r}{J_t + J_p} \quad (15)$$

#### D. Active Rectifier Condition

Active rectifier is represented as 6 pulse rectifier with 6 switching conditions. According to figure 1, the switching conditions are based on the respond of controller's signal,  $u_a$ ,  $u_b$ , and  $u_c$ . As shown in figure 3, The controller's response is compared to carrier signal (green line) in PWM. If the response is higher than the carrier, PWM's value is 1, otherwise, if the response lower than the carrier signal, the

PWM's value is 0. The switch is on or off by the value of PWM. If the PWMA = 1 PWMB = 1 and PWMC = 0, means  $S_a = 1$ ,  $S_b = 1$ ,  $S_c = 0$ ,  $S_a' = 0$ ,  $S_b' = 0$ ,  $S_c' = 1$ . Then the circuit diagram for this condition is shown in figure 4(a).

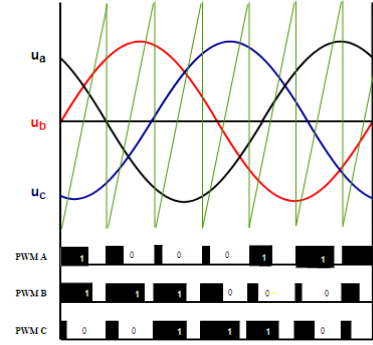


Figure 3 Switching Condition for Active Rectifier

#### E. Combine Circuit Model

According to figure 2, the 6 condition in table 1 can be represented by using the circuit diagram that is showed in figure 4.

From electric circuit analysis, conditions in figure 4(a) and 4(b) represented into matrices as follows

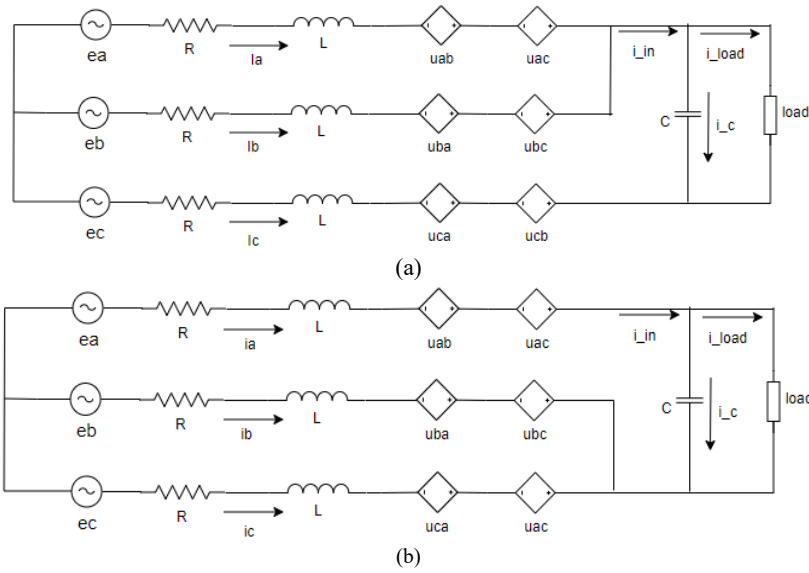
Condition 4(a):

$$\begin{bmatrix} \frac{di_a}{dt} \\ \frac{di_b}{dt} \\ \frac{di_c}{dt} \\ \frac{dv_{dc}}{dt} \end{bmatrix} = \begin{bmatrix} -R_s & R_s & R_s & -1 \\ 2*L_s & 4*L_s & 4*L_s & 4*L_s \\ R_s & -R_s & R_s & -1 \\ 4*L_s & 2*L_s & 4*L_s & 4*L_s \\ R_s & R_s & -R_s & 1 \\ 4*L_s & 4*L_s & 2*L_s & 2*L_s \\ \frac{1}{C} & \frac{1}{C} & 0 & -1 \end{bmatrix} \begin{bmatrix} i_a \\ i_b \\ i_c \\ v_{dc} \end{bmatrix} + \begin{bmatrix} \frac{1}{C} & -1 & -1 \\ 2*L_s & 4*L_s & 4*L_s \\ -1 & 1 & -1 \\ 4*L_s & 2*L_s & 4*L_s \\ -1 & -1 & 1 \\ 4*L_s & 4*L_s & 2*L_s \\ 0 & 0 & 0 \end{bmatrix} \begin{bmatrix} e_a \\ e_b \\ e_c \end{bmatrix} \quad (16)$$

Condition 4(b):

$$\begin{bmatrix} \frac{di_a}{dt} \\ \frac{di_b}{dt} \\ \frac{di_c}{dt} \\ \frac{dv_{dc}}{dt} \end{bmatrix} = \begin{bmatrix} -R_s & R_s & R_s & -1 \\ 2*L_s & 4*L_s & 4*L_s & 2*L_s \\ R_s & -R_s & R_s & 1 \\ 4*L_s & 2*L_s & 4*L_s & 4*L_s \\ R_s & R_s & -R_s & 1 \\ 4*L_s & 4*L_s & 2*L_s & 4*L_s \\ \frac{1}{C} & 0 & 0 & -1 \end{bmatrix} \begin{bmatrix} i_a \\ i_b \\ i_c \\ v_{dc} \end{bmatrix} + \begin{bmatrix} \frac{1}{C} & -1 & -1 \\ 2*L_s & 4*L_s & 4*L_s \\ -1 & 1 & -1 \\ 4*L_s & 2*L_s & 4*L_s \\ -1 & -1 & 1 \\ 4*L_s & 4*L_s & 2*L_s \\ 0 & 0 & 0 \end{bmatrix} \begin{bmatrix} e_a \\ e_b \\ e_c \end{bmatrix} \quad (17)$$

Where,  $R_s$  is Stator resistance,  $L_s$  is stator inductance,  $V_{dc}$  is DC link voltage,  $r_{load}$  is load resistance.

Figure 4. Electric Circuit Diagram (a)  $S_a = 1$   $S_b = 1$   $S_c = 0$  (b)  $S_a = 1$   $S_b = 0$   $S_c = 0$ 

### III. CONTROLLER STRATEGY

As shown in figure 5, The controller is divided by 2 part: double close loop control consist of current control and speed control, and the last part is MPPT.

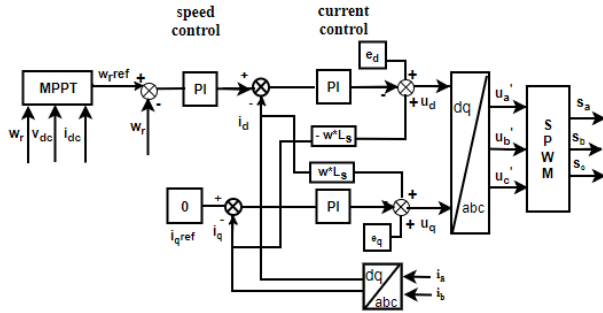


Figure 5. Controller block diagram

#### A. Current Control

For controlling the three-phase current, the transformation into  $i_d$ ,  $i_q$  is needed. The controller control  $i_d$  and  $i_q$  than use PI control to regulate the error. The reference of  $i_d$  is based on the output of speed control. Due to control the unit power factor, the reference of  $i_q$  is set to 0.

After calculating the appropriate  $u_d$  and  $u_q$ , space vector PWM control method could be directly used to calculate the control signal of switches in the main circuit [5]. The calculation is shown in equation (18) and (19).

$$u_d = e_d + \omega_r * L_s * i_q - K_p * (i_d^* - i_d) - \int K_i * (i_d^* - i_d) dt \quad (18)$$

$$u_q = e_q - \omega_r * L_s * i_d - K_p * (i_q^* - i_q) - \int K_i * (i_q^* - i_q) dt \quad (19)$$

#### B. Speed Control

The controller of the speed also use PI control. The input of the control is the error of speed reference from the output of MPPT and the actual rotor angular speed whereas the output is the reference for  $i_d$ . The calculation is shown in equation (20).

$$I_{dref} = K_p * (\omega_r^* - \omega_r) + \int K_i * (\omega_r^* - \omega_r) dt \quad (20)$$

#### C. MPPT

To track the maximum power from the double close-loop controller, a *Perturb and Observe* (P&O) MPPT algorithm is used. MPPT also ensure the turbine to work at its maximum power. P&O algorithm work by changing the control parameter and observe the output change [6]. This algorithm have low complexity, high efficiency, and does not require sensors or system requirements.

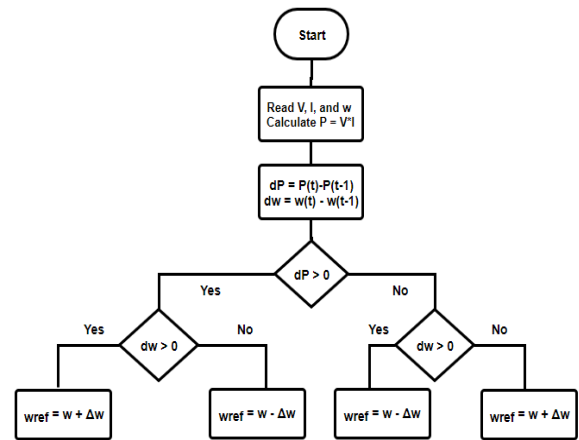


Figure 6. MPPT flowchart

Electric power compared with previous power. If  $\Delta P$  is positive and the speed change is positive, the reference speed will increase. The detail algorithm is shown in figure 6.

#### IV. RESULT

The proposed model in this paper simulated using Simulink MATLAB S-Function block. First, we need doing a test to track maximum power for various wind speed ( $V_w$ ). The test is done by adding continuously the  $\omega_{rref}$  as  $\omega_r$  can't follow  $\omega_{rref}$ . The illustration is shown in Figure 7. From this test, we know where the maximum power is, thus after the MPPT is implemented, we can conclude that the controller and MPPT is work in its maximum power. The test shows the maximum power of 6 m/s, 7 m/s, 8 m/s in Figure 8. The simulation shown the responses of system for various the wind speed are shown in Figure 9. .

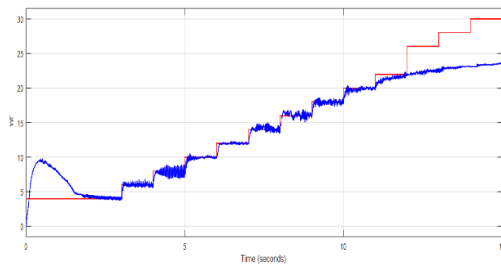
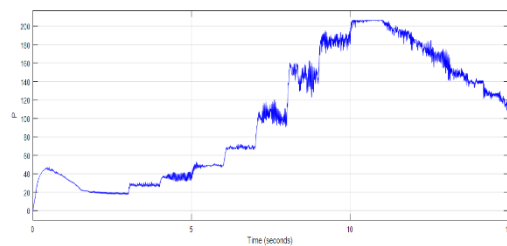
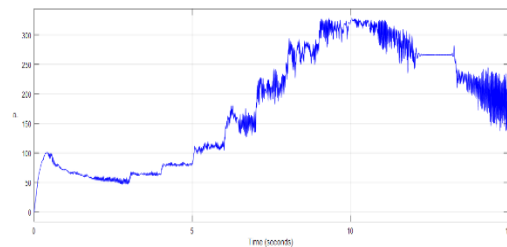


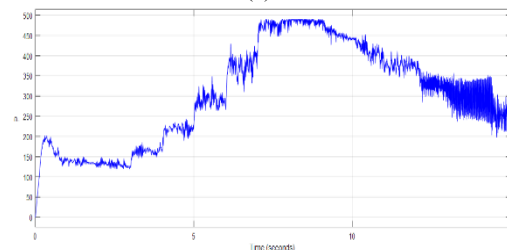
Figure 7.  $w_r$  for MPP testing in  $V_w = 6$  m/s



(a)

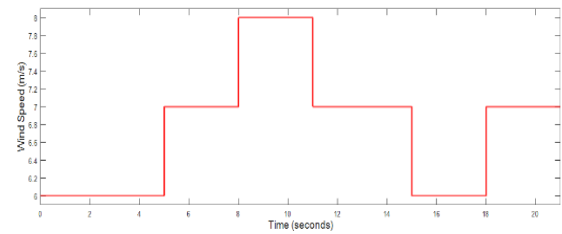


(b)

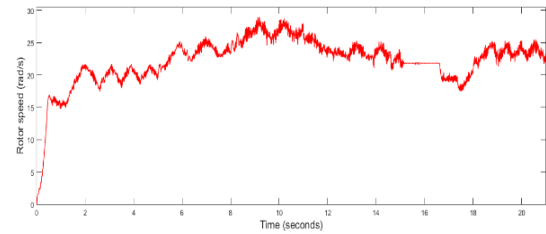


(c)

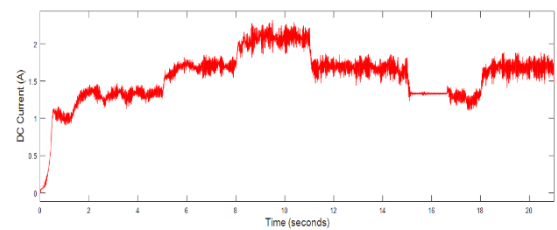
Figure 8. Turbine Power MPP testing (a) 6 m/s, (b) 7 m/s, (c) 8 m/s.



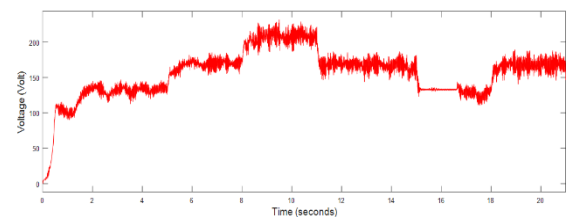
(a)



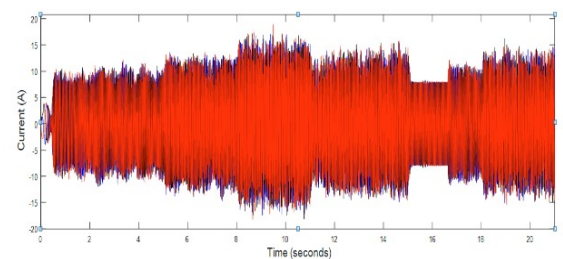
(b)



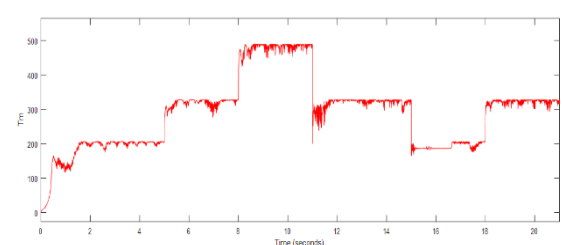
(c)



(d)



(e)



(f)

Figure 9. Wind turbine system with MPPT for various wind speed (a) wind speed (b)  $\omega_r$  (c)  $i_{dc}$  (d)  $v_{dc}$  (e)  $i_{abc}$  (f)  $P$

According to figure 9, The model of active rectifier is successfully simulated. The rectifier has produced DC current and voltage. The rotor speed is also successfully controlled by looking at  $\omega_r$  following the reference that come from the MPPT. When Figure 9(e) is compare to figure 8, the Power's values is equal to the maximum power from the testing simulation. Thus, MPPT algorithm could track its maximum power and perform the turbine rotor speed to work in its maximum power.

#### V. CONCLUSION

This paper proposed a model of active rectifier for small wind turbine which is controlled by speed control and MPPT. The model and controller successssfully simulated using Simulink MATLAB S-Function block. The simulation tested system by giving a various wind speed. The system performed great result either in speed control or in MPPT. The MPPT algorithm forces rotor angular speed to produce a maximum power and the simulation strongly show system work in its maximum. Furthermore, according to simulation, the system is able to be implemented by further improvement.

#### ACKNOWLEDGMENT

This research is funded by Universitas Indonesia research grant of the *Publikasi Internasional Terindeks untuk Tugas Akhir Mahasiswa UI (PITTA)* Nomor: 2439/UN2.R3.1/HKP.05.00/2018 .

#### REFERENCES

- [1] M. Malinowski, "Optimized Energy- Conversion System for Small Wind Turbine," *IEEE Power Electronic Magazine*, p. 16, 2015.
- [2] S. Lechat Sanjuan, "Voltage Oriented Control of Three-Phase Boost PWM Converters," p. 11, 2010.
- [3] A. Omar, F. Khater and A. Shaltout, "Per Unit Modeling of Wind Energy Conversion System Based on PMSG," in *ACCS'017&PEIT'017*, Alexandria, Egypt, 2017.
- [4] P. Vas, *Sensorless Vector and Direct Torque Control*, 1999.
- [5] W. S.-m. Wei Ke-xin, "Modeling and Simulation of Three-Phase Voltage Source PWM Rectifier," *IEEE Computer Society*, p. 982, 2008.
- [6] M. A. Abdullah, A. Yatim, C. W. Tan and S. R, "A Review of Maximum Power Point Tracking Algorithms for Wind Energy Systems," *Renewable and SUSTainable Energy Reviews* 16, pp. 3220-3227, 2012.
- [7] I. Nurzaman, B. W. Harini, N. Avianto and F. Yusivar, "Implementation of Maximum Power point Tracking Algorithm on Wind Turbine Generator using Perturb and Observe Method," in *International Conference on Sustainable Energy Engineering Application (ICSEEA)*, 2017.
- [8] H. Fathabdi, "Maximum MEchanical Power Extraction from Wind turbines using Novel Proposed High Accuracy Single-sensor-based MAXimum Power Point Tracking Technique," *Energy*, pp. 1219-1230, 2016.
- [9] Y. Xia, K. H. Ahmed and B. W. Williams, "A New MAXimum Power Point Tracking Technique for Permanent Magnet Synchronous Generator Based Wind Energy Conversion System," *IEEE TRANSACTIONS ON POWER ELECTRONICS*, vol. 26, no. 12, pp. 3609-3620, 2011.
- [10] M. S. A. S. R. G. F. Yusivar, "Stability Analysis of DC-link Voltage Control on Autonomous Micro Hydro Power Plant System," p. 500, 2014.



# **AUTHORS' BACKGROUND**

Your Name	Title*	Research Field	Personal website
Ni Luh Gayatri Dharmaraditya	Master Student		-
Lazarus Stefan	Master Student		-
Feri Yusivar	Associate professor		

\*This form helps us to understand your paper better, **the form itself will not be published.**

\*Title can be chosen from: master student, Phd candidate, assistant professor, lecture, senior lecture, associate professor, full professor

# Stator Flux Oriented Control of Three-Phase Induction Motor with Improved Decoupling Scheme

Irvan Arif, Bernadeta Wuri Harini, and Feri Yusivar

Department of Electrical Engineering  
Faculty of Engineering, Universitas Indonesia  
Depok, Indonesia

vanarif.engineering@gmail.com, b.wurihari@gmail.com, yusivar@yahoo.com

**Abstract**—This paper proposes an improved decoupling scheme of stator flux-oriented control for three-phase induction motor. The simulation software used in this paper is MATLAB Simulink®. The result of the simulation indicates that this stator flux-oriented control can control the speed of the rotor angle and stator magnetization current successfully. The angular velocity of 120 rad/s achieved by settling time 2 seconds in critically-damped response and steady-state error 0.083%. The controller can overcome the external disturbance in the form of load torque of 5 Nm which has been simulated in this paper. The proposed stator voltage decoupling scheme which is used in this simulation is correct and become one of success factor of this control method.

**Keywords**—Induction Motor; SFOC; Decoupling Model; Stator Flux Model

## I. INTRODUCTION

Induction motor is a type of AC motor that is often used by industrial field because it has good self-starting ability, simple structure, low cost of production and maintenance, and reliable [1]. One of the problem of induction motor is that it is difficult to control. Further developments of power electronics and microelectronics open the issue of research and development of induction motor vector control. Some vector controlling techniques that have been proposed before are divided into two, direct vector control and indirect vector control based on field orientation vector. Direct vector control obtains the field orientation vector by using the quantity of stator terminal. In the other hand, indirect vector control obtains the field orientation vector by using slip frequency of machine.

Stator flux-oriented control of induction motor is a type of direct vector control because it uses the quantity of stator terminal. This method has several parts that can be developed, such as decoupling scheme and stator flux model.

This paper describes the simulation of three phase squirrel cage induction motor speed control based on stator flux orientation by using the proposed decoupling stator voltage scheme.

## II. IM MODEL AND DRIVE OPERATING PRINCIPLE

To simulate the three-phase squirrel cage induction motor control, the dynamic model of induction motor is needed. The fundamental behavior of squirrel cage induction motor is usually based on a set of dynamical equations that can be

expressed in different reference frame. In this section, the induction machine model is defined by the stator currents and stator flux as state variables in the stationary  $\alpha$ - $\beta$  reference frame. The dynamic model that is used in this paper is same as in [4]. The following is the dynamic model of three phase squirrel cage induction motor:

$$\frac{di_{\alpha s}}{dt} = (R_s L_s i_{\alpha s} - N_p \omega_r L_m^2 i_{\beta s} - R_r L_m i_{\alpha r} - N_p \omega_r L_r L_m i_{\beta r} - L_r u_{\alpha s})K \quad (1)$$

$$\frac{di_{\beta s}}{dt} = (N_p \omega_r L_m^2 i_{\alpha s} - R_s L_r i_{\beta s} - N_p \omega_r L_r L_m i_{\alpha r} - R_r L_m i_{\beta r} - L_r u_{\beta s})K \quad (2)$$

$$\frac{di_{\alpha r}}{dt} = -(R_s L_m i_{\alpha s} - N_p \omega_r L_s L_m i_{\beta s} - R_r L_s i_{\alpha r} - N_p \omega_r L_s L_r i_{\beta r} - L_m u_{\alpha s})K \quad (3)$$

$$\frac{di_{\beta r}}{dt} = -(N_p \omega_r L_s L_m i_{\alpha s} - R_s L_m i_{\beta s} - N_p \omega_r L_s L_r i_{\alpha r} - R_r L_s i_{\beta r} - L_m u_{\beta s})K \quad (4)$$

$$K = \frac{1}{L_m^2 - L_s L_r} \quad (5)$$

Where:

- $u_{\alpha s}, u_{\beta s}$  = Stator voltages  $\alpha$ - $\beta$  in *stationary reference frame* (Volt)
- $i_{\alpha s}, i_{\beta s}$  = Stator currents  $\alpha$ - $\beta$  in *stationary reference frame* (Volt)
- $R_s$  = Stator resistance (Ohm)
- $R_r$  = Rotor resistance (Ohm)
- $L_s$  = Stator inductance (Henry)
- $L_r$  = Rotor inductance (Henry)
- $L_m$  = Mutual inductance (Henry)
- $\omega_r$  = Rotor angle speed (rad/s)
- $N_p$  = Number of pole pair

Figure 1 below shows the three-phase squirrel cage induction motor speed control based on stator field orientation block diagram with the proposed control algorithm.

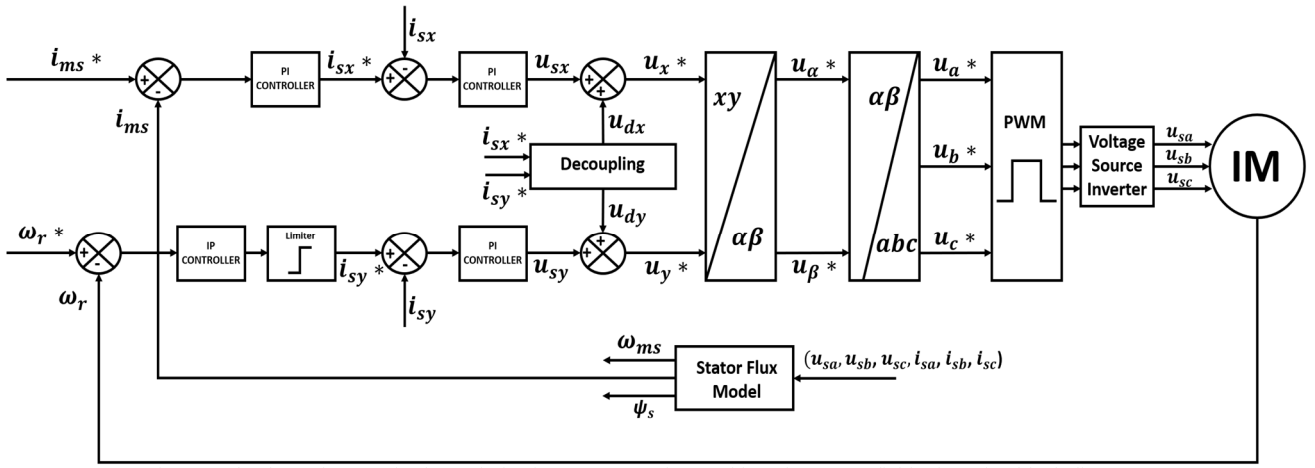


Figure 1 The three phase squirrel cage induction motor speed control based on stator field orientation block diagram

The algorithm inputs are reference rotor speed  $\omega_r^*$  and stator magnetizing current  $i_{ms}^*$ . Main control loop consists of the speed IP regulator, the magnetizing current PI regulator, and the current controllers. The feedback signals of stator magnetizing current  $\hat{i}_{ms}$  and rotor speed  $\omega_r$ , needed for closed-loop control are provided by stator flux model and rotor speed sensor, respectively. The stator flux model utilizes the stator currents  $I_s$  and voltages  $U_s$  as the input variables. Decoupling scheme that is proposed in this paper is described later.

### III. IMPROVED DECOUPLING SCHEME AND STATOR FLUX MODEL

#### A. Improved Decoupling Scheme

Decoupling scheme is a very important part of stator field oriented control. By using an appropriate decoupling scheme, the torque component and flux component can be separated and controlled respectively. In modelling the decoupling equation of induction motor stator voltage, it can be started from the equation of rotor voltage as in the following equation (6)

$$\bar{u}_{r\psi s} = R_r \bar{i}_{r\psi s} + L_r \frac{d\bar{i}_{r\psi s}}{dt} + L_m \frac{d\bar{i}_{s\psi s}}{dt} + j(\omega_{ms} - \omega_r)(L_r \bar{i}_{r\psi s} + L_m \bar{i}_{s\psi s}) \quad (6)$$

In equation (6) there is still a rotor current component, where the component must be eliminated by substituting equation (18) into equation (6), and by assuming the rotor coil of the squirrel cage type is a short circuit then  $\bar{u}_{r\psi s} = 0$ , then a new rotor voltage equation is obtain as follows.

$$0 = R_r \left[ |\bar{i}_{ms}| - \frac{L_s \bar{i}_{s\psi s}}{L_m} \right] + L_r \frac{d|\bar{i}_{ms}|}{dt} - \left( \frac{L'_s L_r}{L_m} \right) \frac{d\bar{i}_{s\psi s}}{dt} + j\omega_{sl} \left[ L_r |\bar{i}_{ms}| - \left( \frac{L'_s L_r}{L_m} \right) \bar{i}_{s\psi s} \right] \quad (7)$$

Then, it is necessary to separate the real and imaginary components from equation (7) to obtain the equation (8) and (9) as follows

$$\frac{L_m}{L'_s} \frac{d|\bar{i}_{ms}|}{dt} + \frac{L_m}{L_s T'_r} |\bar{i}_{ms}| = \frac{di_{sx}}{dt} + \frac{i_{sx}}{T'_r} - \omega_{sl} i_{sy} \quad (8)$$

$$\omega_{sl} \left( \frac{L_m |\bar{i}_{ms}|}{L'_s} - i_{sx} \right) = \frac{di_{sy}}{dt} + \frac{i_{sy}}{T'_r} \quad (9)$$

To obtain the stator voltage equation in the x and y axes it is necessary to substitute equations (22) and (10) into equations (8) and (9)

$$|\bar{i}_{ms}| = \frac{R_s}{\omega_{ms} L_m} \left( \frac{u_{sy}}{R_s} - i_{sy} \right) \quad (10)$$

The three phase squirrel cage induction motor stator voltage equation in the x and y axes are represented by the following equations (11) and (12)

$$u_{sx} = L'_s \frac{di_{sx}}{dt} + \left( \frac{L'_s}{T'_r} + R_s \right) i_{sx} - \left( \omega_{sl} - \frac{R_s}{\omega_{ms} L_s T'_r} \right) L'_s i_{sy} - \frac{L'_s}{\omega_{ms} L_s T'_r} u_{sy} \quad (11)$$

$$u_{sy} = \frac{L'_s \omega_{ms}}{\omega_{sl}} \frac{di_{sy}}{dt} + \left( R_s + \frac{L'_s \omega_{ms}}{\omega_{sl} T'_r} \right) i_{sy} + L'_s \omega_{ms} i_{sx} \quad (12)$$

In equations (11) and (12), it can be seen that there is coupling between the x and y components that can cause nonlinearity. Therefore, we can obtain the stator voltage decoupling equation as in the following equations (13) and (14)

$$u_{dx} = \frac{L'_s}{\omega_{ms} L_s T'_r} u_{sy} + \left( \omega_{sl} - \frac{R_s}{\omega_{ms} L_s T'_r} \right) L'_s i_{sy} \quad (13)$$

$$u_{dy} = -\omega_{ms} L'_s i_{sx} \quad (14)$$

The given stator voltage must satisfy the following equations (15) and (16)

$$u_x^* = u_{sx} + u_{dx} \quad (15)$$

$$u_y^* = u_{sy} + u_{dy} \quad (16)$$

Figure 2 below is the decoupling scheme proposed in this paper.

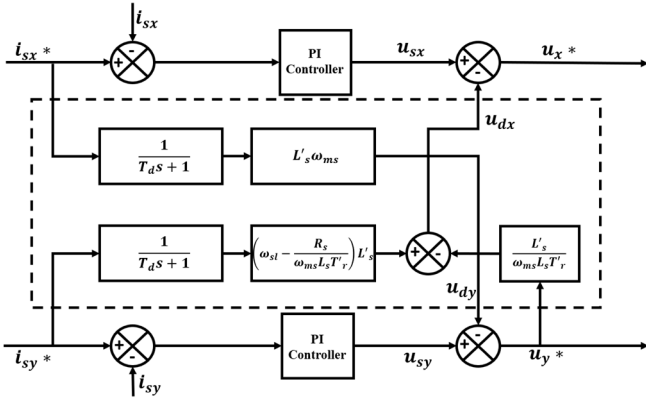


Figure 2 The improved decoupling scheme of three phase squirrel cage induction motor stator voltage

### B. Stator Flux Model

Stator flux model is one of the important parts of stator field oriented control of induction motor. By using the appropriate stator flux model, the calculation results of the parameters required in the control objective will be more accurate and precise. In an attempt to model the statof flux model of three-phase squirrel cage induction motor, it can be started from the three phase squirrel cage induction motor stator voltage as in the following equation (17)

$$\bar{u}_{s\psi s} = R_s \bar{i}_{s\psi s} + L_s \frac{d\bar{i}_{s\psi s}}{dt} + L_m \frac{d\bar{i}_{r\psi s}}{dt} + j\omega_{ms} L_s \bar{i}_{s\psi s} + j\omega_{ms} L_m \bar{i}_{r\psi s} \quad (17)$$

In equation (17), there is still a rotor current component. As it is known that in the three phase squirrel cage induction motor, rotor current component is very difficult to obtain. Therefore, the rotor current component of the equation (17) must be eliminated by substituting the rotor current equation shown in equation (18)

$$\bar{i}_{r\psi s} = |\bar{i}_{ms}| - \frac{L_s \bar{i}_{s\psi s}}{L_m} \quad (18)$$

Substituting equation (18) into equation (17), equation (19) is obtained as the stator voltage equation of the three phase squirrel cage induction motor in which no rotor current component is present.

$$\bar{u}_{s\psi s} = R_s \bar{i}_{s\psi s} + L_m \frac{d|\bar{i}_{ms}|}{dt} + j\omega_{ms} L_m |\bar{i}_{ms}| \quad (19)$$

Then, simplify equation (19) to its real and imaginary component and make it in the x-y stator current equation as in the following (20) and (21) equations.

$$i_{sx} = \frac{u_{sx}}{R_s} - \frac{L_m}{R_s} \frac{d|i_{ms}|}{dt} \quad (20)$$

$$i_{sy} = \frac{u_{sy}}{R_s} - \omega_{ms} L_m \frac{|i_{ms}|}{R_s} \quad (21)$$

To obtain the equation of stator flux model, equation (20) and (21) must be processed to obtain the stator flux model as follows.

$$\frac{d|i_{ms}|}{dt} = \frac{u_{sx}}{L_m} - \frac{R_s}{L_m} i_{sx} \quad (22)$$

$$\omega_{ms} = \frac{1}{L_m |i_{ms}|} (u_{sy} - R_s i_{sy}) \quad (23)$$

$$\psi_s = L_m i_{ms} \quad (24)$$

$$\theta_e = \int \omega_{ms} dt \quad (25)$$

Equations (22) – (25) are the basic equations of stator flux model which are used to calculate the parameters of the three phase squirrel cage induction motor used for control. The representation of the stator flux model in a block diagram can be made from equations (22) – (25). Figure 3 below shows a diagram of the stator flux model of three phase squirrel cage induction motor that is used in this research.

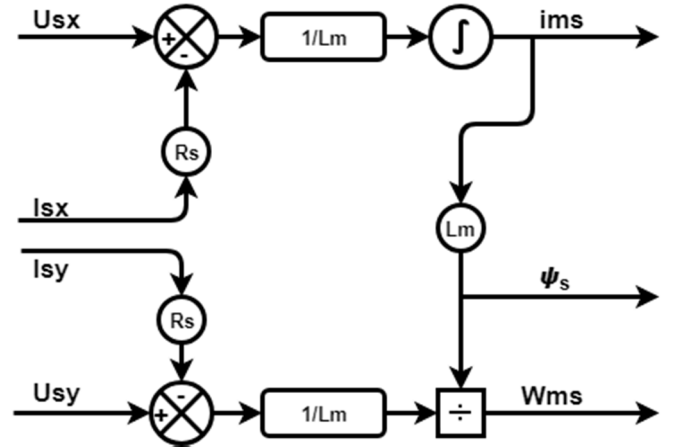


Figure 3 Stator flux model of three phase squirrel cage induction motor

## IV. SIMULATION RESULT

The proposed simulation of three phase squirrel cage induction motor in this paper is simulated by C-MEX S-Function block diagram in MATLAB Simulink. The simulation was run for 10 seconds. Figure 4 below is the simulation block diagram in MATLAB Simulink.

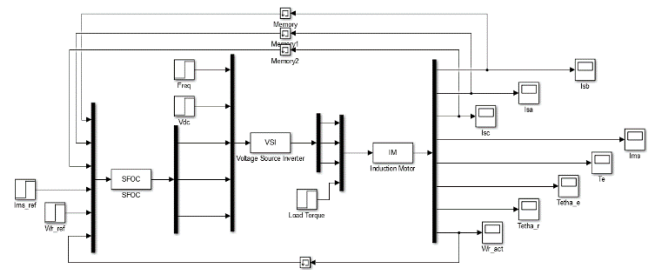


Figure 4 CMEX S-Function Simulation Diagram in MATLAB Simulink

The test was done within two condition testing. For the first segment, system was tested by stating the load torque as 0 Nm, the stator magnetizing current as 1.45 A and the rotor speed as 120 rad/s. This is shown as a no load testing. The second segment was tested by stating the load torque as 5 Nm after 5 seconds of the simulation, the stator magnetizing current as 1.45 A and the rotor speed as 120 rad/s. This is shown as load testing.

The parameter and rating of a three-phase induction motor that is used in this simulation shown in the table below

Table 1 Induction Motor Parameters and Ratings

$V_{rated}$	220 V	$R_r$	1.7979 $\Omega$
$I_{rated}$	5.1 A	$L_s$	0.4633 H
$N_{rated}$	1433 rpm	$L_r$	0.4633 H
$R_s$	2.4057 $\Omega$	$L_m$	0.4531 H

#### A. No Load Testing

Figure 5, 6, 7, and 8 showed the rotor speed, stator magnetizing current, stator voltage of three phase induction motor during the no load testing. Based on figure 5, the response of the rotor speed is critically-damped by settling time of 2 seconds and the steady-state error is 0.083%. Figure 6 showed the response of stator magnetizing current that is successfully controlled by the controller. The response is fluctuated in the range of 1.45 A. Figure 7 showed the response of stator voltage (control signal) during the no load test. The amplitude of control signal is 130 Volt. Figure 8 showed the response of stator current during the no load testing. The amplitude of stator current in steady-state condition is 2 A, still below the maximum current allowed.

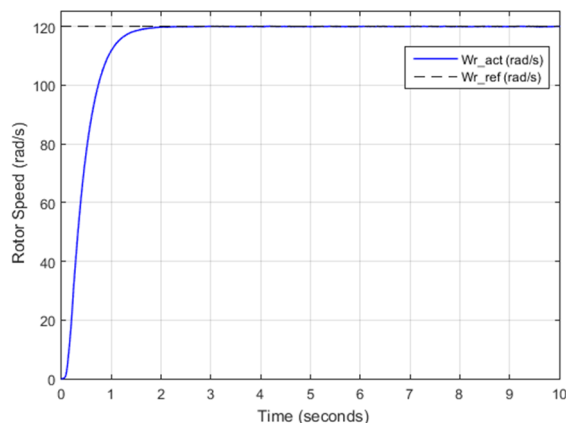


Figure 5 Rotor speed response in no load testing

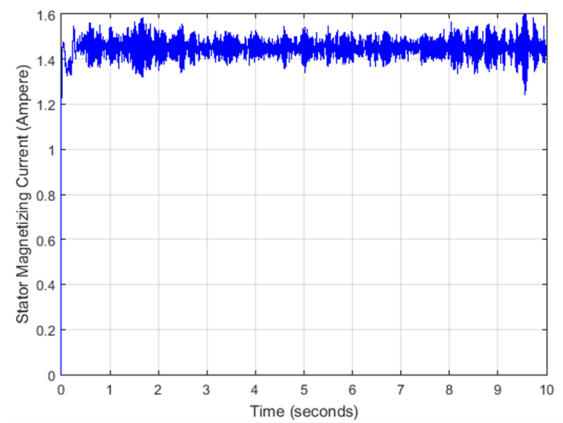


Figure 6 Stator magnetizing current response in no load testing

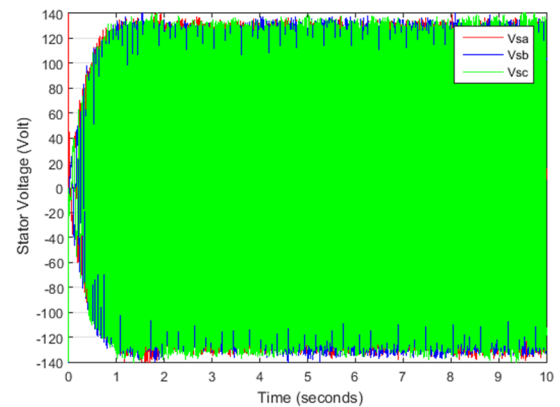


Figure 7 Stator voltage (control signal) response in no load testing

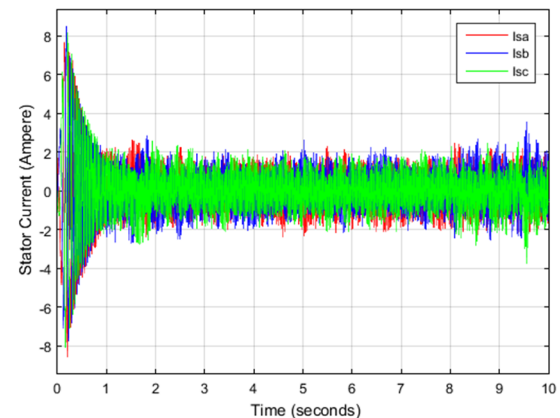


Figure 8 Stator current response in no load testing

#### B. Load Testing

Figure 9, 10, 11, and 12 showed the rotor speed, stator magnetizing current, and stator voltage of three phase induction motor during load testing. Based on figure 9, the response of the rotor speed is critically-damped by settling time of 2 seconds, and when the load torque was changed from 0 to 5 Nm after 5 seconds of simulation, the rotor speed decreased but the controller can handle the load torque and the rotor speed

increased back to 120 rad/s. Figure 10 showed that the response of stator magnetizing current in the load testing is same as in the no load testing. Figure 11 showed the response of control signal (stator voltage) during the load testing. The amplitude of control signal increased from 130 Volt to 150 Volt after the load torque was applied to the system. Figure 12 showed the response of stator current during load testing. The amplitude of stator current increased from 2 A to 4 A after the load torque was applied to the system.

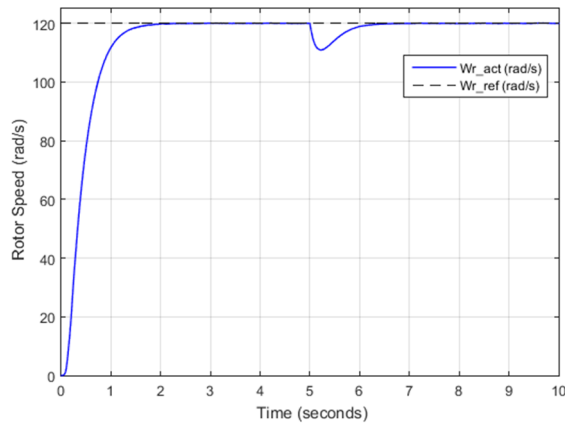


Figure 9 Rotor speed response in load testing

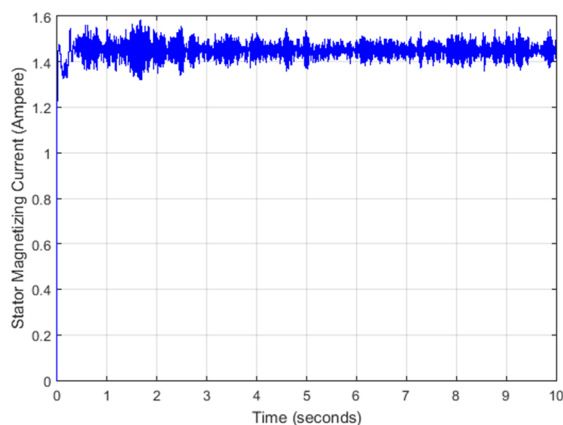


Figure 10 Stator magnetizing current response in load testing

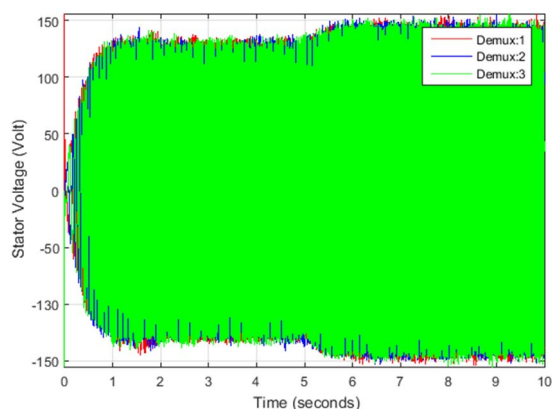


Figure 11 Stator voltage (control signal) response in load testing

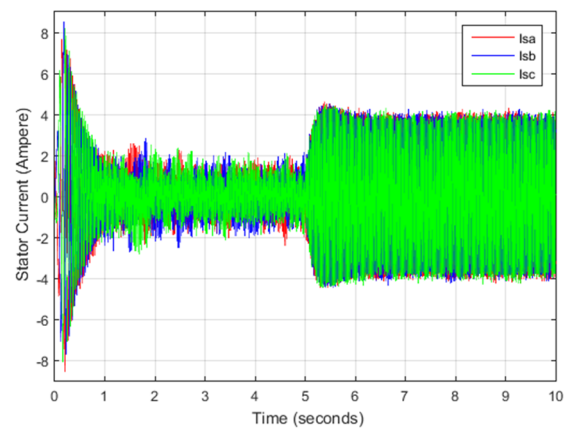


Figure 12 Stator current response in load testing

## V. CONCLUSION

The result of the simulation indicates that this stator flux oriented control with improved stator voltage decoupling scheme is capable to control both speed of the rotor angle and stator magnetization current successfully. The angle velocity of 120 rad/s achieved by settling time 2 seconds in critically-damped response and steady-state error 0.083%. The controller can overcome the external disturbance in the form of load torque of 5 Nm which has been simulated in this paper. The proposed stator voltage decoupling scheme which are used in this simulation is correct and also become one of success factor of this control method.

## ACKNOWLEDGMENT

This research is funded by Universitas Indonesia research grant of the *Publikasi Internasional Terindeks untuk Tugas Akhir Mahasiswa UI* (PITTA) 2018 Nomor: 2439/UN2.R3.1/HKP.05.00/2018

## REFERENCES

- [1] M. Baishan and J. Feng, "Study on Stator Flux Oriented Sensorless Induction Motor Control System," *IEEE*, pp. 758-762, 2014.
- [2] S. Lee, G. Park and M. Jung, "Sensorless Stator Flux Oriented Control of Induction Motors using PLPF with Flux Error Compensator," *IEEE*, 2014.
- [3] V. Staudt and A. Steimel, "Stator-Flux-Oriented Control for Traction Drives," *IEEE*, pp. 779-786, 2015.
- [4] F. Yusivar dan S. Wakao, "Minimum Requirements of Motor Vector Control Modeling and Simulation Utilizing C MEX S-function in MATLAB/SIMULINK," *IEEE*, 2001.
- [5] J. Cherian and J. Mathew, "Parameter Independent Sensorless Vector Control of Induction Motor," *IEEE*, 2012.



# Sensorless PMSM Control using Fifth Order EKF in Electric Vehicle Application

Nanda Avianto Wicaksono

Electrical Engineering,

Universitas Indonesia

Kampus UI Depok 16424, West Java,  
Indonesia

nanda.avianto@esdm.go.id

Bernadeta Wuri Harini

Electrical Engineering,

Universitas Indonesia

Kampus UI Depok 16424, West Java,  
Indonesia

wuribernard@usd.ac.id

Feri Yusivar

Electrical Engineering,

Universitas Indonesia

Kampus UI Depok 16424, West Java,  
Indonesia

yusivar@yahoo.com

**Abstract**—This paper is intended to design a controller and an observer of a sensorless PMSM (permanent magnet synchronous motor) in electric vehicle application. The controller uses the field orientation control (FOC) method and the observer type is the fifth order extended Kalman filter (EKF). The designed controller and observer are tested by varying the elevation angle of the route that is several times abruptly changed. The simulation result shows that the designed controller and observer can respond to the elevation angles given.

**Keywords**—Sensorless PMSM, FOC, EKF, electric vehicle, elevation angle, torque load

## I. INTRODUCTION

The development and utilization of electric vehicles are getting higher along with the increasing awareness of the environmental friendly energy. Consumer users need electric vehicles that can not only be used in the city, but can also be used in the rural and country side. In the rural and country side, one challenge encountered is the ascending route. The elevation angle in the rural and country side is higher than those in the city. The elevation angle in the rural and country side also changes abruptly. Therefore, it takes an electric vehicle that is able to respond to different types of elevation angles.

The elevation angle of an ascending route affects the torque load that is handled by the motor. In combustion vehicle application, the relation between the elevation angle and the torque load was developed by Kamalakkannan [1]. This model can be used in developing the mechanical part of the electric vehicle model.

The motor used is the sensorless PMSM that is equipped with neither the sensor of the rotational speed of the rotor nor the sensor of the rotor/electric angle position [2]. One of them is needed to run PMSM. To obtain the rotational speed of the rotor or the rotor angle position, an EKF observer is used in this design.

The EKF was used in many applications that use sensorless PMSM. The EKF for sensorless PMSM was developed by Zheng et.al [3], Termizi et.al [4], and Walambe et.al [5]. They developed the fourth order EKF that is able to estimate stator currents in dq-axis, rotational speed of rotor, and electric angle position. The fourth order EKF did not estimate torque load. If the torque load changed abruptly, the fourth order EKF could not estimate the rotation speed of rotor and the electric angle position accurately, but it could if the torque load is relatively or slightly constant. Without rotation speed of rotor and electric angle position, field orientation control (FOC) algorithm could not control

PMSM. The developed fourth order EKF was only tested by using one shot of torque load in short term of many seconds. It did not ensure the controller and the observer could work in long term continuously.

In order to respond to the elevation angle of the route that changes abruptly, this paper will develop the fifth order EKF. The fifth order EKF is able to estimate stator currents in dq-axis, rotation speed of rotor, electric angle position, and torque load.

The controller and the fifth order EKF is also tested by varying the elevation angle of the route in long term of several hundred seconds. The elevation angle of the route given is several times changed abruptly.

## II. ELECTRIC VEHICLE MODEL

The electric vehicle model consists of four parts, i.e. the mechanical part, the PMSM part, the controller part, and the fifth order EKF. The block diagram of the electric vehicle model is shown in Fig. 1.

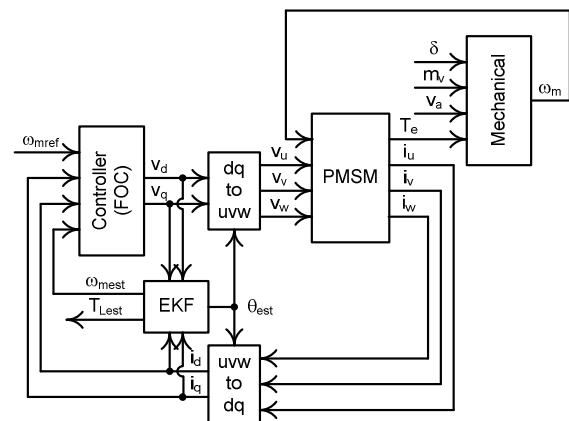


Fig. 1. The electric vehicle model block diagram

### A. Mechanical

In an ascending route, there are four forces that work, i.e. inertia force, gradient force, rolling resistance force, and aerodynamic drag force (see Fig. 2)[1].

The inertia force is a force that works when the vehicle accelerates or decelerates. The inertia force is expressed by

$$f_i = m_v a_v = m_v r_w \alpha_w \quad (1)$$

where  $f_i$  is the inertia force,  $m_v$  is the mass of the vehicle,  $a_v$  is the vehicle acceleration/deceleration in translation movement,  $r_w$  is the wheel radius, and  $\alpha_w$  is the wheel acceleration/deceleration in rotational movement.

The gradient force is a force that works while the vehicle is on an inclined plane. The gradient force is expressed by

$$f_g = m_v g \sin \delta \quad (2)$$

where  $f_g$  is the gradient force,  $m_v$  is the mass of the vehicle,  $g$  is the gravity acceleration, and  $\delta$  is the elevation angle of the inclined plane.

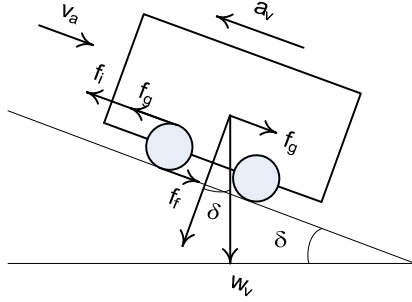


Fig. 2. The electric vehicle on an inclined plane

The rolling resistance force is a friction force between the wheels and the road. The rolling resistance force is expressed by

$$f_f = c_r m_v g \cos \delta \quad (3)$$

where  $f_f$  is the rolling resistance force,  $c_r$  is the friction coefficient between wheel and road,  $m_v$  is the mass of the vehicle,  $g$  is the gravity acceleration, and  $\delta$  is the elevation angle of the inclined plane.

The aerodynamic drag force is a force that works when the vehicle is moving with respect to the surrounding air. The aerodynamic drag force is expressed by

$$f_a = 0.5 \rho_a c_d A_f (v_v + v_a)^2 \quad (4)$$

where  $f_a$  is the aerodynamic drag force,  $\rho_a$  is the mass density of air,  $c_d$  is the drag coefficient of air,  $A_f$  is the front area of the vehicle,  $v_v$  is the vehicle velocity, and  $v_a$  is the air velocity.

By considering the four forces, the total torque load of the wheel is expressed by

$$T_w = r_w (f_i + f_g + f_f + f_a) \quad (5)$$

where  $T_w$  is the total torque load of the wheel and  $r_w$  is the wheel radius.

The wheel and the motor are connected by a gear. The gear is the mechanical part that is used to change the speed and the torque between the wheel and the motor. The relation speeds between the wheel and the motor is expressed by

$$\omega_w = \frac{\omega_m}{n_g} \quad (6)$$

where  $\omega_w$  is the rotational speed of the wheel,  $\omega_m$  is the rotational speed of the motor, and  $n_g$  is the gear ratio.

The relation torques between the wheel and the motor is expressed by

$$\frac{T_w}{\eta n_g} = T_m \quad (7)$$

where  $T_w$  is the torque of the wheel,  $T_m$  is the torque of the motor,  $n_g$  is the gear ratio, and  $\eta$  is the efficiency coefficient of gear.

In rotational movement, the relation between rotational acceleration and torque is expressed by

$$J_m \frac{d\omega_m}{dt} = T_e - B_m \omega_m - T_{m0} - T_m \quad (8)$$

where  $J_m$  is the moment inertia of the motor rotor,  $\omega_m$  is the rotational speed of the motor,  $B_m$  is the friction of the motor,

$T_{m0}$  is the initial torque of the motor, and  $T_m$  is the total torque load of the motor.

By substitution (1)-(7) to (8) obtains the relation between rotational speed and the torque load of the motor is expressed by

$$\left( J_m + \frac{r_w^2 m_v}{\eta n_g^2} \right) \frac{d\omega_m}{dt} = T_e - B_m \omega_m - T_{m0} - \frac{r_w}{\eta n_g} (f_g + f_f + f_a) \quad (9)$$

## B. PMSM

In this paper, the electrical model of PMSM is expressed by [2]

$$\frac{di_d}{dt} = \frac{-R_s i_d}{L_d} + \frac{N \omega_m L_q i_q}{L_d} + \frac{v_d}{L_d} \quad (10)$$

$$\frac{di_q}{dt} = \frac{-R_s i_q}{L_q} - \frac{N \omega_m L_d i_d}{L_q} - \frac{N \omega_m \psi}{L_q} + \frac{v_q}{L_q} \quad (11)$$

$$T_e = N \psi i_q + N L_d i_d i_q - N L_q i_d i_q \quad (12)$$

$$\frac{d\theta}{dt} = N \omega_m \quad (13)$$

where  $i_d$  is the stator current in d-axis,  $i_q$  is the stator current in q-axis,  $v_d$  is the stator voltage in d-axis,  $v_q$  is the stator voltage in q-axis,  $T_e$  is the electric torque that is generated by the PMSM,  $\omega_m$  is the rotational speed of the motor,  $\theta$  is the electric angle position,  $N$  is number of pole pairs,  $R_s$  is the stator resistance,  $L_d$  is the inductance in d-axis,  $L_q$  is the inductance in q-axis, and  $\psi$  is the magnetic flux of the PMSM. The PMSM block diagram is shown in Fig.3.

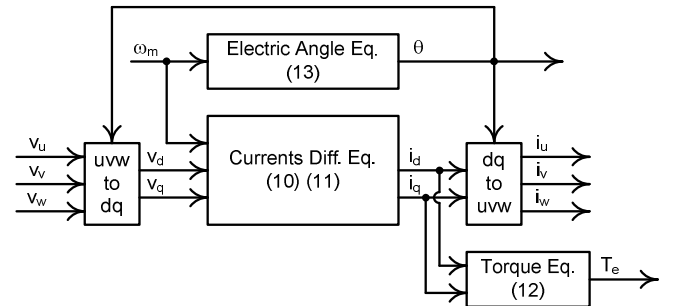


Fig. 3. The PMSM block diagram

## C. Controller

The controller part is composed of speed controller, linear current controllers, and nonlinear decoupling references calculation [3]. The controller block diagram is shown in Fig.4.

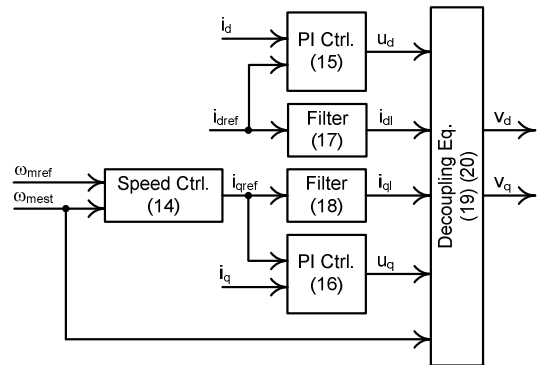


Fig. 4. The controller block diagram

The speed controller uses PI controller. It is expressed by

$$i_{qref} = K_{pw}(\omega_{mref} - \omega_{mest}) + K_{iw} \int_0^t (\omega_{mref} - \omega_{mest}) dt \quad (14)$$

where  $i_{qref}$  is the reference value of the stator current in q-axis,  $\omega_{mref}$  is the reference value of the rotational speed of the motor,  $\omega_{mest}$  is the estimated value of the rotational speed of the motor.

The controller sends the stator voltage references to PMSM. The stator voltage references contained the linear references and the nonlinear references. The linear references are adjusted by two PI controllers that are expressed by

$$u_d = K_{pid}(i_{dref} - i_d) + K_{iid} \int_0^t (i_{dref} - i_d) dt \quad (15)$$

$$u_q = K_{piq}(i_{qref} - i_q) + K_{iiq} \int_0^t (i_{qref} - i_q) dt \quad (16)$$

where  $u_d$  is the linear stator voltage references in d-axis, and  $u_q$  is the linear stator voltage references in q-axis,  $i_{dref}$  is the reference value of the stator current in d-axis,  $i_{qref}$  is the reference value of the stator current in q-axis,  $i_d$  is the actual value of the stator current in d-axis, and  $i_q$  is the actual value of the stator current in q-axis. On the other hand, the nonlinear stator voltage references is to consider coupling mechanism in the PMSM.

The total of the stator voltage references are adjusted by two low pass filters and decoupling equations that are expressed by

$$\frac{di_{dl}}{dt} = \frac{1}{T_d}(i_{dref} - i_{dl}) \quad (17)$$

$$\frac{di_{ql}}{dt} = \frac{1}{T_d}(i_{qref} - i_{ql}) \quad (18)$$

$$v_d = u_d - N\omega_{mest}L_q i_{ql} \quad (19)$$

$$v_q = u_q - N\omega_{mest}L_d i_{dl} - N\omega_{mest}\psi \quad (20)$$

where  $i_{dl}$  is the low pass filter output of the stator current in d-axis,  $i_{ql}$  is the low pass filter output of the stator current in q-axis,  $v_d$  is the total of the stator voltage references in d-axis,  $v_q$  is the total of the stator voltage references in q-axis,  $u_d$  is the linear stator voltage references controller in d-axis,  $u_q$  is the linear stator voltage references in q-axis,  $\omega_{mest}$  is the estimated value of the rotational speed of the motor,  $N$  is number of pole pairs,  $L_d$  is the inductance in d-axis,  $L_q$  is the inductance in q-axis, and  $\psi$  is the magnetic flux of the PMSM.

#### D. EKF

In this research, the fifth order EKF is designed to estimate the stator currents in dq-axis, the rotation speed of motor, the electric angle position, and the torque load.

$$x_k = [i_d \ i_q \ \omega_m \ \theta \ T_L]^T \quad (21)$$

In designing the fifth order EKF, the PMSM model that is used is expressed by

$$\frac{di_d}{dt} = -\frac{R_s i_d}{L_d} + \frac{N\omega_m L_q i_q}{L_d} + \frac{v_d}{L_d} \quad (10)$$

$$\frac{di_q}{dt} = -\frac{R_s i_q}{L_q} - \frac{N\omega_m L_d i_d}{L_q} - \frac{N\omega_m \psi}{L_q} + \frac{v_q}{L_q} \quad (11)$$

$$\frac{d\omega_m}{dt} = \frac{N\psi i_q}{J_m} + \frac{NL_d i_d i_q}{J_m} - \frac{NL_q i_q i_d}{J_m} - \frac{T_L}{J_m} \quad (22)$$

$$\frac{d\theta}{dt} = N\omega_m \quad (13)$$

There are five calculation steps in the algorithm EKF. The five calculation steps are [4,5]

$$x_k^f = f(x_{k-1}^e) \quad (23)$$

$$P_k^f = J_f(x_{k-1}^e)P_{k-1}(J_f(x_{k-1}^e))^T + Q_{k-1} \quad (24)$$

$$K_k = P_k^f (J_h(x_k^f))^T (J_h(x_k^f)P_k^f (J_h(x_k^f))^T + R_k)^{-1} \quad (25)$$

$$x_k^e = x_k^f + K_k (z_k - h(x_k^f)) \quad (26)$$

$$P_k = (I - K_k J_h(x_k^f))P_k^f \quad (27)$$

### III. IMPLEMENTATION AND TEST SCENARIOS

The mathematic model of the electric vehicle is written in the C MEX and simulated by using Matlab/Simulink. The realization of the electric vehicle model is shown in Fig. 5. The parameters of PMSM and mechanical part are listed in Table I and II [6].

TABLE I. PMSM PARAMETERS

Parameters	Quantities	Unit
N	4	pole pairs
$\psi$	0.08975	V.s/rad
$L_d$	0.202	mH
$L_q$	0.29	mH
$R_s$	8.669	m $\Omega$
$J_m$	0.01	kg.m <sup>2</sup>

TABLE II. MECHANICAL PARAMETERS

Parameters	Quantities	Unit
$c_r$	0.014	[-]
$g$	9.81	m.s <sup>-2</sup>
$\rho_a$	1.2041	kg.m <sup>-3</sup>
$c_d$	0.31	[-]
$A_f$	2.11	m <sup>2</sup>
$r_w$	0.2933	m
$\eta$	0.96	[-]
$n_g$	12.5	[-]
$m_v$	900	kg
$v_a$	2	m.s <sup>-1</sup>

The electric vehicle model is tested by two test scenarios. Each scenario of the system is done by varying the elevation angle of the route. The first test scenario represents the elevation angle up and down gradually and the second test scenario gives the abrupt changes of the elevation angle of the route.

In the first scenario, the elevation angle given are 0 deg. between 0-50 sec., then 5 deg. between 50-80 sec. and 10 deg. between 80-110 sec., then 15 deg. between 110-140 sec. and 20 deg. between 140-170 sec., then 25 deg. between 170-200 sec. After that, the elevation angle given was 20 deg. between 200-230 sec., then 15 deg. between 230-260 sec. and 10 deg. between 260-290 sec., then 5 deg. between 290-320 sec. and back to 0 deg. between 320-350 sec.(see Fig. 6).

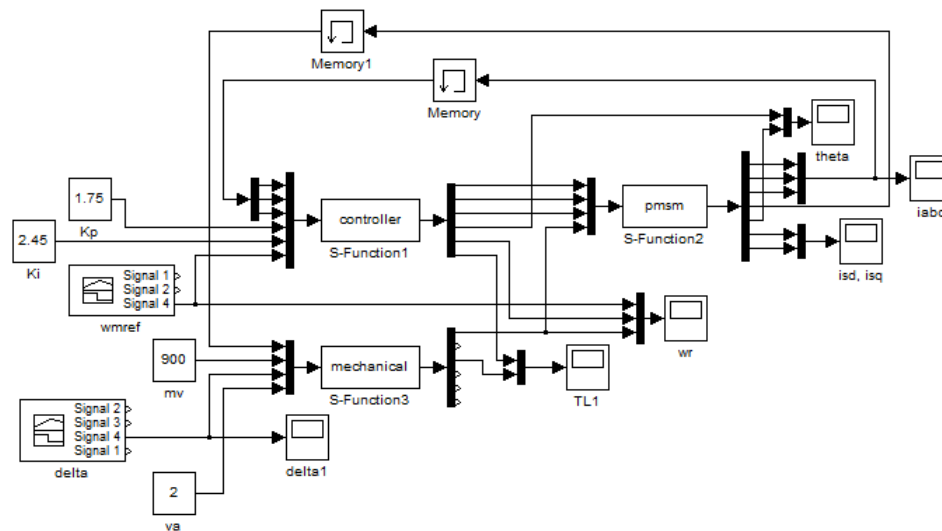


Fig. 5. The implementation of the electric vehicle in Simulink/Matlab

In the second scenario, the elevation angle given are 0 deg. between 0-50 sec., then 22 deg. between 50-80 sec. and back to 0 deg. between 80-110 sec., then 22 deg. between 110-140 sec. and back to 0 deg. between 140-170 sec., then 22 deg. between 170-200 sec, and back to 0 deg. between 200-230 sec, and back to 0 deg. between 230-250 sec. (see Fig. 7).

In both scenarios, the rotational speed of the motor is kept constantly in 200 rad/s as shown in Fig. 8.

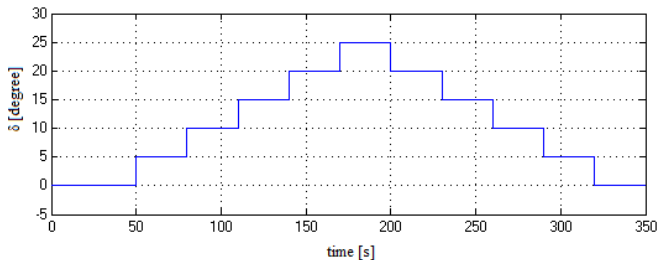


Fig. 6. The elevation angle ( $\delta$ ) in (deg) in the first test scenario

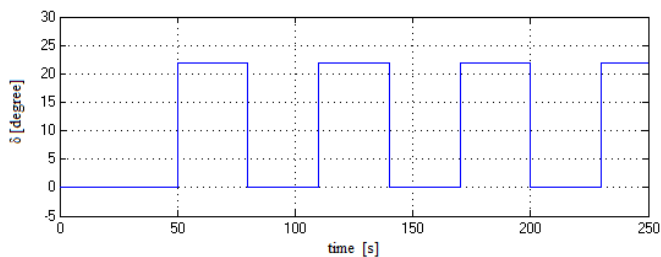


Fig. 7. The elevation angle ( $\delta$ ) in (deg) in the second test scenario

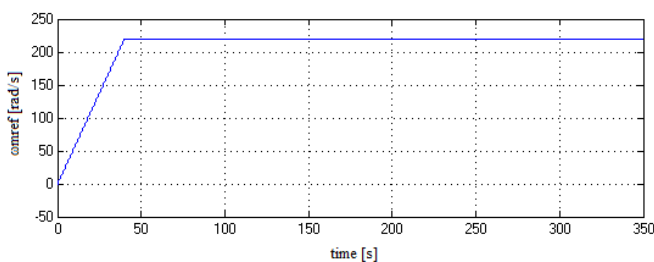


Fig. 8. The speed motor reference

#### IV. RESULT AND DISCUSS

The simulation shows that the controller and the fifth order EKF are able to regulate the actual value and the estimated value of the rotational speed of the motor that are close to this reference value.

The additional elevation angle results in the actual value and the estimated value of the rotational speed decrease in the beginning then follow this reference value. On the other hand, the decrease of the elevation angle results in the actual value and the estimated value of the rotational speed increase in the beginning then follow this reference value (see Fig. 9-12).

Fig. 9 and 10 show that the response of the controller and the fifth order EKF in the first test scenario. Fig. 11 and 12 show that the response of the controller and the fifth order EKF in the second test scenario. These results show that the controller and the fifth order EKF can respond to the changes given.

Fig. 10 and 12 show the magnitude changes of the elevation angle influences the over-shoot transient of the actual value and the estimated value of the rotational speed. The 10 deg. magnitude changes influences the over-shoot transient of 15 rad/s (see Fig. 10). The 22 deg. magnitude changes influences the over-shoot transient up to 33 rad/s (see Fig. 12).

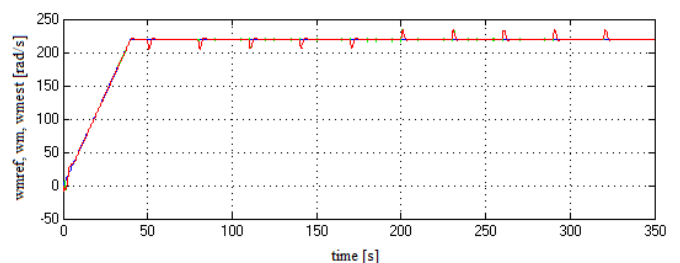


Fig. 9. The reference value (blue), the actual value (red), the estimated value (green) of the rotational speed of the motor in the first test scenario

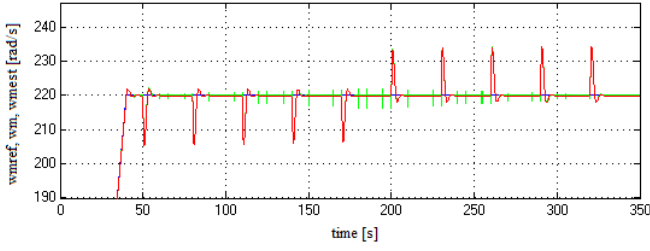


Fig. 10. Zooming the reference value (blue), the actual value (red), the estimated value (green) of the rotational speed of the motor in the first test scenario

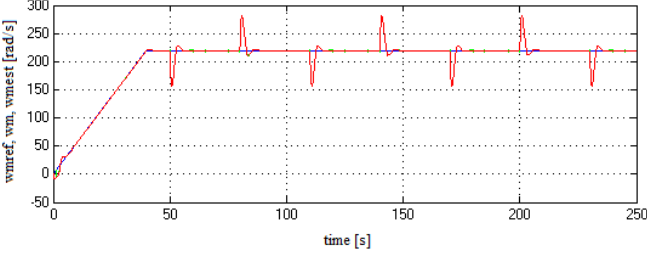


Fig. 11. The reference value (blue), the actual value (red), the estimated value (green) of the rotational speed of the motor in the second test scenario

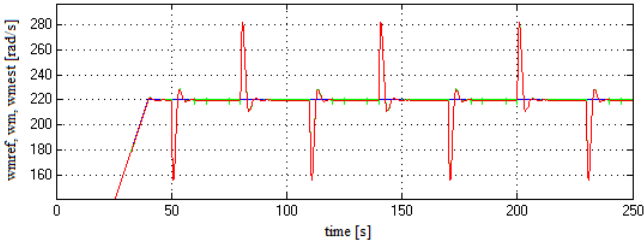


Fig. 12. Zooming the reference value (blue), the actual value (red), the estimated value (green) of the rotational speed of the motor in the second test scenario

Fig. 13 shows the comparison of the actual value (green) and the estimated value (blue) of the electrical angle position in the first test scenario. This result shows the fifth order EKF designed is able to estimate the electric angle position that close to the actual value.

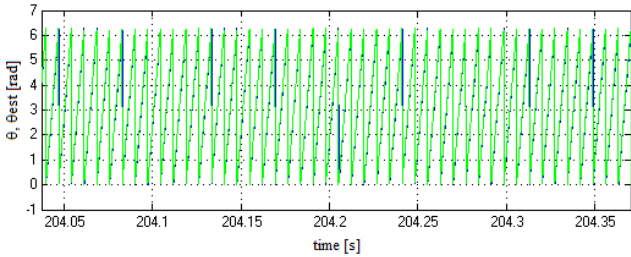


Fig. 13. Comparison of the actual value (green) and the estimated value (blue) of the electrical angle position in the first test scenario

Fig. 14 and 15 show the response of the motor current. The response of the motor current in q-axis follows the changes of the elevation angle. On the other hand, the response of the motor current in d-axis is influenced by nonlinear coupling in PMSM. These results also show the controller and the fifth order EKF can work in the changes given.

Fig. 16 and 17 show the torque load in the mechanical part and the estimated value of the torque load in the fifth order EKF part. The torque load in the mechanical part is represented by green line, and the estimated value of the torque load in the fifth order EKF part is represented by blue

line. Both of the torques are able to respond to the changes of the elevation angle that is given in both test scenarios

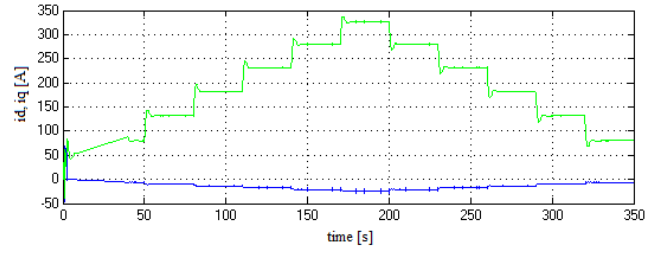


Fig. 14. Motor currents in the first test scenario (id blue, iq green)

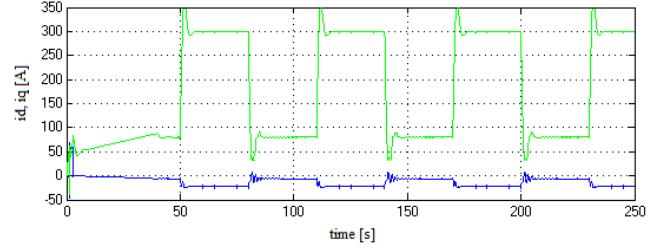


Fig. 15. Motor currents in the second test scenario (id blue, iq green)

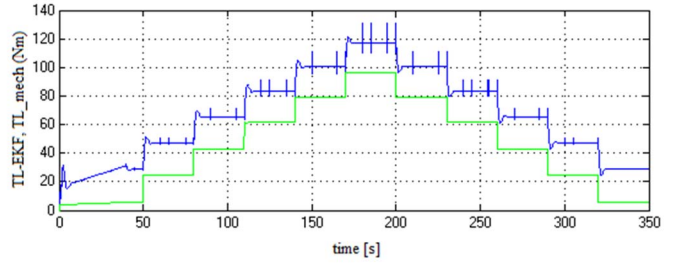


Fig. 16. The estimated value of the torque load in the fifth order EKF part (blue) and the torque load of the mechanical part (green) in the first test scenario

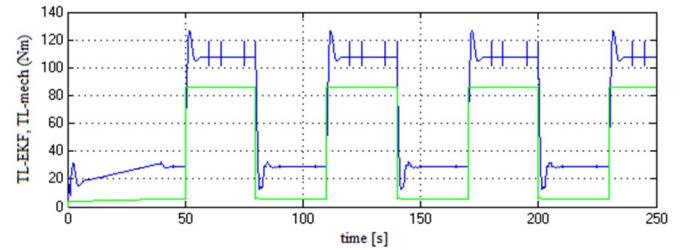


Fig. 17. The estimated value of the torque load in the fifth order EKF part (blue) and the torque load of the mechanical part (green) in the second test scenario

The difference between the torque load in the mechanical part and the estimated value of the torque load in the EKF part is caused by the differences in the definition. The torque load of the mechanical part is expressed by (29).

$$\left(J_m + \frac{r_w^2 m_v}{\eta n_g^2}\right) \frac{d\omega_m}{dt} = T_e - B_m \omega_m - T_{m0} - T_{L-mech} \quad (28)$$

$$T_{L-mech} = \frac{r_w}{\eta n_g} (f_g + f_f + f_a) \quad (29)$$

The estimated value of the torque load in the fifth order EKF part is expressed by (31). The result shows the fifth order EKF designed for the PMSM can be used in the electric vehicle model, without changing the model structure of the observer.

$$J_m \frac{d\omega_m}{dt} = T_e - T_{L-EKF} \quad (30)$$

$$T_{L-EKF} = B_m \omega_m + T_{m0} + \frac{r_w^2 m_v}{\eta n_g^2} \frac{d\omega_m}{dt} + \frac{r_w}{\eta n_g} (f_g + f_f + f_a) \quad (31)$$

## V. CONCLUSION

The controller and the fifth order EKF designed are able to regulate the actual value and the estimated value of the rotational speed of the motor in accordance with the reference value. The fifth order EKF is able to estimate the stator currents in dq-axis, the rotation speed of rotor, the electric angle position, and the torque load accurately although the elevation angle of route was changed several times. The result shows the fifth order EKF designed for the PMSM can be used in the electric vehicle model, without changing the model structure of the observer.

## ACKNOWLEDGMENT

This research was funded by Universitas Indonesia research grant of the Publikasi Internasional Terindeks untuk Tugas Akhir Mahasiswa (PITTA) UI 2018 No.2439/UN2.R3.1/HKP.05.00/2018.

## REFERENCES

- [1] Balaji Kamalakkannan, "Modelling and Simulation of Vehicle Kinematics and Dynamics," Master Thesis, Halmstad University, 2017.
- [2] Bernadeta Wuri Harini, Aries Subiantoro, Feri Yusivar, "Stability Analysis of MRAS Speed Sensorless Control of Permanent Magnet Synchronous Motor," 2017 International Conference of Sustainable Energy Engineering and Application (ICSEEA), Jakarta, 2017.
- [3] Zedong Zheng, Yongdong Li, Maurice Fadel, "Sensorless Control of PMSM Based on Extended Kalman Filter," EPE 2007, Aalborg, 2007.
- [4] Mohamad Syakir Termizi, Jurifa Mat Lazi, Zulkifilie Ibrahim, Md Hairul Nizam Talib, M. J. A. Aziz, S. M. Ayob, "Sensorless PMSM drives using Extended Kalman Filter (EKF)," 2017 IEEE Conference on Energy Conversion (CENCON), pp.145 – 150, 2017.
- [5] Rahee A. Walambe, Aishwarya A. Apte, Jayawant P. Kolhe, Anjali Deshpande, "Study of Sensorless Control Algorithms for a Permanent Magnet Synchronous Motor Vector Control Drive," 2015 International Conference on Industrial Instrumentation and Control (ICIC), pp.424-428 India, 2015.
- [6] Abi Iqbal Prasetyo, "Simulasi Penerapan Motor Listrik Permanen Magnet pada Mobil Listrik Jenis City Car," Bachelor Thesis, Electrical Engineering Universitas Indonesia, 2016.

## APPENDIX

$$\mathbf{x}_k = [i_d \quad i_q \quad \omega_m \quad \theta \quad T_L]^T \quad (A1)$$

$$f_1 = i_d - \frac{R_s i_d \Delta t}{L_d} + \frac{N \omega_m L_q i_q \Delta t}{L_d} + \frac{v_d \Delta t}{L_d} \quad (A2)$$

$$f_2 = i_q - \frac{R_s i_q \Delta t}{L_q} - \frac{N \omega_m L_d i_d \Delta t}{L_q} - \frac{N \omega_m \psi \Delta t}{L_q} + \frac{v_q \Delta t}{L_q} \quad (A3)$$

$$f_3 = \omega_m + \frac{N \psi i_q \Delta t}{J_m} + \frac{N L_d i_d i_q \Delta t}{J_m} - \frac{N L_q i_q i_d \Delta t}{J_m} - \frac{T_L \Delta t}{J_m} \quad (A4)$$

$$f_4 = \theta + N \omega_m \Delta t \quad (A5)$$

$$f_5 = T_L \quad (A6)$$

$$\mathbf{J}_f = \begin{bmatrix} J_{f11} & J_{f12} & J_{f13} & J_{f14} & J_{f15} \\ J_{f21} & J_{f22} & J_{f23} & J_{f24} & J_{f25} \\ J_{f31} & J_{f32} & J_{f33} & J_{f34} & J_{f35} \\ J_{f41} & J_{f42} & J_{f43} & J_{f44} & J_{f45} \\ J_{f51} & J_{f52} & J_{f53} & J_{f54} & J_{f55} \end{bmatrix} \quad (A7)$$

$$J_{f11} = 1 - \frac{R_s \Delta t}{L_d} \quad (A8)$$

$$J_{f12} = \frac{N \omega_m L_q \Delta t}{L_d} \quad (A9)$$

$$J_{f13} = \frac{N L_q i_q \Delta t}{L_d} \quad (A10)$$

$$J_{f14} = 0 \quad (A11)$$

$$J_{f15} = 0 \quad (A12)$$

$$J_{f21} = -\frac{N \omega_m L_d \Delta t}{L_q} \quad (A13)$$

$$J_{f22} = 1 - \frac{R_s \Delta t}{L_q} \quad (A14)$$

$$J_{f23} = -\frac{N L_d i_d \Delta t}{L_q} - \frac{N \psi \Delta t}{L_q} \quad (A15)$$

$$J_{f24} = 0 \quad (A16)$$

$$J_{f25} = 0 \quad (A17)$$

$$J_{f31} = \frac{N L_d i_q \Delta t}{J_m} - \frac{N L_q i_q \Delta t}{J_m} \quad (A18)$$

$$J_{f32} = \frac{N \psi \Delta t}{J_m} + \frac{N L_d i_d \Delta t}{J_m} - \frac{N L_q i_d \Delta t}{J_m} \quad (A19)$$

$$J_{f33} = 1 \quad (A20)$$

$$J_{f34} = 0 \quad (A21)$$

$$J_{f35} = -\frac{\Delta t}{J_m} \quad (A22)$$

$$J_{f41} = 0 \quad (A23)$$

$$J_{f42} = 0 \quad (A24)$$

$$J_{f43} = N \Delta t \quad (A25)$$

$$J_{f44} = 1 \quad (A26)$$

$$J_{f45} = 0 \quad (A27)$$

$$J_{f51} = 0 \quad (A28)$$

$$J_{f52} = 0 \quad (A29)$$

$$J_{f53} = 0 \quad (A30)$$

$$J_{f54} = 0 \quad (A31)$$

$$J_{f55} = 1 \quad (A32)$$

$$\mathbf{J}_h = \begin{bmatrix} 1 & 0 & 0 & 0 & 0 \\ 0 & 1 & 0 & 0 & 0 \\ 2 & 0 & 0 & 0 & 0 \\ 0 & 2 & 0 & 0 & 0 \\ 0 & 0 & 2 & 0 & 0 \\ 0 & 0 & 0 & 2 & 0 \\ 0 & 0 & 0 & 0 & 2 \end{bmatrix} \quad (A33)$$

$$\mathbf{Q} = \begin{bmatrix} 0 & 0 & 0 & 0 & 0 \\ 0 & 0 & 0 & 0 & 0 \\ 0 & 0 & 0 & 0 & 0 \\ 0 & 0 & 0 & 0 & 0 \\ 0 & 0 & 0 & 0 & 0 \end{bmatrix} \quad (A34)$$

$$\mathbf{R} = \begin{bmatrix} 2 & 0 \\ 0 & 2 \end{bmatrix} \quad (A35)$$



# SIZING OPTIMIZATION AND OPERATIONAL STRATEGY OF HRES (PV-WT) USING DIFFERENTIAL EVOLUTION ALGORITHM

Ilham Pakaya

Electrical Engineering Dept.

University of Muhammadiyah Malang

Jl. Raya Tlogomas No. 246, Malang

[ilham@umm.ac.id](mailto:ilham@umm.ac.id)

Zulfatman Has

Electrical Engineering Dept.

University of Muhammadiyah Malang

Jl. Raya Tlogomas No. 246, Malang

[zulfatman78@gmail.com](mailto:zulfatman78@gmail.com)

Annas Alif Putra

Electrical Engineering Dept.

University of Muhammadiyah Malang

Jl. Raya Tlogomas No. 246, Malang

[annasalif2013@webmail.umm.ac.id](mailto:annasalif2013@webmail.umm.ac.id)

**Abstract** - The instability of energy resources and corresponding cost of the system are the main two problems for designing the hybrid solar-wind power generation systems. The configuration of the system must have a high reliability on the power supply availability but with a minimum cost. The purpose of this paper is to find the most optimum or balanced configuration between technical reliability and total annual cost for the PV module number, the wind turbine number, and the battery number. The appropriate strategy of load management is needed by adjusting the potential energy resource to the load power demand. Loss of Power Supply Probability (LPSP) is a method to determine the ratio of power generation unavailability by the system configuration which used as technical analysis. Annualized Cost of System (ACS) is a method to determine the total annualized cost of the project lifetime which used as economic analysis. The result from the simulation showed that the Differential Evolution (DE) algorithm can be an alternative method to find the best configuration with a low number of LPSP and ACS. Since DE has a better efficacy and faster time to find global optimum than other algorithms.

**Keywords** - LPSP, ACS, Differential Evolution.

## I. INTRODUCTION

Nowadays, renewable energy is considered as an alternative energy to replace fossil fuel which starts to rareness. But, the main problem of renewable energy is the availability of the energy really depends on the weather condition that can intermittently change every time.

A system uses only one type of energy resource disposed to has not maximum result to fulfill the load demand. It leads to over-sizing components (unnecessary components) and life-cycle cost [1-4]. Therefore, by combining two or more resource of renewable energy can complement the drawbacks in each individual energy source.

Due to intermittent sunlight intensity and wind speed, the generated energy in each time has a big influence on the system reliability toward the power supply availability. Therefore, a proper power management strategy is needed to determine the size of the components. The reliability level of hybrid renewable energy system can be known with LPSP method. LPSP is a method to determine the ratio of power supply unavailability that is produced by system configuration. LPSP is used as a technical analysis.

Besides a technical analysis, economic analysis is an aspect that is important as well as technical analysis. An economic analysis is used to understand how much cost the configuration system has. ACS becomes an economical analysis method in this paper.

Finding the most optimum system configuration consider both a technical aspect and economical aspect, an optimization method or optimization algorithm is needed in

search of the global optimum e.g. genetic algorithm (GA), particle swarm optimization (PSO) algorithm and differential evolution (DE) Algorithm [5-14].

In [5-6] [8], which used genetic algorithms to size optimal PV/Wind/batteries hybrid systems by minimizing LPSP and the ACS. The studied showed genetic algorithms made possible to calculate the number of the components of the optimal configuration which ensure a cover of the load with an acceptance of an LPSP. However, to create the program of GA is not easy. PSO is easy to code but weak in search of global optimum [6-7]. Meanwhile, DE has a high efficacy and be able to find global optimum faster than other algorithms [7-14].

Based on the background above, the propose this paper determine the best configuration system in hybrid renewable energy generation (PV-wind turbine) with optimal LPSP and ACS using DE algorithm.

## II. METHODOLOGY

### A. Hybrid Component Design

Hybrid renewable energy system consists of PV panel, wind turbine, battery, inverter, battery charge controller and others. The schematic diagram of the system in this paper is shown in Fig. 1.

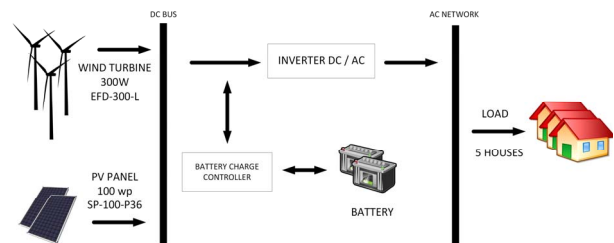


Fig. 1. Schematic Diagram of Hybrid Renewable Energy System

#### 1) PV Array

The power supplied by the panels can be calculated as a function of the solar radiation by using the following formula [4][7]:

$$P_{pv} = P_{N-pv} \times npv \times \frac{G}{G_{ref}} \times [1 + K_t(T_c - T_{ref})] \quad (1)$$

Where,  $P_{N-pv}$  is rated power under reference condition, in this paper uses a 100 wp PV panel,  $npv$  is PV module number,  $G$  is solar irradiation ( $W/m^2$ ),  $G_{ref}$  is solar irradiation under reference condition ( $1000 W/m^2$ ),  $T_{ref}$  is cell temperature under reference condition ( $25 ^\circ C$ ),  $K_t$  is the temperature coefficient of the maximum power ( $-3.7 \times 10^{-3} (1/^\circ C)$ ). The cell temperature  $T_c$  can be calculated as the equation below.

$$T_c = T_{amb} + (0.0256 \times G) \quad (2)$$

where  $T_{amb}$  is ambient temperature.

#### 2) Wind Turbine

The energy that is caught by the blades can be calculated as the equation below [15]:

$$P = \frac{1}{2} \cdot \rho \cdot A \cdot v^3 \cdot C_p \quad (3)$$

where  $\rho$  is air density ( $\text{kg/m}^3$ ),  $A$  is intercepting area of the rotor blades ( $\text{m}^2$ ),  $v$  is wind speed ( $\text{m/s}$ ), dan  $C_p$  is power coefficient of a wind turbine. The theoretical maximum value of the power coefficient is 0,593, also known as Betz's coefficient. But, in the reality, the value of power coefficient is between 0,35-0,45 [15].

*Cut-in speed* ( $v_c$ ) is the lowest wind speed ( $v_R$ ) where the turbine starts to rotate and produces an energy. *Cut-out speed* is the highest wind speed. *Rated output speed* is wind speed between *cut-in speed* and *cut-out speed* where the power output reaches the maximum power and is called *rated power output*. The power output in terms of wind speed can be estimated using the equation below [15]:

$$P_w(v) = \begin{cases} \frac{v^k - v_c^k}{v_R^k - v_c^k} \cdot P_R & v_c \leq v \leq v_R \\ P_R & v_R \leq v \leq v_F \\ 0 & v \leq v_c \text{ dan } v \geq v_F \end{cases} \quad (4)$$

Where  $P_R$  is *rated power* and  $k$  is Weibull shape factor. The total of  $P_w$  will be multiplied by the number of the wind turbine ( $nwt$ ).

### 3) Battery

Batteries have a big role in the off-grid hybrid renewable energy system and also have a big share of initial cost [15]. Batteries are used as backup storage when the produced energy is larger than the energy from the load demand.

The storage capacity of the battery ( $C_B$  (Ah)) can be calculated according to the following relation [7][16]:

$$C_B = \frac{E_L \times A_D}{V_B \times (DOD)_{\max} \times \eta_{inv} \times \eta_B} \quad (5)$$

where  $E_L$  is daily load (Wh). The autonomous days ( $A_D$ ) is the number of days that the battery will be capable to supply the load if the renewable sources are bad [4][7].  $V_B$  is battery voltage (Volt),  $DOD_{\max}$  is the maximum depth of discharge,  $\eta_{inv}$  is inverter efficiency dan  $\eta_B$  is battery efficiency.

### 4) Inverter

The Inverter is one of the important components in the hybrid renewable energy system. An Inverter can convert DC current from PV and wind turbine to become AC current which is needed for the load demand.

An inverter must be able to capable of handling the AC load when it reaches a maximum point. Thus, designing the capacity of the inverter can be assumed 20% higher than maximum AC load from the entire load demand [4].

### 5) Battery Charge Controller (BCC)

Battery Charge Controller acts as the interface between batteries and individual generator and DC bus. BCC protects the batteries both from overcharging and deep discharging. BCC shall switch off the load when the batteries reach the certain state of discharge. BCC shall switch off the batteries from the DC bus when it is fully charged.

Determining the capacity of BCC according to the battery voltage and the output power from the wind turbine and PV panel. The capacity of BCC is 20% larger than the output power from the wind turbine and PV panel.

## B. Meteorological Data

The area which is chosen by this paper at the Third Campus of University of Muhammadiyah Malang (UMM) lies on the geographical coordinates of  $7^{\circ}55'14.8''$  S and  $112^{\circ}35'55.4''$  E. The solar irradiation and wind speed data are gotten from NASA Surface Meteorology and Sun Energy, that is <https://eosweb.larc.nasa.gov>. The solar irradiation data is shown in fig.2 and the wind speed data is shown in fig. 2.

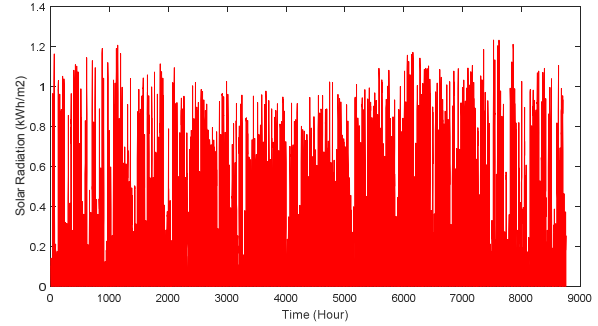


Fig. 2. Solar Irradiation Data during One Year

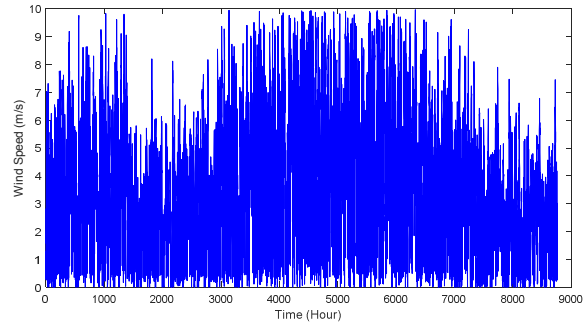


Fig. 3. Wind Speed Data during One Year

The ambient temperature data in that area will be assumed. The highest temperature occurs in the middle of the day and the lowest temperature occurs in the middle of the night.  $T_{amb}$  will be assumed constantly during a year. The daily  $T_{amb}$  is shown in Fig. 4.

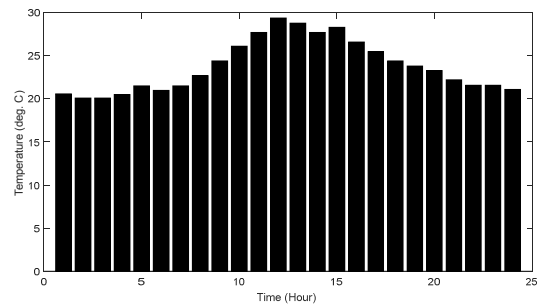


Fig. 4. Daily Ambient Temperature

## C. Load Profile

The number and capacity of batteries depending on the load profile. Moreover, the maximum load and the characteristic of consumers affect the reliability of the system such as the sizing of the components and the electricity price [7].

The load profile which is used in this research is rural load characteristic. The average user of electricity is assumed 2 kWh per day, which is sufficient for the basic load household. The number of houses is assumed to be 5. The load profile of the rural area in hourly is shown in Fig. 5.

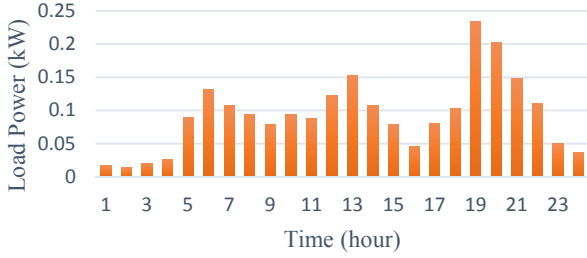


Fig. 5. Load Profile of Rural Area

#### D. Power Management Strategy

The Uncertainty of renewable energy source makes the power management strategy to become very complex, especially when the source of energy must match the time distributions of load demand. Because of limited renewable energy resource from generated power, the generator's capacity cannot directly increase to match the increasing demand. Therefore, having a power management strategy is very important in the hybrid renewable energy system. The following conditions will be considered to create power management strategy [4][7]:

- Condition 1  
The excess of generated energy from a renewable source which has already fulfilled the load is used to charge the battery.
- Condition 2  
The renewable source is not enough to provide energy for the load. The energy which is stored in the batteries is used to supply (discharging) the load.
- Condition 3  
The renewable source fails to provide energy for the load and the stored energy from the battery is also depleted. In this condition occurs a blackout.

The flowchart from several conditions is shown in Fig. 6.

#### E. Optimization Criterion

##### 1) Power Reliability Analysis based on LPSP Concept

LPSP is a probability of insufficient power supply when the hybrid generation system and the stored energy from batteries are unable to fulfill the load demand. If LPSP is 0 means that the load will be fully satisfied. On the contrary, if LPSP is 1 means that the load will never be satisfied. The Objective function of LPSP time-0 to time- $T$  can be described as the equation follow [5]:

$$LPSP = \frac{\sum_{t=0}^T \text{Power failure time}}{T} = \frac{\sum_{t=0}^T \text{Time}(P_{\text{available}}(t) < P_{\text{needed}}(t))}{T} \quad (6)$$

where  $T$  is the total hour. *Power failure time* or blackout time is defined as the time when both the hybrid generation system and the energy from batteries are unable to fulfill the load demand. The power which is needed by the load can be described by the following equation:

$$P_{\text{needed}}(t) = \frac{P_{\text{AC load}}(t)}{\eta_{\text{inverter}}} \quad (7)$$

and the power available from the hybrid system can be described by the following equation:

$$P_{\text{available}}(t) = P_{\text{pv}}(t) + P_{\text{wt}}(t) + E_b(t) - E_{b\text{min}} \quad (8)$$

where  $P_{\text{pv}}(t)$  is the power produced by PV panels time- $t$ .  $P_{\text{wt}}(t)$  is the power produced by wind turbines time- $t$ .  $E_b(t)$  is the stored energy from batteries time- $t$ .  $E_{b\text{min}}$  is the minimum energy stored in the batteries.

#### 2) Economic Analysis based on ACS Concept

The economic analysis in this research uses the concept of (ACS). The annualized cost of the system consists of *annualized capital cost* ( $C_{\text{acap}}$ ), *annualized replacement cost* ( $C_{\text{arep}}$ ) and *annualized maintenance cost* ( $C_{\text{amain}}$ ). Table 1, shows the data cost information and lifetime from the component used by the system. ACS can be described by the following equation [5]:

$$ACS = C_{\text{acap}} + C_{\text{arep}} + C_{\text{amain}} \quad (9)$$

##### a) Annualized capital cost ( $C_{\text{acap}}$ )

$C_{\text{acap}}$  consists of the cost of each component and the installation cost. It is calculated using the equation:

$$C_{\text{acap}} = C_{\text{cap}} \cdot CRF(i, Y_{\text{proj}}) \quad (10)$$

where  $C_{\text{cap}}$  is the initial capital cost for each component, US Dollar.  $Y_{\text{proj}}$  is the lifetime of the component, year. CRF is the capital recovery factor. The Equation of CRF is calculated by:

$$CRF(i, Y_{\text{proj}}) = \frac{i \cdot (1+i)^{Y_{\text{proj}}}}{(1+i)^{Y_{\text{proj}}} - 1} \quad (11)$$

where  $i$  is the annual real interest rate. Can be described by the following expression below:

$$i = \frac{i' - f}{1 + f} \quad (12)$$

where  $i'$  is the nominal interest rate and  $f$  is the annual inflation rate.

##### b) Annualized Replacement Cost

Annualized replacement cost is the annualized value for all replacement cost of the hybrid system during the project lifetime. In this study, the battery is the only component which must be replaced periodically during the lifetime of the project.

$$C_{\text{arep}} = C_{\text{rep}} \cdot SFF(i, Y_{\text{rep}}) \quad (13)$$

where  $C_{\text{rep}}$  is the replacement cost (battery), US Dollar.  $Y_{\text{rep}}$  is the lifetime of the component, year.  $SFF$  is sinking fund factor.  $SFF$  can be described by the following equation:

$$SFF(i, Y_{\text{rep}}) = \frac{i}{(1+i)^{Y_{\text{rep}}} - 1} \quad (14)$$

##### c) Maintenance Cost

Maintenance cost of the hybrid system is gradually increased in every year because of inflation. Thus, the maintenance cost is given as the equation below:

$$C_{\text{amain}}(n) = C_{\text{amain}}(1) \cdot (1+f)^n \quad (15)$$

where  $C_{\text{amain}}(n)$  is the maintenance cost for the year- $n$ .

TABLE I. THE SYSTEM COMPONENTS' COST AND LIFETIME

Component	Initial Capital Cost	Replacement Cost	Maintenance Cost (1st year)	Lifetime (Year)	Interest Rate $i'$ (%)	Inflation Rate $f$ (%)
<b>PV Panel</b>	1000 US\$/kW	-	10 US\$/kW	20	12	4
<b>Wind Turbine</b>	1000 US\$/kW	-	30 US\$/kW	20		
<b>Battery</b>	1500 US\$/kAh	1500 US\$/kAh	50 US\$/kW	4		
<b>Inverter</b>	300 US\$/kW	-	10 US\$/kW	20		
<b>BCC</b>	250 US\$/kW	-	7,5 US\$/kW	20		

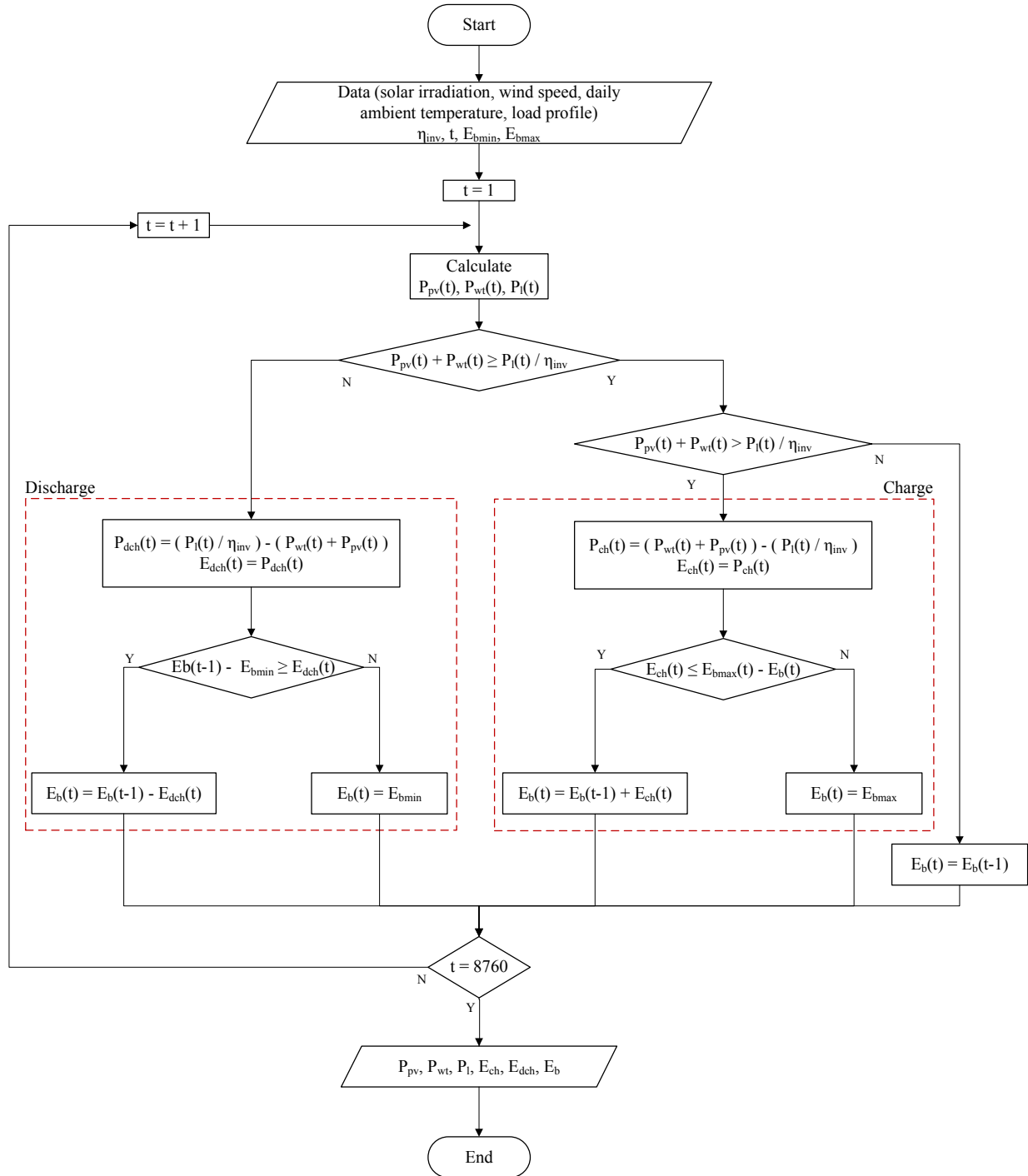


Fig. 6. Flowchart of Power Management Strategy

### F. Multi-Objective Optimization

Optimization of the hybrid renewable energy system is categorized as a multi-objective problem. Linear scalarization is one of the most popular approaches because of its simplicity. This method converts the multi-objective problem into a single objective problem. The fitness function can be calculated as [7]:

$$fitness = \min \left\{ \sum_{i=1}^k w_i \frac{f_i(x)}{f_i^{\max}} \right\}, w_i \geq 0 \text{ \& } \sum_{i=1}^k w_i = 1 \quad (16)$$

where  $x$  is the decision variable vector,  $w_i$  is the weight of importance of each objective,  $k$  is the number of objectives,  $f$  is the objective function and  $f_i^{\max}$  is the upper bound of  $i$ -th objective function.

In this studied, LPSP and ACS are equally important criterions to find the optimum system configuration. Thus, the weight ( $w_i$ ) for both objectives is 0.5 [7].

### G. Optimization using DE Algorithm

DE algorithm was invented by Rainer Storn and Kenneth Price in 1995 [9][10]. This algorithm is categorized as an evolutionary algorithm [14]. Evolutionary algorithm mimics the evolution theory from Darwin where each of the individuals in the population evolves from one generation to the next generation. This mimic process is analogized by the process such as mutation, crossover, selection.

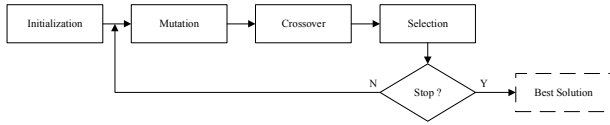


Fig. 7. Block Diagram of DE Algorithm

#### 1) Initialization

The first process in initialization is determining the lower bound  $U_L$  and the upper bound  $U_B$  in every parameter with initial vector  $D$ -dimensions. Next, generate the number randomly in every  $j$  from  $i$  vector in  $g$ -generation or iteration. The initialization process can be calculated as [13][18].

$$X_{j,i,0} = rand_{ij} [0,1] \cdot (U_{Bj} - U_{Lj}) + U_{Lj} \quad (17)$$

with  $i = \{1, 2, 3, \dots, NP\}$  and  $j = \{1, 2, 3, \dots, D\}$ .  $NP$  is the number of population.  $D$  is the number population in every population. The vector's result from initialization process above is called parent vector.

#### 2) Mutation

Biologically, "mutation" means characteristic's changed of a chromosome. In the context of evolutionary computing paradigm, mutation is also seen as a change of information with a random element. The parent vector will be combined with a mutant vector. A mutant vector  $V_{i,g}$  is expressed by the following equation [9][13].

$$V_{i,g} = X_{r1,g} + F \cdot (X_{r2,g} - X_{r3,g}) \quad (18)$$

where  $i, r1, r2, r3 \in \{1, 2, 3, \dots, NP\}$  are random indexes, integer, and different.  $F$  is a scale factor that impacts the difference vector  $(X_{r2,g} - X_{r3,g})$ .

#### 3) Crossover

The purpose of crossover or recombination is to increase the diversity of the population. Recombination creates a trial vector or offspring vector  $U_{i,g}$ . It is calculated as [17]:

$$U_{i,g} = (U_{1i,g}, U_{2i,g}, \dots, U_{ni,g}) \quad (19)$$

where:

$$U_{i,g} = \begin{cases} V_{j,i,g} & \text{if } (rand_j(0,1) \leq CR \\ & \text{or } j = j_{rand} \\ X_{ji,g} & \text{others} \\ & j = 1, 2, \dots, n \end{cases} \quad (20)$$

where  $rand_j(0,1)$  is the uniform random number with an interval of  $[0,1]$  and newly formed in every  $j$ .  $j_{rand}$  is an integer random number starts from 1 to  $D$  and newly formed in every  $i$ .  $CR$  is a crossover rate.

#### 4) Selection

Selection process chooses the best vector among a parent vector  $X_{i,g}$  and the offspring vector  $U_{i,g}$  according to their fitness value. For example, if we have a minimization problem the selected vector can be calculated as [9][17]:

$$X_{i,g+1} = \begin{cases} U_{i,g} & \text{if } f(U_{i,g}) \leq f(X_{i,g}) \\ X_{i,g} & \text{others} \end{cases} \quad (21)$$

A vector which has a smaller fitness value will survive and will become a new parent vector in the next generation  $X_{i,g+1}$ .

DE algorithm is a simulation tool to help in search of the process from various configurations in the hybrid renewable energy system based on LPSP and ACS. DE algorithm will select a configuration which has a lowest-balanced number of LPSP and ACS. However, there is some minor modification for determining the evaluation value that configurations. The value of LPSP is much smaller than ACS. This case makes LPSP has a small effect on the evaluation value. Thus, ACS will be modified into the cost of electricity (US\$/kWh). The DE's parameters in this study are shown in Table 2 below. The flowchart of sizing optimization using DE algorithm is shown on Fig.8.

TABLE II. DE'S PARAMETERS

Number of Populations $NP$	10
Dimintions $D$	3
Mutation Scale $F$	0.7
Crossover Rate $CR$	0.7
Max. Iterations	50

In this study, there are four different types of mutation's strategy, those are [13-14]:

- DE/rand/1  
 $V_i = X_{r0} + F(X_{r1} - X_{r2})$
- DE/current-to-rest/1  
 $V_i = X_i + (X_{best} - X_i) + F_i(X_{r1} - X_{r2})$
- DE/best/1  
 $V_i = X_{best} + F(X_{r1} - X_{r2})$
- DE/best/2  
 $V_i = X_{best} + F_i(X_{r1} - X_{r2} + X_{r3} - X_{r4})$



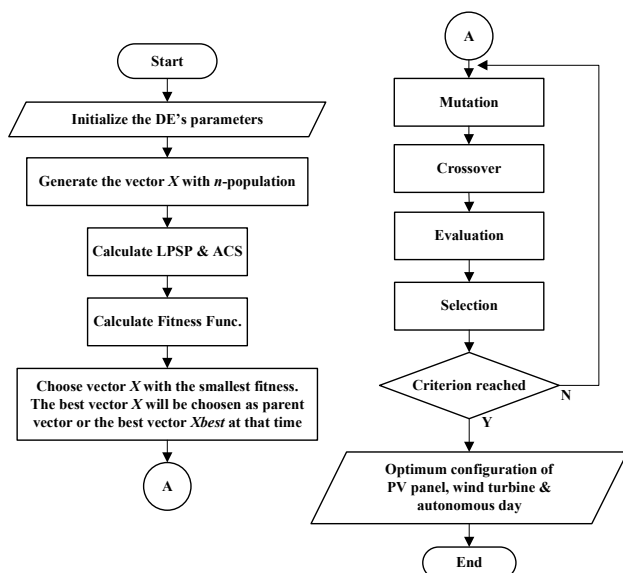


Fig. 8. Flowchart of Sizing Optimization using DE Algorithm

### III. RESULT

#### A. The Result of the Entire System

There are two types of simulations do in this study. First, optimization based on one objective only (LPSP and ACS). Second, optimization using DE algorithm. The results are tabulated in Table 3 below:

TABLE III. THE RESULT OF ENTIRE SIMULATIONS

Configuration	PV Panels	Wind Turbine	Autonomous Day
Based on LPSP Only	28	7	2
Based on ACS Only	4	10	0
DE Algorithm	22	2	1

Then, all of the configurations are reevaluated to understand how many hours of the blackout will probably occur and how much money is needed to build the configuration. On Table 3, configuration based on LPSP only is considered as Configuration I, configuration based on ACS only is considered as Configuration II and configuration from DE algorithm is considered as Configuration III.

TABLE IV. THE RESULT OF REEVALUATION

Configuration	Blackout Time (Hour/Year)	Total Annualized Cost (US\$)
Configuration I	8	1,962.23
Configuration II	4454	725.23
Configuration III	269	1,240.41

From the table above, Configuration I has the fewest blackout time during a year, but it needs a big amount of annualized cost to build the configuration. This configuration is ineffective from the perspective of the economy. Because there is a big possibility of unnecessary operational and lifecycle costs. Meanwhile, Configuration II has a smallest annualized cost. However, the blackout time is exceedingly big. This configuration is not good in term of power supply reliability.

The final decision towards the configurations above, Combination III is the most balanced configuration in terms

of power supply reliability as well as economic's perspective. By choosing the Configuration III, it only needs to increase 71% of the annualized cost from Configuration II and the blackout time can be reduced up to 94%. Rather than increasing the annualized cost by 170% just to reduce the blackout time become 99% by choosing the Configuration I.

#### B. Performance Test from The Algorithm's Result

From Explanation above, the most optimum configuration is the Configuration III or the algorithm's outcome. This configuration has 22 PV panels, 2 wind turbines and 1 autonomous day. Fig. 9 shows a circle diagram of power contribution produced by each component. As can be seen, PV energy is the biggest power contributor for the hybrid system. It means that the solar energy has a big potential amount of energy in the area. Followed by the battery and the least is wind energy. Meanwhile, Fig. 10 shows the contribution of each of the component's initial cost.

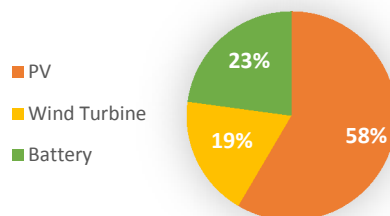


Fig. 9. The Components' Contribution Power

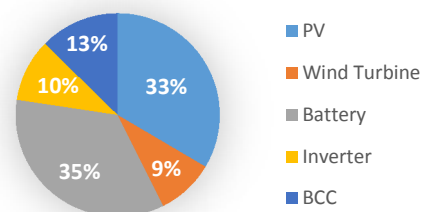


Fig. 10. The Initial Cost Contribution

TABLE V. THE RESULT OF ENTIRE PERFORMANCE TEST OF SYSTEM CONFIGURATION

PV Panel		Inverter	
Numbers	22	Initial Cost	655 US\$
Initial Cost	2,200 US\$	Capacity	2.1818 kW
Produced Energy	4045.597 kWh	BCC	
Wind Turbine		Initial Cost	830 US\$
Numbers	2	Capacity	3.324 kW
Initial Cost	600 US\$	Annualized Cost	
Produced Energy	1295.153 kWh	Initial	653.8 US\$
Battery		Replacement	334.4 US\$
Capacity	1522,3 Ah	Maintenance	252.2 US\$
Initial Cost	2,283.5 US\$	Blackout Time	269 Hours
Used Energy	1581.064 kWh		



### C. Comparison

In this study, the performance's result from the DE algorithm is compared with the PSO. The number of populations is ten and the number of iterations is 50 for both algorithms. The results are tabulated in Table 6 below.

TABLE VI. THE COMPARISON'S RESULT BETWEEN DE AND PSO

Algorithm	Best Configuration (npv nwt ad)	Evaluation Value	Time (Second)
DE	22 2 1	0.3707	25.52
PSO	20 3 1	0.3744	25.70

From the table above, DE finishes the simulation slightly faster than PSO with 0.18 second of difference. The DE's evaluation value is also smaller.

Meanwhile, Fig. 11 and. Fig. 13 are shown the convergence graphic of DE and PSO, respectively. DE reaches the convergence point before 15th iterations, while PSO reaches more than 15th iteration. It can be concluded that DE has a better way to find the global optimum than PSO due to DE has a more efficient code. Thus, DE can become an alternative method to find the best configuration for a hybrid renewable energy system.

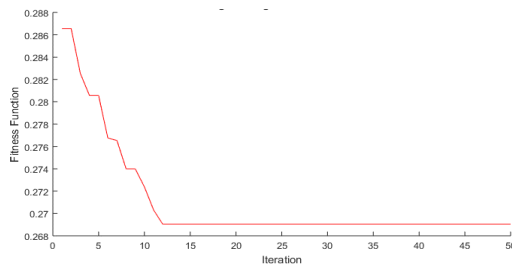


Fig. 11. The DE Convergence Graphic

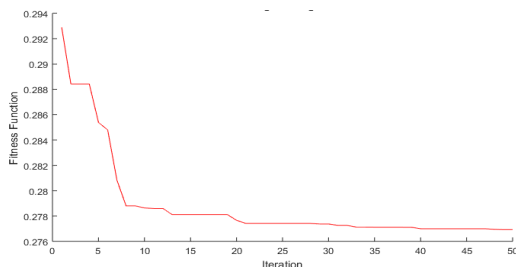


Fig. 12. The PSO Convergence Graphic

### IV. CONCLUSION

The result of this study shows that sizing optimization in a hybrid renewable energy system with only one aspect or one objective leads to unbalanced between power supply reliability and lifecycle cost. Therefore with the use of DE algorithm, the sizing optimization can reach a power supply reliability well with a minimum cost. The performance of DE algorithm in sizing optimization is also better than other algorithms, especially PSO. DE can finish the simulation slightly faster and better in search of global optimum than PSO. Thus, DE can be an alternative method to find the best configuration for a hybrid renewable energy system.

### REFERENCES

- [1] Getachew Bekele, Getnet Tadesse. 2011. "Feasibility Study Of Small Hydro/PV/Wind Hybrid System For Off-Grid Rural Electrification In Ethiopia", Elsevier Applied Energy 97 (2012) 5–15.
- [2] S. Wijewardana. 2014. "Research and Development in Hybrid Renewable Energy Systems", International Journal of Emerging Technology and Advanced Engineering Volume 4, Issue 2, February 2014.
- [3] O. Erdinc, M. Uzunoglu. 2011. "Optimum Design Of Hybrid Renewable Energy Systems: Overview Of Different Approaches", Elsevier Renewable and Sustainable Energy Reviews 16 (2012) 1412–1425.
- [4] Abdel Kareem Daud, Mahmoud S, Ismail. 2012. "Design of Isolated hybrid Systems Minimizing Costs and Pollutant Emissions", Renewable Energy 44 (2012) 215-224.
- [5] Hongxing Yang, Wei Zhou, Lin Lu, Zhaohong Fang. 2007. "Optimal Sizing Method For Stand-Alone Hybrid Solar-Wind System With LPSP Technology By Using Genetic Algorithm", Elsevier Solar Energy 82 (2008) 354–367.
- [6] K. Chandrasekar, N. V. Ramana. 2011. "Performance comparison of DE, PSO, and GA approaches in Transmission Power Loss minimization using FACTS Devices", International Journal of Computer Applications (0975 – 8887) Volume 33– No.5, November 2011.
- [7] Hanieh Borhanazad, Saad Mekhilef, Velappa Gounder Ganapathy, Mostafa Modiri-Delshad, Ali Mirtaheri. 2014. "Optimization of the micro-grid system using MOPSO", Elsevier Renewable Energy 71 (2014) 295-306.
- [8] A. Kaabeche, M. Belhamel, and R. Ibtouen. 2010. "Optimal Sizing Method For Stand-Alone Hybrid PV/Wind Power Generation System", Revue des Energies Renouvelables SMEE'10 Bou Ismail Tipaza (2010) 205 – 213.
- [9] Rainer Storn, Kenneth Price. 1996. "Differential Evolution – A Simple and Efficient Heuristic for Global Optimization over Continuous Spaces", Journal of Global Optimization 11: 341–359, 1997
- [10] Dervis Karaboga, Selcuk Okdem. 2004. "A Simple and Global Optimization Algorithm for Engineering Problems: Differential Evolution Algorithm", Turk J Elec Engin, VOL.12, NO.1 2004
- [11] Chuan Lin, Anyong Qing, Quanyuan Feng. 2010. "A Comparative Study of Crossover in Differential Evolution", J Heuristics DOI 10.1007/s10732-010-9151-1.
- [12] Ali Musratt, Patrick Siarry, Pant Millie. 2011. "An Efficient Differential Evolution Based Algorithm for Solving Multi-Objective Optimization Problems", Elsevier European Journal of Operational Research 217 (2012) 404–416 .
- [13] Swagatam Das, Ponnuthurai Nagarathnam Suganthan. 2011. "Differential Evolution: A Survey of the State-of-the-Art", Ieee Transactions On Evolutionary Computation, Vol. 15, No. 1, February 2011.
- [14] Mandar Pandurang Ganbavale, A. Vasan. 2013. "Differential Evolution using Matlab", Birla Institute of Technology and Science, Pilani. Hyderabad Campus.
- [15] Binayak Bhandari, Shiva Raj Poudel, Kyung-Tae Lee, Sung-Hoon Ahn. 2014. "Mathematical Modeling of Hybrid Renewable Energy System: A Review on Small Hydro-Solar-Wind Power Generation", International Journal Of Precision Engineering And Manufacturing-Green Technology Vol. 1, No. 2, Pp. 157-173.
- [16] A. Kaabeche, M. Belhamel, and R. Ibtouen. 2010. "Optimal Sizing Method For Stand-Alone Hybrid PV/Wind Power Generation System", Revue des Energies Renouvelables SMEE'10 Bou Ismail Tipaza (2010) 205 – 213.
- [17] Irmaduta Fahmiari, Budi Santosa. 2014. "Aplikasi Algoritma Differential Evolution Untuk Permasalahan Kompleks Pemilihan Portfolio", Institut Teknologi Sepuluh Nopember Surabaya

# Indoor Agriculture: Measurement of The Intensity of LED for Optimum Photosynthetic Recovery

Benediktus Anindito  
Faculty of Computer Science  
Narotama University  
Surabaya, Indonesia

benediktus.anindito@narotama.ac.id

Moh Noor Al-Azam  
Faculty of Computer Science  
Narotama University  
Surabaya, Indonesia

noor.azam@narotama.ac.id

Adri Gabriel Sooi  
Faculty of Informatics Engineering  
Widya Mandira Catholic University  
Kupang, Indonesia

adrigabriel@gmail.com

Aris Winaya  
Faculty of Agriculture and Animal  
University Muhammadiyah of Malang  
Malang, Indonesia

winaya@umm.ac.id

Mochamad Mizanul Achlaq  
Faculty of Computer Science  
Narotama University  
Surabaya, Indonesia

mochamad.mizanul@narotama.ac.id

Maftuchah  
Faculty of Agriculture and Animal  
University Muhammadiyah of Malang  
Malang, Indonesia

maftuchah\_umm@yahoo.com

**Abstract**—Indoor agriculture has begun in urban areas. With the narrowness of land and the model of vertical house development, makes this method of indoor agriculture has become a trend in several big cities in the world. Meanwhile, the one that is always needed by every plant is photosynthesis, and every natural photosynthesis of plants continually requires abiotic components of visible light from sunlight. That's why the indoor agriculture requires a replacement source of the sun with artificial sunlight. We can make this artificial sunlight from several light sources, such as incandescent lamps, compact fluorescent lamps (CFL), or the latest with Light Emitting Diode (LED). In this paper, we measured the intensity of light generated from several LEDs with some radiation distance to obtain the optimal energy for plants photosynthesis.

**Keywords**—component, formatting, style, styling, insert (key words)

## I. INTRODUCTION

Because the more narrow and expensive in the urban land that can be used to create a house and its yards, it makes people prefer the concept of small home development or with the concept of vertical development.

The development of housing with such a concept makes the availability of land for planting plants becomes difficult, and people can no longer plant the plants in their yard. Moreover, this makes the indoor farming has been a big concern in urban areas these days.

The natural visible sunlight is one of the essential factors for plant growth. In locations where sunlight as a natural light source is not sufficient for optimum plant growth, a replacement light source may be used[1].

There are several ways to get traditional artificial light sources, such as the use of incandescent, halogen, fluorescent, mercury, High-Pressure Sodium (HPS) and Low-Pressure Sodium (LPS) lamps[2].

The use of these lamps can produce high light intensity but is very inefficient because it requires high electrical energy. Besides these types of lamps also produce high heat -so for indoor use, it will require adequate cooling.

In general, the lighting in an urban home needs averages 50% of the electricity consumption[3]. So when applied these traditional lamps -which require such tremendous power as a light source of the solar substitutes, it will increase the need for electrical energy very significant.

Meanwhile, the need for light intensity for photosynthesis of each plant is many. Some require high intensity, and some are not. Therefore, the selection of lamp power used should also be considered so that this artificial light source has high electrical energy efficiency.

## II. LIGHT EMITTING DIODE

Optoelectronic technology developed rapidly since the mid-1980s. One of these developments is that it has significantly improved the brightness and efficiency of LEDs.

LEDs are one type of the semiconductor diode, which consists of the semiconductor chip with a p-n junction -that formed when p-type and n-type p-type semiconductors are referred to as p-n junction diodes. The p-n junction diodes are made of semiconductor materials such as silicon, germanium, and gallium arsenide (figure 1).

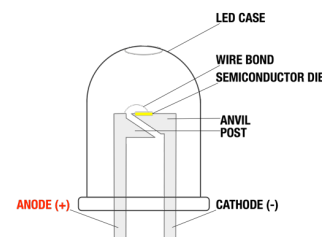


Fig. 1. Light Emitting Diode (LED)

With this p-n connection, the electric current will flow smoothly from the p-side (anode), to the n-side (cathode), and not in the backward direction. When electrified, the electrons and holes (the absence of the electron in a particular place in an atom) flow to the p-n junctions of the electrodes. Then, when the electron fills the hole, it falls to a lower energy level and releases energy in the form of photons[4].

The wavelength or color emitted by the photon on the LED has a relatively broad spectrum of possibilities. This wavelength depends on the bandgap energy on the substance that helps the p-n junctions. Some materials can radiate in near-infrared light, visible or almost ultraviolet light [4], [5].

At the beginning of the mid-1980s, GaAlAs (gallium aluminum arsenide) materials were developed to anticipate fast growth in LED use. The use of GaAlAs material provides better performance than previously available LEDs. The need for LEDs with lower voltages ultimately results in overall

power savings. LEDs with low power can finally be easily connected with Pulse Width Modulation (PWM) to be multiplexed making it suitable for use as outdoor advertising boards.

During this 1980s development period, LEDs are also designed to be barcode scanners, data transmission at fiber optic systems, and medical devices.

The modern improvements in crystal growth and optical design have enabled LEDs in the primary color spectrum -red, green, and blue. So by using the PWM on these three primary colors of LEDs as the base colors, other colors can be made more easily. Therefore currently, the use of LEDs as the basis for the visual display of electronic devices is widespread to use. Telecommunication products, automotive applications, traffic control devices, and colorful message boards, even LED TVs are also commercially available.

Table 1 is a list of some common LED types and the resulting colors [3], [4].

TABLE I. COMMONS TYPE OF LED

Wave Length	Color	Substrate
730 nm	Far-Red	GaP
700 nm	Red	GaP
660 nm	Red	GaAs
650 nm	Red	GaAs
630 nm	Orange-Red	GaP
610 nm	Orange	GaP
590 nm	Yellow	GaP
585 nm	Yellow	GaAs
565 nm	Green	GaP
450 nm	Blue	GaN/SiC

Why are the use LEDs preferred? Comparing with the light range of 8,000 hours of fluorescent lamps, exceedingly a 1,000 hours of incandescent light's, LEDs have a very much longer life of 100,000 hours. In addition to its long life, LEDs have many advantages over conventional light sources. These advantages include small size, a specific wavelength, low thermal output, customizable intensity and light quality, and high photoelectric conversion efficiency. These advantages make LEDs perfect for supporting plant growth in controlled environments such as plant tissue culture spaces and growth spaces.[4]

### III. LED FOR ARTIFICIAL SUNLIGHT

The question that often arises when discussing the ideas of LED as a substitute for sunlight for the plant photosynthesis is, can LEDs replace the sunlight? The sunlight is polychromatic while light from LED is monochromatic, so is it can do the substitution?

#### A. The Sunlight and Plant photosynthesis

Sunlight reaches the earth in a vast spectrum. Starting from below 200 nm to more than 2000 nm[6]. This spectrum or wavelength of the sunlight generally can be divided into three areas (figure 2):

- Ultra Violet ray, which is an invisible light for human eyes, with wavelengths below 380 nm. This region of light spectrum consists of several types, namely:

- Ultraviolet C, i.e., light with the wavelength of 200 nm to 280 nm. This light is harmful to plants because it has high toxicity. UVC from the sun usually never reach the surface of the earth because the ozone layer blocks it.
- Ultraviolet B or light with the wavelength from 280 nm until 315 nm. Although this light is not harmful to plants, it can cause the color of the plants to fade.
- The wavelength from 315 nm to 380 nm referred to as ultraviolet A (UVA), this light does not affect (both positive or negative) on plants.

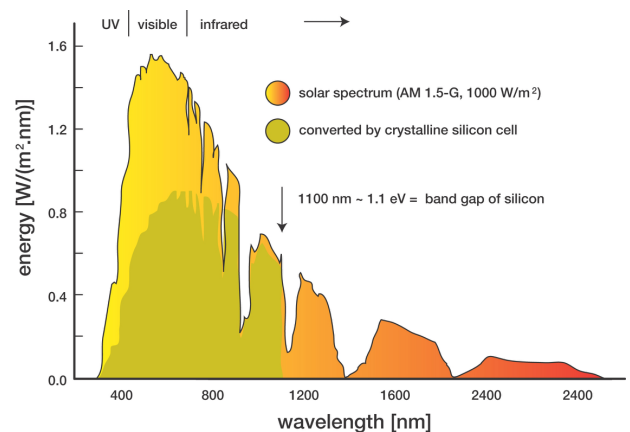


Fig. 2. Sunlight Spectrum[6]

- The visible light, which is the light that can see by the human eyes. For plants photosynthesis, is divided into several areas and benefits:
  - The wavelength from 380 nm to 400 nm as ultraviolet A or the beginning of visible light. At this wavelength, the process of light absorption by plant pigments (chlorophyll and carotenoids) begins.
  - Visible light at the wavelength of 400 nm to 520 nm containing purple, blue and green. At this spectrum peak absorption by chlorophyll occurs and this spectrum has a strong influence on vegetative and photosynthesis.
  - Visible light at the wavelength from 520 nm until 610 nm, that containing green, yellow, and orange light. At these wavelengths are less absorbed by plant pigments, the lesser effect on vegetative and photosynthesis.
  - The visible light at the wavelength of 610 nm to 720 nm contains the red light. Plants again absorb the light at this wavelength and considerably affects vegetative growth, photosynthesis, flowering, and proliferation.
- Infrared light, which is also a not visible light to the human eye with wavelengths higher than 720 nm.

- At the wavelength of 720 nm to 1000 nm, known as far-red or infrared light, this light affects the germination and flowering of plants, although only a small amount of absorption occurs in this band.
- Wavelengths above 1000 nm, all absorption at this spectrum will be converted into heat. So the plants do not use it.

### B. LEDs and photosynthesis of plants

Plants always need light throughout their lives. Starting from the first time when it is yet a sprout, until becoming a flowering and producing as an adult plant. There are three light parameters required by all plants, namely quality, quantity and duration[1], [7]:

- The quantity of light or intensity is the primary parameter that affects photosynthesis. Photochemical reactions within the plant cells require the energy of that light to convert CO<sub>2</sub> to carbohydrates. So the intensity of the lights will determine the success of this reactions.
- The quality of light or spectral distribution refers to the distribution of the light spectrum, i.e., which part of the emission is in the wavelength region of light. These wavelength regions are divided into blue, green, red regions and invisible wavelength regions. The quality of light also affects the shape of plants, development, and flowering (photomorphogenesis)[7].
- The duration of light or photoperiod is how long the plant accepts the light with a certain quantity and quality as above. This duration especially needed at the time of plants in the flowering phase, so the flowering time on plants can be controlled by arranging photoperiod [7].

Light sourced from the LEDs can meet the first parameter and the second parameter required by the plant as above. The intensity of light can be generated by using a substantial LEDs power to produce sufficient light intensity. Alternatively, it could also by using some LEDs light sources.

Meanwhile, the photoperiod is very easy to set. Since the LEDs as a light source is dependent on the presence of electric current, so long as there is an electric current in the house, the photosynthesis of agriculture in this room can also be done.

Which then becomes the question is, whether the LEDs can replace the quality of light such as sunlight?

In some studies, it was found that in conducting photosynthesis, plant chlorophylls responded most strongly to red and blue regions. Although plants receive all the spectrum of sunlight, plants do not use the entire spectrum for photosynthesis. Photosynthesis absorbs only light with a wavelength of 400nm up to 700 nm -which is part of human-visible light[1], [5],[7].

Chlorophylls (chlorophyll a and b) are the essential actors in photosynthesis (figure 3), although they are not the only chromophores. Plants also have other photosynthetic pigments, known as antenna pigments (such as carotenoid  $\beta$ -carotene, zeaxanthin, lycopene, and lutein), which participate in the absorption of light and play an essential role in photosynthesis[8],[9],[10].

From figure 3 and Table II, can be seen that in the photosynthesis plants not all spectrum of light is needed, also not all the visible light spectrum is absorbed by chlorophyll and antenna, only a part is required.

TABLE II. WAVE LENGTH OF LIGHT FOR PHOTOSYNTHESIS

Wave Length (nm)		Known As	V/I	Absorb by Plant
200	280	Ultraviolet C	I	N
280	315	Ultraviolet B	I	N
315	380	Ultraviolet A	I	N
380	400	Ultraviolet A	V	Y
400	520	Purple, Blue, Green	V	Y
520	610	Green, Yellow, Orange	V	Y (but lesser)
610	720	Orange, Red	V	Y
720	1000	Infrared	I	N

(V)isible, (I)nvisible, (Y)es, (N)o

The chlorophyll A absorb more in purple, blue, and red. Meanwhile, the chlorophyll B absorb more in blue and red. Last, the antenna absorbs the purple, blue, and a little green.

As we know above, that the photosynthesis process does not require a full-spectrum visible light, that is why the light from LED can be used as artificial sunlight for photosynthesis. Meanwhile, the LEDs can generate sufficient light at specific wavelengths, turn on and turn off very quickly, then the photosynthesis of plants linked with the solid state LED characteristics is an energy-saving way to indoor agriculture with the low power consumption.

Other artificial light sources do not easily achieve this way.

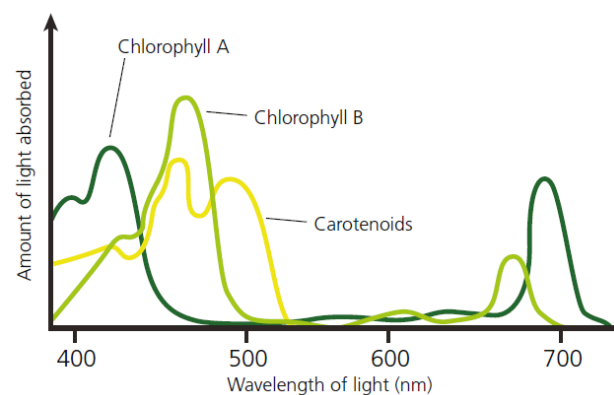


Fig. 3. Spectral Absorption by Plants[6]

## IV. MEASUREMENT OF LED LIGHT INTENSITY

Our experiment on Automatic Plant Acclimatization Chamber (APAC) uses LEDs as the light source -for replacement of sunlight[11]. This experiment aims to create a smart Plant Growth Chamber, which can simulate a specific micro-climate in a specified location and period automatically.

The use of LEDs in this experiment becomes mandatory because only LEDs can be used as artificial light sources with the ability to turn on and turn off quickly. Other light sources take time to reach the maximum of intensity that can be generated.



Besides, only LEDs that can reduce the intensity of light with a simple microcontroller. The intensity reduction in this experiment uses Pulse Width Modulation (PWM) and then reduce the LED duty cycle to decrease the intensity of the generated light and increase the duty cycle to raise it -up to 100% duty cycle for maximum LED light intensity.[12]

This APAC Experiment uses High Power LEDs (HP-LED) with the following specifications:

- light color : 6000 - 6500 Kelvin
- voltage : 9.5 - 12 volts DC
- input current : 900 mA
- light intensity : 800 - 1000 lumens
- view angle : 120 degrees

HP-LED is one type of LED that has higher power and brightness compared to conventional LEDs that require little power and produce less brightness. The conventional LED has an input current 20 mA and principally LED with input current higher than 20 mA is called as HP-LED. Currently, HP-LED widely applied to the headlamp of the car, flashlight, lighting fixtures, and so forth.[13]

HP-LED is an energy-efficient building block that produces ideal lumen output for the latest lighting applications. HP-LED offers the best possible solid-state light source[14].

#### A. Experiment Setup

For this measurement of the intensity of HP-LED, we prepare a chamber of 2 meter by 2 meter as the place of the experiment. This chamber is designed not to reflect the inner-sourced light, and also can not penetrate the light from outside sources. Therefore, the chamber gives the black color of the inner walls (figure 4)



Fig. 4. Darkbox Design

HP-LED will be placed right at the top center of the box as a light source. Some TSL2561 sensors packaged in an array of sensors, placed on board as a luminosity sensor. This boards can be raised or lowered as needed near or away from light sources. Before the actual measurement, the reading results of each TSL2561 sensor were recorded first as a comparison when reading TSL2561.

#### B. LED Radiation Pattern

The specifications of the HP-LED makers that used in this experiment said that its view angle is 120 degrees. So, that when HP-LED is installed in height 1 meter from the sensor so that when described in triangle form will be like in figure 5

The calculation of the width of light to be received from

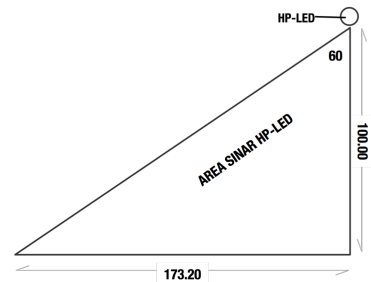


Fig. 5. 2D of Light Area

HP-LED can be calculated by the trigonometric formula: tangent (equation 1).

$$\tan \theta = \frac{\text{Opposite}}{\text{Adjacent}} \quad (1)$$

So if the HP-LED is at an altitude of 1 m (100 cm), then the spread of the light of the HP-LED has the radius of 173.20 cm or a diameter of 336.40 cm.

The measurement with the TSL2561 sensor produces an image of the radiation pattern as shown in Figure 6.

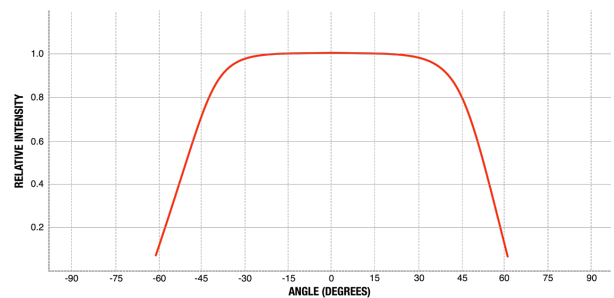


Fig. 6. HP-LED Radiation

#### C. LED Intensity

The intensity of the light is measured by how many luminous fluxes are scattered in specific areas. The amount of light generated by the light source will illuminate the surface fainter if spread over a larger area, so the illumination is inversely proportional to the area where the luminous flux is maintained constant[15].

One lux equals one lumen in square meters or  $1 \text{ lx} = 1 \text{ lm/m}^2$ . The flux of 1,000 lumens, if concentrated in an area of 1-meter square, then it illuminates the area of the square meter with the illumination of 1,000 lux. However, the same 1,000 lumens, if spread over 10 square meters, will produce only 100 lux illuminations.

Regarding calculating the extent of this HP-LED ray, since the rays creating a form of a circular area, the counting base used is the circle area (equation 2).

$$L = \pi \cdot r^2 \quad (2)$$

Since the radius of the light depends on the distance between the HP-LED and the floor, by decreasing equation 1,  $r$  can be obtained by equation 3.

$$r = \tan \frac{\theta}{2} \cdot t \quad (3)$$

So the formula of this area of the HP-LED ray can be calculated directly with equation 4.

$$L = \pi \cdot \left( \tan \frac{\theta}{2} \cdot t \right)^2 \quad (4)$$

Finally, the HP-LED Illuminance at a certain height can be calculated by equation 5.

$$lx = \frac{lm}{\pi \cdot \left( \tan \frac{\theta}{2} \cdot t \right)^2} \quad (5)$$

Where  $lm$  is the flux produced by HP-LED,  $\theta$  is the angle of the HP-LED light beam and  $t$  is the HP-LED height from the base (in meter).

Figure 7 shows the results of the measurement of light intensity compared with the calculation using the formula above.

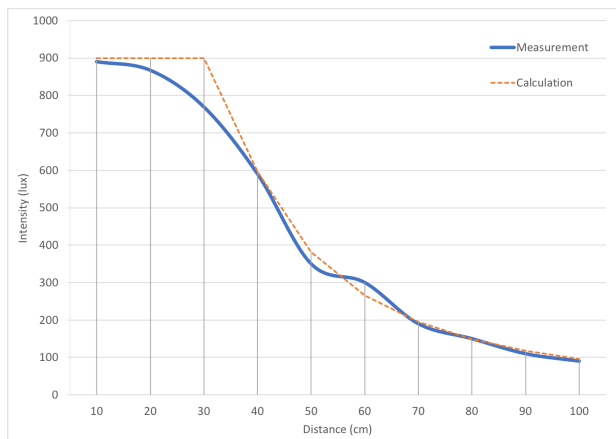


Fig. 7. Lux Calculation (red) and Experiment (blue)

#### D. Tropical Illuminance vs LEDs

In some research reports the average sunlight illumination that occurs around Indonesia can reach 60,000 lux [16], [17]. This magnitude can rise or fall depending on the weather and the position of the sun on the location where the measurement has been done.

However, for the needs of plant photosynthesis, some studies note that it takes around 400 to 600 lux [18].

To be able to achieve the needs of photosynthesis, it is enough to need an LED with a power of 10 watts and placed at an altitude of 40 to 50 cm above the plant. However, this amount will -of course, increasing when the placement of LEDs is more than 50 cm, and plants that require lighting are in the area more than 2.35 square meters.

This means, the need for electric power for photosynthesis needs of plants in the room can be regulated by increasing or decreasing the distance of the LED from the plant. This power requirement will also decrease if the transmitting angle of the LED beam can be reduced and directed to the required location.

#### V. CONCLUSION AND FUTURE WORKS

Plants do not require the entire spectrum of light obtained from sunlight. Plants require only light with a wavelength of 400-700 nm, known as photosynthetically active radiation (PAR). While the LEDs can emit light with a specific wavelength -according to the base material that the manufacturer is making. Therefore, LED is the first artificial light source which can be controlled by an actual spectral composition for the plant.

By using LEDs, the wavelength of light required by plants in it photoreceptors will always be met with the artificial light. Adjustment of the intensity and wavelength of light from these artificial sunlight sources will be able to optimize production as well as to influence the morphology and composition of the plants.

The placement of LEDs positions for specific plants can also be easily arranged, tailored to the specific needs of the plant. Besides LEDs can also be easily integrated into a digital control system, facilitating complex lighting programs such as various spectral compositions during the photoperiod or by the plant development stage.

This experiment needs to be strengthened by the measurement of the light intensity generated by the LED array (multiple LEDs) in some radiation area. The addition of LEDs at a certain distance, of course, does not increase the intensity of light in areas with linear quantities.

For electric power savings, this study should also be followed by conducting another experiment to measure the impact of increasing the voltage and the need of electric current by the LED compared to the intensity of the light generated. Optimizing the use of electric power by LEDs can be achieved by providing a specific voltage for specific intensity needs as well.

Also on the use of PWM to reduce the intensity of LED light. There are still unanswered questions as to whether reducing the duty cycle to reduce the intensity of this light further saves the power than reducing the voltage as the plan above.

#### REFERENCES

- [1] D. Singh, C. Basu, M. Meinhardt-Wollweber, and B. Roth, "LEDs for energy efficient greenhouse lighting," *Renew. Sustain. Energy Rev.*, vol. 49, pp. 139–147, Sep. 2015.
- [2] O. Ransen, "Candelas Lumens And Lux.", 2nd ed. S.I.: Owen Ransen, 2017.
- [3] W. N. W. Muhamad, M. Y. M. Zain, N. Wahab, N. H. A. Aziz, and R. A. Kadir, "Energy Efficient Lighting System Design for Building," 2010, pp. 282–286.
- [4] S. Cangeloso, TotalBoox, and TBX, *LED Lighting: A Primer to Lighting the Future*. Maker Media, Inc, 2012.
- [5] N. Yeh and J.-P. Chung, "High-brightness LEDs—Energy efficient lighting sources and their potential in indoor plant cultivation," *Renew. Sustain. Energy Rev.*, vol. 13, no. 8, pp. 2175–2180, Oct. 2009.
- [6] Joshua S. Stein Ph.D., "Solar Energy And Our Electricity Future," presented at the Renewable Energy Short Course, Burlington, VT, USA, 26-Jul-2011.
- [7] J. N. Nishio, "Why are higher plants green? Evolution of the higher plant photosynthetic pigment complement," *Plant Cell Environ.*, vol. 23, no. 6, pp. 539–548, Jun. 2000.
- [8] H. G. Choi, B. Y. Moon, and N. J. Kang, "Effects of LED light on the production of strawberry during cultivation in a plastic greenhouse and in a growth chamber," *Sci. Hortic.*, vol. 189, pp. 22–31, Jun. 2015.
- [9] R. Wojciechowska, O. Długosz-Grochowska, A. Kolton, and M. Żupnik, "Effects of LED supplemental lighting on yield and some



- quality parameters of lamb's lettuce grown in two winter cycles," *Sci. Hortic.*, vol. 187, pp. 80–86, May 2015.
- [10] A. C. Apel and D. Weuster-Botz, "Engineering solutions for open microalgae mass cultivation and realistic indoor simulation of outdoor environments," *Bioprocess Biosyst. Eng.*, vol. 38, no. 6, pp. 995–1008, Jun. 2015.
- [11] M. N. Al-Azam, M. M. Achlaq, A. Nugroho, A. Gabriel Sooi, A. Winaya, and Maftuchah, "Broadcasting the Status of Plant Growth Chamber using Bluetooth Low Energy," *MATEC Web Conf.*, vol. 164, p. 01029, 2018.
- [12] Y. Gu, N. Narendran, T. Dong, and H. Wu, "Spectral and luminous efficacy change of high-power LEDs under different dimming methods," 2006, p. 63370J.
- [13] J. Barbosa, D. Simon, and W. Calixto, "Design Optimization of a High Power LED Matrix Luminaire," *Energies*, vol. 10, no. 5, p. 639, May 2017.
- [14] C. Darujati and M. Hariadi, "Facial motion capture with 3D active appearance models," 2013, pp. 59–64.
- [15] A. Amoozgar, A. Mohammadi, and M. R. Sabzalian, "Impact of light-emitting diode irradiation on photosynthesis, phytochemical composition and mineral element content of lettuce cv. Grizzly," *Photosynthetica*, vol. 55, no. 1, pp. 85–95, Mar. 2017.
- [16] A. Zain-Ahmed, K. Sopian, Z. Zainol Abidin, and M. Y. H. Othman, "The availability of daylight from tropical skies—a case study of Malaysia," *Renew. Energy*, vol. 25, no. 1, pp. 21–30, Jan. 2002.
- [17] R. Rahim, "Daylight Measurement Data in Makassar-Indonesia," in *Sustainable Environmental Architecture (SENVAR)*, ITS - Surabaya, 2010.
- [18] G.-X. Yang, G.-X. Chi, and J.-Z. Jiang, "A case study for the design of visual environment of a control room in a power plant," *Light. Res. Technol.*, vol. 17, no. 2, pp. 84–88, Jun. 1985.

# Quasi Z-Source Inverter as MPPT on Renewable Energy using Grey Wolf Technique

Quota Alief Sias

Department of Electrical Engineering  
Universitas Negeri Malang  
Malang, Indonesia  
quota.alief.ft@um.ac.id

Irawan Dwi Wahyono

Department of Electrical Engineering  
Universitas Negeri Malang  
Malang, Indonesia  
irawan.dwi.ft@um.ac.id

Irham Fadlika

Department of Electrical Engineering  
Universitas Negeri Malang  
Malang, Indonesia  
irham.fadlike.ft@um.ac.id

Arif Nur Afandi

Department of Electrical Engineering  
Universitas Negeri Malang  
Malang, Indonesia  
an.afandi@ieee.org

**Abstract** — Z-Source Inverter (ZSI) is famous power converter who has capability to deal with voltage sags, improved power factor and wide voltage range of output. Quasi Z Source Inverter (QZSI) is the modern ZSI who has continuous current of input and can reduce stress of the passive component. This paper proposes simple boost QZSI circuit as Maximum Power Point Tracking (MPPT) using Grey Wolf Optimization (GWO) algorithm in photovoltaic system. Grey Wolf algorithm has been compared with the Perturb and Observed (P&O) technique for gaining the maximum power from the sun. Both techniques can get the optimum power of solar panel not only at constant sun light condition but also under varying irradiance levels. The value of average power obtained from GWO technique is greater than P&O. Although the value of solar radiation changes, the output voltage remains stable and both algorithms carry on obtaining optimal power of the sun.

**Keywords** — GWO, MPPT, QZSI

## I. INTRODUCTION

One of the cleanest renewable energy sources and now being widely applied is solar panel technology [1]. This technology can be applied almost all over the world as long as there is sunlight. Photovoltaic (PV) technology is widely used by people all over the world in the last decade because of its simplicity as renewable energy. This is also to be the most popular topic research because of its unique characteristics. Using simple resistive loads, photovoltaic operates at different voltage levels depended on load values under constant sunlight and constant temperature conditions. There is only one point of voltage and current in operating area that produces the most optimal power and it is called the Maximum Power Point (MPP). So this technology generally requires a power conditioner that holds the voltage remain to the optimal point for the purpose of gaining the optimal power. The DC-AC converter or inverter is required as a power conditioner because the solar cells produce DC voltage while almost all existing loads require AC voltage.

Electrical system using solar panel has a lot of configurations such as using battery or not, using MPPT or not, using DC or AC loads and so on. This paper just explain simple solar panel

system without battery and using three phase AC load because almost electrical grid presently use alternating current system. Because using AC loads, Inverters or the DC-AC converter is used in this research. This paper explain QZSI for implementing MPPT and apply GWO as the recent intelligent algorithm to gain the optimum power of the sun.

## II. PHOTOVOLTAIC SYSTEM AND QUASI Z SOURCE INVERTER

### A. Varying Irradiance Levels and MPPT on PV System

The power of solar panels is depended on the sun irradiance levels [1]-[5]. Fig.1 shows that the higher the irradiance of sunlight, the greater the power will be gained. From the P-V graph of Fig. 1, there is one point represent the highest power of the sun. This MPP is obtained from one specific value of voltage and one specific value of current stated at I-V graph. The PV System generally used MPPT as power conditioner to force the operating value of current and voltage to the MPP.

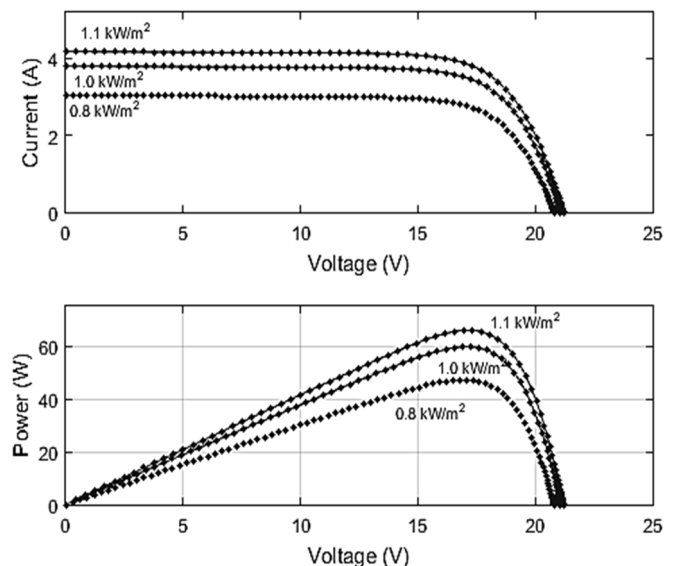


Fig. 1. I-V and P-V characteristic curves of solar panel at varying irradiance

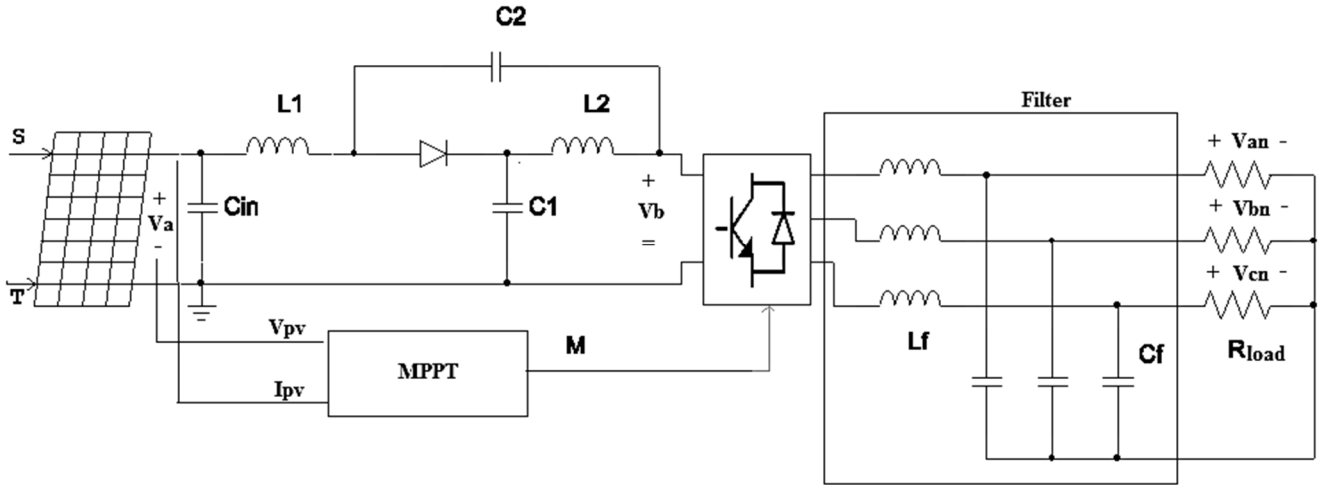


Fig. 2. Simple Boost QZSI circuit as MPPT of Photovoltaic Technology

The results of research show that MPPT implementation is able to absorb sun energy by 99% [2]. The common MPPT technique and the simple one is Perturb and Observe (P&O) technique. It has high efficiency and does not require tuning parameters periodically [3]. P&O is a very simple technique because it does not require knowledge of the curves of solar panel characteristics [4]. P&O can also be implemented at affordable price using arduino microcontrollers [5]. The simple explanation of the P&O technique is shown in Fig.3. The basic principle of this technique is measure the gradient  $m = \Delta P / \Delta V$  from the power and voltage characteristic curve. The gradient will be zero at MPP ( $\Delta P / \Delta V = 0$ ). Operating voltage value of P&O should be increased to get the maximum power when having positive gradient ( $\Delta P / \Delta V > 0$ ) and vice versa.

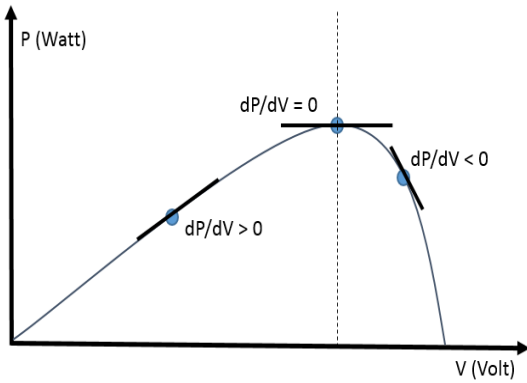


Fig. 3. Basic principle of P&amp;O technique

Fig.4 shows the flow diagram of the P & O technique. Adjusting the operating voltage value on the converter is done by increasing or decreasing the duty cycle. The P & O process is very simple because it only requires voltage and current sensors so that the value of the power generated will also be known. Voltage and power are measured and compared to the results of previous measurements so that the gradient  $dP/dV$  of the curve is obtained. This gradient of the curve will generate a new duty cycle value and the process will be repeated.

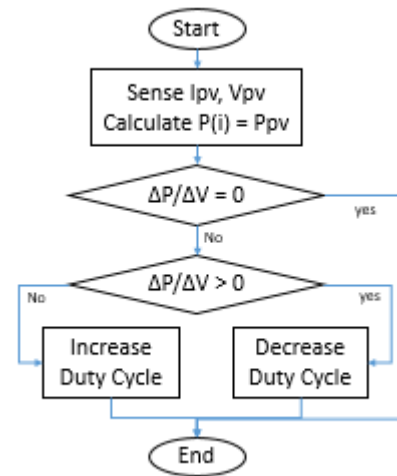


Fig. 4. Flow diagram of P&amp;O technique

### B. Simple Boost Quasi Z Source Inverter

QZSI is the development of ZSI topology which can reduce passive component stress and has continuous input current features [6]-[8]. This paper use the simple boost control to get the higher output voltage. QZSI is an inverter that has two operating conditions, shoot-through and non-shoot-through conditions [8]-[11]. In shoot-through state, condition of the diode is off (open circuit) while in non-shoot-through state, the diode is on (close circuit). QZSI has two important parameters: shoot-through duty cycle and modulation index and has relationships as in (1), (2) and (3) [9].

$$\frac{V_{pn}}{V_b} = \frac{M}{2} \quad (1)$$

$$\frac{V_b}{V_a} = \frac{1}{1-2D} \quad (2)$$

$$M \leq 1 - D \quad (3)$$

The modulation index  $M$  is used to control output AC phase neutral voltage  $V_{pn}$  as in (1) and transfer function of  $V_b/V_a$  in DC port is controlled by shoot-through duty cycle  $D$  as in (2). The relationship between parameters  $M$  and  $D$  for simple boost control is given by (3). From (2), the value of  $1-2D$  can not be empty so that the operating value  $D$  is from 0 to 0.5. Thus from (3), the value of  $M$  is limited only in the range 0.5 to 1.

TABLE I. COMPONENTS OF CIRCUIT

Parameter	Value
$C1, C2$	1 mF
$L1, L2$	1 mH
$R_{load}$	25 $\Omega$
$C_{in}$	5 $\mu$ F

The value of modulation index  $M$  generally has a constant value to maintain the constant output AC voltage. Because the sunlight is not constant in nature, this paper propose to change the value of  $M$  to get the better output voltage. This paper implements the P&O and Grey Wolf methods to adjust the value of  $M$ . QZSI can also be used as MPPT on PV System to ensure maximal conversion efficiency [10][11]. The circuit used in this paper is shown in Fig.2 and all the component values are stated in the Table 1.

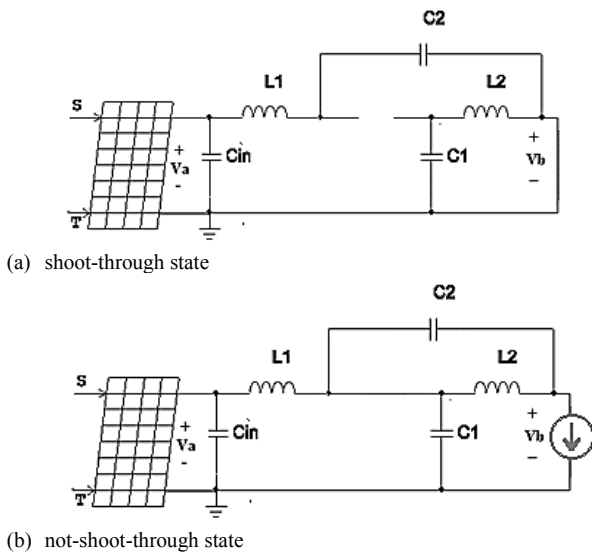


Fig. 5. Operation conditions of the QZSI

In shoot-through state shown in Fig 5a, diode is off and the output voltage  $V_b$  is zero (short circuit). In this condition,  $V_{carrier} > V_p$  and  $V_{carrier} > V_{ref}$  ( $V_a, V_b, V_c$ ) shown in Fig.6 so that the diode is reversed biased. The period in this state is defined as  $T_{st}$  and for non-shoot-through state defined as  $T_{nst}$ . Total period in one cycle is  $T = T_{st} + T_{nst}$ . Shoot-Through duty cycle  $D$  is defined as shoot-through periode divided by total periode ( $D = T_{st}/T$ ).

In non-shoot-through state shown in Fig 5b, the inverter is operated normally since the diode is on (forward biased). Considering the average voltage across the inductor in one cycle of switching periode is zero, so the relationship of output voltage  $V_b$  to input voltage  $V_a$  is obtained as (2). It can be

noticed from (2) that the voltage boosting is obtained by using shoot-through state between upper and lower switches of an inverter leg.

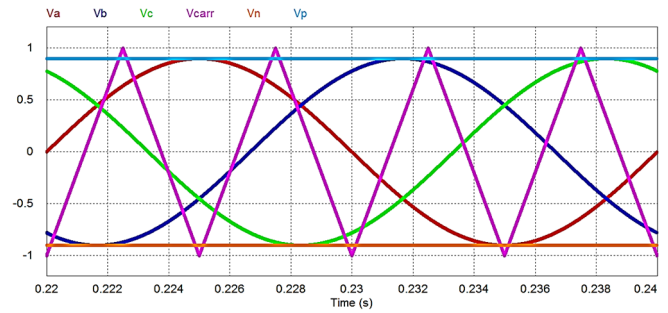


Fig. 6. Illustration of switching pattern of QZSI using Simple Boost Control

### III. MPPT DESIGN USING GREY WOLF TECHNIQUE

The evolutionary methods as meta-heuristic algorithm are usually used to solve optimization problems. They continue to be developed in order to improve the performance of the previous techniques for example the Harvest Season Artificial Bee Colony (HSABC) algorithm proposed on 2013 which can be faster than Genetic Algorithms (GA) on the emission and economic dispatch problem [12]. P&O as the most simple MPPT technique is also developed for time to time to get the better results without the evolutionary method for the first generation [13] and the popular one is MPPT using the evolutionary technique in the recent studies [14].

Grey Wolf algorithm, optimizer published on 2014, has good competitive results compared to the other algorithms for solving 29 benchmarked test functions [15]. It can also be used to solve the real problem such as in PV modeling because of the limited information from the manufacturer datasheet [16]. GWO can also be used as MPPT compared to Improved-PSO (IPSO) method in DC system [14]. This paper explain MPPT using GWO and QZSI for the AC loads. The GWO technique inspired by hunting mechanism of grey wolves and their leadership hierarchy in nature [14]-[16]. GWO algorithm has three main steps of hunting process: tracking, pursuing and attacking. On pursuing process, the encircle behavior can be modeled in (4) and (5).

$$D = |C \cdot Xp(t) - X(t)| \quad (4)$$

$$X(t+1) = Xp(t) - A \cdot D \quad (5)$$

where  $A$ ,  $C$  and  $D$  represent GWO coefficient vectors as in [14],  $Xp$  is the position vector of the prey,  $X$  indicates the position vector of grey wolf. And  $t$  is the current iteration. The vectors  $A$  and  $C$  are calculated in (6) and (7). During iterations, the value of  $a$  is linearly decreases from 2 to 0 and the components  $r_1, r_2$  are random vectors in  $[0, 1]$ .

$$A = 2 \cdot a \cdot r_1 - a \quad (6)$$

$$C = 2 \cdot r_2 \quad (7)$$

The first step for implementing GWO for MPPT is defining the duty cycle  $d$  as a grey wolf and modify (5) to become (8). The value  $A$  and  $D$  is calculated by the previous equations. The optimal power can be obtained by iteration process of

calculating  $d$ . The fitness function of calculating power is defined by (9) and the number of iteration is represented by  $k$  and the current number of grey wolves is indicated by  $i$ . Flow diagram of Grey Wolf Technique and the iteration process are shown in Fig.7.

$$d_i^{k+1} = d_i^k - A \cdot D \quad (8)$$

$$P(d_i^{k+1}) > P(d_i^k) \quad (9)$$

This paper use the P&O and GWO techniques as MPPT by controlling and iterating the modulation index  $M$  of the QZSI. The initial value of  $M$  in P&O is 0.75 because the operating value is limited from 0.5 to 1. GWO Technique use three grey wolves, and the initial value is 0.6, 0.75, and 0.9. P&O use the gradient concept and the GWO use (4)-(9) for each iteration to adjusting modulation index  $M$  until converge state.

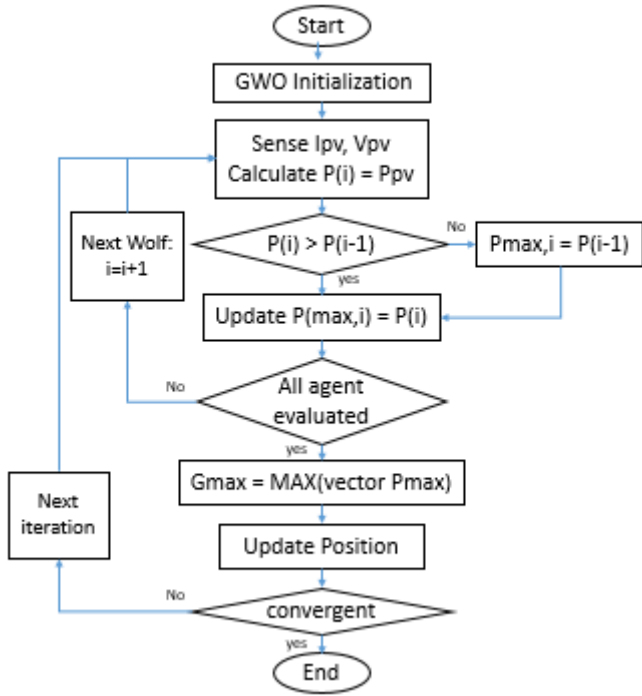


Fig. 7. Flow diagram of Grey Wolf technique

#### IV. SIMULATION RESULTS AND ANALYSIS

The performances of both MPPT methods (P&O and GWO) are pointed in Standart Test Condition (STC) at the first analysis. And the final, both MPPT methods are also be compared under varying condition of sunligh levels. The iteration process of adjusting modulation index  $M$  of QZSI by P&O is stated by the red line in Fig.8. The initial value of  $M$  is 0.75 as stated before and the iteration process has brought it to the steady value of  $M$  at 0.6. GWO method, using three grey wolves in different initial values of  $M$  (0.6, 0.75 and 0.9), stated by the blue line shows the fast iteration process and converge and steady before 0.5 s.

##### A. Output Power Performance under Constant Irradiance

In STC (25°C and 1kW/m<sup>2</sup>), The PV model used in this paper has the 60 Watt peak for optimal power same as in [13]. The performance results of both MPPT are shown in Fig.9.

P&O obtain 51,41 W (85.4%) and GWO has higher result at 53.65 W (89.1%) of the optimal power 60,21 Watt. Much power gained has been lost when the process of iteration before the steady state. After converged, both techniques give the same power gained result up to 99% after 0.2 s. From average power obtained, it can be conclude that the GWO method has the higher efficiency than the P&O technique.

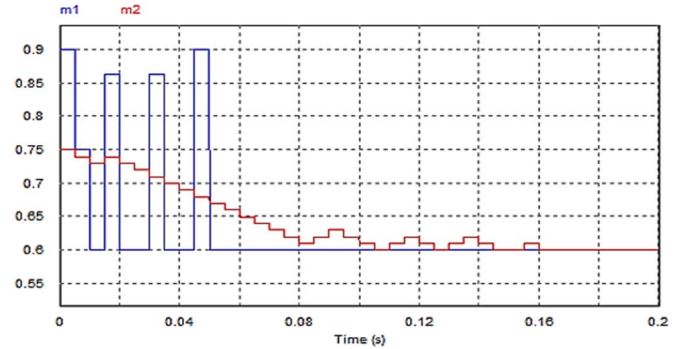


Fig. 8. The index modulation performances of QZSI by P&O (red line) and GWO (blue line) under STC.

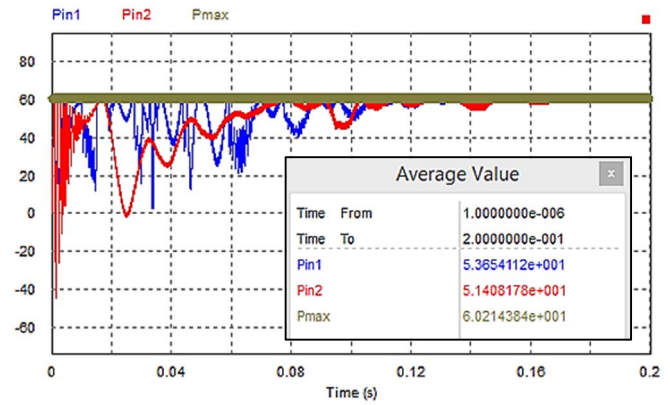


Fig. 9. The performances of QZSI by P&O (red line) and GWO (blue line) under STC.

##### B. Output Power Performance under Varying Irradiance

Both methods P&O and GWO are tested under varying sunlight levels by the suddenly changing the irradiance upper and lower the STC. First, the initial of optimal power from the highest irradiance is settled in 65 Watt and 47 Watt for the lowest irradiance. The conditions is settled by changing the irradiance from the highest power to the lowest, going to the STC and finally from the lowest to the highest one.

Fig.10 and Fig.11 explain the output voltage of three phase system performance using LC filter or only the capacitive filter. Using the balance three phase load 25 Ω, both MPPT methods generate the balance voltage output. Although the power and irradiance conditions are changed rapidly, voltage output performances from both MPPT methods are excellent because they still constant or remain stable. Fig.12 make the clear point that both MPPT methods can be used to obtained the optimal power. P&O obtain 54.31 W (97.61%) and GWO still has higher result at 54.34 W (97.66%) of the optimal power 55.64 Watt.



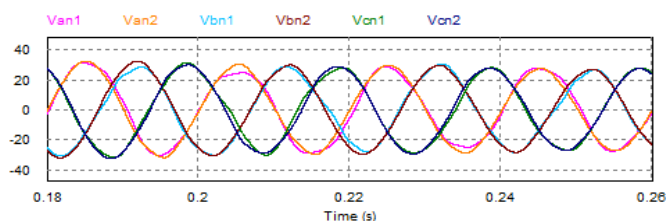


Fig. 10. Voltage performances of QZSI using LC filter

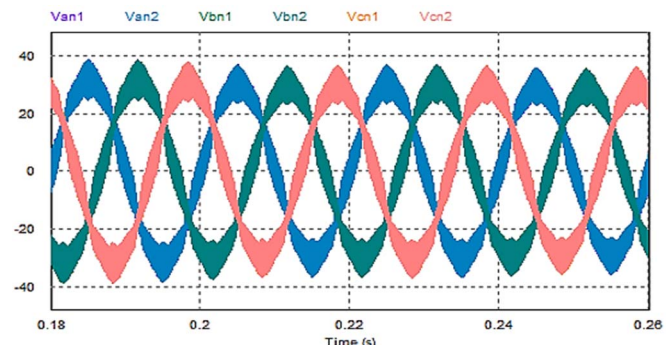


Fig. 11. Voltage performances of QZSI using only capacitive filter

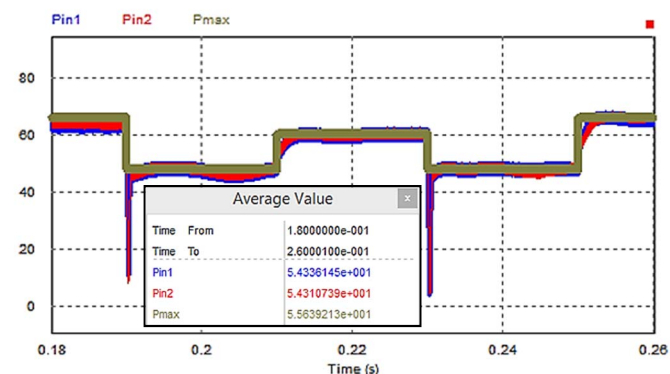


Fig. 12. Output power performance of QZSI by P&amp;O (red line) and GWO (blue line) under varying irradiance.

## V. CONCLUSION

Both techniques P&O and GWO can be used as MPPT in QZSI implementation and have good performance for gaining the optimal power under constant and varying irradiance levels. GWO are faster to converge so that the performance of average power output value is also more higher than P&O. Under constant irradiance level, GWO have obtain 3.7 % more power than P&O. Under varying irradiance level, GWO have obtain 0.05 % more power than P&O. Although the value of solar radiation changes, the output voltage of QZSI remains stable and both algorithms carry on obtaining optimal power of the sun.

## ACKNOWLEDGMENT

This paper is part of the research supported by Universitas Negeri Malang, Malang, Indonesia, for the PNPB Research Program issued on the letter number 21.2.6/UN32.14/LT/2018. The authors would also like to express the sincere gratitude to

all contribution of the Electrical Engineering Department and the Electric Energy Conversion laboratory, Universitas Negeri Malang, Malang, Indonesia.

## REFERENCES

- [1] E. I. Batzelis, G. E. Kampitsis, S. A. Papathanassiou, and S. N. Manias, "Direct MPP calculation in terms of the single-diode pv model parameters," *IEEE Transactions on Energy Conversion*, vol. 30, no. 1, pp. 226-236, August 2014.
- [2] V. C. Sontake, and V. R. Kalamkar, "Solar photovoltaic water pumping system-A comprehensive review", *Renewable and Sustainable Energy Reviews*, 59, pp.1038-1067. January 2016.
- [3] E. Dallago, A. Liberale, D. Miotti and G. Venchi, "Direct MPPT algorithm for PV sources with only voltage measurements," *IEEE Transactions on Power Electronics*, vol. 30, no. 12, pp 6742-6750, December 2015.
- [4] M. A. Elgendy, B. Zahawi, and D. J. Atkinson, "Assessment of Perturb and Observe MPPT algorithm implementation techniques for PV pumping applications," *IEEE Transactions on Sustainable Energy*, vol. 3, no. 1, pp 21-33, January 2012.
- [5] M.K.D. Ulaganathan, C. Saravanan, and O. R. Chitrnanjan, "Cost-effective Perturb and Observe MPPT method using arduino microcontroller for a standalone photo voltaic system," *International Journal of Engineering Trends and Technology (IJETT)*, vol. 8, no. 1, pp. 24-28, February 2014.
- [6] J. Liu, J. Hu, and L. Xu, "Dynamic Modeling and Analysis of Z Source Converter—Derivation of AC Small Signal Model and Design-Oriented Analysis," *IEEE Transactions on Power Electronics*, vol. 22, no. 5, pp 1786-1796, September 2007.
- [7] J. Anderson and F. Z. Peng, "Four quasi-Z-source inverters." In *Power Electronics Specialists Conference, 2008. PESC 2008. IEEE*, pp. 2743-2749. IEEE, 2008.
- [8] J. Liu, S. Jiang, D. Cao, and F. Z. Peng, "A digital current control of quasi-Z-source inverter with battery," *IEEE Transactions on Industrial Informatics*, vol. 9, no. 2, pp. 928-937, May 2013
- [9] D. Sun, B. Ge, D. Bi and F. Z. Peng, "Analysis and control of quasi-Z source inverter with battery for grid-connected PV system," *International Journal of Electrical Power & Energy Systems*, vol 46, pp. 234-240, March 2013.
- [10] J. Khajalehi, M. Hamzeh, K. Sheshyekani and E. Afjei, "Modeling and control of quasi Z-source inverters for parallel operation of battery energy storage systems: Application to microgrids," *Electric Power Systems Research*, vol. 125, pp. 164-173, August 2015.
- [11] R. Sathishkumar, V. Malathi and E. Sakthivel, "Real Time Implementation of Quasi Z-Source Inverter Incorporated with Renewable Energy Source," *Energy Procedia*, vol. 117, pp. 927-934. June 2017
- [12] A. N. Afandi, I. Fadlika and A. Andoko, "Comparing Performances of Evolutionary Algorithms on the Emission Dispatch and Economic Dispatch Problem," *TELKOMNIKA (Telecommunication Computing Electronics and Control)*, vol. 13, no. 4, pp. 1187-1193, December 2015.
- [13] Q. A. Sias and I. Robandi, "Recurrence Perturb and Observe algorithm for MPPT optimization under shaded condition," *2nd International Seminar on Intelligent Technology and Its Applications (ISITIA)*, pp. 533-538, July 2016.
- [14] S. Mohanty, B. Subudhi and P.K. Ray, "A new MPPT design using grey wolf optimization technique for photovoltaic system under partial shading conditions," *IEEE Transactions on Sustainable Energy*, vol. 7, no. 1, pp. 181-188, January 2016.
- [15] S. Mirjalili, S. M. Mirjalili and A. Lewis, "Grey wolf optimizer," *Advances in engineering software*, vol. 69, pp. 46-61, March 2014.
- [16] Darmansyah and I. Robandi, "Photovoltaic parameter estimation using Grey Wolf Optimization," *3rd International Conference on Control, Automation and Robotics (ICCAR)*, pp. 593-597, April 2017.



# Analysis of Waveform of Partial Discharge in Air Insulation Measured by RC Detector

Michael Stevano Sinurat  
School of Electrical Engineering and Informatics  
Institut Teknologi Bandung  
Jl. Ganesha 10, Bandung, 40132, Indonesia  
michaelstevano90@gmail.com

Umar Khayam  
School of Electrical Engineering and Informatics  
Institut Teknologi Bandung  
Jl. Ganesha 10, Bandung 40132, Indonesia  
umar@hv.ee.itb.ac.id

**Abstract**—This study discusses the measurement of Partial Discharge (PD) in air insulation. Partial Discharge Measurement is very important to know the condition of electrical equipment. The cause of partial discharge is not only old equipment, but also from set-up errors and insulation problems. In this research partial discharge measurement was performed by using electrical methods. Electrical method use RC Detector. The modeling of partial discharge was done by using needle-plane electrode distant 1 cm in air insulation. Partial discharge measurement parameters include the measurement of Background Noise (BGN), Partial Discharge Inception Voltage (PDIV) and PD Waveform. The Partial Discharge measurement result show that  $V_{pp}$  of BGN ON is higher than  $V_{pp}$  of BGN OFF. The negative PDIV signal first appeared for the RC Detector at a voltage 3.55 KV and Positive PDIV at 4.01 KV. Negative and positive PD waveform for RC Detector at 5 KV, 5.5 KV, 6 KV, 6.5 KV and 7 KV respectively, it has been found that the fall time is greater than the rise time, and peak to peak voltage ( $V_{pp}$ ) will be greater when the applied voltage is greater.

**Keywords** — *partial discharge, air insulation, rc detector.*

## I. INTRODUCTION

Partial Discharge (PD) can occur in solid insulating materials, liquid insulation materials and gas insulation materials. In general, Partial Discharge can be caused by the local electrical stress concentration in insulation. There are 3 main things that can be the source of the occurrence of PD, the Internal PD (the presence of a cavity between dielectrics or within a particular dielectric), and Corona PD (occurs around the conductor) and Surface PD (occurs on the surface due to contamination) [1-2].

Diagnosis of electrical equipment is necessary to prevent breakdown or equipment damage which can cause a sudden power system disturbance. Partial Discharge Measurement is one of the methods of used to diagnose high voltage electrical equipments in order to assess the condition of electrical equipments. In general, the problem occurs in electrical equipment that has long been used. Damage to electrical equipment, 80% are caused by the insulation problem. The insulation problem can disturb the reliability of the equipment or the electrical system reliability itself. To prevent the power system disturbance, the power system monitoring is needed to maintain the quality of the electrical equipments insulation. This study aims at determining the characteristics of partial discharge measured using the RC Detector. Characteristics of Partial Discharge includes measurement of BGN, PDIV and PD waveform. Partial discharge measurements were

performed by modeling the needle-plane electrode [3-5]. In this research will discuss about experiment setup and PD measurement results by using RC Detector.

## II. PARTIAL DISCHARGE MEASUREMENT SYSTEM

### A. Measurements Object

PD model used in this research is corona discharge. The partial discharge signal is generated by an artificial PD source using a needle-plane electrode 1 cm apart. The diameter of the needle used was 1 mm with 3  $\mu$ m needle tip and needle angle 30°. The needle - plane electrode model is shown in Fig. 1.

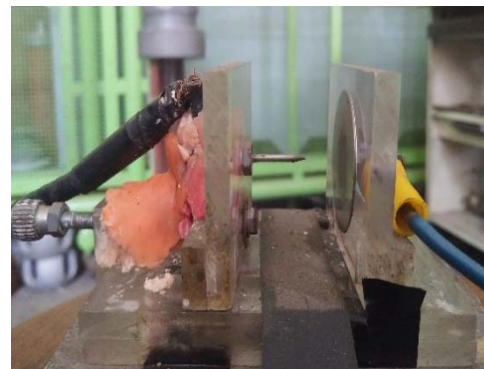


Fig 1. Electrode needle-plane

### B. Partial Discharge Sensor

In this study, partial discharge measurement was performed by using RC detector. The types of sensors used in the measurement of partial discharge are shown in the Fig 2.

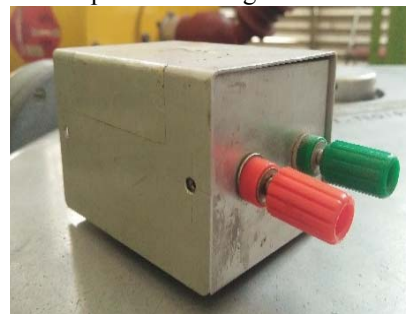


Fig 2. RC Detector sensor

### C. Experimental setup

The experimental setup is shown in Fig. 3. The high voltage test source comes from a 200V / 100 KV transformer

with a power capacity of 5 KVA. After that the transformer is connected to a 6.1 K $\Omega$  resistor to limit the current flowing in the circuit.

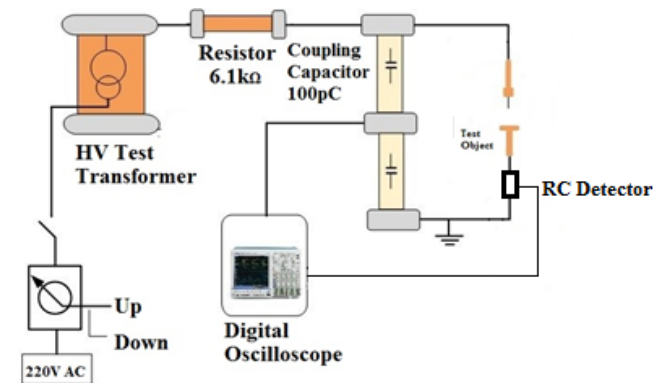


Fig 3. PD measurement setup

#### D. Partial Discharge Measurements

Partial discharge measurements were performed using RC Detector. The data of PD measurement were taken averagely 40 times with 5 variations of voltage level that is 5 KV, 5.5 KV, 6 KV, 6.5 and 7 KV. The Data obtained from each measurement was saved in csv format. This data were processed using Microsoft Office Excel software and plotted using OriginPro 2016 software [6-7]. The characteristics observed in this measurement are:

- BGN OFF and BGN ON
- PDIV (Partial Discharge inception voltage) Positive and Negative
- Positive and Negative Partial Discharge waveform.

### III. MEASUREMENT RESULTS

#### A. Background Noise

BGN measurements aims at determining the amount of noise that is present at the time of measurement in the laboratory.

##### 1) Background Noise OFF

The main purpose of BGN OFF measurement is to determine the noise condition when the measurement circuit is still in Off mode. The BGN OFF condition of RC Detector is shown in Fig. 4. Vpp (mV) shows magnitude of background noise.

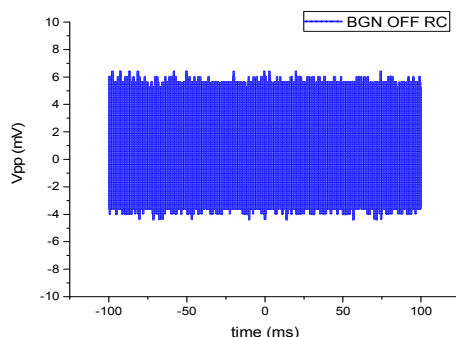


Fig 4. Background Noise OFF of RC Detector

The noise read by oscilloscope as shown in Fig 4. above comes from the environment around the experiment execution, in the form of electric engine sound or interference from electromagnetic waves of equipments in the laboratory. BGN OFF measurements are shown in Table 1.

TABLE 1. V PEAK-PEAK BACKGROUND NOISE OFF OF RC DETECTOR

Vpp Bgn Off			
Sensor	Vpp (mV)	Vmax (mV)	Vmin (mV)
RC Detector	11.32	6.68	-4.64

On measurement of BGN OFF the magnitude of peak to peak voltage (Vpp) detected by RC Detector is 11.32 mV.

##### 2) Background Noise ON

The Measurement of BGN ON aims at determining the noise condition when the voltage source is turned on but still in condition 0 KV. In this experiment, BGN ON was taken when the system condition was not really at 0 KV, but at 1.3 KV. This happens because the voltage regulator used cannot be fixed at the position of 0 KV. BGN ON condition of RC Detector sensor is shown in Fig 5.

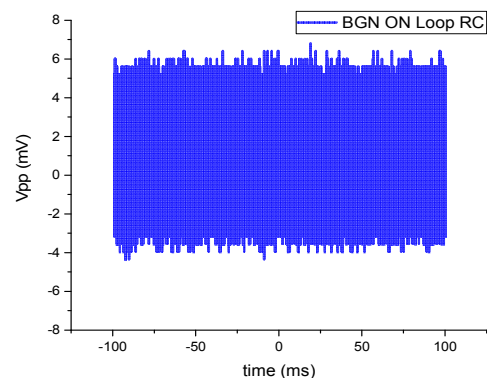


Fig 5. Background Noise ON of RC Detector

The measurements of BGN ON of RC Detector are shown in Table 2.

TABLE 2. V PEAK-PEAK BACKGROUND NOISE ON OF RC DETECTOR

Vpp BGN On			
Sensor	Vpp (mV)	Vmax (mV)	Vmin (mV)
RC Detector	11.36	6.72	-4.64

On measurement of BGN ON the magnitude of peak to peak voltage (Vpp) detected by RC Detector is 11.36.

From the measurement results obtained, Vpp of BGN ON is higher than Vpp of BGN OFF. Background noise observation becomes a parameter in the observation of the wave that appears on the oscilloscope. The objective is to avoid the error of taking observation of partial discharge wave data.

### B. Partial Discharge Inception Voltage (PDIV)

PDIV is the voltage at which PD activity appears for the first time when the source voltage is increased gradually. In this study PDIV observed is negative PDIV and positive PDIV. In this experiment, PDIV was observed 40 times and then averaged.

#### 1) Negative Partial Discharge Inception Voltage

Negative PDIV is the first negative PD signal to appear. Fig 6. shows the negative PDIV waveform detected by the RC detector.

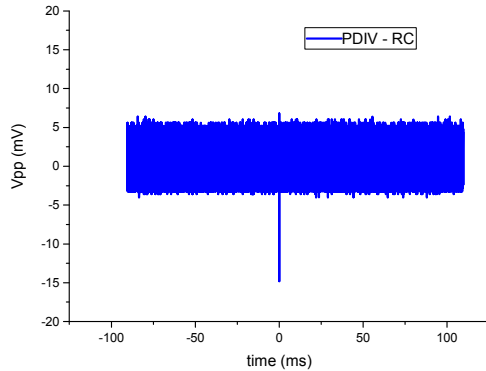


Fig 6. Negative PDIV Measured by RC Detector

The negative PDIV signal first appeared for the RC Detector at a voltage 3.55 KV. Table 3. shows the  $V_{min}$  and  $V_{pp}$  PDIV signals for RC Detector.

TABLE 3. VOLTAGE,  $V_{MIN}$  AND  $V_{PP}$  NEGATIVE PDIV

Negative PDIV			
Sensor	Voltage (KV)	$V_{pp}$ (mV)	$V_{max}$ (mV)
RC	3.55	22.28	- 16

On the measurement, the magnitude of negative PDIV  $V_{pp}$  for RC Detector is 22.28 mV.

#### 2) Positive Partial Discharge Inception Voltage

Positive PDIV is the first positive PD signal to appear. Fig 7. shows the positive PDIV waveform detected by the RC Detector.

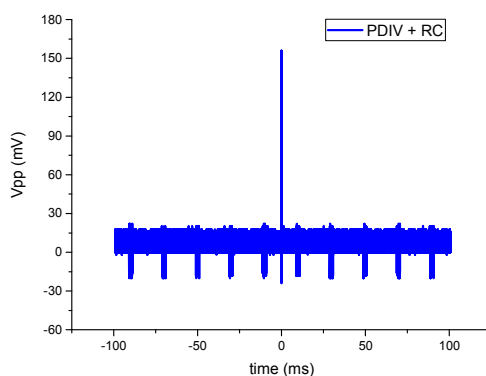


Fig 7. Positive PDIV measured by RC Detector

The positive PDIV signal first appeared for the RC Detector at a voltage of 4.01 KV. Table 4. shows the  $V_{min}$  and  $V_{pp}$  PDIV signals for RC Detector.

TABLE 4. VOLTAGE,  $V_{MAX}$  AND  $V_{PP}$  POSITIVE PDIV

Positive PDIV			
Sensor	Voltage (KV)	$V_{pp}$ (mV)	$V_{max}$ (mV)
RC	4.01	180.05	156

On the measurement, the magnitude of positive PDIV  $V_{pp}$  for RC Detector is 180.05 mV. The data show that the positive PDIV voltage is slightly higher than the negative PDIV which means that the negative PD will appear earlier than the positive PD.

### C. Partial Discharge Waveform

There are two PD waveforms namely negative PD waveform which occurs in negative cycle and positive PD waveform which occurs in positive cycle. PD waveform measurement was taken 40 times. The waveforms needed include the waveforms of positive PD and negative PD for the RC Detector by 5 variations of voltage starting from 5 KV, 5.5 KV, 6 KV, 6.5 KV and 7 KV.

The PD waveform parameter is the time rise ( $t_r$ ), time fall ( $t_f$ ) and amplitude ( $V_{pp}$ ). The rise time usually calculated from 10-90% Amplitude and time fall is calculated from 100-10% Amplitude.

#### 1) Negative PD Waveform measured by RC Detector

Fig 8. shows the negative PD waveforms detected by using the RC Detector at 5 KV.

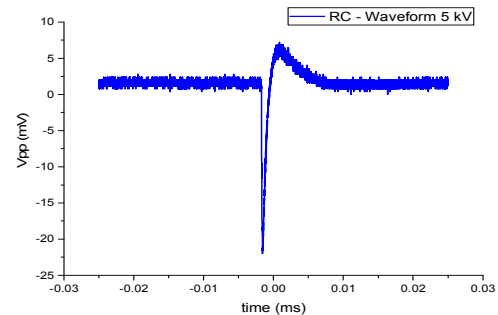


Fig 8. Negative Partial discharge waveform measured by RC Detector at 5 KV

Table 5. shows the rise time and standard deviation of the negative waveform detected by using the RC Detector at 5 variations of voltage level.

TABLE 5. The Rise Time of the Negative PD Waveform Measured by RC Detector

Rise Time Negative PD Waveform		
Voltage	Rise Time (nS)	Std
RC 5 KV	77.39	10.78
RC 5.5 KV	90.92	16.33
RC 6 KVV	104.27	17.90
RC 6.5 KV	106.89	16.33
RC 7 KV	103.41	18.99

Fig 9. shows the rise time graph of the negative PD waveforms detected by using the RC Detector at 5 variations of voltage level.

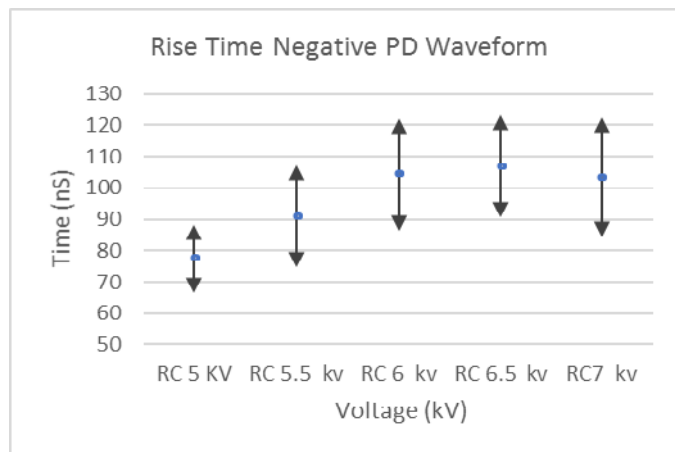


Fig 9. Rise Time Negative PD Waveform

Table 6. shows the fall time and standard deviation of the Negative waveform measured by RC Detector at 5 variations of voltage level.

TABLE 6. The Fall Time of the Negative PD Waveform Measured by RC Detector

Fall Time Negative PD Waveform		
Voltage	Fall Time (nS)	Std
RC 5 KV	706.38	23.02
RC 5.5 KV	737.47	35.45
RC 6 KV	717.56	35.37
RC 6.5 KV	648.86	75.52
RC 7 KV	622.73	87.43

Fig 10. shows the fall time graph of the negative PD waveforms detected by using the RC Detector at 5 variations of voltage level.

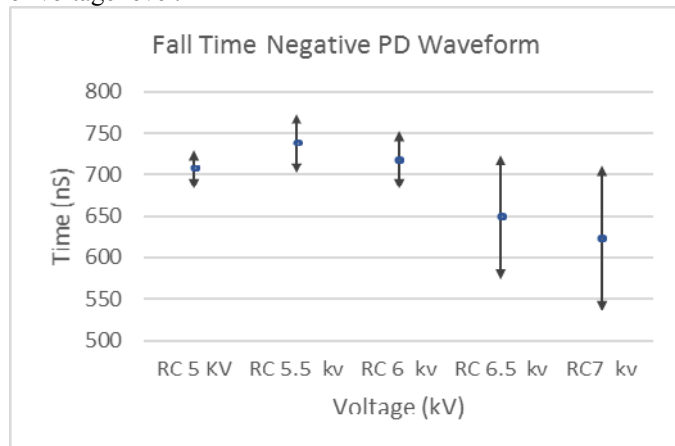


Fig 10. Fall Time Negative PD Waveform

Table 7. shows the Vpp and standard deviation of the negative waveform detected by using the RC Detector at 5 variations of voltage level.

TABLE 7. The Vpp of the Negative PD Waveform Measured by RC Detector

Vpp Negative PD Waveform		
Voltage	Vpp (mV)	Std
RC 5 KV	27.05	1.03
RC 5.5 KV	27.57	3.74
RC 6 KV	29.89	1.27
RC 6.5 KV	39.14	1.95
RC 7 KV	40.82	1.82

Fig 11. shows the Vpp graph of the negative PD waveforms detected by using the RC Detector at 5 variations of voltage level.

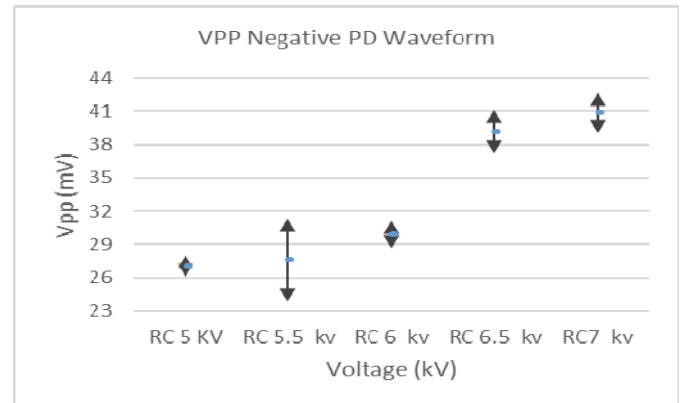


Fig 11. Vpp Negative PD Waveform

## 2) Positive PD Waveform measured by RC Detector

Fig 12. shows the positive PD waveforms detected by using the RC Detector at 5 KV.

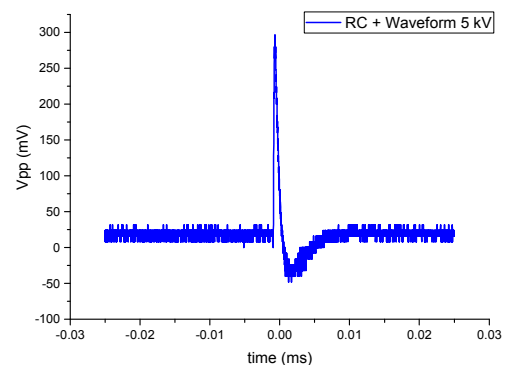


Fig 12. Positive Partial discharge waveform measured by RC Detector at 5 KV

Table 8. shows the rise time and standard deviation of the positive waveform detected by using the RC Detector at 5 variations of voltage level.

TABLE 8. The Rise Time of the Positive PD Waveform Measured by RC Detector

Rise Time Positive PD Waveform		
Voltage	Rise Time (nS)	Std
RC 5 KV	133.12	7.45
RC 5.5 KV	133.18	5.65
RC 6 KV	130.97	5.91
RC 6.5 KV	128.02	6.62
RC 7 KV	131.96	4.77

Fig 13. shows the rise time graph of the positive PD waveforms detected by using the RC Detector at 5 variations of voltage level.

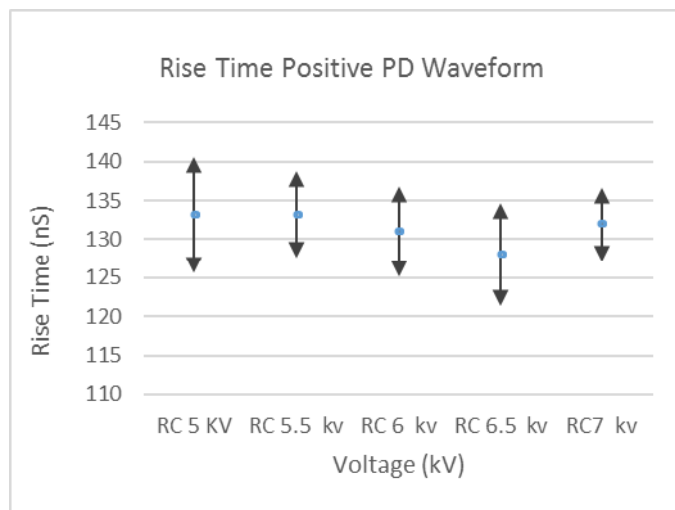


Fig 13. Rise Time Positive PD Waveform

Table 9. shows the fall time and standard deviation of the positive waveform measured by RC Detector at 5 variations of voltage level.

TABLE 9. The Fall Time of the Positive PD Waveform Measured by RC Detector

Fall Time Positive PD Waveform		
Voltage	Fall Time (nS)	Std
RC 5 KV	710.99	20.01
RC 5.5 KV	713.67	20.58
RC 6 KV	698.77	23.91
RC 6.5 KV	696.95	20.12
RC 7 KV	705.38	12.93

Fig 14. shows the fall time graph of the Positive PD waveforms detected by using the RC Detector at 5 variations of voltage level.

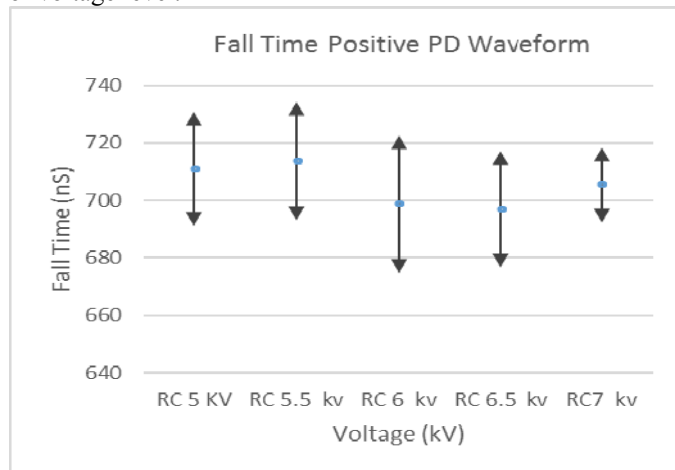


Fig 14. Fall Time Positive PD Waveform

Table 10. shows the Vpp and standard deviation of the Positive waveform detected by using the RC Detector at 5 variations of voltage level.

TABLE 10. The Vpp of the Positive PD Waveform Measured by RC Detector

Vpp Positive PD Waveform		
Voltage	Vpp (mV)	Std
RC 5 KV	449.60	64.97
RC 5.5 KV	476.60	89.63
RC 6 KV	524.80	97.27
RC 6.5 KV	647.40	48.04
RC 7 KV	740.00	34.04

Fig 15. shows the Vpp graph of the Positive PD waveforms detected by using the RC Detector at 5 variations of voltage level.

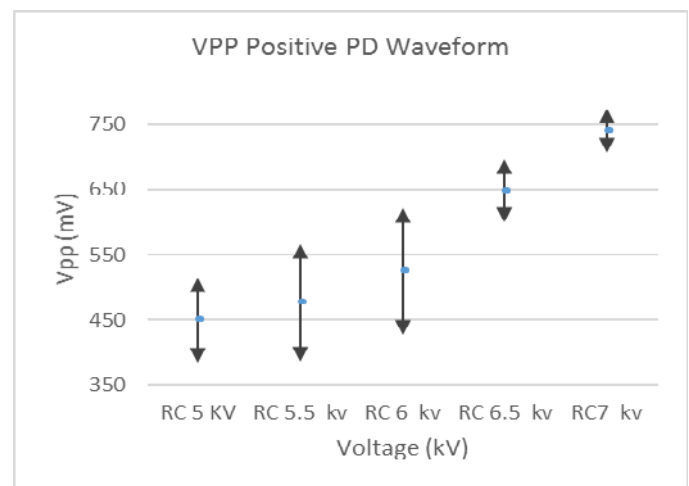


Fig 15. Vpp Positive PD Waveform

#### IV. ANALYSIS AND DISCUSSION

##### A. Background Noise

Based on the measurement results of BGN OFF, it was found that the peak to peak voltage for RC Detector is 11.32 mV. Based on the measurement results of BGN ON, it was found that the peak to peak voltage for RC is 11.36 mV. From the measurement results obtained, Vpp of BGN ON is higher than Vpp of BGN OFF because on the measurement of BGN ON there has been a flowing voltage of 1.2 KV, therefore it can be said that the measurement of BGN is influenced by applied voltage flowing in the experimental circuit.

##### B. PDIV (Partial Discharge Inception Voltage)

From the measurement results, the negative PDIV appears at a voltage of 3.55 KV for RC Detector. The positive PDIV appears at a voltage of 4.01 KV for RC Detector.

These results indicate that positive PDIV is slightly higher than negative PDIV which means negative PD will appear earlier than positive PD. In the needle – plane electrode, a nonhomogeneous electric field occurs at the tip of the needle electrode. The increase in voltage on the needle electrode will raise the strength of the non-homogeneous



electric field around the tip of the needle. The increase of electric field strength will result in the increase of ionization energy of gas molecule ( $U$ ), thereafter there will be the ionization of gas molecules locally around the tip of the needle. This ionization causes gas molecules to release electrons to produce positive ions and free electrons. These ionized free electrons move and have kinetic energy according to equation 1.

$$U = e \cdot V = \frac{1}{2} m_e \cdot v_e^2 \quad (1)$$

where  $e$  is the charge of electrons,  $V$  is the potential difference between the two electrodes,  $m_e$  is the mass of the electron, and  $v_e$  is the velocity of the electron. The greater ionization energy causes more electrons to escape from their bonds. Free electrons produce ionization and pound free air molecules. If the free electron kinetic energy is higher than the ionization energy of the gas molecule, then the gas molecules will ionize into positive ions and produce new free electrons. This happens repeatedly which will cause the occurrence of many positive ions and further trigger the occurrence of avalanche electrons which will finally result in the occurrence of PD.

In the negative cycle, the needle electrode is negative-polarized, and according to Coulomb's law, the ionized electron will move away from the needle electrode and accelerate the appearance of larger avalanche electrons. The appearance of larger avalanche electrons in a shorter time causes PD to occur more easily in the negative cycle. This is what causes the negative PDIV value to be lower than the PDIV positive value.

### C. Partial Discharge Waveform

From the measurement results of negative and positive PD waveform for RC Detector at 5 KV, 5.5 KV, 6 KV, 6.5 KV and 7 KV respectively, it has been found that the fall time is greater than the rise time. This is because the impulse shape of the PD is composed by two types of carriers, namely negative charge carriers (electrons) and positive charge carriers (ions). Thus, the electron mass is lighter resulting in greater electron mobility than the ion, the amount of current is higher due to the electrons but it exhausts soon and contributes to the rise time region to be smaller, whereas the ion-induced currents are smaller and flow in longer periods so that ion-induced currents contribute to the region fall time to be bigger. From the measurement results, it has also been found that the peak to peak voltage ( $V_{pp}$ ) will be greater when the applied voltage is greater. The measurement results indicate that the Partial discharge  $V_{pp}$  is influenced by the voltage applied to the measurement.

## V. CONCLUSION

This study discusses the characteristics of partial discharges measured by using RC Detector in air insulation. The characteristics observed in this measurement are BGN OFF, BGN ON, PDIV Positive, PDIV Negative, Positive Partial Discharge waveform and Negative Partial Discharge waveform. The results of this research is based on Background Noise measurement, it was found that peak to peak voltage for BGN ON is higher than the peak to peak voltage for BGN

OFF, based on PDIV measurement, the positive PDIV voltage is slightly higher than the negative PDIV which means that the negative PD will appear earlier than the positive PD and based on PD Waveform measurement, it was found that the higher applied voltage the higher value of peak to peak voltage required for the partial discharge on each sensor.

## REFERENCES

- [1] Umar Khayam, "Modul Praktikum Lab Diagnosis Tegangan Tinggi, ITB, 2016.
- [2] Suwarno, "Diagnosis of High Voltage Equipments. Bandung", Penerbit ITB, 2014.
- [3] Nhet Ra, Umar Khayam, "Measurement of Partial Discharge In Needle-Plane Using RC Detector, HFCT And Antenna Sensors", International Conference On Electric Vehicular Technology And Industrial, Mechanical, Electrical And Chemical Engineering, 2015.
- [4] Nhet Ra, Umar Khayam, "Partial Discharge Measurement of 4 Types of Electrodes Configuration in Air Insulation using High Frequency Current Transformer Sensor", International Conference On Electric Vehicular Technology And Industrial, Mechanical, Electrical And Chemical Engineering, 2015.
- [5] Mukhlisah Yunus, Fendi, Umar Khayam, "Effect of the Presence of Metal Box on Partial Discharge Detected by Internal Loop Antenna", International conference on Electrical Engineering and Computer Science, 2017.
- [6] Deny Tri Laksono, Umar khayam, "Comparison of Peak to Peak Voltage and number of Partial Discharge Detected by HFCT and Loop Antenna in Metal Enclosed High Voltage Equipment", International Conference on High Voltage Engineering and Power System, 2017.
- [7] Dede Furqon, Rachmat Sannia Putra, Umar Khayam, "Design of Ultrawide Band Partial Discharge Detector using Pi Attenuator and Ultrawide Band Amplifier", International Seminar on Intelligent Technology and its Application, ISITIA-RCEEE 2017, Surabaya, Indonesia, 28-29 Agustus 2017.



# Application of Ultra-Wideband Double Layer Printed Antenna for Partial Discharge Detection

Yuda Muhammad Hamdani, Umar Khayam

Sekolah Teknik Elektro dan Informatika (STEI)

Institut Teknologi Bandung (ITB)

Bandung, Indonesia

yudahamdani@students.itb.ac.id, umar@hv.ee.itb.ac.id

**Abstract-** Partial discharge (PD) is a local electrification phenomenon that partially connects insulation between the conductors and occurs either on the surface of the conductor or inside the insulation (void). During the PD there are several phenomena that accompany the occurrence of PD, such as impulse currents, heat radiation, electromagnetic waves, mechanical waves and chemical processes. This phenomenon is detected and measured to know the existence of PD. One of the PD measurements is ultra high frequency (UHF) method, by measuring the waves generated by PD using antenna. One of antenna having good characteristics is UWB double layer printed antenna. In this paper the application of ultra-wideband double layer printed antenna for partial discharge detection is reported. The application of antenna on PD measurement, shows that the antenna is able to detect PD. The characteristics of PD: PDIV, PDEV, PD waveform are measured using this antenna. Ultra-wideband (UWB) double layer printed antenna is an antenna developed from a square microstrip antenna with symmetrical T-shaped tethering. The proposed antenna is implemented on Epoxy FR-4 substrate with permittivity of 4.3, thickness of 1.6mm, and 72.8mm x 60.0mm in size. The VNA testing of the antenna shows that the antenna bandwidth is from 50MHz to 2.30GHz. The measured results of PD wave are PDIV, PD waveform and PDEV.

**Keywords-**Partial discharge; UWB antenna; UHF.

## I. INTRODUCTION

Partial Discharge (PD) is a local electrification phenomenon that partially connects insulation between conductors and occurs both on the surface of the conductor and inside the conductor (void). This discharge may occur in a conductor (conductor) in a short time, either at close range or at a great distance. PD can occur in solid insulating materials, liquid insulation materials and gas insulation materials. In general, PD can be caused by the local electrical stress concentration in isolation. There are three main things that can be the source of the occurrence of PD, which is Internal PD (the presence of a cavity between dielectrics or within a particular dielectric), Corona PD (occurs around the conductor) and Surface PD (occurs on the surface due to contamination).

During the occurrence of PD, there are several phenomena that accompany the occurrence of PD, such as impulse currents, hot light radiation, electromagnetic waves, mechanical waves, and chemical processes.

This phenomenon is captured to know the existence of PD. The measurement and diagnosis of a non-electric PD is a measurement that does not measure electrical quantities. The concept of non-electric PD measurement is to use a number of sensor equipment and conversion devices from sensors into measurable quantities on measuring instruments such as spectrum analyzers, PD detecting, and oscilloscopes. PD causes electromagnetic waves in which this wave propagates from inside the source of the outgoing material PD. One method of PD measurement is the UHF method, the wave measurements induced by the partial discharge.

This study is an antenna investigation from the beginning of the design to the application of the antenna on the partial discharge measurement. The design of the previously researched reference antennas was re-experimented with PD measurement applications. Antenna design for the purposes of partial discharge measurements is numerous, such as antenna loops, bowtie antenna. However, the performance of the antenna still has its weaknesses in terms of antenna working frequency. The working frequency of the antenna is a parameter that must be considered because the partial discharge has a frequency that must be adjusted by the antenna to be designed. The antenna to be designed should match the antenna characteristics for the partial discharge measurement application. UHF band electromagnetic (EM) wave (300 MHz – 3 GHz) is characteristic PD emission at gas insulation substation (GIS). So far various types of antennas and sensors have been developed to detect PD [1-5]. However, the sensors bandwidth characteristics are still cut into various frequency ranges. This is not same at a certain frequency range. The antenna working frequency is expected to have the same range as the partial discharge frequency range or even more widely. Benefits obtained are, the antenna is able to perform partial discharge measurement applications on all types of isolation with just one antenna.

This research method uses a reference from the antenna form that has been studied with characteristics suitable for

partial discharge measurement applications. The antenna as a sensor acts to receive EM waves. A good sensor should operate at the frequency generated by the PD which located on UHF band (300 MHz – 3 GHz). In this study the one of the antenna is UWB double layer printed antenna. The antenna reference is simulated in antenna design and simulation (ADSS) to obtain parameter results such as return loss and VSWR. The ADSS results are compared with the previously researched reference results. From the obtained frequency results are appropriate, the next step of the antenna is fabricated and tested to obtain data from the form of measurement based on vector network analyzer (VNA). The results of the VNA test compared to the simulated antenna reference results, the VNA test results should not be too much different or maybe the result can be just the same. The next test is antenna testing for partial discharge measurement. The working frequency of antennas in the partial discharge range makes the antenna capable of measuring the partial discharge.

## II. DESIGN OF ANTENNA

### A. Reference Antennas

The Antenna is one of the sensors used in PD measurement using UHF method. In this study the one of the antenna is UWB double layer printed antenna [6]. Figure 1 shows the antenna design, dimensions of the antenna, either on the patch, substrate, or groundplane. UWB double layer printed antenna proposal is then implemented on epoxy FR-4 substrate with a permittivity of 4.3 with a thickness of 1.6mm, and of 72.8mm x 60.0mm in size.

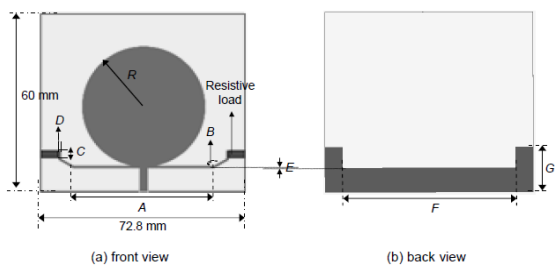


Figure 1. Antenna design.

The reference antenna shape has a wide band yield of 50MHz-5GHz that is capable of being implemented to detect PD signals. The frequency of the PD signal is in the 300MHz-3GHz range. This indicates that the antenna bandwidth is still suitable for PD measurements. Figure 2 shows the result of VSWR measurement of the antenna.

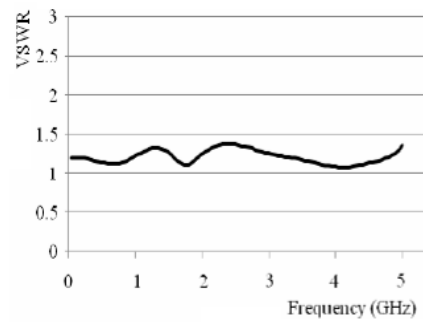


Figure 2. VSWR of proposed reference antenna with optimum dimension.

### B. Simulation of Reference Antennas

The design is simulated again in using ADSS. Software is used to test each form of the antenna so that working frequency range of the antenna obtained. This simulation shows the result of antenna parameter the return loss and VSWR show the working frequency range of an antenna. The result of return loss measurement and VSWR is based on simulation software.

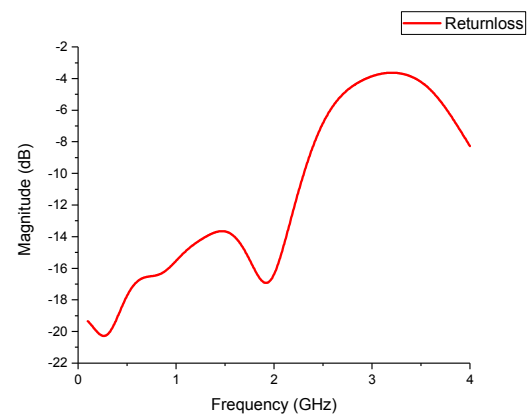


Figure 3. The simulation result of antenna return loss.

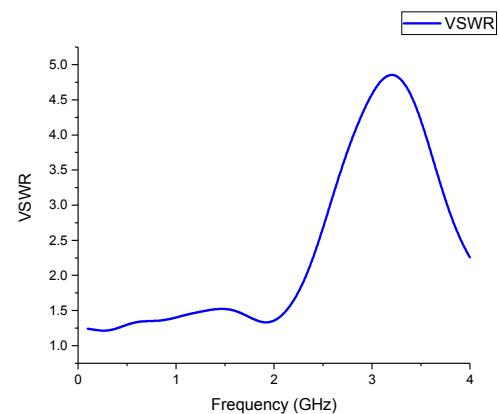


Figure 4. The simulation result of antenna VSWR.

Figure 3 and 4 show the simulation results using ADSS. The working frequency range (VSWR < 2 and return loss < -10dB) of the antenna is 50MHz-2.30GHz. The frequency

results are already able to detect the PD signal since the PD signal frequency range still exists in the antenna's frequency range. The comparison of simulation results using ADSS differs from the antenna reference simulation result, the reference antenna is capable of working frequency 50MHz-5GHz, while the antenna simulation using ADSS is only 50MHz-2.30GHz. This is because of that there are several unknown dimensions in the reference. However, the result can still be in working frequency which is feasible to be used for partial discharge measurement.

### C. Fabrication of Reference Antennas

Fabrication is process where the antennas that have been simulated on the software begin to be made the original form. Antenna material made from PCB makes antenna easy to fabricate. Other components also have a connector sma as a connector to an oscilloscope, and resistor 82 ohm as resistor loading on the antenna. The following is the shape of the result of the fabrication of antenna in figure 5.

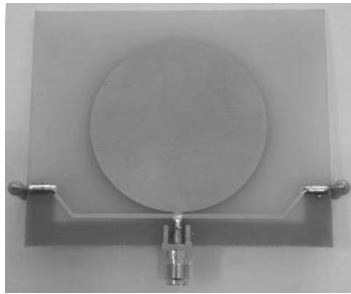


Figure 5. Front view of the antenna.

### III. TEST OF ANTENNA USING A VECTOR NETWORK ANALYZER (VNA)

The antenna is tested using VNA. The test check the working frequency range of the fabricated antenna. It is then compared with the simulation result. simulation results of antenna working frequency of 50MHz-2.30GHz. The VNA result should be the same or close to the result of the antenna simulation in the software. Figure 6 shows a series of antenna testing using VNA.

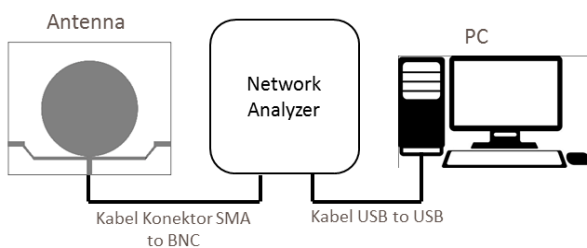


Figure 6. Antenna Testing circuit using VNA.

VNA test results show return loss and VSWR approaching simulation results. Figure 7 and Figure 8 show the return loss and VSWR obtained from VNA testing.

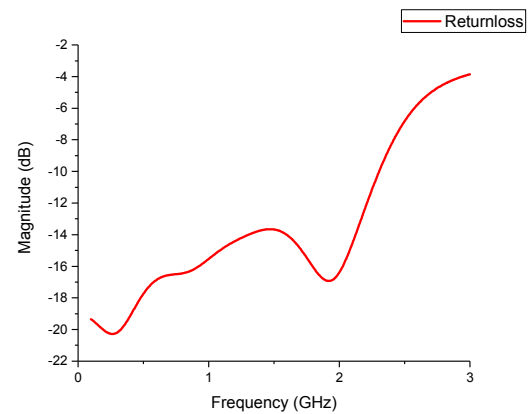


Figure 7. The return loss of antenna using VNA.

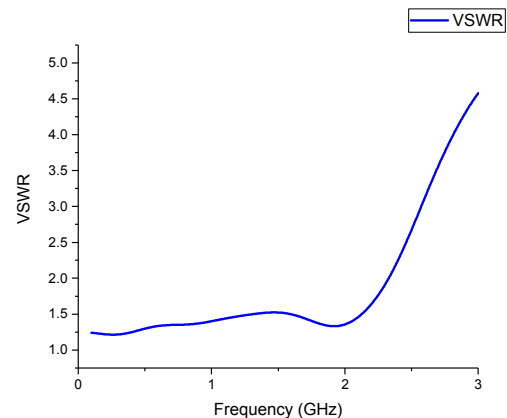


Figure 8. VSWR of the antenna using VNA.

The test results indicate the working frequency range of antenna that has been in fabrication reach 50MHz-2.34GHz. This indicates that the results of the simulation using the software show results that are not much different from when the antenna has been fabricated and tested using VNA.

### IV. EXPERIMENTAL SETUP FOR PARTIAL DISCHARGE DETECTION

The antennas designed in this experiment calculate the benefits of efficiency, and the effectiveness of partial discharge detection so that an antenna can only receive waves from the front only by making a copper-like cube that resembles a bird cage. In Figure 9 shows the partial discharge experiment, the electrodes of plates with 5mm acrylic insulation media are obtained at breaks of 9.12 volts in multimeters or 36.48 kV. PD experiments performed using voltages smaller than (80% x 36.48 kV), or about 29.18 kV and on a 7.30-volt multimeter, this is the maximum limit value for injection into the system. Figure 10 shows a series of PD tests using antenna. While in figure 11 shows the location of each component on the test in the laboratory.

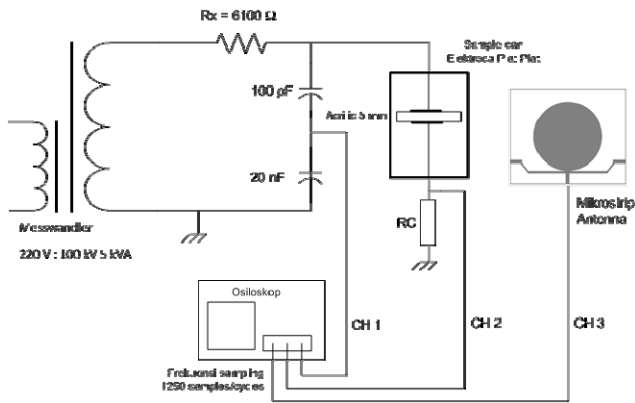


Figure 9. The PD test circuit using antenna sensors

The oscilloscope as a partial discharge wave measurement tool to see PD signal waves. In the oscilloscope, there are three channel probes used. Channel 1 (CH1) is used for the channel from the step-up transformer source. Channel 2 (CH2) is used for detecting impedance sensor measurement. Channel 3 (CH3) is used for antenna sensor measurements.

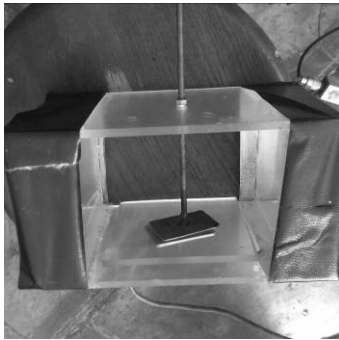


Figure 10. Source of PD



Figure 11. PD testing in laboratory.

## V. MEASUREMENT RESULT AND DISCUSSION

### A. Background noise measurement results of PD (Background ON and Background OFF)

Accurate experimental results are obtained primarily related to the partial discharge waveform, first observed in the background noise test circuit with the oscilloscope. The first measurement is the background noise in the position of the AC high-voltage source from the step-up transformer at the

OFF position, the AC voltage source signal (red color graph), the signal captured by the antenna sensor (blue graph) and the signal captured by the RC detector colored blue) as follows in figure 12.

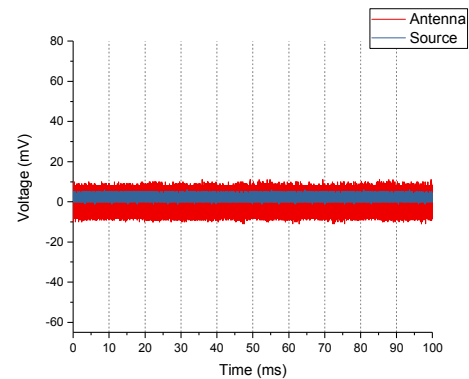


Figure 12. Background noise OFF.

Figure 12 shows the background noise signal when the voltage regulator has not been turned on. This is necessary to know the amount of noise signal coming from the external system. Before the test voltage source turned on it was already seen there is noise that is read on the oscilloscope. The oscilloscope-readable noise is derived from the environment around the experimental execution, in the form of the electric engine sound or interference from electromagnetic waves of equipment in the laboratory. Further observed when the source voltage is switched on to the test circuit.

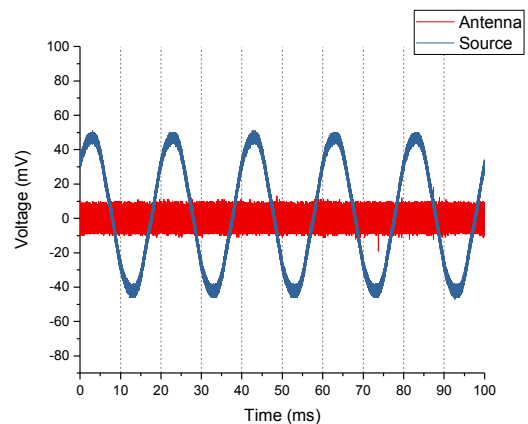


Figure 13. Background noise ON

Figure 13 shows the signal data of the AC voltage source (blue graph), the signal captured by the antenna sensor (red graph), the background noise signal is known when the voltage regulator is turned on. This is necessary to know the amount of noise signal generated by the internal system. The background noise (BGN) measurement is performed before starting the experiment to distinguish between the noise signal and the partial discharge signal to be measured. Once the voltage source is turned on, there is little change in the more noise emerging. Observation background noise becomes a

parameter in the observation of the wave that appears in the next oscilloscope. The purpose to avoid taking data partial discharge wave that was only limited to noise.

#### B. PDIV measurement results

Observation of the partial discharge inception voltage (PDIV), the source voltage is increased gradually and observations are made on the channel oscilloscope 3. Figure 14 shows the signal data of the AC voltage source (blue graph), the signal captured by the antenna sensor (red graph). When the voltage reaches 18 kV (readings of a 4.5 volt multimeter) appears a negative PDIV signal. This occurs because, at half the negative cycle, the partial discharge is generated by electrons derived from field emissions arising from the surface of the electrode. If further observation turns out this also happens in some other negative wave cycle. This signal exceeds the value of background noise on the negative cycle so it can be ascertained that this is a partial discharge wave signal.

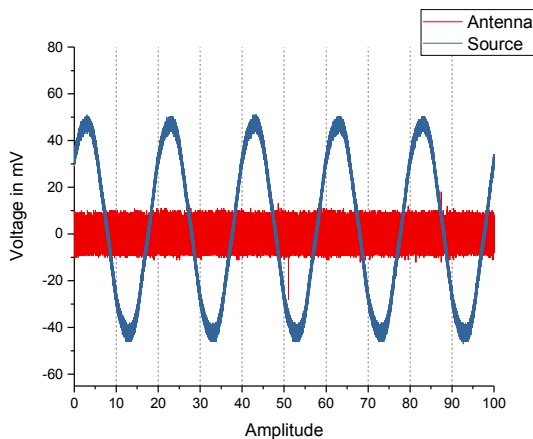


Figure 14. PDIV waveform

Figure 14 shows a negative PDIV signal. This PD signal is the first PD signal to appear on the negative side. The first partial discharge signal that emerges is a negative PD signal. If further observation turns out this also happens in some other negative wave cycle. This signal exceeds the value of background noise on the negative cycle so it can be ascertained that this is a partial discharge wave.

#### C. PD Waveform Results ( Rise Time and Fall Time )

Figure 15 shows that the shape of the partial discharge signal and waveform appearing is not too disturbed by noise in the test circuit. In general, we can observe the basic form of partial discharge signal in the experiment.

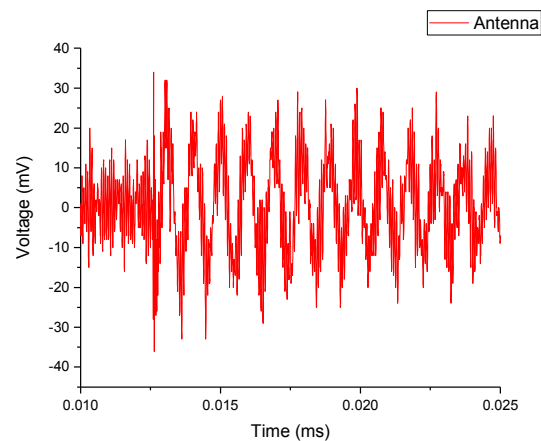


Figure 15. PD waveform measured by antenna at 5.9 kV

Partial discharge waveform can be split into the two-time rise and time fall. Generally, the rise time for partial discharge waves is from 10% to 90% of the peak. While the time fall ranging from 100% to 90%. In addition to being divided into time rise and time fall, the partial discharge waveform can also be divided into two currents due to the flow of electrons and currents due to ion movement. The electrons flow quickly and only in a short time. While the ion currents move slowly and in a relatively long time. This explains the shape of a partial discharge signal that has a sharp rise at the beginning and drops gently after it reaches its peak.

#### D. Partial Discharge Extinction Voltage (PDEV) Results

The voltage source during the occurrence of PD and the voltage source is lowered gradually, it will get the voltage value when the PD will disappear gradually in the positive PD and followed by the negative PD. However, in experiments with plate electrode to plate with acrylic, it cannot be distinguished PDEV negative and PDEV positive because it occurs at a narrow voltage or occurs at about the same time at the source voltage of 19.6 kV for PDEV antenna. Figure 16 shows the PDEV results on the antenna.

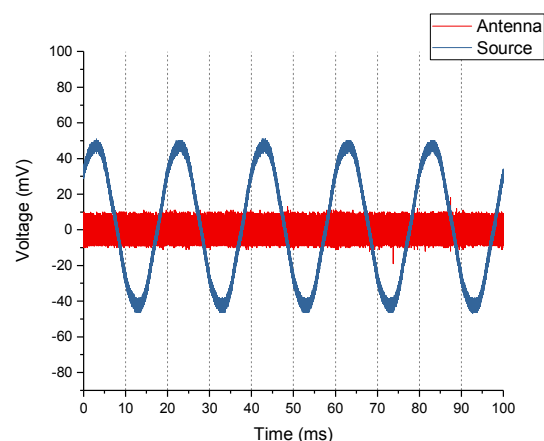


Figure 16. PDEV waveform

## VI. ANALYSIS AND DISCUSSION

The ultra-wideband double layer printed antenna has been tested. Test antenna such as simulation on software ADSS, measurement with VNA and measurement partial discharge detection.

The first, the antenna has been tested on software ADSS for get data of return loss and VSWR. The results of return loss and VSWR antenna have a good frequency for detecting partial discharge 50MHz-2.30GHz. this results indicated antenna can used measurement for partial discharge detection.

The second, after simulation in ADSS, next step is fabrication of antenna and then testing antenna with VNA. The result VNA for antenna have range frequency in 50MHz-2.34GHz. it mean, result of measurement in simulation and VNA not much different value.

And the last experimental, the antenna used to measurement partial discharge. We know the antenna has frequency in 50MHz-2.30GHz. Frequency of partial discharge detection is 300MHz-3GHz. The PD detection range is in the antenna frequency range. Therefore the antenna can be used to detect partial discharge. The result of partial discharge, such as background noise, PDIV, PDEV and PD waveform result is successful to detection with the antenna. The background noise signal is known when the voltage regulator is turned on. This is necessary to know the amount of noise signal generated by the internal system. The background noise (BGN) measurement is performed before starting the experiment to distinguish between the noise signal and the partial discharge signal to be measured. Once the voltage source is turned on, there is little change in the more noise emerging.

Observation of the partial discharge inception voltage (PDIV), When the voltage reaches 18 kV (readings of a 4.5 volt multimeter) appears a negative PDIV signal. This occurs because, at half the negative cycle, the partial discharge is generated by electrons derived from field emissions arising from the surface of the electrode. If further observation turns out this also happens in some other negative wave cycle. This signal exceeds the value of background noise on the negative cycle so it can be ascertained that this is a partial discharge wave signal.

Partial discharge waveform can be split into the two-time rise and time fall. Generally, the rise time for partial discharge waves is from 10% to 90% of the peak. While the time fall ranging from 100% to 90%. In addition to being divided into time rise and time fall, the partial discharge waveform can also be divided into two currents due to the flow of electrons and currents due to ion movement. The electrons flow quickly and only in a short time. While the ion currents move slowly and in a relatively long time. This explains the shape of a partial discharge signal that has a sharp rise at the beginning and drops gently after it reaches its peak.

The voltage source during the occurrence of PD and the voltage source is lowered gradually, it will get the voltage

value when the PD will disappear gradually in the positive PD and followed by the negative PD. However, in experiments with plate electrode to plate with acrylic, it cannot be distinguished PDEV negative and PDEV positive because it occurs at a narrow voltage or occurs at about the same time at the source voltage of 19.6 kV for PDEV antenna.

From the measurement results partial discharge can be stated that the ultra-wideband double layer printed antenna can be included in the classification of one type of partial discharge detection.

## VII. CONCLUSION

The results of several experimental tests that have been done, both on antenna design and antenna testing on the partial discharge measurements in the laboratory, have good results, both in terms of antenna parameters to partial discharge measurements. following the conclusions of the experiments that have been done:

1. The antenna design made has different results on antenna parameters both return loss and VSWR, this is because there are several dimensions of the reference antenna unknown size
2. Antenna designs are made capable of performing partial discharge measurements since the range of antenna receives is in the partial discharge frequency range.
3. The ultra wide band double layer antenna can perform partial discharge detectin and measurements: PDIV, PD waveform and PDEV.

## REFERENCES

- [1] Fauzi Ashari, Umar Khayam, "Design and Fabrication of Vivaldi Antenna as Partial Discharge Sensor", 4<sup>th</sup> International Conference on Electric Vehicular Technology (ICEVT 2017), pp. 76-78, Bali, Indonesia, October 2-5, 2017.
- [2] Fauzi Ashari, Umar Khayam, "Design and Fabrication of Log Periodic Antenna as Partial Discharge Sensor", 4<sup>th</sup> International Conference on Electric Vehicular Technology (ICEVT 2017), pp. 79-81, Bali, Indonesia, October 2-5, 2017.
- [3] Abrar Hakim, Umar Khayam, "Simulation of Goubau PCB Antenna as Partial Discharge Detector", International Conference on High Voltage Engineering and Power Systems, ICHVEPS 2017, Bali, Indonesia, October 2-5, 2017.
- [4] Hanalde Andre, Primas Emeraldi, Ariadi Hazmi, Eka Putra Waldi, Umar Khayam "Long Bowtie Antenna for Partial Discharge Sensor in Gas-Insulated Substation", International Conference on High Voltage Engineering and Power Systems, ICHVEPS 2017, Bali, Indonesia, October 2-5, 2017.
- [5] Umar Khayam, FI Fatoni, "Design and Application of Loop Antenna for Partial Discharge Induced Electromagnetic Wave Detection", The 6<sup>th</sup> International Conference on Electrical Engineering and Informatics (ICEEI), Langkawi, Malaysia, November 25-26, 2017.
- [6] Roy B. V. B. Simorangkir, Achmad Munir. Numerical Design of Ultra-Wideband Printed Antenna for Surface Penetrating Radar Application. TELKOMNIKA, Vol.9, No.2, August 2011, pp. 341~350.



# Reliability Analysis of Randu Garut 3 Distribution System Using Section Technique Method

Jimmy Trio Putra

Department of Electrical Engineering and Informatics  
Universitas Gadjah Mada  
Yogyakarta, Indonesia  
jimmytrioputra@ugm.ac.id

Raka Trialviano Bagus

Department of Electrical Engineering and Informatics  
Universitas Gadjah Mada  
Yogyakarta, Indonesia  
trialvianoraka@gmail.com

**Abstract**— In a distribution system, reliability index is significant to calculate system performance in continuously distribute the electricity power to consumers. Feder analysed by researcher is the main electricity distributor in Tambak Aji industrial area, a developing industrial area. This research is needed to be conducted to ensure the frequent blackout is known and minimalized along with increasement of load number in the feeder. Using section technique method which divides feeder section based on sectionalizer number and detailed calculation in each load point, device failure rate, the length of conductor, and disturbance repairment duration. It was obtained Randu Garut 3 feeder reliability index of SAIFI of 1.759 faults/year, SAIDI of 4.547 hours/year as CAIDI of 2.585 hours/year.

**Keywords**—CAIDI, reliability, SAIDI, SAIFI, Section Technique

## I. INTRODUCTION

Electrical power system's ability to provide sufficient supply with satisfying quality is main role of electrical producer [1]. As the demand of electrical power goes higher, the system is demanded to has reliability in electrical power providing and distribution. Disturbance or damage in system will widely affect reliability value and also make load released thus black out is happened.

To determine reliability level of electrical power distribution, medium voltage network's role is crucial. The electric power distribution systems contributes about 80-90% of the customer reliability problems in general [1-3]. There are some number of factors that may cause abnormal system conditions (or fault conditions) and result in customer interlude, for example contact of animals and trees with distribution equipment, lightning and wind storms as examples of bad weather, distribution equipments with aging condition and lack of maintenance and traffic accidents [4-7].

Electrical system disturbance that resulted in blackout gives losses in consumer's side. According to PT PLN (Persero) West Semarang region data, there is big growth of customer number from 2016 until February 2018 as many as 3645 customer or 3,7%. This is caused by increasement of people's life rate and batch of developments in industrial sector by government, especially West Semarang Government. Thus, there is demand of electrical power system that is standard-fulfilled quality by electrical provider.

This research is done in electrical power main feeder in industrial and office complex region with small number of customer and big number of devices. Beside that, load of Randu Garut 3 feeder will increase in the next few years caused by development of industrial sector in Tambak Aji

region.. This industry will suffer considerable losses if black out occurs, in which the activities will be halt and the product will be damaged or defect. Types of customer are divided in to two: medium and low voltage customer. Furthermore, Randu Garut 3 feeder is frequently disrupted causing circuit breaker in substation works/trips, then 19 blackouts occur during 2017.

Some studies proposed methods for evaluating the reliability of distribution system, for example [8] with quantitative method based on the reliability characteristics of basic system components. There were also a three-state Markov model composed post-fault switching actions [9], a Markov modelling approach by researcher [10]. Researcher [12] with restoration times models for distribution systems faults, meanwhile [11] with a Failure Modes and Effects Analysis (FMEA) technique, and [13] with models for equipment aging. To improve the accuracy of the reliability assessment, historical outage data were directly incorporated into some algorithms [14].

Nowadays, studies to assess reliability of power distribution system with distributed generation [20], [21]. Reference [15] proposed an assessment of reliability that take in to consideration the characteristics of energy released by renewable energy generation such as solar and wind generation. Reference [16] used clustering algorithm using clustering algorithm, output of the unconventional units were correlated with hourly load and designated into certain states. Reference [17] proposed a method to evaluate reliability of a distribution system with wind turbine generators using a simulation of time sequential A six state model of WTG with joint effects of wind speed and forced outage is developed by authors.

This research used section technique method in calculating load point reliability index and analyze reliability index of distribution system in Randu Garut 3 feeder, PT PLN (Persero) west Semarang Region. This method is similar to FMEA method which counts reliability of a system based on effects of failure with the system and how it will affect the load point. This method is similar to FMEA method, system reliability determined by measuring and observing the impact of deterioration in system and load point. Identification of aftermath of an individual failure is conducted systematically by analysing the situation of occurred problem [18]. Section method divides calculation in every section thus analysis was done in detail, fast, simple and accurate. Beside that, obtained system reliability index will be compared with SPLN 68-2-1986 standard and 2018 PT. PLN (Persero) West Semarang's target. Used indexes were SAIFI (System Average Interruptions Frequency Index), SAIDI (System Average Interruption Duration Index) and CAIDI (Costumer Average Interruption Duration Index).

## II. SECTION TECHNIQUE METHOD

### A. Section Technique

Section Technique Method is a structured method to analyse and evaluate system that can be used to find reliability index of distribution system. In this method, system is divided in to several smaller parts or sections first, thus the probability of miscalculation will be minimized and time cost will be reduced [18].

Reliability of a distribution system is based on how is the failure effect from an individual device will affect the system operation. This effect is identified systematically by analysing how is the consequences toward all of the customers in distribution network. Then each of the device failure will be analysed in one load point in the system thus the load point that is disturbed frequently will be found. Flowchart of section technique method is attached in Fig. 1.

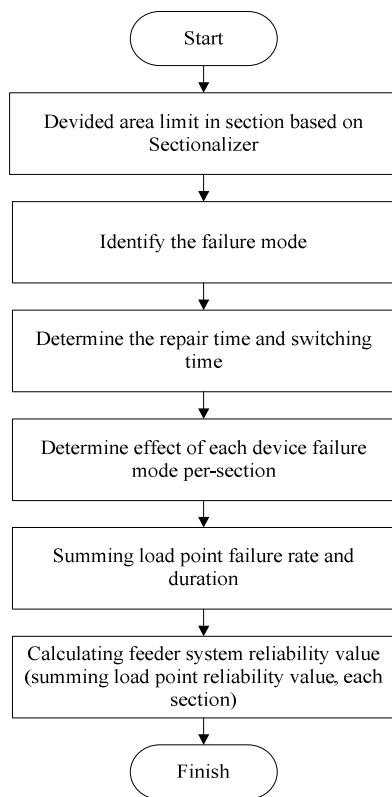


Fig. 1. Flowchart of Section Technique Method

### B. Reliability Index

Reliability of consument service is able to be stated in several indexes, which the three most often used are SAIFI, SAIDI and CAIDI. Below are needed data to find the three indexes, such as:

#### 1) Failure Rate

Failure rate is average value from number of failures in a certain observed time (T), and is stated in failure rate in a year. In an observation, failure rate is stated as below:

$$\lambda = \frac{f}{T} \quad (1)$$

#### a) Load point Failure Rate

The sum of all equipment failure rates will affect the load point, is calculated by the equation:

$$\lambda_{LP} = \sum_{i=k} \lambda_i \quad (2)$$

#### b) Load point Disturbance Duration

The sum of the repairing/switching duration with multiplying the rate of failure of all the equipment affecting the load point, calculated by the equation:

$$ULP = \sum_{i=k} \lambda_i . r_j \quad (3)$$

#### 2) System Average Interruption Frequency Index

SAIFI is defined as the average number of system failures that occur per customer served by the system per unit time (generally per year), calculated by the equation:

$$SAIFI = \frac{\sum NLP . \lambda_{LP}}{\sum N} \quad (4)$$

#### 3) System Average Interruption Duration Index

SAIDI is the average value index of the duration of system disruption for each consumer for a year, calculated by the equation:

$$SAIDI = \frac{\sum NLP . ULP}{\sum N} \quad (5)$$

#### 4) Customer Average Interruption Duration Index.

CAIDI is an index value of the average duration of consumer disturbance each year, informing the average time to normalize the interruption of each customer within a year. Equation in calculating CAIDI:

$$CAIDI = \frac{SAIDI}{SAIFI} \quad (6)$$

## III. TEST SYSTEMS

The data needed in finding the reliability value of the distribution system include outage and repair duration. Both values are obtained with reference to SPLN No. 59 of 1985 as in Table I and Table II. Whereas, the feeder shown in Fig. 2. is supplied from Randu Garut with an installed transformer of 60 MVA. The load served by these feeders are industrial, commercial and residential. There are 43 load points of 1 phase and 3 phase distribution transformer which are low voltage customer type with power below 197 kVA and 25 circuit breaker. The total load of both low and medium voltage is 138 customers. This feeder is divided into 95 lines with a total length of 8.72 km. The data used in this study based on real data taken at PT. PLN (Persero) West Semarang.

TABLE I. FAILURE INDEX AND REPAIR TIME OF MEDIUM VOLTAGE

Overhead Medium Voltage	
Sustained failure rate ( $\lambda$ /km/yr)	0.2
r (repair time) (hour)	3
re (switching time) (hour)	0.25

TABLE II. DATA OF DEVICE OUTAGE, REPAIR AND SWITCHING

Devices	$\lambda$ (unit/year)	r (hr)	rs (hr)
Transformer	0.005	10	0.15
Circuit Breaker	0.004	10	0.25
Sectionalizer	0.003	10	0.15
Recloser	0.005	10	0.25

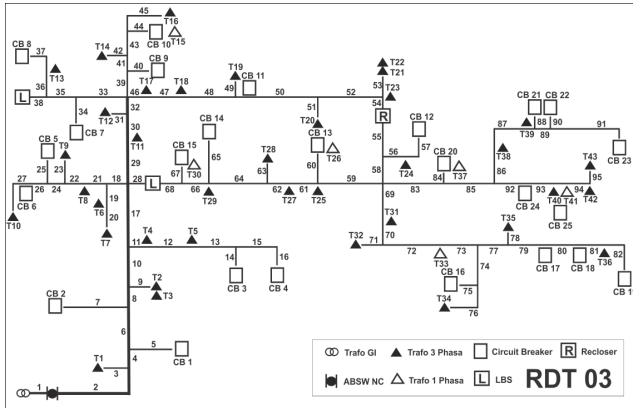


Fig. 2. Single line diagram of Randu Garut 3

#### A. Area Limit with Sectionalizer

The distribution network of Randu Garut 3 is divided based on the number of sectionalizers attached. The feeder has 3 sectionalizers in the form of 2 load break switches; mounted in normally close and 1 reclose. Thus, the feeder has 2 sections with a radial configuration as shown in Fig. 3. and Fig. 4.

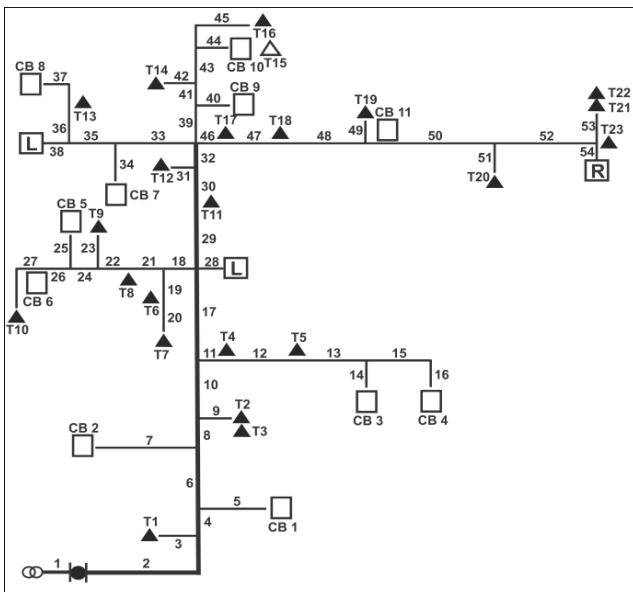


Fig. 3. Section 1 Randu Garut 3

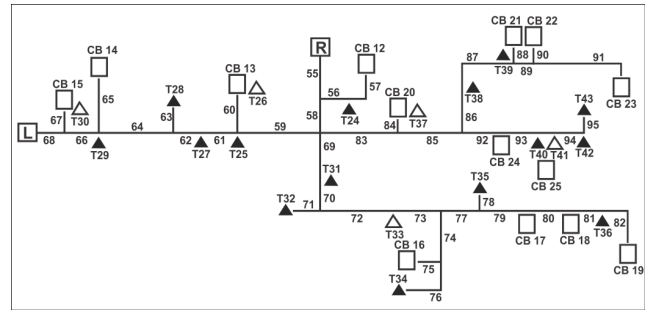


Fig. 4. Section 2 Randu Garut 3

## IV. RESULTS AND DISCUSSION

Reliability analysis was conducted based on data that has been obtained by using data length of lines and data of customer number per load point. The reliability of each section is described as follows:

#### A. Section 1

The effect of a device failure in the system can be seen in the list of failure modes Table III.

TABLE III. SECTION I FAILURE MODE LIST

Disturbance Numbers	Device	Load Point affected by Repair Time	Load Point affected by Switching Time
1	ABSW	CB 1-CB 25 + LP 1-LP 43	-
2	Recloser	CB 1-CB 25 + LP 1-LP 43	-
3	CB 1	CB 1	-
4	T1	LP 1	-
5	L1	CB 1-CB 25 + LP 1-LP 43	-

TABLE IV. FAILURE DURATION AND RATE LOAD POINT SECTION I

Load Point	Failure Duration and Rate Load Point	
	$\lambda$ (fault/year)	U (hours/year)
CB 1	0.982	3.03
?		
CB 11	0.982	3.03
CB 12	0.978	2.99
?		
CB 25	0.978	2.99
LP 1	0.983	3.04
?		
LP 23	0.983	3.04
LP 24	0.978	2.99
?		
LP 40	0.978	2.99
LP 41	0.978	2.99
LP 42	0.978	2.99
LP 43	0.978	2.99

Table III. shows some samples because the number of equipment that had CB as many as 11, 23 transformers, and 54 lines. Next, calculate the value of failure rate and the duration of failure of each load point. Failure rate and failure duration can be seen in Table IV.

From Table IV. It was obtained  $\lambda$  for CB1 to CB12 of 0.982 fault/year and  $\lambda$  for CB12-CB25 of 0.978, the meaning of CB here is that the load point failure rate is in medium voltage customers, whereas LP is low voltage customers and the difference in value of 0.005 was caused by section difference, because the calculation occurred in section 1 then the failure of load point in section 2 in the form of CB and LP was not counted.

Taken one case on CB1,  $\lambda$  CB1 was obtained from the sum of equipment failure rate affecting CB1 and multiplication of failure rate with length of lines. From Table IV. also obtained the value of U for CB1 of 3.03 faults/year. ULP1 is obtained from the sum of multiplication product  $\lambda$  of equipment with repair time or switching time in which the equipment is affecting CB1. Multiplication by repair time or switching time depends on the condition of the equipment, whether the equipment must be off or only experience switching time condition during interruption. This can be seen in Table V.

In section 1, the conditions experienced by all existing equipment are only repair conditions and no equipment was subject to switching time conditions, due to the equipment and the substation were close in distance so that if an interruption happened, it cannot be backed up and the disturbance must be repaired first to the voltage from the new substation can be supplied again, so to find U in Table IV. condition used is repair time condition. By knowing index of reliability of load point can be obtained index of reliability section.

Based on Table VI, it was obtained SAIFI and SAIDI in section I with value 0.9798043 fault/year for SAIFI and 3.00804 hours/year for SAIDI. SAIFI for CB1 was obtained from multiplying the number of consumers on the load point by  $\lambda$  CB1 then dividing it by the total customer.

TABLE V. DISTURBANCE DURATION AND FAILURE RATE SECTION I

Device	$\lambda$ SPLN	Length of lines	$\lambda$ LP (fault/year)	r SPLN	ULP (hr/year)
ABSW	0.003	-	0.003	10	0.03
Recloser	0.005	-	0.005	10	0.05
LP (T)	0.005	-	0.005	10	0.05
L1	0.2	0.21	0.042	3	0.126
2					
L47	0.2	0.05	0.01	3	0.03
L48	0.2	0.1	0.02	3	0.06
L49	0.2	0.03	0.006	3	0.018
L50	0.2	0.2	0.04	3	0.12
L51	0.2	0.04	0.008	3	0.024
L52	0.2	0.15	0.03	3	0.09
L53	0.2	0.05	0.01	3	0.03
L54	0.2	0.04	0.008	3	0.024
TOTAL $\lambda$ LP			0.983	TOTAL ULP	3.04

TABLE VI. SAIFI AND SAIDI PER LOAD POINT SECTION I

Load Point	Numbers of Cons.	Numbers Of Cons. x $\lambda$ LP	Numbers Of Cons. x ULP	SAIFI	SAIDI
CB 1	1	0.982	3.03	0.007116	0.021957
CB 2	1	0.982	3.03	0.007116	0.021957
CB 3	1	0.982	3.03	0.007116	0.021957
2					
CB 25	1	0.978	2.99	0.007087	0.021667
LP 1	1	0.983	3.04	0.007123	0.022029
LP 2	3	2.949	9.12	0.02137	0.066087
LP 3	1	0.983	3.04	0.007123	0.022029
2					
LP 36	5	4.89	14.95	0.035434	0.108333
LP 37	1	0.978	2.99	0.007086	0.021666
LP 38	15	14.67	44.85	0.106304	0.325000
LP 39	4	3.912	11.96	0.028347	0.086666
LP 40	1	0.978	2.99	0.007086	0.021666
LP 41	1	0.978	2.99	0.007086	0.021666
LP 42	10	9.78	29.9	0.070869	0.216666
LP 43	1	0.978	2.99	0.007087	0.021667
Total				0.979804	3.00804

### B. Section 2

The effect of system device failure in section 2 is shown in failure mode list in Table VII.

TABLE VII. FAILURE MODE LIST OF SECTION 2

Disturbance Numbers	Device	LP affected by Repair Time	LP affected by Switching Time
1	Recloser	CB 12-CB 25 + LP 24-LP43	CB 1-CB 11 + LP 1-LP23
2	CB 12	CB 12	-
3	T24	LP 24	-
4	L55	CB 12-CB 25 + LP 24-LP43	CB 1-CB 11 + LP 1-LP23

Table VII. are some of the only equipment samples that can be displayed because the tables are too long, in fact that there are 14 CB, 20 Transformers and 40 lines. Next, calculate the value of failure rate and the duration of failure of each load point. The value of failure rate and duration of failure can be viewed in Table VIII.

TABLE VIII. LOAD POINT FAILURE DURATION AND RATE OF SECTION 2

Load Point	Load Point Failure Duration And Rate	
	$\lambda$ (fault/year)	U (hours/year)
CB 1	0.777	0.19425
?		
CB 11	0.777	0.19425
CB 12	0.781	2.392
?		
CB 25	0.781	2.392
LP 1	0.777	0.19425
LP 22	0.777	0.19425
?		
LP 23	0.777	0.19425
LP 24	0.782	2.402
?		
LP 43	0.782	2.402

By knowing load point reliability index, section 2 reliability index can be obtained and is shown in Table IX.

TABLE IX. SAIFI AND SAIDI PER LOAD POINT IN SECTION 2

Load Point	Numbers of Cons.	Numbers of Cons. x $\lambda$ LP	Numbers of Cons. x ULP	SAIFI	SAIDI
CB 1	1	0.777	0.19425	0.005630	0.001407
CB 2	1	0.777	0.19425	0.005630	0.001407
CB 3	1	0.777	0.19425	0.005630	0.001407
?					
CB 25	1	0.781	2.392	0.00565	0.017333
LP 1	1	0.777	0.19425	0.005630	0.001407
LP 2	3	2.331	0.58275	0.016891	0.004222
LP 3	1	0.777	0.19425	0.005630	0.001407
?					
LP 43	1	0.782	2.402	0.005666	0.017405
Total				0.78001	1.5398

Based on Table IX, SAIFI and SAIDI in section 2 can be obtained with a value of 0.78001 fault/year for SAIFI and 1,5398 hours/year for SAIDI. After knowing the reliability index value of each section, value of index reliability of feeder network system can be obtained by summing index reliability of each section. The calculation can be seen in Table X.

TABLE X. INDEX OF TOTAL RELIABILITY

Section	Index of Total Reliability	
	SAIFI	SAIDI
I	0.979804	3.0080
II	0.78001	1.5398
Total	1.759814	4.5478

The value of SAIFI and SAIDI was obtained by summing the magnitude of the reliability index of each section. For analyzed feeder, it was obtained SAIFI value of 1.759814 faults/year and SAIDI value of 4.5478 hours/year. The value of CAIDI was obtained by dividing the SAIDI value by SAIFI, so the result of the calculation is shown in Table XI.

TABLE XI. CAIDI VALUE

Section	Index of Reliability (CAIDI)
I	3.07004504
II	2.01160328
Total	2.58427267

Furthermore, to determine whether the analyzed that is Randu Garut 3 included in the category of reliable feeder or not, the researcher did two comparison of reliability values that have been obtained with certain standard reliability values, among others:

a) Standards established by PT. PLN (Persero) in accordance with SPLN No. 68-2 Year 1986 on "Level of Security Guarantee of Power System Part Two" which states that the radial configuration network system with PBO (Recloser).

b) Target of Rayon Semarang Barat 2018.

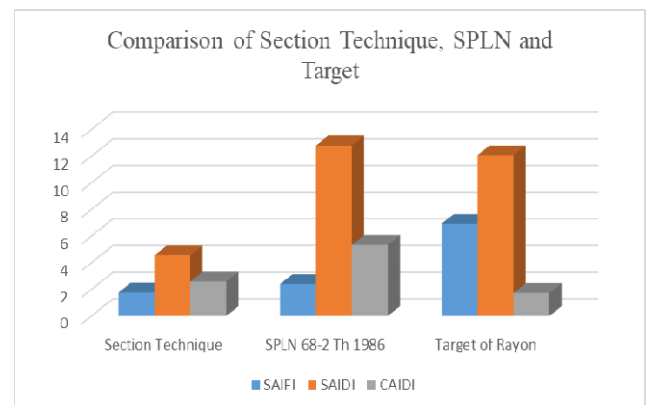


Fig. 5. Comparison of Section Technique, SPLN and Target of Rayon

Shown in Fig. 5. Comparison of section technique method with SPLN No. 68-2 in 1986 and 2018 Target of West Semarang Region, SAIFI and SAIDI reliability index obtained by section technique method was smaller, it means that the reliability value of Randu Garut was higher. While the value of CAIDI obtained was lower than SPLN No. 68-2 in 1986 and higher than the 2018 target.

## V. CONCLUSION

Section technique method is used to analyze distribution system reliability in Randu Garut 3 feeder, total reliability values obtained were SAIFI INDEX of 1.75981884 faults/year, SAIDI index of 4.57712319 hours/year and CAIDI index 2.58427267 hours/fault. Obtained overall reliability index using section technique method was better from PLN standard and target of West Semarang Region in 2018, except for CAIDI value which surpass target of West Semarang Region in 2018. Thus, section technique method is able to become solution in determining reliability index of particular distribution system. In addition, it can be concluded that the longer the lines of the distribution network and the more components of the equipment on the system, the greater the likelihood of failure occurring resulting in blackout at the load point which may decrease the reliability of the feeder.

## REFERENCES

- [1] R. Billinton, R. N. Allan, "Reliability Evaluation of Power Systems", Plenum Press, Second Edition, 1996.
- [2] R. E. Brown, A. P. Hanson, H. L. Willis, F. A. Luedtke, M. F. Born, "Assessing the Reliability of Distribution Systems", IEEE Computer Applications in Power, January 2001, pp. 44-49.
- [3] R. E. Brown, "Electric Power Distribution Reliability", Marcel Dekker, Second Edition, 2009.
- [4] Chow 95 M-y. Chow and L.S. Taylor. "Analysis and Prevention of Animal-Caused Faults in Power Distribution Systems." IEEE Transactions on Power Delivery, Vol. 10, No. 2. 1996. pp.995-1001.
- [5] C. M. Warren, 'The Effect of Reducing Momentary Outages on Distribution Reliability Indices.' IEEE Transactions on Power Delivery, Vol. 14, No. 1, January 1999, pp. 250-255.
- [6] D. E. Parrish, 'Lightning Faults on Distribution Lines,' IEEE Transactions on Power Delivery, Vol. 4, No. 4, October 1989. pp. 2179-2186.
- [7] Brow 97 E. Brown, S. Gupta. R. D. Christie, S. S. Venkata, and R. Fletcher, Distribution System Reliability Assessment: Momentary Interruptions and Storms.' IEEE Transactions on Power Delivery, Vol. 12, No. 4, October 1997. pp. 1569-1575.
- [8] P. Gaver, F. E. Montmeat. and A. D. Patton, Power System Reliability: I Measures of Reliability and Methods of Calculation.' IEEE Transactions on Power Apparatus and Systems, Vol. PAS-83, No. 7, July 1964, pp. 727-737.
- [9] J. Endrenyi, 'Three state models in power system reliability evaluation,' IEEE Transactions on Power Apparatus and Systems, Vol. 90, No. 4. July/August 1971, pp. 1909-1916.
- [10] D. O. Koval and R. Billinton. "Evaluation of Distribution Circuit Reliability.' IEEE Transactions on power Apparatus and Systems, Vol. PAS-98. No. 2. March/April 1979. pp. 509-518.
- [11] S. J. Kostyal, T. D. Vismor and R. Billinton, "Distribution System Reliability Handbook. ' Final Report. EPRI EL-81-16-LD. Project 136-1. Electric Power Research Institute. September 1981.
- [12] M.-y. Chow, L. S. Taylor, and M.-s. Chow, 'Time of Outage Restoration Analysis in Distribution Systems,\* IEEE Transactions on Power Delivery, Vol. II. No. 3, July 1996, pp. 1652-1658.
- [13] S. Asgarpour and M. J. Mathine, 'Reliability Evaluation of Distribution Systems with Non-Exponential Down Times,' IEEE Transactions on Power Systems. Vol. 12, No. 2, May 1997, pp. 579-584.
- [14] R. Billinton and R. Goel, 'An Analytical Approach to Evaluate Probability Distributions Associated with the Reliability Indices of Electric Distribution Systems,' IEEE Transactions on Power Delivery. Vol. 1, No. 3, July 1986, pp. 245-251.
- [15] C. Singh and A. Lago-Gonzalez, "Reliability modeling of generation systems including unconventional energy sources," IEEE Transactions on Power Apparatus and Systems, vol. 104, no. 5, May 1985.
- [16] C. Singh and Y. Kim, "An efficient technique for reliability analysis of power systems including time dependent sources," IEEE Transactions on Power Systems, vol. 3, no. 3, pp. 1090-1096, Aug. 1988.
- [17] P. Wang and R. Billinton, "Time-sequential simulation techniques for rural distribution system reliability cost/worth evaluation including wind generation as alternate supply," in IEE Proc. Transmission, Distribution, and Generation, vol. 148, no. 4, July 2001, pp. 355-360.
- [18] Jamaris, "Analisis Keandalan Sistem Jaringan Distrikbusi 20kV di PT. PLN (Persero) Rayon Panam Penyulang 4 Lobak Menggunakan Metode Section Technique dan Metode Reliability Index Assessment (RIA)", Tugas Akhir UIN SUSKA – Pekanbaru, 5 Januari 2016.
- [19] Santoso, R. "Evaluasi Tingkat Keandalan Jaringan Distribusi 20 kV pada Gardu Induk Bangkinang dengan menggunakan Metode FMEA, Jurnal Fakultas Teknik Universitas Riau, 2016. pp 1-7.
- [20] Abdulaziz. A. Alkuhayli, Srinath Raghavan, Badrul H. Chowdhury, "Reliability evaluation of distribution systems containing renewable distributed generations", North American Power Symposium (NAPS) 2012, pp. 1-6, 2012.
- [21] S. Mostafa Elmi, Mojtaba Rafiei, "Effects of reclosing devices and distributed generation (DG) to improve reliability indices in radial distribution lines", Electrical Power Distribution Networks (EPDC) 2012 Proceedings of 17th Conference on, pp. 1-5, 2012.



# Combined Computational Intelligence Approach for the Power System Optimization Problem

Arif N. Afandi  
Electrical Engineering  
Universitas Negeri Malang  
Malang, Jawa Timur, Indonesia  
an.afandi@um.ac.id

Irham Fadlika  
Electrical Engineering  
Universitas Negeri Malang  
Malang, Jawa Timur, Indonesia  
irham.fadlika.ft@um.ac.id

Langlang Gumilar  
Electrical Engineering  
Universitas Negeri Malang  
Malang, Jawa Timur, Indonesia  
langlang.gumilar.ft@um.ac.id

Yuni Rahmawati  
Electrical Engineering  
Universitas Negeri Malang  
Malang, Jawa Timur, Indonesia  
yuni.rahmawati.ft@um.ac.id

Quota Alief Sias  
Electrical Engineering  
Universitas Negeri Malang  
Malang, Jawa Timur, Indonesia  
quota.alief.ft@um.ac.id

Irawan Dwi Wahyono  
Electrical Engineering  
Universitas Negeri Malang  
Malang, Jawa Timur, Indonesia  
irawan.dwi.ft@um.ac.id

Yunis Sulistyorini  
Mathematics Education  
IKIP Budi Utomo  
Malang, Jatim, Indonesia  
yunis.sulistyorini@gmail.com

Farrel Candra WA  
SPAES Research Center  
Batu, Jawa Timur, Indonesia  
farrel.candrawinata@gmail.com

Michiko Ryuu Sakura A  
SPAES Research Center  
Batu, Jawa Timur, Indonesia  
michiko.ryuusakura@gmail.com

**Abstract**—A power system optimization is one of the major problems in the operating performances of the existing system. This problem takes place on the various technical cases to get optimal conditions of the system. Moreover, many approaches have been implemented to carry out the solution under operational constraints. This paper presents Thunderstorm Algorithm (TA) and Artificial Salmon Tracking Algorithm (ASTA) for defining the optimal strategy of the power system optimization based on the unit commitment. Both algorithms are tested on the IEEE-62 bus system, whereas, results show that ASTA and TA can be combined together to solve the power system problem. These algorithms have been applied to predict the power consumption and it has good performances while searching for the optimal solution. These results also show that the economic dispatch problem is conducted to the power production while the algorithm is performed in good characteristics.

**Keywords**—algorithm; dispatch; emission; optimization; power

## I. INTRODUCTION

One of the optimization problems on the power system operation is a unit commitment (UC) which is consisted of the various generating unit combination. The UC is used to fulfill the energy customer service which is correlated with the total power demand. Technically, the power demand is one of the most considerations on the power production. This factor is associated with energy usages on the consumer site patterns related to the UC over the day, night, week, seasons and holidays. Deal with this condition, a demand forecasting strategy is a very important policy to meet the power production in the behavior of the energy players. In addition, the optimal power production is also urgent to cover all possible combination between existing power plants as a unit commitment. The UC is commonly approached using an economic dispatch (ED) problem [1]–[7] while the optimal allocation of power outputs belongs to the various generators available to serve the load [8]–[11] considering

also an emission dispatch (EmD) problem for decreasing pollutants [6], [12]–[14].

Presently, the ED and EmD are an important optimization problem in the power system operation which can be solved using various techniques. An intelligent computation (IC) is more popular than classical approaches to carrying out this problem [7], [9], [15]–[20]. Since an early idea of the IC, many methods have been proposed based on own inspirations [13], [21] and many natural phenomena or biological processes have been also adopted as the inspiration [12], [21], [22]. Currently, many algorithms have also been proposed which are conducted to phenomena or entities in nature [22]–[26]. These versions have been advanced to increase computational performances through hierarchies and procedures for sequencing orders of the algorithm [8], [14], [27]. In line with previous efforts, this paper presents an emphasizing of thunderstorm mechanism and salmon tracking applied to the power system problem considered various operational limitations.

## II. ALGORITHMS OVERVIEW

Many computational bits of intelligence are developed based on the natural phenomenon and behavior [21], [28]–[31]. In these works, one other is adopted from thunderstorm mechanisms which are recognized by cloud shapes and a pre-signal. In nature, these mechanisms are mitigated from the charge ignition for the interaction between the negative charge [30], [32], [33]. In detail, the Thunderstorm Algorithm (TA) is depicted in Fig. 1 with transforming structures in computation processes are Cloud Phase: Streamer Phase; and Avalanche Phase [8], [11], [34]. This figure illustrated a striking propagation from the sky to earth as a charge moving direction.

In particular, artificial salmon tracking algorithm (ASTA) is also presented in these studies which are designed as given Fig. 2. ASTA is adopted from behaviors of Salmon fish in nature while the salmon run is the

moving time migrated from the ocean, swim to the upper reaches of rivers where spawning on gravel beds [35]. Many works were explored and developed to understand the migration situation [28], [29], [31], [35]. In these works, ASTA is presented in computational parameters cover salmon number, surviving factor, mouth river, tracking round, migrating period. As given in Fig. 2, these parameters are covered for Exploring behaviors and Surviving behaviors.

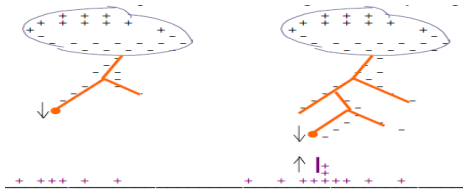


Fig. 1. Illustration of the striking propagation

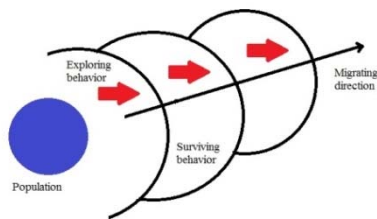


Fig. 2. Principles of the artificial salmon tracking algorithm

### III. METHOD AND APPROACH

Many technical problems are approached using a model which is used to fit the data, simulation, and forecasting. A model can also be used to plan the amount of evaluation required to meet desired levels in various fields [1]–[5]. In addition, the model is used to find the optimal allocation of the UC among the various generators available to serve the load [8]–[11], [34], [36]–[38]. Recently, many strategies are developed to explore a UC considering the fuel cost, emission, transmission line losses, weighting factors, and others [5], [23]–[25]. In these works, the UC covers ED and EmD problems as discussed in [6], [12]–[14] and integrated to become an economic and emission dispatch (EED) problem under operational limitations [14], [25], [39]–[41]. Furthermore, many works have used the EED to describe some economical measurements on the desirable targets [4], [14], [38], [42], [43]. In these studies, the EED is formulated using mathematical statements for defining the objective function and technical constraints [6], [10], [26], [39] considering the IEEE-62 bus system as a sample model of the power system. This model consists of 62 buses; 89 lines; and 32 load buses. This system is also supported by 19 generating units. In addition, this system is constrained by 10% of the loss limit; 0.5 of the weighting factor; and 0.85 kg/h of the emission standard; 5% of voltage violations; 95% of the power transfer capability; and banded on upper and lower power limits.

Moreover, TA and ASTA are designed based on its structures and procedures whereas both interactions are illustrated in Fig. 3. TA is implemented on a standard model of the power system based on the sequencing orders as depicted in Fig. 1 while ASTA uses Fig. 2 for the

processes. In these works, TA is compiled using the cloud phase; streamer phase; and avalanche phase in terms of 1 of the avalanche; 25 of the cloud charge; 100 of the streaming flow; and 4 of the hazardous factor. On the other hand, ASTA is also compiled based pseudo-codes covered for the salmon number, surviving factor, mouth river, tracking round, migrating period. In details, ASTA is presented using 100 of the salmon number, 0.25 of a surviving factor, 100 of the mouth river, 100 of the tracking round, 1 of the Migrating period, and 50 of the population. Based on Fig. 3, the procedures are subjected to the Objective function, TA processes, Unit Commitment, ASTA processes, and the updating processes.

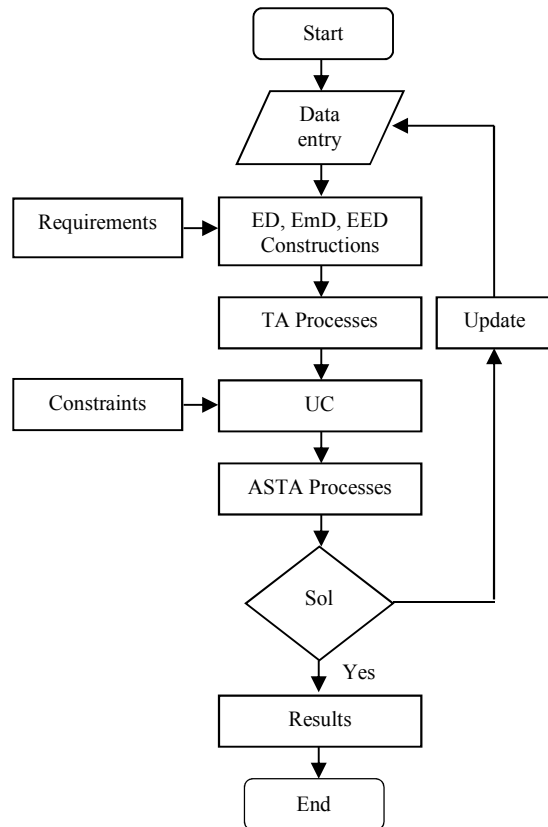


Fig. 3. TA and ASTA interaction

### IV. RESULTS AND DISCUSSION

In this section, the system is modeled using IEEE-62 bus system with main parameters of generating units are listed in Table I. This table informs for the coefficients and power limits. Moreover, graphical performances of the computation are given in Fig. 4 and Fig. 5. From these figures, it is known that Fig. 4 illustrates a computational convergence speed which is searched in 17 iterations while these compiling processes need 82.1 s. Moreover, the optimal solution of the EED is 12,005.6 \$/h after started at 17,408.2 \$/h at the first step. This characteristic also describes that the computation is performed in smooth and stable processes with the consuming time is given in Fig. 5. In total, this simulation is completed in 533.3 s. In these works, the simulation is addressed to evaluate a computing ability while searching the optimal solution of the EED problem as the optimal power production based on the IEEE 62 bus system considering several requirements and constraints. By considering 2,221.2 MW of the power

load, the system has produced 2,387.9 MW from existed generating units. It means that this operation has 166.7 MW of the total power loss or around 6.9%.

TABLE I. GENERATING UNIT COEFFICIENTS

Gen	Fuel Cost			Emission			Limit	
	a (\$/MWh <sup>2</sup> )	b (\$/MWh)	c	$\alpha$ (kg/MWh <sup>2</sup> )	$\beta$ (kg/MWh)	$\gamma$	Pmin (MW)	Pmax (MW)
G1	0.00700	6.80	95	0.0180	-1.8100	24.300	50	300
G2	0.00550	4.00	30	0.0330	-2.5000	27.023	50	450
G3	0.00550	4.00	45	0.0330	-2.5000	27.023	50	450
G4	0.00250	0.85	10	0.0136	-1.3000	22.070	0	100
G5	0.00600	4.60	20	0.0180	-1.8100	24.300	50	300
G6	0.00550	4.00	90	0.0330	-2.5000	27.023	50	450
G7	0.00650	4.70	42	0.0126	-1.3600	23.040	50	200
G8	0.00750	5.00	46	0.0360	-3.0000	29.030	50	500
G9	0.00850	6.00	55	0.0400	-3.2000	27.050	0	600
G10	0.00200	0.50	58	0.0136	-1.3000	22.070	0	100
G11	0.00450	1.60	65	0.0139	-1.2500	23.010	50	150
G12	0.00250	0.85	78	0.0121	-1.2700	21.090	0	100
G13	0.00500	1.80	75	0.0180	-1.8100	24.300	50	300
G14	0.00450	1.60	85	0.0140	-1.2000	23.060	0	150
G15	0.00650	4.70	80	0.0360	-3.0000	29.000	0	500
G16	0.00450	1.40	90	0.0139	-1.2500	23.010	50	150
G17	0.00250	0.85	10	0.0136	-1.3000	22.070	0	100
G18	0.00450	1.60	25	0.0180	-1.8100	24.300	50	300
G19	0.00800	5.50	90	0.0400	-3.000	27.010	100	600

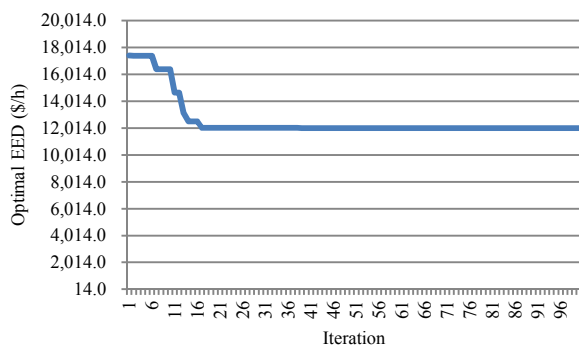


Fig. 4. Computational speed of the optimal solution

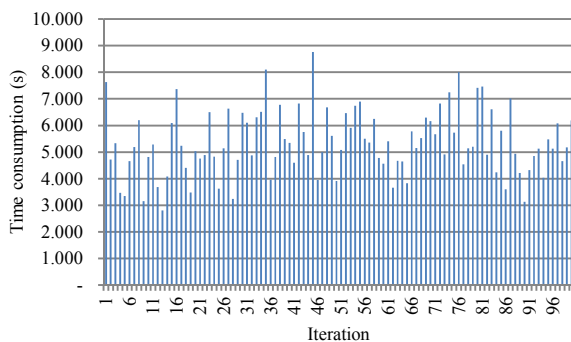


Fig. 5. Computational time consumption

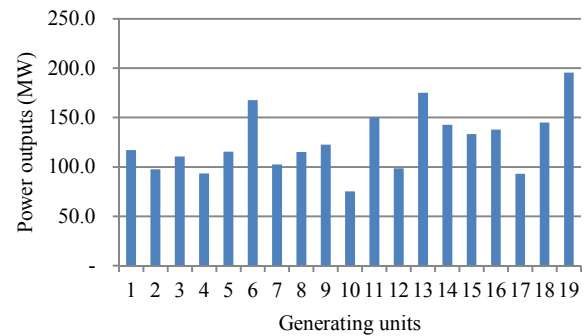


Fig. 6. Individual generating unit commitment

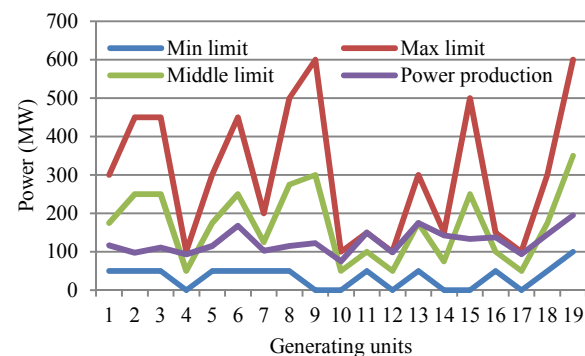


Fig. 7. Power production evaluation

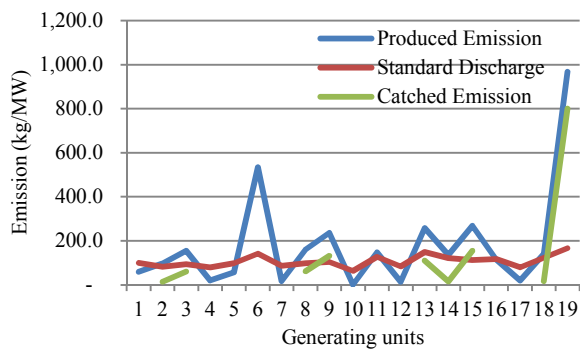


Fig. 8. Emission effects of generating units

TABLE II. OPERATING COST OF GENERATING UNITS

Gen	Power (MW)	Fuel cost (\$)	Emission Compensation (\$)	Operating Cost (\$)
G1	117.2	988.1	0	988.1
G2	97.5	472.3	10.6	482.9
G3	110.6	554.9	45.2	600.1
G4	93.4	111.2	0	111.2
G5	115.6	631.8	0	631.8
G6	167.5	914.3	293.8	1,208.1
G7	102.6	592.6	0	592.6
G8	115.0	720.2	46.8	767.0
G9	122.6	918.3	98.8	1,017.1
G10	75.3	107.0	0	107.0
G11	150.0	406.3	15.6	421.8
G12	98.7	186.2	0	186.2
G13	175.0	543.1	82.5	625.7
G14	142.5	404.4	11.4	415.8
G15	133.2	821.2	116.1	937.3
G16	137.9	368.6	0	368.6
G17	93.2	110.9	0	110.9
G18	144.8	351.1	12.4	363.5
G19	195.3	1,469.3	600.6	2,069.9
Total	2,387.9	10,671.8	1,333.8	12,005.6

As the implication of this unit commitment, generating units also produce individually power outputs within various portions of the pollution as detailed in Fig. 6. In addition, the system operation is also required by many conditions and situations. By considering the operating in terms of maximum, minimum, and middle limits, the power production is evaluated as depicted in Fig. 7. This figure informs the condition of each generating unit on the base of the power capability to give a contribution to the UC. In particular, caused by over standard productions, the generating unit gives an environmental effect as illustrates in Fig. 8. These emissions should be filtered at generating units around 1,778.4 kg/h. In total, generating units release in 3,398.6 kg/MW of the emission even it is permitted only 1,029.7 kg/MW under an emission standard. Economically, the system is optimized in 12,005.6 \$/h for the operating cost covered the fuel procurement and the emission compensation. In particular, Table II presents the details of the operating fee. The fuel consumption needs 10,671.8 \$/h while 1,333.8 \$/h is used for the pollutant compensation. This table also informs that generating units take place on different power capacities to cover the total load demand. Moreover, the system has

released the pollutant in various results over under environmental standard. Several generating units are still operated with the lower pollution is associated with the emission compensation fee.

## V. CONCLUSION

In general TA and ASTA can be combined to solve the problem applied to an IEEE-62 bus system. These algorithms have used to search the optimal balance of cost and emission aspects. Results show that the problem is carried out in various power outputs, emission discharges, and optimized operating costs while the optimal point is obtained. Moreover, real applications are devoted.

## ACKNOWLEDGMENT

The authors gratefully acknowledge the support of Universitas Negeri Malang, Indonesia, for the PNPB Research Grant issued on 21.2.6/UN32.14/LT/2018.

## REFERENCES

- [1] A. N. Afandi, "Optimal scheduling power generations using HSABC algorithm considered a new penalty factor approach," in *The 2nd IEEE Conference on Power Engineering and Renewable Energy (ICPERE) 2014*, 2014, pp. 13–18.
- [2] S. Chandra, V. Kothari, and M. Sharma, "A model for controlling variance in the Artificial Bee Colony algorithm," in *2015 International Conference on Advances in Computing, Communications and Informatics (ICACCI)*, 2015, pp. 263–269.
- [3] A. N. Afandi, *Optimal Solution of the EPED Problem Considering Space Areas of HSABC on the Power System Operation*, vol. 7. 2015.
- [4] N. Tutkun, O. Can, and A. N. Afandi, "Low cost operation of an off-grid wind-PV system electrifying residential homes through combinatorial optimization by the RCGA," in *2017 5th International Conference on Electrical, Electronics and Information Engineering (ICEEIE)*, 2017, pp. 38–42.
- [5] M. El-Shimy, M. A. Attia, N. Mostafa, and A. N. Afandi, "Performance of grid-connected wind power plants as affected by load models: A comparative study," in *2017 5th International Conference on Electrical, Electronics and Information Engineering (ICEEIE)*, 2017, pp. 1–8.
- [6] A. Gupta, K. K. Swarnkar, and K. Wadhvani, *Combined Economic Emission Dispatch Problem using Particle Swarm Optimization*, vol. 49. 2012.
- [7] S. Fadil and B. Urazel, "A security constrained environmental/economic power dispatch technique using F-MSG algorithm for a power system area including limited energy supply thermal units," *International Journal of Electrical Power & Energy Systems*, vol. 56, no. Supplement C, pp. 185–197, Mar. 2014.
- [8] A. N. Afandi and Y. Sulistyorini, "Thunderstorm Algorithm for Determining Unit Commitment in Power System Operation," *Journal of Engineering and Technological Sciences*, vol. 48, no. 6, pp. 743–752, Dec. 2016.

- [9] Y. Li, S. Miao, X. Luo, and J. Wang, "Optimization model for the power system scheduling with wind generation and compressed air energy storage combination," in *2016 22nd International Conference on Automation and Computing (ICAC)*, 2016, pp. 300–305.
- [10] A. N. Afandi, I. Fadlika, and A. Andoko, "Comparing Performances of Evolutionary Algorithms on the Emission Dispatch and Economic Dispatch Problem," *TELKOMNIKA (Telecommunication Computing Electronics and Control)*, vol. 13, no. 4, pp. 1187–1193, Dec. 2015.
- [11] A. N. Afandi *et al.*, "Designed Operating Approach of Economic Dispatch for Java Bali Power Grid Areas Considered Wind Energy and Pollutant Emission Optimized Using Thunderstorm Algorithm Based on Forward Cloud Charge Mechanism," *International Review of Electrical Engineering (IREE)*, vol. 13, p. 59, Feb. 2018.
- [12] A. N. Afandi, Y. Sulistyorini, H. Miyauchi, G. Fujita, X. Z. Gao, and M. El-Shimy, "The Penetration of Pollutant Productions on Dynamic Generated Power Operations Optimized Using a Novel Evolutionary Algorithm," *International Journal on Advanced Science, Engineering and Information Technology*, vol. 7, no. 5, pp. 1825–1831, Oct. 2017.
- [13] A. N. Afandi, "Solving Combined Economic and Emission Dispatch Using Harvest Season Artificial Bee Colony Algorithm Considering Food Source Placements and Modified Rates," *International journal on electrical engineering and informatics*, vol. Vol. 6, p. 267, Jul. 2014.
- [14] M. S. Syed, A. R. Syed, and Y. S. Rao, "A novel seeker optimization approach for solving combined economic and emission dispatch," in *2013 International Conference on Power, Energy and Control (ICPEC)*, 2013, pp. 371–376.
- [15] A. N. Afandi, I. Fadlika, and Y. Sulistyorini, "Solution of dynamic economic dispatch considered dynamic penalty factor," in *2016 3rd Conference on Power Engineering and Renewable Energy (ICPERE)*, 2016, pp. 241–246.
- [16] F. H. Aghdam and M. T. Hagh, "Security Constrained Unit Commitment (SCUC) formulation and its solving with Modified Imperialist Competitive Algorithm (MICA)," *Journal of King Saud University - Engineering Sciences*, Aug. 2017.
- [17] L. Wu, J. Gao, Y. Wang, and R. G. Harley, "A survey of contingency analysis regarding steady state security of a power system," in *2017 North American Power Symposium (NAPS)*, 2017, pp. 1–6.
- [18] A. N. Afandi, "Weighting Factor Scenarios for Assessing the Financial Balance of Pollutant Productions and Fuel Consumptions on the Power System Operation," *Wseas Transactions On Business And Economics*, vol. 14, 2017.
- [19] D. Arengga, W. Agustin, Y. Rahmawati, S. Sendari, and A. N. Afandi, "SPEKTRA fast and smart software for renewable energy management," *IOP Conf. Ser.: Earth Environ. Sci.*, vol. 105, no. 1, p. 012077, Jan. 2018.
- [20] A. R. Bergen and D. J. Hill, "A Structure Preserving Model for Power System Stability Analysis," *IEEE Transactions on Power Apparatus and Systems*, vol. PAS-100, no. 1, pp. 25–35, Jan. 1981.
- [21] A. N. Afandi, "Thunderstorm Algorithm for Assessing Thermal Power Plants of the Integrated Power System Operation with an Environmental Requirement," *International Journal of Engineering and Technology*, vol. 8, pp. 1102–1111, Apr. 2016.
- [22] A. N. Afandi and H. Miyauchi, "Improved artificial bee colony algorithm considering harvest season for computing economic dispatch on power system," *IEEJ Trans Elec Electron Eng*, vol. 9, no. 3, pp. 251–257, May 2014.
- [23] K. Chandram, N. Subrahmanyam, and M. Sydulu, "Equal embedded algorithm for economic load dispatch problem with transmission losses," *International Journal of Electrical Power & Energy Systems*, vol. 33, no. 3, pp. 500–507, Mar. 2011.
- [24] C. C. Columbus and S. P. Simon, "A parallel ABC for security constrained economic dispatch using shared memory model," in *Controls and Computation 2012 International Conference on Power, Signals*, 2012, pp. 1–6.
- [25] B. Y. Qu, Y. S. Zhu, Y. C. Jiao, M. Y. Wu, P. N. Suganthan, and J. J. Liang, "A survey on multi-objective evolutionary algorithms for the solution of the environmental/economic dispatch problems," *Swarm and Evolutionary Computation*, Jun. 2017.
- [26] M. Zheng, X. Wang, C. J. Meinrenken, and Y. Ding, "Economic and environmental benefits of coordinating dispatch among distributed electricity storage," *Applied Energy*, vol. 210, no. Supplement C, pp. 842–855, Jan. 2018.
- [27] L. Lei and W. Shaoqiang, "An Improved Ant Colony Optimization Algorithm Using Local Pheromone and Global Pheromone Updating Rule," in *2016 International Conference on Intelligent Transportation, Big Data Smart City (ICITBS)*, 2016, pp. 63–67.
- [28] A. B. Kristoffersen, D. Jimenez, H. Viljugrein, R. Grøntvedt, A. Stien, and P. A. Jansen, "Large scale modelling of salmon lice (*Lepeophtheirus salmonis*) infection pressure based on lice monitoring data from Norwegian salmonid farms," *Epidemics*, vol. 9, pp. 31–39, Dec. 2014.
- [29] A. B. Kristoffersen, L. Qviller, K. O. Helgesen, K. W. Vollset, H. Viljugrein, and P. A. Jansen, "Quantitative risk assessment of salmon louse-induced mortality of seaward-migrating post-smolt Atlantic salmon," *Epidemics*, vol. 23, pp. 19–33, Jun. 2018.
- [30] X.-M. Shao, E. H. Lay, and A. R. Jacobson, "Reduction of electron density in the night-time lower ionosphere in response to a thunderstorm,"

- Nature Geoscience*, vol. 6, no. 1, pp. 29–33, Jan. 2013.
- [31] K. W. Vollset, B. T. Barlaup, H. Skoglund, E. S. Normann, and O. T. Skilbrei, “Salmon lice increase the age of returning Atlantic salmon,” *Biology Letters*, vol. 10, no. 1, pp. 20130896–20130896, Jan. 2014.
  - [32] R. L. Holle, “The visual identification of lightning-producing thunderstorm clouds,” in *2014 International Conference on Lightning Protection (ICLP)*, 2014, pp. 58–64.
  - [33] G. Satori *et al.*, “An Overview of Thunderstorm-Related Research on the Atmospheric Electric Field, Schumann Resonances, Sprites, and the Ionosphere at Sopron, Hungary,” *Surv Geophys*, vol. 34, no. 3, pp. 255–292, May 2013.
  - [34] A. N. Afandi, Y. Sulistyorini, G. Fujita, N. P. Khai, and N. Tutkun, “Renewable energy inclusion on economic power optimization using thunderstorm algorithm,” in *2017 4th International Conference on Electrical Engineering, Computer Science and Informatics (EECSI)*, 2017, pp. 1–6.
  - [35] S. L. Haeseker, R. M. Peterman, Z. Su, and C. C. Wood, “Retrospective Evaluation of Preseason Forecasting Models for Sockeye and Chum Salmon,” *North American Journal of Fisheries Management*, vol. 28, no. 1, pp. 12–29.
  - [36] Y. Rahmawati *et al.*, “Developing a simulator of renewable energy as a learning media of energy conversion,” *IOP Conference Series: Earth and Environmental Science*, vol. 105, p. 012079, Jan. 2018.
  - [37] K. B. Debnath and M. Mourshed, “Forecasting methods in energy planning models,” *Renewable and Sustainable Energy Reviews*, vol. 88, pp. 297–325, May 2018.
  - [38] M. EL-Shimy, N. Mostafa, A. N. Afandi, A. M. Sharaf, and M. A. Attia, “Impact of load models on the static and dynamic performances of grid-connected wind power plants: A comparative analysis,” *Mathematics and Computers in Simulation*, Feb. 2018.
  - [39] T. Sabo, “A Survey on Environmental Economic Load Dispatch using Lagrange Multiplier Method,” 2012.
  - [40] N. Ghorbani, E. Babaei, and F. Sadikoglu, “Exchange market algorithm for multi-objective economic emission dispatch and reliability,” *Procedia Computer Science*, vol. 120, pp. 633–640, 2017.
  - [41] S. Ghoshal, D. Maity, S. Banerjee, and C. K. Chanda, “Solution of multi-objective emission economic dispatch using bare bones TLBO algorithm biogeography based optimization algorithm,” in *2017 Second International Conference on Electrical, Computer and Communication Technologies (ICECCT)*, 2017, pp. 1–6.
  - [42] A. N. Afandi, “Optimal scheduling power generations using HSABC algorithm considered a new penalty factor approach,” in *The 2nd IEEE Conference on Power Engineering and Renewable Energy (ICPERE) 2014*, 2014, pp. 13–18.
  - [43] L. A. C. Roque, D. B. M. M. Fontes, and F. A. C. C. Fontes, “A multi-objective unit commitment problem combining economic and environmental criteria in a metaheuristic approach,” *Energy Procedia*, vol. 136, no. Supplement C, pp. 362–368, Oct. 2017.



# Partial Discharge and Breakdown Strength of Plasma Treated Nanosilica/LDPE Nanocomposites

N. A. Awang, M. H. Ahmad and  
Z. Abdul-Malek  
Institute of High Voltage and High  
Current,  
Faculty of Electrical Engineering  
Universiti Teknologi Malaysia  
Skudai, Johor Bahru, Malaysia  
naliaa5@live.utm.my

Z. Nawawi, M. A. B. Sidik,  
M. I. Jambak  
Department of Electrical Engineering,  
Faculty of Engineering  
Universitas Sriwijaya  
Ogan Ilir, West Sumatera, Indonesia  
nawawi\_z@yahoo.com

Aulia, E. P. Walidi  
Department of Electrical Engineering  
Andalas University  
Padang, West Sumatera, Indonesia  
aulia007@gmail.com

**Abstract**— Nanocomposites have been actively studied in recent years as an insulating material due to their excellent in electrical, mechanical and thermal properties. Even though, the addition of nanoparticles into polymer matrices showed better performance in relation to partial discharge (PD) and AC breakdown strength tests. However, the introduction of nanoparticles could lead to the formation of agglomeration of the fillers which may nullify the true capabilities of the composites. Therefore, silane coupling agent was introduced for surface functionalization treatment of the nano filler but among the issues associated are toxicity and complexity. In the present study, atmospheric pressure plasma is proposed to enhance the surface functionalization of the nano filler. This proposed method was used to treat the nanosilica ( $\text{SiO}_2$ ) surfaces to enhance the interfacial interaction between the host (LDPE) and nano filler.  $\text{SiO}_2$  nano filler was added into the LDPE at weight percentages of 1, 3 and 5%. The phase-resolved PD behaviour and Weibull analysis of AC breakdown strength of untreated and plasma-treated LDPE nanocomposites were measured to evaluate the performance of the samples. As results, the plasma treated LDPE nanocomposites experience apparent increments of the PD resistance and AC breakdown strength as compared to the untreated nanocomposites. It is implied that the plasma treatment of nanosilica has contributed to the enhancement of the filler dispersion and eventually reducing the agglomeration.

**Keywords**— Partial discharge, AC breakdown strength, atmospheric pressure plasma; nanosilica; Low Density Polyethylene.

## I. INTRODUCTION

Nowadays, polymeric insulating material for example cross-linked polyethylene has attracted much attention due to superior performances especially in power cable application. However, it is eventually subjected to the degradation processes which one of the root causes is electrical discharge. These discharge phenomenon have been considered for an insulation diagnostics and assessment [1]. This drawback of the existing insulating material has opened to a new research area called nanodielectrics. Generally, the nanodielectrics is the combination of host polymer and nanofillers to improve several physical, chemical and electrical properties such as higher PD resistance, higher breakdown strength, reduced space charge accumulation, low tangent delta and reduced permittivity [2]–[4]. Moreover, nanocomposites were controlled by the interfaces between the host polymer and the nanofiller. In addition, the interfaces determine to the surface compatibility between both polymer matrices and the nano

fillers. Many methods have been introduced to improve the surface compatibility such as silane coupling agent. This method was identified to produce toxic and inappropriate for mass production [5].

There is an alternative method namely atmospheric pressure plasma treatment method to treat the surface of the nanoparticles. This treatment method was able to enhance the interfacial bonding between the nano fillers and polymer matrices [6][7]. In this study, plasma treatment was used to modify the surface of  $\text{SiO}_2$  nanoparticles and the modified nanosilica was augmented into the LDPE polymer to produce plasma treated nanocomposites. Thus, the produced nanocomposites sample were then tested in the laboratory to investigate their PD characteristics and AC breakdown strengths. In addition, the different weight percentages of the treated nanosilica augmented into the LDPE was studied in order to find the optimum formulation. It was believed that the limitation of the existing polymer can be solved using the plasma treated nanocomposites as the solution to enhance the PD resistant insulation for high voltage application.

## II. EXPERIMENTAL

### A. Materials

Low density polyethylene (LDPE) was used as the host polymer in this study. LDPE was produced by Titan Chemical, Malaysia with a density of  $0.922 \text{ g/cm}^3$  and the melting index of 25 g/10min. Silicon dioxide ( $\text{SiO}_2$ ) was used as nanofiller was supplied by Sigma Aldrich with an average particle size of 12 nm.

### B. Plasma Treatment

A plasma chamber was designed for surface treatment of nanoparticles having a dimension of  $180 \text{ mm} \times 180 \text{ mm} \times 100 \text{ mm}$  using two circular plane stainless-steel electrodes with  $90 \text{ mm} \times 10 \text{ mm}$  in diameter. This arrangement of plasma chamber was applied the dielectric barrier discharge (DBD) concept of electrodes configuration. Both the electrodes were covered by a quartz glass material with thickness of 1mm used as DBD to avoid from flashover. The glass material provided as DBD to maintain the plasma from the occurrences of micro discharge.

A carrier gas moves between both electrodes and it was ionized to create plasma discharge. Fine wire mesh was inserted between high voltage and ground electrode in order to obtain a stable glow discharge. The gap spacing was kept

constant at 3 mm. Fig. 1 shows a schematic diagram of the setup for the plasma treatment chamber of the nanosilica nanoparticles. Helium gas with a flow rate of 1 L/min used as the working gas for discharge was supplied by Airgas Sdn. Bhd. The applied voltage between 7 to 8.5 kV<sub>rms</sub> at a frequency 50 Hz was used as a power supply to the plasma chamber. The power consumption of plasma discharge was kept constant between 3 to 15 W.

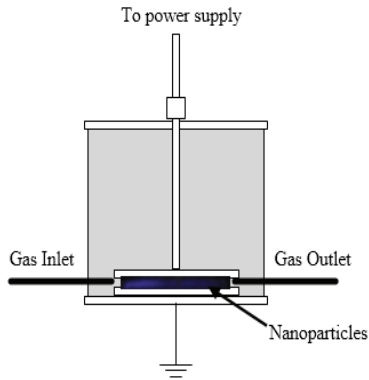


Fig. 1. Schematic diagram of a setup for plasma treatment

The occurrences of filamentary discharge during plasma treatment have been concerned in order to get a homogenous plasma treatment of nanoparticles. To obtain a homogenous and uniform plasma, the nanoparticles were first treated by the atmospheric pressure plasma for 5 minutes and then the nanoparticles were stirred for 30 seconds. This treatment process was repeated 6 times to get the total treatment time of the nanoparticles was 30 minutes [6].

### C. Sample Preparation

For the preparation of nanocomposites, the LDPE and SiO<sub>2</sub> nanofiller was weighted using Radwag, ASX 220 analytical balance to ensure that 100% of LDPE and 1wt%, 3wt% and 5wt% of the total weight of SiO<sub>2</sub>. Then, the compounding process of nanocomposites using the Brabender mixer. LDPE nanocomposites were prepared by melt mixing at 165 °C with a rotational speed of 35 rpm. The mixing time was taken for 2 minutes for each sample. Table I shows the sample code and composition of each sample.

TABLE I. CODE AND SAMPLE COMPOSITION OF EACH SAMPLE

Sample code	Composition		
	LDPE (wt%)	SiO <sub>2</sub> (wt%)	Time treatment (minutes)
A0	100	0	0
B1	100	1	0
B3	100	3	0
B5	100	5	0
C1	100	1	30
C3	100	3	30
C5	100	5	30

After that, LDPE nanocomposites sample had undergone compression process to get the thickness of 100 µm using the Carver hydraulic laboratory press at a temperature of 160 °C.

Preheating process was done in this process for 3 minutes followed by 3 minutes of compression process using 2.5 ton pressure. Table I shows the sample code and composition of each sample. Preheating process was done in this process for 3 minutes followed by 3 minutes of compression process using 2.5 ton pressure.

### D. AC Breakdown Measurements

The experimental test of AC breakdown voltage were conducted. The AC breakdown tests were conducted to observe the breakdown strength of the LDPE containing 1, 3 and 5wt% of untreated and plasma treated SiO<sub>2</sub> nanofiller. The AC breakdown test was based on the American Standard for Testing Materials (ASTM) D149. The measurements of AC breakdown voltage were performed by placing the nanocomposites sample between two 6.3 mm diameter steel ball bearing electrodes immersed in mineral oil in order to avoid from flashover. AC breakdown measurement having an AC voltage with a ramp rate voltage of 1 kV for every 20 seconds was applied to the sample until the breakdown occurred. The totals of 15 breakdown test points were measured on each sample. Fig. 2 shows the experimental setup of AC breakdown tests.

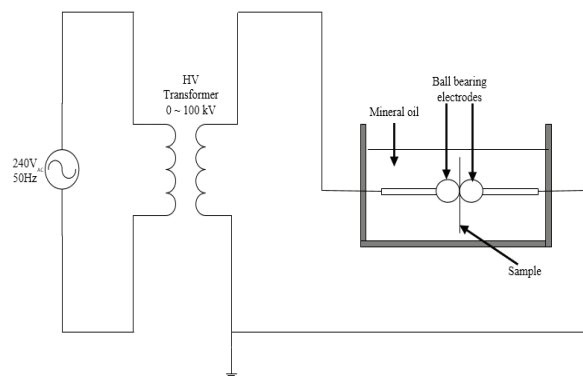


Fig. 2. Experimental setup of AC breakdown tests

### E. Partial Discharge Measurements

Fig. 3 depicts the experimental setup for partial discharge testing. CIGRE Method II test cell was used in this research work to generate PD characteristics in solid insulation. PD measurement has followed the IEC 60270: 2000 standard [8] including preparation of measurement tools as a standard of solid insulating material which stated that the AC voltage of 50 Hz power supply needed to be injected in the solid insulation. The output high voltage transformer was connected to high voltage probe with a ratio of 1:1000 volts. An oscilloscope (Model Tektronix TDS 3034B) requires in this PD setup due to the LAN communication ports availability used to connect with LabVIEW™ program. A 1 nF coupling capacitor was used as a voltage divider to make sure the voltage does not rise on the impedance of PD signals. PD data were analyzed by using a PD program which developed based on the LABVIEW™ software. The voltage was applied up to 4 kV<sub>rms</sub> for 1-hour ageing time of each sample.

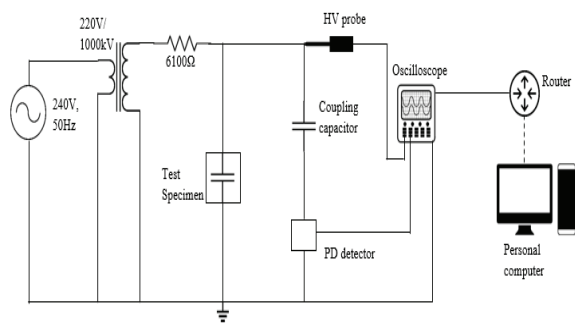


Fig. 3. Experimental setup of partial discharge measurement studies

### III. RESULT AND DISCUSSION

#### A. AC Breakdown Strength

Fig. 4 represents the summary of AC breakdown strength for LDPE containing 1wt%, 3wt% and 5wt% of untreated and plasma treated nanosilica. With the addition amount of nanosilica concentration in LDPE, the AC breakdown strength values increased for both untreated and plasma treated samples compared to pure LDPE sample which were 160.15 kV/mm, 159.78 kV/mm, and 170.71 kV/mm for B1, B3 and B5 samples respectively. For A0 sample, the AC breakdown strength was 155.47 kV/mm. However, AC breakdown strength for the B3 sample almost similar with the B1 sample; it may be caused by the agglomeration of nanofiller that exists in the polymer matrices after blending process. However, it can be clearly noticed that the AC breakdown strength of the plasma treated nanosilica was slightly higher compared to the untreated samples having results of 173.01 kV/mm, 174.70 kV/mm and 176.44 kV/mm for C1, C3 and C5 samples respectively. The highest value of AC breakdown strength was recorded for C5 sample compared to other samples.

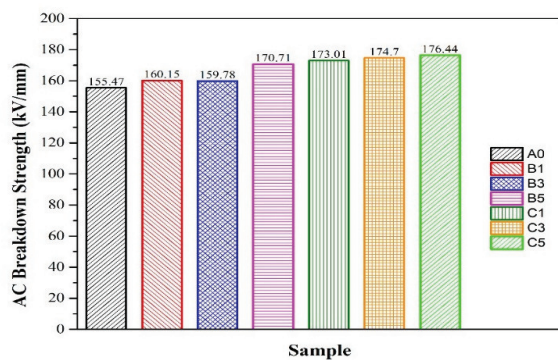


Fig. 4. Comparison of AC breakdown strength for untreated and plasma treated  $\text{SiO}_2$  nanofiller

#### B. Phase-resolved Partial Discharge Patterns

The phase-resolved partial discharge (PRPD) patterns of internal discharge using CIGRE Method II at 4 kV<sub>rms</sub> AC sinusoidal voltage are presented in Fig. 5. Each dot points represent the maximum PD magnitude of all the PD pulses that occur within the first and third quadrants of the voltage waveform. Fig. 5(a) shows the unsymmetrical PRPD pattern of the pure LDPE sample because the positive PD pulse count is higher than negative pulse count for A0 sample and it has

the highest PD magnitude was recorded up to 1800 pC. This is due to the unbalanced electric field at the LDPE nanocomposites sample surface of the positive and negative cycles during PD measurements [9][10].

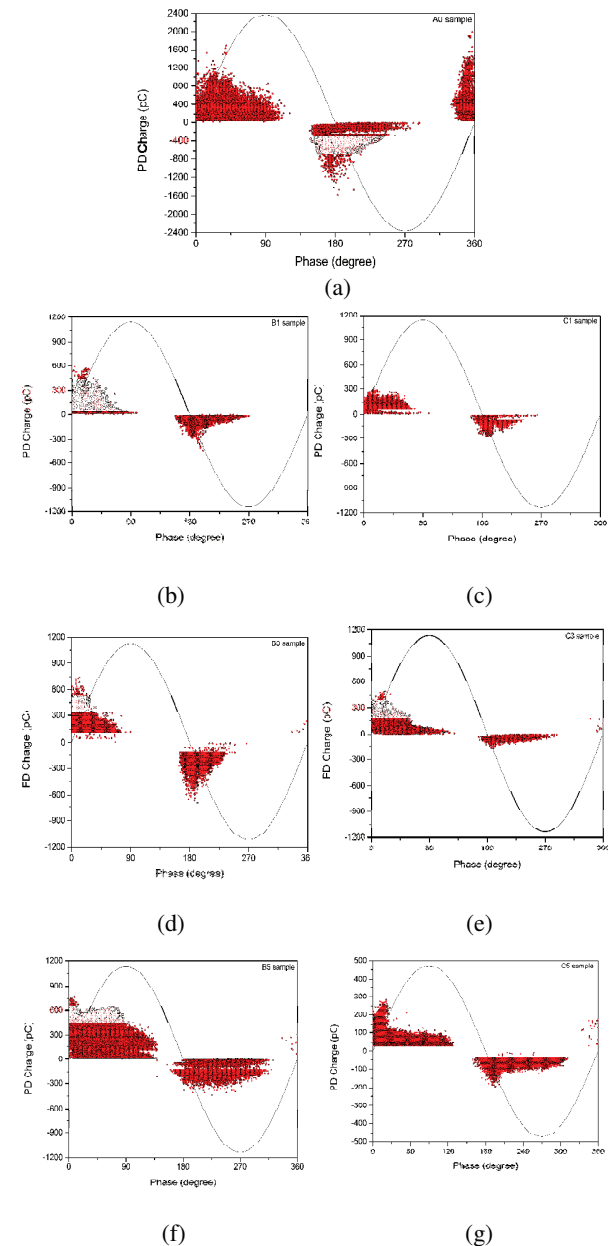


Fig. 5. PD patterns for untreated and plasma treated  $\text{SiO}_2$  nanofiller of (a) A0 (b) B1 (c) C1 (d) B3 (e) C3 (f) B5 and (g) C5 samples under 4 kV<sub>rms</sub> of applied voltage level for one hour ageing time.

In general, the samples containing treated nanosilica show better PD resistance which resulting in lower PD magnitude compared to the A0 sample. For nanocomposites containing 1 wt%, 3 wt% and 5 wt% of untreated  $\text{SiO}_2$  nanofiller into LDPE (C1, C3 and C5 samples), the PD magnitude values are 600 pC, 750 pC and 800 pC. Despite this, the PD magnitude are lower than A0 sample. However, B5 sample depicts the higher PD magnitude among B1 and B3 samples; this is due to the higher filler concentration which contributes to the

space charge trapping [11] also the formation of agglomeration in LDPE nanocomposites sample. It can be seen in Fig. 5(c) and 5(g), the plasma treated nanosilica exhibited the lower PD magnitude rather than untreated nanosilica were 300 pC, 700 pC and 300 pC for C1, C3 and C5 samples; it may be caused by the enhanced the interfacial bonding between nanofiller and polymer matrices after plasma treatment of nanosilica. Nonetheless, for the C3 sample the PD magnitude was larger than C1 and C5 sample. It may be associated with the poor dispersion of the nanosilica particles and incompatible interfaces between nanoparticles and polymer matrices which eventually led to the larger PD magnitude.

### C. Characterization of Nanoparticles

The morphological analysis of Field Emission Scanning Emission Microscope (FESEM) was carried out to analyze the filler dispersion of SiO<sub>2</sub> nanoparticles inside the host polymer and the results were depicts in Fig. 6. Observation shows that there are many severe agglomerations were found in the B5 nanocomposite sample compared to the C5 sample as marked as the red circles.

Fig. 6(b) shows the sizes of agglomeration are relatively smaller than that in the nanocomposites with the untreated SiO<sub>2</sub> nanoparticles in Fig. 6(a) which can be the reason for the improvement in AC breakdown strength and PD suppression. In general, the dispersion was improved when the nanofiller was treated with the atmospheric pressure plasma.

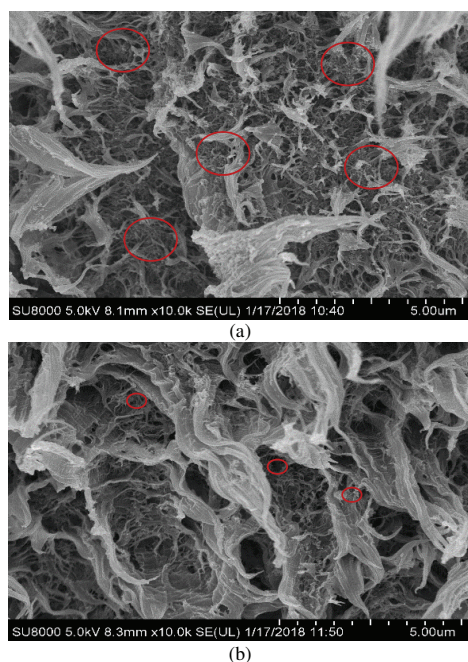


Fig. 6. FESEM images of cross-section of (a) B5 and (b) C5 nanocomposites samples

### IV. CONCLUSION

The partial discharge and AC breakdown strength characteristics of LDPE nanocomposites with different filler loading have been experimentally investigated. Outcomes from this study; the partial discharge resistance and AC breakdown strength have been improved when SiO<sub>2</sub> nanoparticles were treated with the atmospheric pressure

plasma. Higher the nanosilica concentration, higher the AC breakdown strength for both untreated and plasma treated nanocomposites. In addition, C5 sample has the highest AC breakdown strength among the samples. In addition, the PRPD pattern of C5 sample has been plotted and discussed. It showed that lower PD magnitude as compared with B5 sample. The cross-sectional FESEM images clearly showed that the treated sample has better filler dispersion as compared to untreated sample. It is implied that the plasma treatment method is appropriate to be applied in producing nanocomposites as well as improving some of the electrical properties.

### ACKNOWLEDGMENT

The authors would like to acknowledge Universitas Sriwijaya and Universiti Teknologi Malaysia for providing research grants with vote numbers; 4B340, 4B342, 13H98, 4B278 and 4B279.

### REFERENCES

- [1] F. N. Musa, N. Bashir, and M. H. Ahmad, "Electrical treeing performance of plasma-treated silicone rubber based nanocomposites," in *ICHVE 2016 - 2016 IEEE International Conference on High Voltage Engineering and Application*, 2016.
- [2] Wei Yan, B. T. Phung, Zhaojun Han, and K. Ostrikov, "Reinforced insulation properties of epoxy resin/SiO<sub>2</sub> nanocomposites by atmospheric pressure plasma modification," in *2012 IEEE International Power Modulator and High Voltage Conference (IPMHVC)*, 2012, pp. 391–394.
- [3] M. Musa, Y. Z. Arief, and M. H. Ahmad, "Influence of Nano-Titanium Dioxide (TiO<sub>2</sub>) on Electrical Tree Characteristics in Silicone Rubber Based Nanocomposite," in *In Electrical Insulation and Dielectric Phenomena (CEIDP)*, 2013, pp. 498–501.
- [4] M. Ahmad *et al.*, "A New Statistical Approach for Analysis of Tree Inception Voltage of Silicone Rubber and Epoxy Resin under AC Ramp Voltage," *Int. J. Electr. Eng. Informatics*, vol. 4, no. 1, pp. 27–39, 2012.
- [5] F. Musa, N. Bashir, M. Ahmad, Z. Buntat, and M. Piah, "Investigating the Influence of Plasma-Treated SiO<sub>2</sub> Nanofillers on the Electrical Treeing Performance of Silicone-Rubber," *Appl. Sci.*, vol. 6, no. 11, p. 348, 2016.
- [6] W. Yan and Z. Han, "Silica Nanoparticles Treated by Cold Atmospheric-Pressure Plasmas Improve the Dielectric Performance of Organic-Inorganic Nanocomposites," *ACS Appl. Mater. Interfaces*, vol. 4, pp. 2637–2642, 2012.
- [7] W. Yan, B. T. Phung, Z. J. Han, K. Ostrikov, and T. R. Blackburn, "Partial discharge characteristics of epoxy resin-based nanocomposites fabricated with atmospheric plasma treated SiO<sub>2</sub> nanoparticles," in *Proceedings of 2011 International Symposium on Electrical Insulating Materials*, 2011, pp. 353–357.
- [8] W. Hauschild and E. Lemke, *High-Voltage Test and Measuring Techniques*, 2014.
- [9] M. Z. H. Makmud, H. A. Illias, and C. Y. Chee, "Partial Discharge Behaviour within Palm Oil-based Fe<sub>2</sub>O<sub>3</sub> Nanofluids under AC Voltage," in *IOP Conference Series: Materials Science and Engineering*, 2017, vol. 210, no. 1, p. 12034.
- [10] H. Illias, Teo Soon Yuan, A. H. A. Bakar, H. Mokhlis, G. Chen, and P. L. Lewin, "Partial discharge patterns in high voltage insulation," in *2012 IEEE International Conference on Power and Energy (PECon)*, 2012, no. May 2014, pp. 750–755.
- [11] M. H. Ahmad *et al.*, "Temperature Effect on Electrical Treeing and Partial Discharge Characteristics of Silicone Rubber-Based Nanocomposites," *J. Nanomater.*, vol. 2015, pp. 1–13, 2015.



Nurhadi  
Electrical Engineering Department  
Universitas Muhammadiyah Malang  
Malang, Indonesia  
nurhadi@umm.ac.id

288

$P=0.9; V_t=1.0; E_B=1.0; f=60 \text{ Hz}$

### III. FUZZY LOGIC BASED PSS

PSS based on Fuzzy logic controller algorithm has been developed. The main objective of the proposed application was intended for stabilizing and improving the damping of the synchronous machine [4]. A speed  $\Delta\omega$  and active power deviation  $\Delta P_e$  are pointed as the controller input. The controller output is forwarded into the exciter module.

As can be seen in Fig. 2, the fuzzy-logic based PSS uses two input parameters including  $K_\omega$  and  $K_p$ , whereas the output parameter,  $K_u$ . The input parameters selection process is generally subjective which demands the previous knowledge of fuzzy control variables (input and output signal).

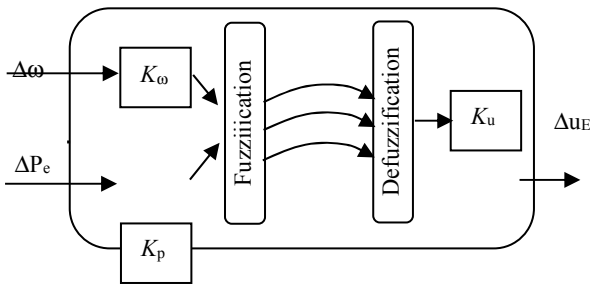


Fig. 2. Schematic diagram of the FLPSS

Using the automatic rule generation and sampled data set generated by using the conventional power system stabilizer, a proper set of rules was obtained [4]. The rule used in all the following are shown in figure 3.

		Active power						
Speed deviation		NB	NM	NS	Z	PS	PM	PB
	NB	NB	NB	NB	NB	NM	NS	Z
	NM	NB	NB	NM	NM	NS	Z	PS
	NS	NB	NM	NS	NS	Z	PS	PM
	Z	NM	NM	NS	Z	PS	PM	PM
	PS	NM	NS	Z	PS	PS	PM	PB
	PM	NS	Z	PS	PM	PM	PB	PB
	PB	Z	PS	PM	PB	PB	PB	PB

Fig. 3. FLPSS rules

### IV. PARTICLE SWARM OPTIMIZATION

In 1995, Kennedy and Eberhart became the pioneers for introducing the Particle swarm optimization (PSO) method [8]. Subsequently, the original Swarm algorithm was modified for improving the performance and adjusting to particular types of problems, the serial version has been implemented previously [9]-[11].

The following are the brief stages of optimization using the PSO algorithm [11]. Consider a swarm of  $p$  particles,

with each particle position describing the possible solution points in the space of the design problem of D. The position  $x_i$  is updated upon each of particle based on the following notation:

$$x_{k+1}^i = x_k^i + v_{k+1}^i \quad (1)$$

with a pseudo-velocity  $v_{k+1}^i$  can be calculated as follows:

$$v_{k+1}^i = \omega_k v_k^i + c_1 r_1 (p_k^i - x_k^i) + c_2 r_2 (p_k^g - x_k^i) \quad (2)$$

Here, subscript  $k$  denote a (unit) pseudo-time increment,  $p_k^i$  denotes the best position of particle  $i$  at time  $k$  (the cognitive contribution to the pseudo-velocity vector  $v_{k+1}^i$ ), while  $p_k^g$  symbolizes the best global position in the swarm at time  $k$  (social contribution).  $r_1$  and  $r_2$  denotes uniform random numbers between 0 and 1. The cognitive and social scaling parameters  $c_1$  and  $c_2$  are systematically selected such that  $c_1 = c_2 = 2$  for allowing the product  $c_1 r_1$  or  $c_2 r_2$  to have a mean of 1.

The particles overshoot the target half the time is the result of using these proposed values which maintains the separation within the group and if there is no overshoot occurred, it will allow for a greater area to be searched.

Fourie and Groenwold generated a comprehensive modification in the original PSO algorithm which permits the transition for searching another result as optimization progresses. This operator decreases the maximum allowed velocity  $v_{max}$ ,  $k$  and the particle inertia  $w_k$  in a dynamic manner, as directed by the dynamic reduction parameters  $k$ ,  $d$ ,  $\omega$ . For the sake of brevity, further details of this operator are neglected.

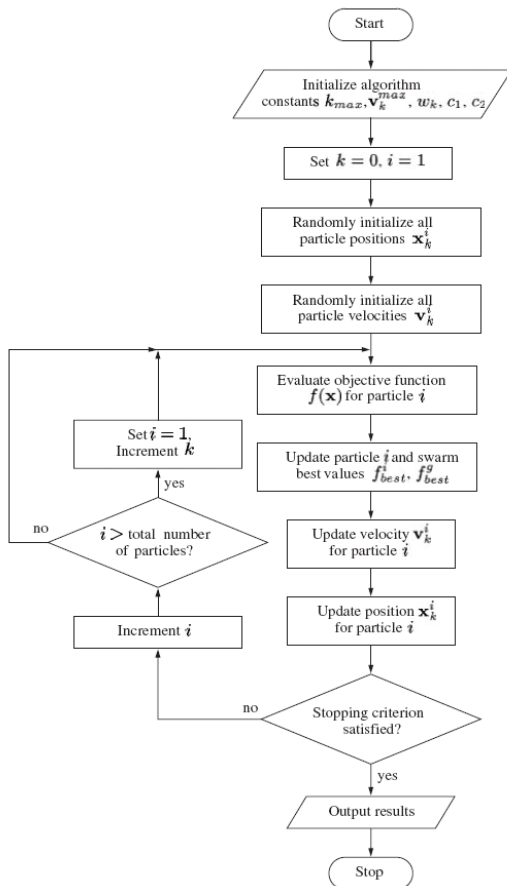
The serial PSO algorithm was performed on a single CPU computer. The total number of particles in the swarm is symbolized by the variable of  $p$ . The significant fitness value from a particular particle at design co-ordinates  $p_k^i$  is presented by  $f_{best}^i$  and the best fitness value in the overall swarm at co-ordinates  $p_k^g$  by  $f_{best}^g$ . At  $k = 0$ , the particle velocities  $v_0^i$ .  $v_0^{maks}$  has its initial value resided within the limits of  $0 \leq v_0 \leq v_0^{maks}$ . The vector  $v_0^{maks}$  is extracted from the fraction of the distance between the upper and lower bounds  $v_0^{maks} = \zeta(x_{UB} - x_{LB})$  with  $\zeta = 0.5$ . The details of PSO algorithm is expounded as follows.

#### 1. Initialize

- Set values constants  $k_{maks}$ ,  $c_1$ ,  $c_2$ ,  $k$ ,  $v_0^{maks}$ ,  $w_k$ ,  $d$ , and  $wd$
- Initialize the maximum dynamic velocity  $v_{max}$ ,  $k$  and inertia  $w_k$
- Set counters  $k = 0$ ,  $t = 0$ ,  $i = 1$ . Set random number seed
- initialize randomly particle positions  $x_{i0} \in D$  in  $R_n$  for  $i = 1, \dots, p$
- initialize randomly particle velocities  $0 \leq v_0 \leq v_0^{maks}$  for  $i = 1, \dots, p$
- Evaluate fitness values  $f_0^i$  using design space co-ordinates  $x_{i0}$  for  $i = 1, \dots, p$



- (g) Set  $f_{best}^i = f_0^i$ ,  $\mathbf{p}^i = \mathbf{x}_0^i$  for  $i = 1, \dots, p$
- (h) Set  $f_{best}^g$  to  $f_{best}^i$  and  $\mathbf{g}_0$  to corresponding  $\mathbf{x}_0^i$
- 2. Optimize
  - (a) Update the particle of velocity vector  $\mathbf{v}_{k+1}^i$  using Equation (2)
  - (b) Update the particle of position vector  $\mathbf{x}_{k+1}^i$  using Equation (1)
  - (c) Update the maximum dynamic velocity  $\mathbf{v}_k^{maks}$  and inertia  $w_k$
  - (d) Evaluate the fitness value  $f_k^i$  using design space co-ordinates  $\mathbf{x}_k^i$
  - (e) if  $f_k^i \leq f_{best}^i$ , then  $f_{best}^i = f_k^i$ ,  $\mathbf{p}^i = \mathbf{x}_k^i$
  - (f) if  $f_k^i \leq f_{best}^g$  then  $f_{best}^g = f_k^i$ ,  $\mathbf{p}^g = \mathbf{x}_k^i$
  - (g) if  $f_{best}^g$  best was improved in (e) then reset  $t = 0$ . Else increment  $t$
  - (h) if  $k > k_{maks}$  go to 3
  - (i) if  $t=d$  then multiply  $w_{k+1}$  by  $(1-w_d)$  and  $\mathbf{v}_{k+1}^{maks}$  by  $(1-v_d)$
  - (j) If stopping condition is fulfilled, then moves to 3
  - (k) Increment  $i$ , if  $i > p$  then increment  $k$ , and set  $i = 1$
  - (l) Go to 2(a)
- 3. Report results
- 4. Terminate

Fig. 4. Serial PSO implementation<sup>11</sup>

#### IV. SIMULATION RESULT

In order to analyze the capability of the PSS method for improving the power system's stability, under small perturbation and large perturbation, the dynamic performance of it was analyzed. The performance of the fuzzy logic-based PSS was thoroughly analyzed for comprehending its capacity with the CPSS method using optimized parameters generated from the phase of compensation technique.

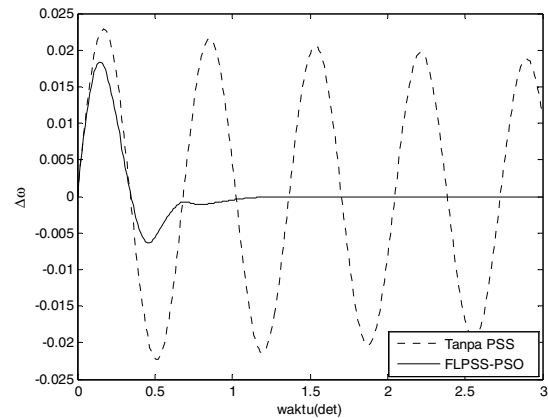
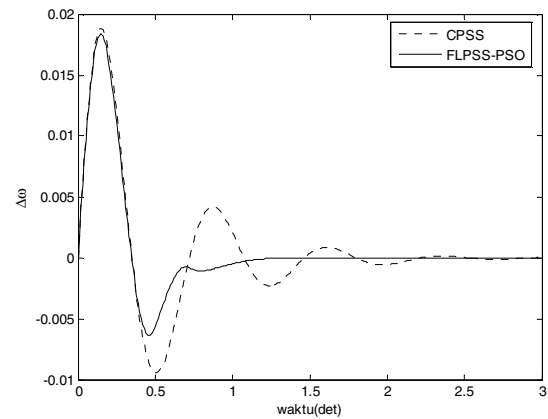
During the nominal operating condition, A small perturbation of step increase in mechanical torque was established. The dynamic responses of the proposed PSS were comparatively analyzed with the CPSS. The proposed PSS generated lower peak over-shoots and damped out low frequency oscillations vastly compared to the CPSS approach which depicted in Fig. 5 and 6. The proposed PSS has a better damped response in overall.

FLPSS tuned PSO with the review of the optimal parameters:

$$Kp = 1,4120 \quad Kw = 0,9592 \quad Ku = 7,5346$$

show results very fast reduction as shown in the figure 5.

When compared between FLPSS and CPSS will have the ability to reduce low frequency oscillations more quickly. It as shown in Figure 6.

Fig. 5. Response to input torque  $\Delta T_m = 1$  puFig. 6. Response to input torque  $\Delta T_m = 1$  pu with Conventional PSS and FLPSS-PSO

The simulation results have shown that the fuzzy logic

controller PSS tuned proposed PSO can be an alternative to dealing with electric power system oscillations. This is shown on the attenuation performed by the controller compared to a system without PSS and PSS with conventional tuned. Selection K and KP through PSO to 30 operations at PSS Fuzzy controller based on input power and speed deviation will produce varying oscillation damping.

## VII. CONCLUSION

The proposed design of optimal PSS controller based on fuzzy showed an effective results and optimal damping so that PSS could become be a stabilizer to handle damping oscillations in electrical power systems. PSS is using Fuzzy controller parameters  $K_p$ ,  $K_\omega$  and  $K_u$  performed using PSO with the fitness function in the form of index performance. Indeed, through this election actually can produce oscillation damping speed deviation highly effective and optimal. The simulation results of the electric power system of single-rail engine has demonstrated the ability infinite optimal stabilizer for damping low frequency oscillations and become an alternative stabilizer.

## REFERENCES

- [1]. Prabha Kundur. (1994). "Power System Stability and Control". McGraw-Hill, New York, Ch.12. pp.817-822.
- [2]. Padiyar, (2008), "Power System Dynamics Stability and Control", BISA Publications, Hyderabad, Ch.8. pp 257-294.
- [3]. Larsen and D. A. Swann. (1981). "Applying Power System Stabilizers". Part I- III, *IEEE Trans. PAS* Vol. 100. no 6. pp 3017-3046.
- [4]. Ruhua You, Hassan J.E, and M. Hasyem N (2002). "An Online Adaptive Neuro-Fuzzy Power System Stabilizer for Multimachine System", *IEEE Transaction On Power System* Vol-18, Febuary,
- [5]. El-Hawary. M. (1998), *Electric Power Applications of Fuzzy Systems*, IEEE Press, New York.
- [6]. Tang K. S., Kim Fung Man, Guanrong Chen, and Sam Kwong. 2001, "An Optimal Fuzzy PID Controller", *IEEE Transactions On Industrial Electronics*, Vol. 48, No. 4, August 2001.
- [7]. J. Kennedy, R. Eberhart. (1995). "Particle swarm optimization," *Proc. IEEE Intl. Conf. Neural Networks*. 4, Nov/Dec . pp 1942 –1948.
- [8]. Ali T. Al-Awami etc, (2005). "Simultaneous Stabilization Of Power Systems Equipped With Unified Power Flow Controller Using Particle Swarm", *15th PSCC*, Liege, 22-26 August 2005
- [9]. Jun-Yi Cao and Bing-Gang Cao. (2006) "Design of Fractional Order Controller Based on Particle Swarm Optimization", *International Journal of Control, Automation, and Systems*. vol. 4, no. 6, pp. 775-781, December.
- [10]. Jaco F. Schuttler. (2005). "Evaluation of a Particle Swarm Algorithm For Biomechanical Optimization", *Journal of Biomechanical Engineering* June, Vol. 127 /465.

# A Design of Coreless Permanent Magnet Axial Flux Generator for Low Speed Wind Turbine

Abdul Aziz Yusuf  
Electrical Engineering  
University of Muhammadiyah Malang  
Malang, Indonesia  
[abdulaziz.yusufumm@gmail.com](mailto:abdulaziz.yusufumm@gmail.com)

M. Irfan  
Electrical Engineering  
University of Muhammadiyah Malang  
Malang, Indonesia  
[irfan@umm.ac.id](mailto:irfan@umm.ac.id)

M. Fattahur Razzaq  
Electrical Engineering  
University of Muhammadiyah Malang  
Malang, Indonesia  
[razzaqfattahur@gmail.com](mailto:razzaqfattahur@gmail.com)

**Abstract** – Most of the available generators in the market are a high speed induction generator which requires high rotational speed and electricity to generate a magnetic field. However, there are very few low-speed generators that exist in the market that available for small energy resources. This paper aims to design and simulate a Coreless Permanent Magnet Axial Flux Generator (PMAFG) for low speed wind turbine. An axial flux generator was designed to have a low speed rotation using a permanent magnet of the type Neodymium Iron Boron (NdFeB). The model was examined with excel to data analyzed. Coreless PMAFG is a generator that is enabled to turn on energy at low speeds. The chosen model was Double Rotor – Single Stator (12 Slots 8 Poles) using Infolytica Magnet software. Finite Element Method (FEM) was employed to analyze the phenomena of the magnetic flux. The test was simulated using static rotation method, which rotated every 3 degrees at 350 rpm with 100 turns and 10, 30, 50, 80 and 100 Ohm of load variations. Compare to the calculation of the design, results of the simulation in terms of voltage, current, power and efficiency had been met with only very small errors.

**Keywords** – low speed generator, double rotor – single stator, NdFeB magnet, finite element method, static rotation.

## I. INTRODUCTION

Wind power plant is a renewable energy source that has not received enough attention from the government. This departs from the understanding of the people who think that Indonesia does not have an adequate wind speed. Indeed, in general the territory of Indonesia has a relatively small potential because it is located on the equator. Even so, in Indonesia there are still areas that have the potential to be built wind power plants, which is a *nozzle effect* area or narrowing between two islands or mountain slopes between which the mountains are close together, including Java, southern and northern Sulawesi, most of the NTT regions, some of the Maluku Islands and Papua with an average wind speed reaching 6 m/s [1].

Wind power plants have construction that is quite unique and has its own aesthetics compared to other power plants, where the construction of wind turbines has four types of components is blades, generators, controllers and data loggers. In this study, focus on generator design and modeling. The most widely available electric generators on the market are high speed radial flux types, where this generator requires gear box transmission to get high speed and also needs the help of supplying the initial electrical energy or excitation voltage to bring up the magnetic field. In addition, most or more than 90% of wind turbines in the world use slip-ring generators that have disadvantages, including: additional costs for slip rings and brush maintenance [2].

Research conducted by Margana for charging 12 volt accumulators, where the generator rotates at a speed of 375 rpm produces a current of 0.11 ampere and a voltage of 11.45 volt. Meanwhile, in the research of Arif Nurhadi, ST, regarding permanent magnet generators 3-phase axial flux that use Fe type permanent magnets rotating at speeds of 100 to 700 rpm produced an AC voltage of 2.7 volts to 33.33 volts. The faster of rotor rotates, the greater the voltage generated [3].

As an alternative solution for that problems, we chose a generator that was easy to make and could be applied at low speeds is the flux axial generator. This flux axial generator use a neodymium iron boron NdFeB type permanent magnet that a rotates at low speed. Flux axial generators are a type of synchronous generator other than the radial flux cylinder type. This generator has a compact construction, disk-shaped and large power density, making it possible to rotate constantly and be able to produce high enough output values at low speed. Based on the simulation of the permanent magnet generator axial flux 12S8P, the generator rotates at a speed of 350 rpm, produces a voltage of 12.8 volts and a current of 45 ampere after being given a load of 10-100 Ohm, by speeds every 3 degrees as far as 120 degrees rounds.

The use of a permanent magnet on this flux axial generator, in order to produce a magnetic field in the air gap without requiring an excitation system for external power. In this type of generator the self reinforcement system is used, this generator rotates at a speed of 100-1000 rpm using 12 pairs of coils and 16 pairs of magnets, called the 12S8P axial flux generator. Seeing from the construction that is simple and efficient in use, a permanent magnet generator is one alternative solution for the process of generating electricity [4].

In the process of converting mechanical into electricity energy, a rotor is needed to drive the energy conversion process. In the rotor there is a magnet that has advantages in its use, that is there is no electrical energy absorbed by the magnetic field system so that there is no loss of electrical energy, which means it can increase the efficiency of the generator. In addition, it can produce a greater torque value than using electromagnets. Another advantage is that it has a greater magnetic flux density than using a non-permanent magnet, and further simplifies construction and maintenance.

## II. RESEARCH METHOD

An analytical design method will be describe in this section. The permanent magnet type used in this project is Neodymium Iron Boron (NdFeB). The design aimed to

determine an initial rotor and stator, coil model and air gap model. In this study the generator designed based on Finite Element Method (FEM) with Infolytica MagNet software. First step to get rename and determine the material used in the generator is initialization and geometry design. It also provide thickness measurement in each part. By these thread, the model can be simulated as well, it covers an important generator components. They are consists of geometry design of stator, rotor, coil, magnet also the both of air gap in rotor and stator [5]. The initialized geometry design of coreless generator permanent magnet of axial flux can be see in figure 1.

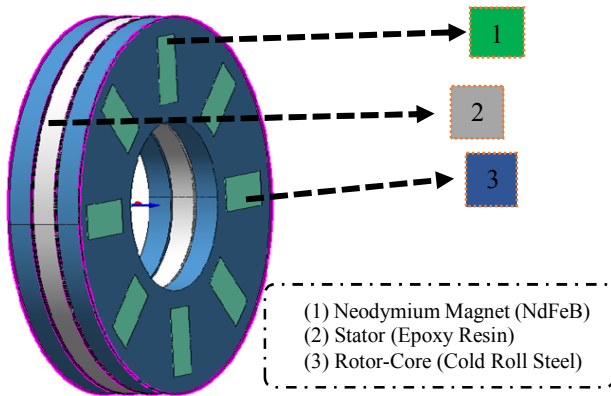


Figure 1. Stator and Rotor Geometry Design GPMAG with MagNet Infolytica Software

We have seen that a torque is generated when a current flows into the motor. In order to understand the relationship between the motor terminal voltage and the current and hereby how there rotational speed is determined, we have to know how electrical power is generated inside the motor, as well as Fleming right-hand rule and the back-emf constant.

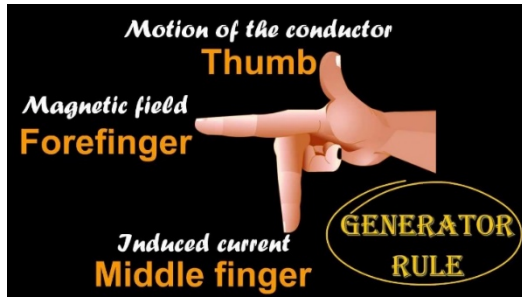


Figure 2. Fleming Right-Hand Rule

As illustrated in figure 2 have the fundamental rules of coreless PMAFG a force works on the conductor, and moves it a speed  $\phi$  to the left. The conductor is moved by the action of the magnetic field and the current. Since the conductor now passes trough the magnetic field a electromotive force  $E$  is generated in the conductor. The magnitude of the force is :

$$E = v B L \quad (1)$$

The directions is determined by Fleming's right-hand rule. Those are the directions in which the electrical power is generated opposite to the direction of the current, so as to oppose it's flow [6].

After to know of fundamental rules it, the coreless PMAFG have a main dimension of a double rotor-singlestator 12 Slots-8 Poles can be determined using the following assumptions :

- Determined the assumptions of outer and inner diameter PMAFG.
- Number of slots-poles, voltage, frequency and speed generator.
- The generator load are known.
- The number of turns per phase per one stator is  $N1$
- The phase stator current in one stator winding is show  $Ia$ .
- The back-EMF (Electromotive Forces) for per-phase and per-one stator windings is show  $Ef$ .

Rules of breakdown for step that above given through to determined assumptions of outer and inner generator, where  $Dout$  is the outer diameter,  $Din$  is the inner diameter of the stator core and  $Kd = Din / Dout$ , if look for  $Kd$  is :

$$Kd = \frac{Rin}{Rout} = \frac{Din}{Dout} \quad (2)$$

After to knowed of the diameter geometry coreless PMAFG, now to discover main important subject of it, which is the number of slots-poles, voltage, frequency and speed of generator, where are the number of poles is  $2p = 16$  pairs and assuming  $kd = Din / Dout = 1/\sqrt{3}$ , and the parameter  $Kd$  available for those previous explanation:

$$kD = \frac{1}{16} \times \left(1 + \frac{1}{\sqrt{3}}\right) \left(1 + \frac{1}{\sqrt{3}}\right)^2 \quad (3)$$

The phase current of serries connected non-overlapping stator windings is:

$$Ia = \frac{Pout}{m1(2V1) \eta \cos \phi} \quad (4)$$

In additions, the number of stator turns per phase and per slots stator are calculated on the basis of line current density with according to eqn below:

$$N1 = \frac{\pi Dout(1+Kd)Am}{4m1\sqrt{2}Ia} \quad (5)$$

Meanwhile, after found the variable related for below should determind value of back-EMF (Electromotive Force) to have generated other variable value. The EMF induced in the stator winding by the rotor excitation system, for according to eqns [7]:

$$Ef = \sqrt{2} nsp N1 kw1 \phi f = \frac{\pi}{4} \sqrt{2} ns N1 Kw1 Bmg D^2 out (1 - k^2 d) \quad (6)$$

While the finite element or mesh is set to 3 mm for the following parts, the are middle stator, double side rotor and magnet. Other than an initial mesh for double side rotor and stator air gap are set to 0.25 mm respectively. In this study, Coreless Generator Axial Flux has design with detail specification. Table 1 shows the design variable of it:

Table 1. The Variable Designs of Coreless Generator

Permanent Magnet Axial Flux	
Design Variable	Initials Value
Magnetic poles	16 Pairs
Magnetic type	Iron Boron NdFeB
Diameter of generator	220 mm
Copper wire diameter	0.8 mm
Number of turns	100 turns
Rotor materials	CR10: Cold Roll 1010 steel
Stator materials	Epoxy resin
Distance air gap rotor and stator	0.25 mm
Number of stator slots	12 Slots
Coil materials	Copper: $5.77e7$ Siemens

### III. RESULT AND ANALYSIS

Figure 3 showed the result of flux linkage GMPAF 12 Slots 8 Poles based on simulation respectively. Flux linkage is a flux that is connected or flowing from rotor to the stator or reverse it. Flux linkage value is to determine the voltage produce by the generator. While each coil voltage is the voltage generated by each coil, in other words it is the voltage of each phase [8].

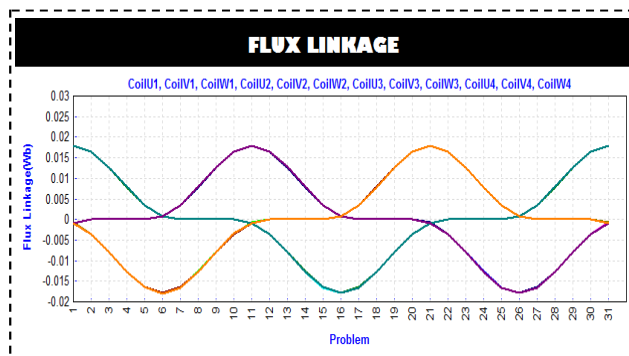


Figure 3. Results Graph of Flux Linkage GMPAF 12 Slots 8 Poles in Infolytica MagNet Software

The picture below is figure 4 showed the result of voltage line to line relations based on simulation respectively. The voltage has appearances of effect rotations of the rotor to arounded stator. Voltage value is to determine of the flux linkage produce by the rotation rotor. While each coil voltage is the voltage generated by each coil, in other words it is the voltage of each phase. The graph it shows the result of voltage per 3 degrees and average voltage

generator permanent magnet axial flux 12 slots 8 poles.

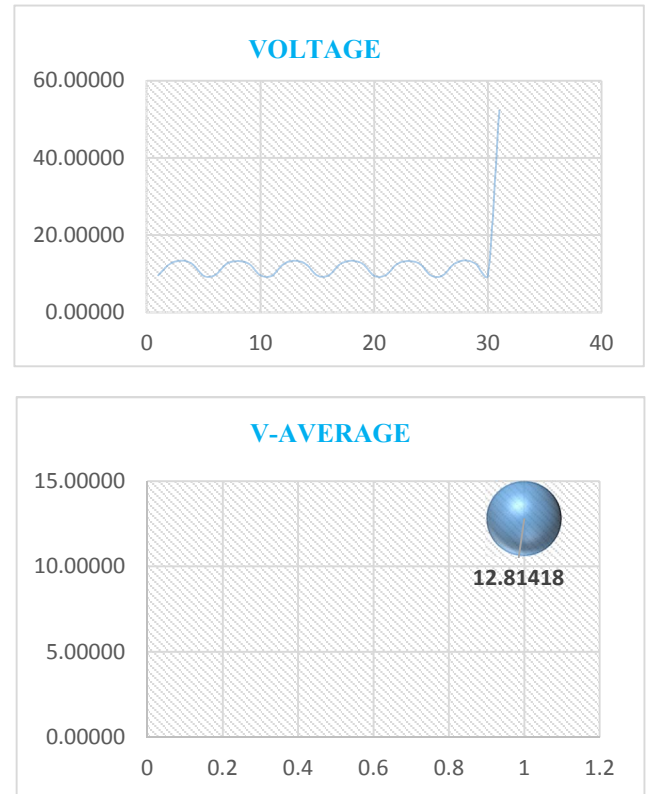


Figure 4. Results Graph of Voltage Line to Line and Point of Voltage-Average Coreless GMPAF 12 Slots 8 Poles

In the figure 5 showed that the output power generated come from the output voltage multiplied by the root of two then divided by the load. The loads assigned to this axial generator is diverse which is (10, 30, 50, 80 and 100  $\Omega$ ). The power generated at each load, then average so that obtained concrete results on each loaded. It's better understand the results of each output power, it is expressed as percent, where (10  $\Omega$  = 57 % ; 30  $\Omega$  = 19 % ; 50  $\Omega$  = 11 % ; 80  $\Omega$  = 7 % ; 100  $\Omega$  = 6 %). From the results of those data seen, the smallest load value is 10  $\Omega$  to got the greatest power, while the largest load is 100  $\Omega$  got the least power. So it can be concluded that, the smallest load of the output power is generated by higher generator, and greatest load gived when the power output by generator is smaller.

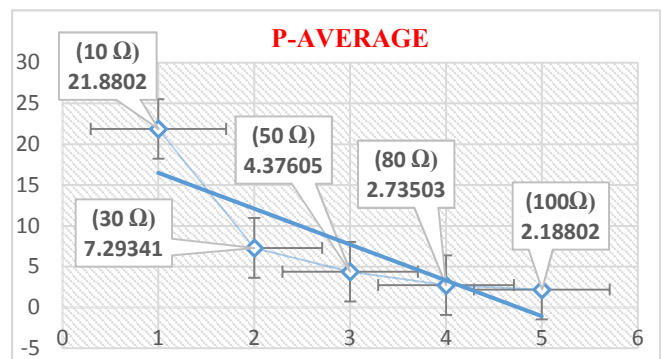


Figure 5. Graph of Output-Power Coreless GMPAF 12 Slots 8 Poles



As for figure 6 below shows that the output current generated come from the output voltage divided by loads. The loads assigned to this axial generator is diverse which is (10, 30, 50, 80 and 100  $\Omega$ ). The current generated at each load then x average so that obtained concrete results on each loaded. It's better understand the results of each current output, it is expressed as percent where (10  $\Omega$  = 57 % ; 30  $\Omega$  = 19 % ; 50  $\Omega$  = 11 % ; 80  $\Omega$  = 7 % ; 100  $\Omega$  = 6 %). From the results of those data seen, the smallest current value is 10  $\Omega$  to got the greatest current, while the largest current is 100  $\Omega$  got the least current. So it can be concluded that the smallest current output is generated by higher of generator, and greatest current gived when the current output by generator is smaller.

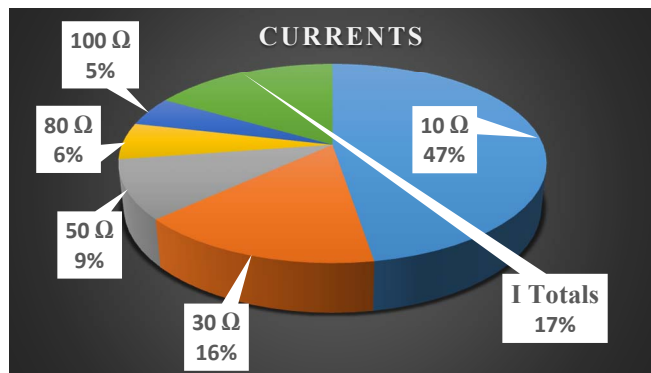


Figure 6. Results Graph of Current-Average with Loads (10, 30, 50, 80 and 100  $\Omega$ )

The next picture there is an efficiency which is, the ability of generator to generates electricity, which is obtained from the output power divided by the input power generator. This is an axial generator has various efficiencies obtained in loads variations is (10, 30, 50, 80 and 100  $\Omega$ ).

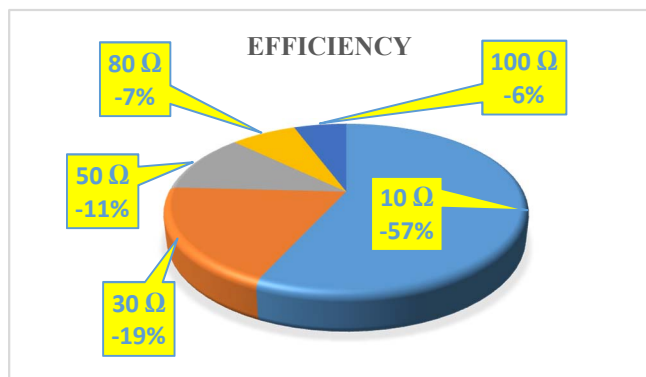


Figure 7. Graph of Efficiencies with Loads Variation (10, 30, 50, 80 and 100 Ohm)

#### IV. CONCLUSION

An analytical design and simulation is presented in this study. It has been provided a low speed electric coreless PMAFG that suitable for low speed wind turbine application. In term of accuracy of simulation and generator construction, the magnet type of Neodymium Iron Boron (NdFeB) and other variables are mentioned (generator diameter, number of turns, poles of magnet and etc) are considered.

This study is a variation speed of generator for rotation per minutes (Rpm) and much turns of coil also be simulated. Advantages of the desain have been result much more better than previous research wich is, Margana for charging 12 volt accumulators, where the generator rotates at a speed of 375 rpm produces a current of 0.11 ampere and a voltage of 11.45 volt, whole this model of coreless PMAFG had been produces a voltage of 12.8 volts and a current of 45 ampere after being given a load of 10 - 100 Ohm. These got generates result of voltage, current, power and efficiency. When voltage be appeared got an affect of rotor rotation has toward induction for stator that have it. Furthermore, since power showed those have a loads generator and the last got a current those the division for both of it. Furthermore, the efficiency of coreless PMFAG could be appeared from divided of power input and output generator.

#### ACKNOWLEDGEMENTS

The authors wishes to express their gratitude and appreciation to God, Parents and Major of Electrical Engineering University of Muhammadiyah Malang for providing facilities, support for this work and hopefully can be useful it.

#### REFERENCES

- [1] Kecil Lentera, "Potensi Angin Sebagai Pembangkit Listrik Tenaga Bayu (PLTB)".
- [2] Rahmat Hamidi M, "Potensi Pengembangan PLTB di Indonesia", Sekretariat Kabinet Republik Indonesia, 18 Juli 2018.
- [3] Jati Waluyo Dimas, Sukmadi Tejo, Karnoto. "Perancangan Generator Fluks Aksial Putaran Rendah Magnet Permanen Neodymium (NdFeB) Dengan Variasi Celah Udara".
- [4] (Hari Prasetijo, Sugeng Waluyo, 2015).
- [5] Irfan M, AH Ermanu, Suhardi Diding, Kasan Nur, Effendy Machmud, Pakaya Ilham, Faruq Amrul. "A Design of Electrical Permanent Magnet Generator for Rural Area Wind Power Plant". In: International Journal of Power Electronics and Drive System (IJPEDS).
- [6] T. Kenjo and S. Nagamori, "Permanent Magnet and Brussless DC Motor". Oxford University Press, 1985.
- [7] Gieras F. Jacek, Wang Rong-Jie, Kamper J. Maarten. "Axial Fux Permanent Magnet Brushless Machines". Kluwer Academic Publishers, New York, Boston, Dordrecht, London, Moscow.
- [8] Chapman, S.J, Induction Motors, "Electric Machinery Fundamental 4". (2012).





# Design of Hybrid System Power Management Based Operational Control System to Meet Load Demand

Nurhadi Nurhadi

Electrical Engineering Department  
University of Muhammadiyah Malang  
Malang, Indonesia  
nurhadi@umm.ac.id

Fachmy Faizal

Electrical Engineering Department  
University of Muhammadiyah Malang  
Malang, Indonesia  
fachmyfaizalp@gmail.com

Zulfatman Has

Electrical Engineering Department  
University of Muhammadiyah Malang  
Malang, Indonesia  
zulfatman@umm.ac.id

**Abstract**— Renewable energy is unlimited sources of energy such as wind, solar, water, etc., which can be employed as unlimited resources of renewable power plants. However, the difficulty of being raised, due instability of the renewable energy resources (RER) that may increase their generation costs, etc. This study presents a design of power management of a hybrid system based on operational control system due to load demand. In this study, power management of hybrid system used 3 renewable energy power plants that are photovoltaic (PV), wind power (WP), and microhydro power plant (MHPP). While battery is employed as storage system. Main focus of the work is to determine the activation of each plant using Artificial Neural Network (ANN) method to fulfill the load demand. Matlab Simulink is employed to developed and simulate the ANN on the system. From results of the simulation can be concluded that ANN can reach target accuracy level in 80%. However, when interconnecting the entire plant, the ANN experienced a misreading due to the voltage drop in each generator that affected the ANN input.

**Keywords**— energy management, hybrid system, artificial neural network, operational control system, load demand

## I. INTRODUCTION

Renewable energy (RE) is unlimited sources of energy such as wind, solar, water, etc., which can be employed as unlimited resources of renewable power plants. This power plant has advantages such as low pollution, low operational costs and abundant resources, but also has disadvantages such as generous cost generation, difficult to generate due to the non-constant renewable energy resource (RER). Thanks to its superiority, research on the RE field is essential for future energy resources.

Photovoltaic (PV) or solar power plants have advantages such as abundant solar energy resources and low maintenance costs, but have disadvantages such as the irradiation of the sun. Wind Power or wind power plants (WP) also have advantages such as wind resources are abundant and environmentally friendly. As with PV, WP also has a disadvantage due to wind resources that are not constant. To overcome the non-constant input, it can be used Micro Hydro Power Plant (MHPP) as auxiliary power plant with additional battery as storage.

RER integration such as PV systems with diesel generators in hybrid power systems is widespread throughout the world thanks to its economic and technical aspects [1]. Lots of research on operational hybrid control system to optimize the power generated. Yusof and Ahmad use Fuzzy logic to optimize battery usage based on state of charge (SOC) in order to back up the system when there is a lack of energy in PV and WP [2]. Trifkovic examined power management using 5 core components (PV, wind

turbine, electrolyze, water storage and fuel cell) using predictive control model [3]. While Dufo-Lopez *et al.* [4] was trying to minimize costs by adding batteries. Other study also discussed about hybrid method wind power and solar generations [5],[6], [7], [8]. Another study was about hybrid system for PV and diesel generation [9]. However, most of those researchers discussed about RERs with relatively constant sources.

In order to overcome some problems that caused by various value of RER, artificial intelligence method can be employed in order to analyze and predict the RER changes. Thus, the output from the plant will be more efficient and can cover load demand. Therefore, the method of Artificial Neural Network (ANN) is needed because this method can analyze and predict the changes that occur in RER using thoughts that approximate human thinking. Thus, the operational problems of these plants can be overcome.

Thus, the purpose of this study is to design a hybrid power management system for PV, WP, and MHPP based on operational control system to meet load demand using ANN. Hopefully, this system can streamline output from the hybrid power plant.

## II. METHOD

The modeling system here aims to model each plant in order to operate in accordance with the intended objectives of the researcher. In general, diagram block of the whole system is expressed as in Fig. 1.

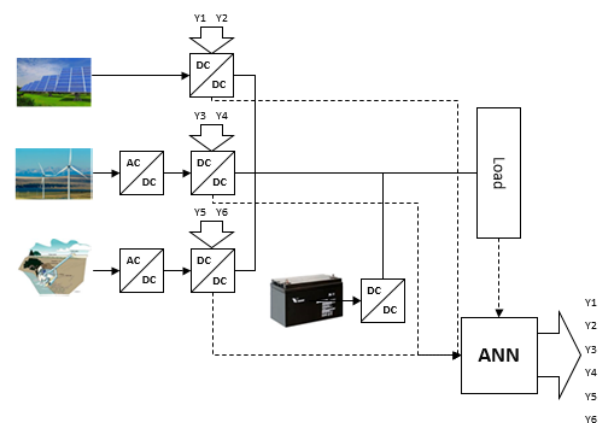


Fig. 1. Block Diagram of Hybrid system

### A. Converter Model

In this study, there are two converters employed namely Boost Converter and Buck Converter as can be seen in Fig. 1. The boost converter is formulated as follows:

$$V_{out} = \frac{V_{in}}{1-D} \quad (1)$$

$$L_{min} = \frac{(1-D)^2 * D * R}{2 * f} \quad (2)$$

$$C_{min} = \frac{D * V_{out}}{V_r * R * f} \quad (3)$$

While the buck converter using the following formula:

$$D = \frac{V_{out}}{V_{in}} \quad (4)$$

$$L_{min} = \frac{(1-D)^2 * R}{2 * f} \quad (5)$$

$$C_{min} = \frac{(1-D) * V_{out}}{8 * V_r * L * f^2} \quad (6)$$

where:

$V_{out}$  = Output voltage (V)  
 $V_{in}$  = Input voltage (V)  
 $D$  = Duty Cycle (%)  
 $L_{min}$  = Minimum Inductor Value (H)  
 $C_{min}$  = Minimal Capacitor Value (F)  
 $R$  = Resistor Value ( $\Omega$ )  
 $f$  = Switching frequency (Hz)  
 $V_r$  = Voltage ripple (V)

### B. PV System Model

The PV system model is provided by Matlab PV Array in Fig. 2 with the following specifications:

Fig. 2: PV Array Parameters

### C. WP System Model

The wind power system is described by the following formula:

$$P_m = C_p \left( \frac{1}{2} \rho A V^3 \right) \quad (7)$$

$$T_r = \frac{C_p \left( \frac{1}{2} \rho A V^3 \right)}{\omega_R} \quad (8)$$

where:

$P_m$  = Turbin Power (Watt)  
 $C_p$  = Power Coefficient  
 $\rho$  = Air Density (kg / m)  
 $A$  = Turbine sectional area (m2)  
 $V$  = Wind Speed (m / s)  
 $T_r$  = orque wind turbine (Nm)  
 $\omega_R$  = Wind turbine rotation speed (rad / s)

### D. MHPP System Model

In MHPP modeling, the model is made simpler to reduce the complexity by using synchronous generator. Fig. 3 and Fig. 4 below are the MHPP system model and parameters in Matlab Simulink [10].

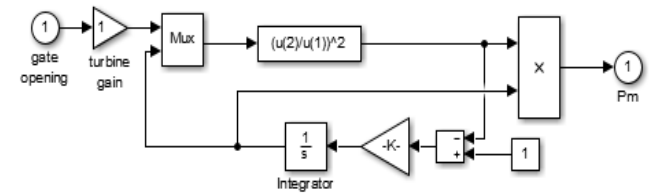


Fig. 3. MHPP Generator Modeling

Fig. 4. Synchronous Generator Parameters

### E. ANN Design

In order to design ANN, there are 2 things to be considered, those are the data training and the data test. The data training is used to determine the weight value required by ANN, while the data test is used to validate the ANN output with the desired target. The following steps are the process of designing the ANN in Matlab Simulink:

#### 1. Specify ANN input variable

The ANN model consists of 8 types of inputs: Time, V PV, P PV, V Wind, P Wind, V PLTMH, P PLTMH, and Load. V PV is PV voltage, P PV is PV power, V Wind is WP voltage, P Wind is WP power, V PLTMH is MHPP voltage, P PLTMH is MHPP power, and Load is load power. In Fig. 5 below presents the ANN structure with 8 inputs, 5 nodes of single layer, and 6 outputs, in which each input serves to regulate the output of the generator.

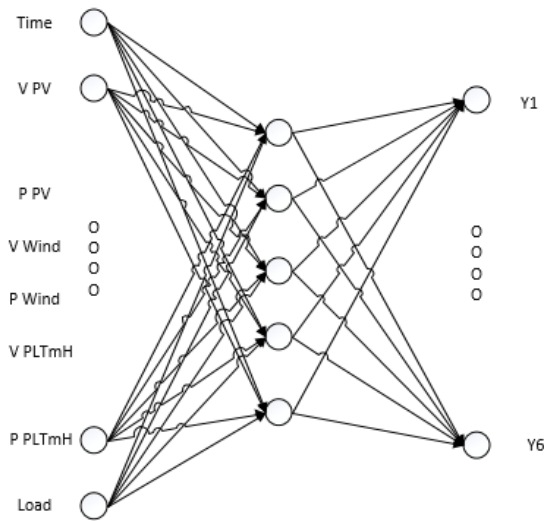


Fig. 5. ANN structure

## 2. Data Normalization

After getting data from the desired variable, the next step is to normalize the data. Normalization of the data is done by using the formula:

$$X' = \frac{0.8 * (X - b)}{(a - b)} + 0.1 \quad (9)$$

where:  $X'$ : Normalized Result Data  
 $X$ : Original data / initial data  
 $A$ : Maximum value of original data  
 $B$ : Minimum value of original data

## 3. ANN Training

After normalizing the data, the next step is to train the ANN using the normalized results data. After training the ANN, the ANN modeling is obtained.

## 4. After obtaining the ANN modeling from Matlab, the next step is to test and to compare the ANN output with the target during training.

## III. RESULTS AND DISCUSSION

In order to simulate the design maximum power value of generators must be defined. TABLE 1 shows the maximum power value of each generator created. In the PV system, there are 40 panels worth 350W that are arranged in parallel and series (8x4). The WP has a maximum power of 25 KW at a wind speed of 12m/s. while the MHPP runs constantly to power 50KW.

TABLE 1: Power Configuration

Configuration	Total Power	Note
PV	13,2 KW	in 1000w/m <sup>2</sup>
Wind Power	25 KW	in 12m/s
Micro Hydro	50 KW	Constant
Battery	12 KW	-

TABLE II: Target Output of ANN

No	PV Out	PV Charge	Wind Out	Wind Charge	Micro Out	Micro Charge
1	1	0	0	0	0	1
2	1	0	0	0	0	1
3	0	0	0	0	1	0
4	0	0	0	0	1	0
5	0	0	0	0	1	0

TABLE III: ANN output at test

No	PV Out	PV Charge	Wind Out	Wind Charge	Micro Out	Micro Charge
1	1	0	0	0	0	1
2	1	0	0	0	0	1
3	0	0	0	0	1	1
4	0	0	0	0	1	0
5	0	0	0	0	1	0

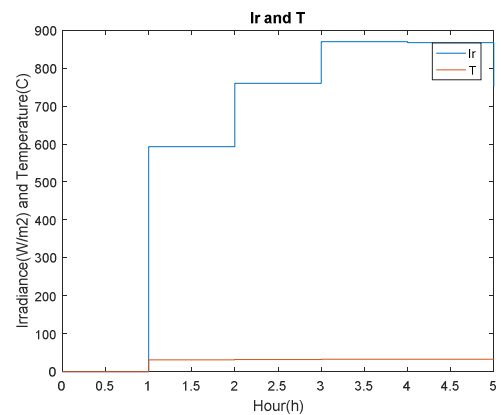


Fig. 6 : Irradiance dan Temperature Input

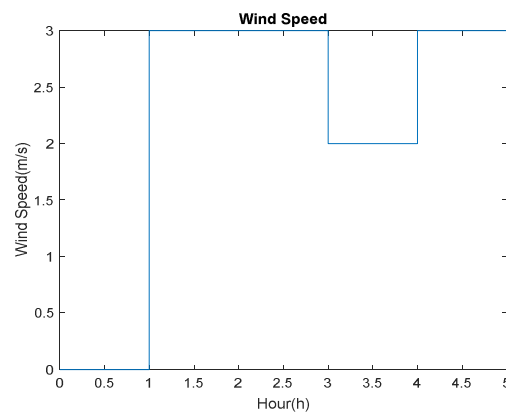


Fig. 7. Wind Speed Input

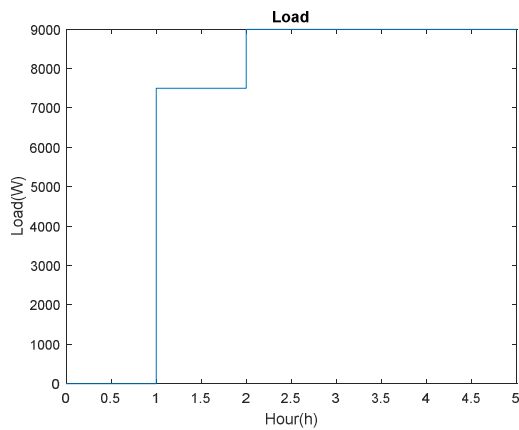


Fig. 8. Load Data

From TABLE II and TABLE III, it can be concluded that ANN output has an accuracy of 80%. From 5 experiments only 1 target that cannot be achieved, that is in data number 3. This can happen because when process of making ANN at Matlab, data number 3 very rare. When ANN looks for a weighted value, the weights match the data that often appears or can be called "Behavior Data". Thus, ANN can be inferred always looking for the weighted value of the dominant data.

Fig. 6, Fig. 7, and Fig. 8 are the data used to test the management of the hhybrid system. As seen at 2<sup>nd</sup> to 5<sup>th</sup> hours, the irradiance value of PV continued to rise from 600 W/m<sup>2</sup> to 900 W/m<sup>2</sup>, while the wind input was small. In WP modeling, in order to produce maximum power required input of at least 10 m/s. In Fig. 8, the load value increased from 2<sup>nd</sup> to 5<sup>th</sup> hours.

Fig. 9 is the output from Y1 to Y6, it is shown that at the 2<sup>nd</sup> to 4<sup>th</sup> hours, there were many changes in output. The output value at each Y1 to Y6 were 1 and 0. By comparing Figs 6, 7, 8 and 9, it can be concluded that at 2<sup>nd</sup> to 3<sup>rd</sup>, the PV produced enough power to supply the load, but at 3<sup>rd</sup> until 5<sup>th</sup> hours, the PV lacked of power despite its large irradiance value (900 W/m<sup>2</sup>). This is due to since the 3<sup>rd</sup> to 5<sup>th</sup> hour, the load value also went up which causes the PV drop its voltage.

Y1 is the output of ANN for PV Load, meaning that PV runs to supply the load. From Fig. 10 it can be seen that Y1 often occurs switching at 2<sup>nd</sup> to 4<sup>th</sup> hours. This occurs because the PV output was maximal and attempts to supply the load, but the PV output had been affected by the load (voltage drop occurs). Hence, the switching on Y1 was not inevitable. Y2 is the output of ANN for the PV charge, which means that the PV runs to supply the battery. Y2 was always zero due to insufficient PV power for charging.

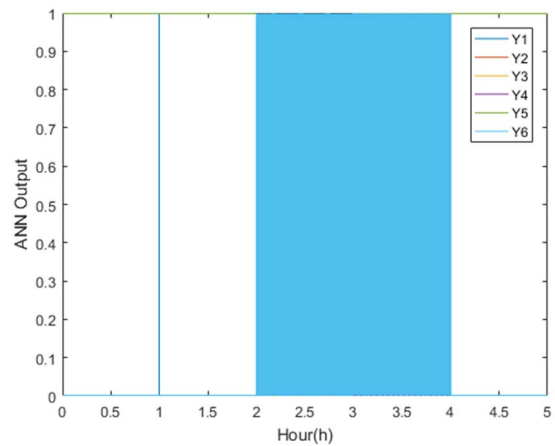


Fig. 9. ANN output

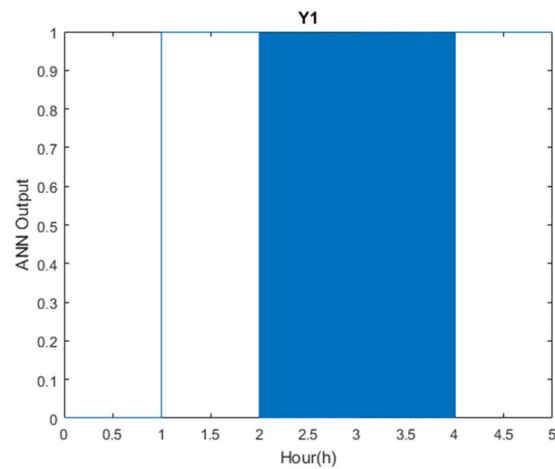


Fig. 10. Output Y1 ANN

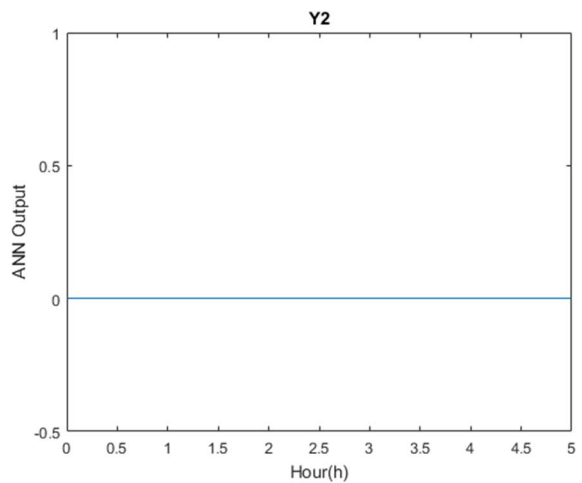


Fig. 11. Y2 ANN output

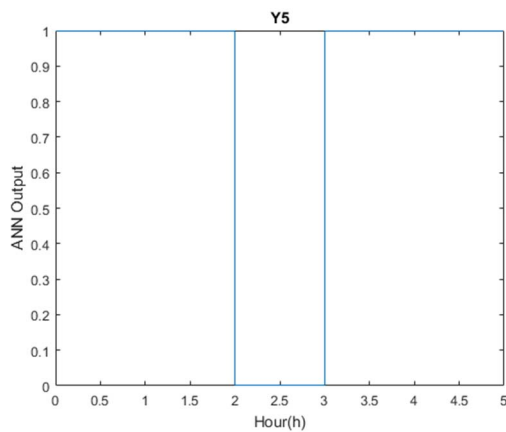


Fig. 12. Y5 ANN output

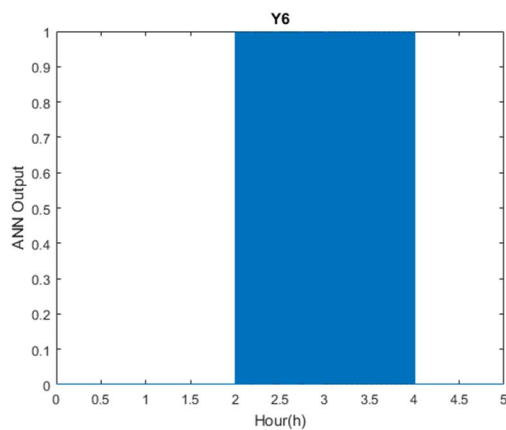


Fig. 13. Y6 ANN output

Y5 is the output of ANN for MHPP load, meaning that the MHPP was running to supply the load. From Fig. 12 it can be seen that at 2<sup>nd</sup> to 3<sup>rd</sup> hours, Y5 output was 0. This occurred because the PV Power output was good enough which derived the MHPP to be off. When the PV (Y1) was on, the MHPP should not be on. This is the same target as when ANN training.

Y6 is the ANN output for MHPP charge as in Fig. 13, meaning that MHPP run to charge the battery. At 2<sup>nd</sup> to 4<sup>th</sup> hours, Y6 was charging. But there was a lot of switching due to the effect of the load installed and the maximum PV output.

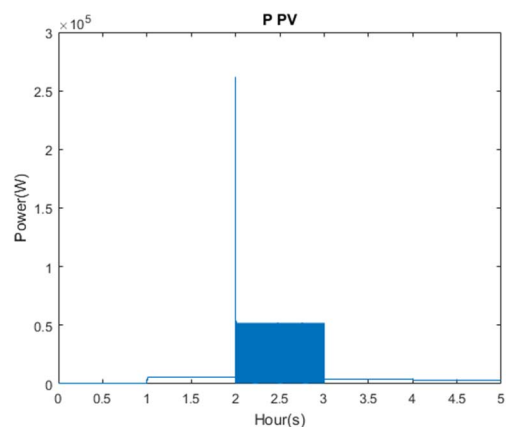


Fig. 14. Power Output of PV

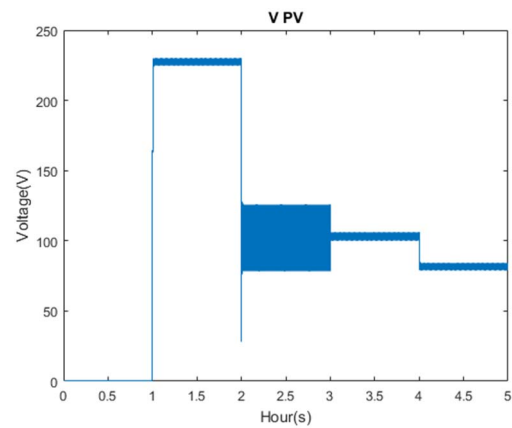


Fig. 15. Voltage Output of PV

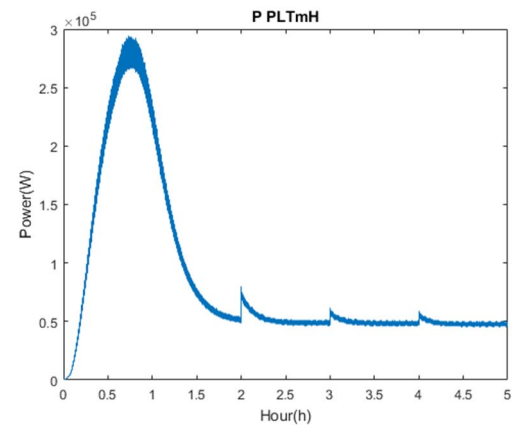


Fig. 16. Power Output of MHPP

Fig. 14 and Fig. 15 show that the PV has a voltage around 82V to 230V, but the PV power can be maximized at 2<sup>nd</sup> to 3<sup>rd</sup> hours. While at 3<sup>rd</sup> to 5<sup>th</sup> hours the PV power dropped. This corresponds to Fig. 6, the  $I_r$  value was rising from 760 W/m<sup>2</sup> to 870 W/m<sup>2</sup> from 2<sup>nd</sup> to 3<sup>rd</sup> which causes the PV power value increased. When the clocks 3, 4 and 5 the values of  $I_r$  were raised from 870 W/m<sup>2</sup>, 861 W/m<sup>2</sup>, and 751 W/m<sup>2</sup>, respectively. But the load value (Fig.8) at 3<sup>rd</sup> to 5<sup>th</sup> hours was also increased, causing the PV to not supply the load. This causes the PV output to drop.

Fig. 16 shows instantaneous spiked during the 2<sup>nd</sup>, 3<sup>rd</sup> and 4<sup>th</sup> hours. This is due to the load changes. At the 2<sup>nd</sup>, 3<sup>rd</sup> and 4<sup>th</sup> hours there were load release and load connection so that the time at which discharge and load connections occurred together which causes instantaneous power spike. In Fig. 17, the voltage values of the MHPP were further down due to the increasing value of the load (Fig. 8) at 2 to 5. In the WP as in Fig. 19, the output power and voltage were very small. This is because the wind velocity input that cannot meet the cut-in zone that causes the turbine does not rotate because the power of WP cannot exceed the load demand, then T3 and Y4 will always be zero as in Fig. 19 and Fig. 20.



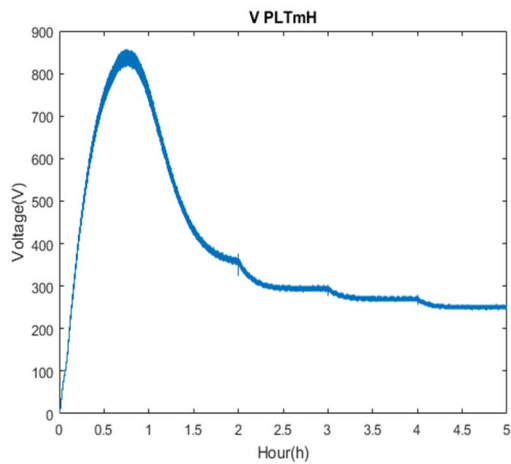


Fig. 17. Voltage Output of MHPP

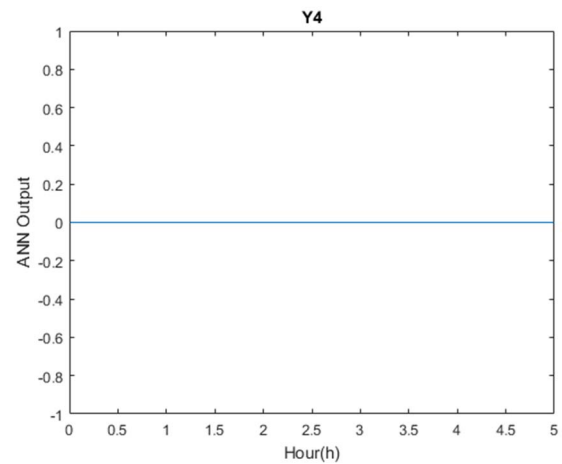


Fig. 20. Output Y4 ANN

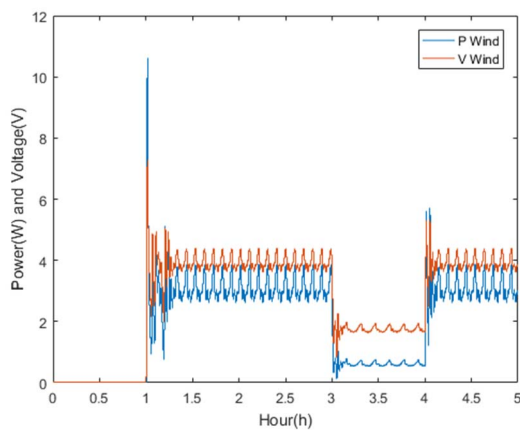


Fig. 18. Power Output and Voltage of WP

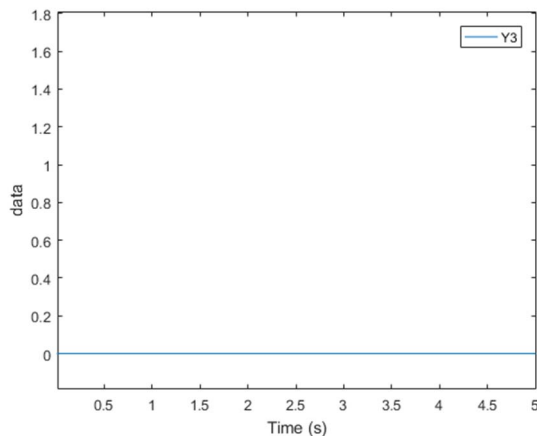


Fig. 19. Output of Y3 ANN

#### IV. CONCLUSION

Hybrid power management system has been successfully implemented on the 3 types of renewable energy sources, and the system was meet the load demand with accuracy in around 80%. Moreover the system can supply the load on demand, even though condition of the source were changing. However, ANN has an error when the generator is interconnected with the load. This was due to the drop of voltage causing the ANN to be misread.

#### REFERENCES

- [1] M.F.M. Yusof and A.Z. Ahmad (2016), "Power Energy Management Strategy of Micro-grid System", Proc. of IEEE International Conference on Automatic Control and Intelligence Systems.
- [2] M. Trifkovic, M. Sheikhzadeh, K. Nigim, P. Daoutidis (2012), "Hierarchical control of a renewable hybrid energy system". Proc. of IEEE Conference on Decision and Control.
- [3] R. Dufo-Lopez, J.L. Bernal-Agustin, J.M. Yusta-Loyo, J.A. Domingues-Navarro, I.J. Ramirez-Rosado, J.L. Ismael Aso (2011), "Multi-objective optimization minimizing cost and life cycle emissions of stand alone PV-Wind-Diesel system with batteries storage". Applied Energy, Vol. 88 No. 11, pp. 4033-4041
- [4] A. Al-Alawi, S.M. Al-Alawi, S.M. Islam (2007), "Predictive control of an integrated PV-diesel water and power supply system using an artificial neural network". Renewable Energy, Vol. 32, No. 8.
- [5] P. Badoni and S.B. Prakash (2014), "Modelling and simulation of 2 MW PMSG wind energy conversion system". IOSR-Journal of Electrical and Electronics Engineering, Vol. 9, No. 4, pp. 53-58.
- [6] Miharja, Farid, "Perencanaan dan manajemen pembangkit listrik tenaga hybrid (angin/surya/fuel cell) pulau Sumba menggunakan software homer". ITS
- [7] Insan, Ivan Ahsanul. (2016). "Optimalisasi dan simulasi maximum power point (MPPT) pada solar-Wind turbine menggunakan metode incremental conductance". UMM
- [8] A.S. Kumar, T. Cermak, S. Misak (2015), "Modelling and simulation of 12Kw direct friven PM Synchronous generator of Wind Power". Proc. of 2015 3<sup>rd</sup> International Conference on Control, Engineering, and Information Technology.
- [9] M. Ammar, P. Jagadeesh, K. Tamer, E. Wilfried (2015), "A review od process and operational system control of hybrid photovoltaic diesel generator system", Renew. and Suistainable Energy Reviews . Vol. 44(c), pp. 436-446.
- [10] Mulyadi, Riyan (2016), "Analisa sistem integrasi Kontrol eletronic load controller dan flow control valve pada PLTmH". UMM.

# ON THE USE OF HILBERT TRANSFORM METHOD FOR ENVELOPING PARTIAL DISCHARGE SIGNAL DETECTED BY USING VARIOUS SENSORS

Umar Khayam

School of Electrical Engineering and Informatics  
Institut Teknologi Bandung  
Indonesia  
[umar@hv.ee.itb.ac.id](mailto:umar@hv.ee.itb.ac.id)

Arpan Zaeni

School of Electrical Engineering and Informatics  
Institut Teknologi Bandung  
Indonesia  
[arpanzaeni@gmail.com](mailto:arpanzaeni@gmail.com)

**Abstract** — Partial discharge diagnosis in the insulator which is applied in some power apparatus has an important role in maintaining the reliability of high voltage equipment in a power system. Partial discharge diagnosis has three main steps, one of them is signal processing that can be done with enveloping especially for partial discharge signal obtained from measurement using UHF PD sensors like Loop Antenna and HFCT. There are several methods we can use to perform signal processing of PD signals. Enveloping method that used in this research is by using Hilbert transform method which applied to signal output from some Partial Discharge Sensors. After we do the envelop process to that signal we can easily determine the important quantities of the signal such as rise time, fall time, pulse width, and peak voltage. That quantities are very important for the next step of the Partial Discharge diagnostic signal Process.

**Keywords** --- Partial discharge diagnosis, UHF PD sensors, signal processing, Hilbert Transform

## I. INTRODUCTION

Base on IEC 60270, Partial Discharge is a local electrical annihilation in isolation that does not fully connect the two conductors, this can occur either near or between the conductor. Generally Partial discharge exist as a result of the local electrical stress concentration in isolation or on the surface of the insulation. the presence of partial discharges inside the insulator is one of the earliest indications indicating that the insulator begins to degrade or begin to deteriorate. If the presence of Partial discharge is not detected early, the insulator will suffer damage causing disruption of the system as a whole. Therefore partial discharge diagnosis become one of the best method to know the condition of insulator.

Partial discharge diagnosis has three main steps that is PD detecting, Signal Processing, and judgement system. Partial discharge can be detected by various sensors, one of them is

using UHF sensors like HFCT dan Loop Antenna. UHF PD detection has some advantages that is its high sensitivity, its avoidance from the low-frequency noise, and its wide and high enough frequency band ranging from 300 M to 3 GHz [1, 2]. UHF detection was first successfully implemented for Gas Insulated Substations (GIS) [3] and is increasingly employed for power transformers because of its relative immunity to interference and ability to provide information on the defect location [4–6]. But detection using UHF PD detector have a result in a hard-to-observe waveform which make us difficult to determine the important magnitudes of a wave. therefore we need an advanced process which one of them is enveloping the signal. enveloping the PD signal has several methods. The method to be used in this research is Hilbert transformation method.

## II. HILBERT TRANSFORM

Hilbert Transform method is a common and very efficient technique for enveloping signal. This method is done by shifting a 90 degree phase and summing the phase shifted with original signals. The Hilbert transform is typically implemented as an FIR (Finite Impulse Response) filter so the original signal must be delayed to match the group delay of the Hilbert transform. This process can be followed by absolute and then peak hold functions, the latter is often implemented as a one pole IIR filter [7].

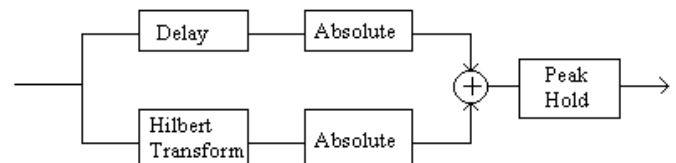


Figure 1. Idea of Hilbert Transform Method

The following diagram gives an idea of how the envelope approximation process works by Hilbert Transform Method

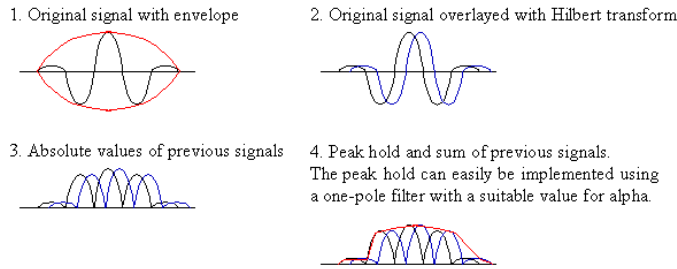


Figure 2. Approximation process of Hilbert Transform Method [7]

Hilbert Transform methods include making analytical signal from the input signal through a Hilbert transform. Analytical signal is a complex signal, where the real part is the original signal, and the imaginary part is the Hilbert transform of the original signal [8].

The algorithm of the envelop detector using this method is shown in Following Figure.

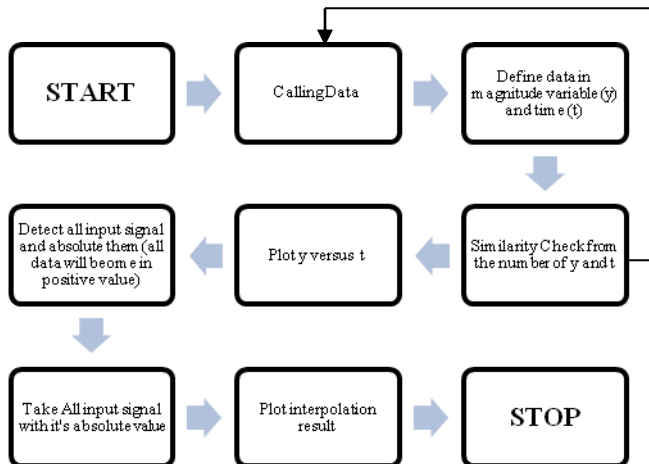


Figure 3. Algorithm of Hilbert Transform Method [8]

The following equation shows how the coefficients of the FIR filter implementation of the Hilbert transform are calculated.

$$h(n) = \frac{2}{n * \pi} * \sin^2\left(\frac{n * \pi}{2}\right)$$

for  $n = \pm 1, \pm 2, \pm \frac{N}{2}$  and  $h(0) = 0$  for  $n = 0$

The one pole IIR filter is defined by the following equation :

$$y(n) = x(n) + a * y(n-1), \text{ where } 0 < a < 1.0$$

Another option for detecting the envelope is to use the square root of the energies of the original and the Hilbert transformed signals, as follows :

$$\text{Envelope} = \sqrt{\text{Hilbert}^2 + \text{signal}^2}$$

In general, this will give similar results to the absolute value technique but can be more run-time efficient.

### III. HILBERT TRANSFORM ENVELOPING IMPLEMENTATION

Base on Algorithm in figure 3 we can make hilbert transform script in Matlab.

```

1 - clc;clear;
2 - load dataku.txt dataku;
3 - t = dataku(:,1); % waktu
4 - y = dataku(:,2); % signal amplitude
5 - hil=abs(hilbert(y));
6 - %menampilkan gambar sinyal asli
7 - figure(1);
8 - plot(t,y,'r-');
9 - hold on;
10 - plot(t,hil,'b--');
11 - hold off;
12 - title('Sinyal orisinil beserta envelopnya','FontSize',18);
13 - xlabel('t');
14 - ylabel('Magnitude');
15 - legend('Original','Envelope');
  
```

Figure 4. Script of Hilbert Transform Method in Matlab

Input data that will be inserted into this hilbert transform method is a csv file obtained from the detection of PD signal by using some detector that has been integrated with the computer. Detector we will use include detecting impedance, HFCT, and loop antenna. Computers that are integrated into the detection circuit must have software that can take wave data for very small time units. Software used in this research is freewave software.

#### 3.1 Hilbert Transform Implementation for PD signal Detection Using Detecting Impedance

Detecting impedance is one of the most efficient PD detector because detecting with this tool can make us get PD signal with relatively easy to be analyzed. The following figure show the PD signal output in oscilloscope that we get from detection use Detecting Impedance.

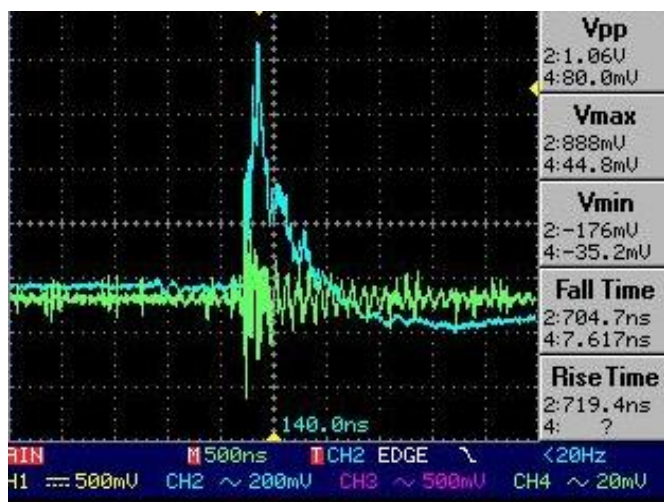


Figure 5. PD signal detection using Detecting Impedance (blue) compared with UHF PD signal (green)

After Detecting Impedance detect the signal then we take that csv data signal which show the relation from time versus magnitude. Then that data will become the input for Hilbert transform script we make. The following figure show the result from enveloping that signal using Hilbert Transform.

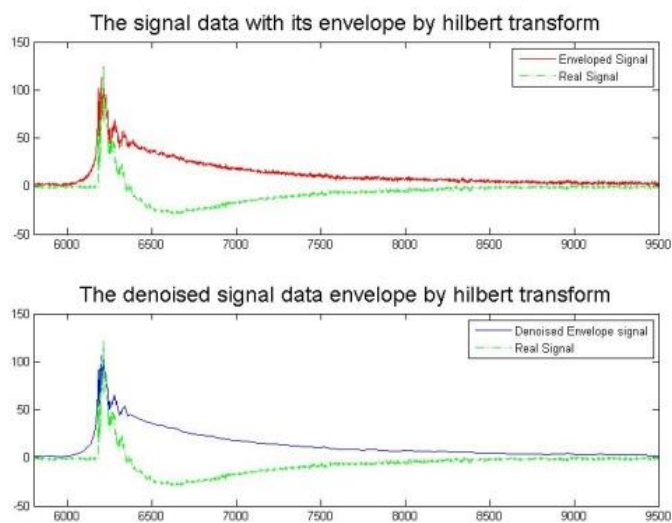


Figure 6. Hilbert Transform Enveloping result for PD signal detection using Detecting Impedance

### 3.2 Hilbert Transform Implementation for PD signal Detection Using HFCT

PD detection using HFCT will produce the signal which higher frequency than the signal we get from detecting Impedance. The Following figure show the PD signal result detection using HFCT.

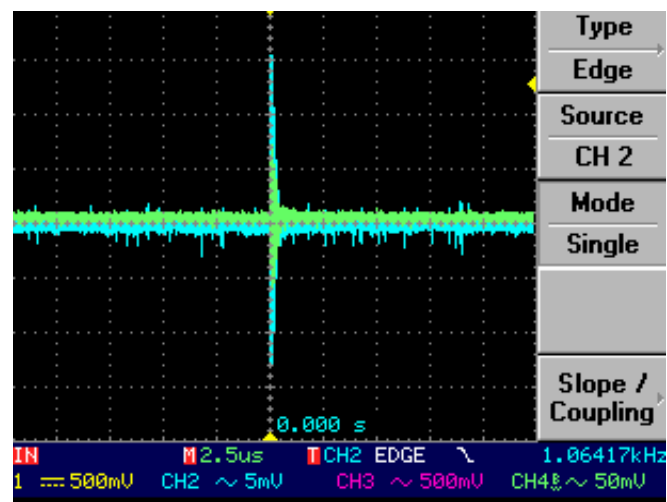


Figure 7. PD signal detection using HFCT (blue)

Same as detection process using Detecting Impedance before, after PD signal successfully detected by HFCT we take data signal in the form of csv file for input to Hilbert Transform script. The following figure show the result from enveloping that signal using Hilbert Transform.

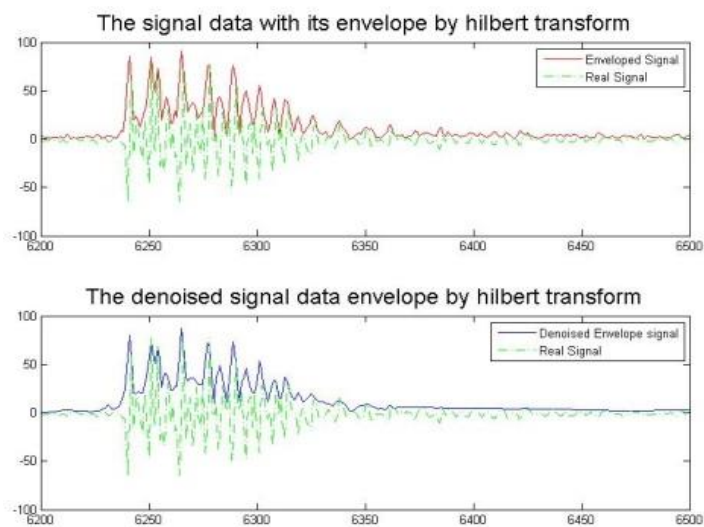


Figure 8. Hilbert Transform Enveloping result for PD signal detection using HFCT

### 3.3 Hilbert Transform Implementation for PD signal Detection Using Loop Antenna

The third detector we use is loop Antenna. Same as PD detection using HFCT, Loop antenna produce the signal which higher frequency than the PD signal from Detecting Impedance. The Following figure show the PD signal result detection using Loop Antenna.

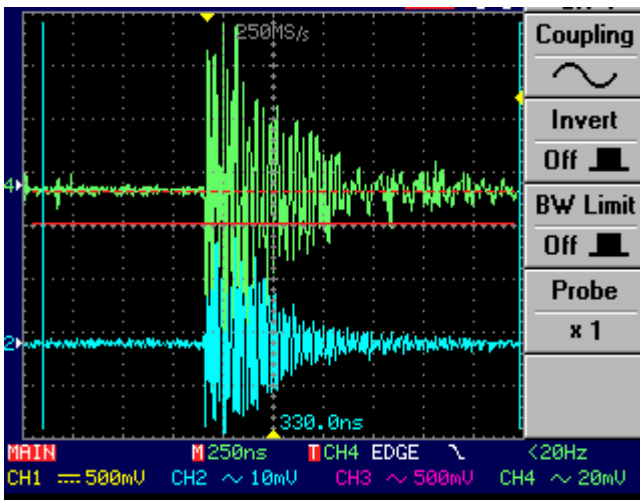


Figure 9. PD signal detection using Loop Antenna (blue)

As we see in that figure, loop antenna produce PD signal with higher frequency. The following figure show the result from enveloping that signal with hilbert transform method.

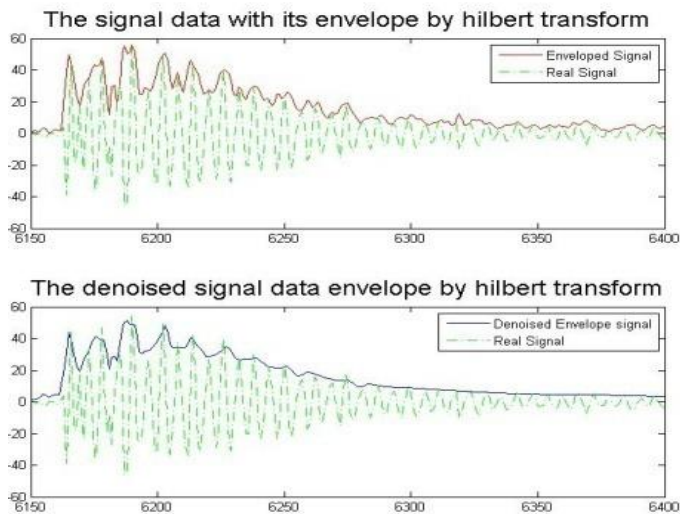


Figure 10. Hilbert Transform Enveloping result for PD signal detection using Loop Antenna

#### IV. DISCUSSION

Based on the PD detection we do, we find that some detector such as HFCT and loop antenna produces PD signal which is difficult to be analyzed. So enveloping that signal can make us easier to determine the important quantities especially rise time and fall time. The Following table show the summary of quantities that we get from the experiment before.

Output PD Signal	Original	Hilbert Transform
Rise Time	140 ns	300 ns
Fall Time	100 ns	224 ns

(a)

Output PD Signal	Original	Hilbert Transform
Rise Time	90 ns	40 ns
Fall Time	260 ns	68 ns

(b)

Output PD Signal	Original	Hilbert Transform
Rise Time	36 ns	124 ns
Fall Time	60 ns	212 ns

(c)

Table 1. Enveloping result : (a) DI ; (b) HFCT; (c) Loop Antenna

Base on that table, we know that Hilbert Transform Method give different and unstable result for each sensors. it can happen because enveloping PD signal using this method still has not only one extreme points for HFCT and Loop Antenna so it is relatively more difficult to obtain rise time and fall time of the captured PD signal. This is due to the oscillation of the captured PD signal have not a relatively permanent value decreasing or permanently increasing, but rather random (up and down) so that the cusp of this signal is also random (up and down). For Detecting Impedance, due to oscillations below the zero point, through the Hilbert transform all these values will be lifted to positive values, and interpolated their peak points. That process caused the PD signal has a long pulse width with a relatively higher fall time value.

#### V. CONCLUSION

The conclusion of this research are :

1. UHF PD sensors give the result of PD signal which have difficult to be analyzed, so we must process the signal to get the important quantities.
2. One of Signal Processing that we can do to process PD signal is enveloping using Hilbert Transform method.
3. Enveloping using hilbert transform will produce the signal with higher value of rise time and fall time for PD signal detected by Detecting Impedance and Loop Antenna.



## REFERENCES

- [1] R. Kuppaswamy and P. Coquelin, "Power transformer assetmanagement on-line partial discharge measurement-a new approach," IEEE Conf. Electr. Insul. Dielectr. Phenomena (CEIDP), pp. 445 – 448, 2005.
- [2] M. Muhr and R. Schwarz, "Partial discharge measurement as aDiagnostic Tool for HV-Equipments," IEEE 8th Int'l. Conf. Propertiesand applications of Dielectric Materials, pp. 195–198, 2006.
- [3] SELLARS A.G., FARISH O., HAMPTON B.F., PRITCHARD L.S.: 'Usingthe UHF technique to investigate PD produced by defectsin solid insulation', IEEE Trans. Dielectr. Electr. Insul., 1995,2, (3), pp. 448–459
- [4] JUDD M.D., YANG L., HUNTER IAN B.B.: 'Partial dischargemonitoring for power transformers using UHF sensorspart 1: sensors and signal interpretation', IEEE Electr. Insul. Mag., 2005, 21, (2), pp. 5–14
- [5] JUDD M.D., YANG L., HUNTER I.B.B.: 'Partial dischargemonitoring for power transformers using UHF sensorspart 2: field experiences', IEEE Electr. Insul. Mag., 2005,21, (3), pp. 5–13
- [6] ASCHENBRENNER D., KRANZ H.G., RUTGERS W.R., AARDWEG P., VANDEN P.: 'On line PD measurements and diagnosis on powertransformers', IEEE Trans. Dielectr. Electr. Insul., 2005, 12,(2), pp. 216–222
- [7] EkaAnnisAmbarani, ReviAldrian, Arpan Zaeni, "Diagnosis Partial Discharge pada Media Jarum-Plat denganpemrosesansinyalberbasis Envelop", STEI, ITB, Bandung, 2014.
- [8] Arpan Zaeni, Umar Khayam "Designing, Simulating, and Manufacturing Envelope Detector to Analyze Partial Discharge Waveform", STEI, ITB, Bandung, 2015



# CIRCUIT SIMULATION FOR WIND POWER MAXIMUM POWER POINT TRACKING WITH FOUR SWITCH BUCK BOOST CONVERTER

1<sup>st</sup> Machmud Effendy  
Electrical Department  
Muhammadiyah University of Malang  
Malang, Indonesia  
machmud@umm.ac.id

2<sup>nd</sup> Khusnul Hidayat  
Electrical Department  
Muhammadiyah University of Malang  
Malang, Indonesia  
khoesnoelhidayat@gmail.com

3<sup>rd</sup> Nuralif Mardiyah  
Electrical Department  
Muhammadiyah University of Malang  
Malang, Indonesia  
diyah\_syk@yahoo.co.id

**Abstract**— Wind turbines have maximum mechanical power at certain wind speeds. Maximum power point tracking (MPPT) is an electronic system capable of extracting maximum wind turbine power. The purpose of this research is to improve wind power efficiency through MPPT wind power design with four switch buck-boost converter and Fuzzy control algorithm. Fuzzy control has two inputs are power changes and voltage changes and one output feeding to the pulse width modulation generator to control FSBB. Simulation results with Matlab simulink shows that wind power without MPPT produce 89% power efficiency, wind power MPPT with two switch buck-boost converter yield 90% power efficiency and emerging high ripple current. The last simulation of wind power MPPT with FSBB produces the highest efficiency of 91% with low ripple current.

**Keywords**—wind turbine, mppt, four switch buck-boost converter

## I. INTRODUCTION

Wind power is one of the power plants that use renewable energy. Wind power produces no pollution and no emissions [1]. MPPT is a technology to increase wind power efficiency by determining maximum power point at certain wind speed. There are two main components of MPPT that is DC to DC converter and control algorithm. The DC to DC converter circuit is widely used for MPPT technology in wind power [2]. Two switch buck-boost converter is a cascaded converter of Buck-Boost Converter that serves to raise and lower the input voltage [3,4].

Four switch buck-boost (FSBB) converter is the development of two switch buck-boost (TSBB) converter, where the output voltage FSBB always positive [5,6]. The FSBB converter uses four MOSFETs as the electronic switch replaces the diode function in the two switch buck-boost converter circuit, so the FSBB converter circuit has higher power efficiency than the two buck-boost converter switches. This is because the cut off voltage in the MOSFET is smaller than the forward diode voltage [7].

There is a lot of study wind power MPPT using control algorithm like fuzzy, neural network etc [8-12]. The result of the research is to know the response of the system when it reaches the maximum power point. In this paper, wind power MPPT is developed using the TSBB converter and FSBB converter, while the control algorithm uses fuzzy logic. The current study aims to reduce power losses and improve the efficiency.

## II. RESEARCH METHOD

The design of wind power MPPT based on fuzzy control using FSBB is illustrated in Figure 1. The design consists of permanent magnet synchronous generator (PMSG), the wind turbine, rectifier AC (alternating current) to DC (direct current), FSBB converter, the load resistor and fuzzy controllers. FSBB converter is modulated by PWM generator.

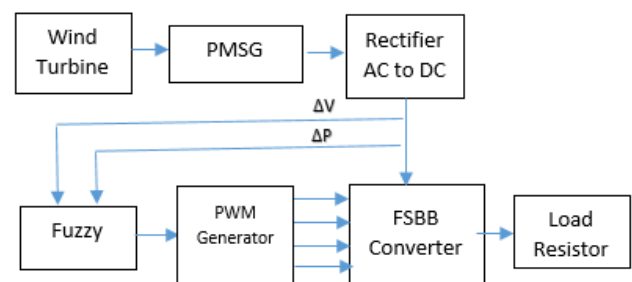


Figure 1 Design of wind power MPPT

### A. Wind Turbine

The characteristics of the wind turbine can be seen from the relationship between rotor speeds with turbine mechanical power. The mechanical power of the wind turbine for each wind speed has a maximum point at a given rotor speed, as illustrated in figure 2

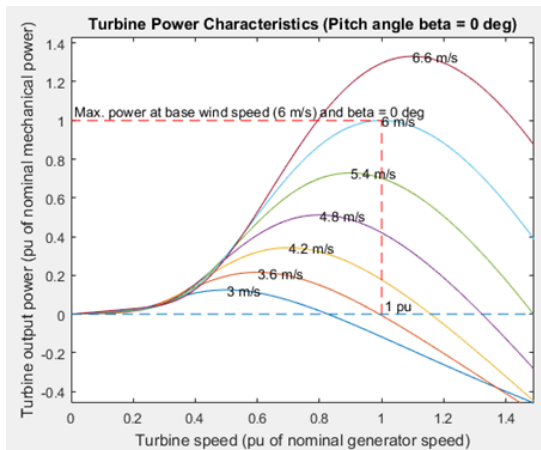


Figure 2. The power characteristics of wind turbines

Mechanical power in wind turbine  $P_m$  is a function of air density  $\rho$ , tip speed ratio (TSR)  $\lambda$ , the pitch angle  $\beta$ , radius propeller  $R$ , and wind speed  $v$  [13].

$$P_m = 0.5 \cdot \pi \cdot \rho \cdot C_p(\lambda, \beta) R^2 \cdot v^3 \quad (1)$$

The relationship between the power coefficient, TSR, and pitch angle of the  $C_p$  wind turbine ( $\lambda, \beta$ ) is written as [13]:

$$C_p(\lambda, \beta) = c_1 \left( \frac{c_2}{\lambda_t} - c_3 \beta - c_4 \right) e^{-\frac{c_5}{\lambda_t}} + c_6 \lambda \quad (2)$$

$$\frac{1}{\lambda_t} = \frac{1}{\lambda + 0.08\beta} - \frac{0.035}{\beta^3 + 1} \quad (3)$$

The value of  $C_1$ - $C_6$  depends on the characteristics of the wind turbine. TSR is the ratio between rotor speed  $\omega_m$  and wind speed, written by the formula [8]:

$$\lambda = \frac{\omega_m \cdot R}{v} \quad (4)$$

#### B. Four Switch Buck-Boost Converter (FSBB)

The buck-boost converter is one type of DC to DC Converter circuit that has an output voltage greater or less than the input voltage. The output voltage is of the opposite polarity the input. The two switch buck-boost converter (TSBB) is the development of buck-boost converter. The output voltage has the same polarity as the input voltage. TSBB uses diodes and transistors for switching as shown figure 3.

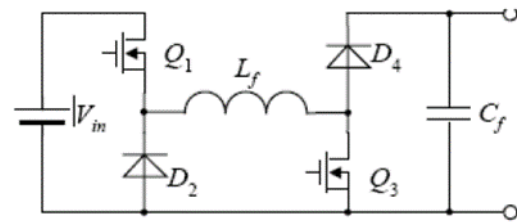


Figure 3 Two Switch Buck-Boost Converter

FSBB and TSBB have the same output voltage polarity as the input voltage. TSBB uses two diodes and two transistors, FSBB uses four transistors. The main advantage of an FSBB is that the voltage drop across the low-side transistor unipolar MOSFET can be lower than the voltage drop across the power diode of the TSBB. The FSBB has greater power efficiency than TSBB

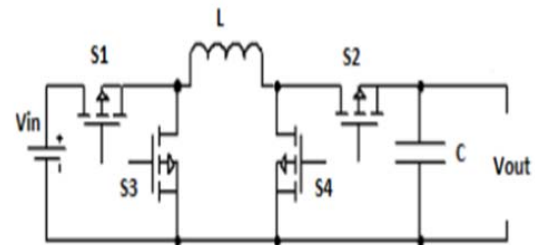


Figure 4. Four Switch Buck -Boost Converter

The output voltage of FSBB is written as [5]:

$$V_{out} = \frac{V_{in} \cdot D}{1-D} \quad (5)$$

Where  $D$  is the duty cycle value

The output current of FSBB Converter is written as:

$$I_{out} = \frac{I_{in} \cdot D}{1-D} \quad (6)$$

The amount of peak to peak ripple current  $\Delta I$  and voltage  $\Delta V_c$  is written as:

$$\Delta I = \frac{V_{in} \cdot D}{f \cdot L} \quad (7)$$



$$\Delta V_c = \frac{I_{out} \cdot D}{f \cdot C} \quad (8)$$

Where  $f$  is the switching frequency.

There are 3 modes of operation with 4 possible switches, as shown in table 1

Table 1 Switching States of the FSBB

Mode	S1	S2	S3	S4
Buck		1		0
Boost	1		0	
Buck				

Mode	$S1$	$S2$	$S3$	$S4$
Boost				

FSBB Converter uses Buck-Boost mode. The charging process occurs when the switches  $S1$  and  $S4$  become ON state, the  $S2$  and  $S3$  OFF are in OFF state. The current passes through the inductor and at the same time the capacitor voltage is directly connected to the load. FSBB operates in discharging process when switches  $S2$  and  $S3$  become ON state, the  $S1$  and  $S4$  are in OFF state. The voltage produced by the inductor is applied to the load and the capacitor.

### C. Fuzzy Logic Controller

Fuzzy controller for Wind power MPPT shown in figure 5.

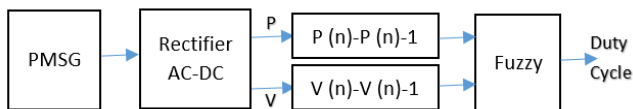


Figure 5 Scheme of the Fuzzy Control

Figure 6 illustrates the fuzzy set of the  $P(n)-P(n-1)$  input which contains five triangular membership functions.

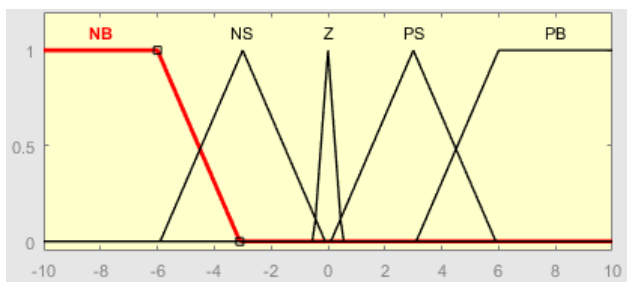


Figure 6 Member function of  $dP$

Figure 7 illustrates the fuzzy set of the  $V(n)-V(n-1)$  input which contains five triangular membership functions

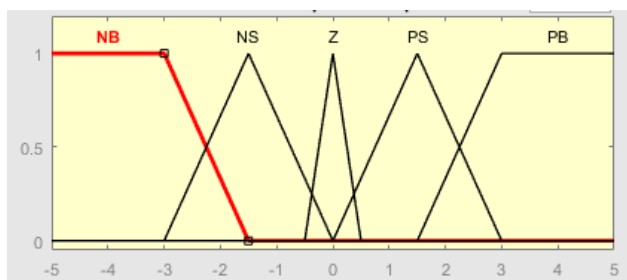


Figure 7 Member function of  $dV$

Figure 8 illustrates the fuzzy set of the duty cycle output which contains five triangular membership functions.

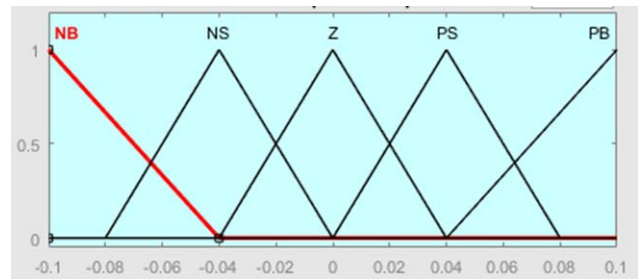


Figure 8 Member function of Duty Cycle

Determination of the rule-base of IF-THEN in the controller contains all the information to control the parameters and is based on perturb and observe, as shown in Table 2.

Table 2 Fuzzy Rules

Fuzzy Rules	$P(n)-P(n-1)$					
		NB	NS	ZE	PS	PB
$V(n)-V(n-1)$	NB	NB	NS	ZE	PS	PB
	NS	NS	NS	ZE	PS	PS
	ZE	ZE	ZE	ZE	ZE	ZE
	PS	PS	PS	ZE	NS	NS
	PB	PS	PS	ZE	NS	NB

### III. RESULT AND DISCUSSION

The design of wind power MPPT with four switch buck-boost converter as shown in figure 1 is simulated using matlab. Design parameter of wind power MPPT is shown in table 2.

Table 2. Design parameter of wind power MPPT

Variable	Parameter
Wind Turbine	$P_m = 200$ W
PMSG	200V 50Hz 220W
FSBB	$L = 2$ mH $C = 10\mu F$ MOSFET $R_{don} = 0.1$ ohm $F = 60$ kHz
Load	$R = 30$ ohm

The circuit simulation for wind power MPPT is explained in more detail in figure 9.

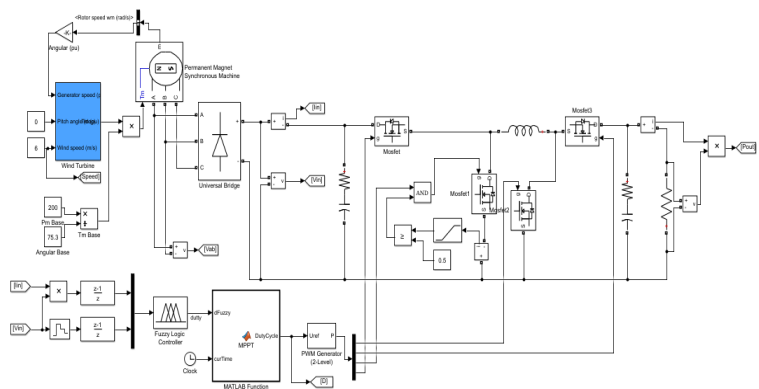


Figure 9 Schematic of wind power MPPT in Matlab

The first simulation is to test wind power without MPPT, wind turbine operated with speed 6 meter/second. Figure 10 shows the result of the simulation. The load power is 177 Watt. There is 27.5% power loss from a maximum power of 200 Watt wind turbines.

Figure 11 shows the simulation results of wind power MPPT with TSBB. The load current is 177 Watt, there is 15% power lost from 200 Watt wind turbine mechanical power.

The last simulation is to test the fuzzy MPP-based wind power using four buck-boost converter switches.

Figure 12 shows the result of the simulation. The load power loss is 9% of the wind turbine's mechanical power of 200Watt.

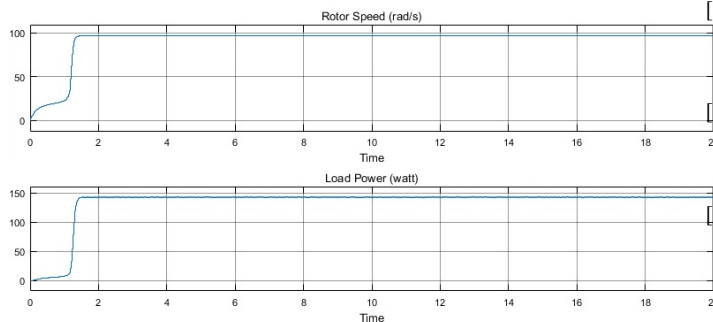


Figure 10 The Simulation of wind power without MPPT

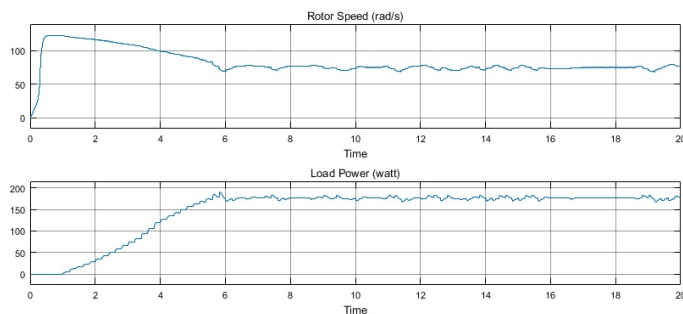


Figure 11 The Simulation f wind power MPPT with TSBB

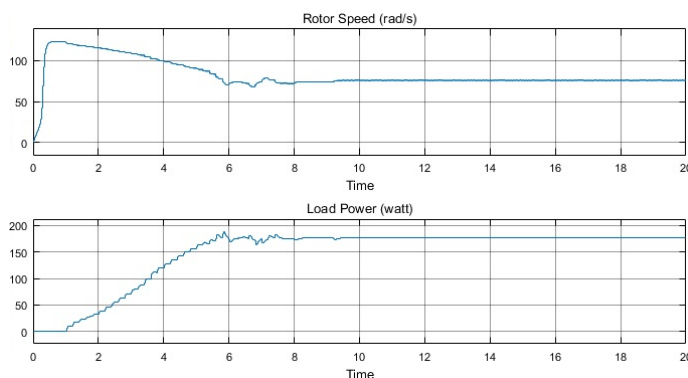


Figure 12 The Simulation of wind power MPPT with FSBB

#### IV. CONCLUSION

The simulation of wind power MPPT with four switch The simulation results show that wind power MPPT using four switch buck-boost converter is better than wind power MPPT using two switch buck-boost converter. TSBB efficiency in wind power MPPT produces 85% and current ripple appears on the load, while the FSBB produces 91% efficiency with smaller current ripple at the switching frequency of 60kHz.

#### ACKNOWLEDGMENT

We would like to thank the Electrical Department Muhammadiyah University of Malang for supporting this project.

#### REFERENCES

- [1] Chen, Blaabjerg. —Wind farm-A power source in future power systems—. Elsevier Renewable and Sustainable Energy Reviews 13 (2009) 1288–1300. 2009
- [2] Koutroulis, Eftichious. Kalaitzakis, Kostas. 2006. —Design of a MPPT System for Wind-EnergyConversier Applications—. IEEE Transactions on Industrial Electronics, vol.53 (2006) 0278–0046
- [3] Rayen., Hariharan., Elavazhagan, Kamalendran N., Varadarajan R., "Dental management of hemophiliac child under general anesthesia", Journal of Indian Society of Pedodontics and Preventive Dentistry, ISSN : 0970-4388, 29(1) (2011) pp.74-79.
- [4] Shanthi., Revathy, Devi A.J.M., Subhashree, "Effect of iron deficiency on glycation of haemoglobin in nondiabetics", Journal of Clinical and Diagnostic Research, ISSN : 0973 - 709X, 7(1) (2013) pp.15-17.
- [5] S Krishnaveni and M.Rasu, "Analysis of Four Switch Positif Buck Boost Converter Based On Mode Selection Circuit For Portable Battery Applications", IEEE Sponsored 2nd International Conference onInnovations in Information Embedded and Communication System, Vol 10 No.20,ISSN 0973-4562, pp 16571-16576, 2015
- [6] Lingeswara.K, K.Prakash,S.P.Vijayaragavan,"Analysis and Design of Four Switch Buck Boost Converter for DC-DC Power Supply Application", IJAREEIE, Vol.4 Issue 6,pp 5618-5629, June 2015
- [7] Rich nowakowski and Ning Tang, *Efficiency of synchronous versus nonsynchronous buck converter*, Analog Aplication Journal of Texas Instrument Corporated, 2009
- [8] Khalil, Lee , Seok . *Variable speed wind generation based on FLC for MOPT* , 35th Annual IEEE Power Electronic Specialists Conference. Jerman. 2004.
- [9] Adzic, Ivanovic, Adzic. Maximum Power Search in Wind Turbine Based on Fuzzy Control. *Journal Acta Polytechnica Hungarica*. 2009; 6(1): 131-149
- [10] CY Lee, YX Shen, Jung CC. Neural Networks and PSO Based MPPT for Small Wind Power Generator. *World Academy of Science, Engineering and Technology*. 2009; 60: 17-23.
- [11] Yilmaz, Ozer. Pitch Angle Control in Wind Turbine Above the Rated Wind Speed by Multi-layer Perceptron and RBFNN. *Elsevier: Expert System with Applications*. 2009; 36: 9767-9775.
- [12] Lin, Hong. A New Elman Neural Network-Based Control Algorithm for Adjustable-Pitch Variable Speed WECS. *IEEE Transactions On Power Electronics*. 2011; 66(2): 1847-1853.
- [13] Burton, Sharpe , Jenskin , Borsanyi ,;Wind Energy Handbook. West Sussex: John Wiley & Sons. 2001

# Modulation Strategies for Indirect Matrix Converter: Complexity, Quality and Performance

Hendril Satrian Purnama

Department of Electrical Engineering  
Universitas Ahmad Dahlan  
Yogyakarta, Indonesia  
lfriyan220@gmail.com

Tole Sutikno

Department of Electrical Engineering  
Universitas Ahmad Dahlan  
Yogyakarta, Indonesia  
tole@ee.uad.ac.id

Mochammad Facta

Department of Electrical Engineering  
Universitas Diponegoro  
Semarang, Indonesia  
mochfacta@gmail.com

**Abstract**—In general, there are two main classifications in matrix converters. The most common known type is conventional matrix converter (CMC) or direct matrix converter (DMC). The other type is indirect matrix converter (IMC). A brief review for modulation strategies are provided in this work for modulation methods for IMC such as carrier-based modulation and space vector modulation (SVM). A sinusoidal current waveform is produced on the input and output sides to implement the modulation method. In the conclusion the modulation methods will be compared based on performance, theoretical complexity, and some other parameters.

**Keywords**—AC-AC conversion, carrier-based modulation, indirect matrix converter, pulse width modulation, space vector modulation.

## I. INTRODUCTION

Matrix Converter (MCs) usually is made from an AC-AC converter which includes the array bidirectional switches. This array is useful to connect main power supply to the load. At this connection circuit, there is no DC-link or energy storage elements [1]. The MCs have a great demand because of their superior function such as: (1) dc link capacitor is removed, (2) a sinusoidal waveform at both input and output terminal, (3) bidirectional power-flow capability, (4) power factor at input side is adjustable, (5) less weight and volume in design, and (6) long life usage [2], [3].

Basically, there is no limitation of frequency for MCs, however the output amplitude is limited to be smaller than input. Modulation technique can be used to solve this limitation problem [4]. There are two modulation strategies commonly used for MCs [5] namely: (1) method for carrier based modulation [6], and (2) space vector modulation (SVM) [2].

This paper briefly explains the most relevant strategies in modulation for IMC and provides the complexity and performance comparison of modulation strategies.

## II. IMC WORKING PRINCIPLE

Common circuits of MCs are usually known in two types of topologies i.e. (1) the conventional matrix converter (CMC) and (2) the indirect matrix converter (IMC). The first IMC topology was proposed by Kolar et al [7], and then developed by another researcher in [8]–[12], the basic principle of IMC are constructed from bidirectional current source rectifier (CSR) and voltage source inverter (VSI) without the use of any intermediate energy storage element [13] [14], as shown in Fig. 1. Commutation in zero

current for IMC applies together with the rectifier circuit and this circuit gives lower losses during switching and reliable topology.

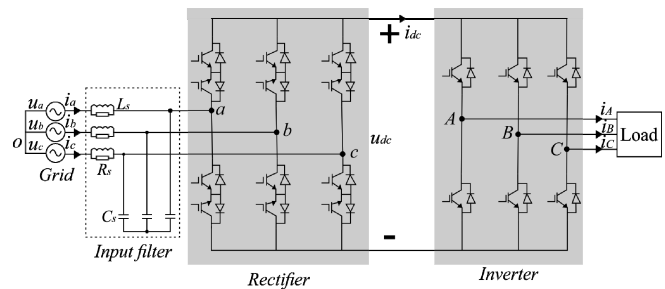


Fig. 1. Schematic diagram of IMC.

The indirect modulation separates each control on input current and output voltage side. The separation or it is also known as a decoupled strategy is carried out by decoupling transfer function  $\mathbf{T}$  of MCs into first transfer function for rectifier and the second transfer function for inverter [15].

Where:

$$\mathbf{T} = \mathbf{I} * \mathbf{R}$$

$$\begin{bmatrix} S_{aA} & S_{bA} & S_{cA} \\ S_{aB} & S_{bB} & S_{cB} \\ S_{aC} & S_{bC} & S_{cC} \end{bmatrix} = \begin{bmatrix} S_7 & S_8 \\ S_9 & S_{10} \\ S_{11} & S_{12} \end{bmatrix} \cdot \begin{bmatrix} S_1 & S_3 & S_5 \\ S_2 & S_4 & S_6 \end{bmatrix} \quad (1)$$

In equation (1), inverter switches  $S_7$ – $S_{12}$  and rectifier switches  $S_1$ – $S_6$ . Result to the product and sum of the input phases. As the equivalent circuit is observed from phase A of inverter output, then two switches  $S_7$  and  $S_8$  of phase A at half bridge are connected directly to phase a, b and c at input side through six switches on rectifiers [16].

## III. GENERAL CLASSIFICATION OF MODULATION STRATEGIES FOR MCs

Fig. 2 shows the classification of modulation methods developed for the IMC. Basically the most well known modulation on MCs is Pulse width modulation (PWM). PWM is classified into two type of modulation strategies, i.e. carrier-based and space vector modulation (SVM) [5]. Carrier-based modulation method is the simplest approach, while the SVM method has an elegant and powerful solution for IMC. The modulation method for IMC was very interested to developed, several method was developed for IMC modulation method proposed in [6], [13], [17]–[21], [21]–[24]



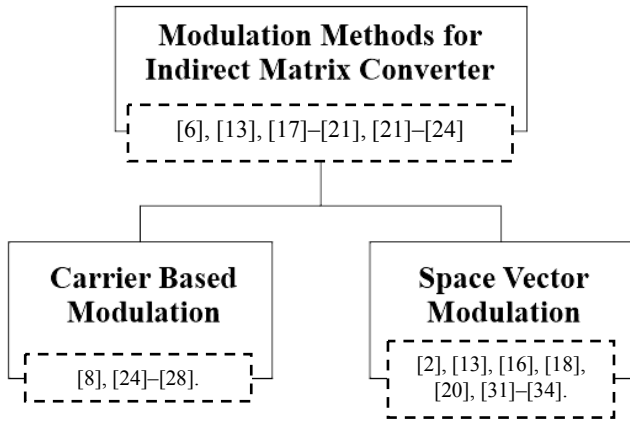


Fig. 2. Summary of modulation strategies for IMC.

#### IV. CARRIER-BASED MODULATION FOR IMC

The first research about carrier-based modulation for MC was proposed by Yoon *et al* [6], by changing the carrier of slope and using voltage offset. By using this techniques, synthesize product of unity power factor in sinusoidal input currents and desired output voltages is implemented. A carrier based PWM for IMC was proposed by Wang [17], where the algorithm of the carrier-based modulation is enhanced in two techniques. The first technique makes a continuous modulation function for all throws based on the designed sinusoidal input current. The switching functions are intended to focus on the zero current commutation which has derived from the modulation functions. More details about this method can be found in [17] and [25]. Different research about carrier-based modulation also proposed in [8], [24]–[28].

#### V. SPACE VECTOR MODULATION FOR IMC

SVM techniques for MCs are known in two different strategies. The first strategy is indirect space vector modulation taking the consideration of a virtual dc link and the second is direct space vector modulation presenting direct conversion [29], [30]. The first research about indirect space vector modulation or it is also known as indirect SVM was proposed by Borojevic *et al* [18], where matrix converter was constructed to combination circuit. This circuit, as it is shown in Fig. 3, synthesis CSI as current source inverter and VSI as voltage source inverter in the connection to a virtual dc link. Three phase inverter stage has six switches,  $S_7$ – $S_8$  for VSI and also other six switches,  $S_1$ – $S_6$  for rectifier circuit [15]. Other research about indirect SVM method are also proposed in [2], [13], [16], [18], [20], [31]–[34].

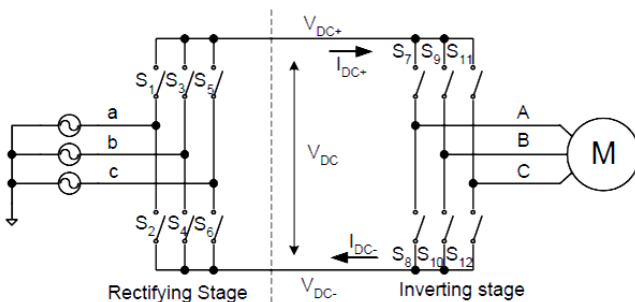


Fig. 3. The equivalent circuit for indirect modulation

Space vector PWM implemented rectifier-inverter in the indirect modulation technique. Three half bridges is not obligatory to follow as an output in this topology, so that only eight switches are possible to apply in the combinations. In Fig. 4(a), this proposed combination can be alienated into six active nonzero output voltage vectors i.e.  $V_1$ – $V_6$  and two zero output voltage vectors  $V_0$ .

The proposed virtual rectifier avoid an open circuit by using nine switching combinations. In this combination, six active nonzero input current vectors from  $I_1$ – $I_6$  and three zero input current vectors  $I_0$  are implemented. The implementation scheme is shown in Fig. 4(a). Current  $I_1$  (ab) gives indication that input phase a is bonded to the positive rail of the virtual DC-link  $V_{DC+}$ , then the input phase b is tied to the negative rail  $V_{DC-}$ . The last connection scheme is shown in Fig. 4(b).

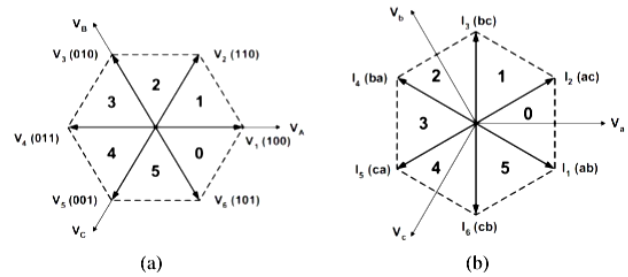


Figure 4: (a) inverter voltage hexagon. (b) rectifier current hexagon.

#### VI. COMPARISON OF THE MODULATION STRATEGIES

The presentation of modulation strategy discussed in this paper will be compared by considering the following parameters, including: (1) Complexity appeared in theory, (2) current quality at load side, (3) dynamic behaviour and response, (4) resonance of input filter, and (5) performance of the system under unbalanced voltage condition at input side.

##### A. Theoretical Complexity

In terms of complexity, carrier-based modulation are considered as a simple technique to generate pulses for gate drive in bidirectional power switches, although they are involve many equations[35]. While the SVM method has very complex to implement if we compare this with the carrier-based method or any other control method[5].

##### B. Quality of Load Current

From several observation in[5], [6], [13], [16], [17], [19], [21], [23], [28], we found that the quality of load current of the carrier-based modulation method and SVM method for MCs is deliver the high quality current to the load. That means quality of load current is not a big problem in the context of MCs.

##### C. Dynamics Behaviour and Response

The dynamic behaviour and response are important result parameter for some modulation and control method. While the dynamic response of carrier-based modulation method and SVM method is pretty good. Therefore from several observation for dynamic response parameter, we found that the control method like a direct torque control (DTC) and predictive control method has a better result on dynamic response parameter[5],[36].



#### D. Resonance of Input Filter

The significant issue in MCs when it is implemented and operated is a resonance of the input filter. A very significant impact on the input filter performance is the characteristic of the modulation method[36]–[39], an important observation not previously concerned. As a result, the modulation method works with a fixed switching frequency, in this case SVM method, have made resonance decreased in the input filter. While a Carrier-based modulation method has the input current with strong resonances in the input filter. This behaviour can be significantly improved and it must be considered at input current side.

#### E. Performance of the System Under Unbalanced Input Voltage Condition.

One of the most significant issues in influencing the performance of MCs is the input voltage condition[40], because of direct power conversion which implies instantaneous power transfer. From several observation through reference[30], [40], [41], [42], we found that the SVM method has a better solution for solving the unbalanced input voltage condition, while the carrier-based modulation has respectable result, although the carrier-based modulation does not need any extra algorithm as the unbalanced condition occurred in input voltage [42].

Based on observations from several references for these modulation methods, we can observe and analysis the comparison of the carrier-based modulation and space vector modulation for IMC. The comparison of these modulation methods has presented in Table I.

TABLE I. Comparison of Modulation Strategies for IMC

Parameter	Modulation method for IMC	
	Carrier-Based Modulation	Space Vector Modulation
Theoretical complexity	very simple	very complex
Quality of load current	good	very good
Dynamic response	good	good
Resonance of input filter	medium resonance	very low resonance
Performance under unbalanced input voltage condition	respectable	very good

#### VII. CONCLUSION

In recent years the development of MCs area is still interesting, especially in the scope of modulation method for IMC. There are two modulation strategies generally used for MCs namely: carrier-based modulation and space vector modulation. These methods have a different theoretical principles and also different complexity stages.

With the results written in this paper, carrier-based modulation have advantages especially on the level of complexity, where this method has the lowest level of complexity when compared to other methods including the SVM method. While the SVM method has an elegant and powerful solution for IMC. For the future observation, the

comparison and the assessment of the method may include more advanced technical aspect.

#### ACKNOWLEDGEMENT

This research was supported by Electrical Engineering Research Group of Ahmad Dahlan University.

#### REFERENCES

- [1] E. Yamamoto *et al.*, "Development of MCs and its applications in industry," *IEEE Ind. Electron. Mag.*, vol. 5, no. 1, pp. 4–12, 2011.
- [2] D. Casadei, G. Serra, A. Tani, and L. Zarri, "Matrix converter modulation strategies: a new general approach based on space vector representation of the switch state," *Ind. Electron. IEEE Trans.*, vol. 49, no. 2, pp. 370–381, 2002.
- [3] J. W. Kolar, T. Friedli, J. Rodriguez, and P. W. Wheeler, "Review of three-phase PWM AC-AC converter topologies," *IEEE Transactions on Industrial Electronics*, vol. 58, no. 11, pp. 4988–5006, 2011.
- [4] J. Lettl and D. Kuzmanovic, "Matrix Converter Induction Motor Drive Employing Direct Torque Control Method," *PIERS Online*, vol. 6, no. 8, pp. 711–715, 2010.
- [5] J. Rodriguez, M. Rivera, J. W. Kolar, and P. W. Wheeler, "A review of control and modulation methods for matrix converters," *IEEE Trans. Ind. Electron.*, vol. 59, no. 1, pp. 58–70, 2012.
- [6] Y. D. Yoon and S. K. Sul, "Carrier-based modulation technique for matrix converter," *IEEE Trans. Power Electron.*, vol. 21, no. 6, pp. 1691–1703, 2006.
- [7] J. W. Kolar, M. Baumann, F. Schafmeister, and H. Ertl, "Novel Three-Phase AC-DC-AC Sparse Matrix Converter Part I: Derivation, Basic Principle of Operation, Space Vector Modulation, Dimensioning," *Appl. Power Electron. Conf. Expo. 2002. APEC 2002. Seventeenth Annu. IEEE*, 2002.
- [8] K. Zhou and D. Wang, "Relationship between space-vector modulation and three-phase carrier-based PWM: A comprehensive analysis," *IEEE Trans. Ind. Electron.*, 2002.
- [9] J. Holtz and U. Boelkens, "Direct Frequency Converter with Sinusoidal Line Currents for Speed-Variable ac Motors," *IEEE Trans. Ind. Electron.*, 1989.
- [10] L. Wei and T. A. Lipo, "A novel matrix converter topology with simple commutation," *Conf. Rec. - IAS Annu. Meet. (IEEE Ind. Appl. Soc.)*, 2001.
- [11] J. W. Kolar, F. Schafmeister, S. D. Round, and H. Ertl, "Novel three-Phase AC-AC sparse matrix converters," *IEEE Trans. Power Electron.*, 2007.
- [12] C. Klumpner and F. Blaabjerg, "Modulation method for a multiple drive system based on a two-stage direct power conversion topology with reduced input current ripple," *IEEE Trans. Power Electron.*, 2005.
- [13] P. C. Loh, F. Blaabjerg, F. Gao, A. Baby, and D. A. C. Tan, "Pulsewidth Modulation of Neutral-Point-Clamped Indirect Matrix Converter," *IEEE Trans. Ind. Appl.*, vol. 44, no. 6, pp. 1805–1814, 2008.
- [14] Lixiang Wei, T. A. Lipo, and Ho Chan, "Matrix converter topologies with reduced number of switches," in *2002 IEEE 33rd Annual IEEE Power Electronics Specialists Conference. Proceedings (Cat. No. 02CH37289)*, 2002, vol. 1, no. 1, pp. 57–63.
- [15] Han Ju Cha, "Analysis and Design Of Matrix Converters for Adjustable Speed Drives and Distributed Power Sources," *Texas A&M Univ.*, no. August, 2004.
- [16] P. Chlebis, P. Simonik, and M. Kabasta, "The Comparison of Direct and Indirect Matrix Converters," vol. 1, no. January 2010, pp. 310–313, 2010.
- [17] B. Wang and G. Venkataramanan, "A carrier based PWM algorithm for indirect matrix converters," in *PESC Record - IEEE Annual Power Electronics Specialists Conference*, 2006.
- [18] D. Borjoević, "Space Vector Modulated Three-Phase to Three-Phase Matrix Converter with Input Power Factor Correction," *IEEE Trans. Ind. Appl.*, vol. 31, no. 6, pp. 1234–1246, 1995.
- [19] T. D. Nguyen and H.-H. Lee, "Modulation Strategies to Reduce Common-Mode Voltage for Indirect Matrix Converters," *IEEE Trans. Ind. Electron.*, vol. 59, no. 1, pp. 129–140, 2012.
- [20] X. Li, Y. Sun, J. Zhang, M. Su, and S. Huang, "Modulation Methods for Indirect Matrix Converter Extending the Input Reactive Power Range," *IEEE Trans. Power Electron.*, vol. 32, no. 6, pp. 4852–

- 4863, 2017.
- [21] M. Jussila and H. Tuusa, "Space-vector modulated indirect matrix converter under distorted supply voltage - Effect on load current," *PESC Rec. - IEEE Annu. Power Electron. Spec. Conf.*, vol. 2005, no. 1, pp. 2396–2402, 2005.
  - [22] T. Friedli, M. L. Heldwein, F. Giezendanner, and J. W. Kolar, "A high efficiency indirect matrix converter utilizing RB-IGBTs," *PESC Rec. - IEEE Annu. Power Electron. Spec. Conf.*, pp. 3–9, 2006.
  - [23] M. Jussila, M. Salo, and H. Tuusa, "Realization of a three-phase indirect matrix converter with an indirect vector modulation method," *IEEE 34th Annu. Conf. Power Electron. Spec. 2003. PESC '03*, vol. 2, pp. 689–694.
  - [24] P. Kiatsookkanatorn and S. Sangwongwanich, "A unified PWM method for matrix converters and its carrier-based realization using bipolar modulation technique," *IEEE Trans. Ind. Electron.*, 2012.
  - [25] F. Gruson, P. Le Moigne, P. Delarue, A. Videt, X. Cimetieffe, and M. Arpillière, "A simple carrier-based modulation for the SVM of the matrix converter," *IEEE Trans. Ind. Informatics*, 2013.
  - [26] L. M. Tolbert and T. G. Habetier, "Novel multilevel inverter carrier-based PWM method," *IEEE Trans. Ind. Appl.*, 1999.
  - [27] A. Hassanpoor, S. Norrga, H. P. Nee, and L. Angquist, "Evaluation of different carrier-based PWM methods for modular multilevel converters for HVDC application," in *IECON Proceedings (Industrial Electronics Conference)*, 2012.
  - [28] S. M. Ahmed, A. Iqbal, H. Abu-Rub, J. Rodriguez, C. A. Rojas, and M. Saleh, "Simple carrier-based PWM technique for a three-to-nine-phase direct ac-ac converter," *IEEE Trans. Ind. Electron.*, 2011.
  - [29] F. Gruson, P. Le Moigne, P. Delarue, M. Arpillière, and X. Cimetieffe, "Comparison of losses between matrix and indirect matrix converters with an improved modulation," in *IEEE International Symposium on Industrial Electronics*, 2010.
  - [30] G. T. Chiang and J. I. Itoh, "Comparison of two overmodulation strategies in an indirect matrix converter," *IEEE Trans. Ind. Electron.*, 2013.
  - [31] M. Y. Lee, P. Wheeler, and C. Klumpner, "Space-vector modulated multilevel matrix converter," *IEEE Trans. Ind. Electron.*, 2010.
  - [32] D. O. Neacsu, "Space Vector Modulation - An Introduction," *IEEE Annu. Conf. Ind. Electron. Soc.*, 2001.
  - [33] J. Wang, B. Wu, D. Xu, and N. R. Zargari, "Indirect space-vector-based modulation techniques for high-power multimodular matrix Converters," *IEEE Trans. Ind. Electron.*, 2013.
  - [34] M. Hamouda, H. F. Blanchette, K. Al-Haddad, and F. Fnaiech, "An efficient DSP-FPGA-based real-time implementation method of SVM algorithms for an indirect matrix converter," *IEEE Trans. Ind. Electron.*, 2011.
  - [35] L. Helle, K. B. Larsen, A. H. Jorgensen, S. Munk-Nielsen, and F. Blaabjerg, "Evaluation of Modulation Schemes for Three-Phase to Three-Phase Matrix Converters," *IEEE Trans. Ind. Electron.*, 2004.
  - [36] M. Rivera, P. Correa, J. Rodriguez, I. Lizama, and J. Espinoza, "Predictive control of the indirect matrix converter with active damping," in *2009 IEEE 6th International Power Electronics and Motion Control Conference, IPEMC '09*, 2009.
  - [37] M. Rivera, C. Rojas, J. Rodriguez, P. Wheeler, B. Wu, and J. Espinoza, "Predictive current control with input filter resonance mitigation for a direct matrix converter," *IEEE Trans. Power Electron.*, 2011.
  - [38] M. Rivera, J. Rodriguez, B. Wu, J. R. Espinoza, and C. A. Rojas, "Current control for an indirect matrix converter with filter resonance mitigation," *IEEE Trans. Ind. Electron.*, 2012.
  - [39] J. I. Itoh, K. Koiwa, and K. Kato, "Input current stabilization control of a matrix converter with boost-up functionality," in *2010 International Power Electronics Conference - ECCE Asia -, IPEC 2010*, 2010.
  - [40] F. Blaabjerg, D. Casadei, C. Klumpner, and M. Matteini, "Comparison of two current modulation strategies for matrix converters under unbalanced input voltage conditions," *IEEE Trans. Ind. Electron.*, vol. 49, no. 2, pp. 289–296, 2002.
  - [41] J. I. Itoh, K. Koiwa, and K. Kato, "Input current stabilization control of a matrix converter with boost-up functionality," in *2010 International Power Electronics Conference - ECCE Asia -, IPEC 2010*, 2010, pp. 2708–2714.
  - [42] Y. Yoon and S. Sul, "Carrier-based modulation method for matrix converter with input power factor control and under unbalanced input voltage conditions," *Power Electron. Conf. APEC 2007*, pp. 310–314, 2007.

# Review on Adjustable Speed Drive Techniques of Matrix Converter Fed Three-Phase Induction Machine

Arsyad Cahya Subrata  
Department of Electrical Engineering  
Universitas Ahmad Dahlan  
Yogyakarta, Indonesia  
[arsyadcahya@gmail.com](mailto:arsyadcahya@gmail.com)

Tole Sutikno  
Department of Electrical Engineering  
Universitas Ahmad Dahlan  
Yogyakarta, Indonesia  
[tole@ee.uad.ac.id](mailto:tole@ee.uad.ac.id)

Aiman Zakwan Jidin  
Department of Electronics & Computer  
Engineering Technology  
Universiti Teknikal Malaysia Melaka  
Malacca, Malaysia  
[aimanzakwan@utem.edu.my](mailto:aimanzakwan@utem.edu.my)

Auzani Jidin  
Department of Power Electronics and  
Drives  
Universiti Teknikal Malaysia Melaka  
Malacca, Malaysia  
[auzani@utem.edu.my](mailto:auzani@utem.edu.my)

**Abstract**—Adjustable Speed Drive (ASD) fed Matrix Converter is an interesting topic and is widely discussed in several articles. ASD provides many advantages, especially in the industrial sector because it increases work efficiency so as to reduce production costs. The induction machines construction is sturdy and its relatively inexpensive maintenance makes it more desirable in industrial process applications. Whereas the Matrix Converter (MC) construction without dc-link capacitors makes it more compact compared to conventional converters. This article discussed the ASD control modulation technique by using MC on a three-phase induction motor.

**Keywords**—Adjustable Speed Drive (ASD), Matrix Converter (MC), Three-Phase Induction Machine, Space Vector Modulation

## I. INTRODUCTION

Adjustable Speed Drive (ASD) on the induction machine is an interesting topic and is widely discussed in several articles. ASD is an electromagnetic system that is suitable to be implemented in industrial applications [1]. The application of ASD on an induction machine provides an increase in power consumption efficiency, so as to provide benefits, especially in the industrial sector and other sectors that use induction machines as a driving motor [2], [3]. ASD provides a continuous speed control circuit on an induction machine. This system optimizes industrial processes and reduces production costs and energy consumption costs.

An induction machine is an interesting choice in the industrial field because it is easy to maintain and a simpler and more robust physical form [4]. Another advantage of the induction engine is the DC engine in terms of size, efficiency, cost, service life and maintenance [5]. Induction machines are generally more desirable in industrial applications than other types of machines. The induction

machine has a constant input supply voltage and the frequency operates at a constant speed. Nearly 60% -65% of the electricity resources are consumed by electric motor drives. In conventional methods, induction motors are combined with other equipment which causes energy waste. Motor speed control by the converter saves energy up to 20% [6]. Therefore a system that is capable of controlling machine speed is needed.

Induction machine speed is controlled by changing the frequency and voltage values. The most promising possibility to change motor speed is to vary the frequency. The current is also controlled by voltage so it offers the possibility to control voltage and change the good frequency [7]. This is achieved by using conventional inverter and converters. The AC-DC-AC converter consists of a controlled or uncontrolled converter, inverter and a dc-link capacitor connected between the converter and the stage inverter. The input supply is connected to the converter while the load is connected to the inverter side [8]. However, the use of conventional inverters and converters as the induction engine speed controller has various problems, among them, are expensive main components and relatively large physical structures. In 1980, Alesina and Venturini introduced an AC-AC converter topology composed of nine bidirectional switches in the form of a 3\*3 matrix known as the Matrix Converter (MC), which is more efficient compared to conventional AC-DC-AC converters. Modeling results conducted by B. Geetha Lakshmi et al, ASD using MC operates well and reduces interharmonics when compared to conventional AC / DC / AC conversion methods.

The simple MC design, not using large dc-link capacitors as energy storage and ease of control of power factor input makes it an advantage that is more concise and practical. Another advantage of MC is that it has a more dynamic performance compared to conventional AC-DC-AC converters [9]. MC becomes an alternative to back-to-back converters because it converts the AC voltage directly

into AC output voltage. The advantage of using MC between is not having a large dc-link capacitor, providing bi-directional power flow, input current and output in the form of sinusoidal waves, input power factor is controlled, high power density, four quadrant operations, regeneration capabilities, concise and simple design [10], [11]. The MC parts are shown in Figure 1. The first part is a three-phase AC power supply. The second part is the MC input filter which functions to filter the input current and produce the capacitive voltage source needed by the MC. The third part is the MC itself.

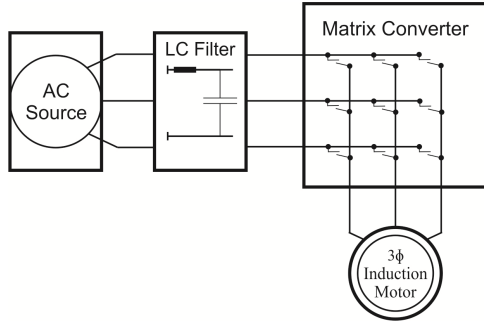


Figure 1. General Matrix Converter

Applications in the industry require AC-AC power conversion. AC-AC converters take power from one AC system and send to another AC system in the form of a wave or amplitude and frequency or phase difference. The AC-AC converter is clarified into two categories: Direct converter and Indirect converter [12]. In general, MC topology is divided into two major parts, namely Direct Matrix Converter (DMC) and Indirect Matrix Converter (IMC). An ASD control with MC on three-phase induction machines uses several modulation strategies. This article discusses the strategy of space vector modulation (SVM) for the control of three-phase induction machines in DMC and IMC.

## II. SPACE VECTOR MODULATION ON DMC

The DMC shown in Figure 2 does not require two AC-DC and DC-AC conversion stages. This converter converts AC directly into AC and hence, it eliminates the unnecessary conversion processes [13]. DMC contains a bidirectional matrix switch that interconnects each phase of input with output. Three-phase induction motor connected to the DMC with nine bidirectional switches. The symbol of  $S_{ij}$  ( $i=a, b, c$  and  $j=A, B, C$ ) represents the ideal bidirectional switch, where  $i$  is the output voltage index and  $j$  is the input voltage index. Then  $[V_i]$  is used as a vector from the input voltage.

$$V_i = V_{ims} \begin{bmatrix} \cos(\omega_i t) \\ \cos(\omega_i t - \frac{2\pi}{3}) \\ \cos(\omega_i t - \frac{4\pi}{3}) \end{bmatrix}$$

Then  $[V_o]$  is used as a vector from the output voltage.

$$V_o = V_{oms} \begin{bmatrix} \cos(\omega_o t) \\ \cos(\omega_o t - \frac{2\pi}{3}) \\ \cos(\omega_o t - \frac{4\pi}{3}) \end{bmatrix}$$

$$V_o = [M][V_i]$$

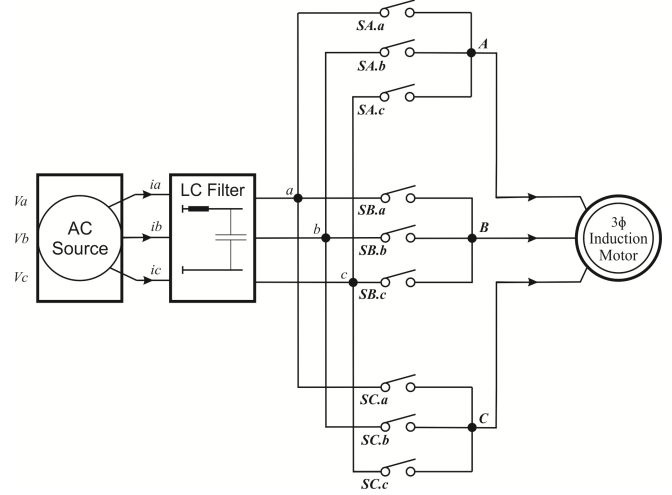


Figure 2. DMC Topology

When the input current is  $[I_i]$  then the output current is

$$I_i = [M]^T [I_o]$$

$[M]^T$  represents the transposed of the matrix  $[M]$ . When commuting, bidirectional switches must meet the following conditions.

- Each input phase voltage is not connected to the same output line to avoid short-circuit.
- The output phase is not opened to prevent interference with inductive loads.

By defining the transfer function every bidirectional switch is as

$$S_{ij}(t) = \begin{cases} 1, & S_{ij} \text{ closed} \\ 0, & S_{ij} \text{ open} \end{cases}$$

Where,  $i \in \{a, b, c\}$ ,  $j \in \{A, B, C\}$

These two conditions are expressed by

$$S_{aj} + S_{bj} + S_{cj} = 1; j \in \{A, B, C\}$$

Under these circumstances, 3\*3 MC only allows 27 switching of 512 combinations. Each T only switches one  $S_{ij}$  ( $j = a, b, c$ ) to ensure a closed loop load current. The switching frequency  $f_s = f_o / 2\pi$  must have a value twenty times higher than the maximum input  $f_i f_o$  ( $f_s \gg 20 \times \text{Max}(f_i f_o)$ ).

During the T period (sequential period) which is equal to  $1/f_s$ , the amount of conduction time used to synthesize the same output phase must be the same as  $T_a$ . Now the time  $T_{ij}$  is called modulation is defined  $t_{ij} = m_{ij} \cdot T_s \cdot t_{ij} = m_{ij} T_s$ .

According to [14], Direct Matrix Converter topology has the following features:

- It has a sinusoidal input current and output voltage
- It uses bidirectional switches that allow energy regeneration to the source.
- It allows adjustment of the input power factor of the converter, power factor is easily achieved.
- It is more compact on physical size and more cost-effective because it does not use DC energy storage links.

Research conducted by [15] controls SVM in DMC by applying the following formula:

$$\underline{x} = \frac{2}{3} (\underline{x}_1 + a \cdot \underline{x}_2 + a^2 \cdot \underline{x}_3) \text{ and } a = e^{j\frac{2\pi}{3}}$$

The output voltage vector reference  $\underline{v}_0$  and the input current  $\underline{i}_i$  are represented in the following formula:

$$\underline{v}_0 = \frac{2}{3} (v_a + a \cdot v_b + a^2 \cdot v_c) = v_0 \cdot e^{j\alpha_0}$$

$$\underline{i}_i = \frac{2}{3} (i_A + a \cdot i_B + a^2 \cdot i_C) = I_i \cdot e^{j\beta_i}$$

The specified switching condition produces 27 configurations for the 3\*3 structure on the MC. The reference voltage vector  $\underline{v}_0^*$  is obtained from two adjacent vector directions. This direction corresponds to the configuration pair  $\pm 1, \pm 2, \pm 3, \pm 7, \pm 8, \pm 9$ . Similarly the current reference vector  $\underline{i}_i^*$  is obtained from two directions located on both sides of the vector and obtained with a configuration of  $\pm 1, \pm 4, \pm 3, \pm 6, \pm 7, \pm 9$ . The chosen configuration pair is that which appears from both lists, in this case, the configuration pair is  $\pm 1, \pm 3, \pm 7, \pm 9$ . Therefore the four configurations used depend on the  $K_v$  sector where the desired output voltage  $\underline{v}_0^*$  vector and  $K_i$  sector are the reference vectors of the input current  $\underline{i}_i^*$ .

Stationary and voltage vector representations that are recorded  $K_v$  for voltage and  $K_i$  for current are shown in Figure 3.

The duty cycle is calculated by the following formula:

$\alpha_0$  is the angle between the desired output voltage vector and the line for the sector.

$\beta_i$  is the angle between the desired input current vector and the line for the vector.

$\cos(\theta_i)$  is the input power factor.

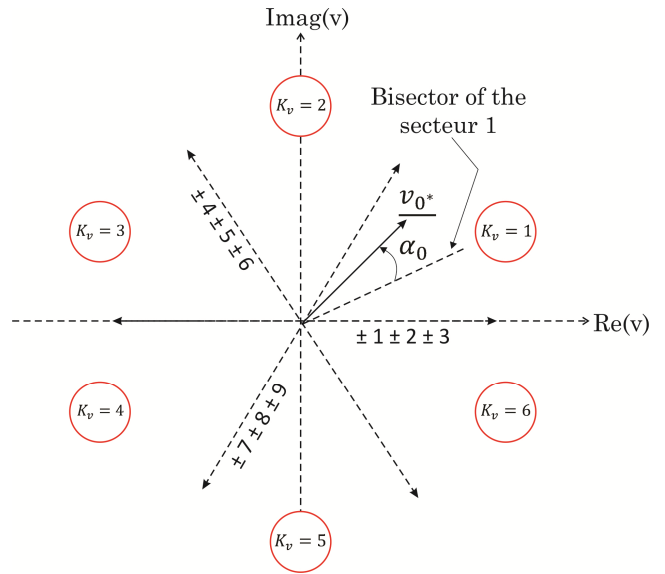


Figure 3. The direction of output voltage vector and output current vector

$$\begin{cases} \delta_I = (-1)^{K_v+K_i} \cdot \frac{2}{\sqrt{3}} \cdot q \cdot \frac{\cos(\alpha_0 - \frac{\pi}{3}) \cos(\beta_i - \frac{\pi}{3})}{\cos(\theta_i)} \\ \delta_{II} = (-1)^{K_v+K_i+1} \cdot \frac{2}{\sqrt{3}} \cdot q \cdot \frac{\cos(\alpha_0 - \frac{\pi}{3}) \cos(\beta_i + \frac{\pi}{3})}{\cos(\theta_i)} \\ \delta_{III} = (-1)^{K_v+K_i+1} \cdot \frac{2}{\sqrt{3}} \cdot q \cdot \frac{\cos(\alpha_0 + \frac{\pi}{3}) \cos(\beta_i - \frac{\pi}{3})}{\cos(\theta_i)} \\ \delta_{IV} = (-1)^{K_v+K_i} \cdot \frac{2}{\sqrt{3}} \cdot q \cdot \frac{\cos(\alpha_0 + \frac{\pi}{3}) \cos(\beta_i + \frac{\pi}{3})}{\cos(\theta_i)} \end{cases}$$

The duration of the zero vector to complete the modulation period is given with the following formula:

$$\delta_0 = 1 - (\delta_I + \delta_{II} + \delta_{III} + \delta_{IV})$$

### III. SPACE VECTOR MODULATION ON IMC

The IMC shown in Figure 4 has a rectification process (AC-DC) and an inversion process (DC-AC). In other words the IMC performs a two-stage conversion. This converter has a rectifier and inverter but does not have the DC storage energy. IMC is classified based on topology and number of devices used. In general, IMC consists of a bidirectional current rectifier following a standard Voltage Source Inverter (VSI). IMC gets a lot of attention and there are some innovative topologies that reduce the number of switches, namely sparse, very sparse and ultra-sparse MC [16].

It is assumed that the three-phase input voltage is given in the following equation:



$$V_{sa} = V_m \cos \theta_a = V_m \cos(\omega_i t)$$

$$V_{sb} = V_m \cos \theta_b = V_m \cos\left(\omega_i t - \frac{2\pi}{3}\right)$$

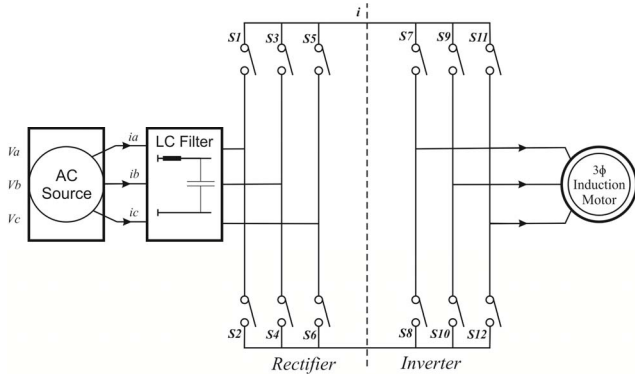


Figure 4. IMC Topology

$$V_{sc} = V_m \cos \theta_c = V_m \cos\left(\omega_i t + \frac{2\pi}{3}\right)$$

On the load side:

$$I_A = I_0 \cos \theta_{0a} = I_0 \cos(\omega_0 t + \varphi_0)$$

$$I_B = I_0 \cos\left(\omega_0 t + \varphi_0 - \frac{2\pi}{3}\right)$$

$$I_C = I_0 \cos\left(\omega_0 t + \varphi_0 + \frac{2\pi}{3}\right)$$

The final formula shows the current in the load. Where  $\omega_0$  and  $\omega_i$  are the frequency of the input and output angles. Whereas  $\varphi_0$  is the initial electric angle of the phase A output current. Then  $V_m$  and  $I_0$  are the peak amplitude of the input voltage and the output current.

However, the IMC at low voltage transfer ratios still has several problems and methods need to be developed to improve the output waveform so as to optimize operating performance. The method to improve the output waveform is categorized into two, namely the control algorithm, which is used to compensate for various non-linear factors, and the modulation strategy. In commutation and semiconductor loading schemes, IMC has a more simple commutation because of its two-stage structure, but it sacrifices more electrical devices connected and produces higher semiconductor losses and lower efficiency compared to DMC.

According to the research conducted by [17] applying SVM to IMC, the space vector diagram in SVM is shown in Figure 5, where six active vectors switching ( $\vec{i}_1 \sim \vec{i}_6$  or  $\vec{u}_1 \sim \vec{u}_6$ ) dividing the complex field into six sectors. The three desired output voltages or input current vectors are located in certain sectors and are synthesized by two adjacent active vectors and zero vectors. Then the duty

cycle vector is calculated according to the volt-second balance or the balance of the capacitor charge.

Assume the vector input voltage is denoted as  $\vec{u}_i = U_{im} e^{j\alpha_i}$  where  $U_{im}$  and  $\alpha_i$  is the position of amplitude and angle  $\vec{u}_i$ . The desired vector input  $\vec{i}_i = I_{im} e^{j\varphi_i}$  lying in the sector  $I = (\varphi_i \in [-\frac{\pi}{6}, \frac{\pi}{6}])$  as shown in Figure 5 (a), the cycle duty vector cycle used is

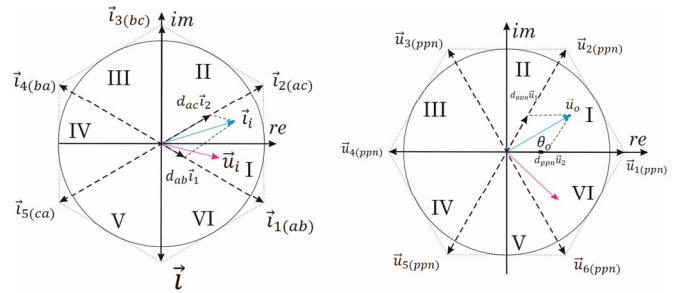


Figure 5. Diagram of space vector on IMC, (a) rectifier stage, (b) stage inverter

$$\begin{cases} d_{ab} = m_i \sin\left(\frac{\pi}{6} - \varphi_i\right) \\ d_{ac} = m_i \sin\left(\frac{\pi}{6} + \varphi_i\right) \\ d_{ro} = 1 - d_{ab} - d_{ac} \end{cases}$$

Where  $\varphi_i$  is the position of the angle  $\vec{i}_i$ ,  $m_i$  shows the receiver modifier index, and  $0 \leq m_i \leq 1$ .

As shown in Figure 5 (b), it is assumed that the desired output voltage vector is  $\vec{u}_o = U_{om} e^{j\theta_o}$  is also located in sector  $I = (\theta_o \in [0, \frac{\pi}{3}])$ , duty cycle the one from the vector used is

$$\begin{cases} d_{pnn} = m_o \sin\left(\frac{\pi}{3} - \theta_o\right) \\ d_{pnn} = m_o \sin(\theta_o) \\ d_{ro} = 1 - d_{pnn} - d_{pnn} \end{cases}$$

Where  $\theta_o$  is the angle position  $\vec{u}_o$ ,  $m_o$  s the inverter modulation index, and  $0 \leq m_o \leq 1$ .

A combination of rectifier and inverter modulation process, the final duty cycle is written as

$$\begin{cases} d_{ab,pnn} = d_{ab} d_{pnn} = k \sin\left(\frac{\pi}{6} - \varphi_i\right) \sin\left(\frac{\pi}{3} - \theta_o\right) \\ d_{ab,pnn} = d_{ab} d_{pnn} = k \sin\left(\frac{\pi}{6} - \varphi_i\right) \sin(\theta_o) \\ d_{ac,pnn} = d_{ac} d_{pnn} = k \sin\left(\frac{\pi}{6} + \varphi_i\right) \sin\left(\frac{\pi}{3} - \theta_o\right) \\ d_{ac,pnn} = d_{ac} d_{pnn} = k \sin\left(\frac{\pi}{6} + \varphi_i\right) \sin(\theta_o) \\ d_o = 1 - d_{ab,pnn} - d_{ab,pnn} - d_{ac,pnn} - d_{ac,pnn} \end{cases}$$



Where  $k = m_r m_o$ . o make it simpler,  $m_o$  is set to one and all modulation indices used to modulate the inverter are set to one in the following section.

Then to get the desired output voltage and input current, it must be satisfactory

$$k = m_r = \frac{q}{q_{\max} \cos(\phi_i)}$$

Where  $q$  is the voltage transfer ratio, and  $q_{\max} \left(\frac{\sqrt{3}}{2}\right)$  shows the maximum linear voltage transfer ratio;  $\phi_i$  is the input power factor angle, and  $\phi_i = \varphi_i - \alpha_i$ .

Usually, in the rectifier stage, only active vectors are active (eg  $\vec{i}_{1(ab)}$  and  $\vec{i}_{2(ab)}$ ) are used to reduce turnover time. The dc-link voltage  $U_{dc}$  only consists of two voltage line-to-line input segments  $U_{ab}$  and  $U_{ac}$ . Therefore,  $d_{r0}$  must be distributed to  $d_{r0(ab)}$  and  $d_{r0(ac)}$  as follows

$$\begin{cases} d_{r0(ab)} = d_{r0} + d_{r0(ab)} \\ d_{r0(ac)} = d_{r0} + d_{r0(ac)} \\ d_{r0(ab)} + d_{r0(ac)} = 1 \end{cases}$$

where  $d_{r0(ab)}$ ,  $d_{r0(ac)}$  are the duty cycles  $\vec{i}_{1(ab)}$  and  $\vec{i}_{2(ab)}$  after distribution, respectively; and  $d_{r0(ab)}$ ,  $d_{r0(ac)}$  must meet the following limits.

$$\begin{cases} d_{r0} = d_{r0(ab)} + d_{r0(ac)} \\ d_{r0(ab)} \geq 0, d_{r0(ac)} \geq 0 \end{cases}$$

One of the most commonly used ways to distribute zero vectors is that  $d_{r0}$  is divided into  $d_{r0(ab)}$  and  $d_{r0(ac)}$  in proportion as

$$\begin{cases} d_{r0(ab)} = \frac{d_{r0}}{d_{r0(ab)} + d_{r0(ac)}} d_{r0} \\ d_{r0(ac)} = \frac{d_{r0}}{d_{r0(ab)} + d_{r0(ac)}} d_{r0} \end{cases}$$

#### IV. COMPARISON BETWEEN DMC AND IMC FED THREE-PHASE INDUCTION MACHINE

The main strategy of ASD driven by the MC is to maintain the current and engine flux at the desired value [18]. In the case of induction motor control, DMC and IMC have several differences in output voltage and power losses that affect the efficiency of the motor. DMC has better supply current and voltage transfer characteristics, smaller voltage losses, and losses. The sinusoidal output wave needed for the working conditions of the ASD system is better. DMC works effectively when given a large modulation index. But when working at low voltages, IMC has superior performance [19]–[21]. Comparison between DMC and IMC in three-phase induction machines is seen in Table 1.

Table 1. Comparison between DMC and IMC

ASD on Induction Machine	DMC	IMC
Supply Current Quality	HIGH	LOW
Voltage Loss	LOW	HIGH
Power Loss	LOW	HIGH
Low Voltage Performance	LOW	HIGH
Large Modulating Index Performance	HIGH	LOW
Sinusoidal Waveforms for working condition	HIGH	LOW

#### V. CONCLUSION

This article discusses the comparison between DMC and IMC by implementing an SVM strategy when performing ASD on an induction motor. From several articles found, ASD using DMC has advantages compared to IMC. Although DMC dominates the advantages of various characteristics, IMC shows superiority when working at low voltage. This shows that the DMC and IMC have their respective advantages in different conditions. Therefore, the application of ASD on an induction motor uses one of the two topologies that have been discussed according to their individual needs.

#### REFERENCES

- [1] K. C. Roy, "Investigations on Matrix Converter for Induction Motor Drive during Abnormal Conditions," pp. 1–4, 2014.
- [2] K. Quiraishi and Dr. S. P. Dubey, "Comparative Analysis on Matrix Converter Fed Induction Motor With No Load and Load Condition," vol. 2, no. 4, pp. 331–334, 2014.
- [3] E. P. Wiechmann, S. Member, R. P. Burgos, and S. Member, "Continuously Motor-Synchronized Ride-Through Capability for Matrix-Converter can-Speed Drives," vol. 49, no. 2, pp. 390–400, 2002.
- [4] P. Karlovský and J. Lettl, "Application of MRAS Algorithm to Replace the Speed Sensor in Induction Motor Drive System," *Procedia Eng.*, vol. 192, pp. 421–426, 2017.
- [5] A. Bhavssar and P. Khampariya, "Induction Motor Fed by Matrix Converter , Modeling , Simulation and Implementation," no. 4, pp. 1079–1083, 2017.
- [6] D. Sri Vidhya and T. Venkatesan, "Quasi-Z-Source Indirect Matrix Converter Fed Induction Motor Drive for Flow Control of Dye in Paper Mill," *IEEE Trans. Power Electron.*, vol. 33, no. 2, pp. 1476–1486, 2018.
- [7] G. Kohlrusz and D. Fodor, "Comparison of Scalar and Vector Control Strategies of Induction Motors," *Hungarian J. Ind. Chem. Veszprém*, vol. 39, no. 2, pp. 265–270, 2011.
- [8] S. P. Karthikeyan, "A Technology Review on Matrix Converter," no. Mc, pp. 4–6, 2017.
- [9] E. E. M. Mohamed and M. A. Sayed, "Matrix converters and three-phase inverters fed linear induction motor drives-Performance compare," *Ain Shams Eng. J.*, 2016.
- [10] B. Geethalakshmi, K. Babu, and S. S. Santhoshma,

- “Analysis of interharmonics in conventional and matrix converter fed adjustable speed drives,” *India Int. Conf. Power Electron. IICPE*, 2012.
- [11] S. Pan, “High Performance Digital Control Techniques,” vol. 4, no. 1, pp. 1–22, 2008.
- [12] S. K. Bhavithra and M. Balasubramanian, “Matrix Converter Fed Induction Motor Drive,” vol. 24, no. 3, pp. 776–781, 2016.
- [13] D. S. Vidhya and T. Venkatesan, “A Review on Performance Analysis of Matrix Converter Fed AC Motor Drive,” vol. 7, no. 1, 2016.
- [14] D. NNADI and C. OMEJE, “Steady state analysis of a three phase indirect matrix converter fed 10 HP, 220 V, 50 Hz induction machine for efficient energy generation,” *Turkish J. Electr. Eng. Comput. Sci.*, vol. 24, pp. 3877–3897, 2016.
- [15] L. Rmili, S. Rahmani, F. Fnaiech, and S. Member, “Space Vector Modulation Strategy for a Direct Matrix Converter,” 2013.
- [16] T. Shi, X. Zhang, S. An, Y. Yan, and C. Xia, “Harmonic suppression modulation strategy for ultra-sparse matrix converter,” *IET Power Electron.*, vol. 9, no. 3, pp. 589–599, 2016.
- [17] X. Li, Y. Sun, J. Zhang, M. Su, and S. Huang, “Modulation Methods for Indirect Matrix Converter Extending the Input Reactive Power Range,” *IEEE Trans. Power Electron.*, vol. 32, no. 6, pp. 4852–4863, 2017.
- [18] R. Prasad, K. Basu, K. K. Mohapatra, and N. Mohan, “Ride-through study for matrix-converter adjustable-speed drives during voltage sags,” *IECON Proc. (Industrial Electron. Conf.)*, pp. 686–691, 2010.
- [19] P. Chlebis, P. Simonik, and M. Kabasta, “The Comparison of Direct and Indirect Matrix Converters,” vol. 1, no. June, pp. 310–313, 2010.
- [20] M. Jussila and H. Tuusa, “Comparison of Direct and Indirect Matrix Converters in Induction Motor Drive,” *IECON 2006 - 32nd Annu. Conf. IEEE Ind. Electron.*, pp. 1621–1626, 2006.
- [21] A. Trentin, P. Zanchetta, L. Empringham, L. De Lillo, P. Wheeler, and J. Clare, “Experimental Comparison between Direct Matrix Converter and Indirect Matrix Converter Based On Efficiency,” *IEEE Energy Convers. Congr. Expo.*, pp. 2580–2587, 2015.

# A Survey on Topologies and Controls of Z-Source Matrix Converter

Tri Wahono

Department of Electrical Engineering  
Universitas Ahmad Dahlan  
Yogyakarta, Indonesia  
triwahono060@gmail.com

Tole Sutikno

Department of Electrical Engineering  
Universitas Ahmad Dahlan  
Yogyakarta, Indonesia  
tole@ee.uad.ac.id

Nuryono Satya Widodo

Department of Electrical Engineering  
Universitas Ahmad Dahlan  
Yogyakarta, Indonesia  
nuryono.sw@ee.uad.ac.id

Mochammad Facta

Department of Electrical Engineering  
Universitas Diponegoro  
Semarang, Indonesia  
mochfacta@gmail.com

**Abstract**—This paper describes the Z-source matrix converter (ZS-MC) topology which specifically discusses topology and control on the ZS-MC. There are two topologies on the ZS-MC, namely Z-source direct-MC (ZS-DMC) and indirect-MC (ZS-IMC). The difference of each of these topologies is in the number of switching mosfets, where ZS-DMC put on nine switches, while ZS-IMC eighteen switches. ZS-IMC topology overcomes the limitations of traditional MC voltage reinforcement and accommodates the operation of buck and boost converter by reducing the number of switches and providing high efficiency.

**Keywords**— Z-source matrix converter (ZS-MC), Z-Source direct matrix converter (ZS-DMC), Z-Source Indirect matrix converter (ZS-IMC), Topologies, Modulation, Control

## I. INTRODUCTION

There are several converter techniques, namely ac-to ac converters which are often called cyclo-converter, dc-to-dc converter, dc-to ac inverter, and rectifier ac-to dc from some of these techniques, how it works with directional models. The classification of the model is a weakness that can only work in one direction, so there are still many stress losses [1]. Therefore the emergence of a matrix converter, matrix converter topology is promising for universal power conversion. The converter matrix offers several significant advantages, like a power factor that can be adjusted. ac-to ac matrix converter topology provides a transformation system for both amplitude and frequency simultaneously in multi-phase voltages without the use of energy storage [2]. Matrix converter can produce sinusoidal signal input current and output frequency higher than input frequency [2][3]. There are two matrix converter topologies including direct matrix converter (DMC) and indirect matrix converter (IMC), DMC can convert voltage and current in one step by using a bidirectional switch that is controlled [4].

As an alternative IMC has a two-stage power conversion with an input stage with six bidirectional switches. The constraints on this topology are voltage reinforcement. therefore z-source topology has high performance and can operate at various load susceptibility [5], by implementing the Z-source network to the conventional three-phase matrix converter utilizes the boost operation, so that the transfer ratio of voltage reached by combining the two topologies to design the Z-source matrix converter (ZS-MC).

ZS-MC does not use a complicated turnover strategy because the Z-source matrix converter intentionally employs the short circuit that is avoided in the conventional matrix [6][7]. Z-source matrix converter is divided into two, namely Z-source indirect matrix converter (ZS-IMC) and Z-source direct matrix converter (ZS-DMC). The operation of the ZS-MC is explained by two modes, such as shoot through zero states and non-shoot through the states. In this paper discusses topology and control in ZS-MC. Section II discusses ZS-MC method, by applying Z-source to utilize the voltage ratio gain feature. Section III discusses ZS-IMC which explains the configuration, control, modulation, and the development of ZS-IMC which is quasi Z-source indirect matrix converter. For section IV discusses the ZS-DMC which consists of configuration, control, and modulation. In section V it represents the two topologies, ZS-IMC topology overcomes the limitations of traditional MC voltage reinforcement and accommodates the operation of buck and boost converter by reducing the number of switches and providing high efficiency.

## II. Z-SOURCE MATRIX CONVERTER TOPOLOGIES

ZS-MC is a new topology that implements the Z-source network (ZS-N), to overcome the limitations of the voltage transfer ratio that has been carried out on conventional matrix converters. The converter uses an exclusive impedance network on the main circuit of the converter to the main power source to create the operation of buck and boost [8]. Deploying the ZS-N to utilize the voltage ratio gain feature is intended to remove complicated switching strategies because ZS-MC deliberately uses the short circuit that is avoided in conventional matrix converters. Fig.1 is a scheme of ZS-MC.

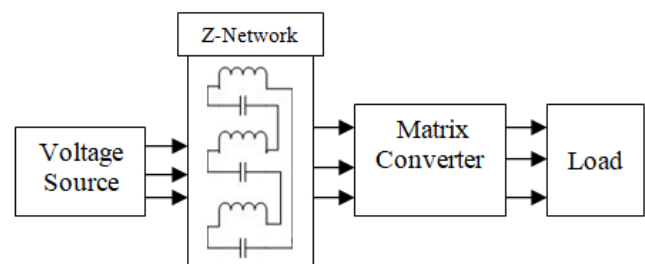


Fig. 1. ZS-MC scheme

Fig. 2 shows the structure of the ZS-MC. There are two structure, namely ZS-IMC and ZS-DMC. The ZS-IMC has been possibly developed as Quasi ZS-IMC.

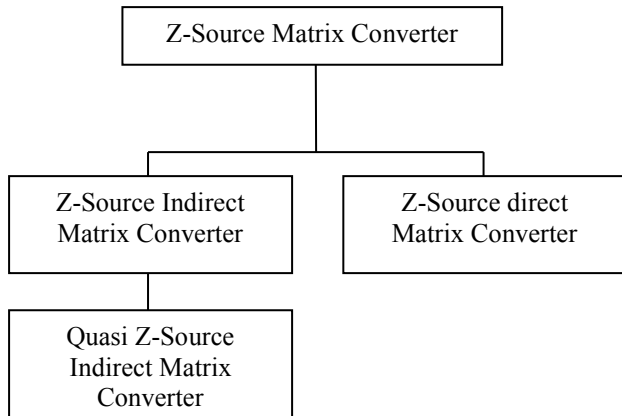


Fig. 2. ZS-MC classification

### III. Z-SOURCE INDIRECT MATRIX CONVERTER

ZS-IMC has 18 bidirectional switches that convert voltage and current in one step as development for a choice to matrix converter. This configuration is made of two conventional converters combined together; this indirect converter circuit has two stages. The first stage is the rectifier and the second stage is the inverter. Two switching cells form rectifier for the proposed topology.

#### A. Configuration of ZS-IMC

The topology of ZS-IMC is illustrated in Fig 3. The fundamental idea of the ZS-IMC is a separation in three stage for AC/AC conversion: In the Z-source, the rectifier stage is constructed from six switches, two directions are constructed with 18 switch directions [9][10], while the inverter level has six feedback. a two-port circuit consisting of a capacitor separator  $L_4$  and  $L_5$  and  $C_4$  and  $C_5$  connected, form X is used to provide the source of the combined impedance of the router level to the inverter stage, section  $S_1$  is used bidirectional [11].

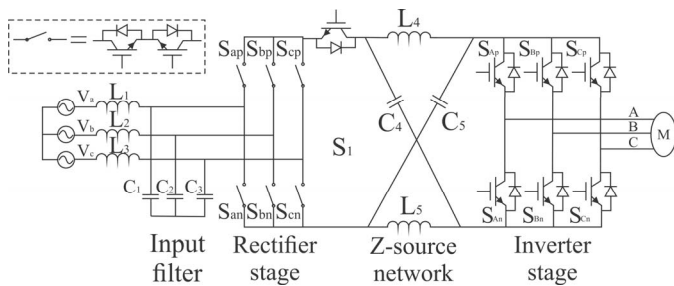


Fig. 3. Topology configuration of ZS-IMC [11].

#### B. Control of ZS-IMC

The ZS-IMC consists of three parts: the source-side Matrix Converter, Z-source network, and matrix converter side-load [2], [12], [13]. The most important aspect of ZS-MC is to execute the operation of buck and boost converter. The topology can increase and decrease the output voltage

compared to the input voltage. Each ZS-IMC utilizes 18 ac switches, so in practical it will be difficult to direct implementation [14]. However, this gave us the finishing point for the proposed topology and assisted us to conclude several practical ZS-MCs. Fig. 4 shows an example of simplified ZS-MC, where the MC source-side in Fig. 3, substituted by three-phase AC switch symbolized as  $S_0$ . When  $S_0$  is stored, then the operation of simplified ZS-MC is the same as traditional VS-MC procedure [9], [15]. An active voltage and zero voltage to the shoot-through status load is produced and included in the PWM MC, and the  $S_0$  is in off position during the shoot-through status. As the interval of the shoot-through become longer, then the output voltage becomes greater and increase. The proposed mechanism clearly reduces the number of switches, compared to the combination shown in Fig. 4.

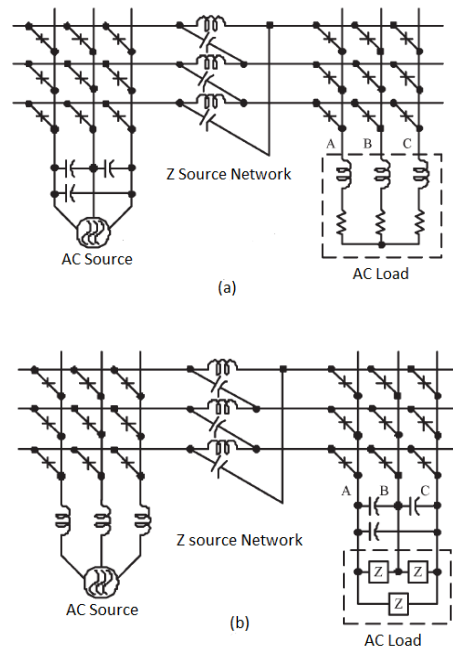


Fig. 4. ZS-IMC (a) Voltage-fed, (b) Current-fed [16].

#### C. Modulation Techniques on ZS-IMC

Modulation techniques used in ZS-IMC use carrier-based pulse width modulation (PWM) compared to space vector modulation (SVM) techniques. Another technique proposed with space vector, in the switching period to minimize harmonic generation in the output waveform. therefore it takes overmodulation, the result of over modulation on the inevitable low-order harmonics produced in the output. Harmonic generation in the vector space d2-q2 results in increased losses. minimize harmonic attention as the desired output is in the over modulation area [17].

The development of ZS-IMC that has been carried out by [18] is a Quasi-Z-source indirect matrix converter (QZS-IMC). By utilizing the Z-source network to integrate filter functions so that they do not require an input filter. The QZS-IMC topology is shown in fig. 5. From this series it can be seen that there is a combination of one switch two inductors  $L_1$  and  $L_2$  and capacitors  $C_1$  and  $C_2$ . It can overcome the voltage ratio, consisting of two stages of

correction and inversion stage. But the results are not easy for system integration and manufacturing processes.

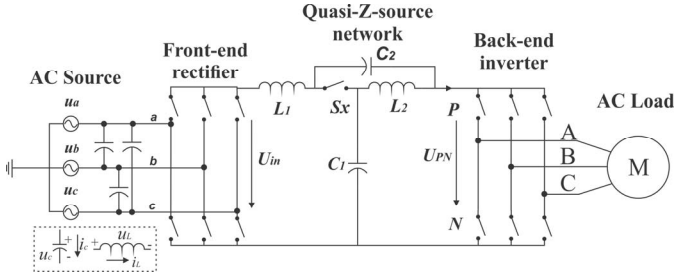


Fig. 5. Quasi Z-Source Indirect Matrix Converter

#### IV. Z-SOURCE DIRECT MATRIX CONVERTER

ZS-DMC has nine bidirectional switches that convert voltage and current in one step. The basic configuration of ZS-DMC [19][20]. It consists of ZS-N and three phase matrix converter connected between load and Z-source. The matrix converter has nine bidirectional switches and each bidirectional switch has two IGBT connected in anti-parallel [21]. The ZS-DMC is explained by two modes i.e. shoot through zero and non-shoot through state [8].

##### A. Configuration of ZS-DMC

The configuration of ZS-DMC shown in Fig. 6, has three main parts, namely, the AC input source, Z-source network, and load. A different level for step-up the voltage on the output side is executed by making a control mechanism the short circuit between the input phases. The ZS-N contains six capacitors, six inductors, and three bidirectional switches. All three switches must have the same status [22].

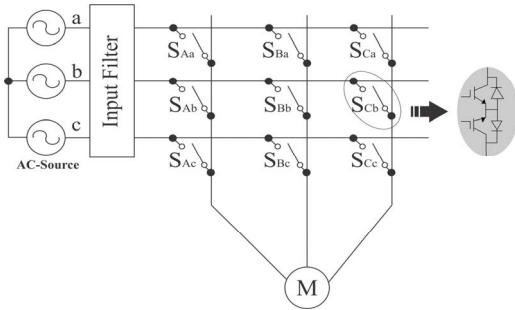


Fig. 6. Main circuit of Z-source direct matrix converter [23]

##### B. Control of ZS-DMC

The utilize the boost feature, ZS-DMC mechanism is carried out in two different states i.e. a shoot-through zero state as in Fig. 7 and a non-shoot-through state as shown in Fig. 8 [24]. During the shoot through the state, switches S1, S2, and S3 are off, which is  $S_z=0$  for boosting operation. During the non-shoot through state, switches S1, S2, and S3 are on, which is  $S_z=1$  for normal operation [25]. It is assumed that the inductors L1, L2, and L3 have the equal inductance value and capacitor C1, C2 and C3 are in identical capacitance. By this configuration, the symmetrical-N is created.

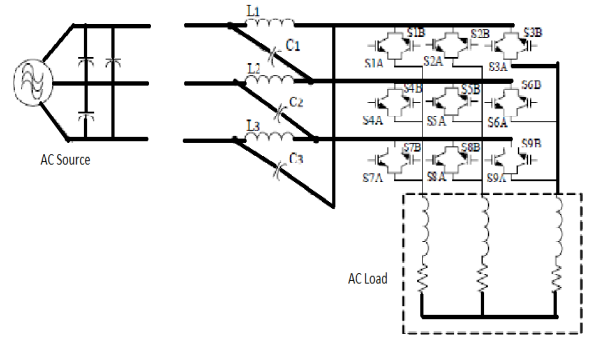


Fig. 7. ZS-DMC in shoot through zero state

Fig. 7 shows the configuration of the shoot-through state for the proposed topology at interval of  $T_0$  during a period of switching process [26]. The matrix converter by design is short-circuited and all switches S1, S2 and S3 are in off position. In Fig. 7, the reconfiguration of equivalent circuit deduces the voltage transfer ratio, by making assumption that there is a symmetrical three-phase system and expansion of input and output voltages.

ZS-DMC is in the non-shoot-through state at  $T_1$  interval during a period of the switching process,  $T$  [27][28]. Fig. 7 shows the configuration circuit for the non-shoot-through state.

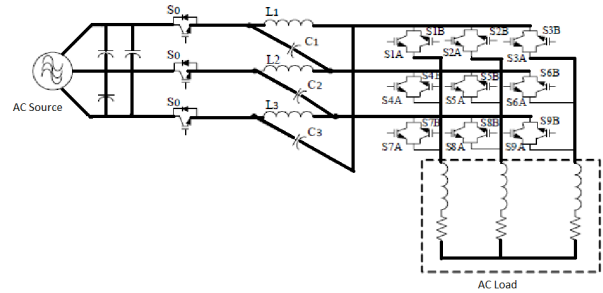


Fig. 8. ZS-DMC in non-shoot-through-state

##### C. Modulation Techniques on ZS-DMC

ZS-DMC uses the modulation space vector method. According to the principle, where each two-phase input does not get a short circuit and must make a closed loop formation. For six active vectors and three zero vectors, there are nine switches to use. Improved performance of ZS-DMC using a different PWM modulation method. have the appropriate PWM schema that is capable of achieving the maximum susceptible output voltage. Minimize harmonics at the output and input currents, providing maximum efficiency [29]. ZS-DMC is the distribution of shoot through the traditional PWM modulation concept. In this section the carrier PWM and space vector based on pulse width modulation schema (SVPWM) [30]. By comparing the two modulations, the THD input current and THD voltage from the SVPWM scheme is 1.2% and 8% lower than PWM, so it shows that SVPWM is suitable for ZS-DMC.

Both of the topologies, ZS-IMC and ZS-DMC in each configuration and control using SVPWM modulation are presented in Table I.



TABLE I. Comparison between ZS-IMC and ZS-DMC of topologies using SVPWM modulation

Type	Configuration	Control
<b>ZS-DMC</b>	by two modes, Shoot through zero state and Non-shoot through state	ZS-DMC has nine bidirectional switches that convert voltage and current in one step
<b>ZS-IMC</b>	two stage rectifier and inverter	Each ZS-IMC requires an 18 ac switch, which makes it difficult to use directly

## V. CONCLUSION

This manuscript outlines a literature review on different Z-source matrix converter (ZS-MC) topologies, including Z-source indirect matrix converter (ZS-IMC) and Z-source direct matrix converter (ZS-DMC). ZS-IMC topology overcomes the limitations of traditional MC voltage reinforcement and makes the operation of buck and boost by decreasing the number of switches to obtain high efficiency, reliability and low cost. ZS-IMC topology is very suitable for research and applied in industry.

## ACKNOWLEDGMENT

This research was supported by Electrical Engineering Research Group Ahmad Dahlan University

## REFERENCES

- [1] T. Friedli and J. W. Kolar, "Milestones in Matrix Converter Research," *IEEE J. Ind. Appl.*, vol. 1, no. 1, pp. 2–14, 2012.
- [2] R. Ghoni, A. N. Abdalla, S. P. Koh, and H. F. Rashag, "Issues of matrix converters : Technical review," vol. 6, no. 15, pp. 3576–3588, 2011.
- [3] P. W. Wheeler, J. Rodríguez, S. Member, J. C. Clare, L. Empringham, and A. Weinstein, "Matrix Converters: A Technology Review," vol. 49, no. 2, pp. 276–288, 2002.
- [4] N. Nie, "Matrix Converter : Circuit Topology , Model , and Analysis," pp. 5918–5923, 2015.
- [5] E. Babaei and E. Shokati Asl, "A new topology for Z-source half-bridge inverter with low voltage stress on capacitors," *Electr. Power Syst. Res.*, vol. 140, pp. 722–734, 2016.
- [6] A. P. Li, "Z -Source Converters : Topologies , Modulation," vol. 65, no. 10, pp. 8274–8276, 2018.
- [7] X. Fang and Z. Chen, "Current-Fed Z-Source Matrix Converter," pp. 93–96, 2009.
- [8] R. Bharani, V. V. Adhisree, B. Amman, E. District, and T. Nadu, "Performance Analysisi of Z-source Matrix Converter by Implementation Different PWM Schemes," pp. 1–9.
- [9] T. Friedli, J. W. Kolar, J. Rodríguez, and P. W. Wheeler, "Comparative Evaluation of Three-Phase AC – AC Matrix Converter and Voltage DC-Link Back-to-Back Converter Systems," vol. 59, no. 12, pp. 4487–4510, 2012.
- [10] A. Ammar, S. Member, H. Y. Kanaan, S. Member, N. Moubayed, S. Member, M. Hamouda, and S. Member, "A Technology Survey of Matrix Converters in Power Generation Systems," 2017.
- [11] W. Song and Y. Zhong, "A Study of Z-Source Matrix Converter With High Voltage Transfer Ratio," pp. 8–13, 2008.
- [12] F. N. Luca Zarri, Giovanni Serra, *Control of Matrix Converters*. 2007.
- [13] S. H. Hosseini, J. Nabati, and A. Mirlou, "Generalized Single Phase Z-Source Matrix Converter," pp. 404–408, 2011.
- [14] F. Z. Peng and S. Member, "Z-Source Inverter," vol. 39, no. 2, pp. 504–510, 2003.
- [15] A. Hakemi and M. Monfared, "Very high gain three-phase indirect matrix converter with two Z-source networks in its structure," 2017.
- [16] B. Ge, Q. Lei, S. Member, W. Qian, and F. Z. Peng, "A Family of Z-Source Matrix Converters," vol. 59, no. 1, pp. 35–46, 2012.
- [17] M. Chai, D. Xiao, R. Dutta, and J. E. Fletcher, "Space vector PWM techniques for three-to-five-phase indirect matrix converter in the overmodulation region," *IEEE Trans. Ind. Electron.*, vol. 63, no. 1, pp. 550–561, 2016.
- [18] M. Li, Y. Liu, H. Abu-rub, and S. Member, "Optimizing Control Strategy of Quasi-Z Source Indirect Matrix Converter for Induction Motor Drives," no. Dmc.
- [19] L. Rmili, S. Rahmani, and K. Al-haddad, "A review of Indirect Matrix Converter Topologies," vol. 1, no. June, pp. 30–37, 2015.
- [20] M. Su, Z. Zhao, H. Dan, T. Peng, Y. Sun, R. Che, F. Zhang, and Q. Zhu, "Modified modulation scheme for three-level diode-clamped matrix converter under unbalanced input conditions," pp. 1–9, 2018.
- [21] E. Karaman, F. Niu, and A. M. Trzynadlowski, "Three-Phase Switched-Inductor Z-Source Matrix Converter," pp. 1449–1454, 2012.
- [22] Z. Wang, Y. Guo, Y. Guo, W. Deng, and X. Wang, "Study of Quasi Z-source Direct Matrix Converter based on New Strategy of Dual Space Vector Modulation," pp. 2–7, 2017.
- [23] S. B. Omar Ellabban, Haitham Abu-Rub, "Z-Source Matrix Converter : An Overview," vol. 8993, no. c, 2015.
- [24] K. Park, S. Member, K. Lee, S. Member, and F. Blaabjerg, "Improving Output Performance of a Z-Source Sparse Matrix Converter Under Unbalanced Input-Voltage Conditions," vol. 27, no. 4, pp. 2043–2054, 2012.
- [25] H. M. Nguyen, H. Lee, and T. Chun, "Input Power Factor Compensation Algorithms Using a New Direct-SVM Method for Matrix Converter," vol. 58, no. 1, pp. 232–243, 2011.
- [26] C. N. El-khoury, H. Y. Kanaan, I. Mougharbel, and K. Al-haddad, "Implementation of a Series Z-source Very Sparse Matrix Converter in a PMSG-based WECS," 2018.
- [27] M. Guo, Y. Liu, and B. Ge, "Optimum Boost Control of Quasi-Z Source Indirect Matrix Converter," vol. 0046, no. c, 2018.
- [28] R. Prasad, K. Basu, K. K. Mohapatra, M. Ieee, N. Mohan, and F. Ieee, "Ride-Through Study for Matrix-Converter Adjustable-Speed Drives during Voltage Sags," pp. 686–691, 2010.
- [29] C. S. A. Sekhar, R. Hemantha, V. Raghavendrarajan, and M. Sasikumar, "Space Vector Modulation Based Direct Matrix Converter for Stand-Alone system," *Int. J. Power Electron. Drive Syst.*, vol. 4, no. 1, pp. 24–35, 2014.
- [30] J. Rodriguez, M. Rivera, J. W. Kolar, and P. W. Wheeler, "A review of control and modulation methods for matrix converters," *IEEE Trans. Ind. Electron.*, vol. 59, no. 1, pp. 58–70, 2012.



# High Frequency Multiplier by cascading diode with high order bandpass amplifier multiple times

Kittipong Tripetch

Division of Electronic and  
Telecommunication Engineering,  
Faculty of Engineering and  
Architecture

Rajamangala University of technology  
Suvarnabhumi, Nonthaburi, Thailand

[kittipong.tripetch.mr@ieee.org](mailto:kittipong.tripetch.mr@ieee.org)

Banchop Sancharoen

Division of Electronic and  
Telecommunication Engineering,  
Faculty of Engineering and  
Architecture

Rajamangala University of technology  
Suvarnabhumi, Nonthaburi, Thailand

[bjsdata@hotmail.com](mailto:bjsdata@hotmail.com)

Dr. Somporn Sriwattanapon

Division of Electronic and  
Telecommunication Engineering  
Faculty of Engineering and  
Architecture

Rajamangala University of technology

**Abstract**—It might be well known that frequency multiplier can use diode for frequency multiplication. The infinite harmonic can be generated using diode with sinusoidal input signal. The output of the frequency multiplier can be seen as a modulated wave if it is not a good result. This paper propose the high frequency multiplier by cascading diode with high order bandpass amplifier multiple times. Novel high frequency BJT bandpass amplifier based on regulated cascode cascade with common gate amplifier is proposed with experimental results.

**Keywords**—BJT Frequency Multiplier, BJT Bandpass amplifier, Diode Frequency Multiplier

## I. INTRODUCTION

In microwave theory community, it is well known that frequency tripler can be designed for Tera-hertz heterodyne systems at 750 GHz since 1992 [1]. The design and evaluation of frequency doubler circuit which has an input frequency at 40 GHz and output frequency at 80 GHz is reported since 1999 [2]. Frequency doubler circuit which is not use diode frequency multiplier is published in [3] by using current –reuse circuit design techniques. The frequency doubler circuit which is fabricated in 0.13 micron SiGe BiCMOS process have been published since 2008 [4]. The first millimeter wave Schottky diode frequency doubler in 0.13 micron CMOS technology is published since 2009 [5]. Schottky diode is broadly used in frequency multiplier for terahertz applications at 2.4 THz local oscillator. The theory based on drift diffusion equation is used in device simulator to plot sinusoidal signal graph at 1.2 THz [6]. Technology of low power terahertz sources is reviewed Chattopadhyay [7].

Because it is well known that the highest oscillation frequency of signal can be generated by the circuit called simple CMOS cross-coupled oscillator. The author can prove in [8] that simple CMOS cross-coupled oscillator with 0.5 micron CMOS process can be designed to oscillate at frequency 2.5 MHz as a triangular wave. Why do we must multiply a signal with a circuit called a frequency doubler and a frequency tripler circuit even though we can use VCO as a frequency multiplication circuit? The answer is that inductor or capacitor could not be tuned without series MOSFET switch. The condition of oscillation of the whole oscillator circuit can be changed as a result of switch parasitic capacitances. Instead, this paper use only one diode cascade with bandpass amplifier to select only high harmonic frequency of output current which is generated from a diode exponential behavior as a function of voltage drop of anode

and cathode terminal itself. But the problem is if you select harmonic frequency of the diode too high, the amplitude of the signal may be divide with too much number as a factorial. As a result, the output amplitude is too low for an oscilloscope to detect and display. Usually, it is in the order of millivolt. For example, the 10<sup>th</sup> harmonic frequency which can be written as

$$\frac{\cos^{10}(\theta t)}{10!} = \frac{\cos^{10}(2\omega t)}{3,628,800}$$

$$\frac{\cos^{10}(\theta t)}{10!} = \left( \frac{1}{3.628 \times 10^6} \right) \left[ \frac{1}{512} \cos(10\theta t) + \frac{10}{12} \cos(8\theta t) + \frac{45}{512} \cos(6\theta t) + \frac{120}{512} \cos(4\theta t) + \frac{175}{256} \cos(2\theta t) + \frac{91}{256} \right] \quad (1)$$

## II. DERIVATION OF TIME DOMAIN RESPONSE FROM

### THE PROPOSED CIRCUIT BLOCK DIAGRAM

From semiconductor theory which was published since 2010 [10]. The diode current can be written as an exponential equation as follow.

$$I = qA \left( \frac{D_p}{L_p} p_n + \frac{D_n}{L_n} n_p \right) \left( e^{\frac{qV}{kT}} - 1 \right) = I_s \left( e^{\frac{qV_D}{kT}} - 1 \right) = I_s \left( e^{\frac{V_D}{V_T}} - 1 \right) \quad (2)$$

It is defined in SPICE model of diode that  $I_s$  is reverse leakage current which is usually in the range  $10^{-12} - 10^{-15}$  ampere. But this constant is not useful if diode is used as frequency multiplier because it is a multiplying factor which make the diode output current to have low amplitude. From datasheet which the author search from Google, it indicates that the leakage current can be maximized in diode datasheet as high as 100nA. The operating temperature is 27 Celcius or 300K to computed thermal voltage of the diode and transistor. The bias of the anode terminal is a cosinusoidal signal and dc bias by resistive divider which should be 1.009 volt for 11 GHz transition frequency so that collector current can be selected to be 8 mA so that base emitter voltage drop of BJT high frequency transistor is 0.813 V so that transistor can operate at maximum transition frequency according to Intersil datasheet. From collector current versus maximum forward current gain ( $h_{FE}$ ) graph, it indicates that at collector current equal with 8 mA  $h_{FE}$  should be 80. Thus, diode current can be designed to be 100 microampere which should be equal with base current. The diode voltage drop can be

compute to be 0.197 if reverse leakage current of microwave Schottky diode is 50nA.

$$I = I_s \left( e^{\frac{V_D}{V_T}} - 1 \right) = (5 \times 10^{-8}) \left( e^{\frac{1.009 \cos(\theta t) - 0.813}{25.875 \times 10^{-3}}} - 1 \right)$$

$$I_{Diode} = (5 \times 10^{-8}) \left( e^{38.9951 \cos(\theta t) - 31.420} - 1 \right) \quad (3)$$

$$V_T = \frac{kT}{q} = \frac{(1.38 \times 10^{-23} \text{ J/K})(300 \text{ K})}{1.6 \times 10^{-19} \text{ C}} = 25.875 \times 10^{-3} [\text{J/C} = \text{V}] \quad (4)$$

Figure1 shows diode current with and without resistive bias with linear scale for y axis. Graph indicates that diode current is peaking at 68.83 microampere. Figure2 shows diode current with and without resistive bias with logarithm scale for y axis. Graph in figure2 shows that the diode current look likes cosinusoidal signal if the y axis use logarithm scale.

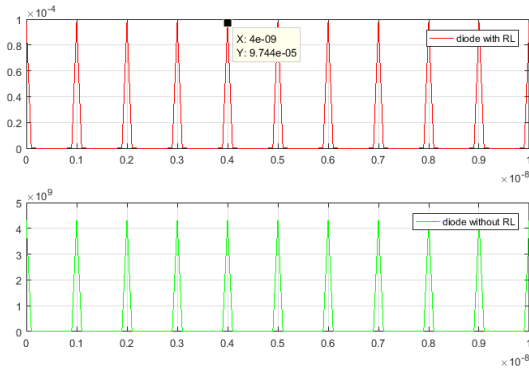


Fig.1 Diode current with and without resistive bias  
(linear scale for y axis)

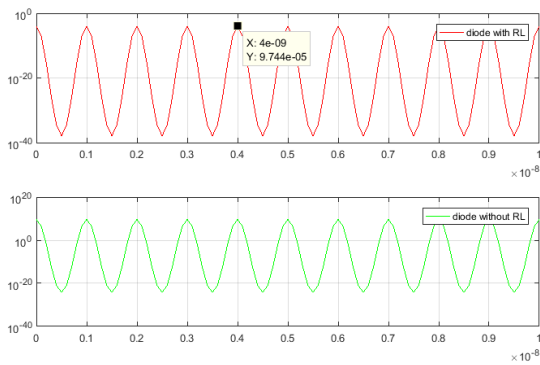


Fig.2 Diode current with and without resistive bias  
(logarithm scale for y axis)

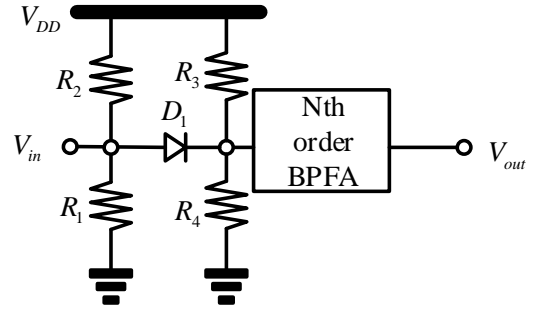


Fig.3 Circuit Block Diagram of Frequency Multiplier

Circuit block diagram of frequency multiplier which has high frequency diode and resistive divider dc bias cascading with block diagram of Nth order bandpass amplifier (BPFA) is shown in figure3. The circuit block diagram of frequency multiplier maybe impractical without good bandpass amplifier circuit. For this paper, simple common emitter with resonance circuit load is the first attempt to derive equation in frequency domain by multiplying transfer function of diode current with transimpedance amplifier to implement output voltage. Output voltage signal can be plotted by using partial fraction expansion of the frequency domain function and inverse's Laplace transform of the partial fraction form.

Thermal voltage can be determined by assume that operating room temperature is 27 degree Celcius so that thermal voltage can be computed as in equation (4)

By using diode current equation and infinite series of Euler constant exponent with x, it can be written as follow

$$e^x = 1 + x + \frac{x^2}{2} + \frac{x^3}{3!} + \frac{x^4}{4!} + \frac{x^5}{5!} + \frac{x^6}{6!} + \frac{x^7}{7!} + \frac{x^8}{8!} + \frac{x^9}{9!} + \frac{x^{10}}{10!} + \dots + \frac{x^n}{n!} \quad (5)$$

$$I_{Diode} = (5 \times 10^{-8}) \left( e^{38.9951 \cos(\theta t)} e^{-31.420} \right)$$

$$I_{Diode} = (5 \times 10^{-8}) \left( 2.2618 \times 10^{-14} \right) \left[ 1 + \left( \frac{38.9951 \cos(\theta t)}{1!} + \frac{(38.9951 \cos(\theta t))^2}{2!} + \frac{(38.9951 \cos(\theta t))^3}{3!} + \frac{(38.9951 \cos(\theta t))^4}{4!} + \frac{(38.9951 \cos(\theta t))^5}{5!} + \frac{(38.9951 \cos(\theta t))^6}{6!} + \frac{(38.9951 \cos(\theta t))^7}{7!} + \frac{(38.9951 \cos(\theta t))^8}{8!} + \frac{(38.9951 \cos(\theta t))^9}{9!} + \frac{(38.9951 \cos(\theta t))^{10}}{10!} + \dots \right) \quad (6)$$

The term such as a  $\cos(\theta t)$  is an exponent with 1,2,3,4,...n in infinite Euler's series. But the equation can be expanded until the 10<sup>th</sup> harmonic due to the laborious of algebra of trigonometry.

$$I_{Diode} = (5 \times 10^{-8}) \left( e^{38.647343 \cos(\theta t)} e^{-31.420} \right) \left( 1 + \frac{(38.9951 \cos(\theta t))^2}{2} + \frac{(38.9951 \cos(\theta t))^3}{3!} + \frac{(38.9951 \cos(\theta t))^4}{4!} + \frac{(38.9951 \cos(\theta t))^5}{5!} + \frac{(38.9951 \cos(\theta t))^6}{6!} + \frac{(38.9951 \cos(\theta t))^7}{7!} + \frac{(38.9951 \cos(\theta t))^8}{8!} + \frac{(38.9951 \cos(\theta t))^9}{9!} + \frac{(38.9951 \cos(\theta t))^{10}}{10!} \right) \quad (7)$$

Expansion terms by terms inside the bracket of equation (7) can be written as follow.

$$I_{Diode} = (1.1309 \times 10^{-21}) \left( 1 + 38.9951 \cos(\theta t) + 760.3089 (0.5 \cos(2\theta t) + 0.5) + 9882.7740 (0.25 \cos(3\theta t) + 0.75 \cos(\theta t)) + 96,344.940 (0.125 \cos(4\theta t) + 0.5 \cos(2\theta t) + 0.375) + 751,396.1161 (0.0625 \cos(5\theta t) + 0.3125 \cos(3\theta t) + 0.625 \cos(\theta t)) + 4,883,461.115 \left( 0.03125 \cos(6\theta t) + 0.1875 \cos(4\theta t) + 0.46875 \cos(2\theta t) + 0.3125 \right) + 27,009,698 \left[ 0.015625 \cos(7\theta t) + 0.109375 \cos(5\theta t) + 0.328125 (3\theta t) + 0.546875 \cos(\theta t) \right] + 132,604,964.5 \left[ 7.8125 \times 10^{-3} \cos(8\theta t) + 0.0625 \cos(6\theta t) + 0.21875 \cos(4\theta t) + 0.4375 \cos(2\theta t) + 0.2734375 \right] + 574,549,316.9 \left[ 3.90625 \times 10^{-3} \cos(9\theta t) + 0.03515625 \cos(7\theta t) + 0.140625 \cos(5\theta t) + 0.328125 \cos(3\theta t) + 0.7109375 \cos(\theta t) \right] + 2,240,460,807 \left[ 1.9531 \times 10^{-3} \cos(10\theta t) + 0.01953125 \cos(8\theta t) + 0.087890625 \cos(6\theta t) + 0.234375 \cos(4\theta t) + 0.68359375 \cos(2\theta t) + 0.35546875 \right] \right) \quad (8)$$

Multiply all terms inside bracket with number and grouping cosinusoidal function which has the same angle so that the diode current equation can be written in a more compact form.

The total terms of harmonic and dc term are enumerated to be 37 terms.

$$I_{Diode} = (1.1309 \times 10^{-21}) \left( \begin{aligned} & \left( 1 + 380.15445 + 36,129.3525 \right) \\ & + \left[ 1,526,081.598 + 36,259,169.98 \right] \cos(\theta t) \\ & + \left[ 796,413,802.5 \right] \cos(2\theta t) \\ & + \left[ 38.9951 + 7,412.0805 + 469,622.5726 \right] \cos(3\theta t) \\ & + \left[ 14,770,928.59 + 408,468,655 \right] \cos(4\theta t) \\ & + \left[ 380.15445 + 48,172.47 + 2,289,122.398 \right] \cos(5\theta t) \\ & + \left[ 58,014,671.97 + 1,531,565,005 \right] \cos(6\theta t) \\ & + \left[ 2,470.6935 + 234,811.2863 \right] \cos(7\theta t) \\ & + \left[ 8,862,557.156 + 188,523,994.6 \right] \cos(8\theta t) \\ & + \left[ 12,043.1175 + 915,648,9591 \right] \cos(9\theta t) \\ & + \left[ 29,007,335.98 + 525,108,001.6 \right] \cos(10\theta t) \\ & + \left[ 46,962.25726 + 2,954,185.719 + 80,795,997.69 \right] \cos(11\theta t) \\ & + \left[ 152,608.1598 + 8,287,810.281 + 196,915,500.6 \right] \cos(12\theta t) \\ & + \left[ 422,026.5313 + 20,198,999.42 \right] \cos(13\theta t) \\ & + \left[ 1,035,976.285 + 43,759,000.14 \right] \cos(14\theta t) \\ & + \left[ 2,244,333.269 \right] \cos(15\theta t) \\ & + \left[ 4,375,844.002 \right] \cos(16\theta t) \end{aligned} \right) \quad (10)$$

The number inside brackets can be added after grouping harmonic frequency. This function should be time domain function. The second step is to transform it by Laplace's transform before cascading with bandpass amplifier transfer function in frequency domain. The third step is determine the unknown of the partial fraction expansion if it is needed before simulation with MATLAB.

$$I_{Diode} = (1.1309 \times 10^{-21}) \begin{pmatrix} [834, 235, 564.6] \\ + [423, 716, 657.2] \cos(\theta t) \\ + [1, 591, 917, 352] \cos(2\theta t) \\ + [197, 623, 833.7] \cos(3\theta t) \\ + [555, 043, 029.7] \cos(4\theta t) \\ + [83, 797, 145.67] \cos(5\theta t) \\ + [205, 355, 919] \cos(6\theta t) \\ + [20, 621, 025.95] \cos(7\theta t) \\ + [44, 794, 976.43] \cos(8\theta t) \\ + [2, 244, 333.269] \cos(9\theta t) \\ + [4, 375, 844.002] \cos(10\theta t) \end{pmatrix} \quad (11)$$

$$I_{Diode}(t) = \begin{pmatrix} 9.43437 \times 10^{-13} + (4.7918 \times 10^{-13}) \cos(\theta t) \\ + (1.8002 \times 10^{-12}) \cos(2\theta t) + (2.2349 \times 10^{-13}) \cos(3\theta t) \\ + (6.2769 \times 10^{-13}) \cos(4\theta t) + (9.4766 \times 10^{-14}) \cos(5\theta t) \\ + (2.3223 \times 10^{-13}) \cos(6\theta t) + (2.3320 \times 10^{-14}) \cos(7\theta t) \\ + (5.0658 \times 10^{-14}) \cos(8\theta t) + (2.5381 \times 10^{-15}) \cos(9\theta t) \\ + (4.9486 \times 10^{-15}) \cos(10\theta t) \end{pmatrix} \quad (12)$$

From Laplace's table, Laplace's transform of cosine function is not different from bandpass amplifier function when damping factor is equal to zero which is written as follow.

$$f(t) = B \cos(2\pi ft) \rightarrow F(s) = \frac{sB}{s^2 + (2\pi f)^2} \quad (13)$$

Taking the Laplace's transform term by term with a total of 11 terms can be written as follow.

$$I_{Diode}(s) = \begin{pmatrix} \frac{9.43437 \times 10^{-13}}{s} + (4.7918 \times 10^{-13}) \left( \frac{s}{s^2 + (2\pi f)^2} \right) \\ + (1.8002 \times 10^{-12}) \left( \frac{s}{s^2 + (4\pi f)^2} \right) + (2.2349 \times 10^{-13}) \left( \frac{s}{s^2 + (6\pi f)^2} \right) \\ + (6.2769 \times 10^{-13}) \left( \frac{s}{s^2 + (8\pi f)^2} \right) + (9.4766 \times 10^{-14}) \left( \frac{s}{s^2 + (10\pi f)^2} \right) \\ + (2.3223 \times 10^{-13}) \left( \frac{s}{s^2 + (12\pi f)^2} \right) + (2.3320 \times 10^{-14}) \left( \frac{s}{s^2 + (14\pi f)^2} \right) \\ + (5.0658 \times 10^{-14}) \left( \frac{s}{s^2 + (16\pi f)^2} \right) + (2.5381 \times 10^{-15}) \left( \frac{s}{s^2 + (18\pi f)^2} \right) \\ + (4.9486 \times 10^{-15}) \left( \frac{s}{s^2 + (20\pi f)^2} \right) \end{pmatrix} \quad (14)$$

The simple bandpass amplifier can be seen in figure4. It was published since 1986. Its transfer function can be derived as follow.

$$\begin{aligned} \frac{V_{out}}{V_{in}} &= \frac{s^2 C_\mu}{s^3 a_3 + s^2 a_2 + s a_1 + a_0} \\ a_3 &= [(C + C_\mu)(C_\pi r_{bb} + C_\mu r_{bb})] \\ a_2 &= \left[ (C + C_\mu) \left( \frac{r_{bb}}{r_\pi} + 1 \right) + \left( \frac{1}{r_o} + \frac{1}{R} \right) (C_\pi r_{bb} + C_\mu r_{bb}) \right] \\ a_1 &= \left[ \left( \frac{1}{r_o} + \frac{1}{R} \right) \left( \frac{r_{bb}}{r_\pi} + 1 \right) + \frac{(C_\pi r_{bb} + C_\mu r_{bb})}{R} - C_\mu r_{bb} \right] \\ a_0 &= \frac{\left( \frac{r_{bb}}{r_\pi} + 1 \right)}{R} \end{aligned} \quad (15)$$

All coefficients of denominator polynomial are defined as a function of small signal parasitic capacitances, resistances, as well as passive elements. If resistive dividers are equal, thus the base current of BJT transistor should be equal with diode current. Thus, the common emitter amplifier with resonance circuit load can act as transimpedance amplifier so that the input can be diode current signal instead of voltage signal. Based emitter of diode could not be derive with diode current signal because diode current could not flow into resistive divider bias circuit to transform current signal into voltage signal.

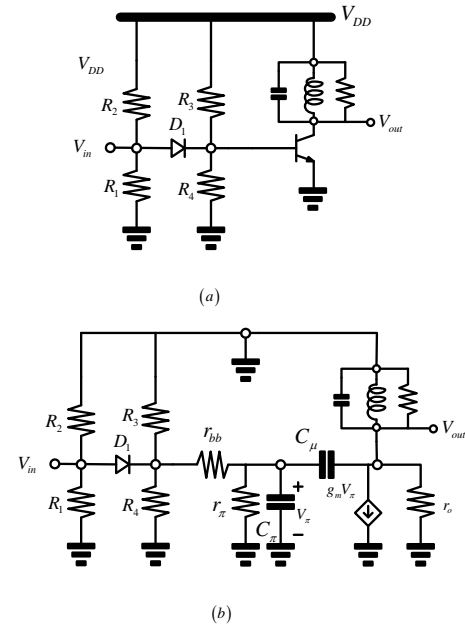


Fig.4 Circuit Block Diagram of Frequency Multiplier  
(a) with transistor level connection of transimpedance amplifier  
(b) small signal equivalent circuit of BJT transistor

Diode current signal can be written as follow

$$I_d = \frac{V_1 - V_2}{r_{bb}} \quad (16)$$

Current which follows through base resistance should be equal with current flow through pi resistor add with pi capacitor add with myu capacitor. After collecting terms, node voltage  $V_1$  which is base terminal of BJT equivalent circuit can be written as follow

$$V_1 = V_2 \left( \frac{r_{bb}}{r_\pi} + 1 + s(C_\pi r_{bb} + C_\mu r_{bb}) \right) - V_{out}(s C_\mu r_{bb}) \quad (17)$$

Performing KCL with another node which is other side of base resistor which is called  $V_2$  which can be written as follow.

$$V_2 = V_{out} \left[ \frac{s^2 C_L + s \left( \frac{1}{r_o} + \frac{1}{R_L} + 1 \right) + \frac{1}{L}}{s^2 C_\mu - s g_m} \right] \quad (18)$$

$$V_1 = V_{out} \left[ \frac{s^3 [C_L (C_\pi r_{bb} + C_\mu r_{bb}) - C_\mu^2 r_{bb}] + s^2 \left[ C_L \left( \frac{r_{bb}}{r_\pi} + 1 \right) + \left( \frac{1}{r_o} + \frac{1}{R_L} + 1 \right) (C_\pi r_{bb} + C_\mu r_{bb}) + C_\mu g_m \right] + s \left[ \left( \frac{1}{r_o} + \frac{1}{R_L} + 1 \right) \left( \frac{r_{bb}}{r_\pi} + 1 \right) + \frac{(C_\pi r_{bb} + C_\mu r_{bb})}{L} \right] + \frac{\left( \frac{r_{bb}}{r_\pi} + 1 \right)}{L}}{(s^2 C_\mu - s g_m)} \right] \quad (19)$$

The coefficients which multiplied with numerator polynomial and denominator polynomial can be grouped as to reduce the size of the equation as follow.

$$\begin{aligned} V_1 &= V_{out} \frac{s^3 b_3 + s^2 b_2 + s b_1 + b_0}{(s^2 C_\mu - s g_m)} \\ b_3 &= [C_L (C_\pi r_{bb} + C_\mu r_{bb}) - C_\mu^2 r_{bb}] \\ b_2 &= \left[ C_L \left( \frac{r_{bb}}{r_\pi} + 1 \right) + \left( \frac{1}{r_o} + \frac{1}{R_L} + 1 \right) (C_\pi r_{bb} + C_\mu r_{bb}) + C_\mu g_m \right] \\ b_1 &= \left[ \left( \frac{1}{r_o} + \frac{1}{R_L} + 1 \right) \left( \frac{r_{bb}}{r_\pi} + 1 \right) + \frac{(C_\pi r_{bb} + C_\mu r_{bb})}{L} \right] \\ b_0 &= \frac{\left( \frac{r_{bb}}{r_\pi} + 1 \right)}{L} \end{aligned} \quad (20)$$

The transimpedance gain can be derived by substitute equation (18) and equation (19) into (16) which can be written as follow.

$$\begin{aligned} I_d r_{bb} &= V_1 - V_2 \\ I_d r_{bb} &= V_{out} \frac{s^3 b_3 + s^2 b_2 + s b_1 + b_0}{(s^2 C_\mu - s g_m)} - V_{out} \left[ \frac{s^2 C_L + s \left( \frac{1}{r_o} + \frac{1}{R_L} + 1 \right) + \frac{1}{L}}{s^2 C_\mu - s g_m} \right] \\ I_d r_{bb} (s^2 C_\mu - s g_m) &= V_{out} \left[ s^3 b_3 + s^2 (b_2 - C_L) + s \left( b_1 - \left( \frac{1}{r_o} + \frac{1}{R_L} + 1 \right) \right) + \left( b_0 - \frac{1}{L} \right) \right] \\ A_{transimpedance} &= \frac{V_{out}(s)}{I_d(s)} = \frac{r_{bb} (s^2 C_\mu - s g_m)}{\left[ s^3 b_3 + s^2 (b_2 - C_L) + s \left( b_1 - \left( \frac{1}{r_o} + \frac{1}{R_L} + 1 \right) \right) + \left( b_0 - \frac{1}{L} \right) \right]} \end{aligned} \quad (21)$$

The transimpedance function of equation (21) can be simplified by grouping pole polynomial with variable  $f$  and grouping zero polynomial with variable  $d$  which can be written as follow.

$$\begin{aligned} \frac{V_{out}(s)}{I_d(s)} &= \frac{r_{bb} (s^2 C_\mu - s g_m)}{\left[ s^3 f_3 + s^2 f_2 + s f_1 + f_o \right]} = \frac{(s^2 d_2 - s d_1)}{\left[ s^3 f_3 + s^2 f_2 + s f_1 + f_o \right]} \\ d_2 &= r_{bb} C_\mu, d_1 = r_{bb} g_m, f_3 = b_3, f_2 = (b_2 - C_L) \\ f_1 &= \left( b_1 - \left( \frac{1}{r_o} + \frac{1}{R_L} + 1 \right) \right), f_o = \left( b_0 - \frac{1}{L} \right) \end{aligned} \quad (22)$$

Output voltage of BJT amplifier with resonance circuit load can be written as a function of diode current by multiplying transfer function on the right hand side of equation (21) with diode current in equation (14) as follow.

$$V_{out}(s) = \frac{(s^2 d_2 - s d_1)}{\left[ s^3 f_3 + s^2 f_2 + s f_1 + f_o \right]} I_d(s) = \left[ \frac{9.43437 \times 10^{-13}}{s} + (4.7918 \times 10^{-13}) \left( \frac{s}{s^2 + (2\pi f)^2} \right) + (1.8002 \times 10^{-12}) \left( \frac{s}{s^2 + (4\pi f)^2} \right) + (2.2349 \times 10^{-13}) \left( \frac{s}{s^2 + (6\pi f)^2} \right) + (6.2769 \times 10^{-13}) \left( \frac{s}{s^2 + (8\pi f)^2} \right) + (9.4766 \times 10^{-14}) \left( \frac{s}{s^2 + (10\pi f)^2} \right) + (2.3223 \times 10^{-13}) \left( \frac{s}{s^2 + (12\pi f)^2} \right) + (2.3320 \times 10^{-14}) \left( \frac{s}{s^2 + (14\pi f)^2} \right) + (5.0658 \times 10^{-14}) \left( \frac{s}{s^2 + (16\pi f)^2} \right) + (2.5381 \times 10^{-15}) \left( \frac{s}{s^2 + (18\pi f)^2} \right) + (4.9486 \times 10^{-15}) \left( \frac{s}{s^2 + (20\pi f)^2} \right) \right] \quad (23)$$

Multiplying terms by terms between brackets of equation (23) so that pole polynomial can be seen as eleven brackets as follow. For compactness in multiplication, let define variable name ten variables as follows.

$$\begin{aligned} V_{out}(s) &= \frac{(s^2 d_2 - s d_1)}{\left[ s^3 f_3 + s^2 f_2 + s f_1 + f_o \right]} = \left[ \frac{9.43437 \times 10^{-13}}{s} + (4.7918 \times 10^{-13}) \left( \frac{s}{s^2 + \theta_1} \right) + (1.8002 \times 10^{-12}) \left( \frac{s}{s^2 + \theta_2} \right) + (2.2349 \times 10^{-13}) \left( \frac{s}{s^2 + \theta_3} \right) + (6.2769 \times 10^{-13}) \left( \frac{s}{s^2 + \theta_4} \right) + (9.4766 \times 10^{-14}) \left( \frac{s}{s^2 + \theta_5} \right) + (2.3223 \times 10^{-13}) \left( \frac{s}{s^2 + \theta_6} \right) + (2.3320 \times 10^{-14}) \left( \frac{s}{s^2 + \theta_7} \right) + (5.0658 \times 10^{-14}) \left( \frac{s}{s^2 + \theta_8} \right) + (2.5381 \times 10^{-15}) \left( \frac{s}{s^2 + \theta_9} \right) + (4.9486 \times 10^{-15}) \left( \frac{s}{s^2 + \theta_{10}} \right) \right] \\ \theta_1 &= (2\pi f)^2, \theta_2 = (4\pi f)^2, \theta_3 = (6\pi f)^2, \theta_4 = (8\pi f)^2, \theta_5 = (10\pi f)^2 \\ \theta_6 &= (12\pi f)^2, \theta_7 = (14\pi f)^2, \theta_8 = (16\pi f)^2, \theta_9 = (18\pi f)^2, \theta_{10} = (20\pi f)^2 \end{aligned} \quad (24)$$

[illegible]

The second step of partial fraction expansion is to determine zero polynomial by convolving each brackets of polynomial 143 times. The third step of partial fraction expansion is to group the coefficients which has the same polynomial order so that every addition of coefficients in front of each polynomial can be grouped for compactness.

$$\begin{aligned}
[s^2 + \theta_1][s^2 + \theta_2] &= [s^2 + (\theta_1 + \theta_2)s^2 + \theta_1\theta_2] \\
[s^4 + (\theta_1 + \theta_2)s^2 + \theta_1\theta_2][s^2 + \theta_3] &= s^6 + [(\theta_1 + \theta_2) + \theta_3]s^4 + [(\theta_1 + \theta_2)\theta_3 + \theta_1\theta_2]s^2 + (\theta_1\theta_2\theta_3) \\
[s^4 + (\theta_1 + \theta_2)s^2 + \theta_1\theta_2][s^2 + \theta_3] &= s^6 + [\theta_{a1}]s^4 + [\theta_{a2}]s^2 + (\theta_{a3})
\end{aligned}
\tag{26.1}$$

$$\begin{aligned}
\left[ s^6 + [\theta_{a1}]s^4 + [\theta_{a2}]s^2 + (\theta_{a3}) \right] \left[ s^2 + \theta_4 \right] &= \begin{bmatrix} s^8 + [\theta_4 + \theta_{a1}]s^6 + [\theta_{a1}\theta_4 + \theta_{a2}]s^4 \\ + [\theta_{a2}\theta_4 + \theta_{a3}]s^2 + [\theta_{a3}\theta_4] \end{bmatrix} \\
\left[ s^8 + [\theta_4 + \theta_{a1}]s^6 + [\theta_{a1}\theta_4 + \theta_{a2}]s^4 \right. \\ \left. + [\theta_{a2}\theta_4 + \theta_{a3}]s^2 + [\theta_{a3}\theta_4] \right] &= \begin{bmatrix} s^8 + [\theta_{a4}]s^6 + [\theta_{a5}]s^4 + [\theta_{a6}]s^2 + [\theta_{a7}] \end{bmatrix}
\end{aligned} \tag{26.2}$$

$$\begin{aligned} \left[ s^8 + [\theta_{a4}]s^6 + [\theta_{a5}]s^4 + [\theta_{a6}]s^2 + [\theta_{a7}] \right] \left[ s^2 + \theta_5 \right] &= \begin{bmatrix} s^{10} + [\theta_5 + \theta_{a4}]s^8 \\ + [\theta_{a4}\theta_5 + \theta_{a5}]s^6 + [\theta_{a5}\theta_5 + \theta_{a6}]s^4 \\ + [\theta_{a6}\theta_5 + \theta_{a7}]s^2 + [\theta_{a7}\theta_5] \end{bmatrix} \\ &= \begin{bmatrix} s^{10} + [\theta_5 + \theta_{a4}]s^8 + [\theta_{a4}\theta_5 + \theta_{a5}]s^6 \\ + [\theta_{a5}\theta_5 + \theta_{a6}]s^4 + [\theta_{a6}\theta_5 + \theta_{a7}]s^2 + [\theta_{a7}\theta_5] \end{bmatrix} \\ &= \begin{bmatrix} s^{10} + [\theta_8]s^8 + [\theta_{a9}]s^6 \\ + [\theta_{a10}]s^4 + [\theta_{a11}]s^2 + [\theta_{a12}] \end{bmatrix} \end{aligned} \quad (26.3)$$

$$\begin{aligned} \begin{bmatrix} s^{10} + [\theta_{a8}]s^8 + [\theta_{a9}]s^6 \\ + [\theta_{a10}]s^4 + [\theta_{a11}]s^2 + [\theta_{a12}] \end{bmatrix} \begin{bmatrix} s^2 + \theta_6 \end{bmatrix} &= \begin{bmatrix} s^{12} + [\theta_6 + \theta_{a8}]s^{10} + [\theta_{a8}\theta_6 + \theta_{a9}]s^8 \\ + [\theta_{a9}\theta_6 + \theta_{a10}]s^6 + [\theta_{a10}\theta_6 + \theta_{a11}]s^4 \\ + [\theta_{a11}\theta_6 + \theta_{a12}]s^2 + [\theta_{a12}\theta_6] \end{bmatrix} \\ \begin{bmatrix} s^{12} + [\theta_6 + \theta_{a8}]s^{10} + [\theta_{a8}\theta_6 + \theta_{a9}]s^8 \\ + [\theta_{a9}\theta_6 + \theta_{a10}]s^6 + [\theta_{a10}\theta_6 + \theta_{a11}]s^4 \\ + [\theta_{a11}\theta_6 + \theta_{a12}]s^2 + [\theta_{a12}\theta_6] \end{bmatrix} &= \begin{bmatrix} s^{12} + [\theta_{a13}]s^{10} + [\theta_{a14}]s^8 + [\theta_{a15}]s^6 \\ + [\theta_{a16}]s^4 + [\theta_{a17}]s^2 + [\theta_{a18}] \end{bmatrix} \end{aligned} \quad (26.4)$$

$$\begin{aligned} \left[ \begin{array}{l} s^{12} + [\theta_{a13}] s^{10} + [\theta_{a14}] s^8 + [\theta_{a15}] s^6 \\ + [\theta_{a16}] s^4 + [\theta_{a17}] s^2 + [\theta_{a18}] \end{array} \right] \left[ s^2 + \theta_7 \right] &= \left[ \begin{array}{l} s^{14} + [\theta_7 + \theta_{a13}] s^{12} + [\theta_{a13} \theta_7 + \theta_{a14}] s^{10} \\ + [\theta_{a14} \theta_7 + \theta_{a15}] s^8 + [\theta_{a15} \theta_7 + \theta_{a16}] s^6 \\ + [\theta_{a16} \theta_7 + \theta_{a17}] s^4 + [\theta_{a17} \theta_7 + \theta_{a15}] s^2 \\ + [\theta_{a18} \theta_7] \end{array} \right] \\ \left[ \begin{array}{l} s^{14} + [\theta_7 + \theta_{a13}] s^{12} + [\theta_{a13} \theta_7 + \theta_{a14}] s^{10} \\ + [\theta_{a14} \theta_7 + \theta_{a15}] s^8 + [\theta_{a15} \theta_7 + \theta_{a16}] s^6 \\ + [\theta_{a16} \theta_7 + \theta_{a17}] s^4 + [\theta_{a17} \theta_7 + \theta_{a15}] s^2 \\ + [\theta_{a18} \theta_7] \end{array} \right] &= \left[ \begin{array}{l} s^{14} + [\theta_{a19}] s^{12} + [\theta_{a20}] s^{10} + [\theta_{a21}] s^8 + [\theta_{a22}] s^6 \\ + [\theta_{a23}] s^4 + [\theta_{a24}] s^2 + [\theta_{a25}] \end{array} \right] \\ &\quad \left[ + [\theta_{a51}] s^2 + [\theta_{a52}] \right] \\ &\quad \left[ \begin{array}{l} + [\theta_{a49} d_2] s^8 + [-\theta_{a49} d_1] s^7 \\ + [\theta_{a50} d_2] s^6 + [-\theta_{a50} d_1] s^5 \\ + [\theta_{a51} d_2] s^4 + [-\theta_{a51} d_1] s^3 \\ + [\theta_{a52} d_2] s^2 + [-\theta_{a52} d_1] s \end{array} \right] \end{aligned} \quad (26.9)$$



Second line in equation (25) can be multiply bracket by brackets. A total of 13 brackets can be enumerated for second line.

$$\begin{aligned} & \left[ (3.5213 \times 10^{-4}) s(s^2 d_2 - s d_1) s[s^2 + \theta_2][s^2 + \theta_3][s^2 + \theta_4] \right. \\ & \left. \times [s^2 + \theta_5][s^2 + \theta_6][s^2 + \theta_7][s^2 + \theta_8][s^2 + \theta_9][s^2 + \theta_{10}] \right] \\ & \left[ s^4((3.5213 \times 10^{-4}) d_2) - s^3((3.5213 \times 10^{-4}) d_1) \right] = [s^4(\theta_{b1}) - s^3(\theta_{b2})] \end{aligned} \quad (27.1)$$

$$[s^4(\theta_{b1}) - s^3(\theta_{b2})][s^2 + \theta_2] = \begin{bmatrix} s^6(\theta_{b1}) - s^5(\theta_{b2}) \\ +s^4(\theta_{b1}\theta_2) - s^3(\theta_{b2}\theta_2) \end{bmatrix} \quad (27.2)$$

$$\begin{aligned} & \begin{bmatrix} s^6(\theta_{b1}) - s^5(\theta_{b2}) \\ +s^4(\theta_{b1}\theta_2) - s^3(\theta_{b2}\theta_2) \end{bmatrix} [s^2 + \theta_3] = \begin{bmatrix} s^8(\theta_{b1}) - s^7(\theta_{b2}) \\ +s^6(\theta_{b1}\theta_3 + \theta_{b1}\theta_2) \\ -s^5(\theta_{b2}\theta_3 + \theta_{b2}\theta_2) \\ +s^4(\theta_{b1}\theta_2\theta_3) - s^3(\theta_{b2}\theta_2\theta_3) \end{bmatrix} \\ & \begin{bmatrix} s^8(\theta_{b1}) - s^7(\theta_{b2}) \\ +s^6(\theta_{b1}\theta_3 + \theta_{b1}\theta_2) \\ -s^5(\theta_{b2}\theta_3 + \theta_{b2}\theta_2) \\ +s^4(\theta_{b1}\theta_2\theta_3) - s^3(\theta_{b2}\theta_2\theta_3) \end{bmatrix} = \begin{bmatrix} s^8(\theta_{b1}) - s^7(\theta_{b2}) + s^6(\theta_{b3}) \\ -s^5(\theta_{b4}) + s^4(\theta_{b5}) - s^3(\theta_{b6}) \end{bmatrix} \end{aligned} \quad (27.3)$$

$$\begin{aligned} & \begin{bmatrix} s^8(\theta_{b1}) - s^7(\theta_{b2}) + s^6(\theta_{b3}) \\ -s^5(\theta_{b4}) + s^4(\theta_{b5}) - s^3(\theta_{b6}) \end{bmatrix} [s^2 + \theta_4] = \begin{bmatrix} s^{10}(\theta_{b1}) - s^9(\theta_{b2}) + s^8(\theta_{b1}\theta_4 + \theta_{b3}) \\ -s^7(\theta_{b2}\theta_4 + \theta_{b4}) + s^6(\theta_{b3}\theta_4 + \theta_{b5}) \\ -s^5(\theta_{b4}\theta_4 + \theta_{b6}) + s^4(\theta_{b5}\theta_4) - s^3(\theta_{b6}\theta_4) \end{bmatrix} \\ & \begin{bmatrix} s^{10}(\theta_{b1}) - s^9(\theta_{b2}) + s^8(\theta_{b1}\theta_4 + \theta_{b3}) \\ -s^7(\theta_{b2}\theta_4 + \theta_{b4}) + s^6(\theta_{b3}\theta_4 + \theta_{b5}) \\ -s^5(\theta_{b4}\theta_4 + \theta_{b6}) + s^4(\theta_{b5}\theta_4) - s^3(\theta_{b6}\theta_4) \end{bmatrix} = \begin{bmatrix} s^{10}(\theta_{b1}) - s^9(\theta_{b2}) + s^8(\theta_{b7}) \\ -s^7(\theta_{b8}) + s^6(\theta_{b9}) - s^5(\theta_{b10}) \\ +s^4(\theta_{b11}) - s^3(\theta_{b12}) \end{bmatrix} \end{aligned} \quad (27.4)$$

$$\begin{aligned} & \begin{bmatrix} s^{10}(\theta_{b1}) - s^9(\theta_{b2}) + s^8(\theta_{b7}) \\ -s^7(\theta_{b8}) + s^6(\theta_{b9}) - s^5(\theta_{b10}) \\ +s^4(\theta_{b11}) - s^3(\theta_{b12}) \end{bmatrix} [s^2 + \theta_5] = \begin{bmatrix} s^{12}(\theta_{b1}) - s^{11}(\theta_{b2}) + s^{10}(\theta_{b1}\theta_5 + \theta_{b7}) \\ -s^9(\theta_{b2}\theta_5 + \theta_{b8}) + s^8(\theta_{b7}\theta_5 + \theta_{b9}) \\ -s^7(\theta_{b8}\theta_5 + \theta_{b10}) + s^6(\theta_{b9}\theta_5 + \theta_{b11}) \\ -s^5(\theta_{b10}\theta_5 + \theta_{b12}) + s^4(\theta_{b11}\theta_5) - s^3(\theta_{b12}\theta_5) \end{bmatrix} \\ & \begin{bmatrix} s^{12}(\theta_{b1}) - s^{11}(\theta_{b2}) + s^{10}(\theta_{b1}\theta_5 + \theta_{b7}) \\ -s^9(\theta_{b2}\theta_5 + \theta_{b8}) + s^8(\theta_{b7}\theta_5 + \theta_{b9}) \\ -s^7(\theta_{b8}\theta_5 + \theta_{b10}) + s^6(\theta_{b9}\theta_5 + \theta_{b11}) \\ -s^5(\theta_{b10}\theta_5 + \theta_{b12}) + s^4(\theta_{b11}\theta_5) - s^3(\theta_{b12}\theta_5) \end{bmatrix} = \begin{bmatrix} s^{12}(\theta_{b1}) - s^{11}(\theta_{b2}) + s^{10}(\theta_{b13}) \\ -s^9(\theta_{b14}) + s^8(\theta_{b15}) - s^7(\theta_{b16}) \\ +s^6(\theta_{b17}) - s^5(\theta_{b18}) + s^4(\theta_{b19}) \\ -s^3(\theta_{b20}) \end{bmatrix} \end{aligned} \quad (27.5)$$

$$\begin{aligned} & \begin{bmatrix} s^{12}(\theta_{b1}) - s^{11}(\theta_{b2}) + s^{10}(\theta_{b13}) \\ -s^9(\theta_{b14}) + s^8(\theta_{b15}) - s^7(\theta_{b16}) \\ +s^6(\theta_{b17}) - s^5(\theta_{b18}) + s^4(\theta_{b19}) \\ -s^3(\theta_{b20}) \end{bmatrix} [s^2 + \theta_6] = \begin{bmatrix} s^{14}(\theta_{b1}) - s^{13}(\theta_{b2}) + s^{12}(\theta_{b1}\theta_6 + \theta_{b13}) \\ -s^{11}(\theta_{b2}\theta_6 + \theta_{b14}) + s^{10}(\theta_{b13}\theta_6 + \theta_{b15}) \\ -s^9(\theta_{b14}\theta_6 + \theta_{b16}) + s^8(\theta_{b15}\theta_6 + \theta_{b17}) \\ -s^7(\theta_{b16}\theta_6 + \theta_{b18}) + s^6(\theta_{b17}\theta_6 + \theta_{b19}) \\ -s^5(\theta_{b18}\theta_6 + \theta_{b20}) + s^4(\theta_{b19}\theta_6) - s^3(\theta_{b20}\theta_6) \end{bmatrix} \\ & \begin{bmatrix} s^{14}(\theta_{b1}) - s^{13}(\theta_{b2}) + s^{12}(\theta_{b1}\theta_6 + \theta_{b13}) \\ -s^{11}(\theta_{b2}\theta_6 + \theta_{b14}) + s^{10}(\theta_{b13}\theta_6 + \theta_{b15}) \\ -s^9(\theta_{b14}\theta_6 + \theta_{b16}) + s^8(\theta_{b15}\theta_6 + \theta_{b17}) \\ -s^7(\theta_{b16}\theta_6 + \theta_{b18}) + s^6(\theta_{b17}\theta_6 + \theta_{b19}) \\ -s^5(\theta_{b18}\theta_6 + \theta_{b20}) + s^4(\theta_{b19}\theta_6) - s^3(\theta_{b20}\theta_6) \end{bmatrix} = \begin{bmatrix} s^{14}(\theta_{b1}) - s^{13}(\theta_{b2}) + s^{12}(\theta_{b21}) \\ -s^{11}(\theta_{b22}) + s^{10}(\theta_{b23}) - s^9(\theta_{b24}) \\ +s^8(\theta_{b25}) - s^7(\theta_{b26}) + s^6(\theta_{b27}) \\ -s^5(\theta_{b28}) + s^4(\theta_{b29}) - s^3(\theta_{b30}) \end{bmatrix} \end{aligned} \quad (27.6)$$

$$\begin{aligned} & \begin{bmatrix} s^{14}(\theta_{b1}) - s^{13}(\theta_{b2}) + s^{12}(\theta_{b21}) \\ -s^{11}(\theta_{b22}) + s^{10}(\theta_{b23}) - s^9(\theta_{b24}) \\ +s^8(\theta_{b25}) - s^7(\theta_{b26}) + s^6(\theta_{b27}) \\ -s^5(\theta_{b28}) + s^4(\theta_{b29}) - s^3(\theta_{b30}) \end{bmatrix} [s^2 + \theta_7] = \begin{bmatrix} s^{16}(\theta_{b1}) - s^{15}(\theta_{b2}) + s^{14}(\theta_{b1}\theta_7 + \theta_{b21}) \\ -s^{13}(\theta_{b2}\theta_7 + \theta_{b22}) + s^{12}(\theta_{b21}\theta_7 + \theta_{b23}) \\ -s^{11}(\theta_{b22}\theta_7 + \theta_{b24}) + s^{10}(\theta_{b23}\theta_7 + \theta_{b25}) \\ -s^9(\theta_{b24}\theta_7 + \theta_{b26}) + s^8(\theta_{b25}\theta_7 + \theta_{b27}) \\ -s^7(\theta_{b26}\theta_7 + \theta_{b28}) + s^6(\theta_{b27}\theta_7 + \theta_{b29}) \\ -s^5(\theta_{b28}\theta_7 + \theta_{b30}) + s^4(\theta_{b29}\theta_7) \\ -s^3(\theta_{b30}\theta_7) \end{bmatrix} \\ & \begin{bmatrix} s^{16}(\theta_{b1}) - s^{15}(\theta_{b2}) + s^{14}(\theta_{b1}\theta_7 + \theta_{b21}) \\ -s^{13}(\theta_{b2}\theta_7 + \theta_{b22}) + s^{12}(\theta_{b21}\theta_7 + \theta_{b23}) \\ -s^{11}(\theta_{b22}\theta_7 + \theta_{b24}) + s^{10}(\theta_{b23}\theta_7 + \theta_{b25}) \\ -s^9(\theta_{b24}\theta_7 + \theta_{b26}) + s^8(\theta_{b25}\theta_7 + \theta_{b27}) \\ -s^7(\theta_{b26}\theta_7 + \theta_{b28}) + s^6(\theta_{b27}\theta_7 + \theta_{b29}) \\ -s^5(\theta_{b28}\theta_7 + \theta_{b30}) + s^4(\theta_{b29}\theta_7) \\ -s^3(\theta_{b30}\theta_7) \end{bmatrix} = \begin{bmatrix} s^{16}(\theta_{b1}) - s^{15}(\theta_{b2}) + s^{14}(\theta_{b31}) \\ -s^{13}(\theta_{b32}) + s^{12}(\theta_{b33}) - s^{11}(\theta_{b34}) \\ +s^{10}(\theta_{b35}) - s^9(\theta_{b36}) + s^8(\theta_{b37}) \\ -s^7(\theta_{b38}) + s^6(\theta_{b39}) - s^5(\theta_{b40}) \\ +s^4(\theta_{b41}) - s^3(\theta_{b42}) \end{bmatrix} \end{aligned} \quad (27.7)$$

$$\begin{aligned} & \begin{bmatrix} s^{16}(\theta_{b1}) - s^{15}(\theta_{b2}) + s^{14}(\theta_{b31}) \\ -s^{13}(\theta_{b32}) + s^{12}(\theta_{b33}) - s^{11}(\theta_{b34}) \\ +s^{10}(\theta_{b35}) - s^9(\theta_{b36}) + s^8(\theta_{b37}) \\ -s^7(\theta_{b38}) + s^6(\theta_{b39}) - s^5(\theta_{b40}) \\ +s^4(\theta_{b41}) - s^3(\theta_{b42}) \end{bmatrix} [s^2 + \theta_8] = \begin{bmatrix} s^{18}(\theta_{b1}) - s^{17}(\theta_{b2}) + s^{16}(\theta_{b1}\theta_8 + \theta_{b31}) \\ -s^{15}(\theta_{b2}\theta_8 + \theta_{b32}) + s^{14}(\theta_{b31}\theta_8 + \theta_{b33}) \\ -s^{13}(\theta_{b32}\theta_8 + \theta_{b34}) + s^{12}(\theta_{b33}\theta_8 + \theta_{b35}) \\ -s^{11}(\theta_{b34}\theta_8 + \theta_{b36}) + s^{10}(\theta_{b35}\theta_8 + \theta_{b37}) \\ -s^9(\theta_{b36}\theta_8 + \theta_{b38}) + s^8(\theta_{b37}\theta_8 + \theta_{b39}) \\ -s^7(\theta_{b38}\theta_8 + \theta_{b40}) + s^6(\theta_{b39}\theta_8 + \theta_{b41}) \\ -s^5(\theta_{b40}\theta_8 + \theta_{b42}) + s^4(\theta_{b41}\theta_8) \\ -s^3(\theta_{b42}\theta_8) \end{bmatrix} \end{aligned}$$

$$\begin{aligned} & \begin{bmatrix} s^{18}(\theta_{b1}) - s^{17}(\theta_{b2}) + s^{16}(\theta_{b1}\theta_8 + \theta_{b31}) \\ -s^{15}(\theta_{b2}\theta_8 + \theta_{b32}) + s^{14}(\theta_{b31}\theta_8 + \theta_{b33}) \\ -s^{13}(\theta_{b32}\theta_8 + \theta_{b34}) + s^{12}(\theta_{b33}\theta_8 + \theta_{b35}) \\ -s^{11}(\theta_{b34}\theta_8 + \theta_{b36}) + s^{10}(\theta_{b35}\theta_8 + \theta_{b37}) \\ -s^9(\theta_{b36}\theta_8 + \theta_{b38}) + s^8(\theta_{b37}\theta_8 + \theta_{b39}) \\ -s^7(\theta_{b38}\theta_8 + \theta_{b40}) + s^6(\theta_{b39}\theta_8 + \theta_{b41}) \\ -s^5(\theta_{b40}\theta_8 + \theta_{b42}) + s^4(\theta_{b41}\theta_8) \\ -s^3(\theta_{b42}\theta_8) \end{bmatrix} = \begin{bmatrix} s^{18}(\theta_{b1}) - s^{17}(\theta_{b2}) + s^{16}(\theta_{b43}) \\ -s^{15}(\theta_{b44}) + s^{14}(\theta_{b45}) - s^{13}(\theta_{b46}) \\ +s^{12}(\theta_{b47}) - s^{11}(\theta_{b48}) + s^{10}(\theta_{b49}) \\ -s^9(\theta_{b50}) + s^8(\theta_{b51}) - s^7(\theta_{b52}) \\ +s^6(\theta_{b53}) - s^5(\theta_{b54}) + s^4(\theta_{b55}) \\ -s^3(\theta_{b56}) \end{bmatrix} \end{aligned} \quad (27.8)$$

$$\begin{aligned} & \begin{bmatrix} s^{18}(\theta_{b1}) - s^{17}(\theta_{b2}) + s^{16}(\theta_{b43}) \\ -s^{15}(\theta_{b44}) + s^{14}(\theta_{b45}) - s^{13}(\theta_{b46}) \\ +s^{12}(\theta_{b47}) - s^{11}(\theta_{b48}) + s^{10}(\theta_{b49}) \\ -s^9(\theta_{b50}) + s^8(\theta_{b51}) - s^7(\theta_{b52}) \\ +s^6(\theta_{b53}) - s^5(\theta_{b54}) + s^4(\theta_{b55}) \\ -s^3(\theta_{b56}) \end{bmatrix} [s^2 + \theta_9] = \begin{bmatrix} s^{20}(\theta_{b1}) - s^{19}(\theta_{b2}) + s^{18}(\theta_{b1}\theta_9 + \theta_{b43}) \\ -s^{17}(\theta_{b2}\theta_9 + \theta_{b44}) + s^{16}(\theta_{b43}\theta_9 + \theta_{b45}) \\ -s^{15}(\theta_{b44}\theta_9 + \theta_{b46}) + s^{14}(\theta_{b45}\theta_9 + \theta_{b47}) \\ -s^{13}(\theta_{b46}\theta_9 + \theta_{b48}) + s^{12}(\theta_{b47}\theta_9 + \theta_{b49}) \\ -s^{11}(\theta_{b48}\theta_9 + \theta_{b50}) + s^{10}(\theta_{b49}\theta_9 + \theta_{b51}) \\ -s^9(\theta_{b50}\theta_9 + \theta_{b52}) + s^8(\theta_{b51}\theta_9 + \theta_{b53}) \\ -s^7(\theta_{b52}\theta_9 + \theta_{b54}) + s^6(\theta_{b53}\theta_9 + \theta_{b55}) \\ -s^5(\theta_{b54}\theta_9 + \theta_{b56}) + s^4(\theta_{b55}\theta_9) - s^3(\theta_{b56}\theta_9) \end{bmatrix} \end{aligned}$$

$$\begin{aligned} & \begin{bmatrix} s^{20}(\theta_{b1}) - s^{19}(\theta_{b2}) + s^{18}(\theta_{b1}\theta_9 + \theta_{b43}) \\ -s^{17}(\theta_{b2}\theta_9 + \theta_{b44}) + s^{16}(\theta_{b43}\theta_9 + \theta_{b45}) \\ -s^{15}(\theta_{b44}\theta_9 + \theta_{b46}) + s^{14}(\theta_{b45}\theta_9 + \theta_{b47}) \\ -s^{13}(\theta_{b46}\theta_9 + \theta_{b48}) + s^{12}(\theta_{b47}\theta_9 + \theta_{b49}) \\ -s^{11}(\theta_{b48}\theta_9 + \theta_{b50}) + s^{10}(\theta_{b49}\theta_9 + \theta_{b51}) \\ -s^9(\theta_{b50}\theta_9 + \theta_{b52}) + s^8(\theta_{b51}\theta_9 + \theta_{b53}) \\ -s^7(\theta_{b52}\theta_9 + \theta_{b54}) + s^6(\theta_{b53}\theta_9 + \theta_{b55}) \\ -s^5(\theta_{b54}\theta_9 + \theta_{b56}) + s^4(\theta_{b55}\theta_9) - s^3(\theta_{b56}\theta_9) \end{bmatrix} = \begin{bmatrix} s^{20}(\theta_{b1}) - s^{19}(\theta_{b2}) + s^{18}(\theta_{b57}) \\ -s^{17}(\theta_{b58}) + s^{16}(\theta_{b59}) \\ -s^{15}(\theta_{b60}) + s^{14}(\theta_{b61}) \\ -s^{13}(\theta_{b62}) + s^{12}(\theta_{b63}) \\ -s^{11}(\theta_{b64}) + s^{10}(\theta_{b65}) \\ -s^9(\theta_{b66}) + s^8(\theta_{b67}) \\ -s^7(\theta_{b68}) + s^6(\theta_{b69}) \\ -s^5(\theta_{b70}) + s^4(\theta_{b71}) - s^3(\theta_{b72}) \end{bmatrix} \end{aligned} \quad (27.9)$$

## REFERENCES

- [1] A. Rydberg, B. N. Lyons, S. U. Lidholm, "On the development of a high efficiency 750 GHz Frequency Doubler for THz Heterodyne systems", *IEEE Transactions on Microwave theory and techniques*, Vol. 40, No.5, May 1992, pp.827-830
- [2] D. W. Porterfield, T. W. Crowe, R. F. Bradley, N. R. Erikson, "A high-power fixed-tuned millimeter-wave balanced frequency doubler", *IEEE Transactions on Microwave theory and techniques*, Vol. 47, No.4, April 1999, pp. 419-425
- [3] K. Yamamoto, "A 1.8V operation 5 GHz band CMOS Frequency Doubler using current-reuse circuit design technique", *IEEE Journal of Solid-State Circuits*, Vol.40, No.6, June 2005, pp. 1288-1295
- [4] U. R. Pfeiffer, C. Mishra, R. M. Rassel, S. Pinkett, S. K. Reynolds, "Schottky Barrier Diode Circuits in Silicon for future millimeter-wave and terahertz application" *IEEE Transactions on Microwave Theory and techniques*, Vol.56, No.2, February 2008, pp. 364-371
- [5] C. Mao, C. S. Nallani, S. Sankaran, E. Seok, K. K. O, "125 GHz Diode Frequency Douler in 0.13 micron CMOS", *IEEE Journal of Solid-State Circuits*, Vol. 44, No.5, May 2009, pp. 1531-1538
- [6] J. V. Siles, J. Grajal, "Physics-based design and optimization of Schottky diode frequency multipliers for Terahertz Applications", *IEEE Transactions on Microwave Theory and Techniques*, Vol.7, July 2010, pp. 1933-1942
- [7] G. Chattopadhyay, "Technology, Capabilities, and Performance of Low Power Terahertz Sources", *IEEE Transactions on Terahertz Science and Technology*, Vol.1, No.1, September 2011, pp. 33-53
- [8] N. Alijabbari, M. F. Bauwens, R. M. Weikle, "Design and Characterization of Integrated Submillimeter-wave Quasi-Vertical Schottky diodes", *IEEE Transactions on Terahertz Science and Technology*, Vol.5, No.1, January 2015, pp. 73-80
- [9] I. Mehdi, J. V. Siles, C. Lee, E. Schlecht, "THz diode technology: Status, Prospects, and Applications", *Proceedings of the IEEE*, Vol.105, No.6, June 2017, pp.990-1007
- [10] Ben. G. Steetman, Sanjay Banerjee, "Solid State Electronic Devices", 5<sup>th</sup> edition, copyright 2000, pp. 177

# Bioelectrical measurement for sugar recovery of sugarcane prediction using artificial neural network

Sucipto, S  
Agroindustrial Technology  
Universitas Brawijaya  
Malang, Indonesia  
ciptotip@ub.ac.id

Widaningtyas, S  
Agroindustrial Technology  
Universitas Brawijaya  
Malang, Indonesia  
shintawidya1435@gmail.com

Supriyanto, S  
Biosystem and Mechanical Engineering  
Institut Pertanian Bogor  
Bogor, Indonesia  
supriyantoku@gmail.com

Arwani, M  
Agroindustrial Technology  
Universitas Brawijaya  
Malang, Indonesia  
m.arwani94@gmail.com

Al Riza, D F  
Agricultural Engineering  
Universitas Brawijaya  
Malang, Indonesia  
dimasfirmanda@ub.ac.id

Somantri, A S  
Indonesian Center Agricultural Post  
Harvest Research and Development  
Bogor, Indonesia  
assomantri@yahoo.com

Hendrawan, Y  
Agricultural Engineering  
Universitas Brawijaya  
Malang, Indonesia  
yusuf\_h@ub.ac.id

Yuliatun, S  
Indonesian Sugar Research Institute  
Pasuruan, Indonesia  
simping7@gmail.com

**Abstract**— One of the problems in the sugar industry is lack of low cost, simple and accurate measurement techniques for sugar recovery of sugarcane in the field or laboratory. This study investigated the potential using of bioelectrical properties as a non-destructive technique for this purpose. A parallel plate capacitor was developed to measure the bioelectric properties of sugarcane in a lateral and longitudinal position of the samples. Eighteen internode samples from 3 sugarcane varieties were measured within 0.1-10 kHz frequency range of LCR meter and then was analyzed sugar recovery in the laboratory. The result showed that in the lateral position are more capacitive and resistive than the longitudinal position. Artificial neural network (ANN) was developed for prediction of sugar recovery as a function of bioelectrical properties. The best ANN model produces a high accuracy in the lateral bioelectrical measurement position with a correlation coefficient ( $R$ ) > 0.90 and mean square error (MSE) < 0.05. It showed that the ANN model based on bioelectrical properties had the potential to be developed as a simple technique to predict the sugar recovery of sugarcane.

**Keywords**—ANN, Bioelectrical measurement, Sugar recovery, Sugarcane

## I. INTRODUCTION

Sugarcane is an important raw material to produce several types of sweetener through a long process in the sugarcane industries. One of the limitations in the sugarcane industry is the lack of reliable and low cost technique to measure the sucrose content from standing sugarcane in the field or stalk sample in the laboratory. This technique would be a useful for the breeding program during sugarcane growth in field, evaluation of the input sugarcane for a fair payment to the farmers in the sugar factory and precision agriculture of sugarcane quality.

In standard practice, the quality of sugarcane was determined using sugar recovery. In Indonesia, sugar recovery measured based on °Brix (soluble solids content of sugarcane is determined from the refraction index of the light passed through the stalk sample) and %Pol (the percent sucrose is determined from rotated polarized light when is passed along the sample) which are measured in laboratory through sugarcane juice samples. Therefore, the measurement of sugar recovery in the laboratory is take a

long time and not applicable in field, because it need a preparation of sugarcane juice.

Mat Nawi [1] reviewed the potential method for measuring sugarcane quality in the field such as refractometry, polarimetry, chromatography, biosensor, wet chemical, and spectroscopy. All the methods mentioned above other than spectroscopy was need sugarcane juice, and therefore are not appropriate for in field measurement. Spectroscopy method using NIR revealed the accurate prediction, however need a high skilled operators and may not be a proper technology.

Bioelectrical properties of the agricultural products has been proven as a reliable, simple and non-destructive sensing technique [2, 3]. This method based on the electrical properties of the material and describes the electric field or material interaction [2, 4]. Naderi-Boldaji [5] revealed that the bioelectrical properties can be used as parameter for the non-destructive measurement of sugar concentration in sugarcane. They used dielectric power of sugarcane to predict sugar concentration by mean of multiple linear correlation. In addition, the bioelectrical properties are applied in prediction moisture content of sugarcane using a simple quadratic function [6].

Initial research have been standardized the bioelectrical properties measurement at frequency below 1 kHz to measure sugar recovery of sugarcane [7]. However, there is not yet a robust model to predict sugar recovery of sugarcane. Therefore, to build a robust predictive model, artificial neural network (ANN) was used. ANN theory, generally accepted as a useful tool for the recognition of various patterns [8]. ANN modelling has been proven as reliable predictive formulation in a various studies such as predicting water content of Sunagoke moss [9], water status of plants [10] and sugar yields during hydrolysis of lignocelluloses biomass [11].

This research aimed to develop a low cost, reliable and non-destructive system for sugar recovery of sugarcane based on the bioelectrical properties measurement and also to develop predictive models of sugar recovery using bioelectrical properties.

## II. MATERIALS AND METHODS

### A. Sample Preparation

Sugarcane sample were taken from 3 commercial varieties of BL, PS 864, PS 862 at Indonesian Sugar Research Institute Pasuruan, East Java, Indonesia. These samples were selected according to their variety of sucrose content (low, mid and high) with early and late maturity to capture a wide range of variation. In addition, the samples were randomly taken from the different zone of the field with 3 stems were taken from each variety without time delay and transferred to the laboratory for bioelectric properties and sugar recovery measurements.

Sugar content usually decreases along the stem height [1], hence the stem samples were cut for three internodes (bottom, mid and top). On the other hand, there are early and late maturing sample. Therefore in total, 18 internode were measured from 3 varieties. For each internodes was re-cut into two paired-samples using a cutter, one was used for bioelectrical measurement and the other one for sugar recovery measurement in laboratory.

### B. Instrumentation Setup and Measurement Principle

The bioelectrical properties were measured at 100 Hz, 120 Hz, 1 kHz and 10 kHz using LCR Meter (BK Precision 879b) connected with a pair of parallel plate. In this study, a parallel plate was constructed by printed circuit board with diameter of 3 cm and the gap between parallel plates was diameter of sample. A sample was placed between parallel plate in lateral position and maintained at 30°C during measurement using thermometric cooler (WAECO). The capacitor is formed by a combination of sample and air as the dielectric. The conductive plates selected from copper material due to its consistency which would not be easily ionized as a factor that will maintain the measurement using capacitive properties. The measurement of bioelectrical properties including inductance (L), resistance (R) and capacitance (C) was repeated six times for each frequency. Therefore, for each sample was obtained 24 dataset and in total there are 432 dataset.

The primary point in measuring bioelectrical properties is the capacitance of the sample. The capacitance of the sample measure was described by Equation 1.

$$C = \epsilon A / d \quad (1)$$

Where C is capacitance (F), A is the area of plates (m<sup>2</sup>), d is the gap between parallel plates (m), and  $\epsilon$  (F/m) is the complex relative permittivity of the substance between parallel plates. When a sample is placed between a pair of parallel plate, capacitance of probe will be changed. In addition thickness of sample will affect the bioelectrical properties.

### C. Laboratory Measurement of Sugar Recovery of the Sugarcane Samples

The laboratory measurement for °Brix and %Pol measurement was conducted according to [5]. Each one of the pair internodes samples were milled and crushed by a small mill (A11 analytical basic mill, IKA®-Werke GmbH & Co. KG, Germany) and then squeezed and centrifuged for extraction of juice. For refractometer (°Brix) test, the juice

sample was clarified through a Whatman filter paper. For polarimetry (%Pol) test, lead acetate was added to the juice sample with 0.02 g ml<sup>-1</sup> concentration and the mixture was clarified by a filter paper. °Brix and optical rotation were analyzed by a digital refractometer (model HI 96801, Hanna instruments, USA) with a range of 0-85° and an accuracy of 0.2 °Brix and a high speed polarimeter (model P8000, Kruss optronic Co., Germany) with a range of ±90° optical rotation, an accuracy of ±0.003° and a tube volume of 5 ml, respectively. %Pol was calculated from °Brix and the degree of optical rotation (OR). The sugar recovery (SR) of sugarcane was calculated using Equation 2.

$$SR = 0.78 (\%pol - 0.4(^{\circ}brix - \%pol)) \quad (2)$$

### D. Artificial Neural Networks Modelling

ANN have been shown to be successful as predictive tools in a variety of ways such as predicting the level of some event outcome [12]. Comparative studies made by researchers suggest that ANN compare favorably with conventional statistical pattern recognition methods [8]. A three layers of ANN structure has been developed for predicting sugar recovery of sugarcane, namely input layer, hidden layer(s) and output layer.

The number of neurons in the input layer was determined by the number of input features obtained from bioelectrical properties. Prior to develop ANN model, selecting feature that are suitable for an application is one of the most critical parts to improve the accuracy and speed of prediction system. There are three category of feature selection, namely filter methods, wrapper methods, and embed methods. In this study, the simplest filter methods namely linear regression was carried out to select the features that is suitable for sugar recovery prediction. The selected features was then applied to the input layer of ANN model, there are capacitance and resistance. Learning rate and momentum were chosen at 0.1 and 0.9, respectively based on the results of preliminary runs. Five models of hidden nodes architecture were developed, i.e. 10, 20, 30 and 40 within one and two hidden layers. The output layer consisted of single neuron namely sugar recovery corresponding to the input features. The activation function namely *logsig*, *tansig* and *purelin* were used to optimize the prediction accuracy. Mean square error (MSE) and correlation coefficient (R) were used to determine training and testing performance of ANN models.

## III. RESULT AND DISCUSSION

### A. Characteristic Sugar Recovery of Sugarcane

Laboratory result of sugar recovery measurement (Fig. 1) revealed that the lower internode has a higher sugar recovery than the upper one. This is due to the lower internode (older) contain more sugar than the younger one [13]. According to Indonesian Sugar Research Institute, PS 862 has a higher sugar content than the other varieties.

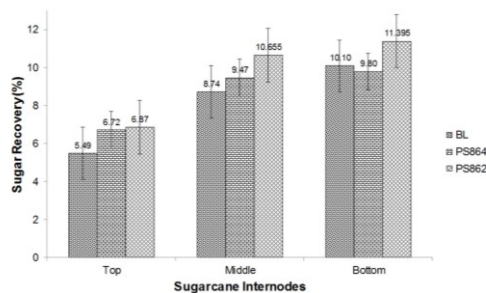
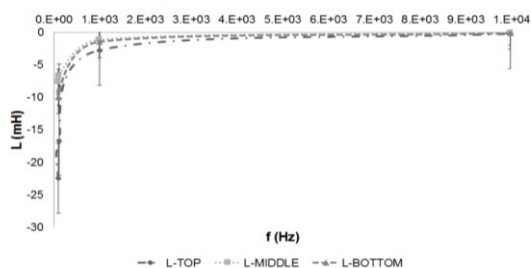


Fig. 1. Sugar recovery distribution in various internodes within three varieties.

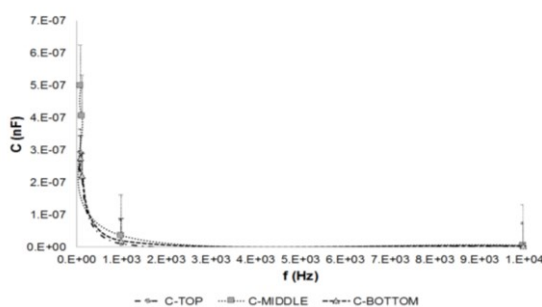
### B. Bioelectrical Characteristic of Sugarcane

Bioelectrical properties of sugarcane were measured within various frequency. Frequency changes in the dielectric material affect the molecular condition [3]. According to Faraday's law, inductance defined as an electromotive force (EMF) generated to counter a given change in the negative electrode, hence in the Fig. 2A shown a decreased of EMF.

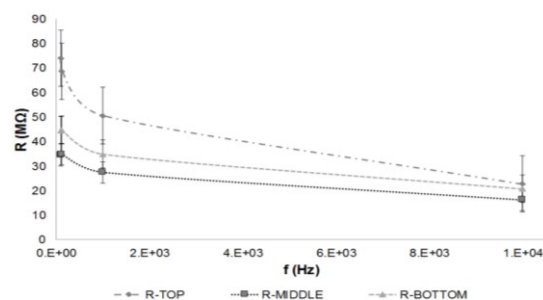
High frequency caused a short time of polarization, hence the polarization does not occur completely without sufficient times [14]. Therefore, the increasing frequency will lead to the decrease in the total polarization. This is produce a low capacitive phenomena in the sample (Fig. 2B). On the other hand, the change of frequency also affect to the condition of ion the sample. Therefore, produced a rapid mobility of dipole due to electrode polarization within high free water state also produce a low resistance (Fig. 2C). The electrical circuit model of sugarcane was constructed in a resistor-capacitor relation suitable with Zhang model.



(A)



(B)



(C)

Fig. 2. The bioelectrical properties of the samples: (A) inductance (B) capacitance and (C) resistance within frequency range of 0.1-10 kHz..

### C. Artificial Neural Network Prediction Model

The normalized dataset was used to determine an optimal proportion of data training and data validation. Data training of 66.67% was obtained the higher correlation coefficient (R). According to [15], the optimal training process can use different data groups by changing the percentage of data and evaluate with the highest regression. A sensitivity analysis performed to determine the best ANN model. In this stage, the sensitivity analysis was carried out using twenty combinations of node in the hidden layer. The sensitivity analysis of ANN was depicted in Table I.

TABLE I. ANN SENSITIVITY ANALYSIS

Topology	MSE Validation	R Validation
2-40-40-1	0.1476	0.7543
<b>2-30-40-1</b>	<b>0.04</b>	<b>0.9175</b>
2-20-40-1	0.2452	0.7136
2-10-40-1	0.2117	0.6586
2-40-1	0.1068	0.7372

The best ANN model is 2-30-40-1 (2 input nodes, 30 nodes in hidden layer 1, 40 nodes in hidden layer 2 and 1 output node) (Fig. 3) with MSE and correlation coefficient (R) are 0.04 and 0.9175 respectively. According to [16], sometimes ANN with more hidden layer can generalize better than simple ANN with low hidden layers. Increase number of hidden layer can inhibit the rate of convergence. Following is the phase of convergence on the best topology with 5000 iterations.

The best ANN model was yet convergence (Fig. 4). This showed the complexity of dataset, so the convergence was slow, even though the target has been achieved. One of the factors that affect the convergence is determination of momentum constant ( $\mu$ ) and learning rate. Learning rate is inversely proportional to the changes of weight and MSE, hence it is takes a longer time. Appropriate momentum constant can be used to offset the learning rate, and avoid a fluctuation of weight changes [8, 9]. The best combination of results obtained from the parameters of 0.1 learning rate and 0.9 momentum constant ( $\mu$ ). The best ANN model can be applied to predict sugar recovery of sugarcane in an interactive application.

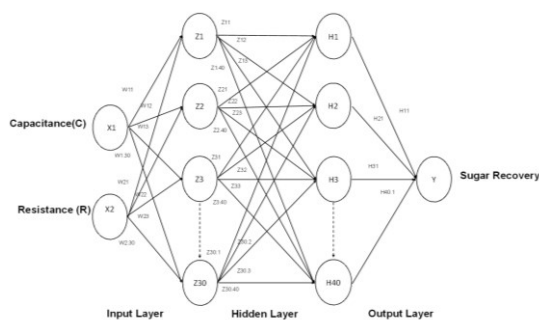


Fig. 3. Selected ANN model

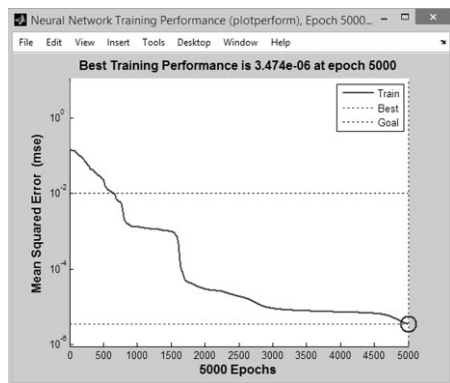


Fig. 4. Generated error in selected ANN model

#### D. Comparison of Lateral and Longitudinal Bioelectric Measurement

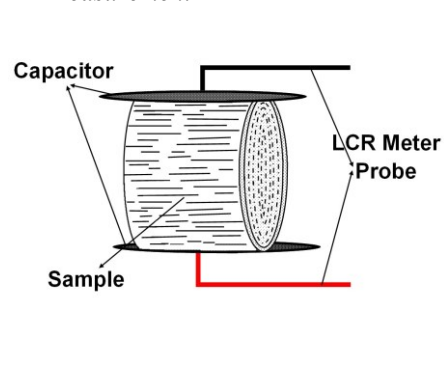


Fig. 5. Lateral position of the sample

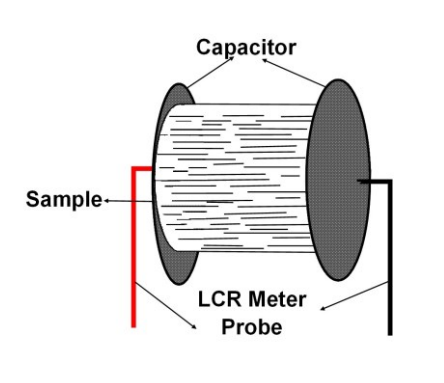


Fig. 6. Longitudinal position of the sample

Initial research bioelectrical properties has been measured in the longitudinal position within the direction of

fibre (Fig. 5). On the other hand, in this research, bioelectrical properties was measured in the lateral position (Fig. 6). Therefore, the resistance of will be slightly higher, caused by resistance of the fibre. According to [2], structure as well as the geometry of material as well as the placement of sample will affect the bioelectrical properties.

TABLE II. BIOELECTRICAL PROPERTIES OF SUGARCANE IN LATERAL POSITION

Node	Frequency (kHz)	Capacitance (nF)	Resistance (kΩ)
Top	0.1	0.0000002922	74079.30
	1	0.0000000099	50605.75
	10	0.0000000012	22731.08
Middle	0.1	0.0000004987	34528.48
	1	0.0000000342	27454.41
	10	0.0000000031	16174.33
Bottom	0.1	0.0000002750	44628.68
	1	0.0000000184	34899.83
	10	0.0000000021	20730.83

TABLE III. BIOELECTRICAL PROPERTIES OF SUGARCANE IN LONGITUDINAL POSITION

Node	Frequency (kHz)	Capacitance (nF)	Resistance (kΩ)
Top	0.1	0.000002367	3112.44
	1	0.000000220	1891.98
	10	0.000000043	1007.19
Middle	0.1	0.000001847	3827.80
	1	0.000000181	2360.46
	10	0.000000036	1250.52
Bottom	0.1	0.000001707	4449.65
	1	0.000000175	2779.80
	10	0.000000033	1415.23

Table II shows the values of bioelectrical properties of lateral measurement tend to be larger than the longitudinal measurement (Table III). Longitudinal measurement result such as capacitance (C), there is the same higher at a frequency of 1 kHz, 10 kHz respectively and another frequency have capacitance gap between  $1 \times 10^{-9}$  to  $1 \times 10^{-6}$  nF. The resistance of lateral measurement is greater longitudinal ones by approx. 1 kΩ. Those results show some tissue layer on stem of sugarcane acts as a capacitor and resistor, so the electric current in the form of a wave has disruption in wax layer of the flow paths, as well as some membrane resistance at intracellular and extracellular of the stems [2, 17]. The cell wall of each layer in stem of sugarcane is very influential on the resistance at lateral position, because on each layer of sugarcane is perpendicular to direction of electric current, so it has high resistance. On the other hand, at longitudinal position sugarcane stems was placed in a parallel position to the electric current, hence there is a little resistance to the electric current flowing through the tissue. The results of measurements bioelectrical properties certainly affect the prediction of sugar recovery of sugarcane. Prediction sugar recovery of sugarcane using ANN in longitudinal model



produce the best topology at 3-30-40-1 MSE and R are 0.0104 and 0.97733 respectively. On the other hand, the best results were obtained on the lateral measurement topology at 2-30-40-1 with MSE and R were 0.04 and 0.9175 respectively. Although in terms of topology ANN lateral measurement results are simpler with 2 inputs, but the complexity of the data inputs affect the results of prediction.

#### IV. CONCLUSION

Bioelectrical properties using a parallel plate capacitor were assessed for rapid and simple measurement of sugar recovery of sugarcane. Sugar recovery was affected the bioelectrical properties, hence the bioelectric model of sugarcane become a resistor-capacitor (R-C) series. There are two model of measurement procedure, which are lateral and longitudinal position of the samples. The first one shown that there is more capacitance and resistance produced by the samples than the last one, which affect the prediction model. ANN model was used to predict sugar recovery based on the bioelectrical properties of the samples. The best ANN structure is 2 input, 30 nodes in first hidden layer and 40 nodes in second hidden layers, also 1 prediction network output (sugar recovery of sugarcane). The sugar recovery of sugarcane was strongly predicted by bioelectrical properties data (MSE of 0.04). Finally, ANN models based on the bioelectrical properties has been proposed to develop an accurate, simple and reliable technique for sugar recovery of sugarcane measurement.

#### ACKNOWLEDGMENT

The authors acknowledgment the financial support from Indonesian Agency for Agricultural Research and Development at Partnership Research Corporation and National Agricultural Development Program No. 123/TL.220/I.1/3/ 2014.k.2014. The authors also thank to Universitas Brawijaya who help this publication.

#### REFERENCES

- [1] Mat Nawi N, Chen G, Jensen T, et al. Prediction and classification of sugar content of sugarcane based on skin scanning using visible and shortwave near infrared. *Biosyst Eng* 2013; 115(2): 154-161.
- [2] Nelson SO. Dielectric properties of agricultural materials and their applications. London, UK: Elsevier Inc. 2015: p.292-292.
- [3] Nelson SO and Trabelsi S. Factors Influencing the Dielectric Properties of Agricultural and Food Products. *J Microw Power Electromagn Energy* 2012; 46(2): 93-107.
- [4] Sucipto S, Djatna T, Irzaman I, et al. Application of Electrical Properties to Differentiate Lard from Tallow and Palm Oil. *Media Peternak* 2013; 36(1): 32-39.
- [5] Naderi-Boldaji M, Fazeliyan-Dehkordi M, Mireei SA, et al. Dielectric power spectroscopy as a potential technique for the non-destructive measurement of sugar concentration in sugarcane. *Biosyst Eng* 2015; 140: 1-10.
- [6] Taghinezhad J, Alimardani R and Jafari A. Development of a capacitive sensing device for prediction of water content in sugarcane stalks. *Int J Adv Sci Technol* 2012; 44: 61-68.
- [7] Sucipto S, Al Riza DF, Hasan MLA, et al. Effect of sample size, frequency, and temperature on the bioelectrical properties of sugarcane (*Saccharum officinarum* L.) for rapid prediction of sugarcane yield. *Industria* 2016; 5(3): 140-148.
- [8] Hendrawan Y and Murase H. Neural-Intelligent Water Drops algorithm to select relevant textural features for developing precision irrigation system using machine vision. *Comp Elec Agric* 2011; 77(2): 214-228.
- [9] Hendrawan Y and Murase H. Bio-inspired feature selection to select informative image features for determining water content of cultured Sunagoke moss. *Expert Syst Appl* 2011; 38: 14321-14335.
- [10] Hendrawan Y and Al Riza DF. Machine Vision Optimization using Nature-Inspired Algorithms to Model Sunagoke Moss Water Status. *Int J Adv Sci Eng Inf Technol* 2016; 6(1): 45-57.
- [11] Vani S, Sukumaran RK and Savithri S. Prediction of Sugar yields during hydrolysis of lignocellulosic biomass using artificial neural network modeling. *Bioresour Technol* 2015; 188:128-135.
- [12] Basheer IA and Hajmeer M. Artificial neural networks: fundamentals, computing, design, and application. *J Microbiol Methods* 2000; 43(1): 3-31.
- [13] Cardozo NP and Sentelhas PC. Climatic effects on sugarcane ripening under the influence of cultivars and crop age. *Sci Agric* 2013; 70(6): 449-456.
- [14] Yang J, Zhao KS and He YJ. Quality evaluation of frying oil deterioration by dielectric spectroscopy. *J Food Eng* 2016; 180: 69-76.
- [15] Li X, Chen F, Sun D, et al. Predicting menopausal symptoms with artificial neural network. *Expert Syst Appl* 2015; 42(22): 8698-8706.
- [16] Dixit PM and Dixit US. Modeling of metal forming and machining processes : by finite element and soft computing methods. Springer. 2010.
- [17] Ando Y, Mizutani K and Wakatsuki N. Electrical impedance analysis of potato tissues during drying. *J Food Eng* 2014; 121: 24-31.

# Implementation of MEMS Accelerometer for Velocity-based Seismic Sensor

Amalia C. Nur'aidha  
Physics Master Program

Brawijaya University  
Jl. Veteran Malang 65145, Indonesia  
amaliacemara@student.ub.ac.id

Sukir Maryanto  
Dept. of Physics

Brawijaya University  
Jl. Veteran Malang 65145, Indonesia  
sukir@ub.ac.id

Didik R. Santoso\*  
Dept of Physics

Brawijaya University  
Jl. Veteran Malang 65145, Indonesia  
dieks@ub.ac.id

\*Corresponding Author

**Abstract**— Micro Electro Mechanical System (MEMS) accelerometer is commonly used as acceleration-based vibration sensor. The MEMS accelerometer is small device, simple in the implementation design, and relatively inexpensive. But in some fields of application, due to low frequency operation and also small magnitude of the measured signal, for example in seismology, velocity-based vibration sensor is usually more desirable than acceleration-based sensor. In this research, a velocity-based vibration sensor has been developed using MEMS Accelerometer device e.g. MMA7361L. The acceleration-based vibration signal from the MMA7361L is converted into a velocity-based vibration signal by using an integrator circuit module. This module is assembled by using a band-pass filter and an integral-amplifier. The laboratory test shows that the developed sensor system could detect both low and high-frequency vibration signals in velocity-based with good result. The sensor system has a frequency range of 0.02Hz to 148Hz. It is wider frequency than the geophone (seismic sensor), thus the velocity-based MEMS sensor system has capability for geophone replacement.

**Keywords**—MEMS accelerometer, velocity-based sensor, integrator

## I. INTRODUCTION

A vibration sensor for detection seismic wave is called a seismic sensor. It is a main component in seismology, which normally used for monitoring seismic activities and seismic explorations [1]. The sensor able to transfer the ground motion into electrical signals [2]. A seismic sensor serves as velocity or acceleration of ground vibrations which is on the surface of the earth [3]. Several seismic sensors have been developed based sensing of an accelerometer, piezoelectric, electromagnetic, capacitance, and others [1].

Usually, the seismic sensors were often used for seismic exploration is geophone. It is one type of electromagnetic spring sensors, which the working principle of it is velocity-

based vibration. Geophone sensor has good linearity and has a relatively low ground noise. However, it has a problem that the limited linear frequency range above natural frequency, usually at 4-12Hz [4].

Recently, great interest of an alternative technology in seismic sensor is MEMS accelerometer device. It is a microchip shaped and acceleration-based sensing device [5]. MEMS accelerometer sensor has ability to detect vibrations-acceleration in broad frequencies, e.g. at 0-800Hz [7]. Unlike geophone which is works above the resonance frequency of velocity, MEMS accelerometers work under the resonant frequency of acceleration. Because of MEMS accelerometer is acceleration-based sensor, it is suitable for strong motion vibration (seismic) sensor, e.g. for high magnitude and high frequency signals [9]. For weak and low-frequency signals, when ground motion occurs at almost the constant velocity the MEMS accelerometer sensor maybe no detects the signals. It is disadvantage of using MEMS accelerometer as acceleration-based sensor for seismic signals. Therefore, in this research we propose a simple method and circuit to convert acceleration-based sensor to velocity-based sensor of the MEMS accelerometer device. So that the weak and low frequency vibration seismic signal can be detected by using MEMS accelerometer based sensor.

## II. METHODS

Fig. 1 shows the block diagram of the integrated sensor system developed in this research. In this research, used MEMS Accelerometer MMA7361L sensor in the form of IC chip. MMA7361L are analog sensors fabricated by Freescale Semiconductor. The MMA7361L sensor enables signal conditioning and g-select to select two sensitivities (1.5g and 6g), with a maximum sensitivity of 800mV / g@1.5g. In addition, the MMA7361L sensor has three working components vertically and horizontally (x, y, and z) [10]. In this study only used the z component that moves vertically. The output then connected to the conditioning circuit.

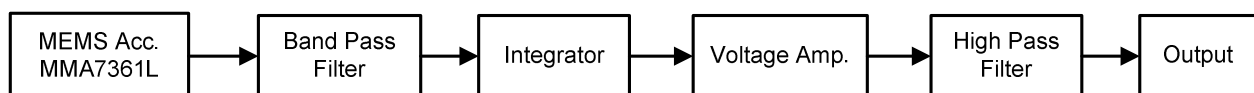


Fig. 1. Block diagram of velocity-based vibration sensor system

Before developing the signal conditioning circuit of the MMA7361L sensor first the geophone sensor simulated to determine the frequency response into the reference (Fig. 2a). Based on Fig. 2a it appears that geophones work at high frequencies with a frequency range at 10Hz until 100Hz and it cannot respond to vibrations when below 10Hz. Geophone inability to respond to frequencies below 10 Hz because the signal recorded is passed on a high pass to reduce the noise around the sensor. Moreover, it cannot be done bandwidth expansion to very low frequencies. Furthermore, Fig. 2a

shows that if the low frequency recorded by geophone its amplitude will decrease [5]. It indicated the geophone deficiency which makes opportunity for MEMS Accelerometer sensor already has a wider frequency bandwidth. The MMA7361L frequency response in Fig. 2b range at 0.01Hz to 200Hz. These show that a flat response amplitude in acceleration. Furthermore, an integral process needed to convert the signal from acceleration into velocity. Then it will be amplified and filtering to obtain the desired frequency range.

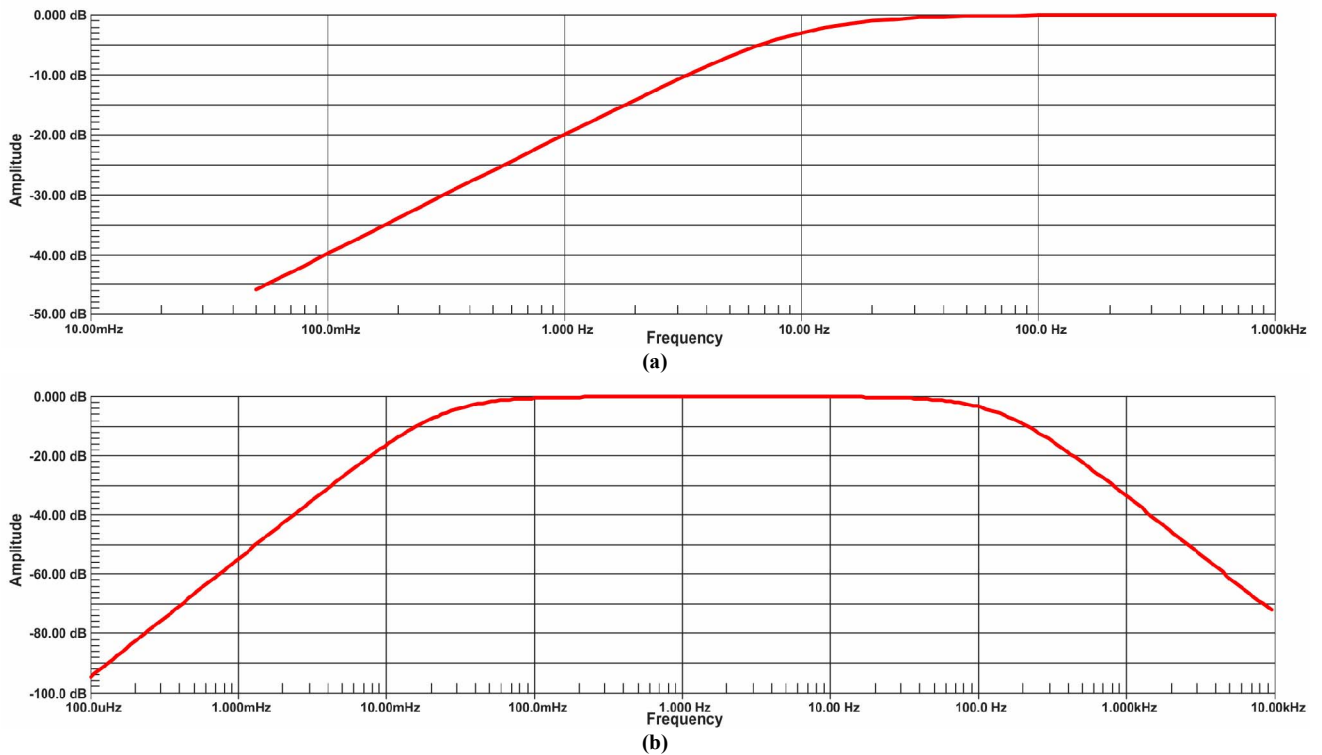


Fig. 2. Frequency response of (a) Geophone and (b) MEMS accelerometer

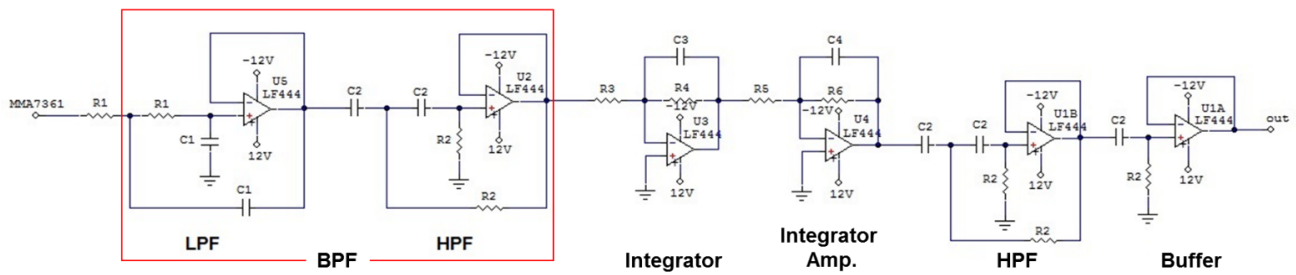


Fig. 3. The signal conditioning circuit for the vibration sensor

Implementation of the block diagram of Fig 1 showed by a circuit in Fig. 3. The circuit in Fig. 3 is composed of the Band Pass Filter (BPF) series which consist by Low Pass Filter (LPF) and High Pass Filter (HPF) circuits then it assembled by the integrator, amplifier, High Pass Filter, and buffer series. The LPF and HPF circuits which form the BPF series is designed based on Sallen-Key second order filter and using the LF444 IC. LF444 is a low power op-amp IC and has a bandwidth up to 1MHz, besides LF444 it is also built from 4 op-amps in one IC [11]. Each  $f_{c-LPF}$  and  $f_{c-HPF}$  values are determined by Equation (1) and (2). Both of these frequencies become more specific by setting the value of ( $R_1$ ,  $C_1$ ) and ( $R_2$ ,  $C_2$ ).

$$f_{c-LPF} = \frac{1}{2\pi\sqrt{R_1 R_1 C_1 C_1}} = \frac{1}{2\pi R_1 C_1} \quad (1)$$

$$f_{c-HPF} = \frac{1}{2\pi\sqrt{R_2 R_2 C_2 C_2}} = \frac{1}{2\pi R_2 C_2} \quad (2)$$

Then BPF series connected to the integrator circuit. The function of integrator circuit is to change the acceleration signal into velocity signal. Basic the integrator circuit (Fig. 4) has assembled by placing the capacitor (C) in the feedback

loop. If the circuit assumed as an ideal op-amp, then the Equation 3 is used [12].

$$I_R = I_c$$

$$\frac{V_{in}}{R} = -C \frac{dV_{out}}{dt} \quad (3)$$

Integral from 0 to  $t$  then Equation (3) become Equation (4)

$$\int dV_{out} = -\int \frac{V_{in} \tau}{RC} d\tau \quad (4)$$

$$V_{out} = -\frac{1}{RC} \int_0^t V_{in}(\tau) d\tau + V_{out}(0)$$

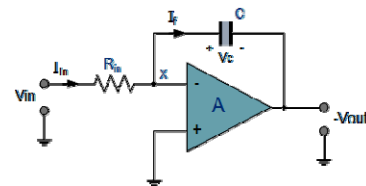


Fig. 4. Ideal integrator circuit

Frequency domain analysis obtained by expressing impedance feedback component in the complex plane, then the transfer function can thus be written as Equation 5. Equation 5 shows that different phase  $90^\circ$  between the input and output occurs at all frequencies.

$$\frac{V_{out}}{V_{in}} = -\frac{Z_c}{Z_R} = \frac{j\omega C}{R} = \frac{j}{\omega RC} \quad (5)$$

For DC signals at  $\omega = 0$  and unlimited gain in the integrator circuit become equivalent like an open circuit. The slackening of feedback from the capacitor made drift in

output voltage due to the input DC voltage had offset. The problem can be solved by connecting a resistor  $R_f$  in parallel with the feedback capacitor (C) (Fig. 5) so obtained the equation (6) [13].

$$V_{in} = A \sin(\omega t) \quad (6)$$

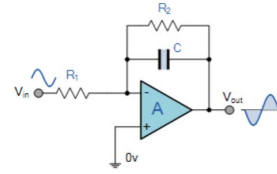


Fig. 5. Integrator circuit

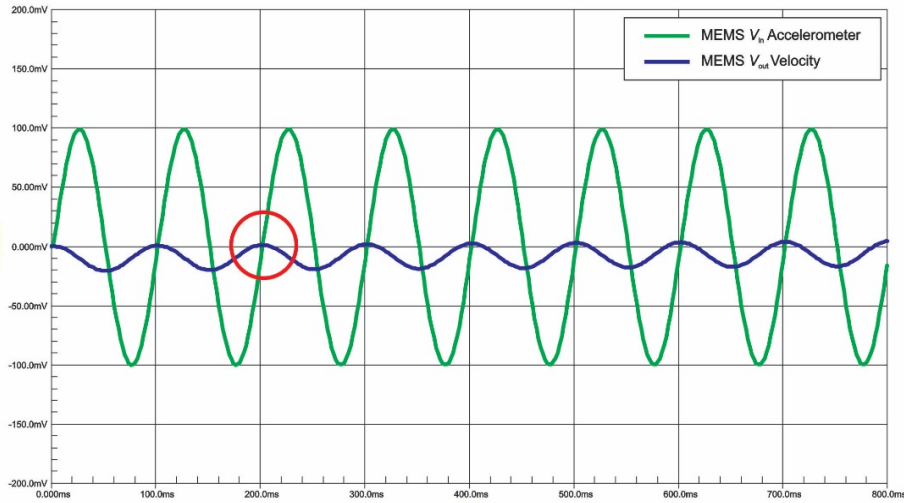


Fig. 6. Response signal input (green line) and output (yellow line) of MEMS-integrator circuit.

The simulation result using integrator circuit as shown in Fig. 6. An input signal has an acceleration (green line) then given integrator circuit so that the output signal becomes the velocity signal (yellow line). The circle sign in Fig. 6 shows the signal change from the acceleration into the velocity signal. The integrator circuit built on this research uses LF444 IC just like in previous LPF and HPF circuit.

$$V_{out} = \int V_{in} dt = \int A \sin(\omega t) dt = -A \cos(\omega t) \quad (7)$$

Then the velocity signal result from integrator circuit will be connected to the integrator amplifier circuit. The function of the integrator amplifier to amplify the output voltage of the integrator circuit. In this research, the Integrator amplifier circuit is built using LF444 IC. Determination of the gain is given by equation 8 and setting ( $R_5$ ,  $R_6$ ) value to obtain the more specific gain value.

$$A_v = \frac{R_6}{R_5} \quad (8)$$

Then, the amplifier output voltage connected to the HPF circuit for passing the high frequency and reduce the incoming mechanical noises. Last, there is a buffer circuit that used to keep the voltage always stable. The output of the signal conditioning circuit will be connecting to the S5000 Pico-scope (4 channels) which an entire Pico-scope process controlled by its software already installed on the computer.

### III. RESULT AND DISCUSSION

Implementation of the sensor and signal conditioning circuit that has been developing printed on PCB (Fig. 7). The

MMA7361L sensor attached to the cantilever beam that used for the sensor test tool. Based on Fig. 7a, there are three output channels (x, y, and z components) from the sensor but in this research only used one channel (z or vertical component). The z component has three pins that consisting of one pin for z output and two other pins as a power supply (ground and 5V). The output from the sensor connected to the signal conditioning module (Fig. 7b). The module consists of three circuits include the low-frequency velocity circuit, high-frequency velocity circuit, and acceleration signal conditioning circuit. Those three circuits are consist of BPF, integrator, integrator amplifier, HPF, and buffer. Except, for the acceleration signal conditioning circuit is not equipped by the integrator circuit because it's just used as a comparison.

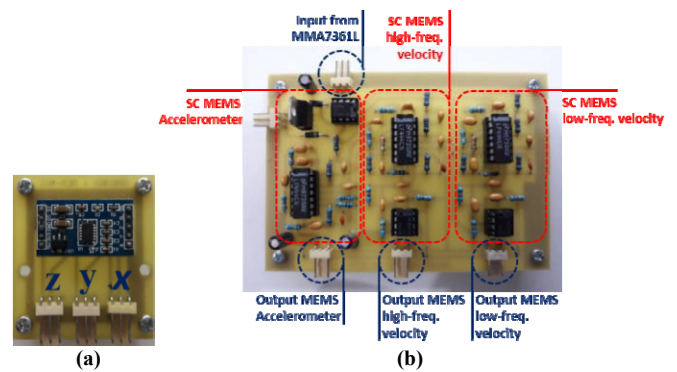


Fig. 7. Design result on PCB (a) MEMS accelerometer MMA7361L sensor and (b) integrated signal conditioning circuit

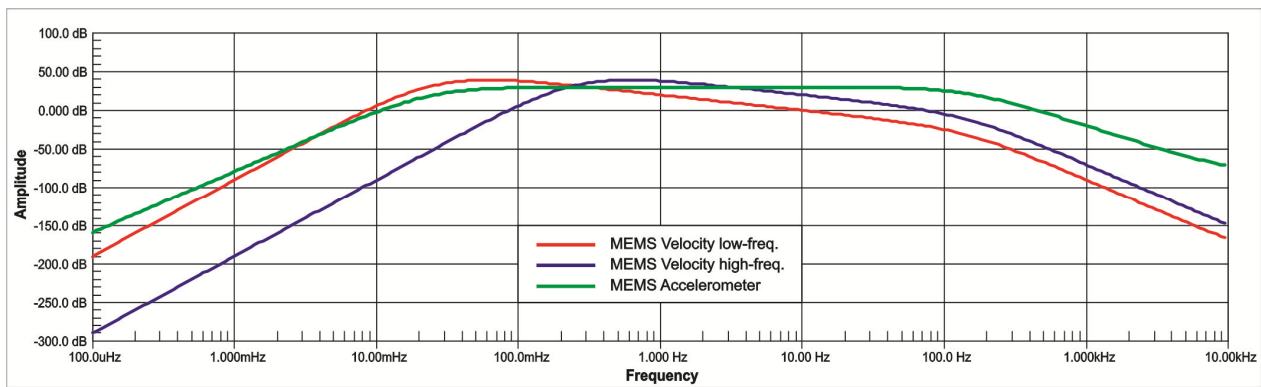


Fig. 8. Frequency responses from MEMS velocity low-frequency (green), high-frequency (red), and MEMS accelerometer (blue)

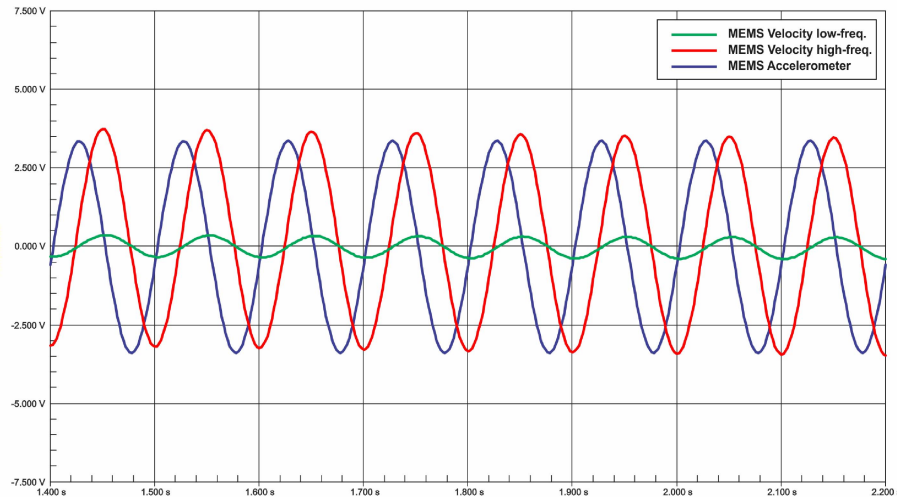


Fig. 9. Signal responses from MEMS velocity low-frequency (green), high-frequency (red) and MEMS accelerometer (blue)

Several simulations are performed to determine the performance of the sensor system has been built based on the circuit in Fig. 3. This performance determination is done by setting the values of  $R_1 = 3.3\text{k}\Omega$ ;  $C_1 = 330\text{nF}$ ;  $R_2 = 680\text{k}\Omega$  and  $C_2 = 10\mu\text{F}$ , the LPF cut-off frequency value is 146Hz and HPF cut-off is 0.02Hz. With these results, the sensor system has a frequency range from 0.02Hz to 146Hz. This frequency range has used for low-frequency velocity circuit in signal conditioning module. Meanwhile, for the high frequency velocity circuit used  $R_1 = 3.3\text{k}\Omega$ ;  $C_1 = 330\text{nF}$ ;  $R_2 = 680\text{k}\Omega$  and  $C_2 = 10\mu\text{F}$  and it has a frequency range from 0.2Hz to 146Hz (Fig. 8). This range frequency usually designed for seismic sensors in general. Moreover, Fig. 9 shows the result of the simulation high and low-frequency output signals from signal conditioning velocity module then compared them with the high-frequency output from MEMS accelerometer circuit. While the signal voltage gain in this research refers to the equation 8 and setting the value of  $R_5 = 10\text{k}$  and  $R_6 = 330\text{k}\Omega$  thus gaining has obtained by 33 times (30dB).

The velocity signal response test from the sensor system observed by attaching the MMA7361L sensor on the cantilever beam by moving the cantilever edge so that obtained high and low-frequency vibrations. Fig. 10a shows the high-frequency output signal from the high-frequency velocity circuit gets maximum amplitude when the sensor system given by a high-frequency vibration type. Similarly, output amplitude response of the low-frequency velocity circuit indicates the presence of low-frequency signal response with maximum amplitude at the peak signal. It happens when high-frequency vibration propagates always

be followed by low-frequency vibration so that the sensor system successfully respond to the low-frequency vibration that oscillation with high-frequency. Meanwhile, for the signal response of high-frequency acceleration circuit has a fluctuated amplitude which reaches the maximum amplitude for a moment then gradually decreases. Then it is also done for low-frequency vibration in the signal response test. Fig. 10b shows the output signal response of low-frequency velocity circuit. The output signal amplitude is equal to acceleration circuit response and still response to the high-frequency vibrations oscillation with the low-frequency vibrations given during the test.

The signal response test result of the velocity-based MEMS sensor system with various vibration frequencies show that the sensor system was able to respond well to all signal frequencies. Next, the sensor system has tested by comparing signal response with the geophone. Fig. 11a is the testing result for high-frequency vibration, seen at the high frequency both velocity-based MEMS sensor system and geophone having the same amplitude value. It shows that at a high-frequency the velocity-based MEMS sensor system can detect vibration well and its ability is proportional to the geophone. Meanwhile, for the result of a low-frequency vibration response has shown in Fig. 11b where at this frequency velocity-based MEMS sensor system has greater amplitude value than geophone. It is due to the geophone is unable to detect low frequencies below 10Hz whereas the velocity-based MEMS sensor system has detectability ranging from 0.02 Hz.

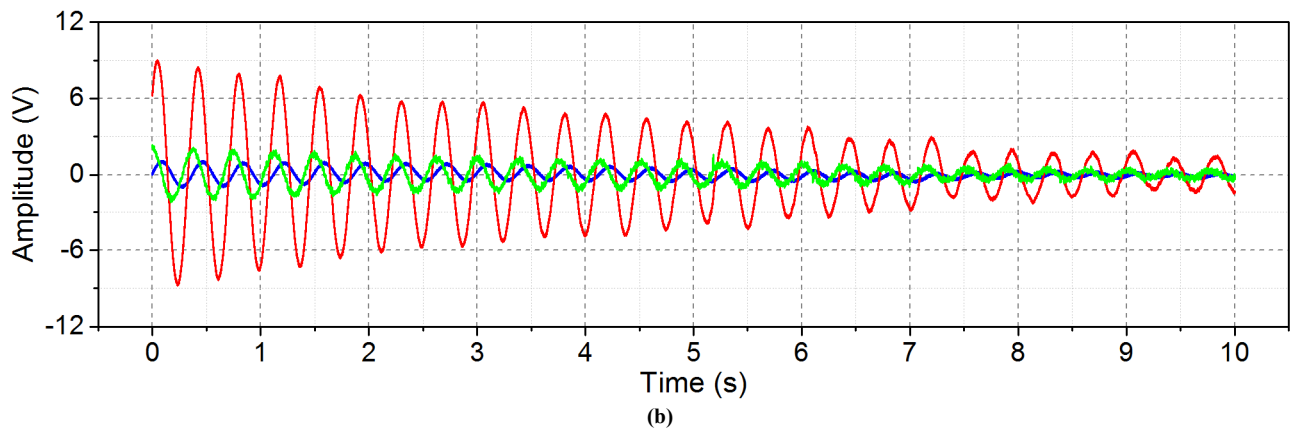
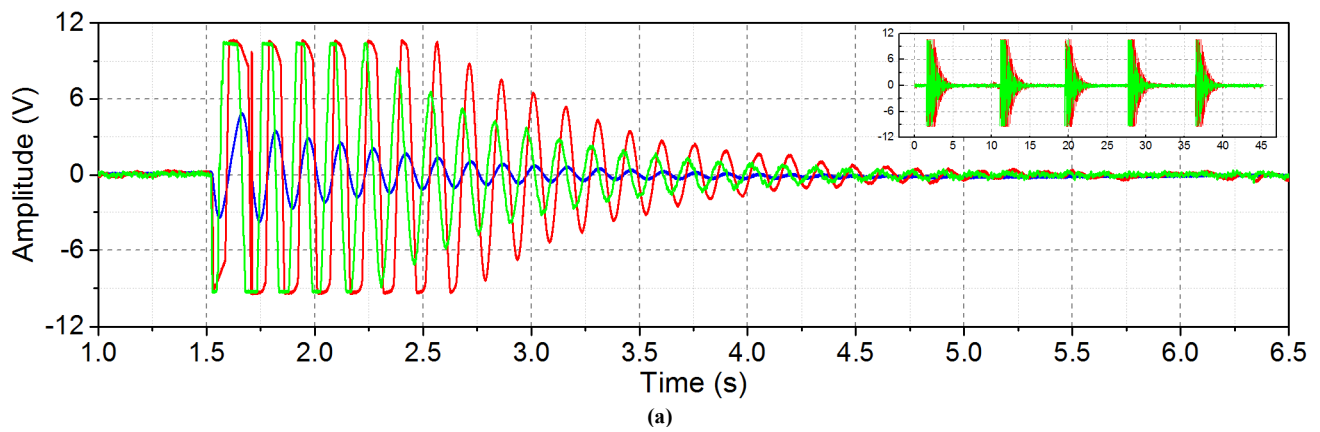


Fig. 10. Signal response of (a) high frequency and (b) low frequency vibrations from signal conditioning high-frequency velocity (red), low-frequency velocity (blue) and MEMS accelerometer (green) circuits.

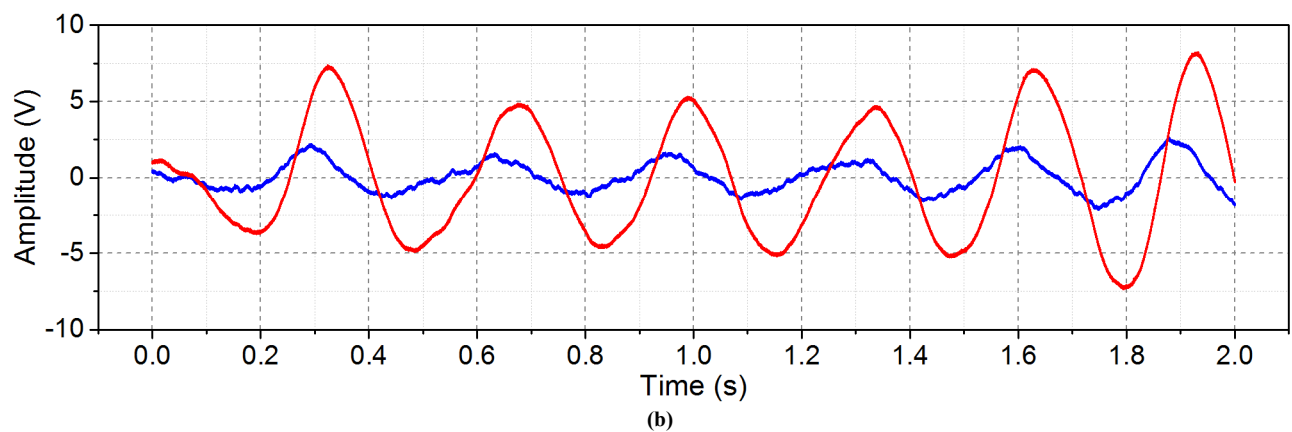
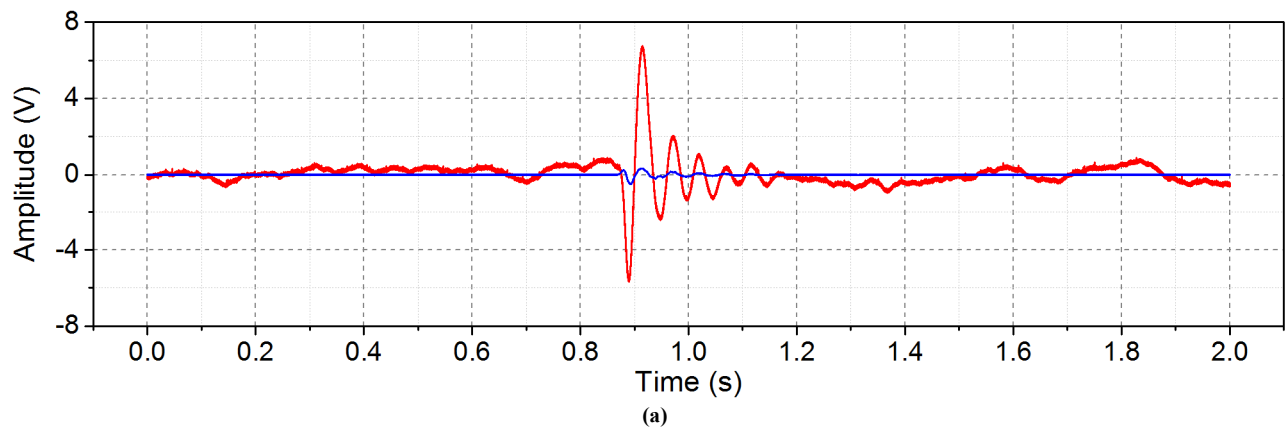


Fig. 11. Comparison (a) high-frequency and (b) low-frequency of velocity signal from velocity-based MEMS (red) and geophone (blue) sensor system.



## IV. CONCLUSION

This research has successfully developed MEMS Accelerometer MMA7361L sensor as a velocity-based vibration sensor by designing a signal processing module capable of converting acceleration signal into velocity signals. The velocity signal output from the sensor system is more stable than geophone output. This based on the amplitude response test results for both sensors while given by the low and high-frequency vibration. As geophones as this system have also been able to detect low-frequency signals that oscillate along with high-frequency vibration signals and vice versa. Other capabilities of this system that has a frequency range from 0.02Hz to 146Hz. The frequency range of the velocity-based MEMS wider than the geophone that has a frequency range from 10Hz to 100Hz. According to these, the velocity-based MEMS system is better able to detect low-frequency vibration signals. The low-frequency vibration signals required for data in monitoring seismic activity. Therefore, the velocity-based MEMS system is suitable as the seismometer especially velocity-based seismometer.

## ACKNOWLEDGMENT

The authors would like to thank to all members of Measurement Circuit and System Research Laboratory, Brawijaya University, and who has supported the implementation of this research.

## REFERENCES

- [1] T. Deng, D. Chen, J. Wang, J. Chen, dan W. He, "A MEMS based electrochemical vibration sensor for seismic motion monitoring," *J. Microelectromechanical Syst.*, vol. 23, no. 1, hal. 92–99, 2014.
- [2] G. Li *et al.*, "A MEMS based seismic sensor using the electrochemical approach," *Procedia Eng.*, vol. 47, hal. 362–365, 2012.
- [3] G. Li, J. Wang, D. Chen, J. Chen, L. Chen, dan C. Xu, "An electrochemical, low-frequency seismic micro-sensor based on MEMS with a force-balanced feedback system," *Sensors (Switzerland)*, vol. 17, no. 9, 2017.
- [4] R. Brincker, B. Bolton, A. Brandt, B. Allé, dan D.-O. M., "Calibration and Processing of Geophone Signals for Structural Vibration Measurements," in *Experimental Mechanics*, 2010, hal. 1–5.
- [5] M. Hons, "Seismic sensing: Comparison of geophones and accelerometers using laboratory and field data," 2008.
- [6] M. S. Hons, R. R. Stewart, G. Hauer, D. C. Lawton, dan M. B. Bertram, "Accelerometer Versus Geophone Response - A Field Case History," 2008, no. June.
- [7] J. Lainé dan D. Mougenot, "A high-sensitivity MEMS-based accelerometer," no. November, 2014.
- [8] J. Laine dan D. Mougenot, "Benefits Of MEMS Based Seismic Accelerometers For Oil Exploration," in *Transducers & Eurosensors*, 2007, hal. 1473–1477.
- [9] T. Aizawa, T. Kimura, T. Matsuoka, T. Takeda, dan Y. Asano, "Application of MEMS accelerometer to geophysics," *Int. J. JCRM*, vol. 4, no. 2, hal. 33–36, 2008.
- [10] D. R. Santoso, S. Maryanto, dan A. Nadhir, "Application of Single MEMS-accelerometer to Measure 3-axis Vibrations and 2-axis Tilt-Angle Simultaneously," *TELKOMNIKA*, vol. 13, no. 2, hal. 442, 2015.
- [11] Texas Instruments, "LF444 Quad Low Power JFET Input Operational Amplifier LF444 Quad Low Power JFET Input Operational Amplifier," 1995. .
- [12] P. Tapashetti, A. Gupta, C. Mithlesh, dan A. S. Umesh, "Design and Simulation of Op Amp Integrator and Its Applications," no. 3, hal. 12–19, 2012.
- [13] R. Hossain, M. Ahmed, H. U. Zaman, dan M. A. Nazim, "A Comparative Study of Various Simulation Software for Design and Analysis of Operational Amplifier Based Integrator Circuits," hal. 278–282, 2017.

# Monitoring The Usage of Marine Fuel Oil Aboard Ketapang-Gilimanuk Ship Based on Internet of Things

**Sarman**

*Master Student of Electrical Engineering Program UNISSULA  
Semarang, Indonesia  
sultanarman8888@gmail.com*

**Arief Marwanto**

*Post Graduated Study – Dept. Of Electrical Engineering  
Univ. Islam Sultan Agung (UNISSULA)  
Semarang, Indonesia  
arief@unissula.ac.id*

**Suryani Alifah**

*Post Graduated Study – Dept. Of Electrical Engineering  
Univ. Islam Sultan Agung (UNISSULA)  
Semarang, Indonesia  
suryani.alifah@unissula.ac.id*

**Abstract**—The development of the shipping industry in Indonesia has continued to increase over the past 10 years due to the sabotage principle. This development can be seen from the increasing number of national vessels. The number of national vessels becomes wider from 6,041 units in 2005 to 24,046 units in 2016. The more number of vessels owned makes monitoring the operational performance of the vessel difficult because each ship has different travel routes. This research made tools that can monitor the performance of ships especially the use of MFO aboard the ship from a distance. The sensors used to measure the volume of MFO in the tank on board are HC-SR04 ultrasonic sensors and potentiometer pendulum sensors. The data from the sensor was processed by Arduino Uno microcontroller. This study would compare the performance of ultrasonic sensors and potentiometer pendulum sensors mounted on MFO oil premises. The study was conducted by measuring the position of the ship horizontally, right and left tilted with a slope level of 30 degrees and 45 degrees. The result of this research is that the potentiometer pendulum sensor was better when MFO surface condition was flat with the average of error sensor 1.60%, while HC-SR04 ultrasonic sensor has an average of error for 2.87%. However, on the skewed surface conditions of MFO, the usage of HC - SR04 ultrasonic sensors was better with average of error for 3.21%, while the potentiometer pendulum sensor had an average of error for 8.66%.

**Keywords**—*Arduino Uno Microcontroller, Ultrasonic Sensor, Potentiometer Pendulum Sensor*

## I. INTRODUCTION

The development of the shipping industry in Indonesia has continued to increase in the past 10 years. This development can be seen from the increasing number of national vessels. The number of national vessels increases from 6,041 units in 2005 to 24,046 units in 2016 [1]. The number of ships owned by ship owners in Indonesia is more and more after the existence of Law No. 17 of 2008 which is about the sabotage principle. Sabotage principle is a way of empowering national sea transport that provides a conducive climate in order to promote the transport industry in the waters, among others, in the field of taxation, and capital in the procurement of vessels and the existence of long-term contracts for transport in waters [2].

The more number of vessels owned makes its own problems for ship owners. One of the problems faced is the way to monitor the performance of the vessel because each ship has different travel routes. During this monitoring of the ship is done by analyzing data from records made by ABK.

This method has a weakness of human error made (by ABK) in making report

## II. BACKGROUNDS

Many data reported by ABK to the ship owner company. One of the data reported was the use of Marine Fuel Oil (MFO). MFO usage reports are important because they affect production cost calculations by management. In order to avoid reporting errors on the use of MFOs on board, this study made a tool that could monitor the use of MFOs aboard the ship from a far-distance.

Research on making wireless ship balance monitoring system has been done by [3]. The sensor used to read the slope of the ship is the IMU sensor. The data from the IMU sensor is sent via Bluetooth to the android system. This system can be used with a maximum distance of 30 meters. Another study was to measure temperature and humidity in agriculture [4]. The module used to measure temperature and humidity is DHT11. Data from DHT11 is sent via Short Message Service (SMS) when there is data request via SMS. In addition, the built system can send SMS automatically to the farmer when the soil moisture is less and the system turns on the pump automatically to water the ground.

Previous studies related to the monitoring of fuel consumption were volume monitoring and water clarity in Lab View based tanks with Ni Myrio controller [5]. Other studies monitored the volume of water in the tank using ultrasonic sensors and water clarity using turbidity sensors. Readout data from the sensor is sent to personal computer (PC) via wireless. The result of SRF 04 ultrasonic sensor reading in the form of volume displayed in PC as simulation of water level condition in tank. While the readout data from turbidity sensor is displayed on the PC in the form of nominal score of water clarity.

## III. SYSTEM MODEL

This study calculated MFO consumption on board by measuring tank volume from MFO using HC - SR04 ultrasonic sensor and potentiometer pendulum sensor. Data from HC - SR04 ultrasonic sensor and potentiometer pendulum sensor. Data from HC - SR04 ultrasonic sensors and potentiometer pendulum sensors were converted by microcontroller into the use of MFO. Data on the amount of use of MFOs remotely sent over the internet using ESP 8266 so that the usage of MFO on board can be monitored from different computers where using the internet network. The architecture system built on this research can be seen in Fig. 1.

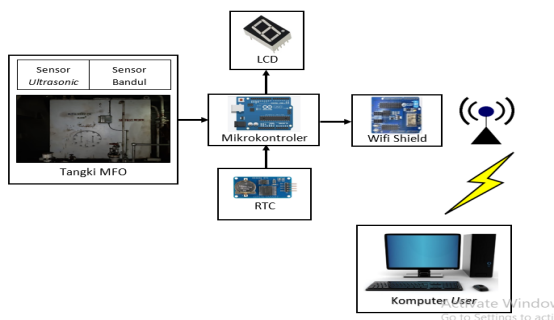


Fig. 1. Architecture System

#### IV. DESIGN MODEL

The design used in this study can be seen in Figure 2. The working of the system is that HC - SR04 ultrasonic sensor and potentiometer pendulum sensor will read the height of MFO in the tank continuously. Data from HC - SR04 ultrasonic temperature sensors and potentiometer pendulum sensor are transformed firstly by Arduino Uno into digital through ADC. Data that has been digital are processed inside the Arduino Uno to be the MFO volume data present in the tank. The volume and time information data from the RTC is sent continuously to the remote user's computer via Wi-Fi Shield ESP 8266 and to the LCD via I2C. Then, LCD and the user's computer display the MFO volume data.

Fig 2. Shows the diagram block, this study used hardware which has the following functions:

1. Ultrasonic sensor is a measure of MFO surface distance with position of ultrasonic sensor being placed.
2. The potentiometer pendulum sensor is a measure of MFO surface distance with the position of the potentiometer pendulum sensor being placed.
3. RTC is a timing information system related to seconds, minutes, hours, days, months, and years when taking the data.
4. The controller is the overall system control center. The controller processes the data from the potentiometer pendulum sensor and the ultrasonic sensor and the timer system from the RTC which is then sent to the LCD and the user's computer.
5. Wi-Fi shield 8266 is as a medium of wireless communication between the microcontrollers to the internet.
6. I2C (Inter-Integrated Circuit) is a serial communication media with a cable between microcontroller to LCD.
7. The LCD is the display of MFO volume near the MFO tank.
8. The user's computer is a remote view of MFO volume (from a distance).

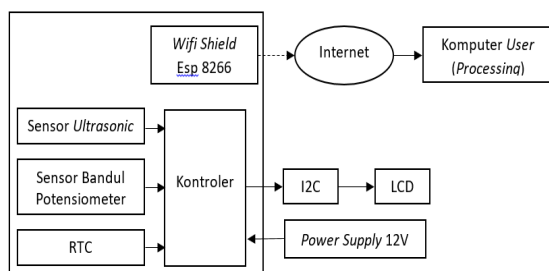


Fig. 2. Hardware Designing Block Diagram

The controller used is Arduino Uno microcontroller module. Arduino Uno microcontroller is a module in which already consists of a minimum system of a microcontroller, ATMEGA 328 series of microcontroller, digital input and output pins, analog input pins, and utility pins. Microcontroller connections with other hardware can be seen in Table 1. The plan used is a miniature tank from the actual MFO tank, as shown in Figure 3.

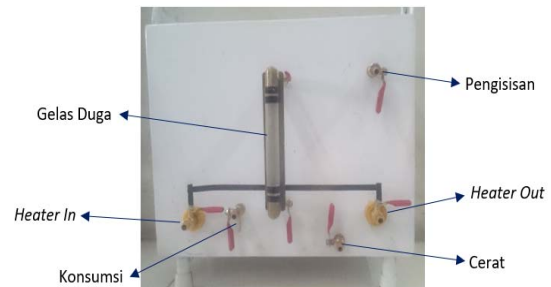


Fig. 3. MFO Miniature Tank

#### V. RESULTS AND ANALYSIS

The test was done by using two types of sensors to measure the volume, namely HC - SR04 ultrasonic sensor and potentiometer pendulum sensor. In addition to using 2 types of sensors, testing was also done with a flat, sloping, and wavy MFO surface as shown in Figure 4

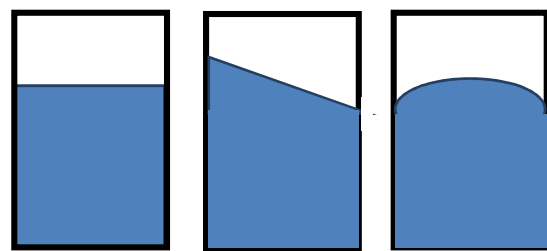


Fig. 4. MFO's Flat, Sloping and Wavy Surfaces

Test results from this research can be seen in Table I and Table II. Based on test results data for HC-SR04 ultrasonic sensors, it is seen that if using HC-SR04 ultrasonic sensor either with flat position, 300 right tilted, 450 right tilted, 300 left tilted, and 450 left tilted on MFO surfaces produced the same output, which was the fuller of MFO volume inside the MFO miniature tank then the better of the sensor readings. This is seen when the volume on the MFO miniature tank showed 13 liters, it was at average of error for 2.09%. Otherwise, the less volume of MFO made the bigger of the error reading. When the volume on the MFO miniature tank showed 9 liters, it was at average of error for 5.68%. The HC-SR04 ultrasonic sensor would have an increasing error when the surface of the MFO was wavy that was 11.09% in average.

Test results for potentiometer pendulum sensor with MFO flat surface position, 300 right tilted, 450 right tilted, 300 left tilted, and 450 left tilted had the same output with HC-SR04 ultrasonic sensor which was the fuller of MFO tank filled then the lower error that happened. When the maximum volume tested in this study was 13 liters, the average of error occurred was 2.95%. Otherwise, when the less MFO tank filled made

the larger of the error that occurred which was 14.31% in average.

TABLE I. RESULT DATA OF ULTRASONIC SENSOR TESTING

MFO Surface	Prediction Glass (Liter)	HC – SR04 Ultrasonic Sensor (Liter)	Error (%)
Flat	9	9,42	4,46
	10	10,32	3,10
	11	11,30	2,65
	12	12,27	2,20
	13	13,26	1,96
30° Right Tilted	9	9,50	5,26
	10	10,32	3,10
	11	11,28	2,48
	12	12,22	1,80
45° Right Tilted	9	9,61	6,35
	10	10,33	3,19
	11	11,28	2,48
	12	12,32	2,60
30° Left Tilted	9	9,47	4,96
	10	10,35	3,38
	11	11,32	2,83
	12	12,3	2,44
45° Left Tilted	9	9,59	6,15
	10	10,31	3,01
	11	11,33	2,91
	12	12,37	2,99
Wave	9	10,52	14,45
	10	11,45	12,66
	11	12,21	9,91
	12	13,34	10,04
	13	14,19	8,39

TABLE II. RESULT DATA OF POTENTIOMETER PENDULUM SENSOR TESTING

MFO Surface	Prediction Glass (Liter)	Potentiometer Pendulum Sensor (Liter)	Error (%)
Flat	9	9,10	1,10
	10	10,08	0,79
	11	11,15	1,35
	12	11,54	3,99
	13	13,10	0,76
30° Right Tilted	9	7,98	12,78
	10	9,02	10,86
	11	10,23	7,53
	12	11,22	6,95
45° Right Tilted	9	7,65	17,65
	10	8,87	12,74
	11	10,01	9,89
	12	11,45	4,80
30° Left Tilted	9	8,1	11,11
	10	9,13	9,53
	11	10,37	6,08
	12	12,89	6,90
45° Left Tilted	9	7,78	15,68
	10	8,89	12,49
	11	10,11	8,80
	12	11,15	7,62
Wave	9	9,78	7,98
	10	10,95	8,68
	11	12,03	8,56
	12	13,11	8,47
	13	14,21	8,52

In addition, in the usage of potentiometer pendulum sensor was occurred a bigger error when the MFO surface position was more skewed when the right side tilted to 45° then the average of error that occurred up to 9.64%. In the 30° tilted, the average of error was 7.68%. The comparison for the wave MFO surface showed that the potentiometer pendulum sensor was better with an average of error for 8.44%, while the HC-SR04 ultrasonic sensor's average of error was 11.09%.

The results of comparing HC-SR04 ultrasonic sensors with potentiometer pendulum sensor indicated that the potentiometer pendulum sensor was better when the MFO surface was flat with an average of error 1.60%, while the mean of error for the HC-SR04 ultrasonic sensor was 2.87%. But when in a sloping position, the usage of HC-SR04 ultrasonic sensors was still better than the potentiometer pendulum sensor. The average of error from HC-SR04 ultrasonic sensor when in a sloping position was 3.21%, mean error for potentiometer pendulum sensor with tilted MFO surface position was at 8.66%.

The results of this study with the best results occurred when the potentiometer pendulum sensor was used to measure the volume of MFO in flat surface conditions with the error of 0.76%. And the worst result occurred when the potentiometer pendulum sensor was used to measure the volume in 45° right tilted condition by 17.65%.

## VI. CONCLUSION

Based on the results of the tests conducted, this study can take some conclusions:

1. Prototype to monitor MFO volume on board by using HC-SR04 ultrasonic sensor and potentiometer pendulum sensor. Test results show that both sensors can transmit data in the form of volume.
2. The usage of the sensor that will be used depends on the location of the ship's operation. If the ship's operation location is not too wavy, it is better to use a potentiometer pendulum sensor than the HC-SR04 ultrasonic sensor because the error result is smaller. But if the ship's location is operating in big waves then it is better to use a potentiometer pendulum sensor because the HC-SR04 ultrasonic sensor produces a big error when the MFO tank is tilted.

## ACKNOWLEDGMENT

The research has been developed under theses supervision project for master student in Post Graduated Study – Department of Electrical Engineering UNISSULA.

## VII. REFERENCES

- [1] M. IDRIS, "https://finance.detik.com". [ONLINE]. Available: <https://finance.detik.com/berita-ekonomi-bisnis/d-3651543/industri-pelayaran-ri-makin-menggeliat-dalam-10-tahun>. DIAKSES [31 MARET 2018]
- [2] UNDANG - UNDANG NO 17 TAHUN 2008.
- [3] A. A. SAPUTRA, E. MARDIANTO, DAN A. H. ADIKORO, "Sistem Monitoring Dan Sistem Penyeimbang Berat Muatan Kapal Ferry Sebagai Antisipasi Kecelakaan", Politeknik Elektronika Negeri Surabaya, SURABAYA, 2013
- [4] K.V.D. SAGAR, M.R. CHOWDARY, S. MAHESH, DAN K.R. RAO, "SMART CROP MONITORING AND FARMING USING INTERNET OF THINGS WITH CLOUD", *Journal of Advanced Research in Dynamical and Control Systems*, Issue : 02-Special Issue, Pages: 265-272, 2018

- [5] E. N. DIANSYAH, "*Rancang Bangun Alat Sistem Monitoring Volume Dan Kejernihan Air Pada Tangki Berbasis Lab View Dengan Kontroller Ni Myrio*", Universitas Muhammadiyah Malang, Malang, 2017
- [6] ANONYMOUS, " <https://kitskart.com> ". [ONLINE].  
AVAILABLE : <https://kitskart.com/product/arduino-uno-r3-smd-development-board/>. DIAKSES [6 MEI 2018]

# Design of Low Noise Micro Liter Syringe Pump for Quartz Crystal Microbalance Sensor

Ridha N. Ikhsani  
Department of Physics  
Brawijaya University  
Malang, Indonesia  
ridha.fisika@gmail.com

D.J. Djoko H. Santjojo  
Department of Physics  
Brawijaya University  
Malang, Indonesia  
dsantjojo@ub.ac.id

Setyawan P. Sakti  
Department of Physics  
Brawijaya University  
Malang, Indonesia  
sakti@ub.ac.id\*

**Abstract**—An injection pump was a critical aspect in the used of Quartz Crystal Microbalance (QCM) biosensor or chemical sensor in liquid. It is required that the pump should have variable speed and doesn't introduce pressure noise to the QCM sensor. In this work, the pump was developed using a micro stepper motor with a microliter syringe. The mechanical transmission transforms the rotational displacement of the motor into a translational displacement of the syringe. The flow rate of the injection pump could affect the signal pattern indicated by a signal spike or instability of the sensor resonance frequency. The developed system successfully minimized the spike signal and improved the stability of the sensor resonance by the used of the microliter syringe pump with optimizing the reaction chamber of the QCM sensor. The flow rate of the pump can be controlled with a minimum speed of 0.7  $\mu\text{L}/\text{second}$  for water. At low flow rate, there was a negligible or none of the spike signal observed during the injection and ejection of the liquid. However, at a high flow rate, few signal spikes may be observed.

**Keywords**—Microliter syringe pump, stepper motor, QCM, flow rate.

## I. INTRODUCTION

As one of the ultra mass-sensitive sensor, the Quartz Crystal Microbalance (QCM) sensor have been used in many applications such as for biosensors applications [1], [2]. The response of frequency change from the QCM sensor caused by a mass change on top of the sensor surface. The QCM as a biosensor works in a liquid environment [3]–[6]. In this experiment, one of the sensor surfaces is put in contact with buffer or sample solution. The buffer and sample solution covered the whole side of the sensor surface. On the other hand, the other side of the sensor surface is in contact with the air.

For sensor preconditioning, immobilization or reaction, buffer or sample solution was injected into the sensor surface. There are two methods for injecting the buffer or sample solution of target molecules on top of the sensor. A flow injection method [7] or the liquid drop method [8]. Although these methods are suitable for injection the buffer or sample solution, both methods have significant shortcomings.

The flow injection system required a complex handling system, and also a short pressure change at the sensor surface. The injection method with a microliter syringe pump has been reported in previous work [9], the injection speed also affected the resonance frequency of the sensor. The small spike signal or noise was detected. Optimizing the injection method is needed to minimize the existence of the spike and to simplify the handling system. On the other hand,

the liquid drop method suffered from a compressional wave or disturbance to the sensor [10]. Usually, a significant change in the sensor resonance frequency was observed at the time of liquid drop.

In the present study, we developed a controllable and low noise microliter syringe pump which can be used to fill the QCM sensor surface in the adjacent reaction cell. The pump was designed for injecting and ejecting the buffer or sample solution with a few disturbance on the frequency responses by minimizing the hydrostatic pressure changes. The microliter syringe pump system was developed and controlled by using a microcontroller. A simple user interface was designed to control the movement of the microliter syringe pump. The used of software to control the system minimized the complexity of the electronics circuit and also providing connectivity with the acquisition software for further development. In addition, the new design of cell reaction chamber is utilized to minimize the spike signal of the frequency response. The speed of a micro stepper motor, which meant the injection or ejection flow rate, was varied during the experiment to investigate the effect of flow rate.

## II. SYSTEM DESIGN AND METHOD

### A. Hardware and software design

In this experiment, the system of microliter pump was developed using a microliter syringe. The syringe stroke was controlled using a 42BYGH-48 stepper motor linear actuator, with a mechanical transmission system. The motor speed and direction were controlled by using a PIC18F45K50 microcontroller. The stepper motor driver DRV8255 was used to drive a motor stepper with PWM micro stepping. The communication between the computer software and the pump system was done using the USB interface. A USB CDC protocol was used for the communication between the microliter pump device and the computer.

The command from the computer was sent to the microcontroller in the pump system using a defined data format and translated by the microcontroller to control the system. The integrated pump system consists of a mechanical part for microliter syringe pump, oscillator circuit subsystem which can be connected directly to the cell reaction with QCM Sensor inside of the chamber, directions control subsystem, frequency counter subsystem, and frequency capture program. The block diagram of a measurement system for QCM sensor including a microliter pump is illustrated in Fig.1.



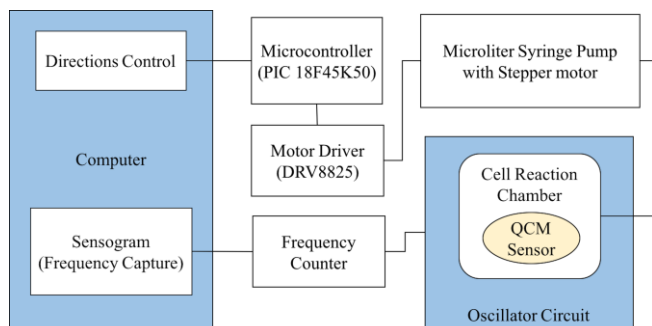


Fig. 1. Block diagram of the measurement system for the QCM sensor.

A disposable syringe with a maximum volume of 100  $\mu\text{L}$  was used as a pump. The syringe has a stroke length of 85 mm. The maximum stroke length of the microliter syringe pump system is 60 mm in parallel with a maximum volume of 75  $\mu\text{L}$ . The mechanical transmission transforms the rotational displacement of the motor into a translational displacement of the syringe. The maximum distance of the displacement transducer was set according to the syringe length. An emergency stop was placed to stop the displacement transducer movement to protect the syringe stroke movement. The design of the microliter pump with a micro-stepper motor and a syringe is presented in Fig. 2.

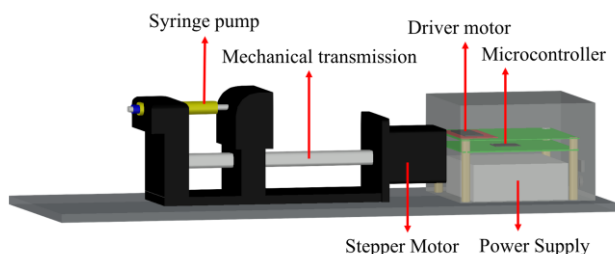


Fig. 2. Design of microliter injection pump.

The PIC 18F45K50 and other electronic part and the system power supply was packed and integrated into the mechanical translator unit. It is placed directly behind the motor stepper unit and spared the space in another end for the reaction cell installation.

The reaction cell made from PMMA (Poly Methyl Methacrylate) and PLA (Poly Lactic Acid). The central part of this reaction cell is a reaction chamber on top of the sensor surface. The liquid inlet and outlet in the edge of the chamber were connected to the tilted injection channel. The position of the inlet and outlet channel was placed far from the center of the sensor disc. The reaction cell is depicted in Fig. 3.

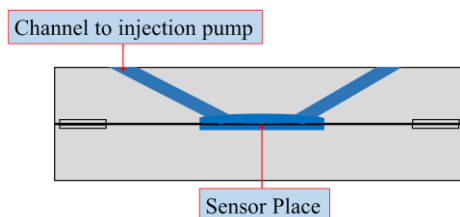


Fig. 3. Design of cell reaction in the experiment (front view).

The sensor was mounted inside of the cell reaction. A silicon ring was used as a damper and spacer to minimize mechanical stress during installation in the cell reaction and sealed the liquid in the reaction chamber.

A simple user interface was developed to control the syringe pump. The interface is depicted in Fig. 4. The software primarily comprised of directions and flow rate control. The user sets the flow rate of the pump by inputting the value of the desired liquid volume per minute in  $\mu\text{L}$ . The minimum value of the volume to be injected 10  $\mu\text{L}$ , and the maximum volume is 75  $\mu\text{L}$ .

The movement of the pump was started when the user presses the direction button (REVERSE button or FORWARD button). Rapid filling and disposal of the reaction chamber were facilitated by FILL UP SYRINGE and FULL DISPENSED buttons.

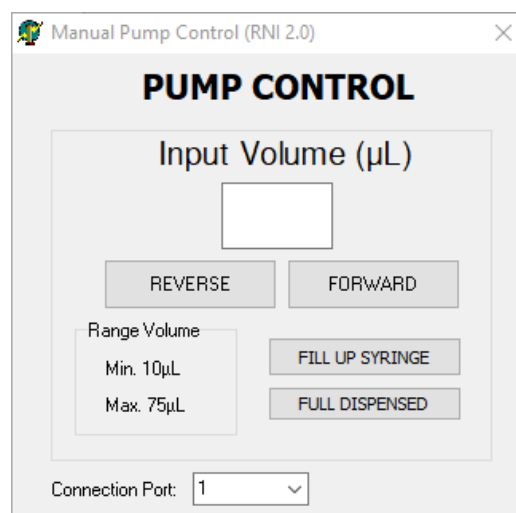
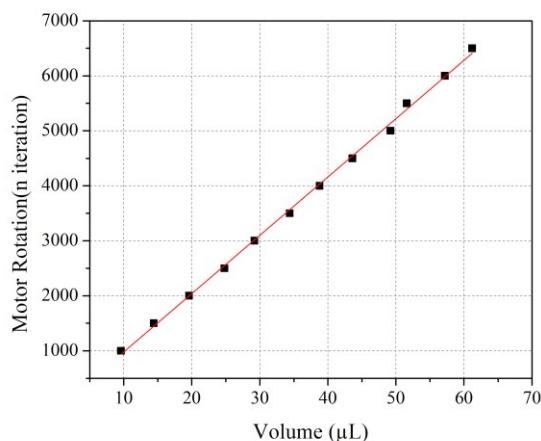
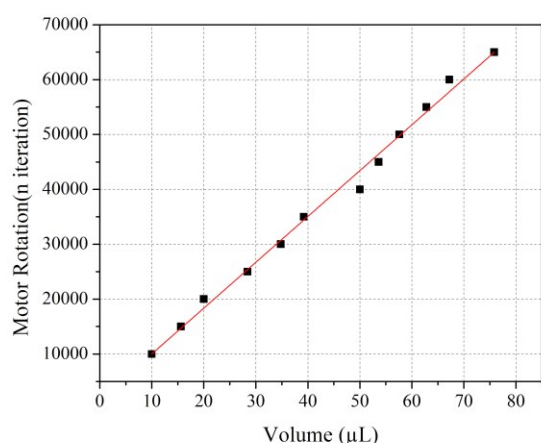


Fig. 4. The user interface of the microliter syringe pump system.

### B. Microliter Pump Calibration

The developed injection system using the syringe pump was calibrated using the volumetric method. Calibration was done using a digital balance with a resolution of 2 mg. The volume was converted from the measured water mass based on the water density at room temperature.

The calibration was done by varying the motor speed. The mass of the ejected water from the syringe pump was weighted using the balance. The amount of the water was determined by the motor speed and time. The ejected water was weighted using the balance and then converted as volume. The results of the volume calibration process are shown in Fig. 5, and Fig. 6.

Fig. 5. Volume calibration for injection speed at a 6.3  $\mu\text{L}$  per second.Fig. 6. Volume calibration for injection speed at a 0.7  $\mu\text{L}$  per second.

### C. Experimental System Setup

The complete setup of the system for the experiment was presented in Fig. 7. It consists of the designed injection pump, the reaction cell, and a frequency counter. The outlet of the syringe pump was connected to the reaction cell to the inlet port by using a silicone hose and a needle.

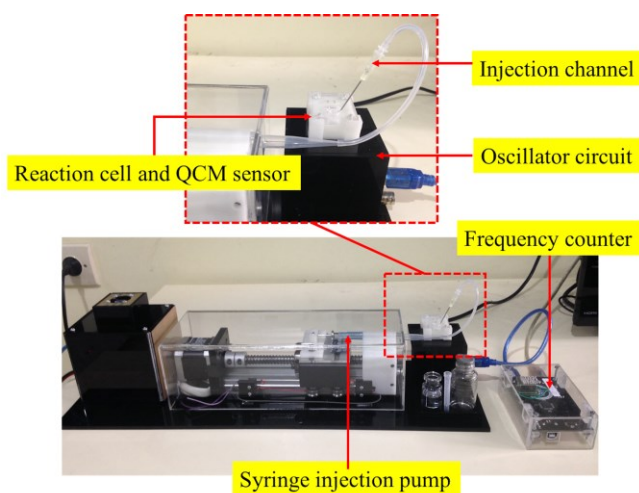


Fig. 7. Photograph of the system

Under the reaction cell, there was an oscillator which able to drive the sensor in contact with air as well as in contact with water. The oscillator was connected to the frequency counter.

### III. RESULT AND DISCUSSION

The pump effect to the sensor was measured by varying the water flow rate injected and ejected into and from the reaction chamber. Initially, the reaction chamber was filled with water to bring the state of the sensor into a condition of one sensor surface in contact with water. After the new resonance frequency in contact with water was reached, the sequence of injection and or ejection was done.

The resonance frequency of the sensor was recorded during the injection and ejection process. The frequency resolution of the frequency counter was 1 Hz. Therefore, any change of the resonance frequency of the sensor equal to or higher than 1 Hz can be measured. Frequency measurement was done every second.

After a stable resonance frequency when the sensor in the reaction cell was observed, a 30  $\mu\text{L}$  water was injected into the reaction chamber to cover the sensor surface with water. The sensor surface gradually contacts with water in parallel with the injected water. The transition of the surface contact of the sensor from entirely in contact with air and totally in contact with water affect the sensor resonance frequency. The resonance frequency of the sensor was rapidly decreased as the resonance frequency of the sensor change according to the Kanazawa-Gordon equation [11]. After the sensor surface was fully covered with water, a new resonance frequency of the sensor was reached. The new resonance frequency was indicated by a constant value of the recorded frequency. Fig. 8 shows the frequency transition of the sensor in contact with air and in contact with water.

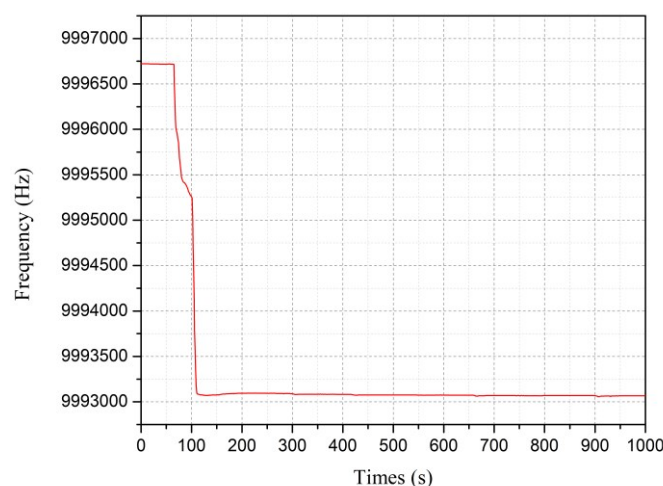


Fig. 8. Sensor resonance frequency during the transition from contacting with air and water

After the resonance frequency was steady, an amount of 10  $\mu\text{L}$  water was injected into the reaction cell. This injection pushes the water to flow into the reaction chamber. The excess water went out onto the outlet. The change in the water flow caused a small pressure change on the sensor surface which affect the resonance frequency of the sensor.

Fig. 9. and Fig. 10. shows the response frequency of the sensor during the injection and ejection process.

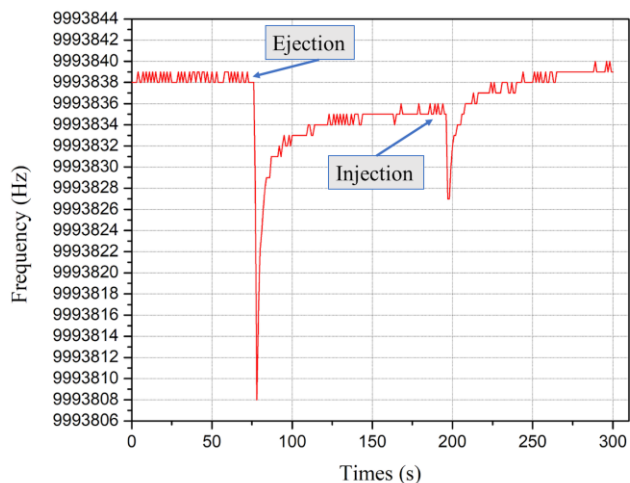


Fig. 9. Sensor resonance frequency caused by 10  $\mu\text{L}$  water injection and ejection at a speed of 6.3  $\mu\text{L}$  per second.

At the event of water injection, the frequency counter recorded a change of the resonance frequency of the sensor. The frequency of the sensor was abruptly decreased, and followed by a gradual increase of the sensor resonance frequency back to the initial frequency.

The similar response was observed during the reverse direction of water flow. When the water was ejected out, the resonance frequency of the sensor changed in a short time resulted in a small spike and then followed by a returning resonance frequency to the initial frequency.

Fig. 9. shows the resonance frequency of the sensor during injection and ejection of 10  $\mu\text{L}$  water at a speed of 6.3  $\mu\text{L}$  per second. During the injection and ejection process, there is no frequency spike, or noise detected. It means that the pressure change caused by injection and ejection speed of 6.3  $\mu\text{L}$  per second does not affect to emersions of frequency spike or noise. However, we found a decreasing frequency during the injection and ejection process. A short frequency change was observed about 20-30 Hz during the first ejection sequence of 10  $\mu\text{L}$  water. After the ejection process was stopped, the resonance frequency reverts to the initial frequency with 2 Hz different. In the injection process, the short frequency change was observed around 10 Hz. After the injection was stopped, the resonance frequency was changed to the first initial frequency with the same value.

The same response is also observed during the injection and ejection process of 10  $\mu\text{L}$  water at a speed of 0.7  $\mu\text{L}$  per second. During the injection and ejection process, the short frequency change was also observed. The resonance frequency decreases during its process. However, after the injection and ejection process, the resonance frequency reverts to the initial frequency with the same value, as shown in the Fig. 10.

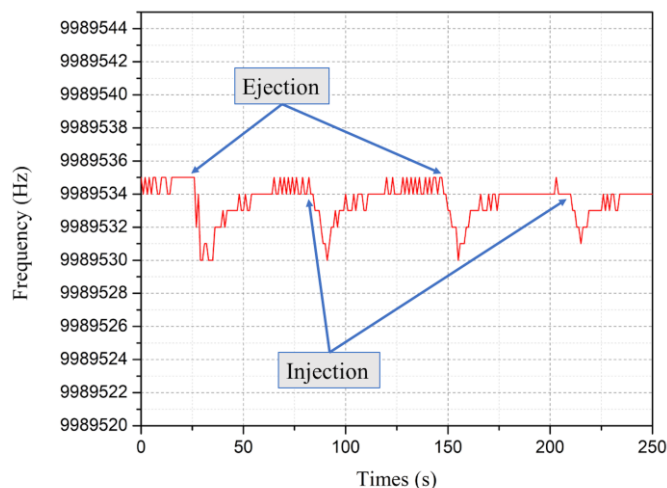


Fig. 10. Sensor resonance frequency caused by 10  $\mu\text{L}$  water injection and ejection at a speed of 0.7  $\mu\text{L}$  per second.

The resonance frequency change of the sensor, during water ejection at the flow rate of 6.3  $\mu\text{L}$  per second was higher than the resonance frequency change caused by the injection of 0.7  $\mu\text{L}$  per second. At 6.3  $\mu\text{L}$  per second, the frequency change caused by ejection was 30 Hz, on the other hand, the frequency change was 5 Hz at an ejection speed of 0.7  $\mu\text{L}$  per second. Meanwhile, the resonance frequency change from the sensor during water injection was also slightly higher at speed 6.3  $\mu\text{L}$  per second, than the water injection speed of 0.7  $\mu\text{L}$  per second. The frequency change was only 4-5 Hz at an injection speed of 0.7  $\mu\text{L}$  per second. At the 6.3  $\mu\text{L}$  per second, the frequency change during water injection was 7 Hz. The higher flow rate theoretically resulted in a pressure change on the sensor surface. The change in pressure on the sensor surface nor other liquid property change during the water flow resulted in a frequency change of the sensor. This result was similar to the other works about resonance frequency effect of syringe pump [9], and a relationship between gas pressure and a frequency sensor [12]. The stability of the sensor resonance in contact with liquid is better compared to work done with a 35MHz QCM sensor [13] and comparable with the work done using 9MHz QCM sensor [14].

The experiment shows that a higher flow rate resulted in a bigger frequency spike during injection and ejection. Therefore, it is necessary to control the flow rate to minimize the frequency spike. During the use of the sensor system for biomolecule reaction, it should be noticed that the frequency change in within 100 seconds after the injection and ejection should consider the effect of the liquid flow on the sensor surface. To minimize the effect one should consider using a slowest liquid flow rate.

#### IV. CONCLUSION

The microliter pump using a syringe injection was successfully developed and its flow rate effect to the QCM sensor was examined. The microliter pump system was able to inject or eject a liquid to the sensor system with a flow rate of 0.7 and 6.3  $\mu\text{L}$  per second. Both water injection and ejection slightly affected the resonance frequency of the sensor. Higher flow rate resulted in a higher frequency change caused by a short pressure change. The flow rate of less than 0.7  $\mu\text{L}$  per second affects to the resonance

frequency of the sensor by 5 Hz at a water ejection and 4-5 Hz at water injection.

#### ACKNOWLEDGMENT

The authors would like to express their gratitude to Collaborative Research Center for Advanced System and Material Technology (CRC-ASMAT) and Sensor Technology Laboratory, for their help during the experiment of this work. This work was part of a research project funded by the Ministry of Research, Technology and Higher Education of the Republic of Indonesia under the HIKOM research grant scheme.

#### REFERENCES

- [1] S. Kurosawa, J.-W. Park, H. Aizawa, S.-I. Wakida, H. Tao, and K. Ishihara, "Quartz crystal microbalance immunosensors for environmental monitoring," *Biosens. Bioelectron.*, vol. 22, no. 4, pp. 473–481, Oct. 2006.
- [2] P. F. Höök and M. Rudh, "Quartz crystal microbalances ( QCM ) in biomacromolecular recognition," *bisensor*, no. March, 2005.
- [3] K. Zhang *et al.*, "A microfluidic system with surface modified piezoelectric sensor for trapping and detection of cancer cells," *Biosens. Bioelectron.*, vol. 26, no. 2, pp. 935–939, Oct. 2010.
- [4] R. L. Caygill, G. E. Blair, and P. a Millner, "A review on viral biosensors to detect human pathogens," *Anal. Chim. Acta*, vol. 681, no. 1–2, pp. 8–15, Nov. 2010.
- [5] J. W. Thies, P. Kuhn, B. Thürmann, S. Dübel, and A. Dietzel, "Microfluidic quartz-crystal-microbalance (QCM) sensors with specialized immunoassays for extended measurement range and improved reusability," *Microelectron. Eng.*, vol. 179, pp. 25–30, 2017.
- [6] Z. A. Talib, Z. Baba, Z. Kurosawa, H. A. A. Sidek, A. Kassim, and W. M. M. Yunus, "Frequency Behavior of a Quartz Crystal Microbalance (QCM) in Contact with Selected Solutions," *Am. J. Appl. Sci.*, vol. 3, no. 5, pp. 1853–1858, 2006.
- [7] M. Michalzik, R. Wilke, and S. Büttgenbach, "Miniaturized QCM-based flow system for immunosensor application in liquid," *Sensors Actuators B Chem.*, vol. 111–112, no. SUPPL., pp. 410–415, Nov. 2005.
- [8] S. P. Sakti, N. Chabibah, S. P. Ayu, M. C. Padaga, and A. Aulanni'am, "Development of QCM Biosensor with Specific Cow Milk Protein Antibody for Candidate Milk Adulteration Detection," *J. Sensors*, vol. 2016, pp. 1–7, 2016.
- [9] R. N. Ikhsani and S. P. Sakti, "Flow rate effect of syringe pump on quartz crystal microbalance sensor resonance frequency stability," in *Proceeding - 2016 International Seminar on Sensors, Instrumentation, Measurement and Metrology, ISSIMM 2016*, 2017.
- [10] R. Lucklum, S. Schranz, C. Behling, F. Eichelbaum, and P. Hauptmann, "Analysis of compressional-wave influence on thickness-shear-mode resonators in liquids," *Sensors Actuators A Phys.*, vol. 60, no. 1–3, pp. 40–48, May 1997.
- [11] K. Keiji Kanazawa and J. G. Gordon, "The oscillation frequency of a quartz resonator in contact with liquid," *Anal. Chim. Acta*, vol. 175, pp. 99–105, 1985.
- [12] A. Wessels, B. Klöckner, C. Siering, and S. R. Waldvogel, "Practical strategies for stable operation of HFF-QCM in continuous air flow.," *Sensors*, vol. 13, no. 9, pp. 12012–12029, 2013.
- [13] J. Liang, J. Zhang, W. Zhou, and T. Ueda, "Development of a Flow Injection Based High Frequency Dual Channel Quartz Crystal Microbalance," *Sensors*, vol. 17, no. 5, p. 1136, 2017.
- [14] L. Rodriguez-Pardo, A. M. Cao-Paz, and J. Fariña, "Design and characterization of an active bridge oscillator as a QCM sensor for the measurement of liquid properties and mass films in damping media," *Sensors Actuators, A Phys.*, vol. 276, pp. 144–154, 2018.

# Appropriate Sets of Criteria for Innovation Adoption of IS Security in Organizations

Sandy Kosasi

STMIK Pontianak

Pontianak, West Kalimantan, Indonesia

sandykosasi@yahoo.co.id

Vedyanto

Santu Petrus Junior High School

Pontianak, West Kalimantan, Indonesia

vedy91@gmail.com

I Dewa Ayu Eka Yuliani

STMIK Pontianak

Pontianak, West Kalimantan, Indonesia

dewaayu.ekayuliani@gmail.com

**Abstract**—Determining sets of criteria and alternatives becoming main priorities is essential to guarantee the success of innovation adoption of Information System (IS) security. The goal of this research was to select and determine important entities as representation of each criterion for managers in making decisions of innovation adoption of IS security. This research applied Technology-Organization-Environment (TOE) Framework, and Human-Organization-Technology-Fit (HOT-Fit) Model to map relative importance variables of criteria and alternatives. AHP Approach was applied for computation simulation to determine priorities of criteria and alternatives. Results show that a principal criterion is manpower of organizations. The eigen factor score is 4.398. Moreover, alternatives covering complexity, financial resources, intensity of competition, and CIO innovativeness have these respective eigen factors scores: 4.326, 9.307, 4.376, and 4.545.

**Keywords**—IS Security; Innovation Adoption; TOE Framework; HOT-Fit Model; AHP Approach

## I. INTRODUCTION

IS (Information System) security becomes an old problem of any organizations. It is an inherent part of all organizational activities. Even small weaknesses of IS can bring failure of organizational operation [1]. Therefore, more organizations cooperate to get ISO certificate of IS security like ISO27001 [2]. Securing IS is the challenge of each organization since data security as well as availability and integrity of information are immensely influenced by complexity of environmental changes, interrelationships, uncertainties, and dependencies on Information Technology (IT). Securing IS can be actualized through determination of policies, procedures, and mechanisms of information flows of organizational structures to prevent exploitation of vulnerability of threats and risks [3].

Moreover, applying IS security system is influenced by capabilities to adopt innovation of IS security for organizational needs. The reason is that each organization has dissimilar characteristics of work culture which is in line with

certain needs of IS security [4]. Most organizations only rely on renewal of security and individual willingness to make new trials without analyzing the needs appropriately [5]. Innovation adoption of IS security is a complex process. Consequently, numerous organizations face difficulties of applying steps with policies, procedures, and mechanisms properly. Besides, steps of developing and implementing IS security adopted by individuals and organizations are still low [6]. Thus, it is of great importance to comprehend why users accept or reject organizational IS security [7].

There have been previous studies discussing innovation adoption of IS security. However, literature specifically exploring models of innovation adoption of IS security in certain organizational levels is rare to find. Previous studies mostly emphasize needs of building and maintaining competitive, operational strengths of IS security. Effectiveness of innovation adoption of IS security is prone to depend on humans, technology, and policies through TOE Framework [8]. Innovation adoption of IS security is strategic and brings significant effects on the success of implementing IS through relationships of humans, technology, organizations, and environment [9]. However, the lack of preparation of understanding adoption of IS security can become primary hindrance of achieving the success of securing the IS assets [10]. In addition, TOE Framework is frequently used and maximized in adopting innovation of IS security in organizations. IS security is also an internal need and involves external parties when representing the systematic innovation adoption of IS security [11].

Adoption innovation of IS security in organizations fails if there are mistakes of determining sets of criteria appropriately [12]. Applying this adoption requires careful considerations of selecting sets of criteria with critical, strategic roles based on specification of organizational needs [13]. It is noted that complexity of selecting and determining sets of criteria exists as organizations have different management and behavior [13]. This statement is supported by previous studies affirming that most organizations only seek easiness by making

replication of existing models directly without strategic considerations of organizational contents [14, 15, 16, 17].

Such the occurrence creates the failure since it is admitted that all criteria are the same and can contribute to conformity of innovation adoption of IS Security. Therefore, in order to make this process successful, strategic decision making is needed to determine proper and important sets of criteria and alternatives for organizations. Different organizations can have different strategic decisions.

Needs of criteria in this research applied dimensions of TOE Framework [18, 19]. They were completed with HOT-Fit Model [20] consisting of technology, organizations, environment, and humans. Meanwhile, alternatives (relative advantage, compatibility, complexity, security concern, presence of champions, infrastructure, top management support, organizational size, financial resources, mimetic pressure, coercive pressure, intensity of competition, vendor support, perceived technical competence of IS staff, employees' IS knowledge, clinical IT experts, and CIO innovativeness) used the variable of each dimension [21, 22].

The research aimed to select and determine sets of criteria which are the most appropriate with the most important alternatives as representation of categories of criteria based on TOE Framework and HOT-Fit Model. This was to ensure readiness of applying innovation adoption of IS security. In order to determine decisions on mainly prioritized factors, AHP Approach method was used.

AHP Approach is also an alternative way to solve various kinds of problems of organizational needs. It can be used to represent decision makers' views of individual institutions. AHP Approach focuses on changes due to different hierarchies created by different people. This method gives 3 advantages such as implementation of empirical cases leading to intuitive solutions, complexly manipulated results, and relative importance of numerous criteria [23].

Computation through AHP Approach is hierarchical when representing functional types of interrelationships. Therefore, complicated cases with multi-criteria can be decomposed into detailed decision elements. Hierarchical models are linearly structured from common decision elements until the most concrete, controllable factors at each bottom level in the form of a decision alternative [24]. Benefits of AHP Approach are that: (a) hierarchical structures as consequences of selected criteria and subcriteria are deep; (b) validity can be computed with the limitation to inconsistent tolerance of selected criteria and alternatives; (c) output tenacity through analyses of sensitivity is measureable [25].

## II. THEORETICAL BACKGROUND

Information is a principal asset of organizations and requires protection. It is crucial for organizations to secure all IS assets due to possible malicious attacks and unauthorized use of access [26]. Protection of the whole IS assets is the form of anxiety because it brings significant impacts on sustainability of organizational activities, and develops and implements system [27]. Protective actions include the use of antivirus, firewall, filter, intrusion detection system,

encryption, authorization mechanisms, authentication system, and proxy devices. Furthermore, providing the training and education on IS security system can help to eliminate IS threats [28].

Possessing IS security is compulsion. Each organization must always secure information assets. IS security should have orientation on perspectives for users. It expedites transaction and exploration of decision making. The foci are security, availability, and integrity [29]. As the consequence, system vulnerability is enhanced [30]. Nonetheless, assuring the success of adoption and implementing IS security in organizations can be actualized through combination of complex practices of TOE Framework and HOT-Fit Model. In fact, full commitment of the whole staff and management levels of organization units is needed [31]. Previous scientific contributions sustainably indicate that the weakest tab of each plan or IS security procedure is the use of computers per se [32].

Implementation of each model of innovation adoption of IS security pertains to strategic decisions of mapping and determining essential sets of criteria based on characteristics and attitude of organizations [33]. Adoption of IS security is fundamental. It should be actualized in organizations. Based on perception of models of innovation adoption of IS security, organizational and individual levels should be analyzed [34].

## III. RESEARCH METHOD

The source of data was the survey through the use of questionnaires sent to all selected respondents by using online, electronic media. This research involved analysis units of organizations. The eighty-five respondents were managers or directors of IT department of palm oil plantation industries working in West Kalimantan Province. Purposive sampling technique was in use to collect data. The computation was through Likert Scales [35]. Data obtained from online questionnaires were completed with in-depth interviews [35]. In order to enhance validity and reliability of collected answers, these interviews were conducted with several selected respondents in groups. The communication was through the application of Whatsapp.

Results of processed data were analyzed by using AHP Approach. This is to support steps of strategic decision making and appropriate sets of criteria of IS security adoption. This approach creates the form of simulation enabling the best choice of sets of criteria and alternatives. Such the model is in forms of hierarchical structures of criteria and alternatives, and is considered through inconsistent tolerance and analysis of sensitivity [36]. The first step is calculation covers definition of problems, goals, and final results. Other steps comprise decomposition of problems in forms of hierarchies and decision elements, paired comparison of decision elements in forms of matrices, estimation of relative weight of decision elements, and examination of hierarchical consistency [37].

The goals need to be divided into subgoals with specific measurement. The hierarchies include goals, criteria or objective levels, and alternatives. Every set of criteria can further be divided into more detailed levels. After all criteria are identified, scores are related to above levels. Relative



scores obtained for choices are measured based on hierarchical levels. Next, scores are synthesized through models. Composite scores of choices at levels and overall scores appear as a result of this process. The measurement is relative for each level and produces matrix scores. However, the results should be consistent. Thus, examination of inconsistency should be conducted to find out and identify possibilities of mistakes of data inputs. A matrix (i,j) is considered to be consistent if the whole elements follow transitivity. Guidelines showing whether Consistency Index (CI) have consistent matrices should exist (see Table I) [38].

TABLE I. BASIC SCALES OF THE ORDER OF IMPORTANCE

Order of Importance	Definition
1	As important as others
3	Moderately important
5	Strongly important
7	Very strongly important
9	Extremely important
2,4,6,8	Scores between two adjacent computations
Reciprocal	If Element i has one of the scores above in comparison to Element j, Element j has a reverse score.

A matrix created as a result of random comparison is absolutely inconsistent. The limit of stated inconsistency is measured through Consistency Ratio (CR). Comparison of CI and Random Index (RI) produces reference scores and determines consistency levels of matrices. CR is computed with this formula:  $CR = CI/RI$  (see Table II). Meanwhile, CI is obtained through this formula:  $CI = (\lambda_{max} - n)/n - 1$ . However, RI is the stated average of consistency becoming the standard of computation of CR. Next, CR of paired matrices is examined. If CR is greater than 0.1, paired comparison should be recalculated until CR is less than or equals to 0.1 [39, 40].

TABLE II. AVERAGES OF CONSISTENCY (RI)

N	RI
1	0.00
2	0.00
3	0.58
4	0.90
5	1.12
6	1.24
7	1.32
8	1.41
9	1.45
10	1.49
11	1.51
12	1.48
13	1.56
14	1.57
15	1.59

#### IV. RESULTS AND DISCUSSION

Determination of sets of criteria and alternatives started with formulation and determination of a number of criteria through previous results using TOE Framework and HOT-Fit Model. All criteria referred to research results [21, 22]. They were processed again to produce the order of importance. Main criteria were initially considered.

The order of importance of criteria was related to palm oil plantation industries in West Kalimantan Province. The adoption success of IS security referred to combination of TOE Framework and HOT-Fit Model with dimensions of Technology (T), Organization (O), Environment (E), and Human (H). Meanwhile, the variables were (1) relative advantage, (2) compatibility, (3) complexity, (4) security concern, (5) presence of champions, (6) infrastructure, (7) top management support, (8) organizational size, (9) financial resources, (10) mimetic pressure, (11) coercive pressure, (12) intensity of competition, (13) vendor support, (14) perceived technical competence of IS staff, (15) employees' IS knowledge, (16) clinical IT experts, and (17) CIO innovativeness. These seventeen instruments were alternatives of criterion (see Figure 1).

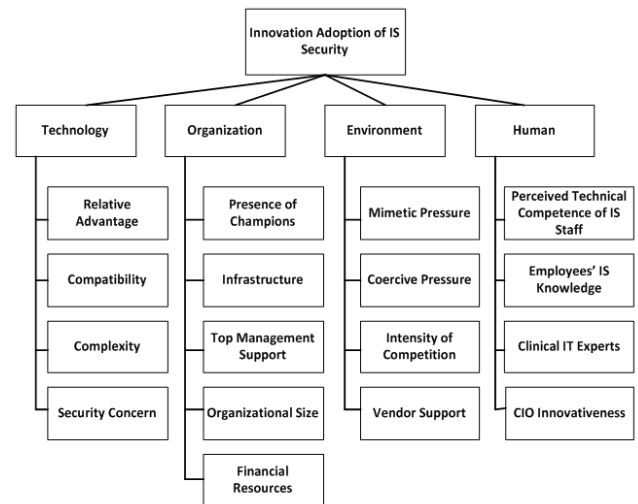


Fig. 1. Hierarchy Model of Criteria and Alternatives

The model of multicriteria combining TOE Framework and HOT-Fit Model began with paired comparison applied to determine weight of criteria and alternatives measured based on subjective preferences of decision making. Comparative Scales 1-9 were used. Next, examination of consistency of paired comparison matrices was conducted. If the ratio is greater than 0.1, paired comparison should be recalculated until it is less than or equals to 0.1 (consistent). Similar steps were applied to comparison matrices among alternatives. Following these, totals of multiplication results of weight of criteria and alternatives were sought.

Outcomes of hierarchical criteria of (a) technology and organization, (b) technology and environment, (c) technology and human, (d) organization and environment, (e) organization and human, and (f) environment and human are consecutively 0.053, 0.057, 0.136, 0.086, 0.182, and 0.136. After conducting

the calculation, eigen factors of technology (0.084), organization (0.175), environment (0.224), and human (0.517) appear. CR levels of all criteria were measured afterwards to indicate comparison of valid results and actual conditions. CR is comparison of CI and RI. CI is obtained through this formula:  $CI = (\lambda_{max} - n) / (n - 1)$ , whereas RI is the score determined with AHP Approach. 4x4 matrices used in this research should have scores which are less than 9%. RI used is 0.90.

Based on computation, it is found that CI equals to 0.071 (7.08%) and CR equals to 0.079 (7.87%). Therefore, strategic decisions of IS security adoption should firstly emphasize human or manpower in comparison to other criteria. As it can be seen from Table III, obtained eigen factors of human criterion is 4.398. Referring to calculation results, the human criterion possesses the highest score. Thus, innovation adoption of IS security requires mapping of organizational staff's abilities to be in line with factors of technology, organization, and environment.

TABLE III. MEASUREMENT OF CRITERION CONSISTENCY

Criterion	T	O	E	H	Total	Summary
T	0.084	0.058	0.075	0.129	0.346	4.111
O	0.253	0.175	0.112	0.172	0.712	4.078
E	0.253	0.349	0.224	0.129	0.955	4.263
H	0.337	0.524	0.896	0.517	2.274	4.398
Total	0.927	1.105	1.307	0.948	4.287	16.849
L-Max						4.212

Every criterion has a different probability level based on business patterns of societies. People's readiness and willingness to accept changes of system and mechanisms of adoption of IS security are priorities. The willingness should be strengthened with strong motivation to accept and implement IS security for the success of organizations. Also, it is important for the staff to have technical skills of IT so that conformity of perception of business needs and IS security exists. The staff should further have mastery of knowledge on structures and mechanisms when securing IS assets. Moreover, there should be security experts improving staff's knowledge. Hence, the staff can work with updated IT in clear organizational structures and controlled environment. Next, consistency of the whole alternatives referring to criteria was measured.

Based on calculation of the eigen factor of technology criterion, obtained scores of these variables: Relative Advantage (R), Compatibility (C1), Complexity (C2), and Security Concern (SC) are respectively 0.070, 0.170, 0.288, and 0.472. Meanwhile, CI = 0.063 and CR = 0.070 (6.95%) result in acceptance. A strategic decision of technology criterion is on complexity with eigen factor = 4.326. Other strategic decisions of security concern, compatibility, and relative advantage can be seen from Table IV.

TABLE IV. COMPARISON OF ALTERNATIVES BASED ON TECHNOLOGY CRITERION

Technology Alternatives	R	C1	C2	SC	Total	Summary
R	0.070	0.043	0.096	0.079	0.287	4.100
C1	0.280	0.170	0.096	0.157	0.704	4.132
C2	0.210	0.511	0.288	0.236	1.245	4.326
SC	0.420	0.511	0.575	0.472	1.979	4.192
Total	0.981	1.235	1.055	0.944	4.214	16.751
L-Max						4.188

Next, in terms of organization criterion, eigen factors of Presence of Champions (PC) (0.395), Infrastructure (I) (0.239), Top Management Support (TMS) (0.163), Organizational Size (OS) (0.120), and Financial Resources (FR) (0.084) were found. Other outcomes show that CI = 0.010 and CR = 0.009 (0.91%) resulting in acceptance. A strategic decision on organization criterion is on financial resources with eigen factor = 9.307. Other strategic decisions of presence of champions, infrastructure, organizational size, and top management support are indicated in Table V.

TABLE V. COMPARISON OF ALTERNATIVES BASED ON ORGANIZATION CRITERION

Organization Criterion	PC	I	TMS	OS	FR	Total	Summary
PC	0.395	0.717	0.978	0.040	0.042	2.171	5.502
I	0.132	0.239	0.652	0.060	0.021	1.103	4.617
TMS	0.066	0.060	0.163	0.024	0.042	0.354	2.175
OS	0.132	0.119	0.033	0.120	0.028	0.431	3.604
FR	0.197	0.060	0.081	0.359	0.084	0.781	9.307
Total	0.921	1.195	1.906	0.602	0.217	4.841	25.204
L-Max							5.041

Following these, measurement of alternative consistency of environment criterion shows that eigen factors of Mimetic Pressure (MP), Coercive Pressure (CP), Intensity of Competition (IC), and Vendor Support (VS) are consecutively 0.099, 0.171, 0.277, and 0.453. CI = 0.010 and CR = 0.009 (0.91%) indicate acceptance. A strategic decision of environment criterion is on intensity of competition with eigen factor = 4.376. It is continued with vendor support, coercive pressure, and mimetic pressure (see Table VI).

TABLE VI. COMPARISON OF ALTERNATIVES BASED ON ENVIRONMENT CRITERION

Environment Criterion	MP	CP	IC	VS	Total	Summary
MP	0.099	0.057	0.139	0.113	0.408	4.121
CP	0.297	0.171	0.092	0.151	0.711	4.163
IC	0.198	0.512	0.277	0.226	1.214	4.376
VS	0.396	0.512	0.555	0.453	1.916	4.232
Total	0.990	1.253	1.064	0.943	4.249	16.892
L-Max						4.223

Finally, measurement of alternative consistency of human criterion yields eigen factors of Perceived Technical Competence of IS Staff (PTCISS), Employees' IS Knowledge (EISK), Clinical IT Experts (CITE), and CIO Innovativeness (CIOI) are 0.091, 0.153, 0.217, and 0.538 in order. Meanwhile, CI = 0.075 and CR = 0.083 (8.28%) were found and acceptance was confirmed. A strategic decision of human criterion is on CIO innovativeness with eigen factor = 4.545. Others are clinical IT experts, perceived technical competence of IS staff, and employees' IS knowledge (see Table VII).

TABLE VII. COMPARISON OF ALTERNATIVES BASED ON HUMAN CRITERION

Human Criterion	PTCISS	EISK	CITE	CIOI	Total	Summary
<b>PTCISS</b>	0.091	0.077	0.072	0.135	0.375	4.100
<b>EISK</b>	0.183	0.153	0.108	0.179	0.624	4.067
<b>CITE</b>	0.274	0.307	0.217	0.108	0.906	4.182
<b>CIOI</b>	0.366	0.460	1.083	0.538	2.448	4.545
<b>Total</b>	0.915	0.998	1.480	0.960	4.352	16.894
<b>L-Max</b>						4.224

## V. CONCLUSION AND FUTURE RESEARCH

Research results were used to explore and determine sets of criteria and alternatives becoming priorities of innovation adoption of IS security. Through AHP Approach, the most crucial criteria are readiness and capabilities of the human to conduct such adoption and most crucial criteria with eigen factor 4.398 area readiness. However, the most essential alternatives are complexity, financial resources, intensity of competition, and CIO innovativeness with these respective eigen factors 4.326, 9.307, 4.376, and 4.545.

All of these variables are principal criteria and, therefore, should be seriously concerned to adopt innovation of IS security especially for palm oil plantation industries in West Kalimantan Province. Orders of criteria and alternatives should be applied as they are name of changes are allowed. Sets of criteria are inappropriate for other industries. This research can be enhanced through engagement of more specific respondents based on clusters of management levels in organizations.

## REFERENCES

- [1] D. Tunçalp, "Diffusion and Adoption of Information Security Management Standards across Countries and Industries," *Journal of Global Information Technology Management*, Taylor & Francis Group, 17, 2014, pp. 221-227.
- [2] International Organization for Standardization (ISO), "The ISO survey of certifications," Retrieved from [https://isotc.iso.org/livelink/livelink/fetch/-8853493/8853511/8853520/18808772/00.Executive\\_summary\\_2016\\_Survey.pdf?nodeid=19208898&vernum=-2](https://isotc.iso.org/livelink/livelink/fetch/-8853493/8853511/8853520/18808772/00.Executive_summary_2016_Survey.pdf?nodeid=19208898&vernum=-2)
- [3] A.E.D. Albuquerque Junior, and E.M.D. Santos, "Adoption of Information Security Measures in Public Research Institutes," *JISTEM- Journal of Information Systems and Technology Management*, 12(2), 2015, pp. 289-315.
- [4] S. Chatterjee, S. Sarker, and J.S. Valacich, "The Behavioral Roots of Information Systems Security: Exploring Key Factors Related to Unethical IT Use," *Journal of Management Information Systems*, 31(4), 2015, pp. 49-87.
- [5] K. Hwang, and M. Choi, "Effects of Innovation-Supportive Culture and Organizational Citizenship Behavior on E-Government Information System Security Stemming from Mimetic Isomorphism," *Government Information Quarterly*, 34(2), 2017, pp. 183-198.
- [6] M.A. Hameed, and N.A.G. Arachchilage, "A Conceptual Model for the Organisational Adoption of Information System Security Innovations," *Journal of Computer Engineering & Information Technology*, 6(2), 2017, pp. 1-10.
- [7] J. Shropshire, M. Warkentin, and S. Sharma, "Personality, Attitudes, and Intentions: Predicting Initial Adoption of Information Security Behavior," *Computers & Security*, 49, 2015, pp. 177-191.
- [8] T. Herath, H.S. Herath, and J. D'Arcy, "Managing Security in Organizations: Adoption of Information Security Solutions," *SIGMIS-CPR*, 2017, pp. 87-88.
- [9] H. Ahmadi, O. Ibrahim, and M. Nilashi, "Investigating a New Framework for Hospital Information System Adoption: A Case on Malaysia," *Journal of Soft Computing and Decision Support Systems*, 2(2), 2015, pp. 26-33.
- [10] M.A. Hameed, and S. Counsell, "Assessing the Influence of Environmental and CEO Characteristics for Adoption of Information Technology in Organizations," *Journal of Technology Management and Innovation* 7(1), 2012, pp. 64-84.
- [11] M.A. Hameed, and N.A.G. Arachchilage, "A Model for the Adoption Process of Information System Security Innovations in Organisations: A Theoretical Perspective," *Australasian Conference on Information Systems*, 2016, pp. 1-12.
- [12] K.P. Kiilu, D.M. Nzuki, "Factors Affecting Adoption of Information Security Management Systems: A Theoretical Review," *International Journal of Science and Research (IJSR)*, 5(12), 2016, pp. 162-166.
- [13] H. Ahmadi, M. Nilashi, O. Ibrahim, T. Ramayah, M.W. Wong, M., Alizadeh, ... and A. Almaee, "Exploring Potential Factors in Total Hospital Information System Adoption," *Journal of Soft Computing and Decision Support Systems*, 2(1), 2015, pp. 52-59.
- [14] O.J. Opala, and S.M. Rahman, "An Exploratory Analysis of the Influence of Information Security on the Adoption of Cloud Computing," *8th International Conference on Systems Engineering (SoSE)*, IEEE, 2013, pp. 165-170.
- [15] R. Baskerville, P. , Spagnoletti, and J. Kim, "Incident-Centered Information Security: Managing a Strategic Balance between Prevention and Response," *Information & Management*, 51(1), 2014, pp. 138-151.
- [16] M. Nilashi, H. Ahmadi, A. Ahani, O. Ibrahim, and A. Almaee, "Evaluating the Factors Affecting Adoption of Hospital Information System Using Analytic Hierarchy Process," *Journal of Soft Computing and Decision Support Systems*, 3(1), 2016, pp. 8-35.
- [17] H. Gangwar, H. Date, and A.D. Raoot, "Review on IT Adoption: Insights from Recent Technologies," *Journal of Enterprise Information Management*, 27(4), 2014, pp. 488-502.
- [18] L.G. Tornatzky, and M. Fleischer, "The Processes of Technological Innovation," Lexington Books Lexington, MA, 1990.
- [19] J. Baker, "The Technology-Organization-Environment Framework," *Information Systems Theory*, Springer, 2012.
- [20] M.M. Yusof, J. Kuljis, A. Papazafeiropoulou, L.K. Stergioulas, "An Evaluation Framework for Health Information Systems: Human, Organization and Technology-Fit Factors (HOT-Fit)," *Int. J. Med. Inform.*, 77(6), 2008, pp. 386-398.
- [21] M. Nilashi, H. Ahmadi, A. Ahani, R. Ravangard, and O. bin Ibrahim, "Determining the Importance of Hospital Information System Adoption Factors Using Fuzzy Analytic Network Process (ANP)," *Technological Forecasting and Social Change*, 111, 2016, pp. 244-264.
- [22] H. Ahmadi, M. Nilashi, and O. Ibrahim, "Organizational Decision to Adopt Hospital Information System: An Empirical Investigation in the Case of Malaysian Public Hospitals," *International Journal of Medical Informatics*, 84(3), 2015, pp. 166-188.

- [23] R. Sharda, D. Delen, and E. Turban, "Business Intelligence and Analytics: Systems for Decision Support," Tenth Edition, Prentice-Hall, Inc., 2014.
- [24] P. Kishore, and G. Padmanabhan, "An Integrated Approach of Fuzzy AHP and Fuzzy TOPSIS to Select Logistics Service Provider," *Journal for Manufacturing Science and Production*, 16(1), 2016, pp.51-59.
- [25] V.L. Sauter, "Decision Support Systems for Business Intelligence," Second Edition, John Wiley & Sons, Inc., 2011.
- [26] N.A.G. Arachchilage, C. Namiluko, and A. Martin, "A Taxonomy for Securely Sharing Information among Others in a Trust Domain," 8th International Conference for Internet Technology and Secured Transactions (ICITST), IEEE, 2013, pp. 296-304.
- [27] Q.J. Yeh, and A.J.T. Chang, "Threats and Countermeasures for Information System Security: A Cross-Industry Study," *Information & Management*, 44(5), 2012, pp. 480-491.
- [28] N.A.G. Arachchilage, S. Love, and K. Beznosov, "Phishing Threat Avoidance Behaviour: An Empirical Investigation," *Computers in Human Behavior*, 60, 2016, pp. 185-197.
- [29] Z.A. Soomro, M.H. Shah, and J. Ahmed, "Information Security Management Needs More Holistic Approach: A Literature Review," *International Journal of Information Management*, 36(2), 2016, pp. 215-225.
- [30] A. Vance, P.B. Lowry, and D.W. Wilson, "Using Trust and Anonymity to Expand The Use of Anonymizing Systems that Improve Security across Organizations," *Security Journal*, 30(3), 2017, pp. 979-999.
- [31] H. Ahmadi, M. Nilashi, L. Shahmoradi, and O. Ibrahim, "Hospital Information System Adoption: Expert Perspectives on an Adoption Framework for Malaysian Public Hospitals," *Computers in Human Behavior*, 67, 2017, pp. 161-189.
- [32] P. Gillingham, "Decision-Making about the Adoption of Information Technology in Social Welfare Agencies: Some Key Considerations," *European Journal of Social Work*, 2017, pp. 1-9.
- [33] Z. Yang, A. Kankanhalli, B.Y. Ng, and J.T.Y. Lim, "Analyzing the Enabling Factors for the Organizational Decision to Adopt Healthcare Information Systems," *Decision Support Systems*, 55(3), 2013, pp. 764-776.
- [34] E. Ziemba, "The ICT Adoption in Enterprises in the Context of the Sustainable Information Society," *Federated Conference on Computer Science and Information Systems (FedCSIS)*, IEEE, 2017, pp. 1031-1038.
- [35] J.W. Creswell, "Research Design: Qualitative, Quantitative, and Mixed Methods Approaches," Fourth Edition, California: SAGE Publications, Inc., 2014.
- [36] T.L. Saaty, "Decision Making For Leaders: The Analytic Hierarchy Process for Decisions in a Complex World," Third Revised Edition, RWS Publications, 2012.
- [37] M.S. Pieter, I.I. Lamia, and F.Y. Wattimena, "Decision Support System in Giving Recommendation for Flat Screen Television Purchase Using Analytical Hierarchy Process Method," *Second International Conference on Informatics and Computing (ICIC)*, IEEE, 2017, pp. 1-5.
- [38] S. Lee, W. Kim, Y.M. Kim, and K.J. Oh, "Using AHP to Determine Intangible Priority Factors for Technology Transfer Adoption," *Expert Systems with Applications*, 39(7), 2012, pp. 6388-6395.
- [39] C.N. Castillo, F.K. Degamo, F.T. Gitgano, L.A. Loo, S.M. Pacaanas, N. Toroy, ... and C.O. Ocampo, "Appropriate Criteria Set for Personnel Promotion Across Organizational Levels Using Analytic Hierarchy Process (AHP)," *International Journal of Production Management and Engineering*, 5(1), 2017, pp. 11-22.
- [40] U. Yudatama, B.A. Nazief, and A.N. Hidayanto, "Strategic Decisions in the Implementation of Information Technology Governance to Achieve Business and Information Technology Alignment Using Analytical Hierarchy Process," *Information Technology Journal*, 16(2), 2017, pp.51-61.

# Self-Efficacy a Critical Factor of Information System: An Investigation using DeLone McLean

Tri Lathif Mardi Suryanto  
Information System,  
Faculty of Computer Science  
Universitas Pembangunan Nasional  
"Veteran"  
Jawa Timur  
Surabaya, Indonesia  
trilathif.si@upnjatim.ac.id

Djoko Budiyanto Setyohadi  
Informatic Engineering,  
Faculty of Industrial Engineering  
Universitas Atma Jaya Yogyakarta  
Yogyakarta, Indonesia  
djoko.bdy@gmail.com

Akhmad Fauzi  
Management Department,  
Faculty of Economics Business  
Universitas Pembangunan Nasional  
"Veteran"  
Jawa Timur  
Surabaya, Indonesia  
akhmadfauzi@upnjatim.ac.id

**Abstract**– This paper examines what influences Attitude toward usage (ATU) as the expectation of the application of Employee Information System (EIS) with high success rate, this research is observed through cognitive value using approach theory of information system success model DeLone and McLean Model (DMM) and affective value using the Human Resource quality theory (HRQ) and the Self-Efficacy (SE) model. The overall data was obtained by providing questionnaires to employees at the Higher Education and using WarpPLS and SEM as a method of analysis. This study found that, because the EIS was positioned as a compulsory system, our study showed that only Self-Efficacy would affect Attitudes toward the Use of EIS. The quality of human resources, as other Affective factors, has no effect on Attitudes towards usage of EIS.

**Keyword**–Employee Information System, DeLone and McLean Model, Attitude toward Usage, Self-efficacy.

## I. INTRODUCTION

News and information changing process from analog to digital format have been invading many Higher Education. Moreover, digitalization is a must, and it requires Higher Education to prepare the critical information system such as Communication and Information Service (CIS) which can simplify their employee's workload.

Employee Information Sistem (EIS) is a vital information system which built for reducing employee's workload to fix employee management issues. In a short, Employee Information Sistem (EIS) can be used to raise employee's performance [1] [2] [3].

The previous scholar reported that many advantages could be obtained. However many studies show that some treatment should be performed. Therefore some research should be conducted before. Since applying EIS can be failed when it is utilized because there is retention from some employee who is doesn't able or doesn't want to re-learn

something digitalized. Age and education background is an example of the understanding gap about EIS implementation at the Higher Education.

This research is aimed to investigate the specific problems at implementing EIS. The structured point of view also is performed particularly about implementation EIS and the Higher Education, by using DeLone and McLean Model (DMM) theory [4] [5] which is modified by other researchers [1] [2] [3] [6] [7] [8] [9]. It is crucial and common to get an appraisal from an employee who is working with EIS at the Higher Education, so Attitude toward Usage (ATU) has to be highlighted [10] [11] [12] [13] [14], especially for limited research in Higher Education. Shortly, is research is aiming for testing and analyzing empirical evidence about factors which influencing ATU to EIS.

## II. LITERATURE REVIEW

At the beginning of the information success study, the system applied in the organization is commonly decided to succeed or fail to supply. In many research objects, there is a lot of evidence about successful information system applied research using ISS DeLone dan McLean model theory [4] [5]. ISS DMM is a model adoption framework to provide a definition of success in the application of IS that comprehensively covers many different perspectives to evaluate IS, then provides appropriate action recommendations [6] [7]. It is vital that Investation of Information Technology (IT/IS) should be aligned to the operation in the organization. The owner expects that the goals of the implementation are achieved correctly. However, there are many problems IT/IS regarding investation of IT/IS in organizations, so the application of IT/IS fails. It is caused by retention of the user. The previous researchers show how important the examination of user's behavior. Furthermore, the user's behavior should be viewed as the usefulness and affective point of view.

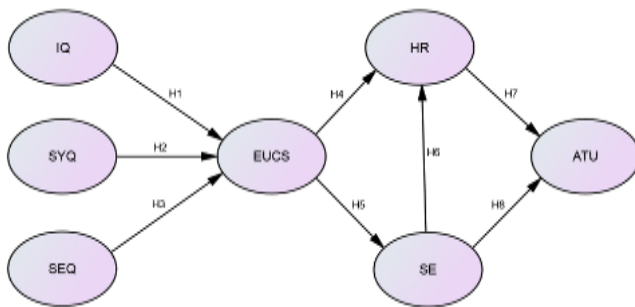
According to the problem of finding strong factors of IT/IS, many portions, particularly on the personal aspect, should be taken into consideration. This portion includes user's satisfaction about the system applied [15] [16], personal human resource qualities [17], the ability to believe

about their skill to finishing their works [18] [19] and their attitude about IT/IS applied. [10] [11] [12] [13] [14].

According to the result of the previous researcher, this study is developed and performed. Furthermore, the some of them are used as a foundation of the model when the investigation is done.

### III. RESEARCH METHOD

The variables compiled obtained from the results of the literature study are then built to become a hypothesis model seen in Figure 1, this process needs to describe variables and answer research questions, we use a quantitative data collection model.



Pict 1. Research Model Hypothesis

#### A. Survey Participant

Both primary and secondary data are used using Hair formula [20] and stratified random sampling method, we got 100 respondents who are Higher Education employee.

#### B. Measurement Scale

Implemented success scale proposed by DeLone and McLean Model [4] [5] which in next situation is adapted by [1] [2] [6] [7]. At the measurement of ATU evolving research is done by [11] [10], so in the end, it has many variables which are concluded in this research using three reflective variables about ATU.

#### C. Instrument

As explained above, this research instrument is designed and built by modified DMM theory which makes 3 supported variable of DMM which is information quality has five indicators; system quality has 5 indicators service quality has 5 indicators, and EUCS has 5 indicators. The modification used in this theory is by adding HR Variable which has 3 instruments and SE which has 5 instruments. The last one is ATU variable which used as an investigated variable in this research, it has 5 instruments.

### IV. RESULT AND DISCUSSION

After the amount of the sample is determined, we spread the questionnaire, then the data collected is discussed and displayed in this part.

#### A. Data Analysis

In table 1 we display respondent's background summary that we collected from offline spreading by probability sampling technique and doing disproportionate stratified random sampling closure which producing 100 respondents. The amount of sample used here is the minimal sample amount which has counted before by Hair Closure [20].

Personal data	%
Age	
< 30	49
31 until 40	20
41 until 50	14
> 50	17
Gender	
Female	41
male	59
Education	
Doctorate	7
Master	50
Bachelor	39
Senior high school	4
Profession	
Campus officials	10
Lecturer	48
Staff	42
Ability computer	
Distress	11
Average	61
Satisfying	28

As we can see at table 1, the summary of respondent's background is mostly male by 59%, the average age of the respondents is 20-33 which is millennial age, where millennial generation in the digital era is a productive age for using and understanding Communication and Information technology well. The education background of our respondents get a perfect point by 50% respondents is post graduated, by average 48% respondents is lecturer who has a post-graduate degree and having the ability to using a computer for work as much as 61%. Self-efficacy or ability to feel able to complete the task of using a computer contributes fully in the process of collecting data obtained from interviews and questionnaires. So that we can conclude that the results of the respondents collected are suitable for research purposes.

#### B. Measurement Model

This research is using WarpPLS closure to doing evaluating and observing measuring instruments reliability and determining construct validation. Also determining significance level of a coefficient model to testing the hypothesis [21] [22] [23].

Figuring	Outcome	Perception
Average path coefficient	0.296	Acceptance
Average R-squared	0.357	Acceptance
Average adjusted R-squared	0.345	Acceptance
Sympson's paradox ratio (SPR)	1.000	Acceptance
R-squared contribution ratio (RSCR)	0.987	Acceptance
Statistical suppression ratio (SSR)	0.875	Acceptance
Nonlinear bivariate causality direction ratio	0.938	Acceptance
Average block VIF (AVIF)	1.948	Ideally
Average full collinearity VIF (AFVIF)	2.730	Ideally
Tenenhaus GoF (GoF)	0.485	Ideally



Tabel 3. Combined loadings

	InQ	SyQ	SeQ	EUCS	HR	SE	ATU
InQ1	0.823						
InQ2	0.831						
InQ3	0.840						
InQ4	0.834						
SyQ1		0.739					
SyQ2		0.773					
SyQ3		0.807					
SyQ4		0.761					
SyQ5		0.776					
SeQ1			0.813				
SeQ2			0.806				
SeQ3			0.824				
SeQ4			0.791				
SeQ5			0.743				
EUCS1				0.792			
EUCS2				0.861			
EUCS3				0.765			
EUCS4				0.775			
EUCS5				0.755			
HRQ1					0.830		
HRQ2					0.834		
HRQ3					0.757		
SE1						0.759	
SE3						0.877	
SE3						0.801	
ATU1							0.876
ATU2							0.861
ATU3							0.893
ATU4							0.793
ATU5							0.904

In table 2 and 3, to set multi-collinearity from the collected, we do observation by using Average Full Variance co-linearity Inflation Factor (AFVIF) [24] [25]. By observing AFVIF, we get 2.98 points which means if AFVIF points are below 3.3. Accordingly, there is no multi-collinearity in the hypothetical model. Moreover, the used data have no bias. It is important to notice that in table 2, the score gained by APC, ARS, and AARS is accepted, and another important point is AFVIF and GoF is fulfilled by the model. In figure 3 combined loading is presented as a validation measurement with the terms > 0.70, from all available indicators that meet confirmatory research testing.

Table 4 is the outer from Latent Variable Coefficients which giving the results about the critical point from R-squared, Composite reliability, Cronbach's alpha, Average variances extracted, and Full collinearity VIFs. R-squared point gained is concluded as every endogen variables are accepted and also suitable for the rules agreed in the R-

squared coefficient point which has been customized is above 0.02 [26] [27].

Tabel 4. Latent Variable Coefficients

	InQ	SyQ	SeQ	EUCS	HR	SE	ATU
R-squared coefficients				0.756	0.210	0.425	0.038
Adjusted R-squared coefficients				0.749	0.194	0.419	0.018
Composite reliability coefficients	0.900	0.88	0.896	0.892	0.849	0.854	0.937
Cronbach's alpha coefficients	0.787	0.83	0.855	0.849	0.732	0.743	0.916

In the CR and CA point we got the suitable point which is CR and CA point is as much as or above 0.6-0.7 [20] [28] [29]. Meanwhile, the other important point is AVE get a good point which makes it acceptable and the research can be continued as well. This means that in Table 4 it provides a numerical explanation that the reliability of the question is considered capable of representing the respondent's will and the variables used are considered appropriate to explain the model

Table 5. Correlation Variable

	InQ	SyQ	SeQ	EUCS	HR	SE	ATU
InQ							
SyQ							
SeQ							
EUCS	0.241	0.360	0.155				
HR				0.205		0.005	
SE				0.425			
ATU					0.003	0.035	

Effect size [22] [23] is the part to explaining the impact caused by testing important parameter. Referring to effect size, Cohen categories (1988) stated that there are 4 effect size categories, i.e. weak  $d=0.00-0.10$ , medium  $d=0.10-0.25$ , strong  $d=0.25-0.40$ , and very strong  $d=>0.40$ . Furthermore, we can see an effect sizes on Table 6, i.e., variable InQ → EUCS, variable SyQ → EUCS, and effect size variable SeQ → EUCS, by means the connection between SyQ and EUCS is make the strongest connection between three exogen variables.

Table 6. Result Hypothesis

H	Correlation	$\beta$	P	Result
H1	InQ → EUCS	0.316	<0.001	Support
H2	SyQ → EUCS	0.441	<0.001	Support
H3	SeQ → EUCS	0.202	0.025	Support
H4	EUCS → HR	0.447	<0.001	Support
H5	EUCS → SE	0.652	<0.001	Support
H6	SE → HR	0.017	0.451	Not Support
H7	HR → ATU	-0.094	0.186	Not Support
H8	SE → ATU	0.203	<0.001	Support

In the other side, the role of EUCS variable to influencing variable HR and variable SE, variable EUCS has the more significant impact to variable SE with effect size score as much as 0.425 compared by its impact to HR which gaining effect sizes score as much as 0.205. By this, we need to pay more attention to the connection between EUCS and HR variable.

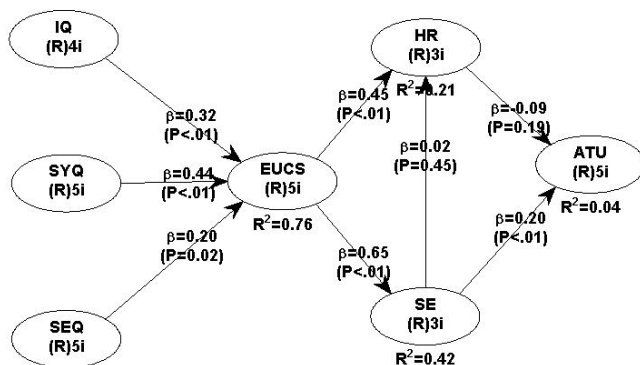
Table Result of Hypothesis Testing is explaining the connection between exogen variables, moderating variables, and endogen variables. To make it more comprehensive, we display it also in Results of Evaluating Model Hypothesis picture. It has been discussed before that H1 has a positive impact and also influencing, empirical evidence between  $\ln Q \rightarrow EUCS$  shows that H1 point is ( $\beta = 0.32$ ,  $p < 0.01$ ) which means H1 is acceptable.

Further, H2 is positive and giving the impact also; empirical evidence shows that the connection between  $SyQ \rightarrow EUCS$  showing the H2 point is as much as ( $\beta = 0.44$ ,  $p < 0.01$ ) which means H2 is acceptable. Further, H3 is positive and giving impacts, the empirical evidence between  $SeQ \rightarrow EUCS$  shows the score of H3 is as much as ( $\beta = 0.20$ ,  $p < 0.01$ ) which means H3 is acceptable.

Further, H4 is positive and giving impacts, the empirical evidence between  $EUCS \rightarrow HR$  showing the result H4 point as much as ( $\beta = 0.45$ ,  $p < 0.01$ ) which means H4 is acceptable. Further, H5 is positive and giving impacts, the empirical evidence between  $EUCS \rightarrow SE$  is showing the score H5 is as much as ( $\beta = 0.65$ ,  $p < 0.01$ ) which means H5 is acceptable.

In H6, it's positive and giving impacts also, the empirical evidence is showing the connection between  $SE \rightarrow HR$  is showing H6 score as much as ( $\beta = 0.02$ ,  $p < 0.45$ ) which means H6 is not acceptable. Further, H7 is positive and giving impacts also, the empirical evidence between the connection of  $HR \rightarrow ATU$  showing H7 score is as much as ( $\beta = -0.09$ ,  $p < 0.19$ ) which means H7 is not acceptable. H8 is positive. It implies that SE will influence ATU. The connection of  $SE \rightarrow ATU$  is reflected by H8. Since, the result H8 point is ( $\beta = 0.20$ ,  $p < 0.01$ ), it means that H8 is acceptable.

From the explanation that has been done before, the following is a picture from the calculation of the model using the WarpPLS 5.0 tool.



Pict 2. Results of Evaluating Model Hypotesis

### C. Findings and Discussion

The critical result of this research is how DMM theoretic models [4] [5] can give the impacts to Attitude toward Usage (ATU). This result is established by observing the affective point, i.e., Human Resource Quality (HRQ) [17] and Self-Efficacy (SE) [18]. Both of them is derived from Technology Acceptance Model Theoretical Model (TAM) [12] [13] [14].

There is no previous research which is focused on developing countries such as Indonesia particularly on discussing the impact of the use of Employee Information System (EIS) DMM to HR, and SE and finally at ATU. This research's result is in line with the previous result especially the scientific contribution concerning user satisfaction when they use Information System [1] [2] [3] [9]. This study shows that the perception of system quality, information quality, and service quality experienced are the important factors in the point of view the user. In the end, these factors can be used to encourage the employees to reach the satisfaction while using EIS as work tools. Another finding of this research, the connection between HR and SE is proven, and they have significant impacts. This research's result is in line with the previous result [1] [2] [17].

At the other observation from this research's results, we find that the connection between SE is not determining of human resource quality is raising and also HR that proven that has not many impacts to ATU which means an employee doesn't need higher educational level only to use mandatory EIS system. It is different than SE which have the specific contribution to ATU, SE is having significant impacts scoring and also tent to be useful to expand, which means a confident employee can finish their works is giving the contribution to successful implied EIS.

### V. MANAGERIAL IMPLICATIONS

In general, the study found that computer user satisfaction and Self-Efficacy had a positive relationship with Attitudes to Use, but specifically Self-Efficacy was the most dominant effect on attitudes toward use. Therefore, the Higher Education that will implement our EIS is very supportive to be able to pay attention to the Employee's Self-Efficiency, just as providing EIS pre-implementation and training implementation as a self-development program that is implemented periodically. The self-development can be programmed such as increased confidence, increased computer skills, and increased knowledge about IT / IS will greatly assist employees to improve Self-Efficacy and ultimately enhancing the Self-Efficacy capability in employees greatly fosters development Higher Education.

### VI. CONCLUSION

Investigation of human factor in the evaluation using the DeLone and McLean model is still interesting. In our research, Affective factor is one of human variable, which is closed to DMM model. Furthermore we find that there are two affective factors in DMM i.e. self-Efficacy and Human resource quality. Since EIS is positioned as a mandatory

system, our study shows that only Self-Efficacy which will influence the Attitude toward Usage of EIS. Human resource quality, as the other Affective factor, has no influence to Attitude toward Usage of EIS.

## REFERENCE

- 1) Suryanto, T. L., Setyohadi, D. B., & Faruqi, A. (2016). Analysis of the Effect of Information System Quality to Intention to Reuse of Employee Management Information System (Simpeg) Based on Information Systems Success Model. *MATEC Web of Conferences Journal*, 58.
- 2) Suryanto, T. L., Setyohadi, D. B., & Wibowo, N. C., (2017). Empirical Investigation on Factors Related to Individual of Impact Performance Information System. *Proc. EECSI 2017, Yogyakarta, Indonesia*, 19-21 September 2017. 978-1-5386-0549-3/17/\$31.00 ©2017 IEEE
- 3) Urbach, N., & Müller, B. (2012). The Updated DeLone and McLean model of information systems success. In *Information systems theory* (pp. 1e18). Springer.
- 4) Al, Y. (2015). Evaluation by users of an industrial information system (XPPS) based on the DeLone and McLean model for IS success, 26(0), 903–913.
- 5) Bossen, C., Groth, L., & Jensen, F. (2013). Evaluation of a comprehensive EHR based on the DeLone and McLean model for IS success: Approach, results, and success factors. *International journal of medical informatics*, 82, 940–953.
- 6) DeLone, W.H., & McLean, E.R. (1992). Information systems success: The quest for the dependent variable. *Information Systems Research*, 3(1), 60-95.
- 7) DeLone, W.H., & McLean, E.R. (2003). The DeLone and McLean Model of Information Systems Success: A Ten-Year Update. *Journal of Management Information Systems*, 19(4), 9–30
- 8) Robo, Salahudin., Setyohadi, D. B., Santoso, A. Joko., (2018). An Identification of Success of Academic System Application Using DeLone and McLean Design (Case Study at Wira Husada school of health science Yogyakarta), 2018 International Conference on Information and Communications Technology (ICOIACT), 827-832.
- 9) Montesdioca, G. P. Z., Maçada, A. C. G., (2015). Quality Dimensions of the DeLone-McLean Model to Measure User Satisfaction: an Empirical Test on the Information Security Context. 2015 48th Hawaii International Conference on System Sciences. 5010-5019
- 10) Hair, J.F., Ringle, C.M. & Sarstedt, M. (2011). PLS-SEM: Indeed a silver bullet. *Journal of Marketing Theory and Practice*, 19(2), 139–152.
- 11) Kock, N., & Lynn, G.S. (2012). Lateral collinearity and misleading results in variance-based SEM: An illustration and recommendations. *Journal of the Association for Information Systems*, 13(7), 546-580.
- 12) Lindell, M., & Whitney, D. (2001). Accounting for common method variance in cross-sectional research designs. *Journal of Applied Psychology*, 86(1), 114-121.
- 13) Esposito Vinzi, V., Chin, W.W., Henseler, J. & Wang, H. (2010). *Handbook of Partial Least Squares: Concepts, methods and applications*, Berlin, Heidelberg: Springer.
- 14) Kock, N. (2011b), Using WarpPLS in e-collaboration studies: Mediating effects, control and second order variables, and algorithm choices. *International Journal of e-Collaboration*, 7(3), 1-13.
- 15) Kock, N. (2013b). Using WarpPLS in e-collaboration studies: What if I have only one group and one condition? *International Journal of e-Collaboration*, 9(3), 1-12.
- 16) Wooldridge, J.M. (1991). A note on computing r-squared and adjusted r-squared for trending and seasonal data. *Economics Letters*, 36(1), 49-54.
- 17) Cohen, J. (1988). *Statistical power analysis for the behavioral sciences*. Hillsdale, NJ: Lawrence Erlbaum.
- 18) Dillon, W.R., & Goldstein, M. (1984). *Multivariate analysis: Methods and applications*. New York, NY: Wiley.
- 19) Peterson, R.A., & Yeolib, K. (2013). On the relationship between coefficient alpha and composite reliability. *Journal of Applied Psychology*, 98(1), 194-198.
- 20) Doll, W.J. Xia, W., & Torkzadeh, G. (1994). A confirmatory factor analysis of the end-user computing satisfaction instrument. *MIS Quarterly*, 18(4), 453–461.
- 21) Leclercq, A. (2007). The perceptual evaluation of information systems using the construct of user satisfaction: case study of a large French group. *The DATABASE for Advances in Information Systems*, 38(2), 27–60.
- 22) Yusoff, Y. M., & Ramayah, T. (2011). FACTORS INFLUENCING ATTITUDE TOWARDS USING ELECTRONIC HRM, 1510–1520.
- 23) Bandura, A., 1982. Self-efficacy mechanism in human agency. *Am. Psychol.*, 37: 122-147
- 24) Li, Yan , Yanqing Duan, Zetian Fu, and Philip Alford. "An empirical study on behavioural intention to reuse e-learning." *British Journal of Educational Technology*, 2011.
- 25) Veneziano, V., Mahmud, I., Khatun, A., & Peng, W. W. (2014). Usability Analysis of ERP Software: Education and Experience of Users' as Moderators, (1001).
- 26) Hong, J., Tai, K., & Methodology, A. (2011). Applying the Technology Acceptance Model to Investigate the Factors Comparing the Intention between EIVG and MCG Systems, 29–30.
- 27) Davis, F.D., 1986. A technology acceptance model for empirically testing new end-user information systems: Theory and results. Ph.D. Thesis, Sloan School of Management, Massachusetts Institute of Technology, Cambridge, MA., USA.
- 28) Davis, F.D., 1989. Perceived usefulness, perceived ease of use and user acceptance of information technology. *MIS Quart.*, 13: 319-340.
- 29) Venkatesh, V. and F.D. Davis, 2000. A theoretical extension of the technology acceptance model: Four longitudinal field studies. *Manage. Sci.*, 46: 186-204.

# Improvement of Information Technology Infrastructure in Higher Education using IT Balanced Scorecard

Clara Hetty Primasari  
Department of Information Systems  
Universitas Atma Jaya Yogyakarta  
Yogyakarta, Indonesia 55281  
clara\_hetty@staff.uajy.ac.id

Djoko Budiyo Setyohadi  
Magister Teknik Informatika  
Universitas Atma Jaya Yogyakarta  
Yogyakarta, Indonesia 55281  
djoko.bdy@gmail.com

**Abstract**— Today the use of Information Technology (IT) in business is a must since IT is useful to obtain competitive advantage. It can be achieved by alignment of IT and business, which is performed by developing a good IT infrastructure. Higher educational organization is one of business which requires competitive advantage to compete with their competitors. However, there are some problems encountered. These include the lack of a systemic approach to IT implementation, the lack of awareness to use IT, the lack of commitment and the leader's interest to implement IT, the weakness of technical support for IT implementation, poorly targeted staff development, lack of ownership and insufficient funds. Furthermore, an evaluation is needed to determine the condition of IT infrastructure problems to deal with issues faced by a higher education organization. Balanced Scorecard is potential framework for analyzing IT infrastructure since it is one of the well-known performance measurements which embrace the important aspect in business. To do performance evaluation in the IT of higher education organization, Balance Scorecard perspective needs to be customized since IT division is more likely to serve internal rather than external parties commonly. The results of this study are expected to give an illustration of the state of IT infrastructure governance of higher education according to four perspectives in IT Balanced Scorecard. Based on this illustration, it can be identified critical recommendation to IT Infrastructure governance in higher education.

**Keywords**— *Improvement; IT Infrastructure; Governance; IT Balanced Scorecard; Higher Education*

## I. INTRODUCTION

Information Technology has been widely used by many parties such as organizations, institutions, companies, educational institutions, and so on to support its business processes. Information and business technologies are closely related, and an institution cannot be a competitive institution if Information Technology and business are not aligned [1]. The alignment between business and Information Technology has proven to have a positive relationship to the performance of an institution [2].

Information Technology occupies a vital position in the process of economic globalization and is a necessity in every developing country [3]. In Education, Information and communication technologies can facilitate education and teaching and learning processes [4]. In the implementation of teaching and learning process, administration, and all academic activities within the university, good IT infrastructure is required. The quality and quantity of infrastructure need to be considered for improvements in productivity and efficiency [5].

In developing countries, generally, there are some problems related to the application of IT infrastructure in higher education. These include the lack of a systemic approach to IT implementation, lack of awareness to use IT, lack of commitment and the leader's interest to implement IT, lack of technical support for IT implementation, poorly targeted staff development, lack of ownership and insufficient funds [6]. An evaluation is needed to find out what specific issues faced by an educational institution in the governance of its IT infrastructure.

There are various frameworks that many previous researchers have found to measure performance, but their effectiveness depends on how qualitative and quantitative perspectives are handled in the relevant context [7]. Kaplan and Norton introduced the Balanced Scorecard as a performance measurement. The purpose of the method is not only limited to make financial evaluation alone but also to measure an important aspect of the business, such as customer satisfaction, internal processes, and the ability to innovate [7]. Martinsons et al. in [8] suggested that the four Balanced Scorecard perspectives need to be modified to fit the IT performance. They argue that a company's IT division usually serves more internal rather than external parties and the project is intended for the benefit of both end users and organizations as a whole.

Based on the above considerations, then selected IT Balanced Scorecard as a framework that used for analysis of IT infrastructure at Higher Education. This research used some Key Performance Indicator (KPI). KPI is the measures used to realize the goals that have been determined. KPIs typically include capability indicators, implementation, and IT resource capabilities [9]. This research resulted in exposure to the state of IT infrastructure in higher education according to the four IT Balanced Scorecard perspectives such as Corporate Contributions, User Orientation, Operational Excellence, and Future Orientation [10]. This was known by the points obtained for each KPI in each IT BSC perspective. By using these points, it could be broken down which KPI that earned good or bad points. These results would be justified by interviews with IT divisions so it could be sorted out several aspects from four IT BSC Perspectives that need to be improved. The main contribution of this research is constructing managerial implication for IT Infrastructure in private higher education based on justification result. Managerial implication contains some recommendations to IT Infrastructure governance for private higher education.

The paper proceeds as follows. In the following section, we first present the Balanced Scorecard application to various institutions such as profit and non-profit or educational institutions. Also Balanced Scorecard that applied to IT Problems called IT Balanced Scorecard. Then, the methodologies used in this research. Following that, result and discussions that consist of result of IT Infrastructure of private university assessment using IT Balanced Scorecard and Report and findings analysis. The next section is Managerial Implication containing recommendations for findings in IT Implementation in private university. The last section is the conclusion of this research.

## II. LITERATURE REVIEW

Performance and management measurement is the heart of an organization that wants to be looked transparent, efficient, effective, and successful in its operations [11]. Performance measurement is developed as a means to monitor and maintain organizational controls to ensure that an organization can execute strategies that lead to the achievement of overall goals [12]. One of the tools for performance measurement that is widely used by researchers in the world is the Balanced Scorecard. The Balanced Scorecard developed by Kaplan and Norton allows managers to view business from four essential perspectives [13]. Such perspectives include customer perspective, internal perspective, innovation and learning perspectives, and financial perspective. Combining these four perspectives, the Balanced Scorecard helps managers understand relationships to go beyond traditional notions of functional boundaries and lead to better decision-making and problem solving [13].

Balanced Scorecard is widely applied in companies or institutions that are oriented to profit, but do not rule out applied to non-profit organizations or educational institutions. The University as an educational institution requires appropriate tools and models to ensure the bounded plans and processes and the effectiveness of graduates into the world of work to demonstrate university performance [14]. There are several studies in the implementation of Balanced Scorecard in education such as research conducted by [15] applying Balanced Scorecard for business school and resulted in finding that Balanced Scorecard approach is suitable for high education situation and allow alignment of various sizes with the mission and unique strategy. Hladchenko in [16] compares the application of the Balanced Scorecard to higher education institutions in Austria and Germany and concludes that the Balanced Scorecard provides a systemic view of strategy for institutions. BSC ensures a full complex framework for strategy implementation and control and sets the ground for further learning in institutional strategic management processes by the "plan-do-check-action" scheme. Philbin in [17] conducted a study to identify how university management can be improved by applying performance measurements with the Balanced Scorecard. The university feels the benefits of a scorecard report that provides specific information for institutional research development and teaching capabilities and this has an impact on improvements in the decision-making process. The Balanced Scorecard is also applied in schools in Iran and concluded that the application of BSC compared to other strategic planning models is more effective and efficient for solving the problems of educational organizations [18].

Balanced Scorecard is also applied to IT problems. The IT division within an organization typically provides services for the internal organization, and it makes IT Balanced Scorecard (IT BSC) slightly different from the usual Balanced Scorecard. Grembergen and Bruggen introduced the IT BSC consisting of four perspectives: User Orientation, Operational Excellence, Future Orientation, and Business Contributions.

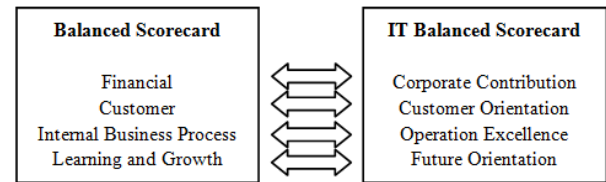


Fig. 1. Comparison of Balanced Scorecard with IT Balanced Scorecard (Grembergen and Bruggen, 1997)

Each perspective in the IT BSC should be translated into metrics and measures that can assess the current situation. This assessment process should be periodically reproduced and coordinated with pre-set objectives. The important thing about IT BSC is that in IT BSC the cause and effect relationship is built and the connection between two types of measurement such as output measurement and performance drivers is clarified [7].

## III. METHODOLOGY

The institution to be analyzed was one of the private universities in Yogyakarta, Indonesia named Universitas Atma Jaya Yogyakarta (UAJY). UAJY was chosen because it was one of the popular private universities in Indonesia and the IT implementation represent the implementation of IT infrastructure governance in higher education. Research methodologies used in this research shown in Figure 2 and explained as follows:

### 1) Organization/Institution Analysis

This research began with the analysis of institutions to be studied. This analysis is started by determining the Key Performance Indicator (KPI) for each IT Balanced Scorecard Perspective. The analysis involved identifying the aspects to be measured in each balanced scorecard perspective. Each measured dimension would be used as a KPI.

### 2) Literature Studies and Determining KPI

To facilitate the determination of KPIs, besides studying the institutions to be analyzed, also by looking for similar research that had been done by previous researchers. KPIs used in this research was determined by comparing previous literature studies related to this study. The KPIs for each of the perspectives were adapted from [19].

### 3) Data Collection

After determining KPI for each perspective, each KPI was converted in the form of questionnaire question which then distributed by convenience sampling method to 30 respondents consisting of staffs and lectures from various faculties and units in UAJY. Not only with questionnaires, but data collection was also conducted by interviews with IT Head, deputy head of IT User Services Department, several staffs, and lecturers.

### 4) IT Infrastructure Analysis using IT BSC

The results of the questionnaire were used to build the IT BSC that would be analyzed and combined with the results of interviews to obtain the results of the analysis. IT BSC

was developed using Balanced Scorecard online tool. IT BSC analysis produced IT BSC Report.

#### 5) Report and Finding Analysis

IT BSC Reports were then analyzed and matched the results with findings from the questionnaire results and interviews with IT Head, deputy head of IT User Services Department, several staffs, and lecturers.

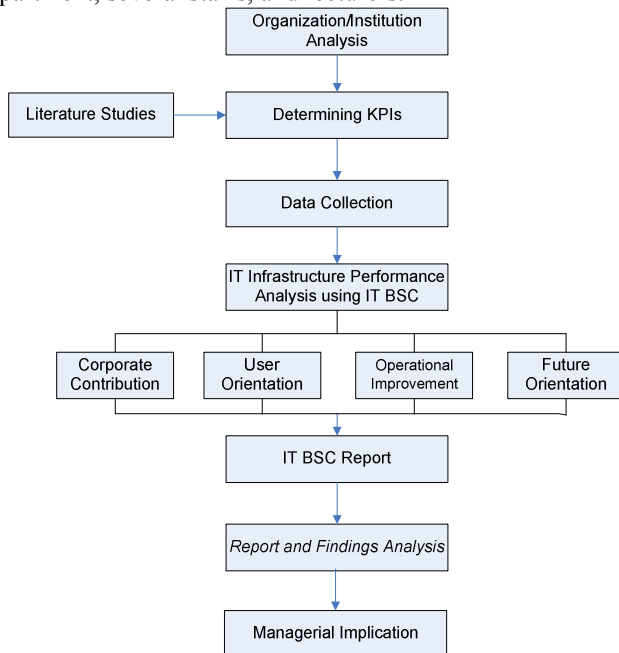


Fig. 2. Research Methodologies

#### 6) Managerial Implication

Analysis of reports and findings is classified which were positive and negative. The positive things found should be kept, while the negative ones must be corrected. These two resulted in suggestions and recommendations for governance of IT infrastructure in the future.

### IV. RESULT AND DISCUSSION

#### A. Results of Assessment with IT Balance Scorecard

Table 1 shows IT Balanced Scorecard report that was generated from questionnaire result. We can see value from each perspective and KPIs. Perspective value ranged from 1-100%, while KPIs from 1-5. The higher the value, the higher or better the value for the perspective or the related KPI. From the report in table 1, it can be seen that the perspective that obtains the best or most significant result is the corporate contribution and the smallest or the worst is the future orientation

KPI with the most significant value is the Business Value of IT Unit, and the lowest is the skill of IT employees. This report will be adjusted to the existing findings and analyzed the cause with information from the interview. It is done to obtain suggestions for improvement and what needs to be maintained and improved for better performance in the future.

TABLE I. IT BALANCED SCORECARD REPORT

Indicator	Desc	Value	Target
<b>Perspective Corporate Contributions</b>		70,00%	
IT Cost Control	KP-1	3,73	5
IT and Business Goals	KP-2	3,6	5
Business Value of IT Function	KP-3	4,17	5
Effectiveness of IT Unit	KP-4	3,7	5
Total performance in group		70,00%	

<b>Perspective User Orientation</b>		66,04%	
Product quality	OP-1	3,67	5
User Contribution	OP-2	3,53	5
User Satisfaction	OP-3	3,5	5
User Interaction with IT Unit	OP-4	3,87	5
Total performance in group		66,04%	
<b>Perspective Operational Improvement</b>		67,29%	
Effectiveness of app development	PO-1	3,47	5
System Maintenance Intensity	PO-2	3,7	5
Effectiveness of Service Functions	PO-3	3,87	5
Repair Accuracy	PO-4	3,73	5
Total performance in group		67,29%	
<b>Perspective Future Orientation</b>		59,58%	
Training Budget for IT personnel	OM-1	3,33	5
IT Personnel Expertise	OM-2	3,30	5
The budget for IT R&D	OM-3	3,33	5
IT Product Innovation	OM-4	3,57	5
Total performance in group		59,58%	
Total performance in IT Scorecard		66%	

#### B. Report and Findings Analysis

The results of IT BSC report were then justified by interviews with some related parties such as the head and deputy head of IT Division as well as some staff and lecturers in UAJY.

##### 1) Corporate Contribution

For Corporate Contributions perspective, there are some KPIs such as IT Cost Control, IT and Business Goals, Business Value of IT Function and effectiveness in IT Unit.

Corporate contributions are embodied in IT Division's strategic plan. There are four focused Strategic Plan of IT Division, including:

1. Improve supporting facilities of Technology-Based Learning Activities. The indicator has not established yet but what is done now is optimizing the use of Learning Management System (Moodle), then improving the WIFI coverage, so that the learning process more convenient.
2. Improve integrated university administration services. This action is done through the internal systems of UAJY such as SIKEU, SISPRAS, SPKP, and others. The indicator of success is that all built systems can be used maximally.
3. Increase infrastructure such as internet reinforcement, building connections, and server capabilities.
4. IT Human Resource Development which performed regularly by training and certification.

IT cost control has been done through the UAJY Financial Information System called Sistem Informasi Keuangan (SIKEU). Based on [20], an effective Cost control system should comply with cost control framework that consists of three criteria:

- a. Systematic and detail Work Breakdown Structure (WBS)

WBS used for cost control must follow a systematic structure. Activities should be partitioned into easy-to-manage elements so that budgets and expenses can be easily controlled. Besides, WBS must also be broken down into various depth levels. The depth level can be made into three levels.

- b. Proper Cost Code

The cost code used in a system must be flexible, following the WBS and accounting code. The cost structure code should have the ability to tackle the



things that increase in the future. Besides the cost code must also be adjusted with the WBS and accounting code.

c. **Employ Earned Value Concept**

Earned value is the performance measurement to report the status of a project regarding both cost and time on a given date. By employing the earned value concept, cost status at given progress can be identified. By identifying the cost status, management can obtain information about the total actual expenditure of each item under the predefined budget.

Based on observations and interviews with SIKEU users, SIKEU has met the three criteria of cost control framework above. However, the users still complain caused by the bug of the system, such as:

- a. Error in system navigation links so the user should re-login to continue their process,
- b. Bug regarding deleting data since when the user wants to delete one data all of the data are deleted
- c. the input process is difficult to be performed caused the data should be inputted one by one.

For IT Investment, it has been in line with existing budget in SIKEU, but it has never been held a calculation about benefits and profits of IT implementation in UAJY. The obstacle of the investment is that the technology used by IT Division is still relatively new, so it feels quite expensive. Beside that, the budget for the technology is limited, and the investment process is long enough.

2) *User Orientation*

For User Orientation perspective there are some KPIs such as Product Quality, User Contribution, User Satisfaction, and User Interaction with IT Division.

To gain user satisfaction, IT Division always strives to make quality products. Products produced by IT Division are tailored to the needs of users. Applications that have been made include:

- a. for staff and lecturers: SIKEU (finance information systems (IS)), SIMKA (personnel IS), SPKP (employee performance appraisal IS) in which there is a presence system with a fingerprint, and ATMAREWARDS (rewards for the use of e-learning sites).
- b. for students: SIATMA (academic IS), SIKMA (student IS), and ATMAREWARDS
- c. for external and alumni: PMB Online (admission IS), and SIMPONI (alumni portal IS).

From the user side, users feel helped by the SIKEU, fingerprint Presence Systems, and other applications created by IT Division. This condition is proven since there are only 10% of respondents who feel that the application produced by IT Division has not suitable with their needs.

When the application is developed, users are involved to ensure the quality of the systems. The user involvement embraces to various management level, from staff up to managerial level. During the development process, users are always included in each stage of application development so that the quality of the application is maintained and the resulting application can be defined as user preferences. Before the application developed, interviews were done to the user about the expected specifications and functions of the system. After that, the application is developed until completed. Subsequently, it is tested to the user to get feedback. Improvements are always made based on user's

feedback until the user feels that the system is ready and fit by their wishes.

Constraint related to the user is that some users are reluctant to switch to the new system because they are comfortable with the old system. The problem about new technology is although new technology mainly succeeded in delivering managers' desired sense to the change process, generating engagement and spirit, it did so while provoking a sense of frustration and anxiety with the technology itself [21]. This condition happens at SIMKA. Users still feel comfortable to use old system although the old system used has not been integrated with other systems that exist in the university, and its functions are not complete compared to the system that has been developed by IT Division.

In addition to system development, user interaction with IT Division occurs in handling customer complaints. 97% of respondents feel that users can quickly obtain answers from complaints or questions in the use of existing systems, through helpdesk ([ksi.uajy.ac.id/helpdesk](mailto:ksi.uajy.ac.id/helpdesk)) with a response speed within 24 hours assisted by student staff team.

3) *Operational Improvement*

For Operational Improvement perspective, there are some KPIs such as Effectiveness of application development, Systems maintenance facility, Effectiveness of service function, and Repair Accuracy. Based on the questionnaires, only 10% of users were dissatisfied with the system developed by IT Division. This situation proves that system development has been effective, but still needs some evaluation about what makes users dissatisfied. According to Helpdesk, 97% of users are satisfied with the complaint response or IT Helpdesk. To improve the quality of service to the user, IT Division uses helpdesk information system based on a ticket system. Any User Repair / Request Advice will be provided with a unique ticket number that can be used to monitor progress and follow-up provided online. IT Division delivers complete archives and history of all User Repair / Suggestions. Submitted forms on hours and days of work will be responded to promptly on the hours of the working day, while forms submitted outside of these hours will be handled at the earliest on the next business day. IT Helpdesk guarantees maximum problem resolution within 48 hours or 2 days from the time of the complaint. Not only fast, but improvements made by the IT team are also accurate and effective according to the problems experienced by users. For complaints that related to other units, IT Division will give it to another unit. Complaints are also documented in regular reports per month.

Maintenance that has been done tends to improve if there is something problematic. Maintenance is done based on the unit request. Examples of maintenance were done when the server down, then identified the cause because it turns out quite a lot of users. The solution was to replace or add the server. If there was damage to the goods and must be replaced or add new, it was not the responsibility of IT Division, but the procurement part.

4) *Future Orientation*

For Future Orientation perspective, there are some KPIs such as Training Budget for IT Personnel, IT Personnel Perspective, Budget for Research and IT Development, and IT Product Innovation. IT Personnel Expertise is good because IT personnel followed rigorous selection before they accepted to work and they always get training

routinely. The conducted training for IT Personnel is done sufficiently as it is targeted and as it is required. Training budget is affordable by the provided budget at SIKEU.

IT Division's staff are spread in every faculty and library to help and support IT in every unit in UAJY. What remains an obstacle is the lack of staff.

Innovation and development are always pursued by IT Division, and its budget comes from the research budget of LPPM (Research unit in UAJY). The innovation of IT products still exists and begins with informal research using the latest technologies.

From justification above, can be sorted out several aspects from four IT BSC Perspectives that need to be improved to form recommendation to management. Aspects that need to be improved such as calculation about benefits and profits of IT implementation, users' complaints about system's bugs., users that comfortable with old systems so that they do not want to use new systems, the use of new technology that considered expensive, and the lack of IT staff. Beside drawbacks above, there are some aspects that have done well such as good IT cost control, consistency to use new technology, consistency to make sure product's quality, and effective and fast user complaints handling.

In the next section, managerial implication is constructed based on the above drawbacks and what have been done well in IT Implementation in UAJY. Managerial implication contributes recommendations to management for highlighted aspects explained before.

## V. MANAGERIAL IMPLICATION

From the findings for each of the perspectives, then it is known things need to be improved and maintained in the implementation of UAJY's IT infrastructure governance. Things that need to be maintained include:

### 1) IT Cost Control

IT cost control has been done very well using SIKEU. All expenses for IT division and even all units in UAJY have been registered and used by the budget listed on SIKEU. Good cost control will make the effectiveness of budgetary usage thereby reducing the possibility of wasted costs that should be allocated to more productive things. Some recommendation for cost control system (SIKEU) are:

- a. Evaluate the use of SIKEU regularly either by spreading questionnaires or by interviewing some random users.
- b. Perform technical improvements by user's complaints
- c. The addition of automatic data input feature with import excel or csv file so that user can enter some data at once with the provided format.

### 2) The use of new technology

IT Division always tries to use new technology in every developed product. Recommendation for this usage are:

- a. Before using new technology, it must be ensured in advance that the technology can truly support and contribute more value on the built services, so the technology used can be beneficial and not just a waste of money.
- b. The use of new technology should be accompanied by regular training of staff related to the new technology to be used.

### 3) Quality products

IT Division always strive to create quality IT products and services. Recommendations of product quality include

- a. Retaining user involvement in every phase of information system development. User involvement is critical to maintaining the quality of a product especially when the product has been launched and used by users in general.
- b. Always make improvements according to user input. Feedback from users during product creation will minimize the possibility of complaints and changes as well as add functionality when the product is launched.

### 4) Effective and fast user complaints handling

Besides the good things that need to be maintained above, there are some things that should be taken into consideration, i.e.:

*1) The indicator has not established for strategic plan especially Improving supporting facilities of Technology-Based Learning Activities.*

Some recommendations are:

- a. Should be created an indicator of success for the strategic plan of the improvement of technology-based learning support facilities to spur and become the motivation to achieve the target.
- b. Indicator created can be used to facilitate evaluation because the evaluation points have been identified. This indicator can make management know things that are lacking and need to be improved or upgraded from a strategic plan.

*2) Calculation of the benefits and profits of IT implementation in UAJY has never been done.*

Some recommendations are:

- a. Benefit and profit calculations should be created to measure the success of IT implementation. The results of the calculations can be used to determine the achievement in the short, medium, or long term.
- b. Calculation result could be used to determine the steps and strategies to be taken whether it is in line with the goals and vision and mission of IT Division.

*3) The technology used by IT Division is still relatively new, so it feels quite expensive.*

In the use of new technology, the most important thing is to ensure maximal perceived benefits. Some recommendations are:

- a. Before deciding the use expensive technology, consideration should be given to the advantages and disadvantages of using the technology. Should be considered if the price of the implementation of the technology is high but the benefits are good for institutional progress,
- b. Making price comparisons from some suppliers of the technology to be used. Choose a supplier or vendor that provides the best price and warranty.
- c. Should be given understanding to other parties authorized for monitoring/controlling the budget to understand that the implementation of the new technology will indeed contribute and bring positive impact to the institutional progress.

*4) Some users are reluctant to switch to the new system because they are comfortable with the old system.*

The key to successful application utilization apart from product quality is also found in the successful socialization of its use. Recommendation to this aspect is:

- a. To convince and encourage every user such as staff, lecturers, and students is required exemplary and influence from the leader. Leaders must be able to give a strong influence so that all parties under it are also encouraged to use information systems developed by the IT division.

#### 5) Lack of IT staff.

Related to the lack of staff at IT Division, there are several recommendations:

- a. It is expected to ensure the number of staff by the needs of IT Division both with proper division of tasks so that there is no overlap, or with recruitment.
- b. For recruitment can be done by requesting the HR Division to be able to prioritize hiring for IT staff so that they can immediately obtain staff without reducing the process of recruitment itself.

The above recommendations were made in accordance with what is need to be improved (drawbacks) and what is need to be maintained (good things) known from points obtained for each KPI in each IT BSC perspective justified with interview result. Recommendations were constructed in detail and adjusted with highlighted drawbacks and positive things found in IT BSC result. Recommendations would be managerial implication for IT Infrastructure governance in private higher education.

It is required awareness from various parties to the implementation of IT in UAJY. Not only the IT division alone improves itself, but must also be accompanied from the awareness of other related units and which used systems from the IT division.

## VI. CONCLUSION

The governance of IT infrastructure in UAJY has been analyzed using IT Balanced Scorecard. This research resulted in several points obtained for each KPI in each IT BSC perspective. From these points could be broken down which KPI is good and bad. Next process was justifying and analyzing each KPI result with interview with IT Division. From the results of the analysis found some things that need to be maintained and upgraded from IT Infrastructure governance in UAJY. The overall result of IT Balanced Scorecard for IT governance in UAJY is good with 66% value. Some things that need to be maintained and improved based on the result of Balanced Score Card analysis, such as IT Cost Control, The use of new technology, Quality products, User engagement in app development, and effective and fast user complaint handlings. Other than that, things to note such as Indicator has not established for strategic plan especially Improving supporting facilities of Technology-Based Learning Activities; Calculation of the benefits and profits of IT implementation in UAJY has never been done; Technology used by IT Division is still relatively new, so it feels quite expensive; and some users are reluctant to switch to the new system because they are comfortable with the old system.

## ACKNOWLEDGMENT

This research was supported by Lembaga Penelitian dan

Pengabdian Masyarakat (LPPM) Universitas Atma Jaya Yogyakarta.

## REFERENCES

- [1] L. Aversano, C. Grasso, and M. Tortorella, "Managing the alignment between business processes and software systems," *Inf. Softw. Technol.*, vol. 72, pp. 171–188, 2016.
- [2] S. Charoensuk, W. Wongsurawat, and D. B. Khang, "Business-IT Alignment: A practical research approach," *J. High Technol. Manag. Res.*, vol. 25, no. 2, pp. 132–147, 2014.
- [3] S. Mitić, M. Nikolić, J. Jankov, J. Vukonjanski, and E. Terek, "The impact of information technologies on communication satisfaction and organizational learning in companies in Serbia," *Comput. Human Behav.*, vol. 76, pp. 87–101, 2017.
- [4] F. Hamidi, M. Meshkat, M. Rezaee, and M. Jafari, "Information technology in education," in *Procedia Computer Science*, 2011, vol. 3, pp. 369–373.
- [5] A. Mitra, C. Sharma, and M.-A. Véganzonès-Varoudakis, "Infrastructure, information & communication technology and firms' productive performance of the Indian manufacturing," *J. Policy Model.*, vol. 38, no. 2, pp. 353–371, 2016.
- [6] C. Sife, A.S.;Lwoga, E.T; Sanga, "New technologies for teaching and learning: Challenges for higher learning institutions in developing countries," *Int. J. Educ. Dev. using ICT*, vol. 3, no. 2, 2007.
- [7] W. Van Grembergen, R. Saull, and S. De Haes, "Linking the IT Balanced Scorecard to the Business Objectives at a Major Canadian Financial group," *J. Inf. Technol. Case Appl. Res.*, vol. 5, no. 1, pp. 23–50, 2003.
- [8] J. Keyes, *Implementing the it balanced scorecard, aligning it with corporate strategy*. 2005.
- [9] ISACA, "CoBIT 4.1," *IT Gov. Inst.*, pp. 1–29, 2007.
- [10] W. Van Grembergen and S. De Haes, "Measuring and Improving IT Governance Through the Balanced Scorecard," *Inf. Syst. Control J.*, vol. 2, no. 1, pp. 34–42, 2005.
- [11] S. Hamid, Y. M. Leen, and S. H. Pei, "Measuring the performance and excellence of academicians through the e-Balanced Scorecard (e-BSC)," in *Information Management in the Modern Organizations: Trends and Solutions - Proceedings of the 9th International Business Information Management Association Conference*, 2008, vol. 1–2, pp. 713–717.
- [12] A. Zangouinezhad and A. Moshabaki, "Measuring university performance using a knowledge- based balanced scorecard," *Int. J. Product. Perform. Manag.*, vol. 60, no. 8, pp. 824–843, 2011.
- [13] R. S. Kaplan and D. P. Norton, "The balanced scorecard: Measures That drive performance," *Harvard Business Review*, vol. 83, no. 7–8, 2005.
- [14] M. Fooladvand, M. H. Yarmohammadian, and S. Shahtalebi, "The Application Strategic Planning and Balance Scorecard Modelling in Enhance of Higher Education," *Procedia - Soc. Behav. Sci.*, vol. 186, pp. 950–954, 2015.
- [15] C. Papenhausen and W. Einstein, "Implementing the Balanced Scorecard at a college of business," *Meas. Bus. Excell.*, vol. 10, no. 3, pp. 15–22, 2006.
- [16] M. Hladchenko, "Balanced Scorecard – a strategic management system of the higher education institution," *Int. J. Educ. Manag.*, vol. 29, no. 2, pp. 167–176, 2015.
- [17] S. P. Philbin, "Design and implementation of the Balanced Scorecard at a university institute," *Meas. Bus. Excell.*, vol. 15, no. 3, pp. 34–45, 2011.
- [18] H. Tohidi, A. Jafari, and A. A. Afshar, "Using balanced scorecard in educational organizations," in *Procedia - Social and Behavioral Sciences*, 2010, vol. 2, no. 2, pp. 5544–5548.
- [19] R. Alit and F. P. Aditiyawan, "Pengukuran Kinerja Organisasi Teknologi Informasi Menggunakan It Balanced Scorecard ( Studi Kasus : Universitas Pembangunan Nasional ' Veteran ' Jawa Timur )," *SCAN - J. Teknol. Inf. DAN Komun.*, vol. XI, no. 3, 2016.
- [20] C. Charoenngam and E. Sriprasert, "Assessment of Cost Control System: A Case Study of Thai Construction Organizations," *Eng. Constr. Archit. Manag.*, vol. 8, no. 5/6, pp. 368–380, 2001.
- [21] N.-S. Reynolds, "Making sense of new technology during organisational change," *New Technol. Work Employ.*, vol. 30, no. 2, pp. 145–157, 2015.

# A Conceptual Framework of Cloud-Based Mobile-Retail Application for Textile Cyberpreneurs

Nik Zulkarnaen Khidzir  
Global Entrepreneurship Research and  
Innovation Centre / Faculty of Creative  
Technology and Heritage  
Universiti Malaysia Kelantan  
Kota Bharu, Kelantan, Malaysia  
zulkarnaen.k@umk.edu.my

Wan Safra Diyana Wan Abdul Ghani  
Faculty of Creative Technology and  
Heritage  
Universiti Malaysia Kelantan  
Bachok, Kelantan, Malaysia  
wsdiyana@gmail.com

Khairul Azhar Mat Daud  
Faculty of Creative Technology and  
Heritage  
Universiti Malaysia Kelantan  
Bachok, Kelantan, Malaysia  
azhar.md@umk.edu.my

**Abstract**— Cloud-based m-retail application is commonly used by internet retailers and cyberpreneurs for conducting online business operations. The emergence of third-party e-commerce platforms along with incentives from Malaysian government has easily enabled the utilization of mobile marketplace app among both Malaysian sellers and customers. As m-retail has just started to gain attention in Malaysia, more works must be done to overcome the academic research limitations in terms of technological and non-technological perspectives. Meanwhile, textile and apparel products are among the most popular to be sold via the internet in addition to the growing number of related businesses. The uses of latest technology such as cloud-based mobile-retail application may help business owners to sustain for business survival. In designing a mobile applications for specific users, a thorough investigation must be performed. A conceptual framework of the apps might be helpful in providing a general overview of required elements for developing a successful mobile-retail applications. Extensive literature reviews, qualitative analysis, interviews and questionnaires have been conducted in designing and validating the proposed framework. The analysis results shows mean values from the survey are  $> 3.5$  for the core element variables in this research. Thus, the statistical analysis validation results indicates the importance of the element as the fundamental component for the proposed framework. Therefore, this paper intends to propose a conceptual framework of cloud-based mobile-retail application specifically to be used by textile cyberpreneurs which might be helpful for related key players.

**Keywords**— *mobile retail; mobile application; cloud-based mobile application; textile cyberpreneurship; conceptual framework.*

## I. INTRODUCTION

Internet retailers are facing new challenges in conducting business nowadays. Apart from using common websites to sell their products, they are now given a few other choices of retail platforms to engage with potential customers. As mobile devices are greatly used nowadays for multiple purposes, the internet retailers must take advantages of this phenomenon to expand their business opportunities and engage in mobile retail (m-retail) activities. Textile and apparel products are among the most popular to be sold in Malaysia via the internet [1]. Some of the well-known textile brands have managed to create their own mobile applications for selling purpose while some others have utilized the existing mobile marketplace applications that are provided by third-party electronic commerce (e-commerce) merchants. The basic functionality of these applications or apps is to enable the sellers to promote and sell their products, while

the customer may use them to search and buy the required items from the seller.

In Malaysia, the e-commerce and mobile commerce (m-commerce) technologies have always been encouraged to be scrutinized and utilized by Malaysian entrepreneurs. Malaysian government has offered various incentives that are related to empower the usage of latest information and communication technologies (ICT) among businesses which include e-commerce and digital entrepreneurship industries [2]. The microentrepreneurs and small and medium enterprises (SME) are also invited to embark into the state-of-the-art technology utilization in targeting for business growth through several programmes such as eUsahawan [3], eRezeki [4] and SME Cloud Adoption [5]. Besides, the improvement of network infrastructure by telecommunication industries has enabled the internet retailing activities to flourish among Malaysians.

As the number of mobile devices users is increasing in Malaysia [6], the possibility for the users to shop or sell by using mobile devices is somewhat high. Moreover, the existence of social media has indirectly promulgated the chances to conduct internet retailing among individuals and businesses. Social media is a powerful marketing tool [7] and very common to be used by Malaysian retailers for online business purpose [8]. Whilst social media too have launched their own mobile apps, the m-retail activities might also escalate among mobile device users, be it customers or sellers. Along with the emergence of mobile marketplace apps and easy payment gateways, m-retail is a promising sector with a lot of opportunities for businesses.

Nonetheless, academic researches about m-retail or mobile shopping (m-shopping) are quite limited in Malaysia [9][10]. This may happen as a result from the e-commerce and m-commerce statuses which had only started to rise recently [11]. In order to accelerate the adoption of e-commerce among businesses, Malaysian government had introduced National eCommerce Strategic Roadmap [11] that emphasized the importance of technology utilization for economic growth. Generally, for a technology to be utilized by business owners or personnel, their needs must be identified and aligned with the business tasks that will be performed via the technology. If the technology or application is usable and helpful in fulfilling their needs, the chance to use it is higher. Hence, a thorough investigation must be conducted to understand the needs of business owners before developing a specific mobile app that can enable m-retail activities. For any information system (IS) or application to be practically implemented, a conceptual view or framework of the app shall be created as a reference to

smoothen the development process. Therefore, this paper intends to present a general conceptual framework of mobile retail application that employs cloud technology specifically for Malaysian textile e-commerce entrepreneurs or cyberpreneurs.

## II. CLOUD-BASED M-RETAIL APPLICATION

### A. Mobile Cloud Computing

Mobile cloud computing is a paradigm that combines both traits of mobile computing and cloud computing into its operations [12]. Mobile computing emerges to support the existence of mobile devices that can be used for communication purposes and information retrievals nowadays. The functionality of mobile devices has expanded aligned with the requirements of users who are always on-the-go and needs to be connected to the Internet. Several major changes have been done in mobile device designs to accommodate current user's activities in terms of screen size, input mechanisms, quality of camera and other smartphone features. The device is becoming more sophisticated day by day to enhance the user's experience while utilizing the technology. As mobile computing provides underlying technology for wireless data transmission by mobile device such as smartphones and tablets, the performance of mobile devices is still unquestionably deficient in terms of battery consumption, limited memory and storage capacity. If an application continuously runs on the mobile device, it is possible for the performance to drop significantly due to its limitations. Hence, to overcome this issue, cloud computing might be the proper solution in which the previous heavy loads that were encountered by mobile devices are now transferred to the cloud for processing. With this, the performance of mobile devices can be improved whilst the cloud takeovers the duties.

Cloud services are commonly offered via software as a service (SaaS), platform as a service (PaaS) and infrastructure as a service (IaaS). The business owners will be attracted to use cloud due to several reasons. First, by using cloud, they do not have to worry about storing a physical server since the cloud is managed by service providers. Second, the fees of cloud are charged according to pay-per-use basis [13], thus reducing the operational cost. Next, the cloud is scalable and flexible to expansion or reduction wherein is convenient for business owners who are likely to expand their businesses and need a bigger cloud size in the future. In all, coupled with traits of mobile computing, the benefits of mobile cloud computing will be advantageous to business owners and mobile device users as shown in Table 1.

### B. Mobile-Retail Application

A mobile application or a mobile app is usually installed on a mobile device to operate with specific functionalities. It is normally built and classified as either native app or hybrid app based on the choice of development team.

For m-retail application, the basic role of the app is to enable mobile retail transactions to be performed by the user. The business owners may encounter several options to utilize m-retail app for their businesses. They may choose to develop their own m-retail app or simply use the existing mobile marketplace apps that are offered by third-party e-

commerce merchants such as Lazada, Zalora, Shopee, Carousell and eBay. Currently, these apps are normally operated by utilizing cloud-based services for better performance on service provider's site. M-retail apps can be downloaded via Google PlayStore or Apple iOS for free and can also be used by both sellers and customers. Nevertheless the operational functionalities of apps for sellers are normally more complex than the apps for customers. This is because the sellers have to fulfill tasks such as managing customer orders, updating inventory and sometimes analyzing sales through the app. On the other hand, the customers may only place orders and view order status by using the app apart from updating user account information.

TABLE I. BENEFITS OF MOBILE CLOUD COMPUTING [14]

Benefits of Mobile Computing	Benefits of Cloud Computing
<u>Mobility</u> The user can perform tasks anywhere via the use of mobile device and network connection	<u>Accessibility</u> The data can be accessed by the user anytime and anywhere through network connection
<u>Time saving</u> Tasks can be conducted whenever the user is connected via network	<u>Storage capacity</u> The cloud can store huge data more than a personal computer
<u>Convenience</u> The mobile device user can perform various online activities regardless of time and location	<u>Data protection</u> The data is safely stored in cloud with disaster backup recovery services
	<u>Scalability</u> The cloud can be expanded according to the requirements of user
	<u>Eco-friendly</u> Only necessary resources are utilized for processing, thus saving the energy

## III. TEXTILE CYBERPRENEURSHIP

In Malaysia, textile industry has been ranked as 10th major export contributors in 2015 [15], thus making it as one of the most profitable sectors for the country. Aligned with the growth of fashion or apparel sectors since Second Malaysia Plan (1971-1975), many entrepreneurs from small to big enterprises have taken opportunities in venturing into the industry whilst contributing for the country's economy. Moreover, the advancements of technology nowadays have easily boosted the sales of apparels and garment products in Malaysia, especially via internet retailing. According to Euromonitor [16], the Malaysian clothing and footwear specialist retailers alone had gained RM 13,923 million of sales in 2012 with 20.69% contribution from overall non-grocery retailers. These impressive numbers have indicated the strong outlook of textile and fashion industry in retail sector. Nonetheless, competitions between fashion brands are very tough in this dynamic industry. Some have been very successful while some have not, thus quitting from the businesses. For the remaining survivors, it is essential to strategize the long-term plan by taking homage of trading opportunities via various state-of-the-art technologies such as e-commerce, m-commerce and cloud-based services. Nowadays, textile internet entrepreneurs or cyberpreneurs are using multiple selling channels for their online businesses. This includes social media platforms, websites, e-commerce merchants' channels and m-retail apps.

#### IV. METHODOLOGY

In order to develop any IS or application, a proper plan with a thorough analysis must be conducted to ensure the usability and success of the application. The traits of every required element must be defined. For this study, the theoretical definition of IS is used as a major reference. One of the accepted definition of information system is "...a computer system that stores data and supplies information, usually within a business context. Information systems often rely on databases. A system of people, procedures, and equipment, for collecting, manipulating, retrieving, and reporting data". [17]. A mobile app can be considered as an IS but is supported by different technologies and environment unlike web or desktop applications. Still, the major components to make an app are similar to other systems which are people, technology and procedures. Based on these elements, the basis of conceptual framework is developed and then elaborated based on several related theories, models or concepts. Figure 1 illustrates an overview research methodology for this study.

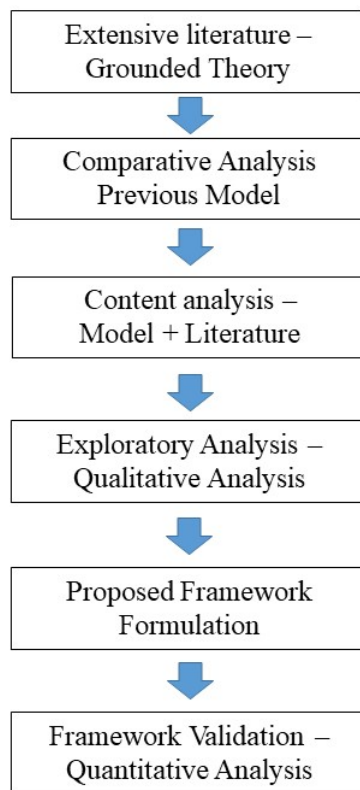


Fig. 1. Conceptual Framework of Cloud-Based M-Retail Application for Textile Cyberpreneurs

Extensive literature reviews were also performed to understand the background of study. By following methods suggested by Doherty and Ellis-Chadwick [18], a collection of related articles, documents from official websites of Malaysian government authorities and other reliable sources was collected and analyzed to suit with the study context. Previous works that are related to conceptual framework development for mobile application were also studied. Keywords like "mobile retail", "mobile shopping", "mobile application framework" and "textile industry" were used for

searching purpose. Content analysis was then conducted by using coding method in which the selected documents were segregated based on code. The unrelated articles or documents were put aside from further analysis.

In understanding the tasks that are normally performed by textile cyberpreneurs, interviews with three textile cyberpreneurs were conducted. Several questions that are related to activities of textile cyberpreneurs for managing their online businesses were asked. Their profiles and background were also inquired. The recorded data was then analyzed and six finalized characteristics of task have been identified as "ubiquitous sales order management, customer information management, product information management, payment information management, sales orders analysis and fashion trends forecasting" [19]. These activities are expected to be conducted by textile cyberpreneurs while using the m-retail application.

For deeper knowledge on technology elements, interviews with three experts or practitioners on mobile cloud technology have been performed and discussed. Based on the data analysis, it can be concluded that four major characteristics of cloud-based m-retail application are "ubiquitous services, reliable services, facilitating resources improvement and scalable services". [19]

The results from review of literatures, exploratory and qualitative data analyses were merged for the purpose of developing a conceptual framework. For validating the proposed framework, quantitative method is used by distributing questionnaires to textile cyberpreneurs.

A unique data collection instrument were develop in order to validate the proposed framework. 600 set of questionnaires were distribute to various industries players, cyberpreneurs and online cyber communities to validate the component of the proposed framework.

#### V. PROPOSED CONCEPTUAL FRAMEWORK

The conceptual framework encompasses interrelated IS elements that could make a successful cloud-based mobile application, especially for textile cyberpreneurs in managing internet retail transactions. The retail management tasks which are going to be conducted by textile cyberpreneurs must be supported by several elements, particularly human elements, technology elements and application quality elements as illustrated in Fig. 2.

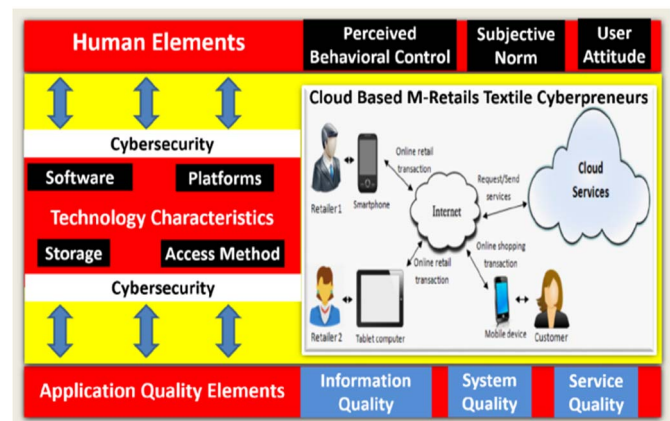


Fig. 2. Conceptual Framework of Cloud-Based M-Retail Application for Textile Cyberpreneurs



The human elements are derived from Theory of Planned Behavior (TPB) [20] that emphasizes human behavior as predictors for technology adoption. Thus, perceived behavioral control, subjective norms and user's attitude shall be examined. TPB has been widely used in many researches on studying the relationships between human beliefs, intention and action in various purposes. For an app to be successfully utilized, the role of people is very important. Hence, human traits must be analyzed and understood.

Meanwhile, the application quality elements are derived from Information System Success (ISS) model [21] that posits quality as essential to ensure technology utilization. DeLone and McLean [21] had suggested the quality dimensions to be investigated are system, information and service qualities. From the perspective of a system developer, quality shall be the upmost priority in delivering any system or application. By promoting quality traits and interesting up-to-date features like artificial intelligence (AI) mechanisms in an app, the user experience while using the app will be enhanced, thus gaining trusts from the user and potential users.

As intermediary between human and application quality elements, technology elements that consist of software, platforms, storages and access methods must be enabled for smooth transactions. The technology must then be supported by cybersecurity elements [22] to warrant secure data transactions which is very crucial for internet retail. Confidentiality, integrity and availability are among the vital elements of security that must be implemented. Since mobile cloud technology is relatively new, several issues regarding security [23] have always been discussed and raised up in many academic researches. Besides, the limitations of mobile devices such as restricted screen size, battery performance, storage capacity and limited memory shall be also taken into consideration.

In all, the conceptual framework is managed to illustrate a holistic view of important elements and required details for designing a cloud-based mobile application which is to be used by textile cyberpreneurs in managing their online business transactions. The framework may be used as a reference by major players of cloud-based m-retail application industry such as service providers, application developers and marketers for better comprehension of the app elements.

## VI. FRAMEWORK VALIDATION

600 questionnaires were distributed via face-to-face and e-mail invitations to selected textile cyberpreneurs who have either participated at several online businesses festivals or have been listed in the directory of Perbadanan Usahawan Nasional Berhad (PUNB). 411 questionnaires were returned but only 348 were usable for data analysis after the process of removing outliers and missing data. Table II summarise the demographic descriptive analysis results for the validation of the framework through statistical empirical analysis.

TABLE II. DEMOGRAPHIC DESCRIPTIVE ANALYSIS RESULTS

Characteristics	Demographics Profiles	Percentage
Gender	Male	15.5 %
	Female	84.5 %
Ethnicity	Malay	84.5 %

Characteristics	Demographics Profiles	Percentage
	Chinese	6.9 %
	Indian	4.3 %
	Others	4.3 %
Age	20 or less	12.9 %
	21 – 25	33.9 %
	26 – 30	21.0 %
	31 – 35	15.5 %
	36 – 40	11.2 %
	41 and above	5.5 %
Textile products	Clothes	89.7 %
	Carpets	4.9 %
	Curtains	5.2 %
	Bedclothes	4.9 %
	Table spreads	4.3 %
	Others	7.2 %
Mobile device type to conduct online business	Smartphone	90.2 %
	Tablet Computer	38.8 %
	Others	2.9 %
Website to conduct online business	Yes	56.6 %
	No	43.4 %
Social media channels to conduct online business	Facebook	87.1 %
	Twitter	14.4 %
	Instagram	71.0 %
	WhatsApp	61.2 %
	WeChat	33.9 %
	Others	1.1 %
	Not using any	3.7 %
Knowledge on cloud-based m-retail application	Heard about it	87.9 %
	Use it	47.1 %
Possess own version of cloud-based m-retail application	Yes	16.1 %
	No	83.9 %

The textile products that are mostly sold by respondents are clothes (89.7%), followed by other than listed textile products (7.2%), curtains (5.2%), bedclothes (4.9%), carpets (4.9%) and table spreads (4.3%). In terms of devices that are utilized for online retail, 314 respondents use smartphones (90.2%), 135 use tablet computers (38.8%) while the remaining 10 use other types of mobile device (2.9%). More than half (56.6%) of respondents possess their own websites for their business while the remaining (43.4%) do not. The finding also shows that social media has been used by respondents for their online retail where 87.1% use Facebook, 71% use Instagram, 61.2 % use WhatsApp, 33.9% use WeChat, 14.4% use Twitter and 1.1% use other platforms. Only 3.7% of respondents do not use any social media platforms for their businesses. The low adoption issue of cloud-based m-retail application among Malaysian textile cyberpreneurs has been acknowledged via the demographic data where only 47.1% has utilized the application and only 16.1% have their own version of mobile app.

From the developed framework, the tested variables were the elements of human, procedure and application quality that consist of user attitude, perceived behavioral control, subjective norm, task characteristics, technology characteristics, information quality, system quality and service quality. On the other hand, the elements of cybersecurity were not tested due to technical aspects of framework which are not suitable to be investigated from textile cyberpreneurs. It is assumed the security mechanisms are crucial to be implemented with no compromises.

In measuring the variables, five-point Likert scale was used where 1 = strongly disagree and 5 = strongly agree. Most of the questionnaire items were adapted from the previous relevant studies as shown in Table III. Only items for task characteristics and technology characteristics were

newly developed based on the earlier interview results with experts and real-life practitioners.

The reliability of items for each construct was measured by determining the value of Cronbach's Alpha. All variables have been found to exceed 0.85, which are good enough based on the recommendation by Nunnally and Bernstein [28]. The specific reliability result for each variable is shown in Table IV.

In order to examine the agreements of respondents, the mean value for each variable is determined. It has been found that the mean value for the variables were ranging from 3.58 to 4.17 as presented in Table V. From the perspectives of textile cyberpreneurs, the user's attitude and task characteristics are the most important elements from the framework. Both variables have shared the highest mean value of 4.17. Meanwhile, information quality has been ranked the lowest with mean value of 3.58. Nonetheless, all values have shown the inclination towards the agreement as they have approached the value of 4. In all, the elements from the proposed conceptual framework are proven to be essential from the perspective of textile cyberpreneurs.

TABLE III. QUESTIONNAIRE ITEMS AND CORRESPONDING REFERENCES

Variable	No. of items	References
Attitude	5	[24] [25]
Subjective norm	5	[25]
Perceived behavioral control	4	[26]
System quality	5	[27]
Information quality	5	[27]
Service quality	4	[27]
Task characteristics	6	Newly developed
Technology characteristics	4	Newly developed

TABLE IV. RELIABILITY TEST RESULT

Variable	No. of items	Cronbach's Alpha
Attitude	5	0.950
Subjective norm	5	0.946
Perceived behavioral control	4	0.902
System quality	5	0.962
Information quality	6	0.979
Service quality	4	0.970
Task characteristics	6	0.940
Technology characteristics	4	0.862

TABLE V. MEAN VALUES AND RANK OF VARIABLE

Variable	No. of items	Mean	Rank
Attitude	5	4.17	1
Subjective norm	5	3.90	5
Perceived behavioral control	4	3.74	7
System quality	5	4.08	3
Information quality	5	3.58	8
Service quality	4	3.82	6
Task characteristics	6	4.17	2
Technology characteristics	4	3.97	4

## VII. CONCLUSION

The proposed conceptual framework can be served as a guideline in understanding the requirements to develop a mobile cloud application specifically for textile cyberpreneurs. As retail transactions can be done via mobile devices nowadays, the essential elements that must be looked

upon are included in the framework to illustrate a holistic viewpoint which is required by service providers and application developers. However, the framework is still in preliminary stage. Therefore, more works must be conducted to assess the framework's feasibility in the future especially in assessing the technical aspects of the application. Furthermore, a mobile app prototype shall be developed based on the proposed framework to examine and validate its usability among the textile cyberpreneurs through case study.

## ACKNOWLEDGMENT

This paper is prepared under Malaysian Ministry of Higher Education's FRGS Grant Nos. R/FRGS/A02.00/01167A/002/2015/000294 and MyBrain15 MyPhD scholarship. Special thanks to all research team for giving full support to this research project.

## REFERENCES

- [1] Goi C-H. M-Commerce: Perception of Consumers in Malaysia. *Journal of Internet Banking and Commerce*, 21:S5, pp. 1-11, 2016.
- [2] Malaysia Digital Economy Corporation. Building An Inclusive Digital Future. Available: <https://www.mdec.my/building-an-inclusive-digital-future>, 2017.
- [3] Malaysia Digital Economy Corporation. eUsahawan - Pemangkin Pendapatan Digital. Available: <https://eusahawan.mdec.my/eusahawan.html>, 2017.
- [4] Malaysia Digital Economy Corporation. eRezeki - Now everyone can benefit from the digital economy. Available: <https://erezeki.my/en/home/>, 2017.
- [5] Malaysia Digital Economy Corporation, Cloud Computing Adoption Programme. Available: [http://www.mscomalaysia.my/cloud\\_sme](http://www.mscomalaysia.my/cloud_sme), 2016.
- [6] Malaysian Communications and Multimedia Commission. Statistical Brief Number Seventeen Hand Phone Users Survey 2014, 2015.
- [7] Syed Ahmad S. F. and Murphy, J. Social Networking as a Marketing Tool: The Case of a Small Australian Company, *Journal of Hospitality Marketing & Management*, 19:7, pp. 700-716, 2010.
- [8] Hassan, S. Shiratuddin, N., Hashim, N. L., Ab Salam, S. N. and Sajat, M. S. Social Media as Persuasive Technology for Business: Trends, and Perceived Impact in Malaysia. Available: [http://www.skmm.gov.my/skmmgovmy/media/General/pdf/SocialMedia\\_in\\_Biz\\_UUM\\_SKMM.pdf](http://www.skmm.gov.my/skmmgovmy/media/General/pdf/SocialMedia_in_Biz_UUM_SKMM.pdf), 2016.
- [9] Wong, C. H., Lee, H. S., Lim, Y. H., Chua, B. H., Chai, B. H. and Tan, G. W-H. Predicting the consumers' intention to adopt mobile shopping: an emerging market perspective, *International Journal of Network and Mobile Technologies*, Vol. 3 No. 4, pp. 24-39, 2012.
- [10] Wong, C. H., Tan, G. W-H., Ooi, K-B. and Lin, B. Mobile shopping: The next frontier of the shopping industry? An emerging market perspective, *International Journal of Mobile Communications*, Vol 13, Issue 1, pp. 92-112.
- [11] Ministry of International Trade and Industry. NATIONAL eCOMMERCE COUNCIL (NeCC). 2015. Available: <http://www.miti.gov.my/index.php/pages/view/3071?mid=409>, 2015.
- [12] Khan, A. U. R., Othman, M. and Madani, S. S. A Survey of Mobile Cloud Computing Application Models, *IEEE Communications Surveys & Tutorials*, Vol. 16, No. 1, pp. 393-413, 2014.
- [13] Prasad, M. R., Gyani, J. and Murti, P. R. K. Mobile Cloud Computing: Implications and Challenges, *Journal of Information Engineering and Applications*, Vol. 2, No. 7, pp. 7-15, 2012.
- [14] Ghani, W. S. D. W. A., Khidzir, N. Z., Guan, T. S. and Daud, K. A. M. Enterprise Mobile Cloud Application for Textile Cyberpreneurs : Big Data Issues , Challenges and Opportunities Enterprise Mobile Cloud Application for Textile Cyberpreneurs : Big Data Issues , Challenges and Opportunities, In *Proceeding of 9th International Conference on IT in Asia 2015 (CITA'15)*, pp. 38-41, 2015.
- [15] Malaysia External Trade Development Corporation. Textiles and Apparel. Available: <http://www.matrade.gov.my/en/foreign-buyers-section/69-industry-write-up--products/722-textiles-and-apparel>, 2016.

- [16] Euromonitor International. World Retail Data and Statistics 2014, 8th Edition, pp. 189-192, 2014.
- [17] Joshi, G. Information Technology for Retail, New Delhi, India: Oxford University Press, ch. 2, pp. 23-24, 2009.
- [18] Doherty, N. F. and Ellis-Chadwick, F. E. New perspectives in internet retailing: a review and strategic critique of the field, *International Journal of Retail & Distribution Management*, Vol. 34 Nos 4/5, pp. 411-428, 2006.
- [19] Khidzir, N. Z., Ghani, W. S. D. W. A. and Guan, T. T. Cloud-Based Mobile-Retail Application for Textile Cyberpreneurs : Task-Technology Fit Perspective Analysis, In *Proceedings of the International Conference on High Performance Compilation (HP3C-2017)*, Computing and Communications, pp. 65-70, 2017.
- [20] Ajzen, I. From intentions to actions: A theory of planned behaviour in J. K. (Eds.), & J. Beckman, *Action-control: From Cognition to Behavior*, Heidelberg: Springer, pp. 11-39, ch.2, 1985.
- [21] DeLone, W. H. and McLean, E. R. The DeLone and McLean model of information systems success: a ten-year update, *Journal of Management Information Systems*, Vol. 19, No. 4, pp. 90-30, 2003.
- [22] Khidzir, N. Z., Ismail, A. R., Daud, K. A. M., Ghani, M. S. A. A., Ismail, S. and Ibrahim, A. H. Human Factor of Online Social Media Cybersecurity Risk Impact on Critical National Information Infrastructure, Nicholson D. (eds) *Advances in Human Factors in Cybersecurity. Advances in Intelligent Systems and Computing*, vol 501. Springer, Cham, pp. 195-207, 2016.
- [23] Khan, A. N., Mat Kiah, M. L., Khan, S. U. and Madani, S. A. Towards secure mobile cloud computing: A survey, *Future Generation Computer Systems*, Vol. 29, Issue 5, pp. 1278-1299, 2014.
- [24] Al-Najjar, G. M. *Mobile Information Systems: An Empirical Analysis of the Determinants of Mobile Commerce Acceptance in Jordan*, Ph.D thesis, Universiti Utara Malaysia, 2012.
- [25] Md Nor, K. and Pearson, J. M. An Exploratory Study Into The Adoption of Internet Banking in a Developing Country: Malaysia. *Journal of Internet Commerce*; Vol. 7, No.1, pp. 29-73, DOI: 10.1080/15332860802004162 , 2008.
- [26] Shih, Y. Y and Fang, K. The use of a decomposed theory of planned behavior to study internet banking in Taiwan. *Int. Res.* Vol. 14, No. 3, pp. 213- 223, 2004.
- [27] Chen, L. Y. Determinants of m-shopping quality on customer satisfaction and purchase intentions: the IS success model perspective, *World Review of Entrepreneurship, Management and Sust. Development*, Vol. 9, No. 4, pp. 543 - 558, 2013.
- [28] Nunnally, J. C and Bernstein, I. H. *Psychometric Theory*. New York: McGraw Hill, 1994..

# Implementation of Winnowing Algorithm for Document Plagiarism Detection

1<sup>st</sup> Nurissaidah Ulinnuha

Department of Mathematics  
Universitas Islam Negeri Sunan Ampel  
Surabaya, Indonesia  
nuris.ulinnuha@uinsby.ac.id

2<sup>nd</sup> Muhammad Thohir

Department of Arabic Language  
Universitas Islam Negeri Sunan Ampel  
Surabaya, Indonesia  
muhammadthohir@uinsby.ac.id

3<sup>rd</sup> Dian Candra Rini Novitasari

Department of Mathematics  
Universitas Islam Negeri Sunan Ampel  
Surabaya, Indonesia  
diancrini@uinsby.ac.id

4<sup>th</sup> Ahmad Hanif Asyhar

Department of Mathematics  
Universitas Islam Negeri Sunan Ampel  
Surabaya, Indonesia  
hanif@uinsby.ac.id

5<sup>th</sup> Ahmad Zaenal Arifin

Department of Mathematics  
Universitas PGRI Ronggolawe  
Tuban, Indonesia  
az\_arifin@unirow.ac.id

**Abstract**— The rapid development of the internet influences information availability. It makes easier for someone to do the plagiarism of a work. The rise of information available online makes the habit of copy-paste without mentioning the reference to become easy so that scientific work unwittingly becomes the result of plagiarism from other scientific works. Plagiarism prevention efforts are involving in various sector. Designing and developing plagiarism checker applications is the purpose of this paper. Specifically by knowing the percentage of similarity between the original document and the test document. This research using Winnowing algorithm because it can detect plagiarism in documents up to sub-section of the document. This research using three validates consisting of computational mathematicians, software engineering experts, and users to test the application feasibility. The experiment uses several scenarios and the result of effectiveness evaluation yields 82% sensitivity, 100% specificity, and 91% accuracy. The implemented system works effectively so the system can be used to detect document plagiarism.

**Keywords**—Plagiarism Detection, Research and Development, Winnowing Algorithm.

## I. INTRODUCTION

The rapid development of information technology has an impact on the rapid dissemination of information. One example is the rapid development of the internet. This causes more and more information available and facilitates a person in making plagiarism [1][2][3]. The number of plagiarism cases by academics became a tragedy in Indonesia's education. The scientific work that made unconsciously becomes the result of plagiarism from other scientific works.

There are several online plagiarism checkers that used to detect plagiarism but are less effective considering the limitations of pages offered, such as Viper. According to Sunu [4], Viper only able to detect a maximum of 8 pages with long checks up to 20 minutes with good computer specifications and super fast internet connection. There is also Turnitin with a payment every year which is not cheap for university campuses in developing countries like Indonesia [5][6][7].

Plagiarism detection is actually a part of pattern recognition[8][9]. In this paper, the plagiarism detection application is built using Winnowing algorithm which is one part of the pattern recognition as a search algorithm for the same document. The system accepts inputs in the form of a text document with a .pdf or .txt extension and afterwards

search for resemblance to the document database. Documents with similarity levels exceeded the threshold will be displayed in the system. The input of the Winnowing algorithm is document string and output of the hash value used as the document fingerprint. According to Niwattanakul, et al [10]. Fingerprints of both documents are processed with Jaccard's coefficient similarity function to get a percentage of document similarity. Data used in this study is the big data in university digital library in one of Indonesian University.

Winnowing algorithm is used as an algorithm to calculate text similarity in a document because Winnowing algorithm can cut the processing time of large files by utilizing the rolling technique of the hashing process [3][11]. In addition, the value of Winnowing algorithm's similarity accuracy is not only influenced by the input value of k-gram, but it is also influenced by the input window value that serves to separate the hash results on each gram.

This research aims to design and develop plagiarism detection application and to know the percentage of similarity between documents tested with Winnowing algorithm. In the end, plagiarism applications are expected to be used by many people.

## II. PRELIMINARIES

### A. Plagiarism

Plagiarism is an act of misappropriation, theft/robbery, publication, statement or declaring a person's own thoughts, writings or creations that the other person has intentionally or unintentionally without the reference [12].

Classification based on the proportion or percentage of words, sentences, hijacked paragraphs [13] divided into:

1. Minor plagiarism : < 30%
2. Medium plagiarism : 30-70%
3. Major plagiarism : > 70%

### B. Winnowing Algorithm

Winnowing Algorithm [11][14] is an algorithm used in plagiarism detection including similar small parts in many of documents. The input of this algorithm is a text document processed to produce an output of hash values collection called fingerprint. This fingerprint is used as the basis of comparison between text files that have been entered and used in plagiarism detection.

In general, the working principle of document resembling algorithm is described in Figure 1 :

- Remove whitespace insensitivity, such as spaces or punctuation.
- Forming a gram chain of size k.
- Calculating hash values of each gram.
- Divide into a particular window.
- Selecting some hash values into document fingerprinting.
- Determine the percentage of similarity between two documents with the Jaccard Coefficient equation

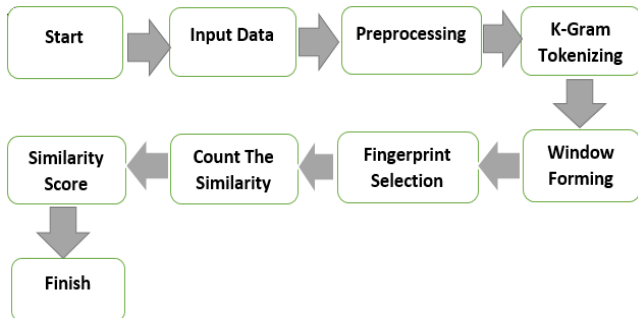


Figure 1. The Steps of Winnowing algorithm

The detailed steps of applying Winnowing algorithm are as follows [11] :

#### 1. Preprocessing

The preprocessing is done in two steps: first, eliminating irrelevant characters in text documents, such as punctuation marks, spaces and second, changing the capitalization. Example, a sentence is given:

"Penelitian ini menggunakan algoritma Winnowing."

After preprocessing, i.e. deleting spaces and punctuation marks, and converting all the letters into small and normal letters (not bold, not tilted and not underlined), resulting is in the following text:

Penelitianinimenggunakanalgoritmawinnowing

#### 2. K-gram Method

The K-gram method [15][16] is a method used in the process of tokenization or separation of text, by forming substring along the character k of a string. Example: Cut a string along k. The value of k is 7. From the above sentence example, the result obtained as Figure 2.

penelit	eneliti	nelitia	Elitian	Litiani	itianin	tianini
aninime	ninimen	inimeng	nimengg	imenggu	menggun	engguna
Ggunaka	gunakan	unakana	nakanal	Akanalg	kanalgo	analgor
Algorit	lgoritm	goritma	oritmaw	Ritmawi	itmawin	tmawinn
Awinnow	winnowi	innowin	nnowing			

Figure 2. The result k-gram with k=7

#### 3. Rolling Hash

The hash function [17] is a function that receives a string input of arbitrary length and converts it into a fixed length output string. The output of the hash function is called hash-value or message digest. Hash

value size generally smaller than the original string size.

The hash method equation is given by:

$$H(c_1c_2c_3) = c_1 * b^{k-1} + c_2 * b^{k-2} + \dots + c_{k-1} * b^1 + c_k \quad (1)$$

where:

c = value of ASCII characters (decimal)

b = basis (prime)

k = sum of character (character index)

The advantage of rolling hashes is for the next hash value. To get the hash value of the k-grams method, the following hash rolling equation is used:

$$H(c_2c_3c_4) = (H(c_1c_2c_3) - c_1 * b^{k-1}) * b + c_{k+1} \quad (2)$$

Using Equation (2) can save computational time when calculating the hash value of a gram. The result of calculating the hash value in gram is shown in Figure 3. Each number indicates the hash value of a gram.

119231	112854	117772	112856	117786	117272	122286	113275
110291	118844	116065	118663	115536	117083	112963	118109
113854	116411	124069	116436	108841	114495	109590	116736
109754	117232	115597	121649	122295	117677		123506
116937	112547	125607	116678	120502			

Figure 3. The result of hash calculation each gram

#### 4. Window Forming

The window is a grouping of several hash values with the specified size. From the window that has been formed, the smallest hash value on each window is selected to be the fingerprint of each document. The number 112854 is the smallest hash value of the window [119231, 112854, 117772, 112856, 117786].

The distance of fingerprint arrangement will be measured using the Jaccard coefficient with other fingerprint documents tested at a similarity level. The smaller the distance, the greater the level of similarity of the document.

#### 5. Fingerprint Document

The fingerprint is a technique that aims to prevent unauthorized copying of a digital content. Fingerprints are not easily detected because they are designed in ways that make digital content difficult to fabricate [18].

Document fingerprinting is a method that can be used to detect document resemblance. Winnowing algorithm uses a fingerprint as a keyword used as a reference to look for similarities with the document being tested. The hash value of the document is divided using window w before determining the fingerprint of both the original document and the test document.

#### 6. Jaccard Coefficient

Jaccard Coefficient is an equation used to find the degree of similarity between two text documents on Winnowing algorithm. This step is done by calculating the hash value and selecting the smallest fingerprint of two text documents[11]. The equation of Jaccard coefficient is given by:

$$Similaritas_{(d_i, d_j)} = \frac{|W(d_i) \cap W(d_j)|}{W(d_i) \cup W(d_j)} \quad (3)$$

where:

$W(d_i)$  = smallest fingerprint text document 1  
 $W(d_j)$  = smallest fingerprint text document 2

### III. RESEARCH METHOD

#### A. Development Model

This research is a type of Research and Development (R&D). The ways undertaken in this development study include several phases[19], i.e:

1. Formulating potentials and problem.
2. Collecting data from university digital library
3. Product design
4. Design validation
5. Revised product design
6. Usage trial of small group product
7. Product revision
8. Usage trial of large group product
9. Product revision
10. Mass production

#### B. Trial and Evaluation Product

The trial and evaluation product is intended to collect the data used as a basis for determining the effectiveness and attractiveness of the developed plagiarism detection application. Data obtained from trials are used to refine and enhance plagiarism detection applications. The trial will test the quality of the applications empirically.

##### a. Trial and Evaluation Design

The trial and evaluation design intended to get feedback directly from the user about the product quality being developed. Prior to testing, first create a design or draft application design that will be developed. First, the design of the application discussed in a Focus Group Discussion (FGD) with people who are considered experts and have competency in the field of computational mathematics and in the field of software engineering. After the application design as FGD results are completed, the next step is the implementation of the program which then through the process of consulting with computer programming experts. The results of consultation with computer programming experts is a product revision. The next phase is usage trials of a large group of university lecturer as a user application. Trials aim to improve the product so that when developed or used, the product has been completely valid and has a certain quality.

##### b. Subject Test

A subject test is a group of academic lecturers. The first phase is small group trials with two lecturers research subjects with areas of computational mathematics expertise and in the field of software engineering. The second phase is large group trials with 19 lecturers.

##### c. Type of Data

The data collected in this study is:

- (1) Data on the process of developing plagiarism detection applications in accordance with predetermined development procedures, including data containing input from computational mathematicians and software engineering experts.
- (2) Application feasibility data based on the assessment results. The data includes:
  - (a) Qualitative data: the value of each assessment criteria.
  - (b) Quantitative data: assessment score.

##### d. Data Collection Instruments

###### (1) Assessment of Small Group Test

In computational mathematics instruments, the components used are effectiveness, correctness, termination, efficiency, and complexity as shown in Table 1. In the instruments of software engineering experts, good application criteria can be reviewed from components of application compatibility, feature completeness, and application display as shown in Table 2.

TABLE 1. GUIDANCE INSTRUMENT EXPERT OF COMPUTATION MATH

No	Aspect of Assessment	Point of Instrument	Number of Point
1	Effectiveness	1, 2, 3	3
2	Correctness	4	1
3	Termination	5	1
4	Efficiency	6	1
5	Complexity	7, 8	2

Data obtained from computational mathematicians and software engineers assessment in the form of numbers. The number converted into qualitative data based on the scoring of results. The media score was analyzed by searching for average ratings. The questionnaire instruments were arranged using a Likert scale with a rating scale of 1 to 5.

TABLE 2. GUIDANCE INSTRUMENT SOFTWARE ENGINEERING EXPERT

No	Aspect of assessment	Point of Instrument	Number of Point
1	Corresponding	1, 2, 3, 4, 5	5
2	Feature Completeness	6,7,8,9,10,11,12	7
3	Display	13,14,15,16,17, 18,19,20,21	9

###### (2) Assessment of Large Group Test

Another name of the instrument for application feasibility is called usability evaluation. Usability evaluation aims to find out how well the application can be operated by the user. The first step in the evaluation of usability is to give tasks to the user while interacting with the system being tested. After all tasks have been completed by the user, the next step is to give a questionnaire containing questions that represent the five aspects of usability.

Questionnaires containing questions that represent the five aspects of usability, namely ease of learning (learnability), memorability, efficiency, errors, and



satisfaction[20] as shown in Table 3. The learnability aspect is an aspect that measures the ease of the user performing simple tasks when first using the application. Memorability aspect is done to measure the speed of the user in remembering the design and function of the application. The aspect of efficiency is used to measure the speed of the user in the work of a task. Errors aspect is used to see the possibility of user error. Satisfaction is an aspect that measures the level of user satisfaction in using the application.

TABLE 3. GUIDANCE INSTRUMENT OF ASSESSMENT FOR ASPECT USABILITY

No	Aspect of assessment	Point of Instrument	Number of Point
1	Learnability	1, 2, 3	3
2	Efficiency	4, 5, 6, 7	4
3	Memorability	8,9,10,11,12	5
4	Errors	13, 14, 15, 16, 17, 18, 19, 20	8
5	Satisfaction	21,22,23	3

TABLE 4. GUIDELINES

Qualitative Data	Score
SS (Strongly Agree)	5
S (Agree)	4
CS (Quite Agree)	3
TS (Not Agree)	2
STS (Strongly Disagree)	1

The questionnaire has 23 questions that have represented the five aspects of usability given to the respondents.

#### e. Data Analysis Technique

This research uses descriptive analysis according to the development procedure performed. The first phase of development is done by collecting the reference material plagiarism system. The next step is designing and manufacturing the application followed by small group test for input suggestion improvement for the application. The last phase is a user's feasibility rating.

Analytical steps to determine the application feasibility is done as follows:

1. Change the assessment in qualitative form to quantitative with the provisions in Table 4
2. Calculating the score per item question using the formula:

$$\text{score} = \frac{1 \cdot n_{STS} + 2 \cdot n_{TS} + 3 \cdot n_{CS} + 4 \cdot n_{S} + 5 \cdot n_{SS}}{n} \quad (4)$$

Where:

- $n_{SS}$  = the number of respondents strongly agree
- $n_{S}$  = the number of respondents answered agree
- $n_{CS}$  = the number of respondents answered quite agree
- $n_{TS}$  = the number of respondents answered disagree
- $n_{STS}$  = the number of respondents answered strongly disagree

$n$  = the number of respondents.

3. Calculate the average score using the average score formula =  $\frac{\sum x}{N}$ , where  $\sum x$  = the total score of all questions and  $N$  is the number of respondents
4. Change the average score to a qualitative score with the assessment criteria in Table 5.

TABLE 5. CLASSIFICATION OF WITNESSES CONCLUSIONS OF USABILITY EVALUATION RESULT

Value	Conclusion
0% - 20%	Strongly disagree that the application is very easy to understand and understand
21% - 40%	Do not agree that the application is very easy to understand and understand
41% - 60%	Simply agree that the application is very easy to understand and understand
61% - 80%	Agreed that the application is very easy to understand and understand
81% - 100%	Strongly agree that the application is very easy to understand and understand

## IV. RESULT OF DEVELOPMENT

### A. User Interface

In the main application view, there are two main menus namely Data Input menu and Process menu. There are two options for input user document data. The first option copies the text from the input document. The next step, click the Plagiarism Detection button. When any document in the database document has similarity level above the threshold, i.e. 30%, the system will switch from the Input Data menu to the Process menu. However, if the similarity of the input document is below the threshold, a dialog message will appear stating that no database document is similar to the input document.

On the Process menu page, list of the similar document will be shown. On this page, documents have been sorted in descending order based on similarity level. The smaller the value of the similarity level, the more different the two documents. The Process menu page is shown in Figure 4.

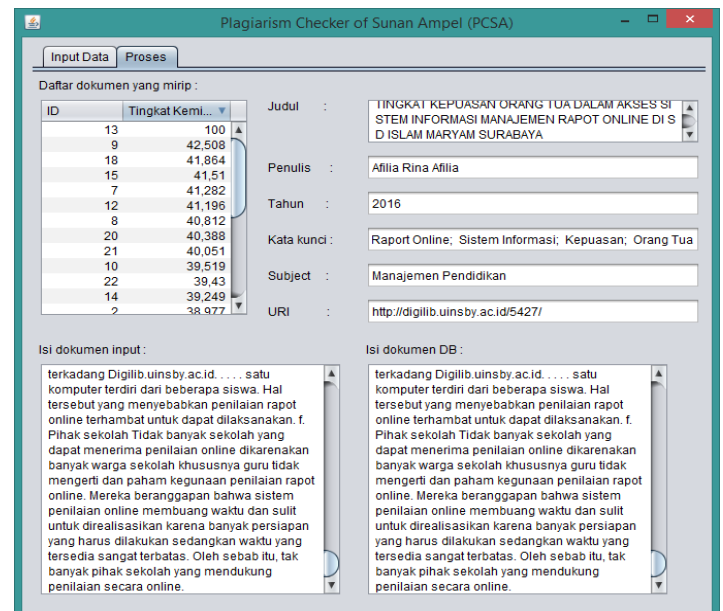


Figure 4. Display of Process menu page

### B. Presentation of Product Test Result Data

#### a) Validation of computational mathematics experts

The instrument for validating algorithm consists of 8 questions. Comments and suggestions obtained from computational mathematicians validation serve as a basis for improving the

efficiency of the algorithm before the application is tested to the user. A scoring diagram per aspect by a computational mathematician is shown in Figure 5.

The maximum score of the overall ideal answer is 40, whereas the computational mathematician assigns 34. The results obtained from the computation mathematician's validation questionnaire are 85% with the description that the application's algorithm eligible for use with slight revisions. Based on the eligibility criteria, Winnowing algorithm that applied to the plagiarism detection application is valid and feasible to use. However, there are several revisions needed to improve the efficiency of the algorithm.

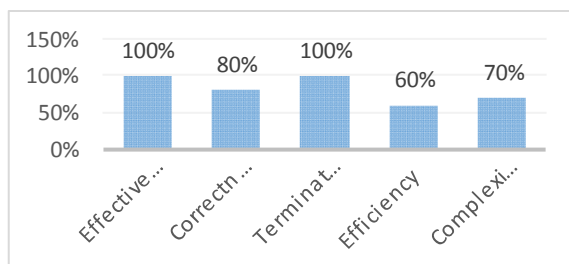


Figure 5. Application appraisal diagram of a computational mathematician

#### b) Validation of Software Engineering Expert

Data validation test results of software engineering experts obtained from two experts in the field of software engineering. Comments and suggestions that obtained from software engineering experts will be the base to improve application performance before application are tested to users.

The result of calculation for the whole item question is 86,67%. Based on the eligibility criteria, the application is reviewed from application compliance, feature completeness, and display. The result shows that application included invalid qualification and eligible to use. However, there are several revisions needed to improve application performance.

#### c) User Validation

User trials are conducted after obtaining valid results against trials that have been done by computational mathematicians and software engineering experts. Diagrams showing user ratings by aspect. From the assessment of large group trial data, it can be seen that the average aspect assessment is 92.27%. Based on the eligibility criteria, the plagiarism detection application included in the qualification is valid and feasible to use.

#### C. Presentation of Data Testing

The purpose of testing to ensure whether the application is built in accordance with the analysis and design done so that the desired goal is achieved. Based on the results of system testing, it can be deduced that functionally, the system can produce the expected output. To summarize the

process, the input document involved is an abstract document.

Table 6 describes the application successfully through the testing phase. Applications can detect the resemblance of test documents derived from database documents with full 100% resemblance scores. Applications can detect the resemblance of test documents whose contents come from some of the contents of the database document. The application can detect the resemblance of test documents whose contents come from database documents even though there are grammatical changes. Applications can accurately detect the resemblance of test documents that are composite content from two database documents.

TABLE 6. SUMMARY OF OUTPUT TESTING DOCUMENTS

No	Type of Test	Level of Change	Result
A	<b>System Test</b>	-	100%
B.	<b>Result Test</b>		
1	Full abstract	100%	100%
2	Partially abstract	40%	41%
		60%	59%
		80%	78%
3	Abstract grammar changes	40% modified grammar and 60% content	61%
		60% modified grammar and 40% content	47%
		80% modified grammar and 20% content	36%
4	Combined abstract	60% abstract 1 40% abstract 2	49% abstract 1 40% abstract 2
		40% abstract 1 60% abstract 2	40% abstract 1 48% abstract 2

Detection of similarity testing by manipulating the document through several scenarios ranging from 100% to 20% similarity level, generating a similarity level of documents of 90.12%. The application can detect the resemblance of test documents whose contents come from the database document despite any grammatical changes. Applications can accurately detect the resemblance of test documents that are composite content from two database documents.

#### D. Measuring Effectiveness

Winnowing method was tested on 100 abstract documents. 50 of the 100 abstract documents are plagiarized in different ways such as simple copy paste, altering some terms with synonyms and altering sentence structure (paraphrase) from a repository document. To mention the plagiarized document, given a limit of 30%. Therefore, if the similarity level between the two documents is more than 30%, then the system considers the input document as a plagiarized document.

To evaluate the effectiveness of the implemented system, three common parameters were used for testing: sensitivity, specificity, and accuracy.

$$\text{Sensitivity} = \frac{TP}{TP+FN}$$

$$\text{Specificity} = \frac{TN}{FP+TN}$$

$$\text{Accuracy} = \frac{TP+TN}{TP+FP+FN+TN}$$

Where :

- True Positive (TP) : the documents which are copied and are recognized as copies
- False Positive (FP) : the documents which are not copied but are recognized as copies
- False Negative (FN) : the documents which are copied but are recognized as the originals
- True Negative (TN) : the documents which are not copied and are recognized as the originals

TABLE 7. PERFORMANCE EVALUATION OF WINNOWER ALGORITHM

	Sensitivity	Specificity	Accuracy
Winnower algorithm	82%	100%	91%

Results of performance evaluation of Winnower algorithm shown in Table 7. Sensitivity score is 82%, which means the system ability to detect plagiarism to give a positive result for plagiarism document of 82%. The specificity score is 100%, which means the system ability to perform plagiarism detection to give negative results on the document is not plagiarism of 100%. The accuracy score is 91%, which means the system's ability to correctly detect all documents tested by 91%. It means that the implemented system detects copy paste, synonym replacement and active to passive active conversion with good performance.

## V. CONCLUSION

This application can be used and developed to detect document plagiarism, especially scientific papers. Application development conducted several tests, that is: (1) Tests conducted by computational mathematicians obtain a feasibility level of 85%. (2) Tests conducted by software engineering experts obtain a feasibility level of 86.67%. (3) Tests conducted by the user obtain a feasibility level of 92.27%. (4) The test results are similarities with several engineering scenarios tested with Winnower algorithm of 90.12%. (5) The document plagiarism detection system using Winnower algorithm yields 82% sensitivity, 100% specificity, and 91% accuracy. The system works effectively so it can be used to detect document plagiarism.

## ACKNOWLEDGMENTS

The authors are grateful to the Ministry of Religious Affairs of the Republic of Indonesia and Sunan Ampel State Islamic University for their support and cooperation.

## REFERENCES

- [1] R. V Smith, L. D. Densmore, and E. F. Lener, "Ethics and the Scientist," pp. 79–91, 2016.
- [2] S. Solarino, *Ethical Behavior in Relation to the Scholarly Community: A Discussion on Plagiarism*. Elsevier Inc., 2015.
- [3] R. Sutoyo, I. Ramadhani, and A. D. Ardiatma, "Detecting Documents Plagiarism using Winnower Algorithm and K-Gram Method," in *Cybernetics and Computational Intelligence (CyberneticsCom)*, 2017 IEEE International Conference on, 2017, pp. 67–72.
- [4] S. Wibirama, "Viper: cara mudah mendeteksi plagiarisme," 2013. [Online]. Available: <http://wibirama.staff.ugm.ac.id/2013/01/29/sunu-wibirama-viper-cara-mudah-mendeteksi-plagiarisme/>. [Accessed: 29-May-2018].
- [5] B. Marsh, "Turnitin . com and the scriptural enterprise of plagiarism detection," vol. 21, pp. 427–438, 2004.
- [6] G. P. V and J. D. Velásquez, "Engineering Applications of Artificial Intelligence Docode 5 : Building a real-world plagiarism detection system," *Eng. Appl. Artif. Intell.*, vol. 64, no. July 2016, pp. 261–270, 2017.
- [7] S. Vie, "A Pedagogy of Resistance Toward Plagiarism Detection Technologies," *Comput. Compos.*, vol. 30, no. 1, pp. 3–15, 2013.
- [8] S. Xie, M. Imani, E. R. Dougherty, and U. M. Braga-neto, "Nonstationary Linear Discriminant Analysis," pp. 161–165, 2017.
- [9] Q. Li, S. Authentication, and C. Technology, "Chapter 4 Non-Stationary Pattern Recognition," pp. 61–73, 2012.
- [10] S. Niwattanakul, J. Singthongchai, E. Naenudorn, and S. Wanapu, "Using of Jaccard Coefficient for Keywords Similarity," in *Proceedings of the International MultiConference of Engineers and Computer Scientists*, 2013, vol. I.
- [11] S. Schleimer, D. S. Wilkerson, A. Aiken, and U. C. Berkeley, "Winnower: Local Algorithms for Document Fingerprinting," 2003.
- [12] N. Kock and A. Chandra, "Dealing with Plagiarism in the Information Systems Plagiarism and Ways to Address Them," vol. 27, no. 4, 2003.
- [13] S. Sastroasmoro and A. Einstein, "Beberapa Catatan tentang Plagiarisme \*," pp. 239–244, 2007.
- [14] N. Elbegbayan, "Winnower, a Document Fingerprinting Algorithm." Linkoping University, pp. 1–7, 2005.
- [15] A. Putera *et al.*, "K-Gram As A Determinant Of Plagiarism Level In Rabin-Karp Algorithm," vol. 6, no. 07, 2017.
- [16] G. Myles, "k-gram Based Software Birthmarks," in *ACM Symposium on Applied Computing*, 2005, pp. 314–318.
- [17] Z. Fuyao, "A String Matching Algorithm Based on Efficient Hash Function." .
- [18] S. J. (Eds. H.C.A. van Tilborg, "Encyclopedia of Cryptography and Security," no. D, p. 838, 2011.
- [19] B. Metode, P. Kuantitatif, and K. Dan, *Sugiyono Metode Penelitian Kuantitatif Kualitatif Dan R D DOWNLOAD*. 2017.
- [20] J. NIELSEN, "Usability 101: Introduction to Usability," 2012.

# Shortest Route at Dynamic Location with Node Combination-Dijkstra Algorithm

\*Note: Sub-titles are not captured in Xplore and should not be used

line 1: 1<sup>st</sup> Achmad Fitro  
 line 2: *Magister Program of Information System*  
 line 3: *School of Postgraduate Studies, Diponegoro University*  
 line 4: Semarang, Indonesia  
 line 5: afi.subarjo@gmail.com

line 1: 2<sup>nd</sup> Suryono  
 line 2: *Lecture Magister Program of Information System*  
 line 3: *Faculty of Information System*  
 line 4: Semarang, Indonesia  
 line 5: suryonosur@gmail.com

line 1: 3<sup>rd</sup> Retno Kusumaningrum  
 line 2: *Lecture Magister Program of Information System*  
 line 3: *Faculty of Information System*  
 line 4: Semarang, Indonesia  
 line 5: retno@live.undip.ac.id

**Abstract**— *Online transportation has become a basic requirement of the general public in support of all activities to go to work, school or vacation to the sights. Public transportation services compete to provide the best service so that consumers feel comfortable using the services offered, so that all activities are noticed, one of them is the search for the shortest route in picking the buyer or delivering to the destination. Node Combination method can minimize memory usage and this method is more optimal when compared to A\* and Ant Colony in the shortest route search like Dijkstra algorithm, but can't store the history node that has been passed. Therefore, using node combination algorithm is very good in searching the shortest distance is not the shortest route. This paper is structured to modify the node combination algorithm to solve the problem of finding the shortest route at the dynamic location obtained from the transport fleet by displaying the nodes that have the shortest distance and will be implemented in the geographic information system in the form of map to facilitate the use of the system.*

**Keywords**— *Shortest Path, Algorithm Dijkstra, Node Combination, Dynamic Location (key words)*

## I. INTRODUCTION

In the world of technology which is very rapid development, a lot of information contains in an internet both spatial and textual information. The information can be combined into spatial queries or called Geographic Information Systems (GIS) [1]. Geographic Information Systems are widely used in information technology such as information on flood-prone areas, land matching to plants, tourism, searching for company location or searching for a person's location [2].

Geographic Information System is a very useful tool for spatial analysis that provides functionality for storing, capturing, analyzing and displaying geographic information [3]. However, GIS can also manipulate and display all forms of geo-referenced information efficiently so that it can give a decision to the user [4]. One example is the information used by the user in showing the decision to guide the trip by showing which route or path to go through to reach the destination by displaying information through the website or mobile device [5]. There are two points to be considered in the process of making decisions about the route of the road on GIS [6], namely: location type and the shortest route search.

A static location is a location that has unchanging coordinates such as gas station locations, hotels, hospitals and companies. While the dynamic location is the location where the coordinates may change at any time such as the car or the location of someone who is always on the move [7]. One company that needs this decision is a public transport company like a taxi, where the administrator can monitor the fleet and guide the route to the taxi customer. In addition, the shortest route search is now also very popularly used by companies to assist in the delivery of products to consumers [8], construction of apartments to regulate the exit points of development materials [9] as well as a private person who travels.

With the increasing number of users search the shortest route then some researchers use algorithms to overcome the problem including algorithms A\*, Dijkstra algorithm and Ant Colony algorithm. Based on existing shortest path search algorithms, the researchers compete each other in providing the shortest route to static locations, especially dynamic locations, where the algorithms are tested by detailing the shortest route information with the fastest time and accuracy in the search for the shortest route where the destination location moves constantly.

The shortest route search by using Dijkstra algorithm is very popular than other algorithms where Dijkstra algorithm uses greedy principle, that is the steps chosen with minimum weights that will connect between the selected vertices with the other node [10] so that it can provide information the fastest and shortest route. The previous research concludes that Dijkstra's algorithm provides the shortest path information with faster search than the A\* algorithm and the Ant Colony algorithm [11],[12],[13],[14].

Dijkstra's algorithm is very fast in searching the shortest route on the undigraph model (not directed) [15]. Dijkstra's algorithm, however, has algorithmic changes for some improvements in optimizing the search for the diagraph model, including: 1. increasing the effectiveness of the diagraph output to avoid infinite looping 2. the algorithm will notice adjacent nodes in the shortest path search, and 3. considering many vertices that can separate labels simultaneously [16]. However, this algorithm does not discuss the memory used in the shortest route search so that researchers have an alternative in an effective and efficient search by combining Dijkstra algorithm with Node



Combination algo-rithm, where Node Combination is an algorithm that has easy to understand steps and smaller memory us-age compared to Dijkstra's algorithm, and the Node Combination algorithm can be applied to Dijkstra's algorithm [17].

Based on the background that has been described, the researcher will modify the node combination algo-rithm to solve the problem in the storage of the nodes passed in the search for the shortest route.

#### A. Geolocation

Geolocation is a technique of identifying geographical location in the real world that comes from an inter-net-connected object, such as a mobile phone, radar or computer. [18],[19]. In geolocation itself there is the simplest form, where geolocation involves a set of geographical coordinates that are closely related to the use of the system in positioning such as a street address at a location [20].

For geolocation or position, search engines often use radio frequency location (RF) methods, such as Time Difference Of Arrival (TDOA) for precision. TDOA systems often use mapping or other geographic information systems. If GPS signals are not available, geolocation apps may use information from cell towers to triangulate position estimates, methods that are not as accurate as GPS but have improved considerably in recent years. This is different from previous location radio technology, such as Direction Finding where the bearing line to the transmitter is reached as part of the process. The word geolocation also refers to the latitude and longitude coordinates of certain locations standardized by ISO / IEC 19762-5: 2008 [21].

#### B. Google Maps API

Google Map API (Application Programming Interface) is one of the advantages provided by google to access data from google map and google local search. Application Programming Interface is a documentation that consists of interface, function, class, structure and so on to build a software. With this API, it allows the programmer to develop a software to be integrated with other software. API can be said to link an application with other applications that allow programmers to use the system function. This process is managed through the operating system. The advantage of this is to allow an application with other applications to interact and interact. The programming language used by google map consisting of html, javascript, ajax, and xml, allows to display google maps on web pages.

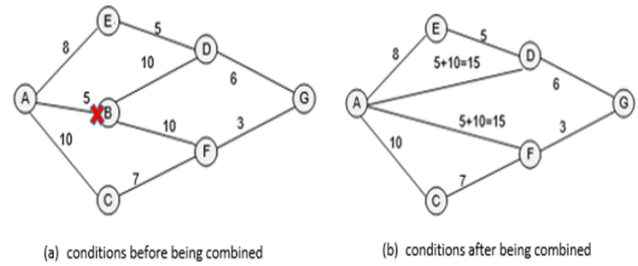
By using the google map API, we can display the digital map on its own website page. In order for this API application to appear, it is necessary to have a key API that is a unique code that is generalized by google map to recognize a number of utilities for manipulating maps and adding content in maps through various services, allowing the creation of powerful map applications on web pages [22],[23].

#### C. Node Combination Algorithm

Node combination has a search system by combining all nodes and still maintaining a labeling set such as Dijkstra's algorithm which will be depicted in "Fig. 1" [24],[17] Suppose all nodes are connected to a rope and will be pulled

slowly, over time all nodes will converge into one where the string will see the shortest strap.

Fig. 1. An example of a combination of nodes



The shortest path search steps using a combination node can be explained by pseudocode to be described in Table 1

TABLE I. PSEUDOCODE ALGORITHM NODE COMBINATION

Algoritma Node Combination (G,s)	
1	$W[s,u] := 0, v_u := v_s, V := V - \{s\}$ /* Initialization */
2	while $W[s,u] < \infty$ and $ V  > 0$
3	$V := V - \{u\}$ /* Node Combination */
4	for each $j$ in $V$
5	$W[s,j] := \min \{W[s,j], W[s,u] + W[u,j]\}$ /* updating edge weights */
6	$v_u :=$ the nearest neighbor of $s$ in $V$ /* finding the nearest neighbor */
/* at the end of the algorithm, the sth row in $W$ contains the corresponding distances */	

#### D. Node Combination-Dijkstra Algorithm

Node Combination-Dijkstra algorithm is algorithm developed by writer in search of shortest route by adopting Node Combination search method that is combining one node with other node and modification in case of storage node which will be explained by pseudocode in Table 2.

TABLE II. PSEUDOCODE ALGORITHM NODE COMBINATION-DIJSKTRA

Algoritma Node Combination-Dijkstra (G,s)	
1.	$W[s,u] := 0, v_u := v_s, P[u] := [s], V := V - \{s\}$ /* Initialization */
2.	while $W[s,u] < \infty$ and $ V  > 0$
3.	$V := V - \{u\}$ /* Node Combination */
4.	for each $j$ in $V$
5.	If $W[s,u] + W[u,j] < W[s,j]$
6.	Then $P[j] := P[u] \cup \{j\}$ , /* updating path */
7.	$W[s,j] := W[s,u] + W[u,j]$ /* updating edge weights */
8.	$v_u :=$ the nearest neighbor of $s$ in $V$ /* finding the nearest neighbor */
/* at the end of the algorithm, the sth row in $W$ contains the corresponding distances */	

## II. DATA

The data used for this study is the location of places in the city surabaya which is interconnected between one point with another point with information weight / distance in meters, latitude longitude coordinates, and address which will be explained in Table 3.

TABLE III. CORDINAT POINTS

No	From	To	Coordinat	Weight	Address
1	A	B	"-7.274982997930746, 112.72668129821636"	1692.91	Jl. Pasar Kembang Kec. Sawahan, Kota SBY, Jawa Timur
		D	"-7.274982997930746, 112.72668129821636"	954.0145	
		E	"-7.274982997930746, 112.72668129821636"	728.3023	
		G	"-7.274982997930746, 112.72668129821636"	2103.285	
2	B	A	"-7.272939639599, 112.741873330076"	1692.91	Jl. Basuki Rahmat Embong Kaliasin, Genteng, Kota Surabaya
		C	"-7.272939639599, 112.741873330076"	826.8011	
		M	"-7.272939639599, 112.741873330076"	2451.245	
		J	"-7.272939639599, 112.741873330076"	1692.327	
3	K	I	"-7.283092639519452, 112.75612122436382"	785.2675	Bank Antardaerah. PT - Pucang Anom Timur Jl. Pucang Anom Tim. No.19, Surabaya
		J	"-7.283092639519452, 112.75612122436382"	483.4498	
		N	"-7.283092639519452, 112.75612122436382"	1374.426	
		M	"-7.283092639519452, 112.75612122436382"	1624.072	
4	L	I	"-7.269129757840544, 112.77423149963238"	1759.133	Jl. Raya Dharma Husada Indah Mulyorejo, Kota SBY, Jawa Timur
		B	"-7.269129757840544, 112.77423149963238"	2451.245	
5	M	L	"-7.262233296342604, 112.76127106567242"	1624.072	Jl. Kedung Tarukan No.86C Pacar Kembang, Tambaksar
		K	"-7.262233296342604, 112.76127106567242"	1374.426	
6	N	G	"-7.290867201464144, 112.74645163518085"	1388.481	STIE YOUTH SURABAYA JL Bung Tomo, No. 08, Kavling 8 Surabaya
		O	"-7.290867201464144, 112.74645163518085"	727.7807	
7	O	N	"-7.2973737545443966, 112.74739577275409"	727.7807	Jl. Ngagel Rejo Kidul 54-38 Ngagelrejo, Wonokromo, Kota Surabaya
		P	"-7.2973737545443966, 112.74739577275409"	1439.804	
8	P	O	"-7.309256355149782, 112.74233176213397"	1439.804	Bendul Merisi Wonocolo, Kota Surabaya
		Q	"-7.309256355149782, 112.74233176213397"	760.3496	
9	Q	P	"-7.306617217538221, 112.7359802911867"	760.3496	Jl. Raya Malang - Surabaya Wonokromo, Kota Surabaya
		H	"-7.306617217538221, 112.7359802911867"	790.3205	
10	C	B	"-7.266213519414126, 112.73869759460308"	826.8011	Jl. Tegalsari No.25 Tegalsari, Kota Surabaya
		D	"-7.266213519414126, 112.73869759460308"	1670.288	
11	D	A	"-7.26697979135388, 112.7235913934312"	1670.288	Jl. Petemon No.5 Petemon, Kec. Sawahan, Kota Surabaya
		F	"-7.26697979135388, 112.7235913934312"	954.0145	
12	E	A	"-7.278729130708208, 112.72127396484234"	728.3023	Jl. Putat Jaya 30 Putat Jaya, Kec. Sawahan, Kota Surabaya
		F	"-7.278729130708208, 112.72127396484234"	1539.035	
13	F	E	"-7.292266031440466, 112.72410637756207"	1539.035	Jl. Mayjen Sungkono 75-143 Gn. Sari, Dukuh Pakis, Kota Surabaya
		G	"-7.292266031440466, 112.72410637756207"	1090.059	
14	G	A	"-7.292436304316622, 112.73397690673687"	2103.285	Bubur Ayam Rasa Darmo, Wonokromo, Surabaya
		F	"-7.292436304316622, 112.73397690673687"	1090.059	
		N	"-7.292436304316622, 112.73397690673687"	1388.481	
		H	"-7.292436304316622, 112.73397690673687"	807.5721	
15	H	Q	"-7.299672841676093, 112.73449189086773"	790.3205	Jl. Joyoboyo Sawunggaling, Wonokromo, Kota Surabaya
		G	"-7.299672841676093, 112.73449189086773"	807.5721	
16	I	L	"-7.2796019598365245, 112.76230103393414"	1759.133	Jl. Raya Menur Manyar Sabrangan, Mulyorejo, Kota Surabaya
		J	"-7.2796019598365245, 112.76230103393414"	698.3279	
		K	"-7.2796019598365245, 112.76230103393414"	785.2675	
17	J	B	"-7.278750570426501, 112.75603539367535"	1692.327	Jl. Dharmawangsa No.97 Kertajaya, Gubeng, Kota Surabaya
		I	"-7.278750570426501, 112.75603539367535"	698.3279	
		K	"-7.278750570426501, 112.75603539367535"	483.4498	

## III. RESULT AND DISCUSSION

### A. Dynamic Location Search

Determination of coordinates on the built system uses a geolocation where the identification or estimation of the real-world geographical location of an object such as a mobile phone. Determination of coordinates on this system is the basic system built to sync the object coordinates with the coordinates that already exist in the system.

Locations generated from geolocation are not all coordinates listed on the location data in this shortest route search information system so that the determination of coordinates generated from the geolocation with the coordinates present in the system will be calculated for the closest search of the coordinates to the coordinates present in system.

The algorithm for calculating the coordinate distance of one with the other coordinates will be written in the Table 4 about pseudocode distance calculation.

TABLE IV. PSEUDOCODE DISTANCE CALCULATION

```

function jarak ($lat1, $lon1, $lat2, $lon2, $hasil)
1  $skordinat= $lon1 - $lon2;
2  $jarak = sin(deg2rad($lat1)) *
    sin(deg2rad($lat2)) + cos(deg2rad($lat1)) *
    cos(deg2rad($lat2)) * cos(deg2rad($skordinat));
3  $jarak = acos($jarak);
4  $jarak = rad2deg($jarak);
5  $smili = $jarak * 60 * 1.1515;
6  $hasil = strtoupper($hasil);
7  if ($hasil == "K") {
8  return ($smili * 1.609344)
9  } else if ($hasil == "N") {
10 return ($smili * 0.8684);
11 } else {
12 return $smili; }
13 end

```

After the calculation of the algorithm it will get the distance between the coordinates of one with the coordinates in the system then, the location is given the coordinates that have the closest distance so that the location will be initialized as a starting point in the search for the shortest route. "Fig. 2" is an example of the position of the geolocation represented by the letter "P" with the graph contained in the system.

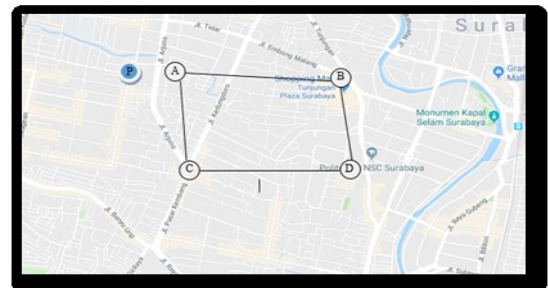


Fig. 2. Position of geolocation with graph.

From "Fig. 2" we can conclude that the position of the geolocation is initialized starting point is at point "A" because that point has the most shortest distance.

### B. Implementation of Node Combination-Dijkstra Algorithm

The Node Combination-Dijkstra algorithm has a base that the initial node will find the closest vertices to the destination node, when it finds the nearest node, the node will be joined with the next node until the end result of this system will be a node that informs the shortest distance between the initial node with the destination node along with the points that have been passed.

For the application of Node Combination-Dijkstra algorithm will be described in Table 5 where the authors will calculate into the assessment matrix starting from point I with the goal to point C. with this matrix the writer can show that the Node Combination-Dijkstra algorithm has the same calculation pattern with Node Combination but the algorithm can also save the history passed.

Initials :  $W[s, u] := 0$ ,  $vu := vs$ ,  $P[u] := [s] := [1]$ ,  $V := V - \{s\}$



TABLE V. THE ROUTE SEARCH MATRIX FROM POINT I TO POINT C

Step	Start	From I to C																
		A	B	C	D	E	F	G	H	I	J	K	L	M	N	O	P	Q
1	I =698										698 {I,J}	785 {I,K}	1759 {I,L}					
2	J =785		698+1692 =2390 {I,J,B}									698+483 =1181 > 785 Then 785 {I,K}	1759					
3	K =1759		2390										1759		785+1374 =2159 {I,K,N}			
4	L =2159		2390											1759+1624 =3383 {I,L,M}	2159			
5	N =2390		2390 {I,J,B}											3383		2159+727 =2886 {I,K,N,O}		
6	B =2886	2390+1692 =4083 {I,J,B,A}		2390+826 =3216 {I,J,B,C}										3383		2886		
7	O =3216	4083		3216 {I,J,B,C}										3383		4325	2886+1439 =4325 {I,K,N,O,P}	

From Table 5 it can be concluded that the system of finding the shortest route from point I to point C can be reached through the point I-J-B-C with a distance of 3216 meters.

### C. System Analysis

To prove that the system has chosen the shortest route, a few alternate paths from the starting point are located at point I with the end point at point C. Alternative routes that can be passed will be explained in Table 6.

TABLE VI. ROUTE SEARCH ALTERNATIVES

Nomor Alternatif	Start	End	Route	Jarak yang ditempuh
Alt. 1	I	C	I-J-B-C	3216 (m)
Alt. 2			I-K-J-B-C	3786 (m)
Alt. 3			I-L-M-B-C	6660 (m)
Alt. 4			I-L-M-B-A-D-C	10150 (m)
Alt. 5			I-K-N-O-P-Q-H-G-A-D-C	11409 (m)

In Table 6 we can see that there are several alternatives in route determination and we can conclude that the shortest route search system using the Node Combination-Dijkstra Algorithm selects the first alternative with a distance of 3216 meters which is the shortest distance among other alternatives, and also, the system can record the history of the nodes passed the

### CONCLUSION

This research has presented the shortest route search system by modifying the combination node algorithm to the dynamic location used in general such as mobile phone online transportation. From the test result of the system, the node combination-dijkstra algorithm can give optimal result in the shortest route search on the dynamic location applied in surabaya city that shows the route search from point I to point C is 3216 meters for the distance with I-J-B-C route.

### REFERENCES

- [1] Jie, Z., Jin, P., Zhang, Q., dan Wen, R., 2014, Exploiting location information for web search, Computer in human behavior 30, 378-388
- [2] Pugas, D.O., Somantri, M., and Satoto, K.I. 2011. Pencarian Rute Terpendek Menggunakan Algoritma Dijkstra dan Astar (A\*) pada SIG Berbasis Web untuk Pemetaan Pariwisata Kota Sawahlunto.

- [3] Rikalovic, A., Cosic, I., dan Lazarevic, D., 2014, GIS Based Multi-Criteria Analysis for Industrial Site Selection., *Procedia Engineering* 69 (2014) 1054-1063.
- [4] Church, R.L., 2002, Geographical information systems and location science, *Computers & Operations Research* 29 (2002) 541-562.
- [5] Krichen, S., Faiz, S., Tlili, T., and Tej, K. 2014. Tabu-based GIS for solving the vehicle routing problem. *Expert systems with application* 41 (2014) 6483-6493.
- [6] Bo, H., Liu, N., dan Magesh, C., 2006, A GIS supported Ant algorithm for the linear feature covering problem with distance constraints, *decision support system* 42, 1063-1075.
- [7] Yin, X., Ding, Z., dan Li, J., 2008, A Shortest path algorithm for moving objects in spatial network databases., *Progress in Natural Science* (2008) 893-899.
- [8] Soltani, A.R., Tawfik, J.Y., Goulernas., dan Fernando, T., 2002, Path planning in construction sites : performance evaluation of the Dijkstra, A\*, and GA search algorithm, *Advanced engineering informatics* 16, 291-303.
- [9] Aleksandar, R., Ilija, C., Djordje., dan Lazarevic., 2013, GIS Based Multi-Criteria Analysis for Industrial Site Selection, *Procedia Engineering* 69, 1054-1063.
- [10] Peyer, S., Rautenbach, D., Vygen, J., 2009, A generalization of Dijkstra's shortest path algorithm with applications to VLSI routing, *Journal of Discrete Algorithms* 7 (2009) 377-390.
- [11] Choubey, N., Bhupesh., dan Gupta, K.R., 2013, Analysis of Working of Dijkstra and A\* to Obtain Optimal Path, *International Journal of Computer Science and Management Research* Vol 2 Issue 3 March 2013 ISSN 2278-733X.
- [12] Dramski, M., 2012, A comparison between Dijkstra algorithm and simplified ant colony optimization in navigation, *Scientific Journals* 29 (101), pp. 25-29.
- [13] Pratiarso, A., Hadi, M.Z.S., Yuliana, M., and Wahyuningdiyah, N. 2010. Perbandingan Metode Ant Colony Optimization dan Dijkstra untuk Pengembangan Sistem Pengiriman Barang di Kantor Pos Area Surabaya Timur Berbasis J2ME. ISSN: 2088-0596 (2010). EEPIS.
- [14] Santoso, L.W., Setiawan, A., dan Prajogo, A.K., 2012, Performance Analysis of Dijkstra, A\* and Ant Algorithm for Finding Optimal Path Case Study: Surabaya City Map, Informatics Department, Faculty of Industrial Engineering.
- [15] Chen, Y.Z., Shen, S., Chen, T., dan Yang, R., 2014, Path Optimization Study for Vehicles Evacuation Based on Dijkstra algorithm, *Procedia Engineering* 71 159 – 165.
- [16] Shu-Xi, W., 2012, The Improved Dijkstra's Shortest Path Algorithm and Its Application, *Procedia Engineering* 29 , 1186 – 1190.
- [17] Lu, X., dan Camitz, M., 2011, Finding the shortest paths by node combination, *Applied Mathematics and Computation* 217, 6401–6408.
- [18] Ciavarrini, G., Luconi, V., and Vecchio, A. 2017. Smartphone-based geolocation of internet hosts. *Computer Networks* 116 (2017) 22-32.
- [19] Cui, Y., An, R., Kartik, B, and Ariyur. 2015. Cellphone Geolocation Via Magnetic Mapping. *Automatica* (2015) 70-79.
- [20] Gustafsson, F. Geolocation-Maps, Measurements, Models, and Methods. Division of Automatic Control, Department of Electrical Engineering, Linköping University, Sweden.
- [21] Dodsworth, E and Nicholson, A. 2012. Academic Uses of Google Earth and Google Maps in a Library Setting. *Information Technology And Libraries*.
- [22] Kiraly, A and Abonyi, J. 2015. Redesign of the supply of mobile mechanics based on a novel genetic optimization algorithm using Google Maps API. *Engineering Applications of Artificial Intelligence* 38 (2015) 122-130.
- [23] Yang, S.Y and Hsu, C.L., 2015. A location-based services and Google maps-based information master system for tour guiding, *Computers and Electrical Engineering* 000 (2015) 1-19.
- [24] Cantone, D., and Faro, S. 2004. Two-Levels-Greedy: a generalization of Dijkstra's shortest path algorithm. *Electronic Notes in Discrete Mathematics* 17 (2004) 81-86.
- [25] Fitro, A., Bachri, S.O., Purnomo, A.I.S and Frendianata, I. Shortest Path Finding in Geographical Information Systems using Node Combination and Dijkstra Algorithm, *International Journal of Mechanical Engineering and Technology* 9 (2), 2018. pp. 755–760.

# Analysis of Consumer Confidence on Mobile Commerce in Indonesia

<sup>1st</sup> Andhika Galuh Prabawati

Master of Informatics Engineering  
Atma Jaya University Yogyakarta  
Yogyakarta

line 5: andhika.prabawati@gmail.com

<sup>2nd</sup> I Putu Angga Widyana

Master of Informatics Engineering  
Atma Jaya University Yogyakarta  
Yogyakarta

line 5: putuanggasaham11@gmail.com

<sup>3rd</sup> Suyoto\*

Master of Informatics Engineering  
Atma Jaya University Yogyakarta  
Yogyakarta

suyoto@staff.uajy.ac.id

**Abstract**— *The rapid development of mobile-based information technology, can change an existing business process. Such as loss of distributors in a single chain of business processes. Mobile Commerce industry is getting a good condition to grow. With the decrease in Mobile communication costs, more and more people are using mobile computing devices that can connect to the Internet. There are several M-Commerce applications in Indonesia, namely Lazada, Tokopedia, Buka Lapak, Shopee and etc. The existence of these applications in Indonesia traders switches to online stores. This study takes three examples of M-Commerce applications in Indonesia with the top three criteria in terms of the best reviews and the highest number of reviews. The results of the sampling application are Lazada, Tokopedia and Buka Lapak. The process of collecting data taken will be analyzed to know about the level of consumer confidence in an M-Commerce application. This is evidenced by a collection of examples of online stores that exist in M-Commerce applications that inform ratings, discount information, and existing features. The results obtained from this research is, consumer confidence can be seen from the review feedback that exists in each - each M-Commerce. Many discounts and low prices have no effect on consumer buying interest in the online store. The researcher's suggestion is to reward the most traded buyers with points that can be redeemed for certain goods, discounted goods or subsidized postage.*

**Keywords**—*Mobile Commerce; business process; online stores; Industrial Information System*

## I. INTRODUCTION

The rapid development of mobile-based information technology, can change an existing business process. Such as loss of distributors in a single chain of business processes. Sellers can directly communicate and handle to consumers. Sellers can also control stock and understand the trends that exist in society. The Mobile Commerce (M-Commerce) industry is getting good conditions for growth, and some new applications from Mobile Trade are emerging. With the decrease in Mobile communication costs, more and more people in many countries are moving using mobile computing devices that can connect to the Internet. These devices are widely applied to personal communication, website browsing, and scheduling, play a more important role in people's lives, and provide more commercial opportunities for Mobile Commerce development [1].

In Indonesia, many M-Commerce applications are superior and often used by the public, such as Lazada, Tokopedia, Buka Lapak, Shopee and so forth. M-Commerce has a different way of marketing strategy. With available M-Commerce applications in Indonesia, the sellers switch to online stores. In its application, the sellers can be found in some M-Commerce. In research Puspha P.V, examines the characteristics of buyers who make transactions with different mobile commerce. In his research, he observed a

real pattern of traction in customers using mobile commerce [2]. A research conducted by A. Hussain, measured the perceived usefulness of mobile commerce application performance in the aspect of effectiveness, efficiency and satisfaction to improve the receipt of the application and user loyalty or seller [3].

## II. LITERATURE REVIEW

### A. Mobile Commerce

Mobile Commerce is the development of E-commerce that utilizes the smartphone as the medium with the principle of mobility. Mobile commerce as a further development on the mobility side of e-commerce. As a trusted transaction service through mobile devices to exchange services and services both between consumers, merchants, and financial institutions. During a transaction or cash flow carried out by a mobile device, it will be categorized as mobile commerce [4]. Mobile commerce can also be interpreted as a platform where users can buy products using mobile devices connected via wireless data connections [5]. The difference between mobile shopping and mobile shopping is in customer's mobile shopping using a mobile device (mobile) while they're shopping online they can use mobile devices and stay like pc [6]. And so in order to increase or influence a customer's trust, M-Commerce application must provide a quality system, information, and service to promote user's comfort in purchasing [7][8]. M-Commerce becomes a new innovation in trading and also part of electronic commerce [9]. In the future, M-Commerce continues to grow in the market with the knowledge developed from longitudinal research on how people relate to M-Commerce from time to time can provide a significant advantage [10].

### B. Customer Behavior

In a study conducted by T.Lei, writing that personalized service can influence the habits of customers in shopping through M-Commerce, some of the components that affect the Social Environment, Content Services, Interface Design [11]. Customer behavior and Feedback can be obtained through data sources, including structural and unstructured data. It is important to optimize user engagement and user attitudes toward products and services [12]. Consumer habits need to be analyzed with the aim of predicting and promoting products intelligently and in accordance with the target [13].

### C. The Development of M-Commerce in Indonesia

There are four elements that influence the development of M-Commerce in Indonesia, namely Information Technology Infrastructure, M-Commerce Knowledge Level in Indonesia [14], Online Traction of Trustworthiness and Information Supply Limitation [15].

#### D. Determinants of Purchase's Continuance Intention

According to S. W. Chou, satisfaction factors, beliefs, learning, habits, and quality of product information examined from cellular services have been studied based on factors such as playfulness, perceived ease of use (EOU), attitudes, and subjective norms [16]. A study shows that purchasing intentions have been determined by three factors such as trust, flow and perceived usefulness [17]. According to C. Chang online purchases are considered as loyalty influenced by direct satisfaction and perceived value based on the context of web and mobile use [18]. Purchasing intentions as electronic loyalty influenced by flow, perceived ease of use, and perceived usefulness have been reviewed based on determinants such as system quality, information quality, service quality, perceived usefulness, perceived ease of use, perceived risk, and satisfaction perceived [19].

### III. RESEARCH METHOD

Step in doing this research can be seen from **figure 1**, that is a flow of research process.

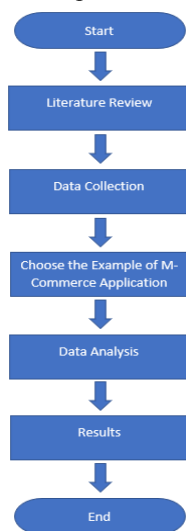


Fig. 1. Research Method

Researchers collected M-Commerce applications, from ten apps are taken rating and total reviewers. The data is taken three M-Commerce again. The criteria are the rating and the most total reviews. Rating rules taken from 4 - 5 scale, total reviews above 500,000 viewers [20]. Data was taken on March 12, 2018, with Play Store source.

The expected results of the research conducted is from the data obtained, researchers know the characteristics of sellers and buyers in online stores. In addition, researchers also want to see how big the level of confidence of buyers in online stores.

### IV. DISCUSSION

#### A. Data retrieval

Table I shows those applications with high ratings are directly proportional to a large number of reviewers.

TABLE I. M-COMMERCE INDONESIA

M-Commerce	Reviews / Rating (1-5)	Total Reviewers
Lazada	4.3	1,323,186
Tokopedia	4.3	725,763
Shopee	4.2	460,449
Elevenia	4.1	96,166
Blibli	4.1	136,000
BukaLapak	4.4	539,072
Matahari Mall	3.9	38,454
Alfacart	3.8	9,110
Blanja.com	3.7	8,048
JD.Id	4.3	81,891
Bhinneka	3.1	77

#### B. Selecting a 3 M-Commerce as an Example

Data were taken on Monday, March 12, 2018, is sourced from existing data in the Play Store. The three (3) M-Commerce are selected to be studied they are Lazada, Tokopedia, and BukaLapak. Here is an explanation of the results of the observations obtained.

##### 1) Lazada

- There are 2 language features (Indonesian & English)
- High rating
- Many Discounts
- Payment can be made periodically (installments).
- The stock is not displayed, but the maximum purchase limit is 5 pcs for all items.
- At the time of making the purchase will go through 3 processes namely the delivery process, payment process, and review process.
- In the sending process to enter data correctly if the contents of the "\*" of the data must be filled, if it is advanced to the payment process ..
- On the payment process will make the selection of payment according to the options listed.
- For payment, there is a choice of pay where the payment is made when the courier to send the goods to the destination and the goods have come to the consumer who made the purchase of goods.
- The Review Process will display Details of the purchase and will proceed with order confirmation.

##### 2) Tokopedia

- There are 2 language features (Indonesian & English)
- Payment can be made periodically (installments).
- The level of consumer confidence is higher, judging by the positive reviews.
- Stock not shown
- Product information shown is the number of sold, who saw the goods, insurance, dam Weight of goods.

- At a time of purchase will do login first. To do list login can enter through facebook, google, and Email.
- Purchase data must be filled correctly and accordingly
- Purchase data for address can directly connect to the maps application to get clarity of location for delivery of goods.

### 3) BukaLapak

- There is only one language.
- Offer many discounts
- Payment can be made periodically (installments).
- The displayed stock is visible
- Purchase Data (address and phone number) must be filled in correctly. Example: phone number must be filled Indonesian phone code. The address in the content must contain the word "Street, Jl." If it does not exist then the input in the user's content is considered invalid.

### C. Data Analysis

Researchers took 30 online stores randomly on three (3) M-Commerce. Tabel II shows the strengths and weaknesses of each M-Commerce in Indonesia.

TABLE II. ONLINE SHOP LIST

No	Store Name	Application	Price	Discount	Rating
Needs of Women (Cosmetics, Shoes, Clothes, Bag)					
1	Pluvia Shoes (Flat Shoes Slip On Kanvas)	Lazada	90000	55%	77%
		Tokopedia	100000	-	98.68 %
		BukaLapak	100000	-	95%
2	Beauty Bonney(Nature Republic Aloe Vera Soothing Gel 92% 300Ml)	Lazada	100000	14%	97%
		Tokopedia	85800	-	100%
		BukaLapak	85800	-	95%
3	Velopestore(Women's Trousers)	Lazada	82600	26%	70%
		Tokopedia	97200	-	99.19 %
		BukaLapak	100000	-	98%
4	Batik Er 25(Square Hijab)	Lazada	90500	30%	0%
		Tokopedia	88300	0%	100%
		BukaLapak	100000	45%	100%
5	Tokohita(Women's Kulot Pants)	Lazada	100000	-	37%
		Tokopedia	90000	-	100%
		Buka Lapak	90000	-	99.90 %
6	Sweet Honey (Rattan Bags)	Lazada	100000	-	0
		Tokopedia	100000	-	0
		Buka Lapak	90000	10%	100%
Baby Needs					
7	Indo Ultimate (Baby Carrier)	Lazada	94490	42%	83%
		Tokopedia	100000	-	92.11 %
		BukaLapak	97600	-	89%

No	Store Name	Application	Price	Discount	Rating
8	Faradisa Batik(Child Batik Clothes)	Lazada	100000	-	100%
		Tokopedia	100000	-	92.98 %
		BukaLapak	100000	-	97%
9	Kembarshop (Baby Gift Wrap)	Lazada	100000	54%	79%
		Tokopedia	84000	-	96.91 %
		BukaLapak	84000	-	100%
10	Lolibi (Baby Bottle)	Lazada	100000	20%	95%
		Tokopedia	99300	-	100%
		Buka Lapak	99300	-	97%
11	Bloombing Deal(Glass Bottle)	Lazada	100000	55%	89%
		Tokopedia	100000	-	100%
		Buka Lapak	100000	-	98%
12	BabyManiaShop(Apron Breastfeeding )	Lazada	100000	40%	90%
		Tokopedia	95500	-	99.46 %
		Buka Lapak	95500	-	95%
13	BabyKlik(Pijamas)	Lazada	91300	19%	91%
		Tokopedia	100000	-	98.61 %
		Buka Lapak	86780	5%	99%
Needs of Men (Bag, Wristwatch, Clothes)					
14	Raja OB(Sling Bag USB Port charger smart backpack B295)	Lazada	96400	66%	79%
		Tokopedia	100000	-	97.82 %
		BukaLapak	100000	-	95%
15	Resinda Fashion Store (Men's Pants)	Lazada	94100	50%	72%
		Tokopedia	100000	-	100%
		Buka Lapak	100000	-	90%
16	Rafflesia Outdoor (Purse and Bag)	Lazada	100000	-	71%
		Tokopedia	97100	-	72.73 %
		Buka lapak	100000	-	90%
17	Keyshima (Batik Shirt)	Lazada	100000	52%	53%
		Tokopedia	80900	-	100%
		Buka Lapak	90090	-	100%
18	Saver Store (Wristwatch)	Lazada	100000	20%	75%
		Tokopedia	66700	-	100%
		Buka Lapak	65000	-	96%
19	Nee Cloth (Shirt)	Lazada	100000	-	77%
		Tokopedia	100000	-	89.47 %
		Buka Lapak	100000	-	0%
20	Sumber Tas Grosir (Backpack)	Lazada	100000	46%	78%
		Tokopedia	100000	-	100%
		Buka Lapak	100000	-	100%
21	Redwingmitary (Backpack)	Lazada	100000	-	73%
		Tokopedia	50000	-	100%

No	Store Name	Application	Price	Discount	Rating
		Buka Lapak	48000	-	98%
22	Mutiar Alkes (Hot Water Bag)	Lazada	100000	42%	90%
		Tokopedia	75000	-	93,10 %
		Buka Lapak	75000	-	99%
Other Equipment					
23	TokoEELIC (Table Lamp Learning Architects RJ800)	Lazada	81700	58%	80%
		Tokopedia	95800	-	99,57 %
		BukaLapak	100000	-	98%
24	Modemku Mega Sarana(Mini ature Dewaruci Ship)	Lazada	89500	76%	81%
		Tokopedia	100000	-	97.96 %
		BukaLapak	100000	-	100%
25	Roemahsula p(A Magician)	Lazada	100000	-	75%
		Tokopedia	85700	-	92.98 %
		BukaLapak	89300	-	97%
26	Galeri Medika (Electric Massage Device)	Lazada	98700	-	92%
		Tokopedia	87100	-	95,40 %
		Buka Lapak	100000	-	96%
27	GlobalNetLi ve (Stick the Old Man)	Lazada	100000	32%	91%
		Tokopedia	86700	-	91,30 %
		Buka Lapak	82400	5%	100%
28	Innofoto(Wa ll Clock)	Lazada	95600	71%	83%
		Tokopedia	100000	-	95,79 %
		Buka Lapak	75000	-	97%
29	Alfaindo(Bo x Store)	Lazada	100000	33%	89%
		Tokopedia	95000	-	98.14 %
		Buka Lapak	95000	-	96%
30	OfficeExpres s(Strapp ler Kangoro)	Lazada	62500	-	82%
		Tokopedia	100000	-	97,22 %
		Buka Lapak	99700	-	97%

## V. RESULT

Researchers calculate the average price sold on each M-Commerce. Figure 2 shows the price average diagram of the online shop. The diagram shows that the highest price is Lazada rather than Tokopedia and Buka Lapak. TABLE II shows Lazada offers the most discounts, but the price after the discount is not much like the normal price of tokopedia and Buka Lapak.

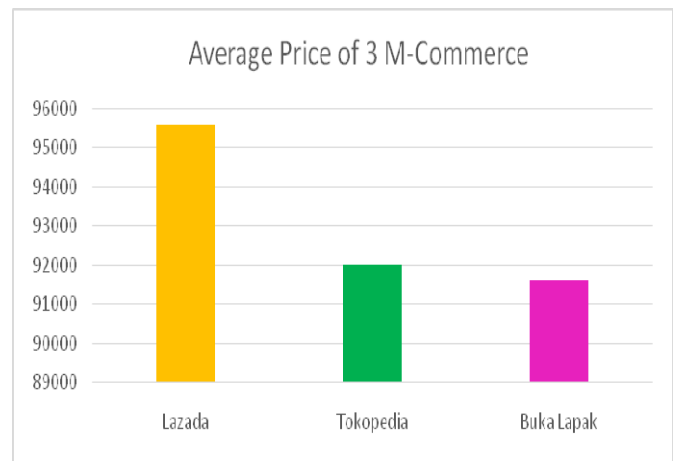


Fig. 2. Average Price of 3 M-Commerce

In addition, the average rating of each store on M-Commerce is also calculated. Tokopedia's results are superior among the other two (2)M-Commerce. Figure 6 shows that Tokopedia does not offer many discounts, but its rating is the highest. The strategies of the three existing M-Commerce examples can be studied further.

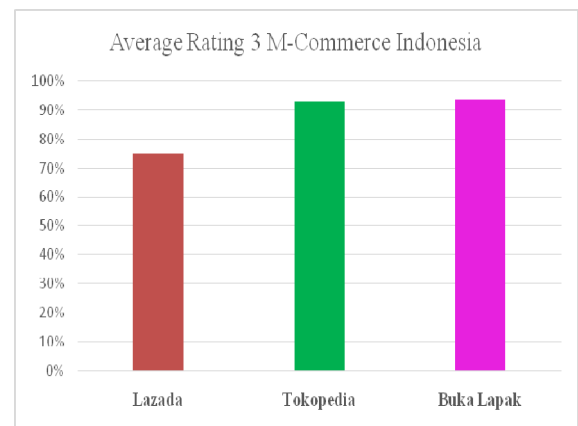


Fig. 3. Average Rating 3 M-Commerce Indonesia

### A. Characteristics of Buyers and Sellers in Indonesia

On Research Prof. Shanti, says everyone's habits are different. In his research also mentioned the population of gender also affect the habit of shopping online[21]. In Indonesia, sellers easily offer their products on more than one M-Commerce app[22].

Table II shows that many sellers in Indonesia offer more products on more than one M-Commerce. At Lazada, many discounts are always there in every item sold, but it did not affect the rating obtained. Because of that, then buyers in Indonesia are also often moving around in buying a product in more than one M-Commerce. A trend in Indonesia many M-Commerce are competing to attract a lot of consumers, strategies that also do diverse. Trust one of the important strategies that need to be done.

## VI. CONTRIBUTION AND IMPLICATION

Effective strategies can result in more customers, but greater costs. However, it can produce "goodwill" in the long run [23]. This research is seen if the marketing method by offering more discounts cannot attract more consumers. The



confidence of every store in M-Commerce is also one factor of the many interests of the buyers. Suggestions that can be given to researcher's M-Commerce especially in Indonesia is to add or adopt from the current trend developing. Suppose, M-Commerce application that tracking the most number of transactions on the consumer then provide points that can be exchanged with certain goods, discounts, or subsidized shipping cost. In terms of the seller, also awarded for sellers who sell the most goods and have the highest rating by giving "Highlight" the name of the store and its products on the main page. Other studies, also reinforce that the packaging of the information presented is also very influential on consumer interest to visit existing M-Commerce [24]. Consumer confidence can maintain long-term trading competition. Each M-Commerce must also have controls on the comments section of every item and store listed in M-Commerce. The comment section is one part that is first read and reviewed by every consumer who will buy a product [22]. Other research also needs to study the inhibiting effects of an M-Commerce business process. The goal is to see how much customers trust, and how many products are purchased and the number of transactions made by consumers[25].

The novelty found in the paper written is that there has never been a study comparing consumer confidence from M-Commerce in Indonesia. M-Commerce retrieval can be from the top three rating and viewers, namely Lazada, Tokopedia, and Buka Lapak with the acquisition of rating 4.3 with viewers 1,323,186 (Lazada), rating 4.3 with viewers 725,763 (Tokopedia), rating 4.4 with viewers 539,072 (Buka Lapak). Data samples taken were sellers who sold the same product in the three M-Commerce.

## VII. CONCLUSION

From the results and discussions obtained, there are several conclusions that can be taken. The trust of an online store is crucial in the marketing strategy of an online business. In the above data, a good belief can be seen from the feedback review every M-Commerce. Examples of existing M-Commerce also show that many discount offers have no effect on the number of sales and good reviews from consumers. When viewed from the price, indicating that consumers are not affected by the low prices and discounts offered. Reasonable price and brand from M-Commerce Application are also considered by consumers before purchasing goods. In addition to having the right strategy, it is also necessary to know the inhibiting factors in doing the strategy. It can also add new ideas in strategies to conduct business processes from M-Commerce. Looking at M-Commerce in the future will continue to grow from time to time.

## REFERENCES

- [1] L. Pucong, Z. Yuansheng, and Z. Wenqiang, "Analysis of Mobile Opportunistic Commerce Value Chain," *2015 2nd Int. Conf. Inf. Sci. Control Eng.*, pp. 132–136, 2015.
- [2] P. V. Pushpa, "Customer Context Based Transactions in Mobile Commerce Business Environment," *Proc. - 13th IEEE Int. Conf. E-bus. Eng. ICEBE 2016 - Incl. 12th Work. Serv. Appl. Integr. Collab. SOAIC 2016*, pp. 208–213, 2017.
- [3] A. Hussain, E. O. C. Mkpogioju, N. H. Jamaludin, and S. T. L. Moh, "A usability evaluation of Lazada mobile application," *AIP Conf. Proc.*, vol. 1891, 2017.
- [4] I. Nabhani, "M-Commerce Adoption and Performance Improvement : Proposing a Conceptual Framework," vol. III, no. 4, pp. 1–9, 2015.
- [5] I. P. Chiang and Y. S. Liao, "Exploring the key success factors of mobile commerce in Taiwan," *Proc. - 26th IEEE Int. Conf. Adv. Inf. Netw. Appl. Work. WAINA 2012*, pp. 369–374, 2012.
- [6] J. H. Wu, L. Peng, Q. Li, and Y. C. Chen, "Falling in love with online shopping carnival on singles' day in China: An uses and Gratifications perspective," *2016 IEEE/ACIS 15th Int. Conf. Comput. Inf. Sci. ICIS 2016 - Proc.*, 2016.
- [7] D. I. Sensuse, I. T. Handoyo, W. R. Fitriani, A. Ramadhan, and P. Rahayu, "Understanding Continuance Intention to Use Mobile Commerce : A Case of Urban Transportation Service," 2017.
- [8] S. Assegaff, D. Zaenal Abidin, and K. Kunci, "Jurnal Teknologi dan Sistem Informasi User Behavior in Adopt Mobile Commerce (Scale Development: Perspective of Trust and Risk)," vol. 3, no. 3, pp. 320–325, 2017.
- [9] L. Priyambodo, F. Tjiptono, and Suyoto, "M-Commerce in Indonesia : Problems and M-Commerce in Indonesia : Problems and Prospects," *Int. J. Comput. Appl. Inf. Technol.*, vol. 1, no. II, pp. 71–76, 2012.
- [10] R. Blaise, M. Halloran, and M. Muchnick, "Mobile Commerce Competitive Advantage: A Quantitative Study of Variables that Predict M-Commerce Purchase Intentions," *J. Internet Commer.*, vol. 17, no. 2, pp. 96–114, 2018.
- [11] T. Lei and J. W. Cao, "The Relationship Study between the Mobile Commerce Personalized Service Scene and Customer Behavior," *Proc. - 2014 7th Int. Symp. Comput. Intell. Des. Isc. 2014*, vol. 2, pp. 467–471, 2015.
- [12] X. Deng, "Big Data Technology and Ethics Considerations in Customer Behavior and Customer Feedback Mining," pp. 3842–3845, 2017.
- [13] R. Mahajan, "Customer Behavior Patterns Analysis in Indian Mobile Telecommunications Industry," *IEEE Access*, no. April 2013, pp. 1165–1169, 2016.
- [14] W. R. Advanced and I. Network, "With Real-time Advanced Inexpensive Network Computing," pp. 6–11, 2014.
- [15] J. Weiyn, T. A. Napitupulu, and Harisno, "The relationship between the high usage of mobile chatting with M-Commerce progress: A case of Indonesia," *Proc. - 11th 2016 Int. Conf. Knowledge, Inf. Creat. Support Syst. KICSS 2016*, pp. 1–5, 2017.
- [16] S. W. Chou and C. S. Hsu, "Understanding online repurchase intention: social exchange theory and shopping habit," *Inf. Syst. E-bus. Manag.*, vol. 14, no. 1, pp. 19–45, 2016.
- [17] T. Zhou, "Understanding continuance usage intention of mobile internet sites," *Univers. Access Inf. Soc.*, vol. 13, no. 3, pp. 329–337, 2014.
- [18] C. C. Chang, "Exploring mobile application customer loyalty: The moderating effect of use contexts," *Telecomm. Policy*, vol. 39, no. 8, pp. 678–690, 2015.
- [19] N. P. Rana, Y. K. Dwivedi, M. D. Williams, and V. Weerakkody, "Investigating success of an e-government initiative: Validation of an integrated IS success model," *Inf. Syst. Front.*, vol. 17, no. 1, pp. 127–142, 2014.
- [20] M. Naili, A. Boubetra, and A. Tari, "Mobile commerce websites ranking," *Proc. - 2014 8th Int. Conf. Next Gener. Mob. Appl. Serv. Technol. NGMAST 2014*, pp. 43–47, 2014.
- [21] P. S. Verma, "Association Between Shopping Habit and Demographics of M-Commerce user 's in India using Two way ANOVA," pp. 38–43, 2017.
- [22] Q. Li, M. Gu, K. Zhou, and X. Sun, "Multi-Classes Feature Engineering with Sliding Window for Purchase Prediction in Mobile Commerce," *Proc. - 15th IEEE Int. Conf. Data Min. Work. ICDMW 2015*, pp. 1048–1054, 2016.
- [23] J. Choi and D. L. Nazareth, "Repairing trust in an e-commerce and security context: An agent-based modeling approach," *Inf. Manag. Comput. Secur.*, vol. 22, no. 5, pp. 490–512, 2014.
- [24] N. Shin, D. Kim, S. Park, and J. Oh, "The moderation effects of mobile technology advancement and system barrier on M-Commerce channel preference behavior," *Inf. Syst. E-bus. Manag.*, vol. 16, no. 1, pp. 125–154, 2018.
- [25] M. Maity and M. Dass, "Consumer decision-making across modern and traditional channels: E-commerce, M-Commerce, in-store," *Decis. Support Syst.*, vol. 61, no. 1, pp. 34–46, 2014.

# Social Media and User Performance in Knowledge Sharing

Setiawan Assegaff 1<sup>st</sup>  
Dept. Of Information System  
STIKOM Dinamika Bangsa  
Jambi, Indonesia  
setiawanassegaff@stikom-db.ac.id

Akwan Sunoto 2<sup>nd</sup>  
Dept. Of Information System  
STIKOM Dinamika Bangsa  
Jambi, Indonesia  
akwan@stikom-db.ac.id

Hendrawan 3<sup>rd</sup>  
Dept. Of Information System  
STIKOM Dinamika Bangsa  
Jambi, Indonesia  
hendrawan@stikom-db.ac.id

Xaverius Sika 4<sup>th</sup>  
Dept. Of Information System  
STIKOM Dinamika Bangsa  
Jambi, Indonesia  
xaveriussika@stikom-db.ac.id

**Abstract**—The aimed of this study is to investigate the impact of social media utilization on student's performances for knowledge sharing in teaching and learning progress. A research model using the Task-Technology Fit Theory as a basis and three hypotheses developed for this study. Model and hypotheses then tested and validated using data obtained from a survey of respondents. The survey was conducted for students at a university in Indonesia. About 103 questionnaires filled out by members of the university, 75 questionnaires declared valid and used for further analysis. Data were analyzed using Smart Partial Least Square (Smart PLS). This study reveals that student performance and Knowledge Sharing impact by technology characteristic and social media utilization

**Keywords**— *Knowledge Sharing, Social Media, User Performance, Task-Technology Fit Theory*

## I. INTRODUCTION

Today's, social media has undergone tremendous development; more and more social media applications are created and developed. Some of the quite popular social media applications are Facebook, Twitter, and Instagram. In 2014, the estimated the number of active users of social media applications in the world is about 1.9 billion people and was estimated in 2018 to be 2.67 billion people. In Indonesia, the number of active users in social media is estimated to be on the number 96.01 million people in the year 2016 (statista.com, 2016). This amount is expected to increase in subsequent years.

Social media is growing rapidly due to the features offered felt quite potentially provide benefits to users [1]. In addition, the application's ability to collect millions of people in one large virtual community makes this application a powerful weapon for those who have an interest in a great community. In its later development, social media has been utilized by the user in many aspects of human life. Social media was used in commerce, social, political and education. In education, it is quite a lot of educational institutions whether formal or non-formal use social media application to support their academic activities [2].

One of the social media features that potential to be used in teaching and learning activities is a virtual community (virtual group) [2]. The virtual community enables the gathering of a group of people who has the same interest [3]. Where the member of the group is facilitated to be able to interact, collaborate and communicate through a variety of

features provided by the social media application [4, 5]. In Educational context, the academic community is believed as one of the most important elements in helping student and lecturer to create intensive interaction. The intensive interaction among students and professors in the community allow them more intense on the process of transfer the formation and knowledge. The exchange of knowledge is one of the keys to creating new skills and competencies.

Nonaka (expert in the field of Knowledge Management) state that the exchange of knowledge can only come through interaction and collaboration activities [6]. Through interaction and collaboration activities the exchange of knowledge between experts and talent would occur. Further, Nonaka argues that new knowledge is only created through interaction and collaboration [6].

Many organizations in the world have proved that the transfer of knowledge is one of the most effective activities in creating new high skill [7]. We can see how organizations increasingly realize the importance of knowledge sharing interaction in an effort to bring a huge benefit to the improvement and creation of new knowledge [8, 9]. Thus we can conclude that the interaction and collaboration is key to the creation of powerful beings are competent [10]. In this study, we would like to investigate whether the use of social media for knowledge sharing activities can improve the performance of students and what factors impact the utilization of social media?

## II. RESEARCH METHOD

### A. Model and Hypotheses Development Social Media

Kaplan and Heinlein define social media as a collection of internet-based applications that provides web 2.0 interactive services among individuals and communities to interact, discuss, create and modify contents. Social media is now believed to be a tool that provides tremendous potential for the organization to improve the performance of the company [11]. To get the maximum benefit from the potential of the social media, the companies develop strategies to use social media in their business activities. Hanna et al (2011) proposed a concept to develop a strategy for the utilization of social media within an organization that they are familiar with the term "social media ecosystem". In the concept in the organization need to understand that the

use of social media in supporting the activities organized needs to be aligned, by appropriately combining social media how traditional and virtually in achieving organizational goals.

Razmerita et al., 2009, proposed several technologies in social media that can be used in optimizing knowledge sharing, namely:

- *A personal webpage* is a tool that can improve the organization and presentation of information and share with the community.
- *Personalized search tools* provide the facility to search for and share information.
- *A social bookmarking* tool that makes it easy for community members to share bookmarks of interest among the members.
- *The personalized live discussion forum* is a tool that can guide in analyzing, evaluating, displaying and sharing of information among member of communities.
- *the virtual world* is a tool that encourages community members to share their knowledge.
- *Blogs and wikis* is a supportive tool for editing, viewing, organizing information or knowledge by individuals or collaborate with others.

The tools above are part of social media technologies and services that could be an option for us in optimizing individual knowledge sharing activities with community members. Unlike the traditional tools for knowledge sharing, social media-based technology services supporting the process of interaction, collaboration more interactive and intensive, thus enabling the sharing of knowledge that is richer in content and more intensive [5]

Research in the field of social media and knowledge management that has to produce some advantage knowledge this time includes conceptual models, case studies, empirical studies. One of the studies related to the social media and knowledge management conducted by Razmerita et al. (2009). In their study, they found that there is the same principle between social media and knowledge management in sharing the information. Social media has shown a positive role in knowledge management. In others research conducted in social media and knowledge management, some researchers have managed to identify the benefits obtained through the use of social media in knowledge management. However, although in principle social media are believed to synergize with knowledge management the researchers also found the constraints faced in the implementation of social media in knowledge management. Knowledge management in social media can be supported through a variety of tools that allow creating, code, organize, and share knowledge, but also to socialize and improve personal network and collaborate in order to organize and create new knowledge.

### Knowledge Sharing

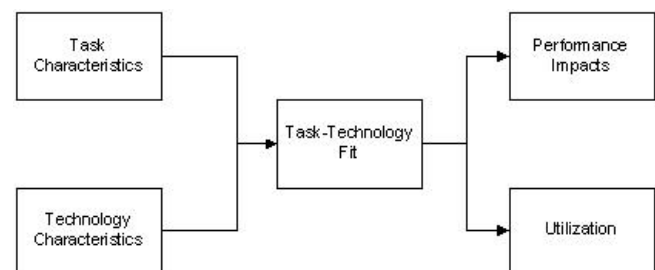
Knowledge sharing is a major activity in the knowledge management area. Knowledge sharing allows individuals in an organization to work together to exchange information, ideas, suggestions, ideas, and experiences that ultimately creating the formation of a new knowledge [1, 3-5].

Knowledge sharing is a mechanism of the spread of knowledge held by the organization to all members of an organization. One of the leading theories relating to knowledge creation comes from Nonaka (2008). Another expert in Knowledge Management Srivastava et al. (2006), defines knowledge sharing as sharing expertise, information, advice, and ideas among individual to another's individual within an organization [7]. In his theory, Nonaka argues that knowledge is created only from the interaction between people or between organizations.

### Task-Technology Fit Theory

This study using the Theory of Task-Technology Fit (TTF) as a basic reference in resolving the issues raised. Task-Technology Fit (TTF) is one of the theories that was built to evaluate the positive impact of the utilization of computer technology which was first introduced by Goodhue and Thomson in 1995. The TTF provides a theoretical basis to determine whether a technology can provide a good impact on user performance through evaluation of conformity between task characteristic and the technology used to complete the task [12].

Task technology fit is a theory that was developed to evaluate the suitability of the duties of a person in an organization with the technology used in these duties. This theory was originally developed by Goodhue and Thomson in 1995. In TTF there are four main pieces of theoretical constructs proposed such as; Task characteristic, Technology characteristic, utilization and performance impact. Goodhue and Thomson in TTF theory suggested that the performance of someone will affect by the characteristic of technology and the utilization of technology for his work.



Source: Goodhue and Thompson, (1995)

Fig. 1 Task-Technology Fit Theory (TTF)

Goodhue and Thomson in 1995 develop a concept for measuring the TTF by using eight factors: quality, locatability, authorization, compatibility, eases of use/training, production timeliness, reliability systems, and relationship with users. Base on the previous research that applies this theory, this theory has been proven able to explain and predict the impact of information technology on the performance of the user. In the beginning, this theory is used to evaluate the performance at the individual level but on the advanced development, this theory was also applied to evaluate the level group of the user which use of information technology. Since the beginning of development, this theory has been applied to various types of information technology, including electronic commerce systems. In the Previous study, researchers generally collaborate theory with other relevant theories or enrich the understanding of technology

utilization. Some researchers explore the theory with new relevant factors to investigate the impact of factors with TTF to getting better understanding impact the use of information technology [13-16]. In developing research instruments researchers using Linkert scale. Where each factor was measured by using 2 to 10 pieces of the question, and with a response using 7 Linkert the scale of strongly agrees to strongly disagree.

#### Model and Hypotheses Development

The following figures (fig.2) shows the relationship between variables that developed for this study. In our research model, we would like to investigate the impact of task-technology fit and social media utilization in student performance for knowledge sharing. The research model contains one independent variable "perceived task-technology fit" and has two dependent variables is the "Social Media Use", and "Student Performance Impact"

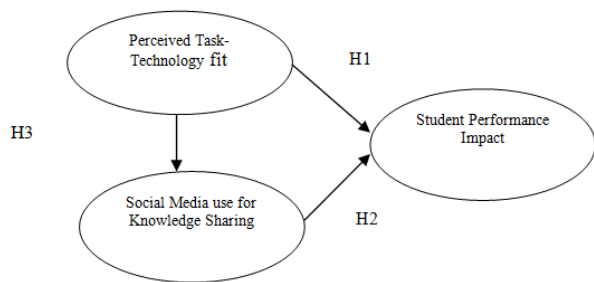


Fig. 2 Research Model

Hypotheses developed for this study are:

**H1:** *Perceived task-technology fit positively influence student performance impact*

**H2:** *Social media use influences positively impact student performance.*

**H3:** *Perceived task-technology fit positively influences the use of social media*

#### Research method

##### A. Participant

Data collection was conducted by direct questionnaire distribution to the respondents. Data collection was using the instrument that contains 10 of the questions. Questionnaires were distributed to students in a university. A total of 75 respondents from 103 respondents who answered the questionnaire. The respondents who participated in the survey consisted of 72% male and 28% female.

##### B. Research Instrument

The instrument applied in this study was developed base on the Task-Technology Fit Theory. Modifications to construct and indicators did to make sure the instrument in meeting the need within the research context. The propose of this study is to examine the relationship between the three constructs are "fit technology task", "social media utilization" and "student performance impact" in the sharing of knowledge. The definition of constructs and their referral sources are described in Table 1.

TABLE I Variable in Research Model

Variable name	Definition	Source
Perceived Task-Technology Fit	User perception related to social media for knowledge sharing	Larsen et al, 2009; Goodhue and Thomson, 1995
Utilization	The use of social media by student	Larsen et al, 2009; Goodhue and Thomson, 1995
Student Performance Impact	Student Performance impact by using social media for knowledge sharing	Larsen et al, 2009; Goodhue and Thomson, 1995

Each construct is measured with indicators using a Likert scale. A scale developed in five levels of ratings, with the following explanation, starting from 1 = strongly disagree to 5 = strongly agree on points. The indicators used in this study are described in the Appendix.

#### C. Data Analysis

Smart PLS used to evaluate the developed research model. Structural Equation Model (SEM) approach applies to validate the research model. SEM was used because of its ability to test a causal relationship between the constructs that contain a number of indicators [17]. There are two major steps undertaken in analyzed data, first conduct model of measurement assessment, the aims of this activity is to ensure that each construct and indicators on the research instrument have met the criteria [18]. The next activity has conducted an evaluation of structural models. In this stage, the hypothesis will be testing along with the model fit assessment.

### III. RESULT AND ANALYSIS

Table 2 below illustrates the profile of the respondents who participated in this study. Respondents came from a college in Indonesia. Data collected by distributed the questionnaire to students. A total of 103 respondents participated in filling out the questionnaire and 75 questionnaires declared valid can be used for further analysis.

TABLE II Demography Characteristic of Respondent

Characteristics of demography	Number of respondents	Percentage
<b>Gender</b>		
Man	54	72%
Woman	21	28%
<b>Age</b>		
20 years and under	14	18%
20-25 years	50	67%
25 years and older	11	25%

### A. Evaluation of Measurement Model

Each construct in the research instrument should be evaluated to check their validity and reliability. It is intended that all constructs that exist meet the standards that have been agreed so it proved valid and reliable. Reliability can be ensured by checking the value of Composite Reliability and Average Variance Extracts (AVE) of each construct. Table 5 below shows that the value of CR and AVE for all constructs is above 0.8 and 0.6. It is indicated that all constructs are reliable. The next reliability test will be performed by internal reliability test of the constructs; this is conducted by evaluating the value of alpha Cronbach. The results of data analysis showed that the Cronbach alpha of each construct is above the 0.7, which indicates the level of reliability is good [19].

TABLE III Model Fit Indicator

	R-Square	Cronbach's Alpha	Commonality	Redundancy
SPI	0.446	0.8347	0.6666	0.2382
SMU	0.402	0.7635	0.6825	0.275
TTF	0	0.7807	0.687	0

The next process is to make sure that all constructs are valid. Two evaluations names convergent validity and discriminant validity will apply in this stage. The first step is to evaluate the value of the loading factor. Table 4 describes the resulting test that all the indicators have factor loading values above 0.6, this indicates that all the indicators met the standards. The indicators meet standard if the construct loading factor value of each indicator above 0.6 [19].

TABLE IV Loading and Cross Loading Factor

	Performance Impact	Social Media Use	Task-Technology Fit
PI1	0.9382	0.6326	0.4551
PI2	0.8715	0.5892	0.6946
PI3	0.6434	0.3012	0.2032
PI4	0.7828	0.4503	0.3496
SMU1	0.5368	0.7907	0.4646
SMU2	0.5216	0.9106	0.6013
SMU3	0.5107	0.7701	0.4997
TTF2	0.58	0.6167	0.825
TTF3	0.2717	0.3715	0.7573
TTF4	0.4792	0.5298	0.8982

The final test in measurement model evaluation is checking the feasibility of the discriminant validity. The test can take place by checking the value of AVE each on each construct exist [20]. The AVE value of a construct must be

greater than the AVE value of the existing construct variants. Table 6 shows that the AVE value of each construct has a higher than the value of the other existing constructs. It can be concluded that the AVE value of each construct has already met the criteria.

TABLE V AVE and CR Value of Variables

	AVE	CR	PF	SMU	TTF
PI	0.666	0.887	0.816		
SMU	0.682	0.865	0.826	0.826	
TTF	0.687	0.867	0.828	0.828	0.828

### B. Evaluation of Structural Model

After conducting an evaluation of the measurement model, and get good results. The next agenda is to test the hypotheses. Before hypotheses test is done, it is necessary to implement several steps to validate that research model. The first step is to measure the explainer power level of models by checking the value of the R2. The result of the test that describes in Figure 2 the R2 value of the model is 0.446. It can be concluded that The model has the ability to predict the performance of students in knowledge sharing using social media amounted to 44.6%. It is proved that the model is fit.

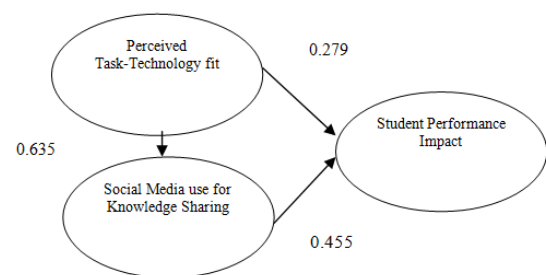


Fig. 3 Evaluation of Research Model

In conducting hypotheses testing, this study uses p-value as indicators. The result of testing is described in Table 6 below. P Value for each hypothesis is: H1 = 0.0001, H2 = 0.0001 H3 = 0.0001. The result shows all of the hypotheses are supported.

TABLE VI Hypotheses Result

Hypotheses	Path Coefficient	T-stat	P-Value	Result
H1	0.279	9.800	0.0001	Significant
H2	0.635	12.99	0.0001	Significant
H3	0.455	5.895	0.0001	Significant

$DF = 72$  ( $DF = N - K$ ) ( $75 - 3 = 72$ ),  $N$  = number of samples  $K$  = number of variables (constructs)

## IV. DISCUSSION

The purpose of this research is to have a better understanding on how task-technology fit elements and the utilization of technology (social media) have an impact on user performance (in this context student as user and knowledge sharing is the main activities of performance).



In General, data analysis result shows that both of elements, task-technology fit element, as well as technology utilization element, impact the user performance. This study found that the task elements of task-technology fit significantly affect the performance of students in sharing knowledge using social media. This means students believe social media provide features that can help them to share the knowledge. Students also believe that their knowledge sharing activities is better by using social media. Future more the students also believe that social media have met their needs in knowledge sharing in learning activities in their college.

The study also reveals that students are assured to using a technology (in this case, social media). This is because they believe that social media has the features they need and these features are complete enough to achieve their goal. They feel social media is the right technology for their activity in knowledge sharing. Our study finding is consistent with previous studies that apply TFF [13, 14]. Aljukhadar et al. and Larsen et al. stated that the people will use technology if the technology fulfillment the needs of the users to performing their task.

Future more, our study indicated if the students also felt that using social media increased knowledge sharing performance. Students feel more productive and more effective due to the use of social media. Our findings are relevant to the study done by Larsen et al and Widagdo and Susanto. Where in the study they found that the use of the technology according to user needs will improve the performance of the work / meet the objectives of the work/activities [13, 14].

Based on the results, this study concluded students have performance increase in their sharing of knowledge activities due to the use of social media in teaching and learning environment. The students felt that social media met their needs and have useful features. The findings in this study reinforce the scientific basis that the performance of the individual as a result of the use of technology is significantly influenced by the characteristics of the technology used but it is also influenced by their desire to take advantage of these technologies.

This study has limitations in term of on the number of respondents for the sample. Future studies may consider obtaining a more proportional number of respondents. There are also two important agenda that should be done in future studies, first investigate whether there are any other elements that independently/ dependently affect the performance of users when using technology in addition to the two elements that have been investigated above. Factors that could potentially include "perceive ease of use", this element relates to whether to utilize a technology users find it easy or not much effort is needed. Another agenda is to conduct research in different universities both in terms of culture or kind. Colleges are investigated currently in the Indonesian island of Sumatra that has a relatively distinct culture with universities on the island of Java. Colleges are investigated at the moment is private college course that different with

public universities environment. These differences can affect the results of the study which has been carried out.

## REFERENCES

- [1] A. M. Kaplan and M. Haenlein, "Users of the world, unite! The challenges and opportunities of Social Media," *Business Horizons*, vol. 53, pp. 59-68, 2010.
- [2] K. Silius, M. Kailanto, and A.-M. Tervakari, "Evaluating the quality of social media in an educational context," in *Global Engineering Education Conference (EDUCON), 2011 IEEE*, 2011, pp. 505-510.
- [3] G. Von Krogh, "How does a social software change knowledge management? Toward a strategic research agenda," *The Journal of Strategic Information Systems*, vol. 21, pp. 154-164, 2012.
- [4] J. Hemsley and R. M. Mason, "Knowledge and knowledge management in the social media age," *Journal of Organizational Computing and Electronic Commerce*, vol. 23, pp. 138-167, 2013.
- [5] L. Razmerita, K. Kirchner, and T. Nabeth, "Social media in organizations: Leveraging personal and collective knowledge processes," *Journal of Organizational Computing and Electronic Commerce*, vol. 24, pp. 74-93, 2014.
- [6] I. Nonaka, *The knowledge-creating company*: Harvard Business Review Press, 2008.
- [7] K. M. Bartol and A. Srivastava, "Encouraging knowledge sharing: The role of organizational reward systems," *Journal of Leadership & Organizational Studies*, vol. 9, pp. 64-76, 2002.
- [8] D. Hislop, *Knowledge management in organizations: A critical introduction*: Oxford University Press, 2013.
- [9] M. E. Jennex, S. Smolnik, and D. Croasdel, "Knowledge management success in practice," in *System Sciences (HICSS), 2014 47th Hawaii International Conference on*, 2014, pp. 3615-3624.
- [10] I. Nonaka and R. Toyama, "The Knowledge-creating Theory Revisited: Knowledge Creation as a Synthesizing Process," in *The Essentials of Knowledge Management*, ed: Springer, 2015, pp. 95-110.
- [11] R. Hanna, A. Rohm, and V. L. Crittenden, "We're all connected: The power of the social media ecosystem," *Business Horizons*, vol. 54, pp. 265-273, 2011.
- [12] D. L. Goodhue and R. L. Thompson, "Task-technology fit and individual performance," *MIS Quarterly*, pp. 213-236, 1995.
- [13] M. Aljukhadar, S. Senecal, and J. Nantel, "Is more always better? Investigating the task-technology fit theory in an online user context," *Information & Management*, vol. 51, pp. 391-397, 2014.
- [14] T. J. Larsen, A. M. Sorebø, and Ø. Sorebø, "The role of task-technology fit as users' motivation to continue information system use," *Computers in Human Behavior*, vol. 25, pp. 778-784, 2009.
- [15] S. Mohammadyari and H. Singh, "Understanding the effect of e-learning on individual performance: The role of digital literacy," *Computers & Education*, vol. 82, pp. 11-25, 2015.
- [16] P. P. Widagdo and T. D. Susanto, "The effect of task-technology fit toward individual performance on the Generation X (1956-1980) using information technology," in *Science in Information Technology (ICSITech), 2016 2nd International Conference on*, 2016, pp. 181-186.
- [17] J. F. Hair, C. M. Ringle, and M. Sarstedt, "PLS-SEM: Indeed a silver bullet," *Journal of Marketing Theory and Practice*, vol. 19, pp. 139-152, 2011.
- [18] M.-C. Boudreau, D. Gefen, and D. W. Straub, "Validation in information systems research: a state-of-the-art assessment," *MIS Quarterly*, pp. 1-16, 2001.



Appendix  
Variables and Indicators

Variable	Indicator	Source
Perceived Task-Technology Fit	Social Media application provides functions/features that help me to share information and knowledge with fellow students and professors	Larsen et al, 2009; Goodhue and Thomson, 1995
	Sharing information and knowledge are better by using social media.	Larsen et al, 2009; Goodhue and Thomson, 1995
	Features of social media fit my needs for sharing information	Larsen et al, 2009; Goodhue and Thomson, 1995
utilization	I use social media to share information	Larsen et al, 2009; Goodhue and Thomson, 1995
	I use social media to share knowledge	Larsen et al, 2009; Goodhue and Thomson, 1995
	I use social media to discuss the information and knowledge with others students and professors	Larsen et al, 2009; Goodhue and Thomson, 1995
Student Performance Impact	Sharing of information/knowledge through social media makes my information sharing activities more productive	Larsen et al, 2009; Goodhue and Thomson, 1995
	Sharing of information/knowledge through social media sharing makes me more effective	Larsen et al, 2009; Goodhue and Thomson, 1995
	Social media with information and knowledge sharing services tool improving the quality of my knowledge sharing	Larsen et al, 2009; Goodhue and Thomson, 1995
	I can easily and effectively share information and knowledge through social media	Larsen et al, 2009; Goodhue and Thomson, 1995

# Learning Motivation increased due to a Relaxed Assessment in a Competitive e-Learning Environment

<sup>1,2</sup>Muhammad Said Hasibuan

<sup>1</sup>Dept of Electrical Engineering  
University Gadjah Mada Yogyakarta  
Indonesia, said.s3te15@mail.ugm.ac.id

<sup>2</sup>Institute Business and Informatics  
Darmajaya, Bandar Lampung,  
Indonesia  
msaid@darmajaya.ac.id

<sup>2</sup>Onno W Purbo

Institute Business and Informatics  
Darmajaya  
Bandar Lampung, Indonesia  
onno@darmajaya.ac.id

**Abstract**— In this work, e-learning is used to increase learners' motivation and competence in addition to learning complementary environment. This work is based on the 7-years of hybrid e-learning classes on Operating System, Computer Network, Network Security, Network Management subjects at 3 Indonesian universities, namely, Surya University, STKIP Surya, and IBI Darmajaya. Most of STKIP Surya's students are from Papua and need more attention and motivation than others. Relaxed assessment processes are performed on each module in addition to mid term and final exams. On average, there are 12-18 modules in each subject matter. To motivate the learners, they may perform as many exams as ones' wish to attained the highest possible mark within the semester on all exams and quizzes. Relaxed assessment processes to attained maximum grades seems to increase the learners' motivation as some learners' retrying in exceeding 50 times for the 100 questions final shown in the Level of Competency (LoC) measurement. In addition, to anticipate, any cheating, eliminate remedial and cost savings, all exams are done on moodle via web. Such method of a whole semester relaxed assessment equipped with about 2000-6000 questions bank per subject and is for the first time performed in Indonesia. This study is also found an increase in the majority of learner's understanding on the subject is very good without remedial. Thus, e-learning seems not only complement learning processes but also able to motivate and to improve the competence of learners as well creating healthy competitive environment among learners.

**Keywords**—*E-learning, Relaxed Assessment, motivation, Level of Competency*

## I. INTRODUCTION

Implementation e-learning in campuses seems to be steadily increased as more universities own and run e-learning websites. The current use of e-learning is normally as a complement to the learning process to deliver teaching materials [1]. Low motivation, urge to learn and boredom are observed in learners while accessing e-learning sites [2].

Previous researches have been done to improve the learners' motivation, such as using a learning style detection approach

[3][4][5][6]. The results showed that the learners' motivation learning style was raised.

The learners' motivation is dynamic, various aspects, such as, the learning subject, pressure and urge to learn may contribute to it. Thus, competency achievement pace may be different for different topic and learner. Methods needs to be examined to maintain and to push the motivation, pressure as well as urge to learn.

This work is based on our experience in seven (7) years implementation of hybrid e-learning classes on Operating System, Computer Network, Network Security, Network Management subjects at 3 Indonesian universities, namely, Surya University, STKIP Surya, and IBI Darmajaya. A relaxed assessment processes are performed on each module of the subject in addition to mid term and final exams. On average, there are 12-18 modules in each subject matter.

## II. MATERIAL AND METHOD

### A. Development of E-Learning

Development of e-learning has been increased and resulting several studies. Several researches have been done to optimized the e-learning processes. Some of the main obstacles in using e-learning, i.e., boredom, demotivation and eventually leads to drop out [7][8][9] needs to be overcome.

One possible cause of boredom and lack of motivation and thus drop out is the lack of personalization given to learners [10][11]. Thus, ability to suite each learners' pace in learning would be substantial.

### B. Taking Research Data

This work use e-learning website build on Moodle Learning Management System (LMS) at <http://lms.onnocenter.or.id/moodle/> for computer network Surya University course and network management IBI

Darmajaya graduate course, and <http://lms.stkipsurya.ac.id> for computer network STKIP Surya course. In our sample classes, there are 17 students participate in computer network class in Surya University, 35 students participate in computer network class in STKIP Surya, and 31 graduate students in network management class at IBI Darmajaya.

The learners' profile of these three (3) universities is fairly different. The majority of STKIP Surya learners is from Papua, Eastern Indonesia islands, and some from Riau islands. The one from Papua and eastern Indonesia may need more attention as well as different approach to motivate and to increase urge to learn. While the majority of Surya University students are from Jakarta and java families. The IBI Darmajaya graduate students are a little bit older than the other two universities and mainly workers, teachers in South Sumatera and surrounding areas.

### C. Research Data Retrieval Process

Research data is taken from the eighteen (18) quizzes, mid test and final exam in the course. A sample of one semester running course was taken in three (3) different universities. The learner may took the exam multiple times within the semester. Since ample questions available in the question bank, a relaxed assessment may be performed. In contrast to conventional assessment, in a relaxed assessment process, the learners may perform as many exams as ones' wish to attained the highest possible mark within the semester on all exams and quizzes. To anticipate, any cheating and eliminate remedials, all exams are electronically performed on moodle via web. In addition, exam time is limited to one (1) hour for 100 questions for mid and final exams.

Since all processes including assessments are electronically performed on moodle. Thus, no paper based processes are involved. Learners may performed their assessment at anytime and anywhere including from their comfort home. It, in turn, significantly reduces campuses' operating costs. to increases competitiveness, intermediate attained mark is weekly published on the web available for all learners as well as public to see. It, in turn, significantly increase pressure among learners to perform much better in each quiz and exam.

Since the exams may be electronically performed many times, the total processed marks reaches a large number of data. For example, one of the student Yomilera Yikwa from Papua took 49 times mid term exam and 121 times final exam. The Level of Competency (LoC) measurement will later clearly show that a more relaxed assessment enable learner's motivation and pressure to learn the subjects.

### D. Research Data Evaluation

This paper, Computer Network course at STKIP Surya, Surya University and Network Management graduate course at IBI Darmajaya will be closely examined and compared. These three courses are fairly similar in content, number of quizzes with 2000 questions bank. We will be closely examined and compare the attempts and, thus, learner's motivation to reach highest mark.

Conventional LoC measurement in normal assessment

process may measure the level of learners' competency. In contrast, LoC measurement in a relaxed assessment processes may also evaluate learners' persistence and pressure to reach the highest mark which is not embedded in a more conventional learning method. The persistence measurement may be for the first time realized in formal Indonesian e-learning environment.

## III. RESEARCH METHOD

The Methodology Research conducted in this study can be seen in Figure 1.

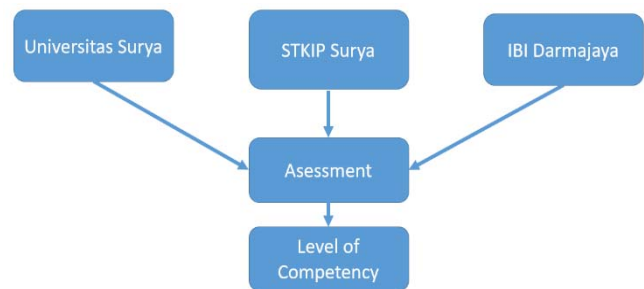


Figure 1 Research Method

Figure 1 shows the used research method to do Student Assessment Evaluation (SAE) in three (3) campuses. In a relaxed assessment process, the students may perform as many exams as ones' wish to attained the highest possible mark within the semester on all exams and quizzes. Such approach is used in the attempt to increase the learners' motivation as well as providing pressure and urge to learn to the learners. The Level of Competency (LoC) measurement will shows that such approach significantly improve competency attained and remove any remedials in the process.

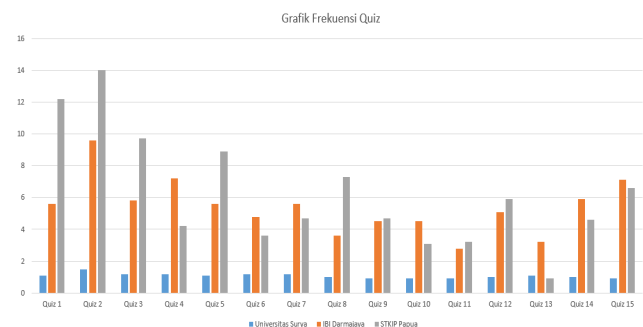


Figure 2 Average Attempts per Quiz of 3 Campuses

Figure 2 shows the average number of attempt performed per learner perquiz in 3 campuses for computer network course in STKIP Surya and Surya University and Network Management in IBI Darmajaya. The figure clearly show significantly more attempt performed by learners at STKIP Surya as compared to the other 2 campuses. Papuan and Eastern Indonesian learners must struggle to do more quizzes to achieve good grades. Quiz re-attempt process is very easy and no cost within the e-learning system. Quiz results can immediately be seen by the learner upon quiz submission. This directly motivates learners to achieve higher marks. Motivation may be internally driven from within learner-self and externally by seeing other learner's mark.

The learners at IBI Darmajaya requires much lower number of attempts perquiz as compare to STKIP Surya at achieve highest marks. It doesn't mean the the learners at IBI Darmajaya is not motivated. It is to say, the learners at IBI Darmajaya require less number of attempt to reach high mark as compare to STKIP Surya.

Unlike STKIP Surya and IBI Darmajaya, many learners at Surya University achieve good mark in their first attempt in each quiz. In other words, not many learners at Surya University re-attempt the quiz after their first attempt. In rare occasion, the learner at Surya University re-attempt their quiz up to five (5) times. Most Surya University student, reach high mark after their first attempt

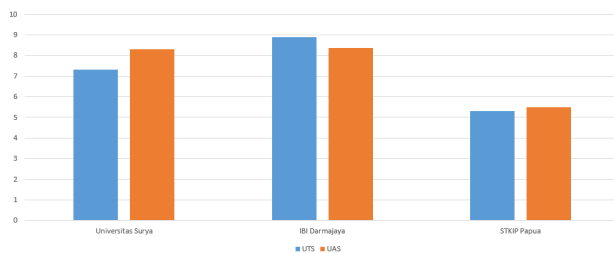


Figure 3 Average Mid Semester and Final Exam mark of the 3 campuses

Figure 3 shows the average Mid Semester and Final Exam mark of the 3 campuses. The comparison shows learners at IBI Darmajaya achieve an average better mid term mark and lower in final exam. In contrast to the other 2 campuses, average mark at Surya University shows a significant increase in final exam as compare to mid term exam. A somewhat increase of average final exam mark is also observed in STKIP Papua.

We may note that on-line exam schedule is fairly relaxed and not at all overlap with other exam schedule of other courses. Thus, during mid term on-line exams, students is fairly relax and no pressure from exams and assignments. However, at the end of semester, most students are normally working under pressure to complete the assignment and exams of other courses.

Figure 2 and 3 show clearly that the motivation and spirit to learn much increase as learner may see the result of their exam immediately after completing the exams. In contrast to conventional assessment proses, it requires longer time to obtain the results. Such long waiting time is one of discouraging aspect in the learning processes.

Immediate release of mark of all quiz, mid term, and final increase motivation and feedback to the learner to concentrate their learning effort. In this study, the number of attempts to do the exams is not limited within the semester. In addition, since only the highest mark is taken into account for the final mark of each quiz, it significantly boost the motivation of the learners to re-attempt the exam and to learn.

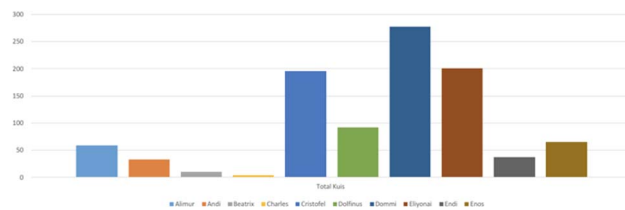


Figure 4 Total Quiz enrolled in 1 semester by STKIP Surya Student

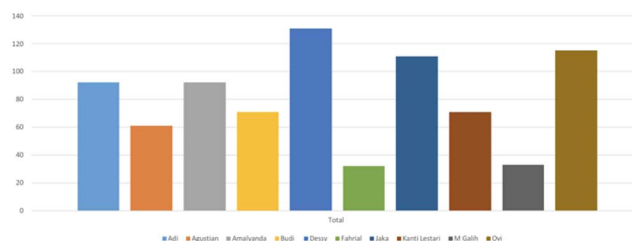


Figure 5 Total Quiz enrolled in 1 semester by IBI Darmajaya Student

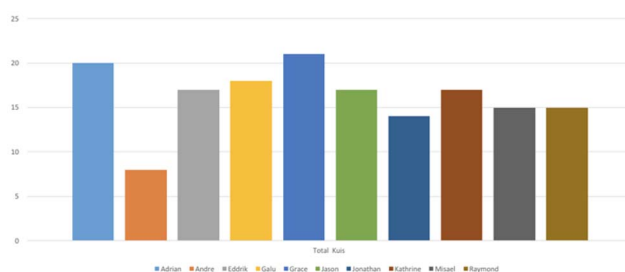


Figure 6 Total Quiz enrolled in 1 semester by Surya University Student

Figure 7,8 and 9 show a sample growth of mark in a single quiz with multiple attempts of one students of STKIP Surya (Figure 7), IBI Darmajaya (Figure 8), and Surya University (Figure 9) who do the exam multiple attempts. The Figures clearly shows an increase trend from its initial attempt to to final attempts and all consistent for all three (3) universities. Thus, it indicate the relaxed assessment process facilitate an increase in level of competency in its particular subject assess in the quiz.

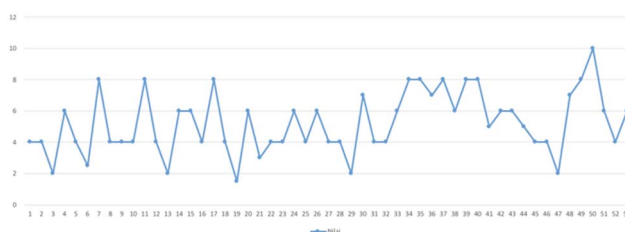


Figure 7 Relax Assessment Quiz 1 STKIP Papua Student

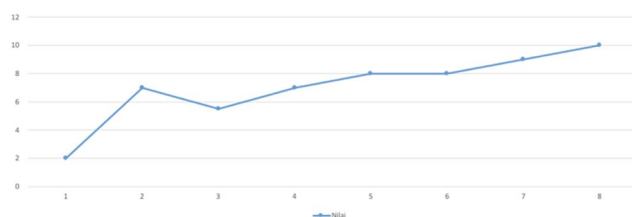


Figure 8 Relax Assessment Quiz 1 IBI Darmajaya Student



Figure 9 Relax Assessment Quiz 1 Surya University Student

The influence of teaching materials to improve the motivation of learning becomes one of next issue that needs to be investigated.

#### ACKNOWLEDGMENT

This work was supported by Ristek Dikti of the Ministry of Research and Higher Education of the Republic of Indonesia under Doctoral Research Grant.

#### REFERENCES

#### IV. RESULT DISCUSSING

This study found that:

1. E-Learning may be used beyond complementing learning processes.
2. A relaxed assessment method allowing learner to perform as many exams as ones' wish to attained the highest possible mark. This, in turn, enables learner's motivation, persistence and create urge to learn the subjects. Such method is for the first time performed in Indonesian universities.
3. Unlike conventional assessment method, whole semester relaxed assessment method allow us to measure learners' increase in motivation and persistence in LoC Measurement.
4. The use of e-learning adding a significant amount of benefits including anytime and anywhere learning environment to the learners while not increasing, in fact, reducing, campuses' operating costs.
5. Allowing students to perform unlimited attempts and taking into account only the highest mark of each quiz seems to be significantly boost the motivation to re-attempt the exam and to learn, and, in turn, increase the average achievable mark without having remedial.
6. Relaxed Assessment processes with unlimited attempts allowing those who are motivated and wants to struggle to be able to achieve good grades. It is rare in conventional learning environment.

Further research related to learning agent to be explored to provide recommendation of teaching materials in accordance with the evaluation results.

- [1] T. Bourlova and M. Bullen, "The impact of e-learning on the use of campus instructional space," *Adv. Web-Based Learn. - Icwl 2005*, vol. 3583, pp. 397–405, 2005.
- [2] H. Imran, M. Belghis-Zadeh, T.-W. Chang, Kinshuk, and S. Graf, "PLORS: a personalized learning object recommender system," *Vietnam J. Comput. Sci.*, no. AUGUST, 2015.
- [3] M. P. P. Liyanage, K. S. L. Gunawardena, and M. Hirakawa, "Using Learning Styles to Enhance Learning Management Systems," *Chapter I*, vol. 07, no. 02, pp. 1–10, 2014.
- [4] P. S. MS Hasibuan, LE Nugroho, "Learning Style Model Detection Based on Prior Knowledge in E-learning System MS," in *2017 Second International Conference on Informatics and Computing (ICIC)*, 2018, pp. 2–6.
- [5] I. Hussain, "Pedagogical Implications of VARK Model of Learning," *J. Lit. Lang. Linguist.*, vol. 38, no. 2000, pp. 33–37, 2017.
- [6] N. bin A. Rashid *et al.*, "Summative EEG-based Assessment of the Relations between Learning Styles and Personality Traits of Openness," *Procedia - Soc. Behav. Sci.*, vol. 97, pp. 98–104, Nov. 2013.
- [7] M. S. Hasibuan and L. Nugroho, "Detecting Learning Style Using Hybrid Model," *2016 IEEE Conf. e-Learning, e-Management e-Services Detect.*, pp. 107–111, 2016.
- [8] R. Habibi, D. B. Setyohadi, and K. I. Santoso, "Student learning styles and emotional tendencies detection based on Twitter," *2017 4th Int. Conf. Inf. Technol. Comput. Electr. Eng.*, pp. 239–243, 2017.
- [9] A. Bruun and J. Stage, "Human-Computer Interaction – INTERACT 2015," *Human-Computer Interact. - INTERACT 2015, Vol. 9297*, vol. 9297, no. SEPTEMBER, pp. 159–176, 2015.
- [10] S. V Kolekar, R. M. Pai, and M. Pai, "Prediction of Learner 's Profile Based on Learning Styles in Adaptive E-learning System," *iJET*, vol. 12, no. 6, pp. 31–51, 2017.
- [11] J. Jun, "Understanding dropout of adult learners in e-learning.," no. 1, p. 158, 2005.



# Development of Mobile Based Educational Game as a Learning Media for Basic Programming in VHS

Hakkun Elmunsyah<sup>1\*</sup>, Gradiyanto Radityo Kusumo<sup>2</sup>, Utomo Pujianto<sup>3</sup>, Didik Dwi Prasetya<sup>4</sup>

Electrical Engineering Department  
Universitas Negeri Malang  
Malang, Indonesia

<sup>1</sup>hakkun@um.ac.id; <sup>2</sup>radityogrady@gmail.com; <sup>3</sup>utomo.pujianto.ft@um.ac.id; <sup>4</sup>didikdwi@um.ac.id

**Abstract**—The purpose of this research is to develop mobile based education game which will be used as the learning media of basic programming for grade X VHS student as well as to know the its eligibility level. The developed education game consists of four basic programming competencies. This learning media is developed using ADDIE model with waterfall model for the flow development. The validation process involved 2 material experts, 1 media expert, and two groups of eligibility testing. The type of data is qualitative and quantitative with the method of data collection is questionnaire. The measurement uses five scale of likert. This study concluded that the developed educational game are valid and eligible to be used as a basic programming learning media.

**Keywords**—Educational Game, Mobile, Basic Programming, VHS.

## I. INTRODUCTION

Students of computer and information technology in vocational high school (VHS) are demanded to have the basic skill in programming. In fact, some schools depends on BSE (*Buku Sarana Elektronik*) which is unpracticable and not suitable with the 2013's curriculum 2013 (revision 2017). Furthermore, the other obstacles are related to the limitation of material source. The limited material source come from their teacher without other learning media as the material source[1].

The conventional learning process only focus on students' cognitive aspects. The teacher uses a book as the main source of information. As a result, the student may feel bored to the subject[2]. It may directly affect the student's learning outcomes. Based on observation, in 1<sup>st</sup> daily test (3<sup>rd</sup> and 4<sup>th</sup> competency) only 27% of 60 students passed those daily test and in 3<sup>rd</sup> daily test (6<sup>th</sup> competency) only 45,9% of students passed those daily test. It has been proven that the conventional learning process method still give a problem to student learning outcomes.

One of ways to enhance the leaning outcome is the use of learning media. Learning media may enable student self motivation to study and understand the material [3]. The form of learning media can be picture, audio, video, animation, props, simulation tool, education game, and other media.

Educational game is one form of learning media which combine education with entertainment. In an educational game consist of multimedia elements such as picture, audio, and animation. Learning process through educational game media can help student more interested to study and make student feel pleases without fell coercion to study. Playing games makes them more enthusiastic, relaxed, happy, and

comfortable in following the lessons[4]. On the other side, the usage of smartphone increase time by time. Based on the quistionaire, 59 of 60 Vocational High School students already have a minimum Android Jelly Bean smartphone. Unfortunately, the increase of smartphone users is not maximally used in learning process by teacher. Therefore, mobile based learning media can be implemented as the potential sollution for improving the learning process. The development of this media using ADDIE model (Analysis, Design, Development, Implementation, and Evaluation).

## II. THEORETICAL BASIS

### A. Research and Development

Research and development is a research method to produce a product and test the effectivity of this product[5]. Effectivity test is needed through a research to test the product which is can make this product can be usefell in wide society. The research activity get information about user needs and data analysis, while the development activity produce learning tools referring to the previous stage.

ADDIE stands for Analyze, Design, Develop, Implement, and Evaluate is a research and development model by Dick and Carey. The consept is being applied for constructing performance-based learning. ADDIE serves as guiding framework for complex situations, appropriate for developing educational products, and other learning resources[6]. The whole procedure of ADDIE model can be seen at Figure 1.

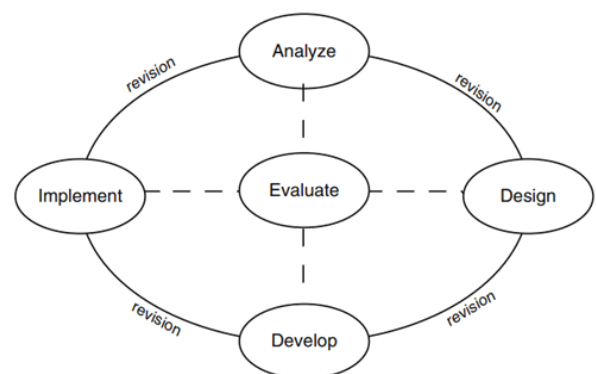


Fig. 1. ADDIE model



### B. Basic Programming Subject

Basic programming is one of compulsory competency for computer and information technology VHS-students. In the structure of curriculum 2013 (revised in 2017), basic programming subject classified in basic group of vocation program (C2), consist of basic, must be passed by X grade before go deep into their competency skills.

The basic competency of this subject are 1) Applying flow of computer program logic; 2) understanding software for programming language; 3) applying flow of programming with structure of computer programming language; 4) applying the used of data type, variabel, constant, operator, and expression; 5) applying operation of arithmetic and logic; 6) applying the branching structure control in programming language; 7) applying looping structure control in programming language; 8) analyze the usage of array to save the data in memory; 9) applying the usage of function; 10) applying user interface in application; 11) applying any kind of control structure in user interface application; 12) analyzing the construction of simple application with user interface based; 13) evaluating debugging in simple application; and 14) evaluating installer package in simple application.

### C. Educational Game

Game is a system with artificial conflict where the player can interact with the system by using certain rules. Rules limit the player behavior and determine player. Game is used to play and use the certain technique and method which can give joyfull and inner satisfaction to its users[7].

Game with educational content better known as educational game. Educational game boost students' interest through the pleased material subject, to ease the students understanding. Educational game is a game for teaching the player [8]. Game with education genre intensively refers to the content and propose of the game[9].

## III. RESEARCH METHOD

In this paper, the model of research and development model which used are ADDIE model. This model is used due to its detail process as well as easiness for implementation. There are five steps in this method and will be explain in the following sub-sections.

### A. Analyze

Analyze is a step to analyze the needs and to adjust the real condition in field. In this step the activity consist of analyze the learning process, analyze the need, also analyze the competency and current curriculum.

### B. Design

Design step have to give solution in the form of prototype or product depiction which will be developed. In this step the prototype be made related with formulation of learning goal, material lesson, form of exercise, also the content of game (storyboard, flowchart, game asset) which will be developed. In this step, the formulation of material lesson take 4 competency, there are 1) applying the use of data type, variable, constant, operator, and expression; 2) applying operation of arithmetic and logic; 3) applying the branching structure control in programming language; and

4) applying looping structure control in programming language. Material referred to module, book, and internet source. The design of game flowchart is showed in Figure 2. Asset of game consist of character, background, item, sound effect, and etc.

### C. Development

Development step is a step where the product of educational game will be developed based on the developed prototype. Here, the main procedure is that to produce the content also develop the proponent learning media. This model give depiction the flow of product development sequentially which is start from 1) analyze; 2) design; 3) coding; and 4) testing.

In this step, alpha testing procedure is implemented to minimalize the failure in product and make sure game can be work suitable with gameplay and all of game asset can be work with well before tested to expertise / validator.

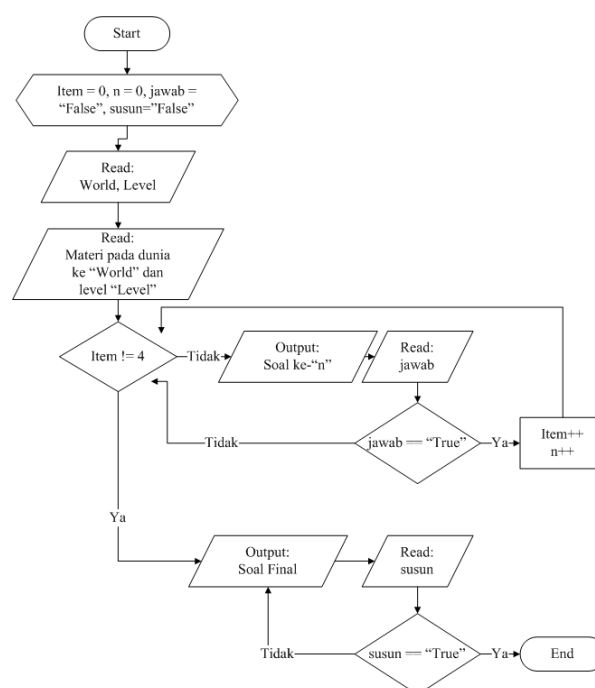


Fig. 2. Flowchart

### D. Implementation

In implementation step, product should be validated by expertise / validator. Afterwards, product can be implemented and tested to students.

In validation process involves two experts: media and material experts. The propose of validation process is giving response or suggestion related to the product which being developed. Material expertises will judge the content and context of material lesson in product. Media expertise will judge functionality of the product.

Feasibility testing is executed by the VHS students. Eligibility testing done in 2 groups: big (30 students) and small groups (10-15 students) [5].

### E. Evaluations

In research and development ADDIE model, evaluations step is the final step in whole of procedure. Basically,

evaluations step is always repeated. If there is any kind of improvement or mismatch solution in every step of development, the data can be used as revision data through the development of the product.

#### F. Research Data

Based on preliminary observation data done to 60 student as respondents and 4 schools, the result are:

- Students have obstacles related to their logic skill.
- Students who passed basic programming subject only 25-40%.
- Students claim content in their modul and BSE less interactive, ilustratif, and only make bored.
- 59 of 60 student already have smartphone with minimal operating system are Android Jelly Bean.
- The current curriculum is curriculum 2013 revision 2017.

#### G. Data Collection

In this research, the used data are quantitative data and qualitative data. The method of data collection are questionnaire which is validate by advisors before given to expertise and respondent. The type of used questionnaire is closed-questionnaire and open-questionnaire with measurement scale are likert scale consisting of five categories of choice [10]. Closed questionnaire are the questionnaire with the amount of item and alternative response already decided, so the respondent enough to choose under the real condition. Open questionnaire used to give response from respondent such as review / suggestion / comment which can be respond freely.

The data analysis uses the formula percentage, where the results of these calculations were used to see the validity and eligibility of this product. Equation 1 is used to determine the percentage of validity and eligibility for this product in each question and Equation 2 is used to determine the percentage of validation and eligibility for this product in total [11]. Table I shows the classification of validity level criteria and Table II shows the classification of eligibility level criteria.

TABLE I. VALIDITY CRITERIA BASED ON PERCENTAGE

Percentage (%)	Validity Criteria
85,01 – 100,00	Very Valid, or can be used without revision
70,01 – 85,00	Valid Enough, or can be used but need little revision
50,01 – 70,00	Less Valid, suggested not to used because need huge revision
01,00 – 50,00	Not Valid, or forbidden to used

TABLE II. ELIGIBLTY CRITERIA OF LEARNING MEDIA

Percentage (%)	Validity Criteria
82 – 100	Very Eligible
63 - 81	Eligible
44 - 62	Less Eligible
25 - 43	Not Eligible

$$V = TSe / TSh \times 100\% \quad (1)$$

Description:

V = Validity based on percentage

TSe = Total of empirik score

TSh = Total of maximal score

$$V = (\sum TSe) / (\sum TSh) \times 100\% \quad (2)$$

Description:

V = Validity based on percentage

$\sum TSe$  = Amount of total empirik score

$\sum TSh$  = Amount of total maximal score

## IV. RESULT AND DISCUSSION

The game interface of the mobile based educational game of basic programming subject for X grade is presented in Figure 3.

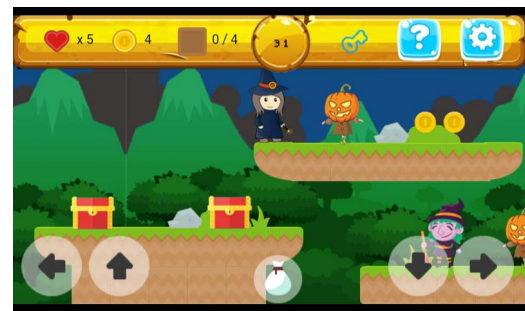


Fig. 3. Game Interface

Mobile based education game of basic programming has been developed used game engine software (Construct 2), Adobe photoshop CS6 is used to create game asset, Format Factory is used to change audio format, and Microsoft Office Visio 2007 as software used to make flowchart. This education game consist 4 competency with the final product is .apk extension and the minimum spesification product for the smartphone are:

- 1 GB RAM.
- Android Jelly Bean.
- Smartphone screen resolution are 480 x 800 pixel.
- 80 MB. of smartphone memory

Media expert validation data were obtained from questionnaire given to the lecturer from Universitas Negeri Malang. The media validation process take 2 times in validation with the final results are shown in Table III.

According to table I on the validity criteria, the results obtained from the media expertise as a whole stated that the learning media used in the learning process are very good. In 1<sup>st</sup> validation, the average score obtained 84,5% with small revisions should be done. The contain should be revised are (1) usability, (2) visual, and (3) layout and interface with the suggestions by the validator are (1) change game welcoming background, (2) give notification when the item are less, and (3) replace the controller. Based on those

result and suggestion, we take revisions in our product and done the 2<sup>nd</sup> validation. In 2<sup>nd</sup> validation, the average score of the whole aspect of the assessment obtained 98,5%. Hence, it can be said that the media used in learning process are valid and don't require any revision.

TABLE III. MEDIA EXPERT VALIDATION

No	Assessment Aspect	$\Sigma Tse$	$\Sigma Tsh$	V (%)	Criteria
1	Software Engineering	64	65	98,5	Very Valid
2	Communication Visual	68	70	97,1	Very Valid
3	Learning Design	20	20	100	Very Valid
Amount		152	155		
Average				98,5	Very Valid

Material expert 1 validation data were obtained from questionnaire, given to the lecturer from Universitas Negeri Malang. The final results of material validation 1 are shown in Table IV.

TABLE IV. MATERIAL EXPERT 1 VALDATION

No	Assessment Aspect	$\Sigma Tse$	$\Sigma Tsh$	V (%)	Criteria
1	Learning Design	103	105	98	Very Valid
2	Communication Visual	19	20	95	Very Valid
3	Software Engineering	10	10	100	Very Valid
Amount		132	135		
Average				97,8	Very Valid

Material expert 2 validation data were obtained from questionnaire given to a VHS teacher, It takes two time of validation process in material expertise 2. The final results of material validation 2 are shown in Table V.

TABLE V. MATERIAL EXPERT 2 VALDATION

No	Assessment Aspect	$\Sigma Tse$	$\Sigma Tsh$	V (%)	Criteria
1	Learning Design	99	105	94,3	Very Valid
2	Communication Visual	19	20	95	Very Valid
3	Software Engineering	9	10	90	Very Valid
Amount		127	135		
Average				94,1	Very Valid

According to table I on the validity criteria, the results obtained from the material expertise as a whole stated that the material in learning media used to the learning process is very good. The average score of the whole aspect of the assessment obtained 97,8% from material expertise 1 and 94,1% from material expertise 2. Hence, it can be said that the material in media used for learning process are valid and don't require any revision.

Small group testing assess 15 VHS students using questionnaire The final results of small group are shown in Table VI.

The obtained results shows that the educational game used to the learning process is very good and eligible. The average score of the whole aspects is 89,5%. Hence, it can be said that the product are eligible and no revision needed.

TABLE VI. SMALL GROUP TESTING ASSESSMENT

No	Assessment Aspect	$\Sigma Tse$	$\Sigma Tsh$	V (%)	Criteria
1	Learning Design	882	975	90,5	Very Valid
2	Communication Visual	918	1050	87	Very Valid
3	Software Engineering	884	875	91	Very Valid
Amount		2684	3000		
Average				89,5	Very Valid

Big group assessment were obtained from questionnaire, is given to 30 VHS students. The final results of small group are shown in Table VII.

TABLE VII. BIG GROUP TESTING ASSESSMENT

No	Assessment Aspect	$\Sigma Tse$	$\Sigma Tsh$	V (%)	Criteria
1	Learning Design	1793	1950	92	Very Valid
2	Communication Visual	1893	2100	90,1	Very Valid
3	Software Engineering	1881	1950	92,9	Very Valid
Amount		5497	6000		
Average				91,7	Very Valid

According to Table II, the results obtained from the big group assessment testing shows that product of educational game used to the learning process is very good and eligible. The average score of the whole obtained-assessment aspects is 91,7%. Hence, it can be said that the product are eligible and don't require any revision for learning process.

## V. CONCLUSION

The developed mobile based educational game is a new innovation of learning media for VHS students. This media consist of 4 competency of basic programming subject. Based on experiments, it can be drawn that the developed educational game is eligible to use in learning process of basic programming.

## REFERENCES

- [1] Pebruanti, L., and Munadi, S. 2015. Pelajaran Pemrograman Dasar Menggunakan Modul Improving Motivation And Learning Outcomes In Basic Programming Using Modules In SMKN 2 Sumbawa. Jurnal Pendidikan Vokasi, 5(3), pp.365–376.
- [2] Prasetyo, L. A. 2015. Pengembangan Game Edukatif “Merakit Komputer Yuk!” Sebagai Media Pembelajaran Pengenalan Perangkat Keras dan Perakitan Komputer Untuk Peserta Didik SMK Kelas X di SMK Batik Perbaik Purworejo. Yogyakarta: FT UNY.

- [3] Ayuningsih, S. 2015. Pengembangan Media Pembelajaran Interaktif Menggunakan Adobe Flash CS3 Pada Mata Pelajaran IPS Materi Keadaan Alam di Indonesia Kelas VII. Yogyakarta: UNY.
- [4] Heriyanto, A., Haryani, S., and Sedyawati, S. M. R. 2014. Pengembangan multimedia pembelajaran interaktif berbasis education game sebagai media pembelajaran kimia. *Chemistry In Education*, 3(1), pp. 1–8.
- [5] Sugiyono. 2013. Metode Penelitian Pendidikan (Pendekatan Kuantitatif, Kualitatif, dan R&D). Bandung: Alfabeta.
- [6] Branch, R. M. 2009. *Instructional Design: The ADDIE Approach*. London: Springer.
- [7] Wulandari, A. D. 2012. Game Edukatif Sejarah Komputer Menggunakan Role Playing Game (RPG) Maker XP Sebagai Media Pembelajaran di SMP Negeri 2 Kalibawang. Yogyakarta: FT UNY.
- [8] Putra, D. R. 2016. Pengembangan Game Edukatif Berbasis Android Sebagai Media Pembelajaran Akuntansi Di Kelas Xi Ips Sma Negeri 1 Imogiri Pada Materi Jurnal Penyesuaian Perusahaan Jasa. *Fakultas Ekonomi Universitas Negeri Yogyakarta*, pp. 1–199.
- [9] Trisna, P., Permana. H., Darmawiguna, I. G. M., Windu, M., and Kesiman, A. 2014. *JA-KO Balinese Pizza : Game Edukasi Interaktif Jaringan Komputer*. 3rd ed, pp. 80–87.
- [10] Widoyoko, E. P. 2017. *Teknik Penyusunan Instrumen Penelitian*. Yogyakarta: Pustaka Pelajar.
- [11] Akbar, S. 2013. *Instrumen Perangkat Pembelajaran*. Bandung: PT. Remaja Rosdakarya.

# Incident and Service Request Management for Academic Information System based on COBIT

Indra Kharisma Raharjana  
Information Systems  
Universitas Airlangga  
Surabaya, Indonesia  
indra.kharisma@fst.unair.ac.id

Ibnu Ibadillah  
Information Systems  
Universitas Airlangga  
Surabaya, Indonesia  
ibnu-ibadillah-  
fst13@fst.unair.ac.id

Purbandini  
Information Systems  
Universitas Airlangga  
Surabaya, Indonesia  
purbandini@fst.unair.ac.id

Eva Hariyanti  
Information Systems  
Universitas Airlangga  
Surabaya, Indonesia  
eva.hariyanti@fst.unair.ac.id

**Abstract**— This paper explores application of Incident and Service Request Management for academic services. We are using Control Objectives for Information and Related Technologies (COBIT) framework as basis for determining the activities in Incident and Service Request Management. The COBIT itself is an IT governance framework included incident handling and service requests, also providing incident response and service request decisions. The software will be developed as a proof of concept that it brings benefits to academic service operations. For most academic services in university, encountered a problem such as incidents reports or a request for services are not immediately addressed, took a long time to respond, or even lost and left unreadable. It is a good idea to standardize incident management and plant it into academic information systems to enforce its application. In software development, we perform five development stages: requirement analysis, system design, stakeholder confirmation, system development, and system evaluation. In requirement analysis stages, we elicited features from activity describe in COBIT and customize it based on interviews and observation. We design use case diagram, use case scenario and database design in system design stages. In stakeholder confirmation stages, a meeting with the stakeholders held and discuss whether the system complies with the requirements or not. system adaptations are made to answer stakeholders concern. System development is conducted based on confirmed system design. Stakeholder evaluated after they follow the case simulation session. Stakeholders provide an evaluation of the system according to their role, based on their experience when using the system in the simulation session. User experience (UX) aspects are also evaluated based on user's interaction with the system. User experience results obtained meet all aspects, including useful, usable, desirable, findable, accessible, credible, and valuable. The evaluation with stakeholder demonstrates the improvement of academic service quality and user satisfaction of the proposed Incident and Service Request Management system solution.

**Keywords**— Academic Information System, COBIT, Incident management, Incident reporting system, Service request, Software development

## I. INTRODUCTION

The handling of incidents that occur in organizations is usually carried out based on the experience of existing staff. Differences in staff experience, lack of proper management makes incident handling fail to achieve the expected quality of

completion [1]. The issue of time in handling incidents and service requests is an important concern for organizational management [2] [3], it is expected that incident handling and service requests can be made as short as possible.

These management issues of incident and service requests occur in many business domains, including Higher Education. The application of academic information system nowadays has become mandatory and inevitable for universities [4] [5] [6]. But most academic information systems are still focused on the main processes of universities. Incident and Service Request Management has not been a major concern of academic information systems.

Incidents in academic information systems may be incidents related to IT systems (e.g. error when input value to academic information system) or within academic scope (e.g. collision lecture schedules, damaged classroom facilities). Service requests are limited to requests for services that are often handled by academics, such as classroom usage requests.

This paper proposes to adopt best practice from incident management framework to academic information system. There are several frameworks that deal with incident management, such as COBIT (Control Objectives for Information and Related Technologies) [7] and ITIL (Information Technology Infrastructure Library) [8]. In this study, we will focus on using the COBIT framework as the basis for determining the activities that need to be done. The implementation of the framework has been proven to improve the maturity of organizational governance [7][8][9] [10].

The purpose of this research is to establish incident management and service request mechanisms for academic services. The software development will be done as a proof of concept [11][12]. Requirement Elicitation, Software Design, Stakeholder validation, software development, and software testing will be done in this study to develop Incident and Service Request Management software.

## II. METHODS

The focus of this research is to design the incident and service request management system for academic services based on the COBIT 5 framework. Case studies were conducted at the Faculty of Science and Technology

Airlangga University (FST UNAIR).

#### A. Requirement Elicitation

The system requirements are identified through interviews and observation. Interviews were conducted to identify the parties involved in the incident handling, service request, problems, and constraints. Observations are made to observe directly any incident handling and service requests activities, as well as the assignment of responsibilities.

Process adjustments in academic services are designed considering COBIT. System requirements of the academic service information system were made based on the activities in Manage Service Requests and Incidents Audit/Assurance Program in COBIT framework [7]. Incidents management and service request process has several activities, namely:

1) *Define incident and service request classification schemes*

2) *Record, classify and prioritize requests and incidents*

3) *Verify, approve and fulfill service requests*

4) *Investigate, diagnose and allocate incidents*

5) *Resolve and recover from incident*

6) *Close service requests and incidents*

#### B. System Design

The system built on a web platform. In system design include use case diagram, use case scenario, and database design.

1) *Use Case Diagram*: This diagram illustrates the system user actors involved in the incident management and service request process as a functional model of the system.

2) *Use Case Scenario*: Use Case Scenario is based on steps in the incident management and service requests process in the Faculty of Science and Technology. This scenario contains the activities that are performed by each actor into the system.

3) *Database Design*: The design of the database done by using two models: Conceptual Data Model (CDM) and Physical Data Model (PDM).

#### C. Confirmation of System Design to Stakeholder

At this stage a discussion with the head of academic administration at FST UNAIR conducted. System design and mockup presented to get feedback from stakeholder [14]. System is designed based on information obtained from interviews, observations, and best practices from COBIT.

#### D. System Development

A web-based system will be developed to implement the design. Implementation is made based on the system design. Functional testings are performed according to system design

specifications. Some of the possible cases of incident and service requests are tested in the system. It is used to assess whether the system is acceptable to use.

#### E. Evaluation

Simulation session is put into practice to evaluate incident and service request management. In addition, evaluation is done to see the user experience aspects such as usable, useful, desirable, accessible, credible, findable, and valuable [15][16] [17].

### III. RESULTS AND DISCUSSION

#### A. Results of Requirement Identification

Interviews were conducted with the head of academic administration in FST UNAIR to identify the parties involved in the flow of incident and service requests.

Observations are made to observe directly every activity of incident handling and service request. Observations were made at the FST UNAIR.

Students, lecturers, and employees can report incidents or requests a service. Such complaints may be non-normal events or also a request to a service. Academic officer will process the report. If the academic officer does not handle the case then the escalation is executed, structurally to the vice deans or functionally to the IT department.

We mapped the roles directly related to the incident management and service request process on FST UNAIR using RACI (Responsible, Accountable, Consulted, and Informed) Chart/ A responsibility assignment matrix [7] [8]. These roles are needed to determine the responsibility for implementing incident management and service requests.

TABLE I. RACI CHART

No	Activity	academic officer	IT department	Vice Dean
1	Prioritize incidents and Service Requests	R	I	I
2	Handling requests and incidents	R	-	C
3	Identify incidents	R	I	I
4	Investigation and Diagnosis	I	C	I
5	Resolve and recover from incident	R	I	I
6	Close service requests and incidents	R	C	I

R = Responsible, A = Accountable, C = Consulted, I = Informed:

To aligning the current system with COBIT, COBIT key management practices are use as an ideal activity baseline. System functional requirements are translate from COBIT 5 activities (Table II).



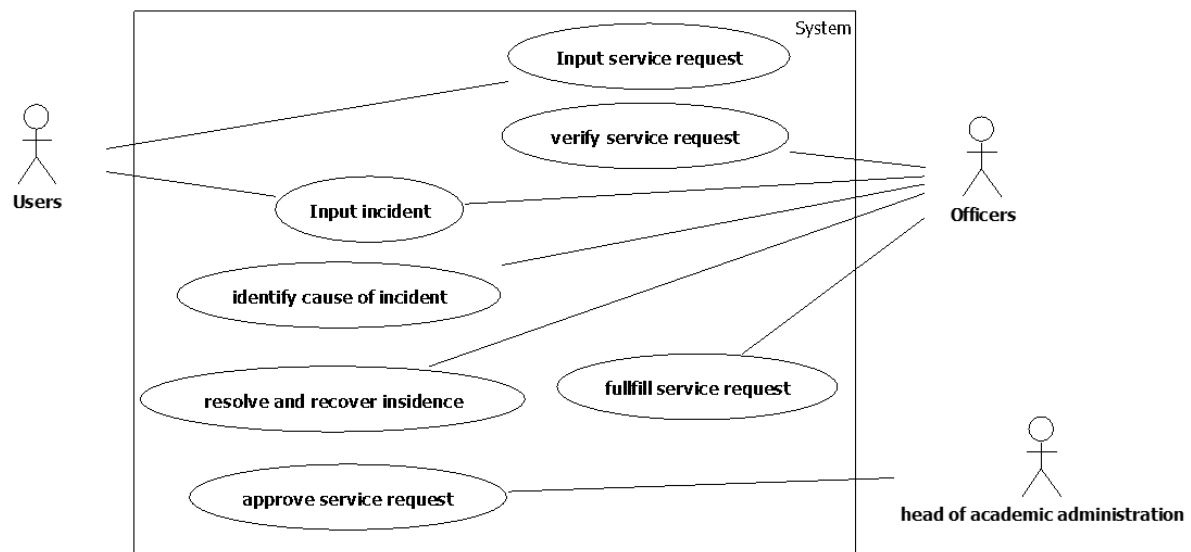


Fig. 1. Use Case Diagram

TABLE II. FUNCTIONAL REQUIREMENTS

No	Activity	Feature
1	Record, classify and prioritize requests and incidents	User may input service request and incident data
2		Users can input data according to type and category
3		Academic officers can give priority estimation to incidents and service requests
4	Verify, approve and fulfill service requests	academic officers verify service requests
5		Head of academic approves the service request
6		academic officers fulfill service requests
7	Investigate, diagnose and allocate incidents	academic officers identify the cause of the incident
8		academic officers recording new incidents
9		academic officer assign a person for incident handling
10	Resolve and recover from incident	academic officer record incident solution
11		academic officers record recovery actions
12		academic officers record incident settlement
13	Close service requests and incidents	academic officers provide notification of service request and incident settlement
14		academic officers close service requests and incidents report

### B. System Design

Use case diagrams were made based on identified functional requirements. Each feature in the use case describes its activity in more detail in the use case scenario. The system activity described in the use case scenario becomes the basis for the database design.

### C. Confirmation to Stakeholder

Based on system design, we created mockup of desired system. So it can get comprehensive feedback from stakeholders. With the mockup, we discussed with stakeholders to make adjustments to the system design.

The results of these confirmations include simplification of activities and roles according to scope. It is also to overcome problems of volatility or policy that change at any time. The system should be made simple, in order to easily adapt to regulatory changes. Yet, it must accord with the COBIT best practices.

Use case diagram changes are made to facilitate the stakeholder request. the revised version of the use case diagram is depicted in figure 1. There are some features from the functional requirement that are merged or eliminated. for example, priority estimation is not done by academic officers, but done by the system according to incident or service request category. assign a person for incident handling feature is deleted. all the features of the Resolve and Recover from the Incident activity are combined into one feature to simplify the process. notification of service request and incident settlement are done by the system if already resolved by officers. service requests and incidents are automatic closes if resolved by officers.

### D. System Development

System design that has been improved according to the results of confirmation with stakeholders then implemented into a web-based system. The feature implementations are shown in Fig. 2. Fig. 2(a) and 2(b) are displaying the User Interface of incident report feature and resolve/recover incident feature respectively.

Functional testing on the system is done by giving a number of inputs on the system which is then processed in accordance with its functional requirements to see whether the system

produces the desired output. We implemented black-box testing for functional testing on the system. Software developers perform functional testing based on use case scenario documents.

#### E. Evaluation

Stakeholder's simulations session are used to evaluate the system. Stakeholders consisting of vice dean of academic (1 person), head of academic administration (1 person), and users who have conducted incident / service request reporting (8 person). Stakeholders are required to run the application in accordance with their respective roles with case studies of incident management and service requests.

The results of stakeholder evaluations are as follows: vice dean of academic provides improvements to the terms that have not standardized according to the guidelines of the existing procedures at the university, so it needs to be followed up by discussing with the university quality assurance team. Head of academic administration says that this application helps because the results can be directly printed for use as a report, but it also allows further developed by other programmers because the source code is available. Other users suggest that this application can be developed for other university department as well, and integrated with the campus information system services.

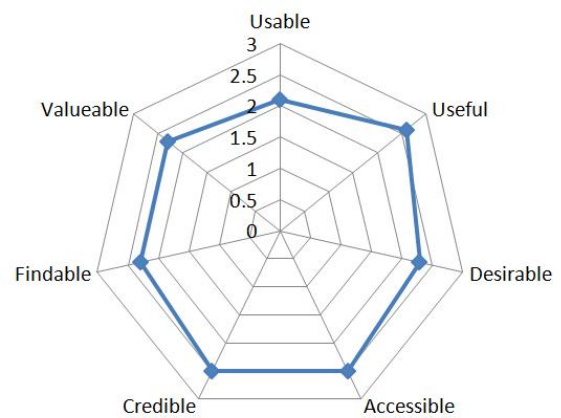


Fig. 3. Evaluation result

User experience aspect such as usable, useful, desirable, accessible, credible, findable, and valuable are also evaluated. Evaluation is done by stakeholders who are involved in the simulation session. Stakeholders fill out the questionnaire to determine the level of agreement on the user experience aspect. The questionnaire uses a Likert scale with 4 attributes: strongly agree to strongly disagree. Numbers are assigned to

(a)

(b)

Fig. 2. Screenshot of the systems. (a) UI for input of incident report. (b) UI for resolve and recover incident.

responses (0 to 3). Result of evaluation can be seen in fig. 3. All attribute providing good result; all respondent agrees that all aspects of users experience are in good form/design.

#### IV. CONCLUSION

Incident and service request management systems are built based on COBIT, where adapts to the needs and business processes of the existing system. The system is designed with consideration of the scope and needs of the organization. These include simplifying activities, as well as considering human resource needs.

The system design is confirmed to stakeholders before it is created, so that the system that created really suits the needs of the user. System testing is done to ensure all functions run as expected. Based on test results, all functions run as expected and no bugs or errors are found.

Simulation sessions are done by running some cases of incident reporting into the system. These simulations are done by stakeholders to evaluate the system. The stakeholder also valued user experience aspect of the system, such as: usable, useful, desirable, accessible, credible, findable, and valuable.

The results of the evaluation confirm the contribution of this study, the application of incident and service requests management in the academic information system can improve the quality and user satisfaction. It also improves the incident management process within the organization integrated into the academic information system.

#### REFERENCES

- [1] Santiago Melián-González and Jacques Bulchand-Gidumal, "Information technology and front office employees' performance," *International Journal of Contemporary Hospitality Management*, vol. 29, no. 8, pp. 2159-2177, 2017.
- [2] Iveth Tello, Christian Ruiz, and Sang Guun Yoo, "Analysis of COBIT 5 Process "DSS02 - Manage Service Requests and Incidents" for the Service Desk Using Process Mining," in *2018 International Conference on eDemocracy & eGovernment (ICEDEG)*, Ambato, Ecuador, 2018, pp. 304-310.
- [3] Jian-Guang Lou et al., "Experience report on applying software analytics in incident management of online service," *Automated Software Engineering*, vol. 24, no. 4, pp. 905-941, 2017.
- [4] Ajeng Savitri Puspaningrum, Siti Rochimah, and Rizky Januar Akbar, "Functional Suitability Measurement using Goal-Oriented Approach based on ISO/IEC 25010 for Academics Information System," *Journal of Information Systems Engineering and Business Intelligence*, pp. 68-74, 2017.
- [5] Armanda Prastiyan Pratama, Nukleon Jefri Nur Rahman, Aji Prasetya Wibawa, and Tinton Dwi Atmaja, "IT service management based on service-dominant logic: Case Academic Information System State University of Malang," in *2017 3rd International Conference on Science in Information Technology (ICSITech)*, Bandung, Indonesia, 2017, pp. 517-520.
- [6] Kridanto Surendro and Olivia, "Academic Cloud ERP Quality Assessment Model," *International Journal of Electrical and Computer Engineering*, vol. 6, no. 3, pp. 1038-1047, 2016.
- [7] ISACA, *COBIT 5: Enabling Processes*.: ISACA, 2012.
- [8] ITIL, *ITIL Service Design*.: TSO, 2011.
- [9] Indra Kharisma Raharjana, Ayundha Puspadini, and Eva Hariyanti, "Information Technology Supplier Management in Hospitals," *Bulletin of Electrical Engineering and Informatics*, vol. 7, no. 2, pp. 306-313, 2018.
- [10] Heru Nugroho and Tutut Herawan, "Enterprise Architecture Characteristics in Context Enterprise Governance Base On COBIT 5 Framework," *Indonesian Journal of Electrical Engineering and Computer Science*, vol. 3, no. 1, pp. 240-248, 2016.
- [11] Heru Nugroho and Kridanto Surendro, "Vocational Higher Education Governance Recommendation Based On Cobit 5 Enabler Generic Model," *Indonesian Journal of Electrical Engineering and Computer Science*, vol. 1, no. 3, pp. 647-655, 2016.
- [12] Riza Afriza Islami, I Made Sukarsa, and I Ketut Adi Purnawan, "Information Technology Governance Archetype in an Indonesian University," *Indonesian Journal of Electrical Engineering and Computer Science*, vol. 12, no. 7, 2014.
- [13] Indra Kharisma Raharjana, *Pengembangan Sistem Informasi Menggunakan Metodologi Agile*. Yogyakarta: depublish, 2017.
- [14] Ira Puspitasari, Reza Pramudhika, and Indra Kharisma Raharjana, "Pasienesia: A mobile based e-patient social network: Promoting empowerment among patients who experience similar diseases," in *2017 Second International Conference on Informatics and Computing (ICIC)*, Jayapura, Indonesia, 2017.
- [15] Indra Kharisma Raharjana, "Memprioritaskan Kebutuhan Perangkat Lunak Menggunakan Model Kano Dengan Menampilkan Rancangan Antarmuka Perangkat Lunak," in *Seminar Nasional Matematika dan Aplikasinya 2013*, Surabaya, Indonesia, 2013.
- [16] Boris Alexandre, Emanuelle Reynaud, François Osiurak, and Jordan Navarro, "Acceptance and acceptability criteria: a literature review," *Cognition, Technology & Work*, vol. 20, pp. 165-177, 2018.
- [17] Andrew R. McUine, "Developing a Questionnaire with the Intent of Measuring User Experience in Test Trials of Low-Cost Virtual Reality," Oregon State University, Thesis 2017.

# Applying IT Services Business Relationship Management on Security Outsource Company

Indra Kharisma Raharjana  
Information Systems  
Universitas Airlangga  
Surabaya, Indonesia  
indra.kharisma@fst.unair.ac.id

Susmiandri  
Information Systems  
Universitas Airlangga  
Surabaya, Indonesia  
susmiandri-13@fst.unair.ac.id

Army Justitia  
Information Systems  
Universitas Airlangga  
Surabaya, Indonesia  
army-j@fst.unair.ac.id

**Abstract**— Most outsource security companies have not implemented information technology optimally. A company must implement information technology that is oriented to customers and stakeholders to be competitive. Outsourcing security companies need to apply a systematic approach for managing customer-oriented services. In this study, we implemented business relationship management based on Information Technology Infrastructure Library (ITIL) framework to develop a service strategy, especially for an outsourced security company. There are 5 stages of activities carried out, namely identifying stakeholders, defining business outcomes, establishing strategic and funding requirements, defining business cases, and validating business activity patterns. Verification and revision of customer requirement analysis are performed to validate and evaluate the results. The result of implementing business relationship management is the recommendations of four IT services that suits the organization. The four IT service recommendations are websites, CRM services, monitoring services, and ordering services. Business case documents for each service have been created to identify business impacts and risks.

**Keywords**— *relationship management, service strategy, ITIL framework, customer requirements analysis, IT service strategy.*

## I. INTRODUCTION

Outsourcing is the process of hiring labors or services from a party outside a company to perform a specific task [1]. Companies tend to hire outsourced employees on the grounds of cost savings, focus on business strategy, gain professional labor, and use of the latest technology [2]. Outsourcing companies are required to always have a competitive advantage as more and more similar competitors company.

Currently, many security outsourcing companies engaged in the provision of labor [4]. This competition makes the company must be competitive, for that customer requirement analysis becomes important [5]. Information Technology (IT) services adoption in organization is believed to provide a competitive advantage [3]. Unfortunately, IT adoption rate in these companies are very low. IT is mostly only used for administrative activities, not yet integrated with business processes [6]. It can lead to ineffective service quality and low competitiveness.

When implementing IT services, organizations need to know their customers' requirements. IT services implemented should not only focus on the technology, must also pay attention to the quality of service and customers relation [7]. Customer requirement analysis is a systematic way of exploring customer requirements and expectations.

Customer requirement analysis can be done using the Kano[5], data analysis[8] and quality function deployment[9]. However, these methods can only identify and prioritize customer needs, not focus on preparing strategies and recommendations for the implementation of IT services. Information Technology Infrastructure Library (ITIL) framework provides practical guidance on IT service governance[10]. ITIL has been commonly used in various industries because it is considered to reduce the failure of the implementation of IT services, improve service and customer satisfaction and save costs[11]. Business Requirement Management (BRM) in the ITIL framework discusses how to connect service providers and customers at a strategic and tactical level so that service providers can understand customer needs for IT services [12].

In this study we propose for applying IT Services Business Relationship Management for identifying Customer Requirement Analysis in security outsourcing company, so the company can plan IT requirement in integrating its business process. This study applies the method of Business Relationship Management in the Information Technology Infrastructure Library (ITIL) framework to perform customer requirement analysis. We use one security outsourcing company as a case study of IT services business relationship management. because it only uses one company as the case study, the results of this study may not be generalized to all outsourced security companies.

## II. METHODS

This research method has several procedures including identifying stakeholder, define the business outcome, specify strategic requirement and funding, define business case, validated business activity pattern, and verification and revise customer requirement analysis. The procedure is illustrated in Figure 1.

### A. Identify Stakeholder

This stage aims to find out stakeholders who are involved and influential. The input of this stage is information about who are the parties or stakeholders involved in business activities. Information about the parties and stakeholders involved is obtained through interview. Stakeholder mapping analysis is conducted for stakeholder classification [13]. Stakeholders are classified into 3 groups: stakeholder salience, dependency level, and stakeholder power interest grid. After the grouping, the next step is to determine the most prioritized

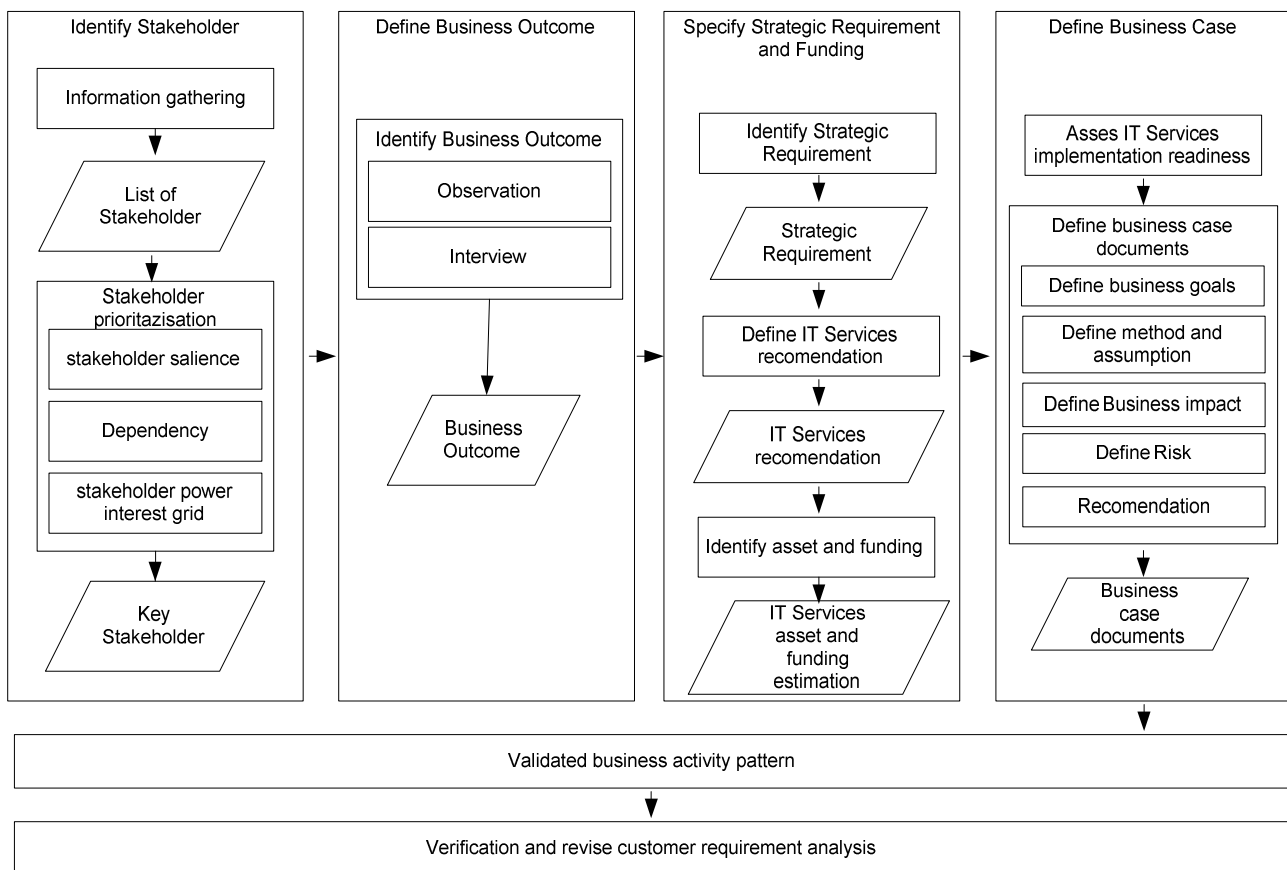


Fig. 1. Step of Customer Requirement Analysis

stakeholders by selecting the stakeholders who belong to all the groups, called key stakeholder.

#### B. Define Business Outcome

The purposes of this stage is to determine what business outcome should be met by IT services. Key stakeholders are interviewed to get information on the business outcome should be implemented, the constraint to be faced, the desired requirements, and expectations of each key stakeholder on IT services. The value to be achieved by the IT services must be ensured during the interview. So the IT services can have value for each key stakeholder and reduce the constraints.

#### C. Specify Strategic Requirement and Funding

This stage aims to identify strategic requirements and funding requirements. The input for this stage is a detailed list of the business outcome obtained in the previous stages. Discussions with key stakeholders are done to establish a long-term strategic requirement. Appropriate IT service recommendations are made based on the results of discussions and best practice studies. Details of the funding and assets required for the implementation of IT services are estimated to get a complete picture.

#### D. Define Business Case

A business case is a decision support and planning tool to project the consequences of a business action taken [14]. Business cases are used as materials to support decision-

making and planning related to the application of IT service recommendations. business case documents created for prioritized IT services. The document contains business objectives, limitations, business impacts, risks of implementing each IT service, and recommendations to avoid risks.

#### E. Validated business activity pattern

This stage is done to know the pattern of business activity in order to estimate the workload of each IT service. The analysis is done by looking at business case documents to find out which business activities are related and knowing who the users are from each IT service. Interviews with users of IT services to gather information about the pattern of business activity.

#### F. Verification and revise customer requirement analysis

At this stage, the verification of the results of customer requirements analysis conducted. The verification process involves managing director and customer. Through interviews and form verification by stakeholder, about the appropriateness of the results, with the opinions and expectations of both parties.

### III. RESULTS

#### A. Identify Stakeholder

There are 14 stakeholders involved in the service or business activity. The party is president director, marketing

TABLE 2 LIST OF THE BUSINESS OUTCOMES

Name	Business Outcomes
President Director	1. IT Services that can help monitor Key Performance Indicator.
Marketing Department	1. IT Services to support marketing 2. IT Services that allow to build trust and good relations with customers and prospective customers
Finance Department	1. IT services that can assist in managing payroll 2. IT services that can be a reminder of customers to make payments 3. IT Services that applied were able to notify automatically who are the customers who have made the payment and display some payment details
HRD Department	1. IT services that can help organize shifts for workers security 2. IT services that can help facilitate the making of a report of security personnel work portion. 3. IT services that can help the recruitment process 4. IT Services to create alternative communication methods to expand access to field coordinator.
The Field Coordinator	1. IT Services that can help monitor the labor security 2. IT services that can add access to communication with the customer for better and efficient monitoring
Customer	1. IT services that can simplify the process of absentee 2. IT services that can be used to mreview the performance of the security 3. IT Services that can facilitate in obtaining general information of outsource company 4. IT Service which can provide alternate communication with the marketing department 5. IT services that are able to provide an alternative way to process bookings 6. IT Services to provide information nical regarding payment

TABLE 3 LIST OF IT SERVICES RECOMMENDATION AND STRATEGIC REQUIREMENT THEY CAN ACHIEVE

Strategic requirements that can be met	Recommended IT services
1. IT Services that can facilitate in obtaining general information of outsource company 2. IT services to support the existence of organisation to be more recognized	Website
1. IT Services which can help the process of recruitment guard	Recruitment Service
1. IT Services that can build trust and rapport with customers and prospective customers 2. IT Services that can increase access to communications with customer in order to create a process monitoring better and more efficient	Customer Relathionsip Management (CRM) service
1. IT services that provide to review the performance of the security 2. IT services can assist monitoring labor security	Monitoring Service
1. IT services can help arrange shifts for workers security 2. IT services that can facilitate the attendance 3. IT services memperm already preparing reports on the long or the work portion of the labor security, for the benefit of the payroll	Labor Arrangements Service
1. IT services that can provide information about the payment details 2. IT Services that applied were able to notify automatically who are the customers who have made payments 3. IT Services can be a reminder of the customer to make payments	Payment Services
1. IT services are able to provide an alternative way for the ordering process more efficient	Ordering Service

department, legal department, human resources department, finance department, supervisor, security labors, customer, paid media, regulators, tax directorate, notary firm, competitor, and Indonesian Security Services Company Association.

From stakeholder mapping analysis using stakeholder salience, dependency, and stakeholder power interest grid [13], showed that there are 8 key stakeholders. Namely: president director, marketing department, legal department, human resource department, finance department, supervisor, security labor, and customer.



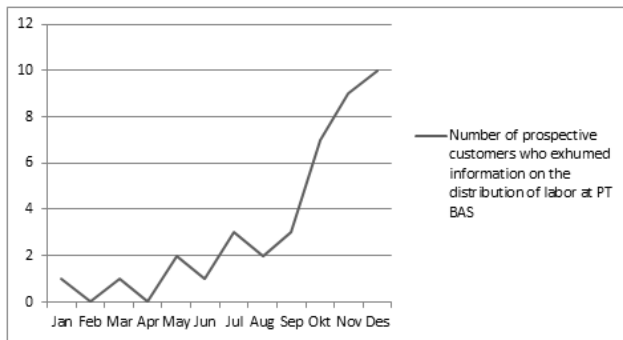


Fig. 2. Pattern of Business Activity for Website

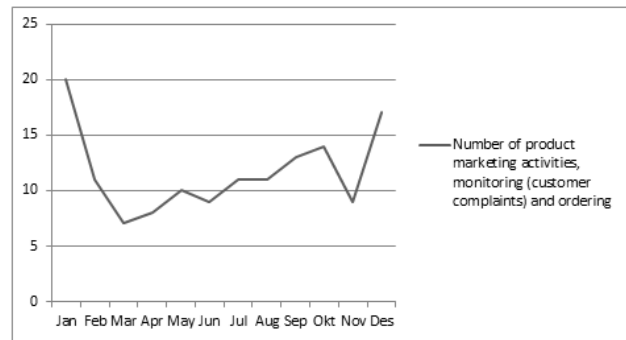


Fig. 3. Pattern of Business Activity for CRM Service

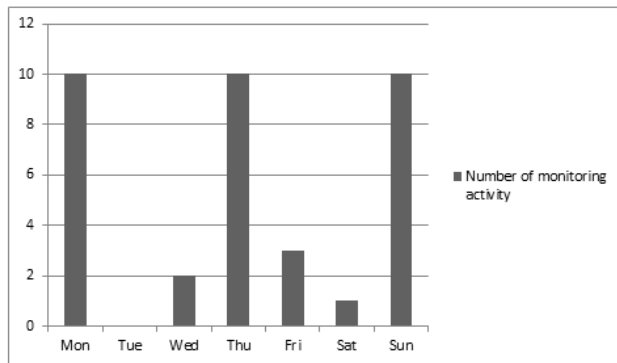


Fig. 4. Pattern of Business Activity for Monitoring Service

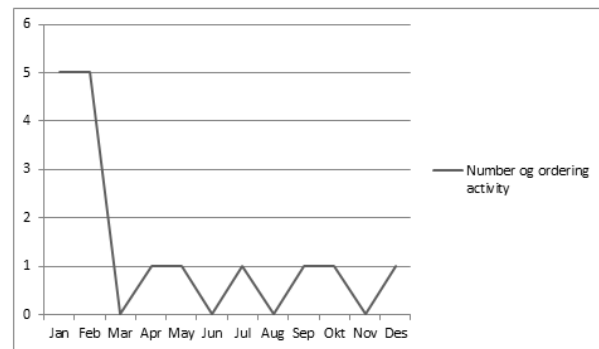


Fig. 5. Pattern of Business Activity for Ordering Service

### B. Define Business Outcome

Interviews were conducted with 8 key stakeholders. Table 2 is a list of the IT services business results expressed by key stakeholders.

### C. Specify Strategic Requirement and Funding

After discussions with stakeholders (security outsource company and customer), the strategic requirement is determined based on business outcomes. Once the list of strategic requirements has been obtained, the next to do is casting ideas of IT Services to be recommended. The list of IT services recommendations from the strategic requirement depicted in Table 3. Estimation of the assets and the funds required to implement the recommendations of the IT services are calculated.

After a detailed estimation of IT services, assets and funds are completed, the next step is to conduct an interview with the finance department to determine the readiness of IT services related to their implementation. At present, the organization prioritizes four IT service recommendations: Websites, CRM services, monitoring services, and booking services.

### D. Define Business Case

In this stage, the business case documents were created. The business case documents were prepared by defining business objective, the business case boundary, business impact, the risk and contingencies for each IT services.

### E. Validated business activity pattern

The website Business activity was extracted from information regarding the distribution of labor services performed by prospective customers who ask about the distribution system of labor services offered. From interviews obtained information about the number of potential customers who inquire about the employment service delivery system (depicted in Figure 2).

Business activities related to the implementation of CRM services were marketing, monitoring, and reservations. Number of product marketing activities, monitoring, and ordering is depicted in Figure 3. Based on the results of an analysis of factors that may affect changes in the pattern of business activity, it can be estimated that the workload of CRM services is mostly used at the beginning of the year, followed by end-of-year usage.

Number of monitoring activity is shown in Figure 4. Based on number of monitoring activity and the results of an analysis of factors that may affect changes in the pattern of business activity, it can be estimated that the workload of monitoring services will be widely used on Mondays, Thursdays, and Sundays. However, due to the possibility of unannounced monitoring that can be made at any time due to a customer complaint, the performance of the monitoring service should also remain good on other days.

Booking service is used to simplify the ordering process of labor security guard. Number of ordering activity is depicted in Figure 5. The results of the analysis of factors that may affect

the pattern of business activity, it can be estimated that the workload of the booking service will be widely used in January and February, however, due to the possibility of many orders also in other months, of the booking services in other months should also remain good.

#### F. Verification and revise customer requirement analysis

The data from the customer requirements analysis results are shown to perform verification processes involving the company and its customers. The verification process performed on the organization involves the head of HRD. From the results of interviews and filling the verification form, obtained information that the results of customer requirement analysis that has been shown, in accordance with expectations. Head of HRD said that the results of a customer requirement analysis can be a consideration and a good source of information to make the implementation of IT services in the company. In addition, the recommended IT services also fit the requirements and conditions of the organization.

The subsequent verification process is done to the customer. From the interview result, it is found that the result of customer requirement analysis has succeeded in defining and conveying requirement from customer side. The recommended IT service also can fulfill customer requirement.

#### IV. DISCUSSION

The stakeholder continuously involved through interviews, and discussions so we get feedback needed. There are several obstacles in conducting this research, such as difficult access to interviews with customers, because of this limitation there was only one customer to be interviewed in this study. The interview was also conducted with one representative from each section or division at the organization. Other obstacles that arise are data and documents are classified to parties outside the organization. We cannot analyze documents or data to ensure the course of business and financial conditions.

This study is a continuation of the study [6] which aims to identify IT strategic requirement, especially for security outsource company. both studies apply the process from ITIL framework. Previous studies [6] focused on the strategy management for IT services process, while this study focused on the process of business relationship management.

This study applied business relationship management as an IT service life cycle strategy. In contrast with the previous study [15] [16] that used the business relationship management concept in the organization that had implemented IT services. this study explores the application of business relationship management to organizations that have not implemented IT. the challenge is to provide understanding to stakeholders regarding the benefits and strengths of IT in providing competitive advantages within the organization.

Furthermore, several matters related to information technology governance and information technology service management can be done in security outsource companies to strengthen competitive advantage. for example, designing enterprise architecture planning [17] [18], creating standard operating procedures for service implementation [17], applying

checklists for crucial matters [18], or strengthening governance in the organization [19] [20].

#### V. CONCLUSION

This study demonstrates that the process of service strategy for business relationship management that exist in the cycle service strategy on the ITIL framework, can be used as a basis in the manufacture of strategy and planning for the implementation of IT services, in accordance with the requirements of the company and its customers, which it has yet to implement a service IT. The results of this study may not be applied to all the outsourcing company. This is because of differences in business processes that are running and the problems faced by each company. Therefore, it needs adjustment to find out the outline of the requirements of the outsourcing company and its customers, in order to determine which strategy is general and flexible, so it can be applied to all outsourcing companies.

#### REFERENCES

- [1] F. Malik, B. Nicholson and S. Morgan, "Assessing the Social Development Potential of Impact Sourcing," in *Socially Responsible Outsourcing*, Springer, 2016, pp. 97 - 118.
- [2] M. Belcourt, "Outsourcing — The benefits and the risks," *Human Resource Management Review* 6, pp. 269 - 279, 2006.
- [3] Purwanidjati and S. Rahayu, "Penerapan Sistem Outsourcing di Perusahaan Swasta dalam Perspektif Perlindungan Hukum Hak-Hak Pekerjaan Kontrak," *Jurnal Hukum*, pp. 1-16, 2010.
- [4] T. Wang and P. Ji, "Understanding Customer Needs through Quantitative Analysis of Kano's Model," *International Journal of Quality & Reliability Management*, pp. 173-184, 2009.
- [5] M. Marrone, F. Gacenga, A. Cater-Steel and L. Kolbe, "IT Service Management: A Cross-national Study of ITIL Adoption," *Communications of the Association for Information Systems*, pp. Vol. 34, Article 49, 2014.
- [6] L. Wijaya, I. K. Raharjana and E. Purwanti, "Strategic Management for IT Services on Outsourcing Security Company," *Journal of Information Systems Engineering and Business Intelligence*, pp. Vol. 4, No. 1, pp. 46 - 56, 2018.
- [7] R. Kurniawati and A. D. Manuputty, "Analisis Kualitas Layanan Teknologi Informasi dengan Menggunakan Framework Information Technology Infrastructure Library V.3 (ITIL V.3) Domain Service Transition (Studi Kasus pada Customer Service Area Telkom Salatiga)," *Jurnal Teknologi Informasi-Aiti*, pp. 31-45, 2013.
- [8] J. Sipatuhar, "Analisis Kebutuhan Pelanggan Potensial Produk PT. HM. Sampoerna, Tbk Cabang Medan," *Jurnal Ekonomi Universitas Sumatera Utara*, pp. 1-54, 2009.
- [9] A. Alexander, W. Didik and J. Budiman, "Analisis Kebutuhan Konsumen dan Rekomendasi Perancangan Perumahan dengan Luas Bangunan," *Jurnal Universitas Petra*, pp. 1-8, 2015.
- [10] L. A. K. Wardani, Murahartawaty and L. Ramadani, "Perancangan Tata Kelola Layanan Teknologi Informasi Menggunakan ITIL versi 3 Domain Service Transition Dan Service Operation Di Pemerintah Kota Bandung," *Journal of Information Systems Engineering and Business Intelligence*, pp. 81-87, 2016.
- [11] S. Sebaaou and M. Lamrini, "Implementation of ITIL in a Moroccan company: the case of incident management process," *International Journal of Computer Science Issues*, pp. Vol. 9, Issue 4, No. 3, pp. 30 - 36, 2012.
- [12] M. B. Al Mourad and M. Hussain, "The Impact of Cloud Computing on ITIL Service Strategy Processes," *International Journal of Computer and Communication Engineering*, pp. Vol. 3, No. 5, 2014.

- [13] I. M. Ari and Purwatiningsih, "Analisis Stakeholder Mapping: Studi Kasus pada Professional Products Division L'ORÉAL Indonesia Periode Januari – Juni 2013," *Jurnal Ekonomi Universitas Indonesia*, pp. 1-19, 2013.
- [14] OGC (Office of Government Commerce), ITIL Service Strategy, London, 2011.
- [15] R. A. T. & S. E. Ramadhan, "Perencanaan Business Realationship Management pada PPTI Stikom Surabaya menggunakan ITIL V3," *Jurnal Sistem informasi & Komputer Akuntansi*, pp. 1-6, 2016.
- [16] A. F. Putri, "Pembuatan Portfolio Layanan TI Bidang Akademik, Kemahasiswaan, Keuangan, dan Sarana Prasarana Berdasarkan Service Strategy ITIL V3 (Studi Kasus: Institut Teknologi Sepuluh Nopember).," Surabaya, 2017.
- [17] I. Safarina, I. K. Raharjana and E. Purwanti, "Perencanaan Arsitektur Perusahaan untuk Pengelolaan Aset di PT. Musdalifah Group menggunakan Kerangka Kerja Zachman," *Journal of Information Systems Engineering and Business Intelligence*, vol. 1, no. 2, pp. 59-72, 2015.
- [18] I. N. Aulia, I. K. Raharjana and Purbandini, "Perencanaan Arsitektur Perusahaan pada Bagian Instalasi Rawat Jalan dengan Kerangka Kerja TOGAF ADM Studi Kasus Rumah Sakit Jiwa Menur Surabaya," *Journal of Information Systems Engineering and Business Intelligence*, vol. 3, no. 1, pp. 52-60, 2017.
- [19] I. K. Raharjana, A. Puspadini and E. Hariyanti, "Information Technology Supplier Management in Hospitals," *Bulletin of Electrical Engineering and Informatics*, vol. 7, no. 2, pp. 306-313, 2018.
- [20] B. P. Santoso, E. Hariyanti and E. Wuryanto, "Penyusunan Panduan Pengelolaan Keamanan Informasi untuk," *Journal of Information*, vol. 2, no. 2, pp. 67-73, 2016.
- [21] H. Nugroho and K. Surendro, "Vocational Higher Education Governance Recommendation Based on Cobit 5 Enabler Generic Model," *Indonesian Journal of Electrical Engineering and Computer Science*, vol. 1, no. 3, pp. 647-655, 2016.
- [22] R. A. Islami, I. M. Sukarsa and I. K. A. Purnawan, "Information Technology Governance Archetype in an Indonesian University," *TELKOMNIKA (Telecommunication, Computing, Electronics and Control)*, vol. 12, no. 7, pp. 5636-5644, 2014.
- [23] R. Ramadhan, T. Amelia and E. Sutomo, "Perencanaan Business Realationship Management pada PPTI Stikom Surabaya menggunakan ITIL V3," *Jurnal Sistem informasi & Komputer Akuntansi*, pp. 1-6, 2016.
- [24] B. A. Firsas, "Pembuatan IT Service Portfolio berdasarkan Service Strategy ITIL V3 (Studi Kasus: Dinas Kependudukan dan Pencatatan Sipil Kabupaten Jember)," Surabaya, 2015.

# Design and Implementation of the Culinary Recommendation System Using Sentiment Analysis and Simple Adaptive Weighting in Bengkulu, Indonesia

Yudi Setiawan<sup>1</sup>, Boko Susilo<sup>1</sup>, Aan Erlanshari<sup>1</sup>, Sumitra J Firdaus<sup>1</sup>, Evi Maryanti<sup>2</sup>

<sup>1</sup>*Department of Informatics, Faculty of Engineering*

<sup>2</sup>*Department of Chemistry, Faculty of Mathematics and Natural Sciences*

*Universitas Bengkulu*

Jl. W.R Supratman Kandang Limun Bengkulu 38371, Indonesia

ysetiawan@unib.ac.id, boko.susilo@unib.ac.id, aan\_erlanshari@unib.ac.id, sumitra.firdaus77@gmail.com, evimaryanti82@yahoo.com

**Abstract**— In 2017, the minister of Indonesia tourism stated that everyone who travels spends his time for culinary about 30-40%. The key point in increasing the tourism income; especially from the culinary sector is about how to inform and promote the wealth of Indonesia culinary to all travellers. The information system of Bengkulu tourism has been developed in the previous study. However, that system has not been able to provide the best culinary recommendations to the travellers. This study focuses on designing and implementing the recommendation system of Bengkulu culinary by using sentiment analysis and simple adaptive weighting (SAW). The recommendation offered is based on the user review and criteria as well. The user review will be classified into positive, negative and neutral reviews by the sentiment analysis method. If the user needs culinary information based on criteria, the system will provide a recommendation and rank of culinary by using simple adaptive weighting. These criteria used are the average price, opening hours, facilities, distance from a central city, and transportation as well. Sentiment analysis method obtains the accuracy of recommendation classification at 79% while the recommendation rank obtained by the SAW method is 90.83%. These results show that the proposed method has a potential for assisting the travellers to gain the best culinary recommendation, especially in the Bengkulu area.

**Keywords**— Culinary, Tourism, Recommendation System, Sentiment Analysis, Simple Adaptive Weighting

## I. INTRODUCTION

Tourism is an activity directly involves and helps the community in managing some benefits especially in the local economy aspect for local communities and governments. However, the Central bank of Indonesia (BI) stated that the economic growth of Bengkulu province is the lowest compared the other provinces in Sumatra Island. Whereas in the economy sector, Bengkulu has a great potential to be more developed. Until 2016, there was not seen yet the supporting from the tourism sector to the regional economy [1].

Bengkulu province has the lowest economic growth of tourism, whereas it has many tourist destinations with the stunning natural attractions that have great potential to develop and expose [2]. Moreover, the culinary has a strong magnet that can attract tourists for coming in Bengkulu, Indonesia. However, some of the culinary places haven't been well-known by Bengkulu people itself, even by the tourists who are coming to Bengkulu. Therefore, an information system is needed to provide the explanation and optional recommendation what the best culinary place which can be reached by tourists and Bengkulu people as well.

Sentiment analysis (SA) known as opinion mining is a method for analysing public opinion, sentiments, evaluation, or emotion on an entity such as product, service, organisation, individual, issue, topic and others [3]. Having travelled, tourists oftentimes will share their experiences by uploading captured moments and information into many social media. Of course, this big data will be hard to understand by people looking for the best recommendation for tourism. These experiences can be analysed by using sentiment analysis for obtaining the summary information and a recommended

destination [4]. Naïve Bayes is one of the sentiment analysis algorithms. Naïve Bayes process involves items describing that may be recommended; comparing items to the other (items or users); and automatically in response to feedback on the desirability of items that have been presented to the user [5].

Convolution Neural Network (CNN) has been quite reliable proved and fast in classifying complex and detail objects to obtain the information about Indonesian food for tourists. By using CNN method, the classification process runs accurately. So that, the detailed information such as the forms, names and food ingredients are generated appropriately [6]. It is proved by the accuracy rate of 70% with 500-times iteration.

In other studies, semantic analysis algorithm is used to measure the words in two texts. The rate of tourism destination is created by comparing the dataset of the travel blog to make the review quality is better [7]. The semantic algorithm is used as knowledge in Tourism Mobile Recommender System (RSs) for providing information about the tourism destination [8]. The tourists can make travel planning based on some criteria such as distance and variety places [9].

Recommendation system for choosing the hotels in Yogyakarta based on simple adaptive weighting achieved more objectively of weighting value than that of direct weighting [10]. An information sharing system such as social media, blogs and website can support the government to promote all about tourism destination, heritage and culinary as well. Photos and videos shared via Apps will be a trending topic [11].

In this study, Sentiment Analysis and Simple Adaptive Weighting algorithms are implemented to design the

recommendation system of Bengkulu culinary. Thus, the information is gained easily for assisting the tourists and Bengkulu people itself. The structure of this paper is organised as follows. Section II describes the experimental method followed by implementation and discussion in Section III. The last section presents the conclusion of this study.

## II. METHOD

### A. Sentiment Analysis

Text pre-processing is the initial process to prepare the text to be ready data for further process. The text should be separated on several different levels. A document can be broken down into chapters, sub-chapters, paragraphs, sentences and ultimately into pieces of words/ tokens. Furthermore, the presence of digit numbers, capital letters, or other characters are removed and changed in this stage [12]. Sentiment analysis process including pre-processing, calculation of probability, classification, gain the alternative result and the data rank as a recommendation result as shown in Fig.1.

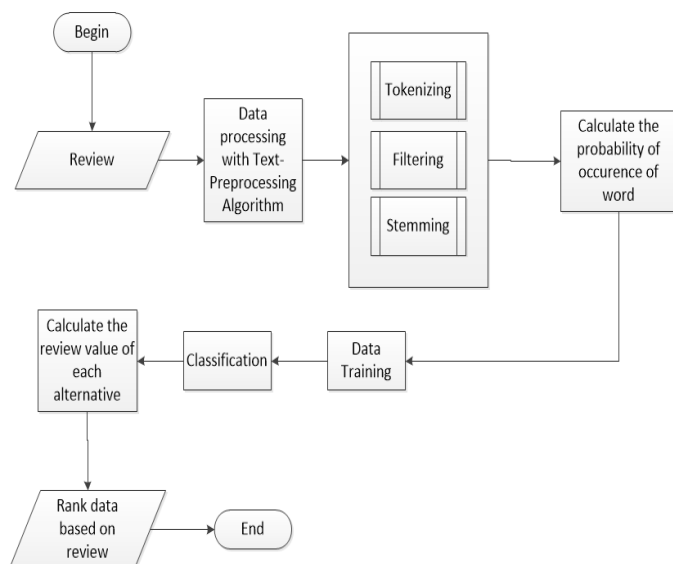


Fig. 1. The flowchart of sentiment analysis in culinary recommendation system

The text pre-processing in sentiment analysis consists of three stages as following described.

#### 1) Case Folding and Tokenizing

Case folding changes all the letters in the document into lowercase, only the letter 'a' up to the letter 'z' allowed. Characterisation letters are omitted and considered as a delimiter. The tokenizing is the stage to enter the string based on the compiled word [12].

#### 2) Filtering

Filtering is the stage of taking important words from tokenising stage results by using a stop-word algorithm (removing the less important words) [12]. Stop-words are non-descriptive words that can be removed in the bag-of-words approach.

#### 3) Stemming

Stemming is the stages of finding the basic word of each word results from the filtering process [12]. The process of stemming in Indonesian text is more complicated since there are variations of affixes that should be removed to get the root word of a word. This algorithm refers to the rules of KBBI (Indonesian language dictionary) which grouped allowed affixes or unauthorized affixes [13].

### B. Naïve Bayes Algorithm

Naïve Bayes is a machine learning method that uses probability calculations. The algorithm takes advantage of the probability and statistical methods proposed by British scientist Thomas Bayes, predicting future probabilities based on past experience. There are two stages in classifying the documents. The first stage is training documents that have known its category. While the second one is that of documents that unknown its category.

### C. Simple Adaptive Weighting (SAW)

Simple Additive Weighting (SAW) is also known as terms weighted summation approach. The basic concept of SAW is to find the weighted sum of performance ratings on each alternative on all attributes. The SAW method requires the process of normalising the X results of the sciences that can be compared with all the alternate ratings available [14]. Simple adaptive weighting process is depicted in Fig. 2.

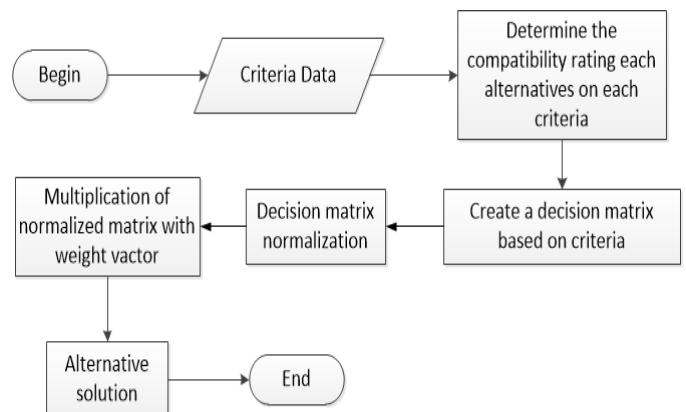


Fig. 2 Flowchart of simple adaptive weighting

The process of simple adaptive weighting is started by inserting criteria data which is subsequently undergo processed to determine the compatibility rating each alternative on each criterion for making the decision of normalisation matrix and then giving an alternative solution.

## III. IMPLEMENTATION AND DISCUSSION

Bengkulu culinary recommendation system is implemented for desktop and mobile using internet browser. Sentiment Analysis and Simple Adaptive Weighting algorithm are embedded in the system as knowledge in providing the culinary recommendation. The user interface is coded in Bahasa, and there are two actors that can access this system namely end users (visitor) and administrator.

### A. System User Interface

The homepage shows the variety of culinary places in alphabetical order. There is also informing the most popular destination and culinary place most opened by visitors. Moreover, a search box is available used to search the culinary place by inputting the keywords. The homepage of end-user interface is presented in Fig. 3.

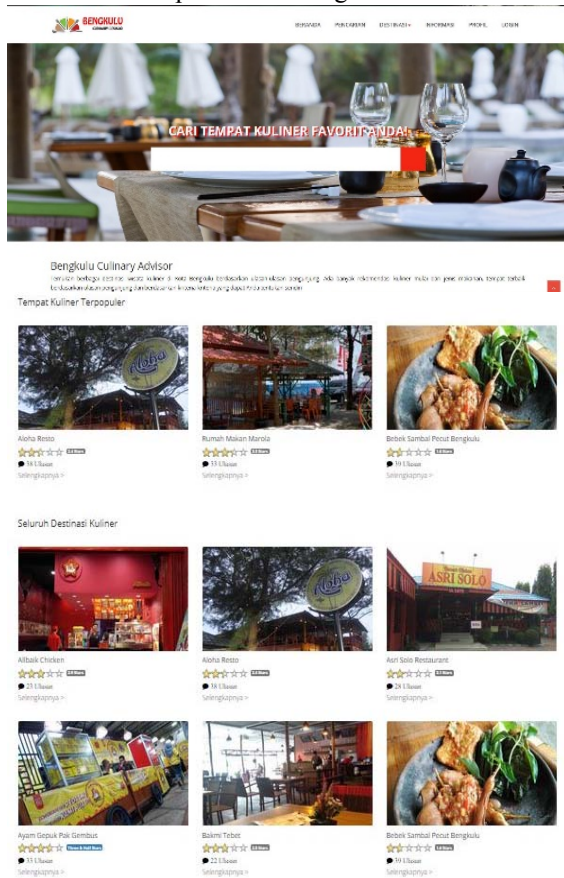


Fig. 3 Home Page Interface of Bengkulu Culinary Recommendation System

Search results are sorted from the highest rating obtained by measuring the ratio of positive reviews to the number of reviews on that culinary place.

The searching using data filtered will show the culinary place based on the selected filters and sorted by SAW value as shown in Fig. 4. These filters including prices, open hour, distance from the central city, and transportation availability.

On the administrator home page, there are several menus consists of users data menu, location data, password data, set criteria data, alternative table data, data, tokenising data, data filtering and stemmed data as displayed in Fig. 5.

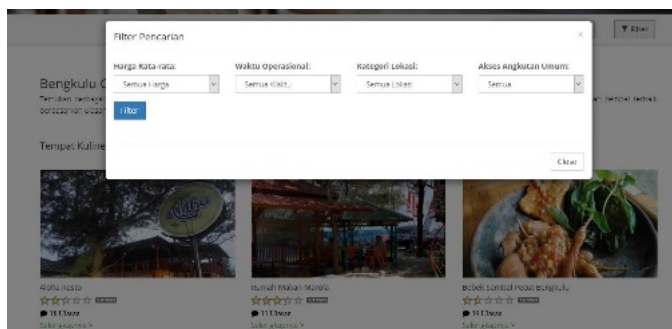


Fig. 4 The Search Filter of Culinary Recommendation System

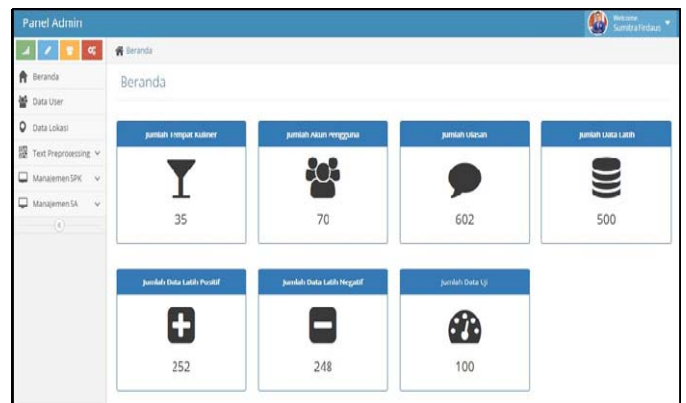


Fig. 5 Administrator interface

### B. Sentiment Analysis for Review Classification

The dataset page displays the entire number of reviews, consisting of training data and test data. This page is used to determine whether training data as positive training data or negative ones. The frequency term page presents a dictionary of words derived from all reviews which training data that has been broken down into words per word. On this page each term (word) has a number of occurrences in each positive training or negative training.

The sentiment classification page displays testing data that has been classified as positive or negative. Furthermore, on this page is also available the button to test sentiment against unclassified reviews as shown in Fig. 6.

No	Lokasi	Ulasan	Positif	Negatif	Status	Tindakan
1	Albaik Chicken	fasilitasnya yang ada well cocok banget untuk anak kos di akhir bulan, ambil pake 6500 ya	0.0327679	0.0229751	positif	<a href="#">Detail</a>
2	Aloha Resto	harga makanannya kurang cocok untuk kecil mahasiswa ya 7000000000 mahal	0.101968	0.130082	negatif	<a href="#">Detail</a>
3	Bakmi Tebet	cocok untuk nongkrong anak lala jaman now	0.0278483	0.0141287	positif	<a href="#">Detail</a>
4	Rumah Makan Jam Gadang	rencanakan barengannya makanan di sini apalagi gado rendangnya relay sangat enak	0.12726	0.0918938	positif	<a href="#">Detail</a>
5	Bombora Bar & Resto	Tidak ada nasi tidak disarankan untuk mahasiswa kelaparan	0.0248447	0.0675575	negatif	<a href="#">Detail</a>
6	Aloha Resto	Makanannya enak tapi harganya kurang cocok untuk anak kos.	0.13741	0.148525	negatif	<a href="#">Detail</a>
7	Bencodex Coffee House	Makanannya sangat enak ditambah lagi tempatnya sangat bersih untuk anak kosnya teman dekat	0.138214	0.0800187	positif	<a href="#">Detail</a>

Fig. 6 Classification Page of Sentiment Analysis Process

### C. Simple Adaptive Weighting Process

The SAW table page displays SAW tables consisting of alternate tables, yield matrices, normalisation matrices and culinary ranking tables which have been calculated by SAW method. Criterion is the basis assessment in determining the priorities order of culinary selection. There are two types of criteria in SAW method namely benefit and cost. A criterion is classified as a benefit since it provides benefits to decision makers, while criteria as a cost since criteria raise the cost for decision makers. The Table 1 shows the weighting of data criteria used such as price, open hour, facilities, distance from the central city, available transportation.



TABLE I  
THE WEIGHTING OF DATA CRITERIA

No	Code	Criteria	Attribute	Weight (w <sub>j</sub> )
1.	C1	Open hour	Benefit	0.2
2.	C2	Average prices	Cost	0.4
3.	C3	Facilities	Benefit	0.2
4.	C4	Distance from central city	Cost	0.1
5.	C5	Availability of transportation	Benefit	0.1
Total				1

The complete ranking result is shown in Fig. 7. The first culinary priority is occupied by Kedai Bandung with the preference value of 0.733. The second priority is KFC Bencoleen Mall with the preference value of 0.693 while the third priority is Waroenk R.A with the preference value of 0.68.

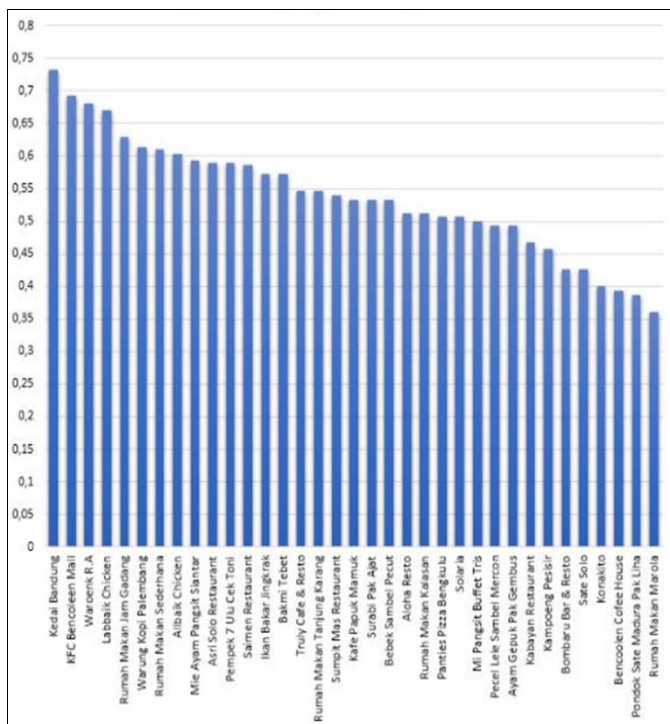


Fig. 7. Culinary recommendation system result ranking

#### D. System Evaluation

In this study, a user-based evaluation is conducted in order to uncover usability problems. Then, users participate in a satisfaction questionnaire to observe user-based evaluation. The questionnaires are then distributed to the respondents. The technique of selecting respondents is done randomly so that 30 samples are obtained from the general public. Before performing the calculations by using Likert Scale, the interval should be looking for firstly.

The rating category of the culinary recommendation system is valued in the range of 1-5. The highest value is 5 while the lowest is 1 with the number of classes and students are 5. The interval value can be calculated using (1). The calculation obtains interval values of 0.8 so that it can be generated the rating category as shown in Table 2. Table 3 presents the calculation results of questionnaire answer for 30 samples.

$$i = \frac{\text{highest value} - \text{lowest value}}{\text{classes}} = \frac{5 - 1}{5} = 0.8 \quad (1)$$

TABLE II  
INTERVAL RANGE OF CATEGORIES

Interval	Category
4.24 – 5.04	Excellent
3.43 – 4.23	very good
2.62 – 3.42	Good
1.81 – 2.61	Fair
1.00 – 1.80	Poor

TABLE III  
THE RESULTS OF USER CONVENIENCE VARIABLES

No	Assessment	Frequency of Answer					
		M	Excellent	Very Good	Good	Fair	Poor
1	Ease of operating the system.	4.4	13	16	1	0	0
2	Ease of searching for a culinary place using search queries	4.6	20	8	2	0	0
3	Ease of getting culinary recommendations based on rating reviews	4.67	20	10	0	0	0
4	Ease in getting the desired culinary information	4.5	15	15	0	0	0
Number of answer frequencies			68	49	3	0	0
Average percentage			56.67%	40.83%	2.5%	0%	0%
Average category total			4.54				
Category			Excellent				

From the number of answers, the score is calculated by multiplying each number of answers with each weight of the answer.

Excellent	13 x 5	=	65
Very Good	16 x 4	=	64
Good	1 x 3	=	3
Fair	0 x 2	=	0
Poor	0 x 1	=	0
Total			132

The above calculation obtained the number of scores for component 2 is 138, for component 3 is 140, and component 4 is 135. The total score is divided by the total number of answers. In this study, the number of respondents in the general public is 30, so the value of the score will be divided by 30. M value for each component variable is presented below.

$$m_1 = \frac{132}{30} = 4.4 \quad m_2 = \frac{138}{30} = 4.6 \quad m_3 = \frac{140}{30} = 4.67$$

$$m_4 = \frac{135}{30} = 4.5 \quad m_{\text{average}} = \frac{4.4+4.6+4.67+4.5}{4} = 4.54$$

Based on Table II, the value of 4.54 falls within the interval 4.24 - 5.04 categorised as "excellent". The percentage for approval level of displayed variable can be done by comparing the total score of each component with the expected maximum score (assuming the respondent chooses the answer of SB, so 5 x 30 = 150).

$$\text{Component 1 : } \frac{132}{150} \times 100 \% = 88\%$$

Component 2 :	$\frac{138}{150} \times 100 \%$	=	92%
Component 3 :	$\frac{140}{150} \times 100 \%$	=	93.33%
Component 4 :	$\frac{135}{150} \times 100 \%$	=	90%
Average			90.83%

From the above calculation, it can be concluded that the percentage of respondent's approval to ease of operating the system is 88%. Ease of searching culinary place using search query obtains the percentage of 92%. Ease of getting culinary recommendations based on rating reviews obtains the percentage of 93.33%. The percentage of ease in getting the desired culinary information is 90%. The average percentage of this system is 90.83%.

In this study, a total of 500 data which consists of 250 positive and 250 negative data are used for classification training process based on Naïve Bayes classifier. Then, the classification testing process by involving 100 data is conducted and obtains the accuracy rate of 79%.

#### IV. CONCLUSION

Bengkulu culinary recommendation system has been developed to assist traveller/tourists and Bengkulu people itself in finding culinary information in easy and efficient based on user review and criteria. Sentiment analysis classifies the user review into positive, negative, and neutral classes which obtain the accuracy rate of 79%. While simple adaptive weighted provides the culinary recommendation based on some criteria and obtain the approval average percentage of 90.83% from 30 respondents. These results indicate that the developed system has a great potential to be implemented for reducing time in finding the culinary place, especially in Bengkulu area. Some observed issues during the testing process need to be addressed in future work. Moreover, this system will be designed in many languages to globalise the proposed application.

#### ACKNOWLEDGEMENT

The authors would like to thank the Directorate General of Higher Education, Ministry of Research, Technology and Higher Education, Republic of Indonesia for financial support of this research.

#### REFERENCES

- [1] E. Poerwanto, "BI: Pertumbuhan Ekonomi Wisata Bengkulu Terendah se Sumatera | Portal Berita Bisnis Wisata." [Online]. Available: <http://bisniswisata.co.id/bi-pertumbuhan-ekonomi-wisata-bengkulu-paling-rendah-di-sumatera/>. [Accessed: 11-Apr-2018].
- [2] Suwarni and A. Soleh, "Membangun Bengkulu Melalui Peningkatan Sektor Pariwisata," presented at the Seminar Nasional Riset Inovatif Ii, 2014.
- [3] B. Liu, *Sentiment Analysis and Opinion Mining*. Morgan & Claypool Publisher, 2012.
- [4] Y. H. Gu *et al.*, "Sentiment analysis and visualization of Chinese tourism blogs and reviews," in *2018 International Conference on Electronics, Information, and Communication (ICEIC)*, 2018, pp. 1–4.
- [5] M. J. Pazzani and D. Billsus, "The Adaptive Web," 10th ed., Springer.
- [6] R. P. Prasetya and F. A. Bachtar, "Indonesian food items labeling for tourism information using Convolution Neural Network," in *2017 International Conference on Sustainable Information Engineering and Technology (SIET)*, 2017, pp. 327–331.
- [7] D. M. Ramadhani, C. Rahmad, and F. Rahutomo, "Tourism destination rating system based on social media analysis (proposal and dataset development in Indonesian language)," in *2017 International Conference on Sustainable Information Engineering and Technology (SIET)*, 2017, pp. 41–46.
- [8] D. Gavlasab, C. Konstantopoulos, K. Mastakas, and G. Pantziou, "Mobile recommender systems in tourism," vol. 39, no. March 2014, pp. 319–333.
- [9] H. Kurdi and N. Alnashwan, "Design and implementation of mobile cloud tourism application," in *2017 Computing Conference*, 2017, pp. 681–687.
- [10] A. Syafrianto, "Penerapan Algoritma AHP dan SAW Dalam Pemilihan Penginapan Di Yogyakarta," vol. 17, no. Desember 2016, pp. 7–12.
- [11] Y. Setiawan, B. Susilo, A. Erlanshari, and D. Puspitaningrum, "Design Dan Implementasi Sistem Informasi Pariwisata Berbasis Konten Sebagai Startup Lokal Bengkulu," presented at the Seminar Nasional Teknologi Informasi, Universitas Tarumanagara, 2017.
- [12] R. Feldman and J. Sanger, *The Text Mining Handbook*. Cambridge: University Press.
- [13] L. Agusta, "Perbandingan Algoritma Stemming Porter Dengan Algoritma Nazief & Adriani Untu K Stemming Dokumen Teks Bahasa Indonesia," in *Konferensi Nasional Sistem dan Informatika 2009*, Bali, 2009, pp. 196–201.
- [14] S. Kusumadewi, S. Hartati, A. Harjoko, and R. Wardoyo, *Fuzzy Multi-Attribute Decision Making (FUZZY MADM)*. Yogyakarta: Penerbit Graha Ilmu, 2006.

# Success Factors of Human Resource Information System Implementation: A Case of Ministry of State-owned Enterprise

Wita Puspitarini, Putu Wuri Handayani, Ave Adriana Pinem, Fatimah Azzahro

Faculty of Computer Science

Universitas Indonesia

Depok, Indonesia

wytter@gmail.com, putu.wuri@cs.ui.ac.id, ave.pinem@cs.ui.ac.id, azzahro.fatimah@cs.ui.ac.id

**Abstract**—This study aims to analyze factors influencing the successful implementation of Human Resources Information System (HRIS) at the Ministry of State-Owned Enterprises (MSOE). There are 22 factors influence the success of HRIS implementation that are categorized into 4 dimensions, namely human, organization, technology and environment based on DeLone & McLean information system success model, HOT (human-organization-technology) fit model and TOE (technology-organization-environment). This research use quantitative method approach and data collection is gathered using questionnaire. Method of data analysis using Entropy method to calculate the weight of success factors and dimensions, and rank factors and dimensions. There are 99 respondents of the HRIS users provided data through the questionnaires distributed to them. This study shows that the dimensions influencing the success of HRIS implementation at the MSOE in priority order are technology, human, environment and organization. In addition, there are 5 factors selected with the highest weights namely information quality, service quality, top management support, system quality and social influence.

**Keywords**—success factor, human resource information system, state-owned enterprise, Entropy

## I. INTRODUCTION

One initiative of e-government implementation at the Ministry of SOE (State-Owned Enterprises) is the use of Human Resource Information System (HRIS) or known as Human Resource Portal. The system was built in 2007 on a web-based basis with funds sourced from the State Budget. Unfortunately, in 2007 when the Human Resource Portal was built, the Ministry of SOE did not have information technology planning that can be used as a standard reference in the manufacture of information systems, therefore the development of Human Resources Portal only meets the needs at that time. Human Resource Portal is used as a tool for collecting data of the Board Directors/Candidates of Board of Directors, Board of Commissioners/Candidates of Board of Commissioners, and Supervisory Board/Candidate of Supervisory Board of SOEs electronically. Then, submission of electronic data from each SOEs to the MSOE has been strengthened by the Regulation of the Minister of SOE No.

PER-18/MBU/10/2014 on the Delivery of Data, Reports and Documents of SOE Electronically. Under this regulation, SOEs are required to submit reports, data and documents to the Minister of SOE and/or echelon I and II officials of the MSOE electronically through the information system provided by the MSOE.

Stakeholder Human Resource Portal, among others are internal parties (i.e MSOE) and external (i.e SOEs). Internal user come from the MSOE is Deputy Assistant of the Executive Resources Management of MSOE as the owner of basic tasks and functions within the MSOE as well as responsible for the policy of filling and managing and presenting the data. In addition, Deputy Assistant Data and IT with MSOE is responsible for developing and maintaining information systems and data security. External users are parties that come from SOEs called admin Human Resource (HR) SOE. Deputy Assistant of Executive Resources Management of MSOEs explains that the data of the Board of Directors and Board of Commissioners/Supervisory Board of SOEs in Human Resources Portal has not yet existed so that Human Resource Portal cannot be used by Deputy Assistant Executive Resources Management of MSOEs to monitor the term of the Board of Directors and Board of Commissioners/Supervisory Board of each SOE and stipulates the candidates for the Board of Directors and Board of Commissioners/Board of Supervision of SOEs in a timely manner. Based on the identification of the above problems, compiled the formulation of the problem set forth in a research question. The research question is "What are the factors influencing the successful implementation of HR Information System at the MSOE?" This research on the MSOE is expected to provide reference to the high ranking official of the MSOE in determining the steps of applying HRIS at the MSOE in accordance with the results of this study.

This paper covers 6 sections of literature study and research methodology that are discussed in Section 2 and Section 3. Results, discussion and research implications are discussed in Section 4, Section 5 and Section 6. The last section discusses on the conclusions from this research.

## II. LITERATURE STUDY

According to [2], HRIS is defined as an integrated computer system designed to carry out many tasks related to

the flow of information within the organization as it relates to its human resources. HRIS could manage data with functions such as storage, analysis, manipulation, retrieval, dissemination, and control. HRIS is not limited to an integrated system and technology, but HRIS also includes employees, policies, working procedures and data required to manage HR related functions [3].

One of the HRISs included in Magic Quadrant Gartner is SAP (System Application and Product in Data Processing) HR (Human Resource). SAP is one of ERP (Enterprise Resource Planning) that offers a variety of information technology solutions to integrate business processes and support the company's operational activities. Using this SAP HR, a company can manage human resources more regularly and can be used for decision-making tools and performance measurement of human resources. This module provides access to all HR data and transactions in one location. So, it can be a tool for managing the roles and responsibilities of organizations that help in creating the corporate management structure and position within the organizational structure.

### III. METHODOLOGY

This research is a quantitative research by using questionnaire to get data. The technology that becomes the object of research is HRIS at the MSOE or known as Human Resource Portal. The population of this study is all employees within the Unit of Deputy Assistant of Executive Resources Management of SOE and Admin HR SOEs. Before the questionnaires were distributed, the questionnaire readability test was performed by distributing draft questionnaires to 5 respondents be tested for their readability. Respondents were asked to provide inputs and responses to the draft questionnaire. With the test of legibility, it can be known whether the draft questionnaire can be clearly understood by the respondent therefore it can be improved before disseminated to the respondent in line with the sample research for data collection. Data processing is performed by using Entropy. All the variables to determine the success factors used in this study are grouped according to the existing dimensions of the research [4] with the HOT Fit model and the TOE framework. Table 1 explains the list of success factors of HRIS.

Table 1 List of Success Factors of HRIS

No	Dimension	Success Factor	Definition
1	Human	System Use	Identify the extent to which the use of information systems can affect user needs
		Perceived Ease of Use	Ease of use of information systems for the purpose in accordance with the wishes of users
		Perceived Usefulness	Benefits of information systems for users associated with increased productivity

No	Dimension	Success Factor	Definition
			(performance) and effectiveness
		Innovativeness of Senior Executives	Leadership of the organization plays an important role in the use of information systems
		IT Capabilities of Staff	The adoption of information systems is supported by the capabilities and competencies of staff in the IT department
		Performance Expectancy	Users believe that using an information system will help it to achieve a profit in its performance
2	Organizational	Relative Advantage	The use of information systems will improve the effectiveness and productivity of the organization
		Top Management Support	Leaders of the organization support the adoption of information systems by providing adequate facilities
		Centralisation	Every decision is made by the leadership of the organization. Centralization of information systems related to decisions for initiation, adoption and application of innovation.
		Formalisation (Procedure/ Rules/ Government Regulation)	Information systems are supported by regulated rules (formal procedure/ regulation/rules) of an organization for the smooth flow of work
		Perceived Cost	The adoption of information systems allows the cost of implementing information systems and lower innovations
3	Technological	Information Quality	The level of output quality in the form of information generated by the information system
		System Quality	System quality measures typically focus on system performance characteristics
		Service quality	<ul style="list-style-type: none"> <li>Quality of service provided when users experience difficulties</li> <li>Users feel that the</li> </ul>

No	Dimension	Success Factor	Definition
			information system suits the needs of the users
		IT Infrastructure	<ul style="list-style-type: none"> <li>The organization has been supported by either local area network or internet network</li> <li>The organization has supported adequate software and hardware for the adoption of information systems</li> </ul>
		Compatibility	Adoption of information systems in accordance with organizational goals, and support (compatible) with the existing process
		Complexity	The ability of complex information systems already includes many organizational processes
4	Environmental	Situational Normality	Success in the use of information systems will be achieved when the existing environmental conditions support for the system
		Competitive Pressure	Conditions where the organization must adopt the information system due to competition with other organizations to improve the quality of the organization.
		Technology Vendor support	Adoption of information systems based on support services from selected technology vendors
		Supporting Facilities and Infrastructure	Users consider the facilities and infrastructure provided by the organization to support the use of information systems
		Social Influence	It is the degree to which users perceive that the importance of other people's existence in using the new information system will affect the user

Questionnaires in this study are distributed in the form of links from google docs and hardcopy. The reason to use these links because respondents have different offices location and there is a time constraint to get answers from respondents quickly. The instrument used in the questionnaire is respondents' profile and a list of success factor statement of HRIS. In the form of respondent data, the respondents are

asked to fill in information on gender, education, respondent's position and respondent's division. In the next section, it contains success factor statements. Each success factor is represented by 4 questions, therefore there are a total of 34 proposed statements being submitted. The respondents should provide his/her judgment on the statements on the most appropriate choice based on an ordinal scale. The ordinal scale in this questionnaire has 5 categories: 1 = very unimportant, 2 = unimportant, 3 = neutral, 4 = important, and 5 = very important.

#### IV. RESULTS

##### 4.1. Respondents Demographics

This study obtained 118 questionnaires that have been filled either through hard copies, soft copies or online forms. Out of 118 questionnaires, there are 10 questionnaires whose respondents came from the same SOE and 9 questionnaires from SOEs that under process of restructuring or liquidation. Thus, there are 99 questionnaires that come from valid respondents in accordance with the method of purposive sampling. Out of the 99 respondents consisted of 9 respondents from the MSOE and 90 respondents came from the Admin of HR SOEs. Table 2 described the demographics of respondents.

Table 2 Respondent Demographics

Demographic		Number of Respondents	Percentage
Gender	Men	64	64.65%
	Women	35	35.35%
Age	<17 years	0	0.00%
	17-25 years	2	2.02%
	26-35 years	35	35.35%
	36-45 years	37	37.37%
	> 45 years	25	25.25%
Education	High School	0	0%
	Diploma	10	10.10%
	Bachelor	51	51.51%
	Master	38	38.39%
	Doctoral	0	0%
Institution	MSOE	9	9.10%
	SOEs	90	90.90%
Position	Staff	51	51.52%
	Head of sub-field or Assistant Manager or equivalent	13	13.13%
	Head or Manager or equivalent	34	34.34%
	Assistant department or General manager	1	1.01%



Demographic		Number of Respondents	Percentage
	or equivalent		
Division/ Working Unit	HR	95	95.96%
	Other divisions	4	4.04%
Experience using HRIS	1 year	2	2.02%
	2 years	7	7.07%
	3 years	22	22.22%
	> 3 years	68	68.69%
The most frequently used feature in SISDM	Personal data	23	23.23%
	Organization data	0	0.00%
	Recapitulation	0	0.00%
	Talent Pool	31	31.31%
	Data of Directors, Commissioners or Supervisory Board and Corporate Secretary	45	45.45%

#### 4.2. Criteria Measurement using Entropy

This method is used for the weighting of existing dimensions and criteria. The steps taken to weight the entropy method are as follows [5]:

- Normalization of the matrix of the questionnaire results (initial data), i.e. subtract all criteria with the maximum value or the highest value. In this study normalization is done by making the matrix of results from the assessment of respondents. Each value on the matrix is then subtracted by the highest value used in this questionnaire. The reduction result is expressed by  $X_{ij}$ . Normalization is done after obtaining the total sum of each subtraction value in the matrix.
- The value of step 1 divided by the total value of all criteria. Next divide each value of the  $X_{ij}$  matrix by the total number of matrix values with the following formula:

$$P_{ij} = \frac{x_{ij}}{\sum_{i=1}^m x_{ij}}, \forall i, j \quad (1)$$

With: m = number of respondents (99)

n = number of criterias (22)

- Determine the value of Entropy, dispersion and weight of each of the following criteria:
  - Calculate the Entropy value of each criterion with the following formula:

$$E_j = \frac{1}{\ln M} \sum_{i=1}^m P_{ij} \ln P_{ij}, \forall j \quad (2)$$

$E_j$  = Entropy values based on normalized data per criterion.

- Calculate the dispersion value of each criterion with the following formula:

$$d_j = 1 - E_j, \forall j \quad (3)$$

- Calculates the weight of each criterion by the formula:

$$W_j = \frac{d_j}{\sum_{j=1}^n d_j}, \forall j \quad (4)$$

The result of weight calculation on 22 criterias in this research is shown by using 6 decimals for displaying data. Table 3 describes the final weighting of each criterion.

Table 3 Value of Criteria's Weight

Rank	Criteria	Dimension	Weight
1	Information Quality	Technology	0.046958
2	Service quality	Technology	0.046929
3	Top Management Support	Organization	0.046644
4	System Quality	Technology	0.046639
5	Social Influence	Environment	0.046639
6	Compatibility	Technology	0.046486
7	IT Infrastructure	Technology	0.046385
8	Situational Normality	Environment	0.046368
9	Complexity	Technology	0.046360
10	Supporting Facilities and Infrastructure	Environment	0.046357
11	Competitive Pressure	Environment	0.046285
12	Perceived Cost	Organization	0.046002
13	Relative Advantage	Organization	0.045603
14	Perceived Ease of Use	Human	0.044696
15	Perceived Usefulness	Human	0.044628
16	System Use	Human	0.044551
17	Innovativeness of Senior Executives	Human	0.043973
18	IT Capabilities of Staff	Human	0.043918
19	Performance Expectancy	Human	0.043918
20	Technology Vendor support	Environment	0.043700
21	Formalisation	Organization	0.043642
22	Centralisation	Organization	0.043321

Table 3 shows that the highest weights are the Information Quality criteria with the weight of 0.046958. This indicates that the HRIS user of the MSOE assumes that the quality of information issued by HRIS is the most important factor in the implementation of HRIS.

#### V. DISCUSSION

Based on Table 3, the final weight of each dimension shows that the dimension that influences the success factors of



HRIS implementation of the MSOE is the technology dimension (weight 0.279757). The results of this study are in line with [4]. The difference between this study and the results of the study by [4] is the order of dimensions numbered 2, 3 and 6, which in this study dimension sequences are technology, human, environment and organization. In previous research the dimension sequences were technology, organization, human and the last environment. However, the success of the HRIS technology dimension of the MSOE is highly dependent on the organization, especially the top management support factor.

Technology is considered an important part that can give a big influence on the HRIS implementation. In addition, it is known that the technological dimension is considered by respondents to have a high level of importance realized from the average value of respondents to 6 criteria that are entirely above 4. In accordance with the results of the questionnaire about user expectations in the development of HRIS, information quality and service quality are the dominant factors in the technological dimension, followed by system quality, compatibility, IT Infrastructure and complexity.

The second greatest weight after the technological dimension is the human dimension. In the human dimension, there are 6 factors where the average value of the scale in this dimension is 3.5. The order of weight criteria on the human dimension is perceived ease of use with weight 0.044696 which illustrates that HRIS MSOE gives ease of use of information system for the purpose which according to user desire. The second sequence is the perceived usefulness criterion with a weight of 0.044628. This illustrates that HRIS MSOE has benefits for users in improving performance. The ranking of the three HRIS success factors in the human dimension is system use with weight 0.044551, this illustrates that HRIS MSOE can identify the extent to which the use of information systems can affect user needs. Innovativeness of senior executives (weight 0.043973) describes the leadership that plays an important role in the use of HRIS in the MSOE. The IT capabilities of staff criteria weighs 0.043918 where users feel that HRIS has adopted capabilities that support staff competencies. And the last is the criteria of performance expectancy (weight 0.043918) where users who believe in HRIS can help improve their work.

Based on the weight of criteria or factors in the environmental dimension is social influence which describes the HRIS user assumes that HRIS MSOE has a complex function that can cover many organizational processes especially in facilitating data collection and search of SOEs talent for prospective Board of Directors or Board of Commissioners. The next factor is situational normality which illustrates that HRIS can support policies or regulations applied by the MSOE.

#### VI. IMPLICATIONS

This research could identify the success factor needed in implementing HRIS at the ministry level. The results of this study can be an evaluation and input for the MSOE that the success factors of the implementation of HRIS in accordance

with the expectations and objectives of making HRIS MSOE, where the dimension of the most influential on the successful implementation of HRIS MSOE is a technology with the criteria of quality information. Thus, the MSOE can improve the quality of information from HRIS by updating the data periodically through the admin HR MSOE in accordance with existing legal umbrella.

#### VII. CONCLUSION

Based on the results of the analysis, the factors that influence the success of HRIS implementation of the MSOE are information quality, service quality, support of top management support, system quality and social influence. Future research is expected to use the recommendation of human resources experts to develop HRIS in the future so that the quality of HRIS could be more improved. Expectations for HRIS MSOE based on user feedback are data updates, feature development, setting of usage procedures, system improvements and ease of use.

#### ACKNOWLEDGEMENT

We want to convey our gratitude to the Directorate of Research and Community Engagement Universitas Indonesia for the Program Hibah Publikasi Internasional Terindeks untuk Tugas Akhir Mahasiswa (PITTA), grant No. 1889/UN2.R3.1/HKP05.00/2018.

#### REFERENCES

- [1] Laudon, K., & Laudon, J. (2012). *Management Information Systems Managing the Digital Firm*. New Jersey: Pearson Prentice Hall.
- [2] Roach, C. (2017). Human Resource Information Systems. Dalam *Global Encyclopedia of Public Administration, Public Policy, and Governance* (hal. 1-8). Cham: Springer International Publishing.
- [3] Hendrickson. (2003). Human Resource Information Systems: Backbone Technology of Contemporary Human Resources. *Journal of Labor Research*, 381-394.
- [4] Alam, M., Masum, A., Beh, L.-S., & Hong, C. (2016). Critical Factors Influencing Decision to Adopt Human Resource Information System (HRIS) in Hospitals. *PLoS ONE* 11(8): e0160366.
- [5] Hsu, P., & Hsu, M. (2008). *Optimizing the information outsourcing practices of primary care medical organizations using entropy and TOPSIS*. *Quality & Quantity*, 42(2), 181-201.
- [6] Alshibly, H. (2011). Human Resource Information System Success Assessment : An Integrative Model. *Australian Journal of Basic and Applied Science*, 157-169.

# Factors Affecting Users' Purchase Intention and Attitudes towards Mobile Advertising: a Tokopedia Case Study

Clarita Nainggolan  
Faculty of Computer Science  
Universitas Indonesia  
Depok, Indonesia  
clarita.nainggolan@gmail.com

Fatimah Azzahro  
Faculty of Computer Science  
Universitas Indonesia  
Depok, Indonesia  
azzahro.fatimah@cs.ui.ac.id

Putu Wuri Handayani  
Faculty of Computer Science  
Universitas Indonesia  
Depok, Indonesia  
putu.wuri@cs.ui.ac.id

**Abstract**— The growing number of mobile users encourages companies to take advantage of these opportunities to improve their marketing strategy. One of the marketing strategies that can be done through mobile devices is mobile advertising. However, the problem is that many users still consider mobile advertising as spam and many companies do not know how to start mobile advertising. While to start mobile advertising, must first understand the attitude of mobile users themselves. Therefore, this study aims to analyze the factors that can affecting Tokopedia application user's attitude to mobile advertising seen from affective and cognitive side. Additionally, this study aims to analyze the impact of mobile advertising on purchase intention of users to purchase products or services offered through mobile advertising. This research uses quantitative approach which is done by collecting respond from 565 Tokopedia application user's. The data is then analyzed using CB-SEM method using AMOS 21. Based on the results of analysis, the writers found that perceived ease of use, perceived usefulness, positive emotions, and negative emotions affect the user's attitude towards mobile advertising. Next, attitude also has an effect on user's purchase intention on advertised products or services.

**Keywords**— *Attitude, cognitive, affective, mobile advertising, m-commerce, purchase intention*

## I. INTRODUCTION

The number of internet users in Indonesia on mobile devices continues to increase and is expected to reach more than 113 million users by 2022 [1]. The rapid growth of mobile users and the development of mobile technology, opening up new opportunities for advertising by using mobile devices. By 2018, mobile advertising is predicted to beat desktop advertising and give the largest contribution of 50.2% to encourage the growth of internet advertising [2].

According to Asia Pacific AppsFlyer Sales Director, Paul Michio McCarthy, there is fundamental challenge that advertisers often faced: how to provide relevant advertising to specific people that can improve the sales percentage [3]. Mobile advertising can certainly respond to these challenges because the characteristics of mobile devices are very important and individualized. Thus, it can help retailers, service providers, and manufacturers to provide more relevant offer [4].

Mobile advertising, a subset of mobile marketing, is one form of advertising that use mobile devices [5]. Mobile advertising is among the popular way to introduce and sell products to public [6]. One of the challenges in using mobile advertising is the number of users who feel disturbed by the existence of mobile advertising such as SMS, email, and banners [7]. Additionally, many e-commerce companies do not know how to implement mobile advertising correctly [3].

Therefore, one of the early step that companies need to take is to analyse what factors can influence mobile phone users to accept mobile advertising positively. These factors may become one of the critical success factor that companies needed to develop their target sales [8].

There are several studies related to user behavior and mobile advertising acceptance. Most of the research explore users' attitude towards mobile advertising by using Technology Acceptance Model (TAM). For example, research conducted by Mohd Syuhaidi Abu Bakar and Rosmiza Bidin (2014) used TAM theory to conduct research on mobile advertising in Malaysia [9]. They found that mobile advertising behaviour and acceptance factors can affect teenagers in Malaysia in using mobile advertising to purchase movies ticket offered in mobile advertising. In addition, Olarte et al. (2016) was extending the concept of TAM by combining perceived usefulness and perceived ease of use factors into cognitive factors and adding affective factors such as positive emotions and negative emotions [10]. These factors used to predict users' behaviour towards mobile ads and their desire to receive mobile ads. Meanwhile, Liu et al. (2012) conducted a study related to the acceptance factors of advertising in general by employing infotainment factor, irritation and credibility factor [11].

Research conducted by Liu et al. (2012) and Olarte et al. (2016) limit their discussion in the factors that can affect users' adoption in mobile advertising, while research from Kim, S., & Yoon, J. (2014) may provide further explanation regarding the relationship of behavioural factors and acceptance to the purchase user intention in making purchases using mobile advertising [11], [10], [12]. This research extends the concepts of several prior research on mobile advertising and m-commerce. Combining the cognitive and affective factors, this research tries to identify the determinant of users' attitude towards mobile advertising and how users' attitude may or may not influence their purchase intention. This paper proceeds as follow. In the next section, we introduce the concept of mobile advertising and provide an overview of its characteristics. We then describe the concept of cognitive, affective and conative in the context of mobile advertising. Then, we develop a conceptual framework that consist of 8 hypotheses explaining the interrelationships between proposed factors. Finally, the paper concludes with a discussion of findings and subsequent implications.

## II. LITERATURE REVIEW

### A. Mobile Advertising

The marketing strategy through mobile phones is currently the most promising approach for the company as it

allows to reach the right audience with the right time and place [13]. The advent of mobile advertising allows advertisers to provide more personalized advertisement to users at the right time and place [13]. Additionally, mobile advertising allows users to compare product and price quickly before they decide to make a purchase [14]. By utilizing mobile advertising in communication strategies, retailers, service providers, and manufacturers to deliver more dynamic offers and campaigns [6]. One of the unique characteristics of mobile advertising is it has a high response rate, can be accessed anytime and anywhere, and has a low cost [15]. According to Salo and Tahtinen, there are three main characteristic of mobile advertising, namely personal, interactive, and context dependent [16].

### B. Attitude and Purchase Intention

In order to understand users' attitude, Fishbein (1967) proposed to investigate the three components on attitude: cognitive, affective, and conative. The cognitive component represents our thoughts, beliefs, and ideas about something. Next, the affective component represents feelings or emotions that something evokes. Lastly, the conative component represents the tendency to act in certain ways toward something. In this study, cognitive component is represented by perceived usefulness and perceived ease of use. Additionally, the affective component of attitude is represented by positive and negative emotions, while the purchase intention represents the conative component of attitude.

According to Manojehri, user's attitude towards mobile advertising can provide information for the company related to users' interest towards their products and services [17]. Additionally, it can also provide the information of users' estimated budget that will be allocated to purchase their product [17]. Moreover, prior research conducted by Fawzy found that there is correlation between attitude and user intentions [18]. In 1980, Ajzen and Fishbein also conducted research that suggested that one's intention to buy or use a product is determined by their attitude towards it before buying or using the product. Thus, it can be concluded that attitude is an important factor that can affect one's intention to buy or use certain products or services. The analysis of users' attitude is important but sometimes quite difficult to understand because of the increasingly complex technology and functionality of the mobile service [19]. Therefore, more researches are needed to comprehensively understand how users' attitude are built.

## III. HYPOTHESES DEVELOPMENT

This research tried to examine the cognitive, affective and conative phase on accepting mobile advertising in Tokopedia users. First, the cognitive aspect is represented by perceived ease of use and perceived usefulness constructs. Second, the affective aspect is measured by utilizing positive emotion, negative emotions, and attitude towards mobile advertising. Lastly, purchase intention is used to represent the conative aspect. Figure 1 illustrate the study's research model that was developed based on previous research. Eight hypotheses are proposed and described in detail below.

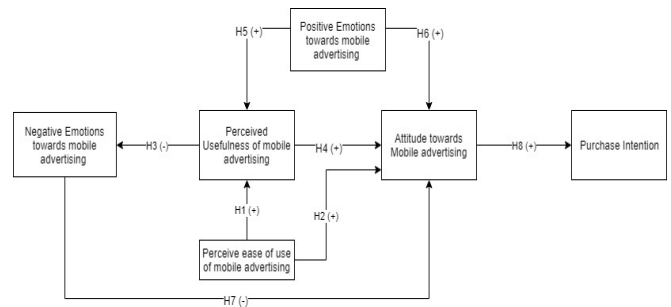


Fig. 1. Proposed Research Model

### A. Perceived ease of use of mobile advertising

Davis defines perceived ease of use as an assessment of how much effort should be put to adopt new technologies [20]. Despite the high level of mobile penetration in developing countries, m-commerce applications are considered as relatively new technology and quite challenging to be operated, especially for inexperienced users [21]. Therefore, new technologies should be easy to learn and use by users. If a technology is easy to operate, then users will be able to more easily perceive the benefits provided by the technology. In the context of mobile advertising, mobile advertising technology that easier to operate will help user to reap the benefits of the advertisement. For example, users can experience the great benefits of mobile advertising that provide automatic discount coupon recommendations when compared to mobile advertising discounts through banners. Additionally, the ease of use of mobile advertising will also affect users' attitude towards mobile advertising. Therefore, these hypotheses are proposed:

H1: Perceived ease of use will positively influence users' perceived usefulness toward mobile advertising

H2: Perceived ease of use will positively influence users' attitude toward mobile advertising

### B. Perceived usefulness of mobile advertising

Perceived usefulness is one of the TAM (Technology Acceptance Model) variables that provide an important influence on the acceptance of a new technology (Davis, 1989). In the context of m-commerce, perceived of usefulness can be defined as the extent to which consumers believe that by using m-commerce their performance can be improved [22]. Thus, it can also be concluded that in the context of mobile advertising, perceived usefulness can be defined as the extent to which consumers believe that by using mobile advertising, their performance can be improved. Thus, consumer can benefit from mobile advertising.

Additionally, Grant and O'Donohoe found that adolescent consumers are very sensitive to the perceived usefulness of mobile advertising [23], [24]. Perceived usefulness is an important factor because according to Tripathi and Siddiqui (2008), consumers may feel disturbed if the offered mobile advertising is not useful or incompatible with the information they are looking for [24]. Based on this study, it can be said that perceived usefulness has influence on consumers' negative feelings towards mobile advertising. Brehm and Brehm (1981) describe the relationship between perceived usefulness with irritation (negative emotions) through reactance theory. In those theory, it is argued that irritation is

the tendency of users to reject ads given because they found that the ads are annoying. Parreño et al. proves that perceived usefulness can reduce the irritation of the user against mobile advertising [24]. Based on the review, the authors propose that perceived usefulness negatively affects consumer's irritation (negative emotions) on mobile advertising because the greater perceived usefulness then it will reduce the negative feelings of consumers to the ads provided. Those, these following hypotheses are developed:

H3: Perceived usefulness will negatively affect users' negative emotions toward mobile advertising

H4: Perceived usefulness will positively affect users' attitude toward mobile advertising

#### C. Positive and negative emotions toward mobile advertising

Kolsaker & Drakatos (2009) found that only users with strongly positive emotions over their devices can maximize the benefits of mobile advertising [25]. When users provided with more relevant and credible content, then the user will further benefit from the mobile ad. Moreover, positive emotions such as desire and affection can have a positive effect on mobile advertisers' attitude [10]. According to Moorman et al., positive emotion such as entertainment can have a positive effect on users' attitudes toward mobile advertising. Meanwhile, Tsang et al. found that irritation as one of the negative emotions can negatively affects the attitude towards mobile advertising. Negative emotions can be assessed from the level of stress and frustration perceived by consumers related to a particular technology [26]. Therefore, the authors draw the hypothesis as follows:

H5: Positive emotions will have positive effect on users' perceived usefulness toward mobile advertising

H6: Positive emotions will have positive effect on users' attitude toward mobile advertising

H7: Negative emotions will have negative effect on users' attitude toward mobile advertising

#### D. Purchase intention on mobile advertised product

In the mobile advertising context, many studies argue that attitude is the determinant of users' acceptance of mobile advertising [13]. Fishbein and Ajzen (1975) define attitude as the tendency of one who can direct them to respond to objects, ideas, or opinions. Prior research also found that attitude can influence the intention of teenagers in Malaysia to buy movie tickets [9]. Thus, this following hypothesis is proposed:

H8: Attitude positively influence users' intention to purchase products that have been offered in mobile advertising

### IV. METHODOLOGY

#### A. Instrument Development

Questionnaire is utilized to collect data by measuring six variables that examined in this research, namely, perceived usefulness, perceived ease of use, positive emotions, negative emotions, attitude, and purchase intention. The indicators of each variable are developed based on previous research and then translated to Bahasa Indonesia. Five-point Likert scales are employed to indicate the respondent's levels of agreement or disagreement with each statement. Table I shows the example of indicators for negative emotions' construct. To maintain the meaning of original instruments,

readability test was conducted before starting the data collecting process.

TABLE I. INDICATORS FOR NEGATIVE EMOTIONS' CONSTRUCT

Code	Indicators
NEG 1	I think the mobile advertising at Tokopedia apps are <b>misleading</b>
NEG 2	I think the mobile advertising at Tokopedia apps are <b>irritating</b>
NEG 3	I think the mobile advertising at Tokopedia apps are <b>confusing</b>
NEG 4	I think the mobile advertising at Tokopedia apps are <b>distracting</b>
NEG 5	I think the mobile advertising at Tokopedia apps are <b>disturbing</b>

#### B. Data Collection

The sample of this study was Tokopedia users in Indonesia that bought product/services through mobile advertising. The data were collected via an official online survey questionnaire by using Survey UI domain (<http://kuesioner.cs.ui.ac.id/KuesionerHalodoc/>). Participants were recruited via popular social networking sites for Tokopedia users such as Facebook, Line Square, Whatsapp, Twitter, Instagram, dan LinkedIn. Limited gifts were offered to encourage participation. After deleting duplicates and incomplete responses, 509 valid surveys remained. Table II summarizes the demographics of the respondents.

TABLE II. DEMOGRAPHY OF RESPONDENTS

Demographic	Category	Frequency	%
Gender	Male	225	44%
	Female	283	56%
Age	<20	117	23%
	20-30	357	70%
	31-40	30	6%
	>40	4	1%
Type of mobile advertising that often used	Banner Tokopedia	436	86%
	Push notification	6	1%
	SMS advertising	66	13%
Last time shopping due to mobile advertising	< 3 months	360	71%
	3-7 months	95	19%
	8-12 months	26	5%
	> 12 months	27	5%
Frequency of shopping through mobile ads	0-5 times	405	80%
	6-10 times	55	11%
	> 10 times	48	9%

### V. RESEARCH RESULTS

The study is conducted in quantitative approach to identify the relationships between variables introduced in prior section. AMOS 21.0 is employed to analyze the research model depicts at Figure 1.

#### A. Measurement Model

To evaluate the proposed model, we employ the two-stage model-building process for applying SEM. First, the measurement model is measured by examining the reliability and validity of constructs. Table III show the results of reliability and validity testing by ensuring each construct has loading factors more than 0.70. Additionally, the Cronbach's Alpha (CA) and Composite Reliability (CR) should be more than 0.70, while the Average Variance Extracted (AVE) can not be lower than 0.50 [27]. Next, the structural model is evaluated and described in the next section.

TABLE III. THE RESULTS OF RELIABILITY AND CONVERGENT VALIDITY TESTING

Variable	Items	Loading Factors	AVE	CR	CA
Perceived usefulness	PU2	0.722	0.977	0.853	0.994
	PU3	0.737			
	PU4	0.793			
	PU5	0.725			
	PU6	0.816			
Purchase intention	PI1	0.708	0.980	0.826	0.993
	PI2	0.729			
	PI3	0.712			
	PI4	0.775			
	PI5	0.735			
	PI6	0.782			
Positive emotions	PE5	0.768	0.743	0.859	0.852
	PE6	0.705			
	PE7	0.749			
	PE8	0.756			
	PE9	0.779			
Negative emotions	NE2	0.727	0.986	0.798	0.995
	NE3	0.721			
	NE4	0.823			
	NE5	0.727			
	ATT10	0.711			
Attitude	ATT3	0.774	0.765	0.888	0.927
	ATT4	0.764			
	ATT5	0.805			
	ATT6	0.733			
	ATT7	0.758			
	ATT8	0.829			
	ATT9	0.75			
	PEOU3	0.718			
Perceived ease of use	PEOU4	0.761	0.976	0.736	0.987
	PEOU5	0.794			

### B. Structural Model Evaluation

The evaluation of structural model consists of three distinct steps. First, we need to estimate the model's overall goodness-of-fit. The values of all fit indices were better than the recommended values, which demonstrate a good fit between the model and data (see Table IV). Next, each  $R^2$  value for endogenous variable should be identified as can be seen in Table V. PU has  $R^2$  value of 0.463 that shows that PU variable can be explained by its exogenous factors up to 46.3% and the rest of it explained by other factors outside model. Then, NEG variable has  $R^2$  value of 0.002 while ATT and PI have  $R^2$  value of 0.622 and 0.655 respectively. Therefore, one can conclude that PI and ATT variable have strong correlation with its exogenous variables.

TABLE IV. THE FIT INDICES FOR MEASUREMENT MODEL

Fit index	Chi Square	RMSEA	GFI	CFI	NFI
Recommended value	>0.05	< 0.07	>0.90	>0.90	>0.90
Model value	0.065	0.023	0.973	0.996	0.98

TABLE V.  $R^2$  VALUE FOR ENDOGEN VARIABLES

Endogen Variables	$R^2$
Perceived Usefulness (PU)	0.463
Negative Emotions (NEG)	0.002
Attitude (ATT)	0.622
Purchase Intention (PI)	0.655

AMOS 21.0 is utilized to perform one-tailed hypothesis testing. The significant path coefficients ( $p \leq 0.05$ ) appear to support the proposed model. Table VI shows the result of

hypothesis testing. From 8 initial hypotheses, 1 of them are rejected while the rest are accepted.

TABLE VI. HYPOTHESES TESTING

Hypotheses	Attributes	Estimate	p	p/2	Results
H1	PU <--- PEOU	0.298	0.002	0.001	Accepted
H2	ATT <--- PEOU	0.322	0.003	0.0015	Accepted
H3	NEG <--- PU	-0.065	0.116	0.058	Rejected
H4	ATT <--- PU	0.234	0.001	0.0005	Accepted
H5	PU <--- PE	0.528	0.005	0.0025	Accepted
H6	ATT <--- PE	0.28	0.006	0.003	Accepted
H7	ATT <--- NEG	-0.031	0.004	0.002	Accepted
H8	PI <--- ATT	0.298	0.002	0.001	Accepted

## VI. DISCUSSION

This study examines users' attitude towards mobile advertising and how the attitude can affect users' purchase intention towards the products or services offered through the mobile advertising. To analyze users' attitude towards mobile advertising, the authors investigate the cognitive, affective, and conative aspects of mobile advertising. Cognitive aspects help author to understand users' attitude by investigating perceived ease of use and perceived usefulness. Meanwhile, the affective aspects are investigated by using positive emotions and negative emotions towards mobile advertising.

The first hypothesis draws a positive relationship between perceived ease of use on perceived of usefulness. This hypothesis is accepted and supported by research of Alicia et al which found that perceived ease of use has a great influence on the benefits or usefulness perceived by users [13],[28]. This will also be affecting users' desire to adopt mobile services.

As for the second hypothesis, the authors propose that perceived ease of use has positive effect on users' attitude. This hypothesis is also accepted and supported by research Olarte et al. which suggests that the higher perceived ease of use will bring more positive user's attitude towards technology [10]. This is because internet and smartphone technology can help companies understand the character of every customer, from demography to the needs of the customer. The ads provided will be tailored to the characteristics of the customer and can improve the attitude of the customer against the advertisement [28].

As for the third hypothesis, the authors propose the hypothesis that perceived usefulness negatively affects negative emotions of users. However, the authors found different things after testing because this third hypothesis was rejected. Based on the research of Edward et al., it suggests that the negative feelings of a person can be affected by the laying and positioning of the ad. If an ad is positioned in the right place, then it will reduce the annoyance perceived by users [29]. So, it is possible that Tokopedia users do not feel disturbed by mobile advertising because of the right placement of its ads.

In the fourth hypothesis, the authors propose a hypothesis that perceived usefulness can provide a positive influence on users' attitude towards mobile advertising. After the test, this hypothesis is accepted and also supported by the research of

Parreño et al. which suggests that perceived usefulness can influence attitude because users can carry their mobile phones at all times thus giving users extra privileged to access the promotions offered as well can increase the chance to access useful information [24]. Nowadays, many advertisers in Indonesia are developing content marketing that is marketing step to give advertisement through which more interesting, useful and informative to attract more audience [28].

In the fifth hypothesis, the authors propose a hypothesis that positive emotions have a positive effect on perceived usefulness and this hypothesis is accepted. The results of this hypothetical test also supported by Kolsaker & Drakatos (2009) that found that only users who have strong emotions to their devices, who can feel the tremendous benefits of mobile advertising it receives [25]. This emotion is derived from the properties of an interactive mobile device that increases the commitment and desire of users to disseminate information related to products or services through their social media. This is in accordance with the behaviour of the Indonesian people towards advertising, most of the audience has a level of patience that is directly proportional to the quality of the ad content displayed. Highly-weighted and high-interest ads will make your audience more patient and get the most out of the ads [3].

In the sixth hypothesis, the authors propose a hypothesis that positive emotions have a positive effect on the user's attitude and this hypothesis is accepted. The results of this hypothesis test are also supported by Park & Salvendy's research which revealed that positive emotions are related to desire and affection that can positively influence the attitude of mobile advertising related users [10], [30]. In providing ad content it is necessary to analyse the emotions to be conveyed through the ad, the emotion can be fear, humour, fantasy and other feelings. It is used to support the user's attitude toward advertising, if the audience receives positive feelings from the advertisement then the probability of receiving advertising message will be greater to be accepted.

In the seventh hypothesis, the authors propose that negative emotions can negatively affect the user's attitude and this hypothesis is accepted. The results of this hypothesis are also supported by Tsang et al. which revealed that negative emotions negatively affect attitude toward mobile advertising [26]. Similar to positive emotions, negative emotions also give big influence on attitude. Indonesians are very sensitive to the presence of an advertisement, especially the placement and positioning of ads in the applications. Advertisement that gives users negative feeling are mainly because of the inadequate position that make the audience not paying attention to the advertisement.

In the eighth hypothesis the authors propose that attitude gives a positive influence on users' purchasing intention towards products or services offered on mobile advertising, and this hypothesis is also accepted. The results of this hypothesis testing are also supported by Fishbein & Ajzen (1975, 1980) which reveal that attitude can affect purchase intention [9]. This happened due to Indonesian behaviour towards mobile advertising that are strongly influenced by the development of Internet technology and smartphones and also influenced by the content provided by ads.

## VII. THEORETICAL AND PRACTICAL IMPLICATION

In terms of theoretical implication, this study complements previous research by providing attitude evaluation from two sides, namely cognitive and affective. The previous research often only focused on one aspect, so it cannot see users' attitude comprehensively. In addition, this study also provides a further description of the conative aspects of users' attitude by using users' purchase intention factor. Meanwhile, from the practical side, this research provides benefits to mobile advertising providers, especially Tokopedia. These results can help Tokopedia in developing strategies for mobile advertising development by prioritizing factors that can improving users' attitude. Additionally, this research can also benefit the advertising agencies and consultants because they can develop mobile advertising in accordance with the attitude of users so as to increase the purchase intention of users of the products or services offered through developed ads. In addition, mobile advertising providers can use cognitive factors such as perceived usefulness and perceived ease of use, and affective factors that are positive emotions and negative emotions to become the criteria in measuring the effectiveness of advertising channels, especially in mobile advertising.

## VIII. LIMITATION AND CONCLUSION

Based on the research results, we found that cognitive factors and affective factors influence users' attitude towards mobile advertising. This study also found the relationship between positive emotions and perceived usefulness. Additionally, we also found that user attitude is one of the antecedent of users' purchase intention to buy products advertised in mobile application. Lastly, this study found that perceived usefulness does not affect users' negative emotions towards mobile advertising.

All the findings of this study may be explored and implemented by any companies that used mobile advertisement to attract customers. Still, this study has several limitations. First, we did not incorporate actual action of users. Second, the demography of respondents did not represents all users characteristics of Tokopedia. Thus, the results of this study may not have represented Tokopedia users' attitude in general. Further data collection needs to be conducted in order to improve the results of this study. Moreover, future research must explore other factors that can affect users' attitude towards mobile advertising such as subjective norms and users' characteristic. One can utilize systematic search to find the right keywords to get additional factors that may influence users' attitude towards mobile advertising.

## ACKNOWLEDGMENT

We want to convey our gratitude to the Directorate of Research and Community Engagement Universitas Indonesia for the Program Hibah Publikasi Internasional Terindeks untuk Tugas Akhir Mahasiswa (PITTA), grant No. 1889/UN2.R3.1/HKP05.00/2018.



## REFERENCES

- [1] Statista, "Number of mobile phone internet users in Indonesia from 2015-2022 (in millions).", 2018. [Online]. Available: <https://www.statista.com/statistics/558642/number-of-mobile-internet-user-in-indonesia/>. [Accessed: 12-Jan-2018].
- [2] Zenith, "Global mobile advertising expenditure to overtake desktop in 2018," 2018. [Online]. Available: <https://www.zenithmedia.com/global-mobile-advertising-expenditure-overtake-desktop-2018/>. [Accessed: 12-Jan-2018].
- [3] Daily Social, "Melihat Efektivitas Iklan Mobile dari Pola Pengguna Aplikasi di Indonesia," 2016. [Online]. Available: <https://dailysocial.id/post/melihat-efektivitas-iklan-mobile-dari-pola-pengguna-aplikasi-di-indonesia>. [Accessed: 19-May-2018].
- [4] D. Grewal, Y. Bart, M. Spann, and P. P. Zubcsek, "Mobile Advertising: A Framework and Research Agenda," *J. Interact. Mark.*, vol. 34, pp. 3–14, 2016.
- [5] Wikipedia, "Mobile Advertising." [Online]. Available: [https://en.wikipedia.org/wiki/Mobile\\_advertising](https://en.wikipedia.org/wiki/Mobile_advertising). [Accessed: 13-Jan-2018].
- [6] J. Martins, C. Costa, T. Oliveira, R. Gonçalves, and F. Branco, "How smartphone advertising influences consumers' purchase intention," *Journal of Business Research*, 2018.
- [7] MaxManroe.com, "Menelusuri Potensi Perkembangan Mobile Advertising di Indonesia," 2018. [Online]. Available: <https://www.maxmanroe.com/menelusuri-potensi-perkembangan-mobile-advertising-di-indonesia.html>. [Accessed: 20-May-2018].
- [8] Q. Min, S. Ji, and G. Qu, "Mobile Commerce User Acceptance Study in China: A Revised UTAUT Model," *Tsinghua Sci. Technol.*, vol. 13, no. 3, pp. 257–264, 2008.
- [9] M. S. A. Bakar and R. Bidin, "Technology Acceptance and Purchase Intention towards Movie Mobile Advertising among Youth in Malaysia," *Procedia - Soc. Behav. Sci.*, vol. 130, pp. 558–567, 2014.
- [10] C. Olarte-Pascual, J. Pelegrín-Borondo, and E. Reinares-Lara, "Cognitive-affective model of acceptance of mobile phone advertising," *E a M Ekon. a Manag.*, vol. 19, no. 4, pp. 134–148, 2016.
- [11] L. Zhang, J. Zhu, and Q. Liu, "A meta-analysis of mobile commerce adoption and the moderating effect of culture," *Comput. Human Behav.*, vol. 28, no. 5, pp. 1902–1911, 2012.
- [12] S. Kim and J. Yoon, "Consumer acceptance of mobile advertising: Focus on mobile users in South Korea and Russia," *Inf.*, vol. 17, no. 1, pp. 23–34, 2014.
- [13] A. Izquierdo-Yusta, C. Olarte-Pascual, and E. Reinares-Lara, "Attitudes toward mobile advertising among users versus non-users of the mobile Internet," in *Telematics and Informatics*, 2015, vol. 32, no. 2, pp. 355–366.
- [14] W. E. Nwagwu and B. Famiyesin, "Acceptance of mobile advertising by consumers in public service institutions in Lagos, Nigeria," *Electron. Libr.*, vol. 34, no. 2, pp. 265–288, 2016.
- [15] Z. Fang, Y. Yang, F. M. Deng, and J. Cai, "Research Advances in Mobile Advertising Areas," *Appl. Mech. Mater.*, vol. 248, pp. 555–558, 2012.
- [16] J. Salo and J. Tähtinen, "Special Features of Mobile Advertising and Their Utilization," in *Encyclopedia of E-Commerce, E-Government, and Mobile Commerce*, 2006, pp. 1035–1040.
- [17] N. N. Manochhri and Y. S. Alhinai, "Mobile-phone users' attitudes towards' mobile commerce & services in the Gulf cooperation council countries: Case study," in *5th International Conference Service Systems and Service Management - Exploring Service Dynamics with Science and Innovative Technology, ICSSSM'08*, 2008.
- [18] S. F. Fawzy, E. Mohamed, and A. Salam, "M-Commerce adoption in Egypt: An extension to theory of reasoned action," *Bus. Manag. Rev.*, vol. 6, no. 1, pp. 2–3, 2015.
- [19] Z. I. Saleh and A. Mashhour, "Consumer Attitude towards M-Commerce: The Perceived Level of Security and the Role of Trust," *J. Emerg. Trends Comput. Inf. Sci.*, vol. 5, no. 2, pp. 111–117, 2014.
- [20] X. Zhang and K. Xiong, "A Conceptual Model of User Adoption of Mobile Advertising," in *2012 International Conference on Computer Science and Electronics Engineering*, 2012, pp. 124–127.
- [21] F. Liebana-Cabanillas, V. Marinkovic, and Z. Kalinic, "A SEM-neural network approach for predicting antecedents of m-commerce acceptance," *Int. J. Inf. Manage.*, vol. 37, no. 2, pp. 14–24, 2017.
- [22] T. Tsu Wei, G. Marthandan, A. Yee Loong Chong, K. Ooi, and S. Arumugam, "What drives Malaysian m-commerce adoption? An empirical analysis," *Ind. Manag. Data Syst.*, vol. 109, no. 3, pp. 370–388, 2009.
- [23] I. Grant and S. O'Donohoe, "Why young consumers are not open to mobile marketing communication," *Int. J. Advert.*, vol. 26, no. 2, pp. 223–246, 2007.
- [24] J. M. Parreño, S. Sanz-Blas, C. Ruiz-Mafé, and J. Aldás-Manzano, "Key factors of teenagers' mobile advertising acceptance," *Ind. Manag. Data Syst.*, vol. 113, no. 5, pp. 732–749, 2013.
- [25] A. Kolsaker and N. Drakatos, "Mobile advertising: The influence of emotional attachment to mobile devices on consumer receptiveness," *J. Mark. Commun.*, vol. 15, no. 4, pp. 267–280, 2009.
- [26] M. M. Tsang, "Consumer Attitudes Toward Mobile Advertising: An Empirical Study," *Int. J. Electron. Commer.*, vol. 8, no. 3, pp. 65–78, 2004.
- [27] J. F. Hair, C. M. Ringle, and M. Sarstedt, "PLS-SEM: Indeed a Silver Bullet," *The Journal of Marketing Theory and Practice*, vol. 19, pp. 139–152, 2011.
- [28] Brightstars, "Inilah Tren Digital Marketing Advertising di Indonesia," 2016. [Online]. Available: <http://www.brightstars.co.id/blog/inilah-tren-digital-marketing-advertising-di-indonesia/>. [Accessed: 19-May-2018].
- [29] S. M. Edwards, H. Li, and J.-H. Lee, "Forced Exposure and Psychological Reactance: Antecedents and Consequences of the Perceived Intrusiveness of Pop-Up Ads," *J. Advert.*, vol. 31, no. 3, pp. 83–95, 2002.
- [30] T. Park and G. Salvendy, "Emotional Factors in Advertising Via Mobile Phones," *Int. J. Hum. Comput. Interact.*, vol. 28, no. 9, pp. 597–612, 2012.

# Analysis of Electronic Medical Record Reception using Expanded Technology Acceptance Model

Indra Kharisma Raharjana  
Information Systems  
Universitas Airlangga  
Surabaya, Indonesia  
indra.kharisma@fst.unair.ac.id

Faisal Apriyana  
Information Systems  
Universitas Airlangga  
Surabaya, Indonesia  
faisal-a-10@fst.unair.ac.id

Taufik  
Information Systems  
Universitas Airlangga  
Surabaya, Indonesia  
taufik@fst.unair.ac.id

**Abstract**— Information technology in the health sector has the potential to increase the quality of patient care by improving process efficiency, reducing errors and reducing costs. But this potential cannot be achieved if there is rejection from stakeholders. In this study, we examine the information technology acceptance model in the medical field. We use Moores's model that was developed from Davis's Technology Acceptance Model by adding the variables that determine the success of information technology acceptance. The variables are divided into two categories: information quality consisting of accuracy, content, timeliness, and format. The Enabling factors consisting technical support and self-efficacy. The case study was conducted among medical personnel at a Hospital in East Java. The subject of research is the use of the electronic medical record. Data were obtained through a questionnaire. Then the data is processed with Partial Least Squares algorithm using PLS software. As a result of the sixteen hypotheses proposed there are fourteen hypotheses accepted and the overall model deemed appropriate.

**Keywords**— *Technology Acceptance Model, Health Service, Electronic Medical Record, IT adoption.*

## I. INTRODUCTION

Today, information technology (IT) has provided benefits in many areas, including health. Institutions of health care providers such as hospitals use IT in health to improve the quality of their services. IT in the health sector such as electronic medical records (RME) has the potential to improve the quality of patient care by improving process efficiency, reducing errors and reducing costs [1]. Despite the many advantages, its application still encounters many problems. In Indonesia only 48% (1257 of 2588) hospitals that have a hospital management information system. In addition, the use of IT in the health field of medical personnel often gets a rejection [2]. Many believe that IT will provide benefits if received and used properly by users [3][4]. Stakeholder readiness and managerial decisions will bring better organizational performance, especially in the case of IT adoption [5].

It is important to know the definition of user acceptance from IT and what variables affect it. The exact definition of IT user acceptance will be the benchmark that illustrates IT's success. Therefore, research on acceptance theory of IT users is needed. Theory of Reasoned Action (TRA) and Theory of Planned Behavior (TPB) are models in the field of social

psychology that proved successful in explaining behavior. TRA explains that behavior is influenced by intentions that have multiple variables [6]. TPB has a behavior control variable that explains that the behaviors performed are also influenced by the existing situation [7]. In addition to TRA and TPB, the theory that explains user acceptance is the Technology Acceptance Model (TAM). In a study of comparisons of these three theories on the use of internet banking representing IT [8], it is evident that TAM is better at explaining the variance in overall model behavior and suitability.

In TAM, user acceptance is defined by the attitude in using a technology which then affects intention of use. And the factors that influence attitudes in using a technology are perceived usefulness (PU) and perceived ease of use (PEOU). PU is defined as the level of trust in a technology that using such technology will improve performance at work. PEOU is defined as the level of confidence, how easy the technology to use [9]. TAM is widely used in areas such as economics, education, industry, and health. While research TAM on IT in the field of health has been done and provide good results in predicting and explaining the acceptance of medical personnel to the use of IT in the field of health. This was stated by [10] who conducted reviews on more than 20 studies related to the theory of user acceptance of IT in the medical field including TAM, TAM added another variable or commonly called an expanded TAM and TAM's predecessor theories are TRA and TPB.

The expanded TAM in the field of health was developed in order to obtain a model suitable for the medical field. An example of research on TAM in the field of health that has been done is the research of [11] which adds variable quality information, service quality and system quality on the TAM model. Another extended TAM example is a study by [12] that add subjective variable norms, drawings, job relevance, output quality, demonstrable results, experience, and volunteerism. While in this study tested the expanded TAM model belonging to [13] because the model is systematic, intuitive and in accordance with case studies in this study that the use of IT is applied in compulsory rather than voluntary.

In Moores's models[13], TAM's expanded declared PU and PEOU a factor affecting user acceptance. PU and PEOU are also influenced by information quality and enabling factors. The quality of information is defined as the accuracy of

information and the absence of false information (accuracy), what kind of information is presented (content), information is presented in a format that is easy to read (format), and timeliness when the information is needed (timeliness). Enabling factors are defined to be the provision of assistance if there is difficulty in using technology (technical support), the ability of users in using the technology (self-efficacy). User acceptance is defined with attitudes in using technology and technological conformity by means of a user's preferred work (compatibility).

This study was also conducted to confirm research on TAM models by Moores[13]. The TAM model illustrates the factors related to IT user acceptance in the health field and how it relates. This study examines the relationship between variables on the Moores TAM model. The case study used is the acceptance of RME technology by medical personnel at one of the Hospital in East Java Indonesia.

This research uses a survey method with the questionnaire as a research instrument. The question on this research questionnaire is similar to that of Moores research but has been translated into Bahasa (Indonesia Language). The TAM model used is also the result of Moores research. Samples are medical personnel using RME at a Hospital. The number of samples was determined by using Slovin equation [14]. After the data obtained a multivariate analysis to test the model. Multivariate analysis technique used is Partial Least Squares (PLS) software. After the model is evaluated with PLS, model interpretation is done to find out the user acceptance picture on the research object. The goal of this study is to measure the suitability of Moores' expanded TAM model with the case study of RME acceptance by medical personnel at Indonesian Hospital.

## II. METHODS

### A. TAM Model

Moores proposed a TAM model applied to health care. The advantage of the Moores model is to use only the important variables that allegedly affect user acceptance. The Moores model retains PU and PEOU as the variable that determines the acceptance of IT users. The size that is considered as a form of acceptance is the use of the system (use), attitude to the system (attitude) and compatibility. The variables that affect PU and PEOU are information quality and enabling factor. Factors of experience using the system are also included in the model to know its relation to change of belief and satisfaction over time.

Each variable is explained by several indicators. Except for the variables of system usage, the indicators are a discourse that describes the feelings or circumstances felt by the users of the system. The indicators in this study are indicators used in Moores research and translated into Bahasa (Indonesian Language).

The model made this model based on Moores research. In Moores research, there is Behavioral Intention to Use (USE) variable but since the use of RME in this study is required by the Hospital, this variable is not included in the model. Moores states that if the use of the system is not an independent variable or in this case, its use is required, this variable has no longer logical validity, so the relationship between this variable

and other variables has no meaning. Moreover, in his hypothesis Moores gives an exception to the hypothesis regarding the use of the system, he states unless the system's use is required.

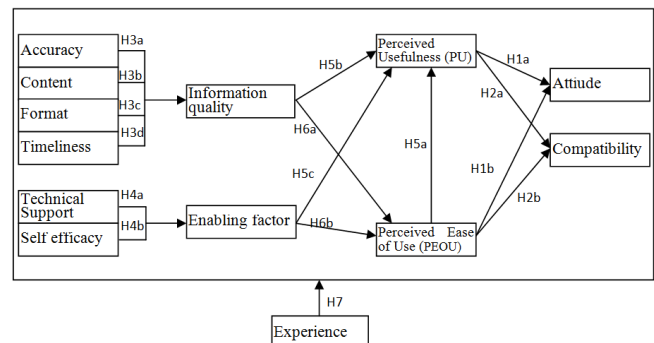


Fig. 1. Model to be tested

The hypotheses to be tested in this study include:

**H1a.** Attitudes will be affected significantly and positively by perceived usefulness;

**H2b.** Compatibility will be affected significantly and positively by perceived ease of use.

**H3a.** The quality of information will be affected significantly and positively by accuracy;

**H3b.** The quality of the information will be affected significantly and positively by the content

**H3c.** The quality of the information will be affected significantly and positively by the format;

**H3d.** The quality of the information will be affected significantly and positively by the timeliness

**H4a.** Possible factors will be affected significantly and positively by the technical support;

**H4b.** Possible factors will be significantly and positively influenced by self-efficacy;

**H5a.** Perceived usefulness will be affected significantly and positively by (a) perceived ease of use;

**H5b.** Perceived usefulness will be affected significantly and positively by the quality of information;

**H5c.** Perceived usefulness will be affected significantly and positively by possible factors;

**H6a.** Perceived ease of use will be significantly and positively influenced by the quality of information;

**H6b.** Perceived ease of use will be significantly and positively influenced by possible factors;

**H7.** Experience in using the system has a significant moderation effect on each IT acceptance component.

### B. Questionnaire

In this study used a list of questionnaire statements on Moores research translated into Bahasa Indonesia. Respondents were asked to provide a score indicating the suitability of each

statement and what respondents felt using a Likert scale of 1 (disagree) to 7 (strongly agree). This study uses an odd scale with a value that is in the middle means neutral that is scale 4. Using a neutral scale means the data obtained is close to the perceived truth of the respondent. The seven-figure scale is more than any other scale that is often done in various studies such as three, four or five. The use of a seven scale in addition to aiming to equal Moores's research is easier than that so that the data obtained represent more of the diversity present in the population or the actual state.

TABLE I. QUESTIONNAIRE BASED ON VARIABLES

Variable	Indicator of the variable in the form of a statement
Accuracy	RME is accurate.
	I am satisfied with RME accuracy.
	Overall, I believe the information provided by RME.
Content	RME provides the information I need.
	The information content suits my needs.
	RME provides reports that I will use.
	RME provides sufficient information.
	Overall, the information content suited my needs.
Format	The Layout format of the screen makes it easy for me to read the information displayed.
	The information displayed is clear.
	Overall, I think the output is displayed in a useful format.
Timeliness	I get the information I need on time.
	RME provides up-to-date information.
	Overall, the information I needed was always available when I needed it.
Technical Support	One particular person (or group) is available to help with hardware difficulties.
	One particular person (or group) is available to help with system difficulty.
	Special directive instructions related to RME are available to me.
	Overall, I've been given sufficient support in the use of RME.
Self-efficacy	I feel comfortable using RME myself.
	I can easily operate my own RME.
	I can use RME, even when nobody shows how to use it.
	Overall, I am confident in my ability to use RME.
PU	Using RME on my work allows me to complete tasks faster.
	Using RME improves my work performance.
	Using RME allows me to increase productivity.
	Using RME improves the effectiveness of my work.
	Using RME makes my job easier.
	Overall, RME is useful for my work.
PEOU	Learn how to operate RME is easy for me.
	It's easy to make RME do something I want to do.
	My interaction with RME is clear and understandable.
	RME is flexible in interacting.
	It is easy for me to become an expert in using RME.
Attitude	Overall, RME is easy to use.
	In using RME I feel joy.
	In using RME I feel happy.
	In using RME it is frustrating.
Compatibility	In using RME I feel satisfied.
	Using RME fits perfectly with the way I work.
	Using RME fits perfectly to my working style.
	Overall, using RME matches all aspects of my work

Questionnaires were given to respondents who were medical personnel using RME at a Hospital. The questionnaire was given along with cover letters and filling instructions. After two weeks, the questionnaire will be reassembled. Then

the results of the questionnaire data in the recapitulation in a spreadsheet program to further process with PLS program.

The study took place from November 3, 2014, to November 16, 2014. With the help of the head of Poli Department, research instruments in the form of paper questionnaires were given to medical personnel using RME. The questionnaire is accompanied by an explanation of the research objectives and instructions for using the filling. Respondents were given two weeks to fill and collect back to head Poli Department. The questionnaire used amounted to sixty-six to forty-seven doctors and nineteen nurses in Poli. A comparison of the number of doctors and nurses who were respondents is presented in Figure 2.

After two weeks after the questionnaire was distributed, the questionnaires were reassembled to obtain the necessary data for the study. Of the sixty-eight questionnaires distributed were obtained twenty-two reassembled questionnaires, fourteen questionnaires from doctors and eight questionnaires from nurses. Based on the percentage return of the questionnaire, more nurses returned the questionnaires than the doctors. Except for personal data, all the points in the questionnaire have been filled out. Because personal data is only filled with name data and do not fill data about the experience using the system. The H7 hypothesis that the influence of experiential variables on all variables on the model is not discussed in the study.

### characteristics of respondents

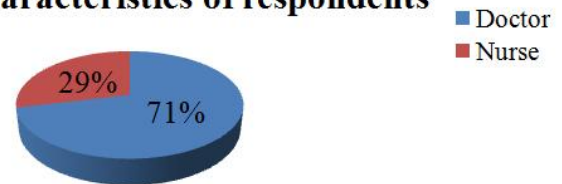


Fig. 2. characteristics of respondents

## III. RESULTS AND DISCUSSION

### A. Evaluation of Measurement Models

The model was tested by using two kinds of evaluation ie evaluation of measurement model and evaluation of the structural model. Both are done by first doing the calculation of PLS algorithm with the help of PLS program. Evaluation of the first measurement model is to evaluate the loading factor value. In the calculation result of PLS algorithm of load factor value from accuracy\_3 indicator correlated with accuracy variable, k\_akurasi\_3 indicator correlated with the variable of information quality and indicator attitude\_3 correlated with attitude variable less than 0,6 which is criterion from acceptable loading factor value.

Since the loading factor value of the accuracy\_3 indicator correlated with the accuracy variable is 0.4433 means that the information provided by RME is free from error is not an indicator of the accuracy variable. Since the loading factor value of the k\_akurasi\_3 indicator correlated with the variable of quality of information is 0.2958. it means that the information provided by RME is free from error is not an indicator of the variable quality of information. Since the

loading factor value of the attitude\_3 indicator that correlates with the attitude variable is 0.2572 means that the statement that using RME is frustrating is not an indicator of the variable of information quality.

The next step, the accuracy\_3 indicator, k\_akurasi\_3 indicator, and the attitude\_3 indicator are removed from the model and then recalculated. When compared, it will be seen that the loading factor value of each indicator after the recalculation becomes increased.

TABLE II. EVALUATION RESULT OF COMPOSITE RELIABILITY AND AVE

Variable	AVE	Composite Reliability
PEOU	0,7126	0,9367
PU	0,7283	0,9412
Accuracy	0,8509	0,9195
Technical Support	0,7014	0,9033
Enabling factor	0,6241	0,9292
Self-efficacy	0,8017	0,9416
Compatibility	0,9169	0,9707
Timeliness	0,8062	0,9258
Content	0,7152	0,9258
Information quality	0,609	0,9526
Attitude	0,8668	0,9513

The evaluation of the next measurement model is the evaluation of composite reliability and AVE evaluation. The composite reliability value received is more than 0.7 and the AVE value received is above 0.5. The evaluation results of composite reliability and AVE are presented in Table 2.

Based on table 2, no variables were found that did not meet the criteria. Each variable has a value of composite reliability above 0.7 which means any reliable variable. Each variable has an AVE value above 0.5 which means that every indicator variable and variable proves valid.

### B. Evaluation of Structural Model

The structural model evaluation consists of two stages: evaluating the value of standardized path coefficients and evaluating the GoF value. The value of standardized path coefficients between variables is presented in Table 3.

TABLE III. PATH BETWEEN VARIABLE COEFFICIENT VALUE

Variable	Path Between Variable Coefficient Value
PEOU -> PU	0,6785
PEOU -> Compatibility	0,5023
PEOU -> attitude	0,3308
PU -> Compatibility	0,3366
PU -> attitude	0,5039
Accuracy -> Information quality	0,2022
Technical Support-> Enabling factor	0,4786
Enabling factor-> PEOU	0,8559
Enabling factor-> PU	-0,4221
format -> Information quality	0,2614
Self-efficacy -> Enabling factor	0,6165
timeliness -> Information quality	0,2438
Content -> Information quality	0,4204
Information quality-> PEOU	-0,0172
Information quality-> PU	0,6308

Based on table 3 there are two paths that have a standardized path does not meet the criteria. The value of standardized path results from the enabling factor to PU and information quality to PEOU is less than 2.0. The two paths that do not meet these criteria, it is mean that the two paths have weak interdependent relationships. To calculate the GoF value required *communality* and  $R^2$  generated by PLS program, the value is presented in Table 4.

TABLE IV. COMMUNALITY AND  $R^2$ 

Variable	Communality	$R^2$
PEOU	0,7126	0,7114
PU	0,7283	0,5607
Accuracy	0,8509	0
Technical Support	0,7014	0
Enabling factor	0,6241	0,9997
Format	0,811	0
Self-efficacy	0,8017	0
Compatibility	0,9169	0,6074
Timeliness	0,8062	0
Content	0,7152	0
Information quality	0,609	0,9998
Attitude	0,8668	0,5997
Means	0,7620	0,3732

By the formula (1) can be calculated the value of GoF namely:

$$GoF = \sqrt{\text{Communality} \times R^2}$$

$$GoF = \sqrt{0,762008333 \times 0,373225}$$

$$GoF = 0,5332$$

Because GoF values meet criteria (greater than 0.36), it means the model in this study can be called overall a good model.

TABLE V. SIGNIFICANCE OF HYPOTHESIS

Hypothesis	Path between variables	t value	Hypothesis test results
H1(a)	PU -> attitude	3,9636	accepted
H1(b)	PEOU -> attitude	2,2593	Accepted
H2(a)	PU -> Compatibility	4,6836	accepted
H2(b)	PEOU -> Compatibility	5,8789	accepted
H3(a)	Accuracy -> Information quality	15,1705	accepted
H3(b)	Content -> Information quality	26,6447	accepted
H3(c)	format -> Information quality	12,7567	accepted
H3(d)	timeliness -> Information quality	24,0762	accepted
H4(a)	Technical Support-> Enabling factor	24,1617	accepted
H4(b)	Self-efficacy -> Enabling factor	19,5425	accepted
H5(a)	PEOU -> PU	4,3342	accepted
H5(b)	Information quality-> PU	5,3563	accepted
H5(c)	Enabling factor-> PU	1,9807	accepted
H6(a)	Information quality-> PEOU	0,1798	rejected
H6(b)	Enabling factor-> PEOU	13,0459	accepted



### C. Hypothesis Testing

A hypothesis test is done by comparing the value of  $t$  arithmetic to the value of  $t$  table. A hypothesis described in a path is considered significant if it has a value of  $t$  arithmetic greater than the value of  $t$  table. With a real level of 5% obtained  $t$  table value of 1.96. While the value of  $t$  arithmetic obtained from the calculation of bootstrapping with 500 samples. The result of comparison of  $t$  value arithmetic with  $t$  table used as hypothesis significance test can be seen in table 5. Based on the comparison between the value of  $t$  arithmetic with  $t$  table there are fourteen hypotheses accepted and one hypothesis rejected. Graphical representation can be seen in figure 3.

### D. Discussion and limitations

What is worth noting is that this study only studies the phenomenon of electronic medical records by doctors and nurses in a single hospital. Some limitations that arise are the quality of medical record application and its application in hospitals is also a dominant factor affecting the results of this study. Besides that, we cannot measure the experience factor in the study because the respondents choose to empty experience field for some reason.

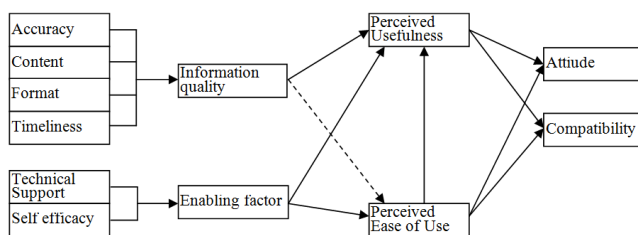


Fig. 3. Result of PLS analysis. Note: Significant paths shown in bold.

Of the sixteen hypotheses proposed there are fourteen accepted hypotheses, one untested hypothesis, and one rejected hypothesis. The untested hypothesis is that experience in using the system has a significant moderating effect on each component of information technology acceptance (H7). The rejected hypothesis is that perceived ease of use will be significantly and positively influenced by the quality of information (H6a).

The results obtained have similarities with the results of the previous Moore studies [13], especially for the level of IT acceptance for healthcare with low experience. Information quality equally has no significant effect on Perceived Ease of Use. In Moore model, the user with high experience, Information quality has a significant influence on Perceived Ease of Use.

## IV. CONCLUSIONS

We measure the level of IT adoption, especially medical records in a hospital using TAM model. The results obtained are the characteristics and factors of application of medical record according to TAM in revealed. The results of the study state that the factors that influence the acceptance of IT, especially the use of hospital medical records are Content, Timeliness, Technical Support, Self-efficacy, and Accuracy.

The only unacceptable hypothesis is Information Quality to Perceived Ease of Use. However, information quality remains significant for Perceived Ease of Use. For further research can confirm the results by taking a larger sample size and covering hospitals that are throughout Indonesia so that the model tested can describe the conditions that occur in Indonesia.

## REFERENCES

- [1] D. Blumenthal and J. P. Glaser, "Information technology comes to medicine," *The New England journal of Medicine*, vol. 356, no. 24, pp. 2527-2534, 2007.
- [2] A. K. Yarbrough and T. B. Smith, "Technology acceptance among physicians: a new take on TAM," *Medical Care Research and Review*, vol. 64, no. 6, pp. 650-672, 2007.
- [3] I. K. Raharjana, A. Puspadini and E. Hariyanti, "Information Technology Supplier Management in Hospitals," *Bulletin of Electrical Engineering and Informatics*, vol. 7, no. 2, pp. 306-313, 2018.
- [4] I. Puspitasari, R. Pramudhika and I. K. Raharjana, "Pasienesia: A mobile based e-patient social network: Promoting empowerment among patients who experience similar diseases," in *Informatics and Computing (ICIC), 2017 Second International Conference on*, Jayapura, 2017.
- [5] U. Muawanah and Gunadi, "Information Technology Adoption, Corporate Governance, and Bank Performance," *Journal of Information Systems Engineering and Business Intelligence*, vol. 4, no. 1, pp. 11-17, 2018.
- [6] Fishbein, Martin and I. Ajzen, *Belief, attitude, intention, and behavior: An introduction to theory and research*, Reading, MA: Addison-Wesley, 1977.
- [7] I. Ajzen, "The theory of planned behavior," *Journal of organizational behavior and decision process*, pp. 197-211, 1991.
- [8] Yousafzai, Y. Shumaila, G. R. Foxall and J. G. Pallister, "Explaining internet banking behavior: theory of reasoned action, theory of planned behavior, or technology acceptance model?," *Journal of applied social psychology*, vol. 40, no. 5, pp. 1172-1202, 2010.
- [9] F. D. Davis, "Perceived Usefulness, Perceived Ease of Use, and User Acceptance of Information Technology," *MIS Quarterly*, pp. 319-340, 1989.
- [10] R. J. Holden and B.-T. Karsh, "The Technology Acceptance Model: Its past and its future in health care," *Journal of Biomedical Informatics*, vol. 43, pp. 159-172, 2010.
- [11] F.-Y. Pai and K.-I. Huang, "Applying the Technology Acceptance Model to the introduction of healthcare information systems," *Technological Forecasting & Social Change*, vol. 78, p. 650-660, 2011.
- [12] W. G. Chismar and S. Wiley-Patton, "Test of the technology acceptance model for the internet in pediatrics," in *the AMIA Symposium*, 2002.
- [13] T. T. Moores, "Towards an integrated model of IT acceptance in healthcare," *Decision Support Systems*, vol. 53, p. 507-516, 2012.
- [14] N. Setiawan, "Penentuan Ukuran Sampel Tabel Krejcie-Morgan: Telaah Konsep dan Aplikasinya," Universitas Padjadjaran, Bandung, 2007.



# Implementation Strategy of Knowledge Management System: A Case of Air Drilling Associates

Siti Hadjar  
Faculty of Computer Science  
Universitas Indonesia  
Depok, Indonesia  
sitihadjar@gmail.com

Putu Wuri Handayani  
Faculty of Computer Science  
Universitas Indonesia  
Depok, Indonesia  
putu.wuri@cs.ui.ac.id

Riri Satria  
Faculty of Computer Science  
Universitas Indonesia  
Depok, Indonesia  
ririsatria@gmail.com

Ave Adriana Pinem  
Faculty of Computer Science  
Universitas Indonesia  
Depok, Indonesia  
ave.pinem@cs.ui.ac.id

**Abstract**— Just as companies in the oil and gas industry, Air Drilling Associates (ADA) also feel the urgency to utilize Knowledge Management to facilitate resilience in a dynamic and competitive business environment. By the end of 2016 ADA introduces the ADA Knowledge Base, a Knowledge Management System, for employee to be utilized as a platform for sharing experiences and learning. However, up to one year since its introduction, the employee participation rate in ADA Knowledge Base is still low. A strategy is required for the implementation of a Knowledge Management System that is part of support for Knowledge Management. This study conducted by using Soft System Methodology approach and Knowledge Management theory. Respondents such as upper management, middle management and staff from the organization has been interviewed. The result defined three steps and sixteen activities for the company to implement the Knowledge Management System.

**Keywords**—Knowledge Management, Knowledge Management System, Implementation Strategy, Soft System Methodology

## I. INTRODUCTION

Several companies in the oil and gas industry have realized that knowledge management implementation is needed as a key strategy to address global competition and to improve competence in meeting business challenges [1]. The operational processes and equipment between each oil and gas companies is not too much different [1]. So, the competition in this industry precisely lies in the application of technology and the use of knowledge at the right time through the right people and the right place in the right way.

Air Drilling Associates (ADA) as one of the companies engaged in the oil and gas industry, feel the same urgency. This company is one of the largest drilling service providers for the oil and gas energy industry. The limited number of similar service providers makes ADA quickly become the leader of the oil and gas industry in the countries where they operate including USA, Canada, Iceland, Indonesia, the Philippines, New Zealand and Papua New Guinea. Nevertheless, the company's management recognizes the importance of updating business strategies to survive and secure the market.

With diverse educational backgrounds and work experience of the employees, the company considers it important to ensure that every operational employee has a uniform knowledge of their services. As stated in the organization document regarding quality guidance, the company should ensure that employees have the appropriate knowledge, skills, experience and behavior to meet business objectives and customer needs both in the short and long term. The employee turnover rate, especially the operational employees in charge of the project, which is quite high during the last three years also becomes the management consideration in deciding to develop a system to manage the experience and knowledge of the employees. It is also expected that the experience of each employee does not go with the employees when they no longer work for the organization.

One of the efforts taken to achieve this is by developing Standard Operating Procedure (SOP) for each service. The organization also develops a web-based knowledge management system named ADA Knowledge Base. However, it is unfortunate that since its introduction, the employees' participation rate on the Knowledge Base, especially in contributing and sharing experience is still low. This is measured by comparison between the number of articles published in the system with the number of projects in the organization. This comparison is measured and presented in one of the meetings, to record the End of Well Report (EoWR) which is the experience and learning of each well drilling operations into the ADA Knowledge Base.

Then underlying formulation of question in this research which is how the implementation strategy of knowledge management system that can be applied in the environment of Air Drilling Associates. This paper has a systematic writing where sections 2 and 3 illustrate the literature study and methodology. The results of the analysis and discussion of the study are described in Sections 4. The implications of the study and conclusions are given in Sections 5 and Section 6.

## II. LITERATURE STUDY

Knowledge management is a systems approach to identifying, validating, capturing and processing knowledge

and then organizing knowledge elements into knowledge assets for business function and decision-making operations [3]. Knowledge management handles some organizational issues such as diminishing employee experience, disruption in human resources balance due to mergers and acquisitions, and unplanned skill needs. Knowledge management is the activities of discovering, collecting, sharing and applying knowledge to enhance the impact of knowledge on achieving the goals of an organization [4]. Knowledge management also defines as a systematic and integral approach that makes it possible to identify, manage and share knowledge within an organization, and to connect people to create new sets of useful knowledge for organizational purposes [5]. From a business point of view, knowledge management of an organization is used to achieve business value and generate a competitive advantage. From the three descriptions can be concluded that knowledge management is the process of managing knowledge by capturing, collecting and sharing, used to achieve organizational goals.

#### A. Knowledge Management Foundations

The foundation of knowledge management is an organizational aspect that supports knowledge management practice in the short and long term. Hence, the successful implementation of knowledge management system is strongly influenced by the existence of knowledge management foundation in an organization. Table 1 shows the relationship of each aspect of the foundation with each associated attribute identified from the knowledge management foundation theory by Irma Becerra-Fernandez and Rajiv Sabherval [4].

TABLE I. KM FOUNDATIONS AND THE ATTRIBUTES

Attributes
<b>Infrastructure</b>
Organization Culture
[OC1] Encouragement for creation and sharing knowledge
[OC2] Understanding the value of KM practice
[OC3] Management support for KM at all levels
[OC4] Reward system for KM practices
Organization Structure
[OS1] Organizational hierarchical structure
[OS2] The organizational structure can facilitate knowledge management through the Community Practices
[OS3] Specific structures and roles that support knowledge management
IT Infrastructure
[ITINF] The existence of IT infrastructure to support capabilities provided in four important aspects: reach, depth, wealth, and aggregation
Common Knowledge
[CK1] Common language and vocabulary
[CK2] Recognition of individual knowledge domain
[CK3] Knowledge mapping
[CK4] Organization's ability to recognize the value of new

information from the external environment

#### Physical Environment

[PE1] Availability of physical facilities as knowledge-sharing locations; meeting room, open workspace

#### Mechanism

[MEC1] Organizational or structural tools used to promote knowledge management

[MEC2] Defining Standards and policies

[MEC3] On-the-job training, face-to-face meeting, employee training, initiation process for new employees

#### Technology

[TECH] Development of information systems to facilitate knowledge exchange, and information repositories

### III. METHODOLOGY

#### A. Soft System Methodology

This research used qualitative research with soft system methodology approach. Soft system methodology consists of seven stages in a cycle [6] ; (1) Define the problem (2) Create the rich picture (3) Define the root definition of the relevant system. Root definitions should be formulated appropriately to understand the essence of the relevant system and adapt CATWOE (Customers, Actors, Transformation processes, World views, Owners, and Environmental constraints) factors (4) Construct the concept of root definitions into the conceptual model (5) Compare the model with the real world to explore the situation (6) Formulate changes from situations that are the issues being addressed (7) Implement the change process.

#### B. Data Collecting

The data was obtained by interview. Interviews were conducted with top management, mid management, and operation staffs. The top management interviews are directed to the President Director and the Air Drilling Associates Director. Interviews on mid management are conducted with employees at the Manager's level, regarding the understanding of the organization's mission and strategy vision and operational project coordination. Operational interviews are addressed to office staff and field operational staff as users.

Based on previous literature study we constructed the indicators for KM Foundation attributes in Table 1. Then, analysis conducted by following seven steps of soft system methodology. An implementation strategy Knowledge Management System will be formulated from the results of the analysis.

### IV. ANALYSIS AND RESULTS

Development strategy of applying knowledge management system in Air Drilling Associates by using Soft System Methodology with the following stages:

#### A. Define the problem

##### 1) First Analysis (Intervention)

The first step in the introduction of problematic situations is defining three parties that play important role within the problem. The three parties are:

- Client: employee of Water Drilling Associates. The Knowledge Base is a knowledge management system

used to support knowledge management activities in ADA with an aim to facilitate employees in finding solutions to problems in their daily task.

- Practitioner: is a person or group of people who conduct the study with the Soft System Methodology.
- Owner Issues: The party acting as the owner of the issue is a person or group of interested persons or affected by the situation or the impact of the result of an improvement effort on the problematic situation.

## 2) Second Analysis (Social)

The introduction of real-world situations, especially the social aspect is essential to understand the general social situation. There are three social elements of concern in this stage [13]:

- Roles: As a company, Air Drilling Associates provides facilities for employees to carry out knowledge management practice as an effort to improve operational performance.
- Norms: Norm is the expected behavior associated with the role. To implement knowledge management, the organization developed knowledge base system to facilitate its employees in finding solutions to problems in their daily task.
- Values: Referring to the Quality Manual document, where the company must ensure that employees have the appropriate knowledge, skills, experience and behavior to meet business objectives and customer needs for both in the short and long term, the management that represented by a CEO, instructed the operational division to record End of Well Report (EoWR) of each well drilled into the Knowledge Base. The purpose is to help each EoWR in learning the drilling activities in other wells.

## 3) Third Analysis (Politics)

The third step in the defining the problem is by incorporating the political situation. This analysis focuses on the study of issues of power affecting the sustainability of the organization. These issues are divided into two categories:

### a) Disposition of power

- The highest authority in the organization is hold by a Chairman
- An organizational structure is designed to define the roles and responsibilities
- A CEO has authority over all operational decisions in all operational areas worldwide through Operational Directors in each region
- Operational areas are divided into three regions. Each region is managed by a Director of Operations
- Operational Director oversees the varying number of Project Managers in each region, depending on the business units and services available in the relevant region

### b) Nature of power

- The Project Manager has the authority to control the operational activities, to conform to the client's requests and as per the company's quality of service standards.
- The Project Manager could encourage employees to follow instructions from the superior

- The Director of Operations has the authority to monitor and assess the performance of operational activities through the Project Manager.

## B. Describe the problem in the form of rich picture

Rich picture is a tool for expressing important relationships in a situation as well as to provide something that can be presented as a basis for discussion [13]. Figure 1 illustrates the relationship and implementation issues of management information systems in Air Drilling Associates.

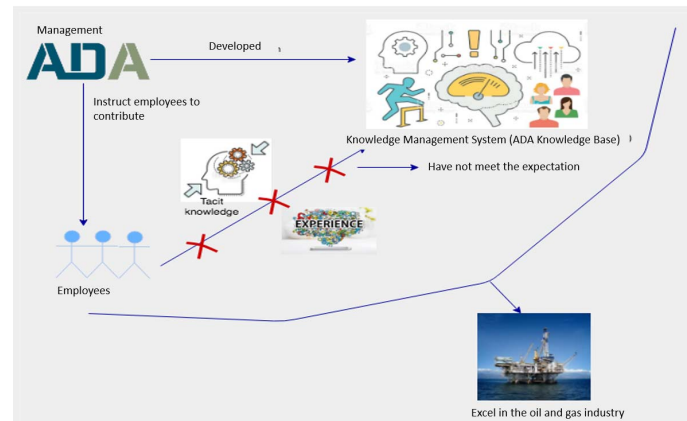


Fig. 1. Rich Picture of the Problem

## C. Define Root Definition and CATWOE (Customers, Actors, Transformation processes, World views, Owners, and Environmental constraints)

A root definition is a literal statement of a system relevant to the real-world situation in which the transformation process in an organization is reflected. Related to this transformation process, inside a root definition it must describe the what (P), how (Q) and why (R). The root definition formulation that includes the three factors is:

"A system for improving the utilization of knowledge management systems (P) by implementing knowledge management system implementation strategies (Q) to achieve the utilization of knowledge management systems in accordance with management provisions in order to provide the best services to clients and achieve competitive advantage in the oil and gas industry (R)."

To test the root definition of the PQR formulation, CATWOE analysis was performed. It is intended to review the root definition to be really describes a system of relevant activities. This analysis is shown in Table II.

## D. Developing a Conceptual Model

The first step is to evaluate the current knowledge management practices in in organization. This information is collected from interviews and observation in the identification of things related to knowledge management. Table 3 shows the current knowledge management activities in ADA based on interviews and observations. Following the root definition that has been compiled in the previous section and current practices of knowledge management activities presented in Table 3, we compiled them into a conceptual model which is presented in Figure 2. There are twelve activities to be performed.

Once validated by the expert, this conceptual model will form the basis of the formulation of the application of the

knowledge management system. In drafting a conceptual model, the authors follow the steps suggested by [13].

TABLE II. CATWOE ANALYSIS

Aspect	CATWOE Analysis
Customer	All employees of Air Drilling Associates
Actors	All employees of Air Drilling Associates
Transformation	Knowledge management systems that have not been well implemented (I) -> Apply a knowledge management system implementation strategy (T) -> Recommended knowledge management system (O)
Worldview	Providing the best services to clients to achieve competitive advantage in the oil and gas industry through the utilization of knowledge management
Owners	All employees of Air Drilling Associates
Environmental Constraints	Employee contributions that do not match the expectations of the board of directors

TABLE III. TABLE I CURRENT KM PRACTICE

Current Condition
<b>Infrastructure</b>
<b>Organization Culture</b>
Employees have been accustomed to sharing knowledge and experience
Employee has sought knowledge from external sources
Not yet have procedures governing communication between departments/divisions
There is no specific budget allocation for knowledge management activities
Support from management to improve knowledge management activities is required the involvement of all parties, socialization and incentives
There has been no assessment of employee participation on ADA Knowledge Base
<b>Organization Structure</b>
There is no special division that regulates and controls the activities of knowledge management and utilization of system
Each division has a closed discussion group
<b>IT Infrastructure</b>
ADA adopts cloud computing. By subscribing to the Cloud computing service model, the Software as a Service (SaaS) and Platform as a Service (PaaS) company employs the resources provided by the service provider
<b>Common Knowledge</b>
Categories of expertise based on competence and division
<b>Mechanism</b>
Socialization related to the utilization of knowledge management system only at the beginning of implementation
KMS is not integrated with other systems
Lack of employee skills in putting ideas into writing
Lack of employee confidence in sharing
There has been no reciprocity for participating staffs
<b>Technology</b>
Discovery process in ADA Knowledge Base is still manual

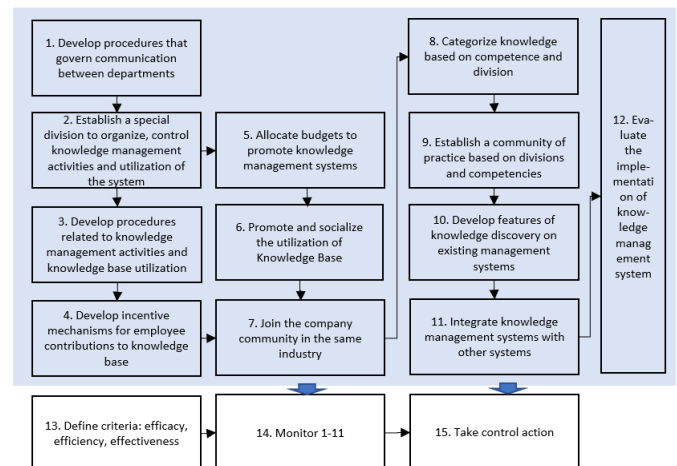


Fig. 2. Conceptual Model

#### E. Compare the model with the real world to explore the situation

The twelve activities in the conceptual model are used to discuss real-world problematic situations by comparing them conceptually with real-world problematic situations. Table 4 describes the comparison.

#### F. Validate the implementation strategy

Furthermore, the conceptual model that has been compiled is validated by the expert. The result of the validation process are as follows:

- Before applying knowledge management system, it is necessary to identify the current knowledge management practices in the company. The first is not required because communication procedures should be included in standard operational procedures integrated between departments.
- Formulating KPIs as a form of compensation of employee contributions to ADA Knowledge Base.
- The seventh activity does not provide significant benefits because each company in the related community will not discuss the lessons learned or the knowledge and experience they have gained during carrying out a project within the community in question. This is because knowledge is considered a corporate asset that must be protected.
- The fourth activity can be omitted, because it is part of the third activity

- Conducting training as part of socialization.
- Adding an activity for preparing system requirements to support knowledge management activities.
- Continuous improvement of knowledge management governance is required to improve knowledge management practices.

Figure 3 shows the revised version of the conceptual model.

#### G. Implement the change process.

Adopting the Regulation of State Minister of Administrative Reform and Bureaucratic Reform Number 14 of 2011 on Guidelines for Implementation of Knowledge Management Program, knowledge management system implementation strategy in Air Drilling Associates is divided into three phases, namely Planning, Implementation and Evaluation. This strategy can be seen in the Figure 3. The first stage is a planning that consists of three activities. Identification of knowledge management practices can use the results from Tables 3 and Table 4 and can also be re-analyzed by the implementation team. The second stage is

an implementation that contains activities carried out for the development of concepts, systems and integration with other existing systems. The last stage of evaluation is to ensure the quality standards of each activity as well as improvements that can enhance the quality.

#### V. IMPLICATIONS

The practical implications of this research can be used by ADA and organizations in the Oil and Gas industry. The results of the conceptual model identification state that the organization should develop procedures and rules related to knowledge management practices including reward mechanisms in the process of sharing knowledge. In addition, the establishment of a special division that regulates knowledge management practices is deemed to be necessary. One form of management commitment is the provision of budget in the implementation of knowledge management also needs to be considered.

TABLE IV. THE COMPARATION OF CONCEPTUAL MODEL AND CURRENT PRACTICES

Activity	Current Practice	Actors	Result
1	Not yet have procedures governing communication between departments / divisions	Management	The existence of written documents in the form of procedures that regulate communication between departments / divisions
2	There is no special division that regulates and controls the activities of knowledge management and utilization of knowledge management systems	Management	A special division to regulate and control knowledge management activities and utilization of knowledge management system (ADA Knowledge Base)
3	Lack of employee skills in putting ideas into writing. Lack of employee confidence in sharing	Formed Knowledge Management Division	The existence of written documents in the form of procedures related to knowledge management activities and utilization of ADA Knowledge Base
4	There has been no reciprocity for participating royals	Formed KM Division	The existence of written documents in the form of incentive mechanism to contribute employees to ADA Knowledge Base
5	There is no specific budget allocation for knowledge management activities	Formed KM Division	There is a special allocated budget for promoting knowledge management systems
6	Socialization related to the utilization of knowledge management system only at the beginning of implementation	Formed KM Division	Promotion and socialization program
7	Seek knowledge from external sources	Management	Being part of the oil and gas industry community
8	Categories based on competencies and divisions are formed among employees subjectively	Management	Categories of knowledge
9	Each division has a closed discussion group	Management	Community of Practice
10	Discovery process in ADA Knowledge Base is still manual	Management	Automated knowledge discovery process
11	Knowledge management system is not integrated with other systems	Management	Easier access to knowledge management systems
12		MP Division is formed	Supervised knowledge management system implementation



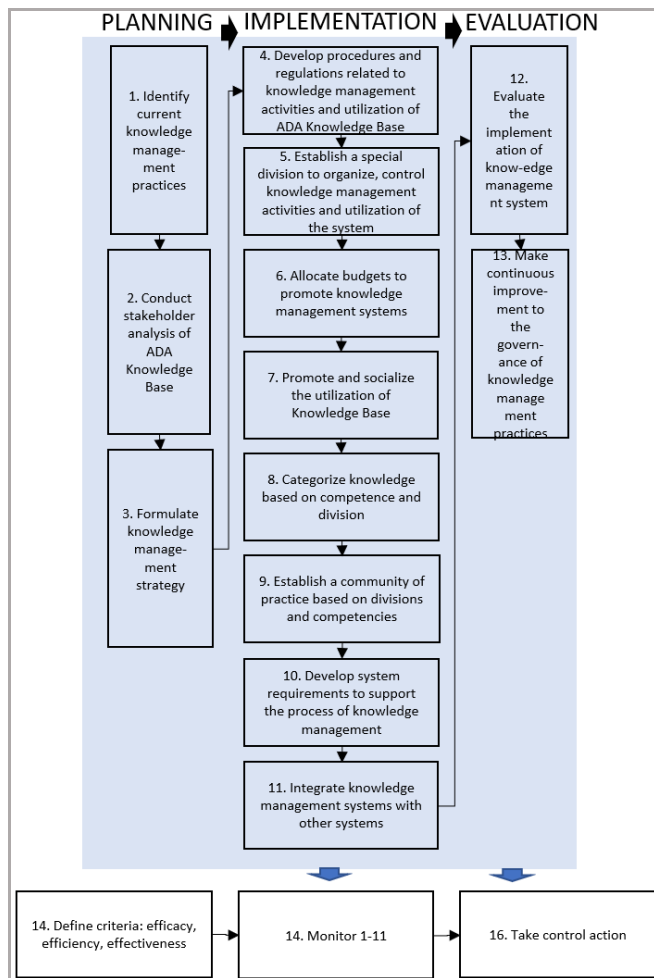


Fig. 3. Revised Conceptual Model

## VI. CONCLUSION

The purpose of this research is to formulate the implementation strategy of knowledge management system that can be applied in the environment of Air Drilling Associates. Based on analysis and result, the implementation strategy for the organization are categorized in three steps which are planning, implementation and evaluation.

Planning steps conducted as the preparation of the implementation steps. In the implementation steps, the organization will be defined and developed the concept and build the knowledge management system. However, the practices of involving in other communities from other company seem to be difficult since every company perceived their knowledge as an important asset. The third

step is evaluation that conducted to evaluate the implementation of ADA Knowledge Base and make continuous improvement to the governance of knowledge management practices

## ACKNOWLEDGEMENT

We want to convey our gratitude to the Directorate of Research and Community Engagement Universitas Indonesia for the Program Hibah Publikasi Internasional Terindeks untuk Tugas Akhir Mahasiswa (PITTA), grant No. 1889/UN2.R3.1/HKP05.00/2018

## REFERENCES

- [1] C. Ramanigopal, "Knowledge Management For The Oil and Gas Industry: Opportunities and Challenges," *Advances In Management*, 2013.
- [2] K. Dalkir and M. Beaulieu, *Knowledge Management in Theory and Practice*, vol. 3, London:: The MIT Press, 2017.
- [3] S. Mohapatra, A. Agrawal and A. Satpathy, "Designing Knowledge Management Strategy," in *Designing Knowledge Management-Enabled Business Strategies*, Springer International Publishing, 2016.
- [4] I. B. Fernandez and R. Sabherwal, *Knowledge Management: System and Processes*, New York: Routledge, 2015.
- [5] M. M. Sbaffoni, *Knowledge Management: Basic Approches and Definitions*, 2010.
- [6] M. Jackson, *Systems Thinking Creative Holism for Managers*. , John Wiley & Sons, Ltd, 2003.
- [7] E. G. Ochieng, O. O. Ovbagbedia, T. Zuofa, R. Abdulai, W. Matipa, X. Ruan and A. Oledinma, "Utilising a Systematic Knowledge Management Based System to Optimise Project Management Operations in Oil and Gas Organisations," 2016.
- [8] H. S. Tooranloo, A. S. Ayatollah and S. Alboghobish, "Evaluating Knowledge Management Failure Factors Using Intuitionistic Fuzzy FMEA Approach," *Knowledge Information System*, 2016.
- [9] S. Mazzoni, F. Ferrazza, G. Giudicati and F. Capriotti, "Knowledge Management in Eni: Workflow and Case Histories in Nothern Italian District (DICS)," in *13th Offshore Mediterranean Conference and Exhibition*, Ravenna, Italy, 2017.
- [10] A. Sutriyono and Elidjen, "Design of Knowledge Management System in PT Premier Oil Indonesia," in *International Conference on Information Management and Technology (ICIMTech)*, 2016.
- [11] R. M. Grant, "The Development of Knowledge Management in the Oil and Gas Industry," *Universia Business Review*, 2013.
- [12] N. H. Saad, R. A. Alias and A. A. Rahman, "Soft System Methodology: A Conceptual Model of Knowledge Management Systems Initiatives," in *4th International Joint Conference*, 2013.
- [13] P. Checkland and J. Poulter, *Learning for Action: A Short Definitive Account of Soft Systems Methodology and its Use, for Practitioners, Teachers and Students*, Chicester: John Wiley and Sons, Ltd, 2006.



# The Utilization of Ontology to Support The Results of Association Rule Apriori

1<sup>st</sup> Dewi Wardani  
 Department of Informatics  
 Universitas Sebelas Maret  
 Surakarta, Indonesia  
 dww\_ok@uns.ac.id

2<sup>nd</sup> Achmad Khusyaini  
 Department of Informatics  
 Universitas Sebelas Maret  
 Surakarta, Indonesia  
 achmadk@students.uns.ac.id

**Abstract**—Association rule is one of the data mining techniques to find associative combinations of items. There are several algorithms including Apriori, FP - Growth, and CT-Pro. One of the advantages of the Apriori algorithm is that it produces many rules. To improve its result, one of the methods is by using the semantic web technology. This work proposes how the hierarchical type of ontology can be utilized by the Apriori algorithm to improve the results. The Apriori with ontology implements the Interestingness Rule (IR) which is a parameter to determine the degree of association between combinations of items in a dataset. The series of experiments show that the proposed idea can improve the results compare to the default Apriori algorithm.

**Keywords**—Association Rule, Apriori, Ontology, Interestingness

## I. INTRODUCTION

Data mining (DM) is the process of finding patterns or interesting information in selected data using a particular technique or method. The association analysis or association rule mining is a data mining technique for finding associative rules between a combination of items. Association rule analysis is also known as one of the data mining techniques that became the basis of one of the other data mining techniques [1]. Apriori algorithm is an algorithm for finding frequent itemsets patterns on association rules. The main steps in Apriori algorithm are: first, look for frequent itemset (set of items that meet the minimum support) of the transaction database, second eliminate the itemset with low frequency based on the predetermined minimum level of support. Next, building the association rule of the itemset that meets the minimum confidence value in the database [2].

The main problem of applying conventional methods of association rule by using Apriori algorithm is [3]: 1) Produce many rules, so that the process of tracing information becomes difficult within the scope of the rule that becomes widespread. 2) Produce many unattractive rules in high numbers resulting in a meaningless rule. 3) Long-running time process. If the database is used in large numbers and varies, it will take a long time to run the algorithm.

Semantic Web is an approach developed specifically on the World Wide Web (WWW) technology that aims to enrich the information provided so that it becomes better in defining it.

Semantic Web allows a web to become more intelligent because it has a knowledge base (knowledge base) in it in the form of ontology. In the semantic web technology, ontology serves as the core (core technology) so that it can be called as semantic web ontology [4]. Ontology is a set of hierarchically structured terms to describe a domain that can be used as the basic framework of a knowledge base [5].

The development of ontology aims to capture knowledge into a format that can be used in the system. Next, by populating the knowledge base to get the instances to fill the knowledge base. The benefit of ontology is to explain a domain of knowledge; provide a hierarchical structure of concepts to explain a domain and how they relate [3].

One of the technologies to improve the default Apriori is by using semantic web technology which applied knowledge base in the form of ontology. By using the domain ontology, it has a positive impact to support the association rule, which can do the pruning on the rule that is not interesting [6]. By using ontology can improve knowledge discovery process in association rule [7]. Ontology is used to support data integration process mining, that is combining knowledge domain into data mining process [8]. The ontology in the hierarchy approach can simplify all data components to a certain level of form so that they can be comprehensively understood. Then the data is classified according to its category to facilitate the searching of information in the dataset.

This research considers the lack of application of conventional association rule method using Apriori algorithm and excess ontology. Hence, required a merger between association rule and ontology. The use of ontology is expected to provide a solution to the problem of conventional association rule methods, namely: the problem of producing multiple rules and producing many rules that are not interesting in high numbers. The main novelty in this work is how to combine the hierarchical ontology into the Apriori algorithm, and compose the new IR formula as well.

## II. RELATED WORK

A work that the using an ontology domain has a positive impact to support association rule. It can anticipate the existence of ambiguous data, reducing the results of the rule so

that more accurate [6]. The other study found a diverse collection of ontology entries on the KDD process. Tests were conducted on two domains, namely medical and sociological fields [7].

The research by Mahmoodi et al. [3] provides information on the use of association rule model with ontology as the solution to solve the problem of tracing information on factors that cause cancers. Test obtained results with clinical databases show that the prediction model according to the desired goal is to produce the best rules. The application of association rule with ontology gives a good impact in the search results of the rule becomes more accurate, unlike the results using only the Apriori algorithm. The test results obtained show that the prediction model according to the desired goal can produce the best rules. Therefore, the method of combining the Apriori algorithm and the concept of ontology gives a good impact in the search results of the rule more accurate, in contrast to the results using the Apriori algorithm alone.

The other work suggested that the proposed method which combined the using ontology is more efficient than other association rule methods. The number of rules generated can be reduced even in a large number of datasets [9].

A similar work which used the association rule mining with ontology (ARMO) method gives more efficient results than other association rule methods. The number of rules generated can be reduced though on the number of large datasets. The results of this study suggest that the proposed method can reduce the rule results produced from the association rule mining process on a large number of datasets [10].

In the other previous study [8] that using the ontology domain has a positive impact to support association rule. It can do the pruning on the rule that is not interesting. It also can anticipate the existence of ambiguous data, and reduce the results of the rule so that more accurate. The model seeks to separate the independent sub-processes of the DM process and combine the mining results.

### III. CONSIDERED PROBLEM AND THE APPROACH

The main proposed idea in this work is to implement the modified interestingness rule (IR) formula. Here, it is assumed that the ontology is consists of classes with no hierarchy among them. Each of class is a single stand class. All individuals of each class is a group hierarchy under the class. Therefore, the graph of ontology is a simple one.

The Apriori algorithm will be implemented with ontology and by considering the value of support and calculation of IR value. This IR value is used to improve the results of the rule search between items in the dataset. The formula calculates the following IR values which modified and inspired from [9], that the IR is customized for three itemsets A, B and C:

$$IR = \left[ \log(2 \times Trans(A, B)) + \log(1 \times Trans(C)) \right] \times \left[ \frac{Trans(A, B, C)}{Total_{trans}} \right]$$

where  $Trans(A, B)$  is the number of stransactions from itemset A and B,  $Trans(C)$  is the number of transactions from

itemset C, and  $TotalTrans$  is the total number of transactions in the database.

## IV. EXPERIMENT AND RESULT

### A. Dataset

This experiment uses two real datasets: 1. Student data (actual data from students of Universitas Sebelas Maret), 2. Internet movie database data (IMDB). The student data provides information about the student's personal and academic data. Examples of student data include student name, the tuition class (UKT), scholarship id, study program, faculty, address, place of birth date (TTL), cumulative grade point (GPA), senior high school, study duration, entry point, parent income, etc.

The IMDB dataset provides information on films from around the world, including those involved in it from actors/actresses, directors and writers. In IMDB data there are some attributes such as director name, genre, movie title, country, number review, budget, etc.

Data with some attributes will be elected again at the preprocessing data stage. Preprocessing data is done by selecting the attributes that will be used. At this stage, it is also done refinement of data contents if the data is not complete. Data that is empty or less complete will be selected so that not included in the data processing. Completed data will be adjusted. Therefore, a program can understand the data.

### B. Ontology Development

At this stage will be designed ontology based on the used dataset. The design of ontology is based on hierarchy ontology approach. The ontology hierarchy approach aims to simplify all data components to form certain levels so that they can be comprehensively understood. Then, the data is classified according to the category. Examples of hierarchical forms of student data ontology can be seen in Figure 2 and Figure 3 below:

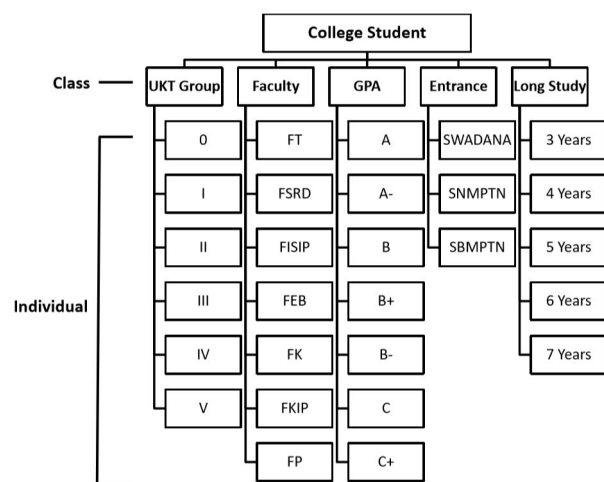


Fig. 1. Ontology of Student

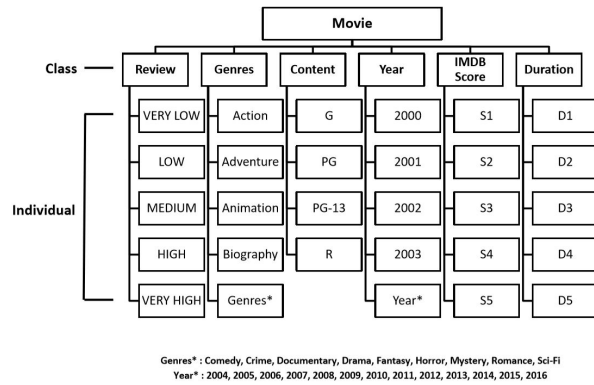


Fig. 2. Ontology of IMDB

### C. Experimental setting

A few attributes are written in the abbreviation for the shake of name simplification. Such as, A means GPA 3.69 – 4.00, FEB means Faculty of Economics and Business, etc. The scenario of the experimental is as below described in Table 1. Each experiment performers two type of experiment: Association Rule Apriori (ARA) and Association Rule Apriori with Ontology (ARAO).

TABLE I. THE SCENARIO OF EXPERIMENTAL

Code	Dataset	Amount	Support	Confidence	IR
1	Student	1000	0.2	0.5	0.1
2	Student	1000	0.2	0.3	0.05
3	IMDB	1000	0.2	0.5	0.1
4	IMDB	1000	0.2	0.3	0.05
5	Student	100	0.25	0.1	0.1
6	Student	100	0.2	0.1	0.1
7	Student	100	0.15	0.1	0.1
8	IMDB	2000	0.2	0.5	0.25

### D. The results

TABLE II. THE RESULT OF EXPERIMENT 1

No	ARAO	No	ARAO
1	(B+), III → SNMPTN : 1*	1	(FKIP), III → SNMPTN : 0.76 *
2	V → SWADANA : 1	2	5 TH, III → SNMPTN : 0.59
3	(B), III → SNMPTN : 0.99	3	(B+), SWADANA → V : 0.58
4	(B+), SNMPTN → III : 0.99	4	(B), SWADANA → V : 0.56
5	(B), SNMPTN → III : 0.99	5	(FISIP), III → SNMPTN : 0.54
6	4 TH, SNMPTN → III : 0.99		
7	SNMPTN → III : 0.99		
8	III → SNMPTN : 0.98		
9	SWADANA → V : 0.98		
10	4 TH, III → SNMPTN : 0.97		
11	(B+), 4 TH → SNMPTN : 0.77		
12	4 TH → III : 0.75		
13	(B+) → III, SNMPTN : 0.74		
14	(B+) → SNMPTN : 0.74		
15	(B+) → III : 0.74		
16	4 TH → III, SNMPTN : 0.73		
17	4 TH → SNMPTN : 0.73		

18	(B) → SNMPTN : 0.64		
19	(B) → III : 0.64		
20	(B) → III, SNMPTN : 0.63		
21	III, SNMPTN → (B+) : 0.59		
22	SNMPTN → (B+), III : 0.59		
23	4 TH, SNMPTN → (B+) : 0.59		
24	SNMPTN → (B+) : 0.59		
25	III → (B+), SNMPTN : 0.58		
26	III → (B+) : 0.58		
27	4 TH → (B+) : 0.56		
28	III → 4 TH : 0.5		

The highest score of information can be obtained from table 2 as follow:

(i). ARAO produces fewer number of rules than ARA. The rules that ARAO generates are 5 rules while ARA has 28 rules.

(ii) In ARA, a combination of item “V → SWADANA” is obvious information. Subjectively, this rule is not interesting. Meanwhile, in ARAO, one item appears “(B+)” as an additional item from the combination of items V and SWADANA so that it becomes more interesting.

TABLE III. THE RESULT OF EXPERIMENT 2

No	ARA	No	ARAO
1	(B+), III → SNMPTN : 1*	1	(FKIP),
2	V → SWADANA : 1		III → SNMPTN : 0.76 *
3	(B), III → SNMPTN : 0.99	2	5 TH, III → SNMPTN : 0.59
4	(B+), SNMPTN → III : 0.99	3	(B+), SWADANA → V
5	(B), SNMPTN → III : 0.99	4	(0.58)
6	4 TH, SNMPTN → III : 0.99		(B), SWADANA → V : 0.56
7	SNMPTN → III : 0.99	5	(FISIP),
8	III → SNMPTN : 0.98		III → SNMPTN : 0.54
9	SWADANA → V : 0.98	6	(FEB), 3
10	4 TH, III → SNMPTN : 0.97		TH → SNMPTN : 0.51
11	(B+), 4 TH → SNMPTN : 0.77	7	(FSRD),
			III → SNMPTN : 0.47
12	4 TH → III : 0.75	8	4 TH,
13	(B+) → III, SNMPTN : 0.74		SWADANA → V : 0.45
14	(B+) → SNMPTN : 0.74	9	(FKIP),
15	(B+) → III : 0.74		SWADANA → V : 0.45
16	4 TH → III, SNMPTN : 0.73	10	(FKIP), 4 TH → III : 0.41
17	4 TH → SNMPTN : 0.73		(FKIP), 4
18	(B) → SNMPTN : 0.64	11	TH → SNMPTN : 0.41
19	(B) → III : 0.64		(FEB),
20	(B) → III, SNMPTN : 0.63	12	SWADANA → V : 0.41
21	III, SNMPTN → (B+) : 0.59	13	(FEB), 4
22	SNMPTN → (B+), III : 0.59		TH → SNMPTN : 0.38
23	4 TH, SNMPTN → (B+) : 0.59	14	(FK), III → SNMPTN : 0.35
			(B),
24	SNMPTN → (B+) : 0.59	15	(FKIP) → SWADANA : 0.3
25	III → (B+), SNMPTN : 0.58		(B+), (FEB) → V : 0.29
26	III → (B+) : 0.58	16	(B), (FKIP) → 4 TH : 0.29
27	4 TH → (B+) : 0.56	17	(FISIP), 4 TH → III : 0.29
28	SNMPTN → 4 TH : 0.5		(B), (FKIP) → V : 0.29
29	III, SNMPTN → 4 TH : 0.5	18	(FISIP), 4
30	(B+), SNMPTN → 4 TH : 0.5	19	TH → SNMPTN : 0.29
31	III → 4 TH : 0.5	21	(B+),
32	SNMPTN → 4 TH, III : 0.49		(FEB) → SWADANA : 0.29
33	III → 4 TH, SNMPTN : 0.49	22	3 TH,
34	(B+) → 4 TH : 0.48		SWADANA → V : 0.28
35	4 TH → (B+), SNMPTN : 0.43	23	(FP), III → SNMPTN : 0.27
36	(B+) → 4 TH, SNMPTN : 0.37	24	5 TH,
			SWADANA → V : 0.23
37	III, SNMPTN → (B) : 0.32	25	
38	SNMPTN → (B) : 0.32		
39	SNMPTN → (B), III : 0.31		

40	III→(B) : 0.31		
41	III→(B),SNMPTN : 0.31		

The highest score of information can be obtained from table 3 as follow:

(i). ARAO produces fewer rules than ARA. The rules generated by ARAO are 25 rules while ARA has 41 rules.

(ii). Similar with the result of table 2. In ARA, a combination of item “V→SWADANA” subjectively is not an interesting rule. In ARAO, one item appears “(FEB)” as an additional item from the combination of items “V and “SWADANA”. Hence, it becomes more attractive.

TABLE IV. THE RESULT OF EXPERIMENT 3

No	ARA	No	ARAO
1	LOW→S3 : 0.85*	1	Comedy , LOW→S3 : 0.82 *
2	S3→LOW : 0.82	2	(R) , LOW→S3 : 0.75
3	(PG-13),S3→LOW : 0.79	3	(PG) , LOW→S3 : 0.65
4	(PG-13),LOW→S3 : 0.78		
5	Action,LOW→S3 : 0.78		
6	Action,S3→LOW : 0.73		
7	(PG-13)→S3 : 0.71		
8	(PG-13)→LOW : 0.71		
9	Action→S3 : 0.71		
10	Action→LOW : 0.67		
11	Action→(PG-13) : 0.63		
12	(PG-13)→LOW,S3 : 0.56		
13	LOW→(PG-13) : 0.56		
14	S3→(PG-13) : 0.53		
15	Action→LOW,S3 : 0.52		
16	LOW,S3→(PG-13) : 0.51		
17	(PG-13)→Action : 0.5		

The highest score of information can be obtained from table 4 as follow:

(i). ARAO produces fewer rules than ARA. The rules that ARAO produces are 3 rules while ARA is 17 rules.

(ii). In ARA, the highest score combination of item is “LOW→S3”. Meanwhile, a more information with the addition term Comedy is obtained from ARAO, “Comedy , LOW→S3”. Hence, it is more interesting

TABLE V. THE RESULT OF EXPERIMENT 4

No	ARA	No	ARAO
1	LOW→S3 : 0.85*	1	Comedy , LOW→S3 : 0.82 *
2	S3→LOW : 0.82	2	(R) , LOW→S3 : 0.75
3	(PG-13),S3→LOW : 0.79	3	(PG) , LOW→S3 : 0.65
4	(PG-13),LOW→S3 : 0.78	4	(R) , Action→LOW : 0.37
5	Action,LOW→S3 : 0.78	5	(R) , Action→S3 : 0.36
6	Action,S3→LOW : 0.73	6	Adventure , LOW→S3 : 0.36
7	(PG-13)→S3 : 0.71	7	(PG),Adventure→LOW : 0.35
8	(PG-13)→LOW : 0.71	8	Drama , LOW→S3 : 0.3
9	Action→S3 : 0.71	9	(PG) , Adventure→S3 : 0.28
10	Action→LOW : 0.67		
11	Action→(PG-13) : 0.63		
12	(PG-13)→LOW,S3 : 0.56		
13	LOW→(PG-13) : 0.56		
14	S3→(PG-13) : 0.53		
15	Action→LOW,S3 : 0.52		
16	LOW,S3→(PG-13) : 0.51		
17	(PG-13)→Action : 0.5		
18	LOW→(PG-13),S3 : 0.44		
19	S3→Action : 0.43		

20	S3→(PG-13),LOW : 0.42		
21	LOW→Action : 0.42		
22	LOW,S3→Action : 0.39		
23	LOW→Action,S3 : 0.33		
24	S3→Action,LOW : 0.32		

The highest score of information can be obtained from table 5 as follow:

(i). ARAO produces fewer rules than ARA. The rules that ARAO produces are 9 rules while ARA has 24 rules.

(ii). Similar with the result of table 4. In ARA, the highest score combination of item is “LOW→S3”. Meanwhile, ARAO obtained “Comedy , LOW→S3”. Hence, it is more interesting

TABLE VI. THE RESULT OF EXPERIMENT 5

No	ARA	No	ARAO
1	(B+)→III : 0.79	1	(FSRD) , 5 TH→III : 0.4
2	(FISIP)→III : 0.68	2	(B) , (FISIP)→5 TH : 0.37
3	4 TH→III : 0.64	3	(B-) , (FSRD)→5 TH : 0.34
4	5 TH→III : 0.63	4	(FISIP) , 5 TH→III : 0.34
5	(B)→III : 0.62	5	(B+) , 4 TH→III : 0.33
6	(FISIP)→(B) : 0.57	6	(FISIP) , 4 TH→III : 0.32
7	4 TH→(B) : 0.56	7	(B+) , (FISIP)→III : 0.32
8	(B)→5 TH : 0.5		
9	5 TH→(B) : 0.49		
10	III→5 TH : 0.48		
11	III→(B) : 0.47		
12	(B)→(FISIP) : 0.42		
13	(B)→4 TH : 0.4		
14	III→(FISIP) : 0.38		
15	III→4 TH : 0.35		
16	III→(B+) : 0.33		

The highest score of information can be obtained from table 6 as follow:

(i). ARAO produces fewer rules than ARA. The rules generated by ARAO are 7 rules while ARA has 16 rules.

(ii). ARA obtained the rule “(B +) → III” which is also found in the 7<sup>th</sup> place of ARAO. Meanwhile, ARAO obtained a more interesting rule, “(FSRD) , 5 TH→III”, because the other term “FSRD” which is absent in ARA, is obtained in ARAO.

TABLE VII. THE RESULT OF EXPERIMENT 6

No	Apriori	No	ARAO
1	(FISIP)→III : 0.68	1	(FSRD) , 5 TH→III : 0.4
2	5 TH→III : 0.63	2	(B) , (FISIP)→5 TH : 0.37
3	(B)→III : 0.62	3	(B-) , (FSRD)→5 TH : 0.34
4	(B)→5 TH : 0.5	4	(FISIP) , 5 TH→III : 0.34
5	5 TH→(B) : 0.49	5	(B+) , 4 TH→III : 0.33
6	III→5 TH : 0.48	6	(FISIP) , 4 TH→III : 0.32
7	III→(B) : 0.47	7	(B+) , (FISIP)→III : 0.32
8	III→(FISIP) : 0.38		

The highest score of information can be obtained from table 7 as follow:

(i). ARAO produces fewer rules than ARA. The rules generated by ARAO are 7 rules while ARA has 8 rules.

(ii). Similar with the result of table 6. ARA obtained the rule “(FISIP)→III” which is also found in the 4<sup>th</sup> place of ARAO. Meanwhile, ARAO obtained a more interesting rule, “(FSRD) , 5 TH→III”, because the other term “FSRD” is obtained in ARAO.

TABLE VIII. THE RESULT OF EXPERIMENT 7

No	ARA	No	ARAO
1	(B-)→5 TH : 0.85	1	(FSRD) , 5 TH→III :0.4
2	(B+)→III : 0.79	2	(B) , (FISIP)→5 TH :0.37
3	(FSRD)→III : 0.77	3	(B-) , (FSRD)→5 TH :0.34
4	(FSRD)→5 TH : 0.77	4	(FISIP) , 5 TH→III :0.34
5	(FISIP)→III : 0.68	5	(B+) , 4 TH→III :0.33
6	4 TH→III : 0.64	6	(FISIP) , 4 TH→III :0.32
7	(B),5 TH→III : 0.64	7	(B+) , (FISIP)→III :0.32
8	5 TH→III : 0.63		
9	(B)→III : 0.62		
10	(FISIP)→(B) : 0.57		
11	V→(B) : 0.56		
12	4 TH→(B) : 0.56		
13	V→5 TH : 0.56		
14	(B),III→5 TH : 0.52		
15	5 TH,III→(B) : 0.5		
16	(B)→5 TH : 0.5		
17	5 TH→(B) : 0.49		
18	(FISIP)→5 TH : 0.49		
19	III→5 TH : 0.48		
20	III→(B) : 0.47		
21	(B)→(FISIP) : 0.42		
22	(B)→4 TH : 0.4		
23	(B)→V : 0.38		
24	III→(FISIP) : 0.38		
25	5 TH→V : 0.37		
26	III→4 TH : 0.35		
27	5 TH→(FISIP) : 0.35		
28	III→(B+) : 0.33		
29	5 TH→(FSRD) : 0.33		
30	5 TH→(B-) : 0.33		
31	(B)→5 TH,III : 0.32		
32	5 TH→(B),III : 0.31		
33	III→(FSRD) : 0.26		
34	III→(B),5 TH : 0.24		

The highest score of information can be obtained from table 8 as follow:

(i). ARAO produces fewer rules than ARA. The rules generated by ARAO are 7 rules while ARA has 34 rules.

(ii). Similar with the result of table 7. ARA obtained the rule “(B-) → 5 TH” which is also found in the 3<sup>rd</sup> place of ARAO. Meanwhile, ARAO obtained a more interesting rule, “(FSRD) , 5 TH→III”, because the other term “FSRD” is obtained in ARAO.

TABLE IX. THE RESULT OF EXPERIMENT 8

No	ARA	No	ARAO
1	(LOW)→S3 : 0.7	1	(VERY_LOW),
2	Action→S3 : 0.69		Comedy→S3 :0.3
3	(PG-13)→S3 : 0.67	2	(PG-13),(VERY_LOW)→
4	S3→(LOW) : 0.65		Comedy:0.24
5	(R)→(LOW) : 0.64	3	(MEDIUM) , Action→S3 :0.23
6	(R)→S3 : 0.63	4	(PG) , Adventure→S3 :0.22
7	(PG-13)→(LOW) : 0.6	5	(MEDIUM),(PG-13)→Action :0.21
		6	(MEDIUM), (PG-13)→S3 :0.21

The highest score of information can be obtained from table 9 as follow:

(i). ARAO produces fewer rules than ARA. The rules that ARAO produces are 6 rules while ARA has 7 rules.

(ii). ARA obtained “(LOW) → S3”. Whereas, ARAO obtained “(VERY\_LOW), Comedy→S3”

(iii). The combination of items produced by ARAO appears several items that are not in ARA, namely: “MEDIUM”, “VERY LOW”, “Adventure”, “Comedy”.

TABLE X. THE COMPARISON OF THE NUMBER OF THE OBTAINED RULES

Experiment	Apriori	Apriori with Ontology
1	28	5
2	41	24
3	17	3
4	24	9
5	8	7
6	16	7
7	34	7
8	7	6

From experimental results 1 to 8 can be concluded:

- ARAO generates fewer rules than ARA as explained in Table 10.
- The use of minimum support, confidence, and IR parameters and the amount of data used can affect the number of generated rules.
- Rules that have high confidence or IR value will always appear even if the minimum parameter value is changed.
- The results of experiments 1 and 2 return pretty similar rules as well as experiments 3 and 4. For the experimental 1 and 2, the most top rule is “III → SNMPTN”. For the experiment 3 and 4, the highest rule is “LOW → S3” (rating at level 3). Until the experiment 4 can be concluded that Apriori with ontology reduces trivial rules (have a meager score). Therefore the number of obtained rules is diminished.
- The experimental 5,6 and 7 show that the result of combining items using Apriori with ontology is more consistent although the minimum support values are various: 0.25,0.20, and 0.15. Also, the testing of the default of the Apriori algorithm with a minimum value of support of 0.25 and 0.20 there are items still trimmed, in example the item “FSRD”, and only appear when the minimum condition of support is 0.15. Whereas in Apriori with an ontology for “FSRD” item always seems at the minimum value of support equal to 0.25 and 0.20.
- Rules that have consequence non-item “III” in experimental 5,6 and 7 the result of the default Apriori algorithm shows that the rules which have 2 until 16 rules. Whereas, in Apriori with ontology has 2 rules with a combination of more complex items. It makes easier in the process of tracking information.
- From experiment 8, it is also can see, in case that to reduce the number of the obtained rule only by increasing the minimum support and confidence as has shown in the default Apriori algorithm, the

obtained rules are not interesting. Comparing to the obtained rules of Apriori with ontology.

#### V. CONCLUSION AND FUTURE WORK.

This research has proposed the utilization of ontology to improve the result of association rule of Apriori algorithm. The ontology is a simply hierarchical ontology. The IR is calculated based on three itemsets. From the obtained results of this study, the utilization of ontology in Apriori can facilitate the tracking of information because it produces fewer amount rules compared to the default Apriori algorithm. The obtained rules of Apriori with ontology are generally also more interesting compare to the result of the default Apriori algorithm.

In the near future study is expected to use more complex ontology which perhaps influences the formula of IR. The use of more efficient IR formulas and measurements of the level of interrelationship of more item combinations, is also the task which should be solved soon.

#### REFERENCES

- [1] J. Han, J. Pei, and M. Kamber, *Data mining: concepts and techniques*. Elsevier, 2011.
- [2] R. Agarwal, R. Srikant, and others, "Fast algorithms for mining association rules," in *Proc. of the 20th VLDB Conference*, 1994, pp. 487–499.
- [3] S. A. Mahmoodi, K. Mirzaie, and S. M. Mahmoudi, "A new algorithm to extract hidden rules of gastric cancer data based on ontology," *SpringerPlus*, vol. 5, no. 1, p. 312, 2016.
- [4] T. Berners-Lee, J. Hendler, O. Lassila, and others, "The semantic web," *Scientific american*, vol. 284, no. 5, pp. 28–37, 2001.
- [5] B. Swartout, R. Patil, K. Knight, and T. Russ, "Toward distributed use of large-scale ontologies," in *Proc. of the Tenth Workshop on Knowledge Acquisition for Knowledge-Based Systems*, 1996, pp. 138–148.
- [6] I. N. Ferraz and A. C. B. Garcia, "Ontology in association rules," *SpringerPlus*, vol. 2, no. 1, p. 452, 2013.
- [7] V. Svátek, J. Rauch, and M. Ralbovský, "Ontology-enhanced association mining," in *Semantics, Web and mining*, Springer, 2006, pp. 163–179.
- [8] P. Ding, S. Jun-yi, and Z. Mu-xin, "Incorporating domain knowledge into data mining process: An ontology based framework," *Wuhan University Journal of Natural Sciences*, vol. 11, no. 1, pp. 165–169, 2006.
- [9] T. Bharathi and A. Nithya, "Enhanced Way of Association Rule Mining With Ontology," *International Journal Of Engineering And Computer Science*, vol. 5, no. 10, 2016.
- [10] B. S. Balasubramani, V. R. Shivaprabhu, S. Krishnamurthy, I. F. Cruz, and T. Malik, "Ontology-based urban data exploration," in *Proceedings of the 2nd ACM SIGSPATIAL Workshop on Smart Cities and Urban Analytics*, 2016, p. 10.



# *DETERMINATION OF ROUTER LOCATION FOR OPTIMIZING COMPUTER NETWORK USING DOMINATING SET METHODS*

Nova El Maidah  
Faculty of Computer Science  
University of Jember  
Jember, Indonesia  
nova.pssi@unej.ac.id

Ivan Destioviko Hardja  
Faculty of Computer Science  
University of Jember  
Jember, Indonesia  
destioviko@gmail.com

Slamin  
Faculty of Computer Science  
University of Jember  
Jember, Indonesia  
slamin@unej.ac.id

**Abstract**— The aims of this research is to develop a system to determine an optimal router location in a computer network. The router location is optimal if the computer network need the minimal number of router without losing the network connectivity. The methods used in order to optimize the router location are dominating set and Greedy algorithm. The data is the router location of computer network in University of Jember. The result showed that the optimal router needed in the networks is 4. These routers were found by using the determination system that implement Greedy algorithm to find the minimum number of dominating set.

**Keywords**— Router, Dominating Set, Greedy algorithm

## I. INTRODUCTION

Implementation of lectures at University of Jember (UNEJ) performed with integrated information system call Sistem Informasi Terpadu (SISTER) UNEJ. SISTER UNEJ is an application that operate using the internet. SISTER UNEJ help lectures to record student and lecturer attendance, archiving subject matter, do the exam, quiz, or evaluation, even do online lectures. With SISTER UNEJ, lectures can be done anywhere at any time as long students and lecturer have access to the internet. To attend attendance, student must scan QR code with SISTER for Student application on their smart phone. The smart phone used must be connected to the internet through the access point of each room where lecture conducted. So that student attendance can be recorded in SISTER UNEJ, lecturers must attend attendance by login in to the subject of lecture conducted. And also lecturers must be login using the internet through the access point of each room where lecture conducted.

In its implementation there are some limitations in SISTER UNEJ used. One of the limitations is the ability of access to the internet. Along with the increasing level of demand and the increasing number of network users who want a form of network that can provide maximum results both in terms of efficiency and improvement of network security itself. One of them is a hotspot that is much popular today. Because of its easy and inexpensive usage in the use of media or devices. Hotspot no longer requires too many cables to be able to share data. Because hotspots rely on wireless transmission media using signals. Hotspot itself requires hardware that can support data sharing without using a cable, hotspot router. A router is a device that sends data packets through a network or the Internet to its destination, through a process known as routing. Routers can be used to connect several small networks to larger networks, called Internetworks, or to divide large networks into several

subnetworks to improve performance and also simplify management.

Disruption in internet use that often occurs, among other because of the large number of users who access it at the same time. And router position is also sometimes a problem because it cannot access the internet properly. For example, the position of the router is outside the class which is blocked by a thick wall. Sometime here is another access point with another service set identifier (SSID) from another room detected in the room. Positioning and exact positioning access point are taken into account in order to keep the network maximizing its reach with good fixed network connectivity [1]. It takes the right strategy to determine the position and distance between routers in a area, in order to function every router is maximized. Some researches on router locations determination were done by several authors such as in [2] and [3].

In this study graph theory is used to describe and determine the location of the router hotspot so that the internet network can be used optimally. Placing a router in a strategic place is also expected to minimize the number of hotspot routers that are used so as to reduce the usual procurement of goods and the use of electricity. Optimal position of the router at the University of Jember are represented in graphical form with the route location as a point. The graph is then analyzed using Set Dominate to determine the location and number of routers to be installed. The router is described as a point and the distance between the routers as a line.

Dominating Set is applied to the search point of router location University of Jember to find out which Router dominating other router. Search point dominates using the Greedy algorithm. The Greedy algorithm is one of the most commonly used algorithms in mathematics and computer science. Algorithm Greedy is a type of algorithm that uses a problem-solving approach by finding the maximum value while at each step. This maximum value is known as the local maximum. The Greedy algorithm usually provides a solution that approaches the optimum value in a reasonably fast time.

This study aims to optimize the location of the Router at the University of Jember by using Dominating Set. The search algorithm used to solve the problem is the Greedy algorithm.

## II. RESEARCH METHOD

### A. Design of System

This study is done by implementing Greedy algorithms and one of topics in Graph theory, namely, Dominating Set to solve the problem. Its was conducted by creating an information system for determining the dominating set on the router graph at the University of Jember. This Information System was built to find out the domination nodes on the router graph as a representation of router location at the University of Jember. The node used is the location of the router and the line between the nodes of the router.

The predominant set is a subset of  $V'$  from the set of points ( $G$ ) where the points that are not on  $V'$  are directly connected to a minimum of one point on  $V'$ . The smallest size of the dominating set is called the domination number denoted by  $\gamma(G)$  [4]. The upper limit of the domination number is the number of points on the graph [5]. If there is at least one point needed for domination in graph, then  $1 \leq \gamma(G) \leq n$  for every graph with a  $n$  order. To find out the optimization in determining the dominating set in any graph by followed Equation (1), where  $p$  is the number of points in any graph,  $\Delta(G)$  is the greatest degree in any graph, and  $\gamma(G)$  is approximate number of Dominating Sets.

$$\lceil 1/(1+\Delta(G)) \rceil \leq \gamma(G) \leq p - \Delta(G) \quad (1)$$

Greedy Algorithm is a type of algorithm that uses a problem solving approach by looking for a maximum temporary value at each step. This maximum value is known locally as local maximum. In most cases, Greedy algorithm will not produce the most optimal solution, so Greedy algorithm usually provides a solution that approaches the optimum value in a fairly fast time. Because of Greedy's nature, the Greedy algorithm is often regarded as an "short sight" and "non-recoverable" algorithm. Therefore, too, the Greedy algorithm is best used on problems that do not attach the optimum solution, and is suitable for simple problems [6].

The Greedy algorithm component consists of: (1) the set of candidate  $C$  which is the set that contains the solution-forming elements; (2) a set of solutions containing the problem solving elements; (3) the selection function for selecting the most likely candidate from the candidate set to be incorporated into the solution set for the optimal solution to be formed (note that the candidate which is already selected in a step will not be considered in the next step); (4) a feasibility function is a function that checks whether a selected candidate will lead to a viable solution, that candidate together with the set of selected solutions will not violate the prevailing constraints on the problem; and (5) an objective function that maximizes or minimizes the value of the solution [7].

In addition to using the greedy algorithm and dominating sets, this system is made based on the web. system input in the form of router data, user data entered by the system admin, as well as other supplementary data. In addition to the main purpose of determining the location of the installation, this system router also backs up data every time there is a new router data. General description of the system is shown in Figure 1.

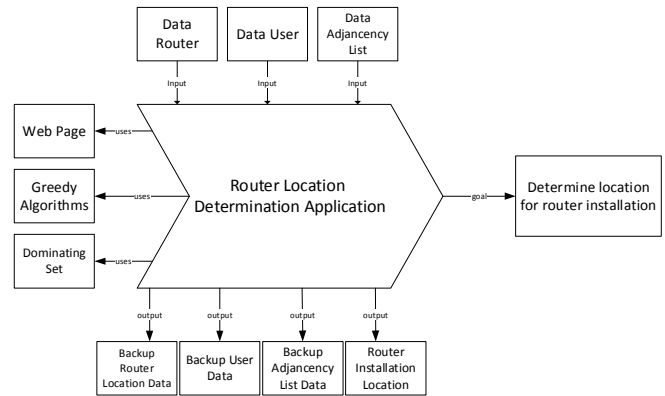


Fig. 1. System Overview

### B. Data Analysis

The data used in this research is the location of routers to be installed at University of Jember and map of University of Jember region obtained from tracking process using Geo Tracker application. Tracking results are then processed using GPS Track Editor. The data then was calculated using Dominating Set and Greedy algorithm. The flow diagram of the routers location determinant information system can be seen in Figure 2.

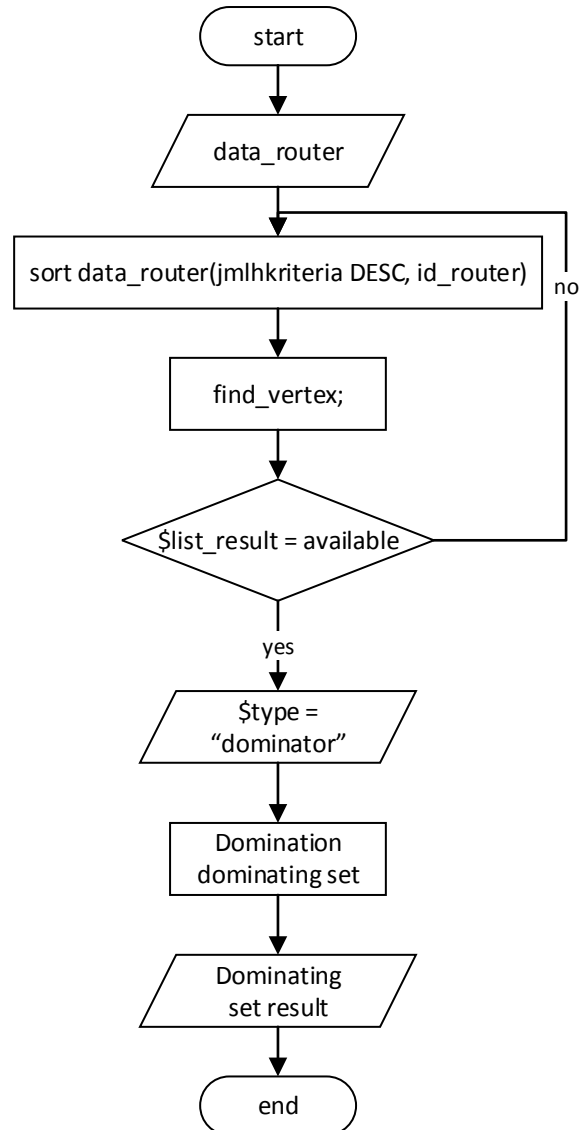


Fig. 2. System Flowchart

For a graph  $G$  with a vertex set  $V$  and an edge set  $E$ , a subset  $S$  of  $V$  is called a dominating set if every vertex  $x$  in  $V$  is either in  $S$  or adjacent to a vertex in  $S$ . The domination number, denoted by  $\gamma(G)$ , is the minimum cardinality of the dominating set of  $G$  [4]. The upper bound of the dominating number is the number of nodes (order) in the graph [5]. if at least one node is need to dominate other nodes in graph, then  $1 \leq \gamma(G) \leq n$  for any graph of order  $n$ . To know whether the dominating set of any graph is optimal or not, we follow the Equation (2), where  $n$  is the order of the graph,  $\Delta(G)$  is the maximum degree, and  $\gamma(G)$  is the dominating number.

$$\lceil n/(1+\Delta(G)) \rceil \leq \gamma(G) \leq n - \Delta(G) \quad (2)$$

Greedy algorithm is applied to the system to determine the dominating number. Greedy Algorithm is an algorithm that uses a problem solving approach by searching temporary maximum value. This value is known as *local maximum*. In many cases, Greedy algorithm does not provide the most optimal solution. However, this algorithm usually provides solutions that close to the optimum value in a fairly fast time. Because of the Greedy nature, the Greedy algorithm is often regarded as a "short sight" and "non-recoverable" characteristic algorithm. Hence, the Greedy algorithm is best used on issues that are not concerned with the optimum solution, and are suitable for simple problems.

Simple Greedy algorithm is used to find dominating number  $\gamma(G)$  as minimal as possible for graph  $G$  of order  $n$  and size (the number of edge)  $m$ . It can be shown that the upper bound is  $\gamma(G) \leq n + 1 - \sqrt{2m+1}$ . Let  $V = \{1, 2, 3, \dots, n\}$ , and  $S = \emptyset$ . Greedy algorithm adds an edge to  $S$  in every step until obtaining a minimal dominating set. A node  $j$  is covered if  $j \in S$  or any neighbour of  $j$  is in  $S$ . Any node which is not covered is called uncovered node [8].

### III. IMPLEMENTATION OF SYSTEM

System developed refers to the waterfall model [9]. The development process is carried out gradually from the previous stage and runs sequentially. The first stage must be completed first, then proceed with the next stage. In general, the stages in the waterfall model are divided into 5 stages: needs analysis, system design, implementation, testing and maintenance included in the flow diagram Figure 3. This model was chosen because it is easier to manage and more detailed to build the system.

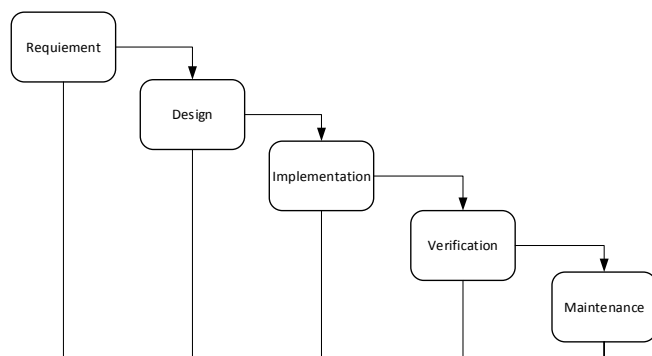


Fig. 3. Waterfall Model [9]

The application of router location determination is a web based system which implements Dominating Set and Greedy algorithm to determine the location of the router. Data input

is sourced from router data, user data, as well as neighboring router data. In addition to determining the exact location for the installation of the router, this system can also backup location data router, user data, and point neighbor data.

Features provided in this system are login, router data management, neighbour node data management, displaying greedy algorithm and dominating set calculation results, user management, and displaying router data. This system can be accessed by three types of users, namely superadmin, admin router, and graph admin. The access rights to the features for these three users are as illustrated in Figure 4.

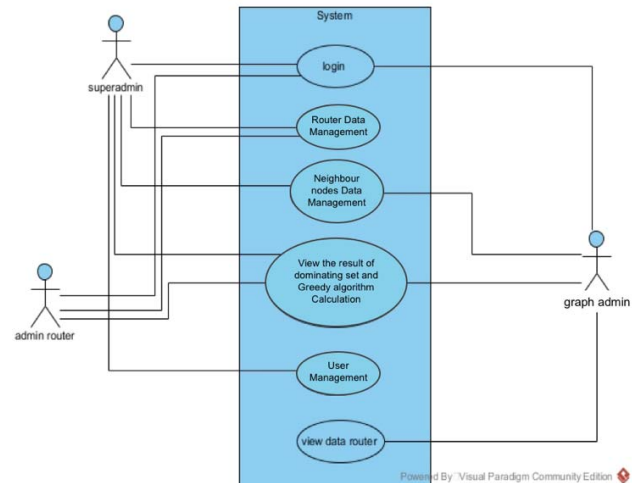


Fig. 4. Usecase Diagram of System

### IV. RESULT AND DISCUSSIONS

The implementation of dominating sets on the system determination of the router location is related to the purpose of this research, that is, to provide a recommendation for the location of the router to be installed in the area of University of Jember. To achieve the purpose, this system has a main feature that is the determination of the router location. This feature applies the calculation of dominating set by searching dominating nodes using Greedy algorithm. The data used in this feature is the node data of router and neighbor node. The data of neighbour node is obtained from the node of router associated with other router.

The process of determining the routine layout of the collection of dominance on the graph is to determine the graph representation of the University of Jember land. Representation of the graph at the University of Jember produces 26 points as in Figure 5. In addition to displaying in the form of images, each node also shows the latitude and longitude position of the node.

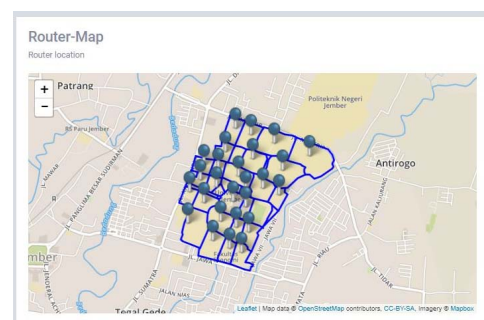


Fig. 5. Map of The Router Location

The first stage is sorting vertex based on the number of the most neighboring points sorted from the largest to the smallest. The first stage of determining vertex can be seen in Table 1. Its indicates that the Router with id 14 and 18 which has the highest number of neighbors in all existing Vertices, has 6 neighbors, while the number of neighbors with the least number of IDs is Router 4, 5, 11, 16, 20, 22 with only 2 neighbors.

TABLE I. VERTEX SEQUENCE

Id_Router	Number of neighbors	latitude	longitude
14	6	-8.16329911	113.716636
18	6	-8.16209903	113.717698
21	5	-8.1628743	113.719811
23	5	-8.16415934	113.718406
26	5	-8.16509391	113.71626
1	4	-8.16661257	113.712999
6	4	-8.16693118	113.716493
7	4	-8.16651699	113.715348
8	4	-8.16520011	113.714168
12	4	-8.16406376	113.715048
13	4	-8.16275748	113.715198
19	4	-8.16098392	113.719211
24	4	-8.16436112	113.717151
25	4	-8.16548685	113.717172
2	3	-8.16661257	113.712999
3	3	-8.16840205	113.715988
9	3	-8.16443015	113.713151
10	3	-8.16357523	113.7139
15	3	-8.16155741	113.71572
17	3	-8.16038918	113.717537
4	2	-8.16870472	113.716861
5	2	-8.16728164	113.717398
11	2	-8.16252384	113.714157
16	2	-8.1599219	113.716421
20	2	-8.16187601	113.721771
22	2	-8.16463724	113.719586

The next second step is to determine the dominator point based on the list of neighboring points, if the list of neighboring points has not been dominated by other points then that point becomes a dominator. The second stage of determining the dominator point can be seen in Table 2. The list that is marked by red is the neighbor list that has the dominator point as the Router id whose list of neighbors has been dominated by other points cannot be used as dominators, because it can be said dominator if the Router ID has a neighbor list that is not dominated by other points. The Dominator Router Id is marked with a blue color of 5, namely 14, 1, 4, 16, 20.

TABLE II. DOMINATOR POINTS

Id_router	Number of neighbors	list	declaration
14	6	12,13,18,23,24,26	dominator
18	6	14,15,17,19,21,23	not
21	5	18,19,20,22,23	not
23	5	14,18,21,22,24	not
26	5	7,8,12,14,24,25	not
1	4	2,7,8,9	dominator
6	4	3,5,7,25	not
7	4	2,6,8,26	not
8	4	1,7,9,12	not
12	4	8,10,13,26	not
13	4	11,12,14,15	not
19	4	17,18,20,21	not
24	4	14,23,25,26	not
25	4	6,23,24,26	not
2	3	1,3,7	not
3	3	2,4,6	not
9	3	1,8,10	not
10	3	9,11,12	not
15	3	13,16,18	not
17	3	16,18,19	not
4	2	3,5	dominator
5	2	4,6	not
11	2	10,13	not
16	2	15,17	dominator
20	2	19,21	dominator
22	2	21,23	not

The third stage then searches for points that have not been dominated by dominator points. The point is marked with yellow which can be seen in Table 3. Its shows the router id that has not been dominated by the dominator point, marked in yellow. Router IDs 6, 25, 10, 11, 22 are router ids whose list is not dominated by the router id that is router id 14, 1, 4, 16, 20. The purpose of finding this remaining point is to find the router id that has not been dominated by the dominator point where this remaining point can later be used as another dominator point.

TABLE III. RESIDUAL POINT

id_router	Number of neighbors	list	declaration
14	6	12,13,18,23,24,26	dominator
18	6	14,15,17,19,21,23	no
21	5	18,19,20,22,23	no

23	5	14,18,21,22,24	no
26	5	7,8,12,14,24,25	no
1	4	2,7,8,9	dominator
6	4	3,5,7,25	no, the rest
7	4	2,6,8,26	no
8	4	1,7,9,12	no
12	4	8,10,13,26	no
13	4	11,12,14,15	no
19	4	17,18,20,21	no
24	4	14,23,25,26	no
25	4	6,23,24,26	no, the rest
2	3	1,3,7	no
3	3	2,4,6	no
9	3	1,8,10	no
10	3	9,11,12	no, the rest
15	3	13,16,18	no
17	3	16,18,19	no
4	2	3,5	dominator
5	2	4,6	no
11	2	10,13	no, the rest
16	2	15,17	dominator
20	2	19,21	dominator
22	2	21,23	no, the rest

The fourth stage is to find the domination point from the point in the third stage of determining the remaining points that produce router id 6, 25, 10, 11, 22. The fourth stage to find the domination point can be seen in table 4. The dominator is router id point 6 and 10, while router id 22 becomes the dominator itself because the router id of the 22 list neighbor is not dominated by the remaining router id, id 6, 25, 10, 11.

TABLE IV. RESIDUAL POINT OF THE DOMINATOR

id_router	Number of neighbors	list	keterangan
6	1	3,5,7,25	residual dominator
25	1	6,23,24,26	no
10	1	9,11,12	residual dominator
11	1	10,13	no
22	0	21,23	stand along

In the development of the router determination system, the comparison of manual and system calculations is the same. Here is a calculation of dominating sets to assess the optimization of the result of dominating node. The number of routers is 26, with the largest degree is 6, as well as the estimated number of dominating number is 8. By following Equation (2), we have:

$$\lceil 26/(1+6) \rceil \leq 8 \leq 26 - 6 = 4 \leq 8 \leq 20$$

From the calculation,  $4 \leq 8 \leq 20$  where 4 is the minimum number of dominating number, 8 is the dominating number generated from Greedy algorithm calculation, and 20 is the maximum number of dominating number. It can be concluded that the node obtained by using the Greedy algorithm has been optimal, since it is the minimum number. The location of the router which is represented by the dominating node can be seen in Table V and mapped as in Figure 6.

Column Id Router in Table 1 shows the location of router that dominate other nodes which is illustrated as a blue (larger) dot in Figure 4. While column List in Table 1 shows which routers are dominated by dominating router which are illustrated as green (smaller) dots in Figure 4.

TABLE V. ROUTER LOCATION OBTAINED BY DOMINATING SET

Id_Router	List	Latitude	Longitude
1	2,7,8,9	-8.166612574832754	113.71299868449572
4	3,5	-8.168704716603795	113.71686106547716
10	9,11,12	-8.163575232750972	113.71389990672472
14	12,13,18,23,24,26	-8.163299109598052	113.71663575991988
16	15,17	-8.159921895592236	113.71642135083677
20	19,21	-8.161876010321398	113.7217713519931
22	21,23	-8.164637243098513	113.71958618983629
25	6,23,24,26	-8.16548684934311	113.71717220172289

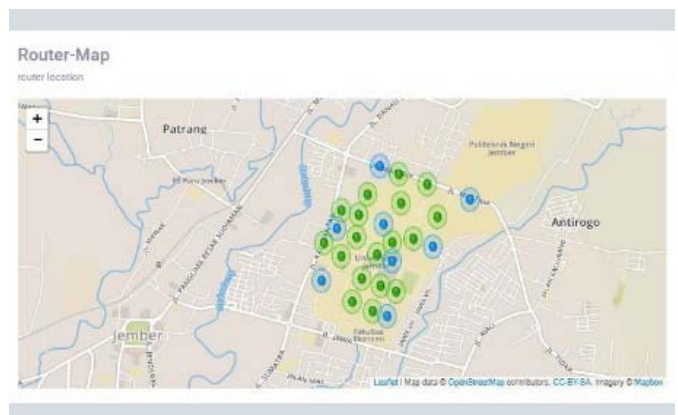


Fig. 6. Router Mapping

## V. CONCLUSION

The Greedy algorithm is implemented in the system to determine dominating set as a representation of router location of computer network in University of Jember. From the calculation, it is obvious that  $4 \leq 8 \leq 20$  where 4 is the minimum number of Dominating Set, 8 is the Dominating set generated from the Greedy algorithm calculation, and 20 is the maximum number of Dominating Set. It was concluded that the point finding result using the Greedy algorithm was optimal, since the number of Dominating Set found from the Greedy algorithm calculation approached the minimum number of Dominating Set.

## REFERENCES

- [1] I. F. Akyildiz, X. Wang, and W. Wang. "Wireless Mesh Networks: a Survey". *Computer Networks* 47(4) (2005) 445-487.
- [2] M. B. Hosseini, F. Dehghanian, M. Salari, "Selective capacitated location-routing problem with incentive-dependent returns in designing used products collection network", *European Journal of Operational Research*, in press.
- [3] H. Guo, X. Wang, H. Cheng, M. Huang, "A location aided controlled spraying-routing algorithm for Delay Tolerant Networks", *Ad Hoc Networks*, Vol. 66, pp. 16-25, November 2017.
- [4] S. Alanko, S. Crevals, A. Issopoussu, P. Ostergard, and V. Petterson. "Computing The Dominating Number of Grid Graph", *The Electronic Journal of Combinatorics*, 2011, vol. 18, issue 1, pp. 141-159.
- [5] T. W. Haynes, S. T. Hedetniemi, and P. J. Slater, 1998, "Fundamentals of Domination in Graphs, Monographs and Textbooks in Pure and Applied Mathematics, Vol. 208, Marcel Dekker Inc., New York.
- [6] T. H. Cormen, C. E. Leiserson, R. L. Rivers, and C. Stein, 2009, *Introduction to Algorithms*, Massachusetts, MIT Press.
- [7] Ardiansyah, F. S. Efendi, Syaifullah, M. Pinto, Pujiyanto, H.S. Tampake, "Implementasi Algoritma Greedy untuk Melakukan Graph Coloring: Studi Kasus Peta Propinsi Jawa Timur", *Jurnal Informatika*, Vol. 4, No. 2, pp. 440-448, Juli 2010.
- [8] W. Alfari, "Pencarian Jalur Terpendek Pengiriman Barang Menggunakan Algoritma A\* (Studi Kasus Kantor Pos Besar Medan)", *JURIKOM*, Vol. 3, No. 1, pp. 90-95, February 2016.
- [9] I. Sommerville, 2011, *Software Engineering (Rekayasa Perangkat Lunak)*. Jakarta: Erlangga.



# Evaluating The Semantic Mapping

Dewi Wardani  
 Department of Informatics  
 Universitas Sebelas Maret  
 Surakarta, Indonesia  
 dww\_ok@uns.ac.id

**Abstract**—The increasing of the importance of links in the network of data influences the idea that links should be considered more in the mapping relational to graph model. Semantic abstraction gaps often occur during the mapping process where the link in the real world is mapped as a node in a graph model. This paper focused on evaluating the result of mapping and converting without losing the semantics. We propose the evaluation of our approach by using *schema.org* as the semantic standard. The experiments in three data sets show that the semantic mapping approach is pretty effective. We obtain quite good score matching without considering the gap index (the average is 0.6922) and with considering the gap index (the average is 0.5264) and the average precision score, 0.7042, is pretty good too.

**Keywords**—*Semantic Mapping, relational model, graph model, schema.org*

## I. INTRODUCTION

The idea of the inventor of Semantic web is to create the web of data [1]. Sometimes, it is called the network of thing [2]. The data will be equal to a thing than a string or the other data types. The main idea is to make data more connected, meaningful and understandable on the machine side. For this purpose, we need the conceptualization of thing like in the real world. In both theory and practice, preparing data which meet the need of semantic web is the bottom block in this technology architecture. As the connected data, we don't see them as a stand-alone data but as a subgraph. We can see that the data model of the semantic web is a graph-based data model [3] [4]. Graph model itself has been proven useful to help solving some tasks [5] [6]. In this model, we will have not only a network of a node but also a network of a link. Links will be more important to the network of data, and link mining will be important in the near future [7].

Lots of data exist in many domains such as a structured and an unstructured type, yet the model is not semantic web friendly. Especially, the structured data in the relational model, it has huge and broad-area user and has been used successfully for a long time [8]. It also has a high-quality information in the sense that it has the main information in almost all applications. This type of data cannot be ignored as a data source for the semantic web. Concerning its importance, we need to map the relational model to a graph model first, which semantic web friendly and much expressive to represent knowledge in the real world [9]. Later on, it can be mapped to the other model or language such as RDF or OWL. Direct mapping to RDF or OWL is out of the focus of this work.

The mapping relational to graph model usually is a naïve converting process, which put all tuples in each relation as a node and the foreign key as a link between two nodes, but not few scientific papers are written for this approach. Almost all ended their work until a relational model is converted to a graph model, without considering the semantics of the real world. Although a graph model basically has no schema, but the mapping process should be started from the schema, and the rest populated data will be following the schema. In summary, up to our knowledge, the semantic mapping which has been proposed [10] is the first work which maps with considering the higher abstraction of the relational model and has shown good performances comparing the naïve model. Showing good performances is not enough to acknowledge the model keeps up the semantic of the real world. Measuring its effectiveness in the sense not losing the semantics of model is an important issue. On the other side, there is no work which measures whether the result graph model keeps up the semantic of the real world.

The main goal of this work is **to evaluate the effectiveness of the semantic mapping approach by comparing the result with the vocabulary in the *schema.org* (<http://schema.org>), a general ontology created by experts as the standard evaluation score**. The remaining sections are organized as follows: section two explains the related work. Section three summarizes the mapping approach from the previous work [10]. Section four describes the evaluating method to examine whether the graph keeps up the semantic of the real world. We conduct and discuss the result of experiments in section five. Finally, the conclusion and discussion our the near future work in section six.

## II. RELATED WORK

In a previous work [11], the goal of the authors is to improve the performance in querying the graph model data. The approach aggregates the populated data into one node as far as it's possible in all possibility search queries to reduce the query traversal time. In our point of view, aggregating the data into one node might cause the semantically lose, the node does not have specific semantics. The node is only a bag for holding data. The other work [12], transforms the relational model to graph model based on dependencies between each attribute of the relation. It is similar to the earlier approach which the semantics of relation will be lost, and there is a possibility of graph data redundancy. In general, we think that the mapping process should not only focus on consuming the data, but also can support the mining of the link or other extended works that possibly only can work better by using the graph model data.

Some other works, convert the relational model to RDF or OWL [13] [14] [15] [16] [17] [18], but almost all focus on direct converting without considering the higher abstraction of a relational database. This is what we mean that the converting process has a potential to semantically lose. In general, the earlier works focus on mapping the data, attributes and relation, but still missed in considering the scheme which is the representation of semantic abstraction of the real world.

The network of data can have multiple types of links and complex dependency structures. This fact is a motivation of our work, that mapping relational to graph should keep up the possibility of the heterogeneous network. In the naïve mapping process to graph model, usually the Foreign Key (*FK*) is mapped as a link, but this rule is not enough for keeping the semantics of a heterogeneous network. In this work, we exploit deeper the link structure to be used in our mapping approach without semantically lose and keep up the graph model like in the real world.

### III. LINK STRUCTURE IN RELATIONAL MODEL

We proposed the semantic mapping which to our knowledge is the first work mapping relational model to graph model which consider the semantic of links. Previous work ignored the semantic issue of the link that has more than two nodes as the link as well. In graph point of view, it is normal that a link connects to more than two nodes. In the real world is also very common that a relationship relates to more than two things. In this part we summarize some definitions of our previous work [10] as below:

**DEFINITION 1 (The Relational Model).** Let  $S(R_1, R_2 \dots R_i)$  be a relational model which consists of a set of Relations,  $i$  is the degree of relation, a set of Primary Key ( $PK(PK_1, PK_2 \dots PK_{iPK})$ ), a set of foreign key ( $FK(FK_1, FK_2 \dots FK_{iFK})$ ) and others sets of integrity constraints ( $IC$ ). Each Relation consists of a set of attributes,  $R(A_1, A_2 \dots A_j)$ ,  $j$  is a degree of attributes.  $r$  is a relation instance of  $R$ , a set of tuples  $r(t_1, t_2 \dots t_i)$ . Each  $n$ -tuple,  $t$  is an ordered list of  $r$  values,  $t=(t_1, t_2 \dots t_n)$ , each value  $v_n$  is a value of attribute  $A_j$ .

**DEFINITION 2 (The Link Structure).** Let  $FK_i \rightarrow_j$  be a foreign key which connects relation  $R_i$  to relation  $R_j$ .  $m$  is the number of in-link and  $n$  is the number of out-link where  $m \geq 0$ ,  $n \geq 0$ .

A number of in-links of Relation  $R_i$  as  $m_i$  and a number of out-links of Relation  $R_i$  as  $n_i$ , within assumption there is no cycle relationship.

$$m_i = \sum n_j \quad (i) \quad n_i = \sum m_j \quad (ii)$$

**DEFINITION 3 (The Relation Type Set).** Let  $L$  be a set of link structure information of relation  $L=L_1, L_2 \dots L_i$ , each  $L_i$  is a list of value  $L_i=(m_i, n_i)$  where  $m_i$  is the number of in-link of  $R_i$ ,  $n_i$  is the number of out-link of  $R_i$  and let  $RSink$ ,  $RSource$  and  $RHub$  are a list of relation  $R_i$  which satisfies  $L$  data. If in the relation  $R_i$ ,  $m_i=0$  then  $R_i$  is a  $RSink$ . If in the relation  $R_i$ ,  $m_i=0$  then  $R_i$  is a  $RSource$ , otherwise the relation  $R_i$  is a  $RHub$ . Each relation type set ( $RSink$ ,  $RSource$ ,  $RHub$ ) is a set of Relation  $R_i$ .

**DEFINITION 4 (The graph model).** Let  $G$  be a graph model of a relational model  $S$ , is a set of node  $N$  and a set of edge  $E$ , a directed property graph  $G(N, E)$  where  $N$  is a set of node  $N=(N_1, N_2 \dots N_i)$  and  $N \in (RHub, RSource)$ . Each  $N_i$  is a set of attribute and its value  $N_i=(A_i, V_i)$ . The edge is defined as (i)  $(\vec{N}_k, N_l) \in E$  if there is a  $fk$  between two relations  $R_l - \vec{fk} - R_k$ . The label of the edge is a combination of the label of two relations  $R_l R_k$ . (ii)\*  $\vec{N}_r \in E$  where  $R_r - \vec{fk} - (R_l, R_k)$  and  $R_r \in (RSource)$  hence the form of the subgraph is  $N_l^A - \vec{N}_r - (N_k^H)$ . Each edge  $N_r$  has a set of attribute and its value  $N_r=(A_j, V_j)$ . The label of the edge is the combination of the name of the relation and the name of hub relation  $N_r N_k^H$ . (iii)  $(N_r) \in HE$  where  $HE$  is HyperEdge and where  $R_r - \vec{fk} - (R_1, R_2 \dots R_i)$  and  $R_r \in (RSource)$  hence the form of the subgraph is  $N_r - \vec{HE} - (N_1, N_2 \dots N_i)$ .  $N_r$  has a set of attribute and its value  $N_r=(A_j, V_j)$ . The label of the hyperedge is the name of the relation  $N_r$ .

\*)  $N_l^A$  is the node as an Authority and  $(N_k^H)$  is the node as a Hub. The weight of Authority  $A_i$  means how famous node  $N_i$  is referenced by the other nodes. The weight of Hub  $H_i$  means how often node  $N_i$  refers to the other nodes. Between two nodes  $N_l$  and  $N_k$  we calculate which node has the greater weight of authority  $\nabla A_i = A_i - H_i$ .  $N_l^A$  draws the direction of an edge. Here are the formulas to find the type of node whether as an authority node or a hub node.

$$A_{R_i} = \sum \text{outlink}_{R_j} \quad (iii) \quad H_{R_i} = \sum \text{inlink}_{R_j} \quad (iv)$$

$g$  is a graph data,  $g=(n, e)$  which following  $G=(N, E)$  as a graph model.

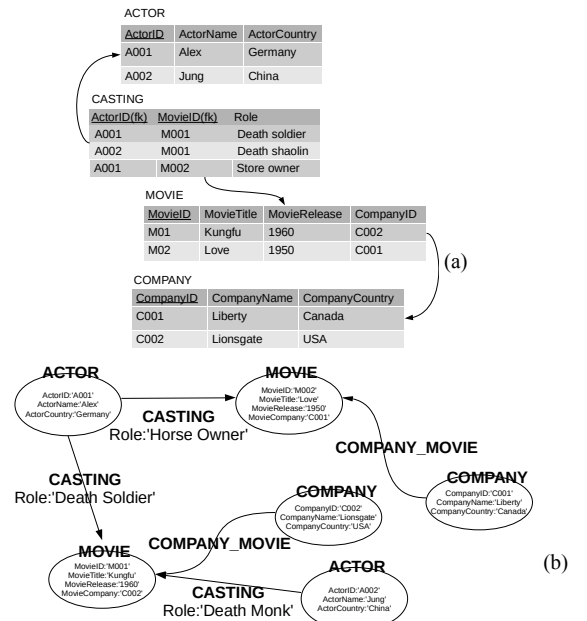


Fig 1. The example mapping and converting (a) relational model to (b). a property graph model based on the approach of the previous work [10]

Figure 1 shows that the approach mapping returns a relational model to a property graph. Figure 1 is the result example of the Semantic Mapping. We can see that RSink is relation Actor and Company. RHub is relation Movie and RSource is relation Casting. Therefore, Casting becomes a link and the others become nodes. Based on our above definitions, the direction of all links are provided as well and is drawn in Fig 1.b.

#### IV. EVALUATING THE SEMANTIC MAPPING

To measure the effectiveness the mapping approach which is explained in section 3, we will compare the result of our graph model with vocabulary and conceptualization of the real world which is formed in the ontology. The measuring process basically is a matching process between our graph model with a graph model of ontology. We use *schema.org*, a famous general vocabulary ontology. We define the graph model in Ontology, in DEFINITION 5 (for the sake of easy reading, we continue the definition and formula numbering from the section 3).

**DEFINITION 5 (The graph of ontology).** Let  $O$  be an ontology which consists a set of classes  $C_1, C_2, \dots, C_n$  in hierarchy format. It has an index of the cluster of class  $i$  where  $i=0, 1, \dots, j$ . Each class  $C_n$  can have another set of subclasses  $C_1, C_2, \dots, C_m$  in each index. Class (domain)  $C_D$  is connected to another class (range)  $C_R$  through object property  $OP_a$  or data property  $DP_b$ . Hence, a subgraph of ontology is  $C_D \circ \tilde{P}_x \circ C_R$  where  $P_x \in (\tilde{OP}_a, \tilde{DP}_b)$ .

The special case in *schema.org*, it has class ACTION which especially describes what entities do. In reality, the class is a relationship therefore it should be as a property. The role class domain and object property are reversed. Hence, the subgraph under the class ACTION is  $P_x \circ \tilde{C}_D \circ C_R$

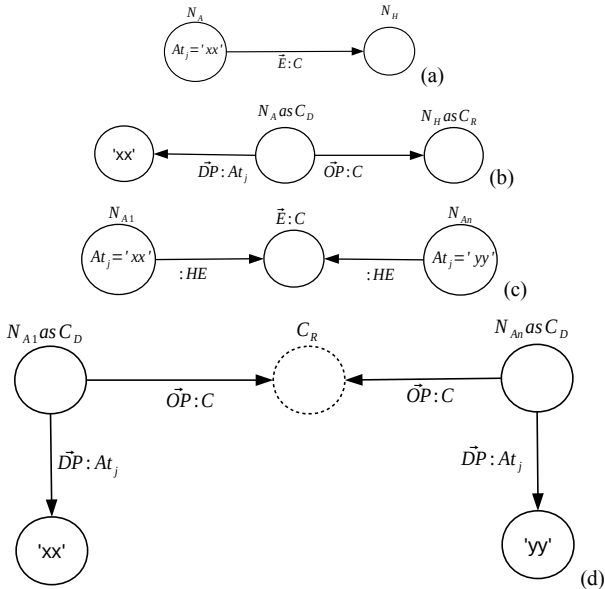


Fig 2. A subgraph type 1 and 2 (a) in our graph model (b) when it's formed in a subgraph of ontology. A subgraph type 3 (c) in our graph model and (d) when it's formed in a subgraph of ontology  $n$  is a number of the authority node  $N_A$ .

We will measure whether the links  $\tilde{E}$  which are obtained by our approach match with the properties  $\tilde{P}$  in ontology. To measure it, we should concern also the nodes which are connected by the link. The link can be varied in the heterogeneous network. The same or similar link does not always connect to the same nodes. Hence, we will match each path of link  $N_A \circ \tilde{E} \circ N_H$  in our graph model with path subgraph of property  $C_D \circ \tilde{P}_x \circ C_R$  in the ontology. In conceptual point of view, actually  $DP_b$  is more matched with attribute  $At_j$  in node  $N_i$ , but in this work we follow formalization of ontology that only matching process  $\tilde{E}$  to  $\tilde{P}$  not  $At_j$  to  $\tilde{P}$ . The best score of similarity matching will be obtained if the path  $N_A \circ \tilde{E}$  is matched with  $C_D \circ \tilde{P}$  in the same index cluster of a class of ontology. Therefore, we use  $d$  as a distance factor to calculate the class gap between the matching result of  $S(N_A, C_D)$  and  $S(\tilde{E}, \tilde{P})$ . Considering that  $C_R$  usually cross the hierarchy of ontology then we avoid similarity  $S(N_H, C_R)$  and avoid the distance factor between  $\tilde{E}$  and  $N_H$ .

#### V. EXPERIMENT AND RESULT

We conducted experiments for three data sets, (1) The artificial movie database, (2) The example problem in [11], to compare the difference result with our approach and (3) The real data set of IMDB (<http://www.imdb.com/>). The measuring process focused on measuring link in the graph result. We implemented two ways experiment: experiments with and without considering the *gapindex* between the link and the node within class and property network of ontology. We use the famous matching score, cosine similarity to calculate the content similarity. The same syntax might have two different meanings or different syntax might have the same meaning, therefore, we use WordNet (<http://wordnet.princeton.edu/>) similarity too. We also calculate the precision score to measure the relevance of the experimental result. In all experiments, we differentiate score between with (with d) and without considering the distance measure and

##### A. The Artificial Movie Database

It has 10 relations, *ACTOR*, *AWARD\_WINNER*, *CASTING*, *CATEGORY\_WINNER*, *COMPANY*, *DIRECTOR*, *LOCATION*, *MOVIE*, *MOVIE\_FESTIVAL* and *PRODUCTION*.

By using our approach 3 relations (*CASTING*, *AWARD\_WINNER*, *PRODUCTION*) turn out as links and the rest 7 relations turn out as nodes. *CASTING\_ACTOR* is a link type2. Whereas *AWARD\_WINNER* and *PRODUCTION* are a link type3. In the real world, it's also correct that *CASTING*, *AWARD\_WINNER* (win specific festival) and *PRODUCTION* (the process of movie making) are relationships and are not entities. The others, *MOVIE*, *COMPANY*, *CATEGORY\_WINNER*, *DIRECTOR*, *ACTOR*, and *LOCATION* are entities. A link *COMPANY MOVIE* is a link type1, which is the only one real link within relational model.

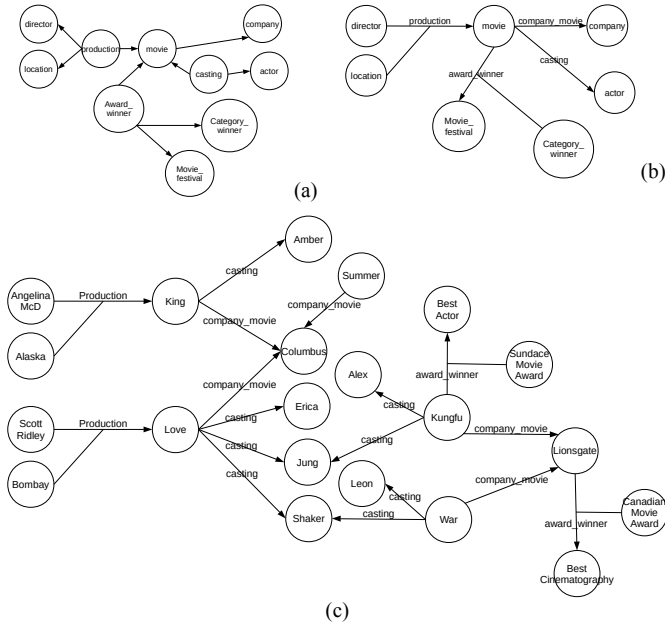


Fig 3. (a) The graph model of naïve approach, (b) The graph model of our approach, (c) The mapping result of graph data

TABLE I. THE MATCHING SCORES OF THE ARTIFICIAL MOVIE DATABASE

Link	WordNet Matching Score		Cosine Matching Score	
	without $d$	with $d$	without $d$	with $d$
COMPANY_ MOVIE	0.6861	0.3430	0.6034	0.3017
CASTING_ A CTOR	0.7380	0.7380	0.8535	0.8535
AWARD_ WI NNER	0.8150	0.8150	0.7831	0.7831
PRODUCTIO N	0.8218	0.4109	0.7628	0.3814

On average  $gapindex$  is 1. For an example in the link  $\bar{E}$  *COMPANY\_MOVIE*, which the authority node  $N_A$  is *COMPANY*, the domain class  $C_D$  *COMPANY* is located upper 1 index hierarchy from the domain class of the relevant property  $\bar{P}$ , but in the same cluster. We can describe this situation is that the  $N_A$  match with subclass-of  $C$  but the link  $\bar{E}$  is connected to the class  $C$ . In the link *CASTING\_ACTOR*, there is no  $gapindex$ , the authority node  $N_A$  *MOVIE* is in the same class cluster. It means that the path  $N_A \circ \bar{E}$  match with path  $C_D \circ \bar{P}$  within one hierarchy class cluster.

We also calculate the precision score, we obtained on average is 0.6483 for WordNet similarity and on average is 0.7739 for cosine similarity. The matching score will be decreased but the relevance of a link  $\bar{E}$  in our graph model with a property  $\bar{P}$  of ontology is maintained stable. This situation often occurs, also in the other 2 data sets. Hence, the precision score is still pretty good, even though the matching score is decreased. It indicates that the link which is obtained by the semantic mapping approach is valid enough. The result

from both WordNet similarity and cosine similarity are pretty good and also good for the precision score. It indicates that the approach is promising.

### B. The Social Database

It has 5 relations, *USER*, *FOLLOWER*, *TAG*, *BLOG* and *COMMENT*.

TABLE II. THE MATCHING SCORES GRAPH MODEL OF THE SOCIAL DATABASE

Link	WordNet Matching Score		Cosine Matching Score	
	without $d$	with $d$	without $d$	with $d$
TAG_ COMM ENT	0.7205	0.3602	0.7071	0.3535
FOLLOWER_ BLOG	0.8705	0.8705	0.6034	0.6034

The precision score on the average is 0.7916 for WordNet similarity and on average is 0.5833 for cosine similarity. 2 relations (*FOLLOWER*, *TAG*) turn out as links and the rest 3 relations turn out as nodes. Both are links type2. In the real world, it's also acceptable that, *FOLLOWER* (action to follow) and *TAG* (commenting action) are a relationship between entities and not the entity. The others, *USER*, *COMMENT*, and *BLOG* are entities. The matching score and precision score are all pretty good.

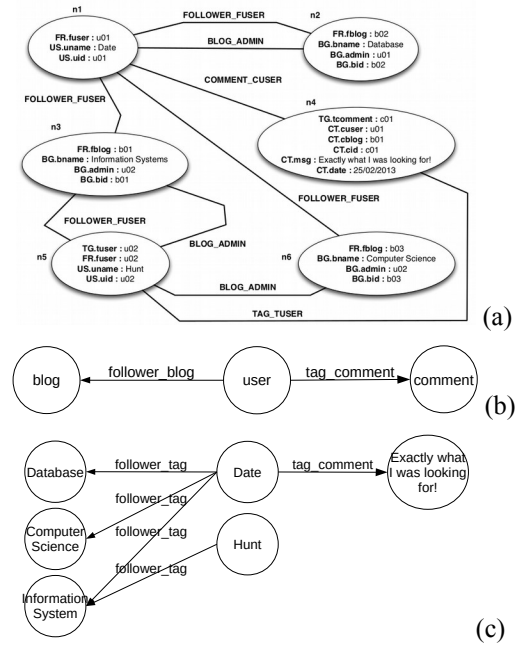


Fig 4. (a) The graph model of [11], (b) The graph model of our approach and (c) The mapping result of graph data

### C. The IMDB Data Set

It is the real movie data set. It has 21 relations, *CHAR\_NAME*, *COMPANY-NAME*, *COMPANY\_TYPE*, *COMPLETE\_CAST\_TYPE*, *INFO\_TYPE*, *KEYWORD*, *KIND\_TYPE*, *LINK\_TYPE*, *NAME*, *ROLE\_TYPE*,

AKA\_NAME, TITLE, CAST\_INFO, MOVIE\_COMPANIES, AKA\_TITLE, COMPLETE\_CAST, MOVIE\_INFO, MOVIE\_INFO\_IDX, MOVIE\_KEYWORD, MOVIE\_LINK and PERSON\_INFO.

TABLE III. THE MATCHING SCORES GRAPH MODEL OF THE SOCIAL DATABASE

Link	WordNet Matching Score		Cosine Matching Score	
	without $d$	with $d$	without $d$	with $d$
NAME_AKA_NAME	0.6333	0.3166	0.3535	0.1767
CAST_INFO	0.6461	0.6461	0.4259	0.4259
MOVIE_COMPANY	0.5671	0.5671	0.6025	0.6025
COMPLETE_CAST_TYPE	0.3809	0.3809	0.7041	0.2347
MOVIE_INFO_INFO_TYPE	0.5512	0.5512	0.6666	0.3333
MOVIE_INFO_IDX_INFO_TYPE	0.5512	0.5512	0.6666	0.3333
MOVIE_KEYWORD_KEYWORD	0.6666	0.6666	0.8535	0.8535
MOVIE_LINK_LINK_TYPE	0.3430	0.1715	0.7041	0.3520
PERSON_INFO_INFO_TYPE	0.8056	0.2685	0.2499	0.1249
AKA_TITLE_KIND_TYPE	0.6428	0.6428	0.8535	0.4267

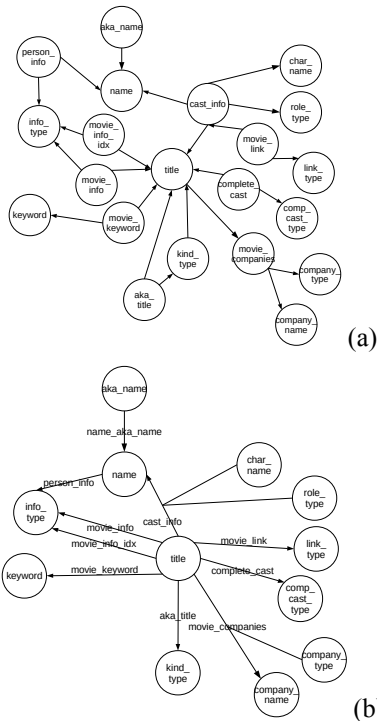


Fig 5. (a) The graph model of naïve approach, (b) The graph model of our approach

The precision score on the average is  $0.6726$  for WordNet similarity and on average is  $0.5700$  for cosine similarity. 8

relations (*CAST\_INFO*, *MOVIE\_COMPANIES*, *COMPLETE\_CAST*, *MOVIE\_INFO*, *MOVIE\_INFO\_IDX*, *MOVIE\_KEYWORD*, *MOVIE\_LINK*, *PERSON\_INFO*) turn out as links and the rest 14 relations turn out as nodes. The matching score and precision score are all pretty good. A few links have low scores. We notice that the low score is caused by a gap of syntax between terms in graph model and the ontology. For an example, in the second experiment for The Social data set, we have a candidate relation has a label *TAG*. *TAG* has information user and their comments. The same description is defined as *COMMENT* or *REVIEW* in the ontology. The same case in the third data set of The IMDB data set, the candidate relation has a label *MOVIE\_LINK\_LINK\_TYPE* and it is a link in IMDB dataset. The same description is defined as URL in the ontology. Those terms refer to the same meaning but as we can see, those terms have a syntax gap.

In the small data set, it might be easier to map manually, but it could be hard and tiring for huge and complex relational model. Although the matching score on the average is not really high but still pretty good, also the precision score is quite high. Therefore, the approach is effective enough to map relational model to graph model without semantically lose than manual semantic mapping especially for a very complex relational schema which probably has hundreds of relation. From the real IMDB data set, we learn that in the complex and huge relational schema there is a bigger possibility many relations which should be mapped as a link, not as a node. Even though the data set of the experiment are the result of this approach [10], but basically all obtained graph models from the other approaches can be evaluated as well.

## VI. CONCLUSION AND FUTURE WORK.

We have proposed the measure to evaluate the semantic mapping, a new approach in mapping and converting relational database model to graph model. The goal of the semantic mapping is to avoid semantics lose by considering semantic abstraction of the real world. This approach exploits the link structure which naturally lies in a relational model and formulate in a few definitions. The experimental result of three data sets included real data set from IMDB data show that this approach is promising, although the matching scores are not really high. Even though some scores are low, but they are investigated correctly as the concept, in the sense links are mapped as properties in comparing ontology. The average of matching scores is similar each other. The average of the matching score without considering the gap of the index is  $0.6922$ , and with considering the gap of the index is  $0.5264$ . On average, the precision score is  $0.6796$ . The average of WordNet similarity is  $0.6517$ , a slightly higher than  $0.5674$  as the average score of cosine similarity. We notice that a gap of the syntax of terms in graph model and ontology causes the low scores.

In the near future, we are going to deploy the graph model which is based on RDF. As both are graph it would be possible to carry out this idea. The most interesting idea is that there is a possibility to introduce a new model of knowledge representation and its implementation. The result of our mapping is a heterogeneous network which really closes with

the real world. We will still exploit the heterogeneous link structure of our mapping result in a few extended works such as using it to improve the inference process and working in retrieval based on link structure.

#### REFERENCES

- [1] T. Berners-Lee and M. Fischetti, *Weaving the Web: The original design and ultimate destiny of the World Wide Web by its inventor*. Harper San Francisco, 1999.
- [2] T. Berners-Lee, J. Hendler, O. Lassila, and others, "The semantic web," *Scientific american*, vol. 284, no. 5, pp. 28–37, 2001.
- [3] C. Bizer, T. Heath, and T. Berners-Lee, "Linked data-the story so far," *Int. J. Semantic Web Inf. Syst.*, vol. 5, no. 3, pp. 1–22, 2009.
- [4] C. Bizer, T. Heath, D. Ayers, and Y. Raimond, *Interlinking open data on the web*.
- [5] W. Chen, L. Cao, X. Chen, and K. Huang, "An equalized global graph model-based approach for multicamera object tracking," *IEEE Transactions on Circuits and Systems for Video Technology*, vol. 27, no. 11, pp. 2367–2381, 2017.
- [6] S. Safaei, P. J. Blanco, L. O. Müller, L. R. Hellevik, and P. J. Hunter, "Bond Graph Model of Cerebral Circulation: Toward Clinically Feasible Systemic Blood Flow Simulations," *Frontiers in physiology*, vol. 9, p. 148, 2018.
- [7] L. Getoor and C. P. Diehl, "Link Mining: A Survey," *SIGKDD Explor. Newsl.*, vol. 7, no. 2, pp. 3–12, Dec. 2005.
- [8] M. J. Cafarella, A. Halevy, and J. Madhavan, "Structured data on the web," *Communications of the ACM*, vol. 54, no. 2, pp. 72–79, 2011.
- [9] C. C. Aggarwal and H. Wang, *Managing and mining graph data*, vol. 40. Springer, 2010.
- [10] D. W. Wardani and J. Kūng, "Semantic Mapping Relational to a Directed Property Hypergraph Model," in *Computer and Information Technology; Ubiquitous Computing and Communications; Dependable, Autonomic and Secure Computing; Pervasive Intelligence and Computing (CIT/IUCC/DASC/PICOM), 2015 IEEE International Conference on*, 2015, pp. 152–159.
- [11] R. De Virgilio, A. Maccioni, and R. Torlone, "Converting relational to graph databases," in *First International Workshop on Graph Data Management Experiences and Systems*, New York, New York, 2013, pp. 1:1–1:6.
- [12] S. Bordoloi and B. Kalita, "Designing Graph Database Models From Existing Relational Databases," *International Journal of Computer Applications (0975–8887) Volume*, vol. 74, pp. 25–31, 2013.
- [13] P. T. T. Thuy, N. D. Thuan, Y. Han, K. Park, and Y.-K. Lee, "RDB2RDF: completed transformation from relational database into RDF ontology," in *Proceedings of the 8th International Conference on Ubiquitous Information Management and Communication*, 2014, p. 88.
- [14] C. Bizer, "D2R MAP - A Database to RDF Mapping Language," in *World Wide Web Conference Series*, 2003.
- [15] S. Rikacovs and J. Barzdins, "Export of Relational Databases to RDF Databases: A Case Study," in *Perspectives in Business Informatics Research*, Springer, 2010, pp. 203–211.
- [16] S. Zhou, "Exposing relational database as RDF," in *Industrial and Information Systems (IIS), 2010 2nd International Conference on*, 2010, vol. 2, pp. 237–240.
- [17] G. Būmans and K. Čerāns, "RDB2OWL: a practical approach for transforming RDB data into RDF/OWL," in *Proceedings of the 6th International Conference on Semantic Systems*, 2010, p. 25.
- [18] N. Konstantinou and D.-E. Spanos, "Creating Linked Data from Relational Databases," in *Materializing the Web of Linked Data*, Springer International Publishing, 2015, pp. 73–102.



# The Role of Social User and Social Feature on Recommendation Acceptance in Instagram in Indonesia

Muhammad Aldi Yusron  
Faculty of Computer Science  
Universitas Indonesia  
Depok, Indonesia  
muhammad.aldi42@ui.ac.id

Putu W. Handayani  
Faculty of Computer Science  
Universitas Indonesia  
Depok, Indonesia  
putu.wuri@cs.ui.ac.id

Qorib Munajat  
Faculty of Computer Science  
Universitas Indonesia  
Depok, Indonesia  
qorib.munajat@cs.ui.ac.id

**Abstract**—This study aims to identify the effect of social features and social users on recommendations acceptance on shopping activities in Instagram. This study uses quantitative approach to process 654 data collected using online questionnaire. The data were analyzed using CB-SEM method and AMOS 21 tools. The results of this study showed that social features and social users give moderating effect on the relationship between social recommendation, cognitive appraisal and affective appraisal. Meanwhile, affective and cognitive appraisal was found to affect purchase intention. The finding shows that the user giving recommendation and the features used to make recommendation can influence the level of recommendation acceptance.

**Keywords**—Social User, Social Feature, Social Recommendation, Purchase Intention, E-commerce

## I. INTRODUCTION

The increasing popularity of social interaction in social networking sites, such as Facebook, Twitter, and Instagram, drove a new form of e-commerce called social commerce [1]. Social commerce allows customers to directly process and develop products in the e-marketplace via social media platforms and social networking sites [2]. Social commerce provides User-Generated Content (UGC) features, such as comments, reviews, ratings, recommendations lists, tags, and user profiles, to allow customers to disseminate information during transactions [3].

One of the social commerce platform that is getting popular in Indonesia is Instagram. Instagram is a photo and video sharing app that lets users take photos, record videos, apply digital filters, and distribute them to various social networking services or within Instagram

platform [4]. Since Instagram was launched in 2010, Instagram users has been increasing, without exception in Indonesia. In 2017, Instagram officially announced that there are more than 45 million active users of Instagram in Indonesia which significantly increased from 22 million active users in early 2016 [5]. From 45 million users, 80% are users that use their account for business purpose [5].

By the various features provided, users can share information related to products / services they have purchased and users who want to buy a product / service can request opinions from other users. However, not all information provided by other users regarding the product / service is credible and able to influence user to purchase the product / service. It shows that acceptance of recommendations is influenced by several factors.

There are several previous studies related to social commerce and purchasing behavior. Research conducted by Chen et al. [17] combines three SCC categories, namely forums & communities, ratings & reviews, and social recommendation. Chen's [17] study aims to investigate the differences between the three categories of SCC in influencing customer decision-making process for shopping. There is also research from Huang and Benyoucef [2] who aims to identify the user preferences of social features on social commerce sites. The study shows the importance of empirical investigation of users' perceptions of the social feature to improve acceptance of recommendations.

From literature study, it was found that there have been few researches on the effect of social features and social users on the acceptance of recommendations by Instagram users. Therefore, this study aims to find out how the influence of

social features and social users on the recommendation acceptance.

## II. LITERATURE REVIEW

### A. Social Commerce Instagram

Social commerce is about building relationships with customers and not just focusing on selling goods or services alone [7]. Today, what customers say is the key to online marketing activities [8]. Thus, business need to build their social commerce by creating an online shopping experience that involves more customers interaction, so that business can use online testimonials provided by their customers to drive more revenue [8].

Instagram is currently evolving into a social commerce platform where business activity is frequently carried out [7]. In Instagram social networking sites, there are many sellers who offer products in the form of goods or services. There are at least 25 million business accounts registered in Instagram [12]. Most sellers already have websites that are accessible to users from the seller's profile page. Using the website, the sellers can take advantage of the Shop Now feature that can be used by the buyer to directly open the seller's web page. Statistics show that 75% of Instagram users use the feature after seeing an ad uploaded by a business account [12]. With a variety of features available to support the interaction between users, Instagram is becoming a powerful social commerce platform.

### B. Social Recommendation

Social recommendation is the use of social media and social networking sites to get and make recommendations about what to buy [25]. There are several trends in social recommendation. The first trend is peer recommendation. Peer recommendation is recommendation made by peer users. The second trend is influencer marketing. Advertising on social media and social networking sites through influencers is currently becoming a trend [9]. Influencers are people who have a lot of followers or audiences on social media or on social networking sites and they have a strong influence on their followers, such as artists, programmers, bloggers, youtubers, and so on [9]. The third trend is user-generated content (UGC). User-generated content is content that is created by internet user and published publicly in a system [10]. User-generated content has great

marketing potential [10] and able to improve brand image with zero/minimal cost [11].

### C. Social Feature and Social User

Social feature is a feature found on social commerce sites that allow users to interact and share information with other users or create content [2]. Social features become a medium for users to share social information, including recommendations about a product. From the various features in Instagram, there are some features that are classified as social features, such as Instagram Stories, Instagram Photo / Video Post, Instagram Direct, and Instagram Comment. In the context of Instagram as a social commerce, these features allow users to observe the behavior of other users and also to get feedback from other users related to a product or a seller of the product [18].

Social users are users who use social feature of social commerce sites to interact, share information, or create certain content. The term social user is adapted from the social identity term found in Tsai and Bagozzi research [26] which defined social identity as group member identification in the virtual community. In this study, social users are divided into four which are friends, family, acquaintance, and celebrity.

### D. Social Learning Theory

Social learning theory is a theory of learning and social behavior that explains how an individual learn new information and behavior by observing and imitating others [16]. There are two dimensions to this theory, namely the cognitive dimension that includes learning of knowledge or skills that builds an understanding and emotional dimension that includes mental, feeling, and motivation [17]. Furthermore, Chen et al. [17] described two dimensions on social learning theory through two variables, namely cognitive appraisal and affective appraisal. Cognitive appraisal refers to a person's evaluation based on utilitarian aspect, whereas affective appraisal is an evaluation based on the emotions, feelings, and reactions experienced by the individual in relation to the observed object [24].

In social commerce, some customers may want to gain more knowledge through existing features to aid their decision making [31]. Such experiences can make customers feel more satisfied, help meet their needs, and increase cognitive attachment [17]. In addition, customers can get social support through interaction with other customers [17]. Such experiences can

satisfy customers's needs of social interactions and thus generate affective attachments. These experiences can trigger customer's intention of buying in social commerce platform [17]. Therefore, this study uses cognitive and affective appraisal to describe the customer decision-making process on social commerce sites.

### III. RESEARCH METHODOLOGY

This research uses quantitative approach with survey method for data collection. The survey contains questions with a choice of answers using a Likert scale from 1 to 5 (strongly disagree, disagree, neutral, agree, strongly agree). Before the survey was distributed, the survey was validated by conducting readability test with 9 sample of respondents from various background of disciplines. Survey then distributed online with target users of Instagram users in Indonesia who have made purchases in Instagram at least once. The data obtained is then processed using CB-SEM (Covariance Based Structural Equation Model).

The research questionnaire is divided into two parts. The first part of the questionnaire contains questions and statements related to the demographics of respondents, such as gender, age, occupation, length of use of Instagram, and frequency of purchases of products / services in Instagram. Meanwhile, the second part of the questionnaire contains statements that represent the factors studied in this study. The statement was adapted from previous related studies. The second part used the Likert scale for the answer.

### IV. RESEARCH MODEL AND HYPOTHESES DEVELOPMENT

The selection of factors and the design of the research model was adapted from the research model of Chen et al. [17]. This research uses one component of SCC, namely recommendations & referrals. Recommendation & referrals is adapted as social recommendation in this study. This research also adds social feature factor from research conducted by Huang and Benyoucef [2] as well as social support factor from Yahia et al research [27] as moderating variables. In this study, the name of social support factor was modified as social users to adjust with this research context. Social users refer to Instagram users, such as friends, family, acquaintances, and celebrities. Fig. 1 shows the research model.

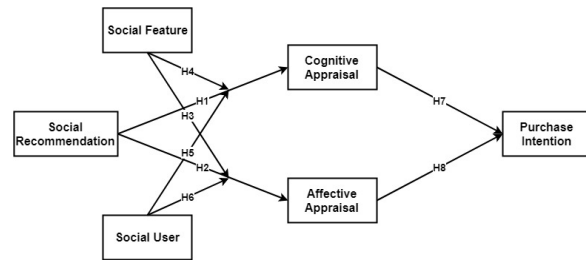


Fig. 1. Research Model

The model illustrates the recommendation acceptance proces in the frame of social learning theory. The formulation of hypotheses in this study will be explained as follows.

#### A. Relationship between Social Recommendation and Cognitive Appraisal

Lee et al. [24] represents cognitive appraisal as an individual's judgment to something, whether it is useful or not. In online shopping, customers have limited information from those provided by the seller. Social recommendation provides additional information for customers so that they can observe and interact further. Such observations or interactions enable customers to learn from other customers who have previously purchased and gained knowledge and information about the product or the respective seller [2]. With such learning, customers can also feel more satisfied because their needs for a knowledge or information can be met [13]. Therefore, a hypothesis that social recommendation positively affects the cognitive appraisal of Instagram users was proposed.

H1: Social Recommendation positively affects the Cognitive Appraisal of Instagram users.

#### B. Relationship between Social Recommendation and Affective Appraisal

Affective appraisal is an evaluation performed by a person based on the person's emotions, feelings, and reactions to something [24]. In social commerce, affective appraisal is related to experiences felt by a person, such as feelings of pleasure, contentment, or relaxation [17]. Social recommendation provides an environment for users to interact with others and exchange emotions, thereby increasing the affective appraisal of discussed matters. Based on this argument, a hypothesis that social recommendation positively affects the affective appraisal of Instagram users was proposed.

H2: Social Recommendation positively affects the Affective Appraisal of Instagram users.

### C. Moderation Effects of Social Feature and Social User

In Instagram, each social feature can provide different functions, information and entertainment to the user. Therefore, the use of social features can affect users in affective and cognitive manners. Based on the argument, social feature was predicted to give moderation effect on the relationship between social recommendation, affective appraisal, and cognitive appraisal of Instagram user was proposed.

Meanwhile, online shopping experiences are also easily affected by personal stories of others, such as family members, friends, acquaintances, or celebrities [6]. Based on a survey conducted by Social Media Link in 2014 with 24,000 respondents, 77% of respondents felt that family members and close friends in social media were the ones who were most influencing to their buying decisions in social commerce. It shows that who gives recommendation influences the acceptance of recommendation. To see how type of users affect the acceptance of recommendation, this study observed how the social user affect the relationship between social recommendation and affective and cognitive appraisal. With that argument, the following four hypotheses were proposed.

H3: Social Feature gives moderation effect on the relationship between Social Recommendation and Affective Appraisal of Instagram Users.

H4: Social Feature gives moderation effect on the relationship between Social Recommendation and Cognitive Appraisal of Instagram Users.

H5: Social User gives moderation effect on the relationship between Social Recommendation and Affective Appraisal of Instagram Users.

H6: Social User gives moderation effect on the relationship between Social Recommendation and Cognitive Appraisal of Instagram Users.

### D. Relationship between Cognitive and Affective Appraisal with Purchase Intention

A person's assessment of a social commerce site and information provided [14] can affect the person's intentions to shop. If a social commerce site is perceived as beneficial to the user, then the user will think that the social commerce site can provide a value for the user [17] which may increase the user's likelihood to make a purchase on the social commerce site [29]. It shows the relation of cognitive appraisal with purchase intention.

In addition to the usefulness aspect, if the use of social commerce sites can make user feel happy, relaxed, or satisfied, then user will think that social commerce sites can provide value to the users [17] which then can increase the likelihood of a purchase on the social commerce site [29]. Based on those arguments, hypothesis that cognitive and affective appraisal positively influence the purchase intention of Instagram users is proposed.

H7: Cognitive Appraisal positively affects Purchase Intention of Instagram users.

H8: Affective Appraisal positively affects Purchase Intention of Instagram users.

## V. RESULT AND DISCUSSION

### A. Demographic of Respondents

The respondents of this study were Instagram users in Indonesia who have purchasing experience in Instagram at least once. Respondents' data were collected from March 7, 2018 to May 14, 2018 and resulted in 684 data. After going through the validation process, there are 658 valid data that can be used. The demographics of this study are presented in the following table.

TABLE I. DEMOGRAPHIC

Demographic Variable		Percent age (%)	Demographic Variable		Percent age (%)
Gender	Male	27.36	Have been using Instagram for	< 6 months	0.76
	Female	72.64		6 – 12 months	3.04
Age (years)	<=20	17.93		1 – 2 years	10.64
	21-30	80.70		3 – 4 years	43.46
	31-40	1.22		5 – 7 years	39.06
	>40	0.15		> 7 years	3.04
Occupation	Student	61.55	Num of purchase made through Instagram	1 - 5	62.15
	Government Employee	2.89		6 – 10	21.73
	Private Sector Employee	26.30		11 – 15	6.23
	Entrepreneur	3.34		16 – 20	2.43
	Others	5.92		> 20	7.45

The information presented in Table I shows that the majority of respondents who completed this research questionnaire is female (72.64%). These results support the results of research

conducted by BMI Research in 2015 which found that the majority of online shopping activities are dominated by women with a percentage of 53% [15]. In addition to gender, the majority of respondents are aged between 21-30, students, and have been using Instagram for more than 3 years. All respondents have experience in making a purchase through Instagram.

### B. Measurement Model

There are three tests conducted on the measurement model, which are convergence validity test, reliability test, and discriminant validity test. Convergent validity test was performed to measure the relationship between the indicator and its construct [32]. According to Hair et al. [22], to achieve convergent validity, the value of the average variance extracted (AVE) of a variable must be greater than 0.5. Each variable in this study has an AVE value in the range of 0.789-0.989. Apart from the value of AVE, convergent validity can also be achieved if the factor loading values of each indicator is greater than 0.7 [21]. If there is an indicator with a factor loading value  $<0.7$ , then the indicator can be erased or set an error variance with a value of 0.01 [30]. Each indicator in this study has a value in the range of factor loading 0.733-0.994. Based on these two results, it can be said that each indicator can represent its latent variable and the model has fulfilled convergence validity test.

The reliability test is performed by evaluating the value of composite reliability (CR) and cronbach's alpha (CA). According to Hair et al. [22], CR and CA values must be greater than 0.7. The calculation results show CR value in the range 0.924-0.996 and the value of CA in the range 0.742-0.880. Thus, it can be said that the construct has a high reliability and the model has met the reliability test.

The discriminant validity test is performed by looking at the AVE root square value which should be greater than the correlation coefficient of each variable [20]. In addition, discriminant validity can also be met by looking at cross-loading of each factor. According to Hair et al. [21], the factor loading of each indicator must be greater than the factor loading of each indicator of another variable. The result shows that each AVE square root value is greater than variable correlation coefficient and each factor loading of an indicator is greater than factor loading of other variable indicator; thus, the model has met discriminant validity test.

After validity and reliability were met, a goodness of fit (GOF) test was required to see the fitness of the model with the existing data [23]. The criteria used are CMIN (P), RMSEA, GFI, AGFI, CFI, TLI, NFI, and CMIN / df [28]. In the first test, the resulting value does not meet the cut-off of each criterion. To make the model fit, the model needs to be changed by adding covariance between variables with other variables, error with other errors, or variables with errors until the model becomes fit based on the largest modification indices (MI) [22]. The results show that almost all criteria have good fit values, except CMIN (P). However, although the CMIN (P) criterion was not fit, the overall model was fit because the study with a sample size more than 250 and observed variables less or equal than 12 will not produce significant CMIN (P) values [22].

### C. Structural Model

Structural model testing is done to examine the hypothesis. The hypothesis submission is done by comparing the p value with the 5% significance level which can be seen from bootstrap confidence in AMOS 21. According to Efron and Tibshirani [19], the hypothesis is accepted if the significance level  $p < 0.05$ . Among the four hypotheses without the proposed moderation effects (H1, H2, H7, H8), the results show that the p values obtained are in the range 0.0003-0.0011, so it can be said that the four hypotheses were accepted. Figure x shows the final research model.

### D. Multi-Group Analysis

Multi-group analysis was conducted to determine the moderation effects of social features and social users (H3, H4, H5, H6). To measure the effect of moderation, SEM was applied to each group by looking at the difference in Chi-square values and the path coefficient [28]. Table II shows the results of multi-group analysis. From the table, we get the result that all hypothesis for moderating effect (H3, H4, H5, H6) were accepted. For relationship between social recommendation and affective appraisal, Instagram Comment (0.83) and friend (0.65) have the highest path coefficient. For relationship between social recommendation and cognitive appraisal, Instagram Photo / Video Post (0.64), Instagram Comment (0.64) and also family (0.68) have the highest path coefficient.

TABLE II. MULTI-GROUP RESULTS

	Social Feature		Social User	
Path	SR-CA	SR-AA	SU-CA	SU-AA
<b>Path coefficient</b>	- Instagram Stories (0.63) - Instagram Photo/Video Post (0.64) - Instagram Direct (0.58) - Instagram Comment (0.64)	- Instagram Stories (0.64) - Instagram Photo/Video Post (0.67) - Instagram Direct (0.54) - Instagram Comment (0.83)	- Teman (0.63) - Keluarga (0.68) - Kenalan (0.66)	- Teman (0.65) - Keluarga (0.64) - Kenalan (0.58)
<b>Chi-square difference</b>	448.363	429.049	440.774	414.300
<b>Cut-off</b>	15.36 (3.84 x 4 difference)		11.52 (3.84 x 3 difference)	
<b>Results</b>	Accepted	Accepted	Accepted	Accepted

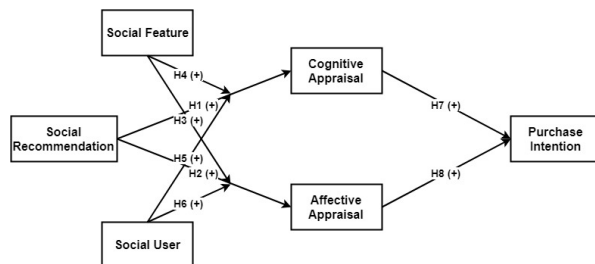


Fig. 2. Final Research Model

### E. Discussion

This study found that social recommendation affects positively Affective Appraisal of Instagram users. Comparing with the research conducted by Chen et al. [17], they found that social recommendation does not have a significant effect on one's cognitive and affective judgments if there are two other SCC components, forums & communities and ratings & reviews. According to Chen et al. [17], the other two components of SCC cause the social recommendation's influence on cognitive appraisal and affective appraisal become weaker. Chen et al. [17] found that if both components are not evaluated then social recommendation will have a significant effect on cognitive appraisal and affective appraisal, as is done in this study. This finding aligns with Chen et al.'s study [17].

This study also found that the features and types of users give moderating effects in the relationship between social recommendation and cognitive & affective appraisal. This means that

the type of features used to provide recommendations and the type of users who provide recommendations affects the level of acceptance of recommendations. It is not surprising that different features generate different influence since each feature has its own characteristics and yields difference entertainment and usefulness level. For example, in Instagram Post, people can view video which is rich in information and more entertaining than text information. Meanwhile, in Instagram Direct Message, there is a limitation in conveying the information thus it has different perceived usefulness and enjoyment than Instagram Post. Those differences influence on how user perceive the recommendation delivered.

As for type of user, it is also intuitive that different user has different effect. For example, it is easier to accept recommendation from someone we know (e.g. family, friends) or someone we respected (celebrity) rather than someone we don't know. This discovery confirms the intuition we have on user's buying behavior and contribute to the theory of user behavior on social commerce sites.

## VI. CONCLUSIONS

This study was conducted with aims to determine the influence of social features and social users on the acceptance of recommendations on online-shopping activities in Instagram. From the analysis, it was found that social feature and social user can influence the acceptance of recommendation. In addition, cognitive and affective appraisal was found positively affecting the purchase intention of Instagram users, where the affective appraisal factor has a greater influence. These findings implied that aside from its function, it is also quite important for social commerce to develop platform that is fun to use to improve affective appraisal which will then influence purchase intention. It is crucial to create social commerce platform with useful and entertaining features which enable users to communicate easily with each other.

## VII. LIMITATION AND FUTURE STUDIES

The scope of this study was to analyse whether types of social features and social users affect the level of acceptance of recommendations. Further research can add more features and type of users to observe in more detail the most effective feature and user in improving acceptance of recommendations. In addition, the majority of respondents from this



study were women, students, and aged between 21-30 years. Further research can balance the demographics of respondents so that it can improve the generalization of the results.

#### ACKNOWLEDGEMENT

This study was supported by PITTA Research Grant No. 1890/UN2.R3.1/HKP.05.00/2018 from Universitas Indonesia.

#### REFERENCES

- [1] T. P. Liang and E. Turban, "Introduction to the special issue social commerce: A research framework for social commerce," *International Journal of Electronic Commerce*, vol. 16, no. 2, pp. 5-13, 2011.
- [2] Z. Huang and M. Benyoucef, "User preferences of social features on social commerce website: An empirical study," *Technological Forecasting and Social Change*, vol. 95, pp. 57-72, 2015.
- [3] A. Ellahi and R. Bokhari, "Key quality factors affecting users' perception of social networking websites," *Journal of Retailing and Consumer Services*, vol. 20, no. 1, pp. 120-129, 2013.
- [4] D. Frommer, "Here's How To Use Instagram," 2010. [Online]. Available: <http://www.businessinsider.com/instagram-2010-11>. [Accessed 29 March 2018].
- [5] R. Triwijanarko, "Insight dari 45 Juta Pengguna Aktif Instagram di Indonesia," 2017. [Online]. Available: <http://marketeers.com/45-juta-orang-indonesia-punya-instagram/>. [Accessed 8 March 2018].
- [6] B. Hutchins, "New Science Behind Trust and Recommendations on Social Media [INFOGRAPHIC]," 2015. [Online]. Available: <https://www.socialmediatoday.com/social-networks/2015-03-12/new-science-behind-trust-and-recommendations-social-media-infographic>. [Accessed 12 May 2018].
- [7] B. Gains, "What is Social Commerce – Our Collection of Trends, Statistics, and Examples," 2017. [Online]. Available: <https://www.referralsasquatch.com/what-is-social-commerce/>. [Accessed 17 April 2018].
- [8] M. Koss, "The 4 Social Commerce Trends To Master This Year," 2018. [Online]. Available: <https://www.yotpo.com/blog/the-4-most-powerful-social-commerce-trends/>. [Accessed 17 April 2018].
- [9] J. Michele, "Kenali Apa Itu Influencer Marketing," 2018. [Online]. Available: <https://kumparan.com/sociabuzz-blog/kenali-apa-itu-influencer-marketing>. [Accessed 17 April 2018].
- [10] A. Mustofa, "Memanfaatkan User-Generated Content untuk Marketing," 2017. [Online]. Available: <https://id.techinasia.com/marketing-user-generated-content>. [Accessed 17 April 2018].
- [11] L. Cosseboom, "Apa Arti User Generated Content bagi Media di Indonesia," 2015. [Online]. Available: <https://id.techinasia.com/arti-user-generated-content-media-indonesia>. [Accessed 17 April 2018].
- [12] R. Mathison, "23+ Useful Instagram Statistics for Social Media Marketers," 2018. [Online]. Available: <https://blog.hootsuite.com/instagram-statistics/>. [Accessed 17 April 2018].
- [13] J. Chen and X. L. Shen, "Consumers' decisions in social commerce context: An empirical investigation," *Decision Support Systems*, vol. 79, no. C, pp. 55-64, 2015.
- [14] Y. Lee and K. A. Kozar, "Designing usabel online stores: A landscape preference perspective," *Information & Management*, vol. 46, no. 1, pp. 31-41, 2009.
- [15] Chi, "Terbukti, Wanita Memang Ratunya Belanja Online," 2015. [Online]. Available: <https://www.vemale.com/karir/77916-terbukti-wanita-memang-ratunya-belanja-online.html>. [Accessed 25 May 2018].
- [16] A. Bandura, "Social learning theory of agression," *Journal of Communication*, vol. 28, no. 3, pp. 12-29, 1978.
- [17] A. Chen, Y. Liu and B. Wang, "Customers' purchase decision-making process in social commerce: A social learning perspective," *International Journal of Information Management*, vol. 37, pp. 627-638, 2017.
- [18] Y. Chen, Q. Wang and J. Xie, "Online social interactions: a natural experiment on word of mouth versus observational learning," *Journal of Marketing Research*, vol. 48, no. 2, pp. 238-254, 2011.
- [19] B. Efron and R. J. Tibshirani, *An Introduction to the Bootstrap*, New York: Chapman & Hall, 1993.
- [20] C. Fornell and D. F. Larcker, "Evaluating structural equation models with unobservable variables and measurement error," *Journal of Marketing Research*, pp. 39-50, 1981.
- [21] J. F. Hair, M. Sarstedt, L. Hopkins and V. G. Kuppelwieser, "Partial least squares structural equation modeling (PLS-SEM): An emerging tool in business research," *European Business Review*, vol. 26, no. 2, pp. 106-121, 2014.
- [22] J. F. Hair, W. C. Black, B. J. Babin and R. E. Anderson, *Multivariate Data Analysis*, London: Pearson Education Limited, 2013.
- [23] P. W. Handayani, A. N. Hidayanto, A. A. Pinem, I. C. Hapsari, P. I. Sandhyaduhita and I. Budi, "Acceptance model of a Hospital Information System," *International Journal of Medical Informatics*, vol. 99, pp. 11-28, 2017.
- [24] Y. Lee, A. N. Chen and V. Illie, "Can online wait be managed? The effect of filler interfaces and presentation modes on perceived waiting time online," *MIS Quarterly*, vol. 36, no. 2, pp. 365-394, 2012.
- [25] M. Shadkam and J. O'Hara, "Social commerce dimensions: the potential leverage for marketers," *Journal of Internet Banking and Commerce*, vol. 18, no. 1, 2013.
- [26] H.-T. Tsai and R. P. Bagozzi, "Contribution behavior in virtual communities: cognitive, emotional, and social influence," *MIS Quarterly*, vol. 38, no. 1, pp. 143-163, 2014.
- [27] I. B. Yahia, N. Al-Neama and L. Kerbach, "Investigating the drivers for social commerce in social media platforms: Importance of trust, social support and the platform perceived usage," *Journal of Retailing and Consumer Services*, vol. 41, pp. 11-19, 2018.
- [28] Z. Awang, *A Handbook on Structural Equation Modeling Using AMOS*, Shah Alam: Universiti Teknologi MARA Press, 2012.
- [29] Y. -S. Wang, C. -H. Yeh and Y. -W. Liao, "What drives purchase intention in the context of online content services? The moderating role of ethical self-efficacy for online piracy," *International Journal of Information Management*, vol. 34, no. 4, pp. 313-330, 2013.
- [30] S. H. Wijanto, "Metode Penelitian Menggunakan Structural Equation Modeling dengan LISREL 9," *Jakarta: Lembaga Penerbit Fakultas Ekonomi UI*, 2015.
- [31] N. Hajli, "Social Commerce Constructs and Consumer's Intention to Buy," *International Journal of Information Management*, vol. 35, no. 2, pp. 183-191, 2015.
- [32] W. Widhiarso, "Praktik Model Persamaan Regresi (SEM) melalui Program AMOS," 2009, [Online]. Available: [http://widhiarso.staff.ugm.ac.id/files/widhiarso\\_-\\_teori\\_dan\\_praktek\\_pemodelan\\_persamaan\\_struktural\\_\(sem\).pdf](http://widhiarso.staff.ugm.ac.id/files/widhiarso_-_teori_dan_praktek_pemodelan_persamaan_struktural_(sem).pdf) [Accessed 3 June 2018]

# User Experience Analysis of the Users Babacucu.Com

Taruna Diyapradana  
Zenius Education  
Gajah Unit ABC Building 5 B3 Floor  
Dr. Saharjo Raya Street No. 111  
Jakarta, 12810  
Indonesia  
[Taruna\\_diyapradana@zeniuseducation.com](mailto:Taruna_diyapradana@zeniuseducation.com)

Ahmad Nurul Fajar  
Information Systems Management Department  
BINUS Graduate Program-Master of Information Systems  
Management,  
Bina Nusantara University  
Jakarta, Indonesia 11480  
[afajar@binus.edu](mailto:afajar@binus.edu)

Ditdit Nugeraha Utama  
Computer Science Department  
BINUS Graduate Program-Master of Computer Science  
Bina Nusantara University  
Jakarta, Indonesia 11480  
[ditdit.utama@binus.edu](mailto:ditdit.utama@binus.edu)

Gunawan Wang  
Information Systems Management Department  
BINUS Graduate Program-Master of Information Systems  
Management,  
Bina Nusantara University  
Jakarta, Indonesia 11480  
[gwang@binus.edu](mailto:gwang@binus.edu)

**Abstract**— The Internet has made sharing information easier. By extension, it has also made sharing things easier. The problem is gauging the user experience of free E-commerce websites such as Babacucu.com to see whether people are interested to visit it or not. One of the elements of user experience is usability, and it will be measured in this research. The methods used to measure the usability are questionnaires and usability testing with the users of Babacucu.com website as subjects. The results of this study are the level of usability of Babacucu.com and recommendations on how to improve the site's usability.

**Keywords**— *Usability, Usability Testing, User Experience, Human-Computer Interaction, Usability Evaluation*

## I. INTRODUCTION

In this day, the internet has allowed us to share information quickly and seamlessly. Emails, instant messaging, social media, blogs, all of them to share information with friends and the public. The internet has also revolutionized shopping, where we don't even have to leave our houses to buy things. What the internet has also helped is the sharing of things. That is the base on which Babacucu.com is founded. Babacucu.com is a free e-commerce website, where its users can share their used things that usually would otherwise end up as junk. This website aims to foster a mentality for people to reduce their waste and instead give away things that would otherwise be thrown away. To help push this mentality as well as get the word of the website out, it

is important to have great user experience to keep the visitors happy and draw in more visitors. In website development, good user experience is essential. User experience is essential to influence a user's perspective of a product [1], so a user-friendly and easy to use user experience design is important to give a good perception to website users. With those factors in mind, an analysis on the site of Babacucu.com, a free e-commerce website, is done to see whether the site has good user experience or not. This research will focus on one of the factors in user experience, which is usability. The first question that aims to be answered by this research is 'How well is the usability in the Babacucu.com site?' The usability of this website is of course very important in determining the user's experience while using the website. The second question to ask in this research is 'What recommendations can be given for the improvement in babacucu.com based on the usability?' The data collected in the research will help find the website's problems and see what it lacks, in order to find what we could do to rectify the issues and make the user experience better for site visitors. The aim of this research is to measure how well the usability level in the Babacucu.com site is, based on defined usability factors. This research is also meant to find what recommendations can be given to improve the usability of Babacucu.com. Future development of this website, as well as other similar websites, will hopefully be able to benefit from this research as well.

## II. RELATED WORK

User experience is what users feel before, during, and after they operate a service or a system. This feeling includes emotions, trust, preferences, cognitive impressions, and various other factors [2]. User experience places heavy emphasis on its users' emotions, contrasting with the belief of human-computer interaction that traditionally believes that users must set aside their emotions to work effectively and rationally using a computer [3]. Now, emotions in computer operations is understood as a critical factor in activities related to the computer, therefore it is important to know [4]. The aim of having good user experience is to give users a clear flow of interaction that does not waste their time, with the end result of an intuitive, valuable, and enjoyable website visit so the users are more likely to come back to the site [5]. One of the main factors of a website's success is user satisfaction [6]. Therefore, it is essential for websites to accommodate user needs to convince them to keep using the site and enjoy the services provided. A good user interface results in three things for its users [7]. Good user experience usually results in good businesses. Businesses such as Amazon and Air B n B became giants in their field because of their large investments to provide the easiest to use services for their clients [8]. These days, most frequent users of the internet are more attentive and tend to know which links are more potentially relevant to the task they aim to achieve [9]. That is why a website design that has complete information and content is essential. The four factors that play a part in user experience are branding, usability, functionality, and content [10]. Usability itself is a sub discipline of user experience design. Even though user experience and usability were interchangeable, usability is now an essential part of user experience, though it does not constitute all of user experience [7]. Usability has a narrower concept than user experience, focusing on the achievement of tasks when using the site, while user experience takes into account the whole experience of a site visit, usability being one of them [11]. Though it has strong ties to each other, user experience and usability are ultimately two different things. Usability can be measured accurately using parameters, while user experience is subjective and varies depending on the user [12]. User experience does not only include how easy a system is used like usability that puts emphasis on task achievement in a context, but also how well a system or website can entertain and be enjoyable aside from the conventional measures of satisfaction like effectiveness and efficiency [13]. Where usability answers the question of 'Can users do the task they wish to do?', user experience answers the question of 'Will users have a good experience using the website or product?' [14]. Usability is the capability of a software or site to provide a user-friendly interface. The usability of a site will have a direct influence to its visitor's user experience, therefore, usability is an important factor in website design [15]. Usability also means that the people who use the site can quickly

understand the interface given and able to finish their task properly [16]. In designing an interactive system, usability is one of the main focuses [17]. International standards define usability as how far a product or site can be used by the user to achieve their goals effectively, efficiently, and with satisfaction in a usage context [18]. To create a system or site with good usability, some things must be taken into consideration, namely [19]: In usability, the key is to design a site that's user-centered. A site with good usability is a site with intuitive design and easy to understand, easy and fast task completion, easy to remember, and has low error rates [20]. One of the problems in usability is the disparity between the mental model of the site's designer and the users. Things that the designer find easy might be difficult to users [21]. Here is where ease of use for the users to navigate the website become important. Good usability is proven to increase user satisfaction [22], while a site with bad usability will confuse users and have detrimental effects to the company [23]. With these considerations, good usability must be a priority to businesses with large online presence. In the QUEM (Quantitative Usability Evaluation Model), the factors of usability are understandability, learnability, and operability [24] that are defined as follows [25] such as Understandability and Learnability. The sub factors of the usability factors are explained in the table below [24]. Usability testing is a way to measure the usability of a website with tests done by users. Most usability tests involve scenarios in which a user is asked to perform tasks likely to be done by regular users in using the site [26]. Problems found in the usability testing must be prioritized, and one of the ways is to categorize them based on the four levels of severity: Unusable, severe, moderate, and irritant [27]. One of the ways to measure usability is to use questionnaires. Two examples of these questionnaires are the System Usability Scale (SUS) and the Computer System Usability Questionnaire (CSUQ). The SUS, developed by John Brooke, consists of ten questions with five options for participants ranging from 'strongly disagree' to 'strongly agree' [28]. SUS has some advantages, such as the ease of answering thanks to its small number of questions, able to be applied to a small sample with reliable results, and is valid and able to differ between a usable and unusable system [20]. The CSUQ, designed off of a journal article by James R. Lewis [29] consists of 19 questions regarding the satisfaction of system users with seven options ranging from 'strongly disagree' to 'strongly agree'. Participants are also asked to write down three most positive and three most negative aspects of the system being tested. Usability evaluation also refers to how satisfied a user is in the process of using a product. To gather this information, methods are used to gather feedback from users regarding a website, one of them is usability testing, where both quantitative and qualitative data can be gained [20].

### III. RESEARCH METHOD

This research consists of several steps. From the problem statement, data is needed to answer the questions. The data will be gained from questionnaires and usability tests to measure the usability level of the Babacucu.com website. The design of the questionnaire and usability tests, as well as the execution of both testing methods will be covered in this section. This research uses several variables that play a part in the search of information and conclusion drawing. The variables of this research are as follows: (a). Independent variable: The user experience of Babacucu.com users, and (b). Dependent variable: The usability of the Babacucu.com site. Data for this research will be gathered using questionnaires. The questionnaire will include questions regarding the sub factors of usability mentioned earlier, measured using the Likert scale. The questionnaire will include multiple choice questions and one open-ended question. The questions given in the questionnaire will measure the following elements of usability and its sub factors, based on the frameworks of the SUS (System Usability Scale) [28] and the CSUQ (Computer System Usability Questionnaire) [29] (1). Understandability, such as the website's visual appeal, the effectiveness of text and information, Consistency of visuals and contents, and the considerations for users' boundaries and disabilities, (2) Learnability, such as the effectiveness of tutorials and guides provided, and the satisfaction of facilities provided to new users to learn how to use the site, (3). Operability such as the satisfaction of site navigation, whether the site is enjoyable to use, the completeness of the site's contents, and User support for interaction. The quantitative data gathered from the questionnaire will be used to determine problems in every usability factor. The scores for each sub factor will be averaged to gain a score for each element. The limit of acceptability for the elements are 3.5, where a lower score means there are parts of the site that are unsatisfactory [30]. The questionnaire will be distributed to registered Babacucu.com users in Google Forms, with links given to them in routine weekly emails as part of the Babacucu.com mailing list. In addition to the questionnaire, a usability test is also performed by testing site users to navigate and do tasks users are expected to do in the daily operations of the website. The usability testing is done with the hallway testing method, taking respondents from the members of Babacucu.com and performing the tests in the Babacucu.com office. For the respondents unable to come to the office, a remote usability testing is performed. The tasks evaluated in the usability testing is based on the pages available in Babacucu.com, which include: (a). Reactions of users when they open the Babacucu.com site, (b). Observing how the users navigate the site without a guide, (c). Searching items they want on the Babacucu.co, site, (d). Asking and receiving free products, (e). Measuring time taken for each task and noting difficulties test participants encounter. The usability testing execution is doing with the usability test of Babacucu.com will involve fifteen respondents. Fifteen were chosen to perform the

test because with fifteen users, 90% of usability issues can be found [31]. Usability test participants are Babacucu.com users contacted by the researcher to perform the usability test. Tests are done face-to-face in the Babacucu.com office or remotely using video call applications for participants who cannot make it to the office.

### IV. RESULTS AND DISCUSSION

The results consists of several results that will explained below:

#### 4.1 Questionnaire Result Analysis

First, indicators of the website's usability are analyzed. The aim of this is to give a description of how the questionnaire participants perceive the indicators given. A descriptive analysis is performed by calculating the averages of each indicators based on the usability sub factors. All the questions given in the questionnaire use a Likert scale ranging from 1 (Strongly Disagree) to 5 (Strongly Agree). The limit of acceptable aspect is 3.5, and if an indicator's average falls under that, it means the indicator is deemed unsatisfactory by respondents. The variables of usability tested in the questionnaire consists of three elements, which are understandability, learnability, and operability. Results of the questionnaire are as follows:

Indicator	Likert Scale					Avg
	1	2	3	4	5	
Website is visually appealing	2	8	30	81	92	4.19
	0.9 %	3.8 %	14.1 %	38 %	43.2 %	
Website provides effective text and information	1	8	29	74	101	4.24
	0.5 %	3.8 %	13.6 %	34.7 %	47.4 %	
Visuals and content of website is consistent	1	5	25	80	102	4.3
	0.5 %	2.3 %	11.7 %	37.6 %	47.9 %	
Website considers user disabilities and limitations	2	5	31	75	100	4.24
	0.9 %	2.3 %	14.6 %	35.2 %	46.9 %	
	3	3	33	79	95	4.22
	1.4 %	1.4 %	15.5 %	37.1 %	44.6 %	

Figure 1 : Questionnaire Results for Understandability

The results of the questionnaire shows that from the four indicators in the understandability factor, a majority of participants answered 'Agree' or 'Strongly Agree'. The average of all indicators are 4.23, more than the acceptable limit of 3.5. The largest average is on the 'Effectiveness of text and

information' indicator with 4.27, while the smallest is on 'Site design is visually appealing' with 4.1

Indicator	Likert Scale					Avg
	1	2	3	4	5	
Tutorials and guidelines are effective and easily accessible	2	8	26	69	108	4.28
	0.9%	3.8%	12.2%	32.4%	50.7%	
	4	5	23	75	106	
	1.9%	2.3%	10.8%	35.2%	49.8%	
Facilities provided to learn the website for new users is satisfactory	3	8	20	74	108	4.30
	1.4%	3.8%	9.4%	34.7%	50.7%	

Figure 2: Questionnaire Results for Learnability

In the learnability factor, a majority of participants also answered 'Agree' or 'Strongly Agree'. The average of all indicators are 4.29, more than the acceptable limit of 3.5. The largest average is on the 'The facilities provided to learn the website for new users is satisfactory' indicator with 4.30, while the smallest is on 'Tutorials and guidelines are effective and easily accessible' with 4.28.

Indicator	Likert Scale					Avg
	1	2	3	4	5	
Website navigation is satisfactory	5	7	33	64	104	4.19
	2.3%	3.3%	15.5%	30%	48.8%	
	3	8	27	74	74	
	1.4%	3.8%	12.7%	34.7%	47.4%	
Website is enjoyable to use	4	8	28	68	105	4.23
	1.9%	3.8%	13.1%	31.9%	49.3%	
	4	6	29	68	106	
	1.9%	2.8%	13.6%	31.9%	49.8%	
Website content is complete	5	4	25	73	106	4.27
	2.3%	1.9%	11.7%	34.3%	49.8%	
	5	4	27	65	112	
	2.3%	1.9%	12.7%	30.5%	52.6%	
	3	7	17	74	112	
Good user interaction support	1.4%	3.3%	8%	34.7%	52.6%	4.33
	2	5	38	77	91	
	0.9%	2.3%	17.8%	36.2%	42.7%	

Figure 3: Questionnaire Results for Operability

In the operability factor, a majority of participants answered 'Agree' or 'Strongly Agree'. The average of all indicators are

4.23, more than the acceptable limit of 3.5. The largest average is on the 'Site content is complete' with 4.30, while the smallest is on 'User interaction support is satisfactory' with 4.17. In the end of the questionnaire, respondents are asked to fill in an open-ended question regarding whether they'd like to come back to Babacucu.com and why, as well as their thoughts on the site.

Table 1: Questionnaire Open-Ended Question Results

Answer	Responses	Percentage
Yes	192	90.1%
No	3	1.4%
Maybe	18	8.5%
Total	213	100%

The ones who said they are interested to return are drawn in by the frequency of product giveaways, while the ones who said maybe cite the accessibility of these giveaways that are usually limited to west java and Java. Those who showed no interest in coming back cited the website being unfriendly to users, lack of giveaway information, and unresponsive customer support as issues.

#### 4.2. Usability Testing Analysis

The following table describes the results of the usability testing done, based on the completion success of the tasks and the time taken to complete the test.

Table 2. Usability Testing Results

Respondent	Task							Time
	1	2	3	4	5	6	7	
1	Success	Success	Success	Success	Success	Success	Success	09:57
2	Success	Success	Success	Success	Success	Success	Success	13:27
3	Success	Success	Success	Success	Success	Success	Success	12:16
4	Success	Success	Success	Success	Success	Success	Success	13:53
5	Success	Success	Success	Success	Success	Success	Success	09:19
6	Success	Success	Success	Success	Success	Success	Success	16:16
7	Success	Success	Success	Success	Success	Success	Success	13:33
8	Success	Success	Success	Success	Success	Success	Success	10:19
9	Success	Success	Success	Success	Success	Success	Success	13:47
10	Success	Success	Success	Success	Success	Success	Success	09:17
11	Success	Success	Success	Success	Success	Success	Success	13:28
12	Success	Success	Success	Success	Success	Success	Success	16:20
13	Success	Success	Success	Success	Success	Success	Success	13:00
14	Success	Success	Success	Success	Success	Success	Success	15:37
15	Success	Success	Success	Success	Success	Success	Success	09:52

Legend: ■ Success  
■ Success, with difficulties

The 15 participants of the usability testing managed to complete all tasks given, though some experienced difficulties along the way. Two participants found difficulties in task one, 'Register Account', running into difficulties filling out birthdate and receiving the confirmation email. One participant had complaints in task two, 'Login' because of the forget password feature, that returned their current password instead of giving the option of making a new password or generating a random one, running the risk of security threats. Three participants found difficulties in task three, 'Search and Sort' because of trouble locating the search bar. Four participants were hindered in task four, 'Request Product', running into difficulties finding the 'Request' button and the page loading that took too long. One participant had trouble in task five, 'Filling out request prerequisites' because of loading issues. Seven participants found difficulties in task six, 'Give Product' because they had difficulties finding the 'Give' button, not clicking the confirmation button on the upload page, and difficulties with uploading photos. Two participants had difficulties in task seven, 'Give Products' because of issues in opening the request notifications and long response times.

#### 4.3. Problems and Comments from Participants

From the dimension of understandability, most participants think that the design of the website is already informative and functional. While the design is consistent, some complain that the design is outdated, there are several items in the interface that aren't used, and the overall design is relatively boring. From the dimension of learnability, participants think that the site is easy to learn as-is, though some features are deemed confusing and some shortcuts are unclear. The filters used to arrange the order of items are also hard to understand. From the dimension of operability, many participants had issues with the website's responsiveness, especially to those who has registered to the site and gave away items, receiving notifications. This is an issue because the notifications cannot be deleted and must be read one by one, and having too many notifications will severely impede the site's responsiveness. Another complaint was about the site's forget password policy where users are given their current passwords instead of either given the option to create a new password or given a randomly generated password.

#### 4.4. Usability Issues Classification

From the results gathered in the usability testing and questionnaire, the usability problems in the Babacucu.com website found by test participants can be classified in four levels in the Rubin and Chisnell classification, ranging from irritants to severe issues. The classification is as follows, based on the severity and its related dimension:

Table 3. Usability Issue Classification

Dimension	Name	Description
Irritant	Understandability	Aesthetic issues in the website design
	Learnability	The search bar that is not easy to find
	Operability	Locations of buttons thought to be not intuitive
Moderate	Learnability	Sorting functions that are hard to understand
	Operability	Response time issues in the site
Severe	Learnability	Insecure forget password procedure
	Operability	Severe performance issues for accounts that has a large number of notifications

#### 4.6 Recommendations for Website Usability Improvement

From the issues found by the usability test, the following recommendations can be given to improve the usability of the website. To solve the design issue, the Babacucu.com website should be redesigned so it would be more modern and more dynamic. The position of the search bar should also be adjusted and made bigger to make it more eye-catching, as well as rearranging the other buttons to stand out more. The sorting function should be done to make understanding it easier and simpler. Site optimizing should be done to reduce the long response times. The issues of the forget password procedure can be solved by giving users who ask for their password a randomly generated password or to make a new password. The issue of severe slowdowns when a user has too many notifications can be alleviated by implementing a feature to mass delete notifications.

## V. CONCLUSION

The conclusions able to be drawn from the research performed are as follows:

1. From the three usability dimensions measured in this research, understandability, learnability, and operability, it is found that user satisfaction based on the findings of this research is good, despite the problems found in the usability testing.
2. The measurements of the three usability dimensions based on the questionnaire where understandability gained a score of 4.23, learnability gained a score of 4.29, and operability with a score of 4.23 showed that the respondents graded the website above the acceptable



limit of 3.5, which means that the usability of the website is good.

3. From the data gathered, the operability factor had the most issues and has several problems able to be categorized as severe, disrupting the site's usability.
4. Based on the evaluation from the scores of usability dimensions gathered, the recommendations that can be given for further development of the Babacucu.com website are as follows: (a). Consider redesigning the website to adjust to the complaints such as the confusing interface and ineffective filter options, especially to deal with the issue of requesting passwords and handling of large numbers of notifications, (b). Give better and more responsive user support to user complaints to keep users coming back.

## REFERENCES

- [1] P. Chirita, "Challenges in Streamlining User Experience Design," in *RoCHI 2011*, Bucharest, 2011.
- [2] R. Lin, H. Li, M. Ma and W. Wang, "Study on User Experience and User Cognitive In Product Design," *Applied Mechanics and Materials*, pp. 174-176, 2013.
- [3] S. Brave and C. Nass, *Emotion in Human-Computer Interaction*, New Jersey: Lawrence Erlbaum, 2003.
- [4] P. Zimmermann, P. Gomez, B. Danuser and S. Schar, "Extending Usability: Putting Affect into the User-Experience," in *User Experience Towards A Unified View*, Oslo, 2006.
- [5] Webtrade, "Creating a Good User "UX" Experience," 30 March 2017. [Online]. Available: <https://www.webtrade.ie/blog/creating-a-good-user-ux-experience.3533.html>.
- [6] M. K. Badini, W. Hussain and O. Sohaib, "User Experience (UX) and the Web Accessibility Standards," *IJCSI International Journal of Computer Science Issues*, pp. 584-587, 2011.
- [7] M. Soegaard, "Usability: A part of the User Experience," July 2017. [Online]. Available: <https://www.interaction-design.org/literature/article/usability-a-part-of-the-user-experience>.
- [8] A. Kucheriavi, "Good UX Is Good Business: How To Reap Its Benefits," 19 November 2015. [Online]. Available: <https://www.forbes.com/sites/forbestechcouncil/2015/11/19/good-ux-is-good-business-how-to-reap-its-benefits/#7d4fdbb74e51>.
- [9] D. E. Baird and M. Fisher, "Neomillennial User Experience Design Strategies: Utilizing Social Networking Media To Support "Always On" Learning Styles," *J. EDUCATIONAL TECHNOLOGY SYSTEMS*, pp. 5-32, 2006.
- [10] R. Rubinoff, "How To Quantify The User Experience," 2004. [Online]. Available: [www.sitepoint.com/print/quantify-user-experience](http://www.sitepoint.com/print/quantify-user-experience).
- [11] J. Mifsud, "The Difference (and Relationship) Between Usability and User Experience," 11 July 2011. [Online]. Available: <http://usabilitygeek.com/the-difference-between-usability-and-user-experience/>.
- [12] K. Lipp, "User Experience beyond Usability," University of Munich Media Informatics Group, Munich, 2012.
- [13] N. Bevan and H. Petrie, *The evaluation of accessibility, usability and user experience*, Boca Raton: CRC Press, 2009.
- [14] J. Spool, "The Difference Between Usability and User Experience," 16 March 2007. [Online]. Available: <https://www.uie.com/brainsparks/2007/03/16/the-difference-between-usability-and-user-experience/>.
- [15] B. Beri and P. Singh, "Web Analytics: Increasing Website's Usability and Conversion Rate," *International Journal of Computer Applications*, pp. 35-38, 2016.
- [16] K. K. Tatari and A. Umar, "Appropriate Web Usability Evaluation Method during Product Development," *Blekinge Institute of Technology*, Ronneby, 2008.
- [17] R. Y. K. Isal, I. S. Junus, H. B. Santoso and A. Y. Utomo, "Usability Evaluation of the Student Centered e-Learning Environment," *International Review of Research in Open and Distributed Learning*, pp. 62-82, 2015.
- [18] L. Fennigkoh, "Visual, Perceptual, and Cognitive Factors in Human-Computer Interface Design and Use," *Biomedical Instrumentation & Technology*, pp. 18-23, 2013.
- [19] P. Isaias and T. Issa, "HCI, Usability, and Environmental Concerns," in *Sustainable Design*, London, Springer-Verlag, 2015, pp. 19-35.
- [20] Usability.gov, "Usability Evaluation Basics," 2017. [Online]. Available: <https://www.usability.gov/what-and-why/usability-evaluation.html>.
- [21] S. Federici and S. Borsci, "Usability evaluation: models, methods, and applications," *International Encyclopedia of Rehabilitation*, 2010.
- [22] R. Safavi, "Interface design issues to enhance usability of e-commerce websites and systems," in *International Conference on Computer Technology and Development*, Kota Kinabalu, 2009.
- [23] e. a. Montero, "Quality models for automated evaluation of web sites usability and accessibility. In International COST294 Workshop on User Interface Quality Model," in *International COST294 Workshop on User Interface Quality Model*, Rome, 2005.
- [24] N. Dehbozorgi and S. Jafari, "Proposing a Methodology to Evaluate Usability of E-Commerce Websites: QUEM Model," *International Journal of Computer Applications*, pp. 39-43, 2012.
- [25] N. Prasad and G. Ramesh, "Usability through Design and its Impact on Reusability," *International Journal of Advanced Research in Computer Science*, pp. 80-84, 2015.
- [26] S. Federici and S. Borsci, "Usability evaluation: models, methods, and applications," *International Encyclopedia of Rehabilitation*, 2010. T. Churm, "An Introduction To Website Usability Testing," 9 July 2012. [Online]. Available: <http://usabilitygeek.com/an-introduction-to-website-usability-testing/>.
- [27] J. Rubin and D. Chisnell, *Handbook of usability testing: How to plan, design, and conduct effective tests*, Indianapolis: John Wiley and Sons, 2008.
- [28] J. Brooke, "SUS: a "quick and dirty" usability scale," *Usability Evaluation in Industry*, 1996.
- [29] J. Lewis, "IBM Computer Usability Satisfaction Questionnaires: Psychometric Evaluation and Instructions for Use," *International Journal of Human-Computer Interaction*, pp. 57-78, 1995.
- [30] Y. M. A. Marreez, M. Wells, A. Eisen, L. Rosenberg, D. Park, F. Schaller and J. T. R. Krishna, "Towards integrating basic and clinical sciences: Our experience at touro university nevada," *The Journal of the International Association of Medical Science Educators*, pp. 595-606, 2013.
- [31] L. Faulkner, "Beyond the five-user assumption: Benefits of increased sample sizes in usability testing," *Behavior Research Methods, Instruments, & Computers*, pp. 379-383, 2003..

# A Measurement Framework for Analyze The Influence of Service Quality and Website Quality on User Satisfaction (Case Study: An IT Service in Jember University)

Beny Prasetyo  
Department of Information  
Systems  
Jember University  
Jember, Indonesia  
beny.pssi@unej.ac.id

Fahrobby Adnan  
Department of Information  
Systems  
Jember University  
Jember, Indonesia  
fahrobby@unej.ac.id

Shinta Amalia Kusuma  
Wardhani  
Department of Information  
Systems  
Jember University  
Jember, Indonesia  
142410101077@unej.ac.id

**Abstract** — The information system is a set tools to present information that has been managed well in order to make it easy and useful for its users. One indicator of the successful implementation of information system is how the end-user satisfaction. User satisfaction can be measured using user satisfaction methods. This study aims to develop a measurement framework to measure the user satisfaction of IT services. The measurement framework will be developed using 3 (three) basic theories such as Servqual by Parasuraman, Webqual by Barnes and Vidgen, and Information System Success Model (ISSM) by DeLone and McLean. The model will be applied to a case study that an IT Service called Sistem Informasi Terintegrasi (SISTER) of the Jember University. This measurements using 100 respondents are students as SISTER's users and will be tested using t testing and GAP analysis. Based on the measurement results, the variable service quality has no significant influence on user satisfaction, and another variable is website quality has a significant influence on user satisfaction. Based on GAP analysis, it's found that the average gap value for service quality variable is -1.12, website quality is -1.00, and user satisfaction is -1.00. It means, the service quality that represents the tangible components, reliability, responsiveness, assurance, and empathy of SISTER's provider according the students perceptions are still not good. In the future, SISTER's provider need to improve the quality of measurement items of indicators of reliability, responsiveness, assurance, and empathy if they want to increase the user satisfaction of SISTER.

**Keywords**— measurement framework; user satisfaction; service quality; website quality; servqual; webqual.

## I. INTRODUCTION

Nowadays, information technology (IT) experienced a very significant development. One of the advancements is the presence of the internet. Internet make the people easy to search, exchange, and share information through various online media and device. According to data from Internet World Stats in 2017 [1], Indonesia is the country with the

third most internet users in Asia after China and India. Based on these reports, in the end of 2017 recorded the internet users in Indonesia reached 143.260.000, where the population of Indonesia's people is 266.764.980. It means, among 53.7% people is active to using the internet daily [1].

One of the utilization of IT in education is the existence of information system to support academic activities at universities or others educational institutions. The information system is a set tools to present information that has been managed well in order to make it easy and useful for its users [2]. According to Doll & Torkzadeh (1988) [3], one indicator of the successful implementation of information system is how the end-user satisfaction. User satisfaction can be measured using user satisfaction methods. There are many methods that can be used to measure user satisfaction of an IT service such as End-User Computing Satisfaction (EUCS), Information System Success Model (ISSM) by DeLone and McLean, Servqual, Webqual and others.

Generally, service quality involves a comparison of expectations with performance perceived of a service [4]. Service quality is a measure of how well the service level delivered matches customer expectations. Delivering quality service means conforming to customer expectations on a consistent basis [5]. Servqual is a model of service quality measurement by Parasuraman (1988) which consists of 5 (five) dimensions including: tangibles, reliability, responsiveness, assurance, and empathy [6]. Servqual is widely used by companies to measure the customer satisfaction of the quality of service.

Webqual is a method for measuring the website quality developed by Barnes and Vidgen in 2000 [7]. Webqual is a development product of Servqual that is widely used for measuring the quality of service. While, Webqual is only can be applied for measure the quality of a website or information system or application. According to Barnes and Vidgen (2000) [7], webqual consists 3 (three) dimensions

including usability, information quality, and service interaction.

According to Parasuraman (1988) [6], the quality of a service can be defined as an overall assessment of the service and generally accepted as overall customer satisfaction. Based on these definitions, it can be concluded the quality of service is an assessment of the ability of service provider to meet the customer expectations. If the customer expectations is greater than the performance of a service provider, it will happen to customer dissatisfaction [8].

The quality of IT services depends on the value that IT service brings to the business of both the IT service provider and its customers, but most IT service providers still do not measure IT services quality in detail [9][10]. Many studies IT service quality measurement that focus is still partial for example, only focus on quality of service or its providers, and there is also focus on measuring the quality of website only.

Based on the above research background, this study aims to develop a measurement framework to measure the user satisfaction of IT services. The measurement framework will be developed using 3 (three) basic theories such as Servqual by Parasuraman [6][11], Webqual by Barnes and Vidgen [7][12], and Information System Success Model (ISSM) by DeLone and McLean [14]. Furthermore, the model will be applied to a case study that an IT Service called Sistem Informasi Terintegrasi (SISTER) of the Jember University. This measurements using 100 respondents are students as SISTER's users and will be tested using t testing and GAP analysis. The t-test was conducted to determine the variable or dimension that significantly influence on user satisfaction, while the GAP analysis is used to determine the level of gap between user expectations and the performance perceived of IT services.

## II. THEORETICAL BACKGROUND

### A. Servqual

Servqual was first designed by Parasuraman, Zeithaml, and Berry (1988) to measure the service quality at the expectation and perceived performance, with the level of service quality determined as the difference score between the expectation and performance perceived [6][11]. The Servqual method consists of 5 dimensions, including [6]:

1. Tangibles  
Tangibles dimension represents physical facilities, adequate equipment and staff ability from service provider.
2. Reliability  
Reliability dimension represents service provider's capabilities to provide the promised services with immediately, accurate, and reliable.
3. Responsiveness  
Responsiveness dimension represents the wish of the staff to help customers, and provide solutions with responsiveness

4. Assurance  
Assurance dimension represents the knowledge, capability, and trustworthiness by the staff, free of the dangers or risk.
5. Empathy  
Empathy dimension represents awareness and good communication by the staff, personalized attention, and understanding what the customer needs.

### B. Webqual

Webqual is a development of the Servqual method. This method is used to measure the quality of website [7]. Webqual has undergone changes and developments from Webqual 1.0 and now is Webqual 4.0 [7]

Webqual 1.0 consists 4 dimensions: usefulness, easy of use, entertainment, and interaction. Webqual 2.0 expands the interaction aspects by adjusting the quality of the service, which is divided into three dimensions: quality of website, quality of information and quality of service interaction. Webqual 3.0 improves the existing deficiencies in Webqual 1.0, and Webqual 2.0 by setting 3 dimensions: usability, information quality and quality of service interaction. The latest version, Webqual 4.0 is based on three areas of research: quality of information (from website), interaction quality and usability (from human computer interaction). Barnes and Vidgen (2003) defines the dimensions of Webqual 4.0 as follows:

- a. Usability  
Usability represents user perception of the quality associated with website architecture such as interface, ease of use and navigation.
- b. Information Quality  
Information quality represents user perception of the quality of the content or website information such as the accuracy of the information, format, relevance, and worth it or not information is displayed.
- c. Service Interaction  
Service interaction represents the ability to provide a sense of security when transacting, having a good reputation, having confidence in providing personal information, providing data and information security confidence and good communication between user and website administrator or helpdesk.

## III. METHOD

### A. Conceptual Framework

As described above, this study aims to develop a measurement framework to measure the level of user satisfaction of IT service users based on service quality perceived and website quality perceived. The measurement framework will be developed using 3 (three) basic theories such as Servqual by Parasuraman [6][11], Webqual by Barnes and Vidgen [7][12], and Information System Success Model (ISSM) by DeLone and McLean [14] which will be

combined into a measurement framework. Measurement framework is illustrated as shown in figure 1. There are three variables in the framework are: (1) Service Quality (X1) and (2) website Quality (X2) as independent variable, and (3) User Satisfaction (Y) as Dependent Variable.

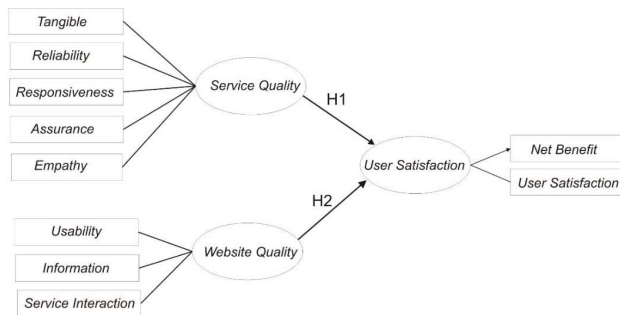


Fig 1. Measurement Framework

Base on the measurement framework, we identified the several hypotheses will be tested on this research. That hypotheses are:

**H1.** Service quality had significantly influence on user satisfaction

**H2.** Website quality had significantly influence on user satisfaction.

### B. Variables and The Operational Definition of Research

The operational definition is a definition that provide that provides an explanation of variables in a measurable form [13]. Based on figure 1, variables, indicators and definition and the reference will be explained in table 1.

Table 1. Operational Definition of Research

Variable	Indicator	Definition	Source
Service Quality	Tangibles	Tangibles represents physycal fascilities, adequate equipment and staff ability from service provider.	[6][15]
	Reliability	Reliability dimension represents service provider's capabilities to provide the promised services with immediately, accurate, and reliable.	[6][15]
	Responsiveness	Responsiveness dimension represents the wish of the staff to help customers, and provide solutions with responsiveness	[6][15]
	Assurance	represents the knowledge , capability, and trustworthiness by the staff, free of the dangers or risk.	[6][15]
	Emphaty	represents awareness	[6][15]

		and communication by the staff, personalized attention, and understanding what the customer needs	
Website Quality	Usability	User perception of the quality associated with website architecture such as interface, ease of use and navigation.	[7][16]
	Information Quality	User perception of the quality of the content or website information such as the accuracy of the information, format, relevance, and worth it or not information is displayed.	[7][16]
	Service Interaction	The ability to provide a sense of security when transacting, having a good reputation, having confidence in providing personal information, providing data and information security confidence and good communication between user and website administrator or helpdesk.	[7][16]
User Satisfaction	User Satisfaction	User satisfaction when using information system	[14]
	Net Benefit	Benefits perceived by users during using information system	[14]

### C. Data Collection

We collect data using a closed questionnaire based on the operational definition table that has been created. We used Non Probability Sampling technique for choosing the sample. Non Probability Sampling does not provide the same opportunity for each element of population to be selected as a sample [17]. A total of 154 students from Jember University which consists 15 faculties became the sample. Sampling is very appropriate beside representing all faculties, the students are also as users of SISTER (Sistem Informasi Terintegrasi) IT service. We distributed the questionnaires by visiting all faculties to meet students. The questionnaire uses likert scale with scale ranges as in table 2.

Table 2. Likert scale of The Questionnaire

Value	Description
1	Very Poor
2	Poor
3	Good
4	Very Good

#### D. Data Analysis Method

After the questionnaire data collected, then the next step is to analyze the data. In this study, we used linear regression method and GAP analysis. Linear regression is used to determine the dimensions or variables of IT services that have significant influence on user satisfaction of IT services. While GAP analysis is to determine the level of gap between user expectation to IT service with actual perceived. The steps of linear regression are:

##### 1. Validity and Reliability Test

Validity and reliability testing of the instruments needs to ensure that the instrument used is valid and reliable. Validity testing used comparison of pearson correlation value with  $r$  table value. While reliability testing using the cronbach's alpha value  $> 0.6$ .

##### 2. T Test

T test is used to partially test the relationship between each independent variables to the dependent variable. T test is often referred as a hypothesized test, because the results of t test are used to answer the hypothesis has been built. An independent variable had significant influence on dependent variable if the significant (Sig.) value  $< 0.05$ .

### IV. RESULTS AND DISCUSSION

#### A. Sample Data

Based on the results of data collection, 154 respondents were obtained. 154 respondents consisting of all faculties in Jember University. Faculty of Computer Science and Faculty of Teacher Training and education become the two faculty with the most respondents which is 24 students or 16% of total sample.

#### B. Linear Regression Analysis

##### 1. Validity and Reliability Testing

Validity testing using pearson correlation coefficient, dimana comparing the value of pearson correlation with  $r$  table value obtained from  $r$  table. Number of samples ( $N$ ) = 154, then degree of freedom ( $df$ ) =  $N-2 = 152$ . Based on  $r$  table, diketahui jika  $df = 152$ , and significance level (2-tailed) 0.05, then  $r$  table value = 0.1330. If the item pearson correlation's value is greater than 0.1330 then it is valid. Hasil lengkap uji validitas dapat dilihat pada tabel 3.

**Table 3.** Validity Testing Results

Dimension	Item Indicator	Pearson-Correlation Value	$r$ Table Value	Result
Service Quality (X1)	Tangible	0.691	0.1330	VALID
	Reliability	0.839	0.1330	VALID
	Responsiveness	0.841	0.1330	VALID
	Assurance	0.722	0.1330	VALID
	Emphaty	0.799	0.1330	VALID
Website Quality	Usability	0.752	0.1330	VALID

(X2)	Information Quality	0.839	0.1330	VALID
	Service Interaction	0.807	0.1330	VALID
User Satisfaction (Y)	User Satisfaction	0.876	0.1330	VALID
	Net Benefits	0.845	0.1330	VALID

Reliability testing aims to test whether the question items in instruments have been reliable and feasible to be a measuring tool. A variable to be reliable if the cronbach's alpha value  $> 0.6$ . Reliability test results for all three variables are described in table 4.

**Table 4.** Reliability Testing Results

Dimension	Cronbach Alpha's Value	Result
Service Quality (X1)	0.798	RELIABLE
Website Quality (X2)	0.826	RELIABLE
User Satisfaction (Y)	0.872	RELIABLE

##### 2. T Test

T test is used to measure the influence of independent variables partially to the dependent variable. According to Sugiyono (2015) [17], terms of an independent variable significantly affects to the dependent variable when:

1. T value  $>$  t table value or significant value (Sig.)  $< 0.05$ , then the variable had significant influence on the dependent variable.
2. T value  $<$  t table value or significant value (Sig.)  $> 0.05$ , then the variable had no significant influence on the dependent variable.

**Table 5.** T Test Results

Dimension	t value	t Table (df = N-3 = 151) $\alpha = 0.05$	Sig.	Result	Hypothesized Result
Service Quality (X1)	0.615	1.655	.539	Significant	Rejected
Website Quality (X2)	8.655	1.655	.000	Significant	Accepted

Based on t test results on table 5, we know that from 2 variables tested, only one variable is Website Quality (X2) had a significant influence on user satisfaction. It can be seen from t value of  $X2 >$  t table value, and Sig value of  $X2 < 0.05$ . It means, based on students perceived as IT service user, they assume that the website quality factor is very influential on their satisfaction when using SISTER. When the Jember University as SISTER's provider improve website quality of SISTER consisting usability, information quality, and service interaction it also increases user satisfaction. Otherwise, if the quality of SISTER's website has decreased, the level of user satisfaction also decreased. Based on table 5, then from the two hypotheses tested only hypotheses 2 (H2) is accepted, and hypotheses 1 (H1) is rejected.

### C. GAP Analysis

GAP analysis to calculate the gap value between expectations and perceived about the overall quality of SISTER. Expectations value is obtained from the maximum value of the measurement instrument, where the maximum value is 4. Perceived value is obtained from the average value of respondents perceptions of each indicator. Gap calculations are performed on each variable. The results of GAP analysis can be seen in table 6.

**Table 6.** GAP Analysis Results

Dimension	Indicator	Value		GAP
		Perceived	Expectations	
Service Quality	Tangible	3.03	4	-0.97
	Reliability	2.90	4	-1.10
	Responsiveness	2.79	4	-1.21
	Assurance	2.92	4	-1.08
	Emphaty	2.75	4	-1.25
	Service Quality (Mean)	2.88	4	-1.12
Website Quality	Usability	3.04	4	-0.96
	Information Quality	3.00	4	-1.00
	Service Interaction	2.97	4	-1.03
	Website Quality (Mean)	3.00	4	-1.00
User Satisfaction	User Satisfaction	2.91	4	-1.09
	Net Benefits	3.08	4	-0.92
	User Satisfaction (Mean)	3.00	4	-1.00

Based on the results of GAP analysis above, the gap value of service quality dimension is -1.12. It means, the average student perception of SISTER service quality is about 2.88 of 4. A GAP analysis results are said to good if the gap value is not more than -1. Thus, based on this results, it can be concluded that the average students has a poor perception on the service quality of SISTER. From the 5 (five) service quality indicators, onlye one indicator that good judgement is tangible where gap value is less than -1. In the future, SISTER's provider need to improve the quality of measurement items of indicators of reliability, responsiveness, assurance, and emphaty if they want to increase the user satisfaction of SISTER.

For the website quality dimension, the gap value is -1.00. It means, that the average students has perceptions of the website quality of SISTER around 3.00. Thus, we can concluded that the average students has a good perception about the website quality of SISTER. From the 3 (three) website quality indicators, all indicators have average GAP is -1.00. It means, currently the user perception on the website quality of SISTER is good enough. But, in the future needs to be improved to be able to reduce the gap value even to 0, where the expectations and perceptions of the quality of website is equal.

For the user satisfaction dimension, the average gap value is -1.00. It means that the average students has

perceptions of satisfaction of SISTER is around 3.00. Thus, based on GAP analysis, it can be concluded that the average students was satisfied overall against SISTER's service.

### V. CONCLUSION

This study resulted in a measurement framework to measure the level of user satisfaction of an IT services by taking a case study is SISTER service of Jember University. The measurement framework developed consists of three dimensions: (1) Service Quality refers to the Servqual method, (2) Website Quality refers to the Webqual method, aand (3) User Satisfaction refers to the Information System Success Model (ISSM) by DeLone and McLean.

That framework is implemented to measure the user satisfaction of SISTER's users. Based on that framework, then proposed 2 hypotheses for this study. Hypotheses 1 is *Service quality had significantly influence on user satisfaction*, hypotheses 2 is *Website quality had significantly influence on user satisfaction*. Based on the measurement results, the variable service quality has no significant influence on user satisfaction, so hypotheses 1 was rejected. Another variable is website quality has a significant influence on user satisfaction, so hypotheses 2 was accepted.

In addition, this study is also calculates gap to determine the quality of SISTER based on comparison of user's perception and user's expectations. Based on GAP analysis, it's found that the average gap value for service quality variable is -1.12, website quality is -1.00, and user satisfaction is -1.00. It means, the service quality that represents the tangible components, reliability, responsiveness, assurance, and emphaty of SISTER's provider according the students perceptions are still not good. In the future, SISTER's provider need to improve the quality of measurement items of indicators of reliability, responsiveness, assurance, and emphaty if they want to increase the user satisfaction of SISTER.

### VI. REFERENCES

- [1] Internet Worldstats, "Internet Usage in Asia, December 2017" [https://www.internetworldstats.com/stats3.htm], Accessed on 19 July 2018.
- [2] Fatta, H. A, "Analisis dan Perancangan Sistem Informasi untuk Keunggulan Bersaing Perusahaan", ANDI, Yogyakarta, 2009.
- [3] Doll, W. J, Torkzadeh, G, "The measurement of end-user computing satisfaction", MIS Quarterly, Vol 12, No 2, 1988, pp. 259-274.
- [4] James J. Jiang, Gary Klein, Neeraj Parolia, Yuzhu Li, "An Analysis of Three SERVQUAL Variations in Measuring Information System Service Quality", The Electronic Journal Information Systems Evaluation, Vol 15, No 2, 2012, pp. 149-162.
- [5] Lewis, R.C, Booms, B.H. "The Marketing Aspecst of Service Quality", American Marketing, 1983, pp. 99-107.
- [6] Parasuraman, A., Zeithaml, V.A., Berry, L.L, "SERVQUAL: A Multiple-Item Scale for Measuring Customer Perceptions of Service Quality", Journal of Retailing, Vol. 64, No. 1, 1988, pp. 12-40.
- [7] Barnes, S, & Vidgen, R, "Web Qual: An exploration of web-site quality", 2000, ECIS Proceedings.



- [8] Barbara, R, Lewis & Vincent W. Michel, "Defining and measuring the Quality of Customer Service", *Marketing, Intelligence & Planning*, Vol.8, No.6, 1990, pp. 11-17
- [9] Spohrer J, Maglio PP, Bailey J, Gruhl D, "Steps toward a science of service systems", *Computer*, Vol. 40, No.1, 2007.
- [10] Lepmets M, Mesquida AL, Cater-Steel, Mas A, Ras E, "The evaluation of the IT service quality measurement framework in Industry", *Global Journal of Flexible Systems Management*, Vol. 5, No.1, 2014, pp.39-57
- [11] Parasuraman, A., Zeithaml, V.A., Berry, L.L., "A conceptual model of service quality and its implications for future research", *Journal of Marketing*, Vol. 49, 1985, pp. 41-50.
- [12] Barnes, S, & Vidgen, R, "Measuring website quality improvements: a case study of the forum on strategic management knowledge exchange", *Industrial Management & Data Systems*, Vol. 103, No. 5, 2003, pp. 297-309.
- [13] Kountur R, "Metode penelitian untuk penulisan skripsi dan tesis edisi revisi", PPM, Jakarta, 2007.
- [14] DeLone, W & McLean, E, "The DeLone and McLean Model of Information System Success: A Ten-Year Update", *Journal of Management Information Systems*, Vol.19, No.4, 2003, pp. 9-30.
- [15] Daniel, Chingang N. & Berinyuy, Lukong P., "Using the SERVQUAL Model to assess service quality and customer satisfaction", UMEA University, 2010.
- [16] Barnes, S, & Vidgen, R, "An Integrative approach to the Assesment of e-Commerce Quality", *Journal of Electronic Commerce Research*, Vol. 3, 2002, pp. 114-127.
- [17] Sugiyono, "Metode Penelitian Kuantitatif dan Kualitatif", Alfabeta, Bandung, 2015.

# Quantitative Strategic Planning Matrix Analysis On The Implementation Of Second Screen Technology

Jarot S. Suroso

Information Systems Management Department,  
BINUS Graduate Program-Master of Information Systems  
Management, Bina Nusantara University,  
Jakarta, Indonesia 11480  
jsembodo@binus.edu

Hitori A. Fatchan

Information Systems Management Department,  
BINUS Graduate Program-Master of Information Systems  
Management, Bina Nusantara University,  
Jakarta, Indonesia 11480  
mas@hitoriaf.net

**Abstract**— A massive technological development requires the company to make strategic changes to compete to survive. In order for companies to survive we need a competitive business advantage to increase Performance Excellence. Similarly, for the PT. Visi Media Asia with its business unit in the field of television, tvOne. In determining and implementing a strategy to compete need to do some analysis. The analytical tool that used in this thesis is IE matrix, SWOT, and QSPM analysis. The internal factor analysis produce the main strength of this company is the company products are loved by people with a score of 0,61. While the company has a major weakness, namely the distribution of technology products is left behind with a score of 0,63. The Merger of internal factors on the company generated an average score of 2,90. External factor analysis (EFAS) generate major opportunities that can be utilized by the company is the development of technology of rapid product distribution with a score of 0,72. While the company's main threat gained from research that people are beginning to switch to digital media than conventional television viewing with a score of 0,63. Merging these two external factors in PT. Visi Media Asia result the average score of 3,12. Based on the SWOT matrix, produced five strategies that can be done by PT. Visi Media Asia on the TV business, tvOne. QSPM processing results is produce the most interesting strategies to be used as a competitive strategy by companies that make technological breakthroughs that can bridging between digital and analog media with TAS value of 7,07.

**Keywords**— *Competitive Strategy, Marketing Strategy, IE Matrix, SWOT, QSPM, Second Screen.*

## I. INTRODUCTION

Television is a medium of information and one way telecommunication since its commercialized in 1920s. Television broadcasting radio waves translated from 54-890 MHz in the form of moving pictures and sound. In line with the times, beginning in the 1980s television can translate digital wave that a wave through the intermediary of electricity supplied by the device such as VCD, DVD, Blu-Ray, etc. Starting in the 2000s a lot of television broadcasting using digital signals by subscribing to a particular provider.

Since this era of digitalization in 2010, the television did not want to miss time, television manufacturers are competing to make smart tv which the audience can interact

with the television (hardware) respectively. Application of the operating system on the television is a smart step manufacturer that television can interact with users, ranging from surfing the Internet, reading gesture user's body, to record the spectacle, take photos, play games, and integrated with other devices such as mobile phones, watches, computers, or smart television other.

But unfortunately, smart television is still not smart enough because it still provides one-way communication, even when connected to the internet, it is because TV broadcasters do not support it. And because of the facilities to make two-way communication is not enough.

Some ways that have been implemented such as a quiz show that using a phone line to communicate with the audience, it is still considered insufficient because only a few viewers who can be contacted, then start in the 2000s, there was an audition of music where the jury is the audience itself by vote the contestants through SMS to the organizers. It is preferred by audience because it can distribute their aspirations to the organizer. Then developed further by making the official account on social media where the audience can communicate as if speaking to a broadcaster, in this way until the time of this thesis, it is very popular.

The development of Internet increasingly attracts the attention of Indonesian people, especially teenagers, they are very close to the device / gadget. As online survey ever undertaken by the Culture Crowd DNA Experts in Indonesia in 2014. A survey of 11,000 students and adolescents aged 13-24 years among the 13 markets find it surprising. In these findings, very significant Indonesian teenagers consume more digital media than other teens in the world. As a result, 69% said they would prefer to ignore the TV than their mobile phone, compared with the global average at 60%. In fact, when they're watching TV, 81% said they always or often using mobile devices when the television is on, compared with a global average of 79%.

Furthermore, the Indonesian people in general spend 181 minutes per day using mobile phones. It is longer than watching TV that only about 132 minutes. In addition, 53% of

respondents said they use their phones to pass the time during commercials are being aired on TV and 40% use mobile phones to stay connected on social media such as Facebook, Path, Twitter, etc. that are not related to what is on TV.

With the second screen technology is expected to screen more interactive spectators to what is being watched and get more information on shows that they are watched, such as watching the previous episode, find out next episode trailers, get behind the scenes information, and so forth. Advertisers are also not hesitate to offer their products because it can target the product information right on target.

## II. LITERATURE REVIEW

Competitive strategy is about being different. This is a deliberate choosing different positions and organize activities that allow you to give a unique value. According to F Rangkuti (2004, p.3), the strategy is a means to an end, while according to Hamel and Prahalad (1995, p.4). Strategi is the action that is incremental (increasing) and continuous and is based on the standpoint of what is expected by the pelanggal future. According to Richard L Daft (2010, p.249) explicitly defines strategy is an action plan that explains about the allocation of resources as well as a variety of activities to deal with the environment, gain a competitive advantage and achieve corporate objectives.

Competitive advantage is what distinguishes one company from another company and give hallmark for the company to meet the needs of the consumer market. Television is a broadcast catcher tool display, in the form of audio-visual and video broadcasting it in broadcasting. The term comes from the Greek tele (distant) and vision (see), so it literally means "look away", because the viewer is away from the TV studio. (Ilham Z 2010: 255).

Meanwhile, according to Adi Badjuri (2010: 39) Television is a media viewing audience once media (audio-visual), which is where people are not just looking at a picture televised, but at the same time hear and digest the narrative of the picture. Based on the description above, it can be concluded that television is one of the electronic mass media to broadcast its broadcast in the form of images or video as well as voice function is to provide information and entertainment to a broad audience.



Fig 1. Second Screen App. when used in watching football broadcast

In the second oxford dictionary screen is a device used while watching television, especially for accessing additional content. Second Screen is the second electronic device used by users to connect into the main screen. The second screen is often used is a smartphone or a tablet, where the special supplementary application allows users to berinteraksi the main screen. Second screen can also be called the Companion screen

## III. METHOD

Research on Competitive Analysis Business Strategy at PT Visi Media Asia if the terms of his approach can be classified as qualitative research. Qualitative research is research that has been limited research goals, but with limitations were revealed as much data about the target of the study (Bungin, 2001: 29). According to their explanations level, this research categorized as a descriptive study. According to Marzuki (2001: 8) states that descriptive research is research done by describing the state of the object or problem and is not intended to take or draw conclusions that are generally applicable. There are six steps required to develop this matrix in QSPM Analysis, they are:

Step 1: Registering a key factor of the strength or weakness of internal and external opportunities or threats in the left column of the matrix. Step 2: Give weight to any external and internal factors. Thickness same as those used in the matrix IFAS and EFAS. Step 3: Checking the second phase (mapping) and identify alternative strategies that can be considered the company to be implemented. Step 4: Setting a value that indicates the appeal of the relative attractiveness of each alternative strategy in a particular cell. Rated appeal are: 1 = not attractive, 2 = somewhat attractive, 3 = quite interesting, 4 = very interesting. Step 5: Calculate the total value of the appeal by multiplying the weight to the value of the appeal. Step 6: Calculating the amount of the total value of the appeal, this amount reveals a strategy which is most interesting in any strategy. The higher the value, the more shows the strategy is attractive and vice versa.

Second Screen Strategy: The strategy centers on the use of smartphones owned by television viewers to expand the

reach of the content of television services so that providers can interact in real time to the audience. Some application on some tv shows, such as: a.Sport Event, b.Drama, c. Game Show, d. Citizen Journalism and e. General Program.

#### IV. RESULTS AND DISCUSSION

Based on the results of questionnaires that have been filled by the VIVA can be seen that there are some internal factors are the weaknesses and strengths as well as external factors are the opportunities and threats in the VIVA group, especially on the business unit tvOne (Table 1).

Table 1. Company's SWOT Mapping

Internal Factors	External Factors
<b>STRENGTHS</b> <ul style="list-style-type: none"> <li>It has a workforce with a good level of education</li> <li>Having advanced technology</li> <li>Products favored people</li> <li>Experience in television media business is quite mature</li> </ul>	<b>OPPORTUNITIES</b> <ul style="list-style-type: none"> <li>Having lots of partner companies</li> <li>The development of rapid content distribution technology</li> <li>Public needs against news higher.</li> </ul>
<b>WEAKNESSES</b> <ul style="list-style-type: none"> <li>Too many employee</li> <li>The geographical location of the manufacturer of less productive workers</li> <li>Distribution technology left behind</li> <li>Lack of exclusive product</li> </ul>	<b>THREATS</b> <ul style="list-style-type: none"> <li>Increased competition similar businesses.</li> <li>Government regulations uncooperative.</li> <li>People are starting to switch to digital media than watching television.</li> </ul>

IFAS (Internal Factors Analysis Summary) matrix, this matrix is based on the identification of the company's internal environmental conditions such as the strengths and weaknesses that are owned by Viva.

EFAS (External Factors Analysis Summary) Matrix is used to determine how much influence from external factors facing the company. EFAS matrix is based on the identification of the external environment such as the opportunities and threats facing the company.

SWOT matrix are concrete steps that should be performed by the company based on the development of IE matrix. Various alternative strategies can be formulated based on the model of SWOT matrix analysis. The main strategies that can be advised there are four kinds, namely: strategy SO, ST, WO and WT. This analysis uses data have been obtained from the matrix of IFAS and EFAS before.

QSPM analysis is the stage of the analysis determining the most competitive strategies of alternatives to the current strategy (Table 2). To simplify the selection of respondents

made the strategy of the 10 strategies that have defined the SWOT matrix will be narrowed down to five options strategies: 1.Empowers partner companies in order to increase the activity or can be absorb labor. 2.Improve and expand product distribution by leveraging existing technology and partner relations firm. 3.Creating a technological breakthrough that bridges between the digital and analog media. 4. Incollaboration with government agencies to produce exclusive content. 5.Empowers partner companies to help improve content distribution technology.

Tabel 2. Strategy Ordered by QSPM Analysis

Rank	Strategy	TAS
1	Creating a technological breakthrough that bridges between the digital and analog media.	7.07
2	Improve and expand product distribution by leveraging existing technology and partner relations firm.	7.03
3	Empowers partner companies to help improve content distribution technology.	6.78
4	In collaboration with government agencies to produce exclusive content.	4.59
5	Empowers partner companies in order to increase the activity or can be absorb labor.	3.97

Based on the results of discussions between the management of PT. Visi Media Asia in cooperation with the vendor PT. XYZ in realizing its strategy, then the application is built tvOne Connect. This application will be a second screen when the audience is or is not watching the tvOne program.

Based on Table 2, the average yield was 0.541 communalities. This value is further multiplied by R2 and rooted. Calculation shows that the value of 0.493 GoF more than 0.36 so that the GoF categorized as large, suggesting that the model is very good (has a high ability) in explaining the empirical data.

The following are the features that are provided tvOne Connect:

##### a.Quiz

This feature allows the viewer tvOne to answer quiz on current events. Each time answering the quiz correctly, then the audience will get a reward in the form of points. Quizzes may include multiple choice questions, and stuffing.

##### b.Poll

This feature allows tvOne to get the audience to give a voice to answer audience questions. Every spectator who answered or to vote will get a reward in the form of points.

#### c. Survey

This feature allows tvOne to provide the questions in accordance with the contents of ongoing events to get reciprocal (feedback) from the audience. This feature may be a reference to research firm to further improve its quality. Every spectator who answers the survey will receive rewards in the form of points.

#### d. Live Streaming

This feature allows the viewer to watch tvOne without using a television device, simply by using the app, viewers can enjoy live broadcasts tvOne. And backed by a live chat feature that allows spectators tvOne at the time that can communicate with each other.

#### e. Video on demand

This feature is a video storage of events tvOne who have been or who are not broadcast OnAir. tvOne connect users can utilize this feature to watch back an interesting event or when the user wants to find an event not to be missed on television.

The performances of Second Screen App Prototypes are shown as Fig 2. Splash Screen, Fig 3. Main Screen, Fig 4. Video on demand list screen tvOne Connect, Fig 5. Video on Demand Screen tvOne Connect, Fig 6. Quiz Screen tvOne Connect, and Fig 7. Login and Register Screen tvOne Connect.



Fig 2. Splash Screen

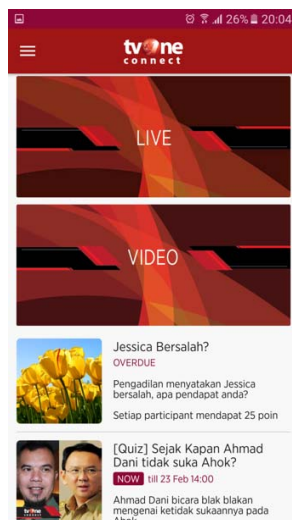


Fig 3. Main Screen



Fig 4. Video on demand list screen tvOne Connect

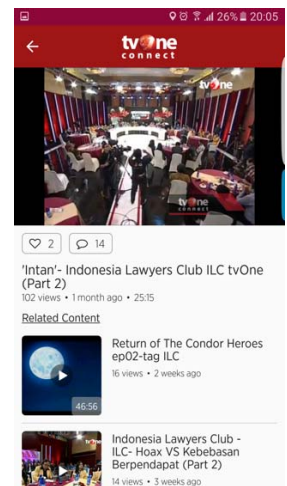


Fig 5. Video on Demand Screen tvOne Connect



Fig 6. Quiz Screen tvOne Connect

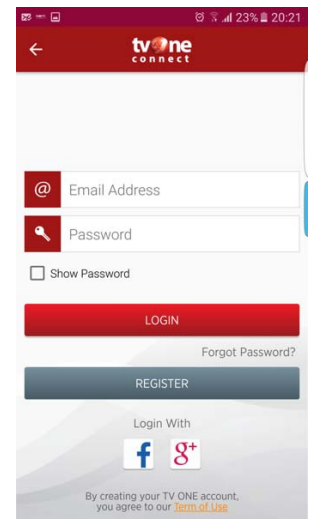


Fig 7. Login and Register Screen tvOne Connect

## V. CONCLUSIONS

1. The results of the analysis of internal and external matrix (matrix IE) showed that the position of tvOne business unit at PT.VISI Media Asia is in cell 2, namely Growth and Build strategy. This result is determined based on the average score of 2.90 on a matrix IFAS and EFAS of 3.12.

2. QSPM analysis results showed that the most competitive strategies to do PT. Visi Media Asia is making a technological breakthrough that bridges between the digital and analog media with the total value amounting to 7.07 Attractiveness Score.

3. Based on the strategy with the greatest TAS value, then the implementation of the second screen technology can be used as a bridge between the analog digital media.

4. Implementation Of Second Screen Technology using Quantitative Strategic Planning Matrix Analysis can be utilised.

## REFERENCES

- [1] Awais, M., & Samin, T. (2012). Advanced SWOT Analysis of E-Commerce. *International Journal of Computer Science Issues*, 569-574. Retrieved from <http://ijcsi.org/papers/IJCSI-9-2-2-569-574.pdf>
- [2] Budiman, T., Suroso, J.S. (2017) *Optimizing IT Infrastructure by Virtualization Approach*. IOP Conference Series: Materials Science and Engineering, Volume 190, Issue 1, 19 April 2017, Article number 012012. ISSN: 17578981. DOI: 10.1088/1757-899X/190/1/012012.
- [3] Denzin, N.K., & Lincoln, Y.S.(2011). Introduction: Entering the field qualitative research. In *Handbook of Qualitative Research* (pp. 1-17)
- [4] Jung, S.C. (2014). The analysis of strategic management of samsung electronics company through the generic value chain model. *International Journal of Software Engineering and Its Applications*, 8(12), 133–142.
- [5] Kothari, C., Kumar, R., & Uusitalo, O.(2014). *Research Methodology*. New Age International.
- [6] Oreski, D. (2012). Strategy development by using SWOT -AHP. *TEM Journal*, 1(4).
- [7] Porter, M. E. (1980). *Competitive strategy: Techniques for analyzing industries and companies*. New York. Porter, M. E. (1996). What is strategy? *Harvard Business Review*, 74(6), 61–78. <https://doi.org/10.1098/rspb.2008.0355>.
- [8] Suroso, J.S. (2016). *Cyber Security for Website of Technology Policy Laboratory*. *Lecture Notes in Electrical Engineering*, Volume 365, 2016, Pages 521-528. ISSN: 18761100. ISBN: 978-981287986-8. DOI: 10.1007/978-981-287-988-2\_58.



# Investment Analysis of Smart Connected Motorbike in Machine to Machine Application in Indonesia

Jarot S. Suroso

Information Systems Management Department, BINUS  
Graduate Program-Master of Information Systems  
Management, Bina Nusantara University, Jakarta, Indonesia  
11480  
jsembodo@binus.edu

Eva Nurul Jamilah

Information Systems Management Department, BINUS  
Graduate Program-Master of Information Systems  
Management, Bina Nusantara University, Jakarta, Indonesia  
11480  
eva.jamiel@gmail.com

**Abstract**— At present the cellular operator is faced with difficult conditions, where the customer growth rate is at its peak. In terms of income, there was also a decline in growth because legacy services (voice & SMS) tended to decline due to threats from OTT. Therefore, a strategy is needed to survive this condition, one of which is to look at the digital market. The digital service business development strategy is carried out to be able to increase the company's revenue through the implementation of Machine to Machine (M2M) services given the promising potential and support of the digital ecosystem. But in reality, the implementation of digital services has not been able to have a significant impact on the company's revenue growth so that a new strategy is needed with a service innovation. This study aims to model M2M digital services into the Smart Connected Motorbike (SCM) service, as well as analyze the service delivery business model in the PT. XYZ so that it is expected to become a new source of income for cellular operators of PT. XYZ. Furthermore, this research will do investment analysis in machine to machine application. Moreover, this research also indicated that this implementation is also feasible to increase the company's earnings.

**Keywords**— Smart Connected Motorbike, Machine To Machine Application, Investment Analysis, Revenue

## I. INTRODUCTION

The global telecommunications industry is currently faced with challenges where the penetration rate of the number of connections for fixed networks has decreased and even tends to be stagnant compared to the penetration rate of the number of connections from mobile networks, especially when comparisons between developed countries and developing countries are due for the construction of a fixed network requires considerable investment costs. This makes the development of mobile networks more of a better choice or alternative related to the required costs and faster time-to-market as shown in Figure 1. In addition, up to June 2014 almost 80% of the world's population has been able to access the 2G mobile network [1].

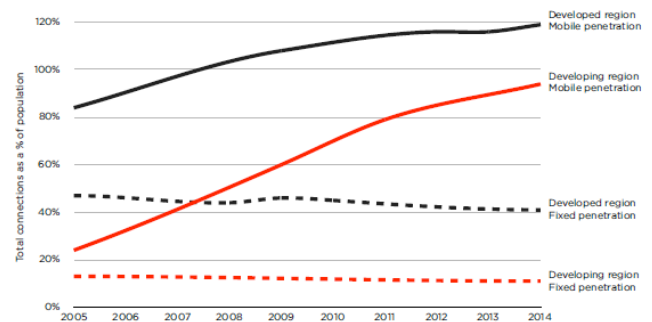


Fig. 1. Penetration of Fixed & Mobile Networks Against Population

This situation also occurred in Indonesia where mobile network penetration grew from 18.76% in 2004 and increased by almost 63% in 2009 which then reached a penetration rate of 91.72% in 2010 or equal to the number of customers of 220 million subscribers. However, even though the penetration of mobile networks can still grow, the most recent problem faced by almost all cellular operators is the fact that there is a decrease in the growth of the number of customers due to the cellular market that has entered the maturity stage or saturation according to the cycle shown in Figure 2. where Indonesia will reach 130% penetration in 2015 with a total of 330 million connections.

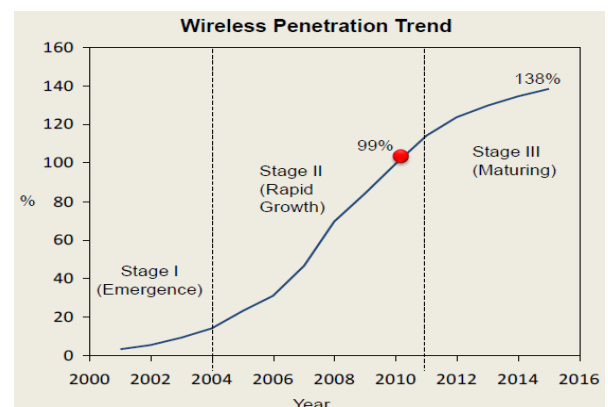


Fig. 2. Mobile Network Penetration Trends reach the Saturation Stage

One of the services included in a digital solution developed by PT. XYZ which has the potential of a rapidly growing business is machine-to-machine (M2M) service technology or also called non-human services. M2M services are services that connect between one device and another device which is usually an application, to exchange information bidirectional and automatically or without human involvement (or with human involvement but very limited) through communication networks so that information from these devices can be utilized by users for the purposes of subsequent business processes, such as for performance and operational efficiency, obtaining equipment statistics, and so on. This research will do investment analysis in machine to machine application. Moreover, this research also indicated that this implementation is also feasible to increase the company's earnings

## II. LITERATURE REVIEW

Figure 3 illustrates simply the wireless M2M service system that is formed by 3 main domains, namely the device (device) along with the sensor module and modem, network (network) that provides connectivity and transmits data, and applications (applications) that process and display data and information

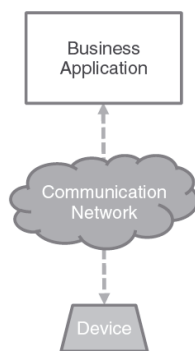


Fig. 3. M2M Service Configuration

Whereas according to the GSMA in explains that IoT is the coordination of several machines, devices or devices connected to the internet network through various network systems. These devices include items that are used daily such as smartphones, tablets and electronic equipment, as well as other machinery such as vehicles, monitors and sensors that are equipped with M2M communication to enable the equipment to send and receive data. In other words, M2M is an integral part of the IoT concept.

From this explanation, the M2M cellular that uses a SIM card is one of the technologies that support the IoT concept as shown in Figure 4. below.

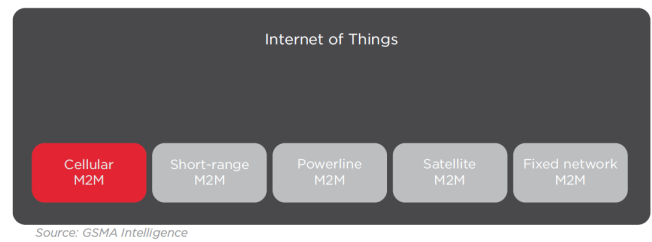


Fig. 4. M2M Position in IoT Coverage

## III. METHOD

At present the telecommunications industry is experiencing a period of stagnation, where the growth in the number of customers has decreased due to the cellular market that has entered the stage of maturity or saturation. Cellular operators globally experienced a downward trend in revenue from legacy businesses such as voice services and SMS (short messaging service), one of the biggest causes of this was the rapid development of OTT (over the top) messaging application services.

As a result of the dynamic changes in the telecommunications business that presents new challenges, the operators of cellular operators are developing several strategies to obtain new sources of income, including the operators of PT. XYZ is by developing innovations in digital services by providing several Value Added Service (VAS) services that rely on existing data services and legacy services.

Therefore PT. XYZ must make different service innovations, integrated by looking at the needs and the market conditions and the technology trends going forward.

In this study, the authors propose a business model for digital services by utilizing M2M technology, namely the Smart Connected Motorbike (SCM) service. This research will use the scientific method approach (scientific method) with the conclusion taking process carried out by deductive method (deductive method) based on the results of the analysis of the business model and the economic feasibility analysis of SCM services. The pattern of research conducted is explanatory and predictive (Figure 5).

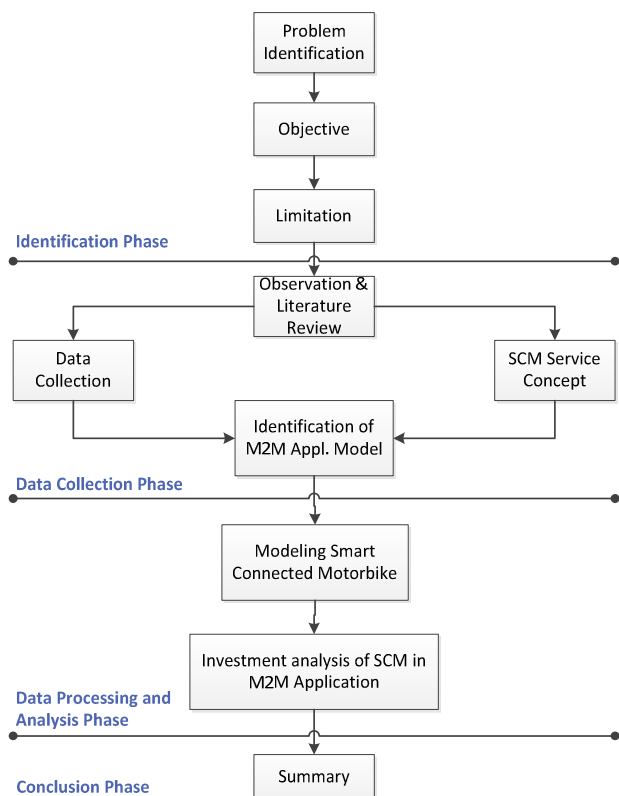


Fig. 5. Framework In The Research

### 3.1. M2M Services System Configuration

To access the features of M2M services for operational purposes, corporate customers and cellular operators can access the platform through desktop web applications (Fig. 6).

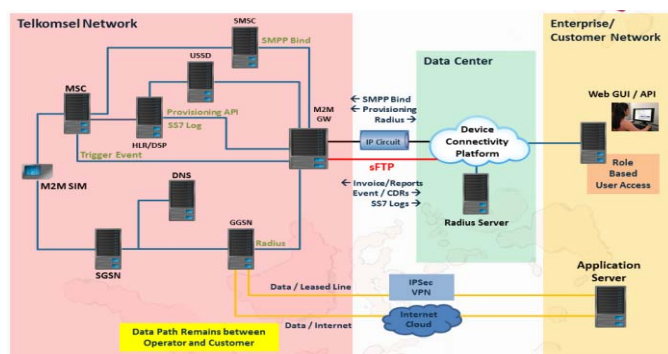


Fig. 6. M2M Platform Configuration System

### 3.2. Smart Connected Motorbike Service Concept

In accordance with the concept of a smart product, a product consists of mechanical and electrical parts, can be transformed into smart connected products (smart connected products) when combined with several other components such as sensors, microprocessors, data storage media, software applications and connectivity, so that it becomes a very

complex system. Apart from that, the concept of smart connected products must have at least 4 (four) new functions or capabilities, namely monitoring, controlling, optimization and independence.

Wireless connection capabilities are able to exchange information between the product and the environment or other systems.

### 3.3. System Architecture of Smart Connected Motorbike Service

This system architecture will enable SCM devices make communication with SCM server and vice versa. In the figure 7 is the architecture model for this service:

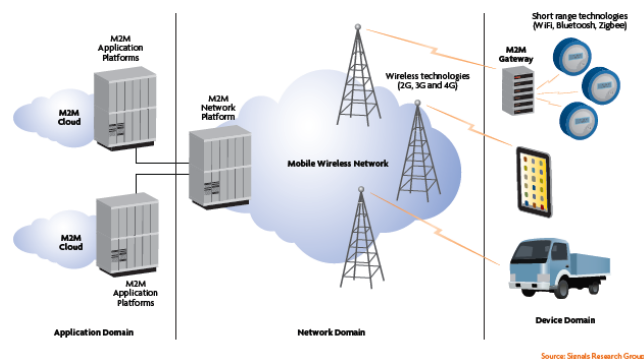


Fig. 7. M2M Service Network Architecture

### 3.4. Business Services M2M

The concept of platform M2M Device Connectivity Platform (DCP) in general which is used to support M2M services is shown in Figure 8. With this platform, the service provider can provide additional services to customers M2M form of several features that may help management of M2M services in addition to providing connectivity services and SIM card.

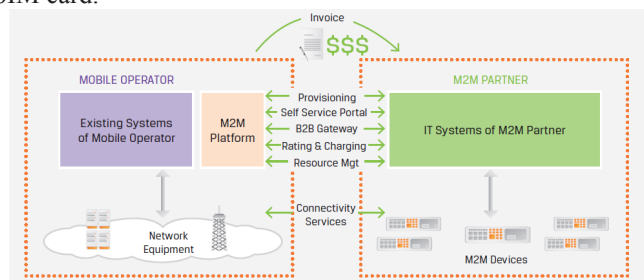


Fig. 8. Configuration Service M2M by M2M Platform DCP .

## IV. RESULTS AND DISCUSSION

### 4.1 Digital Service

There are four (4) digital services become a pillar and developed today to boost the growth of digital ecosystems in Indonesia, namely:

1. Digital Lifestyle, which offers several products concerning the personal segment such as the World Games (mobile game), Payment Gateway Games, Social

- Media Package (social media), media portals, LangitMusik (digital music) and Moovigo (video service portal).
2. Digital Payment & Banking, which offers mobile-based financial services such as mobile banking and mobile e-money.
  3. Digital Advertising, which offers some services targeting corporate customers or SME (small medium enterprise) as LBA (Location Based Advertising), Bulk SMS, SMS Targeted, banners on internet content, Digital Signage and Vending Machine, which is a medium for promoting goods or services to prospective customers
  4. M2M Business, which offers connectivity services to corporate customers for system management Machine-to-Machine (M2M) which runs in the customer's business.

#### 4.2 The concept of Smart Connected Services Motorbike (SCM)

Figure 9. is a simple concept of SCM products use motorcycles that have been installed with the device SCM then connect to the GPS and cellular networks and processed by SCM server, so users can easily take advantage of this service.

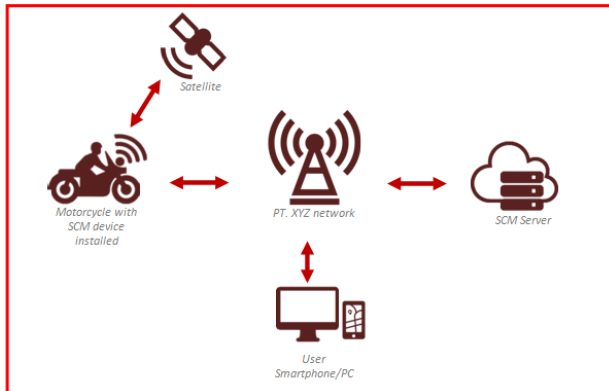


Fig. 9. The concept of Smart Connected Services Motorbike

#### 4.3 Data Estimated Investment Cost (CAPEX)

Data estimated investment cost for the implementation of service delivery Smart Connected Motorbike (SCM) needs to know to determine the economic feasibility of the investment made. The investment costs incurred associated with the implementation of SCM services system is shown in Table 1 below.

**Table 1 –Estimation Data CAPEX Smart Connected Motorbike**

CAPEX	(USD)	(Rupiah)
<b>Device Enabler</b>		
2G Device	20	
3G Device	30	
Gyroscope Sensor	5	
Fuel Pump Connector	2	

<b>Development Cost</b>		
Application Customization		375,660,000
Android		
Application Customization		561,000,000
iOS		
Application Customization		619,240,000
Web Server		
Application Software		104,100,000
License		340,000,000
Professional Services		
<b>Hosting Data Center &amp; Server</b>		
Setup Virtual Machine (VM)		2,000,000
Server		

#### 4.4 Estimated Data Operating Cost (OPEX)

Estimates Data of operational costs (OPEX) on the implementation of SCM services issued regularly shown in Table 2 below.

**Table 2 – Data Estimated Operating Cost (OPEX) Smart Connected Motorbike**

OPEX	(Rupiah)
<b>Hosting Data Center &amp; Server</b>	
Maintenance VM Server	48,000,000
VM Application Server	129,400,000
VM Data Center	185,320,000
<b>Marketing Fee</b>	
Above the line promotion	93,600,000
Below the line promotion	39,000,000

Marketing costs are the costs that used to support pemasaran of SCM services such as promotion Above The Line (ATL) and Below The Line (BTL). Promotion Above The Line (ATL) is the activity of marketing / promotion is usually done by a central management using top-line media in an attempt to form the desired brand image, for example: advertising on television with different versions. ATL nature of the media 'indirect' is about the audience, because it is limited to the reception audience. While the sale Below The Line (Media Line Down) is any marketing or promotional activities conducted at the level of retail / consumer with one of its objectives is to embrace the consumer to be interested in these products, for example: bonus program/gifts, events, coaching consumers and so on other.

#### 4.5 Implementation Model

M2M ecosystem services consist of various businesses, where every business person play at least one business role, could be more. In 2012 the ITU-T (International Telecommunication Union - Telecommunication) recommend the business model for the application of M2M / IOT (ITU-T, 2012). Here's M2M business ecosystem recommended ITU-T as shown in Figure 10.

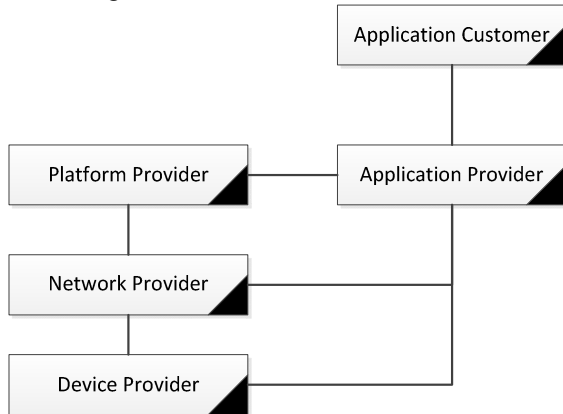


Fig. 10. Bussiness Ecosystem M2M

Here are five (5) business model recommendations issued by ITU-T, as seen in Figure 11.

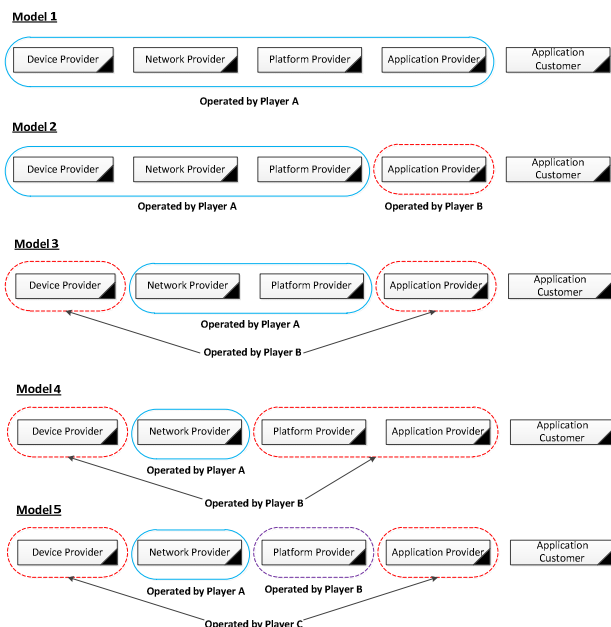


Fig. 11. Bussiness Ecosystem M2M.

#### V. CONCLUSIONS

Based on the analysis that has been done above, we make a conclusion as follow:

1. This study has explained about Investment Analysis of Smart Connected Motorbike in Machine to Machine Application in Indonesia, which obtained data that the

investment in smart connected motorbike application is very good to be done in Indonesia. this is because the growth of motorbikes is very rapid along with the growth of the existing population.

2. Analysis of the business model of this service can also continue to be improved by providing services in the form of added value so as to facilitate motorcycle users in Indonesia to improve security aspects.
3. The organizer can provide subsidies to the selling price of SCM devices so that it is expected for both individual and corporate users.

#### REFERENCES

- [1] Kechiche, Cellular M2M forecasts and Assumptions: 2010-2020, 2014
- [2] BPS. (2014). Data Statistik Transportasi Darat. Badan Pusat Statistik.
- [3] Boswarthick, D., Elloumi, O., & Hersent, O. (2012). M2M Communications: A Systems Approach. John Wiley & Sons Ltd.
- [4] Kechiche, S. (2014, September 23). Cellular M2M forecasts and assumptions: 2010-2020. Retrieved from GSMA Intelligence: <https://gsmaintelligence.com/research/2014/09/cellular-m2m-forecasts-and-assumptions-2010-2020/446/>
- [5] Internal Report. (2015). Digital Service Revenue Report. PT. XYZ.
- [6] Porter, M. E., & Heppelmann, J. E. (2014). How Smart, Connected Products Are Transforming Competition. Harvard Business Review.
- [7] Osterwalder, A., & Pigneur, Y. (2010). Bussiness Model Generation. New Jersey: John Wiley & Sons, Inc.
- [8] Meredith, J. R., & Mantel, S. J. (2009). Project Management: A Managerial Approach 7th Edition. John Wiley & Sons, Inc.
- [9] Grant, R. M. (2010). Contemporary Strategy Analysis. 7th ed. John Wiley & Sons.
- [10] Sullivan, W. G., Wicks, E. M., & Luxhoj, J. T. (2006). Engineering Economy (13th ed.). New Jersey: Pearson Education.
- [11] Sullivan, W. G., Wicks, E. M., & Luxhoj, J. T. (2006). *Engineering Economy (13th ed.)*. New Jersey: Pearson Education.
- [12] Suroso, J.S., Jamilah, E.N. (2017) *Implementation Model of Smart Connected Motorbike Service: An Engineering Economic Analysis of Machine to Machine Application*. Proceedings - 11th 2016 International Conference on Knowledge, Information and Creativity Support Systems, KICSS 2016. 16 June 2017, Article number 7951420. ISBN: 978-150905130-4.
- [13] Sythoff, J. T. (2015). *Cellular M2M Connections - An Analysis of Growth Drivers, Market Segments and Operator Approaches*. London: Pyramid Research, Inc. Retrieved 2015, from dominicgiles.com: <http://dominicgiles.com/swingbench.html>
- [14] Taba, A. S. (2014, December 1). *Kontroversi Layanan OTT*. Retrieved November 29, 2015, from Selular: <http://selular.id/insight/2014/12/kontroversi-layanan-ott/>
- [15] Wyman, O. (2015). Connected Cars & Its New Biz Models: An Opportunity for the French Automotive Industry. Marsh & McLennan.



# Efficiency and Reliability Performance's of the Bioinformatics Resource Portal

1<sup>st</sup> Edy Budiman

dept.of informatics engineering  
universitas mulawarman  
Samarinda, Indonesia  
edy.budiman@fkti.unmul.ac.id

2<sup>nd</sup> Haeruddin

dept.of mathematics education  
universitas mulawarman  
Samarinda, Indonesia  
haeruddin.unmul@gmail.com

3<sup>rd</sup> Andi Tejawati

dept.of informatics engineering  
universitas mulawarman  
Samarinda, Indonesia  
andi.tejawati@gmail.com

**Abstract**—The paper discusses the resource portal of the Borneo's Biodiversity Information System (BBIS) from the point of view of the characteristics of efficiency and reliability performance. Data collection methods and tools use the observation approach that simulates 100 simultaneous users, logging every 10 seconds between random clicks on the URL site. Efficiency testing results based on 27 recommendations from Page-Speed instruments and 19 recommendation parameters from YS-low, obtained average scores on grade A. However, there were still 6 parameters related to system resource issues with score is grade F. Reliability test results referring to Jacob Nelson's equation approaches and Standard TELCORDIA reference. The result shows that the value of  $R = 0.988967$  or the percentage of the reliability value is 98.89% and  $r = 0.011$  or the error rate is 1.1%. The user threshold test results are found when the number increases to 500 users. The success of efficiency testing parameters significantly affects the percentage of performance reliability.

**Keywords**—biodiversity, performance, efficiency, reliability.

## I. INTRODUCTION

Biological diversity (biodiversity) can be translated as all living things on earth, including all plant species, animals and microbes. The species within biodiversity relate to each other and need other to grow or bloom form a living system [1].

Indonesia as an archipelagic country has 13,466 islands, scattered along the tropical equatorial line [2]. One of the largest islands is Borneo known as Kalimantan for the Indonesian territory with high rainfall and humidity, geological events, and geography, Indonesia has many rare plants and species and endemic species that can live and mature.

The greatest challenge in biodiversity management is to maintain a balance between sustainability (ecological) and sustainable benefits (economic). This challenge is not easy to deal with. This is because most of the biodiversity is a cross-border administrative resource and is managed by various parties/sectors. There is considerable pressure from utilization forest and forest products beyond their carrying capacity. Biodiversity is now diminishing on an alarming scale. Species by species disappear faster than the discovery of new species, and also the potential value of the creature for the future just disappears [3],[4], [5].

Regard this, it requires follow-up in the form of data handling and monitoring activities so that the sustainability of the biodiversity of the plant can be maintained for its sustainability, then developed a biodiversity information system of plants in the rain forest of Kalimantan-Borneo in

an effort to integrate the data that has been collected from various sources.

The Borneo Biodiversity Information System (BBIS) that has been built [5], [6], is an open source information system of Borneo island information management systems. The modules developed in BBIS have been able to accommodate all data management and information on biodiversity of plants in the rain forest of Kalimantan, from front desk process to back office (transaction & interaction enabler).

According to Riaz Ahamed's research [7], "Software testing is a critical element of software quality assurance and represents the ultimate review of specification, design and coding. Software testing is the process of testing the functionality and correctness of software by running it. Software testing is usually performed for one of two reasons: defect detection, and reliability estimation" [7].

Further explains that, the problem of applying software testing to defect detection is that software can only suggest the presence of flaws, not their absence (unless the testing is exhaustive) [7]. The problem of applying software testing to reliability estimation is that the input distribution used for selecting test cases may be flawed. The key to software testing is trying to find the modes of failure - something that requires exhaustively testing the code on all possible inputs [7].

One of the software quality benchmarks is ISO 9126 [8], created by the International Organization for Standardization (ISO) [9] and International Electrotechnical Commission (IEC). ISO 9126 defines the quality of software products, models, quality characteristics, and related metrics used to evaluate and define the quality of a software product. The ISO 9126 standard has been developed in an attempt to identify key quality attributes for computer software. Quality factors according to ISO 9126 include Six Quality Characteristics, the model itself is characteristics functionality, reliability, usability, efficiency, maintainability, and portability [10], [11], [12].

This paper will discuss the performance evaluation of a BBIS that focuses on the efficiency and reliability characteristics in software capabilities to maintain certain performance levels, when used under certain conditions, and the efficiency in software capabilities to deliver performance as appropriate and relative to the amount of resources used at the time conditions.



## II. BACKGROUND AND RELATED WORK

### A. Borneo Biodiversity Information System

The development of plant biodiversity information systems in the Borneo island rainforest has been discussed and developed by various approaches and methods, research that has been discussed about; development of plant database management system that discusses plant name taxonomy referring to International Code of Botanical Nomenclature (ICBN) [13], Ethnobotany database: Exploring diversity medicinal plants of Dayak tribe Borneo [14]. Biodiversity information system: Tropical rainforest Borneo and traditional knowledge ethnic of Dayak [15]. Borneo biodiversity in [5], the paper about is Exploring endemic tree species and wood characteristics. The author has also discussed in [6] about the implementation of the six concepts of association owned by Eloquent ORM (i.e. One to One, One to Many, Many to Many, Many Through Many, Polymorphic Relation, and Many to Many Polymorphic Relation) [6].

### B. Network Performance Testing

According to [16], performance tests are used to test each part of the webserver or the web application to discover how best to optimize them for increased web traffic, this is done by testing various implementations of single web pages to check what version of the code is the fastest. This type of test is run without requesting page images in order to concentrate the testing on the code-script and itself [16].

The server performance issues and availability of existing networks in the Borneo area, we have also analyzed and discussed them in previous research, among others; the paper [17], the study was conducted using a mobile device and implemented in seven districts and four points in every district in the city of SAMARINDA, East Borneo. Measurements using the standard quality of TIPHON with some parameters such as end-to-end delay, jitter, packet loss probability and throughput [17]. The paper [18] about the broadband quality of service experience measuring mobile networks from consumer perceived, this paper provides an overview of the quality of service experience from the viewpoint of the customer's perceived of mobile broadband services.

The user perceptions of mobile internet services performance in Borneo on the [19], the study tries to assess the Quality of Service (QOS) for mobile internet services in the ways assessment involves identifying user perception to assess consumer experience of the mobile internet services. The information from the survey pertains to the awareness levels among consumers regarding their data plans overall satisfaction, Indonesia Telecommunication Regulatory Authority (BRTI) and its regulations on QOS [19]. The network performance measurement related to the content of the application has been discussed in the paper [20], this paper discussion of performance rate for implementation of mobile learning in network. And the paper [21] about Mobile learning: Visualizing contents media of data structures course in mobile networks [21].

## III. METHODOLOGY

### A. Data Collection Methods and Tools

The data collection method used is the observation technique, which performs the measurement and direct test of the field using a measuring instrument to test the performance capabilities of BBIS applications that have been developed. The performance characteristic and data collection tool used as follows:

### B. Testing for Characteristic Efficiency

This test uses the GT-Metrix [22], measuring tool developed by GT.net, a Canadian company, which aims to help customer hosting to see website performance, is one tool to check website speed. This tool uses a combination of Google Page-Speed Insights and YS-low to generate value and recommendations.

The basic parameter used is the document size, http request. So as to obtain a predetermined Grade from the measuring instrument. After getting score from test result then calculated percentage with formula of percentage and interpretation according to recommendation of Yahoo Developer Network [23] shown in TABLE I.

TABLE I. DATA ANALYSIS OF GRADE EFFICIENCY TESTING [23]

Score	Grade
A	$90 \leq S \leq 100$
B	$80 \leq S < 90$
C	$70 \leq S < 80$
D	$60 \leq S < 70$
E	$50 \leq S < 60$
F	$0 \leq S < 50$

<sup>23</sup>source: <http://yslow.org/ruleset-matrix/>

### C. Testing for Characteristic Reliability

This test uses the Webserver Stress Tool developed by Paessler AG [24]. Webserver Stress Tool simulates the HTTP requests generated by hundreds or even thousands of simultaneous users, we can test web server performance under normal and excessive loads to ensure that critical information and services are available at speeds end-users expect [24], [25].

The parameters used are failed session, failed pages, and failed hits. The "equation (1)" for calculating the reliability values according to the Nelson [23] model is as follows:

$$R = \frac{n}{n-f} = 1 - \frac{f}{n} = 1 - r \quad (1)$$

Where:  $R$  = Reliability  
 $n$  = Number of workload units  
 $f$  = Total number of failures  
 $r$  = The failure rate

## IV. TESTING AND ANALYSIS

Borneo's Biodiversity Information System (BBIS) was developed using the PHP Framework LARAVEL, which has a Model View Controller design pattern, and Eloquent Object Relational Mapping that can store biodiversity data of plants with the application of six relationship concepts. Implementation of development result Borneo's Biodiversity information system online can be accessed site

URL: <http://borneodiversity.org/>, the BBIS main menu view can be seen in “Fig. 1”.

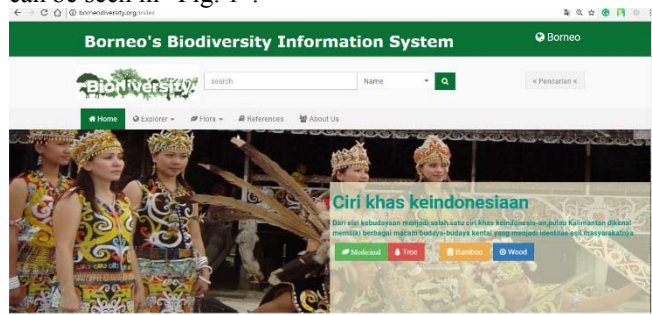


Fig. 1. Webpage of borneodiversity.org

To date, BBIS has stored 233 records of Medicinal Plants, 1482 records of Tree species, 86 records of Wood species and characteristics, 80 records of Bamboo species.

#### A. Analysis of Efficiency Testing

Based on the analysis and calculation of efficiency testing of website:borneodiversity.org using GT-Metrix tool, then the Grade and score as shown in TABLE II for recommendation of Page-Speed and TABLE III for recommendation of YS-low.

TABLE II. PERFORMANCE SCORE OF PAGESPEED PARAMETERS [22]

Recommendation	Grade/Score	Type
Serve scaled images	F (0)	images
Optimize images	F (0)	images
Leverage browser caching	F (0)	server
Minify JavaScript	E (52)	JS
Avoid bad requests	A (92)	content
Defer parsing of JavaScript	A (94)	JS
Minify CSS	A (98)	CSS
Minify HTML	A (98)	content
Specify a character set early	A (99)	content
Specify image dimensions	A (99)	images
Specify a Vary: Accept-Encoding header	B (88)	server
Avoid landing page redirects	A (100)	server
Enable GZIP compression	A (100)	server
Enable Keep-Alive	A (100)	server
Inline small CSS	A (100)	CSS
Inline small JavaScript	A (100)	JS
Minimize redirects	A (100)	content
Minimize request size	A (100)	content
Optimize the order of styles and scripts	A (100)	CSS/JS
Put CSS in the document head	A (100)	CSS
Serve resources from a consistent URL	A (100)	content
Specify a cache validator	A (100)	server
Combine images using CSS sprites	A (100)	images
Avoid CSS @import	A (100)	CSS
Prefer asynchronous resources	A (100)	JS
Avoid a character set in the meta tag	A (100)	content
Remove query strings from static resources	A (100)	content

Based on the analysis and performance test results for Page-Speed presented in TABLE II, the average percentage range of 92-100% (grade A) is available, there are 3 recommendation metrics that are still 0 with grade F (*Serve scaled images*, *optimize images*, and *Leverage browser caching*), and for *Minify JavaScript* metrics obtained 52% value (grade E). So it can be said that the software has a very high efficiency value, from the score obtained then the quality of the software developed from the side of the measurement Page-Speed efficiency mostly get "grade A" if adjusted to the rules recommended [23].

TABLE III. PERFORMANCE SCORE OF YSLOW PARAMETERS [23]

Recommendation	Grade/Score	Type
Add Expires headers	F (0)	server
Use a Content Delivery Network (CDN)	F (0)	server
Make fewer HTTP requests	D (60)	content
Use cookie-free domains	F (0)	cookie
Minify JavaScript and CSS	C (70)	CSS/JS
Avoid HTTP 404 (Not Found) error	A (95)	content
Reduce DNS lookups	A (95)	content
Compress components with GZIP	A (100)	server
Avoid URL redirects	A (100)	content
Make AJAX cacheable	A (100)	JS
Remove duplicate JavaScript and CSS	A (100)	CSS/JS
Avoid Alpha-Image-Loader filter	A (100)	CSS
Reduce the number of DOM elements	A (100)	content
Use GET for AJAX requests	A (100)	JS
Avoid CSS expressions	A (100)	CSS
Reduce cookie size	A (100)	cookie
Make favicon small and cacheable	A (100)	images
Configure entity tags (ETAGS)	A (100)	Server
Make JavaScript and CSS external	(n/a)	CSS/JS

Based on the analysis performance results for YSlow presented in TABLE III generally obtained average percentage range 95-100% (grade A). There are 3 recommendations that are still worth 0 with grade F that is add expires headers, use a CDN and use cookie-free domains, and minify JAVASCRIPT and CSS are 70% (grade C) and Make fewer HTTP requests are 60% (grade D). So it can be said that the software has an average value for testing High category YSlow.

From the score obtained, the software quality developed from the efficiency measurement side (Page-Speed and YSlow) generally get "Grade A", it is stated that the performance analysis of Borneo Biodiversity information system inefficiency characteristics has passed the testing.

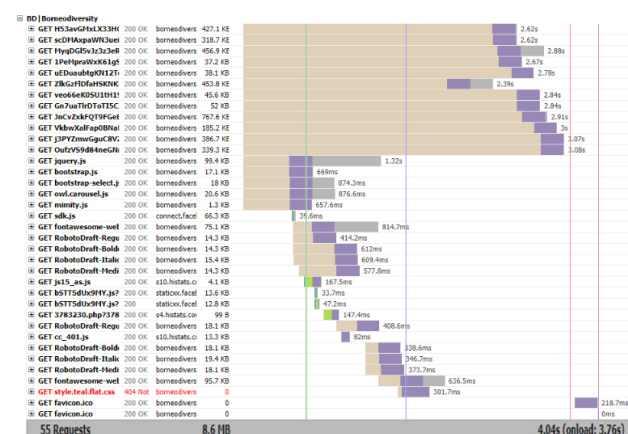


Fig. 2. Response-time load webpage of borneodiversity.org

The Response-time limits to keep the user's attention can wait for the load of the web page is 10s [26]. Whereas according to [27] the best load time a website page is less than 3 second, for an acceptable load time of less than 10s.

The Graph of the response-time measurement shown in “Fig. 2”, obtained the average time load of about 4.04s (onload: 3.76s) with the number of requests of 55 and with the data of 8.6 MB. Based on the data, the time load can be stated to be "accepted" by referring to recommendations J Nielsen [26] for an acceptable time load of fewer than 10s.

### B. Analysis of Reliability Testing

Reliability testing is done using Webserver Stress Tool version 8.0.0.1010 Enterprise Edition (Freeware), with test scenario following [16], as:

- Test Type: CLICKS (run test until 10 clicks per user), the test is finished when each user has initiated the given number of clicks. Clicks tests to test specific URL sequences, on this test URL: <http://borneodiversity.org/>
- User Simulation: 100 simultaneous users – 10s between clicks (Random)
- Logging Period: Log every 10s
- URL Sequencing: Users select URL for each click randomly
- Browser Simulation: HTTP Request Timeout: 120s
- System: Windows 8/2012 V6.2 (Build 9200), CPU Proc. Lev. 686 (Rev. 19971) at 2400 MHz,
- Memory: 445 MB available RAM of 4182 MB total physical RAM, 2852 MB available *Page-file*.

Based on testing the performance of the URL that has been done. The graphs of click time and errors per (URL) in “Fig. 3”, and click time, Hits/s, users / s (all URLs) are shown in “Fig. 4”.

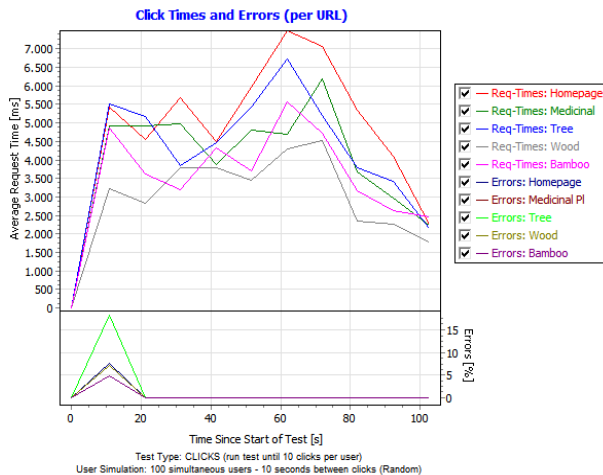


Fig. 3. Click time and errors per (URL)

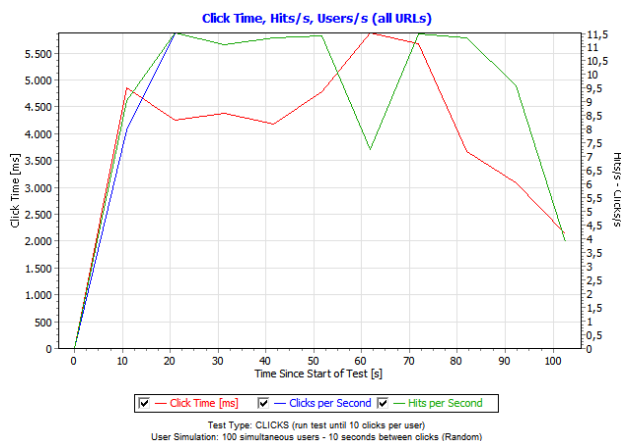


Fig. 4. Click time, hts/s, users/s (all URLs)

Furthermore, the resulting measurement value as presented in TABLE IV.

TABLE IV. WEBPAGE PERFORMANCE RESULTS PER URL WITH 100 SIMULTANEOUS USERS

Page (URL)	Clicks	Errors	Errors (%)	Time Spent (ms)	Avg. Click Time (ms)
Homepage	196	1	0,51	1.067.967	5.477
Medicinal Plant	220	4	1,82	980.660	4.540
Tree	200	4	2,00	923.998	4.714
Wood	204	1	0,49	665.737	3.279
Bamboo	177	1	0,56	689.501	3.918
Sum	997	11	1,1	865.572	4.385

TABLE IV presents the data of simulation result of web page performance with predefined user number, obtained by measurement value of 997 successful clicks with 11 errors, Avg. click times with value between 3.279ms – 5.477ms and Time spent with value between 665.737ms – 1.067.967ms, mean value from Avg. click times is 4,385ms and the mean value of Time spent is 865,572ms.

Calculation of reliability value can be obtained by “equation (1)”, as follows:

$$R = 1 - \frac{f}{n} = 1 - \frac{11}{997} = 1 - 0,011 = 0,988967$$

The result shows that the value of  $R = 0.988967$  or the percentage of reliability value is 98.89% and  $r = 0.011$  or the error rate is 1.1%.

According to TELCORDIA standard that has been discussed by A Asthana and Jack O [28], software reliability success is 95% or 0.95, so based on the benchmark, and from the value of  $R$  obtained then testing Reliability of Borneo's Biodiversity Information System can be stated "accepted" according to TELCORDIA standards.

Additional testing is done to determine the level of ability and threshold of the user on the system, conducted simulation testing by raising the value on the number of users. and the threshold test results are found when the number of users is 500. The test results are presented in TABLE V.

TABLE V. WEBPAGE PERFORMANCE RESULTS PER URL WITH 500 SIMULTANEOUS USERS

Page (URL)	Clicks	Errors	Errors (%)	Time Spent (ms)	Avg. Click Time (ms)
Homepage	958	955	99,69	8.841	2.947
Medicinal	968	965	99,69	9.724	3.241
Tree	1.018	1.014	99,61	15.602	3.901
Wood	1.026	1.020	99,42	18.589	3.098
Bamboo	1.026	1.023	99,71	9.996	3.332
Sum	4996	4977	99,624	12.550	3.303

Reliability value calculation results for 500 users, in TABLE V, the percentage of error rate of 99.624%. Avg. click time of 3.303ms.

### C. Evaluation of Efficiency & Reliability Testing

Borneo's Biodiversity Information System performance analysis from testing of efficiency characteristics (recommendation of Page-Speed and YSlow) which relate to the ability of the software to provide appropriate performance to the number of resources used in certain circumstances still need to be repaired. Such as serve scaled and optimize images, make fewer HTTP requests and use

cookie-domain, minify JavaScript/CSS, use a content delivery network (CDN), and leverage browser caching.

Aspects of reliability characteristics, software capability of the BBIS to maintain its performance when used under certain conditions, by simulating testing on the number of users and click on webpage - URLs randomly. Reliability analysis results show that the software capability of BBIS with 100 user simulation is the highest limit of system capability to the number of user resources, it is highly influenced by the aspect of efficiency characteristics with very low parameter scores, for example on Serve scaled images and optimize images that require high time on-load

## V. CONCLUSION

Borneo's Biodiversity information systems are one of the enterprise-scale systems that represent open-source plant-based taxonomy data, developed by the research team in a follow-up effort to manage the digital inventory of biodiversity data contained in the Rainforest of Borneo Island in terms of its monitoring can be preserved sustainability. The system has a large data content, with diverse types and characteristics of plants, of course, will affect system performance functionality in terms of data accessibility, use of resources, level of efficiency and reliability issues.

The amount of data capacity, writing long and repeatable script code, will have a direct impact on the request, Add Expires headers, and Use cookie-free domains will create long system load time and limited number of users in accessible data. The efficiency aspect must be properly addressed. Inefficient resource use can cause software performance to be sluggish.

## ACKNOWLEDGMENT

This research was financial support by the Directorate General of Research and Development Strengthening of the Ministry of Research, Technology and Higher Education of the Republic of Indonesia in the Beginner Lecturer Research (PDP) scheme. Thanks to the Institute of Research and Community Service or LPPM MULAWARMAN University.

## REFERENCES

- [1] LIPI, *Kekinian Keanekaragaman Hayati Indonesia* [Present status of Indonesian Biodiversity], Kerjasama Kementerian PPN/BAPPENAS, KLH dan LIPI. Indonesian Institute of Sciences knowledges Press. Bogor, 2014.
- [2] Tanzil N, Lembar-Lembar Pelangi: membangun mimpi anak di timur Indonesia, Rb Publishing, 2016.
- [3] BAPPENAS, Indonesia Biodiversity Strategy and Action Plan 2003-2020", IBSAP Dokumen Nasional, Ministry of National Development Planning, Republic of Indonesia, Jakarta, 2004
- [4] BAPPENAS, Indonesia Biodiversity Strategy and Action Plan 2015-2020", IBSAP Dokumen Nasional, Ministry of National Development Planning, Republic of Indonesia, Jakarta, 2016.
- [5] Hairah, U., Tejawati, A., Budiman, E., and Agus, F. (2018). Borneo biodiversity: Exploring endemic tree species and wood characteristics. In Proceeding - 2017 3rd International Conference on Science in Information Technology: Theory and Application of IT for Education, Industry and Society in Big Data Era, ICSITech 2017, (Institute of Electrical and Electronics Engineers Inc.), pp. 435-440. DOI:10.1109/ICSITech.2017.8257152
- [6] Budiman, E., Jamil, M., Hairah, U., Jati, H., and Rosmasari, "Eloquent object relational mapping models for biodiversity information system", 4th International Conference on Computer Applications and Information Processing Technology 2017, CAIPT 2017, in Conf. Rec. IEEE Explore 2018, Institute of Electrical and Electronics Engineers Inc., 2018, pp. 1-5. DOI: 10.1109/CAIPT.2017.8320662.
- [7] Ahamed, S. S. "Studying the feasibility and importance of software testing: An Analysis." arXiv preprint arXiv:1001.4193, 2010. DOI: https://arxiv.org/abs/1001.4193.
- [8] ISO/IEC Standard No. 14598: Information technology – Software product evaluation; Parts 1–6. International Organization for Standardization (ISO) / International Electrotechnical Commission (IEC), Geneva, Switzerland, 1999-2001.
- [9] Ananiadou, S., Thompson, P., Thomas, J., Mu, T., Oliver, S., Rickinson, M., Sasaki, Y., Weissenbacher, D. and McNaught, J., "Supporting the education evidence portal via text mining". Philosophical Transactions of the Royal Society of London A: Mathematical, Physical and Engineering Sciences, vol. 368(1925), 2010, pp.3829-3844.
- [10] ISO/IEC Standard No. 9126: Software engineering – Product quality; Parts 1–4. International Organization for Standardization (ISO) / International Electrotechnical Commission (IEC), Geneva, Switzerland, 2001-2004.
- [11] Neukirchen, H., Zeiss, B. and Grabowski, J., An approach to quality engineering of TTCN-3 test specifications. International Journal on Software Tools for Technology Transfer, vol. 10(4), 2008, p.309.
- [12] Zeiss, B., and Vega, D. Applying the ISO 9126 quality model to test specifications. Software Engineering 2007 105, 231–244, 2007.
- [13] Budiman, E., and Alam, S.N., "Database: Taxonomy of plants Nomenclature for borneo biodiversity information system"2nd International Conference on Informatics and Computing, ICIC 2017, in Conf. Rec. IEEE Explore 2018, Institute of Electrical and Electronics Engineers Inc, 2018, pp. 1-6. DOI: 10.1109/IAC.2017.8280642.
- [14] Haeruddin, Johan, H., Hairah, U., and Budiman, E. Ethnobotany database: Exploring diversity medicinal plants of dayak tribe borneo. In International Conference on Electrical Engineering, Computer Science and Informatics (EECSI), Institute of Advanced Engineering and Science, 2017, pp. 120–125. DOI: 10.1109/EECSI.2017.8239094.
- [15] Dengen, N., Budiman, E., Widians, J.A., Wati, M., Hairah, U., and Ugianto, M., Biodiversity information system: Tropical rainforest borneo and traditional knowledge ethnic of dayak. Journal of Telecommunication, Electronic and Computer Engineering, vol. 10. No. 1-9, 2018, pp. 59-64.
- [16] Paessler, "Webserver Stress Tool", web stress manual: Introduction: Testing Basics, The Network Monitoring Company, p.7. Available at: https://download-cdn.paessler.com/download/webstressmanual.pdf
- [17] Budiman, E., and Wicaksono, O., Measuring quality of service for mobile internet services. Proceeding - 2016 2nd International Conference on Science in Information Technology, ICSITech 2016: Information Science for Green Society and Environment, Institute of Electrical and Electronics Engineers Inc, 2017, pp. 300–305. DOI: 10.1109/ICSITech.2016.7852652.
- [18] Budiman, E., Moeis, D., and Soekarta, R., "Broadband quality of service experience measuring mobile networks from consumer perceived". In Proceeding - 2017 3rd International Conference on Science in Information Technology: Theory and Application of IT for Education, Industry and Society in Big Data Era, ICSITech 2017, Institute of Electrical and Electronics Engineers Inc., 2018, pp. 423–428. DOI: 10.1109/ICSITech.2017.8257150.
- [19] Budiman, E., and S.N. Alam., "User Perceptions of Mobile Internet Services Performance in Borneo." In Proceedings of the 2nd International Conference on Informatics and Computing, ICIC 2017. Institute of Electrical and Electronics Engineers Inc, 2018. p DOI:10.1109/IAC.2017.8280643.
- [20] Budiman, E., Haryaka, U., Watulingas, J.R., and Alameka, F. "Performance rate for implementation of mobile learning in network". In International Conference on Electrical Engineering, Computer Science and Informatics (EECSI), IEEE Xplore, 2017. DOI: 10.1109/EECSI.2017.8239187
- [21] Budiman, E., Haeruddin, Hairah, U., and Alameka, F. (2018). Mobile learning: Visualizing contents media of data structures course in mobile networks. Journal of Telecommunication, Electronic and Computer Engineering, vol. 10. no.1-9, 2018, pp. 81-86.

- [22] <https://gtmetrix.com/>
- [23] <http://yslow.org/ruleset-matrix/>
- [24] <https://www.paessler.com/tools>
- [25] <https://www.bloodypoet.page.tl/Best-AIO-Softwares-ar-.htm>
- [26] Nielsen, J., "Website Response Times", Nielsen Norman Group, 2014. [Online]. Tersedia: <http://www.nngroup.com/articles/website-response-times/>
- [27] Meier, J. D., Farre, C., Bansode, P., Barber, S., & Rea, D., "Quantifying End-User Response Time Goals", Microsoft Developer Network. [Online]. Tersedia: <http://msdn.microsoft.com/en-us/library/bb924365.aspx>
- [28] Asthana, A., Olivieri, J., Quantifying software reliability and readiness, in: 2009 IEEE International Workshop Technical Committee on Communications Quality and Reliability, CQR 2009., 2009. DOI:10.1109/CQR.2009.5137352



# ISO/IEC 9126 Quality Model for Evaluation of Student Academic Portal

1<sup>st</sup> Edy Budiman  
*dept.of informatics engineering*  
*universitas mulawarman*  
Samarinda, Indonesia  
edy.budiman@fkti.unmul.ac.id

4<sup>th</sup> Novianti Puspitasari  
*dept.of informaticsc engineering*  
*universitas mulawarman*  
Samarinda, Indonesia  
miechan.novianti@gmail.com

2<sup>nd</sup> Masna Wati  
*dept.of informatics engineering*  
*universitas mulawarman*  
Samarinda, Indonesia  
masna.wati@fkti.unmul.ac.id

5<sup>th</sup> Muhammad Bambang Firdaus  
*dept.of informatics engineering*  
*universitas mulawarman*  
Samarinda, Indonesia  
bambangf@fkti.unmul.ac.id

3<sup>rd</sup> Joan Angelina Widians  
*dept.of informatics engineering*  
*universitas mulawarman*  
Samarinda, Indonesia  
angel@unmul.ac.id

6<sup>th</sup> Fasa Alameka  
*dept.of informatics engineering*  
*universitas mulawarman*  
Samarinda, Indonesia  
faza.alameka@gmail.com

**Abstract**—The papers discuss and evaluate the quality of student academic portal using ISO / IEC 9126 quality modeling approach. Quality factors are tested and analyzed are characteristics of Usability, Reliability, Efficiency, and Portability, this evaluation is very important, considering the number of users of the portal system so much and growing. One of the efforts to improve and optimize the performance of the academic Information System Management team. Evaluate the quality of the user perception approach 10 principles of usability heuristics and internal site performance testing or web server. The results of analysis and testing of 4 quality characteristics have issued several recommendations for improvement and optimization of the performance of student academic portals.

**Keywords**—ISO/IEC 9126, performance, heuristics, website.

## I. INTRODUCTION

Software quality can be assessed through certain measures and methods, as well as through software tests. The various definitions of software quality depend on which user's point of view defines and views according to their individual needs. According to Crosby [1] defines quality or quality as "conformance to requirements". As long as one can argue about the difference between needs, wants and desires, the definition of quality must take into account the perspective of the user.

The key question for a quality definition is who the wearer is, what matters to them and how does his priority about what method is built, wrapped to support a product. To answer that question, we must recognize the hierarchy of software quality. First, a software product must provide the same function and type of time when the user needs it. Second, the product must be running. If the product has a defect then the product is, of course, no consistency of eligibility. The users will not use it by ignoring the attributes that accompany it. This does not mean that disability is always the main priority in rejecting a product but it will be very important in seeing whether or not it is appropriate.

If the minimum defect rate has not been reached, then there is nothing to consider. Beyond the threshold of quality, however, something related to the consideration and assessment of the defects of a software product as well as its usefulness, suitability, ability, and others depends on the user

looking at and evaluating it including its application and the accompanying software environment [2].

One of the software quality benchmarks is ISO 9126, created by the International Organization for Standardization (ISO) and the International Electro-technical Commission (IEC) [3], [4]. ISO 9126 defines the quality of software products, models, quality characteristics, and related metrics used to evaluate and determine the quality of a software product [3], [4]. The ISO 9126 standard has been developed in an effort to identify key attributes of quality for computer software. Quality factors according to ISO 9126 include six quality characteristics, i.e. Functionality, Reliability, Usability, Efficiency, Maintenance, and Portability.

Comparison of the quality models of McCall, Boehm, Dromey, FURPS, BBN, Star, and ISO 9126 according to [5], the results show that the ISO / IEC 9126 quality model is stated to be more complete and useful. Two main reasons are found in the literature. First, Behkamal [5] states the ISO 9126 model looks more complete than other models and free of other shortcomings. Secondly, Al-Qutaish [6] states that the ISO 9126 quality model is built on international approval.

Website utilization as an online data and information management software has been generated different points of view from the user group (user). To optimize the quality of the website, it is necessary to evaluate the needs of software quality. Website quality evaluation is important to ascertain whether the website has met the needs, expectations and end-user goals.

This paper will discuss and evaluate the quality of one of the student academic portals using the ISO 9126 quality model approach, Quality factors according to ISO 9126 to be discussed and analyzed are quality characteristics, i.e. Usability, Reliability, Efficiency, and Portability, this evaluation is very important, considering the number of users of the system is so many and growing, one of the efforts to improve and optimize the performance of academic management. Evaluation of student academic portals will be analyzed with approaches from user perceptions and portal system applications.



## II. RESEARCH METHODOLOGY

### A. Data Collection Methods

Data collection methods in this paper using:

- Questionnaires, provides a set of questions or written statement to the respondent to be answered. Respondents are students, as many as 120 students as samples will provide a scaled assessment of the student academic portal. The result of the questionnaire will be an assessment for evaluation.
- Observation, conduct testing using a website or web server performance measurement tool to determine the behavior of student academic portals. The tool used is GT-Metrix to test the quality of efficiency and Web Server Stress tools to measure the quality of reliability.

### B. Variables

The variables that will be used in this paper are independent variables. These variables are explained based on the characteristics of the ISO 9126 model with the 10 Heuristic method approach, shown in TABLE I. Variables for testing portal applications using recommendation parameters from Google Page-Speed and YS-low Yahoo.

TABLE I. 10 USABILITY HEURISTICS VARIABLE

Usability Heuristics Variable	Criteria Indicators	Question Number
Visibility of system status	Consistency of view and content	1
	Information Clarity and Status	1
	Feedback System	2
Match between the system and the real world	User Habits Using the System	3
	Color Selection	3
	Use of Words and Languages	4
User control and freedom	Ease of Use	6
	Usage Controls	6
	Operation Cancellation	5
Consistency and standards	Standard Format Design	7
	Standard Formats of Numbers and Alphabets	7
	Color Usage Standards	7
	Consistency of Content and Navigation	9
	Navigation Format Standards	8
Error prevention	Avoiding Error Messages	13
	Use of Keys and Navigation	12
	System Response to Users	12
Help users recognize, diagnose, and recover from errors	Error Information	
	Use of Instructions	11
Recognition rather than recall	Object Clarity and Layout	14
	Ease In Getting Directions	14
	Application of Color In System	14
Flexibility and efficiency of use	Error Message Display	10
	Freedom of Action User Against the System	15
	Availability of Functions	16
Aesthetic and minimalist design	Display Information is Simple and Easy to Understand	18
	Use of Objects and Icons	17
	Menu Order Specifications	18
Help and documentation	Use of instructions on the system	20
	System Navigation Support	19
	Ease of Getting Information	20

### C. Instrument Testing

Testing instruments in the questionnaire uses validity and reliability tests. Testing the validity of data using Pearson product moment correlation coefficient [7], [8]. According to [9] a question is said to be valid and can measure the research variables in question if the validity coefficient is more than or equal to 0.3 to simplify the process of calculating the correlation coefficient, then, Reliability test, this research using Alpha reliability coefficient [10].

Internal reliability testing using to test the consistency of an answer. SPSS provides facility facilities to measure reliability with Cronbach's alpha test statistics. It's suggested that reliability estimates in the range 0.7-0.8 are good enough in basic research. After testing the validity and reliability, the t test item questionnaire will be examined, this test is done to see how big influence between each item refer to [11].

### D. Measurement Scale

Assessment criteria for instruments use a Likert scale [10] giving 5 answer choices. Likert-rating criteria can be seen in Table II.

TABLE II. THE WEIGHT ANSWER QUESTIONNAIRE RESPONDENTS

Answer	Value
Problems at all	0
a little problem that doesn't need to be fixed	1
Small problems whose improvements are low priority	2
Problems that must be fixed and become a high priority	3
Very Important To Fix	4

### E. Testing for Characteristic Efficiency

This test uses the GT-Metrix [12], measuring tool developed by GT.net, this tool uses a combination of Google Page-Speed Insights and YS-low to generate value and recommendations.

The basic parameter used is the document size, http request, so as to obtain a predetermined Grade from the measuring instrument. After getting score from test result then calculated percentage with formula of percentage and interpretation according to recommendation of Yahoo Developer Network [13] shown in TABLE III.

TABLE III. DATA ANALYSIS OF GRADE EFFICIENCY TESTING

Score	Grade
A	$90 \leq S \leq 100$
B	$80 \leq S < 90$
C	$70 \leq S < 80$
D	$60 \leq S < 70$
E	$50 \leq S < 60$
F	$0 \leq S < 50$

### F. Testing for Characteristic Reliability

This test uses the Webserver Stress Tool developed by PAESSLER AG [14]. The tool simulates the HTTP requests generated by hundreds or even thousands of simultaneous users, we can test web server performance under normal and excessive loads to ensure that critical information and

services are available at speeds end-users expect [14].

The parameters used are failed session, failed pages, and failed hits. The “equation (1)” for calculating the reliability values according to the Nelson model [15]. Reliability aspects are tested using the help of the Webserver Stress Tool. Based on the results of the test, you will get successful access data and failed access. The data is then converted into a percentage form. The percentage results are then compared to the TELCORDIA standard. According to TELCORDIA standards, 95% or more of the tests planned for the system must be successful [16].

### III. TESTING AND ANALYSIS RESULTS

#### A. Analysis of Usability Test

Based on the validity and reliability test of the questionnaire that has been disseminated on 120 respondents, The results of the data show that from 20 questionnaire items have a validity coefficient greater than the critical  $r$  that is 0.3, so it can be concluded that 20 other instrument items stated otherwise valid, which means the items used in the questionnaire to measure the indicator can represent the theory and able measure what should be measured, so that it can be included in the next analysis.

The results of reliability test presented on TABLE IV, it is known that the variable usability heuristic approach, all items in the questionnaire indicator is reliable because the value of reliability coefficient greater than 0.70 that is 0.928 which means usability variable heuristic or reliable approach.

TABLE IV. RELIABILITY STATISTICS

Reliability Statistics		
Cronbach's Alpha	Cronbach's Alpha Based on Standardized Items	N of Items
.893	.898	20

According to [11], for hypothesis testing the average of one party either the right or left-handed test, if the value of  $\sigma$  2 is unknown then use the student t-test statistic, with the result for each item of each usability indicator.

The result of calculation with alpha ( $\alpha$ ) = 0.05 and degrees of freedom (DB)  $n-1 = 120-1 = 119$  obtained the table of 1.65776 with the acceptance test criteria  $H_0$  if  $t\text{-count} \leq -t\text{-table} (5\%, 119)$ , reject  $H_0$  in terms of other. If the value of  $t\text{-count} < -t\text{-table} (5\%, 119) = -1.65776$ , then  $H_0$  is rejected means there is no problem on the Student Portal Student item, whereas if  $t\text{-count} > -t\text{-Table} (5\%, 16) = 1.65776$ , then  $H_0$  accepted which means there are problem on student academic portal item. After 20 items were tested using t-test, out of 20 items, there was no problem in student academic portal.

Once known items that have problems then stage next is to determine the level problems. To determine level of the problem, carried out the assessment level of evaluation problem heuristics based on scores maximum of each answer weight. The division of the category level interval the problems are presented in TABLE V.

TABLE V. INTERVAL CATEGORY LEVEL HEURISTIC EVALUATION PROBLEMS

Interval Category		Level of Problems
lower limit	upper limit	
	96	Problems at all
97	192	a little problem that doesn't need to be fixed
193	288	Small problems whose improvements are low priority
289	384	Problems that must be fixed and become a high priority
385	480	Very important to fix

Based on TABLE V, it can provide an assessment of the category of heuristic evaluation problem level on the results of hypothesis research through one sample t-student test, obtained some items on each reusability that there are problems that need to follow-up improvements in the Student Academic Portal. Each item that problem is calculated the value of the score per item then score value compared to TABLE V, then obtained the assessment of heuristic problems based on the scores of each indicator.

TABLE VI. ASSESSMENT OF LEVELS OF HEURISTIC EVALUATION PROBLEMS

Item	Score	Category
20. There is a reminder aid for commands, through online references on student academic portals or others	220	Small Problems that fixes are low priority
5. Users may cancel operations or processes that are running on the student academic portal	205	Small Problems that fixes are low priority
13. The student academic portal system prevents users from making mistakes and will remind them if they make a serious mistake	200	Small Problems that fixes are low priority
18. All the icons on the student academic portal are different conceptually and visually	196	Small Problems that fixes are low priority

Based on TABLE VI, the reusability of the student academic portal is actually not much of a problem that needs to be upgraded. However, there are 4 items that have minor problems that the improvement is a low priority so there is a need for improvement recommendations although having low priority.

TABLE VII. REKOMENDASI SISTEM

Item	Recommendation
20. There is a reminder aid for commands, through online references on student academic portals or others	There is a need for guidance on the use of student academic portal system to facilitate students in using portal both in terms of function and need of usage.
5. Users may cancel operations or processes that are running on the student academic portal	Require optimization in the warning or option if the user wants to cancel the operation or running processes like back or Exit button.
13. The student academic portal prevents users from making mistakes and will remind them if they make serious mistakes	There is a need for a notice on the system, if students access the portal system, a warning when doing something on the system.
18. All the icons on the student academic portal are different conceptually and visually	The use of Icons in the academic portal becomes one of the recommendations for student academic portal can be more easily understood and also not too monotonous.

Based on the findings of the problems in TABLE VI, the recommendation of improvement of academic portal system of students on TABLE VII, presents recommendations that can be used as future reference for the category of problems that the improvement is low.

### B. Analysis of Reliability Test Results

The result of reliability test using Webserver Stress Tool with simulation:

Test Type: CLICKS (run test until 10 clicks per user), User Simulation: 500 simultaneous users - 10 seconds between clicks (Random). The Webpage measurement results (per URL) can be seen on TABLE VIII.

TABLE VIII. RESULTS PER URL

Name URL	Clicks	Errors	Errors [%]	Time Spent [ms]	Avg. Click Time [ms]
Index	140	0	0	520.259	3.716
KHS	155	0	0	547.101	3.530
KRS	137	0	0	415.952	3.036
Curriculum	179	0	0	461.560	2.579
Lecturer Evaluation	136	0	0	363.822	2.675
Sum	747			461.739	3.107

TABLE VIII presents the data of simulation result of web page performance with predefined user number, obtained by measurement value of 747 successful clicks with 0 errors, Avg. click times with value 3.107ms and Time spent with value 461.739ms. Calculation of reliability value according to equation [15]. The result shows that the value of  $R = 1$  or the percentage of reliability value is 100% and  $r = 0.0$  or the error rate is 0%.

According to TELCORDIA standard that has been discussed by A Asthana and Jack O [16], software reliability success is 95% or 0.95, so based on the benchmark, and from the value of  $R$  obtained then testing Reliability of Student Academic Portal can be stated "accepted" according to TELCORDIA standards.

Furthermore, the graph of open requests Transferred data and system memory, CPU load can be seen in "Fig. 1".

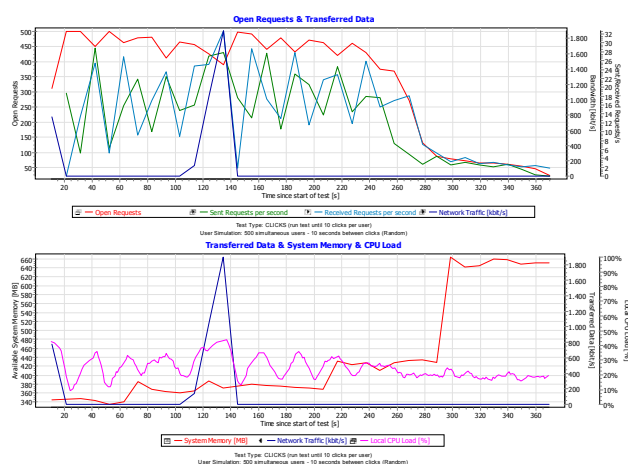


Fig. 1. Requests, Transferred data and system memory, CPU load

Additional testing is done to determine the level of ability and threshold of the user on the system, conducted simulation testing by raising the value on the number of users. and the threshold test results are found when the number of users is 1000. Reliability value calculation results for 1000 users, the percentage of error rate of 99.218%. Avg. click time of 3.624ms

### C. Analysis of Efficiency Test Results

Based on the analysis and calculation of efficiency testing of portal: sia-dev.unmul.ac.id using GT-Metrix tool. The grade and score as shown in "Fig. 2" for the performance of Page-Speed score D (66%) and YS-slow score D(67%).

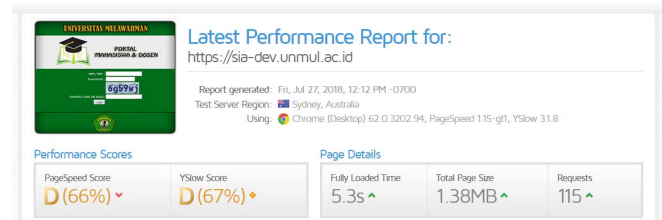


Fig. 2. Performance report of academic student portal

In detail, the performance of the Page-Speed test results is presented in "Fig. 3", and for the details of the YS-low test results are presented in "Fig. 4".

RECOMMENDATION	GRADE	TYPE	PRIORITY
Enable gzip compression	F (0)	SERVER	HIGH
Leverage browser caching	D (63)	SERVER	HIGH
Minify CSS	D (66)	CSS	HIGH
Optimize images	C (77)	IMAGES	HIGH
Avoid bad requests	A (92)	CONTENT	HIGH
Avoid CSS @import	A (92)	CSS	MEDIUM
Minify HTML	A (99)	CONTENT	LOW
Minify JavaScript	A (99)	JS	HIGH
Specify image dimensions	A (99)	IMAGES	MEDIUM
Specify a Vary: Accept-Encoding header	A (93)	SERVER	LOW
Avoid landing page redirects	A (100)	SERVER	HIGH
Defer parsing of JavaScript	A (100)	JS	HIGH
Enable Keep-Alive	A (100)	SERVER	HIGH
Inline small CSS	A (100)	CSS	HIGH
Inline small JavaScript	A (100)	JS	HIGH
Minimize redirects	A (100)	CONTENT	HIGH
Minimize request size	A (100)	CONTENT	HIGH
Optimize the order of styles and scripts	A (100)	CSS/JS	HIGH
Put CSS in the document head	A (100)	CSS	HIGH
Serve resources from a consistent URL	A (100)	CONTENT	HIGH
Serve scaled images	A (100)	IMAGES	HIGH
Specify a cache validator	A (100)	SERVER	HIGH
Combine images using CSS sprites	A (100)	IMAGES	HIGH
Prefer asynchronous resources	A (100)	JS	MEDIUM
Specify a character set early	A (100)	CONTENT	MEDIUM
Avoid a character set in the meta tag	A (100)	CONTENT	LOW
Remove query strings from static resources	A (100)	CONTENT	LOW

Fig. 3. Recommendation and grade of pagespeed results

The performance of the Page-Speed test results on "Fig. 3", there are recommendations of Enable GZIP compression in grade F (0), Leverage browser caching grade D (63), Minify CSS grade D (66), and Optimize images with grade C (77).

PageSpeed	YSlow	Waterfall	Timings	Video	History
RECOMMENDATION		GRADE	TYPE	PRIORITY	
▼ Add Expires headers		F (0)	SERVER	HIGH	
▼ Compress components with gzip		F (12)	SERVER	HIGH	
▼ Use a Content Delivery Network (CDN)		F (10)	SERVER	MEDIUM	
▼ Use cookie-free domains		E (55)	COOKIE	LOW	
▼ Make fewer HTTP requests		B (64)	CONTENT	HIGH	
▼ Avoid HTTP 404 (Not Found) error		A (65)	CONTENT	MEDIUM	
▼ Minify JavaScript and CSS		A (100)	CSS/JS	MEDIUM	
▼ Avoid URL redirects		A (100)	CONTENT	MEDIUM	
▼ Make AJAX cacheable		A (100)	JS	MEDIUM	
▼ Remove duplicate JavaScript and CSS		A (100)	CSS/JS	MEDIUM	
▼ Avoid AlphaImageLoader filter		A (100)	CSS	MEDIUM	
▼ Reduce the number of DOM elements		A (100)	CONTENT	LOW	
▼ Use GET for AJAX requests		A (100)	JS	LOW	
▼ Avoid CSS expressions		A (100)	CSS	LOW	
▼ Reduce DNS lookups		A (100)	CONTENT	LOW	
▼ Reduce cookie size		A (100)	COOKIE	LOW	
▼ Make favicon small and cacheable		A (100)	IMAGES	LOW	
▼ Configure entity tags (ETags)		A (100)	SERVER	LOW	
▼ Make JavaScript and CSS external		(99)	CSS/JS	MEDIUM	

Fig. 4. Recommendation and grade of yslow results

The performance of YS-low test results based on Figure 4, is generally in grade A category, and there is recommendation of Add Expires headers that are still in F grade (0), Compress components with GZIP with grade F (12), Use a Content Delivery Network (CDN) F (10), and Use cookie-free domains grade E (55).

From the score obtained, the software quality developed from the efficiency measurement side (Page-Speed and YS-low) generally get "Grade A", it is stated that the performance analysis of Academic Student Portal in efficiency characteristics has passed the testing.

The Response-time limits to keep the user's attention can wait for the load of the web page is 10s [15]. Whereas according to [17-23] the best load time a website page is less than 3s, for an acceptable load time of less than 10s.

The graph of the response-time measurement shown in "Fig. 5", obtained the average time load of about 5.29s (on-load: 5.09s) with the number of requests of 155 and with the data of 1.4 MB. Based on the data, the time load can be said to be "accepted" by referring to recommendations J Nielsen [15] for an acceptable time load of fewer than 10s.

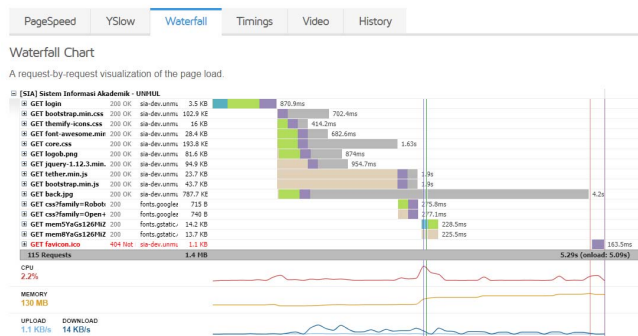


Fig. 5. Response-time load requests webpage of academic student portal

#### D. Portability Testing

Portability test is done by running the application on the browser directly and using the browser tester online at [www.browserstack.com](http://www.browserstack.com). Testing is done on Google Chrome browser, Mozilla Firefox, Internet Explorer, Safari, Opera and on smartphone devices, tablets, and other mobile-based devices. Student portal test results can run without an error. So the quality of portability characteristics is good and fulfilling because the application can run on different browsers without encountered an error.

#### IV. DISCUSSION AND CONCLUSION

Quality factors according to ISO 9126 are discussed and analyzed are quality characteristics of Usability, Reliability, Efficiency, and Portability. Based on the results of analysis and testing that have been done, it can be concluded that:

- Usability Characteristic, recommendations based on Heuristic 10 analysis in the Small Problems category that fixes are low priority.
- Reliability Characteristic, the value of R 100% (accepted), with simulated 500 users. the user's capability and threshold level occurs when simulating 1000 users with a percentage error rate 99.218%.
- Efficiency Characteristic, performance of Page-Speed recommendation score Grade D (66%), and recommendation YS-low score grade D (67%). The response-time obtained the average time load of about 5.29s (on-load: 5.09s) with the number of requests of 155 and with the data of 1.4 MB
- Portability Characteristic, the academic student portal test results can access without an error, the application can run on different browsers without encountered an error.

Knowing the quality of the software can help the Academic Information Systems Division (ICT Team) in assessing the system and improving, planning the determination of future application development cost budgets.

Furthermore, solutions that can be done to optimize performance and improvements on efficiency characteristics that still grade score D, are:

- Enable GZIP compression, Reduce the size of files sent from your server to increase the speed to which they are transferred to the browser, Increase page speed, Cost-benefit ratio: high, Access needed to the .HTACCESS files or server administration files.
- Leverage browser caching, Page load times can be significantly improved by asking visitors to save and reuse the files included in portal.
- Minify CSS, Compacting CSS code can save many bytes of data and speed up downloading, parsing, and execution time.
- Optimize images, Reduce the load times of pages by loading appropriately sized images. Reduce file sizes based on where images will be displayed, resize image files themselves instead of via CSS, save files in appropriate format depending on usage.



- Add Expires headers, expires headers let the browser know whether to serve a cached version of the page, Reduce server load, and decrease page load time.
- Use a Content Delivery Network (CDN), CDNs can give an equally fast web experience to users across the globe.
- Use cookie-free domains, serve static content from a different domain to avoid unnecessary cookie traffic.

#### ACKNOWLEDGMENT

Thank you to the head of the Information and Communication Technology Department of MULAWARMAN University, Head of Informatics Study Program which has supported this research.

#### REFERENCES

- [1] Crosby, Phillip B., *Quality Is Free: The Art of Making Quality Certain*, McGraw-Hill Companies 1979, ISBN: 978-0070145122.
- [2] Humphrey, W. S., *The personal process in software engineering*. In *Software Process*, 1994. 'Applying the Software Process', Proceedings., Third International Conference on the. IEEE, 1994, pp. 69-77.
- [3] ISO/IEC 9126-1, ISO/IEC 9126-1 Software engineering Product quality Part 1: Quality Model, ISO/IEC 2001
- [4] ISO/IEC 9126-2, ISO/IEC, ISO/IEC 9126-2 Software engineering Product quality Part 2: External Metrics, ISO/IEC 2003
- [5] Behkamal, B., Kahani, M., & Akbari, M. K., Customizing ISO 9126 quality model for evaluation of B2B applications. *Information and Software Technology*, vol. 51(3), 2009, pp. 599–609. DOI:10.1016/j.infsof.2008.08.001
- [6] Al-Qutaish, R. E., Quality models in software engineering literature: an analytical and comparative study. *Journal of American Science*, vol. 6(3), 2010, 166–175. Retrieved from <http://publications.rafaelayan.ca/33.pdf>
- [7] Chok, Nian Shong, Pearson's Versus Spearman's and Kendall's Correlation Coefficients for Continuous Data. Master's Thesis, University of Pittsburgh, 2010. (Unpublished) Available at: <http://d-scholarship.pitt.edu/id/eprint/8056>
- [8] Zar, J. H., Spearman Rank Correlation. In *Encyclopedia of Biostatistics*. Chichester, UK: John Wiley & Sons, Ltd. 2005. <https://doi.org/10.1002/0470011815.b2a15150>.
- [9] Kaplan R. M., Saccuzzo D.P., *Psychological Testing: Principles. Applications and Issues*, 3rd ed., Brooks Cole, Pacific Grove, CA. 1993.
- [10] Gliem, J. A., & Gliem, R. R., Calculating, interpreting, and reporting Cronbach's alpha reliability coefficient for Likert-type scales. Midwest Research-to-Practice Conference in Adult, Continuing, and Community Education, 2003.
- [11] Walpole S, McKenna MC. *The literacy coach's handbook: A guide to research-based practice*. Guilford Press, 2012.
- [12] <https://gtmetrix.com/>
- [13] <http://yslow.org/ruleset-matrix/>
- [14] <https://www.paessler.com/tools>
- [15] Nielsen, J., "Website Response Times", Nielsen Norman Group, 2014. [Online]. Tersedia: <http://www.nngroup.com/articles/website-response-times/>
- [16] Asthana, A., Olivieri, J., Quantifying software reliability and readiness, in: 2009 IEEE International Workshop Technical Committee on Communications Quality and Reliability, CQR 2009., 2009. DOI:10.1109/CQR.2009.5137352.
- [17] Budiman, E., and Wicaksono, O., Measuring quality of service for mobile internet services. *Proceeding - 2016 2nd International Conference on Science in Information Technology, ICSITech 2016: Information Science for Green Society and Environment*, Institute of Electrical and Electronics Engineers Inc., 2017, pp. 300–305. DOI:10.1109/ICSITech.2016.7852652
- [18] Budiman, E., Moeis, D., and Soekarta, R., "Broadband quality of service experience measuring mobile networks from consumer perceived". In *Proceeding - 2017 3rd International Conference on Science in Information Technology: Theory and Application of IT for Education, Industry and Society in Big Data Era, ICSITech 2017*, Institute of Electrical and Electronics Engineers Inc., 2018, pp. 423–428. DOI: 10.1109/ICSITech.2017.8257150
- [19] Budiman, E., Haryaka, U., Watulingas, J.R., and Alameka, F. "Performance rate for implementation of mobile learning in network". In *International Conference on Electrical Engineering, Computer Science and Informatics (EECSI), IEEE Xplore*, 2017. DOI: 10.1109/EECSI.2017.8239187
- [20] Budiman, E., and S.N. Alam., "User Perceptions of Mobile Internet Services Performance in Borneo." In *Proceedings of the 2nd International Conference on Informatics and Computing, ICIC 2017*. Institute of Electrical and Electronics Engineers Inc, 2018. p DOI:10.1109/IAC.2017.8280643.
- [21] Budiman, E., Haeruddin, Hairah, U., and Alameka, F. (2018). Mobile learning: Visualizing contents media of data structures course in mobile networks. *Journal of Telecommunication, Electronic and Computer Engineering*, vol. 10. no.1-9, 2018, pp. 81-86.
- [22] Budiman, E., Hairah, U., and Saudek, A., Mobile Networks for Mobile Learning Tools, *Journal of Telecommunication, Electronic and Computer Engineering*, vol. 10 (1-4), 2018, pp. 47-52.
- [23] Meier, J. D., Farre, C., Bansode, P., Barber, S., & Rea, D., "Quantifying End-User Response Time Goals", Microsoft Developer Network. [Online]. Tersedia: <http://msdn.microsoft.com/en-us/library/bb924365.aspx>.

# MEASUREMENT OF IT/IS INVESTMENT ON THE IMPLEMENTATION OF ERP AND THE EFFECT ON COMPANY PRODUCTIVITY

<sup>1)</sup>Qilbaaini Effendi Muftikhali S.Kom., M.Kom

Department of Information System, Faculty of Computer Science, University of Jember  
Jember, Indonesia

[qilbaaini.effendi@unej.ac.id](mailto:qilbaaini.effendi@unej.ac.id)

<sup>2)</sup>Dr. Apol Pribadi, S.T., M. T

Department of Information System, Faculty of Information Technology, Institut Teknologi Sepuluh Nopember (ITS) Surabaya,  
Indonesia

[apolpribadi@gmail.com](mailto:apolpribadi@gmail.com)

Information technology can not be denied in daily activities and is the source of life of some business processes that cause companies to compete in making IT investments. Noted that IT investment increased significantly. However, the data also indicated this investment is not always followed by the achievement of organizational performance. This is known as IT Productivity Paradox, where the benefits obtained do not match what is invested. This phenomenon has long been discussed to this day. IT Productivity Paradox has become an interesting topic in some circles because some findings find different results. Some research proves that investment in IT / IS has driven the performance of the company, while not at other companies. This study aims to determine the phenomenon of IT productivity. The object of research is an organization that has invested and developed ERP system for the last 2 years. The analysis using Information Economics method. The result of investment measurement from this research shows that the application of ERP using Economic Information method in the period of about 2 years shows total project score (64,6) with predicate of influential project. The total score of the project is derived from three aspects of benefits, namely the real aspect, the quasi-real aspect, and the intangible aspect.

**Keywords:** Investment of IS / IT, IT Productivity Paradox, Information Economic

## I. INTRODUCTION

Information technology is undeniably a mandatory requirement that is applied in daily activities and is the life of some business processes in the company. Changes from the manually carried out process have now been computerized in such a way as to cause changes in business processes in each company. This kind of event resulted in companies competing to make IT purchases on a large scale. Recorded in 2015 IT spending in Indonesia was 199 trillion and increased by 8.3 percent increasing in 2016 to 214.4 trillion [1]. This kind of phenomenon is not only for large-scale companies but in the SMEs sector also experiences similar phenomena and Indonesia is listed as the country with the

most investment. Information technology (IT) in a company is said to have a role of competitive advantage, but when companies invest more in the IT field in line with the income that has been obtained by the company.

IT Productivity Paradox is a phenomenon where IT investment carried out by a company does not provide an increase in company productivity [2]. Productivity in a company is not just one of the company's goals but a chain of activities in an organization or commonly called a company's goal in the long run. Maximizing productivity can improve the company's standard of living [3]. The Paradox IT productivity phenomenon is a study that occurs in several companies that have implemented IT in running the company's business processes. Some research shows that from the past 20 years to the present phenomenon the paradox of IT Productivity remains something that is being studied. This study considers that investment in information technology does not have a significant impact in improving corporate finance [4].

Some empirical studies have had difficulty determining the relationship between IT investment and financial performance. The Empirical Study above is proven through some research evidence, this study compares successful users of implementing IT with users less successful in implementing IT. But it is more focused on the successful use of IT, especially to measure the phenomenon of the IT Productivity Paradox. As many as 71 companies examined their financial statements in the last 10 years, the results show that companies that successfully implement IT can be seen in the first 3-4 years, compared to companies that are not successful in implementing IT. The more important thing to note is how to manage IT assets for further investment [5]. Other research shows that there is no positive impact on IS / IT on company performance. This proves the paradox of IT productivity phenomenon in IT investment.

Previous research said the development of research from the IT Productivity Paradox should describe a more detailed explanation of the causes of missmeasurement and mismanagement issues and independent testing of the causes



of the IT Productivity Paradox phenomenon [5]. Missing Measurement of Input and Output is an issue that still occurs to this day as a cause of Paradox's IT Productivity, measurement errors are mainly related to the difficulty of assessing the productivity of the service sector, and the inability of national statistics to take into account the IT contribution qualitatively [2]. In Sims' study [6] stated that there were no significant answers between measurements taken in answering the phenomenon of the Paradox IT Productivity to date. Inappropriate measurement methods will add to the issue of missmeasurement increasingly developing. For example, at present there are too many studies that only use financial methods as a measure, the absence of precision from the measurement method and includes the intangible side, does not include long-term investment and does not analyze the risks of a project [7]. Measuring implementation performance is still being carried out so far but not much is focused on financial and corporate strategy, measurements usually focus on the capability level of an organization [8]. According to the above phenomenon, IT investment requires development to make measurements and evaluate investments in various factors not only in terms of finance, but several related factors must also be involved, such as factors related to IT investment, tangible factors, intangible factors and the risk of IT implementation that has been invested [7]. And these measurements must have several criteria that are measured so that the results of the measurement are more valid and viewed from various aspects [9].

Information Economic is the development of Cost Benefit Analysis that uses multi-criteria aspects in evaluating information technology (IT) investments in terms of tangible and intangible benefits [10]. Information Economic can provide a measurement contribution to the management of the company in managing the investments that have been made and will be done [11]. Information Economic that measures tangible and intangible benefits related to IT investment [12]. Information Economic measures the impact of IT investment by referring to business performance, the advantages of this measurement can evaluate the next investment strategy [13].

Research The development of Enterprise Resource Planning software is growing rapidly in line with the development of the company which was recorded in 2013 with an investment value of Rp.969,12M ERP [14]. This incident describes many companies that implement it to improve their business processes. The development of ERP is still being carried out, but is the investment made in software development in line with the productivity gained by the company. Until now, the measurement of software implementation on each ERP has not been done much and measurements have been carried out to date, it is still only measuring Net Present Value on an information system [15].

Based on the measurement problems above, it was found that there were no measurement tools or frameworks that included measurement of SI / IT investment, until the ERP implementation was always increasing every year, it was

necessary to measure ERP implementation. So this study discusses investment in ERP implementation. Investments are made to contribute more to the company's performance by proving one of the causes of the Paradox IT Productivity, namely output and input mismasurement using the Information Economic approach. Economic Information has the advantages of investing in all the factors that contribute from the tangible and intangible benefits.

## II. RESEARCH METHOD

This research collects two types of data, namely financial and non-financial data. The financial data used in this research is financial report data from 2015-2017. Non-financial data is the result of the questionnaire. The financial report is the main data used to calculate whether the investment is done by the research object because it is used to measure the investment feasibility of ERP. This study takes the object of research company that has implemented ERP for 2 years in Indonesia using information economic. The data has been processed using the method of information economic. By using the method of information economic this research can find tangible benefits, intangible benefits and quasi-tangible benefits.

Information Economic may provide a measurement contribution to the management of the company in managing the investments that have been made and will be made [10]. ISACA said, Information Economic that measures the tangible and intangible benefits associated with IT investment. Information Economic measures the impact of IT investments with reference to business performance, the advantages of these measurements can evaluate the next investment strategy [13].

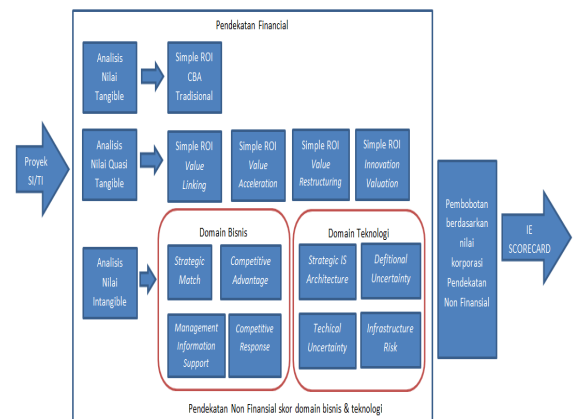


Figure 2.1 Information Economic

- **Collect Data**

Data retrieval is done based on the purpose of the research object environment. Classification of data is taken to collect data related to the implementation of information technology conducted in accordance with the object of research. Data classification is divided into 2 types of data ie financial(tangible benefits and quasi tangible benefits) and non-financial data (intangible

benefits). The following is a classification of benefits :

**Tangible Benefits:** Real benefit or directly affect the organization's profits. Analysis of the tangible benefits or quantitative using simple calculation method Return on Investment (ROI Simple) - Traditional Cost-Benefit Analysis (TCBA).

**Quasi Benefits:** Benefits that directly affect profits but hard to count or otherwise, does not directly affect profits but can be calculated. For example, improving the process of planning, improvement of decision making, and so on. Benefit analysis of the quasi using the calculation of Value Acceleration (VA), Value Linking (VL), Value Restructuring (VR), and Innovation Value (IV): Tangible benefits and quasi tangible benefits using enhanced ROI financial approach, where the results of the assessment results in a monetary value measured by the following formula [9]:

**Enhanced ROI** = Traditional ROI + VL + VA + VR + IV. (1)

**Intangible Benefits:** Benefits not real or that can be seen to have a positive impact for the organization but does not directly affect the profits. For example, enhance the corporate image, increase employee morale, and so on. Intangible values obtained from the questionnaire. Questionnaire using a table of Parker survey. Analysis of the intangible benefits of using two assessments are Business Domain and Technology Domain.

- **Total Score Project**

The project value of IS / IT is measured by the following formula [9]:

**Score Project** = Enhanced ROI + weight of Business Domain + weight Technology Domain. (2)

### III. RESULT AND DISCUSSION

The analysis in this study begins by classifying the collected data. Then process with information economic method. Information Economic processing there are 3 stages of financial benefit processing (Tangible Benefit and Quasi Tangible Benefit), Intangible Benefit and Total Score Project.

Table 3.1 Classification Benefit  
**COST**

NO	Information	Classification	
		Value	Aspect
1.	Development Project Cost	Financial	Tangible
2.	On-Going Cost	Financial	Tangible
BENEFIT			
1.	Reduce the cost of shipping documents	Financial	Quasi-tangible
2.	Project Cost	Financial	Quasi-

3.	Efficiency up to 30% reduce the cost of operational error	Financial	tangible Quasi-tangible
	Questionnaire (Business Domain and Technology Domain)	Non-Financial	intangible

#### A. Collected Data

The following is a classification of data using the methods of information Economic:

- **Tangible and Quasi Tangible Benefit**

Tangible benefits or direct benefits directly affect the company's profits, these benefits are identified from the impact of the implementation of a technology. The tangible benefits of ERP implementation are evident in the reduction of shipping costs made by the organization.(see table 3.2).

Quasi Tangible benefit are a difficult profit to calculate but have an impact on the implementation of ERP. This section explains about category of benefits ERP implementation as *Value Linking (VL)*, *Value Acceleration (VA)* and *Innovation Valuation (IV)*. The benefits of value linking are illustrated in the table below (see table 3.2)

Table 3.2 Benefit Tangible

BENEFIT	TOTAL COST
TANGIBLE BENEFIT	Rp. 9.560.000
QUASI TANGIBLE	
VALUE LINKING	Rp. 22.710.870.000
VALUE ACCELARATION	Rp. 9.576.000.000

The table above is a table that contains the benefits of implementing ERP. The benefits are classified into 2 parts tangible benefits derived from benefits directly after the implementation of ERP during 2015-2017 with a total of Rp. 9,560,000 and the benefits of Quasi tangible for 2015-2017 years amounted to Rp. 32,286,870,000.

- **Intangible Benefits**

Intangible benefits can be obtained by filling in a questionnaire consisting of two domains: business domain and technology domain.

#### B. Tangible Benefit and Quasi Tangible Benefit

The processing of tangible and intangible benefits is part of the processing of information economic methods. This data processing uses Enhanced ROI as illustrated in the table 3.3.

Table 3.3 Score ROI

INVESTMENT COST	RP. 13.882.500.000		
COST	2015	2016	2017
VALUE LINKING	2.034.000.000	7.272.000.000	13.404.870.000
VALUE ACCELERATION	1.560.000.000	2.400.000.000	5.616.000.000
TANGIBLE BENEFIT	3.700.000	4.960.000	2.480.000
ON-GOING COST	0	19.595.000.000	12.090.000.000
CASH FLOW	3.597.700.000	-9.918.040.000	6.933.770.000
TOTAL CASH FLOW			613.430.000
ROI 1 YEAR			2%
ROI			4%

The table above explains the ROI calculation process that has been 2 years after the implementation of ERP. ROI calculation is obtained through the company's cash flow for 2 years. Return on investment for 2 years is 4%.

- Measurement Enhanced ROI

$$\text{Enhanced ROI} = \left( \frac{\text{Yearly cash flow}}{\text{development cost}} \right) \times 100\% \quad (3)$$

$$\text{Enhanced ROI} = \left( \frac{\text{Rp. 598.430.000}}{\text{Rp. 13.882.500.000}} \right) \times 100\%$$

$$= 2\%$$

Table 3.4 Predicate ROI

SCORE	0	1	2	3	4	5
SIMPLE ROI	<0%	1%-299%	300%-499%	500%-699%	700%-899%	>900%

The results of Enhanced ROI calculations are generated that in the last 2 years is worth 2%, if ROI is a whole is worth 4%. These calculations are the result of tangible and quasi tangible benefits in ERP implementation. Below is a score determination of ROI score. The value of ROI in the implementation of ERP 2% then the score on the implementation of value 1 with the quadrant of ROI value (1% - 299%). These results indicate that the value of Return on Investment is too small in the implementation of ERP conducted for 2 years.

### C. Intangible Benefit

For data not directly related to finance, but related to the benefits obtained organization related ERP implementation. In this study, non financial data consists of two things namely questionnaire and determination of company domain weight.

- Result of Questionnaire

Table 3.5 Result of Questionnaire

FACTOR	SCORE
<b>BUSINESS DOMAIN</b>	
STRATEGIC MATCH (SM)	3,3
COMPETITIVE ADVANTAGE (CA)	4,3
MANAGEMENT INFORMATION (MI)	4
COMPETITIVE RESPONSE (CR)	3,7
PROJECT/ORGANIZATIONAL RISK (OR)	2,3
<b>TECHNOLOGY DOMAIN</b>	
STRATEGIC IS ARCHITECHTURE (SA)	4,3
DEFINITIONAL UNCERTAINTY (DU)	0,3
TECHNICAL UNCERTAINTY (TU)	2
IS INFRASTRUCTURE RISK (IS)	1,7

The table above shows the results of a questionnaire consisting of 2 business and technology domains that are disseminated, the questionnaire is filled in by at least 3 parties who have authority in ERP implementation

- Company Domain Weight

The weighting of the firm's factors is the determination of the organization's quadrant position. This determination is done by interviewing several related parties and determining the company's line culture. Results of interviews about the organization in quadrant 2 (strategy). The table below shows that the ERP assessment indicator has been adjusted to the conditions of the company. Here is an indicator of ERP valuation according to the value of each sub domain in table 3.6.

Table 3.6 Quadrant Strategy

	LIKELY VALUE	SCORE
<b>BUSINESS DOMAIN</b>		
A. ROI	Medium	2
B. STRATEGY MATCH	High	4
C. COMPETITIVE ADVANTAGES	High	6
D. MANAGEMENT INFORMATION	Medium	2
E. COMPETITIVE RESPONSE	High	4
F. PROJECT/ORGANIZATIONAL RISK	Low	-1
<b>TECHNOLOGY DOMAIN</b>		
A. DEFINITIONAL UNCERTAINTY	Medium	-2

<b>B. TECHNICAL UNCERTAINTY</b>	Low	-1
<b>C. STRATEGIC IS ARCHITECTURE</b>	Low	1
<b>D. IS INFRASTRUCTURE RISK</b>	Low	1
<b>TOTAL SCORE</b>		20
<b>TOTAL RISK</b>		-4

$$(2,5 \times 20) + (2,5 \times -4) = 40 \quad (5)$$

- The lowest value is achieved when all variable value (20) reaches the lowest value (0) and the risk variable (-4) reaches the highest value (5).

$$(0 \times 20) + (5 \times -4) = -20 \quad (6)$$

Based on Likert scale with already know the highest value, the lowest value, and the middle value hence the table predicate score of the project.

#### D. Total Score Project

Table 3.7 Total Score Project  
Information Economic Scorecard

Faktor	Business Domain					Technology Domain					Total
<b>Bobot Corp rate Value Score Factor</b>	2	4	6	2	4	-1	1	-2	-1	1	
<b>Total Score Project</b>	1	3,3	4,3	4	3,7	2,3	4,3	0,3	2	1,7	
<b>Manfaat (+)</b>	2	13,2	25,8	8	14,8	-	4,3	-	-2	-	<b>64,6</b>
<b>Risiko</b>						2,3		0,9		1,7	
<b>TOTAL</b>											

Based on the Total Score Project 3.7 table above, it is obtained the calculation value of Information Economic 64.6. Details of the value of each sub domain can be seen in the table, the value in the table shows the value of each sub domain from the benefits of implementing ERP. The benefits of implementing ERP valued at 69.8 and the risk of implementing ERP is worth -5.2, from the above value shows that the implementation of ERP can provide many benefits from the company. After getting the IE value above, it is ranked to show the feasibility of ERP implementation.

Regarding strategic quadrant, predicate is determined based on likert scale as project predicate scale. Likert scale is used to measure attitudes, opinions, and perceptions of a person or group of people. With Likert scale then the variable to be measured is translated into indicator variable.

- The highest value is achieved when all the variable values (20) reach the highest value (5) and the risk variable (-4) reaches the lowest value (0).

$$(5 \times 20) + (0 \times -4) = 100 \quad (4)$$

- The middle value is achieved when all the variable values (20) and the risk variable (-4) reach the lowest value (2.5).

Table 3.8 Predicate Project Score

PROJECT SCORE	PREDICATE
71-100	Very Influential
41-70	Influential
11-40	Quite Influential
(-21) - 10	Less Influential
(-50) - (-20)	Very less Influential

Based on the analysis of investment feasibility using Information Economic method within a period of approximately 2 years shows the total score of the ERP project (64.6). The total score of this project is derived from three aspects of benefits, namely tangible aspects, quasi-tangible aspects, and intangible aspects.

Tangible aspects and quasi-tangible aspects are aspects that are calculated by the amount of financial benefits that occur when the ERP implementation. Benefits such as project cost efficiency up to 30%, reduction of shipping costs, company operating cost savings resulting from mistakes in the preparation of financial statements. The calculation of those benefits is used to calculate the ROI value in the ERP implementation. The simple ROI of ERP implementation for two years is 4%, ROI per year reaches 2%. The value of ROI is converted into value according to ROI score table is worth. The intangible aspect is obtained from the perception aspect of employees who know ERP more and understand financially. Perception assessment is done by charging quivery consisting of business domain and technology domain. The value of the business domain 59.5 and the technology domain is 3.1, then the value of the intangible aspect is 62.6. The total project score in ERP investment is 64,6 with project predicate which is **influential** in company operation and has big benefit.

ERP implementation in a company is something that provides more benefits in the company's operations, so every company that has implemented ERP must measure the investment feasibility that has been given both before and after implementation. The measurement must use the right method to produce measurement results that have benefits and evaluation for the company. The above research shows that ERP implementation that has been done and measured using information economic methods is the right thing and can be measured by 2 types of data, financial and non-financial. In addition to this method also measures in terms of tangible, quasi tangible and intangible and the measured domain is from the business domain and domain technology.

Therefore, this method can be suggested for measuring technology investments that have been implemented.

#### IV. CONCLUSION

This research is to make measurement of ERP investment that has been done in the span of 2 years. Measurement is using the method of economic information to determine the feasibility of investment. The results of this study based on the analysis of investment feasibility using Information Economic method within a period of approximately 2 years shows the total score of the project (64.6). The total score of this project is derived from three aspects of benefits, namely tangible aspects, quasi-tangible aspects, and intangible aspects. These results illustrate that the implementation of ERP has a predicate project that INFLUENCES in the company's operations and has great benefits. Based on the results of measurements using the Information Economic method the company can evaluate the information system that has been applied using the method. The evaluation can be seen in terms of intangible benefits that measure several aspects ranging from strategy to the company's technology architecture. This shows that measurement using the Information Economic method is quite effective and efficient, because it provides a comprehensive evaluation in terms of tangible and intangible. Tangible and intangible aspects based on measurements have been made, for further research it is recommended to measure IS / IT investments in terms of variables that affect ERP implementation.

#### ACKNOWLEDGMENT

This work can not possibly be solved without the intervention of Allah SWT. I am especially like to thanks my supervisor, Dr. Apol Pribadi Head of Magister Information System for support, guidance, and motivation. Nobody has been more important to me in the pursuit of this paper than the members of my family. I would like to thank my parents and my brother; whose love and guidance are with me in the whatever I pursue. They are the ultimate role models.

#### REFERENCES

- [1] "infokomputer.com," 13 oktober 2016. [Online]. Available: <https://www.infokomputer.com/tag/investasi-ti/>. [Accessed 8 february 2017].
- [2] E. Brynjolfsson, "The productivity paradox of information technology," *Communications of the ACM*, vol. vol. 36, no. pp, pp. 66-77, 1993.
- [3] U. Essays, "The Information Technology Productivity Paradox Analysis Economics Essay. [online].," 2013. [Online]. Available: Available from: [https://www.ukessays.com/essays/economics/the-information-technology-productivity-paradox-analysis-](https://www.ukessays.com/essays/economics/the-information-technology-productivity-paradox-analysis-economics-essay.php?cref=1)
- [economics-essay.php?cref=1](https://www.ukessays.com/essays/economics/the-information-technology-productivity-paradox-analysis-economics-essay.php?cref=1). [Accessed 11 March 2017].
- [4] C. K. T. M. A. Barua, "Information Technology and bussiness value : an analytic and empirical investigation," *Information Systems Research*, vol. 6, no. 1, pp. 3-23, 1995.
- [5] T. S. a. B. Dehning, "Does successful investment in information technology solve the productivity paradox?," *Information & Management*, no. 38, pp. 103-117, 2000.
- [6] M. H. a. J. M. Sims, "Information technology (IT) productivity paradox in 21st Century," *International Journal of Productivity and Performance Measurement*, vol. 64, no. 4, pp. pp. 457-478, 2013.
- [7] p. C. a. J. D. a. N. Tangjitprom, "survey on available method to evaluate IT investment," *Electronic Journal Information Systems Evaluation*, vol. 19, no. 1, pp. 71-82, 2016.
- [8] F. A. P. A. P. H. J. S. Galih Yudha Saputra, "PENGUKURAN KINERJA SISTEM TEKNOLOGI INFORMASI E-KTP PADA KANTOR KECAMATAN PAKIS KABUPATEN MALANG MENGGUNAKAN FRAMEWORK COBIT," in *Prosiding Seminar Nasional Ilmu Komputer dan Teknologi Informasi*, 2017.
- [9] F. A. a. N. H. Arshad, "Value Delivery of Information Technology Investment: A Conceptual Framework," *International Journal of Computer Theory and Engineering*, vol. 6 no 2, pp. 150-154, 2014.
- [10] B. R. a. T. H. Parker M., *Information Economics: linking business performance*, New Jersey: Prentice Hall, 1988.
- [11] L. W. S. a. Yulia, "ANALYSIS OF THE IMPACT OF INFORMATION TECHNOLOGY INVESTMENTS-A SURVEY OF INDONESIAN UNIVERSITIES," *ARPN Journal of Engineering and Applied Sciences*, vol. 9, no. 12, pp. 2404-2410, 2014.
- [12] ISACA, *CGEIT : Certified in the Governance of Enterprise IT 7th edition*, USA: ISACA, 2015.
- [13] F. S. a. N. S. a. A. H. A. a. A. A.-M. A.-G. a. Z. U. a. F. A. B. a. M. H. Junejo, "Comparative Study from Several Business Cases and Methodologies for ICT Project Evaluation," (*IJACSA*) *International Journal of Advanced Computer Science and Applications*, vol. 6, no. 7, pp. 420-427, 2016.
- [14] F. D. A. Putri, "industri bisnis," 01 april 2013. [Online]. Available: <http://industri.bisnis.com/read/20130401/105/5897/enterprise-resources-planning-nilai-investasi-di-indonesia-rp097-triliun>. [Accessed 21 August 2018].
- [15] A. R. G. S. T. M. W. Puty Mairawati, "Analisis Kelayakan Investasi untuk Penerapan Enterprise Resource Planning : Studi Kasus," in *Seminar dan Konferensi Nasional IDEC*, Surakarta, 2018.

# Analysis on Customer Satisfaction Dimensions in Peer-to-Peer Accommodation using Latent Dirichlet Allocation: A Case Study of Airbnb

Kevin M. Situmorang., Achmad N. Hidayanto., Alfian F. Wicaksono., Arlisa Yuliatwati  
Faculty of Computer Science – Universitas Indonesia  
kevin.mahendra@ui.ac.id, nizar@cs.ui.ac.id, alfian@cs.ui.ac.id, arlisa@cs.ui.ac.id

**Abstract**— Customer satisfaction becomes a key influencer for people's habits or daily activities. One of the examples is in the decision-making process about whether they will use specific products or services. People often need other's review or rating about what they are going to use or consume. In this research, by using customer's online review that available from Airbnb website, we try to extract what are the most talked factors about peer-to-peer accommodation, and how customer sentiment about them. We use Latent Dirichlet Allocation (LDA) to extract that factors and conduct sentiment analysis by utilizing semantic analyzer from Google Cloud NLP. We analyze which factors that has more effect on customer satisfaction, not only in general but more specific based on customer gender and tourism destination object. The result shows that factors related to social benefit and service quality have impact on customer satisfaction, moreover different customer gender and different tourism object destination bring different sentiment among customer. We also find several factors that can be improved by the owner of the accommodation to improve customer satisfaction toward their services.

**Keywords**—Customer Satisfaction, Sentiment Analysis, Peer-to-Peer Accommodation, Latent Dirichlet Allocation

## I. INTRODUCTION

SHARING economy is a peer-to-peer activity to get, to give, or to share things or services through online platform [1] [2]. Collaborative consumption which is based on the concept of sharing economy has brought the society into a new level of consumption pattern. One of the instance of this business model is peer-to-peer accommodation which known as the introduction of Airbnb in 2008 [3]. It is said that peer-to-peer accommodation offering another solution for travelers who want unique experience in choosing accommodation. Physically, Airbnb does not own any assets, which are the accommodations (room, house, hotel, etc.). Airbnb becomes an intermediary between the owners of the accommodations and the customers. The accommodations registered in Airbnb website are available for rent by customers and the process basically goes like the offline accommodation reservation.

Customer or user satisfaction is defined as subjective evaluation from customer or user whether specific product or service have satisfied their expectation [4]. This evaluation is important for others who are willing to use

specific services or products. For example, in the field of peer-to-peer accommodation, before deciding to stay in a specific place, people need to know how well the service quality of both the accommodation and the staff are. Therefore, good experience will bring positive word-of-mouth that will take effect on the increase of company sales and profits [5]. Since customer satisfaction is beneficial for all stakeholders in this peer-to-peer accommodation case, it is important to identify in what factors customers satisfied with certain products or services.

Previous research found that *service quality*, *staff hospitality*, *reputation of the accommodation*, and *security* become the affecting factors for customer satisfaction, specifically related to peer-to-peer accommodation [4]. Additional factors such as *enjoyment*, *social benefits*, *economic benefits*, *sustainability*, *amenities*, and *location benefits* are also identified to be important [2] [3] [6] [7] [8]. Generally, these previous researches used quantitative, qualitative, or combination of using questionnaire and focus group to gather what are important factors behind customer satisfaction. In this method, to avoid useful information are not captured from the questionnaire, we need to involve expert in the construction of each question [9].

In the era of social media, User Generated Content (UGC) as an expression of products or services are useful for companies to know customer's acceptance of their products [10]. In the case of Airbnb platform, this information can be obtained from customer's online review. Realize that trust factor also affecting customer's decision, Airbnb managed to provide only useful reviews and ratings from previous customers through their policy, i.e. (1) deleting reviews that are not represent to customer's personal experience, (2) reviews that are promised by specific reward, and (3) reviews that are driven by the threat of extortion [11]. Airbnb also describe their extortion policy to prevent the creation of any reviews that violates three points above. By utilizing this relevant review data, our main goal is to automate the process of identifying the affecting factors for customer satisfaction, specifically in the domain of peer-to-peer accommodation.

As mentioned in previous research about customer review data [9], customers may not explicitly mention specific dimensions of customer satisfaction in their review. Instead, they indirectly describe other indicators or attribute represent those dimensions. By employed Latent Dirichlet Allocation (LDA) as topic modeling method, this research

This work was supported by Universitas Indonesia under PITTA Grant 2018, with the contract number 1862/UN2.R3.1/HKP.05.00/2018



was able to extract hidden dimension affecting visitor satisfaction towards online hotel reviews that were not found by using traditional method. We adopt this method to extract hidden topics from Airbnb's customer review data as the affecting factors for customer satisfaction. Generally, our experiment tries to figure out the answer of these questions:

- What are the factors or dimensions that affecting customer satisfaction in peer-to-peer accommodation?
- How better are the extracted factors compared to previously identified (in previous research)?
- What is the heterogeneity of perceptions for different groups of customers and different groups of tourism destination object?
- What are the most affecting factors for customer satisfaction based on regression analysis?
- What is the relationship between online rating provided by Airbnb with the customer satisfaction?

We organize the rest of this paper as follows: Section II explains the literature review, continued by research method in Section III. Section IV describes the result and discussion, then the last section brings the conclusion.

## II. LITERATURE REVIEW

### A. Extract Hidden Topics through Latent Dirichlet Allocation

In this research, we want to automatically extract that factors by utilizing Latent Dirichlet Allocation (LDA) as one of techniques for identifying hidden topics from unstructured data. This technique is an efficient unsupervised technique since it can handle not only large data but also periodically and sparse data [12]. By the assumption that each document is made up of topics with certain proportion, LDA tries to find the topics stored in a document.

Here is the outline of topic modeling using LDA [9] [12]:

1. A corpus is a collection of  $m$  documents represented in  $C = \{D_1, D_2, D_3, \dots, D_m\}$ . Each document  $D_d$  consist of  $n$  terms represented in  $D_d = (w_1, w_2, w_3, \dots, w_n)$ . There are  $p$  topics, represented in  $T = \{T_1, T_2, T_3, \dots, T_p\}$ .
2. LDA step by step:
  - a. A document-term matrix is decomposed into two matrices:  $M_1$  which is the document-topic matrix and  $M_2$  which is the topic-term matrix.
  - b. Each term then is randomly assigned to a topic. The assignment will be updated based on the multiplication of  $P_1$  and  $P_2$  until it reaches certain convergence limits.  $P_1$  and  $P_2$  respectively are:
    - $P_1$  or  $P(\text{topic } T | \text{document } D)$  is the proportion of terms in a document assigned to a topic  $T$ .
    - $P_2$  or  $P(\text{word } w | \text{topic } T)$  is the proportion of topic  $T$  to all documents  $D$  derived from term  $w$ .
  - c. In LDA, parameter  $\alpha$  represents the document-topic density while  $\beta$  parameter represents the topic-term density. The higher value of parameter  $\alpha$  indicates that the higher number of topics are construct a

document (and vice versa). The higher value of parameter  $\beta$  indicates that a topic is composed of more terms (and vice versa).

3. Other important issue in LDA technique is to determine the number of topic to be extracted [13]. We use harmonic mean method to estimate marginal likelihood of each LDA model, as done by [14].

### B. Sentiment Analysis using Google NLP API

Sentiment analysis or opinion mining is a process of analyzing opinion, sentiment, evaluation, reaction, and emotion towards specific person, organization, issue, or event [10]. As mentioned in [10], sentiment analysis can be differentiated in several levels, they are:

1. *Document level analysis*. This level of analysis classifies documents into positive, negative, or neutral sentiment based on analysis of the whole content of document that talks about specific entity or product, not about comparison of entities or products.
2. *Sentence level analysis*. In this level, we analyze whether a sentence belongs to positive, negative, neutral, or does not belongs to any sentiment.
3. *Aspect or entity level analysis (feature-based opinion mining)* [15]). The analysis is conducted towards a specific opinion which is consists of opinion target and sentiment of related opinion. Opinion target can be a specific entity and/or specific aspect being talked in that opinion. For example, the sentence "*The iPhone's call quality is good, but its battery life is short*" has "*call quality*" and "*battery life*" as its opinion targets. And evaluation "*good*" and "*short*" for each mentioned target respectively.

After obtaining the list of hidden topics using LDA from the review document collection as the opinion targets, we try to classify each topic into positive, negative, or neutral sentiment as the evaluation of the targets. We utilize Google Cloud NLP API<sup>1</sup> to get the sentiment score. The API provides several methods for text analysis and annotation, one of them is *Sentiment Analysis* method. This method provides sentiment score of a passage that indicates the passage's overall emotion. The sentiment score is ranged between -1.0 (negative sentiment) to 1.0 (positive sentiment). For example, a sentence "*bathroom outside is incredible!*" scored 0.6 and has positive sentiment by using this Google API's method.

## III. RESEARCH METHOD

### A. Data Collection and Text Preprocessing

We use Scrapy<sup>2</sup> combined with Airbnb's API to gather customer review data from Airbnb website. Since Airbnb does not provide gender information, we also use Genderize<sup>3</sup> to identify gender of each customers. We need to

<sup>1</sup>[https://cloud.google.com/natural-language/docs/basics#interpreting\\_sentiment\\_analysis\\_values](https://cloud.google.com/natural-language/docs/basics#interpreting_sentiment_analysis_values)

<sup>2</sup> Python based framework for extracting data from website (<https://scrapy.org/>)

<sup>3</sup> This tool determine gender based on the first name. (<https://genderize.io/>)

know whether a customer is male or female to analyze customer satisfaction based on gender.

We filter the whole data in several steps as follows:

1. Choose the review data which gender is identified. We obtain 32,072 reviews i.e. 45.73% reviews from male customer and 54.27% reviews from female customer.
2. Choose review in English since about 88.22% reviews are written in English. We obtain 27,711 reviews.
3. Choose review that associated with tourism object destination based on the accommodation distance from tourism object (no more than 30 km). Our final data is 24,911 reviews.

We then do several preprocessing steps to transform our textual data into numerical data by following these steps.

1. Replace numerical text that refers to currency with 'price-indicator' notation, for example Rp 8000, 150k, \$50.
2. Tokenization based on whitespace character to get list of single terms or tokens.
3. Part-of-Speech Tagging to identify the class of each term, e.g. noun, verb, adjective, etc.
4. Obtain base form of each term through lemmatization to reduce the number of unique terms obtained from the whole review data.
5. Named Entity Recognition using NLTK<sup>4</sup> for identifying the kind of entity owned by each term. There are nine provided entities, they are *organization*, *person*, *location*, *date*, *time*, *money*, *percent*, *facility*, *gpe* [16]. We add one more identifier to represent people's name that refers to name of the accommodation's host. The identifier is 'pname-indicator'.
6. Noun extraction by only selecting terms that belongs to noun class since they more representing a specific topic compared to those that belong to other classes.

After these steps, we construct bag-of-words for each document, containing 14,263 terms/words. Each document is represented into a vector  $D[(A_1, B_1), \dots (A_m, B_m)]$  where  $m$  is the number of terms (14,263),  $A_i$  is identity number of terms  $i$ , and  $B_i$  is frequency of term  $i$  appears in document  $D$ .

### B. Topic Extraction using LDA

We use Gensim<sup>5</sup> to build LDA model and get numbers of topics from Airbnb's given customer review data. One of the parameters needed to build LDA model is the number of topic. We do experiment on 31 number of topics, started from 20 to 50 and choose the best option. For each number of topics, we build its LDA model and evaluate the harmonic mean value of its log likelihood. From this experiment, the highest value is -1,946,092, reached when we use 43 topics.

From LDA model, each of 43 topics is represented by several most contributing words together with their proportion into related topic, not explicitly by the name of

topics. For example, Table I shows list of words representing certain topic with proportion of each word. By investigating the logical relationship of all contributing words, we try to find a specific topic name for each topic. We also recheck thoroughly into sample of documents to see the usability or context of the words in documents. For example, topic #18 is named as "*friendly host*". There are eight topics that their name cannot be identified because the contributing words relatively not connected each other. We named these topics under the name *Unidentified #1* to *Unidentified #8*. We also choose six words (as seeds) manually to represent each topic since there are several words that are not related into topic they represent. The bold and italic words in Table I shows the selected seeds for topic "*friendly host*".

Each document is associated to topics by considering the probability of each topic in each document through the seeds. We choose some topics for each document which probability exceed a specific threshold to avoid not relevant assignment from a document into specific topics. The threshold value is calculated from the total probability value of each topic in specific document divided by the number of known topics associated with specific documents. From this process, the result shows that the topics which names cannot be identified are relatively have small distribution among the whole documents. This indicates that customers relatively talk less about these topics or dimensions. As the result, we ignore these eight dimensions so there are 35 remaining topics to be analyzed.

### C. Analysis of Dimensions based on Statistical Analysis

After obtaining 35 topics, we then evaluate how customer sentiment towards these topics. Generally, we differentiate our analysis on following aspects:

#### 1) Analysis of Sentiment for Each Dimensions

We start our analysis on aspect level by using sentiment analyzer tools provided by Google Cloud NLP to identify the sentiment of each sentences. We choose sentences which contains at least one seed word and run the sentiment analyzer to get the sentiment of these sentences. Overall result using sentiment analyzer from Google Cloud NLP shows that from the collection of sentences containing seeds, 4% of them are identified as neutral sentiment, 6% as negative sentiment and 90% as positive sentiment.

The next step is to determine the sentiment of each dimension through their seeds. We divide sentences based on their related dimension and reanalyze the sentiment score obtained in previous step using Google Cloud NLP API.

TABLE I  
EXAMPLE OF TOPIC WITH LIST OF CONTRIBUTING WORDS  
(TOPIC #18 / FRIENDLY HOST)

Contributing Word	Proportion (%)	Contributing Word	Proportion (%)
<b><i>pname-indicator</i></b>	19	<b><i>person</i></b>	2.3
minute	8.8	holiday	2
<b><i>family</i></b>	8.6	Place	1.8
<b><i>friend</i></b>	5.3	year	1.7
time	4.8	company	1.7
<b><i>people</i></b>	3.9	contact	1.6
<b><i>thank</i></b>	3.6	child	1.6
kind	3.2	clean	1.4
nature	3.1	message	1.3
trip	3.1	lot	1.1

<sup>4</sup> Natural Language Toolkit, a python-based platform for NLP task (<https://www.nltk.org/>)

<sup>5</sup> Python based library for topic modeling (<https://radimrehurek.com/gensim/>)

### 2) Analysis of Dimensions based on Specific Groups

We analyze customer sentiment not only generally towards the whole dimensions but try to explore the heterogeneity of dimensions within the different groups of customers (e.g. female vs male) [9] and added more analysis for different groups of tourism object destination (e.g. sea, culture, and city). Through this step, combined with statistical test, we want to know how significance is the different of male and female customers sentiment towards each dimension. We have the similar objective with the analysis of groups of tourism destination objects, we want to measure how significance is the difference of customer sentiment of sea, culture, and city tourism object towards of the 35 dimensions.

### 3) Analysis on Online Rating Dimensions

Airbnb website provide two kinds of online rating, they are overall customer rating ranged from 1 to 100 and specific rating for six aspects (*cleanliness, arrival, accuracy, location, value, and communication*) ranged from 1 to 10. We run stepwise regression analysis to identify the most significant dimensions affecting customer satisfaction.

We normalize the overall customer rating into 0 to 10 and this value is chosen as the dependent variable, while the rating value for another six aspects as the independent variable. We run stepwise regression based on (1) and (2).

$$y_i = \hat{y} + e_i \quad (1)$$

$$\hat{y} = b_1x_{1i} + b_2x_{2i} + b_3x_{3i} + b_4x_{4i} + b_5x_{5i} + b_6x_{6i} \quad (2)$$

The variable  $y_i$  represents overall customer satisfaction, while  $x_{1i}$  to  $x_{6i}$  represents customer rating towards *cleanliness, accuracy, value, communication, arrival, and location* respectively, and  $e_i$  represents normally distributed residual error value. The result of this analysis is useful to identify which dimensions provided by Airbnb website that have the most effect on the customer satisfaction.

## IV. RESULTS AND DISCUSSION

### A. The Extracted Dimensions and Their Comparison to Previous Research

Based on the result of topic modeling using LDA, we obtained the total of 35 most discussed topics or dimension among customer review. Our result actually is also agreed upon previous research [6] [7] [8] [9] [17]. This is shown by the result of the calculation of Jaccard Coefficient<sup>6</sup> to get the proportion of overlapping topics obtained by LDA and topics obtained by previous research. The total score is 0.68, so there are more than 50% topics that are also identified as affecting factors in customer satisfaction. Table II shows the comparison of the topics obtained by using LDA with previous research ordered by the proportion or distribution of each dimension towards the whole review document. Furthermore, our experiment using LDA can identify more affecting factors for customer satisfaction compared to previous research result.

Additional result based on Table II, we find that dimensions related to host or staff of the accommodation

TABLE II  
TOPICS OBTAINED BY USING LDA AND OBTAINED FROM PREVIOUS RESEARCH (ORDERED BY TOPIC'S PROPORTION TOWARDS DOCUMENTS)

Topic/ Dimension's Name	Previous Research	LDA
Host Service	X	V
Welcoming Host	V	V
House	V	V
Staff Service	X	V
Villa	V	V
Experience	V	V
Transportation Rental	X	V
Friendly Host	V	V
Apartment	V	V
Driver	V	V
Price Value	V	V
Bathroom	V	V
Arrival Experience	X	V
Booking Experience	X	V
Amenities	V	V
Garden	X	V
Beach Vibe	X	V
Hospitality	V	V
Closeness to Shops	V	V
City View	X	V
Easy to Find the Location	V	V
Closeness to Restaurant	V	V
Style and Decoration	X	V
Room Maintenance	V	V
Cultural Experience	V	V
Hangout	V	V
Activity	V	V
Natural Beauty	X	V
Community	V	V
Insider Tip	V	V
Communication	V	V
Public Transportation	X	V
Help Locals	V	V
Bedroom	V	V
Dining	V	V

has relatively high proportion among the whole customer reviews. These dimensions include *host service, welcoming host, staff service, and friendly host*. Generally, they can be categorized as *social benefits* and *service quality*. *Social benefits* also bring significant effect on customer satisfaction since customers also enjoy their experience live with locals [8]. Moreover, most of the *service quality* focuses only on services provided by host instead of service quality of Airbnb platform. Specifically, customer concern mostly about the accommodation itself, including the hospitality and service given by accommodation host or staff rather than about the Airbnb platform. Furthermore, we cannot find any topics related to Airbnb platform from the result of topic modeling using LDA.

### B. General Customer Sentiment and based on Specific Groups Towards Each Dimension

#### 1) Customer Sentiment Towards Each Dimension

We have already got the result of sentiment analysis of all sentences containing the seeds. Based on the seeds, we classify the sentences based on their dimension to know the sentiment towards each dimension. All dimensions are identified to be indicator of positive word of mouth. There are four dimensions, such as *hospitality, communication, cultural experience, and garden* which reach the highest sentiment score, i.e. 0.7. These dimensions close to *social benefits* aspect, which is in line with the result described in previous subsection that customer's social experience defines their satisfaction.

<sup>6</sup> Jaccard =  $\frac{|\text{Topics obtained by LDA} \cap \text{Topics obtained by previous researcher}|}{|\text{Topics obtained by LDA} \cup \text{Topics obtained by previous researcher}|}$

### 2) Customer Sentiment based on Customer's Gender

We start with the identification of the proportion of each dimension toward customer's gender before identifying the sentiment. Through *t*-test<sup>7</sup>, the result shows that there are 10 topics that significantly different among male and female customers. They are *cultural experience*, *experience*, *host service*, *price value*, *staff service*, *welcoming host*, *apartment*, *driver*, *friendly host*, and *transportation rental*. Since mean value of topic distribution towards male customer is higher than female, it indicates that male customers pay more attention to these factors in determining their satisfaction towards the peer-to-peer accommodation.

We divide the documents into those who authored by male customers and those by female customers then analyze the sentiment for each dimension independently based on customer's gender. All topics get positive sentiment but there are some differences between male and female customer. By using *t*-test, the result shows that there are 9 topics that are identified as significantly different between male and female customer. They are *booking experience*, *host service*, *activity*, *amenities*, *bathroom*, *house*, *transportation rental*, *villa*, *welcoming host*. The *t*-test result also shows the mean value of sentiment on each topic among female customers is higher than the mean value of sentiment on each topic from male customers. This result indicates that sentiments given by female customers are more positive compared to those from male customers.

### 3) Customer Sentiment based on Tourism Destination Object

In this part, we analyze how the distribution of each topic among sea, culture, and city tourism object. By using ANOVA test we obtain 21 topics that has significant difference between the three categories of the tourism object destination. These topics are *amenities*, *apartment*, *experience*, *friendly host*, *hospitality*, *host service*, *house*, *price value*, *staff service*, *transportation rental*, *welcoming host*, *room maintenance*, *arrival experience*, *booking experience*, *bathroom*, *communication*, *community*, *cultural experience*, *driver*, *garden*, *style* and *decoration*. This significant difference indicates that in different tourism destination object, customers talk about different things.

We separate the documents into those who talks about sea, city, and culture tourism destination object then analyze the sentiment of each topic towards these categories independently. There are 11 topics that significantly different among those three categories. They are *arrival experience*, *driver*, *host service*, *house*, *amenities*, *experience*, *transportation rental*, *booking experience*, *friendly host*, *beach vibe*, *staff service*. All topics are identified as positive sentiment scored from 0.3 to 0.7. From this result we can conclude that in different tourism object, customer have different sentiment towards related dimensions.

### C. Analysis on the Relationship between Online Rating with The Sentiment of Extracted Dimension

From the six aspects provided by Airbnb website as the dependent variables (*cleanliness*, *arrival*, *accuracy*, *location*, *value*, and *communication*), the result of regression

TABLE III  
STEPWISE REGRESSION MODEL

Model	$R^2$	Adjusted $R^2$	F	Sig.
1 <sup>a</sup>	0.5178	0.5175	2014	< 0.001
2 <sup>b</sup>	0.6279	0.6275	1582	< 0.001
3 <sup>c</sup>	0.6809	0.6804	1333	< 0.001
4 <sup>d</sup>	0.6981	0.6974	1083	< 0.001
5 <sup>e</sup>	0.702	0.7012	885	< 0.001
6 <sup>f</sup>	0.7062	0.7053	749.7	< 0.001

Note:

<sup>a</sup> Predictors: (Constant), *cleanliness*, *accuracy*

<sup>b</sup> Predictors: (Constant), *cleanliness*, *accuracy*

<sup>c</sup> Predictors: (Constant), *cleanliness*, *accuracy*, *value*

<sup>d</sup> Predictors: (Constant), *cleanliness*, *accuracy*, *value*, *communication*

<sup>e</sup> Predictors: (Constant), *cleanliness*, *accuracy*, *value*, *communication*, *arrival*

<sup>f</sup> Predictors: (Constant), *cleanliness*, *accuracy*, *value*, *communication*, *arrival*, *location*

analysis shows that there is a strong relationship between these variables and the overall customer rating as dependent variable by using significance level 0.1%. Table III shows that the highest  $R^2$  value is obtained by the model which includes all of six dependent variables. This indicates that those six aspect or dimension from Airbnb website also affecting customer satisfaction.

By using Durbin-Watson test (the value is 2.01 and  $p=0.824$ ), it shows that residual error mentioned in Equation (1) is independent and does not have effect on customer satisfaction. Moreover, *cleanliness* is the most affecting dimension on customer satisfaction since it has the highest beta coefficient as shown in Table IV. The most affecting aspect for customer satisfaction ordered by their beta coefficient are *cleanliness*, *value*, *accuracy*, *communication*, *arrival*, and *location* respectively, and the regression model for customer satisfaction ( $\hat{y}$ ) is shown in (2).

$$\hat{y} = 0.36 + 0.31 * cleanliness + 0.2 * accuracy + 0.24 * value + 0.1 * communication + 0.09 * arrival + 0.08 * location \quad (3)$$

We also try to correlate the sentiment score we have obtained for each extracted dimension from LDA model with the overall customer rating from Airbnb website. We want to determine whether the customer's sentiment described in review data is as good as Airbnb's overall customer rating. We transform the sentiment result of each dimension into a rating value from 1 to 10 by using (4) [16]:

$$Rating = \left( \frac{P}{P+N} \times 9 \right) + 1 \quad (4)$$

Variable  $P$  represents the number of positive sentiments, while negative sentiment is represented by  $N$ . The rating of overall topics reaches above 8 and more than 50% of the topics reach above 9. The average of this customer

TABLE IV  
COEFFICIENT OF DEPENDENT VARIABLE FOR REGRESSION MODEL

Variables	Unstandardized		Standardized Beta Coeff.	t	Sig.
	B	Std. Error			
(Constant)	0.36	0.15		2.43	< 0.05
Cleanliness	0.26	0.02	0.31	17.29	< 0.001
Accuracy	0.18	0.02	0.20	10.38	< 0.001
Value	0.22	0.02	0.24	12.15	< 0.001
Communication	0.12	0.02	0.11	5.90	< 0.001
Arrival	0.10	0.02	0.09	4.96	< 0.001
Location	0.07	0.02	0.08	5.19	< 0.001

<sup>7</sup> We use  $p$  value 0.05 and confidence interval 95% for running *t*-test

satisfaction rating is 93.55, and it almost the same compared to customer rating that available at Airbnb website, which is 93.33.

## V. CONCLUSION

Our study tries to automate the process of extracting dimensions of customer satisfaction in peer-to-peer accommodation domain, specifically based on Airbnb case. The result shows that we can automatically find the dimensions through topic modeling using LDA from the collection of customer review data. There are several undiscovered dimensions that affecting customer satisfaction from previous research that use survey at limited sample.

On the analysis of heterogeneity of perception on different groups of customers, especially based on gender, we find that male customers have more attention toward several factors, while female customers tend to give more positive review than male customer in other factors. In the groups of tourism destination objects, we notice that different tourism object, bring different concern among customers about what factors affecting their satisfaction.

Based on the result of stepwise regression analysis, we know that the whole factors provided by Airbnb online rating significantly affecting customer satisfaction, especially *cleanliness* as the most affecting factor. The accommodation's owner should consider this factor to improve their cleanliness of the accommodation, moreover related to *house, villa, apartment, room maintenance, bedroom, and bathroom* since based on the reviews, customers also talk about these factors.

In general, by using *User Generated Content* data such as customer review, it is possible to extract the hidden dimension that affecting customer satisfaction. Through the utilization of NLP method such as topic modeling by using LDA, there will be no more limitation on the scale of the data since this method can handle large amount of data.

## VI. REFERENCES

- [1] R. Botsman and R. Rogers, *What's Mine Is Yours: The Rise of Collaborative Consumption*, New York: Harper Collins Publisher, 2010.
- [2] J. Hamari, M. Sjöklint and A. Ukkonen, "The Sharing Economy: Why People Participate in Collaborative Consumption," *JOURNAL OF THE ASSOCIATION FOR INFORMATION SCIENCE AND TECHNOLOGY*, pp. 2047-2059, 2016.
- [3] I. P. Tussyadiah and J. Pesonen, "Impacts of peer-to-peer accommodation use on travel patterns," *Journal of travel Research*, pp. 1022-1040, 2016.
- [4] R. K. S. Chu and T. Choi, "An importance-performance analysis of hotel selection factors in the Hong Kong hotel industry: a comparison of business and leisure travellers," *Tourism Management*, pp. 363-377, 2000.
- [5] W. W. Moe and M. Trusov, "The Value of Social Dynamics in Online Product Rating Frums," *Journal of Marketing Research*, pp. 444-456, 2011.
- [6] I. P. Tussyadiah, "An exploratory study on drivers and deterrents of collaborative consumption in travel," in *Information and communication technologies in tourism*, 2015.
- [7] M. Möhlmann, "Collaborative consumption: determinants of satisfaction and the likelihood of using a sharing economy option again," *Journal of Consumer Behaviour*, pp. 193-207, 2015.
- [8] C. P. Lamberton and R. L. Rose, "When is ours better than mine? A framework for understanding and altering participation in commercial sharing systems," *Journal of Marketing*, pp. 109-125, 2012.
- [9] Y. Guo, S. J. Barnes and Q. Jia, "Mining meaning from online ratings and reviews: Tourist satisfaction analysis using latent dirichlet allocation," *Tourism Management*, pp. 467-483, 2017.
- [10] B. Liu, *Sentiment Analysis and Opinion Mining*, Chicago: Morgan & Claypool Publishers, 2012.
- [11] Airbnb, "Apa yang dimaksud dengan Kebijakan Konten Airbnb?," Airbnb, [Online]. Available: <https://www.airbnb.co.id/help/article/546/what-is-airbnb-s-content-policy>.
- [12] D. M. Blei, A. Y. Ng and M. I. Jordan, "Latent Dirichlet Allocation," *Journal of Machine Learning Research* 3, pp. 993-1022, 2003.
- [13] D. M. Blei and J. D. Lafferty, "Text mining: Classification, clustering, and applications. Topic Models.," pp. 71-94.
- [14] T. L. Griffiths and M. Steyvers, "Finding Scientific Topics," *PNAS*, vol. 101 (supl 1), pp. 5228-5235, 2004.
- [15] M. Hu and B. Liu, "Mining and Summarizing Customer Reviews," in *The tenth ACM SIGKDD international conference on Knowledge discovery and data mining*, Seattle WA, 2004.
- [16] S. Bird, E. Klein and E. Loper, *Natural Language Processing for Python - Analyzing Text with Natural Language Toolkit*, O'Reilly Media Inc, 2009.
- [17] J. Hamari, M. Sjöklint and A. Ukkonen, "The Sharing Economy: Why People Participate in Collaborative Consumption," *JOURNAL OF THE ASSOCIATION FOR INFORMATION SCIENCE AND TECHNOLOGY*, pp. 2047-2059, 2015.

# Individual Factors As Antecedents of Mobile Payment Usage

Radinal Setyadinsa  
Faculty of Computer Science  
Universitas Indonesia  
Depok, Indonesia  
radinals@gmail.com

Muhammad Rifki Shihab  
Faculty of Computer Science  
Universitas Indonesia  
Depok, Indonesia  
shihab@cs.ui.ac.id

Yudho Giri Sucahyo  
Faculty of Computer Science  
Universitas Indonesia  
Depok, Indonesia  
yudho@cs.ui.ac.id

**Abstract**— The aim of this research was to discover the stances of individual elements as antecedents of mobile payment usage. Data was gathered by distributing a questionnaire, which in latter steps was analyzed quantitatively. This research collected 90 samples, of whom represented users of a mobile payment service in Indonesia. The collected dataset was statistically analyzed, by employing partial least square structural equation modelling (PLS-SEM), aided with SmartPLS3.0. The results showed that two types of individual factors, namely individual difference and behavioral belief played significant roles in shaping users' intention to use mobile payments. Individual differences, consisting of mobile payment knowledge and compatibility significantly influenced perceived ease of use. Behavioral belief, such as trust, was shown to significantly influenced perceived usefulness. Finally, perceived ease of use and perceived usefulness concertedly affected mobile payment users' intention to use.

**Keywords**—PLS, SEM, Mobile Payment, Individual

## I. INTRODUCTION

In recent years, more consumers have conducted purchase transactions over the Internet [1], and have led to an increase of customer demands toward a novel payment instrument that allows for mobility to increase convenience, more specifically in small transactions [2]. Since August 2014, the Governor of Indonesia's Central Bank declared the "Non-Cash National Movement" which aims to increase public awareness of non-cash instruments, thereby gradually moving towards a less-cash society.

Despite the ample benefits of using mobile payment services, its adoption in Indonesia is still relatively low. MasterCard Mobile Payments Readiness Index (MMPRI) in 2012 ranked Indonesia 33rd out of 34 countries in the mobile payment readiness survey, placing Indonesia's consumers as 'below average' in terms of familiarity, frequency and willingness to use mobile payment services [3]. This can also be seen in the lack of availability of payment method options using mobile payment or electronic money in Indonesia. Such predicament led the authors to raise the main question in this research, namely, what factors affect Indonesians in using mobile payment services? This research will look more specifically at individual factors and its roles in shaping consumers' behaviors of mobile payment adoption?

There are some previous works that have investigated behavioral aspects of mobile payments adoption. For example, the work of [1] investigated the antecedents of mobile payment and its intention to use in Vietnam, from the perspectives of mobility, convenience, and compatibility. Other researchers focused on comparing individualities and mobile payment system characteristics [4]. Other

researchers, such as [5] focuses on examining the roles of attitude, subjective norm and perceived behavioral control in shaping interests of using mobile payment services.

In this research, individual factor is first loosely understood as anything or circumstance that may influence an individual to do something. This research differs individual factors as individual difference and behavioral belief. Hence, the goal of this study is to elaborate the roles of individual precursors, namely individual difference and behavioral belief, towards consumers' intention to use mobile payment.

## II. HYPOTHESES DEVELOPMENT

Previous studies were analyzed to obtain a theoretical framework for this research. A visual representation of the underlying research model is portrayed in Figure 1. The hypothesis projected herein are elaborated below:

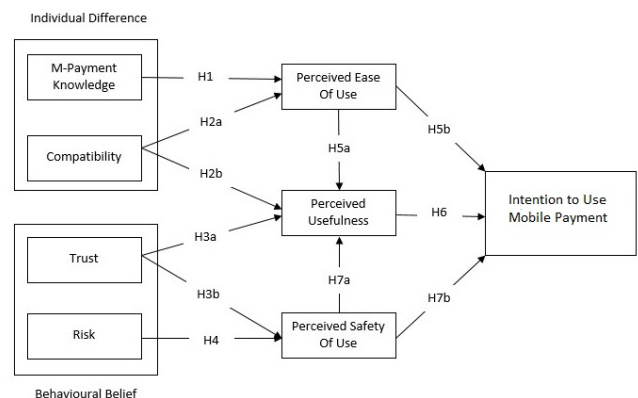


Fig. 1. Underlying Research Model

According to [6], mobile payment knowledge can be defined as knowledge or information concerning the way payment systems are utilized on mobile devices, connected to a mobile communications networks, to induct, approve and approve commercial transactions. Given the popularity of mobile devices, it is very important to understand if those who are users of mobile devices are likely to conduct transactions through mobile payment services. Other research previously conducted has shown the impacts of the level of knowledge concerning mobile payment on the ease of use of mobile payment services [1]. Individuals with higher levels of knowledge concerning mobile payment tend to find the mobile payment service easier to use than those with less knowledge [4]. Customers will find it easier to utilize mobile payment services given a superior degree of knowledge concerning the relevant mobile payment tools [1]. Thus, this research proposes the following hypothesis:



H1: Knowledge concerning mobile payment significantly affects perceived ease of use of mobile payment.

Compatibility can be understood as the operational effectiveness of new services when compared to existing services [7]. Individuals' variety of lifestyles will greatly influence their conclusion of embracing mobile payment services. Mobile payment is an augmentation of conventional Internet-based payments, hence, those who frequently use Internet-based payments tend to have less refusal to accept mobile payment. Such understanding allows for the assumption that perceived compatibility plays a very important role in shaping the intention to adopt a technology. For new services like mobile payment, an individual's ability to assimilate them into their purchasing practices and everyday lifestyle is an eminent element, making it a key success factor of mobile payment services [8]. Therefore, this research proposes the following hypothesis:

H2a: Compatibility significantly affects perceived ease of use of mobile payment.

H2b: Compatibility significantly affects perceived usefulness of mobile payment.

Trust is defined as an individual's willingness to embrace risks with the hopes that their desires are fulfilled [4]. Customers' trust can be identified as an influential factor leading to the triumph of mobile banking, where transactions are conducted on a more vulnerable and uncertain telephone network compared to traditional payment transactions [9]. Transactions made through mobile networks are at risk, with a higher level of uncertainty than any preceding arrangements, thus carrying more risk potentials. Customers who have high trust level on mobile payment services will realize service providers' integrity and reliability; which will augment their intention to use the service [10]. Furthermore, upon conducting transactions, consumers expect personal information to be guaranteed in terms of security, and not be shared with inappropriate parties [11]. Therefore, this study proposes that trusts affect perceived security and perceived usefulness.

H3a: Trust significantly affects perceived usefulness of mobile payment.

H3b: Trust significantly affects perceived security of mobile payment.

Risk relates to the absence of security throughout the payment processes due to mistakes or fraudulent transactions between buyers and sellers [12]. Mobile payment is a form of online transaction that occurs between unknown parties, in which exists financial risks and ambiguity concerning a product's quality. Thus, this research argue that risks affect mobile payment services perceived security.

H4: Risk significantly affects perceived security of mobile payment.

Perceived ease of use is expressed as the level of simplicity and ease to use a particular new system [13]. Hence, it is a vital precursor that affects mobile payment services' intention to use [14]. Perceived ease of use denotes the clarity, understandability, comfortability of users' interactions and experience with the new system [15]. Such understanding allows for the assumption that ease of use is essential precursor influencing new technology acceptance.

Furthermore, perceived ease of use is a factor that shapes perceived usefulness [16].

H5a: Perceived ease of use significantly affects mobile payment's perceived usefulness.

H5b: Perceived ease of use significantly affects mobile payment's intention to use.

Perceived usefulness can be explained as the customer's state of mind concerning the potential of new services in providing benefits and in increasing customers' task performance [17]. According to [18], usefulness can also be understood as customers' believe that adopting new technologies will aid the fulfillment of their expectations. Other research, such as [19] adds that perceived usefulness is a novel amenity that offers more benefits than existing services to those who intend to use it. Therefore, this study suggests that perceived usefulness influences the intention to use mobile payment.

H6: Perceived usefulness significantly affects mobile payment's intention to use.

Perceived security is understood as the confidence that the system ensures confidential user information [20]. Customers will surely pay more attention to security issues in mobile payment services. This becomes an vital component for mobile payment services success [10]. Customers expect that their transaction be accomplished as expected, without data being shared with non-conforming parties [21]. Some even argue that customer security in e-commerce is an important factor because the digital realm carries a higher level of risks when compared to traditional environment [22].

H7a: Perceived security significantly affects mobile payment perceived usefulness.

H7b: Perceived security significantly affects mobile payment intention to use.

### III. RESEARCH METHODOLOGY

This research used a questionnaire-based quantitative approach in gathering data and in conducting hypothesis testing. First of, the variables in the theoretical framework were elaborated to unique question items. Before being disseminated, a readability test was conducted to ensure that all questions were correctly understood. This readability test involved seven individuals whom were active users of mobile payment services. After a thorough revision, the questionnaire was then distributed to the respondents.

The data collection process made use of questionnaires using a survey-form tool with a 6-point Likert scale, having scales that range from strongly disagree to strongly agree. The questionnaire was made using typeform application and then disseminated online through social media. The target of the respondents in this study are those individuals who have previously used mobile payment services.

The questionnaire consisted of 28 questions, representing indicators of eight different variables. The result of this stage is a questionnaire that has been filled by respondents and whose responses were considered as complete and consistent.

Researchers then performed data processing and analysis to test the hypothesis, using Partial Least Square Structural Equation Modeling (PLS-SEM) statistical techniques aided with smartPLS software. Furthermore, data analysis was carried out to test the hypotheses formulated. Then through statistical calculations, the results are discussed by using existing theories as well as previous research results.

#### IV. RESEARCH RESULTS

##### A. Respondents Demography

This research resulted in 90 respondents who filled out the questionnaire. However, only 89 was included to further analysis, because one sample was deemed as invalid due to incompleteness.

The demography of the sample was quite diverse. A majority of them were male (56%) and the rest were female (44%). In terms of age, a large number of those who participated in this study were young adults between 25-35 years old (49%). Most of the respondents held a day job (46%) and all of them (100%) use a smart phone on a daily basis. Finally, a large proportion of them (73%) have previously conducted online transaction and online payment.

##### B. Analysis of the Measurement Model

In this phase, this research will ensure that the data meets all validity and reliability requirements. First, we conducted an examination of the convergence validity. All question items were tested to ensure their loading factor value that represented each indicator on the latent variable were greater than 0.5 [23], [24]. Moreover, the values of Average Variance Extracted (AVE) should surpass 0.5 [24].

This research stumbled upon two indicators that failed meet the Loading Factor threshold, namely H41 and H73. According to [24], indicators that have values of Loading Factor not more than 0.5 should be removed. Upon removal

TABLE 1. ALL INDICATORS LOADING FACTOR VALUES

Variable	Indicator	Loading Factor
Mobile payment knowledge	H11	0.765
	H12	0.796
	H13	0.676
	H14	0.790
Compatibility	H21	0.678
	H22	0.711
	H23	0.875
Trust	H31	0.820
	H32	0.838
	H33	0.804
Risk	H42	0.809
	H43	0.779
	H44	0.822
	H51	0.751
Perceived ease of use	H52	0.744
	H53	0.746
	H54	0.800
	H61	0.822
Perceived usefulness	H62	0.870
	H63	0.875
	H71	0.874
Perceived security	H72	0.823
	H81	0.822
Intention to use mobile payment	H82	0.795
	H83	0.852
	H84	0.615

TABLE II. ASSESSMENT OF CRONBACH'S ALPHA (CA) AND COMPOSITE RELIABILITY (CR)

Variable	CA	CR
Knowledge	0.753	0.843
Compatibility	0.637	0.802
Trust	0.758	0.861
Risk	0.726	0.845
Perceived ease of use	0.758	0.846
Perceived usefulness	0.817	0.891
Perceived security	0.613	0.837
Intention to Use	0.776	0.857

of the two indicators aforementioned, it can be seen that the remaining indicators have met required LF value of greater than 0.5, ensuring the research instrument's convergent validity. All indicators' Loading Factor values are presented in Table 1.

Furthermore, this research also ensured reliability by testing the Cronbach's Alpha (CA) and Composite Reliability (CR) for all indicators. According to [25], a variable is considered to have reliable indicators having CA value exceeding 0.6 and CR value exceeding 0.7. The results are summarized in Table II and presented that indicators reliability in this research have met the requirements.

##### C. Analysis of the Structural Model

In this step of analysis, this research will first test the Coefficient of Determination ( $R^2$ ) prior to testing the hypotheses. The  $R^2$  measures how much a dependent latent variable can be justified by its preceding independent latent variables [26]. The value of  $R^2$  is considered weak if it has a value of less than 0.19, considered medium if it has a value between 0.19 - 0.33, and is considered strong if it has a value between 0.33 - 0.67 [27]. The results in this research showed that three dependent latent variables had strong preceding relationships with its independent latent variables, namely, intention to use, perceived ease of use and perceived usefulness. Additionally, perceived security exhibited a medium strength relationship to its preceding independent latent variables. The results summarizing the coefficient of determination ( $R^2$ ) values are displayed in Table III.

##### D. Hypothesis Testing

An examination of t-statistics values as well as p-values were conducted to test the hypotheses. The hypotheses were tested with a predetermined alpha of 0.05, hence the required t-statistics value should be greater than 1.96. Out of the eleven hypotheses tested, this research resulted in seven hypotheses accepted whereas four hypotheses rejected. A review of the hypothesis's examination product is provided in Table IV. The resulting research model is visually presented Figure 2.

#### V. DISCUSSION

This study found perceived ease of use to positively influenced perceived usefulness alongside intention to use. Mobile payment services are critically questioned by its

TABLE III.  $R^2$  VALUES

Variabel	$R^2$	Category
Perceived ease of use	0.501	Strong
Perceived usefulness (PU)	0.601	Strong
Perceived security	0.302	Medium
Intention to use mobile payment	0.469	Strong

TABLE IV. HYPOTHESES TEST RESULTS

H	Path	T-Statistics	P-Values	Decision
H1	Knowledge → Perceived ease of use	3.607	0.000	Accepted
H2a	Compatibility → Perceived ease of use	2.900	0.004	Accepted
H2b	Compatibility → Perceived usefulness	0.422	0.673	Rejected
H3a	Trust → Perceived usefulness	3.491	0.000	Accepted
H3b	Trust → Perceived security	1.909	0.056	Rejected
H4	Risk → Perceived security	3.738	0.000	Accepted
H5a	Perceived ease of use → Perceived usefulness	2.184	0.029	Accepted
H5b	Perceived ease of use → Intention to use	2.005	0.045	Accepted
H6	Perceived usefulness → Intention to use	2.812	0.005	Accepted
H7a	Perceived security → Perceived usefulness	0.645	0.519	Rejected
H7b	Perceived security → Intention to use	0.573	0.567	Rejected

users in terms of how easy it is to employ. The analysis also yielded that perceived usefulness prejudiced intention to use. The usefulness of services like to mobile payment should be well understood by customers, because it is a critical prerequisite towards adoption. The results in this research also corroborates the arguments of [1] concerning the importance of ease of use in determining the adoption of mobile payment.

Two factors acted as motivators towards perceived ease of use, namely mobile payment knowledge and compatibility. It is safe to assume that mobile device users with higher levels of mobile payment knowledge tend to find the mobile payment service easier to use, when compared to those who lack such knowledge. Mobile device users will experience an easier and more efficient mobile payments transactions, having equipped with a high level of knowledge about mobile payments. In addition, compatibility was also a determinant of ease of use.

Finally, the results showed trust as an antecedent of perceived usefulness. It is known that trusts in payment systems in general, will lessen the necessity to comprehend, govern and supervise activity, enabling users to employ the services easily and efficiently deprived of considerable struggle in translating online services [1]. This research has shown that the same arguments is fitted for mobile payments systems, corroborating trust's role in shaping perceived usefulness in mobile payments.

## VI. RESEARCH IMPLICATIONS

The results in this research provided empirical indications concerning the precursors of perceived ease of use in mobile payments, namely mobile payment knowledge and compatibility. This findings extend our understanding of such antecedent, previously argued by [1], [4]. Additionally, the role of trust in shaping mobile payment's perceived usefulness was corroborated, strengthening the arguments set forth by previous research of similar topic [1].

Furthermore, the robustness of TAM was exemplified in mobile payments circumstances, by showing that perceived

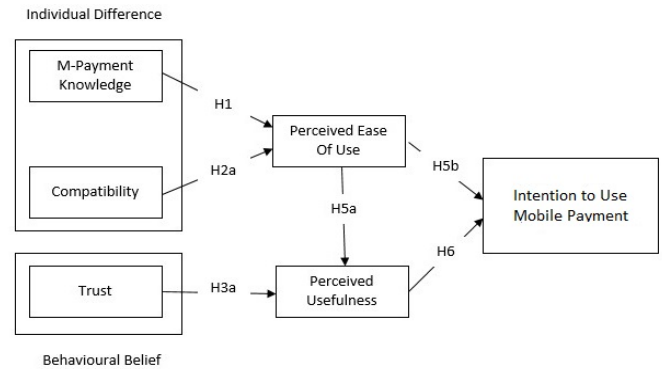


Fig. 2. Resulting Model

usefulness and perceived ease of use both concertedly affected intention to use mobile payments. Such finding validated previous works, such as [4].

Several practical implications are also noteworthy to discuss. First, this research provides insights for organizations offering mobile payment services, more specifically in understanding the way individual factors affected user's intention to use. Those organizations offering mobile payment services should provide ample knowledge for their potential users. The more knowledge an individual has concerning mobile payments leads to a higher perception of ease in using mobile payment services.

Additionally, mobile payment services being offered should ensure compatibility, for example in terms of transaction varieties (purchases, bill payments, etc.) that suit the needs of potential users. These two individual difference factors positively affect perceived ease of use. Furthermore, technological compatibility should also be kept in mind. For example, mobile payment should be offered in platforms compatible with the mobile devices already owned by potential customers.

On the other hand, perceived usefulness was predisposed by an individual's behavioral belief of trust. Organizations offering mobile payment services should strive to continually ensure that their services are safe, reliable, and trustworthy to use, because it will increase users' confidence in the service and their perception of usefulness.

## VII. CONCLUSIONS AND RECOMMENDATIONS

This research was designed to explore the roles of individual precursors of user's intention to adopt mobile payments. The results provided empirical evidences that two types of individual factors, namely individual difference and behavioral belief play significant roles in shaping user's intention to use mobile payments.

Individual differences such as having mobile payment knowledge and ensuring mobile payment compatibility significantly predisposed perceived ease of use. Moreover, behavioral belief, such as trust, was shown to significantly influenced perceived usefulness. Finally, both perceived ease of use and perceived usefulness concertedly affected users' intention to use mobile payment.

## ACKNOWLEDGEMENT

This Research was funded by the 2018 PITTA Grant,  
Universitas Indonesia, Contract Number:  
1887/UN2.R3.1/HKP.05.00/2018

## REFERENCES

- [1] G. Liu and P. T. Tai, "A Study of Factors Affecting the Intention to Use Mobile Payment Services in Vietnam," *Econ. World*, vol. 4, no. 6, pp. 249–273, 2016.
- [2] J. Ondrus and Y. Pigneur, "Towards a holistic analysis of mobile payments: A multiple perspectives approach," *Electron. Commer. Res. Appl.*, vol. 5, no. 3, pp. 246–257, 2006.
- [3] MasterCard, "Mobile payment s Readiness Index," Available: <http://mobilereadiness.mastercard.com/the-index/>, 2012.
- [4] C. Kim, M. Mirusmonov, and I. Lee, "An empirical examination of factors influencing the intention to use mobile payment," *Comput. Human Behav.*, 2009.
- [5] H. Ting, Y. Yacob, L. Liew, and W. M. Lau, "Intention to Use Mobile Payment System: A Case of Developing Market by Ethnicity," *Procedia - Soc. Behav. Sci.*, vol. 224, no. 2016, pp. 368–375, 2015.
- [6] D. L. Amoroso and R. Magnier-Watanabe, "Building A Research Model For Mobile Wallet Consumer Adoption: The Case of Mobile Suica In Japan," *Kennesaw State Univ. Coles Coll. Business, Kennesaw, Georg. USA. Univ. Tsukuba, Grad. Sch. Bus. Sci. Tokyo, Japan*, 2011.
- [7] N. Mallat, M. Rossi, and V. K. Tuunainen, "The impact of use situation and mobility on the acceptance of mobile ticketing services," *Proc. 39th Hawaii Int. Conf. Syst. Sci. Hawaii.*, 2006.
- [8] T. Teo and S. Pok, "Adoption of WAP-Enabled Mobile Phones Among Internet Users," *Omega*, vol. 31, no. 6, pp. 483–498, 2003.
- [9] A. Bhattacharjee, "Individual trust in online firms: Scale development and initial test," *J. Manag. Inf. Syst.*, vol. 19, no. 1, pp. 211–241, 2002.
- [10] D. Gefen, E. Karahanna, and D. W. Straub, "Trust and TAM in online shopping: An integrated model," *MIS Q.*, vol. 27, no. 1, pp. 51–90, 2003.
- [11] T. Zhou, "An empirical examination of initial trust in mobile banking," *Internet Res.*, vol. 21, no. 5, pp. 527–540, 2011.
- [12] W. J. Havlena and W. S. DeSarbo, "On the measurement of perceived consumer risk," *Decis. Sci.*, vol. 22, no. 4, pp. 927–939, 1991.
- [13] F. D. Davis, "Perceived Usefulness, Perceived Ease of Use, and User Acceptance of Information Technology," *MIS Q.*, vol. 13, no. 3, pp. 319–340, 1989.
- [14] G. C. Moore and I. Benbasat, "Development of an instrument to measure the perceptions of adopting an information technology innovation," *Inf. Syst. Res.*, vol. 2, no. 3, pp. 173–191, 1991.
- [15] N. O. Ndubisi and M. Jantan, "Evaluating IS usage in Malaysian small and medium-sized firms using TAM," *Logist. Inf. Manag.*, vol. 16, no. 6, pp. 440–450, 2003.
- [16] F. D. Davis, R. P. Bagozzi, and P. R. Warshaw, "User acceptance of computer technology: A comparison of two," *Manage. Sci.*, vol. 35, no. 8, pp. 982–1002, 1989.
- [17] C. Mathwick, N. K. Malhotra, and E. Rigdon, "The effect of dynamic retail experiences on experiential perceptions of value: An Internet and catalog comparison," *J. Retail.*, vol. 78, no. 1, pp. 51–60, 2001.
- [18] M. Gong and Y. Xu, "An enhanced technology acceptance model for web-based learning," *J. Inf. Syst. Educ.*, vol. 15, no. 4, pp. 365–374, 2004.
- [19] R. Awamieh and C. Fernandes, "Internet Banking: An empirical investigation into the extent of adoption by banks and the determinants of customer satisfaction in the United Arab Emirates.," *J. Internet Bank. Commer.*, vol. 10, no. 1, pp. 1–12, 2005.
- [20] F. N. Egger, "Affective design of e-commerce user interfaces: How to maximize perceived trustworthiness.," *Proceeding CAHD Conf. Affect. Hum. Factors Des. Singapore*, pp. 317–324, 2001.
- [21] R. K. Chellappa and P. A. Pavlou, "Perceived information security, financial liability and consumer trust in electronic commerce transactions," *Logist. Inf. Manag.*, vol. 15, no. 5/6, pp. 358–368, 2002.
- [22] S. Grabner-Krauter and E. Kalusha, "Empirical research in on-line trust: A review and critical assessment," *Int. J. Hum. Comput. Stud.*, vol. 58, no. 6, pp. 783–812, 2003.
- [23] W. W. Chin, "The partial least squares approach for structural equation modeling. In George A. Marcoulides (Ed.)," *Mod. Methods Bus. Res. Lawrence Erlbaum Assoc.*, pp. 295–336, 1998.
- [24] J. Hair, C. Ringle, and M. Sarstedt, "Editorial Partial Least Square: The Better Approach to Structural Equation Modeling," *Long Range Plann.*, pp. 312–319, 2012.
- [25] H. Jogiyanto and W. Abdillah, "Konsep dan Aplikasi PLS (Partial Least Square) untuk penelitian empiris," *Yogyakarta: BPFE-Yogyakarta*, 2009.
- [26] A. Widarjono, "Analisis multivariat terapan dengan program SPSS, AMOS, dan SMARTPLS," *Yogyakarta UPP STIM YKPN*, 2015.
- [27] H. Latan and I. Ghazali, "Partial Least Squares: Konsep, Teknik, dan Aplikasi Menggunakan Program SMARTPLS 2.0 M3," *Semarang Badan Penerbit Univ. Diponegoro*, 2012.
- [28] C. Kim, M. Mirusmonov, and I. Lee, "An empirical examination of factors influencing the intention to use mobile payment," *Comput. Human Behav.*, vol. 26, no. 3, pp. 310–322, 2010.

# Determine supporting features for Mobile Application of NUSANTARA

Dana Indra Sensuse, Ika Arthalia  
Wulandari, Erzi Hidayat, Pristi  
Sukmasetya  
E-Government & E-Business  
Laboratory  
Faculty of Computer Science  
Universitas Indonesia, Depok  
dana@cs.ui.ac.id, {ika.arthalia,  
erzi.hidayat,  
pristi.sukmasetya}@ui.ac.id

Elin Cahyaningsih  
National Civil Service Agency  
E-Government & E-Business  
Laboratory  
Faculty of Computer Science  
Universitas Indonesia, Depok  
elin.cahyaningsih@ui.ac.id

Wina Permana Sari  
Bina Nusantara Institute of Creative  
Technology, Malang  
Sari001@binus.ac.id

**Abstract**—Mobile Application of NUSANTARA which called m-NUSANTARA is an KM tools that design for supporting the KM process in government human capital management. This research is continuation of previous research focusing on the development of a model of knowledge management system for civil servant from three ministries in Indonesia (KEMENPAN&RB, BKN, and LAN) which called Government Human Capital Knowledge Management of Republic of Indonesia (NUSANTARA). Implementation of this KM model is conducted with web system, further development of this system still provides constraints from several sides in providing more optimal service against users requirements as well as limited accessibility and responsiveness. This paper aims to explore the supporting features that will be used to integrate pre-existing systems that build mobile knowledge management applications. Data were collected by interview from each expert in related institution. The CommonKADS method is chosen as a technique to explore the problems and knowledge of each organization. While, SMAPA method is used to validate the result from the experts and end users. Results of this work are determine seven recommended supporting features there are vision and mission view, activity notification, group discussion, search repository, upload document and document activities log.

**Keywords**—knowledge management; knowledge management system; NUSANTARA; SMAPA; CommonKADS;

## I. INTRODUCTION

The management of government human capital (ASN) is essential for the realization of employees with integrity, professional, ethical profession, neutral, and free from political intervention. However the management still has not gained significant results, this is indicated by the ASN performance appraisal results that decline from 2014 KEMENPAN&RB 86, LAN 70 and BKN 65.07 to KEMENPAN 71.12 LAN 70 and BKN 56.54 in 2015. According to the previous study conducted by [1] said that this is due to several factors such as the loss of tacit knowledge, the development of inappropriate knowledge and the incomplete knowledge management process. According to [2], in order to obtain optimal performance then the element of human capital which is the main part in supporting the success of a human capital organization is required to be managed and

employed efficiently. In [3], defines the conceptual model which using ICT utilization by Knowledge Management Systems (KMS) known as Nusantara. The concept of Nusantara proposed as a design of knowledge management system in Indonesia. This method is able to produce the features which needed to support knowledge management process systems. However, utilization of Nusantara which used technology web still has constraints due to limitations of feature web base. Hence, the knowledge information cannot be obtained maximally. Analysis of mobile support is important because the need for knowledge is needed in time, place and every situation.

Nowadays, many web technology which developed to support mobile platform like HTML, HTML5, JavaScript, and CSS to develop mobile application that can run of different platforms and provides JavaScript API's to developers that allow the access to advanced device functionality such as accelerometer, barcode, Bluetooth, Calendar, Camera, Compass, Connection, Contacts, File, GPS, Menu, and Near Field Communication (NFC)[4].

However, it also have limitation include; It does not provide the possibility to have native user interface[5], the performance of the final application is far from the native application[5]. Hence, the feature for mobile Nusantara is considered with native platform to manage information more reliable. CommonKADS methodology is chosen due able to provide a suitable model of requirements for the knowledge-based systems of various knowledge[6] and is also the most established methodology for developing knowledge-based systems[7].

This paper is organized as follows. Section 2 describes supporting theories, section 3 present research methodology and section 4 discusses and analyzes the results of feature for mobile application of NUSANTARA. The last section explains conclusions and analyzes some future work.

## II. LITERATURE REVIEW

### A. Knowledge management (KM)

Knowledge management (KM) is group of activities to discover, capture, share and apply knowledge to gain

organizational objectives using their knowledge[8]. KM also determine as process for identifying, selecting, managing, transmitting, and disseminating information for problem solving, strategic planning and decision making[9]. KM practice can impact human resource management process. It's create, store, distribute and interpret knowledge in every organizational process[10]. Knowledge management in organization are connected to tacit and explicit knowledge. It represents how they were create new knowledge by acquired, represented, exchanged, maintained, integrated process[11]. Based on some definition above it can be conclude that KM is an exploration process of generate, capture, transfer, disseminate and implement knowledge from organizational knowledge resource for problem solving and decision to achieve organizational objectives. Those processes are relies on the organization member. Knowledge management can be successful implemented with human participation process.

### B. Knowledge Management Systems (KMS)

KMS intend to manage knowledge and user to use the knowledge to perform their organizational task[12]. While, according to [13],[8] KMS well known as an IT-based system that used to support, develop and enhance organizational KM process. The process can be applied in some various IT tools and technologies[13]. KMS accommodate some tools and technologies for manage the organizational knowledge asset and KM process which align with organizational business process. This technology is able to integrate knowledge information in KM process[14]. Hence, [8] assume that KMS is a solution to achieve organizational KM process and it

integrates in KM mechanisms and technologies which consist four type as follow:

- a) Knowledge Discovery System: technologies which support activities of creating innovative tacit and explicit knowledge from data and information.
- b) Knowledge Capture Systems: facilitate acquire knowledge both tacit and explicit around people and organizational entities. This system also can collect knowledge from inside and outside organization.
- c) Knowledge Sharing Systems: promote communication activities of tacit and explicit knowledge with using exchange and socialization process.
- d) Knowledge Application Systems: contribute the utilize process of individual knowledge into another individual without directly retrieve or learn the knowledge.

KMS can be represented in various kinds of ICT based on each government KM process which held to manage their organizational knowledge.

### C. NUSANTARA

Government human capital knowledge management of Republic Indonesia (Nusantara) is a knowledge management system for managing the government human resource process. This application used to support the KM process using the information and communication technologies[3]. Result from Nusantara is interpreted with web technology, web based application of Nusantara which consist of some KMS features which have been verified and validates by the experts.

Limitation of work Nusantara is related to the government human capital management which is specific to human resource process and bureaucracy culture in Indonesian government institutions.

### D. CommonKADS

Common Knowledge Analysis and Design System, or CommonKADS in short, is a comprehensive methodology for the developing knowledge-based system [15]. CommonKADS describes the foundation, technique, modeling language and document structure for develop the knowledge based system[16]. This methodology has been widely used for develop many types of system, for example expert system and knowledge management system to solve problem in organizational environment [17]. It also often used for organizational knowledge management system development[18].

Some strength of the commonKADS methodology are flexible to use, represent knowledge (organizational, domain, task, inference), complete, powerful, accurate, comprehensive, represent the KM process and systematic[18]–[29]. CommonKADS is consisted of three layers of model which have relationship among model. Three layers of model of CommonKADS are context layer, concept layer and artifact layer. The more detail of the layer of model respectively is presented in following explanation [30]:

- **Context layer.** This layer of model is consisted of three models, i.e. organizational model, task model, and agent model. Organizational model is used to formulate framework of problems, business processes, stakeholders and potential solutions based real condition within organization environment. Task model is focused on the purpose of business process that related to the required resources, competence, achievement and so forth. Agent model represented assignment of a person, system information, knowledge and culture.
- **Concept layer.** This layer contained two models, including knowledge model and communication model. Knowledge model presents type, rule and structure of knowledge. Communication model describes about the requirement of agents to accomplish their task and knowledge transfer between them.
- **Artifact layer.** This layer is represented by design model which describes technical things of system or software, i.e. architecture, the used algorithm, data structures and hardware.

### E. Previous Study

CommonKADS methodology has been used in several sector such as agriculture[27], [31], tourism [19], education [24], medical [20], [21], industry [18], [28], [25], [29], software development [23], [26] and bioinformatics [22].

GeOasis is one of tourism knowledge based which developed using the CommonKADS methodology to define the ontology of knowledge. This knowledge based provides the tourism information [19]. While, CommonKADS also can be used for determine the requirement analysis [27], share and



transfer natural knowledge engineering in software development [24] and incremental validation process[26].

Other research used CommonKADS to determine the knowledge metamodel, integrates several knowledge, develop expert system, and systematic capture of knowledge expertise[20], [23], [24]. In agriculture sector the CommonKADS develop the design of irrigation system [27], [31]. Hence, this methodology also can define the strategic collaboration of construction virtual business[22]. Then, in medical sector CommonKADS contribute the general framework for the aforementioned problem [20], [21].

### III. RESEARCH METHODS

Methodology of this research consists of five phases, in the first phase of the study literature to build a conceptual foundation of the research study, the next stage is to identify the issue raised in the form of weakness of conceptual design implementation of Nusantara with the web system that has been built.

Next phase we do done the data collection using deep interview to the expert for discovering the requirement of mobile application features related to the expert experiences. The data collection consists of primary and secondary data, primary data in the form of draft results interview conducted against the three state institutions namely LAN, BKN and MENPAN&RB.

The next stage is done by analysis with CommonKADS method to explore the knowledge assets and needs of the system to develop. The elaborations of five model development in CommonKADS are organizational, task, agent, knowledge, communication and design.

Hence, the research result was validated using the SMAPA methods which validated by experts and end users. The validation process used the SMAPA questionnaire instrument. Then, final stage is the conclusion of the research result.

### IV. RESULT AND DISCUSSION

Interview conducted to collect the expert data. While, the respondent distributions are expert from BKN 4 experts, LAN 3 experts and MENPAN&RB 2 experts. The interview result is elaboration of the development of five models: organizational, task, agent, knowledge, communication and design. The Organizational Models (OM) are define problem, context and the solution based on the interview result. The organization model can be seen in Table 1.

Table 1 shows the problems, context organizational and solutions offered to the problem. After the next stage OM is defining the task model. A summary of the modeling agent and not the model elaborated is shown in Table 2. Table II determine each tasks that have been defined are assigned to actors who have received tasks in Table 1. The analysis of tasks and actors is also defined into *use cases* which can be seen is shown in Figure 1. Figure 1 describes the use case of mobile KMS Nusantara which have six actor and six use cases.

The actors are admin, chief of knowledge article, co.admin, validator, expert and visitor, while the use case consist of manage article, manage document, online discussion, find article and document, download document, view article, view user log, manage member, view member list, send message, update expert profile, update validator, give article, document and document verification.

TABLE I. ORGANIZATIONAL MODEL PROBLEM IDENTIFICATION

Organization model	Problems : Worksheet OM-1
Problems	Knowledge management problems 1. Lack of motivation to learn 2. The creation of KM processes and cultural sharing 3. The existing knowledge gap between ASN management staff 4. Not all leaders can be role model 5. Lack of employees who have IT knowledge 6. Lack of commitment both from the side of employees and leaders 7. Loss of expert knowledge Technological problems Lack of IT infrastructure support
Organizational context	External common factors 1. Government and legal regulations 2. Organizational culture factors 3. Uneven employee recruitment rate
Solution	1. Provide an offering of knowledge management tools that are used at any time and at an affordable cost 2. Conceptual costume needs for knowledge management

TABLE II. SUMMARY OF TASK MODEL AND AGENT MODEL

No	Task	Agent	Knowledge Asset
1	Manage validator members, Manage experts, monitor user logs	Chief of Knowledge Officer	Knowledge of validator member data
2	Manage articles, manage documents, conduct discussions to users, search articles	Admin	Document of civil servant manpower management manuscript, document of research journals
3	View the user list and send messages to members	Co. Admin	-
4	Updating profiles, viewing members list, sending messages between members	Expert	Document of civil servant manpower management manuscript, document of research journals
5	Verify documents, view members list, send messages between members	Validator	Information on document data authenticity
6	Download documents, view or read articles	Visitors	-

After defining the task and agent model, the next step is to define the knowledge model. the knowledge model is used Conceptual Modeling Language (CML) as can be seen in Fig. 2.

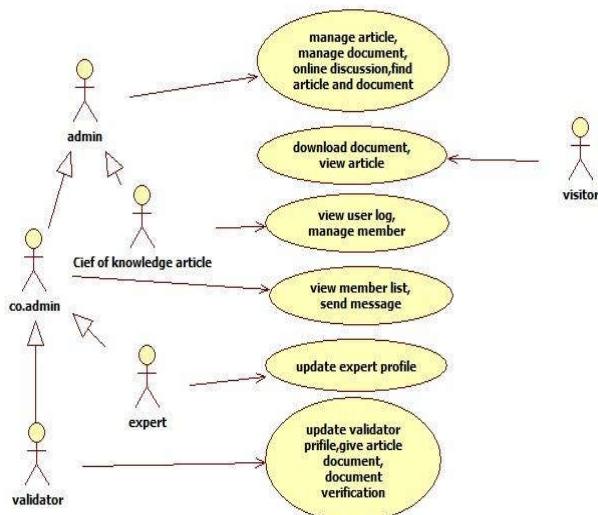


Fig. 1. Use case of mobile KMS Nusantara

Figure 2 show the example of conceptual model which describes in CML 2 languages. Hence, the next phase is determining the communication model; example of communication model can be seen in Table 3.

```

CONCEPT document
DESCRIPTION the attributes of a document
ATTRIBUTES:
    document ID: long
    title: string
    tag: string
    file_name: string
    date: date
    contributor: string
    ...
END CONCEPT document

```

Fig. 2. Example of conceptual model with CML2

Table III describes the example of communication model for each agent which determine in table II. The last stage of the CommonKADS model is a design model, at this stage is defined architecture, system support tools and features that can be used to develop mobile system KMS Nusantara. For interaction component systems can be seen in Fig. 3.

TABLE III. EXAMPLE OF COMMUNICATION MODEL

Communication model	Transaction description worksheet CM-1
Transaction identifier/Name	Management documents
Information object	Information needed to execute system commands are: document id, title, tag, file name, date, contributor, status, year, type, knowledge, source, num download
Agent involved	Admin, Validator, Expert
Communication plant	Expert, admin, validator selects the document manage menu, the document is uploaded read or download

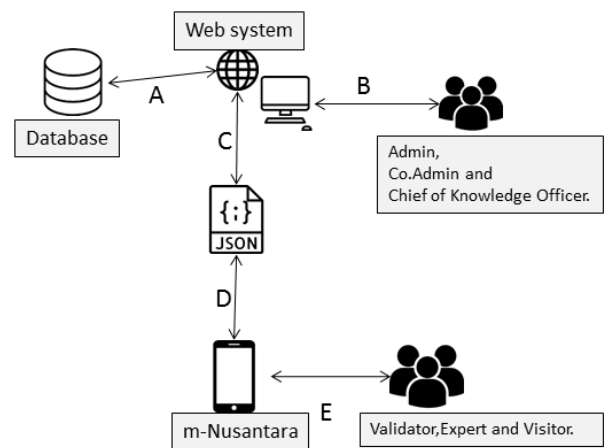


Fig. 3. Interaction among component system mobile KMS Nusantara.

Figure 3 show the interaction among the component system of mobile KMS nusantara based on the database, web system, actors and the mobile application. Each of interaction between point will be describes as follow:

- Interaction A is the communication between the database with the web system, the database using *MySQL* while the web system utilize *PHP* as the source code
- Interaction B display data in the form of web makes it easy for content managers to manage information more effectively.
- Interaction C in obtaining data from storage required "capture data" mechanism using *JSON* format.
- Interaction D data that has been converted into *JSON* form is then captured by *M-Nusantara* mobile app, this mechanism occurs in exchange of data from mobile device to database.

TABLE IV. LIST FITUR MOBILE KMS NUSANTARA

No	List Feature	Information
1	View ASN vision mission	This feature is submitted in the form of a menu that can show the vision of ASN mission
2	Activity notifications and updated information in ASN environment are news articles	This feature deals with providing up-to-date information on ASN developments in the form of notifications on android devices that will be integrated into ASN website pages
3	Group Discussion, chat from chat members.	This feature provides services to users in sharing efforts regarding matters relating to the scope of ASN
4	Searching of data files (repository)	This feature is provided to help find the required archive data in pdf format which can be seen important point2 part of the archive
6	Upload Document	Upload documents are used to store data owned by the practitioner document that will be saved can be a file.
7	Documentation of activities log	This menu aims to document the activities performed, data storage in the form of photos and information about the activities undertaken.

- Interaction E ASN information services obtained by validators, experts and visitors. This service allows users to obtain additional information and features not provided on the WEB Nusantara service.

Besides it also defined supporting features that can support the mobile system on mobile devices KMS Nusantara as seen in table 4.

Table IV determines seven lists of features and brief information above that define based on the CommonKADS analysis. Finally, the last phase is developing the mobile application interface and programming codes. The result of system design can be seen on Fig. 4.

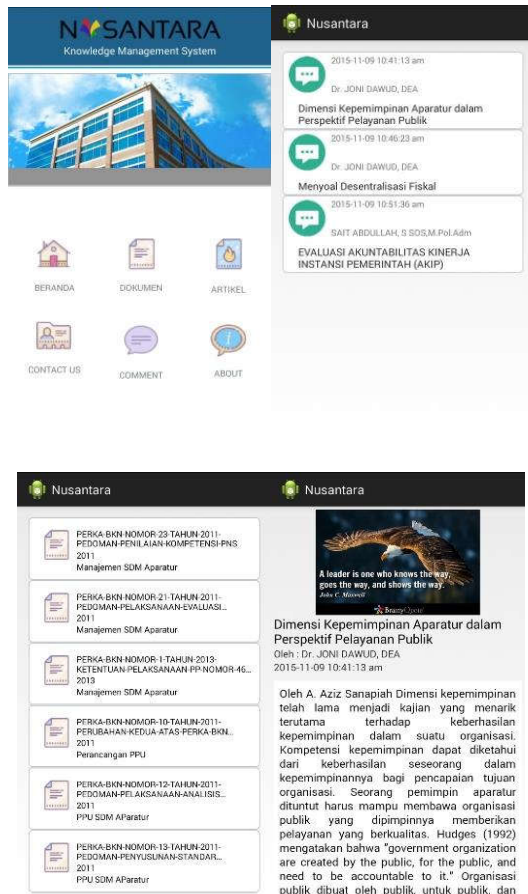


Fig. 4. Mobile application interface of KMS Nusantara.

Figure 4 show the prototype of mobile application interface which is named M-NUSANTARA. In this stage, the prototype was evaluated to measure satisfaction level of user to the application that was developed using NUSANTARA and CommonKADS. SMAPA method was employed as a based to design of questioner with liker scale. The final result was obtained using Aiken method (1).

$$V = \frac{\sum s}{n(c-1)} \quad (1)$$

$$S = r - lo \quad (2)$$

$V$  is value of content validity, where  $s$  is the value of  $r$  that was given by the expert,  $c$  is the highest value validity. Then,  $lo$  is the lowest value which given by the expert and  $n$  is the number of expertise. Coefficient of  $V$  is value from *content validity* which range from 0 to 1. According to six end users and expert samples obtained result can be seen in table 5

TABLE V. CONTENT VALIDITY WITH SMAPA

No	Sub-characteristic SMAPA	Content-Validity(V)
1	Transaction convenience	0.78125
2	Customizing service	0.84375
3	Differentiating function	0.8125
4	Consistency	0.75
5	Efficiency	0.78125
6	Reasonableness	0.75
7	Usability	0.8125
8	Creativity	0.78125
9	Customer Attraction Evaluate	0.875
10	Customer Convenience	0.78125

Table 5 shows result of the SMAPA analysis. Based on the result analysis, customizing service indicator was the highest score (0.84375). It means that mobile NUSANTARA has capability to manage knowledge, otherwise reasonableness and consistency indicator got the minimum score (0.75) due to the incomplete application. The results showed that all of items were obtained were valid, based on Aiken criteria  $>0.75$ .

## V. CONCLUSION

Research finding that seven features that recommended to be implemented in the mobile application of NUSANTARA which called m-NUSANTARA. Those features are ASN vision and mission view, activity notifications and updated information in ASN environment such as a news articles, group discussion, chat from chat members, searching of data files (repository), upload document and documentation of activities log.

The m-NUSANTARA expected to be used as a solution in the management of knowledge in the environment or scope civil state apparatus to manage the expert knowledge. The implementation of m-NUSANTARA in human capital managers (BKN, KEMENPAN&RB and LAN) can disseminate their organizational knowledge to develop the organizational competitive advantages related to the human capital management process.

CommonKADS methodology is used for developing the mobile application features which can give the reliable result of recommended feature align with the expert validation that m-NUSANTARA have a capability to manage the expert knowledge well.

Limitation of this study is specifically used for the human capital management experts which managed by three ministries. Future research can be developing other mobile features and using another approach with widely research area in public or private sector.

## ACKNOWLEDGMENT

The Authors thank to University of Indonesia and Indonesian Higher Education and Research Technology Ministry for facilitate research with research grant of PUPR Research 2016. We are grateful to State Ministry for State Apparatus Reform (KEMENPAN&RB), National Civil Service Agencies (BKN) and National Institute of Public Administration (LAN) for facilitate data research.

## REFERENCES

- [1] E. Cahyaningsih, "A Preliminary Study of Knowledge Management Implementation for Government Human Capital Management," 2016.
- [2] H. Agndal and U. Nilsson, "Generation of Human and Structural Capital: Lessons from Knowledge Management," *Electron. J. Knowl. Manag.*, vol. 4, no. 2, pp. 91–98, 2006.
- [3] E. Cahyaningsih, W. Java, D. I. Sensuse, W. Java, W. C. Wibowo, W. Java, R. Latifah, and W. Java, "NUSANTARA : A New Design of Knowledge Management System in Indonesia," pp. 1–6, 2016.
- [4] W. S. El-Kassas, B. A. Abdullah, A. H. Yousef, and A. M. Wahba, "Taxonomy of Cross-Platform Mobile Applications Development Approaches," *Ain Shams Eng. J.*, 2015.
- [5] W. Tang, J. Lee, B. Song, M. Islam, and S. Na, "Multi-Platform Mobile Thin Client Architecture in Cloud Environment," *Procedia Environ. Sci.*, vol. 11, pp. 499–504, 2011.
- [6] K. Khankasikam, "Knowledge capture for Thai word segmentation by using CommonKADS," *2010 2nd Int. Conf. Comput. Autom. Eng. ICCAE 2010*, vol. 1, pp. 307–311, 2010.
- [7] B. a. Gobin, "Reusing OWL-S to model knowledge intensive tasks performed by Knowledge Based Systems," *Int. Conf. ICT Knowl. Eng.*, no. January 2012, pp. 34–42, 2011.
- [8] Beccera and Fernandez, *Knowledge Management: Systems and Processes*. 2007.
- [9] E. Turban, J. E. Aronson, and T.-P. Liang, *Decision Support System*, 7th ed. 2005.
- [10] D. Palacios-Marques, I. Gil-Pechuán, and S. Lim, "Improving Human Capital Through Knowledge Management Practices in Knowledge-Intensive Business Services," *Serv. Bus.*, vol. 5, no. 2, pp. 99–112, 2011.
- [11] A. Kawtrakul, "Beyond Knowledge Management :," *Knowl. Creat. Diffus. Util.*, pp. 9–15, 2012.
- [12] P. Bera and P. Rysiew, "Analyzing Knowledge Management Systems : A Veritistic Approach," in *Proceeding of the First International Workshop on Philosophy and Informatics*, 2004.
- [13] M. Alavi, D. E. Leidner, and L. Cook, "Review: Knowledge Management and Knowledge Management System: Conceptual Foundations and Research Issues," *MIS Quartely*, vol. 25, no. 1, pp. 107–136, 2001.
- [14] P. Champoux, M. J. Costello, and S. Bourget, "The Canadian Knowledge Management System ( KMS ) within the Land Force Command and Control Information Systems ( LFC2IS )," in *10th International Command and Control Research and Technology Symposium (ICCRTS)*, 2005, pp. 1–13.
- [15] M. Mohanna, "Using Knowledge Engineering for Modeling Mobile Learning Systems," 2015.
- [16] K. Khankasikam, "Knowledge Capture for Thai Word Segmentation by using ComonKADS," in *The 2nd International Conference on Computer and Automation Engineering (ICCAE)*, 2010.
- [17] N. Prat, J. Akoka, and I. Comyn-wattiau, "Expert Systems with Applications An MDA approach to knowledge engineering," *Expert Syst. Appl.*, vol. 39, no. 12, pp. 10420–10437, 2012.
- [18] N. Prat, J. Akoka, and I. Comyn-Wattiau, "An MDA approach to knowledge engineering," *Expert Syst. Appl.*, vol. 39, no. 12, pp. 10420–10437, 2012.
- [19] F. M. Santiago, F. A. López, A. Montejó-Ráez, and A. U. López, "GeoOasis: A knowledge-based geo-referenced tourist assistant," *Expert Syst. Appl.*, vol. 39, no. 14, pp. 11737–11745, 2012.
- [20] Y. H. Tsai, C. H. Ko, and K. C. Lin, "Using commonKADS method to build prototype system in medical insurance fraud detection," *J. Networks*, vol. 9, no. 7, pp. 1798–1802, 2014.
- [21] T. Mawloud, M. M. Djamel, and A. Samia, "An Implementation Tool for the Expertise Model using CommonKADS Methodology," *Int. Conf. Information, Process. Knowl. Manag.*, no. c, pp. 70–76, 2014.
- [22] D. Xavier, F. Morán, R. Fuentes-Fernández, and G. Pajares, "Modelling knowledge strategy for solving the DNA sequence annotation problem through CommonKADS methodology," *Expert Syst. Appl.*, vol. 40, no. 10, pp. 3943–3952, 2013.
- [23] M. Moradi, M. Badja, and B. Vallespir, "Knowledge Based Enterprise Engineering (KBEE): A modeling framework for enterprise knowledge capitalization," *IFIP Adv. Inf. Commun. Technol.*, vol. 338 AICT, pp. 433–440, 2010.
- [24] M. T. Guaglianone and N. Matta, "MNEMO ( Methodology for Knowledge Acquisition and Modelling ): Definition of a Global Knowledge Management Approach Combining Knowledge Modelling Techniques," vol. 4, no. July, pp. 160–169, 2012.
- [25] M. M. Y. Massoud, "Healthcare Collaborative Network Based on Common KADS Methodology," *Proc. - 2015 IEEE Int. Conf. Healthc. Informatics, ICHI 2015*, p. 451, 2015.
- [26] F. Batarseh, "Incremental Lifecycle Validation of Knowledge-Based Systems Through CommonKADS," vol. 43, no. 3, pp. 643–654, 2011.
- [27] S. S. Hasan and R. K. Isaac, "An integrated approach of MAS-CommonKADS, Model-View-Controller and web application optimization strategies for web-based expert system development," *Expert Syst. Appl.*, vol. 38, no. 1, pp. 417–428, 2011.
- [28] M. Hakkak, Y. Zarnegarian, and H. Zarei, "Identifying The Relationship Between Organizational Culture and Knowledge Management," *Glob. J. od Sci. Eng. Technol.*, no. 11, pp. 19–28, 2013.
- [29] R. Rodprasert, T. Chandarasupsang, N. Chakpitak, and P. P. Yupain, "Alternative Design Approach for Energy Management System," *Life Sci. J.*, vol. 11, no. 2, 2014.
- [30] D. E. Avison and G. Fitzgeralds, *Information Systems Development : Methodologies, Techniques, and Tools 4th edition*. 2006.
- [31] A. Nada, M. Nasr, and M. Hazman, "Irrigation Expert System for Trees," *Int. J. Eng. Innov. Technol.*, vol. 3, no. 8, pp. 170–175, 2014.

# Knowledge Management Maturity Assessment in Air Drilling Associates using G-KMMM

Dana Indra Sensuse<sup>1</sup>, Richard Vinc<sup>2</sup>, Ricky Nauvaldy Ruliputra<sup>3</sup>, Siti Hadjar<sup>4</sup>, Jonathan Sofian Lusa<sup>5</sup>, Pudy Prima<sup>6</sup>

Faculty of Computer Science, Universitas Indonesia, Depok, Indonesia  
 dana@cs.ui.ac.id<sup>1</sup>, richard.vinc@ui.ac.id<sup>2</sup>, ricky.nauvaldy71@ui.ac.id<sup>3</sup>,  
 siti.hadjar@ui.ac.id<sup>4</sup>, sofian.lusa12@ui.ac.id<sup>5</sup>, pudy.prima61@ui.ac.id<sup>6</sup>

**Abstract**—Since the early 1990s, companies in the oil & gas industry have realized that their business operations are knowledge-based, where company performance can be derived from faster identification, an assessment of an opportunity, and the speed of an exploitation. The oil & gas industry is one of the leading industries in the application and development of knowledge management; this is caused by changes in market and technology from 1990s to the beginning of the 21st century. Utilizing knowledge management is a must to be able to compete with other oil and gas industry companies. Currently, Air Drilling Associates (ADA) as one of the companies in oil & gas industry already has implemented knowledge management system, but its benefits are far from the expectation. In order to position their efforts and initialize knowledge management, companies need framework to use as a template. The objective of this paper is to measure the knowledge management maturity of Air Drilling Associates and other suggestion related to knowledge management for improvement.

**Keywords**—*knowledge management, knowledge management maturity model, oil and gas industry*

## I. INTRODUCTION

Over the last few years, Knowledge Management (KM) has become one of the success factors of an organization. The main goal of the KM initiative in every organization is to improve the performance of the people involved with the organization [1]. The industrial world is expected to support and use KM to facilitate their resilience in an increasingly dynamic and competitive business environment. Similarly, the oil and gas industry has long utilized KM. According to Robert M. Grant [2], since 1990, the company's interest in KM has been increasing. This is due to technological trends and which reveal many opportunities to exploit existing knowledge in the organization.

Since the early 1990s, companies in the oil & gas industry have realized that their business operations are knowledge-based, where company performance can be derived from faster identification, an assessment of an opportunity, and the speed of an exploitation. In line with previous statements, Zaied, Hussein, and Hassan [3] reveal that the 21st century is an era of economic knowledge, where many organizations have a lot of knowledge that can be used to develop their performance.

The oil & gas industry is one of the leading industries in the application and development of knowledge management; this is caused by changes in market and technology from 1990s to the beginning

of the 21st century. This change encouraged industry to further discuss locations, provide space for environmental responsibility, and develop technology tools in the fields of seismology, drilling, and offshore exploration and production (E&P). The development of information and communication technology (ICT) also enables companies to collect and analyze a huge number of information which enable communication and collaboration among employees in all over the world.

Around the year 2000 to 2010, the Society for Petroleum Engineers (SPE) estimates that there will be 231.000 years of cumulative experience and knowledge that will be lost over the next 10 years as many technical and petroleum engineers will retire [2]. From a different perspective, this urgency is supported by Muthuveloo, Shanmugam, and Teoh [4] who stated that customers will avoid to establish business relationships with company who has employee turnover problem, especially the one in key positions. This tendency is based on customer fears as to whether the organization still has the knowledge required for business continuity and performance, despite the decline of its employees. To address this, a knowledge management is required [5]. Knowledge itself can be a tool for supporting the company's adaptation and survival [6].

To position their efforts and initialize knowledge management, companies need some kind of framework to use as a template [5]. According to Zaied, Hussein, and Hassan [7], KM becomes very important as it can provide assistance to direct organizational and competitive performance. A maturity assessment model is required to measure KM performance. Assessment of KM maturity model will provide the level of maturity of a company so that we can determine the strategy needed to improve it [8].

Air Drilling Associates (ADA) as one of the companies in the oil & gas industry also suffer from the same issues as any other companies in the same industry. Currently ADA already have knowledge management system. The KMS named ADA Knowledge-based were developed to support KM practices in the ADA. Initially, ADA Knowledge Base were specifically expected to improve the operational efficiency of the drilling project at the site where the ADA is operating. Management expects the Project Supervisor of each project to record each End of Well Report into the ADA Knowledge Base as a lesson for the next project. However, the implementation is still considered not as expected. Knowledge transfer from employee-to-

company and among employees does not occur regularly, so there are many insights and opportunities lost in the process. Other than that, ADA must maintain their business continuity process and stay competitive among their competitors who also practice knowledge management. The objective of this study is to measure the KM maturity in ADA and analyze improvement related to KM.

## II. CONCEPTUAL BACKGROUND

### A. Knowledge Management and Knowledge Management System

KM may simply be defined as the management of the activities and the processes that enhance the utilization and the creation of knowledge within an organization, according to two strongly interlinked goals, and their underlying economic and strategic dimensions, organizational dimensions, socio-cultural dimensions, and technological dimensions: (i) a patrimony goal, and (ii) a sustainable innovation goal [5]. Mazzoni, Capriotti, Ferrazza, and Giudicati [7] said that KM covers the whole cycle of knowledge, from knowledge generation, capture, mapping, storage, sharing and capture. The collection of experiences and procedures, their cataloging and conservation is particularly crucial together with the development of new ideas, in a virtuous cycle enabled to valorize and power both single people and the company. Knowledge needs to be managed as it can reside in several different location, including people, artifacts, and organizational entities [9].

As quoted by Ovbagbedia [15], Alavi and Leidner (2001) describe the Knowledge Management System (KMS) as an information technology-based system applied to the development, expansion and support of organizational processes to provide, store, retrieve, alter and use knowledge [9][10]. KMS provides strategic potential for the organization and acts as a decisive source. It is essential to assist the management of key resources and intellectual capital of the organization in creating a competitive advantage [16].

### B. Maturity Model

A development of entities can be simplified and described by using multiple levels of maturity. These levels are characterized based on certain requirements that an entity must achieve. The entity progresses from the bottom to the highest level without skipping a level [12]. In the context of KM, maturity is related to the organizational competency in managing knowledge as organizational intangible asset [11].

### C. Knowledge Management Maturity Model

KM maturity model is the extent to which KM is explicitly defined, managed, controlled, and effected [12]. It describes the stages of growth of KM initiatives in an organization. KM assessment is needed to obtain a KM maturity model. It consists of comparing the tools regarding use cases, principles measured, outputs and contextual factors [13].

Pee and Kankanhalli [12] categorized KM maturity model into two groups, depending on whether or not they are developed based on the Capability Maturity Model (CMM). On their paper, they identified and compared four KMMMs based on CMM, i.e. Siemen's KMMM, Paulzen and Perc's Knowledge Process Quality Model, Infosys' KMMM, and Kulkarni and Freeze's Knowledge Management Capability Assessment Model (KMCA). They also identified and compared six KMMMs that are not based on CMM, i.e. KPMG Consulting's Knowledge Journey, TATA Consultancy Services' 5iKM3, Klimko's KMMM, WisdomSource's K3M, Gottschalk and Khandelwal's Stages of Growth for KM Technology, and VISION KMMM (V-KMMM).

## III. RESEARCH DESIGN

To assess the overall level of Air Drilling Associates, we apply each of the General Knowledge Management Maturity Model elements to each division and unify the final result.

### A. Case Background

Air Drilling Associates (ADA) was founded in 2003 by Chaman Malhotra and Don Wells, the former owners of Air Drilling Services (ADS). It quickly became a leader in SE Asia, Middle East Asia-Pacific region, and in North and South America. The air compression packages provided by ADA operate as stand-alone, self-sustaining operations that are stocked with abundant spare parts and redundancy in mind. ADA probably has the youngest equipment fleet in the industry, with most equipment after 2002. ADA is a world leader in applying air-, mist-, foam-, aerated fluid and other underbalanced techniques for petroleum and geothermal drilling projects.

ADA's vision is "to be the preferred and leading provider of equipment and services for wellbore pressure management while drilling and for commissioning and testing of pipeline and process systems". In order to achieve this, this company has mission of "dedicated to providing innovative drilling and production solutions to our customers in a safe and exceptional level of performance". There are two main departments in ADA; Operational and Finance. Each department is headed by a C-Level leader, Chief Finance Officer and Chief Executive Officer. Headed by a Chairman and Vice Chairman, a CEO oversees three operational directors, each responsible for operational activities in 3 regions; Asia-Pacific, Russia and Europe, Middle East; as well as a Sales Manager and Engineering Manager. A CFO heads a finance director who is responsible for the company's cash flow.

### B. Methodology

General Knowledge Management Maturity Model (G-KMMM) proposed by Pee and Kankanhalli [12] is utilized to measure KM maturity



in ADA. This study performs modeling based on studies and comparisons of pre-existing knowledge management maturity model (KMMM), either based on Capability Maturity Model (CMM, i.e. Siemens KMMM, KPQM, Infosys' KMMM, and KMCA) or not (i.e. Knowledge journey, 5iKM3, K3M, and Stages of Growth for KM Technology). This model was chosen because it covers aspects of people, process, and technology which are important aspects in knowledge management. The model can be seen in Table 1. In this model, the key process areas (KPA) people covers aspects related to organizational culture, strategy, and policy; KPA process includes aspects related to KM activities

such as sharing, application, and knowledge creation; KPA technology covers aspects related to technology and KM infrastructure.

At the *initial* level, the organization only have low level of attention or not at all to manage knowledge formally because it is not considered important for the organization's success and goals. At the *aware* level, organizations have an awareness to manage knowledge formally because they already realize the importance of knowledge for the company, but it is possible that they don't know how to implement it. At the *defined* level, organizations

TABLE I. G-KMMM MODEL [12]

Maturity Level	General Description	Key Process Areas		
		People	Process	Technology
Initial	Little or no intention to formally manage organizational knowledge	Organization and its people are not aware of the need to formally manage its knowledge resources	No formal processes to capture, share and reuse organizational knowledge	No specific KM technology or infrastructure in place
Aware	Organization is aware of and has the intention to manage its organizational knowledge, but it might not know how to do so	Management is aware of the need for formal KM	Knowledge indispensable for performing routine task is documented	Pilot KM projects are initiated (not necessarily by management)
Defined	Organization has put in place a basic infrastructure to support KM	<ul style="list-style-type: none"> <li>- Management is aware of its role in encouraging KM</li> <li>- Basic training on KM are provided (e.g., awareness courses)</li> <li>- Basic KM strategy is put in place</li> <li>- Individual KM roles are defined</li> <li>- Incentive systems are in place</li> </ul>	<ul style="list-style-type: none"> <li>- Processes for content and information management is formalized</li> <li>- Metrics are used to measure the increase in productivity due to KM</li> </ul>	<ul style="list-style-type: none"> <li>- Basic KM Infrastructure in place (e.g., single point of access)</li> <li>- Some enterprise level KM projects are put in place</li> </ul>
Managed	KM initiatives are well established in the organization	<ul style="list-style-type: none"> <li>- Common strategy and standardized approaches towards KM</li> <li>- KM is incorporated into the overall organizational strategy</li> <li>- More advanced KM training</li> <li>- Organizational standards</li> </ul>	Quantitative measurement of KM processes (i.e., use of metrics)	<ul style="list-style-type: none"> <li>- Enterprise-wide KM systems are fully in place</li> <li>- Usage of KM system is at a reasonable level</li> <li>- Seamless integration of technology with content architecture</li> </ul>
Optimizing	<ul style="list-style-type: none"> <li>- KM is deeply integrated into the organization and is continually improved upon</li> <li>- It is an automatic component in any organizational processes</li> </ul>	Culture of sharing is institutionalized	<ul style="list-style-type: none"> <li>- KM processes are constantly reviewed and improved upon</li> <li>- Existing KM processes can be easily adapted to meet new business requirements</li> <li>- KM procedures are an integral part of the organization</li> </ul>	Existing KM infrastructure is continually improved upon

TABLE II. G-KMMM ASSESSMENT INSTRUMENT [12]

Level	Question
<i>KPA: People</i>	
2	PEO2a Is organizational knowledge recognized as essential for the long-term success of the organization?
	PEO2b Is KM recognized as a key organizational competence?
	PEO2c Employees are ready and willing to give advice or help on request from anyone else within the company
3	PEO3a Is there any incentive system in place to encourage the knowledge sharing among employees?
	PEO3b Are the incentive systems attractive enough to promote the use of KM in the organization?
	PEO3c Are the KM projects coordinated by the management?
	PEO3d Are there individual KM roles that are defined and given appropriate degree of authority?
	PEO3e Is there a formal KM strategy in place?
	PEO3f Is there a clear vision for KM?
	PEO3g Are there any KM training programs or awareness campaigns?
4	PEO4a Are there regular knowledge sharing sessions?
	PEO4b Is KM incorporated into the overall organizational strategy?
	PEO4c Is there a budget specially set aside for KM?
	PEO4d Is there any form of benchmarking, measure, or assessment of the state of KM in the organization?
5	PEO5 Has the KM initiatives resulted in a knowledge sharing culture?
<i>KPA: Process</i>	
2	PRO2 Is the knowledge that is indispensable for performing routine task documented?
3	PRO3a Does the KMS improve the quality and efficiency of work?
	PRO3b Is the process for collecting and sharing information formalized?
4	PRO4a Are the existing KM systems actively and effectively utilized?
	PRO4b Are the knowledge processes measured quantitatively?
5	PRO5 Can the existing KM processes be easily adapted to meet new business requirements?
<i>KPA: Technology</i>	
2	TEC2a Are there pilot projects that support KM?
	TEC2b Is there any technology and infrastructure in place that supports KM?
3	TEC3 Does the system support the business unit?
4	TEC4a Does the KMS support the entire organization?
	TEC4b Is the KMS tightly integrated with the business processes?
5	TEC5 Are the existing systems continually improved upon (e.g. continual investments)?

and there is management support that states the KM strategy along with training and incentives. At the *managed* level, KM has become part of the company's strategy along with the model, standard, and KM effectiveness assessment in the company. At the *optimizing* level, KM strongly supports the key business activities of the company along with a voluntary knowledge-sharing culture undertaken by members of the organization.

KM maturity assessment instruments developed by Pee and Kankanhalli [12] are shown in Table 2. These questions are divided for each KPA and the corresponding level. G-KMMM can provide a comprehensive and systematic assessment to be able to identify areas that need to be focused so that the company's performance can continue to increase continuously. Previous studies have also utilized this model to assess KM maturity on firm performance and knowledge creation process [11][14], and to see the effect of organizational culture on KMM [15].

As a comparison, we also assess two other oil & gas companies, namely Royal Dutch Shell and Schlumberger. We chose these two companies because they have succeeded in obtaining MAKE (Most Admired Knowledge Enterprise) awards, an award that seeks to recognize organizations which outperform their peers in creating shareholder's wealth by transforming tacit and explicit enterprise knowledge and intellectual capital into superior products/services/solutions. The data is collected from a review paper by Grant [2].

### C. Data Collection

Data collection is done by interviewing key person from three main divisions in ADA: Sales (SA), Finance (FIN) and Operational (OPS). Due to the peculiarities of the business process and different culture, the results of KM maturity assessment of each division can be different. The results contribute to the general KM maturity assessment on ADA. The G-KMMM assessment instrument is used as interview guidelines.

## IV. RESULT AND ANALYSIS

KM maturity of each division is assessed by evaluating whether a particular practice is performed or not. For every practice that is done then the answer is 'Y', otherwise it will be 'N'. In order to qualify for the level of maturity within the KPA, a division must implement all key practices at that level. For example, the division that practices item PEO2a to PEO4a but not the item PEO4b can be said that it has reached the level 3 of maturity in the People's KPA, as it has not yet implemented all practices that characterize level 4. Table 3 summarizes the maturity ratings of each division.

already have a basic infrastructure that supports KM,

Based on our assessment using GKMMM with the data from Grant's paper [2], both Royal Dutch Shell and Schlumberger belongs to KM maturity level 5. It fulfils all level 5 assessment questions in all of the key process area, which is related to knowledge sharing culture, easy adoption of KM processes to meet new business requirements, and continuous improvement on existing systems. On the other hand, based on interviews, observations and document studies, KM maturity level of ADA is still at level 2. A clearly visible difference between KM practice in Royal-Dutch-Shell-and-Schlumberger and ADA is that both Schlumberger and Shell formed a steering committee with knowledge champion, as well as assign a Chief Knowledge Officer. While in the ADA, the practice of Knowledge Management is still managed by the Operations division whose main focus is to provide the best drilling services, thus KM management is just a side responsibility for the division.

#### A. People Area

All factors why the level of maturity of the people area is still at level 2 are related to the commitment and management support in encouraging KM culture and application in the company's work environment. Starting from the absence of formal KM strategy, lack of clear vision on KM implementation, lack of training or program to increase awareness to KM, no special personnel appointed who has the authority to handle KM, to the fact that there is no incentive system for employees who implements knowledge sharing.

Apart from the existence of the knowledge management system in the company, culture and management support becomes one of the main factors that can initiate and maintain the activities of sharing information between employees, whether one division or cross division.

#### B. Process Area

Assessment in the process area does not produce the same value for the three business units with sales and finance still at level 2, while operations are at level 3. This difference lies in the application of KMS that has improved the quality and efficiency of the work performed by the business unit of the operation, but the impact did not occur on sales and finance business unit. KM implementation becomes important for the operations unit because the team consists of many people and spread so that the KM will improve the work process of the team. This is not the problem in the sales and finance units as they have fewer number of personnel with placements located only in Indonesia, so KM implementation does not have a significant impact. In addition, the process of collecting and sharing information on sales and finance units is not formalized, only limited to non-formal activities. Therefore, the sales and finance

TABLE III. ASSESSMENT RESULT

Item	SA	FIN	OPS	Item	SA	FIN	OPS
<b>People Maturity</b>	<b>2</b>	<b>2</b>	<b>2</b>	<b>Process Maturity</b>	<b>2</b>	<b>2</b>	<b>3</b>
PEO2a	Y	Y	Y	PRO2	Y	Y	Y
PEO2b	Y	Y	Y	PRO3a	N	N	Y
PEO2c	Y	Y	Y	PRO3b	N	N	Y
PEO3a	N	N	N	PRO4a	N	N	N
PEO3b	N	N	N	PRO4b	N	N	N
PEO3c	Y	Y	Y	PRO5	N	N	N
PEO3d	N	N	N	<b>Technology Maturity</b>	<b>3</b>	<b>3</b>	<b>3</b>
PEO3e	N	N	N	TEC2a	Y	Y	Y
PEO3f	N	N	N	TEC2b	Y	Y	Y
PEO3g	N	N	N	TEC3	Y	Y	Y
PEO4a	N	N	Y	TEC4a	Y	Y	Y
PEO4b	N	N	N	TEC4b	N	N	N
PEO4c	N	N	N	TEC5	N	N	N
PEO4d	N	N	N	<b>Overall Maturity</b>	<b>2</b>	<b>2</b>	<b>2</b>
PEO5	Y	Y	Y	<b>Company Maturity</b>	<b>2</b>	<b>2</b>	<b>2</b>

units still cannot be categorized to be in level 3 in the process area.

#### C. Technology Area

Although some divisions can only reach level 2 in other areas, in the area of technology they all reach level 3. This is because the availability of tools that support the practice of KM, i.e. knowledge management system. This KMS is developed with management initiatives that recognize the importance of KM to facilitate corporate resilience in an increasingly dynamic and competitive business environment. The KMS developed is align with the company's commitment to ensure that employees have the right knowledge, skills, experience and behavior to meet business objectives and customer needs both in the short and long term.

Unfortunately, KMS implementation is done without assessing the readiness of the organization in adopting KM. Thus, KM strategy cannot be defined for designing roadmap of KM implementation and planning of KM mechanism, including preparing individual to accept and participate in KM practice.

## V. CONCLUSION

Based on the results of the KMMM assessment, the Air Drilling Associates company is at the level 2 of KM maturity. This result is obtained from the assessment that has been done by considering aspects of people, process, and technology area. It implies that the company is at the aware level where they already realize the importance of knowledge for the company, but it is possible that they don't know yet how to gain the maximum advantage of KM usage.

Other oil and gas companies mentioned earlier has reach maturity level 5. Thus, to be able to compete among competitors, ADA must be able to increase the level of maturity KM to level 5.

The following are suggestions of improvement to achieve knowledge management maturity level 5:

1. Form a division to manage KM daily
2. Appoint a Chief Knowledge Officer
3. Mapping knowledge and establishing Community of Practice based on mapping results
4. Organize regular knowledge sharing sessions; this could be in the form of morning meeting for office and workshop base employee or daily transfer between morning and night shift and vice versa for project base employee
5. Incorporate KM into the overall organization strategy
6. Allocate a special budget for KM
7. Evaluate the KM practice periodically
8. Encourage active KMS utilization; Every contribution to the KMS should be counted and included in the annual performance assessment as one of the performance indicators and awarded with incentives.
9. Integrate KMS with business process; recording the End of Well Report (EoWR) into KMS can be one of the efforts. The company might be able to enforce this by not letting a supervisor to close a project before submitting the EoWR into ADA Knowledge Base.

## ACKNOWLEDGMENT

This work is supported by Hibah PITTA 2018 funded by DRPM Universitas Indonesia No.5000/UN2.R3.1/HKP.05.00/2018.

## REFERENCES

- [1] C. Ramanigopal, "Knowledge Management For The Oil And Gas Industry - Opportunities And Challenges," *Adv. Manag.*, Vol. 6, No. 8, Pp. 3–8, 2013.
- [2] R. M. Grant, "The Development Of Knowledge Management In The Oil And Gas Industry," *Universia Bus. Rev.*, Pp. 92–125, 2013.
- [3] A. Nasser H. Zaied, G. Soliman Hussein, And M. M. Hassan, "The Role Of Knowledge Management In Enhancing Organizational Performance," *Int. J. Inf. Eng. Electron. Bus.*, Vol. 4, No. 5, Pp. 27–35, 2012.
- [4] R. Muthuveloo, N. Shanmugam, And A. P. Teoh, "The Impact Of Tacit Knowledge Management On Organizational Performance: Evidence From Malaysia," *Asia Pacific Manag. Rev.*, Vol. 22, No. 4, Pp. 192–201, 2017.
- [5] M. Grundstein, "Assessing Enterprise's Knowledge Management Maturity Level," *Int. J. Knowl. Soc. Res.*, Vol. 19, No. May, Pp. 380–387, 2008.
- [6] M. Sigala And K. Chalkiti, "Improving Performance Through Tacit Knowledge Externalisation And Utilisation," *Int. J. Product. Perform. Manag.*, Vol. 56, No. 5/6, Pp. 456–483, 2007.
- [7] S. Mazzoni, E. Upstream, D. Ravenna, F. Ferrazza, G. Giudicati, And R. Eni, "Knowledge Management In Eni : Workflow And Case Histories In Northern Italian District ( Dics )," In *13th Offshore Mediterranean Conference And Exhibition*, 2017, Pp. 1–14.
- [8] U. R. Kulkarni And R. St. Louis, "Organizational Self Assessment Of Knowledge Management Maturity," In *Ninth Americas Conferences On Information Systems*, 2003, Pp. 2542–2551.
- [9] I. Becerra-Fernandez And R. Sabherwal, *Knowledge Management: Systems And Processes*. 2015.
- [10] E. G. Ochieng Et AL., "Utilising A Systematic Knowledge Management Based System To Optimise Project Management Operations In Oil And Gas Organisations," *Inf. Technol. People*, 2015.
- [11] B. Hartono, N. Indarti, K. H. Chai, And S. R. Sulistyo, "Knowledge Management Maturity And Firm's Performance: Firm's Size As A Moderating Variable," *Ijee Int. Conf. Ind. Eng. Manag.*, Vol. 2016–Decem, Pp. 1156–1160, 2016.
- [12] L. G. P. Pee And A. Kankanhalli, "A Model Of Organizational Knowledge Management Maturity Based On People, Process, And Technology," *J. Inf. Knowl. Manag.*, Vol. 8, No. 2, Pp. 1–21, 2009.
- [13] Winarni, D. I. Sensuse, E. Cahyaningsih, And H. Noprisson, "Self-Assessment For Knowledge Managemet Strategy Case Study: National Institute Of Aeronautics And Space," *Int. Conf. Inf. Technol. Syst. Innov. (Icitsi)2*, Pp. 44–49, 2017.
- [14] S. Sokhanvar, J. Matthews, And P. Yarlagadda, "Management Of Project Knowledge At Various Maturity Levels In Pmo, A Theoretical Framework," In *Pmi Research And Education Conference*, 2014, No. July, Pp. 27–29.
- [15] H. S. Poor And Z. Lebady, "The Effect Of Organizational Culture On Knowledge Management Maturity," *Palma J.*, Pp. 126–139, 2017.
- [16] Stenmark, D, *Leveraging Tacit Organizational Knowledge. Journal Of Management Information Systems*, 2001.

# Measuring Knowledge Management Readiness of Indonesia Ministry of Trade

Dana Indra Sensuse<sup>1</sup>, Jani Richi R. Siregar<sup>2</sup>, Ronny Ansis<sup>3</sup>, Jonathan Sofian Lusa<sup>4</sup>, Pudy Prima<sup>5</sup>

Faculty of Computer Science

Universitas Indonesia

Depok, Indonesia

dana@cs.ui.ac.id<sup>1</sup>, jani.richi@ui.ac.id<sup>2</sup>, ronny.ansis@ui.ac.id<sup>3</sup>, sofian.lusa12@ui.ac.id<sup>4</sup>, pudy.prima61@ui.ac.id<sup>5</sup>

*Knowledge is one of the important assets for organization. Managing knowledge properly will enable the organization to achieve its objectives effectively and efficiently. Since risk of failed implementation of Knowledge Management (KM) might occur, organization needs to measure their KM Readiness beforehand to successfully implement KM. This study is intended to measure KM Readiness in government agency, namely Directorate of Bilateral Negotiations in Ministry of Trade. The research model for measuring KM readiness was developed based on previous relevant studies. KM enablers, individual acceptance, and KM SECI processes were used to develop the model and research instruments. KM Readiness in government agency was measured by accommodating factor analysis in research model. Data were collected from 53 employees as valid samples. The result shows that KM Readiness level of the Directorate of Bilateral Negotiations in Ministry of Trade is "ready but needs a few improvement".*

**Keywords:** Knowledge Management, KM Readiness, KM Enablers, Individual Acceptance, KM SECI Processes, Government

## I. INTRODUCTION

Directorate of Bilateral Negotiation (DBN) is one instance of government agency in Ministry of Trade. Based on Ministry of Trade Regulation No.8 on 2016, this organization's main task is conducting bilateral trade negotiation with other countries. The purpose of this organization is to achieve trade-deal agreement toward other countries that benefit most for domestic interests.

Negotiation is the key activity in this agency. While conducting negotiations, DBN-Ministry of Trade also coordinates with other government agencies that provide actual information of export-potential commodities along with related strategies. Hence, this organization not only negotiates with other country's representative, but also collaborates with other domestic government agencies.

There are 15 trade negotiations conducted on the last 6 years. However, based on first quarter of 2018 report, there were only 6 (40%) completed trade negotiations, while the other 9 (60%) were still unfinished. This condition becomes one concern of the agency which is needed to be improved by accommodating knowledge management as the solution.

It is unarguable that KM is fundamentally important for organization [1] [2]. Successful KM implementation enable the organization to achieve its objectives more effective and efficient. However, based on [3] and [4], project of KM has failure rate of 70% because many organizations only focused

on theories without concerning the organization's condition when implementing KM. Before implementing KM, assessing organization's KM Readiness is necessary in order to minimize failure risks [1].

There are lot of previous studies about assessment of KM Readiness. The case studies involved private sector companies [2] [5] [6] [7] [8], education institutions such as universities [9] [10] [11] [12] [13], and government institutions [14] [7] [15] [3] [16]. However, among those studies, there is still no discussion about KM readiness' framework to government agency related to negotiation and coordination activities that has been used empirically.

This study is intended to measure KM Readiness in Directorate of Bilateral Negotiation. The research model is developed using Systematic Literature Review [17] [18] toward relevant previous studies. Objectives of this study are: the research model, KM Readiness level, and most determined factor of KM Readiness in this case study.

## II. LITERATURE REVIEW

### A. KM Process

KM is a process that assists an organization to identify, organize, select, deploy and transfer relevant information and skills which are part of the organizational assets of memory, stored in an unstructured way [5]. Transforming the unstructured to become structured pattern enables the organization to: solve its problem, achieve its objectives effectively and efficiently, perform dynamic learning, conduct strategic planning, and make the best possible decision [5]. According to Beccera-Fernandez & Sabherwal, KM is defined as knowledge-related-activities, such as: capturing, discovering, sharing and applying knowledge in order to increase the impact of knowledge use to achieve organization's objectives [5][19]. There are 4 processes in KM, divided by Nonaka-Takeuchi based on knowledge-type transferring, such as: Socialization, Externalization, Combination, and Internalization [5][19].

### B. KM Enabler

Achieving successful KM implementation in organization must consider several aspects. Previous studies suggest that these aspects are pre-conditions to implement KM process successfully. There are KM Infrastructure[11] [13] [20], KM Enablers [2][5][7][8][9][12][14][21], and KM Critical Success Factor (CSF) [3][15][16]. All these studies emphasize socio-

technical perspective and they similarly emphasize factors such as: Organizational Culture, Organizational Structure, and Information Technology. Hence, these 3 factors are relevant to be considered to determine KM Readiness in an organization.

### C. KM Readiness

KM Readiness is defined as a receptive attitude from organization to be involved in KM processes through available sources [8]. KM Readiness is considered as one of indicators and baseline-evaluation to move forward to implement KM, since by knowing KM Readiness, failure risks of KM Implementation are possible to be reduced to minimum [4].

KM Readiness level in this study is determined by using Aydin and Tasci scale [12][23] based on data obtained from survey. Scale measurement can be seen in Figure 1. The scale is given from score 1 to score 5. Score 1 means that factors determine KM are not ready (need some work), while score 5 means fully ready (go ahead).

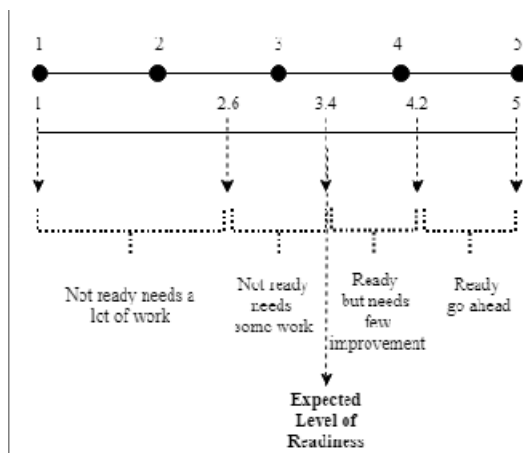


Figure 1 – Aydin & Tasci scale [23]

### D. Individual Acceptance

When it comes to considering people as one of factors which determine implementation of KM, factor of Individual Acceptance comes to place. There are several theories which emphasize that any changes in an organization may be significantly affected by its individual acceptance [14], such as Theory of Reasoned Action (TRA) [24][25], Theory of Planned Behavior (TPB) [26], Technology Acceptance Model (TAM) [27], Unified Theory of Acceptance and Use of new Technology (UTAUT) [28]. This study adopted two factors from UTAUT: Effort Expectancy and Performance Expectancy. UTAUT itself is derived from TAM, TPB, and TRA, while these factors are already proven in previous studies [2] [5] [8] [12] [14] [20] to measure KM Readiness.

## III. METHODOLOGY

### A. Research Model

Based on Systematic Literature Review (SLR) [17] in 17 previous studies [2][3][5][6][7][8][9][10][11][12][13][14][15][16][20][21][29], the proposed research model were developed

to measure KM Readiness. The theoretical framework or the model is displayed in Figure 2. It contains of 3 aspects: KM Enablers, Individual Acceptance toward KM, and KM SECI Process.

KM Enablers in this study's research model contains of 8 variables: Collaboration; Trust; Learning; Management Support; Reward; Decentralization; IT Support; and IT Use. Those 8 variables are categorized into 3 factors, such as: Organization Culture, Organization Structure, and Information Technology. The research model also adopted Individual Acceptance which contains of 2 variables, such as Performance Expectancy toward KM, and Effort Expectancy toward KM. As a dependent variable component, aspect of Intention to be Involved in KM SECI Process contains of 4 dependent variables, such as: Socialization, Externalization, Combination, and Internalization. Figure 2 visualize theoretical framework or research model of this study.

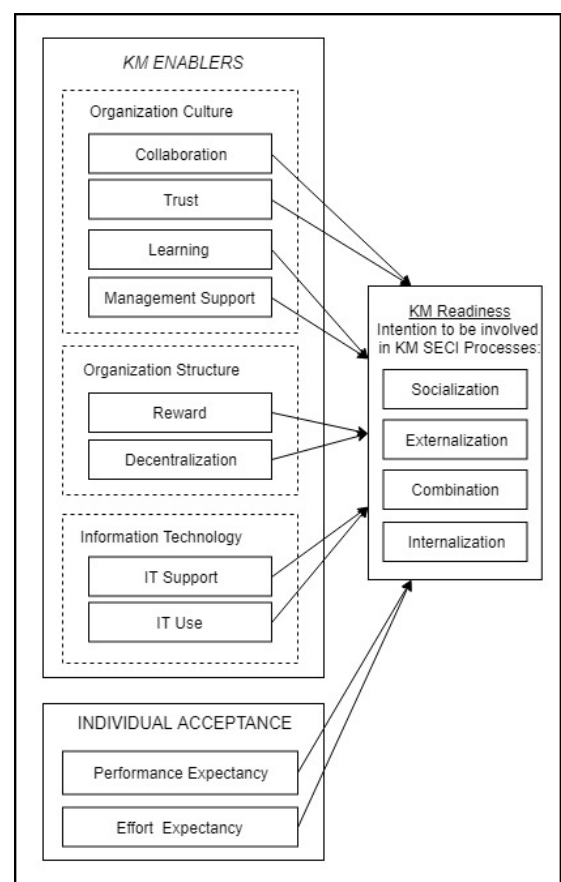


Figure 2 – Research Model KM Readiness in DBN Ministry of Trade

### B. Research Instrument

Research instrument contains of list of questionnaire's questions. It used 5-likert-scale. There are 47 main questions, added with 4 demographic questions. The research instrument is derived from instrument variables. Those 47 questions represented 14 factors, divided into 4 dependent factors and 10



latent factors. The reference for each instrument variable is shown in Table 1.

Table 1 Instrument Variables

No.	Variable	References
1	Collaboration	[5],[7],[8],[12],[14]
2	Trust	[5],[7],[8],[12],[13],[14],[29]
3	Learning	[5],[7],[8],[14],[16],[29]
4	Management Support	[5],[8],[11],[12],[29]
5	Decentralization	[5],[8],[11],[12],[14]
6	Reward	[5],[7],[8],[12],[14],[29]
7	IT Support	[7],[8],[12],[14]
8	IT Use	[8],[9],[12],[14]
9	Performance Expectancy	[2],[5],[8],[9],[12],[14],[20]
10	Effort Expectancy	[2],[5],[8],[12],[14],[20]
11	Socialization	[2],[5],[6],[8],[9],[12],[14]
12	Externalization	[2],[5],[6],[8],[9],[12],[14]
13	Combination	[2],[5],[6],[8],[9],[12],[14]
14	Internalization	[2],[5],[6],[8],[9],[12],[14]

### C. Sample and Data Collection

KM Readiness assessment was conducted in DBN Ministry of Trade by using survey with non-probability sampling, as what Creswell suggests [30]. The online questionnaire was distributed to 70 of total population, then there were only 53 returned and answered. Respondents are categorized based on several demography criteria such as: educational background, working experience (in years), gender, and age.

### D. Validity and Reliability

Before calculating the score of KM Readiness, based on statistic-quantitative methodology [30] and previous studies, both validity and reliability test need to be performed in order to make sure the model along with received data are valid and reliable. Validity test was carried out using convergent and discriminant validity [3][5][12], while reliability test was carried out using composite reliability [3][5][12].

Convergent validity shows that all AVE value for each variable of the model is not less than 0.5 (see Table 2), which is the acceptable value [12]. While discriminant validity (see Table 3) shows that the model is valid based on the criteria of discriminant validity [5][12][30]. Regarding reliability aspect, composite reliability shows that the model is reliable since each CR value is more than 0.7 [3] (see Table 2). Hence the model is considered as valid and reliable.

Table 2 Std Item Loading, AVE, and CR values

Variable	Indicator	Std. Item Loading	AVE	CR
Collaboration	OCC2	0.649	0.563	0.836
	OCC3	0.831		
	OCC4	0.696		
	OCC5	0.810		

Variable	Indicator	Std. Item Loading	AVE	CR
Trust	OCT1	0.906	0.825	0.934
	OCT2	0.876		
	OCT3	0.941		
Learning	OCL1	0.895	0.798	0.922
	OCL2	0.906		
	OCL3	0.879		
Management Support	OCMS2	0.844	0.825	0.903
	OCMS3	0.968		
Decentralization	OSD1	0.914	0.769	0.908
	OSD2	0.954		
	OSD3	0.749		
eward	OSR1	0.864	0.826	0.934
	OSR2	0.917		
	OSR3	0.943		
IT Support	ITS1	0.912	0.734	0.931
	ITS2	0.916		
	ITS3	0.925		
	ITS4	0.847		
	ITS5	0.652		
IT Use	ITU1	0.629	0.656	0.882
	ITU2	0.892		
	ITU3	0.885		
	ITU4	0.806		
Effort Expectancy	IAE1	0.888	0.764	0.907
	IAE2	0.838		
	IAE3	0.895		
Performance Expectancy	IAP1	0.919	0.874	0.954
	IAP2	0.957		
	IAP3	0.928		
Socialization	IS1	0.825	0.596	0.946
	IS2	0.820		
	IS3	0.782		
Externalization	IE1	0.637		
	IE2	0.662		
	IE3	0.675		
Combination	IC1	0.785		
	IC2	0.817		
	IC3	0.742		
Internalization	II1	0.889		
	II2	0.803		
	II3	0.784		

Table 3 Discriminant Validity

	OCC	OCT	OCL	OCMS	OSD	OSR	ITS	ITU	IAE	IAP	Int-SECI
OCC	<b>0.750</b>										
OCT	0.658	<b>0.908</b>									
OCL	0.227	0.398	<b>0.893</b>								
OCMS	0.259	0.153	0.194	<b>0.908</b>							
OSD	0.177	0.101	0.455	0.625	<b>0.877</b>						
OSR	0.312	0.208	0.512	0.664	0.706	<b>0.909</b>					
ITS	0.285	0.307	0.633	0.455	0.511	0.504	<b>0.857</b>				
ITU	0.346	0.347	0.157	0.290	0.148	0.017	0.326	<b>0.810</b>			
IAE	0.438	0.436	0.217	0.391	0.296	0.176	0.304	0.463	<b>0.874</b>		
IAP	0.288	0.280	0.047	0.274	0.006	-0.047	0.075	0.623	0.708	<b>0.935</b>	
Int-SECI	0.272	0.354	0.277	0.226	0.253	0.076	0.298	0.539	0.781	0.619	<b>0.772</b>

#### IV. RESULT AND ANALYSIS

##### A. KM Readiness Level

Measuring the KM Readiness Level was done by calculating total means of each variable. The total means then was mapped to Aydin & Tasci scale level [23]: ready go ahead; ready yet needs few improvements; not ready needs some work; and not ready needs a lot of work.

Calculation of validated and reliable data in this study resulting in level 3.84 of KM Readiness in DBN Ministry of Trade. This level means “ready but needs a few improvements”. Table 4 shows the readiness level for each variable and total as well.

##### B. Factors Analysis

Factors analysis was conducted to get insight of the result. The analysis was done by using SmartPLS 3 as tool. This research model was built also by using SmartPLS 3. The model consists of 11 variables and 47 indicators. Those variables and indicators were tested in term of validity and reliability. Based on validity and reliability test result, out of 47 indicators only 2 of them were eliminated, without eliminating any variable, which means all variables were still intact.

Evaluation of this model was done to predict causality between independent variable and dependent variable. T-Statistic [5] was used to test the hypothesis derived from research model. The hypothesis is accepted if it has a t-static value higher than 1.64 for one-way hypothesis (1-tail) and 1.96 for the two-way hypothesis. alpha value is 5% which means confidence level at 95%. Since mostly of each factor is one-way (1-tail), then the value of 1.64 is used as parameter value.

As displayed in Table 5, this study has found that Effort Expectancy has value of T-Statistic 3.923 which is more than 1.64. This means Effort Expectancy affects employee to be more involved in KM SECI Process.

Table 4 Result of KM Readiness Level for Each Variable and Total

KM Aspects	Variable	Total Mean	Readiness
Organizational Culture	Collaboration	4.26	Ready, go ahead
	Trust	3.90	Ready, but needs a few improvement
	Learning	3.45	
	Management Support	3.65	
Organizational Structure	Decentralization	3.29	Not ready, needs some work
	Reward	2.81	
Information Technology	IT Support	3.27	Ready, go ahead
	IT Use	4.24	
Individual Acceptance	Performance Expectancy	4.46	
	Effort Expectancy	4.18	Ready, but needs a few improvement
Intention to be Involved in KM SECI Process	Socialization	4.14	
	Externalization	4.08	
	Internalization	4.14	
	Combination	4.23	Ready, go ahead
<b>TOTAL</b>	<b>KM Readiness level</b>	<b>3.84</b>	<b>Ready, but needs a few improvement</b>

Table 5 Path Coefficient

Path Correlation	Original Sample (O)	Standard Deviation (STDEV)	T Statistics ( O/STDEV )
Collaboration → Intention to be Involved in SECI (II-SECI)	-0.136	0.132	1.024
Trust → II-SECI	0.019	0.145	0.129
Learning → II-SECI	0.104	0.148	0.704
Management Support → II-SECI	-0.168	0.200	0.838
Reward → II-SECI	-0.033	0.182	0.182

Decentralization → II-SECI	0.107	0.186	0.574
IT Support → II-SECI	0.007	0.165	0.043
IT Use → II-SECI	0.241	0.151	1.593
Performance Expectancy → II-SECI	0.041	0.178	0.233
Effort Expectancy → II-SECI	0.706	0.180	3.923

## V. DISCUSSIONS AND IMPLICATIONS

This study has shown that level of KM Readiness in DBN Ministry of Trade is 3.84 which means “ready but needs few improvement”. This implies that the organization has good start to implement KM successfully. Yet several things need to be improved are: Organizational Culture, Organizational Structure, Information Technology, and Individual Acceptance.

Organizational culture aspect in this study consists of Collaboration, Trust, Learning and Management Support. Among those 4 variables, regarding Table 4, only Collaboration obtained level 4.26 or “ready, go ahead”. Others were relatively same on level “ready but needs few improvement”. Regarding Learning and Management Support variables, which were at level 3.45 and 3.65, this organization needed to improve learning process by conducting more quality-relevant training. It also needed to increase support from management toward employee activity in KM SECI process.

Organizational structure consists of Decentralization and Reward. Both variables were in the same level of “Not Ready, needs some work”. Decentralization was at 3.29 and Reward was at 2.81. Reward was the first lowest level among all variables, while Decentralization was the third lowest. Nevertheless, Reward variable needed the most improvement in this organization to encourage employees to involve better in KM SECI processes. Adding more incentives in KM activity might be one of many ways to improve KM. Decentralization also must be improved by delegating more adequate power regarding decision making in top-down approach. This way might exploit latent potential of each employee to perform better and share their knowledge in organization.

There are 2 variables in Information Technology (IT) aspect: IT Support and IT Use. Apparently, IT-Use had readiness level of “ready, go ahead” at 4.24 (Table 4). On the contrary, IT-Support had readiness level of “not ready, needs some work” at 3.27. From these result, IT-Support needed to be improved. Organization needs to provide better support of IT to their employee to encourage them to involve better in KM SECI process.

Individual Acceptance encapsulated 2 variables: Effort Expectancy and Performance Expectancy. Based on t-statistics value (Table 5), Effort Expectancy variable had strong influence for employee to be involved in KM SECI process, since it had the highest value at 3.923, which is greater than 1.64 as parameter value.

## VI. CONCLUSIONS

The purpose of this study is to assess KM Readiness level of DBN Ministry of Trade. The assessment was carried out by determining the appropriate framework model through literature review of previous relevant studies. The framework model then used to assess KM Readiness. The research model generates several relevant questions in questionnaire which were asked to DBN's employee to obtain their perception.

The result of this study is the KM Readiness level of DBN in Ministry of Trade which is “ready but needs a few improvement”. This study also developed suggestions to the organization to conduct few improvements to successfully implement KM in the future.

## ACKNOWLEDGMENT

This work is supported by Hibah PITTA 2018 funded by DRPM Universitas Indonesia No.5000/UN2.R3.1/HKP.05.00/2018.

## REFERENCES

- [1] D. T. Holt, S. E. Bartczak, S. W. Clark, and M. R. Trent, “The development of an instrument to measure readiness for knowledge management,” *Knowl. Manag. Res. Pract.*, vol. 5, no. 2, pp. 75–92, 2007.
- [2] M. J. M. Razi, N. S. A. Karim, A. R. A. Dahlan, and N. A. Mohamad Ali, “A holistic approach to measure organizational readiness for knowledge management,” *Adv. Sci. Lett.*, vol. 23, no. 4, pp. 2829–2832, 2017.
- [3] A. Hedar, D. I. Sensuse, and P. Sandhyaduhita, “Knowledge management readiness of research agencies: A case of BATAN Indonesia,” *2016 Int. Conf. Informatics Comput. ICIC 2016*, no. Icic, pp. 78–83, 2017.
- [4] P. Akhavan, M. Jafari, and M. Fathian, “Exploring the Failure Factors of Implementing Knowledge Management System in the Organizations,” *J. Knowl. Manag. Pract.*, vol. 6, pp. 1–10, 2005.
- [5] P. A. Nugraha and I. Budi, “Analysis of Knowledge Management Implementation Readiness in A Technology Services Company,” *2017 3rd Int. Conf. Sci. Inf. Technol.*, pp. 602–607, 2017.
- [6] N. Shahriza Abdul Karim, M. Jalaldeen Mohamed Razi, and N. Mohamed, “Measuring employee readiness for knowledge management using intention to be involved with KM SECI processes,” *Bus. Process Manag. J.*, vol. 18, no. 5, pp. 777–791, 2012.
- [7] A. Shajera and Y. Al-Bastaki, “Organisational Readiness for Knowledge Management: Bahrain Public Sector Case Study,” *Build. a Compet. Public Sect. with Knowl. Manag. Strateg.*, 2013.
- [8] M. J. M. Razi and N. S. A. Karim, “Assessing knowledge management readiness in organizations,” *Proc. 2010 Int. Symp. Inf. Technol. - Syst. Dev. Appl. Knowl. Soc. IITSim'10*, vol. 3, pp. 1543–1548, 2010.

- [9] M. J. Mohamed Razi, N. S. Abdul Karim, and N. Mohamed, "Knowledge management readiness measurement: Case study at institution of higher learning in Malaysia," *2011 Int. Conf. Res. Innov. Inf. Syst. ICRIS'11*, 2011.
- [10] L. N. Marouf and N. K. Agarwal, "Are Faculty Members Ready? Individual Factors Affecting Knowledge Management Readiness in Universities," *J. Inf. Knowl. Manag.*, vol. 15, no. 03, p. 1650024, 2016.
- [11] N. K. Agarwal and L. Marouf, "Quantitative and qualitative instruments for knowledge management readiness assessment in universities," *Qual. Quant. Methods Libr.*, vol. 5, pp. 149–164, 2016.
- [12] W. R. Fitriani, A. G. Putra, D. Tanaya, and H. N. Rochman, "Assessing Knowledge Management Implementation Readiness in Faculty of Computer Science , Universitas Indonesia," *Int. Conf. Adv. Comput. Sci. Inf. Syst.*, pp. 171–180, 2016.
- [13] L. Marouf, "Are academic libraries ready for knowledge management?," *Electron. Libr.*, vol. 35, no. 1, pp. 137–151, 2017.
- [14] N. S. Abdul Karim, N. Mohammad, L. M. Abdullah, and M. J. M. Razi, "Understanding Organizational Readiness for Knowledge Management in the Malaysian Public Sector Organization: A Proposed Framework," *2011 Int. Conf. Res. Innov. Inf. Syst.*, pp. 1–6, 2011.
- [15] R. D. Rakhman, A. N. Hidayanto, I. C. Hapsari, P. I. Sandhyaduhita, and I. Budi, "Applying Analytic Hierarchy Process for Measuring Knowledge Management Readiness in Government Institutions," *Int. Conf. Inf. Technol. Syst. Innov.*, pp. 1–6, 2016.
- [16] S. W. Indra, I. Munandar, and I. G. K. Rizal, "Analysis of Knowledge Management Readiness in Government Institution," in *2017 3rd International Conference on Science in Information Technology (ICSITech)*, 2017, pp. 222–225.
- [17] B. Kitchenham *et al.*, "Systematic literature reviews in software engineering-A tertiary study," *Inf. Softw. Technol.*, vol. 52, no. 8, pp. 792–805, 2010.
- [18] D. Moher, A. Liberati, J. Tetzlaff, and D. G. Altman, "Preferred reporting items for systematic reviews and meta-analyses: The PRISMA statement," *Int. J. Surg.*, vol. 8, no. 5, pp. 336–341, 2010.
- [19] I. Becerra-Fernandez and R. Sabherwal, *Knowledge Management: Systems and Processes*. Routledge, 2015.
- [20] R. Jalaldeen, N. Shahriza Abdul Karim, and N. Mohamed, "Organizational Readiness and its Contributing Factors to Adopt KM Processes: A Conceptual Model," *Commun. IBIMA (International Bus. Inf. Manag. Assoc.)*, vol. 8, no. 2009, pp. 128–136, 2009.
- [21] A. Shirazi, S. Mortazavi, and N. P. Azad, "Factors affecting employees' readiness for knowledge management," *Eur. J. Econ. Financ. Adm. Sci.*, vol. 33, no. 33, pp. 167–177, 2011.
- [22] B. Bergeron, *Essentials of Knowledge Management*, vol. 30. 2011.
- [23] C. H. Aydin and D. Tasci, "International Forum of Educational Technology & Society Measuring Readiness for e-Learning: Reflections from an Emerging Country Cengiz Hakan Aydin Deniz Tasci," *J. Educ. Technol. Soc.*, vol. 8, no. 4, pp. 244–257, 2005.
- [24] M. Fishbein and I. Ajzen, "Belief, attitude, intention and behavior: an introduction to theory and research." Reading, MA: Addison-Wesley, 1975.
- [25] B. H. Sheppard, J. Hartwick, and P. R. Warshaw, "The Theory of Reasoned Action: A Meta-Analysis of Past Research with Recommendations for Modifications and Future Research," *J. Consum. Res.*, vol. 15, no. 3, pp. 325–343, 1988.
- [26] I. Ajzen, "The theory of planned behavior," *Organizational Behav. Hum. Decis. Process.*, vol. 50, pp. 179–211, 1991.
- [27] F. D. Davis, "Perceived Usefulness, Perceived Ease of Use, and User Acceptance of Information Technology," *MIS Q.*, vol. 13, no. 3, pp. 319–340, 1989.
- [28] V. Venkatesh, M. G. Morris, G. B. Davis, and F. D. Davis, "User Acceptance OF Information Technology: Toward A Unified View," *MIS Q.*, vol. 27, no. 3, pp. 425–478, 2003.
- [29] K. Mohammadi, A. Khanlari, and B. Sohrabi, "Organizational readiness assessment for knowledge management," *IGI Glob.*, vol. 5, no. 1, pp. 1712–1728, 2010.
- [30] J. W. Creswell, "Research Design: Qualitative, Quantitative, and Mixed Method Approaches." SAGE Publications, p. 548, 2013.

# Personal Extreme Programming with MoSCoW Prioritization for Developing Library Information System

<sup>1st</sup> Gita Indah Marthasari  
Informatika

Universitas Muhammadiyah Malang  
Malang, Indonesia  
gita@umm.ac.id

<sup>2nd</sup> Wildan Suharso  
Informatika

Universitas Muhammadiyah Malang  
Malang, Indonesia  
wsuharso@umm.ac.id

<sup>3rd</sup> Frendy Ardiansyah  
Informatika

Universitas Muhammadiyah Malang  
Malang, Indonesia  
frendy.a@webmail.umm.ac.id

**Abstract**— Software development projects require experience and knowledge of the developer or clients related to the system which will be developed. Unclear clients' needs potentially emerge many changes of needs during the process of development which can not be resolved by using conventional software development methodology. The implementation of the less significant requirements either from the clients or the other stakeholders causes the project development becomes longer. Therefore, a technique is needed to arrange the priority of software requirements. In this paper, we combine personal extreme programming (PXP) methodology with Moscow technique to overcome those problems. PXP is suitable to use in small to medium-sized projects if the clients do not know in detail about the needs in the development of applications, applications needed in relatively quick time, and the development phase is adjusted to use by a single programmer. Moscow technique was used for prioritizing requirements elicited in PXP methodology. Moscow is a method to determine priority needs based on cost, risk, and business value. This technique was applied during the planning phase of PXP to develop library application, thereby it reduced the time of project completion. The result was a library application suited the needs of clients to support business processes at Batu State Attorney's library.

**Keywords**—personal extreme programming, Batu state attorney, library information system, moscow prioritization, test driven development.

## I. INTRODUCTION

Agile Development is a collection of application development methodology which has an incremental and iterative concept [1], [2]. It focuses on processing application and communication with clients. Its goal is to make faster response change and will reduce the completion time of application development projects. The changes are in the form of cost, requirements, schedule, and team members [2]. Examples of methodologies in Agile Development are SCRUM and Extreme Programming (XP) [3], [4]. The comparison between them is that SCRUM focuses on project management and team member [3], while XP focuses on application programming, feedback, and communication with clients. XP is suitable to use in small to medium-sized projects if the clients do not know in detail about the needs in the development of application and application needed in relatively quick time. In the development, the phase in XP practice is adjusted to use by a single programmer called Personal Extreme Programming (PXP) [5], [6]. In PXP, the priority requirements need to be

determined so that the application is completed on time as user's request. The priority setting in PXP is based on technical risk, and business value [7].

State Attorney is one of the institutions that play an essential role in the control of the law and the welfare of the people, especially in the territory of its power in Indonesia [8]. Based on the preliminary survey, we have found a few weaknesses in the service process in Batu State Attorney. One of the weaknesses is found in library services. A member who is going to search for books should look into the catalog in the library. After getting the book code, the member can start searching for books from the shelves according to the code. This sort of searching process can take some time, especially if the book collection is overwhelming. This makes it difficult for members (as prosecutors) when they need a source of information in a short time to support their work. Another problem is the catalog which material made from paper and has a risk of being lost or damaged. When that happens, a librarian has to rewrite each transaction and collection list from scratch, so it takes a lot of energy and time. Besides, the library has no media to remind the members when the duration of the borrowing is up, so they often forget to return the book which potentially lost. The solution to overcome the problems mentioned above is to make an improvement of the library service. Therefore, we need to develop a web-based system to help library management.

The initial stage of creating an application is to clearly define all needs, controls, and functions [9], but it is known that the clients, as well as the users (librarian), do not have a detailed knowledge of the functional requirements for the library application to be developed. As a result, many changes and adjustments of requirements will potentially occur. Changes to needs that have lack significant functionality in the application will increase the project duration. The solution is involving the clients' roles through intensive communication throughout the project. One of the clients' roles is describing all the desirable needs and determining its priority based on the impact on the functionality of the application. Priority setting of requirements also has an impact on project completion time. In the PXP project, clients play an essential role to determine priority. Referring to the needs and clients' requirements, it is necessary to select the appropriate priority method. A quick and easy approach to help clients set priorities is MoSCoW. MoSCoW is a method for prioritizing requirements based on cost, risk, and business

value. These requirements will be grouped into four categories: Must have, Should have, Could have, and Will not have [10], [11]. Therefore, we created a web-based library system by involving the role of clients during the process of making the application. PXP and MoSCoW were used as the development methodology to support the roles of the clients. The result is a web-based library system of Batu State Attorney to assist the performance of library management and the staff and to overcome the problems mentioned before.

## II. RESEARCH METHOD

This research used Personal Extreme Programming (PXP) as the development methodology combine with the MoSCoW as requirements prioritization technique (Figure 1). Overall, we conduct requirements elicitation from clients to identify functional specification of the system then the iteration phase is started. This phase starts with design step and continue until the final step, retrospective, which is the end of iteration stage.

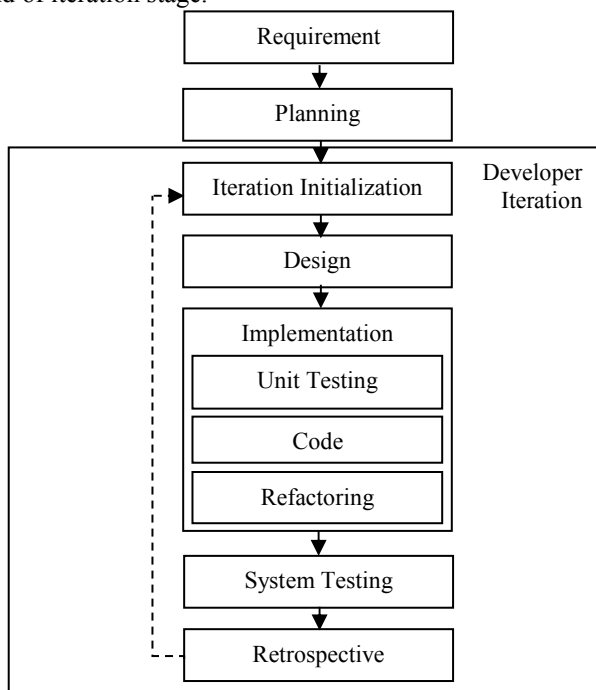


FIG 1. STAGES OF PXP METHODOLOGY [6].

## III. RESULT AND DISCUSSION

### A. Requirements

This stage was done by collecting data at Batu State Attorney Office. We asked the developers and the clients to describe the needs based on the problems encountered. These needs will be converted into a functional specification in the application library. In the PXP methodology, needs refer to user stories written on cards which are called user story cards. The format of the writing is "As [role] I can [action] so [purpose]" [13]. User story criteria are negotiable, estimable, and testable.

### B. Planning

Planning stage describes the procedure on the user story obtained from the requirements stage. We determined the estimated time of implement the user story, the priority needs using Moscow with technical risk criteria, and business value based on [14], [15], and to create a list of release planning. The results of prioritizing Moscow refer to [16] as follows:

Must have criteria lists all of user story meets the criteria of business value and technical risk as follows:

- Registering members, this user story must be implemented in the system. It explains the business processes of borrowing books and to do that a user must be registered as a member.
- Signing up the book, the user story becomes a significant function because it helps the clients' need of storing and backing up book data, searching, and borrowing books.
- Borrowing the book, this user story is the main feature of the system for processing, storing, and backing up data, storing. This functional specification is required for due date notification.
- Automatic reminder messages, this user story also becomes the main feature to prevent members who are late returning the book.
- Book searching by title, this user story helps users finding the availability of books to be borrowed.
- Calculating automatic fines, this user story is essential to help admins calculate the cost of fines for late return of books.
- Notice of due date on the admin side, user story plays a role to help admins view the list of borrowed books that have been in due date which is difficult to do manually.
- New book notification, user story becomes a key feature to make users aware of the latest book list.
- User-specific access, user story restricts and differentiates user permissions.
- Restoring the book, user story must exist as a critical feature of the business process of borrowing books on library applications.
- Registering a new admin, user story stores admin data and permissions to log into the data library in library application.

Should have category is a user story criteria that does not meet the technical risk criteria, but still has business value or can help the business process of library users. User story in the "should have" category is implemented within the specified time frame, but the project is not considered failed even if not implemented. User story included in this category are as follows:

- Changing the website information data, this user story provides library information of Batu State Attorney, such as logos, agency names, addresses, and contacts.
- Reminding due date, user story can help users to see the due date of the borrowing through the application so that they might not forget.
- Proposing a new book, user story helps members submit book suggestions through library application to complete library book collections.



- d. Uploading a book file, this user story is essential as it helps users save book files in softcopy form into the system.

Could have category is a user story that is not included in the criteria of technical risk or business value, but can help to complete the application features. The user story that belongs to this category is viewing a list of new books. The last category is “would not have” criteria that not using user story.

Referring to [17], the result of the release planning list used to develop the application of Batu State Attorney library is shown in table 1.

TABLE 1. LIST OF RELEASE PLAN

	Use Stories	Priority	Point
<b>Iteration 1</b>	Registering the members	Must have	1
	Registering the books	Must have	1
	Inputting the book borrowed	Must have	1
	Automated reminder messages	Must have	1
<b>Velocity</b>			<b>4</b>
<b>Iteration 2</b>	Finding the books based on the title	Must have	1
	Counting the fine automatically	Must have	1
	Accepting the notification of the new books	Must have	1
	Observing the due date of borrowing by admin	Must have	1
<b>Velocity</b>			<b>4</b>
<b>Iteration 3</b>	Registering the new admin	Must have	1
	Special access for a user	Must have	1
	Returning the books	Must have	1
	Changing the website information data	Should have	1
<b>Velocity</b>			<b>4</b>
<b>Iteration 4</b>	Suggesting the new books	Should have	1
	Uploading the book file	Should have	1
	Observing the new books	Could have	1
	Observing the due date of borrowing	Should have	1
<b>Velocity</b>			<b>4</b>

Table 1 shows the results of the release plan list which is determined by the developer along with the clients. There are 4 iterations that must be done in developing the application of Batu State Attorney library. Table 1 shows the title of each user story, each of them has a story point used to describe the difficulty level of working, a user story by the number 1 is estimated to be done within 3 days. One time of iteration has a velocity value of 4, so to complete 16 story points, it takes 4 times of iteration. There is reiteration on iteration development to work on 4 iterations in Table 1.

One iteration development is provided for one time iteration. This paper explains the results of working on the first iteration. Based on the list of planning released in Table 1, the user story done in the first iteration is to register the members, register the books, input the book loans, and automated reminder messages.

### C. Iteration Initialization

Based on the list of planning released in Table 1, the user story done in the first iteration is to register the members, register the books, input the book loans, and automated reminder messages.

### D. Design

Figure 2 shows a database design table for user stories that consist of a member entity for registering the members, a book entity for registering the books, a loan entity for inputting the loan books, and an automated reminder message using an email attribute in a member entity. In the next phase, the developers begin to write the process of program code according to the design that has been made.

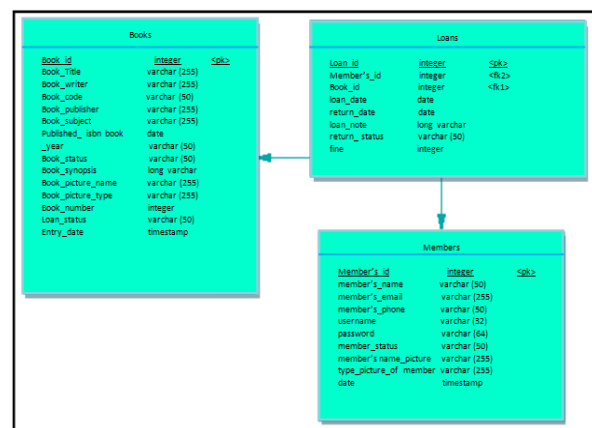


FIG II. DATABASE DESIGN IN THE FIRST ITERATION

### E. Implementation

The implementation of the program using Test Driven Development (TDD) consists of 3 stages: unit testing, code generation, and refactoring. The unit testing results of each user story are shown in Figure 3. Member Controller (Controllermember.php) is used for the user story of member registration, Book Controller (Controllerbook.php) for book registration, Loan Controller (Controllerloan.php) for loaning the book, and Email (Email.php) for automatically sends reminding messages. All codes have passed unit testing shown by value of 100%. The process of completing the program code or code generation is done after the program code of each user story passes the unit testing. Besides, it is also created user views from each user story. The user view in one of the users story is shown in Figure 4.

		Code Coverage					
		Lines		Functions and Methods		Classes and Traits	
Total			100.00%	170 / 170		100.00%	15 / 15
Controllermember.php			100.00%	42 / 42		100.00%	4 / 4
Controllerbook.php			100.00%	61 / 61		100.00%	1 / 1
Email.php			100.00%	22 / 22		100.00%	1 / 1
Controllerloan.php			100.00%	45 / 45		100.00%	4 / 4

FIG III. TESTING RESULT IN FIRST ITERATION

FIG IV. USER VIEW OF REGISTER MEMBER REQUIREMENT

### F. System Test

This stage tests the results of the implementation of features that have been obtained. The test applies the user acceptance test criteria. It is based on the user story. The test is done by the client. The test results are shown in Table 2

TABLE II. USER ACCEPTANCE TEST

Iteration 1			Results	
User Stories	Acceptance test criteria	Priority	Yes	No
Registering the members	Notification of member's data is accepted	Must have	√	
	The account can only be registered by admin			
Loaning the books	Notification of data is successfully saved	Must have	√	
	Loan data can be deleted			
	The loan number by member is only allowed for one time			
Registering the books	Data of the books can be deleted	Must have	√	
	There is an image for the book cover			
Reminder message of the due date of loan	The message is sent by email	Must have	√	
	The message is sent constantly until the book returned			

### G. Restrospective

Based on the results of the first iteration implementation, verification is done at this stage to ascertain whether the realization time is equal to the initial estimation time. The verification results are shown in table 3.

TABLE III. TIME VERIFICATION RESULT ON THE FIRST ITERATION

Iteration 1				
User Stories	Priority	Story Point	Estimation Time	Realization Time
Registering the members	Must have	1	3	3
Registering the books	Must have	1	3	3
The book loans	Must have	1	3	3
Automated	Must	1	3	6

reminder messages	have			
Velocity		4	12	15

### IV. CONCLUSION

Personal extreme programming (XP) could be used to develop an application fast because it could overcome changing requirements flexibly. MoSCoW method was useful in planning and processing which focused on the main needs. The methodology used in this study was personal extreme programming in developing application of Batu State Attorney library which clients were still unfamiliar with software technology. Based on the research that has been discussed, XP is able to meet the needs of clients with the construction of Batu State Attorney library applications to overcome the problems encountered. Batu State Attorney library application which has been built using XP is only based on the client's needs without adding another feature that might be needed in the future. The Moscow approach is able to assist the developers and the clients in determining the priority needs, but it cannot prevent the potential delay time that occurs during the development of Batu State Attorney library applications. It is found that most of the needs have priority "must have" when the determining of Moscow priority is done. However, this makes the processing time longer.

### REFERENCES

- [1] S. Balaji, "Waterfall vs v-model vs agile: A comparative study on SDLC," *WATEERFALL Vs V-MODEL Vs Agil. A Comp. STUDY SDLC*, vol. 2, no. 1, pp. 26–30, 2012.
- [2] D. Greer and Y. Hamon, "Agile Software Development," *Softw. - Pract. Exp.*, vol. 39, no. 7, pp. 701–736, 2009.
- [3] J. Highsmith, "What Is Agile Software Development?," *J. Def. Softw. Eng.*, vol. 15, no. 10, pp. 4–9, 2002.
- [4] V. Devedzic and S. R. Milenkovic, "Teaching Agile Software Development: A Case Study," *IEEE Trans. Educ.*, vol. 54, no. 2, pp. 273–278, 2011.
- [5] R. Agarwal and D. Umphress, "Extreme programming for a single person team," *Proc. 46th Annu. Southeast Reg. Conf. XX - ACM-SE 46*, no. August, p. 82, 2008.
- [6] Y. Dzhurov, I. Krasteva, and S. Ilieva, "Personal Extreme Programming—An Agile Process for Autonomous Developers," *Int. Conf. software, Serv. Semant. Technol.*, no. August 2016, pp. 252–259, 2009.
- [7] K. Beck and C. Andres, *Extreme Programming Explained: Embrace Change*. Addison Wesley Professional, 2004.
- [8] P. R. Indonesia, Keputusan Presiden Republik Indonesia Nomor 86 Tahun 1999 tentang Susunan Organisasi dan Tata Kerja Kejaksaan Republik Indonesia. 1999, pp. 1–13.
- [9] R. Fojtik, "Extreme programming in development of specific software," *Procedia Comput. Sci.*, vol. 3, pp. 1464–1468, 2011.
- [10] I. Stamelos and P. Sfetsos, *Agile Software Development Quality Assurance*, no. February. 2007.
- [11] S. Dimitrijević, J. Jovanovic, and V. Devedžić, "A comparative study of software tools for user story management," *Inf. Softw. Technol.*, vol. 57, no. 1, pp. 352–368, 2015.
- [12] B. W. Boehm, "Software Engineering Economics," *IEEE Trans. Softw. Eng.*, vol. SE-10, no. 1, pp. 4–21, 1981.
- [13] M. Kohn, *User Stories Applied for Agile Software Development*. Boston: Pearson Education, Inc, 2004.
- [14] IIBA, *Agile Extension to the BABOK® Guide*. Toronto, Ontario, Canada, 2005.
- [15] IIBA, *A Guide to The Business Analysis Body of Knowledge*. Toronto, 2015.

- [16] Y. Sugianto, S. Tjandra, and P. Method, "Aplikasi Point of Sale Pada Toko Retail Dengan Menggunakan Dynamic Software Development Method," vol. 8, no. 1, pp. 1–8, 2016.
- [17] H. Rizal, S. Adhy, and P. W. Wirawan, "Perancangan Dan Pembuatan Mobile Learning Interaktif Berbasis Android Dengan Metode Personal Extreme Programming," *J. Informatics Technol.*, vol. 2, no. 3, pp. 1–10, 2013.

# ML-Optimized Beam-based Radio Coverage Processing in IEEE 802.11 WLAN Networks

Mehdi Guessous

*Equipe de Recherche en Smart  
Communications - ERSC (ancien LEC)  
Ecole Mohammadia d'Ingénieurs –  
EMI  
Mohammed Vth University in Rabat  
Rabat, Morocco  
mehdiguessous@research.emi.ac.ma*

Lahbib Zenkour

*Equipe de Recherche en Smart  
Communications - ERSC (ancien LEC)  
Ecole Mohammadia d'Ingénieurs –  
EMI  
Mohammed Vth University in Rabat  
Rabat, Morocco  
zenkour@emi.ac.ma*

**Abstract**— Dynamic Radio Resource Management (RRM) is a major building block of Wireless LAN Controllers (WLC) function in WLAN networks. In a dense and frequently changing WLANs, it maximizes Wireless Devices (WD) opportunity to transmit and guarantees conformance to the design Service Level Agreement (SLA). To achieve this performance, a WLC processes and applies a network-wide optimized radio plan based on data from access points (AP) and upper-layer application services. This coverage processing requires a "realistic" modelization approach of the radio environment and a quick adaptation to frequent changes. In this paper, we build on our Beam-based approach to radio coverage modelization. We propose a new Machine Learning Regression (MLR)-based optimization and compare it to our NURBS-based solution performance, as an alternative. We show that both solutions have very comparable processing times. Nevertheless, our MLR-based solution represents a more significant prediction accuracy enhancement than its alternative.

**Keywords**—Radio Resource Management, Beamforming, Co-channel interference, Machine Learning, NURBS surface, WLAN.

## I. INTRODUCTION

Co-channel interference is one major issue that dense indoor WLAN networks face. To reduce its impact many strategies are adopted: centralized or distributed intelligence processing and decision making, dynamic RRM (dRRM) among others.

The centralized or distributed intelligence processing and decision making ensures that a reliable intelligence is gathered, from APs and new generation WDs, for decision making and that this decision is coherent network wide.

Dynamic RRM is a set of features and techniques that enable the central or distributed WLC optimize the radio resource plan, adapt quickly to radio environment changes, and trigger necessary healing actions to mitigate network issues. Additionally, dynamic RRM optimizes the network capacity by processing effectively new transmission opportunities. It accepts inputs from radio interface (RSSI, SNR, EIRP, noise, etc.), upper application service layers (MAC layer, TCP/IP, etc.), on-field site surveys: passive or active, and design recommendations: standard or per-vendor specifications.

The implementation of dynamic RRM requires deep and feasible approaches to represent and model the network radio coverage. In work [1] and its extension [2], we discuss

different coverage representations and evaluate the corresponding solution models' performance.

The processing of the huge amount of raw data that is input to dRRM requires important network and system resources: sufficient bandwidth, control traffic prioritization in the network, sufficient CPU and RAM to handle intensive computing, and sufficient disk space to store the data and results. In work [3], we present a processing optimized solution of dRRM and discuss its advantages over the previous ones.

Motivated by the advances in machine learning and wide use of its concepts [4], [5], [6] and [7], we investigate in this work how could regression models enhance further our dRRM solution.

In section II, we discuss our Beam-based radio coverage representation of a Wi-Fi Unified Architecture (WUA) which is WLC-based and some important machine learning concepts that are the foundation of this work study. In section III, we compare two Beam-based solution models and show how they could be enhanced thanks to a NURBS-based optimization [3]. In section IV, we discuss an MLR-based alternative to our NURBS-based optimization. In the end, we conclude and further our work.

## II. THEORETICAL BACKGROUND AND RELATED WORK

In this section we recall some important concepts about WUA, discuss our Beam-based radio coverage representation, dRRM solution models, and scope important machine learning concepts that are the foundation of this optimization work.

### A. Wifi Unified Architecture

In standalone AP deployments, dense indoor network capacity does not scale with frequent radio environment changes, number, mobility requirement, and application need of clients. A WLC is required to centralize AP intelligence and build a unified real-time vision of the entire coverage transmit opportunity. This opportunity processing builds on design recommendations, data from the radio interface and upper-layer application services. Some examples of these controllers are: Cisco 8540 Wireless Controller [8] and Aruba 7280 Mobility Controller.

Cisco WUA defines two protocols for the radio raw data exchange between the APs and WLC, on the wired interface, and between the APs themselves, over the air:

- CAPWAP: stands for Control and Provisioning of Wireless Access Points and is used by APs to build a protocol association to a WLC.
- NDP: is the Neighbor Discovery Protocol, it enables the APs to send Over-The-Air (OTA) messages and exchange standard and proprietary control and management information.

In addition to the basic RRM functionality that is described in [9], Cisco APs embark an on-chip RRM advanced feature: CLEANAIR. CLEANAIR, such a Wi-Fi engineer, monitors and measures environment real-time radio characteristics: SNR, interference, noise, etc. and reported them back to the WLC via the already established CAPWAP tunnels. Cisco appliances such as: Cisco Prime Infrastructure (CPI) or Mobility Services Engine (MSE), may extend this feature capability to analytics on Wi-Fi clients' presence, interferers management and heatmaps generation.

Cisco RRM implementation is well discussed in [10]. The idea is to trigger a new RRM Transmit Power Control (TPC) processing when the third neighbor RSSI is stronger than -70dBm and that the current transmit hysteresis is greater than the configured threshold which is by default equal to 6dB. This processing allows an AP to tune its transmit power level to reduce the co-channel interference that the neighboring APs may cause and consequently, eventually, maximize the transmit opportunity toward and from a WD.

But taken alone, it is hard to see how such implementation could hint on the opportunity to transmit at any given coverage point except from the APs? In the next sub-section, we motivate the need for a coverage representation approach and solution model to process this opportunity at every coverage area point.

#### B. Beam-based modelization approach of radio coverage

In a WLC-based WLAN network it is not possible to monitor every coverage area point and report the corresponding measures. Only a set of WDs have this ability: APs and certain Wi-Fi clients with extended capabilities such as Cisco Connected Mobile Experiences (CMX).

It is necessary then, to model the radio coverage and predict the corresponding measures based only on the enabled WDs. In [1] and [2] works, we discuss two major modelization approaches families that may be referred to as "simplistic", Range-based, and "idealistic", Voronoi-based.

The first approach supposes that an AP's coverage corresponds to one of these three ranges: a transmission, interference or no-talk range; that the pattern is omnidirectional in the form of a circle or a disk. In this scheme, the interference at any given point is approximated by the weighted intersection of all the interferers' patterns at this point.

In the second approach, the coverage area is segmented into non-uniform zones in the form of polygons. Each zone corresponds to an AP and its borderlines are proportional to the neighboring APs' transmit power levels. In this scheme, the co-channel interference condition is totally cancelled.

The implementation of the "simplistic" approach is feasible and straightforward, but it has many limitations that burden its performance: non-support of per direction transmit power adjustment, more prone to coverage holes, non-support

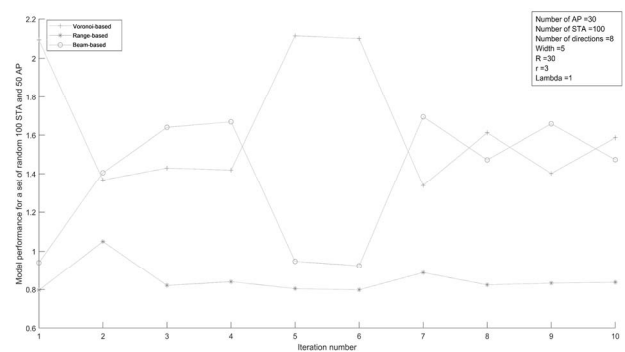


Fig. 1. Voronoi, Range and Beam-based model compared performance

of obstacle detection, non-support of client localization, and non-support of hidden transmit opportunity detection.

The "idealistic" approach is the most performant, but it is not feasible: how could we achieve any polygon propagation pattern? It may be technologically possible but not economically!

In [1] and [2] works, a "realistic", Beam-based approach is presented that is a generalization of the previous two approaches. In this scheme, the AP coverage is the region covered by the beams in the AP's supported transmit directions. The transmit direction and the corresponding power level are tunable which offer two additional degrees of freedom to mitigate a co-channel interference condition especially in comparison with the "simplistic" approach.

In "Fig. 1", we show a compared performance of the three models: Voronoi-based, Range-based and Beam-based, in processing the coverage of a random set of 30 APs and 100 STAs (mobile Stations).

In this simulation, each AP supports 8 transmit directions, "R" is the corresponding transmit power level, "r" represents the sensitivity of an STA at reception, "lambda" reflects the attenuation of a signal from the source to the receiver and "width" is the aperture that characterizes the beam in each direction.

We check that the Voronoi-based model performs better than both Range and Beam-based models. With a "width" value equal to 5, the Beam-based model performs better than the Range-based model.

We show in "Fig. 2", that by tuning, decreasing, beam aperture ("width" value is equal to 0.1) we could achieve an "idealistic"-like performance. In this simulation, the performance of the Beam-based model is better than both the Voronoi and Range-based models.

In "Fig. 3", we show that by increasing the beam "width" significantly (to a value equal to 10 as an example) we approximate our model performance to a "simplistic"-like model performance. In this simulation, the performance of both Beam and Range-based are very comparable.

In "Fig. 1", "Fig. 2" and "Fig. 3", we show that the Beam-based representation model of the coverage generalizes both the Range and Voronoi-based models by tuning the aperture.

For the rest of this work, we set the "width" value to 2 that represents a "realistic" Beam-based representation model of the coverage.

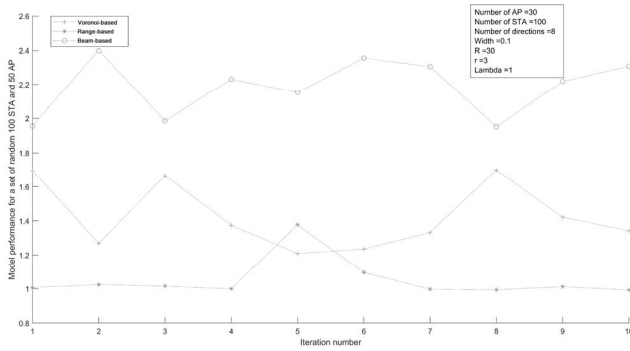


Fig. 2. Near "Idealistic" Beam-based model performance when "width" value is equal to 0.1 unit.

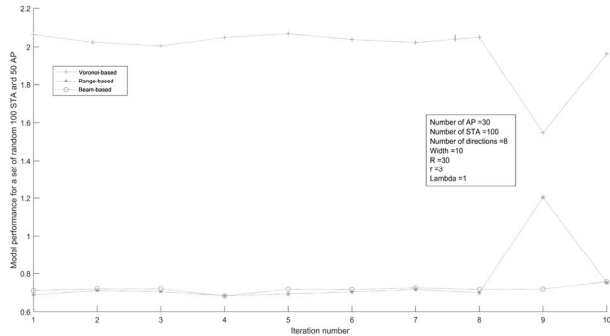


Fig. 3. Near "Simplistic" Beam-based model performance when "width" value is equal to 10 units.

Further, we've implemented a per-AP-power-level-adjustment "supervised" variant of our solution, "WLC2", and proved that it is comparable to a "Cisco"-like implementation that is discussed in detail in [10]. Both "WLC2" and "Cisco" implementation solutions build on the "realistic" Beam-based representation model.

In "Fig. 4", we show an example of a test distribution of a random set of WDs: 30 APs and 100 STAs. At the initialization, the number of the supported AP transmit directions is equal to 8 and each AP power level is set to 30.

In "Fig. 5" and "Fig. 6", We show the transmit opportunity processing results of "WLC2" and "Cisco" solutions respectively. In this simulation, we optimize the number of the APs supported directions and power levels. All the APs have the same optimized number of the supported directions which is equal to 16. Each AP power level may be different from an AP to another. "R" is valued at 99 to denote that this variable is AP and model "WLC2" or "Cisco" dependent. The same power level is applied to all the supported transmit directions of a given AP. We check that both "WLC2" and "Cisco" are of equivalent performance with regards to the transmit opportunity processing results.

To enhance the readability of our results, we shortened the simulation variables names in Table [I].

In Table [II], [III], [IV] and [V], we record the test results for five iterations of the same previous simulation by choosing, at each iteration, a random set of WDs: 30 APs and 100 STAs and measuring "simplistic", "WLC2", "Cisco" and "idealistic" model performance. The "width" is equal to 0.1 and 10 for "idealistic", which is tagged as "Dir1", and "simplistic", tagged as "Dir3", models respectively.

We observe that the processing times are equivalent for both "WLC2" and "Cisco". Even if "Cisco" is more performant, it is more prone to cause coverage holes. "WLC2" measured interference is less than "Cisco" in average.

TABLE I. VARIABLES SHORTENED NAMES

Variable old name	Variable new name
Mean Opportunity (in units)	M.O
Mean Interference (in units)	M.I
Dir. Optimal number	Dir.O
Detected Hole number	H.
Time (seconds)	T.
Relative Processing Time in %	RPT
Performance Score	Perf.
Mean diff to WLC2	M.Diff
Median to WLC2	Med.
Standard deviation To WLC2	Std.

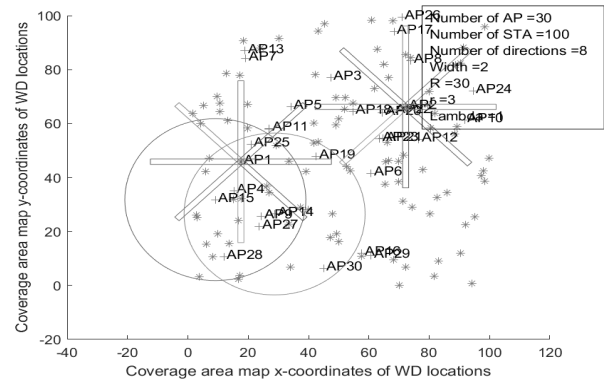


Fig. 4. A distribution example of a random set of WDs: 30 APs and 100 STAs

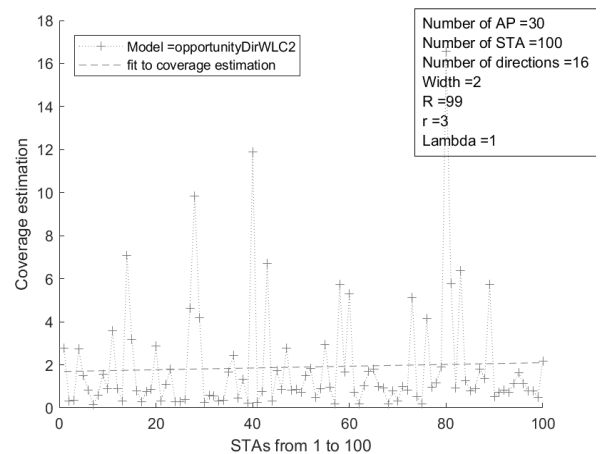


Fig. 5. "WLC2" Beam-based model RRM solution transmit opportunity processing example



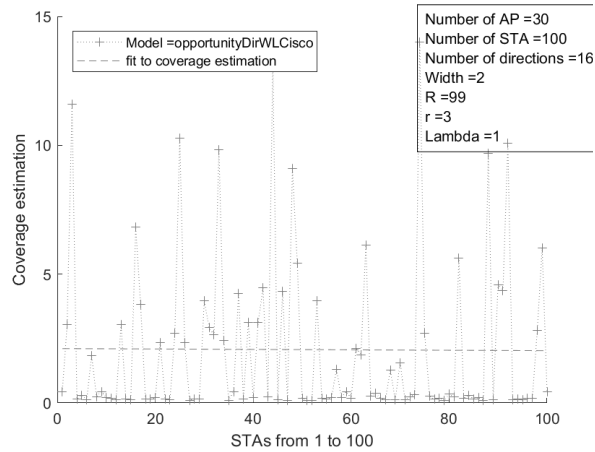


Fig. 6. "Cisco" Beam-based model RRM solution transmit opportunity processing example

TABLE II. BEAM-BASED MODEL PERFORMANCE RESULTS OF "DIR3"

Results: Dir3	Simulation iteration number Settings: AP=30, STA=100, Width=2, R=30, r=3, lambda=1				
	1	2	3	4	5
M.O	0.5	0.3	0.3	0.35	0.3
M.I	150	155	151	149	160
Dir.O	8	16	16	16	8
H.	0	0	0	0	1
T.	25.3856	25.1481	25.0731	25.0016	27.0775

TABLE III. BEAM-BASED MODEL PERFORMANCE RESULTS OF "DIR1"

Results: Dir1	Simulation iteration number Settings: AP=30, STA=100, Width=2, R=30, r=3, lambda=1				
	1	2	3	4	5
M.O	2	1.4	1.5	1.4	1.35
M.I	1.5	1.6	1.5	1.4	1.75
Dir.O	8	16	16	16	8
H.	2	5	2	2	3
T.	26.5227	25.2914	25.0289	24.9015	26.1321

TABLE IV. BEAM-BASED MODEL PERFORMANCE RESULTS OF "WLC2"

Results: WLC2	Simulation iteration number Settings: AP=30, STA=100, Width=2, R=30, r=3, lambda=1				
	1	2	3	4	5
M.O	0.5	0.8	0.4	1	0.5
M.I	40	52	64	60	45
Dir.O	8	16	16	16	8
H.	0	0	0	0	1
T.	82.566	169.5631	209.6245	217.2543	78.6225

TABLE V. BEAM-BASED MODEL PERFORMANCE RESULTS OF "CISCO"

Results: Cisco	Simulation iteration number Settings: AP=30, STA=100, Width=2, R=30, r=3, lambda=1				
	1	2	3	4	5
M.O	5	1	2.5	4	5
M.I	20	75	58	42	15
Dir.O	8	16	16	16	8
H.	5	0	0	3	8
T.	113.1636	179.8094	242.0869	216.0174	73.0206

For the rest of this work, we consider that "WLC2" model is a "realistic" model representation of a coverage area and could constitute a baseline for further optimizations. In one hand, it was proven that Range-based and Voronoi-based models could be generalized to Beam-based equivalents: "Dir3" and "Dir1". In the other hand, working with "width" value of 2, optimizing the power levels and the number of supported transmit directions as per our solution described in [1], we observe a comparable performance between the "WLC2" variant and the Cisco-like implementation of RRM, "Cisco".

In the next sub-section, we introduce a Machine Learning Regression approach that is aimed at optimizing the processing time of our "WLC2" solution. It may eventually, represent an alternative to our NURBS-based optimization that is detailed in [3].

### C. Machine Learning Regression Models

In his book [11], Tom Mitchell describes machine learning in that a computer program, a machine, is said to learn from an experience E with respect to some task T and some performance measure P, if its performance on T, as measured by P, improves with experience E.

A simple form of this learning, focus of this work, is described as "supervised" learning. In this learning, the right answers to some input or training data, are provided in advance. Based on this training data, the inputs and corresponding outputs or "truth", the learning algorithm model parameters are tuned such as to minimize the error between the predicted outputs and the observed "truth".

This "trained" learning, also called hypothesis, is a function, with the previously optimized model parameters, that maps the input variables or features to a predicted outcome.

Supervised learning algorithms could be further classified by the nature of the outcome they work on. If the outcome is continuous then "regression" models are more suitable. For categorical or discrete valued outcomes, "classification" algorithms are more likely.

In our study we work on continuous valued outcomes, then we focus solely on regression models. Many types of regression models exist including: linear regression models (LM), regression trees (Tree), Gaussian process regression models (GPR), support vector machines (SVM), and ensembles of regression trees (Bagged).

To choose between models, we compare their Root Mean Square Error (RMSE) validation score. For all the simulations

of our work, we observe that Coarse Gaussian SVM and Bagged Trees come out with the best RMSE scores. For the rest of our study, we focus solely on these two models.

### III. PROBLEM DESCRIPTION

Simulation results of both RRM implementations: “WLC2” and “Cisco”, were presented in Table [IV] and [V]. For the evaluation of these model performance, we measure the required relative processing time, “RPT”, and the performance score, “Perf.”, given by this formula:

$$Perf. = K_1 * \frac{\sum Interference}{Interference(model) + 1} + K_2 * \frac{\sum Hole}{Hole(model) + 1} + K_3 * \frac{Opportunity(model)}{\sum Opportunity} \quad (1)$$

In Table [VI] and [VII], we summarize these results.

TABLE VI. “WLC2” AND “CISCO” RRM PERFORMANCE AND PROCESSING TIME RESULTS

Results: WLC2 Cisco	Simulation iteration number Settings: AP=30, WD=100, Width=2, R=30, r=3, lambda=1				
	1	2	3	4	5
Perf.	12.22 11.86	10.58 9.02	6.31 7.18	9.29 7.71	11.39 16
RPT	33.34 45.69	42.41 44.97	41.77 48.24	44.96 44.70	38.38 35.64

TABLE VII. “DIR3” AND “DIR1” RRM PERFORMANCE RESULTS

Results: Dir3 Dir1	Simulation iteration number Settings: AP=30, STA=100, Width=2, R=30, r=3, lambda=1				
	1	2	3	4	5
Perf.	8.46 87.18	6.9 110.31	3.87 110.79	6.73 107.04	7.92 84.08

Results’ precision, that measures the gap between the model predicted coverage and the truth, as it might be measured by a specialized equipment such as: Ekahau or AirMagnet, was not considered deeply in this preliminary work. Instead, we consider that the real measure or truth is in between the “simplistic” and “idealistic” measures plots.

Further work may consider processing the raw radio data that is gathered in a laboratory test condition. But as we’ve shown before, tuning parameters of our Beam-based coverage representation may approximate them accurately. Also, we consider that simulating different implementation solutions based on the same modelization foundation would lead to comparable results in a real implementation of the same models.

The measured performance of both solutions “WLC2” and “Cisco” is equivalent and is almost at 10.156 point in average. We check that this performance is better than the “simplistic” case which is at 6.776 point and that the “idealistic” model performance is outstanding at almost 99.88 point.

The measured processing times of both models “WLC2” and “Cisco” are comparable but represent almost 84% of the total required processing time of all the models. This result indicates that both implementations are not scalable regarding the necessary processing time in comparison with the “idealistic” and “simplistic” models.

Because both solutions “WLC2” and “Cisco” are of equivalent performance, for the rest of this work, we focus only on the “WLC2” implementation.

In [3] we propose a NURBS surface-based optimization of the “WLC2” solution processing time. The idea is to process the “WLC2” coverage at only the “control” or “definition” points, and then, the corresponding NURBS surface to find out an estimation of the coverage at the remaining area points. By reducing the number of points “WLC2” processes, we reduce the initial required processing time.

For test purposes, we’ve implemented three variants of this solution: “NURBS1”, “NURBS2”, and “NURBS3”. The difference is in how “definition” points (CP) are chosen. In the first variant, CPs correspond to any random number of the coverage points, STA\_NURBS, weighted by their respective “WLC2” coverage measure. In the second variant, the definition points are the APs. In the third variant, the definition points are the APs but weighted to their optimized transmit power levels. In “WLC2”, transmit power levels are optimized per AP: each AP may have a different transmit power level.

For the same random set of 30 APs, we vary the number of CPs and observe the “NURBS” variants processing time and results precision. In this scheme, the results precision corresponds to the deviation from “WLC2” measurement that is our truth.

In Table [VIII], [IX], and [X], we summarize the results of varying STA\_NURBS number in this range: 100, 500, 1500, 2500 and 10000.

TABLE VIII. “NURBS1” OPTIMIZATION TO WLC2 MODEL PERFORMANCE RESULTS

Results: NURBS1	Simulation STA_NURBS number Settings: AP=30, Width=2, R=30, r=3, lambda=1				
	100	500	1500	2500	10000
M.Diff	41.0604	11.4398	23.5133	<b>0.7598</b>	0.75881
Med.	40.0395	7.5946	19.7305	<b>0.51118</b>	0.43403
Std.	22.8496	19.5894	20.6407	<b>8.4735</b>	3.5212
T.	30.168	136.5365	448.6352	<b>694.6876</b>	1508.60

TABLE IX. “NURBS2” OPTIMIZATION TO WLC2 MODEL PERFORMANCE RESULTS

Results: NURBS2	Simulation STA_NURBS number Settings: AP=30, Width=2, R=30, r=3, lambda=1				
	100	500	1500	2500	10000
M.Diff	48.7473	45.592	57.2992	<b>61.6536</b>	52.5964
Med.	45.9399	42.3936	55.231	<b>60.613</b>	50.065
Std.	23.5647	29.0324	22.7873	<b>24.9228</b>	22.7223
T.	9.3569	9.6129	11.0613	<b>9.1328</b>	5.8624

In Table [VIII], the results show that in general, “NURBS1” processing time and accuracy are increasing with the number of STA\_NURBS. In Table [IX] and [X], the “NURBS2” and “NURBS3” results are not changing considerably because the number of APs is constant. Please note that a high accuracy corresponds to a low mean and a low standard deviation from this mean.

TABLE X. “NURBS3” OPTIMIZATION TO WLC2 MODEL PERFORMANCE RESULTS

Results: NURBS3	Simulation STA_NURBS number Settings: AP=30, Width=2, R=30, r=3, lambda=1				
	100	500	1500	2500	10000
M.Diff	53.9482	49.231	58.0436	<b>62.5081</b>	52.7283
Med.	50.253	46.8791	55.7009	<b>61.2722</b>	50.1472
Std.	23.7241	30.228	23.2916	<b>25.5144</b>	22.8494
T.	1.5346	0.70329	0.93668	<b>0.89961</b>	1.2902

When STA\_NURBS number is at the lowest value, the required processing time represents almost 4.3% of the “WLC2” time, which is an important optimization. But the “M.Diff” representing the mean gap between the “NURBS1” measurement and the truth, is very high at almost 41.06 unit. The standard deviation from this mean is almost 22.84 unit and it is very high. At the highest STA\_NURBS value, the accuracy is very good: the mean is almost equal to 0.75 unit and deviation is only 3.52 unit. But the required processing time is 390% of the “WLC2” time. When STA\_NURBS number is 2500, “NURBS1” performance, time and accuracy, is very close to “WLC2”.

There’s a tradeoff between decreasing the required processing time and increasing the accuracy. For applications that have less constraints on the accuracy, STA\_NURBS number of 500 is an accurate tradeoff. It would require only 19.51% of the “WLC2” initial required processing time. For applications that require a higher accuracy, “NURBS1” is a feasible alternative to “WLC2” in a network with rare radio environment changes.

In dense frequently changing networks, the “WLC2” processing time is not scalable with the number of changes. In these networks “NURBS1”, “NURBS2” and “NURBS3” are powerful and allows fast adaptation to radio environment changes. Upcoming work may spot in detail this “NURBSx” strength that was introduced in [3].

In the upcoming section, we explore an out-of-box MLR-based approach as an alternative to “NURBSx” in improving the coverage prediction accuracy.

#### IV. MLR-BASED OPTIMIZATION SOLUTION

In the previous section, NURBS surfaces helped optimize “WLC2” performance. But this optimization came with a tradeoff between the required processing time and measurement’s accuracy. In this section we propose an alternative out-of-box machine learning approach to improve “NURBS1” accuracy.

Using machine learning algorithms, we predict “WLC2” coverage measurement at a given coverage area point (STA). This value is continuous because it is the resultant sum of continuous, linear, function values. Each of these function

values, corresponds to the effect of a single AP on this coverage area point.

Then, we use supervised regression models to predict interference measurement, the output, at points that are not pertaining to the training set. Our training set represents a 10% random sample record of all the available coverage points. We build our hypothesis on these features: STA index, STA localization coordinates X and Y, first AP of association, corresponding direction, corresponding power level, corresponding load, corresponding reported neighboring APs’ interference, second AP of association, and corresponding direction.

What regression algorithm should we use? For this preliminary work, we’ve chosen to work only with a Coarse Gaussian SVM and Bagged Tree algorithms. These two algorithms have showed the best RMSE validation results for several simulation iterations of the models. “SVM” model has scored an average RMSE of 14.75 point, whereas “Bagged”, 16.03 point.

We train our models using only the training set. Using the trained models “SVM” and “Bagged”, we predict the remaining points that are 90% of the total record set. We use the same training set corresponding “STA index” feature, to predict “NURBS1” values. At the end, we measure the accuracy and time as in the previous section.

In this simulation, the number of the control points or training set samples varies from 40 to 2250 sample. In each iteration, a new set of 10 random APs distribution is processed.

“Fig. 8” shows the per-model required processing time for each test. “WLC2” does not show in this figure because it ranges from 77.6062 to 8496.5513 seconds. The best processing times are recorded for “NURBS” and “Bagged”

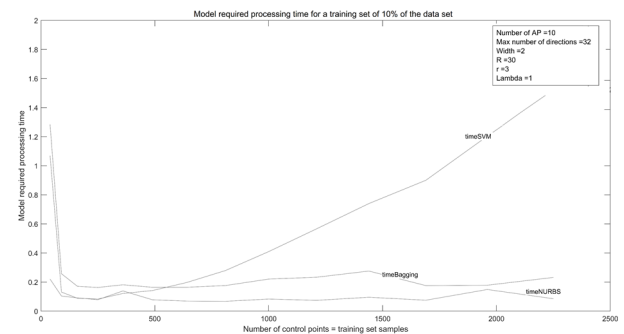


Fig. 8. Plot of models: “SVM”, “Bagged” and “NURBS” required processing time

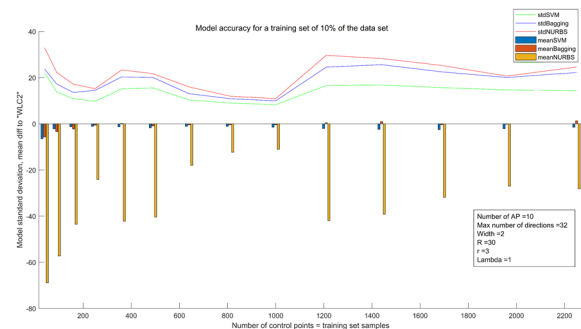


Fig. 9. Plot of models: “SVM”, “Bagged” and “NURBS” accuracy

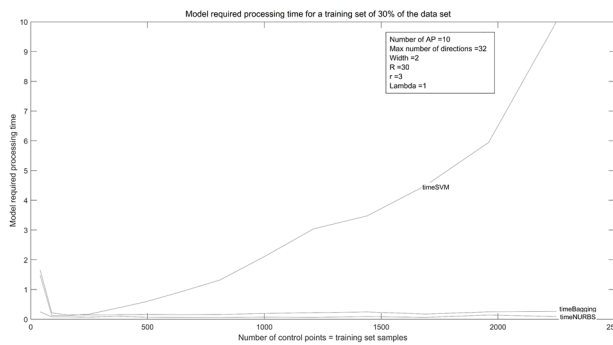


Fig. 10. Plot of models' required processing time when the training set is 30% of the data set

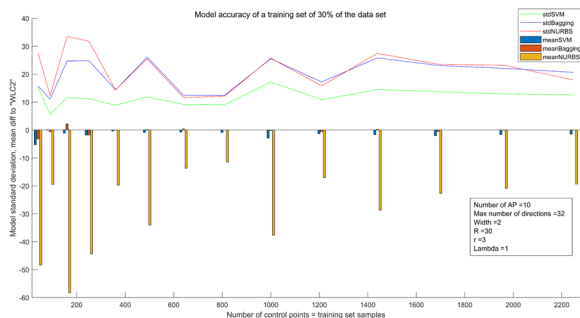


Fig. 11. Plot of models' accuracy when the training set is 30% of the data set

models and seem to be independent from the number of control points. "SVM" time is increasing with the number of control points, but it does not exceed a 1.51 second in time, which is still an important enhancement of "WLC2" solution.

"Fig. 9" shows the accuracy measurement for each test. The "SVM" optimization represents the best accuracy measurement at around 13.77 unit in standard deviation against 18.44 unit in "Bagged" or 21.43 unit in "NURBS".

To confirm our findings tendency, we redo the previous simulation with a large training set of 30% of the total data set. "Fig. 10" and "Fig. 11" show the corresponding required processing time and accuracy respectively.

By increasing the training set to 30% of data set, the "SVM" accuracy that was 76.63% in comparison to its direct challenger "Bagged", is now only 59.52%. Increasing the number of control points seems to have no effect on "Bagged" and "NURBS" as they show a steady pace of both accuracy and time. Instead, "SVM" accuracy has increased remarkably without exceeding the limit of 10 seconds of the required processing time which is acceptable.

## V. CONCLUSION

In this work we've proposed an MLR-based out-of-box alternative optimization approach to Beam-based, representation of radio coverage in IEEE WLAN networks, NURBS-based optimized implementation variant of "WLC2". This has solved an important part of "WLC2" solution scalability issue and opened the possibility to implement new solution variants in further work.

The obtained results have proved that "SVM" solution offers the best tradeoff between the prediction accuracy and

required processing time in comparison with its challengers "Bagged" and "NURBS".

Further work may extend this discussion to model the adaptability to the frequently changing radio environments. In such case, we'll explore in detail advanced concepts behind NURBS surface, ML or deep ML, to implement an efficient incremental processing of the coverage.

In upcoming work, we'll discuss new Beam-based implementation variants: "WLC3" and "WLC4". In "WLC3", we'll try to optimize the transmit power level per AP and per direction. In "WLC4", will process different optimized supported number of directions per AP.

## ACKNOWLEDGMENT

We would thank colleagues: researchers, engineers, and reviewers for sharing their precious comments and on-field experience to improve the quality of this paper.

## REFERENCES

- [1] M. Guessous and L. Zenkour, "Cognitive directional cost-based transmit power control in IEEE 802.11 WLAN," 2017 International Conference on Information Networking (ICOIN), Da Nang, 2017, pp. 281-287. doi: 10.1109/ICOIN.2017.7899520.
- [2] M. Guessous, L. Zenkour, "A novel beamforming based model of coverage and transmission costing in IEEE 802.11 WLAN networks", *Advances in Science, Technology and Engineering Systems Journal*, vol. 2, no. 6, pp. 28-39 (2017).
- [3] M. Guessous and L. Zenkour, "A NURBS Based Technique for an Optimized Transmit Opportunity Map Processing in WLAN Networks," in *Wired/Wireless Internet Communications*, Cham, 2017, pp. 143-154.
- [4] W. M. Campbell, D. E. Sturim, D. A. Reynolds and A. Solomonoff, "SVM Based Speaker Verification using a GMM Supervector Kernel and NAP Variability Compensation," 2006 IEEE International Conference on Acoustics Speech and Signal Processing Proceedings, Toulouse, 2006, pp. I-I. doi: 10.1109/ICASSP.2006.1659966
- [5] S. Wan, M. W. Mak, and S. Y. Kung, "mGOASVM: Multi-label Protein Subcellular Localization Based on Gene Ontology and Support Vector Machines", *BMC Bioinformatics*, 2012, 13:290.
- [6] S. Wan, M. W. Mak, and S. Y. Kung, "Mem-ADSVM: A Two-Layer Multi-Label Predictor for Identifying Multi-Functional Types of Membrane Proteins", *Journal of Theoretical Biology*, 2016, vol. 398, pp. 32-42.
- [7] Lin, W.-H., and Hauptmann, A., "News video classification using SVM-based multimodal classifiers and combination strategies." *Proceedings of the tenth ACM international conference on Multimedia*. ACM, 2002.
- [8] "Enterprise Mobility 8.1 Design Guide," Cisco, 07-Nov-2017. [Online]. Available: [https://www.cisco.com/c/en/us/td/docs/wireless-controller/8-1/Enterprise-Mobility-8-1-Design-Guide/Enterprise\\_Mobility\\_8-1\\_Deployment\\_Guide.html](https://www.cisco.com/c/en/us/td/docs/wireless-controller/8-1/Enterprise-Mobility-8-1-Design-Guide/Enterprise_Mobility_8-1_Deployment_Guide.html).
- [9] "Radio Resource Management White Paper," Cisco, 18-Feb-2016. [Online]. Available: [https://www.cisco.com/c/en/us/td/docs/wireless-controller/technotes/8-3/b\\_RRM\\_White\\_Paper.html](https://www.cisco.com/c/en/us/td/docs/wireless-controller/technotes/8-3/b_RRM_White_Paper.html).
- [10] M. Guessous, "WIFI - Page 2 - @link'blog," *Transmit Power Control in IEEE 802.11 Cisco WLAN networks*, 16-Feb-2017.
- [11] Mitchell, T. M. (1997). *Machine learning*. New York, NY: McGraw-Hill. ISBN-13: 9780070428072; ISBN-10: 0070428077.

# Single-Tone Doppler Radar System for Human Respiratory Monitoring

Rizky Ambarini

Telecommunication Engineering dept.

Telkom University

Bandung, Indonesia

rizkyambarini@student.telkomuniversity.  
ac.id

Aloysius Adya Pramudita

Telecommunication Engineering dept.

Telkom University

Bandung, Indonesia

pramuditaadya@telkomuniversity.ac.id

Erfansyah Ali

Telecommunication Engineering dept.

Telkom University

Bandung, Indonesia

erfansyahali@telkomuniversity.ac.id

Antonius Darma Setiawan

Telecommunication Engineering dept.

Telkom University

Bandung, Indonesia

adsetiawan1701@gmail.com

**Abstract**— Human respiration activities can be identified from the chest wall movement. In developing a non-contacting sensor for human respiration, the chest wall movement can be detected as a Doppler shift. Therefore, the Doppler radar is potential to be implemented for the non-contacting sensor previously mention. In this paper, the Single-Tone Doppler radar which operates at 10 GHz has been studied and proposed for detecting human respiration. The simulation experimental is performed for investigating the capability of the proposed method in detecting the human respiration parameter such as respiration rate and respiration amplitude. The results show that the proposed method is capable to extract the human respiration parameter.

**Keywords**—Doppler radar, continuous wave, small displacement, respiration

## I. INTRODUCTION

Respiration is one of a sign for monitoring human activities. In the medical field, rate and pattern monitoring of human respiration can be used to help in diagnosing pulmonary illness. In the hospital, respiration is mostly detected by a medical device equipment. For example, a silica-nanoparticle thin film is used for developing a sensor chip for respiration. Electrical sensors are widely used also [1].

The pulmonary volumes and capacities of human respiration vary which depends on the size of the lungs, the power of breathing, and the way of breathing. The longer activities, the higher breathing frequency are caused by the strong body movements which are using a lot of oxygen in the muscles which energize the activity [2]. The human respiration model has been studied related to the factors above. Therefore, rate and pattern of human respiration can be used to observe the condition of human health.

There are several concerns in choosing medical measurement devices. In addition to the accuracy of the measurement result, patient comfort in the use of such device, minimal distress, and hygienic measurement are also several matters of the concern, especially for long-term monitoring [3], [4]. Respiratory monitoring can be categorized as a contact or non-contact method. A non-contact method is potentially satisfied all the mention concerns above. This paper analyses the development of a non-contact method for human respiratory monitoring which is based on the radar system.

Radio and detection ranging (Radar) with the high resolution is needed for detecting human respiration. Inspired by an Ultra-Wide Band (UWB) system which can to obtains the high-resolution measurement, several types of research of a UWB radar for detecting human vital signs have been conducted [5], [6]. The experiment results in [5] show that the detection of heart-beat has a very suitable with an Electrocardiograph (ECG) measurement. Meanwhile, the large bandwidth is used, it gives several disadvantages, such as the complexity of its hardware and the problems of its interference. Frequency Modulation Continuous Wave (FMCW) radar system has been investigated for detecting human respiration also [7].

A radar consists of the transmitter and receiver parts. The transmitter output is a radio-frequency wave with a certain frequency which propagates to the target. The receiver is designed to detects the Doppler shift in echoes reflected from moving targets. For example, speedometers, Air Traffic Control (ATC), and detecting small displacement [8]. The Doppler radar is potential to be implemented by using a single-frequency signal which has an advantage for a low bandwidth usage and simple circuit. This paper is focused on the development of a Single-Tone Doppler radar system for human respiratory monitoring. A Single-Tone means that the radar transmits the single-frequency signal by extracting Doppler feature from the target only.

Human respiration activities can be identified by the chest wall movement which is related to the inhale and exhale activities. In the radar system point of view, human chest wall movement which is caused by respiration activities is such a small displacement movement which generates a Doppler shift in a reflected wave. Therefore, a Doppler radar is a great approach for detecting a human respiration monitoring [9], [10].

The radar system which has the capability for measuring a small displacement or vibration of a chest wall movement which relates to the human respiration needs to be studied and developed. An HB100 is a Doppler radar module which operates at a X-Band and developed by AgileSense™. This radar has the frequency of 10 GHz with the wavelength of 33 mm. It consists of a dielectric resonator oscillator, mixer, and a patch antenna. Considering the wavelength of HB100, the phase shift which is caused by the chest wall movement is potential to be detected by using its radar system. However, the capability of Single-Tone Doppler radar at 10 GHz for detecting human respiration needs to be studied first.



Furthermore, the objective of this paper is to study the capability of Single-Tone Doppler radar at 10 GHz for detecting human respiration parameters such as its amplitude and rate.

This paper is organized as follows; Section I describes the background and problem which addressed in this paper, Section II discusses the proposed method in detecting human respiration rate caused by the chest wall movement, Section III discusses the computer simulation using Octave in investigating the proposed method and its results and the last, is Section IV, is for the conclusion.

## II. PROPOSED METHOD

### A. Chest Wall Movement in Human Respiration

The relationship between the human respiration and the chest wall movement can be illustrated in Fig.1. Generally, respiration has a periodic pattern which is related to the inhale and exhale activities and it can be identified by the chest wall movement.  $T(t)$  is an incident of the wave from a signal source,  $R(t)$  is the reflected waves, and  $d_o + x(t)$  is the distance between human and signal source. If the chest wall movement is modeled as a time-varying function of  $x(t)$ , then the propagation distance of the wave as a time-varying also. The movement which is caused by a small displacement of the chest wall movement can be analysed as a certain phase shift on the reflected wave  $R(t)$ .

The magnitude of the phase change which is caused by the small displacement of contraction in respiration is adequately large for measuring chest wall movement in Fig. 1. Let us apply a Doppler radar as the signal source. A Doppler radar transmits a continuous-wave signal, which is reflected by a target and then received and demodulated by a receiver. The position-varying information is demodulated proportionally in the reflected signal when the net velocity is zero. Therefore, the chest wall movement which is caused by the volume change during respiration can be detected by using the Doppler radar motion-sensing system [11].

### B. CW Radar System for Detecting Chest Wall Movement

A block diagram of a CW radar system for detecting a chest wall movement is shown in Fig. 2. The transmitted signal is generated by the oscillator with a certain frequency. Its signal is used for detecting the chest wall movement which is caused by the respiration activities. The transmit signals can be expressed in (1).

$$S_T = A_T \cos(2\pi f t), \quad (1)$$

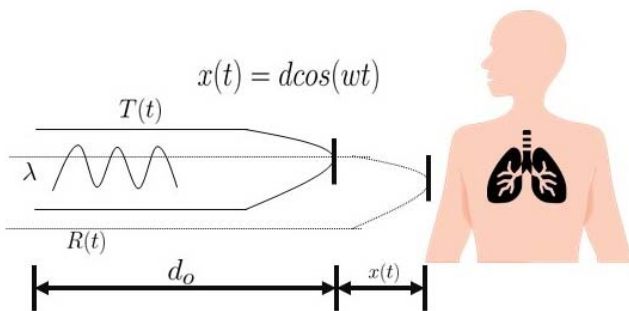


Fig. 1. A periodic chest wall movement which is caused by phase shift.

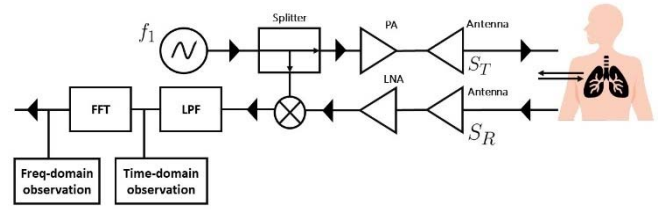


Fig. 2. A block diagram of CW radar system for detecting a chest wall movement.

where  $f$  and  $A_T$  are as a frequency of the transmitted signal and the amplitude of the transmitted signal respectively. The received signal is a reference as a human respiration which is modelled as a sinusoidal pattern. It can be expressed in (2).

$$S_R = A_R \cos\left(2\pi f t + \frac{4\pi}{\lambda} d\right), \quad (2)$$

where  $d$  and  $\lambda$  are the distances between the target and the radar and wavelength of the transmitted signal respectively. If the respiration is modeled as a time-varying function which is caused by the chest wall movement and it has a periodic pattern as shown in Fig. 1, then the received signal is modified which is expressed in (3). In the (3),  $d$  and  $f_i$  refer to the amplitude and the frequency movement due to the respiration activity respectively. After it is amplified by the Low Noise Amplifier (LNA), then the received signal is mixed by the oscillator output. The output of the mixer is shown in (4).

$$S_R = A_R \cos\left(2\pi f t + \frac{4\pi}{\lambda} d \cos(2\pi f_i t)\right). \quad (3)$$

$$S_M = S_T \cdot S_R = \frac{A_M \cos(4\pi f t + \frac{4\pi}{\lambda} d \cos 2\pi f_i t) + A_M \cos(\frac{4\pi}{\lambda} d \cos 2\pi f_i t)}{A_M \cos(\frac{4\pi}{\lambda} d \cos 2\pi f_i t)}. \quad (4)$$

The mixer output  $S_M$  is similar to the narrow-band frequency modulation signal [12]. Therefore, the spectrum of  $S_M$  is influenced by the amplitude of the respiration pattern.

$$S_{LPF} = \sum_{n=0}^{\infty} A_n \cos(2\pi n f_i t) \quad (5)$$

The Low Pass Filter (LPF) output of Doppler radar which is shown in (5) represents as a respiration which is detected by the radar system.

The index  $n$  represents the frequency of each component at the LPF output. The index  $A_n$  represents the amplitude of each component. The harmonic component which is shown in (5) will rise if the amplitude of the respiration pattern  $d$  is increased. From the LPF output, it can be identified that the respiration pattern is associated by the respiration rate with the fundamental frequency of the LPF output and the amplitude of the respiration by the number of the harmonic frequency comes out significantly. The representation of the LPF output is more convenient if it is in the frequency-domain. Therefore, the Fourier Transform is needed for processing the LPF output data. After it is converted into the digital signal, then it needs the Fast Fourier Transform (FFT) computation for obtaining the representation of frequency-domain.



TABLE I. THE NUMBER OF RESPIRATORY FREQUENCY BY AGES.

Groups	Ages	Frequency rate (times/ minute)
Newborn	Under 1 year old	44
Infants	Under 2 years old	50
Toddlers	Under 6 years old	25
Children	Under 15 years old	20
Adults	Above 15 years old	16

### III. RESULT AND DISCUSSION

A computer simulation which is using Octave is performed for investigating the proposed Doppler radar in detecting human respiration. The simulation is performed for the following purpose: observing the performance of the proposed radar in detecting different respiration rate, observing the performance of the proposed radar in detecting different respiration amplitude, and observing the performance of the proposed radar in detecting several real cases of human respiration rate. The simulation refers to the specification of the HB100 module. A Single-Tone Doppler radar system generates and transmits a single-frequency electromagnetic wave with the frequency of 10 GHz.

In this paper, several respiration patterns with the different rate and amplitude are simulated and analysed both in time and frequency domain. In this experiment, the target object is located around 3 m from the CW radar system. Related to the equation of (2), the frequency of transmit signal  $f$  is set to 10 GHz.  $A_R$  and  $f_i$  are a varied rate which will be simulated. The information of the target positions data is required for detecting the small displacement on the target. Refers to the Table I, the normal respiration rate which is caused by the age, from an adult to an infant, it has ranged from 16 to 50 times per minutes. The simulation selects three-different respiration rates: 16, 20, and 30 times per minute. It represents the normal respiration rate of adult, child, and baby.

The LPF output in *time-domain* for the three-different respiration rate is shown in Fig. 3. On this figure, the simulation is performed by taking the example of the respiration rate  $f_i$  of 0.26 Hz, 0.33 Hz, and 0.5 Hz. This example is equaled to the 16, 20, and 30 times per minute of the normal respiration rate. The result in Fig. 3 indicates the LPF output for the three-different respiration rates. The rhythmic of the human respiration for the three-different respiration rates produce an LPF output with the different pattern. Furthermore, it can be analysed that the respiration condition is from the pattern of an LPF output. However, the frequency-domain representation of an LPF output is more suitable to obtains more accurate information about the rate. As shown in Fig. 2, the Fast Fourier Transform (FFT) computation is used to achieve the frequency domain representation of an LPF output.

The LPF output in *frequency-domain* for the three-different respiration rate which has the same case as a simulation in Fig. 3, is shown in Fig. 4. The spectrum of LPF output has been represented in normalized value. Normalization is done by dividing the spectrum of an LPF output with the maximum of its absolute value. The proposed of radar system can to detect the three-different pattern rates. A 0.26 Hz, 0.33 Hz, and 0.5 Hz of respiration rates which have been simulated, it has a different pattern in the frequency domain. The respiration rate can be determined from the

frequency which is associated with the peak spectrum of the fundamental frequency component.

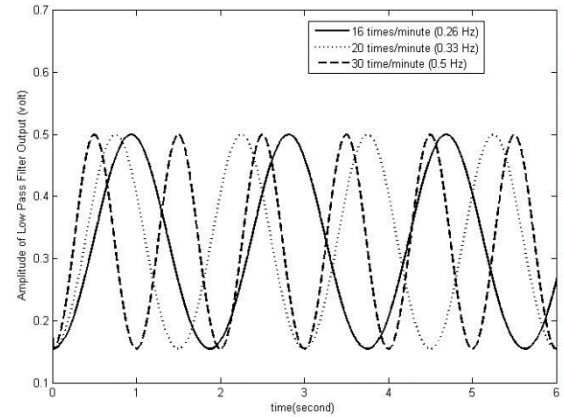


Fig. 3. An LPF output in the time-domain which represents a three-different of respiration rate.

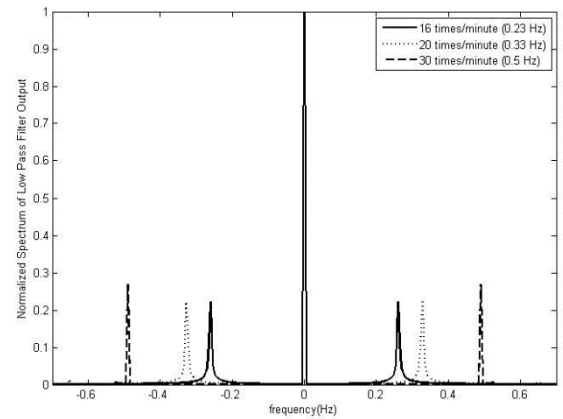


Fig. 4. An LPF output in the frequency-domain which represents a three-different of respiration rate.

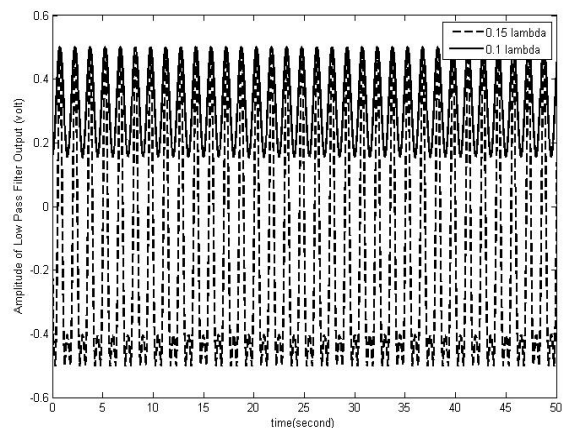


Fig. 5. An LPF output in time-domain for two-different respiration amplitude.

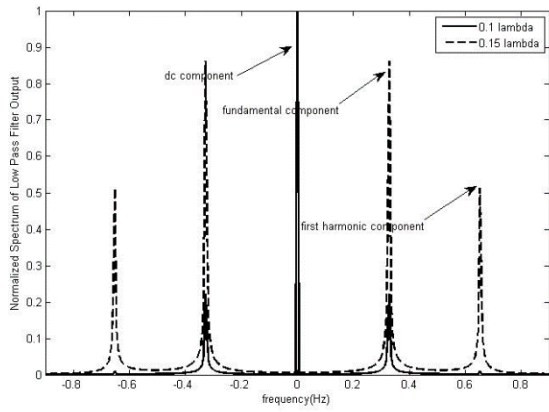


Fig. 6. An LPF output in frequency-domain for two-different respiration amplitude with the respiration rate of 0.33 Hz.

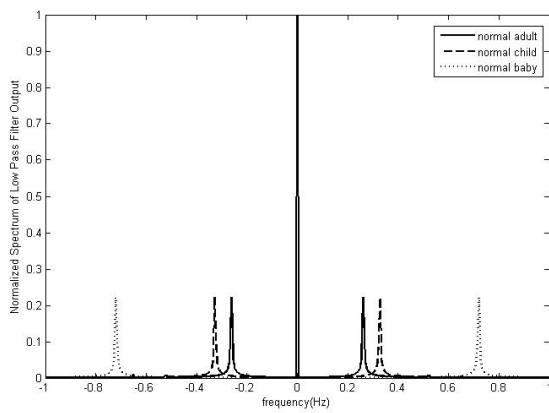


Fig. 7. The normalized spectrum of LPF output for several human respiration cases.

The LPF output for two-different amplitude respiration rate in *time-domain* is shown in Fig 5. The amplitude of  $0.1 \lambda$  and  $0.3 \lambda$  are simulated at the same respiration rate of 0.33 Hz. The result shows that the respiration amplitude has influenced the peak-to-peak value of the LPF output. The high amplitude will cause the high peak-to-peak value and vice versa.

The LPF output for two-different amplitude respiration in *frequency-domain* is shown in Fig. 6. The result is taking from the same simulation case within Fig. 5. In the spectrum of  $0.3 \lambda$ , the first harmonic component (0.66 Hz) appears either the fundamental component (0.33 Hz) also. However, the harmonic components are not for the low amplitude ( $0.1 \lambda$ ) significantly. By increasing the respiration amplitude, it has been affected by increasing the appearance of the harmonic component. The appearance of the frequency harmonic in high respiration amplitude causes the increase of the bandwidth of the power spectrum. By increasing the respiration amplitude, it may be caused by the high activity or illness. Therefore, the appearance of the harmonic component can be used to identify it.

The speed of human respiratory rate is caused by the several factors; age, gender, and activities [2]. The simulation has been performed for detecting the respiration pattern for several different ages group. As shown in Fig. 7, the simulation takes a sample by a baby, child, and adult rate respiration. By the normalized spectrum of an LPF output, the frequency of the baby case is around 0.72 Hz, while for the

child is around 0.32 Hz, and for the adult is around 0.26 Hz. By the time age is changing, the rate of respiration is changing [13]. For the grouping of human rate respiration rate by ages at times per minute is shown in Table I [2].

The effect of the respiration amplitude to the LPF output has been analysed from the power spectrum's perspective. The effect of the respiration amplitude to the power spectrum of the LPF output is shown in Fig. 8. The higher respiration amplitude which is caused by the LPF output has the higher power spectrum level than the lower amplitude. In the previous result, it has been discussed that the higher respiration amplitude increases the harmonic component existence at the spectrum of the LPF output. Furthermore, it affects the increase of the bandwidth and power spectrum of the LPF also.

#### IV. CONCLUSION

The first stage on developing proposed Single-Tone Doppler Radar for the human respiration monitoring has been conducted by the performing Octave simulation which is used for investigating the capability of the proposed Single-Tone Doppler Radar in detecting rate and magnitude of human respiration. The time-domain and the frequency-domain analysis have been conducted in this study. The simulation is performed by taking several cases with the different respiration parameters. The simulation results on Single-Tone Doppler Radar at 10 GHz show that the proposed radar system has the capability to detect the human respiration parameter, such as respiration rate and the amplitude of the chest wall movement. Due to its function to detect the respiration rate and amplitude, the *frequency-domain* observation is more suitable than *time-domain*. The respiration rate can be determined from the fundamental frequency component of the LPF output. The respiration amplitude can be determined from the total power spectrum of the normalized output of the LPF.

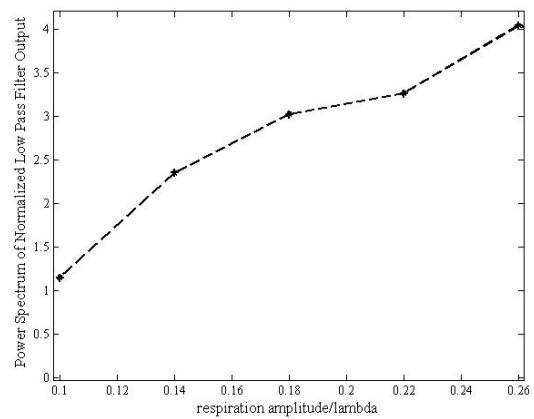


Fig. 8. A power spectrum of normalized LPF output.

## REFERENCES

- [1] K. Shinya, D. Yuya, and F. Minoru, "Silica nanoparticle-based portable respiration sensor for analysis of respiration rate, pattern, and phase during exercises," *IEEE Sensors Letters*, vol. 2, 2018.
- [2] W. Lilis, R. A. Syaichu, and R. P. Hidayat, "Model development of air volume and breathing frequency in human respiratory system simulation," *Elsevier Procedia*, pp. 260–268, 2011.
- [3] X. Yuyong, C. Shiqiam, D. Xingji *et al.*, "Accurate measurement in doppler radar vital sign detection based on parameterized demodulation," *IEEE Transactions on Microwave Theory and Technique*, vol. 65, no. 11, pp. 4483–4492, November 2017.
- [4] T. Jianxuan and L. Jianshan, "Fast acquisition of heart rate in noncontact vital sign radar measurement using time-window-variation technique," *IEEE Transactions on Instrumentation and Measurement*, vol. 65, no. 1, pp. 112–122, January 2016.
- [5] M. Leib, W. Menzel, B. Schleicher and H. Schumacher, "Vital signs monitoring with a UWB radar based on a correlation receiver," *Proceedings of the Fourth European Conference on Antennas and Propagation*, Barcelona, Spain, 2010, pp. 1-5.
- [6] C. H. Hsieh, Y. F. Chiu, Y. H. Shen, T. S. Chu and Y. H. Huang, "A UWB Radar Signal Processing Platform for Real-Time Human Respiratory Feature Extraction Based on Four-Segment Linear Waveform Model," in *IEEE Transactions on Biomedical Circuits and Systems*, vol. 10, no. 1, Feb. 2016, pp. 219-230.
- [7] T. Kiuru *et al.*, "Movement and respiration detection using statistical properties of the FMCW radar signal," *2016 Global Symposium on Millimeter Waves (GSMM) and ESA Workshop on Millimetre-Wave Technology and Applications*, Espoo, 2016, pp. 1-4.
- [8] P. A. Lynn, *Radar Systems*. Macmillan Education, 1987.
- [9] C. Will, K. Shi, R. Weigel, and A. Koelpin, "Advanced template matching algorithm for instantaneous heartbeat detection using continuous wave radar systems," 2017, pp. 1–4.
- [10] L. Jianshan, "Microwave doppler radar sensor for detection of human vital signs and mechanical vibrations," *University of Florida*, 2005.
- [11] H. Ming-Chun, L. J. J., X. Wenyao *et al.*, "A self-calibrating radar sensor system for measuring vital signs," in *IEEE Transactions on Biomedical Circuits and Systems*, May 2016, pp. 352–363.
- [12] M. Shalaby, M. Shokair, and N. W. Messiha, "Modelling and simulation of narrow band electromagnetic interference in millimeter wave massive mimo systems." National Radio Science Conference, March 2018, pp. 149 – 156.
- [13] A. C. Guyton and J. E. Hall, *Textbook of Medical Physiology*, 11th ed., R. Gruliow, Ed. Elsevier Saunders, 2006.

# Dual Frequency Continuous Wave Radar for Small Displacement Detection

Andarining Palupi  
School of Electrical Engineering  
Telkom University  
Bandung, 40257 INDONESIA  
andariningpalupi@student.telkomuniversity.ac.id

Dharu Arseno  
School of Electrical Engineering  
Telkom University  
Bandung, 40257 INDONESIA  
darseno@telkomuniversity.ac.id

Aloysius Adya Pramudita  
School of Electrical Engineering  
Telkom University  
Bandung, 40257 INDONESIA  
pramuditaadya@telkomuniversity.ac.id

Antonius Dharma Setiawan  
School of Electrical Engineering  
Telkom University  
Bandung, 40257 INDONESIA  
adsetiawan1701@gmail.com

**Abstract**— In several field such as structure health monitoring, landslide monitoring and medical measurement, small displacement is used as the indicator of any problem that may rise in such fields. High resolution radar system is required for small displacement detection in millimeter of centimeter scale. Continuous wave (CW) radar with its narrow bandwidth feature, has a simpler system comparing with other radar system. However, the modification is needed to present the ability of CW radar in detecting small displacement. In this paper, dual frequency CW radar was investigated and proposed for small displacement detection. Computer simulation has been conducted to study the capability of the proposed radar system. The result shows that the dual frequency CW radar at 10.525 GHz is capable to detect a small displacement in millimeter scale. The frequency difference of the radar signal needs to be adjusted to avoid the ambiguity in the detection result.

**Keywords**— *continuous wave (CW) radar, small displacement, dual frequency.*

## I. INTRODUCTION

Small displacement is used to identify any problem that may rise in several field such as landslide monitoring, structural health monitoring and medical measurement. Radar system was studied to be implemented in detecting small displacement. Some studies have been developing the Synthetic Aperture Radar (SAR) system that applied to detect a landslide [1-3]. SAR technology uses pulse waveform that having ultra-wideband (UWB) characteristic [4]. UWB characteristic provides a fine resolution and an accurate sensing. However, a wideband radar signal usage, gives some consequences, such as increasing the realization complexity and giving interference in mitigations problems.

A feasible way to distinguish between received and transmitted radar signal is by recognizing the change of echo signal frequency in receiver. It is known as doppler effect [5]. The change of this sinusoidal echo signal gives impact to its phase. From the phase data, the displacement is potential to be estimated. Phase component processing have been studied for high accuracy detection in radar system. Phase repetition for large target distance, become limitation that need to be considered. Doppler radar can be realized using Continuous Wave (CW) radar system, Frequency Modulation Continuous Wave (FMCW) radar system and Impulse radar system. CW radar system has a narrower bandwidth and simpler among other radar system that previously mentions.

CW radar can only detect a dynamic target such as vibration. A vibration may be viewed as time varying small

displacement event that occurred on an object. According to this fact, on CW radar advantages feature such as narrow bandwidth and simple structure, CW radar system is potential to be developed as the radar system for small displacement detection. However, a modification of CW radar system is required to develop its capability in detecting small displacement. HB100 is a CW radar module that operates at 10.525 GHz [6]. Due to the transmitted frequency, the transmitted signal that has a wavelength of 28.5 mm. The objective of this research is to investigate the potential of HB100 to be used in developing CW radar system for small displacement. The theoretical and simulation investigation is then discussed in this paper as the preliminary step in developing prototype of the proposed radar system that based on HB100.

This paper proposed a modification scheme for CW radar which deals with small displacement detection. The dual frequency CW radar system was investigated and proposed for small displacement detection. The theoretical and computer simulation have been performed to study its ability in detecting a small displacement.

This paper is organized into four sections. Introduction section discusses about the background and problems that addressed in this research. Section II explains the proposed method and the theoretical overview. The simulation and its result are discussed in section III and the last is conclusion.

## II. PROPOSED METHOD

The proposed modification takes place on transmitter and receiver part. In transmitter part, we used two sinusoidal signal generators with different frequency, respectively as  $f_1$  and  $f_2$ . The modification in receiver is mainly done on the postprocessing of Low Pass Filter (LPF) output. The block diagram of the proposed dual frequency CW radar is depicted by Fig.1. Summation of sinusoidal signals from generator is then transmitted to the target and amplified by the power amplifier (PA). The transmitted signal of the proposed radar can be written as (1).

$$S_{TX} = A_0 \cos(2\pi f_1 t) + A_0 \cos(2\pi f_2 t), \quad (1)$$

$A_0$  is the amplitude of the transmitted signal and  $t$  is the time of since the signal is transmitted until received. The square block in Fig.1 illustrates the target where small displacement is occurred. The transmitted signal that arrived at the target is reflected to the radar and received at receiver

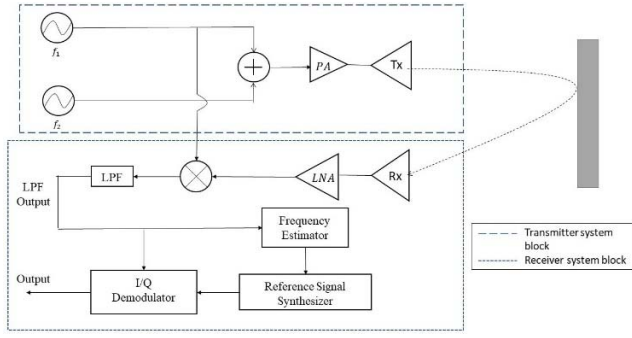


Fig. 1. Block diagram of Dual Frequency Continuous Wave Radar.

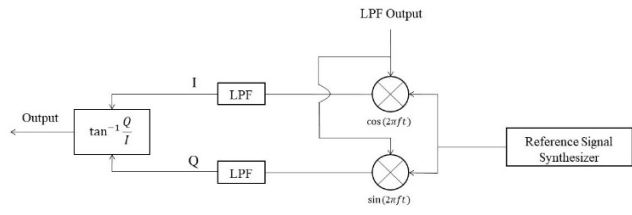


Fig. 2. Block diagram of I/Q demodulator.

side. The received echo signal is amplified by the low noise amplifier (LNA), and can be expressed as (2).

$$S_{Rx} = A_1 \cos\left(\frac{2\pi 2d}{\lambda_1} + 2\pi f_1 t\right) + A_2 \cos\left(\frac{2\pi 2d}{\lambda_2} + 2\pi f_2 t\right), \quad (2)$$

$A_1$  and  $A_2$  are the amplitude of the echo signal with the frequency of  $f_1$  and  $f_2$ , respectively.

The echo signal is mixed with the signal from oscillator 1 ( $f_1$ ). Then, the LPF output contains sinusoidal echo signal and direct current (DC) component, it can be written as (3).

$$S_{M0}(t) = A'_1 \cos\left[2\pi(f_2 - f_1)t + \frac{2\pi 2d}{\lambda_1}\right] + A'_2 \cos\left(\frac{2\pi 2d}{\lambda_2}\right), \quad (3)$$

The displacement data can be obtained from the phase shift data  $\left(\frac{2\pi 2d}{\lambda_1}\right)$  of the sinusoidal echo signal, with  $d$  is the displacement range that occurred, and  $\lambda_1$  is the wavelength of the signal. The sinusoidal echo signal is shown in (4).

$$S_{LPF}(t) = A_L \cos\left[2\pi(f_2 - f_1)t + \frac{2\pi 2d}{\lambda_1}\right]. \quad (4)$$

$A_L$  is the amplitude of sinusoidal component of echo signal. The frequency estimator detects the frequency value  $(f_2 - f_1)t$  or can be written as  $df$ , of sinusoidal component. Then, the reference signal synthesizer generates sin and cos signal with the value of frequency that has been obtained in the frequency estimator. The frequency estimation can be performed by applying the Fast Fourier Computation of the LPF output. The frequency estimation must be done before the proposed radar is operated to detect the small displacement. The reference signal is a sinusoidal signal of LPF output when the transmitter is directly connected to receiver, this connection named as a loopback connection. The reference signal is decomposed in two orthogonal signals, with the amplitude of  $A_r$ , then are written as (5) and (6).

$$S_{ref_I}(t) = A_r \cos[2\pi(f_2 - f_1)t]. \quad (5)$$

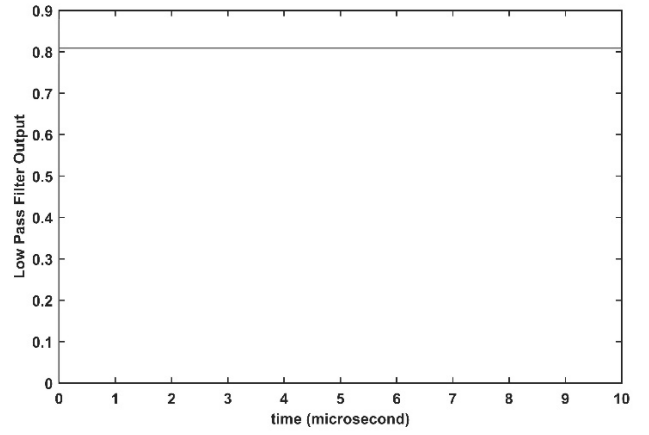


Fig. 3. Single frequency LPF output.

$$S_{ref_Q}(t) = A_r \sin[2\pi(f_2 - f_1)t]. \quad (6)$$

Those sinusoidal signals, sin and cos, are then used in I/Q demodulation process. I/Q stands for in-phase and quadrature, which means there are two sinusoidal signals with  $90^\circ$  phase difference [7]. The block diagram of I/Q demodulator can be shown in Fig.2. The  $S_{ref_I}(t)$  is reference signal for in-phase (I) and  $S_{ref_Q}(t)$  is reference signal for quadrature (Q).

Those two reference signals are then mixed with LPF output in (4) and the results are expressed as (7) and (8), with the value of amplitude are  $A_I$  and  $A_Q$  for in-phase and quadrature signal, respectively. The LPF at in-phase and quadrature section is used to eliminate the higher frequency component, then the LPF output at both section is written as (9) and (10). These LPF outputs are contain the data of the displacement ( $d$ ).

$$S_I(t) = A_I \cos[4\pi(f_2 - f_1)t] + A_I \cos\left[\frac{2\pi 2d}{\lambda_1}\right]. \quad (7)$$

$$S_Q(t) = A_Q \sin[4\pi(f_2 - f_1)t] + A_Q \sin\left[\frac{2\pi 2d}{\lambda_1}\right]. \quad (8)$$

$$S_{LPF_I}(t) = A_o \cos\left[\frac{2\pi 2d}{\lambda_1}\right]. \quad (9)$$

$$S_{LPF_Q}(t) = A_o \sin\left[\frac{2\pi 2d}{\lambda_1}\right]. \quad (10)$$

The phase shift degree can be determined by performing arcus tangent calculation of LPF output of in phase and quadrature sections. Finally, the phase detector output computation is done referring to (11).

$$S_{PD}(t) = \tan^{-1} \left[ \frac{S_{LPF_I}(t)}{S_{LPF_Q}(t)} \right]. \quad (11)$$

### III. RESULT AND DISCUSSION

This system is simulated by MATLAB software. Refers to HB100 module [6], the transmitted frequency ( $f_1$ ) of this system is 10.525 GHz. By shifting the second frequency ( $f_2$ ), the bandwidth of the system is obtained with the value of  $df$ . The initial distance between target and radar is assumed to be known. In this simulation the initial distance is set to be 2.85 m, as the experiment of the radar are going to be done in a room.

If the system only use a single transmitted frequency ( $f_1$ ),  $f_2$  is equal to zero, then the LPF output in Fig.1 is in a form of direct current (DC) signal. The DC signal of LPF output is

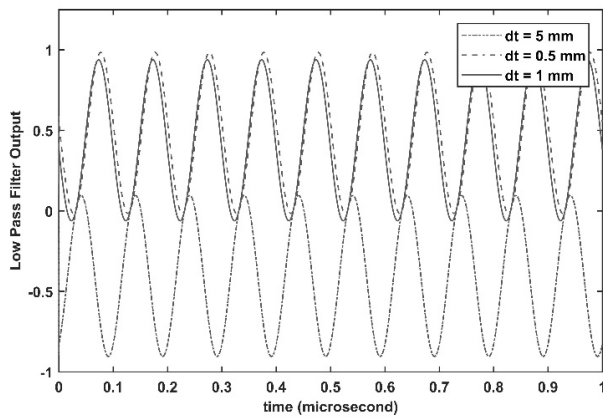


Fig. 4. Dual frequency LPF output.

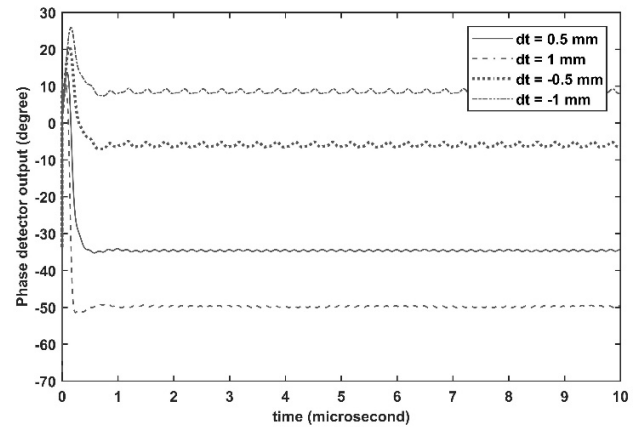


Fig. 6. Phase detector output of dual frequency CW radar.

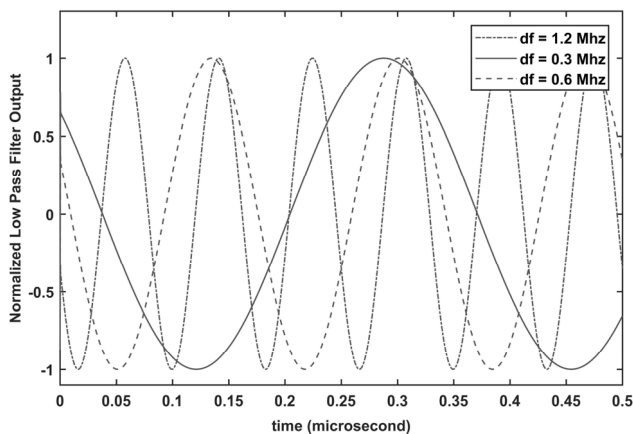


Fig. 5. Normalized dual frequency LPF output.

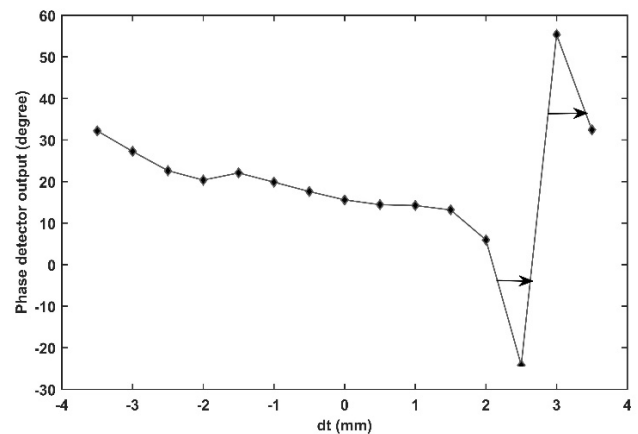


Fig. 7. Phase detector output of dual frequency CW radar with 0.3 MHz bandwidth.

shown in Fig. 3. The phase data is implicitly contained in its DC signal, then the phase data is difficult to be extracted from there. For phase component detection, the sinusoidal output is needed to be generated. By modifying the transmitter with dual frequency, the LPF output on Fig.1 is then in a sinusoidal form. Afterward, the phase data can be determined using I/Q demodulator.

Fig.4 shows the LPF output of Dual Frequency CW radar that proposed. In this result the value of  $df$  is set to 0.3 MHz and the simulation is performed for three different small displacement values ( $dt$ ). These three LPF output in Fig.4, are having the same frequency with different phase with each other. This phase shift contains the displacement data of the target. But, the displacement data cannot be directly obtained from this LPF output, because the LPF output is still in time domain. In order to make the result clearer and simpler, the normalization of LPF output is done. Normalization is a wave function scaling, so that all the probabilities are add to 1.

The normalized LPF output with different value of  $df$  is shown in Fig.5. The frequency of LPF output is proportional to  $df$ . A large  $df$ , causes a high frequency on LPF output and vice versa. The value of  $df$  give consequences to the overall bandwidth of the proposed radar system, therefore the value of  $df$  is expected to be small as possible.

Fig.6 shows the phase detector output for several different value of displacement ( $dt$ ) with the value of  $df$  is 0.3 MHz. As expecting a small value of  $df$ , this value is chosen due to the narrowest bandwidth obtained from the simulation result in

MATLAB. There are four value of displacements, 0.5 mm, -0.5 mm, 1 mm, and -1 mm. The magnitude of the phase detector output should be the same if the magnitude of  $dt$  is also the same. For a sample, in Fig.6, the phase detector output of 0.5 mm displacement is around  $-35^\circ$ . But, on -0.5 mm displacement, the phase detector output is not  $35^\circ$ , it is around  $-5^\circ$ . This kind of thing is happened because of the normalization process that affect the phase detector output.

The frequency difference adjustment is done by shifting the  $f_2$ . Fig.7 and Fig.8, show the phase value in 0.3 MHz and 1.2 MHz bandwidth, respectively. The ambiguity of the phase degree is shown by the arrow in both figures, where one value of phase detector degree has more than one value of displacement ( $dt$ ). Linearity relation between phase detector output and displacement ( $dt$ ), determine the range of displacement detection which can be supported by the proposed radar. The relationship between phase detector output and displacement ( $dt$ ) in Fig.8, is more linear than in Fig.7. It is mean that the bandwidth ( $df$ ) affects to the range of displacement detection. For a certain purpose of displacement detection, the difference between dual sinusoidal signal in transmitter should be selected properly to increase the linearity of phase detector output and minimizing the ambiguity in detection result.

#### IV. CONCLUSION

In this paper, the dual frequency CW radar was proposed. The proposed radar is developed by conducting system



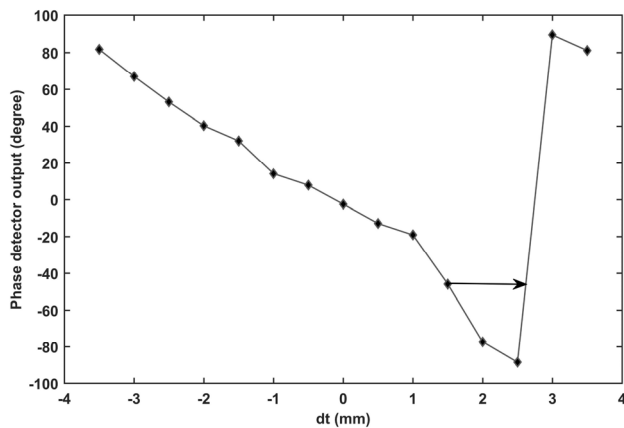


Fig. 8. Phase detector output of dual frequency CW radar with 1.2 MHz bandwidth.

modification of CW radar in transmitter and receiver part. In transmitter part, we used two sinusoidal signal generators with different frequency to obtain the sinusoidal output in conventional CW radar. In receiver part, the modification is done in postprocessing of the LPF output by adding the phase detection computation. Theoretical and simulation were conducted to study the capability the proposed radar system. The result shows that the proposed modification is capable to detect a small displacement in millimeter scale. The result shows that any value of displacement can be detected. In avoiding the ambiguity of phase detector output and arranging the range of small displacement detection, the bandwidth ( $df$ ) needs to be adjusted. The smaller the bandwidth, the higher the ambiguity probability.

#### REFERENCES

- [1] M. Manunta, R. Castaldo, V. De Novellis, P. Lollino, and P. Tizzani, "Integration of SBAS-DInSAR and in-situ observations for 3D numerical optimization modelling: The case study of Ivancich landslide (Assisi, Italy)," in *IEEE Geoscience and Remote Sensing Symp. (IGARSS)*, Milan, Italy, July 2015, pp. 1397-1400.
- [2] Y. Rauste, H. Bt. Lateh, Jefriza, M. W. I. W. Mohd, A. Lönnqvist, and T. Häme, "TerraSAR-X Data in Cut Slope Soil Stability Monitoring in Malaysia," *IEEE Transactions on Geoscience and Remote Sensing*, vol. 50, no. 9, pp. 3354-3363, September 2012.
- [3] A. Novellino, F. Cigna, A. Sowter, M.F. Syafiudin, D. Di Martire1, M. Ramondini, and D. Calcaterra1, "Intermittent small baseline subset (ISBAS) InSAR analysis to monitor landslides in Costa Della Gaveta, Southern Italy," in *IEEE Geoscience and Remote Sensing Symp. (IGARSS)*, July 2015, pp. 3536-3539.
- [4] V. T. Vu, T. K. Sjögren, M. I. Pettersson, A. Gustavsson, and L. M. H. Ulander, "Detection of Moving Targets by Focusing in UWB SAR—Theory and Experimental Results," *IEEE Trans. on Geosci. and Remote Sens.*, vol. 48, no. 10, pp. 3799-3815, October 2010.
- [5] IISC BANGALORE, (2013) Continuous wave and frequency modulated radar. [Online]. Available: <http://nptel.ac.in/courses/101108056/module2/lecture4.pdf> [Accessed January 10, 2018].
- [6] *HB100 Microwave Sensor Module 10.525GHz Microwave Motion Sensor Module*, ver 1.02 ed., Singapore Technologies Electronics, Satcom and Sensor Systems.
- [7] J. Kirkhorn, IFBT, NTNU, *Introduction to IQ-demodulation of RF-data*, September 15, 1999.

# A New Method for Minimizing the Unnecessary Handover in High-Speed Scenario

Yew Hoe Tung  
Faculty of Engineering  
Universiti Malaysia Sabah  
(UMS)  
Johor Bahru, Malaysia  
htyew@ums.edu.my

Muhammad Haikal Satria  
Faculty of Engineering  
Universiti Teknologi Malaysia  
(UTM)  
Johor Bahru, Malaysia  
haikalsatria@biomedical.utm.my

Rindu Nurma Illahi  
Faculty of Engineering  
Universiti Teknologi Malaysia  
(UTM)  
Johor Bahru, Malaysia  
rindunurmaillahi@gmail.com

**Abstract**— The application of Wireless Local Area Network (WLAN) is limited to indoor or pedestrian walking speed environment because the small WLAN coverage will lead to the growth of unnecessary handover rate in high-speed scenario. The previously proposed traveling distance prediction based handover methods assumed mobile terminal (MT) travels at a constant speed is impractical as most of the MTs may not be traveling at constant speed in real environment. These methods have poor performance in case of acceleration because MT will leave the network earlier than the estimated time. In this paper, a new traveling distance prediction based handover scheme that is aware of MT's speed changes is proposed to overcome the limitation of the existing methods. The proposed scheme is adapted to the MT velocity and acceleration or deceleration rate. The numerical result shows that the performance of the proposed scheme is better than the existing handover methods in high-speed scenario. It keeps the probability of unnecessary handover within the user acceptable level in high-speed scenario.

**Keywords**—WLAN; high-speed scenario; velocity; unnecessary handover; vertical handover.

## I. INTRODUCTION

The next generation wireless technology will be focused on ubiquitous access over heterogeneous wireless technologies [1]. The network service is no longer restricted by particular wireless technology. To achieve this, an efficient seamless handover mechanism to switch the mobile terminal (MT) amongst the different wireless technologies is needed to ensure that the MT is continuously connected to the most appropriate network at anywhere.

The existing wireless technologies can be divided into two groups; Third Generation Partnership Project (3GPP) and non-3GPP. Interoperation between 3GPP (2G, 3G and 4G cellular network) and non-3GPP (WLAN, WiMAX, etc.) network candidates is called vertical handover. It can be achieved by using the Media Independent Handover (MIH) [2]. MIH provides information services to discover the neighboring network information, even service to report the link quality and command service to control and manage the network selection [2].

Horizontal handover process is much straightforward contrasted with vertical handover process since it just includes a solitary system. MT can choose the best Base Station (BS) by comparing the measured Received Signal Strength (RSS) of different BSs. The horizontal handover is necessary if the RSS of existing connected BS drops below the predefined RSS threshold and the targeted BS RSS value

is greater than predefined RSS threshold and RSS of the existing connected BS.

WLAN is the most preferable amongst the heterogeneous wireless networks because of its high bandwidth capacity and low access cost. However, the WLAN application is always restricted to the indoor or low speed environment. This is because the small WLAN coverage leads to high number of unnecessary handovers, especially in high-speed scenario. Unnecessary handover occurs when traveling time within WLAN coverage ( $t$ ) is less than the total handover latency enter ( $T_i$ ) to and leave ( $T_o$ ) from WLAN cell ( $t < (T_i + T_o)$ ) where MT does not get any benefit from WLAN cell. High number of unnecessary handovers will interrupt the connection and also induce call drop.

In this paper, a new traveling time prediction based handover method is proposed for minimizing the number of unnecessary handovers to WLAN in high-speed scenario.

## II. RELATED WORKS

Authors in [3] proposed a RSS threshold based handover plan to permit MTs access to WLAN and 3G arrange in consistent way. This scheme made two RSS thresholds. The first threshold is 3G→WLAN threshold and the second one is WLAN→3G threshold. MT initiates handover from 3G network to WLAN if measured WLAN RSS value is greater than 3G→WLAN threshold. When currently attached AP's RSS signal drops below the WLAN→3G threshold, MT performs handover to 3G network. The weaknesses of this scheme are high handover rate and ping-pong impact because of the fluctuation of RSS value caused by channel fading, MT portability, and shadowing [4].

Authors in [5] proposed a dynamic RSS threshold in view of the MT's speed and handover latency to limit the likelihood of handover disappointment from WLAN to 3G systems. In this scheme, MT handovers to WLAN whenever the WLAN is available because it assumed handover failure probability from 3G to WLAN is zero as WLAN cell is covered by 3G cellular network. The primary drawback of this scheme is execution corrupts when the MT's traveling time inside the WLAN coverage is not as much as the handover latency.

The speed based vertical handover algorithm [6-8] defined a speed threshold for WLAN. The MT performs handover to WLAN if and only if the traveling speed is lower than the predefined threshold. The authors in [6-8] defined WLAN speed threshold at 5 m/s and below. In [9, 10], authors presented a Fuzzy based handover algorithm

with the If-Else rule, “If MT speed is low then WLAN-reject is low; otherwise WLAN-reject is high”. The application of WLAN is restricted to low traveling speed or indoor environment such as shopping complex, hospital, airport and home. In fact, the coverage radius of WLAN is more than 50 meters at outdoor environment. For example, IEEE 802.11n coverage radius is up to 100 meters.

Authors in [11] presented a dwell timer based scheme for vertical handover between WLAN and cellular networks to reduce the number of unnecessary handovers. MT will initiate dwell timer after MT first detects the measured RSS value is less than the predefined RSS threshold. MT compares the measured WLAN RSS value with the predefined RSS threshold consecutively until predefined dwell time period expired. If measured RSS is always less than the predefined RSS threshold during the dwell time period, MN initiates the handover to cellular network. Otherwise, it will persist with WLAN. The fixed dwell timer proposed in [11] had successfully reduced the number of unnecessary handovers. However, in high-speed scenario, time taken by MT to cross the WLAN coverage might less than the predefined dwell timer. Therefore, there will be high number of handover failures and unnecessary handovers in high-speed scenario.

For reducing the number of unnecessary handovers, authors in [12] and [13] presented the handover necessity estimation methods. Figure 1 shows the scenario of traveling distance prediction in WLAN. These methods trigger handover to WLAN if and only if the estimated traveling distance ( $l$ ) is greater than the distance threshold ( $L$ ). The traveling distance ( $l$ ) from  $P_{In}$  to  $P_{Out}$  is given as

$$l = \frac{r^2 - s^2 + d^2}{d} \quad (1)$$

where  $r$  is the radius of WLAN coverage,  $s$  is the distance between  $P_s$  and AP, and  $d$  is distance between  $P_{In}$  and  $P_s$ . The value of  $d$  can be determined by

$$d = v_{P_{In}} (t_{P_s} - t_{P_{In}}) \quad (2)$$

where  $v_{P_{In}}$  represents MT's velocity at point  $P_{In}$ ,  $t_{P_s}$  is time at point  $P_s$ ,  $t_{P_{In}}$  is time MT pass through  $P_{In}$ . The distance threshold with acceptable probability of unnecessary handover ( $L$ ) presented by [12, 13] is expressed in Equation (3).

$$L = 2rs \sin \left( \sin^{-1} \left( \frac{l_{th}}{2r} \right) - \frac{\pi P_u}{2} \right) \quad (3)$$

where  $P_u$  is the predefined tolerable or acceptable probability of unnecessary handover and  $l_{th}$  is distance threshold. The  $l_{th}$  can be calculated by multiplying MT speed  $v_{P_{In}}$  with total handover time,  $T_t + T_o$ .  $L$  is equal to  $l_{th}$  if  $P_u = 0$ . The probability of unnecessary handover of [12, 13] is as expressed in Equation (4).

$$P_r = \frac{2}{\pi} \left[ \sin^{-1} \left( \frac{l_{th}}{2r} \right) - \sin^{-1} \left( \frac{L}{2r} \right) \right] \quad (4)$$

This method maintains the probability of unnecessary handovers within the predefined tolerance. However, this method assumes that MT travels at a constant speed. This assumption is impractical as the speed of MT may not be constant in the real environment. This method will have poor performance if MT accelerates, because MT will leave the WLAN coverage earlier than the estimated time. Therefore, a new prediction method which is aware of MT speed changes is proposed in this work to overcome the limitation of existing methods.

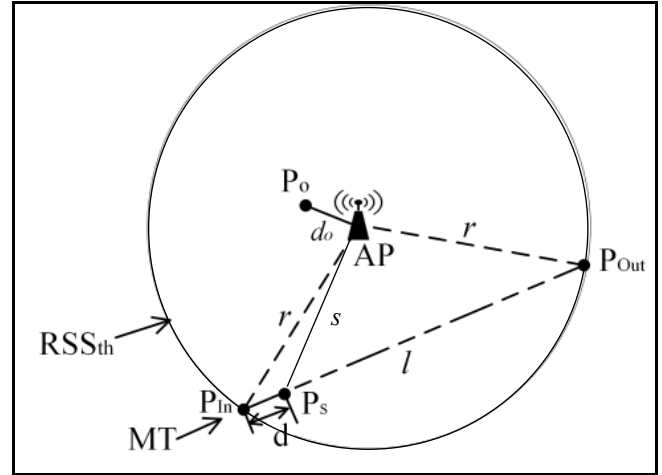


Fig. 1. Traveling distance prediction in WLAN coverage [12].

## I. PROPOSED METHOD

The proposed method is the extension of Yan et al. [12] and Hussain et al. [13] methods. In dynamic speed, the distance  $d$  can be determined by using the kinematic equation [14] where the distance is equal to average speed multiply with time interval. It is given as

$$d = \left| \frac{v_{P_s} + v_{P_{In}}}{2} (t_{P_s} - t_{P_{In}}) \right| \quad (5)$$

where  $v_{P_s}$  and  $v_{P_{In}}$  denotes measured MT velocities at  $P_s$  and  $P_{In}$ , respectively. The MT velocity can be measured by using the velocity estimation technique that is presented in [15]. By substituting (5) into (1), the distance  $l$  can be estimated by using Equation (6).

$$l = \frac{r^2 - s^2 + \left( \frac{v_{P_s} + v_{P_{In}}}{2} (t_{P_s} - t_{P_{In}}) \right)^2}{\frac{v_{P_s} + v_{P_{In}}}{2} (t_{P_s} - t_{P_{In}})} \quad (6)$$

The  $r$  and  $s$  values can be determined by using log-distance path loss model [16]. The distance  $r$  is calculated by using Equation (7).

$$\begin{aligned} RSS_{th} &= P_{TX} - PL_0 - 10n \log \frac{r}{d_0} + \varepsilon \\ \log \frac{r}{d_0} &= \frac{P_{TX} - PL_0 - RSS_{th} + \varepsilon}{10n} \\ r &= d_0 * 10^{\left( \frac{P_{TX} - PL_0 - RSS_{th} + \varepsilon}{10n} \right)} \end{aligned} \quad (7)$$

where  $d_0$  is the reference distance,  $P_{TX}$  represents AP transmit power,  $PL_o$  is the power loss at  $P_o$ ,  $RSS_{th}$  denotes measured received signal strength (RSS) at point  $P_n$ ,  $n$  is the path loss exponent (usually 2 to 4 depending on transmission environment), and  $\varepsilon$  is a zero-mean Gaussian random variable caused by shadow fading. Doppler shift effect in high speed environment can be mitigated by using the Doppler frequency offset estimation and compensation algorithm [17, 18]. The  $s$  value can be calculated by replacing  $RSS_{th}$  in (7) with the measured RSS at point  $P_s$ .

To alleviate the shadowing effect, MT takes numerous RSS samples and the arithmetic mean is evaluated.  $RSS_{th}$  is given by Equation (8).

$$RSS_{th} = \frac{1}{z} \sum_{i=1}^z RSS_i \quad (8)$$

The sample size,  $z$  is adjusted based on the MT's velocity. It is expressed as

$$z = \left\lceil \frac{\gamma}{T_s} \right\rceil \quad (9)$$

where  $T_s$  is RSS sampling time and  $\gamma$  is total sampling period given by Expression (10).

$$\gamma = K * T_m, \quad K \in \{0.1, 0.2, \dots, 0.9\} \quad (10)$$

In the proposed method, MT updates the RSS measurement periodically at time interval of  $T_m$  which is given by  $\frac{D}{v}$  second, where  $D$  is a fixed distance of 1 m. The higher the velocity is, the smaller the  $T_m$  period and sample size. The maximum value of  $z$  is limited to 20 samples to avoid excessive sampling while MT travels at low speed.

Referring to the kinematic equation [14], the relationship between distance, speed, acceleration and time is given as

$$l' = \frac{\alpha \tau^2}{2} + v_i \tau \quad (11)$$

where  $l'$  is traveling distance,  $v_i$  is initial speed,  $\tau$  is traveling time and  $\alpha$  denotes acceleration or deceleration rate. The  $\alpha$  value can be determined by using Equation (12).

$$\alpha = \frac{v_{P_s} - v_{P_{in}}}{\left[ \frac{v_{P_s} - v_{P_{in}}}{\tau} \right]} \quad (12)$$

If  $v_{P_s} = v_{P_{in}}$ , it mean that MT is traveling at a constant speed. MT is accelerating if  $v_{P_s} > v_{P_{in}}$  and decelerating if  $v_{P_s} < v_{P_{in}}$ .

Referring to Equation (11), assuming  $l' = l$ ,  $v_i = v_{P_{in}}$ ,  $\tau = T_i + T_o$  and  $\alpha$  is given by Equation (12), the  $l_{th}$  of the proposed method ( $l_{th,p}$ ) can be determined by using Equation (13).

$$l_{th,p} = \frac{(v_{P_s} - v_{P_{in}})(T_i + T_o)^2}{2 \left[ \frac{v_{P_s} - v_{P_{in}}}{\tau} \right]} + v_{P_{in}}(T_i + T_o) \quad (13)$$

Then substituting (13) into (3), the  $L$  of the proposed method ( $L_p$ ) is given by Equation (14).

$$L_p = 2r \sin \left( \sin^{-1} \left( \frac{(v_{P_s} - v_{P_{in}})(T_i + T_o)^2 + 2v_{P_{in}}(T_i + T_o) \left[ \frac{v_{P_s} - v_{P_{in}}}{\tau} \right]}{4r \left[ \frac{v_{P_s} - v_{P_{in}}}{\tau} \right]} \right) - \frac{\pi P_u}{2} \right) \quad (14)$$

$L_p$  is adjusted dynamically to the MT's velocity and acceleration or deceleration rate. MT triggers handover to WLAN if and only if the estimated traveling distance  $l$  is greater than the distance threshold  $L_p$ .

Figure 2 shows the correlation between acceleration, velocity and distance threshold  $L_p$  with setting of WLAN coverage radius,  $r = 100$  m, total handover time,  $T_i + T_o = 2$  seconds, and acceptable probability of unnecessary handover,  $P_u = 0$ . The higher the MT acceleration rate or velocity is, the greater the distance threshold  $L_p$ . However, the distance threshold introduced by [12] and [13] methods is fixed where  $L$  is equal to  $L_p$  ( $\alpha=0$ ) all the time even though the MT accelerates, because these methods do not account for the changes of velocity and MT is assumed travel at the constant velocity.

The probability of unnecessary handover of the proposed method ( $P_{r,p}$ ) can be calculated by replacing  $l_{th}$  and  $L$  in Equation (4) with  $l_{th,p}$  and  $L_p$ , respectively, yields;

$$P_{r,p} = \frac{2}{\pi} \left[ \sin^{-1} \left( \frac{l_{th,p}}{2r} \right) - \sin^{-1} \left( \frac{L}{2r} \right) \right] \quad (15)$$

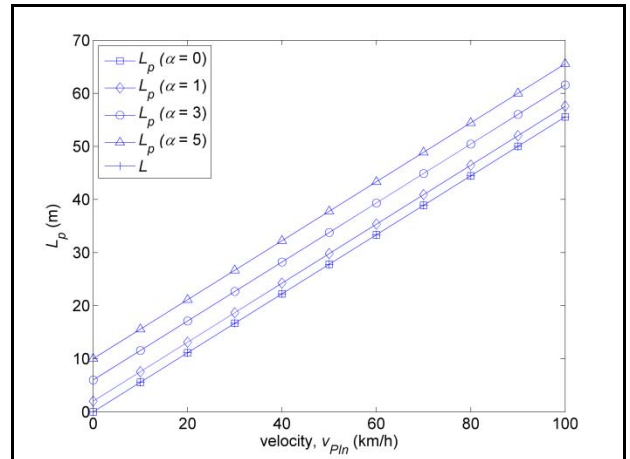


Fig. 2. The correlation between the acceleration rate, velocity and distance threshold  $L_p$  ( $r = 100$  m,  $T_i + T_o = 2$  sec,  $P_u = 0$ ).

## II. PERFORMANCE ANALYSIS AND DISCUSSION

The performance of the proposed method is compared against the approaches in [12] and [13]. In this experiment, the deceleration scenario is omitted because it provides MTs longer traveling time within WLAN coverage and has no impact on unnecessary handover. The simulation parameters are listed in Table 1.

Table 1 Simulation parameters used in the experiment.

Parameter	Value
$\alpha$	0, 1, 3, 5 m/s <sup>2</sup>
$v_{PIn}$	10 to 100 km/h
$r$	100 m [12, 13]
$P_u$	0.02 or 2% [12, 13]
$T_i + T_o$	2 s [12, 13]

Figure 3 shows the probability of unnecessary handover of Yan et al. [12], Hussain et al. [13] and the proposed methods. As shown in Figure 3, Yan et al. [12] and Hussain et al. [13] methods keep the probability of unnecessary handover within the predefined tolerable value ( $P_u$ ) at constant speed ( $\alpha = 0$ ). However, the unnecessary handover probability is up to 35%, 100%, and 165% higher than  $P_u$  at the acceleration rate of  $1\text{m/s}^2$ ,  $3\text{m/s}^2$ , and  $5\text{m/s}^2$ , respectively. The higher the MT acceleration rate is, the higher the unnecessary handover probability for Yan et al. [12] and Hussain et al. [13] methods because MT takes shorter time to cross the WLAN coverage.

In Figure 3, it can be seen that at the acceleration rate ( $\alpha$ ) of  $1\text{m/s}^2$ ,  $3\text{m/s}^2$ , and  $5\text{m/s}^2$ , the proposed method retains the probability of unnecessary handover within the predefined tolerable value ( $P_u$ ), which is 0.02. The numerical result shows that the proposed method outperforms R. Hussain et al. [13] and Y. Xiaohuan et al. [12] methods.

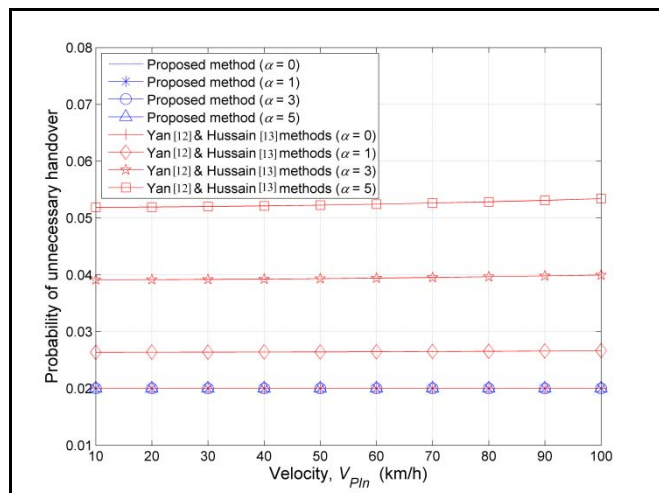


Fig. 3. Probability of unnecessary handover of Yan [12], Hussain [13] and proposed methods ( $P_u = 0.02$ ).

### III. CONCLUSION

This paper presented a traveling distance prediction method to keep the probability of unnecessary handover within the predefined tolerable value ( $P_u$ ) while optimizing the connection time to WLAN in high-speed scenario. The proposed method overcomes the limitation of previous methods which assume the MT traveling in a fixed velocity. The performance of the proposed method is better than the previous methods.

### ACKNOWLEDGMENT

This research is supported by Ministry of Education Malaysia and University Malaysia Sabah, Geran Penyelidikan UMS (SBK0364-2017).

### REFERENCES

[1] A. Ahmed, L. M. Boulahia, Gai, x, and D. ti, "Enabling Vertical Handover Decisions in Heterogeneous Wireless Networks: A

State-of-the-Art and A Classification," *Communications Surveys & Tutorials, IEEE*, vol. 16, pp. 776-811, 2014.

[2] A. De La Oliva, A. Banchs, I. Soto, T. Melia, and A. Vidal, "An overview of IEEE 802.21: media-independent handover services," *Wireless Communications, IEEE*, vol. 15, pp. 96-103, 2008.

[3] A. d. l. Oliva, T. Melia, A. Vidal, C. J. Bernardos, I. Soto, and A. Banchs, "IEEE 802.21 enabled mobile terminals for optimized WLAN/3G handovers: a case study," *SIGMOBILE Mob. Comput. Commun. Rev.*, vol. 11, pp. 29-40, 2007.

[4] M. Kassar, B. Kervella, and G. Pujolle, "An overview of vertical handover decision strategies in heterogeneous wireless networks," *Computer Communications*, vol. 31, pp. 2607-2620, 6/25/2008.

[5] S. Mohanty and I. F. Akyildiz, "A Cross-Layer (Layer 2 + 3) Handoff Management Protocol for Next-Generation Wireless Systems," *Mobile Computing, IEEE Transactions on*, vol. 5, pp. 1347-1360, 2006.

[6] M. Khan and K. Han, "An Optimized Network Selection and Handover Triggering Scheme for Heterogeneous Self-Organized Wireless Networks," *Mathematical Problems in Engineering*, vol. 2014, p. 11, 2014.

[7] T. Janevski and K. Jakimoski, "Mobility sensitive algorithm for vertical handovers from WiMAX to WLAN," in *Telecommunications Forum (TELFOR), 2012 20th*, 2012, pp. 91-94.

[8] H. Tung Yew, E. Supriyanto, M. H. Satria, and Y. Wen Hau, "Autonomous network selection strategy for telecardiology application in heterogeneous wireless networks," *Jurnal Teknologi*, vol. 77, pp. 147-153, 2015.

[9] F. Kaleem, A. Mehbodniya, K. K. Yen, and F. Adachi, "A Fuzzy Preprocessing Module for Optimizing the Access Network Selection in Wireless Networks," *Advances in Fuzzy Systems*, vol. 2013, p. 9, 2013.

[10] H. T. Yew, Y. Aditya, H. Satrial, E. Supriyanto, and Y. W. Hau, "Telecardiology system for fourth generation heterogeneous wireless networks," *ARPJ Journal of Engineering and Applied Sciences*, vol. 10, pp. 600-607, 2015.

[11] S. Dhar Roy and S. R. Vamshidhar Reddy, "Signal Strength Ratio Based Vertical Handoff Decision Algorithms in Integrated Heterogeneous Networks," *Wireless Personal Communications*, vol. 77, pp. 2565-2585, 2014.

[12] Y. Xiaohuan, N. Mani, and Y. A. Sekercioglu, "A Traveling Distance Prediction Based Method to Minimize Unnecessary Handovers from Cellular Networks to WLANs," *Communications Letters, IEEE*, vol. 12, pp. 14-16, 2008.

[13] R. Hussain, S. Malik, S. Abrar, R. Riaz, H. Ahmed, and S. Khan, "Vertical Handover Necessity Estimation Based on a New Dwell Time Prediction Model for Minimizing Unnecessary Handovers to a WLAN Cell," *Wireless Personal Communications*, vol. 71, pp. 1217-1230, 2013/07/01 2013.

[14] D. M. Katz, *Physics for Scientists and Engineers: Foundations and Connections, Extended Version with Modern*: Cengage Learning, 2016.

[15] S. Mohanty, "VEPSD: a novel velocity estimation algorithm for next-generation wireless systems," *Wireless Communications, IEEE Transactions on*, vol. 4, pp. 2655-2660, 2005.

[16] P. Santi, "Modeling Next Generation Wireless Networks," in *Mobility Models for Next Generation Wireless Networks*, ed: John Wiley & Sons, Ltd, 2012, pp. 19-32.

[17] Y. Yang, P. Fan, and Y. Huang, "Doppler frequency offsets estimation and diversity reception scheme of high speed railway with multiple antennas on separated carriages," in *Wireless Communications & Signal Processing (WCSP), 2012 International Conference on*, Huangshan, China, 2012, pp. 1-6.

[18] E. A. Feukeu, K. Djouani, and A. Kurien, "Compensating the effect of Doppler shift in a vehicular network," in *AFRICON, 2013*, 2013, pp. 1-7.



# AUTOMATION SNORT RULE FOR XSS DETECTION WITH HONEYPOT

Syaifuddin  
Faculty of Engineering  
School of Information Technology  
University of Muhammadiyah Malang  
Indonesia, Malang  
Email: saifuddin@umm.ac.id

Diah Risqiwati  
Faculty of Engineering  
School of Information Technology  
University of Muhammadiyah Malang  
Indonesia, Malang  
Email: risqiwati@umm.ac.id

Hanugra Aulia Sidharta  
Faculty of Technology and Design  
Computer Science Program Study  
Bina Nusantara Institute of Creative  
Technology Malang  
Indonesia, Malang  
Email: hanugra.sidharta@binus.edu

**Abstract**— In modern era, data has become precious and important, data leak can lead to high damage to business, impact on losing profit. To avoiding those problems, organization need equip with updated security tools to protecting data and network. As computer network growing rapidly, currently security become important to prevent from attack, both from outside and inside the network. In line with that, new vulnerability grown on everyday basis and resulting increment number of intrusion and attack. Unfortunately, each intrusion and attack have a different pattern and unique behavior, continuous development and research on intrusion detection is mandatory. By statistic, in 2017 attack associated with XSS attack is grew 39% compared with 2015

**Keywords:** Network attack, IDS, XSS

## I. INTRODUCTION

Number of device connected and tethered to computer network growing every day. With technology explosion, almost every person has a PC, laptop or smartphone that starve to connect with internet. This led with increment number of attack on computer network. estimated reaching 580 million number of occurrence. [1] Cyber-attack can spread fast on computer network, on 2004 some researcher found swarm of botnet with estimated roughly up to 25.000 bots with capability transmit junk data around 5 Gbps, sufficient to make computer network on several company become offline. [2]

Intrusion Detection System (IDS) and Intrusion Prevention System (IPS) have been used thoroughly on industrial network. Intrusion Detection is processing to monitor and observe on computer network for unrecognized threat, illegal activities. IDS also can inspect network traffic, to preventing system being target from attacker, such as DDOS attack.[3] IDS/IPS used to identify malicious activity and abnormal activity in network system. With effective IDS, should be have knowledge to detect several type of attack, its variant, several possible technique to evasion attack. [4]

With current IDS/IPS, system just can handle passive intrusion, but with adding honeypot, system can act as an active defender, or act as a decoy, so when there is intrusion, intruder is attack on honeypot as decoy, not real server or real network.[5]

XSS or Cross Site Scripting in one of most common technique used to hack with exploiting application layer. In 2017, attack to web is associate with XSS is grew 39% compared with 2015[6]. XSS also origin of many other attack, such as information disclosure, credential stolen, and content spoofing. XSS attack is simple but yet effective, just by insert malicious script exploit on URL parameter, cookies, database query [7]

## II. BACKGROUNDS

This section expounds the details of the relevant information relating to the paper's topic.

### A. Concept of Intrusion Detection System (IDS)

IDS or Intrusion Detection System is specific device or software with capability to monitor and observe network activity inbound and outbound through system, and recognize compromising pattern that may indicate system is under attack by someone, or someone attempt to compromise network. [8]

Snort is a popular open source IDS/IPS which can utilize for protecting system from attacker. Developed by Martin Roesch in 1998 with C language. Snort can run on almost every computer architecture and OS (Operating System). Snort IDS is real time-based alerting, it monitors and observe anomalies in traffic packet comparing it with rules. Rules in Snort IDS is user friendly and easy to modify. With basic component such as : Packet Decoder, Preprocessor, Detection Engine, Logging and alerting system, and output module. [9]

Snort utilizing rules and compare it with data packet from traffic onto network. Figure 1 is shown basic rule Snort IDS, which divided into two logical part: rule header, and rule option. Figure 2 is shown each field from rule header part, that contain criteria definition. Criteria definition use for comparing data between rule and data packet from network. Rule option following rule header and they are within pair of parentheses. Or in simple word, each option of rule contains 2 parts: keyword and argument. Keyword option extract from arguments with emblem colon. And argument is option inside the emblem double quote, each rule separated with semicolon

Rule Header	Rule Options
-------------	--------------

Fig. 1. Snort IDS rule structure



Action	Protocol	Source Address	Source Port	Direction	Destination Address	Destination Port
--------	----------	----------------	-------------	-----------	---------------------	------------------

Fig. 2. Snort IDS rules header structure

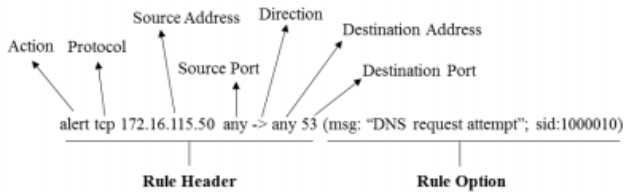


Fig. 3. Example snort IDS

Example of snort IDS rule shown on Figure 3, this rule will triggered general alert with condition: if there is tcp protocol request from source IP address: 172.16.115.50 with any port sent to any IP address with destination port is 53. If this rule triggered will show message: "DNS request attempt", this rule will have saved as sid:1000010

Advantage using IDS can summarize as [10]

1. IDS can detect attack and variant security breach flawlessly
2. Identify harm and affected system.
3. IDS do not suffer with harmful security.
4. Act as quality control for security model and implementation
5. On each suspected attack, IDS will save pattern and behavior for future prevention system.
6. IDS can observe and analyze activity on computer or network.
7. IDS could check system configuration even through vulnerabilities for integrity system.
8. Estimate and analysis abnormal or irregular service.

### B. Honeypot

Honeypot develop by Lance Spitzner, founded in 1999 as honeynet project in nonprofit research. Honeynet design to attract intruder, act as a trap for unauthorized communication on network. Honeypot also can used to learn intruder behavior and intrusion pattern.[11]. Besides that, honeypot can dig various tools used by hacker, even can examine social network of intruder.

Main feature of honeypot is on accuracy from data collection. Unlike most IDS system, honeypot examine only on known attack. Honeypot cannot directly protect on system, unlike IDS that can by pass interception techniques to monitor entire network[5]

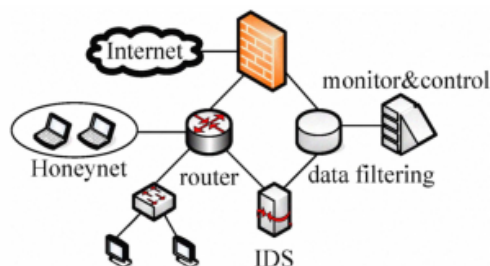


Fig. 4. Honeypot system structure

In Figure 4 shown honeypot system structure, honeypot not really protect network, this system act as a decoy. So, hacker is attack honeypot, not the real system. Unfortunately, honeypot can't be running standalone on system, honeypot need defense with firewall also IDS. Honeypot server act as security policy core, access control, provide security protection through security check, such as traffic analysis, hole detection, pattern matching. Meanwhile IDS support on rapid transform from static to dynamic protection.

### Advantages of honeypot

1. Data collection: normally honeypot collect most data, this system provides a lot of useful information. With these data we can know hacker profile, pattern, how they interact with system.
2. Resource: with honeypot sysadmin can studying on hacker without exposing real system, and minimalizing compromised system
3. Honeypot provide prevention compromised system.

### Disadvantages:

1. Honeypot is worthless if there is no attack on system
2. While there is no activity, honeypot essentially have no use.
3. Honeypot can have misused to attack another machine on another network
4. While honeypot can act as decoy, but there is varying level of risk compromised on security

To overcome those issue, author suggested develop honeypot to dynamic and hybrid model.[12]

### C. Cross Site Scripting (XSS)

According to Web Hacking Incident Database, most popular attack is SQL Injection, XSS (Cross Site Scripting) and DoS (Denial of Service) [7]. XSS attack first discussed in Computer Emergency Respond Team (CERT) back on 2002. [13]

Cross Site Scripting (XSS) is application level code injection type security vulnerability. It may occur while server program uses unrestricted input through HTTP request, or database without any validation. With these vulnerability, hacker can get sensitive data, such as cookies, session log. On figure 5, illustrated sequence XSS attack to some server program. Example on untrusted blog, some user wants to check latest command, legitimate user sent HTTP request for view latest command. Site will respond those request, but due database server already infected with XSS, sensitive information leak to attacker web server.

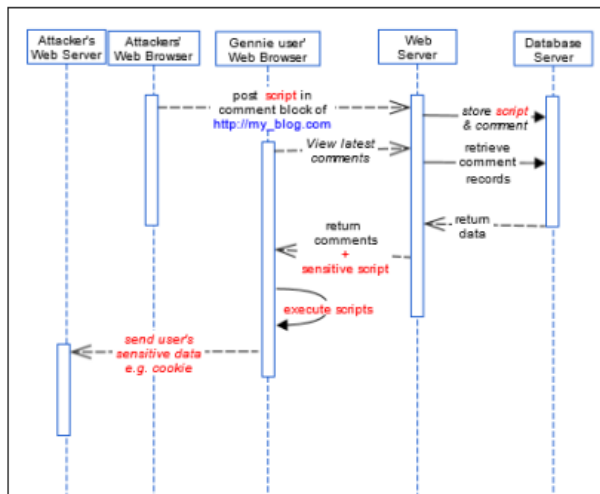


Fig. 5. Sequence diagram to represent XSS attack scenario

### III. RELATED WORKS

Previously, there were several researchers that focused on snort IDS to detect network probe attack, with snort IDS can detect 100% network probe attack based on MIT-DARPA 1999. [9] Khamphakdee et al suggest improving snort IDS with other attack, such as: DOS, U2R, R2L, XSS.

Garg et al research IDS detect attack using signature from malicious and harmful attack. Signature base IDS used to detect known attack, and unknown attack detect with Anomaly based IDS. Garg emphasize due IDS need update frequently due system need to familiar with new attack and threat. [10] Alam et al investigate possibility splitting traffic between snort sensor using policy based splitting mechanism. System will adapt adjusting with incoming traffic dynamically, with this policy will shift traffic load from one sensor to another sensor for improving system performance. [14] Zhai et al, successfully implement IPS based on snort on windows platform. Snort successfully implement by utilize between snort and IPSec [15]

Chawda et al introduce novel dynamic and hybrid model for analyze pattern, characteristic, and track internet thread, such as worm. Data collected from passive fingerprint tools (POf) and active probing such as Nmap [12]. From survey conducted by Cambell et al shown since 2006 honeypot research begin in line with increment number of PC or laptop connected with network, but since 2013 there is another device begin to hook up with internet, smartphone begin to replace PC or laptop. [1] Comparing with other defense strategy and mechanism, honeypot is superior due simple, more flexible during configuration, and consume less resource.[5]

### IV. SIMULATION SCENARIO

On our research, we use several PC with different OS on each PC as figure 6. Attacker PC user OS Back Box. Second PC act as honeypot server, this PC also can listen to network. Third PC as IDS server to filter all packet on network between all PC.

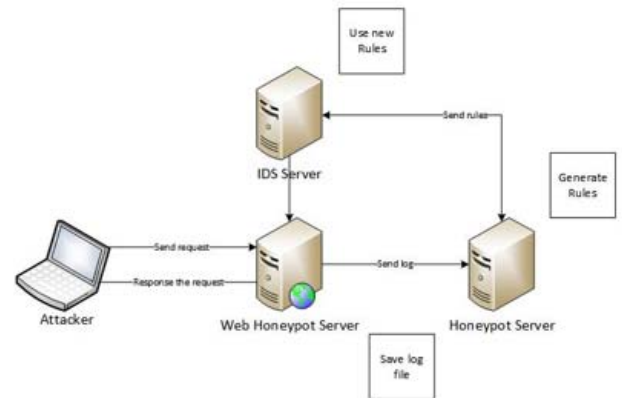


Fig. 6. Honeypot and IDS server topology

In these research IDS server will tell another server if there is breach on server. Rule will continuously update while there is attack on server while current attack is not on list of rules. Assume attacker already succeeded brake into server, all activities record on honeypot log. Malicious script that run on honeypot will become reference for making new IDS rule. Several data also gathered as part new rule, such as: IP address, port number, port protocol service requested, url request from attacker. To manage all of those data we develop program, with those programs will make IDS rule automatically

Step per step algorithm we use to make auto generate IDS rules

1. When honeypot receive HTTP request, honeypot server will listen to specific service and port. To help detect illegal script we filter URL request packet converted to hex. Example, "<script></script>" will be converted to "%3Cscript%3E%3C%2Fscript%3E".
2. Program will check whether those request packet contain illegal activities or not. If there is no illegal suspect than packet will redirect to normal web page. But if there is detected anomalies, honeypot will record log and URL request.
3. URL and tag from XSS will separate and save on another log file
4. Those log file will compare with snort rule, if there are new illegal activities, system will add new rule automatically. IDS server will update that information gradually.

### V. SIMULATION RESULTS

In this research we simulate with 200 XSS attack samples, each attack will record on honeypot. XSS attack list method collected from xxsed.com, owasp.org and cyclist github sample. From each attack we check whether those logs can use to generate rule for XSS attack. But due special character limitation, and there is too many variate XSS attack not all attack succeed generate automatic rule. Below several rule that succeed make by system.

TABLE I. SNORT RULE

No	Rules Snort
1	Alert tcp \$EXTERNAL_NET any -> \$HOME_NET any (msg:"XSS attempt: script injection detected "; flow:to_server,established; content:"Alert(%22XSS_BY_C37HUN%22)"; classtype:attempted-admin; sid:1000001;)
2	Alert tcp \$EXTERNAL_NET any -> \$HOME_NET any (msg:"XSS attempt: script injection detected "; flow:to_server,established; content:"Alert%281%29"; classtype:attempted-admin; sid:1000002;)
3	Alert tcp \$EXTERNAL_NET any -> \$HOME_NET any (msg:"XSS attempt: script injection detected "; flow:to_server,established; content:"Alert(document.cookie)"; classtype:attempted-admin; sid:1000003;)

Data on table 1 is example of rule that succeed generate by system. But not all rules can succeed generate automatically. This suspect due rules on snort server is case sensitive.

```

root@ubuntu: /etc/snort
Action Stats:
Alerts:      0 ( 0.000%)
Logged:      0 ( 0.000%)
Passed:      0 ( 0.000%)
Limits:
Match:       0
Queue:       0
Log:         0
Event:       0
Alert:       0

```

Fig. 7. Snort report on first attack

```

root@ubuntu: /etc/snort
Total:      4826
-----
Action Stats:
Alerts:      174 ( 3.605%)
Logged:      174 ( 3.605%)
Passed:      0 ( 0.000%)
Limits:
Match:       0
Queue:       0
Log:         0
Event:       0
Alert:      174

```

Fig. 8. Snort report on second attack

We conduct 2 phase XSS attack, first attack is occurred when snort data is blank, meanwhile on second attack snort data already updated with data form first attack. From figure 7, when IDS not have information about XSS attack, IDS not alerting if there is XSS attack. But this anomaly detected from honeypot log. From this data IDS data updated for XSS attack. After updated with data from first attack, on figure 8 as second attack, snort already know there is an attack. Snort alerting IDS if there is occur XSS attack, and IDS filtering packet from those attack. From 200 XSS attack, 174 attempts is blocked by IDS, but there is 26 attack miss but from snort stat cannot detect it. Suspect this occur due another variant of XSS attack or due case sensitive on snort rule

## VI. CONCLUSIONS

According to the experiment result, automatic rule for XSS attack is succeed. From 2 phase XSS attack, snort rule succeeds generated base on first phase XSS attack. Comparing between 2 phase, on first phase there is no XSS attack succeed blocked, from 200 XSS attack attempt, not single attack is succeeding to block. On second phase IDS succeed blocked 174 XSS attack from 200 XSS attack, its mean 87% attack succeed blocked by IDS. Automatic rule is succeeding generated base on honeypot log data based on first attack

Although automatic rule is succeeding to generate, there is 13% attack is slip from IDS, suspect this caused by case sensitive snort rule. We propose for attack testing do numerous time, also need to develop rule for another attack, such as DOS, U2R, R2L

## REFERENCES

- [1] R. M. Campbell, K. Padayachee, and T. Masombuka, "A survey of honeypot research: Trends and opportunities," *2015 10th Int. Conf. Internet Technol. Secur. Trans. ICITST 2015*, pp. 208–212, 2016.
- [2] Y. Al-Nashif, A. A. Kumar, S. Hariri, G. Qu, Y. Luo, and F. Szidarovsky, "Multi-level intrusion detection system (ML-IDS)," *5th Int. Conf. Auton. Comput. ICAC 2008*, pp. 131–140, 2008.
- [3] S. Bajpai and A. Gupta, "A genetic annealing based new approach for IDS," *Proc. 2017 Int. Conf. Intell. Comput. Control Syst. ICICCS 2017*, vol. 2018–Janua, pp. 42–45, 2018.
- [4] S. Roschke, C. Willems, and C. Meinel, "A security laboratory for CTF scenarios and teaching IDS," *ICETC 2010 - 2010 2nd Int. Conf. Educ. Technol. Comput.*, vol. 1, pp. 433–437, 2010.
- [5] J. Bao, C. P. Ji, and G. Mo, "Research on network security of defense based on honeypot," *ICCSM 2010 - 2010 Int. Conf. Comput. Appl. Syst. Model. Proc.*, vol. 10, no. Iccasm, 2010.
- [6] Guy Podjarny, "XSS Attacks: The Next Wave | Snyk." [Online]. Available: <https://snyk.io/blog/xss-attacks-the-next-wave/>. [Accessed: 02-Aug-2018].
- [7] B. Jacob, "Automatic XSS detection and Snort signatures / ACLs generation by the means of a cloud-based honeypot system," no. December, 2011.
- [8] J. Xi, "A design and implement of IPS based on snort," *Proc. - 2011 7th Int. Conf. Comput. Intell. Secur. CIS 2011*, pp. 771–773, 2011.
- [9] N. Khamphakdee, N. Benjamas, and S. Saiyod, "Improving intrusion detection system based on Snort rules for network probe attack detection," *2014 2nd Int. Conf. Inf. Commun. Technol. ICoICT 2014*, pp. 69–74, 2014.
- [10] A. Garg and P. Maheshwari, "Performance analysis of Snort-based Intrusion Detection System," *ICACCS 2016 - 3rd Int. Conf. Adv. Comput. Commun. Syst. Bringing to Table, Futur. Technol. from Around Globe*, pp. 0–4, 2016.
- [11] M. Baykara, "A Survey on Potential Applications of Honeypot Technology in Intrusion Detection Systems," *Int. J. Comput. Networks Appl.*, vol. 2, no. 5, pp. 203–211, 2015.
- [12] K. Chawda and A. D. Patel, "Dynamic & hybrid honeypot model for scalable network monitoring," *2014 Int. Conf. Inf. Commun. Embed. Syst. ICICES 2014*, no. 978, 2015.
- [13] I. Yusof and A. S. K. Pathan, "Preventing persistent Cross-Site

Scripting (XSS) attack by applying pattern filtering approach,”  
*2014 5th Int. Conf. Inf. Commun. Technol. Muslim World, ICT4M 2014*, 2014.

- [14] M. S. Alam, Q. Javed, M. Akbar, M. R. U. Rehman, and M. B. Anwer, “Adaptive Load Balancing Architecture for SNORT,” pp. 48–52.
- [15] J. Zhai and K. Wang, “Research on applications of honeypot in Campus Network security,” *Proc. 2012 Int. Conf. Meas. Inf. Control. MIC 2012*, vol. 1, no. Mic, pp. 309–313, 2012.

# Substrate Integrated Waveguide Bandpass Filter with Complementary Split Ring Resonator at 2.45 GHz

Dian Widi Astuti

Department of Electrical Engineering  
Universitas Mercu Buana  
Jakarta, Indonesia  
dian.widiastuti@mercubuana.ac.id

Sis Yasin Darmanik

Department of Electrical Engineering  
Universitas Mercu Buana  
Jakarta, Indonesia  
darmanik.frankfurt@gmail.com

Muslim

Department of Electrical Engineering  
Universitas Mercu Buana  
Jakarta, Indonesia  
muslim@mercubuana.ac.id

Mudrik Alaydrus

Department of Electrical Engineering  
Universitas Mercu Buana  
Jakarta, Indonesia  
mudrikalaydrus@mercubuana.ac.id

**Abstract**— Interferences between two applications should be avoided by using a filter. At present, the miniaturized filter is one of the requirement besides good quality and low insertion loss. The sixteenth-mode substrate integrated waveguide (SMSIW) is proposed by using a complementary split-ring resonator (CSRR) to fulfill miniaturized of filter. The filter design used two of sixteenth-mode SIW (SMSIW) that reduced 15/16 of the circular regular SIW. The frequency center filter design is at 2.5 GHz. The simulation result shows insertion loss value at 0.2 dB and return loss value at 29 dB, while for the measurement result gives insertion loss value at 0.7 dB and return loss value at more than 15 dB. It shows the measurement results give good value with the simulation results.

**Keywords**— bandpass filter, complementary split ring resonator, microstrip filter, sixteenth-mode SIW

## I. INTRODUCTION

The modern wireless communication not only requires high performance filters and low-cost fabrication but also needs the compact dimensions of filter. Therefore, many researches were developed using methods to get the compact dimensions, one of which is split ring resonators (SRRs) besides using high permittivity [1] or coupled resonator [2]. SRRs was introduced by Pendry et al [3] in 1999 and it has interested greatly among researchers in electromagnetics communities. The SRR could be applied as the synthesis of metamaterials with negative effective permeability and left-handedness (LH). In 2004, Falcone et al introduced a duality argument, a complementary split-ring resonators (CSRRs) as new metamaterial resonators. CSRRs structure have been proven effectively to evince negative permittivity. The signal propagation is blocked around their resonance frequency [4]. The integration of CSRR and SIW structure can improve the performance of filter [5, 6] besides using defected ground structure (DGS) [7]. For the first time, SIW was introduced by Deslandes et al in 2001 [8, 9]. SIW could be implemented for microwave components.

SIW has gained interest because of its several pre-eminence such as high-quality factor, low-loss, compact, simple integration with other planar circuits such as antenna, amplifier, mixer and so on in one substrate. SIW can be implemented to antennas, filters, couplers, transition, mixers, amplifier and so on. The performance such as dimensions

and bandwidth are also important when we design SIW structure. The improvement of the compact SIW structure with various waveguide topologies has recently been performed using the substrate-integrated folded waveguide (SIFW) for realization bandpass filter as presented in [10]. A metal septum between dual layer substrate permit folding of the waveguide width that minimizes the dimension by a factor of more than two at the expense of slightly larger losses. Besides SIFW, the half-mode SIW (HMSIW) also can minimize dimensions of nearly 50% as a common SIW [11].

The implementation CSRR to the SIW filters structure gives the improvement of filter such as the insertion loss and return loss value either can minimize SIW filter as presented in [12]. By utilizing CSSR array loaded at HMSIW structure, a miniaturized bandpass filter is achieved [13]. While in [14, 15], a quarter-mode SIW (QMSIW) and an eighth-mode SIW (EMSIW) is used by combining low temperature co-fired ceramic (LTCC) to minimize of wideband bandpass filter. The EMSIW also can be used to reduce the dimensions of filter by a factor 7/8 as shown in [16].

This paper presents sixteenth-mode SIW (SMSIW) loaded with CSRR such as shown in [17] for designing bandpass filter for short range device (SRD) application. The SRD frequency application is 2.4 – 2.483 GHz. Usually at the lower frequency need a wide bandpass filter dimension rather than at the higher frequency but by using SMSIW and CSRR method the dimension more 15/16 compact than common SIW filter.

## II. CIRCULAR WAVEGUIDE AND SIXTEENTH MODE SUBSTRATE INTEGRATED WAVEGUIDE

### A. Circular Waveguide

Firstly, we observe a circular waveguide with an inner radius  $a$ , as shown in Figure 1. This metal pipe supports transversal electric (TE) and transversal magnetic (TM) waveguide modes. The cylindrical coordinates are appropriate with the cylindrical geometry itself.



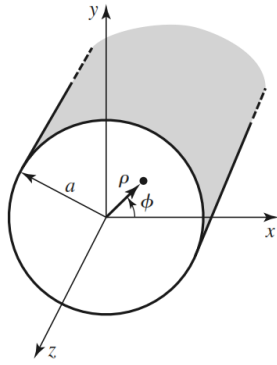


Fig. 1. Geometry of circular waveguide. [18]

The cutoff frequency for TM mode is

$$f_{c_{nm}} = \frac{k_c}{2\pi\sqrt{\mu\epsilon}} = \frac{p_{nm}}{2\pi a\sqrt{\mu\epsilon}} \quad (1)$$

where the several values of  $p_{nm}$  are shown in Table 1.

TABLE I. VALUE OF  $p_{nm}$  FOR TM MODES OF A CIRCULAR WAVEGUIDE [18].

$n$	$p_{n1}$	$p_{n2}$	$p_{n3}$
0	2.405	5.520	8.654
1	3.832	7.016	10.174
2	5.135	8.417	11.620

For the TM modes of the circular waveguide, the lowest cut-off frequency for TM<sub>01</sub> mode, with  $p_{01} = 2.405$ .

### B. Sixteen Substrate Integrated Waveguide (SMSIW)

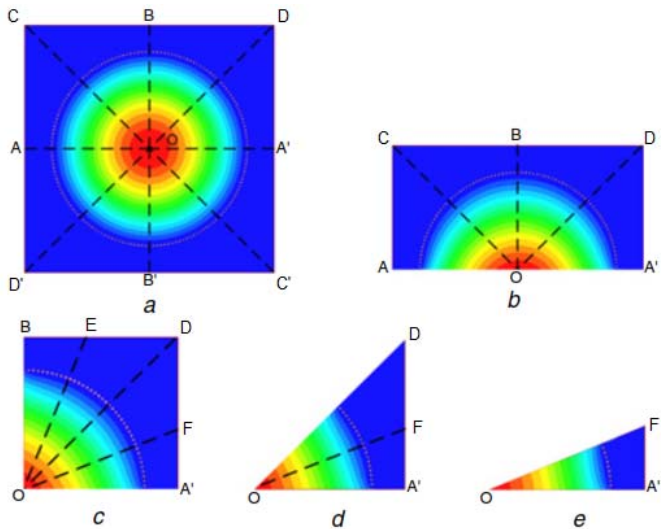


Fig. 2. Simulated electric field distribution with perfect magnetic walls of (a) Common Circular SIW, (b) HMSIW, (c) QMSIW, (d) EMSIW, (e) SMSIW. [17]

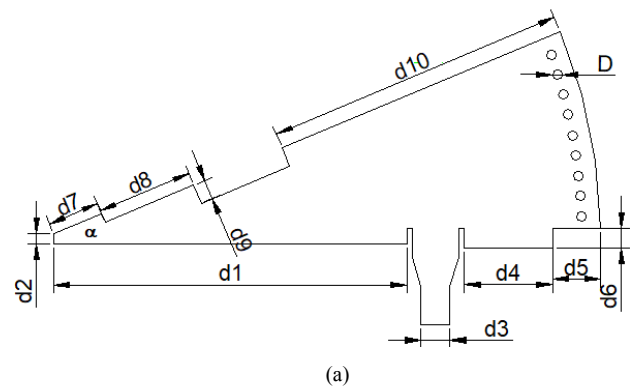
The magnitude of electric field distribution of the TM<sub>010</sub> mode in a common SIW circular cavity, HMSIW, EMSIW, and SMSIW is shown in Figure 2. By bisecting the common SIW circular cavity in Figure 2(a) with another fictional magnetic wall, from A to A', the HMSIW is generated as referred to Figure 2(b). It means the dimensions of the HMSIW is a half of the common SIW circular cavity. As well as the QMSIW is realized by cutting the dimensions HMSIW along fictional magnetic wall from O to B, as shown in Figure 2(c). If the dimensions of QMSIW cuts with another fictional magnetic wall from O to D, the EMSIW will be achieved, as referred to Figure 2(d). The SMSIW is obtained by half-reduction of EMSIW along fictional magnetic wall from O to F, as referred to Figure 2(e). Hence, the SMSIW can be reduced 93.75% compared with common SIW cavity, without changes its resonant frequency. Hence the SMSIW can be applied design for compact microwave component such as a filter.

## III. DESIGN OF BANDPASS FILTER

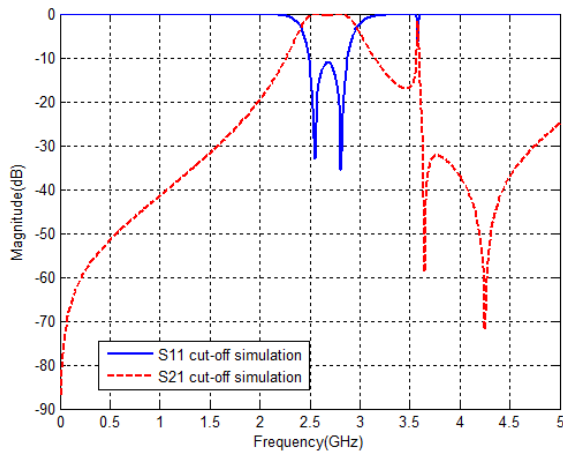
### A. Sixteenth Mode Substrate Integrated Waveguide Circular Cavity

The bandpass filter is designed by using Rogers RT/Duroid 5880 substrate. It has a dielectric constant ( $\epsilon_r$ ) of 2.2, thickness 1.575 mm and loss tangent ( $\tan \delta$ ) 0.0004. In order to make the SMSIW circular cavity, it can be equivalent to common metallic cavity the condition of  $D/d_p \geq 0.5$  and  $D/\lambda_0 \leq 0.1$ . It is to ensure minimum leakage of energy, where  $D$  is the diameter of metallic holes,  $d_p$  is the distance between two adjacent metallic holes and  $\lambda_0$  is the free space wavelength.

Figure 3(a) shown the structure for SMSIW circular cavity with an angel  $\alpha = 22.5^\circ$  and radius  $a = 27.4$  mm. Frequency cut-off can be achieved by equation (1). While Figure 3(b) shows the simulation result of frequency cut-off SMSIW circular cavity. Actually the insertion loss,  $S_{21}$  and the return loss,  $S_{11}$  have good value but the frequency requirement is not suitable with SRD application, and the spurious response occurs at the transmission parameter.





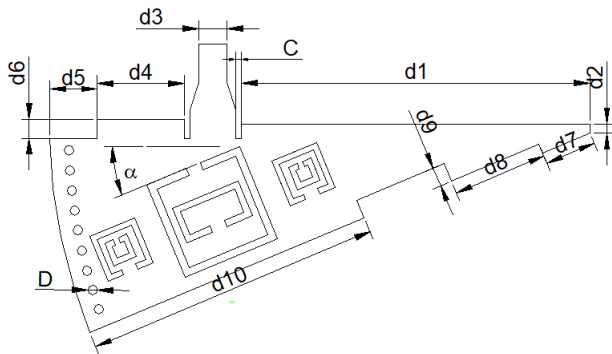


(b)

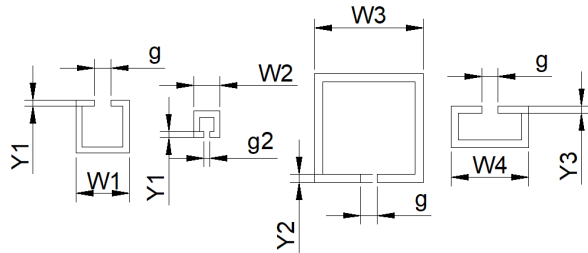
Fig. 3. (a) Proposed design structure of SMSIW, (b) Simulation result of SMSIW circular cavity.

### B. Complementary Split Ring Resonator

Figure 4(a) shows the design of the SMSIW with CSRR. Bandpass filter uses three coupled CSRR that is etching at the top layer. While the detail of parameter CSRR is shown in Figure 4(b).



(a)



(b)

Fig. 4. (a) Design of proposed CSRR-loaded SMSIW (b) Dimension parameter of CSRR.

The parameter values of design are given in Table 2, to fulfil the specification of the bandpass filter for SRD application, which works at 2.4 – 2.483 GHz. The specification was achieved by optimization performed the full-wave electromagnetic simulator-Ansys HFSS v15.

TABLE II. DIMENSION OF BANDPASS FILTER WITH SMSIW CSRR (ALL PARAMETER IN MM)

	Size		Size		Size
d1	18.4	d8	5	W4	3.78
d2	0.5	d9	1	g	0.8
d3	1.5	d10	15.6	g2	0.7
d4	4.6	D	0.6	Y1	0.3
d5	1.9	W1	2.58	Y2	0.4
d6	1	W2	1.28	Y3	0.35
d7	2.75	W3	5.28		

## IV. RESULT AND DISCUSSION

The prototype of bandpass filter is shown in Figure 5. The slot of CSRR are etched at copper layer at the top layer while the bottom layer is a ground layer. The bandpass filter has the symmetrical configuration with two port. The impedance of each port is 50  $\Omega$ .

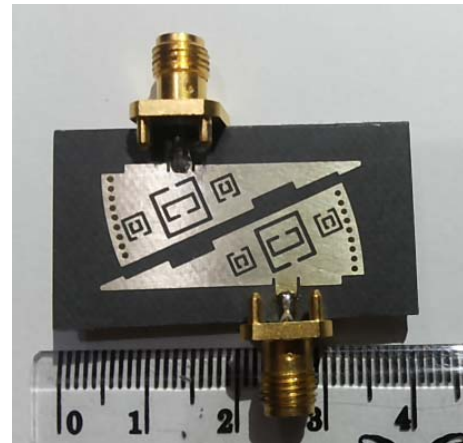


Fig. 5. Prototype of the SMSIW with CSRR.

The fabricated SMSIW bandpass filter with CSRR is measured by using Vector Network Analyzer, Anritsu MS 2026A. Figure 6 shows the comparison of the simulation and measurement results. The dash lines are the simulation results while the solid lines are the measurement. The insertion loss value for the simulation is 0.2 dB and it occur the degradation to 0.5 dB when fabricated. The return loss value is 29 dB for the simulation results and decrease to 17 dB when fabricated. The simulation and the measurement results quite precise as shown by achieving idle values for frequency center and the range of bandpass. Table 3 shows the resume of simulation and fabrication bandpass filter with SMSIW circular cavity.

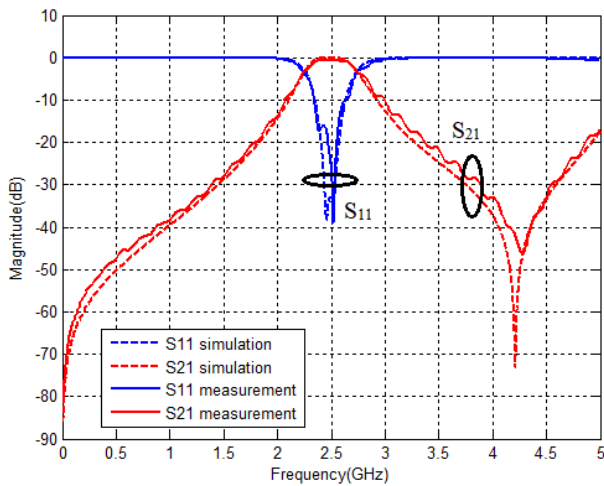


Fig. 6. Simulation and measurement results of SMSIW circular cavity.

TABLE III. COMPARISON BETWEEN SIMULATION AND MEASUREMENT RESULTS OF SMSIW CIRCULAR CAVITY

Parameter	Simulation	Measurement
Pass Band	2.4 – 2.6 GHz	2.4 – 2.6 GHz
Frequency center	2.5 GHz	2.5 GHz
Bandwidth	200 MHz	200 MHz
Insertion loss	0.2 dB	0.7 dB
Return loss	29 dB	17 dB

The overall dimensions of fabricated of SMSIW circular cavity with CSRR has dimension  $33.4 \text{ mm} \times 21.85 \text{ mm} \times 1.575 \text{ mm}$  include two port for microstrip feed lines. While for excluding the two port, it has dimension  $28.6 \text{ mm} \times 13.86 \text{ mm} \times 1.575 \text{ mm}$  which is equivalent to  $0.2383\lambda_0 \times 0.1155\lambda_0 \times 0.0131\lambda_0$ .

## V. CONCLUSION

The reduction dimensions of bandpass filter by using SMSIW with CSRR is achieved 93.75%. The simulation and measurement results gives the insertion loss values below 1 dB and the return loss values more than 15 dB. The little bit of discrepancy between simulation and measurement is mostly due to changes of parameter design when the layout design is converted to fabricate, but the overall results give recommendation for microwave applications.

## ACKNOWLEDGMENT

The authors are very grateful to Indonesia Ministry of Research, Technology and Higher Education, RISTEKDIKTI for supporting and funding this research in skema PDUPT (2018).

## REFERENCES

- [1] D. W. Astuti, Juwanto and M. Alaydrus, "A Bandpass Filter Based on Square Open Loop Resonators at 2.45 GHz" in 2013 IEEE 3rd International Conference on Instrument, Communications, Information Technology and Biomedical Engineering., pp. 147-151.
- [2] M. Alaydrus, D. Widiastuti and T. Yulianto, "Designing Cross-Coupled Bandpass Filters with Transmission Zeros in Lossy Microstrip" in 2013 IEEE 5th Int. Conf. on Information Technology and Electrical Engineering, pp. 1-4.
- [3] J. B. Pendry, A. J. Holden, D. J. Robbins, and W. J. Stewart, "Magnetism from conductors and enhanced nonlinear phenomena," IEEE Trans. Microw. Theory Tech., vol. 47, no. 11, pp. 2075–2084, Nov. 1999.
- [4] F. Falcone, T. Lopetegui, J. D. Baena, R. Marques, F. Martin, and M. Sorolla, "Effective negative-epsilon stopband microstrip lines based on complementary split ring resonators," IEEE Microw. Wireless Compon. Lett., vol. 14, no. 6, pp. 280–282, Jun. 2004.
- [5] W. Che, C. Li, K. Deng, and L. Yang, "A Novel Bandpass Filter Based on Complementary Split Rings Resonators and Substrate Integrated Waveguide," Microwave Optical Technology Letter, vol. 50, no. 3, pp. 699-701, March 2008.
- [6] Q. L. Zhang, W. Y. Yin, S. He, and L. S. Wu, "Compact Substrate Integrated Waveguide (SIW) Bandpass Filter with Complementary Split-Ring Resonators (CSRRs)," IEEE Microwave Wireless Compon. Lett., vol. 20, no. 8, pp. 428-428, Aug 2010.
- [7] D. W. Astuti, A. Jubaidillah, and M. Alaydrus, "Substrate Integrated Waveguide Bandpass Filter for VSAT Downlink," in 2017 IEEE 15th International Conference on Quality in Research (QIR): International Symposium on Electrical and Computer Engineering., pp. 101-105.
- [8] D. Deslandes, K. Wu, "Integrated microstrip and rectangular waveguide in planar form," IEEE Microwave and Wireless Compon. Lett. 2001, Vol. 11, No. 2, pp. 68–70, Feb. 2001.
- [9] D. Deslandes, and K. Wu, "Integrated Transition of Coplanar to Rectangular Waveguides," in 2001 IEEE MTT-S International Microwave Symposium Digest., Vol. 2, pp 619-622.
- [10] N. Grigoropoulos, B. S-Izquierdo, and P. R. Young, "Substrate integrated folded waveguides (SIFW) and filters," IEEE Microwave Wireless Compon. Lett, vol. 15, no. 12, pp. 829-831, Dec. 2005.
- [11] Y. Wang, W. Hong, Y. Dong, B. Liu, H. J. Tang, J. C. Chen, X. Yin, and K. Wu, "Half mode substrate integrated waveguide (HMSIW) bandpass filter," IEEE Microw. Wirel. Compon. Lett., vol. 17, no. 4, pp. 265–267, Apr. 2007.
- [12] Y. D. Dong, T. Yang, and T. Itoh, "Substrate Integrated Waveguide Loaded by Complementary Split-Ring Resonators and Its Applications to Miniaturized Waveguide Filters," IEEE Trans. on Microw. Theory and Techniques. vol. 57. no. 9, pp 2211-2223. Sept. 2009.
- [13] L. Qiang, Q. Sun, W. Zhao, W.-B. Qin, J.-K. Wang, "A Miniaturized Bandpass Filter Based on Half-Mode Substrate Integrated Waveguide Loaded by Complementary Split-Ring Resonators," in 2010 Proc. IEEE International Conference on Ultra-Wideband., vol. 2, pp 1-4.
- [14] Z. Xiangjun, G. Yongxin and Wangfei, "Minimization of Wideband LTCC Bandpass Filter Using QMSIW and EMSIW Cavities," in 2015 IEEE MTT-S International Microwave Workshop Series on Advanced Materials and Processes for RF and THz Applications (IMWS-AMP), pp 1-2.
- [15] S. Chengtian, D. Yabo, Z. Xiangjun, Z. Yanming, and Z. Yong, "Compact wideband LTCC bandpass filter exploiting eighth-mode SIW loaded with CSRR," Microw. Opt. Technol. Lett., vol. 56, no. 9, pp. 2164–2165, Sept. 2014.
- [16] Y. Zhu, "A Source-Load Coupled Bandpass Filter using One-Eight Mode Substrate Integrated Waveguide Cavity," in 2014 XXXIth URSI General Assembly and Scientific Symposium (URSI GASS), pp. 1-4.
- [17] A. R. Azad and A. Mohan, "Sixteenth-mode substrate integrated waveguide bandpass filter loaded with complementary split-ring resonator," Electr. Lett., vol. 53, no. 8, pp 546-547, April 2017.
- [18] D. M. Pozar, Microwave Engineering. 3rd. ed, New York, USA: Wiley, 2004. pp. 121-130

# UUID Beacon Advertisements For Lecture Schedule Information

Wiwin Agus Kristiana  
Faculty of Computer Science  
Narotama University  
Surabaya, Indonesia  
wiwin.agus@narotama.ac.id

Aryo Nugroho  
Faculty of Computer Science  
Narotama University  
Surabaya, Indonesia  
aryo.nugroho@narotama.ac.id

Mochamad Mizanul Achlaq  
Faculty of Computer Science  
Narotama University  
Surabaya, Indonesia  
mochamad.mizanul@narotama.ac.id

Cahyo Darujati  
Faculty of Computer Science  
Narotama University  
Surabaya, Indonesia  
cahyo.darujati@narotama.ac.id

Benediktus Anindito  
Faculty of Computer Science  
Narotama University  
Surabaya, Indonesia  
benediktus.anindito@narotama.ac.id

Moh Noor Al Azam  
Faculty of Computer Science  
Narotama University  
Surabaya, Indonesia  
noor.azam@narotama.ac.id

**Abstract**—Smartphone users are increasingly diverse in using their phones. Some tasks that monitored through the bulletin boards or computer screens, lately it can be done anywhere with a mobile phone while on the move. Similarly, the features in smartphones are increasingly following the development of communication technology. One of them is Bluetooth version 4, which currently can always be available on all types of smartphones. Even for entry-level phones that commonly used by students, nowadays are equipped with the new version of Bluetooth. In this paper discussed the application of BLE or Bluetooth Low Energy, which is part of Bluetooth version 4, to provide the information about availability, lecture schedule, and lecture room at the University Narotama. By using this BLE communication technology all smartphones equipped with BLE, enabling the NARO-MOBILE application and residing in the campus environment, will receive all the latest information provided by SIMNARO - Narotama University Management Information System, in a real-time.

**Keywords**—*Internet of Things, IoT, Internet, Bluetooth, Bluetooth Low Energy (BLE)*

## I. INTRODUCTION

Narotama University is one of the private universities in Indonesia located in Surabaya City. Pawiyatan Gita Patria Foundation in 1981 developed this university for the first time, by beginning the establishment of law faculty in cooperation with lecturers from the Airlangga University.

As one of the 3,276 private universities in Indonesia [1], Narotama has relatively rapid development. Since the late the 1990s, Narotama has launched information technology-based services for all its stakeholders. SIMNARO (Sistem Informasi Manajemen Narotama or Narotama Management Information System) is the name of the developed system which currently has some essential services.

The SIMNARO essential services as follows:

- Academic information system, which is the primary foundation of services to the students. In this system, the students can plan their lectures, choose their classes and get much information about the course that followed.
- ELINA or E-Learning Narotama is an application that uses the Content Management System (CMS) Moodle to use as a basis for online learning over the Internet [2].

- Sistem Informasi Sumberdaya Terintegrasi (SISTER or Integrated Resource Information System), which is a system from the Ministry of Research Technology and Higher Education (Kementerian Riset Teknologi dan Pendidikan Tinggi - Ristekdikti) that is unity in SIMNARO services.
- Quality Assurance Information System, also as one of the primary system because Narotama University has complied with ISO 9001: 2008

As the development of SIMNARO services, this paper has piloted a way to broadcast information to all SIMNARO users in a campus environment via Bluetooth Low Energy (BLE) directly to their smartphone. This method is thought to be quite effective rather than placing information on a bulletin board or asking students to access a server to get the information they need all the time.

## II. BLUETOOTH LOW ENERGY

Bluetooth Special Interest Group (SIG) has defined BLE as part of Bluetooth version 4 which has lower power requirements than previous classical versions of Bluetooth. BLE uses a frequency that is also used by Bluetooth classic, which is 2.4 GHz. Nevertheless, BLE is not compatible with standard Bluetooth in its communications [3].

BLE is primarily designed to transfer data with a small size of data and sparse sending, usually is a simple data, so that the power required is minimal. This design is of course very different from the traditional Bluetooth design, which commonly used earlier. To accommodate the connection between the old model and the new one, Bluetooth SIG then introduces two kinds of trademarks. The first is Bluetooth Smart (BS) for devices that only support BLE, and the second is Bluetooth Smart Ready (BSR) for tools that can work either in Bluetooth classic mode or Bluetooth Low Energy mode.

Currently, a lot of different types of accessories that collaborate with mobile devices such as smartphones, tablets, and notebooks have long used BLE in their standards. Personal devices like smartwatches or others wearable devices are also equipped with Bluetooth 4.0 or later also it has BLE functionality.

Currently, a lot of different types of accessories that collaborate with mobile devices such as smartphones, tablets, and notebooks have used BLE in their standards. Personal devices like smartwatches, smart shoes or others wearable devices are also equipped with Bluetooth 4.0, or later to make

it has BLE functionality. Even on medical devices, BLE also used to help people to live more comfortable and healthy.

The iBeacon is the famous technological name that uses BLE. It introduced by Apple Inc. in middle of 2013. BLE on this device is used to broadcast unique information to the nearest mobile device that has also been equipped with BLE [4]. Equalized to the classical Bluetooth, the iBeacon signal using BLE is expected to have the same coverage area but with lower power consumption.

The application of Indoor LBS or Location Based Services is one of the examples of comprehensive implementation of BLE in iBeacon. The applications inside the BLE observer device (usually smartphone devices) will calculate the strength of RSSI (Received Signal Strength Indication) the BLE signal it receives and then compared to the signal strength during the transmission performed by BLE Broadcaster[3]. The relative distance between the BLE observer and the BLE broadcaster could calculate by using the RSSI or Isotropic loss of free-space radiation calculation (equation 1)[3].

$$\text{RSSI (dBm)} = -10n \log_{10} (d) + A \quad (1)$$

The BLE observer receives all signals transmitted by all nearby BLE broadcasters. Therefore, it is necessary to identify a specific signal received from the BLE broadcaster. Thus, each BLE broadcaster continually sends data in its particular Universal Unique Identifier (UUID) form.

In addition to sending the data in the form of UUID as above, BLE broadcaster also transmits its signal strength. Of all these identifications, the application on the BLE observer can calculate the relative distance of all BLE broadcasters around it.

Currently, most smartphones, with the latest iPhone, Windows Mobile, Blackberry and Android operating systems, are equipped with Bluetooth version 4 compatible with BLE technology. Therefore, all smartphones can perform collaborative operations with iBeacon [3] [5].

#### A. The BLE Stack

BLE has two complementary layers to accommodate the highest performance (Figure 1) and is attributed to the lower layer and the upper layer. These two layers are separated by an adjustable control function from the higher layer to do something on the lower layer.

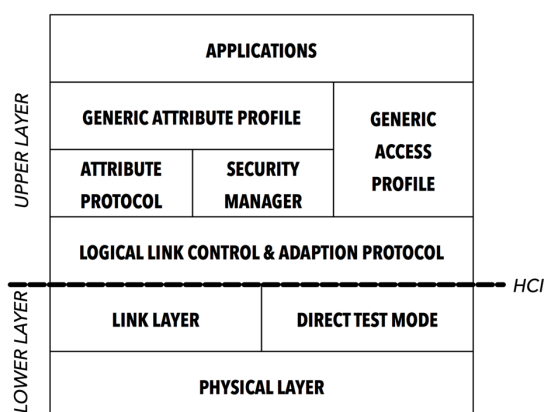


Fig. 1. Bluetooth Low Energy Stack[3-5]

Physical is the most bottom layer, contains an analog communication circuit, and capable of doing the modulating and demodulating analog to digital and vice versa. The radio frequency used is the ISM (Industrial, Scientific, and Medical) band of 2.4 GHz, and partitioned into 40 channels, ranging from 2.4000 GHz to 2.4835 GHz.

Link Layer is the part that interacts directly with the physical layer. This layer is the only real-time hard drive constrained layer of the entire protocol stack since this layer must be responsible for meeting all the time requirements defined by the Bluetooth 4.0 Core specification. Therefore, this layer is usually isolated from the higher layer of the protocol stack by providing an interface that hides the complexity and real-time requirements of the layers above it.

The Link Layer is the element that interacts instantly with it is below layer, that is the physical layer. This layer is the only real-time hard drive layer of the entire protocol stack because this layer must be responsible for meeting all the time requirements specified by the Bluetooth 4.0 core specification. Consequently, this layer usually is isolated from the higher layers of the protocol stack by providing an interface that hides the complexity and real-time requirements of the layers beyond it.

The Logical Link Control and Adoption Protocol have two primary functions, namely multiplexer protocol that gets data from layers above it and then packs it in standard BLE format and vice versa. This layer also performs the fragmentation -if the packet obtained from the above it is more than 27 bytes and then forwarded to the layer below it, and conducts recombination -if it is received from the layer below it some packets and then made a whole package for the layer above it [6-9].

The Attributes Protocol is a manageable stateless client/server protocol used by a BLE device. In the BLE, each device is a client, server, or also perhaps a combination of both, no matter whether it is a master or a slave. A client is a machine that requests data from the server, and a server is a device that gives the data to the client. Each server contains data organized in the form of properties, each of which is assigned a 16-bit attribute, a UUID or Universally Unique Identifier, a pair of permissions information, and multiple of values [9].

The Security Manager Protocol is a combination of a protocol and a series of security algorithms that will conduct the protocol stack capabilities to deliver and exchange security keys. This protocol would enable the device to transfer data securely through an encrypted communication, to ascertain the trust of the identity of the remote device, as well as to mask the Bluetooth Address if it needed.

Generic Attribute Profile is above of ATT. The job is adding hierarchy and data abstraction model above ATT. From the one side, this protocol can be avowed the backbone of BLE data transfer because it describes how the data is prepared and transferred within the applications. GATT represents a general data object that can frequently be used by multiple applications profiles that are known as GATT-based profiles. GATT keeps the same client/server architecture on the ATT layer, but the data is packaged in services, consisting of one or more characteristics. Each characteristic can be recognized as the integration of a piece of user data along with metadata, which includes the description information such as properties, usernames, sections, et cetera. [6-9]



The Generic Access Profile determines how the devices interact with each other at a lower level, beyond the actual protocol stack. GAP can be considered to define the top BLE control layer, given that it determines how the device carry out the control methods such as the discovery of the equipment, connection, the establishment of security, and more, to ensure interoperability and to enable data communication to take place between devices from various vendors. GAP assign different device rules and concepts for organizing and standardizing low-level operation of devices, such as roles and interactions, operational and transition modes, operational procedures for achieving consistent communication, and security aspects, including security modes and processes, also the additional data formats for data non-protocol.

### B. Universal Unique Identifier (UUID)

iBeacon is the first BLE Beacon technology released by Apple. Therefore most beacons take inspiration from the iBeacon data format. In general, the beacon will broadcast four data similar to figure 2. [8][9]

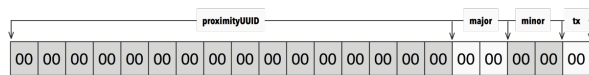


Fig. 2. BLE UUID Format[3-5]

- UUID: 16 bytes of unique data that identifies which beacon that transmit.
- Major: 2 bytes decimal number that could be used to determining the subset number of a large group of beacons within an area.
- Minor: 2 bytes decimal number that could be used to identifying a specific beacon.
- PWR: 1 byte TX power level, indicating the signal strength of the BLE device when transmitted.

The UUID, Major, and Minor data can be used as the location information where is the BLE broadcaster located. Meanwhile, using the PWR information, the application can be calculated relative distance between BLE broadcaster and BLE observer with the calculation of RSSI in equation 1.

By using the calculation of triangulation, the data from several BLE broadcasters that received by the BLE observer can be a clue the current location of the BLE observer somewhere in the room.

### III. UUID ENCODE DESIGN

This research modifies UUID, Major, and Minor contents to broadcast much variety of information through the BLE, especially the information about the status of the courses required by lecturers and students within the Narotama campus.

Meanwhile, the width of the UUID is only 16 bytes in single broadcasting. That is why the data must be encoding first before it broadcasted. The apps that exist within the smartphone as a BLE observer then must first translate the UUID data before it is displayed on the screen.

From some studies, the distance of the BLE signal is limited to only about 20 meters from the broadcaster[3] and will be shorter if there are obstacles around the location. Therefore, broadcasting information with BLE requires multiple BLE broadcasters in one area. This situation occurs in the possibility of overlapping information received by BLE observer from more than one BLE broadcaster. Therefore, the UUID design should be able to anticipate this possibility, so the app does not need to store and display previously received information, which can make the CPU and memory smartphone exhausted.

Figure 3 shows the block diagram of the UUID format used.



Fig. 3. Modified UUID

- DEPT, a 1 byte, is a code of the Department corresponding to the UUID. This information will use by apps to determine whether the UUID data transmission needs to be saved and displayed or forget. This data must be compared to the lecturer or student identification number based on the settings that made by the user.
- CIDN, 3 bytes, is representing the Course Code Identification Number just like the course code in SIMNARO. The name of the course will be stored in SQLite at mobile devices and must be updated by the application if needed.
- LID, 4 bytes, is the Lecturer ID. The LID is representing the staff number ID of Narotama University that all Narotama lecturer also has it. Just like the CIDN, the full name of lecturer will be stored at SQLite and updated by the application if required.
- ROOM, 2 bytes or 4 digit hexadecimal, representing the classroom number. The standard of Narotama in room number is one digit alphabet (A to Z) as the building code and followed by floor and room number. As an example, there is a room on building A at 7th floor and room number 3, so it has called A-701. Therefore the UUID is encoded in 2 forms, the first hexadecimal is the ASCII code for the building alphabet ("A" or 0x41 to "Z" or 0x5A) and then followed by the next three hexadecimal as the numerical (0 through 4095) that representing floor and room number.
- CODE, 1 byte, is representing the Status Code of the class. The code are "0x10" for the class is available, "0x11" class is pending, "0x12" the class is moved, and "0x1F" the class already begins.
- The rest of 5 bytes UUID not used.

Meanwhile, the Major and Minor data fields, which previously used to identify of the grouping of the beacons within a broad group, in this model of information it will use as the data ID of the broadcasted information. This data ID is

required to anticipate the possibility if the data is received more than once by the BLE observer at the smartphone. When it happens, the apps do not necessarily process it as the new information.

In the making of the data ID, it uses two digits of the year followed by two digits of the month and then followed by two digits of the date, and at the end, there will be a sequence number from 0 to 999. This data format is in the decimal form, of course, it has to convert in hexadecimal before its use as the data major and minor. For example, the 157th data that submitted on June 1, 2018, will have the data ID 180601157 or 0xAC3C145 in hexadecimal. So it will be written 0x0AC3 as major and 0xC145 as a minor.

#### IV. THE BROADCASTER

This research used some prototype computer Raspberry Pi 3 which already equipped with Bluetooth version 4 for the broadcasters (figure 4).

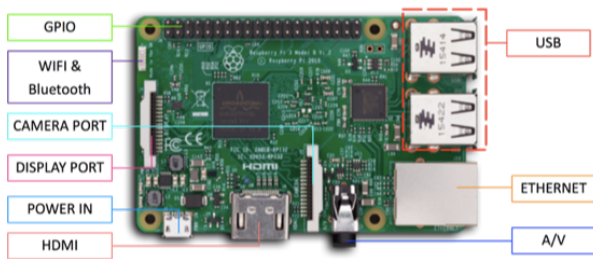


Fig. 4. Raspberry Pi 3 model B

##### A. The Hardware and Network

Raspberry Pi is a single-board prototype computer that low-cost, and high-performance that developed by the UK-based Raspberry Pi Foundation. This foundation concentrates on placing digital power in the hands of people around the world so that the entire world community can understand and shape the ever-growing digital world, can solve their problems, and can use the digital power for their future work.

One that the foundation does is to promote the teaching of basic computer science in schools, especially in developing countries, using this low-cost computer.

The newest version is the Raspberry Pi series 3 model B+, which equipped with:

- A 64-bit quad-core ARM Cortex-A53 CPU with speed at 1.4GHz;
- 802.11ac WiFi LAN;
- Bluetooth 4.2;
- Gigabit Ethernet;
- Power-over-Ethernet support;
- Improved PXE network and USB mass-storage booting; and
- Advanced thermal management

This new Raspberry Pi still carry out 1 GBytes of Random Access Memory (RAM) and also still has four USB slots, HDMI output, and 3.5 mm jack for audio. Besides, for digital communication, this board is provided with 40 pins General-Purpose Input/Output (GPIO) that supports standard communication protocols such as Inter-Integrated Circuit (I2C) and Serial Peripheral Interface (SPI).[10] [11].

The network topology that established in this research using the scheme like figure 5. All BLE broadcasters (Raspberry Pi) not connected as one network of the server farm. It protected from another network to direct access. The access to the BLE broadcaster will be allowed only from the broadcast management server.

The UUID and data ID are constructed on the broadcast management server. It calculates based on the information give by SIMNARO server, the time of the server, and the sequence number of the constructed data broadcast.

The constructed UUID and data ID then will be kept by the broadcast management server to broadcast several times and to several BLE broadcasters as long as the data has permission to transmit. One of the parameters is when the constructed data do not exceed the schedule of the lecture.

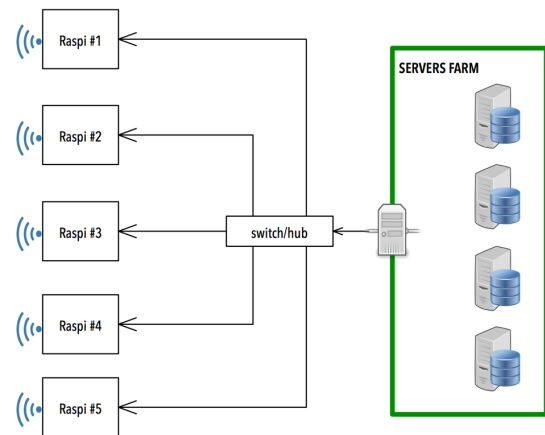


Fig. 5. Experiment Network Topology

##### B. The Logical

In this study, each Raspberry Pi -that acting as a BLE broadcaster, are installed the Application Programming Interface (API) that uses the Python programming language, as the standard programming language for Raspberry Pi [12], and comes with the Django framework for APIs could be accessed by methods communication Hypertext Transfer Protocol (HTTP) [13]. For security reasons, this API is created only accessible by the IP address of the broadcast management server via the Transport Control Protocol (TCP) connection using port 8080.

As described above, the broadcast management server responsible for creating the UUID and the data ID before it sent to Raspberry Pi and then broadcast via BLE. Therefore, the API on Raspberry Pi will only get only three parameters, which are the UUID, the data ID, and the MD-5 hash of all parameters as the security and error protection. The data ID that received by API then will be translated into Major and Minor fields in the data beacons. Meanwhile for the



transmitting signal data field will be filled with the value of 0x00.

When all data ready, these data beacons are broadcasted by Raspberry Pi via the Blue-Z library -the Linux kernel standard library for Bluetooth communication.

The flowchart application for API inside the Raspberry Pi is in figure 6.

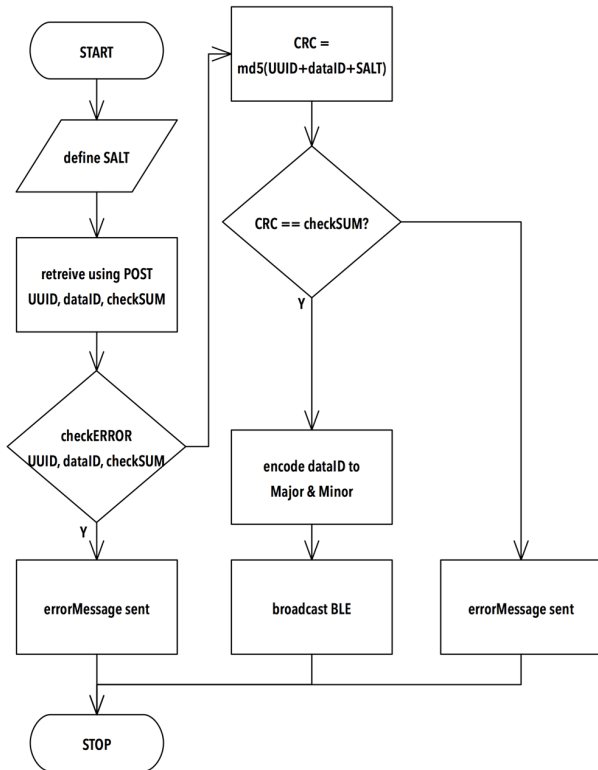


Fig. 6. The Flowchart of BLE Broadcaster

The API will start working when receiving access requests from the broadcast management server. The first API will define a static SALT variable that contains a case-sensitive token. This token must be the same as that in the broadcast management server. Next, the API will perform data retrieval via HTTP with the POST method. API does not access with other methods.

Then the data that has been taken by the API then checked on the variables named UUID, dataID, and CheckSum. All of these variables must be filled with value and should not be empty or contain spaces.

The next step is to calculate the MD-5 hash from the combined the value of UUID, dataID, and the SALT, which is then compared to the contents of the CheckSum variable. If the value is the same, then the process can proceed, but if not then an error message is sent to the sender server, and then the program stops.

If the process passes on, then the dataID separated into 2 bytes data Major and 2 bytes data Minor. As mentioned earlier, Major and Minor data will be as the primary key whether the BLE observer has received the same information or not.

The process then will be ended by broadcasting all the information above and the API back standby receiving requests from the broadcast management server.

## V. THE OBSERVER

In this experiment, we do testing a BLE observer using Xiaomi Redmi 5A smartphone that already equipped with Bluetooth 4.1, using the Android 7.1.2 (Nougat) operating system[14]. These experiments include receiving BLE data signals that are UUID, Major, Minor, and TX strength, as well as translation of UUID into the information displayed on the screen

On the application development side of this research using hybrid programming with Cordova framework[15] and assisted with some plugins that have been available in the market. The main reason for the use of hybrid programming in this experiment is the speed of application development, and the testing does not require advanced programming[16],[17].

### A. The Logical

Figure 7 shows the application logic flowchart on the smartphones.

This application starts by checking on the Bluetooth device. If the device is not active, then the application will show the permission request to the user to activate it, and if the user then allows it then the next step is to turn the Bluetooth device on and then back to the first step, but if the user does not allow it, then the application will stop.

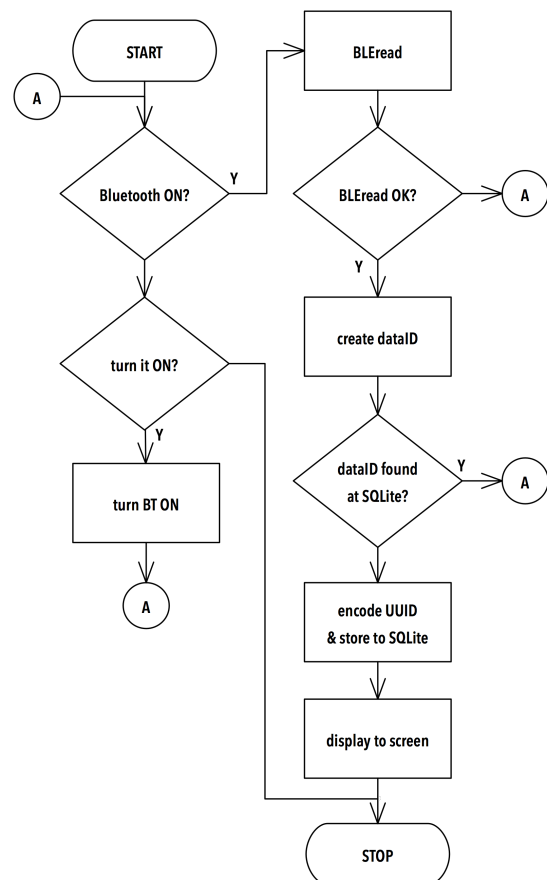


Fig. 7. The Flowchart of BLE Observer

Once the Bluetooth is detected, the next is application execute the method of BLE data read. If this method fails to get the data, it is mean there is no BLE signal captured. Then the application will repeat to the first step. If the method succeeds, then the return value of this method would contain BLE data. The application will get a set of information related to UUID, Major, Minor, and RSSI.

Next, the Major and Minor fields will be translated into the dataID. The results of this translation then use to query in SQLite. If the query found the same of the dataID, it is mean the data is already in the SQLite so then the application will return to the beginning at the origin of the application. If the dataID is not found, then the application will continue in the next step.

When the dataID is not found in SQLite, it means that UUID is not received by BLE observer yet. Therefore UUID needs to decoded to get the required information and store it in the SQLite.

The final step in this application is to show everything that is in SQLite to the screen display. Moreover, the last, application will return to the first step.

### B. The Test Result

In this experiment, the testing of the system is performed by broadcasting several times of data when the smartphone at some locations that covered by the BLE signal. Then observed the BLE signal receiving by the device both when the smartphone is in still position or a move.

The Testing proves that the BLE broadcaster can send the information well, both when smartphones are in a state of immobile, or when the smartphone is in a state of reasonable moves. In all condition, the smartphone can receive the information that broadcasted by Raspberry Pi, decode the UUID to the information, and then display it on the screen.

Figure 8 is the screenshot of smartphones acceptance of the information.



Fig. 8. The Screenshot of Smartphone

Besides testing the concept of broadcasting data via BLE, in this testing also recorded the average RSSI of BLE signal received by the smartphone as the BLE observer and the estimated distance between the smartphone to the Raspberry Pi as a BLE broadcaster without considering the obstacles that exist between them (table 1).

As can be seen in Table 1, the signal strength will decrease if the smartphone away from the Raspberry Pi location. However, in some locations, the declining of the signal can also be caused by an obstacle between the smartphone and Raspberry Pi.

TABLE I. RSSI AND APPROXIMATE DISTANCE

Location	BLE #1	BLE #2	BLE #3	BLE #4	BLE #5
#1	10 m -66dBm	15 m -85dBm	20 m -90dBm	> 30 m N/A	> 30 m N/A
#2	5 m -57dBm	10 m -80dBm	20 m -87dBm	> 30 m N/A	> 30 m N/A
#3	10 m -70dBm	10 m -88dBm	10 m -84dBm	> 30 m N/A	> 30 m N/A
#4	10 m -79dBm	5 m -56dBm	10 m -89dBm	> 30 m N/A	> 30 m N/A
#5	15 m -87dBm	10 m -83dBm	5 m -73dBm	> 30 m N/A	> 30 m N/A
#6	15 m -81dBm	10m -85dBm	15 m -90dBm	20 m -89dBm	20 m N/A
#7	20 m -80dBm	15 m -87dBm	20 m -95dBm	20 m -87dBm	20 m N/A
#8	>30 m N/A	20 m N/A	20 m N/A	15 m -78dBm	15 m -70dBm
#9	>30 m N/A	> 30 m N/A	>30 m N/A	15 m -80dBm	15 m -78dBm
#10	>30 m N/A	> 30 m N/A	>30 m N/A	10m -78dBm	15 m -74dBm
#11	>30 m N/A	> 30 m N/A	>30 m N/A	5 m -55dBm	20 m -85dBm
#12	>30 m N/A	> 30 m N/A	>30 m N/A	10 m -63dBm	5 m -58dBm

## VI. CONCLUSION AND FUTURE WORKS

In this experiment, we have created the mechanism of broadcasting the status and schedule of lectures by using BLE media at Narotama University. This method is sufficient for lecturers and students to know their course schedule without having to move from their positions. With the regular basis broadcasting, no information not received by the students or lecturers as long as they stay within the campus - at an affordable location with BLE broadcaster signals.

Also, because of there is no human involvement required concerning sending or receiving information in this system, the possibility of information being undelivered for the reasons of forgetfulness -as the human nature, can be avoided.

Broadcasting systems that use BLE can load with various data for various purposes, but because of UUID's limited capacity, it is necessary to design the UUID as encoded information as flexible as possible, for all information broadcasting purposes.

The future work of this research is to change the UUID design so that it can be more flexible for the whole purpose of broadcasting information inside the Narotama campus. Because the information required is not just about the schedule and status of the course, but also for other information that supports university roadmaps to become leaders as

universities using information and communication technology.

It even better if we could utilize this system for indoor LBS system too. It because naturally, BLE can use to show the location of a device relative to something around it. So we can have two systems on the same devices.

Other future works that can be developed from this paper are using this encoded UUID concept to broadcast all types of information in a limited location. For example, this encoded UUID concept can be used for communication between sensors and array actuators in a large data center.

## REFERENCES

- [1] Kemristekdikti, Statistik Pendidikan Tinggi Tahun 2017, PT 17, Indonesia, pp. 15, 2017. <https://ristekdikti.go.id/epustaka/buku-statistik-pendidikan-tinggi-2017/>
- [2] L. de la Torre, M. Guinaldo, R. Heradio, and S. Dormido, "The Ball and Beam System: A Case Study of Virtual and Remote Lab Enhancement With Moodle," *IEEE Transactions on Industrial Informatics*, vol. 11, no. 4, pp. 934–945, Aug. 2015. <http://ieeexplore.ieee.org/document/7120976/>
- [3] M. N. Al-Azam, B. Anindito. "BLE Observer Device Menggunakan Raspberry Pi 3 untuk Menentukan Lokasi BLE Broadcaster." [BLE Observer Device Using Raspberry Pi 3 to Determine the BLE Broadcaster Location], *Prosiding SNATIF, Indonesia*, 2016, pp. 181–188, 2016. <http://jurnal.umk.ac.id/index.php/SNA/article/view/646> [in Bahasa Indonesia]
- [4] S.M.H. Sharhan, S. Zickau. "Indoor mapping for location-based policy tooling using bluetooth low energy beacons." *Wireless and Mobile Computing, Networking and Communications (WiMob) Proceedings*, 19–21 October 2015 (Abu Dhabi, United Arab Emirates, 2015). IEEE, pp. 28–36, 2015. <http://ieeexplore.ieee.org/document/7347937/>
- [5] Y. Yang, Zhouchi Li, K. Pahlavan. "Using iBeacon for intelligent in-room presence detection". *Cognitive Methods in Situation Awareness and Decision Support (CogSIMA) Proceedings*, 21–25 March 2016, San Diego, CA, USA, 2016. IEEE, pp. 187–191, 2016. <http://ieeexplore.ieee.org/document/7497808/>
- [6] J. Nieminen, T. Savolainen, M. Isomaki, B. Patil, Z. Shelby, C. Gomez. "IPv6 over BLUETOOTH(R) low energy." *Internet Engineering Task Force (IETF), RFC7668*, 2015. <https://tools.ietf.org/html/rfc7668>
- [7] R. Tabata, A. Hayashi, S. Tokunaga, S. Saiki, M. Nakamura, S. Matsumoto, "Implementation and evaluation of BLE proximity detection mechanism for pass-by framework." *International Conference on Computer and Information Science (ICIS)*, 26–29 June 2016, Okayama, Japan, 2016. IEEE, pp. 1–6, 2016. <http://ieeexplore.ieee.org/document/7550872/>
- [8] M. N. Al-Azam, M. M. Achlaq, A. Nugroho, A. Gabriel Soai, A. Winaya, and Maftuchah, "Broadcasting the Status of Plant Growth Chamber using Bluetooth Low Energy," *MATEC Web of Conferences*, vol. 164, p. 01029, 2018. <https://doi.org/10.1051/mateconf/201816401029>
- [9] K. Townsend, R. Davidson, Akiba, and C. Cuff, "Getting started with Bluetooth low energy: tools and techniques for low-power networking", Revised First Edition. Sebastopol, CA: O'Reilly, 2014. <http://shop.oreilly.com/product/0636920033011.do>
- [10] M. M. Achlaq, M. N. Al-Azam, A. Winaya, Maftuchah, "Nawala Mangsa 2.0—Weather Station with BLE Broadcaster", *Journal of Telematics and Informatics (JTI)*, Vol 6, No 2, June 2018, 2018. <http://section.iaesonline.com/index.php/JTI/article/view/448>
- [11] E. Upton, G. Halfacree. "Raspberry Pi user guide." New Jersey: Willey Publishing. pp. 4. 2014. <https://www.wiley.com/en-us/Raspberry+Pi+User+Guide%2C+4th+Edition-p-9781119264361>
- [12] S. Monk, "Programming the Raspberry Pi: getting started with Python, Second Edition." New York: McGraw Hill Education, 2016. <https://www.amazon.com/Programming-Raspberry-Pi-Second-Getting/dp/1259587401>
- [13] C. Darujati, M. Hariadi. "Facial motion capture with 3D active appearance models". *The 3rd International Conference Instrumentation, Communications, Information Technology, and Biomedical Engineering (ICICI-BME)*, 7–8 November 2013 (Bandung, Indonesia, 2013). IEEE, pp. 59–64, 2014. <http://ieeexplore.ieee.org/document/6698465/>
- [14] A. Nugroho, S. Sumpeno, M. H. Purnomo, "Visualizing Interaction in Catfiz Indonesian Messenger Using Graph Coloring", *NICOGRAPH International* 2015, pp. 1234–1237, 2015. [https://www.researchgate.net/publication/279200763\\_Visualizing\\_Interaction\\_in\\_Catfiz\\_Indonesian\\_Messenger\\_Using\\_Graph\\_Coloring](https://www.researchgate.net/publication/279200763_Visualizing_Interaction_in_Catfiz_Indonesian_Messenger_Using_Graph_Coloring)
- [15] J.M. Wargo. *PhoneGap essentials: Building cross-platform mobile apps*. Boston: Addison-Wesley (2012). pp. 45. <https://www.amazon.com/PhoneGap-Essentials-Building-Cross-platform-Version/dp/0321814290>
- [16] Cordova. Cordova plugin for ibeacon. Mobile apps with HTML, CSS & JS [online] from <https://www.npmjs.com/package/cordova-plugin-ibeacon>. [Accessed on 7 December 2017]
- [17] T. S. Sollu, Alamsyah, M. Bachtar, and A. G. Soai, "Patients' Heart Monitoring System Based on Wireless Sensor Network," *IOP Conference Series: Materials Science and Engineering*, vol. 336, p. 012009, Apr. 2018.

# Comparative Performance Analysis of Linear Precoding in Downlink Multi-user MIMO

Subuh Pramono

Department of Electrical Engineering  
Universitas Sebelas Maret  
Surakarta, Indonesia  
subuhpramono@staff.uns.ac.id

Eddy Triyono

Department of Electrical Engineering  
Politeknik Negeri Semarang  
Semarang, Indonesia

**Abstract**—This paper investigates the comparative performance of linear precoding schemes. The linear precoding schemes are including block diagonalization (BD), zero forcing (ZF), and maximum ratio transmission (MRT) in downlink multi-user MIMO. This work delivers the performance of linear precoding in term of achievable sum rate and bit error rate (BER) with a variation of the signal to noise ratio (SNR) and the number of transmitter-receiver antennas. We suppose that the transmitters have a complete channel state information. The results show that the MRT precoding yields better bit error rate than both the BD and ZF precoding schemes. However, the ZF precoding generates better achievable sum rate than the MRT precoding. In the other side, the MRT precoding also outperforms when the number of active users is bigger than  $K_{\text{cross}}$  while the number of active users is less than  $K_{\text{cross}}$  the ZF precoding is still dominant.

**Keywords**—precoding, maximum ratio transmission, zero forcing, block diagonalization, BER, sum rate

## I. INTRODUCTION

Recently, the number of users on mobile communication system is exponentially increasing. Users need a higher data rate (gigabit per second), low latency and full mobility communication services. Mobile communication technology has to transform their infrastructure to accommodate the demands. Mobile communication system is now moving into 5<sup>th</sup> generation. The 5<sup>th</sup> generation is operating on the millimeter wave spectrum to reach a wider bandwidth but there are some wave propagation challenges. In addition, the 5<sup>th</sup> generation also deploys the newest subsystems on its infrastructure, one of them is an antenna subsystem. The newest mobile communication technology is implementing a multiple-input multiple-output (MIMO) antenna subsystem. The MIMO antenna is transformed into a massive MIMO antenna when a large number of the antenna in one transmitter. The massive MIMO have some advantages in term of channel capacity, spectral efficiency, interference minimization and link reliability [1]. The massive MIMO has been a hot issue of research due to its capability to increase capacity, spectral, reliability and minimize the interference. The transmitter is equipped with large number antennas (massive MIMO) serves a several single or multiple receiver antennas users, it is called a multi-user MIMO. Several users are served simultaneously, there is multipath between transmitter and receiver. Interference could potentially appear under these conditions.

The advancement of massive MIMO could be realized by adding a precoding/beamforming subsystem. The precoding plays a key role in multi-user MIMO signal processing. The precoding consists of two types which are non-linear and linear. Many previous studies have reported the performance of both non-linear and linear precoding in multi-user MIMO. The authors in [2] delivered the performance of zero forcing precoding. In [3], the authors analyzed the comparison between vector normalization and matrix normalization for maximum ratio transmission precoding. Meanwhile, the author in [4] investigated the performance of minimum mean-square error (MMSE) detector and zero forcing in term of spectral efficiency in downlink massive MIMO. In [5], the authors discussed the performance of statistical and imperfect channel state information (CSI) combination for non-linear precoding in downlink massive MIMO. In [6], the authors optimized the average minimum mean square error (AMMSE) detector with imperfect CSI in multi-user MISO (multiple-input single-output).

This paper investigates the linear precoding with complete channel state information-transmitter (CSIT) in downlink multi-user MIMO. Linear precoding is including block diagonalization (BD), maximum ratio transmission (MRT) and zero-forcing (ZF).

This paper is organized as follows. The introduction, previous works, and background of this research are delivered in section I. The multi-user MIMO system model of this work is detailed in section II. The results and discussion of linear precoding performance will be presented in Section III. Section IV will conclude this work.

## II. SYSTEM MODEL

This work uses a single cell model. Fig 1 depicts the single cell model. The transmitter is equipped with multiple antennas. The transmitter has perfect CSI for all users. The channel of multi-user MIMO uses Rayleigh channel model. The channel that coupling the transmitter and the users is depicted in Fig. 2. In addition, the precoding position is also shown in Fig. 2. The system model of this work in detail is described in Fig. 3.

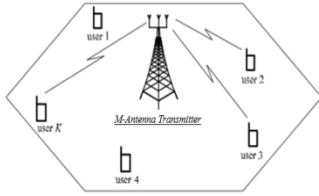


Fig. 1. Multi-user MIMO transceiver (single cell)

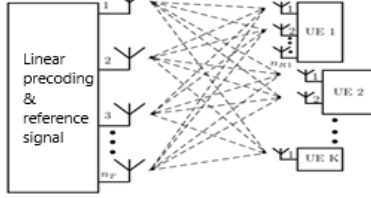


Fig. 2. Precoding subsystem

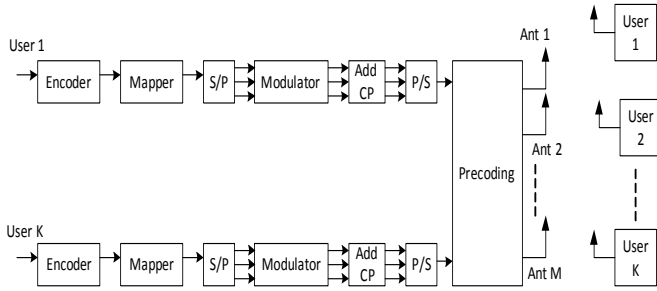


Fig. 3. Multi-user MIMO system model

Consider the downlink multi-user MIMO channels with K-single antennas users are served by a transmitter that equipped with M antennas. The transmitter simultaneously serves K number of  $J_k$  antennas users. The channel matrix between the  $k^{\text{th}}$  user to the transmitter is modeled as follows [3][7]:

$$H_k = \begin{bmatrix} h_{11} & h_{12} & \dots & h_{1M} \\ h_{21} & h_{22} & \dots & h_{2M} \\ \vdots & \vdots & \ddots & \vdots \\ h_{J_k 1} & h_{J_k 2} & \dots & h_{J_k M} \end{bmatrix} \quad (1)$$

$$H = [H_1^T H_2^T H_3^T \dots H_{k-1}^T H_k^T]^T \quad (2)$$

where,  $H_k \in \mathbb{C}^{J_k \times M}$  is multi-user MIMO channel matrix response between the transmitter and  $k^{\text{th}}$  user.  $H$  is the multi-user MIMO system channel matrix.  $Y_k$  is the received signal of  $k^{\text{th}}$  user which is formulated by [7]:

$$Y_k = H_k P_k S_k + H_k \sum_{a=1, a \neq k}^K P_a S_a + n_k \quad (3)$$

$S_k$  is the  $k^{\text{th}}$  user transmission symbol vector with a set  $[S_k^1 S_k^2 S_k^3 \dots S_k^{r_k}]$ .  $n_k$  is the  $k^{\text{th}}$  user additive white Gaussian noise (AWGN) with  $\sigma^2$  variance and zero-mean.  $P_k$  is the precoding matrix for  $k^{\text{th}}$  user.  $P = [P_1 P_2 P_3 \dots P_{k-2} P_{k-1} P_k]$  is a set of precoding multi-user MIMO system.  $S = [S_1^T S_2^T S_3^T \dots S_{k-1}^T S_k^T]^T$  is a set of transmission symbol of system.

Block diagonalization consists of two single value decomposition (SVD) operations. The first SVD operation will

eliminate the multi-user interference (MUI) from the other users. The second SVD operation is applied in parallel user's data stream to maximize the precoding gain.

$$\tilde{H}_k = [H_1^T \dots H_{k-1}^T H_{k+1}^T \dots H_K^T]^T \quad (4)$$

$$H_i P_k = 0, i \neq k \quad (5)$$

SVD decomposition of  $\tilde{H}_k$  is described as follows:

$$\tilde{H}_k = \tilde{U}_k \tilde{\Sigma}_k [\tilde{V}_k^{(1)} \tilde{V}_k^{(0)}]^H \quad (6)$$

Where  $\tilde{V}_k^{(0)}$  is a singular matrix with zero singular value and  $\tilde{V}_k^{(1)}$  is a singular matrix with non-zero singular value.

$$P = [\tilde{V}_1^{(0)} \tilde{V}_1^{(1)} \tilde{V}_2^{(0)} \tilde{V}_2^{(1)} \dots \tilde{V}_{K-1}^{(0)} \tilde{V}_{K-1}^{(1)} \tilde{V}_K^{(0)} \tilde{V}_K^{(1)}] \quad (7)$$

$$y = HPS + n = \begin{pmatrix} H_1 P_1 & H_1 P_2 & \dots & H_1 P_K \\ H_2 P_1 & H_2 P_2 & \dots & H_2 P_K \\ \vdots & \vdots & \ddots & \vdots \\ H_K P_1 & H_K P_2 & \dots & H_K P_K \end{pmatrix} S + n \quad (8)$$

$$= \begin{pmatrix} H_1 P_1 & 0 & \dots & 0 \\ 0 & H_2 P_2 & \dots & 0 \\ \vdots & \vdots & \ddots & \vdots \\ 0 & 0 & \dots & H_K P_K \end{pmatrix} S + n$$

Maximum ratio transmission (MRT) and zero forcing (ZF) precoding have been often implemented for multi-user MIMO signal processing because of a good performance and implementation simplicity. The precoding weight of ZF and MRT can be formulated by as follows, respectively [7][8].

$$W_{ZF} = H^H (HH^H)^{-1} = f_1 f_2 f_3 \dots f_K \quad (9)$$

$$W_{MRT} = H^H = f_1 f_2 f_3 \dots f_K \quad (10)$$

with K (the number of active users) and a large number of N (the number of antennas at the transmitter), the signal to interference plus noise ratio of  $k^{\text{th}}$  user, ZF and MRT precoding, is formulated as follows, respectively[7]:

$$SINR_{ZF, k^{th} user} = \frac{P_d(N-K)}{K} \quad (11)$$

$$SINR_{MRT, k^{th} user} = \frac{P_d N}{K(P_d + 1)} \quad (12)$$

Every active user in downlink multi-user MIMO has an achievable sum rate that is described as follows:

$$R_k = \text{Log}_2(1 + SINR_k) \quad (13)$$

The achievable sum rate of K users is formulated as :

$$R_{sum, K users} = K * \text{Log}_2(1 + SINR_k) \quad (14)$$

Formula (14) was applied in zero forcing, maximum ratio transmission, and block diagonalization precoding, there were described as follows, respectively[7][8]:

$$R_{ZF} = K * \text{Log}_2(1 + SINR_k^{ZF}) \quad (15)$$

$$R_{ZF} = K * \text{Log}_2\left(1 + \frac{P_d(N-K)}{K}\right) \quad (16)$$

$$R_{MRT} = K * \text{Log}_2(1 + SINR_k^{MRT}) \quad (17)$$

$$R_{MRT} = K * \log_2 \left( 1 + \frac{P_d N}{K(P_d + 1)} \right) \quad (18)$$

$$R_{BD} = w_{s,H_j} p_{j=0,i \neq j} \max \log_2 \left| I + \frac{1}{\sigma_n^2} H_s P_s W_s^* P_s^* \right| \quad (19)$$

### III. RESULTS AND DISCUSSION

In section III, this work delivers the performance of linear precoding in term of bit error rate (BER) and sum rate with a variation of SNR, a number of transmitter antennas, and a number of users.

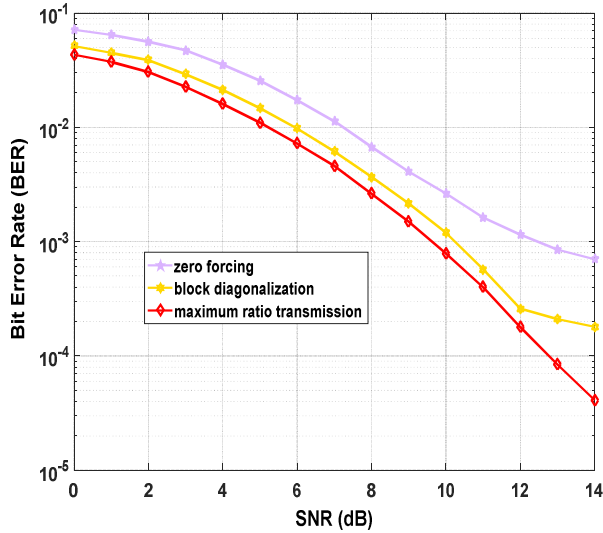


Fig. 4. BER performance with (2,2) x 4 antenna configuration

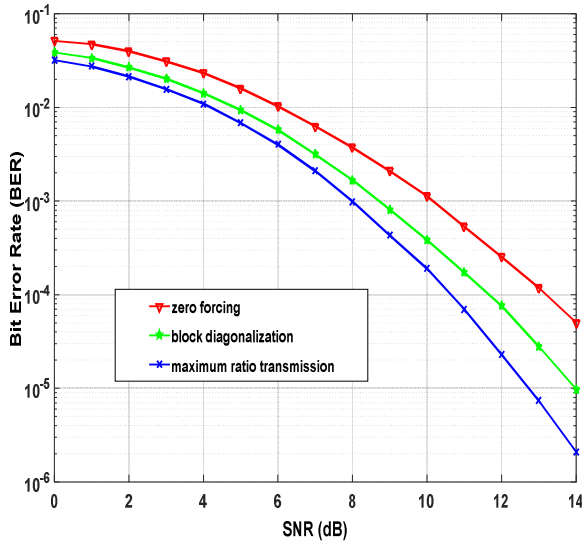


Fig. 5. BER performance with (3,3) x 6 antenna configuration

The results in Fig.4 and Fig.5 depict the comparison of BER performance of BD, ZF, and MRT precoding. The BER performance with variation of a transmit signal to noise ratio (SNR) is plotted. In Fig.4, we use the antenna configuration (2,2) x 4, while Fig.5 uses a (3,3) x 6 antenna configuration,

respectively. We can see from Fig.4 and Fig.5, a bigger number of transceiver antennas produce better BER, at specific SNR 12 dB the (2,2) x 4 antenna configuration generates BER  $1.34 \cdot 10^{-4}$  (MRT) and the (3,3) x 6 antenna configuration yields BER  $1.87 \cdot 10^{-6}$  (MRT), respectively. There is about  $10^{-2}$  of BER refinement. The MRT precoding also needs lower SNR than the ZF and BD precoding. For specific BER  $10^{-4}$  at the (3,3) x 6 antenna configuration, MRT precoding needs about 10.3 dB of SNR while ZF and BD need about 13.5 dB and 11.6 dB. There are 3.2 dB and 1.3 dB of precoding gain. Furthermore, the MRT also has a lower computational complexity.

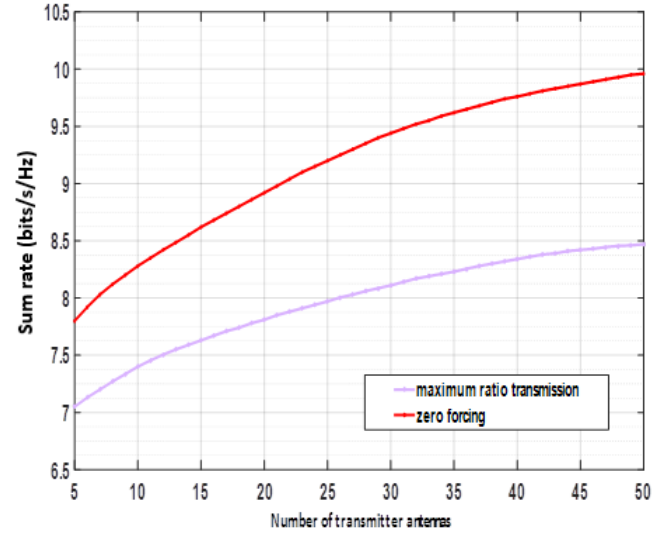


Fig. 6. Performance of achievable sum rate versus the number of transmitter antennas

Based on Fig.6, the results depict the performance of the achievable sum rate for both ZF and MRT precoding. Increasing the number of transmitter antennas lead the achievable sum rate will increase. In addition, a comparison of two precoding schemes indicates that ZF precoding yields higher sum rate than maximum ratio transmission precoding in multi-user MIMO system with equal power per user on downlink transmission.

In Fig 7, we illustrate the achievable sum rate as a function of the transmit SNR for both ZF and MRT precoding in downlink multi-user MIMO. We use the number active user ( $K$ ) = 4 and the number of transmitter antennas ( $M$ ) = 6. The MRT precoding outperforms at the low SNR, particularly 0 to 9.2 dB. The SNR 9.2 dB to be a turning point, ZF precoding gives better performance than MRT precoding at SNR 9.2 to 15 dB.



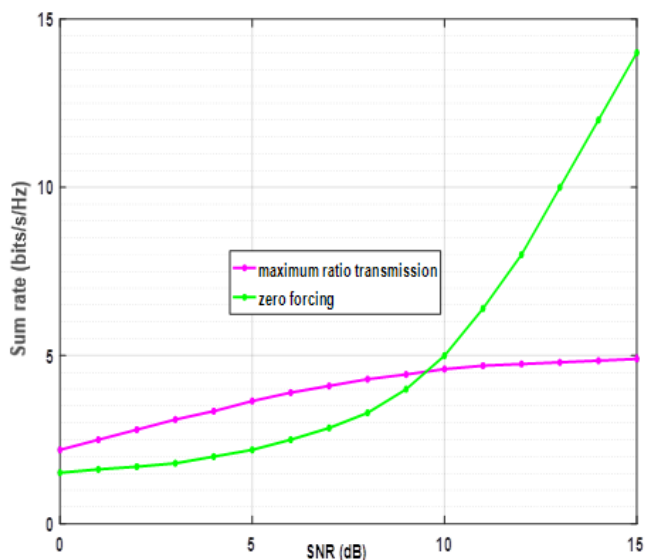


Fig. 7. Performance of achievable sum rate with a variation of SNR

Fig. 8 shows the comparison of the achievable sum rate as a function of a number of active users for both MRT and ZF precoding schemes with  $-6$  dB of power transmit SNR in downlink multi-user MIMO. As mentioned previously, in low SNR categories, the MRT precoding generates a better result with the number active users are larger than  $K_{\text{cross}}$  point,  $K_{\text{cross}}$  point was the number of active users that caused the curve of MRT and ZF were crossed. The MRT precoding performs increasingly as  $K$  increases. Whereas, the ZF precoding performance decreases as  $K$  increases.

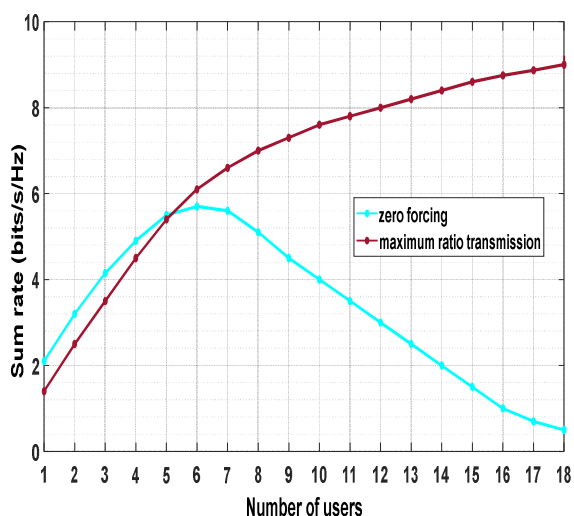


Fig. 8. Performance of achievable sum rate versus the number of active users

#### IV. CONCLUSIONS

This paper provides the comparison and analysis of linear precoding in single cell downlink multi-user MIMO. The investigated parameters are the bit error rate and the achievable sum rate with a variation in the number of active users and signal to noise ratio. Simulation results show that the MRT precoding scheme creates a better bit error rate. Meanwhile, The ZF precoding scheme gives better achievable sum rate. In addition, when a large number of active users is achieved (active users  $> K_{\text{cross}}$ ) that the MRT precoding yields better achievable sum rate than the ZF precoding.

#### REFERENCES

- [1] J.C. Guey, P. K. Liao, Y.S. Chen, A. Hsu, C. H. Hwang, G. Lin, "On 5G radio access architecture and technology [Industry Perspectives]," IEEE Wireless Communications, vol. 22, no. 5, October 2015.
- [2] L. Zhao, K. Zheng, H. L. H. Zhao, W. Wang, "Performance Analysis for Downlink Massive MIMO System with ZF precoding," Transactions on Emerging Telecommunications Technologies, vol.8, no.3, pp. 390-398, 2014.
- [3] Y. G. Lim, C. B. Chae, G. Caire, "Performance Analysis of Massive MIMO for Cell-Boundary Users," IEEE Transactions on Wireless Communications, vol.14, no.12, pp. 6827-6842, 2014.
- [4] H. Quoc Ngo, "Massive MIMO: Fundamentals and System Designs," Linköping University, Sweden, 2015.
- [5] S. Qiu, D. Chen, D. Qu, K. Luo, T. Jiang, "Downlink Precoding with Mixed Statistical and Imperfect Instantaneous CSI for Massive MIMO Systems," IEEE Transactions on Vehicular Technology, vol. 67, no. 4, pp. 3028 – 3041, 2018.
- [6] H. Joudeh, B. Clerckx, "AMMSE Optimization for Multiuser MISO Systems with Imperfect CSIT and Perfect CSIR," Proceedings of IEEE Global Communications Conference, pp. 3308 – 3313, 2014.
- [7] Y. Zhang, J. Gao, Y. Liu, "MRT precoding in downlink multi-user MIMO systems," EURASIP Journal on Wireless Communications, vol. 241, October 2016.
- [8] C. D. Ho, H. Q. Ngo, M. Matthaiou, T.Q. Duong, "On the Performance of Zero-Forcing Processing in Multi-Way Massive MIMO Relay Networks," IEEE Communications Letters, vol. 21, no. 4, pp. 849 – 852, 2017.

# Application of LoRa WAN Sensor and IoT for Environmental Monitoring in Riau Province Indonesia

Evizal Abdul Kadir<sup>1</sup>, Akmar Efendi<sup>2</sup>, Sri Listia Rosa<sup>3</sup>

<sup>1,2,3</sup>Department of Informatics Engineering, Faculty of Engineering, Universitas Islam Riau  
Jl. Kaharuddin Nasution, Pekanbaru, Riau, Indonesia 28284  
email: evizal@eng.uir.ac.id, akmarefendi@eng.uir.ac.id, srilistiarosa@eng.uir.ac.id

**Abstract** — Land and forest fires especially in Riau Province, Indonesia, have affected the length and breadth of Indonesia. The fires are normally hampered by seasonal dry conditions such as El Nino effect. In addition, the haze has affected the neighboring countries such as Malaysia, Singapore and south of Thailand. The effects of haze on human health as reported in that particular year were about 20 million people have suffered from respiratory problems and serious deterioration in overall health. There were other effects on environment, economy, flora and fauna in Southeast Asia region due to this disaster. This research proposes to develop a smart monitoring system using Long Range Wide Area Network (LoRa WAN) with low power wireless data communication and Internet of Things (IoT) technology. With LoRa technology, data can be transmitted up to 30 miles which is worthwhile to cover some of Riau Province that have been badly impacted by this disaster. In this article propose to develop sensors system that capable of detecting land and forest fire. The sensors will be located at several locations that has badly impacted previously. LoRa IoT Technology will be deployed to provide a platform for connecting the sensors. An early indication of land or forest fires is vital for quick prevention before they become uncontrollable and overwhelming. The design and development of LoRa sensors give high feasibility to overcome current issues in Riau Province because of land and forest fire.

**Index Terms** — LoRa WAN, IoT, Sensors, Monitoring

## I. INTRODUCTION

Indonesian suffer from badly haze due to land and forest fires that happen almost every year. The location of Indonesia at equatorial causes this country to have longer dry season spans from April to October. Riau province is one of the state that has high threat to land and forest fire due to peatland, particularly in industrial forest areas. Most of the fires occurring in peat forests are serious due to the characteristics of peat which is easily flamed due to continuous dry season. It has been reported that the total economic loss for Riau province in year 2015 due to this disaster was about USD1.65 billion. More worst when it has huge impact on local environment, flora, fauna and human health. Elderly people and children are severely affected due to haze. Furthermore, the impact of this land forest fire is not only in Indonesia or Riau Province but also has caused deterioration in air quality and human health problem in others countries like Malaysia and Singapore. Current detection method is using satellite to detect any hotspot of land and forest fires. Such data however may not sufficient as the satellite cannot provide fine hotspots detection at other potential areas. The local authorities are normally depending on the satellite imagery to make a

decision or report from local community and company that operation exploiting the lands [1, 2].

Rapid development and evolution in wireless network technology has dramatically changed and improved the natural environmental monitoring system from satellite to ground level detection methods such as Wireless Sensor Network (WSN) [3, 4]. New data for environmental applications and vital hazard warning such as land and forest detection and flood detection can be provided by such systems. The advantages of ground level detection can be categories in three aspects [5-7]: Sensor Nodes; low-cost, low power, robust, low pollution and environmental disturbance; Communication; low data rate, long range and error detection and correction; Computing; small OS for nodes, microcontrollers and low power system. With the emergence of IoT and Long Range (LoRa) Technology [8-10], the wireless sensor network and connectivity become more reliable, robust and quicker. With these technologies, a smart monitoring system for land and forest fire detection can be developed [11-13].

Therefore, in this research focus on developing ground level smart monitoring system to detect and monitor the environmental behavior in term of temperature, humidity and gasses. Proposing a new technology for monitoring system using low power wireless data communication with LoRa-IoT technology. The integration of sensors with LoRa technology would have an effect to local community where people could access the information through developed real-time database in anytime. This ground level detection method will be deployed in other areas, regions and states in Indonesia. It is anticipated to be quicker and cheaper solution than to satellite data acquisition and this would definitely be beneficial to social welfare and economy development. In addition, the development of real-time database would also require some support from them as a policy maker to understand how the system works and also understand the pattern of the results so that an appropriate action can be taken.

## II. LORA WAN MONITORING SYSTEM DEVELOPMENT

Monitoring system is widely use in detection of object or parameters that require continuous in time. Nowadays, many kind of monitoring system based on aim and objective as well as parameters to be monitor. Environmental monitoring for

fire detection is implemented in some of institution or agency to monitor latest status of environmental. Current technology using is mostly from satellite data to detect hotspot of fire, this technology has some weakness and limitation such as only detect when fire already happen and in some case for example in bad weather or cloudy then satellite unable to penetration of cloud and image will not update. New method proposes in this system is use LoRa wireless sensor and IoT. LoRa sensor deploy in the area with high risk of fire to collect data such smoke detection, temperature, particle changing, etc. All the information collected by sensors send to sensor base station as gateway to transfer data collected from monitoring system (data center) because the distance between sensor base station to monitoring system very far away up to 200 km in some area to monitor. To achieve accurate data large number of LoRa sensors will deploy around the area because long range sensor be able to transmit data up to 15 km, mean a base station covering 15 km radius. LoRa sensor based on IoT technology that recently many industries introduced because of advantage long range and low power. Beside LoRa sensor, in every base station attached with high definition camera to analyze sky (environmental) image before and after fire then training data to analyze any changing of environmental image.

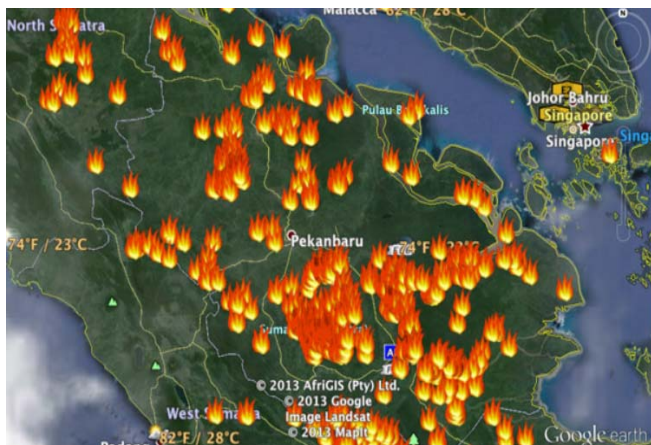


Fig. 1. Riau map and number of hotspots based on satellite image [4].

The selected sites which is high potential for forest fire decided as shows in Fig. 1, where the systems will be installed were chosen by previously obtained the approval of the local authorities such as Riau Local Council and the Ministry of Environment and Forestry Indonesia. Again, the established links between Islamic University of Riau with local authorities is necessary for integrating them into decision making process, facilitating the access for installation, monitoring, data analysis and reporting. Developing ground level smart monitoring land and forest fires using LoRa-IoT technology, an early indication can be obtained which improve the decision making in preventing the disaster. This design acquires new design and development with latest wireless LoRa-IoT technology and signal propagation study.

The setup of sensor base stations at difference area to collect information from LoRa sensor and IoT network deploy surrounding. Fig. 2 shows a proposed LoRa WAN sensor deploy and data network diagram for environmental monitoring. Information collected by sensor base station will keep in internal database then send to monitoring system (data center), because of sensor base station locate in rural

area that far away up to 200 km then solar panel system will use as power supply for system. Latest technology of communication system also proposes such as 4G technology or even 5G technology for future in order to achieve real-time data to display to monitoring system.

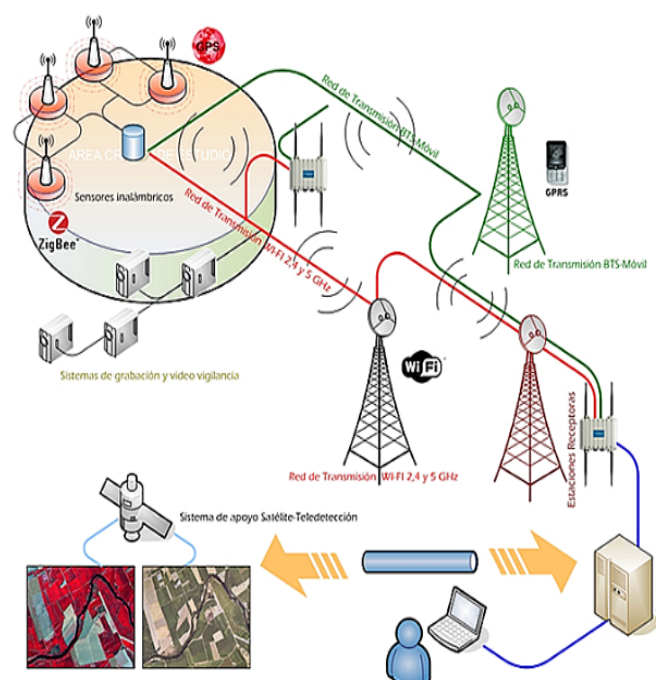


Fig. 2. Proposed LoRa WAN sensor for environmental monitoring.

The sensors be able to detect and gives early warning before fire is happen to authority for prevention action. Next step more sensors and sensor base station setup to cover entire of Riau Province and this project as prototype system to setup in others province in Indonesia. The proposed scenarios of LoRa sensors also opens to analyze behavior and changing of environmental before and after fire by image processing, analyze particle detection, sensor data's and new method of data communication system.

### III. LoRa WAN SOLUTION FOR MONITORING SYSTEM

Proposed solution for LoRa WAN networks employ the robust LoRa modulation by Semtech technology in order to get long range operation. There is standardize by the LoRa alliance, which has defined frame formats, provisioning, medium access, management messages and security mechanisms, device management. Fig. 3. shows illustrates that LoRa WAN networks form a star topologies around gateways, which act as packet forwarders between end devices and a central network server (NS). The NS is responsible for handling MAC layer processing and acts as a portal between applications running on end devices and application servers (APs). The LoRa WAN standard defines three classes for end devices of networking topology in order to cater to a number of different scenarios which are A, B, and C [14].

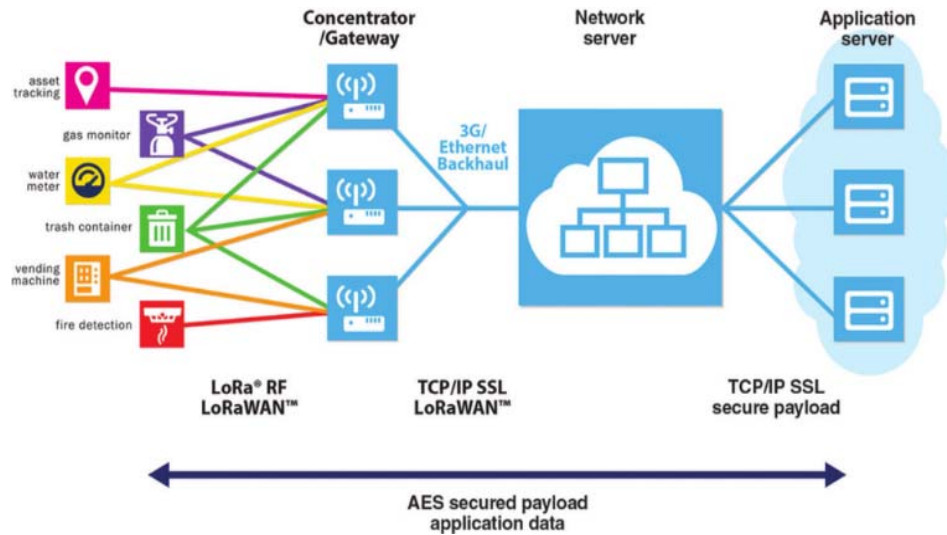


Fig. 3. Overview of the LoRa WAN hierarchical architecture based on Semtech proposal

The A class of end devices have their own transceivers in deep sleep for the majority of the time and wake up infrequently to transmit data toward the NS. The wireless medium access in LoRa WAN network follows an ALOHA scheme, which does not employ listen before talk, and is therefore subject to restrictions in most areas in the world while use it. For example, in Europe, the 868-MHz band consists of a number of sub-bands where Radio Duty Cycle (RDC) restrictions range from 0.1% to 10% with 1% being most common [15].

#### A. LoRa WAN Sensor Node

Solution for the LoRa node as point to collect data of environmental from the sensors installed and the protocol stack of the backbone network to transfer data from the node is shown in Fig. 4. Currently, most of commercially LoRa node (sensor) that available solutions follow by many of system is based on Semtech application notes, whose architecture and block diagram of the system as graphically depicted in Fig. 4. In this case the network backbone use is the internet or at least an intranet network. In this proposed environmental system proposed network is by radio communication which 4G or 5G technology.

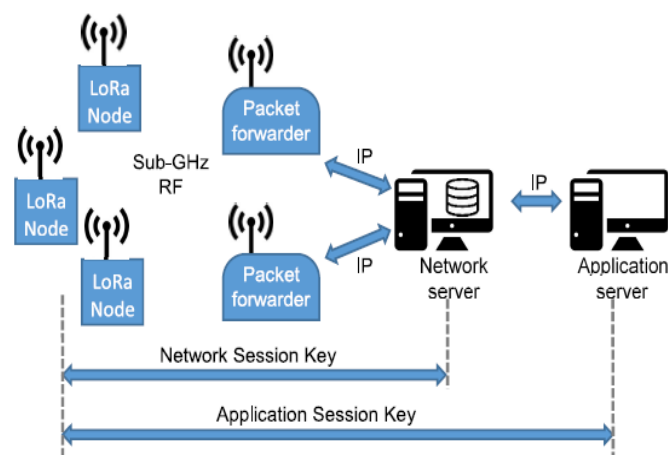


Fig. 4. Overview of the LoRa WAN hierarchical architecture based on Semtech proposal

The network gateway forward from LoRa WAN message based on data collected from LoRa node toward network servers can be one or more. The network server authenticates the received message and further forward the user payload to a single or several application servers to make sure all the data collected from the sensors node is stored in database. The application server used is for in charge of admitting nodes to the network and takes care of encrypting or decrypting user data sent and received to or from the end device. In the end, the application server forward node data from the sensors to a user server that actually implements the final user application. Additional to this scenario of proposed network is a network controller, whose aim is collecting reports related to the network status and be able to modify the LoRa WAN network accordingly for example changing the data rate supported by end devices and implementing an Adaptive Data Rate (ADR) scheme as well as can complement the network servers [16].

#### B. LoRa WAN Networking Architecture

Proposed scenarios of networking architecture in this LoRa WAN as stated in previous section is a network level architecture compatible with regular internet standards for example Internet Protocol version 6 (IPv6), would be highly desirable for a quick integration of the whole LoRa WAN system and its single end nodes within the fast and heterogeneous IoT ecosystem. However, LoRa WAN technologies are highly constrained regarding their transmission capabilities as limited bitrate and reduced packet size. Hence, the straight integration of IPv6 datagrams into LoRa WAN packets is not trivial and compression mechanisms are necessary. Based on this proposed solution is providing IPv6 connectivity to LoRa node by using an LoRa WAN link, but using a Multi-Access Edge Computing (MEC) based architecture to allow this integration by using LoRa technology as accessing network as shows in Fig. 5. The MEC node performs the packet translation tasks for the compression or decompression in order to interconnect the LoRa and IPv6 network segments the bidirectional flows can be established between LoRa WAN and IPv6 nodes [17].



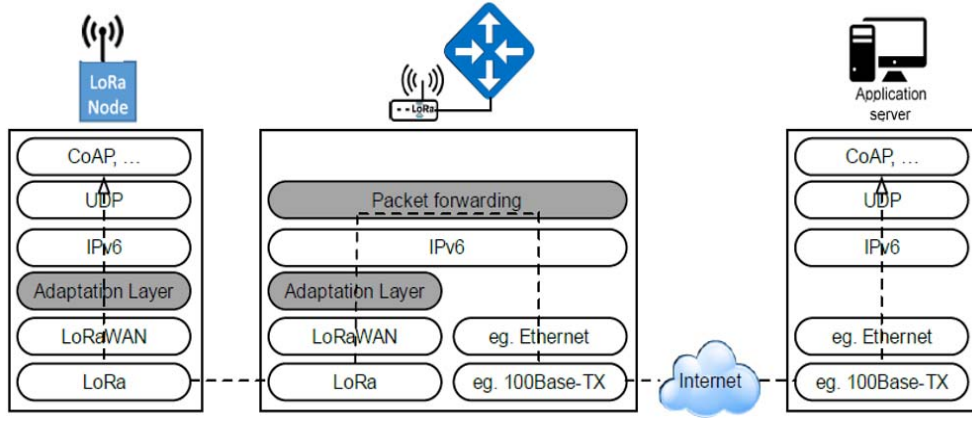


Fig. 5. Architecture of the IPv6 over LoRa WAN networking solution

The proposed solution can contribute of this LoRa WAN network such as:

- A real implementation of IPv6 over LoRa is developed and tested.
- A LoRa node test bench is deployed for providing environmental datas with IPv6 connectivity through LoRa WAN links.
- A base IoT environment for smart environmental data services are setup, which is ready for user to use it.

The other proposed solution for a LoRa WAN network is based on a star-of-stars topology composed of three basic elements in end of devices, a gateways and central network server as shows in Fig. 6 is end-devices, which may correspond to any input such as LoRa node sensors or actuators, communicate with the network server through one or more gateways, while the network server sends LoRa data to end-devices through a specific gateway. End-devices use the LoRa physical layer to exchange data with the gateway, while the gateway and the network server communicate over an IP-based protocol stack [18].

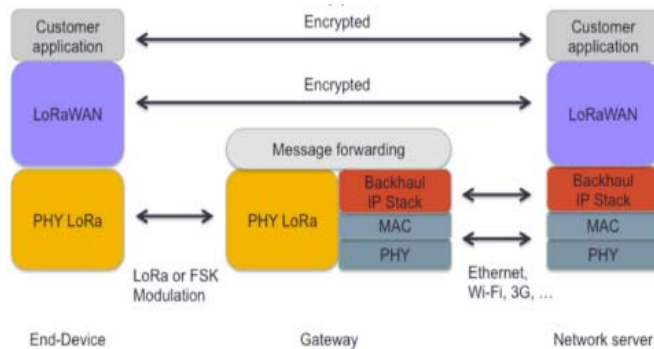


Fig. 6. LoRaWAN (a) system and (b) protocol architecture

### C. LoRa Physical error model

After LoRa Physical (PHY) error model the interleave, the output data are whitened in order to boost the entropy of the information source. Note that in the Bit Error Rate (BER) in simulations the information bits are drawn from a uniform distribution, therefore the entropy of the information source is already at its maximum. Before passing the whitened bit stream to the modulator, it is reverse gray mapped first. This produces a sequence of integers, which are fed to the LoRa

WAN sensor node. At the LoRa sensor node, a sequence of  $N$  time-shifted complex baseband up-chirp samples is generated via a phase accumulator as given by (1), where  $N$ , the number of samples data per baseband symbol, is equal to  $2SF(f_s/BW)$ . The input integer determines the time-shift of the up-chirp [14].

$$m(i) = \begin{cases} \exp(-j\pi), & \text{if } i = 0 \\ m(i-1) \exp(jf(i)), & \text{if } i = 1, \dots, N-1 \end{cases} \quad (1)$$

where the instantaneous frequency  $f(i)$  is given by

$$f(i) = -\pi + \frac{i}{N} 2\pi, \text{ for } i = 1, \dots, N-1. \quad (2)$$

Next, the samples of the LoRa WAN symbol are sent over the Additive White Gaussian Noise (AWGN) channel for a given signal to noise ratio (SNR) as per

$$c(i) = m(i) + \sqrt{\frac{E_s}{2\text{SNR}}} [\mathcal{N}(0; 1) + j\mathcal{N}(0; 1)], \quad \text{for } i = 0, \dots, N-1 \quad (3)$$

where  $\mathcal{N}(0; 1)$  is the standard normal distribution and SNR

$= 10\text{SNR}_{\text{dB}}/10$ . Note that the energy per symbol is equal to one for the LoRa WAN sensor node.

In the end at the receiver, the LoRa demodulator employs correlation based on demodulation where the received symbol is correlated to all known LoRa symbols. The decision on which symbol was sent, is made by selecting the LoRa symbol with the maximum correlation value. After demodulation, the receiver chain is the reverse of the sender chain. The error rate is measured in the information bits, after error correction of the data demodulation.

## IV. CONCLUSION

LoRa WAN system is developed for the environmental monitoring system because applicable for long range sensing up to several miles. Proposed solution for development of the LoRa WAN application in environmental monitoring system as discussed, LoRa node and point to collect data from the sensors installed sent the data to the application server through the IPv6 networking with physical layer used 4G or 5G technology. With the proposed system environmental data can be sent to the application server in minimum time to achieve real time monitoring system.

## ACKNOWLEDGMENT

Authors would like to say thank you very much to RISTEKDIKTI Indonesia for funding this research with grant No. 142/KONTRAK/LPPM/2-2018 and Universitas Islam Riau for support the facilities.

## REFERENCES

- [1] A. P. Vayda, "Explaining Indonesian Forest Fires: Both Ends of the Firestick," *Human Ecology: Contemporary Research and Practice*, pp. 17-35, 2010. Springer Science+Business Media
- [2] N. Yulianti, H. Hayasaka, and A. Usu, "Recent Forest and Peat Fire Trends in Indonesia The Latest Decade by MODIS Hotspot Data," *Global Environmental Research*, vol. 16, no. 22, pp. 105-116, 2012.
- [3] R. Khajuria and S. Gupta, "Energy optimization and lifetime enhancement techniques in wireless sensor networks: A survey," in *International Conference on Computing, Communication & Automation*, 2015, pp. 396-402.
- [4] A. L. Kakhandki, S. Hublikar, and P. Kumar, "An efficient hop selection model to enhance lifetime of wireless sensor network," in *2017 Innovations in Power and Advanced Computing Technologies (i-PACT)*, 2017, pp. 1-5.
- [5] C. Chee-Yee and S. P. Kumar, "Sensor networks: evolution, opportunities, and challenges," *Proceedings of the IEEE*, vol. 91, no. 8, pp. 1247-1256, 2003.
- [6] D. E. Boubiche *et al.*, "Advanced Industrial Wireless Sensor Networks and Intelligent IoT," *IEEE Communications Magazine*, vol. 56, no. 2, pp. 14-15, 2018.
- [7] L. Jie, H. Ghayvat, and S. C. Mukhopadhyay, "Introducing Intel Galileo as a development platform of smart sensor: Evolution, opportunities and challenges," in *2015 IEEE 10th Conference on Industrial Electronics and Applications (ICIEA)*, 2015, pp. 1797-1802.
- [8] A. J. Wixted, P. Kinnaird, H. Larijani, A. Tait, A. Ahmadiania, and N. Strachan, "Evaluation of LoRa and LoRaWAN for wireless sensor networks," in *2016 IEEE SENSORS*, 2016, pp. 1-3.
- [9] A. Lavric and A. I. Petrariu, "LoRaWAN communication protocol: The new era of IoT," in *2018 International Conference on Development and Application Systems (DAS)*, 2018, pp. 74-77.
- [10] D. F. Carvalho, A. Depari, P. Ferrari, A. Flammini, S. Rinaldi, and E. Sisinni, "On the feasibility of mobile sensing and tracking applications based on LPWAN," in *2018 IEEE Sensors Applications Symposium (SAS)*, 2018, pp. 1-6.
- [11] H. C. Lee and K. H. Ke, "Monitoring of Large-Area IoT Sensors Using a LoRa Wireless Mesh Network System: Design and Evaluation," *IEEE Transactions on Instrumentation and Measurement*, pp. 1-11, 2018.
- [12] E. A. Kadir, A. Siswanto, and A. Syukur, "Performance analysis of wireless LAN 802.11n standard for e-Learning," in *2016 4th International Conference on Information and Communication Technology (ICoICT)*, 2016, pp. 1-6.
- [13] E. A. Kadir, "A reconfigurable MIMO antenna system for wireless communications," in *2017 4th International Conference on Electrical Engineering, Computer Science and Informatics (EECSI)*, 2017, pp. 1-4.
- [14] F. V. d. Abeele, J. Haxhibeqiri, I. Moerman, and J. Hoebeke, "Scalability Analysis of Large-Scale LoRaWAN Networks in ns-3," *IEEE Internet of Things Journal*, vol. 4, no. 6, pp. 2186-2198, 2017.
- [15] N. A. B. Zainal, M. H. Habaebi, I. Chowdhury, and M. R. Islam, "Sensor node clutter distribution in LoRa LPWAN," in *2017 IEEE 4th International Conference on Smart Instrumentation, Measurement and Application (ICSIMA)*, 2017, pp. 1-6.
- [16] M. Rizzi, P. Ferrari, A. Flammini, and E. Sisinni, "Evaluation of the IoT LoRaWAN Solution for Distributed Measurement Applications," *IEEE Transactions on Instrumentation and Measurement*, vol. 66, no. 12, pp. 3340-3349, 2017.
- [17] R. Sanchez-Iborra, J. Sánchez-Gómez, J. Santa, P. J. Fernández, and A. F. Skarmeta, "IPv6 communications over LoRa for future IoT services," in *2018 IEEE 4th World Forum on Internet of Things (WF-IoT)*, 2018, pp. 92-97.
- [18] N. Sornin, M. Luis, T. Eirich, T. Kramp, and O. Hersent, "Lorawan specification," *LoRa alliance*, 2015.



# Co-channel Interference Monitoring based on Cognitive Radio Node Station

**Arief Marwanto**  
Dept. of Electrical Engineering –  
Post Graduated Study,  
Faculty of Industrial Engineering  
Univ. Islam Sultan Agung  
(UNISSULA)  
Semarang – Indonesia  
arief@unissula.ac.id

**M Ulin Nuha**  
Electrical Engineering  
Student, Faculty of Industrial  
Engineering  
Univ. Islam Sultan Agung  
(UNISSULA)  
Semarang – Indonesia  
ulin.cenx9395@gmail.com

**Jenny P Hapsary**  
Dept of Electrical Engineering  
Faculty of Industrial  
Engineering  
Univ. Islam Sultan Agung  
(UNISSULA)  
Semarang – Indonesia  
jenny@unissula.ac.id

**Daniel Triswahyudi**  
PT Polytron Electronic  
Indonesia Staff, Kudus  
Indonesia

**Abstract** —Most of installation on wireless LAN on the building is not considering location and geographic space are which probable co-channel interference among near-far wi-fi stations. The use of the same channel which causes of receiver stations experiences of error transmission and delay among data transmission. To analyze this drawbacks, cognitive radio (CR) is adopted which able to monitoring co-channel interference on wi-fi stations. Node MCU Arduino is used to proposed cognitive radio terminal which able to analyzed and monitoring co-channel interference among wi-fi stations known as *co-channel monitoring cognitive radio* (CCMCR). One of the CR task is ability to sensing the whole spectrum channel that operated in certainty frequency. Node MCU is sensed the energy power of the wi-fi stations and converted by analog-to-digital converter which detected power level of the received signal strength indicator (RSSI). The proposed model is examined by indoor experiments which obtained 63.8% co-channel average and adjacent-channel is 36.1%. Thus the proposed CCMCR node station is able to monitor co-channel interference and adjacent-channel as well. Therefore, the results could be used as the basic analysis for the development and installation of wi-fi stations in the building.

**Keywords:** *cognitive radio, spectrum sensing, software defined radio, co-channel interference*

## I. INTRODUCTIONS

Increasingly widespread use of wi-fi users that utilize the 2.4 GHz frequency, such as in offices, computer labs, and high rise buildings, resulting in negative impacts due to unlicensed band frequency of 2.4 GHz, resulting in co-channel interference between users [1]. Co-channel is a fellow radio wave signal operating on the same channel frequency, consequently the client device will encounter an error when translating the same information code [2].

Co-channel occurs when using a channel that does not have enough distance between channels. Co-channel can decrease access point performance in transmitting and receiving signals, access point will lose power and can lose database, consequently error on bits of information being sent, so that the recipient client finds error, or delay in sending data[3]. When the co-channel happens it will decrease the quality of service on the wireless LAN. Steps prevent co-channel on wireless LAN, using technological

breakthroughs such as Cognitive Radio (CR) to improve the quality of service.

In [4] cognitive Radio is an intelligent wireless communication system capable of being aware of the conditions of the surrounding environment and using the "understanding-by-building" methodology to learn from the environment and adapting its internal status to statistical variations in the coming radio frequency (RF) stimulant by making changes to certain operating parameters such as transmission power, carrier frequency, or modulation strategy. While in [5] wireless network and wireless network optimization by minimizing roaming is analyzed. Examination is done by measuring bandwidth, measuring the speed and stability of data transfer during roaming. Moreover, speed and stability of transfer with wireless network system are measures. However, performance testing of each access point which is determined the quality of overall signal and co-channel is not considered. While in [6] has introduced access point interference among wi-fi networks. Interference measurement has proposed by experiencing on topology networks which setup onto bandwidth, signal and noise measurements. Unfortunately, individual measurements that officially done are not consider link budget analysis, co-channel interference, RSSI and energy signal measurements.

Research conducted by [7] explains the Bluetooth technique operates in the 2.4 GHz frequency band which is the same as IEEE 802.11b or Wi-Fi. During Wi-Fi and Bluetooth technologies are used simultaneously at the same time, the chances of interference are enormous because they operate in the same frequency band of 2.4 GHz. The method used is the measurement to determine the effect of Bluetooth interference on IEEE 802.11b WLAN performance system (Wi-Fi). The parameters used are transmission time and throughput. Based on these parameters, it is found that interference effect can affect the feasibility of a Wi-Fi network service. However, monitoring and co-channel interference are not involving in this experiments. In order to investigate the performance of the hotspot, [8] has investigate adjacent signal interference (Co-Channel Interference) which degrade the received signal quality. Interference measurement has been done through six experiments through an implementation on an infrastructure topology, interference measurements can be seen from Quality of service with three parameters such as bandwidth measurement, signal

measurement, and noise measurement. Moreover, in [7] has investigate measurement analysis inside the building has done which determined the effect Bluetooth interference with some of the IEEE 802.11b Wi-Fi parameters that expressed by throughput based on data rate changes. Based on the throughput, the value of delay and jitter are obtained. The results show that the presence of Bluetooth is very influential on Wi-fi which expressed by throughput. Whereas, the effect of throughput is the value of throughput decreases as the increase in distance among the transmitter and receiver. The constraints faced by internet service provider (ISP) in Yogyakarta was interference has been reported by [9]. Most of ISP uses uncertified wireless devices therefore, the equipment is not fully utilized on 2.4 GHz frequency. They proposed transmit power supervision which lead to monitoring the used of frequency 2.4 GHz that to operate the wireless internet network. However, depth interview methods have been used and measurements are not considering in this investigate. Moreover, [10] has proposed bandwidth analysis which perform wi-fi signal quality. The good performance has shown by bandwidth levels is not significantly differ from that leased. However, only bandwidth that measured in this work. Cognitive radio (CR) for dedicated spectrum has been investigated by [11] which discuss about how the ability of spectrum sensing using matched filter method on cognitive radio to detect the presence of user primary on FM Radio channel using three Power Spectral Density (PSD) i.e. PSD Periodogram, Welch and Thomson Multi-taper with MATLAB. However, simulation methods are used which perform spectrum sensing detection on FM radio channels.

## II. CO-CHANNEL DETECTION AND SOFTWARE RADIO MODEL FOR SPECTRUM SENSING MECHANISM

One of the cognitive radio components are sensing capability to the surrounding environment. For the cognitive radio primary transmission, two capabilities of sensing and transmit are needed, therefore NodeMCU ESP8266 which acts itself as a sensor node which can be used as access point (AP) or as a station (STA) which is configured as CR primary transmission known as co-channel monitoring cognitive radio (CCMCR). One NodeMCU ESP8266 is used as a AP and a STA for this CCMCR model. As shown in Figure 1, NodeMCU ESP8266 is connected to the PC as CR station (CCMCR). It is observed and monitoring by sending primary transmission of power and receiving any information of the power levels (RSSI level) from the surrounding environment. In the surrounding of CCMCR node, some wi-fi stations installed which continuously transmit their power levels to the surrounding nodes. The CCMCR node will received channel information based on the received power level from the surrounding wi-fi stations.

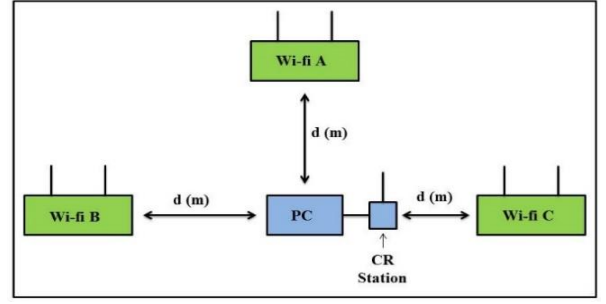


Fig. 1 Co-Channel Detection Model using CCMCR

Assumed that CCMCR is a single user primary wireless networks which observable co-channel activities on wi-fi stations. The power level of the wi-fi stations transmission is denoted by  $P_T$  [12]

$$P_T(\text{dB}) = 10 \log_{10} P_{\text{Signal}} \quad (1)$$

$P_i$  signal is the maximum allowable signal power of wi-fi in decibel (dB) for this frequency spectrum as primary user power level [13]. It is involving measurements at various distances indicates that pathloss values are random and distributed log-normal. In a single CCMCR path of the Tx - Rx, the received  $P_i$  suffered from the noise and path loss [14]. For the link budget measurement, the distance of wi-fi stations to the CCMCR station is considering path loss factor which can be obtained by [15]

$$L_{\text{CCMCR}} = 20 \log_{10} \left\{ \frac{\lambda}{4\pi d_0} \right\} - 10n \log_{10} \left\{ \frac{d_0}{d_{\text{wi-fi}}} \right\} \quad (2)$$

The received signal strength indicator (RSSI) received from wi-fi stations based on free-space path loss. The distance by Friis transmission equation for free space propagation can be found as [16]

$$d_{\text{CCMCR}} = \sqrt{\frac{P_t G_t G_r \lambda^2}{(4\pi)^2 P_r}} \quad (3)$$

Based on [17] and [12] the detection power received at CCMCR is

$$P_{R(\text{CCMCR})}(i) = P_{T-\text{CCMCR}}(\text{dBm}) - 20 \log_{10} \left\{ \frac{(4\pi^2 * ((d_0(i) - d_{\text{wi-fi}}(i)) * 2))}{\lambda_{\text{CCMCR}}} \right\} + \sum_{i=1}^I \left\{ \right. \\ \left. + N_i(0, \sigma)(i) \right\} \quad (4)$$

Where  $P_{R(\text{CCMCR})}(i)$  is the received power;  $\lambda_{\text{CCMCR}}$  is the wavelength of CCMCR node;  $\lambda(i)$  is the wi-fi wavelength,  $P_{T-\text{CCMCR}}(\text{dBm})$  is the power transmit of the CCMCR as the primary transmission;  $d_{\text{wi-fi}}(i)$  is the radius distance between wi-fi stations and CCMCR node;  $P_{T(\text{wi-fi})}(i) \text{ dBm}$  is the power transmit of wi-fi stations;  $N(t)(i)$  is the additive white noise with noise and variance. Therefore, the detection co-channel interference among wi-fi stations at the CCMCR node given as [4]

$$P_{T(\text{co-channel Interference})}(dB)(i) = P_{T(\text{wi-fi})}(dB)(i) - P_{R(\text{CCMCR})}(dB)(i)$$

In the next stage, NodeMCU digitized the received power level based on the magnitude square (FFT) and the software passed received signal strength as digitation format, as shown in Figure 2. A piece of packets or stream data is translated from the received signal levels using ADC block module. ADC then sampled and quantized the magnitude square signal and pass it into baseband processing which are written using C#. For further processing, magnitude square signal then digitized into FFT bins. As shown in Figure 2 which describes the software component architecture of the Node MCU- ESP8266. The Board Manager and the Arduino IDE are used to compile an Arduino C/C++ source file down to the target MCU's machine language as down-conversion processing such as modulation, signal processing and digitizing of the packets.

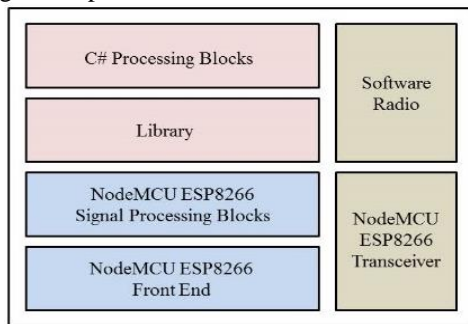


Fig. 2. Proposed of software defined radio co-channel detection monitoring cognitive radio (CCMCR) for Cognitive Radio Component

Furthermore, in Figure 3 shown that received signal level that creates an energy change is received through radio software. The received data adjusts the software that passes the square of the magnitude of the signal strength received from the wi-fi antenna and translates into the current data packet as digitized.

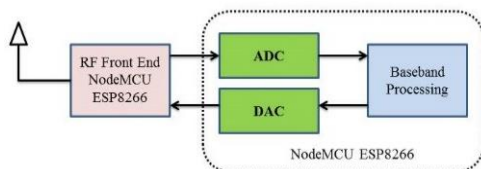


Fig. 3. Software Radio (SR) model for CCMCR node

Figure 3 describes front end software radio architecture and develop using C# (dot Net frameworks) which consist of signal processing blocks library and communicator library in Arduino NodeMCU esp8266. Moreover, the CCMCR node consist of two main boards, the first ESP8266 and Arduino board which the specification as follows: The maximum sampling rate of NodeMCU is 2,5 kHz; Voltage: 3.3V; Wi-Fi Direct (P2P), soft-AP; Current consumption: 10uA~170mA; the clock speed: 80~160MHz; +19.5dBm output power in 802.11b mode; 802.11 support: b/g/n;

### III. POWER MEASUREMENT MODEL ON COGNITIVE RADIO STATION

Figure 4 shows that measurement of power level at CR node station. Radiated power of the electromagnetic spectrum has been detected by antenna. Moreover, the radiated power passes through ADC for sampling level of the signals which perform magnitude square of the signals. The magnitude square form of fast fourier transform (FFT) is conversion onto information as follows: SSID, RSSI value (dB) and channel number.

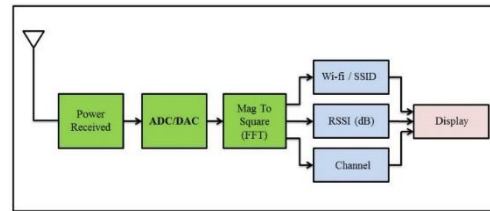


Fig. 4. Blok Diagram Power Received Measurements

The magnitude square form of fast fourier transform (FFT) is conversion onto information as follows: service set identifier (SSID), Received signal strength indicator (RSSI) value (dB) and channel number. The display is presented as numerical, potential co-channel interference and chart of the signals information.

### IV. SOFTWARE DEFINED RADIO FOR CCMCR SYSTEM MODEL

The proposed model is developed based on the C# software which working through back-office systems. It proceeds the computation process such as modulation, demodulation, signal processing, analog to digital conversion, digital to analog conversion, etc. Its combined with Arduino IDE C/C++ which located on front-office which represented the algorithm of the proposed model.

Figure 5 describe the proposed design of the software radio for CCMCR monitoring node station.

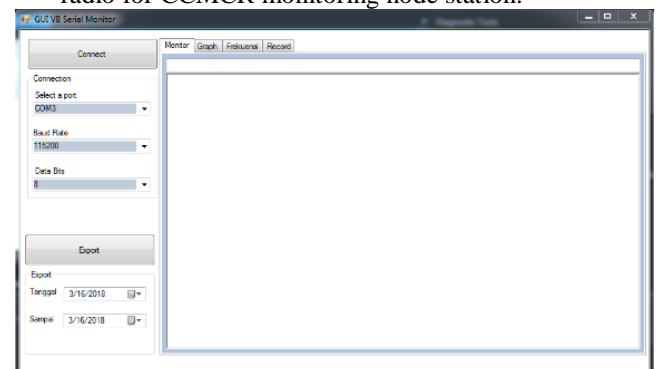


Fig. 5. Proposed GUI of software radio design for CCMCR node station.

The GUI interface consists of three groups of boxes, such as group box connection, group box export, and group box of visual.

### V. EXPERIMENTAL SETUP

Indoor testing is configured by considering attenuation of the materials and shadowing effects of the signals. Indoor testing is done with the aim of obtaining more complex signal characteristics and to know the effect of unauthorized placement of wi-fi by the administrator. Therefore, the

characteristic study of received signal power level can be analyzed more deeply. Testing in the building will also be known type of wi-fi and channel is the most widely used. for further research, if the wi-fi node whose channel is accessed by many users is known by CR node, dynamic spectrum access can be applied in the future wi-fi system.

The cause of signal attenuation or pathloss is the amount of power lost in a certain distance is an important component in obtaining information about the power level received by the CCMCR station. Furthermore, the presence of shadowing is characterized by the average variation of pathloss between the transmitter and the receiver at a location which remains well known to the monitoring station.

The large number of frequencies that will lead to co-channel is an important ingredient that the monitoring system should be aware of. This test will prove how the co-channel occurs and find a solution to the bad power levels received due to co-channel, here are the outlined of floor plans and indoor test locations is shown in Figure 6.

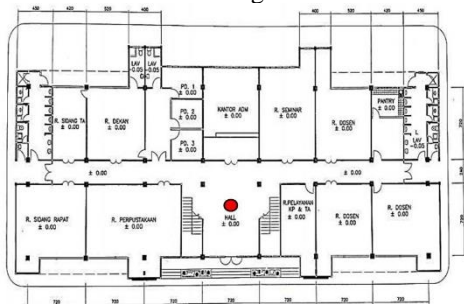


Fig. 6. 1st Floor Indoor Testing Planning

The test was conducted in the 1st floor FTI building which has an area of 4000m<sup>2</sup>. The large number of indoor access points triggers the use of frequencies on the wireless that allow co-channel to occur. To know the performance quality of wireless LAN service based on the bad power level due to the influence of co-channel. The received signal strength score indicator (RSSI) received from the transmitter emitted by wi-fi stations, so that there are some detected wi-fi based on the distance.

## VI. RESULTS AND ANALYSIS

The following figures shows the results indoor testing of CCMCR monitoring.

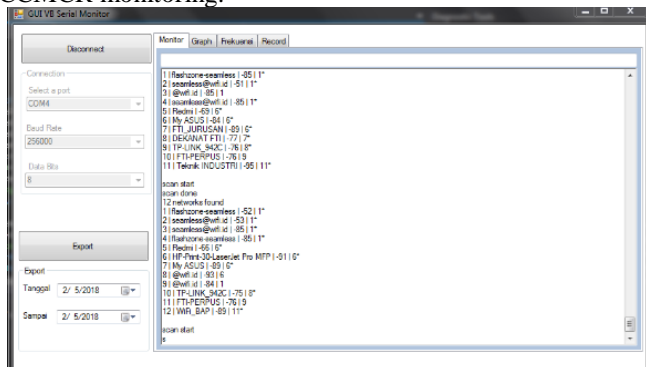


Fig. 7. GUI Monitor Indoor Testing

Figure 7 is the result detection at FTI 1st floor building indicating the existence of co-channel in wireless LAN network, because there is no distance of channel frequency usage, as described in following table:

TABEL 1 CO-CHANNEL OBSERVATION RESULTS BETWEEN THE ACCESS POINT IN THE BUILDING

No	SSID	Channel	RSSI (dBm)
1.	Flashzone-seamless	1	-85
2.	seamless@wifi.id	1	-85
3.	@wifi.id	1	-85
4.	flashzone-seamless	1	-52
5.	seamless@wifi.id	1	-53
6.	HP-Print-30-LaserJet Pro MFP	6	-91
7.	@wifi.id	6	-93

Another detection that CCMCR stations can utilize in the use of wireless LAN frequencies in addition to co-channel is the adjacent channel, which encounters signal coverage between the access points where the power from the nearest transmitter interferes with the work of the receiver when it receives the signal from the remote transmitter as a result reduce the quality of performance on the access point, the following in Table 2:

TABEL 2 ADJACENT-CHANNEL OBSERVATION RESULTS BETWEEN ACCESS POINTS IN THE BUILDING

No	SSID	Ch	RSSI (dBm)
1.	HP-Print-30-LaserJet Pro MFP	6	-91
2.	@wifi.id	6	-93
3.	TP-LINK_942C	8	-75
4.	FTI-PERPUS	9	-76
5.	Wifi_BAP	11	-89

In Figure 7, it is detected that channel 1 has shown the overlap of signal coverage because there is no spacing in the channel usage. The use of a channel combined with an RSSI value indicates that the higher the histogram indicates the received power level the better and vice versa, are outlined in table 3 below:

TABEL 3 STATUS INDICATOR OF OVERLAPPING CHANNELS

No	Channel	Status	RSSI (dBm)
1.	1	Flashzone-seamless	-85
		seamless@wifi.id	-85
		@wifi.id	-85

In Figure 8 is the result of detection of channel frequencies used by some access points. The color indication of detected SSID indicates the use of channel on access point detected by CCMCR station and frequency value indicator, which is described in the following table:

TABLE 4. FREQUENCY AND CHANNEL OBSERVATION RESULTS ON INDOOR TESTING

Ch	SSID	RSSI (dBm)	Co-channel	RSSI (dBm)
1	flashzone-seamless	-75	flashzone-seamless	-75
	seamless@wifi.id	-74	@wifi.id	-75
	@wifi.id	-75	seamless@wifi.id	-74
	flashzone-seamless	-52	flashzone-seamless	-52
	seamless@wifi.id	-53	seamless@wifi.id	-53
6	HP-Pront-30-LaserJet Pro MFP	-90	HP-Pront-30-LaserJet Pro MFP	-90
	seamless@wifi.id	-90	seamless@wifi.id	-90

In Figure 9 there is a collection of interrelated organized letters and numbers that can be stored, manipulated and selected based on the same channel and RSSI values, it is intended to know the co-channel information process that occurs in wi-fi stations, the following is described in table 5:

TABLE 5. RECORDING AND STORAGE RESULTS ON INDOOR TESTING

No	SSID	Channels	Frequency (GHz)
1.	flashzone-seamless	1	2.412
2.	seamless@wifi.id	1	2.412
3.	seamless@wifi.id	1	2.412
4.	flashzone-seamless	1	2.412
5.	HP-Print-30-LaserJet Pro MFP	6	2.437
6.	@wifi.id	6	2.437
7.	@wifi.id	1	2.412
8.	TP-LINK_942C	8	2.447
9.	FTI-PERPUS	9	2.452
10.	Wifi_BAP	11	2.462

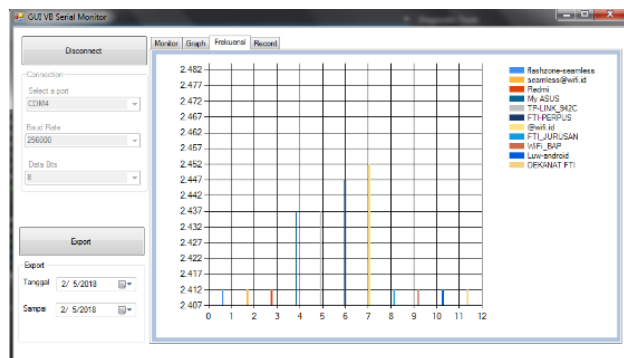


Fig. 8. Frequency and channel observation results on Indoor Testing

To avoid the occurrence of co-channel then the use of frequencies on the access point is a good on channels number of 1, 6, and 11.

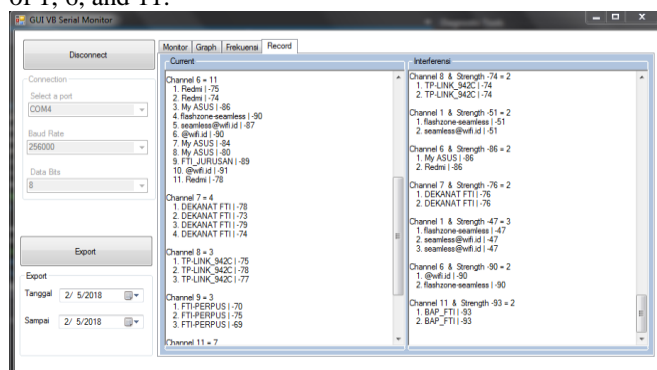


Fig. 9. Recording and storage results on Indoor Testing

## VII. CONCLUSION

1. Prototype for co-channel monitoring has been successfully developed using NodeMCU ESP8266 and C# software.
2. This prototype is able to fulfill one of the functions of cognitive radio that is detecting the power level around it
3. Prototype development and software radio support could well detected co-channel and adjacent channel on intended wi-fi stations
4. Developed software radio can also monitor the magnitude of power levels, frequencies, interferer channels and overlap channels in monitoring area.
5. Dynamic spectrum access is recommended to optimize the performance of the access point so that the co-channel and adjacent channel do not interfere with the performance of the access point. Further research could be conducted in order to optimizing the access point performance during heavy burden traffic and occurring heavy co-channel interferer using cognitive radio systems.
6. It's good before placing the access point, power level measurement and determination of the distance is determined first, so the performance of access point can be optimal. These tools and software can be used to determine optimal access point installation.

## VIII. REFERENCES

- [1] S. Padiaditaki, "Interference-aware adaptive spectrum management for wireless networks using unlicensed frequency bands," 2012.
- [2] H. Chen, *Next Generation Wireless Systems and Networks and Networks*. 2006.
- [3] S. Haykin, "Cognitive Radio : Brain-Empowered," vol. 23, no. 2, 2005.
- [4] A. Marwanto, S. K. Syed Yusof, and M. H. Satria, "Orthogonal Frequency-Division Multiplexing-Based Cooperative Spectrum Sensing for Cognitive Radio Networks," *TELKOMNIKA (Telecommunication Comput. Electron. Control.*, vol. 12, no. 1, p. 143, 2014.
- [5] A. E. Prasetyo, M. Stefanus, A. Wiem, and A. Herusutopo, "Dengan Minimalisasi Roaming Di Binus Square," pp. 611–624.
- [6] P. Studi, T. Informatika, F. Sains, D. A. N. Teknologi, U. I. Negeri, and S. H. Jakarta, "PENGUKURAN INTERFERENSI PADA ACCESS POINT ( AP ) UNTUK MENGETAHUI QUALITY of SERVICE ( QoS ) NURMALIA," 2010.
- [7] Y. Ikawati, N. A. Siswandari, and O. Puspitorini, "ANALISA INTERFERENSI ELEKTROMAGNETIK PADA PROPAGASI Wi-Fi INDOOR," pp. 1–5, 2011.
- [8] J. Jenderal, A. Yani, and N. Palembang, "PERFORMANCE HOTSPOT UNIVERSITAS BINA DARMA."
- [9] W. Studi, K. Yogyakarta, J. Medan, M. Barat, N. Jakarta, and T. Fax, "Penggunaan frekuensi 2.4 ghz dalam keperluan internet wireless (studi kasus yogyakarta)," vol. 9, no. 2, pp. 225–244, 2011.
- [10] H. Nugroho, S. A. Siagian, A. Teknik, T. Sandhy, P. Jakarta, and A. Point, "ANALISIS BANDWIDTH JARINGAN WIFI," pp. 35–43.
- [11] S. D. Kandi and R. Fauzi, "ANALISIS KINERJA SPECTRUM SENSING MENGGUNAKAN METODE MATCHED FILTER PADA COGNITIVE RADIO," pp. 72–77.
- [12] A. Marwanto, "Software Defined Radio Design for OFDM Based Spectrum Exchange Information Using Arduino UNO and X-Bee," no. September, pp. 19–21, 2017.
- [13] X. Kang *et al.*, "Optimal Power Allocation Strategies for Fading Cognitive Radio Channels with Primary User," vol. 29, no. 2, pp. 374–383, 2011.
- [14] A. Ghasemi, C. Canada, and E. S. Sousa, "Spectrum Sensing in Cognitive Radio Networks : Requirements , Challenges and Design Trade-offs," no. April, pp. 32–39, 2008.
- [15] M. Ohta, T. Fujii, K. Muraoka, and M. Ariyoshi, "A Novel Power Controlled Sensing Information Gathering for Cooperative Sensing on Shared Spectrum with Primary Spectrum," pp. 111–115, 2011.
- [16] S. Barai, D. Biswas, and B. Sau, "Estimate Distance Measurement using NodeMCU ESP8266 based on RSSI Technique," pp. 170–173, 2017.
- [17] S. John, *Introduction of RF Propagation*, 2005 John Wiley and Sons.



# Simulation of Mobile LoRa Gateway for Smart Electricity Meter

Sugianto  
Department of Electrical Engineering  
Universitas Indonesia  
Jakarta, Indonesia  
sugianto 71@ui.ac.id

Ruki Harwahu  
Department of Electrical Engineering  
Universitas Indonesia  
Jakarta, Indonesia  
ruki.h@ui.ac.id

Azwar Al Anhar  
Department of Electrical Engineering  
Universitas Indonesia  
Jakarta, Indonesia  
azwar.al@ui.ac.id

Riri Fitri Sari  
Department of Electrical Engineering  
Universitas Indonesia  
Jakarta, Indonesia  
riri@ui.ac.id

**Abstract**— LoRa is a viable connectivity technology for smart electricity meter. In addition to measuring electricity usage, a smart electricity meter enables many features for smart grid, safety, etc. LoRa is advertised to be capable in very long range transmission and low power consumption. However, LoRa uses sub 1 GHz unlicensed spectrum. In the era of connected smart things, this spectrum is very crowded and will be even more crowded. In this paper we propose the use of mobile LoRa gateway for smart electricity meter. With mobile LoRa gateway, the transmission range can be decreased. Thus, LoRa end devices can save more power and nearby systems can reuse the same band with less interference. We study the performance via simulation using modified LoRaSim. The result shows that the performance of LoRa mobile gateway can be achieved.

**Keywords**—LoRa, LoRaSim, Smart Meter

## I. INTRODUCTION

Electricity is a very important source of energy in people's lives, whether in the household sector, lighting, communications, industry, and so on. In Indonesia, 43.7 percent of electricity consumers are the household sector. The National Power Utility Company (PLN) is the state-owned enterprise in the electricity sector in Indonesia. Currently PLN has 2 electricity bill payment systems, namely prepaid and postpaid. The number of postpaid users is more than prepaid users. The comparison between postpaid users and prepaid users is 75.7 percent to 24.3 percent [1].

For postpaid customers, PLN needs to conduct periodic checks to verify the accuracy of their electricity meters. This is to ensure that the data counted by the electricity meter is in accordance with the amount of electricity used by the customers. This process is done manually by PLN officer who read directly on the meter located in each house. This reading meter process is less accurate, takes time and costed [2]. In addition, the customer cannot monitor process of recording the electric usage.

The prepaid system was introduced within the last decade to gradually replace the postpaid system. The prepaid system requires newer metering devices which uses GSM/GPRS connectivity to the charging server in PLN's office. It does not need manual work by the officer on-site. To support the upcoming smart grid era [2, 3], where customer can also sell the electricity that they generate (e.g. by solar panel or

generator), and to incorporate additional features such as emergency alarm and smart pricing, smarter electricity meter is required. These features can only be achieved when the metering device is more connected. Initially, the idea of power-line communication was studied [4]. However, it faces many implementation hurdles. One of feasible connectivity technology for this case is LoRa [5, 6]. Based on Indonesia regulation, PLN does not need to get license from regulator to use LoRa technology [2].

Long Range (LoRa) [1] is a spread spectrum modulation technique derived from Chirp Spread Spectrum (CSS) with an integrated Forward Error Correction (FEC). Some features of LoRa are low power, robust long-range coverage, low cost, and geolocation. Several interesting studies have been conducted about LoRa. Wibisono and Permata [2] proposed an advanced metering infrastructure based on LoRa WAN, the result is LoRa WAN can be operated in electricity smart meter. Raju et al [7] provides an overview of the LoRa used in collecting data from various air pollution sensors to be analyzed with pollution monitoring systems. Wei Ma and Liang Chen [8] proposed LoRa use to support intelligent agricultural data collection and equipment control. Nugraha et al [9] did the experimental trial using LoRa for monitoring and tracking patients with mental disorder. Bor et al [10] built LoRaSim as the environment to simulate LoRa to find LoRa is Low-Power Wide-Area Network (LPWAN) scale, and the result show that LoRa Network can scale when they use multiple gateways and/or use the parameter selection of dynamic transmission.

LoRa is advertised to be capable in very long range transmission and low power consumption. However, LoRa uses sub 1 GHz unlicensed spectrum. In the era of connected smart things, this spectrum is very crowded and will be even more crowded [11]. The number IoT units installed in 2020 is more than 20 millions [12] and according to a study by Wi-Fi Alliance [13, 14], additional spectrum between 500 MHz and 1 GHz in various regions are needed to support the expected growth by 2020.

Indeed, to anticipate the high demand of IoT connectivity, many IoT networks needs optimization to be able to effectively use their resource [15]. In this paper we propose the use of mobile LoRa gateway for smart electricity meter. With mobile LoRa gateway, the transmission range can be

decreased by decreasing its power. The requirement for electricity data meter is not real time, so the data transmitted time from LoRa end devices can be set. Thus, LoRa end devices can save more power and nearby systems can reuse the same band with less interference. Hence, it can use the limited unlicensed spectrum and coexist with other users better.

The performance of mobile LoRa gateway is evaluated via simulation. We perform the simulation using LoRaSim [10] which we modified for several scenarios with mobile gateway. In the next section we introduce about LoRa, LoRaWAN, LoRaSim, and electricity smart meter simulation. Section 3 describes scenario of LoRaSim simulator considered in our simulation. Section 4 presents the results and discussion of our simulation. Section 5 presents the conclusion of this paper.

## II. LITERATURE REVIEW

### A. LoRa

Long Range (LoRa) is patented spread-spectrum radio modulation developed by Cycleo (Grenoble, France) and acquired by Semtech in 2012 [16]. LoRa is not suited for video streaming, it is well fit to serve the Internet of Things (IoT) and Machine to Machine (M2M) applications. Packet size of IoT/M2M generally  $< 100$  kbps and implemented for sensors, or meters, while video streaming  $> 1$  Mbps. The range of frequencies of LoRa that can be used is between 137 MHz to 1020 MHz. A LoRa receiver can decode transmission of 19.5 dB below the noise floor.

Some features of LoRa are low power, robust long-range coverage, low cost, and has geolocation. LoRa uses an asynchronous communication method, the nodes power will on when they send data to the gateway and will return to the power saving mode when no data is sent. LoRa coverage up to 30 miles in rural areas and over 2 miles in densely populated urban areas. LoRa operates in unlicensed spectrum and the LoRa protocol is a free royalty which means LoRa is cost less. LoRa geolocation uses Differential Time of Arrival and other hybrid techniques to determine location. The location of node is estimated by the time packet arrival algorithms from the sensor node to multiple gateways.

LoRa has five configuration parameters that have an influence on energy consumption, transmission duration, resilience to noise, robustness and range [10, 17].

- **Transmission Power (TP).** TP on LoRa can be set between -4 dBm and 20 dBm in 1 dB steps. A bigger TP increases the energy consumption, the transmission duration (more faster), resilience, robustness and the range (more wider).
- **Carrier Frequency (CF).** CF can be programmed between 137 MHz to 1020 MHz in steps of 61 Hz. A higher CF increases the energy consumption, the transmission duration (more faster), resilience, robustness and the range (more wider).
- **Spreading Factor (SF).** SF is the ratio between the symbol rate and chip rate. In each symbol, SF determines how many bits are encoded. SF can be set between 6 and 12. A higher SF increases the energy consumption, resilience, robustness and the range

(more wider), while the transmission duration more slower.

- **Bandwidth (BW).** BW is the width of frequencies in the transmission band. BW can be selected from 7.8 kHz to 500 kHz. A higher BW increases the energy consumption, the transmission duration (more faster), resilience, robustness and the range (more wider).
- **Coding Rate (CR).** CR is the FEC rate used by the LoRa modem that offers protection against burst interference. CR can be set to either 4/5, 4/6, 4/7 or 4/8. A higher CR increases the energy consumption, resilience, robustness and the range (more wider), while the transmission duration more slower.

### B. LoRaWAN

LoRaWAN is a communication protocol and system architecture for LoRa network [5, 18]. LoRa nodes are not associated with a specific gateway, but data transmitted from a LoRa node received by multiple gateways. The gateways support bidirectional communication and can process packets sent from LoRa nodes. Fig 1. Shows that each gateway forward the packet to the network server, and the network server forward it to the application server which handles the customer application and presents relevant data. LoRaWAN gateways designed for outdoor or indoor use, and enable for public and private network deployments.

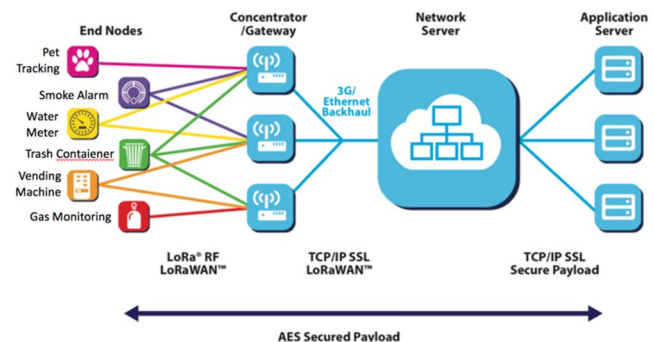


Fig. 1. LoRaWAN Network

### C. LORASIM

LoRaSim is a discrete-event simulator based on SimPy built by Bor, Roedig, Voight and Alonso [10, 19]. LoRaSim is built to simulate the collision of LoRa networks and to analyse the scalability. There are four Python scripts in LoRaSim: `loraDir.py` to simulate a single gateway, `loraDirMulBS.py` to simulate 2 to 24 gateways, `directionalLoraIntf` to simulate nodes with directional antennae and multiple networks, and `oneDirectionalLoraIntf.py` to simulate gateways with directional antennae and multiple networks.

### D. Electricity Smart Meter Simulation

An electricity smart meter simulation that we perform using LoRaSim [10] that we had modified. We modified the placement of nodes and gateway. Nodes in LoRaSim [10] is placed randomly, then gateway is in fixed location. In LoRaSim that we modified, the nodes are in fixed location, and gateway is move from one point to another point. This means that the gateway is mobile.

In this simulation, it is assumed that a residential area consists of 20 houses in each row, if there are 100 houses it will consist of 5 rows of housing and so on as shown in Fig. 2. Each LoRa node will be installed on the electricity meter device in every house. The gateway will be brought by PLN officer using a motorcycle through residential area. Each node will send a packet of electrical data usage (in KWH) to mobile gateway.

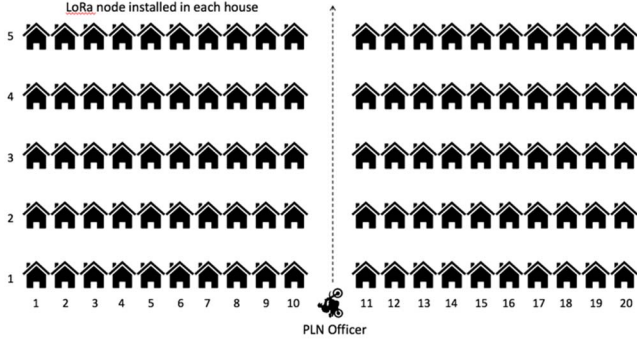


Fig. 2. Residential Area of Simulation

### III. SIMULATION SCENARIO

We modified the LoRaSim simulator as follow: first we define the start position of gateway, then we set the movement of mobile gateway. Second we define the start position of first node and create as many nodes that we want for simulation. The nodes is in fix place position forming like Fig. 2 consists of 20 nodes in each row. Mobile gateway will move from the first row until the last row. To run simulation, we use the expression below:

```
./loraDir.py <Nodes> <AvgSend> <Experiment>
<SimTime> [Collision]
```

Nodes parameter is the number of nodes in one simulation. AvgSend parameter is average of sending interval in milliseconds. Experiment parameter is type of radio setting that used for simulation. The value of experiment setting is 0-5 which every value has embedded parameter setting in LoRaSim. Experiment 0 (Exp 0) use the setting with the slowest data rate. Experiment 1 (Exp 1) is similar to Exp 0, but use a random transmit frequencies. Experiment 2 (Exp 2) use the setting with the fastest data rate. Experiment 3 (Exp 3) use optimize setting per node based on the distance to the gateway. Experiment 4 (Exp 4) use the setting as defined in LoRaWan. And Experiment 5 (Exp 5) is similar to Exp 3, but also optimizes the transmit power. SimTime parameter is the total of running time simulation in milliseconds. Collision parameter is the collision check of simulation. To enable full collision check, set 1, and to enable simplified collision check, set 0.

We choose an electricity meter case study in Indonesia with the assumptions outlined in section 2.4. We run the simulation with modified LoRaSim to evaluate scalability and performance of LoRa deployments. Gateway moves right in the middle of residential area. The simulation example can be seen in Fig. 4. Gateway start position in 2(1), 2(2) gateway is right in the middle of trip, and 2(3) gateway at finish position.

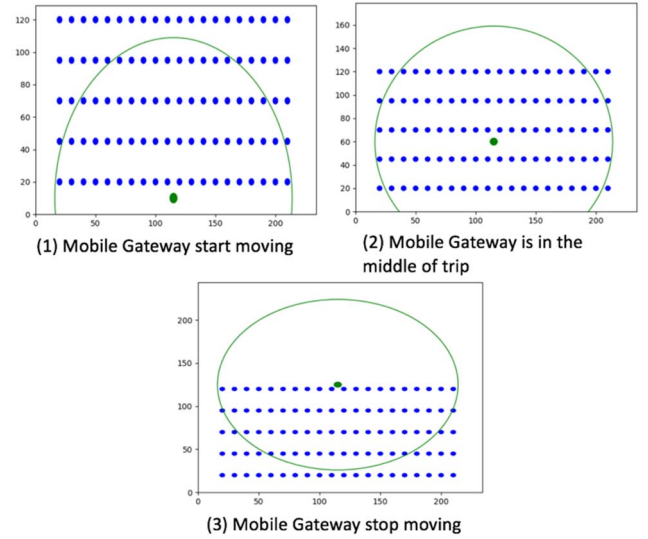


Fig. 3. Simulation Examples of Gateway and Nodes Position in LoRaSim

We run simulation to find Data Extraction Rate (DER) and Network Energy Consumption (NEC). In [10] DER is the ratio of received messages to sent messages over a certain period of time. DER value is between 0 to 1. LoRa deployment is effective when DER value is near to 1. NEC is the energy consumed by the network so the messages can be successfully extracted. The lower NEC value, the more efficient of LoRa deployment.

$$DER = \frac{\sum \text{packet sent} - \sum \text{collision}}{\sum \text{packet sent}}$$

-packet sent: packet sent of each node

-collision: collision occur during sending packets

$$NEC = \frac{\sum_{i=0}^n (t \text{ packet}_i * TxPower_i * V * \text{packet sent}_i)}{1000000}$$

-i: index for node

-n: number of nodes

-t packet: time for packet sent per node

-Tx Power: transmission power

-V: node power

-packet sent: packet sent of each node

The number of nodes in simulation that we use are 100, 120, 140, 160, 180 and 200. We use experiment (Exp) parameter value 3 and 5 which has defined in LoRaSim. As previously explained, in Exp 3 each node has optimized setting based on the distance to the gateway, while in Exp 5 has similar setting to Exp 3 but the transmit power is also optimized. Packet transmission rate ( $\lambda$ ) defined as  $1 \times 10^{-6}$  ms, and packet payload (B) defined as 20 byte. Parameter setting in Exp 3 and Exp 5 shown in Table 1. For average sending packet by LoRa node is 30 s (30000 ms). Our assumption in this IoT era, there are many interferences which can lead collisions. Therefore in our simulations we set 1 to collision parameter. Then we simulate in several scenario. Gateway movement speed based on SimTime parameter value. In any number of nodes (100, 120, 140, 160, 180, 200), the number of rows of nodes (housing) will also

increase, so we add the SimTime in any number of rows that increase.

TABLE I. DEFINED PARAMETER SETTING IN LORASIM

Parameter	Exp 3	Exp 5
TP (dBm)	14	Min (TP)
CF (MHz)	860	860
SF	Best (SF)	Best (SF)
BW (kHz)	Best (BW)	Best (BW)
CR	4/5	4/5
$\lambda$ (ms)	$1 \times 10^{-6}$	$1 \times 10^{-6}$
B (byte)	20	20

We use 3 scenarios to run simulation. In Scenario Number 1 (SN 1) shown in Table 2, we use 100-200 nodes, the average sending interval is set to 30000ms, the Exp is set to 3, and the collision is set to 1. The SimTime for 100 nodes is 6 minutes (360000 ms), SimTime for 120 nodes is 7.2 minutes (432000 ms), SimTime for 140 nodes is 8.4 minutes (504000 ms), SimTime for 160 nodes is 9.6 minutes (576000 ms), SimTime for 180 minutes is 10.8 minutes (648000 ms), and SimTime for 200 nodes is 12 minutes (720000 ms). In Scenario Number 2 (SN 2), we change the speed of mobile gateway by changing the SimTime. SimTime 1 similar to SimTime SN 1, SimTime 2 we increase twice from SimTime 1, and SimTime 3 we decrease twice from SimTime 1. Parameter setting for SN 2 shown in Table 3. In Scenario Number 3 (SN 3), similar to SN 2 but we change the experiment with Exp 5 which has optimized transmit power as shown in Table 4.

TABLE II. PARAMETER SETTING FOR SN 1

Parameter	Scenario Number 1 (SN 1)					
Number of Nodes	100	120	140	160	180	200
AvgSend (ms)	30000					
SimTime (ms)	360000	432000	504000	576000	648000	720000
Exp	3					
Collision	1					

TABLE III. PARAMETER SETTING FOR SN 2

Parameter	Scenario Number 2 (SN 2)					
Number of Nodes	100	120	140	160	180	200
AvgSend (ms)	30000					
SimTime 1 (ms)	360000	432000	504000	576000	648000	720000
SimTime 2 (ms)	180000	216000	252000	288000	324000	360000
SimTime 3 (ms)	720000	864000	1008000	1152000	1296000	1440000
Exp	3					
Collision	1					

TABLE IV. PARAMETER SETTING FOR SN 3

Parameter	Scenario Number 3 (SN 3)					
Number of Nodes	100	120	140	160	180	200
AvgSend (ms)	30000					
SimTime 1 (ms)	360000	432000	504000	576000	648000	720000
SimTime 2 (ms)	180000	216000	252000	288000	324000	360000
SimTime 3 (ms)	720000	864000	1008000	1152000	1296000	1440000
Exp	5					
Collision	1					

#### IV. SIMULATION RESULTS AND EVALUATION

##### A. Scenario Number 1 (SN 1)

We run simulation in several times. The result show DER value is decreasing in some number of nodes (DER Min). It caused by to many collision that occurs during sending packet from LoRa nodes to mobile gateway at a time. As an example in 140 nodes, there is a time that reach 6012 collisions, while the average of the best performance (DER) is around 1000 collisions. When the number collisions are normal, DER value is about 0.9 (DER Max). Overall, the average of DER value (DER Average) from SN 1 results are still above 0.9, except at 200 nodes. With increasing the number of nodes, the energy used also increases. The results of SN 1 are shown in Fig. 4 and Fig. 5.

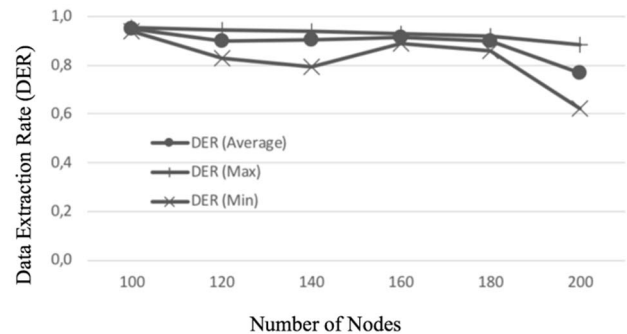


Fig. 4. DER value of SN 1

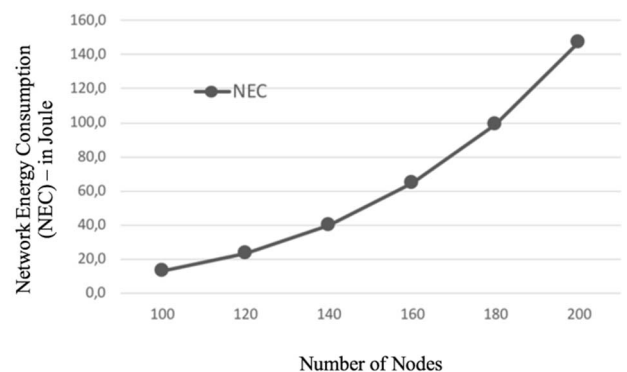


Fig. 5. NEC value of SN 1

### B. Scenario Number 2 (SN 2)

We compare SimTime 1 (V1), SimTime 2 (V2) and SimTime 3 (V3). When the SimTime is increase or decrease twice, the performance does not change too much. The result is still influenced by collisions that occur at a time. But for NEC value, when the SimTime is increase, the energy used is lower than before. And when the SimTime is decrease, the energy used is higher. The results for SN 2 are shown in Fig. 6 and 7.

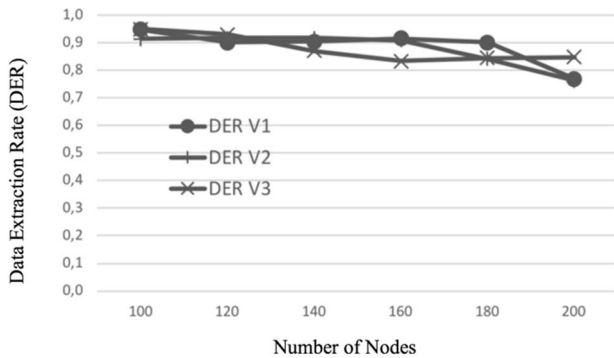


Fig. 6. DER value of SN 2

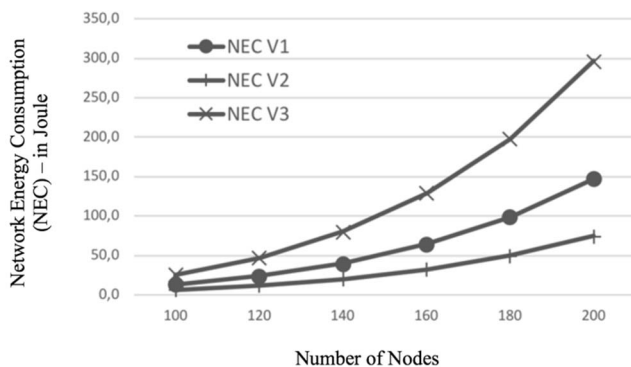


Fig. 7. NEC value of SN 2

### C. Scenario Number 3 (SN 3)

Same results for SN 3 which DER value is influenced by collisions that occur. Different results are on the energy used, using Exp 5 can saves 70-80 percent than using Exp 3. The results of SN 3 are shown in Fig. 8 and 9.

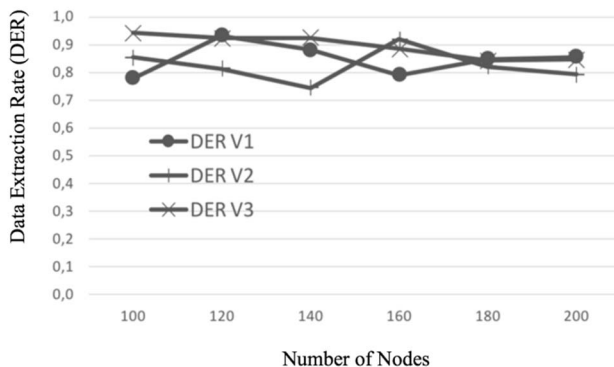


Fig. 8. DER value of SN 3

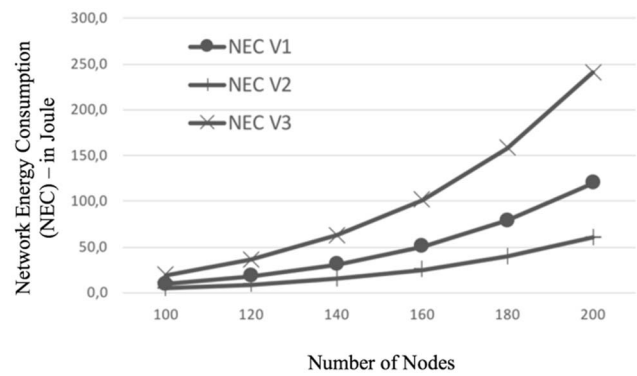


Fig. 9. NEC value of SN 3

## V. CONCLUSION

Based on our work in electricity smart meter simulation with LoRaSim, overall the performance of mobile gateway with LoRa can be achieved, even at a time there is a performance could not be achieved when occur to many collisions. The challenge is to choose a time when the number of collisions that occur is not too much.

When the number of nodes is increase, the energy consumption is also increase. When increasing the simulation time speed, the energy consumption is getting smaller. Optimizing the transmitter power can saves the energy consumptions too.

## ACKNOWLEDGMENT

This research/article's publication is supported by the United States Agency for International Development (USAID) through the Sustainable Higher Education Research Alliance (SHERA) Program for Universitas Indonesia's Scientific Modelling, Application, Research and Training for City-centered Innovation and Technology (SMART CITY) Project, Grant #AID-497-A-1600004, Sub Grant #IIE-00000078-UI-1.

## REFERENCES

- [1] Yukepo. "Indonesia menjadi negara pengguna listrik prabayar terbesar di dunia". in <https://www.yukepo.com/hiburan/indonesiaku/wow-indonesia-menjadi-negara-pengguna-listrik-prabayar-terbesar-di-dunia-kok-bisa-ya/>. Accessed on April 19, 2018.
- [2] Gunawan Wibisono, Gilang Permata S, Awal Awaludin, Paranai Suhasfan. "Development of Advanced Metering Infrastructure Based on LoRa WAN in PLN Bali Toward Bali Eco Smart Grid". 2017 Saudi Arabia Smart Grid (SASG), 2017.
- [3] <http://www.tribunnews.com/bisnis/2016/06/01/pln-luncurkan-smart-grid-dukung-bali-clean-and-green>. Accessed on June 26, 2018.
- [4] <http://journal.ui.ac.id/technology/journal/article/view/157>. Accessed on August 22, 2018.
- [5] Mobile World Live. LoRa Technology: Ecosystem, Applications and Benefits. Semtech Whitepaper. 2017.
- [6] Semtech. Real-world LoRaWAN Network Capacity for electrical Metering Applications. Semtech Whitepaper. 2017.
- [7] Varada Raju, Addala Satya Narayana Varma, Y Satyanarayana Raju. "An Environmental Pollution Monitoring System using LORA". 2017 International Conference on Energy, Communication, Data Analytics and Soft Computing (ICECDS), 2017.
- [8] Yi-Wei Ma and Jiann-Liang Chen. "Toward Intelligent Agriculture Service Platform with LoRa-based Wireless Sensor Network". 2018 IEEE International Conference on Applied System Invention (ICASI), 2017.



- [9] Aswin Tresna Nugraha, Nur Hayati, Muhammad Suryanegara. "The experimental Trial of LoRa System for Tracking and Monitoring Patient with Mental Disorder". 2018 International Conference on Signlas and Systems (ICSigSys).
- [10] Martin Bor, Utz Roedig, Thiemo Voigt, Juan M. Alonso. "Do LoRa Low-Power Wide-Area Networks Scale?". In MSWiM '16 Proceedings of the 19th ACM International Conference on Modeling, Analysis and Simulation of Wireless and Mobile Systems, 2016. New York: ACM Press. pp. 59-67.
- [11] Ruki Harwahu, Alfian Parsekal, Riri Fitri Sari. LoRaWAN Performance Evaluation with Optimized Configuration. International Journal of Future Generation Communication and Networking. Pp. 51-68.
- [12] <https://www.gartner.com/newsroom/id/3598917>. Accessed on June 27, 2018.
- [13] <https://www.wi-fi.org/beacon/alex-roytblat/wi-fi-study-reveals-need-for-additional-unlicensed-spectrum>. Accessed on June 27, 2018.
- [14] <http://maravedis-bwa.com/2018/02/20/measuring-the-need-for-more-unlicensed-spectrum/>. Accessed on June 27, 2018.
- [15] R. Harwahu, R. Cheng, C. Wei and R. F. Sari, "Optimization of Random Access Channel in NB-IoT," in *IEEE Internet of Things Journal*, vol. 5, no. 1, pp. 391-402, Feb. 2018.
- [16] Lorient. "LoRa, LoRaWan, and LORIENT.io". in <https://www.lorient.io/lorawan.html>. Accessed on April 19, 2018.
- [17] Thiemo Voigt, Martin Bor, Utz Roedig, Juan Alonso. "Mitigating Inter-network Interference in LoRa Networks". In EWSN '17 Proceedings of the 2017 International Conference on Embedded Wireless Systems and Networks. 2017. New York: ACM Press. 2017. pp. 323-328.
- [18] LoRa Alliance. A Technical overview of LoRa and LoRaWAN. 2015.
- [19] LoRa. in <http://www.lancaster.ac.uk/scc/sites/lora/>. Accessed on April 19, 2018.



# Rain Attenuation Statistics over 5G Millimetre Wave Links in Malaysia

Mustafa Ghanim

Wireless Communication Centre  
School of Electrical Engineering  
Universiti Teknologi Malaysia  
Johor, Malaysia  
mustafa\_online90@yahoo.com

Manhal Alhilali

Wireless Communication Centre  
School of Electrical Engineering  
Universiti Teknologi Malaysia  
Johor, Malaysia  
manhal@ymail.com

Jafri Din

Wireless Communication Centre  
School of Electrical Engineering  
Universiti Teknologi Malaysia  
Johor, Malaysia  
jafri@utm.my

Hong Yin Lam

Faculty of Engineering Technology  
Universiti Tun Hussein Onn Malaysia  
Johor, Malaysia  
hylam@uthm.edu.my

**Abstract**—Millimetre wave band is a solid contender to be utilized for the future 5G wireless systems deployment. Rain-induced attenuation is a major disadvantage at these frequencies. This paper presents statistics of rain-induced attenuation and rainfall data for two years of horizontally polarized links propagating at 38 GHz and 26 GHz over a terrestrial path link of 301 meters. From the analysed datasets, a rain rate around 116 mm/h exceeded at 0.01% of the time of an average year, while the links recorded 16 and 9.5 dB at the same percentage of time for 38 and 26 GHz respectively. The study aims to identify the prediction model that deliver most reasonable predictions for 5G links operating in Malaysian tropical climate. ITU-R P.530-17, Mello's, and Ghiani's models were all examined. Using ITU-R model, relative error margins of around 3.8%, 30% and 49.7% alongside 22.3, 9.5, 33% were obtained in 0.1%, 0.01% and 0.001% of the time for 26 and 38 GHz respectively. Curiously, ITU-R model demonstrates better predictions to measured rain attenuation with lower error probability. This study highlights the need for new prediction models for short path-length 5G links and helps to improve the design of terrestrial links operating at millimetre wave frequencies in tropical regions.

**Keywords**—fifth generation (5G), millimetre wave communication, rain attenuation, prediction models.

## I. INTRODUCTION

For the currently deployed 4th generation of wireless communications, excess attenuation due to rain can be neglected. However, the demand for greater bandwidth by telecommunication providers requires the move to higher frequency bands in the implementation of the next 5th generation (5G) wireless communication [1]. In tropical regions, the occurrence of rain is more frequent, and the effect on radio links becomes dramatically high for frequencies above 7 GHz, due to higher rain intensities [2], [3]. Therefore, it is fundamental to precisely predict rain-induced attenuation for the planning and design of higher capacity point-to-point 5G radio communication system [4]. The 1-minute rain rate statistics and the rain rate exceeded at a certain percentage of the average year are the most broadly utilized parameters to determine the rain-induced attenuation [5], [6]. Numerous models have been created utilizing these parameters to predict the rain-induced attenuation. However, the majority of these models are conducted and focused on the temperate regions [7]. This could create an issue when applied to the tropical countries due to higher rain rates in tropical regions in comparison to temperate regions. To that end, A campaign to measure the rain attenuation statistics was carried in Universiti

Teknologi Malaysia (UTM) [8]. Some of the most widely used prediction models are empirically based, which uses historical databases for given geographical regions [9], while others are physically based, designed to recover the physical attenuation process, which in turns requires more parameters and longer time to process [10]. Many studies have analysed rain attenuation extensively and various models to overcome the issue have been developed [9]–[12] that primarily enhance the ITU-R P. 530-17 [13] for specific scenarios.

This study investigate three established rain attenuation models, selected to address different types and assumptions used while designing the models, namely, ITU-R P. 530-17 [13] which is the most widely used, Mello model [9] which is usually used in tropical regions, Ghiani's model [14] which is a new physical based model.

The following sections are organized as follow: In section II, prediction models used for the estimation of rain attenuation are briefly discussed. Followed by the system setup, and data collection procedure is discussed. Result and discussion section summarize the accuracy of prediction models. Finally, a conclusion is given in section V, and the possible future research based on the findings is presented.

## II. RAIN ATTENUATION PREDICTION MODELS

Rain-induced attenuation usually presented as the product of rain specific attenuation  $\gamma_R$  (dB/km) and the effective propagation path-length  $d_{eff}$  (km) [15]. The rain-induced attenuation,  $A$  (dB), above  $p$  percent of time is then defined as:

$$A = \gamma_R d_{eff} = \gamma_R d * r \quad (1)$$

where,  $d$  is the actual path-length in km, and  $r$  is path reduction factor at  $p$  percentage of time.

In the ITU-R recommendation P.838-3 [15], the technique to calculate the specific rain attenuation from the rain rate was described. The specific rain attenuation,  $\gamma_R$  (dB/km) is computed from the rain rate  $R$  (mm/h) exceeded at  $p$  percent of the time by applying the power-law relationship as,

$$\gamma_R = kR^\alpha \quad (2)$$

where,  $k$  and  $\alpha$  are frequency dependent coefficients. These constants can be found in the recommendation tables. Due to

the rainfall non-uniformity along the propagation path, a reduction factor of the actual link path-length is presented to reduce the effective path length [10]. However, for shorter links the reduction factor takes values larger than unity, to overcome the model's initial design assumptions. Each model addresses this problem in different way. In this paper three different models included, those of the ITU-R Model [13], Mello's model [9], Ghiani's model [14], these models are briefly explained in the following subsections.

#### A. ITU-R P.530.17 model

The ITU-R recommendation [13] presents the rain attenuation, as described earlier in equation 2, depending on the path reduction factor, which considers the time-space variability of rain intensity along path. The following reduction factor is presented

$$r = (0.477d^{0.633} R_{0.01}^{0.073\alpha} f^{0.123} - 10.579(1 - \exp(-0.024d)))^{-1} \quad (3)$$

where,  $r$  is the distance factor,  $f$ , is the frequency in GHz,  $d$ , is the distance. The maximum value of  $r$  is capped at 2.5.

The resulted rainfall attenuation value exceeded at 0.01% of the time in an average year, is scaled by an empirical formula to other percentages of time between 1% and 0.001% by using the following equation:

$$\frac{A_p}{A_{0.01}} = C_1 p^{(C_2 + C_3 \log 10p)} \quad (4)$$

where,

$$\begin{cases} C_1 = (0.07^{c_0})(0.12^{(1-c_0)}) \\ C_2 = 0.855C_0 + 0.546(1 - C_0) \\ C_3 = 0.139 C_0 + 0.043(1 - C_0) \end{cases} \quad (5)$$

and

$$C_0 = \begin{cases} 0.12 + 0.4(\log_{10} \left(\frac{f}{10}\right))^{0.8} & f \geq 10 \text{ GHz} \\ 0.12 & f < 10 \text{ GHz} \end{cases} \quad (6)$$

This model is recommended to be used worldwide, by providing locally measured rain rates, or by using ITU-R maps, it can help in the prediction for any frequency between 1 and 100 GHz with path-lengths up to 60 km.

#### B. Mello's model

This model uses multiple non-linear regressions to obtain the required numerical coefficients from rain rate and rain cell diameter. And was initially designed using the databanks provided the ITU-R. Mello [9] have used similar procedure as done in [13] which is used by the presented ITU-R model, and overcome the limitation of the ITU-R model by using the complete rainfall distribution as the models input, and keep using the reduction factor parameters from the ITU-R model. In order to correct these limitations, a new effective rainfall rate coefficient ( $R_{eff}$ ) was developed., which helps to predict the rain-induced attenuation complementary cumulative distribution function (CCDF) instead of a single percentage of time, and can be computed as:

$$A_p = \gamma_R \cdot d_{eff} = k(R_{eff}(R, d))^\alpha \frac{1}{1 + \frac{d}{d_0(R)}} \quad (7)$$

where,

$$d_{eff} = \frac{1}{1 + \frac{d}{d_0}} d = rd \quad (8)$$

here  $d$  is the link path-length,  $r$  as presented earlier, the path reduction factor. The definition for  $R_{eff}$  and equivalent rain cell diameter  $d_0$  is then given by:

$$R_{eff} = 1.763R^{0.753 + \frac{0.197}{d}} \quad (9)$$

$$d_0 = 119R^{-0.244} \quad (10)$$

Multiple nonlinear regressions are used to obtain the numerical coefficients in Equations (9) and (10), using the databanks provided the ITU-R.

#### C. Ghiani model

Ghiani [14] has developed novel physically based approach to model the rain attenuation affecting terrestrial links. This model is devised by simulating the interaction between terrestrial links and synthetic rain maps, which are specifically exploited to investigate the path reduction factor, considering the spatial inhomogeneity of rainfall along the link. The accuracy of the proposed model was tested against the MultiEXCELL-derived rain attenuation statistics and against the independent set of experimental data integrated in the DBSG3 databank available through ITU-R. The exceeded rain attenuation with  $p$  percentage in an average year can be calculated as

$$A(p, d) = KR(p)^\alpha d[a(d)e^{-b(d)R(p)} + c(d)] \quad (11)$$

where  $R(p)$ , extracted from the local input rainfall CCDFs, is the rain rate exceeded with  $p$  percentage of an average year, coefficients  $a$ ,  $b$ , and  $c$  are defined as:

$$\begin{cases} a = -0.8743e^{-0.1111d} + 0.9061 \\ b = -0.0931e^{-0.0183d} + 0.1002 \\ c = -0.6613e^{-0.178d} + 0.3965 \end{cases} \quad (12)$$

### III. SYSTEM SETUP AND DATA COLLECTION

Two experimental millimetre wave links operates at 26 and 38 GHz were mounted at UTM Johor campus [5]. The links were set between the roof of microwave lab and the second transceiver was installed on a telecom tower with a path-length between the two antennas of 301 meters. Both antennas are covered by radomes to prevent wetting antenna conditions. The Automatic gain control output level of the antenna unit is then connected to a PC using a data acquisition system and the sampling interval was set to 1-second. The logged data then stored into databank using C language written. The data was collected over duration of 24 months and a satisfactory data availability of 99.95% was achieved.

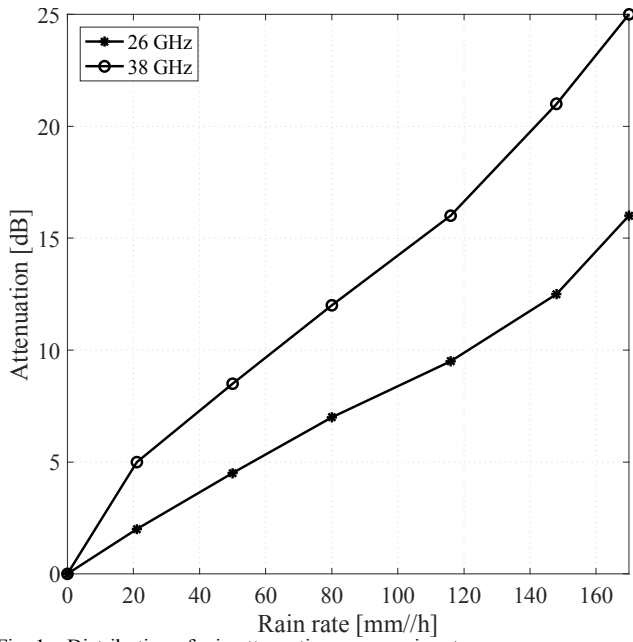


Fig. 1. Distribution of rain attenuation versus rain rate.

A tipping-bucket rain gauge with tip size of 0.2 mm was set up on the same roof. The rain gauge added a time stamp for each tip with 0.1 second resolution. Similar method to calculate 1-minute rain rate used in [16] is used for to present the data in 1-minute integration time. For 0.01% of the time the 1-minute rain rate was found to be around 116 mm/h at the measurement site. Fig. 1 show the rain-induced attenuation versus rain rate for both investigated links of 38 and 26 GHz. The attenuation reaches up to 25 dB on the 38 GHz link, and 16 on the 26 GHz link. This highlight that even with short link distance, that will be used for 5G applications, the rain attenuation should not be underestimated.

#### IV. RESULTS AND DISCUSSIONS

Fig. 2 presents the prediction error plots of ITU-R Model versus rainfall rates for 38 and 26 GHz under horizontal polarization respectively.

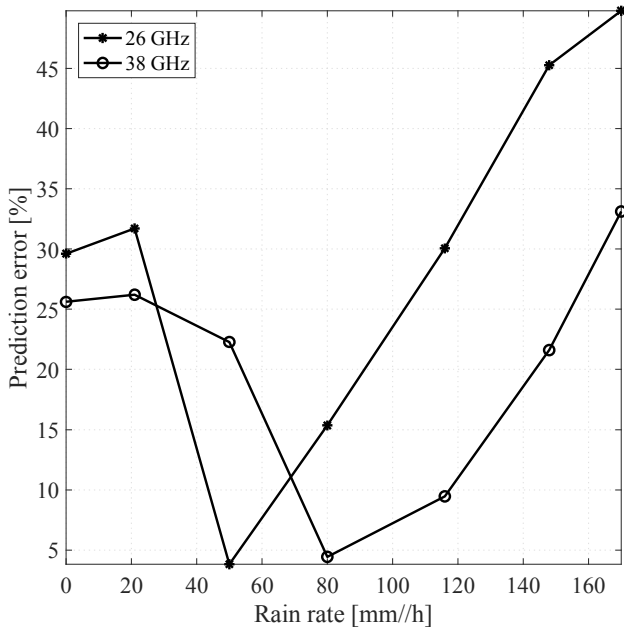


Fig. 2. ITU-R P.530-17 prediction error with rain rate.

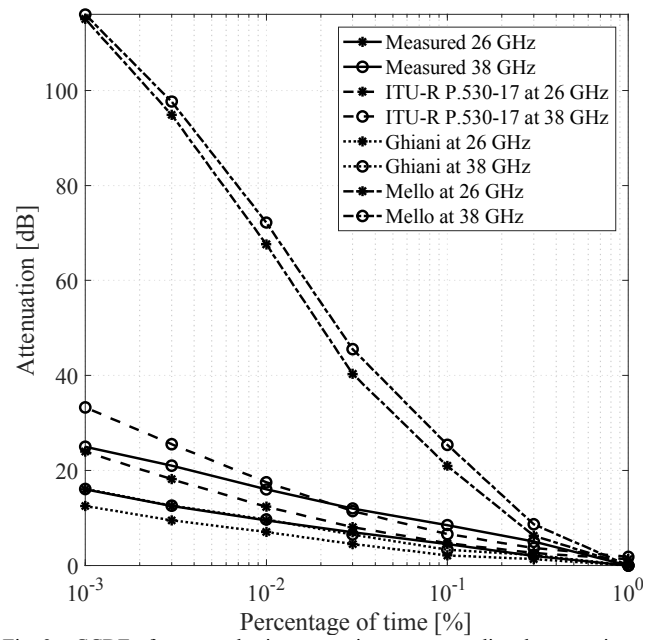


Fig. 3. CCDF of measured rain attenuation versus predicted attenuation at various time percentages for 38 and 26 GHz.

It was found that the error in prediction is higher for 38 GHz link as compared to 26 GHz. The prediction error increases with higher rain rate, due to the initial design of the model based on the data bank from temperate regions, where the rain rates will not reach these high values.

Fig. 3 present comparison between the measured values for 38 and 26 GHz links, and the selected attenuation models. The ITU-R prediction slightly overestimated the rain attenuation and the highest disparity was 8 dB at 38 GHz link. The disparity might be due to the fact that the initial design factors investigated to predict the rain attenuation in the model have not considered the propagation tropical rain. Additionally, ITU-R P. 530-17 is designed for link with path-length longer than 1 km. ITU-R P.530-17, and Ghiani's models give closer estimates to the measured CCDFs of rain attenuation. Large overestimate is shown by Mello's model. The ITU-R model prediction was the most suitable and generated fewer disparities between measured rain attenuation values and the predictions in comparison to other models.

The Mello model shows excessive overestimation. As an example, Mello predicts 25.4, 72.2, 116 dB at 0.1%, 0.01%, 0.001% of the time for 38 GHz link, this might be due to the design of the model based on long-path links.

The relative error figure ( $\varepsilon(p)$ ), is presented to measure the appropriateness for each of the model. And further comparisons are done through the calculation of Standard Deviation (STD) and Root Mean Square (RMS), to examine the performance of the ITU-R, Mello's, and Ghiani's models. The error figure used to examine the accuracy of the prediction models is given by:

$$\varepsilon(p) = \frac{A_{p, \text{predicted}} - A_{p, \text{measured}}}{A_{p, \text{measured}}} \times 100 \quad (13)$$

The calculated  $\varepsilon(p)$ , Standard Deviation (STD) and Root Mean Square (RMS) means for each model are listed in Table I for 26 and 38 GHz respectively.

TABLE I. PERCENTAGE ERROR OBTAINED OVER THE INTERVAL 0.001–1% FOR 26, 38 GHz.

26 GHz			
	ITU-R %	Ghiani %	Mello %
$\epsilon(p)_{mean}$	29.3	32.2	406.43
RMS	32.8	33.9	479.26
STD	16.4	11.4	174.5
38 GHz			
	ITU-R %	Ghiani %	Mello %
$\epsilon(p)_{mean}$	1.8	46.4	218.8
RMS	21.8	47.3	273.1
STD	23.8	10.1	116.9

As can be noted from the table, Mello's model shows higher relative error compared to ITU-R model and Ghiani's models, which is apparent with the increased STD and RMS values. For that, ITU-R, Ghiani's models give better prediction alongside the measured rain attenuation.

#### V. CONCLUSION

Based on the presented results for the described experiment on 26 and 38 GHz links, the rain rate and the induced attenuation are presented for 5G short path-length links. Three well established rain attenuation models were used to compare the predicted results with the measured data. The presented comparison shows that ITU-R P.530-17 model was the most appropriate to be used under the link specification and tropical climate, by giving closer predictions to the measured rain induced attenuation. However, for the lower frequency 26 GHz, the prediction error was slightly lower in comparison with 38 GHz, this might be due to the differences in rain drop size distribution effects on higher frequencies. Additionally, fewer error at low exceedance of time for all the models, and the error increase with time percentages, indicate the differences between the measured and predicted values as the models were initially designed for temperate regions. Ghiani's model followed the ITU-R with close estimate to the measured rain attenuation. In addition, the performed error analyses showed similar judgment. Mello's model fails to adapt to the shorter link path, as it was empirically designed. The study highlights the need for a model that cover shorter path-length 5G links and designed especially for tropical regions. The results presented here could help in the design of a better rain attenuation prediction models for terrestrial links operating at higher frequencies in the tropics.

#### ACKNOWLEDGMENT

This work has been funded by Ministry of Education Malaysia and Universiti Teknologi Malaysia under "FRGS" Vot. No. RJ130000.7823.4F958, and Universiti Tun Hussein Onn Malaysia Tier 1 Grant Vot No. H160.

#### REFERENCES

- [1] T. S. Rappaport *et al.*, "Millimeter wave mobile communications for 5G cellular: It will work!," *IEEE Access*, vol. 1, pp. 335–349, 2013.
- [2] H. Y. Lam, J. Din, and S. L. Jong, "Statistical and physical descriptions of raindrop size distributions in equatorial Malaysia from disdrometer observations," *Adv. Meteorol.*, vol. 2015, pp. 1–14, 2015.
- [3] F. Moupfouma and J. Tiffon, "Raindrop size distribution from microwave scattering measurements in equatorial and tropical climates," *Electron. Lett.*, vol. 18, no. 23, pp. 1012–1014, 1982.
- [4] H. Y. Lam *et al.*, "Impact of Rain Attenuation on 5G Millimeter Wave Communication Systems in Equatorial Malaysia Investigated Through Disdrometer Data," in *EuCAP*, 2017, pp. 1802–1806.
- [5] A. Y. Abdulrahman *et al.*, "Investigation of the unified rain attenuation prediction method with data from tropical climates," *IEEE Antennas Wirel. Propag. Lett.*, vol. 13, no. January 2014, pp. 1108–1111, 2014.
- [6] C. Capsoni, L. Luini, A. Paraboni, C. Riva, and A. Martellucci, "A new prediction model of rain attenuation that separately accounts for stratiform and convective rain," *IEEE Trans. Antennas Propag.*, vol. 57, no. 1, pp. 196–204, 2009.
- [7] L. S. Kumar, Y. H. Lee, and J. T. Ong, "Truncated gamma drop size distribution models for rain attenuation in Singapore," *IEEE Trans. Antennas Propag.*, vol. 58, no. 4, pp. 1325–1335, 2010.
- [8] M. Awang and J. Din, "Comparison of the rain drop size distribution model in tropical region," *RF Microw. Conf. 2004. RFM 2004. Proc.*, no. D, pp. 20–22, 2004.
- [9] L. da S. Mello, M. S. Pontes, I. Fagundes, M. P. C. Almeida, and F. J. A. Andrade, "Modified rain attenuation prediction method considering the effect of wind direction," *J. Microwaves, Optoelectron. Electromagn. Appl.*, vol. 13, no. 2, pp. 254–267, 2014.
- [10] R. Ghiani, L. Luini, and A. Fanti, "Investigation of the path reduction factor on terrestrial links for the development of a physically-based rain attenuation model," *2016 10th Eur. Conf. Antennas Propagation, EuCAP 2016*, no. 1, pp. 2–3, 2016.
- [11] M. Alhilali, J. Din, M. Schönhuber, and H. Y. Lam, "Estimation of Millimeter Wave Attenuation Due to Rain Using 2D Video Distrometer Data in Malaysia," *Indones. J. Electr. Eng. Comput. Sci.*, vol. 7, no. 1, pp. 164–169, 2017.
- [12] H. Y. Lam, L. Luini, J. Din, C. Capsoni, and A. D. Panagopoulos, "Application of the SC EXCELL model for rain attenuation prediction in tropical and equatorial regions," *2010 IEEE Asia-Pacific Conf. Appl. Electromagn. APACE 2010 - Proc.*, 2010.
- [13] ITU-R, "Recommendation ITU-R P.530-17: Propagation data and prediction methods required for the design of terrestrial line-of-sight systems," *Recomm. ITU-R P.530-17*, 2017.
- [14] R. Ghiani, L. Luini, and A. Fanti, "A physically based rain attenuation model for terrestrial links," *Radio Sci.*, vol. 52, no. 8, pp. 972–980, 2017.
- [15] ITU, "P. 838-3 Specific attenuation model for rain for use in prediction methods," *ITU-R Recommendations, P Series Fascicle*. ITU, Geneva, Switzerland, pp. 1–5, 2005.
- [16] M. D. Amico, S. L. Jong, and C. Riva, "Tipping Bucket Data Processing for Propagation Application," in *EuCAP*, 2013, vol. 49, no. 8, pp. 256–260.

# Fuzzy Logic Controller Design for Leader-Follower Robot Navigation

Tresna Dewi, Yudi Wijanarko, Pola Risma, and Yurni Oktarina

*Department of Electrical Engineering*

*Politeknik Negeri Sriwijaya*

Palembang, Indonesia

tresna\_dewi@polsri.ac.id, wijanarko\_yudi@polsri.ac.id, polarisma@polsri.ac.id, and yurni\_oktarina@polsri.ac.id

**Abstract**—Mobile robots are applied everywhere in the human's life, starting from industries to domestics. This phenomenon makes it one of the most studied subjects in electronics engineering. Navigation is always an issue for this kind of robot, to ensure it can finish its task safely. Giving it a "brain" is one of the ways to create an autonomous navigating robot. The Fuzzy logic controller is a good choice for the "brain" since it does not need accurate mathematical modeling of the system. Only by utilizing the inputs from sensors are enough to design an effective controller. This paper presents an FLC design for leader-follower robot. This FLC design is the improvement of FLC application in a single two differential-driven mobile robot. The relation between leader and follower robot is modeled linearly as a spring-damper system. Simulation proves the feasibility of the proposed method in several environment setting, and this paper also shows that the method can be easily extended to one leader and more than one follower's formation. The research in this paper has introduced in the classroom as the teaching-learning media to improve students' involvement and interest in robotics and robotics related class. This paper is also part of our campaign and encouragement for teachers and students to use low-cost and open source software since not all the universities in developing country can afford the expensive high-end software.

**Index Terms**—Fuzzy logic controller, Mobile Robot, Leader-follower formation, Navigation.

## I. INTRODUCTION

Mobile robots are applied everywhere, in industries and domestics, ranging from being a transport robot, a vacuum cleaner, or merely for entertainment purpose, such as a dog robot. A navigation strategy needs to be well designed to ensure the robot functions well. Navigation strategy for the autonomous mobile robot is including target reaching, obstacle avoidance, and wall following. A mobile robot is often applied in an ever-changing dynamic environment that creates complexity for the robot. Motion planning becomes a crucial part of the navigation system to ensure the robot can reach a target or final point, the targets to be intercepted by the robot can be static and dynamic (a moving target) [1]. This motion planning can be generated in real-time (online) or pre-mapped (offline). Real-time motion planning requires a specific intelligence installed on the robot. A planted AI (artificial intelligence) can create a smart robot that works better than the ones without AI.

One of the most applied types of AI is fuzzy logic and has been a well-discussed topic in robotics since introduced by

Zadeh in 1965 [2]. Fuzzy logic enables a linguistic approach to process the uncertain data using designed rules. This method is best for complex systems that are not easy to be modeled with exact mathematics. Rather than going through exact value, the fuzzy logic linguistic set works using IF-THEN rules fed up to an interference engine. The rules are used to encode the behavior of robot motion against the target (static[3] and dynamic target[4]), obstacles and walls found. In this method, even not so effective rules are sufficient enough. A mobile robot is a complex non-linear system and suffers the non-holonomic constraints; therefore a technique like fuzzy logic is very suitable for navigation planning strategy[5]-[11].

The application of a group of simple mobile robots (swarm robot) is better than deploying one sophisticated robot [12]-[17]. The more robots to control the more complex and uncertain the system is, therefore the application of a fuzzy logic controller (FLC) is appropriate in this situation. The controller for one robot can be extended to a group of robots in a leader-follower formation. The controller for leader-follower formation in some cases can be simplified in static controller design [16][17].

This paper proposes a method for motion planning of robots in leader-follower formation by improving/extending the FLC for a single robot. The navigation system is developed by combining several conditions that might be encountered by the robot, such as target reaching, obstacle avoidance, and wall following. The obstacle avoidances are provided by the proximity sensors attached to the robots. The right sensors for both leader and follower are also utilized for wall follower to keep the robot following the walls in a certain distance. The leader is set to reach a static target, while the follower is set to follow the leader by considering the leader as a moving target to pursue. The proximity sensor attached to the front of the follower robot is assigned to keep a safe distance from the leader. The output of the robots is the velocity of the left and right wheels. The system is updated online until reaching the target.

The novelty of this study is the improvement of FLC design for a single robot following a moving target into FLC for a leader-follower formation robot. The feasibility of the proposed method is presented in the simulation with several environment setting using MobotSim [20]. The

relationship between input and output of the system is shown by SCILAB[19]. This research is also to teach the students in robotics class how to design robots controller and to encourage them to be pro-active in learning and designing robots[21][22][23].

## II. MOBILE ROBOTS MODELING

### A. Kinematics Modeling of a Single Robot

Mobile robot considered in this paper is a two wheels differential driven mobile robot, presented in fig. 1. The position and orientation of the robot is  $q = [x \ y \ \phi]^T$ , the translational and rotational velocities are  $\dot{q} = [\dot{x} \ \dot{y} \ \dot{\phi}]^T$ , where  $x$  and  $y$  are robot's position,  $\dot{x}$  and  $\dot{y}$  are translational velocities in  $x$  and  $y$ -axis,  $\phi$  is the orientation of the robot, and  $\omega = \dot{\phi}$  is the rotational velocity.

Robot inverse kinematics is given as

$$\begin{bmatrix} \dot{\theta}_R \\ \dot{\theta}_L \end{bmatrix} = f(\dot{x}, \dot{y}, \dot{\phi}), \quad (1)$$

where  $\dot{\theta}_R = \frac{1}{2\pi r} \cdot v_R$  and  $\dot{\theta}_L = \frac{1}{2\pi r} \cdot v_L$ .  $v_R$  and  $v_L$  are wheel's translational velocities.

Therefore, from eq. 1, robot's velocity is

$$v = r \frac{\dot{\theta}_R - \dot{\theta}_L}{2}, \quad (2)$$

and

$$\omega = \frac{r}{2L} (\dot{\theta}_R - \dot{\theta}_L). \quad (3)$$

where  $L$  is the half width of the robot,  $r$  is the wheels' radius, and  $\dot{\theta}_R$  and  $\dot{\theta}_L$  are right and left wheel's velocities.

Robot presented in fig. 1 suffers the non-holonomic constraint

$$v = \dot{x} \cos \theta + \dot{y} \sin \theta. \quad (4)$$

It means robot only moves in curvature and not in lateral sideward motion, therefore  $0 = \dot{x} \sin \theta - \dot{y} \cos \theta$ .

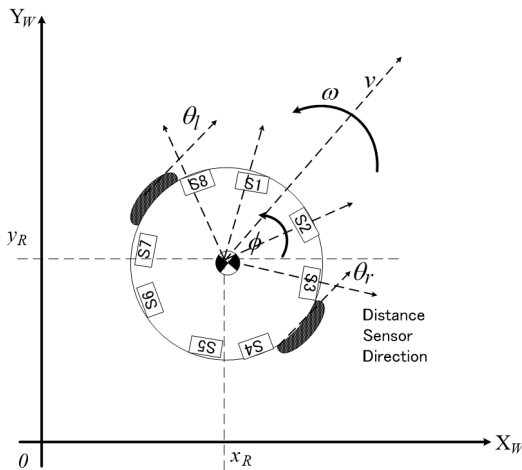


Fig. 1: Single robot in its coordinate frames

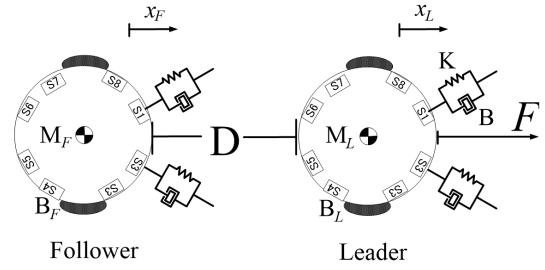


Fig. 2: Leader follower robot spring-damper system modeling

Control input  $v$  and  $\omega$  are defined as

$$\begin{bmatrix} \dot{x} \\ \dot{y} \\ \dot{\phi} \end{bmatrix} = \begin{bmatrix} \cos \theta & 0 \\ \sin \theta & 0 \\ 0 & 1 \end{bmatrix} \begin{bmatrix} v \\ \omega \end{bmatrix} \quad (5)$$

where in this study  $v$  and  $\omega$  is defined as the control inputs.

### B. Leader-Follower Formation Modeling

The dynamics modeling of leader and follower robot relations is considered as a spring-damper system, as shown in fig. 2. This modeling is a representation of proximity sensors attached to the follower [16]. The spring-damper system is also used to model the relation between proximity sensors attached to the leader and the obstacles and walls found. The virtual spring-damper model can be used to describe the flocking robots' behavior where the spring defines the force of attraction to the leader and the damper defines the repelling force.

The dynamics of leader follower robot given in fig. 2 are

#### 1) Leader dynamics

$$F = M_L \ddot{x}_L + B_L \dot{x}_L + B(\dot{x}_L - \dot{x}_F) + K(x_L - x_F), \quad (6)$$

#### 2) Follower dynamics

$$B(\dot{x}_L - \dot{x}_F) + K(x_L - x_F) = M_F \ddot{x}_F + B_F \dot{x}_F, \quad (7)$$

where  $F$  is the force applied to robot leader, the force considered here, is the virtual attraction force produced by the target.  $B$  is the damping constant,  $K$  is the spring constant,  $B_L$  and  $B_F$  are the Coulomb frictions of leader's and follower's wheels.  $M_L$  and  $M_F$  are the mass of leader and follower robot.  $x_L$  and  $x_F$  are the representation of leader and follower displacement along  $y$ -axis.

The distance of leader and follower robot is given by

$$D = \sqrt{(x_L - x_F)^2 + (y_L - y_F)^2} \quad (8)$$

The target is considered to have a virtual force that attracts the leader robot, and the generated leader's trajectory is considered as the virtual reference trajectory for the follower. The error of trajectory tracking between the leader and follower robot can be written as follow.

$$e_{dist} = \begin{bmatrix} e_1 \\ e_2 \\ e_3 \end{bmatrix} = \begin{bmatrix} \cos \phi & \sin \phi & 0 \\ -\sin \phi & \cos \phi & 0 \\ 0 & 0 & 1 \end{bmatrix} \begin{bmatrix} x_L - x_F \\ y_L - y_F \\ \phi_L - \phi_F \end{bmatrix} \quad (9)$$



TABLE I: Rules based for FLC design

No	Input					Output	
	S1	S2	S3	S8	Camera	Left Tire	Right Tire
1	N	N	N	N	Detect	Stop	Stop
2	N	N	N	M	Detect	Stop	Slow
3	N	N	M	F	Detect	Slow	Med
4	N	N	M	N	Detect	Slow	Stop
5	N	M	F	M	Detect	Slow	Med
6	N	M	F	F	Detect	Fast	Med
7	N	M	N	N	Detect	Slow	Slow
8	N	M	N	M	Detect	Stop	Slow
9	M	F	M	F	Detect	Fast	Fast
10	M	F	M	N	Detect	Slow	Med
11	M	F	F	M	Detect	Med	Fast
12	M	F	F	F	Detect	Med	Fast
13	M	N	N	N	Detect	Med	Slow
14	M	N	N	M	Detect	Med	Slow
15	M	N	M	F	Detect	Med	Slow
16	M	N	M	N	Detect	Med	Med
17	F	M	F	M	Detect	Med	Med
18	F	M	F	F	Detect	Fast	Med
19	F	M	N	N	Detect	Fast	Med
20	F	M	N	M	Detect	Med	Slow
21	F	F	M	F	Detect	Fast	Med
22	F	F	M	N	Detect	Slow	Fast
23	F	F	F	M	Detect	Med	Fast
24	F	F	F	F	Detect	Fast	Fast

Note: N is near, M is Medium, F is Far, and Med is medium velocity.

### III. FUZZY LOGIC CONTROLLER DESIGN

FLC designed in this paper is based on the FLC design for a single robot, and the rules-based are kept simple. The spring-damper system is adopted between the leader and follower. The virtual trajectory for the leader is set by an attractive force emitted by the target, and this leader trajectory becomes the reference trajectory for the follower robot. Tracking can be defined as an act of approaching an moving object by matching its location and velocity; therefore follower should match its position and velocity to the leader.

Fig. 3 shows the FLC design proposed in this study where the inputs are from proximity sensors and camera. In this current study, the attached camera is considered to be in two states only, detects or no detection. The camera application for the leader is to recognize the target of the leader robot, and for the follower robot to identify the leader. The camera in this paper has no significant role; however, the inclusion of a camera is to prepare the rules for the real system which is an ongoing project at the moment. Eight proximity sensors

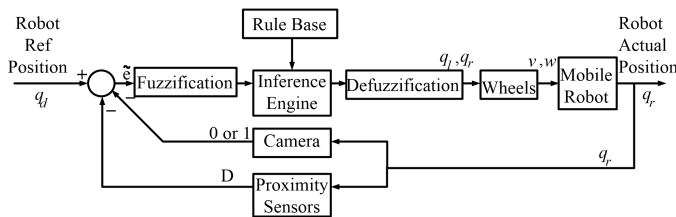


Fig. 3: Diagram block for FLC controller design

are installed on the robot; however, only four are utilized for distance recognition in obstacle avoidance and maintaining the safe distance to leader robot.

FLC is designed by creating a database to define the linguistic variables and fuzzy rules based. Table I shows the rules-based considered in this paper. The linguistic in table I is translated into membership functions of inputs from sensors, given in fig. 4. The fuzzification shown in fig. 3 maps the crisp numbers into a fuzzy set that used to activate the associated fuzzy set. The inference engine handles the way how to combine the rules and represents the knowledge base of the system. The defuzzification converts each of conclusion from inference engines into a single crisp non-fuzzified, and FLC output will be the input to the robots.

Inputs conditions for proximity sensors ( $S1, S2, S3$ , and  $S8$ ) in table I are N for near, M for medium, and F for Far. Near, medium and far show the distance between the robot to obstacles or the follower robot to leader robot. The output results are the wheels' velocity, which is divided into four conditions, stop, slow, medium, and fast. In this paper, camera condition is only limited to 2 states, detection, and no detection, since robot moves if the camera detects the object (leader or target), then the rules simplified only for camera detection.

### IV. RESULTS AND DISCUSSION

The feasibility of the proposed FLC designed is tested in MobotSim software by designing leader-follower robots in several environments. The FLC is designed using MobotSim's built-in BASIC editor. Robots are deployed in an environment including several obstacles which considered as walls, and the target is deemed to have an attractive virtual force. Robots move from start to end points by utilizing distance sensors to keep the safe distance to the obstacles and leader robots.

Robots positioned in the starting points are shown in fig. 6a, 7a, 8a, 9a, and 10a, and robots reaching the target shown in fig. 6b, 7b, 8b, 9b, and 10b. Fig. 6 to 10 show that the leader robots avoid obstacles and keep the distance to the wall in the desired distance, and the follower robots keep the safe distance to the leader while avoiding the obstacles and following the wall at the same time. The robot implemented in this paper is based on the real system, therefore the range of distances considered in this research presented in fig. 4 is also based on the real robot. The robots trajectories show that the follower robot follows the leader from start to end point. The simulation of one leader and one follower can easily extend to more that one followers, as shown in fig. 11.

The material presented in this paper was a part of simulations introduced to students at bachelor level in our Polytechnic. The teaching-learning process is enhanced by involving students' active participation. The enhancement was conducted by introducing several simulation software and encouraging the students to design their robots and environments. The software introduced are low-cost software like this MobotSim and open-source software, since not all the polytechnics in developing country can afford the costly

high-end software. This paper also parts of our campaign and encouragement to teachers and students working with robotics to use low cost and open source software [23].

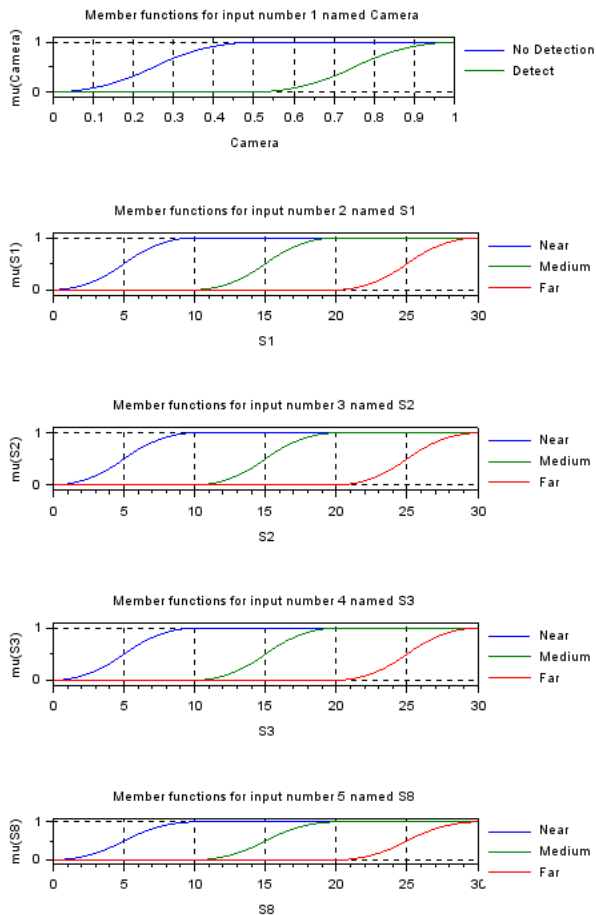


Fig. 4: Membership function of sensors input

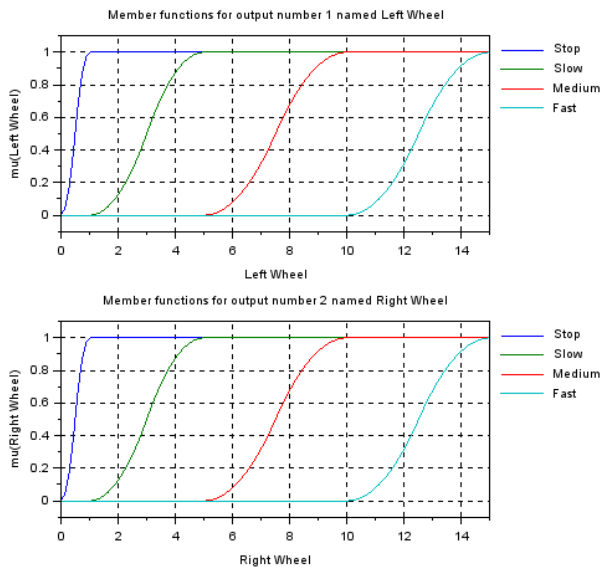
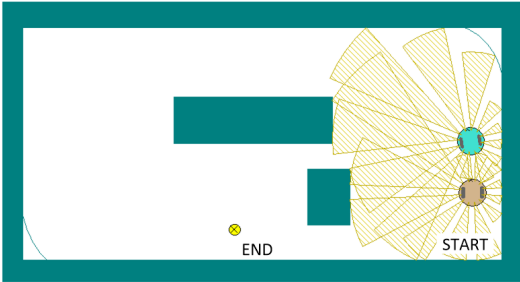
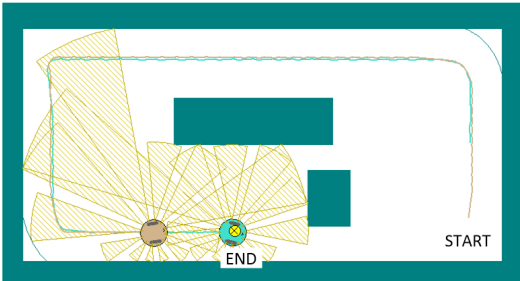


Fig. 5: Output system



(a) Robots in start position

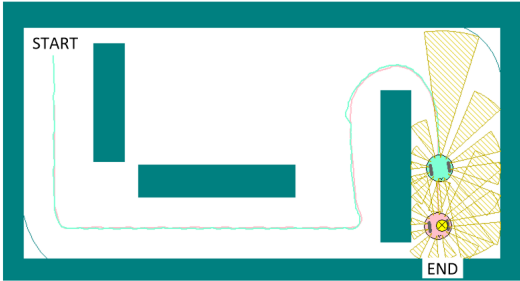


(b) Robots in final position

Fig. 6: Environment 1



(a) Robots in start position



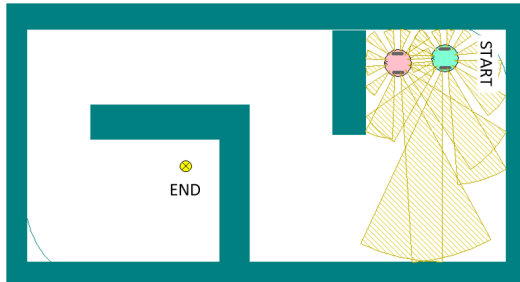
(b) Robots in final position

Fig. 7: Environment 2

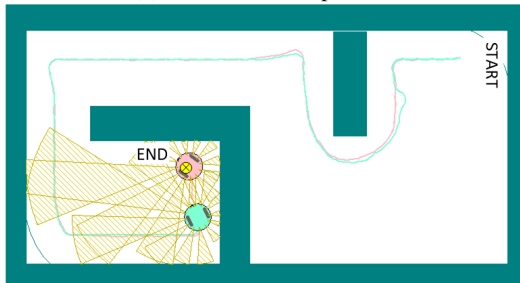
## V. CONCLUSIONS

FLC is a good approach to design navigation system for a mobile robot since this type of controller does not require exact mathematical modeling of the system. The mathematical modeling of a two differential-driven mobile robot suffers the non-holonomics constraint and the sensors attached to cannot be solved by simple mathematical integration. By using FLC, one can take data from sensors as the inputs for the

controller. This paper presents an improvement/extension from FLC design for one robot to leader-follower formation robots. The relation between leader and follower is modeled as a virtual spring-damper system as presented in our previous work [16]. The feasibility of the proposed method is proven by simulations of leader and follower robot in simulation using SCILAB for input-output representation, and MobotSim for showing the implementation to mobile robots. Simulation results show the effectiveness of the proposed method by

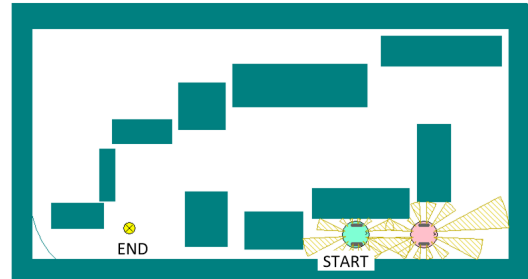


(a) Robots in start position

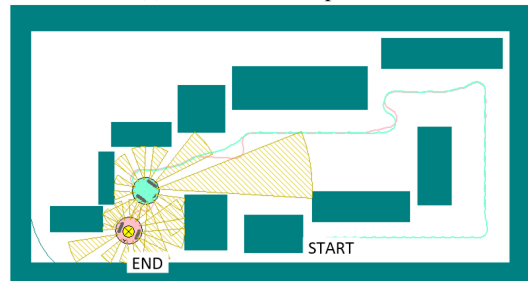


(b) Robots in final position

Fig. 8: Environment 3

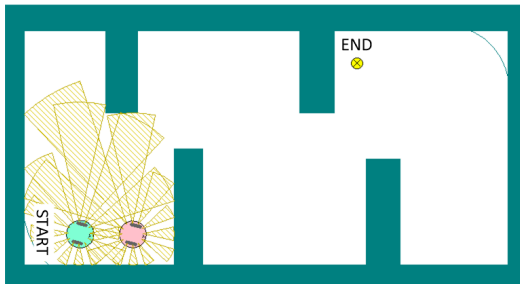


(a) Robots in start position

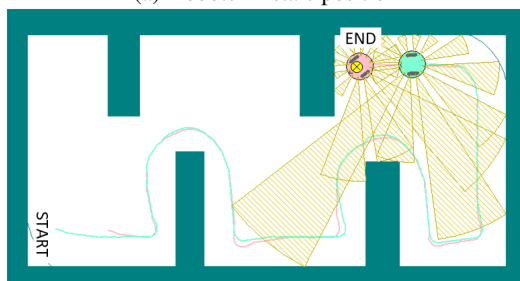


(b) Robots in final position

Fig. 10: Environment 5

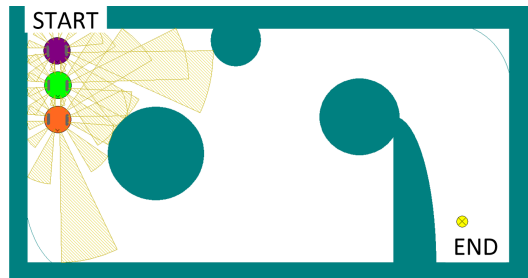


(a) Robots in start position

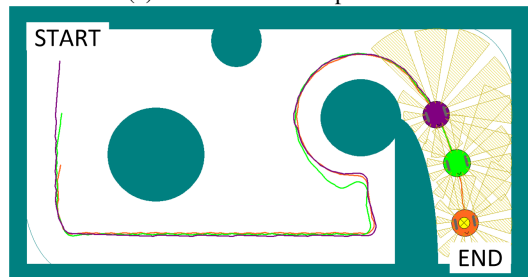


(b) Robots in final position

Fig. 9: Environment 4



(a) 3 Robots in start position



(b) 3 Robots in final position

Fig. 11: 1 leader and 2 followers robot

showing that the follower robot follows the leader in all the environment setting. The proposed method can be easily developed for more than one follower as shown in fig. 11.

The method and software used are also introduced in the author's classroom, as a mean to increase students' involvement in teaching-teaching learning process. By improving the student's involvement, it is also hoped to enhance the creativity and understanding of the students about robotics-related subjects in Politeknik Negeri Sriwijaya. This paper is also part of our encouragement and campaign to encourage teachers and students to use the low-cost, and open source software for teaching-learning process [23], since not all the university and polytechnic in developing countries can afford the costly high-end software.

## REFERENCES

- [1] T. Dewi, N. Uchiyama, and S. Sano, "Service mobile robot control for tracking a moving object with collision avoidance," *2015 IEEE International Workshop on Advanced Robotics and its Social Impacts (ARSO)*, France, 2015, DOI: 10.1109/ARSO.2015.7428197.
- [2] L. A. Zadeh, "Fuzzy Sets. Information Control", vol. 8, pp. 338-353, 1965.
- [3] N. H. Singh and K. Thongam, "Mobile Robot Navigation Using Fuzzy Logic in Static Environments," *Procedia Computer Science*, vol. 125, pp. 11-17, 2018, ISSN 1877-0509, <https://doi.org/10.1016/j.procs.2017.12.004>.
- [4] K. Benbouabdallah and Z. Qi, "Design of a Fuzzy Logic Controller for a Mobile Robot Tracking a Moving Target", *2012 2nd International Conference on Computer Science and Network Technology*, vol. 44, pp. 117-127, 2017. <https://doi.org/10.1016/j.asoc.2016.03.018>.
- [5] S. G. Tzafestas, "Introduction to Mobile Robot Control", 1<sup>st</sup> Edition. Elsevier, pp. 269-305, 2014. <https://doi.org/10.1016/B978-0-12-417049-0.00002-X>. ISBN 9780124171039.
- [6] O. Obe, and I. Dumitrache, "Fuzzy Control of Autonomous Mobile Robot", *U.P.B. Sci. Bull.*, vol. 72, no. 3, Series C, pp. 173-186, 2010.
- [7] H. Omrane, M. S. Masmoudi, and M. Masmoudi, "Fuzzy Logic Based Control for Autonomous Mobile Robot Navigation," *Computational Intelligence and Neuroscience*, vol. 2016, Article ID 9548482, 10 pages, 2016. doi:10.1155/2016/9548482
- [8] A. S. Al Yahmedi and M. A. Fatmi, "Fuzzy Logic Based Navigation of Mobile Robots, Recent Advances in Mobile Robotics", Dr. Andon Topalov (Ed.), 2011, pp. 287-310, ISBN: 978-953-307-909-7, InTech, Available from: <http://www.intechopen.com/books/recent-advances-in-mobile-robotics/fuzzy-logic-based-navigation-ofmobile-robots>
- [9] S. Nurmaini, B. Tutuko, K. Dewi, V. Yuliza, and T. Dewi, "Improving Posture Accuracy of Non-Holonomic Mobile Robot System with Variable Universe of Discourse", *Telkomnika*, vol. 15, no.3, pp. 1265-1279, 2017. DOI: <http://dx.doi.org/10.12928/telkomnika.v15i3.6078>.
- [10] F. Abdessemed, K. Benmahammed, and E. Monacelli, "A Fuzzy-based Reactive Controller for a Non-holonomic Mobile Robot", *Robotics and Autonomous System*, vol. 47, pp. 31-46, 2004.
- [11] A. Pandey, "Path Planning Navigation of Mobile Robot with Obstacles Avoidance using Fuzzy Logic Controller", *2014 IEEE 8th International Conference on Intelligent Systems and Control (ISCO)*, Coimbatore, 2014, 36-41. DOI: 10.1109/ISCO.2014.7103914.
- [12] T. Dewi, N. Uchiyama, S. Sano, and H. Takahashi, "Swarm Robot Control for Human Services and Moving Rehabilitation by Sensor Fusion," *Journal of Robotics*, vol. 2014, Article ID 278659, 11 pages, 2014. <https://doi.org/10.1155/2014/278659>.
- [13] S. El Ferik, M. T. Nasir, and U. Baroudi, "A Behavioral Adaptive Fuzzy controller of multi robots in a cluster space", *Applied Soft Computing*, vol. 44, pp. 117-127, 2017. <https://doi.org/10.1016/j.asoc.2016.03.018>.
- [14] S. K. Pradhan, D. R. Parhi, and A. K. Panda, "Fuzzy Logic Techniques for Navigation of Several Mobile Robot", *Applied Soft Computing*, vol. 9, pp. 290-304, 2009. doi: 10.1016/j.asoc.2008.04.008
- [15] R. Al-Jarrah, A. Shahzad, and H. Roth, "Path Planning and Motion Coordination for Multi-Robots System Using Probabilistic Neuro-Fuzzy," *IFAC-PapersOnLine*, vol. 48, issue 10, pp. 46-51, 2015. <https://doi.org/10.1016/j.ifacol.2015.08.106>.
- [16] T. Dewi, P. Risma, and Y. Oktarina, "Wedge Formation Control of Swarm Robots", *The 14th Industrial Electronics Seminar, Electronic Engineering Polytechnic Institute of Surabaya (EEPIS)*, Indonesia, pp. 294-298, 2012.
- [17] V. Karpov, and I. Karpova, "Leader election algorithms for static swarms", *Biologically Inspired Cognitive Architectures*, vol. 12, pp. 54-64, 2015. <https://doi.org/10.1016/j.bica.2015.04.001>.
- [18] M. A. Molina-Villa, D. R. Avendaño-Flórez, L. E. Solaque-Gusman, and N. F. Velasco-Toledo, "Fuzzy Logic Controller for Cooperative Mobile Robotics Implemented in Leader-Follower Formation Approach," *Revista Facultad de Ingeniería, Universidad de Antioquia*, no. 76, pp. 19-29, 2015.
- [19] <https://www.scilab.org/>, accessed on October 12, 2017.
- [20] <http://www.mobotsoft.com/>, accessed on October 12, 2017.
- [21] P. Shakouri, O. Duran, A. Ordys, and GCollier, "Teaching Fuzzy Logic Control Based on a Robotic Implementation", *IFAC Proceeding Volumes*, vol. 46, issue. 17, pp. 192-197, 2013. <https://doi.org/10.3182/20130828-3-UK-2039.00047>
- [22] A. Pandey, and D. R. Parhi, "MATLAB Simulation for Mobile Robot Navigation with Hurdles in Cluttered Environment Using Minimum Rule Based Fuzzy Logic Controller", *Proceeding of 2nd International Conference on Innovations in Automation and Mechatronics Engineering ICIAME 2014, Procedia Technology*, vol. 14, Vallabh Vidyanagar, 2014, 28-34. <https://doi.org/10.1016/j.protcy.2014.08.005>.
- [23] T. Dewi, P. Risma, Y. Oktarina, and M. Nawawi, "Neural Network Simulation for Obstacle Avoidance and Wall Follower Robot as a Helping Tool for Teaching-Learning Process in Classroom", *Proceeding of 2017 1st International Conference on Engineering & Applied Technology (ICEAT)*, Mataram, 2017, pp. 705-717. <http://conference.fgdt-ptm.or.id/index.php/iceat/index>.

# Arm Robot Manipulator Design and Control for Trajectory Tracking; a Review

Hendra Marta Yudha  
Electrical Engineering Department  
Universitas Tridinanti Palembang  
Palembang, Indonesia  
hendramy@univ-tridinanti.ac.id

Tresna Dewi, Pola Risma, and Yurni Oktarina  
Electrical Engineering Department  
Politeknik Negeri Sriwijaya  
Palembang, Indonesia  
tresna\_dewi@polsri.ac.id, polarisma@polsri.ac.id,  
yurni\_oktarina@polsri.ac.id

**Abstract**—Arm robot manipulator heavily applied in industries ranging from welding, pick-and-place, assembly, packaging, labeling, etc. Trajectory planning and tracking is the fundamental design of an arm robot manipulator. The trajectory is set and determined to satisfy a certain criterion effectively and optimally. Optimization of robot trajectory is necessary to ensure the good quality product and to save energy, and this optimization can be provided by the right modeling and design. This paper presents a review study of arm-robot manipulator design and control for trajectory tracking by investigating the modeling of an arm robot manipulator starting from kinematics, dynamics and the application of the more advanced methods. The idea of this paper comes from the popularity of inverse kinematics among students.

**Index Terms**—Arm robot manipulator; industrial robot; trajectory generation; trajectory tracking.

## I. INTRODUCTION

Robotics and other autonomous systems have been taking an important role in industries and domestic. Robots are machines that have the ability to sense and carry on the assigned test without fatigue. A robot can be fully autonomous and semi-autonomous. Most applied robots are fully autonomous and suffer some issues regarding its properties. Therefore, researchers keep on finding the most efficient and effective way of perfecting autonomous robots applied in industries and finding the most efficient methods for those robots. Arm robot manipulators are designed to replace humans in typical industrial environments that involves dull, dirty, and dangerous environment. Although it is still arguable whether arm robot manipulators are ready to substitute humans, the new revolution of industry, industry 4.0, is already here to prove that a factory needs minimum numbers of human where most of the industrial task are automatically conducted by robots [1] [2].

Arm robot manipulator application in industries ranging from welding, pick-and-place, assembly, packaging, labeling, etc. The commonly applied configurations are SCARA, articulated, cartesian and delta robot. Robot arm manipulator consists of links and joints, and design of links and joints has important roles in controlling robot's trajectory. At the last joint of the robot, an end-effector is attached, and the position of end-effector is an important factor for producing good quality products in industries. The term manipulation

refers to operations conducted by the robot including picking and placing an object, grasping, releasing, interaction with the applied environment and transporting objects within it working space.

Trajectory planning and tracking are one of the fundamental issues in the design of a robot manipulator. The trajectory is set and determined to satisfy a certain criterion effectively and optimally. There are two approaches for arm robot manipulator trajectory tracking [3], by using forward and/or inverse kinematics [4]- [14] in calculating desired joint space, and considering robot dynamics in workspace [14]- [18].

Optimization of robot trajectory is necessary not only to ensure a good quality product but also to save energy used by reducing actuator force, and motion time. Energy saving is important since this type of robot is continuously therefore even a small percentage is matter. The application of PID controller is not enough for optimizing robot trajectories, a further method has to be conducted by applying artificial intelligence such as Fuzzy Logic Controller (FLC) [21]- [23], Neural Networks (NN) [24]- [26], the combination of FLC and NN [27] [28] [29], and Genetic Algorithm (GA) [30] [31].

This paper presents a review study of arm-robot manipulator design and control for trajectory tracking. it investigates the modeling of arm-robot starting from kinematics and dynamics, and the possibility of applying artificial intelligence in creating more effective and efficient system. The idea comes from the famous application of inverse kinematics among students, therefore this paper would like to compare and show method with more advanced method than inverse kinematics in designing and controlling an arm robot manipulator since kinematics ignores the existence of dynamics in joints such as vibration, friction etc.

## II. KINEMATICS OF ARM ROBOT MANIPULATOR

Kinematics is the science that considers the motion of an object (robot) without cares for the cause of that motion. Kinematics studies the position, velocity, acceleration, and other higher derivatives of position with respect to time. Therefore, the study of kinematics refers to all geometrical and time-based properties of motion [33].

An arm robot manipulator is a set of links connected by joints, the lowest part is called the based, and the end

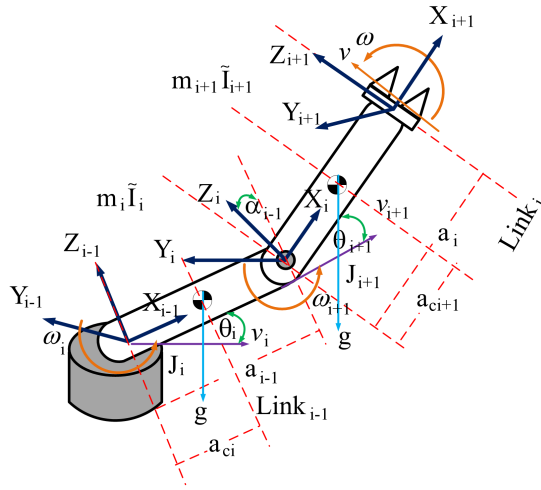


Fig. 1: 2 DOFs revolute arm robot manipulator links

part is called end-effector. The number of joints and how it moves define the degree of freedom (DOF). The joints are characterized as revolute or prismatic joints. Fig. 1 shows 2 DOF robot consists of all revolute joints. A typical applied in industries robot has 5 or 6 joints. In this paper, the kinematics and dynamics are derived from 2 DOF (fig. 1) for the sake of simplicity.

The notations given in fig.1 are

- $X_{i-1}, X_i, X_{i+1}, Y_{i-1}, Y_i, Y_{i+1}, Z_{i-1}, Z_i, Z_{i+1}$  are manipulator coordinate frames.
- $a_{i-1}, a_i, a_{i+1}$ , are the link length,  $\alpha_{i-1}, \alpha_i, \alpha_{i+1}$ , are the link twist,  $d_i$  is the link offset, and  $\theta_i$  and  $\theta_{i+1}$  are the joint angles.
- $J$  is robot's Jacobian matrix;  $J_i$  is link's Jacobian matrix.
- $v_i$  is link's translational velocity and  $\omega_i$  is link's rotational velocity.
- $m_i$  is link's mass.
- $\tilde{I}_i$  is link's inertia
- $a_{ci}$  is the length from link's center of gravity to link's end.
- $g$  is gravitational force.

#### A. Forward Kinematics

There are 2 approaches in calculating the position and orientation of the end-effector, with geometrical approach and algebraic approach. The most applied method, algebraic approach, is by using Denavit-Hartenberg (DH) convention that uses four basic parameters [32]. The distance from  $Z_{i-1}$  to  $Z_i$  measured along  $X_{i-1}$  is  $a_{i-1}$ , the angle between  $Z_{i-1}$  and  $Z_i$  measured along  $X_i$  is  $\alpha_{i-1}$ , the distance from  $X_{i-1}$  to  $X_i$  measured along  $Z_i$  is  $d_i$  and the angle between  $X_{i-1}$  to  $X_i$  measured about  $Z_i$  is  $\theta_i$  [33]. DH representation of fig. 1 is given in table I.

The transformation matrices from base to end-effector is given by

TABLE I: DH-representation

i	$\alpha_{i-1}$	$a_{i-1}$	$d_i$	$\theta_i$
1	0	$a_0$	0	$\theta_1$
2	0	$a_1$	0	$\theta_2$

$${}^{i+1}_i T = \begin{bmatrix} c_{\theta_i} & -s_{\theta_i}c_{\alpha_i} & s_{\theta_i}s_{\alpha_i} & a_i c_{\theta_i} \\ s_{\theta_i} & c_{\theta_i}c_{\alpha_i} & -c_{\theta_i}s_{\alpha_i} & a_i s_{\theta_i} \\ 0 & s_{\alpha_i} & c_{\alpha_i} & d_i \\ 0 & 0 & 0 & 1 \end{bmatrix}. \quad (1)$$

Therefore, the forward kinematics of n-DOF with n-joints is calculated from the base (0) of the robot to the end-effector (n) and given by the matrix

$${}^0_n T = {}^0_1 T {}^1_2 T \dots {}^{n-1}_n T \quad (2)$$

Based eq. 2, the transformation matrix of 2 DOFs manipulator shown in fig. 1 can be written as

$${}^0_1 T = \begin{bmatrix} c_1 & -s_1 & 0 & a_0 c_1 \\ s_1 & c_1 & 0 & a_0 s_1 \\ 0 & 0 & 1 & 0 \\ 0 & 0 & 0 & 1 \end{bmatrix}, \quad {}^1_2 T = \begin{bmatrix} c_2 & -s_2 & 0 & a_1 c_2 \\ s_2 & c_2 & 0 & a_1 s_2 \\ 0 & 0 & 1 & 0 \\ 0 & 0 & 0 & 1 \end{bmatrix}, \quad (3)$$

$${}^0_2 T = \begin{bmatrix} c_{12} & -s_{12} & 0 & a_0 c_1 + a_1 c_{12} \\ s_{12} & c_{12} & 0 & a_0 s_1 + a_1 s_{12} \\ 0 & 0 & 1 & 0 \\ 0 & 0 & 0 & 1 \end{bmatrix} = \begin{bmatrix} r_{11} & r_{12} & r_{13} & p_x \\ r_{21} & r_{22} & r_{23} & p_y \\ r_{31} & r_{23} & r_{33} & p_z \\ 0 & 0 & 0 & 1 \end{bmatrix}. \quad (4)$$

where  $r_{k,j}$  is the rotational elements and  $k$  and  $j = 1, 2, 3$ .  $r_{k,j}$  is calculated using inverse kinematics. The maximum considered DOF is 6DOF, otherwise, it is a redundant robot which kinematics will be different.

From eq. 4, robot's position is

$$\begin{aligned} p_x &= a_0 c_1 + a_1 c_{12}, \\ p_y &= a_0 s_1 + a_1 s_{12}, \\ p_z &= 0 \end{aligned} \quad (5)$$

If all of the coordinate frames in fig. 1 are removed and only the base is consider, robot zero position is  $p_x = a_0 + a_1$ .

#### B. Inverse Kinematics

There are 2 methods to transform a manipulator in Cartesian space into Joints space where the actuators work, namely, geometric and algebraic. For manipulator given in fig. 1, the geometric solution is the easiest way to find inverse kinematics. In this approach, the manipulator is considered in 2D, therefore the considered positions are only  $p_x$  and  $p_y$ , therefore from eq. 4, robot's position is

$$\begin{aligned} p_x &= a_1 c_1 + a_2 c_{12}, \\ p_y &= a_1 s_1 + a_2 s_{12}, \end{aligned} \quad (6)$$

By summing the square of  $p_x$  and  $p_y$ ,  $\theta_2$  is obtained as follow



$$p_x^2 + p_y^2 = a_0^2 (c_1^2 + s_1^2) + a_1^2 (c_{12}^2 + s_{12}^2) + 2a_0a_1 (c_1c_{12} + s_1s_{12}), \quad (7)$$

where based on trigonometric law,  $c_{12} = c_1c_2 - s_1s_2$ ,  $s_{12} = s_1c_2 + c_1s_2$ , and  $c_1^2 + s_1^2 = 1$ . Hence, eq. 7 can be written as

$$p_x^2 + p_y^2 = a_0^2 + a_1^2 + 2a_0a_1c_2, \quad (8)$$

and from eq. 8

$$c_2 = \frac{p_x^2 + p_y^2 - a_0^2 - a_1^2}{2a_0a_1}. \quad (9)$$

Since  $c_1^2 + s_1^2 = 1$ , then

$$s_2 = \sqrt{1 - \left( \frac{p_x^2 + p_y^2 - a_0^2 - a_1^2}{2a_0a_1} \right)^2}. \quad (10)$$

From eq. 9 and 10, there are 2 possible solutions for  $\theta_2$ , that are

$$\theta_2 = A \tan 2 \left( \pm \sqrt{1 - \left( \frac{p_x^2 + p_y^2 - a_0^2 - a_1^2}{2a_0a_1} \right)^2}, \frac{p_x^2 + p_y^2 - a_0^2 - a_1^2}{2a_0a_1} \right). \quad (11)$$

By revisiting and multiplying eq. 7 with  $c_1$  and  $s_1$

$$\begin{aligned} c_1p_x + s_1p_y &= a_0(c_1^2 + s_1^2) + a_1c_2(c_1^2 + s_1^2), \\ -s_1p_x + c_1p_y &= a_1s_2(c_1^2 + s_1^2), \end{aligned} \quad (12)$$

$$\begin{aligned} c_1p_x + s_1p_y &= a_0 + a_1c_2, \\ -s_1p_x + c_1p_y &= a_1s_2. \end{aligned} \quad (13)$$

By combining eq. 13,

$$c_1(p_x^2 + p_y^2) = p_x(a_0 + a_1c_2) + p_ya_1s_2. \quad (14)$$

Therefore,

$$\begin{aligned} c_1 &= \frac{p_x(a_0 + a_1c_2) + p_ya_1s_2}{p_x^2 + p_y^2}, \\ s_1 &= \sqrt{1 - \left( \frac{p_x(a_0 + a_1c_2) + p_ya_1s_2}{p_x^2 + p_y^2} \right)^2}. \end{aligned} \quad (15)$$

Finally, the two possible solutions for  $\theta_1$  are given by

$$\theta_1 = A \tan 2 \left( \pm \sqrt{1 - \left( \frac{p_x(a_0 + a_1c_2) + p_ya_1s_2}{p_x^2 + p_y^2} \right)^2}, \frac{p_x(a_0 + a_1c_2) + p_ya_1s_2}{p_x^2 + p_y^2} \right). \quad (16)$$

Calculating inverse kinematics with the geometric method is very cumbersome, and more DOFs will result in a more cumbersome calculation. Another method is algebraic, by expanding the DH convention, however, for 2DOFs, it is easier with the geometric method.

The position of end-effector shown in fig. 1 is given by eq. 5 and the relationship between joints and end-effector is given by

$$\begin{bmatrix} v \\ \omega \end{bmatrix} = \dot{q}. \quad (17)$$

$v$  and  $\omega$  are the translational and rotational velocity of the end-effector,  $q$  is robot positions.

The objectives of Jacobian implementation is to define joint and workspace velocities, the applied forces and torques, and manipulability properties, and understand the singular configurations.

The first step is to define the orientation of rigid body which consists of the Euler angles  $(\phi, \theta, \psi)$  associated with  $z_0, y_1$  and  $z_2$ . If  $z$  axis is at the base frame considered parallel with the end-effector, and the end-effector position is given in eq. 5. The Euler rotation is

$$\begin{bmatrix} \phi \\ \theta \\ \psi \end{bmatrix} = \begin{bmatrix} \theta_1 + \theta_2 \\ 0 \\ 0 \end{bmatrix} \quad (18)$$

The Jacobian of a 2DOFs manipulator shown in fig. 1 is

$$J = \begin{bmatrix} z_0 \times (p_2 - p_0) & z_1 \times (p_2 - p_1) \\ z_0 & z_1 \end{bmatrix}, \quad (19)$$

where the frame origins are

$$p_0 = \begin{bmatrix} 0 \\ 0 \\ 0 \end{bmatrix}, \quad p_1 = \begin{bmatrix} a_0c_1 \\ a_0s_1 \\ 0 \end{bmatrix}, \quad p_2 = \begin{bmatrix} a_0c_1 + a_1c_{12} \\ a_0s_1 + a_1s_{12} \\ 0 \end{bmatrix}, \quad (20)$$

and the rotational axes given by

$$z_0 = z_1 = \begin{bmatrix} 0 \\ 0 \\ 1 \end{bmatrix}. \quad (21)$$

Therefore, the components of eq. 19 are

$$z_0 \times (p_2 - p_0) = - \begin{bmatrix} 0 & 0 & a_0s_1 + a_1s_{12} \\ 0 & 0 & -a_0c_1 - a_1c_{12} \\ -a_0s_1 - a_1s_{12} & a_0c_1 + a_1c_{12} & 0 \end{bmatrix} \begin{bmatrix} 0 \\ 0 \\ 1 \end{bmatrix},$$

$$z_0 \times (p_2 - p_0) = \begin{bmatrix} -a_0s_1 - a_1s_{12} \\ a_0c_1 + a_1c_{12} \\ 0 \end{bmatrix}, \quad (22)$$

$$z_1 \times (p_2 - p_1) = - \begin{bmatrix} 0 & 0 & a_1s_{12} \\ 0 & 0 & -a_1c_{12} \\ a_1s_{12} & a_1c_{12} & 0 \end{bmatrix} \begin{bmatrix} 0 \\ 0 \\ 1 \end{bmatrix},$$

$$z_1 \times (p_2 - p_1) = \begin{bmatrix} -a_1s_{12} \\ a_1c_{12} \\ 0 \end{bmatrix}. \quad (23)$$

Hence, the Jacobian matrix is

$$J(q)\dot{q} = \begin{bmatrix} -a_0s_1 - a_1s_{12} & -a_1s_{12} \\ a_0c_1 + a_1c_{12} & a_1c_{12} \\ 0 & 1 \\ 1 & 0 \\ 0 & 0 \\ 0 & 0 \end{bmatrix} \quad (24)$$

The translational and rotational velocities of end-effector in fig. 1 are

$$\begin{aligned} v &= J_{v1}\dot{q}_1 + J_{v2}\dot{q}_2, \\ \omega &= J_{\omega1}\dot{q}_1 + J_{\omega2}\dot{q}_2. \end{aligned} \quad (25)$$

where  $J_{v1} = -a_0s_1 - a_1s_{12}$ ,  $J_{v2} = -a_1s_{12}$ ,  $J_{\omega 1} = a_0c_1 + a_1c_{12}$ , and  $J_{\omega 2} = a_1c_{12}$ . The column in Jacobian matrix defines the effect of  $i$ -th joint on the end-effector velocities.

### III. DYNAMICS OF ARM ROBOT MANIPULATOR

Dynamic considers the mathematical equations representing the motion of an arm robot manipulator, which are the motion resulted from the torques applied by the actuators or other external forces applied to the manipulator. The analysis of dynamic starts from a trajectory point or position and calculates the required vector of joint torques. The dynamic analysis also presents the energy needed to move the system.

The generic dynamics of a robot is given by

$$\mathbf{M}(q)\ddot{q} + \mathbf{C}(q, \dot{q})\dot{q} + \mathbf{D}\dot{q} + \mathbf{g}(q) = \boldsymbol{\tau}, \quad (26)$$

$$\mathbf{I}\ddot{\theta} + d\dot{\theta} + mgL\sin\theta = \tau. \quad (27)$$

where  $\mathbf{M}(q)$  is a  $n \times n$ , symmetric and positive definite mass matrix of arm robot manipulator,  $\mathbf{C}(q, \dot{q})$  is a  $n \times 1$  vector  $\mathbf{v}$ , a quadratic functions of the joint velocities,  $\mathbf{D}\dot{q}$  is the friction,  $\mathbf{g}(q)$  is the gravity term,  $\mathbf{I}$  is the inertia matrix, and  $q$  is robot position.

The derivation of the dynamic is coming from kinematic, and from Jacobian in eq. 24, the Jacobian of each robot's link in fig. 1 are

$$J_v^1 = \begin{bmatrix} -a_1s_{12} & 0 \\ a_1c_{12} & 0 \\ 0 & 0 \end{bmatrix}, \quad J_v^2 = \begin{bmatrix} -a_0s_1 - a_1s_{12} & -a_1s_{12} \\ a_0c_1 + a_1c_{12} & a_1c_{12} \\ 0 & 0 \end{bmatrix}, \quad (28)$$

$$J_\omega^1 = \begin{bmatrix} 0 & 0 \\ 0 & 0 \\ 1 & 0 \end{bmatrix}, \quad J_\omega^2 = \begin{bmatrix} 0 & 0 \\ 0 & 0 \\ 1 & 1 \end{bmatrix}, \quad (29)$$

since the z-axes in the frame of link  $i$  and link  $i+1$  are parallel to the same axis of  $\mathbb{F}_0$ , therefore  $\omega$  is considered the same with  $\omega_z$ .

Kinetic energy  $\mathbf{K}$  of the robot in fig. 1 is

$$\mathbf{K} = \frac{1}{2}\dot{q}^T \left[ m_1 J_v^{1T} J_v^1 + m_2 J_v^{2T} J_v^2 + J_\omega^{1T} \tilde{I}_1 J_\omega^1 + J_\omega^{2T} \tilde{I}_2 J_\omega^2 \right]. \quad (30)$$

where

$$J_\omega^{1T} \tilde{I}_1 J_\omega^1 + J_\omega^{2T} \tilde{I}_2 J_\omega^2 = \begin{bmatrix} \tilde{I}_1 + \tilde{I}_2 & \tilde{I}_2 \\ \tilde{I}_2 & \tilde{I}_2 \end{bmatrix}. \quad (31)$$

By neglecting friction, the mass matrix  $\mathbf{M}(q)$  from eq. 26 is

$$\mathbf{M}(q) = \begin{bmatrix} M_{11} & M_{21} \\ M_{12} & M_{22} \end{bmatrix}, \quad (32)$$

where

$$\begin{aligned} M_{11} &= m_1 a_{c1}^2 + m_2 (a_0^2 + a_{c2}^2 + 2a_0 a_{c2} c_2) + \tilde{I}_1 + \tilde{I}_2, \\ M_{12} &= m_2 (a_{c2}^2 + a_0 a_{c2} c_2) + \tilde{I}_2, \\ M_{21} &= m_2 (a_{c2}^2 + a_0 a_{c2} c_2) + \tilde{I}_2, \\ M_{22} &= m_2 a_{c2}^2 + \tilde{I}_2. \end{aligned} \quad (33)$$

The quadratic functions of the joint velocities  $\mathbf{C}(q, \dot{q})$  from eq. 26 is

$$\mathbf{C}(q, \dot{q}) = \begin{bmatrix} h\dot{\theta}_1 & h(\dot{\theta}_1 + \dot{\theta}_2) \\ -h\dot{\theta}_1 & 0 \end{bmatrix} \quad (34)$$

where  $h$  is calculated from the Christoffel symbols  $c_{ijk} = \frac{1}{2} \left[ \frac{\partial M_{kj}}{\partial q_i} + \frac{\partial M_{ki}}{\partial q_j} - \frac{\partial M_{ij}}{\partial q_k} \right]$  as follow

$$\begin{aligned} c_{111} &= \frac{1}{2} \frac{\partial M_{11}}{\partial q_1} = 0, \\ c_{121} &= c_{211} = \frac{1}{2} \frac{\partial M_{11}}{\partial q_2} = -m_2 a_0 a_{c2} s_2 = h, \\ c_{221} &= \frac{\partial M_{12}}{\partial q_2} - \frac{1}{2} \frac{\partial M_{22}}{\partial q_1} = h, \\ c_{112} &= \frac{\partial M_{21}}{\partial q_1} - \frac{1}{2} \frac{\partial M_{11}}{\partial q_2} = -h, \\ c_{122} &= c_{212} = \frac{\partial M_{22}}{\partial q_1} = 0, \\ c_{222} &= \frac{\partial M_{22}}{\partial q_2} = 0. \end{aligned} \quad (35)$$

The gravitational forces working on the robot in fig. 1 is given by

$$\begin{aligned} \mathbf{N}(q) &= \dot{\mathbf{M}}(q) - 2\mathbf{N}(q, \dot{q}) \\ &= \begin{bmatrix} 2h\dot{\theta}_1 & h\dot{\theta}_2 \\ -\dot{\theta}_2 & 0 \end{bmatrix} - 2 \begin{bmatrix} h\dot{\theta}_1 & h(\dot{\theta}_1 + \dot{\theta}_2) \\ -h\dot{\theta}_1 & 0 \end{bmatrix} \\ &= \begin{bmatrix} 0 & -2h\dot{\theta}_1 + h\dot{\theta}_2 \\ 2h\dot{\theta}_1 + h\dot{\theta}_2 & 0 \end{bmatrix}, \end{aligned} \quad (36)$$

which is a skew-symmetric.

Therefore, robot dynamic in eq. 26 can be written as

$$\begin{aligned} M_{11}\ddot{\theta}_1 + M_{12}\ddot{\theta}_2 + c_{121}\dot{\theta}_1\dot{\theta}_2 + c_{211}\dot{\theta}_2\dot{\theta}_1 + c_{221}\dot{\theta}_2^2 + g_1 &= \tau_1, \\ M_{21}\ddot{\theta}_1 + M_{22}\ddot{\theta}_2 + c_{111}\dot{\theta}_1^2 + g_2 &= \tau_2. \end{aligned} \quad (37)$$

The potential energy of each links in fig. 1,  $P_i$ , are

$$P_1 = m_1 g a_{c1} s_1,$$

and

$$P_2 = m_2 g (a_0 s_1 + a_{c2} s_{12}). \quad (38)$$

Therefore, the potential energy  $\mathbf{P}$  of the arm manipulator is

$$\mathbf{P} = P_1 + P_2 = (m_1 a_{c1} + m_2 a_0) g s_1 + m_2 g a_{c2} c_{12}, \quad (39)$$

where

$$\begin{aligned} g_1 &= \frac{\partial \mathbf{P}}{\partial \theta_1} = (m_1 a_{c1} + m_2 a_0) g c_1 + m_2 g a_{c2} s_{12}, \\ g_2 &= \frac{\partial \mathbf{P}}{\partial \theta_2} = m_2 g a_{c2} s_{12}. \end{aligned} \quad (40)$$

Energy kinetic for each links,  $K_i$  are given by

$$\begin{aligned} K_1 &= \frac{1}{2} m_1 a_{c1}^2 \dot{\theta}_1^2 + \frac{1}{2} \tilde{I}_1 \dot{\theta}_1^2 \\ K_2 &= \frac{1}{2} m_2 \dot{\mathbf{p}}_{c2}^T \dot{\mathbf{p}}_{c2} + \frac{1}{2} (\tilde{I}_1 + \tilde{I}_2) \dot{\theta}_2^2 \end{aligned} \quad (41)$$

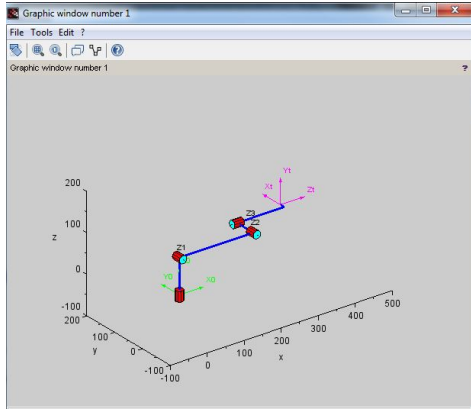


Fig. 2: 4 DOF arm robot simulation in SCILAB

where

$$\dot{\mathbf{p}}_{c2}^T \dot{\mathbf{p}}_{c2} = a_0^2 \dot{\theta}_1^2 + a_{c1}^2 (\dot{\theta}_1 + \dot{\theta}_2) + 2a_0 a_{c2} c_2 (\dot{\theta}_1^2 + \dot{\theta}_1 \dot{\theta}_2) \quad (42)$$

#### IV. SIMULATION AN ARM-ROBOT MANIPULATOR

The arm robot design can be tested in simulation software to ensure the robot follows the reference trajectory. One of open source simulation is SCILAB which is enough to observe robot motion. Fig. 2 shows a 4 DOF arm robot simulated in SCILAB [34].

#### V. DISCUSSION

In designing arm-robot manipulator, there are 2 steps of modeling, the kinematics and dynamics modeling. This section discusses the application of kinematics, and dynamics modeling and the addition of artificial intelligence to create a more effective system.

##### A. Kinematics Modeling

Kinematics modeling is required for designing the motion and trajectory of the robot without considering the dynamics aspect such as force and friction. Kinematics modeling can be tested using simulation to avoid the complexity of the real system in testing the effectiveness of the proposed method. Simulation was conducted by Ceccarelli et al. 2008 utilizing the kinematic design for a manipulator by creating an algorithm for evaluating manipulator workspace [4], Lin et al. 2014 proposed an intuitive kinematic control of a robot via interface with human motion to control a robot directly teleoperated in avoiding obstacle and finishing its task [5], Reihara 2011 analyzed and solved the kinematics problem for an AdeptThree robot arm with the application of DH convention simulated in LabView [6], and Zodey et al. 2014 analyze the kinematics of a robotics gripper by simulating the capability of hand modeling, grasp definition, grasp modeling, grasp analysis and graphic to support the presentation [10].

Donelan 2011 investigated the kinematics singularities of a robot manipulator using Kinematics mapping [7]. Song et al. 2011 presented the cyclic coordinate descent (CCD) for computing inverse kinematics in a multi-joint chain robot [8]. Balkan et al. 2006 classified industrial robots based on

the kinematic and inverse kinematics structure in order to obtain the simplified forward kinematics equations that will lead to simpler inverse kinematics equation [9]. Kucuk et al. 2006 presented kinematics analysis of a Stanford manipulator [11]. Sultan 2006 also presented the analysis of an arm robot manipulator to design an efficient joint trajectory [12]. A complete analysis and design of an arm robot manipulator mounted on a mobile platform is presented by Clothier et al. 2010 by presenting a geometric method in solving the unknown joint angles to control the autonomous positioning of an arm robot, and the type of end-effector used was a gripper [13].

##### B. Dynamics Modeling

Dynamics modeling is necessary to create more effective and efficient arm-robot. Muhammed et al. 2014 proposed a method to minimize energy consumption for an arm robot manipulator by solving robot's inverse dynamic to analyze the forces and torques of each joint and link [14]. Dehghani et al. 2014 proposed a dynamic modeling of a continuum robotic arm that has high adaptation and compatibility with the shape of an object to grasp objects [15].

Cen et al. 2017 discussed the effect of dynamics on forces and torques of an arm robot applied in milling industry by designing a force model. The experimental results showed that the proposed method reduced 50% to 70% error for key characteristic of the robot milling's forces [16]. Bruno et al. 2017 proposed the dynamic model identification of an industrial robot that is linear with respect to the parameters [17]. Paik et al. 2012 designed a humanoid robot by taking the model of a 7DOF arm robot and an 8DOF hand. The proposed model was compatible with the narrating model humanoid, and at the same time powerful and functional to execute various task [18].

##### C. Advance Control

To improve the effectiveness and increase the efficiency, arm robot manipulator trajectory tracking design and control requires more than kinematic and dynamic. The application of advanced control theorem and artificial intelligence are necessary such as adaptive control [19] [20]. Artificial controlled applied in trajectory tracking of an arm robot manipulators are Fuzzy logic controller (FLC) [21] [22] [23], Neural Network (NN) [24] [25] [26], combination of FLC and NN [27] [28] [29] and Genetic Algorithm (GA) [30] [31]. The cumbersome and complication of kinematics and dynamics modeling can be avoided by applying rules-based, and/or learning-based of artificial intelligence.

#### VI. CONCLUSION

Modeling arm robot manipulator is a complicated work, starting from how it moves in kinematics, and how much energy needed in dynamics. This complicated and exhausting work can be avoided by applying artificial intelligence (AI), namely FLC, NN, and GA. By applying AI, the researcher only needs to considered to map the input-output of the

system. However, most of the time, this is not enough, the combination of two types of AI gives a better performance such as ANFIS, and combined the model with forward and inverse kinematics. Arm robot manipulator control and solution is complicated, however, its application is crucial in industries, not to mention, the automatic industry, industry 4.0 is here to create more efficient manufacturing product.

## REFERENCES

- [1] A. Petrillo, F. De Felice, R. Cioffi and Federico Zomparelli, "Fourth Industrial Revolution: Current Practices, Challenges, and Opportunities", *Digital Transformation in Smart Manufacturing*, Dr. Antonella Petrillo (Ed.), InTech, 2018. DOI: 10.5772/intechopen.72304.
- [2] J. E. Agolla, "Human Capital in the Smart Manufacturing and Industry 4.0 Revolution", *Digital Transformation in Smart Manufacturing*, Dr. Antonella Petrillo (Ed.), InTech, 2018. DOI: 10.5772/intechopen.73575. Available from:
- [3] C. Chen and C. Peng (2010). "Coordinate Transformation Based Contour Following Control for Robotic Systems", *Advances in Robot Manipulators*, Ernest Hall (Ed.), InTech, pp. 183-204, 2010. DOI: 10.5772/9541.
- [4] M. Ceccarelli and E. Ottaviano, "Kinematic Design of Manipulators", *Robot Manipulators*, Marco Ceccarelli (Ed.), InTechopen, pp. 49-72, 2008. ISBN: 978-953-7619-06-0.
- [5] H. Lin, Y. Liu, and Y. Lin, "Intuitive Kinematic Control of a Robot Arm via Human Motion," in *Proceeding of 37th National Conference on Theoretical and Applied Mechanics (37th NCTAM 2013) & The 1st International Conference on Mechanics (1st ICM)*, *Procedia Engineering*, vol. 79, pp. 411-416, 2014.
- [6] A. B. Rehiara, "Kinematics of Adept Three Robot Arm", *Robot Arms*, Prof. Satoru Goto (Ed.), pp. 21-38, InTechopen, 2011, ISBN: 978-953-307-160-2.
- [7] P. Donelan, "Kinematic Singularities of Robot Manipulators", *Advances in Robot Manipulators*, Ernest Hall (Ed.), InTechopen, pp. 401-416, 2010. ISBN: 978-953-307-070-4.
- [8] W. Song, and G. Hu, "A Fast Inverse Kinematics Algorithm for Joint Animation", in *Proceeding of 2011 International Conference on Advances in Engineering*, *Procedia Engineering*, vol. 24, pp. 350-354, 2011.
- [9] T. Balkan, M. K. Ozgoren, and M. A. S. Arıkan, "Structure Based Classification and Kinematic Analysis of Six-Joint Industrial Robotic Manipulators", *Industrial Robotics: Theory, Modelling and Control*, Sam Cubero (Ed.), InTechOpen, pp. 149-184, 2006. ISBN: 3-86611-285-8.
- [10] S. Zodey, and S. K. Pradhan, "Matlab Toolbox for Kinematic Analysis and Simulation of Dexterous Robotic Grippers", *Procedia Engineering*, Vol. 97, pp. 1886-1895, 2014. <https://doi.org/10.1016/j.proeng.2014.12.342>
- [11] S. Kucuk and Z. Bingul, "Robot Kinematics: Forward and Inverse Kinematics", *Industrial Robotics: Theory, Modelling, and Control*, Sam Cubero (Ed.), InTechopen, pp. 117-148, ISBN: 3-86611-285-8.
- [12] I. A. Sultan "Inverse Position Procedure for Manipulators with Rotary Joints," *Industrial Robotics: Theory, Modelling and Control*, Sam Cubero (Ed.), InTechopen, pp. 185-210, 2006. ISBN: 3-86611-285-8.
- [13] K. E. Clothier, and Y. Shang, "A Geometric Approach for Robotic Arm Kinematics with Hardware Design, Electrical Design, and Implementation", *Journal of Robotics*, vol. 2010, Article ID 984823, 10 pages, 2010. doi:10.1155/2010/984823.
- [14] A. Mohammed, B. Schmidt, L. Wang, and L. Gao, "Minimizing Energy Consumption for Robot Arm Movement", *Procedia CIRP*, Vol. 25, pp. 400-405, 2014. <https://doi.org/10.1016/j.procir.2014.10.055>.
- [15] M. Dehghani and S. A. A. Moosavian, "Dynamics Modeling of a Continuum Robotic Arm with a Contact Point in Planar Grasp," *Journal of Robotics*, vol. 2014, Article ID 308283, 13 pages, 2014. doi:10.1155/2014/308283.
- [16] L. Cen and S. N. Melkote, "Effect of Robot Dynamics on the Machining Forces in Robotic Milling", *Procedia Manufacturing*, Vol. 10, pp. 486-496, 2017. <https://doi.org/10.1016/j.promfg.2017.07.034>.
- [17] M. Brunot, A. Janot, and F. Carrillo, "State Space Estimation Method for the Identification of an Industrial Robot Arm", *IFAC-PapersOnLine*, Vol. 50, Issue 1, pp. 9815-9820, 2017. <https://doi.org/10.1016/j.ifacol.2017.08.892>.
- [18] J. K. Paik, B. H. Shin, Y. Bang, and Y. Shim, "Development of an Anthropomorphic Robotic Arm and Hand for Interactive Humanoids", *Journal of Bionic Engineering*, Vol. 9, Issue 2, pp. 133-142, 2012. [https://doi.org/10.1016/S1672-6529\(11\)60107-8](https://doi.org/10.1016/S1672-6529(11)60107-8).
- [19] M. Chien and A. Huang, "A Regressor-free Adaptive Control for Flexible-joint Robots based on Function Approximation Technique", *Advances in Robot Manipulators*, Ernest Hall (Ed.), pp. 27-49, 2010. InTech, DOI: 10.5772/9547.
- [20] A. A. Khalate, G. Leena, and G. Ray, "An Adaptive Fuzzy Controller for Trajectory Tracking of Robot Manipulator", *Intelligent Control and Automation*, Vol. 2 No. 4, pp. 364-370, 2011. DOI: 10.4236/ica.2011.24041.
- [21] Z. Zhiyong, Z. JianFeng, H. Lvwen, and L. C., "Trajectory Tracking Fuzzy Control Algorithm for Picking Robot Arm", *International Journal of Control and Automation*, vol. 7, No. 9, pp. 411-422, 2014. <http://dx.doi.org/10.14257/ijca.2014.7.9.35>.
- [22] M. H. Reham, B. Fahmy, and E. Kamel, "Trajectory Tracking Control for Robot Manipulator using Fractional Order-Fuzzy-PID Controller", *International Journal of Computer Applications*, vol. 134, no. 15, pp. 22-29, 2016. DOI: 10.5120/ijca2016908155.
- [23] I. Dumitru, N. Arghira, I. Fagarasan, and S. Iliescu, "A Fuzzy PLC Control System for a Servomechanism", *IFAC Proceedings*, Vol. 43, Issue 22, pp. 69-74, 2010. <https://doi.org/10.3182/20100929-3-RO-4017.00013>
- [24] A. T. Hasan, H. M. A. A. Al-Assadi, and A. A. Mat Isa, "Neural Networks Based Inverse Kinematics Solution for Serial Robot Manipulators Passing Through Singularities", *Artificial Neural Networks - Industrial and Control Engineering Applications*, Prof. Kenji Suzuki (Ed.), InTechopen, pp. 460-478, 2011. ISBN: 978-953-307-220-3.
- [25] E. Mattar, "Robotics Arm Visual Servo: Estimation of Arm-Space Kinematics Relations with Epipolar Geometry", *Robotic Systems - Applications, Control and Programming*, Dr. Ashish Dutta (Ed.), pp. 429-454, 2012, ISBN: 978-953-307-941-7.
- [26] A. Duka, "Neural Network based Inverse Kinematics Solution for Trajectory Tracking of a Robotic Arm", *The 7th International Conference Interdisciplinarity in Engineering (INTER-ENG 2013)*, *Procedia Technology* 12, pp. 20-27, 2014.
- [27] Y. I. AlMashhadany, "ANFIS-Inverse-Controlled PUMA 560 Workspace Robot with Spherical Wrist", *Procedia Engineering*, Vol. 41, pp. 700-709, 2012. <https://doi.org/10.1016/j.proeng.2012.07.232>.
- [28] A. Duka, "ANFIS Based Solution to the Inverse Kinematics of a 3DOF Planar Manipulator", *8th International Conference Interdisciplinary in Engineering, INTER-ENG 2014 Procedia Technology*, Vol. 19, pp. 526-533, 2015, Pages 526-533. <https://doi.org/10.1016/j.procty.2015.02.075>.
- [29] A. Hošovský, J. Pítel, K. Žideka, M. Tóthová, J. Sárosib, and L. Cveticanin, "Dynamic Characterization and Simulation of Two-link Soft Robot Arm with Pneumatic Muscles", *Mechanism and Machine Theory*, Vol. 103, pp. 98-116, 2016. <https://doi.org/10.1016/j.mechmachtheory.2016.04.013>.
- [30] S. Števo, I. Sekaj, and M. Dekan, "Optimization of Robotic Arm Trajectory Using Genetic Algorithm", *IFAC Proceedings Volumes*, Vol. 47, Issue 3, pp. 1748-1753, 2014. <https://doi.org/10.3182/20140824-6-ZA-1003.01073>.
- [31] R. Roy, M. Mahadevappa, and C. S. Kumar, "Trajectory Path Planning of EEG Controlled Robotic Arm Using GA", *Procedia Computer Science*, Vol. 84, pp. 147-151, 2016. <https://doi.org/10.1016/j.procs.2016.04.080>.
- [32] J. Denavit and R. S. Hartenberg, "A kinematic notation for lower-pair mechanisms based on matrices", *Journal of Applied Mechanics*, Vol., 1 pp. 215-221, 1955.
- [33] J. J. Craig, "Introduction to Robotics Mechanics and Control", USA: Addison- Wesley Publishing Company, 1989.
- [34] <https://www.scilab.org/> accessed on May 17th, 2018.

# Vibration Control of Magnetorheological Elastomer Beam Sandwich

Gigih Priyandoko

Department of Electrical Engineering,  
Faculty of Engineering  
Widyagama University  
Malang, Indonesia  
gigih@widayagama.ac.id

Tedi Kurniawan

Faculty of Mechanical Engineering  
Universiti Malaysia Pahang  
Pekan, Pahang, Malaysia  
tedikurniawan@ump.edu.my

Saffirna Mohd Soffie

Faculty of Mechanical Engineering  
Universiti Malaysia Pahang  
Pekan, Pahang, Malaysia  
saffirna@yahoo.com

**Abstract**—A Magnetorheological Elastomer (MRE) is a smart material and that could change their properties by exposure to stimuli such as electric and magnetic fields, stress moisture and temperature. The objective of this research is to develop an MRE as a vibration isolator of a beam sandwich under different currents to get different stiffness of the MRE. An MRE was fabricated by mixing silicon rubber, silicon oil and carbonyl iron particles together and then cured for 24 hours in a circular mold. The experimental result shows that there were decreases in amplitude of the vibration in time and frequency domains when the current applied to the coil is increased.

**Keywords**—Magneto-rheological Elastomer, stiffness control, sandwich beam, vibration isolators.

## I. INTRODUCTION

Sandwich structures are fundamentally utilized in weight sensitive industries such as a car, airplane and marine applications. A sandwich pillar comprises of two lean, hardened and solid confront sheets that are adhesively fortified on the sides of thick, light, powerless center. Confront sheets are utilized to reinforce the sandwich pillar. The center gives bolster for the confront sheets anticipating shear disappointment. The materials of the confront sheets can be metallic and non-metallic. Steel and aluminum are cases of metallic confront sheets whereas fiber strengthened composites are cases of non-metallic confront sheets. Normal center materials incorporate froths, folded sheets, honeycomb sheets and balsa wood [1-2].

Typically, in engineering there was a lot of heavy machinery or structure that vibrates whether on a small or big scale. Vibrations were harmful especially to structures because it can cause structures to fail under very high vibration. Various methods and materials have been proposed to reduce vibration. The methods are broadly classified as a passive, semi-active, or active system [1-5]. These methods use different materials to achieve vibration reduction.

The passive methods use the rubber as the material of choice. However, passive systems are only effective over a very narrow frequency range. As the excitation frequency changes, the vibration reduction effect decreases or even collapses because of mistuning. The semi-active method combines the use of sensors and actuators to vary the properties of an isolator system. On the other hand, the active methods combine the use of sensors, actuators, additional electronics and fluids with controllable properties in solving these problems [6]. In active vibration system, the disadvantages are high consumption of energy and requirement of large activation force. The semi-active method is preferable due to its stability and reliability for both low and high-frequency vibrations.

The high frequency requires low stiffness and low damping vibration isolator while the low-frequency vibration requires high stiffness and high damping vibration isolator [1-7]. Magnetorheological Elastomers (MREs) are a class of smart materials whose stiffness and damping properties can be adaptively tuned to attenuate both low and high-frequency vibration [2-3,6,8-9]. The objective of this research is to develop an MRE as a tunable vibration isolator when different currents are applied to get different stiffness of the MRE.

## II. MAGNETO-RHEOLOGICAL ELASTOMER

Magnetorheological fluids (MRFs) state of matter can be change with the use of different level of magnetic field. The fluids are composed of magnetic particles suspended in viscous fluid. It will have low viscosity with the absence of a magnetic field as the particle is not arranged. To enhance their magnetic susceptibility and reducing their tendency to form an aggregation, the magnetic particle of an MRFs are additionally covered with the special layer. Other substance such as anti-corrosion and anti-sedimentation substance, is added in a small amount. The influence of magnetic field causes changes in the physical properties of MRFs. The liquid returns to its baseline after absent of external magnetic field. One of the disadvantages of the MRFs is the sedimentation [1].

MREs, also known as a magneto-sensitive elastomer, are a class of smart materials whose stiffness and damping properties can be adaptively tuned to attenuate (reduce force/amplitude/effect) both low and high-frequency vibration. It is usually achieved by varying the magnetic flux input and in full active mode using sensors and actuators or semi-active mode [5,10-11]. Also, MREs have an improve properties in new structural materials. They are an intelligent composite material whose physical properties that are sensitive to the effect of the magnetic field. These changes are non-linear, which is completely reversible and occur within several milliseconds. Furthermore, MREs are a solid phase counterpart of MRFs. The liquid carrier is replaced by a solid material elastomer or rubber in the case under analysis. The polymeric matrix that is built inside the material were embedded with good magnetic properties material such as carbonyl-iron [8,12].

There are many benefits to using MRE. They consist of natural or synthetic rubber matrix interspersed with micron-sized (3 to 5 microns) ferromagnetic particles. An elastomer such as rubber is used, on the point that they are generally soft and deformable at room temperature with having the ability to reversibly extend from 5-700% depending on the specific material. In conjunction with the particle structure, the magnetic particle cannot move freely within the matrix due to the elastomer. Thus, no sedimentation presents. On

top of it, with the limitation particles movement result in a quicker response to a magnetic field than in MRFs [13]. MRFs durability is limited due to densification of liquid after many operating cycles. Agglomeration and sedimentation of magnetic particles is no longer a problem in case of MREs. Thermal stability is better where MREs and MRFs have a different operating range which is the essential difference between them [9,11,14].

The fabricated MRE samples are composed of carbonyl iron powder of an approximate diameter of 10  $\mu\text{m}$  dispersed within the room-temperature vulcanizing (RTV) rubber matrix and silicon oil. They are fabricated based on the expertise acquired in the studies as shown in Figure 1.

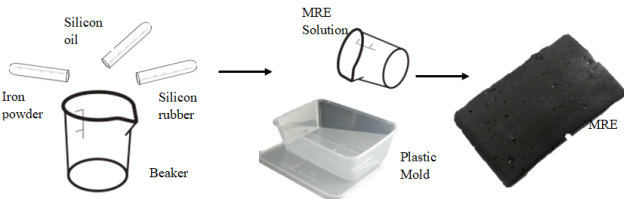


Fig. 1. Fabrication of MRE

### III. VIBRATION ISOLATOR

#### A. Simulation

Finite Element Method Magnetics (FEMM) was an open source finite element analysis software package for solving electromagnetic problems. The program addresses 2D planar and 3D axisymmetric linear and nonlinear harmonic low frequency magnetic and magneto-static problems and linear electrostatic problems. This software was used to help in to design the magnetics circuit in the multi-sandwich vibration isolator by simulating the magnetic field in different types of conditions and parameters.

A setup design is constructed by two materials, where the 304 Stainless steel will be substituted by Aluminum 1100. For aluminum simulation material in FEMM software is shown in Figure 2.

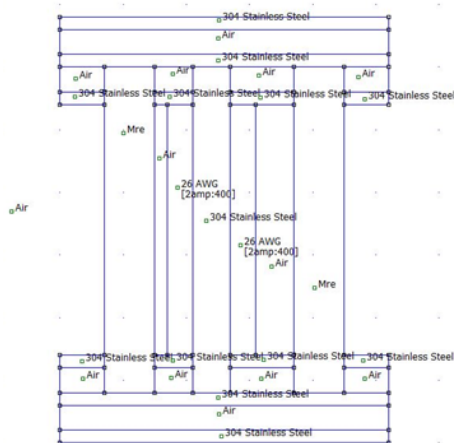


Fig. 2. Model in FEMM using Aluminium material.

Through values of flux density (B) against the field strength (H) a set of curves can produce known as Magnetization Curves, Magnetic Hysteresis Curves or more generally B-H Curves for each sort of core material used as shown in Figures 3a-3c, where FEMM simulation results

without MRE, simulation results using stainless steel and using aluminium materials, respectively.

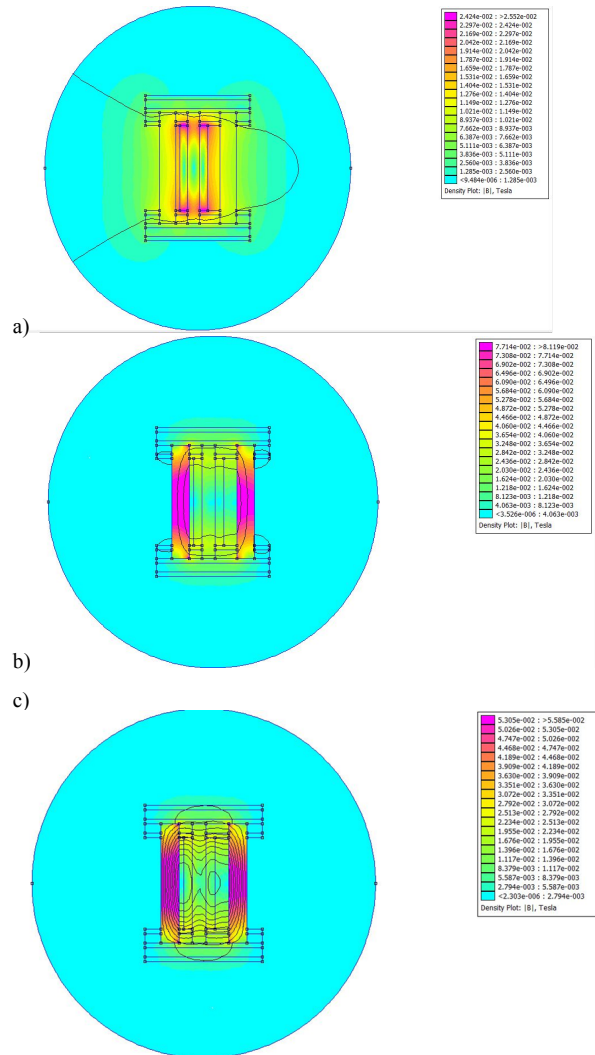


Fig. 3. Magnetics density contour plot

From the figure above, both of the simulations have produced a closed-loop magnetic field strength. The aluminum produces higher magnetic flux than the stainless steel, such that for this research decided to choose aluminum material as the main sandwich plated to be fabricated.

#### B. Fabrication

The beam sandwich is made of two aluminum plates with a pair of aluminum rods which the properties is shown in Figure 4. There were two main materials for the fabrication of the multi-sandwich vibration isolator which were plain carbon steel and aluminum. Plain carbon steel and aluminum were chosen based on its ferromagnetic properties and availability in the market. After each part of the vibration isolator has gone through in processes, the parts are assembled through methods of fitting using bolts and screw. A cross-sectional drawing shown in Figure 4.



### C. Test Setup

Figure 5 shows the experimental setup of the vibration testing on MRE vibration isolator. The DAQ was connected to the laptop and the piezoelectric accelerometer to send the vibration signal to the laptop for processing. The DC power supply supplies current to the DC motor and the electromagnetic coil located inside the vibration isolator. The DC motor is used as disturbances was supplied with a constant voltage at 12V throughout the whole experiment and mounted on top of the vibration isolator. Each time the experiment was conducted, the electromagnetic coil was supplied with 0, 1.0, 1.5 and 2.0 amperes while the DC motor was kept constant DC voltage at 12V. The values and data are recorded inside the laptop using the DasyLab module. The data were analyzed and plotted into graphs for ease of analysis and observing the changes in data. The data were split into the time domain and frequency domain for each current applied for better analysis.



Fig. 4. Cross-sectional Diagram of Vibration Isolator

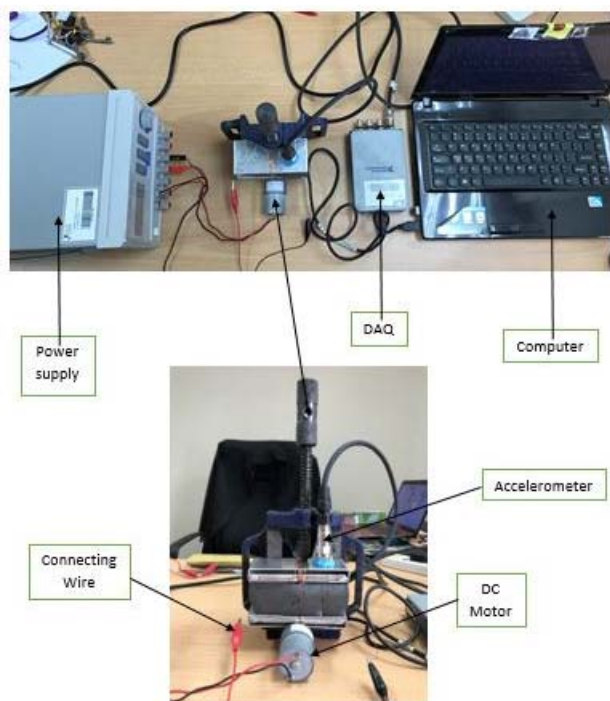


Fig. 5. The experimental setup

## IV. RESULTS AND DISCUSSION

Figure 6 shows the time response of the accelerometer on the vibration isolator when the current applied was 1 ampere. The vibration data are shown to be very useful in analyzing

the vibration of the MRE vibration isolator. It can be seen that averagely the peak for the time domain are in the range of 0.04m to 0.06m. This data might not be representing the whole data because it has been scaled down to plot a clear graph. Figure 7 shows the frequency response of the accelerometer on the vibration isolator when the current applied was 1 ampere. From the figure, it can be seen that the highest peak obtained from the vibration isolator was 0.043m at 420 Hz.

When the current applied to the electromagnetic coils increases, this also increases the magnetic flux density in the effective area of the vibration isolator. This reacts with the carbonyl iron particles in the MRE and increases the stiffness of the MRE which in turn decreases the vibration on the MRE vibration isolator that was made by the 12V DC motor.

Figures 8-9 were the result of gathering data from all the time response graphs and frequency graphs and combining them into two graphs for time and frequency respectively to observe and analyze the difference in amplitude of vibration when the 12V DC motor is providing vibration towards the MRE vibration isolator. From the graph, it was observed that there were slight differences in the amplitude of vibration with each increment of current applied. At some point it was hard to see just by observing the graph as it was not very clear for the time domain, so RMS value was calculated for the entire data for each current applied as shown in Table 1.

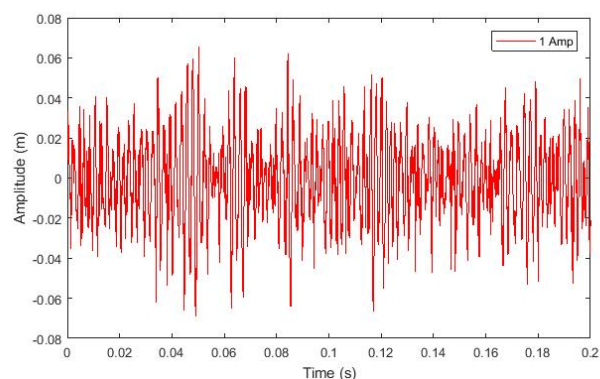


Fig. 6. Time response of vibration isolator at current 1 Amp.

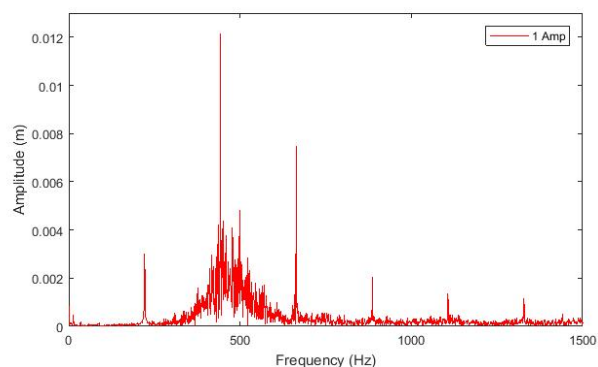


Fig. 7. The frequency response of vibration isolator at current 1 Amp.

TABLE I. RMS VALUE BASED ON EXPERIMENTAL RESULTS

Current (Amp)	RMS Value	
	Time response	Frequency response
0.0	0.0114	0.0102

Current (Amp)	RMS Value	
	Time response	Frequency response
1.0	0.0094	0.0099
1.5	0.0024	0.0082
2.0	0.0014	0.0072

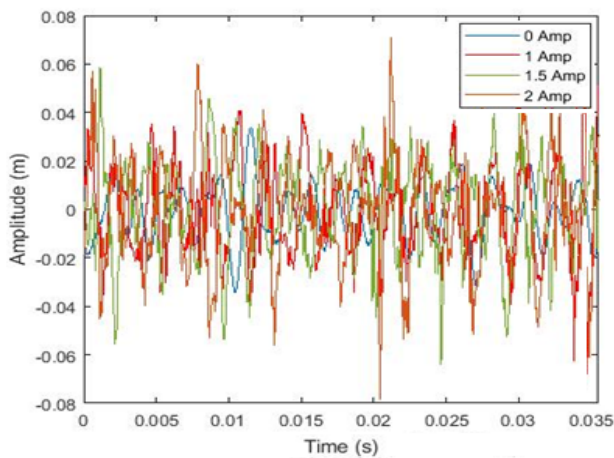


Fig. 8. Time response of vibration isolator at current 0-2 Amp.

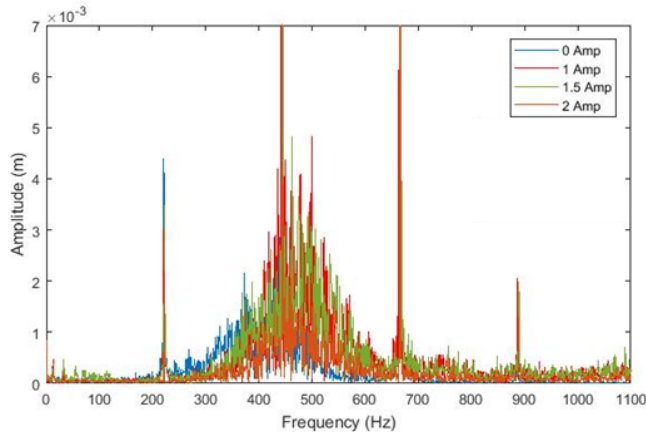


Fig. 9. Time response of vibration isolator at current 0-2 Amp.

## V. CONCLUSION

To conclude from the simulation results obtained, it can be seen that the vibration produced by the DC motor towards the MRE vibration isolator for the sandwich beam is decreasing with each increment in current supplied to the electromagnetic coil. From the experimental results obtained, it can be seen that the peak value for the time and frequency response graphs were decreasing in value as the current applied increased. This was further proven by the RMS value calculated for the time and frequency domains where the value also decreases with each increment of current applied.

This proves that MRE does have the ability to be manipulated by an external magnetic field regarding changing the stiffness and isolating vibration.

## ACKNOWLEDGMENT

The authors would like to thank the Universiti Malaysia Pahang (UMP) for their support in the research work. This research was supported by a UMP research grant (RDU1703148).

## REFERENCES

- [1] M. Behrooz, J. Sutrisno, X. Wang, R. Fyda, A. Fuchs, and F. Gordaninejad, "A new isolator for vibration control," 2011, p. 79770Z.
- [2] Y. Li, J. Li, W. Li, and H. Du, "A state-of-the-art review on magnetorheological elastomer devices," *Smart Mater. Struct.*, vol. 23, no. 12, p. 123001, Dec. 2014.
- [3] H. Deng and X. Gong, "Application of magnetorheological elastomer to vibration absorber," *Commun. Nonlinear Sci. Numer. Simul.*, vol. 13, no. 9, pp. 1938–1947, Nov. 2008.
- [4] N. Hoang, N. Zhang, and H. Du, "A dynamic absorber with a soft magnetorheological elastomer for powertrain vibration suppression," *Smart Mater. Struct.*, vol. 18, no. 7, p. 074009, Jul. 2009.
- [5] J. Yang *et al.*, "Development of a novel multi-layer MRE isolator for suppression of building vibrations under seismic events," *Mech. Syst. Signal Process.*, vol. 70–71, pp. 811–820, Mar. 2016.
- [6] "Magnetorheological elastomer, Sandwich beam, Electromagnet, Free vibration test," *J. Mech. Eng. Autom.*, p. 6, 2016.
- [7] N. H. Rajhan, H. A. Hamid, I. Azmi, and R. Ismail, "Magnetorheological Elastomers: A Review," *Appl. Mech. Mater.*, vol. 695, pp. 255–259, Nov. 2014.
- [8] T. Komatsuzaki and Y. Iwata, "Design of a Real-Time Adaptively Tuned Dynamic Vibration Absorber with a Variable Stiffness Property Using Magnetorheological Elastomer," *Shock Vib.*, vol. 2015, pp. 1–11, 2015.
- [9] Z.-D. Xu, S. Suo, and Y. Lu, "Vibration control of platform structures with magnetorheological elastomer isolators based on an improved SAVS law," *Smart Mater. Struct.*, vol. 25, no. 6, p. 065002, Jun. 2016.
- [10] S. Sun *et al.*, "An adaptively tuned vibration absorber based on multilayered MR elastomers," *Smart Mater. Struct.*, vol. 24, no. 4, p. 045045, Apr. 2015.
- [11] C. Sarkar, H. Hirani, and A. Sasane, "Magnetorheological Smart Automotive Engine Mount," p. 10.
- [12] Yancheng Li, Jianchun Li, and Weihua Li, "Design and experimental testing of an adaptive magneto-rheological elastomer base isolator," 2013, pp. 381–386.
- [13] G. J. Liao, X.-L. Gong, S. H. Xuan, C. J. Kang, and L. H. Zong, "Development of a real-time tunable stiffness and damping vibration isolator based on a magnetorheological elastomer," *J. Intell. Mater. Syst. Struct.*, vol. 23, no. 1, pp. 25–33, Jan. 2012.
- [14] W. H. Li, X. Z. Zhang, and H. Du, "Magnetorheological Elastomers and Their Applications," in *Advances in Elastomers I*, vol. 11, P. M. Visakh, S. Thomas, A. K. Chandra, and A. P. Mathew, Eds. Berlin, Heidelberg: Springer Berlin Heidelberg, 2013, pp. 357–374.

# Magnetorheological Elastomer Stiffness Control for Tunable Vibration Isolator

Gigih Priyandoko

Department of Electrical Engineering,  
Faculty of Engineering  
Widyagama University  
Malang, Indonesia  
gigih@widayagama.ac.id

Tedi Kurniawan

Faculty of Mechanical Engineering  
Universiti Malaysia Pahang  
Pekan, Pahang, Malaysia  
tedikurniawan@ump.edu.my

Efistein A. Naga

Faculty of Mechanical Engineering  
Universiti Malaysia Pahang  
Pekan, Pahang, Malaysia  
efiarch94@gmail.com

**Abstract**—Most of the vibration isolator has fixed stiffness such as a passive vehicle mounting system. Objective of this research is to develop a Magneto-rheological Elastomer (MRE) as a vibration isolator; stiffness of vibration absorber can be controlled by an applied magnetic field. An MRE was fabricated by mixing silicon rubber, silicon oil and carbonyl iron particles together and then cured for 24 hours in a circular mold. The experimental result shows the absorption capacity of the developed MRE is better than the traditional MRE in time and frequency domains.

**Keywords**—Magneto-rheological Elastomer, stiffness control, vibration isolators.

## I. INTRODUCTION

Typically, in engineering there was a lot of heavy machinery or structure that vibrates whether on a small or big scale. Vibrations were harmful especially to structures because it can cause structures to fail under very high vibration. Various methods and materials have been proposed to reduce vibration. The methods are broadly classified as a passive, semi-active, or active system [1-5].

The passive methods use the rubber as the material of choice. However, passive systems are only effective over a very narrow frequency range. As the excitation frequency changes, the vibration reduction effect decreases or even collapses because of mistuning. The semi-active method combines the use of sensors and actuators to vary the properties of an isolator system. On the other hand, the active methods combine the use of sensors, actuators, additional electronics and fluids with controllable properties in solving these problems [6]. Disadvantages of the active vibration system are high consumption of energy and requirement of large activation force. The semi-active method is preferable due to its stability and reliability for both low and high-frequency vibrations. The high frequency requires low stiffness and low damping vibration isolator while the low-frequency vibration requires high stiffness and high damping vibration isolator [1,2,7-11].

The Magnetorheological Elastomers (MREs) are a class of smart materials whose stiffness and damping properties can be adaptively tuned to attenuate both low and high-frequency vibration [1-3,10,12]. The objective of this research is to develop a MRE as a tunable vibration isolator when different currents are applied to get different stiffness of the MRE.

## II. MAGNETO-RHEOLOGICAL ELASTOMER

Magnetorheological fluids (MRF) state of matter can be changed with the use of different level of magnetic field. The fluids are composed of magnetic particles suspended in

viscous fluid. It will have low viscosity with the absence of a magnetic field as the particle is not arranged. To enhance their magnetic susceptibility and reducing their tendency to form an aggregation, the magnetic particle of an MRFs are additionally covered with the special layer. Other substance such as anti-corrosion and anti-sedimentation substance, is added in a small amount. The influence of magnetic field causes changes in the physical properties of MRFs. The liquid returns to its baseline after absent of external magnetic field. One of the disadvantages of the MRFs is the sedimentation [1].

MREs, also known as a magneto-sensitive elastomer, are a class of smart materials whose stiffness and damping properties can be adaptively tuned to attenuate (reduce force/amplitude/effect) both low and high-frequency vibration. It is usually achieved by varying the magnetic flux input and in full active mode using sensors and actuators or semi-active mode [6,9,13]. Also, MREs have an improve properties in new structural materials. They are an intelligent composite material whose physical properties that are sensitive to the effect of the magnetic field. These changes are non-linear, which is completely reversible and occur within several milliseconds. Furthermore, MREs are a solid phase counterpart of MRFs. The liquid carrier is replaced by a solid material elastomer or rubber in the case under analysis. The polymeric matrix that is built inside the material were embedded with good magnetic properties material such as carbonyl-iron [3,14].

There are many benefits to using MRE. They consist of natural or synthetic rubber matrix interspersed with micron-sized (3 to 5 microns) ferromagnetic particles. An elastomer such as rubber is used, they are generally soft and deformable at room temperature. In conjunction with the particle structure, the magnetic particle cannot move freely within the matrix due to the elastomer. Thus, no sedimentation presents. On top of it, with the limitation particles movement result in a quicker response to a magnetic field than in MRFs [4]. MRFs durability is limited due to densification of liquid after many operating cycles. Agglomeration and sedimentation of magnetic particles is no longer a problem in case of MREs. Thermal stability is better where MREs and MRFs have a different operating range which is the essential difference between them [12,13,15].

The fabricated MRE samples are composed of carbonyl iron powder of an approximate diameter of 10  $\mu\text{m}$  dispersed within the room-temperature vulcanizing (RTV) rubber matrix and silicon oil. They are fabricated based on the expertise acquired in the studies as shown in Figure 1.

### III. VIBRATION ISOLATOR

#### A. Simulation

Finite Element Method Magnetics (FEMM) was an open source finite element analysis software package for solving electromagnetic problems. The program addresses 2D planar and 3D axisymmetric linear and nonlinear harmonic low frequency magnetic and magneto-static problems and linear electrostatic problems. This software was used to help in to design the magnetic circuit in the multi-sandwich vibration isolator by simulating the magnetic field in different types of conditions and parameters.

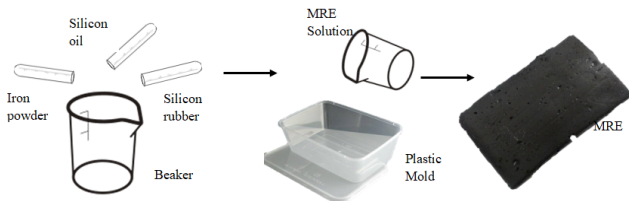


Fig. 1. Fabrication of MRE

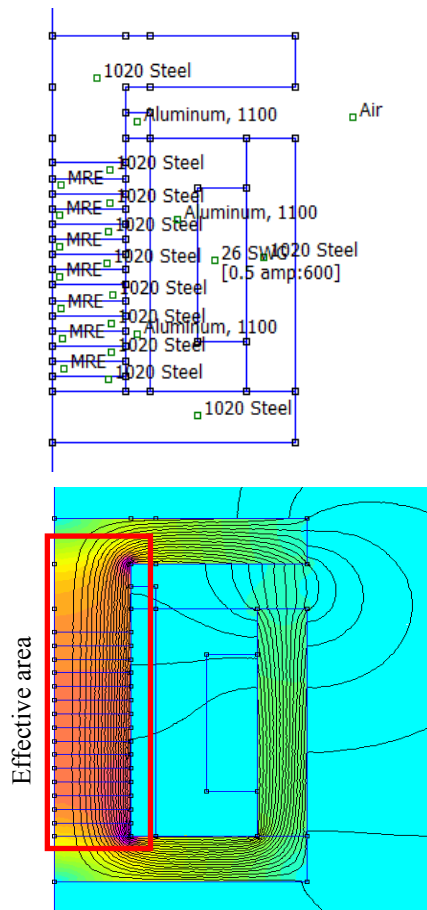


Fig. 2. Magnetics flux density contour plot

After defining the block properties and materials, the software can begin meshing the nodes to start simulating the magnetics circuit in the design that has been plotted and defined earlier. After defining the block properties and materials such as 1020 Steel, Aluminum 6061, copper coils and the air gaps, the FEMM simulation will look like as shown in Figure 2. The contour plot of magnetic flux density

can be shown in the results of the FEMM as shown in the figure. The highest concentration of magnetic flux density was at the area where the MRE was located which was exactly the aim of this design was. This was also achieved by putting steel plates in between the MRE to make a kind of sandwich plate system to drag the magnetic field into the effective area highlighted in the figure. This result will be used to determine the design of the multi-sandwich vibration isolator regarding materials, dimensions of work-piece, and coil properties.

#### B. Fabrication

There were two main materials for the fabrication of the multi-sandwich vibration isolator which were plain carbon steel and aluminum. Plain carbon steel and aluminum were chosen based on its ferromagnetic properties and availability in the market. After each part of the vibration isolator has gone through in processes, the parts are assembled through methods of fitting using bolts and screw. A cross-sectional drawing shown in Figure 3.

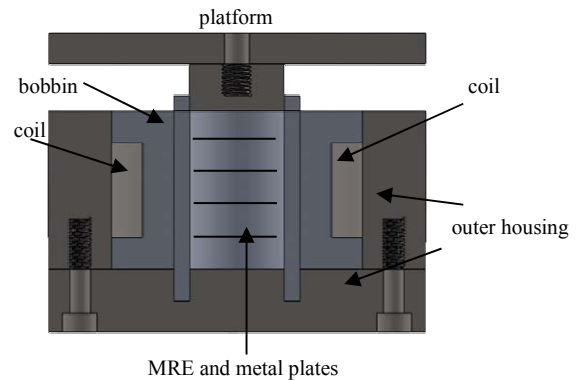


Fig. 3. Cross-sectional Diagram of Vibration Isolator

#### C. Test setup

Figure 4 shows the experimental setup of the vibration testing on MRE vibration isolator. The data acquisition system (DAQ) was connected to the laptop and the piezoelectric accelerometer to send the vibration signal to the laptop for processing. The DC power supply supplies current to the DC motor and the electromagnetic coil located inside the vibration isolator. The DC motor is used as disturbances was supplied with a constant voltage at 12 V throughout the whole experiment and mounted on top of the vibration isolator. Each time the experiment was conducted, the electromagnetic coil was supplied with 0, 1.0, 1.5 and 2.0 amperes while the DC motor was kept constant DC voltage at 12 V. The values and data are recorded inside the laptop using the DasyLab module. The data were analysed and plotted into graphs for ease of analysis and observing the changes in data. The data were split into the time domain and frequency domain for each current applied for better analysis.

### IV. RESULTS AND DISCUSSION

Figure 5 shows the time response of the accelerometer on the vibration isolator when the current applied was 0 ampere. The vibration data are shown to be very useful in analyzing the vibration of the MRE vibration isolator. It can be seen that averagely the peak for the time domain are in the range of 0.05 m to 0.01 m. This data might not be representing the



whole data because it has been scaled down to plot a clear graph. Figure 6 shows the frequency response of the accelerometer on the vibration isolator when the current applied was 0 ampere. From the figure, it can be seen that the highest peak obtained from the vibration isolator was 0.028 m at 1500 Hz.



Fig. 4. The experimental setup

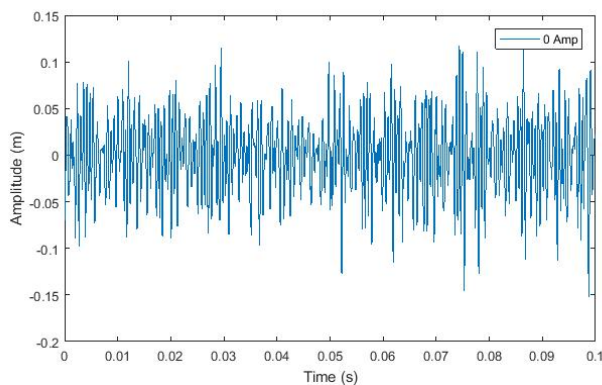


Fig. 5. Time response of vibration isolator at current 0 Amp.

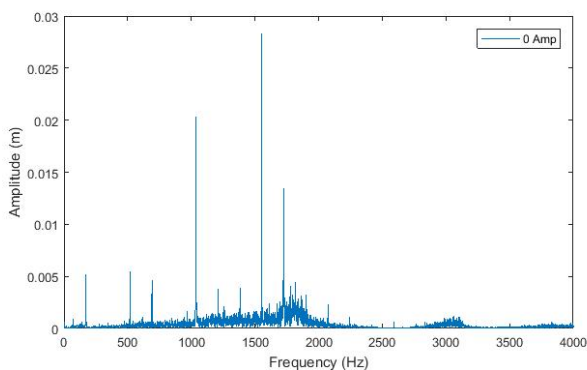


Fig. 6. Frequency response of vibration isolator at current 0 Amp.

When the current applied to the electromagnetic coils increases, this also increases the magnetic flux density in the effective area of the vibration isolator. This reacts with the carbonyl iron particles in the MRE and increases the stiffness of the MRE which in turn decreases the vibration on the MRE vibration isolator that was made by the 12V DC motor.

Figures 7-8 were the result of gathering data from all the time response graphs and frequency graphs and combining them into two graphs for time and frequency respectively to observe and analyze the difference in amplitude of vibration when the 12 V DC motor is providing vibration towards the

MRE vibration isolator. From the graph, it was observed that there were slight differences in the amplitude of vibration with each increment of current applied. At some point it was hard to see just by observing the graph as it was not very clear for the time domain, so RMS value was calculated for the entire data for each current applied as shown in Table 1.

TABLE I. RMS VALUE BASED ON EXPERIMENTAL RESULTS

Current (Amp)	RMS Value	
	Time response	Frequency response
0.0	0.0398	0.0502
1.0	0.0397	0.0499
1.5	0.0391	0.0490
2.0	0.0390	0.0485

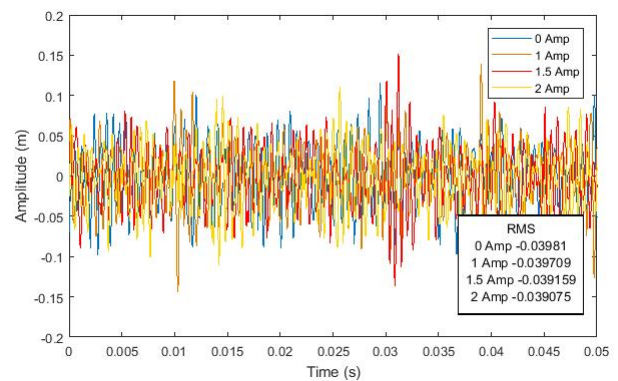


Fig. 7. Time response of vibration isolator at current 0-2 Amp.

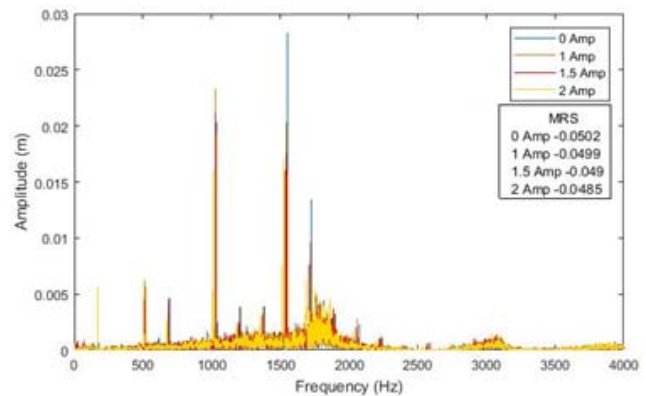


Fig. 8. Time response of vibration isolator at current 0-2 Amp.

## V. CONCLUSION

To conclude from the results obtained, it can be seen that the vibration produced by the DC motor towards the MRE vibration isolator is decreasing with each increment in current supplied to the electromagnetic coil inside the vibration isolator. The vibration isolator that was fabricated was able to focus the magnetic flux density in the effective area of MRE. From the experimental results obtained, it can be seen that the peak value for the graphs was decreasing in value as the current applied increased. This was further proven by the RMS value calculated for the time and frequency domains where the value also decreases with each increment of current applied. This proves that MRE does

have the ability to be manipulated by an external magnetic field regarding changing the stiffness and isolating vibration.

#### ACKNOWLEDGMENT

The authors would like to thank the Universiti Malaysia Pahang (UMP) for their support in the research work. This research was supported by a UMP research grant (RDU1703148).

#### REFERENCES

- [1] Y. Li, J. Li, W. Li, and H. Du, "A state-of-the-art review on magnetorheological elastomer devices," *Smart Mater. Struct.*, vol. 23, no. 12, p. 123001, Dec. 2014.
- [2] H. Deng and X. Gong, "Application of magnetorheological elastomer to vibration absorber," *Commun. Nonlinear Sci. Numer. Simul.*, vol. 13, no. 9, pp. 1938–1947, Nov. 2008.
- [3] T. Komatsuzaki and Y. Iwata, "Design of a Real-Time Adaptively Tuned Dynamic Vibration Absorber with a Variable Stiffness Property Using Magnetorheological Elastomer," *Shock Vib.*, vol. 2015, pp. 1–11, 2015.
- [4] G. J. Liao, X.-L. Gong, S. H. Xuan, C. J. Kang, and L. H. Zong, "Development of a real-time tunable stiffness and damping vibration isolator based on a magnetorheological elastomer," *J. Intell. Mater. Syst. Struct.*, vol. 23, no. 1, pp. 25–33, Jan. 2012.
- [5] X. Liu, X. Feng, Y. Shi, Y. Wang, and Z. Shuai, "Development of a Semi-Active Electromagnetic Vibration Absorber and Its Experimental Study," *J. Vib. Acoust.*, vol. 135, no. 5, p. 051015, Jun. 2013.
- [6] S. Sun *et al.*, "An adaptively tuned vibration absorber based on multilayered MR elastomers," *Smart Mater. Struct.*, vol. 24, no. 4, p. 045045, Apr. 2015.
- [7] N. Hoang, N. Zhang, and H. Du, "A dynamic absorber with a soft magnetorheological elastomer for powertrain vibration suppression," *Smart Mater. Struct.*, vol. 18, no. 7, p. 074009, Jul. 2009.
- [8] M. Behrooz, J. Sutrisno, X. Wang, R. Fyda, A. Fuchs, and F. Gordaninejad, "A new isolator for vibration control," 2011, p. 79770Z.
- [9] J. Yang *et al.*, "Development of a novel multi-layer MRE isolator for suppression of building vibrations under seismic events," *Mech. Syst. Signal Process.*, vol. 70–71, pp. 811–820, Mar. 2016.
- [10] "Magnetorheological elastomer, Sandwich beam, Electromagnet, Free vibration test," *J. Mech. Eng. Autom.*, p. 6, 2016.
- [11] N. H. Rajhan, H. A. Hamid, I. Azmi, and R. Ismail, "Magnetorheological Elastomers: A Review," *Appl. Mech. Mater.*, vol. 695, pp. 255–259, Nov. 2014.
- [12] Z.-D. Xu, S. Suo, and Y. Lu, "Vibration control of platform structures with magnetorheological elastomer isolators based on an improved SAVS law," *Smart Mater. Struct.*, vol. 25, no. 6, p. 065002, Jun. 2016.
- [13] C. Sarkar, H. Hirani, and A. Sasane, "Magnetorheological Smart Automotive Engine Mount," *International Journal of Current Engineering and Technology*, vol. 5, no. 1, 2015.
- [14] Yancheng Li, Jianchun Li, and Weihua Li, "Design and experimental testing of an adaptive magneto-rheological elastomer base isolator," In *IEEE/ASME International Conference on Advanced Intelligent Mechatronics (AIM)* 2013, pp. 381–386. 2013.
- [15] W. H. Li, X. Z. Zhang, and H. Du, "Magnetorheological Elastomers and Their Applications," in *Advances in Elastomers I*, vol. 11, P. M. Visakh, S. Thomas, A. K. Chandra, and A. P. Mathew, Eds. Berlin, Heidelberg: Springer Berlin Heidelberg, 2013, pp. 357–374.



# Improving a Wall-Following Robot Performance with a PID-Genetic Algorithm Controller

Heru Suwoyo

*School of Mechatronic Engineering and Automation,  
Shanghai University,  
Shanghai, P.R China  
herusuwoyo14@yahoo.com*

Chenwei Deng

*School of Information and Communication Engineering,  
Beijing Institute of Technology,  
Beijing, Shi, China  
cwdeng@bit.edu.cn*

Yingzhong Tian

*School of Mechatronic Engineering and Automation,  
Shanghai University,  
Shanghai, P.R China  
troytian@163.com*

Andi Adriansyah

*Departement of Electrical Engineering,  
Universitas Mercu Buana,  
Jakarta, Indonesia  
andi@mercubuana.ac.id*

**Abstract**—*A wall-following robot needs a robust controller that navigate robot based on the specified distance from the wall. The usage of PID controller has been successfully minimizing the dynamic error of wall-following robot. However, a manual setting of three unknown parameters of PID-controller often precisely increase instability. Hence, recently there are many approaches to solve this issue. This paper presents an approach to obtaining those PID parameters automatically by utilizing the role of Genetic Algorithm. The proposed method was simulated using MATLAB and tested in a real robot. Based on several experiments results it has been showing the effectiveness of reducing the dynamic error of the wall-following robot.*

**Keywords**—*Wall-Following Robot, PID Controller, Genetic Algorithm, PID-GA Controller*

## I. INTRODUCTION

A wall-following robot is a robot that has the primary task to follow the wall by maintaining its movement. The robot will move closer to the wall, move forward and move further from the wall when its position is far from the wall, on the predetermined path and close to the wall, respectively. Thus, apparently, by utilizing the mounted distance sensors, the robot has to sense the distance between the wall and itself along the operation. Besides, these distances are processed to generate the proper movement with the involvement of a specific controller. The success of this robot lies in its capability to follow the predetermined path by concerning quickness and accuracy, that apply in automatically wheelchair, electronic goods transportation, and automated guided vehicle (AVG) [1]-[4].

However, the accuracy of all sensors is affected by limited precision. Evenly the best sensors still have a degree imprecision. Consequently, the role of the controller in maintaining the movement has been becoming the core of the problem to be accomplished. There are many control methods have been attempted to address the common issue of the wall-following robot [5], such as Fuzzy Logic [6][7], Genetic Algorithm, Neural Network or hybrid of them [8]. But, most of these approaches have to utilize the orientation sensor featured in the robot (compass, GPS, etc.) [9].

The well-known controller proposed method to address these problems is a PID Controller that generating the proper velocity for each wheel referring to the rule of pulse width modulation (PWM) [10][11]. As known,

generally, the performance of PID-controller lies on a determination of its three necessary parameters. Each parameter of the PID controller has a particular influence on the process. Consequently, their precision should be concerned carefully.

There have been many methods proposed in producing these parameters automatically. The previous PID tuning is using Ziegler-Nichols Algorithm [12]. But the tuning method is needed difficult robot modeling for satisfaction one. In another case, the necessary parameters were obtained automatically involving an algorithm that can derive the original data to be proper optimum parameter respect to the movement. Fuzzy-PID is one of the tuning methods of PID using Fuzzy Logic [13][2]. Tang et al. [14] and Takahashi [15] also proposed a method to tune PID automatically using Neural Network. Unfortunately, these the process is too many computations works that make a control process operated in hard.

This paper proposed a method to improve the performance of a wall-following robot with PID Controller which the parameters tuned automatically by Genetic Algorithm (GA). GA is a metaheuristic inspired by the process of natural selection used to optimize and search for some variables [16] [17].

The robot considered here is a self-designed robot which is completed by some distance sensors. The robot will maneuver use a differential-wheel system of the mobile robot [18]-[20]. These sensors were installed and placed on the precise direction which aims to be ably sensing the left-side, right-side and front-side wall accurately.

This paper is organized as follows. The related basic-knowledge is presented in Section 2. Section 2 also describes the design flow of the proposed method. Section 3 gives the experimental result and discussion. Finally, the experiment will be concluded in Section 4.

## II. METHOD

A designed robot that completed by three distance sensors is used to implement the proposed method. This robot was intended to be able working automatically utilizing the capability microcontroller, Arduino, which calculates the distance and control two DC motors connected to an odometer.

### A. Robot Kinematic Model

Fig. 1 shows the steering system of the nonholonomic wheeled mobile robot. The turning ability is dominantly due to two powered wheels referring to the rule of the differential drive system [17]. The robot has a dimension such as  $L=10$  cm  $R=3.5$  cm

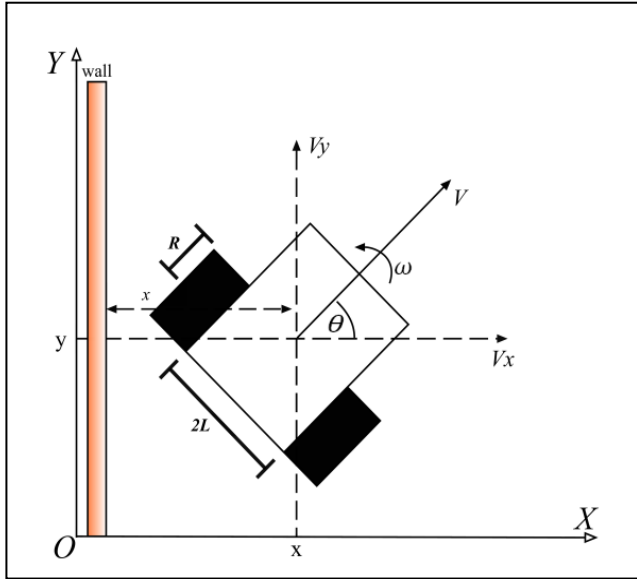


Fig. 1. Robot Pose in a Global Coordinate System

By considering that the robot is operated in a planar environment, the robot's pose  $p$  comprises two-dimensional planar coordinates  $(x, y)$ , and an orientation  $\theta$ . Thus, the prior robot's pose can be described by the following vector,

$$p_{(t)} = [x_{(t)} \quad y_{(t)} \quad \theta_{(t)}]^T \quad (1)$$

Since the linear velocity  $v$  and angular velocity  $\omega$  are considered as the control reference, we have the dynamic,

$$\dot{p} = \begin{bmatrix} \dot{x} \\ \dot{y} \\ \dot{\theta} \end{bmatrix} = \begin{bmatrix} \cos \theta_{(t)} & 0 \\ \sin \theta_{(t)} & 0 \\ 0 & 1 \end{bmatrix} \begin{bmatrix} v \\ \omega \end{bmatrix} \quad (2)$$

where  $\dot{p}$  is the transition of the robot. Then the posterior robot's pose becomes

$$p_{(t+1)} = p_{(t)} + \dot{p} \quad (3)$$

Additionally, involving the term angular velocities for each powered wheels, the control reference can be equated as follows:

$$v = \frac{(\omega_r + \omega_l)R}{2} \quad (4)$$

$$\omega = \frac{(\omega_r - \omega_l)R}{2L} \quad (5)$$

$$\omega_r = vR + \omega L \quad (6)$$

$$\omega_l = vR - \omega L \quad (7)$$

where  $\omega_r$  and  $\omega_l$  are the angular velocity of the right and left the wheel, respectively.

### B. PID-GA Controller Design

PID-controller is a well-known controller widely used to solve a nonlinear problem of the specific system. It adjusts three necessary parameters as condition change dynamically. These non-zero parameters are commonly termed as proportional gain  $K_p$ , integral gain  $K_i$ , and derivative gain  $K_d$  and due to their influence to the output controller, obtaining their accurate values have been regarded as the crucial task of the usage PID controller. These specific values can be obtained by performing particular high-level tuning.

Generally, the optimum setting of these parameters involves the role of accumulated error,  $e(t)$ , which is calculated from actual process value  $p_v$  and predetermined value termed as set point,  $sp(t)$ . Considering  $u(t)$  as the control variable, then the analogy of the PID controller will be depicted as Fig. 2. It can be modeled mathematically as follows [9] [10],

$$u(t) = K_p e(t) + K_i \int_0^t e(\tau) d\tau + K_d \frac{d}{dt} e(t) \quad (8)$$

where  $t$  indicates that the controller is operated in a time domain.

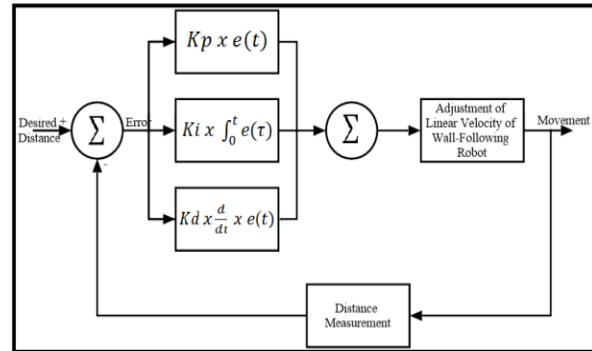


Fig. 2. The PID Controller Diagram

Obtaining the non-zero value of the proper amount of three-term controller  $K_p$ ,  $K_i$  and  $K_d$  have been challenging many researchers. Ineffectively it has been accomplished by manual tuning.

Genetic Algorithm (GA) is an optimization method based on the natural selection process. It modifies the initial population of individual solution till obtained the proper optimum solution to the target system. A term named as fitness function represents the quality of target optimized system. The optimal solution offered by GA can be perceived by adjusting the generated random or known as initial population value with natural process termed as crossover and mutation. To produce the best solution, the process iteration can be predetermined as many as possible [15] [16].

The mobile robot has a task to follow the desired path by maintaining the rotational velocity of each wheel as shown in Fig. 3. These velocities are generated from the linear velocity produced by the PID controller.

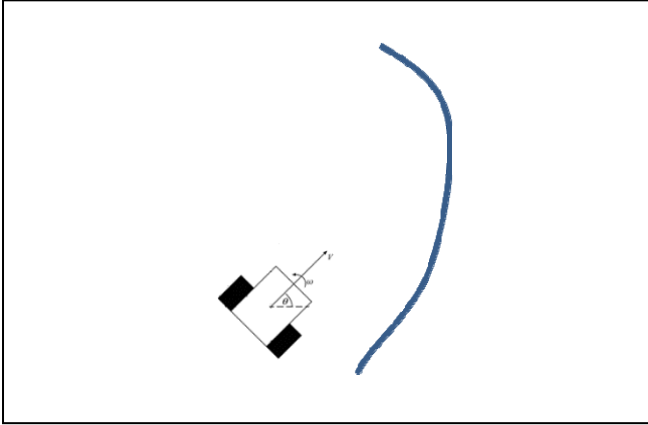


Fig. 3. Wall-Following Process

In order to utilize the general equation of PID, initially the error was designed as follows:

$$e(t+1) = sp - pv(t) \quad (9)$$

Then, considering that the angular velocity  $\omega$  has no much effect to the robot's dynamic error, the angular velocity  $v$  is regarded to be equal as the half of prior orientation. Hence, the PID controller only produces the linear velocity of the robot  $v$  that will be used to obtain each angular velocity of the wheel  $\omega$  by applying (6)-(7).

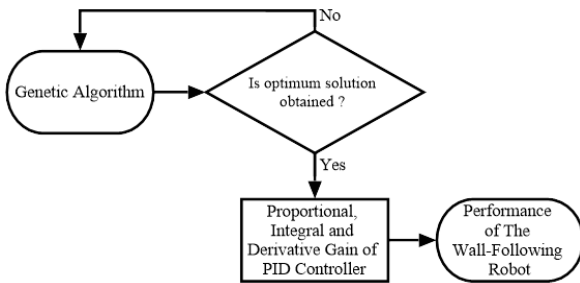


Fig. 4. The PID-GA Controller Diagram

Furthermore, the GA was used to generate three basic parameters of PID (i.e.  $K_p$ ,  $K_i$ , and  $K_d$ ). To know the quality of the gained solution, the fitness function is constructed as follows:

$$\sum_{it=0}^{\max} e(it)^2 \quad (10)$$

where it represents all error along the movement. Each iteration stores an optimum solution of a generation and the next generation will store the new solution if it is better than the previous solution otherwise the process in the current generation will be restarted. The last representation shows us the best solution of three basic parameters of PID controller produced by GA.

Finally, the output of the PID controller  $u(t)$  can be used to recalculate the linear velocity of the stable pose  $e(t) = 0$  denoted by  $v_{st}$ . Then, the final linear velocity  $v(t)$  is derived as follows:

$$v(t) = v_{st} - u(t) \quad (11)$$

### III. RESULTS AND DISCUSSION

The real wall-following robot has been designed and shown in Fig. 5. The proposed method of PID-GA controller was tested by simulating the robot kinematic model using MATLAB.



Fig. 5. The Real Wall-Following Robot

Automatically, a GA has been approached to generating the parameters of the PID controller. The effectiveness includes the quick process and the guaranteed precision. To determine the satisfied parameters, which are non-negative constants, it is required to involve the optimization method. Two different experiments of the wall-following robot performance have been performed either normal with constant linear velocity or controlled by PID-GA Controller.

The mobile robot with different those two type of the controller was positioned at the same coordinate position (8.4,1,π/4). Then, both were operated at the same time span of 100 seconds. The robot should follow the wall in a distance of 6 cm from the wall. By applying 60 iterations or approximately its operation within a minute, the robot performance with the constant linear velocity of 0.15 cm/s is seen in Fig. 6(a). By applying same starting point, the performance of wall-following robot controlled by the GA-PID Controller as seen in Fig. 6(b). The comparison of two different performances can be presented by its generated error on a scale of dm and the last coordinate as shown in Table 1.

Furthermore, the end position that reached by the robot and the total number of errors expressed by (4) have been observed. The position achievement of the robot with PID-GA controller farther from the starting position. It indicates that the robot with PID-GA controller has a better working speed compared to the others. While the value of the total error with PID-GA controller less than other. It also

indicates that PID-GA controller has a better level of following the desired path.

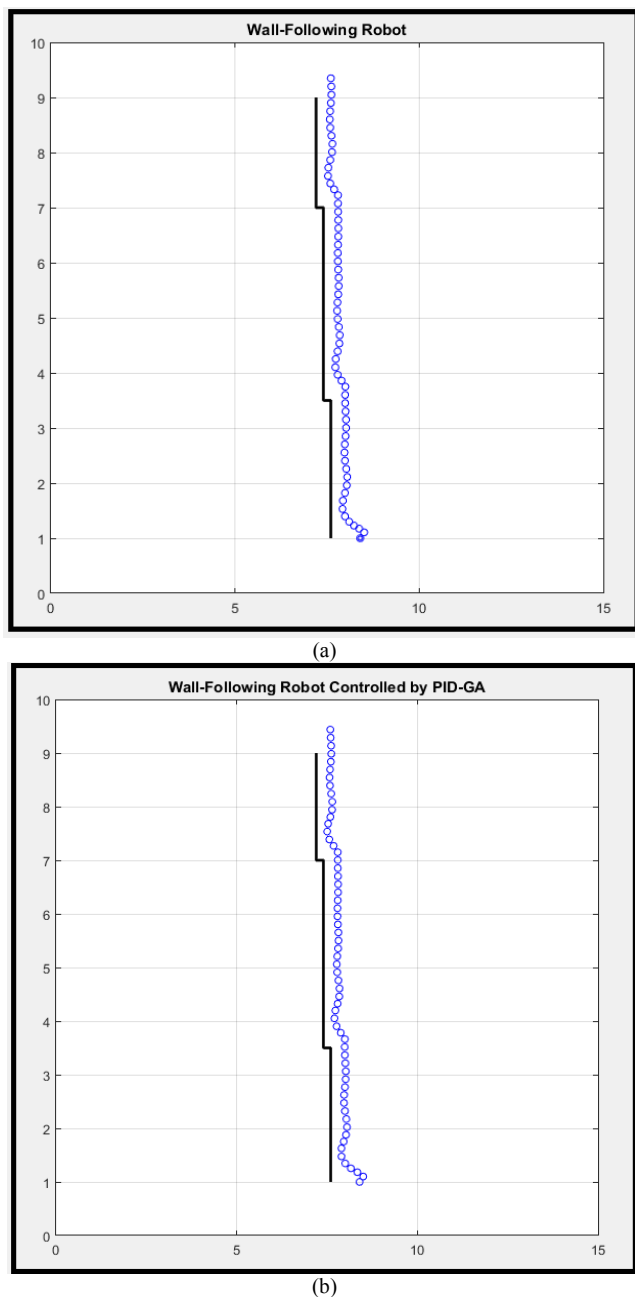


Fig. 6. The Result of the Performance of Wall-Following Robot: (a). PID Controller without GA. (b) GA-PID Controller

TABLE I. TABLE TYPE STYLES PERFORMANCE OF WALL-FOLLOWING ROBOT

Characteristic	Generated Error	Final Position
Normal Movement	0.83625	9.1986
Based on PID-GA	0.78543	9.2867

#### IV. CONCLUSION

The PID-GA Controller has implemented to control the wheeled-mobile robot to follow the desired path along the wall. The role of PID-GA Controller is to produce the proper linear velocity of the wall-following robot. The reduce of the error number shows the effectiveness of the

proposed method. It can be seen from the experimental result that shows the robot has faster speed and smoother movement than the before. The proposed controller able to improve the performance of wall following robot better. The GA able to optimize the PID parameters simpler and with optimization time faster than optimize manually.

#### ACKNOWLEDGMENT

The authors would like to gratefully acknowledge the funding from the Research Program of Electrical Engineering Department, Faculty of Engineering, Universitas Mercu Buana.

#### REFERENCES

- [1] Y. T. Lee, C. S. Chiu and I. T. Kuo, "Fuzzy wall-following control of a wheelchair," Joint 17th World Congress of International Fuzzy Systems Association and 9th International Conference on Soft Computing and Intelligent Systems (IFSA-SCIS), Otsu, Japan, pp. 1-6, 2017.
- [2] A. Adriansyah and H.M.A. Shamsudin, "Wall-Following Behavior-Based Mobile Robot Using Particle Swarm Fuzzy Controller," Jurnal Ilmu Komputer dan Informasi, Vol. 9, No.1, pp. 9-16, 2016.
- [3] A.A. Wardana, A. Widyotriatmo, and A. Turnip, "Wall following control of a mobile robot without orientation sensor," 3rd International Conference on Instrumentation Control and Automation (ICA), Ungasan, Indonesia, pp. 212-215, 2013.
- [4] A. Adriansyah, Y. Gunardi, B. Badaruddin and E. Ihsanto, "Goal-seeking Behavior-based Mobile Robot using Particle Swarm Fuzzy Controller," TELKOMNIKA, Vol. 13, No. 2, pp. 528-538, 2015.
- [5] A. Pandey, S. Pandey, S. and D.R. Parhi, "Mobile Robot Navigation and Obstacle Avoidance Techniques: A Review," International Robotics & Automation Journal, Vol. 2, No. (3), pp. 00022, 2017.
- [6] I. Emmanuel, "Fuzzy Logic-Based Control for Autonomous Vehicle: A Survey," International Journal of Education and Management Engineering, Vol. 2, pp. 41-49, 2017.
- [7] N. P. Varma, V. Aivek and V. R. Pandi, "Intelligent wall following control of differential drive mobile robot along with target tracking and obstacle avoidance," 2017 International Conference on Intelligent Computing, Instrumentation and Control Technologies (ICICT), Kannur, pp. 85-91, 2017.
- [8] N.H. Singh, and K. Thongam, "Fuzzy Logic-Genetic Algorithm-Neural Network for Mobile Robot Navigation: A Survey," International Research Journal of Engineering and Technology (IRJET), Vol. 4, No. 8, pp. 24-45, 2017.
- [9] A. Mohamed., M. El-Gindy and J. Ren, "Advanced control techniques for unmanned ground vehicle: literature survey," International Journal of Vehicle Performance, Vol 4, No. 1, 2018.
- [10] A.S. Wardoyo, S. Hendi, D. Sebayang, I. Hidayat, A. Adriansyah, "An investigation on the application of fuzzy and PID algorithm in the two wheeled robot with self balancing system using microcontroller," In 2015 IEEE International Conference on Control, Automation and Robotics (ICCAR), Singapore, pp. 64-68, 2015.
- [11] I. Ardiyanto, "Task oriented behavior-based state-adaptive pid (proportional integral derivative) control for low-cost mobile robot," 2010 Second IEEE International Conference on Computer Engineering and Applications (ICCEA), Bali, Indonesia, Vol. 1, pp. 103-107, 2010.
- [12] C.B. Prakash and R.S. Naik, "Tuning of PID Controller by Ziegler-Nichols Algorithm for Position Control of DC Motor," International Journal of Innovative Science, Engineering & Technology, Vol. 1, No. 3, pp. 379-382, 2014.
- [13] C.Y. Chou and C.F. Juang, "Navigation of an Autonomous Wheeled Robot in Unknown Environments Based on Evolutionary Fuzzy Control," Inventions, Vol. 3, No. 3, pp. 2-14, 2018.
- [14] Z. Tang, M. Yang, and Z. Pei, "Self-Adaptive PID Control Strategy Based on RBF Neural Network for Robot Manipulator," 2010 First International Conference on Pervasive Computing, Signal Processing and Applications, Harbin, pp. 932-935, 2010.
- [15] K. Takahashi, Y. Hasegawa and M. Hashimoto, "Remarks on Quaternion Neural Network-Based Self-Tuning PID Controller," 2016

International Symposium on Computer, Consumer, and Control (IS3C), Xi'an, China, pp. 231-234, 2016.

- [16] M. Li, C. Wang, Z. Chen, X. Lu, M. Wu and P. Hou, "Path planning of mobile robot based on genetic algorithm and gene rearrangement," 2017 Chinese Automation Congress (CAC), Jinan, China, pp. 6999-7004, 2017.
- [17] D. Sahu and A. K. Mishra. "Mobile Robot Path Planning by Genetic Algorithm with Safety Parameter," International Journal of Engineering Science and Computing, Vol. 7, No. 8, pp. 14723-14727, 2017.
- [18] A.V. Chavan and J. L. Minase, "Design of a Differential Drive Mobile Robot Platform for use in constrained environments," International Journal of Innovations in Engineering Research and Technology (IJIERT), Vol. 2, No. 6, pp. 1-9, 2015
- [19] Y. Gunardi, D. Hanafi, F. Supegina and A. Adriansyah, "Mathematic base for navigation mobile robot using reachability Petri net," Journal of Telecommunication, Electronic and Computer Engineering, Vol. 10, Issue 1-9, pp. 65-69, 2018
- [20] A. Adriansyah, B. Sulle, E. Ihsanto, and Y. Gunardi, "Optimization of circular robot size using behavior based architecture," Journal of Telecommunication, Electronic and Computer Engineering, Vol. 9, Issue 3-7, pp. 67-72, 2017

# A Riview of Solar Tracking Control Strategies

Ali Basrah Pulungan<sup>1,2</sup>

<sup>1</sup> Doctoral Student at Department of  
Mechanical Engineering  
Universitas Andalas  
Padang, Indonesia

<sup>2</sup> Department of Electrical Engineering  
Universitas Negeri Padang  
Padang, Indonesia  
e-mail: alibp@ft.unp.ac.id

Lovely Son

Department of Mechanical Engineering  
Universitas Andalas  
Padang, Indonesia  
e-mail: lovelyson@ft.unand.ac.id

Syafii\*

Department of Electrical Engineering  
Universitas Andalas  
Padang, Indonesia  
e-mail: syafii@eng.unand.ac.id

**Abstract**—This paper presents the use of sunlight trackers to increase the efficiency of solar panels. The sunlight tracking is done by passive and active tracking method with one or two axis. The active trackers use an electrical motor as a driver and can be controlled by a microcontroller or a programable logic controller (PLC) according to the direction of sunlight. The use of this controller in sunlight tracking system performed in real time or periodically. The position of the sun as a controller input can be obtained based on azimuth angle and solar elevation angle or by direct measurement using sensors. From the discussion is obtained an increase of efficiency of 29.37% in average using the active tracker.

**Keywords**— solar cell, tracker, microcontroller, programable logic controller

## I. INTRODUCTION

The depletion of fossil energy sources and the ever-increasing demand for energy have prompted intensive research for the development of renewable energy source that is more efficient and green energy sources. Some renewable energy sources such as wind, micro-hydro, geothermal, biomass, biogas and diesel fuel are used as stand-alone electrical energy sources or interconnected through electricity networks. Solar energy, i.e the sunlight and heat energy has been exploited by humans for a long time by using various technologies ranging from simple to sophisticated. This is due to the fact that the sun as a source of energy can generate more amount of the power until 27.000 times bigger compare to the other sources[1]. The current technology enables to convert the solar radiation into electrical energy known as photovoltaic systems. This conversion system is expected to make a significant contribution which sholved some of the energy problems facing the world today.

The energy conversion efficiency especially in photovoltaic systems is an interesting issue, since the system has a low overall efficiency of less than 20% [2]. The overall increased efficiency of solar panels can be done by maximizing power output, increasing cell efficiency, and implementing a tracking system [3]. The efficiency is also affected by weather conditions, irradiation and temperature levels. For example, clouds that pass through some solar cells or sub-modules will reduce the total output power of the PV arrangement [4].

The use of large-scale PV systems depends on the cost and efficiency of energy conversion. Based on the latest technological developments, the utilization of PV tracking

system is an optimal choice to improve system efficiency and to reduce costs.

## II. SUN TRACKING METHODES

The amount of energy absorbed by the solar panel can be increased through the implementation of a solar tracking system. The sunlight tracking system can be installed by using one or two axis. Actually, the two-axis trackers are most efficient to use but it can increase more complexity. It can be the best choice for locations where the position of the sun continues to change throughout the year in different seasons. While, one axis tracker can be a good solution for places located around the equator that have no significant changes in the sun's position throughout the year [5]. The use of a tracking system will allow PV cells to lead to the sun accurately, which is able to compensate for changes in the height of the sun (throughout the day), to latitude of the sun (during seasonal changes) and to change in azimuth angle. The sun tracking systems using either two axes or one axis can be categorized into two classifications, i.e. passive (mechanical) and active (electrical) tracking methods [6].

### A. Passive (Mechanical) Tracking

The passive trackers work on the principle of thermal expansion. The utilization of solar heat will cause an imbalance in the tracker, so that the movement of the tracer will arise. The level of complexity of passive trackers is lower when compared to the active trackers, but fails to provide high efficiency at low temperatures. In the tropical region with plenty of sunlight available throughout the year and small variations in azimuth angle, it is possible to develop Passive (mechanical) Tracking [7]. In addition, the use of passive tracking fits perfectly with the slow sun movement so as to avoid oscillatory motion [6]. In terms of performance shows that passive trackers can improve PV efficiency and are cheaper in terms of cost, but not widely used by consumers.

Poulek, designed a low-cost passive tracker with one axis using SMA (Shape Memory Alloy). The materials used in the test are NiTi, CuZnAl and CuAlNi, carried out at a short time following the movement of the sun starting at an angle of 60°. The results of the study obtained that this tracker works very well in short testing periods and there is an increase in efficiency of about 2% [8]. However, this tracker design obey to the effect of gear transmission (the self-locking transmission) and cannot be used at an angle position of less than 60°.



Mwithiga et al., has designed and tested a dryer with limited sunlight tracking capability that is manually operated. The drying unit is installed, so that it can face east-west. A disc is used as a position tilt angle regulator with a minimum multiplication of 150. This position would let the collecting plate to be adjusted appropriately to trace the sun during the day. The sun tracking is made with four settings, Dryer is set at  $45^\circ$  to horizontal angle facing east at 8:00 AM. The data was collected by empty drying and coffee dryers. The results showed that the process to dry the coffee beans took 2 until 3 days compared to the drying process without using a tracking system, which took 5 until 7 days. Moreover, the temperature in the room could increased up to the maximum value which is  $70.4^\circ\text{C}$  [9].

Noel Leon et al, conducted a research on Semi-Passive Solar Tracking Concentrator (SPSTC) which aggregated the sunlight with minimum mechanical effort and slight movement. This system consists of Micro-heliostat, Fresnel lens and receiver which is a mirror arrangement positioned above the Fresnel lens. The Micro-heliostat serves to reflect sunlight toward the lens by tracing the path of the sun based on the angle of altitude and azimuth. The test is done by determining the three values of the slope angle with the aim of getting the value of effectiveness on the Fresnel lens and can reduce the influence of blocking and shading on the receiver, so that the amount of solar energy received can be maximized. In this study the effectiveness of Fresnel lenses can still be improved by taking into account the factor of the distance between Micro-heliostat, the number of Micro-heliostat and the slope of the array [10].

Clifford et al., designed a new passive solar tracker modeled by using the computer. This model combines two bimetal strips made from aluminum and steel which is located on a wooden frame, symmetrically on both sides of the horizontal axis. While, the open biometallic strip gets hotter, aluminum is more bending than steel because its thermal expansion coefficient is higher. This bending will cause maximum deflection at the midpoint of the strip, the unbalanced moment and the resulting movement. Then they compared the results obtained from computer models and experiment from bimetal strip deflection due to the effects of thermal radiation. They also observed the required time for solar trackers to accomplish reorientation of the east-west. Both results are similar to each other. The designed solar trackers have potential to increase the efficiency of solar panels until 23%. They also recommend multiple axis system mechanisms for future development [11].

### *B. Active (electrical) Tracking*

The Active Solar Trackers use motors and gear mechanisms as electric actuators to move PV positions. These motors are usually given input by the control signal in the form of the magnitude and direction of tracking to be carried out. The controlling of motor drive can be done by using microcontroller and Programable logic controller (PLC) based on sensor or data which is already available.

Active trackers are claimed to be more accurate and more frequently used and higher efficiency improvements compared to passive trackers [12]. Yet, this tracker requires power and energy consumption.

#### *1) One-Axis System with Microcontroller*

The one-axis system in active tracker has a one-degree freedom movement on the axis rotation, this will make the energy consumption lower than the multi-axis system.

Huang et al., created a three-axis position for tracking system (1S-3P) on the roof of the building. The tracking of sunlight in 1S-3P operation is designed only for three different angles. This tracker, consisting of a simple structure design and a Photovoltage (PV) dc rotator motor. The use of this tracker can increase the generated power by 23.6% compared to conventional tracking systems. The measurement of tracker movement, PV generated power and control algorithm is done by using PIC18F452 microcontroller [13].

J. Beltrán A et al., designed a one-axis sunlight tracking system using two PV modules mounted on a symmetrical structure with a central axis by using a microcontroller as an embedded control system. This sensorless type of tracker operates as an open loop electronic control system. The Tracker control system is oriented to the position of the sun based on the angle of elevation or the sun's inclination to the plane and the angle of the daily movement of the sun or azimuth angle. This tracking system can increase 26% power gain for 8 working hours. This tracker is said to have advantages over closed-loop sensor types, which are not limited by geographic location tracking, this is because the system has been designed and programmed by providing azimuth angle during the day to obtain maximum solar radiation [14].

Tracker with one axis has also been done Priyanjan et al. Trackers designed using a microcontroller as a system control center, from the tests performed, obtained the average value of power generated 13% larger than the fixed position [15].

Abadi. I et al.. created and implemented a single axis solar tracking system oriented to the intensity of solar radiation and ambient temperature. The whole system is controlled by a microcontroller as a main control unit and it worked based on the Fuzzy Logic Controller (FLC). The experimental mechanism is based on a DC motor controlled intelligently by a fuzzy logic controller that drives the prototype according to the input received from the LDR sensor. The tracking system performance was carried out experimentally by comparing the output of energy resulted from two different systems (tracking vs. fixed PV panels), the location of data collection is established in Surabaya - Indonesia. The results showed that the output of energy was increased up to 47 % compared to the fixed system [16].

Adel Abdulrahman et al, designed a single axis sunlight by developing an electromechanical system. The main purpose of this design is to model and create an automatic solar tracking system using an Arduino microcontroller, four LDRs to find the light intensity and two PMDC motors for horizontal and vertical movements. The mechanical component design is focused on static analysis of all parts of the system, such as forces that affect the balance of the tracking system and the calculation of the torque needed to lift the solar panels in the horizontal and vertical axes. In addition, static analysis also considers the wind effect on solar panels. The efficiency of this design is better than fixed PV cells, based on the results of the tests that have been done there is an increase of about 31%. Yet, this can

still be improved by paying more attention to the accuracy of the sensor position [17].

Md. Tanvir Arafat Khan, designed and built a prototype microcontroller based on an automatic tracking system with a control mechanism based on weather conditions and the direction of the sun. The main components used in the prototype are Photo resistors, Microcontrollers and Stepper motors. The solar tracker works with three operating times, i.e. during normal daytime weather, when the sky is cloudy and the two-way rotation i.e. east-west and west-east. This prototype is said to have a simple mechanism for controlling systems at relatively low cost through software-based solutions [18].

Tiberiu Tudorache et al, designed a single-axis solar tracking system using the backs of tilted PV panels and an electric motor as a panel drive on the expected trajectory relative to the Sun's position. The model of tracking system is operated by using a DC motor by an intelligent drive unit according to the received signal obtained from the two simple and efficient light sensors. The minimum energy consumption is received since the electricity supply is only given in the period of movement of PV panels. Instead, the optimum position of the intensity for the signal of light is achieved by maximizing the energy output generated by the PV panel. [19].

Chin CS et al., made a design, model, and test a stand-alone single axis solar tracking. The solar radiation is detected by two light sensors (LDR) placed on the surface of the photovoltaic panel (PV). The intelligent tracking system is operated in different modes to provide the flexibility in the different weather conditions. The PV panel rotates automatically based on the daylight of the sun. This solar tracker system is modeled first using MATLAB™ / Simulink™. The tracker is designed as a single axis tracker having an East-West rotation. The intensity of sunlight is detected using an LDR sensor, which then sends a signal to the microcontroller to rotate the panel using a servo motor. Based on the test results obtained there are irregularities in experimental results with simulation, this can occur due to mechanical friction in the tracking motion [20].

## 2) One-Axis System with Programmable Logic Controller

Al-Mohamad, designed a single axis solar tracking system using a programmable logic-controller (PLC) unit which control the movement of PV modules to follow the direction of solar radiation. The performance of the system has been tested and it can be said that the system worked properly. The movement of the PV module runs smoothly without a lag to the presence of detected radiation. The acquired daily PV power output is increased by more than 20% compared to fixed modules. The PV tracking system can be operated as a stand-alone device and it also can be connected to a personal computer to monitor the entire process and performances via the RS232 serial port. [21]

## 3) Two-Axis System with Microcontroller

Roth et al., Designed and tested a closed-loop automatic two-axis tracker. The amount of sunlight radiation is measured by using a pyrheliometer and two small dc motors is installed there as an instrument to keep the sunlight falling in the middle position of the beam detector. This system get the stability of solar radiation above 140 w/m<sup>2</sup> [22].

Jeng-Nan Juang et al., designed a dual-axis tracking system with real-time semi-portable criteria, increased efficiency by at least 15% and could charge a battery less than eight hours. The motor controller used is The Pololu Dual VNH5019 Motor Shield which allows for controlling two DC motors with Arduino usage. The method used in tracking sunlight is a real-time system, despite the fact that the sun's azimuth does not change significantly in one minute. The sun tracking is carried out in a 12 hour period where the system will check every minute for voltage differences between LDR [23].

SC Ribeiro built innovative solar trackers based on azimuth motion and elevation movements, which main specifications are low cost, small power consumption and flexibility. This platform has two freedom axes with two direct current motors operating in the vertical and horizontal axes controlled by the microcontroller. There are two pairs of LDR for each axis that is vertical and horizontal. The output of the LDR pair is the variable used by the microcontroller to control movement around the vertical axis (azimuth) and horizontal (elevation). This system has been field tested for five days in cloudy winter (end of July and early August 2012), the result is quite good with the total tracker consumption with both motors operating at 67.8 mA. Thus, in such weather conditions there is a relative surplus of 38.98% [24].

Oner et al, designed a solar tracking system which is capable to move on both axes by using a spherical motor controlled by a microcontroller. The spherical motors have the ability to move across both horizontal and vertical axis, compared to using two stepper motors for each axis. The purpose to build this control system is to direct the PV system in such a way that able to face the sun at 90°. The results showed the improvement of the system performance when the tracking systems were used mainly after mid-day during the day compared to fixed-tilt PV panels [25].

Arlikar et al., designed and implemented a three-dimensional two-axis solar tracking system consisting of two stepper motors, two sensors and solar panels. Two stepper motors are Vertical and Horizontal stepper motors are used for 3D movement of solar panels, while each sensor consists of 2 Light Dependent Resistors (LDR). The change of LDR value according to the intensity of the light falling on it which will cause voltage variations. This information will be used by the microcontroller to rotate the stepper motor, so the Panel will always face the sun. It was concluded that 3D solar panels produce more energy than traditional stationary solar panels [26].

## 4) Two-Axis System with Programmable Logic Controller

Abdallah et al., designed and built a two-axis electromechanical solar tracking system, an open-loop control system using a PLC to control the motion of the solar tracker. The PLC programming is based on solar angle analysis and motor speed calculation. This solar tracker works based on the surface position which is defined by the slope of the surface and the azimuth angle of the sun. Two tracking motors are used, one for joint rotation of the north-south horizontal axis and the other for the joint rotation of the vertical axis. Tracking mode is carried out in stages to simplify system work without losing a lot of power and it is very efficient since the amount of power consumed by the

electric motor and the control system will not be more than 3% from the total power obtained by the tracking system. They concluded that the tracking system by using two-axis could increase the daily power up to 41.34% compared to fixed surfaces. [27]

Rosell et al., designed and built systems based on Fresnel concentrators and PV/T collectors using water as a working fluid. The two-axis solar tracking system uses two DC linear actuators to move the concentrator and reed sensor. This system has the characteristics of a fairly simple electromechanical arrangement. The mirror reflects light into focus bands and solar cells. To obtain greater accuracy and to calculate the position of the sun, the PLC system is designed and constructed. Two sensors are positioned to determine the temperature rising in the collector and measure the temperature of the water in and out. Another sensor is used to measure air temperature. The average daily results are measured under different conditions, PV/T system efficiency is affected by flow rates and concentration ratios. The increase of 50% in energy compared to an optimally tilted static surface [28].

Sungur, designed and implemented two-axis solar trackers using electromechanical systems controlled through programmable logic control (PLC). This study is based on the azimuth angle of the sun and the angle of the sun's height is calculated in every hour for each day during the year. The performance measurement of solar panels is carried out in two solar panel conditions, firstly the solar panel is placed in a fixed position and then then it is controlled when it was tracking the sun at azimuth angle and the height of the sun. Based on the data resulted from the measurements, it was shown that a two-axis solar tracking can produce 42.6% more energy compared to a fixed system. [29]

Abu-Khadera et al., Designed a multi-axis solar tracking system that is PLC controlled. They claimed that this system used a simple electromechanical settings, low cost, easy installation and maintenance. The piranometer as a device to measure the availability of solar radiation is installed on a platform on the tracking surface. This study proves that the control programming method works efficiently in all weather conditions regardless of the presence of clouds. The values calculated from the surface position as a function of time are transferred to the PLC program to control the solar position tracking actuator. The motor is used as a solar multi-axis tracking drive, one for rotation with the north-south horizontal axis (N-S) or the east-west axis (E-W, and the other motor for rotating along with the vertical axis. The use of MAST results in an increase in total power output of around 30-45% compared to 320 fixed slope PV cells [30].

### III. DISCUSSION

Taking into account all reviewed articles, a microcontroller or programable logic controller as a control instrument is an option that can be used for active tracking systems, either single or double axis. The use of both passive and active tracers can increase the efficiency of solar panels, with a greater increase in active trackers with an average of 29.37%. The tracking is done in different places with varying weather conditions, the position of the sun can be determined using data obtained by azimuth angle and elevation or through direct detection using sensors.

The use of active trackers has been claimed to be a better tracker in terms of efficiency improvement, but not many discuss that electric motors as active tracking drivers require electrical power. In fact, that the motor power is supplied by the panel itself, this can certainly reduce the power produced by PV. Other problems, the mechanical influence on the device, for example friction, tracking force and oscillation that might arise due to the movement of the tracker which is relatively faster than the relative slow position of the sun. This is an interesting study, how the design of a solar tracking system can produce high efficiency with very low energy consumption, meaning that mechanical losses can be minimized. This problem can be overcome by the development of a tracking mechanism system that integrates electronic control systems in mechanical models, namely aspects of mechanical, kinematic and dynamic structures.

### IV. CONCLUSION

From the reviewed articles, it can be concluded that active trackers are more commonly used than passive trackers. The active trackers can increase efficiency by an average of 29.37%, this tracker consists of one axis and two axis active trackers, generally using a microcontroller or PLC as a controller. The use of this controller allows automatic tracking in real time or periodic.

### RECOMMENDATION

After reviewing various mechanisms for tracking sunlight, the following recommendations should be suggested in the future research:

- There should be another review which includes more papers on the sun tracking system.
- It is necessary to design and construct trackers that integrate electronic control systems in mechanical models i.e. mechanic, kinematic, and dynamic structural aspects to improve efficiency.

### REFERENCES

- [1] Alexandru Catalin, "The Design and Optimization of a Photovoltaic Tracking Mechanism", POWERENG 2009, Lisbon, Portugal, March 18-20, 2009.
- [2] G.Y. Ayvazyan, G.H. Kirakosyan, and A.H. Vardanyan, "Maximum Power Operation of PV system using fuzzy logic control", Armenian Journal of Physics, 2008, Vol 1. pp. 155-159
- [3] Piao, Z.G. Park, J. M. Kim, J. H. Cho, G. B. And Baek, H. L., "A study on the tracking photovoltaic system by program type," Intl. Conf. on Electrical Machines and Systems, vol. 2, pp. 971-973, Sept. 27-29, 2005
- [4] G.K. Singh, "Solar power generation by PV (photovoltaic) technology: A review", Energy 53 (2013) 1-13.
- [5] Muhammad Jamilu Ya'u, "A Review on Solar Tracking Systems and Their Classifications, Journal of Energy", Environmental & Chemical Engineering 2017; 2(3): 46-50
- [6] M.J. Clifford, D. Eastwood, "Design of a novel passive solar tracker", Solar Energy 77 (2004) 269-280
- [7] Harmes Jose Loschi, Yuza Iano, Julio Leon, dkk, "A review on photovoltaic system: Mechanisms and Methods for Irradiation Tracking and Prediction," Smart Grid and Renewable Energy, 2015, 6, 187-208.
- [8] Poulek V, "Testing the new solar tracker with shape memory alloy actors", In: Proceedings of the IEEE first world conference on photovoltaic energy conversion, 1994; Conference record of the

- twenty fourth IEEE photovoltaic specialists conference-1994. Vol. 1. Waikoloa, HI; 1994, p. 1131–1133.
- [9] Mwithiga G, Kigo SN, “Performance of a solar dryer with limited sun tracking capability”, *Journal of Food Engineering* 2006;74:247–52
  - [10] Noel Leon, Hector Garcia, and Carlos Ramirez, “Semi-Passive Solar Tracking Concentrator”, *Energy Procedia* 2014; 57: 275 – 284
  - [11] M.J. Clifford, and D. Eastwood, “Design of a novel passive solar tracker”, *Solar Energy* 77 (2004) 269–280
  - [12] Vijayan Sumathia, , R. Jayapragasha, Abhinav Bakshib, and Praveen Kumar Akellab, “Solar tracking methods to maximize PV system output – A review of the methods adopted in recent decade”, *Energi Terbarukan dan Berkelanjutan Ulasan* 74 (2017) 130–138
  - [13] Huang BJ, Ding WL, and Huang YC, “Long-term field test of solar PV power generation using one-axis 3-position sun tracker”, *Sol Energy* 2011;85(9):1935–44.
  - [14] J. Beltrán A., J. L. González Rubio S. y C. And D. García-Beltrán, “Design, Manufacturing and Performance Test of a Solar Tracker Made by a Embedded Control”, *Fourth Congress of Electronics, Robotics and Automotive Mechanics, CERMA 2007*, 129-134
  - [15] Priyanjan Sharma, and Nitesh Malhotra, “Solar Tracking System Using Microcontroller”, *Proceedings of 2014 1st International Conference on Non Conventional Energy (ICONCE 2014)*; 77: 79.
  - [16] I. Abadi, A. Soeprijanto, A. Musyafa, “Design Of Single Axis Solar Tracking System At Photovoltaic Panel Using Fuzzy Logic Controller”, *5th Brunei International Conference on Engineering and Technology (BICET 2014)* 1-3 Nov. 2014
  - [17] Adel Abdulrahman, Hamoud A. Al-Nehari, Abdulsalam N. Almakhlafy, and Mohammad Baggash, “Design and Implementation of Solar Tracking System”, *International Journal of Engineering and Technical Research (IJETR)* ISSN: 2321-0869 (O) 2454-4698 (P), Volume-4, Issue-1, January 2016. 71-75
  - [18] Md. Tanvir Arafat Khan, S.M. Shahrear Tanzil, Rifat Rahman, and S M Shafiul Alam, “Design and Construction of an Automatic Solar Tracking System”, Dhaka, Bangladesh, *6th International Conference on Electrical and Computer Engineering ICECE 2010*, 18-20 December 2010, 326-329.
  - [19] Tiberiu Tudorache, Liviu Kreindler, “Design of a Solar Tracker System for PV Power Plants”, *Acta Polytechnica Hungarica* Vol. 7, No. 1, 2010, p. 23-39.
  - [20] Chin CS, Babu A, and McBride W, “Design modeling and testing of a standalone single axis active solar tracker using MATLAB/Simulink”, *Renewable Energy* 36 (2011) :3075–3090.
  - [21] Al-Mohamad A, “Efficiency improvements of photo-voltaic panels using a sun-tracking system”, *Applied Energy* 2004;79:345–354
  - [22] Roth P, Georgiev A, and Boudinov H, “Design and construction of a system for Sun-tracking”, *Renew Energy* 2004;29(3):393–402
  - [23] Jeng-Nan Juang, R. Radharamanan, “Design of a Solar Tracking System for Renewable Energy”, *Proceedings of Zone 1 Conference of the American Society for Engineering Education (ASEE Zone 1)* 2014.
  - [24] SC Ribeiro, “Design and development of a low-cost solar tracker”, *Australian Journal of Mechanical Engineering*, Vol 11 No 2, 2013, 139-150
  - [25] Yusuf Oner, Engin Cetin, Harun Kemal Ozturk, Ahmet Yilanci, “Design of a new three-degree of freedom spherical motor for photovoltaic-tracking systems”, *Renewable Energy* 34 (2009) 2751–2756
  - [26] Arlikar Pratik, Bhowmik Abhijit, Patil Manoj, and Deshpande Amruta, “Three Dimensional Solar Tracker with Unique Sensor Arrangement”, In: *Proceedings of the international conference on smart technologies and management for computing, communication, controls, energy and materials (ICSTM)*. 2015; p. 509–513
  - [27] Abdallah S, Nijmeh S, “Two axes sun tracking system with PLC control”, *Energy Conversion and Management* 2004;45:1931–1939.
  - [28] Rosell JI, Vallverdu X, Lecho MA, and Ibanez M, “Design and simulation of a low concentrating PV/thermal system”, *Energy Conversion and Management* 2005;46:3034–3046
  - [29] Sungur Cemil, “Multi-axes sun-tracking system with PLC control for photovoltaic panels in Turkey”, *Renew Energy* 2009;34(4):1119–25.
  - [30] Abu-Khader MM, Badran OO, and Abdallah S, “Evaluating multi-axes sun-tracking system at different.

# Robust and Accurate Positioning Control of Solar Panel System Tracking based Sun Position Image

Lailis Syafa'ah

Electrical Engineering Department  
University of Muhammadiyah Malang  
Malang, Indonesia  
lailis@umm.ac.id

Lailatul Fauziyah

Electrical Engineering Department  
University of Muhammadiyah Malang  
Malang, Indonesia  
fauziyahlailatul17@gmail.com

Zulfatman Has

Electrical Engineering Department  
University of Muhammadiyah Malang  
Malang, Indonesia  
zulfatman@umm.ac.id

**Abstract**—This study contains the robust and accurate positioning control design for solar panel system consisting of elevation and azimuth axis tracker. The ultimate objective of the study is to ensure the solar panel move accurately to follow its tracking reference against mechanical load and other disturbances. The tracking reference was the images of actual sun position. Image processing result as the initial reference and high precision encoder as the controller feedback path were intended to obtain the accurate position of hardware response. Sliding Mode Controller (SMC) with Proportional Integral Derivative (PID) Sliding Surface was employed as control technique that guarantee the solar panel system robust against disturbances or load variation. The proposed method was evaluated through software simulation and hardware validation. The software for the simulation and validation was LabVIEW. While the software for image processing was Vision Assistant. From hardware validation, accuracy of the solar panel system to track the sun position image for elevation and azimuth were 2.622% (0.03007°) and 0.244% (0.00893°), respectively. These results indicate that the solar panel system was available to move accurately to track the sun position both in azimuth and elevation axis.

**Keywords**— Solar tracker, position tracking, image processing, Sliding Mode Controller, PID sliding surface

## I. INTRODUCTION

The most popular research topic on renewable energy is about solar energy that is focused on designing systems to optimize the efficiency of solar energy absorption. One interesting topic is a real time solar tracking system by facing the sun. Solar tracker can increase the output power up to 20-25% for single axis and 30-45% for dual axis. Azimuth & elevation solar tracking allows solar panel to be moved left to right direction by rotating the azimuth plane as well as upwards or downwards in the elevation plane [1, 2]. In this case the control systems is being very important to get the consistency of the system rotation. The precision solar tracking system will give higher efficiency, so the variational method has been applied to get more accurate tracking position. Such as uses the astronomical calculation, GPS, light sensors, until camera with image processing.

The image processing produces higher accuracy on the sun position detection, as known the error values result from the previous simulation study was 0.3688° (azimuth) and 0.3874° (elevation) [3]. In [4], the accuracy of tracking system without being affected by the weather can reach 0.1°. While in the other study [5] by designing system that was capable to detect sun position in cloudy weather can reach 0.04°. These advantages have been compared with the other research method, such as using astronomical calculations the error was 1.0997° (azimuth) and 1.2877° (elevation), LDR which can increase the error in percentages up to 18.13%, while using the photodiodes can reach until 5° error value [3,

6, 7]. These previous results shows that the image processing is capable to result very accurate object identification, because it can provide the sun centroid coordinate pixels precisely in real time. Greater resolution of the camera will provide better performance of solar tracking process [8]. The pixel position of the sun centroid is represented by  $x$  and  $y$  value which is represent the error value from the midpoint of camera frame. These values are used as the initial reference for azimuth and elevation axis to rotate.

The accuracy of the system won't be reached without the precision angle of servo motor rotation although the initial setpoint has very precision value. The servo motor in this system is an actuator that rotates to remove the sun position error. Servo motor is formed from DC motor which is controlled in closed loop system to rotate as much as the reference angle [9]. There are several servo controllers i.e. PID, Fuzzy Logic Controller, Neural Networks, and Line Quadratic-optimal Controller. But these controllers have less resistant to the external disturbance [10]. Moreover the DC motors have the nonlinearity, so the robust controller is needed. Sliding Mode Control (SMC) is one of the popular control strategies and powerfull control technology to deal with the nonlinearity. SMC has two main part, they are the *sliding function* and the *sliding surface*. Precise dynamic model are not required and the control algorithms can be easily implemented. However the parameters design of *sliding function* will affect the robustness of SMC [11].

In this study, Sliding Mode Controller with PID *sliding function* (SMC-PID) was applied to control the angular rotation of the DC motor. The SMC's *sliding surface function* parameters was design to optimized the control robustness. The initial reference is according to the image processing result, while the feedback signal is based on the encoder value. SMC is used to achieve the robustness to the system parameters variation and external disturbances. The main term is to get the most accurate and high precision panel position in order to track the sun position on azimuth and elevation angle.

## II. SYSTEM MODELING

### A. Sun Position Detection

Sun position detection consist of three steps, i.e. vision acquisition (capture the sun image with the camera from MyRIO), vision assistant (image processing), and the determination of the sun pixel position. Camera is used to take the sun picture that will be input for the image processing. The purpose of image processing is to determine the sun centroid location that will be represented in the cartesian coordinate of camera frame by the value of  $x$  and  $y$ .

The vision assistant program as the image processing which shown in Fig. 1, consist of 6 steps, ie. thresholding,

binary inversion, removing small objects, low pass filter, circle detection, and coordinate system determining.

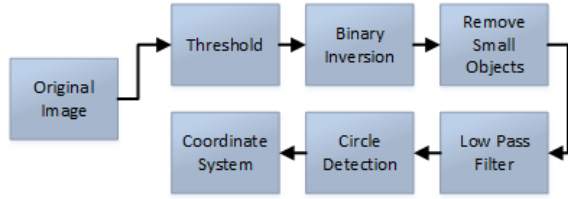


Fig. 1. Vision Assistant Block Program for Sun Detector

There are several image in Fig. 2 which shows the results of each image process sequence. Image (a) shows the original image of sun without cloud around it which will be processed by the vision assistant. Image (b) shows the threshold result which is consist of black and red color. Image (c) shows the binary inversion result which is the brightest area is the sun position area.

Fig. 2 (d) shows the advanced morphology result to remove small objects around the main circle. Image (e) shows the low pass filter result where the less obvious objects will be erased from the image. Then, the image (f) shows the circle detection result, in which we can see the position of the sun circle. The image is processed by coordinate system to obtain the coordinate point of the detected circle from the center frame.

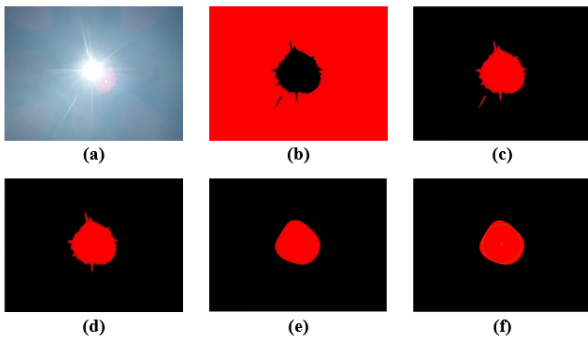


Fig. 2. Sun Detection Process of Vision Assistant

### B. State Space Modeling

The DC motor modeling is a process to obtain mathematical model of the actuator. System identification procedures are performed with LabVIEW's existing features, Identification System in the Control and Simulation Toolkit [12].

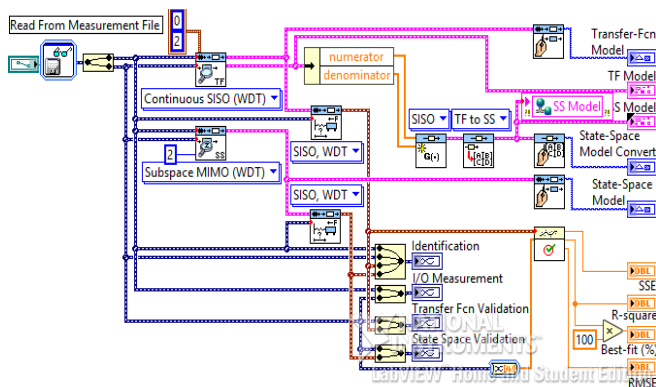


Fig. 3. LabVIEW Validation Program

By using validation process in Fig. 3, which was generated by parameter estimation, the elevation model can approach the real hardware with the percentage of best-fit up to 86.4%. The state equations of the elevation model as result in equations (1) and (2).

$$\frac{dx}{dt} = \begin{bmatrix} -0,618492 & -0,133284 \\ 0,125 & 0 \end{bmatrix} x(t) + \begin{bmatrix} 8 \\ 0 \end{bmatrix} u(t) \quad (1)$$

$$y(t) = [0 \quad 0,014768] x(t) + [0] u(t) \quad (2)$$

While the azimuth model results a better best-fit up to 97.2%, which indicates that the azimuth model has the higher fitness. Because there is no varied mechanical load which affects the system. The horizontal rotational has a stable load in almost all positions. The state equations of the azimuth model are expressed in equations (3) and (4) below.

$$\frac{dx}{dt} = \begin{bmatrix} -0,098421 & -0,051034 \\ 0,0625 & 0 \end{bmatrix} x(t) + \begin{bmatrix} 16 \\ 0 \end{bmatrix} u(t) \quad (3)$$

$$y(t) = [0 \quad 0,00313952] x(t) + [0] u(t) \quad (4)$$

### C. PID Controller

PID controller has many advantages to system respons such as rise time, overshoot, and steady state. The formulation of PID controller is expressed in equation (5).

$$u(t) = K_p e(t) + K_i \int_0^t e(\tau) d\tau + K_d \frac{de(t)}{dt} \quad (5)$$

### D. Sliding Mode Controller

The implementation of SMC based PID sliding surface will be modeled as following block diagram in Fig. 4.

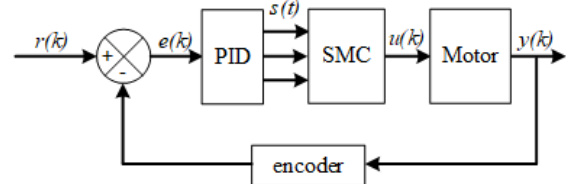


Fig. 4. Block Diagram of SMC-PID

The design is expected to reduce the effects of unwanted disturbances such as load and friction effects. After performing DC motor modeling, the PID will be added to minimize the rotational error between the motor output and reference value. The PID parameter tuning is done by manual tuning in the LabVIEW Control & Simulation toolkit. Then SMC will be applied to the system where the PID will be integrated as the sliding surface optimization of SMC controller intended for the chattering reduction. Basic principle of SMC with PID sliding surface can be seen in Fig. 5.

The  $k_p$ ,  $k_i$ , and  $k_d$  values are the PID parameters as the determinant of the SMC sliding surface value. The mathematical equation is as follows.

$$s(t) = k_p e(t) + k_i \int_0^t e(\tau) d\tau + k_d \dot{e}(t) \quad (6)$$



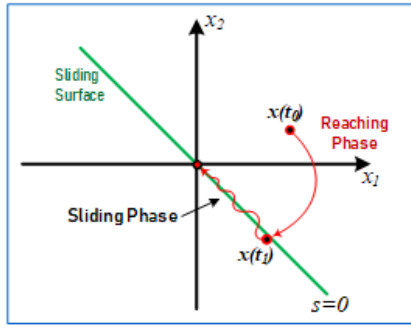


Fig. 5. The Response Illustration of SMC-PID

The first derivative of the sliding surface equation above is expressed in equation (7).

$$\dot{s}(t) = k_p \dot{e}(t) + k_i e(t) + k_d \ddot{e}(t) \quad (7)$$

The difference between the desired value with the actuator's actual position is formulated as the error value. The equation is expressed by equation (8).

$$e(t) = x_r(t) - x_p(t) \quad (8)$$

The second derivative of the error equation above is expressed in the equation (9). This is coming from the second-order model obtained through from the DC motor identification.

$$\ddot{e}(t) = \ddot{x}_r(t) - \ddot{x}_p(t) \quad (9)$$

The present value can be specified using the state space model parameters which is used. The second order of  $x_p$  is presented in equation (10).

$$\ddot{x}_p = -(A\dot{x} + Bx - Cu) \quad (10)$$

The SMC control ( $u_{SMC}$ ) consists of switching control ( $u_{sw}$ ) and equivalent control ( $u_{eq}$ ). The switching control is according to the reaching phase when  $s(t) \neq 0$  while the equivalent control based on the sliding phase when  $s(t) = 0$ . The general equation of SMC is denoted by equation (11).

$$u_{SMC}(t) = u_{sw}(t) + u_{eq}(t) \quad (11)$$

The general switching control formula based on Lyapunov theorem [13] is shown in equation (12). This theorem has been used to reduce the chattering effect which belongs to the usual  $u_{sw}$  formulas.

$$u_{sw}(t) = \tanh\left(\frac{s}{\phi}\right) k_s \quad (12)$$

The complete  $u_{sw}$  formula is expressed in equation (13) by substituting equation (6) to equation (12) above.

$$u_{sw} = \tanh\left(\frac{k_p e(t) + k_i \int_0^t e(\tau) d\tau + k_d \dot{e}(t)}{\phi}\right) k_s \quad (13)$$

Then the equivalent control can be obtained from the derivative of the sliding surface equation. This is obtained by substituting equation (9) and (10) to equation (7). The result is denoted in equation (14).

$$\dot{s}(t) = k_p \dot{e}(t) + k_i e(t) + k_d \{\ddot{x}_r + A\dot{x} + Bx - Cu\} \quad (14)$$

When  $s=s(t)=0$ , the sliding control will be executed because the sliding value has been reached. The equivalent control of SMC can be formed from equation (14) by assume the  $s(t)=0$  that is represented in equation (15).

$$u_{eq} = \frac{(k_p \dot{e}(t) + k_i e(t) + k_d \{\ddot{x}_r + A\dot{x} + Bx\})}{k_d Cu} \quad (15)$$

Those formulas were applied to the LabVIEW which is shown in Fig. 6 below.

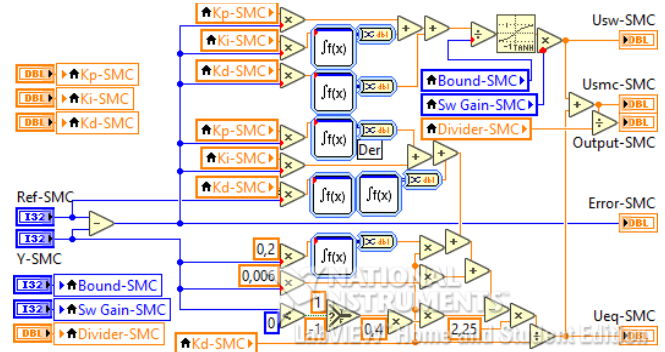


Fig. 6. LabVIEW Program of SMC-PID Controller

#### E. Simulation and Hardware Verification

General block diagram of the solar tracking system and the proposed control scheme can be seen in Fig. 7. below. It shows how the overall system works from input (image) to output (elevation and azimuth position).

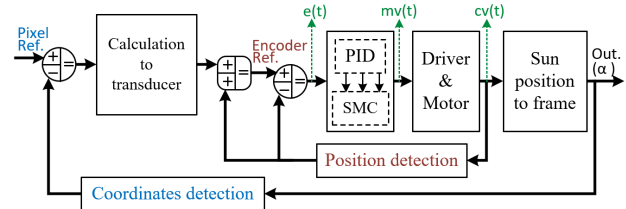


Fig. 7. Block Diagram of The Overall System

The hardware validation process is performed to ensure the simulated SMC-PID design can be applied actually. However, simulation also need to be done before the hardware validation to ensure the proposed algorithms are properly constructed and determine the controller parameters which is implemented to the hardware. The elevation and azimuth position experimental validations are performed separately, using the PID and SMC-PID controllers. Due to the simulation results several parameters value with the best response are obtained and prepared for the hardware validation. Table I and Table II represent the control parameters of PID and SMC controllers, respectively.

TABLE I. PARAMETERS VALUE OF PID GAIN

Parameter	Elevation	Azimuth
Kp	750	1000
Ki	0	0
Kd	350	3700

TABLE II. PARAMETERS VALUE OF SMC-PID GAIN

Parameter	Elevation	Azimuth
Kp	4000	40000
Ki	0	0
Kd	1000	20000
Boundary	15	15
Divider	5	1
Switching gain	10000	500

The hardware used due for the experimental validation is shown in Fig. 8. The main components of the hardware consists of camera, servo motors, encoders, power supply, and electrical module.

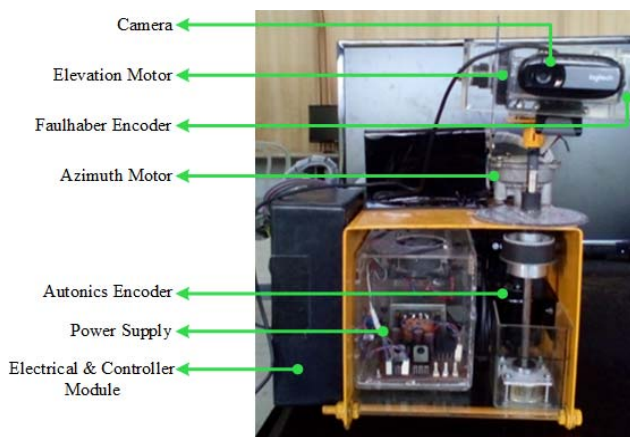


Fig. 8. Prototype of The Elevation and Azimuth Tracker

### III. RESULTS AND DISCUSSION

#### A. Encoder Evaluation

From the test, the elevation angle  $180^\circ$  and the azimuth angle  $360^\circ$  of the prototype were obtained as depicted in Fig. 9 and Fig. 10 below.

Fig. 9. Elevation Angle  $180^\circ$ Fig. 10. Azimuth Angle  $360^\circ$ 

From these results we can obtain the actuator ratio. The elevation actuator rotated  $180^\circ$  when the incremental of faulhaber encoder reached 1272. While the azimuth actuator rotated  $360^\circ$  when the incremental of autonics encoder reached 10840. From those experiments, the encoder and angle ratio of the elevation and azimuth can be formulated with the equation (16) and equation (17), respectively.

$$\frac{\text{elevation angle}}{\text{elevation encoder}} = \frac{180^\circ}{1272} = \frac{1^\circ}{7,067} = \frac{0,1415^\circ}{1} \quad (16)$$

$$\frac{\text{azimuth angle}}{\text{azimuth encoder}} = \frac{360^\circ}{10840} = \frac{1^\circ}{30,111} = \frac{0,0332^\circ}{1} \quad (17)$$

#### B. Sun Position Conversion

Object tracking process was done to obtain the comparison between the pixel values camera to encoder. The object being tracked was the LED (Light Emitting Diode) instead of the actual sun for laboratory scale testing. From the experiment, the error pixel for the initial LED position was 238 (for x value) and 315 (for y value), the hardware should be rotated until the LED reaches the midpoint of the camera frame. To reaches the (0,0) pixel position coordinates the azimuth encoder changed as much as 121 points, while the elevation 54 points. So the pixel to encoder ratio of both axes can be calculated as the equations (18) and (19).

$$\frac{y \text{ value}}{\text{elevation encoder}} = \frac{315}{54} = \frac{1}{0,1714} = \frac{5,8333}{1} \quad (18)$$

$$\frac{x \text{ value}}{\text{azimuth encoder}} = \frac{238}{121} = \frac{1}{0,5084} = \frac{1,9669}{1} \quad (19)$$

#### C. Hardware Validation

Validation of the proposed PID and SMC-PID controllers were confirmed through experiments on the hardware. The experiments were performed for the elevation and azimuth axis separately.

The SMC-PID and PID implementation was done directly to the hardware. The random setpoint signal value was given to analyze the system response in the CW or CCW direction.

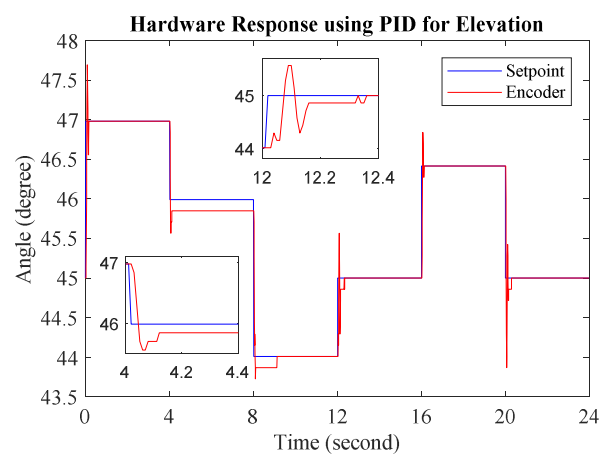


Fig. 11. Elevation Hardware Response with PID Controller

As can be seen in Fig. 11, in the 4<sup>th</sup> second the encoder (position) response with PID cannot reach the setpoint (reference). But, it still can reach the setpoint at the rest of the time with spike in several moments. This deficiency occurs due to PID's inability to withstand the mechanical load beyond the limits.

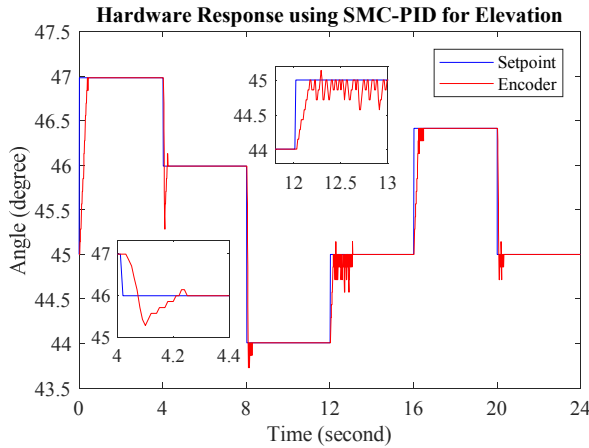


Fig. 12. Elevation Hardware Response with SMC-PID Controller

However, as shown in Fig. 12, the output position of the hardware available to reach the reference in the whole of time without any spikes. The response also maintain in stable in the reference. However, due to drawback of SMC, chattering was exist in certain parts of output response. A higher chattering indicates that the SMC receive a high disturbance. The highest overshoot was at the 4<sup>th</sup> second, but it wasn't as high as PID's overshoot with the error 5 encoder values.

The azimuth axis response with PID and SMC-PID controllers, respectively are shown in Fig. 13 and Fig. 14 below.

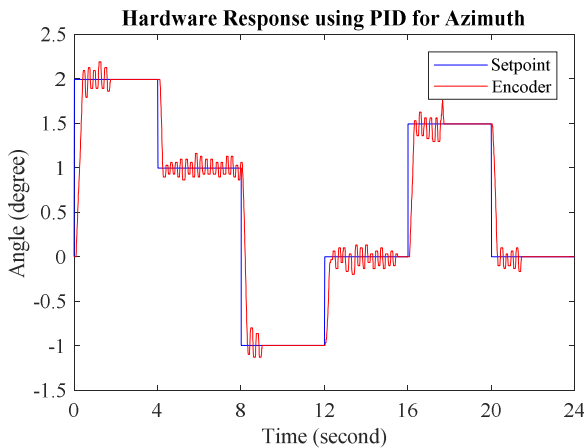


Fig. 13. Azimuth Hardware Response with PID Controller

The output response of the system with PID controller as depicted in Fig. 13, it can be seen that response was capable to reach the reference, but with several oscillations exist in the change of reference. The oscillation was caused by the readability of azimuth sensor was very high. Such that, the small motor rotation which crosses the setpoint (overshoot) reversed the error and caused the oscillation.

While Fig. 14 shows that the output response of the azimuth system with SMC-PID controller can reach the

reference faster than the PID controller. It was due to a high switching gain of the SMC that was capable to increase the system's power to move the hardware faster. However, the SMC switching gain effect occurred continuously, even though it did not out of the reference value. Meanwhile if the switching gain was minimized, it reduced the oscillation, but with a longer rise time. Therefore a manual setting on the switching gain becomes an important point to do.

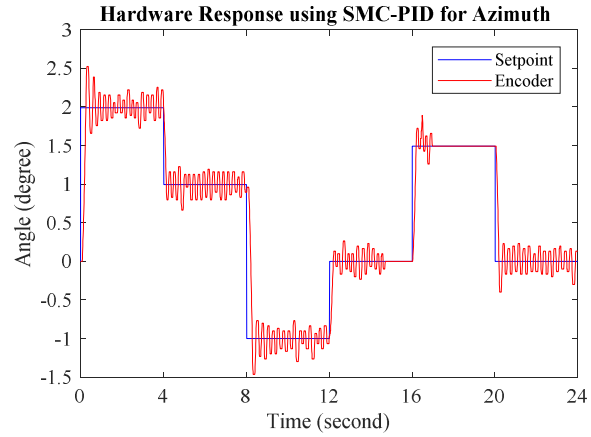


Fig. 14. Azimuth Hardware Response with SMC-PID Controller

#### D. Validation Accuracy

This test was performed to obtain the error value of azimuth and elevation tracking system designed. The position error of the sun image is described in pixels. Then from the pixel error the position error can be calculated using equations (18) to (19) to find out how much the error angle and encoder value that must be driven by the actuator to eliminate all the errors.

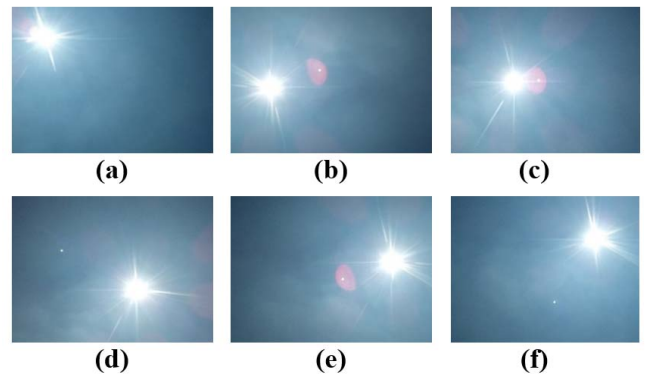


Fig. 15. Varied Sun Position Image

Fig. 15 shows some photos of various sun positions to be tested. Every image has error in elevation and azimuth axis. Each of them has the angle and encoder errors conversion from the detected pixel values. The calculation of encoders (calc.) must be close to the integer values (act.), because the sensor output was read as an integer. The hardware validation process was done by giving the encoder setpoints to the both axis separately.

$$\text{Angle Error} = |\text{Act. Angle} - \text{Calc. Angle}| \quad (20)$$

The Angle Error calculation above is needed to get the error values between the Calculation and Actual Angle. This error was inflicted by the rounding of encoder calculation

(the original conversion results from the pixel error) results to get the actual encoder as the integer values. Then the following graphs show the results of the hardware response with the converted amplitude in angle units.

While in order to calculate the accuracy of position control results that are implemented to the hardware. The average of each error values on both axis (elevation & azimuth) can be calculated by equation below.

$$\text{Average Error} = \left( \sum_{i=1}^n \text{Angle Error} (n) \right) / n \quad (21)$$

The hardware validation results summary can be seen in Table III and Table IV below which shows the elevation and azimuth results, respectively.

TABLE III. VALIDATION RESULT OF ELEVATION (Y)

Image	Pixel	Calc. Angle	Act. Angle	Error (degree)	Error (%)
(a)	211	5,22524°	5,23585°	0,01061°	0,203
(b)	-32	-0,79245°	-0,84906°	0,05660°	7,142
(c)	-18	-0,44575°	-0,42453°	0,02123°	4,763
(d)	-117	-2,89741°	-2,83019°	0,06722°	2,320
(e)	34	0,84198°	0,84906°	0,00708°	0,841
(f)	155	3,83844°	3,82075°	0,01769°	0,461
<b>Average Error</b>				0,03007°	2,622

TABLE IV. VALIDATION RESULT OF AZIMUTH (X)

Image	Pixel	Calc. Angle	Act. Angle	Error (degree)	Error (%)
(a)	-337	-5,68999°	-5,67897°	0,01102°	0,194
(b)	-317	-5,35231°	-5,34686°	0,00544°	0,102
(c)	-127	-2,14430°	-2,15867°	0,01437°	0,670
(d)	126	2,12741°	2,12546°	0,00195°	0,092
(e)	315	5,31854°	5,31365°	0,00488°	0,092
(f)	300	5,06527°	5,08118°	0,01591°	0,314
<b>Average Error</b>				0,00893°	0,244

Analysis of the system accuracy from the data specified in the above table has been done successfully. It can be seen at a glance that most of the azimuth Angle Error are less than the elevation. It can be confirmed by the Average Error rows that shows the azimuth error value is 0,244% with the angle accuracy 0,00893° while the elevation is 2,622% with the angle accuracy 0,03007°. So we can conclude the angle tracking ability of azimuth axis is more accurate than elevation.

#### IV. CONCLUSION

The method applied by using SMC-PID controller can provide the ability of the system to track the sun position image accurately. A more accurate sensor on the azimuth axis causes the angular tracking accuracy is higher. While the mechanical load on the elevation axis can be covered by the controller. This final project results can prove that with the SMC-PID controller, the elevation system can withstand the mechanical load variations in the elevation angle. While for the addition of position sensor (encoder) with high accuracy, the azimuth system can obtain the most high tracking accuracy. The accuracy of solar tracking system is expected to optimize the performance of solar panels without being affected by the mechanical load on the actual system.

#### REFERENCES

- [1] V. Bosetti, "The Future Prospect of PV and CSP Solar Technologies: An Expert Elicitation Survey," *Energy Policy* 49, pp. 308-317, 2012.
- [2] G. J. Prinsloo, Automatic Positioner and Control System for A Motorized Parabolic Solar Reflector, Maitland-South Africa: Stellenbosch University, 2014.
- [3] M. Mirdanies and R. P. Sapura, "Dual-axis Solar Tracking System," in *International Conference on Sustainable Energy Engineering and Application (ICSEEA)*, Indonesian Institute of Sciences (LIPI), 2016.
- [4] M. M. Arturo and G. P. Alejandro, "High-Precision Solar Tracking System," *World Congress on Engineering*, vol. II, 2010.
- [5] C. D. Lee, H. C. Huang and H. Y. Yeh, "The Development of Sun-Tracking System Using Image," *Journal of Sensors*, vol. 13, pp. 5448-5459, 2013.
- [6] A. Zakariah, J. J. Jamian and M. A. Yunus, "Dual-Axis Solar Tracking System Based on Fuzzy Logic Control and Light Dependent Resistors as Feedback Path Elements," *IEEE (SCoReD)*, pp. 139-144, 2015.
- [7] M. Haryanti, A. Halim and A. Yusuf, "Development of Two Axis Solar Tracking Using Five Photodiodes," *IEEE (EECCIS)*, pp. 40-44, 2014.
- [8] H. A. Sohag, M. Hasan, M. Khatun and M. Ahmad, "An Accurate and Efficient Solar Tracking System Using Image Processing and LDR Sensor," *IEEE (EICT)*, pp. 522-527, 2015.
- [9] G. A. Zarkar and S. S. Sankeshwari, "Simulation of DC Servo Motor Position Control using Sliding Mode Technique," *International Journal of Advances in Engineering & Technology (IJAET)*, vol. 7, no. 6, pp. 1882-1888, 2015.
- [10] C. Vivekanandan, R. Prabhakar and D. Prema, "Stability Analysis of a Class of Nonlinear Systems Using Discrete Variable Structures and Sliding Mode Control," *International Journal of Electrical and Computer Engineering*, vol. 2, no. 5, pp. 856-862, 2008.
- [11] T. Chamsai, P. Jirawattana and T. Radpukdee, "Sliding Mode Control with PID Tuning Technique: An Application to a DC Servo Motor Position Tracking Control," *Energy Research Journal*, vol. 1, no. 2, pp. 55-61, 2010.
- [12] M. P. Badramurti, E. A. Hakim and N. A. Mardiyah, "Analisis dan Desain Kontroler Fuzzy-PID pada Plant Motor DC Berbasis Spreadsheet menggunakan Pendekatan Metode Numerik," Muhammadiyah Malang University, Malang, 2017.
- [13] C. C. Soon, R. Ghazali, H. I. Jaafar, S. Y. S. Hussien, S. M. Rozali and M. Z. A. Rashid, "Optimization of Sliding Mode Control using Particle Swarm Algorithm for an Electro-hydraulic Actuator System," *Journal of Telecommunication, Electronic and Computer Engineering*, vol. 8, no. 7, pp. 71-76, 2016.

# *Robust Adaptive Sliding Mode Control Design with Genetic Algorithm for Brushless DC Motor*

Een Utama Putra  
Electrical Engineering Department  
University of Muhammadiyah Malang  
Malang, Indonesia  
putra\_20192@yahoo.co.id

Zulfatman Has  
Electrical Engineering Department  
University of Muhammadiyah Malang  
Malang, Indonesia  
zulfatman@umm.ac.id

Machmud Effendy  
Electrical Engineering Department  
University of Muhammadiyah Malang  
Malang, Indonesia  
machmud@umm.ac.id

**Abstract**— This study aims to design a control scheme that is capable to improve performance and efficiency of brushless DC motor (BLDC) in operating condition. The control scheme is composed of sliding mode controller (SMC) with proportional-integral-derivative (PID) sliding surface. The PID sliding surface is used to improve the system transient response. Then, the SMC-PID is optimized by genetic algorithm optimization for further improvement on the stability and robustness against nonlinearities and disturbances. Chattering problem that appear in the SMC is minimized by employing an adaptive switching gain for the SMC that is integrated with Luenberger Observer. Lyapunov function candidate is applied to guarantee the stability of the system. Simulation on the proposed work is done in Matlab Simulink. Results of the simulation works indicate that the proposed control scheme can improve the transient response, the stability and robustness of the BLDC motor compared to the conventional SMC in the existence of nonlinearities and disturbances.

**Keywords**— BLDC motor, sliding mode control, PID sliding surface, genetic algorithm, adaptive switching gain

## I. INTRODUCTION

Brushless direct current motor (BLDCM) is one of synchronous permanent magnet DC motors. BLDCM is very different from conventional DC motor, since the BLDCM is designed without brush. Without commutation component the motor produces several advantages, such as high efficiency, reducing vulnerability in mechanical components, large torque, longer lifetime, and low noise [1]. Due to their significant role in industrial applications, improvements on the speed control are much needed. Hence, most of researches that discuss the BLDCM speed control are focus on linear and nonlinear modeling and testing with varying loads [2].

Some of the studies that have been done were speed control with fuzzy logic [3], fuzzy PID [4], and Fuzzy Genetics Algorithm [5], where the controller were tested on BLDC linear motor models. The linear model is a model that is only capable presenting the motor when in its maximum performance. But, sometimes with continuous usage it faces some problems, such as friction and the change of parameters that cause the motor no longer linear. These problems were driving several researchers to develop a speed control method based on nonlinear models such as sliding mode control (SMC) [6].

SMC is a control system that has the ability to maintain a system stability in various models with various interference and system parameters. So it is often used in nonlinear models. SMC has a working area on the steady state phase, so that when disturbance occurs and also parameter changes, SMC is able to keep the system performance stable. Recently SMC-PID has been developed, where the SMC sliding surface can be arranged with proportional, integral and derivative parameters. This is done so that the transient response of the system is better than the previous SMC. SMC-PID has proven its performance on conventional DC motors by relying solely on determining PID parameters by trial and error. Unlike conventional DC motors that tend to be easy in parameter determination, BLDCM has a more complicated structure and high nonlinearity level that requires the optimization of parameters for SMC-PID to achieve its best performance [7].

The process of optimizing the PID parameters is done to find the most suitable value to be applied to the system. The genetic algorithm (GA) is used as the optimization method in BLDCM in this research. GA was chosen because it is a modern optimization method that has a high searching capacity, and a heuristic character [8]. With the advantages of the GA method, the determination of the SMC-PID parameter value on the nonlinear BLDCM can be resolved. However, there is still a problem that arises between the advantages of SMC-PID that is the high rate of the chattering when a various disturbance with high magnitude hit the system [9].

The high chattering on the control system is due to the high switching gain of the SMC-PID that should be adjusted against the high magnitude of the disturbance present in the system. Therefore it is necessary to have a Luenberger Observer as a tool to estimate the disturbance in the BLDCM. The estimated value of the disturbance observer is then converted as a determinant of the switching gain of the SMC-PID. Thus, the value of the switching gain that estimates the magnitude of the chattering will adapt in accordance with the value of the disturbance changes received by the system. It's an adaptive robust control scheme that relates to the magnitude of the existed disturbance in the system.

## II. MODELING SYSTEM

### A. State Space Modeling

Modeling is done by state space method where this method is used as a modern method. State space method is

also much done because it is easy in the application of systems that have input and output more than one and easier in terms of computing.

Suppose that the three-phase BLDC motor is controlled by the full bridge driving in the two phase conduction mode [11] as explained below.

$$i_A + i_B + i_C = 0 \quad (1)$$

$$u_{AB} = r_a(i_A - i_B) + L_a \frac{d}{dt}(i_A - i_B) + e_{AB} \quad (2)$$

$$u_{BC} = r_a(i_A + 2i_B) + L_a \frac{d}{dt}(i_A + 2i_B) + e_{BC} \quad (3)$$

Then, subtract equation (2) from equation (3)

$$u_{AB} - u_{BC} = -3r_a - 3L_a \frac{d}{dt}i_B + e_{AB} - e_{BC} \quad (4)$$

$$i_B = -\frac{r_a}{L_a}i_B - \frac{1}{3L_a}(u_{AB} - e_{AB}) + \frac{1}{3L_a}(u_{BC} - e_{BC}) \quad (5)$$

The calculations for the second phase are performed by the same method as in equations (2) and (3).

$$u_{AB} = r_a(2i_A + i_B) + L_a \frac{d}{dt}(2i_A + i_B) + e_{AB} \quad (6)$$

$$u_{CA} = r_a(i_C - i_A) + L_a \frac{d}{dt}(i_C - i_A) + e_{CA} \quad (7)$$

Subtract equation (6) from equation (7)

$$(u_{AB} - e_{AB}) - (u_{CA} - e_{CA}) = 3r_a + 3L_a \frac{d}{dt}i_A \quad (8)$$

$$i_A = -\frac{r_a}{L_a}i_A + \frac{1}{3L_a}(u_{AB} - e_{AB}) - \frac{1}{3L_a}(u_{CA} - e_{CA}) \quad (9)$$

$$u_{AB} = u_{BC} \quad (10)$$

$$e_{AB} = e_{BC} \quad (11)$$

$$u_{CA} = -(u_{AB} + u_{BC}) = -2u_{AB} \quad (12)$$

$$e_{CA} = -(e_{AB} + e_{BC}) = -2e_{AB} \quad (13)$$

The calculation proceeds by substituting equations (10), (11), (12) and (13) in equation (9).

$$i_A = -\frac{r_a}{L_a}i_A + \frac{1}{3L_a}(u_{BC} - e_{BC}) + \frac{2}{3L_a}(u_{AB} - e_{AB}) \quad (14)$$

Other characteristic equation that had by BLDCM is the relation of torque and speed.

$$K_T i - T_L = J \frac{d\omega}{dt} + B_v \omega \quad (15)$$

Or it could be written in another form

$$\dot{\omega} = -\frac{B_v}{J}\omega + \frac{1}{J}(T_e - T_L) \quad (16)$$

where,

$$T_e = K_T i \quad (17)$$

$U_d$  : DC bus voltage.

$e_A$  : Phase back EMF.

$r_a$  : Line resistance of winding,  $r_a = 2R$ .

$L_a$  : Equivalent line inductance of winding,  $L_a = 2(L-M)$ .

$J$  : Rotor moment inertia.

$T_L$  : Load torque

$\omega$  : Rotor speed.

$B_v$  : Viscous friction coefficient.

$K_e$  : Coefficient of line back EMF

$K_T$  : Coefficient of line torque constant

$M$  : Mutual Linkage, assume  $M=0$ .

From the equations that has been elaborated above, the dynamic equations of the BLDC motor is represented in the following state space form.

$$\begin{bmatrix} \dot{i}_A \\ \dot{i}_B \\ \dot{\omega} \\ \dot{\theta} \end{bmatrix} = \begin{bmatrix} -\frac{r_a}{L_a} & 0 & 0 & 0 \\ 0 & -\frac{r_a}{L_a} & 0 & 0 \\ 0 & 0 & -\frac{B_v}{J} & 0 \\ 0 & 0 & 1 & 0 \end{bmatrix} \begin{bmatrix} i_A \\ i_B \\ \omega \\ \theta \end{bmatrix} + \begin{bmatrix} \frac{2}{3L_a} & \frac{2}{3L_a} & 0 \\ \frac{-1}{3L_a} & \frac{1}{3L_a} & 0 \\ 0 & 0 & \frac{1}{J} \\ 0 & 0 & 0 \end{bmatrix} \begin{bmatrix} u_{AB} - e_{AB} \\ u_{BC} - e_{BC} \\ T_e - T_L \end{bmatrix} \quad (18)$$

where  $\theta$  is the rotor position.

From the BLDC equation will be added friction column such as non-linear factor where the factor is a friction that can inhibit the performance of the motor that causes the motor no longer work as a linear system. If column friction is added to equation (18), then the equation becomes as follows. The friction is represented as nonlinearity that exist in the system.

$$\begin{bmatrix} \dot{i}_A \\ \dot{i}_B \\ \dot{\omega} \\ \dot{\theta} \end{bmatrix} = \begin{bmatrix} -\frac{r_a}{L_a} & 0 & 0 & 0 \\ 0 & -\frac{r_a}{L_a} & 0 & 0 \\ 0 & 0 & -\frac{B_v}{J} & 0 \\ 0 & 0 & 1 & 0 \end{bmatrix} \begin{bmatrix} i_A \\ i_B \\ \omega \\ \theta \end{bmatrix} + \begin{bmatrix} \frac{2}{3L_a} & \frac{2}{3L_a} & 0 \\ \frac{-1}{3L_a} & \frac{1}{3L_a} & 0 \\ 0 & 0 & \frac{1}{J} \\ 0 & 0 & 0 \end{bmatrix} \begin{bmatrix} u_{AB} - e_{AB} \\ u_{BC} - e_{BC} \\ T_e - T_L \end{bmatrix} + \begin{bmatrix} 0 \\ 0 \\ 0 \\ -\frac{F_c}{J} \end{bmatrix} \text{sgn}(\omega) \quad (19)$$

Following the complete state equations in (19) for the BLDC motor, the parameters of the motor are given as appeared in Table 1. The parameters are taken from the BLDC motor parameters that was analyzed in the previous research [5].

TABLE I. UNITS FOR BLDC PARAMETERS

Symbol	Parameter	Unit Value
$r_a$	Resistance	0.25 Ohm
$L_a$	Inductance	0.32 mH
$J$	Rotor Inertia	0.00042 Kg-m <sup>2</sup>
$M$	Mutual Linkage	0 mH
$P$	Pole	8 poles
$B_v$	Friction coefficient	0.0096 Nm/(rad/sec)
$K_e$	Back EMF constant	0.65 V/rad/sec
$K_T$	Torque constant	0.0994 Nm/A
$F_c$	Friction column	0.02



### B. Sliding Mode Controller

This study focus on how to design the SMC control system for the BLDC motor that can be shown in the block diagram in Fig. 1. SMC will be the main control system that keeps motor performance from nonlinearity and disturbance. Then the PID sliding surface used which has the advantage of controlling the transient response of the system.

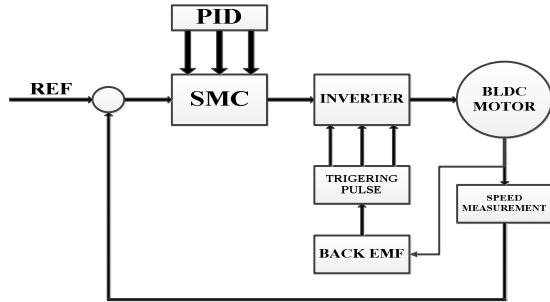


Fig. 1 Blok Diagram System

After performing SMC design with PID sliding surface on BLDC, Optimization will be added to the system to minimize the error of rotation speed between motor output and reference value, the parameter values  $K_i$ ,  $K_p$ , and  $K_d$  will be determined by genetic algorithm. Then the SMC will be applied to the system where the PID will be integrated as the sliding surface of the SMC controller and the system performance monitoring will be performed.

SMC with PID sliding surface will be applied to BLDC 2nd order system, thus yielding the following equation [10].

$$s(t) = K_p e(t) + K_i \int e(t) + K_d \frac{de}{dt} \quad (20)$$

The error occurring due to the difference between the actual value and the desired trajectory is illustrated by (21).

$$e(t) = r(t) - y(t) \quad (21)$$

Where  $e(t)$  is an error obtained from the difference of reference value  $r(t)$  and the system output value  $y(t)$ . If the equation uses 2<sup>nd</sup> order on the model then it can be written on the equation (22).

$$\ddot{e}(t) = \ddot{r}(t) - \ddot{y}(t) \quad (22)$$

$$\ddot{y}(t) = \ddot{\omega} \quad (23)$$

From equation (2), (16) and (17),  $\ddot{\omega}$  can be described as follows:

$$\ddot{\omega} = -A\dot{\omega} - B\omega + Cu(t) - F(t) \quad (24)$$

$$u(t) = v(t) \quad (25)$$

$$A = -\frac{B_v}{J} \quad (26)$$

$$B = -\frac{Kt^2}{JLa} \quad (27)$$

$$C = -\frac{Kt}{JLa} \quad (28)$$

$$F(t) = Te - Tl \quad (29)$$

In general, SMC is described as equation that sums between switching control and equivalent control. Switching control is an adjustment equation when the value of  $s(t) \neq 0$  denoted by symbol  $U_{sw}$  and equivalent control is the adjustment equation when  $s(t) = 0$ .

$$U_{SMC} = U_{eq} + U_{sw} \quad (30)$$

Because of the  $s(t)$  value is equal with 0 it can be assumed that  $s(t) = \dot{s}(t) = 0$  so the derivative of the  $s(t)$  can be written as follows :

$$\dot{s}(t) = K_p \dot{e}(t) + K_i e(t) + K_d \ddot{e}(t) \quad (31)$$

Then it is assumed that the value of the load is 0, and equation (24) is input to change the value of  $\ddot{e}(t)$  it can be written as follows:

$$\dot{s}(t) = K_p \dot{e}(t) + K_i e(t) + K_d (\ddot{r}(t) + A\dot{\omega} + B\omega - Cu(t)) \quad (32)$$

When  $\dot{s}(t) = 0$ , the equivalent control of SMC can be described as

$$U_{eq} = (KdC)^{-1}(K_p \dot{e}(t) + K_i e(t) + K_d(\ddot{r}(t) + A\dot{\omega} + B\omega)) \quad (33)$$

From analysis of Lyapunov stability theory that has been verified, this controller will follow Lyapunov function in equation (34).

$$V = \frac{1}{2} s^2 \quad (34)$$

Where  $V(t) > 0$  and  $V(0) = 0$  for  $s(t) \neq 0$ . The achievement condition will be illustrated in the equation (35).

$$\dot{V}(t) = s(t) \dot{s}(t) < 0 \quad ; s(t) \neq 0 \quad (35)$$

This equation has purpose to ensure the value moving from reaching condition to the sliding phase under stable condition.  $\dot{V}(t)$  must be negative to guarantee the control stability.

$$0 > s(K_p \dot{e}(t) + K_i e(t) + K_d (\ddot{r}(t) + A\dot{\omega} + B\omega - Cu(t))) \quad (36)$$

$$0 > s(K_p \dot{e}(t) + K_i e(t) + K_d (\ddot{r}(t) + A\dot{\omega} + B\omega) - K_d Cu(t))$$

$$0 > s(K_p \dot{e}(t) + K_i e(t) + K_d (\ddot{r}(t) + A\dot{\omega} + B\omega) - K_d C(ueq + usw))$$

$$0 > s(K_p \dot{e}(t) + K_i e(t) + K_d (\ddot{r}(t) + A\dot{\omega} + B\omega) - K_d C(KdC)^{-1}(K_p \dot{e}(t) + K_i e(t) + K_d (\ddot{r}(t) + A\dot{\omega} + B\omega)) + K_d C u_{sw}))$$

$$0 > s(K_p \dot{e}(t) + K_i e(t) + K_d (\ddot{r}(t) + A\dot{\omega} + B\omega)) - sKd C(KdC)^{-1}(K_p \dot{e}(t) + K_i e(t) + K_d (\ddot{r}(t) + A\dot{\omega} + B\omega)) + sKd C u_{sw}))$$

To make sure equation (36) is negative, then the specified of  $u_{sw}$  is

$$U_{sw} = \text{sign}(s)(K_p \dot{e}(t) + K_i e(t) + K_d (\ddot{r}(t) + A\dot{\omega} + B\omega) - Kd C(KdC)^{-1}(K_p \dot{e}(t) + K_i e(t) + K_d (\ddot{r}(t) + A\dot{\omega} + B\omega))) \quad (37)$$

By applying the sign function on the sliding surface so that the equation will be obtained for its switching control:

$$U_{sw} = Ks \operatorname{sat}\left(\frac{S}{\varphi}\right) \quad (38)$$

$$\operatorname{sat}\left(\frac{S}{\varphi}\right) = \left(\frac{S}{\varphi}\right) \quad ; \text{ if } \left|\frac{S}{\varphi}\right| \leq 1 \quad (39)$$

$$\operatorname{sat}\left(\frac{S}{\varphi}\right) = \operatorname{sign}\left(\frac{S}{\varphi}\right) \quad ; \text{ if } \left|\frac{S}{\varphi}\right| > 1 \quad (40)$$

The equation (38), (39), and (40) in practice has a work like prediction control ideal relay. So in this case the sign function can be replaced with the hyperbolic tangent function to improve the performance of hitting control. Where the value of  $Ks$  is the gain of the switching control and  $\varphi$  is the thickness of the boundary layer. So the switching equation can be written:

$$U_{sw} = Ks \tanh\left(\frac{S}{\varphi}\right) \quad (41)$$

To ensure the stability of the proposed control, the Lyapunov function candidate is applied. Various effects of discontinuous function have been reduced by substituting the hyperbolic tangent function with the boundary layer of  $\varphi$ . Results of  $U_{smc}$  in equations (33) and (41) are substituted into equation (30), and (30) is rewritten as follows.

$$U_{smc} = (KdC)^{-1}(Kp \dot{e}(t) + Ki e(t) + Kd (\ddot{r}(t) + A\dot{\omega} + B\omega)) + Ks \tanh\left(\frac{S}{\varphi}\right) \quad (42)$$

### C. Genetic Algorithm

Genetic algorithm (GA) is an optimization algorithm that utilizes genetic and natural selection mechanisms. GA operates with a set of candidate solutions or chromosomes known as the population. Each chromosome consists of a number of numbers that present the solution and can be a binary number.

Population initialization is done to generate the initial solution of a genetic algorithm problem. This initialization is done randomly as much as the desired number of chromosomes / population. Next is calculated the value of fitness and so on is done by using Roulette wheel method, tournament or ranking. Values that have a high fitness will survive in the next generation as Parent. To produce a new generation performed several operations such as selection, crossover and mutation. The procedure will be repeated until found the most optimal solution or after the desired number of generations has been met.

The value of PID which is the coefficient of  $Kp$ ,  $Ki$  and  $Kd$  will be optimized by GA method to ensure maximum control. For GA initialization, we have to define some initial values. Because the performance of a good system control design will depend on how well we determine the initial parameters. The initial parameters of GA are listed in Table II.

The fitness calculations of each chromosome as the selection of objective functions are very important thing. In this study we use SSTE to calculate performance index on controller with equation as follows:

$$SSTE = \sum_{t=0}^N (e)^2 / N \quad (43)$$

TABLE II. INITIAL PARAMETER OF GA

Parameter	Value
Generation	50
Population Size	50
Crossover Method	Crossover Scattered
Maximum Number of Generation	0.8
Selection Method	Tournament
Crossover Probability	0.8
Mutation Type	Uniform Mutation
Mutation Probability	0.1

### D. Luenberger Observer

A linear system that uses a control system must have feedback for comparison with the reference value that will determine the input for the control system. Feedback from the system can be set according to what reference wanted to be given. But to ensure that the feedback output corresponds to the state of the system, it needs a disturbance observer like Luenberger Observer [7].

The problem that arises in SMC control is the existence of a chattering where the value must be adjusted to the biggest disturbance to be received by the motor. This causes the system to perform a large catering even in the minor disturbances. Therefore used Observer that serves to detect disturbance on the motor and then converted to the value of switching gain ( $Ks$ ) on SMC so that the value of chattering will adapt in accordance with the value of disturbance that is received by the plant. Luenberger Observer basic equation is described as follow [12]:

$$\dot{\hat{x}} = A\hat{x} + Bu + L[y - C\hat{x}] \quad (44)$$

with estimation error observer is defined as:

$$\hat{e} = \hat{x} - x \quad (45)$$

$$\dot{\hat{e}} = (A - LC)\hat{e} - Ed \quad (46)$$

$$A - LC = \begin{bmatrix} \frac{-ra}{La} & 0 & 0 \\ 0 & \frac{-ra}{La} & 0 \\ 0 & 0 & \frac{-Bv}{J} \end{bmatrix} - \begin{bmatrix} L1 \\ L2 \\ L3 \end{bmatrix} \cdot [0 \quad 0 \quad 1] \quad (47)$$

$$\lambda I - (A - LC) = \lambda \begin{bmatrix} 1 & 0 & 0 \\ 0 & 1 & 0 \\ 0 & 0 & 1 \end{bmatrix} - \begin{bmatrix} \frac{-ra}{La} & 0 & -L1 \\ 0 & \frac{-ra}{La} & -L2 \\ 0 & 0 & \frac{-Bv}{J} - L3 \end{bmatrix} \quad (48)$$

The polynomial characteristic equation of the Luenberger Observer is the determinant of the matrix in (48).

$$\begin{aligned} \det(\lambda I - (A - LC)) &= \lambda^3 + \lambda^2(-2\rho - \sigma + L3) \\ &+ \lambda(2\rho\sigma + \rho^2 - 2L3\rho) \\ &+ (-\rho^2\sigma + \rho^2L3) \end{aligned} \quad (49)$$

where,

$$\rho = -ra/La \quad (50)$$

$$\sigma = -Bv/J \quad (51)$$

According to the Vieta equation law, the value of the root of the cubic 3 equation is defined as:

$$-(\lambda_1 \lambda_2 \lambda_3) = -\rho^2\sigma + \rho^2L3 \quad (52)$$

$$L3 = \frac{-(\lambda_1 \lambda_2 \lambda_3) + \rho^2\sigma}{\rho^2} \quad (53)$$

Hence, we get the value of L in state Observer

$$L = \begin{bmatrix} 0 \\ 0 \\ \frac{-\lambda_1\lambda_2\lambda_3 + \rho^2\sigma}{\rho^2} \end{bmatrix} \quad (54)$$

where the eigen value of (A-LC) is

$$\text{eig}(A - LC) = [\lambda_1 \ \lambda_2 \ \lambda_3] \quad (55)$$

The difference between the Observer's output value and the actual speed of the motor was used to determine the value of the switching gain in the SMC as shown in the equation (56).

$$U_{SW} = (K_{observer} + Ks)\tanh\left(\frac{S}{\varphi}\right) \quad (56)$$

### III. RESULTS AND DISCUSSION

#### A. SMC-PID-GA in BLDC Motor

Evaluation on the nonlinear BLDC motor was done by equipped with 0.5 N load at  $t = 2$  sec and noise at  $t = 3$ . The noise and the load values influenced the motor characteristics and it was not more than 40% of the input reference.

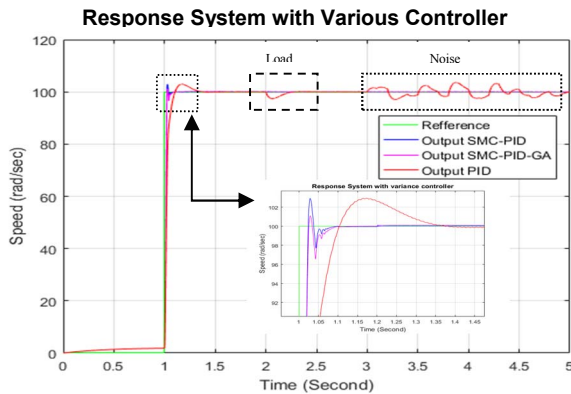


Fig. 2 Comparison of the speed controller on nonlinear BLDC motor with disturbance

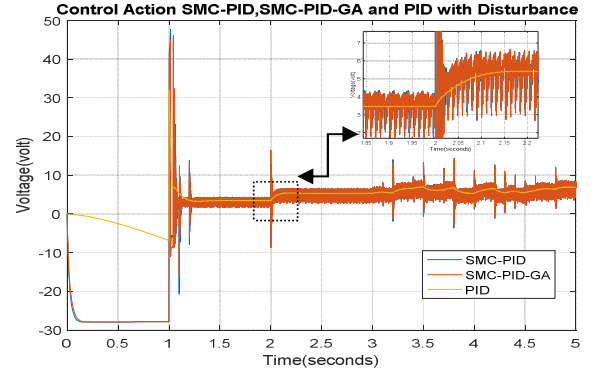


Fig. 3 Control signal of the controller

TABLE III. SYSTEM CHARACTERISTICS

Characteristic	PID	SMC-PID	SMC-PID-GA
Rise Time (sec)	0.04	0.02	0.019
Overshoot (%)	2.9	2.9	1.1
Peak Time (sec)	0.164	0.029	0.03
Settling Time (sec)	0.392	0.132	0.13
SSTE	2.8098	1.269	1.2548

Fig. 2 shows that the performance of the SMC-PID was significantly leading than the PID in both transient and steady state area. It was proven when disturbance occurred at  $t = 2$  second, the SMC-PID keep the system to remain at its reference input and avoid from load perturbation. Similarly, when noise occurs, SMC-PID is able to overcome the interference, such that the system remains in stable condition. Differ from the PID controller that has a big change when the system get the load and noise occurs to the system. This is happened because there was interference on the system. The SMC-PID chattered when the system trajectory was forced to remain on the sliding surface. The SMC-PID control signal as shown in Fig. 3 will remain in chattering condition during the interference, when the interference value is more than the value of switching gain.

Optimizing the value of PID parameters using GA is highly visible from Fig. 2, where the transient response of the system works more optimally although its action control just has a little bit different from the SMC-PID without optimization. In Table III, it is found that the overshoot and error values of the system that generate by GA optimization are smaller than other methods. Compared with previous studies using only conventional SMC on BLDC motors [6], SMC-PID-GA performance is much better especially on the transient response area. Conventional SMC only considers the steady state area aspect, while SMC-PID-GA is developed in addition to steady state performance, the transient response is also noticed, so that all the things that describe the performance of the system on various conditions can be resolved.

#### B. Adaptive SMC-PID-GA

Tests on adaptive SMC will be aimed at the changing of chattering value that will occur in SMC. Luenberger observer will set the value of SMC switching gain so that the

system will perform the chattering according to the number of disturbance that received.

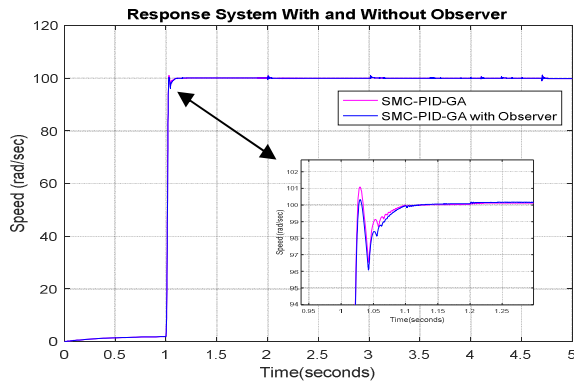


Fig. 4 Response signal of SMC-PID-GA with and without observer

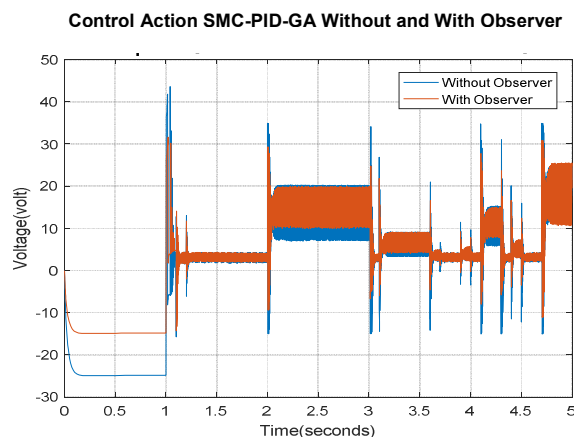


Fig. 5 Control signal with and without observer

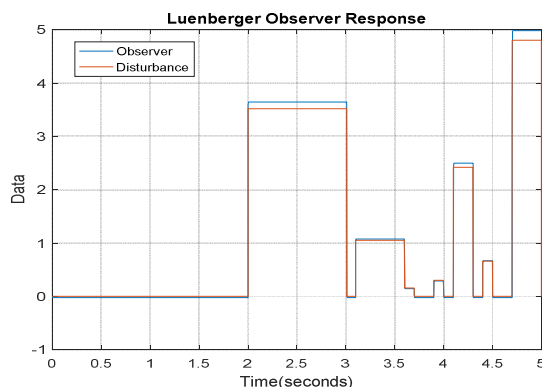


Fig. 6 Disturbance value that estimated by Luenberger Observer

With the observer on the system, it appears that the response of the system as shown in Fig. 4 is not very influential but the disturbance that will be accepted by the system can be detected well by the observer as shown in Fig. 6. The disturbances that have been estimated by Luenberger observer will change the value of SMC switching gain so that seen in Fig. 5 the SMC-PID-GA chattering value varies according to the value of the disturbance that received. This is very important because the higher chattering will result in changes of motor input and there will be vibration in the system. The accuracy of Luenberger observer in estimating

the disturbance is very high, as evidenced by the error between disturbance and observer in SSTE reach 0.0322.

#### IV. CONCLUSION

A robust and adaptive control scheme has been designed and simulated successfully for BLDC motor system. The SMC with PID sliding surface be able to maintain the stability of the system according with the reference point against the disturbance and noise interference. With the addition of genetic algorithm also capable to optimize the SMC-PID performance in area of transient response. Moreover, the inclusion of the Luenberger disturbance observer in the control scheme offer a solution on the problem how to minimize chattering effect on the system, when the disturbance and noise interference changing with uncertain magnitude.

#### REFERENCES

- [1] Varshney, Akash; Gupta, Deeksha; Dwivedi, Bharti.2016. *Speed response of Brushless DC motor using Fussy PID Controller under Varying Load Condition*. JESIT 2017.
- [2] Premkumar,K; Manikandan,B.V. 2015. *Speed control of Brushless DC motor using bat algorithm optimized Adaptive Neuro Fussy Inference System*.Elsevier 2015.
- [3] Usman, Adil, dan Rajpurohit, Bharat Singh. 2016. *Speed Control of a BLDC Motor using Fuzzy Logic Controller*. IEEE 2016.
- [4] Muniraj, Murali dan Arulmozhiyal, Ramaswami. 2015. *Modeling and Simulation of Control Actuation Sytem With Fuzzy-PID Logic Controller Brushless Motor Drives for Missiles Glider Application* .Hindawi Publishing Corporation Volume 2015.
- [5] Deying , Gu, dan Rui , Xia. 2013. *The Speed Control of Brushless DC Motor Based on Fuzzy Genetic Algorithm*. IEEE 2013.
- [6] Galphade, Namita.p; Sankeshwari.Subhash S.2015. *Simulation of BLDC Motor Control using Sliding Mode Technnique*. IJAET 2015
- [7] Chetana, M.Sai; Kumar, K.Ravi; Chakravarthi, Ch.Vishnu.2016. *Comparative Analysis of PID, SMC, SMC with PID Controller for speed control of DC motor*. IJMTST 2016.
- [8] Jaen-Cuellar, Arturo.Y; Romero-Troncoso, Rene de J; Morales Velazquez, Luis; Osornio-Rios, Roque A. 2013.*PID-Controller Tuning Optimization with Genetic Algorithm in servo system*. International Journal of Advanced Robotic System 2013.
- [9] Ayadi, Assil; Smaoui, Mohamed; Aloui, Sinda; Hajji, Soufien; Farza, Mondher. 2018. *Adaptive sliding mode control with moving surface: experimental validation for electropneumatic system*. ELSEVIER 2018.
- [10] Soon, Chang Cee, Rozaimi Ghazali, Hazriq Izzuan Jaafar dan sharifah Yuslinda. 2017. *Sliding Mode Controller Design with Optimized PID Sliding Surface using Particle Swarm Algorithm*. IEEE 2017.
- [11] Shamseldin, Abdelbar Muhammed, dan El-Samahy Adel.A. 2014. *Speed Control of BLDC Motor by Using PID Control and Self-tuning Fuzzy PID Controller* .Elgouna, Egypt : 15<sup>th</sup> International Workshop on Research and Education in Mechatronic (REM).
- [12] Brandstetter, Pavel; Hajovsky, Jiri; Petrtyl, Ondrej. 2016. *Luenberger Observer Aplication in Control of Switched Reluctance Motor*.IEEE 2016.
- [13] Kamal , Md Mustafa; Mathew, Lini and Chatterji ,S. 2014. *Speed Control of Brushless DC Motor Using Intelligent Controllers*. IEEE 2014.
- [14] Sheeba Joice , C., dan Nivedhitha, P. 2014. *Simulation Of Speed Control Of Brushless Dc Motor With Fuzzy Logic Controller*. International Journal of Electrical, Electronics and Data Communication Volume-2.
- [15] Singh, C.P; Kulkarni, SS; Rana, S.C, dan Deo, Kapil. 2014. *State-Space Based Simulink Modeling of BLDC Motor and its Speed Control using Fuzzy PID Controller*. International Journal of Advances in Engineering Science and Technology.
- [16] Zhang , Songmao dan Wang , Yunliang. 2016. *The Simulation of BLDC Motor Speed Control Based-Optimized Fuzzy PID Algorithm*. IEEE 2016.

# Active Fault Tolerance Control For Sensor Fault Problem in Wind Turbine Using SMO with LMI Approach

Nuralif Mardiyah, Novendra Setyawan, Bella Retno, Zulfatman Has  
Department of Electrical Engineering, University of Muhammadiyah Malang, Indonesia  
[nuralif@umm.ac.id](mailto:nuralif@umm.ac.id), [novendra@umm.ac.id](mailto:novendra@umm.ac.id)

**Abstract**— In this paper, we start to investigate the sensor fault problem in a Wind Turbine model with Fault Tolerant Control (FTC). FTC is used to allow the parameters of the controller to be reconfigured in accordance error information obtained online from sensors to improve the stability and overall performance of the system when an error occurs. The design is divided into two parts. The first part is designed Sliding Mode Observer (SMO) based Fault Detection Filter (FDF) to generate a residual signal to estimate fault. FDF is designed to maximize sensitivity fault. The second is a design output feedback control and Fault Compensation to guarantee the stability and performance system from disturbance by ignoring faults.

Moreover, the function of fault compensation is to minimize effect fault of the system. The main contribution of this research is FTC proved to solve the sensor fault problem in a Wind Turbine model. The simulation showed the effectiveness of this method to estimate the fault and stabilized the system faster to a steady condition.

**Keywords**— Fault Tolerant; Sliding Mode Observer; Linear Matrix Inequality; Wind Turbine

## I. INTRODUCTION

Utilization of renewable energy sources is also a suitable solution as a replacement for conventional energy sources that are depleting the number of reserves. Wind energy is one example of an energy source that has shown an increase in the contribution to electricity demand, using renewable energy sources, the use of wind energy, causing decreasing in use of carbon energy [1].

In long-term operation, wind turbine disturbances are considered for various sensors and actuators. To resolve the system errors, a method to compensate for the errors in the system so that the system can have good performance is required. This method is called Fault Tolerant Control (FTC). There are two types of methods in the FTC, namely Passive Fault Tolerant Control Schemes (PFTCs) and Active Fault Tolerant Control Schemes (AFTCS). In PFTCs, the controller parameters are fixed and designed using robust controls to ensure the control system remains capable of resolving errors from system components. In the PFTCs method, no online error information is required for the controller but has an error limit to overcome. While the AFTCS method, the parameters of the controller are reconfigured according to the error

information obtained online to improve the stability and overall performance of the system when an error occurs on the component [2].

The sensor fault case can be classified under sensor saturation, lost sensitivity, and missing measurement. The AFTC scheme for of the actuator or sensor measurement results is based on the error compensation reconstructed with the injection signal. For the sensor fault case such as sensor saturation and lost sensitivity, the AFTC using robust  $H_\infty$  method has been developed in [3]. In fault estimation result from that research, the fault cannot accurately estimate using Luenberger observer with LMI approach. According [4], comparing with another scheme, the sliding mode observer base estimation of fault can make the error estimation can convergence to zero even though the signal fault is time-variant.

In this paper, we design the active fault tolerant control with the sliding mode observer to estimate the fault in the sensor of the wind turbine. Then, output feedback controller based on model reference is designed to control the power of the generator although the wind speed is changing. The fault reconstruction is designed with the LMI approach to reject the fault after its estimated.

## II. THE MATHEMATICAL MODEL OF WIND TURBINE

### A. Wind Model

The main driving force for the wind turbine is a Wind with depends on multiple parameters. Generally, wind model described into two-part, The mean wind model and the stochastic model [5].

In [6], there is three variable that influences the stochastic model of wind. Wind shear which is the effect of wind energy lost at the surface of the earth, tower shadow is the phenomenon when a blade located in front of the tower, the lift on that blade decreases because the tower reduces the effective wind speed. This tower shadow implies that force acting on each blade decreases every time a blade is in front of the tower. An equation describing the wind component is described below

$$v_w(t) = \bar{v}_w(t) + v_{ws}(t) + v_{ts}(t) + v_s(s) \quad (1)$$

In Eq. (1)  $\bar{v}_w$  is the mean wind speed that is occurring in certain intervals;  $v_{ievs}$  and  $v_s$  is the wind shear and tower shade that effect in the wind force in the blade; and  $v_s$  is the stochastic effect in the wind which completely described in [6].

### B. Aerodynamic Model

The aerodynamics model of the wind turbine model is modeled as torque acting in a blade which described below [5]

$$T_d(t) = \frac{1}{2\omega_r} \rho A v_r^3(t) C_p(\lambda(t), \beta(t)) \quad (2)$$

Where  $\rho$  air density,  $A$  is the swept rotor area,  $v_r$  is the wind speed passing through the rotor, and  $C_p(\lambda(t), \beta(t))$  is a mapping of the torque coefficients. The  $C_p$  coefficient modeled as the lookup table depending on the tip speed ratio and the pitch angle.

### C. Drive Train

The purpose of the drive train is to transfer torque from the rotor to the generator. It includes a gearbox that increases the rotational speed from the low-speed rotor side to the high-speed generator side. In this paper, the drive train is modeled by a two-mass model.

$$J_r \dot{\omega}_r(t) = T_d(t) - K_{dt} \theta_{\Delta} + (B_{dt} + B_r) \omega_r(t) + \frac{B_{dt}}{N_g} \omega_g(t) \quad (3)$$

$$J_g \dot{\omega}_g = \frac{\eta_{dt} K_{dt}}{N_g} \theta_{\Delta}(t) + \frac{\eta_{dt} B_{dt}}{N_g} \omega_r(t) - \left( \frac{\eta_{dt} B_{dt}}{N_g^2} + B_g \right) \omega_g - T_d(t) \quad (4)$$

$$\dot{\theta}_{\Delta}(t) = \omega_r(t) - \frac{1}{N_g} \omega_g(t) \quad (5)$$

Where  $J_r$  is the moment of inertia of the low-speed shaft?  $K_{dt}$  is the torsion stiffness of the drive train,  $B_{dt}$  is the torsion damping coefficient of the drive train,  $B_g$  is the viscous friction of the high-speed shaft,  $N_g$  is the gear ratio,  $J_g$  is the moment of inertia of the high-speed shaft,  $\eta_{dt}$  is the efficiency of the drive train, and  $\theta_{\Delta}$  is the torsion angle of the drive train.

### D. Generator Model

The electrical system in the wind turbine and the electrical

System controllers are much faster than the frequency range used in the wind model. On a system level of the wind turbine, the generator and converter dynamics can be modeled by a first-order transfer function

$$\dot{T}_g(t) = -\frac{1}{\tau_g} T_g(t) + \frac{1}{\tau_g} T_{g,ref}(t) \quad (6)$$

where  $T_g(t)$  is the torque in generator and  $T_{g,ref}(t)$  torque reference in generator and  $\tau_g$  is the time constant parameter on the generator.

The power supplied by generator described as below

$$P_g = \eta_g \omega_g(t) T_g(t) \quad (7)$$

Where  $\eta_g$  is the efficiency of the generator.

### E. Pitch Actuator

Pitch actuator system is the hydraulic system that controls the pitch angle in the blade of the wind turbine. The controller is not available. In principle, it is a piston servo system that can be modeled well by a second-order transfer function between the measured angle  $\beta$  and pitch reference  $\beta_{ref}$  [1]

$$\frac{\beta}{\beta_{ref}} = \frac{1}{s^2 + 2\zeta\omega_n + \omega_n^2} \quad (8)$$

where  $\zeta$  is the damping ratio, and  $\omega_n$  is the natural frequency of the pitch actuator.

### F. Linearization

The system has two inputs, the generator torque reference and the pitch angle reference, which are delayed as prior explained. Furthermore, the speed of the wind acts as a disturbance and is an uncontrolled input. The aerodynamic model is affected by the effective wind speed,  $v_r(t)$  affecting the real wind speed,  $v_w(t)$ . If the chosen state variable is  $[T_g \ \dot{\beta} \ \beta \ \theta_{\Delta} \ \omega_g \ \omega_r]^T$  the state space model of the wind turbine is described as following equation

$$\dot{x}(t) = Ax(t) + Bu(t) + Bdv_w(t) \quad (9)$$

Where

$$A = \begin{bmatrix} a_{11} & 0 & 0 & 0 & 0 & 0 \\ 0 & 0 & 1 & 0 & 0 & 0 \\ 0 & a_{32} & a_{33} & 0 & 0 & 0 \\ 0 & 0 & 0 & 0 & a_{45} & 1 \\ a_{51} & 0 & 0 & a_{54} & a_{55} & a_{56} \\ 0 & a_{62} & 0 & a_{64} & a_{65} & a_{66} \end{bmatrix}; B = \begin{bmatrix} b_{11} & 0 \\ 0 & 0 \\ 0 & b_{23} \\ 0 & 0 \\ 0 & 0 \\ 0 & 0 \end{bmatrix}$$

$$Bd = [0 \ 0 \ 0 \ 0 \ 0 \ bd_6]^T$$

And the parameter is described bellow

$$\begin{aligned} a_{11} &= -\left(\frac{1}{T_g}\right) & a_{66} &= -\left(\frac{Bdt + Br}{J_r} + \frac{1}{J_r \partial \omega_r}\right) \\ a_{33} &= -2\zeta\omega_n & a_{32} &= -\omega_n^2 \\ a_{45} &= -\left(\frac{1}{N_g}\right) & b_{11} &= \frac{1}{T_g} \\ a_{51} &= -\left(\frac{1}{J_g}\right) & b_{32} &= -\omega_n^2 \\ & & bd_6 &= \frac{1}{J_r \partial V_r} \\ a_{62} &= \frac{1}{J_r} \frac{\partial Ta}{\partial \beta} & a_{52} &= \left(\frac{Ndt}{J_g N_g} + \frac{Kdt}{J_g N_g}\right) \\ a_{64} &= \frac{Kdt}{J_r} & a_{53} &= -\left(\frac{Ndt + Bdt}{J_g N_g^2} + \frac{Bg}{J_g}\right) \\ a_{55} &= \frac{Bdt}{Bg J_r} & a_{54} &= -\left(\frac{Ndt}{N_g J_g}\right) \end{aligned}$$

In eq (9) there is the nonlinearly term in aerodynamic model of wind turbine. In linearization of wind model, the nonlinearly term of  $\frac{\partial Ta}{\partial \beta}, \frac{\partial Ta}{\partial V_r}, \frac{\partial Ta}{\partial \omega_r}$  directly approximately using parameter identification [5].



### III. FAULT DETECTION WITH SMO

Consider the linear system with the sensor fault is described in the following equation

$$\begin{aligned}\dot{x}(t) &= Ax(t) + Bu(t) \\ y(t) &= Cx(t) + D_f f(t)\end{aligned}\quad (10)$$

where  $y(t)$  is the output of system and  $f(t)$  is the fault that occurs in the sensor of the output state.

In this section, SMO is designed to estimate the faulty in the system. Since  $(A, C)$  is detectable, given SMO the following in equation

$$\begin{aligned}\dot{\hat{x}}(t) &= A\hat{x}(t) + Bu(t) + L(y(t) - \hat{y}(t)) + Gv(t) \\ \hat{y} &= C\hat{x}(t)\end{aligned}\quad (11)$$

Where  $\hat{x}(t) \in R^n$  and  $\hat{y}(t) \in R^n$  represent state and output estimation vector.  $(Vt)$  is switching term of SMO signal. Observer gain  $L$  and  $G$  should be guaranteed the stability of the observer. If Filtering error estimation is given in equation (12) and the derivation in (13)

$$e = x(t) - \hat{x}(t) \quad (12)$$

$$\dot{e} = \dot{x}(t) - \dot{\hat{x}}(t) \quad (13)$$

substitute (10) and (11) into (13) so we have the error dynamics of the observer in equation

$$\dot{e} = (A - LC)e(t) - L(D_f f(t)) + Gv(t) \quad (14)$$

If given the Lyapunov function in equation

$$\dot{V} = \dot{e}^T P e + e^T P \dot{e} + e^T e - \gamma f^T f \quad (15)$$

Substitute (14) into (15) we obtain LMI in equation

$$\begin{bmatrix} Q & PLD_f \\ * & \gamma I \end{bmatrix} < 0 \quad (16)$$

Where  $Q = A^T P + PA - PLC - C^T L^T P$  and  $P^T = P \geq 0$  is the solution of  $Q$ , then the error estimation is asymptotically stable. When the error estimation is convergence to zero the fault estimation given in equation

$$\hat{f}(t) = (y - \hat{y}) \quad (17)$$

### IV. OUTPUT FEEDBACK CONTROL AND FAULT RECONSTRUCTION

In this section, the output feedback control will be design with the model following form. The second order model following form is described in the following equation

$$\begin{bmatrix} \dot{x}_m \\ x_{m+1} \end{bmatrix} = \begin{bmatrix} 0 & 1 \\ -(a * b) & -(a + b) \end{bmatrix} \begin{bmatrix} x_m \\ x_{m+1} \end{bmatrix} + \begin{bmatrix} 0 \\ (a * b) \end{bmatrix} r \quad (18)$$

$$y_r = C x_m$$

where  $a$  and  $b$  are the poles which must be chosen to desire characteristic of the closed-loop system.

If the error system was chosen is between output model reference and output state

$$e_s = y_r - y \quad (19)$$

also, the control signal is below

$$u = K * e + V \hat{f} \quad (20)$$

So, we have the system dynamic become

$$\dot{x} = (A + BVC)x - (BKC + BVC)\hat{x} + BKCx_r + BVD_f f \quad (21)$$

also, the observer

$$\dot{\hat{x}} = (LC + BVC)x + (A - LC - BKC - BVC)\hat{x} + BKCx_r + (LD_f + BVD_f)f \quad (22)$$

If we join the eq.(18),(21) and eq.(22) so we have the augmented dynamic system in equation

$$\dot{\bar{z}} = A_i \bar{z} + B_i \bar{w} \quad (23)$$

Where  $\bar{z} = [x \ x_r \ \hat{x}]^T$ ,  $\bar{w} = [r \ f]^T$  and

$$A_i = \begin{bmatrix} (A + BVC) & BKC_r & -(BKC + BVC) \\ 0 & A_r & 0 \\ (LC + BVC) & BKC_r & (A - LC - BKC - BVC) \end{bmatrix};$$

$$B_i = \begin{bmatrix} 0 & BVD_f \\ B_r & 0 \\ 0 & (LD_f + BVD_f) \end{bmatrix}$$

Consider the Lyapunov function described in the equation below

$$\dot{V} = \dot{\bar{z}}^T \bar{Y} \bar{z} + \bar{z}^T \bar{Y} \dot{\bar{z}} + \bar{z}^T \bar{R} \bar{z} - \rho \bar{w}^T \bar{w} \quad (24)$$

So, we have the LMI in the following equation

$$\begin{bmatrix} (A_i^T \bar{Y} + \bar{Y} A_i) + \bar{R} & \bar{Y} B_i \\ B_i^T \bar{Y} & -\gamma I \end{bmatrix} < 0 \quad (25)$$

where

$$\bar{Y} = \begin{bmatrix} Y & 0 & 0 \\ 0 & Y & 0 \\ 0 & 0 & Y \end{bmatrix}; \bar{R} = \begin{bmatrix} R & 0 & 0 \\ 0 & R & 0 \\ 0 & 0 & R \end{bmatrix};$$

$Y = Y^T \geq 0$  and  $R = R^T \geq 0$  is the solution of error system convergence to zero.

### V. SIMULATION RESULT

#### A. Without Faulty Case

The first step we tested the output feedback controller. In this simulation, the desired power of the generator is  $4 \times 10^6$  Watt with eq.(7) we calculate  $\omega_g(t)$  and  $T_g(t)$  to the model following reference.

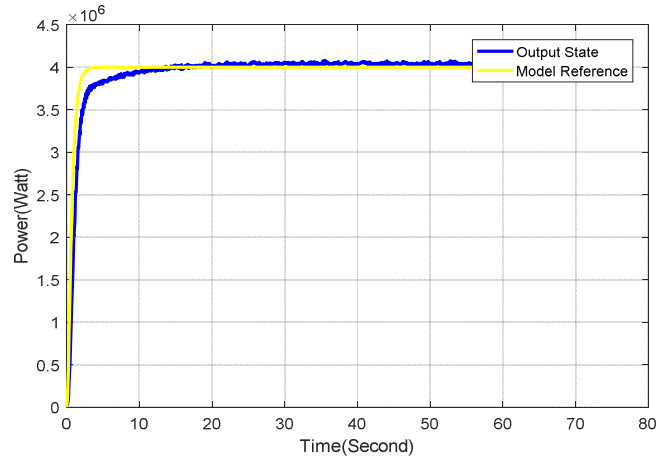


Fig. 1 Generator output power without a faulty case with output feedback controller.

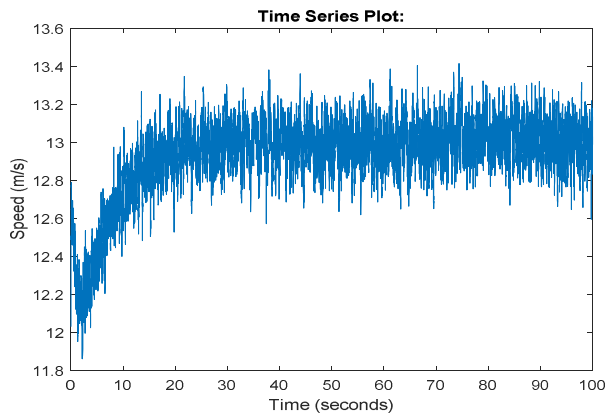


Fig. 2 wind speed

From the simulation, we get that the output feedback control can follow the model reference in 10 seconds with the root mean square error of around 0.132.

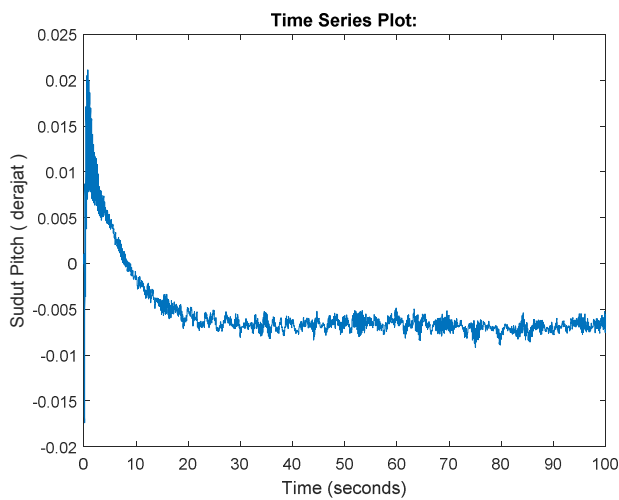


Fig. 3 The angle of pitch signal

FFig. 2 and Fig. 3, its show that the output feedback control with the LMI approach can stabilize the power generator although the wind speed is changing. The robustness from the formulation in LMI shows that the wind speed becomes disturbance successfully handled.

#### B. Faulty Case in One Sensor

In a faulty sensor case, the fault is injected in the second output of the system, i.e.,  $\omega_g(t)$ . From the simulation, it can be shown that the SMO can accurately estimate the fault, its shown from Fig. 4.

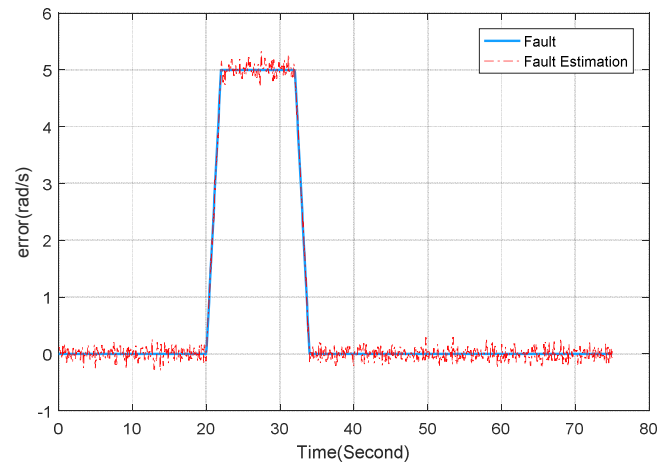


Fig. 4 Comparison of fault and fault estimation using SMO

Fig. 5 shows that the controller responds by comparing when using fault tolerant control and without using fault tolerant control when an error occurs. From the response obtained at that time without fault tolerant control, the output state of the plant had increased and not on the set point due to the giving of the error and just returned to the set points when no error occurred. Meanwhile, when using fault tolerant control when given interference, the response will return to the set points faster 3 seconds when compared with no interference, the response is faster because of the reconfiguration of the control of the addition of set point when the occurrence of errors.

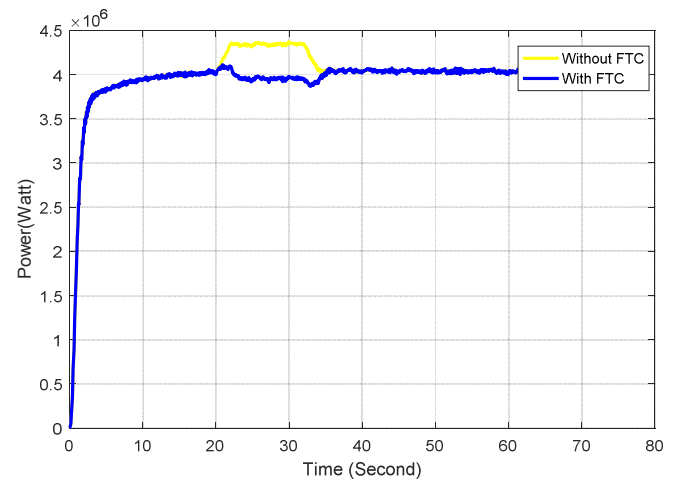


Fig. 5 Comparison with and without FTC

## ACKNOWLEDGMENT

The author would like to give thank to UMM University of Muhammadiyah Malang for providing the facility and support.

## REFERENCES

- [1] P. F. Odgaard, J. Stoustrup, and M. Kinnaert, "Fault-Tolerant Control of Wind Turbines: A Benchmark Model," *IEEE Trans. Control Syst. Technol.*, vol. 21, no. 4, pp. 1168–1182, Jul. 2013. J. Clerk Maxwell, *A Treatise on Electricity and Magnetism*, 3rd ed., vol. 2. Oxford: Clarendon, 1892, pp.68-73.
- [2] M. N. Achmadiyah, R. E. A. Kadir, and A. Jazidie, "Robust H-Infinity Active Fault Tolerant Control for Incomplete Information Problem," 2017, pp. 193–198.
- [3] N. Setyawan, N. A. Mardiyah, M. N. Achmadiyah, R. Effendi, and A. Jazidie, "Active fault tolerant control for missing measurement problem in a Quarter car model with linear matrix inequality approach," 2017, pp. 207–211.
- [4] L. Hao, Y. Ying, Z. Yong, and Z. Zhengen, "Active fault tolerant control with sliding mode observer," 2015, pp. 6259–6263.
- [5] T. Esbensen, B. T. Jensen, M. O. Niss, and C. Sloth, "Joint Power and Speed Control of Wind Turbines," p. 136.
- [6] T. Esbensen and C. Sloth, "Fault Diagnosis and Fault-Tolerant Control of Wind Turbines," p. 177.

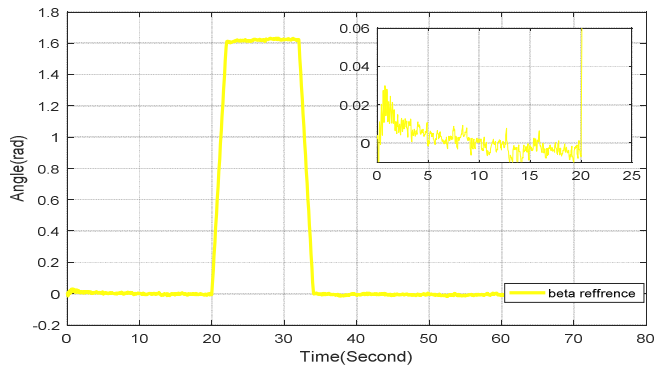


Fig. 6 Angle of pitch signal

## VI. CONCLUSION

After doing the system modeling then do the testing and analysis, it can be taken some conclusions as follows; Design of sliding observer mode used can estimate the fault case at the plant that happened faultily.

Active fault tolerance method is used to overcome the interference and maintain the stability of the system running under the desired output when the interference can be re-stable as when there is no error. Active fault tolerance works successfully in the first second during the interruption.

# Measurement of Thermal Expansion Coefficient on Electric Cable Using X-Ray Digital Microradiography

Yessi Affriyenni  
Department of Physics  
State University of Malang  
Malang, Indonesia  
yessihazrizal@gmail.com

Gede Bayu Suparta  
Department of Physics  
Gadjah Mada University  
Yogyakarta, Indonesia  
gbsuparta@ugm.ac.id

Galandaru Swalaganata  
Department of Mathematics Education  
State Islamic Institute of Tulungagung  
Tulungagung, Indonesia  
galandaru.swalaganata@gmail.com

**Abstract**— Electric cable is a medium to conduct electrical energy. Expansion and contraction caused by thermal changes may result in an aging effect on the cable. This paper presents the way to observe the expansion in electrical cable due to thermal changes using the x-ray microradiography. The observed electric cables were NYA, NYAF, and NYM, each with cross-sectional areas of 1.5 mm<sup>2</sup> and 2.5 mm<sup>2</sup>. The temperature was monitored using a DS18B20 sensor compiled into a microcontroller. In order to process and analyze the cables images, an *ImageJ* software was used. The image differences were compared based on the value of the digital image correlation. The physical analysis was carried out based on Adrian's FWHM and calculated using the regression method. The accurate structural dimension measurement using x-ray digital microradiography is about 50 µm/pixel. The average relative error measured was less than 3%.

**Keywords**— cable, thermal expansion, image correlation, digital microradiograph, x-ray

## I. INTRODUCTION

Electric cable is a medium to conduct electrical energy. Basically, it consists of insulative and conductive parts. The electric cable is characterized by its current conducting capacity (ampacity). The ampacity is affected by the environmental factors such as temperature. The temperature of cable might be changed because of both the response of its resistivity to current changes and the changes in ambient temperature. Expansion caused by thermal changes may result in an aging effect on the cable. Furthermore, it may cause damage [1].

Cable quality is also influenced by its thermodynamics characteristic such as thermal expansion coefficient. The majority of instruments which had been developed to measure this characteristic are dilatometers, comparators, capacitance method, optical interferometry, and thermomechanical analysis but weaknesses are still found [2]. However, these conventional methods cannot detect the expansion of cable installed inside a building, as if it was installed inside the wall or between the ceiling and the roof without destroying the building itself. Thus, we're trying to find a method to detect the change of dimension occurred on the cable using a non-destructive method.

An x-ray micro-digital radiography system has been developed at the Department of Physics, Gadjah Mada University. It is a non-destructive testing method. It comprises a laboratory x-ray generator and an x-ray fluoroscopy image converter. The x-ray generator has a Molybdenum anode target. The x-ray fluoroscopy image converter as image detector comprises a fluorescence screen

in dark cavity which is coupled with a CMOS digital camera to produce digital radiographs [3]. Based on the previous study, the accurate structural dimension measurement using this instrument is about 50 µm/pixel [4].

## II. RESEARCH METHOD

The data was collected in Department of Physics, Gadjah Mada University Yogyakarta including metal cutting, metal drilling, metal welding, data acquisition, and data analysis. The research method followed the flowchart shown in Figure 1. Metal cutting, metal drilling, and metal welding for the heating set were done by following the design shown in Figure 2.

A customized x-ray digital micro-radiography system has been used for data acquisition as shown in Figure 3. The x-ray tube voltage and filament current were set at 40 keV and 30 mA consecutively. The transmitted x-ray from x-ray tube will be partially absorbed by the cable. The passed intensity will form analog radiography image in the fluorescence screens. The image was then captured and converted to be a digital image by CMOS camera. The images were saved in a hard disk of a computer. The images might be displayed and processed for further analysis.

The type of the electric cables for this study was NYA, NYAF, and NYM, which each has two cross-sectional area of 1.5 mm<sup>2</sup> and 2.5 mm<sup>2</sup>. All cables were cut into 120 mm length. The conductor metal of these cables is known to be copper so the range of thermal expansion coefficient should be in the range of  $16 \times 10^{-6}/^{\circ}\text{C}$  to  $18 \times 10^{-6}/^{\circ}\text{C}$  [5]. Every cable was heated from 30°C to 100°C and then their images were collected for each 10°C increment. The temperature changes were monitored by using DS18B20 waterproof temperature sensor compiled into the microcontroller. The measurement results were then displayed on the PC monitor by using the HyperTerminal software [6].

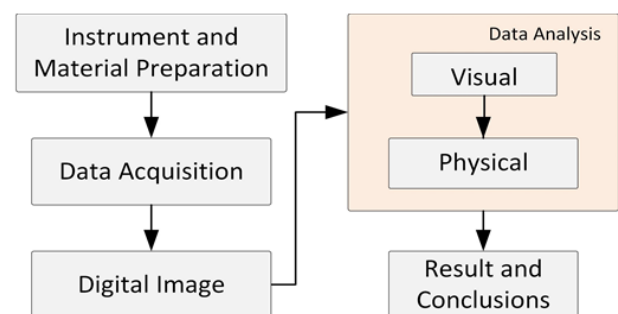


Fig. 1. Flowchart design.

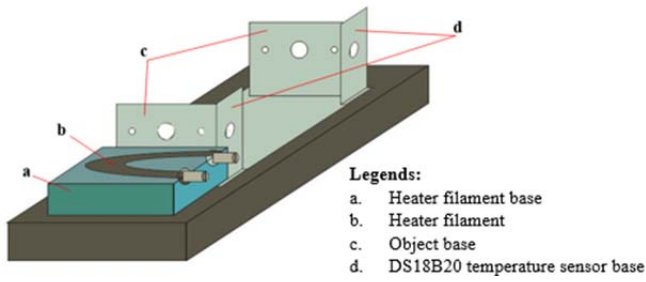


Fig. 2. Heater set design.

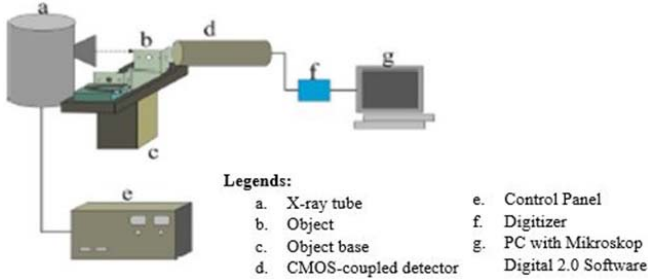


Fig. 3. The x-ray digital micro-radiography system.

In order to process and analyze the radiography images of the cables, an *ImageJ* software was used to analyze the acquired images [7]. Prior, the images were corrected to enhance the visibility and image sharpness.

This software was used for image processing and data analysis. In image processing stage, the images were corrected to remove background values and then added to itself to increase the sharpness [8]. Then, the images were cropped to show the edges only and the process of finding the edge was conducted [9].

Data analysis was conducted in two aspects including visual analysis and physical analysis. Visual analysis was conducted based on image elongation following temperature increment. The image differences were compared based on the value of the digital image correlation (DIC) which has been plugged into the *ImageJ* software [10]. The DIC value measurement follows Eq. 1 which is Pearson's Correlation Coefficient where  $f_i$  and  $g_i$  are the intensity of the  $i^{th}$  pixel in the 1<sup>st</sup> image and 2<sup>nd</sup> image respectively,  $f_{mean}$  and  $g_{mean}$  are the mean intensity of the 1<sup>st</sup> image and 2<sup>nd</sup> image consecutively [11].

The physical analysis was carried out based on Adrian's FWHM [12] to determine the initial and final pixel position of the edges due to temperature changes after the heating process. Position changes were analyzed based on the x-center value of Adrian's FWHM. Metals expansion coefficient was determined using least square fit method (regression method). The equation of thermal expansion is shown in Eq. 2 where  $L$  is the final length,  $L_0$  is initial length,  $\alpha$  is the coefficient of thermal expansion, and  $\Delta T$  is temperature change [13].

$$C = \frac{\sum_{i=1}^n (f_i - \bar{f})(g_i - \bar{g})}{\sqrt{\sum_{i=1}^n (f_i - \bar{f})^2 \sum_{i=1}^n (g_i - \bar{g})^2}} \quad (1)$$

$$L = L_0 + \alpha \Delta T \quad (2)$$

### III. RESULTS AND ANALYSIS

In this study, scanning was done on each object and 5 images were obtained for each 10°C increment. Every obtained image is representing the changes of position due to the changes of temperature. Figure 4a and 4b show the comparison of images before and after subtraction process. Image subtraction was done by subtracting the obtained image with a background image. Plot profiles which are shown in Figure 4c and 4d describe that the background value has been corrected proven by the curve at position range from 0 to 200 coincides with the x-axes in Figure 4d.

Figure 5 shows images and plot profile both before and after addition. The purpose of image addition in this study was to increase the contrast so the edges seemed clearer. Figure 5a and 5b show that there is brightness difference between both images and makes the edges seem clearer. Figure 5c and 5d are the plot profile for the images in Figure 5a and 5b that show no changes in object geometry just the change in gray value. Based on the corrected and normalized radiography images, the image has good contrast so that the edges can be shown clearly.

Table 1 shows image correlation coefficients of images in several temperatures relative to one another for NYA 1.5 object. The DIC value differences signify the geometrical changes occurred, and it is significant at 10°C temperature change from 30°C to 100°C. Other image correlation coefficients for NYA 2.5, NYAF 1.5, NYAF 2.5, NYM 1.5, and NYM 2.5 are not shown because it show the similar trend to Table 1.

TABLE I. IMAGE CORRELATION COEFFICIENTS FOR HEATED NYA, NYAF, AND NYM CABLE

Type	Temperature (°C)							
	30	40	50	60	70	80	90	100
NYA 1.5	1.000	1.000	1.000	1.000	0.999	1.000	1.000	1.000
NYA 2.5	1.000	1.000	1.000	1.000	1.000	0.999	0.999	0.999
NYAF 1.5	1.000	1.000	0.996	0.995	0.983	0.982	0.977	0.966
NYAF 2.5	1.000	0.999	0.990	0.977	0.975	0.975	0.974	0.973
NYM 1.5	1.000	0.997	0.996	0.994	0.985	0.983	0.960	0.947
NYM 2.5	1.000	1.000	0.999	0.998	0.998	0.998	0.998	0.982



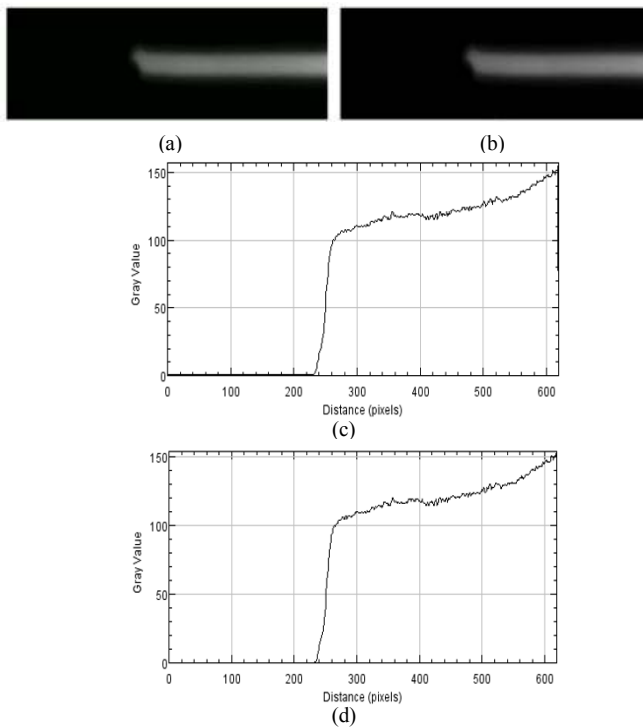


Fig. 4. Example of (a) Image before subtraction, (b) Image after subtraction, (c) Plot profile before subtraction having background gray value of 0, (d) Plot profile after subtraction having background gray value of 1.

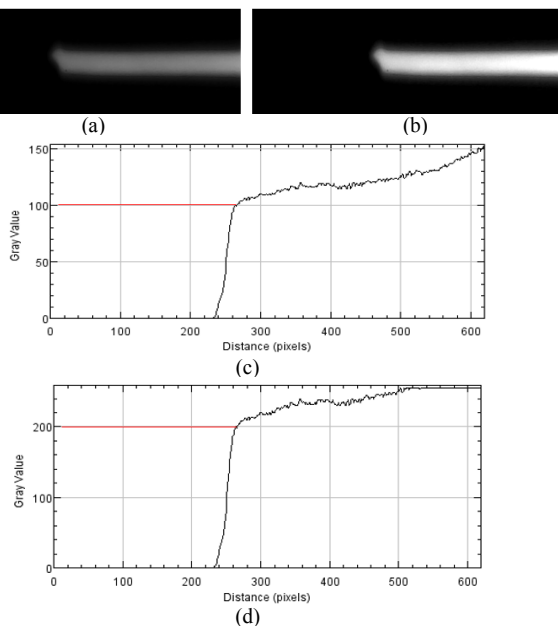


Fig. 5. Example of (a) Image before addition, (b) Image after addition, (c) Plot profile before addition, (d) Plot profile after addition.

Based on Table 1, the image of metal dilation was obtained for each object to show the changes in object geometry caused by its temperature change. Figure 6 shows metal dilation of NYA 1.5, NYA 2.5, NYAF 1.5, NYAF 2.5, NYM 1.5, and NYM 2.5.

The initial position of cable was measured at 30°C temperature using Adrian's FWHM analysis gives the pixel position of the edge and its uncertainty in which it is related to the temperature change. The change of metal length can be observed based on the dilation of peak value on graph

obtained for each temperature that's shown in Table 2 and Figure 7. Calibration procedure yielded on conversion from pixel to c.g.s. unit that is  $220 \pm 5$  pixel equals to 1.5 cm.

Based on the obtained data listed in Table 2, the coefficient of thermal expansion was calculated by using least square fit method or regression method. This method was used because of its capability to determine the uncertainty for minimum length expansion. The linearity for data is shown in Figure 8. Based on the Pearson's  $r$  obtained from the graph, the data were confirmed to be linear so it could be analyzed using the least square method.

The calculated coefficients were then compared with a copper coefficient of thermal expansion range based on [5] that is  $16 \times 10^{-6}/^{\circ}\text{C}$  to  $18 \times 10^{-6}/^{\circ}\text{C}$  since the conductor are all made of copper and shown in Table 3.

Based on the results shown in Table 3, variances still exist in the experiment values but still in the range of the reference value. These might be caused by unknown prior treatment history of the cables in the factory before, whether it was wrought or cast. Furthermore, authors can't control how these cables were treated in the market, how it was rolled, to what degree had it being bent before. These unknown prior histories of specimen might influence the structures of copper. The differences might also be caused by specimen size, heating rate, or thermocouple position.

Based on the research process and the ability of the system to capture metal length changes, authors may state that X-Ray Digital Microradiography built in the department of physics at Gadjah Mada University in Yogyakarta-Indonesia is capable of observing thermal expansion phenomena.

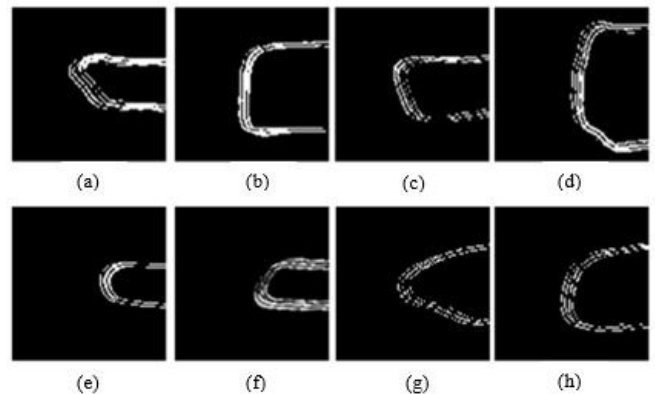


Fig. 6. Conductor dilation from 30°C to 100°C of (a) NYA 1.5, (b) NYA 2.5, (c) NYAF 1.5, (d) NYAF 2.5, (e) NYM 1.5 Blue, (f) NYM 1.5 Black, (g) NYM 2.5 Blue, (h) NYM 2.5 Black.

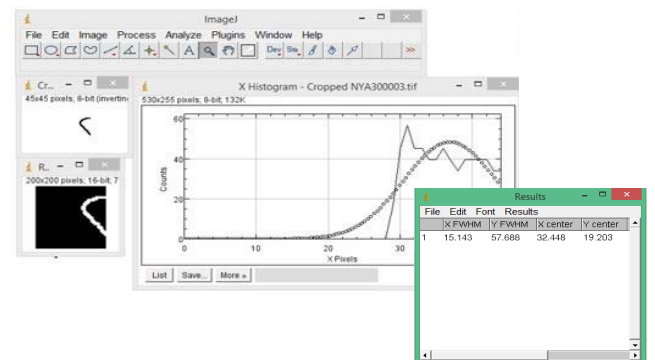


Fig. 7. The image analyzing process on NYA 1.5 at 30°C temperature using Adrian's FWHM plugins.



TABLE II. METALS EDGE'S DILATION. (A) NYA 1.5, (B) NYA 2.5, (C) NYAF 1.5, (D) NYAF 2.5, (E) NYM 1.5 BLUE, (F) NYM 1.5 BLACK, (G) NYM 2.5 BLUE, (H) NYM 2.5 BLACK

$T(^{\circ}\text{C})$	$L_0$ (cm)	$dL$ (cm)
30	12.00 $\pm$ 0.04	0
40	12.00 $\pm$ 0.04	1.32 $\times 10^{-3}$
50	12.00 $\pm$ 0.04	3.71 $\times 10^{-3}$
60	12.01 $\pm$ 0.04	5.73 $\times 10^{-3}$
70	12.01 $\pm$ 0.04	8.03 $\times 10^{-3}$
80	12.01 $\pm$ 0.04	10.41 $\times 10^{-3}$
90	12.01 $\pm$ 0.05	11.80 $\times 10^{-3}$
100	12.01 $\pm$ 0.05	13.17 $\times 10^{-3}$

(a)

$T(^{\circ}\text{C})$	$L_0$ (cm)	$dL$ (cm)
30	12.00 $\pm$ 0.02	0
40	12.00 $\pm$ 0.02	1.67 $\times 10^{-3}$
50	12.00 $\pm$ 0.02	3.94 $\times 10^{-3}$
60	12.01 $\pm$ 0.02	5.52 $\times 10^{-3}$
70	12.01 $\pm$ 0.02	7.04 $\times 10^{-3}$
80	12.01 $\pm$ 0.02	8.68 $\times 10^{-3}$
90	12.01 $\pm$ 0.02	11.85 $\times 10^{-3}$
100	12.02 $\pm$ 0.02	15.14 $\times 10^{-3}$

(b)

$T(^{\circ}\text{C})$	$L_0$ (cm)	$dL$ (cm)
30	12.00 $\pm$ 0.05	0
40	12.00 $\pm$ 0.06	1.87 $\times 10^{-3}$
50	12.00 $\pm$ 0.04	4.13 $\times 10^{-3}$
60	12.01 $\pm$ 0.04	5.84 $\times 10^{-3}$
70	12.01 $\pm$ 0.05	7.61 $\times 10^{-3}$
80	12.01 $\pm$ 0.04	9.99 $\times 10^{-3}$
90	12.01 $\pm$ 0.04	11.97 $\times 10^{-3}$
100	12.01 $\pm$ 0.04	13.88 $\times 10^{-3}$

(c)

$T(^{\circ}\text{C})$	$L_0$ (cm)	$dL$ (cm)
30	12.00 $\pm$ 0.03	0
40	12.00 $\pm$ 0.03	2.43 $\times 10^{-3}$
50	12.00 $\pm$ 0.03	4.16 $\times 10^{-3}$
60	12.01 $\pm$ 0.03	6.31 $\times 10^{-3}$
70	12.01 $\pm$ 0.03	8.55 $\times 10^{-3}$
80	12.01 $\pm$ 0.03	10.64 $\times 10^{-3}$
90	12.01 $\pm$ 0.03	12.25 $\times 10^{-3}$
100	12.01 $\pm$ 0.03	13.80 $\times 10^{-3}$

(d)

$T(^{\circ}\text{C})$	$L_0$ (cm)	$dL$ (cm)
30	12.00 $\pm$ 0.05	0
40	12.00 $\pm$ 0.06	1.68 $\times 10^{-3}$
50	12.00 $\pm$ 0.08	3.78 $\times 10^{-3}$
60	12.01 $\pm$ 0.07	5.91 $\times 10^{-3}$
70	12.01 $\pm$ 0.08	7.64 $\times 10^{-3}$
80	12.01 $\pm$ 0.06	9.57 $\times 10^{-3}$
90	12.01 $\pm$ 0.07	12.06 $\times 10^{-3}$
100	12.01 $\pm$ 0.06	13.86 $\times 10^{-3}$

(e)

$T(^{\circ}\text{C})$	$L_0$ (cm)	$dL$ (cm)
30	12.00 $\pm$ 0.04	0
40	12.00 $\pm$ 0.05	1.60 $\times 10^{-3}$
50	12.00 $\pm$ 0.05	3.27 $\times 10^{-3}$
60	12.01 $\pm$ 0.05	5.37 $\times 10^{-3}$
70	12.01 $\pm$ 0.05	7.51 $\times 10^{-3}$
80	12.01 $\pm$ 0.06	9.59 $\times 10^{-3}$
90	12.01 $\pm$ 0.06	11.28 $\times 10^{-3}$
100	12.01 $\pm$ 0.07	13.36 $\times 10^{-3}$

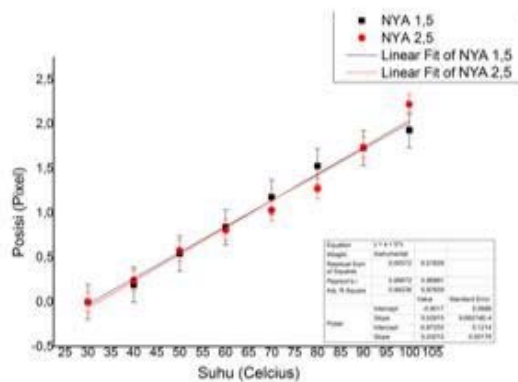
(f)

$T(^{\circ}\text{C})$	$L_0$ (cm)	$dL$ (cm)
30	12.00 $\pm$ 0.05	0
40	12.00 $\pm$ 0.05	2.47 $\times 10^{-3}$
50	12.00 $\pm$ 0.05	4.67 $\times 10^{-3}$
60	12.01 $\pm$ 0.05	6.07 $\times 10^{-3}$
70	12.01 $\pm$ 0.05	8.08 $\times 10^{-3}$
80	12.01 $\pm$ 0.04	10.17 $\times 10^{-3}$
90	12.01 $\pm$ 0.05	12.38 $\times 10^{-3}$
100	12.01 $\pm$ 0.05	14.84 $\times 10^{-3}$

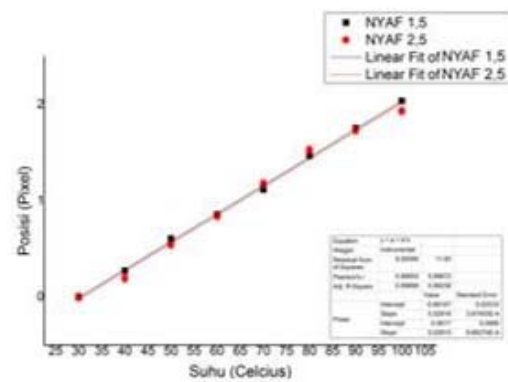
(g)

$T(^{\circ}\text{C})$	$L_0$ (cm)	$dL$ (cm)
30	12.00 $\pm$ 0.07	0
40	12.00 $\pm$ 0.08	2.50 $\times 10^{-3}$
50	12.00 $\pm$ 0.06	4.39 $\times 10^{-3}$
60	12.01 $\pm$ 0.06	5.90 $\times 10^{-3}$
70	12.01 $\pm$ 0.07	7.45 $\times 10^{-3}$
80	12.01 $\pm$ 0.07	10.19 $\times 10^{-3}$
90	12.01 $\pm$ 0.07	12.87 $\times 10^{-3}$
100	12.01 $\pm$ 0.08	14.26 $\times 10^{-3}$

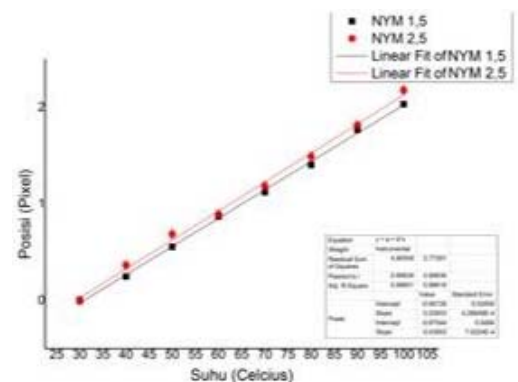
(h)



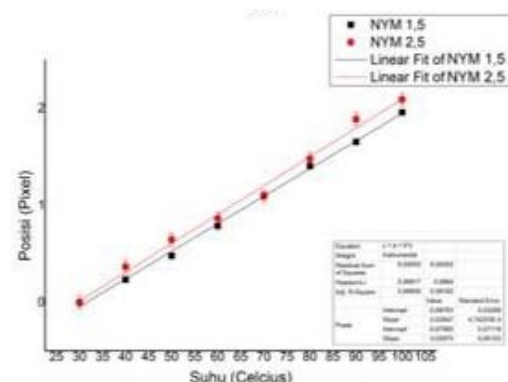
(a)



(b)



(c)



(d)

Fig. 8. Linearity graph of conductor dilation. (a) NYA, (b) NYAF, (c) NYM Blue, (d) NYM Black.

TABLE III. LINEARITY GRAPH OF CONDUCTOR DILATION. (A) NYA, (B) NYAF, (C) NYM 1.5 BLUE, (F) NYM 1.5 BLACK, (G) NYM 2.5 BLUE, (H) NYM 2.5 BLACK

Objects Sizes	Linear Thermal Coefficient	
	1.5 mm <sup>2</sup> ( $\times 10^{-6}/^{\circ}\text{C}$ )	2.5 mm <sup>2</sup> ( $\times 10^{-6}/^{\circ}\text{C}$ )
NYA	$16.6 \pm 0.5$	$17 \pm 1$
NYAF	$16.6 \pm 0.2$	$16.6 \pm 0.4$
NYM	Blue	$16.7 \pm 0.2$
	Black	$16.2 \pm 0.3$
		$17.1 \pm 0.4$
		$16.9 \pm 0.6$

#### IV. CONCLUSION

The developed x-ray microradiography system has been attempted to use for observing metal expansion due to the heating process. From the experiment, the metal expansion can be examined based on the radiographs. Through careful measurement and analysis, it is possible to measure the coefficient of linear thermal expansion with an average relative error of less than 3%. Meanwhile, the measured linear thermal expansion varies in the range of reference values. Improvement may be achieved by better pretreatment, instrument improvements, and proper calibration.

#### ACKNOWLEDGMENT

The authors acknowledged the contribution of Lembaga Pengelola Dana Pendidikan (LPDP) under Ministry of Finance Indonesia for the financial support given to this work in 2016-2017.

#### REFERENCES

- [1] G. F. Moore, *Electric Cables Handbook*. Liverpool: Blackwell Science, 1997.
- [2] S. J. Bennett, "An absolute interferometric dilatometer," *J. Phys. E.*, vol. 10, no. 5, p. 525, 1977.
- [3] G. B. Suparta, A. C. Louk, H. Kurniasari, and G. A. Wiguna, "The use of x-ray micro-digital radiography for clay material inspection," 2014, vol. 9234, p. 92340Y-9234-5.
- [4] A. M. Y. Putranto, "Observation of Linear Thermal Expansion for Aluminium, Iron and Copper Using Digital X-Ray Micro-Radiograph," Gadjah Mada University, 2014.
- [5] F. Cverna, *ASM Ready Reference: Thermal Properties of Metals*. Ohio: ASM International, 2002.
- [6] C. Baumgartner et al., *User's Manual HyperAccess for Windows*. Monroe: Hilgraeve Inc, 2000.
- [7] T. Ferreira and W. Rasband, "ImageJ User Guide," 2012. [Online]. Available: <https://imagej.nih.gov/ij/docs/guide/user-guide.pdf>. [Accessed: 14-Apr-2018].
- [8] G. Swalaganata, Muniri, and Y. Affriyenni, "Moving object tracking using hybrid method," in *2018 International Conference on Information and Communications Technology (ICOLACT)*, 2018, pp. 607-611.
- [9] G. Swalaganata, D. R. Sulistyanningrum, and B. Setiyono, "Super-resolution imaging applied to moving object tracking," *J. Phys. Conf. Ser.*, vol. 893, no. 1, p. 12062, 2017.
- [10] F. Hild and S. Roux, "Digital image correlation," in *Optical Methods for Solid Mechanics*, Weinheim: Wiley-VCH Verlag & Co., 2012, pp. 183-228.
- [11] A. Miranda Neto, A. Victorino, I. Fantoni, D. Zampieri, J. Ferreira, and D. Lima, "Image Processing Using Pearson's Correlation Coefficient: Applications on Autonomous Robotics," in *2013 13th International Conference on Autonomous Robot Systems*, 2013, pp. 1-6.
- [12] A. Martin, "Adrian's FWHM V1.1 code documentation," 2008. [Online]. Available: <https://imagej.nih.gov/ij/plugins/fwhm/>. [Accessed: 14-Apr-2018].
- [13] J. R. Taylor, *An Introduction to Error Analysis: The Study of Uncertainties in Physical Measurements*. Sausalito: University Science Books, 1997.

# A Relative Rotation between Two Overlapping UAV's Images

Martinus Edwin Tjahjadi  
 Department of Geomatics  
 National Institute of Technology  
 (ITN) Malang  
 Malang, Indonesia  
 edwin@lecturer.itn.ac.id

Fransisca Dwi Agustina  
 Department of Geomatics  
 National Institute of Technology  
 (ITN) Malang  
 Malang, Indonesia  
 siscaagustina02@gmail.com

**Abstract**— In this paper, we study the influence of varying baseline components on the accuracy of a relative rotation between two overlapping aerial images taken from unmanned aerial vehicle (UAV) flight. The case is relevant when mosaicking UAV's aerial images by registering each individual image. Geotagged images facilitated by a navigational grade GPS receiver on board inform the camera position when taking pictures. However, these low accuracies of geographical coordinates encoded in an EXIF format are unreliable to depict baseline vector components between subsequent overlapping images. This research investigates these influences on the stability of rotation elements when the vector components are entered into a standard coplanarity condition equation to determine the relative rotation of the stereo images. Assuming a nadir looking camera on board while the UAV platform is flying at a constant height, the resulted vector directions are utilized to constraint the coplanarity equation. A detailed analysis of each variation is given. Our experiments based on real datasets confirm that the relative rotation between two successive overlapping images is practically unaffected by the accuracy of positioning method. Furthermore, the coplanarity constraint is invariant with respect to a translation along the baseline of the aerial stereo images.

**Keywords**— UAV, Relative, Pose, Orientation, Stereoscopic Processing

## I. INTRODUCTION

In supporting a large scale urban city mapping [1] from UAV's images, mosaicking and compositing aerial images [2], as well as stereo matching [3], it is necessary to determine a three-dimensional motion of a rigid object (i.e. a flying UAV platform) from perspective images. A relative orientation process recreates relative translation and angular relationships between two successive overlapping images that existed at the time of photography. A relative orientation consisting of translation and rotation in the stereo images is a prerequisite to retrieve 3D structures from images. The most fundamental problem in geometric computer vision and photogrammetry is a determination of the relative orientation or relative pose from point correspondences between two images.

Numerous works for recovering the position and orientation of stereo images have been shown. Early attempts to reconstruct a scene from the position and rotation from image correspondences utilize projective theory on a coplanarity constraint [4-7]. A solid theoretical foundation about projective significance of the relative orientation matrix was recognized, which is known as the

Fundamental/Essential matrix for describing the geometry of an image pair. Algebraic projective geometry is used to generate polynomial system iteratively to yield an optimal and exact Essential matrix. This method uses 8 point correspondences to the approximate values, then enters into the least squares adjustment with linearized version of the system. One major drawback is the low stability of the system and its use of Gauss-Newton elimination being susceptible to all types of perturbations [8].

Seminal achievements of the scene reconstruction based on this matrix are due to Longuet-Higgins [9] together with Tsai and Huang [10]. They pioneer a further work on the relative orientation improvements. Different strategies and different numbers of minimal correspondences are used to solve the intractable problem using this simplest matrix. For examples, the use of orthogonalization algorithm [11], eigenvectors and eigenvalues [12], singular value decomposition (SVD) [10], quaternions [13], and normalized image coordinates [14] increases the stability and reliability of the resulting matrix. Although an existence of the Essential matrix can be determined with a minimum number of four or fewer point correspondences [15], the most stable and linearly unique solution is given by [14] which use eight point correspondences or more. Other methods using five to seven point correspondences are outlined in [16-18].

Other methods of determining the relative orientation are by exploiting coplanarity condition of the two adjacent images as shown in Fig.1. The geometry of the point correspondence reveals the geometric relations between the scene point and the image points. Assuming the scene point P is static and two images are taken from two different places with a calibrated camera, the relative orientation is described by the two independent sets of exterior orientation parameters (e.g. 6 parameters of each image and thus 12 parameters altogether). Since the scene point object will be reconstructed up to a spatial similarity transformation, which is comprised of seven parameters (i.e. three translations, three rotations, and one arbitrary scale), it means that only 5 parameters out of the 12 total exterior orientation parameters are determinable. This situation is realized by fixing one image (i.e. left image) such that the pose of these images is relatively oriented with respect to each other. Hence, the object points can be reconstructed at an arbitrary scale only up to spatial similarity transformation, or so called a photogrammetric model. Thus, the rotation matrix  $R_2$  of the right image and the direction of the baseline  $b$  connecting two projection center  $O_1$  and  $O_2$  are chosen as the parameters of the relative orientation.

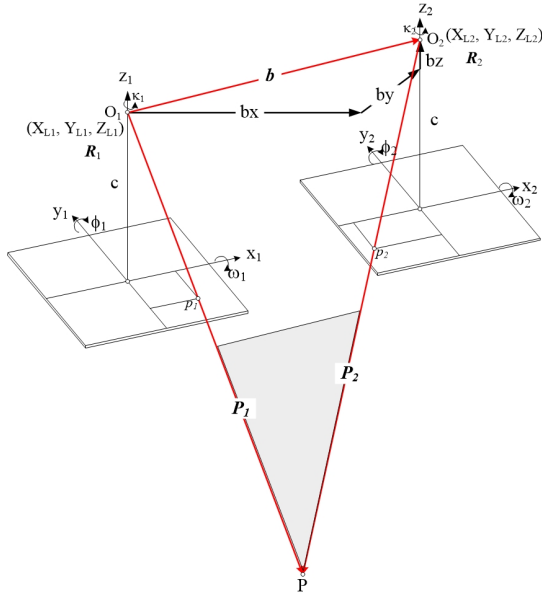


Fig. 1. Relative orientation with a fixed left image

A direct method to determine these parameters based on the coplanarity constraint is reported in [19-24]. It is derived by direct linear transformation (i.e. DLT) from coplanarity condition equation and this method is linear with respect to the 8 unknown parameters [21, 22]. A direct solution for these parameters can be achieved without knowing any approximate values. However, a duality problem of a solution is still exhibited [22]. Attempts to improve the solution are also reported. An alternative approach by imposing four non-linear constraints by deriving inherent orthogonal properties of rotation matrix [20] improves the solution. Another attempt is by adding seven constraints to control and adjust the solution parameters [19]. Six constraints are deduced from the orthogonality of the rotation matrix, and the last one arises from the decomposition of baseline. Furthermore, an attempt to incorporate a RANSAC algorithm in the method to filter out gross errors in the relative orientation solution is also reported by [24].

Instead of decomposing the essential matrix into the rotation and translation parameters of the pose in the direct method, the rotational and translation elements are directly computed into the coplanarity condition. If the epipolar plane defined by the vector of  $\mathbf{b}$ ,  $\mathbf{P}_1$  and  $\mathbf{P}_2$ , which also contain the image point  $p_1$  and  $p_2$ , the computational solution of relative orientation utilizes the condition that an object point  $P$  and the two perspective centers of  $O_1$  and  $O_2$  must lie in a plane (coplanarity constraint). The coplanarity equation is a scalar triple product of a volume of a parallelepiped of these three vectors. If the base of the parallelepiped defined by the any first two out of three vectors and its height by the remaining one, the volume of parallelepiped will be zero if the third vector lies in the plane of the base, making it coplanar with the first two vectors. Direct linear solution of this method uses an extensive algebraic manipulation [21, 22], however a duality of the solution arise due to perturbations in image point coordinates. To remedy the result, further constraints are applied to eliminate the influence of over parameterization of the direct relative orientation model [19, 20, 24]. These improved methods are claimed to be more suitable for UAV flying at low altitudes.

Recent advances in a UAV's low cost direct geo-referencing utilizing a navigational grade of a GPS/GNSS board mounted on the aerial platform [25] provides additional 3D information about geographical coordinates encoded in an EXIF format [26] on each captured images. This low level accuracy of coordinates in geotagged images gives a baseline vector  $\mathbf{b}$  between two successive overlapping images. Since the 3D coordinates of each image are known, therefore the 3D baseline vector between each projection center of each image can be determined. Hence a further constraint on the coplanarity condition can be imposed by these baseline vectors. This paper, therefore, investigates a feasibility of utilizing this vector to determine the relative rotation between two overlapping images. Algebraic manipulations will be elaborated to justify the method in the following sections.

## II. RESEARCH METODOLOGY

The coplanarity condition in Fig. 1 implies a situation in which the object point  $P$  and its corresponding image point  $p_1$  and  $p_2$  on two overlapping images are located on the same plane with the baseline vector  $\mathbf{b}$ . When this condition is achieved, the vector  $\mathbf{P}_1$  will have an intersection with the vector  $\mathbf{P}_2$ , and these vectors together with the baseline vector  $\mathbf{b}$  will be coplanar and the scalar triple product of them is zero. The mathematical model in a determinant form of one pair of corresponding point is given by:

$$\mathbf{F} = \mathbf{b} \cdot (\mathbf{P}_1 \times \mathbf{P}_2) = \begin{vmatrix} b_x & b_y & b_z \\ U_1 & V_1 & W_1 \\ U_2 & V_2 & W_2 \end{vmatrix} = 0 \quad (1)$$

$$\mathbf{b} = \begin{bmatrix} b_x \\ b_y \\ b_z \end{bmatrix} = [X_{L2} - X_{L1} \quad Y_{L2} - Y_{L1} \quad Z_{L2} - Z_{L1}]^T \quad (2)$$

$$\mathbf{P}_1 = [U_1 \quad V_1 \quad W_1]^T = \mathbf{R}_1^T [x_1 \quad y_1 \quad -c]^T \quad (3)$$

$$\mathbf{P}_2 = [U_2 \quad V_2 \quad W_2]^T = \mathbf{R}_2^T [x_2 \quad y_2 \quad -c]^T \quad (4)$$

Equation (1) is the coplanarity condition in the form of a scalar triple product of the volume of a parallelepiped. Its determinant form consists of three vector components of  $\mathbf{b}$ ,  $\mathbf{P}_1$  and  $\mathbf{P}_2$ . A determinable baseline vector of  $\mathbf{b}$  (2) is obtained by extracting geographical coordinates of the two perspective centers of  $O_1$  and  $O_2$  of the left image and the right image respectively. A subtraction of Cartesian coordinates of its geographical ones is sufficient to define the baseline components of the two perspective centers. The Cartesian coordinates are expressed as the  $X_{L1}$ ,  $Y_{L1}$  and  $Z_{L1}$  of the perspective center of the left image as well as the  $X_{L2}$ ,  $Y_{L2}$  and  $Z_{L2}$  of the perspective center of the right image. The vector  $\mathbf{P}_1$  in (3) and  $\mathbf{P}_2$  in (4) represent the object space vector from the image point  $p_1$  and  $p_2$  on the left and the right image respectively. A rotation matrix  $\mathbf{R}$  rotates object space vectors into vectors in the image or model coordinates system. It is a 3 by 3 matrix whose elements constitute the exterior orientation parameters with rotation angles of  $\omega, \phi, \kappa$  [27]:

$$\mathbf{R} = \begin{bmatrix} c\phi c\kappa & c\omega s\kappa + s\omega s\phi c\kappa & s\omega s\kappa - c\omega s\phi c\kappa \\ -c\phi s\kappa & c\omega c\kappa - s\omega s\phi s\kappa & s\omega c\kappa + c\omega s\phi s\kappa \\ s\phi & -s\omega c\phi & c\omega c\phi \end{bmatrix} \quad (5)$$

where the cosine and sine of trigonometric functions are abbreviated to 'c' and 's' respectively.

Here it is assumed that two images have an equal focal length  $c$  and principal point offsets. Also image coordinate on each image have been corrected for the principal point offset. If the left image is fixed and the origin of the local 3D model is located in the projection center of the left image and oriented parallel to its image coordinate system, the exterior orientation parameters can be chosen as  $X_{L1} = Y_{L1} = Z_{L1} = 0$ , also  $\omega_1 = \phi_1 = \kappa_1 = 0$ . Therefore the vector  $\mathbf{P}_1$  can be reduced to:

$$\mathbf{P}_1 = [U_1 \quad V_1 \quad W_1]^T = [\mathbf{I}] [x_1 \quad y_1 \quad -c]^T \quad (6)$$

Now the right image is oriented in the model coordinate system by 3 translations and 3 rotations:  $X_{L2} = b_x$ ,  $Y_{L2} = b_y$ ,  $Z_{L2} = b_z$ , and  $\omega_2$ ,  $\phi_2$ ,  $\kappa_2$ . The vector of  $\mathbf{P}_2$  in (4) can be expanded into:

$$\mathbf{P}_2 = \begin{bmatrix} c\phi_2 c\kappa_2 & -c\phi_2 s\kappa_2 & s\phi_2 \\ c\omega_2 s\kappa_2 + s\omega_2 s\phi_2 c\kappa_2 & c\omega_2 c\kappa_2 - s\omega_2 s\phi_2 s\kappa_2 & -s\omega_2 c\phi_2 \\ s\omega_2 s\kappa_2 - c\omega_2 s\phi_2 c\kappa_2 & s\omega_2 c\kappa_2 + c\omega_2 s\phi_2 s\kappa_2 & c\omega_2 c\phi_2 \end{bmatrix} \begin{bmatrix} x_2 \\ y_2 \\ -c \end{bmatrix} \quad (7)$$

From (7) it is clear that the elements of  $[U_2 \quad V_2 \quad W_2]^T$  are a multiplication of a transposed rotation matrix and a vector of the image coordinates in the right image.

The known baseline vector  $\mathbf{b}$  is defined by the base components of  $b_x$ ,  $b_y$  and  $b_z$  connecting the two perspective center  $O_1$  and  $O_2$ . Suppose the perspective center  $O_2$  is displaced along the baseline toward  $O_1$ , it is clear from the Fig.1 that the vector  $\mathbf{P}_2$  will still be coplanar with the baseline  $\mathbf{b}$  and that the vector will intersect in a point lying on the line between  $O_1$  and  $p_1$ . From a relation of similar triangles, the scale of the model will be directly proportional to the length of the baseline. Therefore, the model coordinate system can be scaled by an arbitrary factor depending of the choice of the baseline length. For simplicity, the longest component of the baseline vector is set to a constant value of  $b'_x$  (i.e.  $b'_x = b_x/b_x = 1$ ). As a consequence of these facts, the other two baseline components are adjusted accordingly into  $b'_y = b_y/b_x$  and  $b'_z = b_z/b_x$ . These divisions mean that a direction of the unit vector of the baseline components remains constant irrespective of the baseline length chosen. Now, three rotation elements only out of five elements of the relative orientation remained. The computational solution of (1) can be simplified into:

$$\mathbf{F} = \mathbf{b} \cdot (\mathbf{P}_1 \times \mathbf{P}_2) = \begin{vmatrix} 1 & b'_y & b'_z \\ x_1 & y_1 & -c \\ U_2 & V_2 & W_2 \end{vmatrix} = 0 \quad (8)$$

The coplanarity condition of (8) is only fulfilled if vector  $\mathbf{P}_1$  and  $\mathbf{P}_2$  intersect in object point P if the position of image point  $p_1$  and  $p_2$ , as well as the orientation parameter of the right image are assumed to be an error free. For each pair of correspondent points one coplanarity equation can be derived. The calculation of the three rotational elements of the relative orientation follows the principle least squares adjustment. The observed quantities are the image coordinates refined for the any systematic error. A general form here,

$${}_r\mathbf{F}_1^0 + {}_r\mathbf{A}_n \quad {}_n\mathbf{v}_1 + {}_r\mathbf{B}_u \quad {}_u\Delta_1 = {}_r\mathbf{O}_1 \quad (9)$$

while  $\mathbf{F}$  is evaluated at the approximate value of (8),  $\mathbf{A}$  is a row matrix which consists of the partial derivatives of  $\mathbf{F}$  with respect to each of the observed quantities,  $\mathbf{v}$  is composed of the residuals to the observation,  $\mathbf{B}$  is a row matrix composed of the partial derivatives of  $\mathbf{F}$  with respect to the rotational elements of parameters,  $\Delta$  is column vector composed of the alteration to the approximate values of the parameters. The subscript  $n$  shows the number of observed values of observable quantities, the subscript  $u$  shows the number of unknown quantities (i.e. 3 rotational parameters), and the subscript  $r$  indicates the number of condition equations where both observed and unknown quantities are present or it equals to the number of correspondences. Since there are four image coordinate measurements for each corresponding point, here  $n = 4r$ . The matrices of each point of observation will be as follows,

$$\mathbf{A}_i = [\partial F_i / \partial x_{1i} \quad \partial F_i / \partial y_{1i} \quad \partial F_i / \partial x_{2i} \quad \partial F_i / \partial y_{2i}] \quad (10)$$

$$\mathbf{B}_i = [\partial F_i / \partial \omega_2 \quad \partial F_i / \partial \phi_2 \quad \partial F_i / \partial \kappa_2] \quad (11)$$

$$\mathbf{v}_i = [v_{x1i} \quad v_{y1i} \quad v_{x2i} \quad v_{y2i}]^T \quad (12)$$

$$\Delta = [\delta\omega_2 \quad \delta\phi_2 \quad \delta\kappa_2]^T \quad (13)$$

where the subscript of  $i$  shows the index of the  $i^{\text{th}}$  correspondence point. Therefore for the number of  $r$  correspondence points, the full matrices would be as follows

$${}_r\mathbf{A}_n = \begin{bmatrix} \mathbf{A}_1 & 0 & 0 & \cdots & 0 \\ 0 & \mathbf{A}_2 & 0 & \cdots & 0 \\ 0 & 0 & \mathbf{A}_3 & \cdots & 0 \\ \vdots & \vdots & \vdots & \ddots & \vdots \\ 0 & 0 & 0 & \cdots & \mathbf{A}_r \end{bmatrix}; {}_r\mathbf{B}_u = \begin{bmatrix} \mathbf{B}_1 \\ \mathbf{B}_2 \\ \mathbf{B}_3 \\ \vdots \\ \mathbf{B}_r \end{bmatrix} \quad (14)$$

$${}_r\mathbf{F}_1^0 = \begin{bmatrix} \mathbf{F}_1^0 \\ \mathbf{F}_2^0 \\ \vdots \\ \mathbf{F}_r^0 \end{bmatrix}; {}_u\Delta_1 = \begin{bmatrix} \delta\omega \\ \delta\phi \\ \delta\kappa \end{bmatrix}; {}_{4r}\mathbf{v}_1 = \begin{bmatrix} \mathbf{v}_1 \\ \mathbf{v}_2 \\ \vdots \\ \mathbf{v}_r \end{bmatrix} \quad (15)$$

In the case of approximately parallel nadir viewing directions, the initial values for linearization of the rotation parameters can be set to zero. The  $\mathbf{F}^0$  is the volume of parallelepiped calculated from the initial values. The approximate values are iteratively improved by the adjusted correction until there is no significant change. The difference coefficient as well as their partial derivatives can be computed using determinants as follows,

$$\partial F / \partial x_1 = (b'_z V_2 - b'_y W_2) \quad (16)$$

$$\partial F / \partial y_1 = (W_2 - b'_z U_2) \quad (17)$$

$$\frac{\partial F}{\partial x_2} = \begin{vmatrix} 1 & b'_y & b'_z \\ x_1 & y_1 & -c \\ r_{11} & r_{12} & r_{13} \end{vmatrix}; \frac{\partial F}{\partial y_2} = \begin{vmatrix} 1 & b'_y & b'_z \\ x_1 & y_1 & -c \\ r_{21} & r_{22} & r_{23} \end{vmatrix} \quad (18)$$

$$\frac{\partial F}{\partial \omega_2} = \begin{vmatrix} 1 & b'_y & b'_z \\ x_1 & y_1 & -c \\ 0 & -W_2 & V_2 \end{vmatrix} \quad (19)$$

$$\frac{\partial F}{\partial \phi_2} = \begin{vmatrix} 1 & b'_y & b'_z \\ x_1 & y_1 & -c \\ -V_2 s\omega + W_2 c\omega & U_2 s\omega & -U_2 c\omega \end{vmatrix} \quad (20)$$

$$\frac{\partial F}{\partial \kappa_2} = \begin{vmatrix} 1 & b'_y & b'_z \\ x_1 & y_1 & -c \\ x_2 r_{21} - y_2 r_{11} & x_2 r_{22} - y_2 r_{12} & x_2 r_{23} - y_2 r_{13} \end{vmatrix} \quad (21)$$

Equations (16) to (21) are partial derivatives with respect to the measurable quantities and unknown parameters. Partial derivatives with respect to the observation of coordinates of the left image are (16) and (17), and of the right image is (18) respectively. Also, partial derivatives of the unknown rotational parameters are expressed in (19) to (21).

### III. RESULTS AND ANALYSIS

Field observations were carried out in Malang city. An array of 30 ground control points (GCPs) is established from a white concentric ring surrounded with dark background for point correspondences (Fig.2). To avoid false matches and to facilitate a possible highest accuracy of image coordinate measurements of GCPs on stereo images, least squares image matching are performed [3] to seek the best matches on stereo images as illustrated in Fig. 3. Furthermore, the matched points of the stereo images are represented in Table 1. The images are calibrated with a fixed focal length of 35mm and the image coordinates are corrected for the principal point offset. Table 1 shows image coordinates of the left and right image in a metric unit instead of pixels.



Fig. 2. GCPs on the Field

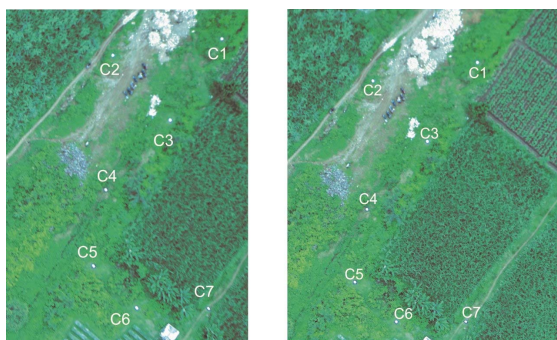


Fig. 3. Some of the correspondence points from cropped stereo images

TABLE I. CORRESPONDENCE POINTS COORDINATES

Point	Left Image		Right Image	
	<i>x (mm)</i>	<i>y (mm)</i>	<i>x (mm)</i>	<i>y (mm)</i>
C1	14.0175	6.5637	7.2925	7.9013
C2	9.9706	5.9494	3.1806	7.1694
C3	12.1038	3.5562	5.3250	4.7850
C4	9.7106	0.9813	2.9463	2.1119
C5	9.2606	-1.8444	2.4706	-0.7519
C6	10.8625	-3.4025	4.1013	-2.3125
C19	3.0850	-0.2513	-3.7700	0.7838
C20	4.7381	0.4644	-2.1375	1.5269
C21	0.2063	3.9688	-6.6509	4.9800
C22	-1.5253	5.4694	-8.3613	6.4506

From the geotagged left image and right image (Fig.3), geographical coordinates are readily available in an EXIF format on each image and they are used to determine projective center coordinates. The result of the projective coordinates of each image is shown in Table 2. It shows a converted Cartesian coordinates from the geographical coordinates. The conversion is performed using widely available open source software.

TABLE II. CARTESIAN COORDINATES IN WGS-84

	Projective Center of Geotagged Images	
	<i>Left Image</i>	<i>Right Image</i>
$X_L$ (m)	674879.6511	674873.7796
$Y_L$ (m)	9121309.6780	9121357.8162
$Z_L$ (m)	809.1911	807.6767

The projective center coordinates of each image in the Cartesian coordinate system are then utilized to calculate the baseline vector components between two images as in (2). If the GCPs are surveyed using geodetic type of GPS, the obtained geographical coordinates can be verified using space resection methods [27-29]. The resection method needs at least three GCPs appeared on both images. The baseline vector is shown in the second column of Table 3. The third column is occupied by the Unit Vector. The unit vector of the baseline is calculated by dividing each component by the length of the baseline  $b$ . Also, the normalized unit vector in the last column is obtained by dividing each unit vector component by the largest element, in this case is  $b_x$ . A result of these calculations is presented in Table 3.

TABLE III. BASELINE VECTOR, UNIT VECTOR, AND NORMALIZED UNIT VECTOR

	Baseline Components		
	<i>Vector (m)</i>	<i>Unit Vector</i>	<i>Normalized Unit Vector</i>
$b_x$	48.1382	0.992159777	1
$b_y$	-5.8715	-0.12101545	-0.12197174
$b_z$	-1.5144	-0.03121277	-0.031459423



A reason to categorize the components into three types shown in Table 3 is to ascertain the influence of the baseline length to the accuracy and stability of rotational parameters of the relative orientation. Due to inaccuracies of the geographical coordinates from the GPS that might influence the resulted rotational parameters, it is a logical decision to decouple its vector components into its unit vectors for maintaining common directions of the baseline vector. To compute the parameters, the vector and the unit vector components in the Table 3 are enter into (1), meanwhile the normalized unit vector components are entered into (8). Iterative least squares adjustments of (9) are used to obtain a solution of (13). Results of the rotational parameters in terms of Euler angles parameterizations are presented in Table 4.

TABLE IV. ROTATION PARAMETERS

	Rotation Elements (degrees)		
	Vector	Unit Vector	Normalized Unit Vector
$\omega_2$	-0.71645164	-0.71645164	-0.71645164
$\phi_2$	2.75634010	2.75634010	2.75634010
$\kappa_2$	-0.65907221	-0.65907221	-0.65907221

Table 4 shows the rotation parameters are remain stable irrespective of the baseline types chosen. It reveals that the rotation parameters are invariant under a change of baseline length as long as its direction of the unit vector remains constant. In other words, imprecisions of the geotagged coordinates in determining the baseline vectors between two images have little or no influence on the numerical stability of the rotation parameters. Evidence shows that all root mean square errors of the projection error on the left image and on the right image for all types are relatively stable of around 0.00171 mm and 0.00168 mm respectively. For example, the projection errors of the type of “unit vector” baseline on both images are illustrated on Table 5.

TABLE V. TYPICAL PROJECTION ERRORS ON TYPE OF “UNIT VECTOR” ON STEREO IMAGES

Point	Projection Error			
	Left Image (x10 <sup>-3</sup> mm)		Right Image (x10 <sup>-3</sup> mm)	
	x	y	x	y
C1	0.1719	1.9986	-0.1233	-1.9490
C2	-0.2971	-3.5082	0.2179	3.4425
C3	0.1526	1.8684	-0.1159	-1.8311
C4	-0.1979	-2.5404	0.1584	2.5028
C5	-0.0026	-0.0351	0.0022	0.0347
C6	0.0823	1.1424	-0.0714	-1.1272
C19	-0.0177	-0.2348	0.0148	0.2337
C20	-0.0243	-0.3163	0.0199	0.3140
C21	0.0762	0.9412	-0.0594	-0.9378
C22	0.0546	0.6594	-0.0416	-0.6579

Based on the small number of projection error presented in the Table 5, it indicates that inaccuracies of the GPS

coordinates from the navigational solutions have little or no influence on the rotation parameter results. No matter what the base line is expressed as a vector, unit vector, or a normalized unit vector, the rotational element results remain stable. For comparison purpose, a classical photogrammetric relative orientation is computed using the same image coordinates as shown in the Table 1. As a rule of thumb, the  $b_x$  component is usually set to 1, and the result of five other parameters is presented in the Table 6.

TABLE VI. PHOTOGRAMMETRIC RELATIVE ORIENTATION PARAMETERS

Parameter	Relative Orientation Value
$b_y$	-0.075552
$b_z$	-0.047
$\omega_2$ (degree)	-0.7164264
$\phi_2$ (degree)	2.7563281
$\kappa_2$ (degree)	-0.6590734

Table 6 shows the result of all parameters of photogrammetric relative orientation. As expected, the base line components of  $b_y$  and  $b_z$  are different from that of the baseline components presented in Table 3, since both are free or unconstrained parameters in a classical relative orientation. On the other hand, all the rotational parameters have very slight differences from that of presented in the Table 4. These very tiny deviations are reasonable since a slight change of the baseline components can change the baseline's direction, and as a result it can also change rotational parameters. Overall, by comparing Table 4 and Table 6, the rotational parameters of the relative orientation are unaffected by a changing of baseline vector components as long as its vector direction is unchanged.

#### IV. CONCLUSION

The most important achievement of this paper is to demonstrate that the rotation parameters of the relative orientation are invariant with respect to the translation along the image projection centers. The relative rotation between two successive overlapping images is practically unaffected by the accuracy of positioning method. Whilst geotagged images are readily available, their coordinates can be utilized to constraint the classical relative orientation computational procedures, hence fewer point correspondences are needed to compute the relative orientation parameters. Constraining baseline parameters of the relative orientation by the navigational grades of GPS coordinates can speed up the computational process and this procedure can readily be integrated into a RANSAC algorithm to produce a faster and more stable direct close form solution of relative orientation.

#### ACKNOWLEDGMENT

The author wishes to express his sincere thanks to Ministry of Research, Technology and Higher Education of the Republic of Indonesia for supporting a research grant “Penelitian Terapan Unggulan Perguruan Tinggi (PTUPT)”, with a contract number of 120/SP2H/LT/DRPM/2018 and ITN.03.0742/IX.REK/2018.

#### REFERENCES

- [1] M. Saadatseresht, A. H. Hashempour, and M. Hasanlou, "UAV Photogrammetry: a Practical Solution for Challenging Mapping

- Projects," *The International Archives of the Photogrammetry, Remote Sensing and Spatial Information Sciences*, vol. 40(1/W5), pp. 619-623, November 2015.
- [2] M. E. Tjahjadi, F. Handoko, and S. S. Sai, "Novel Image Mosaicking of UAV's Imagery Using Collinearity Condition," *International Journal of Electrical and Computer Engineering (IJECE)*, vol. 7(3), pp. 1188-1196, June 2017.
  - [3] M. E. Tjahjadi and F. Handoko, "Precise wide baseline stereo image matching for compact digital cameras," in *2017 4th International Conference on Electrical Engineering, Computer Science and Informatics (EECSI)*, Yogyakarta, Indonesia, pp. 181-186, 2017.
  - [4] C. M. A. V. D. Hout and P. Stefanovic, "Efficient Analytical Relative Orientation," *The ITC Journal*, pp. 304-323, 1976.
  - [5] P. Stefanovic, "Relative Orientation - a New Approach," *The ITC Journal*, pp. 417-448, 1973.
  - [6] E. H. Thompson, "A Rational Algebraic Formulation Of The Problem Of Relative Orientation," *Photogrammetric Record*, vol. 3, pp. 152-159, 1959.
  - [7] E. H. Thompson, "The Projective Theory of Relative Orientation," *Photogrammetria*, vol. 23, pp. 67-75, 1968.
  - [8] U. Helmke, K. Hüper, L. Pei Yean, and J. Moore, "Essential Matrix Estimation Using Gauss-Newton Iterations on a Manifold," *International Journal of Computer Vision*, vol. 74(2), pp. 117-136, 2007.
  - [9] H. C. Longuet-Higgins, "A Computer Algorithm for Reconstructing a Scene from Two Projections," *Nature*, vol. 293(5828), p. 133, 1981.
  - [10] R. Y. Tsai and T. S. Huang, "Uniqueness and Estimation of Three-Dimensional Motion Parameters of Rigid Objects with Curved Surfaces," *IEEE Transactions on Pattern Analysis and Machine Intelligence*, vol. 6(1), pp. 13-27, 1984.
  - [11] J. Weng, T. S. Huang, and N. Ahuja, "Motion and Structure from Two Perspective Views: Algorithms, Error Analysis, and Error Estimation," *IEEE Transactions on Pattern Analysis and Machine Intelligence*, vol. 11(5), pp. 451-476, 1989.
  - [12] S. J. Maybank, "Properties of Essential Matrices," *International Journal of Imaging Systems & Technology*, vol. 2(4), pp. 380-384, September 1990.
  - [13] B. K. Horn, "Relative Orientation," *International Journal of Computer Vision*, vol. 4(1), pp. 59-78, 1990.
  - [14] R. I. Hartley, "In Defense of the Eight-Point Algorithm," *IEEE Transactions on Pattern Analysis and Machine Intelligence*, vol. 19(6), pp. 580-593, 1997.
  - [15] S. Agarwal, H.-L. Lee, B. Sturm, and R. Thomas, "On the Existence of Epipolar Matrices," *International Journal of Computer Vision*, vol. 121(3), pp. 403-415, 2017.
  - [16] D. Nistér, "An Efficient Solution to the Five-Point Relative Pose Problem," *IEEE Transactions on Pattern Analysis and Machine Intelligence*, vol. 26(6), pp. 756-770, 2004.
  - [17] H. Stewénus, D. Nistér, F. Kahl, and F. Schaffalitzky, "A minimal solution for relative pose with unknown focal length," *Image & Vision Computing*, vol. 26(7), pp. 871-877, 2008.
  - [18] J. Philip, "A Non-Iterative Algorithm for Determining All Essential Matrices Corresponding to Five Point Pairs," *Photogrammetric Record*, vol. 15(88), pp. 589-599, October, 1996.
  - [19] Y. Chen, Z. Xie, Z. Qiu, M. Zhang, and S. Zhong, "The model of direct relative orientation with seven constraints for geological landslides measurement and 3D reconstruction," *Earth Sciences Research Journal*, vol. 20(4), pp. F1-F6, 2016.
  - [20] Y. Zhang, X. Huang, X. Hu, Fangqi Wan, and L. Lin, "Direct relative orientation with four independent constraints," *ISPRS journal of photogrammetry and remote sensing*, vol. 66(6), pp. 809-817, 2011.
  - [21] T. Y. Shih, "RLT: A Closed Form Solution for Relative Orientation," *The International Archives of Photogrammetry and Remote Sensing*, vol. 30(B5), pp. 357-364, March 1994.
  - [22] T. Y. Shih, "On the Duality of Relative Orientation," *Photogrammetric Engineering And Remote Sensing*, vol. 56(9), pp. 1281-1283, 1990.
  - [23] L. Chao and Z. Yue, "Approach of Camera Relative Pose Estimation Based on Epipolar Geometry," *Information Technology Journal*, vol. 11(9), pp. 1202-1210, 2012.
  - [24] J. Wang, Z. Lin, and C. Ren, "Relative Orientation in low Altitude Photogrammetry Survey," *The International Archives of the Photogrammetry, Remote Sensing & Spatial Information Sciences*, vol. 39(B1), pp. 463-467, 2012.
  - [25] J. Wang, M. Garratt, A. Lambert, J. J. Wang, S. Han, and D. Sinclair, "Integration of GPS/INS/vision sensors to navigate unmanned aerial vehicles," *The International Archives of the Photogrammetry, Remote Sensing and Spatial Information Sciences*, vol. 37(B1), pp. 963-970, 2008.
  - [26] C. F. Lo, M. L. Tsai, K. W. Chiang, C. H. Chu, G. J. Tsai, C. K. Cheng, N. El-Sheimy, and H. Ayman, "The Direct Georeferencing Application and Performance Analysis of UAV Helicopter in GCP-Free Area," *The International Archives of the Photogrammetry, Remote Sensing and Spatial Information Sciences*, vol. 40(1/W4), pp. 151-157, 2015.
  - [27] M. E. Tjahjadi and F. Handoko, "Single frame resection of compact digital cameras for UAV imagery," in *2017 4th International Conference on Electrical Engineering, Computer Science and Informatics (EECSI)*, Yogyakarta, Indonesia, pp. 409-413, 2017.
  - [28] M. E. Tjahjadi and F. D. Agustina, "Single image orientation of UAV's imagery using orthogonal projection model," in *2017 International Symposium on Geoinformatics (ISyG)*, Malang, Indonesia, pp. 18-23, 2017.
  - [29] M. E. Tjahjadi, "A Fast And Stable Orientation Solution of Three Cameras-Based UAV Imageries," *ARNP Journal of Engineering and Applied Sciences*, vol. 11(5), pp. 3449-3455, 2016.

# Re-Ranking Image Retrieval on Multi Texton Co-Occurrence Descriptor Using K-Nearest Neighbor

1<sup>st</sup> Yufis Azhar

Informatics

Universitas Muhammadiyah Malang  
Malang, Indonesia  
yufis@umm.ac.id2<sup>nd</sup> Agus Eko Minarno

Informatics

Universitas Muhammadiyah Malang  
Malang, Indonesia  
aguseko@umm.ac.id3<sup>rd</sup> Yuda Munarko

Informatics

Universitas Muhammadiyah Malang  
Malang, Indonesia  
yuda@umm.ac.id

**Abstract**— Some features commonly used to conduct image retrieval are color, texture and edge. Multi Texton Co-Occurrence Descriptor (MTCD) is a method which uses all three features to perform image retrieval. This method has a high precision when doing retrieval on a patterned image such as Batik images. However, for images focusing on object detection like corel images, its precision decreases. This study proposes the use of KNN method to improve the precision of MTCD method by re-ranking the retrieval results from MTCD. The results show that the method is able to increase the precision by 0.8% for Batik images and 9% for corel images.

**Keywords**—MTCD, KNN, Image Retrieval

## I. INTRODUCTION

Image retrieval is one of the research topics in the identification of computer pattern and vision. There are numerous previous researches have been conducted on image retrieval system. However, it is still unresolved research topic so far. The retrieval of content-based imagery began in the 1970s when text-based image search was no longer effective [1].

In general, the image retrieval system is built using color, texture, and shape features either separately or in combination have proposed by Minarno [2], [3]. Indexing on CBIR for fast retrieved also have proposed by Munarko [4]. Color features are the most dominant image feature and the easiest to distinguish. J. Huang has proposed image indexing employing a three-dimensional table based on color and distance between pixels. The table describes the spatial relationships in image color alterations. The purpose of color indexing is that the system can distinguish an image with an image stored in the database [5]. Research on texture has also been proposed, both in the field of recognition of clustering patterns, classification and object detection. Julesz conducted, in his research, an analysis of texton interaction to texture discrimination. Moreover, a texton can consist of several pixels. The results of his research revealed that texton only using simple statistical methods was able to provide significant visual perception to distinguish texture [6]. Research on texture has also been conducted by Haralick using the Gray Co-Occurrence Matrix (GLCM). GLCM uses statistical methods of order one and two to produce 14 features, such as mean, variance, correlation, energy, homogeneity and so forth [7].

Jain et al. proposed image retrieval using feature shapes combined with color features to retrieve logo image. Jain's experiments used 400 logo images as data to test the performance of the proposed method. The image retrieval results on two most similar data obtained 99% accuracy [8]. Pradnyana also proposed classification of Endek (balinese

fabric) Image using K-Nearest Neighbor obtained accuracy 91% with k value 3,4,7,8 [9]. Edge detection method one of powerful and simple technique to extract image. Syahrian et al proposed the method to detection cracks using Canny. The results show that the best value for smoothing is 10 and 5 for thresholding in getting not too blurred or to sharp result [10].

Guang Hai Liu developed a research on image retrieval using texton proposed by Julesz. The proposed method is known as Texton Co-Occurrence Matrix (TCM). TCM uses 5 types of texton as kernels to perform feature extraction which generates microstructure maps. There were 2,000 images used as data generated from Corel Dataset and Vistex MIT. The results obtained by TCM in image retrieval ranged from 41% to 43% [11].

Multi Texton Histogram (MTH) has been proposed by Liu to improve TCM performance. The difference between TCM and MTH lies in the type of texton used and the texton shift. MTH uses 4 different types of texton from TCM and switches per two pixels. Meanwhile, TCM shifts its texton per pixel. The MTH test uses Corel 5000 dataset and 10,000 images. MTH testing using Corel 5000 MTH was able to achieve 49.98% precision and 6% recall compared to TCM precision and recall achieved 27.36% and 3.28% respectively. Furthermore, the testing employing Corel 10000 MTH reaches precision of 40.87% and recall of 4.91%, and TCM reaches 20.42% precision and recall of 2.45% [12].

Guang Hai Liu et al. once again proposed an improved image retrieval system using a different approach than MTH. The proposed method is called Micro Structure Descriptor (MSD). MSD uses a 3x3 kernel variation to perform feature extraction. MSD compares the middle value of the kernel with its eight neighbors. Only the neighbor value is equal to the accumulated middle kernel value into a histogram. The MSD test uses Corel 5000 dataset and 10,000 images. At the time of using Corel 5000, MSD was able to produce 55.92% precision and 6.71% recall while testing using Corel-10.000, MSD reaches precision of 45.62% and recall of 5.48% [13].

Human visuals can basically easily distinguish the image edge orientation and color difference in the image. This is behind Guang hai Liu proposed Color difference histogram (CDH) to develop image retrieval system using psychology theory based on human visual perception. CDH is an improvement of MTH and uses the same data as MTH for testing. The results obtained by CDH were better at delivering retrieval results. The precision difference from MTH was 7.39%, and the recall was 0.89% [14].

MSD improvement has been proposed by Minarno et al. in his research using Enhanced Micro Structure Descriptor

(EMSD). EMSD adds an edge orientation feature to the MSD histogram. The performance retrieval test used 300 Batik images as its data, Corel 5000 and Corel 10000. The results obtained by EMSD provided better performance than MSD with 5% precision difference and 1% recall when using Corel 5000. While on the test using Corel 10000, it was found 3% precision difference and 1% recall [15].

MTH repair proposed again by Minarno by adding Gray Level Co-Occurrence Descriptor feature called MTCD. Minarno employed as many as 16 features using Entropy, Energy, Contrast and Correlation using 4 angles of 0, 45, 90 and 135 degree. The study was able to increase the precision by 2.8% for the Batik dataset and 3.4% for the Corel dataset.

This study was proposed to improve MTCD to improve precision by re-ranking index resulted from image retrieval using the KNN algorithm. The results from MTCD testing with KNN increased precision up to 9% for Corel dataset and 0.8% for Batik dataset.

## II. RESEARCH METHOD

### Multi Texton Co-Occurrence Descriptor with KNN

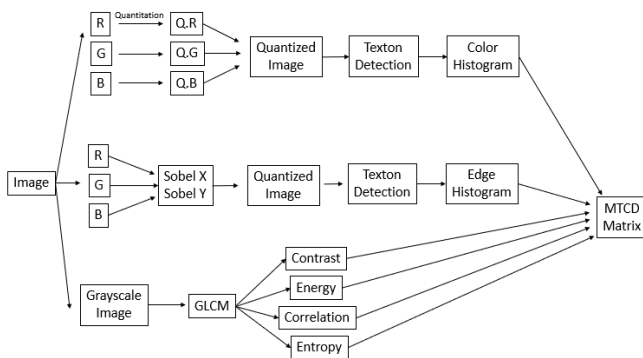


Figure 1. Flowchart of MTCD method

#### a. Extraction of Color Feature

According to Figure 1, it can be seen that an image will go through 3 extraction stages to acquire its features. The first stage is the color feature extraction. To do so, the first image will be broken down into 3 color channels, namely R (red), G (green) and B (blue). Afterwards, each channel will be quantized and then reunited. Following these processes, the texton detection process is completed by using 6 different texton types. A color histogram will then be arranged based on the matrix result of the texton detection process.

#### b. Extraction of Edge Feature

The second stage is edge extraction. The steps are almost identical as color extraction. The image will be split into 3 color channels. Consecutively, by using the sobel, each channel will be converted into grayscale image which will then be quantized and conducted texton detection as in the previous stage. This section will also be optimized in this research. Finally, a border histogram will be constructed.

#### c. Extraction of GLCM Feature

The third stage detects texture using GLCM method. The values which will be extracted through GLCM are energy, contrast, correlation and entropy. Finally, these three features will be incorporated into a 2-dimensional

matrix. This matrix will be used for the preparation of table indexing in image retrieval.

#### d. Re-Ranking KNN

In this study, the proximity between images is calculated using the same method as MTCD, that is modified canberra [16]. The main difference between this study and MTCD is that once the retrieval results are obtained, the KNN method will be applied to re-ranking so that it increases the precision value. Taking the first image of the retrieval result and rearranging the image based on the number of occurrences of most of the images having the same class is the first procedure. Afterwards, the precision value will be calculated by looking at  $r$ -value of the first image,  $r \leq K$ . The proposed redesign model is presented in Figure 2 (a). The first 2nd rank utilizes a B-categorized image.

If an A-class image is used as a query, so the precision value of the retrieval result is 0.67. With KNN, where, the image, with the most emerging class i.e. A image appearing 4 times, will be grouped into one, and placed in the top ranking. Therefore, this process will automatically shift the position of B image to the 5th position (Figure 2 (b)). In this way, the precision value will increase to 1.

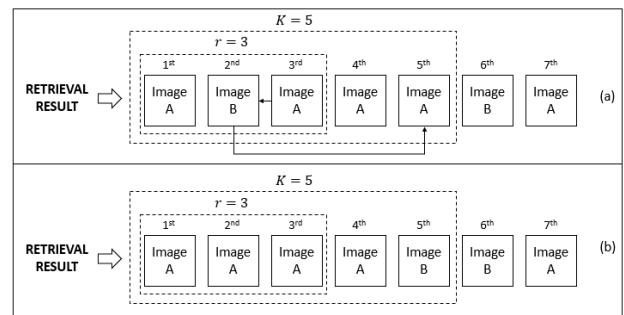


Figure 2. Re-ranking method on the retrieval results using KNN

## III. RESEARCH RESULT AND DISCUSSION

### A. Dataset

In this study, the dataset used consist of 2 types. The first dataset is 300 Batik images divided into 50 categories (each category has 6 pieces of image). This dataset is chosen because the image of Batik has a fairly complex and repeatable detail so that it is suitable for the application of the proposed method. The second dataset used in this study is Corel dataset. This dataset contains 10,000 images divided into 100 categories (each category contains 100 images). Unlike the first dataset which prioritizes the repetition of motifs, the categorization of corel images is based on the appearance of the same objects in an image. The example of categorization in corel dataset is categories of elephant, lion, church, fruit, vegetable, and so forth. It is a challenge to see how well the proposed method identifies the similarity of the objects which appear on two different images. Figures 1 and 2 show an example of the dataset image employed in this study.



Figure 1. Examples of Batik image dataset

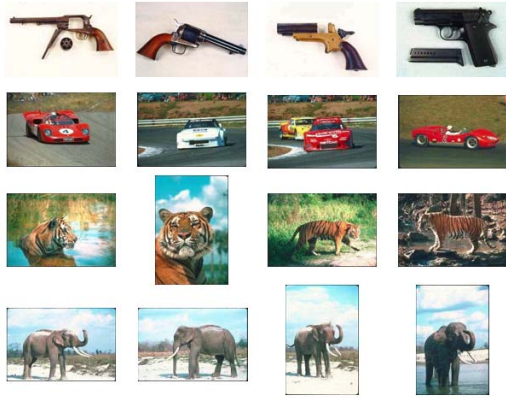


Figure 2. Examples of corel image dataset

In addition to the previously presented discrepancies, the other discrepancies between the two datasets are their dimensions. Batik datasets have the same dimension for all of its image, which is 128 x 128 pixels. As for corel dataset, there are image dimension of 126 x 187 (portrait) and also image dimension of 187 x 126 (landscape). The portrait or landscape image form actually does not affect texton search process, but because there is one dimension of odd value (187), so it needs to have special mechanism before texton search is implemented. This is because texton search is conducted by shifting in every 2 pixels, so if there is one dimension having odd value, there will be 1 row or 1 column that cannot be detected. Figure 3 (a) presents its example result, an image with dimension of 5 x 4. The 5th row cannot be detected by the system because the 6th row does not exist. Therefore, in this study, for any image whose number of rows /columns is odd, 1 additional row/column will be added with 0 for each element as presented in Figure 3 (b).

4	5	4	2
4	2	1	4
5	4	3	4
4	1	4	2
2	4	2	2

(a)

4	5	4	2
4	2	1	4
5	4	3	4
4	1	4	2
2	4	2	2
0	0	0	0

(b)

Figure 3. (a) Image having odd dimension; and  
(b) Additional row for image dimension completion

## B. Testing Results

The proposed method is built using the python programming language. Python is chosen because of the availability of the library to perform image retrieval. In this research, opencv library is used to perform image processing. As for calculating GLCM value, the skimage library is used.

This research uses MTCD method for feature extraction process of an image. This method will extract 3 main features, namely color, edge and texture. To extract color and edge features, Multi Texton Detection (MTD) method is employed. Meanwhile, to extract texture features, it uses GLCM method with specified parameters, energy, contrast, correlation and entropy.

Before applying color and edge extraction, an image will be quantized first. The quantization process is grouping the color ranges in an image into the  $n$  section (bit). In this study, the number of bits used for the color feature is 4 bits for each color channel. As for the edge feature, the number of bits used for is 18. The number of texton used is 6 pieces texton. This is in accordance with the previous research conducted by Minarno [16].

The contribution in this research is the application of KNN algorithm to increase precision value from MTCD method. The classification accuracy of the KNN method depends heavily on the value of  $K$ ; therefore, this study utilizes different  $K$  values for each test scenario. This study uses only precision value because in image retrieval, recall value can not be used as a reference to assess quality of a method. We can just get a high recall value by taking all the image in the database. Another reason is that the image retrieved is small (when compared to the total image overall), the recall value must be very low, so this value is not significant enough to be calculated.

Table 1. Results of precision testing on Batik images

r	K	Precision	
		MTCD	MTCD + KNN
3	5	0.990	<b>0.997</b>
	7	0.990	0.983
	10	0.990	0.977
	12	0.990	0.989
	15	0.990	0.989
4	5	0.980	<b>0.986</b>
	7	0.980	<b>0.983</b>
	10	0.980	0.972
	12	0.980	<b>0.982</b>
	15	0.980	0.980
5	5	0.964	0.964
	7	0.964	<b>0.972</b>
	10	0.964	0.964
	12	0.964	<b>0.970</b>
	15	0.964	<b>0.969</b>

In the first test, Batik image dataset is used as a test object. From each category in the dataset, one image is taken for data testing, and the rest is used as training data. Hence, it produces 50 images for data testing, and 250 images of training data. Each test image is used as a query and calculated precisely from the  $r$  image successfully

retrieved. The mean value of the precision value for each subsequent query will be obtained. This step is repeated as much as six times, so that each image which exist in a category has once become data testing. The precision value of the six tests will then be re-averaged. Table 1 shows that KNN method can increase the precision value of the MTCD method with the proper K value (this study uses 5 different K values). Although the increase recorded in the image of Batik is not very significant, the precision value of MTCD method itself is quite high.

From the test results, when  $r = 3$ , the proposed method can outperform MTCD method for one K-value (i.e. when  $K = 5$ ). Meanwhile, the other four K-values are lower than MTCD method. When the r-value is increased to 4, then there are three K-values which get a higher precision values (i.e. when  $K = 5$ ,  $K = 7$  and  $K = 12$ ). As for  $K = 10$ , the value is lower. Moreover, when  $K = 15$ , the value is the same as MTCD method. When the r-value is increased again to 5, the KNN can increase the MTCD precision value when  $K = 7$ ,  $K = 12$  and  $K = 15$ . As for  $K = 5$  and  $K = 7$ , the precision value is identical to those of MTCD, and none of the K-value results in lower precision values than those of the MTCD method. From this test, it can be concluded that the KNN algorithm can effectively increase the precision value if the value of r is higher. Unfortunately, for the dataset of Batik image, each category has only six pieces of image, if one image is functioned as query, then the remaining images in the database are only 5 images. Therefore, the maximum r-value can be tested only to  $r = 5$ .

Furthermore, in the second test, the image of the corel dataset is employed. In this test, 2 different scenarios are performed. The first scenario, from each category, one random image will be used as data testing, and the rest will be used as data training. Thus, there are 100 data testing and 9,900 training data are obtained. This step will be repeated as much as ten times, then the average precision value of each step will be calculated. Table 2 presents the test results obtained.

Table 2. Results of precision testing for corel dataset (100 data test)

r	K	Precision		Increment (%)
		MTCD	MTCD + KNN	
5	20	0.465	0.572	10
	50	0.465	<b>0.623</b>	<b>15</b>
	100	0.465	0.554	9
12	20	0.359	0.467	11
	50	0.359	<b>0.524</b>	<b>16</b>
	100	0.359	0.488	13

In this test, the r-value used is only two, i.e. 5 and 12. While the K-value used are three, namely 20, 50 and 100. Different r-values are intended to see the consistency of conclusions obtained in the previous test. The greater the r-value, the greater the increment of the precision. From this test, it is found that for  $r = 5$ , there is a precision increase of 15%. As for  $r = 12$ , there is a 16% increase in the precision. It proves that the conclusions obtained in the previous test also apply to this test. This test also obtains the result that

KNN method can increase the precision value of MTCD method for all K-values tested.

The next test scenario still uses the corel dataset. To make it different, there are 50 images taken from each category. Thus, it will get 5,000 data train and 5,000 test data. Moreover, the r-value used is 12. The testing scenario like this is also used by the previous research [16]. Table 3 presents the results of the precision testing obtained.

According to this test, the proposed method again outperformed MTCD method with varying increments, ranging from 5% to 9%. It depends on the K-value used. However, of all K-values tested, the proposed method is always superior.

Table 3. Results of the precision testing of corel dataset (5,000 data test,  $r = 12$ )

K	Precision		Increment (%)
	MTCD	MTCD + KNN	
<b>20</b>	0.288	0.348	6
<b>30</b>	0.288	0.369	8
<b>50</b>	0.288	<b>0.373</b>	<b>9</b>
<b>100</b>	0.288	0.344	5

#### IV. CONCLUSION

From the results of the tests performed, it can be seen that the re-ranking method by using KNN can improve the precision of the MTCD method. Moreover, in testing the parameter of r-value, the results show greater values leading to decreases in the precision value from the retrieval results. On the other hand, the increment of r-value will reinforce the KNN's influence in increasing the precision value of the retrieval results. It happens because the greater the r-value, the more likely the irrelevant image in the retrieval result will be higher. This is where the role of the KNN method is more noticeable because it will decrease the possibility by conducting re-ranking model. Meanwhile, the optimal K-value will be difficult to determine because it depends on the r-value used.

#### REFERENCES

- [1] Y. Rui, T. S. Huang, and S. F. Chang, "Image retrieval: Current techniques, promising directions, and open issues," *J. Vis. Commun. Image Represent.*, vol. 10, no. 1, pp. 39–62, 1999.
- [2] A. E. Minarno, A. S. Maulani, A. Kurniawardhani, and F. Bimantoro, "Comparison of Methods for Batik Classification Using Multi Texton Histogram," *TELKOMNIKA*, vol. 16, no. 3, 2018.
- [3] A. E. Minarno, Y. Minarko, and A. Kurniawardhani, "CBIR of Batik Images Using Micro Structure Descriptor on Android," *Int. J. Electr. Comput. Eng.*, vol. 8, no. 6, 2018.
- [4] Y. Munarko and A. E. Minarno, "HII: Histogram Inverted Index For Fast Images Retrieval," *Int. J. Electr. Comput. Eng.*, vol. 8, no. 5, 2018.
- [5] J. Huang, S. R. Kumar, M. Mitra, and W.-J. Zhu, "Image Indexing Using Color Correlograms," *U.S. Pat.*, vol. 2, no. 12, pp. 12–15, 2011.



- [6] B. Julesz, "Textons, the Elements of Texture Perception, and Their Interactions," *Nat.* 290, no. 5802, p. 91, 1981.
- [7] R. M. Haralick, "Statistical and structural approach to texture," *Proceeding IEEE vol 67 no 5*, vol. 67, no. 5, pp. 786–804, 1979.
- [8] A. K. Jain and A. Vailaya, "Image Retrieval Using Color and Shape," in *Pattern Recognition* 29, 1996, pp. 1233–1244.
- [9] Pradnyana, G. A., Suryantara, I. K. A., & Darmawiguna, I. G. M. (2018). Impression Classification of Endek (Balinese Fabric) Image Using K-Nearest Neighbors Method. *Kinetik: Game Technology, Information System, Computer Network, Computing, Electronics, and Control*, 3(3).
- [10] Syahrian, N. M., Risma, P., & Dewi, T. (2017). Vision-Based Pipe Monitoring Robot For Crack Detection Using Canny Edge Detection Method as an Image Processing Technique. *Kinetik: Game Technology, Information System, Computer Network, Computing, Electronics, and Control*, 2(4), 243-250.
- [11] G.-H. Liu and J.-Y. Yang, "Image Retrieval Based on the Texton Co-Occurrence Matrix," in *Pattern Recognition* 41, 2008, pp. 3521–3527.
- [12] G.-H. Liu, L. Zhang, Y.-K. Hou, Z.-Y. Li, and J.-Y. Yang, "Image Retrieval Based on Multi-Texton Histogram," in *Pattern Recognition* 43, 2010, pp. 2380–2389.
- [13] G. H. Liu, Z. Y. Li, L. Zhang, and Y. Xu, "Image retrieval based on micro-structure descriptor," *Pattern Recognit.*, vol. 44, no. 9, pp. 2123–2133, 2011.
- [14] G.-H. Liu and J.-Y. Yang, "Content-based image retrieval using color difference histogram," *Pattern Recognit.*, vol. 46, no. 1, pp. 188–198, 2013.
- [15] A. E. Minarno, Y. Munarko, F. Bimantoro, A. Kurniawardhani, and N. Suciati, "Batik Image Retrieval Based on Enhanced Micro-Structure Descriptor," in *Computer Aided System Engineering (APCASE)*, 2014, vol. 1, no. Feb, pp. 65–70.
- [16] A. E. Minarno, & N. Suciati, "Image Retrieval Using Multi Texton Co-Occurrence Descriptor". *Journal Of Theoretical & Applied Information Technology*, vol. 67, no. 1, 2014.

# Human Detection using Aggregate Channel Features with Kalman Filtering Image Processing Using Raspberry Pi Camera for Switching Operations of Electrical Appliances

Ramon G. Garcia<sup>1</sup>, Glenn O. Avendaño<sup>2</sup>, Roland Clark Llanes<sup>3</sup>, Patrick Joseph Santos<sup>4</sup>, Mark Angelo Torres<sup>5</sup>, John Jason Zaballero<sup>6</sup>

*Department of Electrical, Electronics, and Computer Engineering  
Mapúa University*

*Intramuros, 1001 Manila, Philippines*

{rgarcia<sup>1</sup> & goavendano<sup>2</sup>}@mapua.edu.ph & {rcsllanes<sup>3</sup> & pjsantos<sup>4</sup> & mantorres<sup>5</sup> & jjmzaballero<sup>6</sup>}@mymail.mapua.edu.ph

**Abstract**— In this paper, Kalman Filter is used to further increase the detection speed of aggregate channel features for human detection image processing. An increase of 83.07% in detection time was observed during the tests. The combined algorithm is then programmed in the Raspberry Pi Microcontroller and camera for the switching on and off operations of electrical appliances. The automation of switching on and off operations of electrical appliances, specifically aircon and lights lead to 18.60% savings in energy. Accuracy tests also show that the combined algorithm has high level of accuracy for human detections.

**Keywords**— *Aggregate Channel Features, Kalman Filtering, Algorithm, Raspberry Pi*

## I. INTRODUCTION

Energy is the ability to do work which is a basic necessity for people. Energy, these days are limited due to the overwhelming consumption which lead to conserving it. In the late 2012, the European Union started to prepare for a potential energy crisis due to their gas supplies that diminished by 30%. Energy conservation is a process of reducing energy consumption by lessening energy service. One type of energy is electricity. Electricity supplies devices, appliances and technologies with an energy for people to work. Many people tend to forget to turn off their appliances due to work and other stuff. Which leads to a large amounts of electricity consumption which cause a waste of electricity and danger due to the appliances overheating. In April 2015, the Bureau of Fire Protection in Davao City reported a fire incident wherein 42 houses and business establishments were razed due to an unattended electric fan that overheated and electrical shorted the circuit. To ease the danger of overheating appliances, the automation of appliances may be applied which can avoid casualties.

Human detection has been an essential improvement on technology that can be implemented for video surveillance. One of the researchers like Rodrigo F.S.C Oliveira et al (2016) conducted a research on human detection on digital videos using motion feature extractors wherein they reduced the false positive detection rate of the algorithm Aggregated Channel Features (ACF). Using motion feature extractors like Motion Boundary Histogram (MBH), Internal Motion Histogram Central Difference (IMHcd) and Weak Stabilized Temporal Difference (WSTD) will improve the detection accuracy and mitigate false alarm emissions which are critical to human detector employment in most of the real-world application. Later on, there were some researchers who developed algorithm on motion detection to determine if there were activities happening. Dr.Virendra Shete et al (2016) proposed a research about a monitoring system that detects motion of any moving object especially humans, and then the CCTV will only start recording video once there is the presence of movement. The algorithm used in their research is the background subtraction that calculates the differences consecutive image. The purpose of their research is to prevent wastage of memory to help the CCTV to record only the area with activities. The research also includes IOT based image processing that allows data to be transferred to any remote server. Cyrel O. Manlises et al introduced a Real-time Integrated CCTV using Face and Pedestrian Detection Image Processing Algorithm for Automatic Traffic Light Transition that uses the viola-jones algorithm which is commonly used for face and pedestrian detection with an accuracy of 90%. The study helps the researchers by introducing image processing for automation of devices such as traffic lights. This study also introduced Python, a powerful programming application that is used for image processing which will be used by the researchers for the programming of their system.

In the past studies, Kalman Filtering and ACF are used as an algorithm separately. In this study, a Raspberry Pi is used for the human detection done by using image processing which uses both Kalman filtering for motion detection and

ACF for human detection as an algorithm; it will also integrate a control system for the automation of appliances, specifically the lights and air-condition units. The proposed system is allocated to be implemented in an office type of environment with space of around 13 square meters in area which at present still implements the manual system. The proposed system will determine the difference in energy consumption between a room installed with the system and a room without the system installed. Furthermore, it incorporates an alarm system that triggers if the system detects an intrusion at a certain range of time, specifically non-office hours thus, enhancing the security level of the room.

The general objective of the study is to implement Human Detection using Aggregate Channel Features (ACF) with Kalman Filtering Image Processing with control system that triggers when a human is detected, and specifically aims for an office or classroom type environment. Specifically, it aims (1) to incorporate human detection algorithm using Aggregate Channel Features for human body recognition and Kalman Filtering Image Processing for human motion detection on a Raspberry Pi Camera module; (2) to implement control measures that will execute appropriate switching actions for lighting and air-conditioning units; and (3) to determine the energy consumption of the system with and without the automation of appliances.

The significance of the study is to further improve the detection time of ACF in human and motion detection image processing by integrating Kalman Filter in the algorithm. The combined algorithm will be then used for the automation of electrical appliances, such as lights and air-condition units thus, eliminating the need of a personnel to manually turn on and off the appliances used which leads to energy savings and effort in the part of personnel. Moreover, the system will also increase the security in the room by integrating an alarm system wherein the alarm will produce a sound when the presence of a human is detected during non-office hours.

The study aims at improving the detection time of ACF in human and motion detection image processing by integrating Kalman Filter in the algorithm. The system focuses on monitoring human presence for switching on and off operations of electrical appliances. Raspberry Pi camera, and micro-controller are employed for the switching on and off operations. Furthermore, energy consumption of the system is also an objective of this study which prompted the researchers to test the system in an office type of environment. Two tests were conducted, one with the system running and another without the system running. To further validate the results, each test was run for a period of 5 days each to simulate the regular working days. The study is limited in an office room setup of 13 square meters with the basic office objects inside. A controlled time table for the movement of persons inside was also followed for the energy consumption test. The study is also limited to some basic electrical appliances found in the office, specifically a 10-watt LED bulb and a  $\frac{3}{4}$  Hp aircon were used.

## II. METHODOLOGY

### A. Conceptual Framework

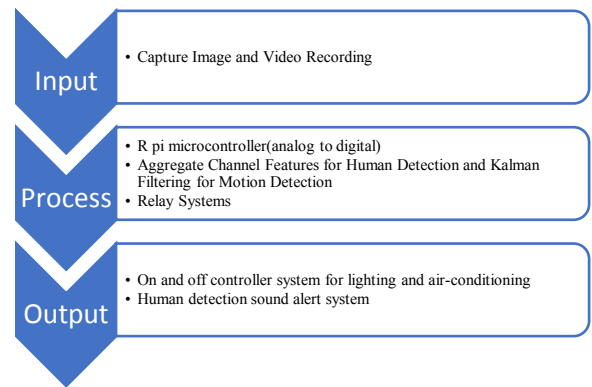


Figure 2.1: Conceptual Framework

The process of the detection of human presence and movement is shown in Figure 3.1. Here, the researchers will design a system utilizing a NOIR R Pi camera module. A Raspberry Pi is employed to the system for the conversion of light into binary numbers. This binary numbers will then be used by the ACF and Kalman filtering image processing for detection of presence and movement of human system. The system will also integrate a relay system for the switching on and off the light and air-condition. A buzzer is also used for additional security that will trigger only if the system detects a presence of human at a certain range of time.

### B. System Flowchart

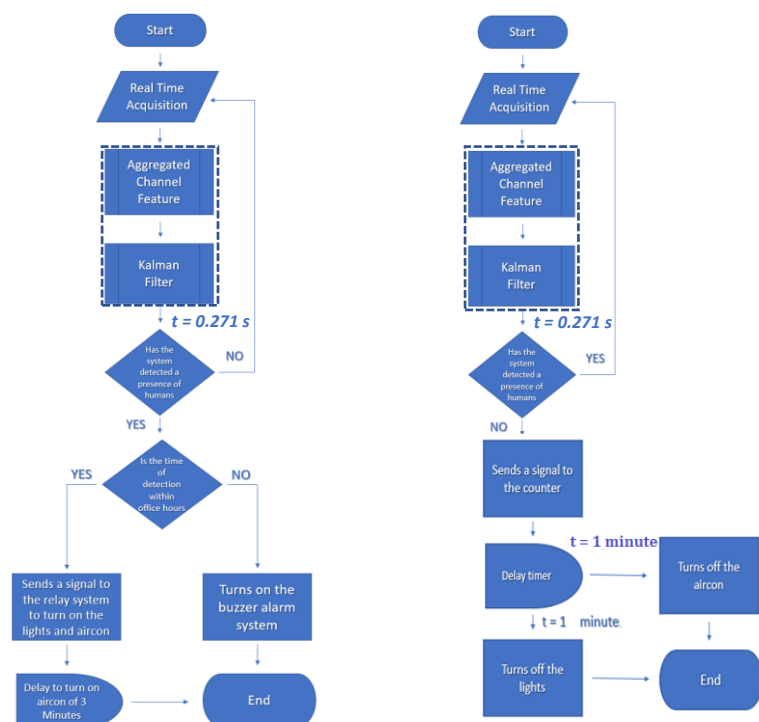


Figure 2.2: System flowchart when lighting and air-conditioning is turned off. (left) and system flowchart when lighting and air-conditioning is turned on. (right)

First, the image and video recording input will be processed in the Aggregate Channel Feature. The ACF commonly involved a Normalized Gradient Magnitude, which is used to extract information from images, the Histogram of Oriented Gradients, which used width and height or image shape for extracting information and last the LUV color channels, which is used to extract a grey image from the captured image. These three processes of image gradient will be used to create the feature vector which is used for human detection. Then the feature vector will be processed in the Kalman filter. The Kalman Filter is a set of mathematical equations that provides an efficient computational (recursive) solution of the least-squares method. The researchers used Kalman Filter for motion detection of humans. The Kalman filter process involves the measurement and time process. The measurement process will be used for computing the actual motion happening while the time update is used to predict the next state of the human moving. If the system has not detected a human, the system will loop back at the capturing process when it has detected a human, the system will move in determining the time of detection. When the time detected is within the office hours, the relay will be activated opening the lights and air conditioning unit while if the time is not within the office hours then the control system for security alarm is turned on.

### C. Block Diagram

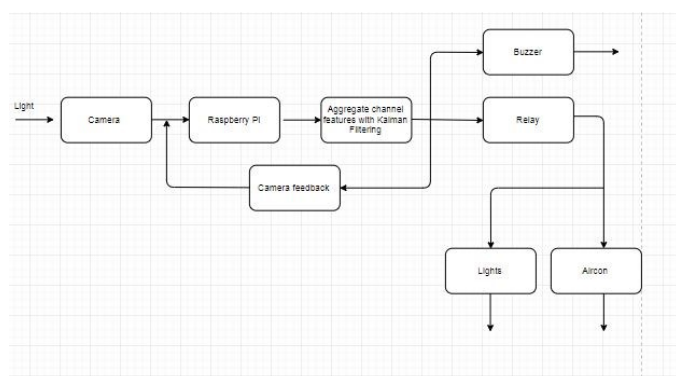


Figure 2.3: Block Diagram of Prototype

This shows the block diagram for the Human Processing using Aggregate Channel Features using Kalman Filtering Image Processing. The system uses a raspberry noir camera, a camera using infrared light for night vision. The input is captured by the noir camera, and which is the captured image and video recordings. Then the data will be processed by using Aggregate channel features and Kalman filtering. Then the system will be divided to two functions, specifically the on and off controller system and the human detection security alert system. The on and off controller system will only be activated in the assigned time serving as an office hour and the air conditioner and light will be relayed while the sound alert system will be activated in the assigned time serving as a non-office hour.

### D. Calibrations

The system will be tested in four ways for calibration. The test will involve camera position, the height of the subject person, position of the subject person, and calibration based on office objects. The position of the camera will be tested using five chosen position within the proposed room set-up which will ensure the most efficient position for the camera.

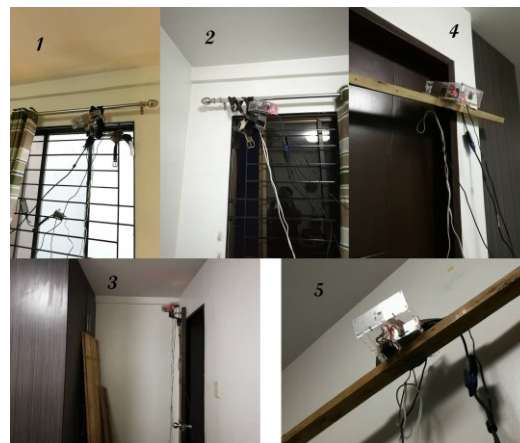


Figure 2.4: Proposed Camera Positions

The camera will be positioned inside the proposed room as shown in figure 2.4. There are five trials in the test. The test will start by guiding three people in the proposed room set-up with the camera in the first position and observing the number of person detected by the system. Then the modal value and the difference are computed. To find the best camera position, the least difference computed will be the best position.

Calibration Based on Camera Position								Difference
Position	No. Of Persons	Control System Status (Number of Trials)					Modal Value	
		1	2	3	4	5		
1	3	3	3	3	3	3	3	0
2	3	2	2	2	2	2	2	1
3	0	0	0	0	0	0	0	0
4	0	0	0	0	0	0	0	0
5	0	0	0	0	0	0	0	0

Table 2.1: Calibration Based on Camera Position



Figure 2.5: Camera View in chosen positions

As shown in Figure 2.5, position 1 is better than position 2 since in position 1, the camera has detected exactly the number of person inside the proposed room which is shown by the green boxes in the feedback video. Moreover, there is an obstruction on the point-of-view of position 3. Therefore, it was automatically neglected. Positions 4 and 5 were also not chosen since the camera does not have a good view of the office.

The distance of the subject from the camera will be tested to ensure that the distance between the subject and the position of the camera will not affect the detection of the system. First, the subject will be position 1 meter away from the camera. Then each position will be tested in five trials if the system detects the subject by observing the on-off controller in the system. After the trials, the modal value of the system is observed. The process will be repeated in the last two positions, 2 meters and 3 meters away from the camera. The parameter calibrated will be the HOG features of the ACF algorithm which focuses on dimensions and shape of the subject.

Calibration Based on Subject Distance								System Control Off Test
Subject	Distance (m)	Control System Status (Number of Trials)					Modal Value	
		1	2	3	4	5		
Humans	1	On	On	On	On	On	On	Yes
	2	On	On	On	On	On	On	Yes
	3	On	On	On	On	On	On	Yes

Table 2.2: Calibration Based on Subject Distance

The height of the subject is tested to ensure that the height of the subject will not obstruct the detection capabilities of the system. The detection capabilities of the system will be tested by observing the on-off controller of the system. There will be 5 trials in the test. After the trials, the modal value of the results will be observed. The parameters that will be calibrated will be the HOG features of the ACF algorithm which focuses on the dimension and shape of the subject.

Calibration Based on Height								System Control Off Test
Subject	Height (ft)	Control System Status (Number of Trials)					Modal Value	
		1	2	3	4	5		
1	2'5	On	On	On	On	On	On	Yes
2	5'	On	On	On	On	On	On	Yes
3	5'1	On	On	On	On	On	On	Yes
4	5'5'	On	On	On	On	On	On	Yes
5	5'6	On	On	On	On	On	On	Yes

Table 2.3: Calibration Based on Subject Height

The office objects will be tested to ensure that the system will not distinguish the subject as a human being. Some objects that can be seen inside the office will be used to determine if the system will detect it as a human being or not.

Calibration Based on Office Objects							
Subject	Control System Status (Number of Trials)					Modal Value	System Control Off Test
	1	2	3	4	5		
Electric Fan	Off	Off	Off	Off	Off	Off	Yes
Lamp Shade	Off	Off	Off	Off	Off	Off	Yes
Computer Chair	Off	Off	Off	Off	Off	Off	Yes
Table	Off	Off	Off	Off	Off	Off	Yes
Small Cabinet	Off	Off	Off	Off	Off	Off	Yes

Table 2.4: Calibration Based on Office Objects

### E. Accuracy test

The accuracy test is for the human detection and motion detection capabilities of the system. This will ensure that the density of the subject will be detected accurately even if the subject is moving or in rest.

Accuracy							Percent Difference
Actual Number Of Person	1	2	3	4	5	Modal Value	
1	1	1	1	1	1	1	0
2	2	2	2	2	2	2	0
3	3	3	3	3	3	3	0

Table 2.5: Accuracy Test

*F. Detection time test*

The detection time test is used to verify if the detection time of the system increased by combining the two algorithms: ACF and Kalman filtering. First, a person will be guided in front of the raspberry pi noir camera then the program will send a measured time for human detection. There will be fifty trials in this test. After the trials, the average detection time will be computed and compared to the reference HOG + Kalman filter algorithm detection time.

Detection Time Test for ACF with Kalman Filtering	
Trial	Time of Detection (s)
1	0.240717
2	0.246077
3	0.353187
4	0.282697
5	0.24069
6	0.275196
7	0.285123
8	0.24169
9	0.280983
10	0.285557
11	0.241787
12	0.281934
13	0.24084
14	0.249491
15	0.242662
16	0.242636
17	0.251199
18	0.263446
19	0.242759
20	0.242328
21	0.289313
22	0.342737
23	0.250601
24	0.342023
25	0.343713
26	0.245951
27	0.340895
28	0.240533
29	0.242359
30	0.24292
31	0.242718

32	0.263533
33	0.256484
34	0.240169
35	0.241004
36	0.359399
37	0.282693
38	0.241469
39	0.279022
40	0.285767
41	0.242145
42	0.283253
43	0.287366
44	0.25339
45	0.253873
46	0.255474
47	0.359583
48	0.255306
49	0.254331
50	0.295456
Time of Detection Average (s)	0.27088958
Time of Detection from HOG + Kalman of Chang Li [5]	1.6 seconds
Percent Difference	83.07

Table 2.6: Accuracy Test

*G. Energy Consumption Testing*

The energy consumption test is to know if the automation of the lights and aircon will lead to the less consumption of electricity. The test will involve a measure of the power consumption of the proposed room with and without the system. The energy consumption will be measured using the electricity meter in the building of the proposed room.

Day	Measured Energy Consumption (KWh) Without the system	Measured Energy Consumption (KWh) With the system
1	9KWh	7KWh



2	9KWh	8KWh
3	8KWh	6KWh
4	8KWh	7KWh
5	9KWh	7KWh
Total	43KWh	35KWh
Difference	8KWh	
Percent Difference	18.6047 %	

Table 2.7: Energy Consumption Test

### III. CONCLUSION

In this study, the researchers were able to design and develop a device that can detect a human being and can send a signal to the relay to turn-on the lights and air-conditioner and to sound an alarm through a buzzer. The system is calibrated to fully utilize the system detection capabilities. The simulated office has an area of 13 square meters. Based on the calibrations, position 1 is the best which can accommodate and cover the room. The Aggregate Channel Features with Kalman filtering is integrated on the system for human and motion detection. The combined algorithm enhanced the speed of detection by 83.07% which was equivalent to 1.33 second faster. The control measures to execute appropriate switching action is incorporated by using materials that has a current rating above 7A to support the air conditioner. The energy consumption of the system is determined to be energy efficient which is proven by using manual computations. The system consumption is about 0.0576 KWh. By using a controlled environment for five days, the energy conserved by using the system is about 18.6047% which translates to 8 KWh saved in five days.

### IV. RECOMMENDATION

To further the study on the system; future researchers may overclock the Raspberry Pi which will improve the microcontroller's computation capability. Overclocking it may also improve its response time. A solid-state relay is also recommended to eliminate the delay of the electromechanically relay. The algorithm also may be combined with other algorithm and may be used with other industrial and automation control for further study.

### REFERENCES

[1] Shah M E Haque. "Human Detection in Surveillance Videos and its Applications". Australia, EURASIP Journal on Advances in Signal Processing., 2013

[2] Sulman N, Sanocki T, Goldgof D, Kasturi R. "How effective is human video surveillance performance?" In 19th International Conference on Pattern Recognition, (ICPR 2008)Piscataway, 2008

[3] P. Chong, Y. H Tay. "A Novel Pedestrian Detection and Tracking with Boosted HOG Classifiers and Kalman Filter" 2016 IEEE Student Conference on Research and Development (SCORED). IEEE, 2016

[4] Jie Zhao, Wei-Jing Liu, Hui-Jia Sun. "A Motion Tracking Method Based On Kalman Filter Combined With Mean-Shift", Proceedings of the 2008 International Conference on Wavelet Analysis and Pattern Recognition, Hong Kong. IEEE, 2008

[5] Changyan Li, Lijun Gui, Yuchen Hu. "A New Method Combining HOG and Kalman Filter for Video-based Human Detection and Tracking", 2010 3rd International Congress on Image and Signal Processing. IEEE, 2010

[6] Prof. Luigi Piroddi, Prof. Marco Targliasacchi. "Pedestrian Detection and Tracking in Low Quality Images with Deep Neural Networks", 2015 pp. 34-35

[7] Rodrigo F. S. C. Oliveira, Carmelo J. A. Bastos-Filho. "Human Detection in Digital Videos Using Motion Features Extractors", 2016 IEEE Latin America Conference on Computational Intelligence (LA-CCI), 2016

[8] Moving Object Detection Using Background Subtraction by S.H. Shaikh 2014 pg 2-5

[9] T. Kokul, A.Ramanan , U.A.J Pinidiyaarachi."Online Multi-person Tracking by Detection Method using ACF and Particle filter". 2015 IEEE Seventh International Conference on Intelligent Computing and Information Systems (ICICIS'15). IEEE, 2015

[10] Virendre V Shete, Niraj Ukende. "Intelligent Embedded Video Monitoring System For Home Surveillance", 2016 International Conference on Inventive Computation Technologies (ICICT). IEEE, 2016

[11] A. Niranjil Kumar, Dr. C Sureshkumar. "Background Subtraction Based on Threshold Detection Using Modified K- Means Algorithm". Proceedings of the 2013 International Conference on Pattern Recognition, Informatics and Mobile Engineering, IEEE, 2013

[12] Hasan Sajid and Sen-Ching Samson Cheung. "Background Subtraction For Static and Moving Camera". Image Processing (ICIP), 2015 IEEE International Conference, 2015

[13] Shu Chang, Xiaqing Ding, Chi Fang. "Histogram of the Oriented Gradient for Face

[14] Kostas Daniilidis and Petros Maragos, "Computer Vision ECCV 2010", 11th European Conference on Computer Vision , Heraklion, 2010, pg 172

[15] "Raspberry Pi Power Consumption Benchmarks" Raspberry Pi® User Guide (2017):

[16] Haier Room Airconditioner Manual (2011) HWR05XC7Manual

[17] Frigidaire Use & Care of Air-Condition (2009)

[18] Amana Package Terminal Air-Conditioner installation instructions & owner's manual (2017)

[19] "The Raspberry Pi Camera Module." Raspberry Pi® User Guide (2017): 223-35.

[20] Cyrel O. Manliseset "Real-time Integrated CCTV using Face and Pedestrian Detection Image Processing Algorithm for Automatic TrafficLightTransition"Humanoid,Nanotechnology,InformationTechnology,Communication and Control, Environment and Management (HNICEM), International Conference , 2016

[21] "Office Space Guidelines" Office Space Guidelines (2018): Web.

# Automatic Estimation of Human Weight From Body Silhouette Using Multiple Linear Regression

Hurriyatul Fitriyah, Gembong Edhi Setyawan  
Computer Engineering, Faculty of Computer Science  
Universitas Brawijaya  
Malang, Indonesia  
hfitriyah@ub.ac.id, gembong@ub.ac.id

**Abstract**—Estimating weight based on 2D image is advantageous especially for contactless and rapid measurement. Several researches used additional thermal camera or Kinect camera, required subjects to do front and side pose and manually extract body measures. This research propose an algorithm to estimate body weight automatically using 2D visual image where subject only do front pose. This research studied 4 features of body measures which are: (F1) height, and width of (F2) shoulder, (F3) abdomen/waist plus arm, (F4) feet. Each feature was simply subtracted based on body proportion where normal body has 8 equal segments. Shoulder is in 2nd segment, abdomen/waist is in 4th segment and feet is in the last segment. Multiple Linear Regression is used to determine weight estimation formula of all combination of 4 features, 15 in total. The highest significance  $R^2$  (0.80) and RMSE 2.68 Kg is given when using all 4 features in the estimation formula.

**Keywords**— *Body weight, Silhouette, Image processing, Multiple Linear Regression*

## I. INTRODUCTION

Image have been used to estimate variables such length, height, distance and area. The estimation required the algorithm to set a pixel-to-cm ratio beforehand. Camera has promoted a non-contact estimation that is essential in non-destructive measurement. It also enable a remote estimation or analysis.

Moreover, researcher has extended the measurement into indirect variables such volume and weight. The estimation basically utilize length or area which then calculate those indirect variables using regression, formulae or an artificial intelligence algorithm.

Research by [1] has uniquely measure volume of a food bowl using cutleries as reference. A pair of chopstick where each was placed on top of the container and on table is proposed to measure its height. Diameter of the container was estimated based on comparison to the actual length of chopstick that was placed on top. Once its diameter and height is estimated, volume of container was calculated using volume of spherical cap formulae.

A volume estimation using image also has been proposed by [2] to measure volume and mass of citrus fruits. The volume is measured in assumption that the fruit was constituted from several elliptical frustums. Each frustums's volume is calculated based on two diameters that was pictured by two cameras in perpendicular arrangement. The mass was measured using correlation formulas between volume to its actual mass and showed high correlation.

The correlation formulas between body traits and body weight has also been proposed by [3]. The research used lateral body surface (BSS) of rabbits to estimate Live Weight (LW) and Carcass Weight (CW) through regression method. Research by [4] investigated 23 indexes from various body surface measure (weight, height, area, difference) of cattle's thorax, abdomen, chest, dorsal and body. A linear regression was also used to find formulas between body weight and the indexes. The research found 6 formulas that has high correlation.

Another recent study that use a regression to estimate weight using anthropometry measurement was suggested by [5]. It used various of regression which were Linear regression, Support Vector Regression, Gaussian Process Regression and Neural Network Regression. The highest accuracy was given by circumference of waist, buttock, thigh and arm, height, gender and ethnicity with confidence interval of 98% with limits of 1.80 Kg and 2.25 Kg when using Gaussian process Regression. The study was used the National Health and Nutrition Examination Survey (NHANES) and US. Army Anthropometry Survey.

The object's weight estimation through image analysis is a helpful method for example when the object are hard to be moved. In emergency room, moving patients to normal scale for weight measurement are mostly harmful to their condition. Whilst weight measurement is essential for calculating dosage of drugs given [6]. Thus research by [7] proposed a bedside weight estimation from abdominal and thigh circumference. The formula for Actual Body Weight (ABW) of male and female are determined by multiple linear regression that was evaluated by correlation for the best formula.

In weight estimation of human body, [8] also investigated 127 combinations ( $2^7-1$ ) from 7 body measures which were height, upper-leg length, calf circumference, upper-arm length, upper-arm circumference, waist circumference, upper leg circumference. The combinations result formulas that was determined using least square method. This study also proposed to use 2D image of human front and side portrait. Since 2D image could not measure circumference, the study propose to measure the width as an equal to diameter of a cylindrical approximation. The study also suggested to take out measurement of calf as this part was poorly affected by loose clothing which hid the actual body measures. List of body surface measures that have been proposed by several researches are shown in Table 1. Those

measures gives insight to what have worked out to estimate human body weight.

All above methods to estimate weight of human body was performed manually in 2D images. Operators still have to count pixels for height, length or circumference manually using visual. In this research, an automatic weight estimation was developed. The developed method would be beneficial for non-contact and computerized measurement of body-weight. The implementation is numerous. It can be applied in health service, public place, surveillance, intruder detection or even for casual implementation in mobile application.

TABLE I  
LIST OF BODY SURFACE MEASURE FOR WEIGHT ESTIMATION

Reference	Body Surface Measure
Giles N Cattermole, et. al., 2016 [9]	Middle-Arm Circumference (MAC)
Robert G. Buckley, et. al., 2011 [7]	– Abdominal Circumference (AC) – Thigh Circumference (TC)
Carmelo Velardo, et. al., 2010 [6]	– Height – upper-leg length – calf circumference – upper-arm length – upper-arm circumference – waist circumference – upper leg circumference
Ana Paula Ferreira melo, et. al., 2014 [10]	Man: – arm circumference – abdominal circumference – calf circumference Women: knee height

The research used only measure of body part that was not affected by loose clothing as suggested by [9]. The actual body weight was measured by normal scale. Each variables were extracted automatically using image processing algorithm. This research utilizes visible light camera, rather than Kinect or thermal camera as in [10] and [11]. The visible light camera is cheaper and simpler to operate.

## II. METHOD

Since the estimation algorithm uses 2D RGB image where people using their regular clothing, body measure chosen should mind this condition. Loose clothing could give additional width to horizontal measures. Hence people were asked to pose straightly towards camera, lay their both hand closely to their body, and stick their leg and feet closely during data acquisition.

Top outfits such shirt or blouse does not add additional width when the arm are placed tightly to the body. Hence horizontal measure in the upper body part such waist or abdominal plus the attached arm in Table 1 were used as features. Arm by itself were not used as features since it is tedious to be segmented as it stick to body. Shoulder horizontal measures also added to feature list as its width is rarely affected by clothing. Nevertheless, a very loose or puffy clothing should be avoided during data acquisition since it would show longer width of shoulder and waist/abdomen even though the arm was placed tightly to the body.

Bottom outfits such trouser and skirt sometimes appears to be loose even when leg were stick closely. Hence horizontal measures in the lower part of body such thigh, upper-leg, calf as in Table 1 were taken out from feature list.

Nevertheless, ankle most of the time shows original width even when the person were wearing foot covers. Height as in Table 1 is used as feature since vertical measure is not affected by clothing. Features for weight estimation using 2D images that was proposed in this study is listed in Table 2.

TABLE II  
LIST OF BODY SURFACE MEASURE FOR WEIGHT ESTIMATION  
IN THIS RESEARCH

F1 Height
F2 Shoulder width
F3 Abdomen/waist plus attached arm width
F4 Feet Width

### A. Features Extraction Using Body Proportion

Distance between person and camera were fixed to 2 meters to ensure standardized pixel size. This research simply used human body silhouette as input. Height is distance between the highest and lowest vertical coordinates of human body silhouette.

To locate shoulder, abdomen/waist plus arm and feet, a human body proportion were used. In normal human, the body is divided into 8 equally vertical segments where shoulder is located in second one-eighth segment, abdomen/waist plus attached arm is located in fourth one-eighth segment, and feet is in lowest one-eighth segment [12]. First and second body feature were assumed to be the largest width in each segment, whilst the third body feature was assumed to be the narrowest in the segment. Figure 1 show the eight segments drawn over an example of human body and its respective features. The border of each segment is shown as line, body features are shown in bolder white line.

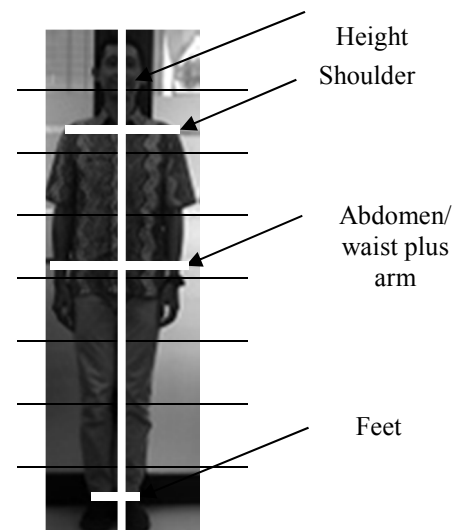


Fig. 1 Eight segments of body part and location of features

The suggested method is simple to implement and require minimum computation. Width of each vertical coordinates were calculated as distance between minimum and maximum horizontal coordinates of the body's edge. The widest width was calculated as maximum of distances in its segment, whilst the narrowest width was calculated as minimum of distance in its segment. The pseudocode for feature extraction is shown in Figure 2.

**Input** human body silhouette  
 Divide silhouette into 8 equal horizontal segments  
 For each segment  
     Count white pixel's width in every rows  
 End  
 Determine shoulder's width as the widest white pixel in 2nd segment  
 Determine abdomen/waist plus arm's width as the widest white pixel in 4th segment  
 Determine leg's width as the narrowest white pixel in 8th segment  
**Output** width of shoulder, abdomen/waist, leg

Fig.2 Pseudocode for feature extraction

### B. Weight Estimation using Multiple Linear Regression

A Multiple Linear Regression predicts future outcome by determining the trend of existing data that has multiple inputs. It assumes that the data has linier trend between inputs and output. The equation for multiple regression is in Equation 1, where  $i$  is number of data,  $b_0$  is regression intercept,  $b_j$  is  $j$ -th predictor's regression slope,  $x_{ij}$  is  $j$ -th predictor for the  $i$ -th observation.

$$Y_i = b_0 + \sum_{j=1}^n b_j x_{ij} \quad (1)$$

The predictor's regression intercept and slope  $b$  is calculated using matrix of predictors  $x$  and actual outputs  $y$  using Equation 2.

$$b = (x^T x)^{-1} x^T y \quad (2)$$

Multiple linear regression from all combination of 4 measures to body weight were investigated. The total combination is 15 as a power-set of 4 minus the null set ( $2^4 - 1 = 15$ ). A coefficient of determination,  $R^2$  was used to measure how well the regression to fit the data. It is a measure of sum-squared of residual (error of estimation) compare to proportional variance of predictors. The value range from 0-1 where the best fit of regression has value of one and the worst is zero. It is calculated using Equation 3.

$$R^2 = 1 - \frac{\sum_{i=1}^n (y_i - \hat{y}_i)^2}{\sum_{i=1}^n (y_i - \bar{y})^2} \quad (3)$$

### III. RESULT AND ANALYSIS

The algorithm was tested in 10 adults male. Some images of human body silhouettes are shown in Figure 3. The silhouettes were made by performing segmentation on human body from its background.

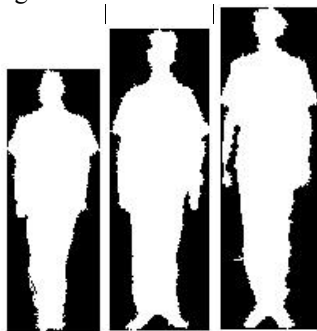


Fig. 3 Some images of human body silhouette

Body features from each silhouette was then extracted using the developed method where the result is shown in Table 3. Each is in standardized pixel unit.

TABLE III  
BODY FEATURE FROM DATA

No	F1	F2	F3	F4	Actual Weight (Kg)
1	176	52	53	15	70
2	192	48	57	26	71
3	192	51	59	20	76
4	197	52	48	19	81
5	198	54	54	17	67
6	209	54	55	16	58
7	194	52	54	22	78
8	185	48	58	21	60
9	200	51	52	15	65
10	197	53	57	25	85

Each feature's correlation coefficient towards actual weight,  $r$ , was calculated. The correlations were tested to check which feature has more similar trend towards actual weight. The rule of thumb in correlation is that  $r > 0.5$  means the correlation is strong. A strong correlation means a change in a feature would result a correct prediction in the actual weight. Although correlation cannot be interpreted as causation, the test can be used to test whether both variables fluctuate together. The result in Table 4 shows that only F4 has strong correlation with the actual weight.

TABLE IV  
CORRELATION BETWEEN FEATURE AND ACTUAL WEIGHT

No	Feature	$r$
1	F1	-0.07
2	F2	0.27
3	F3	-0.06
4	F4	0.54

A linear regression between feature F4 and actual weight are then calculated. It result a weight estimation formula of  $Weight = 47.45 + 1.2 F1$ . This formula was tested in all 10 silhouette and gave RMSE between actual and predicted weight of 6.18 Kg. Although the correlation is low, a weight estimation formula on feature F2 was also calculated. It result a formula of  $Weight = 11.97 + 1.15 F3$  and gave RMSE between actual and predicted weight of 7.15 Kg.

Since RMSE of using one feature is still high, a Multiple Linear Regression using all 15 combination of 4 features is performed. The result of each formula along with  $R^2$  (98% confidence interval) and its Root Mean Squared Error (RMSE) between actual and predicted weight is shown in Table 5.

As listed in Table 5, the highest  $R^2$  belongs to formula number 15 where all features were used in the regression. Formula (15), is then selected as the formula for estimating weight as it gives higher correlation. It uses feature of height, and width of shoulder, waist and feet. The RMSE is 2.68 Kg and the percentage error is 3.8% than the actual weight. The RMSE is similar to study in [5] which in the limit of 1.80 Kg and 2.25 Kg in CI 98%. Although the performance is slightly hinger, this study proposed an automatic and contactless

measurement compare to previous study that require a contact measurement that require longer time to collect all features.

The percentage error is also similar to estimation result conducted by [6] which was  $\pm 5\%$ . Although the performance is similar, but the proposed method in this study excel it since

it only use features from frontal pose of the body compare to study in [6] which use features from side and frontal pose. The plot of estimated weight and actual weight using Formula (15),  $\text{Weight} = -23.62 - 0.37 F1 + 3.34 F2 - 0.93 F3 + 2.33 F4$ , is shown in Figure 4.

TABLE V  
WEIGHT ESTIMATION FORMULA, ITS  $R^2$  AND RMSE

No.	Feature Used	Formula	$R^2$	RMSE (Kg)
1	F1	$\text{Weight} = 72.47 - 0.1 F1$	0.00	7.13
2	F2	$\text{Weight} = 11.97 + 1.15 F2$	0.07	7.44
3	F3	$\text{Weight} = 80.61 - 0.17 F3$	0.00	7.15
4	F4	$\text{Weight} = 47.45 + 1.21 F4$	0.29	6.18
5	F1, F2	$\text{Weight} = 28.30 - 0.18 F1 + 1.51 F2$	0.10	7.62
6	F1, F3	$\text{Weight} = 84.35 - 0.02 F1 - 0.18 F3$	0.00	7.16
7	F1, F4	$\text{Weight} = 41.77 + 0.03 F1 + 1.21 F4$	0.29	6.25
8	F2, F3	$\text{Weight} = 2.87 + 1.21 F2 + 0.11 F3$	0.08	7.43
9	F2, F4	$\text{Weight} = -105.12 + 2.71 F2 + 1.86 F4$	0.62	4.47
10	F3, F4	$\text{Weight} = 101.97 - 1.17 F3 + 1.68 F4$	0.43	13.46
11	F1, F2, F3	$\text{Weight} = 18.40 - 0.18 F1 + 1.57 F2 - 0.12 F3$	0.10	7.61
12	F1, F2, F4	$\text{Weight} = -82.34 - 0.35 F1 + 3.54 F2 + 2.01 F4$	0.71	3.19
13	F1, F3, F4	$\text{Weight} = 107.11 - 0.02 F1 - 1.18 F3 + 1.68 F4$	0.43	5.37
14	F2, F3, F4	$\text{Weight} = -51.20 + 2.48 F2 - 0.87 F3 + 2.16 F4$	0.69	3.96
15	F1, F2, F3, F4	$\text{Weight} = -23.62 - 0.37 F1 + 3.34 F2 - 0.93 F3 + 2.33 F4$	0.80	2.68

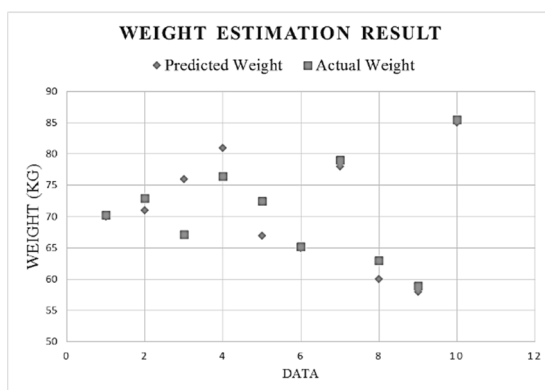


Fig. 4 Result of predicted and actual weight

#### IV. CONCLUSION

An automatic weight estimation using only frontal silhouette of human body has been proposed in this research. The features extracted was chosen where usually it is not be affected by daily clothing that could give additional width. The best estimation formula utilizes feature of height, width of shoulder, abdomen/waist plus arm and feet with high significance  $R^2$ . The developed algorithm enable estimation of human body weight using image that is non-contact and simple. Further investigation to estimate weight in various condition among ages, gender and ethnic should be carried out to test the algorithm in various body silhouette.

#### REFERENCES

- [1] Hippocrate and A. A. Elder, *Master Thesis. Food Weight Estimation Based on Image Processing for Dietary Assessment*, Nara Institute of Science and Technology, 2016.
- [2] M. Omid, M. Khojastehnazhand and A. Tabatabaefar, "Estimating volume and mass of citrus fruits by image processing technique," *Journal of Food Engineering*, vol. 100, pp. 315 - 321, 2010.
- [3] P. Negretti, G. Bianconi and A. Finzi, "Visual Image Analysis to Estimate Morphological and Weight Measurement in Rabbits," *World Rabbit Science*, vol. 15, pp. 37 - 41, 2007.
- [4] R. Gomes, G. Monteiro, G. Assis, K. Busato, M. Ladeira and M. Chizzotti, "Technical note: Estimating body weight and body composition of beef cattle through digital image analysis," *Journal of Animal Science*, vol. 94, p. 5414 - 5422, 2016.
- [5] Ratius, D. Fernandes, B.J. Roque, A. "Height and Weight Estimation From Anthropometric Measurements Using Machine Learning Regressions," in *IEEE Journal of Translational Engineering in Health and Medicine*, vol. 6, 4400209, 2018.
- [6] Dugelay, C. Velardo and J. Luc, "Weight estimation from visual body appearance," in *IEEE International Conference on Biometrics: Theory, Applications and Systems (BTAS)*, 2010.
- [7] R. G. Buckley, C. R. Stehman, F. L. Dos Santos, R. H. Riffenburgh, A. Swenson, N. Mjos, M. Brewer and S. Mulligan, "Bedside Method to Estimate Actual Body Weight in The Emergency Department," *The Journal of Emergency Medicine*, pp. 1 - 5, 2011.
- [8] C. Pfitzner, S. May and A. Nuchter, "Evaluation of Features from RGB-D Data for Human Body Weight Estimation," *IFAC-PapersOnLine*, vol. 50, no. 1, pp. 10148-10153, 2017.
- [9] G. N. Cattermole, G. C. A. and T. H. Rainer, "Mid-arm circumference can be used to estimate weight of adult and adolescent patients," *Emergency Medical Journal*, vol. 0, pp. 1 - 6, 2016.
- [10] A. P. F. Melo, R. K. deSalles, F. G. K. Vieira and M. G. Ferreira, "Methods for estimating body weight and height in hospitalized adults: a comparative analysis," *Brazilian Journal of Kinanthropometry and Human Performance*, vol. 16, no. 4, pp. 475 - 484, 2014.
- [11] J. Kongsro, "Estimation of pig weight using a Microsoft Kinect prototype imaging system," *Computer Electronic Agriculture*, vol. 109, no. C, pp. 32 - 35, 2014.
- [12] B. Bogin and M. I. Varela-Silva, "Leg Length, Body Proportion, and Health: A Review with a," *International Journal of Environmental Research and Public Health*, vol. 7, pp. 1047-1075, 2010.

# Variance and Symmetrical-based Approach for Optimal Alignment of 3D Model

Luh Putu Ayu Prapitasari, Parth Rawal and Rolf-Rainer Grigat  
 Vision Systems Institute  
 Hamburg University of Technology  
 Hamburg, Germany  
 Contact e-mail: putu.prapitasari@tuhh.de

**Abstract**—The concept of building 3D models, known as 3D reconstruction, already exists since the last few decades. However, by manually aligning the objects during acquisition phase does not guarantee that the output, the 3D models, will be perfectly aligned with the computer's world coordinate system. It mainly happens because in real world it is quite challenging to get perfect measurements, especially for the irregular objects. In this paper we address this problem by proposing a method to be used on the post processing phase of the 3D reconstruction process. The method is based on the variance and symmetry of the object's point cloud which is acquired during acquisition. For the evaluation, we applied and evaluated the proposed method to both synthetic and reconstructed 3D models. The results are significant and show that the method capable of aligning the models to a fine resolution of 1' (one minute) angle.

**Keywords**—3D models, Alignment, Variance, Symmetry, Reconstruction

## I. INTRODUCTION

Alignment of a 3D model in 3D reconstruction is an important task and usually done during acquisition or registration phase and later on, for the better output, another alignment procedure could also be done as part of the post processing task [1][2][3][4]. There may be several requirements or problems which arises to the need of aligning a 3D model. One such requirement is optimal dimension measurement from a 3D reconstructed model. In reality, it is almost impossible to align a 3D model to perfection during its acquisition in hardware-wise and some mathematical approaches are definitely required to align it to perfection. Our task is to align the 3D model, software-wise, after acquisition. The method in [5] describes dealing with Continuous Principal Component Analysis (CPCA) for models having two orthogonal symmetry planes passing through an axis and another tool called Local Translational Invariance Cost (LTIC) used when there exists only one or no plane of symmetry. However, our work uses another approach which is quite different from the one proposed in that paper. The unique feature which makes the approach proposed here special is that, there is no featured data such as normal, surface, faces or edges are required to execute the algorithm, which was necessary for the approach listed above. Moreover, unlike some other methods, such as Iterative Closest Point (ICP) [6], which require a reference to align a misaligned model, it is as well not the case in our work.

In the later sections, the working all the four methods in the entire process namely, translation, alignment by variance, alignment by symmetry and classification are described. Testing and evaluation are done in section 4 and in section 5 all the works are then summarized.

## II. CONDITIONS AND ASSUMPTIONS

Apart from the input datasets, there are a few important conditions, criteria and assumptions in the beginning which are important to know before starting the process.



Figure 1. Different objects to be aligned after 3D reconstruction. From top left to bottom right: cube, cylinder, triangle, owl, frog and two owls.

### 2.1. Object Lies on a Plane

The assumption made here initially is that the object lies on a rotating table. It means that there can be only 3 degrees of freedom possible theoretically for the misalignment cases, which are translation in  $X$ -axis and  $Y$ -axis and rotation in  $XY$  plane. In practice, it is possible that the table is not aligned with respect to ground or camera axis and small alignment along other 3 degrees of freedom are also possible. This means that the algorithm can align a model in 2 dimensions in a single implementation. If the object is not lying on a plane, the same algorithm could align it in 3 dimensions on being executed twice, i.e. first aligning along  $XY$  plane and then along  $XZ$  or  $YZ$  plane.

### 2.2. Model is Free from Outliers and Concentrated Noise

Since no information is available about the features of a reconstructed model, it is very important that all outliers and concentrated noise points are removed. If they exist, then it might affect the final alignment in respect to all 3 degrees of freedom.

### 2.3. Criteria and Assumption for Better Human Perception

The algorithms proposed here take care of all ambiguities during alignment, and hence it is necessary to state, how is the model defined for human perception [5]. The human perception model is defined such as: for a specified misalignment range, which is  $45^\circ$  in default case, the model will be aligned to its nearest alignment axis found. This assumption is made considering the fact that humans normally set the object close to its alignment axis even though it is not



possible to align perfectly. As a result, if more than one solutions for alignment have been detected, the algorithm aligns it to the one nearest to the misaligned axis. This solves the problem of ambiguity in alignment.

### III. IMPLEMENTED ALGORITHMS

Following sections show the working of each of the methods pointed in the flow.

#### 3.1. Translation to World Origin

It is possible that the 3D reconstructed point cloud model is lying somewhere in the world frame but not at world origin. The first step is to move the model at world zero such that the center of mass of the object is at world zero. The Z coordinate of all the data points is to be ignored as the object is lying on a plane.

##### Algorithm 1 Method of Variance

```

1: INPUT: point cloud, misaligned range  ▷ misaligned
   range is 45 by default
2: Translate model to world origin
3: procedure VARIANCEALIGNINXY(point cloud)
4:   for  $i := i - n$  to  $i + n$ ,  $i = i + 5$  do  ▷
    $n = \text{misaligned range}$ 
5:     Euclidean transformation of point cloud by  $i$  de-
     grees
6:     Find variance in X direction from YZ Plane
7:   end for
8:   if global maxima exists then
9:      $deg = \text{value of angle with maximum variance}$ ; ▷
     resolution is  $5^\circ$ 
10:  else if global minima exists then
11:     $deg = \text{value of angle with minimum variance}$ ;
12:  end if  ▷  $deg = \text{misalignment in degrees}$ 
13:  repeat above with smaller values of  $n = 1$  and  $n =$ 
     $1/60$  each
14:  until resolution is of  $deg$  is  $1'$ 
15:   $result = \text{Euclidean transformation of point cloud}$ 
     $\text{by } deg \text{ degrees}$ 
16: end procedure  ▷  $result = \text{aligned point cloud}$ 
17: OUTPUT: result, deg

```

The center of mass of object is modeled as the arithmetic means values of X and Y coordinates of all points in the point cloud. As a result, 2 out of 3 degrees of freedom have been found. The next step is to execute translation of point cloud in X and Y coordinate equal to the negative of the mean values of point cloud already found.

#### 3.2. Alignment by Method of Variance

Variance, denoted as  $s^2$ , is a measure of the spread of data from its mean value, which can be defined as follows [7]:

$$s^2 = \frac{1}{n-1} \sum_{i=1}^n (X_i - \bar{X})^2 \quad (1)$$

where in equation 1,  $n$  is the total number of data points,  $X_i$  is the  $i^{\text{th}}$  data point whereas  $\bar{X}$  is the mean of all data points. Note that if the entire dataset of points is transformed to origin from its mean value, then  $\bar{X} = 0$  and the variance in equation 1 changes to equation 2.

$$s^2 = \frac{1}{n-1} \sum_{i=1}^n X_i^2 \quad (2)$$

Equation 2 gives variance along both coordinate axes. If variance is calculated only along the x-axis, then only x component of the dataset X is considered and the equation 2 changes to equation 3.

$$s^2 = \frac{1}{n-1} \sum_{i=1}^n x_i^2 \quad (3)$$

Equation 3 is simple, the sum of squares of x components of all the data points divided by  $(n - 1)$  number of data. This equation is the basis in the approach to align a 3D model by the method of variance. The idea is to rotate the translated model over its entire misaligned range and calculate variance for all the points along X direction from YZ plane. A graph of variance versus angle is formed. The global minima and global maxima values of variance will satisfy the solution for alignment problem. The next step is to resolve ambiguities.

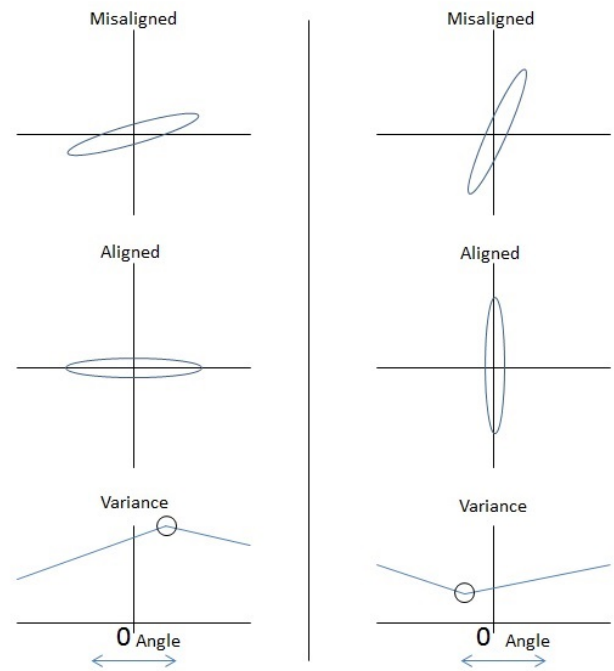


Figure 2. Comparison of two aligned model (resolving ambiguities).

Figure 2 shows an example on resolving ambiguities. In the first case (left), point cloud is more misaligned along X direction where as in second case (right), it is more aligned along Y direction. In the first case (left), alignment will lead to align itself such that variance in X direction is maximum at that angle. However, in second case (right), the variance along X will be minimum. This is also represented in the graph below for understanding. To resolve these ambiguities, both cases have to be dealt with. One of the successful ways to do that is to find whether it has global minima or maxima nearby. Now using this approach, we have resolved the ambiguity and the model is aligned to suit human perception.

Algorithm 1 shows the flow and approach of this method. The first step is to translate the model to world origin as explained in previous section. Next, the translated model is rotated over its entire misaligned range and variance is calculated for all the points along X direction from YZ plane. A graph of variance versus angle is formed. If it has a value of variance as global maxima, the angle at which global

maxima is formed is found out and if it has a global minimum, the angle at which global minima is formed is found out. The reason to do so will be explained in the next section.

For a misaligned range over  $m^\circ$  along both sides, clockwise and counter clockwise, the total number of values of variance obtained are equal to  $\frac{2m}{r} + 1$  where  $r$  is the resolution in degrees. Therefore, the first iteration with  $45^\circ$  and  $r = 5^\circ$  give 19 values of variance. Next, the process is iterated again in steps of  $r = 1^\circ$  from a range equal to angular step size of the iteration before, which is  $m = 5^\circ$  and 11 values of variance with a resolution of  $1^\circ$  are calculated. Once again, a check is made to find out at which angle is global maxima or minima is found. Finally, last iteration is made and end up with a resolution of  $1'$ . The last iteration process will result in 121 values of variance, with  $m = 1'$  and  $r = 1'$ . Now, the value of the global maxima or minima can be found out, and the value of angle at the given value of variance is the misaligned angularity. The point cloud is then transformed with the help of Euclidean Transformation to align itself and form the best possible solution.

The method of variance basically is similar to Principal Component Analysis [8]. It is in our case, however, preferred over PCA because it is easier to resolve ambiguities with variance method. It is to be noted that neither variance nor PCA will work for 3D objects having more than 2 symmetry planes since the variance for such 3D objects will not change on being misaligned. Also, the error points in the point cloud away from the centroid will contribute to erroneous alignment by variance method. For avoiding such failure, a more reliable method of symmetry is used.

### 3. 3. Alignment by method of Symmetry

This approach is totally different from the previous approach of variance. Here, all the points on one side of XY plane are mirrored onto other side and correspondence is established between the mirrored points and points lying in the same side. For each point, a nearest neighbor is found in the mirrored point set. If the object has at least one symmetry plane, the mirrored half will fall exactly on the points lying on other side and distance between nearest neighbor will be ideally zero. The sum of the square of the distances from their respective nearest neighbor gives the squared error. The 3D object is rotated and this procedure is checked, so as the symmetry is found, the 3D object can be transformed to the orientation leading to alignment. The mirroring is explained below with equations in set notations where  $p_i(x_i, y_i, z_i) \in P$ , and  $P$  is  $n \times 3$  data matrix.

$\{P_{x+} | p_i(x_i, y_i, z_i) \in P, i = 1, \dots, n; x_i > 0\}$ ,

$$P' = P_{x+} \begin{bmatrix} -1 & 0 & 0 \\ 0 & 1 & 0 \\ 0 & 0 & 1 \end{bmatrix} \quad (4)$$

$\{P_{x-} | p_i(x_i, y_i, z_i) \in P, i = 1, \dots, n; x_i \leq 0\}$  and by assigning  $P'' = P_{x-}$ , (5)

For each point in  $P''$ , search for a nearest neighbor in  $P'$ .

The squared error ( $e^2$ ) obtained from the algorithm can be formulated in equation as follows:

$$e^2 = \sum_{i=1}^n (p_i - p'_i)^2 \quad (6)$$

In equation **Error! Reference source not found.**,  $p'$  is the nearest neighbor of  $p$ . A summation

of such error along all query points give us squared error ( $e^2$ ).

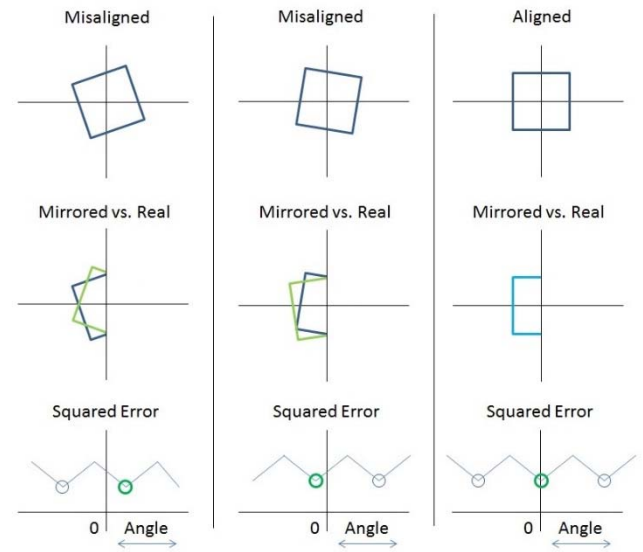


Figure 3. Mirroring, matching and resolving ambiguities.

The algorithm 2 shows the implementation of this approach. The overall procedure is almost same as the one in method of variance. First, we translate the model to world origin. Next, we iterate the method by rotating the model in smaller steps like  $5^\circ$ ,  $1^\circ$  and  $1'$ . Now, after rotating the translated model in definite steps, all the points in the right-hand side of YZ plane i.e. each point  $P_i(x, y, z)$  with  $x > 0$  is mirrored such that  $P_i(x', y', z')$  is  $x' = -x, y' = y$  and  $z' = z$ . In the form of equation, it can be written as:  $\{\forall P_i(x, y, z) \in P, i \in 1, 2, \dots, n | x > 0\}$ ,

$$P' = P \begin{bmatrix} -1 & 0 & 0 \\ 0 & 1 & 0 \\ 0 & 0 & 1 \end{bmatrix} \quad (7)$$

Here  $P$  and  $P'$  are  $n \times 3$  matrices with each row containing 3D points. Take a note that the equation 4 is nothing but simple mirroring of all points about YZ plane. After mirroring, all the points in right side of YZ plane are mapped onto left side. For every point in  $P'$ , a nearest neighbor in left side of YZ plane is searched for  $P$ . This is carried out by the nearest neighbor search (NNS) approach [9]. Upon finding the nearest neighbor, error in symmetry is measured, which is nothing but Euclidean distance between those two points. On completion of the process for all the points, which we term as *squared error*. The squared error so calculated is zero for an ideally symmetrical model. Next, ambiguity is resolved for nearest alignment axis which explained in detail in the next section 3.4. In the end, point cloud is transformed with the help of

Euclidean transformation to align itself and form the best possible solution within a fine resolution of 1'.

### 3.4. Symmetry Detection and Resolving Ambiguities

Figure 3 shows the flow of the algorithm visually. At first, a misaligned input model is given, which is compared with its mirror along YZ plane or Y axis in 2D case. The squared error is minimum when model is symmetric about YZ plane and

#### Algorithm 2 Method of Symmetry

```

1: INPUT: point cloud, misaligned range    ▷ misaligned
   range is 45 by default
2: Translate model to world origin
3: procedure SYMMETRYALIGNINXY(point cloud)
4:   for  $i=i-n$  to  $i+n$ ,  $i=i+5$  do    ▷
      $n$  = misaligned range
5:     Euclidean transformation of point cloud by  $i$  de-
     grees
6:     Find mirror points for all points in point cloud
     in right hand side of YZ plane
7:     Find all the points in original point cloud in the
     left hand side of YZ plane
8:     Find a nearest neighbor for each mirrored point,
     a point in left hand of YZ plane in original point cloud
9:     Find error as Euclidean distance between two
     points
10:    Find squarederror as sum of squares of Eu-
     clidean distances between each pair of nearest neighbor
11:  end for
12:  Find nearest local minima of squarederror
13:  deg = value of angle at local minima
14:  repeat find minimum squarederror for  $n = 1$  and
      $n = 1/60$  each
15:  until resolution is of deg is 1'
16:  result = Euclidean transformation of point cloud
     by deg degrees
17: end procedure    ▷ result = aligned point cloud
18: OUTPUT: result, deg, squared error

```

maximum when it cannot match its mirror model. At the end, nearest angle where the squared error is minimum is found out and the point cloud model is transformed to that angle of rotation. Local minima is considered in this case to resolve ambiguity unlike global minima in the former approach. A suitable explanation to that is because of multiple possibility of existing symmetry planes. The algorithm should be able to align it to any one of them which is found to be nearest. For reconstructed point cloud models, it is very much possible that the squared error at one symmetry plane is much lesser than that to others due to noise and erroneous points, but in order to make the model less dependent on noise, nearest value of local minima is selected even though it is not a global minima. Hence, the alignment axis will change with respect to the orientation of input model which is required to encompass human perception factors. This special feature of this method makes it unique from previous method.

### 3.5. Classification of Reconstructed Models

The value of squared error ( $e^2$ ), even after aligning, in the method of symmetry indicates the error which could be composed of two parts:

- i. Model is symmetric and the squared error ( $e^2$ ) is due to noisy points.

- ii. Model is asymmetric and the squared error ( $e^2$ ) is due to asymmetrical points and noisy points together.

Even though the value is influenced by noisy points, it can be still used to measure symmetry of a reconstructed point cloud model. However, it has to be slightly modified in order to compare the values between different 3D objects.

$$S = \frac{\bar{P}_x}{e^2 \times n^{10}} \quad (8)$$

Equation **Error! Reference source not found.** has been derived based on various observations about relative size of the 3D objects as well as number of points in the point cloud. It is now independent of different models and unique in itself. Basically, the solution to the equation yield a number (for example: symmetrical factor). The symmetrical factor ( $S$ ) values observed from 1 to 10 for reconstructed models and even more for synthetic models. The values 2 and 5 below are calibrated from the testing models. However, they are purely perception based and such parameters can be tuned fine in order to achieve correct classification. For this model, following are the values proposed for classifying reconstructed point cloud model into three different categories:

- 1)  $S \geq 5$ : Reconstructed model is symmetric in one or more number of symmetry planes and alignment is excellent and uses symmetry approach to align.
- 2)  $2 < S < 5$ : Reconstructed model is not symmetric but regular and alignment is very good and uses variance approach to align.
- 3)  $S \leq 2$ : Reconstructed model is irregular and alignment is good and uses again variance approach.

In a way, symmetry factor was a byproduct of method of symmetry alignment. As a result, the same equation can be used to compute symmetry of different models and serve itself as a tool to automatically decide on which method to use for better alignment.

## IV. TESTING AND EVALUATION

The entire evaluation is split into two parts namely, testing and performance. Testing is an important part of evaluation initially and provides a green signal to implement it on real specimens. On successful testing, performance is measured on actual datasets.

### 4.1. Testing

The 3D models from the synthetic testers as shown in figure 4, include a teapot with one plane of symmetry, a perfect cube with four planes of symmetry and a couch again with one plane of symmetry. All the models have different sizes. All these models are aligned by default. The idea is to misalign them with a known angle and apply the algorithms mentioned here to realign them again. In the following table 1, recorded results for 5 different testers by both methods of alignment are shown along with their symmetric values. The term *Size* in the table shows the dimension in centimeter of minimum bounding box in XY plane,  $n$  is the total number of points in the model, *Misalign* is known misalignment applied on test model in degrees, *Align* is result from respective methods,  $t$  is time taken by algorithm in seconds,  $S$  is symmetry factor and *Acc* is accuracy defined as  $\left(1 - \frac{Misalign + Align}{Misalign}\right) \times 100\%$ .

It is to be noted that the model 'perfect cube' fails the alignment algorithm based on variance as expected. Cube has 4 symmetry planes and therefore the variance of all the points along one direction will be constant. This problem is solved when aligned using symmetry approach.

#### 4.2. Performance

The evaluation of six different types of 3D reconstructed models of six real objects, as depicted in figure 1, is done here. Table 1 and 2 show the performance of our algorithm on the reconstructed models. It can be noted again that the method of variance fails to align 'cube'. But then alignment by symmetry aligned it correctly. In other models, the results from both the methods are comparable but the ones by symmetry are found to be better: especially in cases where symmetricity factor is more, such as cube, triangle, cylinder and owl.

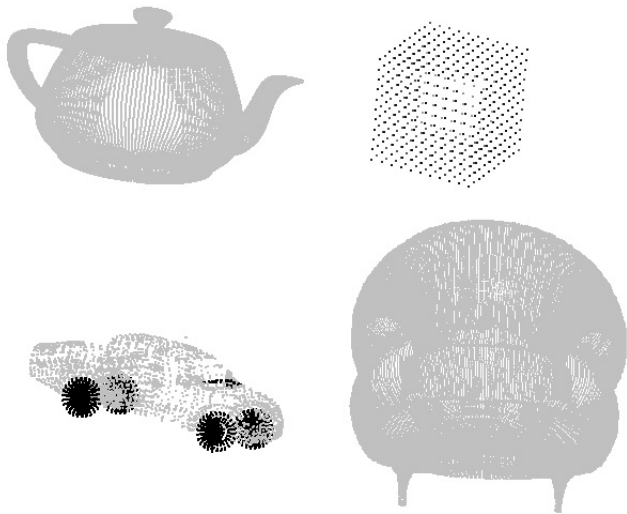


Figure 4. 3D tester models. From top left to bottom right: teapot, perfect cube, car and couch. Source: [10], [11].

As per classification of models on the basis of symmetricity factor ( $S$ ) mentioned in Section 3.5, the six reconstructed models are classified as shown in table 3.

Table 3. Classification of reconstructed models.		
Symmetric	Regular	Irregular
$S \geq 5$	$2 < S < 5$	$1 < S < 2$
Cylinder	Frog	Two Owls
Owl		
Triangle		
Cube		

#### V. CONCLUSION

The entire algorithm of alignment of a 3D reconstructed model is implemented in Matlab R2015b and is successfully tested for misalignments within  $90^\circ$  in XY plane. The results of the reconstructed model are also very satisfying, aligning models to a fine resolution of 1' as shown in Table 1 for the second case, the teapot model, when it is aligned by using the Symmetry method. Also at the end, classification of reconstructed models also value adding. However, it is also observed that the calculation time got increased slowly for models with more than 200,000 points. Important features, limitations and future works are explained in sections below.

#### 5.1. Important Features and Key Points

On a concluding note, the noteworthy features and keypoints of the work are highlighted here:

- Features: (1) robust performance on different misalignment incorporated by human perception factors, (2) does not require featuring information in a model about faces, edges, or their normal, (3) does not require a reference aligned model for aligning procedures, (4) fields good results even with noisy data points.
- Key points: (1) able to align the model by two different possible approaches, symmetry and variance, (2) calculates value of symmetricity factor to give a good comparison between different models, (3) classifies the model, which gives information about how good is alignment axis defined in that case.
- Limitations: (1) involves lot of calculations due to handling of a large number of data points, since down-sampling the point cloud is not a good choice in this case, (2) takes fair amount of time in performing alignment by method of symmetry, (3) uses trial and error approach. It runs a loop and calculates the parameters rather than solving them directly.

#### 5.2. Future Works

The method proposed here to align model in 3 degrees of freedom can also be used to align in 6 degrees of freedom in same steps and the time taken to align in 6 degrees of freedom as a result will be only 2 times to that in 3 degrees of freedom:

- Translate model to world origin in X, Y and Z coordinates (which was only X and Y previously).
- Align model in XY plane.
- Align model in XZ or YZ plane.

One of the limitation is more computation time required, that needs to be considered if the algorithm would be used in real time.

#### REFERENCES

- [1] Aubry, Mathieu, et al. "Seeing 3D Chairs: Exemplar Part-Based 2D-3D Alignment Using A Large Dataset Of Cad Models." Proceedings of the IEEE conference on computer vision and pattern recognition. 2014.
- [2] M. Levoy, K. Pulli, B. Curless, S. Rusinkiewicz, D. Koller, L. Pereira, M. Ginzton, S. Anderson, J. Davis, J. Ginsberg et al., "The Digital Michelangelo Project: 3D Scanning of Large Statues," in Proceedings of the 27th annual conference on Computer graphics and interactive techniques. ACM Press/Addison-Wesley Publishing Co., 2000, pp. 131–144.
- [3] S. Rusinkiewicz, O. Hall-Holt, and M. Levoy, "Real-time 3D Model Acquisition," ACM Transactions on Graphics (TOG), vol. 21, no. 3, pp. 438–446, 2002.
- [4] Van Lierde, Carl, et al. "Method and System for Registration/Alignment Of 3D Digital Models." U.S. Patent No. 9,740,960. 22 Aug. 2017.
- [5] M. Chaouch and A. Verroust-Blondet, "Alignment of 3D Models," Graphical Models, vol. 71, no. 2, pp. 63–76, 2009.
- [6] K.-L. Low, "Linear Least-Squares Optimization for Point-to-Plane ICP Surface Registration," Chapel Hill, University of North Carolina, vol. 4, 2004.
- [7] M. Loeve, "Probability Theory, vol. II," Graduate texts in mathematics, vol. 46, pp. 0–387, 1978.
- [8] I. Jolliffe, Principal Component Analysis. Wiley Online Library, 2002.
- [9] J. L. Bentley, "Multidimensional Binary Search Trees Used for Associative Searching," Communications of the ACM, vol. 18, no. 9, pp. 509–517, 1975.



[10] T. Squid, "3D Models for Professionals, ",  
<http://www.turbosquid.com/>, [Online; accessed 27-July-2018].

[11] The MathWorks, Inc., "Documentation, Matlab," 2018,  
<http://de.mathworks.com/help/matlab/>, [Online; accessed 27-July-2018].

Table 1. Evaluation results of Testers

No.	Misaligned Model	By Variance	By Symmetry	S
1	Model : teapot Size (cm) : $6.5 \times 4$ Points (n) : 41,472 Misalign (°) : 30	t (sec) : 0.59 Align : -29°55' Acc (%) : 99.72	t (sec) : 14 Align : -30° Acc (%) : 100	4.8319
2	Model : teapot Size (cm) : $6.5 \times 4$ Points (n) : 41,472 Misalign (°) : 15	t (sec) : 0.59 Align : -15° Acc (%) : 100	t (sec) : 12 Align : -15°1' Acc (%) : 99.89	21.6290
3	Model : car Size (cm) : $90 \times 37$ Points (n) : 9,218 Misalign (°) : -20	t (sec) : 0.51 Align : 19°53' Acc (%) : 99.42	t (sec) : 3 Align : 19°47' Acc (%) : 98.92	10.1858
4	Model : couch Size (cm) : $90 \times 87$ Points (n) : 146,794 Misalign (°) : -30	t (sec) : 1.15 Align : 29°41' Acc (%) : 98.94	t (sec) : 65 Align : 29°58' Acc (%) : 99.89	35.4026
5	Model : perfect cube Size (cm) : $2 \times 2$ Points (n) : 726 Misalign (°) : 15	t (sec) : 0.45 Align : -12°21' Acc (%) : 82.33 <b>failed</b>	t (sec) : 1 Align : -15°13' Acc (%) : 98.56	7.2817

Table 2. Evaluation results of reconstructed models.

No.	Input Model	By Variance	By Symmetry	S
1	Model : cube Size (cm) : $10.75 \times 10.75$ Points (n) : 130,765	t (sec) : 1.03 Align : 34° <b>failed</b>	t (sec) : 67 Align : -0°28'	5.0545
2	Model : triangle Size (cm) : $9.5 \times 4.5$ Points (n) : 93,490	t (sec) : 0.84 Align : -0°9'	t (sec) : 50 Align : 2°5'	5.1537
3	Model : cylinder Size (cm) : $7 \times 7$ Points (n) : 138,792	t (sec) : 1.05 Align : -2°50'	t (sec) : 60 Align : -6°58'	8.8050
4	Model : owl Size (cm) : $16 \times 11.5$ Points (n) : 111,061	t (sec) : 0.92 Align : -1°41'	t (sec) : 52 Align : -0°12'	6.7110
5	Model : frog Size (cm) : $14 \times 11$ Points (n) : 102,148	t (sec) : 0.90 Align : 9°25'	t (sec) : 49 Align : 11°31'	4.8235
6	Model : two owls Size (cm) : $9 \times 8$ Points (n) : 12,728	t (sec) : 0.44 Align : -24°18'	t (sec) : 6 Align : -21°40'	1.8896

# The Recognition Of Semaphore Letter Code Using Haar Wavelet And Euclidean Function

Leonardus Sandy Ade Putra

Master Programs  
Electrical Engineering of Diponegoro  
University  
Semarang, Indonesia  
leonardusandy@gmail.com

Linggo Sumarno

Department of Electrical Engineering  
University of Sanata Dharma  
Yogyakarta, Indonesia  
lingsum@usd.ac.id

Vincentius Abdi Gunawan

Department of Informatics Engineering  
University of Palangka Raya  
Palangka Raya, Indonesia  
abdi.g05@gmail.com

**Abstract**— Semaphore are one way of communicating over long distances using the semaphore flags. In Indonesia semaphore is used in scout activities as a method to send information in the form of a sentence containing the message. Sending the semaphore letter code tends to be difficult. Based on the need to semaphore learning, this research proposes an algorithm with image processing as a way to correct the movement of the semaphore letter code based on the image obtained by using the webcam. Digital image processing, Wavelet feature extraction, and Euclidean distance function are applied in this study to determine the best recognition rate of variation decimation and distance variation to sending semaphore letter code using the webcam. This study resulted in the best recognition rate of 95.4% in the 1<sup>st</sup> decimation, recognition rate reached 94.6% in decimation 2, and recognition rate reached 94.2% in decimation 3. The result of the introduction of the semaphore letter code is on the introduction of movement as far as 3 to 5 meters.

**Keywords**— Semaphore Flag, Image Processing, Haar Wavelet, Euclidean Function, and Decimation.

## I. INTRODUCTION

Semaphore is one of many ways to communicate over long distances using semaphore flags measuring 45 cm x 45 cm tied to a 60 cm stick [1]. In Indonesia has been applied as one of the skills that every individual must have in scout activities. To communicate with the semaphore, the flag is held in each hand then adjusted in a certain position as in Figure 1, to represent the letter that will be transmitted as a sentence of information. The semaphore flags used in Indonesia are generally red and yellow [2]. Sending information by using semaphore flags is commonly used in the maritime world as the delivery of information between ships, and also used in the scout world as sending the semaphore letter code [1] [3].

In practice to learn the semaphore movement a semaphore sender requires someone who can see whether the position of the sender is proper or not in delivering semaphore codes. This is very necessary because in each semaphore code delivery has a different position for each letter. Thus, this makes less effective learning of semaphore code if done by a single self.

Semaphore movement has been developed in the form of computer programs to be able to support learning the semaphore letter code in the scout world [5].

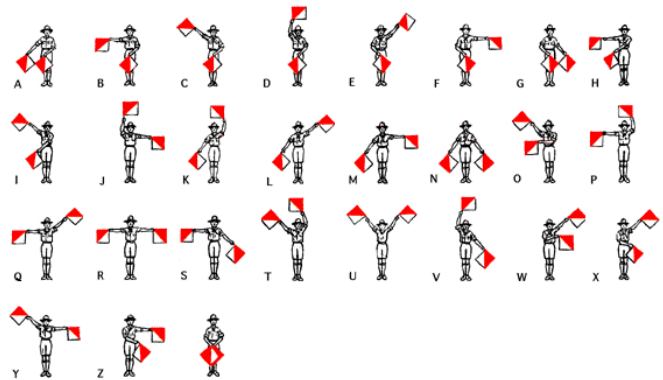


Fig 1. Movement of Semaphore Letter Code [4].

In a previous research [1], the introduction of letters using the Kinect tool with a maximum distance of 2.5 meters and yields a reading rate of 88% and has a weakness that is the length of time used to complete the introduction of letters. Research conducted by [6], semaphore readings obtained a recognition rate of 90% and had constraints in terms of angular readings due to different physical shapes of the sender. Research [5] has succeeded in making computer applications that can help the introduction of the semaphore letters, a weakness in this system is the absence of an instructor role to guide users on using semaphores.

The application of elements of practical and appropriate technology is needed as a supporter as well as an effective solution in solving the problems above, and one of them is by using image processing. Image processing is a generic term for various techniques whose existence is to manipulate and modify images in different ways [7]. The processing of two-dimensional images via a digital computer [8]. Image processing, among others, plays a role in separating the object from the background [9]. The system which will be created can mimic the ability of the human eye to recognize objects in the form of a movement of code delivery that will help humans in learning the delivery as well as receive the semaphore letter code. It can help the user know whether the movement is done right or less precise.

Tests in this study will use variations of distance: 3 meters, 3.5 meters, 4 meters, 4.5 meters and 5 meters and variations of decimation: (1) 32 x 32, (2) 16 x 16, and (3) 8 x 8. This research requires some supporting tools such as webcam [10] [11] which serves to capture motion picture of semaphore letter code, a laptop is then needed to serve as a



place to process images to be recognizable so that the information can be delivered to users and software Matlab as a semaphore letter programming code [12] [13].

## II. RESEARCH METHODS

This study uses variation of distance and decimation to know the effect on the introduction of semaphore letter code. The stages of the introduction phase of the semaphore letter code can be seen in Figure 2. The first process is semaphore letter code capturing using a laptop as a digital data processor machine. The captured image will then enter the preprocessing process and the output of this process will enter the self-extraction process using the Haar Wavelet. The result of the feature extraction will be compared with the data on the database by using the Euclidean. The output of the distance function will display the semaphore letter code on the monitor screen.

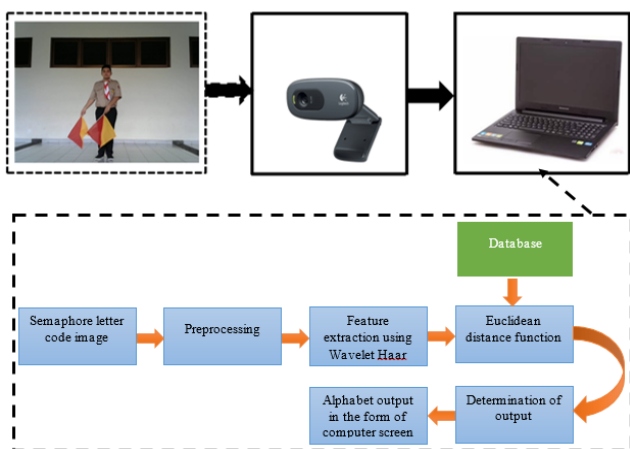


Fig 2. The Flow Diagram of The Semaphore Letter Recognition Process.

### A. Data Collecting

The total of used images for semaphore letters codes is 650 images. The images is obtained from 5 visuals, each of which displays the semaphore letter code from A to Z with variations of distance 3 meters, 3.5 meters, 4 meters, 4.5 meters and 5 meters. Each casted distance produces 26 images, so the images obtained from 1 view is 130 images. As many as 390 image data is used as a database and as many as 260 image data as test data.

### B. Preprocessing

Preprocessing an image is a process aimed to obtain objects contained within the image or to divide the image into several regions of each objects or region (that has) similarities [9]. The preprocessing step is started by converting the RGB image into a HSV image, continued by a process of colour segmentation on the image. The colour segmentation is done to achieve the yellow part of the image as it is on the semaphore flag. The next step is to “crop” and “resize” the image according to the image’s size. The image processing step can be seen on Figure 3.

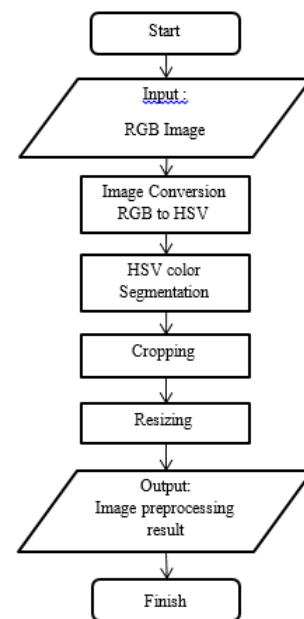


Fig 3. Flow Chart of Image Preprocessing.

Figure 4, shows the RGB image that has been obtained from the webcam will be converted to HSV image, then the image will be preprocessed to obtain the yellow color contained in the semaphore flag. To get the yellow color corresponding to the color on the semaphore flag, researchers used the color-range of the Hue scale of 35-50 on the color scale shown in Figure 5.

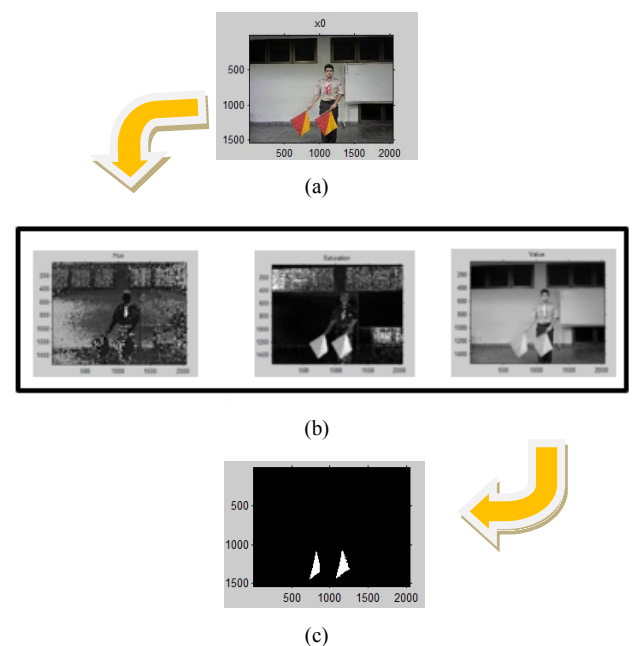


Fig 4. Image Segmentation Process to Yellow Color an Semaphore; (a) RGB Imagery; (b) Results of RGB to HSV Image Conversion; (c) The Image is a Yellow part of The Semaphore Flag.



Fig 5. Hue Scale [14].

### C. Haar Wavelet

Wavelet is defined as a small wave or short wave. The Wavelet's transformation will convert a signal into a Wavelet sequence. The shortwave is a basic function that lies at different times [15], seen in Figure 6. *Haar Wavelet* is the simplest wavelet, introduced by Alfred Haar in 1909. The coefficient of transformation low pass filter (Eq. 1) and high pass filter (Eq. 2) are the base functions of Haar Wavelet. In the image, high pass filters and low pass filters can be represented as 2D matrices. The decomposition of flattening and subtraction that has been done before is actually the same as doing the decomposition (transform) image with Haar Wavelet. Both filters are orthogonal but not orthonormal. The orthogonal and orthonormal tapis Haar are [16]:

$$h_0 = \left( \frac{1}{\sqrt{2}}, \frac{1}{\sqrt{2}} \right) \quad (1)$$

$$h_1 = \left( \frac{1}{\sqrt{2}}, -\frac{1}{\sqrt{2}} \right) \quad (2)$$

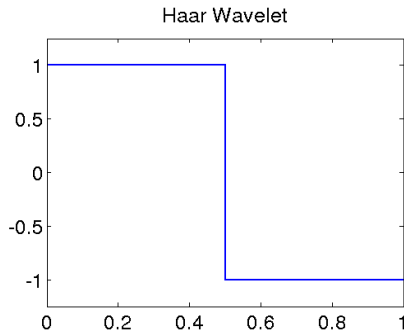


Fig 6. Haar Wavelet [17].

### D. Euclidean Distance

*Euclidean* distance is the most commonly used metric to calculate the similarity of 2 vectors. The smaller the value of Euclidean distance to an object, the higher the level of similarity. The Euclidean distance calculates the roots of squares of differences of 2 vectors [9]. The formula of the Euclidean distance.

$$j(v_1, v_2) = \sqrt{\sum_{k=1}^N (v_1(k) - v_2(k))^2} \quad (3)$$

Where  $v_1$  and  $v_2$  are the two vectors whose distance will be calculated and  $N$  denotes the length of the vector. Distance function will find the difference of the minimum value between data from the self-extraction's output with the data on the database as an output from the recognition of the semaphore letter code.

## III. RESULT AND DISCUSSION

### A. Testing Using Haar Wavelet

Tests are conducted to determine the effect of distance variation and variation of the decimation on the success rate of introducing the semaphore letter code and to know the distance and the value of the decimation that has the optimal success rate. The A letter image on semaphore letter code with many variations of the distances and decimations can be seen on Table I.

TABLE I. THE IMAGE OF THE VARIATION OF DISTANCE TO THE VARIATION OF THE DECIMATION.

Distance (m)	Decimation		
	32 X 32	16 X 16	8 X 8
3			
3.5			
4			
4.5			
5			



























It is seen that the greater the value of the decimation variation, the smaller the pixel level in the image, causing the image to break so that the recognition rate will be lower. The farther the distance is used, the lower the recognition rate. This is because the greater the value of the decimation variation, the decimation experiences repeated convolution and downsampling process as many as the users want, this process resulted in the inserted image to become more blur so that the level of recognition will be lower.

### B. Level of Recognition

At the level of recognition, as many as 260 test data that have been in the process when testing the data will be compared with the data stored in the database. Each value from the Euclidian function on different decimations and

letters with the distance of 3.5 meters can be seen on Table II.

TABLE II. THE DISTANCE VALUE OF EACH LETTER IN THE VARIATION OF THE DECIMATION

Alphabet	Alphabet Image	Decimation		
		32 X 32	16 X 16	8 X 8
A		5.8813	3.1922	1.7176
B		13.0396	7.1204	4.01
C		14.0755	7.6714	4.3012
D		14.2471	7.6805	4.3417
E		14.308	7.9618	4.3566
F		14.5674	7.9912	4.4034
G		14.6888	8.0629	4.4553
H		14.8482	8.0889	4.4855
I		15.412	8.4178	4.7476
J		15.4522	8.5358	4.8693
K		15.5155	8.6081	4.8785
L		15.6003	8.6833	4.899
M		15.6407	8.7063	4.983
N		15.6761	8.7247	5.0259
O		15.7143	8.8532	5.0784
P		15.7575	8.9208	5.3852
Q		16.5466	9.5362	5.7367
R		16.9414	9.7883	5.7376
S		16.9906	9.7974	5.8421
T		17.057	9.8194	5.8652
U		17.0936	9.9489	5.9615
V		17.5923	9.979	5.9867
W		17.6227	10.007	6.0893
X		18.1135	10.2937	6.1237
Y		19.0481	10.458	6.1709
Z		20.05	11.0977	6.3561

From the tests that have been done, the value of variations of the decimation and distance variations that have the best recognition rate can be obtained. The result of the average variation of the decimation and the distance variation which has the best recognition rate can be shown in Figure 7, there are 3 different colors, the blue color represents the result of the influence of the 1st decimation to the distance variation. The red color represents the result of the effect of decimation 2 on the variation of distance and the green color representing the result of the effect of the decimation 3's to the distance variation. The process on the decimation shows that, on decimation 1, image will be processed once on the self-extraction Haar Wavelet process to an image with the size of 32 x 32. On decimation process 2, image will be feature extracted twice so that the image's size will changed into 16 x 16. On decimation process 3, datas will be self-extracted and processed three times and the process will be repeated three times so that the image's size will be 8 x 8.

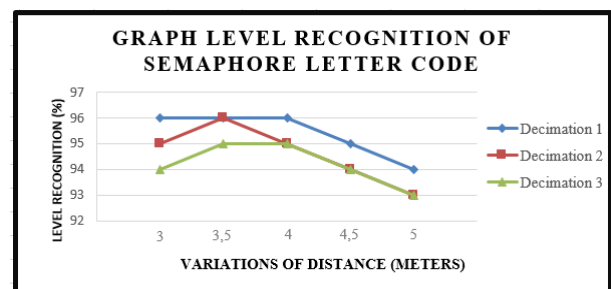


Fig 7. Graph Level Recognition of Semaphore Letter Code.

For example, the effect of decimation variation on the distance can be known in the 1st decimation to get the recognition rate of 96%, for the 2nd decimation gained 95% recognition rate and the 3rd decimation gained a recognition rate of 94%. The greater the value of decimation variation, the pattern recognition rate will be lower, because the greater the chosen decimation value will make the process of repetition of convolution and downsampling more and more in accordance with the variation of the decimation chosen by the user. This will cause the image to be blur and affect the lower recognition rate.

In this study, the percentage of semaphore letters recognition rates on the decimation variation of the overall distance is shown in Table III.

TABLE III. PERCENTAGE OF RECOGNITION RATE

Decimation	Percentage of recognition rate
1	95.4%
2	94.6%
3	94.2%

It is known that at the 1st decimation has the best recognition rate with the percentage of recognition rate of 95.4%.

#### IV. CONCLUSION

In this study, the percentage of the recognition rate of the semaphore letter code in the 1st decimation is 95.4%, the decimation 2 is 94.6%, and the decimation 3 is 94.2%. So the best recognition rate is in the 1st decimation with the

recognition rate at 3 meters distance of 96%, the distance of 3.5 meters by 96%, the distance of 4 meters by 96%, the distance of 4.5 meters by 95%, and the distance of 5 meters by 94 %. The results obtained show that the introduction of the semaphore letter code by using color recognition on the semaphore flag and using Wavelet feature extraction, can result in better recognition rates with longer distances.

## REFERENCES

- [1] A. Rachmad and M. Fuad, "Geometry algorithm on skeleton image based semaphore gesture recognition," *J. Theor. Appl. Inf. Technol.*, vol. 81, no. 1, pp. 102–107, 2015.
- [2] A. Madore, "Make Semaphore Flags," 2015.
- [3] Q. Zhao, Y. Li, N. Yang, Y. Yang, and M. Zhu, "A convolutional neural network approach for semaphore flag signaling recognition," in *2016 IEEE International Conference on Signal and Image Processing, ICSIP 2016*, 2017, pp. 466–470.
- [4] Kualo, "Semaphore." [Online]. Available: <https://www.omniglot.com/writing/semaphore.htm>.
- [5] H. Sinaga, "Learning Application on Signal Scout Semaphore Multimedia And Web-Based Using Computer Assisted Instruction Method," *J. Inf. dan Teknol. Ilm.*, vol. V, no. 3, pp. 160–164, 2015.
- [6] N. Iwane, "Arm movement recognition for flag signaling with Kinect sensor," in *Proceedings of IEEE International Conference on Virtual Environments, Human-Computer Interfaces, and Measurement Systems, VECIMS*, 2012, pp. 86–90.
- [7] R. Gonzalez and R. Woods, *Digital image processing*. 2002.
- [8] A. K. Jain, *Fundamentals of Digital Image Processing*, vol. 14, no. 8. 1989.
- [9] A. S. Abdul Kadir, "Teori dan Aplikasi Pengolahan Citra," no. May, p. 640, 2013.
- [10] D. M. Togasaki *et al.*, "The Webcam system: A simple, automated, computer-based video system for quantitative measurement of movement in nonhuman primates," *J. Neurosci. Methods*, vol. 145, no. 1–2, pp. 159–166, 2005.
- [11] T. L. W. Ce, "HD video desktop collaboration."
- [12] The Mathworks Inc., "MATLAB - MathWorks," [www.mathworks.com/products/matlab](http://www.mathworks.com/products/matlab), 2016. .
- [13] S. E. Lyshevski, "MATLAB Basics," *Eng. Sci. Comput. Using MATLAB®*, pp. 1–26, 2003.
- [14] C. Wikimedia, "File\_HueScale," 2018. [Online]. Available: <https://commons.wikimedia.org/wiki/File:HueScale.svg>.
- [15] L. Sumarno, "Evaluasi Unjukkerja Ekstraksi Ciri Wavelet dalam Pengenalan Huruf Tulisan Tangan Berderau dan Terskala menggunakan Jaringan Syaraf Probabilistik," pp. 1–15.
- [16] D. Putra, *Pengolahan Citra Digital*. Yogyakarta: C.V ANDI, 2010.
- [17] Matematik, "Wavelet and multiscale library - Download," 2017. [Online]. Available: <https://www.mathematik.uni-marburg.de/~waveletsoft/demo.php>.

# Adventure Game Show: Audience Involvement, Destination Image and Audience Behavior

<sup>1</sup>Dwininta Widyastuti  
Faculty of Political and Social Sciences  
University of Indonesia  
Depok, Indonesia  
dwininta.widyastuti@yahoo.com

<sup>2</sup>Irwansyah  
Faculty of Political and Social Sciences  
University of Indonesia  
Depok, Indonesia  
dr.irwansyah.ma@gmail.com

**Abstract**—Currently the popularity of the television programs is on the rise. Entertainment programs attract viewers' attention because they are dominated by games and usually involve physical activities of the game show contestants. The shooting location varied, including adventure tourism destinations comprising natural scenery. This study uses an experimental method to measure the behavior intentions of game show viewers toward adventure tourism screened in the program. This study proves that the relationship of audience involvement and behavioral intentions to travel to tourist destinations is mediated by cognitive and affective images. In particular, cognitive image can significantly correlate to affective image, and both affect behavioral intentions. The medium of television deals with psychological process, so it is found that audience involvement determines audience behavior intentions. Meanwhile, the image of a tourist destination mediates this relationship, giving the perception of cognitive and affective images, hence these two variables are found to be important mediators. Therefore, the management of television programs as a medium of communication need to focus on creating more positive pictures of adventure tourism destinations, which will also lead to the formation of positive affective image. The more beautiful the image of the tourist destination is, the higher travel intentions will be in the future. This study affirms there is a connection between the psychological or emotional dimensions (affective) with intention for visiting tourists.

**Keywords**—Game show, audience involvement, destination image, travel intention, adventure tourism

## I. INTRODUCTION

Television is a medium that acts as a window through which the viewers see the world. Through this medium, the vast world can be brought into everyday life [1]. Television shows screening series of trips to tourism destinations invites viewers to see world's diverse cultures, landscapes and places. These impressions involve audiovisual communication in sophisticated aesthetic and emotional ways [2]. Television broadcasts travel-related programs that comprises specific perspectives on the world and create certain constructs of a particular culture. Call it, a series of travel shows containing pictures and how to get to a particular destination, getting to know the culture and meeting foreigners. These impressions are built in dramaturgic, visual, and auditory ways.

Television shows have been widely recognized for being able to create representations of places around the world [3]. Most of the shows are not intentionally produced to attract viewers to visit a particular destination. It turns out, however, a place illustrated in a movie can be perceived as a product placement that leads to consumers' willingness to

invest certain amount of money to see and experience such place at first hand. This is the reason of the promotion of tourism through television shows.

Tourism is a topic of interesting research, in line with its major contribution in recent decades as one of the fastest growing economic sectors in the world [4]. Promotion of tourist destinations through television shows is considered wide-reaching compared to traditional travel ads and promotions [5]. As a matter of fact, wider audience is not the objective of the marketing campaign. However, the placement of tourist destinations in television shows has the potential to increase curiosity about these tourist destinations among people who are not necessarily the target of traditional advertising [6]. In addition to its excellence compared to traditional advertising, the entertainment television program that features real condition are also more effective in promoting tourism products and destinations rather than movies and soap operas. First, such program costs cheaper than the movie as it does not require an actor or writer, has fewer crews, and its visual editing is relatively uncomplicated. Therefore, tourism induced by the look of reality can be of great help to economically disadvantaged destinations in effective advertising campaigns. The problem of underdeveloped regions being unable to make some investment may be resolved [7].

Another advantage refers to the potential of entertainment television programs to meet the constant quest of authenticity in the postmodern world [8]. Real events can display an authentic "product" image (such as an adventure tourism destination) to the audience. Although viewers generally know that the settings and situations in the entertainment television programs are mostly contrived, the actors and locations are meticulously chosen to show something as if it is natural [9].

## II. LITERATURE REVIEW

A number of studies that have been done previously show a causal relationship between views on reality shows and travel intentions [6] as well audience involvement, cognitive image and affective image [10]. Television-induced travel is indeed a concept that has been explored in the tourism industry [11]. However, research to prove the causal linkage between adventure game shows and the behavioral intentions toward tourist destinations has never been done, especially in Indonesia.

The Indonesian government continues to look for strategies to increase adventure tourism activities in Indonesia as its contribution is significant to state revenues.

Currently, adventure tourism is one of the tourism products developed by the Republic of Indonesia's tourism ministry in the 2016-2019 Priority Tourism Destination Development program and involves the superiority of natural resource tourism attractions owned by Indonesia [12]. In particular, the shows of the game show entertainment genre became one of the shows favored by the Indonesian people. The game show program maintains its position as a program that is in demand by the Indonesian people because the number of viewers is above the average viewer of other television programs in the last three years [13].

Television is known to contribute to the formation of the characteristics of the audience. Television shows resulted in audience involvement in the actors or character's narrative displayed within the program [10]. Audience involvement encourages viewers to perceive the messages conveyed by actors or characters on television shows as genuine information and to use them to broaden audience knowledge, including the knowledge on the tourist destinations featured within. One of the television programs showing a journey in every show is an adventure game show, featuring various tourist destinations.

Television shows are considered as a symbolic stimulus, which can increase audience knowledge including tourism destinations in an area [6]. Later, this knowledge significantly shapes the cognitive and affective images in audience's mind, giving rise to the audience's intentional behavior to visit the destinations described in the television programs [10]. The larger the image of a tourist destination the viewer has, the greater the audience's desire to visit the location featured in the show [6], [11]. As its consequent goal, the viewers want to share similar activities in the tourist destinations in which the television program took place [14].

The causal relationships of audience involvement and the image of the setting of the adventure television program are presented in the research journals. India, a country with abundant adventure tourism destinations, became the filming location of an adventure game show titled "The Amazing Race" [6]. Tourists who watched the show tended to think of India as a travel destination filled with adventurous challenges. Other findings related to television program and audience involvement, tourist destination imagery and travel intentions are presented in a number of studies. The Chinese television program "Where Are We Going, Dad?" caused future behavioral intentions to come to the set [10]. Cognitive image and affective image are known to mediate the relationship between audience involvement and intense behavior for travel to destinations contained in the episodes of this program. A number of destinations being the filming locations of the show were not well-known tourist destinations, but later they turned to attract the attention of viewers who watched the show.

Other research from revealed that the television program "India Celebrity Express" improves and even changes the viewers' knowledge on the state of India, in which the show was set [6]. For example, the show changed viewers' perception of India, such as the poverty rate and the comfort of staying there. This may be due to the fact that the program does not highlight the bad aspects of poverty and comfort in India. This growing knowledge forms the cognitive and affective images of India, which positively increase the desire of the viewers to travel to this country.

Therefore, this research is conducted to fill the gap among the researches related to the causal relationship between adventure game show, the audiences involvement, the image of adventure tourism destination, and the tourists' desire to visit the location. This will explain the management of media in the context of game show television program featuring adventure tourism destination and how it is connected to the audience's travel intention.

Television show featuring reality are judged to have the potential to communicate a more authentic image of a location where the program is set. It is assumed that a show that presents the reality of the contestants' actions in it can change the viewers' perception of the destination which the program shoots. Therefore, the viewers' perception toward the tourist destination may change according to its depiction in the game show. In line with this description, the following are the theoretical hypotheses proposed:

H1: Adventure game TV program causes a difference in the cognitive image, after viewers watched the adventure game show episode.

H2: Adventure game TV program causes the difference in the affective image, after viewers watched the adventure game show episode.

### III. METHOD

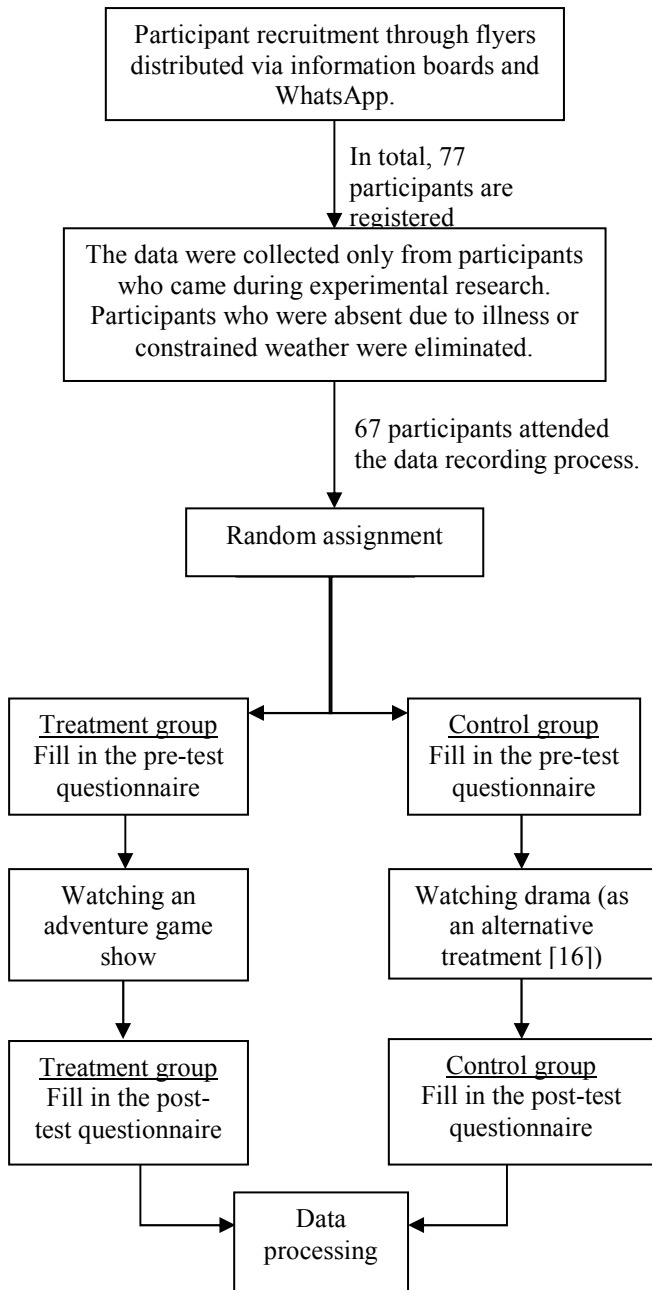
This study uses experimental studies to investigate changes in perception or perception, because this method is able to detect causal relationships between variables involved in research [15], [16]. Data collection in this experimental study was conducted during January to March 2018 at IA STH 6th floor, University of Indonesia (UI) Salemba, Central Jakarta. Participants involved did not get a true explanation regarding the fact that the research was conducted for the purposes of writing an academic thesis; otherwise it was manipulated as an evaluation activity of an adventure television program that has completed its first sequel. Participants were informed that the purpose of this study was to determine the feasibility of the adventure television program in consideration of its second sequel. Manipulation was done so that prospective participants do not have suspicions that they were being involved in a thesis research so as to influence the answers given [6].

This study uses experimental related attributes such as manipulation material in the form of two episodes of "Pro-Warriors" television program, each with a duration of about 25 minutes, questionnaire, participant attendance list, and standard operating procedures. "Pro-Warriors" is the only game show that has a whole episode involving physical activities typical of adventure activities. The shooting location of this television program took the location of tourist destinations in eastern Indonesia which had not been visited by the wider community.

This experimental study uses a random assignment, which is a lottery mechanism that places 67 participants into each group with random methods and accidentally placing participants. The room used as the experimental research location consists of two classes. This research room has been prepared with the same conditions. At the time of the experimental treatment, it was found that there were six participants who had watched the previous "Pro-Warriors"



game show. These participants were eliminated from participation as research participants.



Description: This study eliminates 6 participants because they have already watched the show of "Pro-Warriors". Therefore, this study processed and analyzed data from 61 participants (71.9% of the total participants who signed up)

#### IV. FINDINGS AND RESULT

Preceding the analysis, it is compulsory to test the validity and reliability of research instruments. Based on the data, all experimental research variables are valid and reliable. The KMO & Bartlett's value analysis showed that the audience involvement (0.711) and the cognitive image (0.656) variables were noted to have either high or good validity.

Meanwhile, the validity of affective image variables (0.800) and behavioral intention variables (0.803) were recorded to have very high or very good validity. Furthermore, all variables are very reliable because they have Cronbach's Alpha values above 0.800. The KMO & Bartlett's value of each indicator is valid or above 0.5. The Cronbach's Alpha value of all research indicators is also consistently very reliable or above 0.8.

TABLE I. OUTPUT R SQUARE (COEFFICIENT OF DETERMINATION)

	R Square
Cognitive image	0.229
Affective image	0.361
Behavioral intention	0.621

Source: SmartPLS processed data

The R square value is able to explain the predictive value of the contribution of the independent variable to the dependent variable. Based on the output of R Square in Table 4.32, the contribution of audience involvement to cognitive image is moderate (22.9%); the contribution of viewer involvement to affective image is high (36.1%); and the contribution of viewer involvement to behavioral intention is high (62.1%).

Based on the f square analysis, there are inter-variable relationships that have a weak correlation of latent variables of predictors (exogenous latent variables) at the structural level. That is the relationship of audience involvement and affective image, and the relationship of audience involvement and behavioral intention ( $f^2 < 0.02$ ). Meanwhile, the relationship between cognitive imagery and behavioral intentions was noted to have considerable influence (0.185) for latent variables of predictors (exogenous latent variables) at the structural level. The relationship of cognitive image and affective image (0.431), and the relationship of cognitive image and behavioral intention (0.414) have strong influence of latent variable of predictor (exogenous latent variable) at the structural level.

TABLE II. OUTPUT F SQUARE

	Affective Image	Cognitive Image	Audience Involvement	Behavioral Intention
Affective image				0.414
Cognitive image	0.431			0.185
Audience involvement	0.000	0.297		0.004
Behavioral intention				

Source: SmartPLS processed data

Furthermore, model evaluation is done to find out the result of structural model of this research through bootstrapping with the number of samples assumed as 500. Then an analysis of the path coefficient output data, which aims to re-amplify the analysis of the previous f-square data. The analysis of the path coefficient output data is summarized in the table below:

TABLE III. OUTPUT  $\beta$  SQUARE AND P-VALUE

	$\beta$	t-Statistics	Value of $\alpha$ (Significance) 5%
Audience involvement $\rightarrow$ Cognitive image	0.478	2.742	Supported
Audience involvement $\rightarrow$ Affective image	0.007	0.031	Not Supported
Audience involvement $\rightarrow$ Behavioral intention	0.046	0.405	Not Supported
Cognitive image $\rightarrow$ Affective image	0.598	3.427	Supported
Cognitive image $\rightarrow$ Behavioral intention	0.360	2.234	Supported
Affective image $\rightarrow$ Behavioral intention	0.495	4.103	Supported

Source: SmartPLS processed data

From the calculation of path coefficients with SmartPLS 3.2.7, it was revealed that the coefficient of the audience involvement path to the affective image resulted in a t-statistic value of 0.031 and the engagement relationship of viewers on behavioral intentions of 0.405 (below 1.96) indicating these two inter-variable relations were not significant at 5% significance value. This indicates that their relationship is not proven.

Meanwhile, testing of other cross-variable path coefficients showed a significant relationship because it has a t-statistic value higher than 1.96 at a significance of 5%. The inter-variable relationships that have been shown to be significant are audience involvement on cognitive image (t-statistic = 2.742), cognitive image to affective image (t-statistic = 3.427), cognitive image toward behavior intention (t-statistic = 2.234), and affective image against behavioral intentions (t-statistics = 4.103).

Furthermore, this evaluation is done through Goodness of Fit analysis (GoF) which shows that the structural model analyzed is not fit because it is not in accordance with SRMR criteria  $<0.08$  and NFI  $>0.90$ . There is also an RMS\_theta value higher than 0.12 indicating a lack of conformity. The overall analysis of the Goodness of Fit (GoF) of the model becomes the starting point of the model assessment. If the model does not match the data, then it can be interpreted that the data contains more information than the one presented on the model.

TABLE IV. OUTPUT MODEL FIT

	Estimation Model
SRMR	0.124
NFI	0.488
rms Theta	0.259

Source: SmartPLS processed data

The indirect effect on the causal relationship of audience involvement on behavioral intentions is greater than the value of direct effects. This suggests that the causal relationship between audience involvement and behavioral intentions is mediated by other variables of cognitive image and affective image.

TABLE V. DIRECT AND INDIRECT EFFECTS BETWEEN VARIABLES

Causal Relationship	Standardized Direct Effect	Standardized Indirect Effect
Audience involvement $\rightarrow$ Cognitive image	0.478	N.A.
Audience involvement $\rightarrow$ Affective image	0.007	0.286
Audience involvement $\rightarrow$ Behavioral intention	0.046	0.317

Source: SmartPLS processed data

Therefore, this study yields a model that has been modified to explain the relationship between the variables of audience involvement, cognitive image, affective image, and behavioral intentions. This model summarizes the results of the SEM model test analysis, i.e. the relationship of audience involvement and behavioral intentions mediated by cognitive image and affective image, as follows:

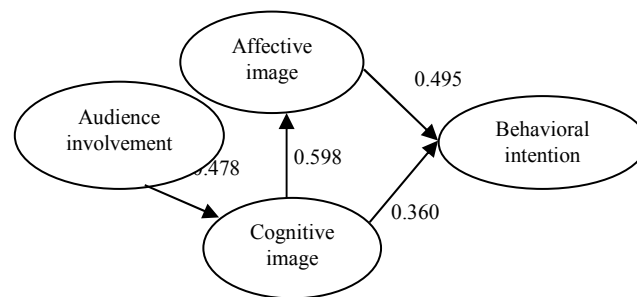


Fig. 1. Models that have been modified (Source: has been reprocessed)

This study proves the effect of adventure game television program on viewers' travel intentions, which are explained by the variables of audience involvement, cognitive image, affective image, and behavioral intentions. The results of the research analysis suggest that the adventure game show can increase the value of audience involvement. The action of a character or an actor in a game show is judged to be a nonsensical "genuine" scene. Physical action performance of adventure game show characters who compete in the outdoors to get the top prize in strict span of time and rules, encourage participants to feel involved or become part of the storyline. These results are consistent with previous research against reality show viewers [6], [10]. It shares similar points because both game show and reality show present the reality of the program participants to the television screen.

Audience involvement encourages viewers to trust the information conveyed in this game show, such as physical and affective conditions (cognitive image and affective image) of the locations in which the program takes place. This is indicated by changes in perceptual values (cognitive image and affective image) of tourist destinations that grows higher after viewers watched the adventure game show. Specifically, the evaluation of cognitive image and affective image shown by viewers after watching a game show matches the conditions displayed in the entertainment program.

These results support previous [6], [10] that the showcasing of reality is able to change the viewer's perception of the tourist destinations according to what appears on the screen. On the other hand, the sensation (felt by tourists) during television viewing is multidimensional which involves symbolic, subjective and emotional values—such as the values described in the cognitive and affective images. This causes such television programs to introduce things such as national culture to the economic perspective of the destinations featured within.

This study did not find whether audience involvement did not cause behavioral intentions. This is considered to occur because the audience require a stage to interpret the image and then personalize the meaning for them to finally decide whether or not they will take the journey. As a result, it takes time for television viewers to decide to actually travel to the tourist destination they have been presented with.

This experimental study also did not find whether audience involvement did not cause affective image. Affective evaluation that refers to the consumer's emotions toward the goal image is not determined by audience involvement. Viewers consider more information about the physical condition of adventure tourism destinations before visiting the site, such as good weather, adequate accommodation, up to the equivalent value of money to get to the tourist destination.

This study also proves the involvement of viewers causing cognitive image of tourist destinations. The relationship is positive and significant, which means that the higher the audience's involvement in the game show television program, the higher the cognitive image of the viewer to the tourist destinations shown.

Furthermore, this study proves that the cognitive image causes the affective image positively and significantly [13]. Therefore, the management of television programs as a medium of communication needs to focus on creating more positive picture of events, which will also lead to the formation of positive affective image of the tourist destinations. The actual or cognitive characteristics of tourist destinations are important because these assessments impact the feelings of television viewers on those destinations.

Cognitive image causing behavioral intentions has been demonstrated in this study. The physical activity shown in the adventure game show does not dampen the viewers' desire to visit the adventure tourism destination, in which the television program is set. Unlike other consumption situations where higher risks prevent consumers from repurchasing a product's service, in adventure travel, higher tourism risks can be attributed to more positive behavioral intentions. Adventure activities are regarded as activities related to identity search.

This study also shows that viewers who like adventure journey want a trip associated with nature. The natural environment is the main motivating factor for reviewing tourist destinations and spreading.

This reinforces the results of the importance of the affective component on the intention to travel tourists to tourist destinations because this component has a strong relationship to travel intentions [17]. Affective image is determined by motivation someone against a place. This

affective image refers to feelings raised by a place because someone wants to feel the benefits of that location [18]. Meanwhile, consumer evaluative responses or those defined as affective imagery depend on their knowledge of objects or cognitive evaluation.

Before making a decision to travel, individuals have considerations to have a location with a more favorable affective picture [19]. For example, by estimating the emotions of him against these tourist destinations. Tourists imagine that these tourist destinations are considered comfortable or attractive. Viewers can take turns visit tourist destinations after watching a video showing the characters in it feel satisfaction being in a tourist destination. Another factor is that video shows display positive interactions between characters and there are significant moments of reflection by viewers. This shows that there is a connection between the psychological or emotional dimensions (affective) with the desire or intention for visiting tourists.

Therefore, the experience that will be enjoyed is taken into account by viewers on an adventure tour. The relationship of audience involvement and behavioral intention to travel to tourist destinations is mediated by cognitive images and affective image [6], [10], [20]. In particular, cognitive images can be significantly correlated with affective images, and both cause behavioral intentions. Television media is related to the journey of psychological processes, so it is found that audience involvement causes the intention of viewer behavior. Meanwhile, tourist destination images mediate this relationship, namely images that provide perception of cognitive images and affective images, so that these two variables are found to be important mediators.

## CONCLUSION

The model test carried out in this study shows that the structural model analyzed is not suitable because it is not in accordance with the criteria so it shows the lack of conformity. The model is not in accordance with the data, then it can be interpreted that the data contain more information than what is presented in the model. Therefore this research proposes the preparation of model-based partial relationships between variables that have been analyzed before. This modified model explains if the relationship of audience involvement and behavioral intentions is mediated by the variables of cognitive image and affective image. The model also confirms that the relationship between audience-variable engagement is only significant to the cognitive image. While the relationship of audience involvement and affective image is weak and insignificant.

Thus, this study reveals that the reality of the competition raised in adventure game show promotes the formation of audience involvement which then correlates with the behavioral intentions, mediated by the cognitive image and affective image. This earlier study revealed that the medium of television concerned with psychological process, so it is found that audience involvement caused audience behavior intentions. Meanwhile, the image of a tourist destination mediates this relationship, giving the perception of the cognitive and affective images, so that these two variables are found to be important mediators. In particular, cognitive image can be significantly correlated with affective image, and both cause behavioral intentions.

## ACKNOWLEDGMENT

This work is supported by Hibah PITTA 2018 funded by DRPM Universitas Indonesia No. 5000/UN2.R3.1/HKP.05.00/2018.

## REFERENCES

- [1] E. Bakoy, "Travel television in a cosmopolitan perspective," Sagepub Journal. Critical Studies in Television: The International Journal of Television Studies Vol. 12 (1) pp. 51–62, 2017.
- [2] A.M. Waade, "Travel Series As TV Entertainment: Genre Characteristics And Touristic Views On Foreign Countries," *Mediekultur* 25 (46) pp. 100–116, 2009.
- [3] E. Sellgren, "Film-Induced Tourism: The Effect Films Have On Destination Image Formation, Motivation and Travel Behaviour," Thesis: Marketing Communication Management, Copenhagen Business School, 2011.
- [4] United Nations The World Tourism Organization (UNWTO), "Internrtional Tourism – Strongest Half-Year Results Since 2010," World Tourist Barometer.
- [5] R. W. Riley and C.S. Van Doren, "Movies As Tourism Promotion: A 'Pull' Factor In A 'Push' Location," *Tourism Management* 13 (3) pp. 267-274, 1992.
- [6] T. Tessitore, M. Pandelaere, and A.V. Kerckhove, "The Amazing Race To India: Prominence In Reality Television Affects Destination Image and Travel Intentions," Elsevier. *Tourism Management Journal* 42 pp. 3-12, 2014.
- [7] S. Hudson and B. Ritchie, "Promoting Destinations Via Film Tourism: An Empirical Identification of Supporting Marketing Initiatives. *Journal of Travel Research* 44, pp. 387-396, 2006.
- [8] R.L. Rose and S.L. Wood, "Paradox and The Consumption Of Authenticity Through Reality Television," *Journal of Consumer Research* 32(2) pp. 284-296, 2006.
- [9] L.K. Lundy, A.M. Ruth, and T.D. Park, "Simply Irresistible: Reality TV Consumption Patterns. *Communication Quarterly* 56(2) pp. 208-225, 2008.
- [10] H. Fu, B.H. Ye, and J. Xiang, "Reality TV, Audience Travel Intentions, and Destination Image," *Tourism Management Journal* 55 pp. 37-48, 2016.
- [11] N. O'Connor , S. Flanagan, and D. Gilbert, "The Integration Of Film- Induced Tourism and Destination Branding In Yorkshire UK," *International Journal of Tourism Research* 10(5) pp. 423-437, 2008.
- [12] Indonesia Ministry of Tourism., "Development of Priority Tourism Destinations 2016-2019," 2016.
- [13] Nielsen Indonesia, "TOP 10 Genre Game Show in 2015-2017," Personal data via email, 2018.
- [14] B.M. Josiam, D.L. Spears, S. Pookulangara, K. Dutta, T.R. Kinley, and J.L. Duncan, "Using Structural Equation Modeling To Understand The Impact Of Bollywood Movies On Destination Image, Tourist Activity, and Purchasing Behavior Of Indians," Sage Publications. *Journal of Vacation Marketing* 21, 2015.
- [15] Irwansyah, "Bipolar Emotional Response Testing of Online News Website Content: Indonesia Case," *International Journal of Social Science and Humanity* 5 (10), 2015.
- [16] J.W. Creswell, "Research Design: Qualitative, Quantitative, and Mixed Method Approaches 3rd Edition," SAGE Publications Ltd. Thousand Oaks, CA, 2008.
- [17] S. Pan, "The Role of TV Commercial Visuals in Forming Memorable and Impressive Destination Images," *Journal of Travel Research* 50 (2), 2011.
- [18] S.M. Gil and J.R.B. Ritchie, "Understanding The Museum Image Formation Process A Comparison of Residents And Tourists," SAGE Journals. *Journal of Travel Research* Vol 47, Issue 4, 2009.
- [19] I.R. Del Bosque, I.R. and H.S. Martin, H.S., "Tourist Satisfaction a Cognitive-Affective Model," *Annals of Tourism Research* 35 pp. 551-573, 2008.
- [20] J.E. Bigne, M.I. Sanchez, and J. Sanchez, "Tourism Image, Evaluation Variables And After Purchase Behaviour: Inter-Relationship," *Tourism Management* 22(6) pp. 607-616, 2001.

# Visual Emotion Recognition Using ResNet

Azmi Najid, Dina Chahyati  
Faculty of Computer Science  
Universitas Indonesia  
Depok, Indonesia  
azmi41@ui.ac.id, dina@cs.ui.ac.id

**Abstract**— Given an image, humans have emotional reactions to it such as happy, fear, disgust, etc. The purpose of this research is to classify images based on human's reaction to them using ResNet deep architecture. The problem is that emotional reaction from humans are subjective, therefore a confidently labelled dataset is difficult to obtain. This research tries to overcome this problem by implementing and analyzing transfer learning from a big dataset such as ImageNet to relatively small visual emotion dataset. Other than that, because emotion is determined by low-level and high-level features, we will make a modification to a pretrained residual network to better utilize low-level and high-level feature to be used in visual emotion recognition. Results show that general (low-level) features and specific (high-level) features obtained from ImageNet object recognition can be well utilized for visual emotion recognition.

**Keywords**— *visual emotion, transfer learning, convolutional neural network*

## I. INTRODUCTION

Visual emotion recognition aims to associate images with appropriate emotions [7]. Humans have an emotional reaction towards images they observed. Every human being have a different emotional reactions to an image. This reaction is very subjective, so it is difficult to collect or label images that correctly represent the emotions of an image. Because of this subjective nature, it is difficult for computers to recognize the emotion of an image.

Along with the development of technology, computing power and data sources are more and more accessible. This development encourages research related to image processing to use deep learning. Deep architecture like deep convolutional neural network needs a big dataset for it to works well [20]. However, this method is difficult to use in visual emotional recognition, since large and confidently labelled data are difficult to obtain. Although You et al., have built a Large-Scale Emotion Dataset [1] consisting of 23,000 images to encourage research related to visual emotion recognition, it is not as large as ImageNet dataset which contain 14 million images [1], [21].

Bigger dataset allows deep neural network to generalize the model to a new data better [19]. Deep convolutional neural network has a very deep number of layers and is able to solve complex problems like ImageNet Object Recognition [2], [19]. Deep architectures such as ResNet can give a good performance for a big dataset like ImageNet, but for a small dataset this model vulnerable to overfitting [4], [19]. To solve the overfitting problem, usually regularization method like dropout, weight decay, and data augmentation is used to reduce generalization error [19]. Another solution to improve performance on a small dataset is to use transfer learning [5], [6]. Transfer learning enable knowledge learned from a task to be used in another task. This knowledge is represented as a network model (pretrained) which was trained on very large

dataset. This pretrained network can be used as a feature extractor or as new network parameter initializer that needs to be fine-tuned later [18]. This method has shown good result [5], and this approach began to be widely used for training relatively small datasets such as the Large-Scale Emotion Dataset [1], [7], [16].

The state-of-the-art method in visual emotion recognition fuses features from the previous layers of CNN to utilize the low-level and high-level feature extracted from the network, but this method needs to train the network from scratch. Training model from scratch especially on a deep CNN takes a long time, compared to using pretrained network. By using pretrained network we can get the generic CNN features that is ready to be used or trained (fine-tuned) in much less time for other task such as visual emotion recognition. Other than that, utilizing pretrained network also showed significant improvement in classification accuracy for small dataset like the emotion dataset [1], [16]. Therefore, to make use of these advantages we will explore on how to utilize low-level and high-level feature obtained from a pretrained deep neural network such as ResNet for our problem.

In this paper, we will report the experimental result of applying transfer learning from ImageNet dataset to Large-Scale Emotion Dataset. We also modify the ResNet architecture in order to better utilized the extracted features from the pretrained network to be used in visual emotion recognition. Important issues addressed is the imbalance class of the dataset, fine-tuning, dropout and model ensembling.

The rest of the paper is organized as follows. We present related works in Section 2. Section 3 describes the proposed method, and Section 4 presents the results of our experiments. Finally, section 5 concludes the works described in this paper.

## II. RELATED WORKS

Visual emotion recognition has been researched extensively [1], [8], [7], [9], [16]. Generally, there has been two approaches on visual emotion recognition, which is using handcrafted features or Convolutional Neural Network (CNN) based features [7]. Both approaches are trying to recognize emotion based on various kinds of low-level and high level features as shown in Figure 1. By low-level features, we mean the saturation, brightness, texture, or dominant colours in the image. Example of high-level feature is the semantics of objects detected in the image (tiger swimming, human swimming, etc).

Rao et al , introduced Multi-Level Deep Representation Network (MldrNet) which uses CNN to obtain low-level feature such as texture and aesthetics using T-CNN and A-CNN [9]. The use of CNN to obtain low level feature is also used by Zhu et al, the difference is that the features are obtained from every convolution layer. The reason is that

every layer in CNN extracts different feature. First few layers of CNN extracts low level feature such as colour and shape, while later layers extracts higher level feature such as semantics of the picture [7]. These feature extracted from each layer are inserted into a Recurrent Neural Network to exploit the dependency from those features.

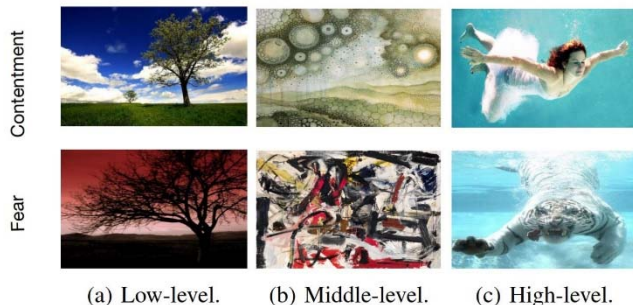


Fig. 1: The same emotion can be evoked from different emotion stimuli. The images in first row are from “Contentment”, and the images in second row are from “Fear”. We can see image emotion is related to many factors, such as low-level features like color (a), middle-level features like texture (b), and high-level features like semantic content (c). [7].

The state of the art method on visual emotion recognition proposed by Zhu et al., incorporate low-level and high-level features obtained from a Convolutional Neural Network (CNN) to perform visual emotion recognition [7]. Features extracted from every layer of the network will then be used to make a prediction, so the network will have predictions based on each feature extracted from every layers of the network. Then these predictions will be combined to make the final prediction of a given image. This model gives the best result compared to other method despite only using shallow network (5 convolutional layer) and trained with random parameter initialization (without using pretrained network) however Yang et al., shows that Transfer Learning using a very deep convolutional neural network significantly improve accuracy in performing visual emotion recognition [7], [16]. Experiment conducted by Yang et al., compare the accuracy between training ResNet from scratch and using pretrained network. The experiment shows that training ResNet with a pretrained network gives 64.67% accuracy while training ResNet from scratch only gives 49.76% accuracy [16].

Training a model using Transfer Learning is easier/faster because we can use “off-the-shelf” CNN features to perform visual emotion recognition, moreover Yang et al., also shows that using a pretrained network can improve the performance of visual emotion recognition [16]. Visual emotion recognition as Zhu et al., described is determined by low-level and high-level features [7], so to recognize emotion of a given image, we will make a modification of a pretrained network to better utilize low-level and high-level features from a network.

### III. PROPOSED METHOD

We proposed to incorporate low-level and high-level features obtained from a pretrained deep CNN. The architecture that we chose as the pretrained model is ResNet-101 [2] trained on ImageNet dataset. The model is evaluated using Hold-Out Validation [4]. Hold-Out Validation divides the dataset into three parts: training set, validation set, and test set. The ratio that we used is 80:5:15 respectively [1].

As mentioned briefly, we will explore four issues related to transfer learning. The first is the imbalance class of the dataset. We solve this issue using weighted sampling technique as described in part A. The second issue is about evaluating how far should we fine-tuned the pretrained model as described in part B, this result will tell us how important extracted feature on some part of the network for recognizing emotion. The third is to address the overfitting issue on a very deep neural network such as ResNet, to overcome this we will evaluate whether dropout will improve the recognition performance, as described in part C. The last issue is about ensembling the ResNet architecture, in this section we will introduce our method on how to incorporate low-level and high-level feature extracted from the pretrained network, this part will be described in section D.

#### A. Sampling

Imbalance class on the dataset causes classes with a small number of data to be recognized not as well as classes with bigger number of data. This experiment attempted to use weighted random sampling technique to load data into a mini-batch to solve the imbalance class problem. The difference between weighted random sampling and simply doing shuffling (random sampling) is, with shuffling the probability of sampling each image is the same regardless of the emotional class, while the weighted random sampling wants to match the ratio of each emotional class to the minibatch. This is done by making the sampling weight inversely proportional to the number of images in a class. We also employ data augmentation to the image so in one iteration the exact same images in class with a small number of data does not appear repeatedly [19], [11].

#### B. Fine-tuning ResNet

ResNet configuration is divided into 4 section of layers, namely L1, L2, L3, and L4. The goal of this experiments is to find out how useful extracted features on some parts of the layer are. We run three experiment on fine-tuning. In the first experiment, only the fully connected (FC) layer is fine-tuned, while the other layers are freezed with the pretrained model. In this model (ResNet-fc), the pretrained model is used as a full feature extractor. In the second experiment, FC and L4 are fine-tuned (ResNet-L4). In the last experiment all layers are finetuned (ResNet). These models are illustrated in Figure 2 below.



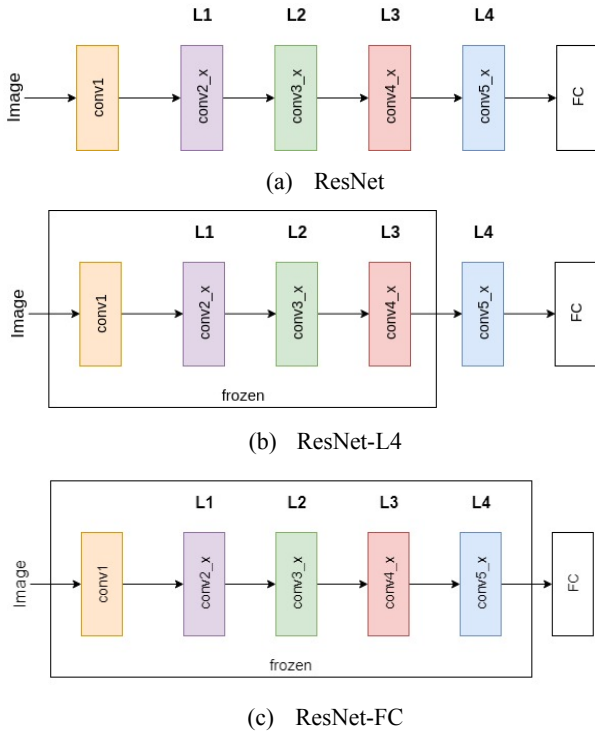


Fig. 2: Three models of fine-tuned experiments

### C. Dropout

ResNet-101 is a "very deep neural network" [2]. This deep architecture has many parameters so it will prone to overfitting and in the last experiments we will see the developed model is suffered from overfitting. Ebrahimi et al., make a modification to the original residual block by adding a dropout layer to prevent this [4], [12], [13]. The dropout layer added in residual block is placed between 3x3 convolution with 1x1 convolution layer as illustrated in Figure 3. In this experiment we compare ResNet-L4 with and without dropout layer. Dropout layer will randomly set entire feature map or channel to be 0 with a probability of 0.5.

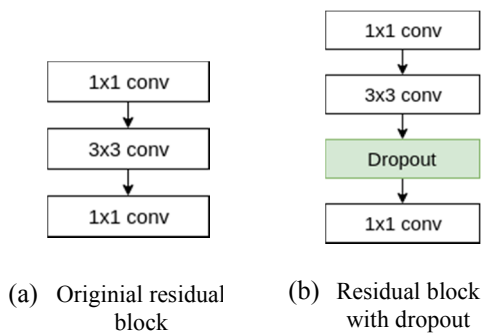


Fig. 3: Dropout experiment

### D. Ensemble Method

Transfer learning is proved to be effective because the extracted feature on pretrained network is transferable for different tasks [5], [6]. Features are transferable because CNN not only extracts specific features (high-level features)

for a task but also extract more general features (low-level features) [5], [6]. Visual emotion recognition is also influenced by low-level and high-level feature as illustrated in Fig 1.

This experiment wants to utilize the extracted features in some parts of ResNet to perform visual emotion recognition. The idea is for the model to have different perspective from low-level and high-level feature on recognizing emotion from an image. To do this, branches from some parts of the network are created to extract different kind of features. Then, prediction from every branch is combined (stacked) by calculating the weighted average from all the predictions. This model is inspired by Zhu et al., the difference is that branches are created from every output of ResNet layers section (section L0, L1, L2, L3, L4) rather than from every convolution layer, because ResNet-101 has too many convolution layer [7]. We will call this model as ResNet-ensemble and is illustrated in Figure 4 below.

$$P(z = c|V) = \frac{\exp(W_c V)}{\sum_k \exp(W_k V)} \quad (1)$$

$$L(V) = -\log(P(z = c|V)) \quad (2)$$

Training ResNet-ensemble is done in two steps. The first step is to train every branch to predict emotion based on a given features. Output of every branch is formed into one dimensional vector  $V$ , then to make a prediction, softmax function is used, Equation 1 [3], [7]. Training is done by minimizing cross-entropy loss in Equation 2 [3], [7]. In this step the trained parameters are the ResNet parameter and the fully connected layers of every branch. In the second step the trained parameters are the the last fully connected layers and also the fully connected layers of every branch.

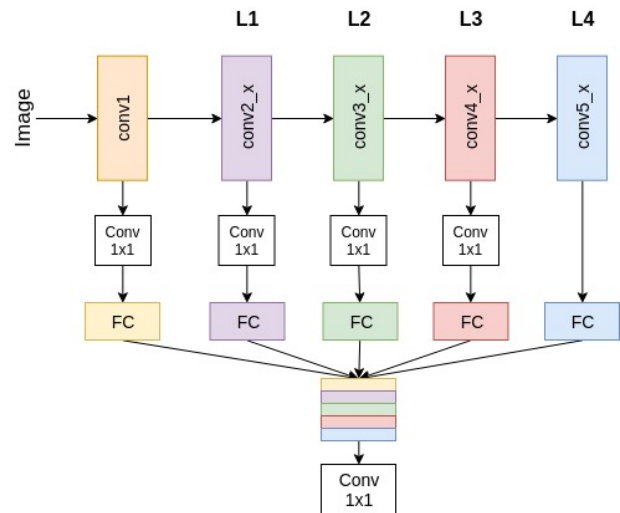


Fig. 4: ResNet-ensemble

For both steps optimization using Stochastic Gradient Descent (SGD) with mini-batch's size 32. The learning rate

of ResNet parameters are  $1e-4$ , and it is smaller than other parameter's learning rate which is  $1e-3$ , that is because we don't want to change the pretrained network parameters too much.

The other ensemble model we developed is done by combining feature extracted from layers section L0, L1, L2, and L3 (ResNet-skip). These features are combined by calculating the weighted average of the activation value on feature map [14, 20]. To calculate this we use ResNet's identity shortcut connection (skipping connection). This network structure can be seen in Figure 5. In order for the feature can be combined, dimension and number of channels ( $C \times H \times W$ ) of a feature map must be the same. To do this we use  $1 \times 1$  convolution to down-sample the feature as ResNet does on the first input of layers section.

The difference between this model and ResNet-ensemble model is that this model is trained in only one step, and also the parameters are trained only on the subsequent layers after combining feature map in the previous layer which is parameter in section L4 and in the fully connected layer (FC) section.

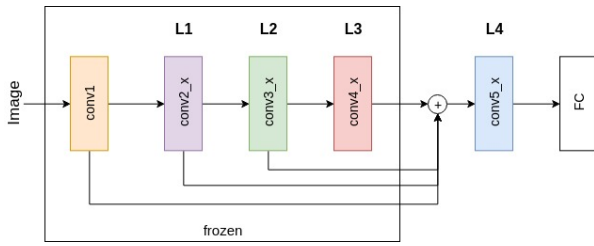


Fig. 5: ResNet-skip

#### IV. RESULTS AND DISCUSSION

In this section, we will present the results of our experiments.

##### A. Experiment Detail

In the process of training, we use the same hyperparameter as the original ResNet parameter with a little adjustment on the hyperparameter value. The model is trained using SGD optimization with momentum = 0.9 (nesterov), weight decay =  $1e-4$ , learning rate =  $1e-4$ , and mini-batch size of 32 for 50 epoch. Our model is implemented using deep learning framework PyTorch on one Nvidia GTX 1070. Performance metric used in this experiment is accuracy, but because there is an imbalance class problem on Large Scale Emotion Dataset [1], we also use macro average true positive rate to see how well the model can learn to recognize all eight emotion class including the emotion class with a small amount of sample.

##### B. Sampling

This sampling experiment was performed on ResNet by simply training the parameter on the replaced classifier. The result is shown in Table I, which tells that the model with weighted sampling gives almost the same accuracy as

shuffling, but the macro average true positive rate (avg-recall) is significantly higher.

Two class that is greatly affected was Fear and Anger. In the dataset of 8 emotion classes, only 4.4% of the images are in Fear class, and only 5.4% is Anger. When we used mere shuffling, the number of images trained for this two classes are small, so their accuracy are only 5% and 10%. By using weighted sampling, the number of images for those two classes are added to match up the number of images in other classes. This method increased the accuracy of the two classes to 27% and 30%.

TABLE I. SAMPLING EXPERIMENT

	accuracy (%)	avg-recall (%)
<b>Shuffling</b>	62.04	51.04
<b>Weighted</b>	62.73	56.44

##### C. Fine-tuning ResNet

The result of fine-tuning is shown in Table II. The ResNet-fc model, only change the classifier of ResNet. ResNet-fc only make use of high-level feature which is extracted for ImageNet object recognition to do visual emotion recognition. That means the accuracy of 62.73 % is obtained using high-level feature for determining semantic content of the image. It shows that semantic content of an image has a big impact in recognizing emotion of an image. The ResNet-L4 and ResNet model give better evaluation result because these model have access to lower-level feature extracted from the earlier layer. So these model can utilize low-level feature like color, brightness, contrast, texture, etc for visual emotion recognition [4], [7], [10].

TABLE II. FINE-TUNING EXPERIMENT

	accuracy (%)	avg-recall (%)
<b>ResNet-fc</b>	62.73	56.44
<b>ResNet-L4</b>	64.95	60.30
<b>ResNet</b>	66.27	62.42

##### D. Dropout

The results of this experiment presented in Table III is contrary to Ebrahimi et al., results. Based on this result we see that dropout does not provide any significant improvement. This is because batch normalization has regularization capability and Ioffe et al., state that in batch normalized network, dropout can be either removed or reduced in strength [17].

TABLE III. DROPOUT EXPERIMENT

	accuracy (%)	avg-recall
<b>ResNet-L4</b>	64.95	60.2
<b>ResNet-L4-dropout</b>	65.04	60.29

##### E. Ensemble Method

The ResNet-ensemble model has more parameters to trained compared to ResNet-skip, so the training time of ResNet-ensemble also takes longer than ResNet-skip. Based on our experiment ResNet-ensemble gives a better result than

ResNet-skip as shown in Table IV Confusion matrix of ResNet-ensemble model can be seen in Figure 6..

TABLE IV. ENSEMBLE EXPERIMENT

	accuracy (%)	avg-recall
<b>ResNet-ensemble</b>	67.74	62.4
<b>ResNet-skip</b>	66.99	62.60

Based on all experiment, the best accuracy (67.74%) is achieved by ResNet-ensemble method using weighted sampling, but as shown in Table IV the avg-recall of ResNet-skip is slightly better than the ResNet-ensemble model. This means that ResNet-skip performs better on small sample emotion such as anger and fear. Confusion matrix for both model can be seen in Figure 6 and 7 below.

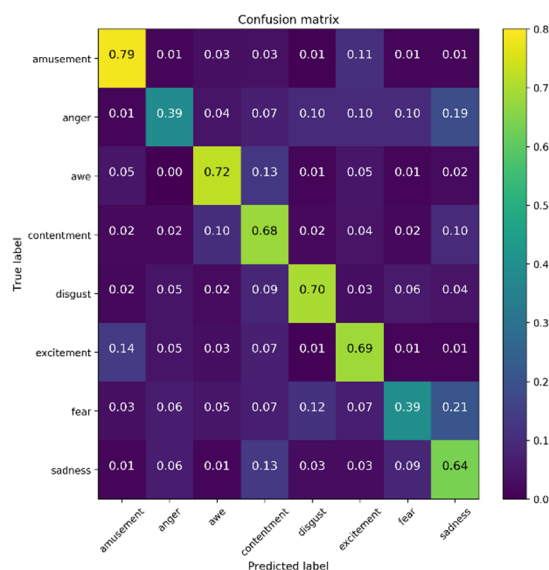


Fig. 6: Confusion matrix of ResNet-ensemble

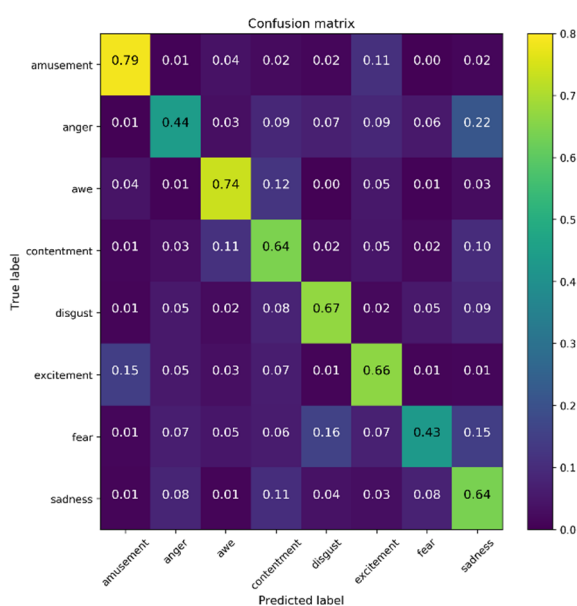


Fig. 7: Confusion matrix of ResNet-skip

All model developed in this experiments has different architecture and parameters to be fine-tuned. Because of this, these model will also have different training time compared to another. Table V present all models performance and their training time per epoch. As presented in Table V, we can see that ResNet-skip performs as good as ResNet-ensemble while spending much less time to trained. ResNet-skip was faster to train because the model only learn parameter on the new skipping connection and the parameter in section L4 of ResNet, while ResNet-ensemble fine-tuned all ResNet parameter in both training step.

TABLE V. COMPARED METHOD

	accuracy (%)	avg-recall	minute/epoch
<b>ResNet-fc</b>	62.73	56.4	4.86
<b>ResNet-L4</b>	64.95	60.3	4.74
<b>ResNet</b>	66.27	62.4	7.98
<b>ResNet-skip</b>	66.99	62.6	4.74
<b>ResNet-ensemble</b>	67.74	62.42	8.60

## V. CONCLUSION

We present a modification of ResNet architecture (ResNet-ensemble and ResNet-skip) to use features from a pretrained network for visual emotion recognition. This modification allows low-level feature and high-level feature extracted from a pretrained network to be utilized better for visual emotion recognition. In our experiment we also show that weighted random sampling can help to improve performance on emotion dataset [1] which has an imbalance class problem. From the fine-tuning experiment we also find that semantic content of an image has a big influence on determining emotion of a given image.

## REFERENCES

- [1] You, Q., Luo, J., Jin, H., Yang, J. (2016). Building a Large Scale Dataset for Image Emotion Recognition: The Fine Print and The Benchmark. *AAAI Conference on Artificial Intelligence*, 30.
- [2] He, K., Zhang, X., Ren, S., Sun, J. (2015). Deep Residual Learning for Image Recognition. *2016 IEEE Conference on Computer Vision and Pattern Recognition (CVPR)*, 770-778.
- [3] PyTorch documentation. (2018). Retrieved from <https://pytorch.org/docs/stable/index.html>
- [4] Chollet, F. (2018). *Deep Learning with Python*. Shelter Island, NY: Manning.
- [5] Torrey, Lisa., Shavlik, J. (2009). Transfer Learning. *Handbook of Research on Machine Learning Applications*.
- [6] Yosinski, J., Clune, J., Bengio, Y., Lipson, H. (2014). How transferable are features in deep neural networks. *Neural Information Processing Systems*, 27.
- [7] Zhu, X., Li, L., Zhang, W., Rao, T., Xu, M., Huang, Q., Xu, D. (2017). Dependency Exploitation: A Unified CNN-RNN Approach for Visual Emotion Recognition. *Proceedings of the Twenty-Sixth International Joint Conference on Artificial Intelligence*.
- [8] Machajdik, J., Hanbury, A. (2010). Affective Image Classification using Features Inspired by Psychology and Art Theory. *Proceedings of the 18th ACM international conference on Multimedia*, 83-92.
- [9] Chen, M., Zhang, L., Allebach, J.P. Learning deep features for image emotion classification, *2015 IEEE International Conference on Image Processing*, 4491-4495.
- [10] Zeiler, M.D., Fergus, R. (2013). Visualizing and Understanding Convolutional Networks. *CoRR*.
- [11] Sun, L. (2017). ResNet on Tiny ImageNet. *Stanford Report*.

- [12] Ebrahimi, S.M., Abadi, H.K. (2016). Study of Residual Networks for Image Recognition. *Stanford Report*.
- [13] Sritasvata, N., Hinton, G.E., Krizhevsky, A., Sutskever, I., Salakhutdinov, R. (2014). Dropout: a simple way to prevent neural networks from overfitting. *The Journal of Machine Learning Research*, 15.
- [14] Ju, C., Bibaut, A., van der Laan, M.J. (2017). The Relative Performance of Ensemble Methods with Deep Convolutional Neural Networks for Image Classification.
- [15] Bamos. (2017). densenet.pytorch. Retrieved from <https://github.com/bamos/densenet.pytorch/blob/master/compute-cifar10-mean.py>
- [16] Yang, J., She, D., Sun, M. (2017). Joint Image Emotion Classification and Distribution Learning via Deep Convolutional Neural Network. *Proceedings of the Twenty-Sixth International Joint Conference on Artificial Intelligence*.
- [17] Ioffe, S., Szegedy, C. (2015). Batch Normalization: Accelerating Deep Network Training by Reducing Internal Covariate Shift. *CoRR*, abs/1502.03167.
- [18] Stanford cs231n lecture notes. [site]. Retrieved from <http://cs231n.github.io/>
- [19] Goodfellow, I., Bengio, Y., Courville, A. (2016). *Deep Learning*. MIT Press.
- [20] Engelbrecht, A.P. (2007). *Computational Intelligence: An Introduction*. Chichester, West Sussex: John Wiley.
- [21] ImageNet. <http://www.image-net.org/>

# A Feature-Based Fragile Watermarking of Color Image for Secure E-Government Restoration

Lusia Rakhmawati<sup>1,2</sup>, Wirawan<sup>1</sup>, Suwadi<sup>1</sup>, Titiek Suryani<sup>1</sup>, Endroyono<sup>1</sup>

<sup>1</sup>Department of Electrical Engineering, Faculty of Electrical Technology, Institut Teknologi Sepuluh Nopember, Surabaya, Indonesia

<sup>2</sup>Department of Electrical Engineering, Faculty of Engineering, Universitas Negeri Surabaya, Surabaya, Indonesia

l1usiarakhmawati17071@mhs.its.ac.id, 2lusiarakhmawati@unesa.ac.id, 1{wirawan, suwadi, titiks, endroyono}@ee.its.ac.id

**Abstract**— this research developed a method using fragile watermarking technique for color images to achieve secure e-government tamper detection with recovery capability. Before performing the watermark insertion process, the RGB image is converted first into YCbCr image. The watermark component is selected from the image feature that approximates the original image, in which the chrominance value features as a watermark component. For a better detection process, 3-tuple watermark, check bits, parity bits, and recovery bits are selected. The average block in each 2 x 2 pixels is selected as 8 restoration bits of each component, the embedding process work on the pixels by modifying the pixels value of three Least Significant Bit (LSB). The secret key for secure tamper detection and recovery, transmitted along with the watermarked image, and the algorithm mixture is used to extract information at the receiving end. The results show remarkably effective to restore tampered image.

**Keywords**— *fragile watermarking, tamper detection, tamper recovery*

## I. INTRODUCTION

In recent years the implementation of Electronic Government (e-government) has been widely used, but the implementation of e-government is still not considered a very important security factor to maintain the integrity, confidentiality, and availability of such digital documents [1]. The integrity aspect relates to the integrity of the data. This aspect ensures that data cannot be altered (tampered, altered, modified) without the permission of the entitled. Some threats to aspects of integrity can be done through access breakthroughs, spoofing, viruses that alter or erase data, and man in the middle attack is attack by inserting themselves in the middle of data transmission [2].

Protection against the attack can be done either by using watermarking technique [1-3], which aims to insert a digital sign (referred to as a watermark) into the origin medium (called host). Watermark is a data string that can be seen (perceptible) or invisible (imperceptible). The invisible watermark can be another image, part of the original image, as well as the original image itself in different sizes [1, 4]. Then the recipient side of the image can be extracted for authenticity of ownership and content integrity.

Current developments, watermarking techniques are also proposed for recovery of tampered digital documents [5-7; 10-12]. In this method not only able to detect the

tampered image, but also can localize the areas and recover it. This method uses the image feature information itself as a watermark. The original image is modified by a particular method, mostly reduced to the corresponding size while still considering the adequacy of information that can represent the original image [5], then inserted to obtain the watermarked image. When there is irresponsible tamper or modification, the watermark can be extracted to restore it.

In addition, several studies have used watermarking techniques for the security of e-government documents. Zhang [6] using encryption and descriptions schemes for the security of e-government documents. However, this scheme is vulnerable to use in distributed networks. Therefore, it is proposed a combination with watermarking technique as an additional layer for document security protection. In Al-Haj et al. method [8] used transform domain as a process for e-government protection. This technique used transform domain, their drawback is on their low capacity. Their weaknesses can be overcome by increasing the storage capacity space by inserting more than one watermark while keeping the image quality of the watermark.

Talking about adding insertion capacity, the use of digital watermarking applications as part of the detection of damage and recovery of digital documents can refer to other pre-existing methods, so that it can be applied to the case of e-government documents. Lin et al. [2] proposes that each block can be validated by using additional authentication data that has been inserted into each block itself, while data recovery is embedded in different blocks. The quality of the recovery image depends on the tampered image, if the damage is reduced, so the quality of the recovery results decreases. Lin et al [10] proposed a hierarchical method by storing watermark in two different region. While He et al. [4] presents a fragile watermarking scheme for self-recovery using neighbouring block methods to recover it.

A representative watermarking technique for tamper detection with restoration capability is Lin's scheme [11], where the insertion process uses a simple technique, LSB (Least Significant Bit). In this method, detection of block damage is done in 3 levels of hierarchy. If not detected at level 1, it will be detected at the next level with probability close to 1. The advantage of this method is effective in terms of memory because it only needs storage for secret keys and simple algorithms to restore the error. In addition to these advantages, there is a weakness in Lin's algorithm,



which is too sensitive to pixel damage. For example, even if only one pixel in a 4x4 pixel block is damaged, the entire block will be detected as a tampered block, so recovery will be made to all pixels in the block, thus adding degradation to the image recovery end result.

The method proposed by He [4], selects important information from an image by performing an average value of 3 x 3 neighbouring blocks, and uses 2 LSB for its insertion process, and works on blocks of smaller size, 2 x 2 pixels, so it can make image resolution better after image recovery. This method works well for collage attacks because it uses the 3x3 neighbourhood as part of the authentication bit. Another method Hassan [13] proposed colour fragile watermarking for image authentication. This method used average intensity in each 2x2 non-overlapping blocks as a watermark for tamper detection and recovery. Using a particular image object as an important part of the authentication process, this method is not quite successful if the modified not certain part, but can damage all parts of the image.

This research takes the idea of the last two methods, [4] and [13], which proposes the development of watermark component selection, the watermark insertion process, so it can be applied to improve the integrity and ability of restoration of damaged colour digital documents. The proposed fragile watermarking technique is discussed in Section II. Section III presents the experimental results and comparative analysis. The conclusion is summarized in Section IV.

## II. PROPOSED SELF-EMBEDDING FRAGILE WATERMARKING SCHEME

In this section, the proposed self-embedding fragile watermarking scheme is described and the block diagram of the system shown in Fig.1. This scheme with watermarking techniques adopted, some important feature information is extracted from the original image as a watermark and reinvested into the image itself into a watermarked image. The watermark image is encoded and transmitted over a communication channel. At the receiving end, modified data is reconstructed using a watermark along with other post-reconstruction methods if the resulting results have not shown good quality.

In general, as shown in Fig. 1, there are four main processes: pre-process the original image, watermark generation and embedding process, tamper detection, and tamper recovery. The detail of proposed technique is described in detail as follows.

### A. Pre-process the original image

RGB color space is not recommended when dealing with computer-based analyzers, RGB is best suited for image display. This is due to the high correlation between components R, G, and B. Numerically the cross-correlation value between component R and G is 0.98, G and B components of 0.94, whereas between B and R has a value of 0.78, so it is not appropriate when used for signal processing especially the use of watermarking techniques. Under the scheme [14], the use of color space that has low correlation can use the YCbCr channel.

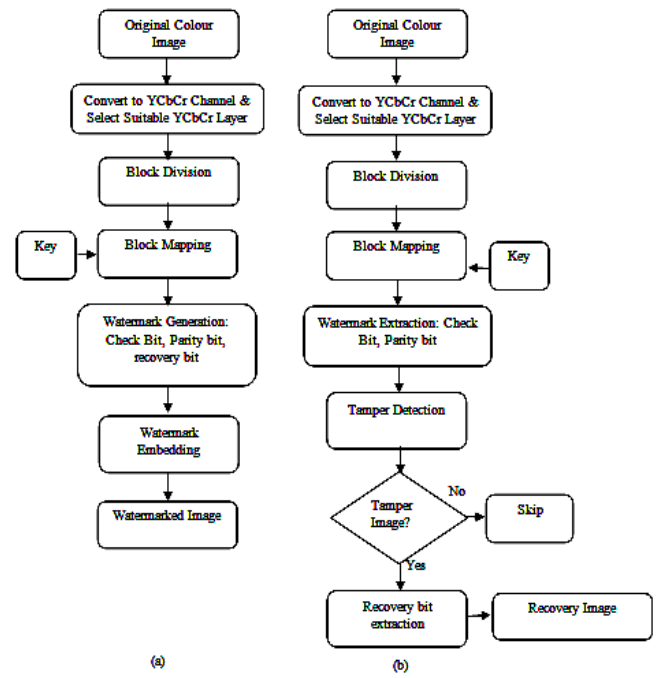


Fig. 1. Block diagram a feature-based fragile watermarking scheme of the proposed method. (a)encoder side; (b) decoder side.

Thus, the proper selection of channels for watermark insertion is required to reduce the degradation of the watermarked imagery. The first thing to do is transform the channel from RGB to YCbCr using equation (1). After that the best channel selection for the insertion process is done. In this research used Cr channel as the place of insertion. Then, by utilizing the block-based watermark method, the channel is divided into 2x2 pixels non-overlapped blocks, which can form a series  $I_t$  ( $t = 1, 2, 3, \dots, N$ ).  $N$  is the total number of blocks in the image.

$$\begin{aligned} Y &= (77/256)R + (150/256)G + (29/256)B \\ Cb &= -(44/256)R - (87/256)G + (131/256)B + 128 \\ Cr &= (131/256)R - (110/256)G - (21/256)B + 128 \end{aligned} \quad (1)$$

Initial process before watermark insertion is done by using 1-D linear transformation [2] as seen in equation (2). This transformation resulted in one-to-one mapping, where the watermark for the tamper recovery process will be inserted.

$$I_t' = [f(I_t) = (k \times I_t) \bmod N] + 1, \quad (2)$$

Where  $\{(I_t, I_t') | t \in [1, N]\}$  is the block number in each 2x2 pixel,  $k$  is a secret key which must be a prime number.

### B. Watermark Generation and Embedding Process

In the proposed scheme, the selected YCbCr channel of the original image  $I$  is partitioned into non-overlapping  $N$  block  $I_t$  ( $t = 1, 2, 3, \dots, N$ ) of size 2x2 pixels. Each block of  $I_t$  is contained four pixels, each pixel is converted to binary bit, 8 bits.

We adopted He's method [4] and Hassan's method [13] for watermark generation by utilizing the original image features, which was used in Rakhmawati [11] for



gray images. As seen in Fig. 3, we generate two watermarks in each 2x2 blocks. Four detection bits  $(c_1, c_2, p_1, p_2)$  and an eight-bit recovery  $(r_0, r_1, r_2, r_3, r_4, r_5, r_6, r_7)$ . The four detection bits replace the 2x2 block in LSB 3, and the recovery bits replace the corresponding block in LSB 2 and LSB 1 by the 1-D transformation. The following algorithm describes watermark generation and embedding.

First, to insert the watermark component, we must create the intensity value of three LSBs in each 8-bits pixel in the 2x2 block to zero, then calculate the average intensity of the five MSBs remaining in each pixel ( $AI_i$ ) as illustrated in Fig. 2. Then through the equation (3), generate the value of  $c_1, c_2$  of each 2x2 block.

$$(c_1, c_2) = ((AI_i)_2 \times K_i) \bmod 2 \quad (3)$$

Where  $K_i$  is key generated randomly of size 20 x 2, it is from 5 MSB which have four pixels and need two check bit, thus the size is 20x2.

Second, to get the value of parity bits can be seen through equation (4) and (5), where  $(r_0, r_1, r_2, r_3, r_4, r_5, r_6, r_7)$  is the binary form of the average intensity  $AI_i$  and also as a recovery bits.

$$p_1 = r_0 \oplus r_2 \oplus r_4 \oplus r_6 \quad (4)$$

$$p_2 = \begin{cases} 1, & \text{if } p_1 = 0 \\ 0, & \text{if } p_1 = 1 \end{cases} \quad (5)$$

After four detection bits and an eight-bit recovery with totally 12-bit watermark are obtained, replace the LSB 1, LSB 2, and LSB 3 of each 2x2 block respectively as shown in Fig. 3.

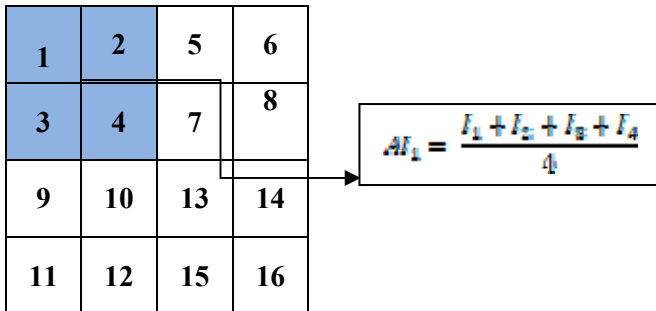


Fig. 2. Illustration watermark generation procedure for 2x2 blocks of 4x4 pixels.

Bit	8	7	6	5	4	3	2	1
Pixel 1						$c_1$	$r_0$	$r_1$
Pixel 2						$c_2$	$r_2$	$r_3$
Pixel 3						$p_1$	$r_4$	$r_5$
Pixel 4						$p_2$	$r_6$	$r_7$

Fig. 3. 12-bit watermark (c, p, r) embedded in pixels 1,2,3,4 of each 2x2 blocks non-overlapping

### C. Tamper Detection

The detection process is done on the receiver side, which basically has a process flow approximately the same as the embedding process on the sender side. The detection process bilaman damage can be explained as follows. 1) the received image is first transform to YCbCr, then the same selected channel that is used in encoder is divided into 2x2 non-overlapping blocks; 2) extract  $c'_1, c'_2, p'_1, p'_2$  in LSB 3 from each block; 3) compare  $c'_1, c'_2, p'_1, p'_2$  with  $c_1, c_2, p_1, p_2$  from original image block. If the four detection bits in each block are not the same, then mark the block as a modified block; otherwise, this block is marked as authentic.

### D. Tamper Recovery

After detection process, the authentic and tampered block can be indicated. In this proposed method only restore the damaged blocks and keep the original block unchanged. For destructed blocks, use the appropriate blocks of one-to-one mapping results as described earlier to obtain the recovery information bit. The next step covers the damaged part by extracting information from the corresponding block, which can be obtained in the last 2 bits in every block.

## III. RESULT AND ANALYSIS

In this section some experiments was conducted to test the extent of success of the proposed method. It was evaluated using the Ministry of Research Technology and Higher Education of the Republic of Indonesia logo as a representative of e-government host image, which has 200 x 200 pixels size. The scheme is evaluated based on the watermark embedding and recovery process.

### A. Watermark Embedding

As mentioned earlier, the selection of watermark components is important to maintain the quality of the watermarked imagery. To evaluate the imperceptibility of the watermarked image can be done by calculating the value of Peak Signal to Noise Ratio (PSNR) which can be seen in equation (6).

$$PSNR(I, I_w) = 10 \times \log_{10} \frac{MAX_I^2}{MSE} \quad (6)$$

Where  $I$  is original image,  $I_w$  is the watermarked image  $MAX_I$  is the maximum possible pixel value of the original image  $I$  and Mean Square Error (MSE) refer to equation (7). In which  $M$  and  $N$  shows the image dimensions.

$$MSE = \frac{1}{MN} \sum_{i=0}^{N-1} \sum_{j=0}^{M-1} (I(i, j) - I_w(i, j))^2 \quad (7)$$



Fig. 4. Test Image (a) original image; (b) watermarked image

In paper [15], it is mentioned that if the larger PSNR values show similarity between the original image and the watermarked image, which has a minimum value of 30 dB as a generally accepted perceptual value.

The PSNR value of the watermarked image will decrease when there is an increase in the number of watermark components. This can be demonstrated from the acquisition of PSNR in the proposed scheme was 36.91 dB for the watermark payload 3 bit per pixel. When compared with the method [4] which was used 2 bit per pixel, the PSNR value larger, that was 42.32 dB. The visual effect of adding the watermark component is shown in Fig. 4.

#### B. Tamper Detection and Recovery

At this stage, the calculation of the performance of the detection process is done by adding degradation as a form of tampered image. In this simulation, we used two type of attacks: the cropped image which are included in the general tamper types [4] and the collage attack. Fig. 5(a) illustrates an example of modification of the watermarked image by removing some of the name information on the logo, tamper detection results in Fig. 5(b), while Fig. 5(c) shows the recovery image. To know objectively, we use the PSNR calculation between the recovery image and the watermark image. The proposed method shows better results, i.e. 37.62 dB, while method [4] produces a PSNR value of 32.40 dB. It shows clearly that in our scheme the tampers can be detected and localized more accurate.

For collage attacks can be done by replacing certain part of the watermarked image with another image, in our experiment we used Chrome's logo of the same size as shown in Fig. 6(a), an example to illustrate the form of collage modification shown in Fig. 6(b), tampered detected area shown in Fig. 5(c), and the recovered image with PSNR 38.87 dB in Fig. 6(d). The results obtained can be seen in Fig. 7, where the PSNR value for cropped modification has a higher PSNR value than the collage modification. In addition, there are differences in graphs that tend to fluctuate for the type of collage attack compared with the type of cropped image. This is due to the high colour degradation difference between the Chrome's logo and the Dikti's logo, so the colour image recognition is more varied.

Furthermore, we compared the proposed scheme with the He's scheme [4] which had modified to RGB image for both types of degradation to show the performance. Fig. 8 and Fig. 9 shows the results of cropping and collage attacks with a tamper region ranging from 5% to 60%. The results show that the proposed scheme gives better results in

recovered image quality which experienced an average increase sharply. In addition, from the PSNR of the recovered image have a greater visual quality, with under 10% cropped attacks have more than 35 dB.

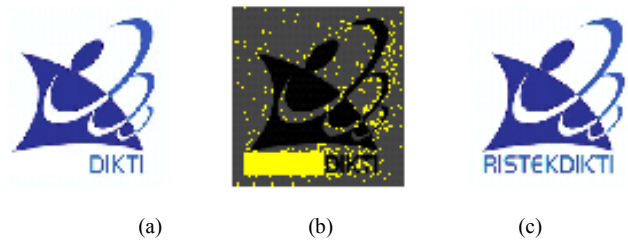


Fig. 5. Test cropped image of proposed method (a) tampered image; (b) tamper detection; (c) recovered image



Fig. 6. Test collage attack of proposed method (a) chrome'logo; (b) tampered image (c) tamper detection; (d) recovered image

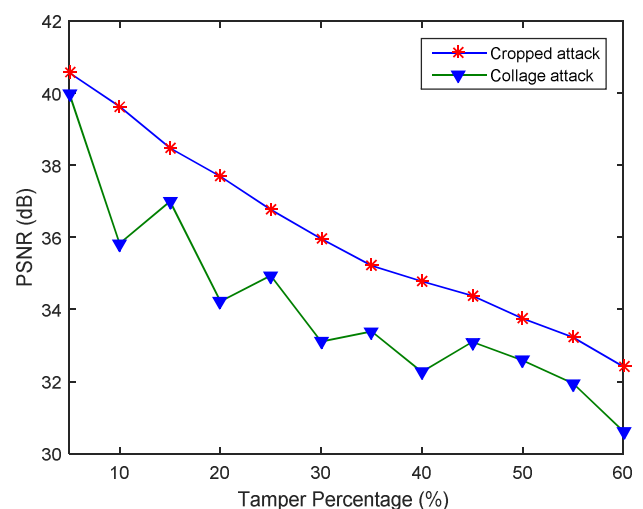


Fig. 7. PSNR of recovered image performance comparison under the collage attack and cropped attack of proposed method

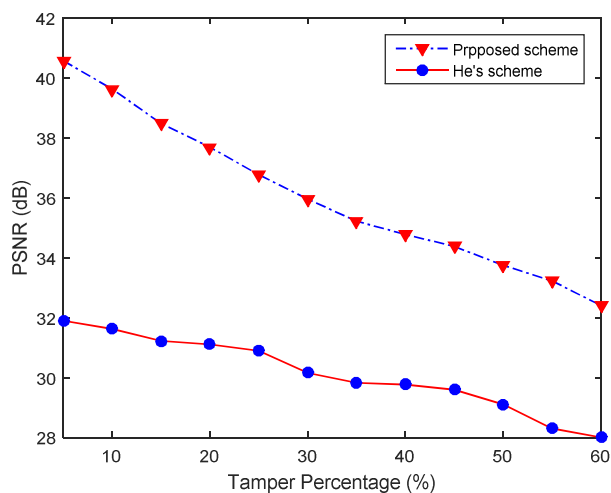


Fig. 8. PSNR of recovered image performance comparison under the cropped attack

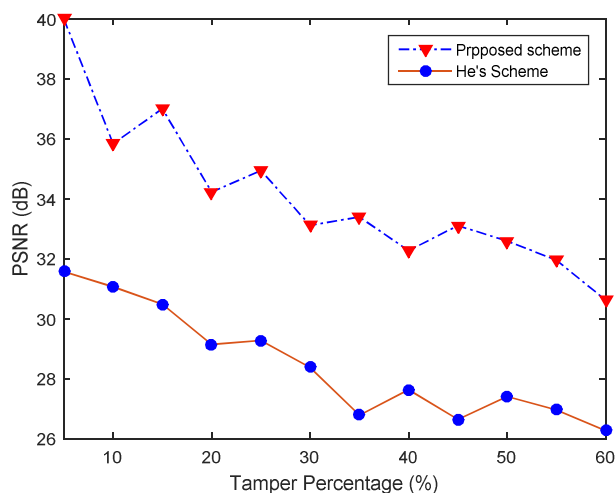


Fig. 9. PSNR of recovered image performance comparison under the collage attacks

#### IV. CONCLUSION

In this paper, we proposed fragile watermarking of color image for secure E-Government restoration in the spatial domain using LSB technique. We generate two watermarks that serve to detect and restore the tampered image. The detection bit is inserted in the 2x2 pixel in current image blocks, while the recovery bit is inserted in the corresponding block as a result of block mapping used 1-D transformation. In addition, the proposed scheme recover deliberate error created to remove image information by extracting the inserted watermark before the image sent. When compared with the methods proposed previously, using 3 bit per pixel, the PSNR of watermarked image normally have around 37 dB. The results show the average value of PSNR increased significantly for both attacks: cropped and collage attacks. In addition, the results indicate that less than 10% of the tampered blocks have been recovered well.

#### ACKNOWLEDGMENT

This research was supported by Institut Teknologi Sepuluh Nopember (ITS) through Laboratory Research Grant (Penelitian Laboratorium) Scheme 2018.

#### REFERENCES

- [1] Bravo-Solorio, S. & A.K. Nandi, "Secure fragile watermarking method for image authentication with improved tampering localisation and self-recovery capabilities", *Signal Processing*, Vol. 91, pp. 728–739, 2011.
- [2] Phen-Lan Lin, Po-Whei Huang, An-Wei Peng. "A fragile watermarking scheme for image authentication with localization and recovery." *IEEE Sixth International Symposium on multimedia software engineering* Washington DC. pp. 146-153, 2004.
- [3] Wu C-M, Shih Y-S. "A Simple Image Tamper Detection and Recovery Based on Fragile Watermark with One Parity Section and Two Restoration Sections". *Optics and Photonics*, vol. 3, no.2, pp. 103–107, 2013.
- [4] He H, Chen F, Tai H, Member S, Kalker T, Zhang J. Performance Analysis of a Block-Neighborhood- Based Self-Recovery Fragile Watermarking Scheme. *IEEE Transaction on Information Forensics and Security*.vol 7, no.1, pp.185–196, 2012
- [5] Qin, C., P. Ji, X. Zhang, J. Dong, and J. Wang, "Fragile Image Watermarking With Pixel-wise Recovery Based on Overlapping Embedding Strategy", *Signal Processing*, Vol. 138, pp. 280–293, 2017.
- [6] Chen,T-Y, M. Hwang, & J. Jan, "A secure image authentication scheme for tamper detection and recovery", *The Imaging Science Journal*, vol. 60, pp. 219–233, 2012
- [7] X. Zhang, G. Han, K. Zou, W. Li, and B. Li., "An Effective Mechanism Based on Watermark for E-government Information", In *Proceedings of the 2007 IEEE International Conference on Convergence Information Technology*, pp. 580-585, 2007.
- [8] Ali Al-Haj , Hussam Barouqa. "Copyright Protection of E-Government Document Images Using Digital Watermarking", *Proceedings of IEEE 3rd International Conference on Information Management*, pp. 441-446, 2017.
- [9] Chen T, Lu H., "Robust Spatial LSB Watermarking of Color Images Against JPEG Compression", *IEEE 5th International Conference on Advance Computational Intelligence ICACI*.pp.872–875, 2012
- [10] Lin PL, Hsieh CK, Huang PW. "A Hierarchical Digital Watermarking Method for Image Tamper Detection and Recovery," *Pattern Recognition*, Vol. 38, No.12, pp.2519–2529, 2005.
- [11] Rakhmawati, Lusia, Wirawan, Suwadi, "Image Fragile Watermarking with Two Authentication Components for Tamper Detection and Recovery", In *Proceedings of 2018 International Conference on Intelligent Autonomous Systems (ICoIAS'2018)*,pp.35-38,2018
- [12] L Rakhmawati and N Rochmawati, " Review of Some Existing Work for Self-Recovery Fragile Watermarking Algorithms", *IOP Conf. Ser.: Mater. Sci. Eng.* 288 012093, 2018
- [13] M. Hamad Hassan, and S.A.M. Gilani. "A Fragile Watermarking Scheme for Color Image Authentication" *Proceeding of World Academy of Science, Engineering, and technology*, Vol. 13, pp.312-316, May 2006.
- [14] L. R. Roldan, M. C. Hernández, J. Chao, M. N. Miyatake and H. P. Meana."Watermarking-based Color Image Authentication With Detection And Recovery Capability", *IEEE Latin America Transactions*, Vol. 14, No. 2, Feb. 2016
- [15] Mousavi, S.M. and A. Naghsh "Watermarking Techniques used in Medical Images : a Survey", *J Digit Imaging*, 2014.

# Aspect-Based Sentiment Analysis Approach with CNN

Budi M Mulyo & Dwi H Widyantoro

School of Electrical Engineering and Informatics

Institut Teknologi Bandung

Bandung, Indonesia

budi.m12@gmail.com, dwi@stei.itb.ac.id

**Abstract**—Lots of research has been done on the domain of Sentiment Analysis, for example, research that conducted by Bing Liu's (2012) [1]. Other research conducted in a SemEval competition, the domain of sentiment analysis research has been developed further up to the aspect or commonly called Aspect Based Sentiment Analysis (ABSA) [2]. The domain problem of Aspect Based Sentiment Analysis (ABSA) from SemEval is quite diverse, all of those problems arise mostly from the real data provided. Some existing problems include Implicit, Multi-label, Out Of Vocabulary (OOV), Expression extraction, and the detection of aspects and polarities. This research only focuses on classification aspect and classification of sentiment. This study uses an existing method of Convolution Neural Network (CNN) method, which was introduced again by Alex K. The study by Alex K reduces the error rate by 15%, compared in the previous year the decrease was only 5%. This research would like to propose CNN methods that have been optimized, and use Threshold (CNN-T) to select the best data in training data. This method can produce more than one aspect using one data test. The average result of this experiment using CNN-T got better F-Measure compared to CNN and 3 classic Machine Learning method, i.e. SVM, Naive Bayes, and KNN. The overall F1 score of CNN-T is 0.71, which is greater than the other comparable methods.

**Keywords**—*Aspect Classification; Sentiment Classification; Deep Learning; Multi-label; Multi-Class; Convolutional Neural Network*

## I. INTRODUCTION

The development of Machine Learning technology is growing rapidly. This development still promises better results, for example Deep Learning. Deep Learning is a concept that relies on features taken from the data. In 2012, Alex K managed to prove that Deep Learning can produce stunning results [3]. Deep Learning in his research uses Convolutional Neural Network (CNN). With those stunning results, many researchers (Google, Stanford, et al) who want to experiment further.

From the SemEval research team in 2014 only two research teams used the Deep Learning method, and the results of the two teams were not good enough [4]. In 2012, Deep Learning represented by ConvNet in 2012 produced a better model but with a different problem domain. The results of ConvNet [3] give the reduction of error results quite drastically. This result compared to previous years, the difference reach 15%. The

developments in 2012 and 2014 should be better, but this is not as expected. Other studies say that this is a matter of improper feature selection that has decreased performance from the previous year [4].

The problem of Aspect Based Sentiment Analysis (ABSA) from SemEval is quite diverse, all of those problems arise mostly from the real data provided. Some existing problems include Implicit, Multi-label, Out Of Vocabulary (OOV), Expression extraction, and the detection of aspects and polarities. The dataset provided is quite implicit because data is taken from real world data with a professional annotator. Multi-labels also become a problem because the dataset in 1 sentence has several different classifications [12]. These different classification problems require separate handling to be solved. The next problem is OOV, this problem is about how the given model can handle the test data which is not in the data during training. In the ABSA competition issue, one of the tasks assigned is Expression extraction. But extraction problem is not explained in this study because the dataset is quite implicit. Aspect and Polarity classification is a major problem in this ABSA competition, this problem is how to conduct training model to classify aspects and polarities.

The classification commonly used for aspects and sentiments is each test data only produces one aspect or sentiment of output. Even though the fact that the sentence can contain several aspects or sentiments. This is the problem that we want to solve with the proposed method. This study also aims to produce a better F-Measure than existing methods, namely CNN and classic Machine Learning.

## II. RELATED WORKS

A lot of research on sentiment analysis has been done, as in Bing Liu's research (2012) [1]. Research outside of SemEval competition to solve the ABSA problem also performed, for example by Taylor (2013) and Susanti Gojali(2016).

Research conducted by Taylor's based on the research by Liu which both use the extraction rule method [14]. The data obtained comes from the scrapping result from TripAdvisor, which contains the dataset Restaurant and Hotel. The results of this study indicate that product reviews contained on the website can be extracted using the Aspect-Based Opinion Mining method. But in the explicit aspect extraction process, it only results in 35% aspect extraction of the whole.

Another study conducted by Susanti said that the sentiment of analysis carried out on documents and sentences did not represent the wishes of the reviewers [15]. Processing at the document level and sentence has not conveyed the polarity of the aspects to be conveyed. This research comes from the construction of extraction rules from grammar, or usually called rule-based. If the dataset has bigger size will be more difficult to extract the aspect, because not all syntax for aspect and sentiment model could be extracted. For example, if there is a word “no” in front, opinion in behind the word, and the length of the sentence is 10, then this method can’t catch this negative value. To improve the results, the deeper rule-making can improve the extraction. But it takes a manual process to capture the aspects that exist in grammar. This manual process requires the of understanding one by one every sentence and lot harder. Their research based on rule-based for extraction, that needs to do a fairly complex manual process which also conducted by other researchers [13], [14], [15], [18], and [19]. Their research also raised ABSA issues, such as Aspect Extraction, Subjectivity Classification and Sentiment.

Recent studies have begun to implement CNN methods into Sentiment Analysis [10], [11]. Research from Kim who conducted several experiments, states that CNN can produce better results than other methods [10]. One of the advantages discussed in his research is that the vector words that have been trained can improve the quality of the model results. Their process also carried out experiments in domain sentiment analysis and question classification.

The most recent result of a successful Sentiment Analysis research is the Recursive Neural Tensor Network (RNTN), which focusing to overcome the problem of negative polarity sentences [9]. The accuracy of predicting fine-grained sentiment labels for all phrases reaches 80.7%, an improvement of 9.7% over the bag of features baselines. This process produce good results, it also because supported by a training model of a Sentiment Treebank. This Sentiment Treebank has a label for each parse tree, which is used for in-depth analysis of the composition effects in sentences. But this study does not use RNTN because of the unstructured dataset.

The results of the CNN-T model are also compared to the classic Machine Learning method, to find out whether the results of this model are better than the existing methods. The methods to be used in classic machine learning are SVM, KNN, and Naive Bayes. SVM uses hyperplane to split between dimensions to select the appropriate class. KNN uses proximity to points to decide class selection. And Naive Bayes uses the co-occurrence and probability functions to find out the appropriate classes.

### III. ARCHITECTURE MODEL

The architecture used has two main processes, namely Modeling and Prediction. Modelling is the architecture that constructs model Aspect and model Sentiment. Different prediction processes were performed on the aspect model and sentiment model. Prediction on aspects is how the aspect model classifies each aspect of the sentence, while the prediction in the sentiment model aims to classify sentence polarity. Fig. 1 illustrates more clearly about the architecture used, from the

input data test and training process, up to the prediction. Area A, is a data training process, Area B is a Prediction process. In this illustration also illustrated that in the middle of the process, there is a process for feature extraction with dashed lines.

The proposed model uses basis of the developed CNN method. This CNN-T model (the proposed model) is a model that collects the output of the CNN training process by taking trade-offs from the correct data and incorrect data. Output the training data is collected according to the label, then selects the best trade-off threshold that separates the correct data and incorrect data. In this way, it could generate more than one class output for one input.

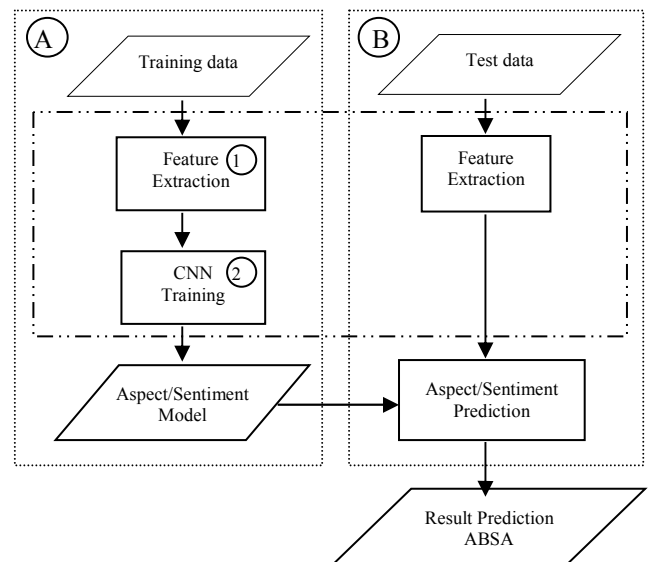


Fig. 1. The Architecture used for handling ABSA problem.

#### A. Modelling

The main problem with ABSA is to classify aspect and sentiment, so that trained model has two models to tackle this problem, namely aspect model and sentiment model. Both models are trained with the same data but each uses a different algorithm. The modeling process consists of two processes, namely Feature Extraction and Convolutional Neural Network (CNN). Feature Extraction is processing to get a feature that exists in the sentences. And CNN reprocesses these representations, to get richer features to fit with labels. The main function in modelling process is to get the optimal representation from sentences in each attribute.

This modeling process includes separating sentences with labels in their respective attributes. Attributes for each dataset is differ depending on the respective domain. If dataset training and dataset test have the different aspect, then this process cannot produce a correct result. The class attribute cannot produce the correct results because there is a possibility that class attributes are not represented during training.

This modelling process consists of two main processes, namely Feature Extraction and Training data with CNN. Feature Extraction is a process to extract training data into the process of construction data in the form of word vector. The



word vector representation for Word Embedding is not constructed from training data. Construction Embedding words require a larger collection of data so that the representation process with existing training data is not enough [4], [6]. The next process is CNN Training which performs reprocessing of representation to take the feature from more varied features.

### 1) Feature Extraction.

Feature Extraction is a process of converting sentences into vectors that represent them. This extraction feature uses Word Embedding as a library which helps representation of sentences. Word Embedding used is Glove from data train on Wikipedia and Twitter domains. The Glove is a library to represent every word with a collection of vectors. Each word in the architecture produces a representation value of 100 vectors, and for each sentence, it will be assumed consist of 100 words for each sentence. If there is a word that is less than 100, it will be padding filled with zero. So every representation of each sentence, yields for outputs that have dimensions of 100 \* 100.

### 2) CNN Training.

The next process is CNN Training, namely Processing Text Representation with the CNN method. As explained earlier, Input data representation of sentences is received by CNN in the form of vector representation. The initial process for training data is split vector representation of each vector with their respective labels. CNN training also needs to be optimized with hyperparameters that must be trained several times to produce optimal parameters.

The Architecture used in this research based on the CNN algorithm as shown in Fig. 2 [10]. This architecture uses 100 \* 100 vector representations as inputs, and the output is (1) generates multi-class outputs for aspect modeling or (2) generates binary classes for sentiment modeling. In this illustration, convolution uses two layers for filters and each layer has 3 regions and 2 filters, while in the real architecture uses the optimal values for each model (aspect / sentiment).

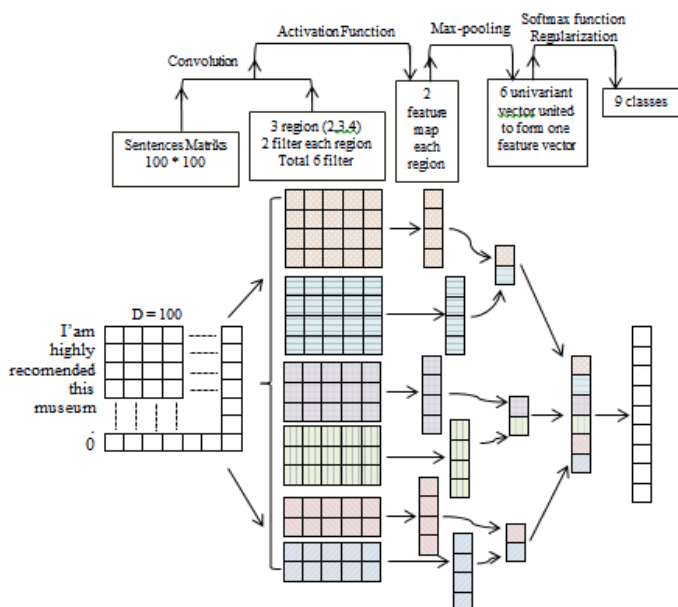


Fig. 2. CNN for the classification of sentences.

Each convolution has its own activation, but all layers in convolution process use the same activation. The activation used in the layers is ReLU which produces the same value as the input, except if the input value is less than 0 then the output is 0. Then the next process is max-pooling which produces a smaller vector. After the process, all the results are combined and represented in the 1 vector. Next process is final activation to generate a representation of each class attribute. The activation used are between softmax or sigmoid, depending on the model that wants to construct. This illustration uses 9 aspect attributes, thus the results output consists of 9 values. Another option can generate one value which is the largest value of all 9 attributes.

The initial process performed for each dataset is almost identical, that process is initializing the attributes for each dataset. Then the next process is the extraction of attributes from the label that has been initialized. Next process enters the training data CNN and performs several times the experiment to produce the optimal hyperparameter [10]. Hyperparameter in question are Filter, Filter Size, Max Pool Size, Drop Out, Epoch, and other parameters. The final activation used is (1) softmax for multi-label classification or (2) Sigmoid for binary classification. Activation produces values in their respective attributes or classified in a class. If generating one value, the closest from its class (binary) of the attributes of will be selected.

The output of this architecture is (1) class name / attribute name or (2) collection of values for a number of attributes. For model CNN-T the output used is the multi-class value. A number of output attributes represent attributes in data training, and class names / attribute names are classification outputs that are automatically selected by the system. All output data from a "set of values for a number of attributes" if combined can visualize the exact results according to the label or not, and choose a better threshold to classify the class (Fig. 4).

The basic process of training this architecture is the Convolution. Equation 1 can simplify the concept of convolution. Convolution is a mathematical process of two functions, which produces a new function that modifies one of these functions. Implementation of Convolution as dull matrix multiplication algorithm asin the equation 1.

$$(f * g)(t) = \int_{-\infty}^{\infty} f(t).g(t - x) \quad (1)$$

The symbol (f) and symbol (g) of the formula are functions, functions (g) which are the inputs and function (f) as filters. With symbol (t) that explains how many times the process is done. Symbol ( $\infty$ ), is an input symbol that can be started from any value that has a positive value up to negative. The last result is the multiplication of function (f) and function (g).

Softmax is an activation that is suitable for the aspect model, which has multi-label attributes. This aspect model can generate an output value of a number of attributes, or class name / attribute name from the largest attribute value.

The results sentiment model has two attributes, positive and negative attributes. These two attributes are very different from



the aspect model. For the aspect model, it has a multi-class attribute. The output of the sentiment model yields only one value, a value ranging from 0 and a maximum value of 1. Sigmoid activation that produces two maximum values, a value of 0 and a value of 1 are two distinct classes. If the value is close to 0, it can be said that the value goes to class 0 and vice versa for class 1. The Threshold from default system for selecting a class is 0.5. If using CNN-T, the threshold value used depends on the exact data in the original training model and the label results.

### B. Prediction

The last process is prediction and get the distribution results for each aspect then this process uses the threshold to classify. This threshold process is different in the sentiment model and aspect model.

Aspect Classification Model takes the biggest attribute value (CNN model). As for the sentiment model to choose the closeness between classes 0 and 1, the threshold used is 0.5. If it is closer to the number 0 then the selected class is class 0, and vice versa for class 1 (CNN Model).

The proposed models is the CNN-T model, which provides a threshold for classify the output. The threshold used is the intersection of each aspect, between the data being correctly fetched and the data being fetched but incorrect. As well as the sentiment model, takes the threshold value that intercepts between data retrieved correct and incorrect. An example is shown in fig. 4 and a detailed explanation is in the subsection.

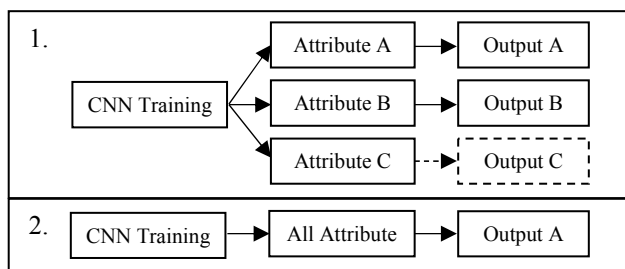


Fig. 3. Illustration of different methods from CNN and CNN-T.

Illustration in Fig 3 part 1 is CNN-T model and second illustration (part 2) is CNN model. CNN training output (CNN-T method) looks for thresholds derived from trade off all data training to classify classes. If it is larger than the threshold then classified to it class. The CNN model classifies data into a class attribute by comparing the value of the attribute generated. Shown in Fig. 3, the illustration could produce 2 outputs or more, i.e. A and B. If Fig. 3 part 2 Output C has a value lower than the threshold, then this sentence is not classified into that class (class C). The CNN model automatically classifies class attributes with the largest attribute values, so this model cannot classify more than one class.

Because input the for training data is a sentence, then the process for prediction is also used a sentence. This study does not focus on the sentiment of defined aspects. This research focuses on making an optimal model, then compared with other comparison models. In short, models that are generated from

aspect and sentiments can stand on their own, regardless of each other's models.

## IV. EXPERIMENT

This experiment shows only the optimal solutions training data. The purpose of this study is not only to produce a good classification, but also to produce a better F1 score than the comparable method. Classic Machine Learning is optimized according to each parameter. The library used is Scikit-learn [16], [17] which also determine optimal parameter value. The next sub-section will explain how the scenario is run and the result of classification report from the experiment.

### A. Scenario Experiment

There are three methods of Machine Learning that used in comparison, there are Support Vector Machine (SVM), Naive Bayes (NB), and K-Nearest Neighbors (KNN). The final result of this study is the comparison of each method using F-Measure as the balance value between Precision and Recall. Dataset Test retrieved for domains ABSA from SemEval 2015 which only used English-language datasets. This research used 2 datasets that different each other. First, the dataset that has the dataset training and test. Second, the dataset that only has the test dataset with a distinct domain. The reason for using the SemEval dataset 2015 because of the annotation process is quite difficult. In the annexation dataset SemEval requires 3 annotators. The first annotator is BRAT (Stenetorp et al., 2012), while the second annotator is tasked with validating the results. When the second Annotator disagrees or unsure of the first Annotator, then there will be decision making by a joint discussion with a third annotator.

This study also tried to conduct experiments to optimization by providing a threshold on the value of model aspects and sentiments. Each Threshold is derived from the exchange of classified data retrieved by the system that correct and incorrect. The value taken is the value that optimizes both data, so that correct data is more retrieved by minimizing the wrong data that retrieved.

### B. Test Results

Fig. 4 is an example of data visualization that consists of the entire data, true data, and false data to retrieve the best value. The x-axis is the value made by the system, while the y-axis is the number of occurrences of data. The value generated by this system is taken from the training process which gives

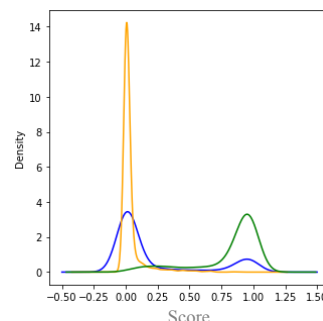


Fig. 4. The Threshold of the restaurant features.

output values between 0 and 1. The green line is the correct data distribution while orange line is the wrong data distribution. Blue line is the overall data, where the data in the visualization has been interpolated by the visualization application. So the data distribution has a value below 0 and a value above 1 that is impossible on the data.

From Visualization (Fig. 4) explain how this data distributed, whether this distribution produces better results or not. Fig. 4 is a visualization representation of how the distribution of data represents for each process. In Figure 4, the data is distributed between classes 0 and 1 in a balanced manner and the intersection of the lines in the middle with small numbers, then this model must provide a better F1 value. Balanced distribution produces better F1 value, because the trade-offs taken will be smaller between the correct data and the wrong data. Fig. 4 is the best balanced visualization, while the remaining visualization is pretty much out of balance.

Test results consist of two main models: Aspect Model and Sentiment Model. The assessment data used for the optimal model is the training data itself. Although the results of training data are good, the results of the data testing can be different.

Table I in the aspect column, the results from CNN and SVM are almost equally good. CNN is a little better than SVM on this restaurant dataset. While the result of laptop dataset, SVM slightly better 0.03 from CNN-T. Abbreviation description for F1 is for F-Measure.

TABLE I. F1 ASPECT AND SENTIMENT

F1	Restaurant		Laptop	
	Aspect	Sentiment	Aspect	Sentiment
SVM	0.64	0.72	<b>0.54</b>	0.77
NB	0.58	0.69	0.49	0.78
KNN	0.56	0.69	0.45	0.75
CNN	<b>0.66</b>	0.72	0.52	<b>0.80</b>
CNN-T <sup>a</sup>	<b>0.66</b>	<b>0.77</b>	0.53	<b>0.80</b>

<sup>a</sup>. CNN-T. (CNN using threshold for each attribute)  
Bold score is the highest score

Table 1 in the aspect column for restaurant datasets and laptop datasets has a small F1 value, between 0.4 and 0.6. This small F1 value is caused by the learning model with (1) limited data and (2) implicit data.

Threshold results for Aspect Model with Restaurant dataset with Ambience, Drinks, Food, Location, Restaurant, and Service order are as follows: 0.1546, 0.066, 0.342, 0.037, 0.164, and 0.1736 respectively. From the set Threshold, the data distribution is not centralized (correct data and incorrect data). The optimal trade-off from threshold is not guaranteed to get a better result of the test data. As seen from table I the results of CNN-T are still better than CNN.

Threshold results of the CNN-T method for Aspect Model on Laptop dataset are better than CNN model. Thresholds of sequential aspects from Connectivity, Design\_Features, General, Miscellaneous, Operation\_Performance, Portability,

Price, Quality, and Usability are as follows 0.0429, 0.13, 0.42, 0.0766, 0.15575, 0.029, 0.0753, 0.13075, and 0.138 respectively. Almost the same as the Threshold Dataset Restaurant, the distribution of the existing data is not completely separate close to the values 0 and 1 but is spread over the side to one side.

Table I in the sentiment column, shows the results from the sentiment model of the CNN model better than other models. The CNN-T model produces a better F1 than the overall model for Restaurant dataset and has a big difference with other models.

The results from CNN-T for Restaurant sentiment are better than the CNN results because of the trade-off distribution that managed to take a more appropriate Threshold. The Threshold Sentiment Restaurant chosen for CNN-T is 0.73, this shows that the sentiment distribution of class 0 exists between 0.5-0.7.

The results of restaurant and laptop sentiments are almost similar although the restaurant sentiment dataset has considerable difference Threshold values between CNN and CNN-T. The Threshold used by CNN-T is 0.713, and the Threshold of CNN is 0.5. The threshold for the laptop dataset from cnn shows that class 0 is wider (class 0 from 0 to 0.713), and class 1 is in the position of 0.713-1.

The results of those models are more focused on the one domain, then SemEval competition raises the other problem that is Out of domains. The competition for this out of domain is provided data test without training data, then the goal is to test this domain with a pre-built model. But Out of domain cannot be implemented into aspect models, only for sentiment models. Because of the different aspects, the aspect model can't be utilized to test the aspect model performance. So the test dataset can only test for the sentiment model. The test dataset for Out Of Domain issues comes from the Hotel test dataset. Training dataset for Out Of Domains comes from restaurant datasets and laptop datasets.

TABLE II. OUT OF DOMAIN RESULT

F1	Hotel
	Sentiment
SVM	0.78
NB	0.79
KNN	0.77
CNN	<b>0.82</b>
CNN-T <sup>a</sup>	0.80

<sup>a</sup>. CNN-T. (CNN using threshold for each attribute)  
Bold score is the highest score

The results in table II (Out of Domain Result) are not different from the results from the table I, where the CNN and CNN-T models still provide better results. The sentiment results in table I overall are better than the aspect models. Implicit data sets make it harder to do a good classification. But, for sentiment with features that only consist of two parts, it could give better rate results.

## EVALUATION AND DISCUSSION

The CNN-T model can extract more than 1 aspect from 1 sentence, the example will be discussed in this section. One example of the sentence is like in sentence 1.

(1) Gorgeous place ideal for a romantic dinner

Sentence 1 should have the label “Ambience” and “Restaurant”. The comparison model that will be discussed here is the CNN model, because this model has similarities with the CNN-T model. The CNN model managed to extract only the “Restaurant” aspect, so that for each sentence only one aspect was obtained. While the CNN-T model succeeded in extracting the correct aspects of “Ambience” and “Restaurant”. The CNN-T process is successful because the sentence produces values that in both aspects exceed the threshold (explained in section III, predictions).

The CNN-T model has the same basis as CNN, so the lack of data and sentences that have implicit properties can reduce the possibility of producing correct aspect predictions.

(2) Excellent food, although the interior could use some help.

The label that should be in sentence 2 are “Ambience” and “Food”. The CNN model produces only one aspect extraction, namely “Food”, but the CNN-T model produces two models namely “Food” and “Service”. The CNN model is less precise because it only produces one extraction, the CNN-T model is also wrong because it produces correct and incorrect aspects of the two extraction results.

## CONCLUSION

The average result of CNN-T from 5 experiments got the best F1 which is 0.71, compared to the other methods, namely CNN (0.7), SVM (0.69), NB (0.67) and KNN (0.64). These results prove the difference between CNN-T is not much different than other compared method. But the CNN-T model has the advantage of being able to extract 1 sentence that has several aspects.

Deep Learning which is represented by CNN and CNN-T gets better results, because the process of capturing the features obtained can take better representation than the classical machine learning method. Deep Learning is very useful for large and complex datasets, with methods that perform calculations in each subsequent layer.

The approach used in Deep Learning provides better results compared to the Classic Machine Learning model. From the entire table I, the CNN-T approach provides fairly good results in general. For a more in-depth assessment of CNN and CNN-T comparisons, the dataset requires greater validation or dataset variation. Although the model of Deep Learning (CNN and CNN-T) is on average only about 0.5 for aspects and 0.8 for sentiment, this result is quite satisfactory with fairly implicit data and little training data.

## REFERENCES

- [1] B. Liu, “Sentiment Analysis and Opinion Mining,”. Synthesis Lectures on Human Language Technologies, vol. 5, no. 1, pp. 1-167, May 2012.
- [2] M. Pontiki, D. Galanis, H. Papageorgiou, S. Manandhar, I. Androutsopoulos, “SemEval-2015 task 12: Aspect based sentiment analysis”, Proceedings of the 9th International Workshop on Semantic Evaluation (SemEval 2015), 2015.
- [3] A. Krizhevsky, I. Sutskever, and G. E. Hinton, “Imagenet classification with deep convolutional neural networks,” in *Advances in neural information processing systems*, 2012, pp. 1097–1105.
- [4] B. Wang, M. Liu, “Deep Learning for Aspect-Based Sentiment Analysis”, pp. 1-9, 2015.
- [5] R. Collobert, J. Weston, L. Bottou, M. Karlen, K. Kavukcuoglu, and P. Kuksa, “Natural Language Processing (Almost) from Scratch,” *J. Mach. Learn. Res.*, vol. 999888, pp. 2493--2537, 2011.
- [6] T. Mikolov, K. Chen, G. Corrado, J. Dean, “Efficient estimation of word representations in vector space”, 2013, [online] Available: <https://arxiv.org/pdf/1301.3781v3.pdf>.
- [7] J. Pennington, R. Socher, C. D. Manning, “Glove: Global vectors for word representation”, The 2014 Conference on Empirical Methods in Natural Language Processing (EMNLP), 2014.
- [8] C. Manning, M. Surdeanu, J. Bauer, J. Finkel, S. Bethard, and D. McClosky, “The Stanford CoreNLP Natural Language Processing Toolkit,” *ACL (System Demonstrations)*, pp. 55–60, 2014.
- [9] R. Socher, A. Perelygin, J. Wu, J. Chuang, C. D. Manning, A. Ng, and C. Potts, “Recursive deep models for semantic compositionality over a sentiment treebank,” in *Proceedings of the 2013 conference on empirical methods in natural language processing*, 2013, pp. 1631--1642.
- [10] Y. Zhang and B. Wallace, “A sensitivity analysis of (and practitioners’ guide to) convolutional neural networks for sentence classification,” *arXiv preprint arXiv:1510.03820*, 2015.
- [11] Y. Kim, “Convolutional neural networks for sentence classification,” *arXiv preprint arXiv:1408.5882*, 2014.
- [12] W. Bi and J. T. Kwok, “Multilabel Classification with Label Correlations and Missing Labels,” in *AAAI*, 2014, pp. 1680–1686.
- [13] T C Chinsha, Shibily Joseph, “Aspect based Opinion Mining from Restaurant Reviews”, *International Journal of Computer Applications*, pp. 0975-8887.
- [14] E. Marrese-Taylor, J. D. Velásquez, F. Bravo-Marquez, and Y. Matsuo, “Identifying Customer Preferences about Tourism Products Using an Aspect-based Opinion Mining Approach,” in *KES*, 2013, vol. 22, pp. 182–191.
- [15] S. Gojali, M. L. Khodra, “Aspect Based Sentiment Analysis for Review Rating Prediction”, *ICAICTA*, 2016.
- [16] F. Pedregosa, G. Varoquaux, A. Gramfort, V. Michel, B. Thirion, O. Grisel, M. Blondel, P. Prettenhofer, R. Weiss, V. Dubourg, and others, “Scikit-learn: Machine learning in Python,” *Journal of Machine Learning Research*, vol. 12, no. Oct, pp. 2825--2830, 2011.
- [17] L. Buitinck, G. Louppe, M. Blondel, F. Pedregosa, A. Mueller, O. Grisel, V. Niculae, P. Prettenhofer, A. Gramfort, J. Grobler, R. Layton, J. VanderPlas, A. Joly, B. Holt, and G. Varoquaux, “API design for machine learning software: experiences from the scikit-learn project,” *CoRR*, vol. abs/1309.0238, 2013.
- [18] D. Ekawati and M. L. Khodra, “Aspect-based sentiment analysis for Indonesian restaurant reviews”, 2017, International Conference on Advanced Informatics, Concepts, Theory, and Applications (ICAICTA), Denpasar, 2017, pp. 1-6.
- [19] Z. Fachrina and D. H. Widyantoro, “Aspect-Sentiment Classification in Opinion Mining using the Combination of Rule-Based and Machine Learning”, 2017, International Conference on Data and Software Engineering (ICoDSE), Palembang, 2017, pp. 1-6.

# Optimal ANFIS Model for Forecasting System Using Different FIS

Deasy Alfiah Adyanti  
Dian Candra Rini Novitasari  
Ahmad Hanif Asyhar

Fajar Setiawan

Department of Mathematics  
Universitas Islam Negeri Sunan Ampel Surabaya  
Surabaya, Indonesia  
deasy\_alfiadyanti@yahoo.co.id, diancrini@uinsby.ac.id,  
hanif@uinsby.ac.id

Department of Forecasting  
Perak Maritime Meteorology Station II Surabaya  
Surabaya, Indonesia  
meteomaritimsby@gmail.com

**Abstract-** Adaptive Network Based Fuzzy Inference System (ANFIS) with time series analysis is one of the intelligent systems that can be used to predict with good accuracy in all fields like in meteorology's field. However, some researches on prediction or forecasting do not emphasize the structure of the ANFIS fuzzy inference system. Thus, in this research, the optimization of the ANFIS model for forecasting maritime weather was carried out by analyzing the exact initialization determination in the three ANFIS fuzzy inference structures, they are grid partition, subtractive clustering, and fuzzy c-means clustering. The input variable used in this research is each variable for the previous two hours, one hour, and at a time and the output of this system is the prediction of one hour, six hours, twelve hours and one day ahead of the ocean current speed (cm/s) and wave height (m) using all three FIS ANFIS approaches. Based on the results, the smallest goal error (RMSE and MSE) of the three FIS ANFIS approaches used for predicting the current speed and wave height, the best model is produced by Subtractive Clustering. It can be seen that Subtractive Clustering produces the smallest RMSE and MSE error values.

**Keywords—** ANFIS, Grid Partition, Subtractive Clustering, Fuzzy C-Means Clustering, Forecasting

## I. INTRODUCTION

Some problems with forecasting require an intelligent system that combines science, techniques, and methods from various sources [1]. The ANFIS with time series analysis is one of the intelligent systems that can be used to predict with good accuracy in all fields [2] [3] [4]. As in the field of meteorology, ANFIS is quite good in forecasting maritime weather system [5].

ANFIS is a method that can handle complex and nonlinear systems through learning algorithms and numerical data (time series) [5], ANFIS can also adapt to atmospheric variables through the neuron system of Artificial Neural Networks (ANN) in ANFIS [5]. This can be seen from researches about predictions using the ANFIS Time Series model. Some of them are research conducted by Agrawal et al on Indian weather forecasting using ANFIS and ARIMA based Interval Type-2 Fuzzy Logic

Model [6]. And then, Babu, et al who comparison of ANFIS and ARIMA model for weather Forecasting [7], then research by Adyanti et al who implements the time series - ANFIS in predicting maritime weather in the Java Sea [5].

Based on the researches that have been developed, maritime weather predictions made only using the model ANFIS design grid partition (genfis1) [5]. Whereas in designing ANFIS models, there are three fuzzy inference system structures namely grid partition (genfis1 function), subtractive clustering (genfis2 function) and fuzzy c-means (FCM or genfis3 function) [3] [8] [9] [10]. The three FIS structures are quite significant to determine the accuracy of ANFIS models [3] because the FIS structure is used to train and test data on ANFIS.

During the training phase, the membership function parameters are iterated until convergence is obtained [11]. This convergence is obtained when the results of the membership function are unchanged and focus on one optimal membership function point. This can be obtained by minimizing the average squared error between output and input. Furthermore, the relationship between input and output from ANFIS is constructed through the FIS structure. FIS structure is obtained by combining the back propagation algorithm and the least squares method [11] [12] [13]. Then the performance of the three models is compared with two statistical criteria, namely RMSE and MSE.

In this research, optimization of the FIS ANFIS model for maritime weather prediction is done by comparing the three FIS ANFIS structures. The purpose of this research was to obtain the best model Ts-ANFIS to predict maritime weather patterns (current speed and wave height) from the comparison of the FIS ANFIS structure. The point taking in this case research was emphasized in one of the coordinates of Gresik waters. The expectations of the researchers from the results of this research are to obtain an effective and efficient forecasting system and be able to assist the shipping of the Gresik coastal community from the results of the ANFIS model which is seen from the point of view of the different FIS ANFIS.

## II. THEORETICAL FRAMEWORK

### A. Artificial Neural Networks and Adaptive Neural Networks

Artificial neural networks (ANN) are one of the artificial representations of human brain neurons [14]. One type of ANN is backpropagation. Then, adaptive neural networks are networks that consist of directional links [13].

### B. ANFIS

ANFIS is a hybrid method of artificial neural networks as an implementation of a fuzzy inference system [15] [16] [17]. The ANFIS method has an architecture that functionally resembles the Sugeno model fuzzy rule base architecture [18] [19]. The ANFIS parameter is divided into two, namely the premise parameter and the consequences that can be adapted to a hybrid algorithm [17].

The ANFIS structure is shown in Figure 1 below:

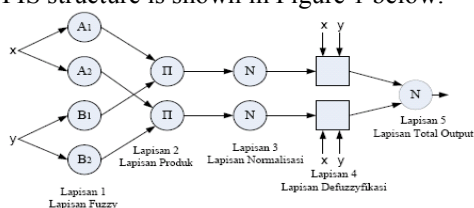


Fig. 1 ANFIS Method Structure

The steps of each layer ANFIS has been described in the theoretical framework of Adyanti et al. [5] [17].

### C. ANFIS Fuzzy Inference System Structure

In ANFIS there are three structures of FIS, they are genfis1 (Grid Partition), genfis2 (subtractive clustering), and genfis3 (FCM clustering) [3] [7], with an explanation of the three structures of the FIS:

- Genfis1 (Grid Partition) applies a grid partition from the input space to produce the initial stage of a FIS. This genfis1 is optimized from various combinations of input variables, a number of data and types of membership functions [8] [9].
- Genfis2 (subtractive clustering) is applied to generate models from data using clustering. The genfis2 clustering algorithm uses a one-pass algorithm to estimate the number of clusters and cluster centers in a set of data but does not perform optimization repeatedly [9] [10] [11] [12]. This function is built based on the subtractive clustering function with the one-pass method and training of input-output data and produces a Sugeno type fuzzy inference system [10].
- Genfis3 (FCM clustering) implements fuzzy c-means as a mechanism for clustering input data and output from this genfis3 is Mamdani or Sugeno [3] [10] [11] [12]. Genfis3 is built based on FIS that uses the FCM function by extracting a set of rules that model data behavior.

### D. Statistical Analysis

In this research two statistical criteria were used for measuring predict performance. They are the root mean

square error (RMSE) and mean square error (MSE). These statistical criteria are used to indicate the accuracy of marine weather prediction [3]. The formula of RMSE and MSE are as follow:

$$RMSE = \sqrt{\frac{1}{n} \sum_{i=1}^n (X_i - Y_i)^2} \quad (1)$$

$$MSE = \frac{1}{n} \sum_{i=1}^n (X_i - Y_i)^2 \quad (2)$$

Where n is the number of data, X and Y are the predicted and actual values.

## III. RESEARCH METHODS

### A. Types of Research

This research is a quantitative descriptive study whose function aspect is applied research. In this study, a comparison of the FIS ANFIS model for maritime weather forecasting systems (current speed and wave height) was compared.

### B. Data Collection and Analysis

Data obtained from BMKG Perak II Surabaya through Automatic Weather System (AWS) record data of 17,520 data from 1 January 2016 to 31 December 2017. Data are time series of current speed and wave height. The data is used as input in the ANFIS process. Time series analysis of current speed and wave height data is converted into three forms, that is, previous two hours, one hour, and at a time. Three forms are used as input in predicting the current speed and wave height. Furthermore, this system output is the prediction of one hour, six hours, twelve hours and the days ahead.

### C. Testing System and Evaluation

The first test is a time series analysis of weather parameters. The time series data from these parameters are divided into two data sections with a ratio of 75: 25 from 17,520. Figure 2 is a flow diagram ts-ANFIS.

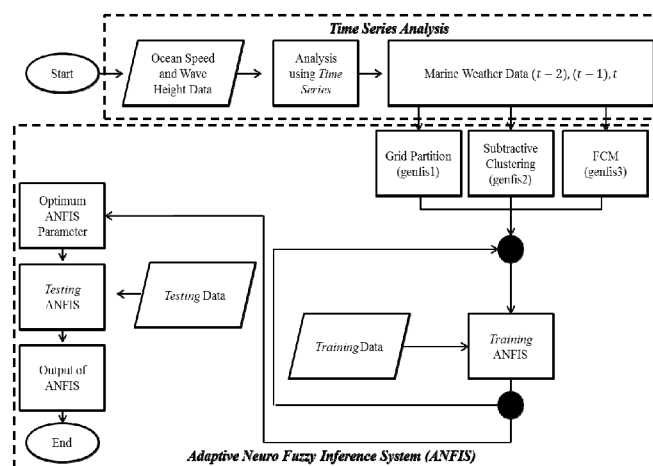


Fig. 2 ANFIS Flow Chart

Following are the steps from the flowchart:

- Maritime weather data in the form of wave height data and current speed data for the past two years.
- The data that has been obtained is then analyzed by the time series by observing input variables and output variables. Then the data is divided into two parts, 75% is used as training data and around 25% is used for data testing.
- All data that has been analyzed is time series processed using ANFIS method using MATLAB.
- In the initial process, training data is managed using ANFIS with initialization of the FIS ANFIS structure, namely *genfis1* (grid partition), *genfis2* (subtractive clustering) and *genfis3* (Fuzzy C-Means clustering).
- Conduct ANFIS training from the three ANFIS fuzzy Inference structures by entering existing training data, then the ANFIS testing phase is by entering testing data.
- Prediction results and statistical criteria are obtained.

#### IV. RESULT AND DISCUSSION

The maritime weather data used is current speed data and wave height data per hour. The data is presented in Table 1.

TABLE I. DATA SAMPLES OF CURRENT SPEED AND WAVE HEIGHT

Date	Time(UTC)	CuSpd (cm/s)	H 1/100 (m)
1/1/2017	0	21.88	0.57
1/1/2017	1	21.36	0.55
1/1/2017	2	20.84	0.54
1/1/2017	3	20.33	0.52

Time series analysis data is used as input variables ( $t - 2$ ,  $t - 1$  and  $t$ ) and output variables ( $t + 1$ ,  $t + 6$ ,  $t + 12$  and  $t + 24$ ). In predicting, three FIS ANFIS structure approaches are used namely *genfis1*, *genfis2*, and *genfis3*. Following are the results of the prediction of current speed and wave height using all three FIS approaches.

##### A. *Genfis1* (Grid Partition)

In conducting the training process in ANFIS, three FISs have the same role of training and testing data to get convergent membership functions. However, the results are adjusted according to orders from ANFIS. The grid partition (*genfis1*) produces an input variable partition where each rule has a zero coefficient on its output. This *genfis1* produces a Sugeno type FIS that models data behavior. To predict the current speed and wave height, several parameters are needed to train and test the ANFIS model.

This parameter is in the form of a membership function of 2 with the "Gaussmf" membership function type and the "Linear" membership function output. The ANFIS training process is determined by parameters that include iteration, target error, level of decline and increase. The maximum iteration is 100, the target error is 0.00001, the initial step size is 0.01, the step size decrease rate is 0.9 and the step size increase is 1.1.

From the parameters that have been determined to predict next hour through the *genfis1* training process, it will stop when the specified goal error value has been reached. For this approach, evaluation of statistical criteria uses RMSE and MSE for prediction of current speed and wave height as in Figures 3 and 4.

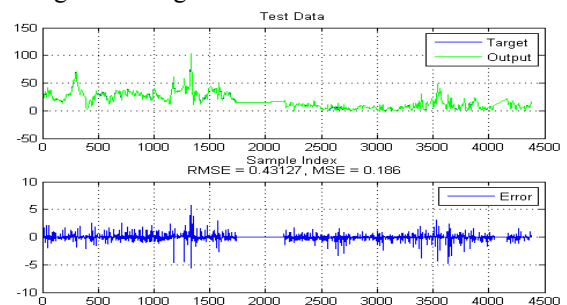


Fig. 3 Prediction of Current Speed an Hour Later

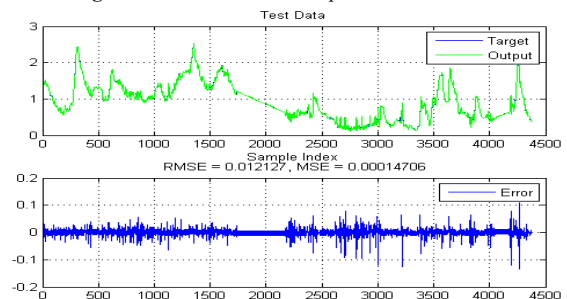


Fig. 4 Prediction of Height Wave an Hour Later

Based on the test results in Figures 3 and 4, it can be seen that the prediction chart from the actual test data (blue line) with the Ts-ANFIS result test data (green line) has the same tendency and the prediction of ts-ANFIS with *genfis1* approach shows the results on the variable current speed and wave height are quite good. It is seen from the results of forecasting that is not so far from the actual data. Then, the biggest error chart of the two variables is located in the range  $[-7; 7]$ . The largest range is in the current speed variable. The RMSE and MSE values as represented in tables 2 and 3.

TABLE II. OCEAN CURRENT SPEED PREDICTION WITH FIS GENFIS1

No	Prediction Time	Number of Validation Data	Predicted Results	RMSE value	MSE Value
1	1 Hour	4380	16.268	0.43127	0.186
2	6 Hours	4380	11.531	3.1344	9.8247
3	12 Hours	4380	5.572	5.8223	33.8995
4	24 Hours	4380	9.698	7.7315	59.7767

TABLE III. WAVE HIGHT PREDICTION WITH FIS GENFIS1

No	Prediction Time	Number of Validation Data	Predicted Results	RMSE value	MSE Value
1	1 Hour	4380	0.39	0.012127	0.00014706
2	6 Hours	4380	0.367	0.081407	0.0066271
3	12 Hours	4380	0.403	0.13814	0.019084
4	24 Hours	4380	0.555	0.21427	0.04591



In table 2 and table 3, the prediction results, the RMSE and MSE values of current speed and wave height are stated. In the tables, it can be seen that genfis1 is quite good at predicting because the results of RMSE and MSE values are good values. Especially the RMSE and MSE value from the wave height, the value is less than 0.05.

### B. Genfis2 (Subtractive Clustering)

In the ANFIS model, the subtractive clustering algorithm is used to design a rule base. Before designing the basic rules of the initial maritime weather variable data (current speed and wave height) are clustered based on the subtractive clustering algorithm. The method of grouping data is based on the degree of membership which includes the fuzzy set as the basis for weighting in clusters by determining the data that has a high potential for the surrounding data [20] [21]. This genfis2 has a pretty good estimate when the input-output is in the form of a time-scale data collection and can estimate the number of clusters and cluster centers in a data set.

Similar to genfis1 (Grid Partition), this genfis2 produces a Sugeno type FIS to model data behavior. The parameters selected for this approach are the number of membership functions in number 2 with the type of membership function "Gaussmf", the output of the membership function "Linear" and the Radius of the influence of 0.55.

The difference in the parameters of genfis2 with genfis1 is the radius of influence, in this research the radius of influence determined is 0.55 with the aim to determine the high potential of a data. The ANFIS training process is determined by the same parameters as genfis1.

In the genfis2 training process, iterations will stop when the specified goal error value has been reached. For this approach, the evaluation of statistical criteria uses RMSE and MSE for the prediction of current speed and wave height as in Figures 5 and 6.

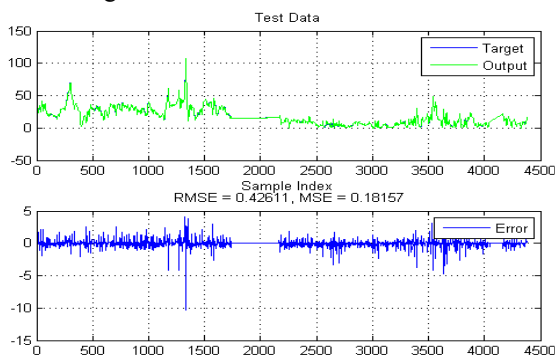


Fig. 5 Prediction of Current Speed an Hour Later

Based on the test results in Figures 5 and 6, as in the previous genfis1, the prediction chart from the actual test data (blue line) with the Ts-ANFIS result test data (green line) has the same tendency. The results of good predictions are also seen in the Ts-ANFIS forecasting with a genfis2 approach. Ts-ANFIS forecasting with the genfis2 approach shows charts of the same pattern between prediction results

and actual data. In this genfis2 approach, the biggest error chart is the current speed prediction with the range  $[-10; 3]$ .

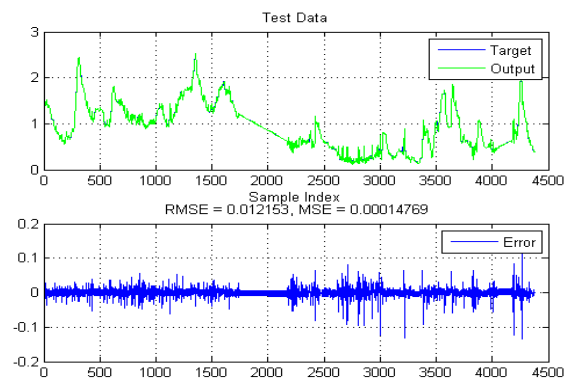


Fig. 6 Prediction of Height Wave an Hour Later

This significant error reduction occurs in a current speed data because the data with the previous data has a far range. Then, in tables 4 and 5 shows the results of the RMSE and MSE values on the prediction of current speed and wave height from the genfis2 approach. When viewed from the genfis1 table, genfis2 is better in forecasting one hour and 24 hours ahead at current speed variables. In wave height forecasting, genfis2 is better than genfis1. So, genfis2 result is relatively smaller than genfis1.

TABLE IV. OCEAN CURRENT SPEED PREDICTION WITH FIS GENFIS2

No	Prediction Time	Number of Validation Data	Predicted Results	RMSE value	MSE Value
1	1 Hour	4380	16.234	0.42611	0.18157
2	6 Hours	4380	11.752	3.2997	10.888
3	12 Hours	4380	5.676	5.9421	35.3083
4	24 Hours	4380	9.932	7.5599	57.1528

TABLE V. WAVE HEIGHT PREDICTION WITH FIS GENFIS2

No	Prediction Time	Number of Validation Data	Predicted Results	RMSE value	MSE Value
1	1 Hour	4380	0.39	0.012153	0.00014769
2	6 Hours	4380	0.37	0.080863	0.0065388
3	12 Hours	4380	0.41	0.13727	0.018843
4	24 Hours	4380	0.57	0.2111	0.044562

### C. Genfis3 (Fuzzy C-Means Clustering)

This genfis3 uses FIS type Fuzzy C-Means Clustering by extracting a set of rules to model data behavior. Input and output variables in this genfis3 are separate from the first rule using FCM as a determinant of the number of rules and functions of membership for antecedents and their consequences. This genfis3 produces a Sugeno or Mamdani type fuzzy inference system to model data behavior. The parameters in genfis3 are the number of membership functions 2 with the type of membership function "Gaussmf", the membership function output is "Linear", the number of clusters is 10, the exponential partition matrix is 2, the maximum number of iterations is 100 iterations and the maximum improvement is 0.00001. The ANFIS training

process is determined by the same parameters as genfis1 and genfis2 parameters.

Like the previous genfis1 and genfis2, the process of training 3 will stop when the specified goal error value has been reached. For this approach, evaluation of statistical criteria uses RMSE and MSE for prediction of current speed and wave height as shown in Figures 7 and 8.

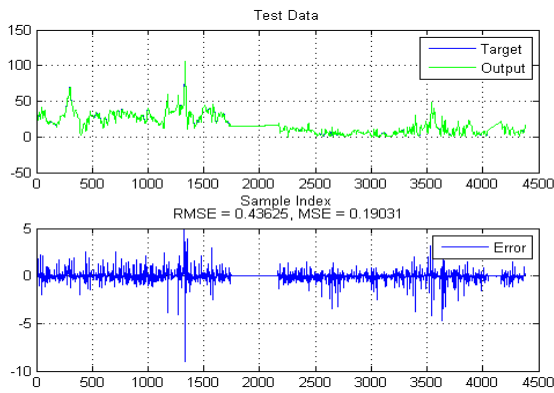


Fig. 7 Prediction of Current Speed an Hour Later

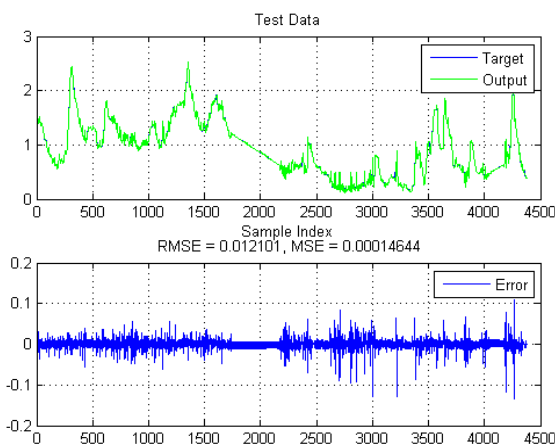


Fig. 8 Prediction of Height Wave an Hour Later

Based on the test results in Figures 7 and 8, the results of the genfis3 approach produce a prediction chart of the actual test data (blue line) with the Ts-ANFIS test results (green line) having a fairly good tendency. Genfis3 also produces good predictions, like genfis1 and genfis2. Genfis3 chart results have the same pattern between prediction results and actual data. However, the chart of errors in genfis3 is a chart that produces the farthest range, is  $[-9; 5]$ . A range error occurs in a current speed variable data.

In tables 6 and 7 show the results of the prediction, the RMSE, the MSE value of the prediction of current speed and wave height. Based on the results of the RMSE and MSE statistical criteria on weather forecasting using genfis3, the largest RMSE and MSE results were obtained. So, based on the range in the error chart, the RMSE and MSE value of genfis3 are not good for forecasting current speed and wave height.

TABLE VI. OCEAN CURRENT SPEED PREDICTION WITH FIS GENFIS3

No	Prediction Time	Number of Validation Data	Predicted Results	RMSE value	MSE value
1	1 Hour	4380	16.23	0.43625	0.19031
2	6 Hours	4380	12.354	3.3237	11.047
3	12 Hours	4380	4.731	5.9516	35.421
4	24 Hours	4380	7.81	7.6473	58.4817

TABLE VII. WAVE HIGHT PREDICTION WITH FIS GENFIS3

No	Prediction Time	Number of Validation Data	Predicted Results	RMSE value	The value of MSE
1	1 Hour	4380	0.39	0.012101	0.00014644
2	6 Hours	4380	0.366	0.080958	0.0065543
3	12 Hours	4380	0.419	0.13741	0.018881
4	24 Hours	4380	0.549	0.21613	0.046712

Of the three FIS approaches used, the membership function which aims to map the value of the membership of a data using the same type of "gaussmf" curve. Because the Gaussian curve is quite a good curve for continuous data. In this research uses marine weather data, it is continuous. Then, the number of membership functions is only two because it does not affect the results of the fuzzification [10]. The fuzzification remains smooth even though the Gaussian set range is wider. Based on the results of the FIS ANFIS approach, the three FIS ANFIS model approaches can be used to predict the current speed and wave height quite good. Meanwhile, to see the model of the FIS ANFIS approach that is best in predicting the current speed and wave height is to look at the results of the error chart of the three FIS approaches shown in Figures 9 and 10.

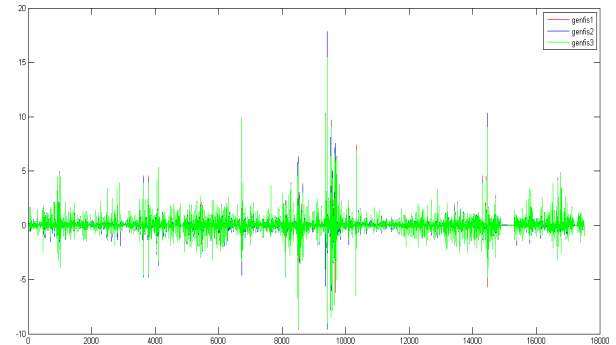
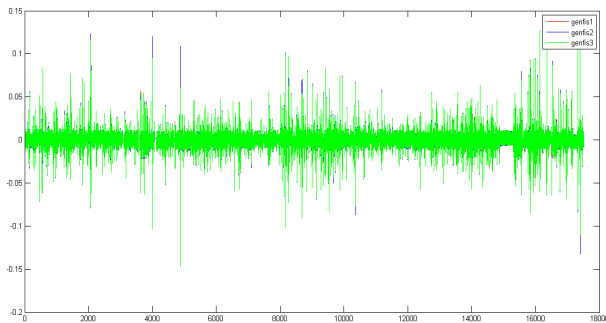


Fig. 9 Chart of Error from Three Generates of FIS to Predict Ocean Current Speed (Red = Genfis1, Blue = Genfis2, Green = Genfis3)

The ts-Anfis model of the three FIS ANFIS is a quite good predictor. Seen in the chart in Figure 3 to Figure 8 the prediction model can follow the pattern every hour of the variable current speed and wave height. On the chart of the three error ANFIS prediction in Figures 9 and 10, it can be seen that the error change pattern does not have a significant difference from the three FIS ANFIS. However, the error value of the current speed is greater than the wave height.

The range of errors seen on the Y-axis of the largest current speed is the range [-10; 3] from genfis3.



**Fig. 10** Chart of Error from Three Generates of FIS to Wave Height Prediction (Red = Genfis1, Blue = Genfis2, Green = Genfis3)

The error value of current speed is large because of the range between the data so far. So, the most optimal FIS ANFIS approach for prediction of current and wave height, it can be seen from the smallest RMSE, MSE values and seen from the range of error testing. From RMSE, MSE, and range of error, the best result for forecasting marine weather is genfis2 or Subtractive Clustering.

## I. CONCLUSION

The results of research on the optimization of the ANFIS model in predicting maritime weather patterns (current speed and wave height) using the FIS ANFIS structure comparison can be concluded as follows:

- a. The data training process using Ts-ANFIS with three FIS-ANFIS approaches produces the smallest goal error value (RMSE and MSE) of 0.186, respectively; 9.8247; 33.8995; and 59.7767 for current speed and 0.00014706; 0.0066271; 0.019084; and 0.04591 for wave heights using the genfis1. And for genfis2 the results of the smallest goal error (RMSE and MSE) are 0.18157, 10.888, 35.3083 and 57.1528 for current velocities and are 0.00014769, 0.0065388, 0.018843, and 0.044562 for wave height. Whereas for genfis3 the results of the smallest goal error values (RMSE and MSE) are 0.19031, 11.047, 35.421 and 58.4817, respectively for current speed and 0.00014644, 0.0065543, 0.018881, and 0.046712 for wave heights.
- b. Based on the results of the smallest goal error (RMSE and MSE) and from range error of the three FIS ANFIS approaches used for prediction of current speed and wave height, the best model is produced by genfis2 (Subtractive Clustering).

## REFERENCES

- [1] M. Ali, R. C. Deo, N. J. Downs and T. Maraseni, "An Ensemble-ANFIS based Uncertainty Assessment Model for Forecasting multi-scalar Standardized Precipitation Index," *Atmospheric Research*, pp. 1-71, 2018.
- [2] K. Prasad, A. K. Gorai and P. Goyal, "Development of ANFIS models for air quality forecasting and input optimization for reducing the computational cost and time," *Atmospheric Environment*, vol. 1, no. 128, pp. 246-262, 2016.
- [3] M. Mostafaei, "ANFIS models for prediction of biodiesel fuels cetane number using desirability function," *Fuel*, no. 216, pp. 665-672, 2018.
- [4] A. Baghban, J. Sasanipour, P. Haratipour, M. Alizad and M. V. Ayouri, "ANFIS Modeling of Rhamnolipid Breakthrough Curves on Activated Carbon," *Chemical Engineering Research and Design*, pp. 1-39, 2017.
- [5] D. A. Adyanti, A. H. Asyhar, D. C. R. Novitasari, A. Lubab and M. Hafiyusholeh, "Forecast Marine Weather on the Java Sea using Hybrid Methods: Time Series - ANFIS," *2017 4th International Conference on Electrical Engineering, Computer Science and Informatics (EECSI)*, pp. 1-6, 2017.
- [6] A. Agrawal and Q. M. F., "Indian Weather Forecasting using ANFIS and ARIMA based Interval Type-2 Fuzzy Logic Model," *AMSE JOURNALS-2014-Series*, vol. 19, no. 1, pp. 52-70, 2014.
- [7] R. Babu, C. B. A. Babu, D. P. Reddy and M. Gowtham, "Comparison of ANFIS and ARIMA Model for Weather Forecasting," *Indian Journal of Science and Technology*, Vol 8(S2), 70-73, January 2015, DOI: 10.17485/ijst/2015/v8iS2/58732, vol. 8, pp. 70 - 73, 2015.
- [8] N. Arora and J. R. Saini, "Time Series Model for Bankruptcy Prediction via Adaptive Neuro-Fuzzy Inference System," *International Journal of Hybrid Information Technology*, vol. 6, no. 2, pp. 51-64, 2013.
- [9] M. Azamathullah, A. A. Ghani and S. Y. Fei, "ANFIS - based Approach for Predicting Sediment Transport in Clean Sewer," *Applied Soft Computing Journal*, vol. 1, no. 12, pp. 1227-1230, 2012.
- [10] R. V. Wasu, "Medium-Term Load Forecasting using Adaptive Neuro-Fuzzy Inference System," *International Journal of Innovative and Emerging Research in Engineering*, vol. 3, no. 1, pp. 610-614, 2016.
- [11] M. W. Dewan, D. J. L. W. Huggett, M. A. Wahab and A. M. Okeil, "Prediction of Tensile Strength of Friction Stir Weld Joints with Adaptive Neuro-Fuzzy Inference System (ANFIS) and Neural Network," *Journal of Mechanical and Industrial Engineering Department*, 2016.
- [12] H. Abbasimehr, M. Setak, and M. Tarokh, "A Neuro-Fuzzy Classifier for Customer Churn Prediction," *International Journal of Computer Applications (0975 - 8887)*, vol. 19, no. 8, pp. 35-41, 2011.
- [13] R. H. Wirasmita, "Sistem Prediksi Intensitas Curah Hujan Menggunakan Algoritma Neuro-Fuzzy (ANFIS)," Universitas Islam Indonesia, Yogyakarta, 2006.
- [14] N. Ghetiya and K. Patel, "Prediction of tensile strength in friction stir welded aluminium alloy using the artificial neural network," *2nd International Conference on Innovations in Automation and Mechatronics Engineering (ICIAME) 2014*, no. 14, pp. 274-281, 2014.
- [15] A. Muslim, "Peramalan Harga Paritas Kedelai Model ANFIS," *Widyaiset*, vol. 17, no. 17, pp. 13-24, 2014.
- [16] I. L. Zulfa and Suhartono, "Peramalan Beban Listrik di Jawa Timur Menggunakan Metode ARIMA dan Adaptive Neuro Fuzzy Inference System (ANFIS)," *JURNAL SAINS DAN SENI ITS*, vol. 4, no. 1, pp. 91-96, 2015.
- [17] H. Koivo, ANFIS (Adaptive Neuro Fuzzy Inference System), Heikki Koivo 2000, 2000.
- [18] S. Barak and S. S. Sadegh, "Forecasting energy consumption using ensemble ARIMA-ANFIS hybrid algorithm," *Electrical Power and Energy Systems*, vol. 1, no. 82, pp. 92-104, 2016.
- [19] H.-T. Ouyang, "Input optimization of ANFIS typhoon inundation forecast models using a Multi-Objective Genetic Algorithm," *Journal of Hydro-environment Research*, no. 19, pp. 16-27, 2018.
- [20] S. Kusumadewi, Analisis & Desain Sistem Fuzzy menggunakan Tool Box Matlab, Yogyakarta: Graha Ilmu, 2002.
- [21] S. Kusumadewi and H. Purnomo, Aplikasi Logika Fuzzy Edisi 2, Yogyakarta: Graha Ilmu, 2013.

# Automated Diagnosis System of Diabetic Retinopathy Using GLCM Method and SVM Classifier

Ahmad Zoebad Foeady  
Dian Candra Rini Novitasari  
Ahmad Hanif Asyhar

Department of Mathematics  
Universitas Islam Negeri Sunan Ampel Surabaya  
Surabaya, Indonesia  
deddyzoebad711@gmail.com, diancrini@uinsby.ac.id,  
hanif@uinsby.ac.id

Muhammad Firmansjah

Department of Eye Health Science  
Medical Faculty, Airlangga University  
RSUD Dr. Soetomo  
Surabaya, Indonesia  
Firmansjah.spm@gmail.com

**Abstract**— Diabetic Retinopathy (DR) is the cause of blindness. Early identification needed for prevent the DR. However, High hospital cost for eye examination makes many patients allow the DR to spread and lead to blindness. This study identifies DR patients by using color fundus image with SVM classification method. The purpose of this study is to minimize the funds spent or can also be a breakthrough for people with DR who lack the funds for diagnosis in the hospital. Pre-processing process have a several steps such as green channel extraction, histogram equalization, filtering, optic disk removal with structuring elements on morphological operation, and contrast enhancement. Feature extraction of preprocessing result using GLCM and the data taken consists of contrast, correlation, energy, and homogeneity. The detected components in this study are blood vessels, microaneurysms, and hemorrhages. This study results what the accuracy of classification using SVM and feature from GLCM method is 82.35% for normal eye and DR, 100% for NPDR and PDR. So, this program can be used for diagnosing DR accurately.

**Keywords**—Diabetic Retinopathy, SVM Classifier

## I. INTRODUCTION

Diabetes mellitus is a chronic metabolic disorder that occurs because the pancreatic system in the body cannot produce enough insulin effectively so that blood sugar levels are not balanced. As a result, there will be an increase in the concentration of glucose in the blood (hyperglycemia). The prevalence rate of this disease is quite high every year. In 2014, the World Health Organization (WHO) noted that the incidence of diabetes mellitus in 18-year-olds was 8.5% of all diabetics worldwide. In 2015 the death rate from diabetes was 1.6 million. However, the highest mortality rate occurred in 2012 which was 2.2 million people from the number of deaths that occur each year [1].

Diabetes mellitus is known as a silent killer because it is often not recognized by patients and can only be known when complications have occurred. One complication due to

diabetes mellitus is Diabetic Retinopathy (DR). This disease spreads to the eye as it makes the sufferer experience visual impairments even to experience blindness. The DR usually attacks diabetics around 10 to 15 years after contracting diabetes [2]. In this case, high glucose levels will normally attack the eye's nerves and cause leakage and swelling of the eye's nerves which will form several components namely microaneurysms, hemorrhages, hard exudates, cotton wool spots, or venous loops [3]. This component becomes the benchmark for the severity of DR.

The identification process has a morphological operation process. Morphological operation is a process to eliminate images that are not needed then information that will be taken more clearly and can be continued in the next process [4]. In this study, a morphological operation used structuring element (SE) which aims to eliminate noise in the background. Wong li yun has succeeded to classifying DR with this morphological operation and backpropagation as a classification method [5]. In this study, the same morphological operation will be used and using SVM classifier because this method faster than backpropagation.

M. Ponni Bala et al explained in his paper that people have abnormalities DR usually characterized by the growth of ocular nerves on the surface of the retina of the eye so that the condition of DR disease is very severe and needs special treatment [6]. WHO stated that in 2002 5% of the world's blindness was caused by DR. It is about 5 million people got blindness [1]. Therefore, to prevent an increase in blindness due to DR, it is necessary to identify early DR diseases based on their severity to reduce worldwide blindness incident.

In this case, the DR has some severity. The severity can be classified into normal, mild, moderate, severe, and proliferative [3]. The easiest way to detect DR disease is to use an image color fundus that can be obtained at hospital. This is possible to obtain the results of microaneurysm (MA) and blood vessel hemorrhages (BV) which is useful to



determine the severity of the infected DR and to find out the initial impact as a sign of DR that attacks the eye. Therefore, it is necessary to detect MA and hemorrhages in the eye so that it can be known the severity of DR. This DR classification is using feature extraction result which is obtained from blood containing features (MA, vessels, and hemorrhages) as a benchmark to determine the severity of DR. The feature that will be detected is BV because it already has MA and hemorrhages and can ease to retrieve data [5].

Before classifying BV, it is necessary to analyze the visual texture of the image obtained using the process available on a computer aided diagnosis system (CAD) in order to determine the severity of the DR through the image color fundus. Some of the steps which are undertaken for the detection and classification of BV using CAD include pre-processing, segmentation, feature extraction, and classification. These steps are done by using several methods to be able to process the color fundus image such as histogram equalization, median filter, binary, morphological operation, GLCM, SVM, ANN, and others.

Several studies have been conducted to detect and classify its features by using the CAD process. A research which was conducted by V. A. Aswale in 2017 on the detection of DR using SVM Classifier and PNN Classifier resulted the 93.33% SVM and 89.60% PNN accuracy. So, it can be concluded that classification with SVM is better than using PNN [7]. Furthermore, the second study regarding SVM was carried out by Md. Hafizur Rahman. It was related to automatic face detection and automatic gender classification using SVM Classifier and Neural Network. The results of the comparison between the two methods resulted in an accuracy of 65% using the Neural Network and 85.5% using SVM [8]. Pooja M. had successfully identified DR using GLCM and the area as feature extraction and SVM as classification. In this paper only classified DR into two classes, that is normal and DR. So, in this study will classify normal and DR then its data will be classified again into NPDR and PDR [9].

Based on previous studies, the CAD process which was used in this research is pre-processing using histogram equalization, and feature extraction using GLCM. In this study, the researcher takes GLCM as a method because it is a feature extraction technique with a second-order statistical feature that performs a probability calculation of an adjacency relationship between two pixels with the distance and a particular angular orientation of the current image [10]. After the statistical feature is obtained through feature extraction using GLCM, its result is used to classify DR based on features of MA, vessel, hemorrhages with the SVM method.

SVM is a pattern recognition method that aims to find the best hyper plane that divides between classes. The SVM method is strongly recommended in the classification of images that focus on the brightness level. Therefore, this method is suitable for determining MA [7]. After the MA was classified using the SVM method, the result focused on the classification of normal, abnormal eyes, non-proliferative diabetes retinopathy (NPDR) and proliferative diabetes retinopathy (PDR). The researcher expects that this study can

contribute to help the medical side detect early MA to find out the level of DR severity.

## II. LITERATURE REVIEW

### A. Diabetes Mellitus

Diabetes Mellitus is a chronic metabolic disorder that occurs because the body's pancreas system cannot produce enough insulin effectively and cause unbalanced blood sugar levels (increased glucose concentration in the blood/hyperglycemia) [11].

### B. Diabetic Retinopathy (DR)

Diabetes Mellitus is a disease of a silent killer. This disease is not recognized by the patient and can be known when complications occurred. One of the complications of diabetes mellitus is Diabetic Retinopathy (DR) [2]. This disease spreads to the eyes and causes the sufferer to experience vision problems even to blindness. High glucose levels will normally attack the eye nerve, causing leakage and swelling of the eye nerve which will form several components such as microaneurysms, hemorrhages, hard exudates, cotton wool spots, or venous loops [5].

### C. Color Fundus Image

Eyes are a human vision organ which is located in a protected cavity like an eyelid [3]. The signs of DR cannot be seen directly but it can be seen through an image called color fundus image. Color fundus image can shown in figure 1.

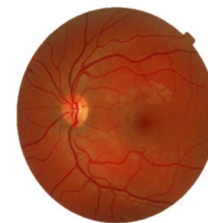


Fig. 1. Color Fundus Image.

### D. Green Channel Extraction

RGB image consists of three channels: red channel, blue channel and green channel. The red channel contains images with high saturation level. The blue channel does not load much information because there is a lot of noise which will have difficulties in finding the desired information, while on the green channel, the contrast level better than others. In this case, it used green channel. This will result clearly visible eye nerve and has more high brightness level than in the red channel and blue channel [7].

### E. Histogram Equalization

The histogram image provides the information related to the pixel intensity deployment in the image. Images that are too light or too dark will have a narrow histogram. Therefore, it is necessary to change the spread of image intensity values

by using the improvement of an image. There are several functions in MATLAB which can be used for image contrast improvement such as *imadjust*, *histeq*, and *adapthisteq*. The contrast improvement has histogram equalization [12]. The purpose of image contrast improvement is to obtain an even histogram distribution. So, each gray level will have the same number of pixels.

#### F. Morphological Operation

Morphological operation is a method used to improve image and can make information clearly visible by removing noise in the image [4]. Structuring element (SE) is one method in morphological operations. SE is a method of image improvement by probe the input shapes in the image matrix which will later be processed to erosion or dilation. SE is often used to remove optical disks (OD) or eliminate noise at the layer and the information obtained more accurate [7].

#### G. Filtering

The median filter method is a filter that serves to smooth and reduce noise or disturbance in the image. This filter is very effective to remove the salt and paper type noise and also to maintain the image detail because it does not depend on the difference of its neighboring values [13].

#### H. Contrast Enhancement

In the process of image repair, there is a function to improve gray scale and true-color images. In this study, the contrast improvement which is used is "*imadjust*" which aims to map the intensity values in the gray scale to obtain better intensity [13].

#### I. Gray Level Co-occurrence Matrix (GLCM)

The technique which is used to derive two-order statistics is to calculate the probability of an adjacency relationship that occurs between two pixels at a certain distance and angular orientation. This method is known as the Gray Level Co-occurrence Matrix (GLCM) [10]. In addition, GLCM can be said to be a second-order statistical feature extraction method which uses a co-occurrence matrix which is an intermediate matrix that represents the neighbor relationship between pixels in images in various orientation directions and spatial distances [14]. To get GLCM feature, there are several ways that can be searched such as energy, contrast, Homogeneity, entropy, and correlation.

Energy denotes the size of the concentration of the pair with a certain gray intensity on the co-occurrence matrix and defined in equation 1.

$$Energy = \sum_{i=1}^L \sum_{j=1}^L p(i,j)^2 \quad (1)$$

The contrast shows the size of the spread of moments of inertia or variation in the image matrix [15] [16]. If the distance is far from the main diagonal of the image matrix, the contrast value of the image is large. Contrast is defined in equation 2.

$$Contrast = \sum_i \sum_j |i - j|^2 p(i,j) \quad (2)$$

Homogeneity shows the degree of homogeneity of an image on a gray scale level. The homogeneous image will have a large homogeneity value [15]. Homogeneity is defined in equation 3.

$$Homogeneity = \sum_{i=1}^L \sum_{j=1}^L \frac{p(i,j)^2}{1 + (i - j)^2} \quad (3)$$

Entropy shows the irregularity of the shape size. Entropy measures information or messages that lost from a transition signal and also calculates image information which is defined in equation 4.

$$Entropy = \sum_{i=1}^L \sum_{j=1}^L p(i,j) (-\ln p(i,j)) \quad (4)$$

Correlation represents the linear dependence measure of the gray currency matrix of the image [15]. It can be defined in equation 5.

$$Correlation = \sum_{i=1}^L \sum_{j=1}^L \frac{(i - \mu_i)(j - \mu_j)p(i,j)}{\sigma_i \sigma_j} \quad (5)$$

#### J. SVM Classifier

SVM is a pattern recognition method that aims to find the best hyper plane that separates the class. Basically, the initial idea of SVM is to maximize hyper plane boundaries because a maximum hyper plane will give a better generalization on the classification method. The hyper plane will be a separator of two classes of data input space is +1 and -1 [17]. Hyper plane will be maximal if the distance between hyper plane and data support vector of each class is optimal. The SVM method is strongly recommended in classifying images that races at the brightness level. Figure 2 shows an SVM illustration with an optimal hyperplane.

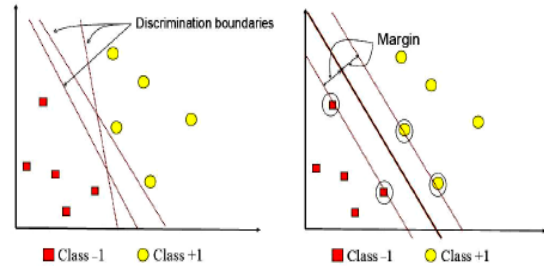


Fig. 2. SVM with the Best Hyperplane that Separates Two Classes

#### K. Confusion Matrix

The confusion matrix is a method which is used to measure the accuracy of a classifier. This method can find out the accuracy, specificity, and sensitivity [18]. To obtain accuracy, specificity, and sensitivity scores, it is necessary to find the True Negative (TN), False Positive (FP), False Negative (FN), True Positive (TP) values on confusion matrix. Confusion matrix table can be shown on table 1.



TABLE I. CONFUSION MATRIX

Actual	Classification	
	+	-
+	True Positive (TP)	False Negatives (FN)
-	False Positive (FP)	True Negatives (TN)

After obtained the value of TP, TN, FP, FN, it can be searched for accuracy, sensitivity, and specificity. That equation defined in equation 6, 7, and 8.

$$Accuracy = \frac{TP + TN}{TP + TN + FP + FN} \quad (6)$$

$$Sensitivity = \frac{TP}{TP + FN} \quad (7)$$

$$Spesificity = \frac{TN}{TN + FP} \quad (8)$$

Accuracy is a success rate in the performed classification. Sensitivity is tinged where people diagnosed the disease is indeed a person who exposed disease. The specificity will be better if normal data is identified normally.

### III. RESEARCH METHODS

#### A. Types of Research

Research on detection of MA, vessels, hemorrhages for the diagnosis of DR severity by using the SVM method is a quantitative descriptive study. It categorized from the aspect of function in this research, It's applied research which aims to assist medical side as alternative detection MA, vessels, hemorrhages to know the severity of DR.

#### B. Data Collection and Analysis

Data color fundus image is obtained from diaretddb with the amount of data as many as 44 data. Data color fundus image will be divided into training and test data. The training data in this study is 6 normal data and 21 DR data. The test data consists in 4 normal data and 13 data DR. The DR data will be subdivided into training data which consists of 18 NPDR data and 2 PDR data, while the test data consists of 12 NPDR data and 2 PDR data. The weakness of data from diaretddb is the absence of labeling for classification. Therefore, labeling in this classification is validated by a doctor from the Dr. Soetomo Surabaya hospital.

Furthermore, the analysis of color fundus image data such as preprocessing process, feature extraction by using GLCM and classification by using SVM. The first step is to improve the image fundus image or color fundus image. Because the color fundus image basically cannot be used as the initial parameter to identify the DR directly. Furthermore, the preprocessing process required stages of improvement including green channel extraction, equalization histogram, optical disk elimination, filtering with a median filter, contrast enhancement, and morphological operation. After the color

fundus image has improved, the next step is to conduct feature extraction by using GLCM. Statistical features that are focused on feature extraction include energy, correlation, contrast, homogeneity, and entropy. This statistical feature is used as input for SVM to classify MA, vessels, and hemorrhages as determinants of the DR severity.

#### C. Testing Data Evaluation

The first test is done by image preprocessing process from color fundus image to get MA feature, vessels, and hemorrhages. Then, the feature is analyzed with texture by using GLCM. Statistical features obtained through feature extraction of GLCM are used as inputs for SVM for MA classification, vessels, and hemorrhages as determinants of DR severity. To achieve the objectives of this research, steps are needed to be sequential and systematic. Figure 3 shows the flowchart of data processing until the classification as a determinant of the severity of DR.

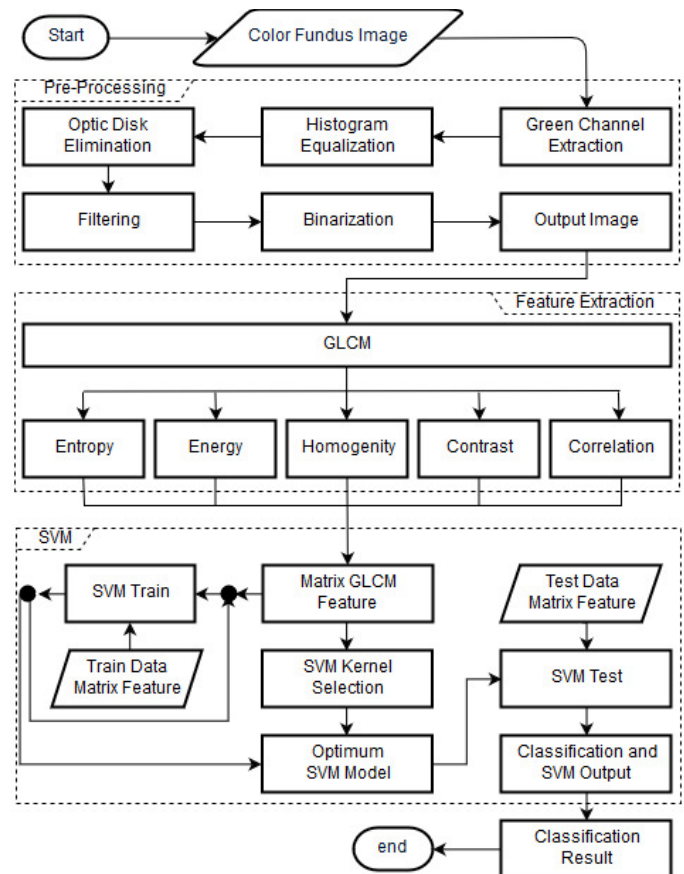


Fig. 3. Flowchart Automatic Detection DR

The steps of automatic detection of DR using SVM as follows:

##### a. Pre-processing

The color fundus image which is obtained from the hospital cannot be used directly as a parameter to identify the DR. Therefore, it is necessary to clarify the components of the DR cause in the eye. So, it can easily be known whether the eye retina has been infected with DR. This image processing stage will be the key to detect DR

in the retina. There are many ways that can be used in this pre-processing stage, such as changing the image to the gray level, contrast settings, and also noise removal.

#### 1) *Green Channel Extraction*

RGB image have three channels such as red channel, blue channel and green channel. The red channel contains images with high saturation level, the blue channel does not load much information because have a lot of noise that will hard to finding the desired information, while on the green channel the contrast level better than others then in this case used green channel. The result is the eye nerve will be clearly visible and has a high brightness level than in the red channel and blue channel.

#### 2) *Histogram Equalization*

Histogram equalization is a technique to adjust the intensity value of the image to be processed in order to get maximum results. In this stage, a contrast-limited adaptive histogram equalization (CLAHE) is used. By using CLAHE, the image will be adjusted to the best contrast level that the result will suitable for processing. But before the CLAHE process is done, first we need complement the image to make the image more clearly when enhanced this contrast.

#### 3) *Optic Disk Elimination*

To eliminate optical disk (OD), then morphology is required to remove the OD on the layer. At this stage structuring element (SE) is required with the default ball-shaped type radius 8. Once the morphology results obtained, the previous image is subtracted with morphological results to produce an image without OD.

#### 4) *Filtering*

The next stage is the filter to remove the background contained in the picture. This stage applies a 3x3 median filter to remove pixels that have low light intensity. The filter result in the morphological stage is to remove noise in the background. In the morphology, the SE used is disk-shaped with a radius 15. Disk-shaped is used because it is more optimal to remove noise than other shaped. After the background has been cleared, the next process is a reduction between the results filtering with morphological results to the remaining components that are useful as a benchmark DR.

#### 5) *Contrast Enhancement*

Furthermore, the next step is to conduct an increase in the brightness of the image so that the components are clearly visible and can be processed to get the classification feature.

#### b. *Feature Extraction*

After the color fundus image has improved, the next step is feature extraction process by using GLCM.

Statistical features that focused on feature extraction are include energy, correlation, contrast, homogeneity, and entropy.

#### c. *SVM classifier*

The vector feature matrix of energy, correlation, contrast, homogeneity, and entropy GLCM is used as training and testing on SVM classifier. The selection of kernel and SVM parameters are needed because the data in this study is in the form of nonlinear data. After obtaining the optimal SVM model through the training process, testing phase is conducted. After the testing phase, the optimum model is detected by DR. Then results of classification are divided into four classifications namely, normal eye, abnormal eye, NPDR, and PDR.

### IV. RESULT AND DISCUSSION

Some process for detecting the severity of DR is required. The process includes pre-processing, feature extraction, and classification. Pre-processing used to improve image quality until the features are clearly visible. Feature extraction used to obtain statistical data from microaneurysms features and hemorrhages features. Classification used to divide into 2 classes, that is Normal-Abnormal (DR) and NPDR-PDR. The DR sample data can be shown on figure 4.

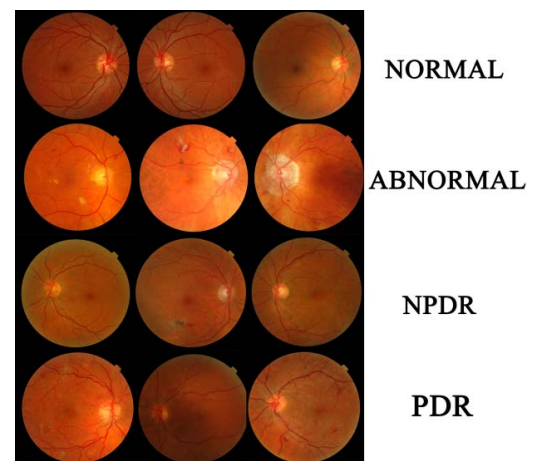


Fig. 4. Sample data of color fundus image

#### A. *Pre-processing*

Pre processing is the first process to obtain the data. Preprocessing data adapted to the available sequence data obtained and good for processing to the next stage. In the preprocessing process starts from the color fundus image, green channel extraction, histogram equalization, optical disk remove, filtering, and contrast enhancement. The results of preprocessing can be shown on figure 5. In Figure 5.a is the color fundus image and the green channel extraction results in figure 5.b. Image quality improvement using histogram equalization on Figure 5.c and then optical disk is eliminated using structuring element in Figure 5.d and followed by median filter to eliminate noise in Figure 5.e looks clearer than previous image and the last step is to increase the contrast of image on Figure 5.f.

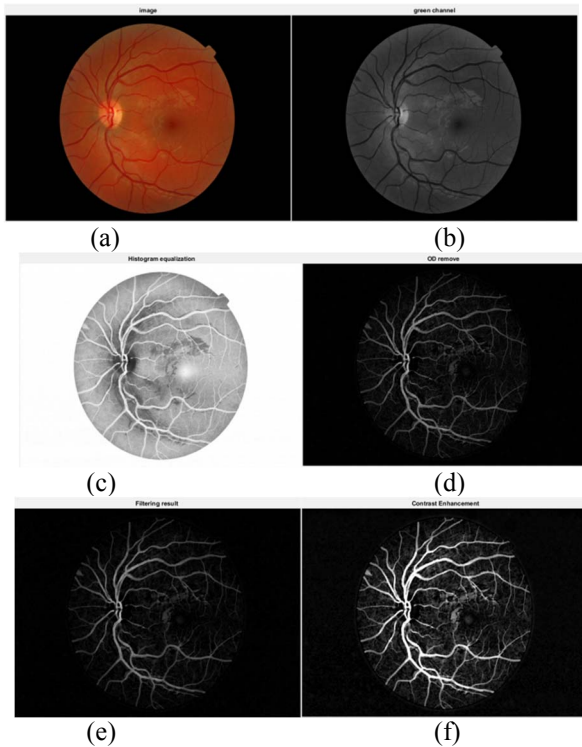


Fig. 5. (a) color fundus image (b) green channel extraction (c) Histogram equalization (d) optic disk elimination (e) filtering (f) contrast enhancement

### B. Feature Extraction

At this stage, the image can be taken by the final of gray scale image, because the GLCM method can only retrieve data from gray scale images. Then the data will be classified using the SVM Classifier. Sample data of this feature extraction can be shown on table 2 and table 3. That statistical data obtained will be processed on the SVM classifier to obtain classification results.

TABLE II. DATA SAMPLE FOR NORMAL AND DR

No.	Feature extraction				Class
	Contrast	Correlation	energy	Homogeneity	
1	0.263659	0.909002	0.581941	0.937558	Normal
2	0.237590	0.923486	0.546646	0.936890	
3	0.261579	0.917437	0.536592	0.934314	
4	0.238781	0.913206	0.535697	0.931708	
5	0.284234	0.924740	0.522379	0.927582	DR
6	0.268286	0.916974	0.533217	0.930133	
7	0.361264	0.907719	0.288979	0.879047	
8	0.260572	0.922748	0.548006	0.933424	
9	0.205339	0.933712	0.563308	0.939471	
10	0.275688	0.912088	0.520706	0.926873	

TABLE III. DATA SAMPLE FOR PDR AND NPDR

No.	Feature extraction				Class
	Contrast	Correlation	Energy	Homogeneity	
1	0.439666	0.859883	0.500604	0.906281	NPDR
2	0.387012	0.864807	0.437227	0.899016	
3	0.413319	0.852143	0.444838	0.896829	
4	0.385913	0.875002	0.539765	0.915449	
5	0.434523	0.863416	0.453694	0.899908	
6	0.428175	0.856331	0.537404	0.914659	
7	0.402631	0.865386	0.509469	0.910613	
8	0.35231	0.862393	0.581968	0.923809	
9	0.46964	0.866296	0.501231	0.909246	PDR
10	0.573235	0.851027	0.208358	0.82974	

### C. SVM Classifier

The input data for the SVM Classifier process is a feature that has been extracted in the GLCM method, which includes contrast, correlation, energy, and homogeneity. Then the results of the classification will be validated using confusion matrix and obtained percentage of accuracy (Ac), sensitivity (Sn), and specificity (Sp). This classification experiment was carried out using various degrees in GLCM. The results of the experiment can be shown on table 4.

TABLE IV. CLASSIFICATION RESULT

Model	Degree	Sp	Sn	Ac
Normal and DR	0°	100%	76.92%	82.35%
	45°	100%	61.53%	72.58%
	90°	100%	53.85%	64.71%
	135°	50%	46.15%	47.06%
NPDR and PDR	0°	91.67%	100%	92.86%
	45°	91.67%	50%	85.71%
	90°	91.67%	50%	85.71%
	135°	100%	100%	100%

From the experimental results in table 4, it can be seen that best results are obtained at 0° GLCM in the Normal-DR class and 135° GLCM in the NPDR-PDR. The best SVM results is True Negative (TN), False Positive (FP), False Negative (FN), True Positive (TP) that can be shown on table 5.

TABLE V. BEST RESULT OF SVM CLASSIFIER

Model	TN	TP	FP	FN
Normal and DR	4	10	0	3
NPDR and PDR	12	2	0	0

Based on the results of the classification in table 4, value of accuracy, sensitivity, and specificity calculated as success standard of the classification experiments presented in table 5. On table 5, there are 3 of the 13 normal data identified as DR. So, total of the data identified as DR is 7 data, which it should be only 4 DR data. it caused sensitivity percentage value of

normal and DR classification is 76.92%. Meanwhile, specificity percentage value of normal and DR classification is 100% because all testing data identified into normal class. So, the accuracy percentage value of normal and DR classification is 82.35%.

On table 2, normal and DR class data are almost same, so DR data has similar characteristics data of normal class which it caused feature extraction data can't divide data into two classes and classifications of normal and DR models get poor sensitivity percentage value.

On table 3, NPDR and PDR data has specificity, sensitivity, and accuracy percentage value is 100%. It caused by the contrast data between NPDR and PDR which can divide data into two classes. In NPDR data contrast is below 0.45, meanwhile in PDR data contrast is above 0.45. So all the data of NPDR and PDR Classification identified equal as initial data.

## V. CONCLUSION

From the results of research on automatic detection of color fundus image with GLCM method as statistical data and SVM classifier, it can be concluded that from the beginning of pre-processing process, feature extraction, SVM classifier to classify between normal people and DR sufferer has an accuracy of 82.35%, and on the classification of patients with NPDR and PDR has an accuracy of 100%. So the SVM classifier method with the data obtained using GLCM can be considered successful for the application of color fundus image as a classification between normal people and people with DR.

## REFERENCES

- [1] World Health Organization, "Diabetes," 15 November, 2017. [Online]. Available: <http://www.who.int/news-room/fact-sheets/detail/diabetes>. [Accessed: 19-Jun-2018].
- [2] N. Gori, "Detection and Analysis of Microaneurysm in Diabetic Retinopathy using Fundus Image Processing," vol. 3, pp. 907–911, 2017.
- [3] A. Sopharak, B. Uyyanonvara, S. Barman, and T. H. Williamson, "Automatic detection of diabetic retinopathy exudates from non-dilated

retinal images using mathematical morphology methods," *Comput. Med. Imaging Graph.*, vol. 32, no. 8, pp. 720–727, 2008.

- [4] R. Srisha and A. M. Khan, "Morphological Operations for Image Processing: Understanding and its Applications Morphological Operations for Image Processing: Understanding and its Applications," *NCVSComs-13*, no. December, pp. 17–19, 2013.
- [5] W. L. Yun, U. Rajendra Acharya, Y. V. Venkatesh, C. Chee, L. C. Min, and E. Y. K. Ng, "Identification of different stages of diabetic retinopathy using retinal optical images," *Inf. Sci. (Ny)*, vol. 178, no. 1, pp. 106–121, 2008.
- [6] C. Aravind, "Automatic Detection of Microaneurysms and Classification of Diabetic Retinopathy Images using SVM Technique," *Int. J. Comput. Appl. Int. Conf. Innov. Intell. Instrumentation, Optim. Signal Process. (ICIIOSP)*, pp. 18–22, 2013.
- [7] V. A. Aswale and J. A. Shaikh, "Detection of microaneurysm in fundus retinal images using SVM classifier," vol. 5, no. 4, pp. 175–180, 2017.
- [8] J. Computing, "An Automatic Face Detection and Gender Classification from Color Images using Support Vector Machine," vol. 4, no. 1, pp. 5–11, 2013.
- [9] P. Maule, A. Shete, K. Wani, A. Dawange, and P. J. V. Shinde, "GLCM feature extraction in Retinal Image," vol. 2, no. 4, pp. 1–8, 2016.
- [10] S. A. SURESH;K, "An Efficient Texture Classification System Based On Gray Level Co- Occurrence Matrix," *Int. J. Comput. Sci. Inf. Technol. Secur.*, vol. 2, no. 4, pp. 793–798, 2012.
- [11] WHO, "Definition, diagnosis and classification of diabetes mellitus and its complications. Part 1: diagnosis and classification of diabetes mellitus provisional report of a WHO consultation," *Diabet. Med.*, vol. 15, no. 7, pp. 539–553, 1998.
- [12] R. Munir, *Pengolahan citra digital dengan pendekatan algoritmik*. Bandung: informatika, 2004.
- [13] A. Usman, *Pengolahan Citra Digital dan Teknik Pemrogramannya*. yogyakarta: graha ilmu, 2005.
- [14] C. Science and S. Publications, "Content Based Medical Image Retrieval with Texture Content Using Gray Level Co-occurrence Matrix and K-Means Clustering Algorithms Department of CIS , PSG College of Technology , Coimbatore , India," vol. 8, no. 7, pp. 1070–1076, 2012.
- [15] R. C. . Gonzalez and R. E. Woods, "Digital image processing," *Nueva Jersey*. p. 976, 2008.
- [16] N. Zulpe and V. Pawar, "GLCM textural features for Brain Tumor Classification," *Int. J. Comput. Sci.*, vol. 9, no. 3, pp. 354–359, 2012.
- [17] E. Prasetyo, *Data Mining, Mengelola Data Menjadi Informasi Menggunakan Matlab*. yogyakarta: ANDI, 2014.
- [18] a. K. Santra and C. J. Christy, "Genetic Algorithm and Confusion Matrix for Document Clustering," *Int. J. Comput. Sci.*, vol. 9, no. 1, pp. 322–328, 2012.

# Development of Discrete-Cockroach Algorithm (DCA) for Feature Selection Optimization

1<sup>st</sup> Yusuf Hendrawan  
Faculty of Agricultural Technology  
Universitas Brawijaya  
Malang, Indonesia  
yusufhendrawan@gmail.com

2<sup>nd</sup> Muchnuria Rachmawati  
Faculty of Agricultural Technology  
Universitas Brawijaya  
Malang, Indonesia  
muchnuria@yahoo.com

3<sup>rd</sup> Muchammad Riza Fauzy  
Graduate School of Technology  
Management  
Institut Teknologi Sepuluh Nopember  
Surabaya, Indonesia  
Muchrizafauzi@gmail.com

**Abstract**— One of the recently proposed algorithms in the field of bio-inspired algorithm is the Hungry Roach Infestation Optimization (HRIO) algorithm. Haven has developed optimization algorithms HRIO that is inspired by recent discoveries in the social behavior of cockroaches. Result showed that HRIO was effective at finding the global optima of a suite of test functions. However, there is no researcher who has observed HRIO for solving discrete feature selection problems. Therefore, we try to develop a discrete-cockroach algorithm (DCA) as the modification of HRIO for optimizing discrete feature selection problem. We test the algorithm to solve feature selection problem in machine vision for predicting water stress in plant using single and multi-objectives optimization. Two objective functions are minimizing prediction error and minimizing the number of feature-subset. The results showed DCA has better performance compared to the existed bio-inspired optimization algorithms such as genetic algorithms (GA) and discrete-particle swarm optimization (discrete-PSO). The performance showed significant difference between DCA and other methods.

**Keywords**— discrete cockroach algorithm, feature selection, multi objective optimization

## I. INTRODUCTION

The natural systems have been one of the rich sources of inspiration for developing new intelligent systems [1; 2]. One of the intelligent system's role is to solve the feature selection problem. In machine learning, discretization and feature selection are important techniques for preprocessing data to improve the performance of an algorithm on high-dimensional data [3]. In this study, a novel artificial intelligence approaches using nature-inspired algorithm for feature selection optimization is proposed. Haven et al [4] have developed optimization algorithms hungry roach infestation optimization (HRIO) that is inspired by recent discoveries in the social behavior of cockroaches. HRIO that has been developed is still used to solve optimization problems in general cases, but there has never been a study that tested the performance of HRIO to solve feature selection issues.

HRIO principle is similar to particle swarm optimization (PSO). There are three factors used by PSO and HRIO, namely inertia, personal influence, and social influence. The difference lies in social influence, where PSO uses global best position while HRIO uses local best position. Obagbuwa et al [5] have developed a dynamic step size adaptation roach infestation optimization (DSARIO) to improve the HRIO swarm stability and enhance local and global search performance. To know the effectiveness of a new

optimization algorithm hence required comparative optimization method that has been widely used in research such as genetic algorithm (GA) and PSO. GA is search algorithms based on the mechanics of natural selection and natural genetics [6]. PSO is an evolutionary computation technique inspired in the behavior of bird flocks which was first introduced by Kennedy and Eberhart [7]. There have been many studies using PSO to solve discrete problems called discrete-PSO [8; 9].

However, there is still no research that tests HRIO performance to solve discrete feature selection problems with single objective optimization [10] and multi-objective optimization [11]. Obagbuwa and Adewumi [12] made modification of social cockroach behaviors, called modified roach infestation optimization (MRIO). The equations in HRIO can be modified to solve the discrete feature selection problem by substituting the algorithm for personal influence and social influence factors with the crossover and mutation methods used in GA. The result shows that MRIO can find global optima of multi-dimensional functions. The objective of this study is developing discrete cockroach algorithm (DCA) as bio-inspired algorithm for solving feature selection problem using single and multi-objective optimization. The DCA is compared with the forefront bio-inspired optimization algorithms i.e. GA and discrete-PSO.

## II. RESEARCH METHODS

Based on the research conducted by Jeanson [13] about characteristics and behavior of cockroaches, there are three simple behaviors of cockroach agents which can be defined as:

1. *Find Darkness*: cockroaches search for the darkest location in the search space as shown in Fig. 1. The level of darkness at a location is directly proportional to the value of the fitness function at that location  $F(x)$ . Perfectly dark condition means that cockroach agent has reached its maximum condition. While perfectly light condition means that cockroach agent has reached a minimum point.
2. *Find Friends*: cockroaches enjoy the company of friends and socialize with nearby cockroaches with the probability per unit time ( $1/\tau_{stop,N}$ ) of stopping when encountering  $N$  friends: 0.49/s for  $N = 1$ , 0.63/s for  $N = 2$  and 0.65/s for  $N = 3$  [13] as shown in Fig. 2. If a cockroach agent comes within a detection radius of another cockroach agent, then there is a probability of  $1/\tau_{stop,N}$  that these cockroaches will socialize (or group). This socializing is emulated in the algorithm by a



sharing of information, where this information is the darkest known location of each individual cockroach agent which can be defined as personal best solution ( $p$ ). In essence, when two cockroach agents meet, there is a chance that they will communicate their knowledge of the search space to each other. They share their knowledge with their neighbors ( $N$ ) and set the darkest local location of the group which can be defined as local best solution ( $l$ ).

3. *Find Food*: when a cockroach agent becomes hungry ( $hunger_i$ ) it searches for food as shown in Fig. 3. The food locations are initialized randomly in the search space. The *Find\_Food* behavior periodically perturbs the population, ideally minimizing the chance of converging to local optima.

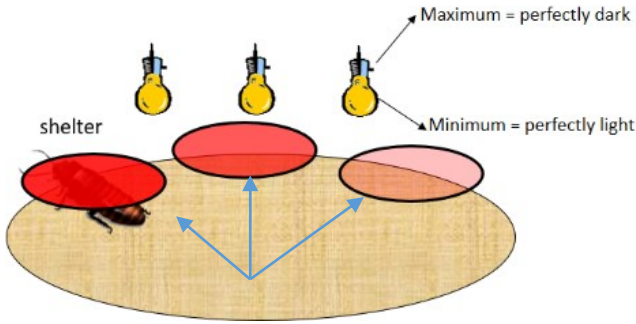


Fig. 1. Find darkness behaviour.

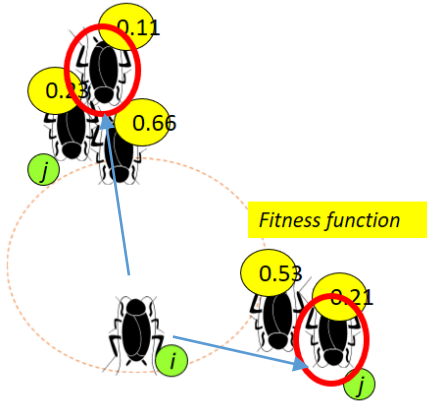


Fig. 2. Find friends behavior.

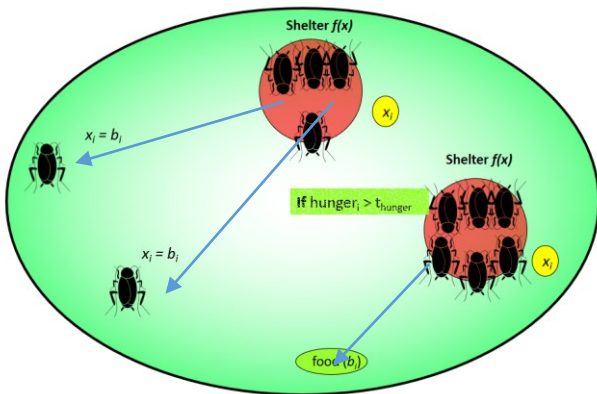


Fig. 3. Find food behavior.

The algorithm of proposed DCA as shown in Fig. 4 are as follows:

1. Initialization of DCA parameters. The maximum iteration ( $t_{max}$ ) is set by the user. In this case we set the global iteration ( $t_{max} = 500$ ). The number of cockroach population ( $N_a$ ) is = 70. For neighbors updating, the parameters are  $A_1 = 0.49$ ,  $A_2 = 0.63$  and  $A_3 = 0.65$ . For hunger updating,  $t_{hunger} = 100$ . The probability of mutation is set ( $w = 0.5$ ). The probability of crossover ( $C_o$ ) is set in various values.
2. Generate cockroach location ( $x_i$ ) randomly and  $hunger_i = rand\{0, t_{hunger}-1\}$ . Each cockroach consist of discrete solution (e.g.  $x_i$ : 0,1,1,0,0,0,0,1,0,0,1,0,...,m), where  $m$  is the number of problem space. Each  $x_i$  in the population represents a candidate solution to the discrete problem.
3. Evaluate each cockroach agent ( $x_i$ ) using fitness function.
4. Update the individual solution  $F(x_i)$ . Individual solution  $F(x_i)$  is calculated according to the fitness value ( $x_i$ ).
5. Calculate neighbors' threshold value ( $d_g$ ):

$$M = [M_{jk}] = \frac{\|F(x_j) - F(x_k)\|}{2} \quad (1)$$

$$d_g = median\{M_{jk} \in M : 1 \leq j < k \leq N_a\} \quad (2)$$

6. Repeat steps 6.1 to 6.4 for those  $x_i$  with partial solutions. Steps 6.1 to 6.8 are as follows:

- 6.1 Updating personal best solution ( $p_i$ ) for the individual cockroach agent. For minimizing objective function:

$$p_i \begin{cases} p_i = x_i & \text{if } F(x_i) < F(p_i) \\ p_i & \text{otherwise} \end{cases} \quad (3)$$

For maximizing objective function:

$$p_i \begin{cases} p_i = x_i & \text{if } F(x_i) > F(p_i) \\ p_i & \text{otherwise} \end{cases} \quad (4)$$

- 6.2 Compute the neighbors ( $N_i$ ) of cockroach  $i$ .

For  $k = 1$  to  $N_a$

$$N_i \begin{cases} N_i = N_i + 1 & \text{if } k : 1 \leq k \leq N_a, k \neq i \text{ AND } M_{ik} < d_g \\ N_i & \text{otherwise} \end{cases} \quad (5)$$

- 6.3 Update the darkest local location or group best solution ( $l_i$ ) according to:

For  $r = 1$  to  $N_i$

$$l_i \begin{cases} l_i = l_{j_r} = \arg \min_k \{F(p_k)\}, k = \{i, j_r\} & \text{if } rand[0,1] < A_{\min\{N_i,3\}} \\ l_i & \text{otherwise} \end{cases} \quad (6)$$

where  $\{i, j\}$  are the indices of the two socializing cockroaches and  $p_k$  is the darkest known location for the individual cockroach agent personal best.

- 6.4 Update roach location ( $x_i$ ):

$$x_i \begin{cases} x_i = C_o \oplus CR(C_o \oplus CR(w \oplus MT(x_i), p_i, l_i)) & \text{if } hunger_i < t_{hunger} \\ x_i = random & \text{otherwise} \end{cases} \quad (7)$$

The update  $x_i$  consists of three components: The first component is  $a_i = w \oplus MT(x_i)$ , which represents the velocity of the cockroach.  $MT$  represents the mutation operator with the mutation probability of  $w$ . In other words, a uniform random number  $rnd[0, 1]$  is generated. If  $rnd[0, 1]$  is less than  $w$  then single insert move mutation operator is applied. The second



component is  $b_i = C_o \oplus CR(a_i, p_i)$ , which is the cognition part of the cockroach agent representing the private thinking of the cockroach agent itself.  $CR$  represents the crossover operator between  $a_i$  and  $p_i$  with the probability of  $C_o$ . Two points crossover (point1 and point2) are selected randomly, where  $point1 < point2$ ,  $point1 > 1$  and  $point2 < m$ . The third component is  $x_i = C_o \oplus CR(b_i, l_i)$ , which is the social part of the cockroach agent representing the collaboration among the group.  $CR$  represents the crossover operator between  $b_i$  and  $l_i$  with the probability of  $C_o$ .

6.5 Evaluate each feature-subset ( $x_i$ ) using fitness function.

6.6 Update the individual solution  $F(x_i)$  based on fitness value.

6.7 Update  $hunger_i$ :

$$hunger_i = hunger_i + rand[0,1] * t_{hunger} \quad (8)$$

6.8 Update iteration-best solution  $T^{TB}$ .

For minimizing objective function:

$$T^{TB} = \arg \min q(F(x_i)) \quad (9)$$

For maximizing objective function:

$$T^{TB} = \arg \max q(F(x_i)) \quad (10)$$

where function  $q(\cdot)$  gives the quality of the solution.

7. Update the total best solution  $T^{TB}$  by the current iteration-best solution  $T^{TB}$ .

For maximizing objective function:

$$T^{TB} \begin{cases} T^{TB} & \text{if } q(T^{TB}) \geq q(T^{TB}) \\ T^{TB} & \text{otherwise} \end{cases} \quad (11)$$

For minimizing objective function:

$$T^{TB} \begin{cases} T^{TB} & \text{if } q(T^{TB}) \leq q(T^{TB}) \\ T^{TB} & \text{otherwise} \end{cases} \quad (12)$$

8. Update best feature-subset.

9. Stopping criterion: the algorithm stops with the total-best solution  $T^{TB}$  and best feature-subset. The search will terminate if the global iteration has been reached.

Testing is done for optimizing feature selection in machine vision for predicting water stress in plant using artificial neural network modeling. Sunagoke Moss is used as the experimental plant to study water stress changes in plant. Bhurga et al [14] have tested the use of leaf color for drought stress analysis in rice. The research demonstrates the capability of machine vision for stress level prediction. Testing procedures includes: first process is image acquisition in a dark chamber as shown in Fig. 5, in which the plant images were captured using digital camera (Nikon Coolpix SQ, Japan) placed at 330 mm perpendicular to the sample surface. The image size was 1024 x 768 pixels. Imaging was done under controlled and well distributed light conditions. Light was provided by two 22W lamps (EFD25N/22, National Corporation, Japan). Light intensity over the moss surface was uniform at  $100 \mu\text{mol m}^{-2} \text{s}^{-1}$  PPF (Photometer, Li6400, USA) during image acquisition. For single objective and multi-objective optimization, total of 212 features are used, consist of color features and textural features from various kind of color spaces e.g. RGB, Lab,

Luv, HIS, HSL, etc. Indriani et al [15] have successfully tested the use of colors and textural features in pattern recognition for biological objects. For modeling the relationship between image features and water stress in plant, artificial neural network (ANN) is used with back-propagation neural network (BPNN) as the learning method. Quiros et al [16] has proven the effectiveness of ANN for pattern recognition using machine vision. The performance of prediction accuracy is measured with root mean square error (RMSE). The number of data used in this study was 500 image data consisting of various water stress condition.

Selection process for selecting relevant image features is done using three nature-inspired approaches i.e. DCA, GA, and discrete-PSO. Multi objective optimization concerns optimization problems with multiple objectives. Barocio et al [17] and Qingqi et al [18] have proven the superiority of bio-inspired algorithms in solving multi-objective optimization. The fitness of multi objective optimization is calculated as follows:

$$function_1 = weight_1 \times RMSE_{(x)} \quad (13)$$

$$function_2 = weight_2 \times \frac{IF_{(x)}}{f_t} \quad (14)$$

$$fitness(x) = function_1 + function_2 \quad (15)$$

where  $RMSE_{(x)}$  is the Root Mean Square Error of validation-set data of BPNN using only the expression values of the selected image features in a subset  $x$ , where  $IF_{(x)}$  is the number of selected image features in  $x$ .  $f_t$  is the total number of image features,  $weight_1$  and  $weight_2$  are two priority weights corresponding to the importance of the accuracy and the number of selected image features, respectively, where  $weight_1 \in [0.1, 0.9]$  and  $weight_2 = 1 - weight_1$ . In this study, the accuracy is more important than the number of selected image features in a feature-subset. Problems solved for single and multi objectives optimization in this study use the same training data. In single objective optimization, the objective function is determined by minimizing prediction error. Whereas in multi objective optimization two objective functions are determined by minimizing prediction errors and minimizing the number of feature-subset.

### III. RESULTS AND DISCUSSION

Figure 6 shows the performance of three bio-inspired optimizations to optimize the feature selection problems in machine vision for single objective optimization. Experimental results show competitive performance among all feature selection optimization techniques. It shows the superiority of DCA, since it achieved better optimization performance as the objective of this research i.e. prediction accuracy of water stress in plant. Based on the observation using some various values of crossover rate ranged from 0.1 to 0.9, GA reached the lowest (optimum) fitness value at crossover rate of 0.5. Discrete-PSO reached the lowest (optimum) fitness value at crossover rate of 0.8. The best fitness plots of the iteration of each optimization method are displayed in Fig. 7 to highlight the search process in each optimization technique. From Fig. 6, the best optimization performance based on

fitness value is achieved with DCA followed by GA, and discrete-PSO.

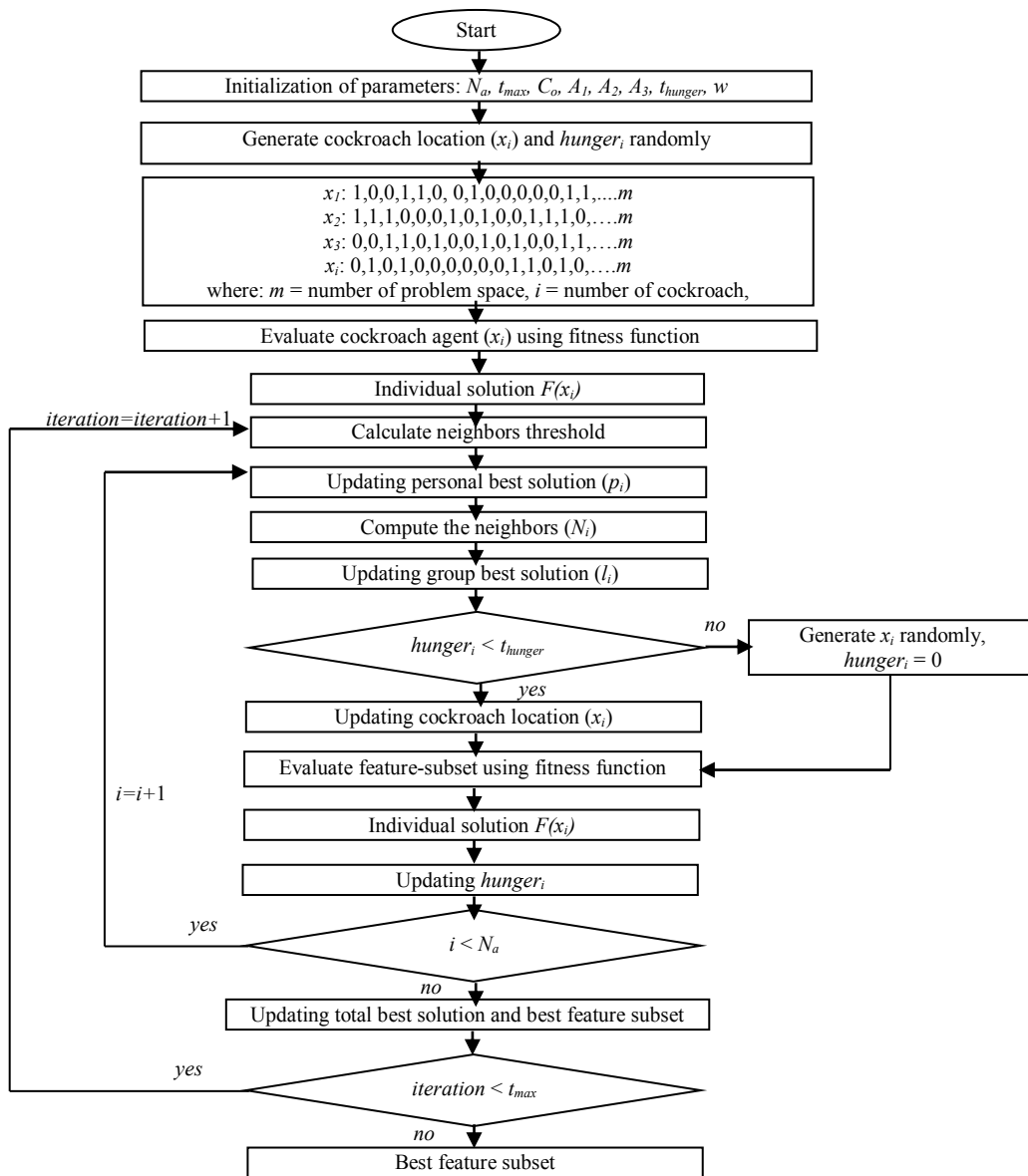


Fig. 4. DCA for discrete-optimization.

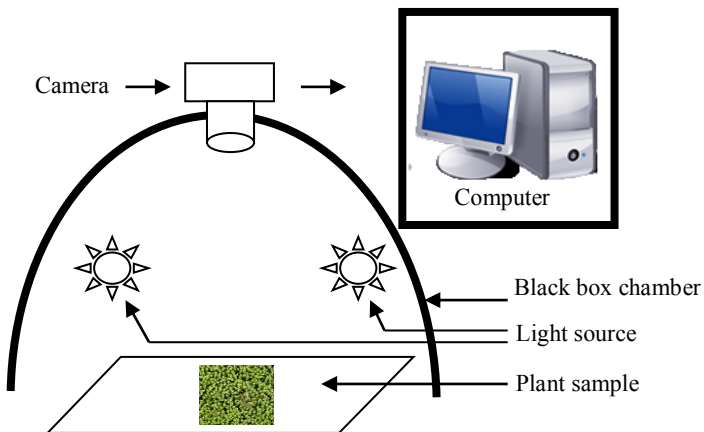


Fig. 5. Procedure of image acquisition and image features extraction

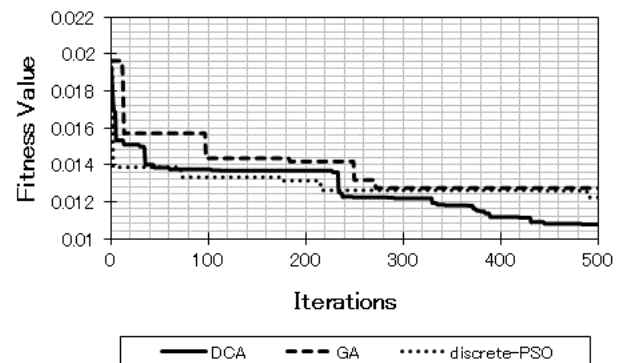


Fig. 6. Performance of single objective discrete-optimization using DCA, GA, and discrete-PSO.

Based on partial analysis using analysis of *t-test* it was shown that there is a significant statistical difference between DCA and other optimization methods at  $\alpha = 0.05$  significant level. Analysis of *t-test* between DCA and GA showed a value of 0.0197, while the *t-test* value between DCA and discrete-PSO showed a value of 0.0143. DCA also showed the least absolute deviation, followed by discrete-PSO, and GA in that order. This implies that DCA showed the highest reliability in optimization process. The results presented in Fig. 6 and 7 clearly show that the DCA have a positive effect on its ability to find global optima for single objective feature selection optimization.

DCA has also been tested using multi-objectives optimization problem [9]. The plots of best fitness values of multi-objectives optimization using all optimization methods are displayed in Fig. 8 to highlight the search process in each optimization method. At the beginning of the iteration, all optimization methods (DCA, GA, and discrete-PSO) were given the same optimization problem which is defined as the initial condition. The fitness value obtained from the initial condition and then normalized by the value of 1.00. During the multi-objectives optimization process the fitness value continues to decrease, searching for the most minimum fitness value. Using the same *weight* parameter ( $weight_1 = 0.9$  and  $weight_2 = 0.1$ ), it shows that DCA has the best performance to minimize the fitness value (normalized fitness value = 0.66), followed by GA (normalized fitness value = 0.67), and discrete-PSO (normalized fitness value = 0.84) in that order, respectively. Figure 9 shows the performance of the discrete optimization method with the first objective function which is to minimize the prediction error (RMSE) of water stress in plant.

For the first objective i.e. minimizing prediction error, based on partial analysis using analysis of *t-test* it was shown that there is a significant statistical difference between DCA and GA method at  $\alpha = 0.05$  significant level, but there is no significant difference between DCA and discrete-PSO. Analysis of *t-test* between DCA and GA showed a value of 0.0382, while the *t-test* value between DCA and discrete-PSO showed a value of 0.2567. Figure 10 shows the performance of the discrete optimization method with the second objective function which is to minimize the number of feature-subset. For the second objective i.e. minimizing number of feature-subset, based on partial analysis using analysis of *t-test* it was shown that there is a significant statistical difference between DCA and other optimization methods at  $\alpha = 0.01$  significant level. Analysis of *t-test* between DCA and GA showed a value of 0.000017, while the *t-test* value between DCA and discrete-PSO showed a value of 0.000162.

Most of all optimization methods can quickly minimize the fitness value at the beginning of 50 iterations, but based on the comparison analysis on the performance of all optimization methods, it shows the superiority of DCA to minimize the fitness value in early iterations, followed by GA and discrete-PSO, respectively. From the results, we can see that, DCA is quicker in locating the optimal solution. DCA has the ability to converge quickly. It has strong search capability in the problem space and can efficiently find optimum solution for multi-objectives optimization. From the results obtained, we can see the advantages of

DCA in solving single objective optimization problems and multi-objective optimization compared to the other two methods, namely GA and discrete-PSO. This is because DCA has the characteristics to move randomly during the *find food behavior* process so it does not get stuck on local optima. This random *find food behavior* is not owned by GA or discrete-PSO. In addition, DCA has a *find friends behavior* process that is neither owned by GA nor discrete-PSO. In this process global optima will be achieved by relying on best solution from its nearest neighbor and not from the best solution of the swarm population as done by discrete-PSO. This can prevent optimization on local optima.

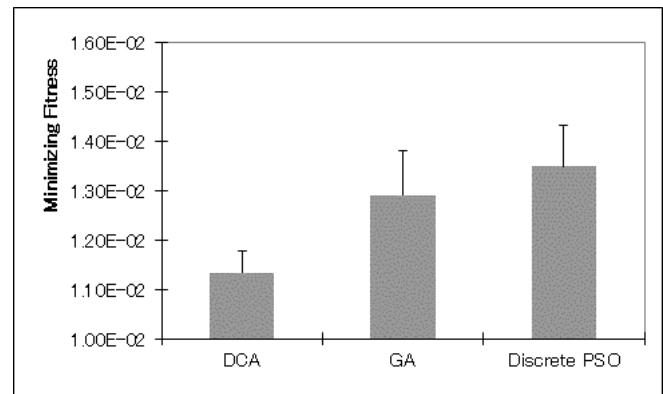


Fig. 7. Comparison of the performance of bio-inspired algorithms for single objective discrete optimization.

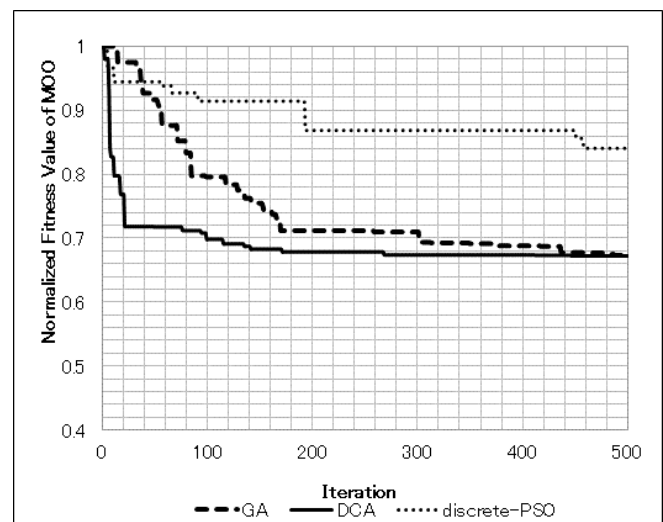


Fig. 8. Performance of multi objectives discrete-optimization (a) DCA; (b) GA; (c) discrete-PSO.

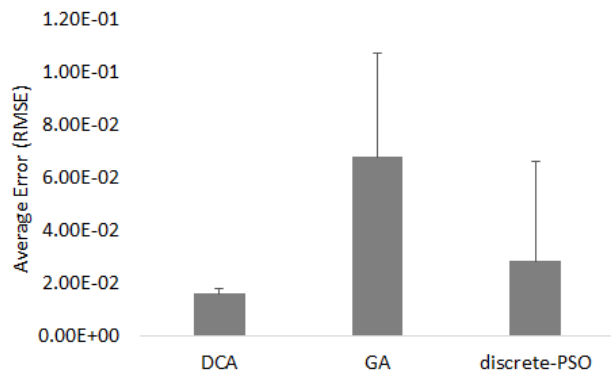


Fig. 9. Performance of multi objectives discrete-optimization for minimizing prediction Root Mean Square Error (RMSE).

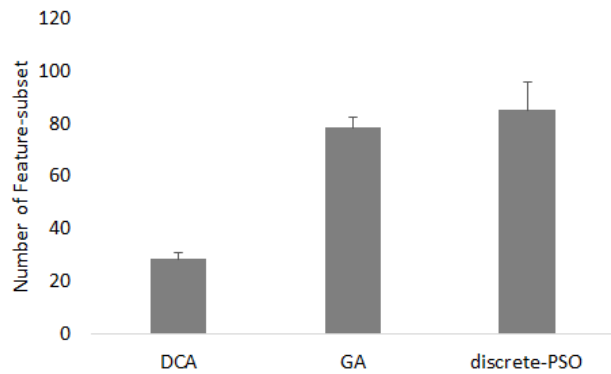


Fig. 10. Performance of multi objectives discrete-optimization for minimizing number of feature-subset.

#### IV. CONCLUSIONS

Discrete cockroach algorithm (DCA) was developed to search optimum solution with the single objective function and multi-objectives feature selection optimization. To test the performance of DCA as optimization method we compare it with two forefront bio-inspired optimization methods i.e. genetic algorithm (GA), discrete particle swarm optimization (discrete-PSO). The achieved optimization results are promising. DCA has the best performance for solving feature selection optimization problems in machine vision for predicting water stress in plant using single objective optimization and also multi-objectives optimization. There is averagely significant difference of feature selection performance between DCA and other optimization methods. DCA has powerful exploration ability to find global optima. Several characteristics make DCA a unique approach: (1) *Find\_Food* behavior that discourages the swarm from converging to local optima; (2) *Find\_Friends* behavior to find global best solution which is determined by a group best solution from the neighborhood of the agents to avoid converging on a sub-optimal solution.

#### REFERENCES

- [1] Hendrawan, Y. and Murase, H., "Neural-Genetic Algorithm as feature selection technique for determining sunagoke moss water content", Engineering in Agriculture, Environment and Food (EAEF); Asia Agricultural and Biological Engineering Association (AABEA) Journal, 3(1), pp25-31, 2010
- [2] Hendrawan, Y. and Murase, H., "Non-destructive sensing for determining Sunagoke moss water content: Bio-inspired approaches", Agricultural Engineering International: CIGR Journal. Manuscript No. 1564, Vol. 13, No.1, 2011
- [3] Tran, B., Xue, B., Zhang, M., "A new representation in PSO for discretization-based feature selection", IEEE Transaction on Cybernetics, 48(6), pp1733-1746, 2018
- [4] Havens, T. C., Spain, C. J., Salmon, N. G., Keller, M., "Roach Infestation Optimization", IEEE Swarm Intelligence Symposium. St. Louis MO USA, September 21-23, 2008
- [5] Obagbuwa, I.C., Adewumi, A.O., Adebisi, A.A., "A dynamic step-size adaptation roach infestation optimization", IEEE International Advance Computing Conference (IACC), Gurgaon, India, February 21-22, 2014
- [6] Goldberg, D. E., "Genetic algorithms in search, optimization and machine learning", Addison Wesley Longman, Inc, United States of America, 1989
- [7] Kennedy, J. and Eberhart, R. C., "Particle swarm optimization", Proceedings of the IEEE International Conference on Neural Networks. Vol 4, pp: 1942-1948, ISBN: 0780327683, Perth, Western Australia November 1995, IEEE, 1995
- [8] Hendrawan, Y. and Murase, H., "Neural-intelligent water drops algorithm to select relevant textural features for developing precision irrigation system using machine vision", Comput. Electron. Agr, 77(2), pp214-228, 2011
- [9] Hendrawan, Y. and Murase, H., "Bio-inspired feature selection to select informative image features for determining water content of cultured Sunagoke moss", Expert Syst. Appl, 38(11), pp14321-14335, 2011
- [10] Hendrawan, Y. and Murase, H., "Neural-discrete hungry roach infestation optimization to select informative textural features for determining water content of cultured Sunagoke moss", Environ. Control Biol, 49(1), pp1-21, 2011
- [11] Hendrawan, Y. and Al Riza, D.F., "Machine vision optimization using Nature -inspired algorithms to model Sunagoke moss water status", International Journal on Advance Science Engineering Information Technology, 6, pp2088-5334, 2016
- [12] Obagbuwa, I.C., and Adewumi, A.O., "Modified roach infestation optimization", IEEE Conference on Computational Intelligence in Bioinformatics and Computational Biology, Honolulu, HI, USA, May21-24, 2014
- [13] Jeanson, R., Rivault, C., Deneubourg, J.L., Blanco, S., Fourniers, R., Jost, C., Theraulaz, G., "Self-organized aggregation in cockroaches", J. Anbehav, 69, pp169-180, 2005
- [14] Bhurga, S., Chaudhury, S., Lall, B., "Use of leaf colour for drought stress analysis in rice", IEEE Fifth National Conference on Computer Vision, Pattern Recognition, Image Processing and Graphics (NCVPRIPG), Patna, India, December 16-19, 2015
- [15] Indriani, O.R., Kusuma, E.J., Sari, C.A., Rachmawanto, E.H., Setiadi, D.R.I.M., "Tomatoes classification using K-NN based on GLCM and HSV color space", IEEE International Conference on Innovative and Creative Information Technology, Salatiga, Indonesia, November 2-4, 2017
- [16] Quiros, A.R.F., Abad, A., Bedruz, R.A., Uy, A.C., Dadios, E.P., "A genetic algorithm and artificial neural network-based approach for the machine vision of plate segmentation and character recognition", IEEE International Conference on Humanoid, Nanotechnology, Information Technology, Communication and Control, Environment and Management, Cebu City, Philippines, December 9-12, 2015
- [17] Barocio, E., Ragalado, J., Cuevas, E., Uribe, F., Zuniga, P., Torres, P.J., "Modified bio-inspired optimization algorithm with a centroid decision making approach for solving a multi-objective optimal power flow problem", IET Generation, Transmission & Distribution, 11(4), pp1012-1022, 2017
- [18] Qingqi, Z., Yanling, Q., Yue, L., Nantian, Q., "Multi-objective mapping for network-on-chip based on bio-inspired optimization algorithms", IEEE Prognostics and System Health Management Conference, Zhangjiajie, China, August 24-27, 2014

# Narrow Window Feature Extraction for EEG-Motor Imagery Classification using k-NN and Voting Scheme

Adi Wijaya  
Electrical Engineering and IT  
Department  
Universitas Gadjah Mada  
Yogyakarta, Indonesia  
adiwijaya@mail.ugm.ac.id

Teguh Bharata Adji  
Electrical Engineering and IT  
Department  
Universitas Gadjah Mada  
Yogyakarta, Indonesia  
adji@ugm.ac.id

Noor Akhmad Setiawan  
Electrical Engineering and IT  
Department  
Universitas Gadjah Mada  
Yogyakarta, Indonesia  
noorwewe@mail.ugm.ac.id

**Abstract**—Achieving consistent accuracy still big challenge in EEG based Motor Imagery classification since the nature of EEG signal is non-stationary, intra-subject and inter-subject dependent. To address this problems, we propose the feature extraction scheme employing statistical measurements in narrow window with channel instantiation approach. In this study, k-Nearest Neighbor is used and a voting scheme as final decision where the most detection in certain class will be a winner. In this channel instantiation scheme, where EEG channel become instance or record, seventeen EEG channels with motor related activity is used to reduce from 118 channels. We investigate five narrow windows combination in the proposed methods, i.e.: one, two, three, four and five windows. BCI competition III Dataset IVa is used to evaluate our proposed methods. Experimental results show that one window with all channel and a combination of five windows with reduced channel outperform all prior research with highest accuracy and lowest standard deviation. This results indicate that our proposed methods achieve consistent accuracy and promising for reliable BCI systems.

**Keywords**—EEG, motor imagery, narrow window, channel instantiation, voting scheme

## I. INTRODUCTION

The term Brain-Computer Interface (BCI) is a system which translate the human brain signals and a communication technique to control a device [1]–[3]. Because of its great potential in areas such as rehabilitation and entertainment, BCI has been studied and developed actively by researchers [4] over the past two decades [5] that is usually recorded using electroencephalogram (EEG) [6]. Motor Imagery (MI) task is one of the most studied types of EEG signals in BCI systems [7]. MI is a mental activity about special motor movement without actual execution [8] or motor output [9]. Many studies have proved that MI plays a crucial role in motor skill learning, prosthesis control and rehabilitation of motor abilities [10].

In BCI, EEG signal is one of the most popular techniques due to low cost and non-invasive nature of EEG [3]. However, the nature of EEG signal has too much noise, [11] non-stationary [12], [13] and subject-dependent [12], [14], [15] that affect the classification results [11]. Therefore, processing of EEG signals, which directly affects the classification accuracy, still represents an important and challenging issue [6]. EEG signal recognition is the key technology of MI-BCI that includes feature extraction and classification [16], [17].

Many studies have been conducted to address those such problems using various signal processing technique such as: time domain, frequency domain, time-frequency domain and spatial domain. Among these approach, time-frequency and spatial domain are commonly used by many studies. These signal processing technique are used as feature extraction and combined with classifier both single classifier or ensemble technique. Several researches also used feature selection since EEG signal recorded with multi-channel.

In spatial domain, Common Spatial Pattern (CSP) is one of most popular technique in EEG based MI classification. Therefore, many studies have been used and improve CSP such as: CSP with sparse time-frequency segment common spatial pattern [18], CSP combined with Differential Evolution as feature selection [19], CSP combined with symmetrical feature [20] and Filter Bank Regularized Common Spatial Pattern [21]. Another approach based on time-frequency signal processing technique by employing three popular wavelet technique has been conducted by [6].

Based on prior research results, CSP still need improvement since CSP very sensitive to noise in nature and often over-fit with small training sets [22]. Existing studies that employed CSP yield excellent accuracy; however, the result still not consistent where some subsets gained low accuracy. Therefore, how to improve the detection performance of EEG based MI is still a challenging issue for the development of BCI systems [22].

In this study, we propose narrow window feature extraction with seven statistical features to tackle non-stationary nature of EEG signal and employing instance-based learning with k-Nearest Neighbor (k-NN) as classifier. K-NN proven as promising classifier in EEG based MI classification [6]. Since instance-based learning need more data, we employ data transformation approach called channel instantiation where EEG multi-channel data transformed into instance which introduced by [22].

The motivation of this work was to analyse the effectiveness of the narrow window feature extraction in channel instantiation approach using k-NN and voting scheme for making accurate and consistent detection of EEG based MI. Another motivation was to analyse a feature reduction with minimum channel by select only motor related activity channels that reduced computation time meanwhile maintain excellent and consistent accuracy. Thus, the proposed method expectedly suitable for reliable BCI systems for further implementation.

## II. RELATED WORKS

EEG based MI classification require two main tasks i.e. feature extraction and classification. In feature extraction, many approaches have been used combined with statistical feature. Since in EEG signal recorded in multi-channel, channel selection also considered by many researchers to reduce computation time yet maintain high accuracy. In this study, the most relevant prior researches are selected as related works based on dataset used (BCI competition III dataset IVa) and method validation with 10-fold cross validation.

In [19], they utilized a differential evolution (DE) based technique to select most relevant features in EEG based MI and CSP as feature extractor (CSP+DE-FS). They achieved excellent accuracy and small standard deviation with 96.02% and 3.77% respectively. However, CSP+DE-FS method is slow compared to the typical feature selection algorithms and the even more slower because of employing DE as a wrapper technique.

Another CSP based feature extraction is used by [21] with improved CSP so called Filter Bank Regularized CSP (FBRCSF). FBRCSF use eighteen selected channel based on the Homunculus Theory and achieve 86.23% and 9.55% for accuracy and standard deviation respectively. FBRCSF not only feature extractor but also classifier based on distance measurement by calculate the distance between each feature vector and each class mean vector. However, FBRCSF need suitable selected parameter set that caused its varying performance.

Another promising study introduced by [18]. They improve CSP with sparse time-frequency segment common spatial pattern (STFSCSP) combined with Discernibility of Feature Sets (DFS) criteria that dedicated for spatial filter optimization and Weighted Naïve Bayesian Classifier (WNBC). They gained excellent result with accuracy about 92.66% and standard deviation about 7.78%. However, the cost of more computation at classification task both in training and testing stages.

A novel feature extraction so called symmetrical feature that built upon CSP (CSP+SF) was introduced by [20]. They achieve 82.06% and 13.4% for accuracy and standard deviation. Although CSP+SF has a robust characteristic of invariant EEG data compared with the previous CSP power band; however, the average results showed that the new feature type has lower performance in terms of power than the original CSP.

Besides CSP, another approach based on signal processing technique by employing three popular technique, i.e.: Empirical Mode Decomposition, Discrete Wavelet Transform, and Wavelet Packet Decomposition has been conducted by [6]. They utilized higher order statistic (HOS) as main feature extractor, k-Nearest Neighbour (k-NN) as classifier and choose only three channels (C3, Cz, C4). Their method achieved excellent result with 92.8% and 2.93% for accuracy and standard deviation respectively. However, their proposed method does not offer the best classification accuracy for all subjects with subject “av” gained lowest accuracy that below 90%.

## III. MATERIAL AND METHODS

### A. Dataset

Dataset IVa from BCI competition III [23] is used in this study. This data set was recorded from five healthy subjects (“aa”, “al”, “av”, “aw”, “ay”). EEG signal recorded for each subject with comfortable chair with their arms resting on the armrests. In this task, all subjects performed three types of motor imageries i.e.: right foot, left hand and right hand. However, for the competition, only right hand and right foot were provided. The recording signals were measured based on extended international 10/20-system with 118 EEG channels. Although signals digitized at 1000 Hz with 16 bit, the data down-sampled at 100 Hz (by picking each 10th sample) also available for analysis. In this study, this 100 Hz down-sampled data is used for EEG based MI classification task. Each subject performed 280 trials in total with the composition for training and testing sets. In this study, although every subject has separate training and testing sets, they were combined into one dataset due to the low number of trials and imbalance between training and testing sets.

### B. Narrow Window Feature Extraction

In this study, narrow window feature extraction approach is used as shown in Fig. 1. This strategy is selected due to tackling the non-stationary nature of EEG signal, where smaller or narrower windows, will exhibit signal stationary [24]. As initial step, original dataset which contains EEG signal is filtered using 4<sup>th</sup> order Butterworth band-pass filter as commonly used in EEG signal processing [14], [25], [26]. EEG signal were filtered in frequency range 8-30 Hz as same range with [19], [27]–[30]. After filtered, a time slot or window between 0.5 – 2 seconds is chosen for further process. This time slot is narrower window than some prior researches, such as: 0.5 – 3.5 seconds [14], 0 – 3.5 seconds [6], [19] and 0.5 – 2.5 seconds [21]. The selected time slot, which is range about 1.5 seconds, consists of 150 data points because 100 Hz down-sampled data is used in this study. These 150 data points then divided into 5 windows for further feature extraction process. So each windows consist 30 data points, which much enough as sample size for statistical calculation.

The next step is conduct feature extraction by using seven statistical features for each window. The following seven statistical features are chosen for EEG based MI classification:

- Mean Absolute Value (mav):

$$mav = \frac{1}{n} \sum_{i=1}^N |x_n| \quad (1)$$

- Root Means Square (rms):

$$rms = \sqrt{\frac{1}{n} \sum_{i=1}^N x_n^2} \quad (2)$$

- Standard Deviation ( $\sigma$ ):

$$\sigma = \sqrt{\frac{1}{n} \sum_{i=1}^N (x_n - \mu)^2} \quad (3)$$



- Skewness:

$$\text{skewness} = \sqrt{\frac{1}{n} \sum_{i=1}^N \frac{(x_n - \mu)^3}{\sigma^3}} \quad (4)$$

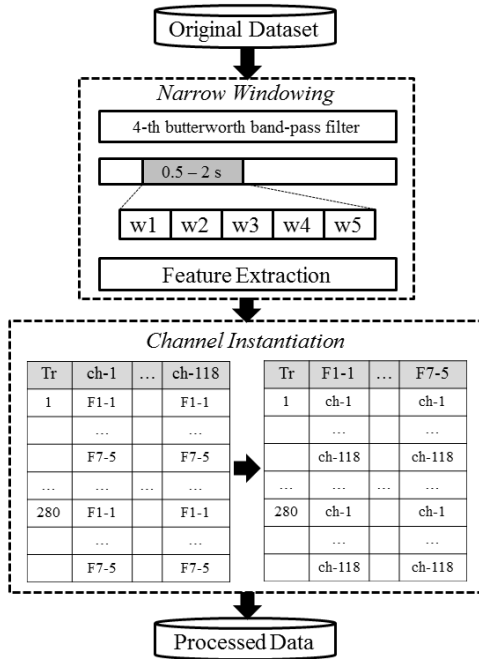


Fig. 1. Narrow window feature extraction and channel instantiation block diagram

- Kurtosis:

$$\text{kurtosis} = \sqrt{\frac{1}{n} \sum_{i=1}^N \frac{(x_n - \mu)^4}{\sigma^4}} \quad (5)$$

- Variance to Means Ratio (vmr):

$$\text{vmr} = \sigma^2 / \mu \quad (6)$$

- Coefficient of Variation (cv):

$$\text{cv} = \sigma / \mu \quad (7).$$

After feature extraction calculated, the next step is channel instantiation step. Channel instantiation means a transformation from column into row, from feature into instance or record. In original dataset, EEG signal were recorded in multi-channel, so the recorded data actually belongs to channel. In this study, each channel has 35 features, comes from 7 statistical features multiple with 5 windows, for each trial. The channel then transformed into row or record and 35 statistical features become column or feature. Since each subject in BCI competition III Dataset IVa has 280 trials, so each subject has 280 x 118 records. In this study, we also use a 17-selected channels (FC3, FC1, FCz, FC2, FC4, C5, C3, C1, Cz, C2, C4, C6, CP3, CP1, CPz, CP2, CP4) since we were only concerned with motor related activity as used by [31] and according to the homunculus theory that represents motor activity area [32].

This dataset transformation based on channel instantiation that proposed by [22]. However, their proposed

method only transform in class level not trial level and then perform classification. In our proposed method, we perform classification in trial level not class level which is a mandatory task that should be performed in BCI competition. This feature extraction and channel instantiation will produce a processed data that will be used further for the classification task.

### C. k-NN and Voting Scheme

Processed data from feature selection stage than feed to 10-fold cross validation (CV) scheme as shown in Fig.2. In 10-fold CV, data will split into 10 subsets mutually exclusive with equal size where nine subsets are used for training and one subset is used for testing and this process repeats 10 times where the testing data is different for each process. As shown in Fig. 2, channel selection is conducted on processed data with 17 channels that related to motor activity.

In 10-fold CV, k-NN is used as classifier since k-NN support incremental learning, able to model complex decision spaces having hyper-polygonal shapes that may not be as easily describable by other learning algorithms such as decision trees and widely used in the area of pattern recognition [33, p. 423]. k-NN searches the pattern space for the k training instance that are closest to the testing instance. These k training instance are the k “nearest neighbors” of the testing instance. Closeness is defined in terms of a distance metric, such as Euclidean distance, Canberra distance, Manhattan distance, etc. In this study, Canberra distance is used as numerical measurement in k-NN parameter. After 10-fold CV conducted, the detected data then saved to MySQL database and then we calculate the accuracy based on voting scheme.

In this voting scheme, the most certain class (class 1 or class 2) detected as a final decision for each trial. Since in this study, one single trial has 118 detected records for all channel scheme and 17 detected records for selected channel scheme. The decision whether class 1 or class 2 based on which channel is most detected to certain class. Since there are 118 channels, we create simple majority voting threshold where detection more than half of 118 for all channel scheme and 17 for selected channel scheme belongs to certain class, so the decision is belongs to its class.

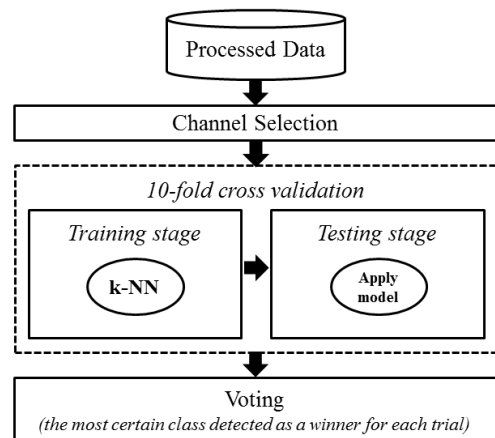


Fig. 2. k-NN detection and voting scheme block diagram

### D. Evaluation

In this study, overall accuracy is used as main evaluation since many prior research used accuracy as main evaluation. This simply calculate based on number of true detection divided to total number of trial. In BCI competition III

dataset IV-a, all subjects (sub-dataset) has 280 trials. Although every subject consisted different train and test sets, they were combined into one dataset due to the low number of trials as used by some prior research [6], [18], [19]. This evaluation calculated after voting scheme is conducted.

#### IV. RESULTS AND DISCUSSION

The experiments are conducted using a computing platform based on Intel i7 CPU and 8 GB RAM with Microsoft Windows 8.1 64-bit operating system. In development tools, Rapidminer 8.1 Educational License and MySQL are used. Matlab R2014b is employed as signal filtering tool and HeidiSQL version 9.4 as MySQL editor for calculating accuracy based on stored data from Rapidminer process with comply to voting scheme.

In this study, we propose two groups based on number of channel used, i.e.: all channels and selected channel. In all channel, only single window of feature extraction is used. Meanwhile in selected channel, a combination of windows are used. Table I and II show the performance results of our proposed methods.

##### A. All Channel Classification Results

In Table I, all single window gain excellent accuracy with 5-th window ( $w_5$ ) gain the best accuracy and lowest standard deviation with 99.71% and 0.16% respectively. All single window gain perfect accuracy for subject “ay”. The  $w_5$  gain most consistent result compared to other single window. This window then used in combination windows scheme which utilize selected channel only.

TABLE I. SINGLE WINDOW WITH ALL CHANNEL

w	Accuracy (%)					Average
	aa	al	av	aw	ay	
w1	97.86	100	99.64	100	100	99.5 ± 0.9
w2	98.21	98.93	100	100	100	99.43 ± 0.82
w3	98.21	99.64	100	100	100	99.57 ± 0.78
w4	98.21	99.64	98.93	100	100	99.36 ± 0.78
w5	99.64	99.64	99.64	99.64	100	<b>99.71 ± 0.16</b>

As shown in Table I, all single window empirically gain excellent and consistent performance with low standard deviation (all below 1%). This findings prove that the narrow window is effective in tackling EEG signal non-stationary [24]. However, this scheme utilize all channels (118 channels). In online BCI system, the using of many channels is not preferable since it will need more resource in EEG signal recording, time and computation [19], etc. Thus, reducing channel is one of solution to tackle those such issues.

##### B. Selected Channel Classification results

Table II presents five our other proposed methods and its results. As shown in Table II, single windows comes from the best windows,  $w_5$  and the rest comes from combination of two until five windows. In these proposed methods, only seventeen channels included in computation. Single window ( $w_5$ ) gain lowest performance both in accuracy and standard deviation. Meanwhile, the performance increase with the number of windows increase. A five windows combination, consists of 1-st, 2-nd, 3-rd, 4-th and 5-th windows ( $w_{12345}$ ),

gain the best performance in matter of highest accuracy and lowest standard deviation with 99.41% and 0.46% respectively. The  $w_{12345}$  with selected channel classification performance almost similar with the best single window ( $w_5$ ) with all channels ( $99.21\% \pm 0.45\%$  vs.  $99.71\% \pm 0.16\%$ ). These findings prove that combination of several narrow window even with minimum channel still gain excellent performance in matter of excellent accuracy and consistent performance in matter of low in standard deviation.

TABLE II. COMBINED WINDOWS WITH SELECTED CHANNEL

w	Accuracy (%)					Average (%)
	aa	al	av	aw	ay	
w <sup>a</sup>	86.79	80.00	91.79	87.14	92.50	87.64 ± 5
w <sup>b</sup>	93.21	95.00	95.71	96.79	97.14	95.57 ± 1.57
w <sup>c</sup>	96.79	97.50	96.79	99.29	98.93	97.86 ± 1.18
w <sup>d</sup>	98.57	99.29	98.57	98.93	99.64	99 ± 0.47
w <sup>e</sup>	98.57	99.29	99.64	98.93	99.64	<b>99.21 ± 0.46</b>

<sup>a</sup> w5, <sup>b</sup> w12, <sup>c</sup> w123, <sup>d</sup> w1234, <sup>e</sup> w12345

In this study, one trial of EEG based MI task has 17 instances to be detected whether class 1 (right hand) or class 2 (right foot). Since one trial has 17 detection results, at least 9 true detections as true detection for corresponding trial. In other word, false detection assigned to corresponding trial when number of misdetection higher or equal to 9. Table III presents averaged number of misdetection distribution among 280 trials for all subjects.

TABLE III. MISDETECTION DISTRIBUTION OF AVERAGED RESULTS FROM ALL SUBJECTS FOR COMBINED WINDOWS WITH SELECTED CHANNEL

range	#misdetection distribution				
	w5	w12	w123	w1234	w12345
0 – 2	41	76.2	105.4	<b>129</b>	<b>150.8</b>
3 – 5	<b>107.2</b>	<b>125</b>	<b>123.8</b>	115.4	102.2
6 – 8	97.2	66.4	44.8	32.8	24.8
>=9	<u>34.6</u>	<u>12.4</u>	<u>6</u>	<u>2.8</u>	<u>2.2</u>
Total	280	280	280	280	280
#True Det.	245.4	267.6	274	277.2	277.8
Accuracy (%)	87.64	95.57	97.86	99	<b>99.21</b>

As shown in Table III,  $w_5$  has highest number of misdetection that caused false detection and decrease its accuracy (range >=9); meanwhile  $w_{12345}$  has lowest number of misdetection. More windows combination increase number of misdetection in lower range (0 – 2 until 6 – 8) that cause increase true detection and finally increase its accuracy (#True Det. divided by Total). In this study, it needs at least 2 narrow windows in order to achieve excellent accuracy (more than 90%). This findings proof that narrow window is still effective although with channel reduction.

In order to analyze the effectiveness of the proposed methods, we compare our proposed methods to the most relevant prior research. Five prior researches, as describe in Section 2, are selected as benchmark and comparison. Table IV presents its comparison.

TABLE IV. PERFORMANCE COMPARISON TO PRIOR RESEARCH

Authors	Method	Accuracy (%)*					
		<i>aa</i>	<i>al</i>	<i>av</i>	<i>aw</i>	<i>ay</i>	<i>average</i>
Baig <i>et al.</i> [19]	CSP+DE-FS	95.8	<u>98.8</u>	<u>89.8</u>	<u>99.2</u>	<u>96.5</u>	<u>96.02 ± 3.77</u>
Kevric and Subasi [6]	MSPCA+WPD+HOS	<u>96</u>	92.3	88.9	95.4	91.4	92.8 ± 2.93
Park S. H. <i>et al.</i> [21]	FBRCSF	91.07	94.64	75	76.78	93.65	86.23 ± 9.55
Miao <i>et al.</i> [18]	STFSCSP	95.2	98.58	79.41	97.78	95.02	92.66 ± 7.78
Park S. M. <i>et al.</i> [20]	CSP+SF	72.62	95.92	63.54	89.85	88.38	82.06 ± 13.4
<i>Proposed Method #1</i>	<i>w5+all-ch+k-NN+VS</i>	<b>99.64</b>	<b>99.64</b>	<b>99.64</b>	<b>99.64</b>	<b>100</b>	<b>99.71 ± 0.16</b>
<i>Proposed Method #2</i>	<i>w5+17-ch+k-NN+VS</i>	86.79	80.00	<b>91.79</b>	87.14	92.50	87.64 ± 5
<i>Proposed Method #3</i>	<i>w12+17-ch+k-NN+VS</i>	93.21	95.00	<b>95.71</b>	96.79	<b>97.14</b>	95.57 ± 1.57
<i>Proposed Method #4</i>	<i>w123+17-ch+k-NN+VS</i>	<b>96.79</b>	97.50	<b>96.79</b>	<b>99.29</b>	<b>98.93</b>	<b>97.86 ± 1.18</b>
<i>Proposed Method #5</i>	<i>w1234+17-ch+k-NN+VS</i>	<b>98.57</b>	<b>99.29</b>	<b>98.57</b>	<b>98.93</b>	<b>99.64</b>	<b>99 ± 0.47</b>
<i>Proposed Method #6</i>	<i>w12345+17-ch+k-NN+VS</i>	<b>98.57</b>	<b>99.29</b>	<b>99.64</b>	<b>98.93</b>	<b>99.64</b>	<b>99.21 ± 0.46</b>

\*bold number means the best results compared to prior researches, underlined number means the best results among prior researches

As shown in Table IV, all prior researches yielded low accuracy for subject “av” (below 90%) and three of them gained wide standard deviation (more than 5%). The best performance from the prior research is hold by Baig *et al.* [19] with 96.02% and 3.77% for accuracy and standard deviation respectively. Compared to our proposed method, especially the proposed methods with selected channel, 4 of 5 our proposed methods outperform all averaged results of the prior researches both in accuracy and standard deviation. Among these results, 2 of 5 our proposed methods outperform not only in averaged result but also outperform in every subjects.

The effectiveness of the proposed methods is a combination strategy from feature extraction scheme until classification scheme. First, the narrow window and its combination in tackling non-stationary EEG signal [24]. Second, the using of higher order statistic (skewness and kurtosis) as statistical feature extraction method [6], mean average value and root mean square [22], [34]. Finally, the using of channel instantiation approach [22] that create more instance that effective for k-NN as instance-based classifier in EEG based MI classification [6].

## V. CONCLUSION

In this study, a combination of narrow window feature selection and seventeen motor related activity EEG channels were used for classification task of MI based EEG signal. A multi-channel with 2-class dataset taken from BCI competition III Dataset IVa is used for this purpose. We conducted and evaluated the proposed methods by using promising approach so called channel instantiation as data transformation, k-NN algorithm and voting scheme for final decision. From the experimental results, all proposed methods with all channel yield excellent accuracy and consistent for all subjects. The proposed methods with selected seventeen channels also effective and gain consistent excellent accuracy with at least three narrow windows combination. These results show that the proposed method has the potential to obtain a reliable EEG based MI classification and can be used practically in online BCI systems such as: controlling a wheelchair, rehabilitation therapies for the stroke rehabilitation or improve motor

rehabilitation outcomes. However, several issue still open for future works such as: a need for automatic feature selection to reduce the computational time and apply model in multi-class EEG based MI classification to test the robustness of the proposed method.

## REFERENCES

- [1] D. H. Krishna, I. A. Pasha, and T. S. Savithri, “Classification of EEG Motor Imagery Multi Class Signals Based on Cross Correlation,” *Procedia Comput. Sci.*, vol. 85, pp. 490–495, 2016.
- [2] J. Minguillon, M. A. Lopez-Gordo, and F. Pelayo, “Trends in EEG-BCI for daily-life: Requirements for artifact removal,” *Biomed. Signal Process. Control*, vol. 31, pp. 407–418, 2017.
- [3] H. Mirvaziri and Z. S. Mobarakeh, “Improvement of EEG-based motor imagery classification using ring topology-based particle swarm optimization,” *Biomed. Signal Process. Control*, vol. 32, pp. 69–75, 2017.
- [4] S. Liang, K.-S. Choi, J. Qin, W.-M. Pang, Q. Wang, and P.-A. Heng, “Improving the discrimination of hand motor imagery via virtual reality based visual guidance,” *Comput. Methods Programs Biomed.*, vol. 132, pp. 63–74, 2016.
- [5] Y. Yu *et al.*, “Toward brain-actuated car applications: Self-paced control with a motor imagery-based brain-computer interface,” *Comput. Biol. Med.*, 2016.
- [6] J. Kevric and A. Subasi, “Comparison of signal decomposition methods in classification of EEG signals for motor-imagery BCI system,” *Biomed. Signal Process. Control*, vol. 31, pp. 398–406, 2017.
- [7] P. J. García-Laencina, G. Rodríguez-Bermudez, and J. Roca-Dorda, “Exploring dimensionality reduction of EEG features in motor imagery task classification,” *Expert Syst. Appl.*, vol. 41, no. 11, pp. 5285–5295, 2014.
- [8] K. McInnes, C. Friesen, and S. Boe, “Specific brain lesions impair explicit motor imagery ability: A systematic review of the evidence,” *Arch. Phys. Med. Rehabil.*, vol. 97, no. 3, pp. 478–489, 2016.
- [9] T. Zhang *et al.*, “Structural and functional correlates of motor

- imagery BCI performance: Insights from the patterns of Fronto-Parietal Attention Network,” *Neuroimage*, 2016.
- [10] H. Burianová *et al.*, “Multimodal functional imaging of motor imagery using a novel paradigm,” *Neuroimage*, vol. 71, pp. 50–58, 2013.
  - [11] L. He, B. Liu, D. Hu, Y. Wen, M. Wan, and J. Long, “Motor imagery EEG signals analysis based on Bayesian network with Gaussian distribution,” *Neurocomputing*, vol. 188, pp. 217–224, 2016.
  - [12] T. Kayikcioglu and O. Aydemir, “A polynomial fitting and k-NN based approach for improving classification of motor imagery BCI data,” *Pattern Recognit. Lett.*, vol. 31, no. 11, pp. 1207–1215, Aug. 2010.
  - [13] S. Chatterjee, N. Ray Choudhury, and R. Bose, “Detection of epileptic seizure and seizure-free EEG signals employing generalised S -transform,” *IET Sci. Meas. Technol.*, vol. 11, no. 7, pp. 847–855, 2017.
  - [14] J. Meng, L. Yao, X. Sheng, D. Zhang, and X. Zhu, “Simultaneously Optimizing Spatial Spectral Features Based on Mutual Information for EEG Classification,” *IEEE Trans. Biomed. Eng.*, vol. 62, no. 1, pp. 227–240, 2015.
  - [15] D. Li, H. Zhang, M. S. Khan, and F. Mi, “A self-adaptive frequency selection common spatial pattern and least squares twin support vector machine for motor imagery electroencephalography recognition,” *Biomed. Signal Process. Control*, vol. 41, pp. 222–232, 2018.
  - [16] L. Duan, M. Bao, J. Miao, Y. Xu, and J. Chen, “Classification Based on Multilayer Extreme Learning Machine for Motor Imagery Task from EEG Signals,” *Procedia Comput. Sci.*, vol. 88, pp. 176–184, 2016.
  - [17] J. S. Suri, A. Kumar, G. K. Singh, and M. K. Ahirwal, “Sub-band classification of decomposed single event-related potential covariants for multi-class brain–computer interface: a qualitative and quantitative approach,” *IET Sci. Meas. Technol.*, vol. 10, no. 4, pp. 355–363, 2016.
  - [18] M. Miao, H. Zeng, A. Wang, C. Zhao, and F. Liu, “Discriminative spatial-frequency-temporal feature extraction and classification of motor imagery EEG: An sparse regression and Weighted Naïve Bayesian Classifier-based approach,” *J. Neurosci. Methods*, vol. 278, pp. 13–24, 2017.
  - [19] M. Z. Baig, N. Aslam, H. P. H. Shum, and L. Zhang, “Differential Evolution Algorithm as a Tool for Optimal Feature Subset Selection in Motor Imagery EEG,” *Expert Syst. Appl.*, vol. 90, pp. 184–195, 2017.
  - [20] S. M. Park, X. Yu, P. Chum, W. Y. Lee, and K. B. Sim, “Symmetrical feature for interpreting motor imagery EEG signals in the brain???computer interface,” *Optik (Stuttg.)*, vol. 129, pp. 163–171, 2017.
  - [21] S.-H. Park, D. Lee, and S.-G. Lee, “Filter Bank Regularized Common Spatial Pattern Ensemble for Small Sample Motor Imagery Classification,” *IEEE Trans. Neural Syst. Rehabil. Eng.*, vol. 4320, no. c, pp. 1–1, 2017.
  - [22] Siuly, H. Wang, and Y. Zhang, “Detection of motor imagery EEG signals employing Naïve Bayes based learning process,” *Meas. J. Int. Meas. Confed.*, vol. 86, pp. 148–158, 2016.
  - [23] B. Blankertz *et al.*, “The BCI competition III: Validating alternative approaches to actual BCI problems,” *IEEE Trans. Neural Syst. Rehabil. Eng.*, vol. 14, no. 2, pp. 153–159, 2006.
  - [24] Siuly and Y. Li, “A novel statistical algorithm for multiclass EEG signal classification,” *Eng. Appl. Artif. Intell.*, vol. 34, pp. 154–167, 2014.
  - [25] L. Sun, Z. Feng, B. Chen, and N. Lu, “A contralateral channel guided model for EEG based motor imagery classification,” *Biomed. Signal Process. Control*, vol. 41, pp. 1–9, 2018.
  - [26] T. Uehara, M. Sartori, T. Tanaka, and S. Fiori, “Robust Averaging of Covariances for EEG Recordings Classification in Motor Imagery Brain-Computer Interfaces,” *Neural Comput.*, 2017.
  - [27] L. Duan, Z. Hongxin, M. S. Khan, and M. Fang, “Recognition of motor imagery tasks for BCI using CSP and chaotic PSO twin SVM,” *J. China Univ. Posts Telecommun.*, vol. 24, no. 3, pp. 83–90, 2017.
  - [28] C. Park, C. C. Took, and D. P. Mandic, “Augmented Complex Common Spatial Patterns for Classification of Noncircular EEG From Motor Imagery Tasks,” *IEEE Trans. Neural Syst. Rehabil. Eng.*, vol. 22, no. 1, pp. 1–10, Jan. 2014.
  - [29] W. Y. Hsu, “EEG-based motor imagery classification using neuro-fuzzy prediction and wavelet fractal features,” *J. Neurosci. Methods*, vol. 189, no. 2, pp. 295–302, 2010.
  - [30] X. Tang, N. Zhang, J. Zhou, and Q. Liu, “Hidden-layer visible deep stacking network optimized by PSO for motor imagery EEG recognition,” *Neurocomputing*, vol. 234, no. December 2016, pp. 1–10, 2017.
  - [31] B. J. Edelman, B. Baxter, and B. He, “EEG Source Imaging Enhances the Decoding of Complex Right-Hand Motor Imagery Tasks,” *IEEE Trans. Biomed. Eng.*, vol. 63, no. 1, pp. 4–14, 2016.
  - [32] C. C. J. M. De Klerk, M. H. Johnson, and V. Southgate, “An EEG study on the somatotopic organisation of sensorimotor cortex activation during action execution and observation in infancy,” *Dev. Cogn. Neurosci.*, vol. 15, pp. 1–10, 2015.
  - [33] J. Han, M. Kamber, and J. Pei, *Data Mining*, 11th ed. Morgan Kaufman, 2011.
  - [34] P. K. Pattnaik and J. Sarraf, “Brain Computer Interface issues on hand movement,” *J. King Saud Univ. - Comput. Inf. Sci.*, 2016.

# Emotion Recognition using Fisher Face-based Viola-Jones Algorithm

Kartika Candra Kirana <sup>1</sup>, Slamet Wibawanto <sup>2</sup>, Heru Wahyu Herwanto <sup>3</sup>

Department of Electrical Engineering

State University of Malang

Jl. Semarang No 5, Malang, Indonesia

[kartika.candra.ft@um.ac.id](mailto:kartika.candra.ft@um.ac.id) <sup>1</sup>, [slamet.wibawanto.ft@um.ac.id](mailto:slamet.wibawanto.ft@um.ac.id) <sup>2</sup>, [heru\\_wh@um.ac.id](mailto:heru_wh@um.ac.id) <sup>3</sup>

**Abstract**—In the form of the image integral, this primitive feature accelerates the performance of the Viola-Jones algorithm. However, the robust feature is necessary to optimize the results of emotion recognition. Previous research [11] has shown that fisher face optimized projection matrix in the low dimensional features. This feature reduction approach is expected to balance time-consuming and accuracy. Thus we proposed emotion recognition using fisher face-based Viola-Jones Algorithm. In this study, PCA and LDA are extracted to get the fisher face value. Then fisher face is filtered using Cascading AdaBoost algorithm to obtain face area. In the facial area, the Cascading AdaBoost algorithm re-employed to recognize emotions. We compared the performance of the original viola jones and fisher face-based viola jones using 50 images on the State University of Malang dataset by measuring the accuracy and time-consuming in the fps. The accuracy and time-consuming of the Viola-Jones algorithm reach 0.78 and 15 fps, whereas our proposed methods reach 0.82 and 1 fps. It can conclude that the fisher face-based viola-jones algorithm recognizes facial emotion as more accurate than the viola-jones algorithm.

**Keywords**—*facial, emotion recognition, fisher face, FLDA, Viola-Jones algorithm.*

## I. INTRODUCTION

The Viola-Jones algorithm is often thought of as a rapid processing for face detection. In this algorithms, AdaBoost algorithms classify the rectangular features in "cascade" stages. The rectangle feature is computed rapidly using an integral theorem every shifting of sub-window. In the form of the image integral, this primitive feature accelerates the performance of the Viola-Jones algorithm. [1] The rate of face detection proceeded in 15 frames per second (fps), thus it supports real-time processing.

Despite image integral can be calculated quickly, the representation of integral is less responsive to changes in face angle[2] [3] [4]. These problems decrease the accuracy. In addition, image integral requires a very large derivative feature to find face boundaries, even for thumbnails [5]. In other research contexts, image integrals cannot identify a problem optimally. For example, [6] explains that river image characteristics are almost identical to other images, such as the ocean. Therefore [6] identifies the river using the modified image integrals based on hydromorphology features. This research segment river from trees, roads, roofs, shore and the

sky using hydromorphology feature until 70%. However, this system distinguishes between sea and river in an accuracy of 68%.

In emotion recognition research, image integrals cannot identify a problem optimally. [7] proposes the Viola-Jones algorithm to detect human emotion in video sequences. Their results show that proposes the Viola-Jones algorithm only reaches the accuracy in 70%. However, their proposed methods can be computed rapidly. [8] also mentioned that the feature integral result does not work well on emotional recognition, thus they combines the Viola-Jones and Edge-Histogram of Oriented Gradient as feature descriptor identify the emotions of the patients. However, Edge-Histogram of Oriented Gradient cannot describe the frequency distribution with the open class.

Image integrals cannot identify the facial emotion optimally because the differences of human expression in showing emotion. For example, uninterested emotions can be marked by yawning (eyes still open). Some others can be marked by falling asleep (eyes closed). Both of these examples have different image integral values, so we need another robust feature in recognizing emotions.

[9] compared textured features in the emotion recognition using Support Vector Machine (SVM). They show that fisher face presents the emotion more represent than gradient and wavelet. However, SVM computes the multi-class classification slowly. [10] proposed the 2D fisher face which is hoped to find the best projection direction matrix. The result shows that 2D fisher face more accurate than Principal Component Analysis (PCA) and 2D-PCA. However, 2D fisher face computes slower than PCA. [11] implements artificial neural networks and fisher face features to recognize emotions in the learning context. They reach an accuracy of 81%. However, they confirmed that the applying of a complex neural network architecture produce an accurate system that computes slowly. Although fisher face optimized projection matrix in the low dimensional features. This feature needs a longer time than the integral features.

The above research [9][10][11] have been shown that the fisher face feature is a robust feature in the facial emotion recognition. However, they consume a longer time than the primitive features. On the other sides, the Cascaded Adaboost algorithm in Viola-Jones algorithms handles the computing

time with reject unnecessary area quickly using hard limit [2][3]. The combination of fisher face and the Cascaded Adaboost algorithm is expected to balance time-consuming and accuracy in facial emotion recognition, thus we propose emotion recognition using fisher face-based viola-jones algorithm. In this study, our contribution is modifying the features of fisher face as a substitute for feature rectangle to detect faces and emotions simultaneously.

## II. FACIAL EMOTION

The emotion can be performed using, gestures, speech, control, and facial expression. However, the most of popular approach in emotion recognition is the acquisition of facial-based features [12]. The emotion is divided into the positive emotion and the negative emotion. The emotion is also divided into neutral, happiness, sadness, anger, fear, surprise and disgust [12]. In this research, we applied our proposed method in the learning environment, thus the basic emotion cannot present the learning specifically. There are two popular learning emotion approaches consisting of Russell's Circumplex approach and the affective and constructive learning-based approach. Russell's Circumplex Approach classify emotion into interest, engagement, confusion, frustration, satisfaction, hopefulness, boredom, and disappointment [13]. In addition, the affective and constructive learning-based approach determine emotions more simply. It separated the emotion into four types. First, the student feels interested in a matter of learning. Second, the student began to have confusion and difficulties. Third, student emotions start negative when feeling there is a frustration in learning. Fourth, shows students gain new insights as the basis for the search for new ideas. [13] [14] [15].

## III. FISHER FACE

Fisher faces or named as fisher linear discriminant is the combination of Principle Component Analysis (PCA) and Linear Discriminant Analysis (LDA). PCA is an unsupervised algorithm, whereas LDA is an unsupervised algorithm. PCA keeps the distribution information but cannot project the optimal matrix. LDA project the optimal matrix under Fisher criterion, but the dimension of the input space is greater than the number of training images, thus it cannot be applied directly. [9] [10] [11]

Projection PCA of the matrix is computed by Equation 1 and projection LDA of the matrix is computed by Equation 2.

$$PCA(\varphi) = \varphi^T S_T \varphi, \quad (1)$$

$$LDA(\varphi) = \frac{\varphi^T S_b \varphi}{\varphi^T S_w \varphi}, \varphi \neq 0, \quad (2)$$

where  $\varphi^T$  is the transpose of the matrix  $\varphi$ . Total scatter matrix  $S_T$  is the summation of the  $S_b$  between-class scatter matrix and  $S_w$  within-class scatter matrix.

$S_b$  between-class scatter matrix is shown as follows:

$$S_b = \frac{1}{N} \sum_{i=1}^C N_c (\mu_i - \mu)(\mu_i - \mu)^T, \quad (3)$$

and  $S_w$  within-class scatter matrix is shown as follows:

$$S_w = \frac{1}{N} \sum_{i=1}^C \sum_{j=1}^{N_c} (x_{ij} - \mu_i)(x_{ij} - \mu_i)^T \quad (4)$$

where if  $N$  present the total of data and  $C$  present the total of class, then  $N_c$  present the total of data in class  $C$ . Meanwhile,  $x$  is the vector and  $\mu$  is the mean of the vector.

## IV. VIOLA-JONES ALGORITHM

In Viola-Jones algorithm, In this algorithms, AdaBoost algorithms classify the rectangular features in "cascade" stages. The rectangular features are calculated using an integral representation which is calculated using Equation 5.

$$W_e = \sum_{y_i \neq k_m(x_i)} w_i^m, \quad (5)$$

where  $W_e$  is the integral of sub window's and  $w_i$  is integral to pixel- $i$ . A number of  $M$  filters are looped at each cascaded stage. The weak classifier ( $k_m$ ) is selected from the pool of the classifier. The weight of the classifier  $w_i$  is updated on each iteration.

## V. METHODOLOGY

### A. Dataset

We captured ten UM's student (six men and four woman with age 18-24 years) in the class using CANON EOS 700D. The camera is placed facing the student at the top of the presentation screen, while the camera and the student sitting position have the different angle of inclination. Video resolution is set 720X1280 pixels in 25 frames per seconds (fps). These videos are converted into the image in 25 frames per minutes, thus there is 100 image of student facial expression. 50 images are set as training data and 50 is set as testing data. In this research, we only capture the two emotion consist of interest and bored in the real class. These both emotions are most commonly found in real class. 'Interest' represents the positive emotion which is described as a state of willingness to process and understand information. Nevertheless, 'bored' represent negative emotion which is described as a state of unwillingness to process and understand information.

### B. Facial Emotion Recognition using Fisher Face-based Viola-Jones Algorithm

The pseudocode Fisher face-based Viola-Jones algorithm is shown in Figure 1. Our contribution is modifying the features of fisher face as a substitute for feature rectangle to detect faces and emotions simultaneously.



```

1 Input: Face image
2 Output: Emotion{Interest,Bored}
3 for i ← 1 to num of sub window's shift do
4   for j ← 1 to num of cascaded stages do
5     for k ← 1 to num of filter do
6       Calculate  $w_e$  fisher face Using Equation (6)
7       update  $w_{face}$  using Equation(8)
8       update  $w_{emotion} = \text{Equation (8)}$ 
9       if  $w_e < w_{face}$  then
10        break for k loop
11       elseif  $w_e < w_{emotion}$  then
12        output = bored
13       else
14        output = interest
15       end if
16     end for
17   end for
18 end for

```

Fig. 1. Pseudocode of Fisher Face-based Viola-Jones Algorithms for Facial Emotion Recognition

Like the original Jones-Viola algorithm, the features on each shifted window are calculated. In this study, we do not present rectangular features, but we modified the Viola-Jones algorithm using the fisher-face feature. Fisher face is a composite of PCA and LDA calculated using Equations 1 and 2 that can be simplified into Equation 6.

$$w_e = J(\varphi) = \varphi^{Fisher} \Lambda \quad (6)$$

At Equation 6, the feature of sub window's  $w_e$  are projected by the matrix  $\varphi$  of fisher's face  $J$ . It calculated using a diagonal eigenvalue matrix  $\Lambda$  that equal to Equation 1 and  $\varphi^{Fisher}$ .  $\varphi^{Fisher}$  eliminates zero eigens and sort in descending order.

A number of  $M$  filters are looped at each cascaded stage. The weak classifier ( $k_m$ ) is selected and the weight of classifier  $\alpha_m$  is calculated by:

$$\alpha_m = \frac{1}{2} \ln \left( \frac{1 - e_m}{e_m} \right). \quad (7)$$

where  $e_m$  is the weight-normalized and it is set as follows :

$$e_m = \frac{w_e}{W}. \quad (8)$$

where  $W$  is a maximum weight. The updated threshold  $w_t$  is updated on each iteration  $m+1$  by:

$$w_t^{m+1} = \begin{cases} w_t^m e^{\alpha_m} & k_m(x_i) \text{ is a miss} \\ w_t^m e^{-\alpha_m} & \text{otherwise} \end{cases}, \quad (9)$$

In this study, there is two threshold  $w_t$  consist of  $w_{face}$  and  $w_{emotion}$ .  $w_{face}$  is the threshold of the face.  $w_{face}$  is compared with the weight of the sub window's  $w_e$ . If  $w_e$  are less than  $w_{face}$ , the sub-windows is rejected as the face. Whereas if  $w_e$  are more than  $w_{face}$ , the sub window is processed in emotion recognition. The procedure of emotion recognition is similar to face detection, However,  $w_e$  are compared with  $w_{emotion}$ .  $w_{emotion}$  is the threshold of emotion. If  $w_e$  are less than  $w_{emotion}$ , the sub-windows is set as bored. Whereas if  $w_e$  are more than  $w_{emotion}$ , the sub window is set as interest.

### C. Evaluation

Series of experiments are conducted to compare the performance of Fisher Face-based Viola-Jones Algorithm and original Viola-Jones Algorithm for the facial emotion recognition. We used original Viola-Jones Algorithm version [7] as a comparison. The emotions ground truth is analyzed manually by an expert. The estimated results are compared with ground truth to obtain the accuracy, precision, and recall which are calculated as follows:

$$accuracy = \frac{TP + TN}{TP + TN + FP + FN} \quad (10)$$

$$precision = \frac{TP}{TP + FP} \quad (11)$$

$$recall = \frac{TP}{TP + FN} \quad (12)$$

where  $TP$  is the number of the interest emotion that classified correctly,  $TN$  is the number of the bored emotion that classified correctly,  $FN$  is the number of interest emotion that classified as bored emotion, and  $FP$  is the number of bored emotion that classified as interest emotion.

## VI. RESULT AND DISCUSSION

In this study, we compare the performance of Fisher Face-based Viola-Jones Algorithm and original Viola-Jones Algorithm for the facial emotion recognition. In this study, we initialize the variables based on [1] and [7] research shown in Table I. We use a base resolution of 24x24 pixels that this bounding box was enlarged up to 50%. We also set 38 layer cascade of classifiers without comparing the best layer values. In addition we implemented 3 stages which are more one stage than [1]. Stage I is used to reject unface area. Stage II is used to update the weight of facial emotion, whereas stage III is used to estimate the emotion using the updated weight.

We evaluated the accuracy, precision, recall, and time-consuming of the system using 50 data of the University of Malang's learning dataset. There are 25 images of students with 'interest' emotions and 25 others have 'bored' emotions in testing data. Moreover, we initialize the 'interest' emotions as a positive class and 'bored' emotions as a negative class. The comparison of evaluation is shown in Table II.

In Table II, we compare our proposed algorithm and the original Viola-Jones algorithms [1][7]. The results show that original Viola-Jones algorithm achieves accuracy, precision, recall, and time up to 0.78, 0.77, 0.80 and 15 fps respectively, whereas our proposed method achieves 0.82, 0.78, 0.84, and 1 fps. These results show that the fisher face-based Viola-Jones algorithm recognizes facial emotion more accurate and precision than the Viola-Jones algorithm. However, our algorithm is 15x slower than the original Viola-Jones. At the same time, the original Viola-Jones algorithm is able to execute 15 frames per second, our algorithm is only able to extract 1 frame every second. The original Viola-Jones system works faster because it uses simple summation based features, while the features we use work twice in PCA and LDA calculations. however, our system is more accurate because the fisher face is able to produce the best vector dimension to represent the face and emotions as described by [9] [10] and [11].

TABLE I. THE INITIALIZATION

Variables	Value
Base resolution	24x24 pixels <sup>a</sup>
Layer cascade of classifiers	38 <sup>a</sup>
Stages	3

<sup>a</sup>. The value set is the same as [1]

TABLE II. THE COMPARISON OF EVALUATION

The Algorithm	Results							
	TP	TN	FP	FN	Accuracy	precision	Recall	Time <sup>c</sup>
Original VJ <sup>b</sup>	20	19	6	5	0.78	0.77	0.80	15 fps
Fisher face-based VJ <sup>b</sup>	21	20	6	4	0.82	0.78	0.84	1 fps

<sup>b</sup>. VJ = Viola-Jones algorithm<sup>c</sup>. time in frame per second (fps)

The example of comparison results in our tests is shown in Figure 2. Figure 2 (a) and Figure 2 (b) show the results of the original Viola-Jones algorithm, while Figure 2 (c) and Figure 2 (d) show the results of the fisher face-based Viola-Jones algorithm. In Figure 2 (a) and 2 (c), both methods can not detect faces that are not facing the camera. However, if the angle of the face is not extreme, both methods can detect the face.

In Figures 2 (b) and 2 (d), both methods can detect two faces that are not facing the camera because the face angle is not extreme. In Figure 2 (b), the viola jones algorithm detects one interested student and one student bored, while in Figure 2 (d), our algorithm detects both students bored. Based on the ground truth by the experts, the two students have an indication of boredom in learning. This is shown by the eyes that did not focus on presentation slides and talk with other students. There is a possibility that the original jones viola detect the emotion of the 2<sup>nd</sup> student emotion as the interest because there is a lot of data of interest trainer which is marked with a smile. Especially for emotional recognition, we find the dominance of the integral area. The analogy of integral dominance is shown in Figure 3.

In the original Viola-Jones algorithm, lip expression is more dominant than the eye expression because the lip changes increase the integral value greater than the eye. This is shown from the comparison between Figure 2 (a) to Figure 2 (b) as changes in eye expression and Figure 2 (a) to Figure 2 (c) as changes in lip expression. While in fisherface, we take the statistical feature on the pixels set as the face, so there is no dominance of certain areas on the face.

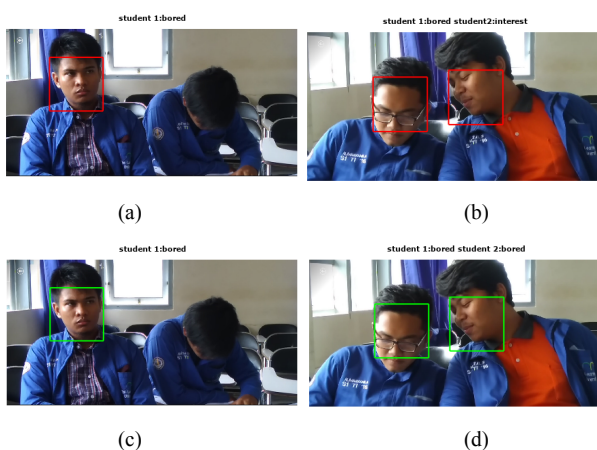


Fig. 2. The Example of Result Comparison (a),(b) Result of [7] Algorithm (c),(d) Result of Our Proposed Method

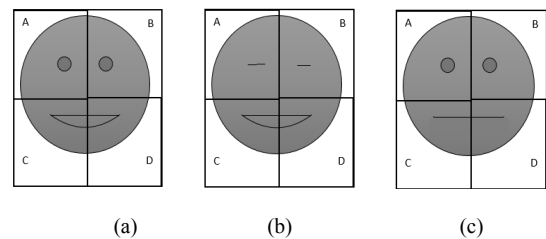


Fig. 3. The analogy of integral dominance

## VII. CONCLUSION

Series of experiments are conducted to evaluate the performance of Fisher Face-based Viola-Jones algorithms. The results show that original viola-jones algorithm achieves accuracy, precision, recall, and time up to 0.78, 0.77, 0.80 and 15 fps respectively, whereas our proposed method achieves 0.82, 0.78, 0.84, and 1 fps. These results shows that the fisher face-based viola-jones algorithm recognizes facial emotion more accurate and precision than the viola-jones algorithm. However, our algorithm is 15x slower than the original viola jones.

In further research, speed improvements are needed. This can be achieved by combining the integral and fisher face concepts which the integrals can be calculated quickly and the fisher face detects facial emotion accurately. In addition, the process of shifting windows is still conventional which is start from left to right. The process of finding the shortest path to the face area can be optimized by a heuristic algorithm.

## ACKNOWLEDGMENT

This research is fully supported by the State University of Malang using PNPB funding. We also thank the Faculty of Engineering for providing the object of study.

## REFERENCES

- [1] P. Viola and M.J. Jones, "Robust Real Time Face Detection" in International Journal of Computer Vision. vol. 57 (2004), pp.137-154.
- [2] D. Peleshko and K. Soroka, "Research of usage of Haar-like features and AdaBoost algorithm in Viola-Jones method of object detection" 2013 12th International Conference on the Experience of Designing and

- Application of CAD Systems in Microelectronics (CADSM), pp. 284-286. Feb. 2013.
- [3] T. Ephraim, T. Himmelman, and K. Siddiqi, "Real-Time Viola-Jones Face Detection in a Web Browser", 2009 Canadian Conference on Computer and Robot Vision, pp. 321-328. 25-27 May 2009.
  - [4] M.V. Alyushin, V.M. Alyushin, and L.V. Kolobashkina, "Optimization of the Data Representation Integrated Form in the Viola-Jones Algorithm for a Person's Face Search," 8th Annual International Conference on Biologically Inspired Cognitive Architectures, *Procedia Computer Science*, vol. 123 (2018), pp. 18-23.
  - [5] A. D. Egorov, D. U. Divitskii, A. A. Dolgih, and G. A. Mazurenko "Some cases of optimization face detection methodes on image (Using the Viola-Jones method as an example)", 2018 IEEE Conference of Russian Young Researchers in Electrical and Electronic Engineering (EIConRus), pp. 1075-1078, Jan. 29 2018-Feb. 1 2018.
  - [6] J. Cuevas, A. Chua, E. Sybingco, and E. A. Bakar, "Identification of river hydromorphological features using Viola-Jones Algorithm", 2016 IEEE Region 10 Conference (TENCON), pp. 2300-2306. November 2016.
  - [7] P. Ithaya Rani and K. Muneeswaran, "Robust real time face detection automatically from video sequence based on Haar features", 2014 International Conference on Communication and Network Technologies, pp. 276-280. Dec. 2014.
  - [8] H. Candra, M. Yuwono, R. Chai, H. T. Nguyen, and S. Su "Classification of facial-emotion expression in the application of psychotherapy using Viola-Jones and Edge-Histogram of Oriented Gradient", 2016 38th Annual International Conference of the IEEE Engineering in Medicine and Biology Society (EMBC), pp. 423-426, Aug. 2016.
  - [9] G. K. Verma and B. K. Singh, "Emotion recognition based on texture analysis of facial expression," 2011 International Conference on Image Information Processing, Himachal Pradesh, 2011, pp. 1-6.
  - [10] Y. Li, W. Yuan, H. Sang and X. Li, "Combination recognition of face and ear based on two-dimensional fisher linear discriminant," 2013 IEEE 4th International Conference on Software Engineering and Service Science, Beijing, 2013, pp. 922-925.
  - [11] S. Wibawanto and K.C.Kirana, "Recognition of Student Emotion based on Matrix-1 Median Fisher's Face and Backpropagation Algorithm," 2017 International Conference on Electrical Engineering and Informatics, pp. 117-122. October 2017.
  - [12] P. Tarnowski, M. Kołodziej, A. Majkowski, and R. J. Rak, "Emotion Recognition using Facial Expressions," International Conference on Computational Science, pp. 1175-1184, June 2017.
  - [13] L. Darling, S. Orcutt, K. Strobel, E. Kirsch, I. Lit, and D. Martin., *The Learning Classroom: Emotion and Learning*, California: Stanford University School of Education, 2010, pp. 90-104.
  - [14] A.R Faria, A. Almeida, C. Martins, R. Gonçalves, J. Martins, F. Branco, "A global perspective on an emotional learning model proposal," *Telematics and Informatics*, 2016, in press.
  - [15] P. Vela, P.A. Vela, R.J. Jensen, *Emotions, Technology, Design, and Learning: Robots, Emotions, and Learning*, Elsevier Inc, 2016, pp.183-197.

# IDEnet : Inception-Based Deep Convolutional Neural Network for Crowd Counting Estimation

Samuel Cahyawijaya  
Institut Teknologi Bandung  
Bandung, Indonesia  
samuel.cahyawijaya@gmail.com

Bryan Wilie  
Institut Teknologi Bandung  
Bandung, Indonesia  
brywilie25@gmail.com

Widyawardana Adiprawita  
Institut Teknologi Bandung  
Bandung, Indonesia  
wadiprawita@stei.itb.ac.id

**Abstract**— In crowd counting task, our goals are to estimate density map and count of people from the given crowd image. From our analysis, there are two major problems that need to be solved in the crowd counting task, which are scale invariant problem and inhomogeneous density problem. Many methods have been developed to tackle these problems by designing a dense aware model, scale adaptive model, etc. Our approach is derived from scale invariant problem and inhomogeneous density problem and we propose a dense aware inception based neural network in order to tackle both problems. We introduce our novel inception based crowd counting model called Inception Dense Estimator network (IDEnet). Our IDEnet is divided into 2 modules, which are Inception Dense Block (IDB) and Dense Evaluator Unit (DEU). Some variations of IDEnet are evaluated and analysed in order to find out the best model. We evaluate our best model on UCF50 and ShanghaiTech dataset. Our IDEnet outperforms the current state-of-the-art method in ShanghaiTech part B dataset. We conclude our work with 6 key conclusions based on our experiments and error analysis.

**Keywords**—crowd counting, inception network, convolutional neural network, deep learning, dense aware, scale adaptive

## I. INTRODUCTION

Crowd counting is a task to perform counting on a large number of specified objects from the given image. In small number object counting, a detection based approach is likely to be used, such method works well in most low-density (sparse) image, but usually failed on a high-density (crowd) image<sup>[9][11][14]</sup>. In crowd counting task, model is developed to fit the dense map of the image and output the total predicted count from the given image. From our analysis, there are two major problems which need to be tackled in order to get better counting estimation. The first problem is scale invariant problem which is caused by variety scale of an object from the given image. The second problem is inhomogeneous density problem which is caused by the difference density level of each crowd image. Both problems lead to the difficulty in choosing the right filter size for each image region.

To handle those problems we bring the idea from inception network. Inception network is divided into several repeatable kind of inception modules. Each inception module lets the network learns the best filter to be used by providing multiple paths of computational graph. Inception network first introduced in 2014 by Szegedy, C. et al.<sup>[1]</sup> and there have been some continuous improvement versions of it, starting from Inception-v1<sup>[1]</sup>, BN Inception<sup>[2]</sup>, Inception-v2 and Inception-v3<sup>[3]</sup>, Inception-v4, Inception Resnet-v1, and Inception Resnet-v2<sup>[4]</sup>. Inception network have been evaluated against ILSVRC dataset and resulting in a really high accuracy.

In this paper, we introduce a novel approach based on Inception Network v1 called Inception Dense Estimator Network (IDEnet). There are 4 main contributions of this works. First, in section III, we show a novel methodology to

apply Inception Network idea in counting task, especially the modification to handle crowd counting task. Second, in subsection IV.B, we report our alternative results that we get when implementing some alternatives of IDEnet architecture. Third, in subsection IV.C, we evaluate our final proposed model with two publicly available crowd counting datasets (UCF50 and ShanghaiTech), and benchmark our evaluation result with other methods. Fourth, in subsection IV.D, we conduct manual error analysis to get more understanding about the counting estimation error.

## II. RELATED WORKS

Works in the crowd counting task can be divided into 2 methods, detection-based and regression-based. We focus our study on regression-based methods because detection-based methods tend to severely suffer in crowd with high occlusion level<sup>[9][11][14]</sup>. Some regression analysis approaches have been conducted for crowd counting tasks. A texture analysis with edge and foreground detection has been conducted<sup>[5]</sup> in 2005. A bayesian poisson regression technique<sup>[6]</sup> has been evaluated on a sparse crowd image in 2009. A multiple texture analysis approach<sup>[7]</sup> has been performed by combining several texture analysis techniques, which are head detection, fourier, wavelet transform, interest point analysis, and GLCM.

Several regression-based methods are designed to be scale adaptive. In order to be scale adaptive, most works implement a multi column network<sup>[8][9][10]</sup>. In multi column network, input image is splited into several different subnetworks, where each subnetwork has different architecture and hyperparameters. The output from subnetworks are then merged to estimate the count. In another work, named Switching CNN<sup>[11]</sup>, the network divided into a switch module and 3 different counting modules. The switch will choose which regressor should be used for the given input image.

Some other regression-based methods utilise spatiotemporal features by using sequence of images to improve the counting quality. Xiong, F. et al.<sup>[12]</sup> utilise convolution LSTM layer in order to process sequence of images into the estimated dense map. Liu, W et al.<sup>[13]</sup> process sequence of images with a siamese network approach where each subnetwork will extract spatial feature from image at time T and then combined with some temporal constraints.

Another approach called scale-adaptive CNN<sup>[14]</sup>, develops a scale adaptive single-column network by utilising pooling, residual, and deconvolution layer. Another work, called Pyramidal CNN<sup>[15]</sup>, is estimating global and local context to achieve better estimation. In Liu et al.<sup>[16]</sup>, dense rank is generated from image and both count and rank are estimated to improve the quality of the model. Another work called DecideNet<sup>[17]</sup>, use an approach similar to a multi column, but some columns interact with another column by sending their output as one of the another column's input.

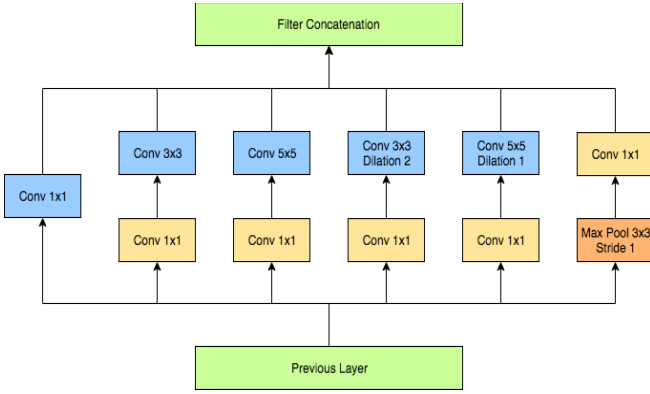


Fig. 1. IDB-v1a module as described in section III.A

### III. PROPOSED METHOD

Our proposed method, Inception Dense Estimator Network (IDEnet), consists of 2 basic building blocks, which are Inception Dense (IDB) and Dense Evaluator Unit (DEU). Combination of several IDBs with an additional pooling layer in the end is called Inception Dense Group (IDG). An IDG is the features extractor module which features will be evaluated into a dense map by a DEU module. Several combinations between each module have been evaluated, each combination and the detail of the complete network architecture are explained below:

#### A. Inception Dense Block (IDB)

IDB is the basic building block of IDEnet. IDB is equivalent to inception module in Szegedy, C. et al.<sup>[1]</sup>. In order to decide the architecture of IDB, analysis through the UCF50 and Shanghai Tech dataset are conducted. From the analysis, we conclude that with image resolution of 1024x1024, the minimum size of recognizable person's head in a photo is around 3 to 5 pixels, while the maximum size of a person's head is between 150 to 200 pixels.

From the above conclusion, we design the minimum size for the convolution filter on IDB to be 3 by 3 and 5 by 5 pixels. To reach filter size of 150 to 200 pixels, we use a 2 by 2 pooling at the end of each IDG and stack up several IDGs so that the network satisfies the equation (1).

$$y = \arg \max_{f(\alpha)} (f(\alpha) * 2^{(\beta-1)}), y \in [S_{min}, S_{max}] \quad (1)$$

Where  $\alpha$  is an IDB filter,  $f(\alpha)$  is the size of an IDB filter,  $\beta$  is the number of IDGs within the designed IDEnet,  $S_{min}$  is the lower bound of the maximum head size, which is 150 pixels, and  $S_{max}$  is the upper bound of the maximum head size, which is 200 pixels.

In this paper, we conduct experimentation with two alternatives of IDB unit. The first alternative consists of 6 different computation units, which is defined as follow: 1x1 convolution, 3x3 convolution, 5x5 convolution, 3x3 convolution with dilation of 2, 5x5 convolution with dilation of 1, and max pooling. The second alternative is the same as inception block on Inception V1<sup>[1]</sup>. The second alternative consists of 4 different computational units, which is defined as follow: 1x1 convolution, 3x3 convolution, 5x5 convolution, and max pooling. We name the first alternative of IDB unit as IDB-v1a and the second alternative as IDB-v1b. The illustration of our IDB-v1a and IDB-v1b are shown in Fig.1 and Fig. 2 respectively.

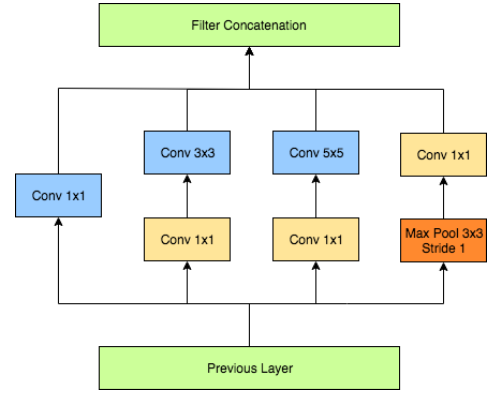


Fig. 2. IDB-v1b module as described in section III.A

#### B. Inception Dense Group (IDG)

An IDG is a sequentially connected IDB units with an additional pooling layer placed after the last IDB. As in the previous analysis in subsection III.A, we design our IDG to satisfy the equation (1). We design slightly different versions of IDG for each version of IDB. We call this IDG as IDG-v1a and IDG-v1b. The illustration of our IDG-v1a and IDG-v1b are shown in Fig. 3.

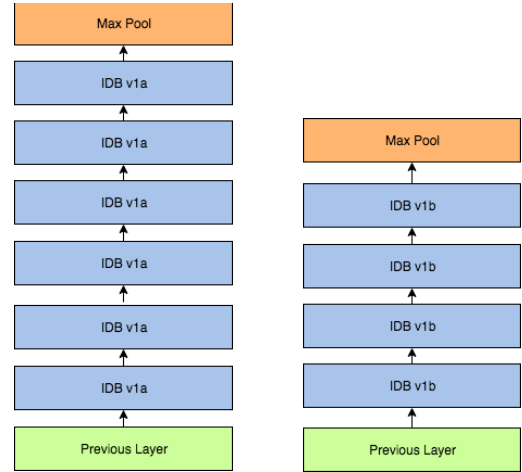


Fig. 3. IDG-v1a (left) and IDG-v1b (right) module

We also design another version of IDG which we called IDG-v1c. When designing IDG-v1c, we start with hypothesis that in order to be scale adaptive, each IDG have to extract feature and perform a counting for the current filter size simultaneously and carry the extracted features and count to the next IDG. In order to carry the extracted features forward, max pooling is widely known to work really well. Although max pooling works really well for forwarding feature to the next layer, in order to carry the count forward to the next layer we should perform a summation pooling instead of max pooling.

By carrying the count forward, the next IDG and DEU module will be able to combine the previous IDG module count with the extracted count from the current IDG module. There is no summation pooling layer in the framework we use when we do our experimentation, we instead use average pooling layer as a replacement, as average operation is basically a summation divided by a constant number. So, from there, we use both average pooling and max pooling at the end of each IDG for carrying the extracted counting and extracted feature from previous IDG layer. The illustration of IDG-v1c is shown in Fig. 4.

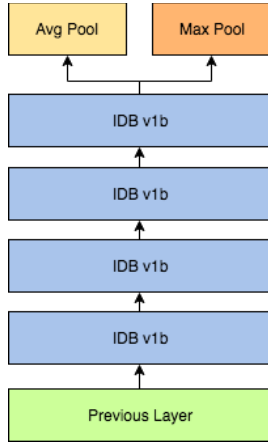


Fig. 4. IDG-v1c: IDG module with average and max pooling

### C. Dense Evaluator Unit (DEU)

DEU is simple regressor module to flatten the multi channel image output from IDG into a single channel image, which represent the dense map result. We flatten the multi channel image into a single channel image by using a 1x1 convolution filter. We also apply a drop out regularization on DEU module to prevent the model from overfitting. The illustration of DEU module is shown in Fig 5.

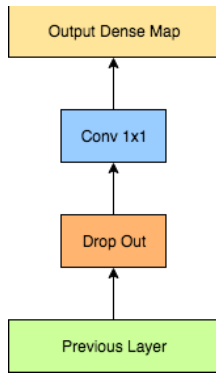


Fig. 5. DEU module to regularize the model and flatten output image into a 1D channel dense map image

### D. Inception Dense Estimator (IDNet)

IDNet consists of several IDGs and DEUs. In this work, we conduct 3 experiments on our IDNet model based on 3 considerations. Each experiment will compare 2 IDNet model and from the result of each experiment, the best IDNet design will be iterated for the next experimentation.

The first consideration is single regression loss versus multiple regression loss approach. In Inception-v1<sup>[1]</sup>, auxiliary classifiers were added into the model to improve the convergence of very deep neural network, prevent gradient vanishing problem, and regularize the model, while in Inception-v3<sup>[3]</sup> the auxiliary classifiers were removed because the auxiliary classifiers didn't give any beneficial impact to the model. We conduct similar experiment with the same idea as in the Inception-v3<sup>[3]</sup>. Our first model will have a multiple DEUs, which named IDNet-v1a, and our second model will have single DEU, which named IDNet-v1b. Both of IDNet-v1a and IDNet-v1b use 4 layers of IDG-v1a as the main computational module and 4 DEUs which each DEU is connected to each IDG-v1a. The illustration for both IDNet-v1a and IDNet-v1b are shown in Fig. 6.

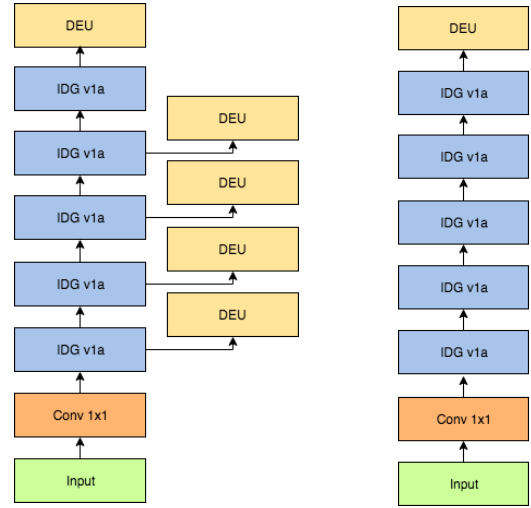


Fig. 6. IDNet-v1a (left) and IDNet-v1b (right)

The second consideration is larger filter size with less pooling layers versus smaller filter size with more pooling layers. We use IDNet-v1b for the larger filter size model, as it turns out giving better result than IDNet-v1a. For the smaller filter size model, we use 5 layers of IDG-v1b as the main computational module with single DEU. We named this model as IDNet-v1c.

The third consideration is related to our own hypothesis as explained in subsection III.B. We compare between IDNet-v1c and another IDNet design which name IDNet-v1d. In this model, we use IDG-v1c which incorporate average pooling and max pooling at the end of the IDG module. The illustration of IDNet-v1c and IDNet-v1d are shown in Fig. 7.

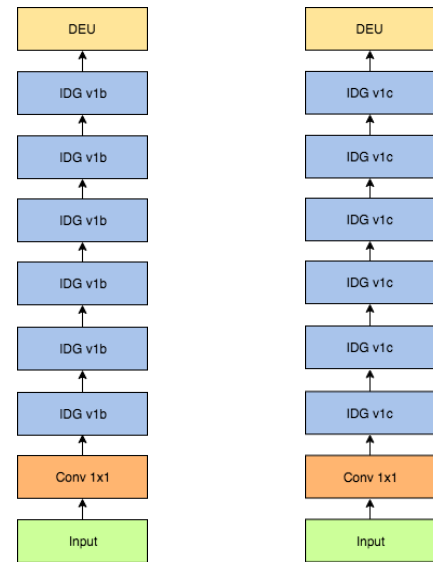


Fig. 7. IDNet-v1c (left) and IDNet-v1d (right)

## IV. EXPERIMENTS

We conduct several experiments to evaluate our IDNet. Each experiment will compare two IDNet models, and from the result of each experiment, the best IDNet design will be iterated for the next experimentation. The best IDNet model from the experiment will then be evaluated on UCF50, ShanghaiTech part A, and ShanghaiTech part B dataset. The detail and result of the experiment are described below:



### A. Experimental Protocol

We conduct 3 types of experiment for deciding the best model of our IDEnet. Each experiment corresponds to each consideration which as described in subsection III.D. The first experiment compares network with single regression loss model and network with multiple regression loss model. The second experiment compares network with larger filter size and less pooling layers and network with smaller filter size and more pooling layers. The third experiment compares network with max pooling layers and network with average pooling and max pooling layers.

In the first experiment we compare IDEnet-v1a with IDEnet-v1b. In the second experiment we compare IDEnet-v1b with IDEnet-v1c. In the third experiment we compare IDEnet-v1c with IDEnet-v1d. We qualitatively compare the model performance by calculating the mean absolute error (MAE) of each model with UCF50 dataset. We split the UCF50 into 90% training set, 5% dev data, and 5% test set. Each image is sliced into a patch of size 224x224. We perform the evaluation to each patch image instead of a single full image. We train each model with 10 epoch training with decayed learning rate start from 0.01 with 0.5 decay rate per epoch. The loss function for single regression loss network and multiple regression losses are defined in equation (2) and equation (3) respectively.

$$loss = \frac{1}{N} \sum_{n=0}^N \sum_{i=0}^W \sum_{j=0}^H |y_{nij} - y'_{nij}| \quad (2)$$

$$loss_{multi} = \sum_{i=0}^X W_i * loss_i \quad (3)$$

where N is the batch size, W and H are width and height of output dense map,  $W_i$  is the loss weight for regression on step i,  $loss_i$  is the single loss for step i,  $y_{nij}$  is the value of pixel (i, j) of the n<sup>th</sup> ground truth dense map, and  $y'_{nij}$  is the value of pixel (i, j) of the n<sup>th</sup> predicted dense map.

### B. Experiments Result and Analysis

TABLE I. EXPERIMENT RESULT

Model Name	MAE Dataset		
	Training	Dev	Test
IDEnet-v1a	90.82	232.41	202.28
IDEnet-v1b	73.53	194.06	202.05
IDEnet-v1c	50.00	45.64	53.98
IDEnet-v1d	48.61	43.50	51.25

From the experiment result on Table. I, we could derive the following conclusions:

1. Multiple regression loss on counting task doesn't improve the convergence of the network nor regularize the network. This result gives consistent conclusion with the removal of auxiliary classifiers as explained on Inception-v3<sup>[3]</sup>.
2. Smaller filter size with more pooling layers works better than bigger filter size with less pooling layers. This probably happens because of the redundant counting performed on same object within the different filter in the same IDG unit. Further analysis is needed to explain this phenomenon.

3. For counting task, combination of average pooling and max pooling perform slightly better than using only max pooling. This answer our hypothesis that have been described in subsection III.B.

From the experiment results and conclusions, we decided to use IDEnet-v1d as our IDEnet-v1, to be evaluated and benchmarked on UCF50 dataset, ShanghaiTech part A, and ShanghaiTech part B dataset. The illustration of IDEnet-v1 is shown in Fig. 8.

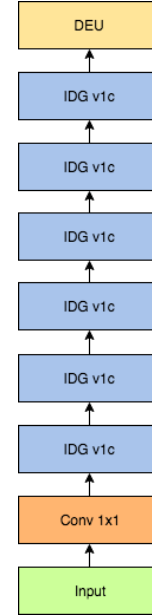


Fig. 8. IDEnet-v1: with DEU and 6 layers of IDG-v1c

We conduct two different preprocessing approaches generating the density map. In the first approach we use the density map directly from the ground truth image. In the second approach, we modify the density map by performing gaussian kernel normalization (GKN) to the ground truth image. By performing GKN, the total sum of the dense image stays the same and this method makes the network learns the dense map better<sup>[8]</sup>.

We evaluate the performance of our IDEnet-v1 by calculating mean absolute error (MAE) and mean square error (MSE). The calculation of MAE and MSE are defined in equation (4) and equation(5) respectively.

$$MAE = \frac{1}{N} \sum_{i=0}^N |y_i - y'_i| \quad (4)$$

$$MSE = \sqrt{\frac{1}{N} \sum_{i=0}^N |y_i - y'_i|^2} \quad (5)$$

where N is the number of samples in the dataset,  $y_i$  is the ground truth count of the i<sup>th</sup> image, and  $y'_i$  is the predicted count of the i<sup>th</sup> image.

### C. Evaluation Comparison

We benchmark the performance of our work with the other works by implementing the standard evaluation protocol on each dataset and use the same formula to calculate the MAE and MSE evaluation metric.

We evaluate our IDEnet-v1 with two different crowd counting datasets. The first dataset is UCF50 from University

of Central Florida and the second dataset is ShanghaiTech dataset from ShanghaiTech University. ShanghaiTech dataset is divided into two different parts, which are called ShanghaiTech part A and ShanghaiTech part B. The statistics of our datasets are shown in Table II.

TABLE II. DATASET STATISTICS UCF50 AND SHANGHAITECH

Dataset	Measure			
	Min	Max	Average	Total
UCF50	96	4633	1279.50	63,974
ShanghaiTech part A	33	3139	501.40	241,677
ShanghaiTech part B	9	578	123.60	88,488

UCF50 dataset contains 50 grayscale crowd images. UCF50 dataset have various density level of the crowd image the image size is not standardized. The statistics of UCF50 dataset is shown in Table II. Evaluation on UCF50 dataset is conducted by performing a 5-folds cross validation on the dataset. We compare our IDNet-v1 with eight existing methods [8][9][10][11][12][14][15][16]. The UCF50 dataset evaluation result is shown in Table III.

TABLE III. EVALUATION METRIC OF THE UCF50 DATASET

Method	Evaluation Metric	
	MAE	MSE
CrowdNet <sup>[8]</sup>	645.00	-
MCNN <sup>[9]</sup>	377.60	509.10
Hydra CNN <sup>[10]</sup>	333.73	425.26
SaCNN <sup>[14]</sup>	314.90	424.80
Switch-CNN <sup>[11]</sup>	318.10	439.20
Pyramidal CNN <sup>[15]</sup>	295.80	320.90
ConvLSTM-nt <sup>[12]</sup>	284.50	<b>297.10</b>
Liu, X et al. <sup>[16]</sup>	<b>279.60</b>	388.90
<b>Ours: IDNet-v1</b>	357.79	513.29
<b>Ours: IDNet-v1 + GKN</b>	368.18	519.12

ShanghaiTech part A and ShanghaiTech part B have several differences<sup>[2]</sup>. ShanghaiTech part A consists of 300 training data of crowd images and 182 test data of crowd images, while ShanghaiTech part B consist of 400 training data of crowd images and 316 test data of crowd images. Another difference is ShanghaiTech part A has unstandardized image size and is retrieved from the internet, while ShanghaiTech part B has a standardized image of 1024x768 and is taken from metropolitan areas in Shanghai.

For ShanghaiTech part A, we compare our IDNet-v1 with five existing methods [9][11][14][15][16]. The ShanghaiTech part A evaluation result is shown in Table IV. For ShanghaiTech part B, we compare our IDNet-v1 with seven existing methods [9][11][13][14][15][16][17]. The ShanghaiTech part B evaluation result is shown in Table V. Our IDNet-v1 unable to achieve the best result in UCF50 dataset and ShanghaiTech part A dataset, but our IDNet-v1 with GKN is able to outperform the state of the art method in ShanghaiTech part B dataset.

TABLE IV. EVALUATION METRIC OF SHANGHAITECH PART A

Method	Evaluation Metric	
	MAE	MSE
MCNN <sup>[9]</sup>	110.20	173.20
Switch-CNN <sup>[11]</sup>	90.40	135.00
SaCNN <sup>[14]</sup>	86.80	139.20
Pyramidal CNN <sup>[15]</sup>	73.60	<b>106.40</b>
Liu, X et al. <sup>[16]</sup>	<b>72.00</b>	106.60
<b>Ours: IDNet-v1</b>	102.95	158.24
<b>Ours: IDNet-v1 + GKN</b>	95.81	153.08

TABLE V. EVALUATION METRIC OF SHANGHAITECH PART B

Method	Evaluation Metric	
	MAE	MSE
MCNN <sup>[9]</sup>	59.10	81.70
Liu, W et al. <sup>[13]</sup>	25.10	45.80
Switch-CNN <sup>[11]</sup>	21.60	33.40
DecideNet <sup>[17]</sup>	20.75	29.42
Pyramidal CNN <sup>[15]</sup>	20.10	30.10
SaCNN <sup>[14]</sup>	16.20	25.80
Liu, X et al. <sup>[16]</sup>	13.70	21.40
<b>Ours: IDNet-v1</b>	15.91	22.85
<b>Ours: IDNet-v1 + GKN</b>	<b>11.32</b>	<b>18.45</b>

#### D. Analysis

We conduct manual error analysis for UCF50 dataset and ShanghaiTech part A dataset. From the manual error analysis, we figure out that our IDNet incorrectly estimates count from the given crowd image because of the following reasons:

1. A very small and occluded human figure
2. A crowd image which are totally different with any other crowd image in the dataset

The first reason is the problem with small pattern size. Small pattern size usually gives a lot of false signal because the same exact pattern is likely to appear in many different places with contrasting signals. One potential solution for this problem is to use a switching mechanism to choose different regression unit for different type of region<sup>[11]</sup>. Another possible solution is to use multiple regression unit and an attention mechanism to pick the correct regression unit. Some examples of the small pattern problem are shown in Fig. 9.

The second problem is a data distribution problem. This problem occurs when the image distribution of the test set is different from the training set, probably because some images are totally different with most of other images. We could solve this problem by adding more similar data into the dataset and balance the distribution of the training set, validation set, and the test set. Further study for systematic dataset assessment is needed to get deeper insight regarding to the data distribution problem. Some example images with distribution problem are shown in Fig. 10.

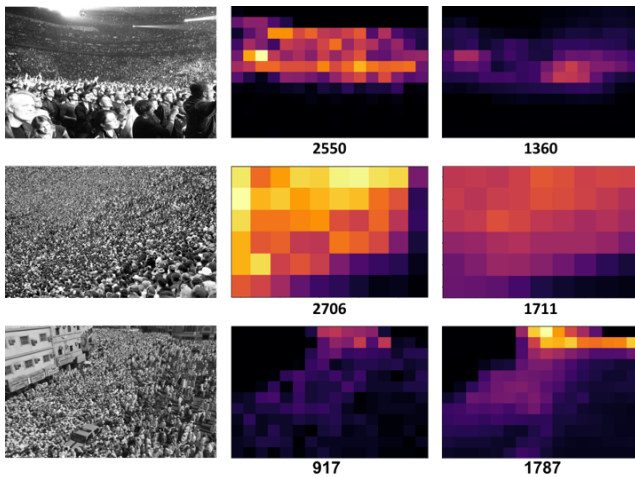


Fig. 9. Small pattern size estimation error. The left image is the input, the center is the ground truth, the right is the prediction. The number below the image represents the ground truth and prediction count respectively.



Fig. 10. Data distribution error. The first row shows images that are totally different from most images on the UCF50 dataset. The other rows show some image groups with similar representation from the UCF50 dataset

## CONCLUSIONS

In this paper we propose an inception based deep learning approach to estimate the crowd density from a crowd image, named Inception Dense Estimator Network (IDNet). Inception based network is very modular so that the network is easily adapted and modified to other image processing task. We evaluated IDNet in UCF50 and ShanghaiTech dataset and our IDNet successfully outperformed the current state-of-the-art method in ShanghaiTech part B dataset.

From our experiments and manual error analysis we found 6 key conclusions, which could be used as a consideration for further research. The 6 key conclusions are as follow:

1. Multiple regression loss on inception based network doesn't give any beneficial impact to the network learning process.
2. Smaller filter size with deeper network works better than bigger filter size with shallower network for crowd counting task.

3. Pooling layer with a combination of average pooling and max pooling works better than pooling layer with only max pooling in crowd counting task.
4. Gaussian Kernel Normalization enables the network to fit the dense map better.
5. Small pattern size and data distribution problems need to be handled in order to achieve a better result.
6. Our IDNet outperforms the state-of-the-art-method in ShanghaiTech dataset part B.

## ACKNOWLEDGEMENTS

The Titan XP used for this research was donated by the NVIDIA Corporation, and this work was also supported by Amazon Web Service (AWS) Educate, and Lembaga Pengembangan Inovasi dan Kewirausahaan Institut Teknologi Bandung (LPIK ITB).

## REFERENCES

- [1] C. Szegedy, W. Liu, Y. Jia, P. Sermanet, S. Reed, D. Anguelov, D. Erhan, V. Vanhoucke, A. Rabinovich, "Going deeper with convolutions," In 2016 IEEE Conference on Computer Vision and Pattern Recognition (CVPR), 2015
- [2] S. Ioffe, C. Szegedy, "Batch normalization: Accelerating deep network training by reducing internal covariate shift," in ICML, 2015.
- [3] C. Szegedy, V. Vanhoucke, S. Ioffe, J. Shlens, Z. Wojna, "Rethinking the inception architecture for computer vision," In 2016 IEEE Conference on Computer Vision and Pattern Recognition (CVPR), 2016, pp 2818–2826.
- [4] C. Szegedy, S. Ioffe, V. Vanhoucke, A. A. Alemi, "Inception-v4, inception-resnet and the impact of residual connections on learning," in AAAI, 2017.
- [5] D. Kong, D. Gray, H. Tao, "Counting pedestrians in crowds using viewpoint invariant training", in BMVC, 2005.
- [6] A.B. Chan, N. Vasconcelos, "Bayesian poisson regression for crowd counting," in 2009 IEEE 12th International Conference on Computer Vision, 2009, pp.545–551.
- [7] A. Bansal, K.S. Venkatesh, "People counting in high density crowds from still images," July, 2015.
- [8] L. Boominathan, S.S.S. Kruthiventi, R.V. Babu, "Crowdnet: A deep convolutional network for dense crowd counting," in Proceedings of the 2016 ACM on Multimedia Conference. MM '16, New York, NY, USA, ACM, 2016, pp.640–644.
- [9] Y. Zhang, D. Zhou, S. Chen, S. Gao, Y. Ma, "Single-image crowd counting via multi-column convolutional neural network," in 2016 IEEE Conference on Computer Vision and Pattern Recognition (CVPR), 2016, pp. 589–597.
- [10] D. Oñoro-Rubio, R.J. López-Sastre, "Towards perspective-free object counting with deep learning", in ECCV, 2016.
- [11] D.B. Sam, S. Surya, R.V. Babu, "Switching convolutional neural network for crowd counting," in 2017 IEEE Conference on Computer Vision and Pattern Recognition (CVPR), 2017, pp.4031–4039
- [12] F. Xiong, X. Shi, D.Y. Yeung, "Spatiotemporal modeling for crowd counting in videos," in 2017 IEEE International Conference on Computer Vision (ICCV), 2017, pp.5161–51699
- [13] W. Liu, K. Lis, M. Salzmann, P. Fua, "Geometric and physical constraints for head plane crowd density estimation in videos," CoRR abs/1803.08805, 2018.
- [14] L. Zhang, M. Shi, Q. Chen, "Crowd counting via scale-adaptive convolutional neural network," 2018, pp.1113–1121
- [15] V.A. Sindagi, V.M. Patel, "Generating high-quality crowd density maps using contextual pyramid cnns," in 2017 IEEE International Conference on Computer Vision (ICCV), 2017, pp.1879–1888.
- [16] X. Liu, J. van de Weijer, A.D. Bagdanov, "Leveraging unlabeled data for crowd counting by learning to rank," in CVPR, 2018.
- [17] J. Liu, C. Gao, D. Meng, A.G. Hauptmann, "Decidenet: Counting varying density crowds through attention guided detection and density estimation," CoRR abs/1712.06679, 2017.

# Multispectral Imaging and Convolutional Neural Network for Photosynthetic Pigments Prediction

Kestrlia R. Prilianti  
Informatics Engineering Department  
Universitas Ma Chung  
Malang, Indonesia  
kestrilia.rega@machung.ac.id

Ivan C. Onggara  
Informatics Engineering Department  
Universitas Ma Chung  
Malang, Indonesia

Marcelinus A.S. Adhiwibawa  
Ma Chung Research Center for  
Photosynthetic Pigments (MRCPP)  
Malang, Indonesia  
marcelinus.setya@machung.ac.id

Tatas H.P. Brotosudarmo  
Ma Chung Research Center for  
Photosynthetic Pigments (MRCPP)  
Malang, Indonesia  
tatas.brotosudarmo@machung.ac.id

Syaiful Anam  
Mathematics Department  
Universitas Brawijaya  
Malang, Indonesia  
syaiful@ub.ac.id

Agus Suryanto  
Mathematics Department  
Universitas Brawijaya  
Malang, Indonesia  
suryanto@ub.ac.id

**Abstract**—The evaluation of photosynthetic pigments composition is an essential task in agricultural studies. This is due to the fact that pigments composition could well represent the plant characteristics such as age and varieties. It could also describe the plant conditions, for example, nutrient deficiency, senescence, and responses under stress. Pigment role as light absorber makes it visually colorful. This colorful appearance provides benefits to the researcher on conducting a non-destructive analysis through a plant color digital image. In this research, a multispectral digital image was used to analyze three main photosynthetic pigments, i.e., chlorophyll, carotenoid, and anthocyanin in a plant leaf. Moreover, Convolutional Neural Network (CNN) model was developed to deliver a real-time analysis system. Input of the system is a plant leaf multispectral digital image, and the output is a content prediction of the pigments. It is proven that the CNN model could well recognize the relationship pattern between leaf digital image and pigments content. The best CNN architecture was found on *ShallowNet* model using Adaptive Moment Estimation (Adam) optimizer, batch size 30 and trained with 15 epoch. It performs satisfying prediction with MSE 0.0037 for in sample and 0.0060 for out sample prediction (actual data range -0.1 up to 2.2).

**Keywords**—convolutional neural network, multispectral digital image, non-destructive evaluation, photosynthetic pigments

## I. INTRODUCTION

Knowledge about photosynthetic pigments composition in a plant is essential due to its vital role in plant development stages. The pigments composition alteration is also known strongly represent the plant responses to internal factors and environmental changes [1]. Therefore, studies to develop an efficient method to describe pigment composition within the plant is one among the important topics in agriculture.

As digital technology is proliferating, a nowadays efficient way in plant evaluation is commonly related to the concept of real time and non-destructive measurement [2]. Digital imaging together with artificial intelligence now become a popular methods to conduct a real-time and non-destructive evaluation [3]. It is now possible to determine and quantify pigments within the plant through its digital image. Moreover, much valuable information could be provided automatically by implementing artificial intelligence method on those quantifications. Such approaches are proven significantly more efficient in cost and time.

Artificial neural network (ANN) is widely used by the agricultural researchers to conduct classification and

prediction on a plant. Some tasks are known to use ANN as the primary data analysis method, e.g, leaf area estimation [4], yield prediction [5], fruit weight prediction [6], leaf chlorophyll prediction [7], and leaf classification [8]. Plant digital image was used as raw data on most of those tasks. Prior to the learning process, the feature extraction step of the digital image must be done. For example: (1) Reference [7] created 19 features from red, green, blue components of RGB color space and hue, saturation, intensity components of HSI color space; (2) Reference [8] used 13 morphological features such as number of boundary pixel, geometric center, number of pixels of the object, etc. Indeed, the accuracy of the ANN model highly depends on the ability of the researcher to determine or create the best features. Therefore, study about feature extraction is one of the critical tasks in developing an ANN model with a digital image as the raw data. Regarding this difficulties, deep learning was created to automate the feature extraction process. It reduces the system dependency on the prior human knowledge and minimizes the human effort to design the feature [9].

Convolutional Neural Network (CNN) is one of the most popular architectures of deep learning. The convolutional term is taken from the morphological image processing technique. Convolutional matrix is applied on an image for edge detection, blurring, sharpening, embossing, and more. In CNN algorithm, convolution is the primary process for each layer. Many CNN projects were aimed to classify digital image based on the object shape. However, some researcher proved that CNN is also superior to classify digital image based on the object color [10,11]. Some CCN projects on plant image are species classification [12,13], phenotyping [14] and disease detection [15]. In this research, CNN was used as the main tools to determine and quantify the pigments contained in the plant to create a novel non-destructive photosynthetic pigments prediction system. The system's input is a multispectral digital image of a plant leaf, and the output is the prediction of three main photosynthetic pigments content. Those pigments are chlorophyll, carotenoid, and anthocyanin. Data of the actual pigment content were provided by conducting spectrophotometry on the plant leaf which the picture was taken by digital camera. Those data were used to train the CNN architecture. Three CNN models with different level of complexity were evaluated to determine the most suitable architecture for pigments content prediction. Moreover, two different optimizers were also compared to acquire the best result.



## II. MATERIALS AND METHODS

### A. Sample Preparation

*Syzygium oleana* and *Piper betle L* leaves were used in the experiment. Variation of carotenoid content was provided by the yellowish *Piper betle L* leaves, and variation of anthocyanin content was provided by the reddish *Syzygium oleana* leaves. There were as much as 444 leaves prepared for the data collection. Each leaf was chosen with the consideration of data variation fulfillment. Color variation, age, and position from the terminal bud were among the contemplations. This is vital concerning that the CNN learning process will rely upon it. Samples were divided into two sets, a training set, and a test set. The training set was used by the CNN architecture to learn the data and create the relationship model whereas the test set was used to evaluate the prediction performance of the model. Each sample will go through two data acquisition process. The first is multispectral digital image acquisition using a digital camera. The other data acquisition was laboratory analysis to identify and measure the pigments contained in each leaf using Spectrophotometry method.

### B. Multispectral Image Acquisition

Photosynthetic pigments only absorb light at a specific wavelength and reflecting others [16], e.g., chlorophyll strongly absorbs the light at 650-700 nm and 400-500 nm wavelength and reflects the light at 560 nm wavelength. This characteristic is utilized in this research to quantify the pigments amount. Therefore, the leaf digital image was taken individually using Pcopixelfly 14 bit CCD camera with Thorlabs visible bandpass filter (Fig. 1). Ten bandpass filters were used in the experiment i.e. 350, 400, 450, 500, 550, 600, 650, 700, 750 and 800 nm. Each filter will pass the light only in a single wavelength which reflected by the sample leaf being analyzed. Tungsten halogen was used as the light source. It provide a wide range of electromagnetic wavelength from 360-2400 nm.

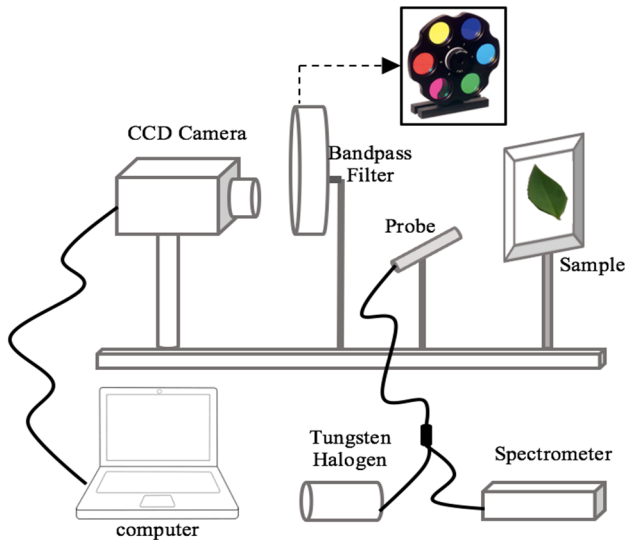


Fig. 1. Data acquisition scheme

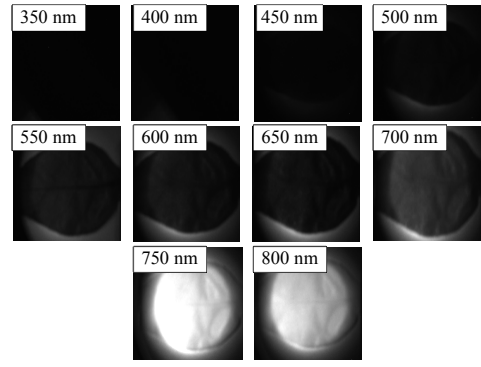


Fig. 2. Example of the leaf multispectral image

The results are 10 images (multispectral image) as seen in Fig. 2. An image with bright appearance indicates that the leaf strongly reflects the light and vice versa. As an example, the image labeled 750 nm shown the brightest color, that is mean the sample leaf strongly reflects the light with a 750 nm wavelength. Image preprocessing was conducted to simplify the input such that CNN algorithm could run faster. Two preprocessing procedures were applied to each digital image, i.e., segmentation and resizing. Segmentation was aimed to extract only the leaf area because the ultimate goal of the experiment is to recognize the color variation. Unlike other common CNN implementation which is focused on the shape recognition, in this research shape was not important otherwise color structure was the most valuable feature. Resizing was aimed to reduce the total amount of the pixel that will proceed in the CNN and to equate the overall size of the input image at once. These images were then used as the input of the CNN.

### C. Pigment Content Measurement

Chlorophyll, carotenoid, and anthocyanin content were measured using non-destructive spectrometer (Ocean Optic USB-4000). The measurement process was done simultaneously with the digital image acquisition (Fig. 1). A leaf sample is exposed to light from the light generator (tungsten halogen) via a probe. In the same time, the probe captured the reflected light and sending it to the spectrometer. The spectrometer then measures the intensity and send it to the computer for the quantification and visualization. Pigments content was then calculated using (1) and (2) for chlorophyll, (3) and (4) for carotenoid and (5) for anthocyanin [17].

$$(Chl)RI_{green} = \left[ \frac{R_{750-800} - R_{430-470}}{R_{520-580} - R_{440-480}} \right] - 1 \quad (1)$$

$$(Chl)RI_{red\ edge} = \left[ \frac{R_{750-800} - R_{430-470}}{R_{659-740} - R_{440-480}} \right] - 1 \quad (2)$$

$$CRI_{green} = [(R_{510})^{-1} - (R_{550-570})^{-1}] * R_{750-800} \quad (3)$$

$$CRI_{red\ edge} = [(R_{510})^{-1} - (R_{700-710})^{-1}] * R_{750-800} \quad (4)$$

$$ARI = [(R_{500-570})^{-1} - (R_{700-710})^{-1}] * R_{750-800} \quad (5)$$

(Chl)RI stands for chlorophyll reflectance index, CRI is carotenoid reflectance index, and ARI is anthocyanin reflectance index. These indices was then used as the output of the CNN representing the pigments content.

#### D. Dataset Preparation

Table 1 describes the dataset structure. Each leaf digital image will be paired with the 5 pigment indices. From those pairs, 80% will be randomly selected as the training set, and the remaining will be the test set.

TABLE I. STRUCTURE OF THE DATASET

Digital Image	leaf1.jpg	...	leaf391.jpg
(Chl)RI <sub>green</sub>	0.45	...	0.89
(Chl)RI <sub>rededge</sub>	1.24	...	1.45
CRI <sub>green</sub>	-0.11	...	0.04
CRI <sub>rededge</sub>	0.84	...	0.03
ARI	0.72	...	0.01

#### E. Design of the CNN Architecture

Three CNN models was implemented and evaluated in the experiment, i.e., ShallowNet, AlexNet and VGGNet. OpenCV library was used to preprocess the multispectral images. For the ShallowNet and AlexNet architectures, multispectral images were resized to 32x32 pixel, and for the AlexNet architecture, the images were resized to 120x120 pixel. Among those three CNN model, ShallowNet is the simplest model and AlexNet is the most complex model.

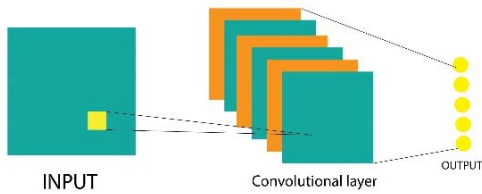


Fig. 3. ShallowNet architecture

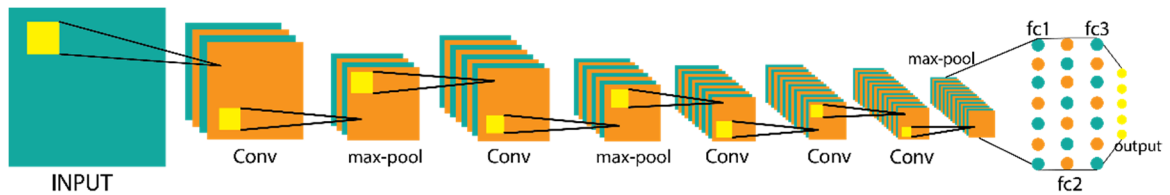


Fig. 4. AlexNet architecture

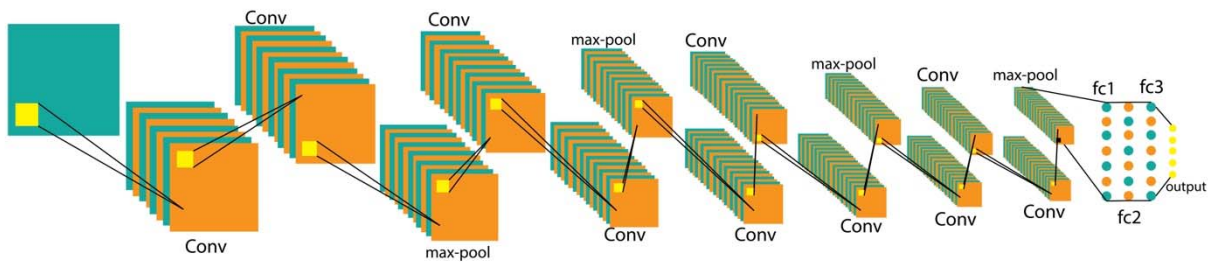


Fig. 5. VGGNet architecture

1) *ShallowNet*: Fig. 3 depicts the architecture of ShallowNet. There was 1 convolution layer with 32 filters in size 3x3 and 1 output layer with 5 nodes. Each node in the output utilizes LeakyRelu activation function and represents the pigment indices.

2) *AlexNet*: Fig. 4 depicts the architecture of AlexNet. There were 5 convolution layers and 3 fully connected layers. Design of each layer can be seen in Table II.

TABLE II. DETAIL OF THE ALEXNET ARCHITECTURE

Hidden Layer		Design
Convolution	1	96 filters in size 11x11 with max pooling in size 3x3
	2	256 filters in size 5x5 with max pooling in size 3x3
	3	384 filters in size 3x3 without pooling
	4	384 filters in size 3x3 without pooling
	5	256 filters in size 3x3 with max pooling in size 3x3
Fully Connected	1	4096 nodes with LeakyRelu activation function
	2	4096 nodes with LeakyRelu activation function
	3	1000 nodes with LeakyRelu activation function

3) *VGGNet*: Fig. 5 depicts the architecture of VGGNet. There were 10 convolution layers and 3 fully connected layers. Design of each layer can be seen in Table III.



### F. Implementation

Python 3 with Tensorflow library and Keras API was used to develop CNN architecture. The experiment was run on the personal computer with 2.3 GHz Intel Core i5, RAM 8 GB DDR3L, and Windows 10 operating system.

TABLE III. DETAIL OF THE VGGNET ARCHITECTURE

Hidden Layer	Design
Convolution	1 8 filters in size 2x2 without pooling
	2 8 filters in size 2x2 with max pooling in size 2x2
	3 16 filters in size 2x2 without pooling
	4 16 filters in size 2x2 with max pooling in size 2x2
	5 32 filters in size 2x2 without pooling
	6 32 filters in size 2x2 without pooling
	7 32 filters in size 2x2 with max pooling in size 2x2
	8 64 filters in size 2x2 without pooling
	9 64 filters in size 2x2 without pooling
	10 64 filters in size 2x2 with max pooling in size 2x2
Fully Connected	1 4096 nodes with Relu activation function
	2 4096 nodes with Relu activation function
	3 1000 nodes with Relu activation function
	4 5 nodes with LeakyRelu activation function

### G. Optimization Method

The optimization algorithm was used to minimize the error function. This function is dependent on the internal parameters (weights dan bias) such that while minimizing the error, the internal parameters are updated as well. Gradient descent is a fundamental technique used to optimize the error function. However, because of its weaknesses, many researchers have developed variants of this technique. Two of the most recent development of gradient descent variants are Root Mean Square Propagation (RMSProp) [18] and Adaptive Moment Estimation (Adam) [19] which were used in this research. The RMSProp optimizer reduces the error function fluctuation caused by stochastic gradient descent technique. It also determines a learning rate value for each parameter automatically. Each internal parameters ( $\omega$ ) are updated using (6), (7), and (8). Whereas  $\eta$  is initial learning rate,  $v_t$  is exponential average of squares of gradients and  $g_t$  is gradient of time t along  $\omega^j$ .

$$v_t = \rho v_{t-1} + (1 - \rho) \cdot g_t^2 \quad (6)$$

$$\Delta \omega_t = -\frac{\eta}{\sqrt{v_t + \epsilon}} \cdot g_t \quad (7)$$

$$\omega_{t+1} = \omega_t + \Delta \omega_t \quad (8)$$

Adam optimizer improves the RMSProp technique. Rather than adjusting the learning rate by the average of the first moment (the mean), Adam makes utilization of the average of the second moments of the gradients (the

variance). This approach makes Adam able to achieve good results faster. The internal parameters ( $\omega$ ) are updated using (9), (10), and (11). Whereas  $m_t$  is the mean and  $v_t$  is the variance of the gradient.

$$m_t = \frac{m_t}{1 - \beta_1^t} \quad (9)$$

$$v_t = \frac{v_t}{1 - \beta_2^t} \quad (10)$$

$$\omega_{t+1} = \omega_t - \frac{\eta}{\sqrt{v_t + \epsilon}} \cdot m_t \quad (11)$$

### H. Performance Indicator

Unlike other common CNN model which is intended to conduct a classification task, the CNN model in this research was aimed to run a prediction task. Therefore, the classification performance indicator such as accuracy, specificity, and sensitivity was not used to evaluate the model. Otherwise, Mean Square Error (MSE) was applied for the evaluation. The MSE calculation is based on (12),  $y_i$  is the actual pigment content (represent by reflectance index),  $\hat{y}_i$  is the prediction of the actual pigment content and  $n$  is the total amount of data.

$$MSE = \frac{1}{n} \sum_{i=1}^n (y_i - \hat{y}_i)^2 \quad (12)$$

## III. RESULT AND DISCUSSION

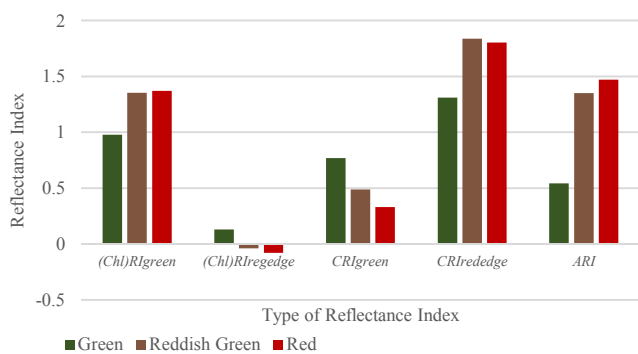
### A. Data Collection

Table IV describes the color distribution of the leaf samples. Yellow and yellowish green is the most challenging sample to collect. In the most plants, those colors will appear in the aging stage. Unfortunately, in the aging stage the structure of the leaf has started to damage as well. Therefore, such leaves will cause improper color variation to describe the pigment content. In this research the yellow and yellowish green samples were obtained from the fresh *Piper betle L* leaves, this kind of plant will produce yellow leaves in the normal stage not only in the aging stage. All samples were come from a several healthy plants.

TABLE IV. SAMPLE DISTRIBUTION

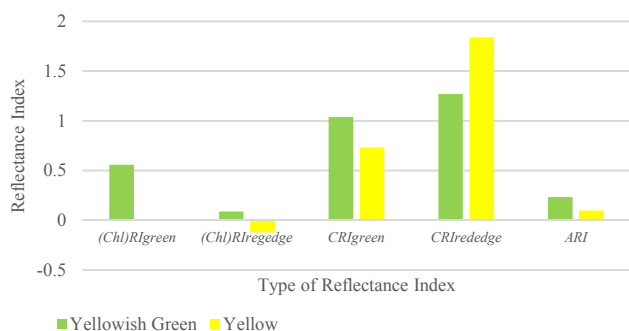
Group of Visual Color	Data Amount
Green	97
Red	90
Yellow	50
Reddish Green	147
Yellowish Green	60

Fig. 6 depicts the pigments content distribution of *Syzygium oleana*. It can be seen that the pigments content of each color category (green, reddish green, and red) confirms the theory that the visual color of leaves could well represent its pigment content. The red leaves seem to have more anthocyanin and less chlorophyll. Otherwise, the green and reddish green leaves seem to have more chlorophyll and less anthocyanin. This data also justify that *Syzygium oleana* is suitable to provide the variation on anthocyanin content data. Table V describes the minimum and maximum value of the pigments content in *Syzygium oleana*.

Fig.6. Pigment content distribution of *Syzygium oleana*TABLE V. THE RANGE OF *SYZYGIUM OLEANA* PIGMENTS CONTENT

Pigment Content Metric	Minimum	Maximum
<i>(Chl)RI<sub>green</sub></i>	0.407663	1.857813
<i>(Chl)RI<sub>red</sub></i>	-0.107580	0.323876
<i>CRI<sub>green</sub></i>	0.157148	0.981661
<i>CRI<sub>red</sub></i>	0.814667	2.226155
<i>ARI</i>	0.283901	1.967888

Fig. 7 depicts the pigments content distribution of *Piper betle L*. As well as on *Syzygium oleana*, the pigments content of each color category (yellowish green and yellow) also confirms the color-pigment content relationship theory. The yellow leaves seem to have more carotenoid and less chlorophyll. All of the leaves seem to have a little amount of anthocyanin. This fact also justifies that *Piper betle L* is suitable to provide the variation on carotenoid content data. Table VI describes the minimum and maximum value of the pigments content in *Piper betle L*.

Fig.7. Pigment content distribution of *Piper betle L*TABLE VI. THE RANGE OF *PIPER BETLE L* PIGMENTS CONTENT

Pigment Content Metric	Minimum	Maximum
<i>(Chl)RI<sub>green</sub></i>	-0.116920	0.793131
<i>(Chl)RI<sub>red</sub></i>	-0.161180	0.161759
<i>CRI<sub>green</sub></i>	0.442079	1.137226
<i>CRI<sub>red</sub></i>	0.511603	1.398290
<i>ARI</i>	0.065826	0.302499

## B. Selection of The Best CNN Architecture

Experiments to determine the best CNN architecture were done by making some changes to the CNN parameters, i.e., optimizer type, number of batch size, and number of the epoch. Adaptive Moment Estimation (Adam) and Root Mean Square Propagation (RMSProp) were selected as variations of the optimizer. Batch size was tried with the size of 30, 60, and 120 while the epoch was tested in the number of 15, 30, and 45.

1) *ShallowNet*: Table VII and VIII summarize the performance of the ShallowNet architecture using MSE as the performance indicator. The lowest MSE (both during training and testing) is obtained while using the Adam optimizer with batch size 30 (see the grayed-out cells). The ideal number of the epoch is 15.

TABLE VII. IN SAMPLE MSE OF SHALLOWNET ARCHITECTURE

Epoch	Batch Size					
	30		60		120	
	Adam	RMSprop	Adam	RMSprop	Adam	RMSprop
15	0.0037	0.0433	0.0373	0.0544	0.0936	0.2938
30	0.0094	0.0086	0.5621	0.0191	0.6551	0.0315
45	0.0047	0.0417	0.4363	0.0164	0.5771	0.0313

TABLE VIII. OUT SAMPLE MSE OF SHALLOWNET ARCHITECTURE

Epoch	Batch Size					
	30		60		120	
	Adam	RMSprop	Adam	RMSprop	Adam	RMSprop
15	0.0060	0.0486	0.0355	0.0661	0.1012	0.2800
30	0.0096	0.0126	0.5380	0.0205	0.6310	0.0330
45	0.0064	0.0417	0.4118	0.0212	0.5531	0.0355

2) *AlexNet*: Table IX and X summarize the performance of the AlexNet architecture. The same as before, it is using MSE as the performance indicator. The lowest MSE (both during training and testing) is obtained while using the Adam optimizer with batch size 30. The ideal number of the epoch is 45 (see the grayed-out cells). Compared to the ShallowNet architecture, the lowest MSE of AlexNet architectures is still greater than the ShallowNet lowest MSE.

TABLE IX. IN SAMPLE MSE OF ALEXNET ARCHITECTURE

Epoch	Batch Size					
	30		60		120	
	Adam	RMSprop	Adam	RMSprop	Adam	RMSprop
15	0.1753	0.3549	0.0658	0.0795	0.1708	0.3494
30	0.1804	0.0244	0.1699	0.3277	0.1694	0.3162
45	0.0061	0.0178	0.0079	0.0545	0.1695	0.0712

TABLE X. OUT SAMPLE MSE OF ALEXNET ARCHITECTURE

Epoch	Batch Size					
	30		60		120	
	Adam	RMSprop	Adam	RMSprop	Adam	RMSprop
15	0.1512	0.3316	0.0677	0.0743	0.1463	0.3362
30	0.1563	0.0219	0.1457	0.3000	0.1456	0.2918
45	0.0074	0.0177	0.0087	0.0512	0.1455	0.0674

3) *VGGNet*: Tables XI and XII summarize the performance of the VGGNet architecture and still using MSE as the performance indicator. The lowest MSE (both during training and testing) is obtained while using the Adam optimizer with batch size 30 (see the grayed-out cells). The ideal number of the epoch is 30. Compared to the ShallowNet and AlexNet architecture, the lowest MSE of VGGNet architectures is still greater than the lowest MSE of the other two CNN models.

TABLE XI. IN SAMPLE MSE OF VGGNET ARCHITECTURE

Epoch	Batch Size					
	30		60		120	
	Adam	RMSprop	Adam	RMSprop	Adam	RMSprop
15	0.0127	0.0318	0.1269	0.1860	0.1712	0.1404
30	0.0086	0.0174	0.0075	0.1107	0.1692	0.1767
45	0.1696	0.0218	0.1692	0.0281	0.1692	0.1924

TABLE XII. OUT SAMPLE MSE OF VGGNET ARCHITECTURE

Epoch	Batch Size					
	30		60		120	
	Adam	RMSprop	Adam	RMSprop	Adam	RMSprop
15	0.0145	0.0306	0.1104	0.1761	0.1472	0.1268
30	0.0099	0.0174	0.0085	0.1066	0.1452	0.1582
45	0.1459	0.0227	0.1451	0.0245	0.1452	0.1680

#### IV. CONCLUSION

The CNN model is proven to be able to find the best color features of leaf multispectral digital images and successfully used it to predict the photosynthetic pigment content. From all experiments with 3 different types of CNN model (ShallowNet, AlexNet, and VGGNet), it was determined that ShallowNet-based architecture be the best architecture for photosynthetic pigment prediction. The architecture reaches lowest MSE while using Adam optimizer and trained with batch size 30 and number of epoch 15 (i.e., 0.0037 for in sample and 0.0060 for out sample). In this case, as the complexity of the CNN architecture is increasing the prediction performance is decreasing. The most straightforward CNN architecture, i.e., ShallowNet was able to model the relationship between visual colors recorded on multispectral digital image and pigments content better than AlexNet and VGGNet.

#### ACKNOWLEDGMENT

This research is partially funded by the Ministry of Research, Technology, and Higher Education of the Republic of Indonesia through a national research grant program year 2018. The authors also acknowledge Machung Research Center for Photosynthetic Pigments (MRCPP) for the support of laboratory facilities.

#### REFERENCES

- [1] S. Sofia, and M.V.M. Teresa, "Quantification of Photosynthetic Pigments of Plants, Water and Sediment Samples in Chirackal and Kattiparambu of Ernakulam District, Kerala," *International Journal of Plant & Soil Science*, vol.12, no.5, pp.1–7, September 2016.
- [2] M.M. Ali, A. Al-Ani, D. Eamus, and D.K.Y. Tan, "Leaf Nitrogen Determination Using Non-Destructive Techniques—A Review," *Journal of Plant Nutrition*, vol.40, no7, March 2017.
- [3] S. Sharma, and C. Gupta, "A Review of Plant Recognition Methods and Algorithms," *International Journal of Innovative Research in Advanced Engineering*, vol. 2, no. 6, pp.111-116, June 2015.
- [4] A. Shabani, K.A. Ghaffary, A.R. Sepaskhah, and A.A. Kamgar-Haghighi, "Using the Artificial Neural Network to Estimate Leaf Area," *Scientia Horticulturae*, vol. 216, pp.103–110, February 2017.
- [5] J.D.R. Soares, M. Pasquala, W.S. Lacerdab, S.O. Silvac, and S.L.R. Donatod, "Comparison of Techniques Used in The Prediction of Yield in Banana Plants," *Scientia Horticulturae*, vol.167, pp. 84–90, March 2014.
- [6] M.R.N. Rad, S. Koohkan, H.R. Fanaei, and M.R.P. Rad, "Application of Artificial Neural Networks to Predict the Final Fruit Weight and Random Forest to Select Important Variables in Native Population of Melon (*Cucumis melo* L.)," *Scientia Horticulturae*, vol.181, pp.108–112, January 2015.
- [7] S.X. Mei, J. Ying-tao, Y. Mei, L. Shao-kun, W. Ke-ru, and W. Chong-tao, "Artificial Neural Network to Predict Leaf Population Chlorophyll Content from Cotton Plant Images," *Agricultural Sciences in China*, vol. 9, no.1, pp. 38-45, January 2010.
- [8] J.I. Arribas, G.V. Sanchez-Ferrero, G. Ruiz-Ruiz, and J. Gomez-Gil, "Leaf Classification in Sunflower Crops by Computer Vision and Neural Networks," *Computer and Electronics in Agriculture*, vol.78, no.1, pp.9-18, August 2011.
- [9] Y.L. Cun, Y. Bengio, and G. Hinton, "Deep Learning," *Nature*, vol. 521, pp.436-444, 2015.
- [10] Z. Cheng, X. Li, and C.C. Loy, "Pedestrian Color Naming via Convolutional Neural Network," in *Proceeding ACCV*, 2016, pp.35-51.
- [11] V.O. Yazici, J.V. Weijer, and A. Ramisa, "Color Naming for Multi-Color Fashion Items," in *Proceeding World CIST*, 2018, pp. 64-73.
- [12] M. Dyrmann, H. Karstoft, and H.S. Midtiby, "Plant Species Classification using Deep Convolutional Neural Network," *Biosystems Engineering*, vol.151, pp.72-80, November 2016.
- [13] M.M. Ghazi, B. Yanikoglu, and E. Aptoula, "Plant Identification using Deep Neural Networks via Optimization of Transfer Learning Parameters," *Neurocomputing*, vol. 235, pp.228–235, April 2017.
- [14] J.R. Ubbens, and I. Stavness, "Deep Plant Phenomics: A Deep Learning Platform for Complex Plant Phenotyping Tasks," *Frontiers in Plant Science* vol.8, pp.1190, July 2017.
- [15] S.P. Mohanty, D.P. Hughes, and M. Salathé, "Using Deep Learning for Image-Based Plant Disease Detection," *Frontier Plant Science*, vol.7, pp.1419, September 2016.
- [16] A.S. Herrera, "The Biological Pigments in Plant Physiology," *Agricultural Sciences*, vol.6, pp.1262-1271. October 2015.
- [17] A.A. Gitelson, and M.N. Merzlyak, "Non-Destructive Assessment of Chlorophyll, Carotenoid, and Anthocyanin Content in Higher Plant Leaves: Principles and Algorithms," *Papers in Natural Resources*, vol.263, pp.78-94, 2004.
- [18] G. Hinton, N. Srivastava, and K. Swersky. Lecture 6a. Class Lecture, Topic : "Overview of Mini Batch Gradient Descent", Computer Science Department, University of Toronto, 2015.
- [19] D.P. Kingma, and J.L. Ba, "Adam: A Method for Stochastic Optimization," in *Proceeding ICLR*, 2015.

# *Application for the diagnosis of pneumonia based on Pneumonia Severity Index (PSI) values*

1<sup>st</sup> Elyza Gustri Wahyuni  
Department of Informatics, FTI  
Indonesian Islamic University  
Yogyakarta, Indonesian  
elyza@uii.ac.id

2<sup>nd</sup> Ahmad Syahriza Ramadhan  
Department of Informatics, FTI  
Indonesian Islamic University  
Yogyakarta, Indonesian  
13523107@student.uui.ac.id

**Abstract**—There have been several studies discussing the diagnosis of pneumonia based on symptoms experienced by patients, some using artificial intelligence methods such as monotonous and non-monotonous methods with mixed results. According to the results of previous studies, there have been no results that can be directly implemented by experts, especially lung specialists in Indonesia. The cause is according to the Indonesian pulmonary doctor, the reference used to diagnose pneumonia patients is to use the Pneumonia Severity Index (PSI) which is it can classify pneumonia levels and determine therapeutic solutions appropriate to the level of pneumonia of patients. Level results according to PSI will be qualitative and unambiguous values so that the Sugeno fuzzy logic method is very suitable to overcome these problems. Application results using Sugeno Fuzzy Logic have been successfully applied to diagnose the level of pneumonia and are matched with PSI Score with a value of 75%, based on four clinical data that have tested at Balikpapan Hospital.

**Keywords**— *Pneumonia, Fuzzy Logic, Sugeno, Pneumonia Severity Index (PSI).*

## I. INTRODUCTION

Pneumonia is a disease that attacks lung tissue with a cough and hard to breathe symptoms [1]. Based on the Guidelines for Diagnosis and Management of Community Pneumonia Indonesia, pneumonia is defined as an acute inflammation of lungs parenchyma caused by a microorganism (bacteria, virus, fungi, parasite) [2].

Even based on the results of Riskesdas 2007, pneumonia ranked second in the proportion of the cause of death the children aged 1-4 years. It is therefore seen that pneumonia is a major health problem in Indonesia [3].

Other research ever conducted by [4] on URI (Upper Respiratory Tract Infection) diagnosis expert system for under five years old, here it is said that children especially the age of toddler is very susceptible to URI disease including Pneumonia and if the delayed subscription risk that will happen very danger. In addition, it is also explained that the application succeeded to be one way to diagnose 7 URI disease including Pneumonia with Certainty Factor method. It's just that this research is not specifically diagnosed with Pneumonia disease.

Subsequent studies were also for the diagnosis of 6 URI of colds, sinusitis, pharyngitis, laryngitis, bronchitis, and pneumonia. As for the data included symptoms are body temperature, the number of a cough in one minute, pain in the head, pain during swallowing, thick and smelly secretions, stiffness, sneezing, throat feels sputum, nausea, nasal congestion, shortness of breath, and pain on the chest. Then after the input is accepted it will be processed by Fuzzy

Mamdani, this research focuses only on the diagnosis of various URI but not specific to Pneumonia [5].

Subsequent research in press [6] focusing on the diagnosis of pneumonia disease level using the Fuzzy Tsukamoto method here focuses on cases of pneumonia that experts say can be classified as "mild" and "severe" which also adjusts cases that often occur. The results of the study using the user accepted test to the expert states that 95% of the results have been accepted by experts so that it can be used as a recommendation for the diagnosis of patients.

From this research try to be developed again for the result obtained really in accordance with the requirement of expert especially Indonesian Lung Specialist. The reference used by Indonesian pulmonary specialist is the value of Pneumonia Severity Index (PSI) which is used to classify Pneumonia level, so to develop previous research this application requires a method that can overcome the qualitative output that is using Fuzzy Sugeno. Fuzzy Sugeno is a method that has tolerance on the data and is very flexible. The advantages of the Sugeno method are intuitive and can provide feedback based on information that is qualitative, inaccurate, and ambiguous. [7].

Expected by developing previous research this application can be useful by lung doctors in diagnosing pneumonia disease accurately and in accordance with the value of Pneumonia Severity Index (PSI).

## II. THEORETICAL FRAMEWORK

### A. Fuzzy Logic

*Fuzzy logic* was introduced for the first time by Lothfi A. Zadeh, a professor from the University of California. Fuzzy logic has a degree of membership in a range 0 to 1, which is different from digital logic or discrete that only has 2 value, 0 and 1. Fuzzy logic is used to translate a unit which is expressed using linguistic language. For the example, we can express a scale of the speed with slow, rather a quick, fast, and very fast [8].

### B. Membership Function

The fuzzy membership function is a curve that shows the mapping of data input to the degree of membership which has the value between 0 to 1. Some of them are mentioned under the following lists [9]:

#### 1. Linear Representation

Linear representation is described as a linear line. There are 2 only ways of possibility:

- The ascension of the set starts from 0 degrees of membership and then move to the right, which is the direction that has a higher domain value.

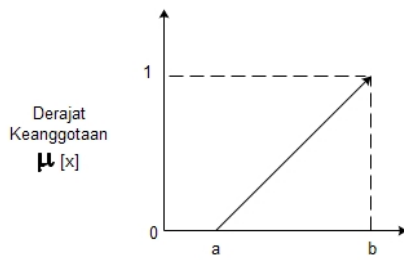


Fig. 1. Representation of uphill curve fuzzy

Membership:

$$\mu [ x,a,b] = \begin{cases} 0; & x \leq a \\ \frac{x-a}{b-a}; & a < x < b \\ 1; & x \geq b \end{cases} \quad (1)$$

- Descension starts from the higher domain, and then move right to the lower domain value.

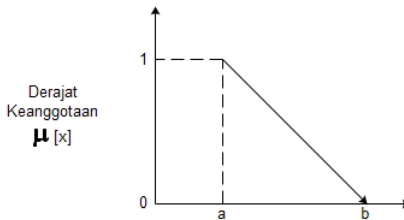


Fig. 2. Representation of downhill curve fuzzy

Membership:

$$\mu [ x,a,b] = \begin{cases} \frac{b-x}{b-a}; & a < x < b \\ 0; & x \geq b \end{cases} \quad (2)$$

## 2. Representation of Triangle Curve

Basically, this curve is a merge of two linear curves.

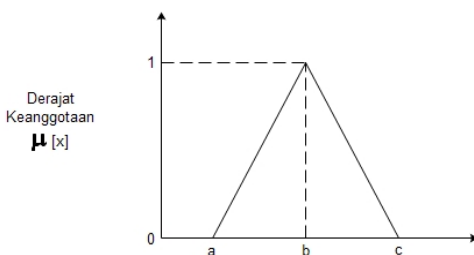


Fig. 3. Representation of Triangle Curve

Membership:

$$\mu [ x,a,b] = \begin{cases} 0; & x \leq a \text{ or } x \geq c \\ \frac{x-a}{b-a}; & a < x < b \\ \frac{c-x}{c-b}; & b < x < c \end{cases} \quad (3)$$

## 3. Shoulder Curve

The area that is made at the center of the variable that is represented as a triangle curve will increase and decrease at the left and right side of it. But sometimes one of the sides of it doesn't change at all.

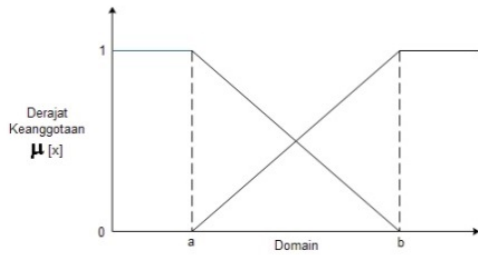


Fig. 4. Shoulder Curve Representation

Membership:

$$\mu [ x,a,b] = \begin{cases} 0; & x \leq a \\ \frac{b-x}{b-a}; & a < x < b \\ 1; & b < x < c \\ 0; & x \geq c \end{cases} \quad (4)$$

## C. Fuzzy Inference System Sugeno Method

The Sugeno method was introduced by Takagi-Sugeno Kang in 1985 [10]. this method is similar to the Mamdani method in many respects. The first two parts of the fuzzy inference process, Fuzzyfication the inputs and applying the fuzzy operator, are the same. The main difference between Mamdani and Sugeno is that the Sugeno output membership functions are either linear or constant.

A typical rule in a Sugeno fuzzy model has the form:

IF Input 1 is X AND Input 2 is Y, THEN output is Z = ax+b+c. (5)

For a zero-order Sugeno model, the output level z is a constant (a = b = c = 0).

Each rule weights its output level, Zi by the firing strength of the rule, Wi. For example, for an AND rule with Input 1 = x and Input 2 = y, the firing strength is:

$$w_i = \text{AndMethod}(F_1(x), F_2(y)) \quad (6)$$

where F1,2(.) is the membership functions for Inputs 1 and 2. The final output of the system is the weighted average of all rule outputs, computed as:

$$\text{Final Output} = \frac{\sum_{i=1}^N w_i z_i}{\sum_{i=1}^N w_i} \quad (7)$$

where N is the number of rules.

#### D. Pneumonia Severity Index (PSI)

The pneumonia severity index (PSI) or PORT Score is a clinical prediction rule that medical practitioners can use to calculate the probability of morbidity and mortality among patients with community-acquired pneumonia [11].

The PSI score is used to classify the Pneumonia level as well as the appropriate type of treatment for the patient [12]. Following table 1, The degree of PSI risk score based on the Indonesian Lung Doctor Association:

TABLE I. PSI RISK SCORE DEGREE

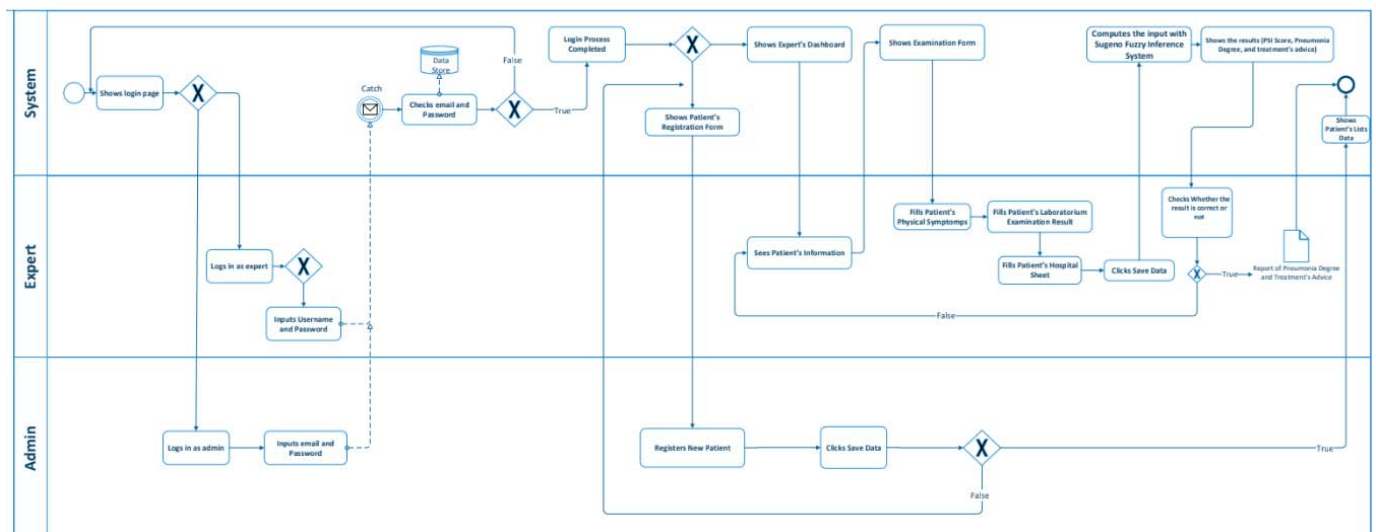
Total Value	Level of risk	Class of risk	Death rate	Type of Treatment
Not Predictable	Low	I	0.1%	Outpatient
<70	Low	II	0.6%	Outpatient
70-90	Low	III	2.8%	Inpatient/ Outpatient
91-130	Moderately	IV	8.2%	Inpatient
>130	High	V	29.2%	Inpatient

<sup>a</sup>. Data were taken from Indonesian Lung Doctor Association guide

#### III. SYSTEM ANALYSIS

It is known that there are 4 steps to determine the disease that is suffered by the patients. They are anamnesis, physical check-up, laboratory check-up, and another step to know the history of the patient's diseases. Anamnesis is a step used by the doctor by asking the patient in order to get to know the symptoms that are happened to the patient. Next is the physical check. Pulse rate, blood pressure, temperature, respiration, and age. Next is laboratory check-up. This is done so that the doctor knows the value of the Blood Urea Nitrogen, Glucose rate, Ph, PaO<sub>2</sub>, Hematocrit, and Sodium. And for the last, to identification the other disease that has been experienced by the patient, we can combine the result of all the steps, or based on the patient's documents.

After all examination results obtained, then the next step all the data entered into the system to be calculated by a Sugeno method, then the system will provide output in the form of diagnosis of URI level and the URI value suffered by the patient. So the doctor can make the output system as an alternative solution to diagnose Pneumonia disease with the value of the PSI Abbreviations and Acronyms. Business process flow can be seen in Figure 5:





L, 40% hematocrit, no pleural effusion, and patient history of disease have impaired consciousness.

The first step calculated by the Sugeno method is Fuzzyfication process that is the calculation contained in the fuzzy set of each variable. The Fuzzification Process of each variable is as follows:

TABLE II. FUZZY MEMBERSHIP VALUE FOR EACH VARIABLE

Variable Name	Low	Moderately	High
Temperature (36)	0.33	0.67	0
Pulse rate (110)	0	0.6	0.4
Respiratory (25)	0	0.5	0.5
Systolic (90)	1	0	0
Age (23)	1	0	0
Blood Urea Nitrogen (20)	0.23	0	
Glucose rate (200)	0	0.38	0.62
PaO2 (70)	0.5	0.5	
Ph (7.4)	0	1	0
Hematocrit (40)	0	1	0
Sodium (135)	0	1	0

The above Fuzzy membership values are obtained from equations of formula 1 through 4, according to the fuzzy set classification each divided into 3, namely: low, moderate and high, except BUN and PaO2 which are only divided into low and high.

The next step is to calculate the Crisp value obtained from the observation of other disease symptoms that may be suffered by the patient, it will be worth 1 if the patient has the symptoms (including the members) and if not then it will be worth 0 (not members), according to the previous patient case example only experience Disturbance of Consciousness so that membership 1 and the other is 0.

TABLE III. CRISP MEMBERSHIP VALUE OF EACH VARIABLE

Variable Name	No	Yes
Pleural Effusion	1	0
Malignancy comorbid	1	0
Liver disease	1	0
Congestive heart	1	0
Cerebrovascular	1	0
Kidney	1	0
Disturbance of Consciousness	0	1

After the Fuzzyfication process of each Fuzzy set gets its own membership value, the next step is to do the composition rule process, that is calculated fire strength ( $\alpha$ ) because the operator used for the rule is "AND" then look for the minimum value of each rule used. Then after the value of  $\alpha$  is obtained, the next step is to find the z value of each rule. There are 21 composition rules, which are adopted from expert knowledge. From the results of the composition of the rules, it is obtained the results of calculating the  $\alpha$  value, z value and the value of defuzzification.

The final stage in the Sugeno method is Defuzzification referring to the formula 7. This process aims to find the weighted average value of the 21 rules by dividing the total value of z from each rule by the total alpha value of predicate ( $\alpha$ ) of each rule. Then get the value as follows:

$$\sum z = 14.95$$

$$\sum \alpha = 0.23$$

$$\text{Defuzzification} = \frac{14.95}{0.23} = 65;$$

The conclusion of the defuzzification result is the final score of 65 which results are matched with Table 1 of the PSI Risk Score Degree, then the patient X belongs to the level I category with low pneumonia level and is recommended for outpatient treatment.

### B. Implementation of system testing

Testing the system is the final stage after getting the calculation of fuzzy Sugeno. This step is performed to test the level of validity and calculation results generated system as well as to test the conformity of results with expert knowledge that refers to the PSI.

The test results of the system by using input data in accordance with the same case example can be seen in figure 6:

Patient Details Data		Laboratorium Results	
id	354000	PH	7.4
Name	Jaka P	Bloode Urea Nitrogen	20
Date of Examination	02 July, 2018 at 02:26 PM	Natrium	135
Temperature	36	Glucose	200
Pulse Rate	110	Hematocrit	40
Respiratory	25	Pao2	70
Age	23	Systolic	90
		pleural effusion	no
Medical Records		Examination's Result	
Disease Level	no	Pneumonia Score	65
Liver Attack	no	Conclusion	light pneumonia
congestive heart Attack	no	treatment advice	outpatient
Serebrovascular Illness	no		
Kidney illness	no		
awareness disorder	yes		

Fig. 6. Sistem Test Result with case Example

The result of the system test in Figure 6 can be concluded that with the input according to the case example get the same output with the manual calculation and the result is also according to the reference value of PSI value used by Indonesian Lung Doctor Association, it can be concluded that the test result of the system is valid.

#### IV. EXPERIMENTAL RESULT

##### A. Testing Effectiveness

This test is done to know the amount of system accurate by comparing the result of the pneumonia severity index and the system's output. Cases were obtained from some patients who experienced Pneumonia in RSKD Balikpapan. The following table is a result of the test.

TABLE IV. EFFECTIVENESS TEST RESULTS

No	Name	PSI	System	Evaluation
1	Patient 1	100 (Moderately)	100 (Moderately)	Appropriate
2	Patient 2	65 (Low)	65 (Low)	Appropriate
3	Patient 3	195 (High)	195 (High)	Appropriate
4	Patient 4	80 (Low)	85 (Low)	Not Appropriate

After comparing the result, the next step is to do the average calculation:

$$\text{Average} = \frac{3}{4} \times 100 = 75 \%$$

By all of the data that has been tested above, it is concluded that the accuracy of the system is amount to 75%.

#### V. CONCLUSIONS

The conclusions obtained from some test results that are tailored to the expert knowledge of pulmonary specialist are:

- 1) The system has been successfully applied to help the expert to diagnose the pneumonia
- 2) Sugeno fuzzy logic has been successfully applied in the decision-making process of pneumonia and is matched with a Severity Pneumonia Index Score of 75% based on test clinical data of patients with pneumonia in Balikpapan Hospital.

#### ACKNOWLEDGMENT

Thank you to the Department of Informatics, Faculty of Industrial Technology, Islamic University of Indonesia, the staff and college teacher.

#### REFERENCES

- [1] Depkes RI. *Pedoman Tatalaksana Penumonia Balita*. Jakarta: Departemen Kesehatan RI Direktorat Jenderal Pengendalian dan Penyehatan Lingkungan. 2007.
- [2] Perhimpunan Dokter Paru Indonesia. *Pneumonia Komunitas Pedoman Diagnosis & Penatalaksanaan Di Indonesia*. 2014.

- [3] [5] Kemenkes RI. Pneumonia Balita. Retrieved September 6, 2017, from Buletin Jendela Epidemiologi: <http://www.depkes.go.id/downloads/publikasi/buletin/BULETIN%20PNEUMONIA.pdf>, 2014.
- [4] Pratiwi, A., Wahyuni, E.G., "Sistem Pakar Diagnosis Ispa Pada Balita Dengan Metode Certainty Factor", *Seminar Nasional Informatika Medis (SNIMED)*. 2016.
- [5] Wiweka, E. P., "Sistem Pakar Diagnosa Infeksi Saluran Pernafasan Akut (ISPA)". 2013.
- [6] Wahyuni, E.G., Ramadhan, A.S., "Sistem Diagnosis Pneumonia Menggunakan Logika Fuzzy Tsukamoto", *The 10th Conference on Information Technology and Electrical Engineering (CITEE 2018)*. 2018.
- [7] Thamrin, F., Sedyono, E., dan Suhartono, "Studi Inferensi Fuzzy Sugeno Untuk Penentuan Faktor Pembebanan Trafo PLN". *Teknologi Informasi*, 2012, pp.1-5.
- [8] Budiharto, W., & Suhartono, D., *Artificial Intelligence Konsep dan Penerapannya*. Yogyakarta: ANDI. 2014.
- [9] Kusumadewi, S., & Purnomo, H., *Aplikasi logika fuzzy untuk mendukung keputusan*. Yogyakarta: Graha ilmu. 2004.
- [10] Sugeno, M., *Industrial applications of fuzzy control*, Elsevier Science Pub. Co., 1985.
- [11] Fine, MJ; Auble, TE; Yealy, DM; Hanusa, BH; Weissfeld, LA; Singer, DE; Coley, CM; Marrie, TJ; Kapoor, WN; et al., "A prediction rule to identify low-risk patients with community-acquired pneumonia". *N Engl J Med*. 336 (4): 243–250. 1997.
- [12] Mark Williams; Scott A. Flanders; Winthrop F. Whitcomb., "Comprehensive hospital medicine: an evidence-based approach". Elsevier Health Sciences. 2007. pp. 273.

# Impact of Matrix Factorization and Regularization Hyperparameter on a Recommender System for Movies

Gess Fathan<sup>1</sup>, Teguh Bharata Adji<sup>2</sup>, and Ridi Ferdiana<sup>3</sup>  
*Department of Electrical and Information Technology Engineering*  
*Universitas Gadjah Mada*  
 Yogyakarta, Indonesia  
[gess.fathan@mail.ugm.ac.id](mailto:gess.fathan@mail.ugm.ac.id), [adji@ugm.ac.id](mailto:adji@ugm.ac.id), [ridi@ugm.ac.id](mailto:ridi@ugm.ac.id)

**Abstract**—Recommendation system is developed to match consumers with product to meet their variety of special needs and tastes in order to enhance user satisfaction and loyalty. The popularity of personalized recommendation system has been increased in recent years and applied in several areas include movies, songs, books, news, friend recommendations on social media, travel products, and other products in general. Collaborative Filtering methods are widely used in recommendation systems. The collaborative filtering method is divided into neighborhood-based and model-based. In this study, we are implementing matrix factorization which is part of model-based that learns latent factor for each user and item and uses them to make rating predictions. The method will be trained using stochastic gradient descent and optimization of regularization hyperparameter. In the end, neighborhood-based collaborative filtering and matrix factorization with different values of regularization hyperparameter will be compared. Our result shows that matrix factorization method is better than item-based collaborative filtering method and even better with tuning the regularization hyperparameter by achieving lowest RMSE score. In this study, the used functions are available from Graphlab and using Movielens 100k data set for building the recommendation systems.

**Keywords**— Recommendation Systems, Collaborative Filtering, Matrix Factorization, Regularization.

## I. INTRODUCTION

The numbers of data that are available in the internet are huge. Recommender Systems help to deal with this issue by giving item recommendations based on the user's preferences. There are many applications of recommendation systems in e-commerce products which consist of music, movies, travel and books.

Collaborative filtering methods are widely used in recommendation systems and is divided into neighborhood-based and model-based. Neighborhood-based collaborative filtering is also called memory-based algorithm. This algorithm works by discovering similarity patterns from users and items' past behavior towards the rating. The neighborhood-based collaborative filtering is divided into user-based collaborative filtering and item-based collaborative filtering. In this paper, the used method is item-based collaborative filtering method because it provides a better accuracy predictions rather than the user-based collaborative filtering [5].

In model-based approach, the models are built with supervised or unsupervised machine learning methods to predict the users' rating that is not rated yet based on the past

rating. There are many methods in this approach including decision tree, naïve bayes, and latent factor models. The latent factor model is called by many researchers as the state-of-the-art recommender system [8-10]. The latent factor method find the latent preferences of users and latent attributes of items from the ratings. Matrix factorization is the mathematical tool that can draw the latent features. Overfitting is one of the problems in recommendation systems. One way to fix this issue is by incorporating the regularization as a parameter in the Matrix factorization model [2].

In this research, GraphLab is used as a tool and Movielens 100k as the dataset. The dataset include the list of movies, users, and ratings given by users. From the dataset, the models will be trained using item-based collaborative filtering and matrix factorization with different values of regularization hyperparameter from GraphLab and compares the results in term of RMSE.

## II. NEIGHBORHOOD-BASED COLLABORATIVE FILTERING

Neighborhood-based collaborative filtering method works by discovering similarity patterns from users and items' past behavior towards the rating and is divided into user-based and item-based collaborative filtering. Item-based collaborative filtering provides a better accuracy predictions rather than the user-based collaborative filtering, therefore item-based collaborative filtering is used [5]. The item-based collaborative filtering is shown in Fig. 1.

In Fig. 1, item 1 is chosen by three users on the left. To find which user this item should be recommend, the system finds similar items which are also chosen by those users, and then determines which other users that also choose those items. In this case, all three items are chosen by user 6. Therefore, item 1 is the best recommendation for user 6. The second best recommendation is to recommend item 1 to user 5, and so on.

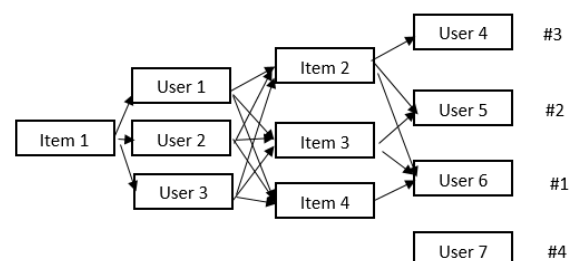


Fig. 1. Item-Based Collaborative Filtering

The models can learn user's behavior from implicit and explicit data. The examples of explicit data are rating of an item given by a user, searching of an item by a user, user preference towards two given items, and list of items that a user likes. While, examples of implicit data are what items a user views, how many times a user looks at an item, items that a user purchased, items that a user has watched or listened to, and items that a user likes or dislikes.

The collaborative filtering methods are suffering from some issues including cold start, scalability, and sparsity.

- Cold start: it requires a huge existing data to gives accurate recommendations.
- Scalability: in a big data era, a big computation power is often needed.
- Sparsity: most active users only rated a small amount of items.

### III. MODEL-BASED COLLABORATIVE FILTERING

The main idea of model-based collaborative filtering approach is to predict the users' rating that is not rated yet based on the past rating. One of the main method in this approach is latent factor model. This method finds the latent preferences of users and latent attributes of items from the ratings [2].

Matrix factorization is the mathematical tool that can draw the latent features. Matrix factorization can help to overcome the issues of neighborhood-based collaborative filtering with combination of good scalability and predictive accuracy. The recommendation items are given if there is high correspondence between item and user's factors. The illustration of matrix factorization is shown in Fig. 2. Fig. 2 characterizes user factors with male and female, and characterizes item features with serious and escapist. In matrix factorization model, the predicted rating is given by the dot product of the movie's and user's locations on the graph. For example, user 6 is expected to love movie 8 and to hate movie 1.

The basic matrix factorization method suffers from the data sparsity or missing values in user-item rating. Some works proposed to overcome this issue by minimizing the objective function or loss function and incorporate regularization to avoid overfitting. There are two approaches to minimize the objective function, stochastic gradient descent (SGD) and alternating least square (ALS).

According to [12], SGD works through iterative process of rating predictions and calculate the prediction error from each iterations. While, ALS minimizing the objective function in one time by fixing one of the parameter then compute the other parameter and vice versa. ALS is better than SGD for model that use implicit data and for parallelization process. However, SGD is generally easier and faster [11].

In the optimized matrix factorization method, regularization addresses the overfit problem. The main idea of regularization is by adding biases to control the magnitude of features to stay low. In this paper, stochastic gradient descent [5] is used to train the model. The optimization is done in parallel over multiple threads. The optimized objective function is shown in equation 1

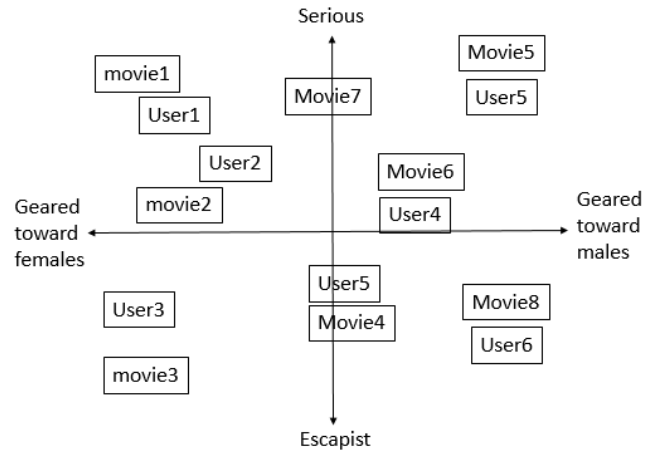


Fig. 2. Matrix Factorization approach

$$\min_{\mathbf{w}, \mathbf{a}, \mathbf{b}, \mathbf{v}, \mathbf{u}} \frac{1}{|\mathcal{D}|} \sum_{(i,j,r_{ij}) \in \mathcal{D}} \mathcal{L}(\text{score}(i,j), r_{ij}) + \lambda_1 (\|\mathbf{w}\|_2^2 + \|\mathbf{a}\|_2^2 + \|\mathbf{b}\|_2^2) + \lambda_2 (\|\mathbf{U}\|_2^2 + \|\mathbf{V}\|_2^2) \quad (1)$$

where  $\mathcal{D}$  is the observation dataset,  $r_{ij}$  is the rating of item  $j$  given by user  $i$ ,  $\mathbf{U} = (\mathbf{u}_1, \mathbf{u}_2, \mathbf{u}_3, \dots)$  shows the latent factors of user, and  $\mathbf{V} = (\mathbf{v}_1, \mathbf{v}_2, \mathbf{v}_3, \dots)$  shows the latent factors of item.  $\mathcal{L}(\hat{y}, y)$  by default is the loss function of  $(\hat{y} - y)^2$ . There are two regularizations in this equation. The first one is  $\lambda_1$  shows the *linear regularization* parameter, and the second one is  $\lambda_2$  the *regularization* parameter.

### IV. RELATED WORK

Sarwar et. al. [11] from University Minnesota compared the effectiveness of recommender systems with collaborative filtering and singular value decomposition (SVD). The study showed that SVD is worse than the traditional collaborative filtering in e-commerce dataset due to the very sparse data. However, SVD works better in MovieLens dataset.

To overcome the sparsity problem, many methods have been applied. A method proposed by Ranjbar et. al. [15] try to overcome this problem through imputation of values to the unknown rating in a matrix factorization-based method. The datasets that were used are MovieLens, Jester, and EachMovie. The proposed method outperformed another methods such as ALS, SGD, RSGD, SVD++ and MULT. Another way to improve the model performance is to incorporate regularization to make the model less likely to overfit [12,14].

A study about comparison of ALS and SGD was done by [13]. The study showed that SGD is faster, easy to implement, and less likely to overfit. However, ALS works better for a large datasets. A study by [9] compares the result between matrix factorization that incorporating regularization without tuning, biases, implicit feedback and temporal dynamic. The temporal dynamic achieved the lowest RMSE (0.8563).

Comparison between GraphLab library and MapReduce library showed that Graphlab works better in terms of accuracy and speed. However, MapReduce worked better for the model with parallelization process like ALS [16].

## V. METHODOLOGY

This section will explain the dataset, tool, and implementations. Each step is described below.

### A. Dataset Description

In this study, Movie Lens – 100k is used as the dataset and it was published by Groupleans research group. The data can be retrieved from <http://grouplens.org/datasets/movielens/100k/s>. This dataset contains 90570 number of observation with 943 users and 1682 movies. Every user has rated minimally 20 movies. This dataset contains detail of users, ratings, and movies. The recommendation systems that are going to build consist of four systems, i.e. item-based collaborative filtering, matrix factorization with regularization hyperparameter =  $1e-8$ , matrix factorization with regularization hyperparameter =  $1e-6$ , and matrix factorization with regularization hyperparameter =  $1e-5$ . We only use User\_id, Movie\_Id, and Rating from the dataset.

### B. Tool

The tool that is going to be used is Graphlab. GraphLab is an open source project with Apache license and was started from Carnegie Mellon University by Prof. Carlos Guestrin in 2009. GraphLab is used for data mining and machine learning tasks. The main benefit of GraphLab is on dealing with big data. Graphlab also offers many methods on recommendation systems such as item-based collaborative filtering, matrix factorization, popularity-based recommender, etc. GraphLab is basically a paid package for python but free for educational purpose for 1 year. The dataset from MovieLens is loaded to GraphLab to build and evaluate the models.

### C. Implementation

The implementation starts from dividing the data into training and testing data using the following codes:

```
train_data = graphlab.SFrame(ratings_base)
test_data = graphlab.SFrame(ratings_test)
```

The next step is to train our item-similarity collaborative filtering and matrix factorization models with different regularization (tuning) hyperparameters using the following codes:

```
item_sim_model = graphlab.item_similarity_recommender.create(train_data, user_id='user_id',
item_id='movie_id', similarity_type='pearson')

matrix_model = graphlab.factorization_recommender.create(train_data, user_id='user_id',
item_id='movie_id', target='rating')

matrix_model2 = graphlab.factorization_recommender.create(train_data, user_id='user_id',
item_id='movie_id', target='rating', regularization=1e-6)

matrix_model3 = graphlab.factorization_recommender.create(train_data, user_id='user_id',
item_id='movie_id', target='rating', regularization=1e-5)
```

The trained models is then used to make predictions of top 5 movies for first 5 users using the following codes:

```
item_sim_recomm = item_sim_model.recommend(users=range(1,6),k=5)
item_sim_recomm.print_rows(num_rows=25)

matrix_recomm = matrix_model.recommend(users=range(1,6),k=5)
matrix_recomm.print_rows(num_rows=25)

matrix_recomm2 = matrix_model2.recommend(users=range(1,6),k=5)
matrix_recomm2.print_rows(num_rows=25)

matrix_recomm3 = matrix_model3.recommend(users=range(1,6),k=5)
matrix_recomm3.print_rows(num_rows=25)
```

The recommendation items are shown in Table I, Table II, Table III, and Table IV and consecutively show the item-similarity collaborative filtering model, matrix factorization with default regularization =  $1e-8$ , matrix factorization with regularization =  $1e-6$ , and matrix factorization with regularization =  $1e-5$ . The top 5 items are recommended for 5 users and will be based on the top prediction score of movie\_id to the user\_id.

The last step in implementations is evaluation. The evaluation method is using RMSE. RMSE evaluates how far the predicted rating is to the real rating in the test set.

TABLE I. RECOMMENDATION ITEMS FROM ITEM-SIMILARITY MODEL

user_id	movie_id	score	rank
1	286	0.807692307692	1
1	294	0.803643724696	2
1	288	0.779352226721	3
1	300	0.7004048583	4
1	117	0.645748987854	5
2	50	1.0	1
2	181	0.886639676113	2
2	121	0.775303643725	3
2	174	0.765182186235	4
2	98	0.706477732794	5
3	50	1.0	1
3	100	0.894736842105	2
3	286	0.807692307692	3
3	294	0.803643724696	4
3	1	0.791497975709	5
4	50	1.0	1
4	100	0.894736842105	2
4	181	0.886639676113	3
4	286	0.807692307692	4
4	294	0.803643724696	5
5	258	0.831983805668	1
5	286	0.807692307692	2
5	294	0.803643724696	3
5	1	0.791497975709	4
5	288	0.779352226721	5

TABLE II. RECOMMENDATION ITEMS FROM MF MODEL 1

user_id	movie_id	score	rank
1	641	5.98897409384	1
1	647	5.96105399673	2
1	1142	5.75104442184	3
1	513	5.68665328567	4
1	1143	5.54071626012	5
2	1084	5.20163165723	1
2	430	5.03280498777	2
2	408	5.00056316648	3
2	479	4.94514080082	4
2	1217	4.90031440687	5
3	1022	8.23701111917	1
3	1129	7.59797196035	2
3	956	7.11752150898	3
3	902	7.07752202396	4
3	896	6.81965915804	5
4	1512	7.15124506448	1
4	512	6.38825682496	2
4	537	6.29441139792	3
4	131	6.10380361174	4
4	960	6.01562090908	5
5	253	6.85750261639	1
5	835	6.34628666137	2
5	647	5.98012734149	3
5	1160	5.91109669898	4
5	1137	5.88876122926	5



TABLE III. RECOMMENDATION ITEMS FROM MF MODEL 2

user_id	movie_id	score	rank
1	580	5.99185414185	1
1	408	5.90874336232	2
1	647	5.81605891456	3
1	171	5.78312789966	4
1	661	5.75177876224	5
2	408	5.97054117118	1
2	345	5.80860196744	2
2	169	5.75896160994	3
2	1367	5.68278216515	4
2	513	5.67374794875	5
3	1065	6.77786777113	1
3	919	6.62959916835	2
3	640	6.60721805637	3
3	902	6.46627381389	4
3	390	6.31030798648	5
4	320	7.02297147308	1
4	543	6.7170946518	2
4	57	6.5523339728	3
4	1137	6.19249375854	4
4	887	6.17432463859	5
5	580	5.66781765912	1
5	640	5.55278543328	2
5	1022	5.44059067618	3
5	1065	5.4394948328	4
5	1240	5.22025699113	5

TABLE IV. RECOMMENDATION ITEMS FROM MF MODEL 3

user_id	movie_id	score	rank
1	313	4.61491753851	1
1	1449	4.60885021967	2
1	318	4.53699675147	3
1	483	4.48800209109	4
1	408	4.48317974052	5
2	1449	4.84868753181	1
2	318	4.76065751669	2
2	483	4.71997261924	3
2	408	4.71627475778	4
2	1524	4.71345534633	5
3	1449	4.81601162013	1
3	313	4.6885892287	2
3	169	4.68405101393	3
3	1524	4.68321508184	4
3	408	4.67280998538	5
4	1449	4.87368424135	1
4	313	4.77035822012	2
4	1524	4.73541900682	3
4	408	4.72595168094	4
4	114	4.71749826745	5
5	1449	4.1318826642	1
5	313	4.07762528156	2
5	318	3.99792723675	3
5	1524	3.99695160604	4
5	114	3.97113763206	5

## VI. RESULT AND DISCUSSION

The RMSE evaluation is shown in Table V :

TABLE V. RECOMMENDATION ITEMS FROM MF MODEL 1

	Item-similarity model	MF model1	MF model2	MF model3
RMSE	3.43530307	1.06577743	1.05890407	0.997194837

The MF model1 is a matrix factorization method with regularization hyperparameter =  $1e-8$ . In model2 and model3, the regularizations are  $1e-6$  and  $1e-5$ . In table 5, MF model3 outperforms the other methods with the lowest RMSE score or highest accuracy. This explains that matrix factorization model with regularization (tuning) hyperparameter will result in better accuracy than that of the item-similarity collaborative filtering model.

## VII. CONCLUSIONS

In this study, item-similarity collaborative filtering method and matrix factorization method with different values of regularization hyperparameters are used. The best recommender model is the one with the lowest RMSE score. The result in Table V shows that matrix factorization with regularization hyperparameter =  $1e-5$  outperforms the other methods in term of RMSE. Therefore, the matrix factorization with the smallest regularization hyperparameter results in better recommendations. For future work, we can incorporate the matrix factorization with more features such as user's gender, user's age and movie genre. The model can also be improved through preprocessing such as using imputation and removing extreme values.

## REFERENCES

- [1] V. Khadse, A. P. S. Basha, N. Iyengar and R. Caytiles, "Recommendation Engine for Predicting Best Rated Movies", International Journal of Advanced Science and Technology, vol. 110, pp. 65-76, 2018.
- [2] Yehuda Koren, "Factorization meets the neighborhood: a multifaceted collaborative filtering model," in Proceeding of the 14th ACM SIGKDD international conference on Knowledge discovery and data mining, New York, NY, USA, 2008, pp. 426-434
- [3] Leon Bottou, "Stochastic Gradient Tricks," Neural Networks : Tricks of the Trade. Vol. 7700, pp. 430-445, 2012.
- [4] Ilhami, Mirza & Suhajito, Suhajito, "Film Recommendation Systems using Matrix Factorization and Collaborative Filtering," International Conference on Information Technology Systems and Innovation (ICITSI), 2014.
- [5] B. Sarwar, G. Karypis, & J. Konstan, "Item-based Collaborative Filtering Recommendation Algorithms, " 10<sup>th</sup> International World Wide Web Conference (WWW10), 2001.
- [6] P. Cremonesi, Y. Koren, & R. Turrin, . "Performance of recommender algorithms on top-n recommendation tasks, " In Proceedings of the fourth ACM conference on Recommender systems - RecSys '10 (p. 39)., 2010.
- [7] G. Jawaheer., P. Weller, & P. Kostkova, "Modeling User Preferences in Recommender Systems: A Classification Framework for Explicit and Implicit User Feedback", ACM Transactions on Interactive Intelligent Systems, 2014.
- [8] J. A. Konstan & J. Riedl, "Recommender systems: From algorithms to user experience", User Modelling and User-Adapted Interaction, 2012.
- [9] Y. Koren, R. Bell, & C. Volinsky, "Matrix Factorization Techniques for Recommender Systems", Computer, vol. 42, no. 8, pp. 30-37, 2009.
- [10] S. Funk, "Netflix Update: Try This at Home," Dec. 2006; <http://sifter.org/~simon/journal/20061211.html>.
- [11] B.M. Sarwar. G. Karypis, J. Konstan, and J. Riedl, "Application of Dimensionality Reduction in Recommender System—A Case Study," Proc. KDD Workshop on Web Mining for e-Commerce: Challenges and Opportunities (WebKDD), ACM Press, 2000
- [12] A. Paterek, "Improving Regularized Singular Value Decomposition for Collaborative Filtering", Proc. KDD Cup and Workshop, 2007.
- [13] L. Zheng. "Performance evaluation of latent factor models for rating prediction". Master's thesis, Beijing University of Posts and Telecommunications, 2015.
- [14] EV Cervantes, LC Quispe, and JO Luna, "Performance of alternating least squares in a distributed approach using graphlab and mapreduce", 2nd Annual International Symposium on Information Management and Big Data, 1478:122, 2015.
- [15] M. Ranjbar, P. Moradi, M. Azami, M. Jalili, "An imputation-based matrix factorization method for improving accuracy of collaborative filtering systems", Engineering Applications of Artificial Intelligence, vol. 46, Issues PA, pp. 58-66, 2015.

# Object Detection of Omnidirectional Vision Using PSO-Neural Network for Soccer Robot

Novendra Setyawan, Nuralif Mardiyah, Khusnul Hidayat, Nurhadi, Zulfatman Has  
Department of Electrical Engineering, University of Muhammadiyah Malang, Malang  
novendra@umm.ac.id

**Abstract**—The vision system in soccer robot is needed to recognize the object around the robot environment. Omnidirectional vision system has been widely developed to find the object such as a ball, goalpost, and the white line in a field and recognized the distance and an angle between the object and robot. The most challenging in develop Omni-vision system is image distortion resulting from spherical mirror or lenses. This paper presents an efficient Omni-vision system using spherical lenses for real-time object detection. Aiming to overcome the image distortion and computation complexity, the distance calculation between object and robot from the spherical image is modeled using the neural network with optimized by particle swarm optimization. The experimental result shows the effectiveness of our development in the term of accuracy and processing time.

**Keywords**—Mobile Robot, Omni-Vision, Particle Swarm Optimization; Neural Network;

## I. INTRODUCTION

In the robotics field, various researchers have been developed to improve the robot ability. Soccer robot competition is a real-world test for the control system, path planning, navigation sensor, and vision system research subject. In past decade, omnidirectional vision or Omni-vision system has become one most important thing in soccer robot system. Omni-vision provides 360 degrees view of the robot's surrounding environment in a single image that can be used to object detection [1], tracking [2], and localization [3].

Generally, Omni-vision system can be established in a various way, such as mechanical servo camera, the spherical lens (fisheye panorama), and hyperbolic mirror. The spherical lens is one of the more accessible and useful ways to provide the Omni-vision, because of the structure have a stable and rigid than using reflection mirror which consists two parts and is fragile [4].

Despite the advantages of full view from the spherical image, a barrel distortion makes object detection or tracking more complicated. The various method has been developed to rectify and restore using some image processing techniques [3], which make computation more complex. Besides that, some calibration technique has been proposed to estimate the correct spherical image model [2].

One artificial modeling technique to calibrate the spherical image is using Neural Network [5]. Since the heuristic method has been widely used to solve many problems [6]. In this paper, we combined PSO to optimize the neural network model to calibrate and modeling the distance between the object and the

robot from the spherical image with some experimental data learning in developing an efficient Omni-vision to recognize and tracking the object.

## II. VISION ARCHITECTURE AND OBJECT DETECTION

### A. Spherical Lens Omnidirection

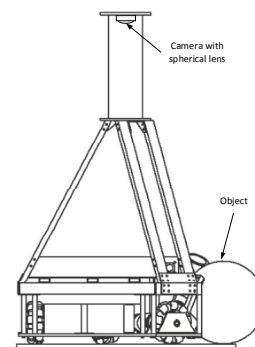


Fig. 1 Omni-vision architecture using aspherical lens

The use Omni-vision in soccer robot, allows the robot to acquire 360 degrees view around its central rotation axis. To provide effective and efficient Omni-vision system, we put the camera with spherical lens in the top of robots. This Omni-vision system allows obtaining the object in the field around the robot without moving itself or its camera.

An Omni-vision system assures an integrated perception of all main target objects in the surrounding area of the robot, allowing more maneuverability. However, it is setup implies higher degradation in resolution when the object is growing away from the robot.

### B. HSV Color Space

In this study, the image captured from the camera with the spherical lens is in the RGB color space. The color components from the image are correlated with the sum of light that reflected by the object. Image segmentation of those color components will be more difficult in this situation [7].

Converting image color space from RGB to HSV color space is chosen because HSV color space describes color more naturally and similarly. According [8], all colored object in the soccer field have far enough distance in HSV color space.

### C. Gaussian Blur

Gaussian blur is an image blurring process using the Gaussian function. This method is widely used to reduce noise

and obscure details on images. Gaussian blur is commonly used in the early stages of digital image processing to improve the structure of the image on an absolute scale.

#### D. Thresholding

Thresholding process usually used in image color segmentation. By using the thresholding process, the desired color interest will be separated by other colors. Pixels with a value between the minimum and maximum threshold values of the object interest will be labeled and colored with the specified value.

$$Dst(x, y) = \begin{cases} ball & ball_{min} < HSV < ball_{max} \\ line & line_{min} < HSV < line_{max} \\ field & field_{min} < HSV < field_{max} \end{cases} \quad (1)$$

In the soccer field, three main objects have a different color, such as the ball, field, and line. Those objects have far enough distance in HSV color space. Thus, the thresholding process in HSV color space can be applied for object detection in soccer field which described in (1).

#### E. Morphological

Morphological is an image enhancement process consisting of a process called opening and closing. The opening operation aims to smooth the contour of the object and eliminate all the pixels that are smaller than the elemental structure of the matrix element. The closing operation aims to smooth the contours of the object and fill the small holes with the elements of the matrix structure. [9]

Image of threshold result of HSV will be done opening and closing process. The opening is a process of erosion and then dilation, and closing is a process of dilation then erosion. Erosion aims to eliminate noise images. Dilation aims to combine the disconnected images due to the elimination of the color limit.

### III. DISTANCE ESTIMATION USING PSO-NN

#### A. Model of Spherical Lens

In previous steps, the distance and angle between the object and the center of the screen have been obtained. However, the distance unit still in the pixel. Therefore, real distance from the spherical image can be estimated using a neural network model. The NN model consists of one input layer, one hidden layer, and one output layer. The mathematical model from the input layer to the hidden layer described in eq:

$$\alpha_j = \sum_{i=1}^N WI_{i,j} X_i + WI_j^b bias_j \quad (2)$$

$$yh_j = \tanh(\alpha_j) \quad (3)$$

Then, the correlation between the hidden layer to the output layer described in eq:

$$\beta_k = \sum_{i=1}^N WO_{i,j} yh_j + WO_k^b bias_k \quad (4)$$

$$yo_k = \tanh(\beta_k) \quad (5)$$

The NN model weight  $WI_{i,j}$ ;  $WI_j^b$ ;  $WO_{i,j}$ ; and  $WO_k^b$  learned by using data pair between input data such as distance in pixel and the output data such as the real distance.

#### B. Adaptive Particle Swarm Optimization

PSO is a population-based optimization search algorithm that inspired by birds flocking behavior. The birds are assumed to be the particle in the PSO algorithm, each particle represented as a solution, the quality of solution determined by the corresponding fitness value. The particle has the best fitness value is a leader of the group.

The algorithm of PSO begins with generating randomize particles and then each particle “fly” in the search space to search some feasible solution. In every generation, the velocity  $V_{id}(t)$  and position  $X_{id}(t)$  updating mechanism each particle is described in

$$V_{id}(t+1) = \omega \cdot V_{id}(t) + c_1 \cdot r_1 (P_{id}(t) - X_{id}(t)) + c_2 \cdot r_2 (G_d(t) - X_{id}(t)) \quad (6)$$

$$X_{id}(t+1) = X_{id}(t) + V_{id}(t+1) \quad (7)$$

Where  $P_{id}(t)$  called personal best position, represent the best fitness value found by particle  $i$  at iteration  $t$  and  $G_d(t)$  called global best, represent global fitness value found by the swarm of the particle. The constants number  $c_1$  and  $c_2$  called acceleration parameter,  $r_1$  and  $r_2$  are independent random number distributed in range  $[0,1]$ , and  $\omega$  is a constant number called inertia parameter.

The main function of the inertia parameter in PSO is to maintain the proportion of exploration and exploitation in every iteration process. An adaptive inertia parameter approach in [11] is adopted in this paper. Inertia parameter updated based on the Percentage of Successful ( $PS$ ) in every iteration. A high value of  $PS$  indicates the particle is moving toward an optimum solution, in contrast, the smaller value indicates that particle is moving around the optimum value without much improvement. The value of  $PS$  can calculate as follows

$$PS = \frac{\sum_{i=0}^n SC_i}{n} \quad (8)$$

where  $n$  is the number of particles and  $SC$  is success count of particle that defined as follow

$$SC = \begin{cases} 1 & J(X_{id}(t)) < J(P_{id}(t-1)) \\ 0 & J(X_{id}(t)) \geq J(P_{id}(t-1)) \end{cases} \quad (9)$$

Using  $PS$ , the following update rule of inertia parameter is

$$\omega = (\omega_{max} - \omega_{min})PS + \omega_{min} \quad (10)$$

#### C. Encoding The Particle

In the previous section, the NN model of the spherical lens has described, a correct model of the spherical lens can be obtained by learned the NN weight  $WI_{i,j}$ ;  $WI_j^b$ ;  $WO_{i,j}$ ; and  $WO_k^b$ . Therefore, in order to obtain the optimum model, the NN weight

$(WI_{1,1} \dots WI_{i,j}, WI_1^b \dots WI_j^b, WO_{1,1} \dots WO_{i,j}, WO_1^b \dots WO_k^b)$  becomes  
particle  $\vec{x} = (WI_{1,1} \dots WI_{i,j}, WI_1^b \dots WI_j^b, WO_{1,1} \dots WO_{i,j}, WO_1^b \dots WO_k^b) = (x_1, x_2, \dots, x_d)$ .

#### D. Objective Function

The objective function is representing the error between the output of the NN model and desired data training. Using the percentage mean square error (PMSE), the best individual particle is the one which results in the minimum PMSE which described in the following equation:

$$J = PMSE = \frac{1}{M \cdot K} \sum_{n=1}^M \sum_{k=1}^K (y_{t_{n,k}} - y_{o_{n,k}})^2 \quad (11)$$

#### E. Update of the personal best and global best position

Personal best position ( $P_{id}(t)$ ) is the best position archived by particle so far and global best position ( $G_{id}(t)$ ) is the best position archived by the swarm of the particle so far at generation. In this paper, the standard method is used to update ( $P_{id}(t)$ ) and ( $G_{id}(t)$ ). Since the NN model problem transformed into minimization of the objective function in (11), the following update mechanism of ( $P_{id}(t)$ ) is

$$P_{id}(t) = \begin{cases} X_{id}(t) & J(X_{id}(t)) < J(P_{id}(t-1)) \\ P_{id}(t-1) & J(X_{id}(t)) \geq J(P_{id}(t-1)) \end{cases} \quad (12)$$

also, the ( $G_{id}(t)$ ) can be obtained as follows

$$G_d(t) = \min(J(P_1(t)), J(P_2(t)), \dots, J(P_d(t))) \quad (13)$$

Completely path planning algorithm using adaptive Gaussian parameter is described in

```

Start
Initialize particle as  $WI_{i,j}; WI_j^b; WO_{i,j};$  and  $WO_k^b$ ;
 $P_i = x_i$ ;
End
While (termination condition is false)
  SC=0;
  For i=1 to number of particle
    For d=1 to n
      Update velocity of particle using Eq. (6)
      Update position of particle using Eq. (7)
      Evaluate particle with objective function using Eq. (11);
    End
  End
  Update  $P_{id}$  and  $G_d$  using Eq. (12) and Eq. (13);
  Update Acceleration parameter using Eq.;
  Update Inertia parameter using Eq. (10);
  Check re-initialization of particle described in Eq.
End
 $(y'_1, y'_2, \dots, y'_n) = G_d$ ;
End

```

Fig. 2 Pseudocode of proposed algorithm

## IV. EXPERIMENTAL RESULT

System tested in a computer with Intel Core i5 3.2 GHz processor and 4 GB of RAM. First, we experimented with object detection such as detecting and tracking a ball and tested how far that ball can be detected. Then after that, training data taking from the real distance between the center of the robot which correlated with the center of the image and the ball.

In object detection, calculation process takes about 50 milliseconds to ball detected. With 23 cm steps, we experimented the camera detection range that can be detected the ball among 23 cm to 483 cm. Fig. 3 shows the experimental process which ball can be detected at least about 22 cm. This experiment is also obtained the correlation data between real distance and in a pixel. In Fig. 5 shows that the correlation is exponentially increased. From that figure, we conclude that the object distance can be accurately measured between 23 cm to 400 cm.

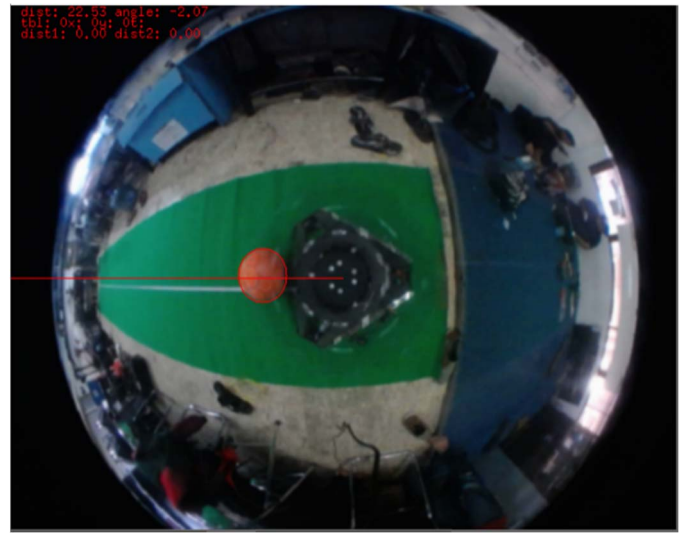


Fig. 3 Ball detection in 22 cm from the center of robot

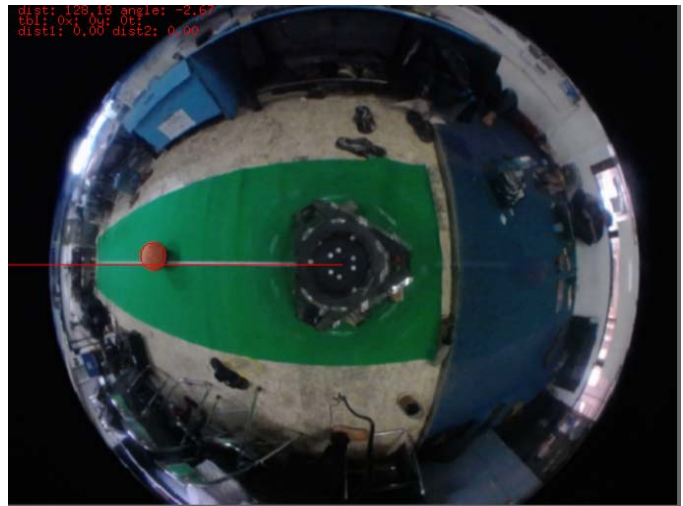


Fig. 4 Ball detection in 128 cm from the center of robot



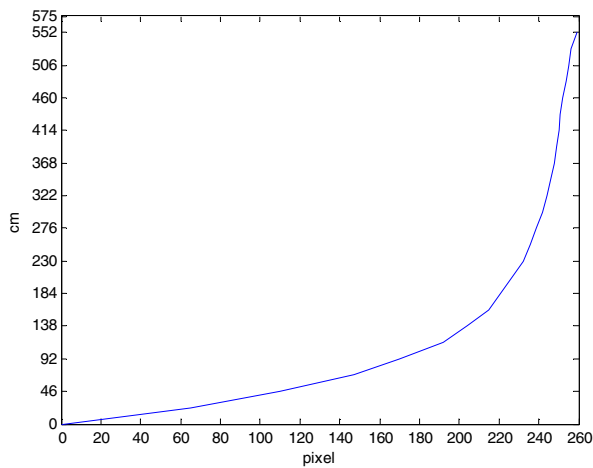


Fig. 5 Object Distance Correlation in cm and pixel

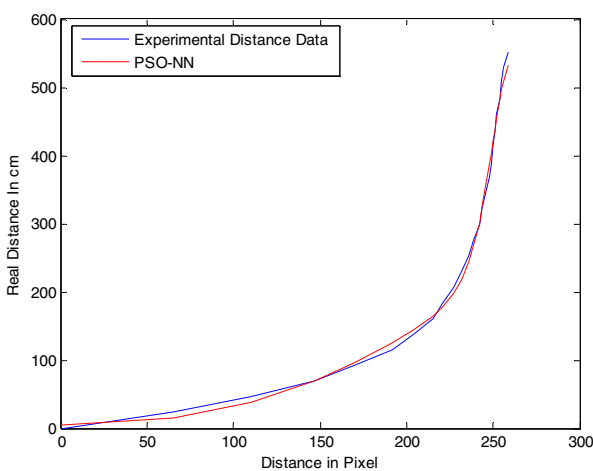


Fig. 6 Distance Comparison between experimental data and PSO-NN model

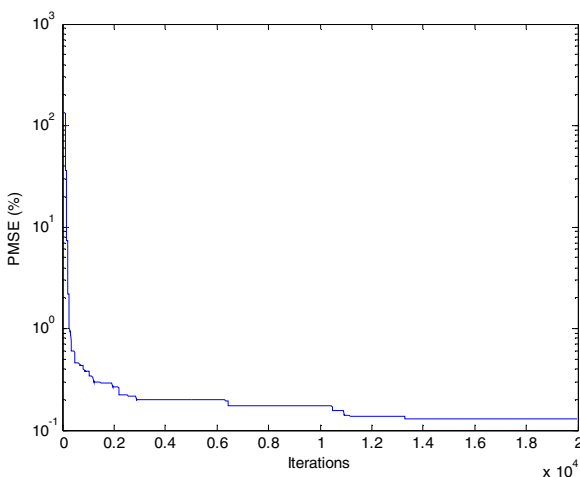


Fig. 7 objective function value in every iteration

The second, experimental object distance data trained by PSO to get the NN forward model. In this experiment, PSO using 30 numbers of the particle, and the acceleration parameters are  $c_1 = c_2 = 2$ . PSO can find the global optimum with 0.11 % of PMSE. Fig. 6 shows that the data resulting from PSO-NN accurately close to experimental data. Under the 14000 iteration PSO can find the global optimum. Fig. 7 shows the convergence speed in  $2 \times 10^4$  iteration.

## V. CONCLUSION

From the experimental data, the object in the soccer field can be detected and tracked. The real distance in cm of the object can be accurately modeled. With our proposed method the object detection and distance computation with omnidirectional vision are effective and efficient in accuracy and processing time.

## VI. ACKNOWLEDGMENT

The author is grateful to UMM (University of Muhammadiyah Malang) Robotics Workshop that contributes to this research. Our acknowledgment also gives to PUSKAREKATEK (UMM Engineering Faculty Research Foundation) for supporting.

## REFERENCES

- [1] D. B. Kusumawardhana and K. Mutijarsa, "Object recognition using multidirectional vision system on soccer robot," 2017, pp. 183–187.
- [2] W. Feng, Y. Liu, and Z. Cao, "Omnidirectional Vision Tracking and Positioning for Vehicles," 2008, pp. 183–187.
- [3] H. Lu, S. Yang, H. Zhang, and Z. Zheng, "A robust omnidirectional vision sensor for soccer robots," *Mechatronics*, vol. 21, no. 2, pp. 373–389, Mar. 2011.
- [4] Z. Cao, S. Liu, and J. Rong, "Omni-directional Vision Localization Based on Particle Filter," 2007, pp. 478–483.
- [5] B. A. Garro and R. A. Vázquez, "Designing Artificial Neural Networks Using Particle Swarm Optimization Algorithms," *Comput. Intell. Neurosci.*, vol. 2015, pp. 1–20, 2015.
- [6] N. Setyawan, R. E. A. Kadir, and A. Jazidie, "Adaptive Gaussian parameter particle swarm optimization and its implementation in mobile robot path planning," 2017, pp. 238–243.
- [7] A. N. Fitriana, K. Mutijarsa, and W. Adiprawita, "Color-based segmentation and feature detection for ball and goal post on mobile soccer robot game field," 2016, pp. 1–4.
- [8] A. K. Mulya, F. Ardilla, and D. Pramadihanto, "Ball tracking and goal detection for middle size soccer robot using the omnidirectional camera," 2016, pp. 432–437.
- [9] Setiawardhana, R. Dikairono, T. A. Sardjono, and D. Purwanto, "Visual ball tracking and prediction with the unique segmented area on soccer robot," 2017, pp. 362–367.

- [10] J. Kennedy and R. Eberhart, "Particle Swarm Optimization," *IEEE Int. Conf. Neural Netw.*, pp. 1942–1948, 1995.
- [11] A. Nickabadi, M. M. Ebadzadeh, and R. Safabakhsh, "A novel particle swarm optimization algorithm with adaptive inertia weight," *Appl. Soft Comput.*, vol. 11, no. 4, pp. 3658–3670, Jun. 2011.



# Decision Support System Scheme Using Forward Chaining And Simple Multi Attribute Rating Technique For Best Quality Cocoa Beans Selection

Januar Adi Putra <sup>1)</sup>, Agustinus Mariano Galwargan <sup>2)</sup>, Nelly Oktavia Adiwijaya <sup>3)</sup>

Faculty of Computer Science,

University Of Jember

Jember, Indonesia

[Januaradi.putra@unej.ac.id](mailto:Januaradi.putra@unej.ac.id) <sup>1)</sup>, [marianogalwargan@unej.ac.id](mailto:marianogalwargan@unej.ac.id) <sup>2)</sup>, [nelly.aa@unej.ac.id](mailto:nelly.aa@unej.ac.id) <sup>3)</sup>

**Abstract**— Cocoa is a crop plantation originating from the tropical forests of Central America and northern part of South America. In general, cocoa grouped into three types namely Forastero, Criollo, and Trinitario which is the result of a cross between Forastero with Criollo. Cocoa (*Theobroma cacao* L.) is one of the commodity that has an important role in the Indonesian economy. The Indonesian's processing directorate, and the programs related to the 2015–2019 development are the Increased Production and Productivity of Sustainable Plantation Crops. This program is conducted to increase the production, productivity of cocoa and other plantation crops. One of the focus activities is Inventory of postharvest data of plantation. In the selection of cocoa beans based on the best quality, Indonesian Coffee and Cocoa Research Center is often missed so that there are some cocoa beans that should not pass the quality but still processed into processed products. In that case we proposed a new scheme for Decision Support System by using Forward Chaining method and Simple Multi Attribute Rating Technique (SMART). The combination of these two methods proved to be able to do a very good selection of cocoa beans. Where the selection is done with two stages proven can really filter the cocoa beans are good for health.

**Keywords**—Cocoa Bean, DSS, Forward Chaining, SMART

## I. INTRODUCTION

Indonesia is one of the world's top cocoa producers after Ivory Coast and Ghana, with 13% of world cocoa production. The production of Ivory Coast and Ghana are 39% and 19% respectively [1]. Therefore, Indonesia's cocoa production is highly calculated in the world cocoa market. Jember Regency is one of the big cocoa bean producing cities in East Java Province. Almost all areas in Jember Regency are plantation area, especially cocoa bean plantation. Plantation in Jember Regency is not a plantation owned by an individual (farmer) but rather a smallholder plantation, which is a collection of small gardens owned by several farmers. The farmers each have a plantation area of approximately 1 - 2 hectares. In quantity, cocoa products in Indonesia at this time the results are quite encouraging, but the quality is not satisfactory. So in the world market is still difficult to compete with products from other countries that have good quality standards. Jember regency, known as a cocoa producer, should be able to improve the quality of cocoa beans into a product in order to compete with other cocoa producing countries. One of the products produced

from the processing of cocoa beans is chocolate. Chocolate with the content of cocoa (cocoa beans) more than 70% also has health benefits, because chocolate is rich in antioxidant content of fenoldan flavonoids that can boost the immune system is very large. With the presence of antioxidants will be able to capture free radicals in the body. Given the various benefits of the importance of the content contained in cocoa beans and derivatives products for the health of the human body, the thing that must be maintained is the selection of cocoa beans with the best quality. Determining cocoa beans with the best quality according to Indonesian's standard must be appropriate with predefined standards and criteria. In the selection of cocoa beans based on the best quality, Indonesian Coffee and Cocoa Research Center is often missed so that there are some cocoa beans that should not pass the quality but still processed into processed products. In addition, the inventory process for managing reports on cocoa beans still uses manual systems that can lead to errors and lack of time efficiency. This manual process is considered inefficient, requiring the system to support the process of selecting the best cocoa beans based on quality. The existence of this system is expected to support the process becomes more optimal and efficient.

Inventory management affects all functions of the cocoa operating system. As a managerial process, an inventory is necessary in a series of planning processes to the elimination of an inventory. However, the reality that occurs in the field of most agencies less attention to the importance of inventory. Based on the explanation of the above problems, a system is needed to assist the selection process of the best cocoa bean selection as well as to manage the digital data inventory for an information presented in graph form showing good quality cocoa quality for health produced from year to year as center evaluation material research coffee and cocoa Indonesia. Utilization of technology that can be used for this problem is to create a system that will be able to combine tools (tools) information systems and models to evaluate the various options. This system is known as Decision Support System (DSS)[2]. In that case we proposed a new scheme for Decision Support System by using Forward Chaining method and Simple Multi Attribute Rating Technique (SMART). Forward Chaining method is run by gathering the facts to draw conclusions. Forward Chaining method is used for the process of determining the quality requirements of cocoa beans based on the beans.

While the Simple Multi Attribute Rating Technique (SMART) method is looking for the weighted summaries and rankings determined through each alternative on all predefined criteria and subcriteria. The Simple Multi Attribute Rating Technique (SMART) method in this research is used for the process of determining specific quality requirements. The combination of Forward Chaining method and Simple Multi Attribute Rating Technique (SMART) is expected to facilitate decision making in making the best decision to determine the best cocoa beans selection based on quality.

## II. METHOD

### A. Decision Support System

Decision Support System (DSS) according to [3], can be described as a system capable of supporting ad hoc data analysis, and decision modeling, decision-oriented, future planning orientation, and use at unusual moments. DSS are tools that an organization uses to support and enhance decision-making activities [4]. Early use of decision support analysis was marketing. DSS was defined by Power [5] as a coordinated collection of data, system, tools and technology, with supporting software and hardware by which an organization gathers and interprets information from business and environment and turns it into a basis for marketing action. Little [6] defined the DSS as a "model-based set of procedures for processing data and judgments to assist a manager in his decision-making."

### B. Forward Chaining

The solution to some problems naturally starts with the collection of information. Reasoning is applied to this information to obtain logical conclusions. For example, a doctor usually begins to diagnose a patient by asking him about the symptoms he or she suffers from, such as high blood pressure, temperature, headache, sore throat, coughing ...etc. Then the doctor uses this information to draw a reasonable conclusion or to establish a hypothesis to explore further. This way of reasoning is called in an expert data driven system, forward-chaining [7].

Forward chaining can also be called advanced trace or search driven data (driven search). So the search starts from the premises or information input (if) first then to the conclusion or derived information (then). Forward Chaining means using the set of conditions-action conditions. In this method, data is used to determine which rule to run or by adding data to working memory to be processed to find a result.

The process of search by forward chaining method departs from left to right, ie from the premise to the final conclusion, this method is often called datadriven that search is controlled by the data provided. Forward chaining is also called advanced reasoning that rules are tested one by one in a certain order. The infrared machine will try facts or statements inside knowledge base in a situation expressed in the IF section rule [8]. If the facts in the knowledge base are in accordance with IF rules, then the rule is stimulated and the next rule is tested. The process of testing the rules one by one continues until one complete round through the entire rule device.

### C. Simple Multi Attribute Rating Technique (SMART)

The Simple Multi Attribute Rating Technique (SMART) is a multi criteria decision making method developed in 1997 by Edward [9][10]. The SMART method is based on the theory that each alternative consists of a number of criteria that have value and each criteria has a weight that describes how important the value of the weight is compared to other criteria. SMART Method is more useful because of its simplicity in responding to the needs of decision makers and how it responds. The analysis involved is transparent so that this approach provides a great understanding of the problem and is acceptable to the decision maker [9][11]. SMART method is used more often because of its simplicity in responding to the needs of decision makers and analyzing responses. SMART uses a linear additive model to forecast the value of each alternative and its decision-making methods are flexible. The steps to solve the SMART method in general are as follows:

1. Determine the problem
2. Determine the criteria to be used
3. Determine alternative to be used
4. Determine the value of scale 0-100 based on priority to assess the weight
5. Give weight to each criteria on each alternative then in normalization. Normalization of weights can be seen in equation 1.

$$nw_j = \frac{w_j}{\sum w_j} \quad (1)$$

annotation:

$nw_j$  = normalization  $i$  criteria

$w_j$  = weighting criteria

$\sum w_j$  = sum of all the criteria

6. Calculate the value of utility by using equation 2.

$$u_i(a_i) = 100 \frac{(C_{\max} - C_{a_i})}{(C_{\max} - C_{\min})} \% \quad (2)$$

annotation:

$u_i$  = utility or sub criteria value of criteria  $i$

$a_i$  = alternatives  $i$

$C_{\max}$  = maximum value of sub criteria

$C_{\min}$  = minimum value of sub criteria

$u_i(a_i)$  = value from alternative  $i$

7. Calculate the final value of each criteria and subcriteria using equation 3.

$$\sum_j = 1/n \cdot u_i(a_i), i=1,2,\dots,k \quad (3)$$

annotation:

$a_i$  = alternatives  $i$

$w_j$  = weighting criteria  $j$

$u_i$  = utility or sub criteria value of criteria  $i$

$u_i(a_i)$  = value of criteria  $i$

#### D. Proposed Scheme

The data analysis phase begins by examining the overall data that has been obtained from the data collection stage. The data is used to select the cocoa beans, the data used are the data of general quality criteria and specific quality criteria. General quality criteria data consist of insects life, moisture content, smelled of smoke, foreign object, and levels of broken beans. Specific quality data consists of the content of moldy bean, slaty bean, the content of insect-damage bean, waste bean, and germinated bean. To obtain the best cocoa beans that meet all the criteria mentioned above, we propose a new Decision Support System Scheme using a combination of Forward Chaining and SMART methods. The initial step is to make selection of cocoa beans by using a general quality test by Forward Chaining method. Cocoa beans that passed the general quality test are then selected again by using specific tests with SMART method with strict feasibility test to produce the best cocoa beans. The proposed Decision Support System Scheme can be seen in Figure 1.

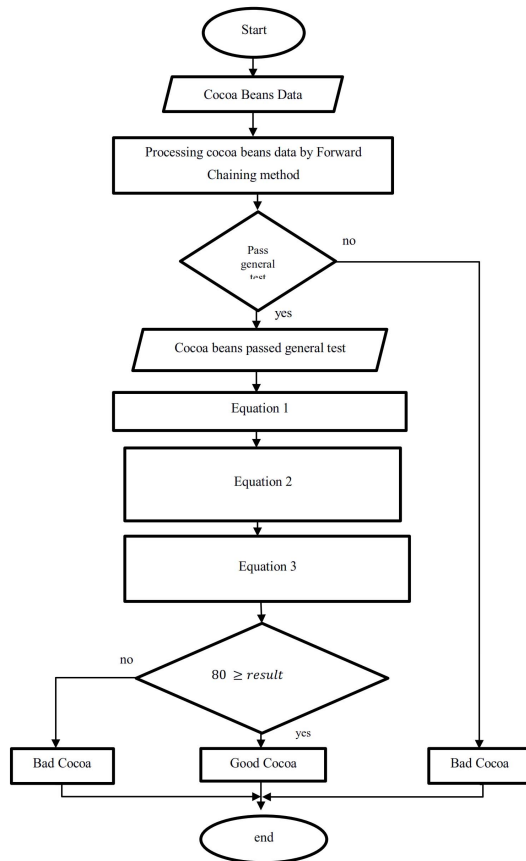


Figure.1 Proposed Scheme

### III. RESULT AND DISCUSSION

System design will be done after the analysis is done. The design is done to provide a general description of the system to be built. This software development adopts the development pattern of waterfall method. Waterfall method is a systematic and sequential method that starts at the level and progress of the system until the analysis, design, code,

test and maintenance. This chapter describes the results of research that has been done and discussion of decision support system that has been made. The discussion was conducted to explain and explain how this study answers the problem formulation as well as the purpose and benefits of this research as what has been determined at the beginning of the study.

#### A. Data Sampling

The sampling data were taken from the Indonesian cocoa research center with the amount of 13 and each cocoa beans were coded. General test criteria data used in making decision support system of quality selection of cocoa beans for health can be seen in Table 1 and the sampling data can be seen in Table 2.

Table 1 General Quality Test Criteria

No.	Type of Test
1	Insects Life
2	Moisture Content
3	Smelled of Smoke
4	Foreign Object
5	Level of Broken Beans

Tabel 2 Sample Data of Cocoa Beans

Cacao Code	Insect Life	Moisture Content	Smelled of Smoke	Foreign Object	Broken Beans
KA_001	No	3,5	No	No	1
KA_002	No	7,6	No	No	1
KA_003	No	4	No	No	3
KA_004	No	4	No	No	2
KA_005	No	7	No	No	4
KA_006	No	4	No	No	1
KA_007	No	4	No	No	1
KA_008	No	5	No	No	2
KA_009	No	3	Yes	No	1
KA_010	No	3	No	No	1
KA_011	Yes	2	No	Yes	2
KA_012	Yes	2	No	Yes	4
KA_013	Yes	3	No	No	3

#### B. General Quality Testing

At the cocoa beans selection stage based on the quality of commonly used Forward Chaining method. Implementation of Forward Chaining Method on Decision Support System for Good Quality Selection of Cocoa Beans is obtained from establishing a complete and good base of rules and knowledge base so that the general quality test process of cocoa bean gets good accuracy. The test mechanism in this decision support system is to do forward reasoning using rules based on a particular order and pattern.

The first step is to determine the criteria that will be tested at the quality selection stage of cocoa beans general test. The data on the general quality test criteria of cocoa beans is shown in Table 3. The second step is to determine the rules to represent knowledge using the production rule method which is usually written in the if-then form. Table 3 describes the quality of cocoa beans based on general quality requirements. The terms in the table are then represented in the facts or Forward Chaining rules that can be seen in Figure 2.

Table 3 General Requirements Good Cocoa Beans

No.	Type of Test	Units	Requirement
1	Insect Life	Beans	No
2	Moisture Content	%	Max 7,5
3	Smelled of Smoke	Beans	No
4	Foreign Object	Beans	No
5	Broken Beans	Beans	Max 2

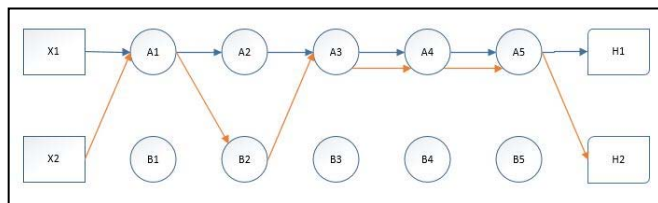


Figure 2 Forward Chaining rule

Annotation:

X1 = Cocoa Beans 1

X2 = Cocoa Beans 2

A1 = No Insect

A2 = Moisture Content  $\leq 7.5$

A3 = No smell of smoke

A4 = No foreign object

A5 = Broken beans  $\leq 2$

B1 = Insect

B2 = Moisture Content  $\geq 7.5$

B3 = Smell of smoke

B4 = Foreign object

B5 = Broken beans  $\geq 2$

The requirements for passing the general test shall meet the five prescribed conditions: no live insects, moisture content  $\leq 7.5$ , no smoke-free beans, no foreign object, and broken beans content  $\leq 2$ . If there is one condition that is not fulfilled, then the cocoa beans otherwise not passed the general test. Table 2 is a sample of cocoa beans data. From the predetermined criteria and rules it can be collected that the cocoa beans that passed the general quality test selection can be seen in Table 4.

Table 1 Cocoa Beans Pass the General Quality Selection

Cocoa Code	Selection
KA_001	Pass
KA_002	No
KA_003	No
KA_004	Pass

KA_005	No
KA_006	Pass
KA_007	Pass
KA_008	Pass
KA_009	No
KA_010	Pass
KA_011	No
KA_012	No
KA_013	No

### C. Specific Quality Testing

After the general test the next step is a specific quality test. This specific quality test is aimed to get the best quality cocoa beans. At the stage of selection of cocoa beans based on specific quality used Simple Multi Attribute Rating Technique (SMART) method. The data criteria used in making decision support system of good quality cocoa beans selection for health at specific selection stage can be seen in Table 5.

Table 5 Criteria, Value and Weight

No.	Criteria	Requirements	Value	Weight
1	Mouldy Cocoa Bean (bean)	0 – 2	0	30
		3 – 4	20	
		> 4	100	
2	Slaty Cocoa Bean (bean)	0 – 3	0	20
		4 – 8	20	
		9 – 20	50	
		> 20	100	
3	Insect-Damaged Cocoa Bean (bean)	0 – 1	0	30
		= 2	20	
		> 2	100	
4	Waste Content (bean)	0 – 1,5	0	10
		1,6 – 2	20	
		= 3	50	
		> 3	100	
5	Germinated Cocoa Bean (bean)	0 – 2	0	10
		= 3	20	
		> 3	100	

The first step in the implementation of the SMART method of cocoa quality selection is to assess each cocoa beans based on predetermined criteria. The rating scale is 1-100 for each criteria. From the assessment conducted by the researchers obtained results as shown in Table 6.



Table 6 Value of each Cocoa Beans

Cocoa Code	Criteria				
	Mouldy bean	Slaty bean	Insect-damaged bean	Waste bean	Germinated bean
KA_001	0	50	20	20	100
KA_004	0	50	100	50	100
KA_006	0	20	0	100	20
KA_007	0	20	0	50	100
KA_008	0	50	100	50	20
KA_010	100	0	0	50	0

The second step is to determine the weight and calculate the value of the weight improvement of each criteria. The weight of each criteria can be seen in Table 5. To calculate the value of weighted improvement is using equation 1, so that we get the weight improvement as in Table 7.

Table 7 New Weight

Criteria	Weight
Mouldy bean(K <sub>1</sub> )	0,3
Slaty bean (K <sub>2</sub> )	0,2
Insect-damaged bean (K <sub>3</sub> )	0,3
Waste bean (K <sub>4</sub> )	0,1
Germinated bean (K <sub>5</sub> )	0,1

The third step is to determine the utility value for each sub criteria using the formula as in equation 2 or directly assign a utility value based on the priority. The result of the preference value is entered in the utility value calculation table. The utility calculation table is shown in Table 8.

Table 8 Utility Calculation

Cocoa Code	Criteria				
	Mouldy bean	Slaty bean	Insect-damage bean	Waste bean	Germinated bean
KA_001	0	50	20	20	100
KA_004	0	50	100	50	100
KA_006	0	20	0	100	20
KA_007	0	20	0	50	100
KA_008	0	50	100	50	20
KA_010	100	0	0	50	0

The fourth step is to calculate the preference value of each cocoa beans by using the utility value that has been obtained previously. To calculate the SMART result is use equation 3. The result of the preference value is entered into Table 9.

Tabel 9 SMART Result

Cocoa Code	value
KA_001	72
KA_004	45
KA_006	84
KA_007	81
KA_008	53
KA_010	65

Table 9 shows the total final value of SMART result calculation. The SMART preference value is the reference used for ranking derived from the total utility value multiplied by the weight of the criteria. SMART calculations that have been obtained then sorted from the largest to the smallest. If the smart results obtained more or equal to 80 then the cocoa beans are considered worthy of specific tests as well as considered as cocoa beans are good for health. But if the smart results obtained less than 80 then the cocoa beans are considered unfit for health. Selection ranking results can be viewed in Table 10.

Tabel 10 Sorting Results

Cocoa Code	SMART result	Rank	Feasibility
KA_006	84	1	Yes
KA_007	81	2	Yes
KA_001	72	3	No
KA_010	65	4	No
KA_008	53	5	No
KA_004	45	6	No

From the calculations that have been done with Forward Chaining and SMART method, the best cocoa beans that passed the general test and specific test are cocoa beans with code KA\_006 and KA\_007 with the final value of 84 and 81.

#### D. System Implementation

The designed Decision Support System is implemented in web form making it easier to access. System is designed using php (laravel framework) and mysql programming language.

#### IV. CONCLUSION

Implementation of Forward Chaining Method in the general test is to check the criteria referring to the Indonesian National Standard on the quality of cocoa beans so that from the facts that have been previously known can produce a new conclusion. Implementation of Simple Multi Attribute Rating Technique (SMART) method in specific test starts from cocoa bean data collection that has passed general test to be processed in specific test phase. After the cocoa beans that have passed the general test have been collected it will be added weight and value for each criteria. Where the assessment criteria refers to the Indonesian National Standard on the quality of cocoa beans. The calculation using the Simple Multi Attribute Rating Technique (SMART) method refers to the utility value of each subcriteria. The combination of these two methods proved to be able to do a very good selection of cocoa beans. Where the selection is done with 2 stages proven can really filter the quality cocoa bean from the not quality one.

#### ACKNOWLEDGMENT

We would like to thank the Indonesian Coffee and Cocoa Research Center for supporting this research.

## REFERENCES

- [1] Icco, "Report on the World Cocoa Conference 2012," *World Cocoa Conf. 19-23 Novemb. 2012*, no. December, pp. 9–13, 2012.
- [2] R. Sugumaran and J. Degroote, *Spatial Decision Support Systems: Principles and Practices*, 1st ed. Boca Raton, FL, USA: CRC Press, Inc., 2010.
- [3] J. H. Moore and M. G. Chang, *Design of Decision Support Systems*, vol. 12. 1980.
- [4] S. Alter, *Decision Support Systems: Current Practice and Continuing Challenge*. 1980.
- [5] D. Power, *Decision Support Systems: Concepts And Resources For Managers*. 2002.
- [6] J. D. C. Little, *Models and Managers: The Concept of a Decision Calculus*, vol. 50. 2004.
- [7] A. Jose and A. Prasad, *Design and Development of a Rule Based Expert System for AACR: A Study of the Application of Artificial Intelligence Techniques in Library and Information Field*. Saarbrücken, Germany, Germany: VDM Verlag, 2011.
- [8] B. H. S. Mzori, "Forward and Backward Chaining Techniques of Reasoning in Rule-Based Systems," no. July, pp. 1–53, 2015.
- [9] Risawandi and R. Rahim, *Study of the Simple Multi-Attribute Rating Technique For Decision Support*, vol. 2. 2016.
- [10] J. M. Taylor and B. N. Love, "Simple multi-attribute rating technique for renewable energy deployment decisions (SMART REDD)," *J. Def. Model. Simul. Appl. Methodol. Technol.*, vol. 11, no. 3, pp. 227–232, 2014.
- [11] F. Amato, V. Casola, M. Esposito, A. Mazzeo, and N. Mazzocca, *A smart decision support systems based on a fast classifier and a semantic post reasoner*, vol. 4. 2013.



# CountNet: End to End Deep Learning for Crowd Counting

Bryan Wilie  
Bandung Institute of Technology  
Bandung, Indonesia  
brywilie25@gmail.com

Samuel Cahyawijaya  
Bandung Institute of Technology  
Bandung, Indonesia  
samuel.cahyawijaya@gmail.com

Widyawardana Adiprawita  
Bandung Institute of Technology  
Bandung, Indonesia  
wadiprawita@stei.itb.ac.id

**Abstract**—We approach crowd counting problem as a complex end to end deep learning process that needs both a correct recognition and counting. This paper redefines the crowd counting process to be a counting process, rather than just a recognition process as previously defined. Xception Network is used in the *CountNet* and layered again with fully connected layers. The Xception Network pre-trained parameter is used as transfer learning to be trained again with the fully connected layers. *CountNet* then achieved a better crowd counting performance by training it with augmented dataset that robust to scale and slice variations.

**Keywords**—transfer learning, crowd counting, deep learning

## I. INTRODUCTION

Crowd counting task in deep learning community is aiming to count every head of a human being present in a crowd shown in a photograph. The crowd in the photo is usually present in a different density, hence the name of the crowd counting, in a dense and sparse crowd. The crowd counting problem is actually a counting problem, done by estimating the number of people in the crowd, in regards to the distribution of the crowd density at one gathering area.

One of the uniqueness in this deep learning task is that not only the whole photograph can be a training data, but also slices of the photograph can represent a whole photograph as a no crowd slices, sparse crowd slices, dense crowd slices, and the mixture of them all. This brings advantage to data collection process. Whilst in another deep learning task, researcher needs to acquire hundred thousands of data, 50 high resolution photograph can already make the same abundances. From this abundances, we can get millions of training data, just by using some augmenting processes.

Besides that, crowd counting is a vast perspective problem. Some of the perspective in the earlier work is the detection [12, 13, 20, 21, 22, 24] and regression [2, 3, 4, 5, 8, 23] network. Detection approach crowd counting is successful for scenes with low crowd density, but the performance on a very dense crowd is still problematic. This happened because on these dense crowd environment, usually only partial of the whole humans are visible, only head to shoulder for horizontally taken photos, and only the top of the head, for a orthogonally taken photos. For this method, parts to be detected by the method is too small, and the counting method will not detect any object that is not a crowd. This is why this method tends to underestimate the counting in a dense crowd settings, and that is still a challenge for the detection method.

While counting by detection needs big part of a human body being located, crowd counting by regression simply estimates crowd counts without knowing the location of each person. Density estimation is sometimes used as an intermediate result, and then using a linear operation, e.g.

sum, a crowd counting method get the overall crowd count results [2, 3]. The regression part, in [5] for example, is using fully CNN model for counting in highly congested scenes. Different with detection based crowd counting, regression based counting tends to overestimate sparse crowd settings counting prediction. This is happening because regression method is trying to find an n-dimensional polynomial function of linear and non-linear relationship between pixels and counting from each of the pixel. The performance of this method relies on the statistical stability of the pixels data. Thus, regression method needs is to explore intrinsic statistical principle of the whole data.

Density estimation method itself is good for regression crowd counting if the intermediate output is handled again by a human processor or processed in an optimized hand engineered feature mapping. As described before, one of feature mapping used is a linear operation, which is to sum each pixels to get the crowd count. This approach should be working smoothly if the density making process could be inversed without a loss, or had an inverse for each pixels translation into the density, or if the blur filtered area's total pixels value can be retained after the filtering process, so that the density making process do not change the ground truth crowd count. Crowd counting is a task with a rich variety of low and high level features and not only has many non-linearity in its inputs, but also has many non-linearity in its outputs. This actually is not a simple counting task, it is actually a task to generalize massive non-linearity provided by differences of the crowd density.

This research approaches crowd counting task as an end to end deep learning process. This process is partly different with some previous implementation of crowd counter. Some implementation only apply deep learning algorithm until it produces the output of predicted density map, thus the title, density estimation, and then sum the predicted density map to get the predicted crowd count. By that term, the algorithm performance is limited by the chosen counting method, and the end to end deep learning process is opening that limit so that the machine can also learn better counting method as well. The limitation is illustrated in Fig. 1, and the end-to-end solution is illustrated in Fig. 2.

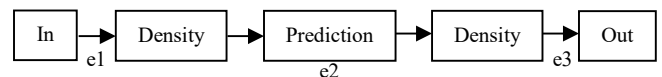


Fig. 1. Previous implementations, introducing errors as e1, e2, and e3

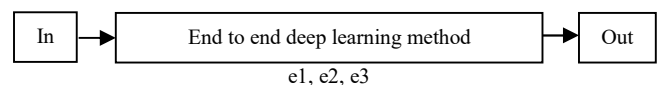


Fig. 2. End to end deep learning implementations.

As we can see on Fig. 1., the previous' implementations introduces three kinds of errors, e1, e2, and e3, from the

density making process, slicing process, prediction process and the output counting process respectively. While the prediction error ( $e_2$ ) is purely handled by the iterative training from the network, other errors such as density making error, slicing error and output counting error is not seen and calculated by the iterative training. That's why the network will have errors at least from the sum of  $e_1$ ,  $e_2$  and  $e_3$ . Different approach in Fig. 2. let the iterative training process see and calculate the counting errors and takes it as loss in a learning process. This way, we let the end-to-end deep learning process also learn from the counting errors by not limiting the potential performances of the counting system. This specific advantage makes the end-to-end approach a more favorable approach for crowd counting.

Although the process tends not to limit the potential performances of the counting system, it needs a network that can generalize well to every linearity and nonlinearity available in the dataset and also a general training data. If the learning algorithm is a large-enough neural network and if it is trained with enough training data, it has the potential to do very well, and perhaps even approach the optimal error rate [15]. This end to end deep learning method can be confidently applied also because the result is not a decision, nor that the prediction error could turn into a fatal error.

Covered in this paper is a crowd counting in a spatial term, not in a temporal term. This paper also redefines regression and detection method as a crowd counting with recognition-priority method, as the result is expected to reflect the ground truth density as close as possible and try to count the crowd with the density prediction being summed. *CountNet* is a counting-priority method and in it, the counting step will be learned by the algorithm itself, not by a hardwired sum method. This is handled by using extra fully connected layers. Extensive data augmentation used is by sampling patches from the multi-scale image representation to make the counting system robust to the scale variation. Our approach is trained and evaluated on the challenging UCF\_CC\_50 extremely dense crowds dataset and has achieved better result.

In summary, we make the below contributions:

- We find that crowd counting task is a problem of finding a generalization of many non-linearly distributed crowd density that can't be counted or categorized easily.
- Based on that understanding, we create an end to end deep learning method, *CountNet*, and tune every hyper parameters of it so that the algorithm can be trained with a good amount of a general kind data, do the model fitting properly, and expect many linearity and non-linearity to be captured by the algorithm.
- Experimental results reveal that our method can achieve a better result on a challenging crowd counting dataset

## II. RELATED WORKS

### A. Crowd Counting by Detection

Earlier works approach crowd counting by detecting the counted crowd. Some of the approaches are using region proposal generators, low-level features [21, 22], binary classifiers like Naive Bayes classifier [24], and Random

Forest [20]. There are also CNN based object detectors [12, 13] used to approach this crowd counting task. Detection based approach is successful for predicting scenes with low crowd density. On the occasions with high crowd density like in our chosen dataset, these approach performances are still not that good. The detection based crowd counting tends to underestimate the crowd counting predictions on the high crowd density, because only part of the whole objects are visible for localization be done by object detectors, or because the object in those highly congested areas are simply too small to be detected.

### B. Crowd Counting by Regression

Counting by regression is not requiring the exact local position of each person in the crowd. In fact, some of the preliminary work use edge and detection features to learn mapping from image patterns to crowd counts. A deep convolutional neural network (CNN) is also used in a switchable training scheme for crowd counting task in [2]. The early approach of crowd counting is using a concatenated deep VGG network and parallel shallow network [3], which at the time, performed the state-of-the-art result. Despite its error to the large crowd dataset, the result is actually precise at some images in the dataset. Some others used a fully convolutional network architecture [5] with a number of max pooling layer and a 2D integrator which is an element-wise sum, to deliver the crowd count, or with a cascaded multi-task learning settings for density estimation [23], or with a combination with Gating CNN [8], which is proven to be specialized in a specific appearance and has the robustness to large appearance changes. Others implemented a multi-scale convolutional neural network to extract scale-relevant features from crowd images using a single column network based on the multi-scale blob [4]. Counting by regression is quite reliable in crowded settings and tends to overestimate predictions in a low crowd settings. This overestimations and errors in the regression based approach mainly come from the statistical stability of the data and the neediness of more instances to help explore intrinsic of that statistical stability principles.

### C. Crowd Counting by Other Methods

Combining the best from both sides, there is an approach that combines results from the regression network and the detection network [11]. This superposition combination method is unique as it trains another network called 'Quality-Net block' to captures the different importance weight of two density maps by dynamically assessing the qualities of the regression prediction and detection prediction for each pixel. This approach also covers the non-linearity introduced by different crowd density that some tried to grasp using a multi-task learning method. Other novel crowd counting approach leverages abundantly available unlabeled crowd imagery in a learning-to-rank framework [19]. This approach learn from unlabeled datasets by incorporating learning-to-rank in a multi-task network which simultaneously ranks images and estimates crowd density maps.

## III. CROWD COUNTING BY COUNTNET

Our solution formulates the crowd counting task as a counting problem, with an understanding of linearity and non-linearity of the training set and test set. From our experiments, we understand that other than the non-linearity

of the features explored by previous' researches, there are also non-linearity introduced by each of different crowd density. To handle the size variations on the dataset, we slice the dataset to a respective size so that all training set and test set are images of typical size. Facilitating those reasons, we need to employ some of preprocessing methods, selecting the best pre-trained model that can generally captures linearity and non-linearity, and also set our learning parameters to maximize our convergence time and result. Those employment are described below.

#### A. Preprocessing

Enhancing features captured by the algorithm, we augment the data with several augmenting technique used before in [3] and some addition of hand-engineered sampling technique designed by ourselves. Features enhancement used here is mainly to handle scale and direction variation and to address dense crowd region.

First we do a multiscale pyramidal scaling from 0.5 to 1.3 with 0.1 steps incremented times the original full scale image resolution. The scaling will make the algorithm more robust to scale variation so that the algorithm can be trained to recognize people in more scale variation. Then the scaled image is sliced in patches of same size, so that the input to the network is in controlled size. After that, the slices then flipped in the left/right direction to further augment the dataset. This data augmentation has obtained us around 2 million slices to train. Before we sample this 2 million, we shuffle all this total sample randomly. By this augmentation, the algorithm trained is more robust to scale and direction variation and then can generalize well to most of the crowd we have in our data.

Second, we sample high relative crowd count patches more often and include also the other levels of relative crowd count patches. In our reported result, we use a maximum of 200,000 slices of training set, consisted of a maximum of 10,000 slices from the lowest relative crowd count patches, 10,000 slices again from the low relative crowd count patches, another 10,000 slices from the medium relative crowd count patches, then 60,000 slices from high relative crowd count patches, and lastly a maximum of 110,000 slices from the highest relative crowd count patches available in our 2 million of total slices. This lowest to highest relative crowd count level is calculated from the maximum and minimum crowd count range divided by five to indicate five categories, lowest, low, medium, high, highest. The highest category's upper bound is a half times the maximum crowd count from all slices. This is done to make space for more data variations from the same crowd count group. From our training results, the sampling method ended up not using 200,000 slices as training sample. This happened because there's not enough slices available from the relative crowd count group. For example, one group only have a 79,776 slices from a maximum of 110,000 slices. We tend to not augment our training set more than what's already done because our infrastructure usage is already approaching its limit from that total training set sampled.

#### B. Xception: Depthwise Separable Convolutions [6]

We have tried several networks to be the main predictor of our end to end deep learning system, and we choose Xception: Depthwise Separable Convolutions [6] network, developed by Keras' own author, François Chollet. Xception

is a convolutional neural network architecture based entirely on depthwise separable convolution layers that map the cross-channels correlations and spatial correlations in the feature maps of convolutional neural networks, entirely decoupled.

The Xception architecture has 36 convolutional layers forming the feature extraction base of the network. The 36 convolutional layers are structured into 14 modules, all of which have linear residual connections around them, except for the first and last modules. In short, the Xception architecture is a linear stack of depthwise separable convolution layers with residual connections. [6]

We also choose this architecture because Xception have one the best top-1 accuracy and top-5 accuracy on the ImageNet validation dataset while also have the lowest parameters count, size, and depth, compared to the recent InceptionV3 and InceptionResNetV2 [7]. By the performance on the ImageNet validation dataset, the network proven to have a good proportion of linear and nonlinear generalization in such a compact parameters count, size and depth.

Our proposed end to end deep learning network will output a predicted count for the input slice. To achieve this, we omit the top layer of the Xception network (by setting the include\_top = False), and add fully connected network sized 1024 with relu activation to introduce non-linearity aspect to the network's final counting, and then add fully connected network sized 256 also with relu activation, fully connected network sized 16, and lastly, a fully connected network sized 1 to output a final predicted count. This final predicted count will be the prediction of the input slice crowd count. The illustration of our proposed end to end deep learning network is shown in Fig 3.

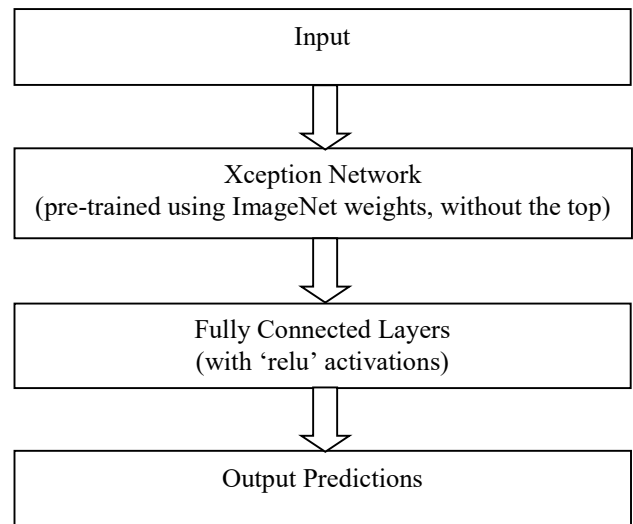


Fig. 3. Our approach of End to End Deep Learning Network

#### C. Learning Parameters

We use cyclical learning rates as described in [10], so that by creating new learning rate policies, our training could converge faster than other linearly and even exponentially decreasing learning rate policies. For the learning rate policies, we choose base learning rate at  $1e-6$ , max learning rate at  $1e-2$ , and gamma of 0.99994 in "exp range" mode. We set step size equal to 2 – 10 times the number of

iterations in an epoch. Number of iterations will be derived from number of total training set data in each epoch divided by batch size. This step size is a representation of half a cycle from a full cycle of a cyclical learning rates. The learning tends to converge at around 3 to 4 epochs, so we train our network for 5 epochs at each of our training, to make sure the convergence happens before the training finished.

#### D. Training Settings

For training purposes, this transfer learning method using pre-trained weights from Xception network to be trained again with the fully connected layers with glorot uniform initializer as the default initializer from Keras. We train our model using maximum of 200,000 samples from lower half of the crowd distribution (to make space for more data variation) and validate our model for each epoch, using around 1,000 samples. The maximum of 200,000 samples then will be trained as 64 mini-batches, and shuffled at each epoch. This training is done for 5 epochs for each fold of the 5 folds cross validation method.

We only train the model until the validation loss converges, as it marks the beginning of overfitting error or variance error. If the validation loss goes lower than the previous validation loss convergence point, we also take that weights as the best weights of the training session. We don't take weights that has bigger validation loss than the convergence points. This way, our model is preserved from the overfitting training result.

### IV. EXPERIMENTAL RESULTS

This end to end deep learning approach is evaluated for crowd counting on the challenging UCF\_CC\_50 [1] dataset, contains 50 grayscale crowd images with various sizes and with number of crowd count per image varies between 96 and 4631 people averaging at 1280 individuals per image.

Similar to recent works, to ensure generalization and exclude overfitting problem from testing trained dataset, our approach is evaluated using 5-folds cross validation method. The whole 50 images from UCF\_CC\_50 dataset is being divided randomly into 5 splits with each splits then containing 10 images. In each of the 5 folds, we consider 4 splits (40 images) for training the end to end deep learning network and 1 remaining split (10 images) to test the network. The maximum of 200,000 slices will be obtained from each of these 40 training images in regards to previously described data sampling and augmentation method. On UCF dataset, this procedures yield around 170,000 slices of training patches per fold. We train our CountNet: end to end deep learning network using Keras [15] and Tensorflow [14] deep learning framework on Tesla V-100 GPU and 64 GB of RAM. Our network was trained using Adam Stochastic Optimizer [17, 18] with learning rate policies later overruled by cyclical learning rates policies, and calculate loss as mean absolute error. The average training time per fold is around 5500 seconds.

#### A. Results

Measuring performance of our approach, we use Mean Absolute Error (MAE) to quantify the error of every predictions made by our approach. MAE computes the mean of absolute difference between the ground truth counts and the predicted counts for all images in this UCF dataset. The

result illustrates that compared to the others implementation that creates a new network, this simple transfer learning method with a network that already has the accuracy proven for ImageNet can achieve a better accuracy than the others.

Our approach contains a random sampling and random initialization, in which making the network prone to robustness error. To completely show the result of our trainings, we use average to describe our MAE. So each trainings has its own MAE, but because we trained it 4 times, we calculate each of our trainings MAE as average MAE from 4 trainings, thus we call it average of 4 MAEs. The average of 4 MAEs is 335.3, with the details of the 4 MAEs in each folds written in Table 1.

TABLE I. 4 TIMES 5 FOLDS TRAINING IN DETAIL

4 Times 5 Folds Training				
5 Folds Training	Training 1	Training 2	Training 3	Training 4
Fold 1	261.8	388.1	445.3	491.8
Fold 2	269.9	287.1	323.9	279.9
Fold 3	239.2	302.3	284.2	215.8
Fold 4	554.2	444.3	494.1	458.7
Fold 5	162.5	321.2	310.4	171.8
<b>5 Folds MAE</b>	<b>297.5</b>	348.6	371.6	323.6
<b>Average MAE</b>	<b>335.3</b>			

Although our proposed method has an average MAE on 335.5, roughly seeing, the MAE is ranging from 300 to 370 and the method have a lowest prediction MAE on 297.5. This shows that our method have certain robustness problem in it. This problem should be addressed in future research so that the estimated predictions have a reliable results.

Below also shown in Fig. 4, is the detailed predicted count for each images in the UCF dataset, compared with its actual count taken from Training 1. Vertical axes is for amount of crowd count in each images. Horizontal axes is for image number in UCF\_CC\_50 dataset. Red lines and dots for prediction counts, blue lines and dots indicates ground truth counts.

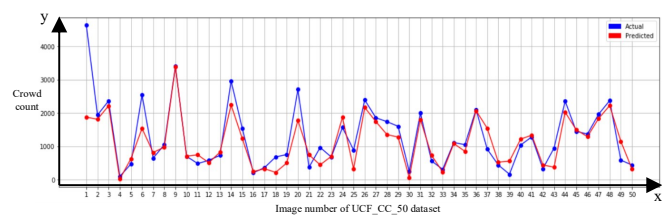


Fig. 4. Training 1 Result: Comparing Prediction and Ground Truths.

Most of the prediction is close to the ground truth counts, but we still see some of the predictions missed the ground truth counts disorderly. This prediction error present mainly because of a lack of training data. We have tried to train the proposed method with our 2 million training data, but we can't go on because of the bottleneck in our infrastructure settings.

### B. Comparison with Some Early Contributions

We compare our proposed method to some of the related work and existing method referenced in this paper. The comparison is shown in Table II.

TABLE II. RESULTS COMPARISON

Methods	MAE
Idrees <i>et al.</i> [1]	419.5
Zhang <i>et al.</i> [2]	467.0
CrowdNet [3]	452.5
MsCNN [4]	363.7
MCNN [25]	377.6
Walach <i>et al.</i> [26]	364.4
Marsden <i>et al.</i> [5]	338.6
Proposed method	335.3

The comparison above shows that the proposed method has already achieved better results when compared to several earlier approach. The proposed method, by the MAE, proved that it is better than: global consistency constraint counts on the head detections from texture elements [1], counting by convolutional neural network (CNN) trained alternatively with crowd density and count [2], counting by using density estimation from concatenated deep and shallow network [3], using multiscale CNN [4], multi-column CNN [25], CNN with layered boosting and selective sampling [26], and Fully CNN architecture [5]. Should the robustness problem be handled in the future, this proposed method could achieve state-of-the-art performance on the crowd counting task.

### V. CONCLUSION

In this paper, we proposed an end-to-end deep learning approach to deal with the crowd counting task. We showed that by using pre-trained network, the Xception network, and adding fully connected network at the top of the pre-trained network, we can achieve a better crowd counting performance by training it with augmented dataset that robust to scale and slice variations. The proposed method has achieved a better result from earlier methods that also tested on the challenging highly dense crowd dataset, the UCF\_CC\_50. Experimental result shows that the proposed method can achieve even better result by addressing the robustness problem on the estimated predictions.

### ACKNOWLEDGMENT

The Titan XP used for this research was donated by the NVIDIA Corporation, and this work was also supported by Amazon Web Service (AWS) Educate, & Lembaga Pengembangan Inovasi dan Kewirausahaan Institut Teknologi Bandung (LPIK ITB).

### REFERENCES

- [1] H. Idrees, I. Saleemi, C. Seibert, and M. Shah, "Multi-source multi-scale counting in extremely dense crowd images," in CVPR 2013
- [2] C. Zhang, H. Li, X. Wang, and X. Yang, "Cross-scene crowd counting via deep convolutional neural networks," in CVPR 2015
- [3] L. Boominathan, S.S. Kruthiventi, and R.V. Babu, "Crowdnet: a deep convolutional network for dense crowd counting," in ACM 2016
- [4] L. Zeng, X. Xu, B. Cai, S.Qiu, and T. Zhang, "Multi-scale convolutional neural networks for crowd counting," in ICCV 2017
- [5] M. Marsden, K. McGuinness, S. Little, and N. E. O'Connor, "Fully convolutional crowd counting on highly congested scenes," in VISAPP 2017
- [6] F. Chollet "Xception: Deep learning with depthwise separable convolutions," in CVPR 2017
- [7] Documentation for individual models, (2018, July 10). Retrieved from <https://keras.io/applications/#xception>
- [8] S. Kumagai, K. Hotta, and T. Kurita, "Mixture of counting cnns: adaptive integration of cnn's specialized to specific appearance for crowd counting," in Machine Vision and Applications 2018
- [9] M. Marsden, K. McGuinness, S. Little, and N. E. O'Connor, "ResnetCrowd: a residual deep learning architecture for crowd counting, violent behaviour detection and crowd density level classification," in AVVS 2017
- [10] L. N. Smith, "Cyclical learning rates for training neural networks," in WACV 2017
- [11] J. Liu, C. Gao, D. Meng, and A. G. Hauptmann, "DecideNet: counting varying density crowds through attention guided detection and density estimation," in CoRR 2017
- [12] S. Ren, K. He, R. Girshick, and J. Sun, "Faster r-cnn: towards real-time object detection with region proposal networks," in NIPS, 2015.
- [13] R. Girshick, "Fast r-cnn," in ICCV 2015
- [14] M. Abadi, A. Agarwal, P. Barham, E. Brevdo, Z. Chen, C. Citro, G. S. Corrado, A. Davis, J. Dean, M. Devin, S. Ghemawat, I. Goodfellow, A. Harp, G. Irving, M. Isard, Y. Jia, R. Jozefowicz, L. Kaiser, M. Kudlur, J. Levenberg, D. Mane, R. Monga, S. Moore, D. Murray, C. Olah, M. Schuster, J. Shlens, B. Steiner, I. Sutskever, K. Talwar, P. Tucker, V. Vanhoucke, V. Vasudevan, F. Viegas, O. Vinyals, P. Warden, M. Wattenberg, M. Wicke, Y. Yu, and X. Zheng. TensorFlow: Large-scale machine learning on heterogeneous systems, 2015. Software available from tensorflow.org.
- [15] F. Chollet. Keras. <https://github.com/fchollet/keras>, 2015.
- [16] A. Ng, Machine Learning Yearning. Deeplearning.ai, 2018
- [17] D. Kingma, and J. Ba, "Adam: a method for stochastic optimization," in ICLR 2015
- [18] S. J. Reddi, S. Kale, S. Kumar, "On the convergence of adam and beyond," in ICLR 2018
- [19] X. Liu, J. v. d. Weijer, and A. D. Bagdanov, "Leveraging unlabeled data for crowd counting by learning to rank," in CVPR 2018
- [20] V.-Q. Pham, T. Kozakaya, O. Yamaguchi, and R. Okada, "Count forest: co-voting uncertain number of targets using random forest for crowd density estimation," in ICCV 2015
- [21] N. Dalal and B. Triggs, "Histograms of oriented gradients for human detection," in CVPR 2005
- [22] P. Sabzmejdani and G. Mori, "Detecting pedestrians by learning shapelet features," in CVPR 2007
- [23] V. A. Sindagi and V. M. Patel, "CNN-based cascaded multi-task learning of high-level prior and density estimation for crowd counting," in AVSS 2017
- [24] A. B. Chan and N. Vasconcelos, "Bayesian poisson regression for crowd counting," in ICCV 2009
- [25] Y. Zhang, D. Zhou, S. Chen, S. Gao, and Y. Ma, "Single image crowd counting via multi-column convolutional neural network," in CVPR 2016
- [26] E. Walach and L. Wolf, "Learning to count with cnn boosting," in ECCV 2016

# Sentiment Analysis Based on Appraisal Theory for Assessing Incumbent Electability

Canrakerta, Pamuji Lasiyanto Putro, Zikri Irfandi, Nur Fitriah Ayuning Budi, Achmad Nizar Hidayanto  
Faculty of Computer Science, Universitas Indonesia  
Depok, Indonesia

canrakerta@ui.ac.id, pamuji.lasiyanto@ui.ac.id, zikri.irfandi@ui.ac.id, nurfitriah@cs.ui.ac.id, nizar@cs.ui.ac.id

**Abstract** — Sentiment analysis is a useful study for determining opinions by classifying text. The document used in the research comes from Twitter about public opinion about community satisfaction related to performance of incumbent. The method used is Appraisal Theory. The data used are 1587 for Jokowi related data, 1774 for Ministry related data, and 1337 government related data. The result of data analysis from this research is that people have positive sentiments for incumbent. Innovation is a term that has the highest positive sentiment, whereas imaging is the term that has the lowest negative sentiment.

**Keywords** — *sentiment analysis; appraisal theory; twitter*

## I. INTRODUCTION

Upcoming general election in 2019 is expected to be the concern of the whole community. No exception for the incumbent who has the opportunity holding the wheels of government for two periods. Incumbent's performance is now a benchmark of electability level to advance in elections in 2019. The level of electability can be reflected from public opinion related to the level of satisfaction with the current government performance [1].

The rapid development of the internet ranges from news media to social media. The most popular social media among mobile internet users in Indonesia includes Facebook, Instagram, Twitter, Google+, Path, Snapchat, Tumblr, and so on [2]. Social media today is not limited to use as a medium of friendship but can also function like other marketing media, advertising, to the delivery of opinions and aspirations [3].

Public opinion related to current government can be seen through social media [4]. One such social media is Twitter. Twitter has the fifth largest number of users in the world, and there are tweets totaling 4.1 billion tweets in 2016 alone [5]. This rapid development made Twitter one of the most fertile places for people to share their opinions on government performance. The opinions of public within Twitter are opportunity for the incumbent to see community satisfaction.

Sentiment analysis is done to view opinions or opinions about a problem. One theory used to derive sentiment analysis is the theory of judgment. Assessment theory is a theory that explains the language used in communicating consisting of feelings and opinions [6]. In this research, sentimental analysis is done to see the opinion of society which is addressed to the incumbent based on Twitter data 2017. The result of opinion measurement can be used as parameter of society satisfaction to incumbent's performance. With the aim that sentiment analysis can be used to measure incumbent electability in Election 2019.

## II. LITERATURE STUDY

### A. Sentiment Analysis

The sentiment analysis, also known as opinion mining, is a study to determine public opinion about services, products, films, and so on. The need for sentiment analysis has become very important [7]. When people will make decisions, they will refer to the opinions of others. Almost all companies conduct market surveys and research to capture public opinion about their products, as well as in government, to see how government performance can be done by studying public opinion [7]. The need for sentiment analysis is growing substantially, especially with the development of social media as a place for society to express its opinions. Sentiment analysis has been widely used to examine social media content. [8] developed a system that can analyze and provide sentiment predictions through social media content in real time using AsterixDB. In addition, [9] proposes one semantic approach to determining user attitudes and business insights based on the results of analytical sentiments from social media in Arabic. Sentiment analysis was also used by [10] which introduced SmartSA, a lexicon-based sentiment classification system for social media genres. [10] hybridizing the general purpose of the lexicon and proven to improve the sentiment of results.

### B. Appraisal Theory

Appraisal theory describes how to use language to communicate with others [11]. Appraisal Theory is a system of interpersonal meaning. Appraisal is used to negotiate social relations between people,



by telling what is felt about things and people to the reader. There are three aspects that were explored in the discussion of the appraisal system, namely attitudes, how the attitude was expressed, and the source of the engagement [12]. As explained below:

1. Attitudes, related to evaluation of objects, character, and feelings. Attitudes are divided into three types of evaluations of attitudes, namely affect (feelings of people), judgment (character of people), and appreciation (value of an item).
2. Appreciation, talking about the opinion of a person both inside and outside a person such as shy, ugly, beautiful and one's behavior in a social context such as heroic, weak.
3. Engagement related to the source of attitude is divided into two types, namely (1) heterogloss (relating to the source of attitudes that come from other than the author) and (2) monogloss (relating to the source of attitudes derived only from the author). Heterogloss is an attitude that is derived not only from the author.

### C. Data Mining

Data mining is the process of finding patterns new, has a meaning, descriptive model, easy to understand and predictive of large-scale data [13]. Data mining can also be interpreted as disciplinary fields from various fields such as statistics, machine learning, information retrieval, pattern recognition and bioinformatics. Data mining is widely used in many domains such as retail, telecommunications finance, social and more [14]. Data mining is part of a process called [13]. Generally, the processes in KDD are:

1. Data Cleansing (to eliminate inconsistent data);
2. Data Integration (merging from various sources);
3. Data Selection (relevant data is taken from the database for analysis);
4. Data Transformation (data is transformed and consolidated into an appropriate form for aggregation);
5. Data Mining (an important process where intelligent methods are applied to extract data patterns);
6. Pattern Evaluation (identifying interesting patterns that represent knowledge based on certain measurements);
7. Knowledge Presentation (visualization techniques and representations of knowledge used to present that knowledge to users).

### D. Text Mining

Text mining is part of data mining activities that focus on textual data. The process of text mining itself is done in phase to get a word from text data that has potential as an attractive variable [15].

Here is a process done in research to get a set of words that have potential as an attractive variable:

1. Cleansing. Cleansing is a process of cleaning up unnecessary words to reduce noise. The omitted words are URL, hashtag (#), username (@username), and email. Additionally, punctuation marks such as dots (.), Commas (,), and other punctuation will be omitted.
2. Case Folding. Case folding is the stage of changing the form of words into the same shape, whether it be all the lower case or the upper case.
3. Stopword Removal. Filtering plays a role to remove the commonly emerging and common words, showing less of relevance to the text. The words to be discarded are defined in the stopword list.
4. Stemming. Stemming is the stage to create a word that affixed back to its original form. example of the word omitted will be "lost".
5. Tokenizing. Tokenizing works to identify words in the text into several sequences that are cut off by spaces or special characters.

### E. Citizen Satisfaction

Satisfaction reflects people's judgment of a product to what extent product performance meets customer expectations [16]. If performance is less than expectations, customers are disappointed. If appropriate, customers are satisfied. If it exceeds then the customer is very happy.

Public satisfaction is the result of opinion and public assessment of the performance of services provided to the apparatus of public service providers. The element of service is a factor or aspect contained in the provision of services to the community as a variable preparation of community satisfaction survey to determine the performance of service units [17].

## III. RESEARCH METHOD

### A. Data Collection

Data collection is done by utilizing data from social media Twitter. With the Twitter API available, the public can tweet crawling based on the required query. In this study, the query used for the data collection phase is the word "jokowi" OR "ministry" OR "government". The three words are considered to have a connection with the object of research and are also a word that is pretty much tweeted by the public in expressing their opinions on Twitter social media. In addition, the tweet used in this study is an Indonesian-language tweet. Table 1 is a detailed amount of data collection based on successful tweets in crawling.

TABLE 1 Number of tweets based on query

Query	Total Tweet
jokowi	1587
ministry	1774
government	1337

### B. Data Preprocessing

Preprocessing data is intended to perform cleansing and transformation of data that has been collected in the previous stage. In this stage, there are several steps taken to obtain the final data used when conducting word weighting and sentiment analysis to assess community satisfaction with the President of the Republic of Indonesia. Figure 1 below explains how the preprocessing data stages are performed.

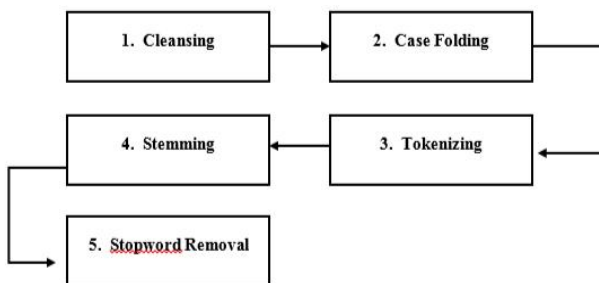


FIGURE 1 Data Preprocessing Stages

The data obtained will be processed firstly in the preprocessing data phase to facilitate the scoring stage based on Appraisal theory. Table 2 is an example of preprocessing data stages.

TABLE 2 Sample Data Preprocessing Stage

Initial Condition	
President @jokowi appears from the car sunroof, Nabire Papua residents welcome him him up to Nabire Regency, fantastic	
Cleansing Results	
The president appears from the car sunroof, Nabire Papua residents welcome him up to Nabire Regency, fantastic	
Case Folding Results	
The president appears from the car sunroof, nabire papua residents welcome him up to nabire district, fantastic	
Tokenizing Results	
president appear from sunroof car residents nabire	papua welcome him up to regency nabire fantastic

TABLE 2 Sample Data Preprocessing Stage (continue)

Stemming Results	
president appear from sunroof car residents nabire	papua welcome him up to regency nabire fantastic

The output of preprocessing data is a collection of words used by researchers to search for terms as an analysis material in scoring season. Table 3 is a term performed after a rational and emotional evaluation.

TABLE 3 Sentiment Terms

No.	Term	Proposed Sentiment
1	Innovation	positive
2	Open	positive
3	Advance	positive
4	Prosperous	positive
5	Phase	positive
6	Appreciation	positive
7	Success	positive
8	Image	negative
9	Deteriorate	negative
10	Abandoned	negative
11	Hate	negative
12	Corruption	negative
13	Lie	negative

### C. Scoring

Based on previous research [6], Figure 2 is a proposed model for the scoring library range that will be used in the study. Based on the range scoring library, then will be calculated every positive or negative terms based on data that has been done preprocessing until the case of case folding.

Attitude		Graduation				Engagement
A1 Value = +2	A1 Value = -2	B1 = A1 + Words Value = +3	C1 = Words + A1 Value = +1	D1 = A1 + Emote Value = +3	D4 = A2 + Emote Value = -3	E
				D2 = B1 + Emote Value = +4	D5 = B2 + Emote Value = -4	
		B2 = A2 + Words Value = -3	C2 = Words + A1 Value = -1	D3 = Emote Value = +1	D6 = Emote Value = -1	
<i>Senang</i> /Happy	<i>Kecewa</i> /Dissapoint	<i>Sangat</i> /Very	<i>Lumayan</i> /Pretty air	:)	- __ -	<i>Sebelumnya</i> /Before
<i>Suka</i> /Like	<i>Nyesel</i> /Regret	<i>Terlalu</i> /Too	<i>Agak</i> /Rather	:D	:(	<i>Sesudahnya</i> /After
<i>Bagus</i> /Good	<i>Jelek</i> /Bad	<i>Benar-benar</i> /Really	<i>Rada</i> /Rather (Informal form)	^ ____ ^	!	<i>Mungkin</i> /Maybe

FIGURE 2 Proposed Model for Range Scoring Library

Here is an example of using scoring library range:

<b>Jokowi</b> has a <b>remarkable innovation</b> for Indonesia.	
T1	A
<b>Abandoned</b> development becomes a <b>government</b> problem	
A	T2
<b>Ministry of Finance</b> has not improved the <b>problem of corruption</b>	
T3	A

**Description:**

- A: Appraisal
- T1: Target 1 (Jokowi)
- T2: Target 2 (Government)
- T3: Target 3 (Ministry)

**Calculation:**

- Targetscore T1 = 3
  - Targetscore T2 = 2
  - Targetscore T3 = 2
  - Total Targetscore = 8 (Positive)
- D. Term Weighting

Based on the predetermined terms, the study will weight each term based on Term Frequency. It is done to calculate the appearance or frequency of a term. Term Frequency is done to see the weight of a term against positive or negative sentiments.

$$w_{\text{tf}_{t,d}} = \begin{cases} 1 + \log_{10} \text{tf}_{t,d}, & \text{if } \text{tf}_{t,d} > 0 \\ 0, & \text{otherwise} \end{cases} \quad (1)$$

## IV. RESULTS AND DISCUSSION

Sentiment analysis based on the Appraisal theory that has been done has several results and conclusions. The first result is the overall total sentiment. Figure 3 is a graph of the overall total sentiment. Based on the figure, it can be seen the term innovation is the highest term value for positive sentiment, while the value of the imaging term is the lowest value for negative sentiment. The second result is the total sentiment based on the predetermined term and the existing target score. These results are used to see how a sentiment is toward jokowi, government, and ministries.

Figure 4 is a graph of total sentiment based on the T1 targetscore. Based on the figure, it can be seen the term innovation is the highest term value for positive sentiment, while the value of the imaging term is the lowest value for negative sentiment. Figure 5 is a total sentiment graph based on T2 target score. Based on the figure, it can be seen the term of appreciation is the highest term value for positive sentiment, while the value of hate and lie term is the lowest value of the term for negative sentiment. Figure 6 is a graph of total sentiment based on the T3 targetscore. Based on the figure, it can be seen the term of openness is the highest term value for positive sentiment, while the term abandoned value is the lowest value for negative sentiment.

The third result is the term frequency based on the specified term. This result shows the term that often arises based on public opinion emotionally to the incumbent. The term frequency can be the basis for the incumbent to make decisions or steps to be taken to improve electability in elections 2019. Table 4 is the value of Term Frequency based on predetermined terms.

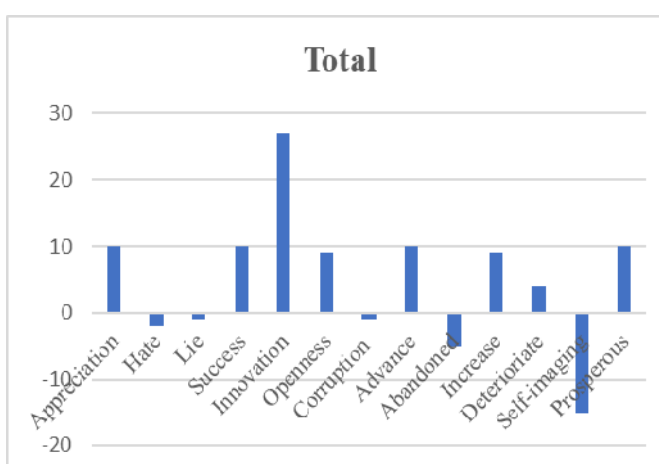


FIGURE 3 Total Overall Sentiment

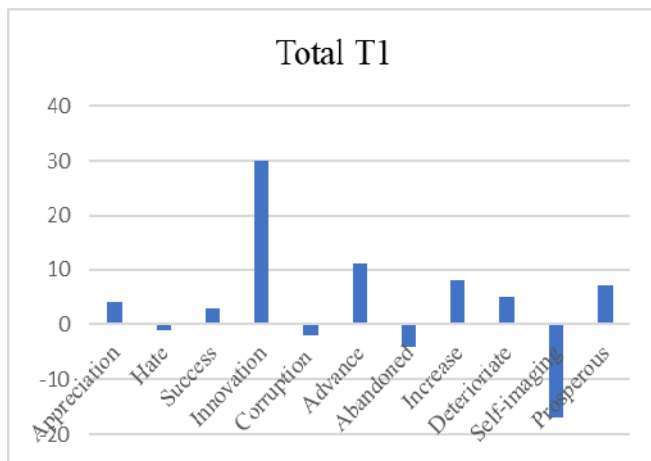


FIGURE 4 Total Sentiment Based on Target Score T1

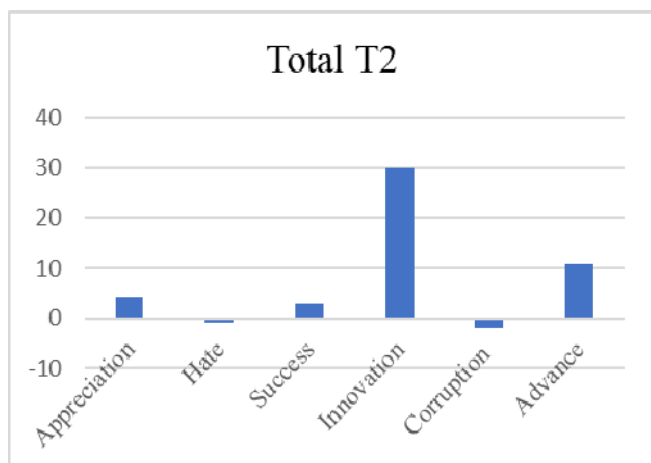


FIGURE 5 Total Sentiment Based on Target Score T2

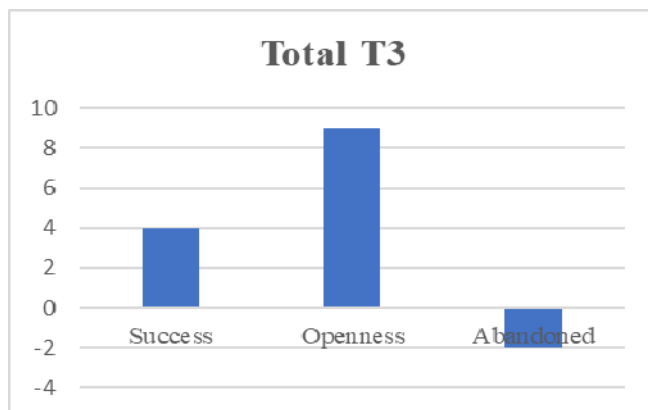


FIGURE 6 Total Sentiment Based on Target Score T3

TABLE 4 The Result of Term Frequency

Term		Term Frequency
Appreciation	10	0.08547
Hate	3	0.025641
Success	10	0.08547
Innovation	27	0.230769
Corruption	2	0.017094
Advance	10	0.08547
Abandoned	6	0.051282
Phase	9	0.076923
Deteriorate	4	0.034188
Image	15	0.128205
Prosperous	10	0.08547
Open	9	0.076923

## V. CONCLUSION

Based on the research that has been done, it can be drawn conclusions as follows. First, public sentiment towards the incumbent has a positive value, with innovation as a term that has the highest positive sentiment value, while imaging is a term that has the lowest negative sentiment value. On the other side, public sentiment towards the President of the Republic of Indonesia, Joko Widodo, also has positive values, with innovation as a term that has the highest positive sentiment value, while imaging is a term that has the lowest negative sentiment value. Another finding of this study shows that public sentiment towards the government also has a positive value, with appreciation as a term that has the highest positive sentiment value, while hate and lying are terms that have the lowest negative sentiment. Finally, this study concludes that public sentiment towards the ministry also has a positive value, with openness as a term that has the highest positive sentiment value, while stalling is a term that has the lowest negative sentiment value.

However, this study considers several limitations, they are (1) the research method used has not been able to capture the slang-word language. Therefore, further research is needed in natural language processing; and (2) this research does not estimate hoax detection on every tweet used as test data.

## ACKNOWLEDGMENT

This research was supported by PITTA Grant Universitas Indonesia contract number 1862/UN2.R3.1/HKP.05.00/2018

## REFERENCES

- [1] A. Buntoro, "Analisis Sentimen Calon Gubernur DKI Jakarta 2017 Di Twitter", vol. 1, no. 1, pp. 32–41, 2016.
- [2] Statista, "Most popular social media of mobile internet users in Indonesia as of January 2016, by age group [online], available at <https://www.statista.com/statistics/279776/preferred-netizen-social-media-in-indonesia-by-age/>", 2017.
- [3] G. Enli, "Twitter as arena for the authentic outsider: exploring the social media campaigns of Trump and Clinton in the 2016 US presidential election", vol. 32, pp. 50–61, 2017.
- [4] S. Hasbullah, D. Maynard, R. Chik, F. Mohd, and M. Noor, "Automated Content Analysis: A Sentiment Analysis on Malaysian Government Social Media", Proceedings of the 10th International Conference on Ubiquitous Information Management and Communication - IMCOM '16, pp. 1–6, 2016.
- [5] Globe, "Indonesia Fifth-Largest Country in Terms of Twitter Users available at: <http://jakartaglobe.id/news/indonesia-fifth-largest-country-in-terms-of-twitter-users/>", 2017.
- [6] Alamsyah, W. Rahmah, and H. Irawan, "Sentiment analysis based on appraisal theory for marketing intelligence in Indonesia's mobile phone market," J. Theor. Appl. Inf. Technol., vol. 82, no. 2, pp. 335–340, 2015.
- [7] M. Kang, J. Ahn, and K. Lee, "Opinion mining using ensemble text hidden Markov models for text classification," vol. 94, pp. 218–227, 2018.
- [8] S. Yoo, J. Song, and O. Jeong, "Social media contents-based sentiment analysis and prediction system", Expert Systems with Applications, vol. 105, no. 102–111, 2018.
- [9] S. Tartir and I. Abdul-Nabi, "Semantic Sentiment Analysis in Arabic Social Media", Journal of King Saud University – Computer and Information Sciences, vol. 29, no. 229–233, 2017.
- [10] A. Muhammad, N. Wiratunga, and R. Lothian, "Contextual sentiment analysis for social media genres", Knowledge-Based Systems, vol. 108, no. 92–101, 2016.
- [11] Read, D. Hope, and J. Carroll, "Annotating Expressions of Appraisal in English," 2005.
- [12] P. K. Orenek, "Emotion Classification of Microblogs Based on Appraisal Theory," no. i, pp. 13–14, 2012.
- [13] J. Han, M. Kamber, J. Pei, "Data Mining concepts and Techniques", Elsevier: USA, 2012.
- [14] Y. Zhao, "R and Data Mining: Examples and Case Studies," no. December 2012, 2015.
- [15] J. Sanger and R. Feldman, "The Text Mining Handbook: Advanced Approaches in Analyzing Unstructured Data". Cambridge University Press: New York, 2007.
- [16] P. Kotler and K. L. Keller, "Marketing Management". Prentice Hall: New Jersey, 2012.
- [17] Peraturan Menteri Pendayagunaan Aparatur Negara dan Reformasi Publik, "Pedoman Penyusunan Survei Kepuasan Masyarakat Unit Penyelenggara Pelayanan Publik", 2017.

# Robust Principal Component Analysis for Feature Extraction of Fire Detection System

Herminarto Nugroho

Department of Electrical Engineering  
Faculty of Industrial Technology, Universitas Pertamina  
Jakarta, Indonesia  
herminarto.nugroho@universitaspertamina.ac.id

Muhammad Koyimatu

Department of Computer Science  
Faculty of Science and Computing, Universitas Pertamina  
Jakarta, Indonesia  
koyimatu@universitaspertamina.ac.id

Ade Irawan

Department of Computer Science  
Faculty of Science and Computing, Universitas Pertamina  
Jakarta, Indonesia  
adeirawan@universitaspertamina.ac.id

Ariana Yunita

Department of Computer Science  
Faculty of Science and Computing, Universitas Pertamina  
Jakarta, Indonesia  
ariana.yunita@universitaspertamina.ac.id

**Abstract**— Fire detection system with deep learning-based computer vision (DLCV) algorithm is considered in this paper. It uses a Charge Coupled Device (CCD) visible light sensor which can be found in closed circuit television camera (CCTV). The performance of the system depends on the number of trained fire image datasets that might lead to the curse of dimensionality. In this paper, we propose a robust Principal Component Analysis (PCA) to tackle the problem by significantly reducing the dimension of such datasets in feature extraction. It is shown that the proposed algorithm increases interpretability while minimizes information loss.

**Keywords**—principal component analysis, the curse of dimensionality, feature extraction, fire detection system, deep learning.

## I. INTRODUCTION

Oil and gas industry demand high safety standard especially to prevent fire disaster which can naturally or technically happen and unavoidably hurt the industry in both human and environmental safety as well as company profit [1]. Therefore, it needs a robust and accurate fire detection system. Fire detection is commonly performed visually by using ultraviolet (UV) camera [2], infrared (IR) camera [3], or visible light camera (VLC) [4]. UV-based and IR-based fire detections have high sensitivity and fast response, yet prone to disturbance from other UV and IR lights [5] [6]. Hence, this paper focuses on the fire detection system based on the VLC which uses a Charge Coupled Device (CCD) sensor.

CCD sensor records a glimpse of fire in the form of video or static images as the data. Computer vision techniques then pre-process the data prior to data training. The data training exploits Deep Learning algorithm to detect whether or not the flame exists in the captured video or images. The algorithm has been implemented to solve many complex problems [7] [8]. It can increase the accuracy of detection from any kind of fire and smoke in the captured video or images [9]. However, it needs a huge number of datasets in order to obtain high accuracy detection and hence costs computationally expensive. Therefore, it is desirable to extract only the important features of the captured videos or images, such that the dimension of the datasets can be

reduced while the most of the information in the data is still preserved.

Many techniques have been developed for feature extraction, such as auto-encoder [10], Isomap [11], nonlinear dimensionality reduction (NLDR) [12], multifactor dimensionality reduction (MDR) [13], and Principal Component Analysis (PCA) [14]. PCA is widely used in feature extraction because it is simpler compared to other techniques. The idea of PCA is to reduce the dimensionality of a dataset, while preserving as much ‘variability’, i.e. statistical information as possible [14]. In this paper, the implementation of a robust Principal Component Analysis (PCA) is proposed to reduce the dimensionality of the fire videos or images.

The organization of this paper is as follows. The fundamental concept of PCA is introduced in Section II. Section III presents the proposed PCA, which is Robust Principal Component Analysis (RPCA). The implementation results of the proposed PCA for fire feature extraction is shown in Section IV. Finally, the conclusion is given in Section V.

## II. PRINCIPAL COMPONENT ANALYSIS

### A. The Basic Mathematical Concept of Principal Component Analysis

Consider a dataset consists of numerical observation data on  $p$  variables, for each of  $n$  individual observation. These data can be defined as  $p \times n$  –dimensional vectors  $x_1, x_2, \dots, x_p$ , or, equivalently, a matrix as follows:

$$\mathbf{X} \in \mathbb{R}^{n \times p}. \quad (1)$$

PCA seeks a linear combination of the column of matrix  $\mathbf{X}$  in equation (1) with maximum variance. Such linear combinations are given by

$$\tilde{\mathbf{X}} = \sum_{j=1}^p a_j x_j = \mathbf{X}\mathbf{A}, \quad (2)$$

where  $\mathbf{A}$  refers to a constant vector consisting  $a_1, a_2, \dots, a_p$ , and  $j$  refers to the index of the variables.

The variance of the linear combination mentioned in equation (2) is given by

$$\text{var}(\mathbf{X}\mathbf{A}) = \mathbf{A}'\mathbf{S}\mathbf{A}, \quad (3)$$

This research is funded by PT. Pertamina (Persero) via Universitas Pertamina selective research grant (UPSKILLING) 2018 with grant number 002/UP-WR3.1.1/SK/III/2018 date March 20, 2018. All source code and images of this research is available on <https://github.com/herminarto/DLCV>



where  $\mathbf{S}$  defines sample covariance matrix associated with the dataset, and  $\mathbf{A}'$  is the transpose of  $\mathbf{A}$ . The covariance matrix  $\mathbf{S} \in \mathbb{R}^{p \times p}$  is a real symmetric matrix which has exactly  $p$  real eigenvalues, and their corresponding eigenvectors can be defined to form an orthogonal set of vectors.

From equation (3), the linear combination of matrix  $\mathbf{X}$  can be found by obtaining a  $p$  – dimensional vector  $\mathbf{A}$  which maximize the quadratic form  $\mathbf{A}'\mathbf{S}\mathbf{A}$ . Note that, for the sake of the existence of the solution, an additional restriction is introduced, which is requiring  $\mathbf{A}'\mathbf{A} = 1$ . Therefore, the optimization problem can be formulated as

$$\max_{\mathbf{A}} (\mathbf{A}'\mathbf{S}\mathbf{A} - \lambda(\mathbf{A}'\mathbf{A} - 1)), \quad (4)$$

where  $\lambda$  specifies a Lagrange multiplier.

The derivative of the cost function in equation (4) with respect to constant vector  $\mathbf{A}$  is given by

$$\frac{d}{d\mathbf{A}} (\mathbf{A}'\mathbf{S}\mathbf{A} - \lambda(\mathbf{A}'\mathbf{A} - 1)) = \mathbf{S}\mathbf{A} - \lambda\mathbf{A}. \quad (5)$$

Then, the optimization problem in equation (4) can be solved by setting equation (5) to a null vector, which produces the equation as follow:

$$\mathbf{S}\mathbf{A} - \lambda\mathbf{A} = \mathbf{0} \Leftrightarrow \mathbf{S}\mathbf{A} = \lambda\mathbf{A}. \quad (6)$$

Hence, it can be found that the constant vector  $\mathbf{A}$  is a unit-norm eigenvector and  $\lambda$  is the corresponding eigenvalue of the covariance matrix  $\mathbf{S}$ .

Given equation (6), the variance of the linear combination in equation (3) can also be defined as

$$\text{var}(\mathbf{X}\mathbf{A}) = \mathbf{A}'\mathbf{S}\mathbf{A} = \lambda\mathbf{A}'\mathbf{A}. \quad (7)$$

Equation (7) implies that finding the largest eigenvalue  $\lambda_k$  and its corresponding eigenvector  $\mathbf{A}_k$  are of interest if we seek the maximum variance of the linear combination.

The full set of the corresponding eigenvector  $\mathbf{A}_k$  is the solution to the problem of obtaining new linear combinations up to  $p$ , as

$$\tilde{\mathbf{X}} = \mathbf{X}\mathbf{A}_k = \sum_{j=1}^p a_{jk}x_j. \quad (8)$$

It maximizes variance, subject to *uncorrelatedness* with previous linear combinations [14]. The linear combination  $\tilde{\mathbf{X}} = \mathbf{X}\mathbf{A}_k$  refers to the principal components (PCs) of the dataset  $\mathbf{X}$  in this paper.

### B. Principal Component Analysis with Standardized Matrix Datasets

The previous subsection presents a mathematical background to implement PCA to find the linear combination of the original variables in dataset  $\mathbf{X}$ . However, PCA does not work effectively if the variables have different measurement units between them. This due to the fact that the properties of PCA have some undesired features when being implemented on a dataset with different measurement units [14].

To overcome this undesirable feature, the standardized version of dataset matrix is used when implementing PCA. Each data element inside dataset  $\mathbf{X}$ , which is  $x_{ij}$  will be both centered and divided by the standard deviation  $s_j$  of variable

$j$ . The mathematical expression of this standardization process is presented as follow:

$$z_{ij} = \frac{x_{ij} - \bar{x}_j}{s_j}, \quad (9)$$

where  $z_{ij}$  is the element of the standardized version of the initial dataset matrix  $\mathbf{X}$ , which is denoted by  $\mathbf{Z}$ . Standardization is useful because most changes of scale are linear transformations of the data, which share the same set of standardized data values [14].

We know that the covariance matrix of a standardized dataset is actually the correlation matrix of the initial dataset, denoted by  $\mathbf{R}$ . Thus, while the original PCA uses covariance matrix  $\mathbf{S}$ , the standardized version PCA uses correlation matrix  $\mathbf{R}$ .

The principal components (PCs) of the standardized matrix  $\mathbf{Z}$  is defined as

$$\tilde{\mathbf{X}} = \mathbf{Z}\mathbf{A}_k = \sum_{j=1}^p a_{jk}z_j. \quad (10)$$

It is important to note that the PCs of the standardized dataset are not directly related to the PCs of the original dataset in equation (8).

In a correlation matrix PCA, the coefficient of correlation between the  $j$ -th variable and the  $k$ -th PC is given by

$$r_{\text{varj.PC}_k} = \sqrt{\lambda_k} a_{jk}, \quad (11)$$

(see [15] for more detailed derivation) which is requiring the normalization  $\tilde{\mathbf{A}}_k' \tilde{\mathbf{A}}_k = \lambda_k$  instead of  $\mathbf{A}'\mathbf{A} = 1$ , where coefficients of the new loading vectors  $\tilde{\mathbf{A}}_k$  specifies the correlations between each original variable and the  $k$ -th PC.

### III. ROBUST PRINCIPAL COMPONENT ANALYSIS

PCA is very sensitive to outliers in datasets. The existence of many outliers in the dataset can hurt the performance of the PCA. Some research activities have been conducted to develop a robust principal component analysis (RPCA). Since the early work by Huber [16] [17], the development of RPCA have been improving really well.

With the increasing need to work in the fast-growing areas of machine learning and image processing, which deal with huge datasets, generates some new development of the method for a robust principal component analysis. Wright [18] defined RPCA as a decomposition of a matrix  $\mathbf{X} \in \mathbb{R}^{n \times p}$  into a sum of two matrix components:  $\mathbf{L} \in \mathbb{R}^{n \times p}$  and  $\mathbf{S} \in \mathbb{R}^{n \times p}$ , where  $\mathbf{L}$  and  $\mathbf{S}$  specify a low-rank component and a sparse component matrix respectively [14].

The idea of decomposing dataset matrix  $\mathbf{X}$  into a low-rank component matrix  $\mathbf{L}$  and a sparse component matrix  $\mathbf{S}$  is to differentiate a general pattern from a disturbance from the whole dataset. The low-rank matrices are associated with a general pattern of the datasets, e.g. a face in facial recognition, or a background image in video CCTV. The sparse matrices are associated with disturbances of the datasets, e.g. shading or expression in facial recognition and a moving object or person inside a video CCTV.

We seek to find the matrix  $\mathbf{L}$  and  $\mathbf{S}$  which minimize a linear combination of two different norms of the low-rank and sparse components, that is:

$$\min_{L, S} (\|L\|_* + \lambda \|S\|_1), \quad (12)$$

where  $\|L\|_*$  indicates the nuclear form of  $L$ , where  $\|L\|_* = \sum_r \sigma_r(L)$  specifies the sum of the singular values of  $L$ ,  $\lambda \|S\|_1 = \sum_i \sum_j |s_{ij}|$  denotes the  $l_1$ -norm of the sparse matrix  $S$ .

Choosing

$$\lambda = \frac{1}{\sqrt{\max(n, m)}}, \quad (13)$$

for solving the optimization problem in equation (12) effectively works in a general setting while capable to recover the low-rank and sparse components with high probability [19]. Another variation of RPCA using the more complex structure of noise can be found in [20]. A comparative study of PCA and RPCA for video surveillance datasets can also be found in [21].

#### IV. FEATURE EXTRACTION: RESULTS AND ANALYSIS

Unlike face or any landscape background, the nature of fire makes it is hard to extract the feature of fire from an image or video. Fire has many distinctive forms and colors. Sometimes, the fire is covered by smoke which makes it more difficult to extract its features. In this section, we present the result of the feature extraction of a dataset containing 10793 RGB images that mostly contain fire, but has 10% outlier images, i.e. images which do not contain fire. The image resolution is  $480 \times 480$  pixels. Thus, these raw images have initially  $3 \times 230400$  feature points each. It is a relatively large feature dimension compared to a small resolution image. This fact shows the importance of feature reduction to save computation power.

##### A. Feature Extraction from the Fire Images Dataset

Let the dataset containing all 10793 RGB images be a matrix  $X$ . It means that  $X$  has 10793 individual image data, in which each image can be defined as a matrix  $Y_n \in \mathbb{R}^{3 \times 480 \times 480}$ . Each image matrix is then reshaped into a matrix  $Y_n \in \mathbb{R}^{1 \times 691200}$ . Thus, the original dataset is defined by matrix  $X \in \mathbb{R}^{10793 \times 691200}$ .

Fig. 1 shows the feature extracted using PCA for different size of components. The bigger the component size is the more feature points extracted. If the number of components is very small, the feature extracted will lose too many information, as shown in Fig. 1 (a). It can be observed that we cannot distinguish the images which consist of fire or not.

Even though Fig. 1 (b) can extract more feature points than (a), it is still difficult to identify fire from the images. This means that 64 extracted feature points are not enough. The different result can be observed if we extract using 128 components. Thus, it becomes clear to identify fire in the images, as we can see in Fig. 1 (c). The more feature points extracted, the clearer the images become, and hence making it easier to spot the fire.

##### B. Reconstruction Process from the Extracted Features

In order to be able to reconstruct the original images from certain principal components (extracted features), we can simply map it back to the original dimension with the transpose of the constant vector, i.e. vector  $A_k'$ .

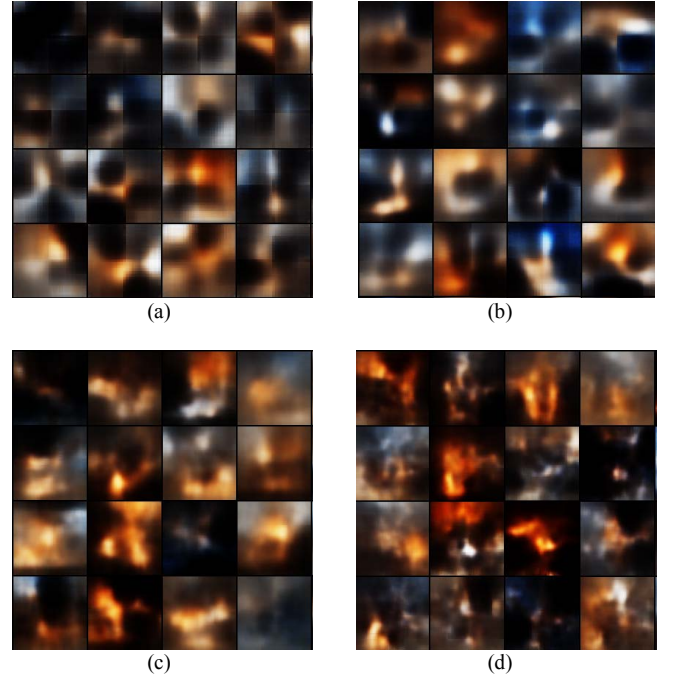


Fig. 1: The resulting feature extracted using Principal Component Analysis with different size of components: (a) 32 components, (b) 64 components, (c) 128 components, and (d) 256 components. The bigger the component size is the more feature points extracted.

Consider the case of PCA with the standardized dataset, in which the extracted feature is given in equation (10), the reconstruction process is then given by

$$\hat{X} = \tilde{X} A_k' = (Z A_k) A_k' + \mu \quad (14)$$

where  $\mu$  is the mean vector required to obtain the final reconstruction of the initial raw datasets.

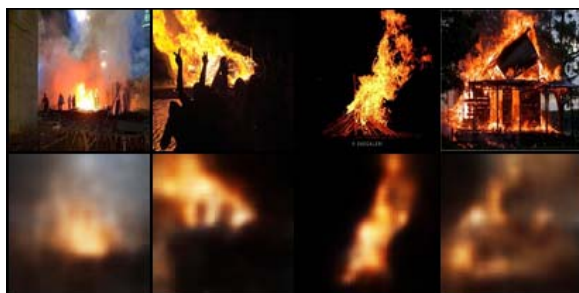
Note that the term  $A_k A_k'$  in equation (14) is the so-called projection matrix of a dataset  $X$ . This means one can project the features extracted using this projection matrix to reconstruct the initial dataset. The perfect reconstruction is obtained when the projection matrix is an identity matrix, i.e. no dimensionality reduction is performed.

Fig. 2 shows the reconstruction result from the features extracted using PCA for two different component size. Both 128 components and 512 components can reasonably be reconstructed. Our goal is to determine the smallest feature points possible without losing too many information from the dataset. By doing so, we can significantly reduce the dimension of the images, yet still get an information-rich dataset. This is very essential in training deep learning.

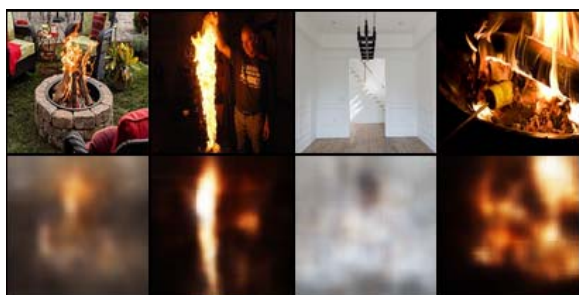
#### V. CONCLUSION

PCA is suitable to extract features from a given fire images dataset. Even though the nature of fire makes hard to extract the feature of fire from an image, PCA can actually extract enough important features. The resulting extracted features then can be reconstructed and still can be distinguished between images which contain fire or not. From this reconstruction images, we can determine the suitable component size of the PCA which results in the smallest feature points without losing too much important information. This suitable component size of the PCA then

can be used to reduce the dataset dimension. For future work, it is interesting to compare PCA to another feature extraction method such as auto-encoder, Isomap, nonlinear dimensionality reduction (NLDR), or multifactor dimensionality reduction (MDR).



(a)



(b)

Fig. 2: Reconstruction result from the extracted features using Principal Component Analysis with different size of components: (a) 128 components, and (b) 512 components.

## REFERENCES

- [1] M. Christou and M. Konstantinidou, "Safety of offshore oil and gas operations: Lessons from past accident analysis.," Publications Office of the European Union, Luxemburg, 2012.
- [2] J. Sun, G. Guo and X. Zhang, "Research on UV Flame Detector," in Instrumentation and Measurement, Computer, Communication and Control (IMCCC), 2014 Fourth International Conference on. IEEE, 2014.
- [3] L. Yang, Z. Guo-Sheng, L. Li-Kun and Z. Chong, "Research on the stability of IUR76-I/IUR76-II test systems for flame detectors and related national standards," in Test and Measurement, 2009. ICTM'09. International Conference on, 2009.
- [4] J. Choi and J. Y. Choi, "Patch-based fire detection with online outlier learning," in Advanced Video and Signal Based Surveillance (AVSS), 2015 12th IEEE International Conference on, 2015.
- [5] G. Monitors, "How to Select a Flame Detector.," 10 July 2018. [Online]. Available: [http://www.gmigasandflame.com/article\\_how\\_to\\_select\\_a\\_flame\\_detector.html](http://www.gmigasandflame.com/article_how_to_select_a_flame_detector.html).
- [6] Spectrex, "Spectrex Flame Detector Range," 10 July 2018. [Online]. Available: <http://www.technoswitch.co.za/wp-content/uploads/2017/01/BR-Spectrex-170130.pdf>.
- [7] X. Wu, X. Lu and H. Leung, "An adaptive threshold deep learning method for fire and smoke detection," in Systems, Man, and Cybernetics (SMC), 2017 IEEE International Conference on, 2017.
- [8] I. T. Jolliffe and J. Cadima, "Principal component analysis: a review and recent developments," *Phil. Trans. R. Soc. A*, vol. 374, no. 2065, 2016.
- [9] K. Ito and K. Kunisch, Lagrange multiplier approach to variational problems and applications, Siam, 2008.
- [10] I. Jolliffe, "Principal component analysis," in International encyclopedia of statistical science, Springer, 2011, pp. 1094--1096.
- [11] P. J. Huber, Robust statistical procedures, Siam, 1996.
- [12] P. J. Huber, "Robust statistics," in International Encyclopedia of Statistical Science, Springer, 2011, pp. 1248--1251.
- [13] J. Wright, A. Ganesh, S. Rao, Y. Peng and Y. Ma, "Robust principal component analysis: Exact recovery of corrupted low-rank matrices via convex optimization," *Advances in neural information processing systems*, pp. 2080--2088, 2009.
- [14] J. Candès, X. Li, Y. Ma and J. Wright, "Robust principal component analysis?," *Journal of the ACM (JACM)*, vol. 58, no. 3, p. 11, 2011.
- [15] Q. Zhao, D. Meng, Z. Xu, W. Zuo and L. Zhang, "Robust principal component analysis with complex noise," *International conference on machine learning*, pp. 55--63, 2014.
- [16] T. Bouwmans and E. H. Zahzah, "Robust PCA via principal component pursuit: A review for a comparative evaluation in video surveillance," *Computer Vision and Image Understanding*, vol. 122, pp. 22--34, 2014.

# Indonesian ID Card Recognition using Convolutional Neural Networks

M Octaviano Pratama, Wira Satyawan, Bagus Fajar, Rusnandi Fikri, Haris Hamzah  
Artificial Intelligence Department  
PT Premier Optima Sattiga  
Jakarta, Indonesia  
{ octav, wrsatya, bagus, rusnandi, haris } @premieroptima.com

**Abstract**— Indonesian ID Card can be used to recognize citizen of Indonesia identity in several requirements like for sales and purchasing recording, admission and other transaction processing systems (TPS). Current TPS system used citizen ID Card by entering the data manually that means time consuming, prone to error and not efficient. In this research, we propose a model of citizen id card detection using state-of-the-art Deep Learning models: Convolutional Neural Networks (CNN). The result, we can obtain possitive accuracy citizen id card recognition using deep learning. We also compare the result of CNN with traditional computer vision techniques.

**Keywords**— Indonesia Citizen Id Card, Deep learning, Convolutional Neural Networks

## I. INTRODUCTION

Indonesian id card is used by various companies with several purposes like for sales and purchasing recording, campus admission system, online booking and other purposes. Almost current input process of id card was done by using manually input from clerk or admin. The lack of this system is not efficient, time consuming and prone to error. There are several techniques involving automatically process of citizen id card recognition like Optical Character Recognition (OCR) [1] to recognize fields value in citizen id card image. Currently the growth of deep learning has become state-of-the-art of various fields like text processing [2], music classification [3] until image recognition [4]. The last aforementioned is used not only to classify or recognize given image but also used to recognize character in image. One of deep learning model that can be used as text recognition in image is Convolutional Neural Networks (CNN) [5]. The performance of CNN to classify or recognize text in image has been proved in various experiments like from Lai [2], The process of recognition character in image starting from extracting text features in images using two layers: Convolutional layers and Sub sampling layer, then it will be forwarded into classification layer: softmax to determine the final class or text in image.

Based on above explanation, this study aim is to create system or model in order to recognize Indonesian citizen id card using one of deep learning technique: Convolutional Neural Networks (CNN). The contributions of this research are: (1) the propose experiments to recognize citizen id card fields like number, name and address using CNN, (2) preprocessing techniques of recognition process, (3) dataset contains alphanumeric character from thousand Indonesian citizen id card. this research is expected can be used by industry to input the fields in Indonesian id card by using automatically input process.

## II. RELATED WORK

TABLE I. RELATED WORK

Ref	Related Work	
	Model	Tasks
[6]	Bileving, RLSA	Indonesian Id Card Detection
[7]	Template Matching	Indonesian Id Card Detection
[5]	Convolutional Neural Networks	Image Recognition
[8]	Histogram	document segmentation using histogram analysis
[9]	Morphological Transformation	Morphological Transformation in Image Procoessing

There are several empirical researches related to image recognition. Most of them used image processing and optical character recognition (OCR) models. Less id card data is required by using OCR and image processing techniques, reversely when using machine learning or deep learning, much data is required in order to be recognized.

## III. METHOD

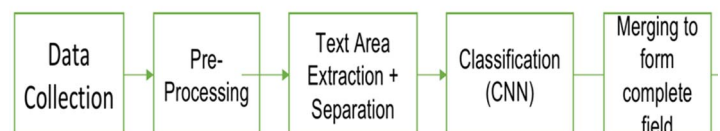


Fig. 1. Workflow of Research

The workflow of method in this research can be seen in figure 1. The process starting from data collection. We collected citizen id card, then thousand citizen id cards are preprocessed using various image processing techniques. After having appropriate pre-processed image, text area in citizen id card is extracted and separate per characters. The next step classification model using Convolutional Neural Networks (CNN) is perfomed to recognize each character in citizen id card. The last step, all of recognized character will be merged to produce complete recognized fields in citizen id card.

For data collection, we collected almost a thousand citizen id card data from various companies. The dataset then pre-processed by using Grayscale techniques to convert RGB layer into grayscale, then thresholding (Eq. 1) is perfomed to convert grayscale image  $G(x,y)$  into binary by selecting appropriate threshold.



$$I(x, y) \begin{cases} 1, & \text{if } G(x, y) > T \\ 0, & \text{otherwise} \end{cases} \quad (1)$$

After having binary image representation of id card, morphological transformation is performed by using dilation, erosion, opening and closing to produce image without noise. The result of pre-processing then forwarded into text area extraction and separation. We used automatically text area separation by forming kernel (the area or box contain character). The kernel is fixed sized move from left to right (Figure 2). We determine the coordinate of fields: id card number, id card name and id card address as follow:

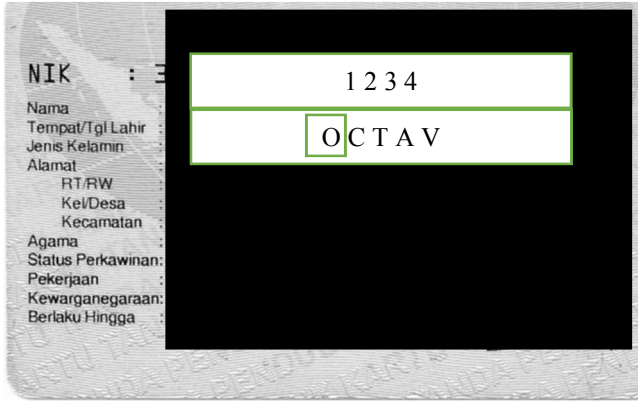


Fig. 2. Citizen Id Card Text Area Extraction and Separation. Box inside name in id card is kernel that move from left to right

When the kernel find character inside of identity card, then it will be crop and save into new file. Let say the name "OCTAV" will be saved into 5 different file JPEG type in the same folder. On the other side, when having name "WIRA" it will be saved into 4 different file JPEG in the same folder but different with the first one. All of the file is scaling into the same size 32 x 32 pixels size. The file is then given a label by annotators in order to be recognized by CNN in the next step. The class label contains 26 label (A – Z) and 10 label (0 – 9) and 1 label whitespace. Total 10.000 character and 10.000 labels  $\{x_i, y_i\}$  is obtained from this process.

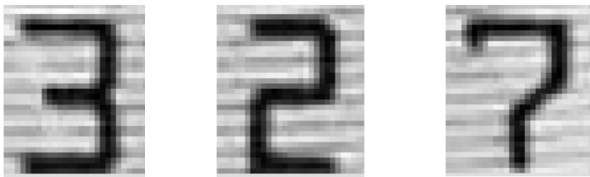


Fig. 3. Image File Containing Number and Character. Left image is annotated with 3, center image is annotated with 2, and the last image is annotated with 7

After obtaining character for each identity card, the data is separated into training data and validation data with weight of separation 70% for training data and remaining for testing data. Training data then forwarded into Convolutional Neural Networks (CNN) architecture (figure. 4) to produce model. The training process using CNN starting from each digits or alphanumeric characters put in input layer, then Convolutional process with 5 x 5 kernels scan through image overlapping from left to right. The result of this process  $S(x, W)$  then put into sub sampling layer which scan by kernels 2 x 2 non-overlapping through image. The result of sub sampling or max pooling  $Z(x, W)$  then put into fully connected layer which

contains Softmax layer the classified into class label prediction.

$$S(x, W) = \sum_{i=1}^n \sum_{j=1}^m x_{ij} W_{(i-m, j-n)} \quad (2)$$

$$Z(S, U) = \sum_{i=1}^n \sum_{j=1}^m S_{ij} U_{(i-m, j-n)} \quad (3)$$

$$\text{Softmax}(z_i) = \frac{\exp(z_i)}{\sum_{i=1}^n \exp(z_i)} \quad (4)$$

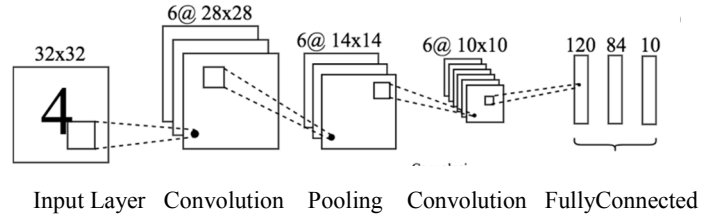


Fig. 4. Convolutional Neural Networks (CNN) architecture which consists of 2 convolutional layers, 2 sub sampling layers and fully connected layer.

The process of training is repetitive until convergence or none of the weight or kernel change. After having appropriate model, measurement evaluation then performed using Precision (Eq. 5), Recall (Eq. 6), and F-Score (Eq. 7). Precision score indicated that item retrieved relevant to query, meanwhile Recall score indicated that item relevant retrieved and F-score is the average of Precision and Recall. After measuring a model, the model can be used to predict unknown or existing id card. The prediction result then combining each other to form the final field recognition of Indonesian citizen id card.

$$\text{Precision} = \frac{|\text{Relevant} \cdot \text{Retrieved}|}{\text{Relevant}} \quad (5)$$

$$\text{Recall} = \frac{|\text{Relevant} \cdot \text{Retrieved}|}{\text{Retrieved}} \quad (6)$$

$$F - \text{Score} = 2 \frac{\text{Precision} \cdot \text{Recall}}{\text{Precision} + \text{Recall}} \quad (7)$$

TABLE II. DESIGN EXPERIMENTS

Model	Feature	Pre-Processing
Convolutional Neural Networks	10.000 Alpha-numeric image	Yes
Convolutional Neural Networks	10.000 Alpha-numeric image	No
Support Vector Machine	Sobel, Gabor Filter	Yes
Support Vector Machine	Sobel, Gabor Filter	No

We used 10.000 alphanumeric character extracted from Indonesian citizen id card with 37 labels (A – Z, 0 – 9, and whitespace). The experiment environment is Python with various libraries like Numpy, Tensorflow, and others. The experiment is tried in GPU computer with CUDA support. Research experiment of this research can be seen in table 2. There are four experiments which involving CNN and SVM models as benchmarking. For CNN model, we used 10.000 alpha numeric image and pre-processing techniques. For benchmarking SVM model, we used 10.000 image extracted using Sobel and Gabor filter features.

#### IV. RESULT AND DISCUSSION

We created 10.000 alphanumeric character dataset derived from Indonesian citizen id card. The dataset is encoded in HDF5 file. The dataset was preprocessed and ready to be used in machine learning or deep learning model. After performing 100 epoch training, we obtained 91% and 90% for training accuracy and validation accuracy using CNN with pre-processing (Figure 5). On the other side we also obtain 64% and 62% for training accuracy and validation accuracy using SVM with pre-processing. Without pre-processing the result of evaluation is below than with pre-processing. The beneficial of Pre-processing to citizen id card image is can remove noise, filter merely appropriate dataset and other.

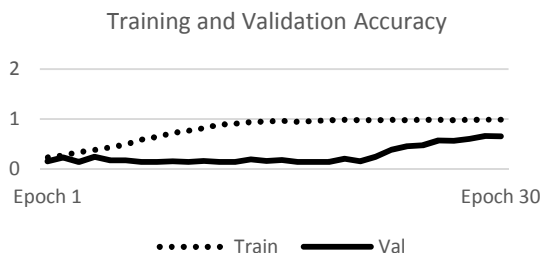


Fig. 5. Training and Validation Accuracy

For measurement evaluation using Precision, Recall and F-score, the complete result can be seen in table 3. CNN result is better than SVM because it consists automatically feature extraction from pre-processed images, reversely in SVM we used manually feature extraction Gabor Feature and Sobel.

TABLE III. MEASUREMENT EVALUATION

Model	Precision	Recall	F-Score	Support
Convolutional Neural Networks	0.84	0.85	0.84	1000
Convolutional Neural Networks (Pre-Processing)	0.89	0.88	0.88	1000
Support Vector Machine	0.62	0.64	0.63	1000
Support Vector Machine (Pre-Processing)	0.71	0.74	0.73	1000

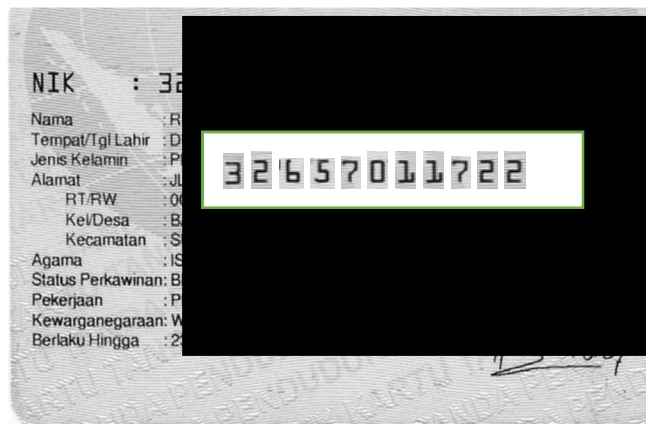


Fig. 6. Recognition result. The field in id card number is recognize one by one using CNN. After obtaining character prediction, then the result is combined to form field result.

We tried to predict complete citizen id card number (16 digits) using CNN. After trying several sampling of

Indonesian citizen id card, from a hundred complete id card, the number of fully correct prediction is 76 meanwhile 24 id card incorrect predicted. The factors affects to incorrectly prediction are: (1) citizen id card is not readable (noise, vanish, or scratch), and (2) citizen id card image is cut off.

TABLE IV. PREDICTION FOR EACH ID CARD

Ground Truth	Prediction	Success
3204090311910003	3204090311910003	Yes
3204092505600001	3204092505600001	Yes
3204091812630002	3204091812630002	Yes
3216037009810006	3216037009810006	Yes

#### V. CONCLUSION

We created dataset of alphanumeric character derived from Indonesian citizen id card which consists of 10.000 images. The dataset was pre-processed using several image processing techniques: Grayscale, binary, morphological transform. the dataset then separated into training, validation and testing which training used for forming a model, validation to validate each epoch training and testing data is used for measurement evaluation. Each result of classification then combining form id card field like name, number or address. After performing 100 epoch training, we obtained 91% testing accuracy. For measurement evaluation, we obtained 0.89, 0.88, and 0.88 using precision, recall and F-score. As benchmarking, we used other model: Support vector machine (SVM). The performance of CNN is better than SVM.

For the future experiments, we plan to use other deep learning model like Recurrent Neural Networks (RNN), Residual Neural Networks (ResNet) [4] or other models. We also to plan augment more and more dataset in order to improve the performance.

#### References

- [1] R. Mithe, S. Indalkar, and N. Divekar, "Optical Character Recognition," *Int. J. Recent Technol. Eng.*, vol. 2, no. 1, pp. 72–75, 2013.
- [2] S. Lai, L. Xu, K. Liu, and J. Zhao, "Recurrent Convolutional Neural Networks for Text Classification," *Twenty-Ninth AAAI Conf. Artif. Intell.*, pp. 2267–2273, 2015.
- [3] M. O. Pratama and M. Adriani, "Music Era Classification using Hierarchical-level Fusion," in *ICACIS 2018*, 2018.
- [4] K. He, X. Zhang, S. Ren, and J. Sun, "Deep Residual Learning for Image Recognition," Dec. 2015.
- [5] A. Krizhevsky, I. Sutskever, and H. Geoffrey E., "ImageNet Classification with Deep Convolutional Neural Networks," *Adv. Neural Inf. Process. Syst.* 25, pp. 1–9, 2012.
- [6] S. Widodo, "Optical Character Recognition for Indonesian Electronic Id-Card Image," pp. 225–232, 2014.
- [7] M. Ryan and N. Hanafiah, "An Examination of



- Character Recognition on ID card using Template Matching Approach,” in *Procedia Computer Science*, 2015, vol. 59, pp. 520–529.
- [8] V. J. Dongre and V. H. Mankar, “DEVNAGARI DOCUMENT SEGMENTATION USING HISTOGRAM APPROACH,” *Int. J. Comput. Sci. Eng. Inf. Technol.*, vol. 1, no. 3, 2011.
- [9] K. Sreedhar and B. Panlal, “ENHANCEMENT OF IMAGES USING MORPHOLOGICAL TRANSFORMATIONS,” *Int. J. Comput. Sci. Inf. Technol.*, vol. 4, no. 1, 2012.

# Sarcasm Detection on Indonesian Twitter Feeds

Dwi A. P. Rahayu

Informatics Department  
University of Muhammadiyah Malang  
Malang, Indonesia  
dwi.ap.rahayu@umm.ac.id

Soveatin Kuntur

Graduate of Informatics Department  
University of Muhammadiyah Malang  
Malang, Indonesia  
kuntursoveatin@gmail.com

Nur Hayatin

Informatics Department  
University of Muhammadiyah Malang  
Malang, Indonesia  
noorhayatin@umm.ac.id

**Abstract.** In social media, some people use positive words to express negative opinion on a topic which is known as sarcasm. The existence of sarcasm becomes special because it is hard to be detected using simple sentiment analysis technique. Research on sarcasm detection in Indonesia is still very limited. Therefore, this research proposes a technique in detecting sarcasm in Indonesian Twitter feeds particularly on several critical issues such as politics, public figure and tourism. Our proposed technique uses two feature extraction methods namely interjection and punctuation. These methods are later used in two different weighting and classification algorithms. The empirical results demonstrate that combination of feature extraction methods, tf-idf, k-Nearest Neighbor yields the best performance in detecting sarcasm.

**Keywords**—social media, negative opinion, sentiment analysis, sarcasm detection, feature extraction

## I. INTRODUCTION

In this modern day, online data grows significantly every minute. Twitter is one of social media which produces millions of data every day. Indonesia ranked as 5<sup>th</sup> biggest country of Twitter users[1]. Thus, Indonesian tweets data is abundant and worth to be analyzed. Twitter limits a message to have a maximum of 280 characters which leads users either be concise or be creative in writing their messages. Most of Indonesian Twitter's users are active and expressive, they can creatively express their tweet on trending topics in that limited number of characters[1]. As part of their creativity, some of them often use sarcasm, i.e. positive words to express negative opinion, in their Twitter message.

Sarcasm or irony has been extensively explored in linguistic and psychology field. Nevertheless, in natural language processing field, detecting sarcasm within a sentence or message is still considered as a big challenge because the lexical features extracted from the sentence do not give enough information to detect sarcasm[2]. The existence of sarcasm can also drop the performance of sentiment analysis techniques[2]. While sarcasm detection is an emerging research field in English natural language processing. There are only very limited researches which focus on sarcasm detection in Indonesian. To the best of our knowledge, there is only one research on Indonesian sarcasm detection using full machine learning algorithm[2]. Therefore, this research aims to fill this gap by proposing a technique in Indonesian sarcasm detection.

This research investigates and detects sarcasm used in Indonesian Twitter feeds on several trending topics in 2018 such as politics, public figure and tourism. Our sarcasm detection technique uses combination of feature extraction method, weighting method and classification algorithm. The writers first use the combination interjection and punctuation,

Bag of Words and Naïve Bayes to detect sarcasm. The combination of interjection and punctuation, tf-idf and k-Nearest Neighbor are employed. We compare these two combinations to get the best technique in detecting sarcasm.

We discuss current techniques used in sarcasm detection in section two, followed by details of our techniques in section three. We then present our experiment data, settings and results in section four, followed by conclusion and future work in section five.

## II. RELATED WORK

Sentiment analysis is a technique to identify people's opinion, emotion towards any situation and attitude. Sentiment analysis is used to determine whether people's opinion or emotion is positive, neutral or negative based on words used in their sentences. Researchers use machine learning to further investigate sarcasm on text data collected from various sources[3][4][5][6].

Some of feature extraction methods used in sarcasm detection on English sentences are punctuation and interjection. Early work on sarcasm detection on Twitter data using punctuation and interjection successfully gained a f-measure score of 0.813[3]. In another work which detects sarcasm in Facebook comment posts, combination of interjection and punctuation with syntactic feature increased the f-measure score into 0.852[4].

Despite many researches have been conducted to detect sarcasm in English, there is only one of a kind on Indonesian. The only machine learning based sarcasm detection on Indonesian social media messages is proposed by Edwin Lunando and Ayu Purwarianti[2]. They used unigram, the number of interjection words, negativity and question word as feature extraction method, then use these features in classifiers such as Naïve Bayes, Maximum Entropy and Support Vector to detect sarcasm. The accuracy of their proposed technique was still very low. This low accuracy was caused by many sarcasm texts in their dataset have no global topic. They also recognized terms using translated SentiWordnet. They translated English SentiWordNet terms into Indonesian using Google Translate which may lead to undetected terms as Indonesian words used in social media are very rich[2].

In this research, we investigate sarcasm detection technique on Indonesian sentences by combining punctuation and interjection feature extraction methods with two different weighting methods and two classification algorithms. Our technique does not involve any translation process to avoid similar problems faced by previous researchers happened[2]. Instead, we use pre-processing and stemming algorithm which are designed for Indonesian. Details of our technique will be further discussed in next section.

### III. PROPOSED TECHNIQUE

Opinions posted in social media can be categorized as positive, negative, and neutral. A positive sentiment can be further classified as actual positive or sarcasm as shown in Fig. 1[2]. Therefore, positive tweets have to be extracted from crawled tweets prior to sarcasm detection process.

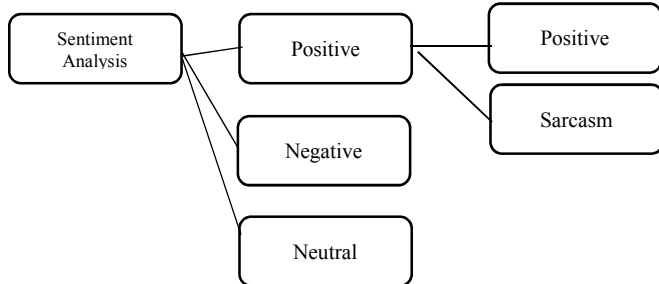


Fig. 1. Levelled method in sentiment analysis [2]

As displayed in Fig. 2, our technique includes two phases. The first phase of our technique preprocesses the tweets and categorizes the sentiment of tweets. This preprocessing technique is very important to extract meaningful words from sentences and discard common words and symbols[7]. In preprocessing, we firstly use a case folding method to make all sentences have a uniform case. We then use a filtering method to remove URLs, mentions, and hashtags within the tweets. We also leverage stemming algorithm on Indonesian, Sastrawi Stemmer, which can be accessed on github[8]. We use this stemmer to remove suffixes and prefixes from words within tweets.

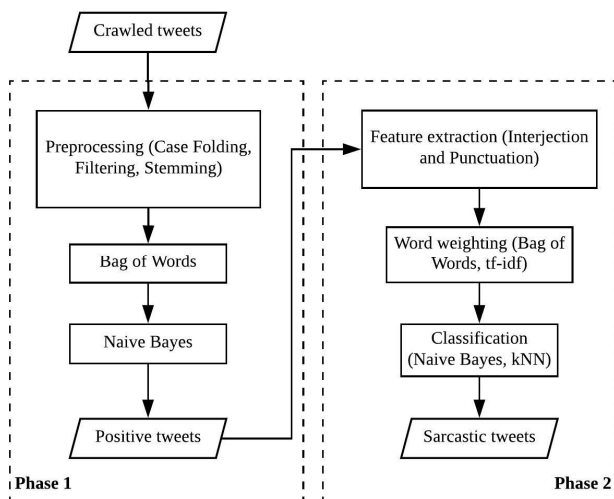


Fig. 2. Sarcasm detection phases

Once all tweets are preprocessed, we use Bag of Words to count the frequency of words and run Naïve Bayes classifier to categorize the tweets as positive, negative and neutral tweets. The positive tweets are then further investigated in the second phase of our technique which detects the sarcasm.

The second phase of our technique combines two feature extraction methods, a word weighting method and a

classification algorithm to extract sarcasm tweets from positive tweets. The feature extraction methods extract any words which indicated sarcasm and any sign that showed emotional suppression. The word weighting method rank preprocessed words based on its importance/frequency within the documents. The classification algorithm categories tweets based on similarity between testing data and training data which contained feature that have implemented.

In this second phase, we use two combinations. These two combinations are summarized in Table I.

TABLE I. SARCASM DETECTION TECHNIQUE COMBINATION

<b>Combination 1</b>	Interjection + Punctuation + Bag of Words + Naïve Bayes classifier
<b>Combination 2</b>	Interjection + Punctuation + tf-idf + Cosine similarity + k-Nearest neighbor

For the first combination, we combine interjection and punctuation in feature extraction process, Bag of Words in word ranking process, and Naïve Bayes in classification process. Interjection extracts any words which indicated to be sarcasm such as “wow”, “anjir”, “anjay”, “njir”. Punctuation extracts any sign indicated emotional suppression such as “!!”, “?!”, “??”. Bag of words weighting method ranks extracted words(features) based on its frequency within the sentence. Naïve Bayes classifies the tweets by calculating the probability of each tweet as sarcasm tweets based on extracted ranked words (features).

We then utilize a different combination in comparison with the first one. This combination also uses interjection and punctuation for feature extraction process. However, instead of using Bag of Words and Naïve Bayes, tf-idf and k-Nearest Neighbor are used instead for word weighting and classification process. Note that tf-idf ranks the words based on its appearance in total documents, whereas k-Nearest Neighbor classifies the tweets by calculating cosine similarity of tweets’ features towards positive and sarcasm tweets in training data set.

### IV. EXPERIMENT

#### A. Dataset and Software

In our experiment we use Indonesian tweets crawled from Twitter. We crawled 2315 tweets on various topics such as public figure, politics, places, and tourism. We crawled tweets which contains trending topics such as “apbd”, “apbn”, “#thepowerofsetnov”, “Jogja Baik Saja”, “Bu Dendy” and “lgbt”. These words are selected based on Indonesian Twitter feed trending topics in 2018.

We divide this data into 1389 training data and 926 testing data. The training data consist of 538 positive tweets, 213 negative tweets, 638 neutral tweets. The positive tweets include 217 sarcasm tweets. In order to develop the ground truth, each tweet is manually labeled as positive, sarcasm, neutral and negative by two linguistic teachers.

These tweets are then preprocessed using case folding, filtering and stemming as discussed in previous section. Table II shows an example of sarcastic tweet and its preprocessed result. The underlined words show the transformation from unprocessed into processed tweets.

We mainly use Python to conduct our study. The first phase of our technique uses Bag of Words method and Naïve Bayes classifier provided in free TextBlob Python library [9]. The second phase of our technique is also implemented in Python. We developed our own code to implement the weighting methods and classifier algorithms.

TABLE II. TWEET PREPROCESSING

Preprocessing Step	Tweet
Initial	"@denradityaa: Gue kalo jadi anak bu dendy pas dimarahin dikasih tiket umroh sampe kiamat kali ya?"
Case folding	"@denradityaa: gue kalo jadi anak bu dendy pas dimarahin dikasih tiket umroh sampe kiamat kali ya?"
Filtering	gue kalo jadi anak bu dendy pas dimarahin dikasih tiket umroh sampe kiamat kali ya
Stemming	gue kalo jadi anak bu dendy pas marah kasih tiket umroh sampe kiamat kali ya

To measure the performance of our technique we use three parameters which are commonly used in information retrieval namely precision, recall and f-measures. Precision shows the fraction of correctly classified tweets out of all retrieved tweets with the reference of ground truth. Recall shows the fraction of correctly classified tweets out of all relevant tweets. f-measure shows harmonic means of precision and recall. These three parameters give better insight of learning performance on internet based phrases than simple accuracy since, commonly, there is a big data imbalance within crawled documents[10].

### B. Experiment Result

The technique performances are measured in three different states. The first measurement is to analyze the performance of first phase of our technique.

TABLE III. SENTIMENT ANALYSIS RESULT

No	Parameter	Score
1	Recall Positive	0.81
2	Recall Negative	0.92
3	Recall Neutral	0.73
4	Precision Positive	0.60
5	Precision Negative	0.87
6	Precision Neutral	0.90
7	f-measure Positive	0.69
8	f-measure Negative	0.89
9	f-measure Neutral	0.81

Table III shows the result of phase 1 of our technique which categorizes crawled tweets into positive, negative, and neutral tweets. Despite high precision of negative and neutral class which is 0.87 and 0.90 respectively, the precision of positive class in this first phase is only 0.60 due to significant number of positive tweets categorized as neutral. The positive recall, negative recall, and neutral recall are 0.81, 0.92, and 0.73, respectively. Those precision and recall scores produces

f-measure of positive, negative and neutral class as 0.69, 0.89 and 0.81 respectively.

These measurement parameter scores show that the combination of Bag of Words and Naïve Bayes is capable to classify each tweet class from the actual tweet class. However, the classification accuracy might be improved further if other word ranking methods is implemented.

We run an experiment on phase 2 of our technique on positive tweets resulted from previous phase. In phase 2, we use two different algorithm combinations as highlighted in Table I to identify tweets which contain sarcasm. Table III shows the combination 1 measurement parameter scores.

TABLE IV. SARCASM DETECTION RESULT – COMBINATION 1

No	Testing	Score
1	Recall Sarcasm	0.92
2	Recall Positive	0.65
3	Precision Sarcasm	0.34
4	Precision Positive	0.97
5	f-measure Sarcasm	0.50
6	f-measure Positive	0.78

As displayed in Table IV, precision of positive class is very high, 0.97. However, the precision of sarcasm class is very low, 0.34. The recall value of positive class and sarcasm class are 0.92 and 0.65 respectively.

These scores show that combination 1 is able to separate sarcasm class from actual sarcastic tweets, however combination 1 is only able to separate very few sarcastic tweets out of all positive tweets. On the other words, there are still many sarcastic tweets which are categorized as positive tweets.

The imbalance of precision and recall of both sarcasm and positive class leads to low f-measure scores. The f-measure score of sarcasm class is 0.50 and the f-measure of positive class is 0.78. These low f-measure scores imply that combination 1 is not able to accurately extract sarcastic tweets. Based on our analysis, Bag of Words might not be a good weighting method for sarcasm detection as it significantly affects the classification result.

The subsequent experiment of phase 2 uses combination 2 to detect sarcastic tweets out of positive tweets. The results of this experiment are shown in Table V. As shown in Table V, precision of positive class is 0.95. It is slightly lower than precision of positive class using combination 1. However, the recall of positive class is 0.82, which is significantly higher than combination 1. The precision and recall of sarcasm class are also better for combination 2. The precision and recall of sarcasm class are 0.74 and 0.92 respectively. These precision and recall scores leads to high f-measure scores. The f-measure score of positive class is 0.88 and the f-measure score of sarcasm class is 0.88. These higher f-measure scores suggest that combination 2 detects sarcastic tweets better than combination 1.

TABLE V. SARCASM DETECTION RESULT – COMBINATION 2

No	Testing	Score
1	Recall Sarcasm	0.92
2	Recall Positive	0.82
3	Precision Sarcasm	0.74
4	Precision Positive	0.95
5	f-measure Sarcasm	0.82
6	f-measure Positive	0.88

The comparison of combination 1 and combination 2 f-measure scores is re-highlighted in Fig 3 to give a better picture of each combination's performance. This comparison shows that the combination tf-idf and k-Nearest Neighbor gives significantly better prediction of sarcastic tweets than the combination of Bag of Words and Naïve Bayes. Combination 2 is 32% more accurate than combination 1 in detecting sarcasm within tweets. The tf-idf methods give smoother rank of words which leads to better features to be selected and used in classification. k-Nearest Neighbor which distinguishes sarcastic tweets based on similar tweets with smallest distance can accurately differentiate sarcastic tweets from positive tweets.

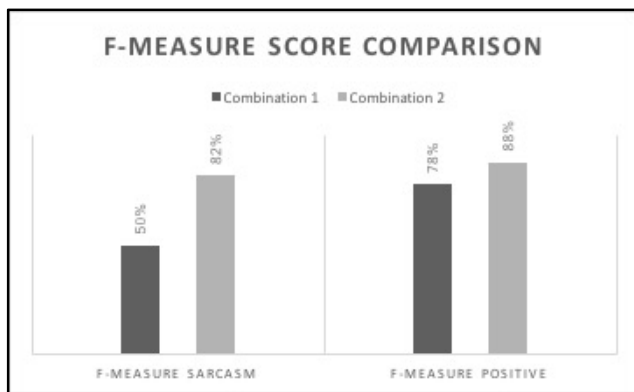


Fig. 3. f-measure of combination 1 and combination 2

Fig. 3 also shows that combination 2 has better f-measure score in detecting positive class than combination 1 even though the difference is not significant. These f-measure scores indicate that combination 2 performs better in both sarcasm and positive tweets detection.

The empirical results shown in this section concludes that the combination of interjection and punctuation, tf-idf and k-Nearest Neighbor is our recommended technique in sarcasm detection on Indonesian Twitter feeds.

## V. CONCLUSION

Sarcasm is very special as it includes words which mean the opposite of what people really want to say. Sarcasm is widely used to mock someone or to be funny. Sarcasm existence within sentiment analysis field becomes important because its appearance influences sentiment analysis accuracy. Sarcasm detection on English messages has been widely researched, however there is very limited research on sarcasm detection in Indonesian. This research proposes a technique which extract positive tweets and further detects sarcastic tweets in Indonesian Twitter feeds.

The first phase of our technique uses Bag of Words and Naïve Bayes to separate positive tweets from crawled tweets of 2018 trending topics. The second phase of our technique analyses two combinations of feature extraction method, word weighting method and classification algorithms performance in detecting sarcastic tweets from previously classified positive tweets.

Empirical results show that combination of Bag of Words and Naïve Bayes that is used in first phase is able to extract positive tweets with f-measure score 0.69. Experiment results on second phase shows that combination of interjection, punctuation, tf-idf and k-Nearest Neighbor can accurately detect sarcastic tweets with f-measure score 0.82. The experiment results also show that this combination outweighs the combination of interjection, punctuation, Bag of Words and Naïve Bayes performance in detecting sarcasm. Thus, our technique is a promising technique to detect sarcasm in Indonesian sentences.

Since sarcasm detection research in Indonesia is currently very limited, there are many open research opportunities in this field. This work in proper can be extended further by combining different word weighting methods and classifiers, as well add more sophisticated feature extraction technique such that more sarcasm is detected.

## REFERENCES

- [1] I. Nurcahyani, "Tiga Karakter Pengguna Twitter di Indonesia," 2015. [Online]. Available: <https://www.antaraneews.com/berita/515549/tiga-karakter-pengguna-twitter-di-indonesia>.
- [2] E. Lunando and A. Purwarianti, "Indonesian social media sentiment analysis with sarcasm detection," *2013 Int. Conf. Adv. Comput. Sci. Inf. Syst. ICACIS 2013*, pp. 195–198, 2013.
- [3] M. Bouazizi and T. Ohtsuki, "Sarcasm detection in twitter: »all your products are incredibly amazing!!!« - are they really?," *2015 IEEE Glob. Commun. Conf. GLOBECOM 2015*, pp. 1–6, 2015.
- [4] M. S. M. Suhaimin, M. H. A. Hijazi, R. Alfred, and F. Coenen, "Natural language processing based features for sarcasm detection: An investigation using bilingual social media texts," *ICIT 2017 - 8th Int. Conf. Inf. Technol. Proc.*, pp. 703–709, 2017.
- [5] M. Hu and B. Liu, "Opinion extraction and summarization on the web," *Aaai*, pp. 1–4, 2006.
- [6] E. Forslid, "Automatic irony- and sarcasm detection in Social media," 2015.
- [7] A. Krouska, C. Troussas, and M. Virvou, "119. The effect of preprocessing techniques on Twitter Sentiment Analysis," *Information, Intell. Syst. Appl. (IISA), 2016 7th Int. Conf.*, pp. 1–5, 2016.
- [8] "Sastrawi stemmer bahasa Indonesia." [Online]. Available: <https://github.com/sastrawi/sastrawi/blob/master/RE-ADME.en.md>.
- [9] S. Loria, "textblob Documentation," 2014.
- [10] G. Hripcsak and A. S. Rothschild, "Agreement, the F-measure, and reliability in information retrieval," *J. Am. Med. Informatics Assoc.*, vol. 12, no. 3, pp. 296–298, 2005.





## Author Index

### A

Abdul Kadir, Evizal  
 Abu Yazid, Mohamad Haider  
 Adnan, Fahrobby  
 Adriansyah, Andi  
 Adyanti, Deasy  
 Afandi, Arif  
 Affriyenni, Yessi  
 Ambarini, Rizky  
 Angkoso, Cucun  
 Anindito, Benediktus  
 Apriani, Ani  
 Arif, Irvan  
 Assegaff, Setiawan  
 Astuti, Dian  
 Azhar, Yufis  
 Azman, Novi

### B

Bintang Dewantoro, Tri  
 Budiman, Edy

### C

Cahyadi, Basri  
 Cahyawijaya, Samuel  
 Canrakerta, Canrakerta

### D

Dewi, Tresna  
 Dharmaraditya, Ni Luh

### E

Effendy, Machmud  
 Elmunsyah, Hakkun

### F

Fahmi, Fitra  
 Fajar, Ahmad  
 Fathan, Gess  
 Fitriyah, Hurriyatul  
 Fitro, Achmad  
 Foeady, Ahmad  
 Frigura-Iliasa, Mihaela

### G

Garcia, Ramon  
 Ghanim, Mustafa  
 Guessous, Mehdi

### H

585 Hadjar, Siti 440  
 100 Hakim, Ermanu 288  
 106 Hamdani, Yuda 266  
 626 Has, Zulfatman 636,642  
 713  
 278 Hasibuan, Muhammad 399  
 653 Hayatin, Nur 54  
 552 Hendrawan, Yusuf 726  
 27 Hetty Primasari, Clara 365  
 249 Humaira, Fitrah 95  
 156 Husain, Ivan 218  
 231 Husniah, Lailatul 60

### I

664 Ikhsani, Ridha 349  
 22 Irwansyah, Irwansyah 690  
 Ismail, Aldi Bayu Kreshnanda 74

### K

16 Kadaryono, Kadaryono 180  
 138,493 Khayam, Umar 303  
 ,499 Khidzir, Nik Zulkarnaen 371  
 11 Kholimi, Ali Sofyan 66  
 743 Kirana, Kartika 738  
 781 Kosasi, Sandy 354  
 Kristiana, Wiwin 574  
 Kusuma, Wahyu 31

### L

Lastomo, Dwi 186  
 Lazarescu, Emil 198

### M

Mahali, Muhammad 129  
 Maidah, Nova 452  
 122 Mardiyah, Nuralif 648  
 471 Marthasari, Gita 540  
 761 Marwanto, Arief 345,590  
 675 Maskur, Maskur 164  
 383 Muftikhali, Qilbaaini Effendi 505  
 719 Mulyo, Budi 707  
 202 Musdholifah, Aina 150

### N

669 Nainggolan, Clarita 429  
 602 Najid, Azmi 696  
 545 Napitupulu, Haposan 175

Nasution, Feldiansyah	35	Setyadinsa, Radinal	517
Nugroho, Herminarto	787	Setyawan, Novendra	765
Nur Amali, Darari	89	Sias, Quota Alief	255
Nur'aidha, Amalia	339	Sidik, Muhammad Abu Bakar	284
		Sinurat, Michael	260
<b>O</b>		Situmorang, Kevin	511
Octavia DP, Yuan	169	Subrata, Arsyad	316
		Sucipto, Sucipto	334
<b>P</b>		Sugianto, Sugianto	596
Pakaya, Ilham	242	Sugihono, Hartawan	144
Palupi, Andarining	557	Sumadi, Fauzi	49
Pinem, Fransiska	116	Suroso, Jarot S	483,488
Prabawati, Andhika	288	Suryanto, Tri	360
Pramono, Subuh	581	Syafii, Syafii	213
Prapitasari, Luh Putu Ayu	679	Syaifuddin, Syaifuddin	565
Prasetya, Didik	85		
Prasetyo, Beny	477	<b>T</b>	
Pratama, M. Octaviano	791	Tjahjadi, Martinus	658
Prilianti, Kestrilia	749	Tripetch, Kittipong	326
Priyandoko, Gigih	618,622		
Pulungan, Ali Basrah	631	<b>U</b>	
Purnama, Hendril	312	Ulinnuha, Nurissaidah	377
Puspitarini, Wita	424		
Putra, Januar Adi	770	<b>W</b>	
Putra, Jimmy	272	Wahono, Tri	316
		Wahyuni, Elyza	755
<b>R</b>		Wahyuni, Evi	160
Raharjana, Indra	408,413	Wardani, Dewi	446,458
	435	Wibowo, Hardianto	134
Rahayu, Dwi	795	Wibowo, Satrio	110
Rahmat, Mohd	1	Wicaksono, Nanda Avianto	236
Rakhmawati, Lusia	702	Wijaya, Adi	732
Ravichandran, Naresh Kumar	7	Wilie, Bryan	776
Riadi, Imam	43		
		<b>Y</b>	
<b>S</b>		Yew, Hoe Tung	561
Sakti Pramukantoro, Eko	70	Yudha, Hendra	612
Sandy Ade Putra, Leonardus	685	Yusron, Muhammad Aldi	464
Sensuse, Dana	522,528	Yusuf, Abdul	292
	534		
Setiawan, Erwin B.	80		
Setiawan, Yudi	419		



# **EECSI 2018 CONFERENCE**

---

Malang, Indonesia

*<http://eecs.org/2018>*